12
1
56
Vol. 63

SAE TRANSACTIONS

Society of Automotive Engineers, Inc.
29 West 39th Street New York 18, New York

C. G. A. Rosen
President

John A. C. Warner
Secretary and General Manager

B. B. Bachman
Treasurer

Norman G. Shidle
Editor

E. D. Allen
Managing Editor

All articles appearing in SAE Transactions are indexed in "Engineering Index."

Copyright 1955, Society of Automotive Engineers, Inc.

Price: $3 to members, $7 to public and college libraries and U. S. Government Agencies, $10 to nonmembers. Foreign: $3 to members, $8 to public and college libraries, $11 to nonmembers.

Photolithographed reproductions can be had of any article published in SAE Transactions. Prices, on quantities of 100 copies or more, varying with number of pages and illustrations, can be obtained upon request from SAE Special Publications Department, 29 West 39th Street, New York 18, N. Y.

SCIENCE - TECHNOLOGY
INFORMATION SERVICE CENTER
LOCKHEED AIRCRAFT CORPORATION
GEORGIA DIVISION

CONTENTS—VOL. 63, 1955

Page

Design, Evaluation, and Selection of Heavy-Duty Rear Axles – K. W. GORDON 5

Simulated Jet Transport Operation – R. D. KELLY and H. B. KASTER 36

Buick's Twin Turbine Dynaflow Transmission – R. J. GORSKY 42

Practical Yardsticks for Deposit Effects – C. A. HALL, J. A. WARREN, and J. D. McCULLOUGH 53

A Cradle for New Power – Chassis Features of the Firebird – ROBERT SCHILLING 63

Pinwheels or Piston? – A Progress Report on Automotive Gas Turbines – W. A. TURUNEN 72

Progress of Torque Converters – E. W. ZINGSHEIM and M. M. SCHALL 84

Coordination of Electric with Other Braking Systems – F. C. HILE 98

Napier Nomad Aircraft Diesel Engine – HERBERT SAMMONS and ERNEST CHATTERTON 107

Designing New Performance into a Special Motor Oil – L. RAYMOND and J. F. SOCOLOFSKY 132

Who Is the Designer – The Stylist or the Engineer? – DUNCAN McRAE and KENNETH E. COPPOCK 145

Size, Structure, and Shape of European Automobiles – LAURENCE POMEROY 159

ABC's of Ultrasonic Inspection – EDWARD F. WELLER, JR. 177

Wear, Scuffing, and Spalling in Passenger-Car Engines – H. A. AMBROSE and J. E. TAYLOR 192

Influence of Lubricant and Material Variables on Cam and Tappet Surface Distress – T. W. HAVELY, C. A. PHALEN, and D. G. BUNNELL 204

Lifters and Lubricants – JOSEPH B. BIDWELL and PAUL VERMAIRE 211

Application of Airborne Radar to Airline Operations – EDGAR A. POST 227

When Are Brakes "Adequate"? – J. G. OETZEL 242

Some Concepts of Knock and Antiknock Action – B. M. STURGIS 253

Basic Facts about Noise as Related to Aviation – ADONE C. PIETRASANTA and RICHARD H. BOLT 265

Why Do Airplanes Make Noise? – ARTHUR A. REGIER 275

Acoustic Design and Performance of Turbojet Test Facilities – R. O. FEHR and B. E. CROCKER 284

Aircraft Noise Problem in Airport Vicinities – C. E. ROSENDAHL 289

Control of Propeller Noise in Turboprop Installations – JOERN SCHMEY and RALPH M. GUERKE 295

An Airplane Manufacturer's Progress with Noise Suppression Devices – ROBERT E. L. FOGLE and HOLDEN W. WITHINGTON 303

Jet Noise – JOHN M. TYLER and EDWARD C. PERRY 308

Designing Adjustable-Speed V-Belt Drives for Farm Implements – WILLIAM SPENCER WORLEY 321

Improvement in Stopping Ability of Trucks in Use on the Highway – F. WILLIAM PETRING 334

The New Look in Lubricating Oils – J. B. BIDWELL and R. K. WILLIAMS 349

Some Factors Affecting the Fatigue Strength of Steel Members – C. W. GADD, J. O. ANDERSON, and DAVID MARTIN 362

Weighing Vehicles Static and in Motion by Electronic Scales – O. K. NORMANN 373

Reverse Thrust for Jet Transports – JOSEPH SUTTER 379

Comparison of Intermediate-Combustion Products Formed in Engine with and without Ignition – WILLIAM C. DAVIS, MARION L. SMITH, EARL W. MALMBERG and JANE ANN BOBBITT 386

The New Chevrolet V-8 Engine – R. F. SANDERS 400

Page

Tractor-Engine Design Requirements for Best Fuel Utilization – H. T. MUELLER and R. E. GISH 420

Structural Design of High-Speed Propellers – F. B. STULEN 429

Carburetor Icing Tendencies of Some Present-Day Fuels and Engines – W. P. DUGAN and H. A. TOULMIN... 442

Tractor Seat Suspensions for Easy Riding – MAX HAACK 452

Flight Load Measurements and Analysis – W. L. HOWLAND and C. J. BUZZETTI 471

Correlation of Engine Noises with Combustion Phenomena – ROBERT MEAGHER, R. L. JOHNSON, and K. G. PARTHEMORE 481

Manufacture of Blades, Buckets, and Vanes for Turbine Engines – A. T. COLWELL 492

Wear Rates of Gears by the Radioactive Method – F. L. SCHWARTZ and R. H. EATON 506

Engine Cranking at Arctic Temperatures – W. E. MEYER, J. J. DeCAROLIS, and R. L. STANLEY 515

Effects of Operational Factors on Structural Fatigue in Fighter Aircraft – GEORGE N. MANGURIAN and PHILIP D. BROOKS 531

New Pontiac V-8 Engine – C. B. LEACH and E. L. WINDELER 545

Temperature Limitations of Petroleum, Synthetic, and Other Lubricants in Rolling-Contact Bearings – ZOLTON N. NEMETH and WILLIAM J. ANDERSON 556

Distribution and Effects of Automotive Exhaust Gases in Los Angeles – GORDON P. LARSON, JOHN C. CHIPMAN, and ERWIN K. KAUPER 567

Automobile Exhaust and Ozone Formation – A. J. HAAGEN-SMIT and MARGARET M. FOX 575

An Inventory of Automobile Gases – DALE H. HUTCHISON and FRANCIS R. HOLDEN 581

Air Pollution Foundation – What It Is and What It Does – W. L. FAITH 587

Some Effects of Engine-Fuel Variables on Exhaust-Gas Hydrocarbon Content – F. G. ROUNDS, P. A. BENNETT, and G. J. NEBEL 591

Flame Photographs of Light-Load Combustion Point the Way To Reduction of Hydrocarbons in Exhaust Gas – J. T. WENTWORTH and W. A. DANIEL 602

Some Early Reminiscences – SIR HARRY RICARDO 620

Control of Residual Stress in Practice – GEORGE SACHS 628

Fuel Properties and Jet-Engine Combustor Performance – C. M. KUHBACH, W. F. RITCHESKE, and K. H. STRAUSS 642

Reserve Tractive Ability and Vehicle Drag Test Codes and Comparative Demonstration of Test Equipment – Report of CIMTC Subcommittee XII – Tractor Test Codes 651

High Supercharging Development of a GM 16-278A 2-Stroke-Cycle Diesel Engine – WARREN G. PAYNE and WOLFGANG S. LANG 676

Effect of Surface Temperature on Wear of Diesel-Engine Cylinders and Piston Rings – H. V. NUTT, E. W. LANDEN, and J. A. EDGAR 694

Development of a New Gas Turbine Super Alloy GMR-235 – D. K. HANINK, F. J. WEBBERE, and A. L. BOEGEHOLD 704

Abrasive Wear of Piston Rings – C. E. WATSON, F. J. HANLY, and R. W. BURCHELL 717

Antiknock Requirements of Passenger Cars – 1953 CRC Survey – H. W. BEST, H. A. BIGLEY, and R. K. WILLIAMS 729

Method of Scavenging Analysis for 2-Stroke-Cycle Diesel Cylinders – W. H. PERCIVAL 737

Symposium – Plastics for Truck Bodies – HIRAM McCANN, DAVID S. BROWN, HENRY JENNINGS, WALTER R. HERFURTH, and STANLEY S. WULC 752

Control of Low-Temperature Sludge in Passenger-Car Engines – R. L. WILLIS and E. C. BALLARD 777

Tire Thump: Its Mechanism and Measurement – DAVID C. APPS and GEORGE M. VANATOR 787

Developments in Explosion- and Fire-Suppression Techniques – GEORGE GRABOWSKI 803

Index 809

Design, Evaluation, and Selection Of

Heavy-Duty Rear Axles

K. W. Gordon, Truck Division, Dodge Bros. Corp., Chrysler Corp.

This paper was presented at a meeting of the SAE Detroit Section, Detroit, Mich., Nov. 1, 1954.

TRUCK rear axles move the loads of a dynamic civilization. This statement in itself may not be very startling, but think – practically every substance and product used today is transported at least part way by truck. Food, clothing, furniture, industrial supplies, and building materials are all sooner or later loaded aboard trucks. And trucks, of course, are driven through rear axles.

Wheels were not always mounted on axles. When man made his first carts, centuries ago, he merely fastened them to the sides of a rough box. Later, as he learned to train animals and put them ahead of the cart instead of himself, he found that a shaft, or axle, connecting the wheels was desirable to help support the heavier loads that then became possible. When buggies and wagons came into use, leaf-spring suspensions were added to smooth out the bumps. With the introduction of engines, the axle took on an added job: to transmit and divide power. Then, of course, improved brakes were required, especially as speeds increased. Now, as engine power continues upward, the role of the heavy-duty truck axle takes on more and more importance.

The tremendous growth of the trucking industry during the past 50 years can be seen in the total United States truck registration figures: 700 in 1904 compared with approximately 10,000,000 in 1954. It is also rather impressive to note that truck drivers represent 8% of the total American labor force, and that trucks carry nearly 80% of the total tonnage hauled in the United States. With regard to heavy-duty trucks (above 2½-ton classification), annual sales have nearly tripled in less than 10 years.

It may be helpful here as a starting point to describe some of the more common uses of these heavy-duty trucks. Trucks engaged in tractor service, typified by the familiar highway freighters, may be called on to do anything from hauling steel over the Pennsylvania hills to speeding perishables over the midwest flatlands. Tank truck duty, in which bulk liquids such as gasoline, fuel oil, or even milk are handled, is another familiar service in the heavy class. Trucks used in the construction industries for transporting earth, gravel, concrete, and other materials constitute a large proportion of heavy-duty operations. Service here may involve

HEAVY-DUTY rear axles are analyzed in this paper – the first L. Ray Buckendale Lecture to be delivered.

The author presents a practical method of evaluating heavy-duty rear axles, with emphasis on performance and axle ratio.

The major part of the paper is devoted to a discussion of the four functions of rear axles, as follows: (1) To carry the load, (2) to transmit driving torque, (3) to allow differential action, and (4) to help stop the vehicle.

The Author

K. W. GORDON (M '52) is project engineer for the Chrysler Corp. Mr. Gordon received a B.S. degree from Western Michigan College in 1943. After graduation he became a junior chemist with the Great Lakes Steel Corp. Mr. Gordon was with the U. S. Air Force as an instructor in radar electronics, and with the Wilson Foundry & Machine Co.

local or long-distance hauls, frequently consisting of one-way payloads and empty return trips. Vehicles for this type of service must not only travel on the highways at a reasonable speed, but often must also be able to negotiate the temporary roads of a construction project, or the steep exit of a gravel pit. In addition to these, there are many other special types such as logging vehicles, mobile cranes and shovels, and special equipment trucks for oil field operations and public utilities.

The axles of all of these vehicles have two major functions in common: to carry the load and to transmit torque. It is not surprising, then, to find that there are certain basic similarities in design and construction, which, in part, are brought about by state laws imposing limitations on allowable axle loading. For 2-axle units (vehicles with front and single rear axles), a practical top gross weight of about 24,000 lb is common when the legal rear-axle load is 18,000 lb. For long life, severe service, or for special purposes, higher-capacity rear axles are available. At the present time, three axles is the largest number commonly used on any power unit, and the practical gross vehicle weight limit is about 40,000 lb within the most common legal limit of 32,000 lb for a tandem axle (two rear axles). The size of the axle alone is impressive: a single rear-axle assembly, complete with tires, wheels, and brakes suitable for an 18,000-lb axle load, weighs a ton – roughly one-third of the total weight of the truck chassis and cab, or two-thirds the weight of an average sized automobile.

It is quite obvious that the selection of a heavy-duty axle requires a discriminating evaluation of the various types and makes available, based on a sound analysis of both present practice and past experience using all of the analytical tools of the designer. It, therefore, seems appropriate that this initial Buckendale Lecture add to the general fund of information by formulating and organizing a practical method of evaluation and selection, by summarizing current design practices, and by describing the many features and functions of axles.

Evaluation and Selection

Evaluation is a process of comparison. An engineer may be called on to evaluate an entirely new axle, to appraise an existing design in a new or different application, or to select the most practical of several different types or makes for a specific purpose. In the last two cases, he would probably review service and sales records to get an indication of operating costs, reliability, adaptability to various types of operation, and popularity with the customer. For all three, his analysis may include an elaborate stress comparison employing specialized mathematics or it may consist of no more than a diagrammatic space layout or perhaps a tabulation of available axle ratios. In many cases, there may be no other course than to test the device, either in the laboratory where accurate control can show up small differences, or in road tests under actual operating conditions.

The analytical treatment of axle components is one of the most desirable and economical methods of evaluation. A simple approach is to tabulate for each unit, major features such as strength, construction, materials, durability, unsprung weight, space requirements, lubrication, maintenance provisions, gear ratios, accessories, type of reduction, type of gearing, nominal load capacity, torque capacity, ring-gear and pinion set, differential, axle shafts, bearings, brakes, tires, wheels, and, of course, costs if available.

Unfortunately, many unpredictable variables exist in axle design that cannot be evaluated with certainty except by direct test. Typical examples can be found in the evaluation of metallurgical refinements and the even less tangible effects of changes in lubricants. The advantages of laboratory tests here include precise control, detection of small differences in results, and the economy of accelerated types of tests. The chief disadvantage, especially where large, heavy-duty axles are concerned, is that very extensive equipment and instrumentation are required. As might be expected, complete axle test facilities are normally limited to the axle specialists.

Road and field tests allow relatively fast correlation of laboratory test results, and are valuable for confirming or rejecting new theoretical design criteria before involving the laboratory in full-scale tests. Once their relationship to actual operating conditions has been established, these criteria can be applied to new designs, which can then be rapidly evaluated in the laboratory. Also invaluable to any type of appraisal are service and sales records accumulated within the industry, which can be extremely useful in the selection of commercially feasible capacities and axle ratios.

In the evaluation or selection of axles, two factors are usually emphasized: performance and axle ratio. These will now be discussed.

Performance Indexes – In an abstract way, the performance potential of a vehicle is defined when the horsepower and total load are known. However, it is the rear axle which translates this into actual miles per hour and ability to accelerate. Throughout the years several indexes of performance have been established. Fundamentally they are all an expression of Newton's second law of motion: $F = MA$. The net force is the difference between the tractive and the retarding forces; mass, of course, is proportional to the total weight of the vehicle; acceleration potential may be expressed as gradeability, activity horsepower, or some other suitable parameter.

Gross vehicle weight (gvw) numerically approaches (but should not exceed) the sum of the front- and rear-axle capacities of the power unit or prime mover. It also equals the empty weight of the power unit plus the allowable payload. *Gross*

combination weight (gcw) is the total weight of the power unit and loaded trailers. At the present time, gcw values recommended by truck manufacturers are approximately twice the gvw of the tractor as a single unit. Both gross vehicle weight and gross combination weight are convertible into mass units and hence become fundamental factors in all performance calculations.

Pounds per horsepower is an easily determined performance index which reflects potential rather than absolute ability. Experience has shown that vehicles whose pounds-per-horsepower ratios are greater than 500 have too high a gcw for their power, and restrict the flow of traffic. Present-day vehicles seldom exceed a maximum of about 400 lb per hp.

Engine displacement per ton-mile is a similar but more abstract factor bearing a closer relationship to vehicle fuel consumption.

Maximum gradeability is another performance parameter which has become well established. It permits direct translation of engine output, load, and gear ratio into an easily understandable dimension – per cent slope or vertical rise per 100 ft. It is, further, a specific application of the factor of pounds per horsepower, and numerically approximates the maximum tractive effort or propelling force at the road-tire contact per 100 lb of gcw.

Maximum road speed is important to both the operator and the designer. The operator considers it nearly as important as load capacity because the product of these two factors is rate of transportation – payload-miles per hour. Since the designer's purpose is to fill the needs of the operator, he is definitely interested in maximum speed and its influence on axle ratio selection.

Axle Ratio Selection – Now that several of the established performance indexes have been reviewed, it may be well to clarify some of the factors in the selection of axle ratios. One of the first requirements is a method of estimating the speed potential of the given vehicle and engine combination. This involves a balance of the vehicle resistance horsepower requirements with the horsepower available from the powerplant. In 1950 Stamm and Lamb presented a paper on the SAE performance prediction procedure,[1] which reduced the equation of vehicle power and resistances to a foundation which is sound both in theory and practice. Up to now, the application of this SAE procedure has involved a series of tedious cut-and-try operations, but refinements have been developed and will be outlined below.

The derivation of the simplified method can be covered briefly by stating that at maximum speed the sum of the resistance horsepowers – air resistance, chassis friction, rolling resistance and, if pertinent, gradeability horsepower – equals the vehicle output horsepower. Since formulas for each of the resistances are suggested by the SAE, construction of a simple graph expressing the equality just given is possible for any selected value of grade. Such a graph is shown in Fig. 1, developed for level road operation. Similar charts can be drawn for any required grade. With them, all that need be known to arrive at an approximation of the maximum potential vehicle speed are the frontal area, gross weight, and net engine horsepower (minus friction horsepower). It then becomes simple enough to select an axle ratio which permits the engine to develop the design output at the anticipated road speed.

Consider a tractor-trailer combination grossing 45,000 lb with a frontal area of 90 sq ft and an engine developing 150 net hp at 3400 rpm. Deducting 10% for chassis friction, approximately 135 hp is left available at the rear wheels. On the vertical (ordinate) scale of Fig. 1, locate 1.5 (135 hp divided by 90 sq ft frontal area). Travel horizontally on the 1.5 line to the 500 line in the family of curves (45,000 gcw divided by 90 sq ft frontal area). Reading down from this point to the horizontal (abscissa) scale, we find a maximum level road speed of 56 mph expected from the truck.

Since we know that the engine speed at maximum power is 3400 rpm, and if we assume a tire size of 10.00/20-12 (which has 500 revolutions per mile or (500) (56)/60 rpm at 56 mph), the axle ratio which will permit the engine to develop the design output at maximum potential road speed is easily fixed. Dividing the desired engine speed by

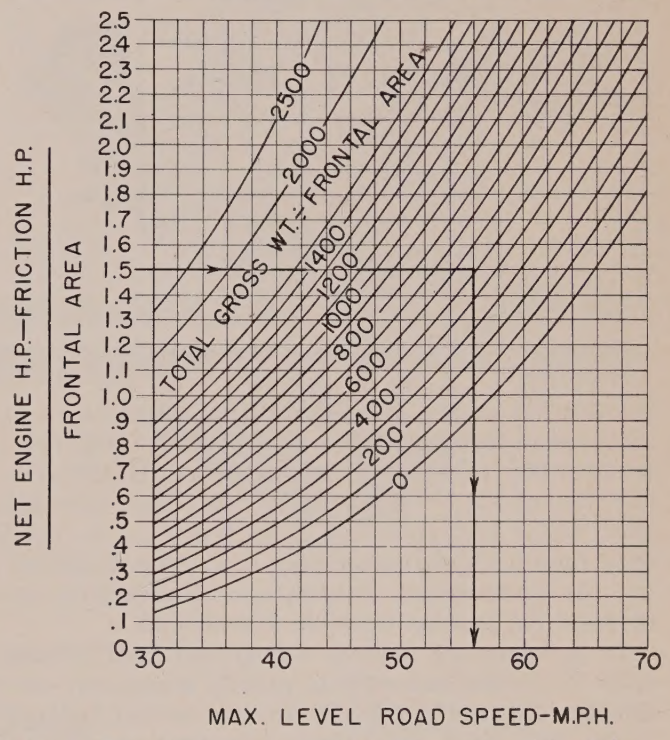

Fig. 1 – Estimating maximum road speed for commercial vehicles (0% grade)

[1] See SAE *Quarterly* Transactions, Vol. 4, April, 1950, pp. 147-157 + (disc) 158-160: "Predicting Road Performance of Commercial Vehicles," by A. F. Stamm and E. P. Lamb.

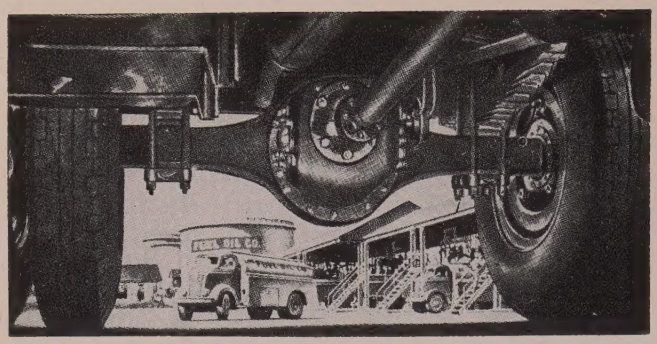

Fig. 2 – Axle viewed from under a loaded truck (Timken-Detroit Axle)

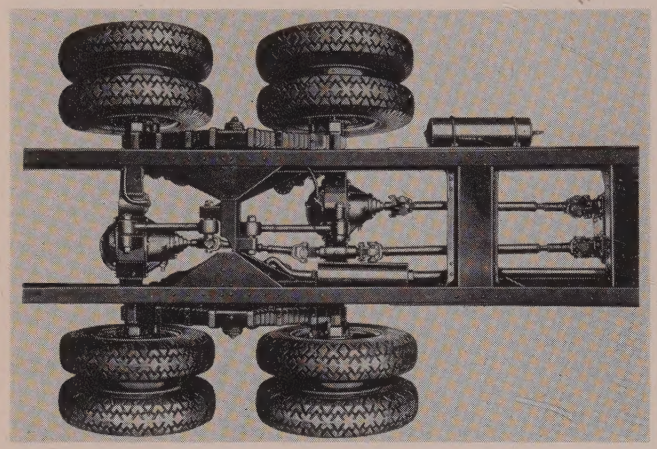

Fig. 3 – Typical tandem axle assembly (TDA)

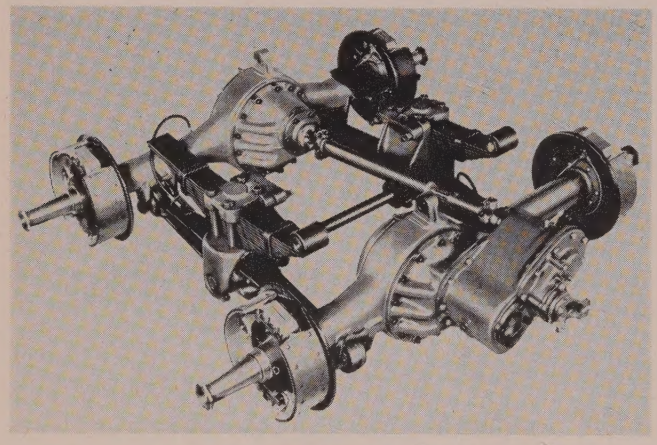

Fig. 4 – Tandem axle design (Eaton)

the desired axle speed, we find that the axle ratio required in this instance is (3400) (60) / (500) (56) or 7.3. The closest commercially available ratio, say, 7.4, would normally be chosen. Thus, the axle ratio which best suits any given truck can be fixed once the major characteristics of the truck, including the horsepower, weight, and gradeability requirements, assume tangible dimensions.

It is becoming widely recognized that trucks must be geared not only to satisfy maximum conditions, but also to reach an economical balance under light-load, level-road operating conditions. An answer is found in the increasing popularity of the 2-speed axle. The two ratios are often selected so as to straddle the optimum single-speed ratio. For example, a 2-speed axle of 6.63/8.51 might be chosen instead of the aforementioned 7.4 single ratio. The slower 8.51 ratio would give increased accelerating ability for heavy hauling, while the fast 6.63 ratio would permit higher road speeds for light operation. Selection of the proper spread between the two ratios is governed, on the one hand, by the diversity of operation, and on the other hand by the available transmission ratios so as to provide the best possible series of gear splits for maximum ease of control. By "gear splitting" is meant the obtaining of two overall gear ratios from each transmission ratio through the use of the 2-speed rear axle; the ideal condition of gear splitting would be an evenly stepped, geometric progression from the highest overall ratio to the lowest. Since present truck transmission ratios approach a geometric progression of about 1.6, a narrow axle ratio spread of 1.3 (as in the example of 6.63/8.51) would achieve excellent gear splitting. From another point of view, a wide spread of 1.5 (such as 6.63/9.92) would yield high tractive potential for heavy hauling but quite ineffective gear splitting. A compromise, which achieves part of each advantage but utilizes neither fully, would be a medium spread of 1.4 (such as 6.63/9.18). Incidentally, a wider spread approximating 2.0 is conceivable and not without merit.

Higher-speed engines, now becoming popular, are bringing new problems to the chassis designer. In direct drive, of course, the axle ratio is the only reduction between the engine and the tires. Inasmuch as maximum road speed and tire size seem to be restricted for the foreseeable future to their present values, the axle ratio presumably will have to increase proportionately with the engine speed. However, in recent years, engine speed increases have already moved the required axle reduction nearly beyond the 7.8 allowed by single-reduction gearing. Double-reduction or 2-speed axles allow somewhat greater reduction but involve cost and space considerations. Somewhat greater reduction with hypoid gearing may be possible by decreasing the maximum transmission ratio, allowing finer-pitched teeth in the ring-gear set.

The advent of these higher-speed engines presents an interesting challenge. With a crankshaft speed of only 4000 rpm, which is scarcely beyond the present range, the selection of a suitable combination of driving ratios in the axle and transmission becomes a difficult compromise for the present drive line arrangement. However, by introducing a reduction gear ahead of the transmission, thereby slowing down the drive line, the drive line problems of the clutch, transmission, and propeller shaft, as well as the rear axle, would remain about as they are today. Capacity would increase only as operators insist upon greater performance – meaning more horsepower. It appears to be a logical predic-

tion that reciprocating engines for heavy-duty trucks which operate at over 5000 rpm will need reduction boxes or underdrive transmissions.

An ideal drive train would automatically match the power source to the load. The propelling force would be instantly adjusted to the best compromise between acceleration and load requirements and the power available. Economy of operation must not be overlooked, either, however. Except in the service of the nation for defense or to protect life and property, trucks – especially of the size of primary concern in this paper – operate to return a fair yield. Economy is thus a matter of greatest concern to the investors.

In economic aspects, ratio selection can be summarized in an expression involving ton-mile-hours per gallon of fuel consumed. Whatever increases the ton-miles or decreases trip time for the same fuel consumed will lower the cost of operation. Increased speed may even compensate for higher fuel consumption. In other words, ratio selections must be justified by providing a maximum in moving material at a minimum overall cost. Truck design engineers must select axles which, rather than accentuating any single factor, achieve the optimum balance of performance, economy, durability, and versatility.

Design Practices

Before going further into the individual features and functions of axles, it may help to stop and take a look at some of the various designs in current use.

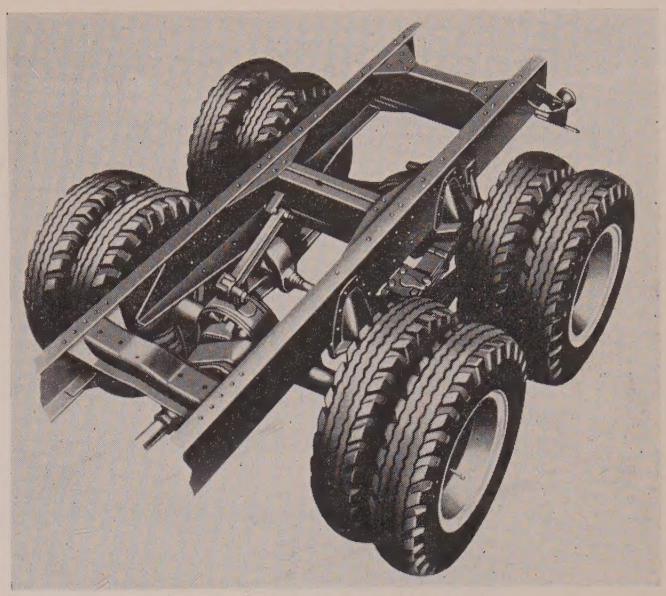

Fig. 5 – Tandem axle assembly (Eaton)

Fig. 2 shows a single rear axle viewed from below a loaded truck. The propeller shaft bringing the engine power into the rear axle and the leaf springs cushioning the load can also be seen.

Fig. 3 is a top view of a truck chassis equipped with a tandem axle. The relationship between the drive line, frame, springs, and tires is clearly shown. With this type of tandem axle, a torque divider is employed to split the power between two propeller

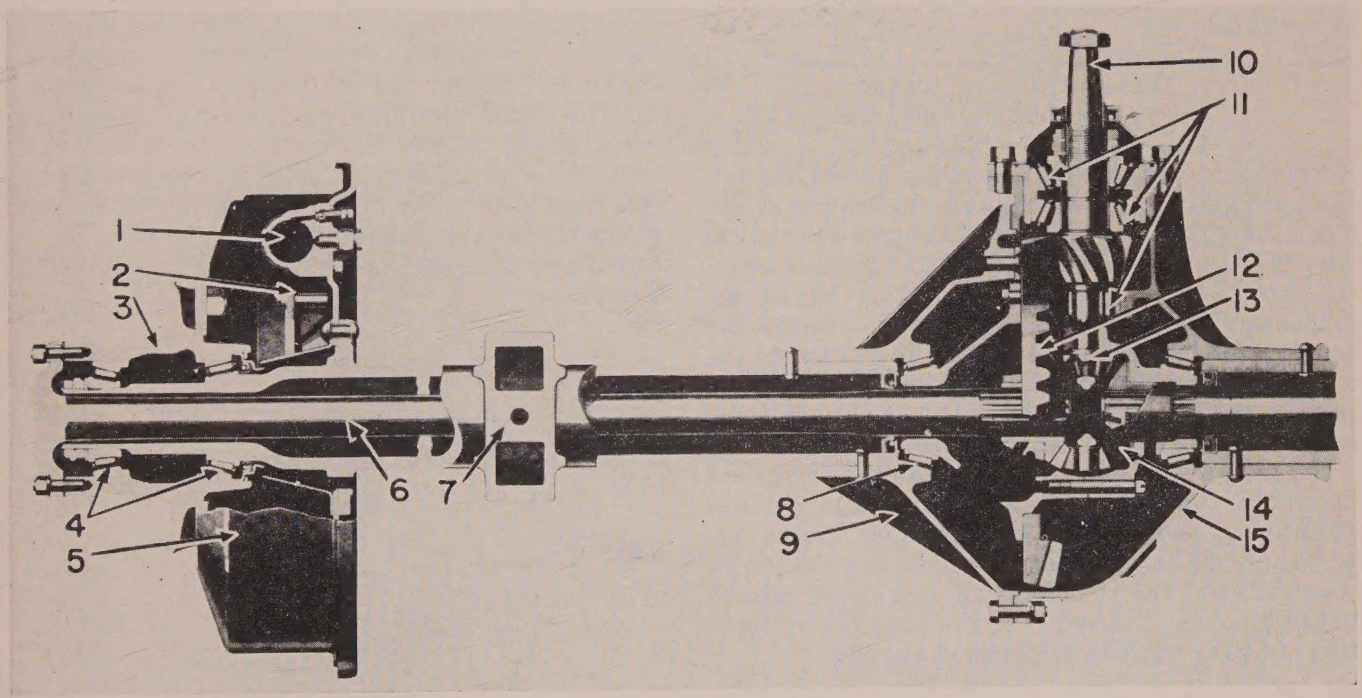

Fig. 6 – Nomenclature of rear-axle parts (TDA)

(1) Brake cylinder
(2) Brake shoe
(3) Hub
(4) Wheel bearings
(5) Brake drum
(6) Axle shaft
(7) Spring seat
(8) Differential bearings
(9) Differential carrier half
(10) Bevel pinion shaft
(11) Pinion bearings
(12) Bevel gear
(13) Differential pinion
(14) Differential side gear
(15) Differential carrier half

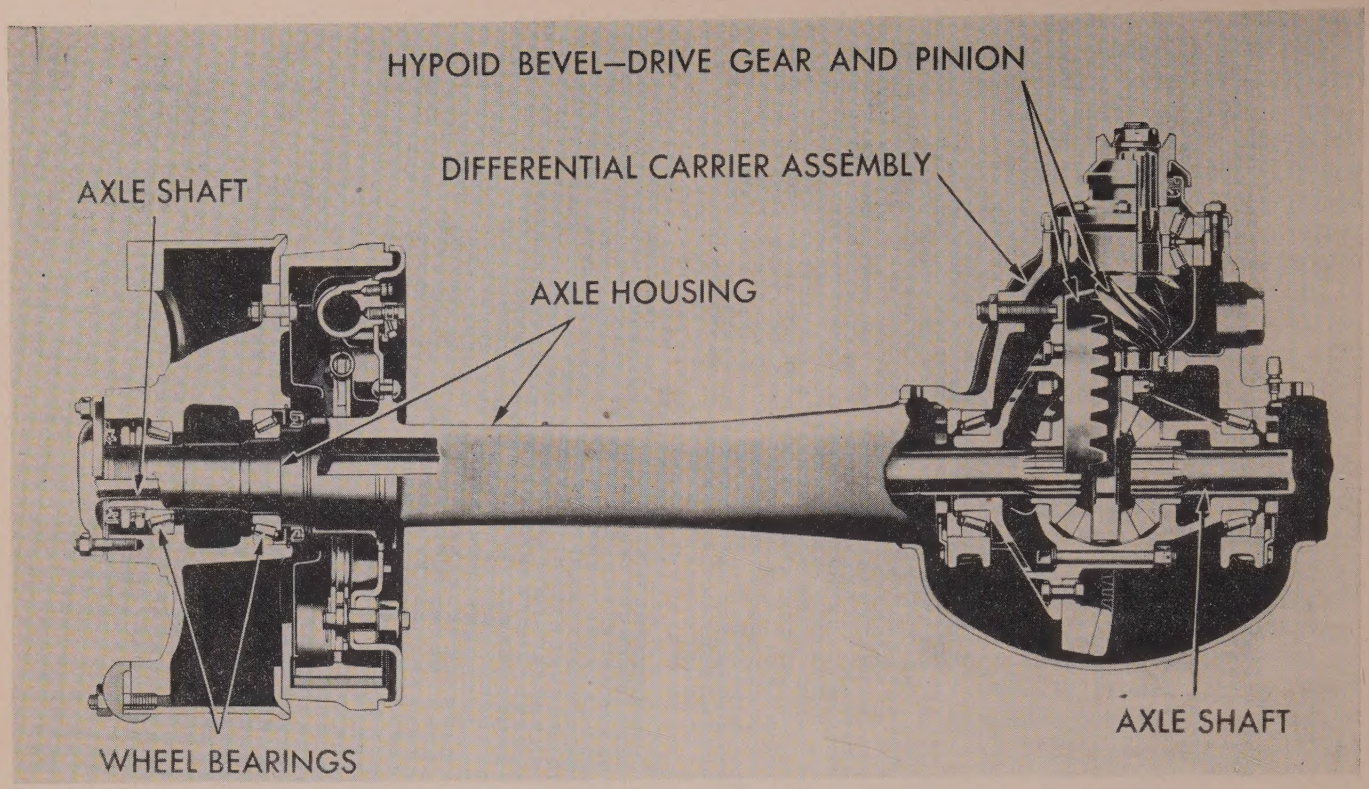

Fig. 7 – Typical rear-axle assembly (TDA)

shafts. Figs. 4 and 5 show another type of tandem axle, in which the torque divider is located at the forward axle, requiring only one shaft from the transmission.

Simply stated, all rear axles have four functions to perform:

1. Carry load.
2. Transmit driving torque.
3. Allow differential action.
4. Help stop the vehicle.

These functions are performed by the several distinct groups of parts which make up the axle. Figs. 6 and 7 are cutaway views of bevel-gear rear axles, showing the various parts involved. The axle housing performs the load-carrying function; the torque is transmitted from the propeller shaft through the bevel pinion, bevel ring gear, and differential to the axle shafts and wheels; differential action, of course, occurs in the differential gears; and the wheel brakes provide the stopping action.

Industry's solutions to the design problems posed by these functions are in many ways similar, permitting correlation of the various design approaches, without having to cope with details of construction. The remainder of this paper will be devoted to the discussion of the four major functions of the rear axle as outlined above.

Load-Carrying Function

Units of primary concern to the load-carrying function are the suspension, wheel hub support, and the axle housing with its varied constructions and strength considerations. Also of concern are the spindle, wheel bearings, spring seats, wheels, and tires.

Suspension – Although the driving and braking torque and thrust must be transmitted to the chassis, it is undesirable to attach the axle rigidly to the frame, for the operating shocks and stresses would be intolerable. Hence, a resilient suspension is used with thrust and torque reactions accommodated by a variety of linkages. The Hotchkiss drive shown in Fig. 8 is widely used on single rear-axle trucks because of its distinct simplicity and cost advantage over other types. The springs take care of longitudinal and lateral alignment as well as torque reaction, and do so with a fair degree of cushioning.

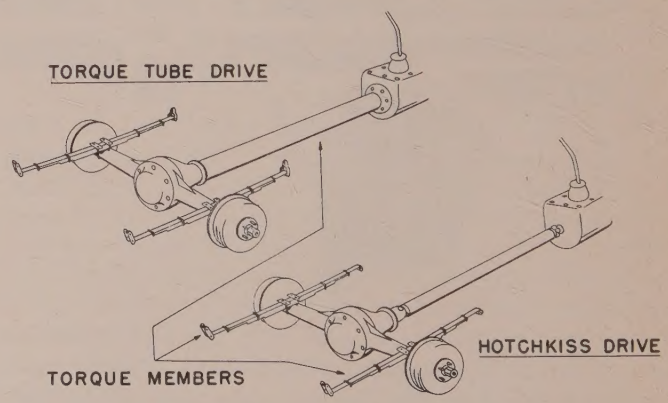

Fig. 8 – Hotchkiss versus torque-tube drive

Perhaps the nearest competitor in simplicity is the torque-tube drive used on some passenger cars and trucks. This drive utilizes the springs in the same way except for torque reaction. The axle housing is free to rotate in saddles attached to the springs, while torsional resistance is provided by a tubular housing, enclosing the propeller shaft, attached rigidly to the axle carrier at the rear and fastened to the frame at the forward end through a large hollow ball and socket enclosing the necessary propeller-shaft universal joint.

In the early days of the industry, radius-rods found application with chain drives where some longitudinal adjustment was desired. As such, they are seldom used today; rather, a modification is found in tandem axles. Tandem axles, or bogies as they are frequently called, are basically just a pair of rear axles suspended from the chassis by an appropriate linkage. A typical present-day suspension is shown separately in Fig. 9, and assembled into a tandem axle in Fig. 10.

The tandem axles, detached completely from the springs, transfer their thrust and torque directly to the frame by means of the radius-rods; hence, the stability of either axle is unaffected by the driving or braking torque of the other. Parallel arm construction and swivel joints are used to permit independent articulation for uneven road conditions. The most obvious advantage of the tandem axle is greater load capacity. Accompanying this is much greater flotation, traction, and inherently (although not always realized) superior riding characteristics. Fig. 11 demonstrates this superior ride. The balanced spring arrangement lifts the frame at its center only one-half the movement of the wheel when encountering an obstruction. Hence, a 10-in. obstruction or depression in the road results in only a 5-in. vertical movement of the frame.

There is, however, one deficiency that has long been recognized – the relative skidding of the two rigidly directed axles of the tandem while cornering. This constitutes a hazard to the control of a fast-moving vehicle, especially when road traction is uncertain. Under the impetus of growing popularity of the tandem axle in highway freight hauling, the problem of improving the basic design of the tandem suspension is receiving more and more serious attention.

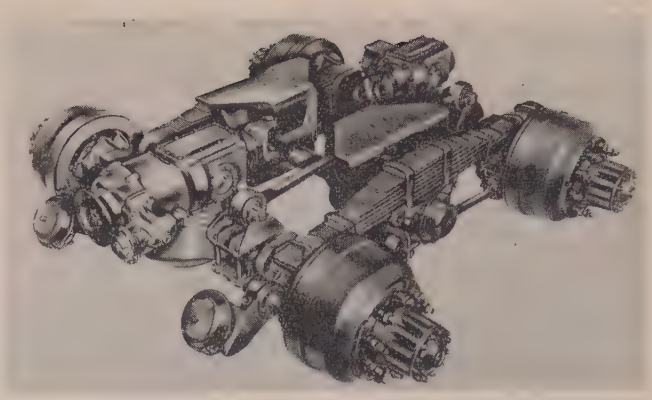

Fig. 10 – Suspension of Fig. 9 assembled into tandem axle (TDA)

Wheel Hub Support – By far the most predominant method of wheel hub support in the heavy vehicle field is the full-floating design sketched in Fig. 12 and illustrated in Figs. 6 and 7. Its important distinguishing feature is that the wheel is supported entirely by the axle housing. Two bearings on the outside of the housing provide alignment and accommodate all loads, even with the axle shaft removed from the assembly. The shaft is thus a purely torsional member and, what is more important, it can be removed without taking off the wheel or impairing load capacity.

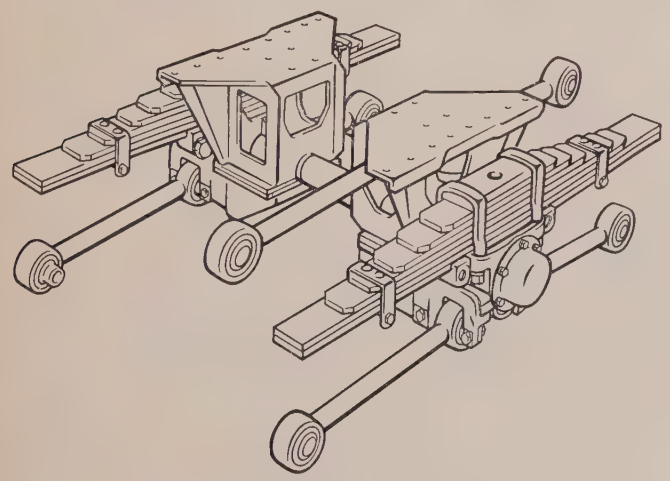

Fig. 9 – Typical tandem axle suspension (TDA)

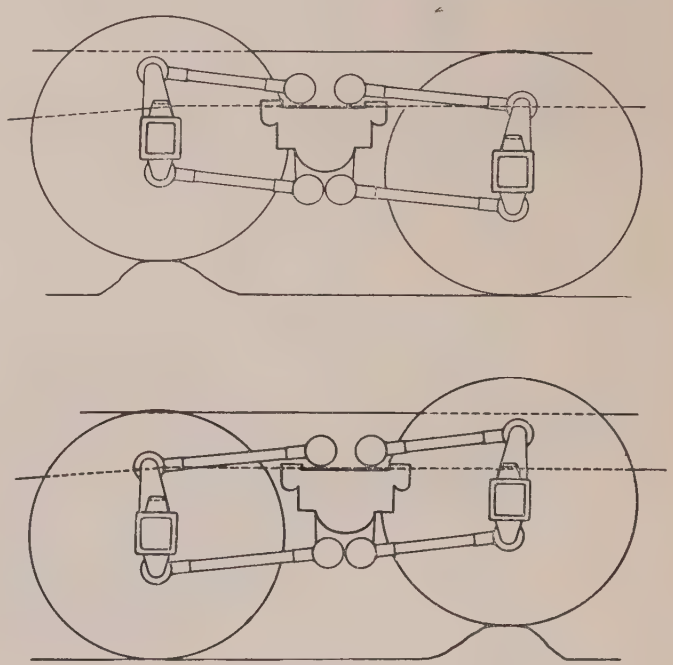

Fig. 11 – Diagram of tandem suspension showing frame movement as half of wheel movement (TDA)

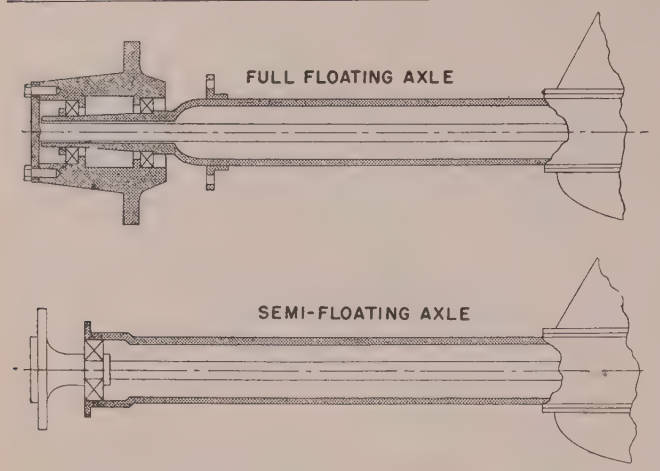

Fig. 12 – Full-floating versus semifloating designs

Passenger cars and light commercial vehicles, accounting for the great majority of vehicles in use, commonly use the semifloating construction. In this, the load is transferred from the axle housing to the wheel through the axle shaft, quite differently from the full-floating axle, where the load never touches the drive shaft. Note that the semifloating axle shaft is subject to continuous *bending* stress as well as torsion. Other types of hub support have been used, but they consist mainly of intermediate variations of these two basic arrangements, both in function and design.

Types of Housing Construction – The individual concepts of different manufacturers have understandably given rise to many variations in axle housing fabrication techniques. The more common housing constructions include forgings, castings, stampings, and expanded tubing.

Axle housings forged from tubular blanks (Fig. 13) are widely used. In this process, SAE 1035 steel plate is formed into welded steel tubing. The central portion of the tube is perforated by a slit, which, after subsequent forging and addition of reinforcing rings, forms the banjo portion. The ends of the tube are swaged to give the desired thickness at the spindle ends and spring pad sections. Backing plate flanges and spring pads are affixed by welding. The housing is heat-treated to about 200 minimum Brinell hardness and machine-

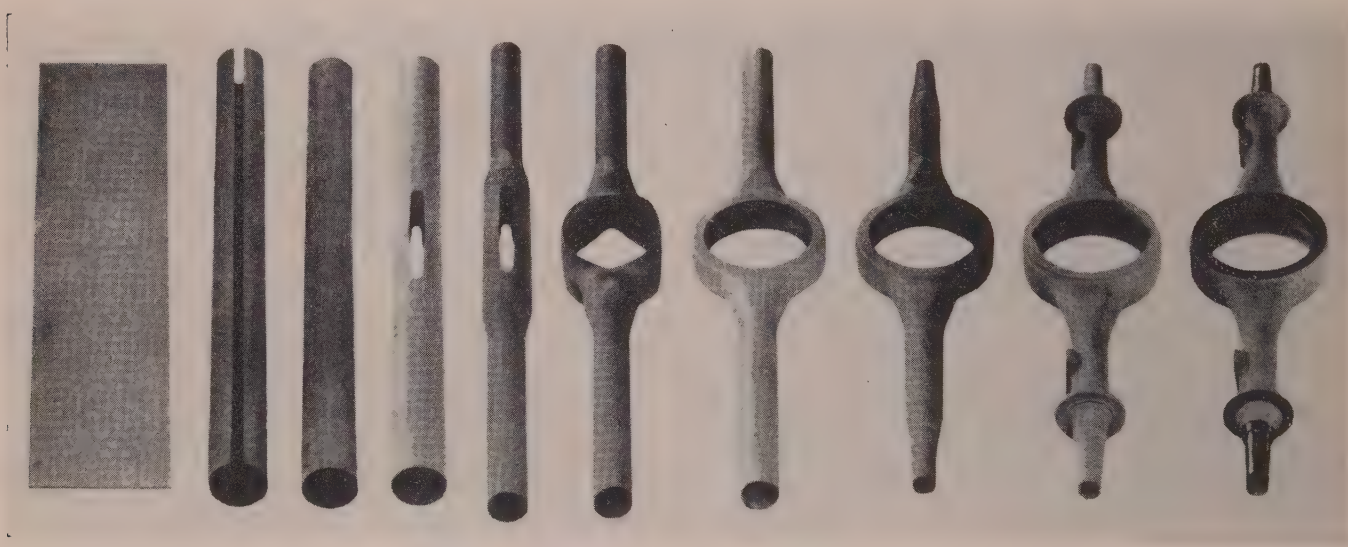

Fig. 13 – Housing forged from tubular blank (Clark)

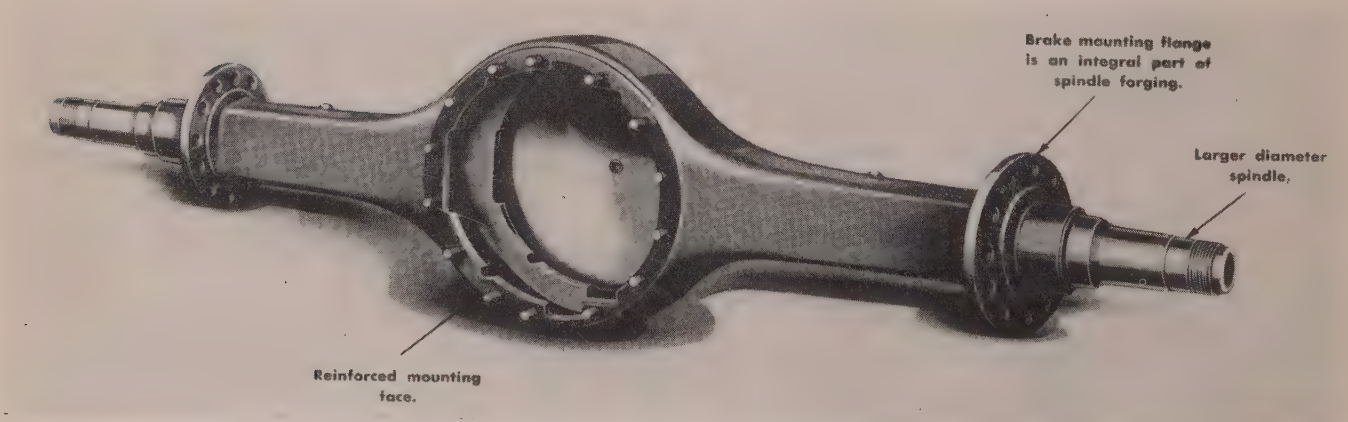

Fig. 14 – Rectangular hot-forged housing with butt-welded upset-forged spindles (TDA)

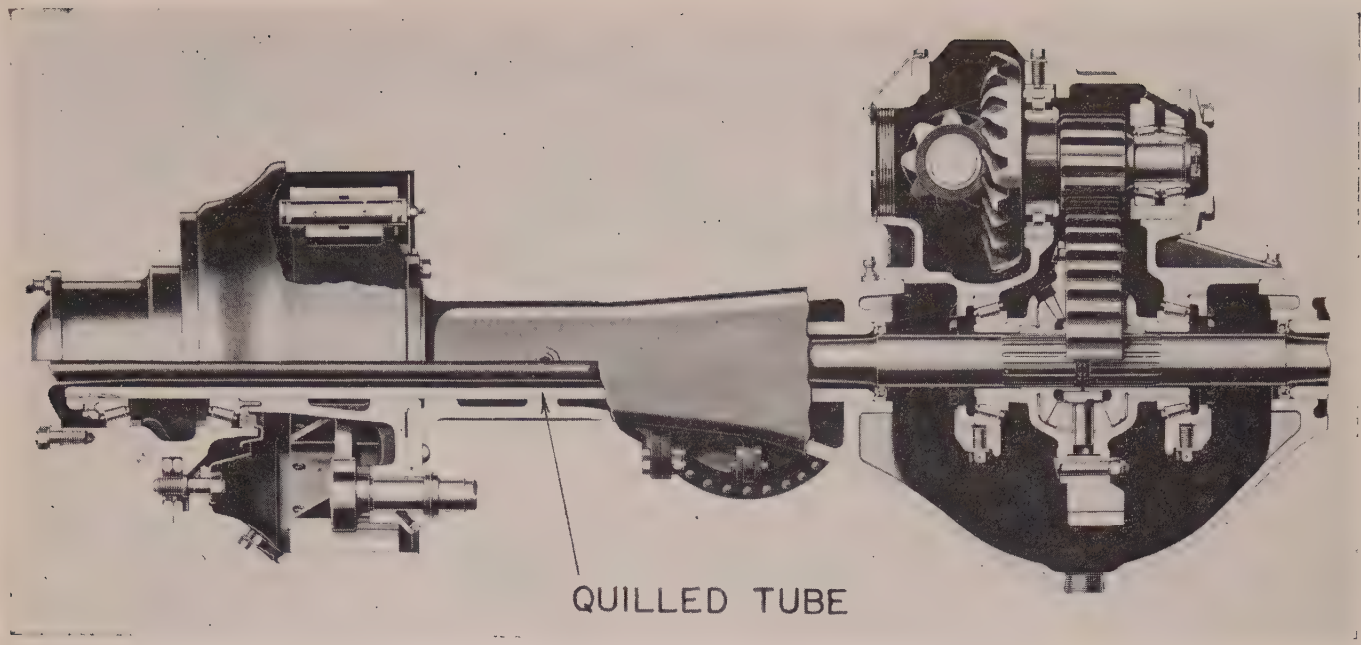

Fig. 15 – Cast housing with quilled alloy-steel tubing (TDA)

finished where necessary. The result is a one-piece, banjo-type, heat-treated housing. Another design (shown in Fig. 14) is hot-forged with partial arms extending slightly beyond the spring seats where the housing section is rectangular. This design, allowing a full-corner rectangular section, consists of top and bottom halves, which are welded on the horizontal centerline of the axle. Upset-forged steel spindles are heat-treated and electrically butt-welded in place. These spindles are made from alloy steel, while the central housing section is SAE 1035 carbon steel. The strongest material is thus used where the stress is greatest.

Cast axle housings (Fig. 15) are frequently found on the heavier commercial vehicles. A common construction is a cast banjo section with partially extended arms into which alloy-steel tubing is quilled at each end. The arms of the casting are rectangular in section, providing a high ratio of strength to metal used. Ribs bored internally support the tube, which is secured axially by dowels. The tube in turn supports the wheel bearings.

The stamped or pressed-steel type widely used for passenger cars, finds modified application to heavy-duty trucks. A typical example of this type (Fig. 16) consists of two identical sections of expanded tubing welded together at the banjo section and having swaged spindles at the outer ends. Reinforcing rings at the banjo section add strength.

Most housings must be designed to permit assembly of the differential carrier complete with ring gear and differential. However, split housings, which do not use a differential carrier assembly as a separate subassembly, are also used. Such an axle is shown in Fig. 17.

Housing Strength – Fig. 18 shows a typical axle as a load-carrying member. The center section of the axle housing accommodates the differential carrier and raises its own special considerations as to deflection and stress. The spindle ends, admitting drive shafts on the inside and accommodating wheel bearings on the outside, are more critical and merit special attention due to several points of local weakness and stress concentration.

Like beams, with their strength dependent upon dimensions, material, and processing, housings are supported at the wheel tread points and loaded at the spring centers. The bending moment between the springs remains uniform and is equal to the product of half the total axle load (neglecting tire and wheel weight) and the distance from the tire center to the adjacent spring center. The resulting stress is, of course, the quotient of this bending moment and the minimum section modulus of the housing between spring centers. For simplicity, this analysis has been based on static conditions.

Usually, the maximum housing stress (excluding spindles) is found between the spring centers,

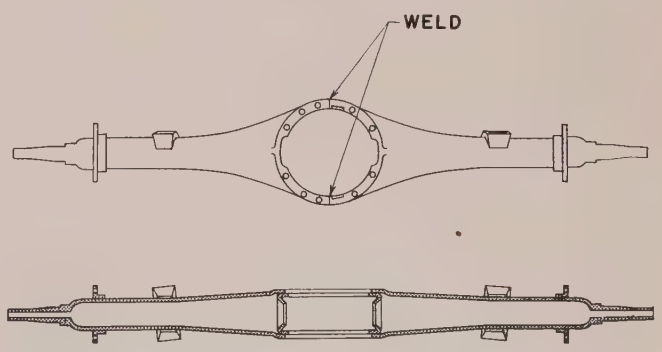

Fig. 16 – Axle housing from two identical sections welded together at banjo

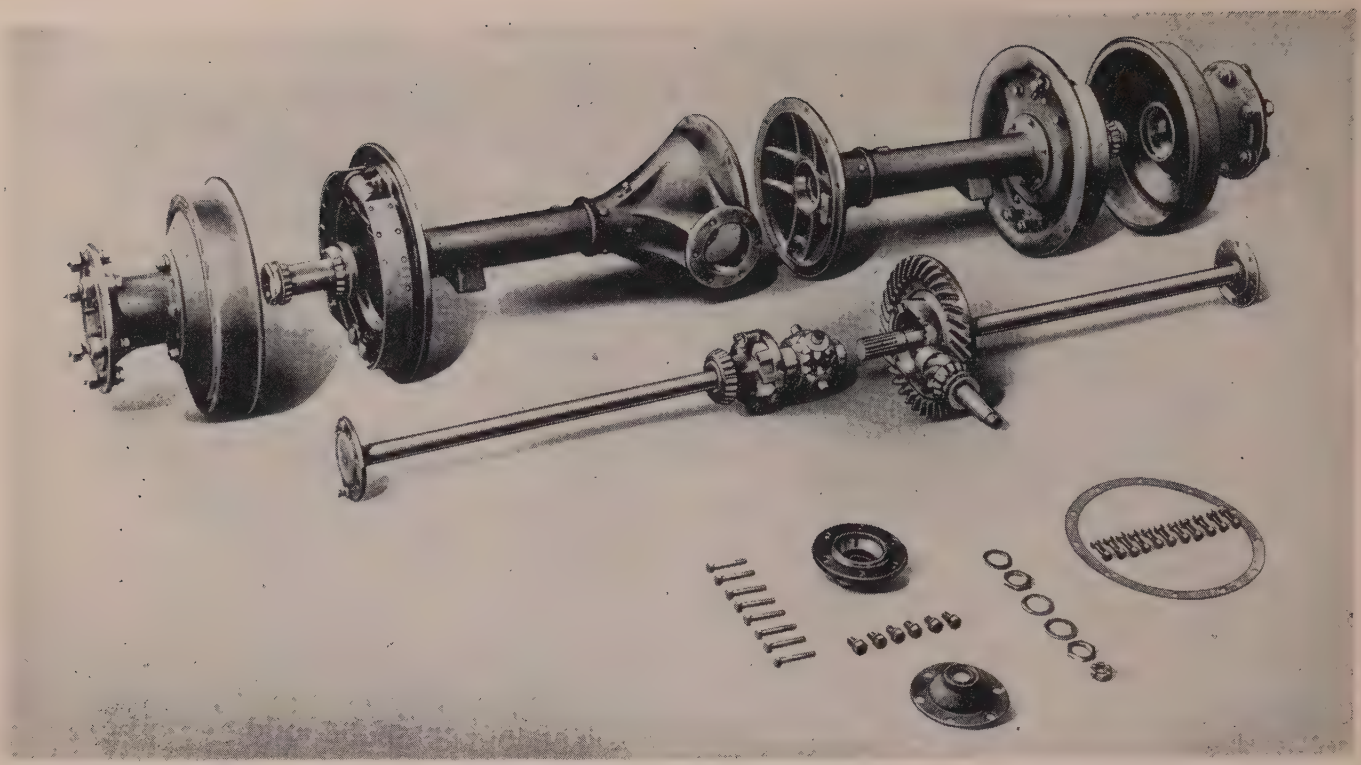

Fig. 17 – Split-type axle housing (TDA)

since the bending moment here is a maximum. However, in some designs, such as those made from tubular blanks, the banjo actually extends outboard of the spring centers, making the minimum section modulus between springs of sufficient magnitude to transfer the critical section to some point outboard of the springs, even though the moment there is less. (The moment arm of an outboard section is simply the distance from the section to the vertical load line of the nearest tread point.)

Note that, while the tread point for single tires lies at the center of the tire, that for dual tires is taken midway between the two tires. Incidentally, most heavy-duty trucks use dual tires for maximum capacity, since they allow a lower platform height than do larger single tires.

Shear stresses, from vertical, tractive, and brake torque loads, exist in the housing outboard of the spring pads, but these are small compared to bending stresses and theoretically, at least, their effect is minute.

Spindle Strength – The wheel spindle of a full-floating axle is actually the extremity of the housing structure. It has at least one critical section, particularly at the inner bearing, where it is subjected to bending forces imposed by combinations of static and dynamic loading. Because accurate prediction of combined dynamic stresses is quite complicated, only static vertical loads and lateral skid loads will be considered first, allowing a safety factor to help over the more obscure points. Static loading produces an upward bending moment on the spindle equal to the product of the load per side and the lateral distance from the tread centerline to the critical section of the spindle. The static stress, then, is this bending moment divided by the section modulus. (Dual tires introduce a certain amount of redundancy, which is neglected.)

Lateral skid forces produce either upward or downward moments on the spindle depending on skid direction. Here the moment equals the product of the load per side, the coefficient of road-to-tire friction, and the loaded radius of the tire. It should be noted that, although a vehicle negotiating a turn experiences a weight transfer to the outside wheel, the skid moment on this side reacts in a direction opposite to the vertical moment, and the two moments tend to offset each other.

Sample Calculations for Housing and Spindle – At this point it is appropriate to illustrate the design methods discussed so far with examples. For the purpose of developing meaningful examples it seems best to define an "industry average" heavy-duty, single-reduction axle. These specifications will then be used in the examples through the rest of the paper.

1. Vehicle – heavy-duty highway tractor-trailer combination.
2. Tye of gearing – single-reduction hypoid.
3. Rear-axle capacity – 22,000 lb.
4. Axle ratio – 7.8.
5. Tire size – 11.00/20.
6. Transmission ratio – 7.5 (in low gear).
7. Net engine torque – 300 lb-ft.
8. Net engine hp – 150.
9. Gross vehicle weight – 28,000 lb.
10. Gross combination weight – 60,000 lb.
11. Frontal area – 90 sq ft.

Gear efficiency, though needed for accurate power requirement calculations, has been omitted to simplify the examples. Some specifications and dimensions necessary for specific examples are included with the lists of symbols when needed. For consistency of symbol usage in all of the examples, subscripts designating the four functions of an axle have been added to the symbols: h for housing and sp for spindle, in the load-carrying function; g for gears and s for shafts, in the torque transmitting function; d for differential; and b for braking. At this point we will consider only the load-carrying function of the housing and spindle.

Housing and Spindle Symbols	Assumed Specifications
P = Rated load capacity, lb	22,000
M_h = Housing bending moment, in.-lb	
Z_h = Section modulus of housing at critica section, in.^{3}	
S_h = Stress at housing critical section, psi	
k = Wall thickness of section (round or rectangular), in.	
D_h = Outside diameter of round housing section, in.	
d_h = Inside diameter of round housing section = $(D_h - 2k)$, in.	
B_h = Outside width of rectangular housing section, in.	
H_h = Outside height of rectangular housing section, in.	
t = Effective tread width, in.	72
s = Distance between spring centers, in.	40
M_{st} = Spindle bending moment due to static weight, in.-lb	
M_{sk} = Spindle bending moment due to skid, in.-lb	
r = Tire loaded radius, in.	20
a = Distance from effective tread line to spindle shoulder, in.	3¼
D_{sp} = Outside diameter of spindle, in.	
d_{sp} = Inside diameter of spindle, in.	
S_{st} = Spindle static stress, psi	
S_{sk} = Spindle skid stress, psi	
Z_{sp} = Section modulus of spindle at critical section, in.^{3}	

Housing sections forged or stamped from SAE 1035 steel and with a hardness of 200 Bhn have a yield strength of 60,000 psi. In order to allow a safety factor of 4 to 1 for dynamic loading (such as striking a bump at high speed), an allowable static stress of $\frac{60{,}000}{4}$ or 15,000 psi is usually specified. For a rigorous design analysis, it is necessary to consider the combined stresses from dynamic bending and lateral skid, as shown later. For comparative evaluations and rapid estimations for preliminary design work, however, the housing and spindle may be analyzed by the following formulas, which will be termed "design approximations."

(D.A. 1) Housing bending moment between spring seat centers:

$$M_h = \frac{P}{2} \times \frac{(t - s)}{(2)} \quad \text{(see Fig. 18)}$$

$$M_h = \frac{22{,}000}{2} \times \frac{72\text{–}40}{2} = 176{,}000 \text{ in.-lb}$$

(D.A. 2) Housing stress and section modulus:

$$Z_h = \frac{M_h}{S_h}$$

For axle design, assuming $S_h = 15{,}000$ psi allowable static stress for forged steel, the minimum allowable section modulus can be calculated:

$$Z_h = \frac{176{,}000}{15{,}000} = 11.7 \text{ in.}$$

From this, section dimensions can be calculated from:

$$Z_h = 0.0982 \frac{(D_h^4 - d_h^4)}{D_h} \text{ for round sections}$$

or:

$$Z_h = \frac{1}{6H_h} [B_h H_h^3 - (B_h - 2k)(H_h - 2k)^3] \text{ for rectangular sections}$$

For axle evaluation, the section modulus is known or can be calculated from the actual dimensions of the axle under study, and S_h determined. As an example, take a rectangular housing section 5¼ in. high and 4⅝ in. wide, with a ½-in. wall thickness.

$$Z_h = \frac{1}{6 \times 5.25} [4.625 \times 5.25^3 - (4.625 - 2 \times 0.50)(5.25 - 2 \times 0.50)^3] = 12.4 \text{ in.}^3$$

Since this is above the minimum allowable section modulus of 11.7 in.^{3}, the section is adequate, and the actual static stress at the critical section is:

$$S_h = \frac{M_h}{Z_h} = \frac{176{,}000}{12.4} = 14{,}200 \text{ psi}$$

which is within the allowable static stress of 15,000 psi.

For housings, we have considered only those stresses resulting from vertical forces (this premise will be substantiated later). For spindles, however, stresses from both vertical and lateral forces must be analyzed. This is because, referring to Fig. 18, while the moment arms for the housing vertical and skid forces are about the same $\left(\frac{t - s}{2} \text{ approximates } r\right)$, the moment arm (r) for the spindle lateral skid force may be about five times the moment arm (a) for the vertical force. Allowable spindle stress and size varies with the spindle material and hardness. Spindles integral with the housing have the same yield stress as the housing (60,000 psi); those made of alloy steel, and heat-treated to a hardness of 300 Bhn, have a yield

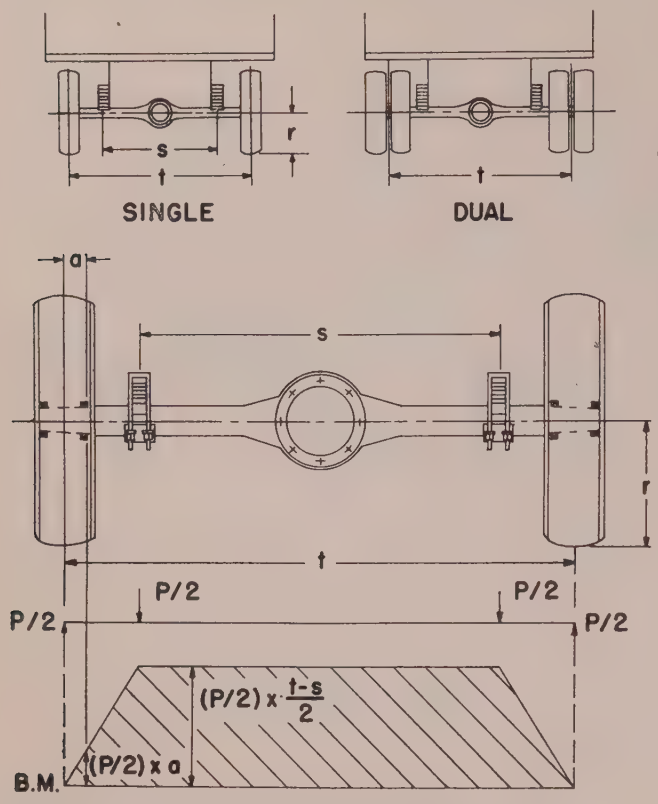

Fig. 18 – Housing as load-carrying member

stress approximating 90,000 psi. On the basis of many comparative analyses, it has been found that a yield strength safety factor greater than 4 to 1 is desirable. Thus, the maximum allowable static stress at the spindle critical section will be set at 12,000 psi.

The location of the spindle critical section is usually at the shoulder for the inner wheel bearing, where high bending moments and stress concentrations exist. In some cases, however, if the spindle section changes abruptly, or is not tapered from the outer bearing to the inner bearing, the critical section may be outboard of the shoulder. For comparative evaluations or rapid preliminary design estimations, the maximum stress may be assumed to be at the shoulder section.

(D.A. 3) Spindle static moment and stress:

$$M_{st} = \frac{P}{2} \times a \quad \text{(see Fig. 18)}$$

$$M_{st} = \frac{22{,}000}{2} \times 3.25 = 36{,}000 \text{ in.-lb}$$

The minimum allowable section modulus for this moment and an allowable stress of 12,000 psi is:

$$Z_{sp} = \frac{M_{st}}{S_{st}}$$

$$Z_{sp} = \frac{36{,}000}{12{,}000} = 3.0 \text{ in.}^3$$

Section dimensions can then be calculated from.

$$Z_{sp} = \frac{0.0982\,(D_{sp}^4 - d_{sp}^4)}{D_{sp}}$$

For evaluation of a given spindle section with 3⅝ outside diameter and 2 7/16 inside diameter, the section modulus may first be calculated:

$$Z_{sp} = \frac{0.0982\,(3.625^4 - 2.44^4)}{3.625} = 3.7 \text{ in.}^3$$

Since this is above the minimum allowable section modulus of 3.0 in.^{3}, the section is adequate, and the actual static stress at the section is:

$$S_{st} = \frac{M_{st}}{Z_{sp}}$$

$$S_{st} = \frac{36{,}000}{3.7} = 9700 \text{ psi}$$

which is well within the maximum allowable static stress of 12,000 psi.

(D.A. 4) Spindle skid moment and stress:

$$M_{sk} = 0.7 \frac{P}{2} \times r \quad \text{(see Fig. 18)}$$

in which 0.7 is the road-to-tire coefficient of friction.

This formula assumes that the maximum spindle stress from lateral skid also is located at the inner wheel bearing shoulder.

When a vehicle is rounding a curve, the resulting weight transfer to the outer wheel makes the lateral force greater than $0.7P/2$; the vertical reaction, however, produces a moment opposing the lateral moment, offsetting the weight transfer effect, and the above formula still holds true as a useful approximation.

$$M_{sk} = 0.7 \frac{P}{2} \times r$$

$$M_{sk} = 0.7 \frac{22{,}000}{2} \times 20 = 154{,}000 \text{ in.-lb}$$

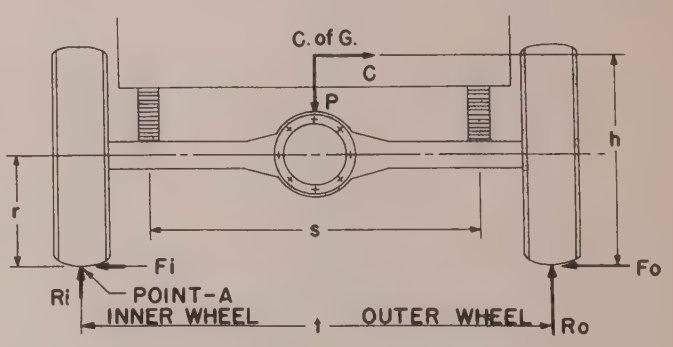

Fig. 19 – Skid loads on full-floating rear axles

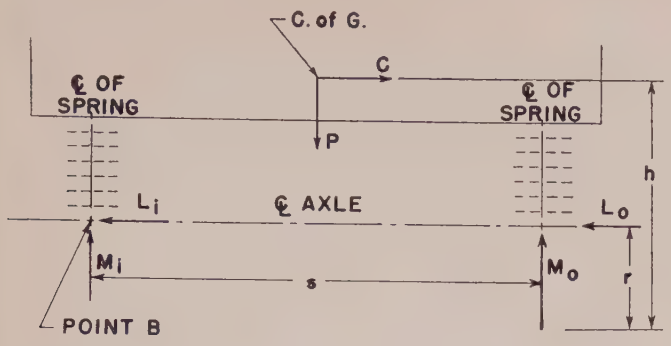

Fig. 20 – Equilibrium diagram of spring suspension forces

Actual analysis of many representative axles indicates a maximum allowable lateral skid stress of 50,000 psi. The minimum allowable section modulus to satisfy this condition is then:

$$Z_{sp} = \frac{M_{sk}}{S_{sk}}$$

$$Z_{sp} = \frac{154{,}000}{50{,}000} = 3.1 \text{ in.}^3$$

The 3.7 in.^{3} actual section modulus selected in D.A. 3 thus satisfies the requirements of both the static and lateral skid conditions. The actual lateral skid stress for the given spindle section with 3.7 in.^{3} modulus is:

$$S_{sk} = \frac{M_{sk}}{Z_{sp}}$$

$$S_{sk} = \frac{154{,}000}{3.7} = 42{,}000 \text{ psi}$$

which is within the allowable 50,000 psi.

Analysis of Axle under Dynamic Conditions – The above design approximations and the bending moment diagram of Fig. 18 are typical of what might be found in textbooks. As already mentioned, they are quite valuable for making preliminary design and evaluation calculations. However, they do not allow for the combined forces encountered under dynamic conditions, such as rounding a curve at high speed where weight transfer and lateral skid forces become very significant. A more exact method of analysis will, therefore, be presented.

We will assume that our "industry average" truck is making a sharp left turn at a high enough speed to bring the wheels just short of skidding. The weight transfer will be to the right, or outer, wheels.

Fig. 19 shows the rear axle under lateral skid load, where:

C = Centrifugal force acting at center of gravity, lb
h = Height of center of gravity above ground line, in.
R_i = Reaction on inner wheel in vertical plane, lb
R_o = Reaction on outer wheel in vertical plane, lb
F_i = Force of friction on inner wheel from lateral skid, lb
F_o = Force of friction on outer wheel from lateral skid, lb

Again, if we assume that the maximum possible coefficient of friction between the road and tires is 0.7, the maximum lateral force at the point of skid for the entire axle is:

$$0.7\,P = F_i + F_o = C \tag{1}$$

Summing the moments about point A of Fig. 19:

$$\Sigma M_a = 0$$

therefore:

$$P \times \frac{t}{2} + C \times h - R_o \times \quad = 0$$

$$R_o = \frac{P \times \frac{t}{2} + C \times h}{t}$$

$$R_o = \frac{P}{2} + C \times \frac{h}{t} \tag{2}$$

Similarly:

$$R_i = \frac{P}{2} - C \times \frac{h}{t} \tag{3}$$

Since the frictional force is equal to the coefficient of friction times the vertical load:

$$F_i = 0.7\,R_i \tag{4}$$

$$F_o = 0.7\,R_o \tag{5}$$

We shall now consider the reaction at the springs, through which the load is transmitted from the body to the axle. Fig. 20 shows an equilibrium diagram of the truck body and springs. From this we will solve for the spring reactions, which in turn will be used to construct a free-body diagram of the axle.

In Fig. 20:

L_i = Lateral component of inner spring reaction, lb
L_o = Lateral component of outer spring reaction, lb
M_i = Vertical component of inner spring reaction, lb
M_o = Vertical component of outer spring reaction, lb

Summing the moments about point B, we find the intersection of the inner spring and axle centerlines:

$$\Sigma M_B = 0$$

therefore:

$$C\,(h - r) + P \times \frac{s}{2} - M_o \times s = 0$$

$$M_o = \frac{P \times \frac{s}{2} + C\,(h - r)}{s}$$

$$M_o = \frac{P}{2} + \frac{C\,(h - r)}{s} \tag{6}$$

Similarly:

$$M_i = \frac{P}{2} - \frac{C\,(h - r)}{s} \tag{7}$$

Summing up the horizontal forces.

$$L_i + L_o = C \tag{8}$$

Now, going a step further, we construct Fig. 21, which is a free-body diagram of the bearing forces acting on the spindle, where:

d = Distance between bearing centerlines, in.

e = Distance from tread load line to inner bearing centerline, in.

From fundamental statics, R_i, the radial load due to the vertical load component on the inner wheel, can be resolved into its two bearing components:

$$R_i \times \frac{e}{d}, \quad \text{and} \quad R_i \times \frac{d-e}{d} \tag{9}$$

similarly, for the outer wheel:

$$R_o \times \frac{e}{d}, \quad \text{and} \quad R_o \times \frac{d-e}{d} \tag{10}$$

The bearing forces resulting from the frictional forces F_i and F_o, respectively, can also be determined by taking moments about bearing centers.

Having developed these formulas, we shall proceed with the calculations, using the values below:

P = Axle load = 22,000 lb

t = Tread = 72 in.

s = Distance between spring centers = 40 in.

h = Height of center of gravity above ground line = 45 in.

r = Loaded radius of tire = 20 in.

d = Distance between bearing centerlines = 5 in.

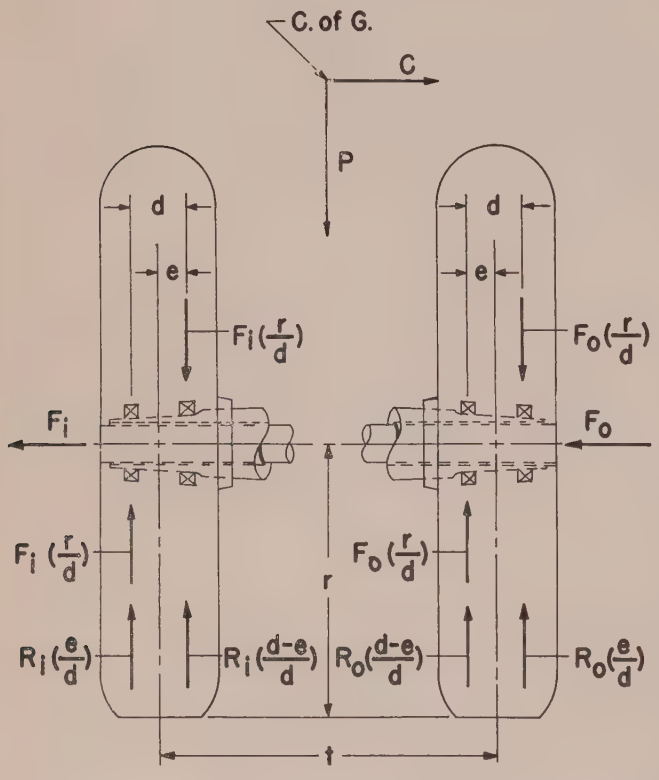

Fig. 21 – Equilibrium diagram of bearing forces on spindle

e = Distance from tread load line to inner bearing centerline = 2½ in., or $\frac{d}{2}$ in this example. (Assuming ¾ in. from centerline of inner bearing to spindle shoulder, this gives the 3¼ in. from load line to spindle shoulder as used in D.A. 3.)

Substituting these values into the equations, we have for the centrifugal force:

$$C = 0.7 \quad P = 0.7 \times 22{,}000 = 15{,}400 \text{ lb} \quad \text{(from eq. 1)}$$

The vertical reaction on the outer wheel is:

$$R_o = \frac{P}{2} + C \times \frac{h}{t} = \frac{22{,}000}{2} + 15{,}400 \times \frac{45}{72} = 20{,}620 \text{ lb} \quad \text{(from eq. 2)}$$

The vertical reaction on the inner wheel is:

$$R_i = \frac{P}{2} - C \times \frac{h}{t} = \frac{22{,}000}{2} - 15{,}400 \times \frac{45}{72} \quad \text{(from eq. 3)}$$

= 1380 lb. (Note that had the weight transfer been slightly greater, so as to unload the inner wheel completely, making $R_i = 0$, the truck would have overturned while rounding this curve.)

The frictional force on the inner wheel from lateral skid is:

$$F_i = 0.7\ R_i = 0.7 \times 1380 = 966 \text{ lb} \quad \text{(from eq. 4)}$$

Frictional force on the outer wheel from lateral skid is:

$$F_o = 0.7\ R_o = 0.7 \times 20{,}620 = 14{,}434 \text{ lb} \quad \text{(from eq. 5)}$$

The vertical component on the outer spring is:

$$M_o = \frac{P}{2} + \frac{C\ (h-r)}{s} = \frac{22{,}000}{2} + 15{,}400\ \frac{(45-20)}{40}$$

$$= 11{,}000 + 9620 = 20{,}620 \text{ lb} \quad \text{(from eq. 6)}$$

For the inner spring:

$$M_i = \frac{P}{2} - C\left(\frac{h-r}{s}\right) = 11{,}000 - 9620 = 1380 \text{ lb} \quad \text{(from eq. 7)}$$

The sum of the horizontal components of the spring reaction is:

$$L_i + L_o = C = 15{,}400 \text{ lb} \quad \text{(from eq. 8)}$$

For the purpose of balancing the thrust forces, which do not affect bending stress, we may assume for the inner spring:

$$L_i = F_i = 966 \text{ lb}$$

and for the outer spring:

$$L_o = F_o = 14{,}434 \text{ lb}$$

which also add up to 15,400 lb.

The outer bearing radial load due to the vertical load component on the inner wheel is, from eq. 9:

$$R_i \times \frac{e}{d} = 1380 \times \frac{2.5}{5} = 690 \text{ lb}$$

Also from eq. 9 the inner bearing radial load

due to the vertical load component on the inner wheel is:

$$R_i \times \frac{(d-e)}{d} = 1380 \times \frac{5-2.5}{5} = 690 \text{ lb}$$

Likewise, from eq. 10 the bearing radial loads due to the vertical load components on the outer wheel are:

$$R_o \times \frac{e}{d} = 20{,}620 \times \frac{2.5}{5} = 10{,}310 \text{ lb}$$

and:

$$R_o \times \frac{d-e}{d} = 20{,}620 \times \frac{5-2.5}{5} = 10{,}310 \text{ lb}$$

The skid moment *forces* on the inner wheel bearings are:

$$F_i \times \frac{r}{d} = 966 \times \frac{20}{5} = 3860 \text{ lb}$$

and for the outer wheel bearings:

$$F_o \times \frac{r}{d} = 14{,}434 \times \frac{20}{5} = 57{,}740 \text{ lb}$$

Referring to Fig. 21, we find that the total radial force on the inner wheel outer bearing is:

$$R_i \times \frac{e}{d} + F_i \times \frac{r}{d} = 690 + 3860 = 4550 \text{ lb}$$

and for the inner wheel inner bearing:

$$R_i \times \frac{d-e}{d} - F_i \times \frac{r}{d} = 690 - 3860 = -3170 \text{ lb}$$

or a total downward force of 3,170 lb.

The total radial force on the outer wheel outer bearing is:

$$R_o \times \frac{e}{d} - F_o \times \frac{r}{d} = 10{,}310 - 57{,}740 = -47{,}430 \text{ lb}$$

or a total downward force of 47,430 lb.

And for the outer wheel inner bearing:

$$R_o \times \frac{d-e}{d} + F_o \times \frac{r}{d} = 10{,}310 + 57{,}740 = 68{,}050 \text{ lb}$$

Fig. 22 shows the equilibrium diagram, the shear diagram, and the bending moment diagram for the forces just calculated for this axle under dynamic lateral skid conditions. Summing up, these forces used in the diagram (with minus signs indicating downward forces) are:

$F_i = 966$ lb
$F_o = 14{,}434$ lb
$L_i = 966$ lb
$L_o = 14{,}434$ lb
$M_i = -1{,}380$ lb
$M_o = -20{,}620$ lb

Radial force on inner wheel outer bearing = 4550 lb
Radial force on inner wheel inner bearing = −3170 lb
Radial force on outer wheel outer bearing = −47,430 lb
Radial force on outer wheel inner bearing = 68,050 lb

In this example the shear is zero and the bending moment constant between spring centers. This is

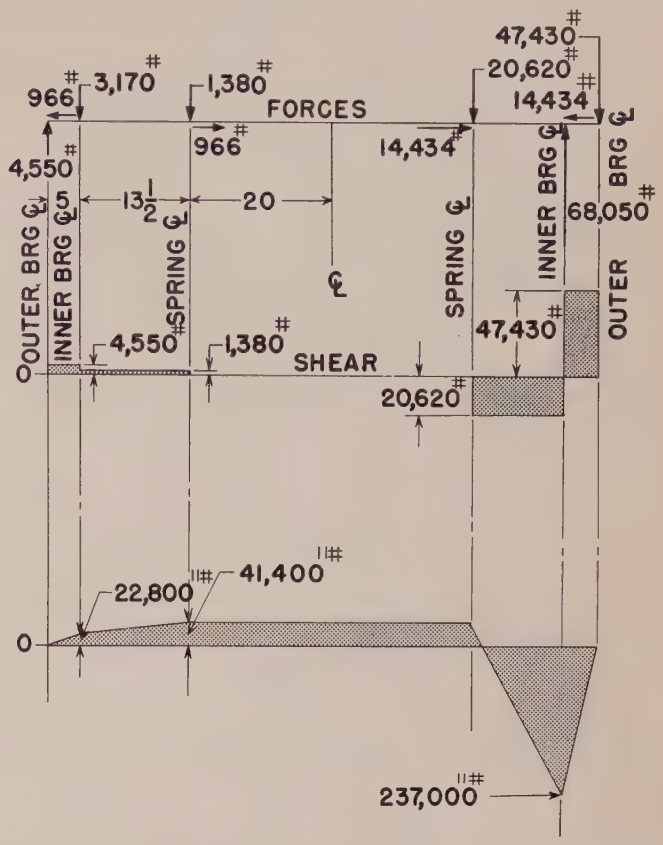

Fig. 22 – Equilibrium diagram, shear diagram, and bending moment diagram for axle under skid load

not always true, but occurs in this case because of the dimensions selected.

In our example the effective tread load line is assumed midway between the bearing centers. If it were located nearer the inner bearing we would find, for lateral skid conditions, that the bending moment in the spindle would be reduced and the bending moment of the housing between spring centers would be increased. Also note that the bearing loads have, for simplicity, been assumed to act on the spindle at the center point of each bearing, whereas actually they are distributed along the length of the bearing.

Comparison of Results of Static and Dynamic Calculations – As seen in Fig. 22, the maximum bending moment in the housing proper of our dynamic example is 41,400 in.-lb. This is less than one-fourth of the 176,000 in.-lb calculated for static conditions under D.A. 1. From this it is apparent that the housing sections near and between the spring pads should be designed for static vertical loading with an ample safety factor for striking bumps; they should not be based on lateral skid calculations.

For spindles, however, the picture is quite different. The maximum spindle bending moment in Fig. 22 is 237,000 in.-lb; that calculated in D.A. 4 was only 154,000 in.-lb. A closer look is thus in

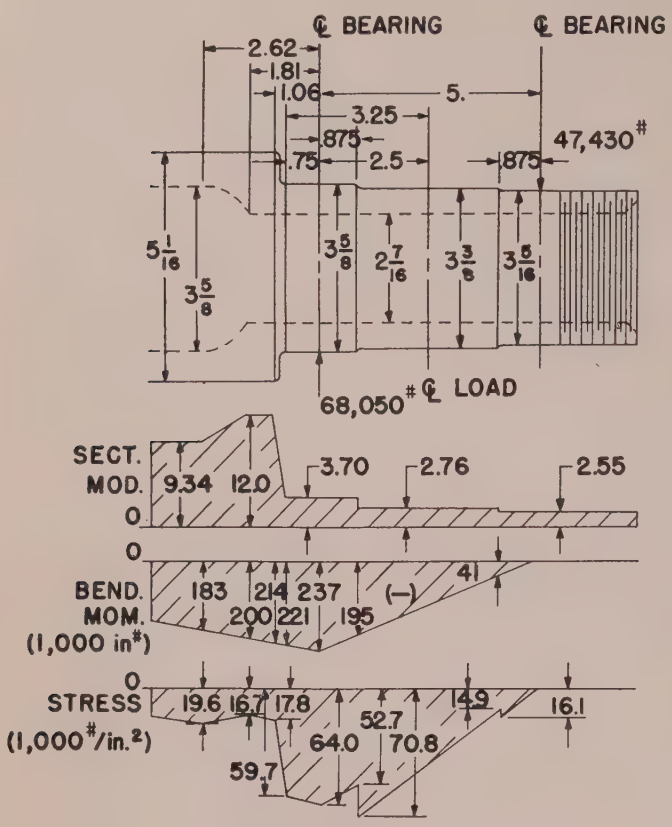

Fig. 23 – Spindle with diagrams for lateral skid

order here. Fig. 23 shows the outer wheel spindle, in which the highest stresses and negative bending moment occur.

A section modulus diagram is drawn under the spindle in Fig. 23; below this is a bending moment diagram; and below this is a stress diagram. Note that the maximum stress does not occur at the inner bearing shoulder, as is often assumed. This is due largely to the fact that the spindle does not taper from the outer bearing to the thicker inner bearing section.

The maximum stress at this critical section is 70,800 psi – almost double the 42,000 psi from D.A. 4, thus emphasizing the need for a more comprehensive analysis for final design than normally given in textbooks. Although the stress found is quite high, it represents an extreme condition, as the truck is about to roll over when rounding a curve. Furthermore, the example is representative of an alloy spindle, which, as previously stated, has a yield strength approximating 90,000 psi.

Stress concentrations at sudden transitions in cross-sections may have an appreciable effect upon spindle performance, particularly at higher hardness; however, the treatment of this added complication was felt to be beyond the scope of this paper.

Wheel Bearings – The inner and outer wheel bearings on heavy truck axles have a spread between centers approximating one-fourth of the loaded radius of the tire. Obviously, the wider the spread the less will be the bearing load created by lateral skid couples. Bearings are usually placed so that the vertical load line passes between them, but closer to the inner than to the outer bearing since the former usually can accommodate higher load. This practice also reduces the spindle moment arm. Tapered roller bearings are employed most frequently because they adapt themselves favorably to the complexity of the various acting forces. Catalogs giving formulas, ratings, and sample calculations are available from manufacturers of bearings.

Spring Seats – Axle housings for vehicles with conventional suspensions are fitted with spring seats to which leaf springs are attached. Obviously, the spring seats and housing at this section must withstand the load to which the U-bolts holding the springs are tightened. The design problem, then, is: how much tension will there be in the U-bolts?

Simply stated, this tensile force must be high enough to flatten the spring against the spring seat so that the spring, when in its extreme deflected position, will not become loose enough to fan-tail. The magnitude of this load for each half of the U-bolt is usually several times the nominal main-spring capacity; this may be appreciated by considering the spring as a composite beam of several leaves, which must be deflected from an unloaded cambered position to a flat beam in the short distance between the U-bolts.

Wheels and Tires – Tire and rim sizes usually limit both the load and torque-carrying ability of the axle. Since Tire and Rim Association Standards have been established to cover these components, they will not be taken up in detail here. However, the attachment of the wheels to the axle does merit consideration. Heavy trucks normally use either cast spoke or disc wheels. The former are made with an integral wheel and hub, and a demountable rim, doing away with the need to carry a spare wheel. Disc wheels, on the other hand, are attached to the hubs with studs.

In the design, evaluation, and selection of axles, consideration must be given to wheel studs, since they govern the wheel and tire mounting, thereby limiting the adaptability of the axle. The most common disc wheel mounting for heavy-duty trucks consists of 10 studs on an 11¼ bolt circle. The bolt circle diameter and the number and size of the studs must, of course, have sufficient strength to match the axle capacity and tire size. An empirical formula based upon experience and usage will guide in the mounting selection, once the maximum tire size has been established. The formula involves two factors: the mounting moment factor and the wheel moment factor.

The mounting moment factor is expressed as a

function of the number of studs, the bolt circle diameter, and the stud size; the wheel moment factor combines tire capacity and loaded radius. The formula, then, simply states that to ensure adequate strength, the mounting moment factor should equal or exceed the wheel moment factor. A list of the factors, calculated for different conditions, is given in Table 1, which is arranged so that any given mounting will accommodate tires above but not below it in the list. An empirical formula, such as this, must be subject to some latitude in application. For example, single rear wheels or strain-drawn studs require more strength, and thus the mounting moment factor should be multiplied by 0.85 in such cases. Another point to note is that an increase in bolt circle is more advantageous than an increase in the number of studs, because a small circle limits the increment of improvement in bearing pressure.

Torque Transmission Function

The second major function of the axle, which we have outlined earlier, is to transmit the driving torque to the rear wheels. The torque handling units of the axle consist of the driving gears and bearings, supports, differential assembly, and axle shaft, each with its own special function and design problems. It is, of course, essential to establish the torque capacity of the axle in a manner consistent with actual operation. Basic items such as engine torque, transmission and axle ratios, and material strength enter directly into the calculations; such considerations as skid torque potential, type of service, manufacturing methods, and maintenance provision influence the selection of safety or service factors. For simplicity, some axle designers rate an axle as adequate for any imposed torque provided that its use is restricted to a certain size tire. However, forward thinking demands a reappraisal which takes into account

Table 1 – Disc Wheel Mounting Guide

Mounting Moment Factor				Wheel Moment Factor			
$MMF = 4.5\ N^{1/2}\ DS$				$WMF = \frac{CR}{1000}$			
No. of Studs (N)	Bolt Circle (D)	Stud Size (S)	MMF	Tire 20 In. Diameter	Capacity (C)	Radius (R)	WMF
				6.00-6	1400	15.9	22
				6.50-6	1700	16.4	28
				7.00-8	2000	16.9	33
				7.50-8	2375	17.6	42
				7.50-10	2700	17.6	48
				8.25-10	2900	18.0	52
				8.25-12	3150	18.0	57
5	8	¾	60				
				9.00-10	3450	18.9	65
10	7¼	⅝	65				
				9.00-12	3850	18.9	72
6	8¾	¾	72				
				10.00-12	4000	19.7	78
				11.00-12	4500	20.1	90
8	10	¾	95				
				11.00-14	4850	20.1	98
				12.00-14	5275	20.8	110
				12.00-16	5675	20.8	118
10	11¼	¾	120				

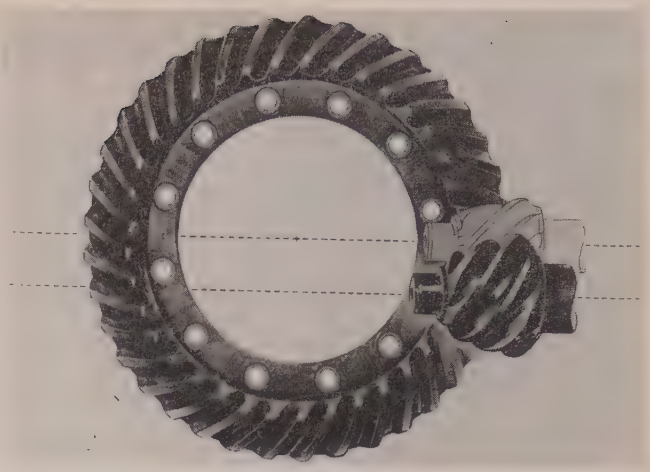

Fig. 24 – Spiral bevel intersecting axes and hypoid nonintersecting axes (TDA)

faster, more powerful engines and increased capacity tires with higher strength cords.

Basically, axles are subject to the same fundamental laws of physics as the simple lever and wedge. Higher-order mathematics, combined with years of experimental and field experience, has established the general proportions of present-day axle drives. The design approximations, presented below, deviate only slightly from these standards.

Before the design of the torque transmitting parts of the axle is gone into further, the various types of gearing and reduction will be briefly described.

Type of Gearing – The nomenclature differentiating between axle types refers specifically to the mechanism providing the right-angle drive from the propeller shaft to the axle. Bevel or hypoid gears (Fig. 24) predominate in this function, although worm drives are also found. Salient differences between the various types are of interest. A spiral angle, common in gearing applications, increases the number of teeth in contact at any given time; this is the primary factor accounting for the superiority of spiral bevel gears over straight bevel gears with respect to smoothness, quiet operation, and lower dynamic stresses. The hypoid system goes a step or two further. Readily identified by its nonintersecting axes, this system can employ a larger pinion than can spiral or straight bevel drives of the same ratio. This gives an added margin of strength, permitting a greater reduction in a given space – the primary reason for their wide preference in truck single-reduction applications. Hypoid systems also exhibit a high degree of smoothness and quietness directly attributable to the offset axes and resulting worm-drive tendencies. However, this same phenomenon produces high sliding velocities between the teeth – distinctly not an advantage. Fortunately, the early development of extreme-pressure lubricants reduced the magnitude of this problem.

The continuous spiral action of worm-gear drives in Fig. 25 provides very quiet operation; but more

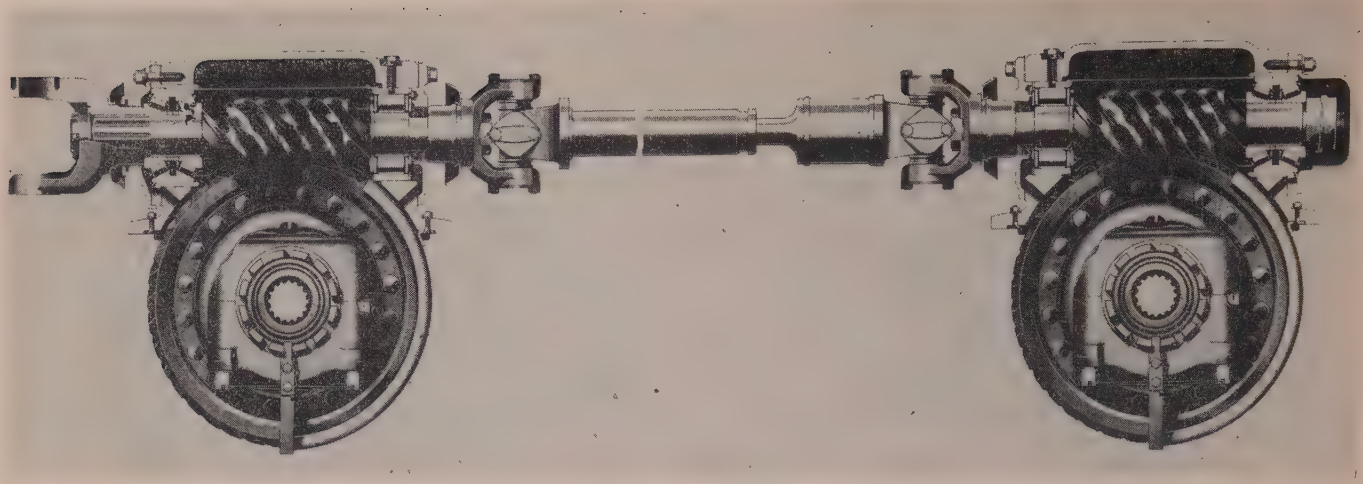

Fig. 25 – Worm-gear drive for tandem axles (TDA)

important to the heavy-axle industry is the long life of the worm gear and its ability to accommodate very high reductions in a single step. Important disadvantages include low mechanical efficiency, higher cost, and the need for considerable space above or below the axle center. Though it conceivably could compete with some double-reduction drives, its use is mainly restricted to a few special applications, such as tandem through-drive axles.

Type of Reduction – The important types of reduction may be grouped into three fundamental classifications: single-reduction, double-reduction, and 2-speed.

Fig. 26 shows a typical single-reduction axle, identified by its single-step reduction. The power-flow path of a single-reduction axle is sketched out in Fig. 27. In the overhung pinion design of Fig. 26, the pinion is mounted behind its supporting bearings A, B, and C, permitting some simplification of construction. Drive pinion bearing spacers and differential bearing adjusters provide

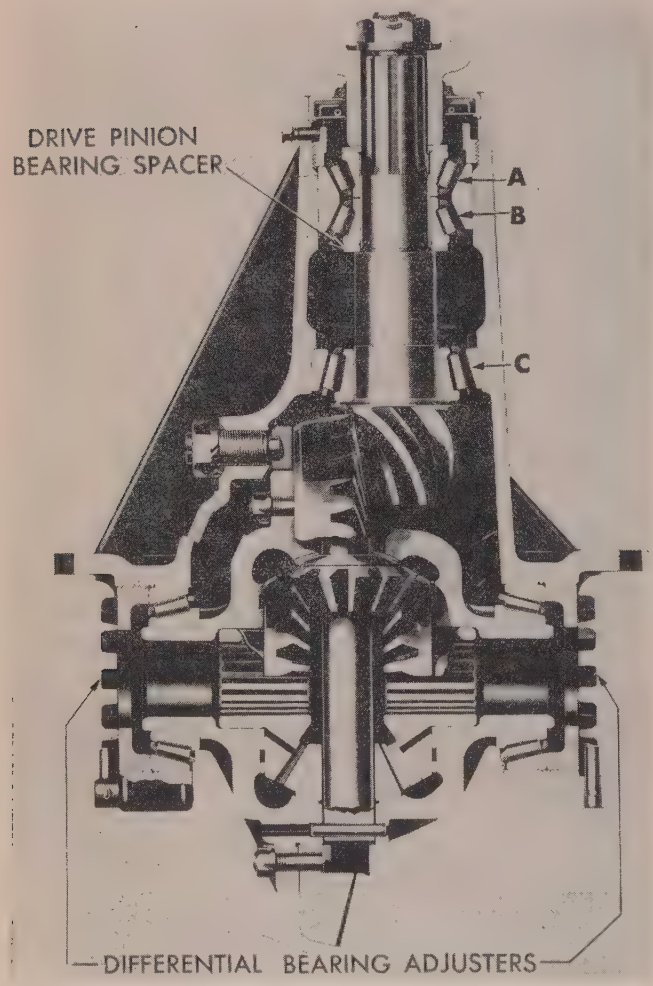

Fig. 26 – Single-reduction axle with overhung pinion

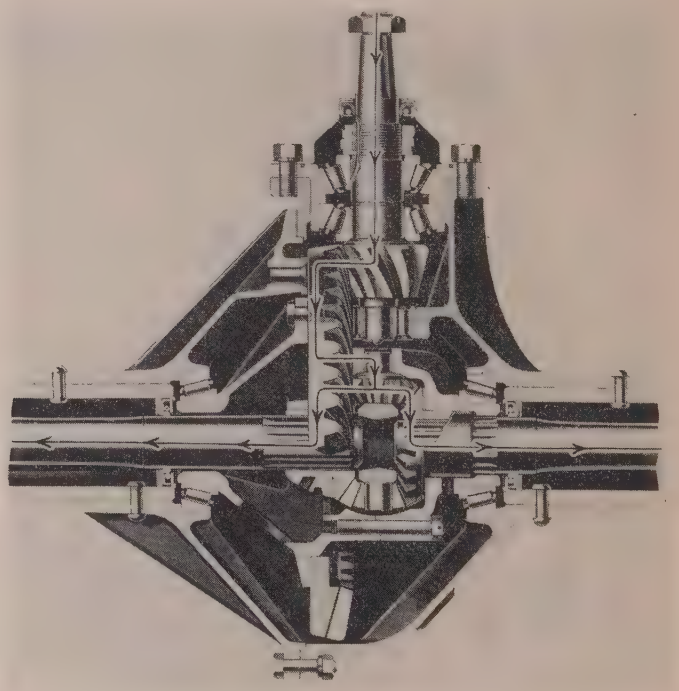

Fig. 27 – Torque travel through single-reduction axle (TDA)

for proper bearing assembly and adjustment. For heavy vehicles a straddle-mounted pinion, as shown in Fig. 28, has the advantage of greater rigidity as well as somewhat lower bearing loads.

The double-reduction drive of Fig. 29 overcomes the ratio limitations of single-reduction drives by introducing a second step – usually spur, helical, or herringbone gears – behind the customary bevel- or hypoid-gear set. The primary advantage of this system is the avoidance of auxiliary transmissions and attendant increased capacity of the drive line; on the debit side is a serious loss of vehicle flexibility. Incidentally, double-reduction gearing of the hypoid-helical type is built not only in the conventional front-mounted design, but also in a top-mounted design; the latter an important spatial consideration in short-wheelbase tractors and in tandem-drive units.

The 2-speed axle effectively combines the advantages of both previous types. High torque multiplication is available at the flick of a button or lever, and yet no sacrifice is necessary in economical highway or light-load operation. The shift is effected by a direct mechanical linkage, by vacuum or compressed air, or electrically.

The power flow of a typical 2-speed design (Fig. 30) is almost identical to that of the double-reduction train except that a speed change is accomplished by a shift collar (dog clutch), which couples one of two second-stage gear sets to the first-stage hypoid-gear set.

In a planetary 2-speed design the maximum reduction is obtained through a planetary-gear set interposed between the ring gear and differential, as shown in Fig. 28. In high speed the sun gear is mechanically locked to the planet carrier, causing the entire output unit to rotate at ring-gear speed. Similarly, in low speed the sun gear is locked to the axle housing, causing the planetary annulus, which is part of the ring gear, to drive the planet carrier through the planet pinions, with resulting lowered speed. The speed change is accomplished by shifting the sun gear axially into engagement with "dogs" in the planet carrier for high, or in the differential bearing support for low.

Drive Pinion Mounting – As noted earlier, a pinion may be overhung or straddle-mounted. Neither method affects the gear geometry, although a straddle-mounted pinion can operate at slightly higher tooth loads and is generally considered superior. The type of mounting does, however, have an obvious effect on bearing loads and on pinion shaft and carrier design. With an overhung assembly it is advisable to space the bearing centers 2.5 times the overhang distance, rear bearing center to load center. Not only does the straddle arrangement allow a more compact structure, but the maximum radial bearing load is substantially half that of the overhung type, while the thrust load remains the same. Serious complexities in the straddle design can stem from the limited space

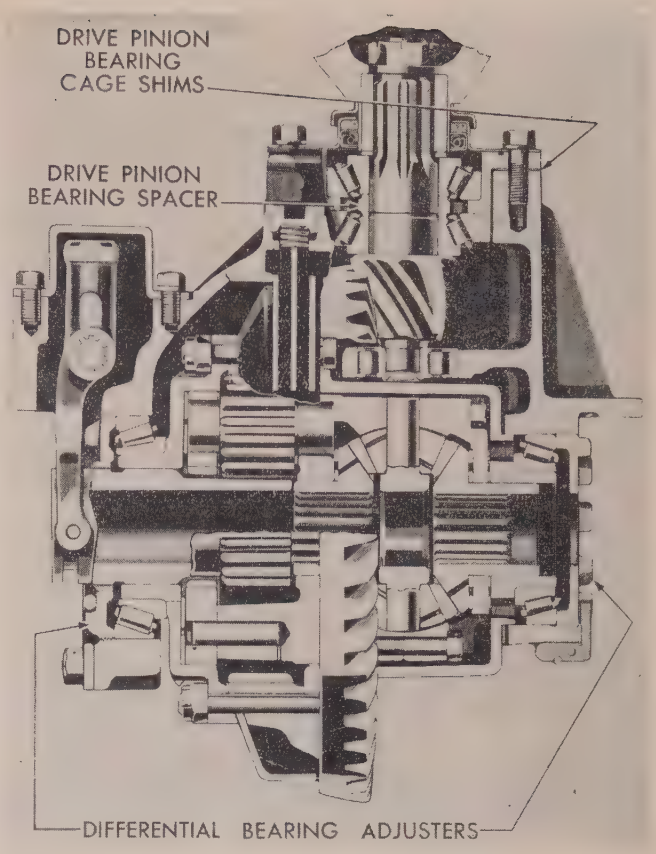

Fig. 28 – Planetary 2-speed train (Eaton)

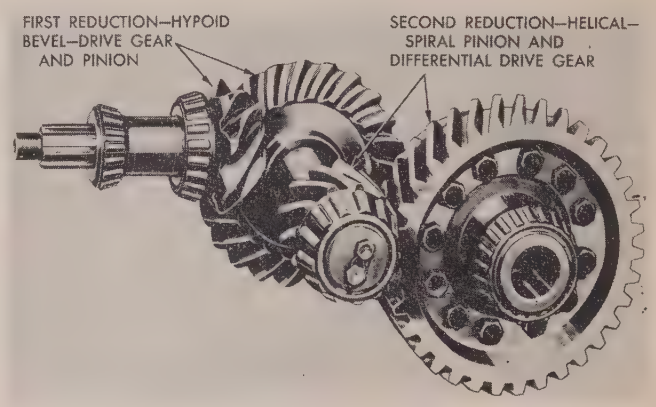

Fig. 29 – Double-reduction gear train (TDA)

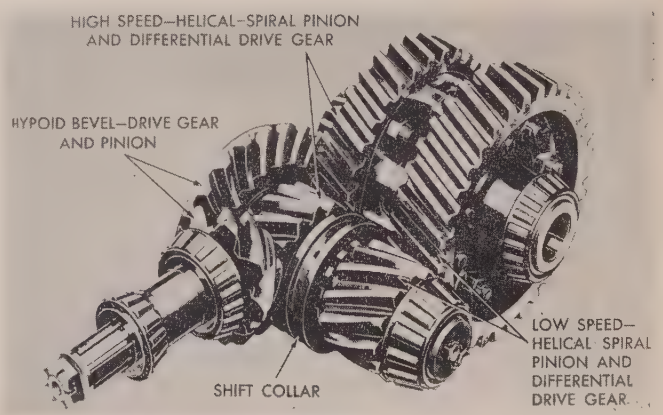

Fig. 30 – Double-reduction 2-speed train (TDA)

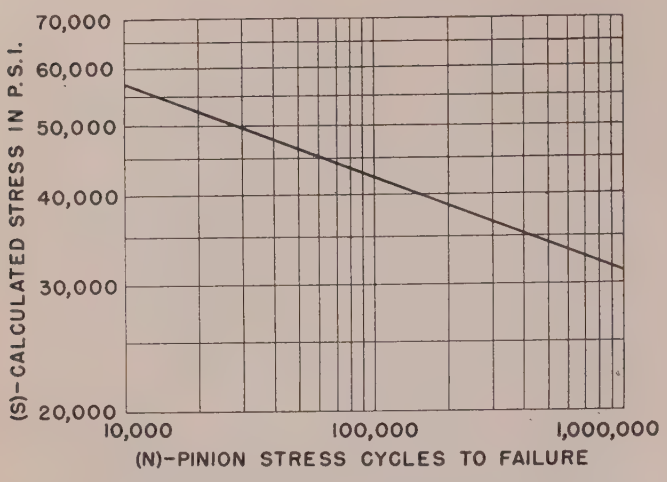

Fig. 31 – Fatigue life chart – spiral bevel rear-axle gears

available between the pinion axis and the ring gear, placing undesirable restrictions on bearing dimensions.

One other aspect of pinion mounting deserving discussion is the position of the pinion axis with respect to the ring-gear axis. In hypoid systems, the pinion may be offset above or below the ring-gear center. In addition, it may be located either to the right or left of the ring gear, depending on the application and desired direction of rotation. The amount of offset is somewhat arbitrary but for heavy vehicles it approximates one-eighth of the ring-gear diameter to minimize sliding velocities. Practically all present single-reduction hypoid designs have the pinion below the gear center and on the right-hand side. A necessary variation occurs in double-reduction and 2-speed axles, where the pinion is above the ring gear and to the left – lest the vehicle end up with one forward (and a mighty slow one at that) and five reverse speeds. The hypoid pinion is usually offset in the direction of gear rotation, and drives with the concave side of the pinion teeth contacting the convex side of the gear teeth, since this achieves the most favorable operation. In any case, the spiral angle should be oriented to direct the pinion thrust outward, away from the ring gear; the usual hypoid pinion spiral is left-handed, rotating counterclockwise as viewed from the rear.

Drive Gears – Hypoid gears are predominantly specified for the right-angle drive from the propeller shaft to the axle. In addition to having offset axes, the hypoid system differs significantly from the spiral bevel system in that the spiral angle of the pinion is greater than the spiral angle of the mating gear, whereas with the spiral bevel system the angles of mating gears are equal. As the spiral angle increases, the circular pitch or distance between the teeth increases, which explains the greater size and strength of hypoid pinions over spiral bevel pinions for the same reduction.

Axle ratio must, of course, be determined from performance requirements. Single-reduction hypoid gears are limited at the present time to a maximum ratio of about 7.8 to avoid excessive weakening of the teeth (this restriction is even more severe for spiral bevel gears). Since the minimum number of pinion teeth is 5 for hypoid gears, ring-gear diametral pitches of about 2.2 to 3.3 are common, the coarser pitches being applicable to the larger gears.

The common gear materials – carburizing grades of chrome-nickel-molybdenum steels – can serve as a basis for preliminary design approximations. It should be noted, however, that the final material selection will rest heavily on fatigue life, and ease of machining and heat-treating, as well as physical properties, availability, and cost.

Ring-gear proportions may be based on compressive tooth load per inch of face, which in current practice is limited to about 12,000 lb per in. for overhung pinion designs and 15,000 lb per in. for straddle-mounted pinions. (Design values are figured for the maximum expected low-gear torque.) This, plus tooth beam strength considerations lead to ring-gear outside diameters (in inches) of about ¼ of the cube root of the ring-gear torque (in pound-inches), and radial tooth face widths of about 1/7 the outside diameter. To be more exact, the "¼" factor actually ranges between 0.23 and 0.27, the lower value being representative of 9-in. ring gears of double-reduction axles and the higher, of 16-in. ring gears of single-reduction axles. Likewise, the "1/7" factor ranges from 1/6 for small gears to 1/8 for the larger gears. The cubic relationship of ring-gear diameter to torque may be seen as a result of three parameters: (1) torque arm (ring-gear radius), (2) tooth width, and (3) tooth form (larger gears are generally straddle-mounted, with coarser pitches).

Compressive Stresses on Gear Teeth – The substantiation for using load per inch of face as a first approximation in design or as a convenient method of comparative evaluation is found in the Hertz equation for bodies under compressive stress. For localized contact stresses of gear teeth, the special case of two cylinders in contact is applicable, and the maximum compressive stress by the basic Hertz equation is:

$$S_c = 0.583 \sqrt{W \left(\frac{1}{R_1} + \frac{1}{R_2}\right) \Big/ \left(\frac{1}{E_1} + \frac{1}{E_2}\right)}$$

where W is the load per inch of face, E_1 and E_2 are the moduli of elasticity, and R_1 and R_2 the radii of curvature of the mating teeth at the contact point. Since for steel gears E_1 and E_2 are 30,000,000 and R_1 and R_2 have a relatively constant relationship, the load per inch of face (W) is the only factor which varies appreciably. Hence this

simple expression of load per inch of face can theoretically be used as a parameter of tooth loading. Incidentally, chemical surface treatment of gear teeth improves wear-in characteristics very considerably.

Sample Calculation for Drive Gear Set – A sample calculation will now be given illustrating the pertinent design approximations useful for evaluation or preliminary design of drive gear sets.

Axle Drive Gear Set Symbols	Assumed Specifications
T_g = Ring-gear torque, lb-in.	
D_g = Ring-gear outer diameter, in.	
w_g = Gear-tooth radial face width, in.	
F_g = Individual compressive tooth load, lb.	
N_g = Number of teeth on ring gear	
N_p = Number of teeth on pinion	5

The maximum torque imposed on the ring gear is the engine torque multiplied by both the transmission ratio and axle ratio, obtained from the specifications of the "average" vehicle.

(D.A. 5) Ring-gear torque:

T_g = Net engine torque $\times$ transmission low-gear ratio $\times$ axle ratio

$T_g = 300 \times 7.5 \times 7.8 = 17{,}600$ lb-ft

$= 210{,}000$ lb-in.

(D.A. 6) Pinion and ring-gear teeth:

$N_p = 5$ or more $\qquad N_p = 5$

N_g = Axle ratio $\times N_p \qquad N_g = 7.8 \times 5 = 39$

(D.A. 7) Ring-gear diameter:

$$D_g = 0.27 \sqrt[3]{T_g}$$

$$D_g = 0.27 \sqrt[3]{210{,}000} = 16 \text{ in.}$$

(D.A. 8) Diametral pitch:

$$\text{Diametral pitch} = \frac{N_g}{D_g} = \frac{39}{16} = 2.5$$

(D.A. 9) Tooth face width:

$$w_g = \frac{D_g}{8}$$

$$w_g = \frac{16}{8} = 2 \text{ in.}$$

(D.A. 10) Individual compressive tooth load:

$$F_g = \frac{2T_g}{(D_g - w_g)}$$

$$F_g = \frac{2 \times 210{,}000}{16 - 2} = 30{,}000 \text{ lb}$$

(D.A. 11) Compressive tooth load per inch face width:

$$\text{Tooth load/in.} = \frac{F_g}{w_g}$$

$$\text{Tooth load/in.} = \frac{30{,}000}{2} = 15{,}000 \text{ lb per in.}$$

Since, as mentioned earlier, the maximum compressive tooth load per inch for an overhung pinion is 12,000 lb per in., D.A. 11 indicates that a straddle-mounted pinion should be used. The alternative to this could be a larger face width or a slightly larger gear diameter.

Allowable Bending Stress in Rear-Axle Gear Teeth – The tooth dimensions not only must be adequate to withstand compressive surface loads, but the beam strength at the tooth base must also be sufficient to transmit maximum power without breaking, even under moderate shock loading.

An empirical equation (developed by Almen and Boegehold), based on test experience and widely used in the industry, for allowable bending stress in rear-axle bevel gears may be expressed as:

$$NS^{7.54} = 10^{39.8}$$

where N is the number of stress cycles in a fatigue testing machine and S is the calculated stress. The equation may be graphed as a straight line on logarithmic scales, as shown in Fig. 31. Of course, one cycle in the machine may equal over a thousand cycles of normal road operation. While the number of stress cycles considered as a satisfactory fatigue life for the pinion may vary somewhat throughout the industry, 300,000 is representative. Transposing the equation and substituting this value for N, we find that the allowable stress is:

$$S = \text{Antilog}\left(\frac{39.86 - \log 300{,}000}{7.54}\right) = 36{,}000 \text{ psi (approx.)}$$

which may be checked by the graph. Since the ring gear has several times as many teeth as the pinion, a given ring-gear tooth will carry load less frequently than a pinion tooth in the same proportion as the number of teeth in the pinion to that of the ring gear. This ratio determines the stress cycles for which the ring-gear teeth are designed. If we consider a ratio of teeth as say 6.5 to 1, the stress cycles required for the ring gear would be:

$$\frac{300\,000}{6.5} = 46{,}000 \text{ cycles}$$

which, referring to the graph again, corresponds to a stress of 47,000 psi.

Since the allowable stress of the pinion tooth is less than that of the ring-gear tooth (36,000 versus

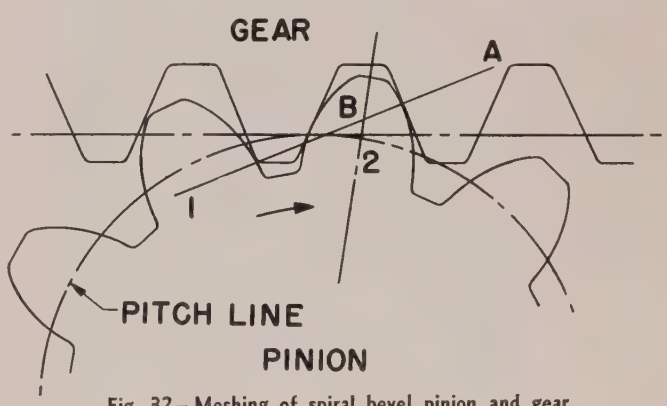

Fig. 32 – Meshing of spiral bevel pinion and gear

47,000 psi in our example), the dimensions affecting tooth beam strength must be greater for the pinion than for the ring gear.

Strength of Spiral Bevel Gear Teeth – Now that we know the allowable bending stresses near the root of the tooth, we shall determine a method of calculating the stress, which in turn will give the required tooth face width for satisfactory beam strength. (A design approximation for this value has already been given in D.A. 9.) A gear and pinion similar to that shown in Fig. 32 is helpful in determining dimensions and visualizing the problem. A pinion tooth is most highly loaded just before the next tooth comes into mesh. Looking at the drawing, we see that as pinion tooth 1 nearly makes contact with a gear tooth, pinion tooth 2 carries the entire load, acting along line *AB*. The pinion tooth stress is a maximum for this condition. Enlarging the view of this one pinion tooth, we have the sketch in Fig. 33.

Since the force along line *AB* may be considered as acting at any point on this line we shall, for simplicity, assume that it acts at point *B*, on the radial centerline of the tooth. Force *AB* may be resolved into its components *YB* and *XB*. The radial component *YB* produces only compressive stresses, which, though tending to reduce the tensile bending stresses at point *O* slightly, is usually neglected. The tangential component *XB* is the significant one,

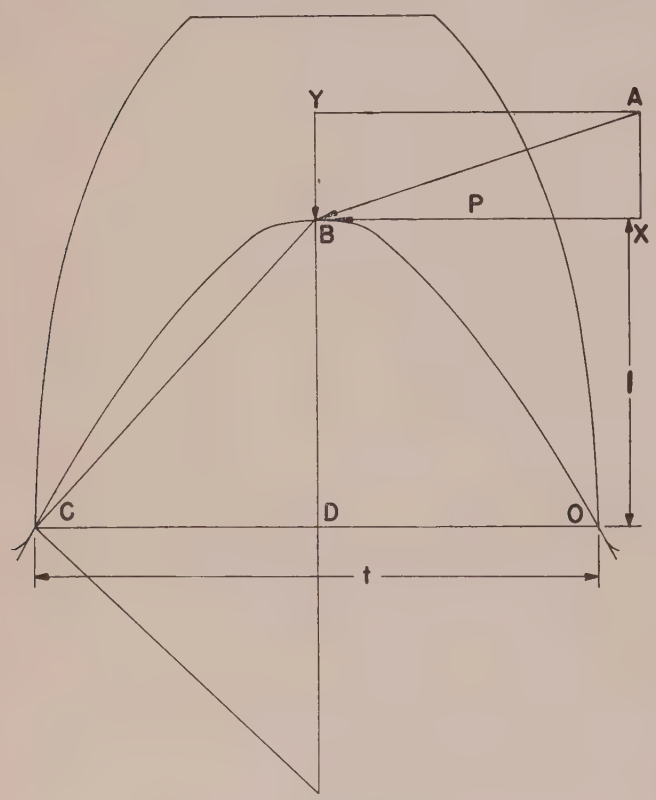

Fig. 33 – Beam strength of pinion tooth

and tends to bend the tooth. The tooth cantilevers from its base *OC*, with its weakest section near the root of the tooth. Accurate determination of the exact location of point *O* is made by drawing a parabola *CBO* having point *B* as its apex, and which is tangent to the tooth surface. The points of tangency locate *O* and *C*. The parabola represents a cantilever beam of uniform strength and therefore the line connecting points *C* and *O* is the critical section at the base of the cantilever.

Stress in the tooth may be expressed as:

$$S = \frac{Pl}{Z} = \frac{6Pl}{Qt^2} \times$$

where *S* is tensile stress at point *O*, *P* is tangential load, *l* is beam length, and *Z* is the base section modulus, which, in turn, is the product of the square of the tooth thickness (*t*) and the equivalent tooth face width (*Q*) divided by 6 (in gearing texts a form factor combining effective beam length and section modulus is often used instead of this formula). A rigidity factor (*f*) has been added to reflect the method of pinion and gear mounting; *f* is considered unity for overhung mountings and 0.80 for straddle mountings.

The equivalent tooth face width is used in place of the actual tooth face width to compensate for the decreasing diameter of the bevel pinion from its front to rear surfaces (see Fig. 34). For convenience, calculations are normally based on the large end of the tooth section. However, since the diameter (which can also be considered as the moment arm of the tooth) decreases and the torque applied remains constant, the tangential load on the tooth increases as we move from the large end of the tooth to the small end. Thus, the actual stress on the tooth is higher than it would be for a parallel-faced spur-gear type of tooth having the same face width. Since, as the above formula indicates, stress varies inversely as the face width, a lower, or equivalent, face width is used in stress calculations for bevel gears. This equivalent face width closely approximates 0.87 times the actual face width, and can be considered as being the face width of a spur pinion having the same strength, diametral pitch, and number of teeth as the spiral bevel pinion.

Using the "industry average" truck specifications, our pinion is required to transmit 300 lb-ft of net engine torque with 7.5 transmission low-gear ratio. If D.A. 5 is applied to the pinion (by eliminating the factor of axle ratio), the pinion torque is calculated to be:

$$T_p = 300 \times 7.5 = 2250 \text{ lb-ft}$$
$$= 27{,}000 \text{ lb-in.}$$

If our layout showed *R* as 1.6, the tangential tooth load would then be:

$$P = \frac{27{,}000}{1.6} = 17{,}000 \text{ lb}$$

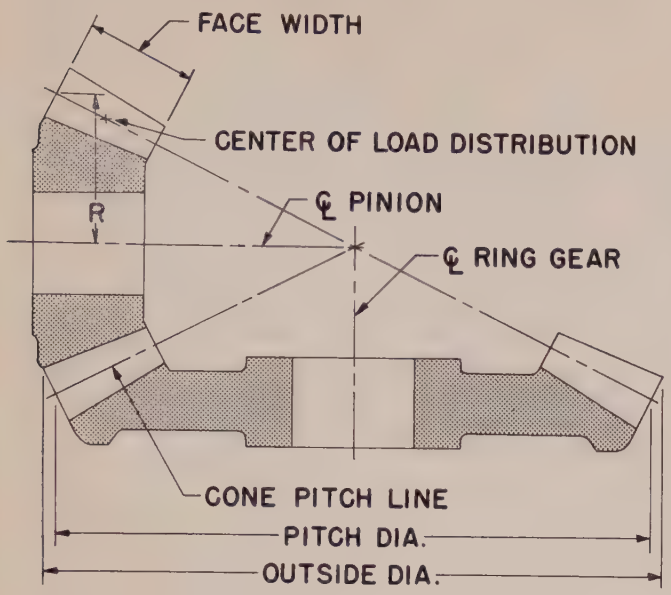

Fig. 34 – Spiral bevel pinion and gear set

Referring to Fig. 33, if the beam length (l) were 0.60 and the tooth thickness (t) were 0.90, we can insert known values in the bending stress equation and solve for the required pinion face width. The allowable stress is 36,000 psi, as previously determined, and a straddle-mounted pinion design will be assumed.

$$S = \frac{6Plf}{Qt^2}$$

$$36{,}000 = \frac{6 \times 17{,}000 \times 0.60 \times 0.80}{Q \times 0.90 \times 0.90}$$

so that:

$$Q = 1.68 \text{ in.}$$

As stated before, the equivalent face width approximates 0.87 times the actual face width, therefore the required actual face width is:

$$1.68/0.87 = 1.93 \text{ in.}$$

This may be rounded off to a nominal 2 in.

Our example has been for the pinion since this is usually more critical than the ring gear. The ring-gear face width, of course, can be calculated by similar means. Further, our example has been for spiral bevel rather than hypoid gears, since the former provide a simpler example. However, since hypoid gears are simply a modification of spiral bevel gears permitting operation on nonintersecting axes, the same allowable stresses and method of calculation can be used as an approximation for hypoid gears. Refinements of the method for hypoid gears may be found in booklets published by the manufacturers of gears and gear cutting machinery. A detailed discussion of gear design may be found in "Marks' Handbook,"[2] "Manual of Gear Design" by Buckingham,[3] and two books by Heldt.[4]

Differential Carrier – The differential carrier (Fig. 35) is, in a sense, part of the axle housing, completing an enclosing structure retaining the lubricant and resisting the weather. Considered separately, however, the carrier is a complex supporting assembly, providing the all-important alignment between the drive gears, the differential assembly, and the main axle housing. The importance of rigidity of mounting to gear durability cannot be over-emphasized: for proper tooth contact, the pinion must not deflect more than 0.003 vertically and 0.010 laterally. In this regard, the ring gear is frequently backed up by an adjustable thrust block adjacent to the point of mesh. This block has a slight clearance that will limit extreme deflection but will not interfere with normal operation. The bearings also contribute much to overall rigidity. Details of design will depend on the main housing and differential construction, maintenance and lubrication provisions, and the obviously important manufacturing procedures and tolerances.

Lubrication – Lubrication of gears and bearings – pinion bearings in particular – must be adequate for all conditions of speed, load, and temperature. This is achieved in practice by a great variety of troughs, grooves, traps, or scrapers incorporated in the carrier assembly to pick up lubricant and deliver it with a reasonably consistent flow to the various parts, such as the drive-pinion and differential bearings. A means of picking up lubricant is shown in Fig. 36. The lubricant is usually a mineral-base oil capable of withstanding temperatures approaching 400 F for limited periods without deterioration. For hypoid gears, with their

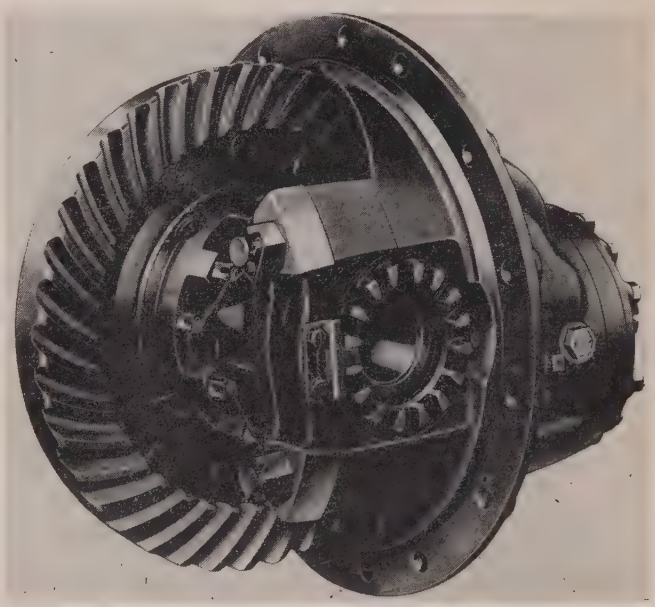

Fig. 35 – Differential carrier (TDA)

[2] See "Mechanical Engineers' Handbook," by L. S. Marks. Pub. by McGraw Hill, New York, 1951.
[3] See "Manual of Gear Design," by E. Buckingham. Pub. by Machinery, New York, 1935-1937. 3 vols.

high tooth loading and sliding velocity, special additives have been developed to produce a lubricant which will maintain the surface film under heavy loads, preventing possible metal-to-metal contact and resultant scoring or welding of the teeth.

Lubrication is a very important subject deserving much fuller treatment than is possible within the scope of this introductory paper. Axle cooling is another subject that can only be directed to the reader's attention. Many variables enter the problem – surface area, volume of lubricant, speed, and atmospheric conditions are but a few.

Bearings – Almost without exception, antifriction bearings are used to support the drive components. Ball, radial roller, and tapered roller bearings are used in a great variety of combinations. The tapered roller has enjoyed the widest favor in axle applications because of its high capacity for both radial and axial loads in a single compact unit. Equally important is its ability to operate at absolutely zero clearance under preload, providing the very maximum in rigidity. The bearings are supplied in a wide variety of standard sizes and capacities and should be selected according to the manufacturer's recommendations. Most catalogs include excellent detailed methods for selecting bearings, analyzing loadings, and predicting life.

Even a tentative selection of bearings will require preliminary layout work. Indispensable information such as the space available for bearing races and location of forces for load determinations can be obtained only after the basic proportions have first been established.

Axle Shafts – Axle shafts can be given a fairly straightforward analysis since they transmit only torque in the full-floating type of construction.

The torque applied to the individual shafts is one-half of the ring-gear output torque due to the dividing action of the differential. (Biasing or locking differentials, of course, demand special consideration.) The basic shaft diameter is obtained from the usual handbook torsional formula. Allowable shearing stress can be taken as 70,000 psi for properly hardened shafts. For rapid estimation the body diameter closely approximates 0.042 times the cube root of the axle shaft torque in pound-inches.

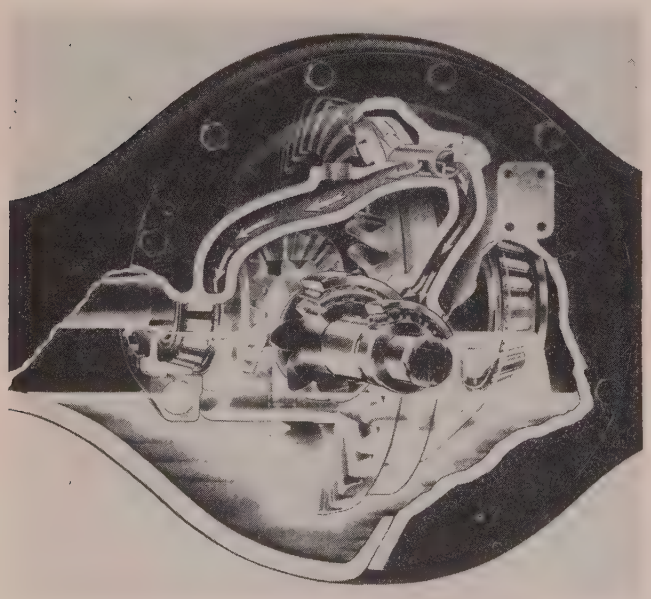

Fig. 36 – Typical lubrication pickup method (Eaton)

Latest manufacturing techniques now make use of precisely controlled flame or induction hardening treatments and shotpeening to gain substantial improvements in fatigue strength – a very important reliability factor. Today, an increasing number of rear-axle shafts are fabricated and hardened from plain carbon steels rather than heat-treated alloy steels. The carbon steel not only is more economical, but, when properly heat-treated, its hard case of 600 Bhn and soft core of 250-300 Bhn is admirably suited to carrying the torsional service stresses. A slightly lower surface hardness gives better impact strength but shorter fatigue life. Of course, the facilities for hardening and minimizing distortion of the carbon steel shafts may be more expensive than for heat-treating alloy shafts. Alloy-steel shafts, normally of molybdenum steels, heat-treated to a surface hardness of 400 Bhn provide exceptional impact strength and good fatigue life.

Special attention must be given to the design of the splines at the differential end of the shaft so that stress concentrations, inevitable at the spline run-out area, do not accelerate fatigue failure. General practice is to select a common nominal spline diameter in which the root diameter is slightly larger than that of the shaft body; the end to be splined is then upset sufficiently to accommodate machining operations. In most heavy-duty applications 16 to 18 splines are used and may be straight-sided, tapered, or involute in cross-section, with a length 1.3 times the spline diameter. The minimum length of spline engagement can be reduced to 0.75 times the spline diameter by the use of short, stubby involute splines fitted to close-tolerance female splines in place of straight-sided long splines with looser fitting tolerances.

The outer end of the shaft may be similarly splined but is more frequently attached to the wheel by means of a flange integral with the shaft and bolted to the wheel hub. The proportions are such that the flange diameter is smaller than the wheel pilot diameter. The attaching bolts must, of course, be of sufficient size and number to withstand the imposed torque. Another design uses a splined flange and hub to transmit torque so the bolts take only end thrust and maintain assembly.

In establishing axle shaft strength, it is considered appropriate to design the shafts (which are relatively easily replaced) with the view of providing a form of "safety fuse" to protect less

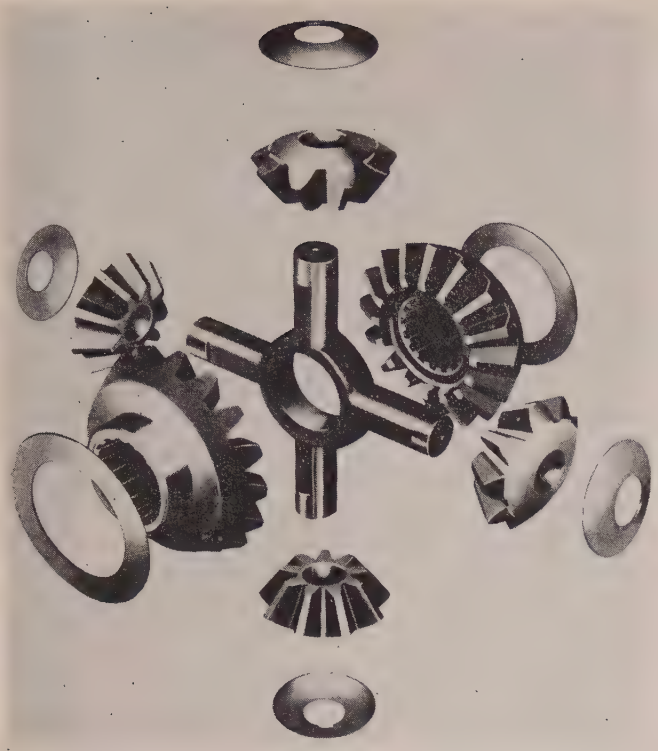

Fig. 37 – Differential pinion and side-gear assembly (TDA)

accessible units in the axle assembly. It is obvious, then, that safety factors must be judiciously selected and adequate comparisons made.

Sample Calculations for Axle Shafts – The following calculations will illustrate axle shaft evaluation and preliminary design technique.

Axle Shaft Symbols	Assumed Specifications
D_s = Shaft body diameter, in.	
T_s = Individual shaft torque, lb-in.	$\frac{1}{2}\ T_g$ = 105,000 (from D.A. 5)
S_s = Allowable stress, psi	70,000
d_s = Diameter of splines, in.	
n = Number of splines	
L_s = Length of splines, in.	

(D.A. 12) Axle shaft diameter:

$$D_s = \sqrt[3]{\frac{T_s}{0.196\ S_s}}$$

$$D_s = \sqrt[3]{\frac{105{,}000}{0.196 \times 70{,}000}} = 2.0 \text{ in.}$$

Spline diameter (d_s) could then be set at about 2.3 in.

(D.A. 13) Spline length:

$$L_s = 1.3\ d_s$$

$$L_s = 1.3 \times 2.3 = 3.0 \text{ in.}$$

Differential Function

The third major function of the rear axle is to allow differential action. As used in this discussion, the differential is ideally a device which will permit a difference between the rotative speeds of the driving wheels, at the same time dividing the driving torque between them equally. The need for the device can be emphasized by pointing out that, in any turn, the outside rear wheel of a truck travels farther than the inner wheel; in a tight turn this may be as much as 30%. The potential effect of this on steering, tire wear, and structural components is obvious.

Conventional Differential Operation – The underlying principle of the conventional bevel-gear differential, which has been known and used since 1827, is shown in Figs. 37 and 38, and can be described very simply: It is a balance lever, the most basic of machines. The lever being the differential pinion (occurring in sets of two or more), which in operation pivots about an axis rotating with the ring gear. Loads on diametrically opposite teeth will always be exactly equal since – again, for emphasis – the pinion is an equal-armed balance lever, hence equal forces will be transmitted unchanged to the axle shaft gears, or differential side gears, also of equal diameter. It naturally follows that equal forces applied to equal moment arms (gear radii) result in equal torques. Going one step further, we find that the pinions can also be defined as idlers; that is, they are completely free to rotate about their axes, changing no torque by so doing. Kinematically, they average the wheel speeds and restrict the ring-gear motion to this average. By virtue of this idler function, the wheel speeds can differ from one another with no significant energy loss.

Notwithstanding the advantage of substantially equal torque at all times regardless of variations in wheel speed, the conventional differential has an inherent deficiency that has caused concern from the first year of its existence. This is, of course, the severe loss of traction which occurs if one wheel encounters poor traction conditions, as evidenced, for example, by the inevitable wheel spinning during icy weather. This phenomenon occurs because the balancing function of the pinions does not permit torque greater than that of the spinning wheel to be applied to the stable

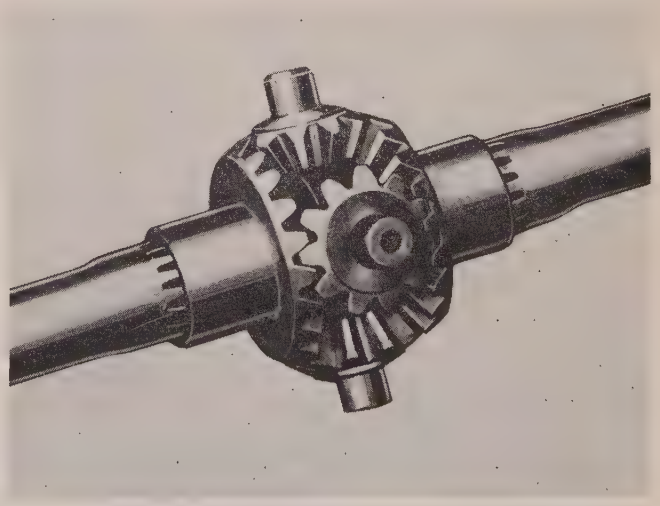

Fig. 38 – Assembled view of differential (TDA)

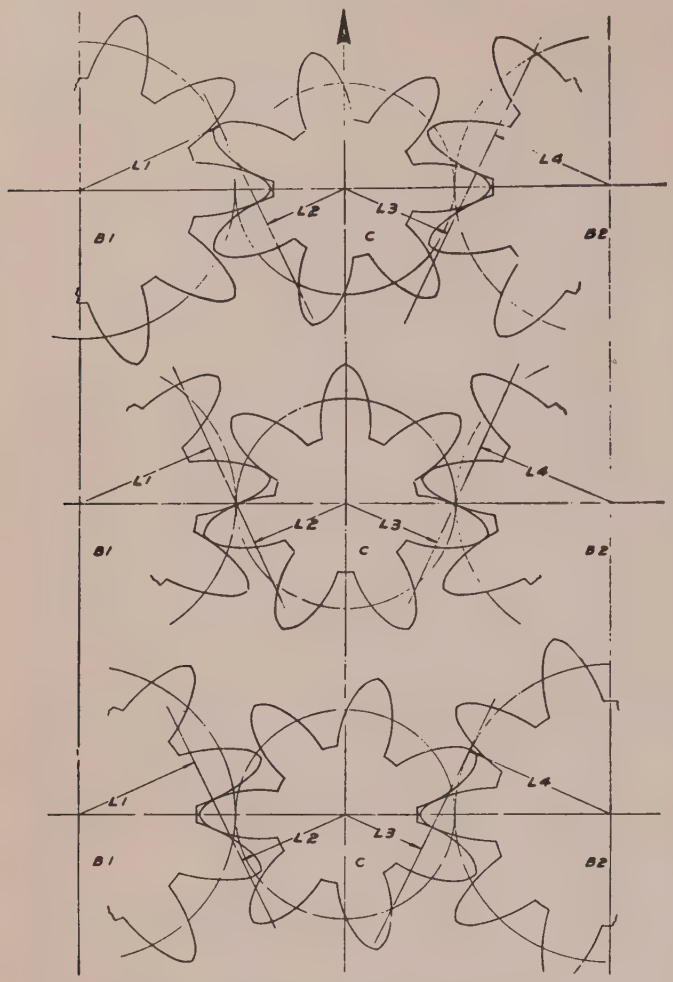

Fig. 39 – Diagram illustrating variation of leverage obtained with torque-biasing differential (TDA)

wheel. For passenger cars such circumstances are not so critical, but for a heavy off-the-road vehicle even a slight loss might initiate spin and cause the vehicle to become mired, where otherwise the stable wheel could have carried it through. The desire to overcome this handicap has resulted in several different designs departing considerably from the conventional and attempting to shift torque automatically from the low to the high traction side. They can be classified under two general headings: torque-bias (partial torque shift) and positive-locking devices (total torque shift).

Torque-Bias Types – One torque-biasing differential (see Fig. 39) incorporates an interesting application of a special gear-tooth contour to an otherwise conventional differential, thereby achieving a torque bias. The effect is to change the function of the differential pinion from that of an equal-armed lever to that of an unequal-armed lever. The center sketch of Fig. 39 shows the condition with both wheels rotating at the same speed, and the pinion acting as an equal-armed lever. In the event that one wheel is unable to take its share of the torque without slipping – the right wheel in the upper sketch and the left wheel in the lower sketch – that wheel will tend to move ahead, rotating the pinion to a position where it acts as an unequal-armed lever, delivering less torque to the wheel with the lowered traction, and more torque to the wheel with good traction. If a wheel should break loose and spin, however, the differential behaves in the conventional manner.

Locking Types – Early developments sometimes incorporated a manually operated dog clutch between the axle shafts and positively drove both wheels whenever it was desirable. However, as would be expected, inevitable evolution has resulted in automatic "clutches," one of which is illustrated in Fig. 40.

This design drives both shafts at the same speed through positively engaged dogs, as long as road conditions permit. During a turn, however, the engaging section of the clutch member (*B* in the diagram) climbs a ramp on the spider and center cam assembly (*A*), releasing the outside wheel and allowing it to freewheel until equal speed conditions are regained. The wheel is connected through the axle shaft to side member *E*, which is splined internally for the shaft and externally for the clutch member; part *C* is a flanged spring retainer for spring *D*. In the event one wheel loses traction completely, the other is positively coupled to the ring gear and transmits all the power that traction conditions will support. Quite apparent in this design, but also true in differentials employing friction for bias, to any degree, is the unbalance of torque developed whenever the wheel speeds differ, even though it may not be required in normal good road operations. This partially defeats the original purpose of the differential, but experience has proved that, in view of the benefits gained, the compromise is warranted under many conditions.

Further discussion of these and other types of differentials may be found in "Automotive Chassis" by Heldt[4] and in "Automotive Differentials" by Buckendale and Boughner.[5]

Differential Gears – For actual design and calculation, only conventional differentials will be discussed. The service conditions have a strong influence upon the selection of material, lubricant, and maintenance provisions. Preliminary considerations for differential gears will, of course, involve the maximum low-gear torque rating, which is the same as for the ring gear. From this it is possible to determine differential-gear sizes and overall space requirements. Since pitch line speeds are low and, in fact, motion is relatively infrequent,

[4] See "Automotive Chassis," by P. M. Heldt. Pub. by Heldt, Nyack, N. Y., 1952; "Torque Converters," by P. M. Heldt. Pub. by Heldt, 1951.
[5] See SAE *Quarterly* Transactions, Vol. 5, July, 1951, pp. 359-375: "Automotive Differentials," by L. R. Buckendale and L. G. Boughner; digested in *SAE Journal*, Vol. 59, May, 1951, pp. 52-57.

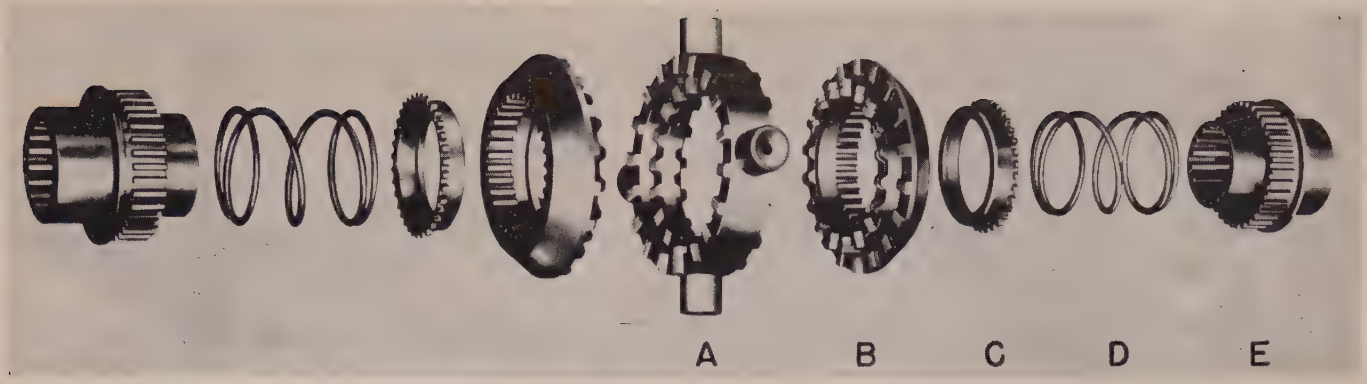

Fig. 40 – Exploded view of locking differential (TDA)

smoothness and quietness are not serious problems in differential gears; hence, straight bevel gears with teeth of the 20-deg American Standard stub-tooth form are generally used.

Current practice for heavy vehicles indicates the use of four pinions with 10 teeth each and side gears with 16 teeth each as a basis for first assumptions. (The number of side-gear teeth must be even to permit alignment and assembly.) The side-gear diameter can be approximated as 1/10 the cube root of the differential torque in pound-inches. Gear-tooth face width is approximately 1/5 the side-gear diameter. These proportions will usually yield an individual tooth loading of about 9000 psi of tooth face. A more detailed tooth analysis can be treated similar to that already covered under ring-gear design.

Pins – The next important consideration is the pinion pin bearing. The diameter of the pin (the bearing surface for the pinion) is generally chosen as a nominal diameter, the pin usually being part of a forged cross in heavy-duty axles. Axial length of the bearing approximates 1.1 x pin diameter, being made as great as possible. These dimensions together yield a bearing stress of approximately 14,000 psi. Lubrication of the differential pinion bearings is accomplished by drilling radial oil holes at the bottom land of one or more pinion teeth or by machining oil flats on the pins or spider cross.

Differential Case – The differential case on which the ring gear is mounted is probably the most complex design item of the differential. It is the actual supporting member for the differential gears and must maintain precise alignment of the differential components, the ring gear, and the axle shafts while transmitting torques and radial loads of high magnitude. The geometrical layout must be symmetrical about the differential axis to provide reasonable balance. The construction must allow reasonably simple adjustments and service procedures. In these respects the ultimate case design will depend greatly upon other major axle components such as the axle housing, differential carrier, bearings, shafts, and drive pinion location. If the axle is of the 2-speed type, compactness may become a main objective and introduce further complications. Evidently, then, a great many unknown factors influence the final construction, and only general suggestions can be noted.

Current case designs generally employ cast malleable iron. The larger units are usually constructed in two sections and bolted together to facilitate assembly. The case is machined to provide bearing and thrust surfaces for the pinions and side gears, and a machined flange is incorporated to mount the ring gear (which is often offset axially to provide a centered location for the main drive pinion).

Thrust washers of bronze or hardened steel are inserted between the case and the differential pinions and gears to prevent wearing away of the case, resulting in drive train slackness. It is claimed by some that phenolic laminated washers have

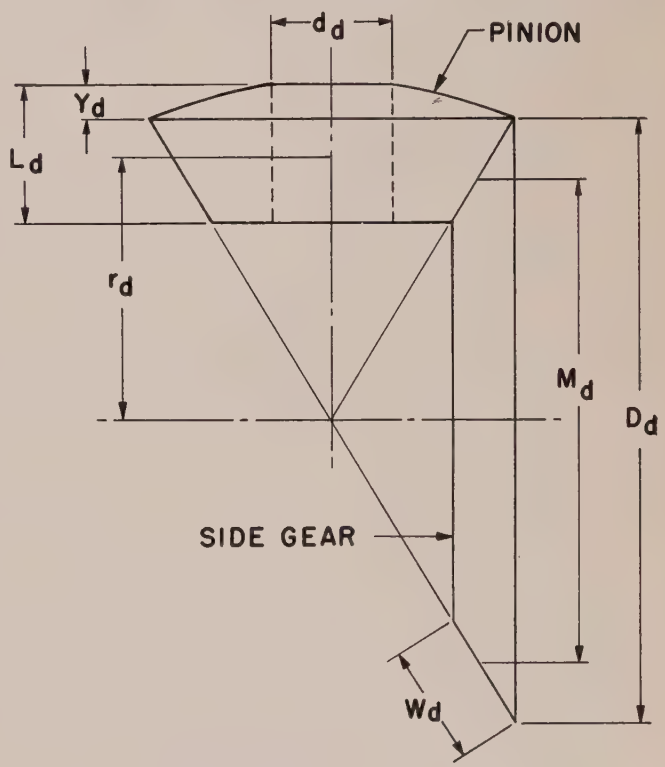

Fig. 41 – Basic layout of differential gears

lower friction and wear rate characteristics than hardened steel.

The differential pinion pins are frequently arranged in the form of a spider, as shown in Fig. 37, or as a single pin extending across the case diameter plus two shorter pins inserted in a central block.

Alignment of the differential within the axle housing is provided by bearings supporting the outer ends of the differential case. These must carry the tangential, radial, and axial loads on the ring gear, loads which must in turn be withstood by the differential case structure.

Sample Calculations for Differential Assembly – Design approximations for a differential assembly are given below; reference to the layout of the basic geometry in Fig. 41 may prove helpful.

Differentia Symbols	Assumed Specifications
T_d = Total differentia torque = Ring-gear torque, lb-in.	210,000
N_d = Number of pinions	4
D_d = Outside diameter of side gear, in.	
M_d = Side-gear mean diameter at midpoint of tooth face, in.	
w_d = Tooth face width, in.	
F_d = Individual tooth load, lb	
d_d = Pinion pin diameter, in.	
L_d = Pinion pin bearing length, in.	1.1 d_d (approx.
r_d = Mean distance of pinion bearing surface from differential axis (or mean radius), in.	$\frac{M_d}{2}$ (approx.)
y_d = Amount of pinion crown, in.	
p_d = Pinion pin bearing pressure, psi	14,000 (approx.)

For a first approximation of side-gear diameter:

(D.A. 14) Side gear diameter:

$$D_d = 0.1 \sqrt[3]{T_d}$$

$$D_d = 0.1 \sqrt[3]{210{,}000} = 6.0$$

The diametral pitch for 16 teeth would then be $\frac{16}{6.0} = 2.7$.

The corresponding pinion diameter for 10 teeth is $\frac{10}{2.7} = 3.70$ in.

The tooth face width, varying from 1/4 to 1/5 the side-gear diameter, may be approximated as:

(D.A. 15) Tooth face width:

$$w_d = 1/5\ D_d$$

$$w_d = 1/5 \times 6.00 = 1.20 \text{ in.}$$

Laying out these dimensions as in Fig. 41 establishes the basic design of the gears. An approximation shows that M_d equals 80% of D_d, or 0.80 x 6.00 = 4.80 in. The mean radius (r_d) to the pinion bearing area equals the distance from the cone center to the midpoint of the bearing area. Allowing a slight increase for a crowned back on the pinion, r_d can be taken for a first approximation as $M_d/2 + 0.20 = 2.60$.

(D.A. 16) Individua tooth load:

$$F_d = \frac{T_d}{N_d M_d}$$

$$F_d = \frac{210{,}000}{4 \times 4.80} = 11{,}000 \text{ lb}$$

(D.A. 17) Tooth face loading:

$$\text{Face load} = \frac{F_d}{w_d} = \frac{T_d}{N_d M_d w_d}$$

$$\text{Face load} = \frac{11{,}000}{1.20} = 9.170 \text{ lb/in.}$$

(D.A. 18) Differential pinion pin diameter and bearing length:

$$d_d L_d = 1.1\ d_d^2 = \frac{T_d}{p_d N_d r_d} \qquad d_d = \sqrt{\frac{T_d}{1.1\ p_d N_d r_d}}$$

(since $L_d = 1.1\ d_d$)

$$d_d = \sqrt{\frac{210{,}000}{1.1 \times 14{,}000 \times 4 \times 2.60}} = 1.11 \text{ in.}$$

Pin diameter can be increased to 1¼ in., a nominal size.

Bearing length of 1.1 d_d gives 1⅜ in.

From Fig. 41 $r_d = \frac{D_d}{2} + y_d - \frac{L_d}{2}$ and y_d (scaled from Fig. 41) = 0.31, therefore $r_d = 2.62$

(D.A. 19) Pinion pin bearing pressure:

$$p_d = \frac{T_d}{N_d r_d d_d L_d}$$

$$p_d = \frac{210{,}000}{4 \times 2.62 \times 1.25 \times 1.375} = 11{,}800 \text{ ps}$$

which is within the allowable design specification of 14,000 psi.

Stopping Function

The last of the rear-axle functions to be discussed is perhaps less conspicuous in its association, but it is none the less important in the business of designing and using axles: namely, brakes, or the stopping function. Many papers have been written and committees organized for the purpose of exploring and defining the answer to the question, "When are brakes adequate?" Part of the complications that arise in answering the question are due to the three approaches to brake capacity that must be taken into account.

First, brakes must develop sufficient torque to stop the truck within a specificed distance. Brake torque output can be determined by test or approximated by calculation.

Second, brakes must have adequate ability to dissipate heat. The energy absorbed in a single stop may be enough to heat 20 lb of water from room temperature to the boiling point. Furthermore, braking horsepower may be as much as 10 times greater than maximum engine horsepower, since a truck requiring over 60 sec to reach its top speed may have to stop in less than 1/10 of this time.

Third, brakes must have acceptable wear characteristics. Thickness and area of lining must bear a relation to the axle load and tire radius which will make for minimum lining wear per stop. While

gross vehicle weight per unit of lining area for heavy trucks approximates 55 psi for current average practice, many other variables enter into this problem and, at present, there is no common agreement on a satisfactory "brake capacity index."

Heavy-duty truck brakes of high torque output must be fitted into a space restricted to about 80% of the nominal tire diameter. Most medium- and heavy-duty trucks use 20-in. tires, with 22-in. also offered in some instances. The most popular brake diameter is thus 80% of this, or 16 in. As truck axles become heavier and their capacity increases, larger wheel cylinders or air brake chambers and attendant wider linings must be used along with more power assistance. In order to increase torque and equalize lining wear without increasing dimensions, brakes having both shoes self-energizing (that is, tending to wrap into the drum) are used. In the case of air brakes, the operating cam is made to push harder on the nonenergized shoe. Still another way of increasing brake capacity is to use a lining with a higher coefficient of friction on the nonenergized shoe. Schematic diagrams of different hydraulic brake types used on heavy-duty trucks are shown in Fig. 42. A sketch of a hydraulic line system illustrating the method of actuation is shown in Fig. 43.

Fully energized designs in common use for hydraulic rear brakes are the dual-primary, duo-servo, and dual types. The first one mentioned has a single cylinder acting on levers, which press against the center of the shoes, the shoes in turn being wedged toward the drum by angled abutment blocks. The second type again has only one cylinder but pushes the toe of the first shoe into the drum, which in turn pushes the toe of the second shoe into the drum. The dual brake uses a cylinder for each shoe. In most cases both cylinders are double-acting so as to give full servo action in both directions of rotation. Differing from these is a single-cylinder Lockheed type in which the cylinder pistons push on the toe of one shoe and the heel of a second, both shoes being provided with separate anchors such that the energization of the first shoe is not passed on to the second. Obviously, a brake with dual-energization develops more torque over one where only a single shoe is energized. Tests and calculations show a torque increase of about 50% to 100%, depending on the type of actuation. Calculation of the torque output of a brake may be relatively complicated when consideration is given to such items as actuation factors, toe and heel angles, brake geometry, and center of drag. Test results may vary widely, depending upon lining coefficients, wear-in, frequency of application, drum speed, speed of application, amount of lining, line pressure, drum and shoe deflections, and thermodynamic properties of the brake. However, careful consideration of fundamentals and of actual test results enables an approximation of torque output to be worked out which will be useful for comparative evaluations and initial design.

For conventional 2-shoe air and hydraulic brakes, the torque is nearly proportional to the piston (or cam) force and the brake diameter. Piston force is the product of line pressure (P) and wheel cylinder piston area (A), while drum diameter may be represented as D. The product of line pressure, piston area, drum diameter, and a brake type factor (K) yields an approximate value

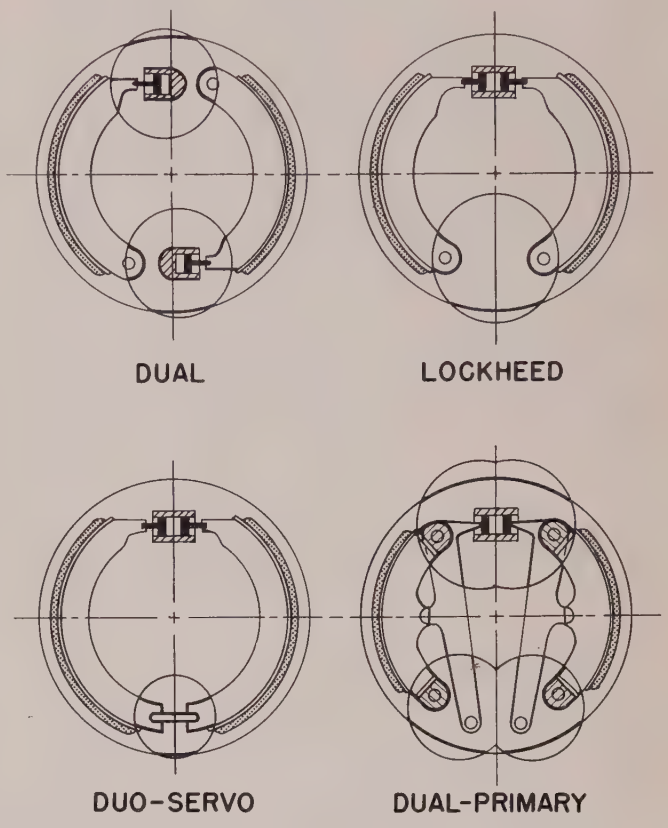

Fig. 42 – Schematic diagrams for hydraulic brake types for heavy-duty trucks

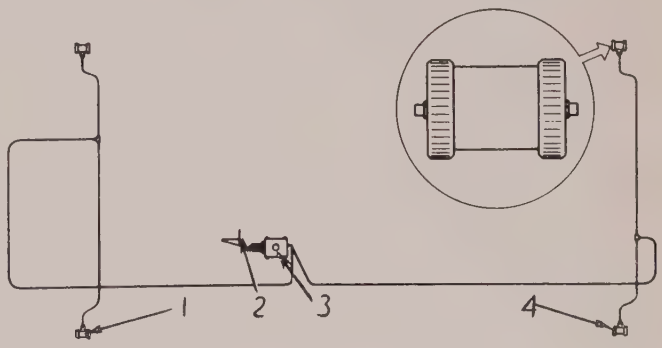

Fig. 43 – Hydraulic line system (TDA)

(1) Front wheel cylinder
(2) Foot pedal
(3) Master cylinder
(4) Rear wheel cylinder

of inch-pounds of brake torque per brake: $K \times P \times A \times D$. Test results and complex mathematical analyses indicate that K approximates unity for single-cylinder Lockheed brakes and 1.5 for dual-energized types. For air brakes the same formula applies, except P and A are air pressure and chamber area, respectively, and a leverage factor of slack adjuster length (L) divided by twice the cam radius ($2R$) is introduced.

Choice of drum diameter and wheel cylinder area is, within limitations, under control of the designer, but the maximum operating hydraulic line pressure for heavy trucks, with power assistance, is limited to from 1500 to 2000 psi. This pressure is dependent on brake pedal push, pedal ratio, master-cylinder piston area, and the amount of power assistance (incidentally, all heavy-duty trucks have some type of power assistance). A 200-lb pedal push is nominal for fast stops with master-cylinder-controlled booster units, while the Public Roads Administration has found some drivers who can exert 390 lb of pedal push.

Once the line pressure has been established for the desired pedal force, the tractive braking effort for the rear axle can be estimated by dividing the sum of $KPAD$ values for each brake by the tire loaded radius. This figure divided by the rear-axle weight will give the braking efficiency of the rear brakes. Braking efficiency is simply a ratio of retarding tractive effort to weight. The front brakes must also be considered for their contribution to the total braking effort. Further, front and rear brakes must be so related that optimum braking balance is obtained, both with the truck loaded and unloaded, and with weight transfer effects taken into account.

As a general rule, the overall braking system should be adequate to provide a deceleration of 14 ft per sec per sec. This represents a braking efficiency of 44% or, in other words, the braking tractive effort between tires and road equals 440 lb per 1000 lb of weight. Some designers prefer to allow for 60% efficiency, and use a proportionately higher value of K in the $KPAD$ formula. Theoretically, if full brake application is instantaneous, a deceleration of 14 ft per sec per sec will produce a stop from 20 mph in 30 ft. For passenger cars and light trucks this distance may be realized or even bettered. However, for heavy, long-wheelbase trucks and tractor-trailer combinations the stopping distance may be as much as 40 and 50 ft, respectively, since transmission of pressures through the comparatively long brake lines require a definite amount of time.

Master-cylinder reserve volume is another problem which requires serious attention. The fluid displaced in the master cylinder is the product of its piston area and stroke. Assume, for example, that the master-cylinder piston and all wheel cylinder pistons (eight on a 4-wheel truck) have diameters of 1¾ in. The brake pedal may have a 9-in. maximum effective travel with 6 to 1 ratio, giving a potential master-cylinder stroke of 1½ in. Since this stroke must be equally divided between eight wheel cylinder pistons, each gets a maximum travel of 3/16 in. Lining wear beyond that accommodated by this travel requires brake adjustment. Hydraulic brakes are usually designed for 1/8 to 7/32 maximum wheel cylinder travel, depending upon brake geometry, size, and type. Heat causes drum expansion and hence creates a need for more reserve. Heavy trucks approach the higher side of the range – usually 3/16 to 7/32 travel. In trucks, contrary to passenger-car practice, front wheel cylinders are usually smaller than rear cylinders, with the master-cylinder diameter equaling the rear wheel cylinder diameter. Air brakes are also limited in chamber stroke and reservoir capacity.

Most axle designs provide for the installation of various types and sizes of brakes, allowing relatively greater freedom of selection than for most other axle components. Further discussion of the braking function of the axle is beyond the scope of this introductory paper; the subject, with particular emphasis on air brakes and air brake systems, does appear to be a fertile and informative topic, however.

Sample Calculation for Brakes – For our example we shall consider brakes of the dual-energized type with hydraulic actuation, and illustrate the calculation of brake torque, wheel cylinder size, and master-cylinder size required to satisfy the stopping requirement.

Brake Symbols	Assumed Specifications
C = Rear-axle capacity, lb	22,000
R = Tire radius, in.	20 for 11.00/20 tire
P_b = Brake line pressure, psi	1700 (500 pedal, 1200 dual booster)
A_b = Rear wheel cylinder piston area, in.²	
B_b = Rear wheel cylinder diameter, in.	
D_b = Maximum brake drum diameter, in.	16½ with 20-in. tires
E_b = Brake efficiency required	44%
T_b = Torque per brake required, lb-in.	
b_b = Master-cylinder diameter, in.	

(D.A. 20) Torque per brake required:

$$T_b = \frac{C}{2} \times E_b \times R$$

$$T_b = \frac{22{,}000}{2} \times 0.44 \times 20 = 97{,}000 \text{ lb-in.}$$

(D.A. 21) Wheel cylinder size:

$$B_b = \sqrt{\frac{4A_b}{\pi}}$$

$$A_b = \frac{T_b}{KP_bD_b} \text{ (since } T_b = KP_bA_bD_b\text{)}$$

$$A_b = \frac{97{,}000}{1.5 \times 1700 \times 16.5} = 2.30 \text{ in.}^2$$

$$B_b = \sqrt{\frac{4 \times 2.30}{\pi}} = 1.72 \text{ in.}$$

A standard diameter of 1.75 in. should be selected.

(D.A. 22) Master cylinder size:

$b_b = B_b$

$b_b = 1.75$ in. diameter

Conclusion

The design, evaluation, and selection of heavy-duty truck axles presents a worth-while challenge to the engineer. With the aid of the scientific methods already available to him, he can continue to make strides forward toward striking an optimum balance of performance, economy, durability, and versatility. With the aid of new theories and methods which he, himself, can develop, these strides toward the optimum may in time bring him close enough actually to reach out and touch that ultimate goal.

Acknowledgment

In the preparation of this paper valuable assistance was given by the members of the Buckendale Lecture Committee: Dale Roeder, L. W. Fischer, E. P. Lamb, A. L. Boegehold, and C. E. Frudden. Illustrations and technical assistance were contributed by the Clark Equipment Co., the Eaton Mfg. Co., the Spicer Mfg. Co., and the Timken-Detroit Axle Co. Appreciation is also expressed to members of the Chrysler Corp. Engineering Division, who contributed their time and experience to the paper.

Additional References

1. "Analytical Mechanics of Gears," by E. Buckingham. Pub. by McGraw-Hill, New York, 1949.

2. "Improved Method for Estimating Fatigue Life of Bevel and Hypoid Gears," by W. Coleman. SAE *Quarterly* Transactions, Vol. 6, April, 1952, pp. 314-331.

3. "Automobile Chassis Design," by R. Dean-Averns. Pub. by Iliffe, London, 1952.

4. "Elements of Motor Vehicle Design," by C. T. B. Donkin. Pub. by Oxford, London, 1935.

5. "Handbook of Engineering Fundamentals," by O. W. Eshbach. Pub. by Wiley, New York, 1936.

6. "Motor Vehicle Engineering – Chassis," by E. Favary. Pub. by McGraw-Hill, New York, 1922.

7. "Gears," by P. S. Houghton. Pub. by Technical Press, London, 1952.

8. "Gear Design Simplified," by F. D. Jones. Pub. by Industrial Press, New York, 1952.

9. "Kent's Mechanical Engineers' Handbook," ed. by C. Carmichael. Pub. by Wiley, New York, 1950. 2 vols.

10. "American Machinist Gear Book," by C. H. Logue. Pub. by McGraw-Hill, New York, 1922.

11. "Rear-Axle Ratio," by R. Mackenzie. *Bus and Coach,* Vol. 21, April, 1949, pp. 131-133.

12. "Epicyclic Gearing," by R. McCrae. Pub. by Draughtsman Pub. Co., London, 1937.

13. "Gears," by H. E. Merritt. Pub. by Pitman, London, 1942.

14. "Development and Lubrication of Automotive Hypoid Gear," by F. F. Musgrave. *Institute of Petroleum Journal,* Vol. 32, January, 1946, pp. 32-44.

15. "Motor Vehicle," by K. Newton and W. Steeds. Pub. by Iliffe, London, 1950.

16. "Machinery's Handbook," by E. Oberg and F. D. Jones. Pub. by Industrial Press, New York, 1949.

17. "Involute Gears," by W. Steeds. Pub. by Longmans, London, 1948.

18. "Commercial Motor Transportation," by C. A. Taff. Pub. by R. E. Irwin, Chicago, 1950.

19. "Radial and Lateral Reactions Acting upon Wheels of Motor Cars," by E. A. Tsudakov. *Engineers' Digest,* Vol. 2, September, 1945, pp. 438-446; November, 1945, pp. 554-559; December, 1945, pp. 612-617; Vol. 3, January, 1946, pp. 18-25.

20. "Hypoid Lubricants for Truck Axles," by E. W. Upham. *Automotive Industries,* Vol. 82, Jan. 15, 1940, pp. 74-75.

21. "Strength-Stress Life of Helical-Gear Teeth," by E. J. Wellauer. Proceedings of Society for Experimental Stress Analysis, Vol. 10, No. 2, 1953, pp. 37-52.

Manufacturers' Publications

Listed here are a few of the many excellent handbooks and pamphlets written and published by the manufacturers of the equipment and mechanisms discussed in this paper.

1. "Brake Design Trends" by B. E. House and R. A. Goepfrich. Pub. by Bendix Aviation Corp., South Bend, Ind., 1944.

2. "Clark Engineering Digest." Pub. by Clark Equipment Co., Buchanan, Mich.

3. "Clark Engineering Manual." Pub. by Clark Equipment Co., Buchanan, Mich.

4. "Eaton Two-Speed Axles." Pub. by Eaton Mfg. Co., Cleveland, Ohio.

5. "Engineering Data." Pub. by Bower Roller Bearing Co., Detroit 14, Mich.

6. Gleason Machine and Gear Pamphlets. Pub. by Gleason Works, Rochester 3, N. Y.

7. "Handbook of Motor Vehicles Used by the United States Armed Forces." Pub. by Timken-Detroit Axle Co., Detroit, Mich.

8. "Hypoid Gears." Pub. by Timken-Detroit Axle Co., Detroit, Mich.

9. "Motor Truck Facts." Pub. by Motor Truck Committee of Automobile Manufacturers Association.

10. "New Departure Handbook," Vol. 2. Pub. by New Departure Division, General Motors Corp., Bristol, Conn.

11. "Timken Engineering Journal." Pub. by Timken Roller Bearing Co., Canton, Ohio.

Simulated Jet

RESULTS from the first year of a simulated jet transport operation provide very encouraging answers to several important questions regarding the practicability of reliable commercial operations across the United States.

When jet transports of American manufacture become available in a few years the high fuel consumption at lower altitudes will make it necessary to cruise at altitudes of 35,000 to 40,000 ft. This will result in a change in cruising levels from the well-explored lower region of "conventional weather" to a higher region of mysterious "jet streams" with velocities sometimes as high as 200 mph. These stratosphere conditions have no known direct relation to the familiar weather of the lower 25,000 ft of atmosphere to which operating experience has been limited in the past.

Before purchasing a fleet of multimillion dollar jet transports, it is essential to find the answers to questions such as the following:

1. Will variation in cruising altitude aid in avoiding unfavorable winds?
2. Will special routing be necessary because of "jet streams"?
3. How shall fuel reserve be planned so that neither safety nor reasonable economy is compromised when fuel for holding or for flight to a distant alternate is required?
4. How reliable will schedules be for jet transports?
5. Is the present Weather Bureau reporting of upper-air wind conditions adequate for the inauguration of civil jet transport services across the United States?

IN order to study the practicability of reliable cross-country commercial jet transport operation, a series of simulated jet flights are in progress. Flights for these hypothetical airplanes are handled by regular United Air Lines dispatchers and are subject to the same delays, traffic restrictions, and holding as other real aircraft in the area.

This paper presents results of the first year of this study and answers questions about such items as: variations in cruising altitude to avoid unfavorable winds, special routing because of jet streams, fuel reserve policy, reliability of schedules, and adequacy of present-day weather reporting.

The Authors

R. D. KELLY (M '29) is superintendent of the Technical Development Division of United Air Lines in California. He attended Franklin College, and received his B.S. degree in Mechanical Engineering from Purdue University in 1925. In 1930 Mr. Kelly took charge of the Instrument Shop of Boeing Air Transport Corp., which was one of the predecessor companies of United Air Lines. Mr. Kelly was transferred to United Air Lines in 1936 as a test engineer.

H. B. KASTER is a research meteorologist for United Air Lines. In 1922, he obtained his B.S. degree in Mathematics and Astronomy from the University of California, where he later obtained his Masters Degree. Mr. Kaster taught at Pomona College, the University of California, and Boeing School of Aeronautics, where he later became Superintendent of Technical Instruction.

Transport Operation

R. D. Kelly and H. B. Kaster, United Air Lines, Inc.

This paper was presented at the SAE National Aeronautic Meeting, New York, April 15, 1954.

After only a very little study it became evident that such questions cannot be answered accurately by using averages, extremes, or frequency distributions of climatological type weather data. Each flight is subjected to variable wind, temperature, and other atmospheric changes from the start of the take-off until it lands at its destination. A surprisingly small proportion of the time may be spent at the maximum cruising altitude.

For instance, on a nonstop flight from New York to San Francisco, the heavily loaded plane will not reach 40,000-ft cruising altitude until near Omaha. The ground air temperature and wind direction and velocity at New York (which may limit either fuel or payload), the winds at lower altitudes for the first half of the trip, the winds at cruising level for the last half of the trip, and the reserve fuel required and the traffic problems at the destination are all important variables which must be worked out for each flight. One or more of these factors may have a maximum or a minimum effect at a time when the other factors are average. Could all factors be adverse at the same time? And could navigation around adverse winds improve the overall performance at these times?

To find a reliable solution to the problem it was decided to consider all of these details as they would have applied to actual specific jet flights, and to make complete solutions for day-in and day-out operations covering each season of the year. To have done this from past records would have been impractical, especially with respect to the air traffic problems and dispatch planning.

Barring actual service tests with real jet aircraft, the most practical plan was to "operate" hypothetical simulated flights each day in accordance with actual winds, temperatures, and altitudes to be encountered in normal coast-to-coast flights over United Air Lines routes. The flights were either nonstop between New York and San Francisco or one stop, using Chicago for that stop. Full flight plans were made for each simulated trip, and regular United Air Lines dispatchers followed them through the actual traffic patterns and terminal conditions from time of departure to destination arrival. No preference was given to the jet in this regard. It was charged with the same ground delays, traffic restrictions, holding, clearance to alternates, and so forth, as being experienced by other aircraft in the area. The only advantage accorded the hypothetical airplane was freedom from mechanical difficulties.

It is hoped that this study made in advance of "freezing" of American jet aircraft designs will be helpful in the finalized design and operational plans.

Results and Conclusions

1. *Wind and Cruising Altitude* – It quickly became apparent that flight planning would be much simpler than expected.

While winds often differ considerably with altitude it was found that a selection of flight levels is rarely necessary in preparing a flight plan. The best altitude is practically always the highest altitude because fuel consumption decreases very rapidly with increase in altitude with the proposed jet transports.

Sometimes a westerly wind is as much as 50 mph stronger at 35,000 ft than at 40,000 ft, and on a few of these occasions it was found that 5 to 10 min could be saved by flight at a level 5000 to 10,000 ft below the maximum cruising altitude possible with the load. However, this gain of a few minutes

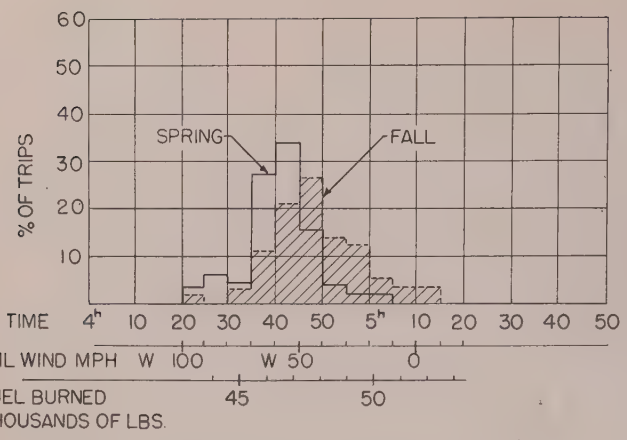

Fig. 1 – Block-to-block performance nonstop eastbound from San Francisco to New York

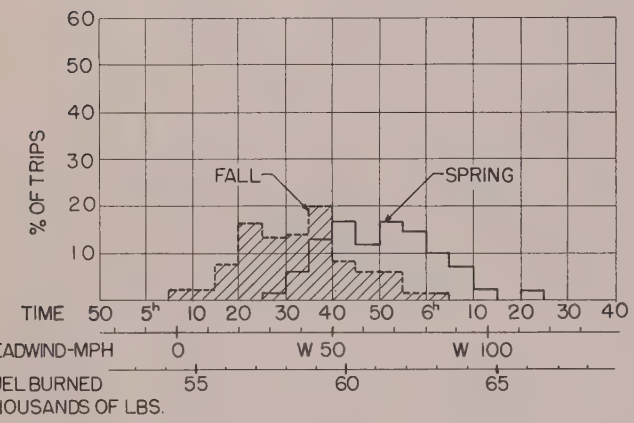

Fig. 2 – Block-to-block performance nonstop westbound from New York to San Francisco

was always at the expense of approximately 500 lb of fuel for each minute of flight time saved.

For this reason all flights were planned to climb as high as possible, as soon as possible, in order to cruise at the highest possible altitude.

2. *Most Efficient Route* – Much effort was made in the beginning to determine the most economical route for each flight by detouring to avoid unfavorable winds or to take advantage of favorable winds. However, it very quickly became apparent that north or south detours were rarely of value. In fact, there were only half a dozen occasions during the entire year when a detour was worthwhile, and the average saving on these few occasions was 5 min flying time.

It is therefore considered highly probable that jet transport flights will all follow an airway or some standard route such as the great circle route. The slight gain occasionally resulting from detouring for more favorable winds does not appear to justify the resulting minor traffic problems.

In general the airflow at 35,000 or 40,000 ft above the United States consists of a nearly straight flow of westerly winds or at times making one meander toward the south then back and to the northeast. The average speed of this broad flow is of the order of 50 to 75 mph. With careful inspection it will be found that within this broad stream there are one or more lines along which the speed appears to be greater than the general flow. With the use of some imagination, these lines of higher speed can be traced clear across the continent and are referred to as "jet streams." Sometimes three or four jet streams appear on the map, but a more conservative analyst may limit the same map to one jet stream.

Few people seem to be aware of the fact that regardless of all of the publicity being given to studies of the jet stream there is no standard definition even among meteorologists. In some circles the term refers to winds above a certain speed. In other cases the term implies a wind shear greater than some specified value which varies with altitude. In still other cases the term is applied to the axis of greatest wind speed regardless of speed or shear.

In localized spots the wind speed along one of these streams on a rare day may flare up to as much as 200 mph. However, this extremely high speed extends for only a few hundred miles along the stream and the speed then tapers off to little more than that of the surrounding westerly flow. Thus, jet streams should be of little significance in the scheduling of 550-mph jet transports over the United States routes.

In practice, if a jet aircraft flies along the axis of one of the areas of high velocity, it will usually be through the area in 20 or 30 min. An increase of 40 to 60 mph in headwind for 20 min adds only a few minutes to the flying time, and this is less than the time required for detouring such an area even if its exact location is known.

When the normal low-velocity jet stream lies along the airway for a considerable distance the decrease in wind speed to either side is so gradual

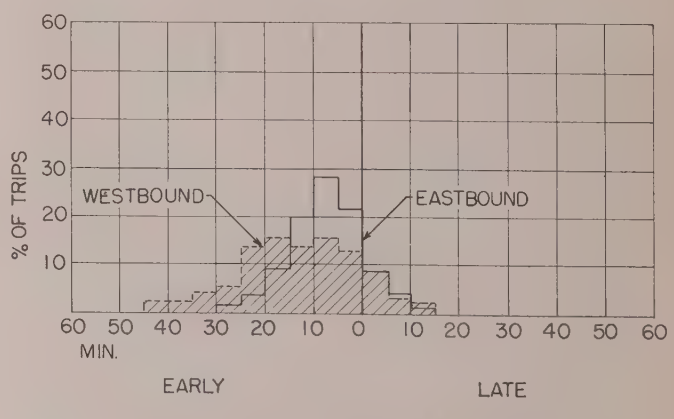

Fig. 3 – Schedule reliability for San Francisco to Chicago and return

that detours nearly always require more time than is gained.

3. *Reserve Fuel Adequacy* – Some of the simulated nonstop flights from San Francisco to Idlewild carried full payload as well as reserve fuel for flight from New York to Washington, D. C., as an alternate.

The fuel reserve policy was the same as for reciprocating-engine-powered transports. This policy was developed through years of experience; but with improvement in landing aids and the shorter time between departure and arrival for jet aircraft, it is possible that a review of the reserve fuel policy with respect to jet aircraft will be worth while. This is emphasized with the jet where the reserve fuel carried in this study averaged more than half the full payload on eastbound flights. Westbound flights into San Francisco carried average reserves approximating one-third the maximum payload.

The amount of reserve fuel actually used was negligible in comparison to the amount of reserve fuel carried.

Flights landed at alternate airports such as Boston, Philadelphia, Cleveland, or Sacramento on eight days during the year, but always at times when such irregularities had been expected and always with more than 1 hr's reserve fuel on board.

During a year's operation, flights were held for 20 to 40 min due to traffic on 16 days, and one flight was held for 1 hr before landing.

All flights which landed at Chicago had 13,000 lb or more fuel on board. Only 2% of Chicago-bound trips used an appreciable amount of reserve fuel, and the greatest amount ever used was 5000 lb.

So far as this study is concerned the fuel capacity of our hypothetical jet transport was more than adequate for operation under present reserve fuel and dispatch policies.

4. *Schedules* – Scheduled flight times, taken as the times which were equaled or bettered 85% of the time, gave the data in Table 1. (Constant thrust was assumed for all flights.)

Table 1 – Scheduled Flight Times

	Summer		Winter		Average for Year	
	hr	min	hr	min	hr	min
San Francisco – Chicago	3	39	3	33	3	36
Chicago – Idlewild	1	38	1	35	1	36
San Francisco – Idlewild Nonstop	4	59	4	48	4	54
Idlewild – Chicago	1	58	2	05	2	02
Chicago – San Francisco	4	13	4	19	4	16
Idlewild – San Francisco Nonstop	5	45	6	03	5	55

Since these times are based on an assumption of constant power, the small differences between winter and summer averages are negligible for schedule purposes.

Figs. 1 and 2 show the distribution of flight times for the nonstop flights during the periods August-September-October and February-March-April, the seasons of weakest and strongest winds, respectively.

Neglecting the 5% of trips at the bottom of the charts, the smallest variation in flight time is found in eastbound flights in the fall. The greatest variation is found in westbound flights in both spring and fall. As mentioned before, these charts are based upon use of constant power.

The middle scale of the three scales at the bottom of these charts shows the approximate mean wind component (the average wind component along the course during climb, cruise, and descent) corresponding to each flight time. It is interesting to note that the extreme values of the wind component affecting the flight are approximately 0 mph and 100 mph but that if the bottom 10% of flights are omitted, the effective wind component for the remaining 90% of flights ranges from 20 mph to 70 mph. A range of only 50 mph for 500-mph jets corresponds to a range in wind of 25 mph for a 250-mph airplane.

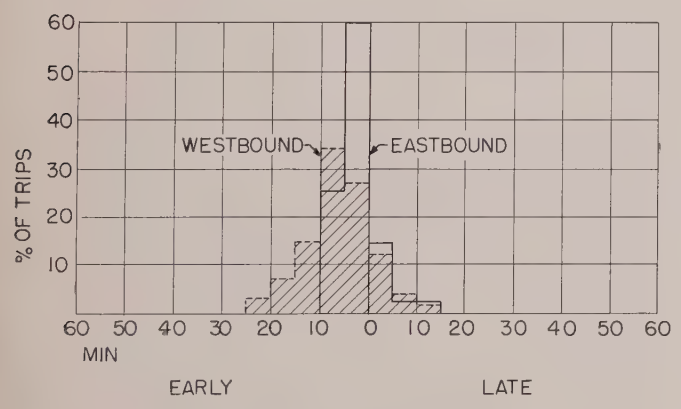

Fig. 4 – Schedule reliability for Chicago to Idlewild and return

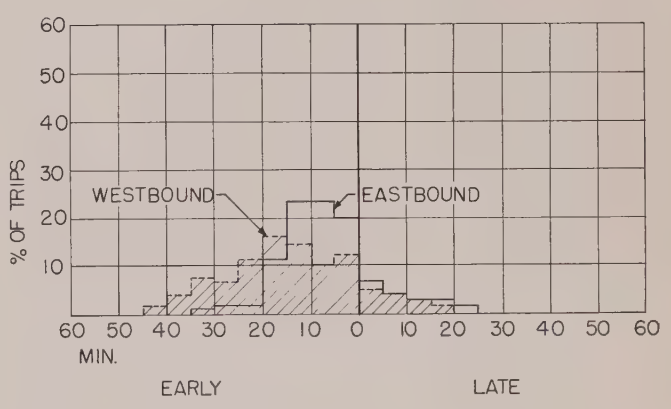

Fig. 5 – Schedule reliability for San Francisco to Idlewild nonstop and return

Table 2 – Refueling Requirements

Refueling Station Flight Segment, Nonstop	Chicago CHI-SFO		Idlewild IDL-SFO		San Francisco SFO-IDL	
	Minimum	Maximum	Minimum	Maximum	Minimum	Maximum
Total Fuel in Airplane at Take-off (Including Reserve for Possible Use at Destination), lb	41,000	50,000	63,000	74,500	55,000	65,000
Fuel in Airplane Before Refueling (Unused Reserve from Previous Trip), lb	−14,500	−13,500	−13,000	−12,000	−8,000	−7,000
Amount Refueled, lb	26,500	36,500	50,000	62,500	47,000	58,000
Amount Refueled, Kerosene, gal	3,960	5,450	7,460	9,340	7,010	8,650
Refueling Flow Time at 250 Gpm x 2 Hoses, min	8	11	15	18⅔	14	17⅓

A scale showing the fuel used is also added at the bottom of each diagram.

A flight time which was equaled or bettered 85% of the time was arbitrarily selected as the "schedule time" for each route, and arrival times were plotted about this schedule time in Figs. 3, 4, and 5. It is assumed that in practice this unexpectedly small range from schedule time would be even further reduced by some adjustment in power for the purpose.

5. *Upper-Air Wind Data* – The number of wind reports from near the 40,000-ft or 35,000-ft levels is much less than those available for lower levels. However, for the purpose of plotting the broad flow of air at these levels, they appear to be more adequate than are the greater number of lower wind observations for plotting the many clockwise and counterclockwise circulations and frontal wind shift lines which clutter the maps for lower levels.

This fact combined with the fact that variation in wind is a much smaller percentage of the airspeed for jet transports than for low-altitude aircraft results in the present observing network being very satisfactory for supplying wind data for jet transport flight planning.

6. *General Comments* – Existing airport runway lengths, corrected for obstructions, were used. These lengths are: San Francisco – 8900 ft, Idlewild – 8800 ft, and Chicago Midway – 6300 ft. Payload restrictions were not encountered at San Francisco. Payload was restricted by several thousand pounds on half a dozen summer days at Idlewild for the transcontinental nonstop trip when unusually high ambient temperatures limited the climb performance.

Operation from Chicago Midway Airport is considered marginal from a safety standpoint. The new O'Hare Airport at Chicago is considered preferable for jet transport operation.

It is of interest to find that the refueling requirements (Table 2) for the jet transport are less than one might assume. Practically all of the reserve fuel for the next trip is already in the airplane – it was left over from the previous trip. The only fuel to be added is the trip fuel.

For example, on the Chicago to San Francisco segment, the most fuel that we ever had to have aboard at take-off was 50,000 lb. But the unused reserve fuel in the airplane upon landing at Chicago from Idlewild has run between 13,500 and 14,500 lb. Therefore, only about 36,000 lb had to be refueled. This represents only 5400 gal of kerosene, which incidentally is just under the total fuel capacity, in gallons, of one of United's DC-7's. Conventional refueling equipment using two-point underwing refueling at only 250 gpm per hose can refuel the airplane with 5400 gal in 11 min. Refueling for the transcontinental nonstop trips will take a little longer, 19 min for the highest headwind Idlewild to San Francisco trip.

The refueling time for Chicago, although shorter, is more critical since in this case it is a through stop. The maximum refueling time instead of the average is the criteria because this occurs on the days when there is the highest headwind and therefore the greatest chance of a late arrival at the destination. These delaying factors should not be permitted to compound.

Scope of Study

Each flight was planned according to the usual wind and weather data available in airline dispatch offices. The reserve fuel included was sufficient to provide for the same holding time and flight to the same alternate airports being specified by the Dispatch Department for DC-6 flights to the same destination.

Six simulated flights were planned each day as follows:

1. Depart San Francisco 0725 PST for Chicago.

2. Depart Chicago 1345 CST for Idlewild.

3. Depart Idlewild 1310 EST for Chicago.

4. Depart Chicago 1450 CST for San Francisco.

5. Depart San Francisco 0830 PST nonstop to Idlewild.

6. Depart Idlewild 1310 EST nonstop to San Francisco.

After each flight plan was completed, the dispatch office at destination was notified of the time of departure, calculated flight time to the check point near the destination, and the calculated amount of fuel on board at the time of arrival over the check point.

At the time of arrival over the check point the receiving dispatcher determined the treatment which would have been given an actual airplane, such as being held in a traffic pattern at a particular altitude, being diverted to an alternate airport, or directed to land at the original destination. The receiving dispatcher then reported the time and place of landing, the time and altitude of any holding, the amount of low-level maneuvering, if any, and whether the runway was wet, dry, or icy.

At the time of writing, these simulated flights have been conducted for approximately 15 months, but the figures accompanying this paper are based upon only the first 12 months of operation.

As indicated earlier, the high speed of jet aircraft results in a small variation in schedules between winter and summer. For this reason it is assumed that the variation in performance from year to year, between one winter and the next for example, will be very small. The simulated flights are being continued; but for the reasons just mentioned, the results for a longer period are not expected to differ noticeably from the results for the first 12 months.

Airplane performance characteristics for the hypothetical jets are close to those which have since been announced by several manufacturers for proposed jet transports.

A few of the basic operating characteristics for the hypothetical jet transports used in this investigation are shown in Tables 3-7.

A full 22,000-lb payload was assumed on all flights except for the nonstop Idlewild-San Francisco flight on 5 days of the year when a reduction of several thousand pounds was necessary because strong headwinds required a large fuel load and a high take-off temperature reduced our permissible take-off weight.

Contrary to some opinions, both outside and within the industry, current jet transports are being planned to carry the reserve fuel for the same amount of holding time as is customary for present transports. This means that they will be able to take their place in traffic patterns without preference and will be able to fly to the same alternates as used by other aircraft.

When an alternate was required the fuel load was as follows:

Climb, cruise, and descent to destination.
5% of above for reserve.
45 min holding over destination.
5 min low-altitude maneuvering.
Climbout and cruise at 20,000 ft to alternate.
Descent to alternate.
45 min fuel in tanks at landing.

If CAVU (ceiling and visibility unlimited) weather exists over the destination, no holding or alternate fuel is required and the following fuel is carried:

Climb, cruise, and descent to destination.
5% of above for reserve.
5 min low-altitude maneuvering.
45 min in tanks at landing.

Table 3 – Maximum Weights

Maximum Take-off Weight, lb	200,000
Maximum Landing Weight, lb	140,000
Maximum Payload, lb	22,000
Maximum Fuel Capacity, lb	85,600

Table 4 – Climb to 35,000 Ft

Take-Off Weight, lb	Time, min	Speed, mph
140,000	16	430
160,000	20	430
180,000	25	432

Table 5 – Cruising Performance

Altitude, ft	Gross Weight, lb	True Air Speed, mph
35,000	140,000	561
	180,000	530
40,000	120,000	557
	150,000	520

Table 6 – Take-Off – Chicago

Temperature, F	Maximum Take-Off Weight, lb
+60 and below	193,000
70	186,500
80	180,000
90	173,200
100	166,000

Table 7 – Take-Off – San Francisco and Idlewild

Temperature, F	Maximum Take-Off Weight, lb
+60 and below	200,000
70	192,200
80	186,000
90	179,800
100	173,600

Buick's Twin

BEGINNING with descriptions of some past and present transmission designs, this paper goes on to describe the twin turbine Dynaflow transmission used in the 1953 Buick models. This design uses the torque multiplying characteristics of a planetary gear set and a hydrokinetic torque converter while retaining the smooth, uninterrupted power flow typical of a fluid torque converter.

A unique feature of this Dynaflow torque converter is that all the power transferred is through the gear set and first turbine at low speeds and gradually and smoothly diminishes as the power transferred through the second turbine increases until it does all the work at higher speeds.

Several vector diagrams analyzing the driving and reaction torques and forces aid in explaining the operation of the twin turbine Dynaflow.

The Author

R. J. GORSKY (M '54) is staff engineer in charge of Buick's Transmission Division in Flint, Michigan. He came to Buick in 1931 as a cooperative student at General Motors Institute. After completing the college graduate training course, he joined the Transmission Division. From 1941 to 1945, he represented Buick at Pratt & Whitney to expedite the manufacture of the aircraft engine Buick was building. Upon returning to Flint, he began work on the development of the Dynaflow.

TRANSMISSIONS are as "old as the hills," and when one reviews some of the many designs experimented with and those used in production, he concludes that there are about as many varieties.

The use of an automotive transmission has always been, and still is required to compensate for the shortcomings of an internal-combustion engine. The internal-combustion engine, as we know it today, cannot run below approximately 400 rpm without stalling; it develops relatively little torque at low speed, where the torque demand is the greatest to obtain good car acceleration; and it cannot be made to run counterclockwise readily to reverse the motion of the vehicle.

Therefore, the primary purposes of a transmission (or a transmission and clutch combination) are to prevent the engine from stalling when the car speed is low or zero; to enable the engine to operate at a higher speed where it develops more power while the transmission multiplies the engine torque for better acceleration; and to reverse the rotation of the driveshaft, using a gear train to provide a means of reversing the vehicle motion. These requirements can be obtained in many ways as one realizes when he sees the many types of transmissions which have been used in the past 50 years.

There are many secondary requirements which are expected of the transmissions of today, such as, ease of operation, smoothness, maximum car performance, best fuel economy, cost of manufacture, and weight. Everyone evaluates these items in a slightly different manner, and no one combination has been arrived at which has the best of all items. Consequently, compromises must be made which result in different transmission designs, and the perpetual argument as to which is the best goes on.

A few of the many transmission designs which have been used are as follows:

The *friction drive,* which has a wide range of torque ratios, infinitely variable, was used in some very early vehicles. It has smoothness of ratio change and could be easily disengaged for neutral and shifted to obtain reverse. However, its shortcoming was durability. Also, for the high-powered engines of today, materials have not been discovered which can endure the pressures required to prevent slippage. This type of drive is used today on some machines which do not require the transmission of much power and which can utilize the desirable characteristics of this design.

Inertia drives have been designed and seem to be more of a novelty than a utility. They require a ratchet mechanism and consequently "free wheel." The public more or less rejected "free wheeling" cars back in the 1930's, and a reliable ratchet mechanism to drive a 4000-lb car would be very bulky.

Electric or magnetic transmissions appeared on the American market years ago but did not stay long. Now they have reappeared in the diesel-electric locomotive field. The evaluation of factors such as initial cost, operating cost, performance, weight, and efficiency have proved that this type of drive for this application is very satisfactory.

Turbine Dynaflow Transmission

R. J. Gorsky, Buick Motor Division, GMC

This paper was presented at a meeting of the SAE Dayton Section, Jan. 19, 1954.

Planetary transmissions were used in many early vintage cars. These generally had one forward-speed, reduction, a direct drive, and a reverse. (As some of you can recall, the reverse was used too frequently to reduce the forward speed of the car when the brake was not very effective.) One forward-speed reduction didn't give much flexibility in performance, and with the general trend of higher engine speeds and higher vehicle speeds, this type of manually operated transmission yielded to the sliding-gear transmission.

The *sliding-gear 3-speed transmission* was used on many early cars and was used practically exclusively during the late 1920's and early 1930's. It was developed into a reasonably simple, durable device which covered a satisfactory ratio range and was manufactured for a relatively low cost. The introduction of helical gears to reduce noise and synchronizers to facilitate shifting were outstanding advancements made in this transmission. Many companies have spent many man-hours and large sums of money in developing this transmission into the smallest, lightest, and lowest cost unit being made today. Practically no development work is being carried on with this transmission, and its manufacturing cost is actually increasing because of the diminishing quantity being made. A friction clutch is used in conjunction with the sliding-gear transmission to enable the gear teeth to be meshed.

We, who have been driving automatic transmissions, realize that operating a synchromesh-equipped car smoothly is an art in manipulating the clutch, throttle, and gearshift lever, while steering the car. (If you question that statement, try driving a synchromesh car, and you will find that that art of operation has become a bit rusty.)

To simplify the operating of a car and to obtain a wider ratio range coverage, the 4-speed "self-shifting transmission" was made by Buick Motor Division and offered as optional equipment on 1938 Buicks and Oldsmobiles. It required a friction clutch which had to be used when the vehicle was started or stopped. Approximately 25,000 units were built during that model year. This transmission was the forerunner of the Hydra-matic transmission which is being built by the Detroit Transmission Division.

Fluid couplings were introduced on the American market in the 1930's. It is their characteristic to transfer very little torque at low speed and slip only only a small amount at higher speed. This enables a vehicle to be brought to a stop without stalling the engine and thereby reduces or eliminates the use of the clutch pedal. It cannot multiply torque; therefore, it must be used in conjunction with gears to provide satisfactory car performance.

The transmission engineer is confronted with the problem of best utilizing the engine power and to do it in a manner which the car buying public finds most pleasing. This includes car performance, fuel economy, smoothness of operation, and a minimum manipulation of controls by the driver.

Hydrokinetic torque converters seem to fill this order in a satisfactory manner in view of their being used in all new automatic transmissions introduced on American-made passengers cars since Buick's introduction of the Dynaflow transmission in 1948.

The hydrokinetic torque converter is not new – it was invented some 45 years ago by Dr. Herrman Foettinger. It was first used as a speed reducer for marine steam turbines, which was before the time of present types of high-speed reduction gear drives.

Torque-converter transmissions have been used for some time in passenger buses. Their principal feature in this application is in reducing driver fatigue and in reducing the time to make a given run. This converter is used for starting purposes only and is locked out after the bus is accelerated to some predetermined speed.

Torque-converter transmissions were used extensively in World War II tanks because of the flexibility they provided and because they required a

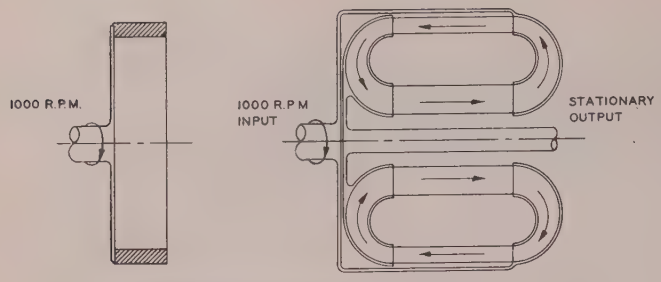

Fig. 1 – Spinning flywheel (left) and fluid coupling (right)

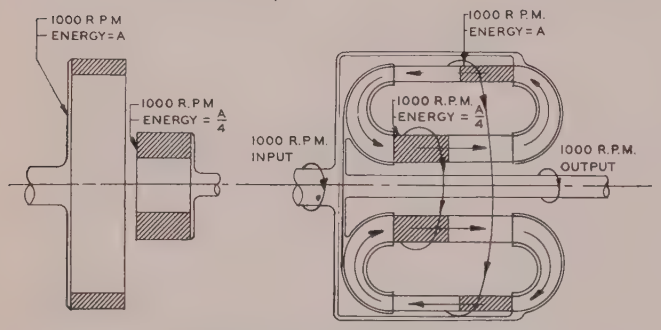

Fig. 2 – Comparison of fluid drive coupling with two flywheels; (left) flywheels, (right) fluid coupling

minimum of attention or manipulation of controls by the tank driver.

To explain how the Dynaflow twin turbine converter functions, it is necessary to understand how a hydrokinetic drive works, that is, how a fluid coupling works and how a torque converter works. If the operating principles are reduced to comparisons with familiar mechanics, the torque converter is easy to understand.

The simple mechanics of a hydrokinetic drive begin with the mechanics of a spinning flywheel (Fig. 1). A spinning flywheel has stored up energy, and if it is stopped, it will exert a force on the mechanism stopping it. Conversely, a force must be exerted against it to get it up to speed again after it has been stopped. A fluid coupling with an engine driving the input member and the output member stalled or stationary is a direct equivalent of this principle.

As an example, let us take a fluid coupling which has the input member running at 1000 rpm and the output member stalled. The input member is nothing more than a centrifugal pump, picking up oil at a small diameter and making it spin along with the vanes in this member. Centrifugal force sends the oil out radially, and the oil leaves the input member at a large diameter in the form of a spinning flywheel rim, a flywheel rim made of oil. The energy in this spinning flywheel rim of oil came from the engine. As noted before, the output member is stationary, so a force will be exerted on its vanes as this spinning flywheel of oil is stopped. The force exerted will depend on the rate at which it is stopped, its mean diameter, and its weight. The fluid then flows from the large diameter of the output member to its small diameter having an inward radial movement and no spinning movement. As it leaves the small diameter of the output member, it reenters the input member to repeat this cycle.

If we examine the action of a fluid drive coupling running efficiently at a higher speed, we will recognize another direct comparison with flywheels (Fig. 2). Let us assume two flywheels are running at 1000 rpm, each weighing the same but having different mean diameters. It is evident that the large-diameter flywheel, while no heavier in total weight than the small one, is more of a flywheel. If the diameter of the larger flywheel is twice as great as that of the smaller flywheel, it will be four times the flywheel though no heavier in total weight. In other words, the energy contained in the larger flywheel is four times greater than that in the smaller one though both weigh the same and run at the same speed.

Let us record another basic fact – if both of these flywheels were to have the same energy, the smaller one would have to run twice as fast as the larger one.

Let us now look at a fluid coupling with both the input member and the output member turning at 1000 rpm and assign a value A to the energy in the oil as it leaves the input member. The energy of this same oil as it leaves the output member will be one-fourth of A, and the difference, or three-fourths of A, will be absorbed by the output member and used as the output driving force.

Actually, the speed of the driven member must lag the speed of the driving member so that the oil will flow and enable the transfer of power from the input member to the output member via the medium of oil. If the speed of the driving and driven members were equal, the counter centrifugal forces of the fluid in the driven member would balance the centrifugal forces of the fluid in the driving member and no fluid flow would result. The amount of lag will depend on the speed and torque being transferred.

That is how the fluid coupling works.

Now, we don't have far to go from here to a simple three-element torque converter (Fig. 3). Let us assume the circulation efficiency to be 100%, and let us take the fluid drive coupling previously mentioned just as it was with the input member running at 1000 rpm and the output member stalled. But let us replace the straight vanes in the output member by strongly curved vanes. We shall make the entrance of vanes so that the oil will be received without splash and strongly curve them backward so that the exit oil will be actually spinning backward – it is a backward spinning flywheel. The

force felt by the converter output member, or turbine, is obviously much greater since it has not only absorbed the energy in stopping the spinning flywheel which entered it, but it has also reversed the direction of spinning.

An appreciable amount of energy would be required by the engine to stop this backward spinning flywheel if it were permitted to impinge directly on the vanes of the input, or pump member. To take care of this condition a stationary member, or stator, is interposed. This member has curved vanes also, so that it again reverses the direction of the spinning oil causing it to spin in the same direction as the pump it enters. The reaction force on this member establishes the amount of torque multiplication the unit is developing. The output torque must always equal the input torque plus the reaction torque on the stator support. The pump member picks up this oil, adds energy to it as it passes from the entrance diameter to the exit diameter, and this cycle continues to repeat itself.

The oil functions in the same manner when the turbine member is permitted to move. The rate of oil flow decreases as the turbine speed approaches the pump speed, and the torque multiplication decreases at the same time. It is this characteristic which enables the engine together with the torque converter to supply maximum torque for starting and accelerating right where it is needed.

At cruising speeds the rate of oil flow through the openings between the vanes, or vortex flow, is small, but the rotary motion of both the pump and turbine is high. Under this condition the stationary member, or stator, would form a very serious obstruction to the flow of oil and cause the efficiency to drop as the speed increases. To prevent this from occurring the stator member is mounted on a freewheel clutch which enables it to change the direction of flow when needed and to free wheel out of the way, or along with the rotary flow of oil, when not needed. Under these conditions of cruising, this design of converter actually functions in a manner similar to a fluid drive.

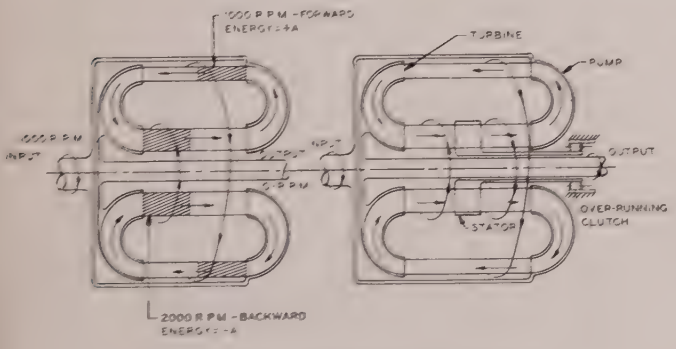

Fig. 3 – Simple 3-element torque converter

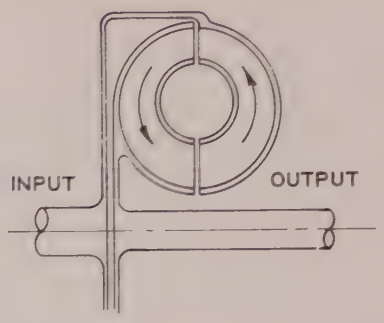

FLUID COUPLING

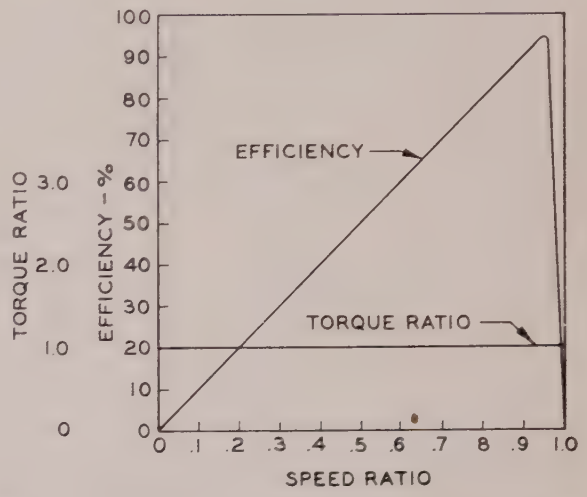

Fig. 4 – Torque ratio and efficiency curves for a fluid coupling

As in any hydraulic device there are flow losses and shock losses in a hydrokinetic drive. To obtain no shock losses it is necessary to have the oil enter each member in a direction parallel to the vane entrance. The absolute direction of oil flow changes as the rotary speed changes in relation to the vortex flow. Therefore, to avoid any shock losses it would be necessary to provide vanes with adjustable entrance angles. This is not practical to do. We approached this end in the original Dynaflow by adding a second stator and a second pump.

The torque ratio and efficiency curves for a fluid coupling show that the torque ratio is always 1/1 (in other words it does not multiply the input torque) and the efficiency curve is inversely proportional to the slip taking place (Fig. 4). As the relative speeds of the elements approach 1/1, the efficiency again falls off to zero because no torque can be transferred, as previously mentioned.

Typical torque ratio and efficiency curves for a torque converter, superimposed on the fluid coupling curves, show that the torque ratio of more than 1/1 can be obtained (or in other words a

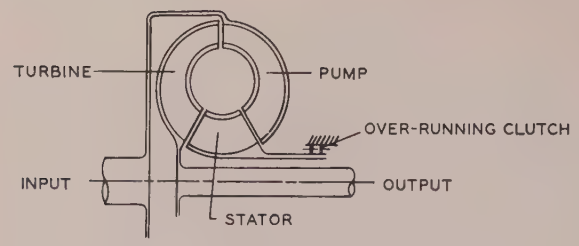

SIMPLE THREE ELEMENT CONVERTER

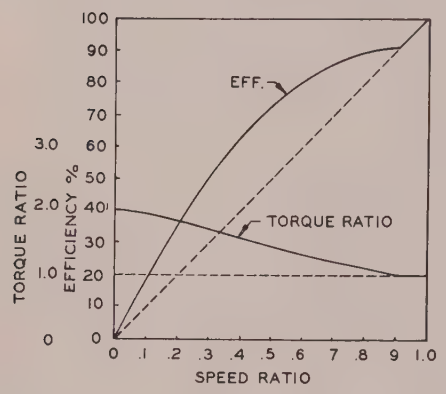

Fig. 5 – Torque ratio and efficiency curves for a torque converter

torque converter can multiply torque) and the efficiency curve rises faster, peaks, and falls off until it reaches the fluid-coupling curve (Fig. 5). At this point the stator element free wheels, and the unit functions in a manner characteristic of a fluid coupling.

Different converter designs will produce different torque ratio and efficiency curves. The original Dynaflow torque converter which consisted of a primary pump, a secondary pump (which was mounted on an overrunning clutch), a turbine, and two stators (which also were mounted on overrunning clutches) was, in a sense, three torque converters and a fluid coupling combined into a single unit (Fig. 6). This resulted in four sets of curves, the most desirable portions of which were utilized. The break points 1, 2, and 3 in the efficiency curve are the points at which the secondary pump stops overrunning the primary pump, the secondary stator starts to free wheel, and the primary stator starts to free wheel, respectively.

To improve the car performance and converter efficiency and to reduce the engine speed for a given car speed the twin turbine dynaflow transmission was introduced on the Buick 1953 models (Fig. 7).

This design utilizes the torque multiplying characteristics of a planetary gear set in conjunction with the torque multiplying ability of a hydrokinetic torque converter and retains the smooth, uninterrupted power flow characteristic of a fluid torque converter. The arrangement of the twin turbine Dynaflow torque converter is unique in that all the power transferred is through the gear set and first turbine at low speeds and gradually and smoothly diminishes as the power transferred through the second turbine increases until it does all the work at higher speeds.

Let us take time out to go over the nomenclature of the twin turbine parts (Fig. 8). The converter pump is driven by the engine and energizes the converter fluid. The first turbine receives the fluid leaving the pump and drives the planetary ring gear through a diaphragm member which is riveted to the ring gear. The second turbine is doweled and bolted to the planet carrier which in turn is splined to the converter output shaft. The stator is mounted on an overrunning clutch which is common to it and to the planetary sun gear.

To explain the operation of this unit let us first review the driving and reaction torques and forces (Fig. 9). At stall, the output shaft and turbines will be stationary – by definition. The engine is driving the converter pump which produces the driving force to the fluid as shown by arrow P. The fluid circulates through the first turbine which is stationary and in so doing imposes a force which is resisted as shown, namely, force T_1.

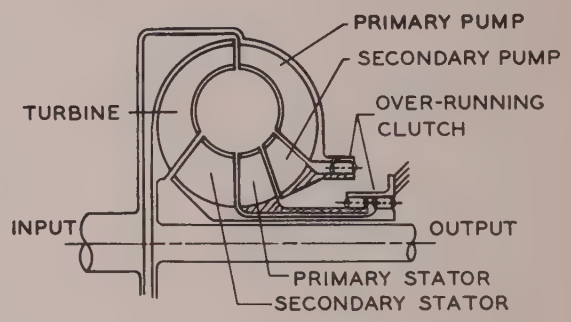

FIVE ELEMENT DYNAFLOW

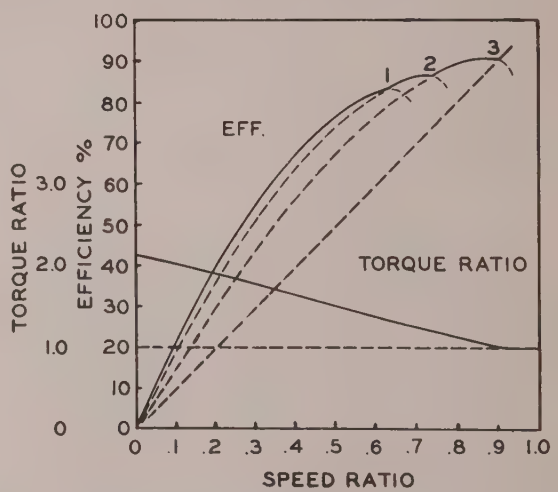

Fig. 6 – Torque ratio and efficiency curves for 5-element Dynaflow

The fluid passes through the second turbine with no appreciable change and on through the stator which redirects it and consequently has a reaction force, as shown by arrow S. The driving force, P, plus the reaction force, S, must always equal the driving forces, T_1 plus T_2. This relationship must always exist. (When it doesn't, one had better take another look at his analysis and calculations.)

The driving force T_1 is fed into the planetary gear set where it is increased by the ratio of 1.6/1. At the gear set, the ring gear, which is connected to the first turbine, is driving; the sun gear is held stationary by the overrunning clutch; and the planet carrier, which is splined to the converter output shaft, is driven by the planet pinion. This arrangement has increased the stall torque ratio from 2.25/1 in the original Dynaflow to 2.45/1 in the present twin turbine Dynaflow and raised the efficiency curve (Fig. 7).

As the car speed increases, the driving force (T_1) on the first turbine gradually decreases as the driving force (T_2) on the second turbine increases (Fig. 10). The latter force on the second turbine is delivered directly to the converter output shaft because the second turbine is secured to the planet carrier which in turn is splined to the main shaft.

As the car speed continues to increase, the driving force on the second turbine (T_2) exceeds that on the first turbine (T_1), and the reaction force on the stator (S) continues to decrease (Fig. 11).

At cruising the first turbine is transferring no power, and the second turbine is transferring all the power (Fig. 12). The stator is taking no reaction and is free wheeling in a clockwise direction as permitted by its overrunning clutch mounting. At this stage the converter is no longer multiplying torque and is operating in a manner similar to a fluid coupling.

So much for the driving forces. Now to describe how these changes take place, a few vector diagrams should be of some assistance (Fig. 13).

With a low member speed, as shown at S_1, and a high vortex flow, as shown at F_1, the vector sum will be O-A. With a high member speed, S_3, and a low vortex flow, F_3, the vector sum will be O-C. The length and direction of the vector sum, or absolute velocity of the oil, will change as the conditions change. The vectors shown are for purposes of illustration and do not necessarily represent true values. The absolute velocity of a particle of oil will be the vector sum of the velocity of the converter member it is leaving, which will be a tangential vector, plus the vortex velocity of the oil in relation to the blade it is leaving. The latter will have a direction parallel to the exit end of the blade. If the member is stationary, the absolute velocity will be the same as the vortex velocity.

As previously mentioned, the pump operates like a simple centrifugal pump, and the absolute velocity of the fluid will be the vector sum of the circumferential speed S of the pump blade which drives the fluid plus the linear speed F of the fluid in relation to the blade. As the pump speed increases and the fluid flow decreases, the vector sum will change in direction and magnitude as shown by vectors A, B, and C. Because of its mass and velocity, this fluid contains energy, which is obtained from the engine.

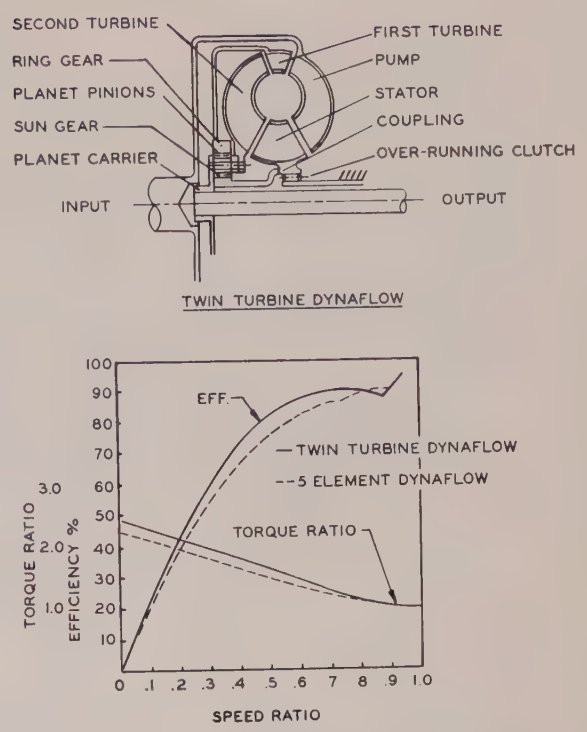

Fig. 7 – Torque ratio and efficiency curves for twin turbine Dynaflow

When the direction of this flow is changed, a force is imparted to the member causing it to change in direction.

A vector diagram showing the oil leaving the first turbine blades will show the amount of directional change of the oil flow (between the pump exit and the first turbine exit) and will consequently indicate the force imparted to this member (Fig. 14).

At stall the turbine speed is zero; therefore, the direction of oil flow will be tangent to the exit end of this blade as shown at F. This results in the largest change in direction between the entering oil and the leaving oil; consequently, it produces the greatest driving force on this member.

The difference in directional change decreases as the first turbine speed increases as shown by the resultant vectors A, B, C, and D. At D the high rotational speed of the first turbine causes the oil to flow between its blades without being changed in direction. At this point it is delivering no drive, and the second turbine blades do all the driving.

The second turbine also has curved blades and

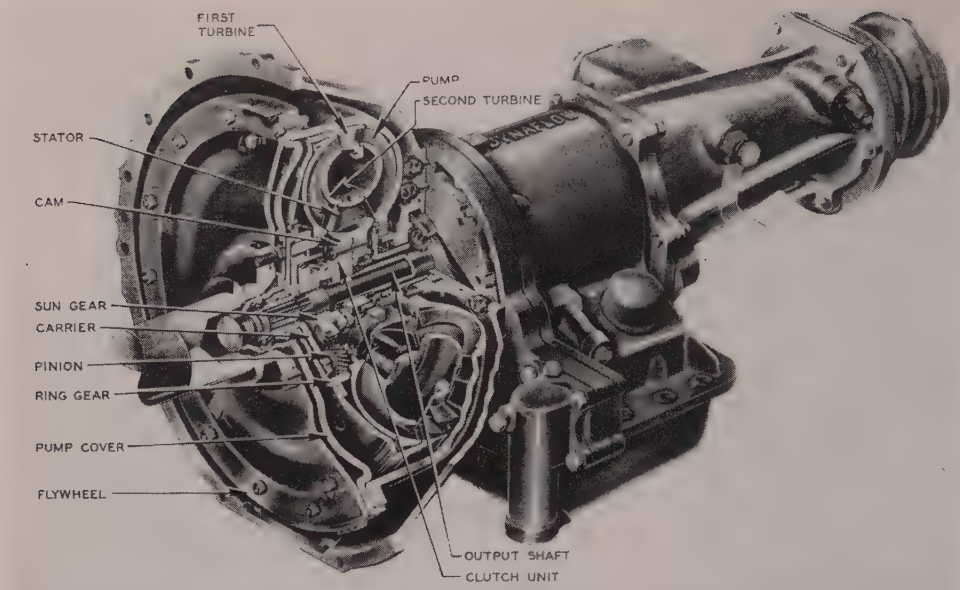

Fig. 8 – Section showing twin turbine parts

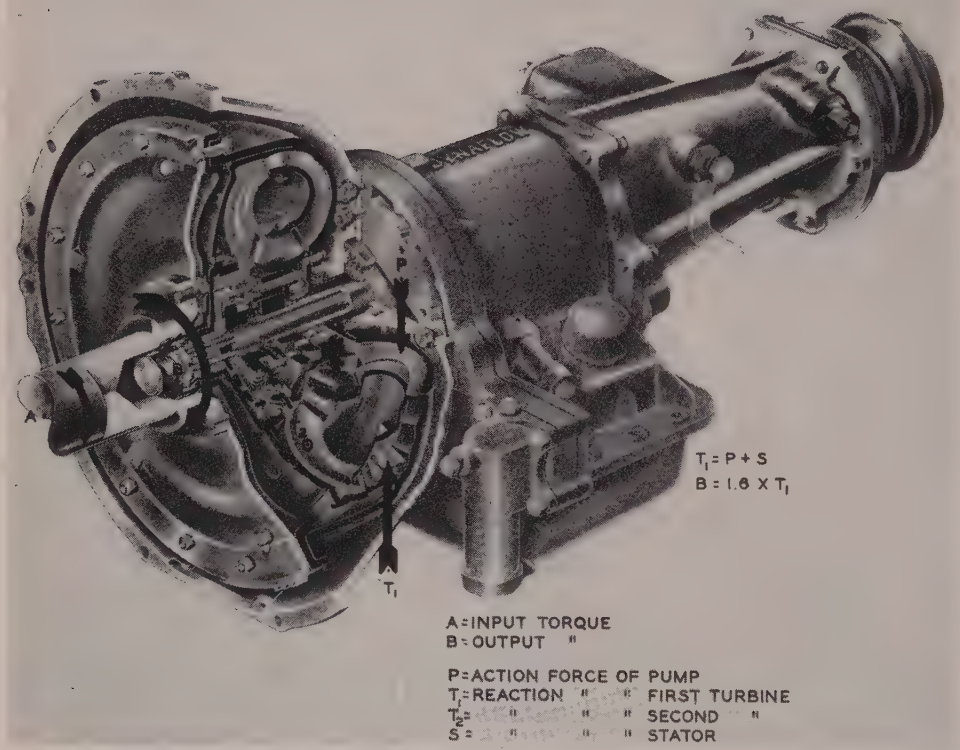

Fig. 9 – High torque drive

has a smaller diameter at its exit end than its entrance end, which further enables it to extract energy from the flowing oil (Fig. 15). This member functions in the same manner as the turbine in the previously mentioned three-element torque converter. The exit oil flow is shown by vector sums, *A*, *B*, *C*, and *D*.

By virtue of the converter planetary gear set which multiplies the first turbine torque by a ratio of 1.6/1, the speed of this member will be 1.6/1 faster than that of the second turbine. It is this relationship which enables the first turbine to reduce its load carrying ability while the second turbine increases its load carrying ability. The *difference* in their speeds is zero at stall and increases as the output shaft speed increases. This feature enables the first turbine to move ahead of the second turbine so that the latter can take the driving force of the fluid and deliver it directly to the converter output shaft.

The fluid leaving the second turbine and entering the stator changes in direction *A*, *B*, *C*, and *D* as

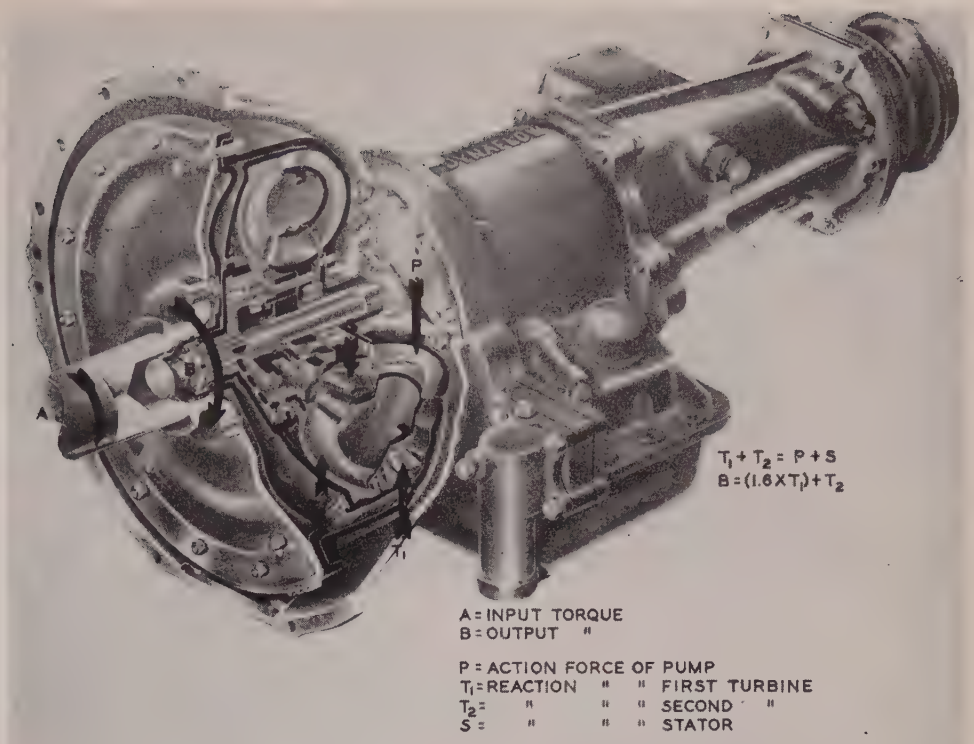

Fig. 10 – First turbine drive

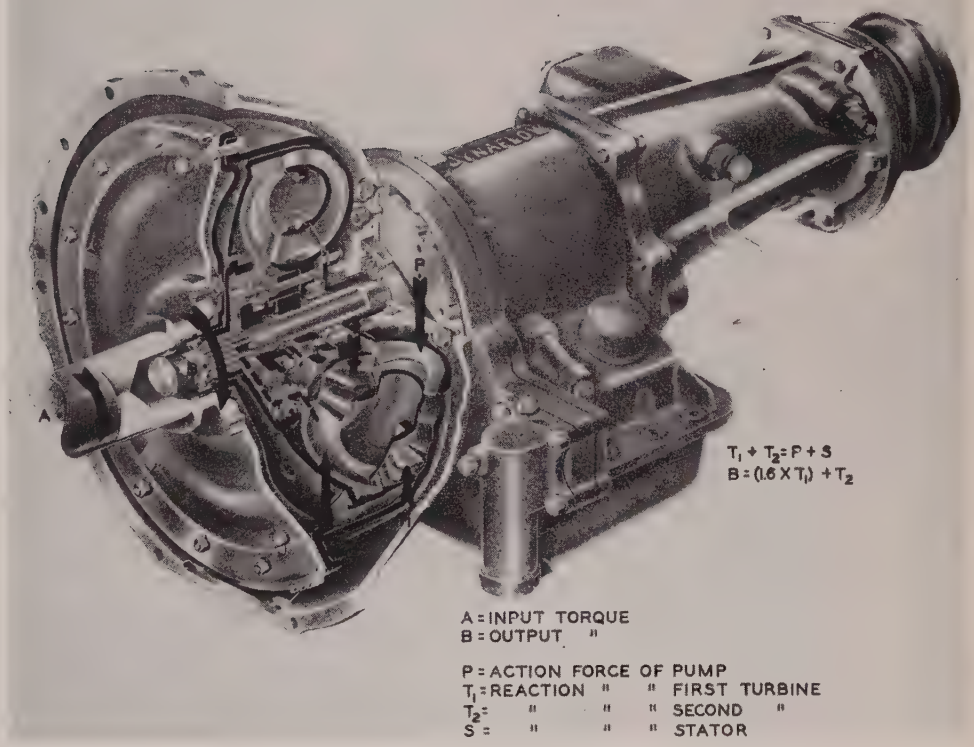

Fig. 11 – Second turbine drive

the car speed increases, thereby imposing a diminishing torque reaction on the stator blades (Fig. 16). When the oil impinges on the back side of the stator blades, as shown at *D*, the stator free wheels along with the oil so that it will not obstruct the fluid flow.

The twin turbine converter has eliminated the "slip" or "buzz-up" sensation and has greatly increased the low-end performance. For example, test results show that a 1953 Buick Roadmaster equipped with a twin turbine Dynaflow, checked against a Buick companion car of the same engine power and car weight, out-distanced the latter by 35 ft, or two car lengths, when accelerated, full throttle, from a standing start to 50 mph in 11.3 sec. This is the result of a more efficient converter

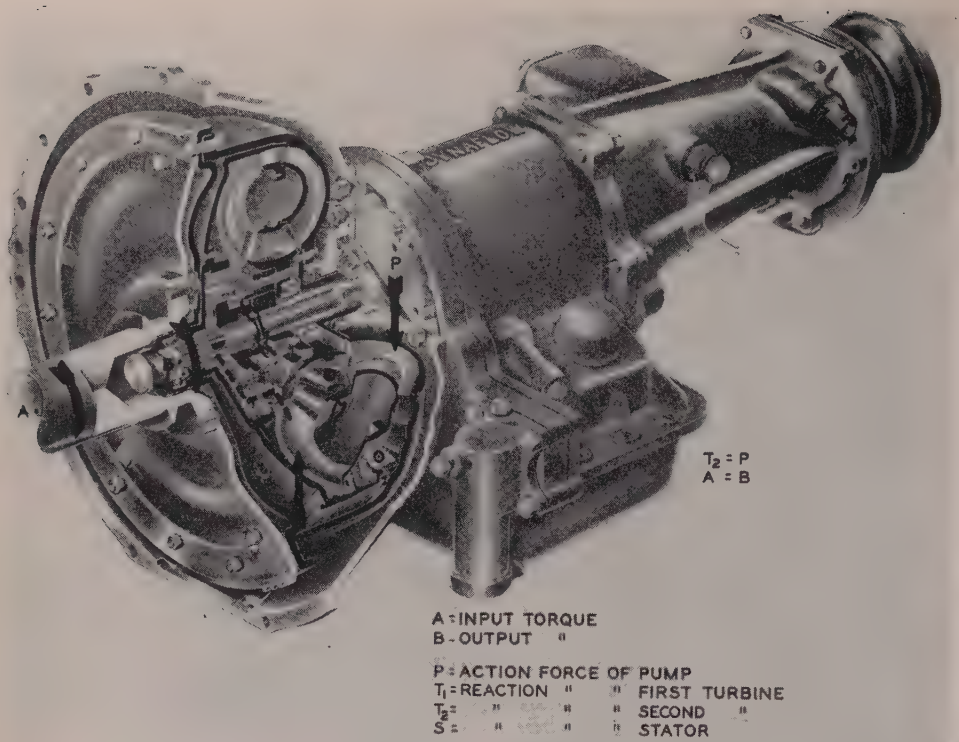

Fig. 12 – Coupling drive

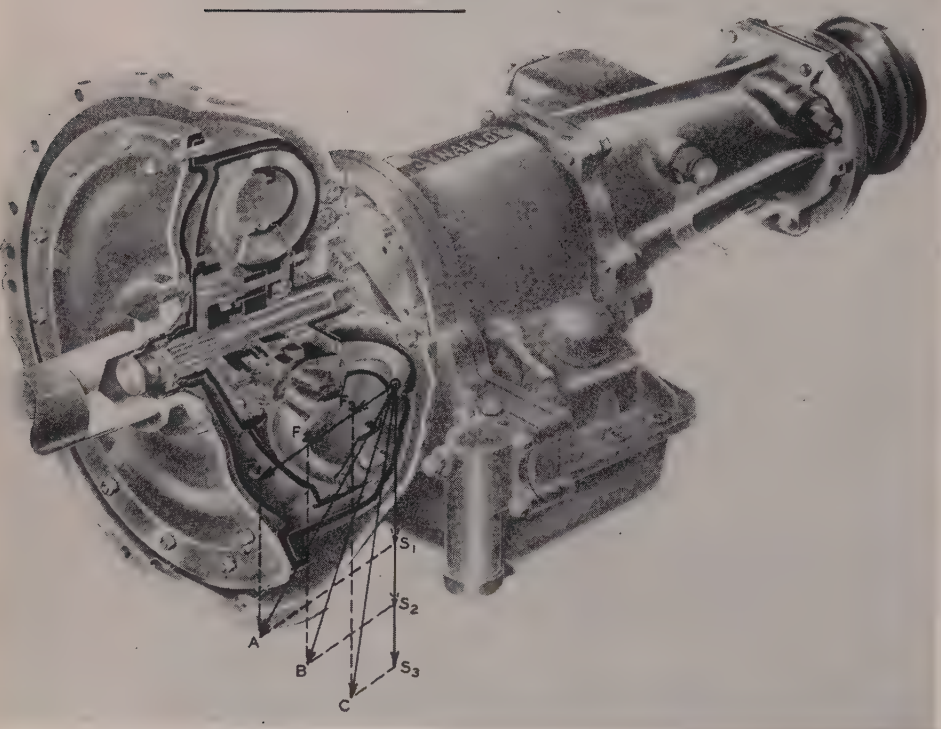

Fig. 13 – Pump vector analysis

design which has retained the smooth uninterrupted power flow to the rear wheels that has been characteristic of all Dynaflow transmissions built. Today, it is the only automatic transmission that has this smoothness of operation, free of automatic shifts, in the driving range from start to cruising speeds.

The complete Dynaflow transmission consists of a torque converter together with a hydraulically operated transmission to obtain the various ranges – park, neutral, drive, low, and reverse (Fig. 17). The torque converter drives the car through a compound planetary gear cluster which is locked up by a multiple disc clutch for all normal operation. When the range selector lever at the steering wheel is set to low range, oil pressure applies the

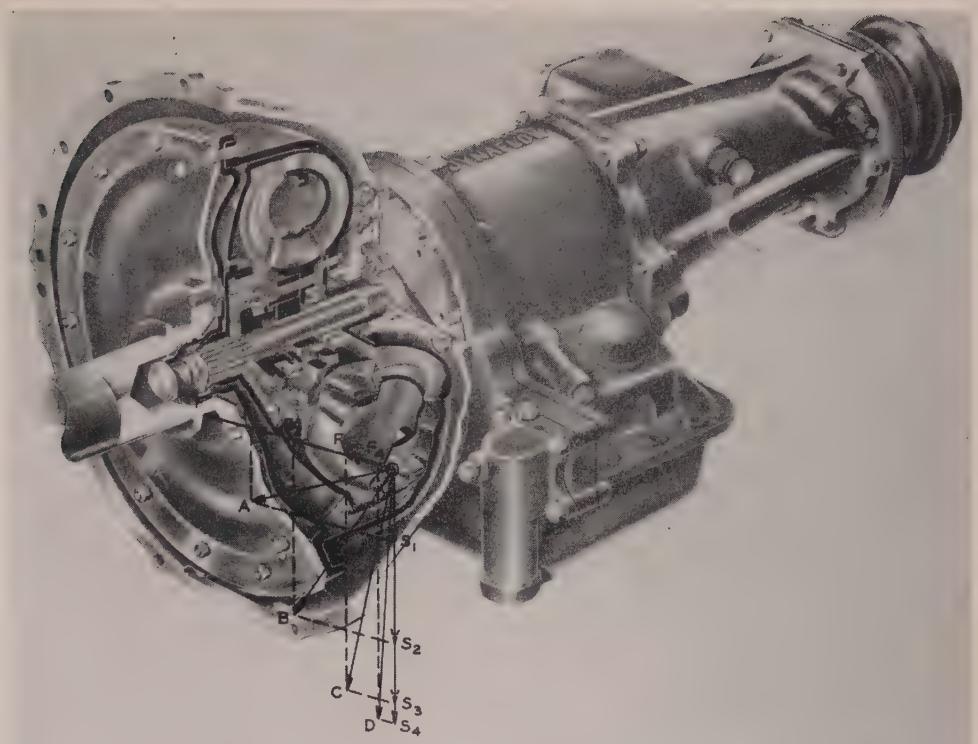

Fig. 14 – First turbine vector analysis

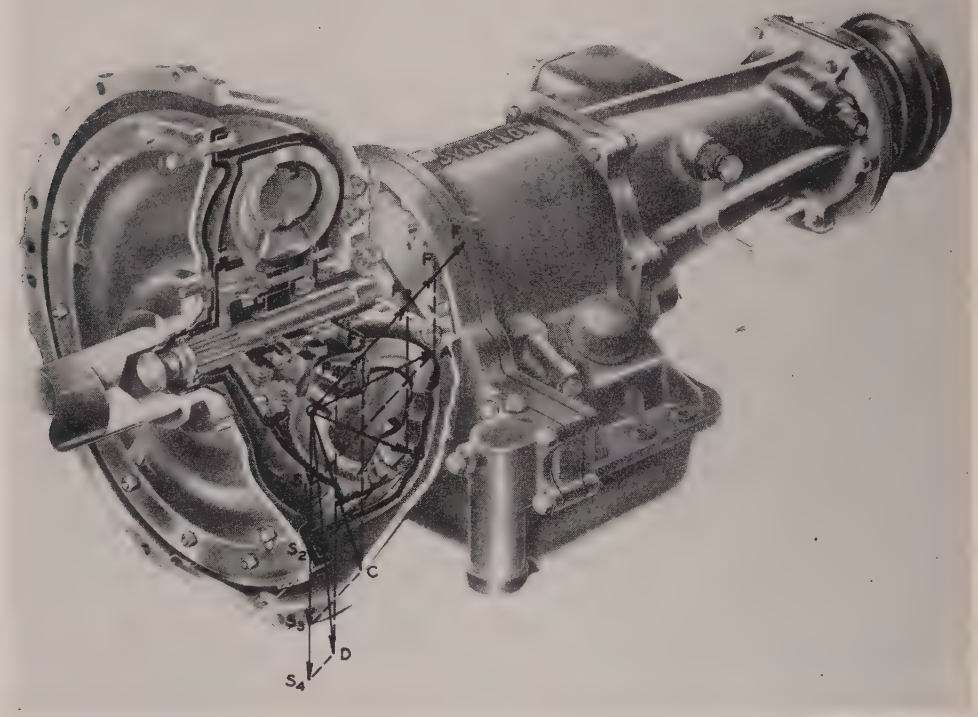

Fig. 15 – Second turbine vector analysis

low band, thereby holding one of the planetary reaction members producing a geared reduction of 1.82/1. Low range is used for emergency power and for increased engine braking while descending long steep grades. Reverse range is obtained in a similar manner by applying the reverse band which locks a different reaction member of the planetary.

To supply oil under pressure to operate the high clutch piston, low and reverse servo pistons, and to circulate oil through the converter and lubrication system, two pumps are used. One is driven at engine speed and the other at propeller-shaft speed. The latter is a small pump which supplies all the oil required when the car speed is high enough for it to do so. The oil from the larger pump is then relieved to the oil suction line so that a minimum amount of power is needed for pumping. The rear pump which is run at propeller-shaft speed pro-

SCIENCE - TECHNOLOGY
INFORMATION SERVICE CENTER
LOCKHEED AIRCRAFT CORPORATION
GEORGIA DIVISION

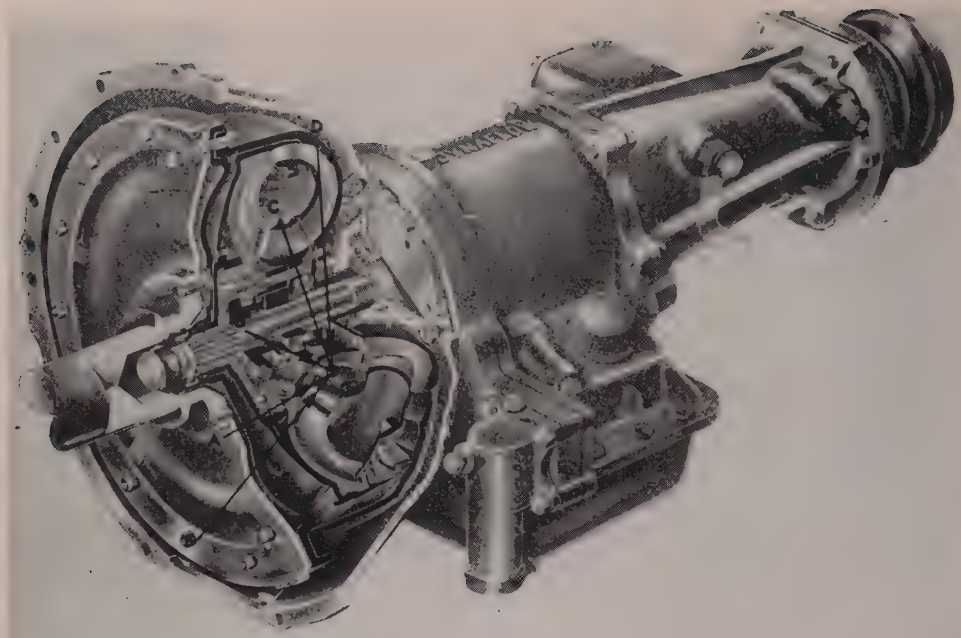

Fig. 16 – Stator vector analysis

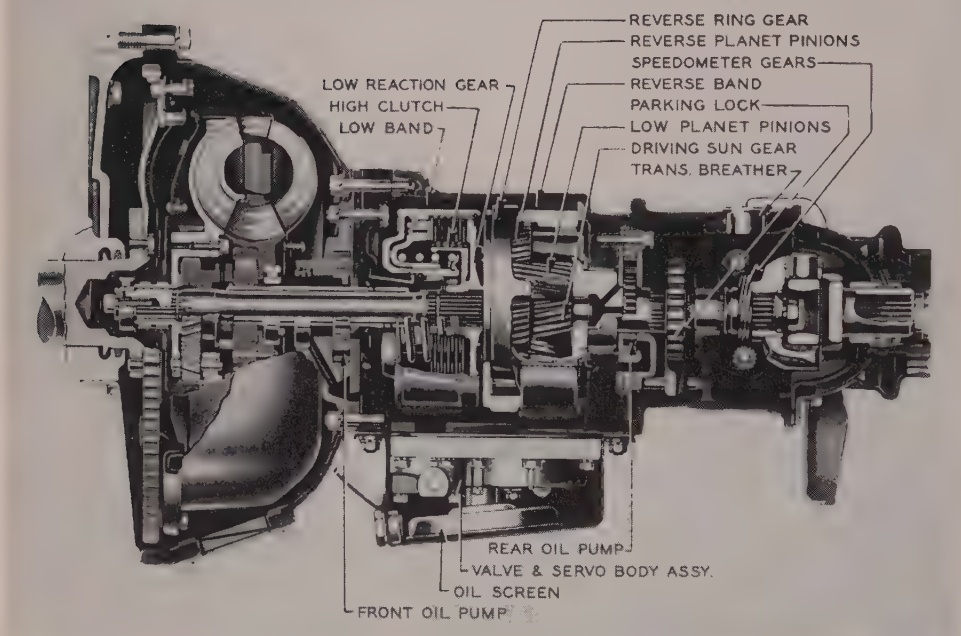

Fig. 17 – Section of complete Dynaflow transmission showing torque converter and hydraulically operated transmission

vides oil pressure to engage the low band to obtain a drive through the transmission when a car needs to be push started, as in the case of a weak battery.

At the rear of the transmission is a parking lock which will rigidly lock the propeller shaft when the car is parked. This takes the place of parking a synchromesh-equipped car "in gear." In addition this enables the engine to be started while the car is held from moving.

A torque converter cannot transmit torque when the pump and turbine members are stationary. Therefore, a car so equipped cannot be held or parked against the engine friction and compression as can be done with a synchromesh-transmission-equipped car.

Since 1948 Buick has built over 1,800,000 torque-converter-type transmissions, which is more than any other passenger-car manufacturer has built. Five other makes of automatic transmissions have appeared on the market since that time – all of which have incorporated a torque converter. From this it certainly appears quite evident that a torque converter has characteristics which meet the fancy of the car-buying public.

Practical Yardsticks For Deposit Effects

C. A. Hall, J. A. Warren, and J. D. McCullough, Ethyl Corp.

This paper was presented at the SAE Summer Meeting, Atlantic City, June 10, 1954.

COMBUSTION-CHAMBER deposits are one of the limiting factors in the utilization of higher engine compression ratios because of their tendency to (1) increase the octane number requirement for the suppression of knock and (2) ignite the fuel-air mixture erratically and thus produce uncontrolled combustion. This latter phenomenon, called deposit-induced ignition (hereafter deposit ignition) may be noticeable as autoignition, wild ping, preignition, or engine roughness.

Due to the importance of the problem, a large number of laboratories have been investigating the effects of various gasolines and lubricating oils. At the present time there are no standardized test

USEFUL test procedures and instrumentation for evaluating the effects of combustion-chamber deposits are described here. A multicylinder deposit-ignition counter has been developed which detects and records the deposit ignition occurring in the individual cylinders of a multicylinder engine. This new instrument measures basic deposit effects over a wide range of engine operating conditions and can be used either in the laboratory or on the road.

The instrument is useful for studying the effects of fuels, lubricants, and additives in multicylinder engines. Since variation among individual cylinders can be detected, the instrument is also useful for studying engine design changes as well as operating conditions.

Road and dynamometer test procedures for evaluating deposit-induced autoignition by the conventional audible method of detection are described along with the effects of several fuel-lubricant-additive combinations.

The Authors

C. A. HALL is a research supervisor of the Ethyl Corp. Research Laboratories. He graduated from Ohio State University in 1937 with a B.S. in M.E. degree, and obtained his M.S. degree in 1941. Mr. Hall spent one year with the Frigidaire Division of General Motors Corp., and the following four years as an instructor in mechanical engineering at Rice Institute. He has been with the Ethyl Corp. since 1942.

J. A. WARREN (M '54) is a research engineer with the Ethyl Corp. Research Laboratories. He obtained a B.S. in Mechanical Engineering from the University of Connecticut, and a master's degree from Yale University. Mr. Warren's past experience includes eleven years of teaching mechanical engineering at Brown University and Yale University; and one and one-half years on the staff of the Automotive Section of the Infantry School at Ft. Benning, Ga.

J. D. McCULLOUGH is assistant head of the Instrumentation Section of the Ethyl Corp. Research Laboratories. He graduated from the University of Cincinnati in 1942 with a B.S. in Electrical Engineering, and received a master's degree in automotive engineering from the Chrysler Graduate School in 1944. Mr. McCullough joined the Engineering Division of the Chrysler Corp. as an instrument engineer in 1942. After four years at Chrysler, he joined the Ethyl Corp., where he has been ever since

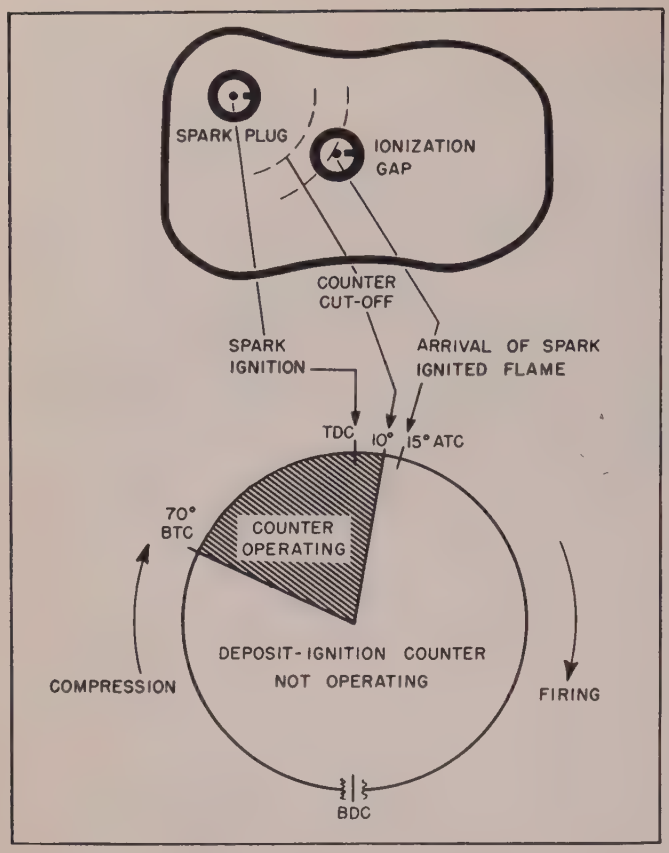

Fig. 1 – Portion of engine cycle during which deposit-ignited flame fronts are recorded—single-cylinder engine. Any deposit-ignited flame front arriving at ionization gap between 70 deg btc and 10 deg atc is recorded by counter

procedures. Instead, there are a variety of methods used by various laboratories. Some are mild procedures and some are severe, and this naturally leads to a variety of results among laboratories. Because of this, there are differences in opinion as to the extent of the deposit-ignition problem. There is, however, a general agreement that test procedures are needed which will provide consistent results in terms of customer-driver reaction to knocking "noises" on the road.

The Ethyl Laboratories have been investigating the effects of deposits for a number of years and have developed certain test procedures for use with a single-cylinder engine, a multicylinder engine on a dynamometer, and passenger cars on the road. Ethyl's procedures, techniques, and instrumentation are described briefly in this paper, along with some typical results obtained on the effects of gasoline, oil, additive, and operating factors. All data are referred to baseline tests which were run with oil 1-A (straight mineral, SAE 20, mixed base) and typical premium-grade gasoline-base stocks. All test fuels contained 3.0 ml tel per gal.

Single-Cylinder Engine Procedure

A single-cylinder engine was selected as a desirable test tool to permit testing of small samples of experimental fuels, oils, and additives under closely controlled operating conditions.

Table 1 – Cycling Deposit-Accumulation Schedule for Single-Cylinder Engine Procedure

	Idle	Full Throttle
Cycle Duration, sec	50	150
Speed, rpm	600	900
Fuel/Air Ratio	0.087	0.077
Ignition Timing	tdc	
Compression Ratio	7.0/1	
Jacket Coolant Temperature, F	150	
Oil Temperature, F	160	
Intake Air Temperature, F	112	
Test Duration, hr	165	

The procedure developed, described in a previous paper,[1] consists of a CFR L-head engine operated under a cycling schedule summarized in Table 1. The test is started with clean combustion chambers, the octane requirement is determined at 24-hr intervals in terms of primary reference fuels, and the test is continued until the requirement stabi-

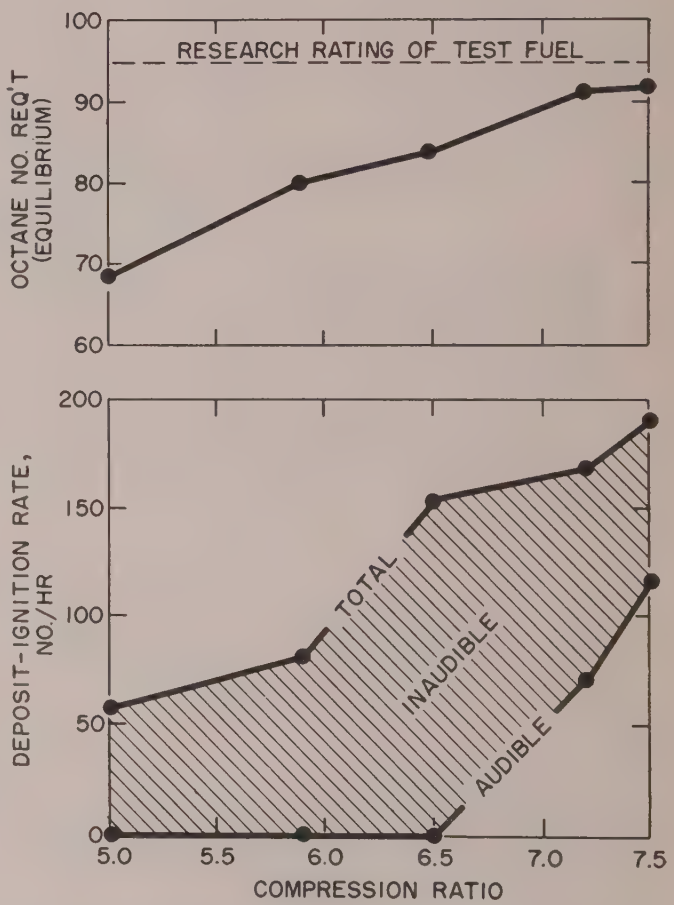

Fig. 2 – Compression ratio effect – single-cylinder engine procedure, fuel 2-A, oil 1-A

lizes. The engine is equipped with special instrumentation to detect and count (1) the total number of engine cycles in which the deposits ignite the fuel-air mixture (total deposit ignition) and (2) the number of these deposit ignitions which result in audible knock. This latter phenomenon is called audible deposit ignition. The special instrumentation is described briefly below.

Total Deposit-Ignition Counter – The deposit-ignition counter for this engine, described in a previous paper,[1] automatically detects and counts uncontrolled combustion arising from ignition by the deposits and differentiates it from normal combustion. This equipment consists of an electronic circuit, an electromechanical recording counter, a camshaft-driven timing device, and an ionization gap in the combustion chamber. Differentiation between normal and uncontrolled combustion is accomplished by making the counter operate only during a selected portion of the engine cycle before the normal spark-ignited flame front arrives at the ionization gap. Fig. 1 shows the relative location of the spark plug and ionization gap, and the portion of the engine cycle in which deposit ignition is recorded.

The engine is operated under conditions such that the spark-ignited flame front arrives at the ionization gap at about 15 deg atc. As shown graphically in Fig. 1, the counter is controlled to record the occurrence of deposit-ignited flame fronts at the ionization gap from 70 deg btc to 10 deg atc (counter cutoff). During this period, deposit ignition may be either inaudible or audible. The counter does not discriminate between these two cases but records all flame fronts, provided they arrive within the specified period. Hence, deposit-ignition rates determined by this equipment are referred to as total deposit-ignition rates. This instrumentation, developed by the Ethyl Laboratories, is now being used, or soon will be, by at least 12 other laboratories.

Audible Deposit-Ignition Counter – Since road evaluation of deposit ignition in passenger cars at the present time depends largely upon audible methods, a counter which counts only those deposit ignitions which are audible was developed for use with the single-cylinder engine. Briefly, this counter, referred to as an audible deposit-ignition counter, consists of a microphone suspended above the head of the engine, the necessary electrical components, and an electromechanical recording counter. The microphone is isolated from external noises by an acoustical baffle. An electrical filter is incorporated which results in the counter being actuated by only the high-frequency disturbances resulting from audible deposit ignitions or from knock. Since fuels of sufficient octane number to prevent knock are used in all tests, the counter supplies an accurate count of only audible deposit ignition.

An acoustical means is provided which permits the sensitivity of the audible counter to be adjusted periodically to a standard. This instrument supplements the total deposit-ignition counter and provides additional information regarding deposit-ignition effects.

The above instrumentation and procedure have been used by Ethyl for evaluating gasoline, additive, oil, and engine factors. The results of some of this work are presented herein to illustrate the usefulness of the procedure and instrumentation.

Compression Ratio Effects – Since deposit ignition is assuming greater importance with the trend to higher compression ratios in passenger-car engines, the effect of changing compression ratio in the single-cylinder engine was examined in a series of full-length tests. For these tests, the operating conditions and schedule were the same as presented in Table 1 except for compression ratio, which was varied from 5/1 to 7.5/1 by changing cylinder-head gasket thickness.

Fig. 2 shows the effect of changing compression ratios on both audible and total deposit-ignition rates, and the equilibrium octane requirement at each compression ratio. Although both the equilibrium octane requirement and the total deposit-ignition rate increased as compression ratio was raised from 5/1 to 7.5/1, none of the deposit ignitions were audible at compression ratios below 6.5/1. As the compression ratio was increased above 6.5/1, the audible deposit ignition also increased with this particular test fuel, as shown in

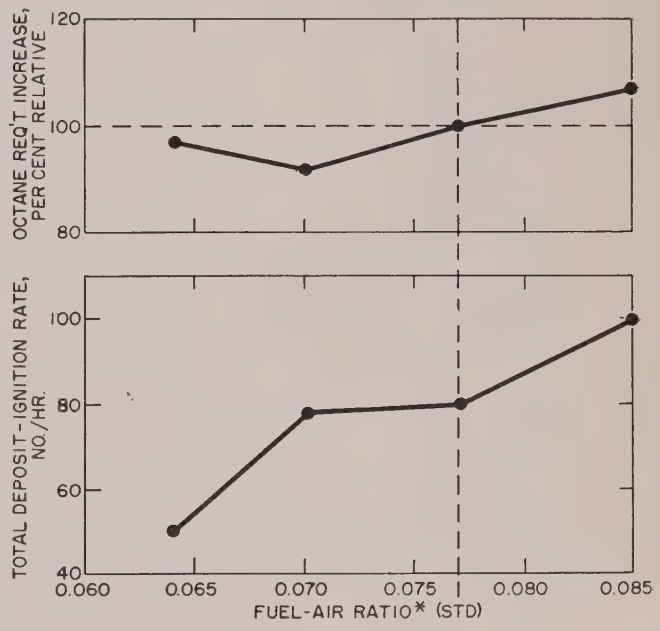

Fig. 3 – Fuel/air ratio effect – single-cylinder engine procedure, fuel 2-A, oil 1-A. Fuel/air ratio (asterisked) during full-throttle 900-rpm portion of test cycle; one complete test run at each fuel/air ratio

[1] See SAE Transactions, Vol. 62, 1954, pp. 40-49: "Deposit-Induced Ignition – Evaluation in a Laboratory Engine," by D. A. Hirschler, J. D. McCullough, and C. A. Hall.

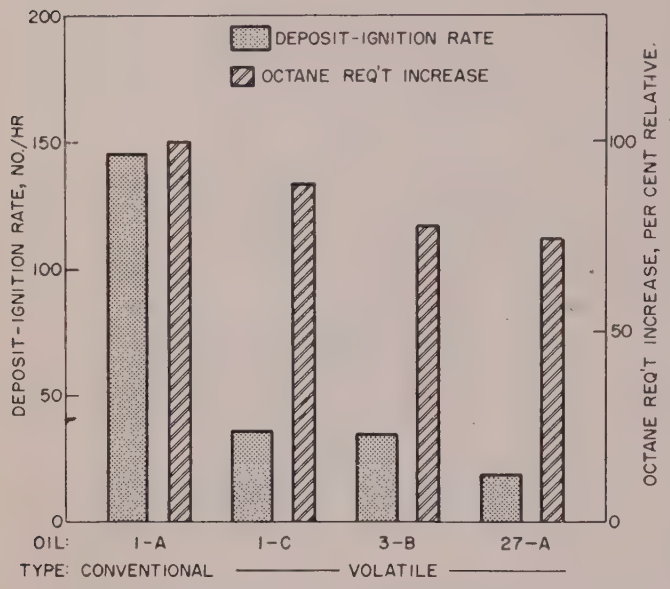

Fig. 4 – Effect of different oils – single-cylinder engine procedure, fuel 2-A

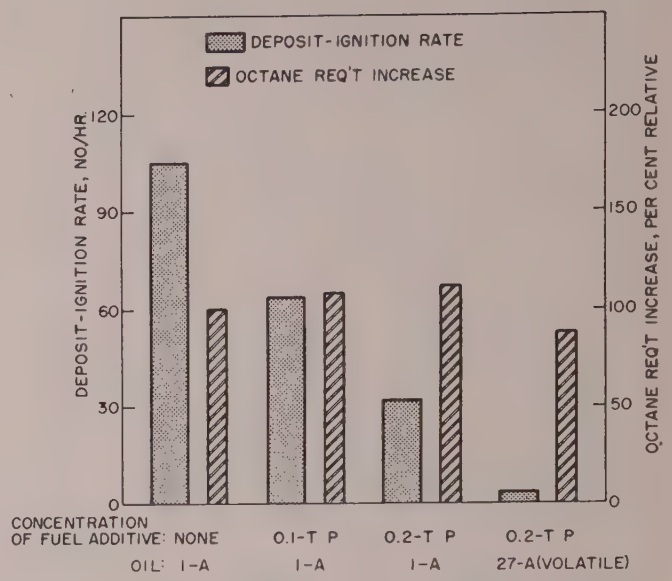

Fig. 6 – Effect of fuel additive N with two different oils – single-cylinder engine procedure, fuel 2-A

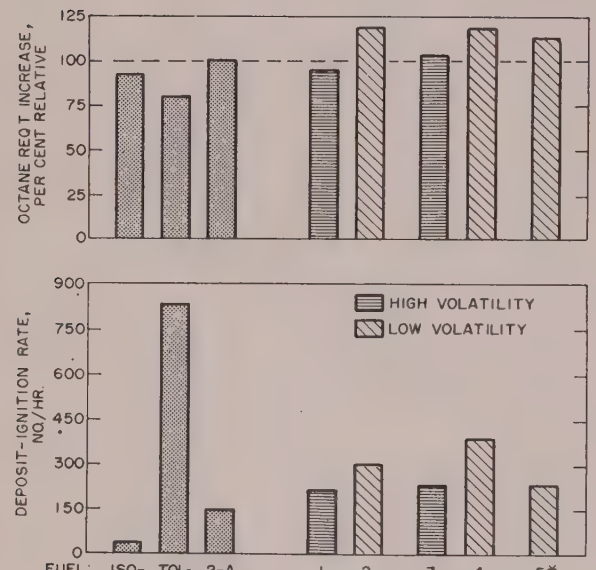

FUEL:	ISO-OCT.	TOL-UENE	2-A COMM'L	1 CAT. CRK'D	2 CAT. CRK'D	3 CAT. REF'D	4 CAT. REF'D	5*
% EVAP AT 330°F:	100	100	89	92	77	92	77	77
90 % POINT °F:	208	227	333	324	382	323	368	362
AROMATICS %:	0	100	21	21	40	41	50	35
OLEFINS %:	0	0	25	41	22	2	2	2
SATURATES %:	100	0	54	38	38	57	48	63

Fig. 5 – Effect of different fuels – single-cylinder engine procedure, oil 1-A. Fuel No. 5 (asterisked) is fuel No. 4 with heavy aromatics replaced with heavy paraffins

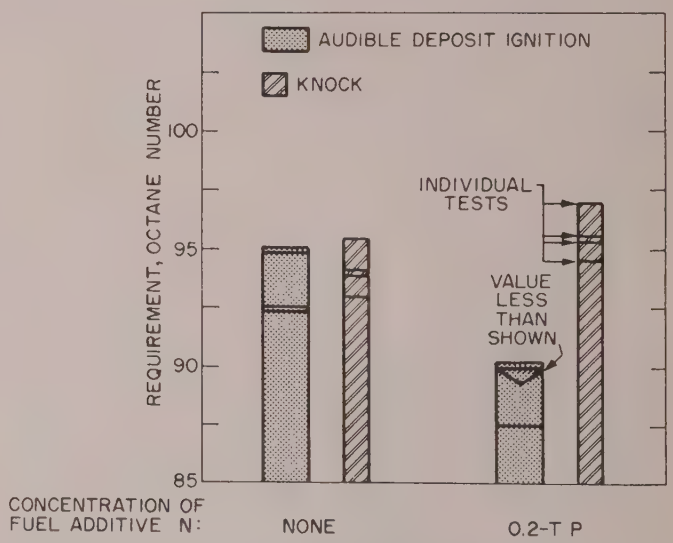

Fig. 7 – Effect of fuel additive N – multicylinder engine dynamometer procedure, engine M, fuel 2-A, oil 1-A

Fig. 2. It was verified that, like knock, the audible deposit ignition caused by a given set of deposits, could be reduced by either increasing the octane number of the fuel or enriching the mixture at full throttle.

Fuel/Air Ratio Effects – It has been pointed out that enriching the fuel/air ratio reduces the audible deposit ignition from a given set of deposits. This results from the increased resistance of the end gas to detonation. Over a long period, however, enriching tends to accentuate the formation of the type of deposits which increase total deposit ignition. This latter effect is shown in Fig. 3 when the engine was run using the cycling procedure outlined in Table 1 with the fuel/air ratio during the full-throttle portion of the cycle adjusted for each test as indicated.

The equilibrium deposits accumulated during prolonged rich-mixture operation not only caused a larger increase in octane number requirement but also were more prone to increase deposit ignition. In order to provide a common basis for comparison, the equilibrium requirement data in all tests were measured at the same standard fuel/air ratio (0.077). Since the audible counter was not available for these tests, no audible data were taken.

Passenger-car carburetors take advantage of these fuel/air ratio effects in that they normally maintain lean ratios during part-throttle cruise conditions where considerable amounts of deposits are accumulated. Furthermore they provide rich mixtures during full-throttle acceleration where maximum audible deposit-ignition tendencies generally occur.

Lubricating Oil Effects – Previous papers[1-6] have reported that deposit ignition and octane requirement increase are reduced as the volatility of the lubricating oil is increased. These findings have accelerated the recent marketing of multigraded, volatile-type oils, such as 5W-20 and 10W-30.

The data presented in Fig. 4 illustrate how this test procedure can differentiate between a conventional, straight mineral, SAE 20 oil 1-A and the newer more volatile oils. The volatile oils reduced deposit-ignition rate approximately 80% and octane requirement increase approximately 20%. The requirement increase data are expressed in percentage values relative to those obtained with the reference oil, 1-A. The volatile oils, which also contain relatively high concentrations of additives, appear to be more effective in reducing deposit ignition than requirement increase.

Fuel Composition Effects – High-octane commercial fuels now in use or planned for the near future contain considerable amounts of catalytically cracked and catalytically reformed stocks. These stocks contain relatively large proportions of aromatics, especially in the higher boiling fractions, in order to provide the necessary high antiknock quality. Because of this trend in the refining industry, it was of interest to obtain some indication of the effects of these two types of refinery stocks on deposit ignition.

It has been shown in a previous paper[1] that base fuel composition is a factor in building the type of deposits that cause deposit ignition. Work with leaded pure hydrocarbons disclosed that the aromatics formed deposits which gave more deposit ignition than other classes of hydrocarbons.

Tests were run on a catalytically cracked stock and on a catalytically reformed stock of similar low-volatility characteristics. Each of these stocks had 77% evaporated at 330 F in the ASTM Distillation Test. Both fuels were also tested after removing some of the higher boiling fractions until 92% was evaporated at 330 F. Thus the high-volatility fuels had only one-third as much material boiling above 330 F as compared with the low-volatility fuels. A fifth fuel blend was made by substituting heavy paraffins for the heavy aromatics in the low-volatility catalytically reformed stock.

Test results are shown in Fig. 5 for these five special fuels with pertinent information concerning volatility and hydrocarbon type of each fuel. In addition, data are presented on two hydrocarbons, isooctane and toluene, and commercial premium grade fuel 2-A. The two hydrocarbons produced the minimum and maximum deposit-ignition rates, respectively, in a group of individual hydrocarbons tested. It may be observed that all of the gasolines were between the two hydrocarbons with respect to deposit-ignition rate. However, deposit-ignition rates were slightly greater for all five special fuels than for commercial fuel 2-A. This latter fuel contains 35% straight run, 40% catalytically cracked, 10% polymer, and 15% butane and pentane.

Increasing the volatility of either the catalytically cracked or catalytically reformed fuels by reducing the quantity of higher boiling fractions resulted in both a lower deposit-ignition rate and a slightly lower octane requirement increase. Also, when heavy paraffins were substituted for heavy aromatics in the low-volatility reformed stock, the deposit-ignition rate was reduced to that of the

---

[2] "Combustion-Chamber Deposits as Related to Carbon-Forming Properties of Motor Oils," by J. D. Bartleson, and E. C. Hughes. Paper presented at meeting of American Chemical Society, Atlantic City, September, 1952.

[3] See SAE Transactions, Vol. 61, 1953, pp. 361-376: "Combustion-Chamber Deposition and Knock," by H. J. Gibson, C. A. Hall, and D. A. Hirschler.

[4] See SAE Transactions, Vol. 62, 1954, pp. 57-65: "Some Effects of Fuels and Lubricants on Autoignition in Cars on the Road," by R. K. Williams and J. R. Landis.

[5] See SAE Transactions, Vol. 62, 1954, pp. 228-242: "Effect of Lubricant Composition on Combustion – Chamber Deposits," by J. G. McNab, L. E. Moody, and N. V. Hakala.

[6] "Crankcase Oil – An Approach to Combustion-Chamber Deposit Problem." by R. L. Overcash, W. Hart, and D. J. McClure. Paper presented at SAE Annual Meeting, Detroit, Jan. 14, 1954.

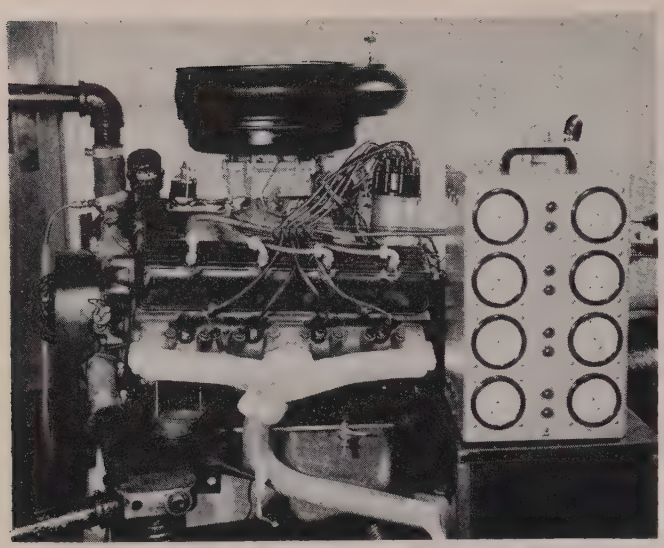

Fig. 8 – Test engine with multicylinder deposit-ignition counter

high-volatility reformed stock. This indicates that deposits formed by the heavy aromatics in the original low-volatility reformed stock (No. 4) caused more deposit ignition than those formed by the heavy paraffins. Octane requirement increase was not, however, significantly affected by replacing the heavy aromatics with the heavy paraffins.

Since the heavy aromatics are desired to meet competitive octane number levels, this points up the need for better oils or a fuel additive or both which will counteract the increased deposit-ignition tendencies.

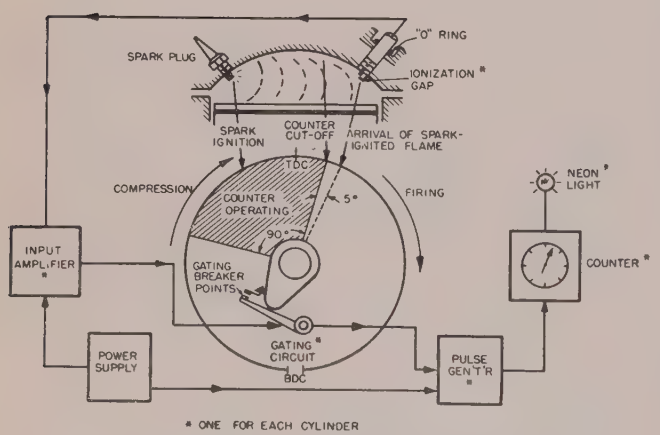

Fig. 9 – Multicylinder deposit-ignition counter

Fuel Additive Effects – The single-cylinder engine procedure has been very useful in screening fuel additives designed to reduce deposit ignition. An example of this type of test work is presented in Fig. 6 which shows the test results on the leaded base gasoline, 2-A, and the same fuel containing two different concentrations of fuel additive N, the concentration of this commercial additive being expressed in terms of theories of phosphorus (0.1 or 0.2-T P). The use of the additive lowered the total deposit-ignition rate by 40% at a phosphorus content of 0.1 theory and by 70% at 0.2 theory. In these tests the additive showed a slight tendency to increase equilibrium octane requirement. Data are also presented which show that the combination of fuel additive N (0.2-T P) and volatile oil 27-A reduced the deposit-ignition rate by 96%. In addition to practically eliminating deposit ignition, this combination also gave a lower octane requirement increase for knock.

Multicylinder Engine Dynamometer Procedures

The single-cylinder test procedure previously described provides reproducible data under controlled conditions. Such a procedure is economical in time, manpower, and equipment, yet it permits the investigator to rank fuels, lubricants, and additives according to their relative merits. A logical extension of such single-cylinder engine tests would involve the same sort of data for present-day passenger-car engines. Dynamometer operation of multicylinder engines can provide data on the effect of engine variables as well as oil-fuel-additive variables, and yet retain the desirable feature of close control of test conditions.

A cycling-type dynamometer test schedule has been developed for use with a modern high-compression V-8 engine. This schedule, summarized in Table 2, consists of short periods of idling, acceleration, road-load operation, and deceleration. The test is started with clean combustion chambers and continues until the audible deposit ignition and octane number requirements have stabilized. Two different methods, described below, have been developed for rating and measuring the effects of the deposits accumulated with this schedule. The methods are referred to as the audible rating method and the deposit-ignition counter method.

Audible Rating Method – This is an aural method whereby the audible deposit ignition and knock requirements were determined by rating with primary reference fuels during the 20-sec acceleration period of the cycling schedule, at which time normal operation was followed except that the throttle was held in its wide-open position. The audible deposit-ignition ratings were made at 5-deg retarded ignition timing every 12 hr. The ratings for knock were made at standard ignition timing every 24 hr. Audible deposit ignition was distinguished

from knock by shutting off the ignition as soon as knock occurred. If the engine continued to run, the knock was considered to be audible deposit ignition.

Fig. 7 illustrates how this procedure and rating method can be used to determine the effect of fuel additives. The use of fuel additive N showed a substantial decrease in audible deposit ignition requirement and a slight increase in knock requirement.

Deposit-Ignition Counter Method – Experience with the single-cylinder total deposit-ignition counter indicated the desirability of similar instrumentation for use with multicylinder engines. If such an instrument could indicate total deposit ignitions in each cylinder, it would be extremely useful in correlating the single-cylinder data with modern passenger-car engines. Such an instrument would also permit the basic measurement of the tendency of deposits to ignite the fuel-air mixture, rather than measurement of a secondary effect such as the audible manifestation. Furthermore, it would provide a continuous record during all engine operation with the test fuel and thereby reduce the necessity for frequent observations with primary reference fuels. The technique could be used by engine builders in studying the influence of various mechanical design factors on undesirable variability of deposit effects among cylinders.

The Ethyl Laboratories recently developed a multicylinder deposit-ignition counter which accomplishes the above objectives. Fundamentally this instrument is similar to that used with the single-cylinder engine described in a preceding section. In spite of its similarity, the design requirements for the multicylinder deposit-ignition counter were much more stringent than for the single-cylinder engine counter. For example, instead of operating at low engine speeds, it was desired to operate over the full load range at speeds from idle to 4500 rpm. It was also desirable to retain the standard centrifugal and vacuum spark advance characteristics rather than operate with fixed spark advance. In addition, because the instrument was to be usable on road-test vehicles, its total power consumption, size, and construction were limited by considerations involving available space in a passenger car.

Fig. 8 shows the multicylinder deposit-ignition counter in use on a dynamometer test stand. The eight individual count indicators are accompanied by eight neon bulbs which, by flashing as a count is recorded, provide an additional indication as to which cylinders are deposit igniting. Either of two separate power supplies may be used with the instrument: a 115-v, 60-cps laboratory source or a 12-v, d-c source to be used for road operation. Four of the special ionization gap transducers may be seen with their shielded connectors extending through the rocker-arm cover. The transducers consist of a model-airplane spark plug located in the end-gas region of the combustion chamber and

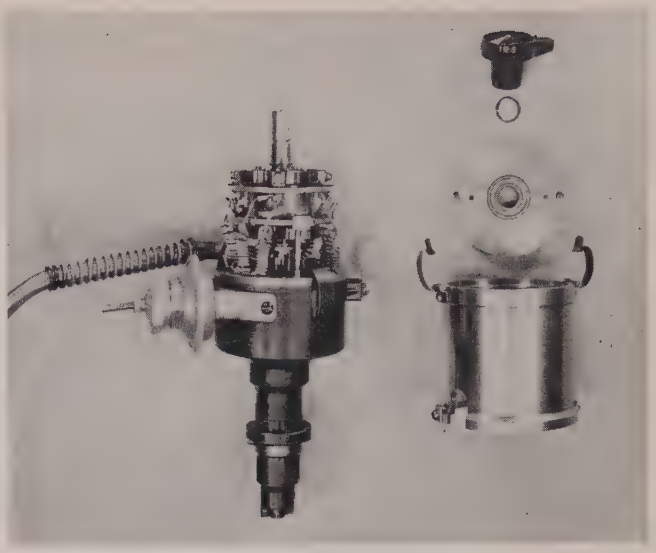

Fig. 10 – Special distributor parts

sealed from the cooling water by a stainless-steel tube whose upper end is fitted with threads to receive the connector shown. The cooling water is retained by means of a neoprene "O" ring surrounding each tube. The end-gas location of the ionized gap, shown schematically in Fig. 9, permits the counting of deposit ignitions originating anywhere in the combustion chamber regardless of the crank angle at which such ignition was initiated.

Since the electrical conductivity of the gap varies due to the presence of ions in the flame front, a voltage pulse is generated in a load resistor placed between the ionized gap and a d-c power supply. This pulse is amplified by the input amplifier and, depending upon the action of the gating breaker points, may cause the pulse generator to advance the counter one digit. The gating breaker points provide the discriminating action to differentiate between normal combustion and deposit-ignited

Table 2 – Cycling Deposit-Accumulation Schedule for Multicylinder Engine Dynamometer Procedure

Cycle Duration, sec	Type of Operation	Speed, rpm	Load
60	Idle	700	No load
20	Acceleration	700 to 2000	Throttle position A[a]
180	Road load	2000 (55 mph)	25 bhp
20	Deceleration	2000 to 700	Closed throttle

Road Load F/A Ratio	0.069
Basic Ignition Timing	5 deg retarded from standard
Jacket Coolant Temperature, F	165
Oil Sump Temperature, F	210
Test Duration, hr	160

[a] Throttle position A gives 1.9 in. of Hg manifold vacuum at 700 rpm.

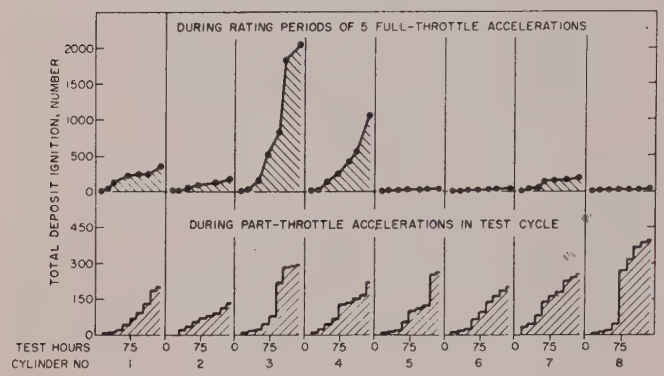

Fig. 11 – Accumulated total deposit-ignition count in various cylinders – multicylinder engine dynamometer procedure, engine M, fuel 2-A, oil 1-A

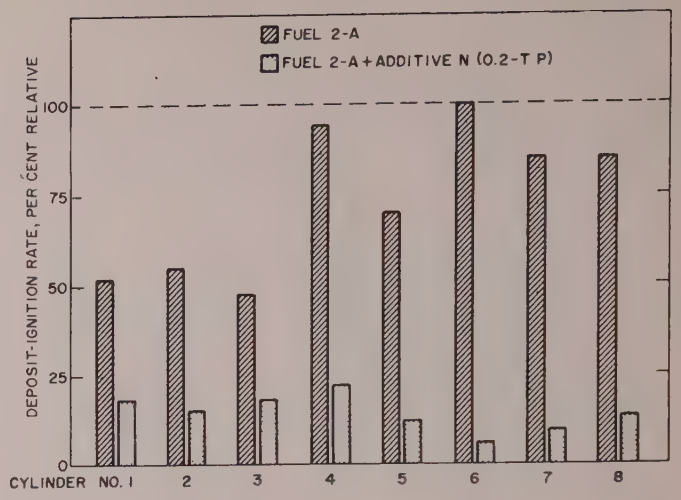

Fig. 12 – Effect of fuel additive N in various cylinders – multi-cylinder engine dynamometer procedure, engine M, oil 1-A. Deposit-ignition count determined during part-throttle acceleration of test cycle on test fuel

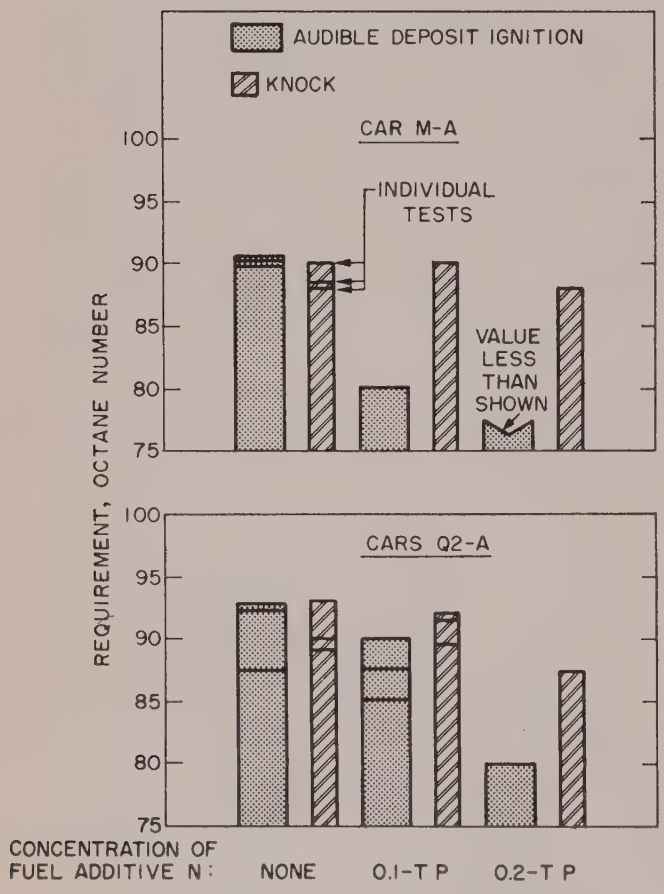

Fig. 13 – Effect of fuel additive N on vehicle fuel requirements – San Bernardino road tests, fuel 21-A, oil 1-A

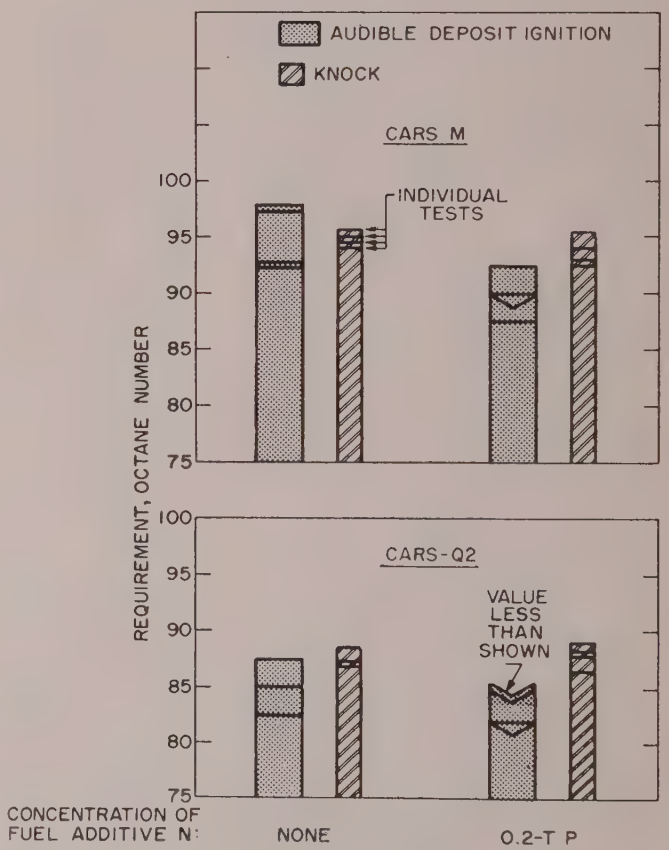

Fig. 14 – Effect of fuel additive N on vehicle fuel requirements – Detroit road tests, fuel 11-A, oil 1-A

combustion. The discriminating action is illustrated in the polar diagram portion of Fig. 9. Any flame front arriving at the ionization gap before the critical crank angle, denoted as "counter cutoff" (shaded portion of polar diagram), will cause the pulse generator to advance the counter one digit. The crank angle at which counter cutoff occurs is set to precede slightly the crank angle at which a normal flame front arrives at the ionization gap. Since the counter does not operate for the duration of the cycle after counter cutoff, the normal spark-ignited flame front does not actuate the counter.

The special gating breaker points are located in a penthouse structure atop the standard distributor shown photographically in Fig. 10. By mounting the special gating breaker points on the proper distributor components, the gating action, corresponding to the shaded area in Fig. 9, advances and retards with the spark-ignition timing. This feature permits the counter to function over the full range of automatic spark advance.

Selection of the crank angle at which counter cutoff occurs was made on the basis of measured flame arrival time under conditions of no deposit ignition (clean combustion chambers). These data, obtained over the full speed and load range, permitted the selection of a crank angle slightly in advance of the normal flame arrival time. Obviously, cycle-to-cycle variations in flame travel time from spark plug to ionization gap precluded an exact setting of such a point. Counter cutoff was therefore selected as 5 deg crank angle before the earliest observed flame arrival time, thus providing a margin of safety for day-to-day variation in test variables.

Fig. 11 shows typical data obtained with the deposit-ignition counter when used in conjunction with multicylinder engine M. The engine was operated on the standard cycling schedule summarized in Table 2. The lower portion of Fig. 11 shows the accumulated number of total deposit ignitions that were recorded by the counter for each individual cylinder as the regular cycling portion of the test progressed. These counts were observed to occur only during the part-throttle acceleration portion of the cycling schedule. Deposit ignition occurred in all eight cylinders with approximately a two to one variation among cylinders. As would be expected, the total count is rather low because no full-throttle operation was encountered.

Multicylinder-engine audible deposit-ignition ratings, both on the road and in the audible dynamometer procedure, are made during wide-open throttle accelerating conditions. In order to obtain comparative data, five full-throttle accelerations were made on the test fuel three times each 24-hr period. The number of deposit ignitions that occurred during these periods was recorded separately from those which occurred during the regular cycling procedure and are shown in the upper portion of Fig. 11. There was much more variation among individual cylinders during these full-throttle accelerations. Furthermore, the total count in some cylinders was much greater than obtained during the part-throttle accelerations even though there were 20 times as many part-throttle accelerations made during the test. In contrast to the part-throttle data, cylinders 5, 6, and 8 had practically no deposit ignition under full-throttle accelerating conditions.

Another interesting observation was that when audible deposit ignition occurred during the full-throttle accelerations, it occurred in one or more of cylinders 1, 2, 3, or 4. Furthermore, when audible deposit-ignition ratings were made with primary reference fuels during full-throttle accelerations, the same four cylinders were the only ones which produced audible deposit ignition. These observations were made by shutting off the ignition when knock occurred and observing the neon lights to determine which cylinders continued to fire. Except for cylinder 7, these audible observations correlate with the deposit-ignition count when both were made under full-throttle accelerating conditions.

The effect of fuel additive N, evaluated with this test technique, is shown in Fig. 12. The data are presented in terms of per cent relative deposit-ignition rate measured during the part-throttle accelerations of the standard cycle. Cylinder 6 had the highest rate of deposit ignition during the baseline test, and this is expressed as 100%. From these data it can be observed that fuel additive N showed a considerable reduction of the deposit-ignition rate in each of the eight cylinders. Similar additive effects were observed under the full-throttle accelerating conditions. This technique makes use of data from all eight cylinders, whereas the audible method is based on the overall audible effects which may be caused by only one or two cylinders.

Road Tests

The final proof of the effectiveness of any gasoline-oil-additive combination must, of course, be made on the road. There are two general types of road evaluations:

1. A limited number of closely controlled tests using test-car drivers and operating over a definite route with the audible deposit ignition and knock observations made under approximately the same weather conditions.

2. A large number of cars operating under a variety of owner-type driving conditions. Although this introduces a number of variables, a statistically sound answer can be obtained if sufficient cars are used.

The data reported are from tests of the "limited number of closely controlled" type, run with modern, high-compression, V-8 engine passenger cars

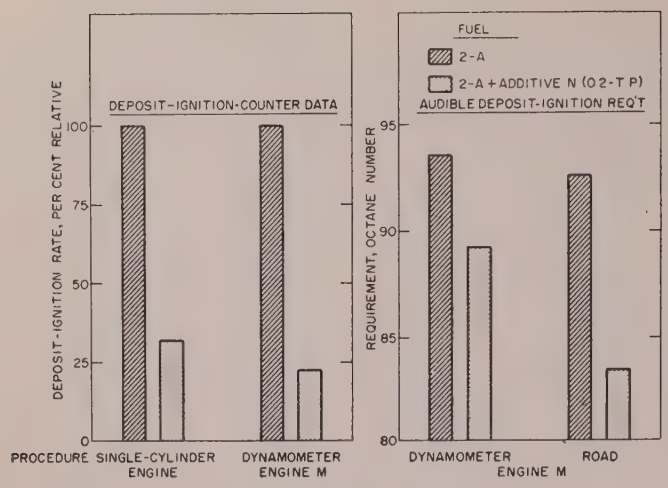

Fig. 15 – Correlation of various test procedures – oil 1-A

at San Bernardino, Calif. and Detroit, Mich. In both localities, combustion chambers were initially clean, and the vehicles were operated over a fixed test route under a moderately low-speed, metropolitan-area driving schedule. Standard ignition timing was used during road operation and measurement of octane requirements for knock. The audible deposit-ignition observations, however, were made with ignition timing retarded 5 deg from the standard setting. This was done to prevent knock from influencing the audible deposit-ignition observations. After deposits had been accumulated for 3000 to 6000 miles, at least five ratings were made per vehicle at intervals of approximately 500 miles. These ratings were made during full-throttle accelerations from 10 to 50 mph under level-road conditions using primary reference fuels. Audible deposit ignition was distinguished from knock by shutting off the ignition as soon as audible knock occurred. If the engine continued to run, the audible knock was considered to be audible deposit ignition.

San Bernardino Road Tests

The San Bernardino road tests were run with the top speed limited to 50 mph, and the four-barrel carburetors on the 1953 cars Q2A were replaced with the 1951 two-barrel carburetors. Because these carburetors provided slightly leaner full-throttle fuel/air ratios, this change increased the audible deposit-ignition tendencies of these vehicles, thereby permitting a more severe test on deposit-ignition suppressing additives. The data presented in Fig. 13 show that while additive N at 0.1 theory phosphorus concentration tended to reduce audible deposit ignition in car M-A, the higher concentration of 0.2 theory phosphorus was considerably more effective in both car makes. Unlike the results obtained from the single-cylinder engine and multicylinder engine dynamometer tests, the additive did not show any tendency to increase the octane requirement for knock during these road tests.

Detroit Road Tests

The Detroit road tests were run with the top vehicle speed limited to 40 mph. The vehicles were operated for a continuous ½-hr period at idle in each 8-hr shift during the knock and audible deposit ignition portion of the test in order to provide a more severe test of the additive. Furthermore, the use of leaner carburetor power jets decreased full-throttle fuel/air ratios 6 and 13% for cars Q2 and M, respectively. Fig. 14 shows the effectiveness of fuel additive N at 0.2 theory phosphorus concentration in lowering audible deposit-ignition requirements without affecting knock requirements. Not only was the audible deposit-ignition requirement reduced, but observations indicated that the frequency with which audible deposit ignition occurred was reduced in about the same order as predicted by the single-cylinder engine.

Thus, the results from these road tests confirm the findings of the single-cylinder engine and multicylinder engine dynamometer test procedures in that the additive was effective in reducing the deposit-ignition tendencies. This correlation of the various procedures is supported also by test data on other fuel-lubricant combinations.

Summary

Useful and practical test procedures along with special instrumentation have been developed for measuring the effects of combustion-chamber deposits on deposit ignition. These laboratory and road test procedures correlate to give consistent directional results as illustrated in Fig. 15.

One of these procedures employs a newly developed multicylinder deposit-ignition counter which detects and counts uncontrolled deposit-ignited combustion in each cylinder. With this instrument, the effect of variations in engine design as well as gasolines, oils, and additives can be evaluated both in the laboratory and on the road. Studies with these procedures have led to the following findings:

1. Refinery trends which increase the aromatics in gasolines, to secure higher antiknock quality, lead to the formation of combustion-chamber deposits which have greater deposit-ignition tendencies. This trend places further emphasis on the need for better lubricating oils or special fuel additives or both.

2. The use of a commercial phosphorus fuel additive will reduce deposit ignition.

3. The new volatile multigraded lubricating oils will reduce deposit ignition.

A Cradle for New Power— Chassis Features of the Firebird

Robert Schilling, Research Laboratories Division, GMC

This paper was presented at the SAE Summer Meeting, Atlantic City, June 9, 1954.

THE Firebird turbopower car not only has an unusual powerplant, it is an unusual car all around. It is neither a passenger car, nor a sports car, nor a race car, but simply a test vehicle built to meet certain specifications. These specifications explain why the car has been built as it is, and they will be discussed before the chassis components are described in detail.

Requirements

From the chassis designer's viewpoint, the outstanding fact about the car is that it weighs about 2800 lb while it has nearly 400 hp available. The car is therefore capable of speeds in excess of 200 mph, and it must be possible to accelerate, drive, and decelerate safely at these speeds. Interpreting this in terms of detailed requirements leads to the following rules:

1. Directional stability at all speeds must be good; maximum cornering ability is not essential since the car will not be used for road races, but the steering must be responsive enough for easy control.

2. The brakes must be unusually good in control and in heat dissipation. In spite of its moderate weight, at the potential top speed the car will have several times the kinetic energy of a Cadillac.

3. There is no need for a smooth boulevard ride or for ability to handle rough roads; the car will be used only on reasonably level surfaces.

4. Road noise and harshness need to meet only minimum standards.

5. Requirements for durability are also moderate; a total life of 10,000 miles on good roads should be sufficient. However, for that mileage the car must be absolutely reliable. Static strength

THIS paper explains how the design problems were solved for the Firebird, a high-power, high-speed, light-weight, turbopowered car.

Broad latitude was allowed the chassis engineer in designing the frame, suspension system, brakes, and steering. The result is the application of many unique features on the Firebird, some of which are used on an automobile for the first time.

The Author

ROBERT SCHILLING (M '28) is head of the Engineering Mechanics Department at General Motors Research Laboratories in Detroit, Mich. He received his early automotive engineering training in his native Germany, where he graduated as a mechanical engineer from the Munich Technical University. He came to the United States in 1927 and began working for Oldsmobile at Lansing, Mich. Mr. Schilling joined the Buick Motor Co. for a short time, and then returned to Oldsmobile. He has been with General Motors Research Laboratories since the end of World War II.

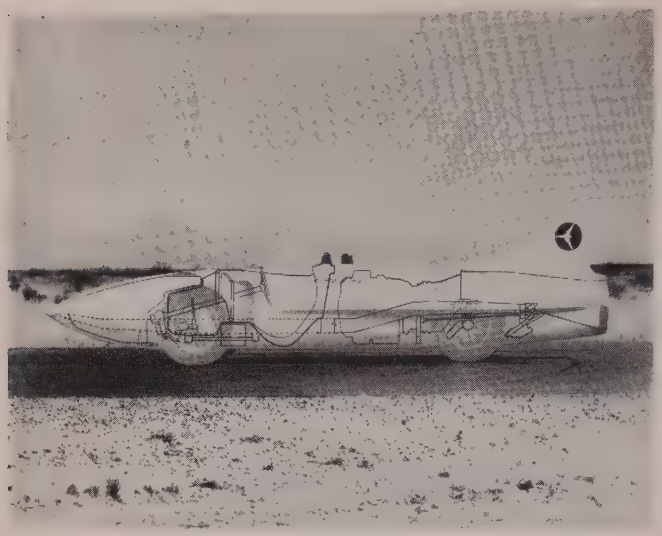

Fig. 1 – Overall view of chassis arrangement. This phantom view shows how the chassis elements are arranged in the body shell and how closely they are fitted to the body contour

should be as high as on normal cars (maximum vertical acceleration equal to $5g$), in order to provide safety on unexpected road waves.

To these performance specifications can be added some general rules which determine the type of elements to be used.

6. Where possible, all chassis parts should be located inside the body skin in order to reduce air drag and to maintain appearance.

7. The car need not be designed for easy production and low cost.

8. In order to take advantage of the opportunity to experiment, as many novel features as possible should be used, as long as final performance is not jeopardized.

The car resulting from these specifications can be seen in Fig. 1 which shows the overall arrangement of the components.

Beginning at the front end, inside the tapered nose section and closely fitting the body contour, is the fuel tank, constructed of glass-cloth reinforced plastic. It has two venting and overflow lines so arranged that it will vent properly even at extreme acceleration or deceleration. Immediately behind it is the steering gear, followed by brake and accelerator pedals which are almost on the front wheel centerline. The driver's cockpit with seat, headrest, and instrument panels reaches nearly to the midpoint of wheelbase. Next follows the turbopowerplant, with transmission and final drive, and at the extreme rear, split-flap air brakes and the exhaust system.

An overall view of the chassis and powerplant appears in Fig. 2. There are three main areas of the car:

1. At the extreme front is the fuel tank space.
2. Next is room for the driver and controls.
3. Almost completely filling the rear half is the powerplant, transmission, and exhaust system.

The main specifications of the car are given in Table 1.

Table 1 – Main Specifications of the Firebird

Overall Length, in.	222.7
Overall Width, in.	80.0
Height to Top of Bubble, in.	41
Height to Top of Vertical Fin, in.	55
Ground Clearance, in.	4½
Wheelbase, in.	100
Thread, Rear, in.	50
Thread, Front, in.	54
Tire Size	6.70-16
Rim Section	5K
Frame – Welded all box member 2 x 5 x 1/16 maximum section	
Front Suspension – Double wishbone, with torsion bar spring and ball joint steering axis	
Rear Suspension – De Dion, longitudinal single-leaf springs with lateral balance beam	
Steering – Recirculating ball type with parallelogram linkage, 20/1 overall ratio	
Brakes – Hydraulic, twin wheel cylinders with all forward energizing shoes. Brake drum of finned aluminum casting on cast-iron insert, 11 x 2.50 in.	
Weight, Empty, lb	2440
Weight, Loaded (Driver and 35 Gal Fuel):	
Front, lb	1315
Rear, lb	1485
Total	2800
Static Ride Deflection:	
Front, in.	2.75
Rear, in.	2.50
Ride Clearance (Front and Rear):	
Bump, in.	2.00
Rebound, in.	2.50

Frame

In Fig. 3, which shows the chassis alone without powerplant, the frame can be clearly seen. Its front is pointed to fit inside the body contour and padded with sheet rubber on the fuel-tank mounting areas. The siderails widen toward the rear and have a long and easy kickup which fits them into the horizontal stub wing surfaces between body and rear wheels. There are a total of six crossmembers, the last one behind the rear wheels. This extends beyond the siderails and carries the hinges and operating elements for the split-flap air brakes. Siderails and crossmembers are all-welded box members with a maximum section of 2 x 5 x 1/16 in. This construction, although expensive to build, results in a frame of high stiffness and low weight.

Wheels and Brakes

The wheel and brake arrangement is unusual for passenger cars; however, it is very similar to one developed by General Motors Engineering Staff for Ordnance vehicles, where it was used to produce a truly waterproof brake. It is used for the Firebird because it results in excellent airflow over the brake drums and therefore in good heat dissipation; the brakes are not made waterproof, but are vented through screened openings in the wheel disc. The exploded view in Fig. 4 shows the components. They are, from right to left:

The *stub drive shaft* with universal joint. Just to the left of the universal joint can be seen the outer race of a ball bearing. This fits into the bore

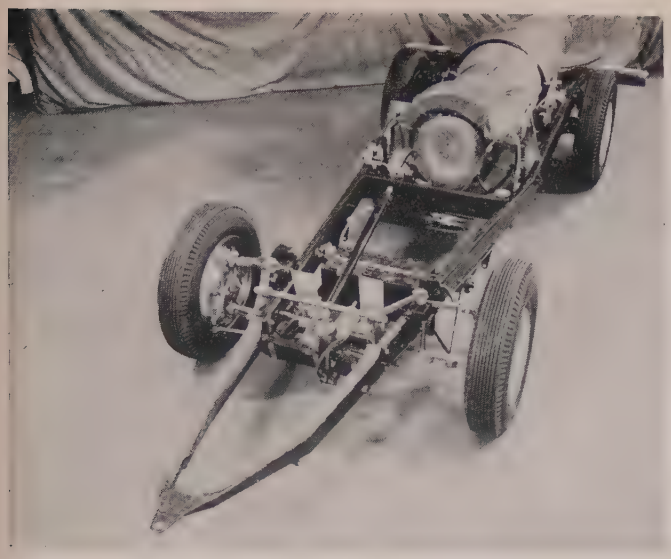

Fig. 2 – Chassis without body, powerplant installed. Powerplant occupies practically all interior space in body shell behind center crossmember. Rear portion of frame siderails is raised and moved out into area of the horizontal stub wings. Front of frame is tapered following the pointed body contour

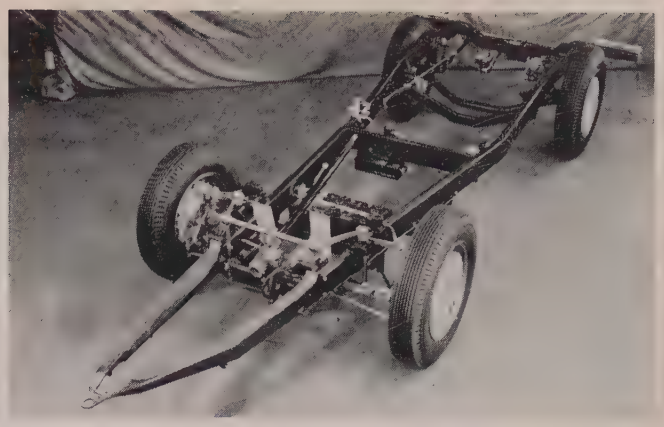

Fig. 3 – Chassis without body and without powerplant. Axle tube and frame rear crossmembers are depressed, and rear springs are moved close to frame siderails to clear powerplant and exhaust system

Fig. 4 – Components of wheel and brake assembly. Compared to the usual arrangement, the order of the parts is reversed: brake drum and backing plate are mounted outside of wheel. Wheel disc is integral with hub, and only the rim is removable

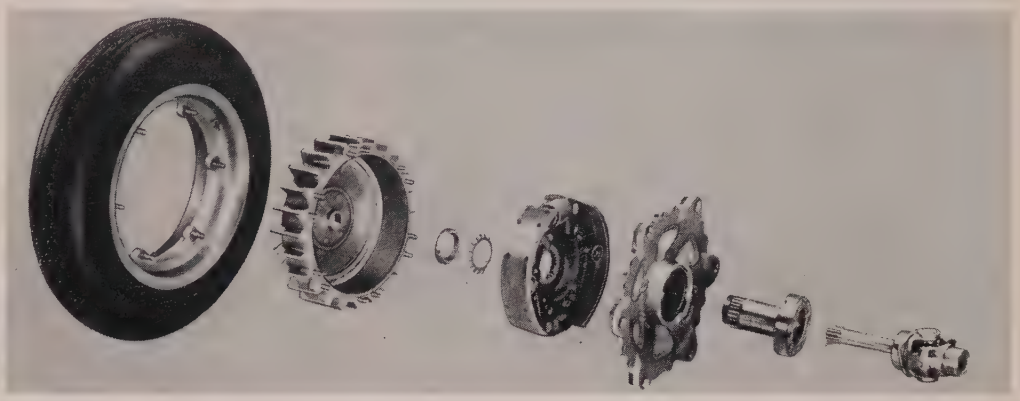

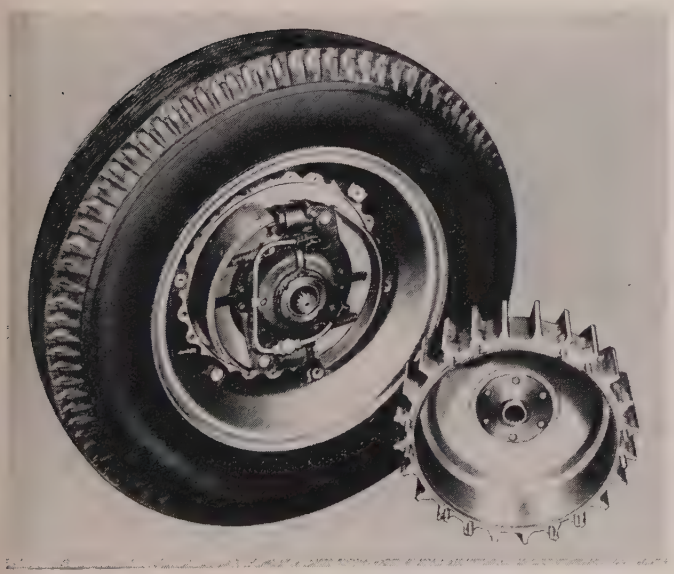

Fig. 5 – Brake assembly. Removal of brake drum exposes brake shoes and wheel cylinder for inspection and service

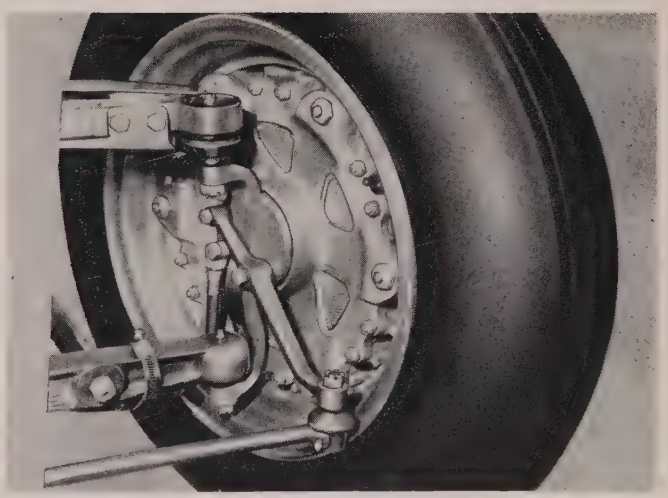

Fig. 6 – Inside face of front wheel. Screened openings in wheel disc permit air to enter interior of brake drum and to cool wheel-cylinder assembly

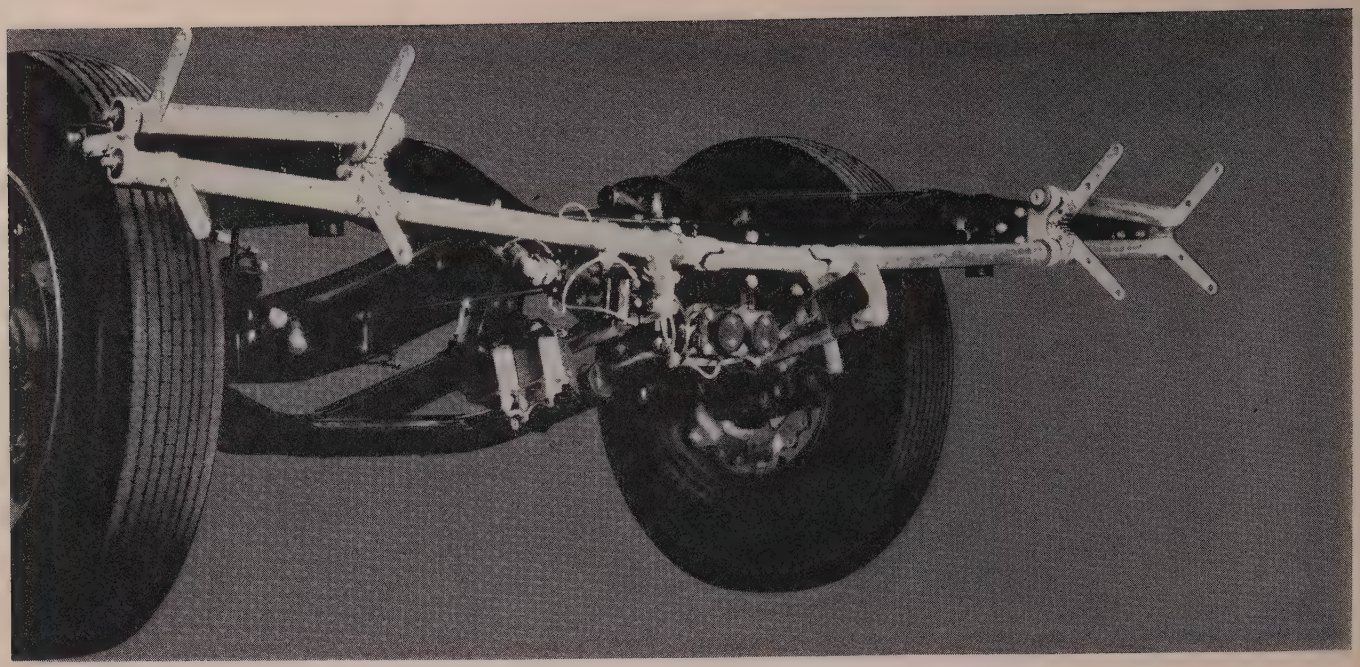

Fig. 7 – Split-flap air brakes. Hinge shafts and actuators for the air brakes are mounted on brackets carried by the rear crossmember

of the *rear wheel spindle* through which the stub shaft passes. This spindle is permanently bolted to the end flange of the axle tube, not shown in this view. For the front wheels, the flanged rear spindle is replaced by the front spindle which has no flange but two extensions connecting it to ball joints which form the steering axis.

The six-spoked *wheel* is an aluminum forging; the wheel bearings and seals are mounted in its bore, so that the whole assembly can be slipped on the spindle.

The *brake cylinder and shoe assembly* is next to fit over the spindle and is seated on the splined portion. It forms a complete preadjusted brake assembly. Brake fluid is admitted from a fitting on the flange of the wheel spindle through drilled passages and through an "O" ring seal located on a flat in the spline area.

A *lockwasher* and *nut* hold the brake assembly and wheel-bearing inner races in place.

The *brake drum* has a cast-iron rubbing surface over which a ribbed aluminum drum is cast; a splined hub is riveted to its center. When assembled to the wheel by six pairs of studs, the drum fits over the brake shoe assembly and engages the splines at the end of the stud drive shaft. Axle-shaft torque is transmitted through the brake drum to the wheel.

The *rim* is also an aluminum forging and fastens with six studs to the wheel, seating radially and laterally on six pads of insulating material which reduce the heat transmitted from the hot brake drum to the rim and therefore to the tire.

These parts can again be seen in Fig. 5 where the brake drum is removed to show the left rear wheel and brake assembly. To the lower right of the wheel spindle is seen the fitting through which brake fluid enters from the spindle, being piped first to the lower and then to the upper wheel cylinder. There is one wheel cylinder for each brake shoe, and all shoes are arranged so that they are energized in forward motion. The brake cylinder and shoe assembly was designed and built by Moraine Products Division.

Fig. 6 is a view of the left front wheel assembly, showing the wheel to rim and wheel to brake drum bolting in more detail. Also visible is the front spindle with its two extensions and the mounting of the steering arm.

Split-Flap Air Brakes

The mechanical brakes would be considered oversize for an ordinary passenger car of the same weight; but at its potential top speed the Firebird has so much kinetic energy that the brake temperature might become excessive during a single stop. The split-flap air brakes described elsewhere have hence been incorporated in the body design.

Fig. 7 shows how they are supported from the rear crossmember so that the braking forces need not be carried by the body structure. The upper and lower hinge shafts each carry two stub arms to which the flap surfaces are bolted; they are forced to rotate in opposite directions by the gear sectors which couple them. Extensions of the lower hinges are coupled by a short universal jointed shaft to assure uniform positioning. They are rotated by a pair of electric screw jack actuators which can open the flaps against the full air drag in 3 sec. Also in the picture, but hard to distinguish,

are the opening relays, limit switches, and pickup for the position indicator.

Front and Rear Suspensions

The front suspension is shown schematically in Fig. 8. It is of the double-wishbone type with a torsion bar spring and ball-joint steering axis. The lower wishbone is horizontal at normal standing height. The upper wishbone is slightly inclined, producing a swing arm of about 110 in. and therefore a rate of camber change of approximately ½ deg per in. The front roll center is 1.9 in. above ground. The raised roll center and camber change action were considered desirable to maintain high cornering power at the front wheels so that the car would not have the slow steering response usually found on parallel-action front suspensions.

Fig. 9 shows a front view of the assembly in which can be seen the wishbone arms and the ball joints connecting them to the front wheel spindle.

The front shock absorber is of the cam-and-lever type with end-to-end valving. This special unit, fitted to the body contour, was designed and built by Delco Products Division. The shock-absorber arm forms the upper wishbone.

Attached to the lower wishbone is a strut leading up to the roll stabilizer bar; it also carries bump and rebound stop pads which contact a frame bracket adjacent to the siderail. The unusual design of these elements keeps all the suspension parts within the body contour except the two wishbones.

The lower wishbone assembly is shown in Fig. 10 in an exploded view. At the left is the wishbone arm, the ball-joint socket at its outer end B, and an eye for mounting of a rubber bushing at the inner end A. The torsion bar spring is inserted into a splined hole near the center of the arm. The other end C of this spring is splined to a trunnion, and both ends are held in place by nuts so that the arm and torsion bar form a triangular wishbone member. The whole assembly oscillates around axis A-C. This rotation occurs in the usual way around the rubber bushing at A in the wishbone arm, but at the rear end of the torsion bar spring C the same rotation results in a windup of the torsion bar spring simultaneously with a rotation of the trunnion around its axis at right angles to the torsion bar spring.

The arrangement of the wishbones on the chassis frame can be seen in the worm's-eye view of Fig. 11. This shows the frame crossmember to which the inner end of the lower wishbone arm is connected and also the location of the torsion bar trunnion in another crossmember immediately below the frame siderails.

Camber of the front wheels is not adjustable but is held between 0 and −½ deg at normal standing height. Caster angle is adjustable from 0 to +3 deg by shifting the front shock absorber along its mounting surface, where it is located by interlock-

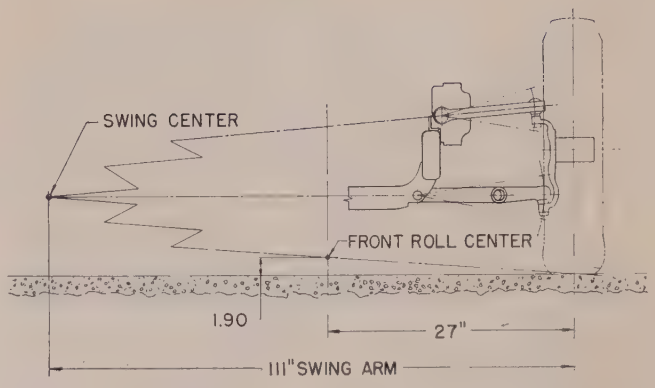

Fig. 8 – Transverse geometry of front suspension. The intersection lines of upper and lower wishbone plane with the transverse plane through the front wheels determine the virtual center of wheel motion and therefore the geometry features of the front suspension

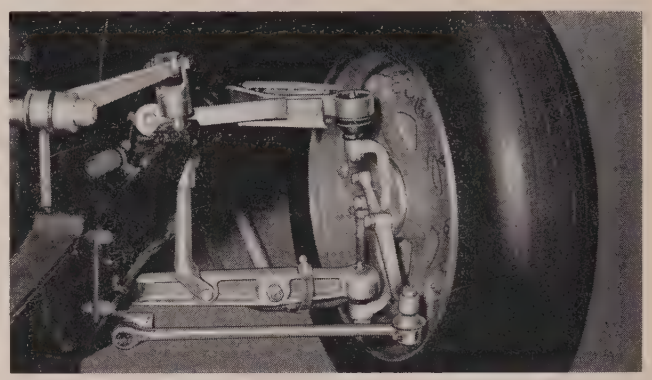

Fig. 9 – Front suspension seen from ahead. Wishbones, wheel spindle, and steering axis ball joints form the suspension linkage. Link from lower wishbone to roll stabilizer bar carries bump and rebound stops; it almost hides the vertical cylinder of the shock absorber

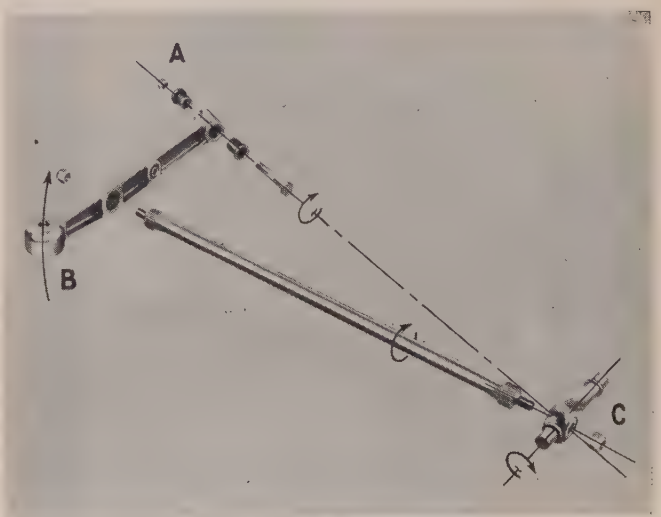

Fig. 10 – Elements of the lower wishbone. The hinge line passes along axis of rubber bushing at A and through intersection point of trunnion axis and wishbone centerline at C

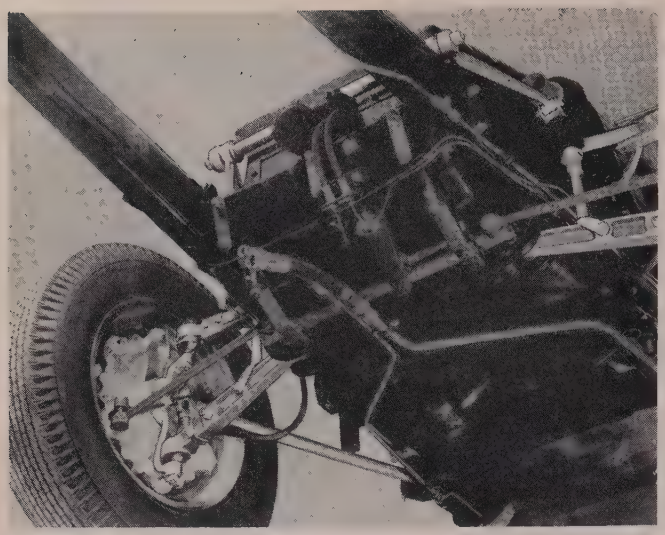

Fig. 11 – Front suspension, view from below. Wishbone arm and torsion bar trunnion are mounted in crossmembers located under the frame siderails

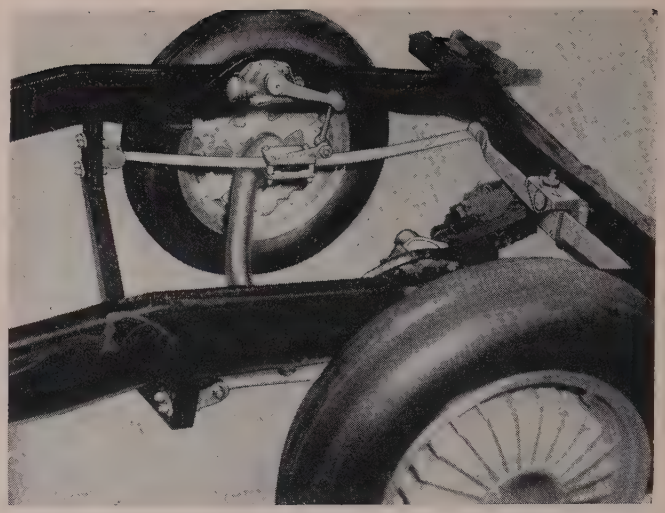

Fig. 12 – Rear suspension, side view. The leaf springs pass over the tubular axle, allowing space for the drive shafts and universal joints not shown. The rear ends of the leaf springs are fastened to the roll balance beam

ing serrations. A setting of $+1\frac{1}{2}$ deg proved satisfactory.

The rear suspension takes the form of a De Dion axle with single-leaf longitudinal springs. Fig. 12 shows an overall view of the installation. There is a tubular axle with integral spring seats, single-leaf longitudinal springs connected at the rear to a balance beam, and cam-and-lever type shock absorbers mounted above the springs. The same elements can also be seen in Fig. 13 which shows the subassembly of axle, springs, and balance beam. This assembly is connected to the frame at three points: the two front spring eyes and the center of the balance beam.

The balance beam was necessary to assure proper car handling in view of the unusual geometry of the car. Because the rear springs are located high inside the body, the rear roll center is almost as high as the center of gravity, but the front roll center is low. If front and rear roll rates were about equal, the rear wheels would then carry too much of the overturning couple under lateral acceleration, causing dangerous oversteer. To avoid this, the front roll stabilizer bar is provided, nearly doubling the front roll rate, and the rear balance beam is used to reduce the rear roll rate to less than 50% of its original value.

This reduction is obtained because the balance beam is free to oscillate about a central longitudinal axis, thereby equalizing the loads at the rear ends of left and right springs. Since it has a cross-section of $\frac{1}{4}$ x 2 in., it is also flexible enough longitudinally to eliminate the need for spring shackles.

A side view of the suspension geometry is shown

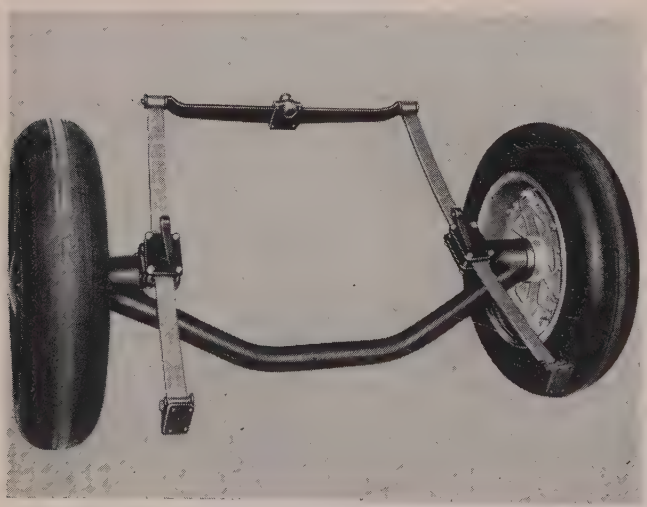

Fig. 13 – Rear axle and spring subassembly. Rear axle, single-leaf springs, and balance beam form a subassembly that is fastened to the frame at three points: the two front spring eyes and the center bearing of the balance beam

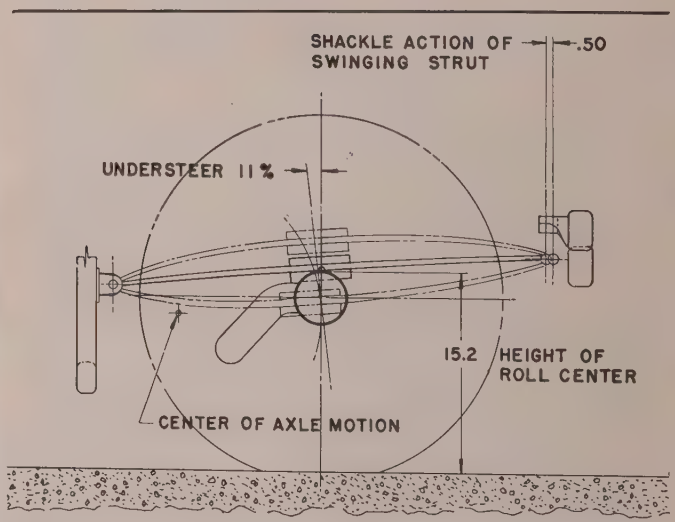

Fig. 14 – Side view geometry of rear suspension. Roll center and roll steer geometry are determined by the position of the rear leaf springs

in Fig. 14; on it can be seen the sloping mounting of the leaf springs, resulting in a roll understeer of 11%. The rear roll center, lying in the plane of the rear spring eyes, is 15.2 in. above ground.

With the high location of the springs and their short length of 34 in., it might be supposed that there could be a tendency to brake hop. However, the spring rates are so high that the windup due to braking thrust remains small. There is no power-hop tendency at all, since the axle-shaft torque reaction is carried by the sprung-mounted final drive, and the rear suspension receives only driving thrust at the wheel center.

Steering Mechanism

The steering linkage is arranged ahead of the front wheels as shown in the worm's-eye view on Fig. 15. It is of the parallelogram type with two idler levers, a connecting link, and tie-rods reaching to the steering arms. The whole linkage is in the plane of the lower wishbone, and the tie-rods have the same length as the lower wishbone. The Pitman arm is parallel to the idler levers and connected to one idler by a short link. The geometry is such that there is no Ackerman toe-out in turns, since for high-speed driving toe-in is required for correct tracking.

The steering gear is of the recirculating ball type of special construction fitted to this chassis. Both steering gear and linkage were built by the Saginaw Steering Gear Division. In Fig. 15 and again in Fig. 16, the gear is shown mounted on a crossmember in the center of the frame with the steering column at a very low angle.

Brake and Accelerator Pedals

To the left of the steering gear in Fig. 16 can be seen the brake pedal and to the right the accelerator pedal. They have the form of treadles with built-in heel rests. Since the driver's seat and headrest are part of the cockpit construction, it was impracticable to provide seat motion for leg room adjustment. Instead the pedals are made adjustable longitudinally. The pedal assembly is shown in more detail in Fig. 17 which shows the pedal bracket carrying the two treadles on lateral extensions. This bracket can slide on its central guide and is locked in place by a latch located in its interior under the central rib. The handle visible at the rear end is used to unlock the latch by a

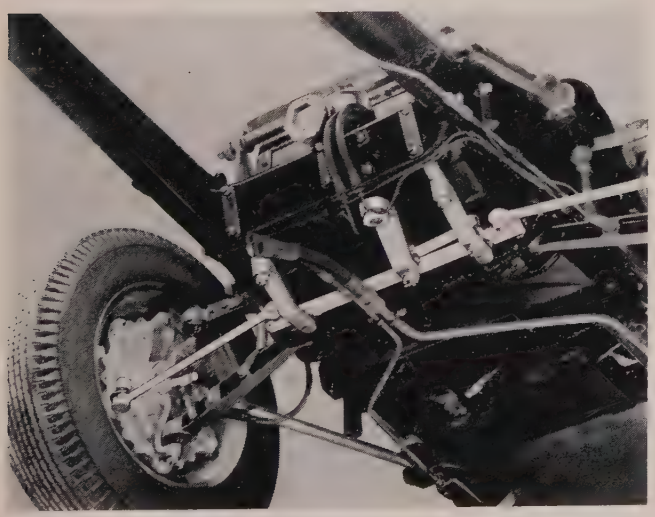

Fig. 15 – Steering linkage seen from below. The Pitman arm appears near the car centerline and is connected to the left idler lever through a short drag link. The two idler levers and crosslink form a parallelogram which supports the tie-rods

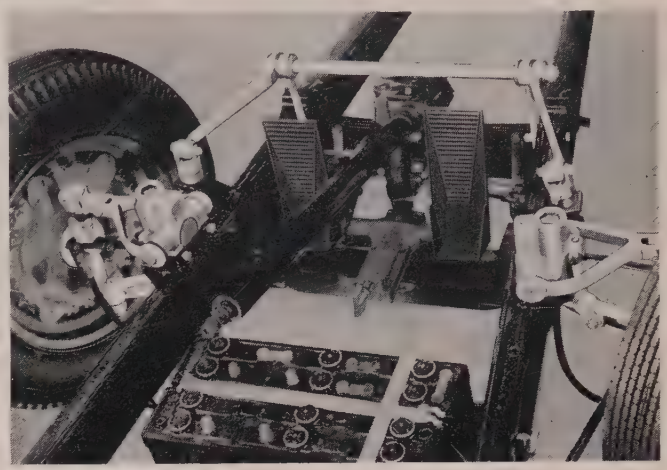

Fig. 16 – Steering gear and pedals seen from above. The two treadle-type pedals are a few inches ahead of front wheel centerline and are placed to left and right of the steering column. The roll stabilizer is arranged to pass in front of the driver's feet

Fig. 17 – Pedal support subassembly. The bracket carrying both pedals, an accelerator transfer cross-shaft, and the brake master cylinder can slide longitudinally and is locked in position by means of the central operating handle

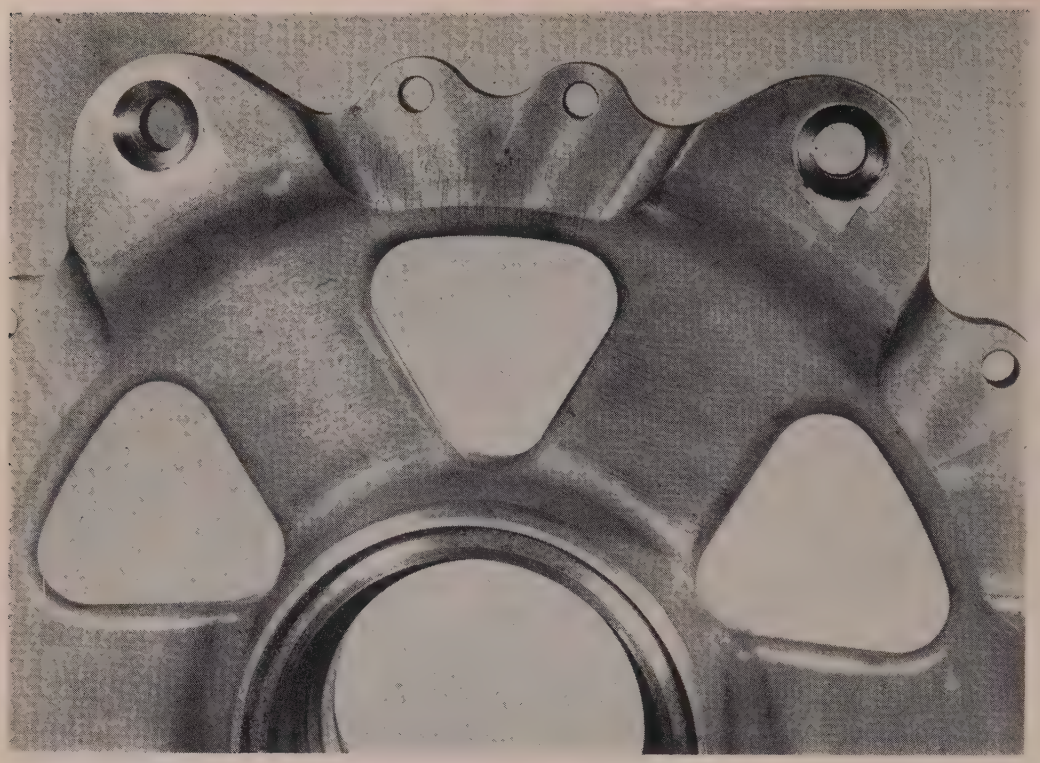

Fig. 18 – Stresscoat pattern of wheel after loading. The first step in checking the durability of the forged aluminum wheel is a stresscoat test which locates the areas of highest stress and permits an estimate of stress magnitudes

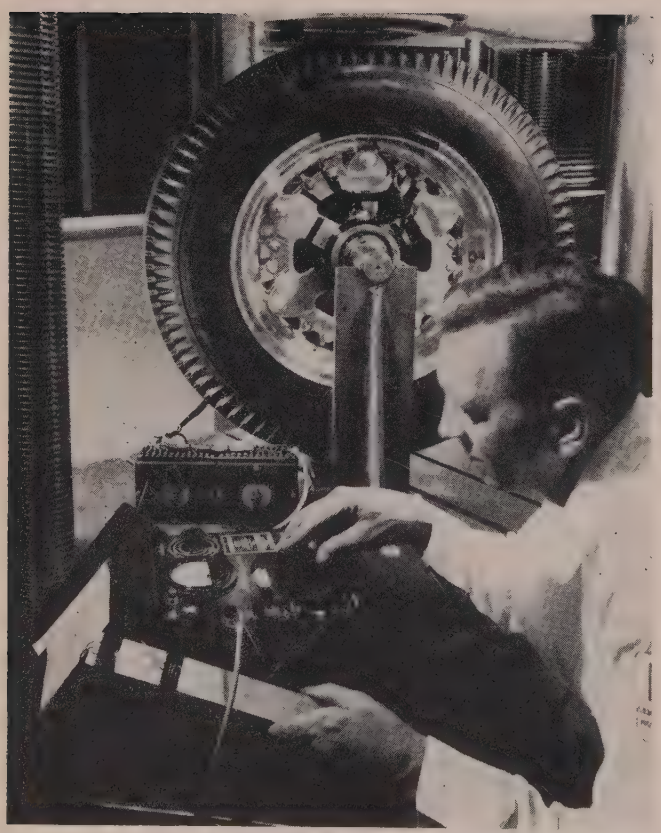

Fig. 19 – Static test of wheel assembly. In a second stage of testing, strain gages are mounted to the points of highest stress, and accurate stress measurements are carried out under various static load conditions

45-deg turn and to slide the pedals into the desired position. Also visible in the picture is an idler shaft operated by the accelerator, which is connected by a universal jointed shaft to a cross-shaft mounted on the frame siderail.

The brake master-cylinder assembly is mounted close to the brake pedal on the pedal bracket and connected by short links. It is also of special design, built by Moraine Products Division. There are two master cylinders in parallel, one operating the front brakes and the other the rear brakes. The two systems are connected by a crossbore in which is located a balance piston with limited travel. This dual arrangement acts like an ordinary single-cylinder system if all brakes are in order, since only a small displacement of the balance piston is required to assure equal fluid pressure front and rear. However, if either the front or rear brake develops a leak so that the pressure in its line drops, the balance piston will travel up to its stop and therefore will not permit the pressure in the intact system to drop. The car in effect has two independent brake systems for safety.

There are no parking brakes in the wheels but a parking lock is incorporated in the transmission and actuated by the transmission shift lever.

Laboratory Testing

It was clear from the beginning of the project that most of the road-test time available should be

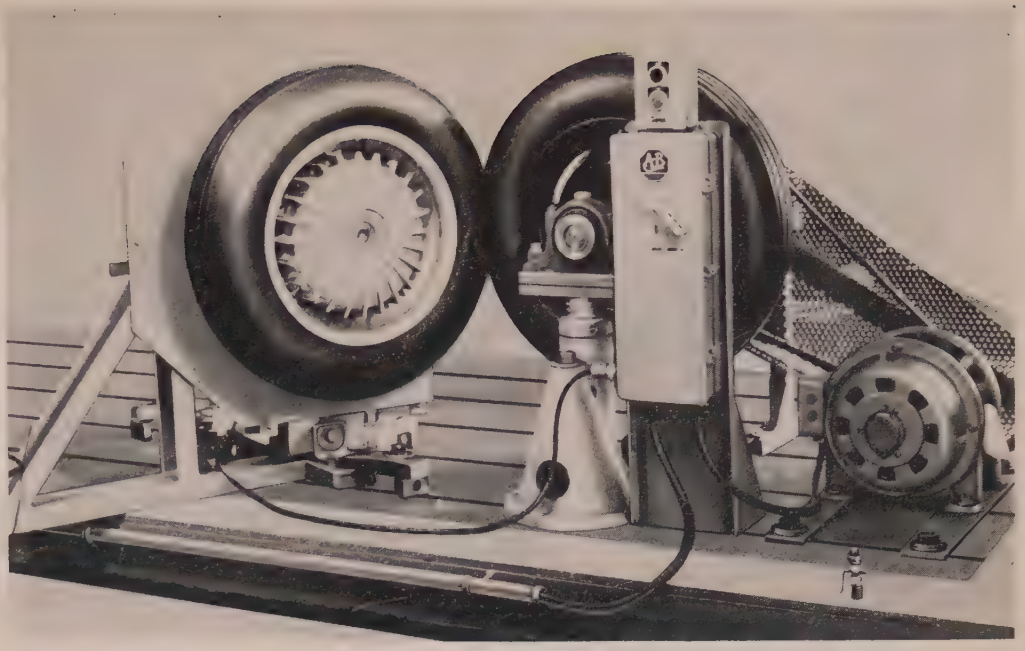

Fig. 20 – Durability test of wheel assembly. Based on the preceding stress measurements (Fig. 19) the loading condition likely to cause earliest failure is selected and reproduced by pressing two wheel and tire assemblies against each other while both wheels rotate

used for work with the powerplant, so that all of the chassis components must function reliably with little road-test development. The novel chassis elements were therefore subjected to laboratory testing to check their functioning as well as their static strength and fatigue durability. Figs. 18-22 show some of these test operations.

It has already been mentioned that a number of components were designed and built by Divisions of General Motors Corp. other than the Research Laboratories. But that is not all; many other Divisions of the Corporation assisted by temporary assignment of personnel to this project or by furnishing information from their own past experimental work. The Firebird chassis, therefore, shows the experience and practices not just of a small staff of men, but of many engineering groups in General Motors.

(Discussion of this paper is on p. 83, following the Turunen paper.)

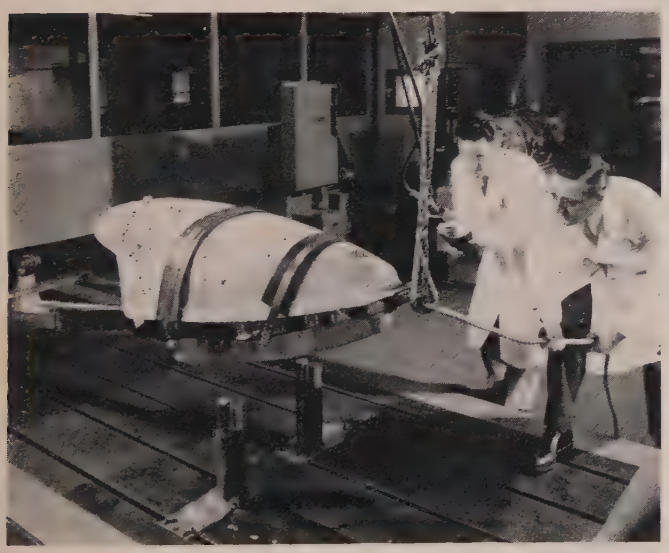

Fig. 21 – Drop test of fuel tank. A fuel tank mounted on a frame segment and filled with water is dropped on four spring plungers so that the maximum deceleration reaches 10g

Fig. 22 – Malfunctioning test of brake system. Complete system is arranged on bed plate, and two strain-gage pressure pickups fitted to front and rear systems. Functioning is checked under various operating cycles, with leaks introduced at various locations

Pinwheels or Pistons?—

A Progress Report

FIVE years ago a paper study[1] was presented before this Society which attempted to evaluate the possibilities of gas-turbine automotive equipment. Since that time an exploratory project on automotive gas turbines has been conducted at the General Motors Research Laboratories. This paper is a summary report of the work thus far accomplished.

The initial paper pointed out the possible advantages as well as the disadvantages of automotive gas turbines. However, as a paper study can only list these factors, it was decided that a small gas turbine would have to be built and tested in order to evaluate these advantages and disadvantages in a particular installation to learn more about the effect of each.

The design of the first Whirlfire engine, the GT-300, was based on the following criteria:

1. The initial study indicated that the area in which the gas turbine might best make its initial

[1] See SAE *Quarterly* Transactions, Vol. 4, January, 1950, pp. 102-115: "Gas Turbines in Automobiles," by W. A. Turunen.

FOR about five years, an exploratory project to study the application of gas turbines in automotive equipment has been conducted at the GM Research Laboratories. This paper summarizes the work thus far accomplished.

Included here are descriptions of the two models of the Whirlfire gas-turbine engine developed and some operating experience obtained with these engines installed in the Firebird turbo-powered car and the Turbo-Cruiser transit bus.

The Whirlfire installations have demonstrated that smooth, reliable operation, with very desirable power and torque characteristics, can be attained. They also indicate that future developments must be directed toward improved fuel economy, reduced acceleration time, and a suitable dynamic braking system.

The Author

W. A. TURUNEN is head of the Gas Turbines Department at General Motors Research Laboratories in Detroit, Mich. He received his B.S. in Mechanical Engineering from Michigan School of Mines and Technology, and his Master's degree in Engineering Administration from Columbia University. With the exception of four years in the Army Engineer Corps, he has been with General Motors since 1939.

on Automotive Gas Turbines

W. A. Turunen, Research Laboratories Division, GMC

This paper was presented at the SAE Summer Meeting, Atlantic City, June 9, 1954.

entry into the transportation field would be in the heavy-duty or commercial installations. It was therefore decided to build a unit which would develop 300 hp at the shaft.

2. It was recognized that problems, some anticipated and some unforeseen, were bound to arise in the development of an engine such as the GT-300. Consequently it was decided to emphasize mechanical simplicity and reliability in the original design rather than strive for the ultimate in fuel economy.

In the interest of simplicity, it was decided that a centrifugal compressor with a design-point pressure ratio of 3.5 would be used. To take advantage of its excellent torque characteristics, the dual turbine arrangement with separate gasifier and power turbines was selected. It was decided that both turbines should be single-stage axial-flow units. The inlet temperature to the gasifier turbine was set at 1500 F for reasonable bucket life. It was felt that a two-bearing gasifier shaft would be extremely desirable; and this consideration, coupled with the problems of critical shaft speeds and adequate bearing life, contributed to the final choice of 24,000 rpm for the design-point gasifier speed. This selection of speed then established the diameters of the compressor rotor and the gasifier turbine. High turbine speed with minimum size and weight was balanced against low rotative speed with decreased bucket stresses and lower gear ratios in the final selection of 12,000 rpm as the design point for the power turbine.

Whirlfire Engine Model GT-300

A schematic of the final mechanical arrangement of the GT-300 Whirlfire engine is shown in Fig. 1. The engine can be conveniently considered as two mechanically independent components, the gasifier or gas generator section and the power turbine-transmission section. The only coupling between the two units is a flexible duct to transmit the working fluid from the gasifier to the power turbine.

The mechanical arrangement of the gasifier is shown in Fig. 2. The prime function of the gasifier is to provide hot compressed gas to the power turbine. In this respect it functions exactly like a small jet engine. Air enters the engine through the splitter-type, glass-fiber-lined silencer. The radial-flow compressor discharges air through the single-outlet air scroll to the combustor. A double-walled elbow directs the hot gas from the combustor into the nozzle box and thence through the nozzle diaphragm and the gasifier turbine.

The combustion chamber is of the side-entrance type, with the inlet located midway between the dome and the outlet. The burner liner is a conventional-domed can type with inlets suitably located for admission of primary and secondary airflow. A duplex-type fuel nozzle built by GM Diesel Equip-

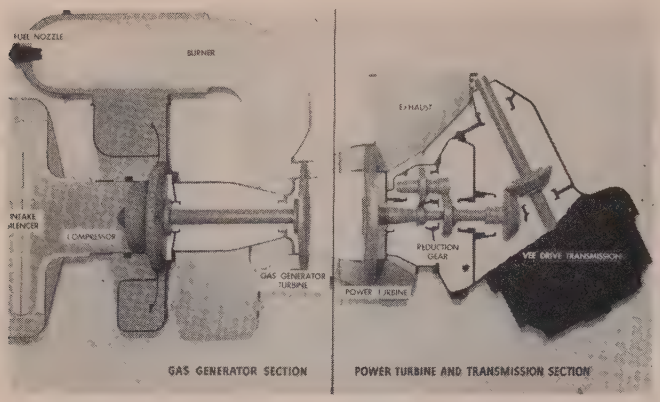

Fig. 1 – Schematic diagram of gas-turbine engine as installed in Turbo-Cruiser

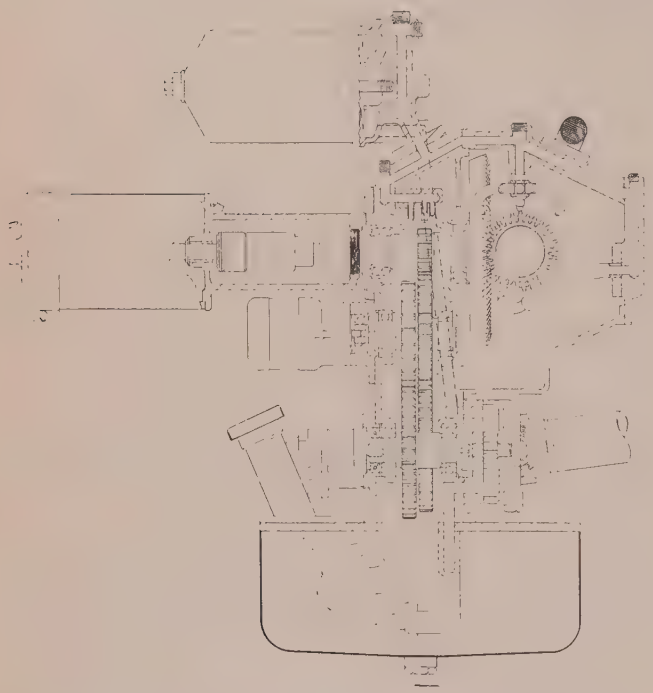

Fig. 3 – Gas generator accessory section of GT-300 engine

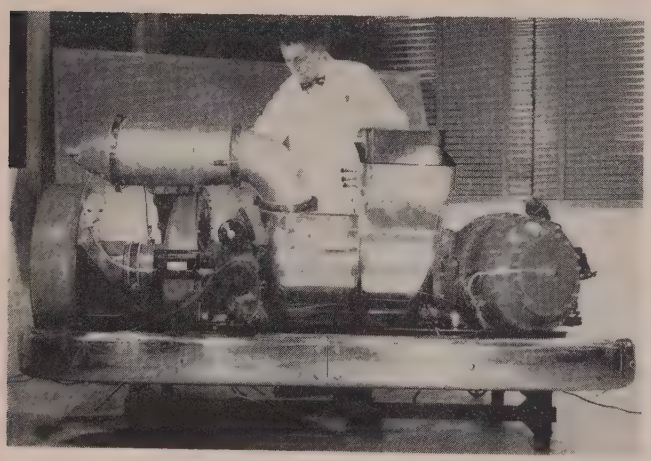

Fig. 5 – GT-300 Whirlfire turbopower unit ready for installation

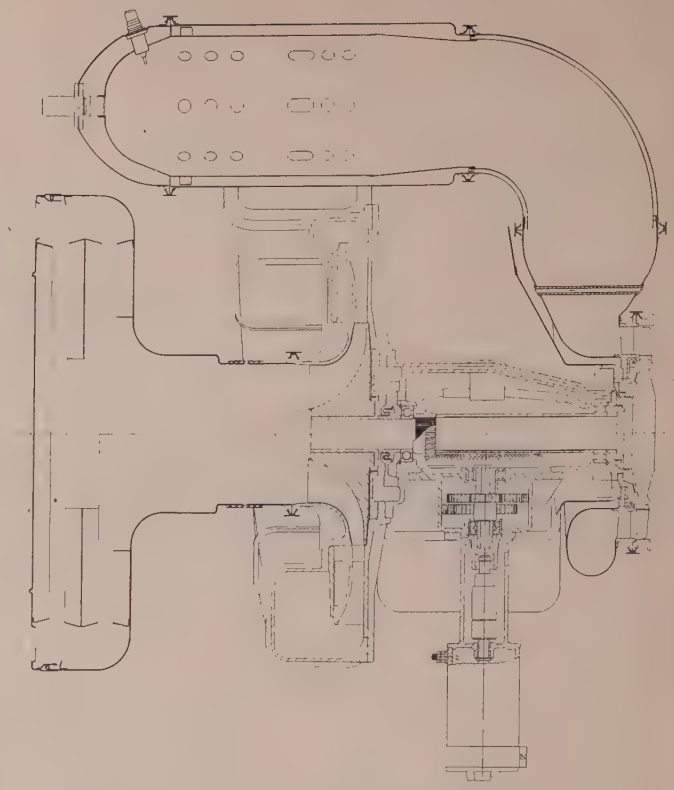

Fig. 2 – Gas generator section of GT-300 engine

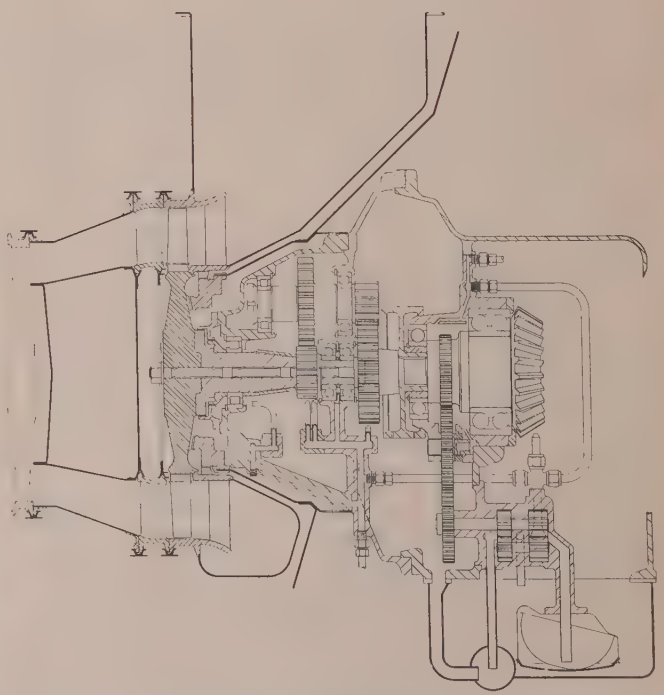

Fig. 4 – Power turbine and reduction gear of GT-300 engine

ment Division is mounted in the center of the burner dome. The AC Spark Plug Division igniter plug, energized only during starting, is mounted on the side of the dome.

The sheet-metal, single-entrance nozzle box is welded to a one-piece cast nozzle diaphragm. The diaphragm, which includes the inner and outer shrouds and vanes, is precision cast as a single unit by the shell-molding process. Seventy-three buckets, precision cast by Fabricast Division of GM, are secured to the turbine disc by means of the familiar fir-tree fastening.

The accessory section of the engine is shown in Fig. 3. All engine-driven accessories are in the gasifier section and are driven from the turbine shaft through a right-angle spiral bevel gear. Thus, the accessories are mounted at right angles to the turbine shaft. A Delco automotive-type starting motor using a conventional engaging mechanism is mounted on the high-speed accessory shaft. This is used only to crank the engine and is disengaged during normal operation. In addition to the starting motor, the accessories include a tachometer-generator, a fuel pump, a gasifier lube pump, a power-turbine lube pump, and a power take-off suitable for driving an electric generator and service air compressor.

The gasifier lubrication system includes an AC full-flow oil filter and provides solid jet lubrication to all high-speed gears and bearings. Gravity scavenging is employed to return oil to the sump in the lower part of the accessory housing.

The general assembly of the power turbine-transmission section is shown in Fig. 4. The construction of the power-turbine nozzle diaphragm and wheel assembly is similar to that used in the gasifier turbine with 61 buckets on the power-turbine wheel. The first pinion of the power-turbine reduction gear is splined on the power-turbine

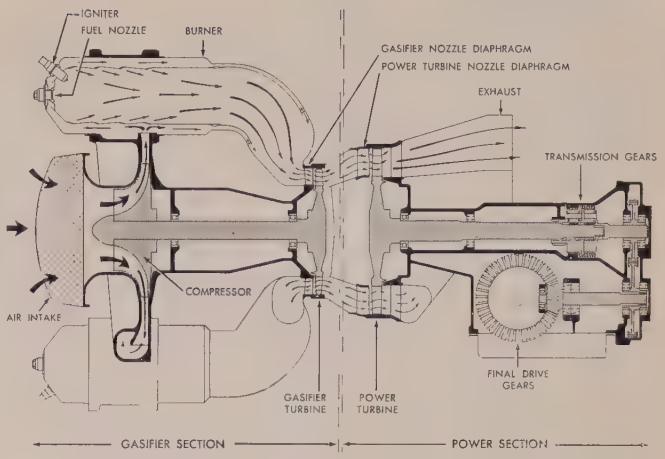

Fig. 6 – Schematic drawing of the GT-302 Whirlfire turbopower unit

shaft. Three jackshafts, equally spaced around the power-turbine shaft, carry the first-stage gears and second-stage pinions.

The Vee-type transmission is an adaptation of the unit used in the GMC transit coaches. The torque converter, which is not necessary with a free-shaft turbine, is removed and replaced by a set of constant-mesh low-drive gears.

The power-turbine exhaust passes into a collector mounted behind the turbine wheel. The entire hot part of the engine is enclosed in an aluminum radiation shield. The cooling air, drawn in over the faces of both turbine discs, is discharged within

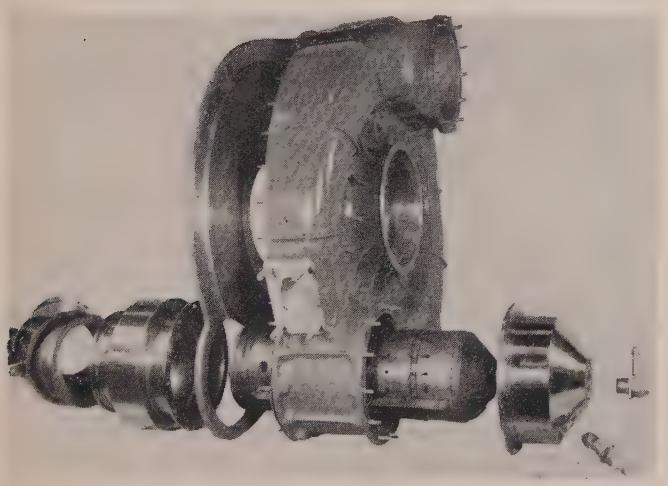

Fig. 7 – View showing integration of combustion chambers with compression housing

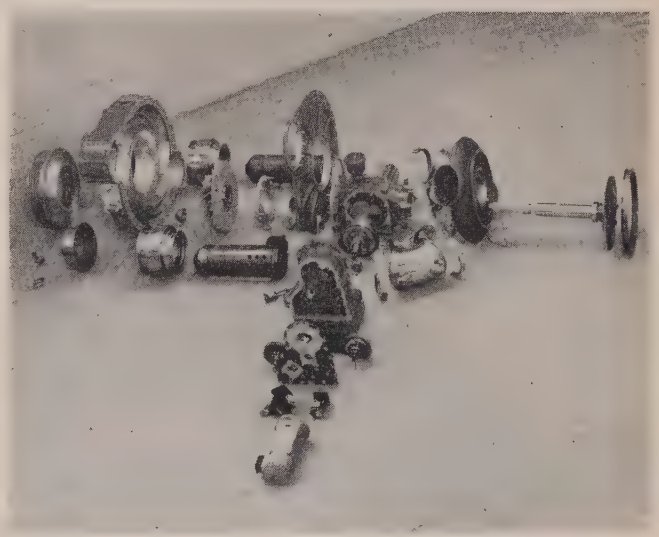

Fig. 8 – View showing all components of the GT-302 gasifier unit

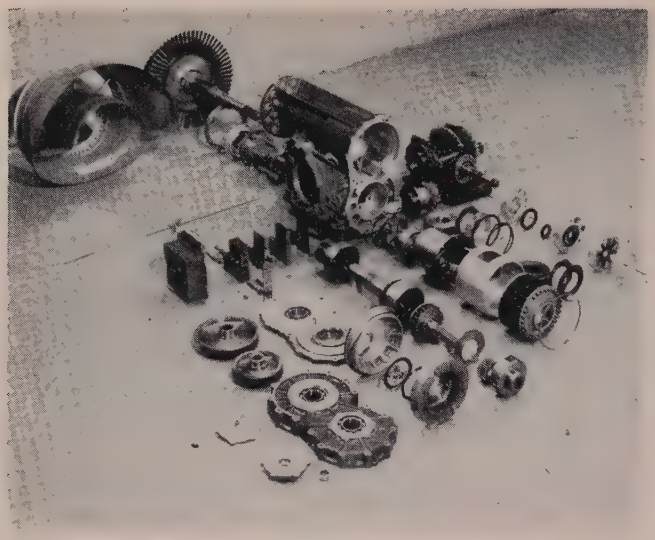

Fig. 9 – View showing all components of the power section of the GT-302

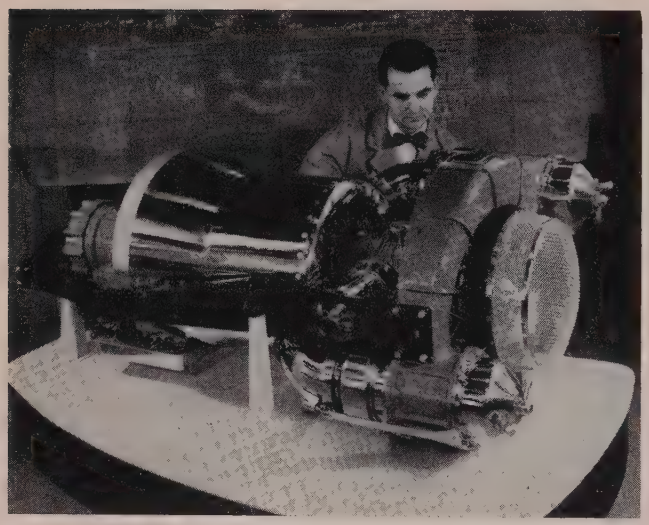

Fig. 10 – Complete GT-302 Whirlfire engine

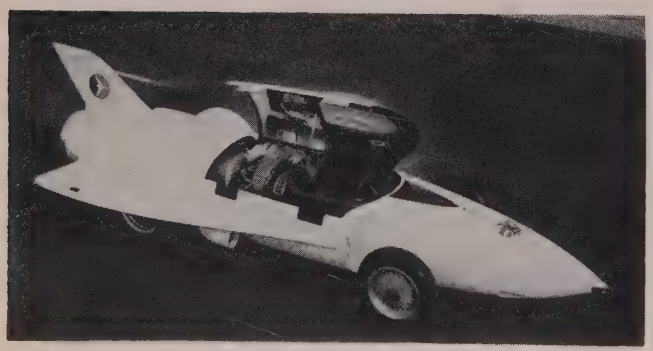

Fig. 11 – View of the GT-302 installed in the Firebird

the radiation shield and is exhausted around the exhaust collector outlet.

The complete GT-300 Whirlfire Turbo-Power unit ready for installation is shown in Fig. 5. The silencer and the two engine sections complete with accessories and instrumentation fittings are mounted on a unit cradle. The whole unit is then mounted in an outer cradle for installation in the Turbo-Cruiser Coach. High-frequency-vibration isolators are provided between the inner and outer cradle to prevent transmission of engine noise to the coach body.

Whirlfire Engine Model GT-302

Before the GT-300 engine could be installed and tested in a vehicle, another version of this engine was built. The new model, designated the GT-302, is shown schematically in Fig. 6. The design objective of this engine, to be installed in the XP-21 Firebird, was to utilize all the major components of the GT-300 engine in as compact a unit as possible without any change in the generally conservative engine design philosophy. The space requirement of the single combustor on the GT-300 was unacceptable, and the new design incorporated a two-burner gasifier unit with a transmission specially designed for the Firebird.

In order to keep the overall size of the engine to a minimum, the combustors had to be kept as close to the shaft centerline as possible. The scheme by which this aim was accomplished is shown more clearly in Fig. 7. The dual-outlet air compressor scroll terminates in cylindrical sections integral with the compressor housing and parallel to the centerline of the turbine shaft. Thus, the compressor housing forms the center section of the outer combustion chamber. The outer combustion-chamber shell is completed by the domed end, the cylindrical expansion-joint section, and the double-walled outlet elbow. The fuel nozzles and igniter plug are mounted as shown on the combustion-chamber dome.

All of the parts and accessories required to complete a GT-302 gasifier assembly are shown in Fig. 8. The screened air inlet incorporates an aluminum finned-tube oil cooler to provide the necessary oil-cooling capacity. The other principal departure from the GT-300 gasifier is the use of a starter-generator, which eliminates the starting-motor engaging mechanism and provides energy to recharge the batteries. The accessory housing and drive assembly was also redesigned to make it more compact.

The power-turbine wheel of the GT-302 engine, shown in Fig. 9, is the same as that used in the GT-300 engine, but the balance of the components for the power turbine-transmission assembly are entirely new. The power-turbine shaft runs on two bearings mounted in a flanged, cylindrical, cartridge-like housing. The turbine rotor and bearing cartridge assembly can be removed from the transmission assembly as a unit.

The transmission assembly, designed by General

Fig. 12 – Turbo-Cruiser coach showing GT-300 engine installed

Motors Engineering Staff Transmission Development Group, provides gear reduction from power-turbine speed to wheel-axle speed with driver-selected gear ranges including "Park," "High," "Performance," and "Reverse." This design successfully resolves unique problems of planetary gear trains and pinion bearings operating at speeds much higher than previously encountered.

No neutral is provided, the transmission remaining in "High" gear when the "Park" pawl is engaged. Thus the power-turbine wheel is always connected to the rear wheels to eliminate the possibility of a turbine runaway that might occur if neutral were provided. This feature is further enhanced by the spring-applied "High"-gear train brake assuring a safe operating condition in the event of hydraulic failure. The "Performance" setting on the transmission provides for acceleration in a lower gear range. Shift to "High" gear occurs automatically at a predetermined speed.

The sun gear for both the low- and high-gear planetary systems is formed directly on the extended power-turbine shaft. Multiple-disc-type holding brakes are used on the high and low planetary systems, and a cone brake is used on the reverse-gear system. A pair of transfer gears on the back side of the transmission between the planetary-system centerline and the output-shaft centerline can be readily replaced to change the overall turbine-to-axle drive ratio.

The right-angle-drive gearing and differential normally housed in the rear axle is enclosed in the transmission housing. However, no differential is used in the Firebird installation. Universal-jointed rear axles transmit the power to the rear wheels and are installed after the powerplant is secured to the chassis. The hydraulic system operates all shifting procedures in addition to providing lubrication and cooling for the complete power turbine-transmission assembly. An externally mounted oil-to-air heat exchanger provides sufficient cooling capacity for all operating conditions.

Firebird Installation

The complete GT-302 Whirlfire engine ready for installation into the Firebird chassis is shown in Fig. 10. The exhaust discharges horizontally in a semicircular annulus above the transmission assembly. All of the hot parts of the engine are enclosed in aluminum radiation shielding ventilated in the same manner as in the GT-300 engine. The gasifier and power sections are independently mounted on a light box-section frame of which the compressor case itself functions as a major crossmember.

The unit construction of the powerplant greatly simplifies vehicle installation. A three-point mounting system utilizing resilient, high-frequency-vibration isolators is employed. Quick-disconnect couplings in the fluid and electrical leads minimize engine installation and removal time.

The engine installed and ready for test operation in the Firebird is shown in Fig. 11. The exhaust

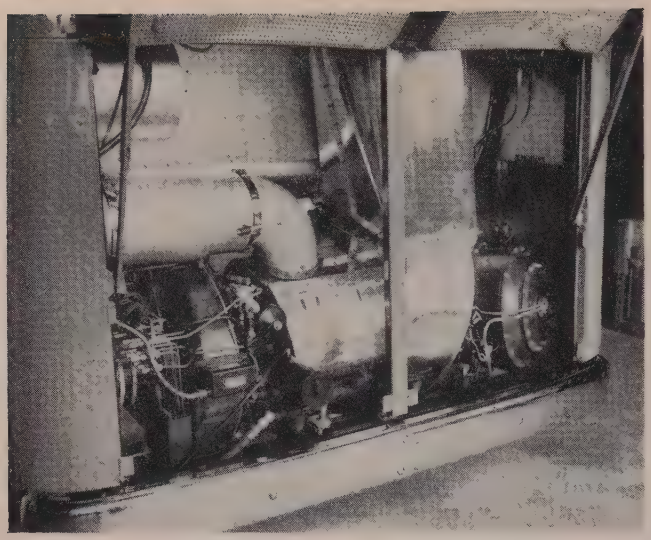

Fig. 13 – GT-300 Whirlfire engine installation

Fig. 14 – Operator's section in Turbo-Cruiser coach

duct extending from the turbine exhaust collector to the rear of the Firebird is supported on the engine frame. The exhaust outlet is sized to minimize engine back pressure and reduce form drag of the body. The engine exhaust collector discharges into the exhaust duct with an eductor effect to carry away ventilating air from the radiation shield and engine compartment.

Turbo-Cruiser Installation

The Turbo-Cruiser bus modified for the GT-300 installation is shown in Fig. 12. The selection of a GMC transit bus to function as a test vehicle was based on several factors. The engine could be installed in the existing engine compartment with ample space for special test instrumentation; the vehicle could be ballasted to represent a wide variety of service conditions with little difficulty; the seating capacity could be used to advantage in demonstrating the new type of powerplant; and finally, plenty of space was available to accommodate special test equipment and observers.

The appearance differs from the diesel-powered unit only in the provision for an exhaust duct discharging through the rear roof crown panel. A closeup of the engine installation is shown in Fig. 13. The gasifier compressor is in the left foreground, the single combustor directly above it, and

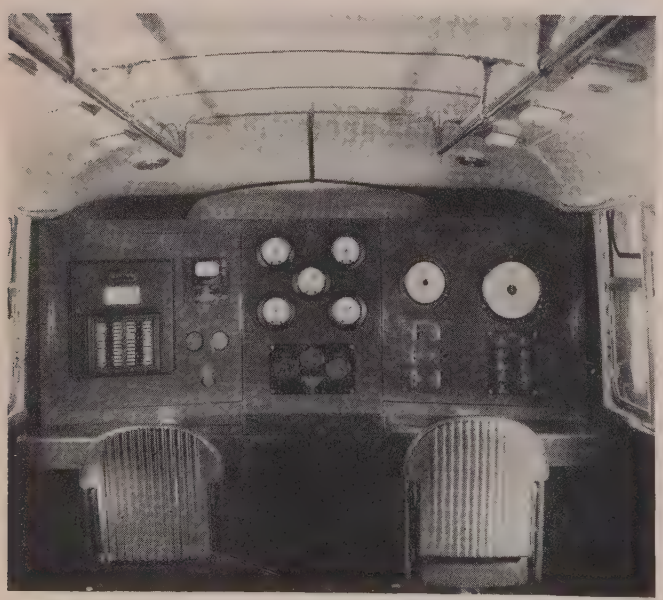

Fig. 15 – Test controls in Turbo-Cruiser coach

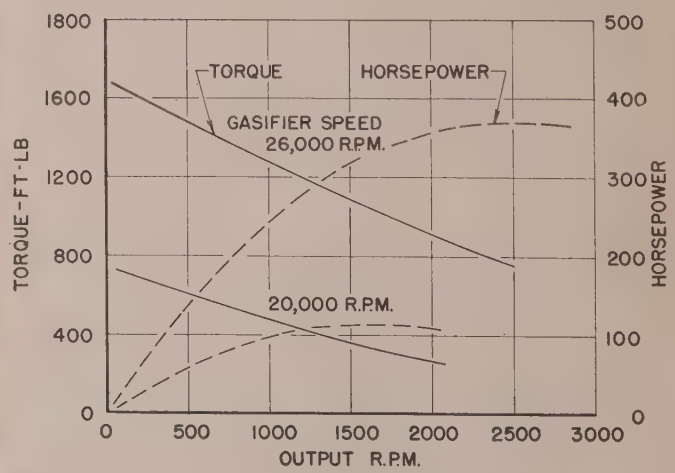

Fig. 16 – Performance curves of Whirlfire turbopower model GT-302

the aluminum-shielded exhaust duct and hot engine section to the right. A portion of the Vee-drive transmission housing can be seen to the far right.

A view of the operator's section of the Turbo-Cruiser is shown in Fig. 14. Very little change was made in the operator's instrument panel. Two oil-temperature indicators were added above the standard instrument panel to supplement the warning-light system used with the diesel installation. An auxiliary instrument panel indicating nozzle-box temperature, gasifier speed, and fuel-system pressure is provided to monitor engine operation and serve as an aid in starting. An emergency-stop button is provided in the event that any undesirable operating condition should be observed.

All special test instrumentation indicators are installed in a console extending across the rear of the coach as shown in Fig. 15. Seats for two observers are provided to expedite data recording. The instruments include a multipoint temperature indicator, vibration meter, speed indicators and counters, fuel- and lube-system pressure gages, and precision multipoint diaphragm pressure gages for high and low ranges. Short-run fuel consumption is measured by a weigh-tank system. The instrumentation is nearly as complete as a standard test cell installation and supplies data not usually obtained from an operating vehicle.

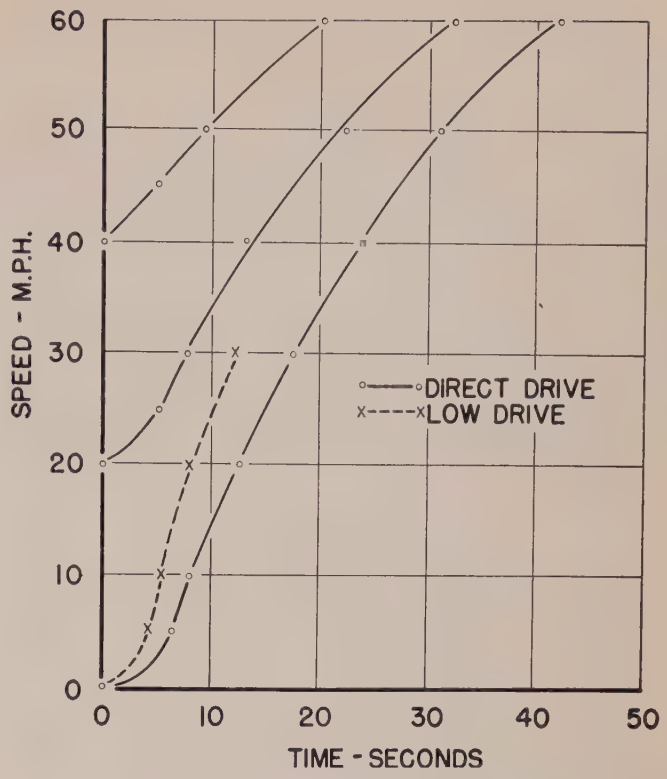

Fig. 17 – Acceleration characteristics of GT-300 Whirlfire Turbo-Cruiser

Operating Experience

Before either the Firebird or the Turbo-Cruiser installations were made, considerable dynamometer testing of both models was accomplished. As both units have the same rotating parts, work on either model was largely applicable to both. However, as operation of a heavy-duty commercial vehicle differs from a light, high-performance vehicle, it was felt that both installations would have to be made to obtain information in both areas. As the Whirlfire engine provided much more power than is desirable in contemporary automobile designs, a new design appeared necessary. Further, this allowed new precepts in chassis design to be tried out, giving information in addition to that obtained from the powerplant alone. As it was felt that this testing would best be accomplished off public highways, a great latitude in design of the Firebird was permitted. Experience to date with the Whirlfire engines is based on over 1000 hr of dynamometer operation and over 2500 miles of test driving in the Firebird and the Turbo-Cruiser. The bulk of the mileage, however, has been in the latter installation.

Fuel Economy

At the outset of the program, it was recognized that many problems would arise in the development of this powerplant. It was decided, therefore, that mechanical simplicity would be emphasized on the first design so that these various problems could be pinpointed. These would then be dealt with in a later design. Consequently, an open-cycle unit without regeneration was built, as high fuel consumption was only one item on the list of anticipated disadvantages of the gas turbine in an automotive installation.

At design point an open-cycle gas turbine with modest operating temperatures and pressures has a brake specific fuel consumption about twice that of its piston-engine counterpart. Further, at part throttle the fuel economy deteriorates more rapidly than in a piston engine. The question immediately arises, "What can be done about this?"

The approaches to improved fuel economy were outlined in the paper presented before this group in 1949 and are essentially unchanged today.

First is a continuing improvement in component efficiencies and a reduction in internal pressure losses. Any improvement in these are immediately reflected in improved specific fuel consumption. Secondly is the raising of operating temperatures. Much work has been done in this area by General Motors Research. A new high-temperature alloy, GMR-235, developed by the Research Metallurgy Department, has shown great promise in raising operating temperatures. This material has been incorporated in the first design and the engine under the present design conditions has shown no indication of being temperature limited. It is therefore felt that much can be gained in this area.

Finally the addition of a heat exchanger or regenerator to recover some of the exhaust heat will further improve fuel economy. The work in this area has been directed toward the development of a light, compact heat exchanger with good effectiveness constructed of noncritical materials. The work at General Motors Research on the Aldip process has shown definite promise toward an effective solution to this problem.

The engine is relatively insensitive to the type of fuel it can consume. A broad range of fuels can be used ranging from gasoline to the diesel fuels. Octane numbers and cetane numbers have no meaning in the gas turbine. The fuel must still possess the same degree of cleanliness as required by piston engines.

Performance

One of the features of the gas turbine that is very desirable in a vehicular powerplant is its favorable torque curve. With the dual- or free-turbine arrangement, the engine produces maximum torque at stall as shown in Fig. 16. This stall torque, which is over twice that of design-point torque, decreases almost linearly with increasing output shaft speed. It will be noted that the horsepower curve does not peak sharply, presenting maximum power over quite a broad range of shaft speeds. At present, the engine, with all accessories loaded and no correction for reduction gearing or ducting losses, is rated at 370 hp.

The maximum torque can be utilized only if the gasifier section is at maximum speed. From a standing start in direct drive, with the gasifier initially idling, a delay in acceleration is experienced which depends on the time required to bring the gasifier to speed. Acceleration characteristics of the Turbo-Cruiser transit bus, shown in Fig. 17, exemplify what can be expected. The overall acceleration time is better than in its commercial counterpart operating under similar conditions. Starting from a standstill in low drive appreciably improves acceleration at low vehicle speed.

The effect of the inertia of the engine rotating parts is evident from the delay in the early part of the acceleration curve. In order to minimize this delay, the moment of inertia of the rotating gasifier components must be kept to a minimum. It now appears that the original design can be improved in this respect. Experience indicates that the limiting acceleration temperature can be raised appreciably above design temperature without any adverse effects. This will also help to decrease acceleration delay.

The acceleration is extremely smooth, entirely without any jerks or jolts. Further, the power is applied so smoothly that the maximum coefficient of traction can be maintained.

Operating Temperatures

Because the combustion and expansion processes in a gas-turbine engine are continuous, the average gas temperatures, and consequently the exposed metal temperatures, are high. The lack of suitable materials long delayed the advent of the gas turbine even though the first patents were taken out prior to those on conventional piston engines. The design operating temperature of the Whirlfire engine was set at 1500 F, as this appeared reasonable in view of long life requirements. Operating experience with the engine, however, has proven that this temperature is very conservative. In spite of high metal temperatures, the installed engine does not pose any heat problems. The aluminum radiation shield which surrounds the hot zone of the engine has proven to be extremely effective. In the Firebird installation the aluminum radiation shield has proven more than adequate to protect the plastic body, in many places less than 1 in. away. The compartment temperature in the Turbo-Cruiser installation is no higher than with the usual diesel installation.

Air Requirements

In order to limit the operating temperatures to obtain reasonable life of the parts exposed to the hot gases, the overall air/fuel ratio of a gas-turbine engine ranges from about 100/1 to 50/1. The specific air consumption of a gas turbine is therefore in the order of four to ten times that of a reciprocating engine, depending on the operating efficiency. The air-handling ducts, both on the inlet and outlet of the engine, are larger in the same proportion and require an entirely new design concept in the engine installation.

The air filtering requirements are considerably less stringent in the gas turbine than in the conventional piston engine. Thus far the engines have been operated entirely without air filters, and the only ill effects noted have been some erosion on the aluminum compressor and diffuser caused by the passage of sand particles. Experience indicates that the air should be strained rather than filtered to keep out the large particles.

Exhaust

The Firebird was not designed to be used on public highways, allowing horizontal discharge of the exhaust gas which is desirable both from an engineering and styling standpoint. However, the hot gases diffuse very rapidly, and at idle one can stand quite close to the outlet without discomfort. The exhaust pipe could be made considerably smaller, even in spite of the fact that all the cooling air of the engine compartment, as well as the engine exhaust, is funneled through it. In this first installation minimum pressure drop is maintained in the exhaust system. Although this is a very desirable condition, it may have been an unfortunate choice in view of the misunderstanding of the problem that this large exhaust may have promoted.

In the transit-coach installation the exhaust is discharged vertically. This appears to be more

practical in commercial-type vehicles. The gas turbine, due to the large volume of excess air required to keep operating temperatures within reasonable limits, has a clear exhaust, free from carbon monoxide. In the Whirlfire installations the exhaust shows no smoke or discoloration through the entire speed range.

Controls

Engine speed and output is regulated in the engines by controlling the amount of fuel supplied to the gasifier section. This is accomplished in both the Firebird and the Turbo-Cruiser installations by a needle-type fuel control valve actuated by a conventional accelerator pedal. Only the transient condition of operation must be monitored, as a sudden surge of fuel to the engine at low speeds could cause an over-temperature condition while the gasifier adjusts its speed to the new fuel setting. A simple acceleration limiter is used which controls the rate at which the fuel is introduced to the engine during speed increases. Essentially this is a fuel bypass regulated by compressor pressure. By adjusting this bypass, the maximum acceleration temperatures and the rate of acceleration can be maintained at any desired level. In both installations, this control has worked very satisfactorily. Speed can be maintained at any desired level without any special precaution. From the operator standpoint the control of the engine is equally as convenient as that of any piston-engine installation.

High-Speed Rotation

One of the first things that strikes the uninitiated about the gas-turbine engine is the high speed of its rotating parts. In working with gas turbines, one uses 1000-rpm increments in the same manner as 100-rpm steps are used with the piston engine. Although the speeds are high, the ratio between idle and maximum speed is about the same as in diesel practice. The idle speed of the gasifier is usually set at about 8000 rpm, and the maximum speed is 26,000 rpm.

The question of gyroscopic effect generally arises in discussion of gas-turbine-powered vehicles. This effect has been minimized in the Whirlfire engines by designing the two turbines to rotate in opposite directions. The gyroscopic moment at design point is thereby reduced to a very small value and is a maximum with the gasifier at maximum speed and the power turbine stalled. The actual magnitude of the gyroscopic effect might best be visualized by assuming a vertical pitch frequency of 100 cpm with an amplitude of 2 in., as might be induced through the suspension of a moving vehicle. Under the most severe conditions, this would result in a gyroscopic moment of 525 in.-lb in the horizontal plane. This would have little effect on control of the vehicle.

Another question that arises is, "How safe is a unit rotating at these speeds?" The shrouds surrounding the turbine wheels on the Whirlfire engine are made from steel forgings heavy enough to contain any bucket fragments. The most serious failure which might occur is a burst turbine disc. To minimize this possibility, the discs are designed with a large margin of safety. With proper design considerations such as these, the gas turbine is as safe as any contemporary engine.

Durability and Maintenance

The Whirlfire engines have proven to be very rugged, and only one major failure has thus far been experienced. A blade of a cast compressor inducer failed after 10 hr of operation on the dynamometer. This condition was remedied by machining the part from an aluminum forging. Since proper forging and machining techniques were established, no further failures have been experienced. One surprising feature of the unit has been its ability to absorb foreign material. On several occasions pieces of special instrumentation have passed through the machine. The turbine buckets were bent, but in no instance did they fail, even after subsequent running of the damaged parts.

The engine is very easy to maintain, as each of the major components can be removed and serviced as a unit. Further, it is possible to replace damaged turbine buckets on the engine without disassembly. The design of the combustion chambers is such that the fuel nozzle and inner liner can be removed, inspected, and reassembled in a few minutes. As the drives for the engine accessories are at right angles to the main shaft, the accessories can be removed individually with little difficulty. This arrangement permits a wide variety of accessories to be used, as length is not a governing criterion. For example, on the transit-bus installation an extension shaft is connected to one accessory shaft to drive a remotely located generator and air compressor.

Noise

Noise level is usually placed high on the list of disadvantages of the gas-turbine engine. In the initial paper study, this disadvantage appeared very significant, based largely on jet-engine experiences. The unmuffled version of the gas-turbine engine is indeed noisy. However, reduction of the noise level of these engines did not pose as great a problem as first anticipated. Most of the noise, at least the most disagreeable noise, emanates from the air inlet to the compressor. This is of high frequency, between 2000 and 7000 cps, and can be very satisfactorily absorbed by many available materials. In the transit-bus installation, a very elementary splitter-type silencer reduces engine inlet noise to an acceptable level. The exhaust noise, on the other hand, is of comparatively low frequency – 150 cps – where a resonator-type silencer would be more effective. In the Turbo-Cruiser, only an intake silencer is used, the exhaust being unmuffled. The results are surprisingly good,

and the noise level of this installation compares rather favorably with its commercial counterpart. The Firebird is entirely unmuffled, and although the noise level is higher than in the muffled bus version, it is not too objectionable, as the body shell attenuates the noise to some degree.

Starting

Both models of the engines are very easy to start. The model GT-300 engine uses a standard 12-v starting motor while the GT-302 installed in the Firebird uses a 24-v starter-generator. In both cases the starting time and sequence is the same. The starting motor and the ignition system are energized. The gasifier section is brought up to 3000 rpm, and the solenoid valve in the fuel line just ahead of the nozzles is opened. Combustion then begins, and the starter is held on until the gasifier reaches about 6000 rpm. The entire sequence requires about 20 sec. Although no extreme-cold-weather starts have yet been attempted, it appears that this engine should be quite easy to start even under subzero conditions.

Braking

Much has been said about the lack of engine braking in the gas-turbine engine, and all the speculation is generally correct. In neither installation, the Turbo-Cruiser or the Firebird, does the engine supply any appreciable braking during deceleration. The Firebird scoots along rather briskly with the gasifier idling once the vehicle is accelerated to speed. This imposes rather severe requirements on the vehicle brakes, and it appears that some sort of supplementary dynamic braking device may be required. One example of this is the flap brake system used on the Firebird.

It is possible, however, to have the engine supply braking in special cases. If the vehicle is descending a steep grade, the transmission can be shifted to reverse. This causes the power-turbine wheel to turn backwards; and, with the gasifier speed selected to maintain proper retarding torque, the vehicle can descend at any speed desired without resorting to the vehicle brakes. This might be very desirable in a commercial vehicle handling heavy loads over steep terrain. In this particular instance, at least, the free-wheeling characteristics are actually an advantage.

Lubrication and Bearings

In a commercial installation with present operating temperatures, the lubrication requirements of the gas turbine do not appear very severe. For one thing, the lubricant is never exposed to the combustion area or to the products of combustion. The oil, in addition to providing lubrication, is used to cool the high-speed bearings. Silver-plated retainers are used in the Hyatt roller bearings and the New Departure ball bearings on both turbine shafts. Bearing experience thus far has been very good as the first failure has yet to occur. In all cases these high-speed bearings are jet lubricated. Oils with rather low viscosity and with little tendency to foam are used, and experience has indicated that commercially available premium motor oils will fill these requirements.

As operating temperatures are increased, the requirements of the lubricant become more stringent, as it then must withstand the "soaking" condition to which it may be exposed. When the unit is shut down, the heat from the hot zones soaks through the shaft into the bearings and may cause the oil to coke if these temperatures rise above the limiting temperature of the oil. On a subsequent start, the coke and carbon would have an adverse effect on the bearing. This condition, however, has never been experienced with the Whirlfire engines. Further, in these engines the oil consumption is so low that it has not been measured. The greatest loss, which is through the breather pipe, has been minimized by proper breather design and location.

Weight

One of the greatest advantages of the gas-turbine engine is its favorable weight/power ratio. The entire power package for the Firebird, which includes the transmission and final drives, weighs only 775 lb and gives the powerplant and drive a weight/power ratio of approximately 2 lb per hp. This ratio is about one-third that of a conventional piston engine and drive. In the Turbo-Cruiser installation, the gas-turbine engine, in addition to supplying nearly twice as much power as the diesel normally used, saves over 1500 lb in engine weight. In both cases this saving in weight has been accomplished without sacrificing strength of the components. Automotive rather than aircraft design practice is followed throughout.

Summary

These investigations to date have not given a clearcut answer to the question whether pinwheels will replace pistons as power for automotive equipment. The problem of powerplants must be reevaluated continuously in the light of new developments and changing requirements.

General acceptance of the gas turbine for roadable equipment is still dependent on future developments. These must be directed toward improved fuel economy, reduced acceleration time, and a suitable dynamic braking system. Other problems that were anticipated are of secondary importance and in some cases nonexistent. The Whirlfire installations have demonstrated that smooth, reliable operation, with very desirable power and torque characteristics, can be attained. These, coupled with the very favorable weight/power ratio, are already applied to advantage in specialized installations. A statement from the first paper on automotive gas turbines still holds true: "In view of the developments which seem sure to materialize, the future of the gas turbine must be contemplated with an open mind and with a degree of optimism."

Report of Oral Discussion on Schilling and Turunen Papers

by J. S. Collman,
Research Laboratories Division, GMC

H. R. Hazard, Battelle Memorial Institute: The rotating speeds of the turbines are noticeably lower than those of contemporary design. Would this lead to more economical fabrication of such high-cost items as reduction gearing, forged compressor rotors, and others? What is the cost outlook for the gas turbine in comparison with other types of prime movers? The heat exchangers which are proposed as a means of improving the fuel economy of the gas turbine are heavy, costly, and difficult to fabricate. Would higher pressure ratios possibly requiring two-stage centrifugal compressors be a more economical means of effecting the desired fuel economy?

I would also like to know what the approximate effect of a 100-deg increase in turbine inlet temperature would be in overall fuel economy, and has the ram pressure recovered in the induction system of the Firebird been considered in its design?

Mr. Turunen: Mr. Hazard's questions would form the basic outline of a very extensive research program. The complete answers to many of these questions are still being sought.

The production cost of the gas turbine has not yet been studied in an all-out effort to reduce costs because it will be necessary first to justify its place in the automotive field. Just as in the automatic transmission field, mechanical and economic problems will be overcome if turbines prove to be desirable and acceptable.

In order to gain full advantage from an increase in compressor pressure ratio, it is necessary to increase the turbine inlet temperature as well. The effect of a 100-deg increase in turbine inlet temperature depends on the design pressure ratio to such an extent that no specific answer can be given. In the present range of operation, a 100-deg increase in turbine inlet temperature might result in as much as 5% decrease in fuel consumption.

The ram air pressure recovery was not considered in the design of the Firebird induction system.

R. E. Smith, ARO, Inc.: Is compressor surge critical in the operation of the fuel control, and how does the acceleration time of the Whirlfire engines compare with present diesel engines?

Mr. Turunen: Compressor surge is not a problem in operation of the fuel control during transient conditions; turbine inlet temperature is the only condition requiring monitoring. All acceleration work to date has been carried out at indicated nozzle-box temperatures of 1650 F or below, which is considered very conservative in view of the thermal properties of the material and the short duration of high temperatures during transient conditions. Acceleration of the gasifier turbine from idle to full speed is accomplished in about 5 sec. This time can be further reduced by allowing higher temperatures during acceleration and also by reducing the moment of inertia of all rotating parts to a minimum.

D. W. Hutchinson, Turbex Corp.: How does the torque response of the Whirlfire engines compare with conventional engines? I am also interested in some of the problems encountered in the planetary gear systems of the transmission.

Mr. Turunen: Full torque is available from the power section as soon as the gasifier turbine has reached maximum speed or in about 5 sec. This compares with approximately 2 sec required by the diesel engine connected to a torque converter transmission to measure full torque output.

The question concerning gearing problems can be answered much more adequately by O. K. Kelley, head of the General Motors Engineering Staff Transmission Development Group.

Mr. Kelley: The speeds encountered in developing a transmission for the Firebird were a far more serious problem than the loads. Surprisingly enough, the most serious operating condition arose during coastdown from full speed. Under this condition the pinions of the planetary system are unloaded permitting the pinion bearing needles to float within the journal space. Centrifugal force cramps the needles to the outermost part of the clearance space resulting in bearing conditions much more severe than associated with full-power operation. This problem was further complicated by the fact that high centrifugal pressure of the lube oil introduced to these bearings forced the oil out of the bearings before it could accomplish its purpose. Several sleepless nights were endured before this problem was satisfactorily solved by proper location of the lube-oil passages and the addition of damping rings to impede the flow of oil from the bearings.

F. E. Moskovics: Is surge or pulsation a problem in design of the fuel control? Is the GM Turbine Development Group cognizant of the work being done by the NACA in developing short axial-flow turbine blades?

Mr. Turunen: Surge or pulsation of the fuel system has presented no problem to date in the development of the fuel control. Compressor surge is an ever-present problem in gas-turbine machinery, but at the modest pressure ratio employed in the Whirlfire engines this condition has not been serious. Close contact is maintained with the NACA Laboratories in order to benefit from all of the development work which is being carried on there, not only in the field of axial-flow turbines but also compressors and other components.

Mauri Rose, Chevrolet Motor Division: As driver of the Firebird, I have been asked most frequently how fast I have really driven the car. The highest speed indicated on the mechanical speedometer has been between 135 and 140 mph and has been limited to this figure largely by the lack of an adequate straightaway test course.

My first impression of the car was the smooth acceleration provided by the turbine in comparison with other high-power cars I've driven. This smooth application of power to the rear wheels greatly increased the potential traction effect which could be applied without skidding the wheels. The steering of the vehicle has been excellent, and the suspension and cornering characteristics are much superior to other cars that I have driven. The effect of the air-brake flaps is not noticeable below 100 mph, but the dual-cylinder hydraulic brakes have proven more than ample to handle the car under any conditions that have been encountered.

Progress of

ALTHOUGH the torque converter was invented almost fifty years ago, its greatest use and largest acceptance by the public has been in recent years.

History of Torque Converter and Converter-Coupling

The torque converter was first developed about 1905 in Germany by Dr. Herrmann Föttinger for a permanent reduction unit between the ship's high-speed turbine and low-speed propeller. This unit, which required an extensive amount of development, was superseded from 1914 onwards by the more efficient herringbone reduction gears which were developed by Sir Charles Parsons in England.

In 1930, A. Lysholm of the Ljunstrom Steam Turbine Co. of Sweden, well-known manufacturers of steam turbines, developed a torque converter of a much smaller size which was suitable for use in automotive vehicles. This unit was used in England in city buses made by Leyland Motors and was known as the Lysholm-Smith converter. The unit consisted of six bladed members and was designed for a manual change to lockout drive. The maximum torque ratio was about 5/1 with a peak efficiency of about 82%.

In 1933, Spicer obtained one of the first produc-

A COMPREHENSIVE survey of torque converters – their history, description, characteristics, and applications – is presented in this paper.

Fluid-flow diagrams, performance curves, and diagrammatic sketches accompanying the text illustrate the various types of torque converters most used.

The many advantages of the torque converter transmission listed in this paper are responsible for its wide use in the industrial, military, and both off- and on-highway installations, as well as the familiar city-bus and passenger-car applications described here.

The Authors

E. W. ZINGSHEIM (M '44) is chief engineer of the Hydraulic Transmission Division of the Spicer Mfg. Division of Dana Corp. in Toledo, Ohio. He studied Mechanical Engineering at Washington University in St. Louis. Mr. Zingsheim worked for the Marmon Motor Car Co. for two years, and then joined the Kluber-Dawson Machine Co. in 1926. He has been with Spicer since 1929, where he began as a designer in the Joint Division.

M. M. SCHALL (M '44) is a hydraulic transmission engineer at Spicer Mfg. Division of Dana Corp. He received his engineering degree from the University of Toledo, in 1937. Mr. Schall worked in the Engineering Department of the Electric Auto-Lite Co. during his senior year in college. He joined Spicer in 1937 as an engineering draftsman. Mr. Schall achieved his present position in 1952.

Torque Converters

E. W. Zingsheim and M. M. Schall,
Spicer Mfg. Division of Dana Corp.

This paper was presented at a meeting of the SAE Philadelphia Section, Feb. 10, 1954

tion converters built by the Leyland company and installed it in a chassis for extensive test work. The unit as built showed some promise, but it was felt that considerable further improvement was necessary to meet the requirements of city-bus operation in this country.

A modified design, which included an automatic change to lockout drive, was built and installed in a rear-engine bus furnished for this purpose by the Yellow Truck & Coach Mfg. Co. The redesigned unit resulted in the Spicer torque converter which has been in active production since 1938.

Sometime later, Twin Disc Clutch Co. obtained a license from the Ljunstrom company of Sweden to build the Lysholm-Smith type of converter for industrial use.

About 1930, in England, P. N. Salerni produced the first converter and coupling in one unit. His first units were single-stage and later two-stage converters in which the reaction members were allowed to move forward independently. In 1941, the J. Brockhouse & Co., Ltd., of England were granted a license for the development and manufacture of this transmission which came to be known as the Brockhouse-Salerni Transmitter. This device was run experimentally in double-decker buses in England.

The first converter-coupling which was made in Germany in about 1934 was the effort of Dr. Föttinger and Professor Spannhake and was known as the Trilok. The unit was tested in a passenger car, but development was curtailed during the war.

The Schneider Brothers, one of whom had worked with Föttinger in Germany, produced a converter-coupling in the United States in 1940. This unit was a single-stage three-element type in which the reaction member rotates freely during the coupling range. The White Motor Co. used this converter in their buses for a short period in a unit known as the White Hydrotork Drive. The converter now has some use in industrial applications.

During World War II there was some development on torque converters and many experimental installations were made in military vehicles. One of the military units that went into production was a tank destroyer built by Buick and was known as the M-18. The torque converter section was of the three-stage Lysholm-Smith type and was manufactured by Spicer. The Detroit Transmission Co. manufactured the three-speed forward planetary transmission which was used behind the torque converter.

During 1946 and 1947, Spicer was in production on its new 16-in. and 18-in. size three-stage bus converters. Among other improvements, the units contained newly designed blade profiles developed at Spicer to increase vehicle performance in the converter range of operation.

Early in 1948, General Motors introduced the Dynaflow transmission in the Buick. This was the first production transmission embodying the torque converter principle for passenger-car use. It was not too long afterwards that other passenger-car manufacturers were announcing their new torque converter transmission.

The Hydrodynamic Drive

In the SAE Hydrodynamic-Drive Terminology, a hydrodynamic drive is defined as a type of drive that transmits power solely by dynamic fluid action

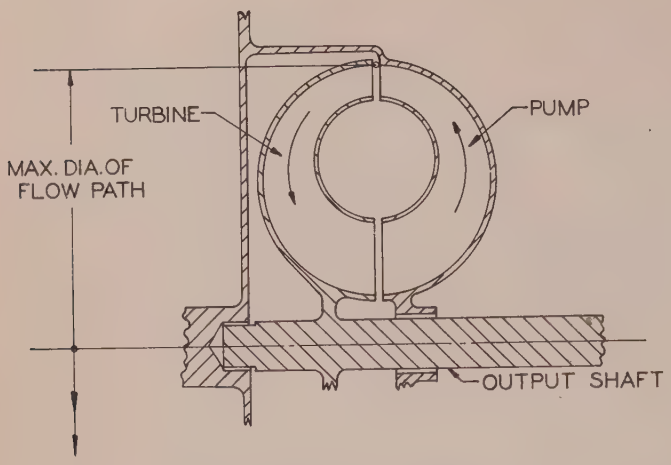

Fig. 1 – Simple fluid coupling

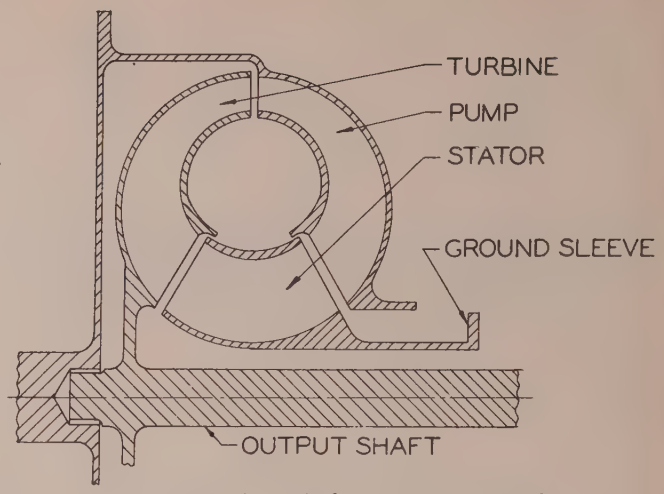

Fig. 4 – Single-phase, single-stage torque converter

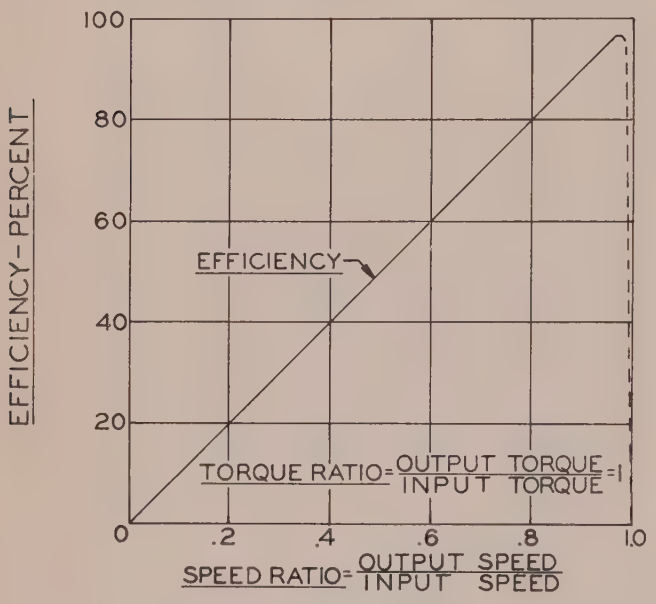

Fig. 2 – Fluid coupling efficiency

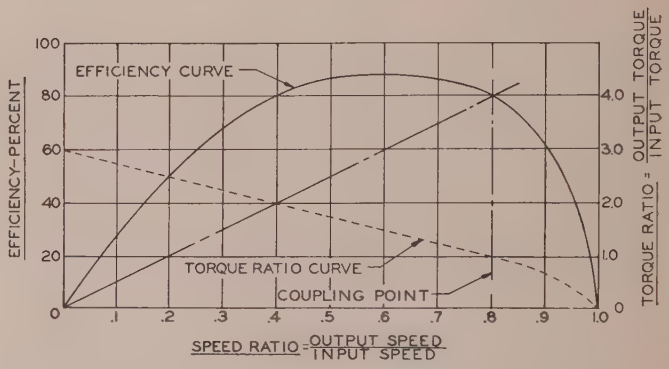

Fig. 5 – Performance characteristics for single-stage torque converter

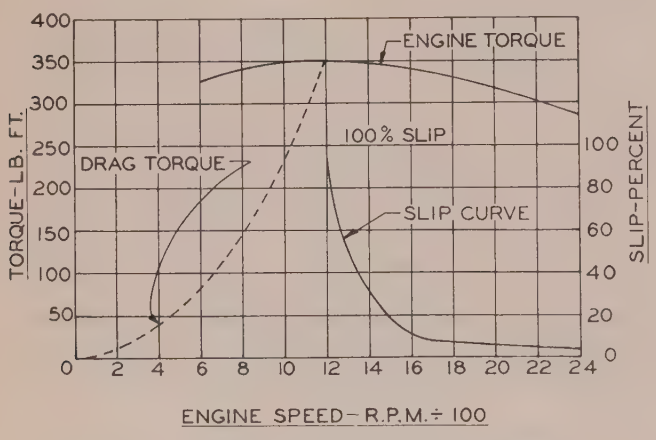

Fig. 3 – Performance curves for fluid coupling

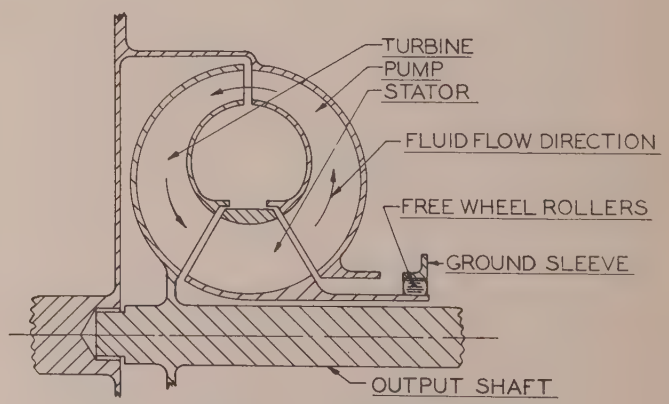

Fig. 6 – Single-stage, two-phase torque converter

in a closed recirculating path.

A hydrodynamic drive transmits torque by changing the rotating momentum of a mass of fluid. Two well-known examples of this principle are the fluid coupling and the torque converter.

A fluid coupling is defined as a hydrodynamic drive which transmits power without the ability to change torque; whereas, a torque converter is a hydrodynamic drive which transmits power with ability to change torque.

Fluid Coupling

Since the fluid coupling (see Fig. 1) is not a torque multiplier, there have to be gears in back of it to produce the different drive ratios required. The hydraulic coupling has a torus-shaped split housing in which the blades or vanes are set radially to the drive shaft. As the pump starts to rotate, the oil is thrown toward the outer rim of the housing and becomes a moving mass. When this mass strikes the stationary blades of the turbine, it exerts a force on them proportional to the weight of the fluid that flows out of the pump every second. This kinetic energy is recovered in the turbine by retarding the forward rotation of the oil which then flows back into the pump and again picks up momentum. Since the blades of the coupling are straight or radial, torque may be transmitted in either direction with the same efficiency.

In normal operation of the fluid coupling, the turbine always turns at a lower speed than the pump, and since both pump and turbine have substantially the same dimensions, the centrifugal force on the liquid in the pump is always greater than that on the fluid in the turbine. This difference between the two centrifugal forces causes the fluid to circulate in the torus.

During steady normal operation, the pump and turbine speeds are nearly equal and there is very little disturbance in the fluid flow as the fluid passes from one element to the other; therefore, rather high efficiencies are possible. The losses occur as slip or difference in revolutions between input and output members. The minimum losses under ordinary working conditions are about 2%.

The efficiency of a fluid coupling when plotted against speed ratio is a straight diagonal line as shown in Fig. 2. Since there is no torque multiplication produced, the efficiency of the fluid coupling is equal to the speed ratio at which the unit is operating. All reduction in speed represents slip or loss.

Typical performance curves for a simple fluid coupling are shown in Fig. 3. In a fluid coupling the stall torque rises as the square of the engine speed. If a torque curve is plotted against engine speed, we obtain a rising logarithmic curve which represents 100% slip. Where this curve crosses the engine torque curve, the maximum starting torque available and the stall speed for the given engine and coupling are indicated. If the vehicle is allowed to accelerate by releasing the brakes, the slip curve will drop from 100% and the vehicle has to be speeded up considerably before the slip drops sufficiently for economical operation.

Torque Converter Operation

The torque converter is an infinite variable torque ratio hydrodynamic drive with the maximum torque ratio usually produced when the output shaft is stalled. The torque ratio falls off smoothly and automatically as the output shaft gains speed. Unlike the simple straight radial blading of the fluid coupling, the torque converter requires carefully curved, smooth, and formed blading to obtain optimum performance characteristics. The blades are usually made of streamline shapes with rounded leading edges to reduce the shock losses for the variable inlet fluid flow velocities. In addition to the pump and one or more turbine members, a stationary reaction bladed member must be added to the fluid circuit to obtain torque multiplication. The reaction member accomplishes this by changing the turbine discharge velocity into additional forward-drive momentum. In the single-stage converters, the reaction member precedes the pump and the forward-drive momentum adds torque to the pump which results in a greater spinning momentum out of the pump than the engine alone could produce.

In the multiple-stage converters the reaction blades normally precede the turbine members. The fluid leaves the reaction blades at a corrected forward angle before entering the turbine blades, thus imparting additional forward momentum to the turbine rotor. The number of stages are indicated by the number of times a different set of turbine blades takes a "bite" at the fluid as it circulates through the closed recirculating path.

By splitting up the turbine into separate bladed stages and interposing suitable reaction blades between the turbine stages, the amount of torque multiplication produced can be increased. The increase in torque multiplication usually results in reduced peak efficiency since rotational losses and fluid entrances and exit losses are increased.

The actual fluid flow directions are dependent on the relative speeds of the pump and turbine; therefore, for each converter there is one particular speed ratio at which the blade angles best suit the fluid flow and peak efficiency occurs. This condition represents the design point of the given torque converter. As the speed ratio changes above or below this point, the shock losses of the fluid entering the blades increase, the converter becomes less efficient, and less torque multiplication is being produced for a given speed reduction.

Thus the torque converter has a certain usable speed ratio range over which it performs efficiently. Once the design point is passed the losses again increase. At the coupling point the output

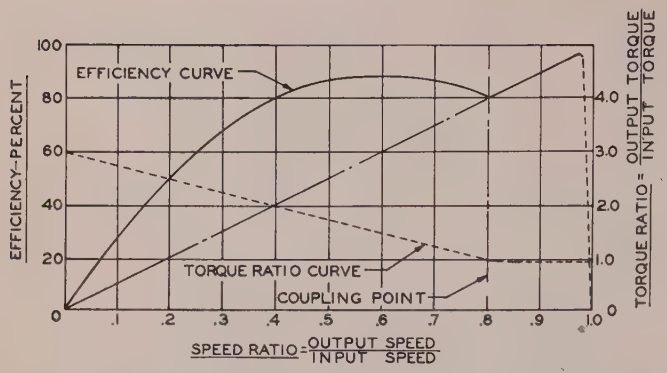

Fig. 7 – Performance characteristics for single-stage, two-phase torque converter

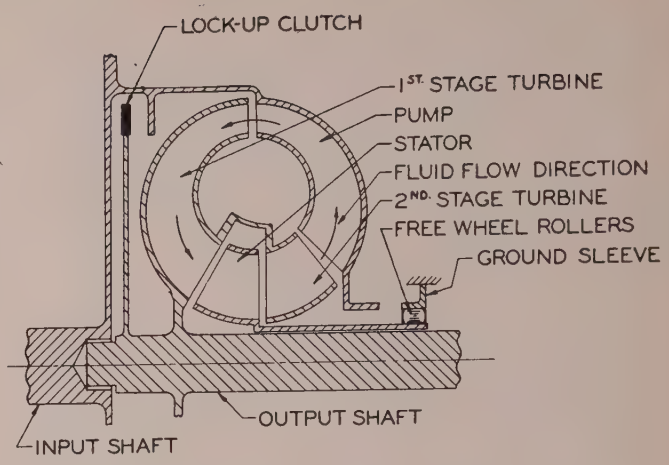

Fig. 10 – Two-stage, four-member torque converter

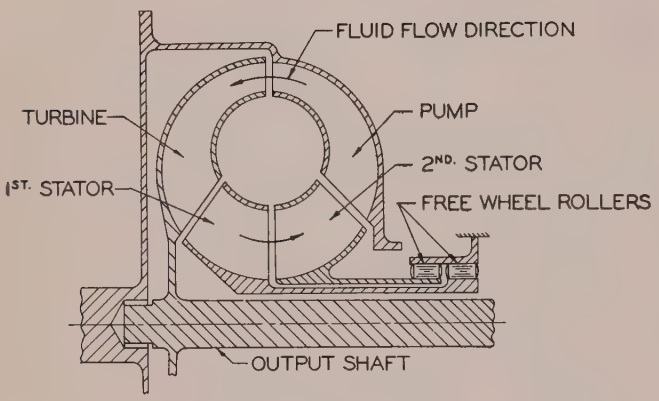

Fig. 8 – Single-stage, four-member polyphase torque converter

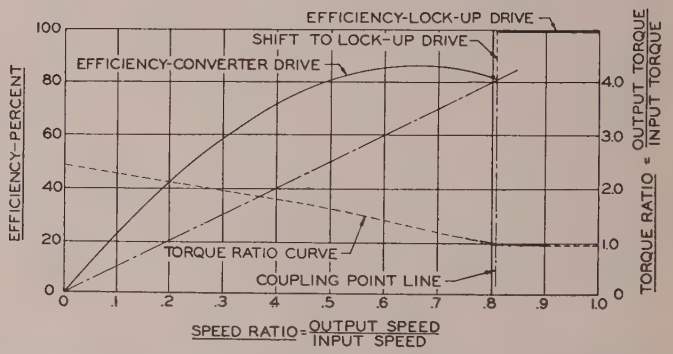

Fig. 11 – Performance characteristics for two-stage, four-member torque converter

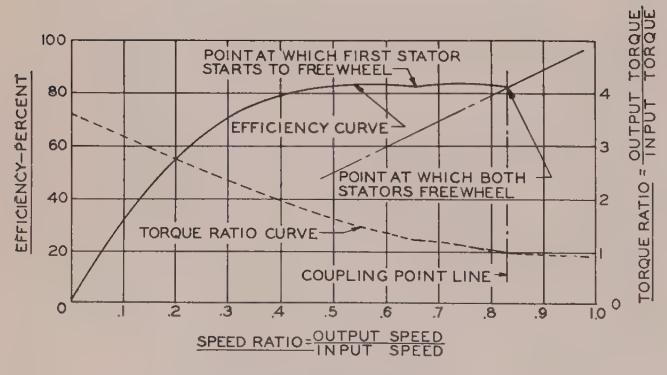

Fig. 9 – Performance characteristics for single-stage, four-member polyphase torque converter

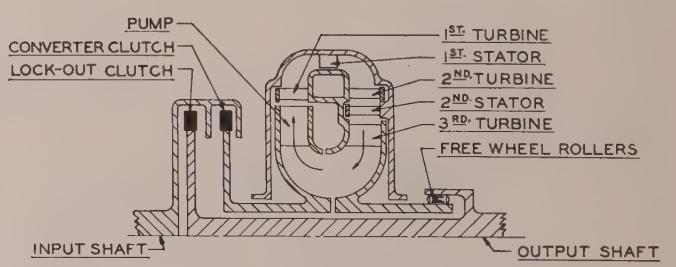

Fig. 12 – Three-stage, stationary-housing torque converter

torque is equal to the input torque, and beyond this point the converter should either be shunted out of the drive or the reaction blading be allowed to rotate in a forward direction to eliminate the shock losses.

Types and Performance Characteristics

Fig. 4 shows a diagrammatic sketch of a single-stage, three-element converter. The typical performance curves for this converter are shown in Fig. 5.

Fig. 6 shows a diagrammatic sketch of a three-member, two-phase converter. The term "phase" as applied to a torque converter refers to the number of times the functional arrangement of a working member changes. In this particular case, the unit acts as a torque converter until the coupling point is reached. Beyond this point, the resultant backing force on the reaction member is negative and the freewheel member or one-way clutch allows the reaction member to rotate in a forward direction. The shock losses from the reaction member are eliminated, and the arrangement becomes similar to a fluid coupling; thus the functions of both converter and coupling are obtained in one unit. Fig. 7 shows the performance curves expected to be obtained from this combination.

Since some of the present production torque converters are of the single-stage, four-member polyphase type, it is worthy to note the construction and performance characteristics of this type of unit. Fig. 8 shows a diagrammatic sketch of this unit. The reaction member is split into two distinct elements which are mounted in series on individual free wheels. In an effort to reduce the shock losses at the blade entrances, the individual reaction members are allowed to freewheel independently when the fluid impinges on the back side of the blades. When the first reaction member starts to freewheel some torque multiplication is produced from the second reaction member, and when both reaction members are freewheeling in a forward direction the unit has the characteristics of a fluid coupling. Fig. 9 shows the characteristics of this four-element, polyphase, single-stage torque converter.

The type of torque converter in one passenger-car unit is interesting since it is the only one that has incorporated the two-stage design. A diagrammatic sketch of the blade arrangement is shown in Fig. 10. The pump is of the rotating-housing type. The reaction member is positioned between the first- and second-stage turbine and is mounted on an overrunning clutch which locks in the torque conversion range. Since a lockup clutch is used for high-speed operation, maximum efficiency in coupling range is not of extreme importance. The reaction member will freewheel in coupling range or when the lockup drive clutch is engaged. Therefore, the reaction member is free to rotate at all times except when torque multiplication is required. The unit has a torque multiplication ratio of about 2.4/1. The performance characteristics for this unit are shown in Fig. 11.

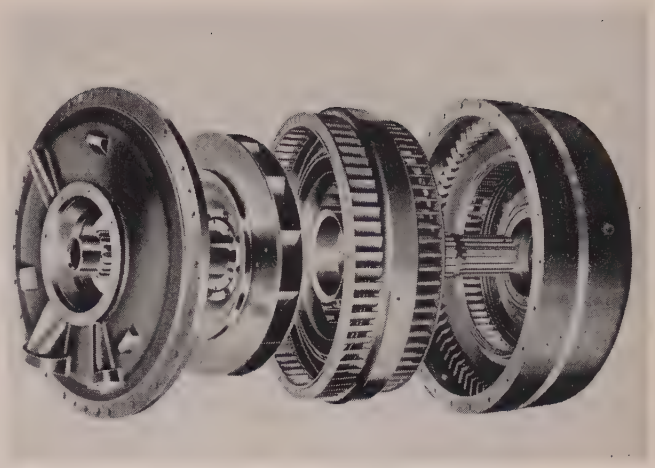

Fig. 13 – Exploded view of torque converter showing input pump at left and output turbine at right

A diagrammatic sketch of a three-stage, stationary-housing torque converter is shown in Fig. 12. (See also Fig. 13.)

In "converter drive" the converter clutch is engaged and rotates the pump which circulates the fluid around the hydraulic case. The fluid leaves the pump with high-velocity head and strikes the first-stage turbine blades, which are located around the circumference of the pump, causing the turbine to rotate in the same direction as the pump. This operation does not utilize all of the kinetic energy stored up in the fluid. The fluid leaves the turbine blades in a backward direction (in relation to pump and turbine rotation), and then enters the first-stage reaction or stator blades, which are secured to the outer circumference of the hydraulic case. The fluid leaves these blades at a corrected angle in a forward direction and strikes the second-stage turbine blades imparting additional forward-drive momentum to the turbine rotor. The above operation is repeated once more before the energy in the fluid is absorbed by the turbine rotor. After passing through the third-stage turbine blades the fluid returns to the pump inlet and the above cycle is repeated.

Fig. 14 shows a schematic diagram for the fluid flow through the three-stage torque converter. Although the blades in the diagram are shown as flat plates, they are actually of streamline shapes with rounded leading edges to reduce shock losses for the variable inlet fluid flow velocities.

Fig. 15 shows the performance characteristics for a three-stage, stationary-housing torque converter.

The stall torque ratio for this particular converter is 6.0/1, with a peak efficiency of 85% at 0.45 speed ratio, and the coupling point is at 0.67

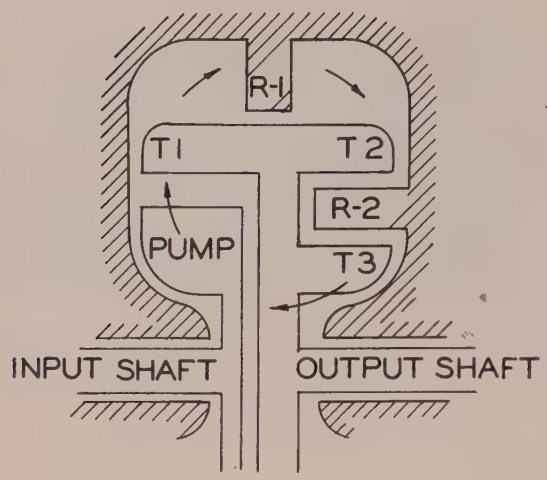

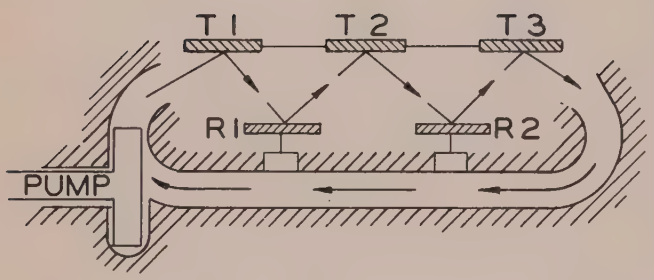

Fig. 14 – Fluid-flow diagram for three-stage converter

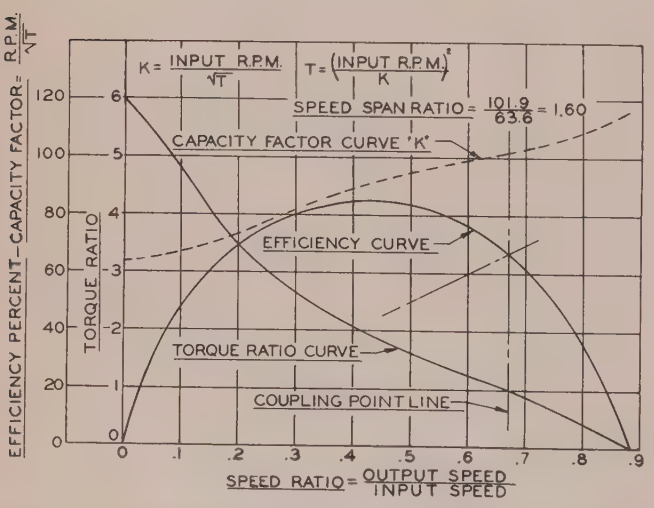

Fig. 15 – Performance characteristics for three-stage torque converter

speed ratio. In this curve we have introduced a capacity factor or K factor curve, which indicates the size or torque-absorption characteristic of the unit. This curve, when used with a similar capacity factor curve for a given engine, enables one to determine vehicle performance curves.

Fig. 16 is a diagrammatic sketch of a two-stage, stationary-housing torque converter. It is similar to the three-stage torque converter shown in Fig. 14 except for one stator member which is positioned between the first- and second-stage turbine blade assemblies.

This type of two-stage torque converter may be designed for improved high-speed operation with a higher peak efficiency and a higher coupling point than the three-stage type. The stall torque ratio is however reduced to about 3 to 4.0/1 and therefore auxiliary gearing should be used in applications where the horsepower/weight ratio is low and where it is necessary to overcome excessive varying road-load requirements.

Torque Converter Performance Curves

Fig. 15 is a performance curve for a three-stage, high-torque-multiplication torque converter. Since the relation of output speed to input speed determines the fluid-flow directions between the various blade stages, the characteristics of a given torque converter are such that torque ratio and efficiency will be constant for each particular speed ratio, regardless of the input torque. The input torque varies directly as the square of the input speed, and the capacity factor K, which is the input speed divided by the square root of the input torque, will also be a constant for any given speed ratio.

Thus, for each particular speed ratio, a given torque converter will have a fixed torque ratio, efficiency, and capacity factor K value. When these three characteristics are known, the performance characteristics of the torque converter with a given engine can be accurately computed.

The shape of the K curve is an indication of the shape of the input speed curve for the vehicle. A rising input speed curve is advantageous for automotive use since the torque conversion range is extended and engine lugging is reduced after a shift to lockout drive.

Fig. 17 is a performance curve of an automotive diesel engine used in bus application. It is important to note that the torque converter is concerned entirely with the net installed torque of the engine, and all accessory and fan losses must be deducted from the gross torque curve.

The computations from converter curve in Fig. 15 and engine curve in Fig. 17 result in the power train performance curves shown in Fig. 18.

With the set of curves shown in Fig. 18, vehicle performance curve may be determined if the axle ratio, tire size, gear ratio, and so forth, are given. Fig. 19 shows the performance curves for a 44-

passenger city bus using the power train shown on Fig. 18. The tire size is 11.00 x 20 and the rear-axle ratio is 4.88. The performance is shown for vehicle operation in converter drive as well as lockout drive, and all curves are shown for full-throttle operation.

Although the coupling point of the converter was reached at 34.5 mph, the governor called for a shift at 27.5 mph. The engine speed increased from 1380 rpm at stall to 2015 rpm at the shift point. The engine speed changed from 2015 rpm to 1120 rpm during the shift from converter to lockout drive. The high starting tractive effort available allows the vehicle to accelerate rapidly through the converter range to speeds where the efficient lockout drive is obtained. The shift out of converter, which in this particular unit occurred at 27.5 mph, was made at 1.4 torque ratio and at about 80% efficiency. The vehicle is geared to give a maximum speed of 52 mph at engine governed speed of 2100 rpm.

Another method for determining vehicle performance is by using the family of performance curves as shown on Fig. 20. These curves are obtained from dynamometer test results, and each converter design has its own individual set of curves. These curves show input torque and output torque at constant engine speeds plotted against output rpm. An engine torque curve may be plotted in the upper set of input torque curves, and by projecting downward in the lower set of curves the output torque may be obtained for the particular input and output speed conditions.

The torque converter may be used as a dynamometer for the engine, and Fig. 20 shows how this is done. The performance of the vehicle is checked under full-throttle conditions by observing input and output speeds. The input speeds are plotted for the corresponding output speeds, and thus the actual input torque that the engine is delivering to the converter may be determined.

The performance of a 36-passenger city bus (Fig. 21) was checked in this manner, and the test results are compared with the calculated results which were based on a higher specified engine torque curve. Fig. 22 shows the comparison of specified engine performance curves versus actual engine performance curves as obtained from tests in the vehicle.

Fig. 23 shows a comparison of the vehicle performance based on the specified engine torque curve versus the actual engine torque curve as obtained by using the torque converter in the vehicle as a dynamometer for the engine.

Torque Converter Applications

By recognizing the limitation of the torque converter, the transmission designer can better suit a

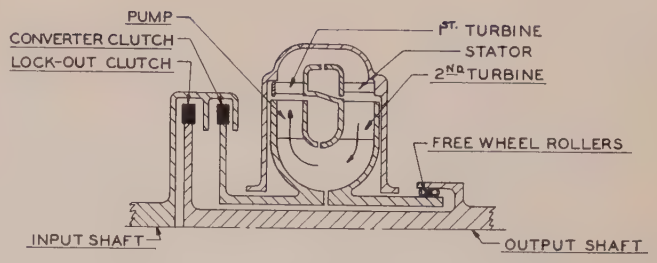

Fig. 16 – Two-stage, stationary-housing torque converter

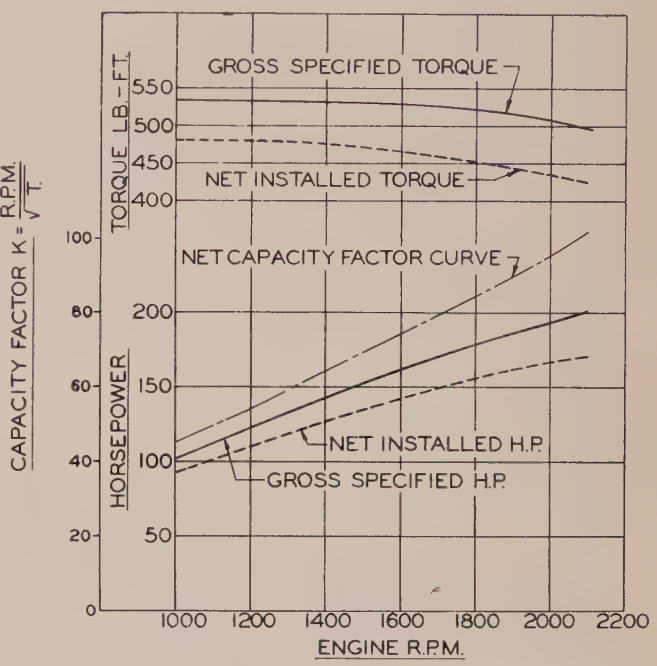

Fig. 17 – Bus diesel-engine performance curves

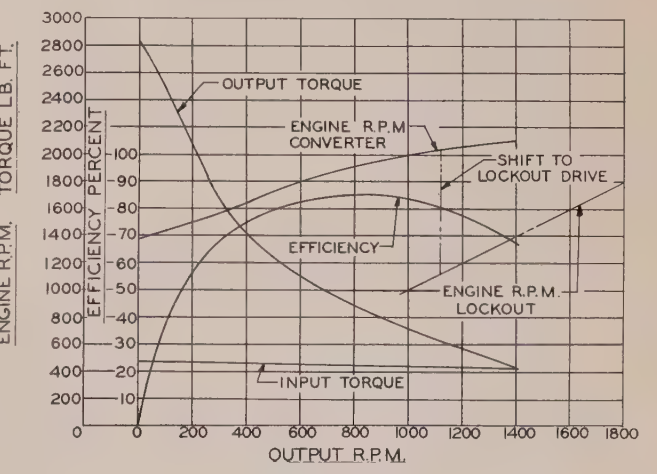

Fig. 18 – Three-stage torque converter with bus diesel engine

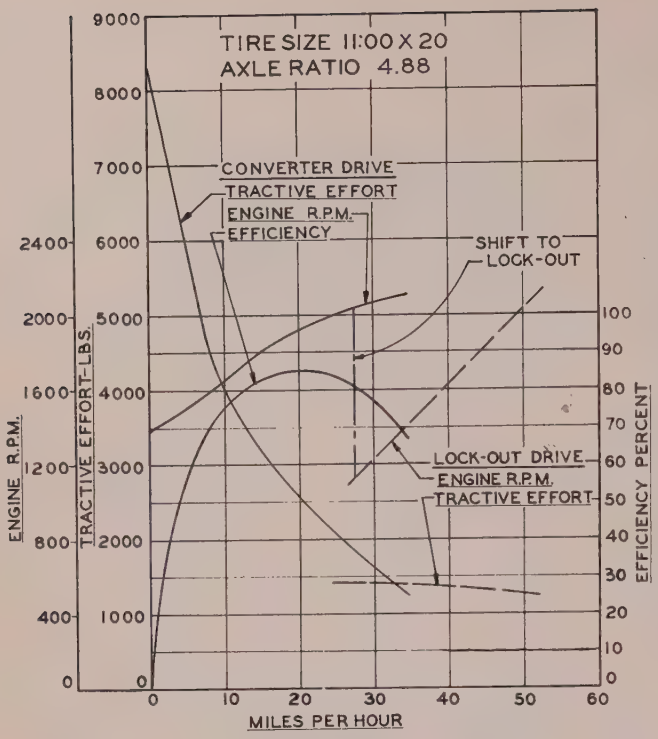

Fig. 19 – Vehicle performance curves for 44-passenger city bus

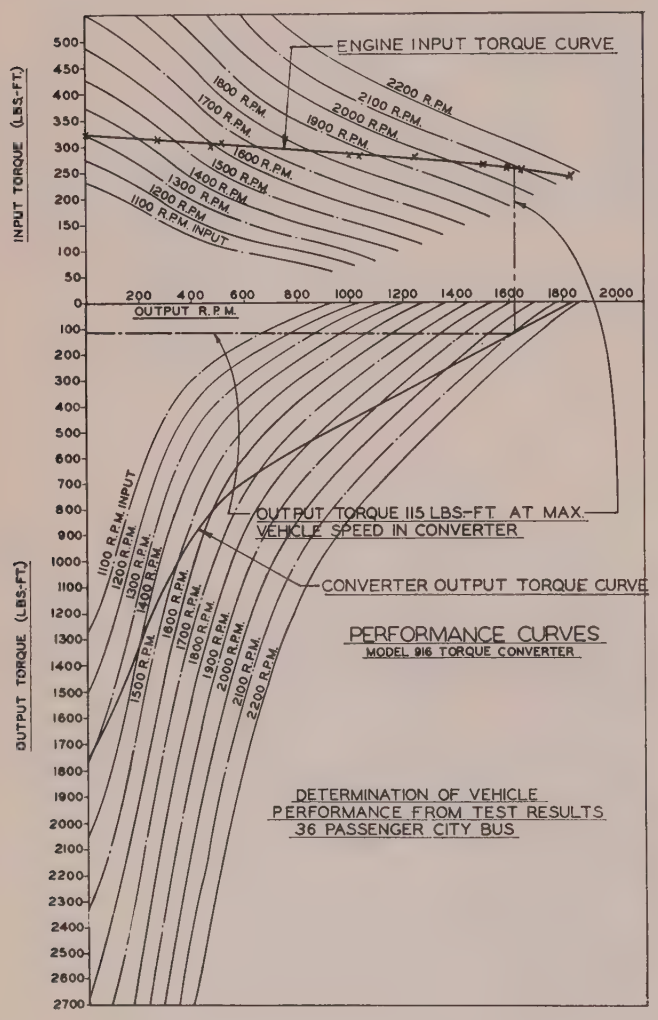

Fig. 20 – Torque converter performance curves

hydrodynamic transmission to the vehicle for its particular application. Some torque converter applications and their particular characteristics are as follows:

City-Bus Applications – One of first applications of the hydraulic torque converter for automotive use was in city buses where the need for this type of unit was very necessary. In congested city traffic, the driver is kept busy operating the vehicle, handling change, and issuing transfers to the passenger. The problem of controlling clutch engagement to permit the smooth starting of the loaded vehicle was a difficult problem to which the drivers could not give their full attention. In rear-engine buses, the engine compartment is too far from the driver to control smooth clutch engagement by engine noise. Therefore, higher engine speeds were used while engaging the clutch to make sure that the engine was not stalled. The enormous number of gear shifts which were required in driving a heavy loaded bus in congested city traffic presented a serious maintenance problem to both the clutch and shifting mechanism.

The introduction of the torque converter for city-bus applications early in 1938 was eagerly welcomed by the public, the driver, and the vehicle operator.

The work required for city-bus operation consists of repeated standing starts and rapid acceleration to keep up with city traffic. The three-stage converter having a high torque ratio range to handle the frequent and rapid changes of tractive effort requirements has proven advantageous for this application. This high torque ratio range in the torque converter with the addition of an automatic lock-out clutch meets the requirements of city-bus operation without the need of auxiliary gear ratios.

Fig. 21 – Spicer 36-passenger test bus with instrumentation

The success of the application of torque converters for city buses is attested by the fact that practically 100% of all the larger units are furnished with a torque converter transmission.

Industrial Applications – There are numerous applications of the torque converter for industrial units, and each application actually requires special treatment and individual analysis. Some applications where torque converters are being tested or are now in effect are cranes, hoists, shovels, switchers, railcars, crawlers, scrapers, track-laying and wheeled tractors, shop lift trucks, and oil-well drilling rigs.

The torque converter will succeed in these applications only if it can show a net savings in cost to the operator. This can be effected as follows: (1) by reducing maintenance and vehicle down-time, (2) by doing more work per day, and (3) by improving fuel economy. Although the torque converter installation reduces driver skill, it cannot get by in commercial and industrial applications simply as a driver convenience.

The industrial applications require smooth, shockless starting and must accelerate under variable load conditions. Such units as tractors which do various types of work like bulldozing, plowing, or scraping must be started and run under conditions where manual shifting under load becomes a difficult task. A shift at these low vehicle speeds usually results in the stalling of the engine. The

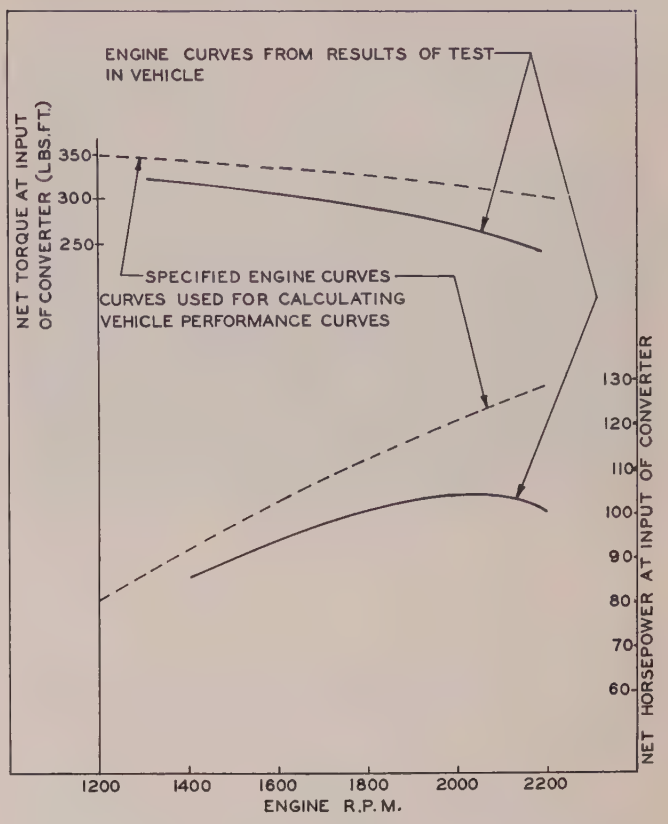

Fig. 22 – Comparison of engine performance curves from tests in vehicle

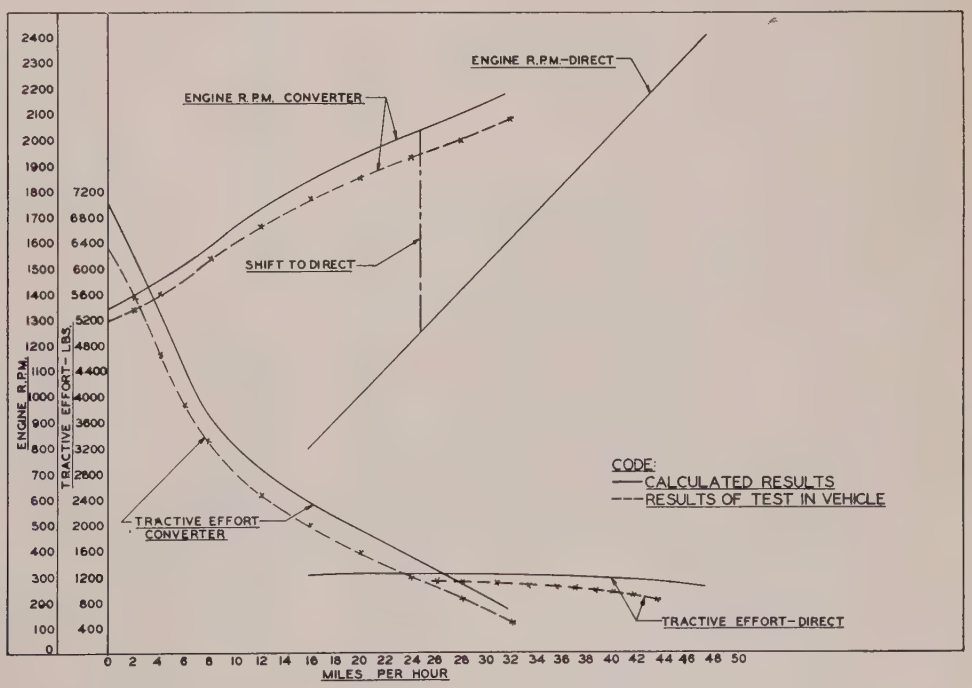

Fig. 23 – Comparison of vehicle performance curves from tests in vehicle

Fig. 24 – 18-ton amphibian tank with torque converter transmission climbing a 60% grade

Fig. 25 – Amphibian tank with torque converter transmission "hitting the beachhead"

torque converter is the natural choice for these applications.

Military-Vehicle Applications – The numerous advantages of the torque converter necessitates the use of this type of unit in the drive line. The problem here is to obtain the almost impossible performance specifications that are usually required. (See Figs. 24 and 25.) In addition to performance, the hydrodynamic drive transmission must have such virtues as minimum maintenance and maximum life, ease of operation, economy, and mechanical reliability. The design of an automatic transmission for a 50- to 60-ton tank with an 800-hp engine that can climb a 60% grade and have a maximum speed of about 45 mph presents a difficult problem for the transmission designer.

Passenger Cars – The modern passenger car has a high horsepower/weight ratio which is increasing each year. These automobiles use a converter-coupling type of transmission with a stall torque multiplication ratio from about 2.0 to 2.5/1, and the units are referred to as low-torque-multiplication converter-couplings. Since they are designed for high peak efficiencies and high efficiencies in the coupling range, low-speed performance is sacrificed in favor of improved performance at small speed reductions. Cruising speeds of the vehicle are obtained at part throttle in coupling range, whereas vehicle acceleration is obtained by opening the throttle and causing the engine to speed up. This results in a lower speed ratio, and torque multiplication is produced at a higher input torque.

The Studebaker and Packard Ultramatic hydrodynamic drives are the two passenger-car transmissions that have a lockup clutch. The lockup clutch connects the pump and turbine, thus eliminating the slip that is always present when the transmission is used as a coupling.

The limitation of torque converter for passenger-car service has necessitated the use of a semiautomatic two- or three-speed transmission behind the unit. By supplementing the planetary gear ratios behind the torque converter, acceleration and gradeability are improved and provision is made for braking on steep hills.

Off-Highway-Truck Converter Application – Torque converters were first introduced in mining trucks in the summer of 1948 for use in the Mesabi Iron Ore Range. The Spicer three-stage, high-torque-multiplication converters were first used with a three-speed manually operated auxiliary gear box. These units were installed in 20-ton trucks having a 275-hp diesel engine. The gear ratios in the three-speed auxiliary gear transmission behind the torque converter were preselected to obtain the required performance. (See Fig. 26.)

The performance of the torque converter trucks was very good in this application. The converter-driven trucks could outperform the standard transmission truck on rolling roads, with their many gradient changes. These loaded vehicles were driven at wide-open throttle with the converter absorbing all the horsepower the engine developed, and vehicle speeds would vary with the changes in the grade. Since no shifting was required by the driver, he could give all his attention to the manipulation of his vehicle.

Later installations included two single-stage converters which were used with two 190-hp diesel engines in a 30-ton tandem-axle truck. The output shafts of the converters were connected to two individual three-speed semiautomatic planetary transmissions.

The use of the torque converter in this applica-

Fig. 26 – Euclid 20-ton mining truck with Spicer torque converter transmission

Fig. 27 – Highway hauler tractor with Spicer "synchro-verter" transmission, 54,000-lb gross combination weight

tion has practically eliminated drive-line maintenance in the differentials, drive axles, and the final drives. The life of these component parts is normally about 5000 hr. The engine life of the converter trucks has also been substantially increased.

The success of the torque converter in this application is noted by the fact that the majority of the trucks that have been delivered to the mining companies in the last few years have been furnished with torque converters.

Panel- and Delivery-Truck Applications – The requirements for this service are similar to a small city-service bus or taxicab since a great percentage of the operation consists of start-and-stop driving. The basic requirements of a transmission for this application are reliability and long life with minimum maintenance. Good acceleration to keep up with city traffic, fairly high efficiency, and weight and cost are also prime considerations. The solution to this transmission problem has been the adoption of the high-production passenger-car type of hydrodynamic drive.

Highway-Tractor-Hauler Application – The application of the torque converter transmission for this field is very promising since it comprises a region where a large volume of production may be expected. The vehicles which come under this classification have a gross combination weight of 35,000 to 60,000 lb. They must be geared for vehicle speeds of 60 to 70 mph and they must be capable of performance in the various types of terrain that are encountered in cross-country operation. These heavy-duty highway tractors have a very small horsepower/weight ratio – about 1300% less than the average passenger car. These vehicles are required to meet extended periods of start-and-stop driving since service requirements are often encountered where routes pass through large cities with congested traffic. This condition together with the maximum vehicle speed and gradeability requirements emphasizes the need for a flexible transmission. The greater the varying grades and the more start-and-stop service that these heavy loaded trucks are subjected to, the more arduous is the job of the truck driver who has continuously to shift gears to meet the variable driving conditions. Many of the transmission combinations for these vehicles on the road today have from 10 to 15 speeds.

There are some experimental torque converter transmission installations being run in actual field service. Although much valuable data is being gathered, it is too early to formulate definite opinions from the results on hand.

Gillan and Coleman have already covered the advantages and disadvantages of a torque converter transmission for heavy-duty tractor trucks.[1] The paper was based on tests of a White 60,000-lb tractor truck which was equipped with a Spicer two-stage converter and five-speed synchromesh transmission. This combination has been referred to as the "synchroverter" transmission. (See Fig. 27.) The torque converter is provided with a "hot shift" hydraulic clutch for lockout drive. The two-stage converter was selected for the improved performance obtained with the high-speed gasoline engines that are used for this application. Since gear ratios are provided behind the torque converter, it is not necessary to obtain the maximum torque multiplication in the hydraulic unit.

An extra feature for this application, which has been very favorably accepted in the field, is the ad-

[1] "Advantages and Disadvantages of Torque Converter Type Transmissions for Medium- and Heavy-Duty Trucks and Tractors in Both Multiple-Stop and Long-Distance Operation," by P. L. Gillan and W. S. Coleman. Presented at SAE Summer Meeting, Atlantic City, June 10, 1953.

dition of hydrodynamic braking. Downhill hydrodynamic braking is obtained when the vehicle is in lockout drive by engaging the converter clutch. This permits the engine, which is being driven by the vehicle, to drive the converter pump which in turn drives the turbine at a racing or no-load condition. The energy required to drive the pump and turbine is the retarding effort or hydrodynamic braking which is in addition to engine braking; it is in the form of heat and is dissipated by the circulation of the converter fluid through the heat exchanger. The use of the augmented hydrodynamic braking allows heavily loaded trucks to descend steep grades in higher gear ratios than normally possible, reduces vehicle brake maintenance, protects the engine from overspeeding, and provides safer control of the vehicle by the driver.

On the basis of the performance requirements that must be met for heavy-duty tractor-trailer service, it seems safe to predict that the future transmissions for this application will incorporate a torque converter in the drive line.

Advantages and Disadvantages of the Torque Converter

For the past few years practically all transmission development included the use of the hydraulic torque converter in the drive line. The general acceptance by the public of the millions of passenger cars equipped with hydraulic torque converters (at optional cost) and the increasing use of torque converters in commercial and industrial applications is tangible proof of the merits of this type of transmission. This general acceptance of the torque converter has been due to its large number of advantages as a power transmitting device.

Some of the advantages of the torque converter may be peculiar to a given type of application. However, the more important advantages that are apparent in the various applications may be summed up as follows:

1. The main advantage of the torque converter is its wide range of variable ratio which enables it to vary speed and torque ratios gradually while under load. This enables vehicles to accelerate under conditions where conventional gear shifting is most difficult.

2. The torque converter is an excellent smooth starting device, far superior to the slipping friction clutch, which makes it particularly suitable for use with automatic and semiautomatic transmissions.

3. The torque converter is an excellent shockless accelerating device which dampens out torsional vibrations automatically in a fluid cushion, thus increasing engine, differential, axle shaft, and gear life. This is of particular importance where diesel engines are used as the power source.

4. The torque converter in the drive line eliminates almost all engine lugging and overspeeding which increases engine life and prevents needless wear and tear on the clutch and entire mechanism.

5. The torque converter enables the engine to operate in a more favorable speed range, which increases the payload or amount of work per unit of time.

6. The torque converter provides downhill hydrodynamic braking (in designs where this feature may be incorporated).

7. The torque converter may be used as a dynamometer for a periodic check of engine performance.

8. The torque converter reduces the mental and physical exertion of driving to a minimum, and consequently the driver can devote his time and attention to the safe control of the vehicle.

9. The torque converter reduces maintenance costs, and by reducing "down-time" to a minimum, availability of the unit to the operator is increased. This is of particular importance in industrial applications where "down-time" on large and expensive equipment is an important factor.

10. The torque converter has a low drag torque at idle speeds, and the engine need not be declutched when the vehicle is idling.

11. The torque converter either eliminates or minimizes gear shifting.

In return for the above list of advantages, the following list of disadvantages are worthy of consideration:

1. Higher first cost. This is generally determined by the specific application since the higher costs may be reflected in the amount of added features such as the addition of a multiple-speed automatic transmission behind the torque converter.

2. Generally some increase in weight.

3. Generally higher fuel consumption. Here again this disadvantage depends upon the particular application. In some industrial applications of the torque converter, more work per day is obtained for the increase in fuel consumption. In passenger-car units a sacrifice in fuel economy has been made to obtain the utmost in smoothness with the minimum requirements of driver attention.

In the Spicer highway-truck application and city-bus application, under certain conditions, indica-

tions are that the torque converter helps to improve fuel economy.

4. The torque converter or converter-coupling cannot compete with gears for continuous steady operation.

Torque Converter Accessories

For satisfactory performance of any hydrodynamic torque converter certain auxiliary accessories are required. A small charging pump, which is usually driven from the engine, is required to maintain a positive pressure in the hydraulic section at all times. Since a small amount of fluid is continuously circulated through a reservoir tank to remove gases, the charging pump serves the purpose of keeping the converter supplied with oil and maintains pressure on the fluid, thus preventing power losses due to cavitation.

A certain amount of heat is generated in any hydrodynamic fluid device, and the torque converter is no exception. The power losses which produce heat in the converter fluid are taken care of by a cooler or heat exchanger in the fluid system. To secure suitable operating conditions a portion of the converter fluid is circulated continuously through the cooler or heat exchanger. The stationary-housing type two- and three-stage converters rely on the natural pressure difference between the converter and cooler for circulation. The rotating-housing type of torque converter (the single-stage converter-coupling type) requires a rather large-capacity circulating pump which may be combined with the charging pump to circulate the converter fluid through the cooler. Some passenger-car torque converters do not have a cooler or heat exchanger but rely on forced air circulation over the converter housing to cool the fluid.

Torque Converter Fluids

Some of the losses in torque converters are made up of flow losses and rotational losses resulting from the shearing action between adjacent layers of oil molecules. These losses can be reduced by using converter fluids of relatively low viscosities. Since these losses are greater for the high torque multiplication type of converters, low-viscosity fluids are more necessary for these units to assure optimum converter performance.

In the first hydrodynamic-drive transmissions for city-bus operation, the hydraulic section was self-contained by three positive-type seals. This permitted the use of a converter fluid of low viscosity and of little lubrication value. The first fluids used consisted of 5% engine oil and 95% kerosene. The viscosity of this fluid was about 28 SUS at 210 F.

In some of the first diesel-engine coaches, the converter fluid system was connected to the engine fuel tank. Insufficient cooling resulted in high fluid temperatures which caused excessive oxidation to the converter fluid. There was considerable variation in the properties of the diesel fuel used, and a breakdown of the fluid caused deposits of sludge or varnish in the fluid system and blocked critical passages in radiators, heat exchangers, injectors, filters, and relief valves.

The oil companies were not interested in developing a special fluid for this operation until a relatively large number of units were in service and production of torque converters for buses had increased. There are now many torque converter fluids approved for the bus-type units. These fluids are blended from low-viscosity mineral oils with suitable additives to assure proper operation in the coach when subjected to extreme conditions. Such properties as gravity, flash point, viscosity, pour point, antifoam, antirust, oxidation stability, and lubricity must be controlled in the converter fluid. However, the sole criterion for final approval of any converter fluid must be field-performance tests in the torque converter itself.

In the passenger-car units and in other units where a common fluid system is used for both the hydraulic section and mechanical section, more emphasis must be placed on the lubricity or load-carrying capacity of the fluid. In addition to the properties listed above, the fluid must also be capable of lubricating such elements as overrunning clutches, bearings or sleeve bearings, and planetary or spiral bevel gears.

SAE automatic torque fluid Type A has been recommended for practically all the passenger-car types of automatic transmissions.

Conclusion

Since the end of World War II the torque converter has made enormous progress for use with almost every type of vehicle application. What future progress can the torque converter make? Certainly, with more research we can look for improvement in performance, and with increasing production and improved production processes the cost premium may be reduced.

The torque converter will continue to make progress in transmission of power applications since it will be used more under conditions where its inherent advantages show up the most. High starting torque developed in torque converter drive enables heavy loads to be rapidly and smoothly accelerated under adverse conditions, while the lockout feature provides full speed operation at maximum efficiency. For any machine or device that must operate under a variable load, the torque converter is the most promising and logical choice.

It is for the vehicles that are the workhorses of the nation that the torque converter offers the most advantages and where the most progress will be made.

Coordination of Electric

THERE can be no question as to the importance of balanced brakes in the operation of any motor vehicle. This is particularly true when applied to articulated vehicles where there is always the danger of jackknifing and where trailer brakes are usually a considerable distance from the control valves on the prime mover, making application time an important consideration. There are, of course, many factors which are oftentimes overlooked that affect brake balance regardless of the brake location or the type of brakes. These are mechanical in nature and controllable by proper maintenance procedures. Such problems must be overcome before "push-button" braking is a desirable feature. They are:

1. Smooth tires on one wheel and good rubber on the opposite wheel.

2. Possibly relining only one brake and then not with the same specification as on the other brake.

3. Possibly the drums are not close to being the same diameter. Perhaps one is concentric, and one is eccentric.

4. Loose wheel bearings.

5. Unbalanced loads over the wheels.

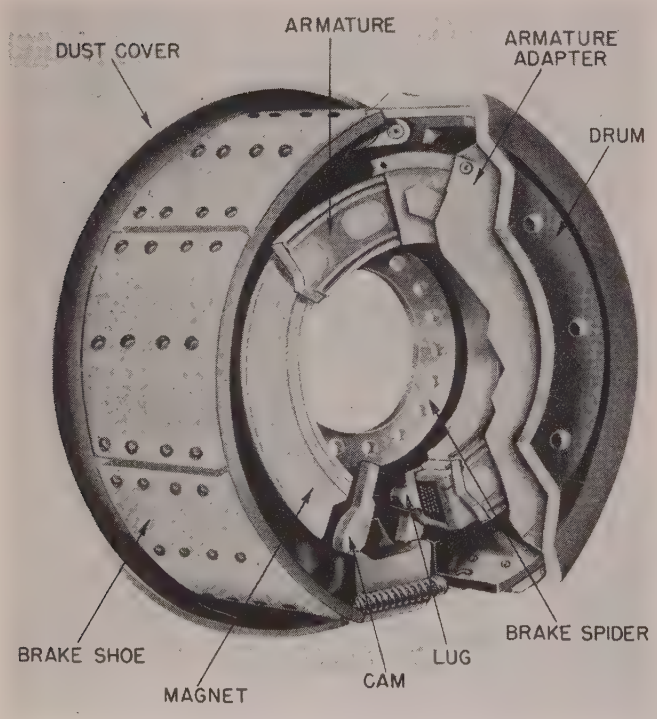

Fig. 1 – Warner electric foundation brake

Braking Problems with Single-Axle Semitrailers

As an example, I recently had the opportunity to inspect the brakes on a single-axle semitrailer. This unit had been an offender particularly with regard to the balancing of the brakes. The brakes, drums, and other components were up to standard. Upon examination, however, the two sets of tires were of a different make, and one set was found to be 1½ in. larger on the OD than the other, even though both sets were of the same size and had what appeared to be the same amount of tread. This 1½ in. on the OD only amounted to approximately ⅝ in. on the static loaded radius, being equivalent to about 2 to 3% difference in the developed force at tires and road. Since the brakes were working near to capacity for the load, the differ-

with Other Braking Systems

F. C. Hile, Warner Electric Brake & Clutch Co.

This paper was presented at the SAE Annual Meeting, Detroit, Jan. 11, 1954.

ence in the loaded radius was just enough to cause the smaller tire to lock the wheel and the larger one not to lock up. When a wheel is locked, the brake becomes a clutch and the tire the brake. A sliding tire has about 40% less friction at the road than a tire just ahead of a slide, which is the maximum obtainable. In the example above, the brake on the wheel having the smaller tire OD did not have the retardation of the other brake, resulting in the unbalanced condition.

To discuss balanced braking, a thorough understanding of the brakes, braking systems, and associated members is necessary. A knowledge must be had of the capabilities and limitations of different

HOW electric-actuated trailer brakes are synchronized with the air, hydraulic, or vacuum braking system as used on tractors is described here.

Brake balance between the electric and other systems used involves balance of brake buildup time. This is done by having the two types of brakes build up simultaneously for their respective axle loads and tire sizes. A load control consisting of a variable rheostat does this job for the electric brakes. It is also used for balancing the electric brakes with the tractor brake system.

The speed and versatility of electricity as used for trailer brakes make possible synchronized braking of combination vehicles without sacrifice of tractor brake speed – all brakes work simultaneously, resulting in shorter stops and less danger of jackknifing.

Other important safety features of the electric brake include: (1) They furnish an independent braking system for the trailer. (2) They are operated by a constant source of power.

The Author

F. C. HILE (M '29) is chief engineer of the Automotive Division of the Warner Electric Brake & Clutch Co. in Wisconsin. He attended Ohio Northern University, and received his B.S. degree in Mechanical Engineering from Tri-State College of Engineering. Mr. Hile was employed by Bendix Products Corp. as a commercial car brake engineer in 1928. He has been with Warner Electric Brake & Clutch Co. since 1941.

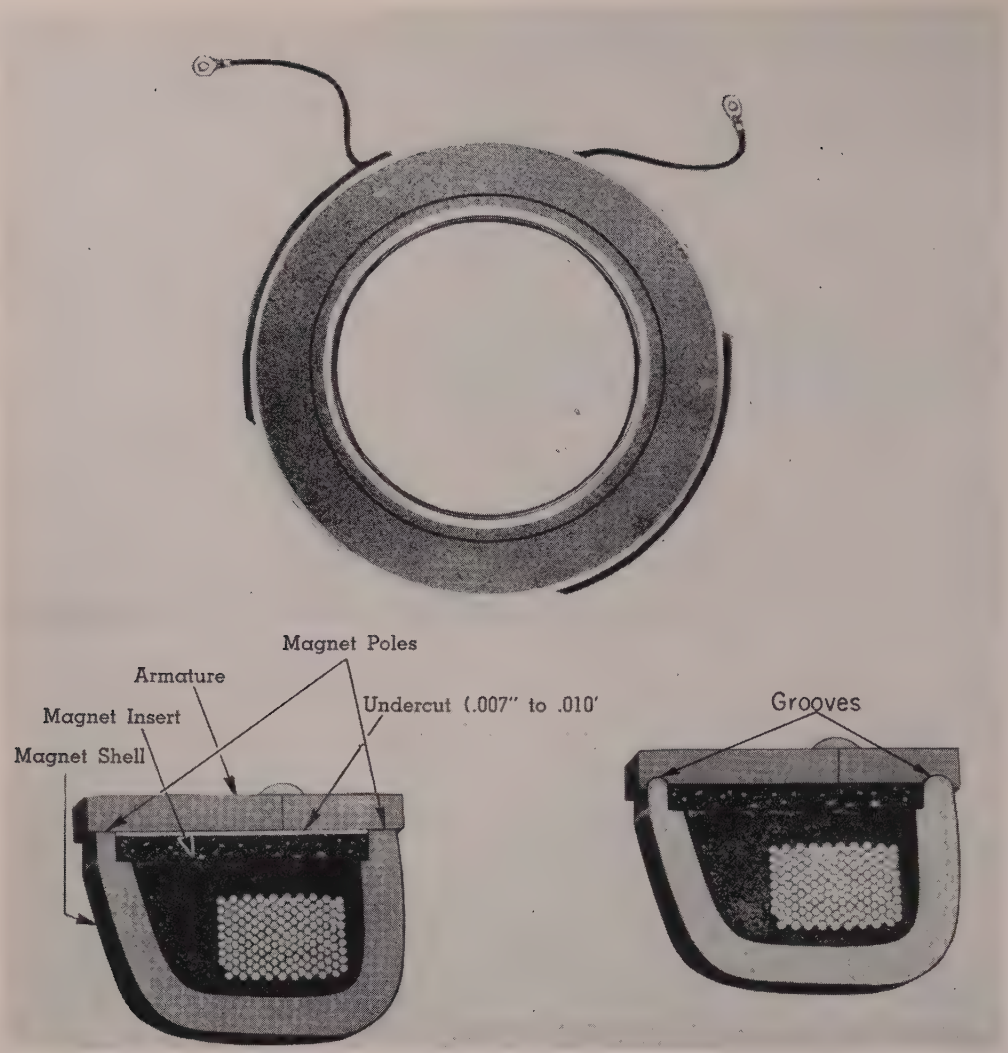

Fig. 2 – Brake magnet

types of brakes and their component parts. I have been asked to discuss the electric trailer brake and its capabilities regarding brake balance with various types of tractor brakes.

Electric Brakes are Popular

During the past several years, electricity as applied to trailer brake systems has received general acceptance because it can be synchronized with either air or hydraulic systems as used on tractors.

Since electricity is the fastest known medium, electric-actuated brakes are fast upon application and release. This reduces the problem of brake balance to one of balancing the brake buildup time, or as it may be termed, brake retardation. This can be accomplished by having the two types of brakes build up simultaneously for their respective axle loads and tire sizes.

The Warner electric foundation brake (Fig. 1) falls in the same category as the air, vacuum, or hydraulic foundation brake because they are all mechanical in nature. The backing plate (or spider), brake shoes (or band), and cams are common to each, with the exception of the hydraulic where the input force to the shoes is from a wheel cylinder.

The actuating means of the electric brake is an electromagnetic clutch formed by the brake magnet (Fig. 2) and armature (Fig. 3). The magnet is of a full circular horseshoe shape, embodying a copper coil held in place with a filler composition, and with a friction material facing. The facing is primarily to retard wear. However, when the magnet and armature seat themselves, this facing acts much in the same manner as the shoe lining does with the drum and gives additional input force to the brake shoes.

The magnet mounts on a circular pilot on the brake spider (Fig. 4) and is free to rotate in either direction a fixed amount. On the back of the magnet

is a lug or trunnion that actuates the cams. The armature face is a segmental ring mounted on flat leaf springs which attach to a mounting ring that is bolted into the brake drum. When the wheel, hub, and drum are on the axle in running position, the armature face ring contacts the magnet face and is depressed approximately $\frac{1}{8}$ in. The purpose of the depression is to keep the armature face in contact with the magnet at all times under a slight tension so it will follow up wear.

From a receptacle at the front of the trailer, two wires (battery and ground) are connected to the two terminals on each brake. From this receptacle to a like unit on the rear of the tractor, a flexible coupling cable is used to carry the electric current from the tractor battery to the brakes and to the ground connection. The brake wire is connected to the hot side of the starter switch, and the ground is made at the battery ground connection. We find that a kingpin and fifth wheel cannot be depended upon to form a satisfactory ground between tractor and trailer. In the tractor circuit an electric controller (graduated rheostat) is used to meter the current to the brakes which on an average is around 3.5 amp per brake for maximum capacity. When the controller is applied, the magnet becomes energized and attracts the armature magnetically. As the wheel rotates, the armature rotates the magnet on its pilot, and the trunnion on the back side of the magnet presses against a cam, which

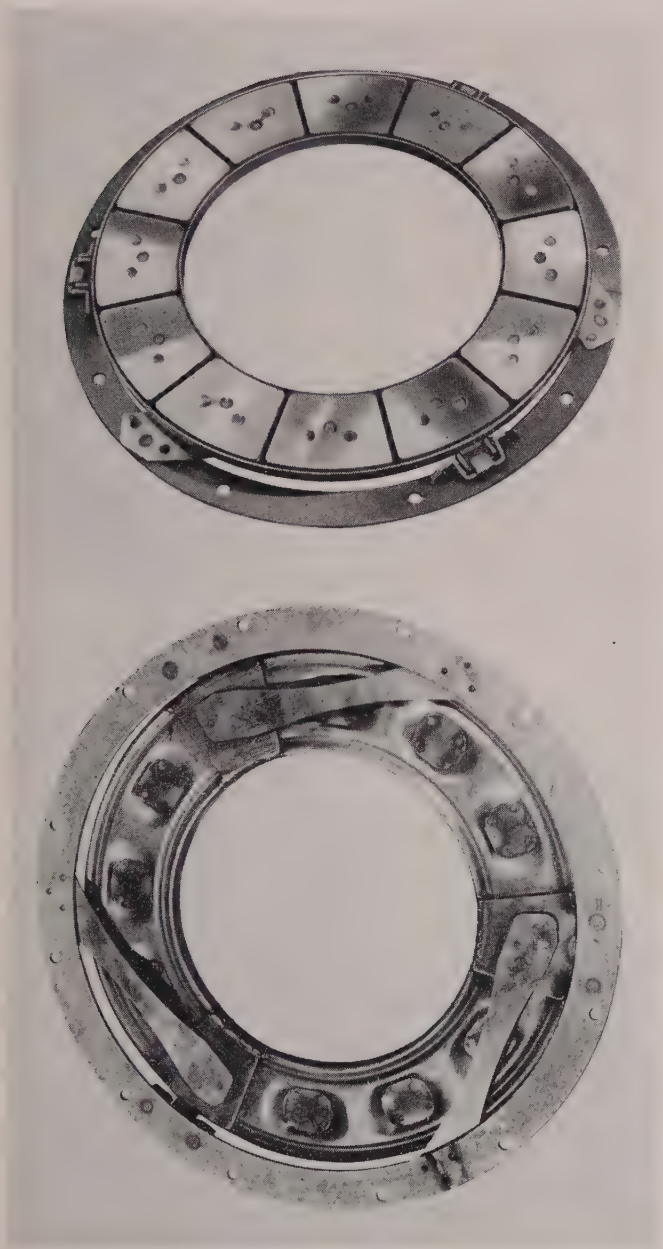

Fig. 3 – Brake armature

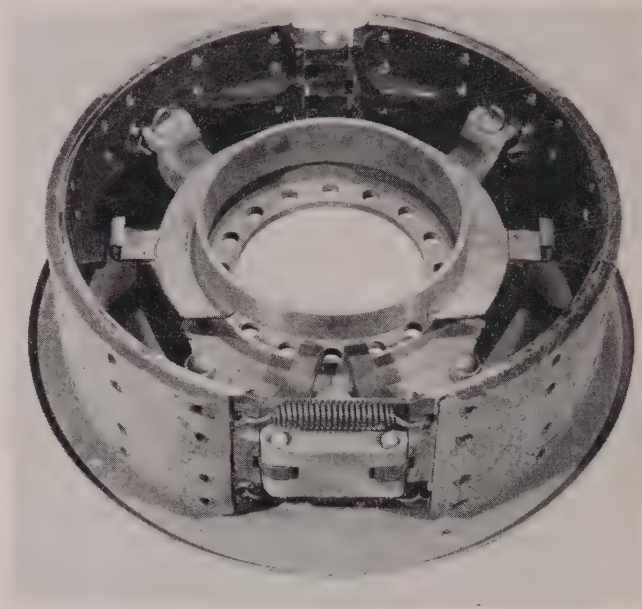

Fig. 4 – Magnet mounted on circular pilot on brake spider

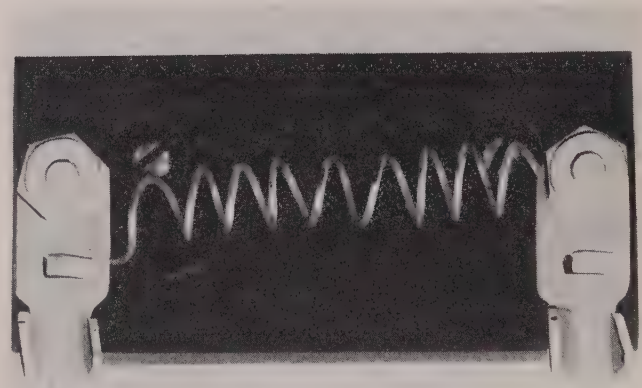

Fig. 5 – Resistor used to adapt 6-v electric brakes to 12- or 24-v systems

Table 1 – Standard Controllers and Adaptions for Electric Brakes

Design Volts	Type Actuation	No. of Brakes	Contact Bank	No. of Resistance Grid Banks	External Resistor Required
6	Hand Air Hydraulic Vacuum	2 or 4	Single	1	None
12	Hand Air Hydraulic Vacuum	2 or 4	Single		1 (2 brake) or 1 (4 brake) As required
6	Hand Air Hydraulic Vacuum	6	Twin	1 (2 brake) 1 (4 brake)	None
12	Hand Air Hydraulic Vacuum		Twin	1 (2 brake) 1 (4 brake)	1 (2 brake) 1 (4 brake)
6	Hand Air Hydraulic Vacuum	8	Twin	2 (2-4 brake)	None
12	Hand Air Hydraulic Vacuum	8	Twin	2 (2-4 brake)	2 (4 brake)
24	Hand Air Hydraulic Vacuum	2 or 4	Single		

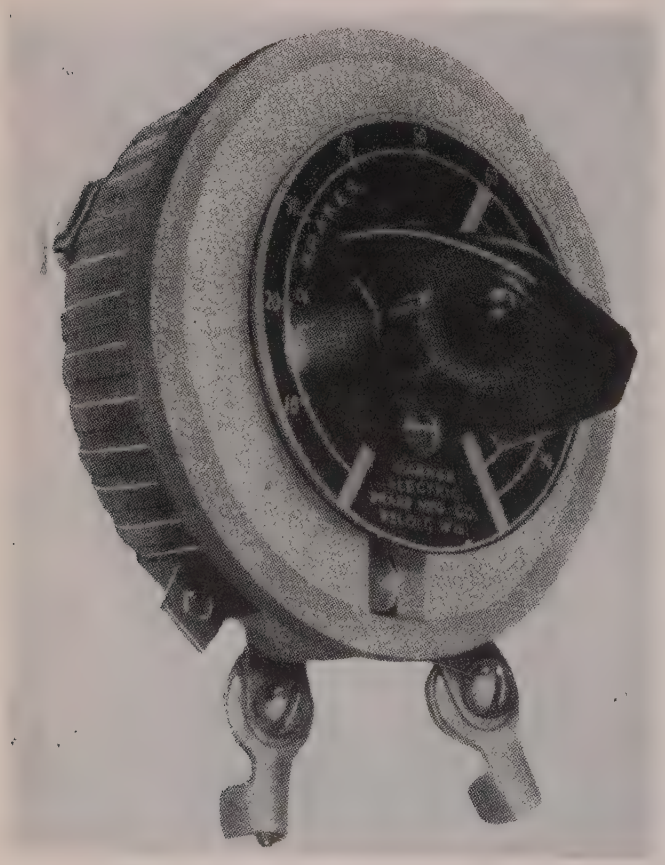

Fig. 6 – Variable rheostat used as load control

in turn pushes against a brake shoe, thus applying the brake.

The power of the magnet, and the pull it exerts on the armature, depends on the amount of current flowing through the magnet coil, which is metered through the controller as required.

Therefore, the medium of "electricity" does no more than energize the magnet, causing the magnet to attract the armature which in turn starts the shoe into the drum through cam action.

Self-Adjusting Brakes

As now designed, the electrically actuated foundation brake is self-adjusting. The fixed full travel of the magnet permits the lining to wear to the rivet heads without a mechanical shoe adjustment. Without a mechanical adjusting means for lining wear, approximately 0.020-in. clearance between new lining and drums is desired. This requires a little more care in fitting the shoes to the drums than on other types of foundation brakes, but it is not difficult with the simplified procedure as outlined in factory instructions.

Warner electric brakes are designed for 6 v, but with the use of resistors (Fig. 5) are adaptable to 12- or 24-v electrical systems. The present commercial controllers have eleven contact steps or graduations and can be actuated mechanically by hand or by air, vacuum, or hydraulic pressure. The same basic controller is used in all methods of actuation but differs where 12- and 24-v ignition systems are used. The present standard controllers and adaptions are charted in Table 1.

It has been explained that, with proper resistance, the 6-v electric brakes are adaptable to 12- and 24-v electrical systems. It is impractical, how-

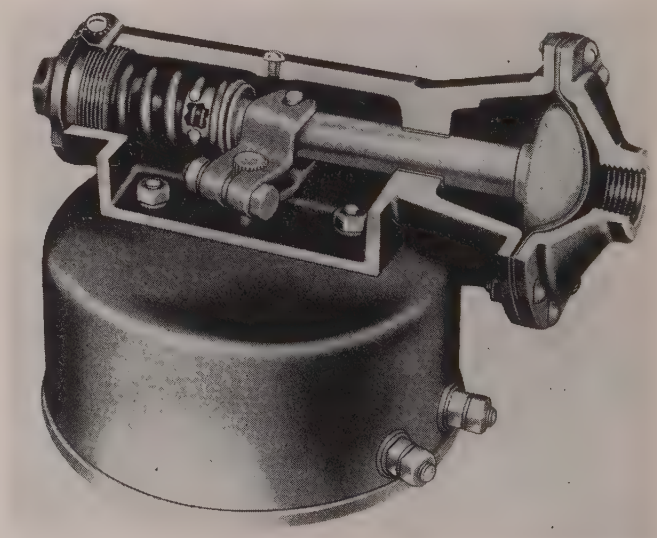

Fig. 7 – Air-actuated electric controller

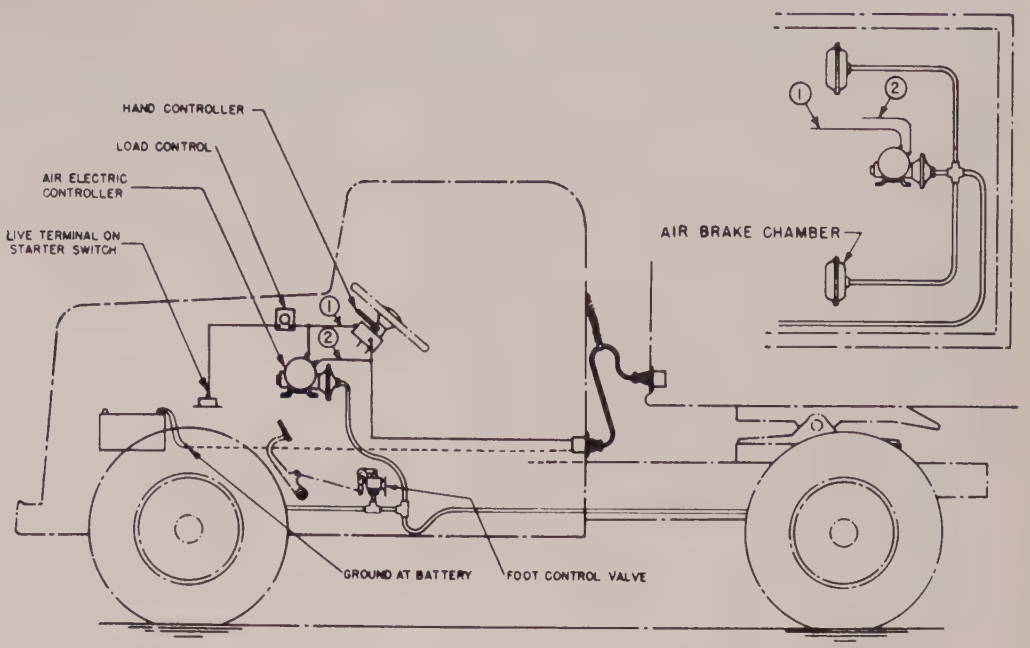

Fig. 8 – Air controller installation diagram

ever, to design all of the necessary resistance into the controller bank, therefore additional resistors must be introduced into the circuit.

For a "single-bank" 12-v controller, the resistor can be located anywhere in the circuit, but for convenience it is usually connected between the battery and the controller.

For "twin-bank" 12-v controllers, used with six- or eight-brake trailers, the proper resistor must be connected between each controller bank and the respective brakes which it operates, because the controllers have only one battery terminal.

Any 6-, 12-, or 24-v tractor equipped with the proper controls can interchange with any 6-v Warner electric-braked trailers. Naturally, the controls would be simplified if 12- and 24-v brakes were desirable, because the controller resistance grids would be designed for the respective voltage and would eliminate the need of external resistors in the circuit. However, this would not permit the use of any tractor having a lower voltage electrical system with a trailer having 12- or 24-v brakes.

How to Balance Electric Trailer Brakes

To balance the electric trailer brakes to varying axle loads and road conditions, the use of a load control (variable rheostat) (Fig. 6) is used in the control circuit. The load control is mounted on the dash in a location convenient to the driver. For single-bank controllers, it should be connected between the battery and the controller. For twin-bank controllers, they must be installed between each controller bank and its respective brakes.

With the proper size of brakes for the load carried and properly installed, it can be assumed that the electric trailer brakes themselves are balanced. The load control is also used in balancing the electric brakes with the tractor brake system.

Brake Synchronization

It has been shown that the speed of electricity affords the versatility necessary to synchronize the electrically actuated trailer brakes with air or hydraulically actuated tractor brakes. It is interesting to note how this is accomplished.

Preferably, the air-actuated electric controller (Fig. 7) and control components are installed on the tractor. The controller may be connected into the tractor air system (Fig. 8), either behind the double check valve in the trailer service line or in the tractor line itself. The controller should be placed in an accessible location and out of the road-splash zone for ease if piping and checking.

Before attempting to balance the electric trailer brakes with the tractor brakes, the tractor air system (including brakes) must be operating at peak performance to obtain the maximum operating efficiency and provide the shortest possible stops. To obtain this peak performance, the following should be checked and adjusted:

1. Proper brake, air chamber, and slack adjuster size for the axle load and required tire size.

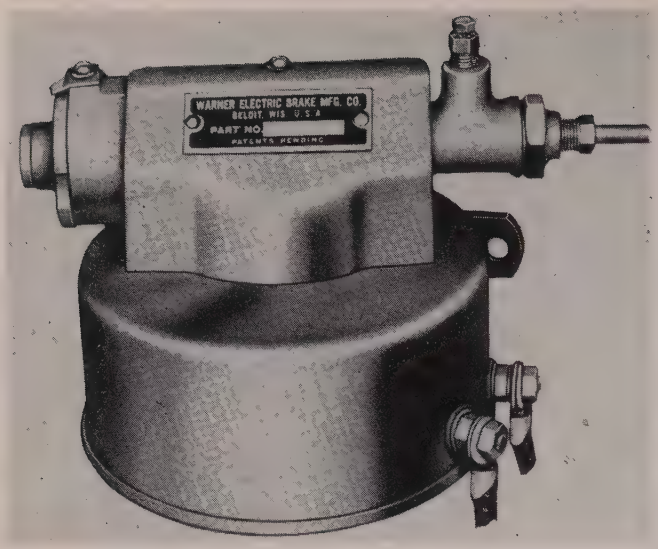

Fig. 9 – Hydraulic-electric controller

2. The slacks must be properly adjusted to provide proper lining-to-drum clearance.

3. With engine running, a minimum air reservoir pressure of 105 psi must be available so 85-90-psi air-brake chamber pressure is obtained on a full air pedal application. If this cannot be achieved, the tractor air system components must be checked, adjusted, and, if necessary, replaced in order to obtain these pressures.

With the tractor brakes in balance and the electric brake circuit completed (between tractor and trailer), run the engine so the tractor ammeter shows the generator charging. By connecting a low reading d-c ammeter in the line at the controller with the load control set at 100%, the controller is then fully applied. The reading on the ammeter will indicate the total amperage being drawn by all brakes. The amperage per brake should be approximately 3.5 amp for each brake in the circuit. (The proper amperage for a given brake size is shown in the maintenance manual.) If the required total amperage for the electric brakes in the circuit is not obtained, the system is checked for loose or dirty connections, broken wires, and proper wire size. In many cases, too small a wire is used. As in the case of a water pipe, for a given pressure, the larger the pipe, the less the resistance, and greater the water flow.

When the electric system has been checked for total amperage, the procedure for balancing with the tractor brakes may begin. With the ammeter in the line and the load control at 100%, an air gage is inserted in the air-brake line at one of the drive-axle chambers. The foot brake pedal is slowly depressed and the amperage increase by step is observed as the air-brake chamber pressure is in-

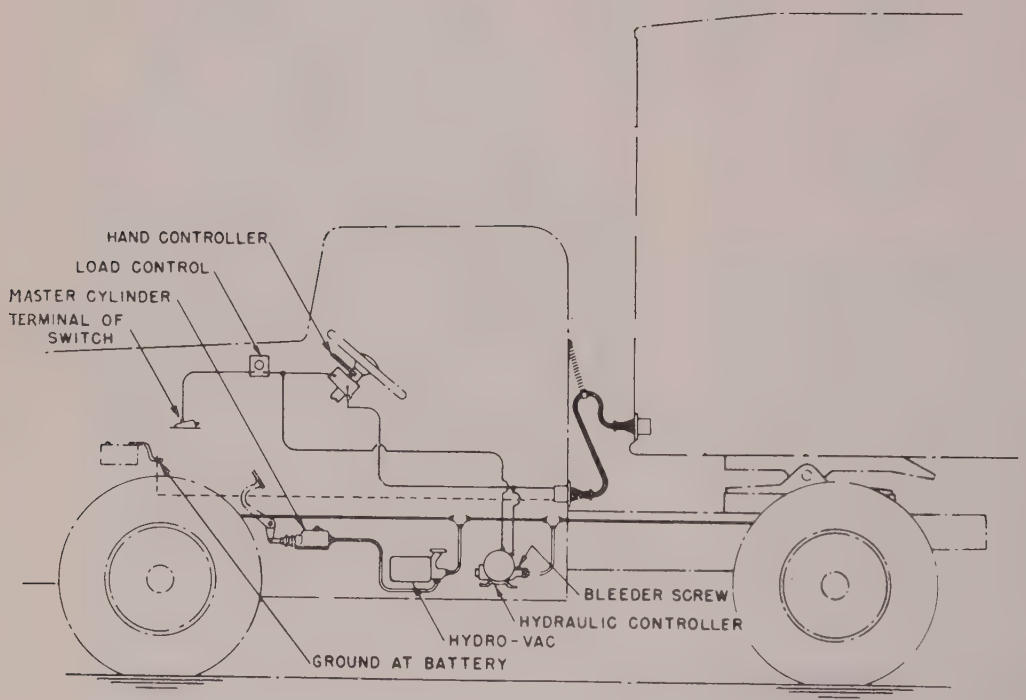

Fig. 10 – Hydraulic controller installation diagram

creased. The controller cover may also be removed and the step increase observed in the blade contact. Ordinarily, the first blade of the air-electric controller should make contact when the air-brake chamber pressure reaches 16-20 psi, and the controller should be full on at approximately 70-psi air-brake chamber pressure. Even though the 85-90-psi air chamber pressure is possible (item 3 above), it reaches about 60-70 psi quickly during an emergency brake application and takes longer to build up to maximum brake chamber pressure. On a full-power emergency stop, the speed of the electric trailer brakes will reduce to a minimum the danger of a full tractor brake application ahead of the trailer brake application. Because the normal air-brake chamber pressure is 20-25 psi for fanning or slowing brake application, 35-45 psi for normal brake application, and 60-70 psi for emergency brake application, the air-electric controller has been designed to provide synchronization and balance under all braking conditions.

There are different load springs available for the air controller. However, due to the small volume of air required to fill the controller chamber, as compared to the brake chambers, the spring must be of sufficient load to approach the balance of the build-up time for the tractor braking system. There is also an adjusting nut on the controller that, when used with the proper spring and the load control, completes the procedure of balancing tractor and trailer brakes.

Because of the speed of electricity, there is a tendency for the electric trailer brake to do more than its share of the braking unless the tractor air-brake system is maintained in top operating condition. To insure balance between tractor and trailer brakes and to take advantage of the safety therein, it is important to correct faulty tractor brake systems rather than attempt to compensate for them with control adjustments in the electric-brake actuating mechanism.

Balancing with Hydraulically Actuated Brakes

Electrically actuated trailer brakes may also be synchronized and balanced with hydraulically actuated tractor brakes. While there are two principal types of hydraulic actuation – straight hydraulic and hydraulic with power assist – the installation of the hydraulic-electric controller (Fig. 9) is the same in both cases. It is connected in the main hydraulic line (Fig. 10) back of the power assist regardless of type. It is important to note that when an air assist is used with hydraulic tractor brakes, the use of the hydraulic-electric controller is recommended in preference to the air-electric controller because in all cases better results are obtained by synchronizing the actuating mediums that directly operate the brakes. While application delay in tractor air-brake systems has been reduced to a minimum, hydraulic actuation more nearly approaches the speed of electric actuation and therefore provides for an overall faster brake.

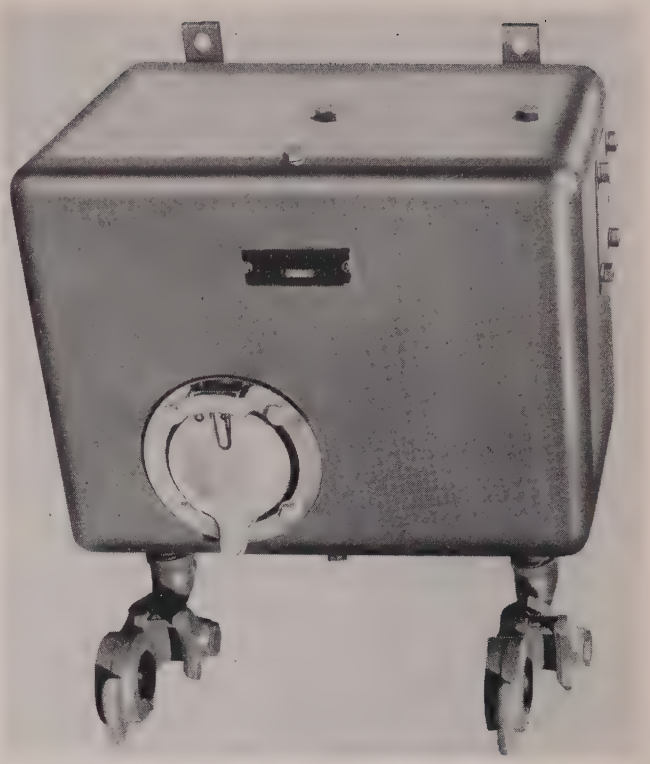

Fig. 11 – Air-electric controller pack

The hydraulic-electric controller employs a hydraulic cylinder, is equipped with a bleeder screw, and has a relatively small displacement with a ½-in. bore and a ⅝-in. maximum stroke. It is as important in synchronizing hydraulic-electric systems to have the hydraulic system operating at peak efficiency as it is to have the air system in top condition when synchronizing air-electric systems. Once synchronized using the proper controller spring, it is seldom, if ever, necessary to make additional controller adjustments. The balancing procedure is identical to that used in balancing air-electric systems, except that a hydraulic pressure gage is used in place of an air pressure gage. The first blade of the controller should make contact at approximately 150-200-psi line pressure. The controller must be full on at full pedal application. Because of the variance in different hydraulic systems, several controller springs of different loads are furnished with each controller so that it can be matched with the particular tractor on which it is installed.

Interchange of Equipment

As the demand for electric brakes increased, the problem of interchange of equipment became more apparent. In large operations where a limited number of electric-brake trailers would require equipping a large number of tractors with control equipment, it became necessary to develop an alternate

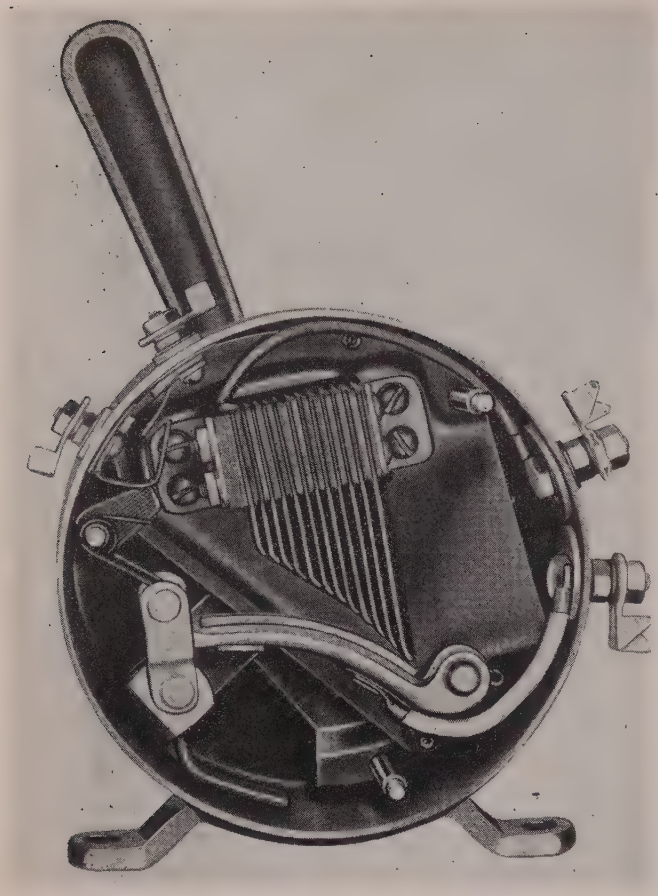

Fig. 12 – Hand controller with cover removed

method of providing control. The problem was solved by mounting the air-electric controller pack (Fig. 11) on the trailer. It was necessary to use a quick release valve and to install a low-pressure switch in the emergency air line on the trailer for independent braking in the event of air failure. With the controller on the trailer, it was only necessary to provide a brake and a ground circuit in the tractor electrical system. The load control, while not absolutely necessary, is in most cases installed on all tractors. All tractors, however, were not equipped with air brakes, and provision had to be made for those having vacuum over hydraulic brakes. A vacuum adapter (similar to Fig. 11) was designed for the standard controller making trailer installation possible. The balancing procedure with this controller is similar to that with the air-electric and hydraulic-electric except that the amperage is checked against the low-pressure air system. The first blade of the controller should make contact at about 2 to 4 in. vacuum, and controller must be full on at full pedal application at 16 to 20 in. vacuum.

The hand controller, which mounts on the steering wheel, is shown in Fig. 12.

Whether air or hydraulic, there is a variance in tractor brake actuating systems, and while it has been possible to compensate for this variance to some extent with the load control, the controller spring and controller adjusting nut must have a general setting for the average tractor. It has been our experience that, in this manner, balance can be attained for all practical purposes. The condition of the tractor braking systems, however, is even more important under these circumstances, and most operators have found regular maintenance schedules to be of substantial value.

Safety, Efficiency, Maintenance

Safety, operational efficiency, and minimum maintenance requirements are objectives toward which all brake manufacturers are directing their efforts. While the attainment of these objectives involves many factors, balanced braking plays a major role.

From the standpoint of safety, the elimination of application delay in the brake systems of articulated vehicles allows all brakes to function simultaneously. Shorter stops may be expected, and jackknifing due to the application of either the tractor or trailer brakes ahead of the other is reduced to a minimum.

It is also pointed out that with all brakes applying and releasing together each is carrying its share of the brake load. This is important from the standpoint of temporary heat-fade and excessive wear that often causes brake failure without warning. Proper loading, driver ability, and sound maintenance, however, are also contributing factors to brake fade and excessive wear.

Other Safety Factors

It has been shown how the versatility of electricity applied to the actuation of trailer brakes make synchronized braking, without the sacrifice of tractor brake speed, possible on articulated vehicles. This discussion would not be complete without mention of two other important safety factors afforded by electric brakes.

1. They furnish an independent braking system for the trailer.

2. They are operated by a constant source of power.

Tremendous advancement has been made in the design of all types of brakes and brake actuating mechanisms, and significant developments will be made in the future through the combined efforts of all brake engineers. There is no question of the superiority of one brake or braking system over another, but rather it is the responsibility of the equipment manufacturer and the operator to apply the proper brake and braking system as indicated by his requirements.

Napier Nomad Aircraft Diesel Engine

Herbert Sammons and Ernest Chatterton,
D. Napier & Son, Ltd.

This paper was presented at the SAE Summer Meeting, Atlantic City, June 10, 1954.

THE Nomad engine has been designed and developed in England by Napier with the object of providing a powerplant which will enable the greatest possible operating economy to be achieved in air transport services, with particular reference to air freighting.

The special suitability of the engine for these purposes arises primarily from its low fuel consumption which remains below 0.35 lb per ehp per hr over the whole useful range of cruising speeds and altitudes, and at some conditions is as low as 0.326 lb per ehp per hr, this corresponding to a brake thermal efficiency of 42%.

The economic value of these low consumptions is emphasized by the use of relatively cheap diesel fuel, although the engine will run equally well on aviation kerosene or on wide-cut gasoline.

Although the engine operates on the diesel cycle, its specific output in terms of power developed per unit of cylinder volume is higher than that achieved

THE Nomad compounded diesel engine described in this paper has been developed by Napier during the past seven years.

Resulting from the combination of a diesel engine with a gas turbine, the engine gives lower fuel consumptions than can be obtained from any other type of powerplant and maintains these consumptions over a wide range of aircraft speeds and altitudes.

These characteristics, which are still further improved by the ability to use cheap fuels, produce an engine making possible extreme economy for air transport purposes and very long-range operations for either military or civil purposes.

The Authors

HERBERT SAMMONS is managing director of D. Napier & Son, Ltd., in Acton, England. In 1922 he was appointed chief designer of Petters Ltd., oil engine manufacturers, of Yeovil, England, where he later became chief engineer. Mr. Sammons was made manager of the Kadenacy Department of Sir W. G. Whitworth, Ltd., in 1934. He has been with D. Napier & Son, Ltd., since 1943.

ERNEST CHATTERTON is chief engineer of the Piston Engine Division of D. Napier & Son, Ltd. He received his degree in engineering from the University of London in 1922. Mr. Chatterton's association with Napier dates back to 1930 when he took charge of experimental design. He became assistant chief designer in 1938, chief development engineer in 1941, deputy chief engineer, and subsequently, in 1949, he was appointed to his present post.

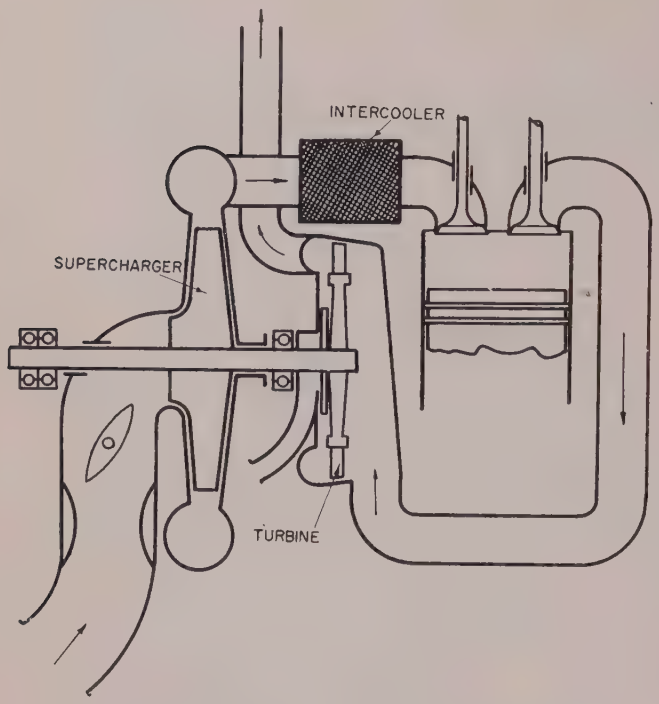

Fig. 1 – Exhaust-driven supercharger on Napier Lion

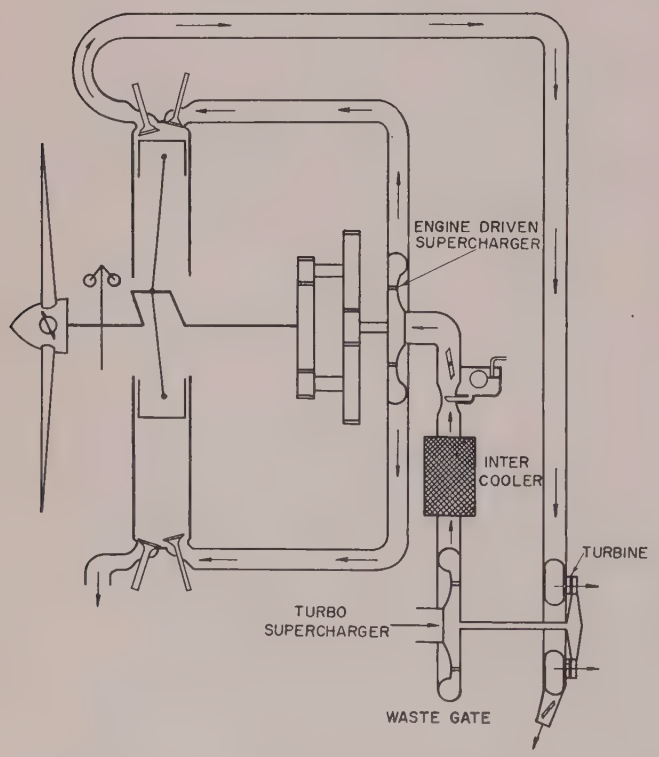

Fig. 2 – Arrangement of General Electric turboblower system

by the gasoline engine even in its most recent stages of development, the power output per cubic inch of cylinder volume under take-off conditions being 1.25 shp for the basic engine and 1.64 shp in its complete form with water injection. Due to these high outputs the specific weight of the engine can be reduced to below 1 lb per ehp.

Briefly then, the Nomad engine may be described as a diesel engine designed particularly for aircraft use, which weighs about 1 lb per hp and has a specific fuel consumption lying between 0.326 and 0.35 lb per ehp per hr over the whole of its useful operating range.

These unique performances are achieved by associating a piston engine with a gas turbine to form a "compound" engine, the operating cycle of which is devised so that each component can make its maximum contribution to the overall results.

The Piston Engine and the Gas Turbine in Partnership – The association of a gas turbine with a piston engine is by no means a recent conception. As early as 1924 a Napier Lion Series V engine was equipped with a turbine in the manner shown in Fig. 1, the exhaust gases being fed into the turbine to provide all the power to drive the engine supercharger.

At a later date during the 1939-1945 war, many engines were installed in operational aircraft fitted with "turbochargers" of the type shown in Fig. 2, in which an exhaust-activated turbine drives a subsidiary blower boosting the air intake of the normal engine supercharger.

While it may perhaps be said that the germ of the compounding principle is contained in these early examples, neither of them can be regarded as a true demonstration of compounding, for in each case the functional conditions of the engine are normal. No attempt is made to adjust these conditions to extract maximum energy from the combination, and the turbine is applied with the primary objective of extending the normal performances of the engine over a greater range of altitudes.

The extent to which this limited objective is achieved, as compared with a normal engine fitted with a two-speed mechanically driven blower, is illustrated in the power curves of Fig. 3, which show that the engine equipped with a turbine is able to maintain a selected cruising boost pressure and, therefore, its cruising power at a sensibly constant value over a wide altitude range.

This result serves to demonstrate the striking effects on engine performance which can be derived from the simplest possible association of a gas turbine with a normal piston engine.

A more recent powerplant which combines a piston engine with turbines is the Curtiss-Wright "Turbo-Compound" engine, which at the present time is installed in the Lockheed Super Constellation and other aircraft. This application differs from the two previously mentioned in that the power produced by the turbines is fed back into

the crankshaft, and the engine may therefore be classified as "compounded."

In this case the 18 cylinders of the 4-stroke gasoline engine are divided into three groups of six, each group feeding a separate turbine geared into the crankshaft system. The basic engine is the C.18.CB Cyclone to which the turbines have been added with the object of recovering as much waste energy as possible from the exhaust gases without disturbance to the established cylinder operating conditions. To avoid any material back-pressure effects the turbines are therefore of the "blow-down" type, which are activated by the impulsive velocities in the exhaust ducts.

No reliable performance data on the Wright turbo-compound engine is available in England, but its extensive and growing use indicates that worthwhile improvements in performance are being achieved. It will, however, be demonstrated later that this type of association between a developed spark-ignition engine and gas turbines is subject to definite limitations which prevent the full virtues of the compounding principle from being realized.

If, however, a piston engine and a gas turbine are designed together in the original inception to produce a true "compound" design, the scope for improved performance becomes much greater, for in this case the cycle of operations can be manipulated to exploit the most valuable features of the piston engine and the turbine which can then be associated together to produce a powerplant possessing strongly defined performance characteristics, which cannot be achieved by any other type of prime mover.

It is the purpose of this paper to analyze the characteristics of the compound engine with particular reference to the Napier Nomad, which is the only existing example of the type, and to indi-

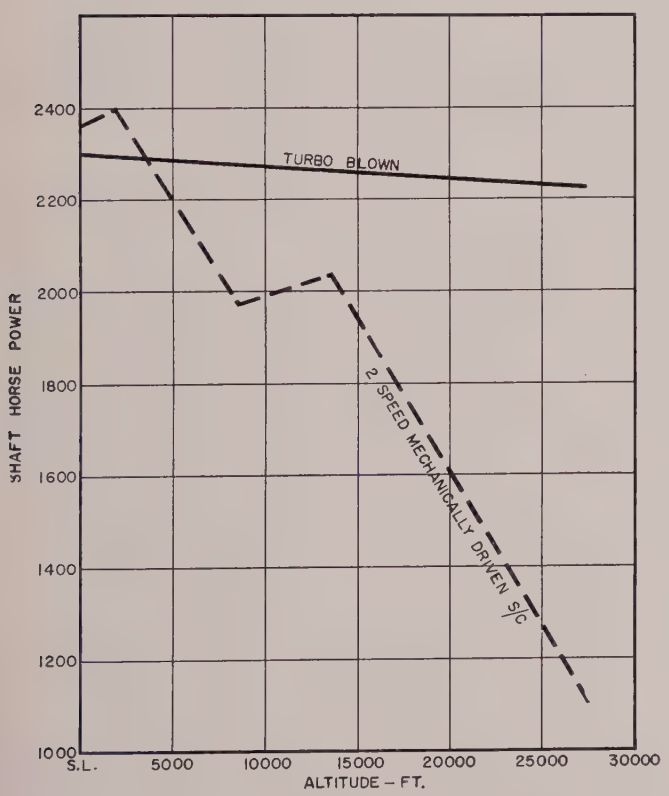

Fig. 3 – Altitude performance of turboblower engines

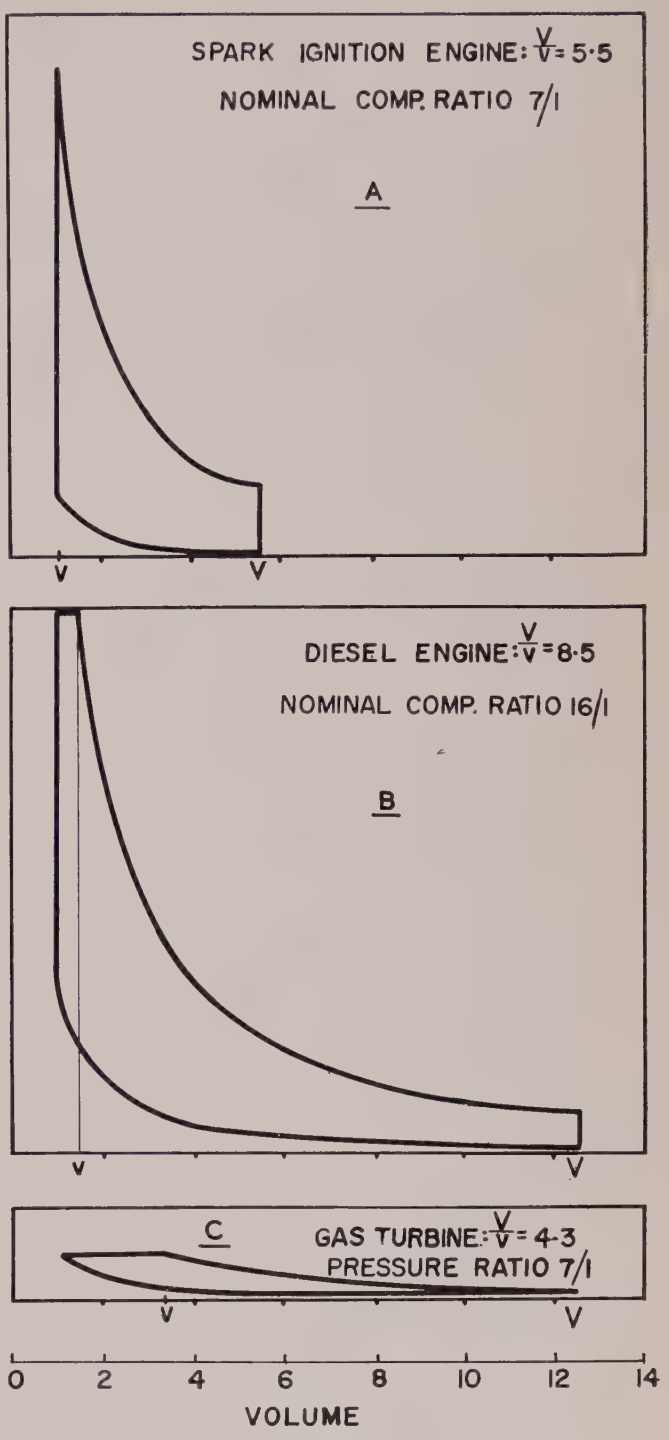

Fig. 4 – Typical indicator diagrams

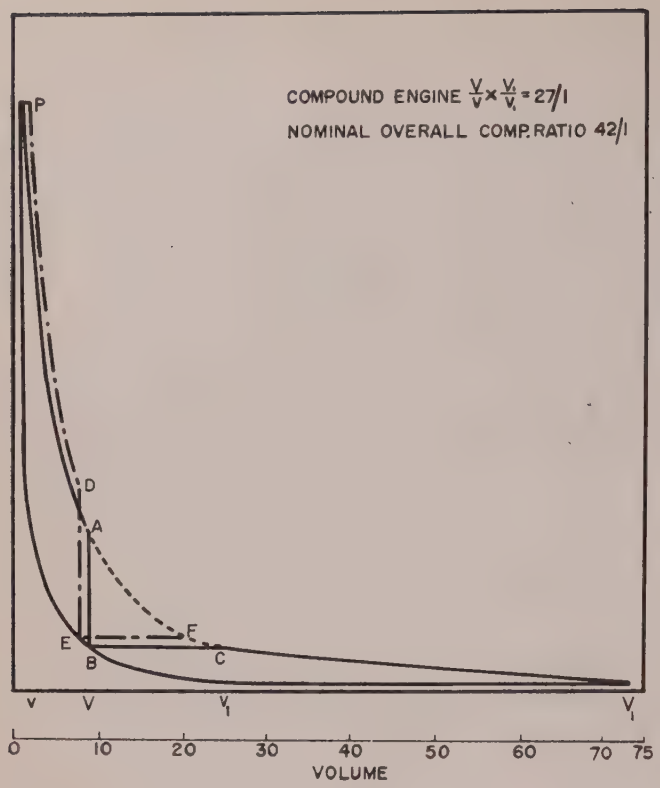

Fig. 5 – Compound indicator diagram

cate the contribution which such an engine can make in modern aviation.

How Compound Cycle Is Derived

If the major functional characteristics of the various types of engine are considered individually, it will be possible to indicate the factors involved in the derivation of the compound cycle and to assess the theoretical basis and practical limitations of this cycle in relation to others.

In broad terms, without too much respect for meticulous detail, the main relevant characteristics of different engines may be summarized as follows:

The Spark-Ignition Engine – The gasoline-burning engine, by its nature, consumes essentially all the air supplied to it, and the power developed by a given size of cylinder is almost entirely dependent on the rate at which it can inhale and reject air. Apart from changes in operational speed, the air quantity can be increased by supercharging, but the extent to which this is possible is limited by detonation and preignition difficulties.

An approximate "indicator diagram" for this type of engine is shown in Fig. 4A. Combustion takes place at constant volume, and the peak temperature of the cycle will be in the region of 4500 F. Basically the thermal efficiency of the cycle is governed by the volumetric ratio V/v, and this again is limited by the occurrence of detonation. Furthermore, if the supercharging pressure is increased to raise the maximum power, the compression and expansion ratios will, in general, require to be reduced to avoid detonation with consequent sacrifices in thermal efficiency over the cruising range of the engine.

It is, therefore, true to say that the destructive phenomenon of detonation is the limiting factor to both the power output and the thermal efficiency obtainable from this type of engine, and most of the spectacular power development demonstrated during the 1939-1945 war resulted directly from the introduction of fuels less prone to detonation coupled with the use of water injection and charge coolers which allowed the charge density to be increased and its temperature reduced, thus keeping within the detonation limits.

Typical performance figures achieved from spark-ignition engines in the more recent phases of their development are given in Table 1.

This type of engine is not amenable to manipulation of its cycle for compounding purposes, for any back pressure imposed in the exhaust system by a turbine will introduce practical difficulties, such as an increase in temperature of exhaust valves, and an increase in the mass and temperature of the residual gases which reduces the volumetric efficiency and raises the charge temperature, thus accentuating the already acute detonation difficulties. The best that can be done with this cycle is the arrangement already referred to as used in the turbo-compound in which a proportion of exhaust-heat recovery is achieved without disturbance to the normal pressure and temperature levels in the engine cylinder.

Although the foregoing remarks all relate to four-stroke engines, a similar situation exists if applied to the two-stroke gasoline-engine cycle.

The Diesel Engine – This engine also attempts to burn all the air which is supplied to it; but as in this case the mixing of fuel with the air has to take place in the cylinder within a maximum period of about 35 to 40 deg of crank rotation, it is not found possible in practice to utilize more than about 80% of the total air trapped in the combustion chamber. For a given maximum power output the cylinder dimensions will therefore need to be larger than in the spark-ignition engine. In the 2-stroke diesel engine a further loss of air occurs because of the necessity for effectively scavenging the burned gases from the cylinder, which implies a wastage of about 40% of the total air throughput which will escape from the exhaust ports or valves during the scavenging process. This air lost during scavenging is not entirely without value for it does act as an internal cooling agent and therefore reduces the thermal loadings on the pistons for a given amount of fuel burned.

As with the gasoline engine, the quantity of air trapped in the engine cylinders can be increased by supercharging, and, as the detonation limitation no longer exists, the degree of supercharge can be increased as dictated by the general balance of the engine design. It will be observed, however,

that in the 2-stroke engine any degree of supercharge can only be effective providing that a corresponding resistance, or back pressure, is offered at the exhaust ports or valves.

The approximate indicator diagram for this cycle is shown in Fig. 4B. Here combustion takes place partly at constant volume and partly at constant pressure, the proportion of fuel burned at constant volume being to some extent controllable and determined by the limitation established by the designer for the maximum cylinder pressure.

Although not strictly correct, due to the portion of constant-pressure combustion, the thermal efficiency for present purposes may again be related to the expansion ratio V/v, which in this case is considerably higher than in the gasoline-engine case with resultant improvement in fuel consumption.

The flame temperature during combustion will also be in the region of 4500 F, but, due to defective air utilization, the heat of combustion is diluted to some extent and the maximum temperature spread over the total air in the combustion chamber will be reduced to about 3300 F.

The diesel engine has not been widely used in aviation, but one engine which saw considerable service before the 1939-1945 war was the Junkers Jumo engine, the results from which are also included in Table 1.

It will be apparent that the cycle of operations described, particularly when referred to the 2-stroke engine, is very much more adaptable for compounding purposes than the spark-ignition case, for the following possible variables exist:

(a) In the absence of detonation or preignition troubles the compression ratio and the degree of supercharge may be varied to suit design requirements.

(b) The maximum cylinder pressures are to some extent controllable by variation in the rate of fuel input.

(c) Back pressures in the exhaust system need not be an embarrassment and are in fact essential when high degrees of supercharge are to be used.

(d) An excess quantity of air, over and above that required for combustion, is passed through the engine, this serving as an internal cooling agent which also reduces the mean temperature of the exhaust gases.

It will be seen later that these possibilities may be turned to very good account in the compound engine, and it may be stated here that the 2-stroke diesel cycle forms the ideal basis for compounding.

The Gas Turbine – Discussion here is limited to the turboprop engine, as it is this arrangement which is of interest relative to the compound case.

The basic cycle on which this engine operates is shown in Fig. 4C. Combustion takes place at constant pressure, and the basic thermal efficiency is again governed by the volumetric expansion ratio which, in the present state of compressor and turbine development, is limited to a lower value than that employed in either the diesel or the spark-ignition motor. If such an engine burned all the air passed through it the temperature of combustion would again be in the region of 4500 F, and this is the continuously maintained temperature at which gases would enter the turbine. This temperature is prohibitive, and with available materials and design technique, the temperature at the inlet to the turbine is limited to about 1500 F. To achieve this reduction in temperature, air to

Table 1 – Comparative Performance of Piston Engines

Type of Engine	Actual Engine	Fuel	Maximum Shp at Take-Off	Maximum Shp per Cu In.	Maximum Shp per Sq In. of Piston Area	Specific Weight at Take-Off, lb per shp	Specific Fuel Consumption, Sea Level at 60% Take-Off Power, lb per shp per hr
Gasoline[a]	Napier Sabre VA	100/130 grade	2550	1.14	5.43	0.976	0.50
Gasoline[a]	Napier Sabre VII	100/130 grade + water injection	3050	1.37	6.5	0.840	0.50
Gasoline[a]	Wright Compound	115/145 grade + water injection	3700	1.11	6.97	0.92	0.400[b]
Two-stroke diesel	Junkers Jumo 205E	Diesel fuel	600	0.59	3.73	1.910	0.345
Compound diesel[a]	Napier Nomad	Diesel fuel	3046	1.22	9.0	1.175	0.359
Compound diesel[a]	Napier Nomad	Diesel fuel + water injection	3480	1.39	10.25	1.027	0.345
Compound diesel[a]	Napier Nomad	Diesel fuel + auxiliary combustion + water injection	3970	1.59	11.70	0.959	0.340

[a] Figures based on total shp.
[b] 51% power, auto-lean mixture.

the extent of about 3½ times the amount actually required for combustion is therefore passed through the engine to provide temperature dilution.

When such an arrangement is associated with a piston engine to form a compound system such high excess air factors become unnecessary, for the reduction in gas temperatures is achieved by virtue of the work done in the piston-engine cylinders and the compressor and turbine dimensions for a given rate of fuel consumed are thereby greatly reduced.

The objection may be raised that the figures here quoted for expansion ratio and turbine inlet temperature in the turboprop engine are lower than some which are projected at the present time. Although this is appreciated it does not affect present considerations relative to the compound cycle, and in any case it will be seen later that most of the developments which permit improved performances of the turboprop are also of direct application to the compound engine.

The Compound Engine – In the compound engine the cycle of operations is shared between a 2-stroke diesel engine and a turbine, exhaust gases from the engine being fed into the turbine. The back pressure imposed by the turbine on the engine cylinders establishes the lower pressure level of the operating cycle in the cylinders and also determines the degree of supercharge necessary to pass the required quantity of air through the engine.

The approximate form of the overall indicator diagram resulting from this combination is shown in Fig. 5, the division of work between the engine and the turbine being indicated by the line ABC, the difference in pressures between points A and B being that which exists between the pressure in the cylinder at the moment of exhaust release and the pressure at inlet to the turbine.

Considering first the characteristics of this complete diagram, it may be said that due to the high degree of compression which takes place outside the engine cylinders it is possible to use an overall compression ratio considerably higher than in the normal diesel engine. Furthermore, the expansion line in the turbine extends down to atmospheric pressure, and the result of these two factors combined is to produce a very high value for the overall expansion ratio. The actual expansion ratio which determines the limiting thermal efficiency, however, is lower than this due to the losses which occur at transfer from the diesel engine to the turbine, and its value may be derived in the following way.

It will be seen that the overall diagram is compounded of two separate ones, first that for the diesel engine which is similar in form to that of Fig. 4B, and second that for the compressor-turbine combination which is similar to that of Fig. 4C. The expansion ratio for the diesel cycle is V/v, and that for the turbine V_1/v_1, so that the actual expansion ratio for the complete cycle is given by the product $(V/v) \times (V_1/v_1)$.

Within practical limits, for a given overall diagram the value of expansion ratio given by the product $(V/v) \times (V_1/v_1)$ and therefore the limiting thermal efficiency of the cycle does not change materially with the position of line ABC indicating the division of work between the diesel engine and the turbine.

But the division of work does exercise considerable influence on the dimensions and weight of the combined unit for a given maximum power, and the selection of the various design constants affecting this point is one of the major problems in the early stages of compound engine design. Some indications of the nature of this problem may be obtained from a consideration of the following points.

Clearly the compound engine is subject to the same practical limitations as apply to other engines, so that the maximum cylinder pressure and the maximum turbine inlet temperature are reasonably well-defined points determined by practice. If now the compound engine operated on an ideal air/fuel ratio and burned all its air, the temperature at point P would be about 4500 F, and corresponding temperatures at various points down the expansion line would be defined. The maximum height for point C on the expansion line would therefore be fixed by the permissible turbine inlet temperature, and this would also establish the supercharging pressure.

But it has been already pointed out that the diesel engine does not consume all the air supplied to it and, furthermore, that in the two-stroke cycle the excess air passed through the cylinders during the scavenging period can be controlled by porting design.

It is, therefore, possible to design the cycle so that the amount of excess air is a relatively high proportion of the total mass flow through the engine, in other words, to operate the engine on a higher overall air/fuel ratio. This excess air will mix with the exhaust gases and reduce their temperature, so that to achieve the same limiting temperature at inlet to the turbine it now becomes possible to raise the position of point C on the expansion line to a new position F, the division of work now being indicated by line DEF. But this adjustment to the cycle has also raised the supercharging pressure so that a greater quantity of air will be trapped in the engine cylinder, thus permitting more fuel to be burned and a greater mean indicated pressure to be developed, as shown by the dotted expansion line.

The thermal loadings in the engine cylinders will set a limit to the extent of this adjustment; but, as a practical point, it may be said that the passage of excess air through the cylinders not only gives ideal scavenging, it also provides a considerable degree of internal cooling, any resulting increase in its temperature being subsequently recovered in the turbine and therefore retained in the cycle. By exploiting this factor it is possible in the compound-

engine cylinder to achieve a rate of fuel burning which is much greater than in the normal diesel engine, with a corresponding reduction in the dimensions and weight of engine required for a given power. This, coupled with the reduced size of compressor and turbine required for a given rate of fuel burning, which has already been referred to in the section on The Gas Turbine, allows the size and specific weight of the compound powerplant to be reduced to values which, when coupled with its high thermal efficiency, render it more suitable than other powerplants for certain applications.

The determination of the appropriate division of work in any particular case, therefore, involves consideration of a range of different overall air/fuel ratios, each involving corresponding adjustments to the size and pressure ratio of the compressor and turbine and the dimensions of the engine cylinders derived from the thermal and mechanical loadings imposed. The lightest possible powerplant results when the best balance between these various factors is established in relation to the design targets.

Some characteristics of the compound engine as demonstrated by the Nomad are given in Table 1 to allow comparison with other types of engine.

Mechanical Arrangements for Compounding

For the purposes of this paper the compound engine is considered to consist of three major mechanical elements, first a 2-stroke diesel engine, second a gas turbine, and third a compressor. Investigators of compounding possibilities have sometimes proposed more complex arrangements involving a relative multiplicity of turbines, compressors, and heat exchangers, designed with the object of extracting maximum possible energy from the fuel burned. In practice it seems unlikely that such complexity would be justified, for the thermal and aerodynamic losses involved in the gas-transfer passages can exert serious influences on the actual results obtained. In any case, such arrangements are ruled out for aircraft purposes on the grounds of bulk and weight, and discussion is therefore limited to possible combinations of the three basic elements concerned. Of these components the piston engine and the turbine contribute to the total power output, but the compressor absorbs power and must be driven.

From the purely mechanical standpoint three possibilities exist and their applicability is considered.

1. *The compressor may be driven by the turbine – all output power being delivered by the piston engine (Fig. 6A).*

This arrangement constitutes in effect a 2-stroke diesel engine equipped with a turboblower. It demands that over the whole operating range the turbine must be in power equilibrium with the compressor. Such a condition is impossible to achieve in practice because, while at full power the turbine can produce power in excess of compressor requirements, at low outputs it cannot satisfy the compressor demands due to the small exhaust energy available from the engine. This arrangement is therefore not applicable.

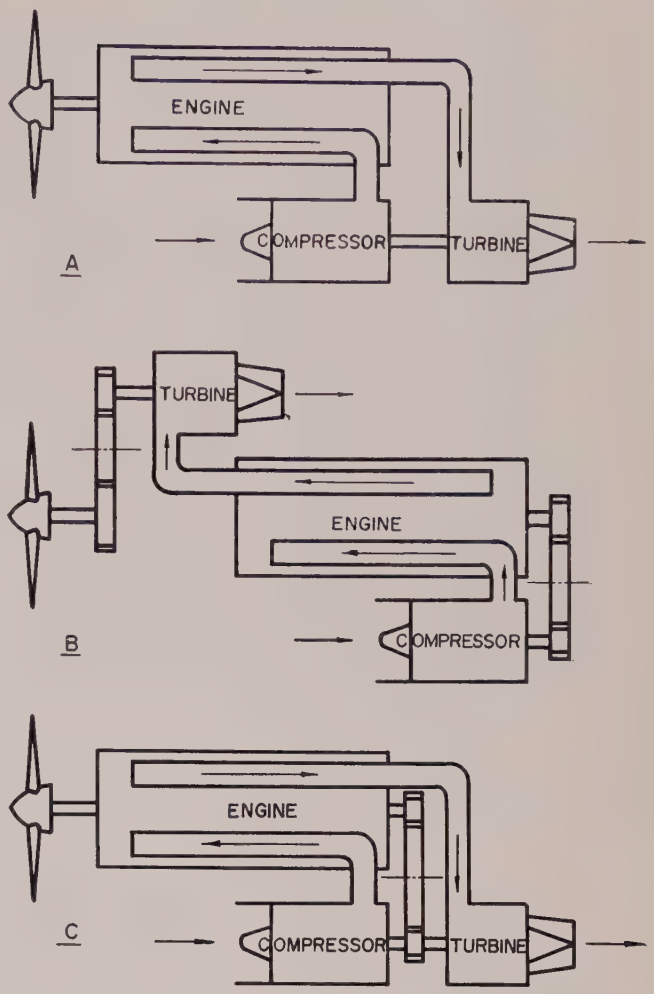

Fig. 6 – Mechanical arrangements for compounding

2. *The compressor may be driven by the piston engine – all output power being taken from the turbine (Fig. 6B).*

In this case the piston-engine-compressor combination operates purely as a gas generator for the turbine. Here the piston engine and compressor must remain in power equilibrium at all operating conditions, and the limitations arising from this requirement give rise to a number of disadvantages.

Firstly, at low power outputs the piston engine is prevented from making the contribution of which it is capable to the total power output, this resulting in very poor thermal efficiencies at part load conditions.

Secondly, due to the steep power law of the compressor against rpm the piston engine at cruising

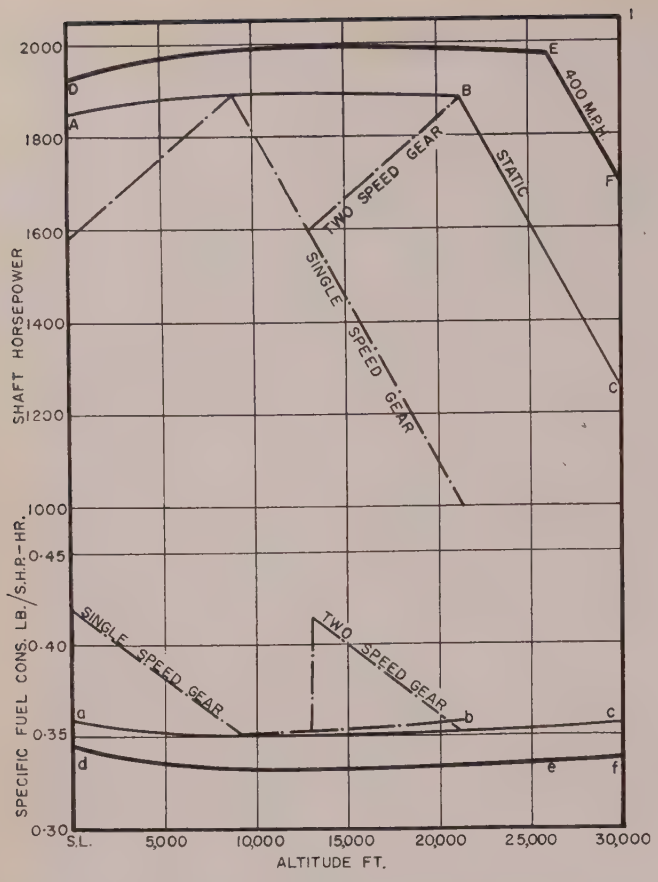

Fig. 7 – Altitude performance with fixed-gear and variable-gear superchargers

conditions requires operation at high piston speeds which results in greater wear and tear than necessary.

A further serious objection to this arrangement exists in relation to the powerplant weight, for it will be seen that two sets of high-ratio reduction gearing are required, one between the compressor and the engine crankshaft and the other between the turbine and the propeller shaft, and both of these are called on to transmit high powers.

3. *All three components may be coupled together to form a common mechanical system (Fig. 6C).*

In this system no requirement exists for power equilibrium between any two components, and this allows the greatest possible flexibility in the choice of operating conditions for best performances over the whole speed range. Furthermore, the lightest possible powerplant results for the compressor and turbine, which have sympathetic characteristics on a speed basis, can be connected solidly together, the reduction gearing connecting them into the engine system being called upon to transmit only the difference in the power produced by the turbine and that demanded by the compressor.

This is the basic mechanical system employed in the Nomad engine.

Altitude Performance – The powerplant layout suggested in Fig. 6C suffers from the defect common to all engines which depend upon a fixed-ratio gear-driven compressor in that its power falls off rapidly as altitude is increased, its power and fuel consumption curves for some part-load condition being of the form shown by the broken lines in Fig. 7. Some improvement may be obtained by the provision of a two-ratio gear between the engine and the turbocompressor set, in which case these results would be modified in the manner shown. A much more satisfying solution to the problem can be obtained if an "infinitely variable gear" is employed, in which case the power and consumption lines can be maintained at sensibly constant values over a wide range of altitudes, as shown by the full lines ABC and abc in the diagram. In fact, the employment of such a gear confers still greater benefits, for it permits the gear ratio at any flight condition to be adjusted to take full advantage of air intake "ram" resulting from forward speed so that at all times the compressor power absorption is kept to a minimum, thus enabling enhanced performances to be obtained, as shown by the lines DEF and def.

A further advantage of the variable gear is that it enables the compressor to be driven up to its maximum speed at any engine rpm, thus permitting greater maximum power altitudes to be achieved at low engine speeds.

Due to certain favorable factors which will be referred to later, it has been found possible to embody such an "infinitely variable gear" in the Nomad engine.

The Napier Nomad Engine

Having discussed briefly the basic problems involved in compounding, it is now possible to examine the practical solutions to these problems as demonstrated in the Napier Nomad and to consider the results obtained from this engine in relation to aircraft requirements.

Mechanical Details – The mechanical layout of the Nomad is shown in Fig. 8, and it will be seen that this follows the arrangement suggested in Fig. 6C, except that an "infinitely variable gear" has been interposed in the gear system between the turbocompressor set and the engine. This permits a range of gear ratios to be selected for any crankshaft speed.

The diesel engine has 12 cylinders in banks of six, horizontally opposed on a six-throw crankshaft, and the cylinder design is of the simplest possible 2-stroke type, using piston-controlled ports with no valve gear of any kind. The loop-scavenging system employed is that in which the incoming air is directed against the cylinder wall with an upward movement towards the combustion chamber, as shown in Fig. 9. This type of airflow not only gives effective scavenging of burned gases from the cylinder, but due to the well-organized flow path it permits high airflows with minimum aerodynamic losses.

The combustion chamber is hemispherical in

form with a centrally disposed injector having one central orifice and five equally spaced radial orifices, the only unusual feature being that the radial sprays are directed at the combustion-chamber walls, experience having proved this to be beneficial.

The injector pumps, which are in blocks of six, are of normal "jerk-pump" design, specially developed to deal with the high outputs and speeds of operation required.

The pistons, which are illustrated in Fig. 10, have Y-alloy bodies but are fitted with austenitic steel tops designed to run at temperatures in the center of the crown between 1100 and 1300 F at full power. Oil cooling is provided behind the piston rings to ensure minimum temperatures at this point.

The unidirectional loadings on the connecting rods resulting from two-stroke operation permit the use of an unusual design, as shown in Fig. 11, both small- and big-end bearings being of the half-bearing or "slipper" type, with light straps as safety devices in the reverse-loading direction.

A further development of this type of bearing is applied at the small end. On this bearing high loadings are experienced accompanied by low rubbing velocities, and due to the unidirectional loadings no separation of the surfaces occurs on a normal bearing to permit the ingress of lubricating oil.

On the Nomad this difficulty has been overcome in the manner illustrated in Fig. 12.

The bearing is divided lengthwise into three sections comprising two outer bearings "X" and a center bearing "Y." The outer bearings are coaxial with each other but their centers are displaced transversely from the centerline of the connecting rod. The axis of the center bearing is similarly displaced on the opposite side of the connecting-rod axis. The three bearings therefore constitute, in effect, two bearings eccentric to one another, their eccentricity being equally spaced about the axis of the connecting rod. In practice the distance between centers of these two bearings is only 0.035 in., but the operation of the arrangement can be best understood if this dimension is greatly exaggerated as shown in B, C, and D of the diagram, from which it will be seen that relief of loading and separation between the surfaces is obtained through the rocking of the connecting rod.

The axial compressor has 12 stages and operates at a maximum pressure ratio of 8.25/1 with an air mass flow of 13 lb per sec, and to extend the operat-

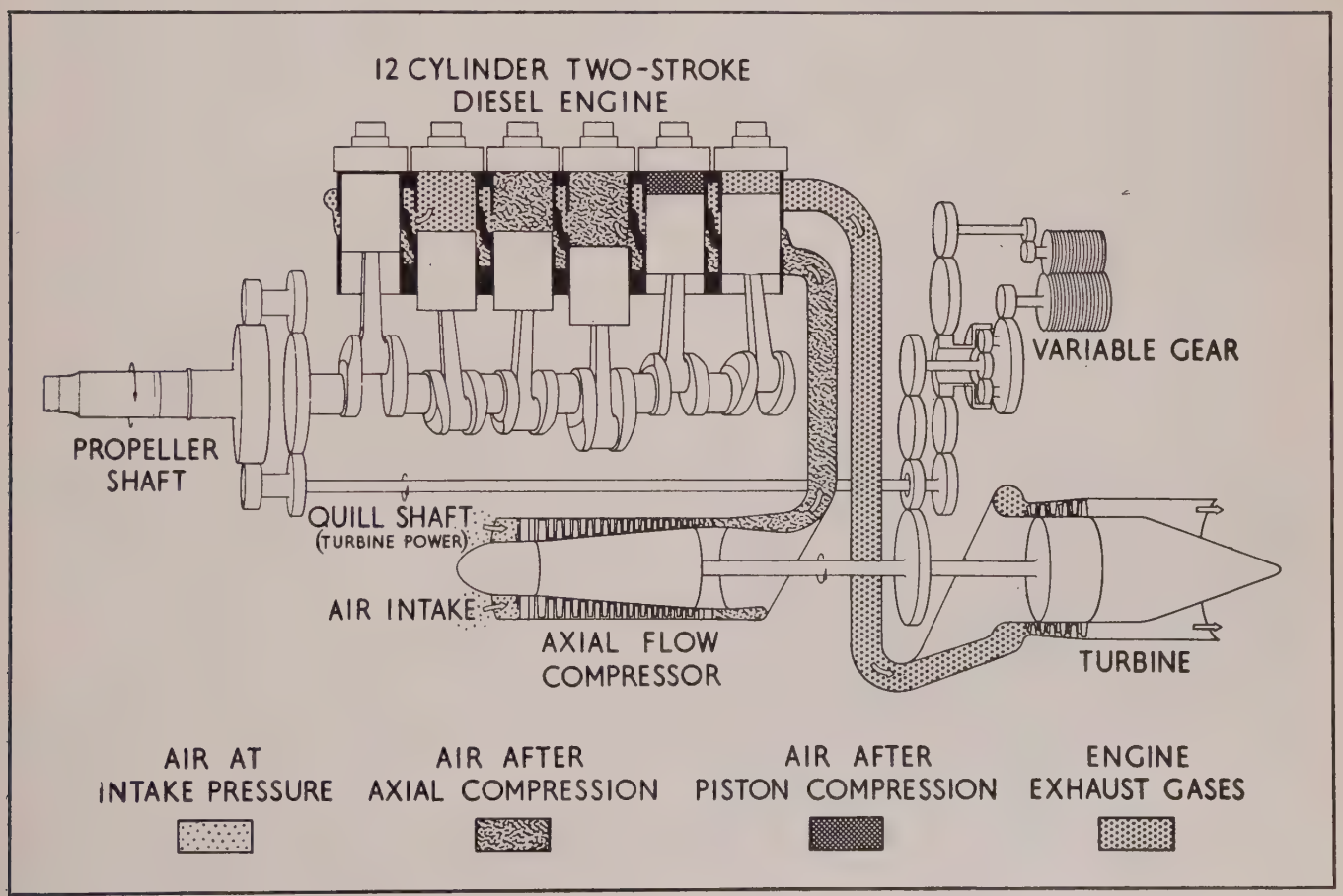

Fig. 8 – Diagram of Nomad engine

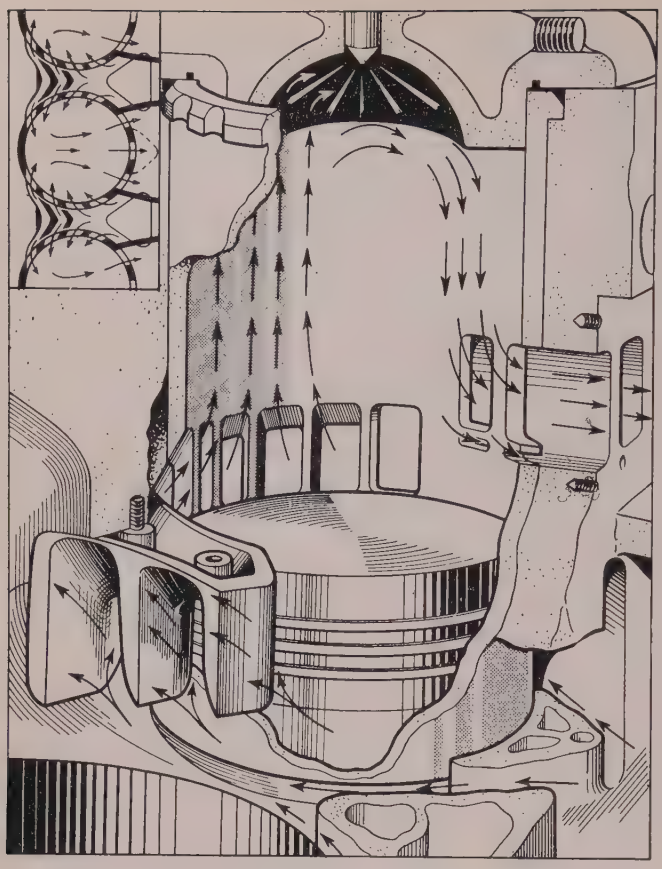

Fig. 9 – Arrangement of engine cylinder

ing range at low-speed end, adjustable inlet guide vanes are fitted.

The adiabatic efficiency of the compressor at take-off (sea-level static) is 85% and its peak efficiency 87.5%.

The three-stage turbine is mounted coaxially with the compressor, and its blading is designed to extract maximum energy from the gases, the residual jet thrusts being small. Its efficiency at take-off (sea-level static) is 84% and 86% at the altitude cruising rating.

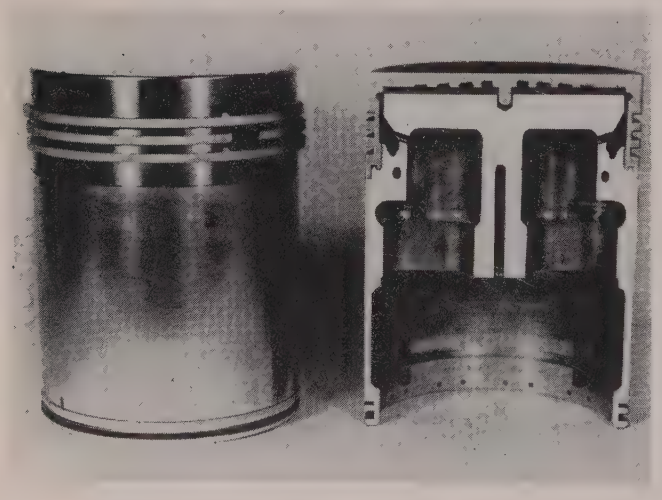

Fig. 10 – Arrangement of piston

Both compressor and turbine are connected into the rear gear casing by shafts having toothed couplings at each end to allow for expansion effects.

The Infinitely Variable Gear – This gear has been designed and developed by Napier to suit the particular requirements of the Nomad application, but the basic scheme was evolved by Dr. Joseph Beier and developed in Germany before the 1939-1945 war. It is an ingenious practical adaptation of the well-known scheme in which two conical members are end-loaded together, the gear ratio being varied by sliding one cone over the other. The actual details of the Beier version of this basic scheme are as shown in Fig. 13. Here a "pack" of discs with narrow conical rims are mounted on a central shaft and spring-loaded to trap between them a series of coned discs carried on a planetary shaft, which is arranged to swing about a fulcrum to obtain changes in gear ratio. By attaching a gear to the planetary shaft meshing with one at the fulcrum, it is possible to arrange a constant mesh gear system so that changes in gear ratio can be made while running. It will be clear that a number of planetary shafts can be similarly disposed around the center shaft, and in the Nomad three sets of planetary discs are used.

This type of gear would normally be classified as a "friction" device; but, in this particular application, the drag force between the discs is obtained by fluid shear of the oil film at the contact points, the end loads being adjusted in relation to the lubrication conditions to obtain the most efficient operation.

A great advantage of this device is that it transmits power through a multiplicity of contact points, the number of which can be varied experimentally to achieve most satisfactory performances.

To reduce the dimensions and weight of the variable gear to a minimum, it is connected into the gear system of the Nomad, as indicated in Fig. 14.

Here the speed-reducing gear for the turbocompressor set is of epicyclic form, the variable-speed device being connected across two members of the epicyclic train. This, in effect, produces two mechanical systems in parallel, only about 30% of the total power flow being transmitted through that part of the system in which the speed-varying device is fitted.

The arrangement of this complete system in the Nomad is shown in Fig. 15.

The Complete Engine – A longitudinal section through the engine is shown in Fig. 16, the layout following closely the diagrammatic arrangement of Fig. 8.

It will be observed that a torsional vibration damper of viscous-fluid type is attached to the free end of the crankshaft. This item is not necessary for any condition of normal operation but is provided to protect the engine in the event of one cylin-

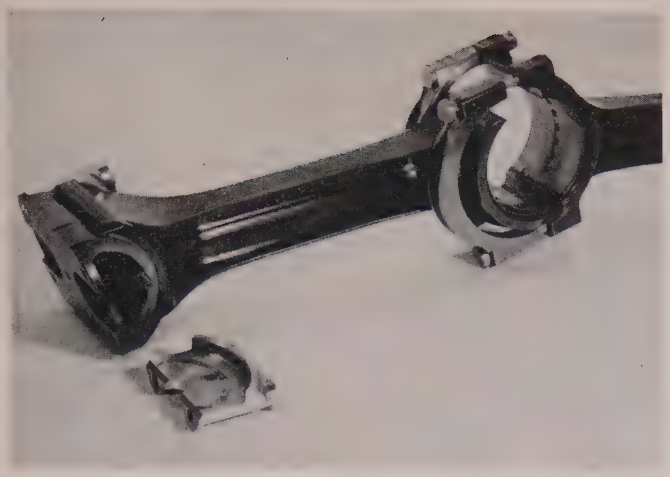

Fig. 11 – Arrangement of connecting rod

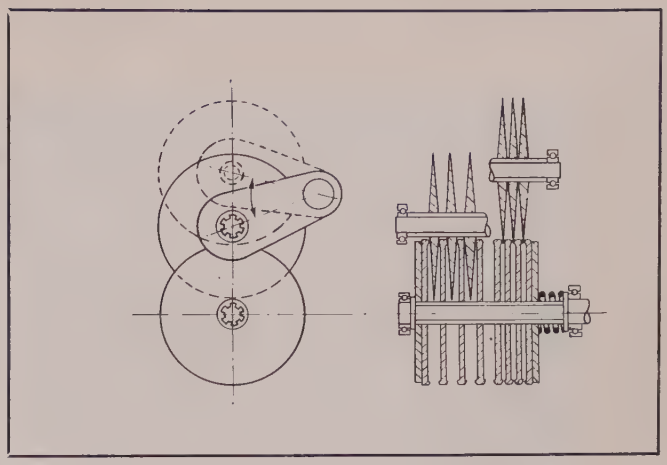

Fig. 13 – Diagram showing operation of variable gear

der "cutting out" due to seizure of a fuel injector pump.

Fig. 17 shows the engine in cross-section and indicates clearly the vertically divided magnesium crankcase and the aluminum cylinder blocks, the whole structure being bolted together by steel through-bolts. It will be seen that dry liners are employed, the liners themselves being of chromium-copper material chromium plated in the bores. The dimensions on this drawing show that the frontal area of the engine is small, in piston-engine terms, the shape being convenient for cowling purposes.

Fig. 18 shows a cutaway drawing from which the main features may be identified. The reduction gear is of conventional form using straight spur gears, two layshafts transmitting power from the engine crankshaft to the output gear, a further two providing the power connection between the output gear and the turbocompressor combination.

Fig. 19 is a photograph from one side and shows that the engine is suspended from four pickup points, two at the front end of the crankcase and two on the rear gear casing. This arrangement is convenient from the installation point of view and gives maximum accessibility, particularly to the compressor and turbine.

Starting is by electric motor, and as the compression ratio in the engine cylinders is insufficient to give self-ignition under these conditions, spark plugs are fitted in each cylinder head activated from a high energy system. These plugs are used only for starting.

A three-quarter front view is shown in Fig. 20.

Engine Operation and Control – The engine is equipped with a single lever control system which relates the variable factors together to produce a

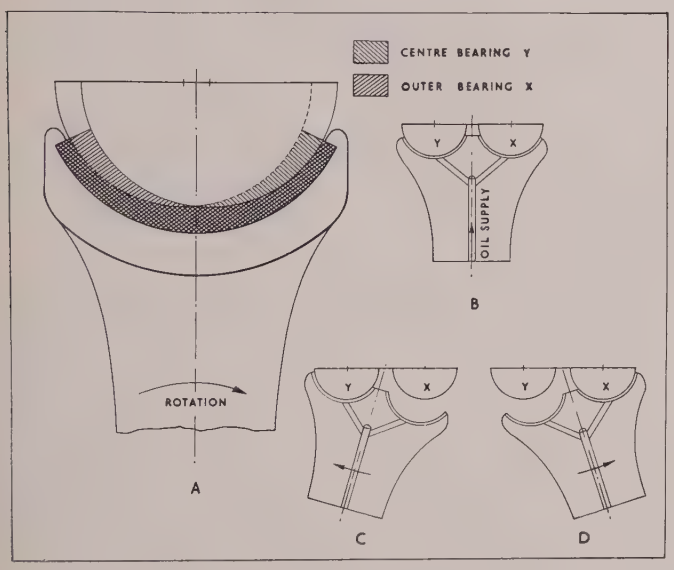

Fig. 12 – Connecting-rod small-end bearing

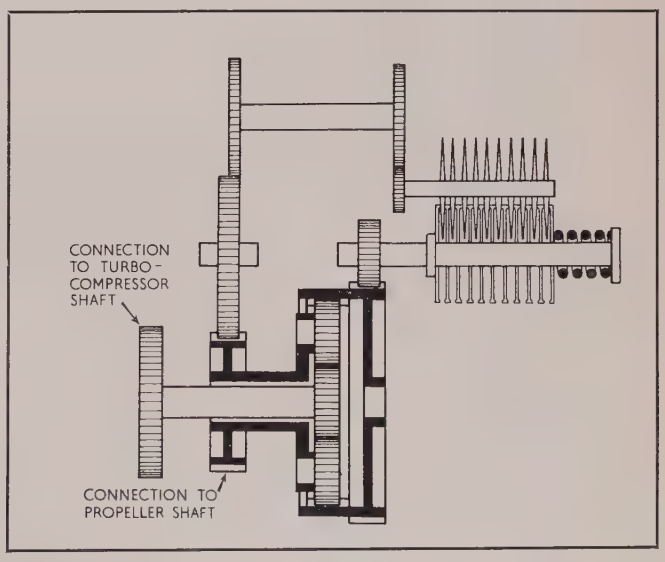

Fig. 14 – Connection of variable gear to epicyclic train

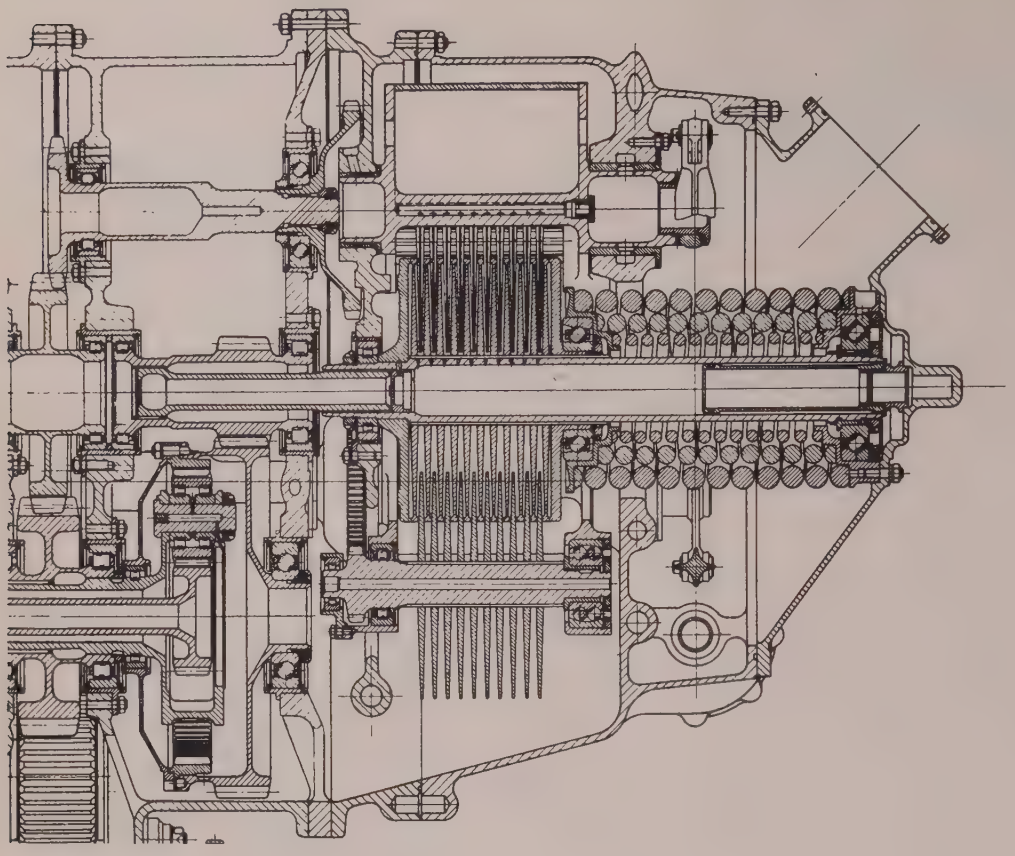

Fig. 15 – Variable gear as fitted to engine

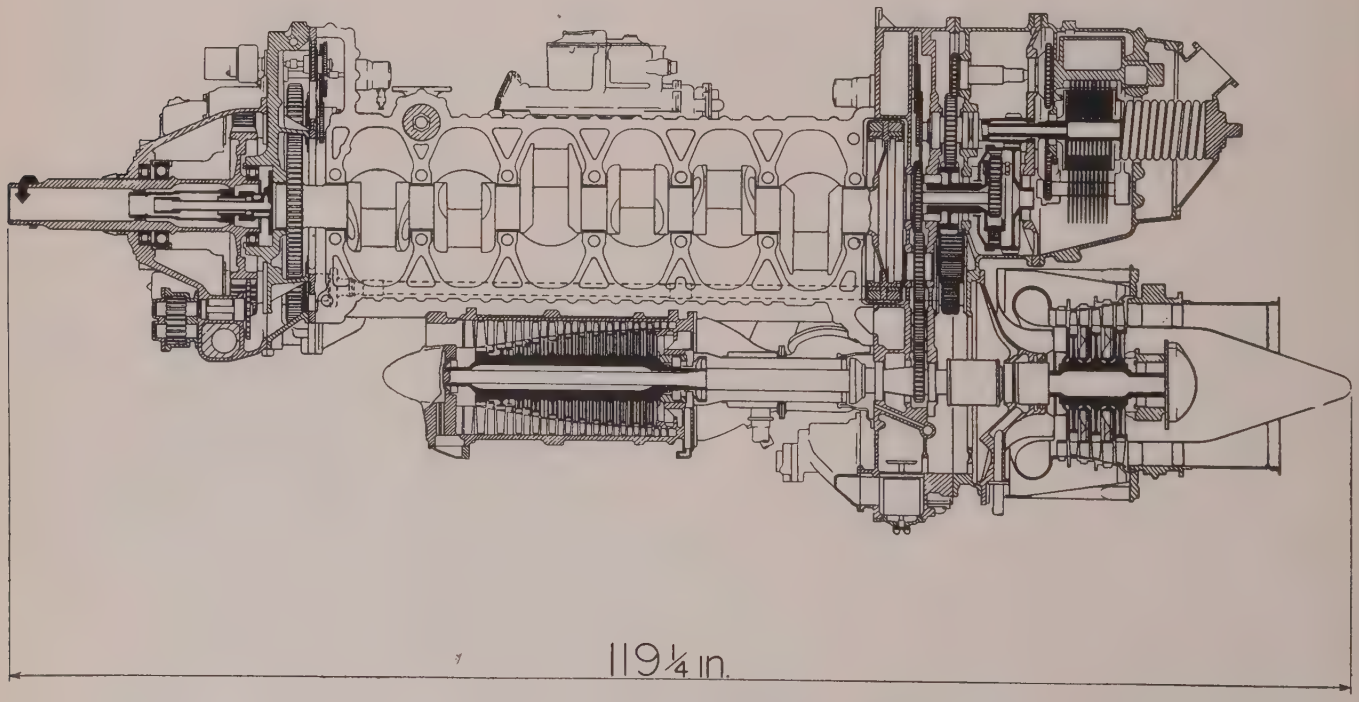

Fig. 16 – Longitudinal section of Nomad engine

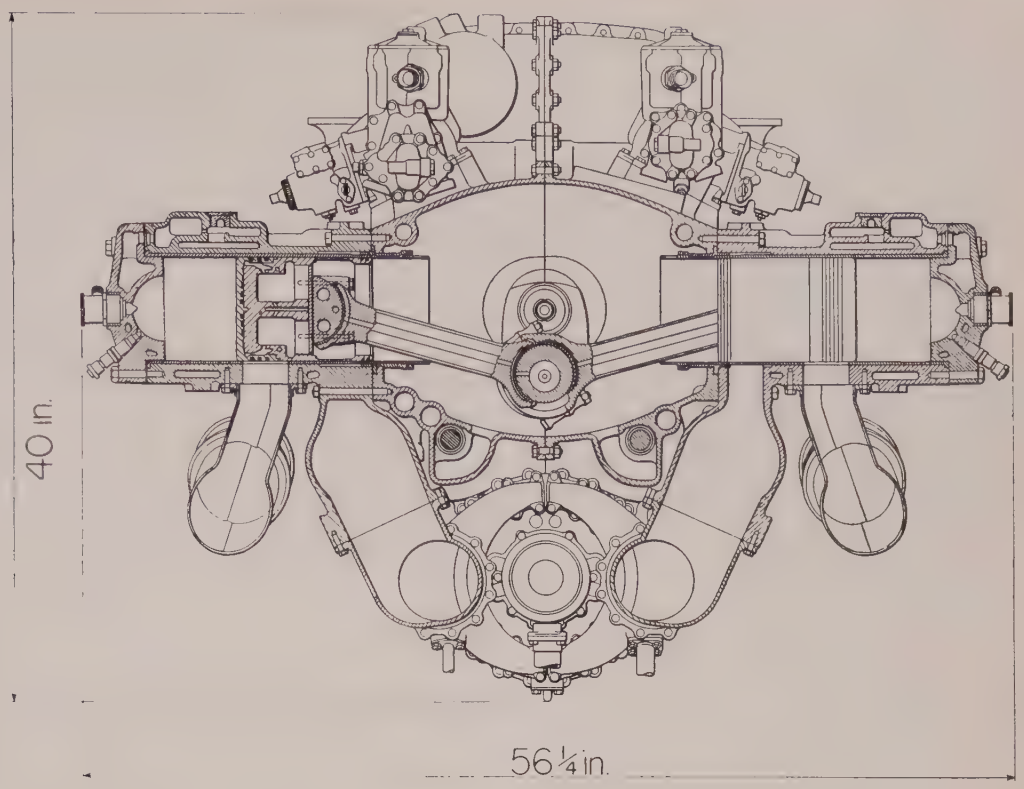

Fig. 17 – Cross-section of Nomad engine

predetermined power law against rpm. The speed function is controlled by a normal mechanically set constant-speed unit varying propeller pitch, each speed selection being mechanically related to a rack setting on the fuel pumps governing the fuel flow, and to a selected boost pressure. The boost pressure setting is applied to a normal type of variable-datum boost-control unit, the servo piston of which operates the setting of the infinitely variable gear, the ratio of which is thereby automatically adjusted to maintain the selected boost pressure. Any selected rpm, fuel flow, and boost pressure are in this way automatically maintained with increasing altitude until the maximum permitted rpm of the turbocompressor set is reached, this corresponding to the maximum power altitude for that particular engine condition. Above this point resetting mechanism is provided which reduces fuel flow in sympathy with decreasing boost. The engine is therefore capable of maintaining a constant selected boost and power with corresponding fuel consumptions over a wide range of altitudes which at 60% of take-off power extends from sea level up to 25,000 ft.

For optimum matching over the full power and altitude range of the engine, a variable-capacity compressor is necessary. This change in capacity is achieved by an automatic device which adjusts the incident angle of the compressor inlet guide vanes to a function of inlet pressure with a variable datum controlled by boost pressure.

Nomad Engine Performances

Brief reference was made in the section on The Compound Engine to some factors influencing the division of work between the diesel engine and the turbine. In the actual case this problem is more complex than was indicated, for there are other aspects of engine performance, such as altitude requirements and the fuel consumptions at part loads, which must also be considered. Taking all the design requirements into account and also taking advantage of considerable experimental data, the major operating factors used in the Nomad and the resulting performances are summarized in the following text.

Take-Off Performance of Basic Engine – The supercharging pressure used in the diesel engine for take-off is 89 psia, this corresponding to a volumetric compression ratio of 3.36/1. When this is multiplied by the actual compression ratio in the engine cylinders based on effective stroke (8/1) we arrive at an overall compression ratio of 27/1.

Allowing for air intake and ducting losses the

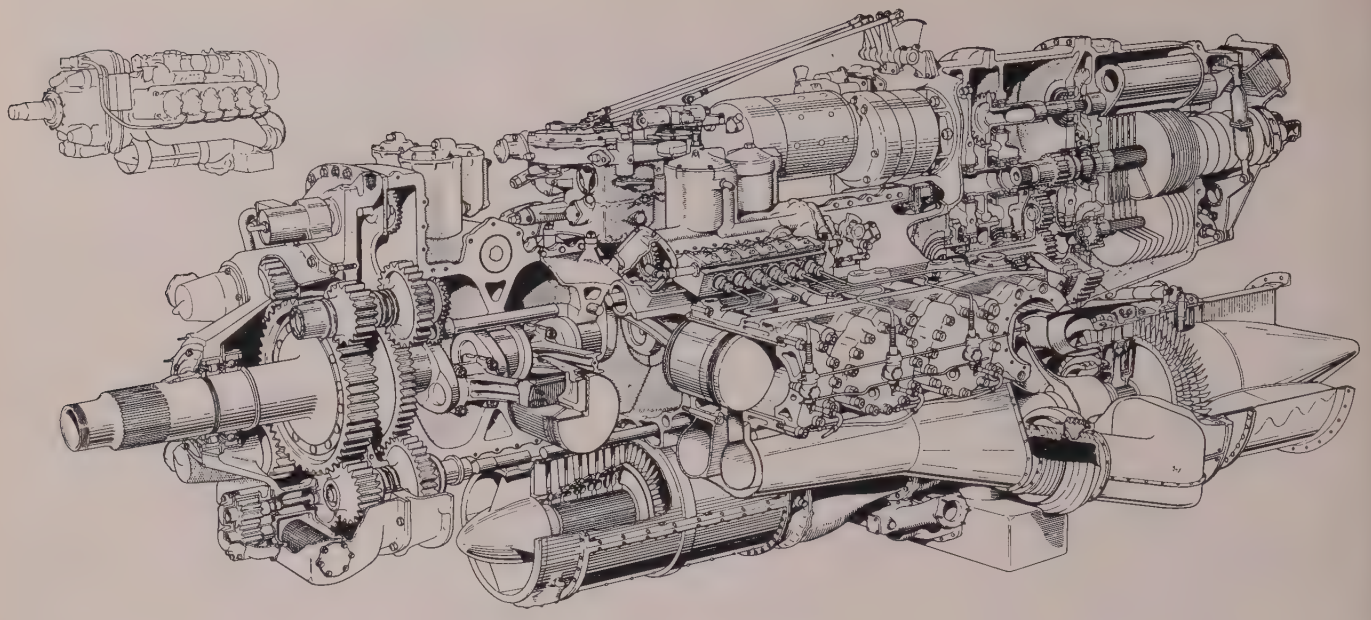

Fig. 18 – Cutaway view of engine

pressure ratio demanded from the compressor to provide the supercharging pressure of 89 psia at sea level is 6.28/1. The maximum pressure ratio of the compressor at its top speed is 8.25/1, and this permits the take-off boost to be maintained up to 7750 ft by variation in gear ratio.

The air/fuel ratio dictated by the cylinder performance requirements is 40/1, corresponding to an air mass flow of 13 lb per sec; and when operating with a maximum pressure limitation of 2200 psi a brake mean effective pressure of 205 psi is developed in the cylinders which have a bore of 6 in. and a total stroke of 7.375 in., giving a swept volume of 2502 cu in.

At the maximum crankshaft speed of 2050 rpm the piston speed is 2520 fpm, and the bhp developed by the diesel engine alone, neglecting any contribution from the turbine, is 2660, or 1.06 hp per cu in.

The ability of the engine to operate at such high outputs is an indication of the benefits derived from the excess air factor, for the recorded piston-ring temperatures at this power are no higher than those on a normal diesel engine developing less than half the power at equivalent piston speeds.

The pressure drop across the engine cylinders at take-off power is 13.0 psi, giving a turbine inlet pressure of 76 psia, and the temperature at the turbine inlet is 1222 F.

The pressure ratio across the turbine at sea level is 4.6/1, and this corresponds to a volumetric expansion ratio of 3.36/1 which when multiplied by the diesel expansion ratio of 8/1 gives an overall

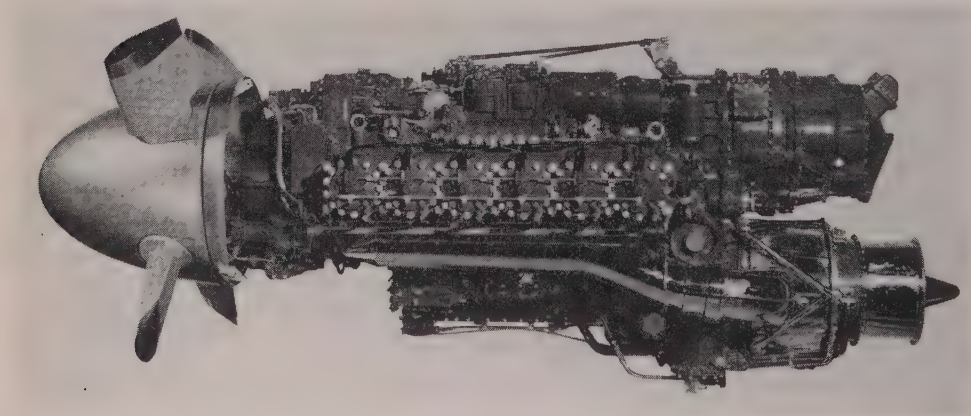

Fig. 19 – Side view of Nomad engine

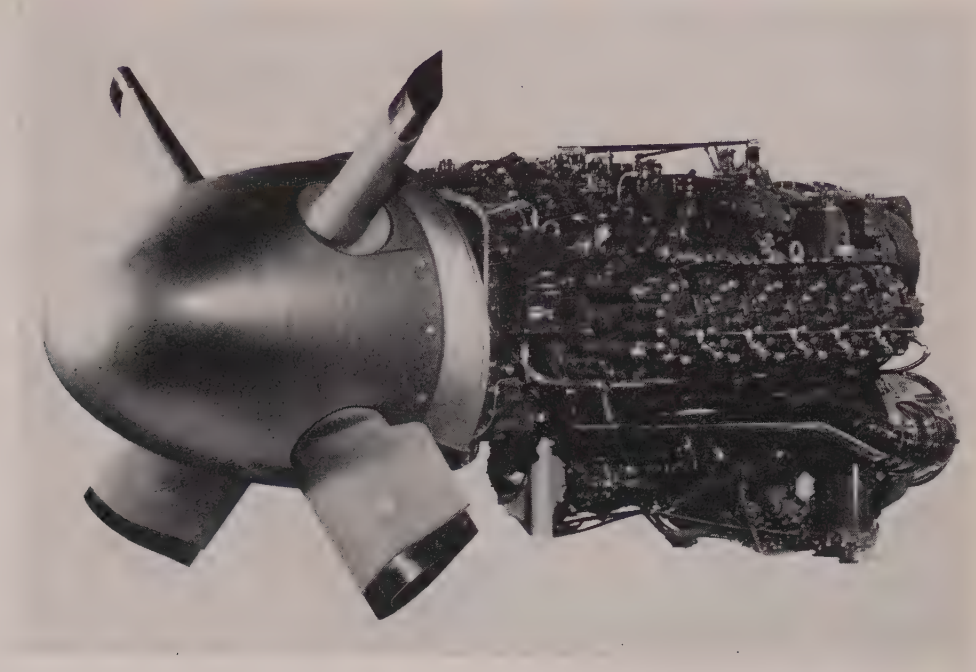

Fig. 20 – Three-quarter front view of Nomad engine

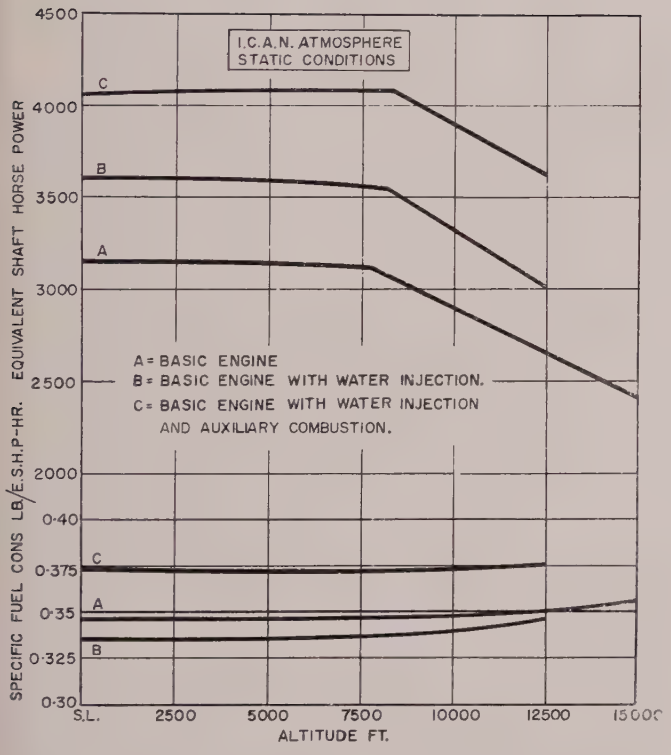

Fig. 21 – Take-off powers against altitude with fuel consumption

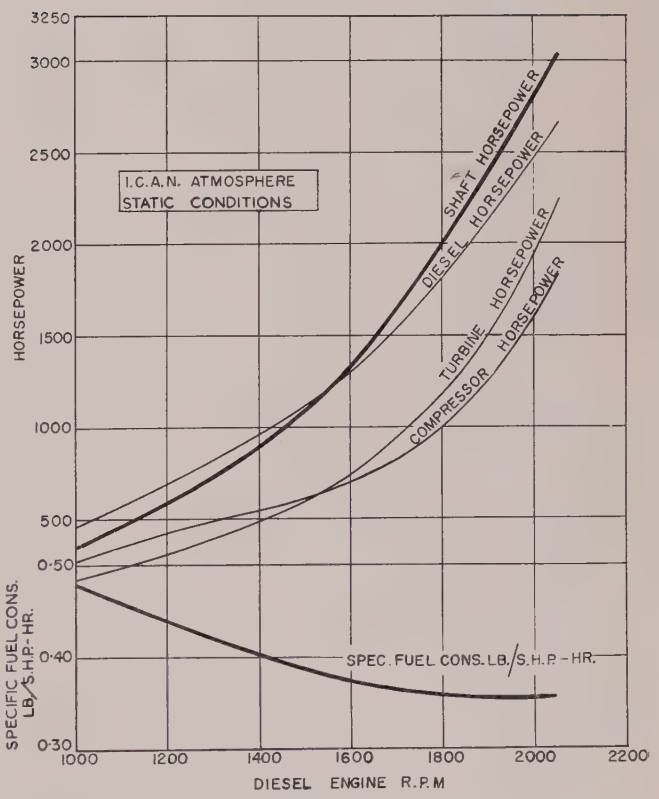

Fig. 22 – Sea-level static interconnection power curve

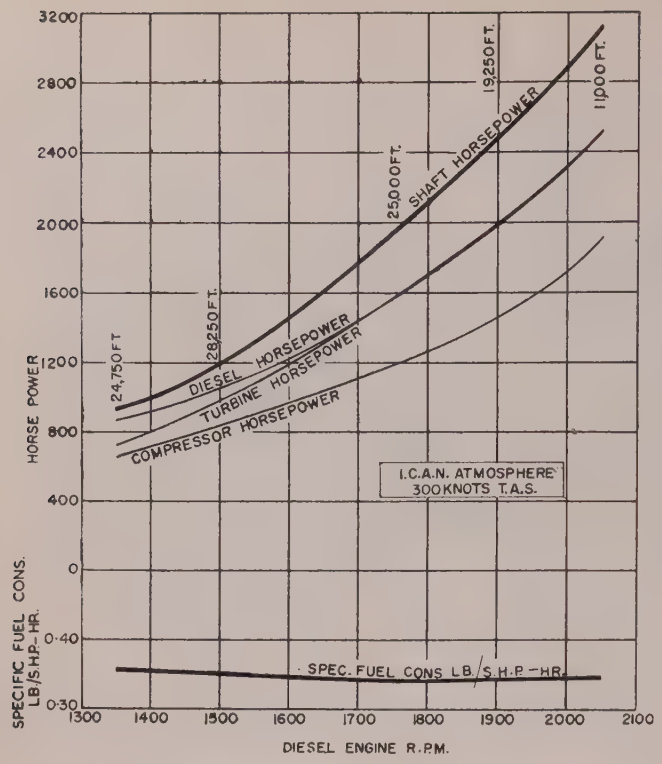

Fig. 23 – Altitude interconnection power curve

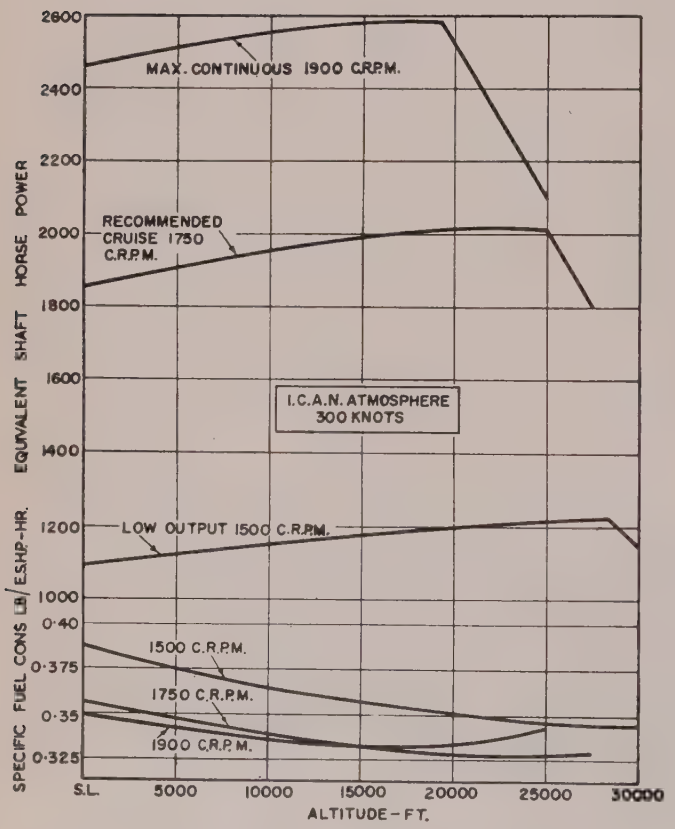

Fig. 24 – Altitude cruising curves with fuel consumptions

expansion ratio of 27/1.

The power developed by the turbine at sea level is 2250 hp of which 1840 hp is absorbed in driving the compressor, so that there is an excess of 410 hp, less a slight power loss of about 20 hp in the variable gear, as an addition to the diesel-engine output. The equivalent horsepower developed by the engine, taking into account the small amount of jet thrust available, becomes 3135 hp or 1.25 hp per cu in.

The net dry weight of the engine is 3580 lb, so that the specific weight is 1.175 lb per hp.

The specific fuel consumption based on the equivalent power is 0.345 lb per ehp per hr.

Take-Off Performance with Water Injection – With the high degree of supercharge used for take-off the charge air temperature is high, about 477 F at sea level. This could be reduced by aftercooling, but this would involve additional bulk and weight together with a serious loss of energy from the cycle. The charge temperature can be reduced most conveniently and its density increased without energy loss by the injection of water into the inlet manifolds, and when this is done a greater quantity of air can be packed into the engine cylinders and the power output still further increased. Using water injection in this way, the equivalent power of the engine is increased to 3580 hp (1.43 hp per cu in.) and the specific weight is reduced to 1.0 lb per hp. The specific fuel consumption is also reduced to 0.336 lb per ehp per hr.

Take-Off Performance with Auxiliary Combustion – A further possibility for increasing the maximum power output arises from the presence of excess air in the exhaust manifold between the engine and the turbine, for, at the expense of a slight increase in the turbine inlet temperature, a small quantity of additional fuel can be injected and burned at this point. This extra fuel is burned at low expansion ratio and therefore at low efficiency, but the effect on the overall specific consumption is small.

This system of auxiliary combustion can be used in association with water injection, and for a turbine inlet temperature of 1377 F the take-off power can be increased to 4100 hp (1.64 hp per cu in.), the specific weight being thereby reduced to 0.93 lb per ehp. The specific fuel consumption in this case is increased to 0.374 lb per ehp per hr.

The take-off performances against altitude for the three conditions referred to are illustrated in Fig. 21.

Cruising Performances at Altitude – The power law to which the engine is controlled over the speed range under sea-level static conditions is shown in Fig. 22, the shape of this curve being devised to maintain optimum thermal efficiency and altitude performance over as wide a range as possible and also to suit control requirement of the propeller.

On the same diagram are shown also the corresponding diesel, turbine, and compressor powers,

and it will be observed that at 1500 rpm the turbine power exactly balances that absorbed by the compressor. At lower engine speeds the power developed by the turbine is below that demanded by the compressor, and this power deficiency has to be fed in from the diesel engine.

The engine rpm at which balance occurs between the turbine and compressor powers varies with altitude and forward speed, but over the useful cruising range the power transmitted through the infinitely variable gear is relatively small.

From the section on Engine Operation and Control it will be clear that as altitude is increased with the engine operating at any point on the interconnection curve, the boost pressure appropriate to that condition will be maintained by progressive adjustment of gear ratio until the limiting rpm of the turbocompressor set is reached, this representing the maximum power altitude for that particular operating condition. Bearing in mind the reduction in compressor work necessary to achieve the selected boost pressure due to forward speed and the improvements in compressor and turbine efficiency derived from increasing altitude, there results a continuous increase in power output until maximum power altitude is reached, with corresponding reductions in specific fuel consumption.

The power interconnection curve extended up to the maximum power altitudes at each value of rpm with a forward speed of 300 knots and the corresponding component powers are shown in Fig. 23. It will be observed that over the whole operating range at these conditions the specific fuel consumption remains sensibly constant between 0.34 and 0.36 lb per shp per hr.

Fig. 24 shows performances at varying altitudes with selected engine ratings, and again the constant values for both power and fuel consumptions are worthy of note. The best fuel economy of 0.326 lb per ehp per hr is achieved at the recommended cruising rating at 22,250 ft where a power of 2027 ehp is developed.

A complete heat balance for this operating point is depicted in Fig. 25, and from this it will be seen that a brake thermal efficiency of 42% is obtained, which is higher than that of any other aircraft engine.

Engine Weights – It is customary to compare weights of engines on the basis of the weight per horsepower produced under maximum power conditions.

This method of comparison is valid for some purposes but does not provide an accurate indication of the effects of the engine weight in flight for it fails to take into account the varying altitude performances of which the engines are capable.

This point is of importance in comparing the Nomad with other types of engine, for its ability to maintain constant power over a wide band of altitudes has the effect of reducing its effective specific weight under operating conditions.

In Fig. 26 a comparison is shown between the

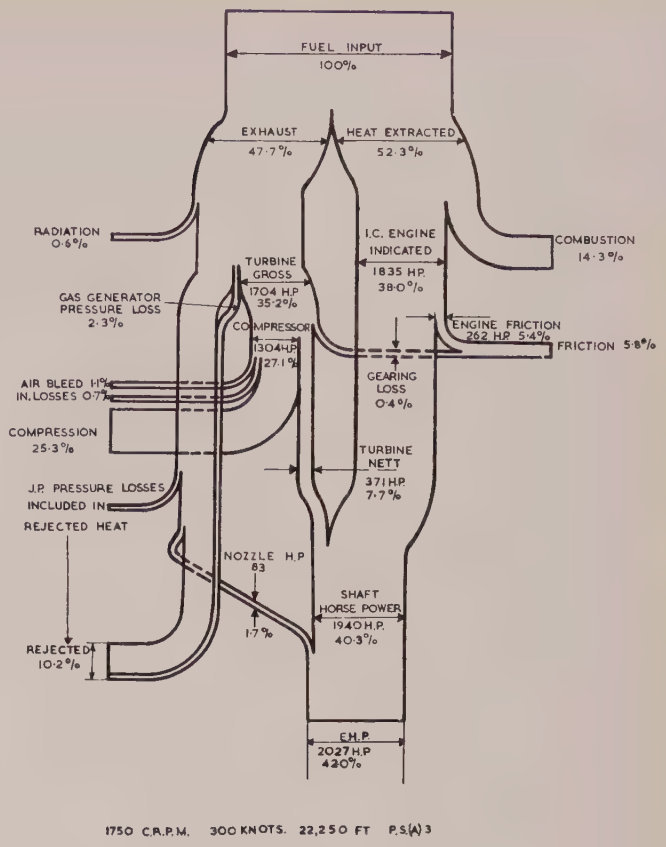

Fig. 25 – Heat balance diagram

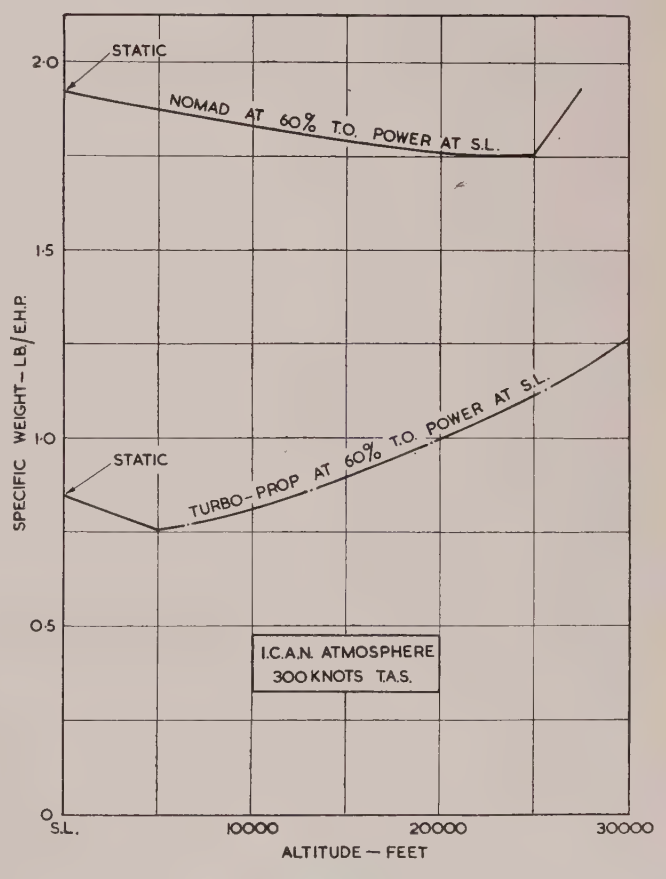

Fig. 26 – Specific weights at altitude

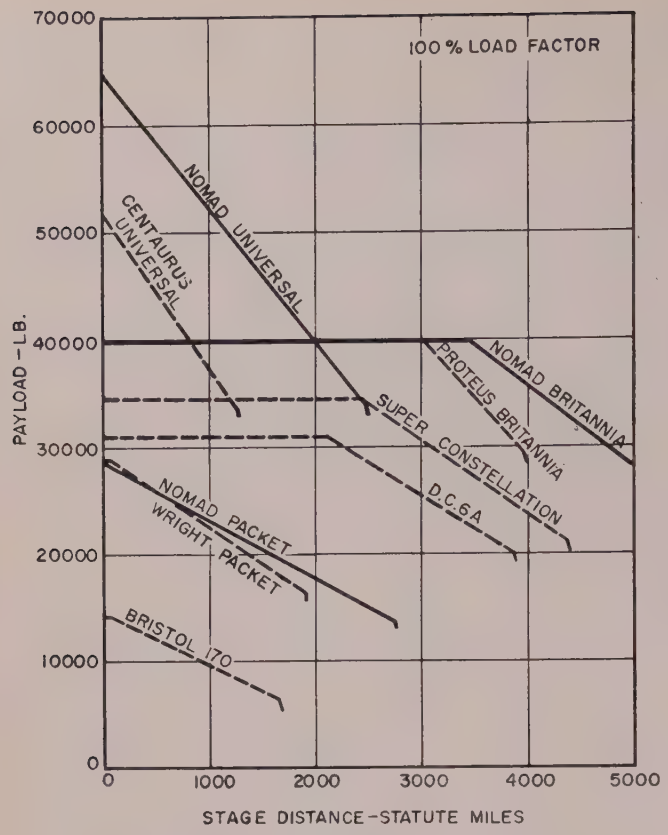

Fig. 27 – Variation in payload with stage distance

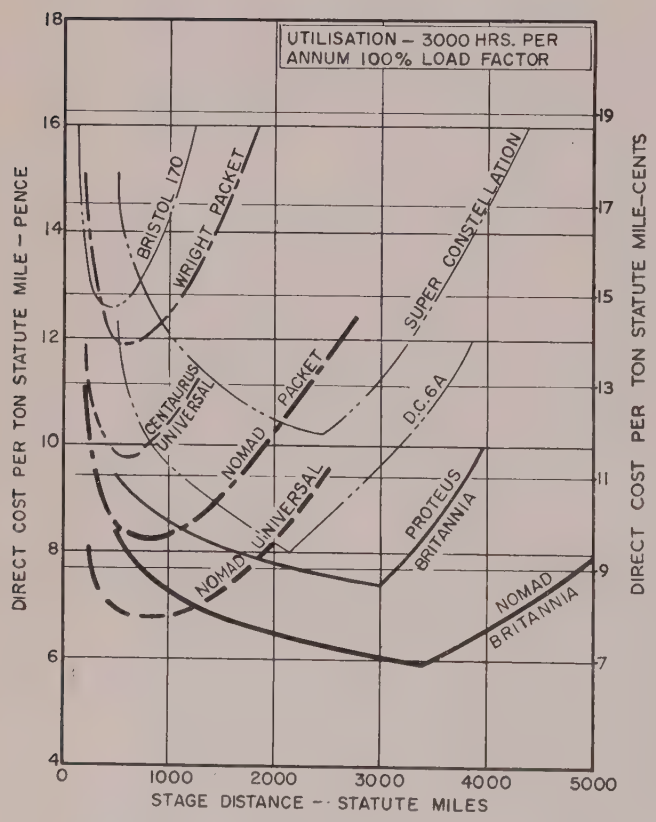

Fig. 28 – Improvement in operating costs per long ton-mile

specific weights under altitude power conditions between the Nomad with a specific weight of 1.17 lb per hp at take-off power and a turboprop engine weighing 0.5 lb per hp at take-off power. Both engines are considered to deliver a cruising power under sea-level static conditions of 60% of the take-off power, this increasing the specific weight figures to 1.9 and 0.83 lb per hp, respectively.

Due to the shapes of the power curves of the two engines against altitude the Nomad specific weight is reduced right up to the critical altitude, whereas the turboprop specific weight increases steadily as altitude is increased.

The difference between the two engines is therefore much less at 25,000 ft than at sea level. This factor must therefore be taken into account when aircraft performance comparisons are made.

General Characteristics – Apart from the performance figures which have been quoted there are two further characteristics which arise from the nature of the operating cycle and which assume some importance.

Firstly, there is extreme adaptability in the matter of fuels. Designed to run on diesel fuel for maximum economy, the engine will operate equally well on kerosene or wide-cut gasoline.

Secondly, the engine is insensitive to increases in ambient temperature, losing less than 2% of its take-off power for each 20 F increase in temperature.

Nomad Engine in Modern Aviation

Consideration of the performance figures which have been quoted demonstrates that the outstanding characteristics of the Nomad engine are its low fuel consumptions, which are maintained unimpaired over a wide range of powers, altitudes, and flight speeds, and its ability to use cheap fuels.

These two factors combine to provide great economy in operation; but apart from this the smaller quantity of fuel consumed, as compared with other engines for a flight of given duration, reduces the proportion of all-up weight of the aircraft absorbed by fuel storage, thus enabling the useful payload to be increased. Alternatively, the original payload may be flown over a greater distance.

There are specific aircraft applications in which these characteristics can display very definite operational advantages over other types of powerplant, and it is necessary to consider these in two categories, those applied to military purposes and those for civil use.

In the military field economy of operation is a secondary consideration; it is the ability to perform a defined operation more effectively which assumes greater importance. On this basis the Nomad engine constitutes the most suitable powerplant for maritime reconnaissance aircraft, which have to undertake prolonged periods of search at low altitudes and low flight speeds at considerable distances from base. Here the long-range propen-

sities of the engine, coupled with the ability to employ any desired type of flight plan without significant change in the quantity of fuel consumed, enable maximum effectiveness of the military operation to be achieved with minimum total duration of flight.

A further military application in which the Nomad shows to advantage is in the tactical role of army support. In such cases the necessity for large apertures in the fuselage for troop and supply dropping makes pressurization difficult, if not impossible, and the ability to carry maximum payloads at altitudes below that at which pressurization becomes necessary is one which is derived directly from the operating characteristics of the engine.

It is in the civil field, however, and particularly in air freighting operations, that the Nomad can make its biggest contribution to aviation at the present time; and it was, in fact, for this purpose that the engine design was originally undertaken.

There can be little doubt that the greatest opportunity for expansion in the aviation industry in the immediate future lies in the development of air freighting services; there are tremendous potential markets in this field which are almost entirely unexplored, even in the United States where more progress has been made than elsewhere.

For freighting purposes economy is the vital factor, and it seems certain that satisfactory operating economy will be achieved only by aircraft designed primarily for freighting. The development of such aircraft is of vital economic importance at the present time, not only in relation to the business which can result from expansion in freighting activities, but also in potential sales of the aircraft concerned. There exist already two such British aircraft which are of noteworthy performance in this particular field, the Bristol Britannia for the longer ranges and the Blackburn Universal Freighter for the shorter routes.

With the cooperation of the aircraft companies concerned, design studies have been made by Napier to assess the effects on operating characteristics of these aircraft if the engines now fitted were replaced by Nomads. In addition, to cater for cases in which the volume of traffic would not justify the use of such large aircraft, a similar study was undertaken relative to a civil version of the Fairchild Packet.

The results of these studies are shown in Figs. 27 and 28. It is not possible here to describe in detail the methods by which these curves have been derived; it must suffice to state that they are based on the standard SBAC method of computation; but the fuel costs which have been used are given in Table 2, being average world prices excluding the United States.

For comparative purposes the characteristics of three other well-known aircraft, the Bristol 170 Freighter, the Lockheed Super-Constellation, and the Douglas DC-6A with their existing engines are also shown on the curves.

Table 2 – Fuel Costs

Aircraft	Engines	Fuel	Fuel Cost per Imperial Gallon	Fuel Cost converted to Cents[a]
Bristol Britannia	Proteus	Aviation turbine fuel	1/10	25.7
Blackburn Universal	Centaurus	Gasoline 100/130 grade	2/7¼	36.5
Fairchild Packet	Wright compound	Gasoline 115/145 grade	2/9	38.5
All three aircraft	Nomad	Diesel fuel	1/8	23.3

[a] Assuming $2.80 per £ sterling.

Fig. 27 shows the change in payload resulting from the fitting of Nomad engines, and Fig. 28 shows the improvement in direct operating costs per British ton-mile.

Examination of these results indicates in no uncertain manner the contribution which the Nomad engine can make to the problem of economical freighting over short or long ranges of flight.

Acknowledgments

The authors wish to express their thanks to the Board of Directors of D. Napier & Son, Ltd. for permission to publish this paper and to the Bristol Aeroplane Co., Ltd. and Blackburn and General Aircraft, Ltd. for their agreement to display the results shown in Figs. 27 and 28. They are also grateful to their colleagues at Napier, who gave assistance in the preparation of the paper.

DISCUSSION

Discusses Advantages of High-Pressure Turbocharging

– Rudolph Birmann
De Laval Steam Turbine Co.

THE individual components of the Nomad engine – that is, the loop-scavenging 2-stroke engine, the low-pressure turbine-driven compressor, and the variable-ratio turbine speed reduction gear – are outstanding developments for which the designers and the manufacturer deserve a great deal of credit. The integration of these three components into a successful aircraft powerplant represents an even greater accomplishment.

The performance figures given in the paper speak for themselves, actually proving that a compound engine of this type can have a definite place in the field of aircraft propulsion, primarily because of its extraordinarily low fuel consumption and its excellent power/weight ratio. The fuel

consumption achieved is far lower than can be expected from the pure gas turbine for many years to come and lower than is possible with the piston type of engine alone. This achievement is made possible by compounding the piston engine with a turbo machine in such a manner that the reciprocating engine handles the high-pressure, high-temperature end of both compression and expansion and the turbo machine handles the low-pressure end. Such compounding takes advantage of the fact that the piston type of engine is the more suitable to cope with high pressures and high temperatures, whereas the turbo machine has a distinct weight, size, and performance advantage in the low-pressure range where the temperatures are comparatively moderate.

Because of the advantages to be derived from compounding the piston engine with the turbo machine, the compound engine has a promising future in the field of aircraft propulsion, and in the form of high-pressure turbocharging compounding it has already gone a long way toward keeping the reciprocating internal-combustion engine competitive with other prime movers in the fields of stationary, marine, and locomotive powerplants.

In all fields of application the future of the compound engine is assured; however, this is only if the engine layout is made as simple as possible to permit the attainment of best possible reliability and low production and maintenance cost. From this point of view it seems regrettable that the Nomad engine is perhaps more complicated than it need be. To reap the advantages of compounding it is not necessary to connect mechanically the exhaust-turbine-driven compressor to the engine crankshaft by means of a variable-ratio reduction gear. The much simpler alternative – that of all output power being delivered by the piston engine – could easily give equally good or even better results, but it is passed over by the authors with the statement that in practice it is impossible to achieve power equilibrium between compressor and turbine over the whole operating range. In reality there are an impressive number of turbocharged two-cycle marine engines in service, which contradicts the authors' misgivings regarding this much simpler compounding arrangement. The high-pressure turbocharging of diesel engines (employing compressor pressure ratios of 3/1) is rapidly coming into use, and judging from experience with heavy-duty stationary engines there is no reason why a similar compound arrangement of an even higher-pressure-ratio turbocharger and a reciprocating engine could not be evolved for aircraft application. As a matter of fact, the development of the Nomad engine has solved the most difficult problems involved – namely, the development of an exhaust-turbine-driven compressor capable of a combined efficiency of over 72% and suitable to produce a compressor pressure ratio of 8.25/1, and the development of a two-stroke engine designed to operate with inlet manifold pressures of 89.0 psia.

It is somewhat puzzling why, after having developed such outstanding components, these components were not combined in a simple, high-pressure-turbocharged engine – in other words, why the development of the Nomad engine was made much more difficult by the introduction of the complicated mechanical connection between the low-pressure turbo machinery and the high-pressure reciprocating engine. This question is justified in view of the outstanding performance already achieved by high-pressure turbocharger-engine combinations. Fuel consumptions as low as 0.306 lb per bhp per hr have been recorded, even though none of the test installations had the advantage of the high pressure ratios and high combined efficiencies of the Nomad turbocompressor. Turbocharged two-stroke engines, in which the turbocharger constitutes the sole source of air supply to the engine and has no mechanical connection of any kind thereto, are in everyday service.

It would be interesting to speculate on what the results would be if the reciprocating and turbo components of the Nomad engine were combined into a straightforward, high-pressure-turbocharged engine, in which the precompressed air was cooled in an intercooler. In such an arrangement the complicated variable-ratio reduction gearing (presently connecting the turbine to the engine crankshaft) would be eliminated and replaced by a simple intercooler. It should be brought out at this point that intercooling would not constitute a serious loss of energy from the cycle, as the authors indicate in the section on Take-Off Performance with Water Injection. As a matter of fact, the great merit of intercooling lies in the reduction of the negative work required for the compression in the engine cylinders – a reduction that can easily amount to much more than the 371 turbine horsepower which is delivered to the engine crankshaft through the reduction gearing. This reduction in the work of compression is the underlying reason for the sensitivity of the thermal efficiency of the diesel cycle to the charge temperature at the beginning of the compression stroke – the lower this temperature, the higher the thermal efficiency.

Straightforward turbocharging, with intercooling, maintaining the present pressure levels employed in the Napier Nomad engine and the turbine and compressor performance presently obtained, would result in numerous advantages over the present Nomad powerplant. It is estimated – on the basis of experience with high-pressure turbocharging of both 2- and 4-stroke engines – that these advantages would be as follows:

1. The entire engine layout would be more simple, correspondingly more reliable, lighter, and cheaper to manufacture.

2. The relationship of turbocharger and engine would not be dictated by considerations of the reduction gear, and the turbocharger could be so located that less frontal area and a more desirable configuration of the engine nacelle would be achieved, and perhaps even provisions for the recovery of pulsating exhaust energy could be accommodated.

3. The turbocharger, in lieu of producing net brake horsepower output, would produce a higher differential between intake and exhaust manifold pressures. This higher pressure differential would make it possible to pass the same amount of scavenging airflow through ports having a smaller area. In other words, the excessive height (63% of the stroke) of the intake and exhaust ports in the Nomad engine could be reduced and the ratio of effective stroke to total stroke made more favorable, thereby resulting in increased engine output and a better engine performance.

4. For the same net total output the thermal loading of the engine would be lowered by bringing about a lowering of the entire internal temperature level in the cylinders; and alternately, for the same thermal loading of the engine, the total output of the engine would be substantially increased.

5. Because of the reduction of the thermal loading (which can be brought about if the total output of the engine is maintained the same), the size, weight, and drag of the cooling radiator would be reduced sufficiently to make up for the weight and drag of the intercooler.

6. For the same total output, the specific fuel consumption would be reduced, probably to less than 0.3 lb per bhp per hr.

The authors deserve unstinted praise and congratulations for successfully going far beyond any previous development of compounding the reciprocating engine with the turbo machine. They are to be particularly commended for their pioneering work in selecting an extraordinarily high pressure level for the thermodynamic division between these

two types of machinery, thereby pointing the way toward further development in high-pressure turbocharging of all types of internal-combustion engines.

Describes Double-Slipper Connecting-Rod Design

– Gregory Flynn, Jr.
Research Laboratories Division, GMC

THE Napier Nomad diesel engine is obviously a most interesting design and represents a remarkable engineering achievement. The paper certainly should prove stimulating to engine designers.

As one who is concerned primarily with the diesel engine I am carefully going to sidestep getting into any arguments between the turbojet, turboprop, and reciprocating-engine airplane drivers. Instead, I would like to confine my remarks to that part of the paper concerning the mechanical features of the diesel engine itself, which I found most interesting.

I have a few questions and some comments to make on various parts which perhaps would best be handled in the order in which they appear in the paper.

1. To accomplish the objectives of Napier as stated in the paper, the highly supercharged, compounded, 2-stroke diesel was, I believe, a wise choice. The compression ratios, pressures, and efficiencies are reminiscent of the work currently being done in France with the Pescara cycle which also uses a highly supercharged 2-stroke cylinder and a gas turbine.

2. The elimination of valve gear is always desirable, but I question the statement about "well-organized airflow path." When the piston is at bottom center the only air that gets "well organized" is that which follows the intake port walls. A good deal of air flows straight through and out the exhaust ports. It has been our experience from many studies of airflow in uniflow and loop-, or cross-

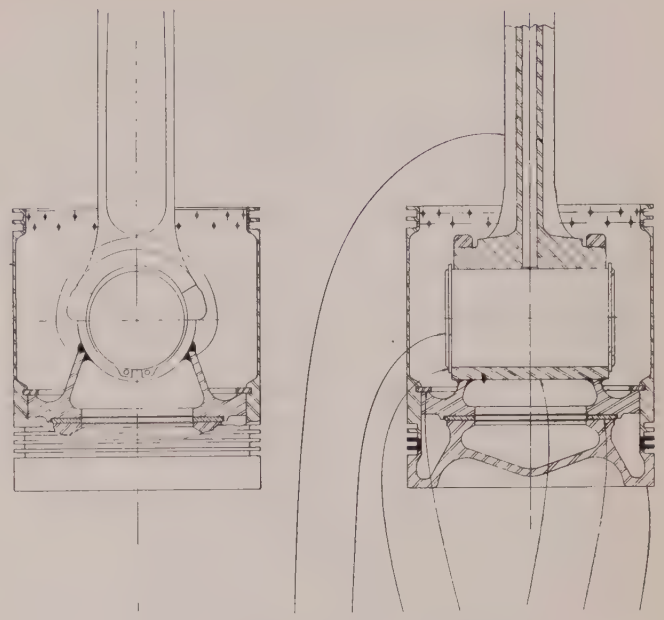

Fig. A – Double-slipper connecting rod

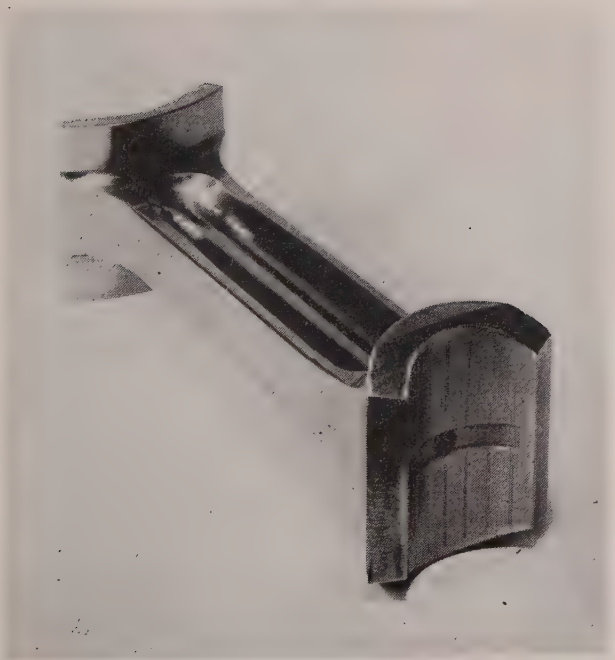

Fig. B – Finished connecting rod

Fig. C – Connecting rod assembled in carrier

Fig. D – Wrist-pin assembly

scavenge, cylinders that the air doesn't always follow the pretty little arrows we designers like to put on the drawings and diagrams. Much of the air is short-circuited directly across the top of the piston. This is perhaps fortunate because some of this "unorganized" air performs a very useful function by cooling the top of the piston which would otherwise be in a very stagnant region if we were to believe the arrows denoting loop scavenge airflow. In any very high-output engine adequate piston cooling is mandatory.

The drawing in the paper shows a secondary row of ports or slots below the exhaust ports proper. I am curious to know if this is correct, and if so, what is the purpose of the slots?

3. With regard to the injection system, the statement is made that it has been found beneficial to "direct the spray at the walls of the combustion chamber." Because of the shape of the chamber this seems to be the only place to squirt fuel. However, there is a generous squish area on the cylinder head so that fuel will be injected into a region of extremely high-velocity airflow as the upward motion of the piston displaces air inward into the hemispherical chamber. Is not this the reason for the beneficial results obtained with the spray angles used and not because fuel is squirted at the chamber walls?

4. The piston design I find interesting since Napier found it necessary to employ steel heads. It has been our experience that for really high loads it is easier to make an all-steel piston which can be made lighter than those of cast aluminum. Adequate oil cooling, however, must be provided. I assume that all the cooling oil is put into the piston through the rod. Is that correct, and if so, how is it distributed in the piston? The drawing is not too clear in this respect. It would also be interesting to know how much oil is used.

The connecting rod is most intriguing. I do not consider the slipper-type crankpin bearing very unusual since we have been using this type of bearing in production diesel engines for many years. A slipper bearing rod permits a much smaller crankcase design than the more conventional articulated aircraft construction and would be the natural choice when space and weight are at a premium.

The wrist-pin bearing is another matter. As stated in the paper, high bearing loads, low rubbing velocities, and no separation of the surfaces is a problem that has plagued us for some time. The wrist-pin bearing is certainly a touchy spot in any two-stroke engine. We are constantly on the brink of trouble as we increase our engine outputs

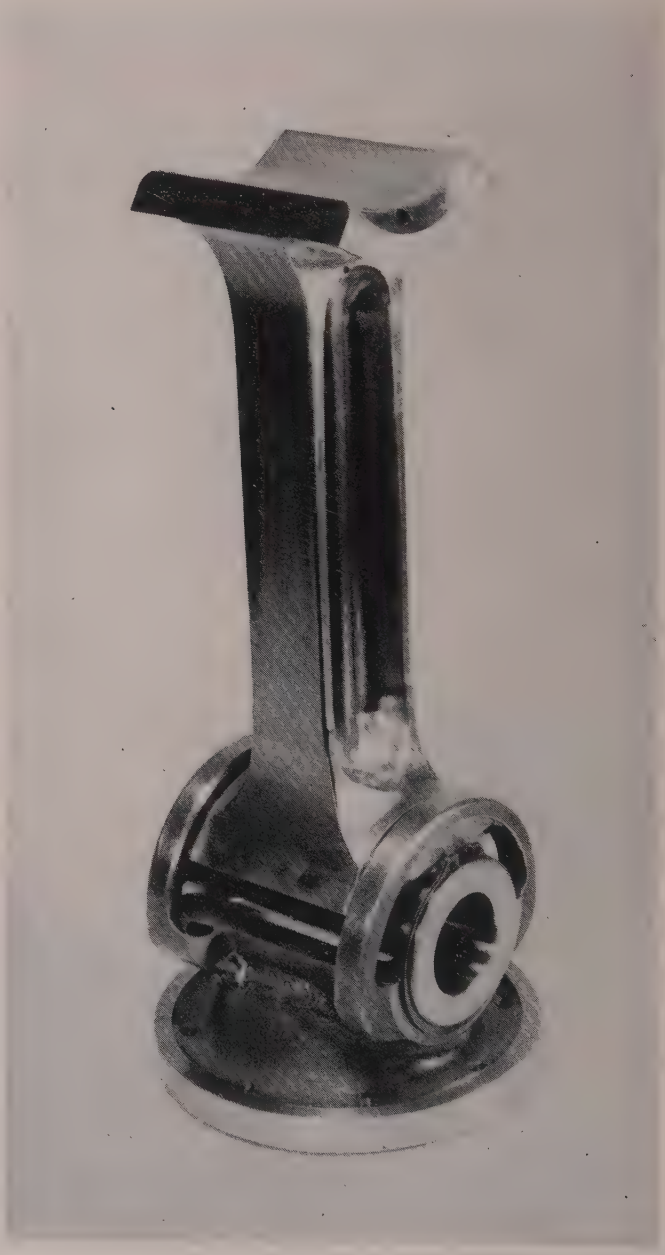

Fig. E – Complete rod, carrier, and wrist-pin assembly

and bearing loads. In some cases it has been necessary to resort to very expensive bearing materials and caution in the choice of a lubricant to obtain satisfactory service.

Several years ago we designed a double-slipper rod for one of our high-output single-cylinder test engines. I thought we were being very smart to achieve a 35% increase in bearing area in the same piston, but it wasn't nearly as clever a trick as that employed by Napier.

Shown in Fig. A is a drawing of a double-slipper connecting-rod design. There were two main purposes for this arrangement. One was to alleviate wrist-pin loading and the other was the elimination of all threaded fastenings in the piston, which explains the choice of a floating piston with a rod, wrist pin, and carrier retained by means of a snap ring.

Fig. B is a photograph of the finished connecting rod. It was originally thought that the rod could be made perfectly symmetrical but because of the interference in the piston, it was necessary to use a reduced diameter on the wrist pin end.

Fig. C shows how the connecting rod is assembled in the carrier. First it is cocked and inserted, then it is straightened up and pulled against the hoops for the insertion of the wrist pin.

Fig. D shows the assembly of the wrist pin itself which holds the connecting rod and carrier assembly together and is retained by two snap rings at the outer ends of the pin.

Fig. E shows the complete rod, carrier, and wrist pin assembly ready to be installed in the piston.

Although this design has been successfully run for many hours of high-load operation, I was not able to sell it to one of our manufacturing divisions.

Everyone knows that to make a bearing work there must be a clearance space provided and a lubricant in the clearance. Increasing area or providing better material as is commonly done just takes the curse off a critical bearing. But providing the clearance so that it may fill with oil as the engineers of Napier have done is a most simple and straightforward engineering accomplishment.

It would be interesting to know what bearing materials Napier used in the connecting-rod bearings and how they are bonded to the rods.

Points Out Nomad's Unusual Combination of Constructions

– Marsden Ware
Packard Motor Car Co.

THIS engine brings to mind previous aircraft diesel engines, prominent among which were the Mercedes Benz, the Junkers Jumo, and the Packard radial diesel engine. All these engines had an impressive although limited service experience. Mercedes Benz engines made several Atlantic flights installed in the Hindenberg airship. The Junkers Jumo powered a considerable number of German fighters. The Packard diesel was used in a number of aircraft and established a nonrefueling record which held for a period of many years. With the performance that is being obtained with the Napier Nomad, those who have previously envisioned the diesel engine playing a prominent part in aircraft may yet find impressive evidence of real usage.

The Napier Nomad engine puts together a number of constructions which are unusual in their combination although not new individually. Among these are: compounding, 2-stroke with loop scavenging, direct fuel injection, compression ignition, high air/fuel ratio.

Unusual and noteworthy mechanical features include: variable-speed supercharger-turbine gearing, variable compressor inlet guides, piston-pin bearing and lubrication, piston construction.

While the Packard radial diesel engine was definitely in the specific weight classification of aircraft engines as of that day, the specific weight of the Napier Nomad is much less than any previous aircraft diesel engine. The Napier Nomad is quite definitely in the modern aircraft engine weight class. The Wright compound gasoline engine shows a specific weight of 1.1 lb per hp, while the Napier Nomad compound diesel engine shows a specific weight of 1.2 lb per hp.

The performance of the engine is quite impressive. The specific constructions used in the cylinder are evidently very important in obtaining the high cylinder performance. The 2-stroke valveless construction avoids questions of exhaust-valve capacity to handle the high heat load. Oil cooling and heat-resisting metals combine to enable the pistons to live with intense heat loading.

There is no end to the questions which may be raised concerning many details which are not included. A few of these are:

How much heat is carried off by oil cooling in the piston or how much oil is circulated through the piston?

What is the oil consumption?

Do you expect still greater specific power with greater air dilution?

What is the limit of air dilution?

What endurance and type test requirements have been met?

Is there a marine version of the engine, and if so, how does it compare with the aircraft engine?

It appears that the ordinary turbocharged diesel is not to be classed as a compound engine, although large increases in power and high expansion ratios are obtained with the turbocharger. Is it appropriate as inferred from the wording in the paper to confine the term "compounding" for actual mechanical power connection of both turbine and engine to the power take-off shaft?

Asks About Nomad's Performance and Reliability

– W. G. Lundquist
Wright Aeronautical Division, Curtiss-Wright Corp.

IN regard to the performance of the engine, the top question which comes to my mind concerns whether or not the experimental testing of the engine has confirmed or disagreed with the performance as projected analytically. I believe I am correct in assuming that the performance curves presented were derived analytically and they do not represent necessarily accomplished test data. To what extent have test data substantiated these curves and are such data available for publication? It would be very interesting to see the correlation.

In regard to the weight of the engine, I cannot make out whether or not the weight comparisons include the weight of the associated liquid cooling radiators, piping, and other installation requirements associated therewith including the weight of the coolant itself. In comparison, all installed weights of the Nomad engine compared with other engines would, of course, have to include such additional weights to give a correct overall comparison. Specifically then, the question is: Do the weights given in this paper include the complete weight of the coolant system and coolant?

Has it been determined what the engine's oil heat rejection is and what oil cooler requirements are necessary?

Obviously, in addition to the weight requirements of the cooling system and the oil cooling system, the frontal area requirements for the coolant and oil radiators will be of great importance in completing any installation comparison.

In regard to mechanical features, several questions occurred as I read the paper. In the first place, what has the

experience been with this engine in regard to the loss of lubricating oil through the exhaust ports and the associated "coking" of these ports due to the leakage of lubricating oil? This has been one of the classical problems associated with the ported 2-stroke engine, and it would be interesting to know what has been experienced with the Nomad.

I note from the engine pictures that the cylinder heads are bolted on. Is the cylinder head to cylinder block joint a metal-to-metal design, or is a gasket used in this place? This is another trouble spot for diesel engines, and it would be interesting to know what experience has been obtained in the case of the Nomad on this item.

I think I would agree with the authors that the field of application for an engine of this type which is designed to have a very high thermal efficiency would be in the so-called air transport category as distinguished from military tactical operations. However, the trend in this field is definitely towards higher subsonic speeds, and in these areas the overall engine efficiency as defined by the miles per gallon yardstick is not a function of internal thermal efficiency of the engine alone but must include the effect on the flight efficiency of the weight and size factors involved in the engine design. For that reason, the more elaborate forms of compound engine have not been too promising in the past, and any consideration of their use must be predicated on the installed net overall efficiency including the induced and parasite drag characteristics of the installed powerplant. For these reasons, the piston-type engines encounter increasing competitive disadvantage as sonic speed is approached. It was for these reasons that we at Wright Aeronautical chose to make the turbo-compound engine the simplest practical form of compound engine which could be accomplished without increasing weight or other drag factors.

Another very important factor involved in the selection and use of an engine, particularly for commercial airlines, is the day-to-day on-schedule reliability which is demanded, and this factor is inherently tied in and controlled by mechanical simplicity or lack of simplicity as the case may be. We have learned very painfully throughout the years that mechanical complications in the basic engine design and the use of accessory components such as complicated fuel and power controls can be a prolific source of operational difficulties and schedule delays in airline operation. In other words, the probable time and cost to an airline operator involved in debugging an engine with such complications will be an extremely important consideration in the selection of the engine for transport use, particularly commercial airline operation. I am certain that this aspect of the Nomad engine has been considered carefully, and it would be interesting to hear what development progress in regard to reliability of external engine accessories has been achieved.

These factors did, in fact, control to a very large extent our thinking during the development of the Wright turbo-compound engine. The turbo-compound engine model currently operating on the airlines (and in United States military operations) was deliberately, therefore, kept as simple design-wise as could be and yet attain a definite beneficial utilization of the compound principle. The engine utilizes no accessory power control whatsoever, being operated exactly as an uncompounded piston engine. To as great an extent as possible, the compounding has been so devised as to add no additional mechanical or thermal load to the cylinders. Actual operating experience has confirmed that this deliberate emphasis on simplicity has been largely instrumental in the acceptance and success of the engine. We have in the past and we still are studying other more complicated types of compounding, and we may yet conclude that further complication may be warranted to achieve further improvements in performance. For that reason, the contribution represented by this paper on the Nomad engine is of great interest to us, and we feel the Nomad project represents a very important contribution to the development of piston aircraft engines. We would like, therefore, to commend the Napier company and others responsible for this project for their farsighted vision in undertaking the project, and we will look forward to the progress which can be made in the future in the field of compound piston aircraft engines.

Dislikes Nomad's Apparent Complexity

– F. W. Kolk
American Airlines

ALTHOUGH I am impressed by the low fuel consumption of the Nomad, I am concerned about the seeming complexity of the engine. The Nomad appears to combine the complexities of both aviation piston engines and gas turbines.

In a new airplane, utilization is very important, and if the plane is not available because of mechanical breakdown or maintenance, the operating cost figures can be very misleading. Utilization is a function of mechanical excellence and complexity. It is thus undesirable to increase the number of components in an engine.

Discusses Point in Theoretical Analysis

– L. C. Lichty
Yale University

THE compound engine developed by Napier is a very worth-while contribution. However, one point of interest in the theoretical analysis appears to be overlooked.

The area, ABCA, on the pressure-volume diagram (Fig. 5) is assumed to indicate the loss of work of the compound cycle because of the process of releasing the gases from the reciprocating engine at P_A to the turbine inlet at P_B by a thermodynamically irreversible process. As a result of this process, the entropy of the medium at point C would be greater than at point A, assuming an adiabatic process. This indicates a larger volume at point C than indicated in Fig. 5, and consequently the expansion curve for the turbine from the corrected location for C to turbine exhaust pressure would be higher than indicated. Thus, some of the loss of available energy caused by the irreversible release process is recovered in the turbine, and the loss of work would be less than indicated by the area ABCA.

For the foregoing reason, point F in Fig. 5 would not lie on the curve AFC, but would be on a similar curve above the curve PD, extended to intersect the turbine inlet-pressure line.

It can be shown that the correct value for V_c might be as much as 6% higher than the value indicated, depending on the pressure drop in the transfer process. Thus it appears the turbine work might be more than 6% higher than indicated in Fig. 5.

The foregoing discussion assumes the expansion processes are adiabatic isentropics. However, if they are actual expansion processes with heat transfer out of the medium, the recovery of some of the indicated loss of work is possible.

Authors' Closure To Discussion

MR. BIRMANN contends that mechanical connection of the turbine to the power output shaft is an unnecessary complication; however, we strongly disagree. Turboblow-

ers are widely used in aircraft engines, and Napier is well aware of what can and cannot be done with them. For aircraft service, connection of the turbine to the output shaft is essential for best flexibility and performance. A turboblower system cannot be designed to produce the equivalent results.

In answer to Mr. Flynn's discussion, more air can be passed through the cylinder with less aerodynamic loss with the Nomad type of flow path. The development of the scavenge system of the engine was based on many thousands of hours of testing and research. The airflow and pressure losses are very much influenced by the directional flow control that can be effected.

The extra row of ports below the main exhaust ports in the cylinders eliminates the tendency for the bridges between ports to distort and cause piston rubbing. In addition, the small ports were found to improve engine performance.

A conical combustion chamber was first tried, but we found that, as the fuel spray angle was widened, better performance resulted. The hemispherical combustion-chamber form was thus a natural development. We do not claim that it is the best possible configuration, but for the Nomad it gives good results.

Regarding the piston design, oil is fed transversely to an annular chamber behind the piston rings. No oil is fed directly to the piston crown, although some of the oil does contact the crown undersurface.

We agree that the design of the connecting-rod bearings is not wholly new, but it does have a number of unusual features. Thin-walled bearings, steel backed with a lead-bronze lining, are used.

In answer to Mr. Ware's questions, the lubricating oil consumption of the Nomad is 8 pt per hr at cruising conditions and 16 pt per hr at full power. Only about half the air is consumed in the engine cylinders. The limitation to using more of the available air is the thermal load on the piston. We expect future development of the piston to make possible higher outputs from the engine.

We have no information on the limit of air dilution nor on the endurance qualities of the engine. There is no marine version of the Nomad engine.

Mr. Lundquist also raises some questions about performance data. All results given in this paper are actual test data, except the curves referring to flight conditions. The weights given are net dry weights and so do not include external separate equipment. This is in accord with the usual practice.

Lubricating oil is lost through the ports during idling conditions, producing a blue haze in the exhaust. There has never been any carbon buildup in the ports; this is probably a result of the temperatures involved. A copper ring is used as the cylinder-head sealing. This was the most satisfactory of several methods tried.

We do not regard the Nomad engine as being complex and think this criticism is not justified, as the Nomad is basically a very simple design. While the Nomad is more complicated than a simple low-powered piston engine, usually the only alternative high-output engines ever suggested are hypothetical engines that have not been built. All engines are very simple in the first design consideration stage; they become complex when built or when they are developed to working reliability.

The turbine and compressor of the Nomad are normal types of rotating machinery that have proved to be reliable. The piston part of the engine is similar to conventional engines and is simple and reliable. The fuel-injection system is basically more reliable than a spark-ignition system.

We agree entirely with the points raised by Professor Lichty.

There were a number of comparatively detailed points of this nature which arose during the preparation of the "indicator" diagrams used for illustrating the paper. A certain degree of simplification was regarded as desirable in order to avoid the necessity for somewhat lengthy explanations. The main purpose of the diagrams was, of course, to indicate the broad principles on which the compound engine operates.

An attempt was made to excuse such slight departures from the truth by the cunning introduction of the phrase, "in broad terms without much respect for meticulous detail."

ORAL DISCUSSION

Reported by Alan R. Schrader
USN Engineering Experiment Station

Carl F. Bachle, Continental Aviation and Engineering Corp.: How is it possible for the engine to operate with gasoline as a fuel?

Reply: The engine was developed to burn gasoline because this was a requirement of the British Ministry of Supply, which considered that the engine should be capable of using fuels available throughout the world. Actually, the engine is very insensitive to fuel quality. This is probably a result of the high degree of supercharging employed.

Mr. Bachle: What is the efficiency of the variable-speed gear?

Reply: The variable-speed drive efficiency ranges from 65 to 92%. For conditions where the efficiency is low, the amount of power transmitted is also low, so power losses are not serious.

Dale H. Brown, General Electric Co.: I note the use of variable compressor inlet guide vanes. What is the flow restriction characteristic of the diesel and the turbine that requires this degree of finesse? How much air does this compressor handle at sea-level take-off?

Reply: The compressor inlet variable guide vanes allow the operating range of the engine to be extended at the low-speed end.

Mr. Brown: Of the air that is delivered by the compressor, it appears that some must go right through the engine. How many pounds of air actually get trapped in the cylinder? Also, this does not look like as positive a scavenge system as the valve-in-head or opposed-piston engine. What is the ratio between the pounds of air trapped and the pounds of residuals left in the cylinder?

Reply: No information is available as to the proportion of air trapped in the cylinder. Data of this sort would be desirable, but we know of no reliable means of obtaining them.

Mr. Brown: Our experience indicates that one to two points of stage efficiency can be realized through use of a shroud on the turbine. What were your considerations in selecting and using an unshrouded wheel?

Reply: We are aware of the slight performance improvement made possible by shrouding the turbine. However, this knowledge was not available at the time of design, and it appears that redesign of the turbine would not be warranted for the small improvement gained.

Mr. Brown: While the turbine-compressor set appears small, it represents a tremendous inertia during starting and acceleration of the engine. What starting power was required? Did the compressor-turbine set require provision for slipping the drive during starting or other high-torque occasions?

Reply: No difficulty has been experienced due to inertia of the rotating parts.

Designing New Performance

FOR a period of approximately three years, starting shortly after the end of World War II, the authors' company marketed a cross-graded SAE 10W-20 engine oil in several selected areas in this country. The oil had a number of then unique properties which led to good customer acceptance in these marketing areas. This early large-scale experiment also demonstrated the practicability of marketing such an oil on a national scale.

With this field experience and with the introduction of new automotive engines having requirements not fully met by conventional oils, the design and development of a special engine oil entered a new phase. A primary and essential objective of this new oil development program was to help ameliorate the harmful effects of combustion-chamber deposits which result in octane number requirement increase (ONRI) and preignition, particularly in the higher-compression-ratio engines which were being aggressively developed by some segments of the automotive industry. These developments in higher-compression-ratio engines involving improved combustion-chamber shapes and mechanical octane numbers, together with new transmission developments, foreshadowed major gains in the efficiency of utilization of high-octane-number gasolines. And, as described by Holaday,[1] advances in petroleum technology have made pos-

CURRENT-production gasoline engines with their greater power and efficiency call for new engine oils having improved performance if the advantages of these new engines are to be fully realized.

The right oil can reduce knock, preignition, and spark-plug fouling, thus increasing engine efficiency. Reduced mechanical and corrosive wear, greater engine cleanliness, and improved starting performance, oil consumption, and fuel economy can also be effected with specially designed lubricants.

This paper describes how one new oil formulation, a blend of selected distillate oils with V.I. improvers and a new detergent-inhibitor combination, has been designed, built, and tested with these desired performance properties in view.

The Authors

L. RAYMOND (M '36) is assistant chief automotive engineer, Socony-Vacuum Oil Co., Inc. He has been engaged in petroleum research since receiving his M.A. degree from Columbia University in 1928, having been connected with the Texas Co. and the Tide Water Associated Oil Co. before joining Socony-Vacuum in 1945.

J. F. SOCOLOFSKY (M '48) is supervisor of the Lubricants Section of Socony-Vacuum Laboratories. He has been engaged in petroleum research since receiving his A.B. in Chemistry from the University of Kansas. Mr. Socolofsky has been with Socony-Vacuum since 1941.

into a Special Motor Oil

L. Raymond and J. F. Socolofsky,
Socony-Vacuum Oil Co., Inc.

This paper was presented at the SAE Summer Meeting, Atlantic City, June 9, 1954

sible lower-cost production of these high-octane-number fuels. However, as also pointed out in Holaday's paper, the principal technical problem confronting technologists working in this field may be said to be combustion-chamber deposits. Holaday stated in this connection:

"... Improved lubricants can contribute to reduced octane number and autoignition requirement, such reductions being equivalent to adding a corresponding number of octane numbers to the fuel. The overall effect is a lower octane number requirement for a given compression ratio."

Allied to this improvement in combustion-chamber deposits was to be a reduction in spark-plug deposits and spark-plug misfiring. Because of its tremendous economic importance, it was, therefore, believed that the first objective of any really new engine oil development should be the improvement in combustion-chamber deposits with its attendant benefits.

A second major objective in the design of the truly new engine oil was considered to be reduced mechanical and corrosive wear. The new overhead-valve V-8 engines are more powerful and, at the same time, more compact and efficient than their predecessors. The trend toward higher specific outputs and speeds from physically smaller engines has meant more heavily loaded parts. These higher loadings have increased the scuffing and wear tendencies of such parts as rings, hydraulic valve lifters, cams, oil-pump drive gears, and bearings. As an example, in the case of hydraulic valve lifters where the cam sweeps across the lifter with line or point contact and where the lifter never leaves the cam at low speeds, the increased loading of a smaller lifter can easily lead to mechanical failure of the lifter and its cam. Thus the requirement for increased protection under borderline (boundary) lubrication conditions to prevent scuffing and welding became an obvious part of the antiwear objective.

At the same time, these higher pressures have made the more heavily loaded parts more susceptible to the destructive effects of the corrosive wear occurring under low-temperature conditions. This acidic corrosion and wear is generally seen at its worst in its attack on the piston rings and cylinders; it leads to loss of power, blowby, high oil consumption, and other manifestations of engine deterioration. Similar corrosion can occur in the close-fitting parts incorporated in hydraulic valve lifters, in which case the effect can either be wear leading to rapid leakage or rust deposits which stick the piston in the hydraulic cylinder, causing the unit to stop functioning as an automatic valve lash adjuster. The minimizing of corrosive wear at low temperatures thus became an integral part of the second major objective of reducing wear.

The third design objective in the development of the new oil was considered as improved engine cleanliness, particularly in low-temperature operation. The new engines with their higher output and greater efficiency operate at lower load factors than

[1] "What Can We Get from Higher-Octane-Number Fuels," by W. M. Holaday. Paper presented at SAE Annual Meeting, Detroit, Jan. 13, 1954.

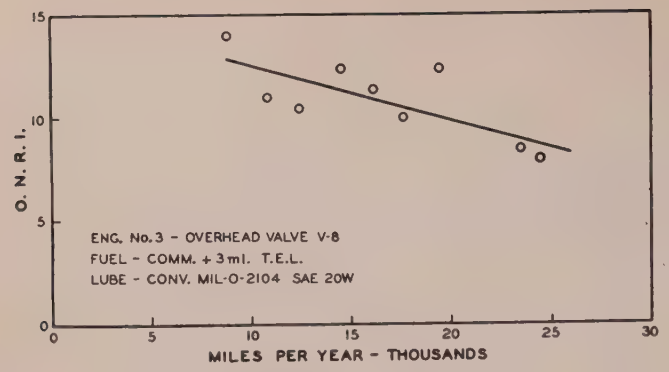

Fig. 1 – Relationship between driving rate in miles per year and ONRI

the old engines under similar service conditions. Because of this, the engines are more susceptible to the formation of the deposits arising from the fuel, particularly in start-stop city-type driving. Also, the newer engines contain parts which, because of their closer fits and finer finish, have a smaller tolerance for deposits before malfunctioning occurs. It appeared necessary, therefore, to keep these newer engines freer from deposits than the older designs of lower specific output.

It was considered that wear and deposits must also be avoided or minimized because, in leading to higher oil consumption, they brought about an increase in combustion-chamber deposits, with an attendant adverse effect on knock, preignition, and spark-plug misfiring.

The fourth and final objective was to design an oil with viscosity, volatility, and pour point characteristics which would permit its use in all areas of the country, regardless of season. In essence, the accomplishment of this objective implied a combination of low oil consumption at high temperatures and easy starting at low temperatures. These desirable performance properties would also result in improved fuel economy through reduced engine friction, particularly during starting and warmup.

The major objectives of this new engine oil development program thus became:

1. Reduced knock, preignition, and spark-plug misfiring.

2. Reduced mechanical and corrosive wear.

3. Increased engine cleanliness.

4. Improved viscosity, volatility, and pour point characteristics to achieve the combination of low oil consumption at high temperatures, easy starting at low temperatures, and improved fuel economy.

Reduced Knock, Preignition, and Spark-Plug Fouling

Our laboratories have been engaged in a large-scale and sustained attack on the first objective of reduced knock, preignition, and spark-plug misfiring, through reduction and change in the combustion-chamber deposits. Published information, including a number of papers presented before the SAE by representatives of the petroleum, automotive, and related industries, has furnished an excellent fundamental background of how combustion-chamber deposits affect knock, preignition, and spark-plug misfiring. The special skills of a petroleum laboratory naturally lie in the field of oil and fuel composition and processing and in additive compounding. However, early in this work, it became apparent that engine make and operating conditions have a significant effect on the formation of combustion-chamber deposits. An example of the effect of engine make is given in the paper by Korp.[2] Some of the data from this paper are repeated in Table 1.

In addition to the difference in average clean requirement, the data show a range in octane number requirement increase (ONRI) from 4½ numbers for car 1 to 12 numbers for car 3. Comparison of the two different fuel-oil combinations for the three cars shows an advantage of 1½ to 4½ numbers in lower ONRI for the experimental combination.

The effect of driving conditions in normal, everyday operation is illustrated in Fig. 1 where ONRI is plotted against miles per year. The cars with the lower mileages per year have the higher ONRI, reflecting the probable influence of short-trip operation on combustion-chamber deposit buildup.

In addition to illustrating the variations arising from differences in engines and operating conditions, these and other data have also proved conclusively that fuels and lubricants can significantly affect combustion-chamber deposits and the combustion phenomena of knock and preignition which are of so much concern. In trying to segregate the influence of the lubricant, one of the steps in the present development was an investigation of the effect of:

a. All distillate versus distillate-bright stock blends.

b. Oil viscosity.

Tables 2 and 3 summarize some of the engine data.

Table 2 demonstrates a considerable increase in ONRI with increasing bright stock content and viscosity. The data under the heading of "Carbon/Lead Salt Ratio" are derived from a special test which has been found to be a useful research tool. It is described in Appendix II. These data indicate that increasing percentages of bright stock lead

[2] "Combustion-Chamber Deposit Studies in Laboratory and Field Tests," by H. J. Korp. Paper presented at CRC Symposium on Combustion Deposits, Detroit, September, 1952.

Table 1 – Road Octane Number Requirement Increase (ONRI)

Car Make[b]	Clean ONR		Average[a] Stabilized Requirements				ONRI Difference Due to Fuel-Lube Combination
			Commercial Fuel-Lube[c]		Experimental Fuel-Lube[d]		
	Average	Range	ONR	ONRI	ONR	ONRI	
1	84	81–86½	88½	4½	87	3	1½
2	73	68–80½	82	9	77½	4½	4½
3	75½	72–81½	87½	12	83	7½	4½

[a] Each fuel-lube combination was run in 30 cars (10 of each make).
[b] Car make code as designated by engine type given in Appendix I.
[c] Commercial premium gasoline (3 ml tel per gal) and SAE 20 high V.I. paraffinic oil (MIL-O-2104 additives).
[d] Unleaded alkylate and SAE 20 naphthenic distillate oil (no additives).

Table 2 – Influence of Lubricant on Combustion-Chamber Deposits and ONRI

Lubricant				Lab Combustion Test,[b] Carbon/Lead Salt Ratio	COT Engine Test[c]		Stabilized Road ONRI, Average 18 Cars[d]
Code[a]	SAE Grade	% Bright Stock	Additive Dosage		ONRI	Deposit Weight, g	
A	10W-20	0	Supplement 1	0.7	1½	3	7
B	10W	10	MIL-O-2104	1.5	4½	5	9
C	20W	30	MIL-O-2104	1.7	6½	6	10
D	30	45	MIL-O-2104	2.0	7	7	—

[a] Lubricant code given in Appendix I.
[b] Laboratory combustion deposits test described in Appendix II.
[c] COT engine test described in Appendix III. Fuel is commercial plus 3 ml tel.
[d] Each oil run to stabilized ONR in nine cars make 1 and nine cars make 3. Fuel is commercial plus 3 ml tel.

Table 3 – Influence of Mineral-Oil Viscosity and Volatility on Combustion-Chamber Deposits and ONRI

Lubricant					Lab Combustion Test,[a] Carbon/Lead Salt Ratio	COT Engine Test[b]	
SAE Grade	Viscosity, SUS at 210 F	V.I.	% Bright Stock	90% Distillation Point, F		ONRI	Deposit Weight, g
10W	44.5	109	0	870	0.7	0	3
30	62.5	95	0	970	0.9	1	3
30	62	98	45	1150	2.3	7	5

[a] Laboratory combustion test described in Appendix II.
[b] COT engine test described in Appendix III. Fuel is commercial plus 3 ml tel.

to higher carbon/lead salt ratios in the deposit. It is theorized that the higher proportion of carbonaceous material is responsible for the higher ONRI observed. This effect of bright stock is also shown in Table 3, in which straight mineral oils are compared. The SAE 10W and SAE 30 grade distillates show 0 and 1 ONRI, respectively, while the SAE 30 blend of distillate and bright stock gives an ONRI of 7. Referring back to Table 2, it should be noted that both the laboratory and the road data show similar trends.

Because the second and third major objectives of reduced wear and increased cleanliness presupposed higher additive concentrations, the influence of additive concentration on ONRI was also studied. Some limited data are shown in Table 4.

These data indicate no significant effect of detergent concentration on ONRI when using commercial gasoline containing 3 ml tel per gal. However, with unleaded alkylate, the nondetergent oil gave a much lower ONRI than the Series 2 oil. It is interesting to note that in tests with unleaded isooctane reported by McNab et al.[3] the addition of a detergent-inhibitor additive increased the ONRI by 7 numbers compared to the base oil. However, with current commercial fuels and with the detergents investigated by the authors' laboratories, differences in additive concentration did not affect ONRI. This observation corroborates earlier data reported by Bassett[4] in which a premium-type oil containing inhibitor only and a Series 2 oil from the same base stocks showed equivalent ONRI and combustion-chamber deposit weight. It is believed that generalizations on the effect of additives are probably premature and that individual results may differ depending on the particular base stocks,

[3] See SAE Transactions, Vol. 62, 1954, pp. 228-242: "Effect of Lubricant Composition on Combustion-Chamber Deposits," by J. G. McNab, L. E. Moody, and N. V. Hakala.

[4] See ASTM Specification Technical Publication No. 102, 1950, "Does Service Performance Justify Higher Quality Lubricating Oils?" by W. B. Bassett. (Presented at ASTM Symposium on High Additive Content Oils.)

Table 4 – Influence of Additives on ONRI

Lubricant			Octane Number Requirement Increase[a]		
Code	SAE Grade	Additive Level	COT Engine[b]	17.6 Engine[b]	Multicylinder Engine[c]
A Base	10W-20	None	1	—	—
A	10W-20	Supplement 1	1½	—	—
D Base	30	None	7	12	4
D	30	MIL-O-2104	7	—	—
D (S-2)	30	Supplement 2	—	11½	12

[a] Engines and test procedures described in Appendix III.
[b] Fuel is commercial plus 3 ml tel.
[c] Fuel is unleaded alkylate.

Table 5 – Effect of Lubricant on Stabilized ONRI in Different Engines, Laboratory and Road Comparison

Lubricant			Laboratory ONRI		Road ONRI			
Code	SAE Grade	Additives	COT	Engine 5[a]	9 Cars[b] Make 1	9 Cars[b] Make 3	21 Cars[c] Make 4	5 Cars[d] Make 5
A	10W-20	Supplement 1	1½	5½	4	10	3½	5
E	5W-20	MIL-O-2104	4	—	3½	11	4	—
B	10W	MIL-O-2104	4½	—	5½	12½	—	—
C	20W	MIL-O-2104	6½	10½	6½	13½	6	8½

[a] Test procedure described in Appendix IV.
[b] Each oil run to stabilized ONRI in each of the nine cars.
[c] Each oil run to stabilized ONRI in seven cars.
[d] Oil A run to stabilized ONRI in two cars, oil C in three cars.

Table 6 – Combustion-Chamber Deposits and ONRI, Effect of Oil Change in "Carboned" Engine

Car		Operation on Conventional SAE 20 Oil		ONR After Changeover to Cross-Grade 10W-20 Oil A		Change in ONR Due to Oil Change
Year	Make	Miles	Stabilized ONR	Miles Operation on Oil A	ONR	
1949	1	51,107	95½	5944	92½	−3
1950	2	7,830	87½	5426	87	−½
1950	2	12,390	90½	4342	86	−4½
1949	3	15,928	91½	3409	86½	−5
1951	3	5,309	92	1332	87	−5
1951	3	4,052	91	4861	89½	−1½
1952	3	7,701	88	1032	86½	−1½
1953	4	7,854	92½	2734	91	−1½
1953	4	8,820	92	4671	91½	−½
1953	4	6,269	90	3203	89½	−½
1953	4	10,258	87	2546	87	0
1952	5	18,214	97	6830	88	−9
1951	7	32,586	93	5499	89	−4

additives, engines, fuels, and test conditions used.

With the above four major quality objectives in mind, an oil formulation comprising a blend of selected distillate oils plus a combination of V.I. improvers and a new detergent-inhibitor combination was designed. Because of its commercial significance to both the automotive and petroleum industries, some of the data on this product, designated as oil A, are discussed in the following sections.

Table 5 illustrates the effect on ONRI of the new type of formulation in comparison with more conventional products. In each case, the new cross-graded product shows a consistent and relatively large gain in reduced ONRI over the more conventional SAE 10W and SAE 20W lubricants, the average reduction being more than 3 octane numbers. In general, oil A shows a small advantage over SAE 5W-20 oil E.

The large effect of engine design on ONRI is shown again in the comparison of the results on cars 1, 3, 4, and 5 – the spreads in ONRI among the four makes being approximately the same as that reported in Table 1.

The new oil A represents a major gain in reduced ONRI, which at one time was thought impossible to accomplish through lubricating oil. Considerable room for improvement still remains and will continue to be the target of major effort.

All of the previous comparisons of ONRI were

Table 7 – Influence of Lubricant on Preignition, Laboratory Engine Tests

Lubricant		Multicylinder Engine 5[a] Stabilized Preignition Requirement (Res. O.N.)	Multicylinder Engine 6[b] % Accelerations Giving Wild Ping	Modified CFR Engine[c] Preignition Counts Per Hour
Code	Type			
A	Cross-grade SAE 10W-20	91½	0	33
—	Conventional-type commercial SAE 20 oils	99	26	170

[a] Test procedure described in Appendix IV.
[b] Test procedure described in Appendix V.
[c] Engine and test procedure similar to that described by footnote 6.

Table 8 – Influence of Lubricant on Preignition and Detonation on the Road

Lubricant		Engine 5[a]			Engine 8[b]
Code	Type	Stabilized Knock Requirement (Res. O.N.)	Wild Pings (Average) Per One Acceleration[c]	After-Running (Switch Off) Per Accelerations[c]	Stabilized Preignition Requirement (Res. O.N.)
A	Cross-grade SAE 10W-20	88½	0.7	0 per 11	92
—	Conventional-type commercial SAE 20 oils	92	3.9	3 per 8	99

[a] Test procedures described in Appendix VI.
[b] Test procedure similar to that described by footnote 7.
[c] Wild ping and after-running tests were made with fuels having octane numbers higher than those shown in column headed "Stabilized Knock Requirement (Res. O.N.)."

obtained starting with engines having clean combustion chambers. Of more immediate importance, although not of greater long-range consequence, is the effect of the change to the new type oil in a "carboned" engine. Information has been obtained on this phase as shown in Table 6.

In each case the oil was changed without any reconditioning of the engine. While the data are not extensive, the trend is consistent and significant in showing a reduction in ONR following the change to oil A. The average reduction in ONR is approximately 3 numbers, while the largest gain is 9 octane numbers. The mileages shown are not those required to effect the change but are the mileages at which the cars could be tested conveniently. It should be noted that in some cases substantial decreases in ONR occurred in relatively short mileages after the change to oil A. With the small number of cars of any one make represented, it is not possible to detect whether there is any trend in the magnitude of the reduction in ONR by car make.

These beneficial results in reduced ONRI are at variance with those reported in a recent paper by Overcash et al.[5] in which it was stated that all distillate oils showed to advantage in reduced ONRI in clean engines whereas no benefit was observed when these oils were charged to a dirty engine. The authors believe that differences in test conditions are probably chiefly responsible for the apparent discrepancy although other factors such as engine make, oil, and fuel may be involved. The data by Overcash et al. were obtained in laboratory tests using a light-duty cycle in which the maximum load was 10 bhp at 2000 rpm for the 6-cyl engine. The authors' data were obtained in road tests in driver-owned vehicles. No restrictions were placed on driving habits except that top speeds were limited to 50 mph. It is known that combustion-chamber deposits, particularly those formed under city driving conditions, are unstable and subject to removal and modification with changes in speed, load, and temperature. Thus, some of the deposits from a previous oil should gradually disappear after a change to another oil. If the second oil had a lower deposition tendency, the ultimate result should be a reduction in combustion-chamber deposit and ONR. This was the case in the data shown in Table 6.

To an increasing extent the new higher-compression-ratio engines are showing serious indications of being preignition-limited, rather than knock-limited.[6, 7] Compared to knock, which responds to spark setting, the control or elimination of preignition due to deposits is much less within the power of the engine designer. In addition, preignition is more objectionable and can be more

[5] "Crankcase Oil – An Approach to the Combustion-Chamber Deposit Problem," by R. L. Overcash, W. Hart, and D. J. McClure. Paper presented at SAE Annual Meeting, Detroit, Jan. 14, 1954.

[6] See SAE Transactions, Vol. 62, 1954, pp. 40-49: "Deposit-Induced Ignition – Evaluation in a Laboratory Engine," by D. A. Hirschler, J. D. McCullough, and C. A. Hall.

[7] See SAE Transactions, Vol. 62, 1954, pp. 57-65: "Some Effects of Fuels and Lubricants on Autoignition in Cars on the Road," by R. K. Williams and J. R. Landis.

Table 9 – Mechanical Wear Tests[a]

Lubricant			Hydraulic Valve Lifter Tests		Timken OK Load, lb
Designation	SAE Grade	Additives	Engine 6	Engine 9	
A	10W-20	Supplement 1	Good	Satisfactory	10
A Base[b]	10W-20	None	Good	Poor	3
A-1[c]	10W-20	Supplement 1	Poor	Poor	35
C	20W	MIL-O-2104	Good	Satisfactory	6
F	20W	MIL-O-2104	Good	Poor	6

[a] Test procedures described in Appendix VI.
[b] Base stock-V.I. improver blend for oil A.
[c] Oil A with different e-p agent.

destructive than knock. For these reasons, the influence of combustion-chamber deposits on preignition and the means for the alleviation of preignition are currently subjects of major interest and effort. The data in Tables 7 and 8 were obtained in four different engines, under different test conditions, and indicate the effect of a major change in oil formulation in alleviating preignition tendencies.

The laboratory test data in Table 7 show that, compared to conventional type SAE 20W oils, oil A gave a much lower preignition requirement (expressed as Research octane number) in one engine, a great reduction in the incidence of preignition in another, and complete elimination of wild ping in a third. Differences in oil performance are also indicated in the road test data in Table 8, the new type oil showing an advantage in several forms of uncontrolled combustion, including reduced knock as shown by lower ONR, fewer wild pings, and no after-running. Experience, based on laboratory and field data, has been that the new type oil A has a more rapid and larger effect on preignition than on knock.

Reduced Mechanical and Corrosive Wear

1. *Mechanical Wear* – Smaller parts, higher loads, and much more severe lubricating conditions have led to a greater number of parts operating under boundary lubrication conditions. The boundary lubrication problem is very complex, the end effects being the result of interrelated and not readily separable factors of design, metallurgy, surface finish, operating conditions, and lubricant. Not much is known about the mechanisms by which these factors bring about the end result of surface distress or metal failure because of inability to reduce the reactions to fundamental parameters of temperature, pressure, time, and so forth. For this reason, most of the research has involved an empirical, rather than a fundamental, approach. In addition to the use of bench-test machines originally developed, in most cases, to measure the extreme-pressure properties of gear lubricants, a number of engine tests have been devised empirically to evaluate one or more of the factors contributing to this problem. Some of these engine tests and their results are described in recent papers by Mougey[8], Bidwell and Vermaire[9], Ambrose and Taylor[10], and Havely, Phalen, and Bunnell[11]. The conflicting nature of these data and the inability to explain or predict the difference in performance illustrate the obscure and complicated phenomena involved. While the present paper cannot shed much light on the mechanisms involved, some of the data obtained by the authors' laboratories on valve lifter wear in two modern overhead-valve V-8 engines are shown in Table 9, the test conditions used being outlined in Appendix VII.

While published data indicate that viscosity has a measurable effect on wear and scuffing under these boundary lubrication conditions, it appears to be a relatively small factor which can be far outweighed by the influence of selected additives. Comparison in Table 9 of the performance of different oil-additive combinations in the two engines indicates that a lubricant which gives good protection in one engine is not necessarily satisfactory in another and that the order of merit of a series of lubricants can vary from engine to engine, confirming the observations of other laboratories. Oil A appears to have the ability to protect adequately both engines under these boundary lubrication conditions.

In view of the differences in behavior of different engines with a common series of lubricants, it would be too much to expect that any given antiwear or antiscuff bench test developed for another purpose would predict performance in any specific engine. As an example, the results on the Timken

[8] "Engine Wear as Affected by Lubricant Composition," by H. C. Mougey. Paper presented at ASTM Symposium on Engine Lubrication, Technical Committee B, ASTM Committee D-2, Atlantic City, July 1, 1953.

[9] See pp. 211-226 of this volume.

[10] See pp. 192-203 of this volume.

[11] See pp. 204-210 of this volume.

machine illustrate this weakness. Oil A-1 with the highest rating in the Timken machine gives the poorest results in both engines 6 and 9, while oils A and C, with relatively low Timken passing loads, are satisfactory in both engines. These data are cited as a cautionary note to other workers in this field, since unwise reliance on bench tests can be an expensive, time-consuming, and unproductive attempt at a shortcut.

2. *Corrosive Wear* – Increased traffic density and greater use of cars for short trips produce conditions which are more favorable to corrosive attack in our higher-horsepower engines. A 1951 survey[12] of car use found that 38% of all trips were for less than 3 miles one way and 63% for less than 6 miles one way. These short trips do not permit reaching high enough jacket temperatures to prevent condensation of corrosive combustion products on the ring and cylinder surfaces, and thus wear is accelerated.

The authors' laboratories have employed both CFR gasoline and diesel engines equipped with radioactive top rings for studies of corrosive wear. Wear data over a range of temperatures on four oils differing in viscosity characteristics and additive level are shown in Fig. 2. It will be noted that, with conventional oils, wear increases appreciably with decreasing temperature and that at the lower temperatures there is a large difference in the wear protection afforded by a straight mineral oil and by a MIL-0-2104 oil of conventional base stock formulation. Increasing the additive dosage of the latter to the Supplemental List 1 level shows a further decrease in wear rate. Comparison of curves 3 and 4 indicates that cross-graded oil A, with its lower viscosity at low temperatures, gives lower wear than the conventional SAE 20W oil of like additive content. It is interesting to note that Hamer et al.[13] reported a similar beneficial effect of low-viscosity oils.

Field performance data are believed to support the temperature effects on wear shown in the laboratory. The field results on three different car makes plotted in Fig. 3 show an inverse relationship between engine wear and total miles driven per year. The greater the annual mileage, the lower the wear. This is to be expected since, in general, the lower-mileage car would usually be the car with the higher proportion of short trips and lower jacket temperatures. The same effect of increased

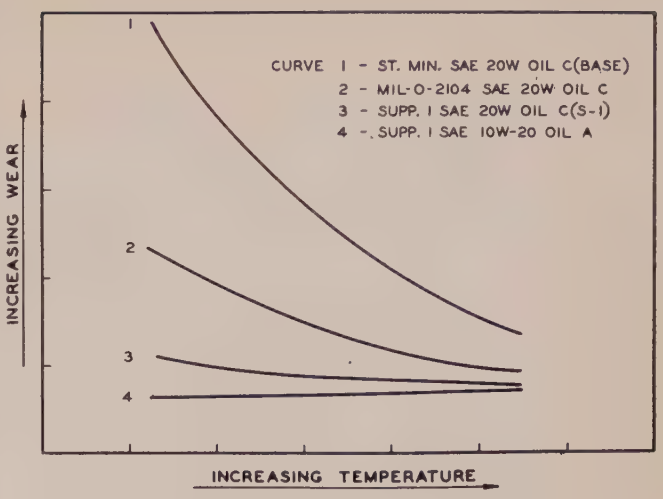

Fig. 2 – Radioactive engine wear tests

wear with the increased number of starts for the same mileage was reported by Pocock.[14]

Engine Cleanliness

In short-trip driving, which constitutes such a large percentage of all trips, the lower temperatures and low load factor of higher-horsepower engines are productive of deposits arising from rich-mixture operation and incomplete combustion of the fuel. On the other hand, the closer clearances of these engines demand greater protection against

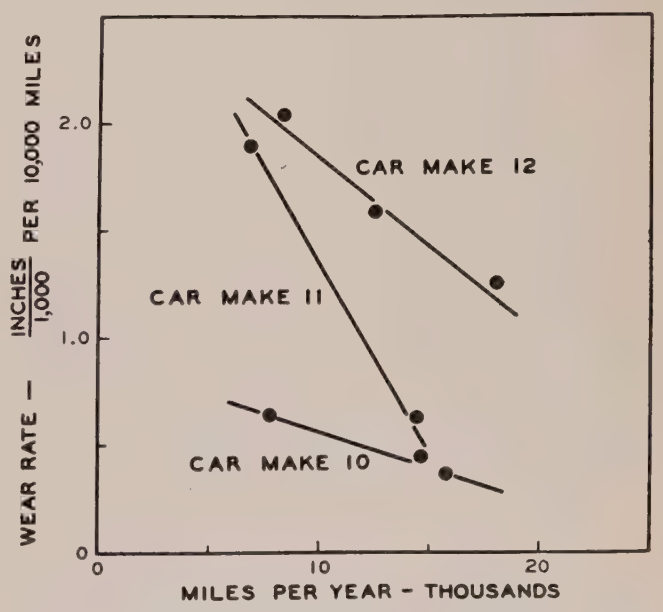

Fig. 3 – Car miles per year versus top cylinder bore wear

[12] See "Automobile Transportation in Defense or War," by W. Owen. Prepared for Defense Transport Administration, Washington, D. C., October, 1951.

[13] "Lubricating Oil Requirements of the Modern Automotive Engine," by J. P. Hamer, T. S. Tutwiler, and C. A. Weisel. Paper presented at ASTM Annual Meeting, Atlantic City, June 29-July 3, 1953.

[14] See SAE Transactions, Vol. 61, 1953, pp. 154-164: "Can All Engine Wear Be Trapped in a Can?" by R. J. Pocock.

Table 10 – 100-Hr Cyclic Engine Test[a]

Lubricant			Engine Cleanliness		
Designation	SAE Grade	Additives	Piston 10=Clean	Overall 100=Clean	Oil Ring Slot Clogging, %
A	10W-20	Supplement 1	5.0	80	5
A-2[b]	10W-20	Supplement 1	3.9	76	15
C	20W	MIL-O-2104	3.3	77	10
E	5W-20	MIL-O-2104	3.0	75	20
G	20W	Antioxidant only	2.5	72	—

[a] Test procedure described in Appendix VIII.
[b] Oil A with different detergent combination.

deposits of varnish- and sludge-forming materials. The solution to this engine protection problem demands additives which are more effective in preventing the formation, agglomeration, and deposition of such harmful products. Because the principal application of these new oils is in gasoline engines, an extensive program involving cleanliness evaluations in a variety of gasoline-engine tests was added to the usual Caterpillar L-1 and Chevrolet FL-2 type tests of detergency. One such cyclic test (see Appendix VIII) conducted under special operating conditions of admittedly high severity has demonstrated in the past that there is much room for improvement in the capacity of engine oils to handle fuel-formed deposits. An example of this is shown in Table 10 where a premium oil G and oils A-2, C, and E, employing conventional-type detergents, all showed a relatively low level of cleanliness protection. As a result of emphasis on gasoline-engine performance, a new type additive combination has been developed for this type of service. The effectiveness of this approach is indicated by the improvement in cleanliness shown by the use of this new additive in oil A.

Low-Temperature Starting and Oil Consumption

The aspect of oil quality which has been receiving the greatest commercial emphasis from industry has been cross-grading, or the increase in viscosity index which permits one oil to span two or more SAE viscosity grades. Thus, products designated as SAE 5W-20 or SAE 10W-30 have been introduced recently by a number of oil companies. These products meet the viscosity specifications of an SAE 5W (or 10W) grade oil at 0 F, and an SAE 20 (or 30) grade oil at 210 F. At present, it is difficult to formulate a practical 5W-30 oil due to technical limitations and cost considerations. Since commercially available SAE 5W-20 oils appear to suffer from high oil consumption while the SAE 10W-30 oils appear to be deficient in low-temperature properties, the lubricant manufacturer who wishes to market a single cross-graded oil for use in all cars under all conditions in all areas finds himself in a dilemma. One method of resolving this dilemma is to start with the premise that the engine does not recognize SAE numbers and that the selection of the preferred viscosity range should be based on engine performance data and engine requirements. With such information available, it should be possible to arrive at the viscosity range which will best serve the greatest number of cars for the greatest part of their operation.

With respect to the low-temperature characteristics, the minimum starting temperatures of four commercial oils ranging from a cross-graded SAE 5W-20 to a conventional high V.I. SAE 20W oil have been derived from the borderline starting curve in the paper by Fleming et al.[15] The data are summarized in Table 11 together with the key viscosity values on the four oils. It will be observed that in a car in good mechanical condition, the SAE 20W oil will permit starting at –3 F_9 the SAE 10W oil at –10 F, and the SAE 5W-20 oil at –23 F. The viscosities and temperatures shown do not provide for the effect of dilution which is always

Table 11 – Influence of Lubricant Viscosity and V.I. on Minimum Engine Starting Temperatures

Oil Designation	E	A	B	C
SAE Grade	5W-20	10W-20	10W	20W
Viscosity, SUS				
0 F	Below 4000	7000	10,000	25,000
210 F	50	55	45	54
Viscosity Index	150	140	110	105
Minimum Starting Temperature, F	–23	–17	–10	–3

[15] See SAE *Quarterly* Transactions, Vol. 4, July, 1950, pp. 410-417: "Performance of High V.I. Motor Oils," by C. L. Fleming, Jr., B. W. Geddes, N. V. Hakala, and C. A. Weisel.

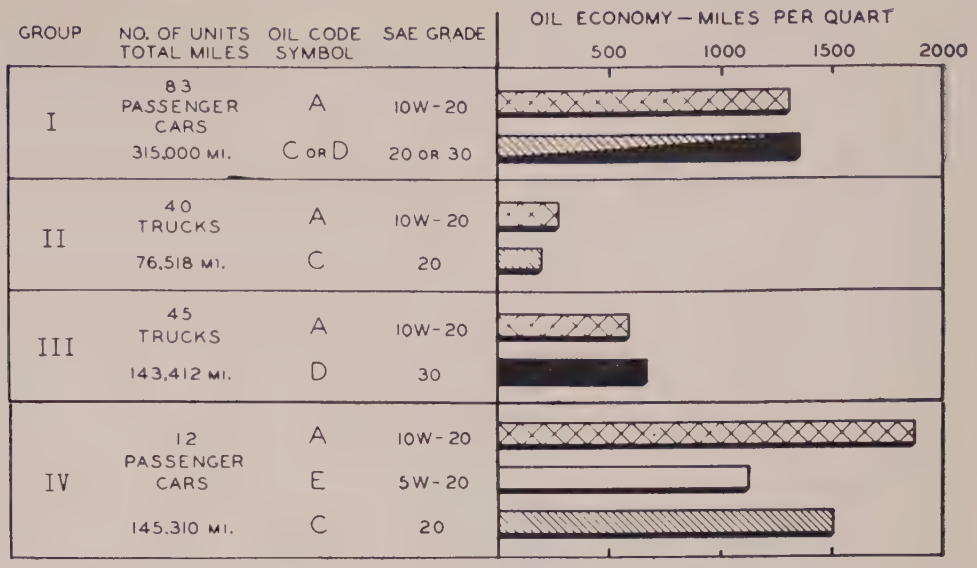

Fig. 4 — Oil consumption in road vehicles

Group I - 1950-53 cars, individually owned and operated. Variable service. Oil A compared to either C or D in each vehicle.

Group II - 1949-53 1/2 ton and 1 ton panel trucks. Multi-stop delivery service. 20 trucks on each oil.

Group III - 1952-53 16,000 G.V.W. trucks. Multi-stop delivery service. 23 on oil A; 22 on oil D.

Group IV - 1950-52 cars, 6 each of 2 makes. Individually owned and operated. Oils alternated in each car.

encountered in engines operating at low temperatures and which tends to lower the minimum starting temperatures. If it is considered that a minimum starting temperature of −15 to −20 F will satisfy the requirements of all but a very small percentage of the cars in this country and that these latter cars can be taken care of by SAE 5W oils, then a product intermediate in low-temperature characteristics between the SAE 10W oil and the SAE 5W-20 oil will be satisfactory. An oil such as oil A which permits starting without dilution at −17 F appears to satisfy this requirement although its viscosity at 0 F does not permit it to be classified as an SAE 5W oil.

At the other extreme, high oil consumption under high-speed and high-temperature driving conditions is an undesirable characteristic. Oil consumption is one of the most difficult performance properties to measure with a satisfactory degree of precision because even small changes in engines, operating conditions, and instrument settings can influence the absolute and relative consumption values in comparing a group of oils or engines. In order to obtain a relatively high degree of precision, the special oil-consumption equipment described in the paper by Snyder et al.[16] has been utilized. This installation makes it possible to switch from one oil to another without shutting down or changing speed or load. An extensive study has been made of the factors affecting oil consumption, and it is planned to present the data in a separate paper. Bearing on the present discussion, the results indicate that variations in individual engines and operating conditions frequently can greatly outweigh oil differences. The two controlling factors affecting differences due to oils are viscosity and volatility.

With respect to the latter factor, it becomes essential to control the minimum flash point. This volatility effect is of particular importance with cross-graded oils which tend to use low-viscosity, low-flash neutrals. While such materials can be employed satisfactorily in finished blends, it becomes difficult to eliminate the more volatile and higher flash components with oils meeting SAE 5W-20 specifications. In this connection, attention should be called to the paper by Hamer et al.[13] in which a V.I. improved oil showed lower consumption in long-mileage road tests than a bright stock blend, both oils having the same SUS viscosity at 210 F and employing the same low-viscosity base stock.

An extensive field test, employing 201 passenger cars and light trucks and more than one million miles of service testing, has been conducted to

[16] See "A Broad Look at Engine-Oil Testing," by G. H. S. Snyder, E. A. Martin, L. Raymond, and J. F. Socolofsky. Pub. by API Division of Refining, New York, May, 1953.

investigate the oil consumption performance of five oils varying from SAE 5W-20 to SAE 30 viscosities. Results of some of these tests are shown in bar-chart form in Fig. 4. It should be noted that oil A (cross-graded SAE 10W-20) is equivalent or somewhat superior in consumption to oil C (conventional SAE 20 of approximately the same SUS viscosity at 210 F as oil A) in each of the comparisons. In the one group of vehicles in which oil A was compared with oil E (SAE 5W-20), oil A showed a significant advantage in better oil economy.

The selection of the viscosity range of any oil, conventional or cross-graded, is a matter for each company's individual choice, based on technical and commercial considerations. Analysis of the low-temperature starting and oil consumption data led the authors' company to the conclusion that a viscosity range of approximately 7000 SUS at 0 F and 55 SUS at 210 F would cover the requirements of all but a very small part of the cars in this country. As technological "know-how" moves forward and as it becomes possible to broaden the viscosity range without adverse effects, it is anticipated that a single oil covering the complete range of starting and oil consumption requirements will be practicable. Until that time it is the authors' opinion that emphasis should be placed on engine requirements rather than on SAE numbers in arriving at the preferred viscosity range.

Conclusions

More powerful and efficient gasoline engines currently in production and in prospect have created new problems and intensified old problems. Engine oils not only improved in present performance properties but having new qualities are essential if maximum performance and protection are to be obtained with these new engines. In addition, the older engines can also benefit from various improvements in oil quality. The authors believe that these considerations lead to new concepts of oil quality which can best be achieved by concentrating attention on the performance requirements of the gasoline engines now in service and to be built, and by disregarding arbitrary classifications or specifications which impose undesirable limitations. The authors have attempted to show how one such completely new oil was designed, built, and tested according to these modern concepts of quality and performance. Differences of opinion undoubtedly exist as to the importance of the different performance properties of an oil. Nevertheless, it is probably recognized that future progress in more efficient engines is most dependent on reductions in knock, preignition, and spark-plug fouling tendencies, toward which the lubricant can make a large contribution, as demonstrated in the present paper. At the same time, reduced mechanical and corrosive wear, increased engine cleanliness, and improved viscosity characteristics with attendant benefits in starting, oil consumption and fuel economy are all important in assuring maximum satisfaction in both new and older cars. Close cooperation between the automotive and petroleum industries in the development of improved engines and oils should lead to large benefits for their mutual customer and should help the continued growth of both industries.

Acknowledgment

Obviously, a work of this magnitude required the cooperative effort of a large number of the authors' coworkers. The number who have made substantial contributions is too great to attempt to mention by name. The authors feel, in presenting this paper, that they are only the spokesmen for this group.

We are also deeply indebted to the numerous individuals in the automotive and associated industries who cooperated so willingly in conducting special engine tests which were such an important part of this program.

APPENDIX I

Tables 12 and 13 describe the lubricants and engines used.

Table 12 – Lubricants

Designation	SAE Grade	Viscosity, SUS at 210 F	V. I.	Approximate Additive Dosage
A	10W-20	55	140	Supplement 1
B	10W	45	110	MIL-O-2104
C	20W	54	105	MIL-O-2104
D	30	62	95	MIL-O-2104
E	5W-20	50	150	MIL-O-2104
F	20W	55	95	MIL-O-2104
G	20W	54	105	Antioxidant only

Table 13 – Engines

Designation	Type
1	8 cyl, in-line, overhead valve
2	6 cyl, L-head
3	V-8, overhead valve
4	6 cyl, overhead valve
5	8 cyl, in-line, L-head
6, 7, 8, and 9	V-8 overhead-valve engines of different makes
10	6 cyl, overhead valve
11	V-8, L-head
12	6 cyl, L-head

APPENDIX II

Procedure – An unleaded gasoline is distilled to the 90% point. The remaining 10% residue[17] is blended with tel (motor mix) to give 2.5 ml per 100 ml of residue. Four grams of this fuel is blended with 1.0 g of the oil to be evaluated.

A weighed Vycor glass crucible (3½ in. high and 1½ in. in diameter) is placed upright in a close-fitting electric furnace. The crucible temperature is

[17] The 10% residue will vary with the composition of the gasoline used and may affect the deposit formation.

Table 14 – Equipment and Procedure for Combustion-Chamber Deposits Tests

	17.6	COT	Commercial Multicylinder
Engine Details			
Cylinders	1	1	6
Bore and Stroke, in.	$2^5/_8$x$3^1/_4$	$2^3/_4$x$2^3/_4$	—
Displacement, cu in.	17.6	16.3	—
Compression Ratio, nominal	7.5	6.5	—
Head Type	Valve-in-head, hemispherical	Valve-in-head, hemispherical	L-head
Test Operating Conditions			
Duration, hr	72	100	96
Engine Speed, rpm	1800	1400	2000
Jacket Coolant Out Temperature, F	175	180	165
Oil Temperature, F	160	150	160
Intake Air Temperature, F	135	Atmospheric	135
Intake Manifold Pressure, in. of Hg abs	20	3	14 (approx)
Load, bhp (approximate)	0.8	0.5	10
Air/Fuel Ratio	13.0	13.0	17.0
Spark Timing, deg btc	20	38	32
Oil-Change Period, hr	24	None	24
Oil Charge	2500 ml	1 qt	5 qt
Octane-Number Requirement Procedure			
Engine Speed, rpm	1200	1400	800, 1000, 1250, 1500
Spark Timing, deg btc	11	26	6, $7^1/_2$, 9, $10^1/_2$
Intake Air Pressure, in. of Hg abs	29	Atmospheric	Atmospheric
Engine Load	Maximum	Max	Max
Air Temperature, F	135	Atmospheric	135
Jacket Coolant Temperature, F	175	180	165
Oil Temperature, F	160	150	160
Air/Fuel Ratio	Approx 13/1 for max knock	13/1	13/1

held at 700 ± 5 F. Five milliliters of the test blend is dropped on the bottom of the heated crucible at a controlled rate over a 45-min period. This is done with a hypodermic syringe mounted on a metering device above the crucible. The resulting deposit is heated 30 min longer, cooled, and weighed.

The deposit is treated with concentrated H_2SO_4 at 1000 F to burn off the carbon and convert the lead salts to the sulfate. The amount of carbonaceous material is determined by difference between the weights of total deposit and $PbSO_4$. The ratio of per cent carbonaceous to per cent $PbSO_4$ in the original deposit is reported.

Repeatability – Based on the average of duplicate tests, the maximum difference between averages will vary as follows:

0.1 for ratios of 0.1 to 1.0
0.2 for ratios of 1.0 to 2.0
0.4 for ratios above 2.0

APPENDIX III

The laboratory test equipment and procedure for the combustion-chamber deposits program are described in Table 14.

APPENDIX IV

The laboratory multicylinder engine procedure for octane-number requirement and preignition is similar to one developed by the du Pont laboratories for preignition studies. A brief outline of engine properties and test conditions is given in Table 15.

Before each run, combustion-chamber deposits were removed and a detonation (knock) requirement was taken on the clean engine accelerating from 850 to 1800 rpm. The engine was then operated (cycling procedure) for 14 hr and another detonation requirement taken. Two hours later, the engine was tested for preignition, employing wide-open-throttle accelerations from 850 to 2600 rpm. Every 2 hr thereafter the engine was tested, alternating detonation (knock) requirements and preignition requirements. The antiknock quality of the rating fuels was increased as the preignition and knock requirements increased. In this way, curves were generated defining the engine's stabilized detonation and preignition requirements. Preignition was detected by thermionic pickup on the S/V en-

Table 15 – Engine Properties and Test Conditions

Engine Type	In-line 8, L-head
Fuel Type	Commercial premium type (3 ml tel per gal)

Continuous Cycling Procedure

	Idle	Part-Throttle Load
Cycle Duration, min	1	3
Speed, rpm	500	1750
Load	Idle	Maintain 20 bhp
Approximate A/F	9/1	14/1

gine analyzer[18] and by a rumbling or thudding noise indicating extremely advanced ignition.

APPENDIX V

The dynamometer test procedure for evaluation of fuels and lubricants with respect to combustion-chamber deposits is shown in Table 16.

Table 16 – Dynamometer Test Procedure

Deposit Schedule	
Engine Speed, rpm	2000
Water Temperature, F	165
Minimum Oil Temperature, F	180
Spark Setting	Mfg. rec. for light load
Load, bhp	10-12
Duration, hr	110

Rating Schedule

Rating every 30 min is as follows:

1. Determine borderline knock.
2. With spark 10 deg retarded from borderline knock, open throttle fully and observe for wild ping or other signs of autoignition for 5 sec.
3. With the throttle still open, advance spark until borderline knock is detected.
4. With the throttle still open, retard the spark 5 deg from borderline and observe for wild ping or other signs of autoignition for 5 sec

APPENDIX VI

Road Preignition Procedure – For each preignition test, the car's detonation ONR was "bracketed" using sensitive reference fuels and full-throttle accelerations (from about 800 to 2000 rpm). Wild pings occurring during accelerations on no-knock reference fuels were counted aurally and recorded. Throughout the test, the S/V engine analyzer was used to assist the observer in detecting preignition. No reference fuels lower in octane number than that required to give true trace detonation were tested.

After the fourth-gear detonation requirement was obtained, the vehicle was accelerated in third gear from 20 to 60 mph on a reference fuel 5 octane numbers above the reference fuel which gave trace knock in the fourth gear. This was done to insure that any preignition encountered would not be knock induced. During this acceleration the observer noted any wild ping and engine roughness or rumbling. At the end of this acceleration the ignition switch was turned off, and any evidence of high-speed after-running was noted. Immediately after the third-gear acceleration, the vehicle was brought to a stop and checked for after-firing at idle with the key off. This third-gear acceleration was then repeated.

[18] "A New Engine Analyzer," by E. A. Martin and J. H. Goffe. Paper presented at SAE Summer Meeting, Atlantic City, June 10, 1954.

APPENDIX VII

Cam and tappet wear test conditions are shown in Table 17.

Table 17 – Cam and Tappet Wear Test Conditions

Engine 8—All engine operation at no load.

1. Break-in

Time, min	Engine Rpm	Jacket Water Temperature, F
15	1500	165 ± 3
30	1500	165 ± 3
30	1800	165 ± 3
45	2000	165 ± 3

2. Run test cycle for 50 camshaft hr
3. Cycle

Time, hr	Engine Rpm	Jacket Water Temperature, F
2	1000	100 ± 3
2	0	65 ± 3 (water circulating)

Engine 9 – All engine operation at no load

1. No break-in
2. Run test cycle to 120 camshaft hr or to failure
3. Cycle

Time, hr	Engine Rpm	Jacket Water Temperature, F
2	1200	170 ± 3
1	0	No external cooling

APPENDIX VIII

The Chevrolet stop-and-go cyclic test is normally run for 100 hr, but it can be extended to 200 hr or more.

Type of Test – Idling, full-throttle acceleration, continuous road load, deceleration with alternate cold and hot conditions.

Cycle Description – Load and speed (temperatures as below) are:

1. 1 min idle at 600 rpm, no load.
2. ½ min acceleration, 600 to 2500 rpm.
3. 2½ min, 2500 rpm continuous at road load.
4. ½ min deceleration, 2500 to 600 rpm against closed throttle.
5. Repeat.

Time and temperature (cycling as above) are:

1. 4-hr period, 200 F jacket outlet, 250 F oil temperatures.
2. 8-hr period, 95 F jacket outlet, 160 F oil temperatures.
3. Repeat.

Oil Charge – 5 qt, make up every 12 hr.

Oil Change at 100 hr.

Fuel – Commercial premium containing 3 ml tel per gal.

Air/Fuel Ratios – Idle 9-9.5/1; full load and throttle 12/1; road load 14.5/1.

Who Is the Designer—the Stylist or the Engineer?

Duncan McRae, Kaiser Motors Corp. and Willys Motors, Inc., and
Kenneth E. Coppock, Fisher Body Division, GMC

This paper was presented at the SAE Summer Meeting, Atlantic City, June 7, 1954.

IN the early and formative years of the automobile industry, the automobile engineer was, in effect, a first-class mechanic with an inventive mind. Little was known of the many technical aspects of engineering, as applied to automobiles, that are today taken for granted.

Chassis were designed to a great degree by trial-and-error method with little, if any, computations used in arriving at a satisfactory structure.

The bodies were almost entirely designed by the draftsman who laid them out and the craftsman who built them.

The problem in the early days was to make a machine which would run – and keep running – for a reasonable length of time before repairs and adjustments were needed.

The body was merely something to sit into so the machine could be operated with some degree of convenience.

Through the years many types of specialization have come into being in the design and engineering of automobiles.

This was a natural evolution. Just as the introduction of steam as a source of power by Watt brought forth through the years the development of the mechanical engineer and the development of electricity by Edison brought forth the electrical engineer, so, too, through the years the automobile industry has brought forth the chassis engineer, the engine expert, the ride engineer, and the body engineer – to name only a few.

Some 30 or more years ago, another force began to be felt in the design of automobiles – and that was the hand of the stylist.

Starting from a modest beginning in the industry, the early stylist was a part of the body engineering group. His function was to assist in the refinement of the body *after* the overall size and shape had been established.

Just as other fields of endeavor have expanded and specialized, so has the stylist function, through the years, expanded and become highly specialized until today the stylist sets the shape of the car *before* the chassis and body engineers really enter the design picture.

The main point that my colleague and I will try to make to you is this: due to the high degree of specialization and the technical skills required both in styling and body engineering, it is essential today that the body engineer have an understanding of the stylist's problems, without being a stylist, and that the stylist have an appreciation of the body

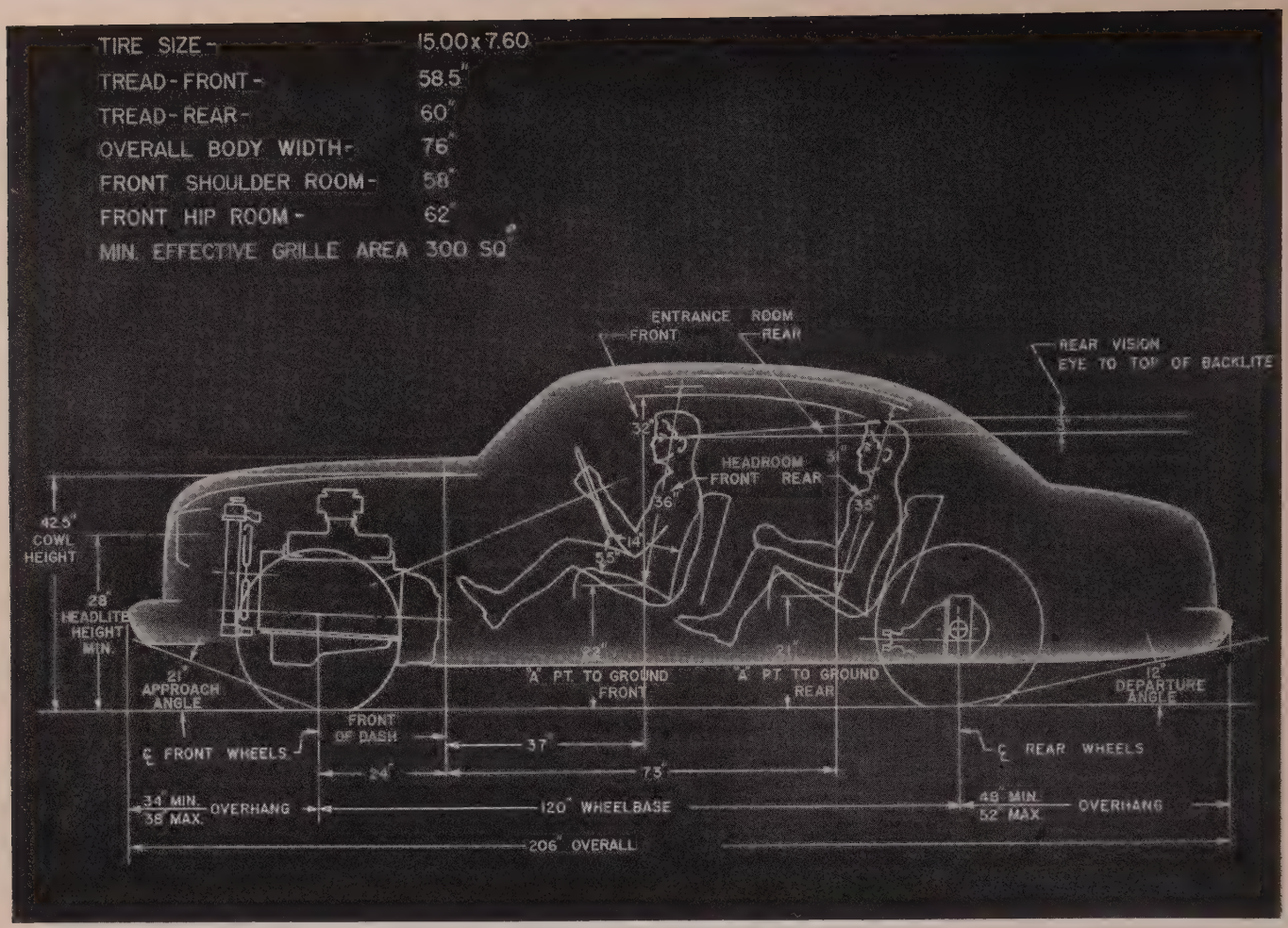

Fig. 1 – Package drawing showing dimensional limitations

engineering problems, but need not be an engineer per se.

In order to emphasize how the stylist and the engineer do and must work together, we will discuss some of the problems and how they are solved in designing an automobile.

Space does not permit us to cover all the problems in designing and engineering a body. However, we have selected some of the main points that have the greatest bearing on styling an automobile.

The first step in the development of an automobile is the establishment of the so-called "package size" of the vehicle. This is generally done by top management since the car is intended to be marketed in a certain price class. The major determining factors of this package size are:

1. The size of the car the new design will replace.
2. The sizes of the competitive cars the new car will be marketed against.
3. The general overall price class the car will be expected to fit into.

Fig. 1 will show you the generally accepted controlling dimensions around which the stylist is expected to render his ideas.

By examination, it will readily be seen that the stylist has considerable latitude for the free play of his imagination.

The chassis components are designed and arranged to provide a framework around which a well-styled car *can* be created. Such items as overall height, hood height, angle of approach, and angle of departure receive particular attention.

Although the design of the chassis necessary to provide a pleasing style is oversimplified in this discussion, it should be emphasized that the styling and design of the body are, to a great extent, dependent upon the advantages that can be provided by the chassis designer. Actually, the chassis design is the result of considerable preliminary collaboration between the chief engineer, the body engineer, and the stylist.

Also, the efforts of the engine designer are toward reducing the height of the engine to provide low overall cowl height. The chassis designer concentrates on a driveshaft location which permits dropping the seats to accommodate lower passenger seating and thereby a lower overall car height. Passenger comfort and ease of vehicle operation

are the important factors in establishing the dimensional limitations around which the stylist must create his design.

Referring again to the simplified form shown in Fig. 1, we have chosen, for the sake of illustration, a car in the medium-price range, having a wheelbase of 120 in. and an overall length of 206 in. The outline enveloping the passenger compartment and chassis components shown in this illustration is the present model or the shape of the car our new design is to replace. You will note that overall height and cowl height have been lowered. To achieve this, it has been necessary to lower the seats and the engine. These are the major design advantages in dimensional limitations which the stylist will have in creating the new design. Shown in chart form are pertinent factors which must also be considered, such as tire size, tread, shoulder room, hip room, overall width, and grille area, which will be required to provide sufficient volume of air to cool the engine.

Passenger comfort will be controlled by head room – front seat and rear seat – and entrance room shown as a dimension from the cushion to the top of the door. The stylist will be given some freedom in selecting the amount of the body which overhangs the front wheel and the amount of body overhanging the rear wheel. However, if he desires to increase the front overhang, he must decrease the rear overhang to maintain overall length of 206 in.

Now that we have set the problem, the next portion of this paper will show you how the stylist arrives at the beautiful creations he is so adept at turning out.

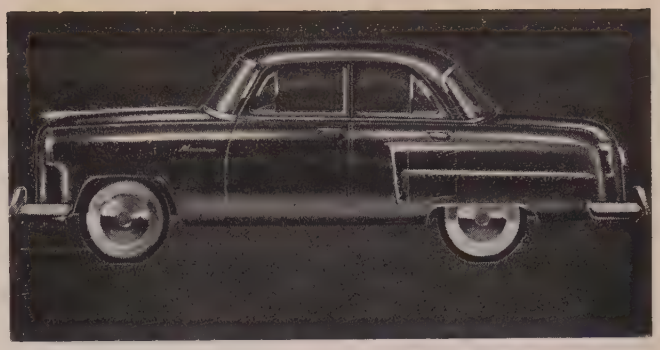

Fig. 2 – Current model

Styling the Car

The automobile styling profession is perhaps the newest addition to the field of arts; and because the automobile stylist is an accepted member of the team engaged in the development of today's motor cars, we should describe the background and requirements of this newcomer:

Above all, the automobile stylist must possess an esthetic sense that enables him to visualize and create in three dimensions – form, shape, and a proportion which will express the desired quality which may be the feeling of massiveness, fleetness, or perhaps the bold mechanical look associated with power and high performance.

He must be complete master of the tools of the

NEITHER stylist nor engineer can be called *the* designer of a new automobile. Rather, as this paper shows, it is the team of stylist and engineer working together which creates a pleasing and practicable design.

This paper is divided into four parts. Mr. Coppock, in the introduction, sets forth the problems involved in car design. How the stylist conceives his ideas for the new body is described by Mr. McRae under the heading "Styling the Car."

Under "Engineering Problems," Mr. Coppock describes the body engineer's part in making the stylist's ideas practicable. Finally, Mr. McRae summarizes the changes made and compares the new model with the current model on which the new design was based.

The Authors

DUNCAN McRAE (CM '54) is chief stylist for Kaiser Motors and Willys Motors, Inc. in Ypsilanti, Michigan. After studying art and engineering for two years at the University of Southern California, Mr. McRae began his styling career as a clay modeler with the Ford Motor Co. in 1939. Since that time he has styled for the Chrysler Corp., headed the Advanced Styling Department for the Kaiser-Frazer Corp. and was supervisor in charge of the Ford Motor Co.'s Exterior Design and Body Development studios.

KENNETH E. COPPOCK (M '46) is assistant chief engineer in charge of the Experimental and Development Section, Trim Engineering, Trim and Hardware Styling, Laboratory and Fisher Body Proving Ground Activity. He attended Albion College in Michigan. Mr. Coppock worked for General Motors in their Styling Section for 14 years, and then transferred to Fisher Body Engineering Division as director of the Experimental and Development Section. He was appointed to his present position in 1949

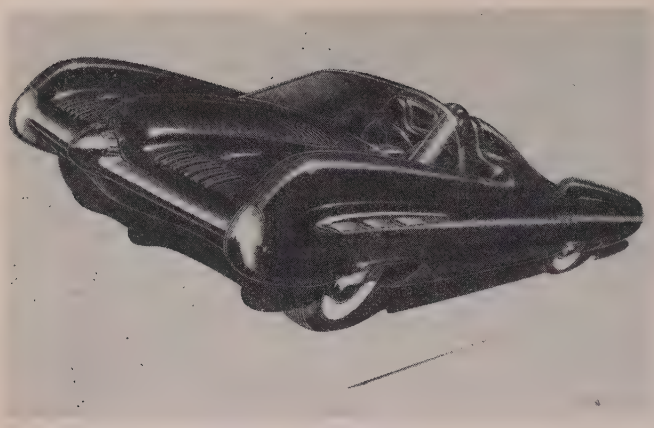

Fig. 3– Idea sketch 1

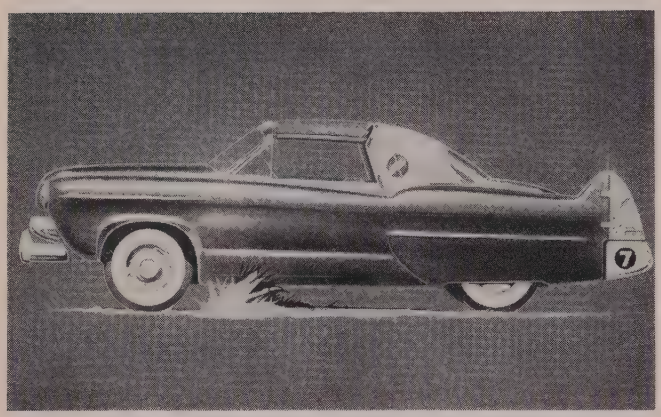

Fig. 4– Idea Sketch 2

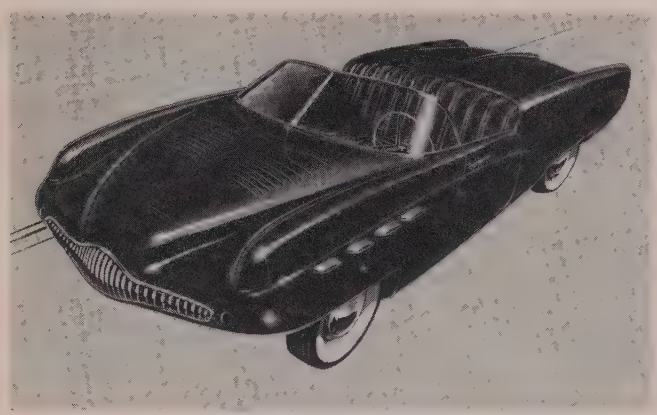

Fig. 5 – Idea sketch 3

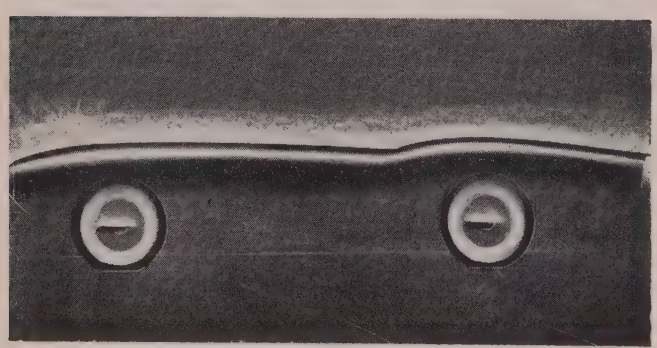

Fig. 6 – Fender silhouette

styling craft so that any concept of surface or shape may easily flow from his brush or sculpturing tool to such perfection that the concept will not be compromised by an easily arrived at solution.

He must be capable of producing quick "thumbnail" sketches, scale drawings, full-size blackboard layouts and illustrations, and finished perspective renderings. He must be a sculptor because he must model his creations in three dimensions from the size of a small instrument panel control knob to the size of the complete automobile itself.

The stylist must have an understanding of product development, production methods, and systems; and most important, he must have a keen sense of interpreting consumer psychology. This background of product development, production methods, and consumer psychology must not inhibit the complete freedom of thought so necessary in the creation of his new product.

The first step the stylist must make in any design program is to list the desired appearance qualities the new car should possess. Often this is most easily accomplished by reviewing in detail the present model since it has been viewed on the highway under all conditions and has been measured against competitive designs.

Fig. 2 illustrates today's product. It appears to be square and box-like – the hood is rather high and short compared to other cars in the same price range – roof and pillars certainly don't reflect the light and airy appearance which has become so popular since the introduction of the hardtop body style. The overall length indicates that we are as long as our competition. Nevertheless, the car seems shorter.

From these observations, we establish the following list of design aims so that all members of the styling group will direct their efforts toward one goal:

1. Eliminate square, box-like appearance.
2. Lower and lengthen hood.
3. Create a light roof effect.
4. Give the feeling of greater overall length.

Occasionally the new package drawing will incorporate dimensional changes which greatly assist the stylist; very often, however, the desired new effects are achieved by illusion resulting from reproportioning of lines, surfaces, and details.

Let us follow the steps and theories used by one styling group as they attempt to create a new car which will fit dimensional limitations of the package drawing and possess the four desired styling features we have listed.

The stylist keeps a file of sketches which represent his thoughts and ideas as shown in Figs. 3, 4, and 5. He draws from this file, often in modified form, lines and surfaces which will answer existing problems.

In order to create an automobile which will look "right," the stylist aims at vital unity – the complete and perfect organization of all units which

make up the whole. To begin, then, we will first establish the most important line – the lower body silhouette, the line that sweeps from the headlights to the taillights. This line is important because it separates the lower body from the roof structure and because it is the longest horizontal line on the automobile. In order to achieve maximum length, we will move the headlight as far forward as possible and move the taillight back. This will give us our greatest overhang at the four corners instead of at the centerline of the car as is found in the older model.

In theory, a straight horizontal line appears longer than a broken line. Yet a straight line possesses neither interest nor direction and tends to contribute to the box-like appearance we wish to eliminate. Because of this, we design the front fender silhouette (Fig. 6) with a slight drop as it extends back and then raise the line as it passes over the rear wheels. This gives us an interesting line which possesses feeling and direction.

The windshield, roof, and window lines are considered next; and because they are so completely dependent upon one another, they must be handled at one time. We definitely want a light upper structure appearance so that the eye will move horizontally from the nose of the car to the rear and not be compelled to travel vertically up and down heavy pillars and thick roof sections, thereby decreasing the illusion of length.

A wrap-around windshield further aids our quest for visual lightness of the upper structure. We will extend the windshield as far as entrance room permits and curve it back into the roof as shown in Fig. 7.

We next make an attempt to lower substantially the hood and rear deck, but we find that due to the angle of both the windshield and backlight, any substantial drop greatly reduces the hood and rear deck length. The lower hood and deck also have a tendency to exaggerate the height of the roof. We, therefore, compromise hood and deck in order to balance the design as shown in Fig. 8.

The lower body line is determined by frame height and ground clearance. We curve it slightly, however, so that it will gracefully follow the rest of the design and blend into the wheel cutouts. These wheel openings, Fig. 9, have been lowered over our previous model in an attempt further to lengthen the car by stressing horizontal areas and by minimization of vertical surface interruptions.

Equal care and consideration is given to all details – always bearing in mind our four design aims. Good styling is not a veneer applied after the design has been created but must be built in as the design progresses. A styling problem is the same whether it concerns the entire body of the automobile or just a small detail such as the steering wheel; design has nothing whatsoever to do with decoration. Rather, design should embrace efficiency, competence, and also stability. This has been our aim in creating the new design shown in Fig. 10.

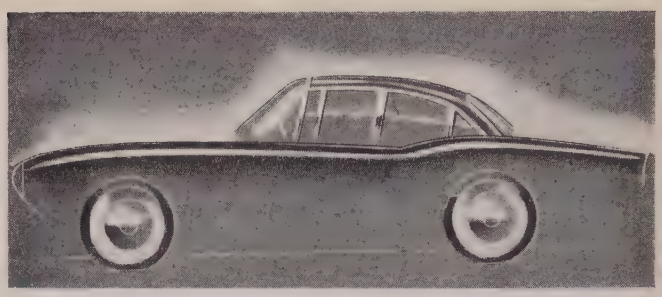

Fig. 7 – Development of superstructure

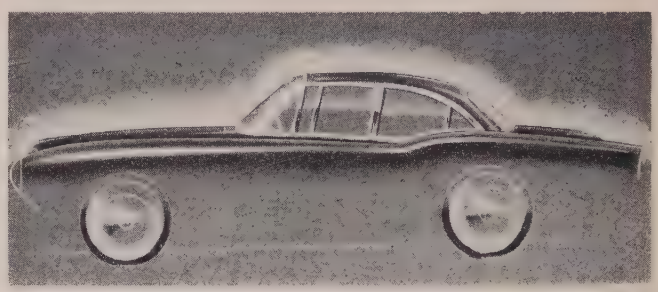

Fig. 8 – Development of hood and rear deck

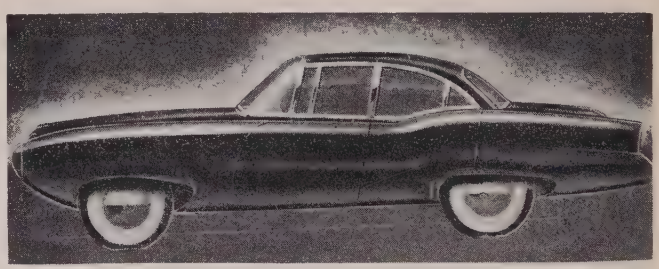

Fig. 9 – Development of wheel cutouts and lower body line

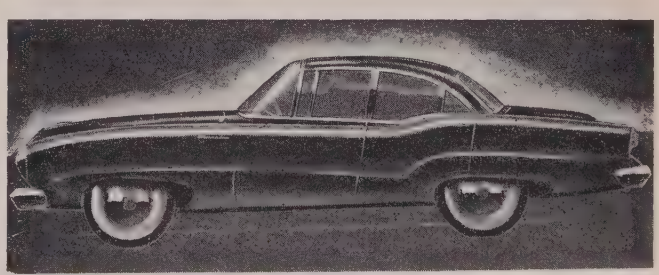

Fig. 10 – Styling proposed design

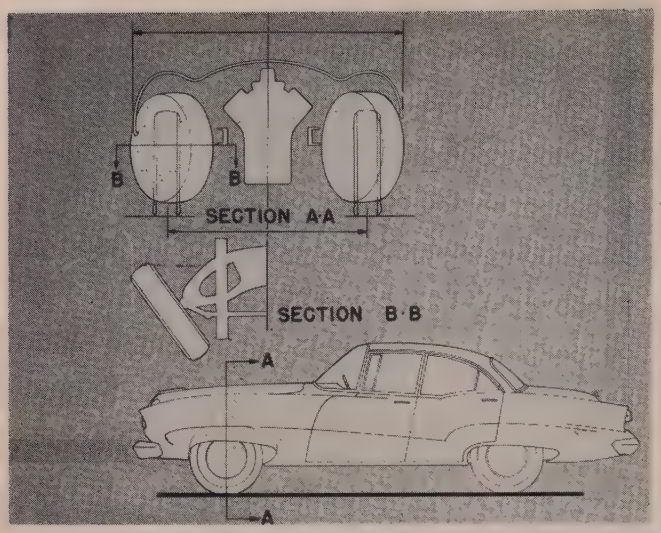

Fig. 11 – Front tire clearance

We now have designed the complete automobile.

Assuming that this design satisfies the styling objectives, we will submit our proposal to the engineering group for their consideration. In actual practice, automobile surfaces of today, with fillets and free-flowing contours, have advanced to a point wherein a side, front, and rear view drawing no longer serves as a suitable conveyance of thought between stylists or between stylists and engineers. Instead, the stylists depend to a great extent upon three-dimensional clay models as an aid in design development and as a medium to relay their thinking. For this study, however, the design must be presented in line drawings only.

The automobile stylist, obviously, is a specialist who contributes to the planning of a project with particular reference to its appearance. This specialization of esthetics that is half gift and half experience cannot exist on its own in the automobile industry without the combined talents of the engineering and production groups. Let us follow the engineers as they pull this dream into a reality.

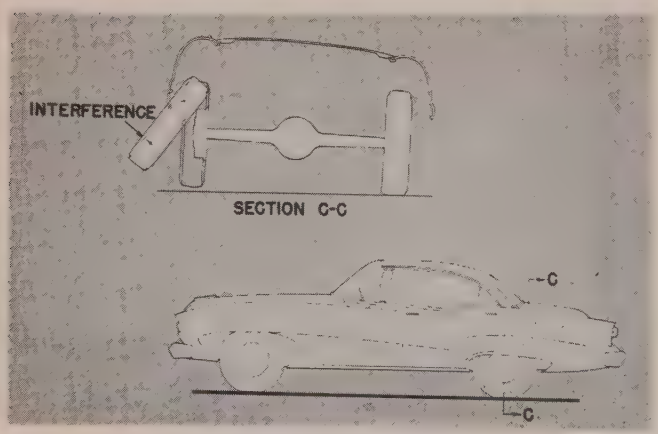

Fig. 12 – Rear wheel clearance

Engineering Problems

We have seen that the stylist, to be successful in arriving at something new and pleasing, must give free play to his imagination until he finds a theme or motif around which he can work his ideas.

The body engineer on the other hand finds that he is faced with a multitude of problems upon receipt of the stylist's drawings and that he must direct *his* creativeness toward making the stylist's concept practicable.

If the body engineer understands that the stylist has a definite purpose in developing his concept of this new car and has had to draw on all his resources of creative talent to bring forth something new and different, he will try to the best of his ability to design his structure within the shape and form established by the stylist.

There are, however, certain fundamental requirements that the body engineer must establish to produce a commercially acceptable product.

The body engineer is responsible to management to see that the body is structurally sound, safe, weatherproof, comfortable, and can be economically manufactured.

I would like to point out here that, by mutual agreement, my colleague has incorporated a number of problems into his design which normally would have been settled at some period during the styling development of this car.

As we go through the discussion of the various engineering problems related to this design, we will make what alterations we find necessary in the car as submitted and finally turn back to the stylist the revised version of his design. This is a very important point, because no one is any better qualified to revise and correct the original design than the one who created it in the first place.

The first point we will consider is the wheel cut line over the front wheel shown in Fig. 11. In the upper part of this picture you will note the cross-section taken through the centerline of the front wheels at A-A. (View B-B is the plan view of the front wheel in full-turn position.) On the left-hand side we see that as the wheel is turned and under a full bounce condition, the tire and the fender interfere.

We have three alternatives to correct this interference:

1. We can narrow the tread; that is, move the tire in toward the centerline.
2. Widen the fender line.
3. Raise the bottom line upward until we reach a point where we have no interference.

Since the overall width of the car (as well as the tread width) was established by management, 1 and 2 are eliminated. The only correction possible in this instance is to raise the fender line (3), as

shown on the right-hand side of view A-A and represented by the dotted line in the side view of the car.

A similar condition exists at the rear wheel (Fig. 12). Although the rear wheel does not change its position in relation to the centerline of the car, except in an extreme roll condition, the tire must be free to clear the fender line and the brake drum for removal purposes. This is shown by Section C-C in Fig. 12. In this case for the same reasons as stated previously we recommend that the fender cut line be raised as shown by the dotted line. In this case the stylist may have the option of adding fender skirts over the wheel opening if he so chooses.

Fig. 13 shows the overall structural concept of the automobile body as the body engineer must consider it. The view at the bottom of the picture shows the frame and body combination subjected to a 1500-lb static load evenly divided between the two seat locations, that is, 750 lb at each of the front and rear seating points. Under these conditions, the structure is to be of such rigidity that it will show a deflection no greater than 0.10 in. taken at the bottom of the frame midway between the centerlines of the wheels. In such a test the spring suspension is blocked out by placing supports from the frame to the ground at the wheel locations as illustrated.

The body is expected to carry from 50% to 60% of this total load and the frame from 40% to 50%. It is generally accepted that if the body structure is sufficiently rigid, it is also adequately strong.

In the upper portion of Fig. 13 is Section F-F taken through the complete body. On the left are two sections, D-D and G-G, taken through the windshield post and the top of the roof at the top of the door opening respectively. These sections have been designed to conform to the original styling version of the body and are found to be inadequate from a stiffness standpoint. The heavy shaded portions of these sections show the main structural members that are considered as body structure.

On the right-hand side are shown the corresponding redesigned sections, D^1-D^1 and G^1-G^1.

When the body engineer determines the structural requirement of a given body, he designs many sections taken at a number of strategic locations throughout the body. These are known as typical sections and serve two purposes. (1) They give all concerned an idea of how the structure is to be assembled, and (2) they are used in determining the potential rigidity of the body structure by determining the sectional properties of each member by establishing the moment of inertia of these sections.

In this discussion we are considering only a few of these sections that will have the greatest effect in the stylist's conception of the car body.

In Section D-D (the original version) we find

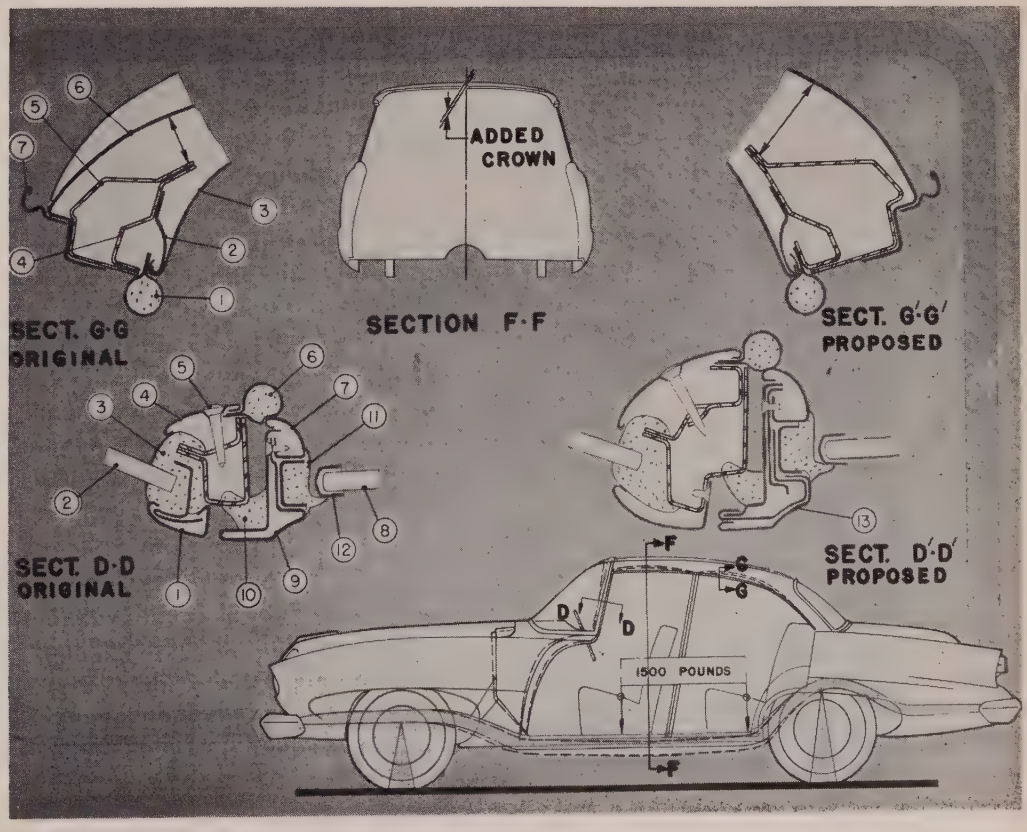

Fig. 13 – Overall body structure

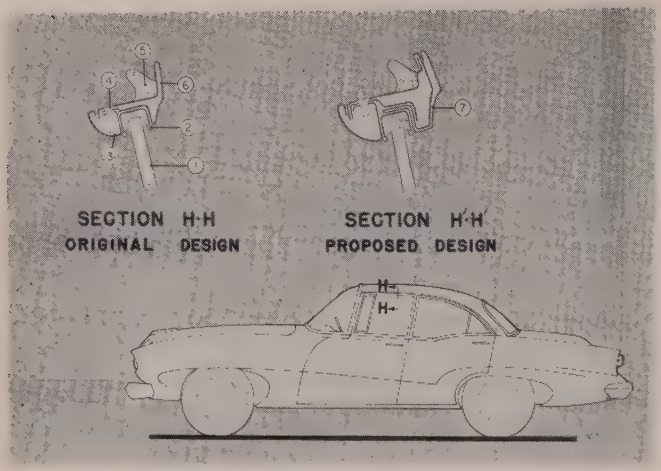

Fig. 14 – Door header construction

that the stylist is striving for a very small windshield pillar and door pillar section. This section consists of the main structural member (shown in shaded area) which is made from two parts of 0.075 gage, spot-welded together, forming a closed box section. The moment of inertia of this section calculates to a maximum and minimum value of 0.035 in.^{4} and 0.028 in.^{4} respectively. By past practice, this value is too low for consideration.

The balance of the parts in the section are as follows:

1. Chromium molding framing the windshield.
2. The windshield glass.
3. The rubber weatherstrip containing the windshield glass.
4. The windshield inner molding.
5. Windshield inner molding retaining screw.
6. The rubber and fabric draft strip or windhose that runs around the entire inner periphery of the door opening.
7. The door window retaining or garnish molding.
8. The door ventilating glass.
9. The door upper frame structure. This is shown as a one-piece rolled section to be made from polished stainless steel and bolted to the door lower panel at the belt line.
10. The rubber weatherstrip that seals the door to the body against wind and rain. This rubber seal also runs around the entire periphery of the door.
11. The rubber weatherstrip for sealing the ventilating glass frame (13) and the door frame.
12. The chrome frame around the ventilating glass (8).

On the right-hand side of Fig. 13 we show the proposed Section D^1-D^1. It will be noted that the structural portion (shaded area) has been increased in area to a considerable degree to bring it within the required value necessary. This section has a moment of inertia of 0.129 in.^{4} maximum and 0.047 in.^{4} minimum, while the gage has been reduced to 0.059 stock. Again the corresponding parts are shown as follows:

1. Windshield chrome frame.
2. Windshield glass.
3. Windshield glass rubber retaining strip.
4. Windshield inner molding.
5. Inner molding retaining screw.
6. Draft strip or windhose section.
7. Door frame inner molding.
8. Door ventilating glass.
9. Door upper frame structure. This has been redesigned to be made integral with the door lower panel inner and outer.
10. The door weatherstripping.
11. The door ventilating glass weatherstripping.
12. The door ventilating glass chrome frame.
13. Chrome scalp to be assembled to the door upper frame after the body has been painted.

For similar reasons we find it necessary to change the roof rail section as shown in Section G-G and G^1-G^1.

Considering Section G-G first, we find that the structural portion consists of Part 4, the roof rail inner panel, and Part 5, the roof rail outer panel, spot-welded together to form a box section. The moment of inertia of this section is found to be 0.139 in.^{4} maximum and 0.075 in.^{4} minimum. This is considered too low a value for this car.

The remaining parts shown in this section are:

1. The windhose or draft strip.
2. The windhose and headlining retainer.
3. The fabric headlining.
6. The roof panel.
7. The roof drip molding that extends over the top of the front and rear doors.

It will be noted that the clearance between the roof panel and the roof rail is shown as being insufficient for proper welding clearance.

Section G^1-G^1 shows the proposed version of this same section. Again it has been necessary to enlarge the roof rail members to bring them up to the proper size for sufficient rigidity. This section now has a moment of inertia of 0.260 in.^{4} maximum and 0.123 in.^{4} minimum. This, by past practice, is considered adequate. Again the numbers indicate the related parts in this section as shown for Section G-G.

Section F-F shows that we propose increasing the thickness of the roof because the roof as shown is believed to be too thin for proper handling in fabrication and assembly. This increase in roof crown also gives us adequate room for welding the roof rail as indicated.

It will be noted in the side view of the car in the lower picture that under the 1500-lb loading, the roof rails and windshield pillars tend to deflect as indicated by the dotted lines.

Fig. 14 shows Section H-H taken through the top of the door and the parts shown are:

1. Door dropping glass.
2. Glass run channel.

3. Door inner finish molding.
4. Door molding retaining screw.
5. Door weatherstrip.
6. Door upper frame.

This door frame section is considered too light, and therefore the proposed design is shown (Section H^1-H^1) to represent what the body engineer feels is the size required for this particular body. It will be noted that a chrome scalp (7) has been added to the proposed section. This proposed design permits the door to be made in two main stampings, an inner panel and an outer panel, and welded together. The chrome scalp is added after painting.

For the windshield my colleague has shown a one-piece "wrap-around" or "panoramic" windshield which is bent in two directions (Fig. 15). There are two very important considerations that must be given to any curved-glass windshield design. (1) The windshield must be optically acceptable, and (2) the windshield must be commercially economical. By experimentation it has been found that a glass bent to approximately a 9-in. radius is optically acceptable if the bent portion is so located that it is viewed by the driver at approximately 90 deg to the tangent of the curvature. As the radius of curvature is increased, the angle of sight becomes less critical.

Windshields, as you know, are required by law to be made of plate safety glass. That is, they must be made of two pieces of plate glass bonded together with a plastic inner liner which prevents the glass from shattering in large slivers when broken. The curved windshield is no exception.

To make a curved windshield the glass is cut to size, and two pieces are coated with a substance to prevent them from fusing together under heat. The glass pieces are then laid together for bending over a fixture to which they will conform to the required shape during the application of intense heat.

As the glass softens from the heat, the weight of the glass causes it to drop slowly into the form until the required amount of bending is attained. The glass is then slowly cooled until it can be handled. After bending, the glass is then laminated with the plastic inner liner and the entire assembly put in a huge autoclave where under heat and pressure a complete bond between the glass and the plastic is achieved.

From this description it can readily be seen that to bend a glass in one direction is not the simplest operation and to bend it in two directions increases the manufacturing hazard of breakage and rejected windshields. Therefore, for economical and manufacturing reasons we propose changing the windshield in this design to a single curvature.

In Fig. 16 we endeavor to show by schematic drawings, which in no way indicate the actual method used, the difference in bending a single

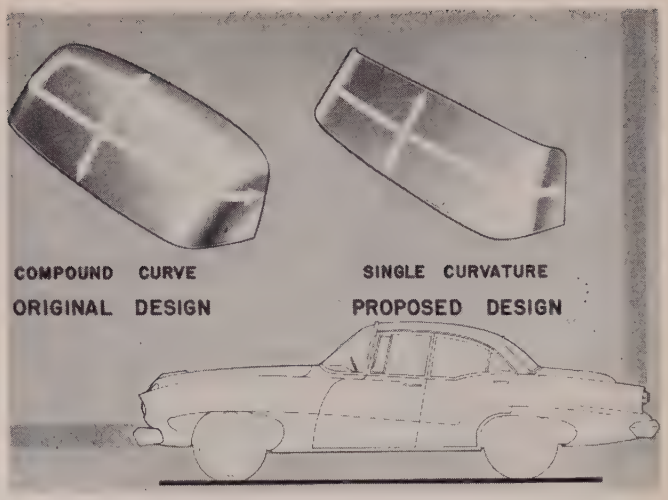

Fig. 15 – Windshield glass design

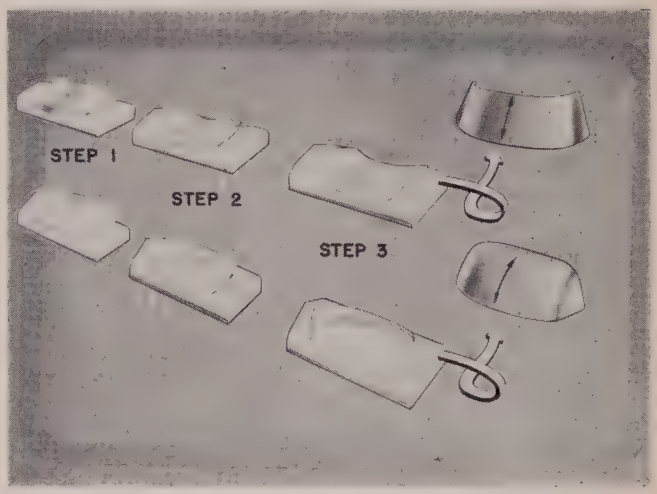

Fig. 16 – Windshield glass bending method

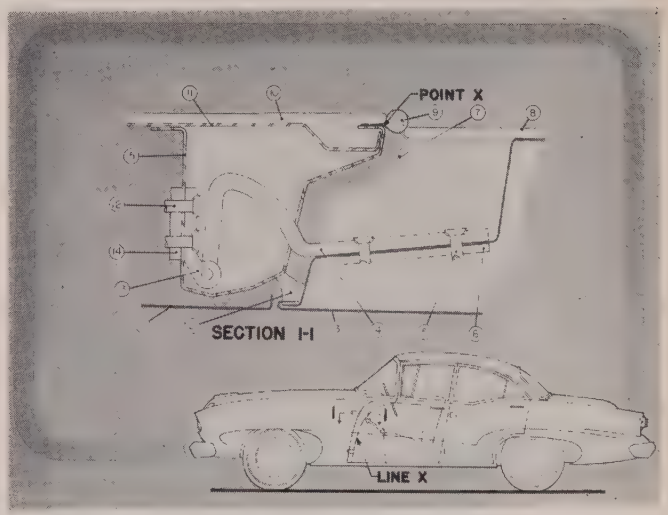

Fig. 17 – Front door hinging

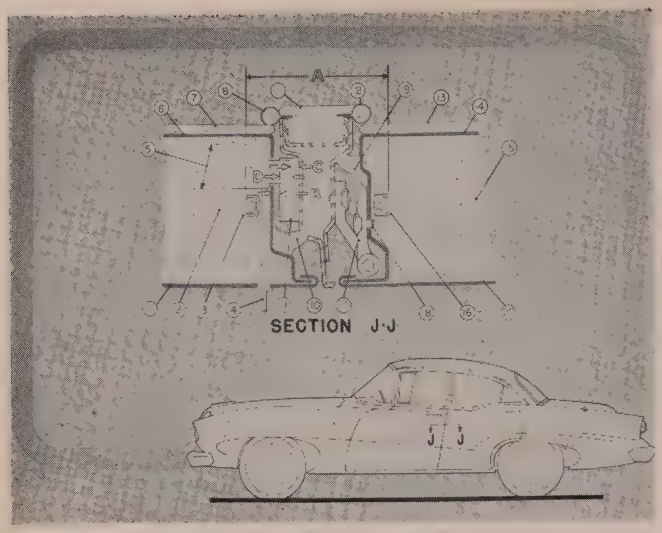

Fig. 18 – Center pillar construction (below belt)

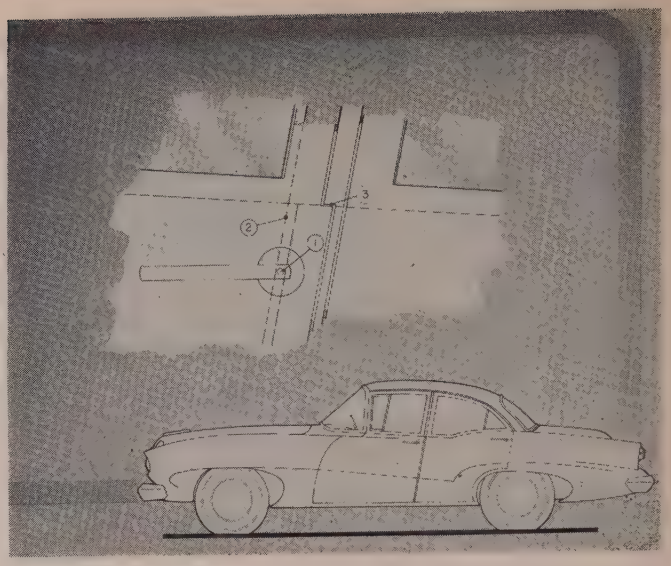

Fig. 20 – Door handle relocation

curvature glass as compared to a compound curvature glass. In Step 1 the glass is laid on the fixture the same for both types of glass. Step 2 shows the glass starting to take form due to the application of heat. Step 3 shows the single curvature glass completely formed to the fixture and ready for cooling while the compound curvature has to be heated considerably more to complete the bending in the other direction. This increases the time of bending appreciably while at the same time poses still greater problems in laminating to the plastic inner liner.

Fig. 17 illustrates a typical front door hinge installation. Section I-I is taken through the upper hinge as indicated and shows the following parts:

1. Front fender surface panel.
2. Door rubber weatherstrip.
3. Front door outer panel.
4. Male hinge strap (door).
5. Hinge strap attaching bolt.
6. Door tapping plate.
7. Door inner panel.
8. Front door trim panel.
9. Front pillar windhose or draft strip.
10. Shroud side trim panel.
11. Shroud side panel.

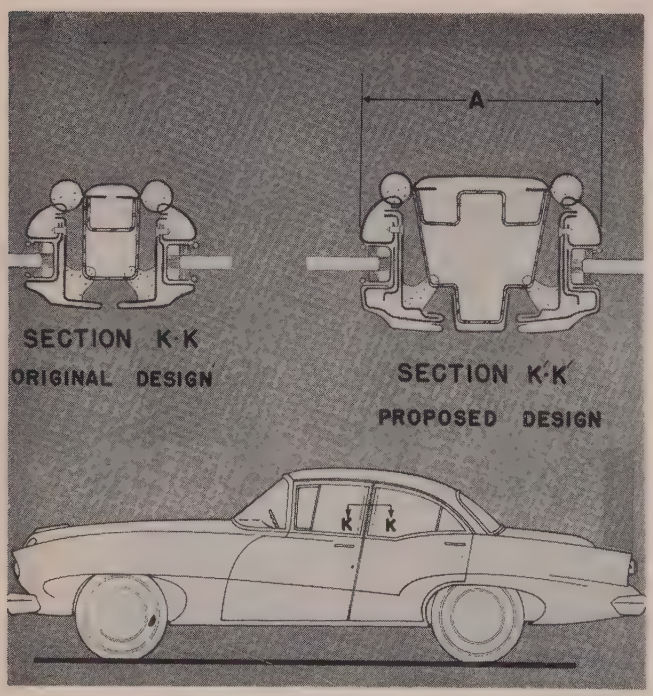

Fig. 19 – Center pillar construction (above belt)

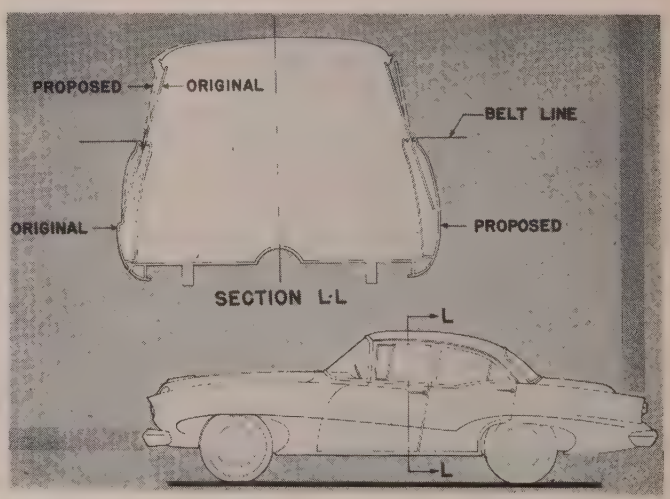

Fig. 21 – Tumble home correction

12. Female hinge attaching bolt.
13. Female hinge strap (pillar).
14. Hinge pillar tapping plate.
15. Front body hinge pillar.

The front door hinge must be rigid enough to support a 200-lb load at the door handle without the door deflecting more than ¼ in. No permanent set should take place under these conditions.

In establishing the pillar inner line X, it is essential that as large a radius as possible be maintained from the base of the windshield to the pillar and at the same time allow adequate room for passenger entrance between the seat and the pillar indicated by the arrow in the lower picture.

Design of Center Pillar

The problems involved in the design of a center pillar (Fig. 18) are probably the most complex in the entire body shell. In this case, the stylist has tried to get a very light pillar between the front and rear door.

To be acceptable, the center pillar as a structural member must be able to support the rear door weight plus 200 lb and at the same time stand considerable torsional loading as the rear door is swung open to its stop position.

The pillar is also expected to give a solid mounting for the front door lock striker. Any undue fore-and-aft movement of the pillar at the lock location could cause the front door to become disengaged.

Section J-J represents the proposed construction for this body. The main structural members are again shown by the shaded portion, and the remaining parts are as follows:

1. Front door outer panel.
2. Front door dropping glass.
3. Glass run channel.
4. Door lock rod from the outside push button.
5. Door lock.
6. Front door inner panel.
7. Front door trim panel.
8. Front door opening windhose.
9. Door lock striker.
10. Front door weatherseal (rubber).
11. Center pillar trim panel.
12. Rear door opening windhose.
13. Rear door trim panel.
14. Rear door inner panel.
15. Rear door dropping glass.
16. Glass run channel.
17. Rear door hinge.
18. Rear door hinge attaching screw.
19. Rear door rubber weatherstrip.
20. Rear door outer panel.

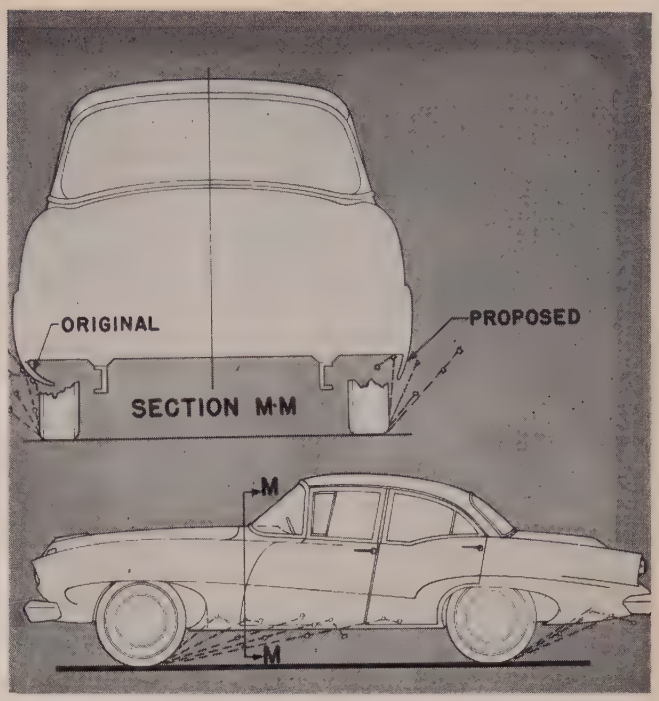

Fig. 22 – Turn under revision

This distance between the two dropping glasses represented by dimension "A" is arrived at in the design of the center pillar after all the parts such as the hinge, lock, striker, and so forth, have been placed in their relative positions and sufficient area is left to get an adequate structural member between them. The most critical dimensions to maintain are the door inner panel clearance to the lock striker "B," the clearance from the lock bolt end to the pillar face "C," and the overlap of the lock bolt to the lock striker "D."

After establishing the conditions of the center

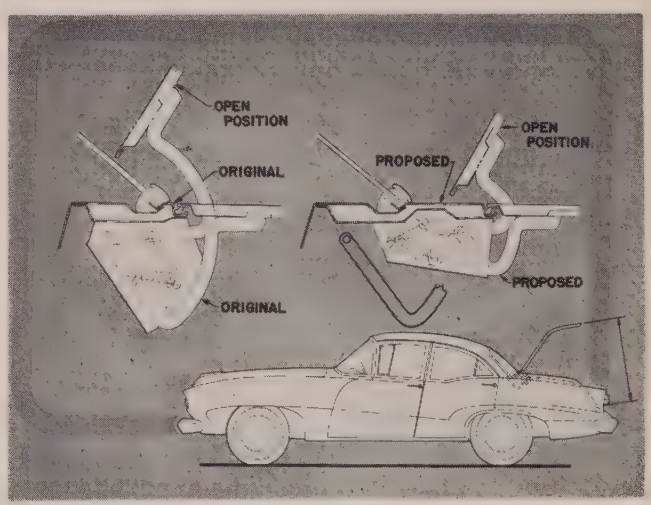

Fig. 23 – Deck lid hinging

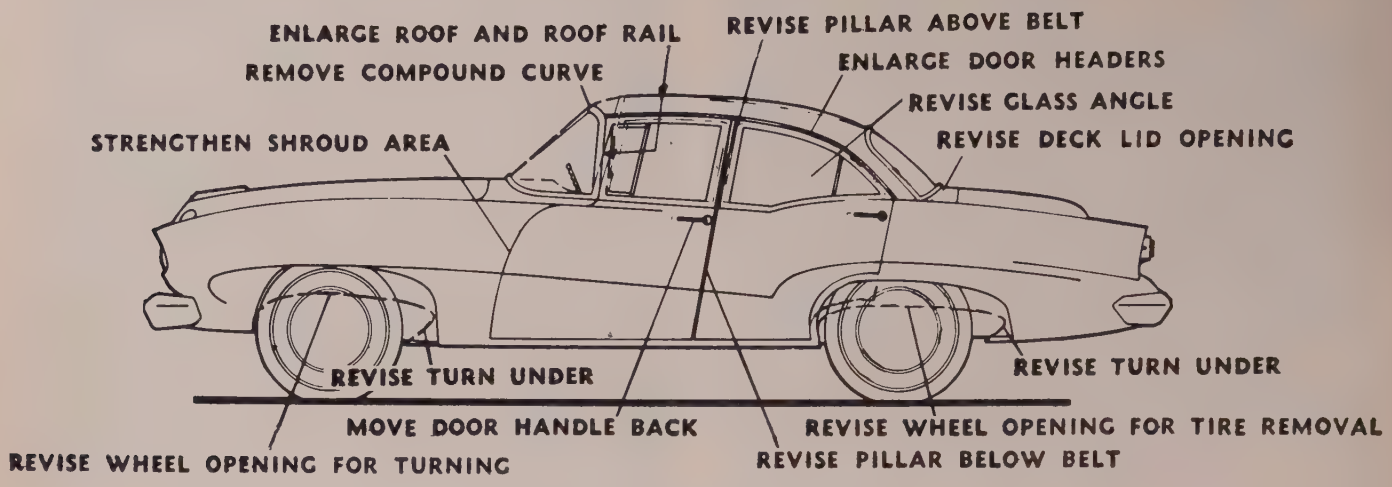

Fig. 24 – Summary of engineering changes

pillar at the door lock area, let us now consider what happens to the pillar above the belt line.

In Fig. 19 we have two sections shown. The one on the left, Section K-K, is taken through the pillar as indicated and shows the design as originally submitted. The main structural member is too small and the distance between the glass runs 2 and 9 is too narrow to satisfy the pillar at the lock area as previously shown. The door construction is the same rolled section as previously referred to and cannot be considered for the reason stated before.

In the proposed Section K^1-K^1 we have enlarged the pillar section to match dimension "A" to the same as established below the belt line.

The door structure has been changed to a stamped construction, and a chrome scalp has been added to the front and rear door outer panels as well as the center pillar outer surface.

The effect of this change on the body design is shown by the dotted lines in the view at the bottom of the picture.

Another appearance change as the result of the center pillar redesign is shown in Fig. 20 where the door handle (1) is relocated rearward due to the increase in the center pillar width and to eliminate interference with the dropping glass.

The dropping glass edge (2) has been moved forward, and an offset (3) in the front door opening line has become necessary.

Turn Under of Body Side Shape

Fig. 21 illustrates what is known as the "turn under" and "tumble home" of a body side shape. Section L-L is taken through the complete body. The upper portion of the section from the roof to the belt line is the "tumble home," the lower portion from the belt to the bottom of the body is the "turn under." In the original design the tumble home is excessive, causing the glass to contact the door outer panel when the glass is dropped completely down. This can be corrected by straightening the tumble home as shown on the left side of Section K-K, or the stylist may have the option of eliminating the offset from the turn under and leaving the tumble home as originally proposed.

Another problem concerning the turn under is shown in Fig. 22. In this case we have taken a section through the body at M-M. In Section M-M the left-hand side indicates the original design where the turn under rolls under the body an excessive amount. This makes it possible for stones and gravel thrown up from the tires to mar the surface of the body as illustrated. On the right-hand side this fault is corrected by moving the lower portion of the body outward so the stones will hit the underneath side causing no damage. This change necessitated removing the points from the front and rear fenders at the rear of each wheel as indicated by the dotted lines in the side-view illustration.

Finally we come to the trunk lid hinging shown in Fig. 23. To achieve the effect of a long rear trunk, my colleague has made the trunk opening adjacent to the base of the back light as shown in the upper left-hand illustration. To hinge the lid to clear the backlight and have sufficient access to the trunk requires an unusually large hinge. By the addition of a panel between the base of the backlight and the trunk lid opening, the hinge is reduced considerably in size. It is proposed that

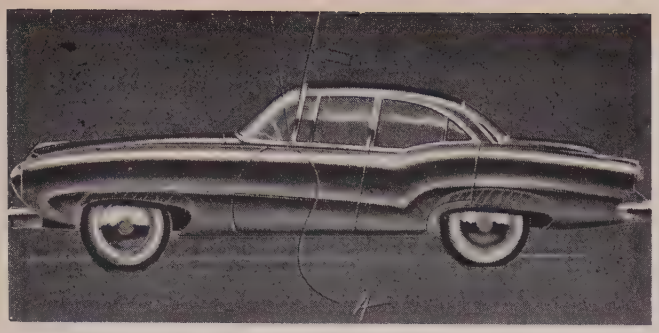

Fig. 25 – Areas of major revision

this panel be incorporated into the style of this car as the large hinge interferes with the luggage space in the trunk and, therefore, is not considered desirable.

Changes Proposed

Let us now summarize the changes we have proposed:

1. Revise front wheel opening for turning.
2. Revise rear wheel opening for tire removal.
3. Enlarge roof and roof rail sections.
4. Enlarge door headers.
5. Windshield compound curve removed.
6. Strengthen shroud area.
7. Center pillar revised below the belt line.
8. Center pillar revised above the belt line.
9. Locate door handle rearward.
10. Glass angle revised in doors.
11. Revise turn under.
12. Deck lid opening revised.

For public acceptance the automobile must be well-styled. For customer satisfaction it is mandatory that the automobile must be well-engineered.

Obviously, the changes we have proposed do affect the appearance to some degree; however, the stylist is a realist and recognizes that he must compromise his ideals with reality. Therefore, my colleague will now show you how he overcomes these obstacles in arriving at his final design.

Summary

Skill and experience play increasingly important roles in these final steps of product development. The original styling goals remain the same, but an entirely new approach to certain details may be necessary to fulfill engineering demands and maintain design unity.

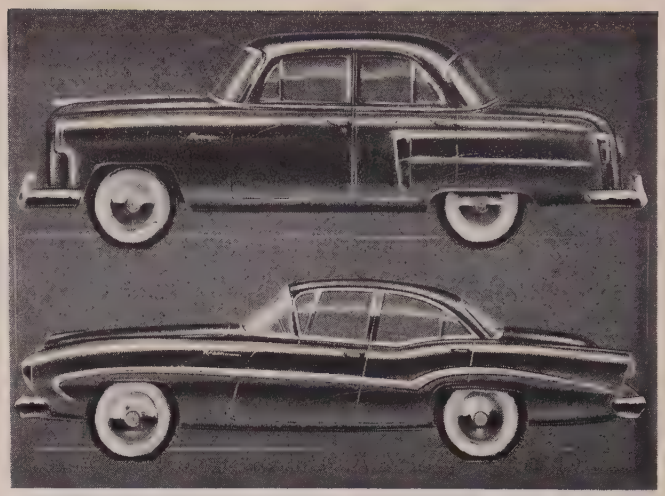

Fig. 26 – Comparison of current and future model

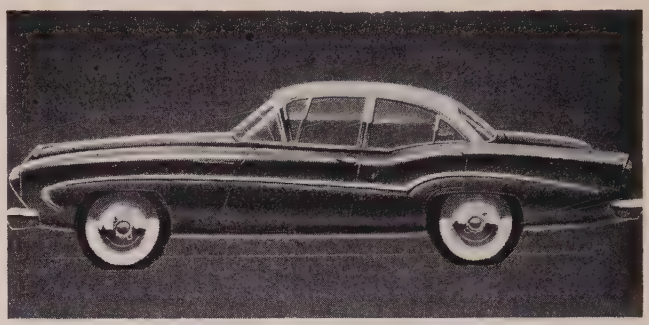

Fig. 27 – Future model

As shown in Fig. 24, only two items seriously threaten the original styling concept. The windshield has been sufficiently modified to force a restyling of the upper structure. The need for raising the wheel cutouts eliminates the horizontal feeling expressed in the original design.

The balance of the engineering changes, while important to the stylist, will not harm the overall design goal; and with these changes, styling advantages can still be achieved over the present production model.

Fig. 25 identifies the changes required in the roof area. By holding point "A" and swinging the header forward until it intersects the flat surface of the windshield angle, windshield visibility is kept to the maximum. The front ventilator wings must be modified to fit and the backlight angles changed slightly. These modifications bring the upper structure back into harmony with the lower body.

The added height of the wheel cutouts coupled with the extended trailing edge leaves an unattractive gap between the wheel and body surface. The best solution is to depart completely from the original shape, let the cutouts follow the periphery of the tire, and use a chrome body side molding to

replace the original offset. The molding will re-establish the horizontal effect lost by raising the cutouts.

Now that the basic styling has been completed and is within the limits of good engineering, let us compare the new model (Fig. 26) with our present vehicle and review the original four aims, which were:

1. Eliminate square box-like appearance.
2. Lower and lengthen hood.
3. Create a light roof effect.
4. Give the feeling of greater overall length.

We believe that we have accomplished our aims. Engineering is satisfied that construction will present no serious problems. Who is the designer – the stylist or the engineer? Together we have arrived at the formula for a new product, a formula created by a team of specialists working to the mutual benefit of all, resulting in an automobile which has improved appearance and new sales appeal.

Together we have designed a new automobile (Fig. 27).

ORAL DISCUSSION

Reported by G. M. Buehrig
Ford Motor Co.

C. C. Dybvig, Spicer Mfg. Division, Dana Corp.: What type of training prepares a person for a styling career and a body engineering career?

Reply: At present, the only school with a course of training in body engineering is the General Motors Institute. The University of Michigan expects to offer training in this field fairly soon. The Art Center School, Pratt Institute, and the Cleveland School of Design are some of the schools offering some training for stylists.

C. W. Phelps, Yale University: Why lengthen the hood for style at the expense of safety, and why place the steering wheel so high that it interferes with vision?

Reply: The longer hood does not necessarily reduce vision or impair safety. The steering wheel is placed as low as possible with adequate clearance to the seat and to be the best compromise for people of different stature.

T. Morris, Ward's Automobile Topics: Why not use a door lock that ties the body structure together?

Reply: Mercedes uses a lock of this type, but it is expensive and has many manufacturing problems because of the exact fit required on the door.

E. P. White, Aluminum Co. of America: What was the anticipated production for the example chosen?

Reply: No figure was used, but it was assumed to be a high production car.

Mr. White: Would the design have been changed if the model were designed for reinforced plastics?

Reply: It might have been.

T. H. Rogers, Goodyear Tire and Rubber Co.: In designing the car, the outside appearance was stressed. How about the inside?

Reply: It would receive equal consideration, but space limitations prevented its being included in this paper.

J. W. Howden, J. W. Howden Co.: It was stated that the easiest place to start a proposed design is with the present model. Why?

Reply: It was stated that the present model was studied and evaluated in setting up the design aims for the new car.

Mr. Howden: Do designers ever start to design a car from "scratch" taking into consideration only function and styling?

Reply: Yes.

Maurice Olley, Chevrolet Motor Division, GMC: Has new design sacrificed head room as compared with old? How will weights compare?

Reply: The car was lowered by floor plan and chassis changes which allow for lower seats. No weights were calculated on this problem, but there is no reason to believe they would vary appreciably.

A. L. Haynes, Ford Motor Co.: Are the relationships with stylists always as smooth as represented in this paper?

Reply: No, not always; however, this relationship is improving. It is expected that the relationship will be improved somewhat by a closer fraternal feeling between the two groups as members of the styling profession become more numerous in the SAE.

W. Lichty, General Motors Institute: Has the elimination of wheel shields been a styling or an engineering decision?

Reply: Styling.

A. C. Bodeau, Ford Motor Co.: How does the stylist inform the body and chassis engineer of styling trends?

Reply: Usually, new ideas in styling appear in sketch form several years ahead of acceptance for a production car.

J. J. Ivancic, White Motor Co.: Will the introduction of fiberglas as a material for bodies allow the stylist to revive designs that were discarded because of sheet-metal limitations?

Reply: Both materials have limitations. The product designer considers the material when developing the design.

Size, Structure, and Shape Of European Automobiles

Laurence Pomeroy, The Motor

This paper was presented at SAE National Passenger Car, Body, and Materials Meeting, Detroit, March 3, 1954.

ECONOMIC conditions in postwar Western Europe are, according to Mr. Pomeroy, responsible for 90% of European cars being smaller, noisier, slightly lighter, but very similar to American cars, and somewhat faster than might be expected.

How the designer ingeniously fits the passenger into the seemingly small space afforded by the European car is described in this paper. Other features of European automobiles discussed are their structure and styling.

The Author

LAURENCE POMEROY is technical editor of *The Motor*. In 1926 he became a sales engineer for E. T. White, Ltd. in London, England. In 1928 he joined Wellworthy, Ltd., as a consulting engineer. Mr. Pomeroy left a consultant position in Germany to join the staff of *The Motor* in 1937.

THE author last had the honor of presenting a paper to the Society nearly 10 years ago in 1946. His subject then was "The Performance of European Economy Cars," and the paper was written almost immediately after the conclusion of a long, exhausting, and ruinous war. In these circumstances he made two statements, of which one has proved true, the other false.

The false statement was, "This competition will be fortified by world developments in motor roads which will mask the inherent limitations of the small car from the aspects of hill climbing and acceleration." Outside America there have, in fact, been few developments in motor roads throughout the world except for perhaps 100 miles of two-lane highway in Belgium and the beginnings of extension to the great autobahn network in Germany. In France under 100 miles of new road have been built since the war, and in England expenditure has been almost entirely confined to the erection of "Danger" and "No Parking" signs.

The true statement was, "Economic factors prescribe that normal European cars should not exceed 2000 lb curb weight and should be capable of at least 30 mpg in day-to-day running. Improved body form would permit such cars to sustain road speeds of 70-80 mph and will make the small economy car increasingly competitive with larger types."

Economic Aspects

During the period from 1946 to 1953, the European car has been a small, light car, and there seems no probability that it will depart from this formula in the next decade. For this reason it is necessary to analyze the economic framework within which

Table 1 – Production of Private Cars in Europe, 1953

United Kingdom	570,000
France	360,000
Germany	355,000
Italy	133,000
Total	1,418,000

Table 2 – Principal Manufacturers by Nationality

United Kingdom	5
France	5
Germany	3
Italy	1

the European automobile industry has to live before considering the strictly engineering aspects of its products.

Western Europe has a population slightly greater than that of the United States, but it is divided into 14 main national units all of which restrict trade across their frontiers by quotas and fiscal devices. These are imposed not solely by greed or from mean-mindedness but primarily to preserve local employment and to conserve a pool of skilled labor upon which survival may depend in case of war. Restrictions are also thought to be necessary for reasons of international currency, which is too large a subject to outline in this paper.

The result of these restrictions is to lower the productivity of Western Europe as a whole, and in comparison with the United States there are also many other factors which tend to reduce the average output per man which becomes available for civilian consumption. In some countries, notably the United Kingdom, the burden of arms is very heavy, and the postwar development costs of only two British jet engines have been paid for by tax money which would have bought one eighth of all the new cars which have been put on to the British market since the war. One 100-hr-type test of a typical jet engine consumes enough fuel to keep 3% of all British cars running for a month. Similar erosions of private buying power by communal needs in respect to rearmament and also to social welfare can be seen in most other European countries. In addition many of them are poor in natural resources (such as thickly populated Italy and sparsely populated Norway) or have a low level of skill, as in Spain. As an approximation, the productivity per head for Western Europe is around one-third that of the United States, and when deductions have been made for armament the percentage is probably even lower. However, even at the stated figure the American must imagine living in a country having roughly the same population as the United States but supported on only one-third the number of work people.

In the realm of transport the position is further influenced by the close network of railway and other public services which have been built up in the past hundred years, and although England has only one-third the population of the United States there are twice as many people carried in railway trains in a year.

It will be plain that the need of an automobile for personal transport is less in Europe than it is in the United States, and the possibility of purchasing and operating one is not only lower now but is likely to be permanently lower.

There is one further aspect of automobile marketing in Europe which will probably have repercussions on the design of private cars in the next decade. It is becoming increasingly difficult for a private person in Europe to buy and operate a car on his personal account.

Few cars can be purchased for less than $1500, and none can be amortized and run for less than $600 per annum. Assuming that few people can devote more than 20% of their net income to an automobile, it follows that ownership of a new car implies a net income of not less than $3000, but this is an absolute minimum. It would be reasonable to take $4000 as a normal base in England, and according to official returns there are only 1.3 million families receiving $4000 or over per annum. On the face of it, new-car buyers cannot exceed this number.

In practice more than 90 European cars out of 100 are purchased with company funds but used for both business and pleasure. This may well lead to three differing points of view which will govern the choice of the make and type of car bought. Companies earning high rates of profit may endow, so to speak, their senior executives with expensive and exotic types of cars which will be regarded as the fruits of office. In other cases the initial price will be considered as of minor importance compared to economy in running and maintenance, that is, the car will be judged as a machine tool. In the third case companies will seek to provide their employees with transport at the bare minimum cost.

To sum up, it is likely that companies will tend either to purchase cars of the smallest and cheapest kind, or alternatively will regard first price as unimportant. It may be that this will reduce the sale of medium-sized, medium-priced vehicles.

The full effect of this change in trading practice has yet to be felt, and it will now be proper to turn from explanation and speculation to some figures of current output. The Western European countries produced in 1953 private cars in the quantities shown in Table 1.

A fair proportion of these cars were exported to countries lying outside Western Europe, and it is probable that the total number of new cars pur-

chased within the European market was but little over one million in the past 12 months.

Hence, in approximate terms the total purchase of Western European cars by the natives of that region is roughly equal to the purchase of Chevrolet products alone of the General Motors group by United States citizens. This being so, it is surprising to observe that there are 50 major makes of car and about 120 distinct design types. A very wide range of vehicles is offered, weight figures running from 1100 to 5900 lb, engine output from 9 to 210 bhp, maximum road speed from 45 to 145 mph and fuel consumption from 40 mpg over long distances down to 10 mpg. Prices vary from $1000 up to $17,000. These numbers and these variations might at first sight seem to make any attempt to analyze European design in general terms quite impossible. Closer inspection of the figures reveals, however, that there is reasonable uniformity between 90% of the cars sold and that these emerge from only 14 principal factories grouped as shown in Table 2.

If we reckon that these produce about 1¼ million units per annum, we have about 90,000 units per annum per organization from the large (by European standards) factories, leaving 150,000 units emerging from the remaining 36 separate manufacturers, or an average of just under 5000 per annum from the specialist makers. Actual outputs in the latter category are a good deal more varied, being from 100 per annum by Ferrari to around 10,000 per annum by Jaguar. In this field the seven-passenger limousine with custom-built body built to run on the Promenade des Anglais at Nice is only comparable with the V-12 overhead camshaft two-seat coupe built to compete in the Mille Miglia in the matter of price extracted from the connoisseur; and so the author proposes largely to ignore this variegated, if fascinating, collection of vehicles and to base this paper on the characteristics of cars bought by average buyers.

Within these limits we have 36 distinctive design types originating from 18 financial entities, of which two in Sweden have a very limited output and two in Czechoslovakia are, strictly speaking, outside the confines of Western Europe and are included only by reason of historic tradition and the present fact that their products are bought in some parts of Western Europe, for example, Belgium.

Car Specifications

Reduced to the essentials of engine output, wheelbase, tread, and weight we can safely say that 90% of the million cars purchased by the average European buyer in the past year, or likely to be bought in the coming year, have specifications as set out in Table 3.

It may be valuable at this point to summarize the findings on the basis of the smallest and largest factors as well as the average and to compare them with a typical American car such as the Chevrolet. (See Figs. 1-5.) In this comparison the 2-CV Citroen is excluded, as it is in effect a special-purpose vehicle, although an extremely popular one. With this qualification we have the data shown in Table 4.

It will be observed that, although average European cars betray variations in engine power of 3/1,

Table 3 – Specifications of Various European Cars

Make and Model	Maximum Bhp	Wheelbase	Tread	Dry Weight, lb
Czechoslovakia				
Minor II	20	91	45	1480
Skoda	32	98	49	1960
Tatra	56	106	51	2680
United Kingdom				
Austin A.30	30	79½	45	1460
Austin A.40	40	92½	49½	2160
Austin A.70	68	99	56	2740
Ford Popular	24	94	45	1670
Ford Prefect	36	87	48	1500
Ford Consul	47	100	50	2450
Ford Zephyr	68	104	50	2600
Hillman Minx	37.5	93	51	2000
Morris Minor	30	86	50½	1750
Morris Oxford	41	97	53	2200
Standard Vanguard	68	97½	50½	2800
Standard 8	26	84	48	1450
Vauxhall Wyvern	40	103	54½	2200
Vauxhall Velox	64	103	54½	2340
France				
Citroen 2 CV	9	93½	49½	1100
Citroen 11 CV	56	114	53	2350
Ford Vedette	60	106	54	2580
Peugeot 203	42	100	52	2000
Renault 4 CV	19	82½	47	1180
Renault Fregate	60	110	55	2420
Simca	45	96	48½	2080
Germany				
D.K.W.	23	88½	49	1750
Ford Taunus	38	98	48	1875
Mercedes-Benz 170	52	112	53	2600
Mercedes-Benz 180	52	104	57	2300
Opel Olympia	45	95	49	2000
Opel Kapitan	65	106	53	2660
Volkswagen	25	94½	51	1540
Italy				
Fiat 500 B	16	79	44	1200
Fiat 1100	36	92	48	1750
Fiat 1400	44	104½	51½	2500
Sweden				
Saab	25	97	46	1680
Volvo	43	104½	51	2130
Average European Car	42.0	95	50	2030

Table 4 – Power and Dimensions of Basic Automobiles

	European			
	Small	Large	Average	Chevrolet
Hp	19	68	42	105
Weight, lb	1180	2800	2030	3400
Wheelbase, in.	79½	112	95	115
Tread, in.	45	56	50	58

Fig. 1 – Side view of 7-seater 120-hp Daimler which is the largest car built in Europe today

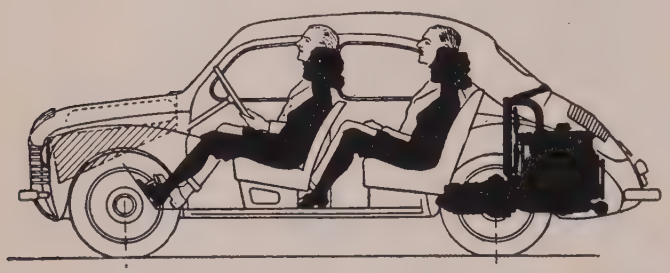

Fig. 2 – Side view of 4-seater 19-hp French Renault with rear engine, the smallest European car in large-scale production

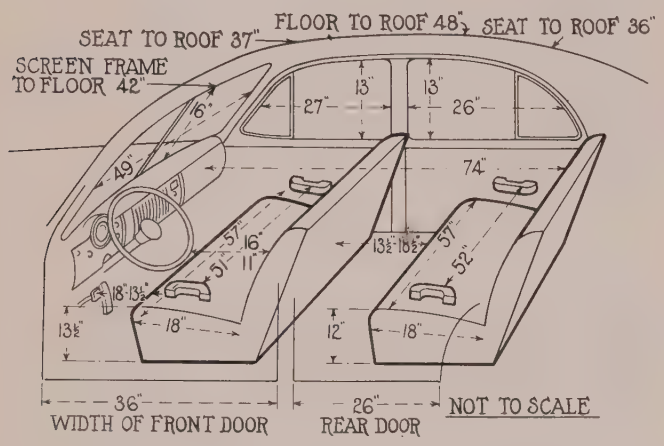

Fig. 3 – Perspective view of Chevrolet body interior

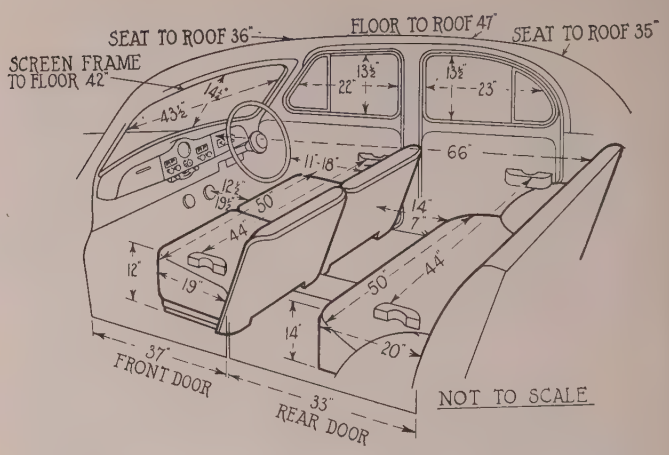

Fig. 4 – Comparative perspective view of 40-hp Austin body interior

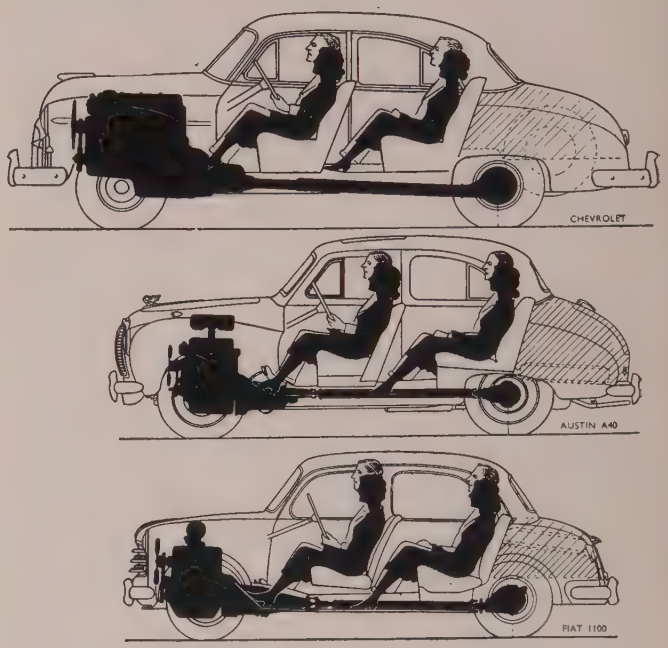

Fig. 5 – Drawings to the same scale of the largest volume produced cars in United States, United Kingdom, and Italy

Table 5 – Body Dimensions of 12 Sample Cars Arranged in Order of Engine Size

Car	Dash to Rear Seat Back, in.	Front Seat Width, in.	Rear Seat Width, in.	Car Width, in.	Seat Height, in.	Floor to Roof, in.	Height, in.
Chevrolet	74	57	57	74	13½	48	66
Renault	60	50	49	56	10	47	59
Standard 8	59	48	47	58	11	48	58
Morris Minor	58	48	47	59	13	47½	58
Fiat 1100	67	47	49	58	13½	46	56
Volkswagen	55	46	52	60	13½	47	59
Austin A. 40	66	50	50	63	12	47	64
Simca	63	51	50	61	10	47	57
Hillman	68	44	49	62	12	48	60
Fiat 1400	67	53	50	65	14	49	58
Ford Consul	72	51	50	64	13	48	60
Renault Fregate	67	57	55	68	12	45	60
Vauxhall Velox	69	53	55	67	14	49	64
Average	64	50	50	62	12½	47	59

Table 6 – Seating and Leg Room (to Nearest ½ In.) on 12 Sample Cars Arranged in Order of Engine Size

Car	Leg Room, Front		Leg Room, Back		Seat Width	
	Min	Max	Min	Max	Front	Back
Chevrolet	13½	18	13½	18	18	18
Renault	17	20	6	9	16½	16½
Standard 8	13	20	8	15	19	18
Morris Minor	14½	17½	7	10	19	18
Fiat 1100	16	20	7	11	17½	19
Volkswagen	12½	19	2	8½	18	19
Austin A. 40	12½	19½	7	14	19	20
Simca	13½	18	8	12½	18	19
Hillman	14½	19½	6½	11½	19	19
Fiat 1400	14½	18½	6	10	19½	20
Ford Consul	13½	18½	8	13	19½	20
Renault Fregate	12	16½	7½	12	20	19
Vauxhall Velox	14	18	7	11	19	19
Average	14	18½	7	11½	18½	19

the changes in weight are as between 1 and 2.4, wheelbase in proportion 1/1.4, and tread as 1/1.25.

Comparing the average European vehicle with the Chevrolet we find wheelbase is in ratio of 1/1.2 and tread ratio is 1/1.16. By contrast in weight there is a difference of 1/1.5 and in engine power of 1/2.5. Finally, and perhaps most important, let us consider the platform area expressed in terms of wheelbase and tread. We then have the smallest European cars with 25 sq ft, the largest with 43½ sq ft, and the average with 33 sq ft. The Chevrolet on the same system of measurement shows 47 sq ft. The platform area therefore of the average European car is 30% less than that of the Chevrolet and of the smallest types 50% less than the Chevrolet. It would thus seem that if the Chevrolet is a 5-6 seater then the smallest European cars would be 3 seaters. In fact, this is not far from the truth, but at least four seats are provided.

Restricted Car Space

Before proceeding to consider the structure and shape of these cars, let us see first how European designers contrive to accommodate four persons within a very restricted space, for the necessity to do this thing powerfully affects both the disposition of the organic units and the structure of the body which encloses and, in modern designs, almost invariably supports them.

As human beings have length, breadth, and height, it may be sensible to compare small European cars with the typical American Chevrolet successively in these dimensions. For this purpose the author has made a selection of typical European cars with engines varying from 45 cu in. up to 130 cu in., wheelbases ranging from 82 in. up to 110 in., and wheel treads from 47 in. up to 55 in. Comprising six British, three French, two Italian, and one German model, they will be treated as a representative team of 12 for the analysis shown in Tables 5-9.

An interesting measurement is the distance between the instrument panel (which is normally on the plane of the leading edge of the front door) and the back of the rear seat.

As can be seen from Table 3 the Chevrolet measures 74 in. whereas the European cars vary between 72 in. and 58 in. The largest of our representative cars therefore is 2 in. shorter than the Chevrolet and the smallest 15 in. shorter; although it is interesting to note that the average of the European team as a percentage of the wheelbase is exactly the same as the Chevrolet. But as the average wheelbases are shorter, the legs of two rows of human beings have to be accommodated in a space which averages 10 in. less than is normal to the U. S. vehicle. Hence a good deal of ingenuity is required from European designers in avoiding rear seats suitable solely for bicrural amputees.

As will be mentioned later, about 4 in. is gained

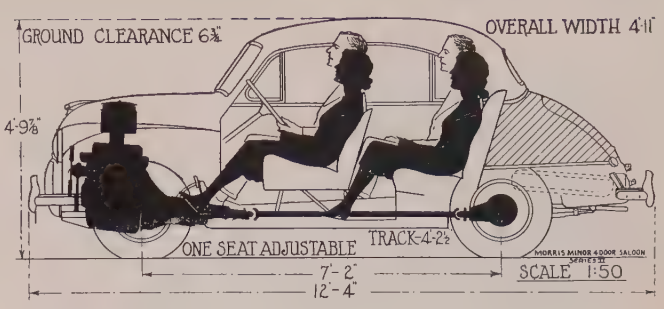

Fig. 6 – Full use made of wheelbase on British Morris Minor car with engine mounted wholly ahead of front wheel centers and pedals encroaching upon the wheel arches

Table 7 – Unused Margins of 12 Sample Cars Arranged in Order of Engine Size

Car	Unused Width	Unused Length	Unused Height
Chevrolet	17	7	18
Renault	6	—	12
Standard 8	10	—	10
Morris Minor	11	—	10½
Fiat 1100	11	—	10
Volkswagen	8	—	12
Austin A. 40	13	5	17
Simca	11	6	10
Hillman	13	4	12
Fiat 1400	12	8	11
Ford Consul	13	2	12
Renault Fregate	11	3	15
Vauxhall Velox	12	8	15
Average	11	5	12

Table 8 – Weight per Cubic Foot of Potential Passenger Space on 12 Sample Cars Arranged in Order of Engine Size

Car[a]	Frontal Area, sq ft	Wheelbase	Cu Ft	Weight, lb	Lb per Cu Ft
Chevrolet	31	9.8	302	3400	112
Renault	20.5	6.84	140	1180	84.5
Standard 8	21	7	147	1450	99
Morris Minor	21	7.17	150	1750	107
Fiat 1100	20	7.75	155	1750	103
Volkswagen	22.5	7.84	177	1540	87
Austin A. 40	25	7.66	192	2160	112
Simca	21.5	8.0	172	1800	105
Hillman	23	7.75	180	2100	117
Fiat 1400	23.5	8.7	204	2500	123
Ford Consul	23.5	8.33	196	2450	125
Renault Fregate	26.5	9.19	244	2420	99
Vauxhall Velox	27	8.8	238	2340	94
Average	23	7.92	180	1953	108.5

[a] Frameless except for Chevrolet.

Table 9 – Brake Horsepower per Square Foot and Related Maximum Speed of 12 Sample Cars Arranged in Order of Engine Size

Car	Sq Ft	Hp	Hp per Sq Ft	Estimated Maximum Speed, mph	Timed Maximum Speed, mph
Chevrolet	31	98	3.13	85[a]	85[a]
Renault	20.5	21	1	58	60
Standard 8	21	26	1.24	62.4	61
Morris Minor	21	30	1.33	64	62
Fiat 1100	20	36	1.8	71	77.5
Volkswagen	22.5	25	1.11	60.5	63
Austin A.40	25	42	1.68	69	69
Simca	21.5	45	2.1	74.5	74
Hillman	23	37	1.61	68.5	67
Fiat 1400	23	44	1 91	69 6	74.4
Ford Consul	23.5	47	2	73	72
Renault Fregate	26.5	57	2.15	75	78
Vauxhall Velox	27	64	2.38	78	80
Average	23	39.5	1.70	68.6	69.8

[a] Within 5% of six United States cars.

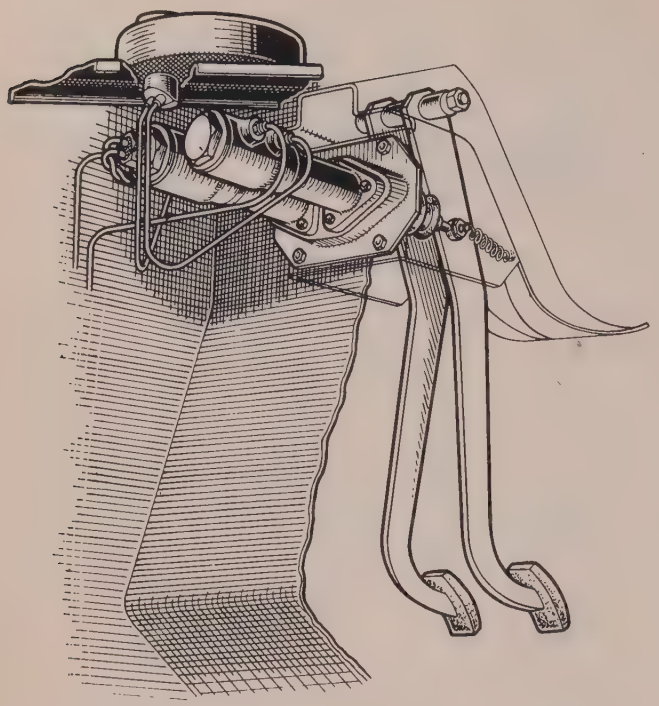

Fig. 7 – Saving of space possible by using pendant pedals and hydraulic brake and clutch gear on British Ford

on European cars by placing the pedals that much nearer to the front-wheel center (Fig. 6). A further 1 or 2 in. can be saved by modifications to pedal mounting and reduced pedal travel (Fig. 7).

Brake-pedal travel is normally confined to between 3 and 4 in., and although this limits the mechanical advantage in relation to the brake shoes with braking areas of around 45 sq in. per 1000 lb unladen weight it is possible to obtain 0.9 *g* stops with pedal pressures not exceeding 100 lb. There remains, however, a deficit of around 6 in. Table 6 shows that there are no major differences between European and a typical American car in respect to the leg room provided for the driver as measured from the leading edge of the front seat to the pedals, and that any difference that there is in respect to length of seat is in favor of the European models. But on the average of 12 typical cars the maximum leg room available in Europe for the rear-seat passengers is 2 in. less than the minimum provided on a Chevrolet.

With the front seat right back the European in an average car has to fit his knees and lower leg into a gap measuring only 7 in. across. It is perhaps primarily for this reason that European cars are less suitable than American for long-distance travel with more than two people aboard.

Having now outlined the effect of short wheelbase upon leg room and seat length, let us look at the picture from the viewpoints of breadth and height.

The Chevrolet, with an overall width of 74 in., will accommodate seats 57 in. wide. The widest of the selected European cars is 68 in. with which it is contrived to offer a seat of similar width. The smallest requires an opening 56 in. wide but will nevertheless embrace a 50-in.-wide seat. It will be seen from the table, however, that there are a number of variations in this matter, and some designers take the view that if there is insufficient space to accommodate three people on one seat then 44 to 48 in. is adequate provision for two persons. In the matter of seat height above the floor there is a considerable uniformity between European and United States practice and fairly close agreement between the figures used by the principal European manufacturers themselves.

It is obvious from a study of the dimensions that humans can in a fair measure be telescoped longitudinally when in a sitting position and compressed laterally. Not much, however, can be done to shorten them in the sitting posture. Thus the figure from floor to interior of the roof is the same (48 in.) for the Chevrolet and for the Standard 8, which is one of the smallest European models, and no designer dare reduce this figure by more than an inch or two. This being so, it is all the more interesting to perceive that there are very big differences in overall height, and this leads us to a further study of how effectively the designer uses the cubic content of a given body space.

This is set out in Table 6 in which unused length between the wheel arches has been computed on the perhaps somewhat rudimentary basis of measuring the difference between the front-wheel arch and the pedal gear. It will be seen that the Chevrolet loses 7 in. in this respect and that it is matched by two European cars with the same figure. On five European cars, however, the pedals are placed either level with, or in some cases ahead of, the wheel arch, and one may regard these as having no unused space lengthwise. The average is 3 in. which shows a gain of 4 in. compared with the American type and which is possible by some constructional features described later in this paper.

There are equally interesting figures in respect to the difference between useful width as determined by the seats provided and the overall width of the vehicle. This, so to speak, unused width amounts to 17 in. in the case of the Chevrolet, whereas on European cars it varies from a minimum of 6 in. to a maximum of 13 in. with an average of 11 in.

Finally, the Chevrolet stands 18 in. higher than the space measured between the floor and the roof; and although there are two European cars which lose 15 and 17 in. in this dimension, a number contrive with only 10 or 12 in., of which at least 7 in. is an unavoidable debit, to provide a minimum ground clearance.

It follows that the floor level on many European

cars must be at hub center, or even a little below. For normal construction a tunnel for the propeller shaft is therefore imperative, but on some of the largest selling cars in Europe it is avoided by placing the engine behind the rear axle and driving the rear wheels through a gearbox mounted immediately ahead of the swinging halfshafts. In fact the largest selling cars in Czechoslovakia, France, and Germany (Tatra, Renault 4 CV, and Volkswagen, respectively) have this form of construction. An alternative, adopted on 40% of the cars bought in Germany before the war and still retained by D.K.W. in that country and by Citroen, which is the second most popular make of car in France, is to use a front-mounted engine in conjunction with front drive. This scheme is also followed by Saab in Sweden.

Important from a spatial point of view is that with all rear-engined and some front-drive cars the engine is placed behind, or in the alternative, ahead of the axle centers. Hence it does not obtrude lengthwise into any useful passenger-carrying area. This feature can also be observed on some cars with conventional drive and propeller shafts, for it was revived so far as in-line engines are concerned by Fiat with their 30-cu in. car in 1937 and is now to be observed on the Morris Minor and Oxford models, to quote but two examples.

The word "revive" is used advisedly, for the 1880 steam-propelled Bollée had a 2-cyl in-line engine mounted ahead of the front wheels with the boiler placed behind the rear wheels. In addition to thus securing the modern feature of a high polar moment of inertia, it is worth while digressing to remark that the Bollée also embraced independent suspension with two transverse leaf springs and rack-and-quadrant steering gear!

Returning to modern times, 12 out of the 36 largest selling models have their engines so disposed that they occupy no potential passenger space.

Thus we can conclude an analysis of the spatial aspect of the European car by saying that on modern designs there is available for seating a length equal to the wheelbase, or possibly slightly more; a width equal to the tread, or possibly slightly more; and a height from floor to roof, which is equal to that available in larger cars, although the overall height of the vehicle is frequently less than 60 in.

Structural Aspects

One consequence of the correspondingly low floor level has already been mentioned. Another is that in order to provide reasonable beam stiffness in the side rail of the frame the floor must be depressed so as to provide some degree of "step down" after the door has been opened. This can lead to considerable design difficulties if the doors, when the car is viewed in plan, have to be placed on a base wider than the wheel tread, for it means that with a conventional frame there must be a very sharp sweep in forward of the frame door pillars, and there is very little space to effect this without sharp angles and local structural weaknesses. This leads us from the consideration of the spatial aspects of the car to a review of the structure.

Large-scale European manufacturers do not depart greatly either in materials or in methods of fabrication from the welded all-steel body which was pioneered by Hudson and Budd in the United States nearly 30 years ago. Indeed much of the plant as well as the technique of body construction has been imported into Europe from America, and any notion that European builders make liberal use of special materials, either in the way of light alloys or plastics, may be dismissed as extravagant. But whereas American cars, with two exceptions, retain a separate frame to which the engine, transmission, and suspension units are attached and upon which the separate body structure is mounted, in Europe a single structure is used by the overwhelming majority of builders. In fact the only cars to use separate frames are those which are continuations of a basic prewar type.

A combined body and chassis construction was used as early as 1903 by Vauxhall and from 1911 to 1924 by Lagonda, but the introduction of the practice for large-scale production must be ascribed to Citroen with their front-wheel-drive model of 1934. In this design, which is still constructed in large numbers after an interval of 20 years, there is considerable use of box sections and but moderate reliance upon stressed panels

Opel in Germany followed Citroen; and Vauxhall, in England, Opel; with Morris and Hillman firmly established with this method of construction in the immediate prewar period. From the beginning it was found possible to save as much as 100 lb in weight on a small car (about 5% of the total) and simultaneously to double torsional stiffness so that 2500 lb per ft for 1 deg distortion can be reckoned as a normal figure.

On many of the earlier examples the designer was concerned to an unnecessary degree with the problems of repair after road accidents. For this reason it was not uncommon to find detachable tubular structures bolted on to the scuttle and projecting therefrom to support the engine and suspension units. These are now disappearing (although retained on the Fiat 1100 introduced in 1953), and it is normal to taper off the structure from windshield height as it projects forwards. There has also been a move in some quarters, notably by Ford and Morris in England and by Citroen in France, to mount the suspension units directly on the scuttle together with the suspension reaction points and to overhang the engine from a "front" mounting which may be placed behind the rearmost cylinder. (See Figs. 8 and 9.) This practice is

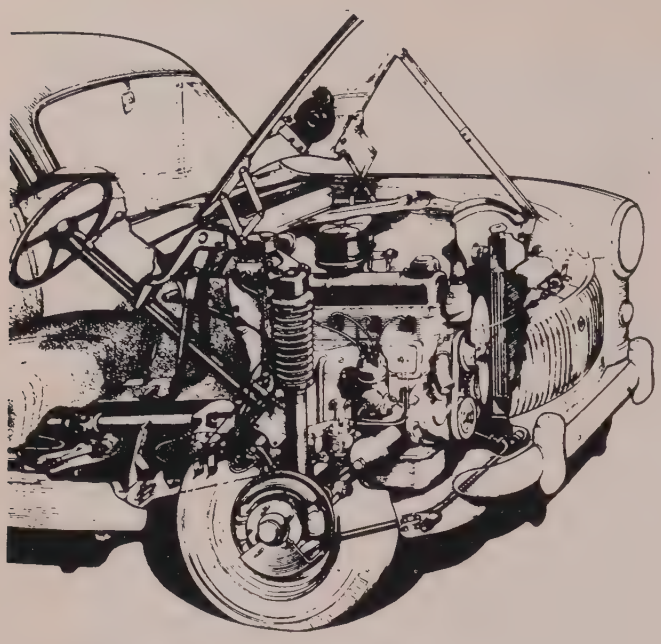

Fig. 8 – Front suspension unit attached to top of cowl structure on British Ford

likely to become increasingly common for it increases the torsional stiffness very substantially and the hood, radiator cowl, and front fenders are simply mud- and weather-excluding unstressed panels. With this class of construction, also, accidental damage is more readily repaired; and there is less likelihood of the main hull suffering from severe distortion, which would lead to the car's being off the road for some time and to a very extensive repair bill.

With the removal of the frame, the complications of side rails at an inconvenient width disappear, but both the floor and the roof are severely stressed. There is indeed a danger of frameless cars becoming two very deeply boxed structures at each end of the car with a somewhat tenuous support between them especially as, for reasons which will be considered later, it is absolutely necessary to provide European customers with four doors, except on the cheapest cars.

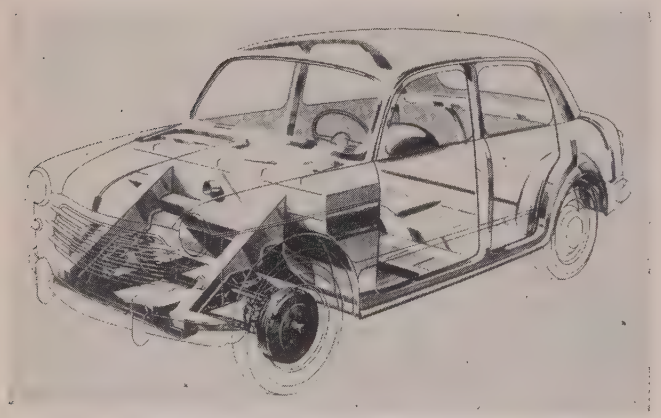

Fig. 9 – Unit construction on 40-hp Italian Fiat with subframe for mounting of engine and suspension units

On the other side of the picture a stiff structure is particularly necessary on European cars for, with the exception of England, they spend much of their life traveling over really rough roads and are subject frequently to cornering loads arising from lateral accelerations of up to 0.5 g. For these reasons it is not uncommon to find that the floor is reinforced with apparently vestigial structures which may retain a major structural purpose. An example is the new 180 Mercedes-Benz. Daimler-Benz has always attached great importance to structural stiffness and for the past 20 years has used deep oval-section frame tubes of almost pure cruciform layout. On the new 180 model the body and chassis are one structure, but the outlines of an X frame can still be discerned and are shown in a drawing (Fig. 10). It is significant that with no engine and transmission change this car is not only much stiffer as a structure but also 10% lighter than the model which it succeeds.

An interesting hybrid construction is adopted by Volkswagen, the leading producer in Germany numerically and one of the largest in Europe. On this car the mechanical units are assembled into a separate frame of platform type with a central tunnel or backbone. This stiffener forms a housing for the control rods and electric wiring, but the presence of this deep tunnel is all the more remarkable since, as before mentioned, the engine is at the back and a perfectly flat floor could have been used if Dr. Porsche had so wished. The body shell is permanently united to the platform at a later stage in the assembly, and the car therefore finishes as a unit body and chassis even if it does not start as such.

On a number of the latest Nuffield models the necessary propeller-shaft tunnel is given the extra function of a stiffening member, but as the backbone so formed has to be open at the bottom the advantages which can be gained from this arrangement are somewhat limited.

Enough has been said to show that European designers are very conscious of the need for stiff structures, but with the moderate engine power and torque at their disposition they are no less sensitive to the matter of weight.

It may be argued that the small size of the European car is favorable to the designer seeking to construct a stiff light-weight structure. On the other hand, thickness of materials cannot be scaled down in proportion to car size, and some items (for example, glass, seats, wheels, instruments, steering wheels, door hinges, and handles) represent a virtually constant weight irrespective of car size. On balance, one would therefore expect European cars

to be slightly heavier than American types in proportion to their size.

It is somewhat difficult to draw definite conclusions in this matter, as almost any criterion upon which one bases the judgment will be unfair to one class of car or another. The author has taken as his standard the greatest cubic content potentially available for passenger carrying. To get an approximate idea of this capacity, he has multiplied the frontal area of various cars by the distance between the wheel centers. This gives a typical American car such as the Chevrolet 302 potentially useful cu ft, or rather more than double the figure obtained on the smallest European cars. On this basis the Chevrolet weighs 112 lb per available cu ft – a figure which is 3% greater than the average for the selected 12 European cars. These, however, vary considerably amongst themselves, the rear-engined 45-cu in. Renault weighing only 84.5 lb per cu ft, whereas the front-engined 122-cu in. model from the same factory weighs 99 lb. Similarly, the 65-cu in. Fiat weighs 103 lb and the 85-cu in. model 123 lb. To sum up, it may be considered creditable that European designers can show a reduction in specific weight in comparison with considerably larger cars, but the differences in this respect between cars built on opposite sides of the Atlantic are not great.

A constructional feature which is of some importance is that, whereas a considerable number of American cars are built with two-door bodies, this type is in Europe virtually confined to cars such as Opel and Ford, which are built in American controlled works, and to the prewar-designed Volkswagen. Most other popular European cars are fitted with four doors, and there is a good dimensional reason why this should be so.

The intended occupant of the back seat on a European car is confronted with a gap between the leading edge of the back seat and the back of the front seat which will not normally be more than 9 in. wide. Entrance to this is complicated by the comparatively low roofline with which he is confronted. A 6-ft-high American has to abase himself but 6 in. to enter a Chevrolet, but the Englishman of 5 ft 10 in. must bow his head by a foot before he can enter a Morris Minor. In these circumstances it is essential to enter the gap at right angles if an unseemly scramble for space is not to be witnessed.

Unfortunately, the provision of four doors considerably weakens the unitary structure, and for a given standard of stiffness, inconvenience of the four-door body must be paid for by greater weight. For given standards of stiffness, all the European cars listed would be a great deal heavier than they are if they had separate chassis frames, and it seems certain that no future European car designed for large-scale production will have a frame with a separate existence from the body.

But in order to meet the technical requirements of a convertible and the commercial requirements

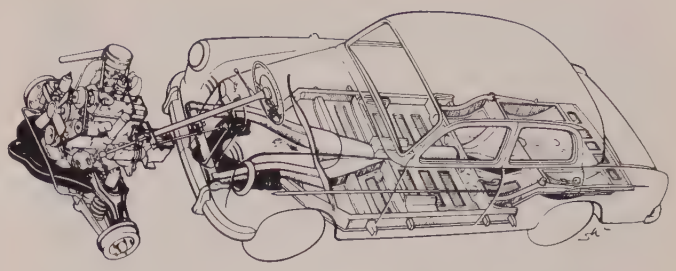

Fig. 10 – Unit construction on 50-hp Mercedes-Benz with subframe for mounting of engine and suspension units and stiffening members formed in floor

of specialist body builders (small in number but large in prestige), it is not uncommon to find that the standard unit-construction model is supplemented by alternatives. Opel, Peugeot, and D.K.W., for example, sell about 10% of their output with folding tops, and the substantial loss of stiffness which follows the removal of the stressed steel roof is made good (but, it must be admitted, only partially) by using a thicker-gage steel for the floor. In Italy there are a number of flourishing specialist body builders, and to meet their needs the Fiat Co. offers a platform-type frame with box-section side rails to provide a measure of stiffening. Vauxhall follows a similar practice for certain export models.

The highly stressed panels of a unitary-construction car are bad offenders as magnifiers of high-frequency noise, and the problem itself has been exacerbated by the position of the front wheels on the modern car which leads to road noise being fed directly into the cowl and driving compartment. A leading British designer once remarked that even if you took the engine and transmission out of his car and let it roll downhill over a rough road surface you still would not be able to hear yourself speak.

In France and Belgium this is held to be an advantage for, it is argued, when so much road noise is inevitable why should one spend time and money on making quiet engines and gearboxes which can be spent to better advantage on improved steering and brakes. This attitude also reflects the Latin view that quiet cars, like daily baths, are an Anglo-American affectation.

In some companies, however, much thought has been given to suppressing road noise, and in the Standard 8 and the Mercedes-Benz 180 cars introduced recently an attempt has been made to isolate both engine and road noise by the use of rubber mountings. The design of the Mercedes-Benz is of particular interest, for as can be seen from Fig. 10 the engine, steering, and suspension units are all mounted in a detachable subframe which is then bolted to the main hull at three points through large rubber buffers. Of the other companies using unitary construction Vauxhall has

Fig. 11 – 35-hp Ford Taunus which has set the pattern for modern European popular-car styling

been notably successful in quieting its cars by the strategic disposition of sound-damping felts and sprayed-on materials.

To sum up, the combination of the body and frame into one single unit offers important advantages in stiffness, strength, and weight reduction, with minor penalties in respect to repair and damage and at the cost of severe but not insuperable difficulties in respect to interior quietness. It is also an arrangement particularly well suited for the modern small car where the front suspension elements can be located immediately upon the cowl and where the width between the doors is greater than the wheel tread.

Let us now review the morphology of the modern European car.

As a bridge between the spatial and constructional aspects of design, which we have just considered, and the aspects of style and shape, which remain to be discussed, it may be sensible to examine the baggage-carrying capacity and the overall proportions of European vehicles.

There is in Europe a widespread myth that American cars are built with excessive fore and aft overhang, but whatever the truth of this proposition in absolute terms it does not stand up under examination when considered in proportion to the wheelbase. On the Chevrolet the overall length is 72% more than the wheelbase, whereas of our sample dozen European cars the A.40 Austin has the highest ratio, with a 70% increase, and the Fiat 1100 the lowest, with 58%. The average of the dozen is 68% – a figure very little different from the Chevrolet. Even when 70% of the aggregate overhang is behind the back axle, considerable ingenuity has to be exercised to offset the limits imposed by modest overall dimensions. It can be reckoned that the covered baggage-carrying space in the European car is between 55 and 65% that of a United States model, but it suffices for all normal needs. Abnormal loads, such as those involved when families are taking an annual holiday, are met very frequently by the use of roof racks. Providing space for the spare wheel presents a particular difficulty, and on the Fiat 1100 it is mounted horizontally in a tray at the back of the rear locker.

A striking space saver is the use of the rear fenders as a cover for double fuel tanks on the Jaguar Mark VII. A somewhat similar scheme has been adopted on the newly introduced British Ford models which have the fuel tank placed on the left-hand side of the luggage locker, thus enabling the depth of the baggage space to be materially increased. On the Vauxhall and Standard Vanguard the tank is wedge shaped and placed just behind the rear seat.

Rear-engined cars present particular problems as they carry their engines in the boot. The Renault relies upon an external roof rack for the carriage of any substantial sized items, but on the Volkswagen a 12 x 37-in. well is placed immediately behind the rear seat. This encroaches upon the leg room available for the driver and passengers and has the further disadvantage of being accessible only by passing baggage through the doors and over the rear seats.

On both the Morris Minor and the Standard 8 the back of the rear seat folds forward so that there is a large unobstructed space from the tail of the car right up to the back of the front seats. On the Standard 8, moreover, the back seats as a whole can be rolled forward, so that with two persons only aboard the car has a luggage space equal to that provided by full-sized vehicles.

Top-hinged luggage-locker lids opening upwards are standard practice, but owing to the comparatively small size of the opening and light weight of the lid it is comparatively rare for spring counterbalancing mechanisms to be employed.

Generous provision for the carriage of small parcels, maps, guide books, and various articles for personal use is given particular attention on European cars, especially those of British origin. A particularly useful feature is the full-width tray mounted beneath the instrument panel, which is to be seen even on very cheap cars such as the Standard 8, Ford Consul, and Morris Minor. Large lockers with lockable lids are common alternatives, and on many cars pockets are provided in the front doors, these being present in a few cases also at the back.

This interest in the carriage of small articles may be explained in part by the comparative narrowness of the cars which results in front seats which afford no surplus space. It is mainly due to the wide use by Europeans of maps and guide books so that they may navigate poorly signposted roads and find their way with the aid of the Michelin Guide to those establishments which provide "a good meal for the district," or "excellent cuisine: worth a detour," or even on occasions to those which offer "memorable meals redounding to the glory of French cooking, fine bottles . . . worth a special journey . . . in these restaurants price has no meaning."

Fig. 12 – 40-hp Fiat showing typical styling, minimum overhang in relation to wheel tread, and nearly as possible flush-mounted windows

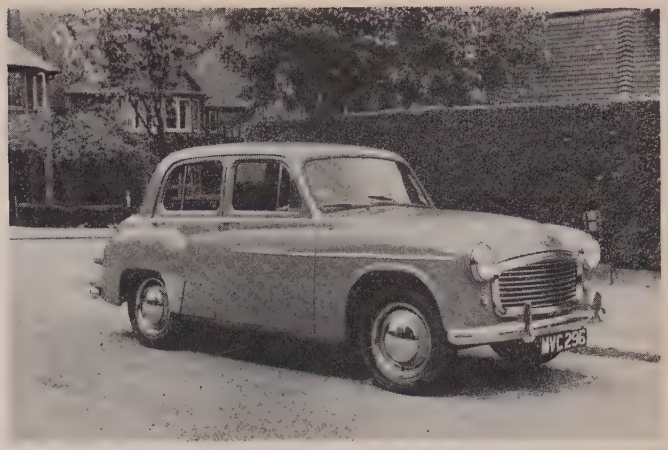

Fig. 13 – 40-hp Hillman Minx showing typical British small-car styling

Let us now turn from the automobile as an instrument of Bacchus and conclude with some observations on European style and shape.

Style and Shape

The small size of European cars makes any effort at ornament a somewhat perilous exercise as there is insufficient mass of motor car to carry any elaboration of chromium-plated strips, panels, and the like. Hence, styling has to be considered more in relation to the basic shape than to any applied features, and here Ford influence has been dominant in the cars designed (as distinct from being built) since the war. The German Ford Taunus model of 1950 was clearly based upon Dearborn thinking, and it was the first European mass-production car which combined full-width treatment of the body with a curved windshield and a hood which sloped down between the front fenders. These basic features have since become the hallmark of the modern European car, and the influence of the Taunus upon, for example, the Fiat 1100 and the British Ford can readily be appreciated by comparing the illustrations of the two cars (Figs. 11 and 12).

This shape is practical, easy to keep clean and simple to repair, but some may consider it excessively box-like in appearance. The alternative of rather more rounded lines can be studied in the illustrations of the Hillman Minx (Fig. 13) which retains a vestige of the long swept fender and of the Renault Fregate (Fig. 14) which is a notable curvilinear project.

The front air intake, which the stylist has built up as a dominant feature on the United States car, is comparatively unobtrusive on European models. (See Fig. 15.) In the extreme of the rear-engined Renault and Volkswagen it is nonexistent, although the former has some slightly suggestive horizontal chromium strips mounted on the nose of the car. On the new Standard 8 with conventional engine position, the air entry is a simple scoop of diminishing cross-section, which is innocent of chro-

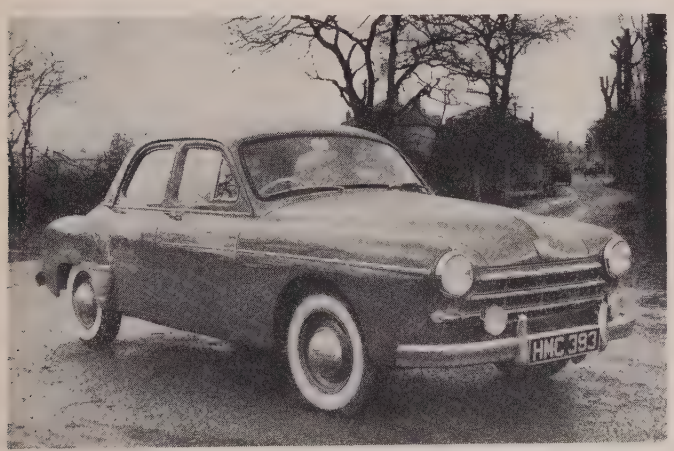

Fig. 14 – Curvilinear styling exemplified by the 65-hp French Renault

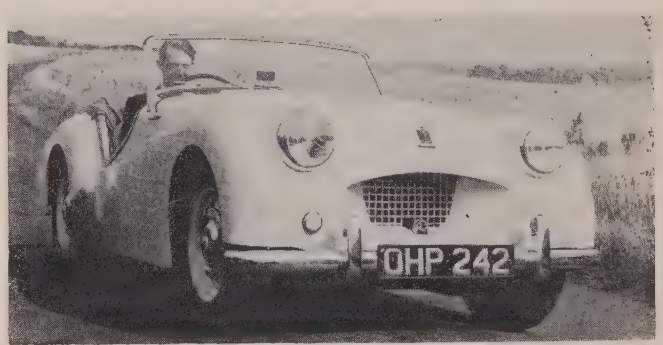

Fig. 15 – A British sports car showing minimum ornament and chrome plating

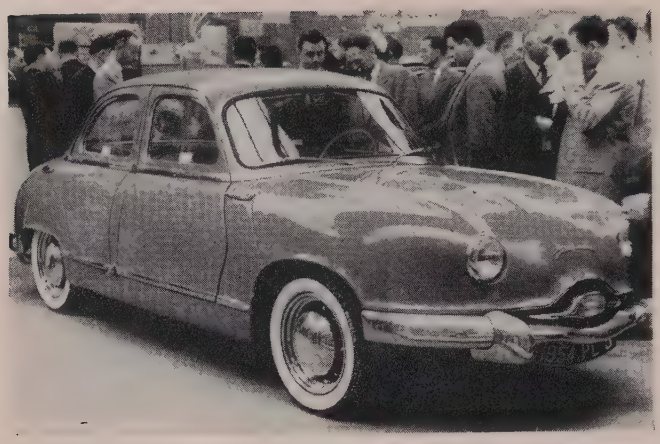

Fig. 16 – The 80-mph, 40-hp French Panhard, the shape of which has been developed by careful drag tests

mium-plated surround or grille. The latest Ford and Fiat cars also show this marked tendency to simplify this particular aspect of external appearance.

For practical reasons one may expect that the squared-up style will eventually be embraced by most manufacturers, although it would seem to be an inherently poor shape from an aerodynamic point of view.

Drag is important on really small cars, for whereas it is rarely possible to drive a 100-mph car for long distances at full speeds it is comparatively easy to hold a 60-mph car at its terminal velocity. As specific consumption tends to rise with the engine running at full throttle and maximum rpm, it follows that the overall miles per gallon on small cars when driven hard is sometimes disappointing.

Much of the drag on a modern motor car would be termed "parasitical" by an aircraft engineer. It rises from protuberances such as door handles, the inset of the windows, and from unavoidable losses through the radiator core and from wind trapping in the wheel arches. Although there are no accurate figures upon which to make a dogmatic statement, it seems likely that these losses are a higher proportion of the total on small European cars than they are on the larger American type. In order, therefore, to retain equality on a basis of road speed in relation to horsepower per square foot of frontal area, it is necessary for the European designer to make strenuous efforts in the reduction of drag wherever this may be possible. It will be seen from Table 9 that compared with the United States vehicle capable of 85 mph on a little over 3 hp per sq ft of frontal area the European average is a little under 70 mph from 1.7 hp per sq ft, which is almost exactly in accordance with expectation on a straight-forward root basis. One may conclude that the European designer has done rather better than to offset the disadvantages inherent in the small car.

This has been achieved more by attention to detail than by any use of radical aerodynamic form. The Fiat 1100 is a particularly interesting example of this fact, for although it is of the square-outline school it shows a road speed substantially in excess of the calculated maximum. On studying details of this model, one discovers that the wheels are set out almost to the full width of the body and the wheel arches are of minimum size. The windows are placed as nearly as possible flush to the outer side of the car, and close study has been made of airflow through the radiator core and out from beneath the hood.

The most advanced European small car from the aerodynamic angle is the newly introduced Dyna Panhard 54 (Fig. 16) which has yet to reach full-scale production. This is a front-wheel-drive model which makes it possible to provide a floor which also acts as a smooth undertray. Great care has been taken to suppress protuberances and to give a well-shaped envelope, and the result is a road speed of 80 mph with only 1.92 hp per sq ft – a gain of 10% over the theoretically computed speed and the equivalent of a drag reduction of one-third compared with the typical United States car.

The profile of the Panhard was developed in two stages. Early tests with one-fifth scale models in the Eiffel laboratory at St. Cyr were supplemented by full-scale tests on the road in which the airflow was recorded by an ingenious installation of 16-mm moving cameras trained on to wool tufts attached to the outer skin. This attack on the drag problem in two stages follows from the European belief that tests on small-scale models have but a limited value.

In 1948, Union Technique de l'Automobile, du Motocycle, et du Cycle published a paper by Romani in which he compared tests made on one-fifth scale models at St. Cyr (having a 6 x 7-ft rectangular working section) with tests made on full-scale cars in the open working section of the Chalais-Meudon wind tunnel, which is an ellipse measuring 52 x 26 ft. Romani points out that even when the drag coefficients obtained by these two methods are comparable, this may be only coincidental and as a result of partial compensation of scale effect.

When full-size cars are tested under simulated road conditions he found that compared to small-scale models:

1. Drag increased appreciably for front-engined cars but remained constant or was even reduced for rear-engined designs.

2. The lift increased considerably for front-engined cars but only slightly for rear-engined vehicles.

3. In every case the resultant acts farther forward under the road condition. This last item is of great significance on light high-speed cars with low drag which may need rear stabilizing fins. Probably such expedients will not be needed on low-

drag cars of limited power and with maximum speeds not exceeding 80 mph.

An important conclusion reached by Romani as a result of the full-scale tests was that poorly designed bumpers and badly positioned front air intakes could result in serious drag losses. Allowing for the power consumed in driving the fan, he found total cooling losses as high as 20% of developed horsepower on cars where a comparatively minor rearrangement of the air intake and radiator core could lower this figure to 10%.

He considered that only limited credence could be given to any tests of one-fifth scale models. With one-tenth scale models he considered the correlation between the model figures and real car must be reckoned as a happy accident.

Dramatic reductions in horsepower needed to propel a car at high speeds have been achieved in Europe by highly specialized vehicles (Fig. 17); and on the Bertone-bodied Alfa Romeo (Fig. 18), as little as 0.6 hp per sq ft is needed to drive a 2800-lb car at a constant 60 mph. Even if we allow production cars a substantial increase upon this figure and reckon upon about 0.8 hp per sq ft at 60 mph, the larger cars on the market (with engines developing 60 bhp and with a frontal area of about 25 sq ft) should do about 85 mph. By the same standards the smallest models, with 20 sq ft of frontal area and approximately 30-hp engines, will have a maximum speed of about 75 mph. These maximum speed figures will offer cruising speeds little different to those utilized on larger cars.

Looking into the future one may expect that European cars will continue the established practice of using a unitary body and chassis, but this may be stiffened by up to say 25% and simultaneously lightened by perhaps 10%, as greater knowledge is accumulated of the stress pattern over the shell. Noise suppression will certainly be improved, at least in England and Germany, and it is likely that the weight penalty arising therefrom will offset the gains achieved by the stress men. On balance it is likely that there will be little change in curb weight, nor can one see any possibility of serious changes in overall dimensions. Many cars are already as small as the human frame permits, and economic facts limit the maximum weight, size, and power which can command a large sale.

Anyone who has followed this paper from the opening words up to this point may well feel that the author has come a long way to spend the funds of his company and the time of his audience in telling them that European cars are like American cars except that they are smaller, noisier, and slightly lighter and faster than might be anticipated. The author offers as excuse that this basic similarity is not generally recognized, and he hopes that his endeavors will be counted as the establishment of truth and not as the utterance of a truism. He will also supplement the information which is relevant to 90% of European output with some brief comments on the field of special-purpose vehicles.

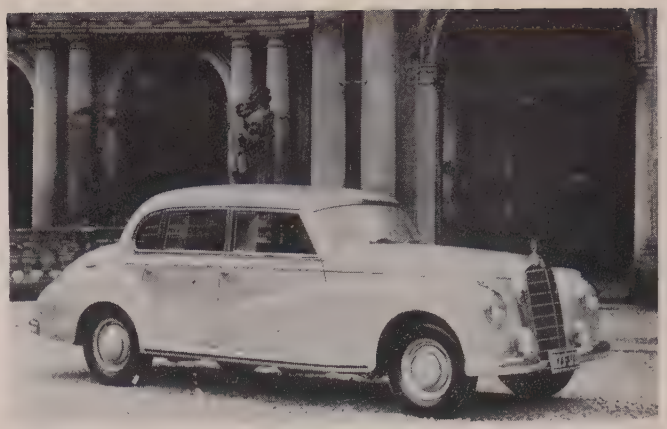

Fig. 17 – Traditional lines combined with low drag offering 100 mph on 115 hp with the largest Mercedes-Benz

The 150,000 cars sold in Western Europe to the more wealthy and discriminating buyers fall into three classes. Much the largest of these is broadly similar to the popular models but with an enlargement of tread, wheelbase, and engine power so as to provide superior standards of performance and comfort. Cars in this category are produced in various factories at the rate of between 5000 and 10,000 per annum and are typified by the Rover and Jaguar Mark VII in England, the Mercedes-Benz 220 and 300 in Germany, the 6-cyl 180-cu in. Citroen in France and the V-6 Lancia in Italy.

With the exception of the Lancia the bodies of these and similar types of vehicle are mounted upon separate chassis frames. This diminishes the capital cost of changes in body style and shape, permits the sale of bare chassis to specialized coachbuilders, and makes a useful contribution to sound damping.

Limited use of aluminum can be seen in this class of business, light-alloy sheet being used for the

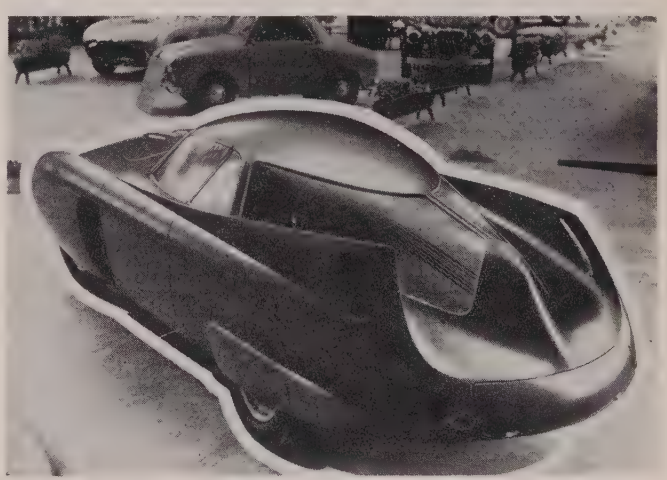

Fig. 18 – A very-low-drag Italian body by Bertone on an Alfa Romeo chassis

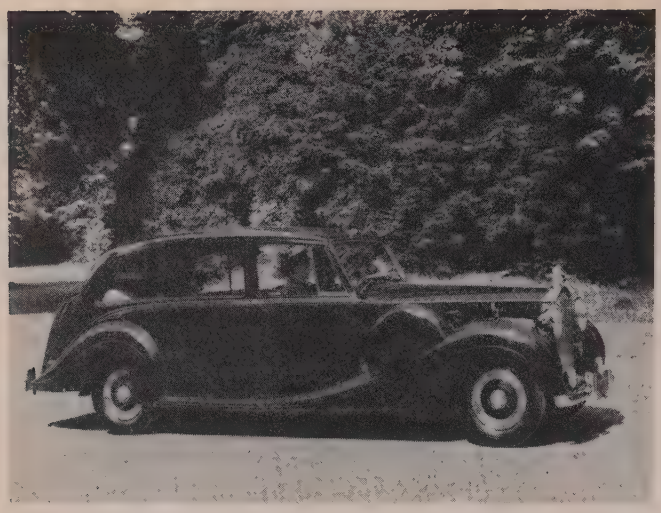

Fig. 19 – A Rolls-Royce with custom-built body exemplifies a British speciality

doors on the Rover and for doors, rear luggage-locker lid, and many other parts by Lancia. On the whole, however, these cars conform to convention in respect to materials, shape, and constructional methods, fully tooled pressed-steel bodies being essential to keep costs within reasonable bounds. As they are sold to a wealthy minority, the styling is designed to appeal to the conservative mind. For this reason it is normal to find that the air intake takes the form of the traditional radiator, even to the provision of a pressed-out dummy radiator cap. Leather upholstery is almost universal, and those built in England are commonly provided with veneered wood for the instrument panel, window surrounds, and so on.

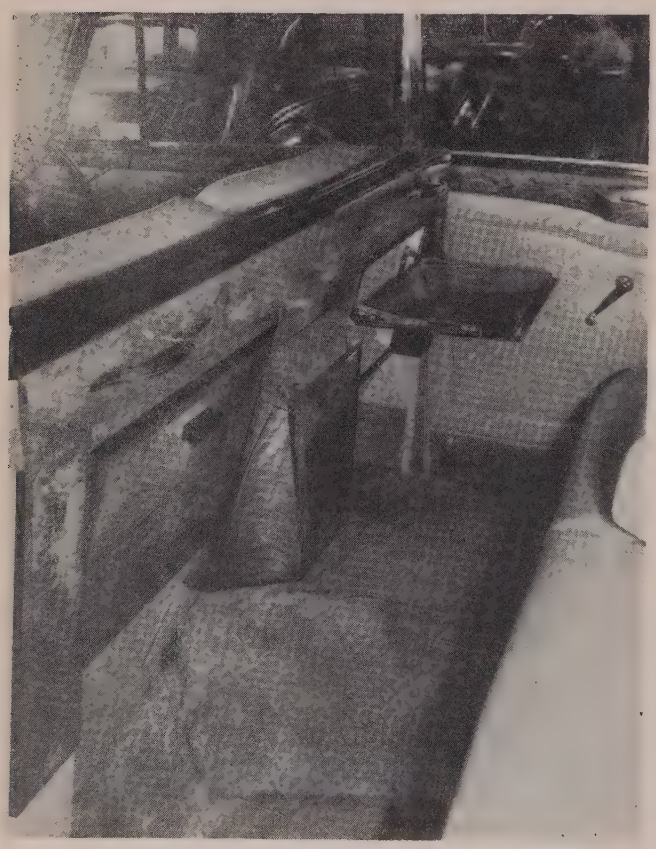

Fig. 20 – Interior of a British custom-built town carriage

As all the cars in this category have front engines and are yet substantially lower than United States vehicles, their ability to carry five or six people is reduced by the inevitable propeller-shaft tunnel. However, few European manufacturers seriously consider the prospect of carrying six people in comfort for long distances.

Probably 120,000 of the residual cars fall into the above group. Of the remaining 30,000 a few, almost entirely of English origin, are very much larger than the standard vehicle, with the rest finding their justification in being very much faster than normal.

England stands alone today in the continued production of a few hundred cars having wheelbases of 130-140 in. and mounting owner-cum-chauffeur driven bodies with a division separating the front compartment from the back. These continue to be triumphs of the coachbuilder's art, and either ash or light-alloy framework is used with quite frequent use of light-alloy panels. (See Figs. 19 and 20.)

Many of these cars are notable for the continued use of razor-edge styling, and although this represents a deliberate rejection of the world trend, the latter is followed in the use of lamps submerged in the fenders, the last being swept through to the back of the motor car but retaining their separate identity.

Imitation radiators are universal, and the internal fittings may perhaps best be indicated by a review of a car which was exhibited at the last London Motor Show. This read, "The big limousine has a long, gradually sloping wing (fender) to reduce the impression of height. This also conceals a running board of a practical width, running boards being essential in this type of car. Two face-forward occasional seats and a polished veneered cabinet for decanters complete the furniture of the division.

"Luggage accommodation is very lavish; the car is shown with four large fitted suitcases plus two smaller matching valises for overnight use. Small articles can be carried in the front-door lockers which give a space measuring 12 x 7 x 10 in. for maps and similar objects."

Of another car it was said, "All interior finishes including the instrument board are covered with red crocodile skin, and fitted suitcases in the compartment behind the seats are made with red crocodile also. A sliding tray on the left of the instrument board contains a hinged-over mirror together with silver cigarette case, compact, lighter, and clothesbrush to match." Special features included a heat-insulated roof, double sealing to the doors, double-width windows with an air space between to

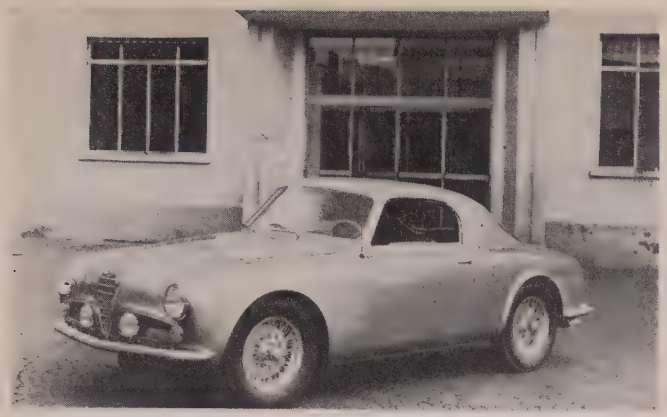

Fig. 21 – A typical Italian fixed-head coupe by Pinin Farina, one of the pioneers of this type of car

Fig. 22 – The use of fins to preserve aerodynamic stability and to act as crash bars by Touring on a Pegaso chassis

prevent misting-up, and on a number of high-priced vehicles the rear window is electrically heated with the same end in view.

These cars are designed and built with the minimum concessions to modern style and constructional methods. What is often thought of as advanced European styling is primarily an Italian concept which has in the past five years established itself as the dominating influence on the high-performance cars built throughout Europe.

The origin of this style can be seen in some stock competition cars built for long distance races between 1937 and 1939, and the bodies built by Superleggera Touring for B.M.W. and Alfa Romeo in 1939 clearly form the inspiration for the Packard Clipper of 1941. In the immediate postwar period the Italians have developed the envelope form so as to provide a highly refined appearance and reasonable aerodynamic efficiency.

These bodies are normally lower than they are wide, of two-door construction, and confined to the carriage of two or three persons, the back seats being clearly for emergency uses only. Although extremely elegant these vehicles have a somewhat limited use and sale, their influence on the outer world and their propaganda value being quite out of proportion to the numbers built, which do not exceed 2000 or 3000 in any given year. The popularization of the Italian form (Fig. 21) is largely due to Porsche in Germany and Jaguar in England. The former, based on Volkswagen components, takes advantage of a rear engine to provide a small two-seater fixed-head coupe of very low drag and excellent appearance, while Jaguar, with a larger 160-bhp engine has popularized the open two-seater of modified Italianate line. In this car the swept fender and dummy radiator betray the fact that it was one of the immediate postwar concepts, whereas on the Austin Healey the hood is swept down between the fenders which form a continuous line from front to back. Cars of this kind are built in considerable numbers, Porsche's output for example amounting to around 4000 a year, Jaguar's a comparable figure, and Austin Healey's scheduled for even larger numbers. Most of these cars are built from steel pressings, and the all-aluminum-paneled body is in Europe like the Prussian's description of the pug in England: "a seldom dog." It has been found that the addition of an undertray materially reduces drag, and speeds of 110 mph with 90-100 hp are now being obtained. With speeds of this order there is little tendency to aerodynamic instability, but a number of European cars can readily be bought which will reach maximum speeds between 120 and 140 mph, and it seems likely that there will be a steady development of substantial tail fins for these vehicles. On the Bertone-bodied Alfa Romeo, for example, shown at the last Italian show, a fin rises to roof height from each rear fender; and on the Touring-bodied Pegaso (Fig. 22) side fins are arched over from the fender into the top of the roof with the object not only of providing a stabilizing effect on the road but a real antiroll bar should the car turn over!

European manufacturers embark upon the construction of special bodies in numbers of 25 per annum upwards, and it is for this reason impossible to do more than summarize the trends in design and the details to be found in the products of the three dozen car manufacturers engaged in this sector of the business, who are supplemented by around two dozen custom body builders.

It seems sensible to end this paper by uniting a brief survey of the specialist market to an assessment of what present-day specialist features may find a place on popular cars within the next five years. We have in the past year been able to see one such transition, for Fiat has followed Mercedes-Benz in providing a transparent baffle at the back of the window in the front door – a device which enables the window to be almost fully dropped at 90

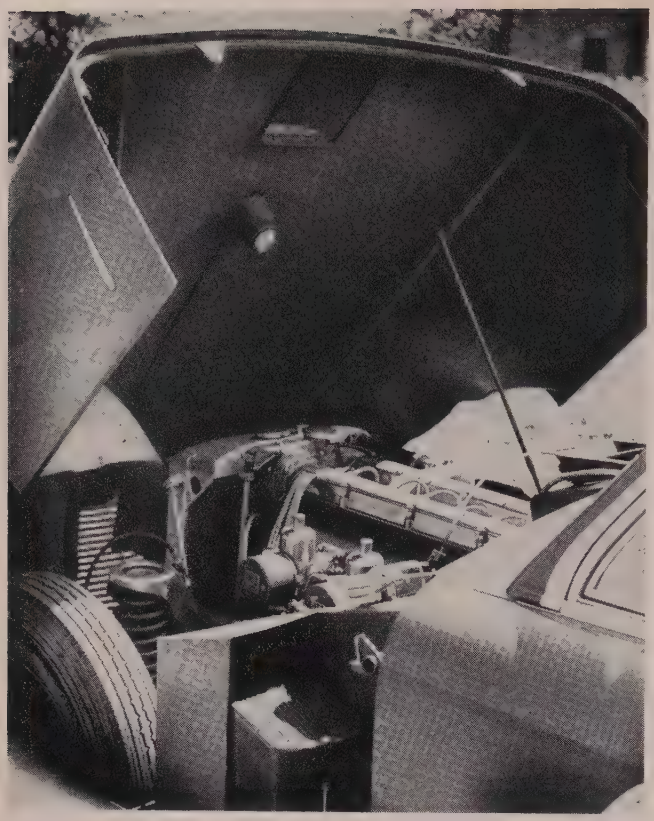

Fig. 23 – One-piece forward-opening hood giving full accessibility for the engine and front suspension element of the Aston Martin

mph without the occupants of the rear seat becoming aware of the fact.

Another minor but useful feature was to be seen on the Jensen 541 at the Earls Court exhibition, as the elliptical air intake on this car could be quite closed by a correspondingly shaped pivoted panel, the pivots being placed off center so that, should the mechanical means provided for opening the orifice fail, wind pressure alone would ensure passage of air through the radiator core. On this car and on the DBII Aston Martin (Fig. 23), the hood and the front fenders are made in one piece pivoted at the fore part. When they are lifted, the engine, front suspension, and steering linkages become 100% accessible.

An alternative can be seen on the Mercedes-Benz 180 and Riley Pathfinder cars, both of which have a pivot on the cowl and thus lift from the front. Both also have a dummy radiator (of the shape traditional to the make concerned) which lifts up with the hood.

A desirable feature standardized on the larger Mercedes-Benz cars are proprietary front seats so shaped that when both are level three people can sit abreast. With only two people it is possible to vary the inclination of the backrest, and on the passenger side a supplementary headrest is provided. When this is attached and the back let down to its maximum angle, a comfortable semireclining position enables the passenger to sleep during long journeys.

It would not seem that there are any constructional features in specialist cars which could be adopted with advantage by the mass manufacturer, but as already mentioned it may be that the latter will refine the shape of his vehicles so as to bring their wind resistance closer to the really aerodynamic types. This could be done with no loss of seating space and with slight if any increase in cost.

These are but a few of the ways in which the specialist car can be of service to the designers of high-production vehicles, but one must recognize that the social and technical needs which the two types serve are widely different. It is therefore logical that the means which are adopted are also far apart.

Whereas, however, in the United States the utility car, built wholly for transport, has almost annihilated the specialized type, in Europe conditions are such that the two are likely to coexist on a sound social and economic basis for many years to come. We may thus expect a continuance of cars produced in large quantities which will be similar to United States vehicles but on a smaller scale and which will be built to serve the same purpose within a restricted fiscal frame. To them will be added a minority of special types which have no counterpart in the New World.

DISCUSSION

Frameless Construction Has Many Advantages

— Maurice Olley
Chevrolet Motor Division

THIS paper contains a lot of information to which we would do well to pay attention.

1. Regarding integral construction, I am glad the author emphasized the obsolete feature of American passenger cars in general, through using the separate chassis frame. Perhaps he didn't put it as bluntly as that, but that is what he meant. We know from experience in Europe that the frameless construction, if only by virtue of the mental exercise involved, leads to a better and lighter car. I have driven frameless cars with well over ten years of war service behind them, which were rusted into a filigree by salt water and neglect along their lower fringes, but still felt solid, and in which the only noticeable change was a decrease in road noise.

I doubt whether 2-door construction is an advantage in a frameless car. Increased width of the door means that

the roof pillar has been moved farther back. Frameless cars, as the author says, are stiff in torsion, but they tend to be flexible in bending, and this tendency is worse in 2-door cars.

The author does not go into detail on the chief problem of the conventional frameless car. This is that the cowl and dash are almost cut in two in their most important portion by the presence of the engine and transmission. The structure is bifurcated from the radiator back to the front seat.

The front-drive and rear-engine cars avoid this difficulty, and some of them at least take full advantage of it by means of a solid crossmember at the bottom of the dash.

2. The author has handed us a lot of useful information on economy of space. It would be interesting if we had comparisons of "useful area" with "total area occupied"—a measure of our efficiency in the use of road space. Probably American cars average 40-45% and European production cars 50-55%.

The various dimensions are not equally important. Height and length are important chiefly for garage space. Length is not important within a few inches in traffic because we have to leave 30 ft or more between cars at 30 mph for safe stopping.

Width is extremely important because of limitations in the width of traffic lanes, and increasing difficulty in estimating the width and the position of the vehicle in the traffic lane on the part of the driver. If we consider the driver sitting at a constant eye height above the fender tops, his chances of knowing where the car stands on the road decrease in proportion to the width of road that he cannot see. This width increases as the tangent of a large angle and therefore much faster than in direct proportion. Thus, a motorcyclist knows exactly where he is on the road, whereas some of our smaller women drivers, on some of our larger cars, quite evidently have only the vaguest idea of where the road is relative to their vehicle.

Another aspect of width is the parking lot difficulty. And this goes double for what the author calls "unused width"; in other words, thick doors. A thick door not only increases the width of the car uselessly, but increases the occupied width by that much more, by the time the doors are open wide enough to allow the occupant to escape. This again depends on the width of the occupant at his or her greatest dimension. And again the women are in real trouble!

ORAL DISCUSSION

Reported by Russell H. Peebles
Hudson Motor Co.

Dave Cliff, Chrysler Corp.: Didn't Dodge and Budd collaborate in pioneering the all-steel body rather than Hudson and Budd?

Mr. Pomeroy: According to a U. S. publication (unnamed) it was Hudson and Budd. I shall investigate further.

Phillip Tabb, Hudson Motor Car Co.: In regard to the low number of sales to individuals, would you comment on the amount of advertising, dealer distribution, dealer attitude, and prevalence of time payments in England and Europe?

Mr. Pomery: Export of automobiles is necessary to sustain the British economy. It is only recently that cars began to appear in automobile show windows for inspection before purchase. Selling policy was, up until the present, that salesmen represented several makes of cars and was actually a "customer's" man, fitting the type of automobile to the demands of the buyer. This policy is changing now, and each company maintains its own sales force. Advertising is extensive by the large companies.

Stewart Lawson, Analysis, Inc.: To what extent are the British developing plastic bodies and aircooled engines?

Mr. Pomeroy: British car makers have not found it necessary to consider plastics because skilled body builders are available and can use simple and inexpensive tools. Cars, therefore, are not exactly alike.

The Volkswagen and Citroen have aircooled engines and Fiat will follow soon. Aircooled engines are noisy but have advantages.

Fred Hoadley, Ford Motor Car Co.: What is your opinion of the new Grand Prix formula?

Mr. Pomeroy: It has stimulated interest in racing cars to the extent that I predict 200-mph cars will be factory-built.

Milton Bald, Hudson Motor Car Co.: Since 90% of European cars are purchased with company funds as "machine tools" and the women have little influence on the purchase, could this be reflected in lesser attention to eye appeal than here, where women have some influence on most car sales? By this I refer to a lesser use of interior and exterior color and less chrome, which we often hear referred to as the continental look.

Mr. Pomeroy: Feminine influence is not as prevalent in British styling as in the U. S. I am reminded of a German car manufacturer who, when I mentioned that a new braking device would be hard for women to work, said, "Pomeroy, we can't stop women from driving, but let's not encourage them."

ABC's of Ultrasonic

IN the past decade the use of ultrasonics has become increasingly important in nondestructive inspection. Its use has resulted in better quality control, faster production rates, reduced inspection costs, and safer plant equipment. Four basically different methods of ultrasonic inspection are in commercial use today. In chronological order of successful application to industrial testing these are:

1. Pulse echo.
2. Resonance.
3. Transmission.
4. Frequency modulation.

Submersion testing is sometimes referred to as another method. It is actually another way of applying one or more of the methods just listed.

The Pulse Echo System

This system locates defects by means of the echo principle which has been used extensively in both sonar and radar. As in these fields, the basic principle of operation consists of the transmission of a pulse of ultrasonic vibrations into the part or medium to be inspected. These vibrations are similar to sound waves except that they are of higher frequency. A measurement is then made of the time intervals between the initial pulse and the arrival of the reflection or echo from the internal defects and from the opposite side.[1, 2, 3] A cathode-ray tube is usually employed for displaying the signals derived from these pulses. The action of the ultrasonic energy can be visualized from Fig. 1. The pulse is impressed on the block of material with the aid of a quartz-crystal transducer, which is a device used to interchange electrical and mechanical vibrations. The crystal is capable of doing this because it is piezoelectric, that is, it changes dimensions when a voltage is applied across its face. If this is a high-frequency alternating voltage, its dimensions are forced to change rapidly and ultrasonic vibrations result. In order to pass the ultrasonic energy into the material, a layer of liquid is required between the crystal and work. Oil is usually employed for this purpose. The pulse of ultrasonic energy begins its travel through the material. Several types of ultrasonic waves are possible. However, the type most commonly used in ultrasonic inspection is the longitudinal or simple compression wave. Fig. 1 shows the ultrasonic pulse traveling through the block without dispersing. In actual practice this is not the case, because the ultrasonic waves spread sideways some as they travel forward. By choosing a high frequency in the range of 500,000 cps to 10,000,000 cps and a suitable transducer, this spreading may be kept to a very few degrees. Thus, it is possible to produce a beam of sound of small cross-sectional area for ultrasonic exploration.

In the pulse echo system the initial burst of ultrasonic energy is indicated at the beginning of a trace on the cathode-ray-tube screen. The pulse

---

[1] U. S. Patent 2,280,226 April 21, 1942, "Flaw Detecting Device and Measuring Instrument," issued to F. A. Firestone.

[2] See *Metal Progress*, Vol. 48, September, 1945, pp. 505-512: "Supersonic Reflectoscope for Internal Inspection," by F. A. Firestone.

[3] See *Metal Progress*, Vol. 48, September, 1945, pp. 513-516: "Supersonic Flaw Detector," by E. N. Simons.

Inspection

Edward F. Weller, Jr., Research Laboratories Division, GMC

This paper was presented at the SAE Summer Meeting, Atlantic City, June 9, 1954.

travels through the material until it hits a discontinuity where part of the energy is reflected, and the remainder continues to travel through the article under test. Ultrasonic waves are transmitted quite readily through solids, but they are nearly 100% reflected at an air boundary. Since flaws are really gas- or slag-filled cavities they distinctly reflect ultrasonic waves, thus permitting detection.

The reflection is picked up by the crystal transducer which now acts as a receiver and is impressed on the oscilloscope screen as a pip. Then, after a further interval of time, the reflection from the face returns and is indicated on the screen. This process is rapidly repeated, usually 60 times per second, to provide a stationary pattern.

Fig. 2 is a block diagram of a typical pulse echo

ULTRASONIC inspection is proving its worth in mass-production industries through better quality control, faster production rates, reduced inspection costs, and safer plant equipment.

This paper describes in detail three types of inspection methods: resonance, reflection, and transmission. Practical inspection instruments utilizing these methods are also discussed.

Some of the applications of ultrasonic inspection include the testing of turbine wheel forgings and other jet engine parts, long rods and bars, bondings between bearings and connecting rods, rubber-to-metal bondings, laminated stock, and inclusions in bolts.

The Author

EDWARD F. WELLER, JR., is assistant department head of the Physics and Instrumentation Department of General Motors Research Laboratories. He received a degree in Electrical Engineering from the University of Cincinnati in 1943. He entered the employ of the General Motors Research Laboratories in 1946, and worked on the development and improvement of instruments required for research within the Laboratories. He was appointed to his present position in 1952.

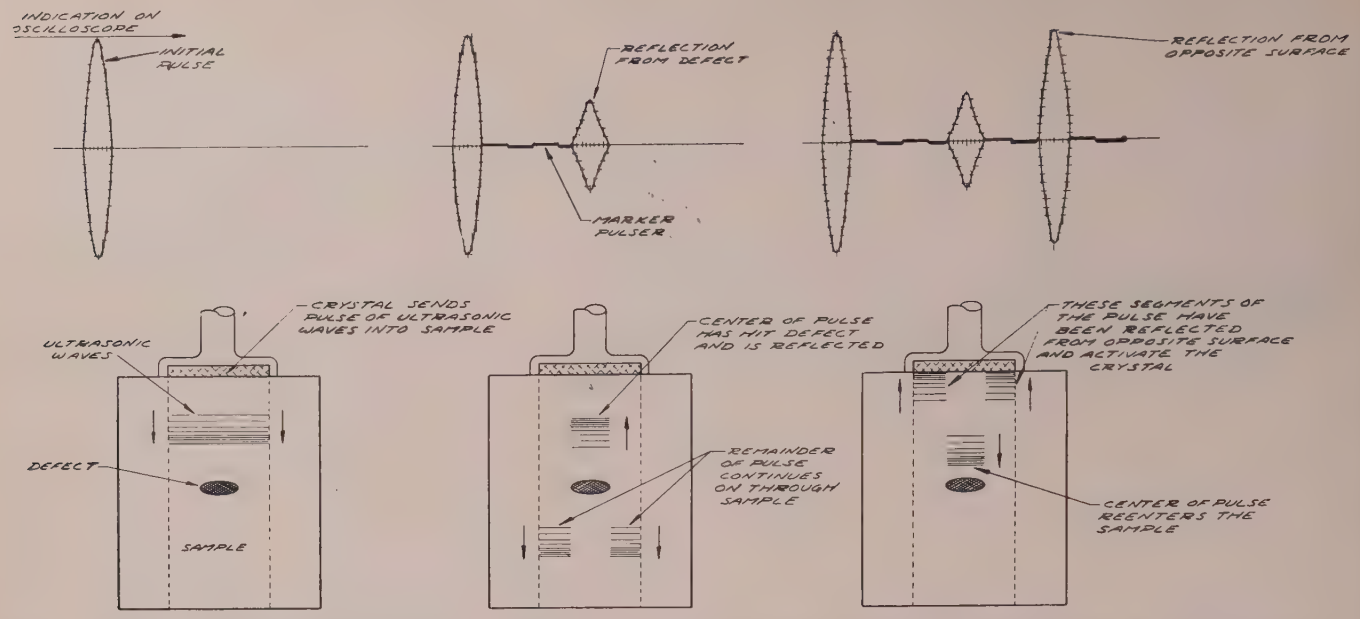

Fig. 1 – Action of a pulse of ultrasonic vibration as it traverses a sample in the pulse echo system. A cathode-ray tube is used to present the information

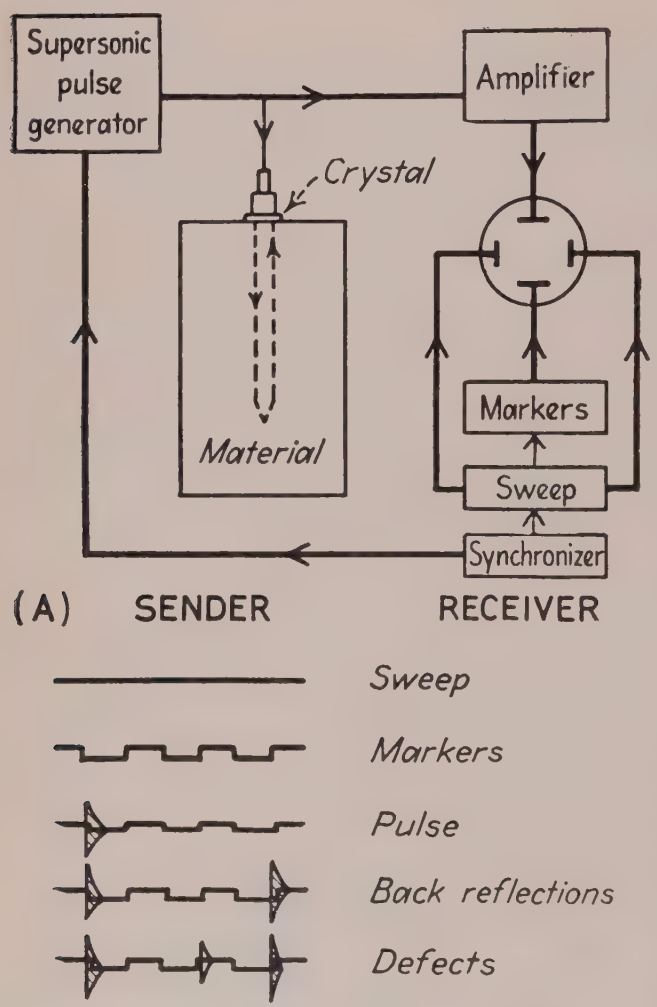

Fig. 2 – Block diagram of the pulse echo system

system. The necessary elements are a supersonic pulse generator for producing the high-frequency pulse, the crystal transducer for converting the electrical vibrations into mechanical vibrations and vice versa, and an amplifier for amplifying the received signals before they are displayed on the cathode-ray tube. In addition to these, a sweep generator is required and a synchronizer to provide a stationary pattern. The marker pulses are used in calibrating the instrument, and, therefore, the location of flaws can be accurately determined.

A typical transducer used for this type of system is shown in Fig. 3. It is necessary for the surface of the material being examined to be relatively smooth in order to provide adequate contact between the crystal and the work.

An actual photograph of the oscilloscope screen of a pulse echo system is shown in Fig. 4. The timing marks have been adjusted so that one cycle is equal to 1 in. Fig. 4 indicates that the flaw is 3 in. from the front surface.

Fig. 5 shows the pulse echo system being used to examine a large steel casting for flaws. The ring bosses undergo severe stress in operation and are being examined to determine if cracks have developed after an experimental test. Fig. 6 shows the crank of a large press being examined for flaws. Periodic examination of crankshafts and other highly stressed parts enables the plant superintendent to predict when the crankshafts require replacement. Inspection tests such as this result in less down-time and safer operation. In order to apply the crystal to the ends of the shafts, it is necessary to clean off the scale and smooth the surface so that adequate contact can be made between the crystal and the shaft. In plants which have been set up for routine inspections, these

Fig. 3 – A typical crystal transducer used in ultrasonic inspection. A transducer is used to interchange electrical and mechanical vibrations

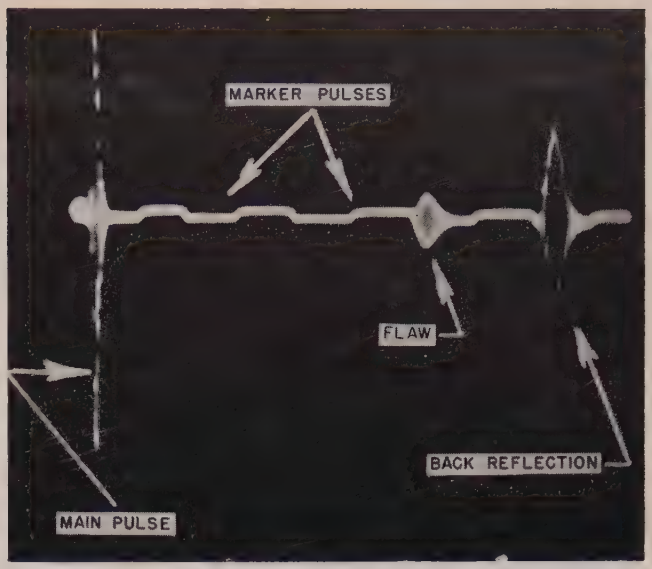

Fig. 4 – Photograph of a pulse echo system cathode-ray screen

shafts have been turned flat before installation. Fig. 7 shows the pulse echo system being used to examine a fabricated traction motor frame. The transducer used is a standard 45-deg-angle crystal which is placed on the top face and sends the ultrasonic energy into the work at approximately 45 deg. Since the welded section is at a 45-deg angle, the ultrasonic wave travels directly into the weld. Applications of ultrasonic inspection such as this result in large savings in inspection time.

Stainless-steel turbine wheel forgings were some of the first production parts to be inspected with the pulse echo system. These wheels spin at high speeds and are highly stressed, necessitating detection of all flaws. Fig. 8 shows a wheel which is being searched on all flat surfaces for defects. This equipment finds flaws which cannot be found in any other way because voids in the original ingot have been forged flat. A master set block such as shown in Fig. 9 is made from a turbine wheel forging containing simulated defects of known size and of known loss of reflection. Since the velocity of sound varies with the material, it is necessary to use the same material for a test block as that used in the part to be inspected. The instrument is calibrated prior to test, and all defects found in a

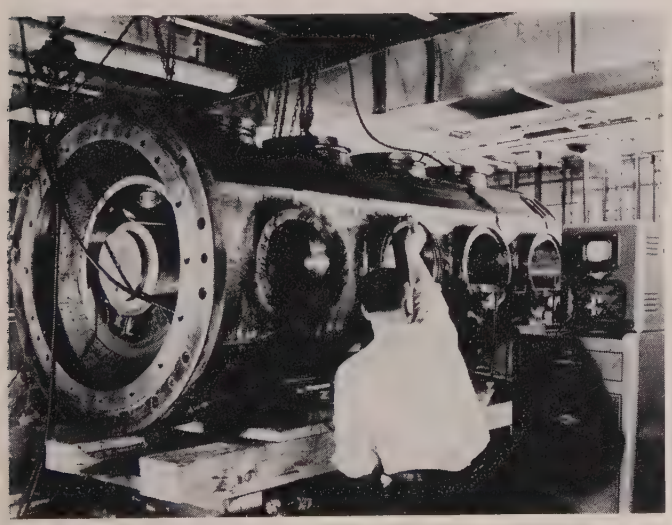

Fig. 5 – The pulse echo system used in examining a highly stressed ring boss on a large casting

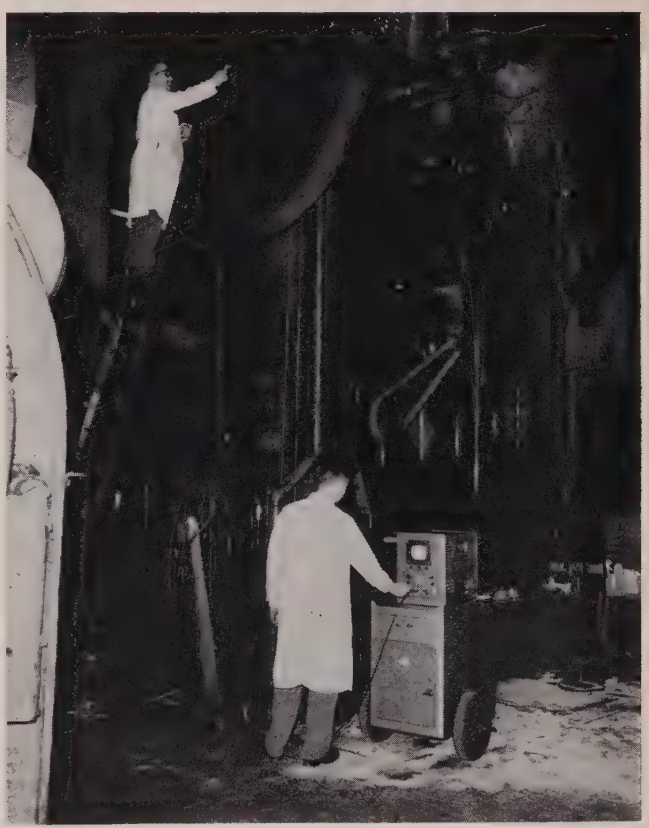

Fig. 6 – Crank of a large press being examined for flaws. Periodic inspection of highly stressed parts improves plant safety and reduces down-time caused by equipment failure

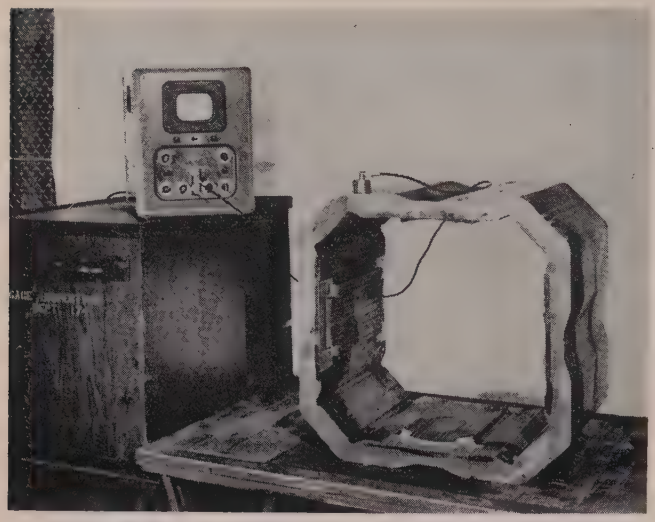

Fig. 7 – Fabricated traction motor frame welds being examined for flaws

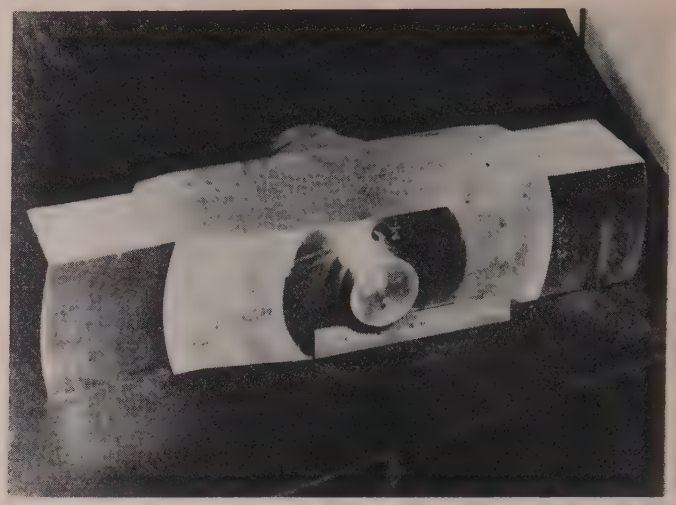

Fig. 9 – A master set block made from a turbine wheel forging containing simulated defects used in calibrating the pulse echo system

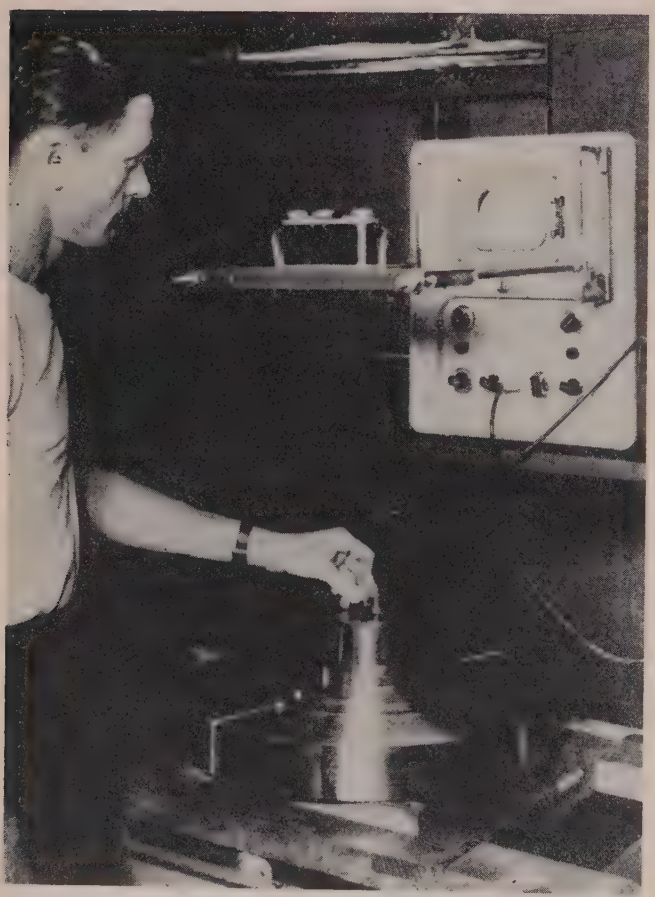

Fig. 8 – Stainless-steel turbine wheel forgings are examined for defects. These forgings were some of the first production parts to be inspected with the pulse echo system

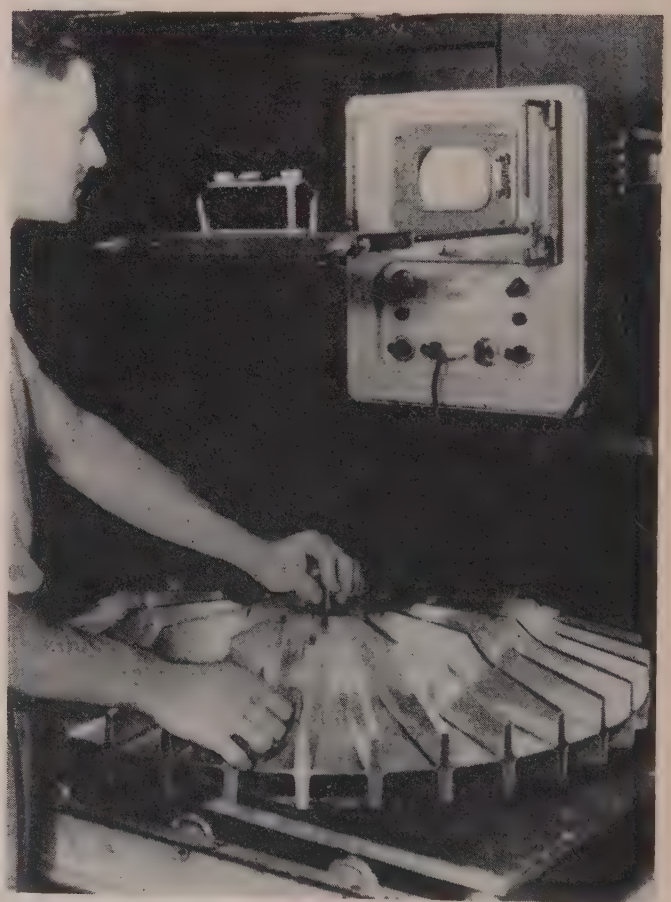

Fig. 10 – Jet engine compressor rotors undergo production-line inspection to determine the material quality

forging are compared to the master set block. Needless to say, the quality of turbine wheels used in jet engines after passing such a test is greatly improved.

Other jet engine parts such as compressor rotors shown in Fig. 10 also undergo production-line inspection to determine the material quality. In this particular test, only the hub area is examined, but it has resulted in reduced spin-test failures.

The pulse echo system can also be successfully used in determining the quality of long rods and bars up to approximately 30 ft. During World War II, one plant was having considerable difficulty in producing tank shafts because of internal defects in the material. The pulse echo system was applied to this problem and resulted in screening out all bars containing flaws such as shown in Fig. 11. The diameter of this bar is approximately 3 in., and it shows numerous cup flaws detected prior to machining operations.

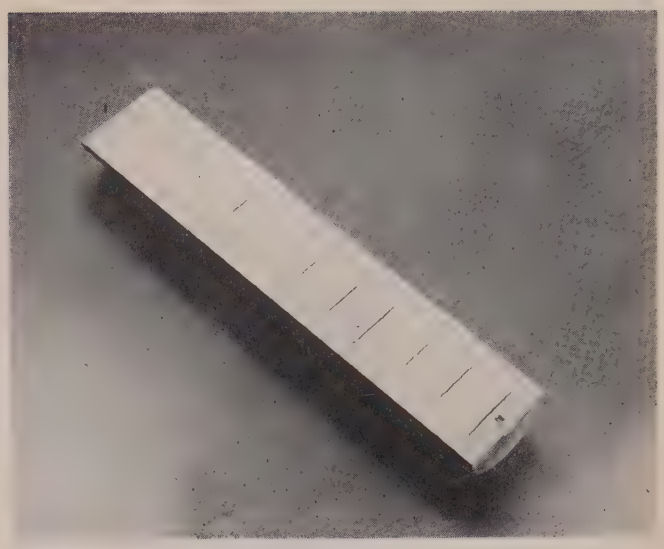

Fig. 11 – Typical flaws readily found in long bars with the aid of pulse echo systems. This bar is 3 in. in diameter

Ultrasonic Resonance Testing

Instead of a pulse of energy being applied to the transducer as in the pulse echo system, the transducer is activated with a continuous voltage of high frequency in the resonance system.[4, 5] The quartz crystal is set into vibration and passes the vibration on to the material against which it is pressed as shown in Fig. 12. The frequency of vibration is then changed by tuning the electronic circuit coupled to the crystal. If the range of frequency which can be supplied by the instrument is proper for the piece which is being tested, a frequency will be found where the part vibrates in resonance. This means that the frequency applied by the crystal is the same as the frequency at which the piece wants to vibrate. The resonant frequency depends on the velocity of sound and thickness of the material. Since the velocity is known, the thickness can be determined from the resonant frequency. Fig. 13 is a view of an early hand-tuned resonant system using a meter to indicate when the resonant frequency is reached. When the resonant frequency is reached, the meter cur-

[4] U. S. Patent 2,431,233, Nov. 18, 1947, "Supersonic Measuring Means," issued to W. S. Erwin.

[5] See *Iron Age*, Vol. 154, Nov. 9, 1944, pp. 59-61: "Supersonic Measurement of Metal Thickness," by W. S. Erwin.

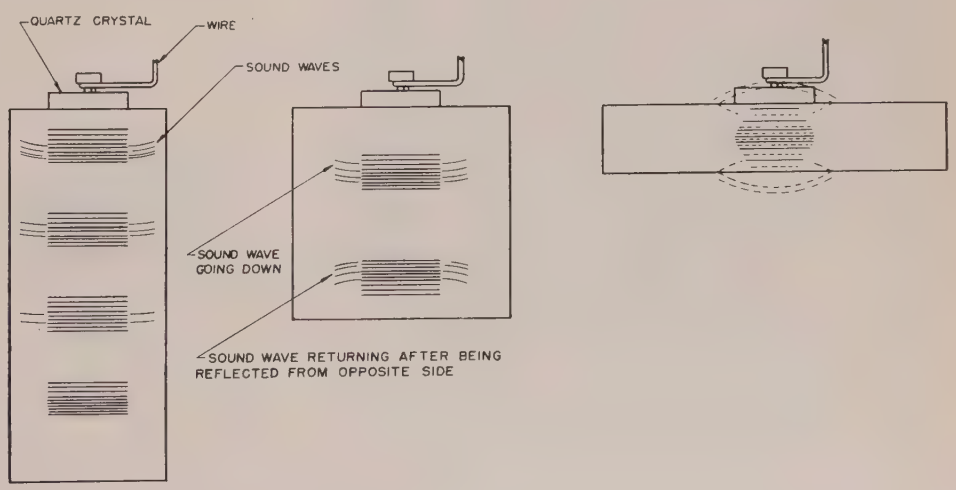

Fig. 12 – The action of a continuous wave of ultrasonic energy traveling down a bar in the resonant system. If the waves are sent out at the proper intervals, they will get back to the crystal at the same instant another wave is being sent out. The waves will build up large vibrations in the sheet. The resonance method measures these intervals to find the thickness of the sheet

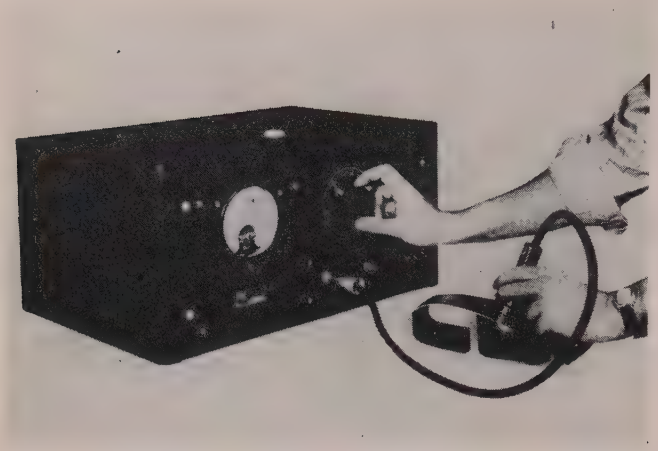

Fig. 13 – A hand-tuned resonance system using a meter to indicate when the resonant frequency is reached. Since the velocity of sound in the material is known, the thickness can be computed from the frequency

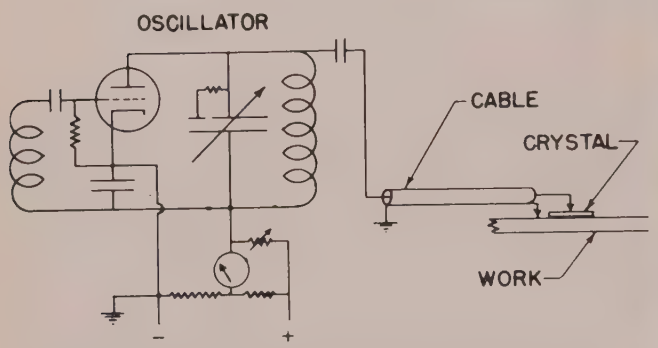

Fig. 14 – Elementary circuit diagram of the resonant system

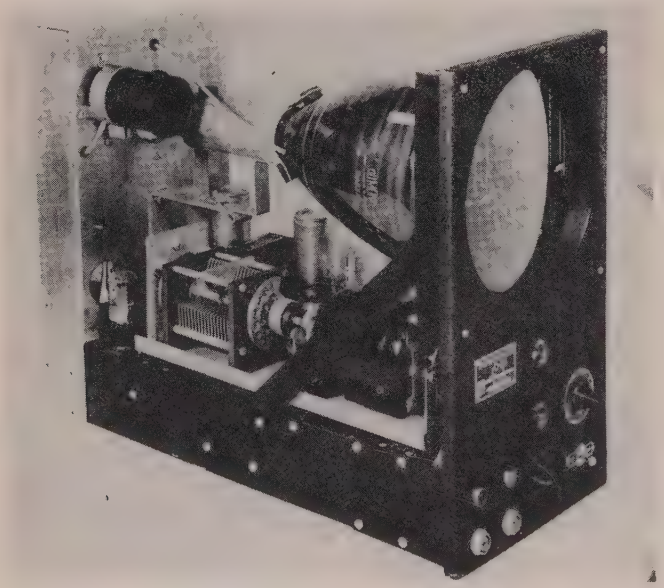

Fig. 15 – Automatic resonant system employing a cathode-ray tube for displaying the information

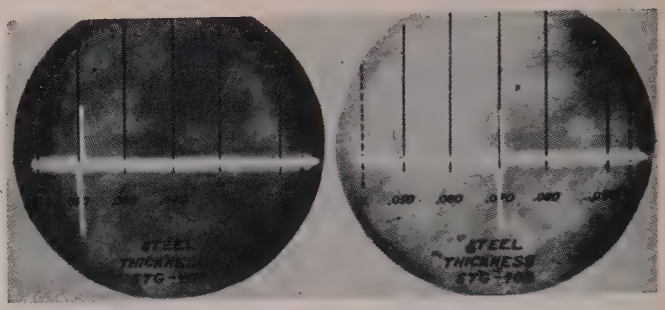

Fig. 16 – Calibrated screen of the resonant system showing indications for two different thicknesses. Left: 0.50-in. steel; right: 0.070-in. steel

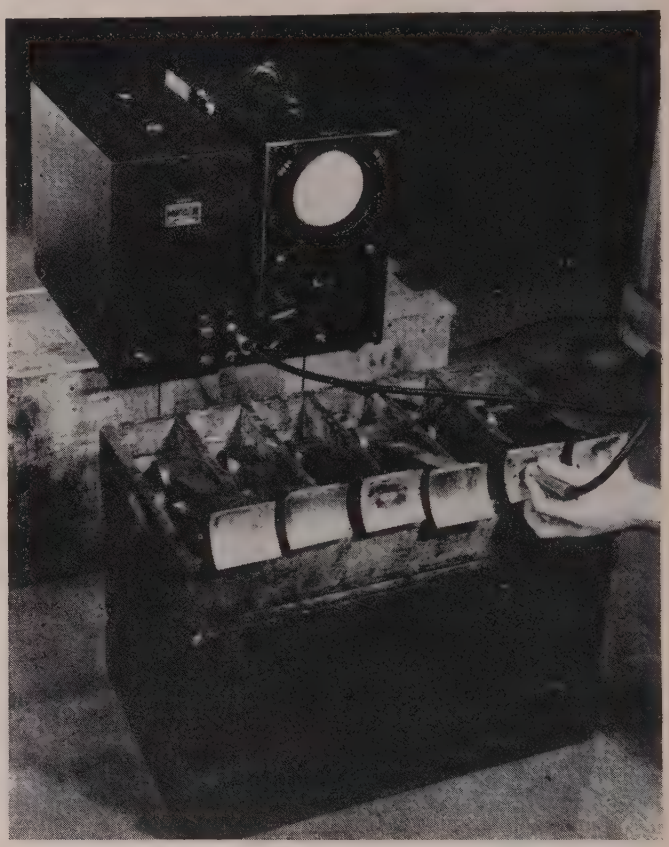

Fig. 17 – The resonant system used in checking bonds between silver bearings and connecting rods

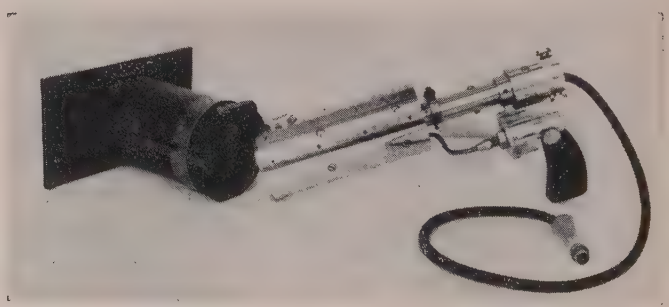

Fig. 18 – A special crystal and holder for examining cylinder-wall thickness

rent increases. A circuit diagram of this unit is shown in Fig. 14. A simple oscillator feeds the crystal which is coupled to the work with a thin film of oil. The resonant system requires that both surfaces be relatively smooth and nearly parallel.

A modified version of this instrument is shown in Fig. 15 wherein the indication is displayed on a cathode-ray tube.[6, 7] A motor-driven condenser continually varies the oscillator frequency through its range. In one range, for example, the frequency is varied from approximately ½ to 1½ megacycles (this is governed by the thickness of the work to be examined). The rotating system also initiates a sweep which is displayed on the cathode-ray tube. When resonance is reached, a vertical deflection such as is indicated in Fig. 16 results.

Fig. 17 shows the use of an early two-unit resonant system in checking the bond between silver bearings and connecting rods.[8] The crystal was ground to fit the bearing surface. Voids in the bond were displayed on the cathode-ray tube by the appearance of indications corresponding to the thickness of the bearing itself. Fig. 18 shows another application in which the resonant system is applied in measuring cylinder-wall thicknesses. A special crystal[9] and holder were made so that the entire surface of the cylinder could be manually scanned. This is a special application and will not work in all cases. Porosity of the casting, rough surfaces on both sides of the cylinder wall, grain size of the material, and lack of parallelism, all limit the usefulness of ultrasonics in many of these applications. Fig. 19 shows the resonant system as used in examining the thickness of a propeller-blade camber sheet. After the propeller blade has been balanced by removing material from the camber sheet, it is inspected to determine if the sheet has been thinned out beyond minimum tolerances. This same inspection also checks the brazed bond between the camber sheet and the forging.

Rubber-to-steel bondings may also be examined. Fig. 20 shows a section of a bond containing a void which was detected by this method. Since the ultrasonic energy is greatly absorbed by rubber, there will be no resonance in the metal where the rubber-to-steel bond is good. Where there is a void, the thickness of the steel alone will be indicated. Fig. 21 shows a void in copper brazing which was located by inspection on the outer surface on one of the sheets. If the material is bonded at all, the strength

Fig. 19 – Resonance system as used in examining the thickness of a propeller-blade camber sheet. The brazed bond between the camber sheet and the forging may also be inspected

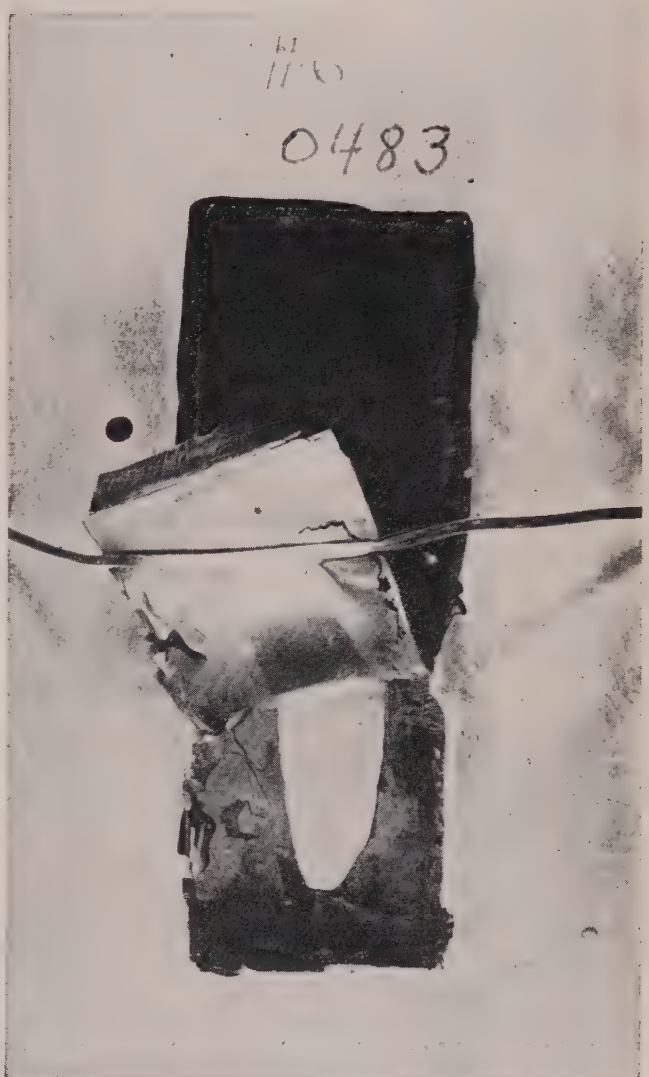

Fig. 20 – Voids in rubber-to-metal bond such as this may be located with the resonance method

[6] U. S. Patent 2,431,234. Nov. 18, 1947, "Automatic Sonic Measuring Means," issued to G. M. Rassweiler and W. S. Erwin.

[7] See *Iron Age*, Vol. 160, July 24, 1947, pp. 48-55: "Automatic Sonigage – New Ultrasonic Testing Instrument," by W. S. Erwin and G. M. Rassweiler.

[8] See *Review of Scientific Instruments*, Vol. 18, October, 1947, pp. 750-753: "Ultrasonic Resonance Applied to Nondestructive Testing," by W. S. Erwin and G. M. Rassweiler.

[9] U. S. Patent 2,485,722, Oct. 25, 1947, "Crystal," issued to W. S. Erwin.

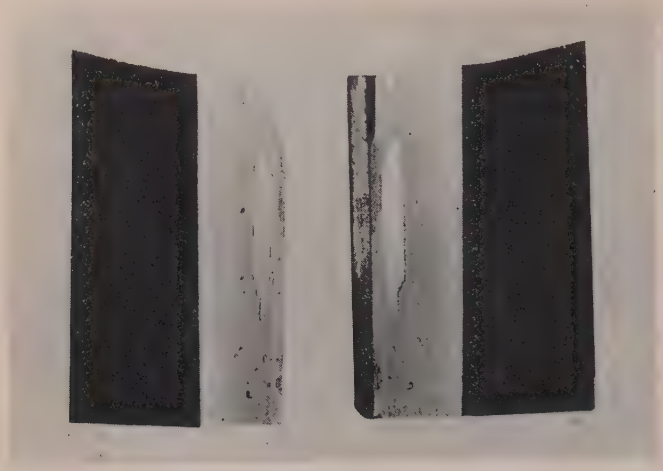

Fig. 21 – This void in copper brazing was located by inspection on the outer surface of one of the sheets

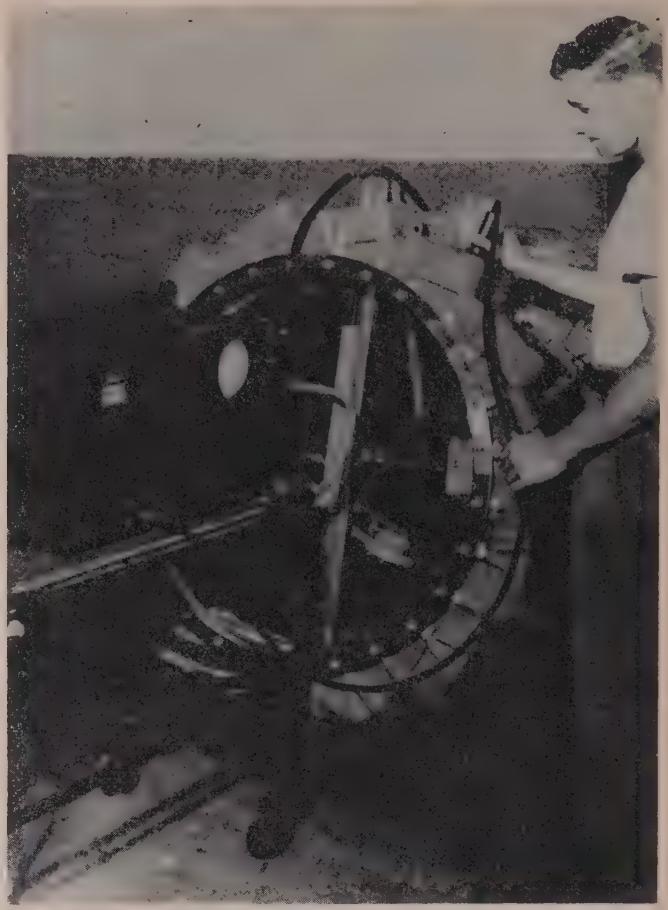

Fig. 22 – The wall thickness of a jet engine diffuser ring being examined with the resonance system

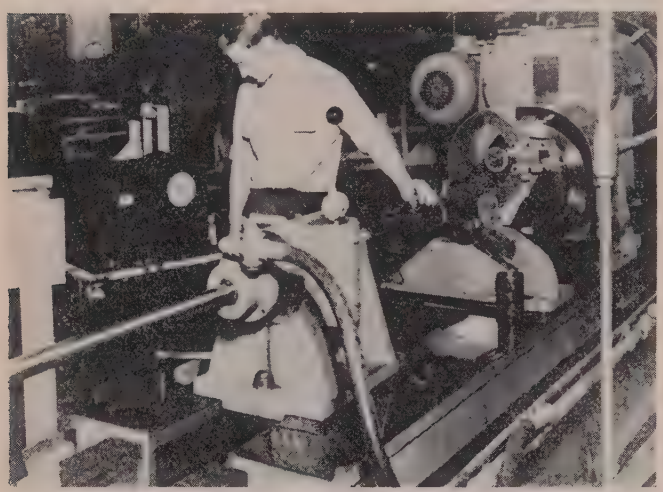

Fig. 23 – The resonance system used in monitoring the wall thickness of a turbine wheel shaft while a gun drill is used to bore out the shaft

Fig. 24 – If the portion under the crystal is sound, the indication corresponding to total thickness is obtained. The black lines in the block are sawcuts

Fig. 25 – If the flaw is parallel to the contact surface, a thickness reading is obtained characteristic of the depth of the flaw

of the bond cannot be determined by this method.

The resonant system has been successfully employed in production-line inspection of jet engine diffuser rings. Fig. 22 shows an early instrument used in inspecting the wall thickness to screen out those castings whose wall thicknesses are below requirements. Wall-thickness determinations within 0.005 in. were made possible on this part.

Another application of the resonant system is shown in Fig. 23 where the wall thickness of a turbine wheel shaft is measured while a gun drill is used to bore out the shaft. Calibration of the instrument by means of master set blocks allows the wall-thickness variations to be determined within 0.005 in. The application of the instrument to this problem allows the machine operator to determine the point at which the cutters become dull and start to run out and thus enables him to know when to change cutters.

While the resonant systems are designed to measure thin sections and usually operate over a range from about 0.015 in. to about 0.400 in., they can be used on sections larger than this, in which case harmonics are used. Fig. 24 shows the resonant system checking a test block. The two black lines are saw cuts, simulating defects. The position of the crystal transducer is over a sound section, and the harmonic indications correspond to the total thickness. Notice the number of vertical deflections present. However, if the crystal is placed over the parallel saw cut, Fig. 25, then a thickness reading is obtained characteristic of the depth of the flaw. Note the change in the number of pips on the scope screen. If the saw cut is not parallel to the surface, no thickness indications appear on the screen as shown in Fig. 26 since no resonance in the material is obtained. The use of this method in production inspection affords a valuable and nondestructive test. Flaws in turbine wheels have been found using this method. The section of a forged billet in which flaws were detected is shown in Fig. 27.

Fig. 26 – If the flaw is not parallel to the surface, no thickness indications appear on the cathode-ray screen

The instruments which have been discussed are of the semiportable type and may be carried to the work. A still more portable resonant instrument in which the indication is an audible signal is shown in Fig. 28. This self-contained instrument may be carried by the operator as he makes a measurement. Fig. 29 shows one of these units being used to examine a welded section in a ship's hull. Fig. 30 shows a special unit which may be carried on the operator's back as he examines the bolt-hole area in rails.

Ultrasonic Transmission Testing

A diagram of the ultrasonic transmission testing equipment is shown in Fig. 31. It consists of sending and receiving crystals with a test tank and an oscillator and detector.[10] Ultrasonic energy is sent

[10] U. S. Patent 2,655,035, Oct. 13, 1953, "Ultrasonic Transmission Testing," issued to W. S. Erwin.

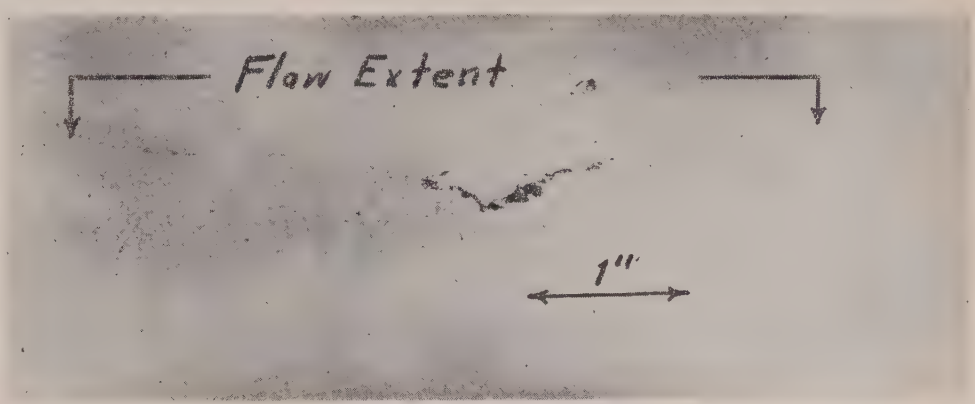

Fig. 27 – Flaws of this type are located in billets being used for forgings with the resonance system

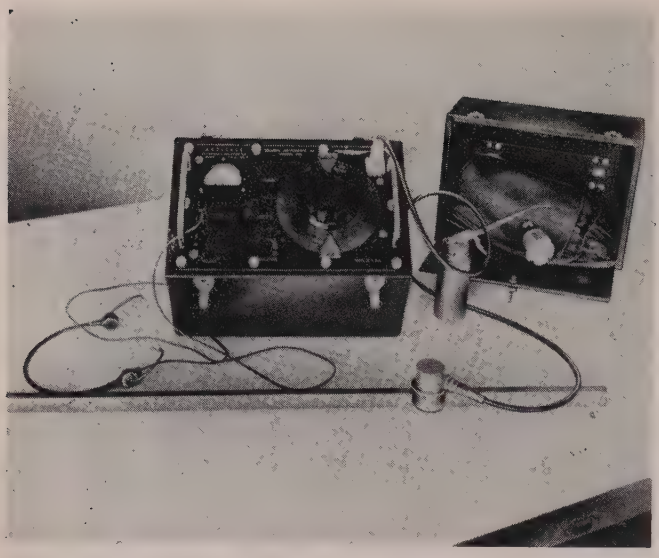

Fig. 28 – Portable resonant system which provides an audible signal as an indicator of resonance

through the piece under test, which is submerged in the tank of liquid, and is picked up and measured at the opposite side. The energy detected by the receiving crystal is an indication of the quality of the piece under test. The oscillator frequency is about 2 megacycles per second. Fig. 32 is a view of the equipment as used in a production setup.

Jigs and fixtures are usually required to center the part under test in the ultrasonic beam. Fig. 32 shows some fixtures used for centering valves in a test tank. It also shows the apertures in front of the crystals to limit the area of the ultrasonic beam so that only the piece to be tested is in the path of the beam. This increases the sensitivity of the system.

Some typical problems in which the transmission equipment has been successfully used are detection of laminated stock, poorly brazed bonds, and inclusions in bolts.

An interesting problem was that of the inspection of a butt-welded center bolt used in an oil-filter assembly. This problem was well suited for the transmission equipment because of the speed at which the examination can be made. A view of this production setup is shown in Fig. 33. This method of inspection permitted checking 1000 bolts in 1¼ hr as compared to 1000 bolts in 10 hr by another method.

One manufacturing plant was faced with the problem of separating a large quantity of bolts containing flaws. Some examples of the separation made possible by the use of this equipment are shown in Fig. 34. A sound bolt is shown on the left. It was possible to detect the narrow filamentary flaws or pipes in the middle bolt, while the cup flaws shown in the right bolt were very readily detected.

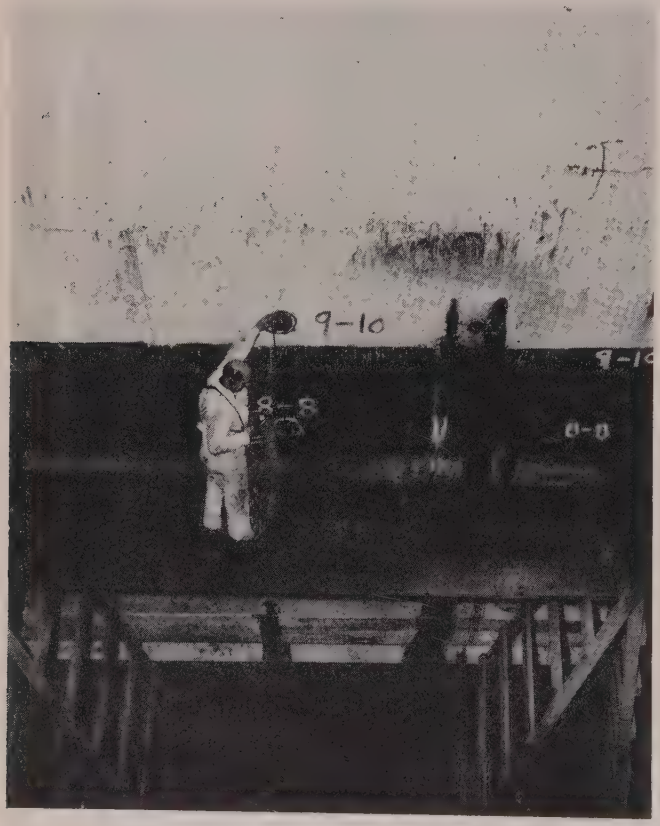

Fig. 29 – Portable resonant system used in examining a welded section in a ship's hull

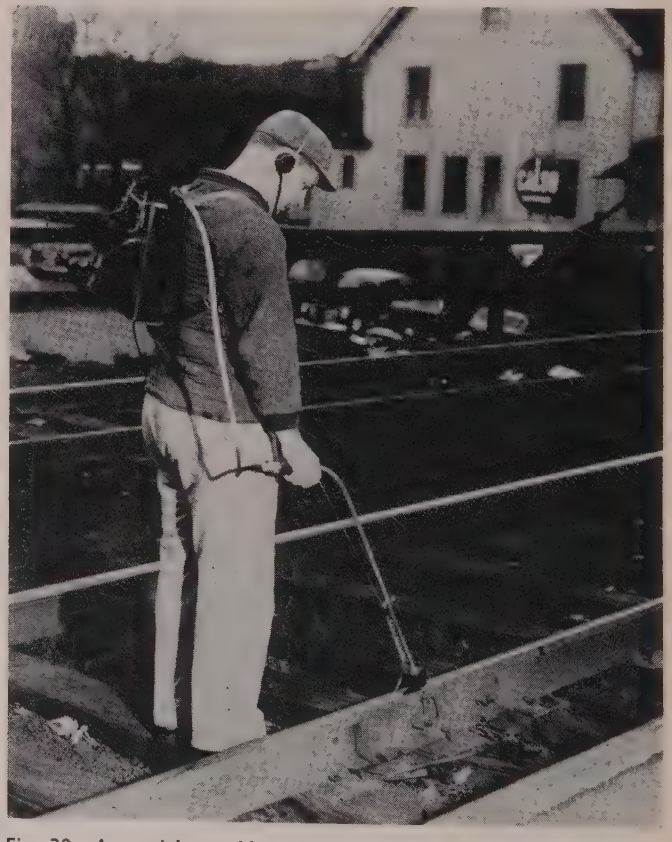

Fig. 30 – A special portable resonant system for examining the bolt-hole area of rails

Fig. 35 shows a cylinder with aluminum cast around it being examined for poor bonds. The crystals are mounted in special holders so that they can be lowered into the test tank, thereby scanning the entire surface of the material under test. In some tests it is necessary to focus the ultrasonic beam in order to concentrate the energy. Lucite lenses afford a simple method for focusing the energy and were used in the examination of the cylinders shown in Fig. 35. The transmission equipment just described employs submersion of the sample, although this is not a requirement of this method. Submersion may also be used with the pulse echo method. Submersion has advantages in some problems as compared to pressing the crystal against the surface. Since it is not necessary for the crystal to touch the test piece, the surface-finish requirements are not as great as in crystal

Fig. 33 – A production setup used in examining a butt-welded oil-filter center bolt. A savings of 8¾ hr in inspecting 1000 bolts resulted from the installation of this equipment

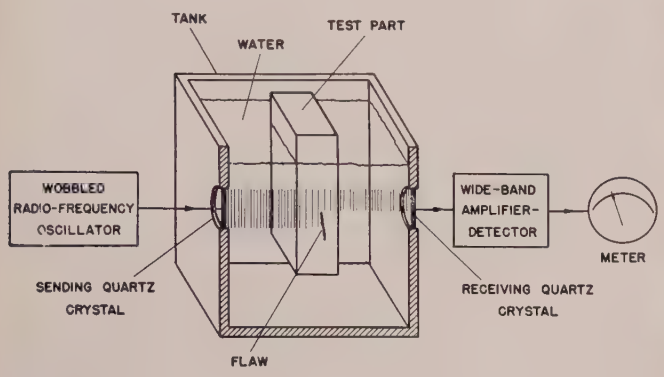

Fig. 31 – Block diagram of the transmission system

Fig. 34 – Examples of bolts sorted with a production setup using the transmission system. Sound bolt is on the left. Pipe flaws were detected in bolt in center, while cup flaws in the right bolt were very easily detected

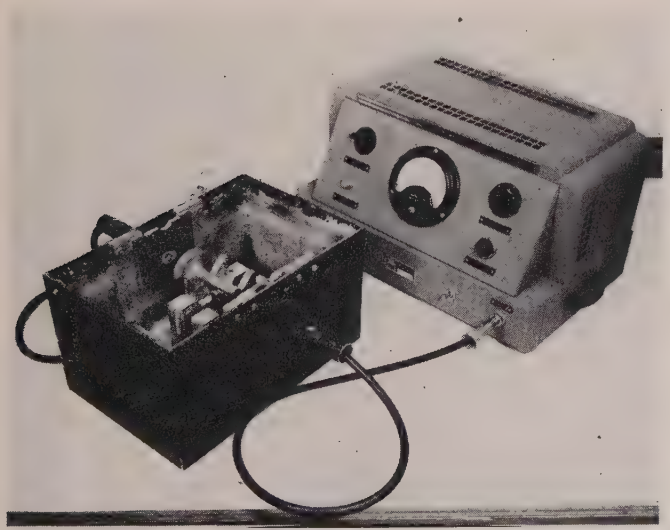

Fig. 32 – Equipment required for production transmission inspection. Special fixtures are used to center the part under test. Note aperture used to limit area of the ultrasonic beam

Fig. 35 – Special crystal transducer holders for examination of bonds between a cylinder and aluminum which had been cast around it. Note special lucite lens to focus the ultrasonic energy

contact systems. Coupling to the work is more uniform from one piece to another, which is particularly important in transmission testing.

Frequency Modulation

A recent newcomer in the ultrasonic inspection field is a system employing frequency modulation equipment in a submersion method.[11, 12] This system operates in a manner similar to the aircraft altimeter. Both the frequency modulation and pulse echo submersion methods have been used in automatic devices for flaw detection in parts with complicated shapes.

Conclusion

While ultrasonic inspection will not solve all problems, it is capable of doing what other nondestructive methods will not do. For instance, it is capable of detecting minute interface defects, while X-ray techniques will only detect volume voids. It will permit detection of deep subsurface defects which the magnetic-particle and liquid-penetrant methods are incapable of doing. The portability of the ultrasonic equipment also makes it very attractive for a large number of inspection problems.

It is obvious from the discussion of ultrasonic inspection techniques presented in this paper that no one method will satisfy all production problems. The problem should be studied carefully to determine which method will effect the best results, since many times two of these methods will perform satisfactorily. Each production application of ultrasonic testing techniques is a project in itself. It is often necessary to build special test fixtures and purchase or build special transducers. Ultrasonic inspection is not a cure-all for production testing, but with a fair chance and plenty of ingenuity, ultrasonic testing can solve many problems. The results should be an improved product at a lower cost.

DISCUSSION

Describes Equipment for Making Permanent Acoustic-Test Records

– W. I. Bendz
Sperry Products, Inc.

MR. WELLER'S paper is a welcome addition to the rapidly growing list of literature on the subject of ultrasonic nondestructive testing.[a-d] While the illustrations cover a representative group of the usual applications of pulse echo type of instrumentation, it may be of interest to include a few other accessories which are now in commercial use and which widen the scope of ultrasonic testing.

Mr. Weller referred to the use of a "standard" 45-deg-angle crystal, and indeed this particular angle transducer so far exceeds the usefulness of all other angles that perhaps it deserves to be called a "standard." However, there are occasions when some other angle may be the solution to a problem. Such a case is illustrated by Fig. A in which search units of 24, 19, and 15.5 deg are used to detect axle cracks in areas which would otherwise be impossible.

[11] U. S. Patent 2,593,865, April 22, 1952, "Ultrasonic Flaw Detector," issued to D. C. Erdman.

[12] See *Nondestructive Testing*, Vol. 11, November-December, 1953, pp. 27-31: "Ultrasonic Inspection Using Automatic Recording and Frequency Modulated Flaw Detector," by D. C. Erdman.

[a] See ASTM Special Technical Publication No. 101, January, 1951, "Symposium on Ultrasonic Testing."

[b] See pp. 240-250: "Ultrasonic Testing and Inspection," by J. C. Smack, in "ASME Handbook – Metals Engineering – Design." Pub. by McGraw-Hill, New York, 1953.

[c] See *Nondestructive Testing*, Vol. 12, May-June, 1954, pp. 29-33: "Immersed Ultrasonic Inspection with Automatic Scanning and Recording or Warning Signal," by John C. Smack.

[d] See ASTM Bulletin No. 198, May, 1954, "Surface Waves at Ultrasonic Frequencies," by E. G. Cook and H. E. Van Valkenburg.

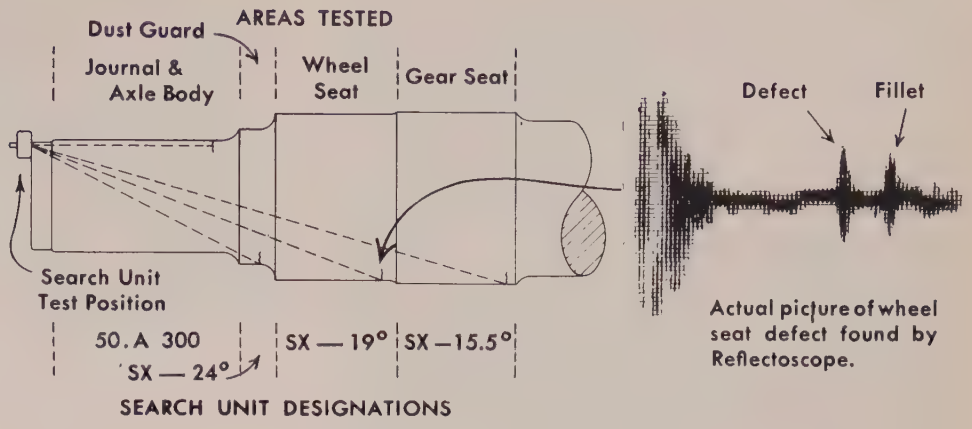

Fig. A – Three angle search units inspect all axle critical areas

One other use for angle beam search units is illustrated by Fig. B which shows a light-weight ultrasonic test car for inspecting the joint area of railroad track. Cracks which may emanate from bolt holes in the rail ends are accurately indicated by the reflectoscope under the operator's canopy.

The point is that angle beam search units are commercially available to fit a very wide variety of testing circumstances.

Another very useful search unit which is a newcomer among the family of angle crystals generates a surface wave.[d] As the name implies, surface waves will travel along a smooth surface of a solid with only small attenuation for many feet. But any scratch or defect in or just below the surface will cause an acoustic reflection which is indicated in the usual manner. Surface waves have been generated on either flat or curved surfaces of solid samples of steel, aluminum, beryllium, magnesium, and titanium.

Commenting on through transmission, it is well to note that the Sperry Type UR reflectoscope can be used with two search units for either reflection or through testing, contact or immersed. Thus, the pulse echo system is also useful to test by through transmission and is employed commercially for testing porous materials, of which grinding wheels are a typical example.

Ultrasonic instrumentation is now commercially available for the purpose of making permanent records of the acoustic test.[e] Fig. C shows a Type UR reflectoscope fitted with an accessory unit for operating an alarm system and any standard pen recorder such as a Brush Model BL-202. If desired, the apparatus will also operate two pen recorders, one printing reflection (echo) signals while the other prints back reflections. In either case the amplitude of recorded line and acoustic signal holds a linear relationship. Adjustments provide for selecting three areas which are penetrated by the ultrasonic beam and for which the recording apparatus is effective. Thus, echo signals from known causes such as holes, shoulders, backface, and so forth, can be excluded from the written record. Also an alarm relay can be set to give a signal at any adjustable level of echo signal amplitude.

Recently, apparatus for automatically scanning jet rotor wheels was completed for the Allison Division of General Motors and is now operating daily for routine inspection of parts. The apparatus also makes a permanent inked record of each part tested, which is a developed plan view on a circular chart. Fig. D illustrates the complete equipment, taken during final test in the laboratory. Sonic inspection of the part takes place in immersion tank 1 which includes a rotating turntable on which the specimen is mounted and search unit positioning head sliding on horizontal ways. Operation of the equipment is vested in console 2 which also houses all electronic units. The reflectoscope visual monitor tube is located at the center top. Pushbuttons and control switches are on the sloping front panel, while all adjustments for controlling calibra-

Fig. B – Ultrasonic inspection car locates defects originating from bolt holes in rail ends using angle beam search unit

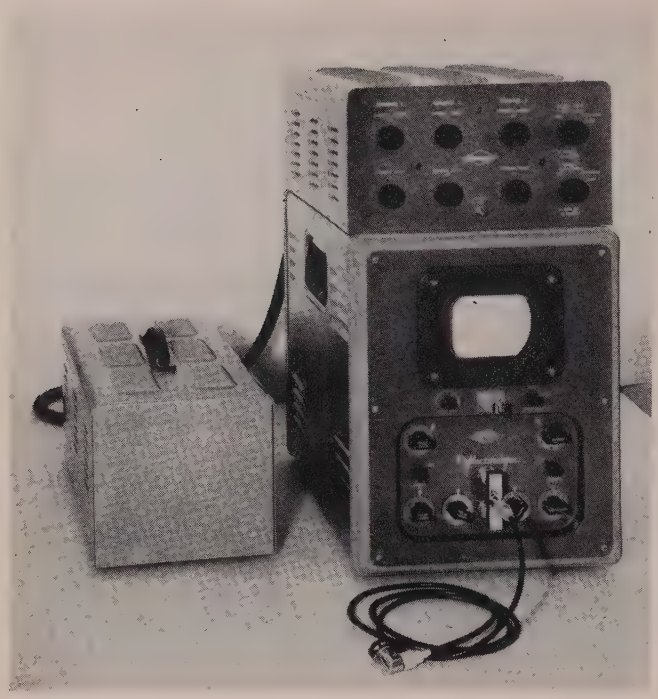

Fig. C – Attachment to reflectoscope will operate direct inking recorder to make permanent test records or operate alarm for defect presence

tion of the reflectoscope are behind the two doors which are normally kept locked. Permanent records are made on recording table 3 which revolves the chart in synchronism with the specimen turntable. All control apparatus for operating the system servo motors is enclosed in cubicle 4. The specimen is aligned on a jigging plate at station 5 prior to being loaded in the testing tank.

A closeup of the actual testing apparatus is given in Fig. E wherein the rotor forging can be seen in the foreground. The search unit is the cylindrical housing shown pointing toward the hub of the rotor. It is rotated to any

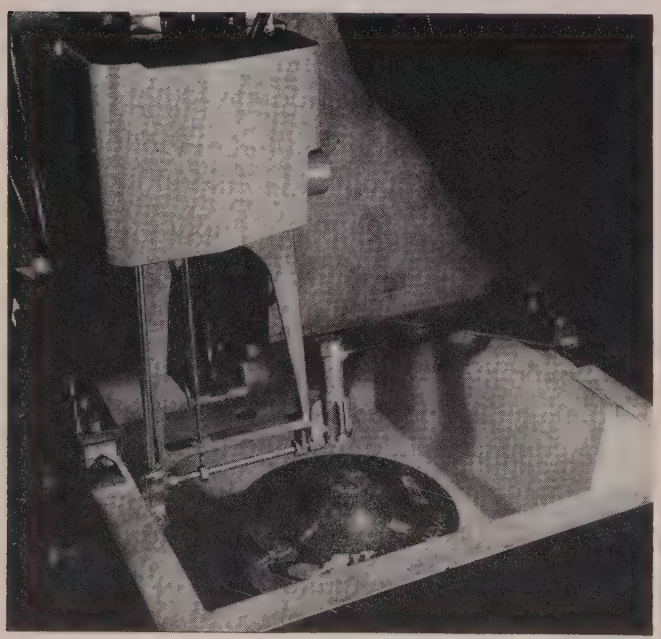

Fig. E – Coordinate positions of search unit provide complete scanning of specimen mounted on rotating table. In service, tank is filled to cover bottom of search unit

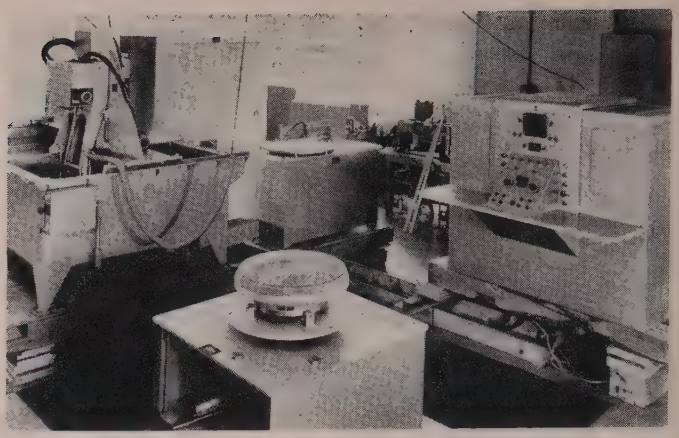

Fig. D – SIMAC apparatus for automatic scanning and testing jet rotor wheels; 1 – inspection tank, 2 – control console and monitor station, 3 – recorder, 4 – control cubicle, 5 – preliminary setup station

required angle by means of the horizontal shaft which is aligned to the crystal face at the bottom of the housing. Horizontal slides for the entire carriage can be seen at sides of the tank, whereas vertical slides for raising and lowering the search unit are hidden behind the vertical supports. The illustration was taken with the tank empty to afford a clearer view.

The recorder table is shown in Fig. F. A circular chart is driven from the same shaft which turns the specimen while a fast-writing pen inks the chart. The pen is traversed radially by a horizontal screw and nut. During the active cycle of the test, a device measures out exactly one revolution of the specimen. During this period the reflectoscope is "connected" to the recorder pen which makes its record on the chart. The reflectoscope is then "disconnected" and the search unit repositioned to the next scanning point. Meanwhile the pen is advanced radially by rotating its lead screw exactly one revolution. In this manner both the ultrasonic scan and chart recording are developed as a series of concentric lines. Fig. G illustrates a typical chart taken on a test specimen previously prepared with several drilled holes. The overlapping marks

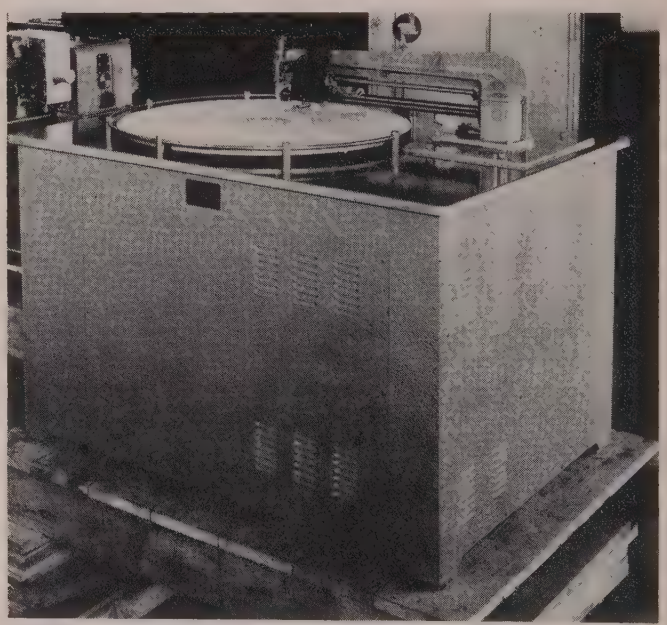

Fig. F – Recorder table for making circular chart which in reality is a developed plan view of the ultrasonic test

Fig. G – Typical chart. Test specimen was prepared with artificial defects to evaluate performance of equipment

which align radially are deliberate check marks which respond to the overall system operation once for each scanning cycle. Thus the permanent record also indicates the reflectoscope performance throughout the test.

Fig. H illustrates the punched tape and "tape reader" which controls the testing program automatically. Sixty holes across the width of the tape are used in a binary code system to operate closed-loop servos so as to program the horizontal, vertical, and angular positions of the search unit, the path length of the ultrasonic beam entering the part, specimen turning speed, ultrasonic power level, and three other detail control functions. The tape is stepped one row of holes for each scanning development. Thus, the length of the tape depends upon the number of scan lines required to test a specimen. When a test is completed, the tape automatically returns to a "home" position in readiness for the next operation.

A closeup of the servo unit for positioning the search unit angle is shown in Fig. I. The servo motor is toward the right with its shaft horizontal and driving into a two-speed gear box which is electrically controlled. The unit directly above the rectangular gear box is a position converter which serves to match the actual position of the search unit angle against the demand of the tape punching. The servo will continue to drive the search unit in the proper direction until the position converter is satisfied that the actual position exactly matches that called for by tape punching. All servos are controlled by magnetic amplifiers, no electronic tubes being used for this purpose.

The apparatus described above is one approach to the problem of automatic scanning. There are other methods. Sperry chose the scheme illustrated for the reason that it is relatively simple and can be maintained by the average personnel employed for plant maintenance. Also, the components are reliable, and satisfactory operating life is expected. The service to date is too short to draw conclusions except in the general way that automatic scanning operations for ultrasonic nondestructive testing have been proven possible, and when given the problem of quantity inspection of like or similar parts, the cost of automation can often be justified.

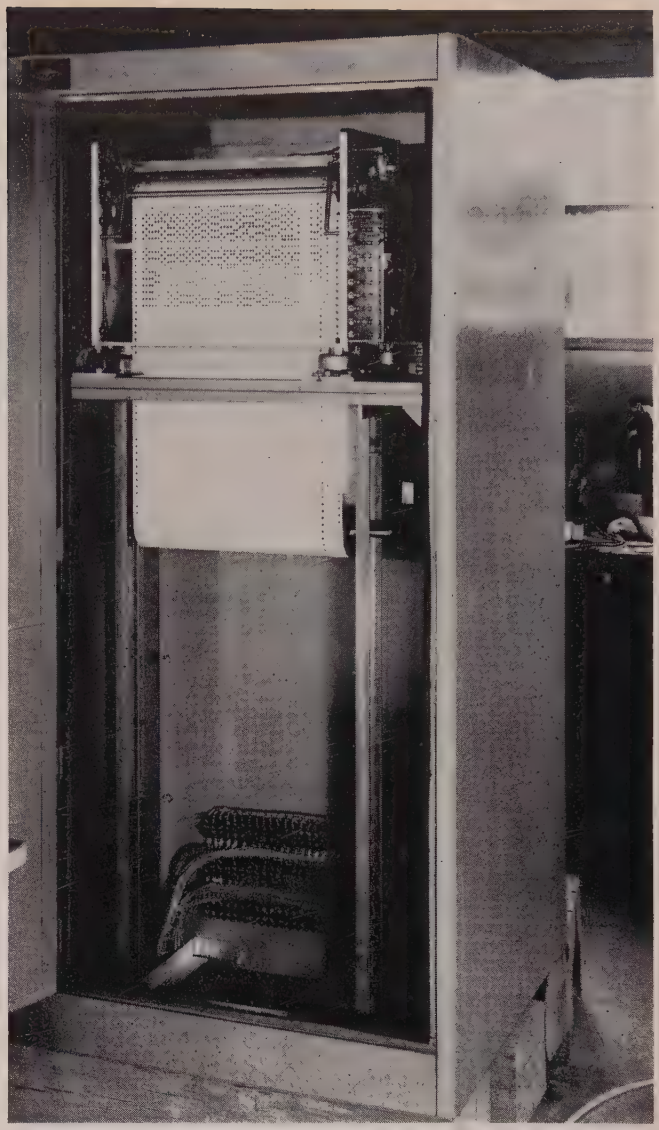

Fig. H – Holes punched in endless "tape" are "read" by this apparatus and control the sequence of all functions required for automatic scanning

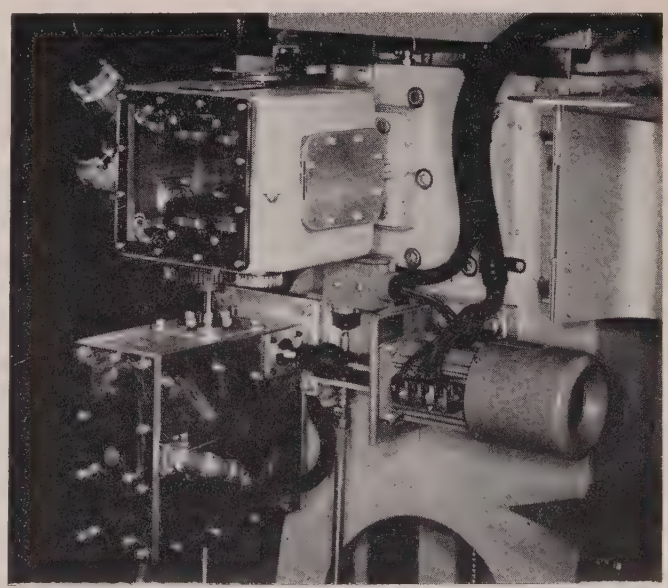

Fig. I – Servo motor and position-checking components for search unit angle positioning

Wear, Scuffing, and Spalling

THE following discussion is generally limited to loss of metal from valve lifters and piston rings during operation in passenger-car engines, the influence of certain types of oil on such loss of metal, and testing methods for evaluation of oils in these respects. The several mechanisms of weight loss may be defined for the purpose of this discussion in the following simple terms:

Wear – to be impaired gradually by use, that is, to lose metal gradually and smoothly by friction.

Scuffing – a type of wear in which the surfaces are roughened.

Spalling – chipping or breaking up of the metal surfaces.

A more detailed discussion of these terms will be given in the appropriate section of the paper.

The study of the influence of lubricants on wear and scuffing is ancient by comparison with the recent flurry of interest in the spalling problem. Spalling of valve lifters may first become evident to the naked eye by appearance of hairline cracks on the surface rubbed by the cam. Following many thousands of stress reversals of this surface, metal flakes from the surface, leaving pits or craters. The pitted surface may wear off a cam nose quite rapidly. Vincent Ayres has presented an interesting discussion of spalling or pitting of valve-lifter faces.[1] He said, in part:

"Tappet-face pitting is a phenomenon associated with tappets having a face material of chilled cast iron. The pitting is a fatigue failure resulting from overstress, and it may be accelerated by corrosive materials present in the crankcase. . . . Wear or scuffing may be reduced by increased load-carrying capacity of the lubricating oil. This improvement may be valid only for steel and hardenable cast-iron tappets and may not reduce fatigue or wear of chilled iron tappets."

While the above opinions have been substantiated by a considerable amount of data available from engine tests, it seems likely that the study of spalling is too new for establishment of a thorough understanding of all the factors involved.

Wear of valve lifters appears to be reasonably reproducible in controlled engine tests. Mougey[2, 3, 4]

Table 1 – Brief Engine Test Conditions

Procedure[a]	Engine Type	Temperature Range	Speed Range	Test Duration
A-1 (2)	V-8, overhead valve	Moderate	Low-moderate	2 hr
A-1 (6)	V-8, overhead valve	Moderate	Low-moderate	6 hr
A-2	V-8, overhead valve	Low	Low	100 hr
A-3	V-8, overhead valve	Moderate-high	Low-high	3000 miles
B-1	V-8, overhead valve	Moderate	Low	100 hr
C-1	6-cyl, L-head	Moderate-high	Low-high	3000 miles
D-1	6-cyl, overhead valve	High	High	36 hr

[a] Letter designates engine make; numbers indicate different test procedure in same engine.

[1] See Eaton Engineering Forum, Vol. XIV, December, 1953, pp. 2-14: "A Question and Answer Discussion of Valve-Gear Problems," by Vincent Ayres.

[2] "Progress Report on API Service Classifications and Designations for Lubricating Oils for Automotive-Type Engines," by H. C. Mougey. Presented at API Lubrication Committee Meeting, White Sulphur Springs, W. Va., May 11-13, 1953.

[3] "Engine Wear, as Affected by Lubricants," by H. C. Mougey. Presented at Symposium on Engine Lubricants, Technical Committee B, ASTM Committee D-2, Atlantic City, July 1, 1953.

[4] See SAE Transactions, Vol. 62, 1954, pp. 196-209: "Forty Years of Progress in Automotive Lubrication – A Look into the Future," by H. C. Mougey.

in Passenger-Car Engines

H. A. Ambrose and J. E. Taylor,
Gulf Research & Development Co.

This paper was presented at the SAE National Passenger-Car, Body, and Materials Meeting, Detroit, March 2, 1954.

RESULTS of a laboratory study of some of the factors causing wear, scuffing, and spalling in passenger-car engines, with emphasis on the lubricating oil variables involved, are reported in this paper, which is part of the Symposium on Cam and Tappet Wear.

The tests show that piston-ring and valve-lifter wear and spalling of some valve-lifter materials seem to be greater with low-viscosity oils such as SAE 5W-20 and 10W.

Certain antiwear lubricating oil additives reduce valve-lifter and ring wear but may increase spalling of chilled iron lifters. However, using an oil with good antiwear properties for engine break-in will not prevent future lifter wear if the engine is operated with an oil of poor antiwear characteristics.

has described laboratory engine test methods for evaluation of the effects of various oils on wear and spalling of valve lifters and wear of piston rings. Additional engine test procedures have been devised. Little has been published on laboratory bench scale tests for measuring the antiwear characteristics of modern motor oils or correlation of such tests with performance of oils in engines.

Description of Engine Tests

The data reported in this paper were obtained from tests conducted in four different makes of en-

Discussion of this and the other papers in the Symposium starts on p. 220.

The Authors

H. A. AMBROSE (M '37) is director of the Product Division of Gulf Research & Development Co. He received a B.S. degree in Chemistry from Norwich University in 1924, and a Ph.D. Degree in Chemistry from the Massachusetts Institute of Technology in 1929. Mr. Ambrose was with the Research Department of the Gulf Production Co. from 1931 to 1933, when he joined the Gulf Research & Development Co.

J. E. TAYLOR (M '37) is director of the Automotive Engineering Division of Gulf Research & Development Co. He joined Gulf Research in 1934 following graduation from the University of Pittsburgh, where he received a B.S. degree in Mechanical Engineering. Mr. Taylor transferred to the Product Development Section of the Gulf Oil Corp. in 1949. Three years later he transferred back, to assume his present position.

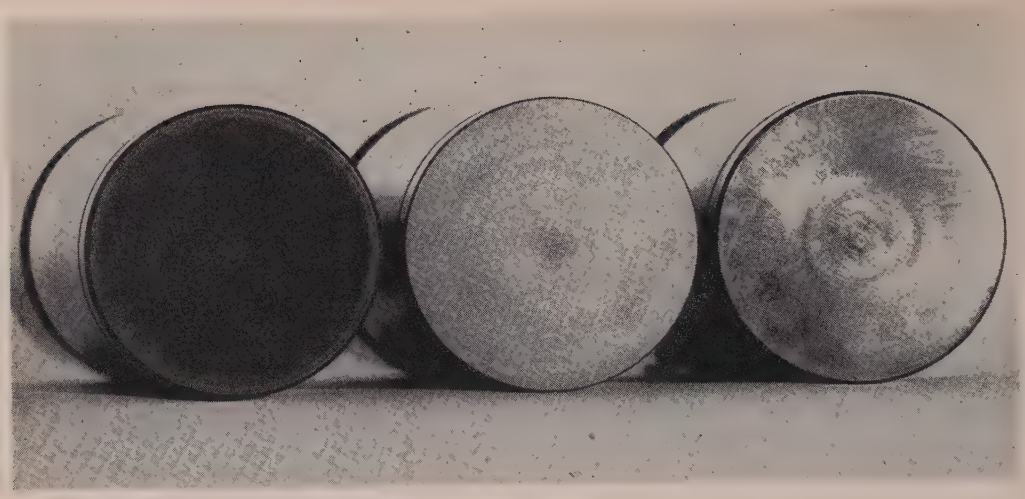

Fig. 1 – Valve lifters from engine make A; left to right: new, slightly worn, badly worn

gines and four different procedures were used for one of these engine makes. A brief outline of the engine test conditions is given in Table 1. More detailed information on the various test procedures is given in the Appendix.

Referring to Table 1, the letter under the heading "Procedure" designates the engine make, and the numbers following the letter indicate different test procedures in the same engine. Procedures A-1 (2) and A-1 (6) are identical except for test duration, the A-1 (2) cycle being repeated three times to obtain procedure A-1 (6).

Procedures A-3 and C-1 were conducted on chassis dynamometers and were intended to simulate, in part, severe high-speed operation in the Appalachian Mountains. These tests consisted of: (1) 1000 miles of simulated city-suburban operation to break in the engine and obtain an oil mileage baseline, (2) 1000 miles of high-speed mountain type of operation to promote cylinder and piston ring wear and scuffing, and (3) another 1000 miles of city-suburban operation to determine if oil consumption was adversely affected by the previous severe operation. The average car speed in these tests was approximately 40 mph, and the test duration was therefore approximately 80 hr.

The standard valve-lifter material for engines A and C was steel and for engines B and D was chilled cast iron. Valve-spring pressures were essentially standard for all tests except for procedure B-1. In this test, spring pressures with valve fully open were maintained approximately 50% above normal.

Table 2 – Oil Code

Code No.	Viscosity	Detergency Level	Detergent	E-P Additive
A-1	5W-20	Series 1	(a)	—
A-2	5W-20	Series 1	(a)	(1)
A-3	5W-20	Series 1	(a)	(2)
A-4	5W-20	Series 1	(b)	—
A-5	5W-20	Series 2	(a)	—
A-6	5W-20	Series 2	(d)	—
A-7	5W-20	Series 1	(a)	(3)
A-8	5W-20	Series 1	(a)	(4)
A-9	5W-20	Series 2	(a)	(1)
B-1	10W	—	—	—
B-2	10W	—	—	(1)
B-3	10W	Series 1	(a)	—
B-4	10W	Series 1	(c)	(5)
C-1	10W-30	Series 1	(a)	—
D-1	20-20W	—	—	—
D-2	20-20W	Series 1	(a)	—
D-3	20-20W	Series 1	(a)	(1)
D-4	20-20W	Series 2	(c)	(5)
E-1	30	Series 1	(a)	—

Test Oils

The data reported in this paper cover tests conducted on a total of 19 different oils. The oil code is presented in Table 2. The test oils cover a range of viscosities from 5W-20 to 30 and a range of detergency levels from none to Series 2. Four different detergent additives and five different e-p additives were employed.

The various letters in the oil code refer to viscosity classifications. All references to viscosity are based on the appropriate SAE classifications.

The term "detergency level" is employed to classify various degrees of detergency, and the level is based on the familiar Series 1 and Series 2 classifications. Although only a detergent code is given, all oils contained sufficient oxidation and bearing corrosion inhibitor to pass the CRC L-4 test.

The term "e-p additive" is employed to connote antiwear additives of various sorts. Although the antiwear properties of all such additives may not be due to extreme pressure characteristics, the term e-p appears to be accepted in the automotive and petroleum industries to connote antiwear characteristics and is employed in this paper for simplicity.

Test Results – Wear

The primary purpose of an engine lubricating oil is to minimize friction and wear in an engine. Ex-

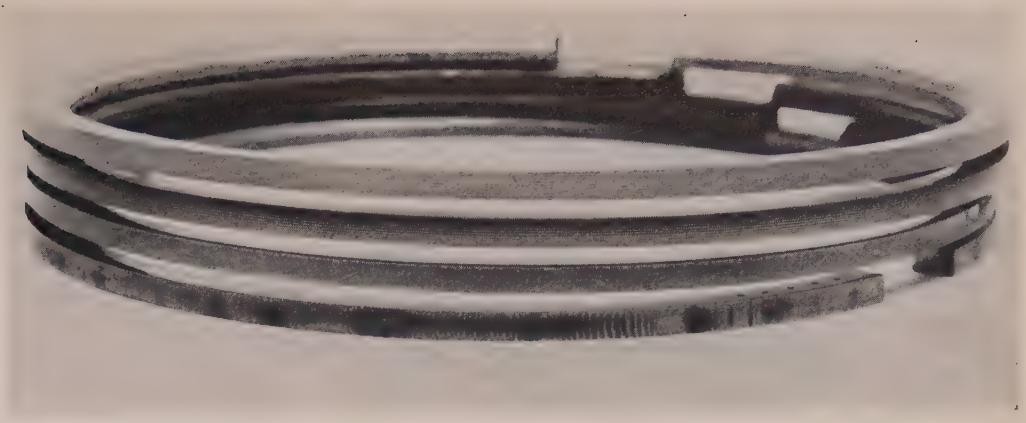

Fig. 2 – Examples of ring wear in engine make C; top to bottom: new, slightly worn, badly worn, scuffed

perience has shown that the valve lifters of modern high-specific-output engines are extremely sensitive to the antiwear characteristics of lubricating oils and that there is a relationship between valve-lifter wear and the wear of other engine parts such as push-rods, rocker arms, timing gears, and oil-pump drive gears. Since valve-lifter wear is an important consideration in engine lubrication, is a good index of wear in certain other parts of the engine, and is relatively easy to measure, it has been adopted as an important criterion of the antiwear characteristics of automotive lubricating oils. In the following discussion on wear, valve-lifter wear is intended to be a measure of the overall antiwear characteristics of engine lubricating oils with the possible exception of piston-ring and cylinder wear; however, data are presented to show the relation between lifter wear and cylinder and ring wear. Where valve-lifter wear measurements are given, they refer to wear in the center position of the lifter since it has been determined that on the average the maximum wear occurs in the center position.

Fig. 1 shows three typical lifters from engine A. The one at the left has not been used; the one in the center was used for 6 hr but shows very little wear; the one at the right is rather badly worn considering the short duration of this test.

Fig. 2 shows several compression rings from engine make C to illustrate the degrees of ring deterioration to be discussed. The top ring is new while the others have been used and are classified as good, worn, and scuffed respectively.

Effect of Test Duration on Valve Lifter Wear – A very short test (2-hr duration) has been used to measure valve lifter wear in engine A. This test employs moderate speeds and temperatures as shown in the Appendix for test procedure A-1 (2). In order to determine whether this 2-hr test was a valid criterion of lifter wear for extended service, data on lifter wear after 2 and 6 hr of operation were obtained on a variety of oils [the 6-hr procedure is a continuation of the 2-hr procedure and is given in the Appendix as test procedure A-1 (6)]. The relationship between the 2-hr and 6-hr tests is shown in Fig. 3. From these data it was concluded that the 2-hr test was a little too short to be conclusive. It was further decided that an oil having good antiwear properties should not allow more than 0.0004-in. wear in the 6-hr test. This latter decision was based on the appearance of lifters in addition to wear measurements.

Table 3 shows the relation between the 6-hr test and a 3000-mile vehicle test using the same engine. Only oils exhibiting reasonably good antiwear characteristics in the 6-hr test were selected for vehicle tests; however, the oils covered a range of viscosities, detergency level, and e-p additives. In no case was the wear in the 3000-mile vehicle test significantly greater than in the 6-hr engine test. These results indicated that the 6-hr test provided a good measure of the long-term antiwear properties of lubricating oils under moderate- to high-temperature operating conditions.

Effect of Oil Viscosity on Valve-Lifter Wear – Since the problem of valve-train wear has been as-

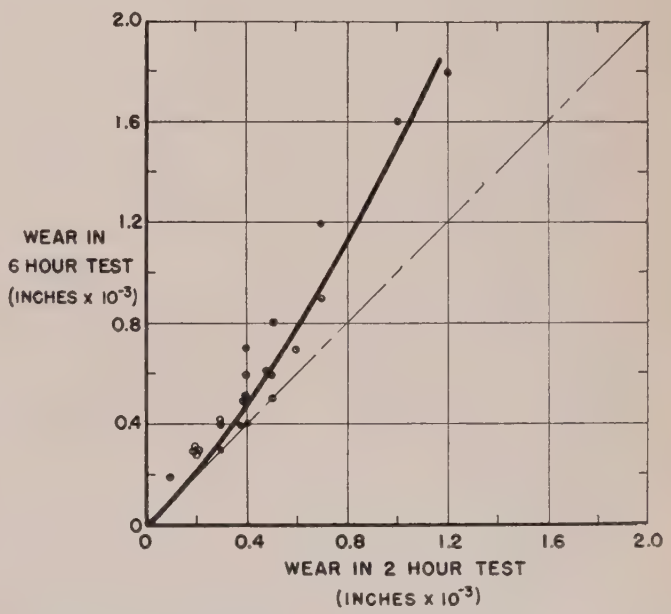

Fig. 3 – Effect of test duration on valve-lifter wear in engine A with various oils

Table 3 – Effect of Test Duration on Valve-Lifter Wear in Engine A

	Oil	Viscosity	E-P Additive	Average Lifter Wear, In. 6-Hr Test A-1 (6)	Average Lifter Wear, In. 3000-Mile Test A-3
Detergent Oils					
	A-2	5W-20	(1)	0.0004	0.0006
	A-3	5W-20	(2)	0.0005	0.0008
	D-2	20-20W	—	0.0004	0.0005
	D-4	20-20W	(5)	0.0004	0.0005
Nondetergent Oils					
	B-1	10W	—	0.0006	0.0005
	B-2	10W	(1)	0.0003	0.0003
	D-1	20W	—	0.0004	0.0005

Table 4 – Effect of Valve Lifter Break-In on Wear in Engine A – Test Procedure A-1 (6)

	In.
Initial Wear After 6-Hr Operation on Oil B-4	0.0004
Total Wear After 6 Additional Hr on Oil A-1	0.0016
Wear Due to Oil A-1	0.0012
Initial Wear After 6-Hr Operation on Oil A-2	0.0004
Total Wear After 6 Additional Hr on Oil A-1	0.0014
Wear Due to Oil A-1	0.0010
Wear Normally Encountered with Oil A-1	0.0014

Table 5 – Effect of Operating Conditions on Valve-Lifter Wear in Engine A – Various Oils

Oil	Lifter Wear, in.		
A-2	0.0004	0.0006	0.0020
B-1	0.0006	0.0005	0.0008
D-2	0.0004	0.0005	0.0009
D-3	0.0003	—	0.0003
Test Procedure	A-1 (6)	A-3	A-2
Test Duration	6 hr	3000 miles	100 hr
Jacket Temperature, F	165	160 200	100
Oil Temperature, F	150 190	130 260	80 135
Speed Range, rpm	900 2000	1000 3500	1000

Table 6 – Effect of Metallurgy on Valve-Lifter Wear

	Oil	Lifter Wear, in. Steel	Hardenable Iron	Chilled Cast Iron
Engine A				
6-hr test [A-1 (6)]	A-1	0.0014	0.0003	0.0003
100-hr test (A-3)	A-1	—	0.0007	0.0009
Engine B				
100-hr test (B-1)	A-2	—	0.0012	0.0030

Table 7 – Relation Between Valve-Lifter Wear and Piston-Ring Wear

Oil	A-1	B-1	A-3	D-2	A-2
Oil Viscosity	5W-20	10W	5W-20	20-20W	5W-20
Detergency Level	Series 1	—	Series 1	Series 1	Series 1
Antiwear Additive	—	—	(2)	—	(1)
Lifter Wear, in. Engine A 6-hr test [A-1 (6)]	0.0014	0.0006	0.0005	0.0004	0.0004
Top-Compression-Ring Weight Loss, g					
Engine C 3000-mile test (C-1)	1.65	0.53	0.10	0.10	0.11
Engine D 36-hr test (D-1)	0.17	0.07	0.04	0.09	0.06
Engine A 3000-mile test (A-3)	—	—	0.33	0.54	0.50

sociated with the introduction of 5W-20 oils a natural question was whether viscosity had any effect on wear. Fig. 4 indicates that higher-viscosity oils (SAE 20-20W and 30) are quite superior to their low-viscosity counterparts (SAE 5W-20 and 10W) in this respect. All oils shown in the figure are comparable except for viscosity.

Fig. 5 again shows the viscosity effect under different operating conditions and using engine B in addition to engine A. Both engines were operated for 100 hr, engine A under low-temperature, low-speed operating conditions (procedure A-2) and engine B under moderate-temperature operating conditions but with abnormally high valve-spring pressures (procedure B-1). In both engines much lower wear was obtained on the 20-20W oil than on the 5W-20 oil. All oils shown on this figure are comparable except for viscosity. They are the same oils of comparable viscosity as shown on Fig. 4 except for the addition of e-p additive (1).

Effect of Valve-Lifter Break-In on Wear – Some people have subscribed to the theory that valve-lifter wear is a break-in problem and that, if the engine is properly broken in on a good oil, subsequent operation on an oil with poor antiwear characteristics would not result in lifter wear.

Consequently, two sets of 6-hr tests were conducted in engine A to test this theory, and the results are presented in Table 4. In the first set of tests the engine was first operated on oil B-4, and the lifters wore 0.0004 in., which is good; however, after operating an additional 6 hr on oil A-1, 0.0012 in. additional wear was experienced. Similar results were obtained when the engine was broken in on oil A-2 and then operated on oil A-1. Since the wear due to operation on oil A-1 in this test is nearly as great as is normally encountered on oil A-1, it can be concluded that such oils will permit rapid lifter wear irrespective of how the engine is broken in.

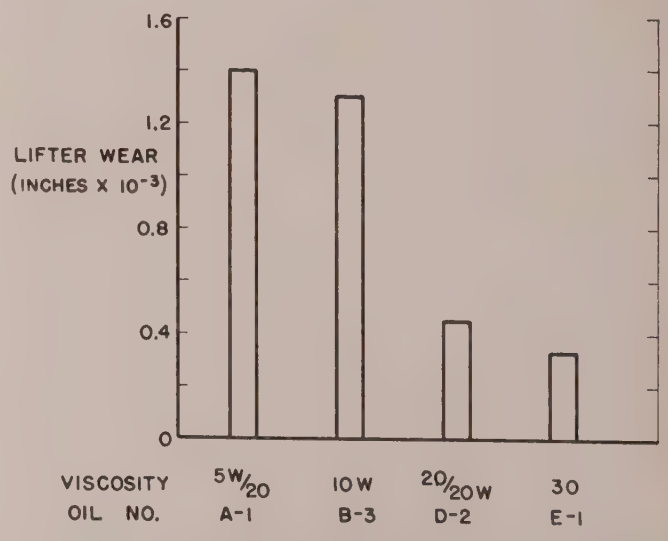

Fig. 4 – Effect of oil viscosity on valve-lifter wear in engine A, 6-hr tests A-1(6), Series 1 detergent oils

Effect of Operating Conditions on Lifter Wear – Table 5 shows the effect of operating conditions on lifter wear in engine A. The pertinent test conditions are given at the bottom of the table. As previously shown, test procedure A-1 (6) and A-3 give essentially the same results on high-quality oils even though A-3 is by far the longer test; however, when oils are tested at low temperatures, quite different results may be obtained. The best example of this effect is shown for oil A-2 which permitted more than three times as much wear in the 100-hr low-temperature test as it did in the 3000-mile (approximately 80 hr) moderate- to high-temperature test. On the other hand, oil D-3 did not allow significant wear in either the 6-hr moderate-temperature test or the 100-hr low-temperature test.

Effect of Metallurgy on Valve-Lifter Wear – Table 6 shows the effect of valve-lifter metallurgy on wear. In the 6-hr test on oil A-1 in engine A, excessive wear occurred when steel lifters were used, whereas extremely low wear occurred when hardenable iron and chilled cast-iron lifters were used. In the 100-hr low-temperature test on oil A-1 in this same engine, hardenable iron appeared to have a slight advantage over chilled cast iron. Steel lifters were not tested for 100 hr on this oil because of the excessive wear that was encountered in the 6-hr test.

In engine B, hardenable iron lifters were significantly better than chilled cast-iron lifters. Since this is an extremely severe test, 0.0012 in. wear in 100 hr is considered reasonable.

Relation Between Valve-Lifter Wear and Piston-Ring Wear – Table 7 presents data to show the relation between valve-lifter wear and piston-ring wear. The oils are arranged in the order of decreasing valve-lifter wear in the 6-hr test in engine A. Although the difference in lifter wear of 0.0001 in. between oils A-3 and D-2 or A-2 is quite small, it is considered significant since these data are the average of a large number of tests.

Top-compression-ring weight loss for the 3000-mile test using engine make C agrees reasonably well with the lifter wear results from engine A since it places the oils in approximately the same order.

In engine D, oil A-1 is the poorest as would be predicted from the lifter wear values in engine A; however, the relative merits of the other oils could not be predicted from the lifter wear values. Of particular significance is the fact that oil A-3 is the best oil in this series in engine D. This same advantage for oil A-3 is shown for the 3000-mile test in engine A.

From these data, it appears that valve-lifter wear data may predict piston-ring wear for extremes in oil quality; however, such data may not be a good index of piston-ring wear when only small differences in valve-lifter wear are obtained.

Relation Between Valve-Lifter Wear and Laboratory Bench Tests – Bench tests have been helpful for investigation of the influence of viscosity and additives on valve-lifter and ring wear. However, none of these tests appears to correlate with spalling or fatigue pitting of valve lifters.

Timken – The results of a few Timken tests are shown in Fig. 6. The OK load by the standard procedure is shown for various 5W-20 oils and one 10W oil plotted against the valve lifter wear obtained in the 6-hr test in engine A [procedure A-1 (6)]. Several of the 5W-20 oils contain e-p additives. There is no correlation evident. Correlation might have been obtained if the Timken had been operated under some other conditions. Rates of wear at constant load might have been in better agreement with the engine tests than OK loads.

Falex – Falex wear tests were run on several 5W-20 oils for 3 hr at 100 lb load following break-in

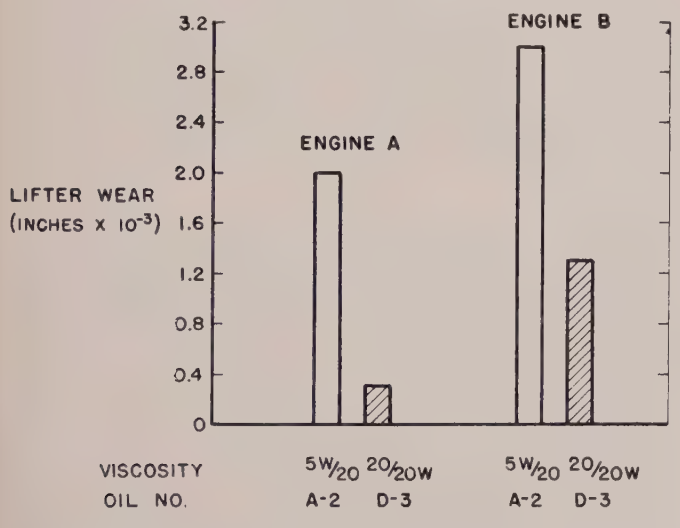

Fig. 5 – Effect of oil viscosity on valve-lifter wear, 100-hr tests, Series 1 detergent oils plus e-p additive (1)

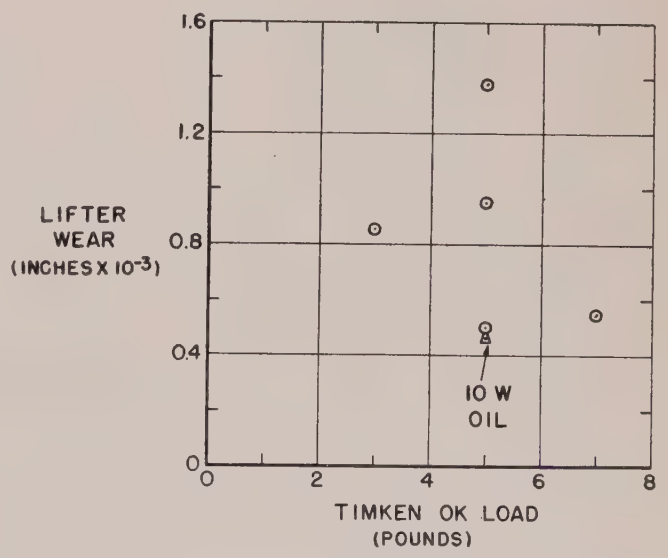

Fig. 6 – Relation between Timken OK load and lifter wear in engine A, 6-hr test A-1(6), detergent 5W-20 oils

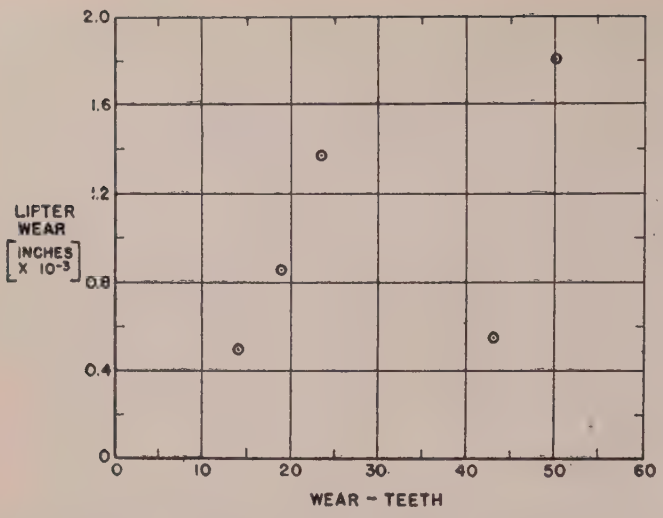

Fig. 7 – Relation between Falex test and lifter wear; Falex test at 100-lb jaw load for 3 hr; lifter test in engine A, 6-hr test A-1(6), detergent 5W-20 oils

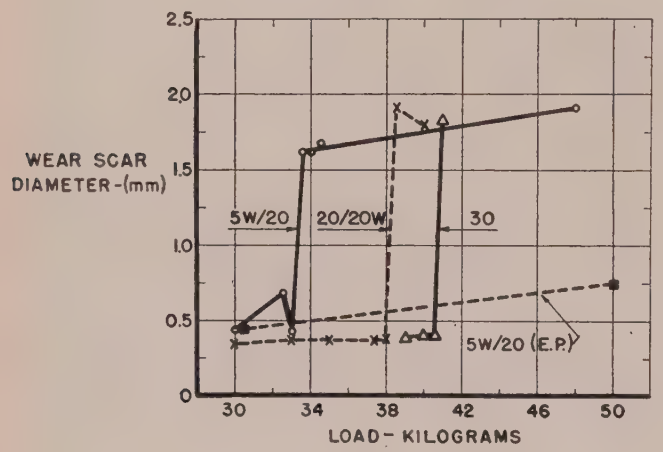

Fig. 8 – Wear versus load for four-ball test, 1 hr at 230 F and 1800 rpm, detergent oils

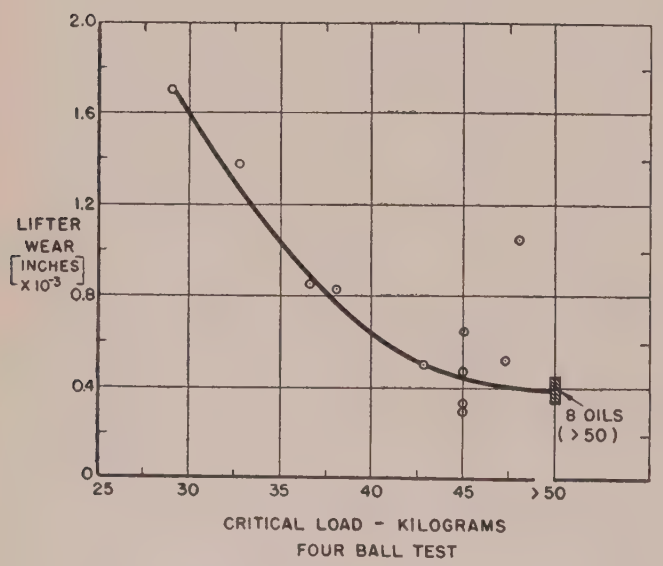

Fig. 9 – Relation between four-ball test and lifter wear; four-ball test for 1 hr at 230 F and 1800 rpm; lifter test in engine A, 6-hr test A-1(6), detergent 5W-20 oils

for ½ hr at 50 lb. The inconclusive results of these tests compared with the 6-hr test in engine A are shown in Fig. 7. Although four of the five oils line up reasonably well, one oil is badly out of line.

Four-Ball Machine – We found that reasonably reproducible results relating viscosity and composition with wear were obtained with the four-ball machine. Results of wear tests run at 1800 rpm and 230 F are shown in Fig. 8. Under these conditions it was found that the wear scar diameter increased sharply from values substantially less than 1 mm below some critical load to values greater than 1.5 mm above the critical load. It was found that this sharp break occurred within a load differential of about 0.5 kg.

Fig. 8 shows this type of data for several oils. It was also found that the formation of large wear scars at loads above the break-point occurs very quickly after the start of the test and is usually accompanied by noise, vibration, and high torque as would be expected with scuffing or high rate of wear. In most cases this instability lasted less than 2 or 3 min, and relatively smooth operation was obtained for the balance of the test. A possible explanation for this behavior is that below the critical load the system is able to prevent metal-to-metal contact on the area provided by plastic deformation of the metal (Hertz line area) even though the unit loads may exceed 200,000 psi. The critical load, then, is the point beyond which the system can no longer support the load on the area available without allowing definite metal contact. Rapid wear, with incipient seizure and surface roughening, then occurs until an area of five to ten times the original has developed, and this new surface is large enough to carry the load without scuffing.

Fig. 9 shows critical load values from four-ball machine tests run at 1800 rpm, and 230 F for 1 hr versus wear of valve lifters during 6-hr tests in engine A [procedure A-1 (6)]. It is readily apparent that the critical loads for SAE 5W-20 oils show good correlation with the wear obtained in engine tests. The 6-hr tests in engine A have not established a definite difference among several of the better oils tested. With the exception of two cases, wear of valve lifters has been low in the 6-hr engine tests for all oils with critical load values above 45 kg.

Cylinder and Ring Wear Machine – Additional wear tests of interest were made with a machine designed specifically for studying the effects of viscosity and composition of oils on scuffing and wear of piston rings. Fig. 10 shows this machine which is a modification of a machine designed by the Perfect Circle Corp. a number of years ago to study ring scuffing. Fig. 11 shows a cross-section of the ring and cylinder specimens. The cylinder section is reciprocated against the ring section through a 5½-in. stroke at a rate of 640 strokes per min. The ring specimen is free to tilt in the directions of travel so that an oil wedge can form between the ring and

cylinder. The ring section can be loaded hydraulically to any desired pressure up to 2500 psi. The oil under test is supplied from lines discharging directly in front of and behind the ring specimen at a rate of 11 cc per hr. The oil is not recirculated.

The cylinder specimens are cut from gray cast-iron castings, rough machined, and then normalized before machining and honing to final size. The ring specimens are cut from commercial cast-iron compression rings. The ring faces are not altered before use. Each ring specimen weighs about 2.2 g. Weight losses are determined with an accuracy of about ± 0.2 mg.

Briefly, the procedure is to test each lubricant in the cylinder and ring wear machine at three or four separate loads, each for a period of 20 and 40 hr. A new piston-ring and sleeve specimen are used at each load for the purpose of obtaining uniformity of test conditions. At the end of 20 hr, the test is interrupted and the ring weight loss measured. The piston-ring specimen is then put back in the machine and the test continued to 40 hr.

Several wear tests by this method are summarized in Fig. 12 for oils containing detergent additives. Addition of an e-p additive to the 5W-20 oil provided a significant reduction in wear (from 5.3 mg in 40 hr for the 5W-20 oil to approximately 1.5 mg for the same oil with the e-p additive). These results are in general agreement with valve-lifter wear data reported earlier in this paper, which show the effects of oil viscosity and e-p agents on wear.

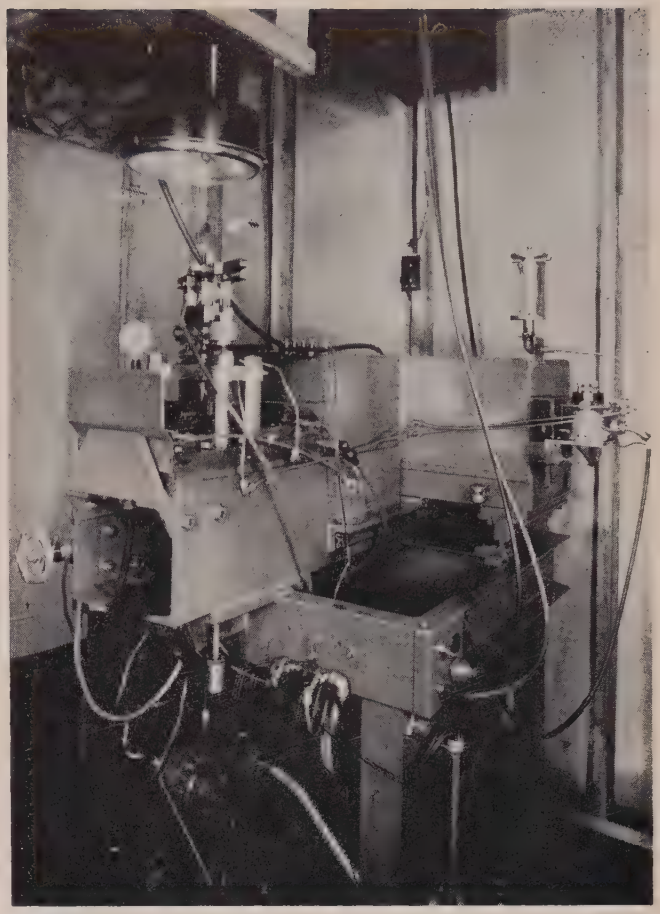

Fig. 10 – Cylinder and ring wear machine

Test Results – Scuffing

Fig. 13 shows the type of valve-lifter failure referred to as scuffing in this paper. The lifter on the left is used but in practically new condition, while the one on the right is scuffed. The term "scuffing" may be a misnomer; however, since we had heard engineers from automotive companies

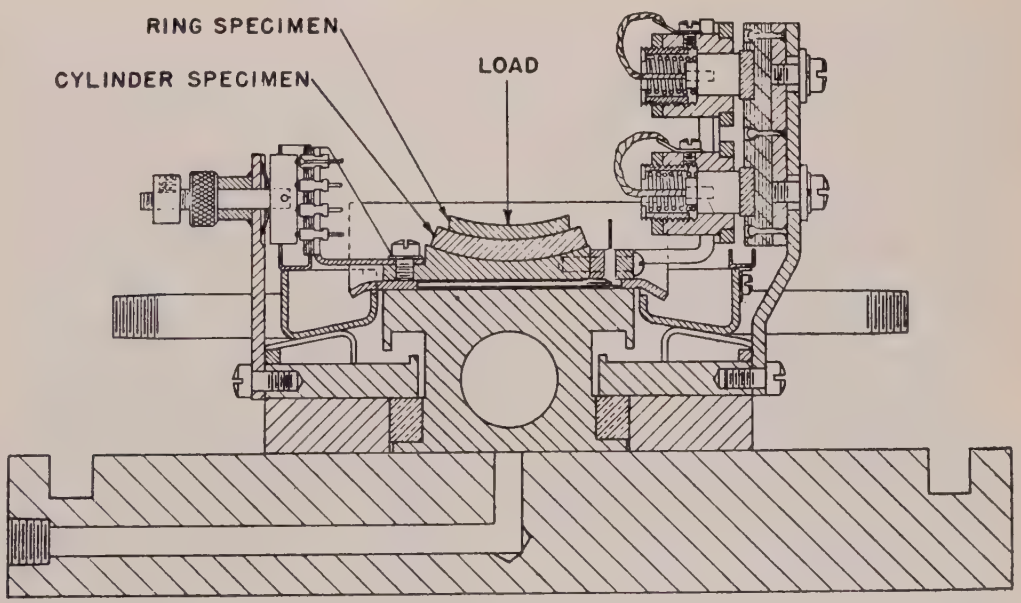

Fig. 11 – Cylinder and ring wear machine – cross - section through ring and cylinder specimens

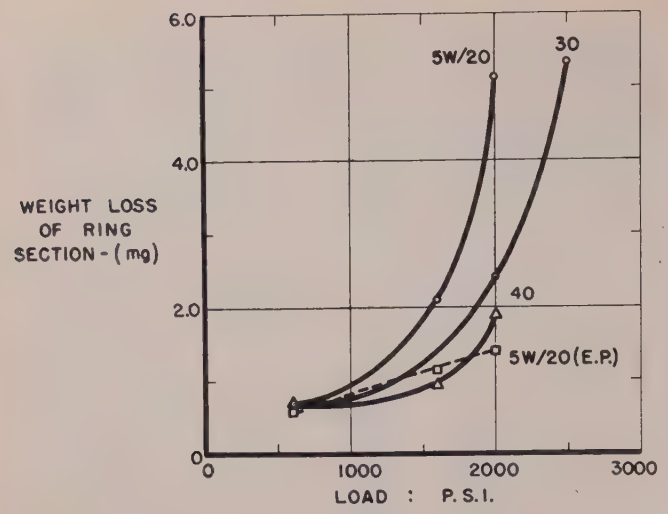

Fig. 12 – Relation between load and wear from 40-hr test in cylinder and ring wear machine with detergent oils of various viscosities

refer to such lifters as "scuffed" lifters and since microscopic examination showed the surface characteristics to be similar to that often referred to as scuffed, we decided to adopt this term to characterize this type of lifter failure. To date, scuffing has been encountered only with steel lifters in engines A and C.

Scuffing appears to be the most serious failure that can occur to a valve lifter since in all cases where scuffed lifters have occurred the mating camshaft lobe was badly worn. Preliminary X-ray investigations and metallographic studies of nonscuffed and scuffed lifters have in general shown a larger amount of cementite (Fe_3C) or similar microconstituent to be present in the scuffed lifters. Since it is well known that iron carbides in general and cementite in particular are extremely hard, abrasive materials, it was theorized that the occurrence and state of distribution of excess cementite is responsible for the accelerated camshaft lobe wear. The excess cementite in the lifters was formed during the carburizing process prior to installation in the engine. Verification of this theory is now being attempted in comparative engine tests.

Scuffed lifters have been encountered on a variety of oils covering a range of viscosities and additives; however, it may be significant that oils permitting this phenomenon were either borderline or relatively poor in antiwear qualities. It is possible that sufficient cementite is present in certain lifters to cause rapid cam wear if the lubricating oil permits the softer metallic constituents in the lifter surface to be worn away preferentially, exposing the cementite as in relief polishing.

Test Results – Spalling

Fig. 14 shows the type of valve-lifter failure referred to as spalling in this paper. The lifter on the left is used but is in practically new condition, while the one on the right is spalled. The spalled lifter surface contains holes of irregular shape that appear to be caused by rupture of the metal below the surface to the point where a small piece of metal is no longer bonded to the body of the lifter and is thrown out during engine operation. We have heard of this phenomenon referred to as fretting corrosion, pressure corrosion, pitting, and just plain "holes in the head," as well as spalling; however, the term spalling seems to suit this phenomenon as well as any of the others and was therefore adopted for our work. The following discussion presents some data on the effect of several lubricating oil and mechanical variables on spalling. In this discussion the evaluation of spalling is

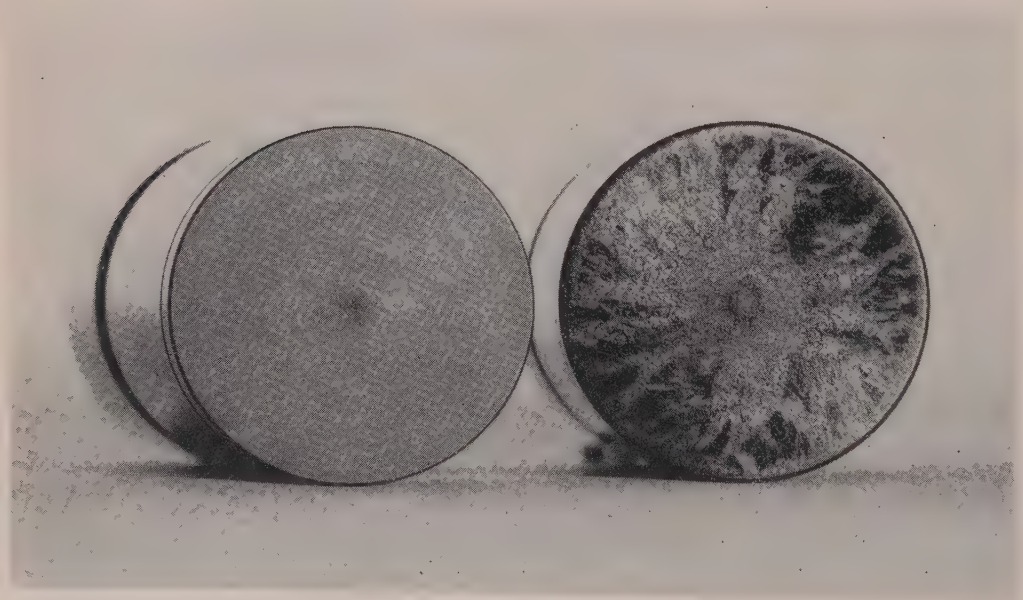

Fig. 13 – Valve lifters from engine make A; left: slightly worn; right: badly scuffed

based on the number of spalled lifters obtained in the various tests. Although this method may be criticized because it does not show the degree of spalling encountered, our experience indicates there is generally a good relationship between the number of spalled lifters and degree of spalling.

Effect of Oil Detergency on Spalling – Table 8 presents data showing the effect of detergency on spalling in engine B (100-hr test) using 5W-20 oils. All oils are made from the same base oil, and detergent additive (a) was employed to attain the two levels of detergency. Comparing oils A-1 and A-5 which do not contain an e-p additive, less spalling was encountered on the Series 2 detergency level oil; however, comparing oils A-2 and A-9 which contain e-p additive (1), more spalling was encountered on the Series 2 oil. These data indicate that the amount of detergent additive (a) contained in an oil has only a small effect on lifter spalling and that the direction of the effect of detergency level may depend on the other additives in the oil.

Effect of E-P Additives on Spalling – Table 9 presents data to show the effect of certain e-p additives on spalling in engine B using 5W-20 oils. Again the base oils are the same, and all contain detergent additive (a) to attain the Series 1 level. The data indicate that more valve-lifter spalling will be encountered on oils containing any of these e-p additives than on the same oil without the additives; however, it is important to remember that these e-p additives greatly minimize valve-lifter, cylinder, and piston-ring wear. Although there is little doubt that severely spalled lifters can damage cam lobes, we have seen numerous cases of badly spalled lifters without any cam damage. Under these circumstances it appears that if a choice must be made between wear and spalling, the oil with good antiwear characteristics should be chosen because of the greater practical significance of the wear problem.

Effect of Oil Viscosity on Spalling – Table 10 presents data to show the effect of viscosity on spalling in engines A and B (test A-2 in engine A

Table 8 – Effect of Detergency on Spalling – 5W-20 Oils, Engine B (V-8)

Oil	E-P Additive	Detergency Level	No. of Lifters Spalled
A-1	None	Series 1	6
A-5	None	Series 2	2
A-2	(1)	Series 1	10
A-9	(1)	Series 2	16

Table 9 – Effect of E-P Additives on Spalling – Detergent 5W-20 Oils, Engine B (V-8)

Oil	E-P Additive	No. of Lifters Spalled
A-1	None	6
A-2	(1)	10
A-7	(3)	16
A-8	(4)	10

Table 10 – Effect of Oil Viscosity on Spalling in V-8 Engines

	Oil	Viscosity	Engine B	Engine A
No Detergent or E-P Additive	B-1	10W	—	0
	D-1	20-20W	0	0
Series 1 Detergency Level, No E-P Additive	A-1	5W-20	5	2
	C-1	10W-30	6	—
	D-2	20-20W	0	0
Series 1 Detergency Level, E-P Additive (1)	A-2	5W-20	10	2
	D-3	20-20W	6	0

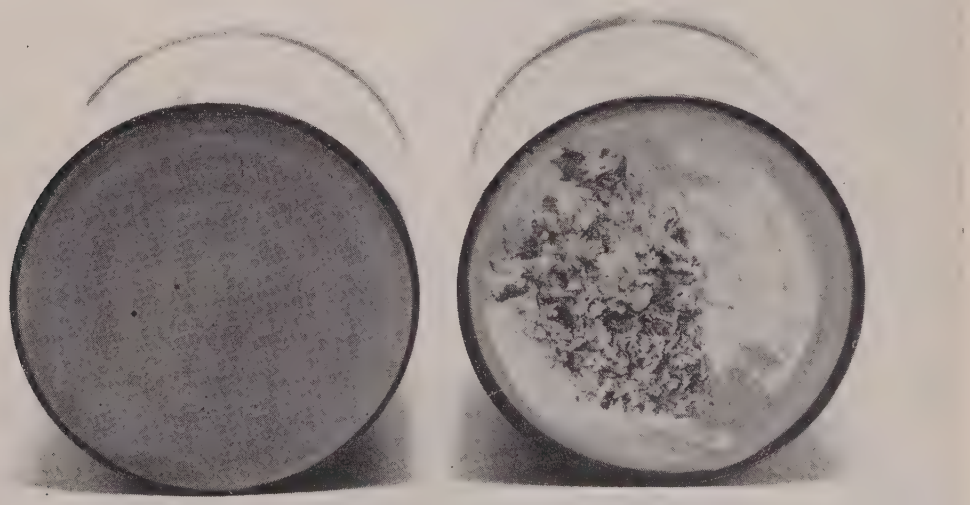

Fig. 14 – Valve lifters from engine make B; left: slightly worn; right: badly spalled

and the standard 100-hr test in engine B). Since data previously presented have shown an effect of detergency level and e-p additives, these data are grouped to eliminate the additive effect. All oils are comparable from the standpoints of crude source, treatment, and detergent-additive type and concentration.

In the first group (no detergent or e-p additive), no effect of viscosity is shown since no spalling was experienced on engine A and the 10W oil has not been tested in engine B.

In the second group (Series 1 detergency level but no e-p additive), a viscosity effect is indicated since no spalling was encountered in either engine on the 20-20W oil, whereas, some spalling was encountered in both engines on the 5W-20 oil. Since essentially the same amount of spalling was encountered on the 10W-30 and 5W-20 oils the indications are that valve-lifter spalling is related to the low-temperature viscosities of oils rather than to their high-temperature viscosities.

In the third group [Series 1 detergency level plus e-p additive (1)], a viscosity effect is again indicated since less spalling was encountered in both engines on the 20-20W oil than on the 5W-20 oil.

Effect of Valve-Lifter Metallurgy on Spalling – A limited number of tests have been run in engines A and B to determine the effect of valve-lifter metallurgy on lifter spalling. In these tests no spalling was encountered on hardenable iron lifters using oils that permitted excessive spalling on steel and chilled cast-iron lifters. These results indicate that a practical and simple cure for valve-lifter spalling is the use of hardenable iron valve lifters.

Conclusions

This paper reports the results of a laboratory investigation of some of the factors responsible for wear, scuffing, and spalling in passenger-car engines with particular attention paid to the lubricating-oil variables involved. Some of these problems have only recently become important, and much more work will be required before sweeping conclusions can be drawn; however, the data obtained to date indicate that the following conclusions may be valid:

1. Wear of piston rings and valve lifters and spalling of certain valve-lifter materials may be significantly greater for oils of low viscosity, such as SAE 5W-20 or 10W, than for higher-viscosity oils, such as SAE 20 or 30 oils of similar formulation.

2. Scuffing of steel lifters invariably results in high camshaft lobe wear. The surface of scuffed lifters generally contains relatively large amounts of materials similar to cementite (Fe_3C) which could be responsible for camshaft wear because of their hard, abrasive nature. While the cementite was formed during the carburizing process, it is possible that lubricating-oil quality contributes to scuffing since this phenomenon has been experienced only with oils having poor or borderline antiwear properties.

3. The inclusion of certain e-p (antiwear) additives in lubricating oils reduces valve-lifter and piston-ring wear but may increase spalling of chilled cast-iron lifters.

4. Valve-lifter wear data predict piston-ring wear for wide variations in oil quality; however, such data may not be a good index of piston-ring wear when only small differences in valve-lifter wear are obtained.

5. The detergency level of oils does not appear to have a definite effect on valve-lifter wear or spalling.

6. Use of an oil with good antiwear characteristics for engine break-in does not guard against future valve-lifter wear if the engine is operated with an oil having poor antiwear characteristics.

7. The spalling and antiwear characteristics of lubricating oils must be evaluated under a variety of operating conditions. Some oils that appear outstanding under certain operating conditions may be relatively poor when tested under different operating conditions.

8. Certain laboratory bench tests show promise for measuring the antiwear characteristics of engine lubricating oils.

9. The general adoption of hardenable iron for valve lifters would simplify the job of developing improved engine lubricating oils. Since these lifters do not spall, various antiwear agents could be added to oils to minimize engine wear and scuffing.

Acknowledgment

The authors acknowledge the cooperation and assistance of the many other Gulf employees who contributed to this program; particularly E. S. Francis, D. W. Gow, W. E. Kramer, C. B. Pattinson, and B. G. Jeske.

Appendix

Engine Test Procedures

Test Procedure A-1 (2), V-8, Overhead-Valve Engine (Engine Make A) –

Time, min	15	30	30	45
Speed, rpm	900	1500	1800	2000
Load	No load			
Jacket Coolant Temperature, F	165 ± 5			
Oil Temperature (Not Controlled), F	160–200			

Test Procedure A-1 (6), V-8, Overhead-Valve Engine (Engine Make A) – This consists of test procedure A-1 (2) repeated three times.

Test Procedure A-2, V-8, Overhead-Valve Engine (Engine Make A) – This consists of test procedure A-1 (6) followed by alternate periods of operation and shutdown as shown in Table 11.

Test Procedure A-3, V-8, Overhead-Valve Engine (Engine Make A) – In this test, the vehicle is operated on a chassis dynamometer for 3000 miles. All driving is done in third gear of the automatic transmission. The first and third 1000-mile periods simulate city-suburban driving to break in the engine and obtain oil mileage records under these driving conditions. In the early part of these periods, engine speeds are maintained in the range of 1500 to 2000 rpm. Speeds are gradually increased in 250-rpm increments until a speed of 3500 rpm is attained at 500 miles. For the remaining 500 miles, the engine is alternately operated on low-, intermediate-, and high-speed schedules (50 miles on each schedule and repeat). Throughout these test periods, frequent decelerations and accelerations are intermixed with level-road operation.

The second 1000-mile period is designed to simulate severe high-speed driving in the Appalachian Mountains. The operating schedule is given below:

1. Two minutes at 3000 rpm – level-road conditions.

2. Two minutes at 3000 rpm – wide-open throttle.

3. Decelerate from 3000 rpm to 1500 rpm.

4. Accelerate at wide-open throttle from 1500 rpm to 3500 rpm.

5. Four minutes at 3500 rpm – level-road conditions.

6. Two minutes at 3500 rpm – wide-open throttle.

7. Decelerate from 3500 rpm to 1500 rpm.

8. Accelerate at wide-open throttle from 1500 rpm to 3500 rpm.

9. Decelerate from 3500 rpm to 1500 rpm.

10. Accelerate at wide-open throttle from 1500 rpm to 3000 rpm.

11. Repeat steps 1 through 10 for a total of 1000 miles.

The engine temperatures attained during the test are shown in Table 12.

Test Procedure B-1, V-8, Overhead-Valve Engine (Engine Make B) – This test is comprised of alternate periods of operation and shutdown as shown in Table 13.

The test is run for 100 hr of engine operating time unless intermediate inspections of lifters and camshaft indicate excessive spalling, scuffing, or wear.

Test Procedure C-1, 6-Cyl, L-Head Engine (Engine Make C) – This test consists of the same city-suburban and mountain-type operation as test procedure A-3. All driving is done in high gear.

The engine temperatures attained during the test are given in Table 14.

Test Procedure D-1, 6-Cyl, Overhead-Valve Engine – The conditions of operation for this test are given in Table 15.

Table 11 – Operating and Shutdown Periods
(Test Procedure A-2)

	Operating Period	Shutdown Period
Time, hr	2	2
Speed, rpm	1000	0
Load	0	0
Jacket Coolant Temperature, F	100	85–95
Oil Temperature (Not Controlled), F	Approx 135	85–95

The above 4-hr cycle is repeated 25 times.

Table 12 – Engine Temperatures
(Test Procedure A-3)

	City-Suburban Cycle	Mountain Cycle
Jacket Coolant Temperature, F	160–180	180–200
Oil Temperature, F	130–220	160–260

Table 13 – Operating and Shutdown Periods
(Test Procedure B-1)

	Operating Period	Shutdown Period
Time, hr	2	1
Speed, rpm	1200	0
Load	0	0
Jacket Coolant Temperature, F	180	125–180
Oil Temperature (Not Controlled), F	Approx 180	125–180

Table 14 – Engine Temperatures
(Test Procedure C-1)

	City-Suburban Cycle	Mountain Cycle
Jacket Coolant Temperature, F	135–170	150–180
Oil Temperature, F	160–225	200 245

Table 15 – Operating Conditions
(Test Procedure D-1)

Time, hr	36
Speed, rpm	3150
Load, hp	30
Jacket Coolant Temperature, F	200
Oil Temperature, F	265 or 280

Influence of Lubricant and Material Variables on Cam and Tappet

UNTIL recently, automotive engines were not difficult to lubricate from the standpoint of protecting the various rubbing metal surfaces from distress. There are a few exceptions to this statement, but for the most part the crankcase oil needed only the load-carrying ability of the uninhibited straight mineral oil from which it was blended. Primary requirements were considered to be prevention of sludge and lacquer, protection against wear when operating at low temperatures, and protection against bearing corrosion. However, at least several of the new overhead-valve V-8 engines have critical areas of lubrication. An example of this is found in the valve train, especially the valve-lifter faces which may become severely distressed. The reasons for this have not yet been firmly established, but a number of changes have been made in going to these new high-output engines which might be expected to have an adverse effect. The valve-spring force has been increased to keep the linkages in the flexible overhead-valve mechanism in contact. For better engine breathing the valve size, lift, and cam ramp severity have been increased. These and no doubt other design changes have resulted in increased severity of the lubrication requirements of some of the modern engines.

This paper is concerned with the interrelationships between lubricants and mating surfaces of the cams and valve-lifter faces. The diverse combinations of materials and mechanical designs chosen by different manufacturers for the construction of these parts is illustrative of the state

AN experimental program to determine the influence of crankcase oils on scuffing and pitting of cams and tappets in overhead-valve V-8 engines is described in this paper, which is part of a Symposium on Cam and Tappet Wear.

Results indicate that certain additives may eliminate, while others actually promote, scuffing and pitting of a particular type of surface. At the same time, the protection afforded a tappet surface by any particular additive depends upon the tappet material. An additive that protects steel lifters from scuffing may cause chilled iron tappets to pit. In the authors' tests hardenable cast iron was found to be the easiest tappet metal to lubricate.

Discussion of this and the other papers in the Symposium starts on p. 220.

The Authors

T. W. HAVELY (J '54) is group leader in charge of research on wear and friction phenomena at the Wood River Research Laboratory, Shell Oil Co. Mr. Havely received his B.S. degree in Mechanical Engineering from the University of Notre Dame in 1947, and has been with Shell since that time.

C. A. PHALEN is a member of the staff of Shell Oil Co.'s Wood River Research Laboratory. He received his B.S. in Mechanical Engineering from Michigan College of Mining & Technology in 1948, and his B.S. degree in Business from Shurtleff College in 1952. Mr. Phalen has been with the Shell Oil Co. since 1948.

D. G. BUNNELL is on the staff of Shell Oil Co.'s Wood River Research Laboratory. He received his B.S. degree in Chemistry from Heidelberg College in Ohio in 1943. He received a B.S. in Chemical Engineering in 1947, and his M.S. in 1948 from Purdue University. Mr. Bunnell has been with Shell since 1948, when he started in the Houston Research Laboratory.

Surface Distress

T. W. Havely, C. A. Phalen, and D. G. Bunnell,
Wood River Research Laboratory, Shell Oil Co.

Paper was presented at SAE Passenger-Car, Body, and Materials Meeting, Detroit, March 2, 1954.

of the art. As shown in Table 1, in eight overhead-valve V-8 passenger-car engines, seven combinations of metals and surface treatments are in use. This is in addition to differences in certain mechanical features, such as the crown of the lifter, taper of the cam, and spring loading. The mating surfaces may be subject to scuffing, pitting, or both; and it has been established that the performance of the valve lifters in service is greatly dependent upon the lubricant used. In fact, there is no better example of the role of the lubricant as a structural material than this application.

Cam and Lifter Face Lubrication

In this investigation, three different engines and six different types of cam and lifter combinations were used. The various test procedures employed in the experimental program are shown in Table 2. For the most part, the test methods were based on procedures followed by the engine builders for studying cam and lifter materials and design. The laboratory test installations are very simple since cam and lifter distress is readily obtained under no-load conditions. Thus dynamometers or power-absorbing equipment is not necessary. Engine speed can have a major influence on the lubrication of cam and lifter. In the test work described here each of the engines was operated at a particular speed that had been found suitable for showing differences in lubricants. Valve-spring load is another important variable in cam and lifter lubrication. From Table 2 it can be seen that engine A was operated at about the maximum valve-spring loading recommended by the manufacturer. Engines B and C, on the other hand, were operated at considerably higher than standard valve-spring loadings to accelerate the lifter face distress. There is, of course, some question about the validity of results obtained by this technique. But the appearance of the lifter faces after test under these accelerated conditions was similar to that in the field after extended running under normal spring loads.

Evaluation of performance is based upon the appearance of the lifter faces. Cams are also inspected and their condition noted, but the lifter face is more satisfactory for evaluating surface distress since a much larger area is involved. Both height loss and weight loss were measured and recorded during the early work. For the most part these measurements were found to be insensitive to large differences in appearance. All physical measurements were abandoned as testing progressed, since it became apparent that both the scuffing and pitting phenomena were best evaluated by visual examination of the surfaces.

Steel Tappets on Hardenable Cast-Iron Cams – Engine A – Considerable experience has been gained on the performance of lubricants with both Parco-treated and untreated steel lifters in this engine. It has been found that these lifters scuff but do not pit under the test conditions used. The scuffing is very difficult to prevent but at the same time is seldom catastrophic in nature. That is, while the surface looks bad, the cam noses are seldom worn off even with extended running.

Lubricant viscosity has little or no influence on

Table 1 – Cams and Tappets in Overhead-Valve V-8 Passenger-Car Engines

Engine	Tappet: Material	Tappet: Crown, in.	Tappet: Coating	Cam: Material	Cam: Taper Angle, min	Cam: Coating	Spring Load at Cam, lb: Valve Closed	Spring Load at Cam, lb: Valve Open
1	Chilled cast iron	0.0020 with ½-in. flat	Ferrox	Drop-forged steel	12.5	Parco	Intake: 112 Exhaust: 75	Intake: 229 Exhaust: 165
2	Hardenable cast iron	0.0025	Parco	Cast iron	7	Parco	162	281
3	Chilled cast iron	0.0020	None	Cast iron	7	Parco	100	225
4	Chilled cast iron	0.0040	Ferrox	Cast iron	7	None	Intake: 97 Exhaust: 92	Intake: 248 Exhaust: 248
5	Carburized steel	0.0015	Parco	Cast iron	6.5	None	92	210
6	Chilled cast iron	Flat	Ferrox	Forged steel	None	None	93	216
7	Chilled cast iron	0.0040	Ferrox	Cast iron	7	None	80	214
8	Hardenable cast iron	0.0040	Parco	Cast iron	7	None	80	214

the performance of these material combinations. SAE 5, 10, 30, and 50 undoped mineral oils gave lifters of unsatisfactory and practically identical appearance. Lubricating oil additives, however, have a profound effect on performance of these materials. Experimental test results are shown in Table 3. The results shown in this table are but a summary of the many compounds tested with this metal combination. They were selected, however, as representing typical performance of the various types of chemical compounds tested. Some sulfur-phosphorus compounds may give excellent protection to the lifters, while others may actually give poorer performance than the base oil. Additives containing only phosphorus behave in a similar manner; some protect the lifters, others do not. Compounds containing only sulfur have invariably been found poor in this application. Table 3 also shows that additives containing chlorine, lead, and a combination of these elements are not satisfactory for the lubrication of these material combinations. On the other hand, it has been found that some carboxylic acids are rather effective. Esters of these acids are in general not effective.

In general, with a given lubricant, the results obtained with treated and untreated lifters were essentially equivalent.

Figs. 1 and 2 illustrate the extremes in appearance that have been observed with lifters of these two types. The photographs represent the range in performance of lubricants from "excellent" to "very poor" on an arbitrary scuffing rating scale of excellent, satisfactory, borderline, unsatisfactory, and very poor. On this scale undoped mineral oil is rated "unsatisfactory" on both treated and untreated lifters.

Parco-Treated Hardenable Cast-Iron Tappets on Hardenable Cast-Iron Cams – Engine A – Of the three types of lifters tested in engine A, Parco-treated hardenable cast iron appeared to be the least influenced by lubricant quality. These tappets are subject to scuffing, but it is believed that, under certain conditions, pitting may also occur.

Although these lifters were less sensitive to lubricant quality than steel lifters in engine A, the relative performance of various additive types remained the same. Base-oil viscosity had no influence on scuffing; sulfur-phosphorus compounds, phosphorus compounds, and carboxylic acids afforded greatest protection; sulfur compounds, combinations of chlorine and lead, and esters gave least protection. The results are summarized in Table 3. In general, all the lubricants gave better performance with these lifters than with the steel lifters. As can be seen from Fig. 3, the extremes of performance obtained during the lubricant testing were not as great as found for either treated or untreated steels (Figs. 1 and 2).

Ferrox-Treated Chilled Cast-Iron Tappets on Hardenable Cast-Iron Cams – Engine B – Chilled

Table 2 – Engine Operating Conditions for Valve-Lifter Surface Distress Tests[a]

	Engine A	Engine B	Engine C	
Cooling Water, In, F	135–140	135–140	135–140	
Cooling Water, Out, F	165–170	180–190	165–170	
Valve-Spring Load at Cam			Exhaust	Intake
Valve Open, lb	243 (210)[b]	330 (214)	290 (165)	(229)
Valve Closed, lb	108 (92)	165 (80)	172 (75)	(112)
Engine Load	None	None	None	
Oil Temperature at Gallery, F	155–165	185–195	190–200	
Engine Speed, rpm	15 min at 1000 30 min at 1500 30 min at 1800 165 min at 2000	1200	3000	
Total Test Time, hr	4	40	200	

[a] Each test is run with new camshaft and lifter set.
[b] Figures in parentheses are maximum standard valve-spring loads at cam.

Table 3 – Scuffing Ratings in Engine A with Hardenable Cast-Iron Cams

Additive Type in SAE 10 Lubricant	Scuff Rating of Lifters[a]: Parco, Steel	Steel	Hardenable Cast Iron
1. None	Unsatisfactory	Unsatisfactory	Unsatisfactory
2. Sulfur-Phosphorus C	Excellent	—	—
Sulfur-Phosphorus E	Satisfactory	Satisfactory	Satisfactory
Sulfur-Phosphorus A	Borderline	—	—
Sulfur-Phosphorus D	Very poor	—	—
3. Phosphate A	Satisfactory	—	—
Phosphate B	Borderline	Borderline	Excellent
4. Sulfur A	Very poor	—	—
Sulfur B	Very poor	Very poor	Borderline
5. Chlorine	Unsatisfactory	—	—
6. Lead	Very poor	—	—
7. Detergent + Chlorine + Lead	Very poor	Very poor	Borderline
8. Acid A	Excellent	Satisfactory	Excellent
Acid B	Borderline	Borderline	Satisfactory
9. Ester	Very poor	Very poor	Borderline

[a] Degree of scuffing in terms of lube performance: excellent, satisfactory, borderline, unsatisfactory, very poor.

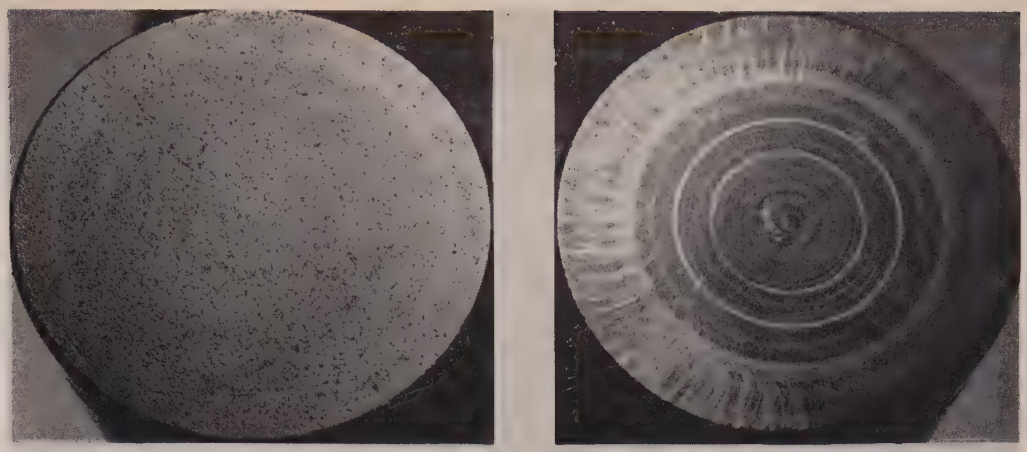

Fig. 1 – Performance extremes with untreated steel in engine A – 4 hr

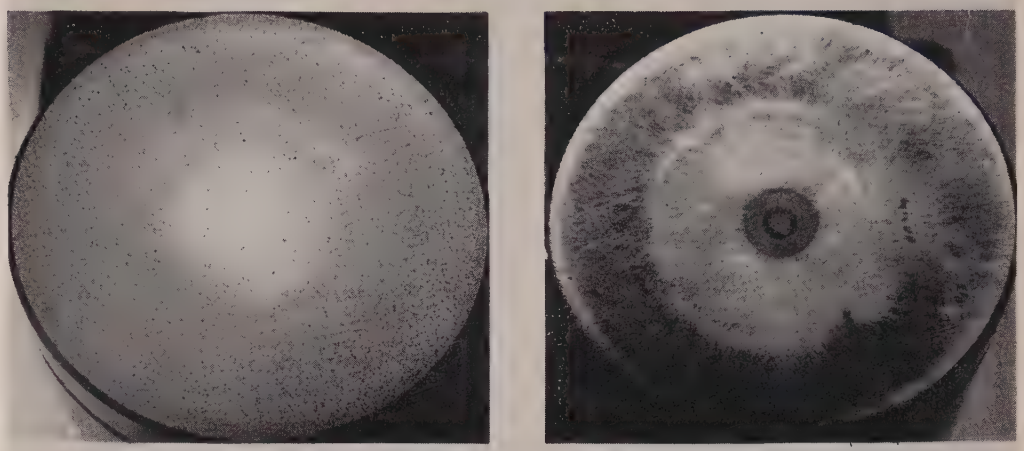

Fig. 2 – Performance extremes with Parco - treated steel in engine A – 4 hr

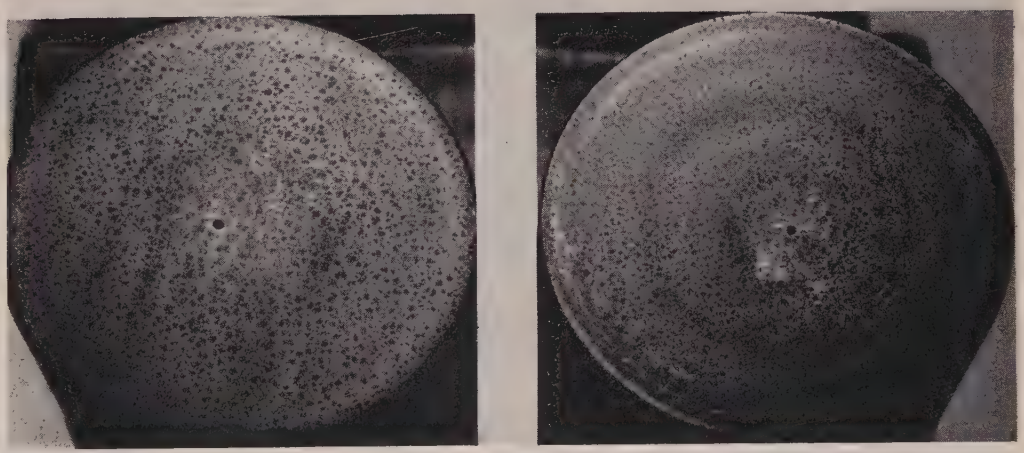

Fig. 3 – Performance extremes with Parco - treated hardenable cast iron in engine A – 4 hr

cast-iron lifters may scuff, pit, or suffer both types of surface distress when tested under the conditions shown in Table 2 for engine B. For this engine, pitting is rated as the percentage of lifters pitted. Scuffing, where observed, is rated light, medium, or heavy. It was found impracticable to apply the more detailed rating scale used with engine A since both pitting and scuffing frequently occur in the same test. The influence of lubricant viscosity has not yet been studied in this engine, but considerable fundamental work has been done by various investigators which shows that increasing viscosity reduces pitting. It is expected this finding will apply to pitting of tappet faces.

From the results in Table 4, it can be seen that SAE 10 high V.I. base oil allows medium scuffing on these lifters but little or no pitting. As shown by the results of the two different proprietary detergent-sulfur-phosphorus compound combinations tested, it is possible to reduce scuffing but at the same time promote severe pitting. On the other hand, both scuffing and pitting may be virtually

Table 4 – Scuffing and Pitting Ratings in Engine B Having Untreated Hardenable Cast-Iron Cams

Additive Type in SAE 10 Lubricant	Cast-Iron Lifters: Ferrox, Chilled Pitting[a]	Ferrox, Chilled Scuffing[b]	Parco, Hardenable Pitting[a]	Parco, Hardenable Scuffing[b]
None	19	Medium	—	—
	0			
Detergent + Sulfur-Phosphorus[c]	87	None	—	—
	100			
Detergent + Sulfur-Phosphorus[c]	6	None	—	—
	0			
Sulfur-Phosphorus A	6	Light	—	—
Sulfur-Phosphorus B	0	Medium	0	None
Sulfur A	0	Heavy	0	None
Phosphate A	0	Heavy	0	None

[a] Per cent of total number of lifters pitted.
[b] Degree of scuffing: none, light, medium, heavy.
[c] Proprietary lubricants; the detergent and sulfur-phosphorus additive in each case are different.

eliminated by selection of the proper additive combination. Table 4 also shows that sulfur-phosphorus compound A slightly improved the resistance to scuffing without promoting pitting, while a low concentration of sulfur-phosphorus compound B gave no improvement in performance over the base oil. A sulfur additive and phosphate A gave heavy scuffing but no pitting.

Fig. 4 illustrates the extremes of lube performance observed with this combination of materials.

Parco-Treated Hardenable Cast-Iron Tappets on Hardenable Cast-Iron Cams – Engine B – In Table 4, results obtained with chilled cast iron are compared with hardenable iron, and, as in engine A, the superiority of the hardenable tappets is demonstrated. It is shown that even lubricants allowing heavy scuffing on the chilled material perform satisfactorily on the hardenable cast iron.

Ferrox-Treated Chilled Cast-Iron Tappets on Steel Cams – Engine C – The results of tests on three lubricants are available from this engine. From the data collected in Table 5, it appears that the two additive oils, one containing a sulfur-phosphorus compound and the other a chlorine-lead type additive, promote pitting compared with the base oil. In regard to scuffing, the sulfur-phosphorus additive resulted in an improvement while the chlorine-lead additive had little effect.

The extremes in lubricant performance with this tappet are shown in Fig. 5.

Bench Scale Evaluation of Lubricants – A number of commonly used bench scale scuffing tests were run in an attempt to determine if any of these simple procedures would predict the performance of lubricants in engines. Using standard test techniques, four-ball wear, four-ball e-p, SAE, Timken, and Falex tests were run and the results compared with those obtained in engine A using Parco-treated steel lifters on hardenable cast-iron cams. As is shown in Table 6, no correlation between the bench tests and engine tests seems to exist. A limited number of comparisons with cams and lifters of other metals shows no better correlation with either scuffing or pitting. This is not surprising since none of the standard bench tests uses the same combinations of metals as the engines. As has been seen from the results of engine testing, the metals have a large influence. Perhaps if the test metals were changed to conform to those being used in the engine and the test techniques modified, a satisfactory bench test could be established.

Discussion

Some of the results of the testing of lubricants in the different engines with various metal combinations are summarized in Tables 7 and 8. Table 7 shows the results obtained in engine A for 27 lubricants tested with untreated steel, Parco-treated steel, and Parco-treated hardenable cast-iron tappets. From this composite of the data, it is apparent that the effectiveness of Parco treatment in reducing scuffing is not clear cut. The superiority of the hardenable cast-iron lifters, however, is clearly illustrated. Seventeen of the lubricants were rated "excellent" and "satisfactory," while none rated "very poor." A graphic illustration of this superiority of hardenable iron is shown in Figs. 6 and 7. Fig.

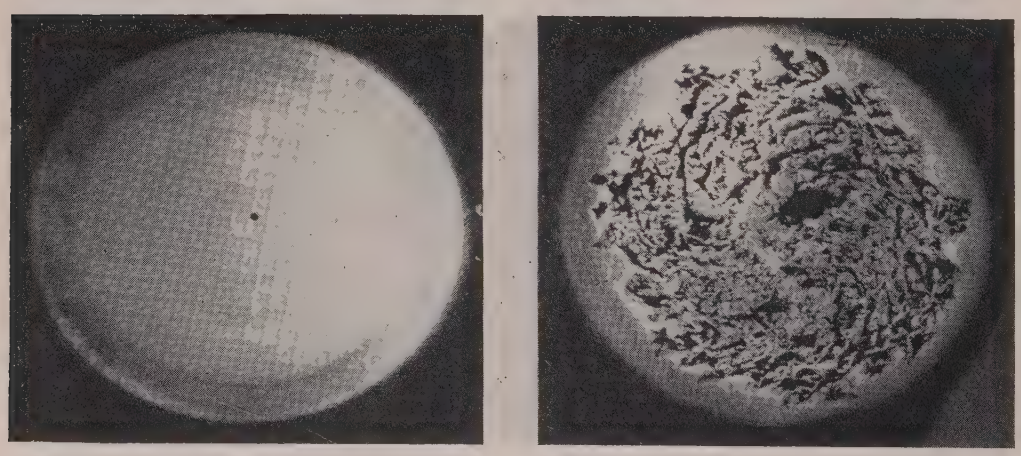

Fig. 4 – Performance extremes with Ferrox-treated chilled cast iron in engine B – 40 hr

6 compares the appearance of untreated steel tappets with hardenable cast-iron tappets using a lubricant giving very poor performance with the former. Fig. 7 compares Parco steel with hardenable cast iron after test on a different lubricant, but again one giving very poor appearing steel tappets. In both cases the hardenable iron lifter surfaces are in good condition.

Table 8 compares the performance of various lubricants in each of the three engines. The ability of a lubricant to protect Parco-treated steel lifter

Table 5 – Scuffing and Pitting Ratings in Engine C

Additive Type in SAE 10 Lubricant	Ferrox Treated Chilled Cast-Iron Lifters on Steel Cams	
	Pitting[a]	Scuffing[b]
None	37	Medium
	50	
Detergent + Sulfur-Phosphorus	81	None
Detergent + Chlorine + Lead	60	Medium

[a] Per cent of total number of lifters pitted.
[b] Degree of scuffing: none, light, medium, heavy.

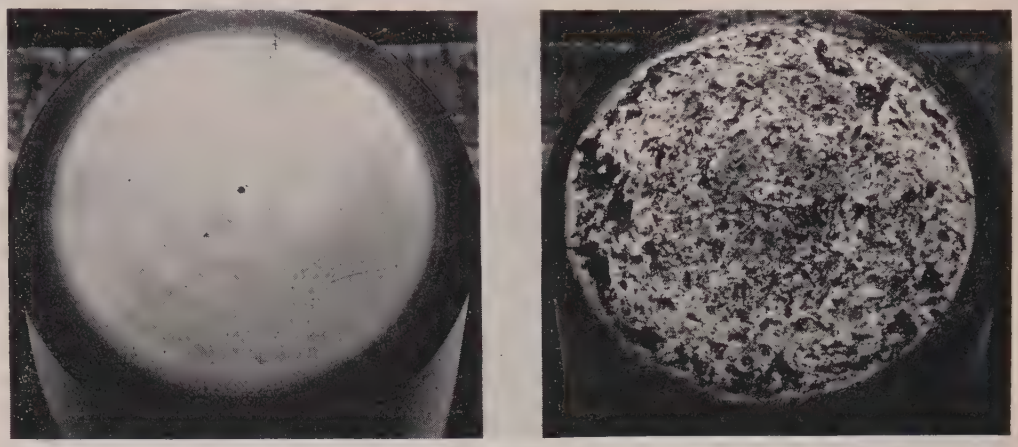

Fig. 5 – Performance extremes with Ferrox-treated chilled cast iron in engine C – 200 hr

Table 6 – Comparison of Engine A Performance with Load-Carrying Ability as Measured in Bench Tests

Additives in SAE 10 Lubricant	Engine A, Parco Steel Lifters,[a] 4-Hr Test	Four-Ball Wear, mm 600 Rpm, 80 C, 2 Hr		Four-Ball E-P, FTP[b]	SAE-L-17,[c] lb	Timken OK,[d] lb	Falex, lb
		15 Kg	50 Kg				
Detergent + Sulfur-Phosphorus	Excellent	0.29	0.49	236	92	15	—
Sulfur-Phosphorus E	Satisfactory	0.26	0.46	272	113	13	900
Phosphate A	Satisfactory	0.35	0.92	236	72	9	1375
Phosphate C	Borderline	0.47	0.53	294	90	15	1950
Chlorine	Unsatisfactory	0.80	1.03	273	89	11	750
Detergent + Sulfur C	Very poor	0.41	0.80	238	134	13	900
Sulfur-Phosphorus D	Very poor	0.56	1.0	234	73	9	—

[a] Cam material is untreated hardenable cast iron.
[b] Flash temperature parameter, a criterion of load-carrying ability. In general, load-carrying ability is proportional to magnitude of number.
[c] CRC L-17-545 conditions except sliding velocity reduced to 81 in. per sec.
[d] Two-pound load increments.

Table 7 – Influence of Valve-Lifter Material on Scuffing in Engine A[a]

Rating	Untreated Steel	Parco Steel	Parco Hardenable Cast Iron
Excellent	—	1	8
Satisfactory	6	3	9
Borderline	9	12	8
Unsatisfactory	3	5	2
Very poor	9	6	0
Totals	27	27	27

[a] Cam material is untreated hardenable cast iron.

Table 8 – Summary Comparison of Lubricant Performance in Different Engines

Additive Type in SAE 10 Lubricant	Engine A	Engine B				Engine C	
	Parco, Steel Lifters	Ferrox, Chilled Cast-Iron Lifters		Parco, Hardenable Cast-Iron Lifters		Ferrox, Chilled Cast-Iron Lifters	
	Hardenable Cast-Iron Cams	Hardenable Cast-Iron Cams		Hardenable Cast-Iron Cams		Steel Cams	
	Scuffing	Pitting[a]	Scuffing[b]	Pitting[a]	Scuffing[b]	Pitting[a]	Scuffing[b]
Detergent + Sulfur-Phosphorus	Excellent	87 100	None	—	—	—	—
Detergent + Sulfur-Phosphorus	Satisfactory	—	—	—	—	81	None
Phosphate A	Satisfactory	0[c]	Heavy	0	None	—	—
Detergent + Sulfur-Phosphorus	Borderline	6 0	None	—	—	—	—
Sulfur-Phosphorus B	Borderline	0	Medium	0	None	—	—
None	Unsatisfactory	19 0	Medium	—	—	37, 50	Medium
Sulfur A	Very poor	0	Heavy	0	None	—	—

[a] Per cent of total number of lifters pitted.
[b] Degree of scuffing: none, light, medium, heavy.
[c] One pitted cam nose.

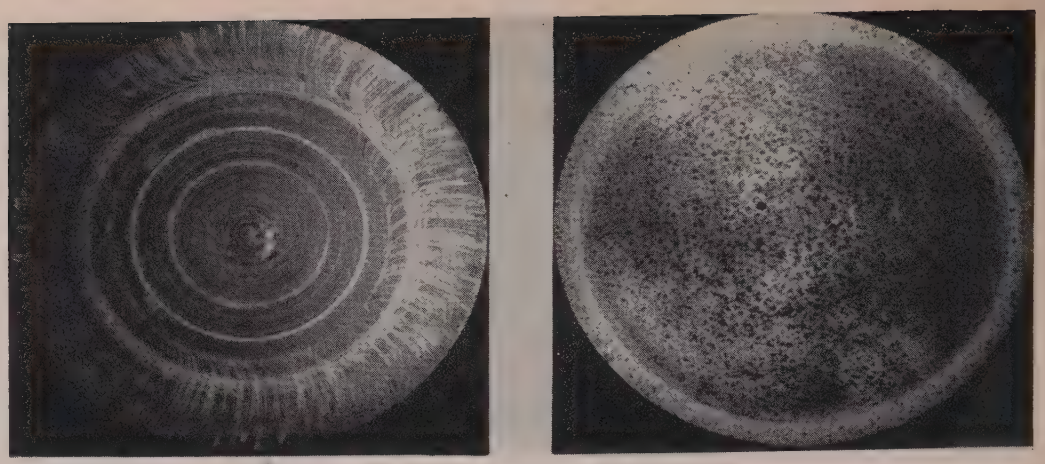

Fig. 6 – Comparison of steel (left) and Parco - treated hardenable cast iron (right) with same lubricant in engine A – 4 hr

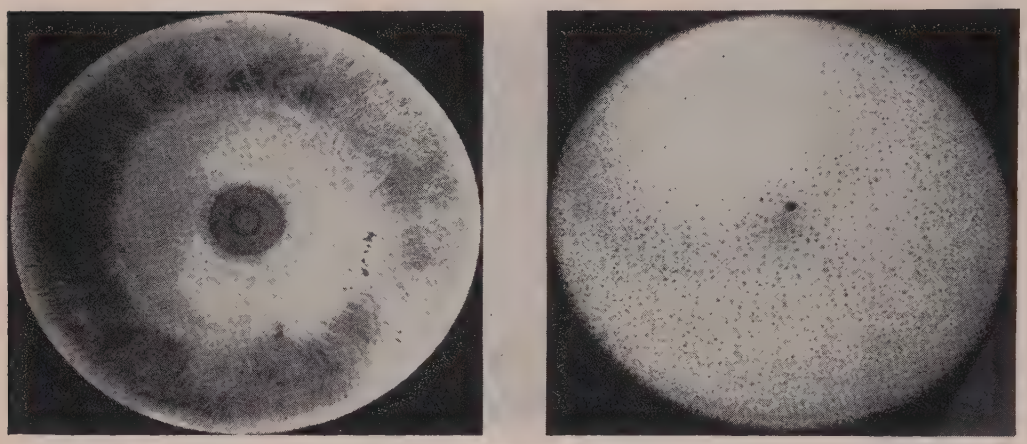

Fig. 7 – Comparison of Parco-treated steel (left) and Parco - treated hardenable cast iron (right) with same lubricant in engine A – 4 hr

faces in engine A is compared with its performance with chilled cast iron and hardenable cast iron in engine B and with chilled cast iron in engine C. From these data it is evident that a lubricant which protects Parco-treated steel lifters from scuffing will probably protect chilled and hardenable iron from scuffing. On the other hand, it appears likely that the ability of a lubricant to prevent pitting of chilled iron lifters is inversely related to its ability to protect against scuffing. Engine C shows the same trend as engine B in this regard, but too few data are available to draw firm conclusions.

On the basis of experience to date it is concluded that chilled cast-iron tappets are the most difficult to lubricate, steel tappets intermediate, and hardenable cast iron least difficult. This conclusion is based on the fact that chilled cast iron is extremely sensitive to lubricant quality in regard to both scuffing and pitting; changes in lubricant additives directed at improving load-carrying ability may lead to pitting. Scuffing with chilled cast-iron lifters is often catastrophic, that is, lifter and cam nose may suffer sufficient loss of lift to prevent the cylinder from functioning. Steel tappets are concluded to be less difficult to lubricate than chilled cast iron because the scuffing is seldom catastrophic. In addition, these lifters are not subject to both pitting and scuffing as are chilled cast-iron lifters and tend only toward scuffing. Hardenable cast-iron tappets are least sensitive to lubricant quality, and while they may scuff and pit under certain conditions a wide range of lubricants will protect them from distress.

On the basis of tests on a wide range of lubricant additive types, it is believed that standard bench tests may give information that is misleading in regard to ability of lubricants to prevent scuffing or pitting of valve lifter faces. For this reason, standard bench tests for load-carrying ability or wear protection should be carefully considered before they are included in specifications against which motors oils are purchased.

About 100 different lubricants have been evaluated in the course of the testing program summarized in this paper. Of the many different types of additive materials evaluated, phosphorus and sulfur-phosphorus compounds appear most suitable for use in motor oil formulations to prevent distress of cams and valve-lifter faces. From the accumulated engine testing it is apparent, however, that a formulation suitable for one metal combination may very well be completely unsatisfactory with another. On the basis of this knowledge, one can appreciate the difficulty in providing one lubricant to satisfy the lubrication requirements of the seven different cam and tappet combinations that exist in the eight overhead-valve V-8 engines of today.

Lifters and Lubricants

Joseph B. Bidwell and Paul Vermaire

Research Laboratories Division, GMC Diesel Equipment Division, GMC

This paper was presented at the SAE National Passenger-Car, Body, and Materials Meeting, Detroit, March 2, 1954.

PREVENTION of wear on rubbing parts has always been the primary function of lubricating oil used in internal-combustion engines. While substantial advances have been made over many years in the quality of oils from the standpoint of oxidation resistance and detergency, the present products available to the motoring public differ markedly in their ability to prevent damage to some critical rubbing parts. The design and material of which the rubbing surfaces are made exert no less influence upon the expected service life. The remainder of this paper will deal with the relation of these two factors – lubricant and design.

Which are the critical rubbing areas where lubricant and design effects are most pronounced? In general, they are the rubbing ferrous parts which are not separated by a hydrodynamic film and therefore operate under conditions of boundary lubrication at least part of the time. Specifically, piston rings and cylinder bores, distributor

RELATIONSHIP of the factors of lubricant and engine design which affect wear of cams, lifters, rocker arms, and rocker shafts is discussed in this paper, which is part of the Symposium on Cam and Tappet Wear.

To reproduce service failures of valve-train parts in the laboratory in a short time, special tests procedures and certain engine modifications were devised for this study.

Results of these laboratory tests, which agree well with data obtained in actual service, are presented here.

The Authors

JOSEPH B. BIDWELL (M '54) is assistant head of the Mechanical Development Department of General Motors Research Laboratories. He received his B.S. degree in Mechanical Engineering from Brown University in 1942. Mr. Bidwell joined General Motors shortly after graduation, and worked on bearings and other engine components. He left in 1944 to work at the Naval Research Laboratory, and returned to General Motors two years later.

PAUL VERMAIRE is a senior engineer on hydraulic valve lifters at Diesel Equipment Division, General Motors Corp. He received a B.M.E. degree from General Motors Institute. Mr. Vermaire also attended Calvin College in Grand Rapids. Before joining the GM Diesel Equipment Division in 1944, he was employed by Fisher Body Division of GM and the American Seating Co. in Grand Rapids.

drive gears, rocker arms and shafts, and cams and valve lifters may exhibit great performance differences as a result of changes in design or oil. In any particular engine design one of these areas will usually be the most subject to wear, and the severity of the wear problem will be found to depend upon the lubricant used. Since an engine cannot be run without a lubricant and the lubricant is not especially useful without the engine, it is always difficult to place the responsibility for wear either on the design or the lubricant – they just will not work together. What is necessary for a solution to these problems is an understanding of the influence of both design and oil composition. The designer must determine if he can reduce severity of operation without sacrifice of performance or life of some other part. Similarly, the lubricant producer should attempt to provide the desired antiwear properties in his products if this can be done. Frequently both courses must be followed.

Service Problems

Though numerous examples of wear on the critical engine parts mentioned above could be considered, we will restrict the following discussion to problems associated with the valve gear – cams, lifters, rocker arms, and rocker shafts. Data obtained both in passenger-car service and from laboratory dynamometer tests will be presented to illustrate lubricant and design effects.

Fig. 1 – Lifters from car A run with three commercial oils; left to right: oil 1, oil 2, oil 3

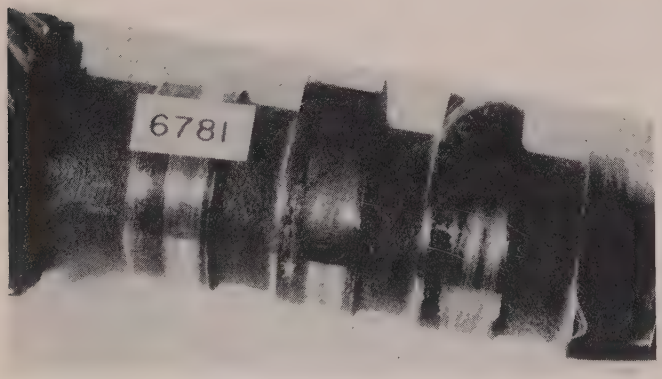

Fig. 2 – Camshaft from car A run with oil 3

The valve lifters shown in Fig. 1 were removed from three cars of make A which were all run under similar service conditions. Many drivers and types of service were involved, and the lubricant used was the only controlled variable. These lifters are all carburized steel hydraulic valve lifters. The first lifter, from test 6775, has run for 13,676 miles with oil 1 and is representative of all of the lifters from this engine. A great deal of wear has occurred leaving a smooth, severely worn surface with a peculiar contour. Lifter 6778 was operated 5686 miles using oil 2. This lifter face still has the matte effect caused by grit blast marks on the original surface. This is indicative of very little wear. In two other cars of the same make run on this same oil, the lifters are in similar condition after more than 50,000 miles on each. The third lifter, 6781, was run with oil 3 for 11,928 miles. The center of the lifter is unworn and grit blast marks are evident, but extensive wear is found just outside of this area. Uniform wear of the lifter face is in itself harmless, but wear of the nature illustrated by lifters numbered 6775 and 6781 generally causes wear of the cam lobes also. Failure of these parts is evidenced by noise and loss of performance. The camshaft, which was taken from the same engine as lifter 6781, is shown in Fig. 2. This illustrates the camshaft failure which follows excessive lifter damage. The lobes exhibit appreciable wear in the nose area, and poor cam contact is shown by the varnish pattern.

We have been operating several cars of make D from the Research Laboratories Garage with a number of different lubricants to determine whether these cars also will demonstrate differences in performance. All of these cars were driven by a large number of drivers for transportation within the city and to nearby communities. No special driving instructions were given, so that a wide variety of service is included. Again, the most pronounced difference between oils has been evident on the face of the valve lifters. Some

Table 1 – Lifter Wear and Pitting in 1953 Car D After 13,000 Miles Using Five Commercial Oils

Oil Used	SAE Viscosity Grade	Number of Cars	Average Wear (0.0001 in.)	Average No. of Pitted Lifters
Oil 4	10W	1	10	1
Oil 2	10W	2	15	1.5
Oil 1	5W and 10W	5	26	5.6
Oil 5	5W and 10W	4	46	5.5
Oil 3	5W – 20W	3	28	9.7

oils greatly accelerate fatigue of the lifter face. Table 1 is a summary of results of these tests. All of the cars were run approximately 13,000 miles under similar conditions. This table makes it clear that lifter pitting in service is definitely a function of the lubricant used. Oils 2 and 4 exhibit very much less lifter pitting and wear than do the others. It is particularly interesting that oil 2 is superior to most other oils, both in car D and car A, even though the geometry and metallurgy of the cams and lifters are different. The next three figures illustrate the appearance of lifter faces run in three of these cars. Fig. 3 is a set of lifters which have been run in a car operating from the Research Garage with oil 2 for 13,333 miles. These lifters exhibit very slight wear and practically no pitting. The lifters shown in Fig. 4, which have run 13,401 miles with oil 1, have been severely pitted in the same kind of operation. The lifters run with oil 3 and shown in Fig. 5 have been run 6500 miles and have a pitted appearance similar to those run with oil 1. The relatively short mileage required to produce this much damage should be noted.

Fig. 3 – Lifters from car D run 13,333 miles with oil 2

All of the above service experience establishes the importance of the lubricant but presents many unanswered questions. How does the lubricant influence lifter fatigue? Is viscosity a critical factor? Are highly additive oils less effective than low? Does specific additive composition exert influence? Is the performance of the lifter and lubricant combination affected by the type of operation? Similarly, there are many questions concerned with design. What is the best metallurgical combination for lifters and cams? For rockers and rocker shafts? What is the best lifter and cam geometry? How should rocker arms be lubricated? Questions like these can only be answered by extensive laboratory testing under conditions which will simulate service failures. Since valve-train parts have been found to be especially subject to wear in service, an engine test has been

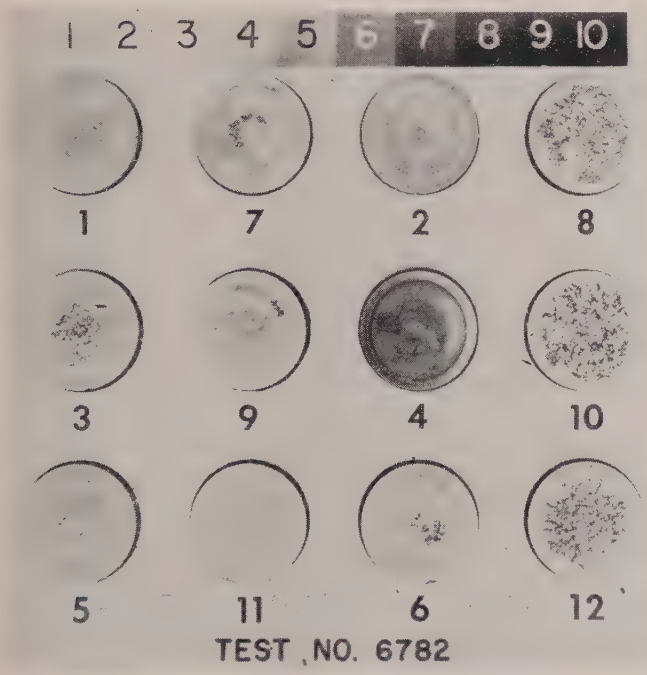

Fig. 4 – Lifters from car D run 13,401 miles with oil 1

Fig. 5 – Lifters from car D run 6500 miles with oil 3

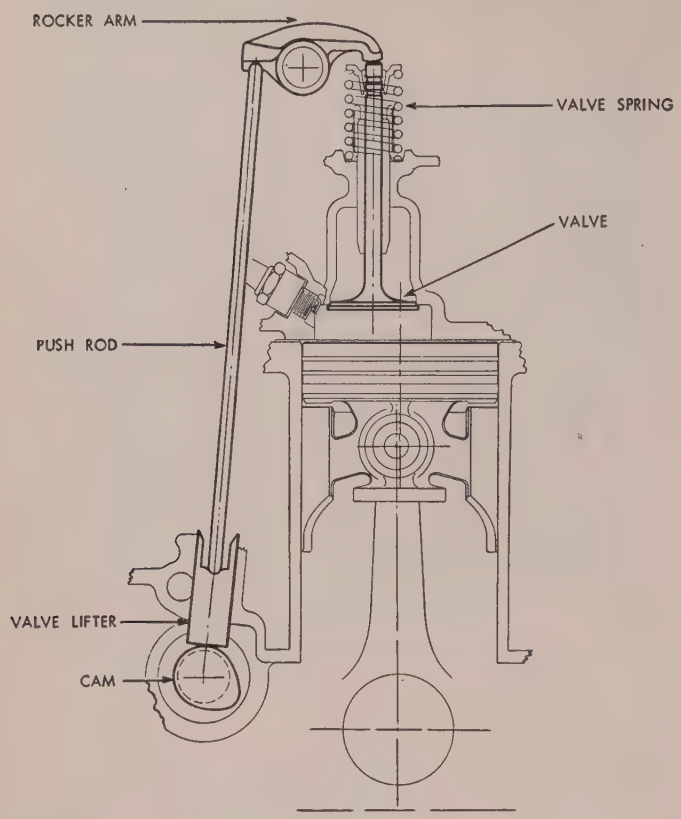

Fig. 6 – Diagram of valve-gear arrangement

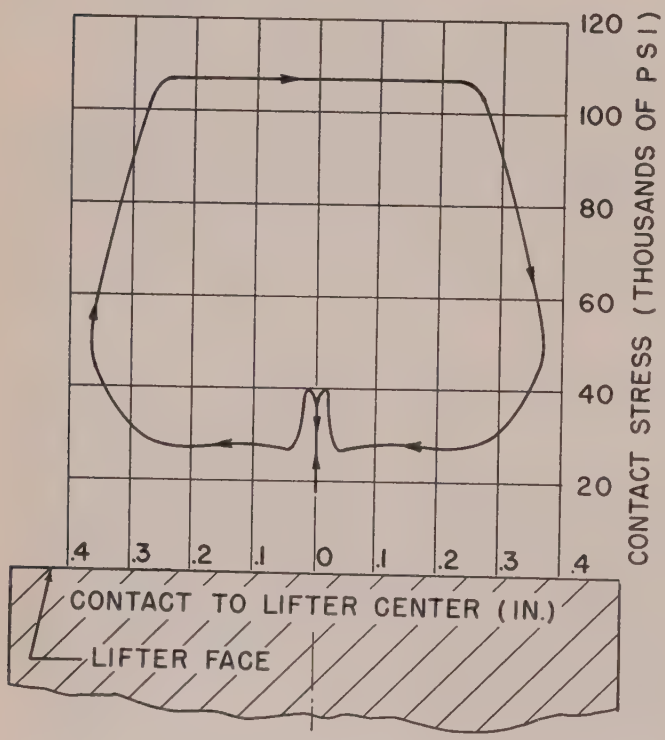

Fig. 7 – Lifter contact stress

developed which will reproduce service failures using valve lifters and rocker arms as the test elements.

Lifter Operating Conditions

Before discussing some of the results of these tests, let us consider the operating conditions of valve lifters and rocker arms. Fig. 6 illustrates the arrangement of these elements. The purpose of the valve lifter is to convert the rotary motion of the camshaft into a reciprocating motion which is transmitted by a push-rod to a rocker arm. This arm changes the direction of motion and operates the engine valves. The valve train is loaded by the valve spring and any dynamic forces arising from accelerations in the system. As a result of the curvature of the cam, the stress in the lifter face is very high, and sliding must occur between cam and lifter under this high stress. The amount of sliding will be affected by rotation of the lifter and by the contour of the lifter and cam, but some sliding must always occur.

Hydraulic valve lifters have made the operation of rocker arms more difficult. With this type of valve lifter the push-rod and rocker arm are subjected to a small load as a result of the spring and the oil pressure inside the lifter even when the lifter is on the cam base circle. The magnitude of the force is perhaps 15 or 20 lb, but this is sufficient to prevent separation of the rocker and shaft, thus prohibiting establishment of a "squeeze" oil film in this area. The rocker arm with a hydraulic valve lifter may be compared to a 2-stroke-cycle piston-pin bushing. In both cases the relative rotation of the parts is insufficient to provide a separating oil film, and since no load reversal occurs to provide a squeeze film, they must operate under boundary lubrication conditions.

The stress at the point of contact between a typical cam and lifter is shown in Fig. 7. This stress is calculated without including inertia effects. Low-speed operation is the most severe with respect to lifter fatigue because the lifter is decelerating at the time of peak stress so that at high speed the forces resulting from this deceleration tend to decrease the load between the lifter and the cam. The horizontal axis represents a section perpendicular to the camshaft axis through the face of the lifter, and the stress is plotted on the vertical axis. When the lifter is on the cam base circle, the oil pressure and the small spring inside the lifter cause a contact stress of about 18,000 psi. As the valve begins to open this stress rises to almost 40,000 psi and then drops as the point of contact moves out from the center and the lifter rises. As the point of contact approaches its farthest outward position, the stress rises rapidly and reaches its maximum value as the point of contact moves inward. The maximum stress of about 106,000 psi remains practically

constant as the point of contact passes center and the valve attains its maximum opening. The order of events then reverses as the valve closes. It can be seen that a large part of the lifter surface is subjected to a high compressive stress. The stress at any point on the lifter surface varies over a range from 0 to its maximum value each time the contact area passes over it. Lubricant reaches the contact area principally by splash. The unit loads are too high to permit full film lubrication with oil of normal viscosity so that some metallic contact occurs. The lifter operating conditions outlined above are conducive to two types of failure – fatigue resulting from cyclic high stressing, and wear resulting from sliding contact under high unit load.

Both wear and fatigue failures of lifters are encountered in service, and we have shown by some service data that both are influenced by the lubricant used. Many design factors are also known to affect severity of lifter operation. Shape of the lifter foot, shape of the cam profile, lifter and cam materials, cam to lifter offset, and valve-spring load are all known to play important parts, though the exact magnitude of their effects are not known. Under boundary lubrication conditions it is well known that the rubbing materials, their surface roughness, loading, oil supply, and lubricant all have a bearing on the success of operation of such parts. For this reason, the ability of the lubricant to provide satisfactory boundary lubrication may be evaluated by operating in the rocker arms.

Geometry and materials used by four car manufacturers for camshafts and valve lifters in their 1953 engines are tabulated in Table 2. The wide variety found in these designs is a good indication that there is no universally accepted solution to the lifter problem. Both crowned and flat lifter faces are used. The crowned lifter with a tapered cam assures positive lifter rotation, reduced sliding velocities, and less severe alignment problems at the expense of increased stress. Many people have proposed alignment as the major factor in promoting lifter fatigue when a flat lifter face is used on a straight cam. This does not appear to be the case in our car D car tests and dynamometer tests, to be described later. This statement is based on three pieces of evidence. First, measurements of several engine blocks indicate that bore squareness is sufficiently accurate so that clearance of the body in the bore will permit alignment. Second, on lifters which do not rotate, the lubrite coating on the body is found intact on the sides of the lifter in line with cam axis. This is evidence that the bore has not exerted a couple in the plane of the cam which would affect the load distribution on the cam. Finally, all of the failures occur first at or near the center of the lifter. It is hardly conceivable that if the bores were restraining the lifters, that they should be always tilted so as to cause higher loads at the lifter center. Rather, you would expect about half of the failures to begin near the edge.

Table 2 – Lifter Materials and Geometry for Four 1953 Cars

	Car			
	A	B	C	D
Camshaft Material	Alloy iron	Steel	Alloy iron	Steel
Lifter Material	Steel	Chilled iron	Alloy iron	Chilled iron
Cam Taper (θ)	0 deg 6 min	0 deg	0 deg 7 min	0 deg
Lifter Radius (R)	65 in.	Flat	35 in.	Flat
Offset (D)	0.122	0	0.073	0.125

Table 3 – 1953 Rocker-Shaft Design for Four 1953 Cars

Engine	Shaft Grooving	Arm Grooving
A	Helical	None
B	None	Axial (5 grooves)
C	Circumferential	None
D	Axial (flat)	Circumferential

A similar diversity of design exists in the case of rockers and rocker shafts. Each manufacturer utilizes a different means of lubricating these parts. These designs are tabulated in Table 3. The oil supply to this point is complicated by the need to restrict the quantity of oil getting on the valve stems. An excessive supply promotes oil consumption. An additional factor does not appear in this tabulation but affects severity of rocker operation. It is eccentricity of the load applied to the rocker bearing. The placement of the load can be such that only a relatively short length of the bearing is useful, causing much more tendency toward wear and scoring than for an equal central load.

Laboratory Tests on Lubricants

In view of the service experience described above, a test procedure was devised which would evaluate oils with respect to their ability to provide boundary lubrication and inhibit fatigue of the lifter face. The 1953 car D engine was selected to serve as the test machine. A great deal of experimental work followed to devise engine modifications and a test schedule which would best reproduce service failures in a short time. Tests were run with jacket water and oil temperatures both high and low, at high and low speed, at steady speeds, and cycled. The procedure finally adopted is simple to perform and produces results in a short time. Modification to the engine consists in only two changes:

1. Increase valve-spring load to 240 lb in the fully open position.
2. Invert the rocker shaft to eliminate the flat

Fig. 8 – Lifters from LS-5 test with mineral-base oil

Fig. 9 – Lifters from LS-5 test with oil 2

in the load area normally used to improve rocker operation.

Table 4 is a summary of the test conditions finally adopted. This test procedure has been designated the LS-5 test. All of the test parts required are standard 1953 car D parts. The camshaft material is steel, and the valve lifters are chilled iron. The rocker shafts are induction-hardened steel under the rocker-arm bearings, and the arms are pearlitic malleable cast iron. The test parts are not specially selected or inspected but are regular service parts.

Table 4 – LS-5 Test Conditions

Engine: 1953 Engine D
Modifications:
Valve-spring load 240 lb open
Rocker shafts installed inverted
Operating Conditions:
Speed – 3150 rpm
Oil sump temperature – 255 F
Jacket temperature – 190 to 200 F
Test duration – 24 hr

Table 5 – Summary of LS-5 Test Results on Several Commercial Lubricating Oils

Oil	SAE Viscosity Grade	Lifters		Rocker Arms	
		Pitting Severity	Wear (0.0001 in.)	Metal Pickup	Wear (0.0001 in.)
Oil 1	40	5	5.5	83	29.5
Oil 2	10W	19	7	21	5
Base Oil	10W	22	10	42	7
Oil 3	5W – 20	52	18.5	8	4.5
Oil 5	5W	61	21.5	37	5.7
Oil 1	10W	75	21.5	80	10.5
Oil 6	10W	92	20	25	5

All of the test results which follow were obtained with the LS-5 procedure run in several different engines. In addition, lifter pitting is a fatigue phenomenon, and considerable scatter can be expected. Therefore, the appearance of any one lifter in a single test may not be representative of the whole group, and all 12 lifters must be considered in evaluating a test. Differences in oil performance are sufficiently pronounced so that discrimination between good and bad is not difficult.

Rocker-arm operation with different lubricants is characterized by varying degrees of wear on the arm and metal transfer from the arm to the shaft. Oils differ markedly in the property, which has been called "e-p property," that prevents this kind of damage to the rocker arm and shaft. Oils which have superior boundary lubricant properties and therefore perform well in rocker-arm operation also provide the necessary protection for distributor drive gears, piston rings, and similar sliding ferrous parts.

Table 5 is a tabulation of the performance of several commercial oils in the LS-5 test. Each oil was run twice and the values for wear and pitting are therefore based on 24 lifters or rocker arms. The column headed "Pitting Severity" is 100 times the ratio of the number of lifters which are pitted to any degree divided by the number of lifters which rotated in that particular test. The reason for dividing by the number of rotating lifters rather than the total number used in the test will be evident later. It is clear that small values of pitting severity are characteristic of desirable oils. The lifter wear figures are the difference in overall lifter length measured at the center of the lifter

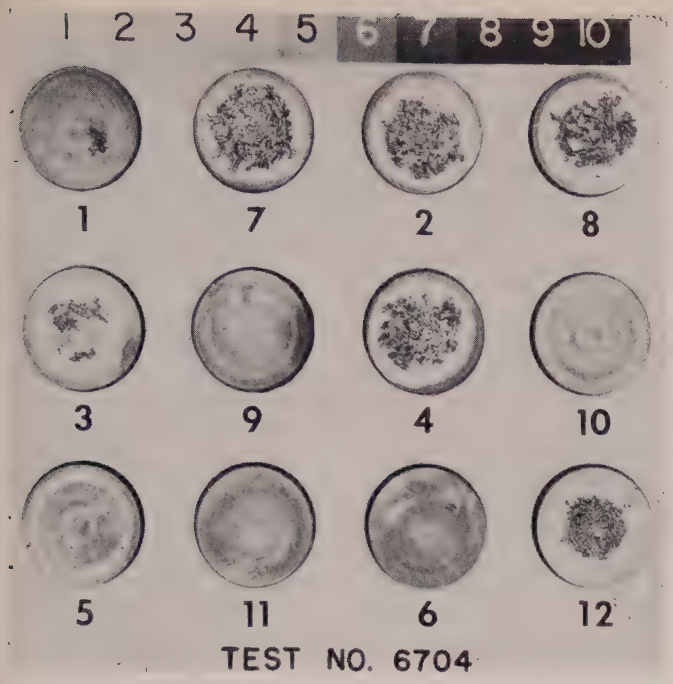

Fig. 10 – Lifters from LS-5 test with oil 1

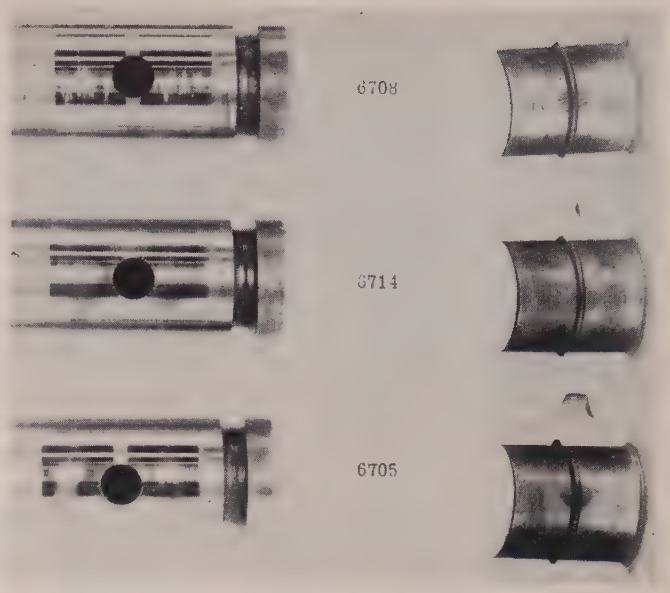

Fig. 11 – Rocker-arm and shaft performance of three oils; top to bottom: base oil, oil 2, oil 1

face. These wear figures do not distinguish between metal lost through fatigue and loss by wear in the usual sense. This distinction can be made by noting the appearance of the lifter face.

Metal pickup from the rocker arm to the shaft is very difficult to evaluate quantitatively. For lack of a better method, the values tabulated are the percentage of arms which exhibit pickup. No attempt has been made to consider the degree of metal transfer, but this factor may be judged from the rocker arm wear figures which are a measure of the wear on the loaded side of the arm. Rocker-shaft wear figures are not given since the shaft frequently is larger at the end of a test as a result of metal transfer.

One of the first conclusions which we reached as a result of our test program was that the ability of an oil to act as a suitable boundary lubricant was not necessarily related to its effect upon lifter pitting. Data from Table 5 illustrate this fact. The SAE 40 grade of oil 1 which produced the least lifter pitting exhibits the worst rocker arm wear and metal transfer. On the other hand, oil 6 which causes almost 100% lifter pitting in this test has relatively little wear and metal transfer. The influence of viscosity is also indicated by the relative performance of the SAE 10W and 40 viscosity grades of oil 1. These tests show a large difference in pitting severity between a high- and low-viscosity oil, but both viscosities give very poor performance on the rocker arms. The viscosity influence on the lifter face may result from hydrodynamic forces which modify the load distribution. Further work on effects of viscosity is required. Knowledge of the influence of V.I. improvers is also important in connection with multiviscosity oils. The results of these 24-hr tests may be compared with the results tabulated in Table 1 obtained in the same engine run in passenger-car service. Oils which demonstrate superior performance in service show a similar superiority in the LS-5 test. Similarly, oils which perform poorly in cars are rated poor by the laboratory test procedure. This correlation permits the rapid evaluation of a much larger number of oils than would be possible in service tests which are more expensive and require longer to complete.

The appearance of some good and bad lifter faces is illustrated in Figs. 8, 9, and 10. These may also be compared to those removed from cars and shown in Figs. 3, 4, and 5. Fig. 8 is a set of lifters run with a mineral-base oil with no additive. These lifters are not pitted but several have failed to rotate. Oil 2 was run with the lifters in Fig. 9. Only one lifter shows distress as a result of pitting, and one more has only rotated for part of the test. In Fig. 10 most of the lifters are pitted – these have been run with oil 1.

The rocker shafts and the loaded area of the rockers run with three representative oils are shown in Fig. 11. The top pair were run with base oil and illustrate the metal transferred from the arm to the shaft by welding. This is one type of arm failure. The overall wear is relatively small, and much larger wear values have been encountered with other oils. The middle shaft and arm were run with oil 2 and have suffered very little wear and metal transfer. This oil also gives satisfactory results

Table 6 – Summary of LS-5 Test Results on Several Oil Additives in a 10W Base Oil

Additive	Lifters		Rocker Arms	
	Pitting Severity	Wear (0.0001 in.)	Metal Pickup	Wear (0.0001 in.)
Zinc dithiophosphate A	0	5	17	4.5
Same plus Supplement 1 addition of sulfonate-type detergent	0	6	8	3.7
None	0	4	79	11.7
Zinc dithiophosphate B	5	5	4	3.2
Phosphorus, sulfur, chlorine inhibitor	10	4	96	14.7
Sulfurized turpene	19	7	62	5.7
Sulfurized olefin	33	10	42	4.2
Phenate-type inhibitor-detergent	50	13	46	4.7

Table 7 – Cold Cycle Test Schedule

Break-In – 2 hr, no load, water out 165 F, oil temp 190 – 200 F

Time, min	Speed, rpm
15	1000
30	1500
30	1800
45	2000

Cycling Schedule – no load, water out 100 F
Each cycle consists of:
2 hr operation at 1000 rpm.
2 hr stopped with cold water running through the block.

Inspections
All lifters and cams are inspected at the beginning and end of each test. The lifters only are inspected after break in and after six cycles.

Running Time
A total of 25 cycles is run. This is a total engine operating time of 50 hr.

Table 8 – Influence of Design and Material on Lifter Performance in Cold Cycle Test with Oil 3

Engine	Lifter Material	Lifters Not Rotating	Number Pitted	Average Wear (0.0001 in.)
A	Chilled iron	0	0	32
	Alloy iron	0	0	10
	Steel	0	16	38
B	Chilled iron	13	1	10
	Alloy iron	1	0	8
	Steel	4	7	19
C	Chilled iron	0	1	30
	Alloy iron	0	0	17
	Steel	1	11	42

with respect to pitting. The third set was run with oil 3 which is satisfactory on the rocker arms, as shown, but causes excessive lifter pitting.

In all of the tests run in engine D an effect of the lubricant upon rotation of the lifters has also been observed. Some oils always cause all of the lifters to rotate while others may permit several to remain stationary or only partially rotate. When the lifter does not rotate, the surface may become scuffed and a shallow notch worn at the center, but no fatigue has yet been observed on lifters which do not rotate. It is for this reason that nonrotating lifters have been excluded in the evaluation of lifter pitting.

The tests which were run on commercial oils involved differences in both additives and base oil. In order to study the additive effect separately, a series of tests were run with several representative types of oil additives in the same 10W base stock. They do not all represent complete engine oils since some have no detergent. These additive compositions are only a few of the many elements used in commercial compounded oils, but they permit us to study the influence of individual materials. Since additives which answer the same general description may possess widely different properties, this data should not be interpreted to infer that the performance of all such materials are alike. The summarized results of these tests are shown in Table 6. It is once more evident that when the oils are arranged in order of pitting severity, the rocker-arm damage is not in the same order. This is more evidence demonstrating the different nature of wear and pitting damage. The two values shown for zinc dithiophosphate represent results with this material obtained from two sources. This particular additive seems to provide excellent wear-control properties, as evidenced by its performance on the rocker arms. It is also interesting to note that all of the commercial oils tabulated in Table 5 which demonstrated satisfactory performance on the rocker arms contained this material as one additive component. From the data given here, it is evident that the zinc dithiophosphates used in these tests do not promote lifter pitting. However, from the tests on commercial oil, it has not been able to prevent lifter pitting when used in usual concentration in combination with some detergents. It is possible that a larger amount would be beneficial. The individual additive material which produced the greatest lifter pitting is the phenate type, which is used in a number of commercial oils. The use of a sulfonate type detergent with the zinc dithiophosphate inhibitor produced a finished oil which has all of the desirable properties so far as wear and pitting are concerned. This formulation is very similar to oil 2, which has demonstrated superior performance in cars A and D.

Laboratory Design Comparison

A considerably different test procedure has been used to evaluate both design and material factors with respect to resistance to pitting and wear under adverse operating conditions and with lubricants which are deficient in boundary film protection. This evaluation has been performed with only one lubricant which has proved to lack the required boundary lubricant and antifatigue properties when used in engine A. The test procedure was developed to produce severe damage to the steel valve lifter used in this engine. This test involves low-speed, low-temperature, cycling operation. The details of the test procedure are shown in Table 7.

All of the tests were run with oil 3. Three engines were used in these tests, one each of makes A, B, and C. All used cast alloy iron camshafts. Valve lifters were made to suit the particular geometry of each engine from three different materials, chilled cast iron, hardened cast alloy iron, and carburized

steel. All lifter faces were subjected to a surface treatment, and the steel lifters were grit-blasted prior to this treatment.

Three tests were run in each engine. Each test used eight lifters of each of two materials so that upon completion of three tests in one engine, 16 lifters of each material had been run. The results of these tests may be used to compare the severity of the three engine designs and to compare the performance of the three materials in each engine. Wear and pitting data from these tests are summarized in Table 8, which also shows the effect of design upon lifter rotation.

In all of the three engine designs run in this test, the hardenable alloy iron lifters suffered the least wear and pitting. In fact, no pitting was encountered with this lifter material in these tests.

One interesting fact which can be seen is the resistance to pitting exhibited by chilled iron under these test conditions. Only two chilled lifters suffered any pitting, and this was slight. A similar resistance under similar conditions was noted in the development of the LS-5 test procedure. It should be noted that these cold cycle test conditions are not the most severe for chilled iron and that this material is subject to fatigue in the usual passenger-car service. The engine design influence on lifter rotation and wear is also clearly shown. Engine B design is such that lifters frequently do not rotate. When rotation does not occur, lifters do not pit. There is some wear on the lifter face, and a groove is worn on a diameter. With this design, pitting can occur if the lifter does happen to rotate. The least wear in all of the combinations tried occurred in engine B with alloy iron lifters. However, wear with this same lifter material was also small in the other two engines.

In all of the engine designs the carburized steel lifters suffered the most damage with respect to pitting, scuffing, and wear. A 100% failure occurred in engine A. It should be noted that, though the steel lifters suffered under these adverse test conditions, when run with suitable lubricants steel lifters may be found superior to the other lifter materials for long service life. The poor fatigue life of these lifters would not be expected in view of the superior fatigue strength of this material as measured in air. This seeming paradox may be explained on the basis that these failures are due to corrosion fatigue and that the steel lifters are more susceptible to corrosion fatigue than chilled or alloy iron under the cold cycling test conditions. Corrosion fatigue is not a corrosion phenomenon in the usual sense. Rather, it is the name given to the influence of the atmosphere or surrounding media upon fatigue life of parts subjected to cyclic stress. The failed part shows no evidence of corrosion but appears as a normal fatigue failure. The appearance of a 100X metallographic section through a chilled iron lifter which has been pitted in an LS-5 test with oil 1 is shown in Fig. 12. This illustrates the nature of the

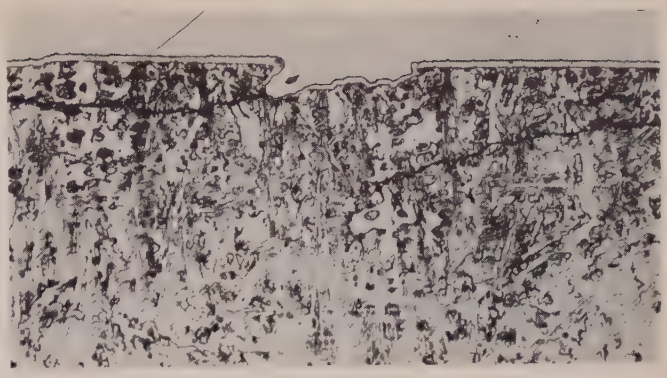

Fig. 12 – Section through fatigued lifter from LS-5 test (reduced from photomicrograph taken at 100X)

subsurface crack. These generally follow a path parallel to the surface. It can be seen that the crack passes directly through some of the carbide particles rather than following a grain boundary. This is typical of fatigue failures. The effect of corrosion fatigue is felt in the reduction in fatigue life of a part when it is run in a medium which promotes failure. The exact mechanism by which this acceleration of fatigue damage occurs is not known. It is evidently related to chemical reactions which take place between the metal and the surroundings. As a consequence, different metals have varying degrees of susceptibility to corrosion fatigue in different media. It is this fact that explains the apparent poor fatigue resistance of steel in the cold test procedure. Iron lifters are less affected by the particular crankcase oil under these operating conditions.

It was stated that, in the development of the LS-5 procedure, several operating schedules were tried. With the chilled iron lifters used in this test the most damage was found when the operating temperatures were high. This difference between the most severe conditions for steel lifters and for chilled iron might be expected as a result of their difference in resistance to chemical attack. In addition to the influence of the test conditions, the camshaft material has a large effect upon the success of lifter operation. Therefore, the results of these few tests are not sufficient to permit final judgment of the relative merits of the three lifter materials employed under conditions other than those encountered in this test. It is necessary to determine the most difficult operating condition for each material combination before this can be done. The performance of the hardened alloy iron is outstanding in the test, however, and it is believed that this material is less influenced by oil quality under other conditions also. Again, however, the large differences which exist between various alloy irons should be anticipated.

Conclusions

From our LS-5 test work it appears that uncompounded mineral oil does not affect fatigue appre-

ciably. It is apparent that either additive material put into the oil or products formed in the crankcase during operation with this type of oil are responsible for the accelerated failure. It is most likely that the corrosion fatigue experienced by valve lifters might also be affecting the fatigue durability of other engine parts, such as piston pins, crankshafts, and connecting rods, which also operate in contact with oil. It appears that selection of materials and attention to design might reduce the boundary lubrication properties required in the oil for successful operation of the cams and lifters, but this change might not permit reduction in the oil quality since boundary conditions also exist on piston rings and distributor drive gears.

Summarizing what we have learned:

1. Influence of lubricating oil upon fatigue and wear of engine parts has been established. Particular additives have been shown to lack boundary lubricant properties and promote lifter pitting.

2. Test procedures for evaluating the boundary lubrication quality and effect of crankcase oil upon lifter corrosion fatigue have been developed and correlation with service failures established.

3. Some design factors have been observed and three lifter materials evaluated with respect to their ability to operate satisfactorily with poor lubricants and under adverse operating conditions.

4. Corrosion fatigue, the cause of accelerated lifter pitting, is under study. An understanding of the mechanism of this phenomenon will permit us to reduce its effect by proper design and lubricant selection.

Increasing the power output of an engine of given displacement necessitates improved breathing and higher maximum speed. Greater valve lift and higher speed require stiffer valve springs to assure that the lifters will follow the cam. These changes accentuate valve train wear problems. It is therefore to be expected that the incidence of these problems will increase. It follows that all possible means – both with design and lubricants – must be studied to permit solution of these difficulties.

Acknowledgment

The cooperation of many people has been essential in the preparation of this copy. H. C. Mougey provided us with an appreciation of wear problems. Numerous people also called particular instances of excessive wear to our attention. We are indebted to A. Elston, J. Altenhoff, and G. Malone for their efforts in conducting laboratory and service tests.

DISCUSSION OF CAM AND TAPPET WEAR PAPERS

Give Results of a Limited Study of Valve-Train Wear

– R. E. Crosthwait, E. A. Martin, and J. F. Socolofsky
Socony-Vacuum Laboratories

VALVE-lifter and camshaft wear in automotive engines is a problem that involves four interrelated factors: (1) metallurgy of valve-lifter and camshaft materials; (2) mechanical load and design of the valve train; (3) valve-train operating conditions, such as oil temperature and speed; and (4) properties of the lubricating oil. One approach to the problem has involved the use of production engines, operating under a specific set of test conditions, to evaluate the performance of lubricating oils.

Our laboratories have conducted a limited study of the valve-train wear problem in two makes of engines operating under test conditions (recommended by the respective builders) which emphasize cam and tappet distress.

Engine A – Since no excessive pitting or scuffing (either of the valve lifters or camshaft) was noted under the test conditions used for this engine, the effect of valve-lifter metallurgy and lube oil composition on valve-train wear was evaluated by measuring lifter height wear. The reproducibility of the test in engine A was good, when considering either the individual valve lifter in each test or the average wear of repeat tests.

The test program in engine A was arranged to evaluate the following types of lube oil additives: (1) oxidation inhibitors, (2) detergents, and (3) so-called "e-p" agents. Fig. A is a graphical presentation of the test results.

Generalizations from the test results in engine A are: (1) valve-lifter metallurgical structure is a major factor in valve-train wear; (2) commercial detergents, oxidation inhibitors, and e-p agents, depending on their chemical

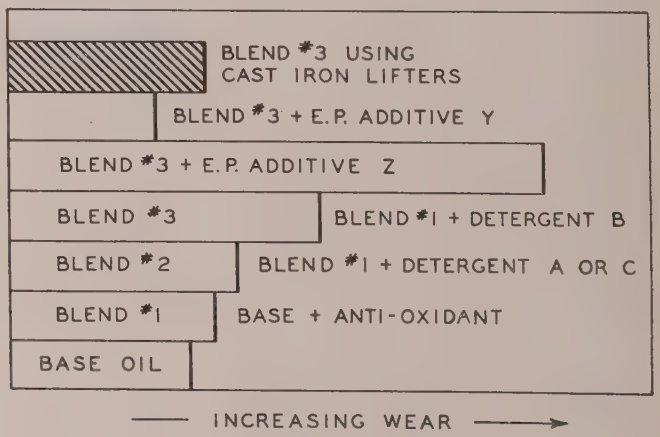

Fig. A – Valve lifter wear

structure, may exhibit no effect, may promote wear, or may reduce wear. Fig. B presents these generalizations in graphical form. They are based on the assumption that no interaction occurred between the various additives utilized.

Engine B – A few lubricant evaluation tests were conducted in engine B. This engine, involving different design and metallurgy and operating under a different set of speed, oil temperature, and valve-spring loading conditions, showed poor correlation with the valve-train wear results from engine A. In addition, engine B gave erratic results with respect to measured wear, observed scuffing, and pitting among the individual lifters.

General – In the course of this investigation it was also found that the usual laboratory bench tests (for wear and e-p properties) were of little value in predicting valve-train wear results.

In conclusion, our limited study of valve-train wear indicates that, although the problem is complex, wear may be reduced by (1) metallurgical changes in valve-train parts and (2) the use of special lube oil additive combinations. In the latter case, however, some additives which reduce wear under one set of test conditions actually promote wear under other conditions. This has been confirmed by other investigators.

Fig. B – Valve lifter wear due to additives or lifter material (hardened cast-iron camshaft)

Table A – Laboratory versus Field Test Lifter Wear in Engine X with Chilled Cast-Iron Lifters

	100-Hr Cyclic Laboratory Test		6000-Mile Field Test	
	Lifter Wear, in.	No. of Lifters Spalled	Lifter Wear, in.	No. of Lifters Spalled
Oil A	0.0056	0	0.0025	13
Oil B	0.0019	1	0.0013	0
Oil C	0.0014	0	0.0049	0

Table B – Laboratory versus Field Test Lifter Wear in Engine Y with Steel Lifters

	100-Hr Cyclic Laboratory Test – Lifter Wear, in.	6000-Mile Field Test – Lifter Wear, in.
Oil A	0.0023	0.0077
Oil B	0.0006	0.0065
Oil C	0.0008	0.0012

Driving Conditions Have Marked Effect on Lifter Wear

– H. L. Yowell
Standard Oil Development Co.

THESE three excellent papers clearly demonstrate that a wealth of basic data has been accumulated at a rapid rate on this problem by both the petroleum and automotive industries. It is certainly comforting to have this "know-how" at an early date and to see it being pooled here today so that it can be utilized to alleviate the valve-train wear problems that have recently plagued both industries.

It is especially fitting that Messrs. Ambrose and Taylor have offered definitions for the types of wear that are encountered in valve trains. Certainly a common language is important in a problem that we are all studying so vigorously. In general, the information presented in these papers agrees with the results that we have obtained in our work. Although there are some points on which we differ with their conclusions, I will not discuss those details in view of the time limitations for these remarks. We have used several of the laboratory engine test methods described in these papers. In addition, we have conducted extensive field tests to determine how well these laboratory methods correlate with field performance. In general, we feel that the correlation of the laboratory engine test data with field data has not been good. For example, Table A shows that engine X, equipped with chilled iron lifters, gave valve lifter wear of 0.0056, 0.0019, and 0.0014 in., respectively, for oils A, B, and C in a 100-hr cyclic engine test. These same oils were field tested in an automobile equipped with engine X in a 6000-mile test in which the driving consisted of approximately 50% city stop-and-go driving and 50% mild intercity driving. The top speed during this test was 45 mph, and the average speed was about 22 mph. Under these conditions, you will note that the values for these three oils were 0.0025, 0.0013, and 0.0049 in., respectively. It is interesting that in two out of the three cases, the field wear was less than in the laboratory engine test. Also it will be noted that oil A gave no evidence of spalled lifters in the laboratory test, whereas 13 of the lifters spalled in the field test. However, this spalling did not increase the lifter wear.

Table B compares the wear obtained in engine Y, which has steel lifters, in a 100-hr cyclic laboratory test and the

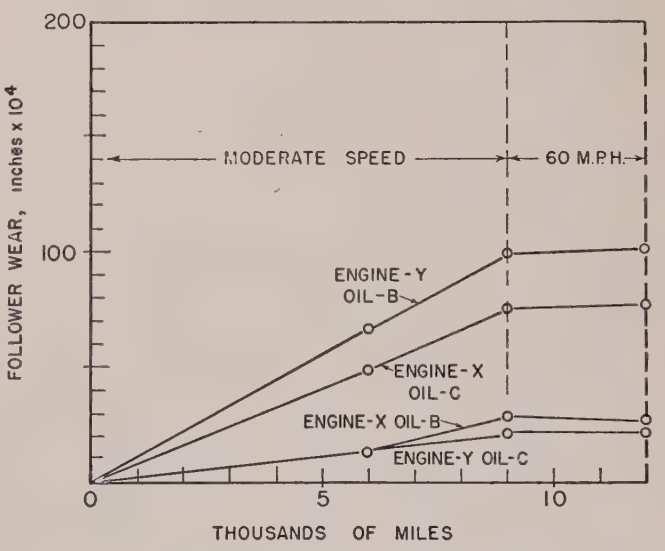

Fig. C – Influence of driving conditions on lifter wear

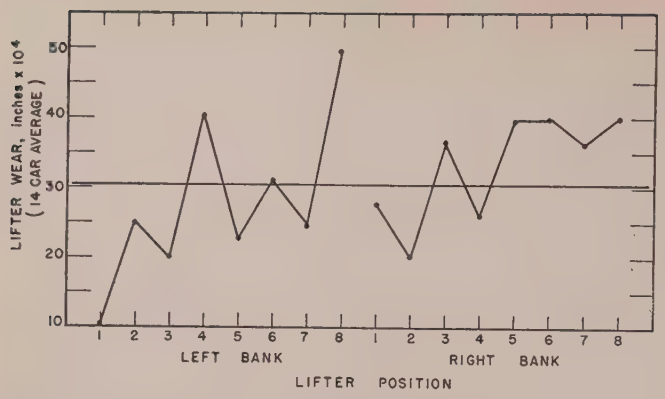

Fig. D – Influence of engine design on lifter wear in engine Y after 6000 miles

Table C – Influence of Break-In on Lifter Wear in 60-Mph Field Tests in Engine X, Chilled Cast-Iron Lifters, Oil F

Lifter Wear Rate, in. per 1000 miles	
With Prior Break-In	No Break-In
0.0002[a]	0.0029[b]

[a] 50,000-mile test.
[b] Cam lobes failed at less than 2000 miles.

Table D – Influence of Metallurgy on Lifter Wear, 6000-Mile Field Test in Engine X with Oil E

Chilled Cast-Iron Lifters		Hardenable Cast-Iron Lifters	
Wear, in.	No. of Lifters Spalled	Wear, in.	No. of Lifters Spalled
0.0032	3	0.0004	0

Table E – Influence of Engine Type on Lifter Wear, 6000-Mile Field Test

	Engine X		Engine Y		Engine Z	
	Lifter Wear, in.	No. of Lifters Spalled	Lifter Wear, in.	No. of Lifters Spalled	Lifter Wear, in.	No. of Lifters Spalled
Oil A	0.0025	13	0.0077	0	0.0007	0
Oil B	0.0013	0	0.0065	0	0.0012	0
Oil C	0.0049	0	0.0012	0	0.0008	0
Oil D	0.0021	0	0.0006	0	0.0008	0

6000-mile field test. Here we see that oils A, B, and C gave values of 0.0023, 0.0006, and 0.0008 in., respectively, in the laboratory while the field test showed values of 0.0077, 0.0065, and 0.0012, respectively, for the same oils. The laboratory test showed oils B and C to be essentially equivalent and superior to oil A. The field test, on the other hand, showed oils A and B to be essentially equivalent and considerably inferior to oil C. In this case, in contrast to the results with engine X, the field wear was considerably higher than the laboratory wear with these oils.

Our field tests have also shown that driving conditions have a marked effect on lifter wear. Fig. C shows that, at moderate driving speeds, the lifter wear increased linearly over a distance of 9000 miles. This was true in both engine X and engine Y with oils B and C. However, when the driving speed was increased to 60 mph, there was essentially no lifter wear regardless of whether the lifters had shown any marked tendency to wear under the moderate-speed driving conditions. This figure also points out the difficulty a petroleum company encounters in lubricating different metallurgy systems. Engine X appears to thrive on oil B and is unhappy with oil C. Engine Y, on the other hand, reacts completely opposite to these two oils. The data in Table C show that engine break-in can have an appreciable effect on lifter wear in 60-mph field tests. This test was carried out in engine X which is equipped with chilled cast-iron lifters. In this case, the break-in consisted of starting the driving at a speed of 35 mph with the speed increasing in increments of 5 to 10 mph per 100 miles of driving until 60 mph was reached. By using this technique, a 50,000-mile test was completed with the lifters wearing at an average rate of only 0.0002 in. per 1000 miles. However, when the cars were started off at 60 mph without break-in, the average lifter wear was 0.0029 in. per 1000 miles, and the cam lobes failed at less than 2000 miles.

We have also found that engine design appears to have some effect on lifter wear. Fig. D shows the wear that is encountered on lifters at the different positions in engine Y in the left and right bank. It will be noted in general that the wear level appears to alternate between the odd and even positions and differs in the two banks. The wear also appears to be progressively greater from the front to back positions. These data represent the average of the lifter wear obtained with seven oils run in duplicate in cars equipped with engine Y. Since this relationship held for 14 cars with seven different oils, it is apparent that design factors are responsible for the different wear levels in the different positions. There was, however, no correlation between the wear of the lifters actuating the intake and exhaust valves. A similar alternating wear relationship was noted in engine X.

As pointed out in the papers, metallurgy is one of the principal factors in lifter wear. Table D shows the results that we obtained with oil E in two cars equipped with engine X. In one car, the regular chilled cast-iron lifters were employed while hardenable cast-iron lifters were placed in the second car. Under identical driving conditions in the same caravan, the chilled cast-iron lifters showed a wear of 0.0032 in. as compared to a wear of only 0.0004 in. on the hardenable iron lifters. Also, three of the chilled cast-iron lifters spalled, whereas none of the hardenable iron lifters spalled.

The influence of engine type and especially valve-train metallurgy on lifter wear is summarized in Table E. Here we see that engine Z, which is equipped with hardenable iron lifters, gave essentially the same low level of wear regardless of the type of oil used. Engines X and Y, however, responded to oils A, B, and C almost completely differently. This further emphasizes the difficulty of producing an oil that will be suitable for both types of engines. Oil D, however, shows that improvements can be made in lubricants to alleviate the valve-train wear of engines with different metallurgy types. Such improvements are needed to lubricate satisfactorily many of the automobiles now on the road. Nevertheless, it appears that the correction that can be obtained by metallurgy far outweighs the improvements that can be made by changes in lubricants.

Data Verify Undesirability Of Rotating Tappet Lifters

– W. S. James
Fram Corp.

TABLE 8 of the Bidwell-Vermaire paper, taken in conjunction with the remarks by H. F. Bryan to the effect that rotating lifters are harmful rather than beneficial, bears close examination.

From Table 2, car B is an engine with zero cam taper, zero offset, and a flat lifter. Cars A and C have cam taper of 6 and 7 min and an offset of 0.122 and 0.073 in. It is interesting to note that engine B has the minimum average wear of the lifters under any condition of material in either the lifter or the cam. It is also to be noted that engine B has the minimum number of pitted tappets under the worst conditions of alloy combinations of camshaft and tappet. Also, that engine B has the least number of pitted tappets when the alloy combination is most favorable. This table definitely points up Mr. Bryan's comments on the undesirability of the rotation of tappet lifters.

Reduced Valve-Spring Weight Gives Increase in Valve Life

– T. A. Scherger
Studebaker Corp.

THE authors have confined the greater part of their discussions to the effect of lubricating oils on lifter and cam failures. Our company recognizes the fact that oils do have an important effect on the life of these highly stressed parts. In our test work we use low-film-strength oil and recommend the improved oils for production and service. Failures of cams and lifters in early-model V-8 production engines were traced to edge riding due to hollow grinding of some cams, which left the sides of the cam high. This condition was aggravated by casting techniques which permitted wide variations in cam locations. Correcting these faults reduced the number of failures but did not eliminate them entirely. Scuffing of the cams at the nose appeared to be the starting point of the failure. This was transferred to the lifter face, and the next step was a complete loss of valve lift. The persistence of this type of failure was practically eliminated by changing the material of the camshaft from cast iron to steel in order to prolong useful cam life. In every case where a lifter failed with cast-iron camshaft the cam also failed, whereas with steel camshaft the lifters could be replaced unless the car had been operated too long with spalled lifters.

Early tests with low-film-strength oils indicated failures were confined to high speeds. It was thought that some of these failures may have been due to false motion of the valve and cam mechanism. High-speed photography was used over the speed range and proved that this was not the case. Studies with strain gages were made to determine whether any excessive cam loading condition may be due to binding of any of the operating parts. There were no indications of the existence of any such condition. Further tests indicated that lifter failures occurred at low engine rpm at less total engine revolutions than at high speed. We consider 3000 rpm the dividing point between low and high speed. This would indicate that the stresses which caused the failures were due to spring loads rather than inertia loads. The loads which caused failures also appeared to be confined to the nose of the cam. That these conclusions were correct was verified by the fact that lighter parts did not materially affect the results obtained. This led us into an investigation of the effect of valve-spring loads on lifter failures. It was found that spring loads could be reduced to the point where lifter failures were eliminated. However, with this condition, valve clatter occurred below the desired top engine rpm. A redesign of the cam contour permitted a reduction in valve open spring load of approximately 30% with no sacrifice in power or in valve clatter speed. This reduction in spring weight reduced the number of valve-lifter and cam failures to where they are negligible, especially with the use of good oils.

A reduction in the cam nose radius gave increased lifter life. Our original cam had a nose radius of 0.264 in. and was changed to a nose radius of 0.176 in. This change in nose radius reduced the scuffing tendency on both the cam and lifter, especially with the steel camshaft. This is contrary to expectations, as the unit loading or stresses should be higher with the small nose radius.

Metallurgical investigations were made in an attempt to obtain materials which would give more satisfactory life. Thus far we have been unable to find any material which surpassed the chilled cast iron when using a steel camshaft. Taper of the cam, used to obtain lifter rotation, is limited due to the danger of obtaining edge riding. Cam finish is important, as rough cams cause high unit load concentrations. Our cams are lubrized to eliminate scuffing tendency on initial run-in.

The greatest increase in valve mechanism life was obtained by a reduction in valve-spring weight and improvement in cam finish in our V-8 engine.

Suggests Flat Cam and Tappet To Reduce Loading and Wear

– H. F. Bryan
International Harvester Co.

WE have had considerable experience with the cam wear problem, having built overhead-valve engines for many years.

Original materials employed were a carburized steel tappet and forged steel camshaft. Later, the tappet material was changed to chilled cast iron in most models and is preferred.

The basic problem is that of two surfaces rubbing together at high velocity under heavy load. In this respect, it is similar to other lubrication problems in an engine. Unit pressure is approximately 139,000 psi and shear stress approximately 42,500 psi. No mention is made in any of the papers of the effect of shear stress on the cam wear problem.

We believe that the solution should be made in the engine rather than by use of special oils, the proper approach being to reduce unit loading and maintain a correct film of lubricant.

To obtain reduced unit pressure, the best procedure is to increase contact area by using a flat cam and tappet. No tappet bore misalignment is allowed. The bearing surface L/D ratio calls for a reduced diameter at the nose.

Tappet rotation is undesirable as it makes oil-film formation difficult due to increased shearing stress and throw-off action. In one application where a 0.001-in. cam taper is used, endurance of tappet faces is much inferior to that obtained with untapered cam design.

Cementite Microstructure Used on Steel Tappet Face

– V. G. Raviolo
Ford Motor Co.

THIS discussion deals with all three papers, although the one by Messrs. Bidwell and Vermaire was received too late for proper study and analysis. I will say of it only that, although the work appears to have been carefully conducted and evaluated, I have some doubt of the validity of the test technique, because of the spring overload that was applied. We are using this technique ourselves, with an eye to its significance in future design conditions. However, in any area as undefined as this one, I am suspicious of any attempt to accelerate the test by changing the design condition, when the effect of the change is not clearly predictable.

The main part of this discussion will center on the metallurgical aspects of the other two papers.

I am indebted to C. L. Stevens, supervisor of our Quality

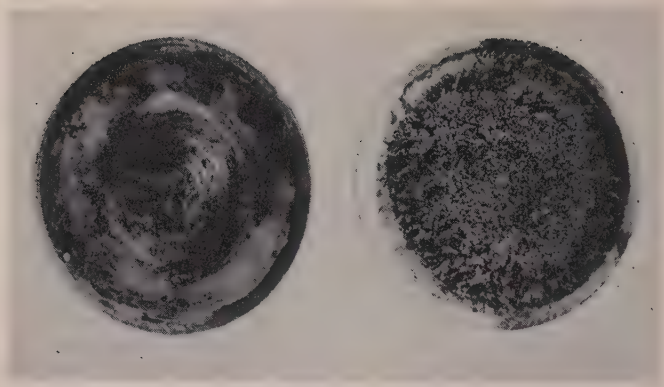

Fig. E – Left: scuffed steel tappet; right: pitted steel tappet

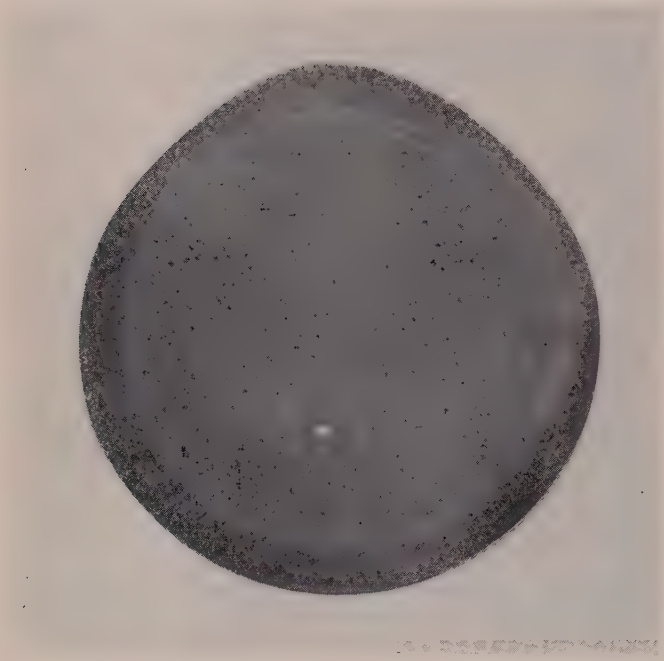

Fig. F – Cam lobe cross-section showing excessive wear

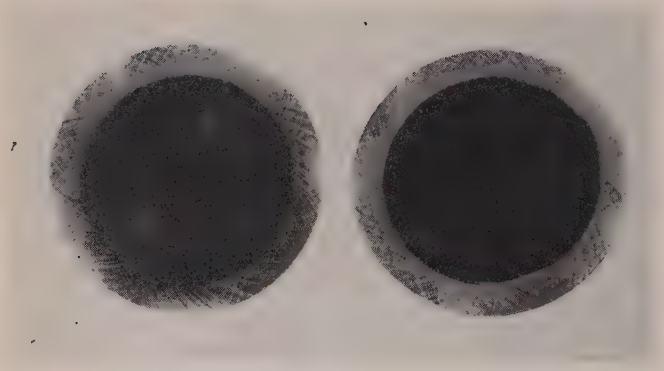

Fig. G – Improved tappets resulting from change in metallurgical process control

Fig. H – Desirable microstructure showing considerable concentration of cementite in matrix of martensite and austenite

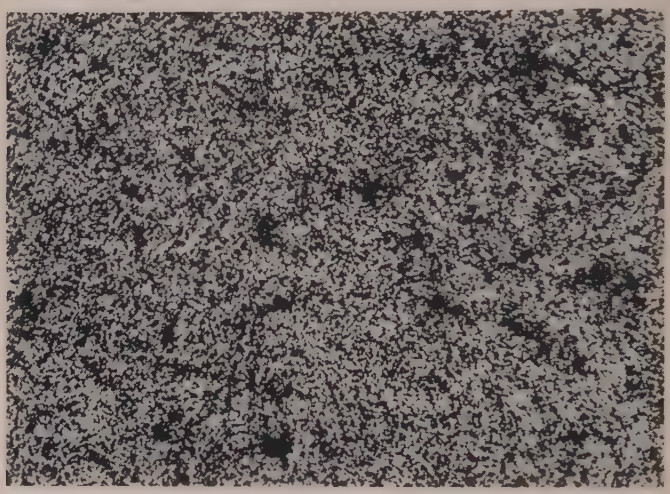

Fig. I – Acceptable microstructure showing higher concentration of cementite than desirable

Fig. J – Unacceptable microstructure where cementite is nearly continuous

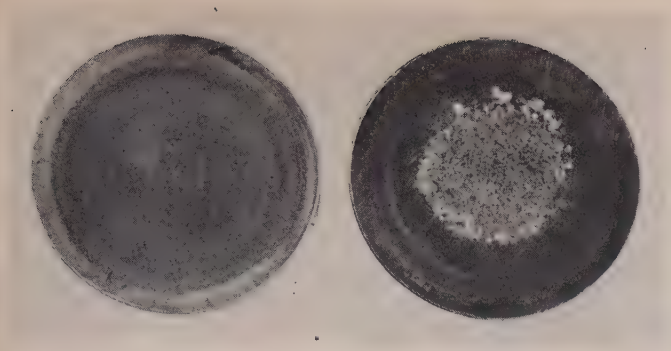

Fig. K – Left: experimental tappet showing neither pitting nor scuffing; right: badly pitted production-processed tappet

Control Laboratory in the Engine and Foundry Division, for the bulk of the metallurgical data I will cite concerning our own tests and experience.

The authors of these two papers have presented us with some truly impressive data, and for this we are grateful. However, I am surprised by some of their conclusions, which I feel are somewhat *too* conclusive. The past literature is meager in data and has not kept pace with the knowledge we've gained over the years. I would like to explore some of these conclusions in the light of our experience.

Messrs. Ambrose and Taylor conclude from four 6-hr tests that rapid tappet wear is not a break-in problem. We have kept careful records, and the distribution of failures does not support this conclusion. An appreciable percentage of failures occur before delivery of the vehicle, and the bulk of failures occur under 300 miles. Failures beyond 500 miles are rarely encountered. This history has been so consistent that we are suspicious of the authors' technique.

Messrs. Ambrose and Taylor also conclude that hardenable iron lifters have an advantage over chilled iron lifters, and that both are far better than steel. This is an oversimplification of a potentially complex study. The variations in analysis and microstructure alone, not to mention processing and design variables, can show a complete reversal of this conclusion, as I will illustrate later. We have had both success and failure in several specific development programs with each of these materials.

They also found cementite to be abrasive, and excess cementite to be the cause of cam lobe wear. On the other hand, Messrs. Havely, Phalen, and Bunnell found that steel tappets scuff but do not pit, and that, in any case, cam lobes are seldom worn.

Let us look further into this problem. Fig. E shows two supposedly identical steel tappets. One of the tappets is scuffed and the other is pitted. We consider both to be typical failures.

Fig. F shows the cam lobe in cross-section. In most cases, we found that scuffing and pitting result in excessive cam lobe wear, as illustrated.

Fig. G shows the excellent results derived from a change in metallurgical process control, by means of which we developed a considerable amount of the supposedly abrasive cementite on the tappet face.

Fig. H illustrates the microstructure we strive to maintain. It contains a considerable concentration of cementite in a matrix of martensite and austenite.

The type of microstructure shown in Fig. I is functionally acceptable, even though the concentration of cementite is greater than we like.

In the structure of Fig. J, the cementite is nearly continuous and extends from 0.002 to 0.003 in. below the surface. Surprisingly, the wearing properties of this surface are very good. However, this type of microstructure is

Fig. L – Microstructure of experimental tappet showing large graphitic areas in matrix of martensite and carbides

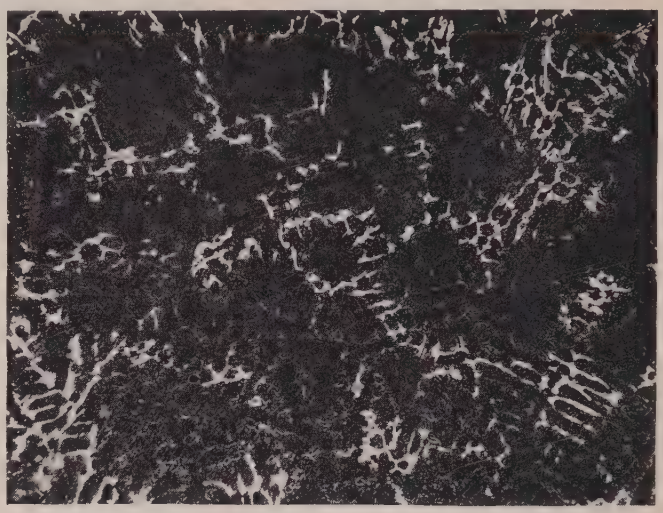

Fig. M – Microstructure of pitted production tappet showing smaller graphite areas and concentrated martensite matrix

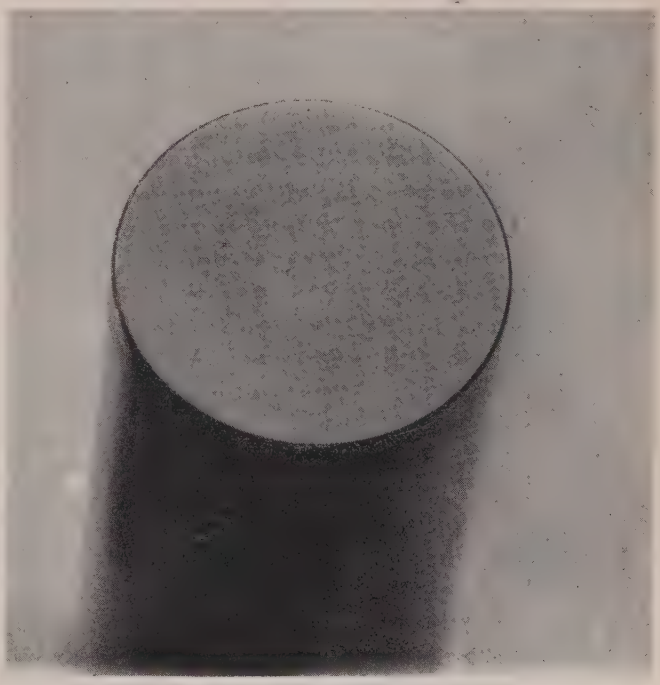

Fig. N – Chilled iron tappet

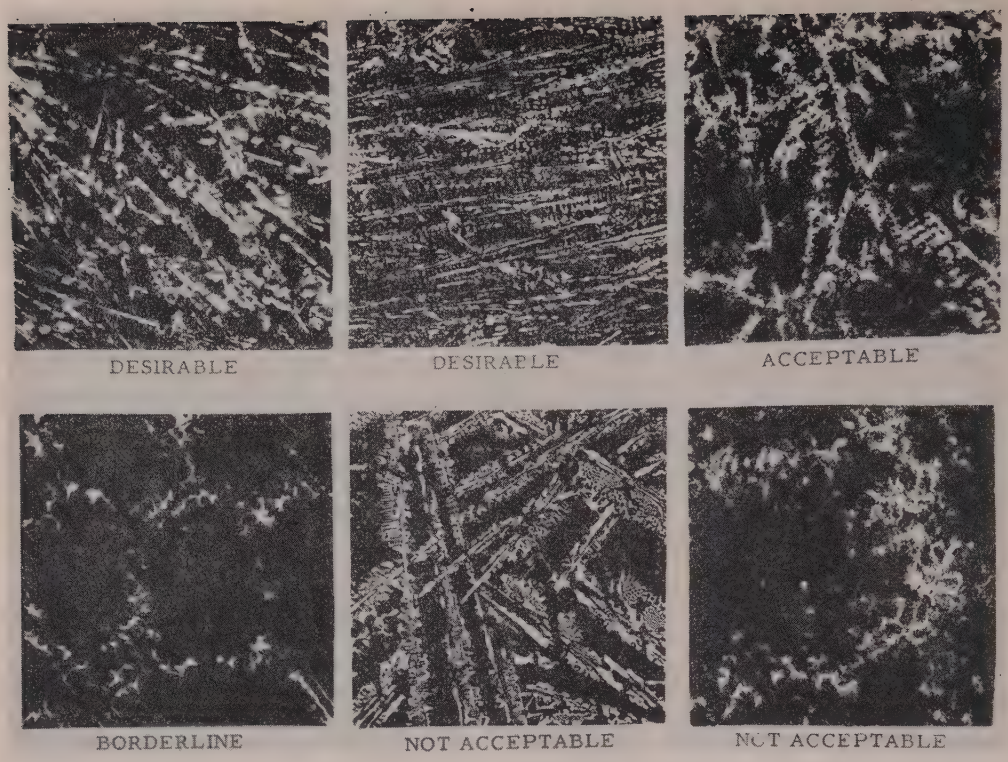

Fig. O – Various kinds of microstructure which can be developed in an unhardened camshaft

unacceptable because of its low impact strength. Let me add that we have worked with steel tappets from three different sources, and we have consistently observed the same results.

Messrs. Havely, Phalen, and Bunnell state that hardenable iron tappets, operating against hardenable iron cams, are subject to scuffing, and that, under certain conditions, pitting may also occur. Fig. K shows two tappets of identical analysis which were tested in the same engine under the same conditions. The one on the left is an experimental tappet, and it shows neither pitting nor scuffing. The one on the right is a production-processed tappet which is badly pitted. Fig. L shows the microstructure of the experimental tappet, in which large graphitic areas are contained in a matrix of martensite and carbides. This tappet was machined from a large slug. Fig. M shows the microstructure of the badly pitted production tappet. The graphite areas are smaller, and the martensitic matrix is concentrated. This tappet was cast closely to size.

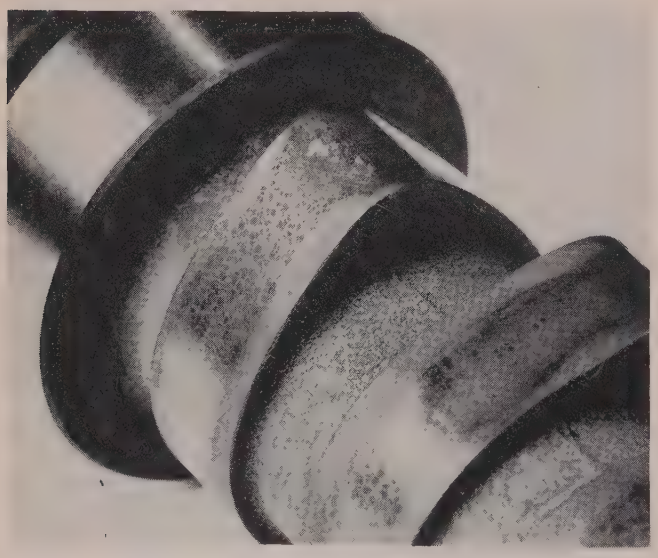

Fig. P – Cam lobe having microstructure shown in lower left corner of Fig. O

We found that the microstructure varied with the rate of cooling. The larger casting resulted in a better microstructure because of its slower cooling rate. By rearranging the analysis, we were able to produce this desirable microstructure in the tappet machined from the smaller slug, with subsequent functional success, as would be expected.

Messrs. Havely, Phalen, and Bunnell also conclude that chilled iron tappets may scuff, pit, or both, and that they are more difficult to lubricate than either steel or hardenable cast iron tappets. This is a contradiction of the conclusion of Messrs. Ambrose and Taylor. Fig. N shows the excellent results that can be achieved with chilled iron tappets. As a matter of fact, our experience has been that, although chilled iron may scuff and pit, we are sure that it takes less effort to develop metallurgical compatibility with chilled iron than with either steel or hardenable iron.

And now for a conclusion of our own and a suggestion to the authors. It is not apparent from either paper that they have considered any cam lobe material other than hardenable iron, and we suggest that they consider unhardened iron. We have found that the hardening process itself introduces variables which are difficult to control, although we have had considerable success with all of the combinations tested by the authors. Fig. O illustrates the various kinds of microstructure which can be developed in an unhardened camshaft. The acceptable microstructures are those in which acicular carbides are evenly dispersed in a matrix of pearlite.

Fig. P shows a cam lobe which has the borderline type of microstructure illustrated in the lower left corner of Fig. O. You will note that the cam nose shows evidences of moderate fatigue. As previously illustrated, small variations in microstructures do not result in destruction of the cam lobe. On the contrary, this iron has high load-carrying ability and self-healing properties. The borderline structure exhibits a tendency toward pitting or surface fatigue, which invariably heals over without affecting the tappet.

Application of Airborne Radar to Airline Operations

Edgar A. Post, United Air Lines

This paper was presented at the SAE National Aeronautic Meeting, Los Angeles, Oct. 7, 1954.

A YEAR ago, we had just completed our technical and operational evaluation of a 5.5-cm airborne weather radar. Members of the flight evaluation team were busy putting together a summary story for presentation before our Flight Operations management on what a radar of this wavelength, designed primarily for weather mapping, would do for airline operations. On March 1, 1954, a detailed report titled "Evaluation of C-Band (5.5-Cm) Airborne Weather Radar" was released covering the flight tests of this radar.

I will cover my subject by first describing very briefly our DC-3 radar installation and explaining how the evaluation program was conducted. I will then cover the operational applications by discussing the conclusions reached as a result of our flight test program and will conclude my paper with a description of a commercial 5.5-cm radar and a discussion of the indicator scope installation and the attention which must be given the scope by a pilot during thunderstorm avoidance operations. I trust those of you who have read our complete report or summaries of this report will bear with me when I draw occasionally from the report in presenting this paper.

Some of you, no doubt, have been asking yourselves the question, "Why did United Air Lines evaluate a 5.5-cm radar?" Let me give you the twofold answer as I see it.

First of all, this evaluation program is typical of the independent development and research programs which are carried on from time to time by United and other scheduled airlines – programs which, in general, are designed to obtain solutions to specific problems facing a given air carrier or, more often, the industry as a whole.

Secondly, with theoretical studies and operational tests of 3- and 10-cm radars indicating that for weather mapping a wavelength somewhere in between would come closer to fulfilling airline weather-mapping radar requirements, United decided it was high time an actual evaluation was made to determine what a radar designed primarily for weather mapping and operating on 5.5 cm would do for airline operations. Before embarking on a multimillion-dollar installation program, we wanted to know if such a radar would permit a pilot to avoid moderate and heavier turbulence, damaging hail, and tornadoes by detouring the hard cores of thunderstorms with small deviations from the flight planned route rather than by wide detours of the entire storm area, and in this process

permit the pilot to see through sufficient heavy rain so that he would not be led blindly into the hard core of a storm.

Description of Aircraft Installation

The RCA experimental 5.5-cm radar, contracted for in October, 1952, was installed in a United DC-3 Cargoliner, which was nicknamed and fondly referred to as "Sir Echo" (Fig. 1). The radome was installed by Douglas Aircraft Co., and the equipment mountings, wiring, wave guide, and the like were installed by United's San Francisco Maintenance Base. The transmitter-receiver unit, synchronizer, and NACA and Ryan gust recorders were installed in the left baggage pit (Fig. 2). The NACA VGH recorder[1] provided a record on photosensitive paper of vertical acceleration, pressure altitude, air speed, and time and event marks. Since the photographic record from this recorder had to be developed and analyzed by NACA, a Ryan recorder was also installed to provide on aluminum foil an immediately available record of acceleration, altitude, air speed, and time and event marks for use in debriefing sessions.

Fig. 1 – Radome installation

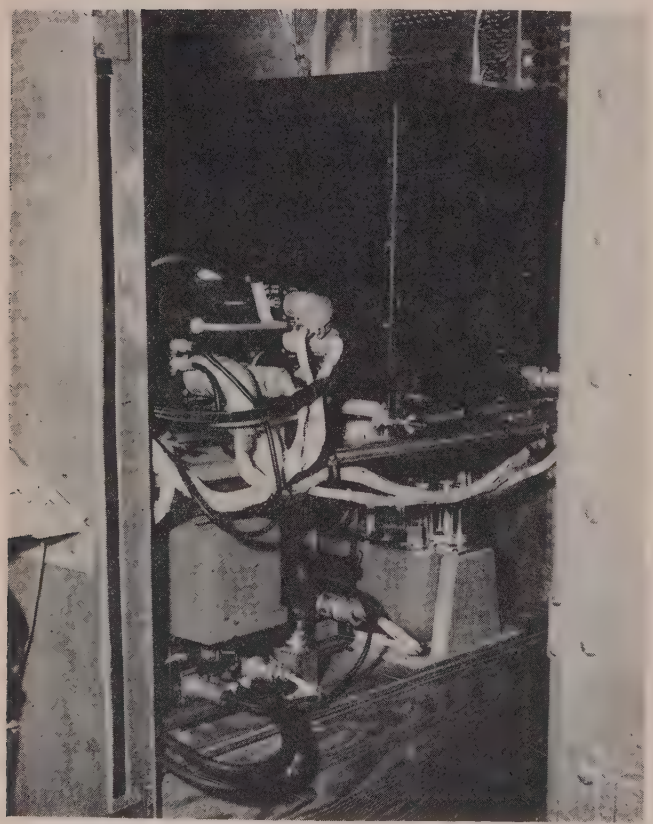

Fig. 2 – Synchronizer and transmitter-receiver units on upper shelf and NACA and Ryan recorders on lower shelf

The radar operator's position was located in the left forward corner of the cabin (Fig. 3). A radar camera and periscope were installed on the radar observer's scope to permit simultaneous viewing and picture taking. A complete set of flight instruments were provided at the observer's position in addition to the radar controls. A second scope was installed in the cockpit between the two pilots and was equipped with a three-eyepiece viewer (Fig. 4).

Both radar scopes were the standard 5-in. diameter military-radar type and presented the radar information as the familiar Plan Position Indication (PPI) display (Fig. 5). In an airborne PPI display, the aircraft is thought of as being at the center of the scope, as shown in Fig. 5, with the antenna cutting horizontal 7½-deg wedge-shaped slices out of the clouds it sweeps through, as shown in Fig. 6. The farther away the storm is, the thicker the slice seen by the radar. Three antenna beams are shown in Fig. 6 to indicate that antenna tilt permits the pilot to select the 7½-deg slice of the storm he wishes to examine.

[1] See NACA Technical Note 2265 (1951), "NACA VGH Recorder," by Norman R. Richardson.

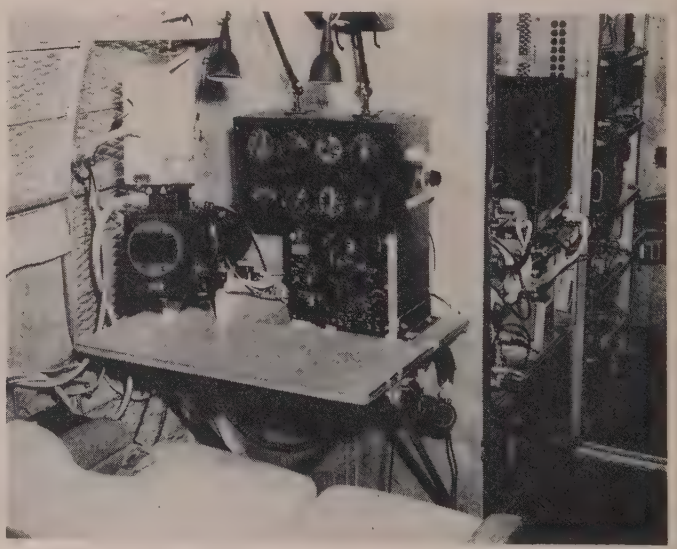

Fig. 3 – Radar observer's position

AN investigation of airborne radar of 5.5-cm wavelength to be used for weather mapping is discussed in this paper.

Results show that radar of this wavelength paints an accurate picture of the weather, thus permitting the pilot to detour a storm area with a minimum increase in flight time or to navigate through a storm while avoiding areas of heaviest turbulence.

In addition, this radar provides warning of hail shafts or tornadoes or of impending collision with terrain; its good terrain-mapping ability enables the pilot to scan an airport area to determine best possible flight paths.

The Author

EDGAR A. POST is superintendent of Navigational Aids at United Air Lines. He graduated with a B.S. in Electrical Engineering from the University of Illinois in 1936. After graduation he joined United Air Lines Communications Laboratory as a field radio engineer. While at United Air Lines he held the positions of radio and communications engineer, assistant and acting superintendent of Aircraft Radio Maintenance, and flight radio engineer. In 1942 he was called to active duty at the Aircraft Radio Laboratory at Wright Field. He returned to United Air Lines in 1945

The antenna installation in the nose of our DC-3 permitted echoes to be seen only in the area 125 deg either side of straight ahead. The concentric circles in Fig. 5 are range marks spaced 2 miles apart. Aircraft movement is always toward the top of the scope, therefore the radar echoes move from the top of the scope toward the bottom while the aircraft is maintaining a constant heading. It has become common practice to refer to the position of radar echoes as "pips" and to identify them in terms of a distance from the center of the display and a clock position. Utilizing this procedure, the cloud echo in Fig. 5 would be referred to as being at 6 to 10 miles centered at twelve-thirty (o'clock) or 12:30.

As shown in Fig. 7, the RCA experimental radar had three ranges: a 10-mile range with 2-mile range marks, a 30-mile range with 5-mile range marks, and a 100-mile range with 25-mile range marks. It will be noted that the 11:30 (eleven-thirty o'clock) echo at 10 miles on the 10-mile range appears closer to the center of the scope on the 30- and 100-mile ranges, although it is the same number of miles from the aircraft, because the range marks have been changed.

Our experimental radar was equipped with isoecho contour circuitry as an aid in locating the areas of most rapid change in precipitation rate. Fig. 8 shows what happens to a simple precipitation echo when the isocircuitry is turned on. For all practical purposes this circuitry displays two rates of rainfall: the lighter rate defined by the outer edge of the echo and the heavier rate by the outer edge of the iso hole.

Evaluation Flight Procedures

Unlike previous thunderstorm probing research by the Thunderstorm Project, American Airlines and the Navy, where pilots went out of their way to find trouble by flying through the cores of thunderstorms, Sir Echo and his crew started out in June, 1953, to prove that thunderstorm conditions could be flown without getting into trouble; "trouble" in this case meaning heavy turbulence, damaging hail, and tornadoes. We knew from previous experience and research that the hard cores

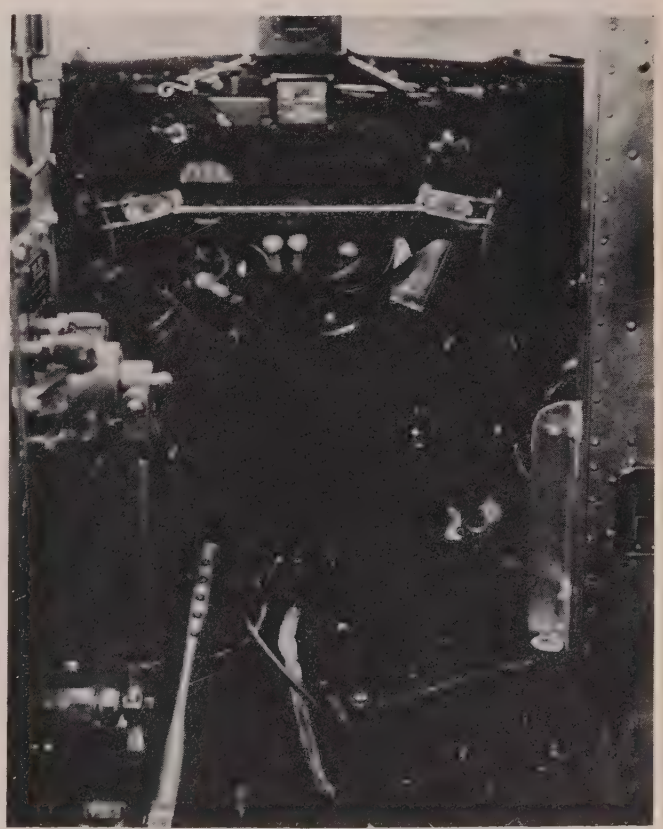

Fig. 4 – Cockpit scope with triple-view hood

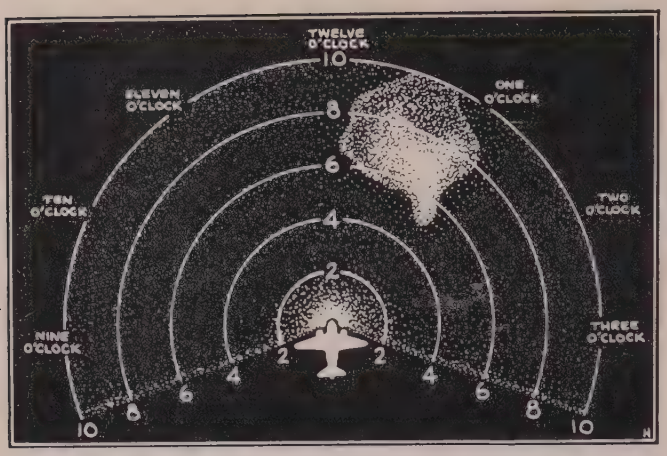

Fig. 5 – PPI scope presentation

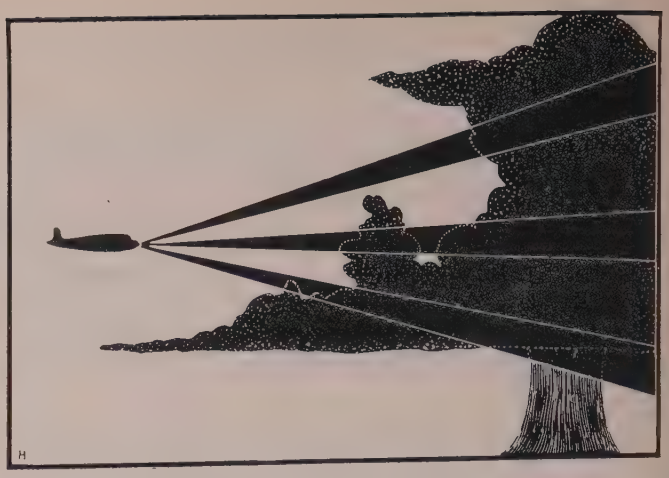

Fig. 6 – Radar beam cutting slices through cloud

of thunderstorms were to be avoided and, from the work done by American Airlines, that heavy turbulence is usually associated with areas of most rapid change in precipitation rate. With isoecho contour circuitry designed specifically to identify these storm areas, we looked forward with confidence to the task ahead.

Operations were conducted out of Denver, and each morning during the evaluation program, the day's weather analysis was discussed by the Captain, Weather Adviser, and Flight Coordinator before a plan of operation was formulated. Flights were usually planned with the goal of having the aircraft arrive in the expected thunderstorm area as the storms were developing.

The flight evaluation team included the Captain, the First Officer, Weather Observer, and Flight Evaluation Coordinator. The cockpit scope permitted the first three crew members to make rapid and continuous comparisons of visual cloud appearances with the radar scope presentations. Notes on these comparisons were logged by the Weather Observer, who also kept a detailed weather log and took Polaroid and 16-mm colored moving pictures of cloud exteriors. The Flight Evaluation Coordinator, in addition to operating the radar, took radar pictures and maintained a detailed log of the settings of the radar controls for use in studying radar photographs during debriefing sessions and in preparing the final report.

The flight evaluation team and Meteorological Adviser met in debriefing sessions following operational evaluation flights, at which time radar-scope photograph negatives were projected and studied and correlated with radar and weather logs, flight tracks, cloud pictures, weather maps, Ryan gust recordings, and personal opinions.

The flight evaluation program began on schedule

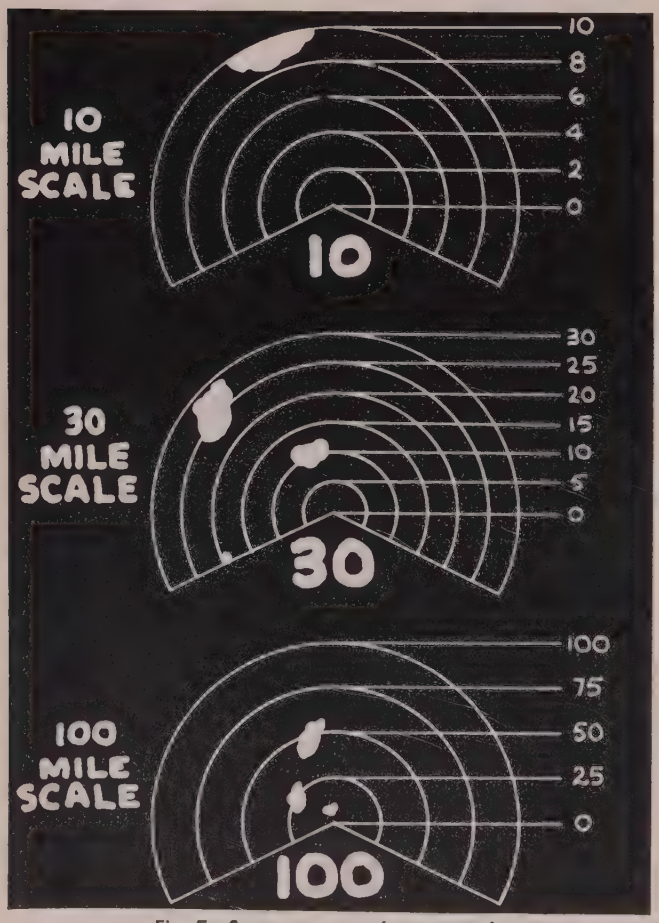

Fig. 7 – Scope ranges and range marks

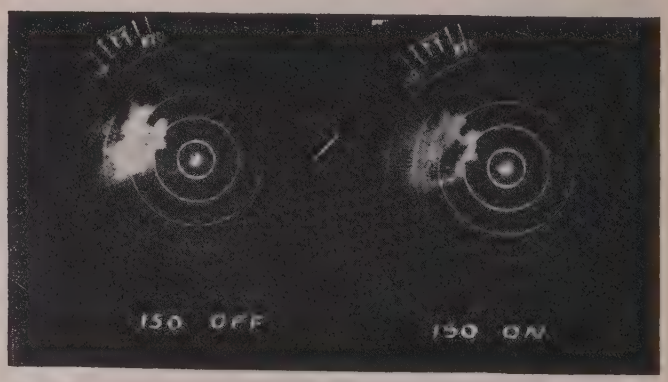

Fig. 8 – Precipitation echoes

on June 1, 1953 and in the next four months 40 technical and operational flights were made totaling 133 hr of flying, 80 of which were in the immediate vicinity of or through corridors of thunderstorms. More than 6000 radar-scope photographs were taken, and over 2500 representative radar and cloud pictures were cataloged in two large albums.

Denver turned out to be a most desirable base of operations that could have been selected, for during the evaluation an abundance of thunderstorms were available within less than 90 min flying time which permitted a sampling of all types of thunderstorms (Fig. 9) except the hurricane and true nocturnal. From a radar evaluation standpoint, we were fortunate to find associated with the thunderstorms we flew more than a normal amount of hail, five cases of known tornadoes, and four cases of cloudburst or near cloudburst rain. As an example of what we found within an hour's flying of Denver, on the afternoon of June 7 there were 50 confirmed tornadoes along and near the mainline airway between Denver and Des Moines.

Now that we've had a quick look at how the United 5.5-cm radar evaluation was conducted, let us take a brief look at the operational conclusions which were drawn from this evaluation.

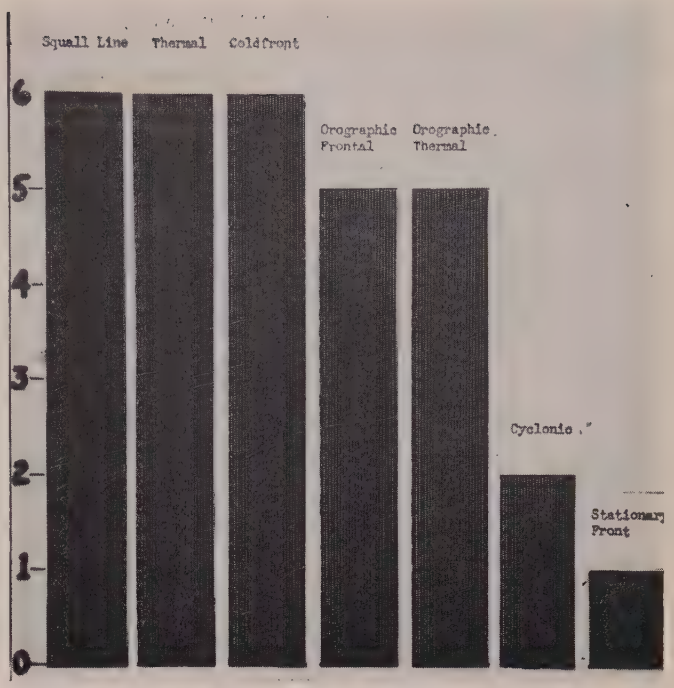

Fig. 9 – Type and number of thunderstorms probed

Operational Conclusions

1. It is a very useful device for safer and smoother navigation of thunderstorm and precipitation areas and will permit a pilot to avoid moderate and heavier turbulence associated with these areas, usually by detours in the order of 5 miles or less from the planned flight path.

2. It will penetrate 15 miles or more of heavy rain equal to or greater than 60 mm per hr and will not lead a pilot blindly into the hard core of a storm (Fig. 10).

3. It provides a satisfactory warning of hail shafts.

4. Even though we were unable to look at a radar picture and say, "Here is a tornado," there is considerable indirect evidence provided by the radar scope which will permit the pilot to avoid these violent storms merely by exercising ordinary good judgment in detouring sharp edged echoes and – probably more important – in being highly suspicious of any fingerlike projections from such echoes.

5. Using the "safety-circle" technique, this radar provides a method of avoiding collisions with ter-

Fig. 10 – Penetration of heavy rain, 5-mile range marks

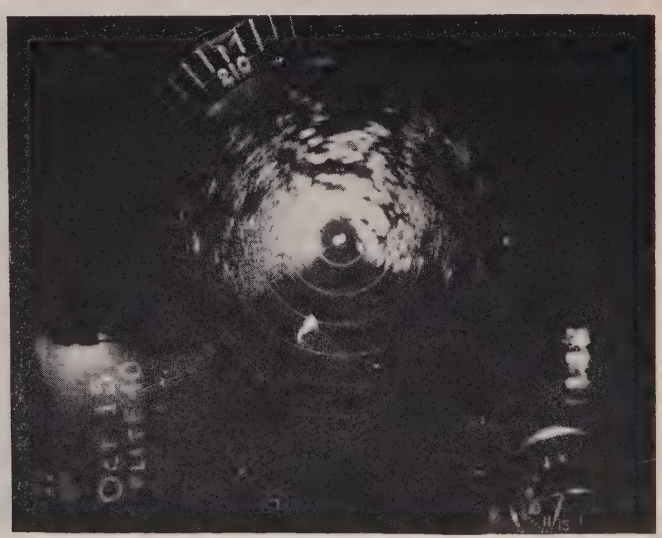

Fig. 11 – Mountainous terrain, 5-mile range marks

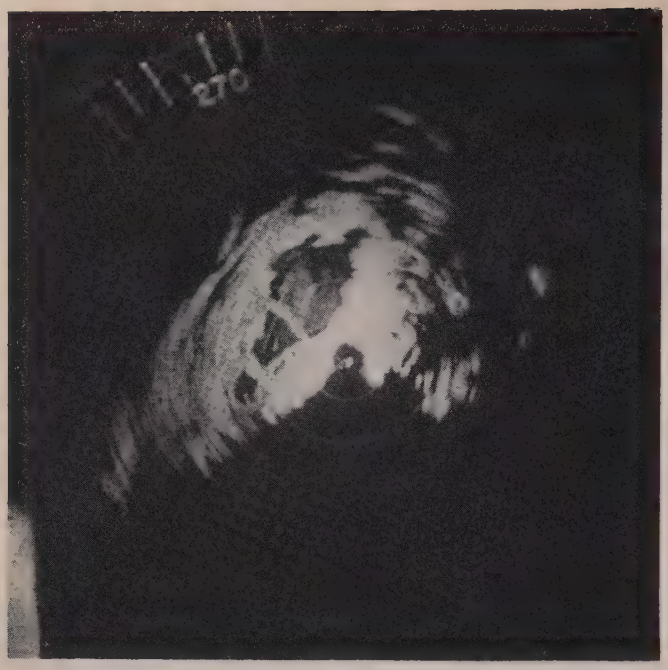

Fig. 12 – Over Oakland ILS outer marker headed west; bay area ahead and to left

rain (Fig. 11). Antenna pitch stabilization is required when using this technique.

6. Terrain mapping capability of this radar is good (Fig. 12).

7. Separation of storm and terrain echoes is feasible without added complexity of circular polarization (Fig. 13). Circular polarization is of no value for distinguishing between hail and rain.

8. The radar has very little, if any, application in avoidance of other aircraft.

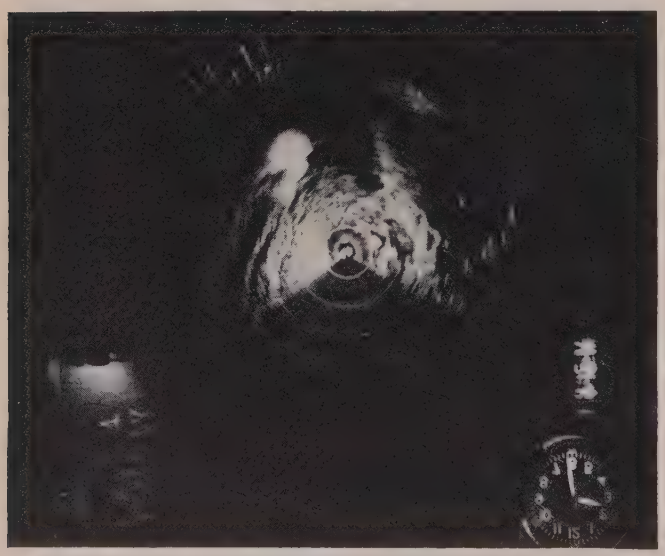

Fig. 13 – Cloud and terrain echoes

Table 1 – Subjective Observations of Turbulence by Weather Observer

Type	Number	Percentage
Smooth	320	55
Slightly rough at times	163	28
Slightly rough	63	11
Moderately rough	34	5.7
Rough	2	0.3
Total	582	100

9. Isoecho contour circuitry is essential for determining which corridors in storm areas may be flown through with safety.

10. The scope display, while not bright enough for all conditions even though a hood was used, is usable until bright storage tubes are in production. The bright storage tube display must be capable of halftone reproduction.

11. Roll and pitch antenna stabilization are necessary to give a stable presentation devoid of serious intermittent ground mapping when observing weather echoes in rough air and to provide a satisfactory display for use of safety-circle techniques for terrain avoidance.

12. A 22-in. antenna provides adequate definition and justifies the installation of radar in aircraft which cannot accommodate a larger antenna.

While we may dispense with most of the just-mentioned conclusions without further explanation, turbulence avoidance and hail detection require additional discussion.

Turbulence

On the subject of turbulence, I wish to point out that during the 31 flights operated under actual storm conditions in close proximity to storm cells, including circumnavigation, VFR traverses under the bases, and IFR penetration through storm clouds, the maximum acceleration recorded by the NACA gust recorder was $-0.97g$. The maximum acceleration recorded on the Ryan recorder during a flight prior to the time the NACA recorder was operative was $1.3g$, which is equivalent to $1.14g$ on the NACA.

Of the 582 subjective observations logged by the weather observer at intervals of 5 to 10 min during the tests, 94% indicated smooth or slightly rough air as shown in Table 1. Only 5.7% were logged as moderately rough and 0.3% as rough. Considering the fact that these observations include those taken in areas where we expected to encounter some rough air, I feel you will agree that this record speaks for itself.

A cursory examination of the gust data derived by NACA from NACA VGH recordings, which were received on July 16, 1954, confirms the above subjective turbulence observations. These gust

data were derived by reading the individual acceleration peaks and the associated air speed and altitude to determine the "derived" gust velocities U_{de} above a 10-fps threshold. The formula below was used to calculate the derived gust velocities as defined by Pratt.[2] These velocities are 50 to 70% larger than the gust velocities computed according to the "effective" gust velocity U_e scale used in past radar evaluations.[3]

$$U_{de} = \frac{2 \Delta n W}{1.47\, m\, \rho_o\, S\, V_e\, K_g}$$

where:

U_{de} = Derived gust velocity, fps
W = Airplane weight, lb
S = Wing area, sq ft
m = Slope of wing lift curve per radian
g = Acceleration due to gravity, ft per sec per sec
$\bar{c}$ = Mean geometric chord, ft
ρ = Mass density of air, slugs per cu ft
ρ_o = Mass density of air at sea level, slugs per cu ft
Δn = Normal-acceleration increment, g units
u_g = Airplane mass ratio, $\dfrac{2W}{\rho m g \bar{c} S}$
K_g = Gust factor (function of u_g) defined by Pratt[2]
V_e = Equivalent airspeed, mph

From the NACA gust data, discussed above, we find that the maximum derived gust velocities encountered during the 35 hr the NACA recorder was in operation were −33.7, −25.2, and +23.9 fps, and the accelerations associated with these gusts were −0.97, −0.67 and +0.78g respectively.

Although the reproduction deadline for this paper prevented any detailed analysis of the NACA gust data, the gust values were tabulated in 1-fps brackets with the results shown in Table 2.

Dividing the computed number of miles flown (4350) during the 35 hr the NACA acceleration data were taken by the number of gusts in each bracket provided points for a curve which indicates the average number of miles flown to exceed a given gust velocity, as shown in Fig. 14. Effective gust velocities (U_e) are also plotted on Fig. 14 and were obtained by dividing the U_{de} figures by 1.6.

The 35 hr of recordings taken with the NACA recorder were taken for the most part while in the immediate vicinity of thunderstorms with the recorder turned off while flying cross-country to and from the storm areas. Although some of the NACA recorded flying was done at distances greater than 5 miles from storm echoes, a great deal was done at distances considerably less; and some flights

Table 2 – NACA Gust Data

Gust Velocity, fps	No. of Gusts Encountered	Gust Velocity, fps	No. of Gusts Encountered
10 – 11	281	18 – 19	11
11 – 12	160	19 – 20	6
12 – 13	101	20 – 21	4
13 – 14	50	21 – 22	2
14 – 15	54	23 – 24	1
15 – 16	28	25 – 26	1
16 – 17	25	33 – 34	1
17 – 18	13		

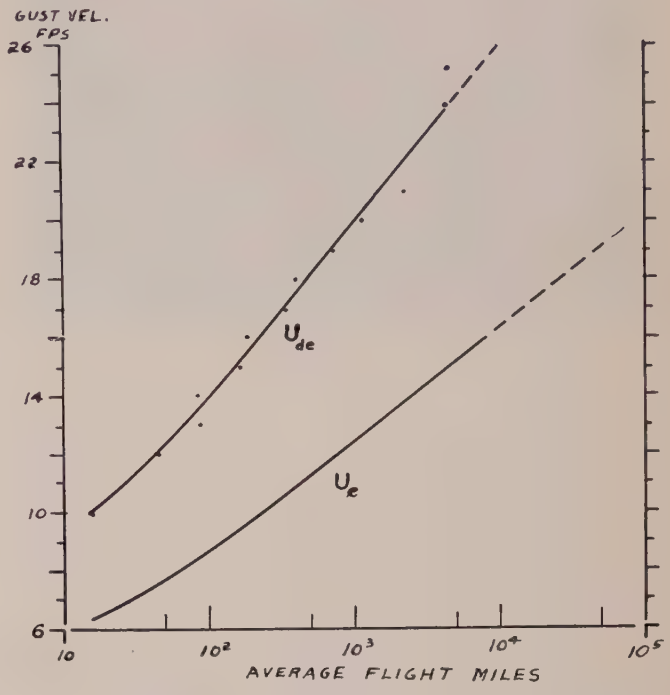

Fig. 14 – Average number of miles flown by UAL to exceed a given gust velocity

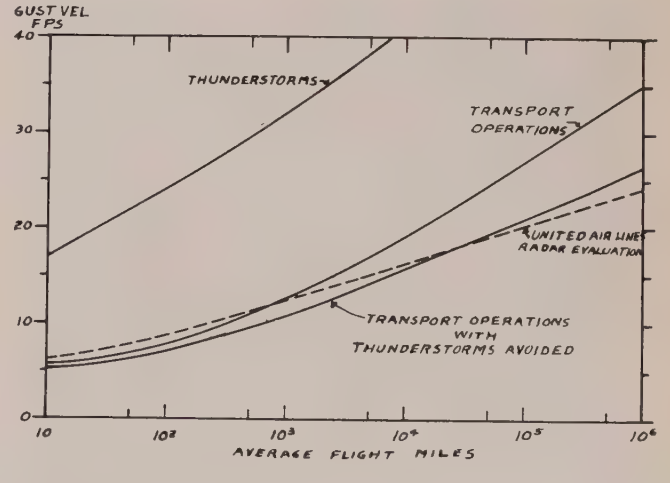

Fig. 15 – Comparisons of gust experience for transport operations with and without thunderstorm flying with UAL thunderstorm experience using radar

[2] See NACA Technical Note 2964 (1953), "A Revised Formula for the Calculation of Gust Loads," by Kermitt G. Pratt.

[3] See American Airlines Flight Engineering Navy Bureau of Aeronautics Contract No. a(s) 9006, Final Report on Task No. 1, 1949, "Development of an Airborne Radar Method of Avoiding Severe Turbulence and Heavy Precipitation in Precipitation Areas of Thunderstorms and Line Squalls."

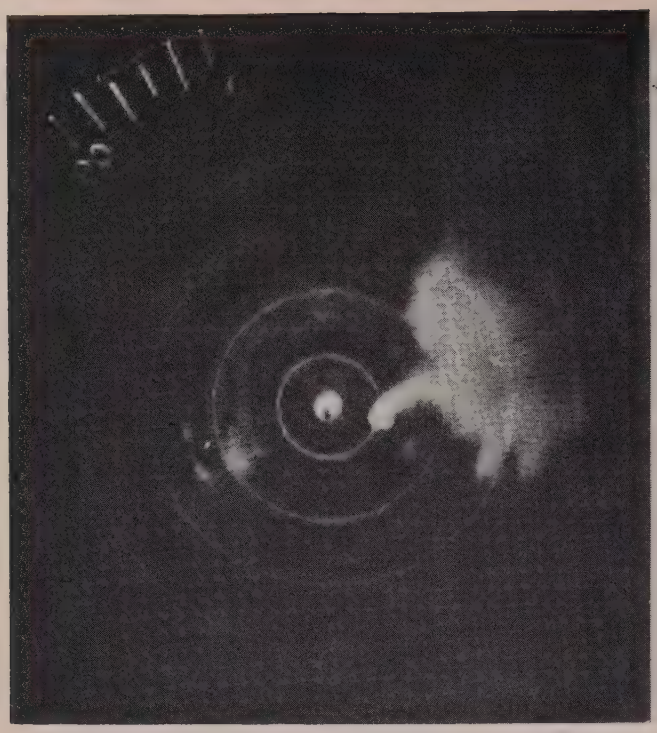

Fig. 16 – Hail echo picture with finger present

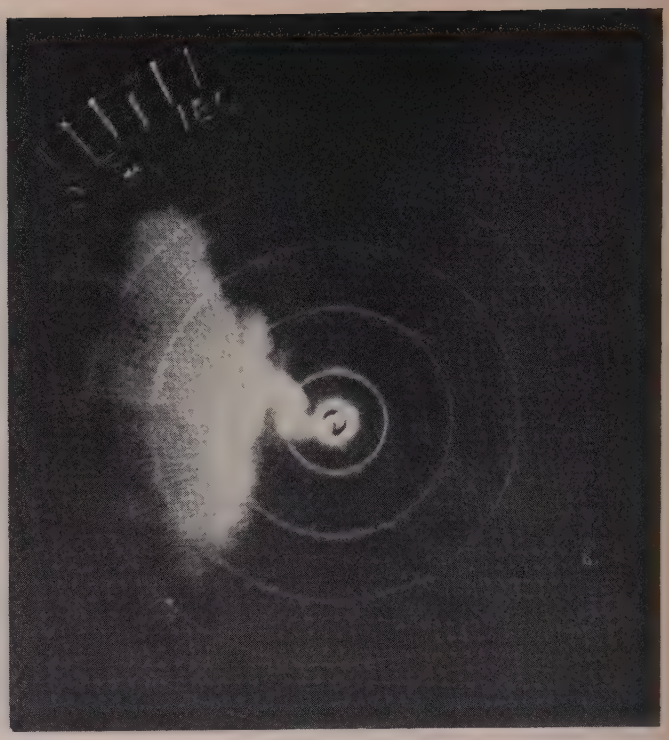

Fig. 17 – Hail echo picture with hooked finger present

were actually made through the nondangerous portions of the echoes as determined from the radar. Some flights were even made in storm areas where considerable turbulence could be expected, just to confirm radar indications; and our gust experience is, therefore, higher than would probably be expected from passenger operations where turbulent areas would be given as wide a berth as practical.

Thus while Fig. 14 includes more and heavier gusts than would probably be encountered in conservative passenger operations, the U_e values fall about where they would be expected when plotted on the curves developed by H. B. Tolefson of the Langley Aeronautical Laboratory.[4] Except for the United data, Fig. 15 is a copy of Fig. 2 from Mr. Tolefson's report.[4]

The left portion of the United curve in Fig. 15 lies above the "Transport Operations" curves, as expected, because practically all the United acceleration records were taken in thunderstorm areas. Since radar was being used to avoid moderate and

[4] See Bulletin of the American Meteorological Society, May, 1953, "Some Possible Reductions in Gust Loads through Use of Radar in Transport Airplanes," by H. B. Tolefson, Langley Aeronautical Laboratory.

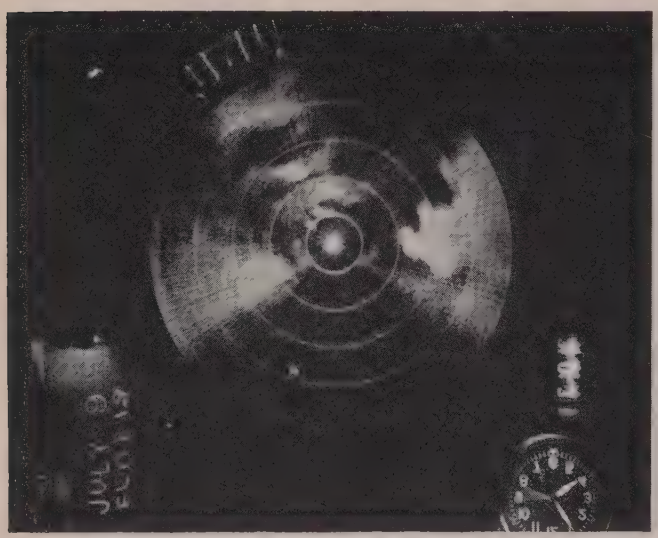

Fig. 18– Hail echo picture with scalloped edge present

Fig. 19 – Hail echo picture with U-shape present

heavier thunderstorm turbulence in most cases, it is significant that the United curve crosses the "Transport Operations" gust curve at 12 fps and the "Transport Operations with Thunderstorms Avoided" curve at 17.5 fps. In other words, Mr. Tolefson's "Thunderstorms Avoided Curve" is conservatively realistic, and a new curve lying below both transport operations curves in Fig. 15 could very probably be drawn for transport operations equipped with weather radar. A more detailed study of our gust data, I believe, will show this to be true.

Hail

Prior to our evaluation program, attempts to detect hail were completely unsuccessful. I, therefore, feel that our conclusion, "It provides a satisfactory warning of hail shafts," is very significant and needs further explanation. Out of 31 thunderstorm flights, 23 encountered hail, saw it, or received ground reports of it. We are confident that no other radar project has ever collected a more comprehensive set of hail pictures. Out of our catalog of hundreds of pictures, we selected 84 to study in detail as representative examples. Of those 84 echoes, a finger (Fig. 16) or a hook (Fig. 17) or both were present in 82. Fig. 18 shows the presence of a scalloped edge, and Fig. 19 shows the presence of a U-shape. Table 3 provides a more complete analysis of our hail experience.

Table 3 – Summary of Hail Echoes as Displayed by RCA Prototype C-Band Radar, June to August, 1953

Echo Forms	Number	Percentage
Hail echo pictures analyzed in detail	84	100
Hail echo pictures with finger or hook present	82	98
Hail echo pictures with finger present	67	80
Hail echo pictures with hook present	57	68
Hail echo pictures with scalloped edges present	32	38
Hail echo pictures with prominent U-shape	25	30
Intensity of Hail Echoes	**Number**	**Percentage**
Weak	4	5
Moderate	31	37
Strong	49	58
Sharp isoecho contour	55	65
Sources of Hail Observations	**Number**	**Percentage**
White patch or streak observed on ground	25	30
Photographed or logged by weather observer on plane	18	21
Observed on windshield of plane	31	37
Reported on ground	10	12

Comparisons with Other Radars

The United evaluation team was interested in comparing our 5.5-cm radar with other radars operating on shorter and longer wavelengths, and we were fortunate in being able to make three comparisons: the first with a Weather Bureau 10-cm ground radar, the second with an airborne APS-42 3.2-cm radar, and the third with an Air Defense Command radar. Since only a single flight was conducted with each type, comparisons were not conclusive, but each turned up information of interest.

At North Platte, one member of the group stayed on the ground to watch the Weather Bureau 10-cm scope while Sir Echo flew overhead, around and through the thunderstorms in the area. Fig. 20 shows the radar echoes seen by Sir Echo and closely confirmed by the Weather Bureau. These echoes were masked by the nearly solid more than 100-mile bank of clouds lying southeast of North Platte (Fig. 21).

Another ground comparison was made with an Air Defense radar. During this comparison, two members of the evaluation team stayed on the ground to view the Air Defense scope and sketch echoes while Sir Echo flew overhead. The echoes on the two scopes were nearly identical, although United actually painted more detail than Air Defense, but this was to be expected because it was closer to the precipitation. No opportunity was afforded to study the Air Defense scope displays of distant precipitation echoes.

Observations of weather echoes on the ground radar scopes lead us to conclude that, while these radars would show severe storms at distances of 100 miles or more, the resolution with their larger antennas is not sufficient to permit ground operators to vector aircraft through narrow corridors between storms when the storms are more than 40 or 50 miles distant. Air Defense controllers confirmed this thinking by informing us that their vectoring service consisted of steering pilots around storms and storm lines and not through them. Thus, we may conclude that ground radar is primarily an effective tool for giving pilots the broad picture but does not provide sufficient detail,

Fig. 20 – North Platte storm echoes, 25-mile range marks

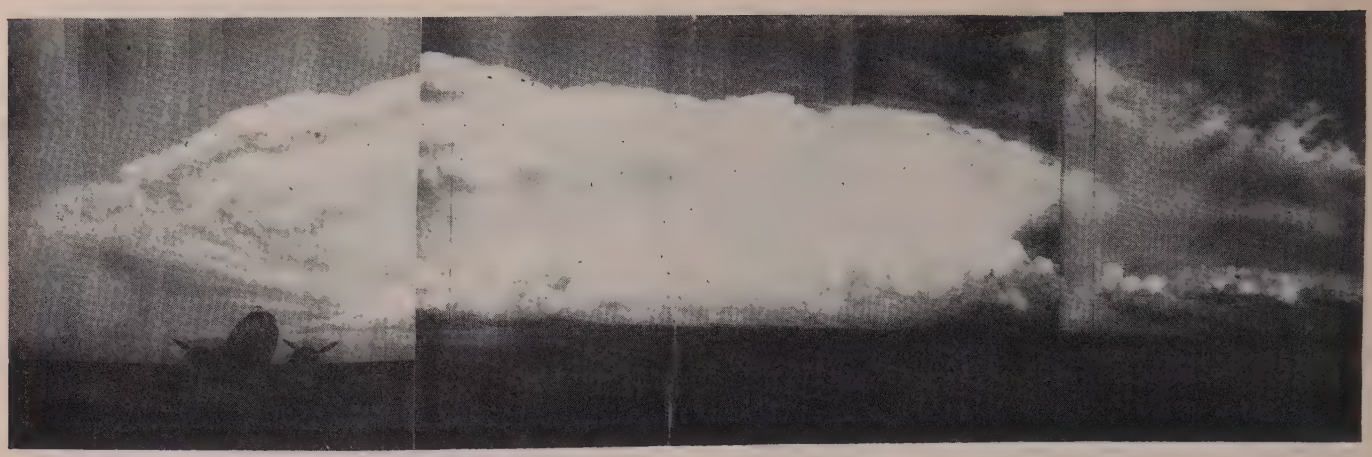

Fig. 21 – Picture of storm southeast of North Platte taken 35 min before scope picture in Fig. 20

particularly on distant echoes, to permit them to be steered through narrow corridors in lines or clusters of thunderstorms. Obviously, airport surveillance radars and other ground radars can be used at short ranges for vectoring aircraft through corridors, but it is impractical from an economic point of view to locate ground radars close enough to provide corridor vectoring service along all airways. A very complicated communications problem would also be presented by such a network of radar stations.

Our third comparison was with an APS-42 3-cm radar installed in a Navy R5D. The most amazing thing about this comparison flight was the weather itself. Unscheduled and unpremeditated, this follow-the-leader flight was set up on the morning of August 9, when there wasn't a cloud in the sky within 300 miles of Denver. That afternoon, within an hour's flying of Denver, an 8-in. cloudburst occurred between Flagler and Burlington which put the Rock Island Railroad tracks under water, washed out highway bridges, and inundated whole ranching communities. Hail fell in several spots. Fig. 22 is one of the pictures taken aboard Sir Echo that afternoon showing a North-South line of storms 140 miles long. This was the longest line of storms brought within view of our scope during the whole summer season.

Although many pictures were taken, I will show only a couple of examples of 5.5- and 3.2-cm comparative radar pictures. The pair in Fig. 23 illustrates overpainting by the 3.2-cm radar picture on the right. Note that where 3.2 cm shows a strong echo ahead and to the left, 5.5 cm paints in only harmless fuzzy, which we had found from experience could be flown through with no difficulty.

In the pair of pictures in Fig. 24, 3.2-cm radar

Fig. 22 – 140-mile line of storms

Fig. 23 – Comparison of 5.5-cm (left) and 3.2-cm (right) pictures taken at same time. Note how 3.2 cm paints large and fairly heavy return where 5.5-cm shows only light rain

Fig. 24 – Comparison of 5.5-cm (left) and 3.2-cm (right) pictures taken at same time with both aircraft in light rain. Big echo on left seems completely distorted on 3.2-cm scope

echoes in the right picture are being attenuated along the left side, and detail is lost in the back of the echo. We found evidence of this in other pictures taken on the flight, and this characteristic is supported not only by earlier 3.2-cm observations made by American Airlines and the Navy but also by simultaneous 3.2- and 10-cm ground observations made by Hal Foster of M.I.T.[5]

I am convinced from our experience as well as the experience of others that if you do not want to be misled by airborne radar weather indications, you had better use a wavelength of 5.5 cm rather than 3.2 cm. Of course, if you plan to avoid all storms by flying around them, 3.2 cm will help you do that.

5.5-cm Commercial Weather Penetration Radar

When asked to prepare this paper, I was requested to describe an airborne radar system. While this could be accomplished by reading the details of the Airline Electronic Engineering Committee's 5.5-cm Weather Penetration Airborne Radar Characteristics, I will instead describe the system being built by RCA to meet these characteristics. A quite similar system, which will be interchangeable electrically and mechanically but operating on a 3.2-cm wavelength, is being built by Bendix Radio Corp. I have selected the RCA system because it operates on 5.5 cm, the wavelength I feel is required for airborne weather radar operations.

The RCA system is made up of five major units for a single-scope installation (six units in a two-scope installation). Total weight of the components is approximately 140 lb with installed weight estimates running from 175 to 200 lb, which, incidentally, do not include weight of additional or larger inverters if they are necessary to provide the radar power. The equipment requires approximately 1000 w of a-c power and 30 w of d-c. 600 va of the a-c power must be 115 v ±5%, 380 to 420 cycles; and the remaining 400 va may be 115 v ±10%, 300 to 1000 cycles.

Figs. 25-30 were furnished through the courtesy of RCA.

Fig. 25 shows the 25-lb antenna with a 22-in.

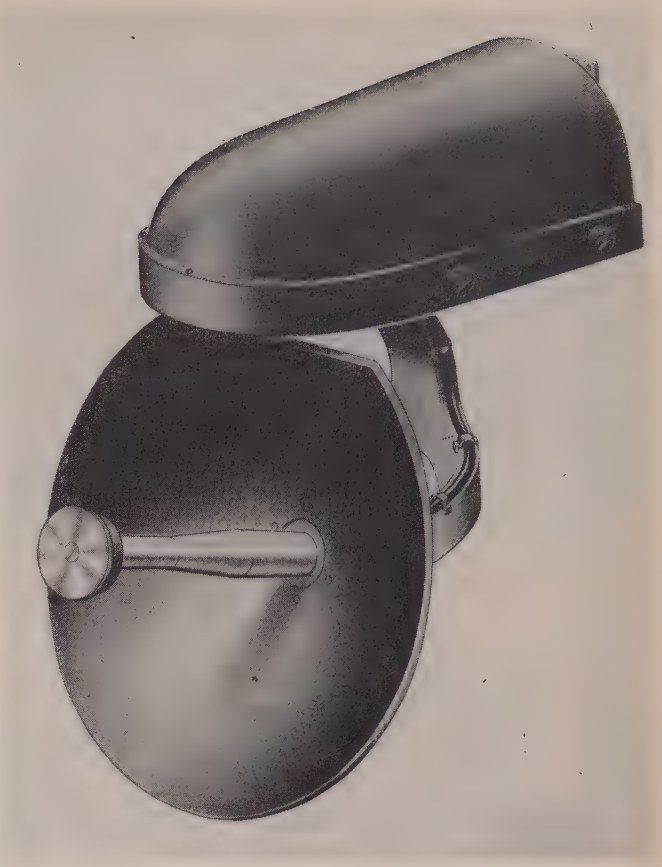

Fig. 25 – Radar antenna

[5] See M.I.T. Technical Report No. 20 (November, 1952), "The Use of Radar in Weather Forecasting with Particular Reference to Radar Set AN/CPS-9," by Hal Foster.

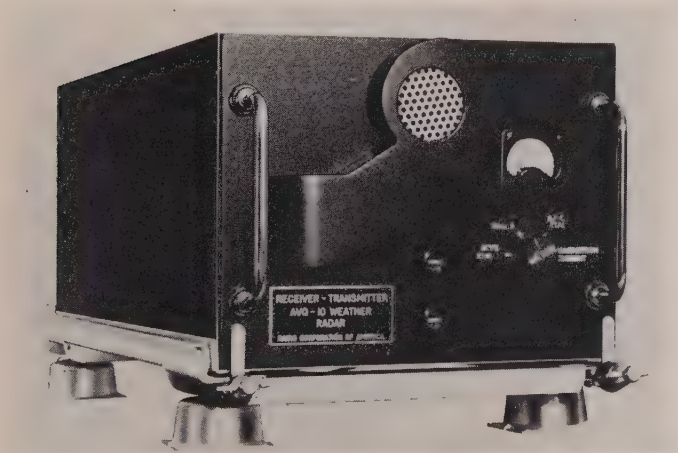

Fig. 26 – Transmitter-receiver unit

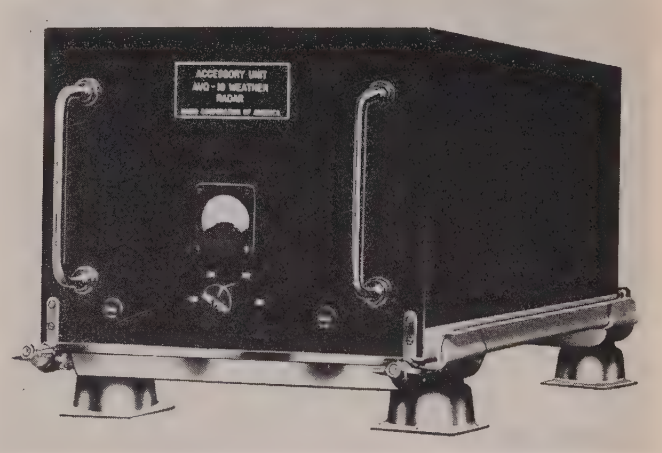

Fig. 27 – Accessory unit

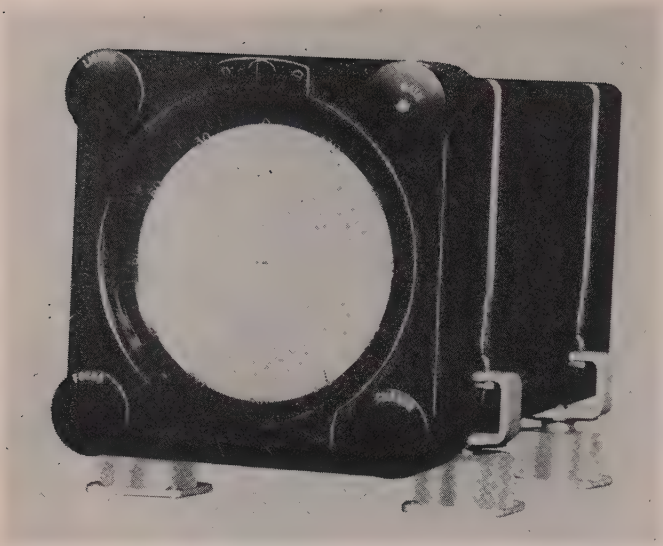

Fig. 28 – Indicator scope

parabolic dish which will give a 7-deg beam width. A 22 x 30-in. elliptical dish can also be used with this antenna mount to give a 5.4-deg horizontal beam width. The antenna is stabilized in roll and pitch, will rotate through 360 deg at 15 rpm, and can be tilted up 10 deg and down 15 deg. Gyro signals from an autopilot, if installed, may be used for antenna stabilization. A maximum of 30 ft of waveguide may be used between the antenna and the transmitter-receiver units.

Figs. 26 and 27 show the transmitter-receiver and accessory units, which weigh 60 and 33 lb respectively. Each unit is 10⅛ in. wide, 19 9/16 in. long, and 7⅝ in. high; and all connections, including a wave guide, are made through connectors at the rear of the units. These units are self-cooling, although apertures are provided for use in aircraft which will use forced-air cooling. Since most of the 1000 w of power consumed by the radar is dissipated in these two units, it is anticipated that the installation of these units in the radio rack will require the use of forced cooling in most aircraft installations.

Fig. 28 shows the indicator scope which is approximately 6¼ in. square by 13½ in. long and uses a standard 5-in. 5FP7A cathode-ray tube. This version is provided with focus, intensity, height, and cursor controls, and the display is a centered PPI type. I envision the production indicator we expect to install will use an off-centered PPI display to make better use of the scope area, with fixed lines radiating from the aircraft's position on the scope (Fig. 29).

Controls have been simplified as much as possible, as shown in Fig. 30. This panel is only 3⅜ x 5¾ x 4½ in. This version carries function (iso-echo), contour and stabilization switches plus tilt and gain controls.

Indicator Scope Installation and Use

Illumination of existing-type cathode-ray tubes is adequate for operation in the cockpit without a hood only during night conditions. During daylight operations, a hood is required in order to permit the observer's eyes to become adjusted to the low light intensities presented on the scope. In view of this fact and until the bright storage display tube becomes available, the scope should be located beside the pilot's seat so that it may be used with a hood and viewed with the pilot's eyes not more than 18 to 20 in. from the scope face. One bright-storage-type display located in the center of the instrument panel will probably be adequate for both pilot and copilot. Until the bright display becomes available, we plan a separate scope for pilot and copilot use.

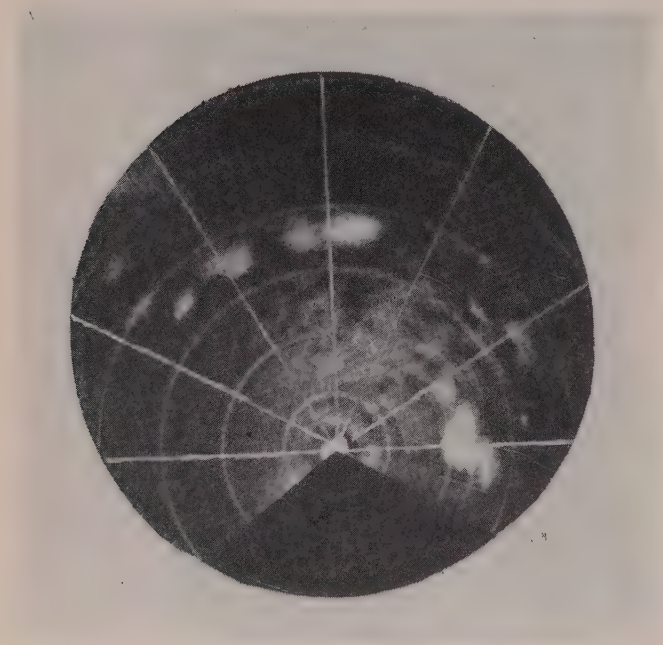

Fig. 29 – Off-centered PPI indicator display

Fig. 30 – Control panel

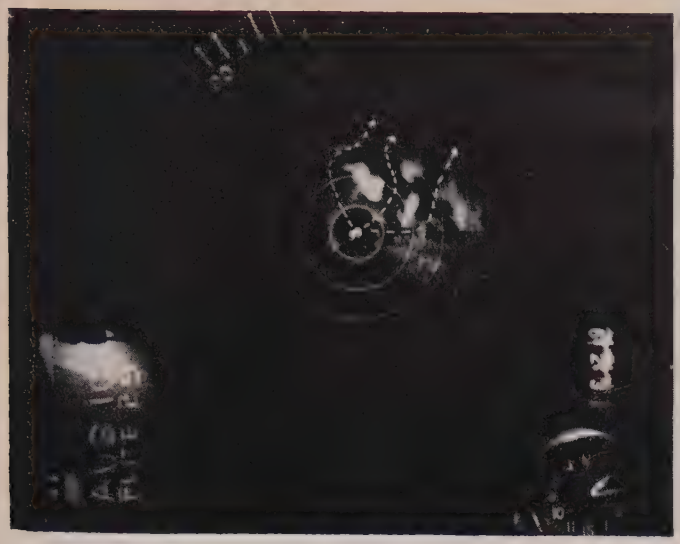

Fig. 31 – Selecting corridor between storm cores

Fig. 32 – Possible departure or arrival routes between storm cores

It is my belief that it is the characteristics of the present-type scope tube that call for almost continuous pilot attention while flying through thunderstorm corridors. A bright storage tube should reduce the attention required. It is the general feeling of those who participated in the United evaluation program that, when actually engaged in the process of penetrating a line of storms, particularly through narrow corridors, one crew member should devote most or all of his time to observing the scope, directing the other crew member where to fly. If an autopilot is being used, the pilot doing the radar observing can also fly the airplane.

Since most storm lines are not very wide when penetrated perpendicularly, the period of time during which one crew member would be devoting most of his time to the radar would be limited, and, therefore, we do not envision any need for a third crew member to maintain the radar watch. Normally, the corridors between storm cores are quite wide, in which case very close attention to the scope is not necessary. This point of view, incidentally, applies to the use of either the present-type display or the future bright-tube display.

Summary

In outlining the United evaluation program and its results and conclusions, I have covered the operational applications of airborne radar. In order that they will stand out better in your memory, let me summarize them for you by answering the question, "What exactly can the pilot do with radar that he hasn't been able to do before?"

1. He can detour a *storm* area after having scanned it from over 75 or more miles away, thus giving him the opportunity to instigate a detour at a point where his flight time will be increased very little.

2. He can *choose* a corridor of the mildest activity or turbulence if penetration of a storm area is desirable or necessary (Fig. 31). Normally a suitable corridor can be found without departing more than 5 miles from the planned flight path.

3. He can scan the *area* around an airport, before taking off or landing, to determine the best possible flight path out of or into that airport (Fig. 32).

4. He can establish his position relative to high terrain or easily distinguishable ground features (Fig. 33).

5. He can give valuable *information* to other

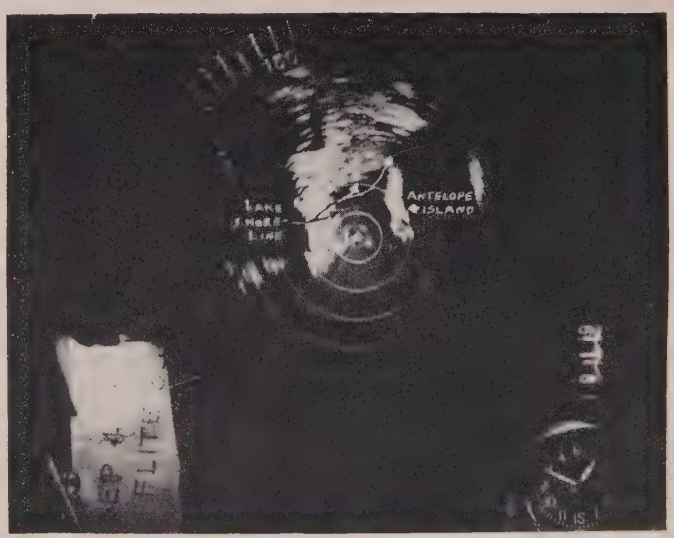

Fig. 33 – Salt Lake Valley looking south from Layton fan marker

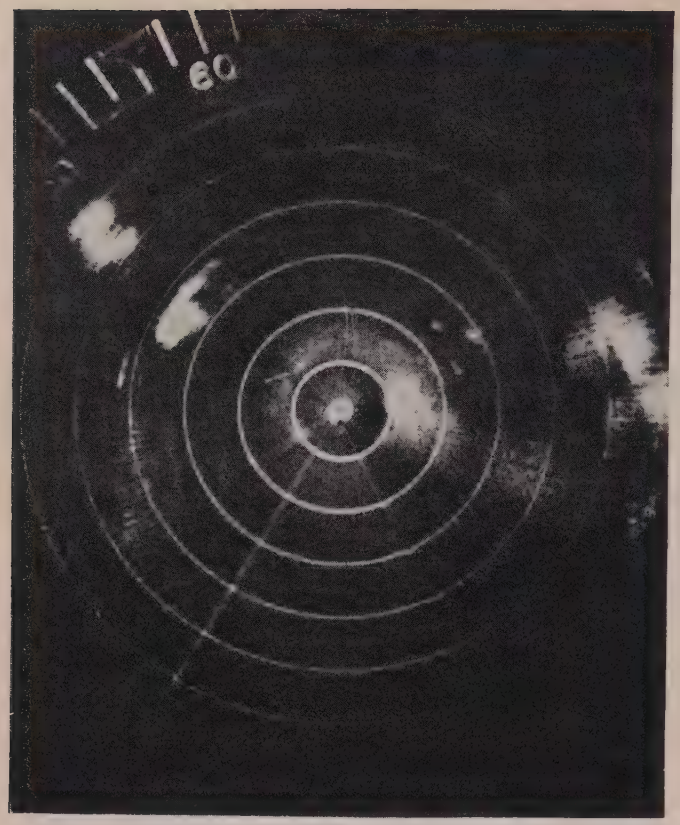

Fig. 34 – 30-mile gap between storm cores which, through windshield, appeared as solid line

Table 4 – Number of Days With Thunderstorms Along Denver-Omaha Airway

Month	Days	Month	Days
January	2	July	28
February	2	August	28
March	5	September	15
April	9	October	4
May	19	November	1
June	30	December	0

aircraft not equipped with radar, thus reducing operational delays during storm seasons (Fig. 34).

The ability of airborne radar to do these five things and in so doing avoid damaging hail and provide the passenger with a relatively smooth ride through thunderstorm conditions, I feel, justifies the installation of airborne radar in airline aircraft, particularly when we consider the amount of thunderstorm activity confronted every year. Table 4 shows the average number of days per month when thunderstorms occur somewhere on or near the airway between Denver and Omaha. It is literally true that we have a daily threat of storms in this sector from June to September, and

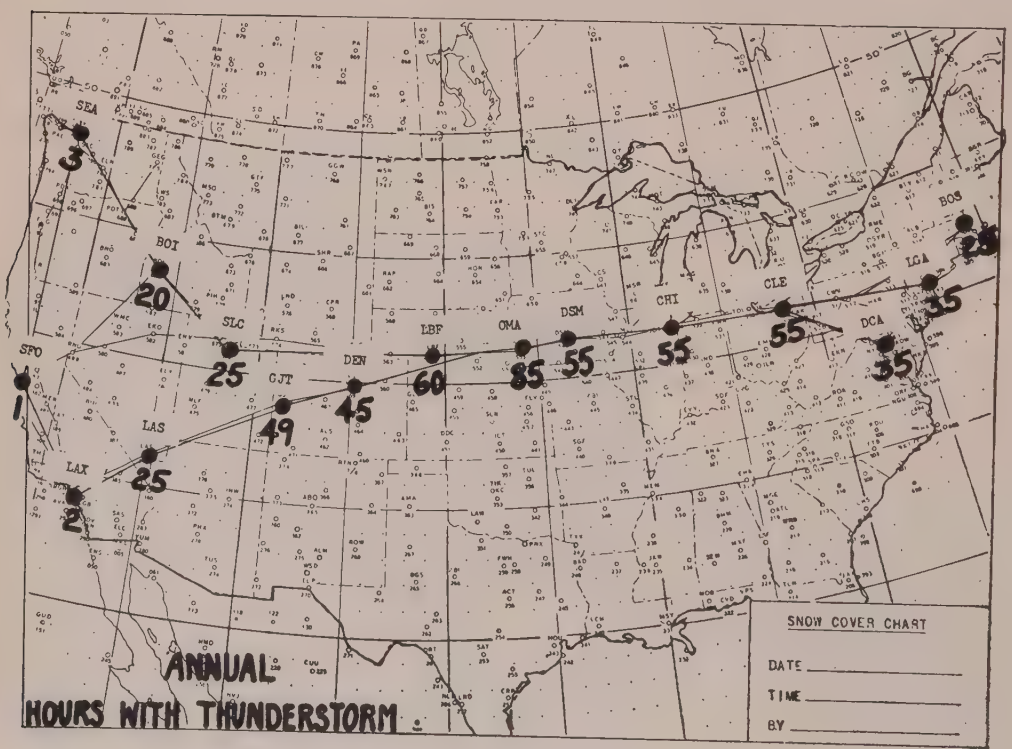

Fig. 35 – Hours per year that thunderstorms occur within 15 miles of airports

Fig. 36 – Airline thunderstorm accidents during 1938-1953

this is only a small segment of the United routes which are plagued with thunderstorms. Fig. 35 shows the number of hours per year in which thunderstorms occur within 15 miles of United's terminal airports.

In weighing the costs of an airborne radar installation in an airline fleet, tangible and intangible savings must be considered. Tangible savings include:

1. Shorter detours and shorter periods of reduced speed in thunderstorm areas.

2. Less holding.

3. Fewer static discharges (lightning strikes).

4. Less hail damage.

5. Probable elimination of airplane structural damage resulting from thunderstorm turbulence (Fig. 36).

United's conservative evaluation of these savings indicates they would pay off installation plus maintenance costs of a fleet radar installation in 10 to 12 years.

In addition to the tangible savings, there are the following nonmeasurable or intangible savings which, I believe you will agree, will reduce the 10- to 12-year amortization period considerably:

1. Customer good will.

2. Improved standing in comparison with carriers not equipped with radar.

3. Missed customer connections.

4. Canceled flights (with loss of revenue).

5. Disruption of operations, including off-line operation and stops, ferrying, added passenger handling costs, and so forth.

I trust that this paper has not given you the mistaken idea that radar is either an infallible crystal ball or a complete answer to the avoidance of all turbulence, for we have only scratched the surface in our radar evaluation. I believe, however, that conservative operating procedures using airborne radar within its limitations will not only contribute tremendously to increased safety, passenger comfort, and schedule reliability, but will also provide the flight crews with a new "tranquillity of spirit" when those thunderclouds loom up ahead. Civil airborne radar is here, bringing CAVU (Ceiling and Visibility Unlimited) weather to the cockpit.

When Are

PRESENT laws call for a single "legal stopping distance" that must be met by all types of vehicles in order for those vehicles to be considered good. However, this stopping-distance requirement cannot always be met by all classes of vehicles on today's highways. General opinion realizes the need for revision of this requirement.

This paper does not specify what revisions should be made, but it does present information pertinent to the consideration of such revisions. The factors affecting brake performance and stopping ability which are discussed here are brake capacity, weight shift, tire capacity, and road condition.

The Author

J. G. OETZEL (M '19) is vice-president in charge of engineering at the Warner Electric Brake & Clutch Co. He received a B.S. in Mechanical and Electrical Engineering from Clemson College in South Carolina. Mr. Oetzel has worked for the General Electric Co., Fairbanks, Morse & Co., and the Atlas Imperial Diesel Engineering Co. He has been with the Warner Electric Brake & Clutch Co. since 1939, when he started as a consulting engineer.

THERE has been considerable controversy about "legal stopping distance." There has been a lot of talk about "hundred-mile-an-hour" cars recently, which naturally raises the question about how quick can they stop. Trucks can go faster than they are now allowed to legally, but is it safe to let them? Can they stop? Highway engineers, in planning for "sight distance," curves, and intersections, need to know what braking distances they can reasonably expect from cars and trucks – present and future. They need to know what is being done normally and now, not necessarily the shortest stop that it is possible to make.

To this end the Bureau of Public Roads has run tests to see what a representative group of vehicles can do in the way of stopping distances, including passenger cars stopping from "high speeds" of 70 to 90 mph. These were mostly privately owned vehicles in ordinary "everyday" service, and the trucks and semis were from regular transport operations. These are good reports and give a great deal of useful information. Whenever such a report is issued, however, it stirs a lot of comment about the number of accidents caused by "inadequate" brakes, but rarely is anything said about the "inadequate" driver.

A recent publication says: "Although a more critical skidding condition usually exists when a surface is wet than dry, about three out of four fatal accidents and two out of three of all accidents occur on dry surfaces. Many of these no doubt could have been avoided if the drivers had been able to *stop a little sooner.*" The major factors which control this ability "to stop a little sooner" are:

1. The driver.
2. Condition of the vehicle.
3. Brake capacity and timing.
4. Weight shift.
5. Tire capacity.
6. Road condition.

Much has been written about the driver and "driver reaction time," but reaction time is only a part of skill and ability in driving. A driver having a relatively long reaction time, which is compensated for by anticipating road and traffic conditions far enough ahead, may be a very safe, accident-free driver. Far more accidents are avoided by "anticipation" than by "quick thinking" on the part of the driver. It is easier to blame the equipment than the driver, and this is often honestly done, where careful and competent analysis will show that the driver was really at fault or, at least, expected too much from his equipment. Of course, he may not have *known* that he was expecting too much, or working his equipment beyond its capacity, or that it was in poor condition, but "ignorance of the law is no excuse."

That it is "easier to blame the equipment" includes the condition of the equipment. While it is not questioned that much of the equipment in daily operation is not in the best of condition, this poor condition is often not the true cause of the accident, the true cause again being traceable to some driver fault. There are no statistics to support

Brakes "Adequate"?

J. G. Oetzel, Warner Electric Brake & Clutch Co.

This paper was presented at the SAE Summer Meeting, Atlantic City, June 7, 1954.

this because in too many cases the necessary skill and ability is not available at the time of an accident to determine the true cause. Mechanical devices, however, are far more predictable than are human beings.

When studies are made and reported on field tests of the stopping ability of a "cross-section" of highway vehicles, the "legal stopping distance" is used to measure whether a vehicle is good or bad. This makes for good or bad publicity, but are "legal stopping distances" right? Is it possible for a single stopping-distance requirement to be met by all classes of vehicles on the highway today? Is it that simple? It has been generally conceded for some time that they need revision. It is not the purpose of this paper, however, to tell what revisions should be made but rather to present some information which may be useful to the consideration of such revisions, as we come now to the remaining factors: brake capacity, weight shift, tire capacity, and road condition.

Years ago, when "30 ft from 20 mph" was set up as the single criterion of stopping ability, it seemed reasonable; but since then weights and speeds have increased, and the articulated vehicles which have come into general use have more complicated braking systems. These changes have forced upon us a realization of the many variables which affect the ability to stop. In fact, some of these variables should be examined even before an attempt is made to determine the torque required of the brakes.

As a start in this direction, Fig. 1 shows the general relationship between rubbing speed and coefficient of friction.[1] While this represents a specific set of conditions, it is useful here to show the general trend of variation in coefficient with rubbing speed which, incidentally, is synonymous with "heat rate." On this chart has been indicated the range of rubbing speed normally used by automotive brakes, by industrial brakes and clutches, and by friction saws which have no teeth, require little pressure, yet cut steel almost like an acetylene torch. This also indicates the difficulties to be expected in clutches and brakes if too high a rubbing speed is used. The lower portion of this curve will be repeated in other charts to serve as a reference or base.

On Fig. 2 the "reference" curve (R) is repeated, and here it should be pointed out that this curve represents "steel on steel." The two dotted curves represent resin-bonded lining on alloy cast iron (often called "semisteel") and also represent two different heat rates. At the same rubbing speed, the heat rate may be changed by changing the unit pressure or the unit inertia or both.

The other three curves of Fig. 2 are from oscillographic records of stops at very high heat rates of the same unit inertia at the same unit pressure but beginning at three different rubbing speeds. These show how the coefficient changes *during* a single application because of the surface temperatures developed. They also show how the coefficient recovers because of the surface temperature becoming lower as the rubbing speed – and consequently the heat rate – diminishes. For two of

[1] This curve was replotted and generalized from "Determination of the Coefficient of Friction of Steel on Steel at High Velocities" by Grotsch and Plake as found in Fig. 11, p. 340 of *American Journal of Physics*, Vol. 17, September, 1949, "What About Friction?" by Frederic Palmer.

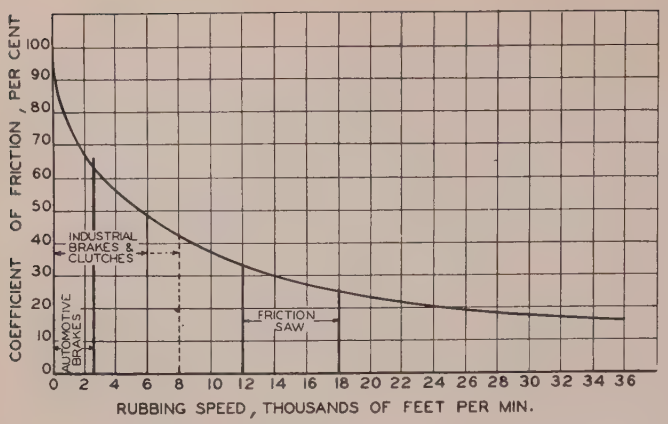

Fig. 1 – Generalized relation between coefficient of friction and rubbing speed, steel on steel

these curves full recovery of coefficient is not attained until after the stop is completed. This is "heat fade" in action. At lower heat rates it may not occur until, after successive applications, sufficient heat has been accumulated to raise the surface temperature to the "fade" point *during* an application.

We have seen that the *trend* of this relationship is the same for brake lining on cast iron as for metal on metal. What about rubber on concrete? Superposed on the reference curve of Fig. 3 are two curves ending at about 3500 fpm. The lower, broken curve is for a locked-wheel slide. The upper, dotted curve is supposed to represent an "impending" slide, but its "trend" indicates that some sliding already is taking place. The other two curves extending beyond 100 mph are for locked wheels at two loadings; the lower, of course, being the heavier loading, the higher heat rate.

Ralph A. Moyer, research engineer, University of California, has shown the difference between "impending" and "locked-wheel" slides, and I am indebted to him for the oscillographic charts of Fig. 4. This shows a *drop* of 37% for wet portland cement concrete for a fixed condition of weight and speed, and of nearly 52% for "wet bleeding asphalt." The speed in this case was 40 mph or 3520 fpm; and from this you can see how it fits into the "trend" picture of Fig. 3, which is from data published by Moyer several years ago.

This analysis shows why a vehicle seems actually to speed up the moment the wheels lock. It also shows the danger that attends the locking of wheels at high speeds and why high-speed "spins" are so "vicious." It has been almost providential that the trends shown for the various materials are so similar. As we learn to provide more heat capacity in our brakes, however, it will be easier to lock wheels at high speeds, so we must pay more attention to the torque capacity of the brakes or to other means of control which will make it difficult – if not impossible – to lock wheels at high speeds. We talk about the ability to "stop a little sooner," but the ability to lock wheels will not necessarily make a shorter stop possible, and it can be even more dangerous. And when you can brake just short of locking wheels, that is the end of the line – unless you throw out an anchor.

Brakes, however, are not the only factor in locking wheels. The center of gravity of a vehicle must be some distance above the road surface so a force-couple is produced between the retarding force at the tire-road contact and the inertia force acting at the center of gravity. In decelerating, this couple tends to depress the front end of the vehicle and to lift the rear end, that is, to add weight at the front end and reduce weight at the rear end. This is commonly referred to as "dynamic transfer," "weight transfer," or "weight shift." The charts pertaining to this are attached as an appendix.

A hypothetical but representative passenger car is shown in Section 10 of the Appendix. Here it must be assumed that the brake torque on each axle must be varied as the weight on the axle

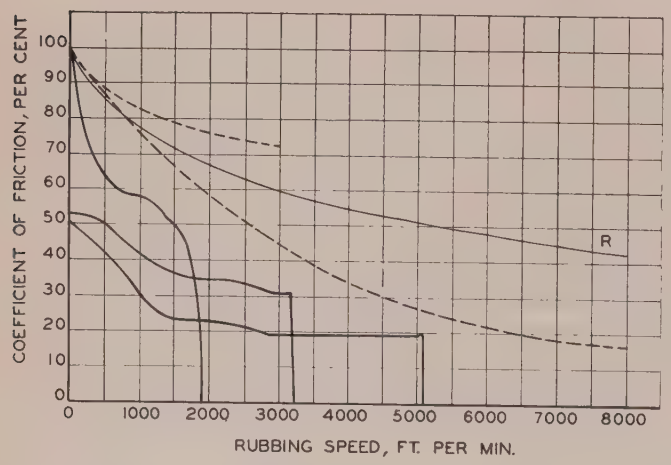

Fig. 2 – Comparison of generalized relation of coefficient of friction versus rubbing speed, with "friction material" on cast iron and changes during three actual stops

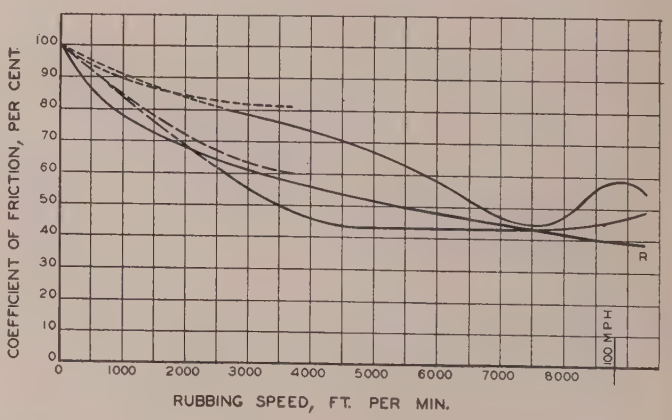

Fig. 3 – Coefficient of friction versus rubbing speed, steel on steel and rubber on concrete. R = reference curve, steel on steel; Dotted = "impending" slide; Broken = locked-wheel slide; Solid = locked-wheel slide to 100 mph at two different loadings

varies. In other words, if the brake torque were constant and based on equal weight and tire-road coefficient on the two axles, the rear wheels would soon lock. This shows why passenger cars generally have adopted "60-40" braking, which is a "practical" compromise. It was also this increase in front braking that was a large factor in getting away from the solid axle with its semielliptic springs and in going to other suspensions which could better withstand the increased braking without affecting the steering geometry. With "60-40" braking a deceleration of about 20 ft per sec per sec can be reached before the rear wheels are on the point of locking up. Slightly more weight on the rear, relative to the front, can bring this to 22.5 ft per sec per sec.

Similarly, Section 5 of the Appendix represents a typical "conventional" truck. With braking based upon the static loading, this truck would lock the rear wheels almost immediately unless some excess front braking is provided. Whether more braking could be used on the front wheels will depend on how much the front suspension could take before the steering is affected. The variables of loading encountered make it impossible to determine accurately the best distribution of braking, and we must rely on the "good judgment" of the designer and manufacturer to effect a practical compromise.

The picture is almost identical for the COE and the 6-wheeler, differing only as affected by the assumed – or actual – height of the center of gravity. In view of this and of the variables of loading, is it surprising that there is a wide divergence of stopping distances in any "cross-section" test under actual operating conditions? Of course, brake sizes, systems, and conditions can further affect this divergence, but my main purpose is to call attention to the fact that other factors help determine how much braking we can put on a vehicle.

Articulated vehicles are considerably more complicated, and, in these, the buildup rate and timing of the brakes on the different axles are important variables in determining the stopping distances. No really adequate picture can be given by such calculations as are presented in Section 11 of the Appendix which illustrates a fairly representative tractor and semitrailer. It does serve to show what must be accomplished in the way of brake torque on the different axles if the shortest possible stopping distance is to be attained. Of course, it presupposes instant buildup of all brakes and no "fading." And a different loading would change everything, so a practical compromise is needed.

No such calculations have been made for the truck and full trailer. *If,* and this is a big "if," *each* unit is correctly braked – taking weight shift into consideration – and the timing and buildup of the brakes are perfectly synchronized, there will be no push or pull on the tow-bar connecting the two. The difficulties in the way of accomplishing this are tremendous, and many practical compromises must be made for a long time to come in seeking

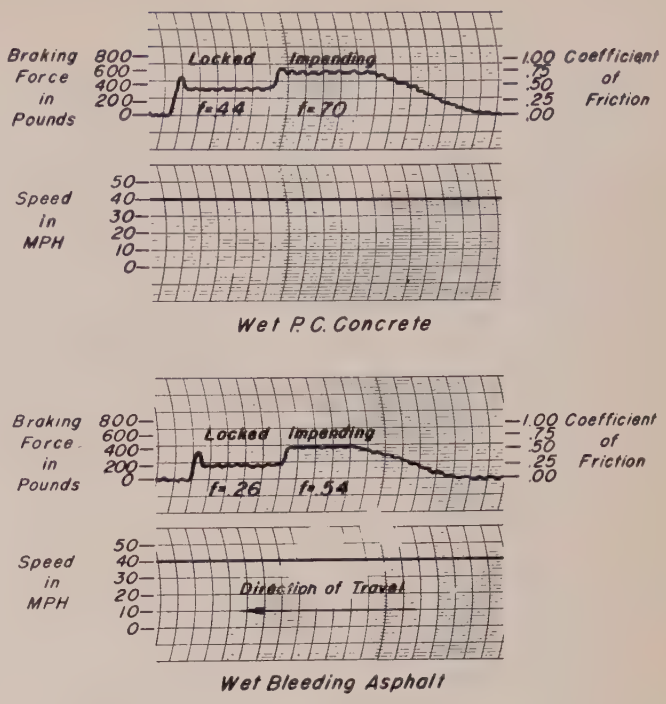

Fig. 4 – Change of tire-road coefficient as brake torque builds up to lock wheel and is released again; from oscillograms of impending skid and locked-wheel conditions

the best middle ground among the many variables.

Passenger cars have a fairly narrow range of loading variables, so it is easier to make a good compromise; thus, passenger cars have generally good brake performance when the brakes are kept in good condition. The fewer the variables, the better the compromise which it is possible to make.

Tire capacity and road condition can be discussed together because we are here concerned with the capacity of the tire to grip the road. This has already been mentioned in connection with the variation of coefficient with speed for different materials. Many tests have been made and many reports written on this subject. Two things, however, can stand repeating. The first is that the published data on road coefficient at the "slide-impending" condition indicate that some sliding is already taking place and that heat is already being generated at the tire-road contact. The second is that more retardation can be accomplished on a wheel that is turning than on one that is locked. Ice conditions are amply covered elsewhere.

So far we have considered factors affecting the attainment of the shortest possible stop, but is the shortest possible stop desirable? The "sports-car fan" wants bucket seats and straps to hold him in them and also a crash helmet. The average American family, however, wants a more comfortable vehicle that you can get in and out of easily. In this kind of car the driver can brace himself on the steering wheel, and anyway he knows what is com-

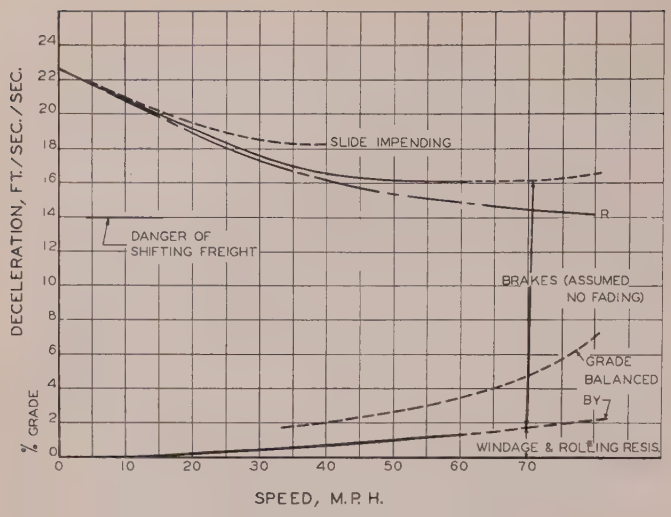

Fig. 5 – Relation of speed to factors producing deceleration for typical 45,000 gvw tractor and van-type semitrailer

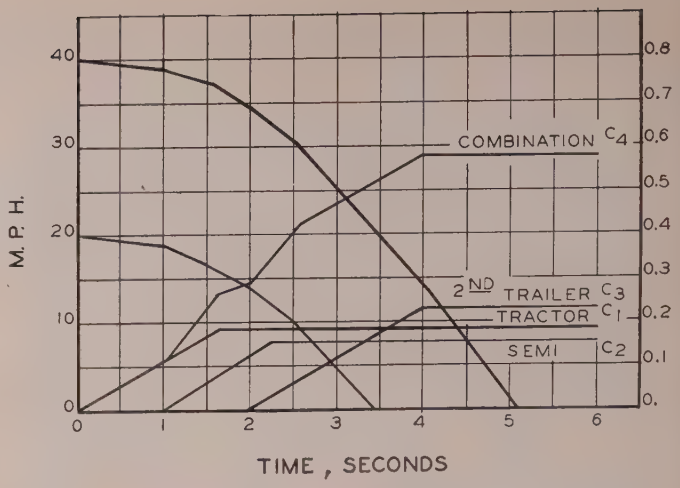

Fig. 7 – Effect of brake timing and rate of buildup on stopping time, Case II

ing. His passenger may be busy talking, or watching the scenery, and may not know the driver is going to "hit the brakes." A deceleration of 10 ft per sec per sec will make a seated passenger lean forward and begin to be uncomfortable to the point that he may criticize the driver. At 12 or 14 ft per sec per sec the passenger is thrown against the windshield or the back of the front seat unless he is well braced. At about the same deceleration – 10 ft per sec per sec – freight begins to shift, and at 14 ft per sec per sec it must be well braced. Incidentally, 10 ft per sec per sec about represents the coefficient of a metal box resting on metal skid rails in a truck or trailer body.

Some of these factors have been put together in Fig. 5 to try to give a little better overall picture. This chart represents a tractor and van-type semitrailer of about 45,000 lb gvw. The reference curve R has been repeated here and this does represent one certain heat rate, but it is not offered as representing this class of vehicle generally. The "slide-impending" curve shown may not represent accurately the tire loading condition for this particular vehicle. In spite of this, the two together may give some idea of the relationship between the two. Now consider the fact that tire loading may raise or lower the "slide-impending" curve and that brake heat rate may raise or lower curve R. When curve R is above "slide-impending" the wheels lock. The "providential" part comes in that the very factors which increase the tire loading also increase the heat rate of the brakes which, on any given vehicle, tends to keep the two in step.

In most of the foregoing we have considered factors which are of use in determining what should be the torque of the brakes on the different axles of a vehicle or train. Suppose for a moment that we assume that 14 ft per sec per sec is the maximum *desirable* deceleration. If the brakes build up instantly and the vehicle reaches that deceleration the instant the pedal is touched and if it can maintain that deceleration throughout the stop, then it

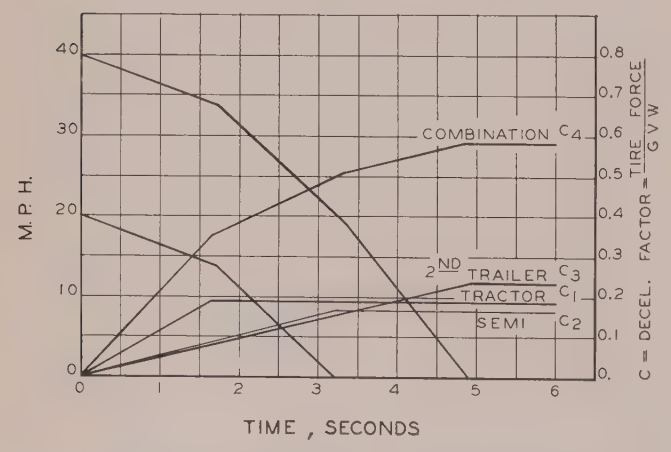

Fig. 6 – Effect of brake timing and rate of buildup on stopping time, Case I

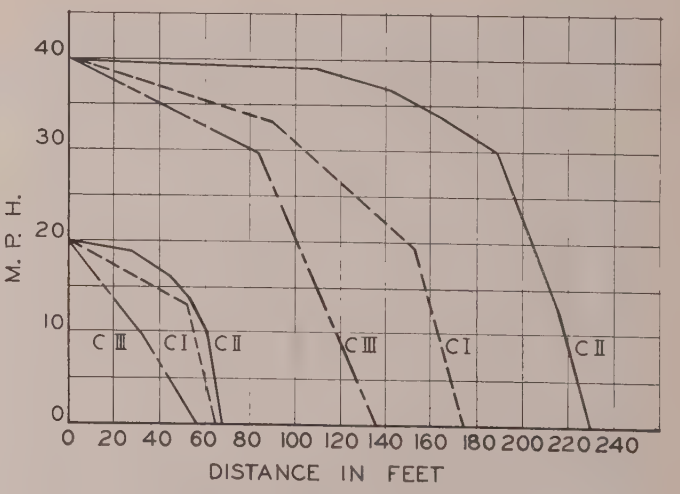

Fig. 8 – Relative stopping distance, Cases I, II, and III

could stop from 20 mph in 30.73 ft and from 40 mph in 122.9 ft. Note that the length of this theoretical stop from 40 mph is just four times as long as the one from 20 mph. It is doubtful if brakes can ever be made to act that fast.

Time is required even for the driver to push the pedal down, and the brake response may not be that fast. To see what happens, let's take a hypothetical tractor-semi-full-trailer train and assume that the brakes on each unit build up as one brake. In Case I (Fig. 6) suppose that they all start at the same instant but build up at different rates to their respective torque values. In Case II (Fig. 7) suppose they build up at the same rate but start at different times as shown in Fig. 6. Maximum deceleration of the combination in these assumed cases is about 18.5 ft per sec per sec.

The distance required to stop is shown in Fig. 8. For Case I the ratio of stopping distance is not 4, as for instant buildup, but is 2.67; while for Case II this ratio is 3.66. Actual measured stops on the highway show such difference in ratio and of much the same order. Even for the passenger cars reported in *Public Roads* for June, 1953, the stops from 40 and 20 mph—as figured from the equations for the "statistical average" and "85 percentile" appearing in Fig. 12 of that article—show ratios of 2.83 for the average, 3.7 for the 85 percentile. It is easy to understand when you remember that the buildup time and rate should be the same for any given vehicle and driver at both 40 and 20 mph. Percentagewise the effect is different at the two speeds. As the ratio approaches 4, a slow buildup or fade—or both—is suspected. Fading may take place on only one axle because rarely do all brakes on the train work at same heat rate, and it is no easy matter to get them to, but it can be done.

While we know we cannot expect an instant buildup, it seems reasonable to predict a buildup time of ¾ sec for all brakes on the vehicle. On this assumption, and using the same braking values as for Cases I and II, Case III is shown in Fig. 9. Here the stops are noticeably shorter, but the ratio drops to 2.38. No claim is made that the decelerations of Cases I, II and III could actually be obtained where weight shift is a factor. The calculations for the charts of these three "cases" have been simplified with a resulting slight loss of accuracy; but, since they are only for comparison with each other and to illustrate certain points, it is felt that this is of little consequence. Plotting the speed-time and speed-distance curves as a series of straight lines makes it a little easier to follow the events.

Still another factor should be remembered in considering field studies of stopping distance, and that is the temperature of the brakes. Some linings have higher friction cold, others have higher friction warm. Either will "fade" at some temperature. Some brakes therefore, will be at their best warm, others, cold; and this is another reason for the wide divergence encountered on such "cross-

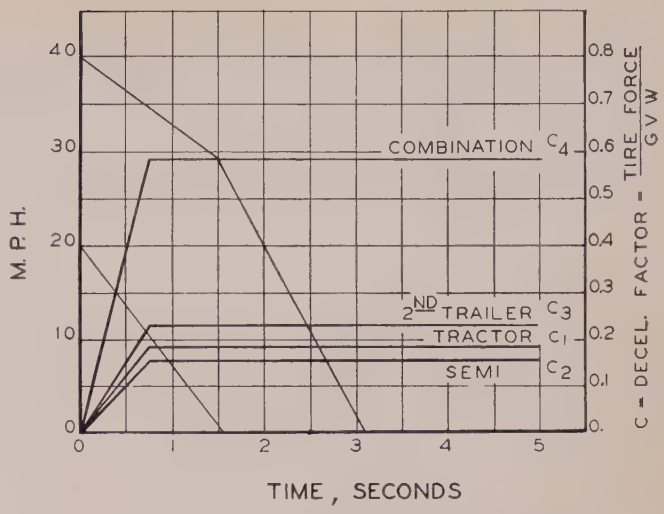

Fig. 9 – Effect of brake timing and rate of buildup on stopping time, Case III

section" tests because of the impossibility of testing each vehicle at its best operating temperature, and the test would not then be representative.

The present stopping requirements of "30 ft from 20 mph" should be relatively easy for the passenger car. The "statistical average" car of the *Public Roads* report could do it in 22.75 ft and the "85 percentile" car in 28 ft. Loading will make some difference, of course, and the cars of the *Public Roads* report probably had little or no load other than the driver and observer. The straight truck is much more affected by loading variables and weight shift. Truck trailers and trains are also much affected by brake timing and rate of buildup.

With identical brakes on two axles of the same static load and on one vehicle, they might be "adequate" as to heat capacity in the hills yet "inadequate" under the weight-shift conditions of a quick stop. The nature of some tandem-axle suspensions causes a transfer of weight from one axle to another that is independent of the vehicle or train as a whole. Brakes on the two axles need to have the same heat capacity for the hills but different torque capacity for the best quick stop.

It is going to be difficult to legislate such factors as weight shift, loading variables affecting the center of gravity, and brake timing and rate of buildup. Improvements are going to take time, but it is hoped that this discussion may point the way to some of these improvements and to a better understanding of the results of these "cross-section" tests. When a brake can lock its wheel, that is the most it can do. It must, first of all, be "adequate" in heat capacity and it may have "adequate" torque capacity even if it cannot lock the wheel. The time that the brakes on one axle go to work relative to the other axles of the train is not a matter of the "adequacy" of the brake but of the system which operates and controls it.

More on Brakes ——→

Appendix to Paper by J. G. Oetzel

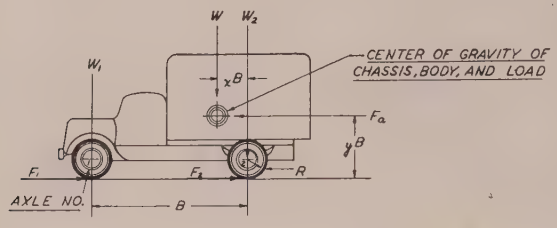

IN THE STATIC CONDITION.

$$W_1 = \frac{WxB}{B} = Wx \qquad W_2 = \frac{W(BxB)}{B} = W(1-x)$$

WHEN DECELERATING AT FT. PER SEC.^{2} = a

$$Fa = Ma = \frac{Wa}{g} = F_1 + F_2$$

THEN, WITH DYNAMIC TRANSFER OF WEIGHT DUE TO DECELERATION:

$$W_{1a} = W_1 + \frac{yBFa}{B} = Wx + yFa = Wx + \frac{yWa}{g} = W\left(x + \frac{ya}{g}\right) \text{---------- 1}$$

AND

$$W_{2a} = W_2 - yFa = W(1-x) - yFa = W(1-x) - \frac{yWa}{g} = W\left[(1-x) - \frac{ya}{g}\right] \text{-- 2}$$

MAXIMUM BRAKE TORQUE WHERE f = ROAD COEFFICIENT:

$$T_1 = \frac{fRW_{1a}}{2} = \frac{fRW}{2}(x+yf) \text{---------- 3}$$

$$T_2 = \frac{fRW_{2a}}{2} = \frac{fRW}{2}[(1-x)-yf] \text{---------- 4}$$

SINCE: $f = \frac{a}{g}$

NOTE THAT: $f(x+yf)+f[(1-x)-yf] = f$

AND: $f - f(x+yf) = f[(1-x)-yf]$

HENCE: $\frac{100f(x+yf)}{f} = \%$ LOAD ON FRONT AXLE ---------- 5

AND: $100 - \frac{100f(x+yf)}{f} = \%$ LOAD ON REAR AXLE ---------- 6

Section 1 – Formulas, 2-axle motor vehicle

Passenger cars, generally, have adopted "60-40" braking; and the example, shown in Section 10, indicates that this is a good practical compromise when "weight shift" or "dynamic transfer" is considered. The formulas of Section 1 apply. The variables encountered in the loading of trucks make it more difficult to find and adopt a similar practical compromise. In the example of Section 5, "40-60" braking might be indicated, but suppose the same chassis were used as a tractor, then what?

It is the purpose of this Appendix to set forth some formulas and examples pertinent to the consideration of the weight shift problem as it affects the torque capacity of the brakes on the various axles, and they are offered only as a start in this direction. They are offered with the hope that they may induce some ideas as to why it may be more difficult for many trucks to make stops as short as passenger cars can make.

They are also offered with the hope of inducing some ideas as to means of controlling the brakes on the various axles just short of "lockup" for reasons apparent from Fig. 4 of the text. As it stands today, the shortest possible stop on a multi-axle vehicle is attained by locking as many wheels as possible in the shortest possible time, then let-

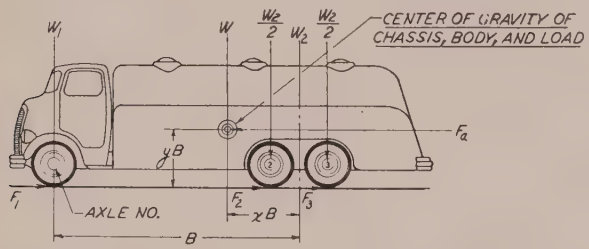

WITH DYNAMIC TRANSFER OF WEIGHT DUE TO DECELERATION:

$$W_1 = W\left(x + \frac{ya}{g}\right)$$

$$\frac{W_2}{2} = \frac{W}{2}\left[(1-x) - \frac{ya}{g}\right]$$

MAXIMUM BRAKE TORQUE AT ROAD COEFFICIENT = f:

$$T_1 = \frac{RW}{2} f(x+yf)$$

$$T_2 = T_3 = \frac{RW}{4} f[(1-x)-yf]$$

LOAD ON AXLE IN PER CENT OF W:

$$\text{FRONT} = \frac{100f(x+yf)}{f}$$

$$\text{REAR (EACH)} = \frac{1}{2}\left[100 - 100f\,\frac{(x+yf)}{f}\right]$$

Section 2 – Formulas, 3-axle motor vehicle

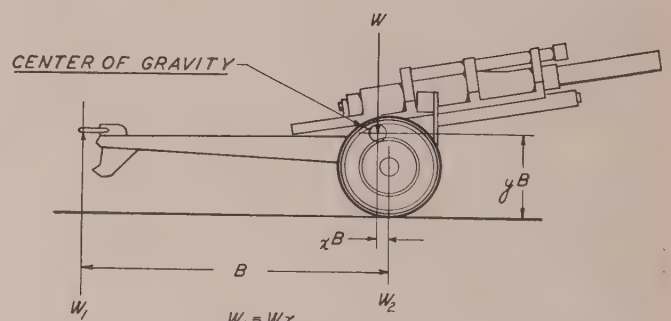

$W_1 = Wx$

$W_2 = W(1-x)$

$W_{1a} = W(x+yf)$

$W_{2a} = W[(1-x)-yf] = W[1-(x+yf)]$

$T_2 = \frac{fRW}{2}[1-(x+yf)]$

LOAD IN PER CENT OF W:

PINTLE: $\frac{100f(x+yf)}{f}$

TIRES (2): $100 - \frac{100f(x+yf)}{f}$

Section 3 – Formulas, single-axle trailer

ting each tire decide for itself how much weight is on it and how much retarding force it can develop. It is expected that it will be a long time before the best answer can be found. In the meantime, it is hoped that a study of the conditions set forth may suggest some reasonable regulations to use while improvements are being made.

Meanwhile a great deal must continue to depend on the competence of our drivers to anticipate conditions far enough ahead that they will never need to use such high deceleration rates as will disturb passengers or shift freight.

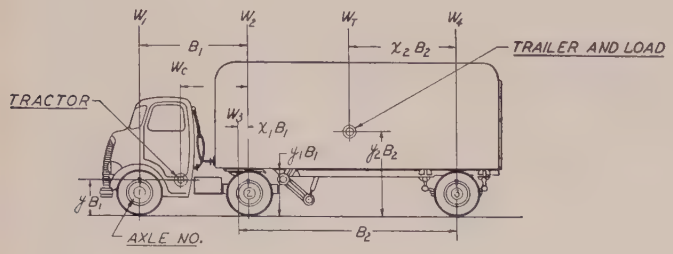

IN THE STATIC CONDITION:

$W = W_c + W_T$

$W_1 = W_c x + W_3 x_1$ $\quad W_2 = W_c (1-x) + W_3 (1-x_1)$

$W_3 = W_T x_2$ $\quad W_4 = W_T (1-x_2)$

WHEN DECELERATING AT FT. PER SEC.^{2} = a

$$W_{1a} = W\left[\frac{W_c}{W}(x+yf)+\frac{W_T}{W}(x_2+y_2 f)(x_1+y_1 f)\right]$$

$$W_{2a} = W\left\{\frac{W_c}{W}[(1-x)-yf]+\frac{W_T}{W}(x_2+y_2 f)[(1-x_1)-y_1 f]\right\}$$

$$W_{3a} = W\left\{\frac{W_T}{W}[(1-x_2)-y_2 f]\right\}$$

$$T_1 = \frac{RW}{2} f\left[\frac{W_c}{W}(x+yf)+\frac{W_T}{W}(x_2+y_2 f)(x_1+y_1 f)\right]$$

$$T_2 = \frac{RW}{2} f\left\{\frac{W_c}{W}[(1-x)-yf]+\frac{W_T}{W}(x_2+y_2 f)[(1-x_1)-y_1 f]\right\}$$

$$T_3 = \frac{RW}{2} f\left\{\frac{W_T}{W}[(1-x_2)-y_2 f]\right\}$$

Section 4 – Formulas, 2-axle tractor and single-axle semitrailer

—EXAMPLE—

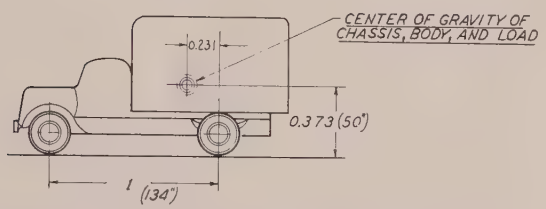

a	f	$f(x+yf)$	$f[(1-x)-yf]$	PER CENT G.V.W. ON FRONT AXLE	PER CENT G.V.W. ON REAR AXLE
3.22	0.1	0.02683	0.07317	26.83	73.17
6.44	0.2	0.06107	0.13888	30.53	69.47
9.66	0.3	0.10287	0.19713	34.29	65.71
12.88	0.4	0.15208	0.24792	38.02	61.98
16.1	0.5	0.20875	0.29125	41.75	58.25
19.32	0.6	0.27288	0.32712	45.48	54.52
22.54	0.7	0.34447	0.35553	49.21	50.79
STATIC DISTRIBUTION OF WEIGHT				23.1	76.9

W = G·V·W·

a = DECELERATION F.P.S.^{2}

f = ROAD COEFFICIENT

R = LOADED RADIUS OF TIRE

AT INCIPIENT TIRE SLIDE:

TORQUE, EACH FRONT BRAKE = $\frac{RW}{2} f(x+yf)$

TORQUE, EACH REAR BRAKE = $\frac{RW}{2} f[(1-x)-yf]$

Section 5 – Example, brake performance for 4 x 2 "conventional" truck, taking weight shift into account

—EXAMPLE—

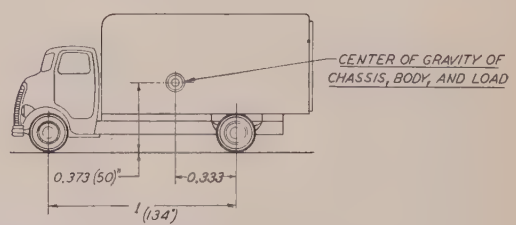

a	f	$f(x+yf)$	$f[(1-x)-yf]$	PER CENT G.V.W. ON FRONT AXLE	PER CENT G.V.W. ON REAR AXLE
3.22	0.1	0.03703	0.06287	37.06	62.94
6.44	0.2	0.08152	0.11828	40.8	59.2
9.66	0.3	0.1334	0.16623	44.5	55.5
12.88	0.4	0.19288	0.20672	48.27	51.73
16.1	0.5	0.25975	0.23975	52.00	48.00
19.32	0.6	0.33408	0.2653	55.7	44.3
22.54	0.7	0.41587	0.2834	59.47	40.53
STATIC DISTRIBUTION OF WEIGHT				33.33	66.66

W = G·V·W·

a = DECELERATION F.P.S.^{2}

f = ROAD COEFFICIENT

R = LOADED RADIUS OF TIRE

AT INCIPIENT TIRE SLIDE:

TORQUE, EACH FRONT BRAKE = $\frac{RW}{2} f(x+yf)$

TORQUE, EACH REAR BRAKE = $\frac{RW}{2} f[(1-x)-yf]$

Section 6 – Example, brake performance for 4 x 2 COE truck, taking weight shift into account

—EXAMPLE—

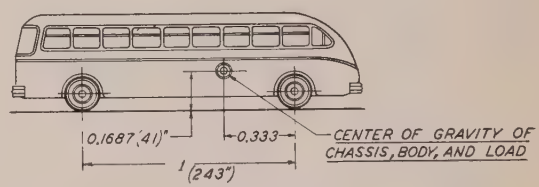

a	f	$f(x+yf)$	$f[(1-x)-yf]$	PER CENT G.V.W. ON FRONT AXLE	PER CENT G.V.W. ON REAR AXLE
3.22	0.1	0.034987	0.064928	35.02	64.98
6.44	0.2	0.07334	0.12651	36.7	63.3
9.66	0.3	0.11494	0.18475	38.01	61.99
12.88	0.4	0.15995	0.24634	39.37	60.63
16.1	0.5	0.2083	0.2912	41.7	58.3
19.32	0.6	0.25999	0.33941	43.37	56.63
22.54	0.7	0.31502	0.38427	45.02	54.98
STATIC DISTRIBUTION OF WEIGHT				33.33	66.66

W = G·V·W·

a = DECELERATION F.P.S.^{2}

f = ROAD COEFFICIENT

R = LOADED RADIUS OF TIRE

AT INCIPIENT TIRE SLIDE:

TORQUE, EACH FRONT BRAKE = $\frac{RW}{2} f(x+yf)$

TORQUE, EACH REAR BRAKE = $\frac{RW}{2} f[(1-x)-yf]$

Section 7 – Example, brake performance for typical bus, taking weight shift into account

More on Brakes ⟶

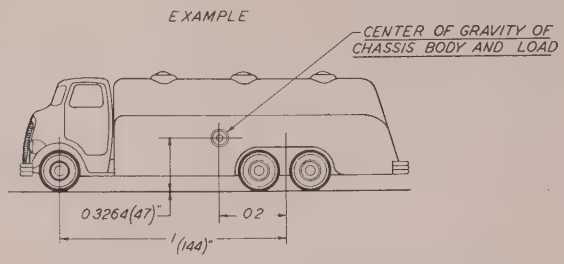

a	f	f(x+yf)	f[(1-x)-yf]	PER CENT G.V.W. ON FRONT AXLE	PER CENT G.V.W. EACH REAR AXLE
3.22	0.1	0.02326	0.07674	23.26	38.37
6.44	0.2	0.05306	0.14694	26.53	36.73
9.66	0.3	0.08937	0.21062	29.79	35.1
12.88	0.4	0.1322	0.2677	33.05	33.47
16.1	0.5	0.1816	0.3184	36.32	31.84
19.32	0.6	0.2375	0.3624	39.58	30.21
22.54	0.7	0.2999	0.4001	42.84	28.58
STATIC DISTRIBUTION OF WEIGHT				20.00	40.00

W = G·V·W·

a = DECELERATION F.P.S.^{2}

f = ROAD COEFFICIENT

R = LOADED RADIUS OF TIRE

AT INCIPIENT TIRE SLIDE:

TORQUE, EACH FRONT BRAKE = $\frac{RW}{2} f(x+yf)$

TORQUE, EACH REAR BRAKE = $\frac{RW}{4} f[(1-x)-yf]$

Section 8 – Example, brake performance for 6 x 4 COE trailer, taking weight shift into account

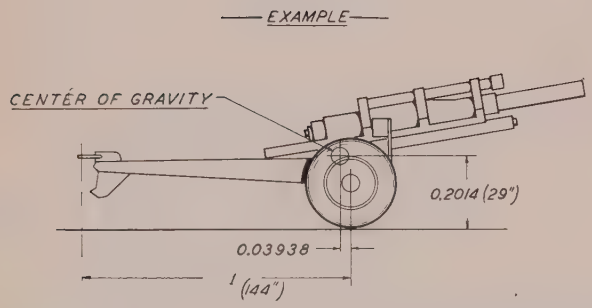

a	f	f(x+yf)	f[(1-x)-yf]	PER CENT G.V.W. ON PINTLE	PER CENT G.V.W. ON TIRE
3.22	0.1	0.00595	0.09405	5.95	94.05
6.44	0.2	0.01593	0.18407	7.96	92.04
9.66	0.3	0.02994	0.27006	9.98	90.02
12.88	0.4	0.04798	0.35202	11.995	88.005
16.1	0.5	0.07004	0.42996	14.001	85.999
19.32	0.6	0.09613	0.50387	16.02	83.98
22.45	0.7	0.1262	0.5738	18.03	81.97
STATIC DISTRIBUTION OF WEIGHT				3.94	96.06

W = G·V·W·

a = DECELERATION F.P.S.^{2}

f = ROAD COEFFICIENT

R = LOADED RADIUS OF TIRE

AT INCIPIENT TIRE SLIDE:

TORQUE, EACH BRAKE = $\frac{RW}{2} f(x+yf)$

Section 9 – Example, brake performance for single-axle trailer, taking weight shift into account

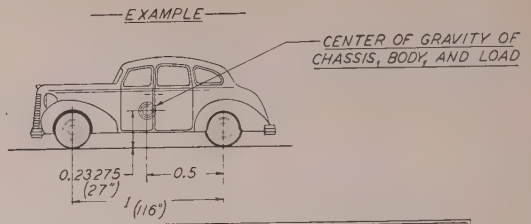

a	f	f(x+yf)	f[(1-x)-yf]	PER CENT G.V.W. ON FRONT AXLE	PER CENT G.V.W. ON REAR AXLE
3.22	0.1	0.05233	0.04767	52.33	47.67
6.44	0.2	0.10931	0.0907	54.65	45.35
9.66	0.3	0.17094	0.12906	56.98	43.02
12.88	0.4	0.2372	0.16276	59.30	40.70
16.1	0.5	0.30817	0.19182	61.63	38.37
19.32	0.6	0.38377	0.21623	63.96	36.04
22.54	0.7	0.46402	0.23598	66.29	33.7
STATIC DISTRIBUTION OF WEIGHT				50.00	50.00

W = G·V·W·

a = DECELERATION F.P.S.^{2}

f = ROAD COEFFICIENT

R = LOADED RADIUS OF TIRE

AT INCIPIENT TIRE SLIDE:

TORQUE, EACH FRONT BRAKE = $\frac{RW}{2} f(x+yf)$

TORQUE, EACH REAR BRAKE = $\frac{RW}{2} f[(1-x)-yf]$

Section 10 – Example, brake performance for passenger car, taking weight shift into account

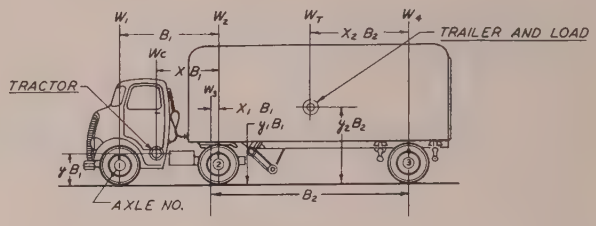

EXAMPLE

W_c = 5916 W_T = 24864 x = 0.537 x_1 = 0.0597 x_2 = 0.5 W_c = 0.1922 W

$W_c x$ = 3180 W = $W_c + W_T$ y = 0.208 y_1 = 0.336 y_2 = 0.387 (65°) W_T = 0.8078 W

$W_c(1-x)$ = 2735 = 30780 B_1 = 134 B_2 = 168

BRAKE TORQUE: (R = LOADED RADIUS OF TIRE)

FRONT WHEEL = $\frac{RWH}{2}$; DRIVE WHEEL = $\frac{RWL}{2}$; TRAILER WHEEL = $\frac{RWN}{2}$

f	A x+yf	B (1-x)yf	C x_1+y_1f	D $(1-x_1)-y_1f$	E x_2+y_2f	F $\frac{W_c}{W}A$	G $\frac{W_T}{W}EC$
0.1	0.5578	0.4422	0.0933	0.9067	0.5387	0.10721	0.0406
0.2	0.5786	0.4214	0.1269	0.8731	0.5774	0.11121	0.05919
0.3	0.5994	0.4006	0.1605	0.8395	0.6161	0.1152	0.07988
0.4	0.6202	0.3798	0.1941	0.8059	0.6548	0.1192	0.10267
0.5	0.6410	0.3590	0.2277	0.7723	0.6935	0.1232	0.12756
0.6	0.6618	0.3382	0.2613	0.7387	0.7322	0.1272	0.15455
0.7	0.6826	0.3174	0.2949	0.7051	0.7709	0.1312	0.18364

f	H f(F+G)	J $\frac{W_c}{W}B$	K $\frac{W_T}{W}ED$	L f(J+K)	M $(1-x_2)y_2f$	N $f\frac{W_T}{W}M$	CHECK H+L+N f
0.1	0.01478	0.08499	0.39456	0.04795	0.4613	0.03726	0.09999
0.2	0.03408	0.08099	0.40723	0.09764	0.4226	0.06828	0.20000
0.3	0.0585	0.07699	0.41781	0.14844	0.3839	0.09303	0.29970
0.4	0.08875	0.07300	0.42628	0.19971	0.3452	0.11152	0.39998
0.5	0.12538	0.06900	0.42962	0.24931	0.3065	0.12379	0.49848
0.6	0.16905	0.06500	0.43692	0.30115	0.2678	0.1298	0.60000
0.7	0.22039	0.06100	0.43909	0.35006	0.2291	0.12955	0.70000

a	f	M.P.H. PER SEC.	PER CENT G.V.W. ON: FRONT AXLE	DRIVE AXLE	TRAILER AXLE
3.22	0.1	2.195	14.78	47.95	37.26
6.44	0.2	4.391	17.04	48.82	34.14
9.66	0.3	6.586	19.50	49.48	31.02
12.88	0.4	8.782	22.19	49.93	27.88
16.1	0.5	10.977	25.076	49.86	25.06
19.32	0.6	13.172	28.17	50.19	21.64
22.54	0.7	15.368	31.48	50.00	18.52
		STATIC	12.73	46.88	40.39

Section 11 – Example, brake performance for 4 x 2 tractor and single-axle semitrailer, taking weight shift into account

Discussion of Paper by J.G. Oetzel

Presents Data on Stopping Distances for Unloaded Vehicles

– C. W. Jackman
Chevrolet Division, GMC

MR. OETZEL'S emphasis on weight distribution and dynamic weight shift points up some of the difficulties encountered in obtaining the most effective brake function on unit vehicles and combinations, the effect on combinations being particularly complicated.

This is further complicated by the fact that the percentage distribution of loading on various axles is usually quite different in an unloaded vehicle than when fully loaded to its rated capacity.

In establishing a distribution of braking effort among the axles of a vehicle or combination, it is desirable to provide for all different operating conditions as well as possible. This does not provide the best brake performance for every operating condition.

High percentage on front wheels would give best performance under many conditions but results in dangerous loss of steering under other conditions.

High percentage on tractor rear wheels is useful under most conditions but may result in fade on long grades, as well as rapid wear and high maintenance costs. Locked tractor rear wheels produce uncontrollable jackknifing.

High percentage on semitrailer wheels reduces wear on tractor brakes and gives good control on moderate stops on dry pavement. Weight transfer makes them less effective for quick stops. Locked trailer wheels produce bad jackknifing on slippery roads.

In order to indicate roughly the conditions which might prevail if the vehicles shown in Mr. Oetzel's paper were unloaded, the figures in Table A are shown.

If we choose a commonly used brake balance of 60% front and 40% rear, it is obvious that front wheels will slide first with full passenger load on a slippery surface. On dry footing, rear wheels will slide first, loaded or not.

To a first approximation, assuming 0.7 maximum adhesion, maximum deceleration will be:

$$\text{Loaded, } \frac{33.7}{40} \times 22.5 = 19 \text{ ft/sec}^2$$

(more refined, 19.9 ft/sec² equivalent to 21.6 ft minimum at 20 mph)

$$\text{Driver only, } \frac{27.1}{40} \times 22.5 = 15.2 \text{ ft/sec}^2$$

(more refined, 17.3 ft/sec² equivalent to 24.9 ft minimum at 20 mph)

We have all experienced this rear-wheel slide while driving alone. It is readily controlled by easing the brakes, but it does limit stopping ability.

Apparently there should never be any difficulty in meeting a 30-ft stopping distance requirement at 20 mph.

Figures for a conventional truck are given in Table B. How shall we balance these brakes? Obviously, if we want to show the best stopping ability, loaded, on dry pavement, it would be about 50% front and 50% rear. But the front springs will not take it. So we usually take about 30% front and 70% rear. This is favorable for steering down slippery winding hills with full load.

Under all other conditions, stopping ability is limited by rear-wheel slide, which is fairly easy to control in a unit vehicle.

With 0.7 maximum adhesion, maximum deceleration will be:

Loaded, 18.0 ft/sec², equivalent to 23.9 ft minimum at 20 mph

Unloaded, 11.8 ft/sec², equivalent to 36.4 ft minimum at 20 mph

At 11.8 ft/sec², the rear wheels are carrying only 36.8% of the weight but are doing 70% of the braking. The deceleration is therefore $36.8 \times 22.5/70 = 11.8$ ft/sec². Stopping distances shown make no allowance for application or buildup time. It would be hard to meet a **40-ft** stopping distance requirement at 20 mph, **unloaded.**

For the loaded combination of the tractor and single-axle semitrailer (Table C): If brake balance is taken as at $0.2g$ loaded, the 34.2% effort on the trailer rear axle is the controlling factor, and maximum deceleration is $22.5 \times 24.6/34.2 = 16.2$ ft/sec², or a minimum stopping distance of 26.5 ft at 20 mph.

(By solving simultaneous equations, we find that 24.6% of the combination weight is on the trailer rear wheels at 16.2 ft/sec² deceleration.)

For the unloaded combination, maximum deceleration is $22.5 \times 18.5/34.2 = 12.2$ ft/sec², or a minimum stopping distance of 35.2 ft at 20 mph. In addition, each 0.1-sec lag in application time adds 2.9 ft to the stopping distance.

Taking 0.3 sec as a reasonable maximum lag time, these stopping distances become:

$$\text{Loaded, } 26.5 + 8.7 = 35.2 \text{ ft}$$
$$\text{Unloaded, } 35.2 + 8.7 = 43.9 \text{ ft}$$

In view of the recent adoption by the National Committee on Uniform Traffic Laws and Ordinances of a scale of stopping distances for passenger cars and trucks, which depends upon gross weight and number of axles and is based upon a realistic interpretation of the tests conducted by the Bureau of Public Roads, it appears certain that closer attention to vehicle stopping distances is to be expected in the near future. An important phrase in the Uniform Code is "Under all conditions of loading" which includes, of course, the curb weight or empty condition. It can be anticipated that brake design engineers, field service engi-

Table A – Per Cent Weight on Front and Rear Wheels Under Various Conditions for Passenger Car

Loaded (5 Passengers)	Front, %	Rear, %
Static	50	50
Deceleration $0.2g$ = 6.4 ft/sec²	54.6	45.4
Deceleration $0.435g$ = 14 ft/sec²	61.1	38.9
Deceleration $0.7g$ = 22.5 ft/sec²	66.3	33.7
Driver Only		
Static	56.6	43.4
Deceleration $0.2g$ = 6.4 ft/sec²	61.2	38.8
Deceleration $0.435g$ = 14 ft/sec²	67.7	32.3
Deceleration $0.7g$ = 22.5 ft/sec²	72.9	27.1

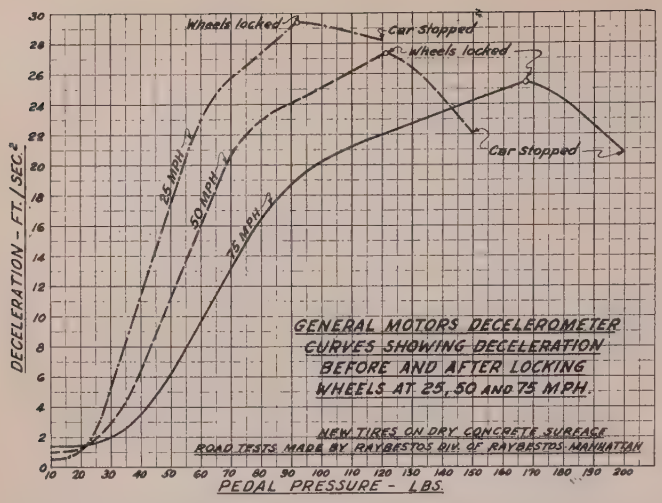

Fig. A – Decelerometer curves showing deceleration before and after locking wheels at 25, 50, and 75 mph (new tires on dry concrete)

Table B – Per Cent Weight on Front and Rear Wheels Under Various Conditions for Conventional Truck

Loaded	Front, %	Rear, %
Static	23.1	76.9
Deceleration $0.2g$ = 6.4 ft/sec²	30.5	69.5
Deceleration $0.435g$ = 14 ft/sec²	39.3	60.7
Deceleration $0.7g$ = 22.5 ft/sec²	49.2	50.8
Driver Only (c.g. lowered also)		
Static	53.3	46.7
Deceleration $0.2g$ = 6.4 ft/sec²	58.7	41.3
Deceleration $0.435g$ = 14 ft/sec²	64.9	35.1
Deceleration $0.7g$ = 22.5 ft/sec²	72.0	28.0

Table C – Per Cent Weight on Each Pair of Wheels Under Various Conditions for Tractor and Single-Axle Semitrailer

Loaded (30,780 lb)	Tractor Front, %	Tractor Rear, %	Trailer Rear, %
Static	12.7	46.9	40.4
Deceleration $0.2g$ = 6.4 ft/sec²	18.1	47.7	34.2
Deceleration $0.435g$ = 14 ft/sec²	24.4	48.8	26.8
Deceleration $0.7g$ = 22.5 ft/sec²	31.5	50.0	18.5
Driver Only (c.g. of trailer lowered also) (10,780 lb.)	(3320 lb)	(5030 lb)	(2430 lb)
Static	30.8	46.7	22.5

neers, and truck operators will find it necessary to give close attention to the problem of brake distribution in order to meet these requirements.

Onset of Sudden Rain Can Cause Dangerous Loss of Traction

– Clyde S. Batchelor
Raybestos Division, Raybestos-Manhattan, Inc.

MR. OETZEL has shown that the maximum deceleration is obtained just before wheel locking. The deceleration curves of Fig. A show the deceleration change occurring due to wheel lock at three different speeds under one set of conditions.

In regard to road traction variable, Mr. Oetzel mentions ice as one of the great traction reducers. Another one which occurs infrequently and is often not recognized is a temporary condition which occurs just at the very beginning of a rain storm. To set the stage for the most dangerous condition, it should not have rained for several days and the road should be a heavily travelled highway with a smooth surface. A sudden rain under these conditions for a period of less than 5 min produces a loss of traction comparable to the slickest ice. Many serious wet-road skids have been attributed to wet roads alone when it was actually a momentary condition. The late Dr. Frederick Stanley analyzed this phenomena and found that oil, road smut, and rain water, in critical amounts, forms an emulsion which creates a continuous lubricating film. As the rainstorm continues, this oil-water slick is washed away, and the original traction of the normal wet-road surface is restored.

How Driver "Anticipation" Helps On Vehicles with Poor Brakes

– A. H. Easton
University of Wisconsin

MR. OETZEL'S reference to driver "anticipation" provides an answer to how drivers are getting by with the equipment that has the poor braking characteristics shown in Mr. Petring's paper.[a] By the same token, the good driver never uses the full brake application except in an emergency. Even though some loads will not permit decelerations of greater than 10 ft per sec per sec, I would say that the driver should have the maximum possible deceleration available in case he absolutely needs it.

The oscillograms shown in Fig. 4 bear out some of the remarks which I made on Mr. Petring's paper regarding the maximum braking available with skid impending.

The author's fine analysis of the weight distribution on a truck-tractor semitrailer unit deserves considerable attention. It is apparent from his calculations that the braking power of the front axle is overlooked on the surfaces of higher coefficients of friction. For example, with a coefficient of friction of 0.6 the weight on the front axle is 28%, and therefore 28% of the braking is available at the front axle as shown in Section 11 of the paper. Again referring to our 1952 units, the front wheels of one of the tractors would not slide under load, the stopping distance using this tractor was 39 ft. The other tractor connected to the same trailer gave a stopping distance of 34 ft, a difference of 5 ft due to the difference in braking at the front wheels.

Author's Closure To Discussion

IN regard to the comments by Mr. Batchelor:

I wonder if all wheels locked, where indicated, or only the rears. I wonder how long it took to build pedal pressure up to the locking point. I wonder if the change in slope (at 16 to 24 ft/sec²) doesn't indicate where "impending slide" began, where the slip between tire and road begins to increase, or if this indicates locking of rears ahead of fronts. I wonder if the rate of pedal pressure buildup was the same for all three speeds and uniform throughout the stop. I wonder if the lower ends of the curves indicate the difference in rolling resistance and windage at the three speeds.

[a] For Petring paper, see pp. 334-348 of this issue.

Some Concepts of

Knock and Antiknock Action

B. M. Sturgis, E. I du Pont de Nemours & Co., Inc.

This paper was presented at the SAE National West Coast Meeting, Los Angeles, Aug. 18, 1954.

ALMOST from their very beginning, the power output and efficiency of spark-ignition automobile engines have been limited by combustion knock. This problem has received a great deal of attention over many years from both the automotive and petroleum industry; and, as the result of improved engine design, improved gasoline refining processes, and the use of antiknock additives, the power and performance of automobile engines have increased enormously. This development reflects great credit to these industries, and there is no reason to doubt that progress in more efficient fuel utilization will continue.

Although the improvement in the mutual adaptation of fuels and engines has been great, its progress has been slowed by the fact that largely empirical methods have been used. This has been necessary because the fundamental nature of the knock process, the differences in hydrocarbon knock behavior, and the way in which antiknocks function have not been understood.

It is evident that a thorough knowledge of the knock process and its causes would facilitate efficient fuel utilization. For this reason a number of investigations of hydrocarbon oxidation and knock have been pursued during the past 30 years in an attempt to secure this knowledge. Development of an understanding of these processes has been slow due to the very rapid and complex nature of the knock reaction, the difficulty of making precise observations of knock in an engine, and the difficulty of reproducing knock outside of engines. Up until the past few years the physical nature of knock and the factors affecting it had been explored, but only a few glimpses into the actual chemical reactions causing knock had been obtained. It is only recently that techniques have been improved, instrumentation refined, and the knowledge of rapid chemical chain reactions developed to the point which has allowed real progress to be made in the study of the chemical reactions occurring in engines. As a result of these recent chemical studies, the picture of the changes which occur in the fuel-air mixture in an engine prior to combustion, the effect of these changes on knock, and the method by which antiknocks function, has become more clear. This paper will describe the present knowledge of these processes.

Physical Aspects of Knock

It has been established that knock takes place in the last portion of the engine charge to burn. In a normal engine cycle the flame is initiated at the spark and travels in a fairly uniform manner across the combustion chamber, compressing the unburned gas before it. This "end gas" receives heat from the advancing flame front. If the temperature and pressure of the "end gas" are below certain critical values, which are dependent on the fuel used and engine operating conditions, the flame front will move forward in a regular manner until all of the fuel is consumed. If, however, the tem-

perature and pressure conditions are sufficiently severe, the rates of the chemical reactions taking place in the unburned charge will increase so rapidly that it will be consumed at a very high rate. This very high rate of burning sets up a shock wave which impinges on the cylinder wall to give the knocking sound characteristic of detonation in an engine. These phenomena are illustrated in Fig. 1. Any condition which raises the temperature or pressure of the engine charge, such as increased compression ratio or intake air temperature, will promote knock. Lengthening the time available for the chemical reactions to take place, such as by increasing the length of flame path or lowering the engine speed, will also tend to increase the tendency for knock to occur. The significance of these factors will not be entirely understood until the nature of the chemical reactions preceding knock is known. These are rather complex, as shown by radiation measurements which often demonstrate the presence of cool flames or blue flames prior to autoignition or knock.

Chemical Reactions Preceding Knock

Evidence of Reaction – The presence of precombustion reactions in engines usually can be observed by three different methods: (1) measurement of cylinder pressure, (2) measurement of radiation, and (3) determination of the presence of fuel oxidation products.

The increase in cylinder pressure which accompanies precombustion reactions is due to a combination of two factors: (a) a release of chemical energy from the fuel which heats and expands the engine charge and (b) an increase in the number of molecules in the system due to the degradation of the fuel by oxidation processes. Fig. 2, taken from Pastell,[1] illustrates the pressure increase due to partial oxidation of a reactive fuel in a motored engine under mild conditions. For air, and for a fuel such as isooctane which does not exhibit a measurable reaction under these mild conditions, the pressure-time curve is symmetrical about the top dead center line. However, for a fuel such as 60-octane-number primary reference fuel which undergoes appreciable precombustion reactions, the pressure curve is not symmetrical. At or near top dead center the pressure curve for the reacting fuel rises above that for the non-reacting fuel and stays above it for the remainder of the expansion stroke. These precombustion reactions can sometimes result in a large heat release and pressure development. Measurements have indicated that as much as 25 to 40% of the total energy available from combustion of some quite reactive hydrocarbon is released before a hot flame appears.[2] Cornelius and Caplan[3] have stated that no losses in power and thermal efficiency of current automotive engines should occur on the road as a result of precombustion reactions since they probably mostly occur after spark ignition rather than during the compression stroke.

If a sensitive radiation detector is placed in the head of a motored engine and the compression

---

[1] See SAE *Quarterly* Transactions, Vol. 4, October, 1950, pp. 571-587: "Precombustion Reactions in a Motored Engine," by D. L. Pastell.

[2] See SAE *Quarterly* Transactions, Vol. 6, July, 1952, pp. 472-487: "Early Combustion Reactions in Engine Operation," by E. B. Rifkin, C. Walcutt, and G. W. Betker, Jr.

[3] See SAE *Quarterly* Transactions, Vol. 6, July, 1952, pp. 488-510: "Some Effects of Fuel Structure, Tetraethyl Lead, and Engine Deposits on Precombustion Reactions in a Firing Engine," by W. Cornelius and J. D. Caplan.

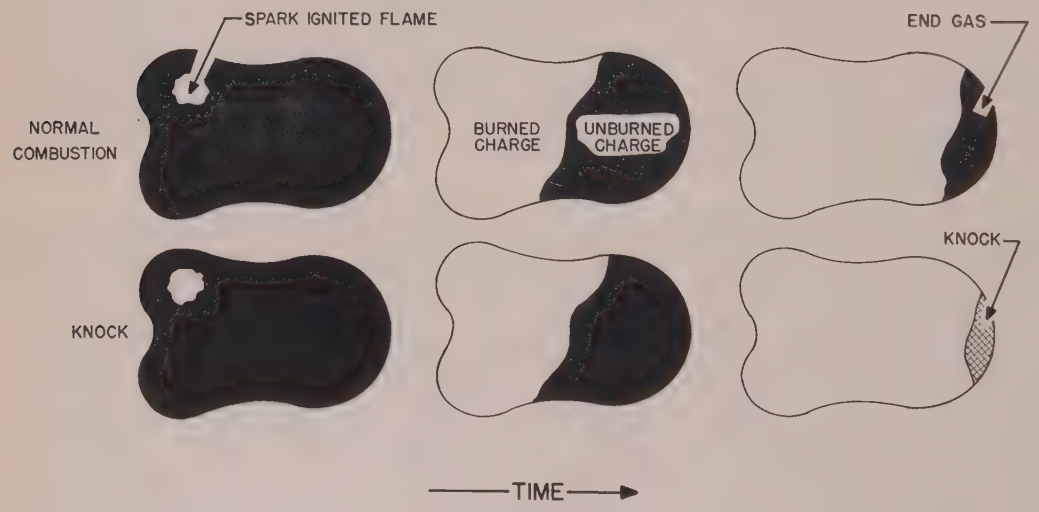

Fig. 1 – Normal and knocking combustion

RECENT improvements in techniques and instrumentation plus further data on rapid chemical chain reactions have made possible a clearer picture of the chemical reactions in engines. This paper describes the present knowledge of the changes in the fuel-air mixture prior to combustion, the effect of these changes on knock, and the method by which antiknocks function.

Knock is controlled by the preflame reactions occurring prior to fuel combustion. These reactions are very complex, but the specific reactions causing knock seem to be simple, probably involving very fast reactions initiated by combinations of only hydrogen and oxygen. Hydrocarbon structure affects the rate of accumulation of enough of the hydrogen-oxygen species to cause knock.

Tel slows the later stages of reaction, probably by deactivating the hydrogen-oxygen groups. The active antiknock species seem to be either lead oxide or metallic lead.

The Author

B. M. STURGIS (M '47) is head of the Combustion and Scavenging Division of the Petroleum Laboratory of E. I. du Pont de Nemours & Co. He received his Ph.D. in Chemistry from M.I.T. in 1936. That same year he joined the Jackson Laboratory of E. I. du Pont de Nemours & Co., working on natural and synthetic rubber problems.

ratio of the engine gradually increased to provide higher peak cycle temperatures and pressures, radiation will appear with most fuel-air mixtures when severe enough conditions are reached. A further increase in compression ratio will increase the intensity of the radiation until, eventually, autoignition and extremely rapid combustion of the charge will occur. This radiation occurs as the result of a cool flame, so called because of its low emissivity and very low heat release compared to a hot flame. The emissivity does, however, signify chemical reactions of sufficient intensity to activate certain oxidized fuel molecules to the point of radiation.

By means of a variety of sampling devices, samples of the fuel-air mixture have been taken from the "end gas" of fired engines and simulated "end gas" of motored engines and analyzed for chemical composition. Using an easily oxidized fuel, a wide variety of oxidation products have been found. The extent of hydrocarbon oxidation is illustrated by the fact that in a motored engine about 70% of n-heptane introduced as a stoichiometric fuel-air mixture was found to have been changed into other products prior to autoignition.

Stages of Precombustion Reactions – The oxidation of most hydrocarbons in engines is known to give rise to a cool flame prior to the formation of a hot flame. Careful investigation with a combination of chemical sampling procedures and radiation measurements has demonstrated that most hydrocarbons go through three or even four stages in their oxidation process. The cool flame is preceded by a period of oxidation in which the intermediates necessary for cool-flame formation are produced. The first evidence of oxidation is usually seen in the engine about 50-75 F below the temperature required for cool-flame formation. Fig. 3 is an ignition diagram for a stoichiometric mixture of n-heptane and air in a motored engine, plotted in terms of temperature and pressure, which shows the regions of pre-cool-flame reaction, cool flames, and hot flames. It can be seen that the curve depicting the points of earliest detectable oxidation is approximately parallel to the lower cool-flame limit curve.

Most hydrocarbons also give rise to a blue flame just prior to autoignition. This is seen more frequently at lean mixtures, although it is believed to be present at all mixture strengths. The blue flame is not just a more intense cool flame but appears to be a somewhat different phenomenon as judged by the shape of the radiation curve and chemical analysis of the products formed in this region.

Reactions Leading to Cool Flames – The complete oxidation of a hydrocarbon, such as occurs

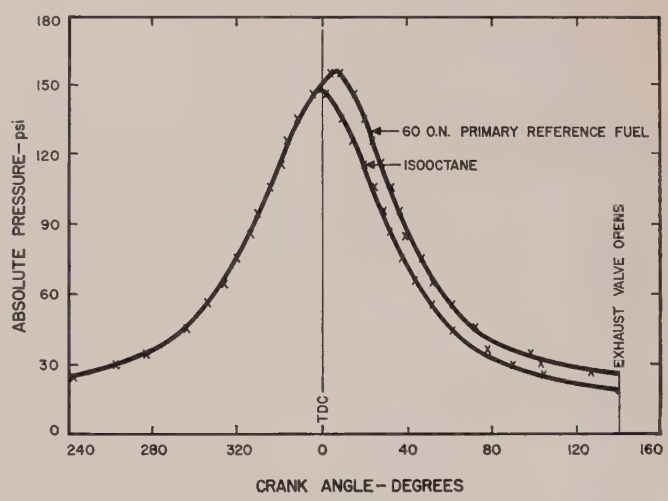

Fig. 2– Pressure-time diagram showing precombustion reactions at 7.0/1 compression ratio, 0.075 fuel/air ratio, 900 rpm, and 300 F inlet mixture temperature

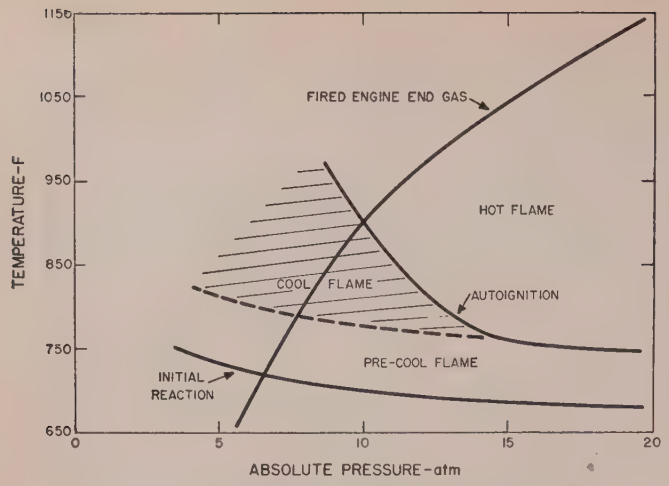

Fig. 3 – Precombustion reactions of n-heptane

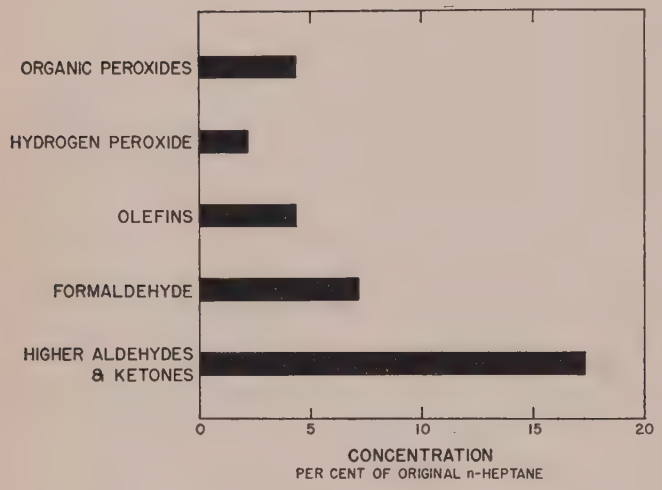

Fig. 4 – n-Heptane oxidation in pre-cool-flame region

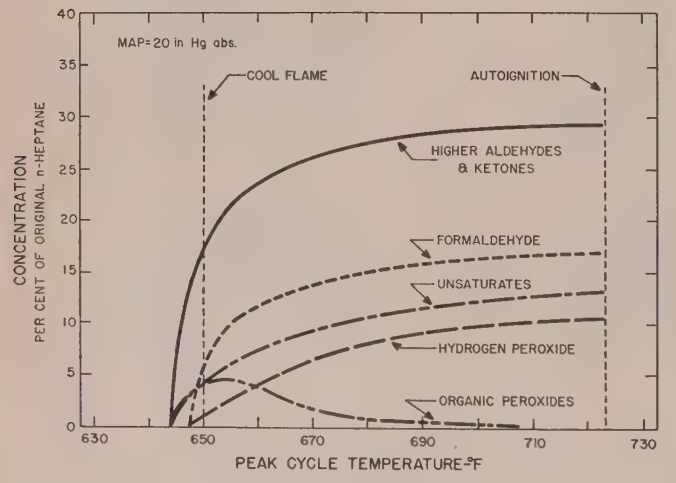

Fig. 5 – Exhaust-gas composition, n-heptane

during its combustion, is a very complex process. The overall equation for the combustion of heptane is

$$\underset{\text{heptane}}{C_7H_{16}} + \underset{\text{oxygen}}{11\ O_2} \longrightarrow \underset{\text{carbon dioxide}}{7\ CO_2} + \underset{\text{water}}{8\ H_2O}$$

This does not occur in one step, but by a series of collisions of oxygen molecules with the heptane molecule to form first a series of intermediate products, such as peroxides, aldehydes, and ketones, and finally ending with carbon dioxide and water. The product first formed by reaction of a hydrocarbon with oxygen is a peroxide.

$$\underset{\text{hydrocarbon}}{C_7H_{16}} + O_2 \longrightarrow \underset{\text{peroxide}}{C_7H_{15}OOH}$$

These peroxides are quite unstable at the elevated temperatures existing in the end gas of an engine and can decompose in several different ways to form more stable compounds containing oxygen, such as aldehydes, R-C-H, or ketones, R-C-R. They

$$\text{R-C-H} \qquad\qquad \text{R-C-R}$$
$$\quad\ \|\ \qquad\qquad\quad \|$$
$$\quad\ O \qquad\qquad\quad O$$

can also decompose to form very reactive materials called radicals, which can promote the oxidation of more molecules of the hydrocarbon. The aldehydes and ketones and other intermediates can react with more oxygen to form, eventually, the end products of oxidation.

Sampling experiments have been carried out in motored CFR engines in which the temperatures and pressures of the entire fuel-air mixtures were varied to simulate the conditions present in the end gas of a fired engine. Davis, Smith, and Malmberg[4] have demonstrated that the same types of oxidation products are formed under these conditions as in the end gas of a fired engine. The samples were analyzed to determine what types of chemical compounds were present. The sample compositions were determined as a function of compression ratio, commencing at engine conditions for which no reaction occurred and continuing up to the point of autoignition of the hydrocarbon-air mixture.

Using a stoichiometric n-heptane-air mixture, no evidence of reaction was observed at low compression ratios. As the compression ratio was increased, a point was reached at which peroxides were just detected. Further increases in compression ratio gave rapidly increasing amounts of peroxides and also rapidly increasing amounts of aldehydes and ketones. Olefins also appeared, probably formed by decomposition of peroxide radicals. Just prior to the formation of a cool flame, hydrogen peroxide appeared. This substance, HOOH is believed to re-

[4] See pp. 386 to 399 of this issue: "Comparison of Intermediate-Combustion Products Formed in an Engine with and without Ignition," by W. C. Davis, M. L. Smith, E. W. Malmberg, and J. A. Bobbitt.

sult from the recombination of active radicals formed by the decomposition of organic peroxides. Considerable concentrations of intermediate oxidation products are formed during this pre-cool-flame reaction period. The concentrations of these intermediates just prior to the appearance of a cool flame, as detected by very sensitive radiation detectors, is illustrated in Fig. 4.

Cool Flames – As the cool-flame boundary is crossed, the original rapid buildup of intermediates slows down, and the curves level off as they approach the autoignition point, as shown in Fig. 5. There is a marked decrease in the amount of organic peroxides present. These results indicate that some sort of reaction inhibition is occurring.

The organic peroxides which are formed originally from the hydrocarbon are believed to decompose in two different ways. The first is a fission of the peroxide molecule to yield two radicals, each of which can help to initiate further oxidation of the hydrocarbon. The second is a thermal decomposition to form the relatively inactive aldehydes, ketones, and olefins. Prior to cool flames the first reaction is the dominant one, but in the cool-flame region the second reaction appears to dominate. These reactions are shown in Fig. 6. This causes the whole oxidation process to slow down during the cool-flame period.

The radiation from cool flames has been shown to be produced by excited formaldehyde molecules. Formaldehyde, HCHO, is the simplest aldehyde and is usually found in considerable amounts in the oxidation products of hydrocarbons. Only a few of the formaldehyde molecules radiate, because in order to do this they must be formed by a special process which imparts to them an excess of energy. This process is believed to be associated with the decomposition of organic peroxides.

In order to study the decomposition of peroxides in engines, small amounts of t-butyl hydroperoxide dissolved in benzene, which acted as an inert solvent under the conditions of the test, were motored through a CFR engine and exhaust samples analyzed for the peroxide and its decomposition products at increments of compression ratio from 4/1 to 14/1. Results of these experiments are shown in Fig. 7. It is seen that at a compression ratio giving a peak cycle temperature of about 650 F the peroxide started to decompose. It reached a maximum rate of decomposition at about 750 F, which was the point at which cool-flame radiation appeared. Most of the products of decomposition were higher ketones; however, small amounts of hydrogen peroxide and formaldehyde appeared prior to the cool flame. Only very small amounts of organic peroxide were sufficient to cause the appearance of a cool flame. These experiments indicate that a cool flame occurs as the result of the decomposition of organic peroxides. The formation of cool flames is a rather complex process, however, since oxygen was found to be necessary.

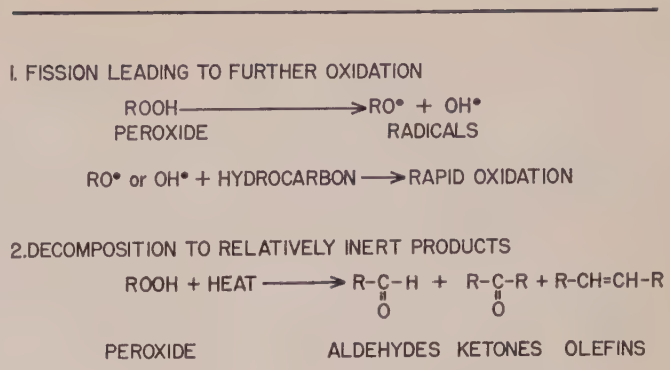

Fig. 6 – Peroxide decomposition

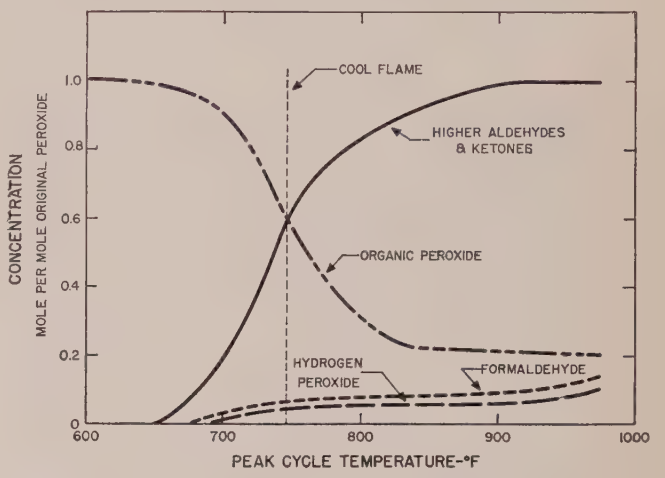

Fig. 7 – Exhaust-gas composition, benzene +0.1% t-butyl hydroperoxide

Table 1 – Effect of Oxygen on Cool-Flame Formation

Atmosphere	Moles Product per 100 Moles Peroxide HCHO	Moles Product per 100 Moles Peroxide H_2O_2	Cool-Flame Intensity
Air	12	10	100
Nitrogen + 0.002% Oxygen	None	None	8

The importance of oxygen was determined by repeating the peroxide decomposition experiments in the presence of nitrogen rather than air. The results given in Table 1 show that in the substantial absence of oxygen, little radiation was observed.

These experiments confirm that cool flames are not the result of peroxide decomposition per se but of further oxidation of the decomposition products.

Although hydrocarbon oxidation preceding combustion in an engine is a very complex reaction, the essential features appear to be the formation and decomposition of organic peroxides and the reactions of their decomposition products to form hydrogen peroxide, formaldehyde, and radicals having high amounts of energy.

Blue Flames – Knock is known to result from an

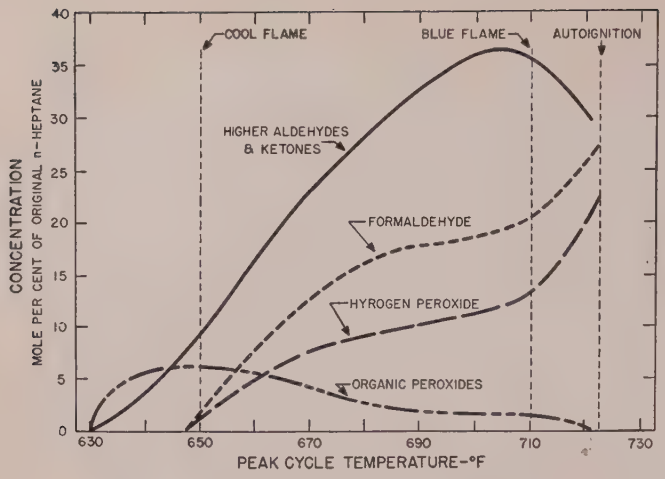

Fig. 8 – Effect of blue flame on exhaust-gas composition, n-heptane

extremely rapid chemical reaction. This reaction is thought to be of the chain-branching type, which means that a number of very reactive radicals interact to produce an ever-increasing number of reactive radicals. The diagram of Fig. 5 does not show this type of a reaction taking place, since the concentrations of the products change but little as autoignition is approached. It was believed that the reason for this is that the very rapid reactions ordinarily take place over a very narrow range of compression ratios just prior to autoignition and that samples of the precombustion reaction products cannot be taken so close to autoignition. It was found that by using leaner mixtures, this pre-autoignition reaction could be slowed down and spread over a greater range of compression ratios so that samples from this region could be taken.

The chemical reaction taking place in this region was accompanied by a bright blue radiation intense enough to be easily seen by the eye looking through a window into the engine combustion chamber. This region of precombustion reaction has been termed the blue-flame region. On a radiation diagram in which radiation intensity was plotted against engine crank angle, the blue flame was indicated by a second radiation peak, later in the engine cycle than the cool-flame peak. Considerable energy was evolved in this region, since the engine would run against its friction without being motored.

Fig. 8 shows the concentrations of intermediate-oxidation products formed in a motored engine with n-heptane at an 0.033 fuel/air ratio under conditions in which a blue flame existed at compression ratios just below autoignition. It is seen that the concentrations of hydrogen peroxide and formaldehyde suddenly increase in the blue-flame region, so that just prior to autoignition the rates of formation of these substances is very rapid. Such a rapid formation of these simple products signifies a large evolution of heat and also formation of a large number of reactive radicals.

The Knock Reaction

Studies of the reactions taking place in the blue-flame region just prior to autoignition indicated that a large number of simple radicals were being formed, some of which combined to form hydrogen peroxide, while others probably reacted to cause autoignition. These radicals could be very simple combinations of hydrogen and oxygen, such as OH′ or HO'_2.

If the knock reaction is a reaction between simple radicals such as these, then hydrogen should also knock in an engine, since it forms the same intermediate radicals when oxidized. In order to determine what similarities exist between hydrogen combustion and hydrocarbon combustion, extensive studies of the combustion characteristics of hydrogen-air mixtures were made in a CFR engine. This investigation by Anzilotti[5] in this country and by Downs, Walsh, and Wheeler[6] in Great Britain, demonstrated that hydrogen knocks in engines and has a good tetraethyl lead response.

The knock resistance of hydrogen compared to a number of hydrocarbons over a range of mixture compositions is shown in Fig. 9. The fuels were rated under identical conditions except for spark advance, which was adjusted to that for maximum power with each fuel. A spark advance of from 28 to 30 deg btdc was used with the hydrocarbon fuels, but with hydrogen the spark was at top dead center because of its much faster flame speed. Hydrogen is seen to fall in the middle of a group of hydrocarbons with respect to its knock resistance and to re-

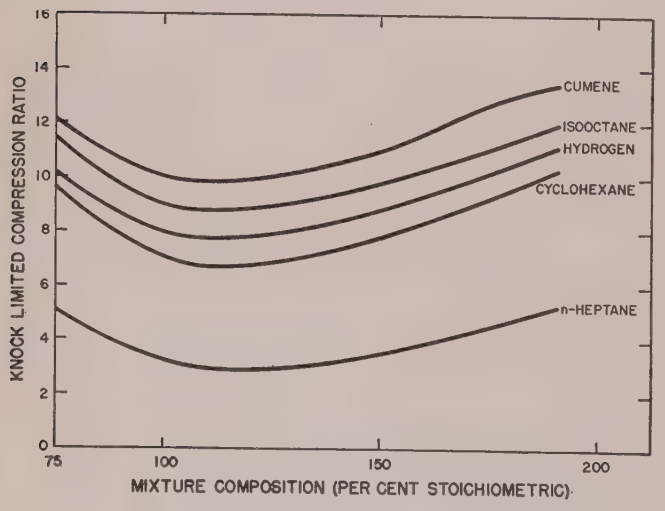

Fig. 9 – Knock resistance of hydrogen compared to hydrocarbons

[5] "Combustion of Hydrogen as Related to Knock. I. Parallel Behavior of Hydrogen and Paraffinic Fuels," by W. F. Anzilotti, G. W. Scott, J. D. Rogers, and V. J. Tomsic. Presented at 124th National Meeting of American Chemical Society, Chicago, Sept. 10, 1953.

[6] See Philosophical Transactions of the Royal Society of London, Series A, Vol. 243, July 19, 1951, pp. 463-524: "Study of Reactions that Lead to 'Knock' in Spark-Ignition Engine," by D. Downs, A. D. Walsh, and R. W. Wheeler.

spond in a similar manner to changes in mixture composition.

Calculations of combustion time showed that the hydrogen combustion was completed in but 29% of the time necessary for isooctane. The effect of the much faster flame speed of hydrogen is beneficial as far as knock is concerned because the residence time of the end gas is much shorter, and, therefore, higher compression ratios can be tolerated without knock. If it were not for this shorter end-gas residence time, hydrogen probably would knock far more readily than any of the hydrocarbons.

The knocking combustion of hydrogen resembles that of paraffinic hydrocarbons in another respect – it responds well to tetraethyl lead. Fig. 10 shows the marked increase in knock-limited compression ratio resulting from the addition of small amounts of tetraethyl lead.

Additional support for the similarity in knock behavior between hydrogen and paraffinic hydrocarbons is seen in the effect of sulfur compounds on their engine performance. Certain types of sulfur compounds act as proknocks in hydrocarbon fuels, while others do not. A series of four different sulfur compounds lined up the same way in hydrogen as in paraffinic hydrocarbon fuels with respect to their proknock effect.

These data all show that the knocking characteristics of hydrogen in an engine are very similar to paraffinic hydrocarbons. It might be deduced, therefore, that the same types of chemical reactions cause knock in both types of fuels. Since with hydrogen these reactions can only be between simple substances containing hydrogen and oxygen, perhaps hydrocarbon knock is the result of reactions of these same substances.

Carbon Monoxide Combustion – If simple radicals containing hydrogen are the cause of hydrocarbon knock, then a fuel which contains no hydrogen, such as carbon monoxide, CO, might be expected to burn in engines without knocking. It has been shown that water enters into the combustion reactions of carbon monoxide, and can contribute hydrogen to the intermediate-combustion products.[7, 8] When tested in a CFR engine, a carbon monoxide-air mixture containing 1.4 mole % water was found to knock but to be more resistant to knock than isooctane.[9] This is illustrated in Fig. 11. The response of the knocking characteristics to mixture composition for this "wet" carbon monoxide was found to be similar to that of isooctane.

It was found impossible to maintain strictly anhydrous conditions in the engine, even though the

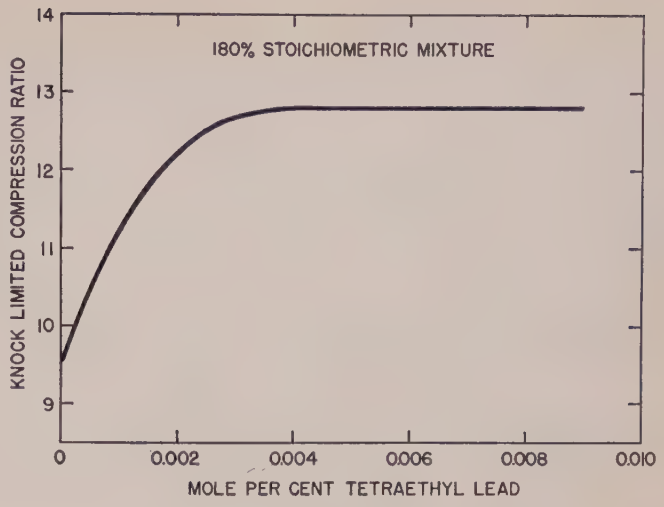

Fig. 10 – Tetraethyl lead response of hydrogen

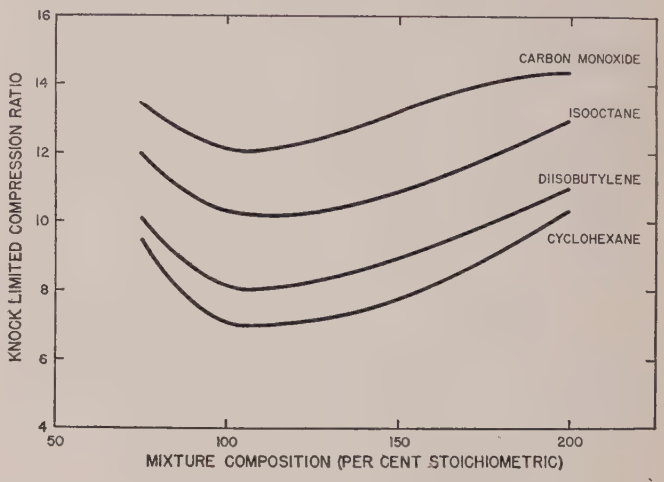

Fig. 11 – Knock resistance of carbon monoxide compared to hydrocarbons

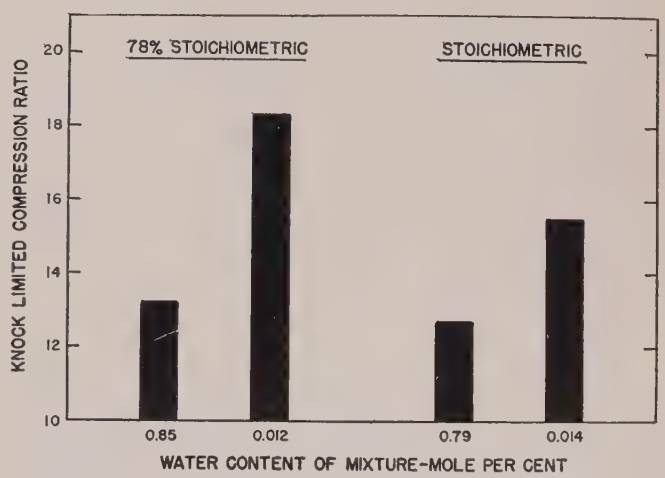

Fig. 12 – Effect of water on knock resistance of carbon monoxide

[7] See "Combustion, Flames, and Explosions of Gases," by B. Lewis and G. von Elbe. Pub. by Academic Press, Inc., New York, 1951.

[8] See *Journal of Chemical Physics*, Vol. 15, 1947, pp. 431-433: "Equilibrium Atom and Free-Radical Concentrations in Carbon Monoxide Flames and Correlation with Burning Velocities," by C. Tanford and R. N. Pease.

[9] "Combustion of Hydrogen and Carbon Monoxide as Related to Knock," by W. F. Anzilotti and V. J. Tomsic. Presented at the Fifth International Combustion Symposium, Pittsburgh, September, 1954.

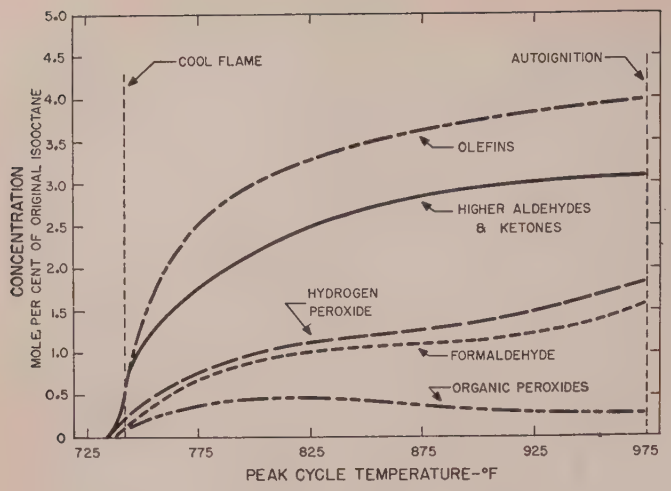

Fig. 13 – Exhaust-gas composition, isooctane

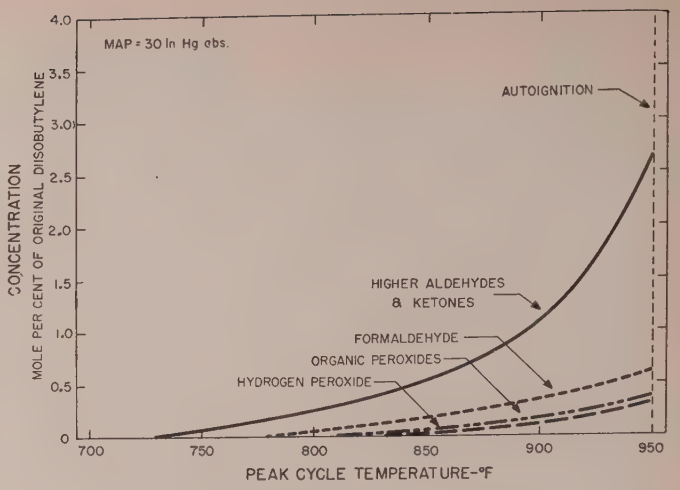

Fig. 14 – Exhaust-gas composition, diisobutylene

fuel, air, and fuel induction system were thoroughly dried, because of trace quantities of crankcase oil which entered the combustion chamber and burned to give water. However, definite trends were established in the knock behavior of carbon monoxide by drying as carefully as practicable and then determining knock-limited compression ratios at various moisture concentrations by adding known amounts of water vapor. As the carbon monoxide-air mixture became drier, the tendency to knock became less as shown in Fig. 12.

These data indicate that it is entirely possible that a perfectly dry carbon monoxide-air mixture would not knock in an engine under any ordinary conditions. This lends further support to the theory that the knock reaction may be related to the presence of simple hydrogen-and-oxygen-containing radicals.

Effect of Hydrocarbon Type

Although the knock reaction may be a rather simple one consisting of extremely rapid production and combination of hydrogen-and-oxygen-containing species, the formation of the critical concentrations of these species necessary to trigger the reaction is dependent upon the structure of the hydrocarbon or other fuel being burned in the engine. It has been seen in Fig. 4 that under the motored engine conditions used, n-heptane started to form oxidation products at the relatively low temperature of 645 F, quickly gave rise to a cool flame, and produced large amounts of reaction products prior to autoignition at 723 F. At this point about 70% of the n-heptane had been converted into other products.

Isooctane, as might be expected from its much higher octane number, acted somewhat differently. Higher temperatures were required for reaction to start, the first evidence of product formation being at nearly 100 F higher temperature than for n-heptane, even though the pressure conditions were more severe due to operation at a higher manifold air pressure.[10] Isooctane oxidized more slowly than n-heptane and produced a much smaller quantity of preflame reaction products, as illustrated in Fig. 13. This slower and less extensive oxidation occurred in spite of the fact that the region of reaction was at a higher temperature than that for n-heptane, and temperature is known to increase the rates of chemical reactions. These facts point both to the greater difficulty of oxygen attack on this hydrocarbon, as predicted by Livingston[11] and to the greater stability of the peroxides which are formed. Some of the organic peroxides are seen to exist clear up to the point of autoignition. Only about 7% of the isooctane was changed into other substances prior to autoignition. These facts combine to explain why isooctane-air mixtures do not autoignite and detonate until a temperature of 975 F is reached. The formation of the critical concentration of the species responsible for knock evidently takes place slowly and is not accomplished until high temperatures are present.

Diisobutylene ordinarily does not give rise to cool flames in engines. The oxidation pattern for this hydrocarbon should, therefore, be quite different from that of the paraffins. Fig. 14 shows that, while oxidation occurred in the same temperature region as isooctane, the vigorous reaction following initiation of oxidation was not present. The reactions were inhibited so that they proceeded very slowly, and no appreciable concentration of products was obtained until just prior to autoignition. The organic peroxides apparently did not undergo the type of decomposition to give cool-flame-forming substances.

Benzene did not form any detectable intermediate

---

[10] See *Industrial and Engineering Chemistry*, Vol. 46, May, 1954, pp. 1024-1029: "Preflame Oxidation of Hydrocarbons in a Motored Engine," by A. J. Pahnke, P. M. Cohen, and B. M. Sturgis.

[11] See *Industrial and Engineering Chemistry*, Vol. 43, December, 1951, pp. 2834-2840: "Correlation of Knock Resistance of Pure Hydrocarbons with Chemical Structure," by H. K. Livingston.

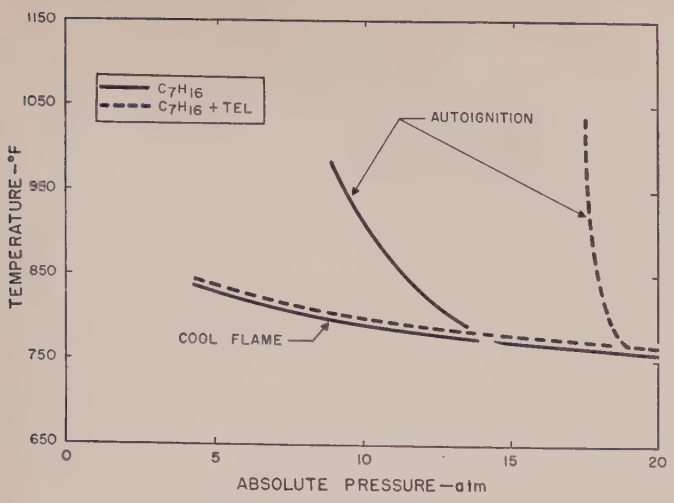

Fig. 15 – Effect of tel on ignition limits of n-heptane

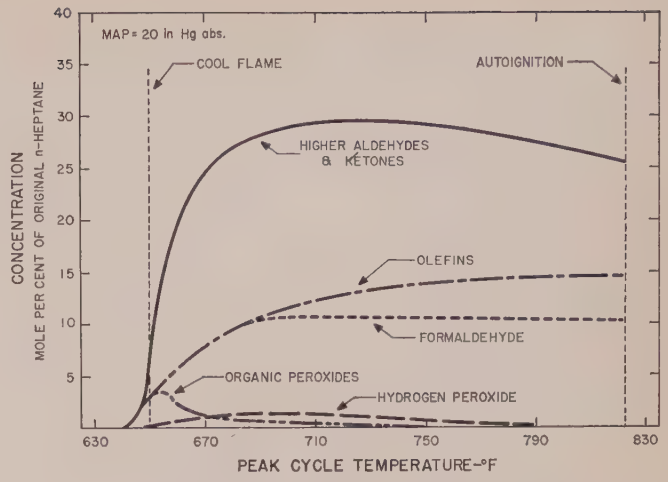

Fig. 16 – Exhaust-gas composition, n-heptane +3 ml tel per gal

products prior to autoignition, indicating that the mode of ignition for this hydrocarbon is vastly different from that for the paraffins. Once oxidation is initiated, it must proceed so rapidly that it is not possible to follow the reaction course by the techniques which have been employed.

Hydrocarbon Blends

In general, olefins blend with paraffins to give higher octane numbers than would be predicted from the octane numbers of the two components. It has been seen that olefins inhibit their own oxidation. They also act to inhibit the oxidation of paraffins with which they are blended. Addition of diisobutylene to n-heptane, for example, raises the engine compression ratios at which oxidation of the heptane is initiated and at which a cool flame appears and slows the cool-flame reaction so that considerably more severe engine conditions are required to produce autoignition. Table 2 illustrates the effects on the precombustion reactions of n-heptane caused by blending with it 23 mole % of diisobutylene.

The blending properties of hydrocarbons can thus be explained by their inhibitory effects on the oxidation reactions of other hydrocarbons.

Action of Antiknocks

Very little has been known concerning the way in which tetraethyl lead reduces the knocking tendencies of fuels. Neither the structure of the active antiknock, the means by which it exerts its effect, nor the steps in the hydrocarbon oxidation reactions which are slowed or altered are definite.

Pastell[1] and Melby[12] have shown that the addition of tetraethyl lead to an oxidizing hydrocarbon usually has very little effect on the point at which a cool flame appears but displaces the autoignition limits to regions of higher temperatures and pressures. This is illustrated in Fig. 15. This would indicate that the early oxidation reactions leading to the formation of organic peroxides are little influenced by tetraethyl lead but that the reactions occurring in the cool-flame region are considerably affected. Tetraethyl lead must be rather selective and influence certain specific reactions rather than the whole oxidation process, since it has been demonstrated that with reactive hydrocarbons the rate of energy liberation due to precombustion reactions is not affected over most of the precombustion period[2] and almost as much pressure is developed due to precombustion reactions[3] in an engine in the presence of tetraethyl lead as in its absence.

More specific information concerning the action of tetraethyl lead has been obtained by repeating the hydrocarbon oxidation experiments in the motored engine in the presence of this antiknock. Fig. 16 shows that the addition of tetraethyl lead to n-heptane at a concentration of 3.0 ml per gal had little effect on the concentrations of total aldehydes and ketones and of olefins formed or on their rates of formation. Thus the reactions leading to the products present in largest amounts took place as usual. The organic peroxide curve also remained practically unchanged. Most striking was the fact that the hydrogen peroxide was almost completely eliminated.

Fig. 17 shows more clearly the relationship between the concentrations of higher aldehydes

Table 2 – Preflame Properties of a Hydrocarbon Blend

Fue	Compression Ratio			Cool-Flame Duration, compression ratios
	First Reaction	Cool Flame	Autoignition	
n-Heptane	5.7	5.9	8.0	2.1
77% n-Heptane 23% Diisobutylene	7.1	7.3	11.2	3.9

[12] See *Journal of the Institute of Petroleum*, Vol. 38, December, 1952, pp. 965-973: "Effects of Fuel Additives on Precombustion Reactions of n-Heptane," by A. O. Melby.

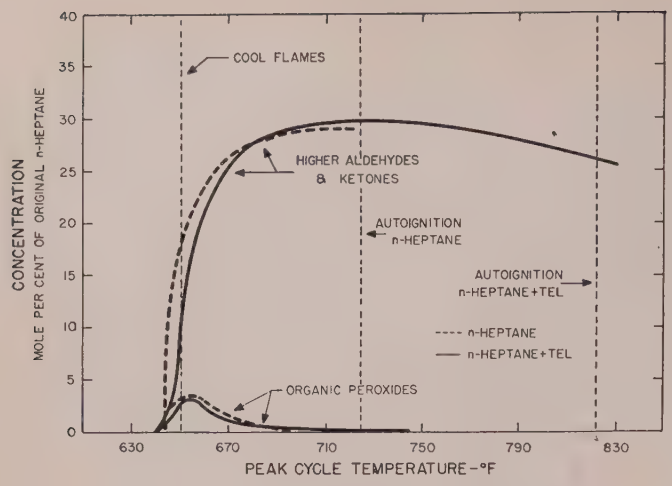

Fig. 17– Effect of tel on n-heptane oxidation

and ketones and of organic peroxides in the presence and absence of tetraethyl lead. It can be seen that up to the point of autoignition of the unleaded hydrocarbon the curves for both fuels are almost identical.

Table 3 compares the concentrations of several classes of intermediates just before autoignition, taken from these same experiments.

It has often been supposed that organic peroxides were the key intermediates in the reactions leading to knock and that they were destroyed by tetraethyl lead. The fact that the rate of buildup of the peroxide concentration and the total amount formed was unchanged by tetraethyl lead shows that this antiknock has little effect on the early hydrocarbon oxidation reactions and does not promote destruction of the organic peroxides formed. To study in more detail the effect of tetraethyl lead on peroxide decomposition, this antiknock at a concentration of 3.0 ml per gal was added to benzene containing 0.1% of t-butyl hydroperoxide. This peroxide solution, mixed with air, was passed

Table 3 – Comparison of Intermediate Concentrations Just before Autoignition for Leaded and Unleaded n-Heptane

Intermediate	Concentration, mole % of n-heptane	
	Unleaded	Leaded 3 ml per gal
Aldehydes and Ketones	29	26
Olefins	13	14
Organic Peroxides	Trace	Trace
Hydrogen Peroxide	11	Trace

through the motored engine, and the exhaust gas was sampled and analyzed. The organic peroxide decomposition curve was identical with the one obtained when the same experiment was carried out in the absence of tetraethyl lead. The small amount of hydrogen peroxide normally formed was completely eliminated, however, and the formaldehyde reduced. This is illustrated in Fig. 18.

It is evident that in n-heptane oxidation tetraethyl lead does not interfere with the reactions leading to the formation of organic peroxides, with the decomposition of these peroxides, or with the reactions leading to the formation of higher aldehydes and ketones or olefins. It appears, rather, to deactivate radicals formed by organic peroxide decomposition which carry out further steps in the reaction, leading to hydrogen peroxide formation or to knock.

It was seen in Fig. 8 that in the "blue-flame" region preceding autoignition the concentration of hydrogen peroxide increased rapidly. This was interpreted to signal the rapid formation of simple radicals of hydrogen and oxygen, such as OH′ and HO_2', some of which combined to form hydrogen peroxide while the remainder initiated the knock reaction. In the presence of tetraethyl lead this rapid increase in hydrogen peroxide concentration in the "blue-flame" region is slowed and delayed. It appears that a primary function of tetraethyl lead may be to deactivate these simple hydrogen-oxygen radicals.

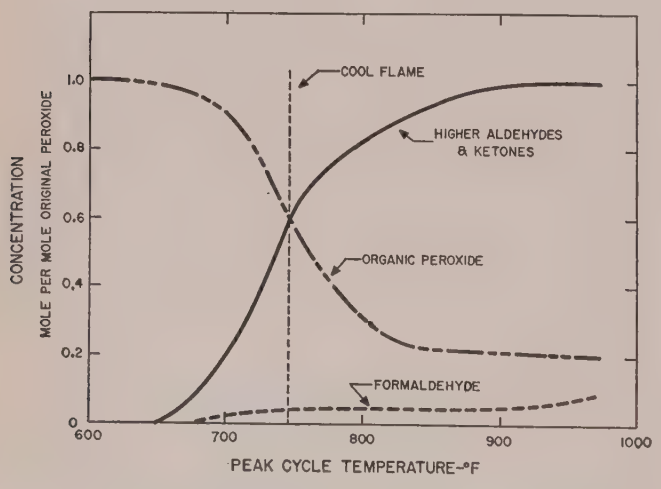

Fig. 18 – Exhaust-gas composition, benzene +0.1% t-butyl hydroperoxide +3 ml tel per gal

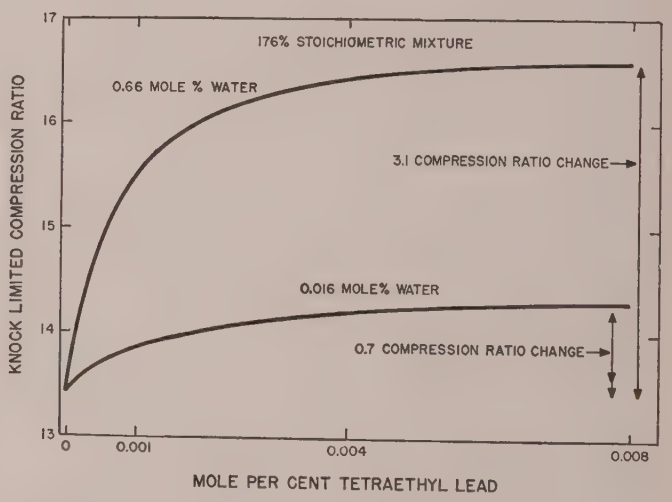

Fig. 19 – Tetraethyl lead response of "wet" and "dry" carbon monoxide

The results obtained using hydrogen as the engine fuel confirms that these types of radicals can be deactivated by tetraethyl lead, since a marked increase in the knock-limited compression ratio of hydrogen-air mixtures was obtained by the addition of small amounts of tetraethyl lead. The radicals present in this system must of necessity be OH′, HO_2′, and H′.

More striking evidence of the role of tetraethyl lead in deactivating hydrogen-oxygen radicals is seen in the response of "wet" and "dry" carbon monoxide to this antiknock. It was shown in Fig. 12 that at relatively low water content the knocking tendency of carbon monoxide increased as the water content increased, indicating that hydrogen-oxygen radical reactions were responsible for knock. In a similar manner, the response of carbon monoxide to tetraethyl lead increased as the water content of the fuel became greater. The relative response of "wet" and "dry" carbon monoxide to tetraethyl lead is shown in Fig. 19.

It is concluded from these data that tetraethyl lead is fairly specific in its action, that it generally is effective only on reactions occurring rather late in the reaction sequence, and that its probable victims are simple hydrogen-oxygen radicals which can, under the proper conditions, initiate reactions so rapid as to cause knock.

The Active Antiknock Material

There has been much dispute as to what material actually acts as the antiknock when tetraethyl lead is added to a fuel. It has been found that tetraethyl lead is largely decomposed rather early in the engine cycle, so that little of it exists as such at the time when the antiknock action is occurring. The initial decomposition product is probably metallic lead. However, at high temperatures in the presence of oxygen, metallic lead would be expected to oxidize quickly to lead oxide.

There is evidence in the literature[13, 14] to indicate that either metallic lead or lead oxide can act as an antiknock if in a very finely divided form. The difficulty lies in introducing these materials into an engine in sufficiently small particle size. Tetraethyl lead represents an ideal way of doing this, since it decomposes at about the right time in the engine cycle to produce very finely divided lead or lead oxide just when needed.

Some light on the identity of the active antiknock was given by a study of the influence of tetraethyl lead, lead oxide, and metallic lead on the explosion temperatures of hydrogen-oxygen mixtures in glass tubes.[5] The addition of very small quantities of tetraethyl lead caused a substantial elevation of the explosion temperature of a stoichiometric hydrogen-oxygen mixture, as shown in Fig. 20. This might be expected, since tetraethyl lead reduced the tendency of hydrogen to knock in an engine. When the inside of the tube was coated with lead oxide, the explosion temperature was increased considerably; a metallic lead coating, however, had no effect on the explosion temperature. These results are illustrated in Fig. 21. The work of Walsh and coworkers[14, 15] in Great Britain has led them to believe that lead oxide may be the active antiknock material. More work is necessary to resolve the identity of the antiknock species and the exact way in which it functions.

Although a complete understanding of the reac-

---

[13] See Philosophical Transactions of the Royal Society (London), Vol. 234, 1935, pp. 434-521: "On the Phenomenon of Knock in Petrol Engines," by A. Egerton and F. L. Smith.

[14] See Proceedings of Royal Society of London, Vol. 215, No. 1123, December, 1952, pp. 454-466: "Inhibiting Effect of Lead Tetraethyl. Part II. Effect of Lead Monoxide on Slow Oxidation of Methane," by D. E. Hoare and A. D. Walsh.

[15] See Proceedings of Royal Society of London, Vol. 215, No. 1121, November, 1952, pp. 175-186: "Inhibiting Effect of Lead Tetraethyl. Part I. Effect of Lead Compounds on Vapor-Phase Slow Oxidation of Diisopropyl Ether and on Ignition of Diethyl Ether," by G. H. N. Chamberlain and A. D. Walsh.

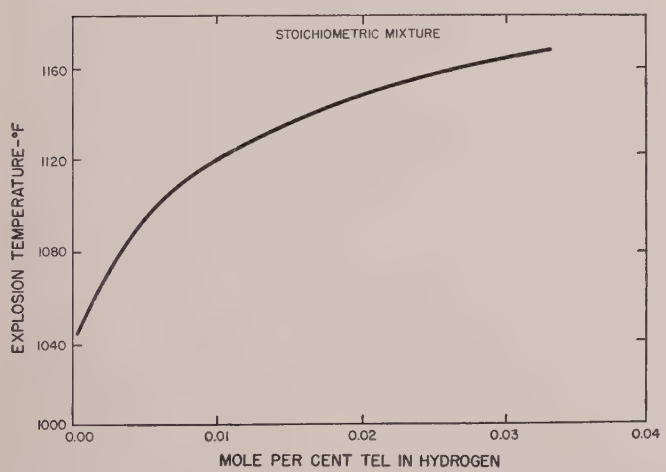

Fig. 20 – Effect of tel on explosion temperature of a hydrogen-oxygen mixture

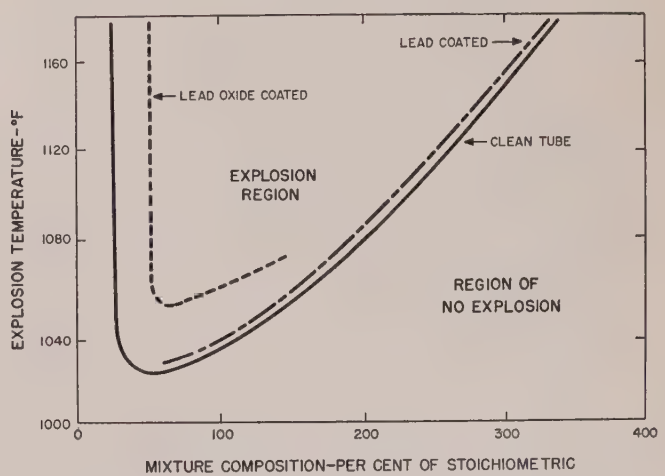

Fig. 21 – Effect of lead and lead oxide on explosion temperature of hydrogen-oxygen

tions leading to knock and methods for suppressing them is not yet available, a great deal of new information has been obtained during the past few years, which is increasing our understanding of these processes. Such information should eventually lead to improved methods for controlling abnormal combustion in engines.

Summary

1. The occurrence of knock in spark-ignition engines operated on hydrocarbon fuels is controlled by the nature and extent of the preflame reactions which occur prior to fuel combustion.

2. Although these reactions are very complex, the specific reactions causing knock are believed to be relatively simple, probably involving very fast reactions initiated by species containing only hydrogen and oxygen.

3. Hydrocarbon structure influences the rate of accumulation of sufficient quantities of the hydrogen-oxygen species to cause knock.

4. Tetraethyl lead does not affect to any extent the early hydrocarbon reactions but slows some of the later stages of reaction, possibly by deactivating the hydrogen-oxygen species.

5. The active antiknock species may be either lead oxide or metallic lead, although experiments seem to favor the former.

Acknowledgment

For the experimental data discussed in this paper, the writer is indebted to W. F. Anzilotti, A. J. Pahnke, C. A. Sandy, and V. J. Tomsic of the du Pont Petroleum Laboratory.

DISCUSSION

Certain Basic Data Are Still Required

— G. A. and E. A. Richardson
Richardson Patent Development

IN discussing this paper, we are well aware of the large amount of detailed investigations which have gone into the background work and particularly into the paper under consideration. Nevertheless certain data of prime consequence are still lacking. Hence, it seems well to recall what was reasonably obvious as much as 32 years ago, was offered to the SAE in paper form 30 years ago, and was published in brief[a] 22 years ago.

Flame propagation, detonation, and dope action were taken up as a preliminary to the discussion of mechanical methods of eliminating detonation so that any fuel, irrespective of its chemical character, might be burned without detonation. The process was covered by a patent controlled by us.[b] Said process was tested before 1936[c] and, within the very limited region of investigation, behaved as claimed. The apparatus used, which failed, was not of the inventor's design or choosing and was unnecessarily complicated.

Change in combustion with temperature requires that we use kinetic theory methods for assigning collision velocity probabilities and recognize that a given collision may be elastic if no energy is absorbed, necessarily inelastic if such can occur. It was further noted that collisions may involve a series of n methods of possible dissociations, each characterized by the energy required to produce it.

At any given temperature, the highest probable velocity of collision will be greater than required for j methods of dissociation (hence, such are possible), but less than that required for the remaining k modes of dissociation. The latter are impossible at the temperature existing. No attempt was made to separate dissociations and reassociations, as the theory was merely a qualitative statement of a more complex series of interactions. However, it was obvious that some higher level of dissociation might make possible a much greater development of energy in combustion, thereby permitting a slow flame to jump to a high-speed detonation.[d]

If a material (dope) were available which would be gaseous before combustion started, dissociate with the absorption of considerable energy at the most critical time during combustion, thereby materially delaying the attainment of the detonation temperature, then a small amount of such substance could serve to prevent detonation by giving time for the flame to cross the combustion chamber.

Unfortunately the very data which would be significant and which were known to be required in 1922—and which should not be too difficult to obtain by persons interested in detonation who have available adequate laboratories—are the data lacking at the present time. What is the dissociation of tetraethyl lead with temperature? How much energy is absorbed at each temperature? What are the ionic products? Also, what is the rate of liberation of energy in the cold-flame reactions, particularly in the gases still ahead of the flame front, and what would be the time-delaying action on temperatures in the presence of the dope? It is of interest that the dope for some reason greatly reduces the quantity of H_2O_2 and its ions present. Likewise the mode of such action would be of interest. Data on the energy of formation of the peroxide and its ions with temperature are required.

Referring to Fig. 15 of the paper, the temperature for so-called autoignition (there is no such thing as autoignition in detonation of the type under discussion[e]) with tel is the same as for C_7H_{16} alone at the cool-flame line, but the density is different. This brings us to the criticism that exhaust-gas compositions are appropriately given in mol per cent, but it is the concentrations in the combustion chamber which are significant. Nothing is said about the influence of these.

We are impressed by the large amount of miscellaneous but presumably interesting information being gathered by such research while, apparently, basic principles seem to be considerably disregarded.

This discussion is made in a spirit of constructive appraisal of this valuable and comprehensive paper. We know how to avoid detonation. Hence, we are not interested parties but merely onlookers in a field which we explored adequately long ago. We trust that our remarks will be received in the spirit in which they are made.

---

[a] See Pennsylvania State College Technical Bulletin No. 16, April 22, 1933, pp. 3-20: "Heating Fuels for Injection Engines," by E. A. Richardson.

[b] U. S. Patent No. 1,876,168, "Process of Preparing Fuels for Use," issued Sept. 6, 1932. Another patent, U. S. Patent No. 2,207,944, "Fluid Actuated Valve," issued July 16, 1940, covers some of the apparatus necessary for effectively carrying on the process. Both patents issued to E. A. Richardson.

[c] See NACA TN 565 (1936), "Influence of Fuel-Oil Temperature on Combustion in a Prechamber Compression-Ignition Engine," by H. C. Garrish and Bruce E. Ayer.

[d] For a detailed development of the theory, see "Introduction to Chemical Physics," by J. C. Slater. Pub. by McGraw-Hill, New York, 1939.

Basic Facts about Noise as Related to Aviation

Adone C. Pietrasanta, Bolt, Beranek, and Newman, Inc.
and
Richard H. Bolt,
Acoustics Laboratory, Massachusetts Institute of Technology

This paper was presented at the SAE National Aeronautic Meeting, New York, April 14, 1954.

THERE are many kinds of noise problems. There are problems concerned with noise from traffic, ventilating equipment, aircraft and aircraft powerplants, industrial machinery, and many other noise-producing devices. Common to all noise problems are certain fundamental aspects and considerations, both physical and psychological in nature. A knowledge of these fundamentals is inherently necessary for a clear understanding of any noise problem. And a clear understanding is a necessary prerequisite to the rational approach and possible subsequent solution of those noise problems which confront us.

The purpose of this paper, therefore, is to present some of the basic facts about noise and noise problems, with particular emphasis on aviation noise problems. It is hoped that this presentation will serve as an introduction to the rest of the papers in this symposium and will lay the groundwork for a better understanding of the relation of the subject matter of the other papers in this symposium to the aircraft noise problem as a whole. Also it is hoped that this paper will aid in the clarification of some of the present thinking on aviation noise problems.

The Nature of Noise – Let us begin with a brief discussion of the nature of noise itself. We might ask ourselves: What is noise? How do we measure it? How can we specify or describe a noise?

Subjectively, noise is any unwanted sound. A sound, and there are an infinite number of sounds, becomes a noise only as the result of a subjective reaction. For instance, the majority of us would agree that the sound from the exhaust of a "souped-up" automobile is definitely noise, yet it might be music to the ears of a hot-rod addict. There is also, of course, a diversity of opinion in this respect concerning music, and it is safe to say that one man's music might be another man's noise.

Noises (and sounds) can be described physically by specifying their sound intensity in watts per square centimeter as a function of frequency. However, the range of sound intensities encountered in practice is so very great – the ratio of some of the highest intensities measured to the faintest intensity that the average ear can hear is about a million billion to one – that it would be extremely awkward and cumbersome to work just with sound intensities. For this reason we usually state not the intensity but the corresponding logarithmic quantity, the *intensity level*[1] in decibels. The intensity level for a sound intensity of I, for instance, is given by

$$10 \log_{10} \frac{I}{I_o} \text{ decibels}$$

[1] The term *level* is ordinarily used when expressing a quantity in decibels.

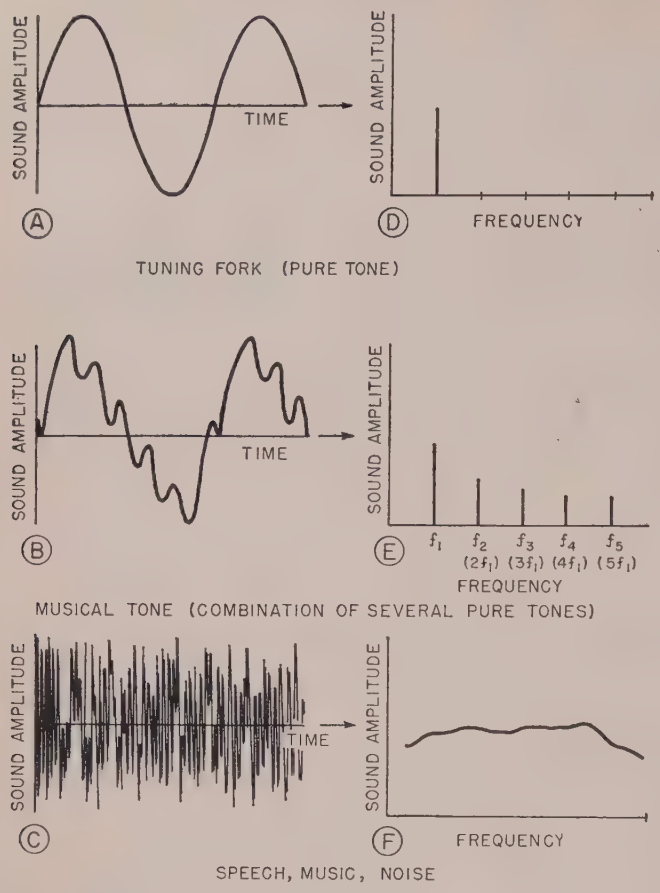

Fig. 1 – Schematic representation of a pure tone, a musical tone, and speech, music, and noise, showing the variation of sound amplitude with time and with frequency

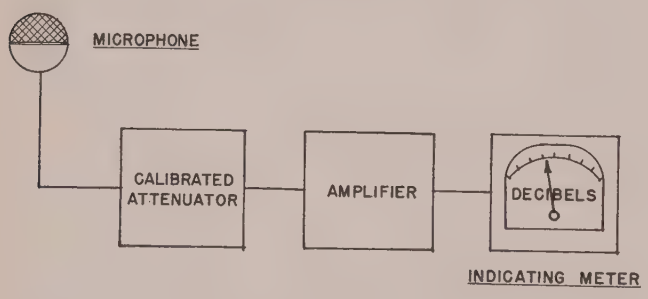

Fig. 2 – Simplified block diagram of a sound-level meter

where I_o is the standard reference sound intensity of 10^{-16} w per sq cm. It is important to note that decibels are used to express the ratio of two intensities; they are not absolute units such as inches, pounds, or gallons and, consequently, are not handled in the same way. A doubling of sound intensity results in an increase in intensity level of 3 db. Hence, if a sound intensity were increased by 100% and the original intensity level were 70 db, it would become 73 db, not 140 db! Likewise, a factor of 10 change is represented by a 10-db change, a factor of 100 by a 20-db change, and so on. Therefore, the range of intensities described above – a million billion to one – could be represented by a range of 0 to 150 db.

Also necessary in the basic description of sounds and noises is the extremely important concept of frequency. We are all familiar with the sound produced by the simple tuning fork. This sound, known as a *pure tone,* is composed of one frequency, the resonant frequency of the tuning fork. A more complex sound is a *musical note,* for example, middle C on the piano, which has a fundamental frequency of about 256 cps, in addition to several harmonic frequencies. In practice one encounters sounds which are much more complex, such as *speech, music,* and a wide range of sounds classed as *noise.* These various kinds of sounds are pictured schematically in Fig. 1. At the left of the figure are plots of sound amplitude as a function of time for a pure tone, a musical tone, and speech, music, and noise. We see that the pure tone is a sinusoid, the musical note is basically sinusoidal with superimposed variations, and the latter class is composed of sound amplitudes which fluctuate randomly with respect to time. To the right in the figure are plotted the sound amplitudes as a function of frequency for these three examples. The pure tone is represented by a single frequency component, the musical note is characterized by several discrete frequencies including a fundamental and its harmonics, and for the third class of sounds we see that the frequency distribution is continuous, with the sound amplitude varying with frequency. Noises which are characterized by sound amplitudes extending over a wide range of frequencies as indicated in Fig. 1 are classed as *wide-band noises.*

Measurement of Noise – The above discussion gives some idea of the physical description of noise. Now, how do we measure noise? A basic sound-measuring instrument is the sound-level meter. It has also been called a "sound meter," a "decibel meter," a "noise meter," and so forth. Essentially it consists of a microphone, a calibrated attenuator, an electronic amplifier, and an indicating meter which reads in decibels (see Fig. 2). The reading obtained on this meter is indicative of the sound energy in the region from 20 to 10,000 cps. This reading is called the *overall* reading and is generally what is meant by the sound-level readings referred to in newspapers and popular magazines. No clue as to the frequency distribution of the noise is given by the overall reading. This one fact points up the limitation of the use of the sound-level meter in aviation noise problems. We saw in our discussion above that complex sounds and, in general, all noises are composed of frequency components distributed over a part or all of the frequency spectrum between 20 and 10,000 cps.[2] Therefore, to understand more completely a

[2] The average human ear has a frequency response of about 20 to 16,000 cps, and one would reasonably suppose, therefore, that measurements should be taken at least up to 16,000 cps. However, the great majority of noise sources radiate very little energy in the frequency range above 10,000 cps.

NOISE has two aspects: (1) subjectively, it is any unwanted sound; (2) objectively, it is characterized by many variables.

The subjective view is important in determining the response of people to aircraft noise and in establishing engineering design objectives for noise control. The engineering of noise control deals with the objective aspect in three parts:

1. The noise source – characterized by its total noise power output and the distribution of this power with respect to frequency and space.

2. The path – propagation in structures, through the air, and over terrain as influenced by properties of materials, geometry, meteorological conditions, and topography.

3. The received noise – its sound level, frequency spectrum, time pattern, and other variables as required to correlate with the subjective response of man in the aircraft, on the line or in the community.

The Authors

ADONE C. PIETRASANTA is an engineer with Bolt, Beranek, and Newman, Inc. He received a B.S. degree in Electrical Engineering from the University of Pittsburgh in 1948, and an M.S. degree in Electrical Engineering from Massachusetts Institute of Technology in 1951. Before joining Bolt, Beranek, and Newman, Mr. Pietrasanta was an instructor with the University of Pittsburgh, and a research and teaching assistant with M.I.T.

RICHARD H. BOLT has been associate professor of physics and director of the Acoustics Laboratory at Massachusetts Institute of Technology since 1946. From the University of California, he received a B.A. degree in 1933, an M.A. degree in 1937, and a Ph.D in 1939. Dr. Bolt was an associate in physics at the University of Illinois during 1940 and research associate at M.I.T. from 1941-1943. He worked for the Office of Scientific Research and Development in London during 1943 and 1944. After that he became chief technical aide with the National Defense Research Committee.

problem involving these or similar noises, the information obtained with a sound-level meter should be *supplemented by a frequency analysis!*

For this purpose one employs an instrument known as a frequency analyzer. A basic analyzer in widespread use today is the octave-band analyzer shown in Fig. 3. It is suitable in the majority of applications where continuous wide-band noises are found. With it one can obtain readings in eight octave bands in the frequency region between 20 and 10,000 cps. Such information enables one to obtain a clearer picture of the distribution of sound energy with respect to frequency.

In noise problems where more detailed information is required it may be necessary to employ frequency analyzers having narrower frequency bands than the octave-band analyzer. Also certain noise problems may require the use of more specialized equipment. A discussion of sound-measuring equipment and details of the basic techniques of noise measurement are given elsewhere in the literature.[3, 4] However, it is well to point out here that accurate measurements are essential to the proper analysis of any noise problem. These can be obtained only by using a reliable calibration technique and having adequate knowledge of the limitations of one's sound-measuring equipment.

All noise problems have a fundamental structure

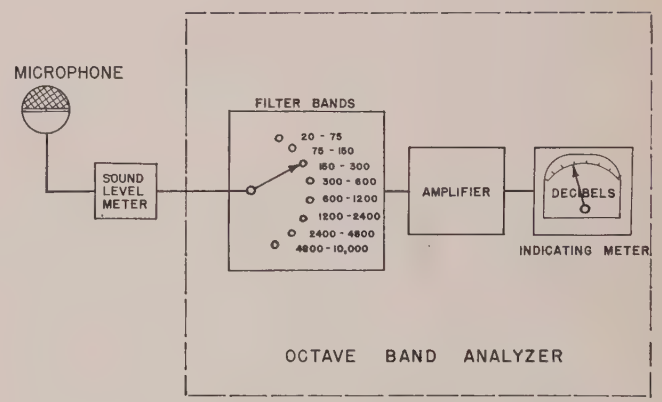

Fig. 3 – Simplified block diagram of an octave-band analyzer and its use in conjunction with a sound-level meter

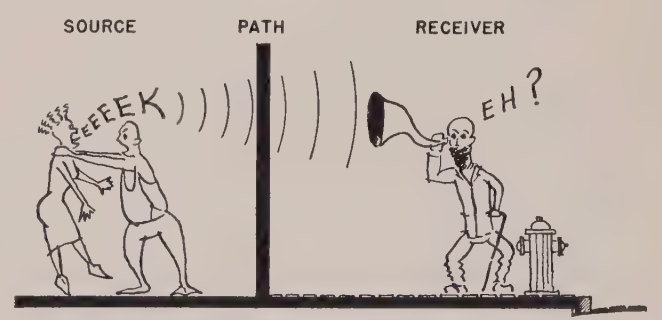

Fig. 4 – Schematic example of the fundamental components of a noise problem – source, path, and receiver

[3] See Proceedings of the Third National Noise Abatement Symposium, 1952, "Industrial Noise Measurement – Scieence or Art?" by J. R. Cox and C. R. Williams.

[4] See "Handbook of Noise Measurement," by A. P. G. Peterson and L. L. Beranek. Published by General Radio Co., Cambridge, Mass., 1953.

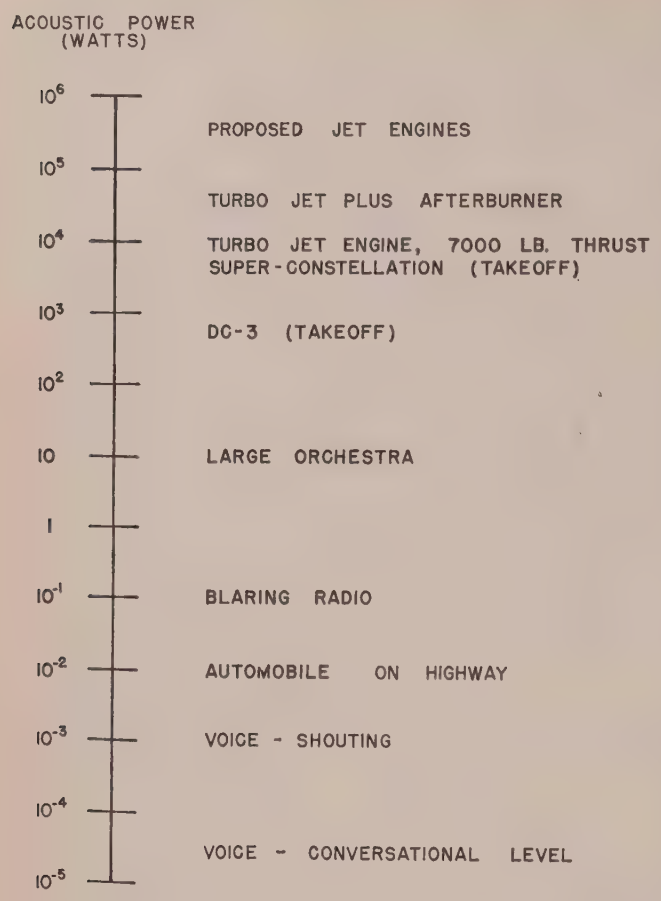

Fig. 5 – Acoustic power in watts of several familiar noise sources

which can be divided into three parts (see Fig. 4). First, and obviously, there must be a *noise source.* This can be a jet engine, a noisy ventilating system, a jazz band, or even a leaky water faucet. Necessary to every noise problem is a *receiver,* someone who hears the noise source and in one way or another experiences a reaction. Finally, the noise must reach the receiver by traveling along some *propagation path.* Each of these components of a noise problem is discussed in some detail below with particular emphasis upon the importance of each to the understanding of the total noise problem.

Properties of a Noise Source

A noise source can be described by specifying three basic quantities:

1. The total acoustic power radiated.
2. The distribution of this power with respect to frequency.
3. The distribution of this power in space, that is, the directivity pattern.

Power Radiated – The fundamental acoustic property of any noise source is its total power output, which is expressed in watts just as we express the power of a light bulb. Fig. 5 indicates the acoustic power output of several familiar kinds of noise sources. For example, a man shouting produces on the average about 1/1000 of a watt of acoustic power, whereas a large orchestra radiates about 10 w. A 7000-lb-thrust turbojet operating at maximum power radiates about 10,000 acoustic watts, and it is estimated that some of the future jet engines now being designed will radiate more than 100 kw of acoustic power.

It is interesting to note that only a very small fraction of the usable power of a noise-producing device is converted to noise. For example, in the case of a turbojet engine, the noise power produced is approximately 1/10,000 of the mechanical power in the jet exhaust stream.

The total power radiated by most aviation noise sources in normal present-day operations is, in general, independent of the noise source environment. In other words, whether a jet engine or a propeller, for instance, is operated in an airframe, in a test cell, or on a test stand in an open field makes little difference with regard to its total acoustic power output. Consequently, the only true comparison of aviation noise sources is a comparison of the total acoustic power output of each. For example, suppose that the sound pressure level measured "near the exhaust" of jet engine A was 150 db, and "25 ft away" from jet engine B was 140 db. To conclude from these measurements that jet engine A is "10 db noisier" than jet engine B is meaningless because the sound pressure level for most aviation noise sources (as will be pointed out later) varies greatly with distance, frequency, and angular location. On the other hand, to compare the total acoustic power output of each (which is independent of angle and distance), that is, to say that "jet C produces 100 w more acoustic power than jet D," is meaningful.

Frequency Spectrum – The power output of a noise source is usually distributed over a range of frequencies. This frequency distribution determines the character or quality of the noise. The characteristic "roar" of a diesel truck or of a jet engine afterburner, for instance, indicates that the frequency spectrum of the noise has a maximum in the low-frequency region. On the other hand, the "hissing" noise of a compressed air jet or the "whine" of an idling turbojet engine is mainly high frequency in nature.

A knowledge of the frequency distribution of noise is essential in the understanding of any noise problem. This is clearly demonstrated by a comparison of the two noise spectra shown in Fig. 6 which were determined by an octave-band frequency analysis. Spectrum A, predominantly low frequency in nature, might be the characteristic roar from a jet engine operating with its afterburner; spectrum B might well represent the whine of a turbojet. It is quite obvious that these spectra differ markedly from one another. However, in this hypothetical case, the reading one would have obtained using a sound-level meter, that is, an "overall" reading, *would have been the*

same for both noises. Thus, a single reading, that is, an "overall" reading, could be very misleading and could result in erroneous conclusions about the nature and extent of a noise problem. It is extremely important to supplement this single meter reading with a frequency analysis.

Directivity – In general, noise sources do not radiate sound in a perfectly uniform way in all directions but in certain preferential directions. A typical directivity pattern of an aviation noise source is shown in Fig. 7 where the noise field surrounding a single-engine jet aircraft operating at military power has been plotted. The noise field (out to 200-250 ft from the aircraft) is represented by equal "overall" sound-pressure-level contours. Similar directivity plots could have been drawn for each octave band of frequency. These additional contour plots would illustrate the variation of the directivity pattern with frequency.

One can obtain various kinds of information from the graphic description of the noise field in Fig. 7. Specifically, one can determine the overall level for any given angle and radius. Also one can examine the manner in which the sound pressure level decreases with increasing distance from the aircraft and how it varies with angle at a fixed radius. In addition, one can see very clearly the angular region in which the noise levels are a maximum. For this particular jet engine noise field the maximum occurs approximately 35 deg from the jet exhaust axis.

This jet aircraft, as well as all jet aircraft, is characterized by a noise field which has a very marked directivity pattern. To emphasize the need for a consideration of the directivity characteristics of an aviation noise source, let us suppose that two men ventured into the noise field pictured in Fig. 7, each armed with a sound-level meter, and took readings at points X and Y. Their readings would have been, respectively, 128 db at Y and 108 db at X. Both men were very careful to take readings at the same distance from the aircraft, yet these readings differed from one another by 20 db! Differences exceeding 20 db could have been measured at different locations on the same radius.

The above example clearly demonstrates that a reading obtained in the noise field surrounding a directive source depends not only upon the distance from the source but upon one's angular location. Therefore, a report that "110 db was measured 200 ft from a Z-34 jet aircraft" is useless by itself because the angular location of the measurement is not specified.

As another example, if for each of two separate aircraft a reading was obtained at a fixed radius and a fixed angle, and these readings were found to be the same, they would not necessarily indicate that these two aircraft were producing the same amounts of acoustic power or that they had the same directivity pattern. These facts can be determined only by obtaining additional measurements, enough to describe the noise field adequately and to determine, by integrating over all angles, the total acoustic power radiated.

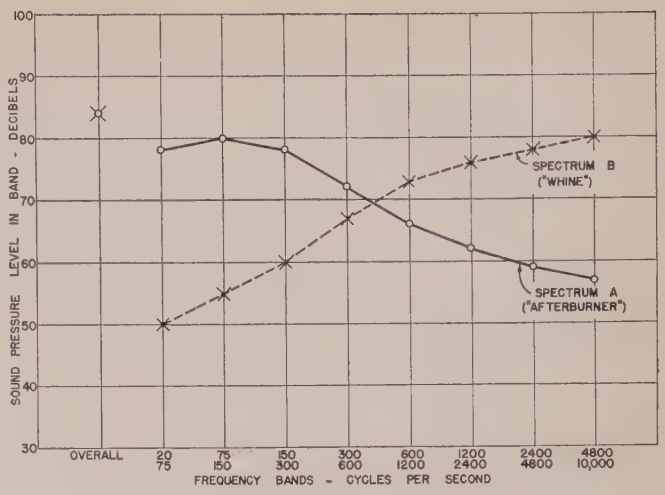

Fig. 6 – Sound pressure levels versus octave bands of frequency for two noises having the same "overall" or sound-level meter reading

Most aircraft noise sources are characterized by noise fields which have pronounced directivity patterns. Typical examples are shown in Fig. 8[5]

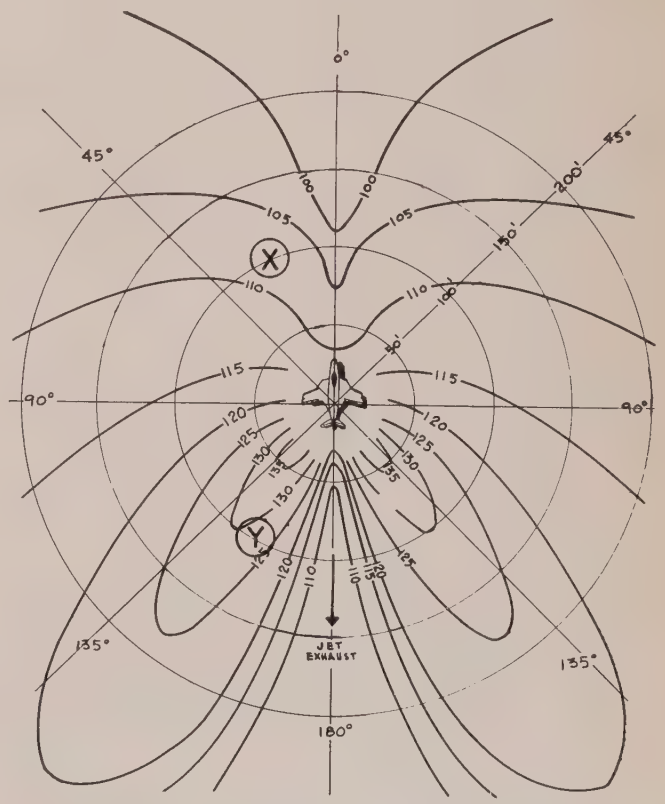

Fig. 7 – Equal overall sound pressure level contours for an F9F-6 jet aircraft operating at military power in a free field

[5] See *Journal of the Acoustical Society of America*, Vol. 25, May, 1953, pp. 367-378: "Physical Characteristics of Aircraft Noise Sources," by H. E. von Gierke.

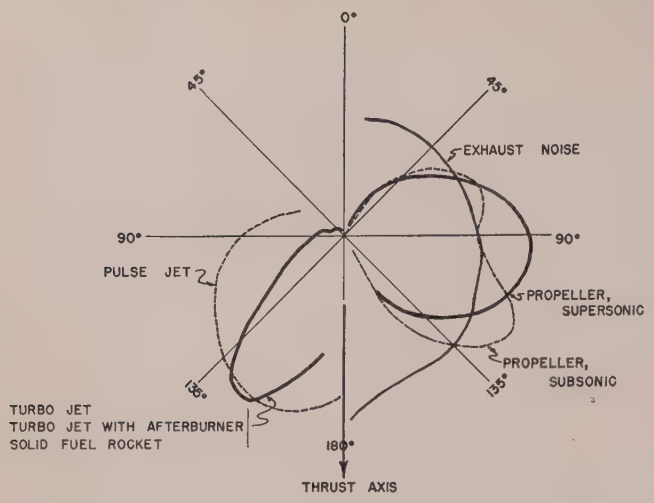

Fig. 8 – Overall directivity patterns for several aviation noise sources. The patterns have been adjusted to show equal maximum values. Zero degrees is in front of the engines

where relative overall levels are plotted as a function of angle for several aviation noise sources. This plot should emphasize the need for a careful study of the noise field in any aviation noise problem.

One might expect that the amount of noise reduction provided by an aircraft muffling device could be reliably determined by measurements at a fixed angle and distance before and after its installation. However, even in this simple case such a technique will not necessarily give the right answer because the directivity pattern or the frequency spectrum may have changed. It is quite possible that the directivity pattern may have been modified, that is, "bent" or "warped," resulting in a decrease in intensity level at some point in the field and an increase at some other location. Also the frequency spectrum of the noise may have changed, resulting in an increase in level at some frequencies and a decrease at others. To determine the effectiveness of a muffling device in reducing the total noise power it is necessary to obtain a sufficient number of measurements to be able to determine the total power radiated before and after installation. A comparison of these two values of power will reveal whether a true change in noise power output has been achieved.

In summary, a noise source can be described completely by specifying its total acoustic power and the distribution of this power with respect to frequency and space. These three acoustic variables in turn depend on the type of engine or other device and the operating conditions of that device. For instance, in the case of jet engines the acoustic power, frequency spectrum, and directivity pattern differ for different types of engines and also vary with the operating conditions of any one jet engine. To complete the picture, therefore, one should not only specify the acoustic power, the frequency spectrum, and the directivity pattern but also the operating condition at which these three quantities were obtained.

The noise produced by aircraft noise sources can, in general, be related to the operating characteristics of these sources. For instance, it has been found that an engineering description of propeller noise, adequate to cover a wide range of normal operating conditions, can be given in terms of (1) blade tip speed, (2) horsepower per blade, and (3) number of blades. For turbojet engine noise one finds empirically that the total noise power can be related to a quantity containing the total mass flow of air and fuel through the engine, the jet exit velocity, the temperature at the jet exit, and the diameter of the jet tail pipe. Such relationships as these can be extrapolated, allowing one to estimate the noise characteristics of aircraft noise sources from their operating characteristics. This is especially important in the design of new engine test facilities or the evaluation of an airport noise problem involving future aircraft. As we gather more and more of this kind of information, our understanding of the basic parameters which affect the noise produced by aircraft noise sources becomes clearer, and the relation of noise characteristics to these parameters becomes more exact.

Propagation of Noise

In any noise problem, once a noise source has been specified, it is necessary to consider the manner in which noise is propagated away from the source. The propagation of sound is influenced by many factors such as the atmosphere, wind velocity and temperature gradients, acoustical treatments, and others discussed later in this paper.

Simple Spreading – The noise radiated from a source spreads out over an increasingly larger area at increasing distances from the source. Because of this spreading, the power is "thinned out." Therefore, the power per unit area, or the intensity, decreases with increasing distance from the source. The intensity of a simple source in free space diminishes to one-quarter each time the distance is doubled, since the area of a sphere increases as the square of its radius. This is called the inverse square law. In Fig. 9 is shown a plot of the variation of sound level with distance from the source. At distances which are greater than several times the largest dimension of the source, in other words, in the "far field," the reduction due to inverse square loss alone is equal to 6 db for each doubling of distance. In the "near field," the variation of sound level with distance is a complex function of the radiation characteristics of a noise source and is shown by the shaded area in Fig. 9.

Influence of the Atmosphere[6] – In addition to

[6] See Proceedings of the Fourth Annual National Noise Abatement Symposium, 1953, "The Physics of Outdoor Sound," by U. Ingard.

simple spreading there is a continuous reduction in intensity attributable to absorption in the air, to bending of the sound by wind velocity and temperature gradients, and to multiple reflections and scattering of the sound from inhomogeneous "pieces of air" associated with turbulence.

The absorption of sound energy in the air is a function primarily of the viscosity of air and the amount of water vapor in the atmosphere. Of the two, the most important effect from the standpoint of practical noise control is that of humidity. Attenuation of sound due to humidity increases with frequency. For 50% relative humidity, for instance, the attenuation at 1500 cps is about 0.3 db per 100 ft, while at 6000 cps it is about 2 db per 100 ft. It must be emphasized that these values of attenuation are realized in addition to the reduction due to the inverse square divergence of sound waves discussed before.

In air, the velocity of sound is proportional to the square root of the absolute temperature. If the temperature is constant, then the velocity of sound will be the same at all points in the medium, and a sound wave traveling away from a noise source will be undistorted. However, if the temperature varies from point to point in the medium, sound waves will follow curved paths, bent in the direction away from the higher temperature and toward the lower temperature.

If the temperature of the atmosphere decreased with height above ground as on a normal summer day, one would expect sound waves to be bent away from the ground in a manner shown in Fig. 10*a*. This bending of the sound waves results in the formation of a shadow zone (indicated by the cross-hatched area) in which the noise levels of the source are very much reduced. At night and during the winter there is generally an inversion of the temperature gradient, and the sound rays are bent downward.

Further irregularities of sound propagation are introduced by the existence of wind velocity gradients. The velocity of sound is effectively changed in a moving medium. Since wind velocity varies with height, refraction effects similar to those caused by temperature gradients will be present. Consequently, sound will bend away from the regions of higher velocity and toward regions of lower velocity. This is indicated in Fig. 10*b* where in the upwind direction a shadow zone similar to that formed by the temperature gradient exists. Downwind from the source the sound is bent downward toward the ground, rather than upward.

The acoustical effect of a wind velocity gradient is not symmetrical as in the case of a temperature gradient. Sound traveling in the direction of the wind will be bent downward, while it will be bent upward in the direction against the wind.

When both wind velocity and temperature gradients exist, it is possible for them to produce canceling acoustical effects. For example, in the direction of the wind, the tendency of the sound to bend downward can be canceled by a negative temperature gradient which would have ordinarily caused a shadow zone. This is indicated in Fig. 10*c*. Downwind the temperature gradient has been canceled by the effect of wind while in the upwind direction the shadow zone has only been intensified.

The primary importance of these wind and temperature effects is the formation of a shadow zone. Sound will not propagate into an ideal shadow zone. However, for frequencies which we are ordi-

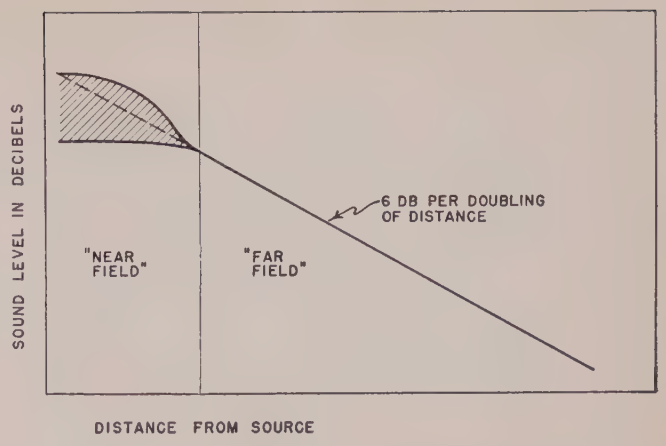

Fig. 9 – Variation of sound level with distance for a distributed sound source showing the near- and far-field dependence

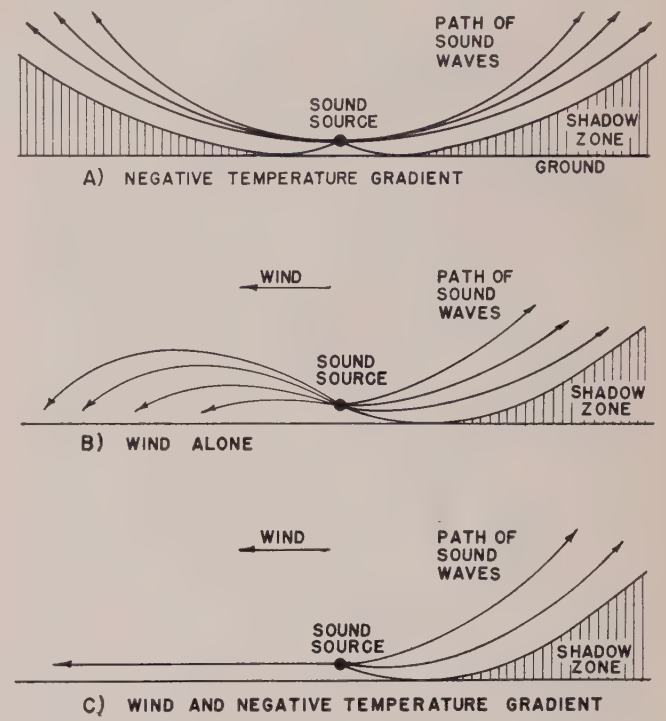

Fig. 10 – Simplified illustration of the effects of wind velocity and temperature gradients on sound propagation

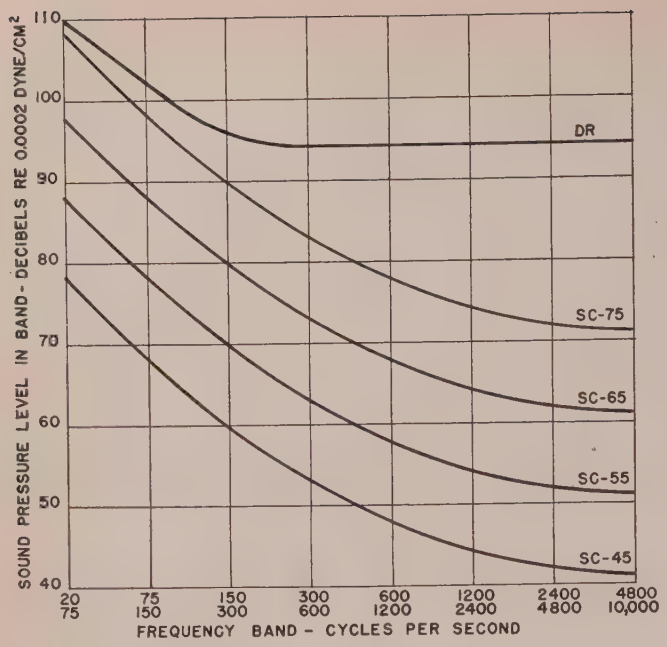

Fig. 11 – Sound pressure levels as a function of frequency for the damage risk (DR) criterion for continuous wide-band noise and several speech communication (SC) criteria

narily interested in, this condition is not fully realized, and a great deal of sound energy will be diffracted into the shadow zone. Of importance are the reductions in the noise levels which can be realized in the shadow zone. As an example, the magnitude of reduction that can be achieved in excess of inverse square for a noise source and receiver both 10 ft above the ground and a wind velocity of approximately 10 mph is of the order of 5 db in the low-frequency region, increasing to 25 db in the 600-1200 cps band, and decreasing to about 10-15 db in the 4800-10,000 cps region. These values of reduction indicate that wind velocity and temperature gradients can appreciably affect the propagation of sound out-of-doors.

It must be emphasized that the effects of atmospheric disturbances on sound propagation are not yet sufficiently well understood to form a solid basis for answering the questions facing us today. Although this problem has been studied extensively, the amount of reliable quantitative information is scanty. Perhaps this is understandable, for the effects of the atmosphere are extremely complicated. This problem is something like weather prediction, a subject which has received vastly more scientific study than sound propagation and is still something less than perfectly certain. The scarcity of available information coupled with the importance of these effects in aviation noise problems strongly suggests the need for more basic research on the subject of atmospheric acoustics.

Influence of Terrain and Building – As sound passes over the earth it is absorbed to some extent by foliage and the soil. These effects will be greatest for sound that grazes the ground and will be least for sound traveling vertically. In addition, these effects are more noticeable as the height and thickness of the foliage is increased. Buildings, tall trees, and other obstacles can block the sound or reflect it out of its original path. This phenomenon is known as shielding and is more noticeable at high frequencies than at low frequencies. At high frequencies the wavelengths are small, and sound is strongly influenced by any barrier in its path. At low frequencies the wavelengths become longer, and a barrier becomes effectively smaller due to diffraction effects. These effects of shielding and terrain attenuation can have considerable bearing on the intensity of aviation noise originating on the ground (for instance, on an airport) which reaches a neighboring community. Reasonable estimates of these effects can be made from available engineering data, although the calculations may become very complicated.

Noise-Control Components – We have been discussing primarily propagation paths which exist out-of-doors. However, indoors, that is, within structures, noise fields can be influenced by noise-control components such as sound attenuating treatments, walls, windows, doors, and so on. Each of these components has an effect on the transmission of sound from a source to a receiver and therefore is a part of the propagation path. Sound attenuating treatments take many forms – there are such configurations as acoustically lined right-angle bends, parallel baffles or splitters, tuned ducts, labyrinths, or water sprays. The proper design and choice of sound attenuating treatments and acoustical components in general form a part of the subject of noise control which will be discussed in some detail in other papers of this symposium.

Geometry can also play an important part in the propagation of sound away from a source. For instance, if, in the basic design of a jet-engine test facility, the exhaust stacks could be pointed away from rather than toward a residential area, an appreciable reduction in jet noise reaching the community could be effected. Also, directing a stack vertically rather than horizontally to utilize its inherent directivity characteristics is sometimes an effective inexpensive means of noise control. One might also seriously consider alternative locations for an engine test facility or for an aircraft run-up area on a plot of land so as to utilize as effectively as possible such factors as wind and temperature gradients for shadow-zone effects, foliage and trees for absorption and scattering of sound, and land contours for possible shielding.

The Effects of Noise on Man

The previous discussion is unimportant unless a receiver – man – hears the noise. The effects of noise on man fall into three categories:

1. The noise may be of sufficient intensity to

have a potential *damaging* effect on the hearing of an individual.

2. The noise may *interfere with speech* communication.

3. The noise may be a source of *annoyance,* particularly in residential communities.

Damage Risk – Prolonged exposures to noises having certain sound pressure levels and frequency characteristics can produce permanent hearing loss. The best estimate of acceptable noise levels for continuous wide-band noise in each of the eight frequency bands between 20 and 10,000 cps which, if exceeded repeatedly and for appreciable periods of time, will give rise to risk of damage to the hearing mechanism, are shown in Fig. 11 by the curve marked DR. The range of susceptibility to damage among individuals, however, varies with people from "tough" ears who can stand levels higher than those indicated by the DR curve, to those people with "tender" ears, most of whom will be protected by the DR curve. Therefore, this curve represents a conservative criterion which, if not exceeded, should prove safe for the large majority (about 95%) of individuals.

Speech Communication – The efficient performance of tasks in many areas associated with aviation noise, for example, the interior of an airplane cabin, the control room of an engine test facility, or even on the deck of an aircraft carrier, is very often dependent on the ability of people to talk to one another. Noise can interfere with man's ability to communicate. An approximate measure of the interfering effect of noise on speech is given by the *speech interference level,* which is the arithmetic average of the sound pressure levels in the three octave bands, 600-1200, 1200-2400, 2400-4800 cps. Engineering knowledge and subjective tests have shown that these three octave bands cover the frequency region most important for the understanding of speech. Curves representing four different speech communication criteria are shown in Fig. 11. These curves are labeled SC-45, SC-55, SC-65, and SC-75, where the number refers to the speech interference level in decibels. Associated with each of these curves is a corresponding communication condition including such factors as the voice level necessary, the distance between a talker and a listener, and the nature of possible communication. This information is tabulated in Table 1.

Annoyance in Residential Areas – Finally, there is the problem of neighborhood reaction to noise. This problem is admittedly complicated, and one might question the validity of any scheme for estimating psychological reactions as subtle as annoyance. However, considerable progress has been made on the basis of empirical correlations, viewed statistically, among a large body of field data. Many types of response, ranging from mild annoyance to vigorous legal action, have been examined together with a wide range of factors that might be related to the response exhibited in each case. One irrefutable fact emerges: *The response cannot be predicted uniquely from a physical description of the noise reaching a receiver.* Instead a study of available evidence indicates that there are at least seven different factors which have a bearing on the interaction of noise with a generalized class of behavior that may be described as "residential living." The role played by each of these factors in contributing to the reaction of a community to intruding noise is discussed below:

1. *Spectrum Character* – An intruding noise spectrum which contains audible pure-tone or single-frequency components is usually more annoying than a spectrum which is reasonably continuous in frequency.

2. *Peak Factor* – A noise which is reasonably continuous in time, at least over periods of a few seconds or more, is less annoying than an impulsive type of noise. Examples of impulsive noises are gun shots, the noise from a drop hammer, and the chatter of a machine gun.

3. *Repetitive Character* – In addition to the short-time peak factor discussed above, the repetitive character of the intruding noise is an important factor influencing the degree of annoyance. A noise which lasts for 20 sec but is repeated every minute is indeed more annoying than the same noise repeated twice a day. A community will tolerate the occasional passage of a jet aircraft overhead, but the frequent passage of such aircraft may lead to strong complaints.

4. *Level of Background Noise* – Tolerance of intruding noise is markedly influenced by the average background noise in the community. Residents in areas with low background noise, such as suburban communities, are more likely to be annoyed by intruding noise of fairly low level than those in urban areas where the background noise is higher and partially or totally masks the intruding noise.

5. *Time of Day* – Intruding noise is usually more tolerable in the daytime than during the sleeping hours of nighttime. At night, the background noise levels from traffic and other sources are usually lower than the corresponding daytime levels, and hence an intruding noise is more notice-

Table 1 – Speech Communication Criteria[a]

Speech Interference Levels, db	Voice Level	Nature of Possible Communication
45	Normal voice at 10 ft	Relaxed conversation (private offices, conference rooms)
55	Normal voice at 3 ft; raised voice at 6 ft; very loud voice at 12 ft	Continuous communication in working area (business, secretarial, control rooms of test cells)
65	Raised voice at 2 ft; very loud voice at 4 ft; shouting at 8 ft	Intermittent communication
75	Very loud voice at 1 ft; shouting at 2 – 3 ft	Minimal communication (danger signals, restricted prearranged vocabulary desirable)

[a] Relation between SC criteria expressed by speech interference levels and the communication conditions for a degree of intelligibility that is marginal with conventional vocabulary and good with selected vocabulary.

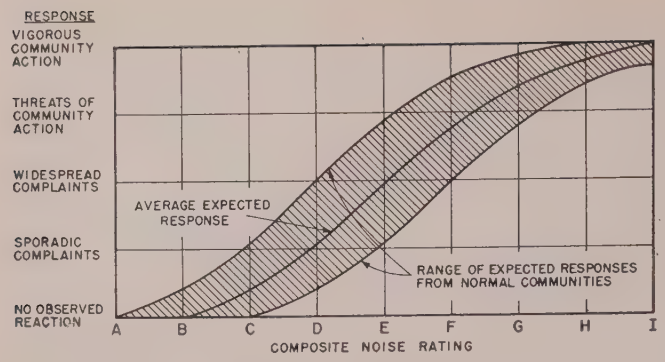

Fig. 12 – Average expected community response to intruding noise as a function of the noise rating

able. Also, interference with sleeping is an important consideration at nighttime.

6. *Adjustment to Exposure* – Residents can become conditioned to intruding noise after repeated exposures. For example, residents close to a railroad can become accustomed to the noise, even though they may be somewhat annoyed during the first few days of exposure.

7. *Intruding Noise Levels* – The actual sound pressure levels as a function of frequency of the intruding noise are, of course, important variables in the problem of estimating neighborhood reaction.

From a careful consideration and a proper weighting of each of these factors one can determine a *noise rating*. This noise rating is a single number which enables one to estimate the statistical range of neighborhood reaction to intruding noise. An empirical relationship has been derived, which has been substantiated by a great number of case histories, which relates the noise rating to the average expected response. This relationship is shown graphically in Fig. 12 where the response, stated in descriptive terms, is plotted as the ordinate and the noise rating as the abscissa. The response scale is a rank order scale ranging from "no observed reaction" meaning that practically no residents are annoyed or disturbed by the noise, to "vigorous community action." Since all communities do not react alike to intruding noise, a "range of expected responses from normal communities" must be specified. This range is shown graphically by the shaded area in Fig. 12.

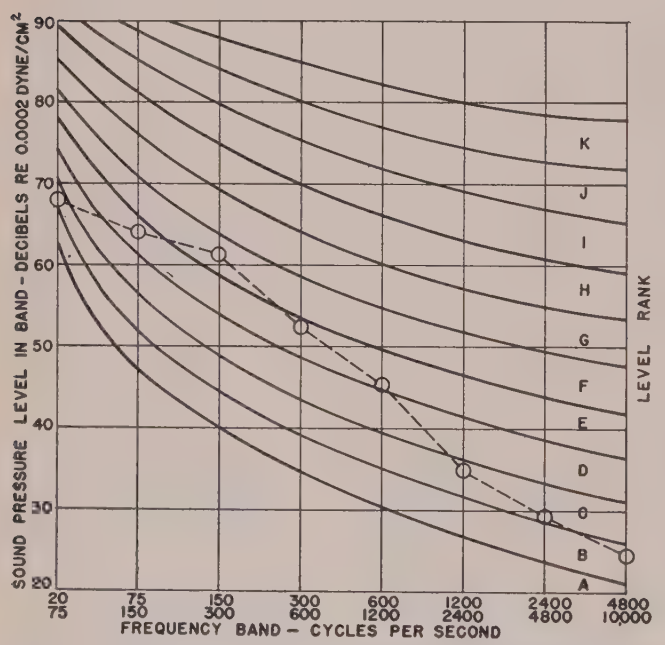

Fig. 13 – Family of curves used to determine the level rank of an intruding noise spectrum. An example of an intruding noise spectrum is the dashed curve which has a level rank of *F* since that is the highest zone into which the spectrum falls

To illustrate the method of estimating the expected response, suppose that in a residential community near an engine test facility the intruding noise spectrum shown by the dashed curve in Fig. 13 was measured. This noise spectrum is shown superimposed on a family of curves which define the "level rank." The ranks are designated by the letters *A* to *K*. The level rank of the noise spectrum is given by the highest area into which the spectrum intrudes in any band. For the spectrum shown in Fig. 13, the level rank is seen to be *F*. This level rank is adjusted upward or downward by an evaluation of the other factors listed previously, resulting in a composite noise rating. Suppose for this example the conditions are such that the level rank *F* must be adjusted downward, resulting in a noise rating of *D*. Consequently a community response of "sporadic complaints" would be expected on the average as a result of operation of the facility.

Summary

Any noise problem is made up of three component parts: a noise source, a propagation path, and a receiver. In the absence of any one of these, a noise problem does not exist. Fundamentally the important single specification of a noise source is its total power. A complete specification includes not only the total power but its distribution with respect to frequency and space. The nature of propagation of sound away from a source depends upon the properties of the propagation path, atmospheric effects, structural geometry and noise-control components. Finally, noise can have several effects on man: it can damage hearing, interfere with speech communication, and cause annoyance.

All of the above factors – relating to the source, the path, and the receiver – must be taken into account if one is to achieve a well-balanced integrated solution to aviation noise problems.

Additional References

1. WADC TR 52-204, 1952, "Handbook of Acoustic Noise Control, Vol. I, Physical Acoustics," by the Staff of Bolt, Beranek, and Newman.

2. WADC TR 52-204, 1953, "Handbook of Noise Control, Vol. II, Noise and Man," by W. A. Rosenblith, K. N. Stevens, and the Staff of Bolt, Beranek, and Newman.

Why Do Airplanes Make Noise?

Arthur A. Regier, Langley Aeronautical Laboratory, NACA

This paper was presented at the SAE National Aeronautic Meeting, New York, April 14, 1954.

THE question "Why do airplanes make noise?" may seem trivial, but it is really at the heart of much of the fundamental research on aircraft noise. The question "Why do propellers make noise?" confounded the experts for many years. The question "Why do jets make noise?" is still one of some controversy and uncertainty. Recent informal conferences at the University of Southampton in England and at the Langley Aeronautical Laboratory of the NACA contained some of the best experts on aerodynamics and acoustics, and yet, one of the questions that was paramount in the discussions was "What is the mechanism of jet noise generation?" Although it is possible often to predict noise levels and obtain "fixes" on the basis of an accumulation of experimental data, one is always likely to make serious errors in extrapolating to other conditions unless one knows why noise is produced. That is the reason for the emphasis on an understanding of the noise-producing mechanism.

It is the purpose of this paper to discuss in engineering language some of the current concepts on the mechanism of aircraft noise generation and to present some of the significant results of recent research on aircraft noise. An attempt will be made

THIS paper presents a brief historical review of the quest for information concerning the mechanism of aircraft noise generation.

It is shown that, after a number of false hypotheses, the noise of propellers was finally traced to the principal aerodynamic loads of the blades. The intensity and characteristics of the noise can now be predicted theoretically from knowledge of the geometry and operating conditions of the propeller.

With regard to jet noise, the picture is not so clear. The actual mechanism of noise generation is still somewhat obscure. Included here is a resumé of United States and British work on determining the actual source of noise. Experiments on devices for reducing noise are also discussed.

The Author

ARTHUR A. REGIER is head of the Vibration and Flutter Branch of the Dynamics Loads Division of the National Advisory Committee for Aeronautics. He graduated from Kansas State College with a degree in electrical engineering in 1935. Mr. Regier joined the Langley Aeronautical Laboratory of the NACA in 1938. In addition to his present duties, he serves as a member of the NACA Special Subcommittee on Aircraft Noise.

SOURCE TYPE	SOURCE NAME	REPRESENTS CHANGE	RADIATION PATTERN	RELATIVE ACOUSTIC EFFICIENCY ($\lambda = 4\pi a$)	SOUND ENERGY FUNCTION OF
	MONOPOLE	VOLUME		1	$\rho A V^3 \left(\frac{V}{c}\right)$
	DIPOLE	FORCE		1/13	$\rho A V^3 \left(\frac{V}{c}\right)^3$
	QUAD-RUPOLE	SHEAR		1/1,000	$\rho A V^3 \left(\frac{V}{c}\right)^5$

Fig. 1 – Characteristics of acoustic noise

to present a unified picture including most of the major aircraft noise sources. The subjects covered include a brief discussion of the relation that the basic elements of acoustics have to various aircraft noise sources, propeller noise theory and application, jet noise and some of the devices that have been investigated in attempts to quiet the jet. A comparison of the intensities of various aircraft noise sources and some remarks on status of research and its application are also included. In such a broad treatment of such a wide field, it is necessary to make certain simplifications which we trust will not offend the experts.

Basic Elements

In order to understand the sources of aircraft noise, it is desirable to relate them to certain basic building blocks of acoustics. We would like to illustrate these acoustic building blocks or sources and give their relations to aircraft noise sources with the aid of Fig. 1. To start with, consider the first four columns in this figure; the last two columns will be explained later.

The first basic building block is the simple source or *monopole* which may be represented by a pulsating sphere that is periodically changing its volume. It sends out sound energy equally in all directions. The monopole source can be related to any part of the aircraft that is emitting fluid in a periodic fashion, such as reciprocating-engine exhaust, pulsejet engines, rough-burning jets and rockets. Such aircraft noise sources are characterized by rather high acoustic efficiency (potent noise makers) and a rather low dependence on velocity as compared to other sources.

The *dipole* which is represented by an oscillating rigid sphere is derived from two monopoles of opposite phase (source and sink) in close proximity. It is the case of sucking and blowing at the same time and may be used to represent a periodic force in a free fluid. The radiation pattern has two lobes with maximums in the direction of the force. The dipole has been extensively used in the theory of propeller noise, and there is some indication that it is related to aerodynamic noise on solid boundaries (cabin noise).

For a number of years, those who did research on the noise of free jets were at a loss as to the source of jet noise, because in such a free jet the forces must be in balance, thereby excluding the dipole, and there are no obvious fluctuating sources of fluid, thereby eliminating the monopole. In fact, there were some elegant arguments to the effect that noise could be produced only at solid boundaries and that a free wake or jet could produce no sound radiation. It was Professor Lighthill of England who first pointed out the possibility of jet noise generation in free jets due to *quadrupole* sources.[1] Although the quadrupole has been used for many years in the theory of light and in wave mechanics, it has been largely ignored in acoustics. There are several kinds of quadrupoles, and the one illustrated schematically on the last line of Fig. 1 represents a type of lateral quadrupole. It is derived from the dipole by placing two equal and opposite dipoles side by side. There is no net force but a shear or moment. The radiation pattern from such a quadrupole is a four-lobe cloverleaf pattern.

The last two columns of Fig. 1 are presented to give a rough indication of the relative efficiencies of these sources and how the acoustic energy may be related to some velocity of the aircraft noise generator. The second last column, labeled relative efficiency, is based on the sound radiation from a sphere oscillating in various modes at a frequency having a wavelength twice the circumference of the sphere.[1] For a given amplitude of the sphere, it may be noted that at the frequency considered the monopole type source has a 1000 times the efficiency of the quadrupole type source. The last column relates the sound energy to the kinetic energy of the aircraft noise source. When one derives the expression for the radiation power of the various acoustic sources, certain relations of frequency and speed of sound appear in the expressions. For example, as shown in the last column of Fig. 1, the speed of sound c appears as the first power in the monopole, as c^3 in the dipole, and as c^5 in the quadrupole. On the basis of dimensional analysis and on the assumption that frequency varies directly as velocity of the aircraft noise generator, one may arrive at expressions such as are given in the last column relating the acoustic energy to physical quantities of the aircraft noise generator. In these relations ρ is the density of the air, V is the velocity of a jet or moving body, A is area, and c the speed of sound in the air.

Experience has shown that a single source or multiple sources in random phase seem to follow the trends with velocity shown in the last column. As is illustrated by the fact that for propeller vortex noise, which is random, the dipole representa-

[1] See Proceedings of the Royal Society, Series A, Vol. 211, March 20, 1952, pp. 564-587: "On Sound Generated Aerodynamically. 1. General Theory," by M. J. Lighthill.

tion indicates that the noise should vary as the velocity to the sixth power; this is borne out by experience. When the source is moving at high velocity or is not of random phase, the sound energy follows entirely different laws. An example of this is the rotational noise of a propeller (to be discussed later); the phases of the dipoles are not random, and the sound energy varies as a much higher power of the velocity.

If a jet can be represented by random phase quadrupoles, one might expect that the sound energy should vary as the eighth power of the velocity. Experience has generally substantiated this for the far-field jet noise. This relation is commonly referred to as Lighthill's eighth-power law.

Propeller Noise

Basis of the Theory – For many years the predominant source of propeller noise eluded the investigators. It was variously ascribed to engine vibration carrying over into the blades, flutter of the blades, unsteady vortex shedding, thickness or blade shape effects, and so forth. Many tests were made with many peculiar configurations and blades of various materials in an effort to obtain a silent propeller. Although the factors mentioned above may contribute to propeller noise, they are generally not the predominant cause of the noise on conventional propellers. Hence, these investigations were largely fruitless.

It was in 1936 that Gutin[2] developed a theory which relates the noise of a propeller directly to the steady aerodynamic loads on the blades. The concepts of this theory are crudely illustrated in Fig. 2. Imagine that the propeller disc is covered with a large number of loudspeakers, oriented in such a way that the axes of the speakers are in the direction of the blade aerodynamic forces. As the propeller rotates, it strikes each speaker in proper phase and gives it an excitation proportional to the aerodynamic load on the blade at that point. It may be noted that when the propeller repeatedly strikes a given speaker, that the speaker vibrates not only at the striking frequency but at many harmonics that are integral multiples of the striking frequency. That is the reason that propeller noise is rich in harmonics.

Since the harmonic output of the speaker is related to the type of blow received, the spectrum of the noise will change with the type of the excitation pulse. For wide pulses the harmonic content would be small, whereas for sharp or impulse-type blows the harmonic content would be large. For practical propellers it has been found that the lower frequencies of the noise are not greatly affected by blade shape or width, but there is some

Fig. 2 – The propeller as a noise source

evidence that the higher harmonics are a function of blade planform.

In the theory it is assumed that each speaker radiates sound as an acoustic dipole. The problem of calculating the sound pressure at any point in space is one of adding up the pressures from all the speakers, taking proper account of the phase differences of the speakers and the time it takes for a signal to pass from each speaker to the observation point. Further details on the application of this theory to various problems are summarized by Regier and Hubbard.[3]

These concepts have been used by the Langley Laboratory of the NACA to develop a method for calculating the sound pressures, not only at large distances from the propeller but also very close to

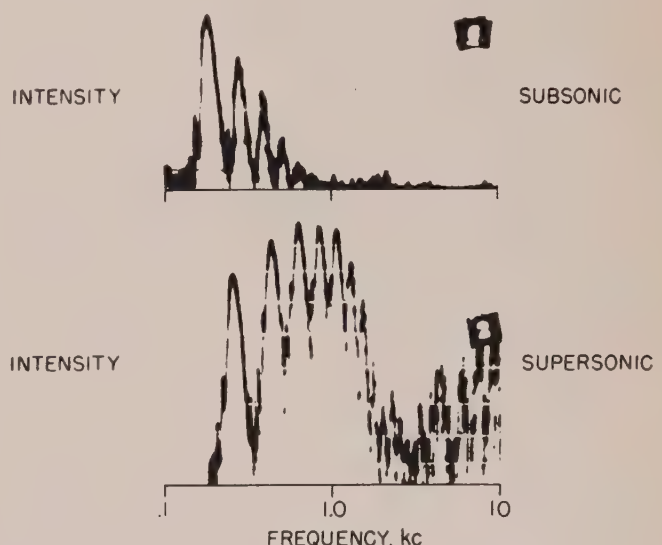

Fig. 3 – Sample propeller noise spectra

[2] See NACA TM 1195 (1948), "On the Sound Field of a Rotating Propeller," by L. Gutin.

[3] See *Journal of the Acoustical Society of America*, Vol. 25, May, 1953, pp. 395-404: "Research on Propeller Noise and Its Reduction," by A. A. Regier and H. H. Hubbard.

[4] See NACA TR 996 (1950), "Free-Space Oscillating Pressures Near the Tips of Rotating Propellers," by H. H. Hubbard and A. A. Regier.

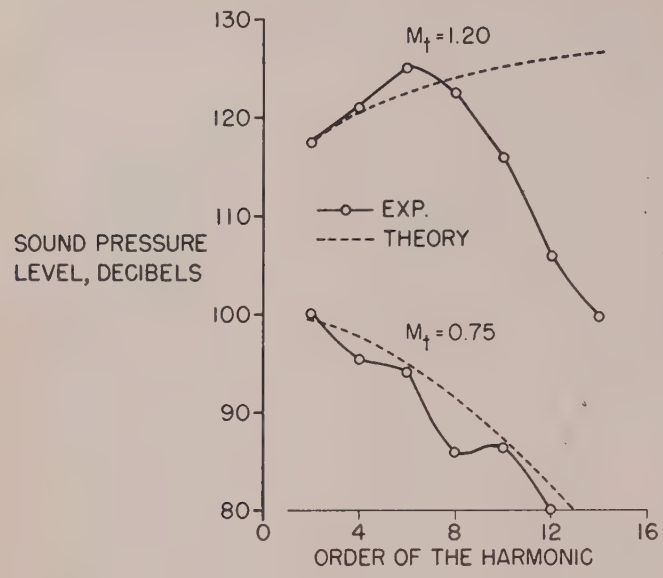

Fig. 4 – Comparison of theory with measured propeller noise spectra

the propeller, in the vicinity of fuselage walls and wings.[4] Comparisons with experiments have shown surprisingly good agreement. We are now confident that we can predict pressures even to within a few inches of the propeller for the lower harmonics of the noise with an accuracy comparable to that which the aerodynamist knows the aerodynamic loads on the blades. These methods have recently been extended to the forward flight case by Garrick and Watkins of Langley[5] and are currently being used by aircraft and propeller manufacturers in trend studies.[6]

Spectra and Comparison with Theory – Some sample noise spectra and comparisons with theory[7] are shown in Figs. 3 and 4. Analyses for both subsonic and supersonic tip speeds are given for a propeller operating on a test stand. It may be noted that at subsonic speeds the fundamental frequency is the most intense component and that at supersonic speed some of the higher harmonics are more intense than the fundamental frequency. Agreement with theory is quite acceptable up to the third or fourth harmonic. The theory overestimates the amplitudes of the higher harmonics of noise at supersonic speeds. Possible reasons for this might be the neglect of blade width and shape effects or effects of finite amplitude of the sound waves.[3]

Application of Theory – Although discussion in detail of the application of propeller noise theory to trend studies is beyond the scope of this paper, a few samples dealing with effects of power, number of blades, rotational tip speed, and effect of forward speed are illustrated in Figs. 5, 6, and 7. Fig. 5 shows how the noise varies when power is held constant, and Fig. 6 shows how the noise varies with power.[8, 9] It may be seen that increasing the number of blades and decreasing the tip speeds are effective ways of reducing the noise. Some preliminary results of calculations made on effect of forward speed[5] are shown in Fig. 7. As forward speed is increased, there is first a decrease in the noise; but at higher speeds there is a con-

[5] See NACA TN 3018, October, 1953, "A Theoretical Study of the Effect of Forward Speed on the Free-Space Sound Pressure Field Around Propellers," by I. E. Garrick and C. E. Watkins.

[6] "Control System and Noise Problems for High-Speed Propellers," by W. H. Clark and J. Schmey. Paper presented at SAE National Aeronautics Meeting, Los Angeles, Oct. 2, 1953.

[7] See NACA TR 1079 (1952), "Sound from a Two-Blade Propeller at Supersonic Tip Speeds," by H. H. Hubbard and L. W. Lassiter.

[8] See NACA TN 2968, June, 1953, "Propeller Noise Charts for Transport Airplanes," by H. H. Hubbard.

[9] See Proceedings of Fourth Annual Noise Abatement Symposium (October, 1953), pp. 81-88: "Airplane and Airport Noise," by H. H. Hubbard.

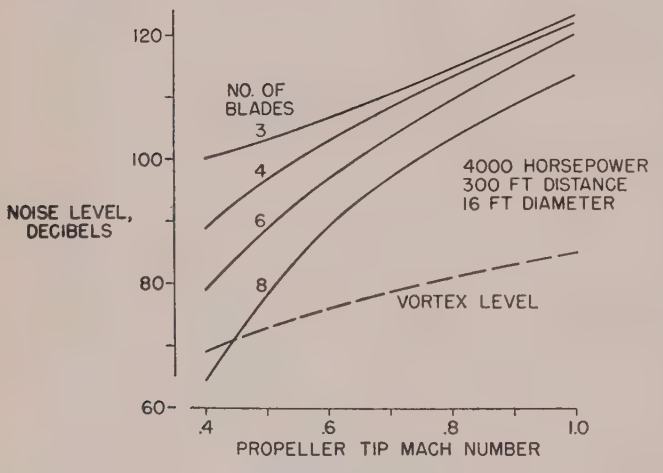

Fig. 5 – Effect of tip speed and number of blades on propeller noise at constant power

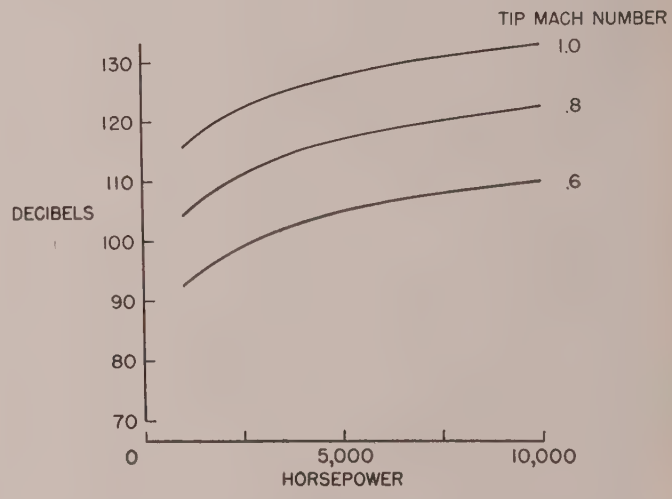

Fig. 6 – Effect of tip speed and power on propeller noise, calculated for four propellers of six blades each, 16-ft diameter at distance of 300 ft. Power is power per engine

siderable increase in noise with the higher frequencies predominating.

The dual propeller may also be treated within the concepts of the propeller noise theory. One of the features of the dual that distinguishes it from the conventional propeller is that the noise is not axially symmetrical but has a maximum in the direction in which the blades overlap, or pass each other, as shown in Fig. 8. The propeller has more harmonics and greater overall noise intensities in the direction of blade overlap. Thus fuselage vibrations may depend on dual propeller phasing.

Jet Noise

Present State of Knowledge – Some information on the present state of knowledge concerning jet noise was discussed in the first part of the paper in connection with the description of the quadrupole and Lighthill's eighth-power law relating sound energy to jet velocity. In this theory the quadrupole strength and the resultant noise intensity are related in some way to the turbulent velocities in the jet $\rho_o v_i v_j$; where ρ_o is the mean density and v_i and v_j are the turbulent velocity vectors. Since the turbulent shearing stresses in a fluid are also related to $\rho_o v_i v_j$, one may crudely say that on the basis of Lighthill's theory the noise intensity should be related to the shearing stresses in the fluid.

Lighthill presents in his theory a rather complicated tensor expression relating noise energy to turbulence; however, it has not been possible to obtain quantitative verification of this theory by experiment, nor is it certain that an experiment can be devised to measure these quantities precisely. This may be further illustrated in comparing propeller noise theory with jet noise theory. The magnitude of the pressure, frequency spectrum, and directional properties of propeller noise may be calculated directly from a knowledge of the aerodynamic pressures on the blade. For a jet this cannot be done as yet. It is not known whether the magnitude of jet noise that is measured is what one might expect from the turbulence in the mixing region of the jet. The theory has, however, given an impetus to research toward obtaining a better understanding of what is happening in the jet and relating this information to the external noise field.

Jet Structure and Its Relation to the Near-Field Noise – To indicate some of the features of the jet mixing region, a shadowgraph picture of a rectangular cold air jet as obtained by G. P. Wood and P. B. Gooderum of the NACA Langley Laboratory is shown in Fig. 9. Some weak shocks are visible near the nozzle, indicating that the flow is slightly above sonic speed. The general mixing of the jet with ambient air is, however, typical of high-velocity subsonic jets. This mixing may be observed at the top and bottom of the jet, starting first as a thin layer and then widening until at a distance of approximately 5 jet diameters the mixing region has entrapped the entire jet. From a measurement of turbulent velocity fluctuations, one reaches the conclusion that the rate of greatest shear is in the region of 2 to 4 nozzle diameters from the exit and hence may be the region which contributes most to the noise. Some confirmation of this is given by Hubbard and Lassiter[10] who show that the

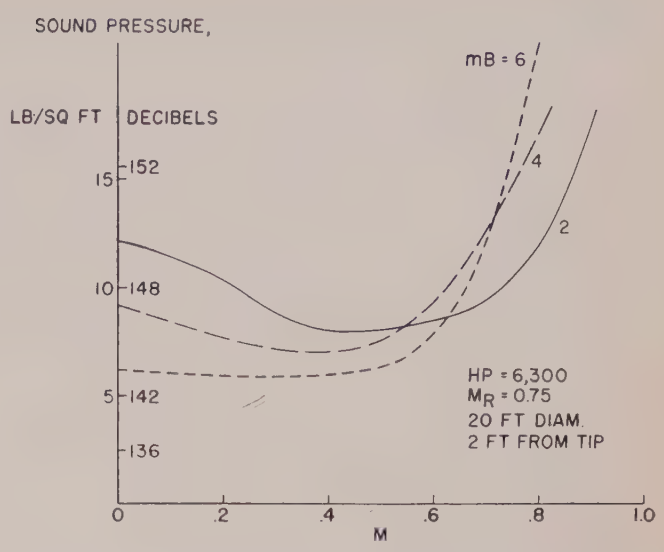

Fig. 7 – Effect of forward speed on sound pressure near the propeller

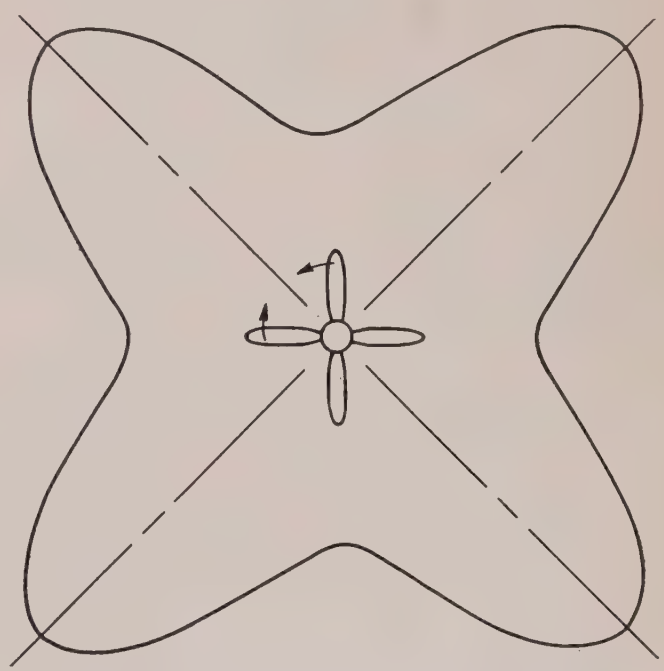

Fig. 8 – Noise intensity pattern about axis of counterrotation propeller

[10] See *Journal of the Acoustical Society of America*, Vol. 25, May, 1953, pp. 381-384: "Experimental Studies of Jet Noise," by H. H. Hubbard and L. W. Lassiter.

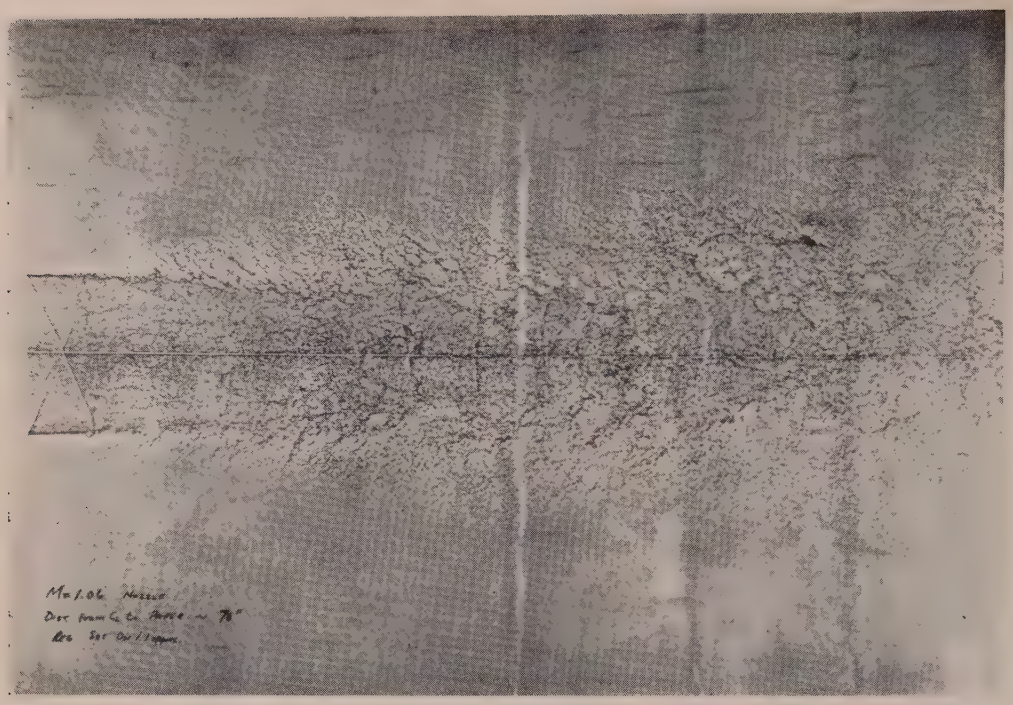

Fig. 9 – Shadowgraph of rectangular air jet at Mach number 1.06

intensity of the noise near the jet was a maximum at 2 to 4 diameters from the nozzle.

Some further information relating the turbulence in the jet to the noise just outside the jet is given in Fig. 10.[10] It may be seen that the predominant frequency of a random spectrum drops off rapidly with distance from the nozzle, which is to be expected as the width of the mixing region widens as shown in Fig. 9. The predominant frequency of the turbulence in the jet and the noise outside correlates well.

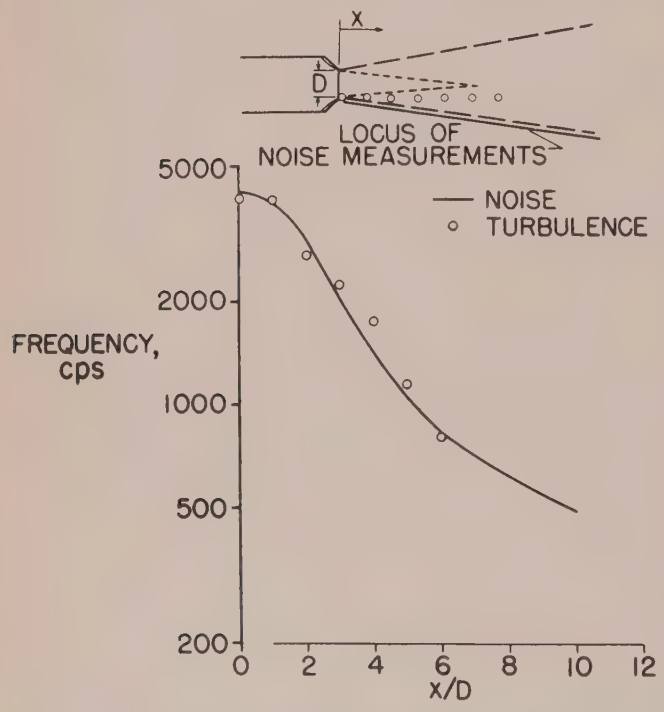

Fig. 10 – Comparison of predominant frequency of turbulence in jet with the noise near jet

There are large differences in the manner in which the noise intensity and frequency spectrum vary with jet velocity when one is near the jet as compared to distances of a hundred or more diameters away. Some of these are consistent with the theoretical concepts and some are as yet unresolved. Further details of some of these problems are discussed in the literature.[11, 12, 13]

Effect of Initial Turbulence, Burning, and Jet Velocity – A number of experiments have been performed at the NACA Langley Laboratory to determine how quiet one can make a jet by reducing the turbulence of the air as it enters the jet. For these tests air was stored in a large tank and exhausted through smooth contoured nozzles.[14] It was found that these jets made a noise comparable in magnitude to that of a smooth operating turbojet of the same size and at similar velocities. Powell[11] has also shown that the noise from jet engines plots along the same curve as obtained for small-scale cold jets.

Some recent laboratory tests on effects of burning on jet noise were made on a model jet by L. W. Lassiter of Langley. Some of the results are shown in Fig. 11. These tests show that when the data

[11] See *Aircraft Engineering*, Vol. XXVI, January, 1954, pp. 2-9: "A Survey of Experiments on Jet Noise," by A. Powell.

[12] See *Journal of the Acoustical Society of America*, Vol. 25, May, 1953, pp. 389-395: "On Noise of Aerodynamic Origin," by O. K. Mawardi and I. Dyer.

[13] See NACA TN 3187 (July, 1954), "Near-Noise Field of Static Jets and Some Model Studies of Devices for Noise Reduction," by L. W. Lassiter and H. H. Hubbard.

[14] See NACA TN 2757, August, 1952, "Experimental Studies of Noise from Subsonic Jets in Still Air," by L. W. Lassiter and H. H. Hubbard.

are plotted on a velocity basis, without regard to burning and gas temperature, all test points fall fairly well along one line. Even though the density of the hot jet is much lower than for the cold jet the noise at a given velocity is approximately the same. Why this is so is still one of the mysteries of the problem.

The conclusion that tentatively may be drawn is that burning noise of a smoothly operating jet does not contribute materially to the total noise and that the predominant source of noise at normal operating speeds is due to the turbulent mixing in the free jet. From Fig. 11, it may be seen that the sound pressures measured at a distance of 150 nozzle diameters fall near a line that has a slope of 4. Since sound energy varies as the square of pressure, these data would indicate an 8th power variation of sound energy with jet velocity. Thus velocity seems to be the most important parameter in jet noise generation.

Devices to Reduce Velocity – This strong dependence of jet noise on velocity has led various investigators to explore devices to reduce jet exit velocity. Some of these devices are shown in Fig. 12. One such device is an oversize pipe to enclose the jet mixing zone. This device generally aggravated noise conditions because of pipe resonances. The converging-diverging aspirators and the diffuser were tested by Westley and Lilley,[15] and they obtained rather indifferent results, except for the overpressured jet. Another device which might have some application to ground run-ups and muffling is the placing of a water-cooled screen in the jet ahead of the region of maximum shear.[13] Some investigators have tried water spray with some success. Although such devices show some promise for possible ground muffling, they do not appear feasible for flight muffling.

Devices to Alter the Jet Mixing – When one works for a time in close proximity to a noisy jet, one becomes obsessed with the idea of stopping the noise by putting things into the jet. Persons have probably stuck everything but the proverbial kitchen sink into the jet at one time or another in an effort to stop the noise. Some of these devices are illustrated in Fig. 13.

It happens that when a jet is operating at pressure ratios above choking, a very intense screech develops which can be eliminated by the insertion of a small object such as the point of a screw driver. Westley and Lilley[15] have explored the effect of such objects as the slotted cylinder and teeth on model jets. These experiments have been extended to full-scale tests by Mr. Greatrex of Rolls Royce[16] and by the Propulsion Laboratory of the NACA at Cleveland. For the model tests,

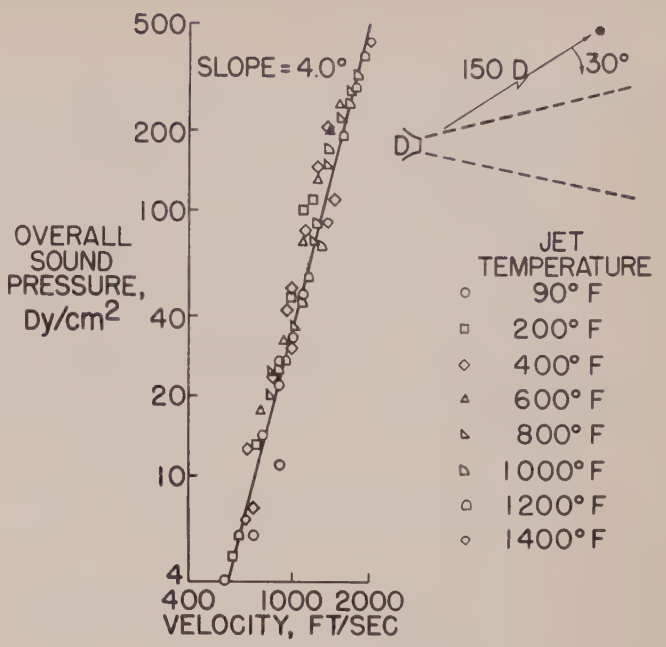

Fig. 11 – Sound pressure at a distance of 150 diameters for a jet operating at various temperatures

it was found that the teeth were very effective in relieving the screech condition at over-pressure or "choked" conditions. The full-scale tests, which were made on engines operating at pressures below "choke," showed that the teeth reduced considerably the low-frequency noise intensity toward the rear of the engine but that they increased the high-frequency noise in the direction perpendicular to the jet. The net result was a shift in the spectrum

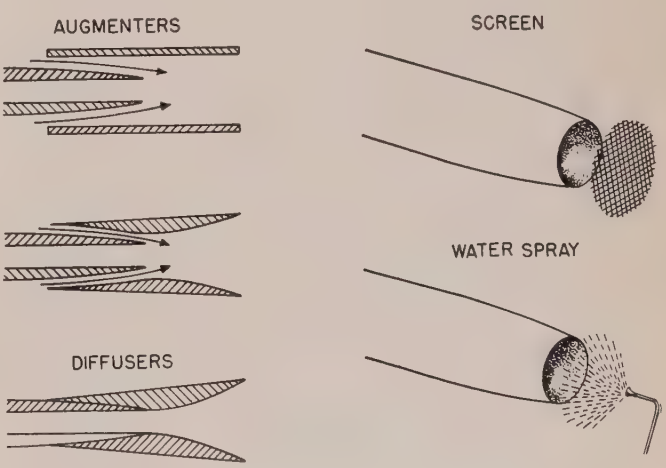

Fig. 12 – Devices for reducing jet velocity

[15] See College of Aeronautics, Cranfield, England, Report No. 53, January, 1952, "Investigation of the Noise Field from a Small Jet and Methods for Its Reduction," by R. Westley and G. M. Lilley.

[16] See *Royal Aeronautical Society Journal*, Vol. 58, April, 1954, pp. 223-231: "Engine Noise," by F. B. Greatrex.

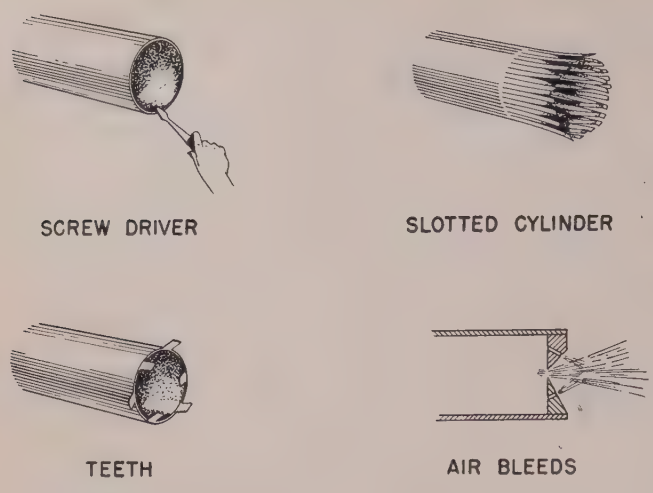

Fig. 13 – Devices for altering the jet mixing region

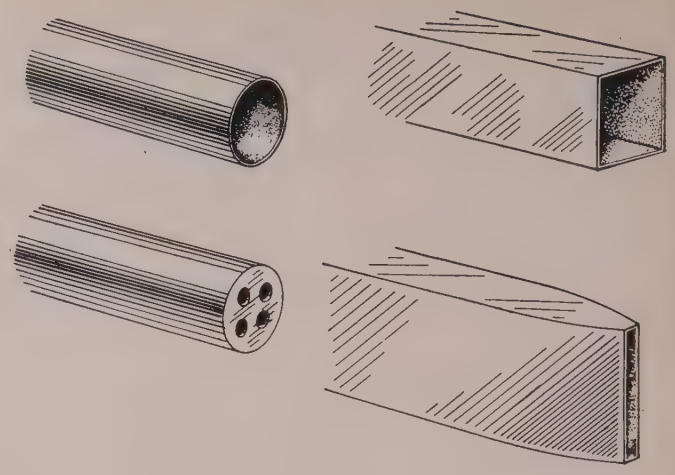

Fig. 14 – Some of nozzle exit shapes investigated

without much change in the total sound energy radiated.

Among devices tested at Langley on model jets were air bleeds. These behaved similar to teeth in relieving the screech condition.[13] Although these devices have not proved too promising, it has been demonstrated that the jet noise spectrum can be changed to a degree. Whether it can ever be changed enough to put it outside the audible range has not been conclusively demonstrated.

During the running of the tests on the large air tank at Langley, a number of different exit shapes were tried. Some of these shapes are shown in Fig. 14. Although this attack on the problem has not been fully explored, the preliminary results were not very encouraging.

Kinetic Energy and Noise

A discussion has been given of some of the things that do and do not appear to affect the noise. Of these, the velocity, whether it be the propeller tip speed or the jet velocity, appears to be of greatest importance. The effect of velocity may be thought of as the product of two factors: (1) the kinetic energy in the wake and (2) an efficiency factor of conversion between kinetic energy in the wake and radiated sound energy. The acoustic power radiated is generally only a small fraction of the kinetic energy of a jet, ranging from about 0.001% to about 1%, depending on approximately the 5th power of the velocity (see Fig. 1 and footnotes [12, 17, 18]). The fraction of the power supplied to propellers that is converted to sound varies from about 0.001% to about 1% for practical propellers. Here, too, the energy converted to sound has a great dependence on the tip speed, ranging from the 3rd to 15th power of the tip speed for various frequency components.

Since the radiated sound energy is a function of the kinetic energy of the propulsive system, it is of some interest to show how the kinetic energy in the jet or slipstream varies with different propulsive units in order to produce 10,000 lb of static thrust. This is shown in Fig. 15. Although it is not possible to draw general conclusions from Fig. 15 regarding the noise, it is of interest that high-velocity rockets produce about 60,000 hp of kinetic energy to develop 10,000 lb of static thrust, whereas the helicopter uses 600 hp to produce comparable thrust. Considering the jets, the afterburner expends much more energy than the bypass to produce the same thrust. From a practical standpoint it must be remembered that it usually takes a heavier and larger propulsive unit to produce the same thrust at lower velocities.

A general summary of the noise levels of various propulsive systems as function of jet or slipstream velocities is presented in Fig. 16. The slope of the line on this figure has been obtained from a consideration that the thrust is equal to ρAV^2 and the sound energy is assumed proportional to ρAV^8 (Fig. 1). Thus, for constant thrust the sound energy is assumed to vary as V^6. (Other laws of variation may be obtained depending on what assumptions are made concerning the dependence of sound energy on the density ρ. The constant K in the equation of the line has been adjusted to fit current noise measurements on jet engines.

It may be seen that although rockets are the

[17] See *Journal of the Acoustical Society of America*, Vol. 25, May, 1953, pp. 367-378: "Physical Characteristics of Aircraft Noise Sources," by H. E. von Gierke.

[18] See WADC Technical Report 52-204, December, 1952, "Handbook of Acoustical Noise Control, Vol. I, Physical Acoustics," by R. H. Bolt, L. L. Beranek, and R. B. Newman.

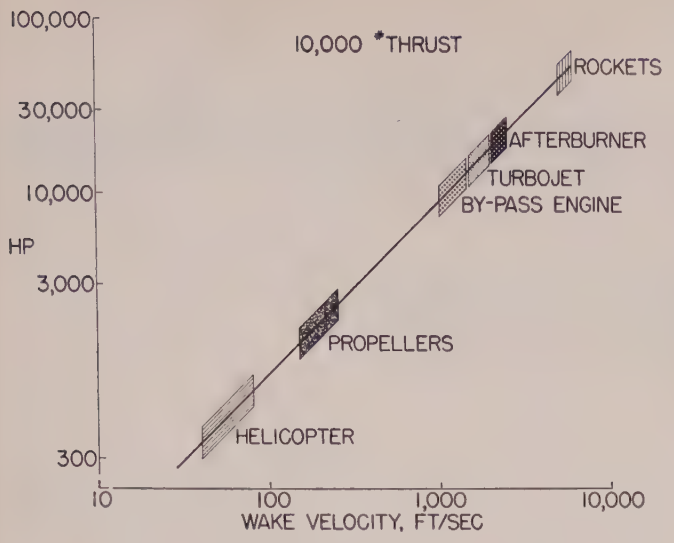

Fig. 15 – Kinetic energy in wake to produce 10,000 lb of static thrust for various aircraft propulsive systems

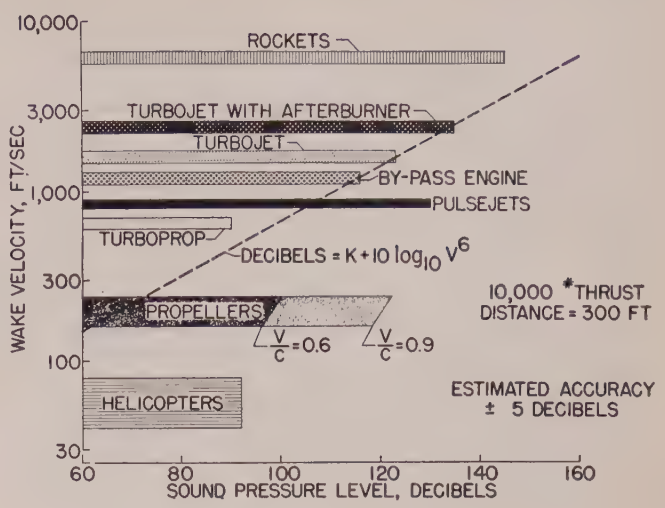

Fig. 16 – Sound pressure levels as function of wake velocity for various aircraft noise sources

noisiest they are not as noisy as one might expect from an extrapolation of jet data. Information for the afterburner and jet was obtained from Greatrex,[16] and there is reason to believe that the bypass engine will have noise levels approximately as indicated. Since the flow of the pulsejet is intermittent, we can expect its noise far to exceed the smooth jet noise curve. Characteristics of this type of noise and a theory based on the monopole source are given in the literature.[19, 20, 21]

The magnitude of noise from the exhaust of the turboprop has been reduced by 10 db from the turbojet curve in Fig. 15 on the assumption that the jet exhaust provides only one-tenth of the total thrust of the turboprop combination. Unpublished measurements made at Langley on a turboprop have shown the exhaust noise to be far below the propeller noise.

It may be noted that for propellers and helicopters the jet or slipstream noise is much lower than the noise actually observed. This is so because the predominant noise is from other sources than the slipstream. For propellers the noise is due to the air loads on the blades as described earlier. The range of noise levels from propellers for a given thrust is quite large depending mainly on tip speed, V/c. For conventional helicopters the noise is primarily engine noise, and its magnitude as given in Fig. 16 is based on unpublished data and information given by Lee Moore.[22]

Conclusion

An attempt has been made to explain the mechanism of aircraft noise generation and to present the current state of knowledge regarding this subject. It has been shown that for propellers the source of noise is well understood and that we can quantitatively calculate the noise intensities and characteristics from a knowledge of the propeller geometry and aerodynamic performance data. Recent research has extended the application of the theory to the near-field noise, the forward-flight case, and the counterrotation propellers.

For jet noise the theory is as yet incomplete. However, a considerable amount of experimental work tends to confirm some of the trends predicted by Lighthill's theory. The NACA is continuing to sponsor university research to throw more light on the mechanism of jet noise generation and is conducting full-scale jet noise tests at the Cleveland Laboratory and model tests at the Langley Laboratory in an effort to obtain a better understanding of the factors that affect jet noise and, if possible, reduce its intensity without impairing performance. At present it appears that the jet exit velocity is the most important factor in jet noise generation.

Additional Reference

NACA RM E54B01, March, 1954, "Tooth-Type Noise-Suppression Devices on a Full-Scale Axial-Flow Turbojet Engine," by Edmund E. Callaghan, W. Howes, and W. North.

[19] See NACA TN 2756, August, 1952, "Noise from Intermittent Jet Engines and Steady-Flow Jet Engines with Rough Burning," by L. W. Lassiter.

[20] See *Journal of the Helicopter Association*, Great Britain, Vol. 7, July, 1953, pp. 32-41: "The Noise of a Pulsejet," by A. Powell.

[21] See *Journal of the Acoustical Society of America*, Vol. 25, No. 3, May, 1953, pp. 417-422: "Noise Characteristics of Pulsejet Engines," by P. S. Veneklasen.

[22] See *Aviation Week*, Nov. 16, 1953, pp. 99-101: "Carriers Outline Helicopter Requirements," by L. Moore.

Acoustic Design

THE attenuation requirements for turbojet test cells vary generally from 20 to 60 db – the lower figure applying to the low frequencies and the upper figure to frequencies of about 1000 cps.[1, 2] Development of acoustic design and acoustic materials since the end of World War II has made it possible to achieve these objectives. Achievement means not only that such noise attenuation can be obtained but also that these installations are practical from the economic point of view.

Economics

It is, of course, very difficult to put any exact cost figures on such sound treatments; but just to give an order of magnitude, the acoustic treatment of test cells for today's size engines may cost anywhere between $500 and $2000 per db attenuation. These figures depend greatly on whether the acoustic treatment is installed in a new test cell, especially designed for this acoustic treatment, or whether the attenuation has to be designed into an already existing test cell that was built to test propellers or reciprocating engines. The number of test facilities to be erected is also important since, in case of larger numbers, it is possible to use mass-production techniques. For example, a large saving was effected in the construction of test cells at the General Electric Evendale, Ohio, plant by large-scale prefabrication. One of the cost-saving methods was the precasting of the concrete next to the construction site. Of influence on the cost is also the availability of space. It is generally less expensive to build horizontal inlet and exhaust ducts than vertical ones. These, however, are often used since space is at a premium in most manufacturing areas. Application of water spray for cooling purposes often reduces the size of the exhaust ducts and makes possible a wider selection of sound-treatment materials.

The attenuation between the test installation and the minimum distance to residential property governs in general the extent of the acoustic treatment which must be installed. This attenuation is calculated from the law of spherical divergence. There will be day-to-day variations from this law due to varying atmospheric conditions. Due to this variation, more sound treatment than calculated from the law of spherical divergence is needed if the test installation must operate at any time. This additional acoustic treatment should give an increase in attenuation of 10 db. If this should not be done, constant monitoring of the noise transmitted into the neighborhood is required. The GE Aircraft

[1] See *Journal of the Acoustical Society of America*, Vol. 24, September, 1952, pp. 480-489: "Acoustic Design of Aircraft Gas Turbine Test Cells," by R. O. Fehr, R. J. Wells, and T. L. Bray.

[2] See *Journal of the Acoustical Society of America*, Vol. 25, May, 1953, pp. 423-428: "Noise Control Measures for Jet-Engine Test Installations," by H. C. Hardy.

THE high noise level associated with turbojet testing creates two noise problems:

1. The reduction of noise in the neighborhood of the installation to an acceptable level.

2. The protection of operating personnel from excessive noise.

Desirable sound levels are established and, on the basis of these levels, specifications are written for the acoustic treatment of the turbojet facilities. The acoustic treatment must not only be satisfactory from the point of view of noise reduction, but it must also be able to withstand the very rigorous operating conditions. High-temperature and high-velocity flow of gases through the exhaust stack makes for these rigorous conditions.

Designs which meet these specifications are discussed in this paper, together with performance data obtained on these designs.

The Authors

R. O. FEHR is a consulting engineer for the Electro-Mechanical Engineering Services Department of General Electric Co. He received a Ph.D. in Electrical Engineering from the Swiss Federal Institute of Technology. Dr. Fehr joined General Electric Co.'s Engineering Laboratory in 1939. He became consulting engineer in 1953. He is past chairman of the Aircraft Industries Association Noise Control Committee.

B. E. CROCKER is a test facilities engineer in the Aircraft Gas Turbine Division of the General Electric Co. He received an electrical engineering degree from Michigan State College in 1949. Mr. Crocker joined General Electric that same year. He is active on the AIA Noise Control Committee, as representative of his Division of the General Electric Co.

and Performance of Turbojet Test Facilities

R. O. Fehr and B. E. Crocker, General Electric Co.

This paper was presented at the SAE National Aeronautic Meeting, New York, April 14, 1954.

Gas Turbine Division has such a system in operation. A microphone is installed in the surrounding area of the plant, and it is connected by telephone lines to a monitoring station within the plant. In addition to this fixed installation, a mobile sound-measuring unit patrols the neighborhood and reports sound levels to the plant by means of radio-telephone.

All these factors which determine the cost of the acoustic treatment are summarized below:

1. Development or production work.
2. New cell, or rebuilt propeller or reciprocating-engine test cell.
3. Horizontal or vertical exhaust and intake ducts.
4. Number of cells to be built simultaneously.
5. Continuous operation or intermittent operations required.
6. Minimum distance to residential property and type of neighborhood.
7. Availability of water for cooling purposes.

Acoustic Specifications

Intake and Exhaust Ducts – First the design objective must be established. This objective is generally the level at residential property in the neighborhood. It is given by curves showing the sound pressure level for one octave band as a function of the octaves 35-75 cps to 4800-9600 cps, and it depends on the ambient level in the neighborhood. Curves of ambient levels are given in Fig. 1. Knowing the minimum distance of the residential property from the test cells, the sound attenuation over this distance due to the law of spherical divergence may be obtained. Adding the decibel value of this attenuation to the desirable decibel sound level at the residence furnishes the design objective for the noise at the exhaust and intake ducts.

The noise level in the test cell is determined from measurements on the engine or for new engines from available graphs of sound power level versus fuel flow.[3] Often data are given for afterburner operation. They may be reduced by about 8 db for operation of the turbojet without afterburner. The duct treatment must then be designed for an attenuation which is given by the difference between the levels in the cell and those which were determined for the exits of the exhaust and intake ducts.

Several corrections must be made to this figure

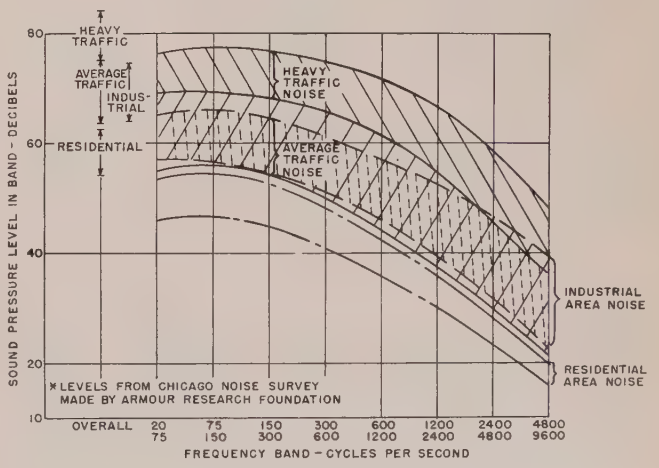

Fig. 1 – Residential sound levels

[3] See Wright Air Development Center Technical Report 52-204 (1952), Handbook for Acoustic Noise Control, Vol. I, Physical Acoustics.

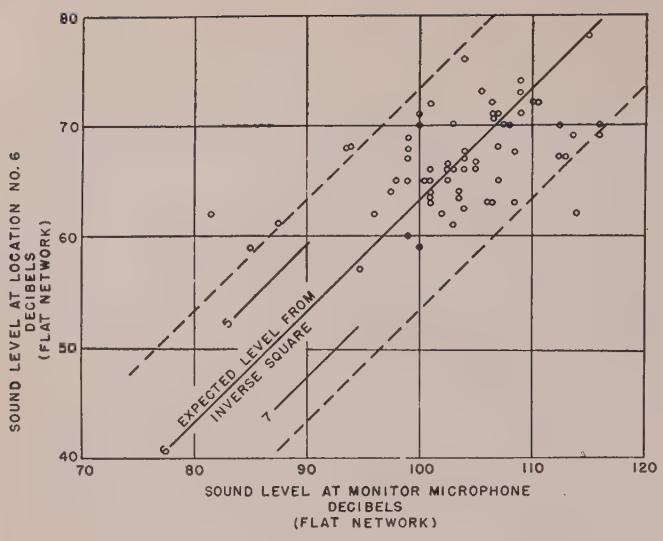

Fig. 2 – Fluctuation of sound attenuation

of attenuation. In many plants more than one test cell is in operation. In this case, the attenuation of each cell must then be increased so that simultaneous operation of these cells is possible without exceeding the design objective. For operation of two cells, the attenuation should be increased by 3 db; for four cells, by 6 db; for ten cells, by 10 db; and so forth. It may be well to set up a testing schedule and to determine how many cells must operate at the same time and then design the sound treatment accordingly.

The change in attenuation due to variation in atmospheric conditions must also be taken into account. A variation of ± 10 db was measured at Evendale, and the points are shown in Fig. 2. The data plotted in this curve were accumulated during 2½ months' operation in the summer months. Greater attenuation than resulting from spherical divergence may be explained by the effects of temperature gradients, wind gradients, absorption on the ground, and absorption due to turbulence. The attenuation due to absorption is considerable for high frequencies, for example, as high as 12 db in the 2400-4800 cps octave for a distance of 1 mile. On the other hand, less attenuation than resulting from spherical divergence may be the result of temperature and wind-velocity gradients. The sound rays are bent downwards when the temperature increases with altitude. This is often the case at night, and hence, the audibility of sound by night may be better than in the daytime. In early spring and in mid-fall, the temperature gradients near the ground have the highest values.[4] This may account for the need of greater care in monitoring the sound levels during these seasons. Observations indicate that the variation of ±10 db measured during the summer months was not exceeded during any other season.

Another correction should be considered to take in account the character of the neighborhood. The design objective is generally given for the very quiet residential neighborhood. For the average suburban residential neighborhood, 6 db may be added to the design objective, and for an urban residential, an increase of as much as 12 db may be made.[5]

Wall Construction – The sound insulation of the walls should equal the sound attenuation through the ducts. For high attenuations, this objective may be achieved with a double partition consisting generally of a concrete wall 1 ft thick and a second wall of cinderblock or sound-isolation panels. In most cases, however, a single concrete wall has proven to be satisfactory.

Window area should be kept to a minimum. If any windows are installed in the wall of the test cell, they should consist of at least three panes of glass with an air space between them. Attention must be paid to the design and construction of doors and of door seals. On many doors, the seal must move into position after closing. The maintenance of this mechanism in a factory is difficult. The most successful installations use double doors with the space between them evacuated.[6]

Test Cell Design

After the acoustic performance specifications have been established, consideration must be given to a design which meets these specifications. Any exhaust duct treatment has to be able to withstand high wind velocities and high temperatures. The exhaust velocities from jet engines are close to sonic, and the temperatures experienced with afterburner operation are about 3200

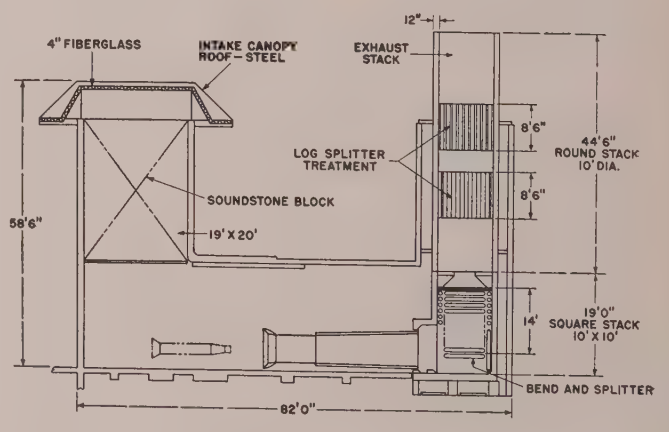

Fig. 3 – Turbojet test cell modified from reciprocating-engine test cell

[4] See *Journal of the Acoustical Society of America*, Vol. 25, May, 1953, pp. 405-411: "Review of Influence of Meteorological Conditions on Sound Propagation," by U. Ingard.

[5] See *Journal of the Acoustical Society of America*, Vol. 23, July, 1951, pp. 435-439: "Levels and Spectra of Traffic, Industrial, and Residential Area Noise," by G. L. Bonvallet.

[6] See Proceedings of National Noise Abatement Symposium, Vol. 2, October, 1951, pp. 21-38: "Physiological and Psychological Effects of Noise," by H. O. Parrack.

F, and without afterburner – "dry" operation – close to 1300 F. Cooling of the hot exhaust gases while passing through the exhaust duct is achieved by augmenting these gases by secondary airflow and sometimes by additional injection of water spray into the duct. Where the water supply is limited, it is often to advantage to design the sound treatment to stand up under temperatures encountered for "dry" engine operation. A water spray is then used only for the short period where the engine is tested with the afterburner. It is good practice to limit temperatures in the exhaust duct to 550 F and to limit the exhaust velocity to 200 fps. It has been found that for higher air speeds, the self-noise of the airstream may exceed the reduction obtainable from the acoustic treatment.

The most common treatments now in use in this country can be divided into:

1. Sound blocks.
2. Straight parallel splitters made from conventional sound-absorbing materials contained in perforated steel sheets.
3. Sine-wave-shaped splitters consisting of baffles filled with sound-absorbing material.
4. Plenums lined with sound-absorbing materials, often in the form of 90- and 180-deg acoustically lined bends.
5. Ducts with attached resonators.

The attenuations which can be obtained with these treatments are available in the literature and in reports. Often it is desirable to make scale model studies of the particular configuration chosen before construction is started.[1, 7]

In the following text, two actually built installations are described, and their measured attenuations are given. They illustrate some of the acoustic treatments outlined above.

Examples of Existing Installations

Modified Test Cell – A turbojet cell which was modified from a reciprocating-engine test cell is shown in Fig. 3. The exhaust duct is made of a haydite concrete pipe 10 ft in diameter which is located within the previously built stack. This was necessary because the originally used portland cement will not withstand the temperatures and pressures in this particular structure where the stack was constructed as part of a building.

Attenuation measurements were made when there was no sound treatment in this stack. The difference between the readings within the cell and outside the stack was due to directivity and spherical divergence. (See Fig. 5.)[8] The readings were taken according to the AIA-En-1 Standard,[9] that is, inside the cell: one nozzle diameter to the side from the nozzle centerline and one nozzle diameter to the rear of the exhaust nozzle; and outside the stack: one stack diameter up and one stack diameter to the side from the centerline of the stack. The acoustic treatment was then installed in the exhaust duct. It consists of a combined bend and splitter treatment and two splitter treatments within the straight section of the stack. The bend splitters are made of logs about 8 in. in diameter and 8 ft long. They are made of fiberglas rolled into a fiberglas cloth, so forming a cylindrical pillow. This pillow is then inserted into the perforated metal cylinder which, in turn, is mounted in racks of structural steel as shown in Fig. 4. These logs can be very easily removed and reinstalled if maintenance should be necessary. They are spaced on about 22-in. centers. They have been in use now with and without afterburners for about 10 months and no failures have occurred to date. Similar installations of parallel batts did not give as good an attenuation and did not stand up as well. The treatment in the straight section of the stack uses the same logs. Here, panel batts are provided as lining of the stack surface. The total attenuation as well as the attenuation of the individual treatments are shown in Fig. 5. The velocity of the stack is about 225 fps, and the temperature of 550 F is obtained by water injection of 250 gpm during afterburner operation.

Fig. 4 – Acoustic treatment consisting of fiberglas log rolled in fiberglas cloth; pillow thus formed is placed in metal cylinder and mounted in steel racks as shown

The acoustic treatment of the intake stack still uses the sound stone blocks which were originally installed for sound treatment when reciprocating engines were tested in this cell. Additional attenuation was obtained by lining a weatherhood

---

[7] See *Journal of the Acoustical Society of America*, Vol. 25, May, 1953, pp. 429-432: "Comparison between Model Study Tests and Field Measurements on Aircraft Test-Cell Silencer," by D. B. Callaway and R. D. Lemmerman.

[8] See *Journal of the Acoustical Society of America*, Vol. 25, May, 1953, pp. 433-437: "Sound Radiation Patterns of Gas Turbine Exhaust Stacks," by R. J. Wells and B. E. Crocker.

[9] See ATC Report No. ARTC-2, "Uniform Practices for Measurement of Aircraft Noise." Published by Aircraft Industries Association, Washington, D. C., Aug. 1, 1952.

protecting the intake duct. The sound stone treatment consists of hollow blocks with an opening of about 11 x 16 in. for the air passage. The treatment of the hood consists of 4-in. fiberglas board attached to an expounded metal screen and covered with fiberglas cloth. A coarse screen holds the cloth and treatment in position. A dimensionally varying air chamber is formed by the treatment and the hood. The sound pressure level beneath the intake stack was measured to be about 10 db below the level measured at the position near the exhaust. The attenuations obtained are shown in Fig. 6. The measurement positions are also shown in the graph. The velocity in the intake stack is about 35 fps.

New Test Cell – A typical design for a test cell specifically built for turbojet operation is shown in Fig. 7. The exhaust system was constructed by using precast concrete sections which were merely set in place. This resulted in a very substantial saving when the cell was built in quantities for production testing. The acoustic treatment of the exhaust consists of sound blocks in the horizontal section, corner treatment similar to the one mentioned above, and parallel panel splitters. The sound blocks are made of haydite aggregate with an alumnite binder. They are made with standard 8 x 8 x 16-in. building-block forms. Their open area is about 40% of the total block. These blocks have proven to have a very low initial cost and are a low-maintenance-cost sound treatment. Many of these cells have now been in operation for more than two years. However, the method of making these blocks and of installing them is very critical. The parallel panel splitters are placed on 8-in. centers and are 4 in. thick with fiberglas wrapped in a fiberglas cloth blanket between perforated steel sheets. Similar panels are used for the treatment of the intake duct. The attenuation for the intake and exhaust duct is shown in Fig. 8.

Conclusions

In the preceding text two actually built installations have been described. There are many other means of acoustic treatment available. Details of these methods may be obtained from the literature or from the catalogs of manufacturers of acoustic materials. The selection of the treatment must be guided by the requirements of the individual case in order to obtain economically the best technical performance.

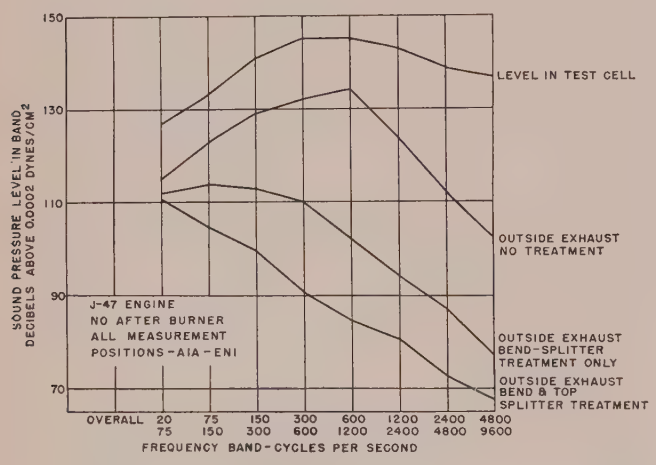

Fig. 5 – Attenuation for modified reciprocating-engine test cell, exhaust duct

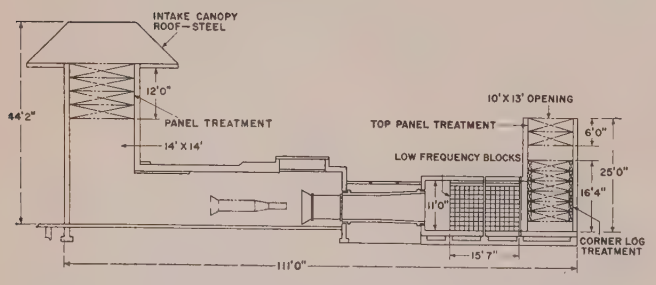

Fig. 7 – Test cell specifically built for turbojet operation

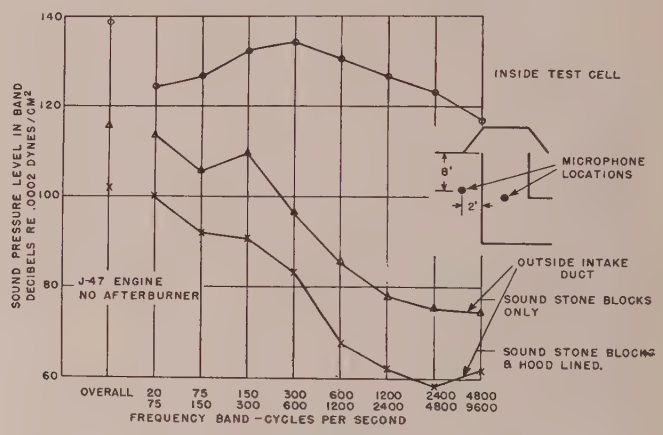

Fig. 6 – Attenuation for modified reciprocating-engine test cell, intake duct

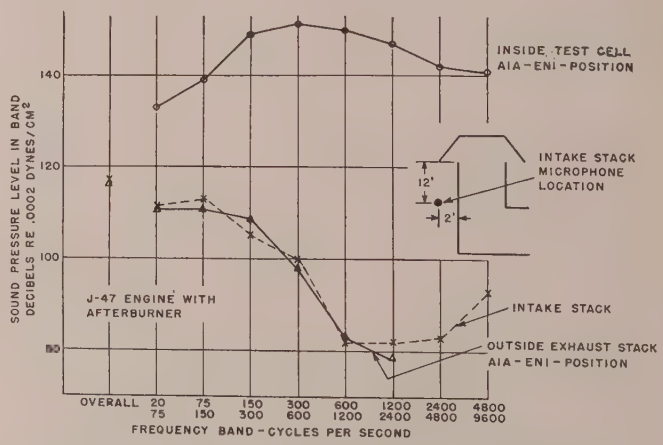

Fig. 8 – Attenuation for new-construction turbojet test cell

Aircraft Noise Problem in Airport Vicinities

C. E. Rosendahl, National Air Transport Coordinating Committee

This paper was presented at the SAE National Aeronautic Meeting, New York, April 14, 1954.

EARLY in 1952, much of the public living near air terminals in the New York-New Jersey metropolitan area was engulfed in semihysterical fright. In a span of only a few months, several transport aircraft had crashed near such airports.

Newark Airport had been closed. Across the Hudson in Queens County, New York, thousands had joined in movements to curtail and even stop operations at LaGuardia and New York International Airports. Aviation is the largest single industry in Queens County, and these great airports are the cornerstone upon which that industry was built. Yet, the air industry, thousands of users of air transport, and our country's whole economy were faced with the awesome threat of having the world's greatest transportation center completely closed to civil air traffic.

Basic Cause of Public Outburst

Although triggered by a mathematically incredible series of accidents, the basic cause of this public outburst lay elsewhere. For some time prior to this almost unbelievable sequence of accidents, in various areas a shift had been taking place in the public's attitude toward air terminal operations.

Traditionally, the average community had sought and fought for location of airfields within its area. Concerted campaigns to have air facilities located convenient to towns and cities had been common. For many years, possession of a conveniently located airport was a hallmark of progress, an unmistakable symbol that the community and its citizens were truly progressive.

Then, through a series of concurrent developments, this picture began to change radically. Communities themselves began to expand rapidly. Some people, for economic reasons, moved closer to airports. Housing developments often enveloped existing airports with their growing residential neighborhoods.

Also concurrently, the traveling and shipping public began to demand increased and better air service. Airplanes became more numerous, larger, faster, their greater powerplants noisier.

During time of war, residents near airports had patiently and patriotically refrained from protest against noise and hazard of military aircraft activities. But, with the war's end, this tolerance did not carry over to the fast-growing operations of nonmilitary aircraft.

In brief, throughout the country, the increasing population near airports was subjected to a growing volume of noisier aircraft. Where formerly communities had sought them, they now fought against having airports located contiguous to their residential and business districts.

With particular respect to the New York-New Jersey metropolitan area, the succession of aircraft accidents merely served to crystallize this already existing and mounting resentment against air terminals and their air operations.

Whereas for years, noise and low flying had been considered mainly as annoyances, now the dominating reaction was FEAR – fear that noisy aircraft would crash in the vicinity. In people's minds, the noisier they were the more hazardous they seemed.

Should we want, we could debate the issue and point out that civil aviation is not the first industry to face mounting community problems as it grew. Nor does it matter, at the moment, that some maintain there may be greater acceptance of aircraft noise and annoyance as younger people and coming generations find aircraft part of their daily lives from the day they are born. In short, we are today faced with a problem that requires action now.

Noise Becomes Major Problem

Though it began as a parasitic or corollary aspect, aircraft noise is currently a major problem. It has served to crystallize the attention of the entire air industry to the very important issue of Community Relations, if you wish, or put another way, the ability and desire of the air industry to be a good neighbor.

To the credit of the civil air industry, the action it took in early 1952, in the areas contiguous to the New York-New Jersey metropolitan airports, to meet the aircraft annoyance problem was vigorous, comprehensive, and unanimous.

NATCC Formed

No more striking evidence of air industry unanimity can be found than the membership list of the voluntarily formed National Air Transport Coordinating Committee (see Table 1) comprising as it does every segment of this great and growing industry.

The purpose of NATCC is to study and analyze certain of the problems arising from the provision of civil air transport service to the New York-New Jersey metropolitan area and to devise the best possible solutions to these problems. Then, through cooperative action by its membership, these solutions are placed in effect as the policy of the agencies and organizations represented on the committee.

True enough, the formation of NATCC was precipitated by a local emergency which threatened to develop into a national crisis. But beyond its local scope, it constitutes an active pilot activity whose experience can be used to advantage by the industry as a whole and by any community or area where similar situations might arise.

New York is looked upon as a proving ground for many new things. The New York area handles the largest volume of traffic; its airports are situated in proximity to highly populated areas; it was the scene of one of the most tragic and unusual experience in civil aviation history. If effective airport community relations in the New York area under such circumstances could be established, they might well serve as a guide and an inspiration for the rest of the country. In brief, "fire fighting" experience in this area might well help "fire prevention" elsewhere.

The NATCC approach to the problem has been two-pronged.

First, we have sought, within the limits of safety and of technological ability, to reduce to an achievable minimum, low, noisy flight over people's homes. Serious effort is being expended also on the matter of controlling noise from ground run-ups. Though they do not have the same psychological effect as noise associated with low flying aircraft, ground run-up noises, also, nevertheless can be most irritating to nearby communities.

Secondly, we have sought to provide interested residents in airport areas with solid, factual information to help them understand and evaluate the air industry's operations from the standpoints of safety, annoyance, economic value, defense value, and the practical aspects of flight. This is not, of course, the occasion for discussion of this phase of the NATCC program, but suffice it to say, the activities of aviation educational and information services constitute a community or public relations project of first magnitude.

As for the main attack on the problem of aircraft noise abatement in airport vicinities, a recent noise abatement study by Trans World Airlines[1] sums up the case rather well as follows:

"Noise and its physiological and psychological

Table 1 – Membership of National Air Transport Coordinating Committee

Air Line Pilots Association
Air Transport Association of America
Aircoach Transport Association, Inc.
Aircraft Industries Association of America, Inc.
Aircraft Owners and Pilots Association
Airport Operators Council
American Airlines, Inc.
American Association of Airport Executives
Capital Airlines, Inc.
Civil Aeronautics Administration
Civil Aeronautics Board
Eastern Air Lines, Inc.
Independent Military Air Transport Association
National Airlines, Inc.
National Business Aircraft Association, Inc.
New York Airways, Inc.
Northeast Airlines, Inc.
Pan American World Airways, Inc.
The Port of New York Authority
Slick Airways, Inc.
Trans World Airlines, Inc.
United Air Lines, Inc.
Allegheny Airlines, Inc.
Colonial Airlines, Inc.
The Flying Tiger Line, Inc.
Mohawk Airlines, Inc.
Northwest Airlines, Inc.
Riddle Airlines, Inc.

[1] See TWA Staff Engineering Report No. 3-2054, April 1, 1953, "Noise Abatement Study."

CONTROL of aircraft noise in airport vicinities lies in two general directions. The first is in control of noise at its source – in the aircraft itself. The second is in the procedural measures in operation of the aircraft and is the subject of this paper.

Measures adopted by the NATCC for application at the major civil airports in the New York-New Jersey metropolitan area are described here. They include:

1. A preferential runway utilization plan.

2. Accelerated climbouts stressing rapid gain of altitude.

3. Restriction of ground run-ups to specified locations.

4. Adoption of procedures particularly adapted to an individual airport.

5. Receipt and analysis of the public's complaints relative to aircraft noise.

6. A public information program designed to acquaint airport neighbors with aircraft matters.

7. Continuous effort at obtaining full compliance with adopted procedures.

The Author

C. E. ROSENDAHL is executive director of the National Air Transport Coordinating Committee. Since his retirement from the Navy in 1946, he has been an aeronautical consultant and a vice-president of the Flettner Aircraft Corp. During his naval aviation duty, Admiral Rosendahl commanded U.S. airships "Los Angeles" and "Akron," and was Chief of Naval Airship Training and Experimentation. He is a Fellow of the Institute of Aeronautical Sciences.

effects are extremely complex and interrelated. Basically, however, two reliefs are well understood and straightforward. These are:

1. Reduce the intensity at the source, and/or
2. Increase the distance between the source and the receiver.

"Obviously, reducing the source intensity would entail tremendous amounts of study, changes in equipment, possibly redesign of certain components such as exhaust systems, propellers, and so forth, and immediately, therefore, appears out of reach. On the other hand, distance is almost [always] to to be had provided performance or other limitations or both of individual aircraft are properly recognized.

"A reasonably valid approximation relating noise and distance is:

'Noise intensity (in terms of energy) varies inversely as the square of the distance from the source, all other factors being equal.'

"For example, if the distance from the source is doubled, the new intensity would be only one-fourth or 25% of the original.

"The other fundamental characteristic is [that] the ear reacts to sound intensity approximately as indicated by a logarithmic scale. For example, if two 100-db sounds are added together, the new intensity is 103 db and not 200 db; and conversely, if the original sound intensity were halved, the ear would recognize only a 3-db reduction (a relatively small change).

"These two fundamentals illustrate that increasing the distance from the source has the greater effect toward reducing sound intensity. It can also be seen that even though the source's intensity may have to be increased to achieve greater height, if the height increase is sufficient, the overall sound intensity to the observer can still be lessened.

"The problem then becomes how this can be done consistent with safe operating procedures."

This ends the quotation from the TWA report.

Increased Distance between Source and Receiver

Fortunately, considerable can be achieved towards aircraft noise annoyance abatement, consistent with safety and good operation, through adoption of certain procedural measures based on increasing the distance between the aircraft as the noise source and the airport neighbor as the receiver. It is such measures upon which NATCC efforts are concentrated. Let us now consider such measures.

When study of the problem began, it was obvious that from the public's standpoint a substantial amount of flight operations in approaching and leaving the terminals could be improved.

For example, some aircraft were making long, low approaches to the airports, requiring use of considerable power. Some were maintaining relatively low altitudes for extended periods after take-off, intent primarily on quickest possible transit to destinations, with rate of climb secondary. Some, in order to get on course as quickly as possible, were executing low-level turns.

All of these practices were well within Federal regulations, and certainly were not conducted with any thought of annoying or frightening air terminal neighbors or other persons. Obviously, they were conducted primarily with economic factors

in mind and with selling speed, the outstanding attribute of travel by airplane.

So, when confronted with the early 1952 situation in the New York-New Jersey metropolitan airport area, the air industry through its newly created NATCC arm adopted certain voluntary remedial operational practices which will now be outlined.

Preferential Runways

First, consistent with safety, it was decided to make maximum possible use of *preferential runways* which would divert numerous operations from residential areas surrounding the airports or route them over water, open areas, or the least congested areas.

It has been long established practice that all landings and take-offs must be made on that runway lying most directly into the direction of the wind. NATCC "preferential" practice is a somewhat new conception in that it permits considerable numbers of landings and take-offs in certain crosswind situations. It is accomplished under standards and procedures which do not violate sound practices and which are in strict accord with pertinent Federal regulations.

Preferential runway utilization is in effect under the following conditions:

1. When weather conditions permit VFR (Visual Flight Rules) operations and when there is no compromise to safety of IFR (Instrument Flight Rules) traffic in the area. VFR require a ceiling of at least 1000 ft and a horizontal visibility of at least 3 miles.

2. When winds are 15 mph or less.

3. When the wind direction is within 80 deg of the heading of the runway, except that when winds are 5 mph or less, the preferential runway may be used when the wind is within 90 deg of the runway heading.

4. When runways are dry and clean.

5. When there are no obstructions adjacent to the runway.

6. When there are no unusual obstructions in the flight path.

7. When the individual pilot concurs. (Nonconcurrence is extremely rare and only for safety reasons.)

There are certain other features which must be understood in connection with the use of runways:

1. When Instrument Flight Rules (IFR) are in effect, it is mandatory that there be used only those runways which have been designated and equipped for instrument operations by the Federal government. IFR are in effect when the ceiling is less than 1000 ft and the horizontal visibility is less than 3 miles.

2. Under IFR conditions, the preferential runway system is *not* in effect.

3. When the wind is over 15 mph, wind *direction* is the determining factor as to what runways are to be used, and the "preferential" system is superseded while such conditions exist.

It must be realized also that under Instrument Flight Rules, the dictates of safety require that all aircraft adhere precisely to fixed instrument paths and to prescribed instrument runways and that such paths necessitate somewhat lower approaches and take-offs than under VFR. Hence, under IFR conditions there will, of necessity for safety's sake, be less separation between aircraft as the noise source and persons living in the vicinities of the instrument runways.

Problem of Crosswind Components

The question is sometimes asked why operations cannot be carried out in higher crosswind velocities and thus possibly permit wider use of those runways labeled "preferential" or most desirable from the standpoint of reduced low flying and noise.

Crosswind components present a problem in air carrier operations for two primary reasons:

1. Aircraft structural limitations.

2. Aircraft controllability features.

When an airplane is landed in a crosswind, generally accepted technique requires that the pilot maintain a drift correction on final approach and that he remove this correction an instant before contacting the runway. Greater stresses are placed on the gear if the drift correction is not removed, and the airplane contacts the runway with the fore-and-aft axis at an angle to the runway. Hence, it is imperative that the airplane be controllable at landing speed to enable the pilot quickly to remove the drift correction. The greater the crosswind, the greater is the amount of controllability required to accomplish this and to maintain the direction of the airplane on the runway throughout the ground roll.

Serious study of crosswind landing gear and techniques has been in progress for years and is continuing. Advances have been made, and more may yet be made. However, the limitations mentioned above as NATCC criteria represent the industry's general agreement as to the maxima consistent with safety that should be permitted in operations of today. These criteria must be predicated on the least capable airplane and on minimum pilot technique. As far as NATCC objectives go, increasing permissible crosswind component values would be most laudable and should provide

an increment to the score achieved by other procedural remedies for our problem. However, this contribution, though valuable, would not wholly solve the NATCC problem. But in no sense should these remarks be construed as minimizing the value of increased crosswind landing improvements.

Training Flights Transferred

Training flights for transport crews and in transport aircraft grow even more important, if possible, as civil aviation expands and progresses. However, only certain training flights of necessity must be performed at such busy civil airports as those in our New York-New Jersey metropolitan area. Hence, under our NATCC program there have been transferred from these metropolitan airports to open areas or other more suitable airports all transport training flights except those required by Federal regulations to be made at these specific airports.

This transfer of training flights has resulted in substantial relief to airport neighborhoods since many of the training flights were legally required, low-level, high-power circling operations over adjacent areas. This one step in this metropolitan area has reduced the number of landings and take-offs so involved by more than 25,000 per year, plus elimination of at least twice as many low-level, high-power circling operations.

Other Aids

We have also applied other ways of increasing the distance between the source and the receiver.

Formerly, even under VFR there were long, low, drag-in approaches. Now, however, during all VFR approaches to Newark, LaGuardia, and New York International Airports, pilots are maintaining altitudes of at least 1200 ft as long prior to landings as the characteristics of their aircraft permit.

The record shows that originally many complaints of low flying and noise annoyance came from areas as far removed as 10 to 15 miles from the terminals, due to long, low approaches to the airports. These long, low approaches have been replaced by those at 1200 ft or higher. A definite proof of our progress has been the virtual elimination of these complaints from points at substantial distances from airports, thus "drying up" previous large complaint areas. These higher approaches with the less power involved also benefit persons much nearer the airport.

Formerly, there were occasional VFR circling approaches at altitudes of only 500 or 600 ft. Now, however, during circling approaches to these terminals, aircraft maintain at least 1200 ft altitude and do not descend below 1200 ft until turning on to base leg, prior to commencing final approach.

Take-off procedures now call for attaining at least 1200 ft altitude as soon as possible.

Each airport has its own peculiarities and at the same time may offer a form of solution of its own. Let me cite briefly a few illustrations of such local situations.

At LaGuardia Airport, take-offs to the southeast on Runway 13 were formerly a major annoyance to the residents of Flushing. Upon examination of the situation, NATCC's Technical Committee found there was a hopeful possibility of solution to this particular situation. This was that such southeasterly take-offs could be diverted from Flushing, down Flushing Meadow Park, without transferring their flight to some other built-up area.

This procedure calls for a slight turn after take-off down the Flushing Meadow Park until an altitude of at least 1200 ft is reached. Following its practice of spot-checking new procedures, our Technical Committee found that the slight turn, in *daylight,* gave relief to Flushing and didn't bother anyone else, but that at *night* it wasn't working too well. It was very difficult for pilots to recognize whether they were over the unlighted Park or over adjacent areas which include high ground on either side and a large cemetery on one border of the open area. Thus, aircraft in short time might unintentionally find themselves over several high-terrain, built-up areas at relatively low altitudes.

Correction of this weakness in this single procedure involved many man-hours of study and survey. We have now come up with what seems to be a practical solution, namely, installation of a vertical light beam at the south end of the Park to guide aircraft over the open area during darkness.

Newark Airport also has its special problems. For example, for the relief particularly of residents of Elizabethport not far off the end of Runway 22, pilots after take-off thereon now turn left (easterly) as soon as practicable, avoiding Elizabethport, and continue the climb over unpopulated areas to at least 1200 ft. To the northward, the Ironbound section of Newark, Kearny, and Harrison complained often of annoyance from planes taking off on Newark Runway 4. Now, after take-off thereon, pilots turn right (east) climbing over the Kearny meadows to at least 1200 ft.

This next item may sound rather simple—and it is.

On the anemometer dial, "calm" winds may fail to register any velocity, but the arrow will nevertheless point in some direction and that direction could have dictated the runway to be used. Now, however, in calm conditions (5 mph or less) at Idlewild, for example, take-offs are made on Runway 25 Left over Jamaica Bay and landings on 4 Right over the same open water area.

Another project for increasing the distance between the aircraft and the airport neighbor was worked out primarily through unceasing efforts of the Air Line Pilots Association and the Air

Transport Association, both cornerstone members of NATCC. It is part of an airport noise reduction proposal by the chairman of the Civil Aeronautics Board and the Administrator of Civil Aeronautics, both also members of NATCC.

This project involves standardization of climbout procedures aimed at producing, with safety, steeper climbout gradients whereby the horizontal distance traveled by the aircraft to an altitude of 1200 ft (or better) is materially reduced. Thus, ascending aircraft should pass over surrounding airport areas at a greater altitude than by previously conventional climbout practices.

The Joint ALPA-ATA Committee, in establishing this new procedure for climbing to 1200 ft, recommended the production of a steeper climb gradient by lesser rates of acceleration after takeoff, lower air speeds, use of higher power settings, and wing flap management consistent with these three features.

Engineers have worked out, for each type of transport plane in use, the saving in horizontal travel to attain 1200 ft altitude when this "preferential climbout" is followed. These calculations show an appreciable saving in all cases but one. These savings, by calculation, run as high as 12,500 ft and even 18,000 ft, or some 2½ and nearly 3½ miles for two particular transports.

This "preferential climbout" is now being implemented in service. Should the results obtained in service even approximate the calculations, a considerable contribution to the noise abatement problem certainly will have been made.

Engine Run-Ups

In the abatement of aircraft ground noise annoyance resulting from engine run-ups at airports, the air industry realizes we have one of the toughest problems of all.

The Port of New York Authority as the airport operator has defined areas for maintenance run-ups where resultant noise should be most effectively controllable and least objectionable to airport neighbors. Use of these prescribed areas is provided in the lease agreements. The designation of run-up areas is predicated on maximum utilization of present and future buildings and field facilities as noise barriers, as far as they may have any such value.

Close contact is maintained with other experimental efforts in this field, such as those of the British. Furthermore, the Port Authority has retained one of the nation's outstanding firms of sound engineers for one of the most intensive airport noise studies ever made. Adaptation of the results of these studies to physical planning and construction at airports is being actively pursued.

After two years of hard work at abatement of aircraft noise around airports, it appears that while other variations may develop, the main possibilities of improvement through procedural measures have been put into effect. Hope for any further gain now lies in obtaining maximum compliance with these voluntarily adopted procedural measures.

Just how effective or successful have these measures been? Well, obviously, it is not possible to compute a precise mathematical value as the index.

However, one indication may be found in the fact that 258,468 take-off and landing operations, or some 47% of all since the system was effectuated, have been conducted over those areas least objectionable to the neighbors of Newark, La-Guardia, and New York International Airports.

It must be understood that the sum total of effectiveness of the NATCC noise and low flying abatement program is not measurable solely in the percentage of preferential runway usage. Actually, the full measure is made up of such percentages plus whatever gains have been made from other alleviating practices such as those already described herein.

Realistically, it must be realized that however effective our program has been to date the noise problem is still with us. That the industry is still up against a tough situation is no more effectively evidenced than in the various pending legal actions aimed at civil air transport operations. As but one example, let me briefly state the so-called Cedarhurst case which lawyers feel may go to the highest courts and set precedents.

The Village of Cedarhurst is a residential community of about 6000 persons located in Nassau County just east of New York City and lies about two miles from the southeast end of one of the principal runways at New York International Airport.

On March 31, 1952, the Village enacted an ordinance declaring in substance that it is unlawful for any persons "to navigate any aircraft within 1000 ft of any dwelling in the Village," or to maintain or use altitudes below 1000 ft over the Village for turning or maneuvering zones, or for the approach or transition zones established for New York International Airport by the Administrator of Civil Aeronautics, and also to carry gasoline or other explosive or inflammable material by air at heights lower than 1000 ft over the Village.

The ordinance prescribes a penalty not exceeding $100.00 for each offense and specifies that its violation shall constitute disorderly conduct.

Comment on such restrictions to air transport is superfluous.

In summary, the airport noise abatement problem has been partially met by a great operational safety record and by such procedural measures as have been outlined herein.

The other side of the coin presents a challenge to the engineer and the scientist in reduction of aircraft noise at its source.

This challenge, too, must be met I believe, if the civil air industry is to live in harmony with its airport neighbors.

Control of Propeller Noise

In Turboprop Installations

Joern Schmey and Ralph M. Guerke,

Propeller Division, Curtiss-Wright Corp.

This paper was presented at the SAE National Aeronautic Meeting, New York, April 14, 1954.

ORIGINS of propeller noise and possible means for its reduction both within and external to turboprop aircraft are discussed here.

Decreasing the tip speed and increasing the number of blades of turboprop propellers result in quieter performance within the aircraft but with a heavy weight penalty. Changes in certain aircraft design parameters, such as increasing clearance between fuselage wall and propeller tips, can also reduce internal noise and vibration.

Improvements in external turboprop noise can be achieved by use of quiet-type propellers, increased rate and angle of climb, preferential runways, adequate airport zoning, and sound-dissipating foliage and ground covers.

The Authors

JOERN SCHMEY is an assistant project engineer in the Experimental Section of the Propeller Division, Curtiss-Wright Corp. He has worked mainly on vibratory stress analysis and acoustical engineering as related to aircraft. Mr. Schmey is a physics graduate of Union College, and has a Master's Degree in Electrical Engineering.

RALPH M. GUERKE is chief experimental engineer in the Propeller Division of the Curtiss-Wright Corp. He received his B.S. degree at M.I.T., where he later obtained his M.S. in Aeronautical Engineering. Mr. Guerke has been with Curtiss-Wright since 1938.

THE noise attributed to the rotation of propellers is comprised of two components known as the rotational and vortex components.[1] Of these, the first is usually the stronger and the one of most concern. It is responsible for the rumbling and roaring characteristic of propeller noise since it is largely comprised of relatively low frequency (50-350 cps) discrete components which are harmonically related to the rate of blade passage.

While the rotational component of propeller noise results from the steady aerodynamic forces on the loaded propeller blade, the vortex component is due to the shedding of vortexes from the airfoil. The latter is distinguishable from the rotational component of propeller noise by reason of its broad band, nondiscrete harmonic content in the frequency range between 600 and 4000 cps. These characteristics of propeller noise are best illustrated in Fig. 1 which reproduces a typical instantaneous frequency spectrum as would be recorded in the vicinity of a rotating turboprop propeller at a representative condition. Another striking difference between the rotation and vortex components of propeller noise can be seen in the relative spatial distribution patterns of Fig. 2. Vortex noise is shown to be a maximum on the axis of propeller rotation while the rotation noise is

[1] See NACA TN 747 (1940), "Propeller Rotation Noise Due to Torque and Thrust," by A. F. Deming.

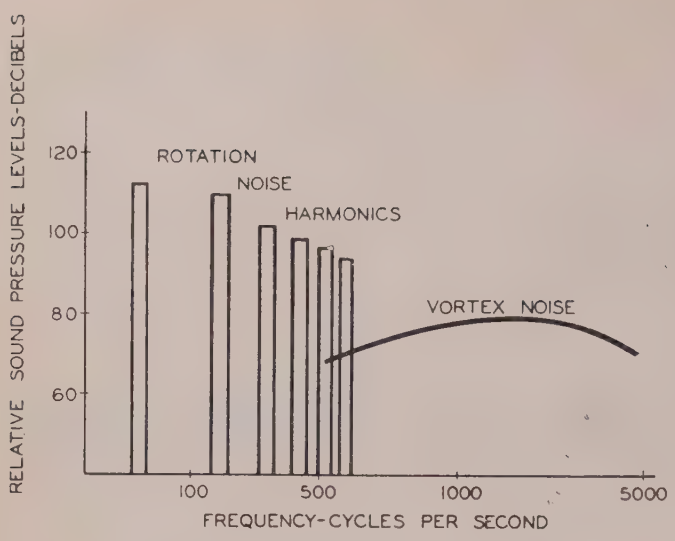

Fig. 1 – Typical turboprop propeller noise spectrum

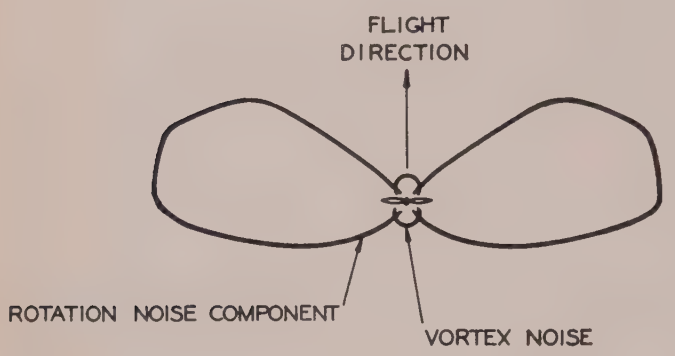

Fig. 2 – Spatial distribution of propeller noise components for typical turboprop propeller

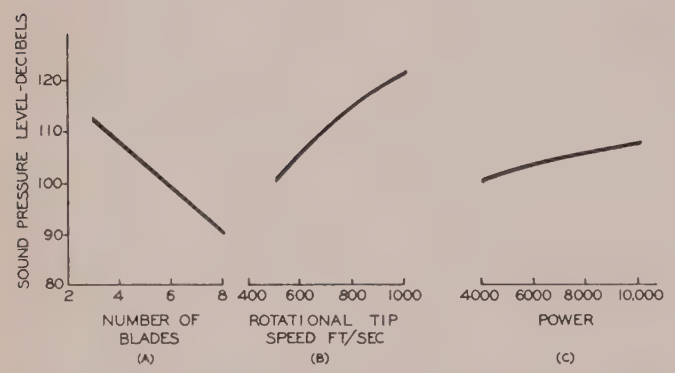

Fig. 3 – Variation of propeller rotation noise with operating parameters of a typical turboprop propeller

strongest in or near the plane of rotation.

The foregoing theories on the origin of propeller noise have found general acceptance as a result of good agreement between experimental and analytical research[2] conducted over a number of years by many investigators. It is applicable to the noise emitted by all propellers including transonic and supersonic types[3] which differ only in magnitude and distribution and not in principle. For these reasons the equipment and procedures for studying and controlling propeller noise, as developed for reciprocating-engine propellers, are generally applicable to the noise generated by the turboprop-powered propellers currently of interest. Due to the considerably higher powers absorbed by the latter, the need for controlling their noise appears to be greater and probably a little more difficult, in view of the economics involved.

In addition to the adverse effect that increasing power has on propeller noise, several other parameters of the propeller configuration influence the extent of propeller noise. These include: (1) the propeller tip speed, (2) the number of blades, (3) blade plan form, and (4) whether dual or single rotation. Since in most applications the rotational component of noise is the most troublesome, the influence of changing (1) and (2) above, as well as power, is shown in Fig. 3 on the total rotational noise component of a conventional propeller.

In Fig. 3*a*, increasing the number of blades is seen to decrease the overall noise output of the propeller. An increase in tip speed has the effect of raising the total propeller sound pressure level, as illustrated in Fig. 3*b*; while in Fig. 3*c*, the total rotation sound pressure level is seen to increase appreciably with increasing power. Blade plan form and especially blade tip shape have frequently been the object of research to determine the contribution of these parameters of propeller design to propeller noise, but to date all evidence seems to indicate that the variations found among conventional blade designs have no significant effect on propeller rotation noise. Even such a drastic difference as square and round blade tip shape has been shown to have relatively little or no effect on the magnitude of propeller rotation noise components. Rigorous testing with model propellers by H. H. Hubbard and A. A. Regier of the National Advisory Committee for Aeronautics indicated no difference in the sound pressure levels,[2] whereas experiments with full-scale propellers and a simulated fuselage conducted by K. R. Jackman of Convair, Division of General Dynamics Corp., showed a few of the lower frequency rotation noise harmonics emitted by the square-tipped blade to be 3 or 4 db greater. In a matter of dual versus single rotation, a thorough study of the rotation noise characteristics of dual-rotation propellers by H. H. Hubbard[4] has shown that there is no material advantage to this configuration over the single-rotation equivalent propeller. Depending on the location of the observer with respect to the propeller, the overall sound pressure level of a dual-rotating propeller was shown to vary between the higher level pro-

[2] See NACA TR 996 (1950), "Free-Space Oscillating Pressures Near the Tips of Rotating Propellers," by H. H. Hubbard and A. A. Regier.
[3] See NACA TR 1079 (1952), "Sound from a Two-Blade Propeller at Supersonic Tip Speeds," by H. H. Hubbard and L. W. Lassiter.
[4] See NACA TN 1654 (1948), "Sound from Dual-Rotating and Multiple Single-Rotating Propellers," by H. H. Hubbard.

duced by the equivalent single-rotation propeller with half the total blades of the dual version to a lower level characteristic of a single-rotation propeller having the total number of blades of the dual version.

There are three distinct noise problems resulting from propeller rotation, and in each case it is the rotational component of the total noise output of the propeller that is the troublesome factor. Without attempting to list them in the order of relative importance, all propeller noise control problems can be classified in one of the following groups: (1) reduction of propeller noise experienced inside the aircraft, (2) minimization of noise external to the aircraft, and (3) control of propeller noise from ground test facilities. This paper discusses the first two of these considerations.

Propeller Noise Problem Inside Aircraft

The noise problems related to the airframe and the space it contains will be considered first, and since the single-engine-type propeller-driven aircraft are not of primary concern, only multiengined airplanes will be discussed. With the latter type of aircraft, the difficulties arising out of the airborne pressure disturbances generated by the rotating propeller are twofold. The first and possibly foremost problem is the structural vibration caused by the pressure waves impinging on the fuselage walls, while the second closely allied problem is the effect of propeller noise on passenger comfort. As shown in Fig. 2, these pressure waves are strongest in the plane of rotation, so that in a multiengine aircraft the walls in the area adjacent to the propellers are exposed to the most severe oscillatory forces.

The extent of the airborne pressure disturbances attributable to the propeller rotation component at the fuselage wall is a function of (1) the propeller design and operating parameters discussed above and (2) aircraft design and operation. Among the latter, the most important airplane design parameter influencing the airborne pressures at the wall is the amount of clearance between fuselage and propeller. Fig. 4 shows the variation of the free-field pressure in or very near the plane of propeller rotation as a function of the distance from the blade tips. At distances greater than about one propeller diameter fore and aft of the plane of rotation, the relieving effect of the increasing tip clearance is considerably less and of little use in effecting sizable reductions in the impinging sound pressure levels.

Another aircraft design feature that might be expected to influence the magnitude of the airborne noise field enveloping the aircraft is the number of nacelles. However, theory as well as experiment has shown that the contribution of the inboard propellers to the total noise dominates over that of the outboard propellers to the extent that the latter do not add materially to the overall airborne noise inside the aircraft.

The effect of airplane forward speed on propeller rotation noise is the factor least well understood. In the past it has usually been the practice to study propeller rotation noise at static airplane conditions because it simplified experimental measurement as well as analytical calculation. Experimental data indicated that at the low forward speeds of aircraft engaged in landing and take-off there was no significant airspeed effect. Even at higher airplane forward speeds the rotation noise was not appreciably different from that at ground operating conditions, and most noise evaluations, whether analytical or experimental, were made in terms of static airplane conditions.

However, with the advent of turboprop-powered flight at cruise speeds in the neighborhood of 0.8 Mach number it has become important to establish to what extent rotation noise is affected by increasing forward speed. With this in mind, I. E. Garrick and C. E. Watkins of the NACA have, from theoretical considerations, developed formu-

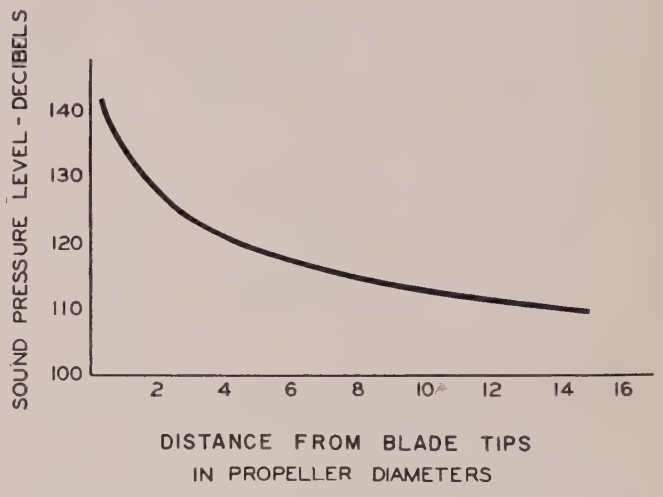

Fig. 4 – Variation of propeller rotation noise with distance from blade tips

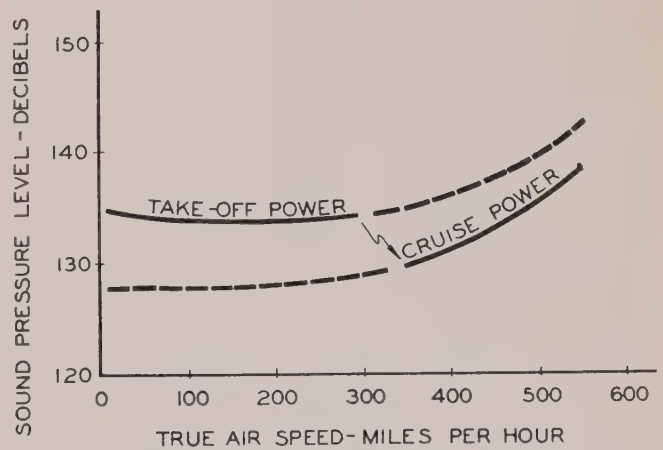

Fig. 5 – Theoretical variation of propeller rotation noise with forward speed for a typical turbopro propeller

las defining propeller rotation sound pressure levels that provide for the effect of forward speed of the aircraft.[5] These relatively complex expressions do not lend themselves to easy interpretation, and rather involved and extensive mathematical manipulations are required before any conclusions can be reached concerning the effect of air speed for a particular set of propeller operating conditions. In view of the importance of the subject and the reliable aerodynamic theory from which the formulas were derived, the Curtiss-Wright Corp., Propeller Division, recently undertook an analytical study with the NACA formula to investigate the effect of forward speed on propeller rotation noise for a number of typical turboprop operating conditions.[6] Among the more important results of this study, it was shown that:

1. As shown in Fig. 5, at sea level and relatively low forward velocities there is a slight tendency for propeller noise to diminish with increasing forward speed, but this relieving effect is not sufficient to be of practical significance.

2. Again in Fig. 5, calculations indicated that as a consequence of high subsonic cruise speeds in excess of 350 mph, the noise level of the first harmonic of propeller rotation noise increases appreciably. For the particular conditions of this figure, considered representative of a typical turboprop transport, the calculated increase in the first harmonic noise level inside the airplane due to the airspeed effect amounts to about 5 db at 0.75 Mach number cruise.

3. While calculation of harmonics higher than the first became increasingly difficult and subject to limitations, based on the simplifying assumptions made in deriving a manageable formula, it can be seen in Fig. 6 that these too indicate an increase as a result of an increase in forward speed.

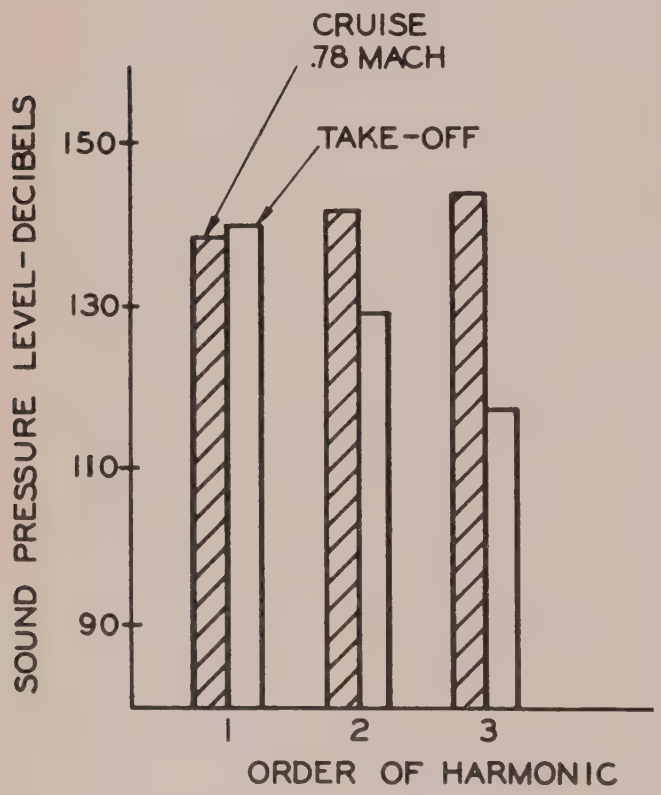

Fig. 6 – Theoretical effect of forward speed on propeller rotation noise harmonics

These results, while analytically accurate within the structure of the simplifying assumptions made in the derivation of the formula, have not been accepted without reservations primarily because the substantial changes predicted have not been aurally observed in military propeller-driven aircraft during high-speed dives. Experimental programs to investigate this unexplored region of propeller noise generation are currently under way by several independent investigators. It is confidently expected that these tests will confirm the qualitative observations and furnish empirical data for the correction of the theoretical formula.

Another way in which the airplane design affects the magnitude of the airborne propeller sound pressure disturbances transmitted through the fuselage and into the cabin space is by means of its inherent structural rigidity, structural and acoustic materials, as well as the fuselage shape.

It is well known that high structural rigidity is the characteristic most effective in reducing low-frequency vibrations of the kind of which propeller rotation noise is comprised. Consequently, the stiffness of panels and frame, especially in the vicinity of the propeller plane, determines, to a large degree, the amount the fuselage responds to propeller rotation noise frequencies and the extent of the aural discomfort from this source inside the airplane. The highest of the rotation noise harmonics and vortex noise are best controlled by the amount of acoustical radiation resistance included in the wall structure of the aircraft. Finally, it has been demonstrated experimentally by H. H. Hubbard and A. A. Regier that the contour of the fuselage in the immediate vicinity of the plane of rotation influences the magnitude of the maximum airborne propeller rotation sound pressure levels. According to their findings, a flat fuselage wall will tend to double the pressure levels on reflection at the fuselage wall as compared to the free-space level.[2] Walls of circular cross-section were found to diminish this effect, providing a more desirable structure from an acoustical consideration.

There is another aircraft design parameter that greatly influences the amount of discomfort suf-

[5] See NACA TN 3018 (1953), "A Theoretical Study of the Effect of Forward Speed on the Free-Space Sound-Pressure Field Around Propellers," by I. E. Garrick and C. E. Watkins.

[6] "Control Systems and Noise Problems for High-Speed Propellers," by W. H. Clark and J. Schmey. Presented at the SAE National Aeronautic Meeting, Los Angeles, Oct. 2, 1953.

fered inside an airplane from propeller noise. As a result of observations by various sources, it is concluded that the characteristic noise of a particular engine type can indirectly affect the subjective response of an observer to propeller rotation noise. An excellent example of this is the disturbing beat frequencies experienced in the past with certain combinations of propeller blade number, engine exhaust frequency, and gear reduction ratio. It will be recalled that there have been a few engine-propeller combinations in the past that were incompatible because of the very strong and objectionable low-frequency engine-propeller beat "noise."

This disturbance is actually of a frequency well below what is usually recognized as the lower limit of human hearing and is perceived only because it is the rate at which the amplitude of an audible frequency is being modulated. What happens is that a strong propeller rotation noise harmonic and a comparably strong harmonic of the engine firing frequency, differing in frequency from the former, alternately reinforce and cancel one another. This interference results in an alternately rising and falling characteristic of the sound pressure level at the observer's ear, leading to the annoying beat sensation.

In general it has been found that the interfering pressure waves must be within about 10 cps in frequency of one another, and both are required to be of an approximately equal and dominant amplitude in order to generate an objectionable beat. These two necessary and sufficient conditions for the generation of beats are made use of in practice to eliminate the disturbance by upsetting either the balance of frequencies or the required amplitude relationship. In the case of a reciprocating engine-propeller combination, a change in blade number or gear reduction ratio is resorted to in order to effect an improvement.

In turboprop engine installations, on the other hand, the nature of the noise spectrum precludes the possibility of a beat disturbance. The noise of the jet exhaust is broad-band and has no discrete or dominant harmonics to contribute to a beat; while the noise from the rotating components such as the compressor, though composed of discrete frequencies, is well beyond the range of strong propeller rotation frequencies.

Another aspect of the manner in which human subjective response to propeller noise is influenced by the type of powerplant has recently been noted. As illustrated in Fig. 7, noise measurements made inside some operational turboprop-propeller-driven aircraft have shown the propeller noise sound pressure levels to be comparable to or even exceed those of the highest powered reciprocating-engine-equipped transports. However, trained observers and crews have agreed that the turboprop-propeller-equipped aircraft are markedly "less noisy" and more comfortable from the standpoint of propeller noise. This would indicate that much of the discomfort from noise generally attributed to the propeller in reciprocating-engine-powered aircraft was actually an indirect consequence of engine noise or structurally transmitted vibration. It has become quite apparent that the subjective interpretations of human hearing to the combination of propeller noise with engine noise is not always in agreement with the objective interpretations of an electronic circuit and voltmeter.

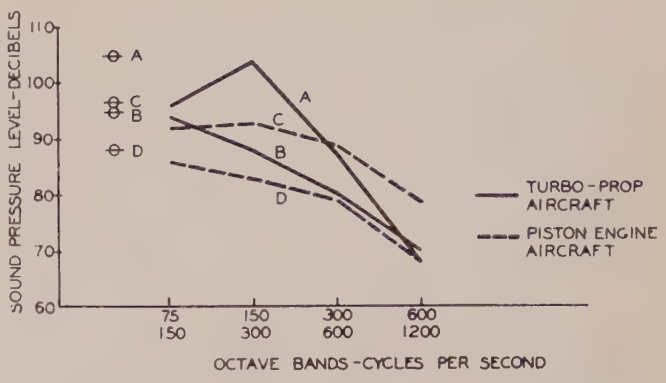

Fig. 7 – Comparison of cabin noise levels of operational turboprop and piston-engine transport aircraft

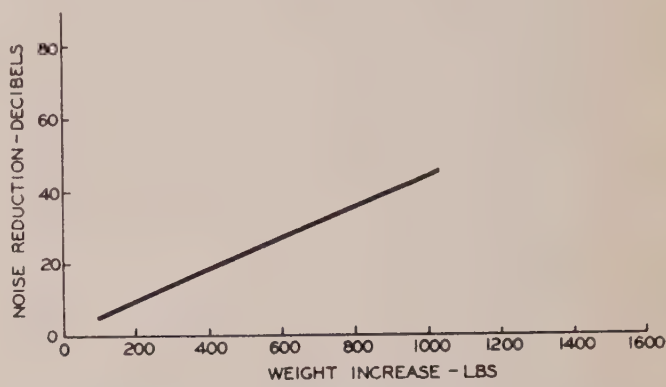

Fig. 8 – Estimated increase of turboprop propeller weight corresponding to reduction in rotation noise resulting from quiet design

The foregoing paragraphs have been devoted to a discussion of (1) the propeller design parameters that control the amount of rotation noise generated and (2) airplane design considerations that determine the ambient propeller noise level inside the airplane and the annoyance resulting from it. It will now be shown how these factors can be applied to control the noise disturbance from propeller rotation if certain conditions are met and related penalties are accepted.

It was seen in Fig. 3 that a decrease in tip speed or an increase in blade number effectively reduces the propeller rotation noise of turboprop propellers. A combination of these two measures is even more effective in controlling the sound pressure amplitudes and might at first appear to be

the answer to the propeller noise problem, but unfortunately this approach is not without disadvantages. If the "quiet"-type propeller equivalent of a conventional propeller configuration is to have a sufficiently reduced tip speed to accomplish a significant noise reduction without a sacrifice in performance, it will in most cases result in a heavier powerplant. To make up for the effect on the aerodynamic performance resulting from the reduced tip speed of the replacement propeller, it is necessary to increase the number of blades or blade activity or both through increases in blade length, width, or section characteristics. These changes in turn seriously effect the airplane design in that they may result in a requirement for a larger landing gear, greater separation of nacelles and fuselage, increased engine mount size and wing structure. In addition, aircraft stability requirements must be provided for. All of these changes tend to add weight to the airplane, and a few will also influence airplane drag and instability.

It would be difficult to estimate the net effect on the total airplane weight accompanying a specific decibel reduction of propeller noise without designing a complete airplane; however Fig. 8 illustrates the estimated propeller weight penalties accompanying a decrease in the amount of propeller rotation noise generated.

It is apparent that the penalty in propeller weight that must be paid for a significant noise reduction is severe. Furthermore to accommodate such a propeller the airplane would probably require very extensive modification, and the overall resulting weight increases would be so large as to approach a prohibitive condition by present standards.

In the case of the typical 4-engine turboprop transport, for example, to reduce the propeller rotation noise by 20 db it is necessary to increase the weight of each propeller by more than 400 lb resulting in almost a 1-ton decrease in airplane payload. It is highly probable that aircraft structural considerations will add even more to the airplane weight as a consequence of the quiet-type propeller configuration, although a minor saving may be realized in the amount of sound treatment and vibration damping normally required.

Appropriate changes in engine gear reduction ratios would also have to be incorporated in the turboprop to accommodate the low-speed-type propellers. In the past this has been a serious obstacle to the reduction of propeller tip speeds in reciprocating-engine installations where practical considerations limited the reduction to a maximum of about 3/1 and an appreciable increase was needed to be effective.[7] In turboprop engines, on the other hand, the corresponding ratios are normally much greater, and only a relatively small change is required to effect a significant change in tip speed. This obstacle to slower-turning propellers is therefore considered to be less of a problem in turboprop applications than it was in the case of reciprocating engines.

The propeller noise level inside an airplane can also be materially reduced by appropriate control of certain aircraft design parameters. Fig. 4 illustrates the theoretical improvement in sound pressure level at the external fuselage wall of a typical turboprop installation resulting from increasing the fuselage propeller tip clearance. In practice, however, it has been found that the reduction in internal aircraft noise may deviate from this due to the inherent response characteristics of the particular airframe to airborne and mechanically transmitted vibration. In any case, increasing the clearance reduces the excitation at the fuselage wall, which is a good start to improving the disturbance from noise and vibration in the cabin.

Propeller tip clearances are normally determined by airplane structural, stability, and performance requirements, with only minor consideration given to measures that compromise the aircraft design and its operating cost in the interest of reduced noise. In the past this has resulted in aircraft having small fuselage tip clearances regardless of the propeller power-absorption capacity. As evidence of this trend in aircraft design it should be noted that while the power ratings of propellers have increased almost tenfold since the first DC-3 airplanes, there has been no corresponding progressive change in fuselage tip clearance to compensate for the much increased oscillating tip pressures.

In the high-speed turboprop transport aircraft of the future, on the other hand, the same design objectives that established the principle of minimum tip clearance for reciprocating-engine aircraft tend to locate the nacelles further outboard so that fuselage-propeller tip clearances are a matter of feet rather than inches. This, as has been seen, is very desirable from the standpoint of internal aircraft noise and vibration resulting from propeller rotation and should ease the problem of noise reduction in commercial turboprop transports.

Another method of alleviating the propeller noise problem within the airplane that has recently been explored with renewed interest and confidence of success is the possibility of effecting a significant reduction in sound level and improving the noise comfort level by synchronizing the phase of propeller rotation in multiengine installations. Development of phasing equipment is in progress, and future testing will establish the magnitude of the possible improvement.

In addition to the foregoing recognized methods of propeller noise reduction inside aircraft, there

---

[7] "Summary of Conference on Aircraft Propeller Noise." Presented at NACA Meeting, Washington, D. C., June 10, 1952.

have been a number of miscellaneous "gimmick" methods proposed in recent years. These have included such things as a slotted blade planform, propeller shroud,[8] electronic means[9] of generating an out-of-phase sound pressure field in the vicinity of the ears, and so forth. In all cases, the weight or complication or both of the associated equipment or techniques or the failure to produce the desired results were such that the method was obviously impractical, but some deserved and have received serious consideration before their unfeasibility was established.

It is apparent then from the foregoing that propeller noise can be reduced materially in turboprop-powered transports through the use of low-rpm, many-bladed propellers. Analytically, it can be shown that these "quiet"-type propellers can be designed to be the aerodynamic equivalent, as far as aircraft performance is concerned, of the conventional configurations they would replace. The airframe design complications and weight penalties that arise out of the installation of such propellers have in the past, however, made their application to reciprocating-engine installations unfeasible. Similarly, little serious consideration is given to the use of "quiet"-type propellers in turboprop applications, and it is unlikely that this situation will be altered in the future unless the operators of aircraft are sufficiently concerned about the noise to accept the penalties involved. To date the initiative has been with propeller manufacturers who have studied the problem but are unable to take more concrete steps since their propeller designs are dictated by the airframe manufacturers who, in turn, are competitively motivated to satisfy the operators' requirements for maximum performance and minimum operating costs. Consequently, emphasis on these qualities is reflected in propeller design and manufacture, and the somewhat higher noise levels are accepted as unavoidable.

Even without the use of "quiet"-type propellers though, expectations are that the discomfort level from noise (and vibration) will be materially improved in the high-speed turboprop transports visualized. For one thing, the absence of the characteristic reciprocating-engine noise and vibrations in the airframe has already been demonstrated to make turboprop propeller-equipped aircraft considerably more tolerable. Furthermore, by reason of performance and stability design considerations, these aircraft will, in all likelihood, incorporate fuselage-propeller tip clearances appreciably greater than those generally used in the past. This will, of course, tend to isolate the critical fuselage wall areas from the severe oscillating

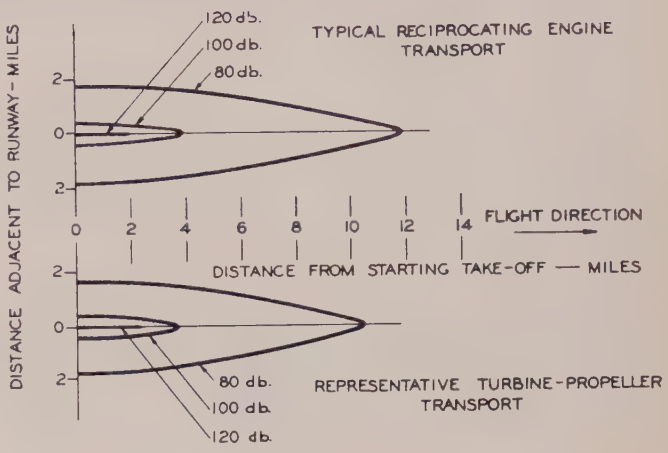

Fig. 9 – Comparison of maximum overall noise patterns during take-off

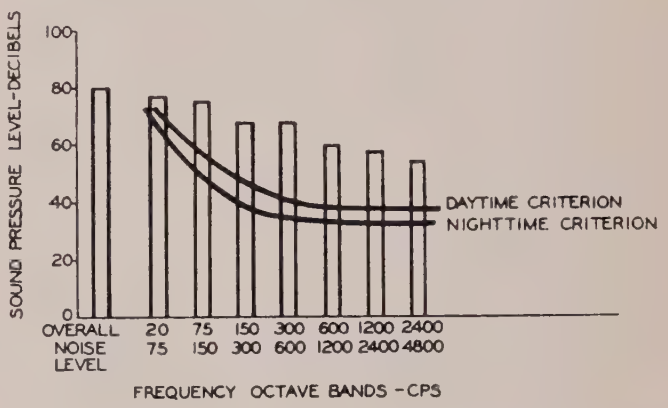

Fig. 10 – Comparison of turboprop aircraft community noise with criteria for acceptable residential noise levels

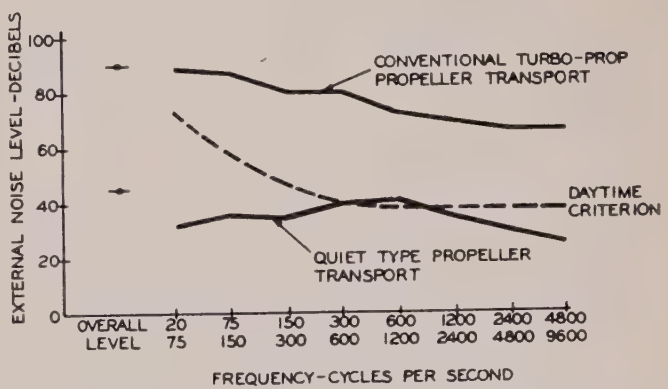

Fig. 11 – Community noise spectra of conventional and quiet-type turboprop propeller aircraft

[8] See NACA TN 2024 (1950), "Sound Measurements for Five Shrouded Propellers at Static Conditions," by H. H. Hubbard.

[9] See *Journal of the Acoustical Society of America*, Vol. 25, November, 1953, pp. 1130-1136: "Electronic Sound Absorber," by H. F. Olson and E. G. May.

pressures in the vicinity of the propeller tips with a substantial improvement in internal noise and resulting vibration.

Aircraft External Propeller Noise Problem

In recent years the concern of the aircraft industry and the aroused opinion of the general public located in the vicinity of airports has steadily increased as a consequence of the greater noise levels created by the aircraft powerplants of increased capacities.

In Fig. 9 a comparison is made between the maximum overall noise patterns in the vicinity of a take-off runway for representative reciprocating-engine and turboprop transport aircraft. It is seen that, except for areas in the immediate vicinity of the runway, the maximum overall community noise resulting from turbine-propeller operations is slightly improved as a consequence of better initial climb performance of this type aircraft.

An indication of the degree of disturbance created at the free-field location of an observer on the ground positioned someplace on the 80-db contour can be obtained from Fig. 10. In this figure the maximum expected turboprop propeller noise spectrum is compared to tentative noise control criteria used by the acoustical consultant firm of Bolt, Beranek, and Newman.[10] The difference between the generally accepted residential daytime noise criterion and the decibel level of the bars, each denoting the extent of the sound pressure of the propeller rotation noise of four engines in the respective octave bands, represents the amount of quieting required to relieve sufficiently the propeller noise problem under this set of conditions. As would be expected, the nighttime criterion poses an even more difficult objective in noise reduction.

The amount by which it is necessary to reduce propeller noise in a given community is dependent on the location of the closest neighbors or residential section with respect to the runways and run-up areas. This of course varies with the particular airport under consideration, but at most of the large, well-established airports in the country the noise problem is of comparable magnitude as a result of similar airport-community geographic locations. Therefore, an effective solution to the problem at any one of these airports could be expected to accomplish the same result at any of the others.

There are two approaches to effecting a solution, or at least an improvement in the external aircraft noise problem. The first is to reduce the noise at the source, and the other consists of secondary control measures that reduce the extent of the disturbance before it reaches the observer. The means by which the amount of noise generated by a rotating propeller can be reduced have been discussed from the point of view of internal aircraft noise. The installation of a "quiet"-type propeller to ease the propeller noise and airborne vibration inside an aircraft will be equally effective in reducing the disturbance created external to the aircraft, as in adjacent communities. This is best illustrated in Fig. 11 where the community noise of a conventional turboprop-propeller-equipped aircraft is compared to an installation of "quiet"-type propellers at the take-off condition. It is readily seen in this figure that the improvement in propeller noise level is appreciable and in most cases would be sufficient to relieve the community noise problem.

The secondary methods and measures of controlling turboprop propeller noise before it reaches the observer include:

1. Increased angle and rate of climb.
2. Use of preferential runways.
3. Adequate zoning of new airports.
4. Generous use of sound-dissipating foliage and ground cover.
5. Use of run-up pens or baffles for ground operation.

A discussion of these approaches to the external aircraft noise problem is beyond the scope of this paper; however, they may be summarized by saying that experience in the past has shown them to be limited in the effectiveness and feasibility of application. For the most part it appears that little lasting improvement has resulted from their application for the conditions of present-day reciprocating-engine propellers, and it is unlikely that any of these measures applied either singly or in combination will be sufficient to control completely the noise of turboprop propellers. In summary, however, it is encouraging to note that the next generation of propeller-equipped transport aircraft are not likely to be greater offenders of community peace and quiet than today's highest powered reciprocating-engine aircraft.

Additional References

1. "Handbook of Noise Measurement," by A. P. G. Peterson and L. L. Beranek. Pub. by General Radio Co., Cambridge, Mass., 1953.

2. NACA TN 2968, June, 1953, "Propeller-Noise Charts for Transport Airplanes," by H. H. Hubbard.

3. WADC TN 52-341 (1952), "Aerodynamic Noise and the Estimation of Noise in Aircraft," by O. R. Rogers and R. F. Cook.

4. "Acoustic Measurements," by L. L. Beranek. Pub. by Wiley, New York, 1949.

[10] See "Final Report on Recommendations for Acoustical Treatment of the Radial-Engine Test Cells," by R. H. Bolt, L. L. Beranek, and R. B. Newman. Pub. by Wright Aeronautical Corp., Wood-Ridge, N. J., April, 1951.

An Airplane Manufacturer's Progress with Noise Suppression Devices

Robert E. L. Fogle and Holden W. Withington,

Boeing Airplane Co.

This paper was presented at the SAE National Aeronautic Meeting, New York, April 14, 1954.

THE airplane manufacturer, as almost every other member of the aircraft industry, is faced with an ever-growing noise problem. Jet-engine thrust increases with each new model; the inevitable byproduct is more and more noise. Intense guided-missile research brings the problem of suppressing the greater noise of rocket and ramjet engines. The growth of residential communities around engine and airplane test facilities has further complicated the problem. As a result we are all in the noise suppression business, whether we like it or not.

Noise control is a negative type of business. A successful noise-control device does not mean greater financial return; but, on the other hand, its neglect can quite likely lead to financial loss

THE efforts of one manufacturer to solve the problem of jet-engine noise suppression when test facilities are near residential communities are reported here.

The authors describe the construction of several suppressors and give data on their effectiveness.

Their experience covers a run-up suppressor and also a portable unit of the water-injector type – both developed for the B-52 airplane, and a water-spray muffler for ramjet engines.

They emphasize the fact that, since World War II, airplane manufacturers have been required to spend more and more time, effort, and money in attempts to cut down the noise produced by airplane and guided missile powerplants. The efforts of their company, they point out, are similar to those of other airplane companies. It appears that the problem is growing. No simple solution is yet in sight.

The Authors

ROBERT E. L. FOGLE is with the Boeing Airplane Co. He received his B.S. from New Mexico A & M and his M.S. from the University of Florida. Previously, Mr. Fogle was supervisor at the Landing Aids Experiment Station in Arcata, California, radio engineer with the Civil Aeronautics Administration, and Navy chief of radar.

HOLDEN W. WITHINGTON is technical staff engineer with the Boeing Airplane Co. He received his B.S. and his M.S. in Aeronautical Engineering from the Massachusetts Institute of Technology. Mr. Withington started at Boeing as supervisor of the Aerodynamics Unit, and then became supervisor of the Powerplant Staff Unit.

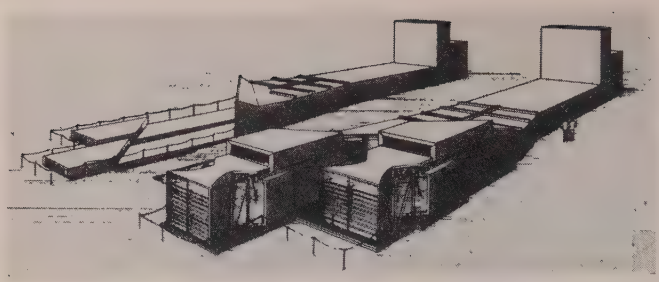

Fig. 1 – General plan of B-52 noise suppressor

through injunction, loss of time, and costly law suits. Naturally, then, the main concern is not to build a bigger and better noise trap but to use the least expensive structure that will do a satisfactory job. Even working under these conditions, the aircraft manufacturers are spending hundreds of thousands of dollars in an attempt to solve their noise control problems.

The following discussion will outline some of the noise problems and the current progress toward their solution that has been made at our Seattle plant.

B-52 Run-Up Suppressor

Experience with some B-47 test airplanes at the Seattle plant early in 1951 indicated that extended running of jet engines at full power could not be tolerated. It was evident that the production of B-52 airplanes in this plant would require some type of noise suppression device to ensure that engine runs could be made at any time as necessary in a production airplane program. The configuration of the B-52 airplane created some interesting problems in the design of a sound suppressor. Eight jet engines in four underslung pods hung on a very flexible wing caused the suppressor configuration shown in Fig. 1 to evolve. Many aspects such as fire hazard, positioning of the airplane, and operation under changing wing fuel loading had to be considered, as well as the acoustical phase, to assure that it would meet the requirements for use by the B-52 airplane.

The general plan of the suppressor is shown in Fig. 1. Essentially, it consists of four separate and distinct mufflers – one for each pod of two engines – grouped to fit the configuration of the B-52 airplane. Each muffler is made up of two units: a steel shell which may be raised from below ground level to enclose the engine pod completely, and a massive concrete tunnel lined with sound-absorbing building blocks and terminated with three 90-deg turns and a vertical exhaust stack.

The steel front portion (Fig. 2) is made of 3-in. channel iron sheathed inside and out with 16-gage steel metal. The inner is perforated with many small holes to allow some sound energy to pass through and be dissipated in Fiberglas wool which fills the cavity between the two walls.

This box-like structure is so arranged that in a position to receive the airplane it is in a pit with the top slightly above ground level. Once the airplane is in position, the structure is raised to surround the engine pod completely. Rubber seals fit tightly against the wing of the airplane. The seals are spring-loaded to allow normal movement of the wing during run-up without injuring the airplane skin or structure while still maintaining a sound-tight seal.

The intake section was designed to be constructed in two stages. The first stage consists of a minimum of acoustic control in the intake duct of each unit. If this was found to be sufficient, well and good. If not, construction would progress to stage two, where a forward structure containing additional acoustic absorbent material would be built. At this time only stage one was completed. Measurements made in the immediate areas around the intake and

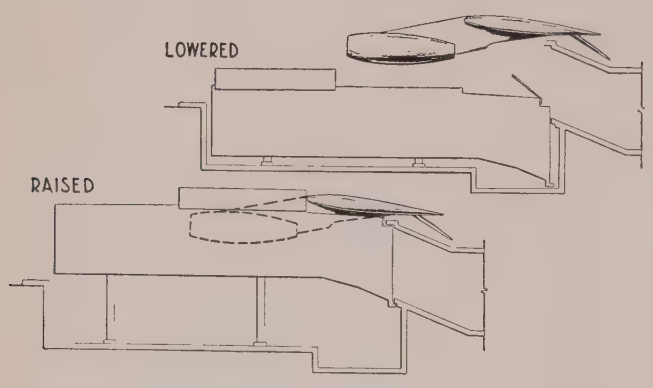

Fig. 2 – Intake section of B-52 noise suppressor showing both lowered and raised position

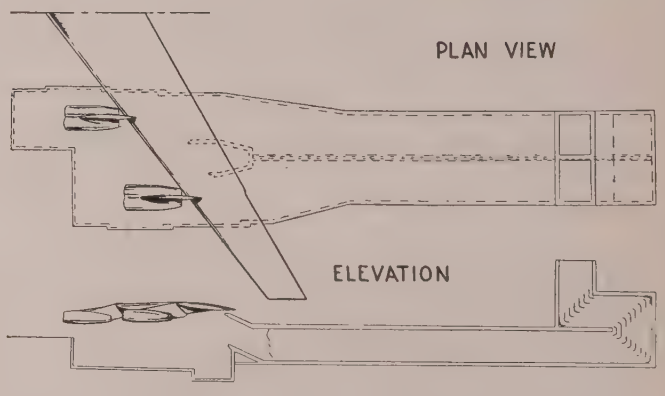

Fig. 3 – Splitter and turning vane details of B-52 noise suppressor

exhaust openings indicate that the intake is radiating at a higher sound level than the exhaust. This means that the intake is now critical and will require additional sound treatment to further lower this sound level in the surrounding community.

Each exhaust tunnel, details of which are shown in Fig. 3, has a cross-section of 12 x 15 ft, and averages 140 ft long. The tunnels are constructed of 10-in. reinforced concrete and completely lined with highly porous cinder building block. When properly cast and installed, these blocks have a good sound-absorbing capacity for this type of material over a fairly wide frequency range. The surface density of the concrete and block wall is high enough to prevent any appreciable radiation of sound through the tunnel walls.

Three 90-deg turns are included, which are very effective in reducing the high-frequency noise. Steel-plate turning vanes have been installed in the turns to smooth out the airflow and lower the back pressure. The measured effect of the turning vanes on the sound level in the nearby community is negligible.

Initial check-out of the suppressor showed poor airflow characteristics and high back pressures. As extensive testing of this suppressor with a B-52 was out of the question, it was decided to construct and test a scale model of one of the tunnels. The test program on this model was both economical and successful in that it showed that certain changes – a vertical splitter along the full length of the exhaust tunnel and corner vanes at the exit – should give quite satisfactory characteristics. The correlation between certain pressure drops and airflow ratios between model and full scale is shown in Fig. 4.

Effectiveness of the Suppressor

In the vicinity of the B-52 ground run-up area are two residential areas. The nearest area is to the north, with some homes as close as 1000 ft. The second community is to the east along the side of a hill overlooking the run-up area, at a distance of 3000-4000 ft. The nearest community is partially surrounded by industrial works, and consequently the residents experience a higher-than-normal ambient noise level. Industrial noises, heavy traffic on nearby arterial streets, and the buzz of light airplanes in the approach pattern of the nearby airfield combine to produce an average daytime ambient noise level of 65-75 db. Bumper-to-bumper traffic through the center of this area during shift changes in the morning, afternoon, and at midnight raises the noise level even higher.

The community to the east is a residential area built on the slope of a hill overlooking the noise suppressor and airplane run-up area. The background noise level here is much lower than that of the other community – about 50-60 db, which is normal for an average residential area. The run-up and takeoff of commercial aircraft from the nearby field occasionally raise the noise level to 70-75 db. Because of its position 200-300 ft above the field, the noise from the run-up area is nearly the same as it is in the much nearer community. Sound energy traveling a free-air path is not dissipated nearly as rapidly as when traveling along the earth's surface.

The overall sound level of two muffled B-52 engines at full power has been measured to be 80-85 db in the two communities. Engines under the same conditions not muffled produce from 92-94 db at the same locations, a 12-14 db difference.

It might be stressed at this point that tolerable noise levels cannot be adequately defined by an overall sound level alone. The frequency distribution of the noise energy must be known. In general, a person is much more tolerant of low-frequency noise than of high frequencies of the same intensity. One commonly used instrument measures the sound level in bands of frequencies by using a series of selective filters. An instrument of this type was used to obtain the sound level shown in Fig. 5,

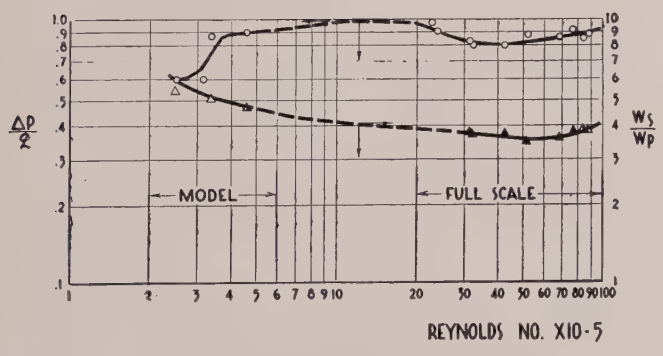

Fig. 4 – Test data showing correlation between pressure drops and airflow ratios – model and full scale

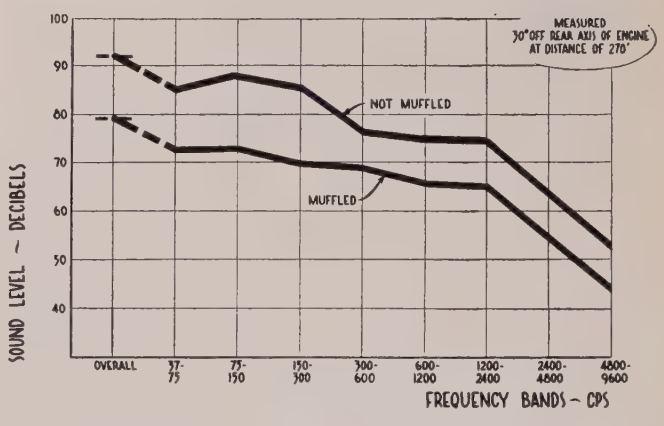

Fig. 5 – Effect of suppressor on noise level of B-52 engine – community noise reduction

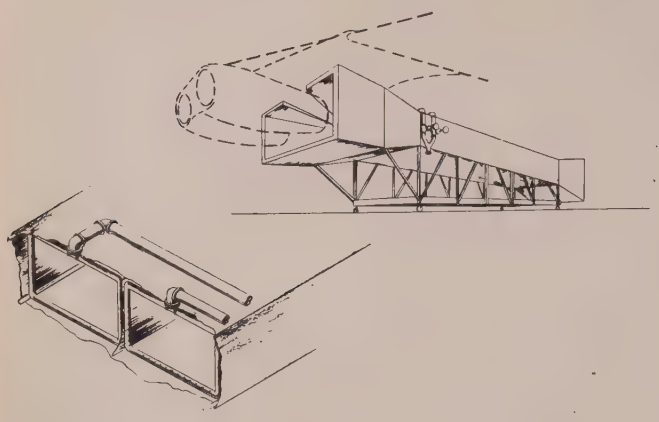

Fig. 6 – Portable water-injection-type jet-engine muffler

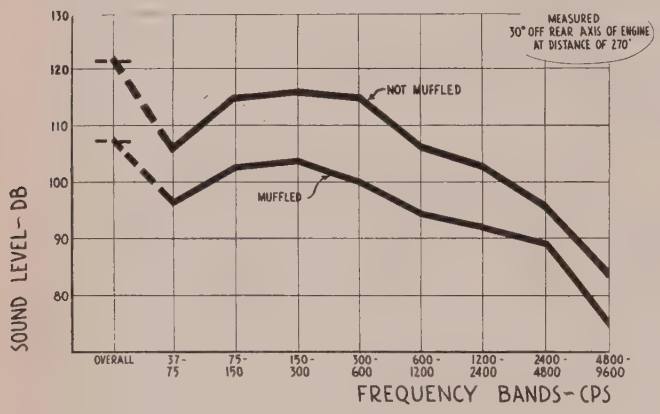

Fig. 7 – Effect of portable suppressor on noise level of B-52 engine

which shows the effect of the suppressor on noise of B-52 engines.

Although we are able to measure the frequency distribution of the noise as well as the overall level, the character and level of sound which will affect a nearby resident is an elusive figure. The problem is a psychological one, dependent upon the attitude and whims of the human mind. Perhaps the only true measure can be one based on the history of complaints from the residents of the community in question.

Unmuffled running of two or more B-52 engines for periods of more than 5-10 min. will bring complaints from these communities even during normal daytime working hours. Any full-power unmuffled running at night, on Saturdays, Sundays, and holidays is sufficient to bring complaints. Engine running time in the suppressor has so far been very limited, but no complaints have been received from the communities during these runs. Engines have been run at high-power settings for periods of more than an hour at a time in a test cell close by with no complaints. This is significant in that this test cell is of very similar construction and produces the same sound level in the communities as those run in the suppressor. We might conclude from this that the level of complaint for these communities lies somewhere between the two curves of Fig. 5. This is true only for these communities and is not necessarily true for any other communities.

B-52 Portable Noise Suppressor

Many conflicting reports have been made about the water-injector type of muffler. There is no agreement on the value of using water to reduce jet-engine noise. However, water injection has generally been used in absorption-type mufflers to cool exhaust gases and decrease gas velocities. Where water has been used, muffler size and weight have been reduced.

The search for a relatively light-weight portable jet-engine muffler – one that could easily be moved from plane to plane as needed – brought on the construction and testing of a simple water-injector type of muffler. It was constructed of heavy-gage sheet metal and angle iron with a cross-section area of 2½ ft and a length of 35 ft. A group of nozzles around the inlet sprays water into the jet exhaust stream. A sketch of the muffler is shown in Fig. 6.

Although the results of sound-level tests of this muffler are not very spectacular, nevertheless they do show that some noise reduction is obtained. The lobe of high noise usually from 30-50 deg off the rear axis, a characteristic of jet engines, was no longer present. The harsh crackling noise usually heard in this area was eliminated. In this area the noise reduction ranged from 10-15 db throughout the audible range, as shown in Fig. 7. Probably because of this, sound levels were measured to be from 1-14 db lower in the surrounding communities, depending upon the location. Noise in an office building 800 ft away was reduced 5-14 db, depending upon the location.

Ramjet Noise Problem

Guided missile powerplant research and testing have recently brought one of the most troublesome noise problems to the airplane manufacturer. The ramjet is a prodigious noisemaker, particularly when running rough, as it so often does under development test conditions. Rough burning produces a low-frequency rumbling noise of very high intensity which shakes houses, rattles windows, and cracks plaster at distances up to two miles. Vigorous complaints have been received in communities as far away as 10 miles under some weather conditions. Many of the complainers thought the house-shaking was caused by an earthquake or bomb.

Water-Spray-Type Muffler

To conduct tests on ramjet engines, a water-spray-type muffler has been constructed. The muffler is a 4-ft tube 40 ft long and turned vertically at

the exhaust end. A bank of nozzles spray water into the duct near the forward end. The unit is track-mounted and is rolled up to enclose the rear portion of the ramjet engine during operation. The general configuration is shown in Fig. 8.

At a distance of 100 ft, the muffler without water injection produced a measured reduction of about 10 db in the frequency range of 150-600 cps. Little effect was noted at other audible frequencies. The addition of the water spray caused a noise reduction of 10-15 db throughout the audible range. Fig. 9 clearly shows the effectiveness throughout the audible band of frequencies. The unmuffled engine had a decided peak of noise output in the 300-600 cps band, which was reduced 15 db.

The effectiveness of the muffler was clearly demonstrated by the complaint record of a series of ramjet tests conducted recently. Two or three complaints were received from a series of ramjet runs utilizing the muffler. One following run without the muffler swamped the company, police, and newspaper telephones with vigorous complaints.

The noise level in the nearest community, a distance of 3500 ft away, during an unmuffled run has been measured as high as 116 db. The sound meter operator reported a most noticeable shaking of the car in which he was sitting. A run immediately following, in which the muffler was used, measured 96 db at the same location. Although this figure is much higher than the maximum level of 72-75 db allowed in a community by some jet-engine manufacturers from their test cell operation, nevertheless few complaints are received by ramjet operation at this level. Probably the most logical explanation is that the ramjet noise is of short duration and occurs infrequently. The average duration of a ramjet test run is 2-3 min. Five runs in a week are considered normal operation.

Ramjet Noise and Weather

Meteorological conditions have been found to have a marked effect on the number and origin of community complaints. Open runs made on days when 1000-2000 ft temperature inversions occur have brought complaints from communities 10-12 miles away. A steep wind gradient brought a flood of complaints from downwind communities at distances of 10-12 miles. Other open runs have brought few complaints. As a consequence, a thorough study of the correlation of sound propagation with local weather conditions is now in progress. It may be possible to predict when weather conditions are favorable for test runs.

To do a thorough job of meteorological and sound-propagation correlation a large number of sound-level measurements must be made at distances up to 8 or 10 miles from the source. As ramjet runs are costly and often bring complaints from irate citizens, it was decided to substitute a sound source which would be more acceptable. Small bombs of the type used in fireworks displays were first tried, but the problems of measuring the short-duration pulses of sound were too large to make it practical. Tests are now in progress using an air-horn of the type used on large ships and at lighthouse sites. There are several advantages: The duration and amplitude of sound energy can be controlled. The frequency is near that of the predominant frequency of the ramjet noise. The tone is not unpleasing to the public. Precise measurements may be made by ordinary sound-level measuring equipment in the communities. The results of these tests should show the relative sound level in the surrounding communities with different meteorological conditions. The measured sound level in the several communities could then be used as a basis for deciding when ramjet runs could be made with the least disturbance to the citizens.

Conclusions

In the years since World War II, the airplane manufacturers have been required to spend more and more time, effort, and money in attempts to cut down the noise produced by airplane and guided missile powerplants. This manufacturer's efforts are similar to those of other airplane companies. It appears that the problem is growing. No simple true solution is yet in sight.

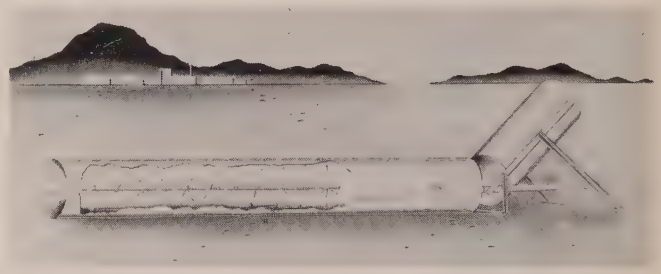

Fig. 8 – Water-spray-type muffler for ramjet

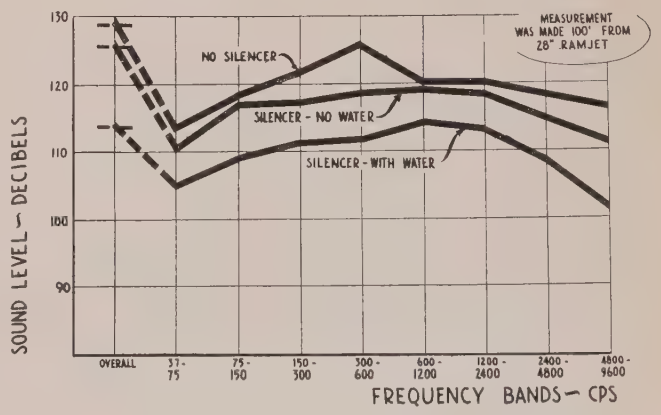

Fig. 9 – Effect of suppressor on ramjet noise level

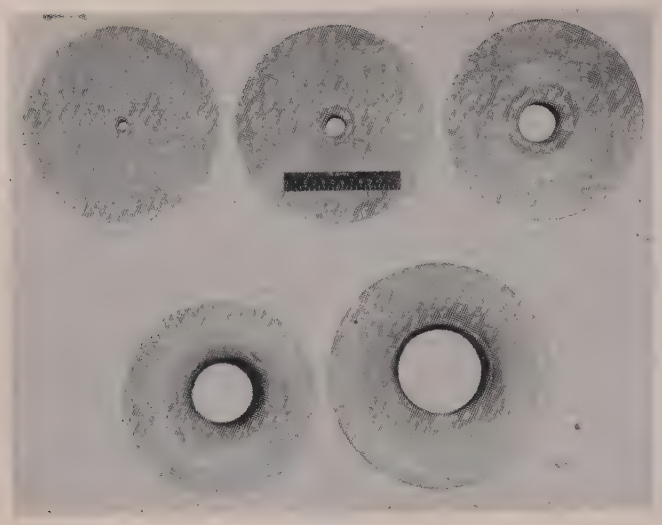

Fig. 1 – Five bellmouth nozzles

JET

RECOGNIZING the need for information of practical use in the design of transport aircraft, our company is actively engaged in the study of jet engine noise. The purpose of this study is to evaluate quantitatively and qualitatively the noise of current models of jet engines and to establish means of predicting the noise of a proposed jet engine. This paper is a report of the progress to date on this study. It is by no means an answer to all of the questions being asked at the present time, but it is believed that certain basic relationships presented here will be of value to the aircraft industry and particularly to those airplane manufacturers working on designs of jet transport aircraft.

This study is presented along several separate lines including the following:

1. Scale-model nozzle studies in a reverberation chamber.
2. Scale-model nozzle studies in an anechoic chamber.
3. Analytical studies of the phenomena of jet noise.
4. Studies of full scale jet engine noise in test cells (reverberant chamber conditions).
5. Free-field studies of jet engine noise.
6. Analytical studies of jet engine noise as a function of jet engine operating conditions.

In carrying out these studies, it has been necessary to develop certain tools and techniques and establish methods of presenting data which would facilitate a practical evaluation of the noise of one jet engine as compared with another. In this presentation it is assumed that the reader is familiar with the current practice of the following:

1. Measurement of sound pressure level (SPL) at a given point in a noise field.
2. Measurement of sound power level (PWL) of a source by summing up the noise intensity levels emanating in all directions from a given source. (PWL values as used in this paper are higher than the SPL values in common usage.)
3. Determination of SPL or PWL per octave, per third octave, per cycle, and so forth, for purposes of analyzing the spectrum of the noise.

SPL is the direct measurement made in a free-field situation and in an anechoic chamber. An anechoic chamber is a chamber with interior surfaces which have practically complete absorption of the sound waves striking these walls. This anechoic chamber is used to provide a space within a noisy working area which has (a) background noise levels low enough to make accurate measurements of noise coming from a source being studied and (b) practically no reflections from the walls of the chamber.

PWL is a measurement of total noise energy or power within a reverberation chamber or is the summation of the total noise emanating from a source.

The most important tool being used in the study of jet engine noise is the scale-model nozzle rig. Rigs of this type include an air supply which facilitates testing many nozzle sizes over a range of nozzle pressure ratios and a range of temperatures which duplicate those of the jet engine to be studied. These rigs include a reverberant chamber for measuring PWL and an anechoic chamber for measuring SPL patterns.

NOISE

John M. Tyler, Pratt & Whitney Aircraft, Division of United Aircraft Corp.
and
Edward C. Perry, United Aircraft Corp.

This paper was presented at the SAE National Aeronautic Meeting, New York, April 14, 1954.

AN analysis of jet engine noise as a function of jet engine design characteristics is presented in this paper along with some thoughts as to possible means for reducing the noise of jet transports for the future.

The authors present a summary of (a) scale-model noise work, (b) full-scale jet engine noise measurements in test cells and free field, and (c) a discussion of information gleaned from comparisons of scale-model work with full-scale engine work.

This paper received the Wright Brothers Medal for 1954.

Instrumentation

Four quantities are necessary to define jet noise. The first is the total acoustical output, or power level. The second is the distribution of the sound energy according to frequency, or the power spectrum. The third is the distribution of the energy in space, or the directivity. The fourth is the distribution of energy with time, or the duration of noise. This last quantity, while important to the airport neighbor, is largely a function of the flight path and was not considered in the program. The power level and power spectrum are most easily measured in a reverberant chamber, but the determination of directivity requires free-field measurements or the use of an anechoic chamber.

The instrumentation used in a large part of this noise study is as follows:

1. Bruel & Kjaer, Massa, Altec, and General Radio microphones and Photocon pressure pickups were used for noise measurements. For small-scale nozzles the Massa 123, which is flat to 20 kc, was used. For high-temperature, high-intensity noise measurements, the water-cooled Photocon pressure pickup was used.

2. Tape recorders were used for jet engine recordings.

3. Direct measurements of noise spectra from scale-model nozzles and data transcription from tapes were accomplished by means of General Radio, Spencer Kennedy, and Bruel & Kjaer filters.

4. The Bruel & Kjaer records were transcribed onto punched cards by means of a telereader. These cards were run through IBM machines which made corrections for instrumentation calibrations and calculated data points for power level and power spectra curves.

Scale-Model Nozzle Studies

Five bellmouth nozzles of different sizes were used to study scale effects. A picture of these nozzles is shown in Fig. 1. The upper nozzles are 1, 2, and 4 in. in diameter, while the bottom two are 7 and 10 in. in diameter. Each nozzle was

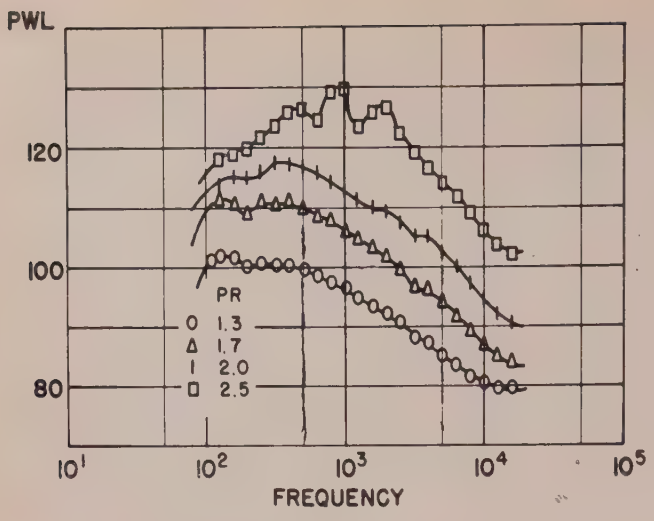

Fig. 2 – Power spectra of the 7-in. bellmouth nozzle

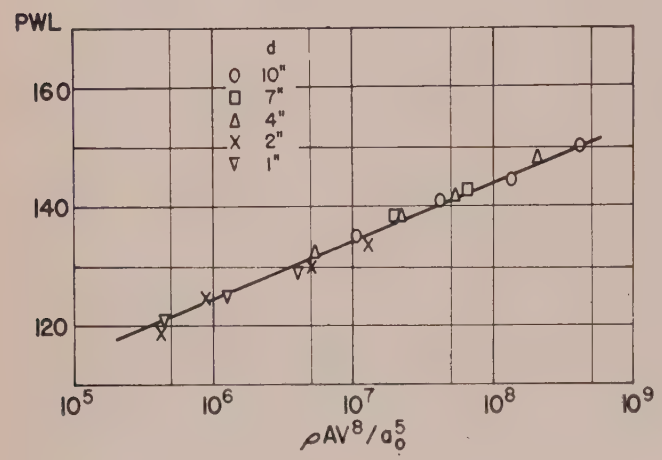

Fig. 3 – Bellmouth nozzle power level versus Lighthill's parameter, $\rho AV^8/a_0^5$

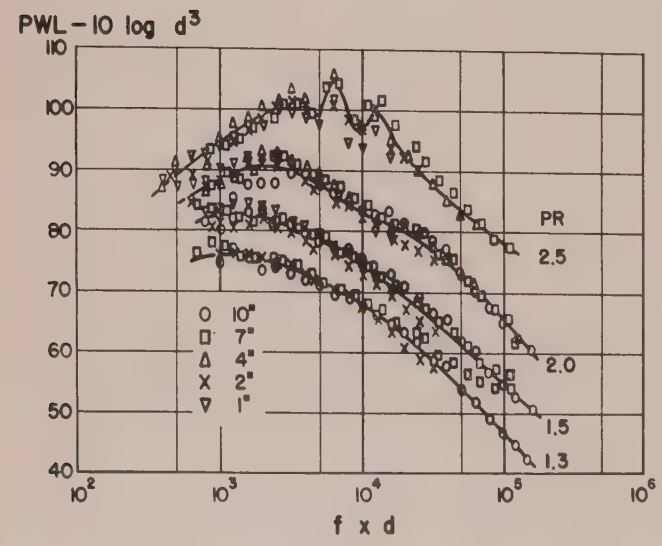

Fig. 4 – Generalized power spectra of bellmouth nozzles

tested at several pressure ratios. The power level spectra of the 7-in. nozzle, which is typical of all five, is shown in Fig. 2. The discrete frequencies which are observed at the higher pressure ratios are a function of shock-wave spacing and will be discussed later. The first objective of these tests was to establish the effect of scale on the overall power level. While the data included a measurement of the overall power level, it was felt that the results would be more accurate if the readings of all the one-third octave filters were added. In most cases this value turned out to be less than 1 db different from the power level measured directly. Since theoretical work of Lighthill had predicted that the acoustic power should be a function of the parameter $\rho AV^8/a_0^5$, the power levels of the five nozzles were plotted against this parameter as shown in Fig. 3. These data are restricted to subsonic flow because the theory is not applicable to supersonic conditions. The discrete frequencies produced at supersonic flow are caused by an entirely different mechanism than that expounded in the theory. The additional noise from discrete frequencies made the supersonic flow points lie somewhat above the line shown in Fig. 3. This line has the theoretical slope of 10 db per decade, which is a striking confirmation of Lighthill's theory. It should be remembered that these nozzles were operated with cold air at subcritical pressure ratios and with a minimum amount of turbulence in the entering air. Under these conditions, which are essentially those assumed in the theory, the power level can be predicted from Lighthill's parameter.

The second objective of the tests was to establish scaling parameters for the noise spectra. It

The Authors

JOHN M. TYLER is chairman of the Noise Committee at Pratt & Whitney Aircraft Division of United Aircraft Corp. He received his M.E. degree from Cornell University in 1927, and did graduate work in Germany from 1931 to 1932. Mr. Tyler started as vibration engineer for General Motors Research Laboratory, and was promoted to assistant section head of the Special Problem Section. He worked for Lycoming Division of Aviation Manufacturing Corp., Hamilton Standard Propeller Division, and was assistant to the president of the Aviation Corp.

EDWARD C. PERRY is with the Research Department of the United Aircraft Corp. His work at the Research Department has included combustion, instrumentation, and jet noise. Mr. Perry attended the California Institute of Technology. He completed his studies at Worcester Polytechnic Institute, receiving his B.S. degree in physics in 1947. After a short time at the National Bureau of Standards and the Naval Gun Factory, he joined United Aircraft Corp. in 1948.

was believed that the frequency was inversely proportional to the size, and therefore the product of frequency and jet nozzle diameter was plotted as the abscissa. The overall power level was shown to be proportional to the area of the jet or to the square of the diameter; therefore, the power level per cycle divided by the cube of the jet diameter was plotted as the ordinate. This plot is shown in Fig. 4. This figure shows that the shape of the power spectrum is the same for all jet diameters tested, but it is a function of pressure ratio. Thus, at a given pressure ratio the entire spectrum of a large jet can be predicted from model data.

Geometry

After establishing the effects of nozzle size on jet noise, it was decided to investigate the effects of nozzle geometry. Several nozzles were constructed having the same exit area but successively greater angles of convergence. A photograph of these nozzles is shown in Fig. 5. The shapes are shown schematically in Fig. 6. The nozzles were tested at several different pressure ratios and the power spectra determined. In this case there was no scaling effect so the spectra are plotted as frequency versus PWL as shown in Fig. 7. It can be seen that the power spectrum is a function of the pressure ratio but is independent of the angle of convergence. Discrete frequencies were again encountered at supercritical pressure ratios.

Discrete Frequencies

In order to study these discrete frequencies in more detail, Schlieren photographs were taken of a jet. Fig. 8 is a Schlieren photograph which shows the variation of shock spacing with pressure ratio. With increased pressure ratio, the shock separation increased, but the frequency decreased. Dr. Powell of England has studied this phenomenon and correlated the ratio of shock spacing to jet diameter with "superpressure." Superpressure is the square root of the difference between the actual pressure ratio and the critical pressure ratio. This correlation is shown in Fig. 9. In addition to measuring the shock spacing from the Schlieren photographs, the spacing was calculated from aerodynamic fundamentals using the method of characteristics. It was estimated that one month of engineering time would be required to make this calculation on a three-dimensional basis. Using a two-dimensional approximation, the calculation was accomplished in a few hours. The resulting curve has the same slope but is displaced from the other curves by an amount which is due to the approximations used in the calculations. While the Schlieren photographs were being taken, the frequencies were measured using a narrow band width filter. Using Powell's theory, shock spacings were calculated from the measured frequencies. As shown in Fig. 9, the shock spacings calculated by

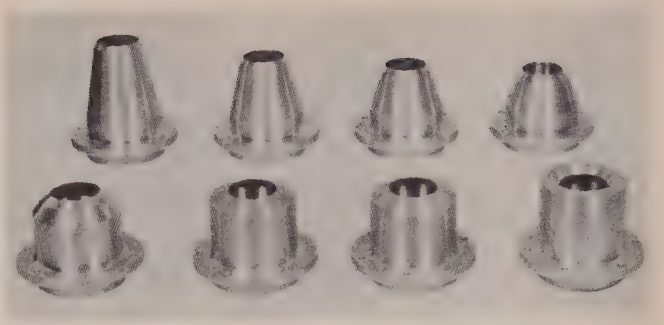

Fig. 5 – Eight conical nozzles with converging angles varying from 15 to 180 deg. The angles of these nozzles are shown in Fig. 6

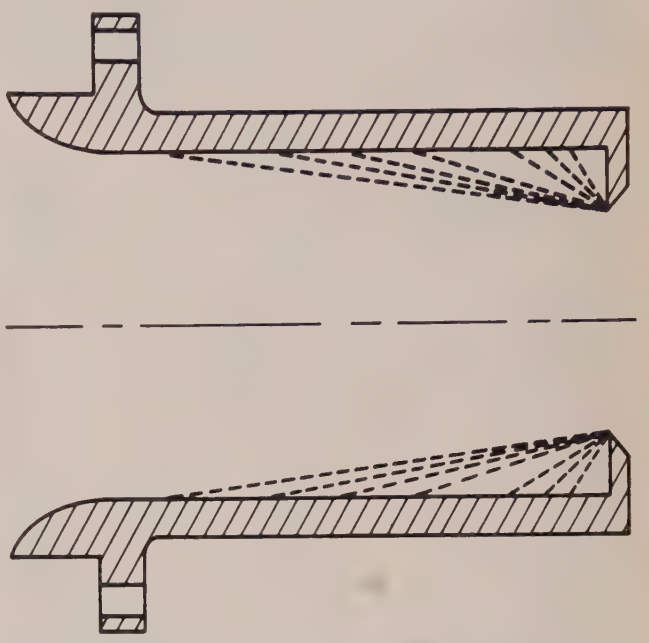

Fig. 6 – Composite drawing of eight conical nozzles at differing angles of convergence

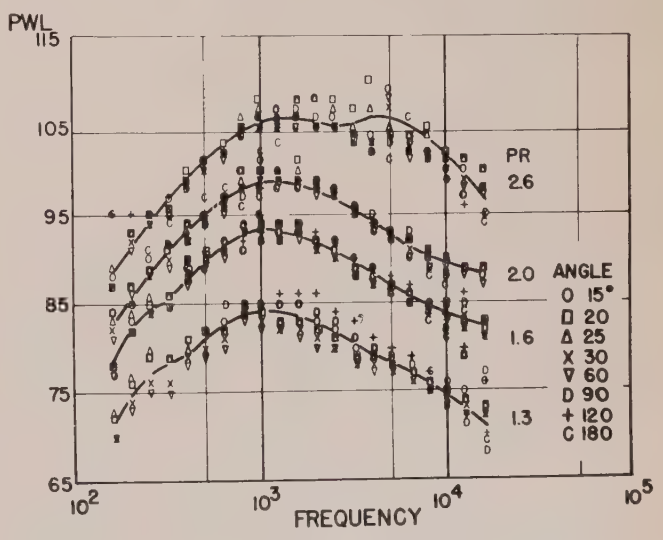

Fig. 7 – Power spectra of converging nozzles

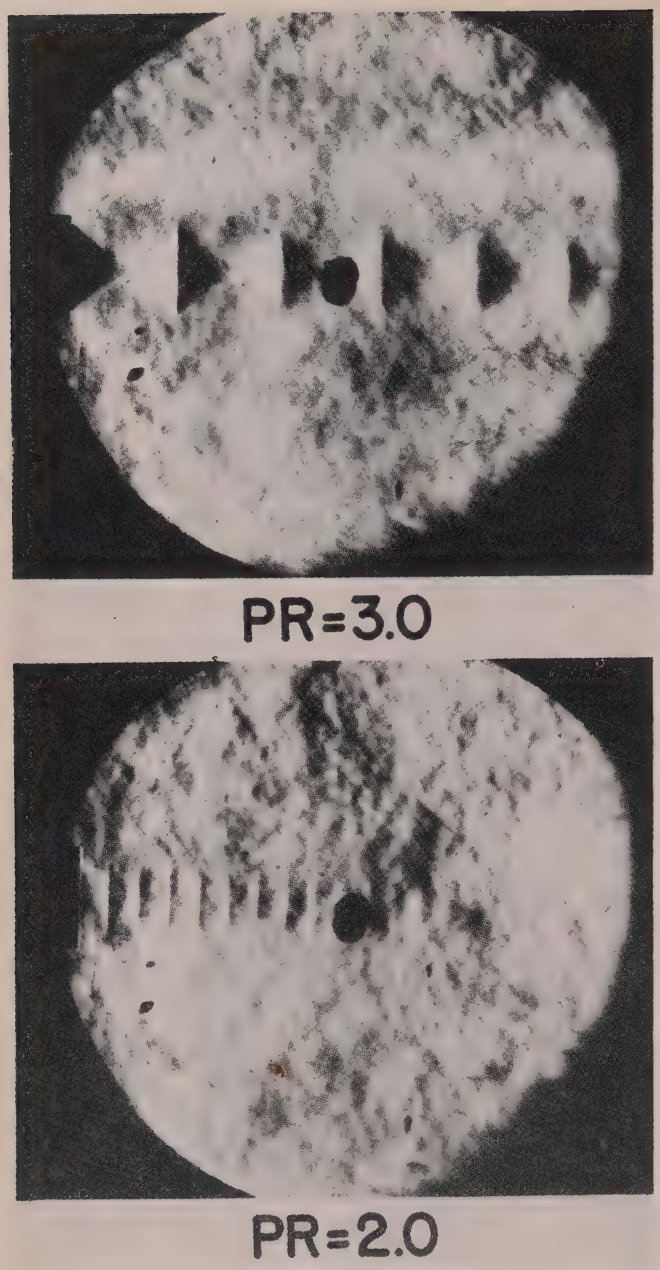

Fig. 8 – Schlieren photographs showing variation in distance between shocks for nozzle pressure ratios of 2 and 3

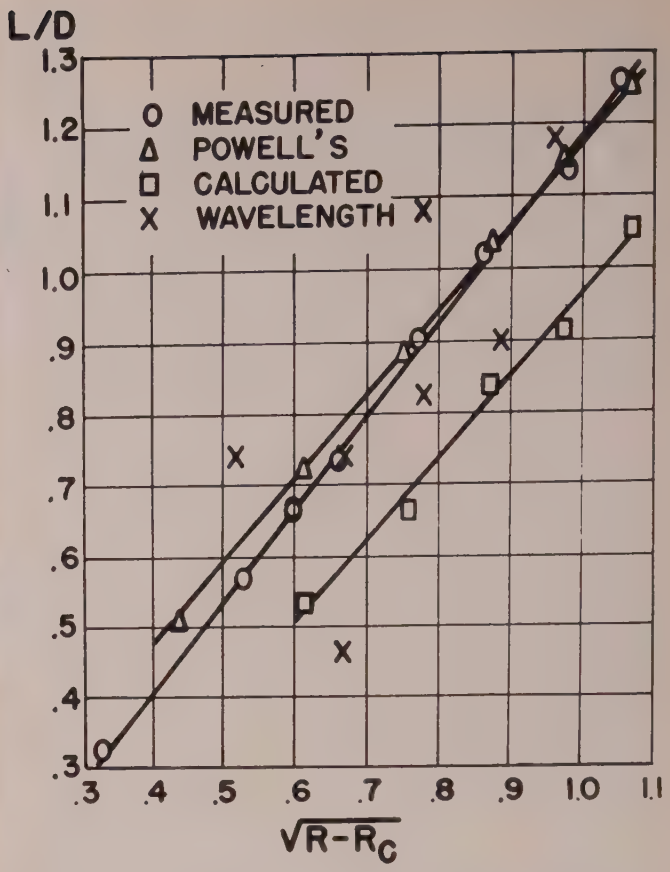

Fig. 9 – Ratio of distance between shocks and nozzle diameter (L/D) versus superpressure

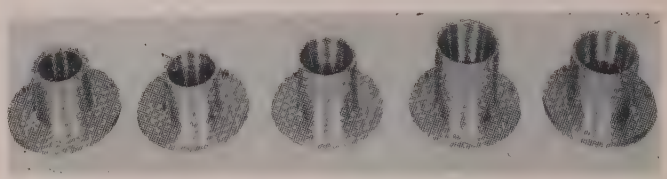

Fig. 10 – Converging-diverging nozzles

this method are also in reasonable agreement with the actual measured spacing. It will be noted that there are harmonics or subharmonics of the frequencies which agree with the measured spacing.

After the tests with convergent nozzles, several convergent-divergent nozzles were designed and constructed. These nozzles are shown in Fig. 10. All the nozzles had a bellmouth inlet and a throat diameter of 1.5 in. The exit ranged from a cylinder to a 40-deg diverging section. The nozzle shapes are shown schematically in Fig. 11. The power spectra of these nozzles at different pressure ratios are shown in Fig. 12. With these nozzles, discrete frequencies were encountered at the lower pressure ratios. In this case there was little or no variation of frequency with pressure ratio. As the pressure ratio was increased, the tone suddenly ceased but reappeared when the pressure ratio was decreased to the same value. It was found that this tone was similar to the jet tone produced by an orifice. Flow

separation occurred at the throat of the nozzle, producing a series of toroidal vortexes. At pressures above critical, the flow separation occurred in the diverging section without the generation of vortexes.

Turbulence

The existence of discrete frequencies will be less important in an actual jet engine than in model nozzles because turbulence in the stream causes a reduction in the amplitude of the pure tones. Turbulence was added in model nozzles by a series of radial blades set in the duct upstream from the nozzles. The effects of turbulence with convergent nozzles are shown in Fig. 13. With the convergent-divergent nozzles the pure tones were more pronounced, and the noise reduction with increased turbulence was correspondingly greater. The effects of turbulence with these nozzles are shown in Fig. 14.

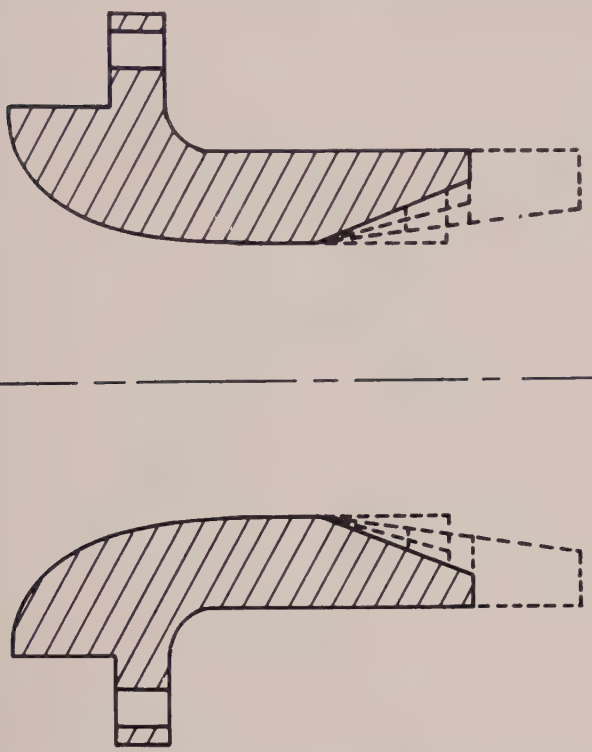

Fig. 11 – Composite drawing of converging-diverging nozzles

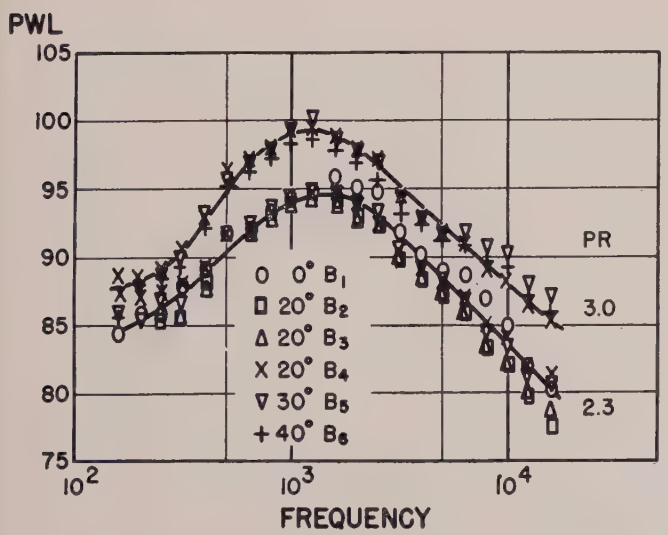

Fig. 12 – Power spectra of converging-diverging nozzles

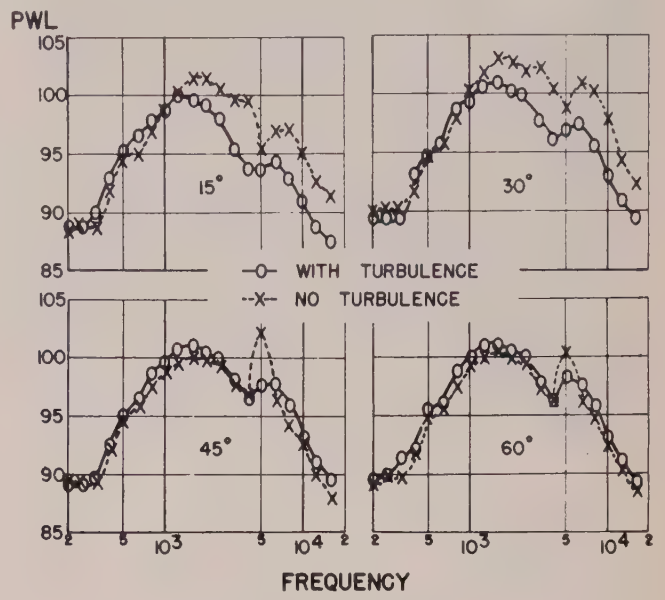

Fig. 13 – Curve showing the effects of turbulence on discrete frequencies generated by converging nozzles at supercritical pressure ratios

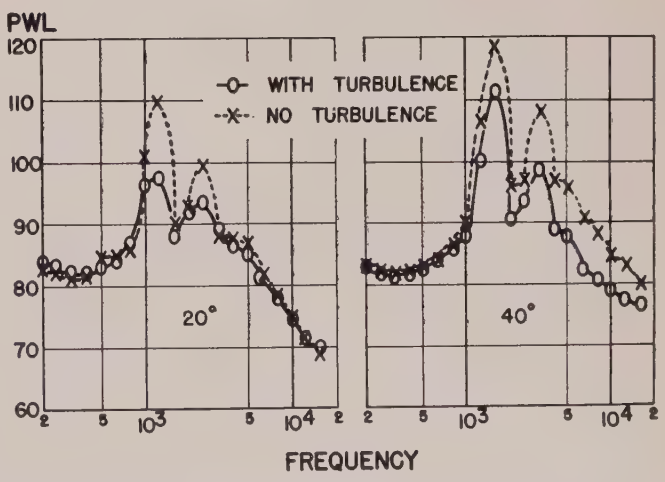

Fig. 14 – Curve showing the effects of turbulence on discrete frequencies generated by converging-diverging nozzles at subcritical pressure ratios

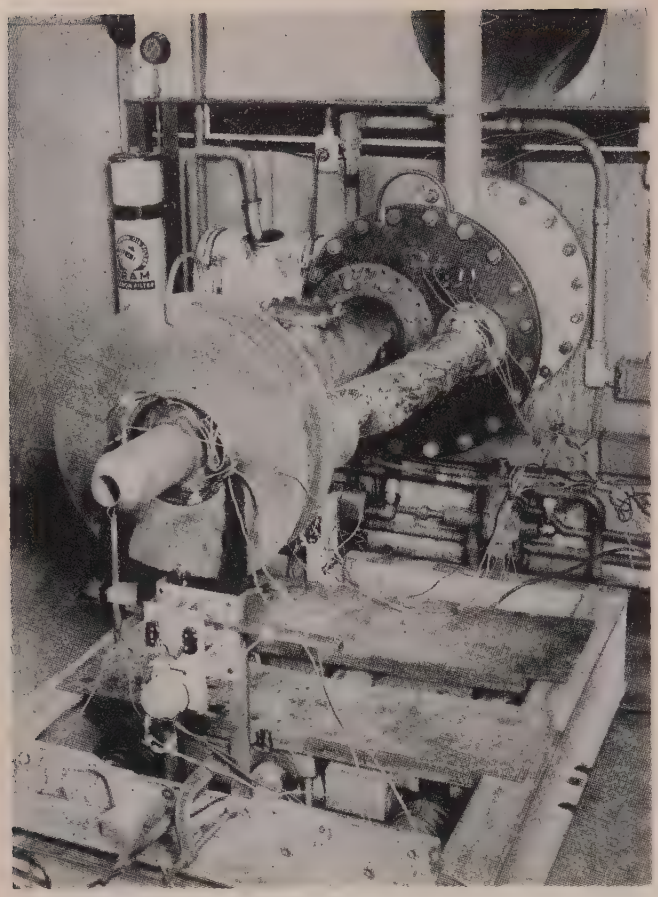

Fig. 15 – Model nozzle test rig

Temperature

Another variable which has an effect on the noise from a nozzle is the jet temperature. To test this effect, a modified turbojet "can" burner was installed upstream from the nozzle. The installation of this can in the rig is shown in Fig. 15. With this burner, it was possible to obtain jet temperatures up to 1600 F. The probe shown in Fig. 15 was used to measure the total temperature and the total pressure profiles of the jet. With this rig, it was possible to vary the temperature without changing the pressure ratio and thus isolate the effects of temperature on the power spectra. The spectra at several different temperatures and at a pressure ratio of 1.7 are shown in Fig. 16. Since the temperature was increased at a constant pressure ratio, the stream velocity was increased, producing an increase in noise. This plot also shows that the peak frequency increased with increased temperature. Actually the entire shape of the spectrum was changed. It can be seen that the temperature also attenuates the discrete frequencies. Fig. 17 shows the effects of temperature when the nozzle is operated at supercritical pressure ratios. It has been shown that the power level of the bellmouth nozzles is a function of Lighthill's parameter $\rho A V^8/a_o^5$ This expression was derived on the assumption that the temperature of the jet was the same as that of the surrounding medium, and, therefore it cannot be used for a hot jet. It can be seen that the most important part of this parameter is the velocity and that jet velocity alone can be used as a reasonable indication of the jet noise. It would be desirable to express this in normal jet engine terms. Basically, engine thrust is the product of mass airflow and velocity, and therefore thrust divided by mass flow is the effective velocity of the jet. Normally, airflow is measured as weight flow. For purposes of this study, thrust divided by weight flow is called "specific thrust." Four different conical nozzles were tested at various pressure

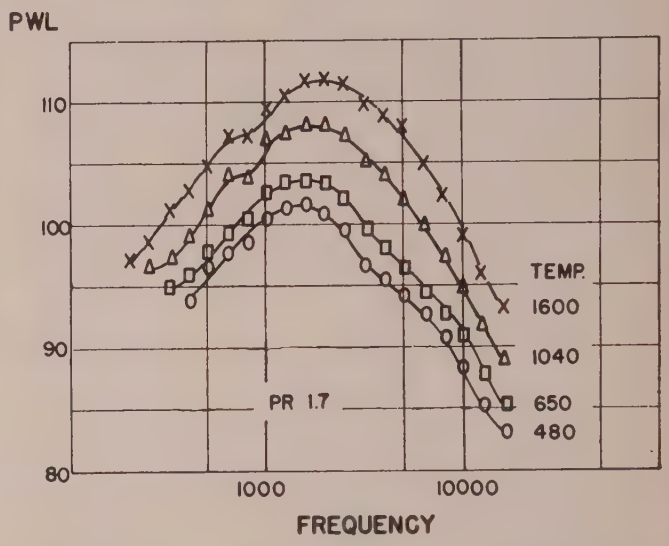

Fig. 16 – Curve showing the effects of temperature on the power spectrum from a conical nozzle at subcritical pressure ratio

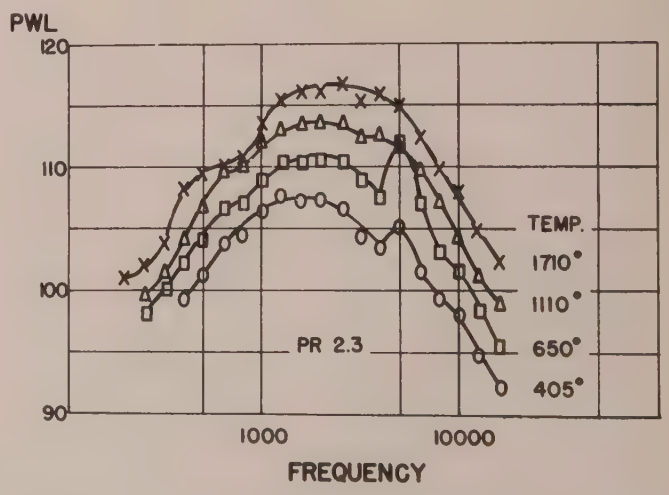

Fig. 17 – Curve showing the effects of temperature on the power spectrum from a conical nozzle at supercritical pressure ratio

ratios and temperatures. The total acoustical power of these nozzles was determined and plotted against specific thrust in Fig. 18. This plot includes data from four different nozzles operated at pressure ratios from 1.3 to 2.8 and temperatures from 100 F to 1600 F. For comparison, the results of the five different bellmouth nozzles are also included. The general adherence to the eighth-power relationship is evident. However, the scatter of the data is not entirely random. It is due to the variation in pressure ratio as is shown in Fig. 19 by a plot of some of the data from Fig. 18. Below critical pressure ratio, the results are essentially independent of pressure. Above critical pressure ratio, the noise level increases with pressure. The eighth-power

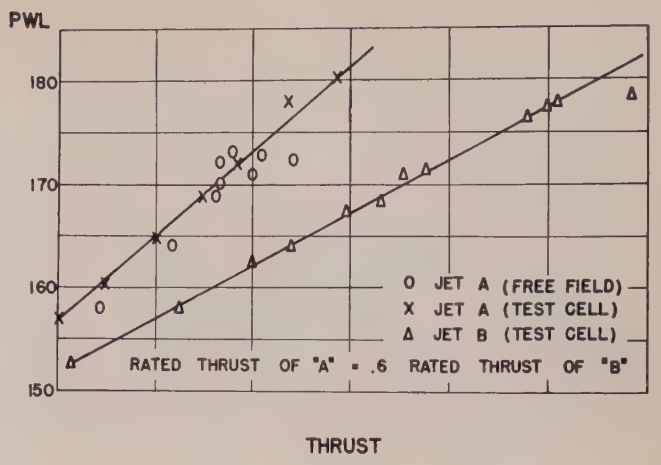

Fig. 20 – Curve showing power level of noise versus thrust of turbojet engines

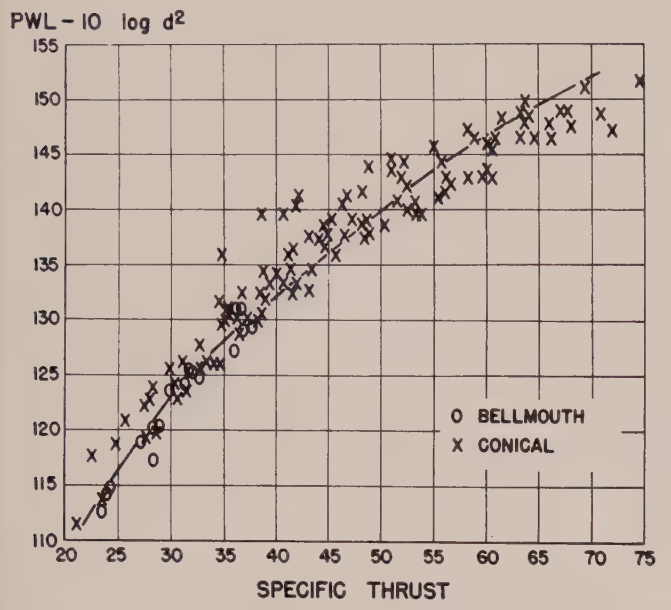

Fig. 18 – Correlation of specific thrust with power level of noise from conical nozzles. The curve is an eight-power variation

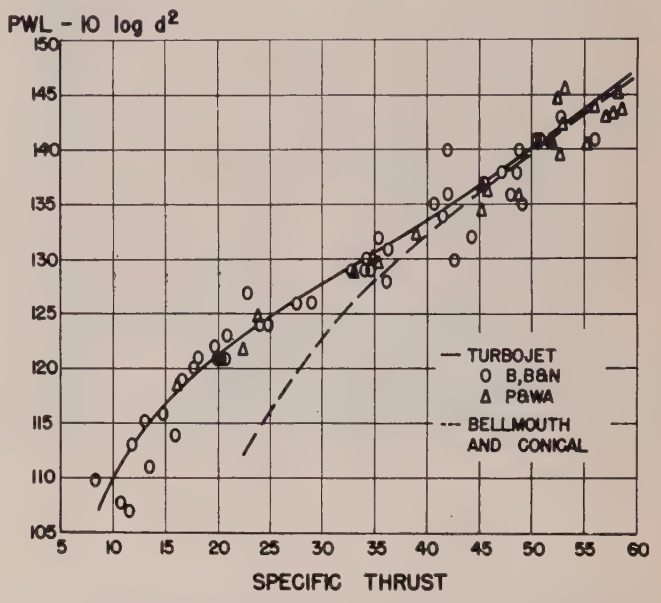

Fig. 21 – Correlation of specific thrust with power level of noise from turbojet engines. The dotted line is the eighth-power variation shown in Fig. 18

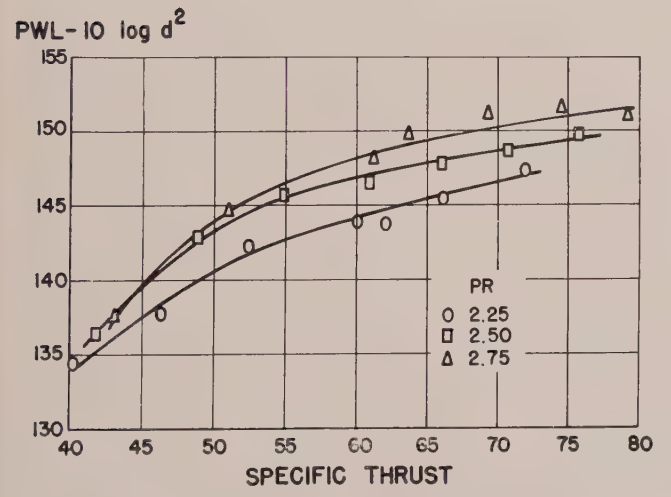

Fig. 19 – Curve showing the effects of pressure ratio on noise output of conical nozzles

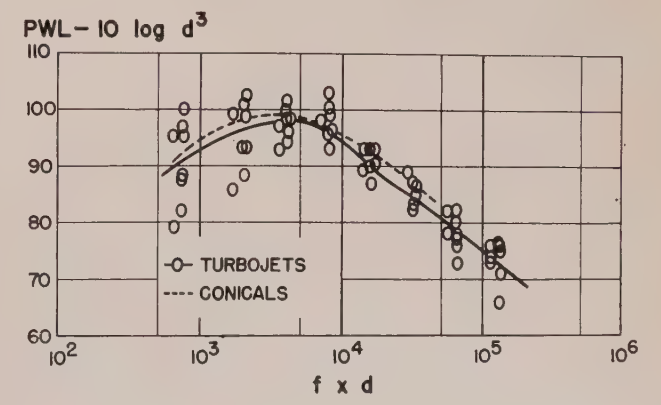

Fig. 22 – Generalized power spectra of turbojet engines and the correlation with hot model nozzles

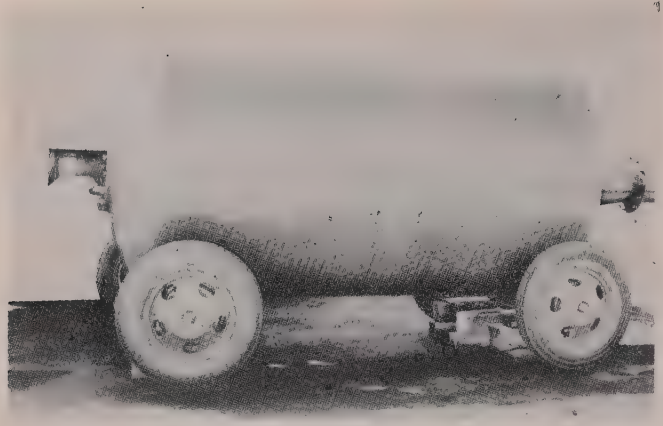

Fig. 23 – Photograph of anechoic tank

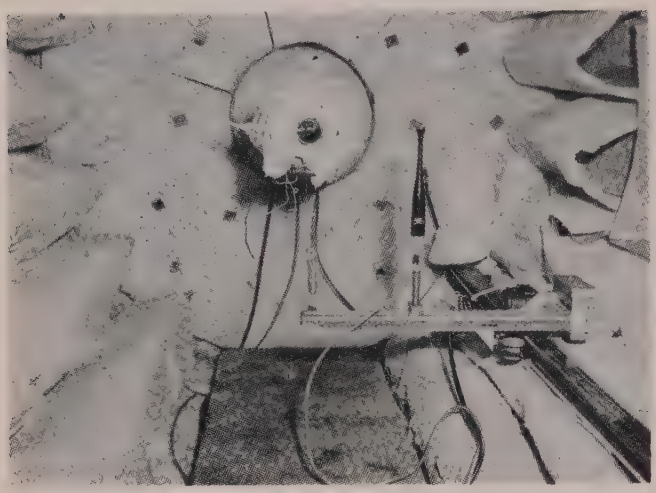

Fig. 24 – Interior of anechoic tank showing test nozzle and microphone

law prediction was based on the assumption that the percentage turbulence remained constant. There is some evidence that this is not true at supersonic velocities, therefore some deviation from the eighth-power law should be expected at supercritical pressure ratios. However, as shown in Fig. 18, there is a general adherence to the eighth-power relationship.

Turbojet Engines

The power levels of two different size engines at various values of thrust are shown in Fig. 20. These data are from test cells and have been supplemented by free-field measurements on the smaller engine. This plot shows that, for a given thrust, the larger engine is approximately 10 db quieter than the smaller engine. It has been possible to explain this difference by computing the jet velocities of the two engines. At a given thrust the airflow of the larger engine is greater than that of the smaller engine and the jet velocity correspondingly less. Since jet noise is largely a function of velocity, the larger engine with lower velocity produces less noise. The specific thrust is a measure of the effective velocity of the jet, and therefore these data were plotted against specific thrust as shown in Fig. 21. In order to supplement the data obtained by Pratt & Whitney Aircraft, data on other manufacturers' engines as reported in the *Journal of the Acoustical Society of America,* May, 1953, by Mawardi and Dyer were used to obtain additional data points for Fig. 21. Additional information on engine operating conditions were obtained from Bolt, Beranek, and Newman to go with these data. From this information it was possible to estimate airflow. With these estimates of airflow and the measured values of thrust, it was possible to compute the specific thrust.

The line drawn through the data in Fig. 21 is the eighth-power curve drawn for the data on bellmouth and conical nozzles in Fig. 18. At the lower values of specific thrust, there is a definite difference between the turbojet and the scale-model nozzle data. This difference is at least partly due to the compressor noise which is included in the engine data. For the high-power conditions, however, the total power level of the noise from a turbojet can be predicted with reasonable accuracy from the model data. The next question is whether or not the power spectrum could be predicted from model data. The variation of the power spectrum with jet temperature for a model nozzle has been shown in Fig. 16. This scale-model curve for the data at 1000 F is shown as a dotted line together with turbojet data in Fig. 22.

Directivity

All of the data presented so far have been power levels or power spectra of the jet noise. Another factor of prime importance is the directivity or the distribution of the sound energy in space. The sound field is normally divided into two regions: the near field and the far field. The near-field noise was studied on a model by the use of an anechoic chamber. A picture of this chamber, which is in the form of a tank, is shown in Fig. 23. The tank is evacuated with a vacuum line shown at the right of the picture. Atmospheric air enters through the bellmouth at the left passing through the nozzle under test. The inside of the tank, with the nozzle and microphone in position, is shown in Fig. 24. The special interior treatment shown is required to obtain the desired inverse-square attenuation within the working area inside the tank. With the microphone traversing mechanism shown in Fig. 24, it is possible to probe the near field and construct maps of isointensity lines. These are of particular importance in connection with studies of failures of airplane structure in the near field. The map for a 1.8-in. diameter nozzle at a 2/1 pressure ratio is shown in Fig. 25. The upper half

of this figure shows a map of the 600 to 1200 cps noise. The lower portion is a plot of the frequencies from 2400 to 4800 cps. These plots may be used to approximate the location of the source of various frequency bands of noise and thereby confirm the fact that the high frequencies are generated close to the nozzle while the lower frequencies are produced several diameters downstream. In some cases a high-frequency lobe in the forward direction was clearly defined.

The far-field noise is measured in free field, that is, in the open, away from reflecting surfaces. Data obtained on a 150-ft circle around a J48 engine in an F9F-5 airplane are shown in Fig. 26. The upper curves are at 80% rpm and the lower ones at 100% rpm. These data demonstrate that the most pronounced variation with rpm is in the low frequencies in the aft direction. The major components of noise are directed along lines at about 30 to 40 deg from the axis of the jet.

Unusual Configurations Tested Including Ducted Fan

A number of ideas in the category of hunches have been tried on the scale-model test rigs. One of the more obvious, to those familiar with the current thinking on jet noise, is the use of an ejector located just downstream from the jet nozzle. The ejector converts high-velocity, low-mass flow into low-velocity, high-mass flow. This is just what theory says is needed to reduce jet noise. A simple cylindrical ejector with a diameter 2.5 times the jet nozzle diameter and a length to diameter ratio of 5 was built and tested. No appreciable noise reduction was found, and it was concluded that the process of mixing in the ejector is just as noisy as the process of mixing without the ejector. Additional tests are being made with other ejector shapes aimed at providing a controlled mixing process. If some ejector design gives a noise reduction and no great loss in thrust, then those problems involving the use of an ejector behind the engine during take-off and climb will have to be considered.

Another idea which seemed to be good before it was tested was the annular nozzle and the flattened nozzle which proved to be quieter on piston-engine exhaust stacks. These designs have had a quenching effect, that is, quick cooling of the thin layer of hot exhaust gases as they mixed with ambient air. However, despite the theory, no appreciable noise reduction was found using these configurations.

The use of fingers in the jet stream as originally tested by Rolls-Royce together with vortex generators inside the nozzle and various other local changes in the shape of the nozzle, including the addition of a diverging section to a straight or converging nozzle, may have the effect of reducing or eliminating discrete frequencies but have no marked effect on the noise spectrum or noise level.

Water has been injected into the hot jet exhaust about one-fourth diameter downstream from the nozzle with no marked reduction of noise even for water flows up to a value equal to the airflow.

Water injection, as used in Pratt & Whitney engines to permit an increase in engine thrust, has no effect on noise. In other words, the noise at a given thrust is the same with water as without water.

Fan or bypass nozzles have been tested over a large range of operating conditions. The results of some of these tests are shown in Fig. 27. It will be noted that the cold outer stream of air has no appreciable effect on the noise level of the hot jet stream. It makes no difference whether the hot inner nozzle is in the plane of the outer nozzle or upstream from the outer nozzle.

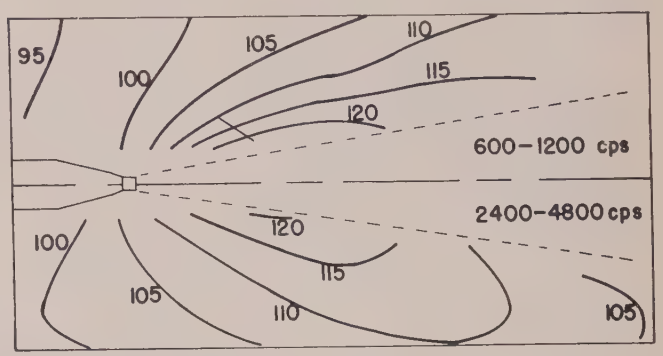

Fig. 25 – Isointensity map of 1.8-in. diameter converging nozzle at a pressure ratio of 2.0

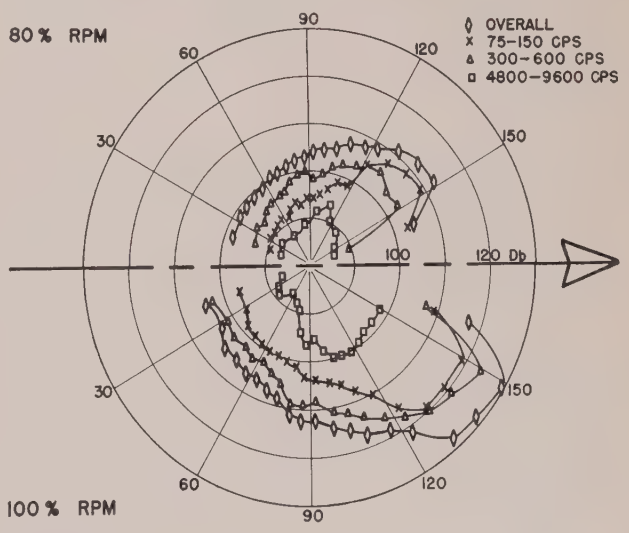

Fig. 26 – Plot of sound pressure levels measured on a 150-ft radius from the exhaust of a J48-P-6

Noise Reduction by Engine Design

As an introduction to this subject, Fig. 28 is presented showing the noise produced by various engines under take-off conditions. These noise levels have been calculated on the basis of the analytical procedures presented, and where noise data are available these values have been verified. It will be noted that when these engines are brought up to take-off thrust they all produce about the same noise levels.

Fig. 29 presents the noise level of these engines in terms of specific thrust. This plot is not very different from Fig. 28, and that is not surprising when it is remembered that a 2/1 change in thrust would change the noise level versus specific thrust only 3 db.

That present engines have about the same noise level results from the fact that these engines are designed to give the highest specific output using the simplest and best design practices. However, should it be necessary to design engines with lower noise levels than present engines, this can be done.

It has been established that the noise power level of jets is roughly proportional to the eighth power of the specific thrust. The most apparent method of noise reduction, therefore, is to reduce the specific thrust. If the specific thrust is reduced, it follows that the airflow through the jet must be increased to maintain the same total thrust. It has been shown in Fig. 20 that a larger engine is appreciably quieter than a smaller engine at the same thrust. This points up one possible method of noise reduction.

In order to correlate noise with a conventional engine design parameter, it would be desirable to work with the noise versus nozzle expansion ratio. Also, in order to present comparisons of take-off noise for various engine designs, it would be desirable to consider these variables in terms of engines all having the same take-off thrust.

Fig. 30 has been drawn to show noise levels at a given thrust, for a series of turbojet engines and two series of turbofan engines, as a function of nozzle expansion ratio. The turbofans have 2/1 and 3/1 airflow ratios, that is, the total airflow through the engine is 2 or 3 times the airflow through the gas-generator portion of the engine. Every point on each curve represents an engine having 100-lb take-off thrust. The fan air nozzle expansion ratios are equal to the gas generator nozzle expansion ratios, and the temperature of the exhaust from the gas generator portion of the engine is constant throughout the chart.

Following down along the jet engine line, the nozzle expansion ratio is reduced, and the engine size increases to maintain the same thrust. Dropping down to the 2/1 turbofan curve, we find a lower noise level as energy is taken out of the gas generator exhaust to drive the fan and the thrust from the fan reduces the thrust required from the jet. Dropping down further to a 3/1 ratio, additional energy is removed from the gas generator exhaust, and additional thrust from the fan allows the jet to be still smaller. However, these reductions are not large compared with the complexity involved and compared with what can be done with a simple jet engine.

The question of whether it would be more desirable from a noise standpoint to have a jet engine with a low nozzle expansion ratio or a turbofan engine with a low expansion ratio involves an analysis of problems beyond the scope of this paper. Obviously comparable low noise levels may be obtained by following either design philosophy.

To pursue further this idea of noise reduction by using less than maximum thrust for take-off, the following is of interest.

1. There is as much as 10 db higher noise level at the neighbor's house when the airplane is in the

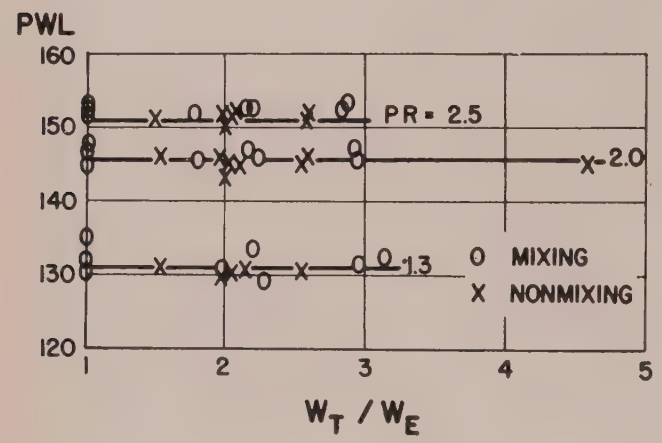

Fig. 27 – Curve showing the effect of cold (200 F) annular air on the power level of noise from a hot (1000 F) jet. W_T = total airflow, W_E = airflow of hot jet

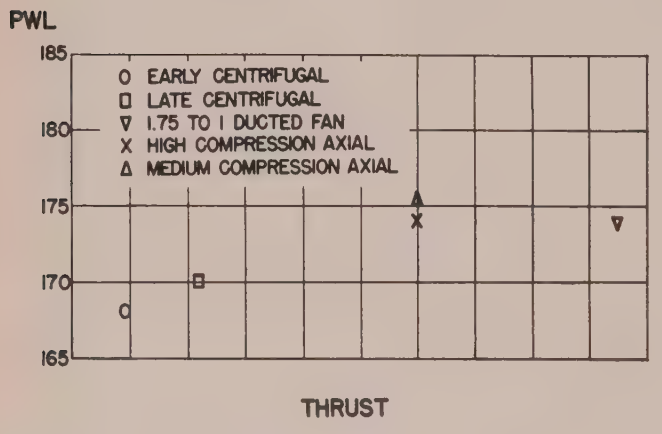

Fig. 28 – Power level of noise from different turbojet engines versus relative thrust category

air at a given distance than when it is on the ground at the same distance. Thus if the thrust is maintained at a high level while the airplane is at or near the ground and then reduced as the airplane starts its climb, the noise level to which the neighbors are exposed will be greatly reduced.

2. Commercial transport airplanes are required to demonstrate satisfactory one-engine-out performance. Thus a four-engine airplane would be required to perform satisfactorily at three-fourths maximum thrust. Four jet engines of the size being considered for proposed jet transports each at three-fourths thrust produce about 7 db less noise than three engines at maximum thrust. A commercial transport airplane could climb at an appreciably reduced noise level by using the one-engine-out thrust schedule in climb but taking the thrust from four engines.

3. As the cruise speeds of transport airplanes increase, the cruise thrust required increases faster than the climbout thrust. This leaves more margin for thrust reduction during climbout for high-speed jet transports.

4. The use of larger engines instead of using water injection, that is, putting the weight into the engine instead of tanks and water, would provide a still greater margin between maximum thrust and climbout thrust and permit climb operation at a lower percentage of maximum thrust.

The above factors, together with others which are being studied, seem to indicate that jet transport operation during climbout, the critical phase from the noise standpoint, at lower specific thrust than now contemplated may prove to be a natural solution to the airport noise problem. In the event of an engine failure or any similar emergency, the full thrust of the engines could be used. At this time the neighbors would be exposed to higher noise levels. However, emergency conditions are so rare that this should not be a difficult problem.

The results of studies along the lines mentioned above, together with a consideration of the relative complexity, size, and efficiency of turbojet and turbofan engines, will indicate which way we should go in the future.

Conclusions

1. A procedure has been established for predicting from scale models the noise power level and power spectra of full-scale jet engines.

2. No quick fix for the quieting of jet aircraft has yet been presented.

3. The noise of jet engines is roughly proportional to the specific thrust to the eighth power.

4. The noise of the turbojet and turbofan engines is a function of the characteristics of gas generator jet stream. It is unaffected by the fan jet stream.

5. A solution to the jet engine airport noise problem may be brought about by other factors which make it possible to operate at low specific thrust during climbout.

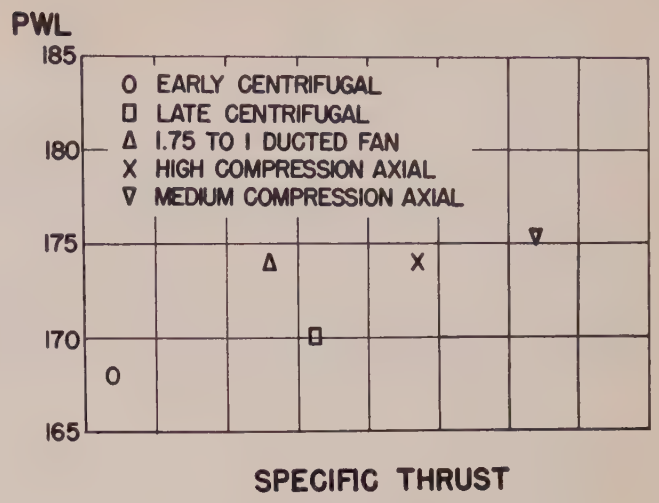

Fig. 29 – Power level of noise from different turbojet engines versus relative specific thrust

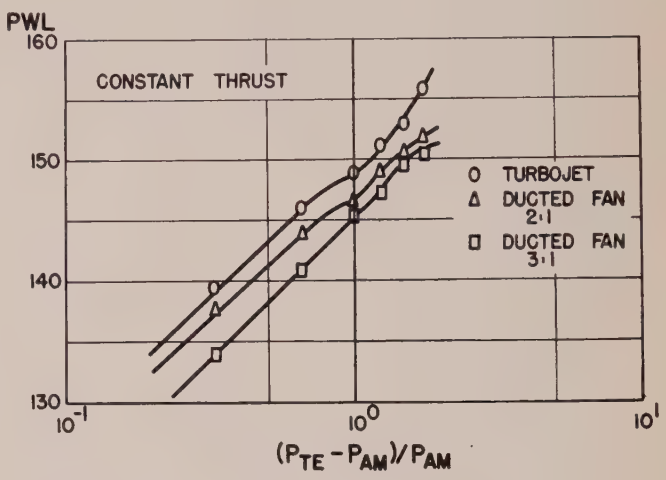

Fig. 30 – Comparison of the power level of noise from jet nozzles of equivalent thrust. P_{TE} = nozzle pressure, P_{AM} = atmospheric pressure

DISCUSSION

Questions Authors' Conclusions on Turbojet and Turbofan Engine Noise

– M. M. Miller
Douglas Aircraft Co., Inc.

I AM reluctant to accept the authors' conclusion 4, "The noise of the turbojet and turbofan engines is a function of the characteristics of the gas generator jet stream. It is unaffected by the fan jet stream." My hesitance is based on one available measurement on an actual bypass engine. The measured sound power level of this engine is very close to the calculated value, using total gas velocity, by either the method of Lighthill or that of the authors. One measurement, of course, proves nothing. It suggests, however, that a more thorough comparison of bypass engines

and their small-scale nozzle simulations is in order before a conclusion is so definitely established.

I am especially concerned because prior to the presentation of the paper, it was reliably reported to me that some engine development policy makers who had advance previews of the conclusions of this paper were interpreting this conclusion to mean that bypass engines have no acoustical advantage over straight jets. It should be remembered that even if conclusion 4 is absolutely correct, the introduction of cold annular air can produce 30 to 40% more thrust for the same noise level than can the pure hot jet.

The true acoustical evaluation of the turbojet versus the turbofan, as viewed by the aircraft manufacturer and the airline operator, can be had only by comparing the sound power level with the maximum available thrust or percentage maximum available thrust and with consideration being given to the weight or drag or both of the engine installation.

We have been studying this paper continuously since its presentation, and it appears that the best criticism will be through the application of the methods of calculation presented to a thorough comparison of straight jet and bypass-type engines. We have started this comparison. In order to complete the study, we must obtain more internal data on current and proposed bypass engines and more specific information from the authors concerning the ejector system they used for the annular cold air tests. We must also determine from them the abscissa scales and specific engines they used for their paper but which were omitted because of security restrictions.

Authors' Methods May Apply in Helicopter Ejector Noise Study

– Stephen du Pont
Doman Helicopters, Inc.

THIS paper is of particular interest in its application to helicopter ejector cooling noise problems.

It would be very interesting to study the conical divergent nozzle mentioned on an exhaust nozzle for engine cooling ejectors and thrust augmentors, and we wonder if the pumping ability of the ejector or thrust of the augmentor would be adversely affected.

The 400-hp Lycoming engine in the Doman helicopter is cooled by exhaust ejectors, and where there is room to install ejectors the project has proved to be a very interesting and inexpensive way to "compound" a helicopter engine, not to speak of the elimination of high-speed fan drive and blades and expensive exhaust turbines. Ejectors are expected to provide an effective muffler to the engine, but results have proved to be disappointing without providing for specific silencing means.

It is interesting that the nozzles Tyler and Perry used in the test are of about the actual size used in full-scale ejectors and thrust augmentors, and therefore the test can be used directly as excellent material for analysis of ejector noise.

Authors' Closure To Discussion

THE following comments are in reply to the discussion by Mr. Miller:

Conclusion 4 is based on the data presented in Fig. 27, taken on a configuration discussed in the last paragraph of the section headed, "Unusual Configurations Tested Including Ducted Fan." These data speak for themselves.

Having nailed down conclusion 4, we have also nailed down the comparison of the noise from a specific turbojet engine versus the noise from a specific turbofan engine. The noise is a function of the gas generator jet characteristics in both cases in spite of many theories to the contrary.

Oral Discussion of Aircraft Noise Symposium Papers

Reported by H. O. Fisher
Port of New York Authority

Question: Is there any information on the effect of turbojet suppressor devices on thrust?

Mr. Regier: NACA's Cleveland lab is setting up a dynamometer to acquire such information. Thrust has not been measured during previous tests in the Cleveland lab because there has been no significant noise reduction, and it was assumed that there was no reason for thrust to be affected materially.

Mr. Withington: Boeing has measured thrust loss in one test operation and found the loss to be about 20% in one cell configuration.

Question: Does radiation from wing surfaces limit effectiveness of the B-52 suppressor?

Mr. Withington: The front end of the suppressor is affected by wing radiation – the front end is, in effect, not a suppressor but a microphone. The rear end, however, is unaffected, and the device as a whole is effective in the direction required.

Dr. Hardy, Armour Research Foundation: Aviation is not the only source of community noise problems. Over the last 15 years, the trucking industry has developed similar problems. Trucks have become noisier, saturation point has been reached, and organized community resistance has developed. Six states have passed legislation concerning this problem, and at least one truck manufacturer has designed a quieter truck.

Question: What dictated choice of length of the B-52 muffler?

Mr. Withington: We don't know exactly – the muffler was a quick and somewhat trial-and-error undertaking. The first time the muffler operated, exhaust gas came out of the intake end instead of the exhaust stack. We then made a model, found it worked well, and followed the model in designing the full-scale muffler. We recommend a model program for the development of any suppressor.

Comment: Other design requirements for multibladed propeller use would raise the weight more than the 400-lb increase per propeller mentioned in one of the papers. Any aircraft manufacturer would be willing to add 400 lb per propeller to reduce noise, but it seems likely that the total increase in aircraft weight would be much greater.

W. C. Lawrence, American Airlines: I think that the bypass engine can be very effective in reducing noise, but the authors seem to consider the bypass engine only slightly better than the straight jet from a noise standpoint.

Mr. Tyler: In the one model of the bypass engine which has been built, the noise was greater at the maximum thrust rating of this engine according to our calculations than for our largest straight jet-type engine. The bypass engine can be built in a quieter version, and the straight jet-type can, too.

Max Miller, Douglas Aircraft Co.: The use of relative thrust rather than specific thrust as a basis for comparison shows the bypass engine to be 6 or 7 db quieter than a straight jet.

Question: How was the level of turbulence determined in the Pratt & Whitney Aircraft experiments?

Mr. Tyler: The first nozzle used was streamlined, then baffles were introduced in subsequent nozzles to induce turbulence.

Designing Adjustable-Speed V-Belt Drives for Farm Implements

William Spencer Worley, Gates Rubber Co.

This paper was presented at the SAE National Tractor Meeting, Milwaukee, Wis., Sept. 16, 1954.

DESIGNING an adjustable-speed propulsion drive for a farm implement used to be a frustrating experience. In the days when the first adjustable-speed drives for combines were being developed – not designed – only the roughest guesses could be made about many of the factors such as what cross-section is required to handle the horsepower? Or, for that matter, what horsepower will be handled? What diameters should be used, and are they large enough? Shall we try 22, 28, 30, or 36 deg included groove angle? How much spring force will be necessary for a spring-loaded sheave? Will it make any difference whether the engine or the driven sheave is spring loaded?

Certainly the agricultural machinery engineers and the belt engineers, too, accomplished much in solving a problem which is plagued with factors which must be compromised. Want more speed variation? Use smaller diameters. Want better service life? Use larger diameters. Want more horsepower? Use higher spring tensions. The belt crushes when you use stronger springs? Use a thicker belt. The thicker belt doesn't give enough variation? Use smaller diameters and a still stronger spring. Belt life goes down? Well, let's back up and get more variation with a lower groove angle. And so on indefinitely, with no way to evaluate except by test the effects of any of the various changes which were considered.

But from the experience and judgment of these engineers there arose a body of knowledge which made it possible, in 1950, for the American Society of Agricultural Engineers to adopt some standards which would begin to tie down some of the factors. They found it possible to agree to adopt a standard 26-deg groove angle and to settle upon four standard belt cross-sections around which to base their designs. Adjustable-speed-drive designing was far from perfected when the standards were adopted, but a solid foundation for developing design formulas and procedures was laid. Belt manufacturers have been able to concentrate on the development of a group of standard adjustable-speed belts and to develop the application data required to permit an intelligent evaluation of the probable performance of a proposed drive without having to resort to extensive testing of each proposal. The Gates Rubber Co. has recently established formulas relating the various factors of an adjustable-speed V-belt drive to the service expectancy of the drive. With these formulas, published here for the first time, the design of an adjustable-speed drive for the propulsion of a farm implement becomes a straightforward process. The designer can now calculate a drive with full confidence that a V-belt of satisfactory quality will give satisfactory service within the limits of the assumptions he must make concerning power requirements and the conditions under which the drive will operate.

It is only fair to point out, however, that not every adjustable-speed problem which can be conceived can be solved. The designer must be prepared occasionally to accept a compromise in some one of his desires as to speed variation, power transmission, or service life. In such cases, the most that these data, or any other, can do is to show quantitatively how these three factors are related and to point the way to that drive which most nearly satisfies the designer's requirements.

We are here concerned with adjustable-speed

propulsion drives and will consider only adjustable-speed drives having two adjustable sheaves. As illustrated in Fig. 1, each sheave has one disc fixed in position on its shaft and one which can move axially with respect to the fixed disc. By arranging them so that the left-hand disc of one sheave moves simultaneously with and in the opposite direction to the right-hand disc of the other, belt alignment is maintained, and the ratio between the pitch diameter of the belt on one sheave and that on the other sheave can be widely varied.

Assuming a constant drive input rpm, the output rpm will vary between the limits established by the high- and low-speed ratio position. The ratio between the maximum driven speed and the minimum driven speed is called the speed variation of the drive and is an important factor in the design. The speed variation determines the relative diameters of the sheaves. The greater the speed variation, the smaller the sheaves will be. With two sheaves of the minimum diameter recommended in the ASAE Standard for V-Belt Drives on Farm Machines, a speed variation of slightly more than 4 is possible. Since the speed variation also determines the ratio of minimum to maximum ground speed in a given transmission gear, a transmission with two or more reductions will be necessary if the range in the ground speed of the implement will be more than 4/1. The designer should establish the speed variation of the drive as low as consistent with the requirements of the gear transmission, yet sufficiently high to give the range in ground speed which will be desirable.

The variation of the adjustable-speed drive should be at least equal to the smallest ratio between the successive gear-reduction ratios in the transmission. If it is not, then there will be a gap in the ground speed corresponding to the high output speed of the drive through the higher gear reduction and that corresponding to the low output speed of the drive through the lower reduction.

The designer may even want to set the variation of the adjustable-speed drive so that there will be an overlap of ground speeds from gear to gear. The graphs in Fig. 2 indicate that three of four propulsion drives in actual use do have speed variation such that there is an overlap in ground speed. This, of course, has the advantage of giving the same ground speeds with either a high-speed setting of the adjustable-speed drive in one gear or a low setting in another gear.

Having established the speed variation required of the adjustable-speed drive, the designer should next consider whether to drive directly from the engine or from a countershaft, which will in turn

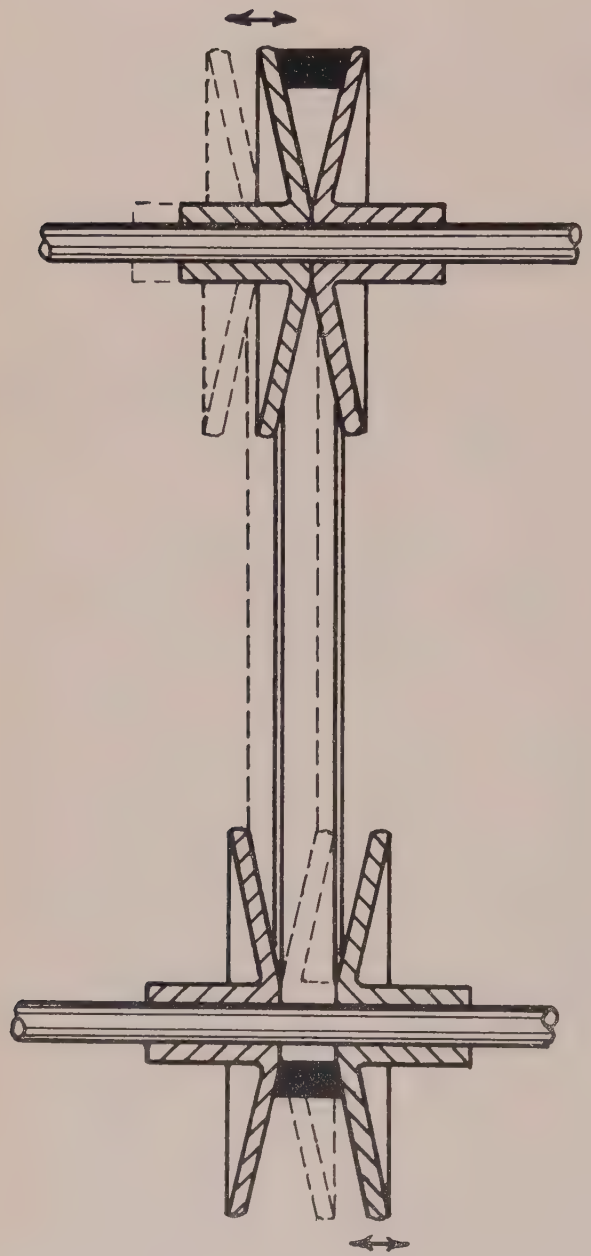

Fig. 1 – Diagram illustrating two adjustable sheaves

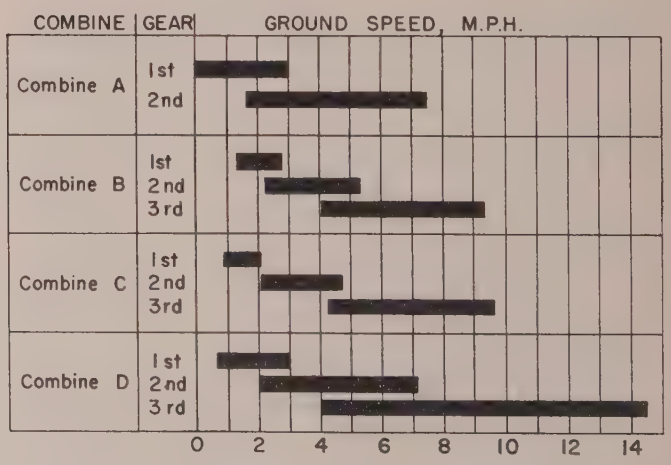

Fig. 2 – Ground speeds of various combines

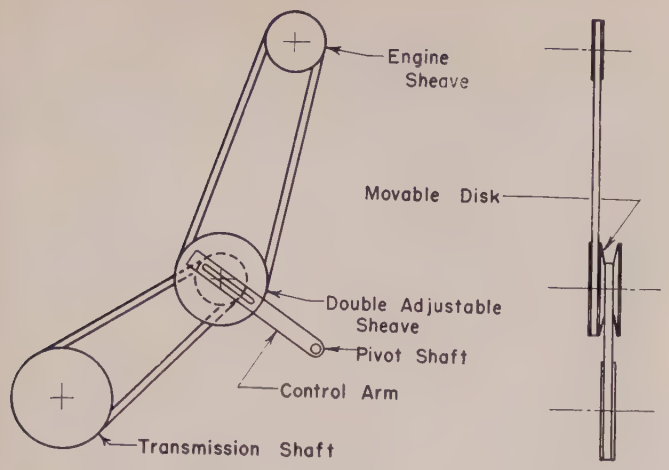

Fig. 3 – Drive using double adjustable-speed sheave with the two movable discs joined

FORMULAS relating the various factors of an adjustable-speed V-belt drive – speed variation, power transmission, and service life – are presented here for the first time. Use of these formulas eliminates previous trial-and-error methods of variable-speed-drive designing.

Following the procedures and data given in this paper, the designer can now calculate a drive knowing that a V-belt of satisfactory quality will give satisfactory service within the limits of certain design assumptions.

The Author

WILLIAM SPENCER WORLEY is assistant chief engineer of the Product Application Division of the Gates Rubber Co. He attended Western State College at Gunnison, Colorado, and the University of Colorado, where he majored in mathematics and physics. Mr. Worley joined the Gates Rubber Co. in 1942, after spending six years in sales work.

be driven from the engine through a conventional flexible power transmission such as a V-belt. This decision is often influenced primarily by the position of the engine with respect to the transmission. When the engine is near the transmission, it is logical to put the driver sheave of the adjustable-speed drive in line with the engine crankshaft. When the engine is some distance away, it is logical to drive from the engine with an ordinary V-belt drive to a countershaft on which the driver sheave of the adjustable-speed drive is mounted. This latter procedure offers some slight design advantage for the adjustable-speed drive since it makes it possible to choose the driver rpm of the adjustable-speed drive to give the best overall performance and escape any possible limitations imposed in running the driver at engine speed.

Some recognition should be made here of one adjustable-speed drive which uses two adjustable-speed belts to span a large distance from engine to transmission and at the same time make an overall reduction in rpm from the engine to transmission. This drive, shown in Fig. 3, uses a double adjustable-speed sheave with the two movable discs joined. This sheave, when the control arm is moved about the pivot shaft, forces one belt deeper into its groove and the other further out. The output speeds are the same as would be obtained by driving from the engine to a countershaft with the fixed diameter sheaves and then using a conventional adjustable-speed drive with driver and driven the same diameter as the double adjustable-speed sheave.

Having decided whether to drive directly from the engine or from a countershaft, the designer should next consider how much power the drive will be required to transmit. The power requirement, of course, will not be constant but will depend on such factors as the terrain, field conditions, the weight of the implement – which on combines or other implements carrying a harvested crop can also vary within wide limits – the ground speed of the machine, and, often, on the method of operation of the machine. Considering the variability in power requirements, we would suggest that the designer choose a number of "typical" situations – say three or four – calculate the power required in each situation, and, to the best of his ability, decide the percentage of the time for which each situation is assumed to exist. This, of course, amounts to replacing the myriad of possible "duty cycles" of the machine with one which may never be exactly met with in practice, but which, if the selection of loads and times is thoughtfully made, will be often closely approached.

In selecting the loads and times, the designer must consider extreme cases ranging from those in which the drive will have to transmit the full power of the engine, through normal operation in good conditions when the drive may handle approximately half the engine power, to the other extreme when little or no power is required.

Emphasis on a drive capable of handling continuously the full power of the engine can lead to drives considerably more expensive than necessary, not only in terms of belt and sheaves, but also in terms of clutches, transmissions, and bearings. On the other hand, ignoring the possibility of difficult conditions can lead to embarrassing comments from users and dealers when really tough weather or crop conditions lead to loads much greater than usual.

The designer would be well advised at this point to decide how much service to expect from the drive. It is probably sufficient to set a lower limit, below which he will agree that the drive will not be satisfactory and should be improved, and an upper limit above which he will feel justified in

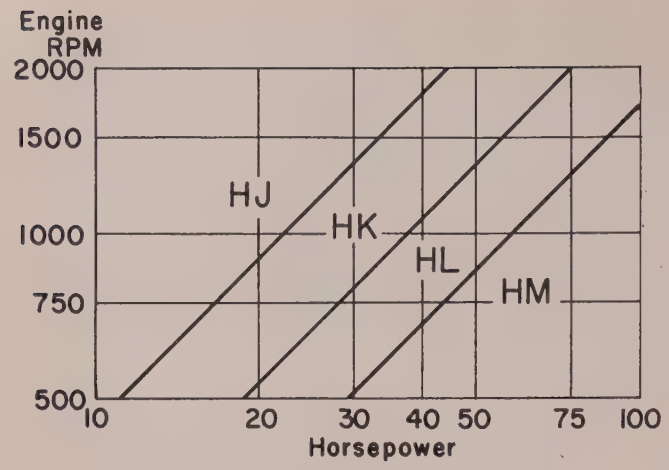

Fig. 4 – Determination of belt cross-section

Table 1 – Pitch-Diameter Change for Various Cross-Sections

Cross-Section	Maximum Pitch-Diameter Change, in.
HJ	4.25
HK	5.14
HL	6.02
HM	6.91

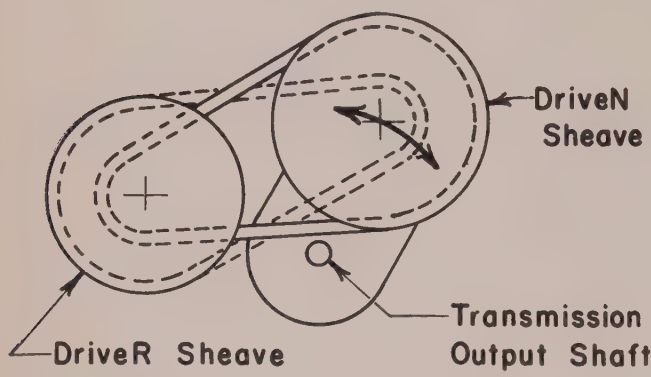

Fig. 5 – Transmission, carrying driven sheave, is pivoted around output shaft for belt take-up

Table 2 – Pitch-Diameter Change to Use When Take-Up is Made on Sheaves

Cross-Section	Pitch-Diameter Change, in.
HJ	3.6
HK	4.5
HL	5.5
HM	6.3

considering a redesign to bring down the service at a decrease in drive cost.

With the loads established, the belt cross-section which will have the best chance of handling the job can be chosen. Fig. 4 is used in making the choice. Opposite the engine rpm on the vertical scale, locate the horsepower loads corresponding to the "typical" situations selected above. If the points all fall between the same two sloping lines, then use the cross-section also indicated between those two lines. If some of the points fall in an area for one cross-section and others in an area for another cross-section, then choose the larger cross-section, provided that the horsepower loads in the larger cross-section area on the chart represent situations which will exist for 10% or more of the time.

With the cross-section established, the maximum difference between the largest and smallest pitch diameter on each sheave is also established. This is called the diameter change, and values are shown in Table 1.

With the diameter change, the designer can determine whether or not it will be possible to use adjustable-speed sheaves of the same diameter, if the driver will run at engine speed; or at what speed the driver should operate if it is mounted on a countershaft. The maximum belt speed and maximum rim speed in feet per minute are given by:

$$\text{Maximum belt speed} = \frac{\pi}{12} K \frac{V}{V-1}(s+r) \qquad (1)$$

$$\text{Maximum rim speed} = \frac{\pi}{12} K \frac{V}{V-1}(S+r) \qquad (2)$$

where:

K = Maximum pitch diameter change (Table 1)
V = Speed variation of drive = S/s
S = Maximum driven speed, rpm
s = Minimum driven speed, rpm
r = Driver speed, rpm

When the drive operates directly from the engine, then, of course, r = engine speed. If this is the case, assume $S = r\sqrt{V}$ and $s = r/\sqrt{V}$ and substitute into equations (1) and (2). If the rim speed is not too high for the sheave material to be used and if the belt speed is not much more than 5000 fpm, then a drive with equal-diameter sheaves will be satisfactory, provided there is no insoluble problem in making the reduction from the output speeds S and s to the wheels of the implement. If either the rim speed or belt speed is too high with the assumed value of S, or if it is not going to be possible to make the reduction required between the driven sheave and the ground wheels, then choose a suitable value for S or s, as the case may be, and compute the other speed from the relation $V = S/s$.

When the driver sheave will operate from a countershaft and it is required to set a suitable value for the driver rpm, r, it is convenient again to assume $S = r\sqrt{V}$, and substitute literally into equations (1) and (2). This gives:

$$\text{Maximum belt speed} = \frac{\pi}{12} K \frac{V+\sqrt{V}}{V-1} r \qquad (3)$$

$$\text{Maximum rim speed} = \frac{\pi}{12} K \frac{V}{V-1}(1+\sqrt{V})r \qquad (4)$$

Solving these equations for r, assuming 5000 fpm belt speed and an acceptable maximum rim speed,

will give two values for r, the smaller of which should be chosen. Then calculate $S = r\sqrt{V}$ and $s = r/\sqrt{V}$, and check to see if the reduction from driven sheave speed to ground wheel speed is practical. If it is, then use the calculated values of S and s; if not, then reduce S to a practical value and calculate $s = S/V$ and $r = S/\sqrt{V}$. By following this procedure, the designer has established the driver rpm and the maximum and minimum driven rpm's in such a way that the largest sheave diameters practical with the chosen cross-section will be used.

But before using the speeds just established to set the diameters of the adjustable-speed sheaves, the designer must decide upon the method he will use to make provision for taking up the belt as it stretches in length and wears down in width during operation. The most satisfactory method, and one to be preferred when it is practical, is simply to arrange for movement of one of the shafts to increase the center distance between the sheaves as necessary. In some implements this has been accomplished simply by moving the engine. In another, the necessary movement is achieved by pivoting the transmission, carrying the driven sheave, around the output shaft of the transmission as shown in Fig. 5.

If it is not possible to make a center distance adjustment to provide for take-up, then it will be necessary to provide for take-up by reserving a part of the diameter change, which would normally be available for speed variation, for take-up. Table 2 gives the diameter changes suggested for use in setting diameters when this course is necessary.

When the values from Table 2 are used, approximately 1½ in. of take-up in belt length will be made available on the sheave. It should be emphasized again, however, that this means of making take-up should be used only after it has been found completely impractical to make take-up by changing the centers.

If it has been found impossible to use sheaves of equal diameters, the designer has still another problem to solve before calculating the sheave diameters. He must allow for calculated belt-length differences at the extreme positions when the maximum diameter of one sheave is greater than that of the other. From the manner in which the maximum and minimum speeds were chosen if the sheaves are unequal in diameter, the driven sheave will be larger than the driver, as illustrated in Fig. 6.

From Fig. 6 it will be seen that the belt length L_2 around the maximum driven diameter and the minimum driven diameter, will be longer than the belt length L_1 around the other extreme diameters. A belt of length L_1 would give the correct maximum driven speed but would not be long enough to go from the minimum diameter of the driver to the maximum diameter of the driven and would, therefore, give a minimum speed somewhat larger than desired.

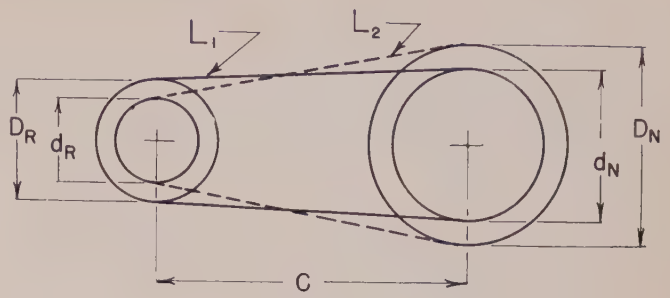

$$(L_2 - L_1) = (D_N - D_R)\frac{(D_N - d_N)}{C} = (D_N - D_R)\frac{K}{C}$$

Fig. 6 – Relationship of belt lengths and sheave diameters where diameters are unequal

If the length L_1 were calculated, one could then use the minimum diameter of the driver sheave, calculate the diameter on the driven sheave at which the belt would run, and then determine the actual low speed which would result and the per cent by which it would be higher than the required low speed. The designer could then assume a low speed the same percentage less than that actually required, substitute this new low speed into the formulas along with the original high speed and driver speed, and arrive at new diameters. The belt length L_1 calculated for these new diameters, would now give a low speed higher than the assumed low speed by the percentage calculated from the original sheave diameters and, therefore, equal to the required low speed. Fortunately, it is possible to apply this rule of false position without having to calculate the belt lengths and diameters. The assumed low speed to use is given by:

$$s_T = s\left[1 - \frac{K(r^2 - Ss)}{1.57\,Cr\,(S + r)}\right] \qquad (5)$$

where:

s_T = Minimum speed to assume for calculating diameters, rpm
s = Required minimum driven speed, rpm
r = Driver speed, rpm
S = Maximum driven speed, rpm
C = Center distance, in.
K = Pitch-diameter change (Table 1 or 2)

Substituting s_T in place of s in equations (6) through (9) give the required pitch diameters for the driver and driven sheaves. The formulas are:

Driver sheave:

Minimum pitch diameter $= Ks(S + r)/r(S - s)$ (6)

Maximum pitch diameter $= KS(s + r)/r(S - s)$ (7)

Check: (Maximum diameter) − (Minimum diameter) $= K$

Driven sheaves:

Minimum pitch diameter $= K(s + r)/(S - s)$ (8)

Maximum pitch diameter $= K(S + r)/(S - s)$ (9)

Check: (Maximum diameter) − (Minimum diameter) = K

where:

K = Pitch-diameter change (Table 1 or Table 2) in.

S = Maximum driven speed, rpm

s = Minimum required driven speed, or assumed from equation (5), rpm

r = Driver speed, rpm

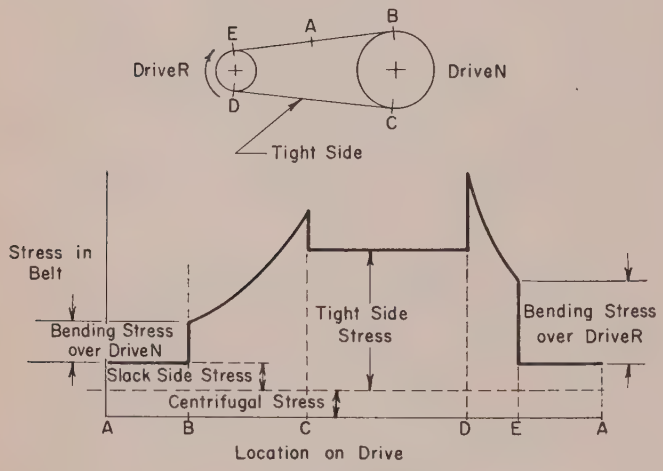

Fig. 7 – Belt stresses

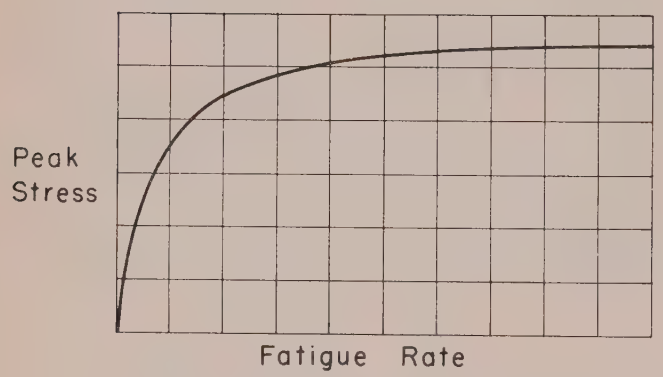

Fig. 8 – Peak stress versus fatigue rate for a typical drive

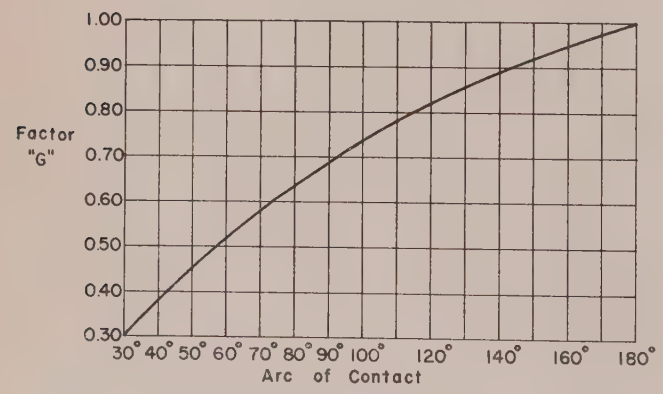

Fig. 9 – Arc correction factor G for fatigue-rate formula

The pitch length of the belt to be specified for the drive is found from this formula:

$$L = 2C + 1.57(D + d) + (D - d)^2/4C \qquad (10)$$

where:

L = Belt pitch length, in.

C = Center distance, in.

D = Maximum pitch diameter of driver sheave, in., equation (7)

d = Minimum pitch diameter of driven sheave, in., equation (8)

If take-up is to be made on the sheaves, the value of pitch-diameter change from Table 2 has been used so far. The minimum diameters for driver and driven sheaves will be used as calculated; and the belt length just calculated is the correct one; but the maximum pitch diameters should now be calculated to their true value, which will be the minimum pitch diameter as calculated with the diameter change from Table 2, plus the actual diameter change from Table 1.

Now that the diameters have been established, the designer turns to consider the service to be expected of the drive. The groundwork for this analysis was set when several "typical" load and speed situations were assumed and each was assigned a certain percentage time of operation. The process now involves analyzing the stresses in the belt in each situation and determining how much each contributes to the ultimate fatigue failure of the belt. Fig. 7 shows how the belt is subjected to stresses from three sources and how these combine to produce a stress peak at each sheave. Each part of the belt is subjected to these peaks as it travels around the drive. We have determined from extensive laboratory and field tests that the peak stress determines the rate at which the belt will fatigue.

The rate is the length, in inches, of a belt which will be completely fatigued in a unit time, which we have taken as 100 hr. Thus, if at one sheave on a drive the peak stress would correspond to a fatigue rate of 40 and at the other sheave the peak stress would correspond to a fatigue rate of 20, then the total fatigue rate for the drive is 60. This means that a 60-in. belt would be completely fatigued in 100 hr. But belt life has been found to be proportional to belt length, so that if the drive actually used a belt 120-in. long the belt life would be 120 in./(60 in./100 hr) or 200 hr. In this sense, we can think of the fatigue rate as the length of belt which will be fatigued each 100 hr, and we can find the life of the belt, in hundreds of hours, by dividing the belt length by the total fatigue rate for the drive. Fig. 8 illustrates the fatigue rate versus peak stress curve for a typical drive.

For adjustable-speed belts, the fatigue-rate equation may be written:

$$\text{Log (fatigue rate)} = 11.111 \log [(HP/SG) + (C_b/d) + C_c S^2] + \log S - C_s \qquad (11)$$

where:

HP = Horsepower load

G = Arc correction factor, Fig. 9

S = Belt speed in thousands of feet per min = $0.262\ dr/1000$

d = Pitch diameter at sheave under consideration

r = Rpm of same sheave

C_b, C_c, C_s = Constants depending on cross-section and are given in Table 3.

For each of the several operating situations, equation (11) is evaluated at each sheave, and the total fatigue rate is found. The total fatigue rate for a lightly loaded situation will be small compared to that for a highly loaded situation, and it is next necessary to take into consideration the per cent of the time at which the drive will operate in each situation. To do so, multiply the total fatigue rate for each operating situation by the per cent of the time at that situation, add up the results, and divide by 100. This gives a total fatigue rate which makes the required adjustment of the fatigue rates for the various times of operation.

The calculated average belt life, in hundreds of hours, is found by dividing the belt length by the total fatigue rate just calculated.

The significance to be given the calculated belt life depends primarily on the accuracy of the load-time cycle in reflecting the actual operation of the implement. A calculated average belt life too low to meet the designer's expectations does not necessarily mean that the drive will be a failure, although, if the working assumptions were carefully made, it will probably be a source of trouble. Neither does it follow that a drive with a high calculated average belt life will be completely trouble-free, although if the assumptions are good, complaints will probably be rare. The designer can only be guided by the calculations and not governed by them.

If it happens that the drive would give hopelessly poor service, then the first thing to check is the choice of cross-section. Review the products of fatigue rate and per cent of time for each operating situation, pick out the one or two highest, and recheck Fig. 4 to be sure that the cross-section used is that recommended for the critical situations. If not, then redesign the drive with cross-section recommended for critical situation.

If the recommended cross-section is used and the drive is still unsatisfactory, then review the diameter calculations in some detail. If rim speed was a limiting factor and the driver operates directly from the engine, consider using higher-strength materials, so that the output speeds can be set to provide sheaves of equal diameter; or putting the driver on a countershaft driven at the correct speed to give equal-diameter sheaves. This last suggestion might also be considered if belt speed was a limiting factor.

If take-up was to have been made on the sheaves, review once more to see if there is some way to get take-up by moving the shafts. This will result in larger diameters.

Table 3 – Constants Used in Fatigue Rate Formula

Cross-Section	C_b	C_c	C_s
HJ	86.31	0.0671	13.3290
HK	151.6	0.0926	14.8862
HL	244.1	0.1217	16.2028
HM	368.8	0.1542	17.3434

Table 4 – Sheave Dimensions and Belt Lengths[a]

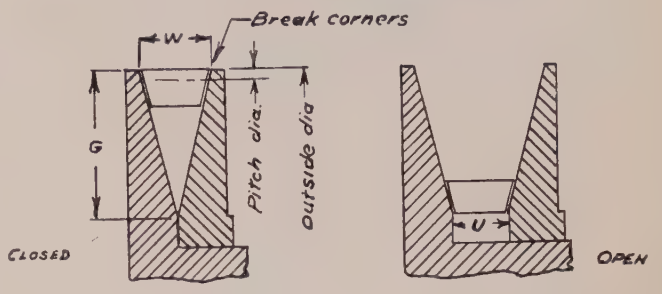

Belt Cross-Section	W ± 0.005 in.	G Maximum Groove Depth, in.	U Maximum Axial Movement, in.	PD to OD, in.	Belt Pitch Length to Effective Length, in.
HJ	1.250	2.71	0.98	0.37	1.16
HK	1.500	3.25	1.18	0.45	1.41
HL	1.750	3.79	1.39	0.52	1.63
HM	2.000	4.33	1.60	0.60	1.88

[a] These data are taken from the ASAE Standard on V-Belt Drives for Farm Machines, adopted in June, 1950.

Table 5 – Belt-Length Allowance for Stretch and Wear

Effective Belt Length, in.	Allowance, in.
25 to 60	$1^{15}/_{16}$
60.1 to 80	$2^{3}/_{8}$
80.1 to 100	3
100.1 to 114	$3^{1}/_{4}$
114.1 to 122	$3^{3}/_{8}$
122.1 to 130	$3^{3}/_{8}$
130.1 to 138	$3^{15}/_{16}$

Finally, if none of the above is possible, consider decreasing the speed variation of the drive. This will give sheaves with larger minimum diameters, but it will also result in less overlap in ground speeds and may necessitate a transmission with an additional gear reduction.

Assuming that sheaves and belt cross-section can be finally determined to give satisfactory life, the designer should next clear up a few details about the sheaves and belt before turning to consider the question of making the drive function as he intends it to. The diameters established thus far are maximum and minimum pitch diameters. The outside diameters of the sheaves can be calculated by adding the value in Table 4 to the maximum pitch diameter of each sheave. Table 4 also gives information on groove top width in the closed position, groove depth, and axial movement of the movable disc.

The belt length established above was the pitch length. Table 4 also gives the amount to be added to the pitch length to get the effective length.

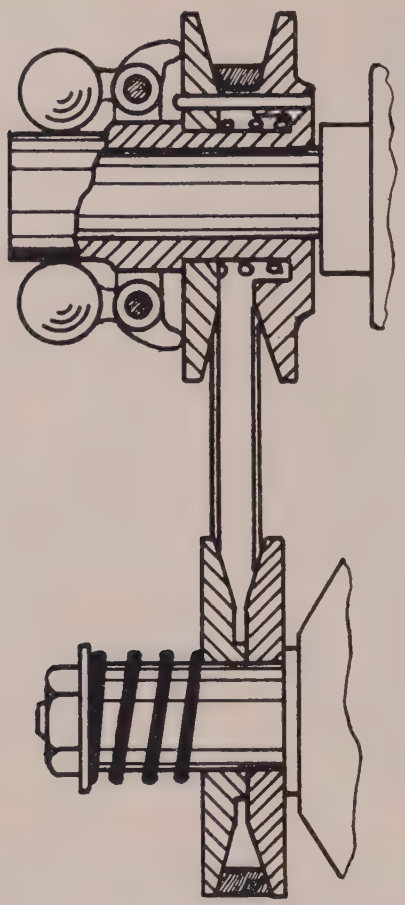

Fig. 10 – Drive with centrifugally loaded arrangement used to locate position of belt in driver sheave. Drive tension is maintained by spring on driven sheave

Table 5 gives the ASAE Standard allowance in belt length to make for belt stretch and wear. This allowance includes the plus manufacturing tolerance as well as an allowance for the stretch and wear of the belt resulting from service on the drive.

No allowance for installing the belt is necessary, because it is possible to open up both sheaves, put the belt on, and then close one sheave up to tension the belt. This, of course, may require disconnecting part of the sheave linkage.

In considering the functioning of the drive the designer has two problems. First, he must provide means by which the output speed of the drive may be set at a desired point; second, he must provide for the discs of the two sheaves to move in such a way that proper belt tension is maintained. On machines with an engine which furnishes power not only to propel the machine but also to perform some other function as well, it is usually desirable to set the engine speed to that of the other function and control the ground speed at constant engine speed. Indeed, it was the requirement for small increments in ground speed at fixed engine speed which led to the first V-belted self-propelled combines.

But there are machines, such as tractors, which might be V-belted and which might have an engine primarily for propulsion. In such a case, it is often desirable to control the ground speed by throttling the engine. Many designs have been worked out for drives in which the position of the belt in the driver sheave is determined by a centrifugally loaded arrangement such that the higher the rpm of the engine, the further out the belt will tend to ride. Fig. 10 shows one such arrangement schematically. Note that the driven sheave is urged to a normally closed position by the spring, which serves to maintain drive tension. Such drives are widely used on motor scooters but could conceivably have even wider application on light tractors.

Assume the drive illustrated in Fig. 10 to be operating at a given throttle setting and engine rpm. If the torque requirement at the ground wheels is increased for some reason, the belt will pull down into the driver sheave and ride further out in the driven, until the torque output of the engine is multiplied sufficiently to handle the increased demand. In doing this, of course, the machine slows down. If the operator wants to maintain ground speed, he does so by increasing the engine speed as the speed ratio of the adjustable-speed drive is changing.

On a machine such as a combine, where it is desired to control the ground speed at fixed engine speed, it is necessary to provide some means of fixing the belt diameter in one sheave. This may be done through a mechanical linkage, which is still common; through a hydraulic positioning cylinder, which is being used to greater extent as hydraulic cylinders take over other such lifting and pushing jobs as positioning the header on a combine; or through an electric motor driving a positioning device, which to our knowledge has not yet been done on production machines. It has been found desirable to fix the diameter of the driver sheave in preference to the driven sheave, since under heavy overloads the belt will pull down into the sheave which is not positively located. If it can pull into the driver, then speed drops off just at a point where maintaining speed is important. If, on the other hand, the belt can pull into the driven, then the speed tends to increase.

With the position of one sheave positively controlled, it is next necessary to provide means so that the belt will be properly positioned on the other sheave to maintain belt tension. We have seen, for example, that if the sheaves are unequal in diameter, a belt which fits the maximum driver diameter and the minimum driven diameter will not fit the other extreme diameters. This means that as the disc on the driver sheave moves its full distance out, the disc on the driven sheave cannot

move its full distance in.

One method of taking care of this problem is a variation of that shown in Fig. 10. The centrifugally loaded sheave is replaced by one which is positively adjusted by mechanical or hydraulic means. The spring then forces the belt to ride at a diameter which is consistent with the diameter of the positively adjusted sheave and the spring force available to tension the belt. This is a widely used method. It is compact, mechanically simple, and comparatively foolproof. It has, however, a few characteristics which are less than ideal. Since the spring changes in length by the amount of axial movement of the disc (from 1 to 1⅝ in., depending on the cross-section) the spring force will not be constant. When the spring is on the driven sheave, as it usually is, the change in spring force results in higher spring force and belt tension at the high-speed position than at the low-speed position. This is just the reverse of the characteristics which would be desired for constant power transmission. For this reason, the springs used must be relatively long, with as low a spring

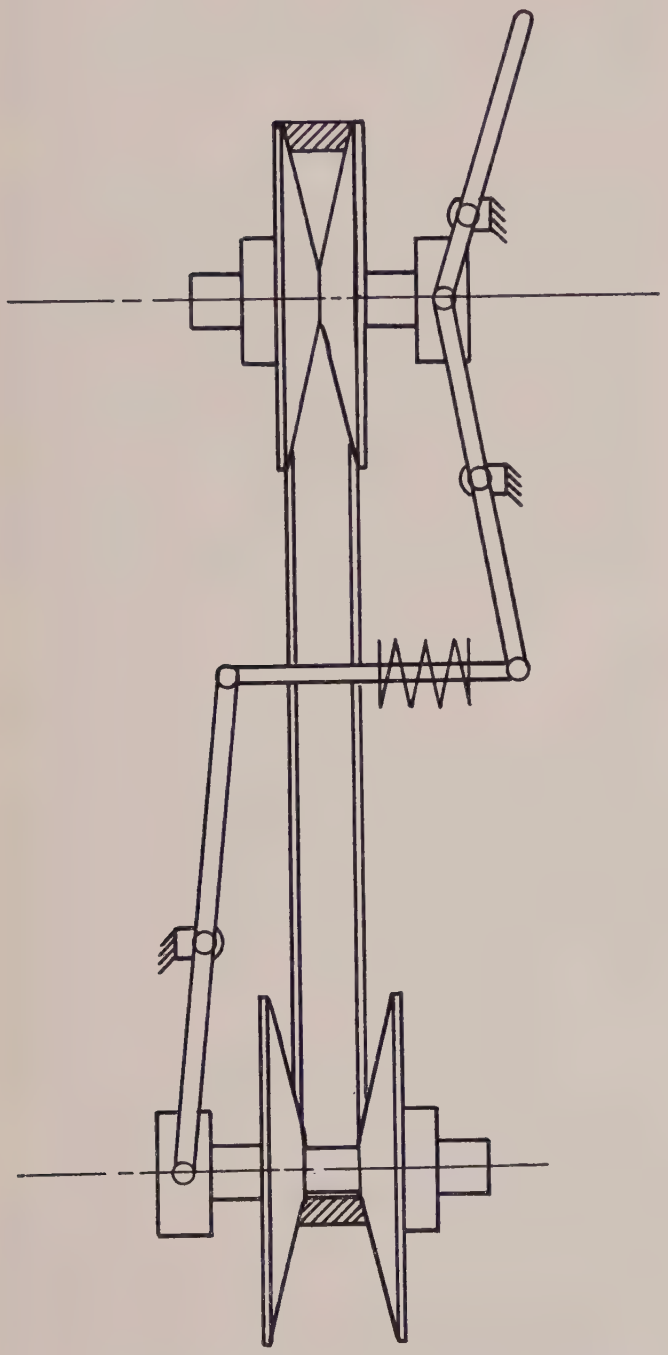

Fig. 11 – An almost solid sheave linkage arrangement where spring compensates only for small difference in lateral movement of the discs

Table 6 – Constant Used in Thrust Formula

	Tension Ratio	Y
Driven Sheave	5	56.37
	9	47.65
Driver Sheave	5	66.02
	9	48.36

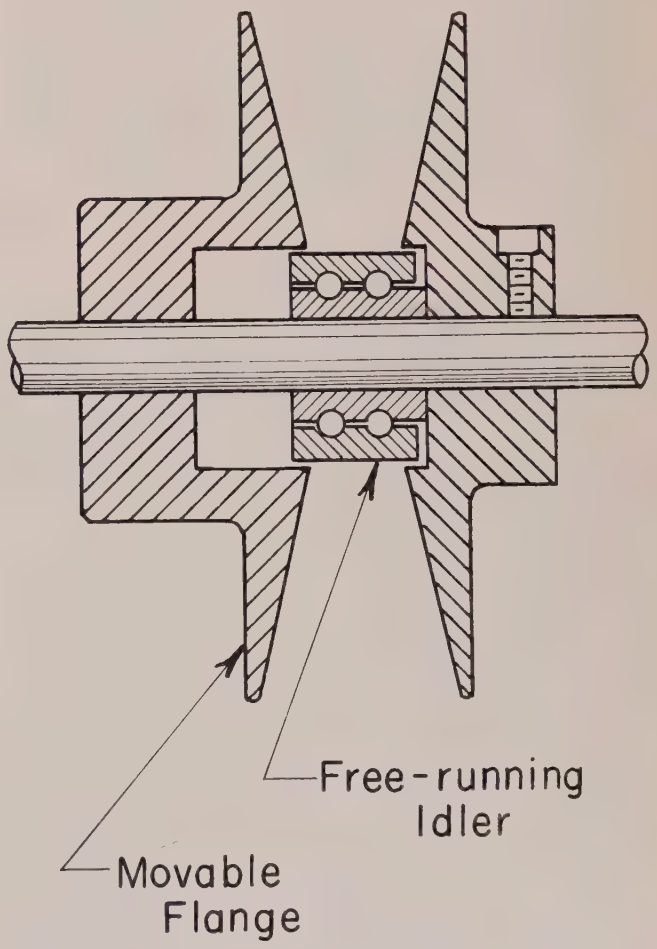

Fig. 12 – Clutch arrangement for adjustable-speed V-belt drives

constant as possible. The spring is chosen so that at low-speed position the tension is sufficient, while at high speed it is not abnormally high.

Fig. 11 is a diagrammatic illustration of another linkage which has also been widely used. This arrangement, although somewhat more complicated and sensitive to adjustment, does have some advantage over the spring arrangement described above. The linkage is almost a solid one. There is, however, a spring interposed at some convenient point. This spring must compensate only for the difference in lateral movement of the discs, which is not very great. This makes it possible to use a short, stiff spring to good advantage. As a matter of fact one design uses the elasticity of the linkage itself with good success.

The simple arrangement shown can, at best, maintain only constant tension at high- and low-speed positions, but other arrangements have been worked out to provide a tension-belt position relation which is more nearly adapted to a constant power requirement. With the sort of linkage drawn in Fig. 11, some provision is necessary to take care of small differences in belt length which occur in manufacturing. A turnbuckle or some similar device does this. It also permits some adjustment of tension and becomes somewhat vulnerable to the tinkering of an unthinking operator.

Regardless of the linkage, the designer will need to know how much thrust will be required of the spring or linkage to maintain sufficient tension. This can be calculated from the following formula, which is based on a 26-deg groove angle:

$$F_s = Y(\mathrm{HP}/S) \qquad (12)$$

where:

F_s = Axial thrust required on movable disc, lb
HP = Horsepower load
S = Belt speed, thousands of ft per min
Y = Constant from Table 6

These constants are given for various tension ratios because the drive will not transmit constant horsepower. The designer does not want to put too strong a spring on the drive for the normal conditions of operation, yet he requires some assurance that there will be sufficient spring force for the operation of the unit at extreme overloads. We recommend calculating the spring pressure required for the normal load the drive will transmit on the basis of a tension ratio of 5. Then check the spring pressure required for the peak loads on the basis of a tension ratio of 9. Calculations should be made at both high- and low-speed conditions, bearing in mind that the maximum torque output of the drive will probably be made from the low-speed position. This will give a range of calculated spring forces which will allow the selection of both the spring rate and the minimum spring force. Since the design of the spring loading arrangement generally fixes the loaded length and not the force, it will be necessary to add an additional 10% to the minimum spring force to compensate for this much variation in the load-deflection characteristics of commercially available springs.

The adjustable-speed V-belt drive lends itself nicely to a simple method for clutching. This method is simply to incorporate a free-running idler, just slightly smaller in diameter than the diameter at the bottom of the groove, into the hub of the movable disc of the driver sheave, as illustrated in Fig. 12. After the sheave disc has been moved into the low-speed position, further axial movement of the disc allows the belt to ride on the idler and disconnects the belt from driving engagement with the sheave. This method of clutching has been successfully used on several production combines.

Although we have so far been concerned primarily with propulsion drives, the data given herewith are equally applicable to any problem requiring an adjustable-speed drive. The procedure for establishing the driven speeds would, of course, be modified to suit the problem; but once the speeds were established, the method for determining the cross-section to use, the diameters of the sheaves, the service to be expected, and the spring force necessary can be applied without modification.

The adjustable-speed V-belt drive has shown itself to be a useful, dependable means for propelling harvesting machines such as combines and corn pickers. We do not feel that this exhausts the field for such drives.

It is our hope that the data we have here presented will serve to stimulate interest in adjustable-speed V-belt propulsion drives for other types of machines and for other applications in which the stepless speed variation of an adjustable-speed drive will offer operational advantages. By using the procedures and data presented herein, the designer can, without need for extensive tests and development, establish an adjustable-speed V-belt drive which will be as compact as possible, give the speed variation required, and perform in a manner and for a length of time satisfactory to his severest critic – his customer.

DISCUSSION

Experimental Data Disagree With Theoretical Results

– Normand E. Morgan
McCulloch Motors Corp.

ALTHOUGH the variable-speed V-belt drive has been successfully applied to various industrial uses and to vehicles of the motor-scooter type as well as to agricultural equipment, its most promising future application may well be in the field of automotive accessory drives. Such a drive is already being manufactured as an integral part of the McCulloch automotive supercharger. The advantages of

driving other engine accessories such as the cooling fan, power-steering pump, and air-conditioning compressor from a similar drive should not be overlooked by the industry.

During the development of our supercharger, a research program on variable-speed V-belt drives was undertaken from which information of considerable interest was obtained. Extensive testing has shown that a serious disagreement exists between experimental data and theoretical considerations such as the Gates Equation [equation (12) of Mr. Worley's paper]. Experimentally it has been found that under some conditions the magnitude of the axial force, which must be applied to the sliding disc of the driver pulley, may be over twice that predicted by theory.

In Fig. A are presented test results of minimum axial force requirement for both the driver pulley and the driven pulley along with curves of predicted axial forces as computed from the Gates Equation and the hoop-tension equation for the same drive. The hoop-tension equation is:

$$F = \frac{(T_1 + T_2)\,\theta}{4 \tan \alpha}$$

where $T_1 + T_2$ is the total tension, θ is the arc of contact in radians, and α is one-half the included groove angle. Although its derivation neglects frictional forces between the belt and the pulley face, the hoop-tension equation appears to be a better approximation to the driver pulley thrust requirement than does the Gates Equation. On the other hand the Gates Equation appears to be quite valid for determining the driven pulley thrust requirement. The computed curves of Fig. A are based on a 30-deg groove angle, 0.4 coefficient of friction (Gates Equation only), 180-deg arc of contact, and a tension ratio of 9. The experimental curves represent data obtained in the laboratory under ideal conditions. In practice, of course, the coefficient of friction, and therefore the axial thrust, may vary considerably with belt and pulley surface conditions.

Although the pulley diameters and belt cross-section used for the test results in Fig. A were somewhat smaller than those which are normally encountered in farm-machinery drives, comparable results have also been obtained on a drive using larger components. In both cases wide ranges of belt speed and effective tension were investigated.

It is of interest to the designer of a variable-speed V-belt drive to know what axial forces must be applied to the sliding pulley discs to produce a change in the speed ratio. In Fig. B is shown a family of curves for conditions of balance at which a small change in the axial thrust on either pulley or a change in the belt tension will result in a speed-ratio change. These curves are from test results on the drive used for the data of Fig. A. It will be noted that the driven pulley thrust required to produce an incremental change in speed ratio decreases as the effective tension increases for constant driver pulley thrust. This fact may appear to be a contradiction of the results expected from theoretical considerations. However, it should be realized that an increase in effective tension under these conditions is accompanied by an increase in tension ratio which apparently has a predominant effect on the axial thrust requirement for balance. In the Gates Equation the effect of tension ratio and other variables is hidden in the factor Y.

It is hoped that this discussion has proved useful to designers of variable-speed V-belt drives and to others interested in the subject. Perhaps it will help stimulate interest in applying this type of drive to new fields where there is need of obtaining a smoothly variable speed ratio with a relatively inexpensive mechanism.

Author's Closure To Discussion

MR. Morgan has presented some very interesting information on the problem of axial thrust required on the sliding discs of a variable-pitch sheave. As he points out, there are many applications for variable-speed V-belt drives out-

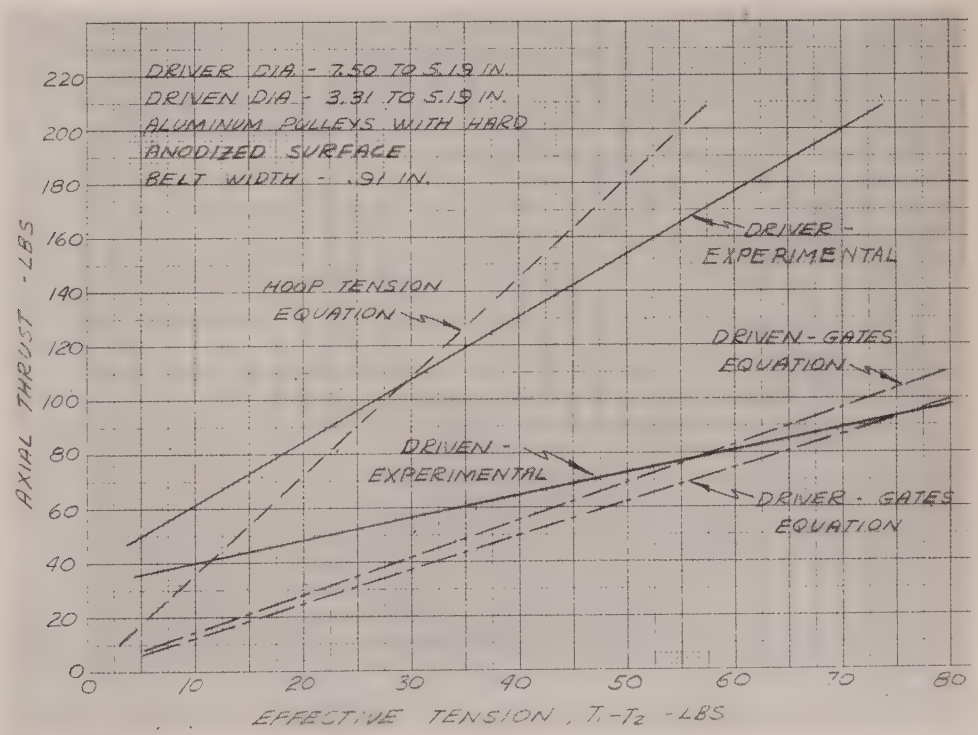

Fig. A – Minimum axial thrust requirement for a variable-speed V-belt drive

side the field of farm implements. The principles presented in the foregoing paper will, of course, apply to the design of any variable-speed drive.

Mr. Morgan refers to equation (12) of the main paper. I will also be concerned with that equation. To make both of these discussions clearer to the reader, it will be helpful to give the equations from which the simplified equation (12) and the values in Table 6 were calculated:

These equations are:

$$\text{DriveN:}\quad F_s = \frac{T_1 - T_2}{2k}\ \frac{1 - \mu_R \tan\alpha}{\mu_R + \tan\alpha}$$

$$\text{DriveR:}\quad F_s = \frac{T_1 - T_2}{2k \tan 2\alpha}$$

Definitions:

$$k = [\ln (T_1/T_2)]/\theta$$

$$\mu = \sqrt{\mu_R^2 + \mu_T^2}$$

$$\mu_T = k (\sin\alpha + \mu_R \cos\alpha)$$

where:

T_1 = Tight side tension, lb
T_2 = Slack side tension, lb
θ = Arc of contact, radians
μ = Coefficient of friction
μ_T = Tangential component of friction
μ_R = Radial component of friction
α = ½ groove angle

Substituting $(T_1 - T_2) = 33$ HP/S, $\alpha = 13$ deg, assuming $\mu = 0.4$, and $k = 0.51$ for a tension ratio of 5 at 180 deg or 0.70 for a tension ratio of 9, reduces the above formulas to those presented in equation (12), with constants as given in Table 6.

Mr. Morgan's Fig. A shows the results of data first presented in his thesis, "Investigation of Variable-Speed-Ratio V-Belt Drives" (University of California, Los Angeles). A review of Mr. Morgan's thesis, and the data presented therein, indeed verifies that the data were obtained under ideal conditions. However, these conditions were not completely specified. With his equipment Mr. Morgan accurately measured $T_1 - T_2$ and axial thrust, but he did not measure $T_1 + T_2$. Instead, he began with axial force well in excess of the minimum, and reduced the force until a condition of "instability" was reached.

Mr. Morgan reports: "This instability was characterized by the slack side of the belt oscillating at a low frequency (about three or four cycles per second), and by a considerable decrease of the angle of contact on a driveN pulley." Mr. Morgan concludes that the vibration of the slack side of the drive indicates a critical tension ratio, and has drawn the curve labeled "Gates Equation" in his Fig. A on the assumption of constant tension ratio.

The frequency with which a running belt vibrates is a function of its mass per unit length, the belt speed, the span length, and the tension in the belt. The criterion of constant frequency of vibration suggests that Mr. Morgan's data actually represent a series of tests run at essentially constant slack side tension and variable effective tension.

In addition to the difference between the tension conditions assumed by Mr. Morgan in constructing Fig. A, and indicated by his criteria of instability, it is felt that Mr. Morgan's data should have been interpreted in terms of a coefficient of friction of 0.5, which has been consistently found in our laboratory testing rather than the more conservative value of 0.4, which was assumed in preparing equation (12) for the use of the designer. Analyzing the driveN experimental curve presented by Mr. Morgan in Fig. A, with the above given formula for a driveN sheave and a coefficient of friction of 0.5, is somewhat difficult, since no data are available as to the exact frequency of vibration of the slack strand of the drive. However, Mr.

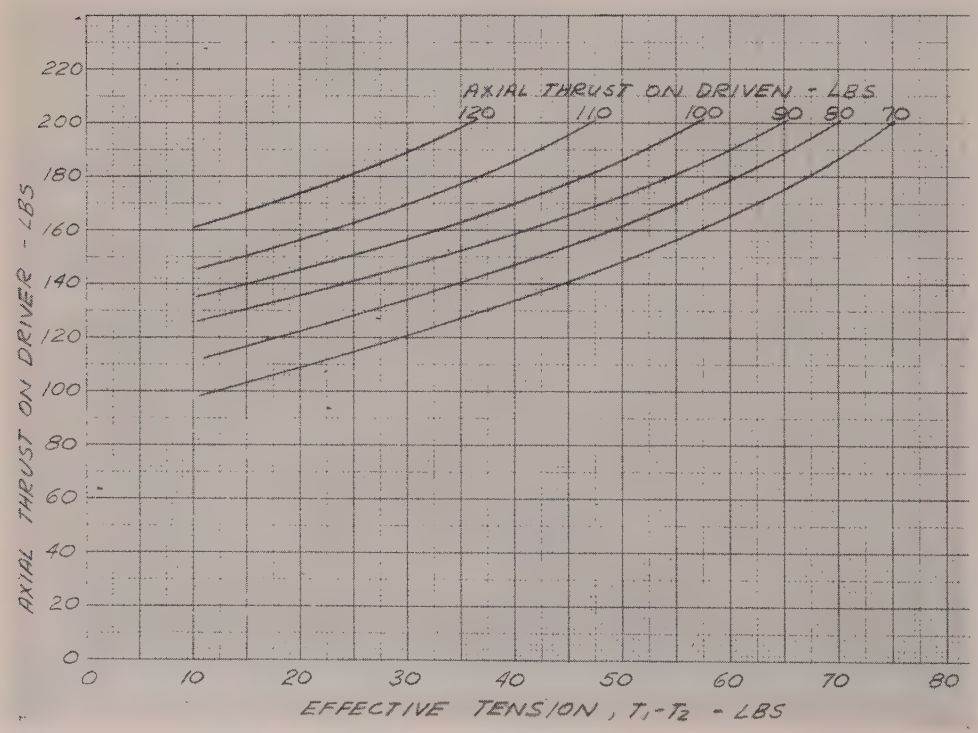

Fig. B – Axial thrust versus effective tension for balance conditions

Morgan's driveN experimental curve can be extrapolated to $(T_1 - T_2) = 0$, at which point $\mu_T = 0$, $\mu_E = 0.5$, and $\frac{T_1 - T_2}{k\theta}$ approaches the limit T_2, which can be assumed to be the constant slack side tension maintained throughout his experiments.

With this as a starting point, T_2 was computed to be 18.9 lb from the extrapolated axial thrust of 32 lb. With this calculated value of T_2, and various values of $(T_1 - T_2)$, the above formula was used to calculate axial thrust required for various values of $(T_1 - T_2)$. The results are given in Table A.

This is a satisfactory agreement, and disposes of the driveN case except for the validity of using Mr. Morgan's axial thrust intercept as a base for calculating T_2.

Mr. Morgan's data were taken at belt speeds ranging from under 1000 to over 7000 fpm. As mentioned above, the belt speed affects the frequency of vibration of a belt span. Table B shows the calculated slack side tension as a function of frequency and belt speed, for the belt used by Mr. Morgan in his experiments.

The value of 18.9 lb calculated for T_2 seems to be reasonable in view of the tensions reported in Table B.

In regard to the data for the driveR sheave, the comments concerning the tension situation which existed in all of Mr. Morgan's experiments still hold. However, Mr. Morgan's discussion does give an opportunity to report some work which was in progress at the time this paper was presented and which has since been completed. This experimental work showed that the stress pattern on a driveN sheave was that which had been assumed in developing the axial thrust formula for a driveN sheave. It further showed that the stress pattern on a driveR sheave, as shown in Fig. 7 of the main paper, is modified at moderate tension ratios such as those used in designing. Incorporating this experimentally determined fact into the force analysis results in the following equation for a driveR sheave:

$$F_s = \frac{T_1\theta}{2} \quad \frac{1 - \mu \tan \alpha}{\mu + \tan \alpha}$$

This formula can be reduced to the following form for design practice, with the assumption, as before, that $\alpha = 13$ deg, $\mu = 0.4$, $T_1 = 33$ HP/S $(1 - e^{-k\theta})$, $k = 0.51$ for a tension ratio of 5 at 180 deg, or 0.70 for a tension ratio of 9:

$$F_s = Y \text{ HP}/S$$

where Y depends on tension ratio and arc of contact according to Table C, which should be substituted for the driveR sheave section of Table 6 in the main paper.

Two sets of Mr. Morgan's data were analyzed using this newly developed equation (with μ taken as 0.5, $\alpha = 15$ deg). One set of data is given in Fig. 12 of Mr. Morgan's thesis, and furnished the driveR experimental line of his present discussion. The other set, taken under conditions of less speed and arc of contact variation, and showing less scattering, is given in Fig. 14 of his thesis. Table D gives the results.

The limits shown above are 0.95 "confidence limits" as derived from a least-square regression on Mr. Morgan's original data. In view of these limits, it is felt that the new formula for the driveR axial thrust is adequate. More detailed analysis of Mr. Morgan's data of Fig. 12 might show considerably better agreement with the new formula. Unfortunately, the need to infer a value of T_2 from the somewhat uncertain frequency of slack side belt vibration makes a more detailed analysis of questionable value. As Mr. Morgan, in his thesis, concludes: "The data obtained did not include the values of total belt tension $(T_1 + T_2)$ . . . any future experimental investigation of variable-speed-ratio V-belt drives should provide means of measuring the total belt tension."

Mr. Morgan's data on axial thrust required at driveR and driveN for balance throw some interesting light on the problem of the force required to shift an adjustable-speed belt drive. While the conditions under which these data were obtained prevent their being used quantitatively, the following qualitative conclusions seem justified, and should be of some value to the designer in evaluating the probable forces required to shift the drive:

If the driveN sheave is spring loaded, the force required at the driveR to shift the drive will be a minimum when there is no power load being transmitted. This minimum force will be somewhat greater than the spring force at the driveN sheave. If power is being transmitted during shifting, more force will be required at the driveR. When maximum power is being transmitted, the force at the driveR may be on the order of three times the spring force at the driveN sheave.

If the driveR sheave is spring loaded, the force required at the driveN to shift the drive will be a maximum when there is no power load being transmitted. This maximum force will never exceed the spring force at the driveR sheave.

Mr. Morgan's interest in this matter, and his cooperation in supplying a copy of his thesis, with details on 235 experimental observations in connection with this rather complex problem, is greatly appreciated. While we have not fully agreed with his interpretation of the data which he collected, we have been impressed with the care, thought, and execution of his testing.

Dietrich Stechert and Floyd Oslund of the Gates Rubber Co. contributed greatly to the review and analysis of Mr. Morgan's data. Their help is gratefully acknowledged.

Table A – Comparison of Calculated DriveN Axial Thrust (On Basis of Constant T_2 = 18.9 lb and Gates Formula) with Experimental Values

	Axial Thrust	
$T_1 - T_2$	Calculated	Measured
10	40.4	40
30	58.0	56
50	76.2	73
70	94.0	90

Table B – Belt Tension as Function of Frequency and Belt Speeds

	Belt Speed, S		
Frequency, cps	1	2	4
2	7.8	14.5	27.7
3	12.7	22.6	42.5
4	18.1	31.4	57.9

Table C – Values of Y for DriveR Sheave (Revision for Table 6)

	Tension Ratio (At 180-Deg Arc of Contact)	
Arc of Contact, deg	5	9
180	93.23	83.91
170	90.16	80.55
160	87.13	77.25
150	84.16	74.01
140	81.24	70.83
130	78.38	67.72
120	75.56	64.67

Table D – Comparison of Calculated DriveR Axial Thrust (Data from Mr. Morgan's Thesis, Figs. 12 and 14) with Experimental Values

	Data of Mr. Morgan's Fig. 12 (T_2 Assumed 21.5, Constant)		Data of Mr. Morgan's Fig. 14 (T_2 Assumed 37.5, Constant)	
$T_1 - T_2$	Calculated	Measured	Calculated	Measured
10	58.8	62 ± 27	89	90 ± 18
30	96.1	108 ± 27	126	126 ± 16
50	133	153 ± 27	163	175 ± 18
70	171	200 ± 27	201	215 ± 22

Improvement Of Trucks

RESULTS of tests conducted on more than 5400 vehicles show that since 1942 there has been considerable improvement in the brake performance of all types of motor vehicles using our highways. A gap existing between the levels of performance of commercial vehicles and passenger cars has been reduced. However, through adequate brake maintenance, the performance of commercial vehicles still can be improved appreciably, and the gap between the performance of trucks and passenger cars can be narrowed still further.

This paper shows the magnitude of past improvement, the current levels of brake performance, and how the brake performance of commercial vehicles can be further improved through maintenance.

IN 1942 the Bureau of Public Roads conducted an extensive study of the brake performance of commercial vehicles and passenger cars selected at random from the everyday traffic. Vehicles of all types were stopped on the highway by a uniformed policeman, weighed and described, and then subjected to at least three emergency stops from a speed of 20 mph. These tests were conducted at eleven locations scattered over the entire country and included nearly 1000 passenger cars and over 3200 commercial vehicles of all types. Late in the fall of 1948 and in 1949 these tests were repeated in Maryland, California, and Michigan. This latter study included tests of 311 passenger cars, 413 single-unit trucks, 401 truck tractors with semitrailers, 54 trucks with full trailers, and 60 truck tractors with semitrailers and full trailers. The studies of vehicles selected at random reveal the levels of brake performance of various types of vehicles as they were found in use on the highway.

In order to determine the improvement in brake performance of commercial vehicles which could be gained through maintenance procedures, a series of controlled tests were run during 1949 and 1950. For these tests a total of 64 trucks of various types were supplied by truck operators from coast to coast. Each vehicle was tested first without any changes being made in the braking system. Thence, any improvements possible through various maintenance procedures were made, and the tests were repeated. The results of these tests emphasize the importance of good brake maintenance.

Improvement Since 1942 (1942 versus 1949)

Since 1942 there has been considerable improvement in the brake performance of the motor vehicles using our highways. This can be attributed to excellent work of both vehicle operators and manufacturers of vehicles and brake equipment. This improvement is clearly illustrated by comparing cumulative frequency distribution curves for the 1949 test results with similar curves plotted from data obtained by the tests conducted in 1942. Figs. 1 through 4 show the comparisons for various types of commercial vehicles. The curves plotted on these figures indicate the percentage of the vehicles that can stop in a given distance or less from a speed of 20 mph. In each figure there are three curves, one for the results of the tests conducted in 1942 at the eleven widely separated locations; another for the tests made in 1942 in just Maryland, Illinois, and California; and a third for the results obtained by tests in 1949 in Maryland, Michigan, and California. A comparison of the two sets of results for 1942 in each example indicates that the smaller sample of tests conducted in 1949 should produce results which represent the general level of brake performance for the entire country.

Fig. 1 shows the cumulative frequency distribution of vehicle stopping distances for 2-axle trucks. Vehicle stopping distance is the distance traveled between the point at which the driver starts to move the braking controls and the point at which the vehicle comes to rest. The curves show that 57% of the 2-axle trucks tested in 1949; 25% tested in Maryland, Illinois, and California in 1942; and 21% tested at all eleven locations in

in Stopping Ability in Use on the Highway

F. William Petring,
Highway Transport Research Branch, U. S. Bureau of Public Roads

This paper was presented at the SAE Summer Meeting, Atlantic City, June 7, 1954.

1942 could stop within 30 ft or less. These curves show, also, the improvement in brake performance in terms of feet. For instance, the best 50% of the 2-axle trucks tested in 1949 could stop within 28 ft or less; while the best 50% tested in Maryland, California, and Michigan in 1942 required up to 38 ft; and the best 50% tested at all locations in 1942 required up to 40 ft to stop from 20 mph. If we wish to investigate the brake performance of these vehicles at the 80- or 90-percentile level, the curves reveal that the magnitude of improvement since 1942 is even greater. Figs. 2, 3, and 4 present similar information for various types of combination vehicles.

Table 1, based on the 50-percentile values of vehicle stopping distance, compares the improvement in performance of passenger cars and several types of commercial vehicles. The percentage of improvement was greater for each type of commercial vehicle than for the passenger cars, with the greatest improvement in the 2-axle truck tractors with 2-axle semitrailers. Other combination units, of which 92% had more than four axles, were the poorest performers and showed the least improvement percentagewise of all the types of commercial vehicles tested.

In comparing the performances of vehicles tested in 1942 and 1949, the validity of the amount of improvement shown for commercial vehicles by the comparisons of cumulative frequency distributions of vehicle stopping distances would be questionable without some consideration of the weight and capacity of the vehicles in each sample. In other words, if the weights of the 2-axle trucks were lighter in 1949 than in 1942 the improvement might be attributed to weight rather than to the braking system. From the tabulation of average gross weights for the various types of vehicles in Table 2, the average weight was generally higher in 1949 than in 1942. However, the reverse is true for the 2- and 3-axle trucks, the 3-axle trucks with 2-axle trailers, and the 3-axle trucks with 3-axle trailers.

In order to show what improvement was made in vehicles of the same capacity and approximate weight, three examples have been prepared. The first example, Fig. 5, compares the average performance observed in 1942 and 1949 for light 2-axle trucks. These vehicles were first classified

The Author

F. WILLIAM PETRING (M '55) is with the Highway Transport Research Branch of the Bureau of Public Roads, conducting motor vehicle performance studies. He received a B.S. in General Engineering from Iowa State College in 1942. Mr. Petring was employed by the National Advisory Committee for Aeronautics where he did research on cooling problems of military aircraft engines. He has been with the Bureau of Public Roads since 1946.

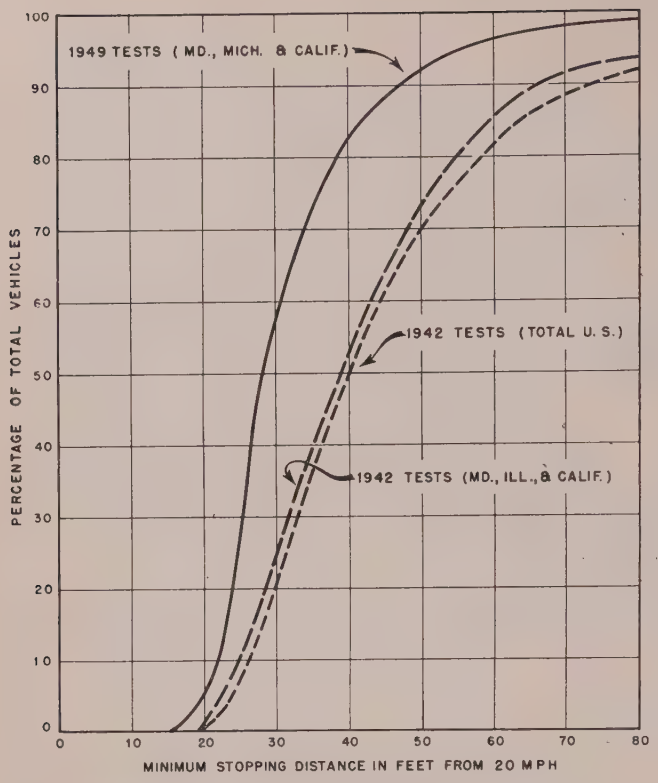

Fig. 1 – Cumulative frequency distribution of vehicle stopping distances of 2-axle trucks selected from everyday traffic

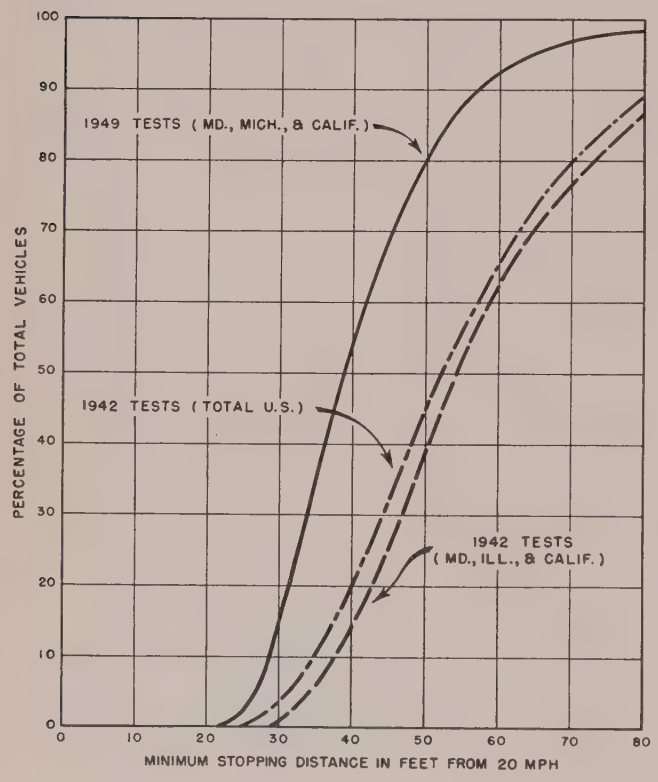

Fig. 2 – Cumulative frequency distribution of vehicle stopping distances of 2-axle truck tractors with 1-axle semitrailers selected from everyday traffic

into weight groups with a range of 5000 lb. An average vehicle stopping distance was then computed for each group and year of study. For any given group, the height of the stippled bar indicates the average stopping distance for the 1942 test vehicles and the hatched bar, the average stopping distance for the 1949 test vehicles. The number of vehicles included in the average is shown beneath each bar. Considering the 15,000- to 19,900-lb group, the average improvement in vehicle stopping distance from 20 mph was 12 ft or a percentage improvement of 22%.

The same type of comparison is presented in Fig. 6 for medium 2-axle truck tractors with single-axle semitrailers and in Fig. 7 for heavy 3-axle truck tractors with 2-axle semitrailers. In each of the three examples very definite improvement is shown for a group of vehicles of the same approximate capacity and weight. The improvements indicated by a comparison of the cumulative frequency curves for a given type of vehicle are unquestionably genuine and show that the operators and manufacturers have been doing something about improving the brake performance of vehicles on the highway.

General Levels of Performance

So far, comparisons of the brake performance of several types of vehicles tested in 1949 have

Table 1 – Comparison of 50-Percentile Values of Vehicle Stopping Distances Observed in 1942 and 1949 for Various Vehicle Types

Type of Vehicle	Stopping Distance, ft		
	1942	1949	Improvement, %
Passenger cars (with hydraulic brakes)	24	20	17
2-axle trucks	39	28	28
2-axle truck tractors with 1-axle semitrailers	54	39	28
2-axle truck tractors with 2-axle semitrailers	65	43	34
All other combination units	66	53	20

Table 2 – Average Gross Vehicle Weights of the Vehicles Tested in 1942 and 1949

Type of Vehicle			Number of Vehicles and Average Gross Vehicle Weight			
			1942		1949	
			Number	Weight, lb	Number	Weight, lb
Single-unit trucks						
2-axle			1231	13,615	367	12,200
3-axle			172	24,716	46	21,100
Truck tractor	Semitrailers					
2-axle	1-axle		1344	28,514	246	30,400
2-axle	2-axle		186	35,098	98	41,500
3-axle	2-axle		59	48,796	57	56,900
Truck	Trailers					
2-axle	2-axle		30	30,120	9	43,100
2-axle	3-axle		15	31,307	2	40,800
3-axle	2-axle		14	47,800	16	46,900
3-axle	3-axle		144	59,528	27	60,000
Truck tractor	Semitrailer	Trailers				
2-axle	1-axle	2-axle	14	39,364	50	58,100
2-axle	2-axle	2-axle	11	56,291	9	63,400
2-axle	2-axle	3-axle	6	53,083	1	94,900

been made with the performance of the corresponding types of vehicles tested in 1942. Fig. 8 compares with each other the performance of the several types of vehicles selected from everyday traffic and tested in 1949. The curves plotted on this figure indicate the percentage of the total vehicles of each type that can stop in a given distance or less from a speed of 20 mph. In the study of these general results it must be kept in mind that the sample of vehicles of each type is made up of various gross weights, capacities, brake types, and conditions of maintenance. The most striking point is the wide variation in the performance of the several types of vehicles. For example, the 50-percentile values are approximately 21 ft for passenger cars, 28 ft for 2-axle trucks, 37 ft for 3-axle trucks, 39 ft for 2-axle truck tractors with single-axle semitrailers, 43 ft for 2-axle truck tractors with 2-axle semitrailers, and 53 ft for all other combination units.

In Fig. 9, the performance of the group of combination vehicles with five or more axles, which had the poorest stopping ability, is broken down for the three major types of vehicles within the group. There was too small a sample of vehicles of each type to obtain reliable characteristic frequency distribution curves, but there is little doubt that the 2-axle truck tractors with single-axle semitrailers and 2-axle full trailers are the worst performers.

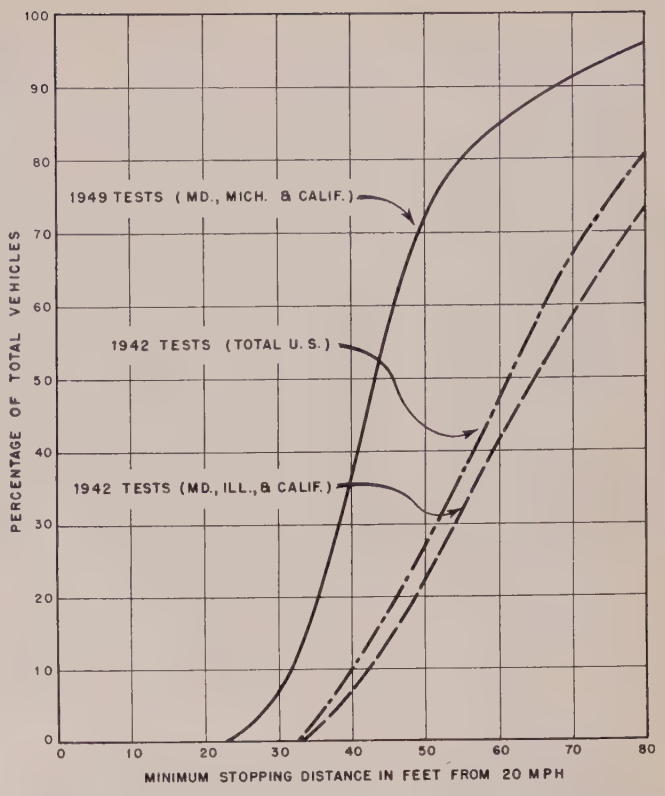

Fig. 3 – Cumulative frequency distribution of vehicle stopping distances of 2-axle truck tractors with 2-axle semitrailers selected from everyday traffic

Table 3 – Average Improvement in Vehicle Stopping Distance by Vehicle Types through Maintenance and Repair of Trucks and Combination Units Selected from Service

Vehicle Type[a]	Number of Vehicles	Average Percentage of Improvement for Initial Speeds of: 20 mph Brake Adjustment Only, %	20 mph Total, %	30 mph, %	40 mph, %
2	4	9.3	10.5	6.2	8.8
2-S1	22	8.9	16.2	16.4	17.6
2-S2	12	6.5	10.2	8.4	11.1
3-S2	4	13.4	17.6	19.6	21.2
3-2	3	12.7	24.7	23.9	22.0
3-3	8	5.7	12.3	11.3	10.0
2-S1-2	8	12.2	21.8	20.4	19.3
2-S2-2	2	10.8	13.6	15.2	13.2
Weighted average	—	9.0	15.3	14.6	15.4

[a] 2 =2-axle truck.
2-S1 =2-axle truck tractor with 1-axle semitrailer.
2-S2 =2-axle truck tractor with 2-axle semitrailer.
3-S2 =3-axle truck tractor with 2-axle semitrailer.
3-2 =3-axle truck with 2-axle trailer.
3-3 =3-axle truck with 3-axle trailer.
2-S1-2=2-axle truck tractor with 1-axle semitrailer and 2-axle trailer.
2-S2-2=2-axle truck tractor with 2-axle semitrailer and 2-axle trailer.

Table 4 – Variation of Improvement Made in Stopping Ability with Vehicle Stopping Distance Measured from 20 Mph for Vehicles Selected from Service

Stopping Distance, Group as Received, ft	Number of Vehicles	Average Stopping Distance as Received, ft	Average Improvement: Brake Adjustment Only, %	Total, %
Under 30	6	26.7	5.8	8.1
30 – 39	18	35.0	5.5	8.7
40 – 49	19	44.2	9.5	13.8
50 and over	20	63.4	10.5	24.1

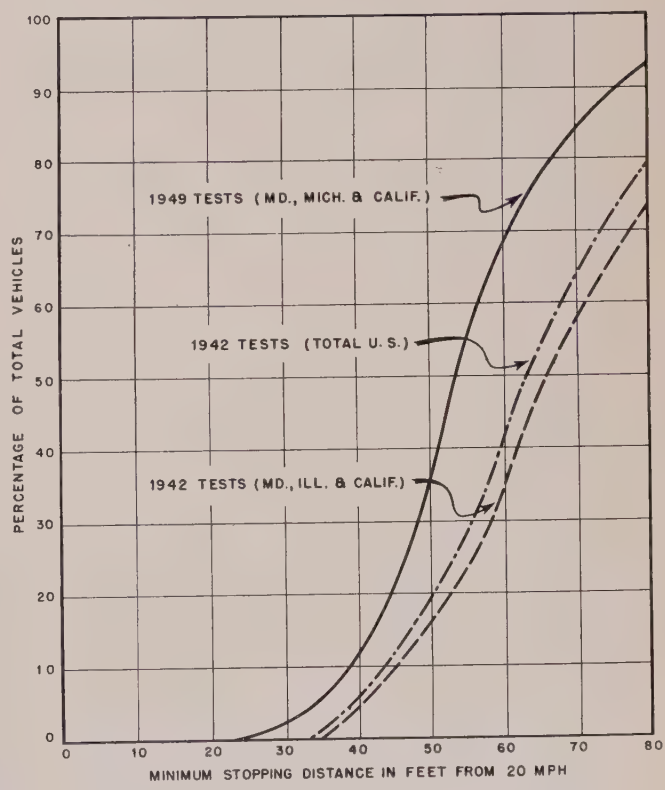

Fig. 4 – Cumulative frequency distribution of vehicle stopping distances of 3-axle truck tractors with 2-axle semitrailers, trucks with trailers, and truck tractors with semitrailers and trailers selected from everyday traffic

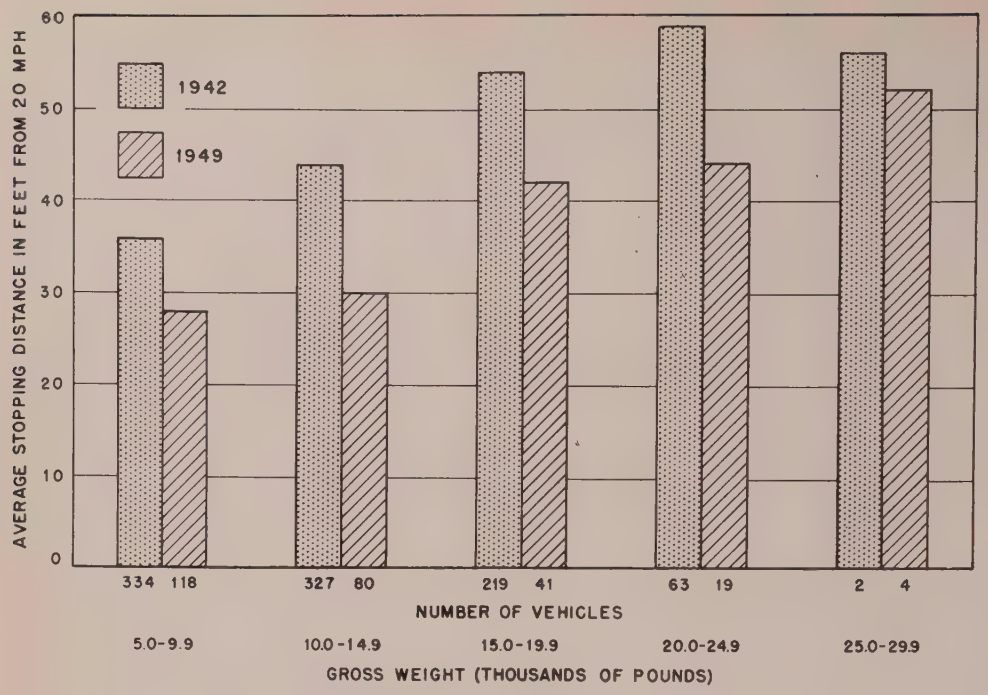

Fig. 5 – Comparison between brake performance observed in 1942 and 1949 for light 2-axle trucks selected from everyday traffic

Improvement Due to Maintenance and Repair

The results of the controlled tests of vehicles furnished by the truck operators clearly indicate that considerable additional improvement in brake performance is possible through maintenance procedures. Fig. 10 presents a general picture of the improvement made in the stopping ability of these vehicles. It is of particular interest to note that only 68% of the vehicles could stop within 50 ft from 20 mph when first tested, but 87% of them could stop in 50 ft or less when returned to the operators.

A summary of the average percentage of improvement in stopping distance is shown by vehicle type in Table 3. Considering the results for the initial speed of 20 mph, it is particularly significant that approximately three-fifths of the average total improvement of 15.3% was accomplished by a brake adjustment which consisted of simply taking up the slack between the brake shoes and the drums. Another point of interest is that the average percentage of total improvement is about the same for all three initial speeds, although there is appreciable variation in the improvement with speed for a few of the vehicle types. One of the largest improvements was for the 2-axle truck tractors with single-axle semitrailers and 2-axle trailers which have been previously singled out as poor performers.

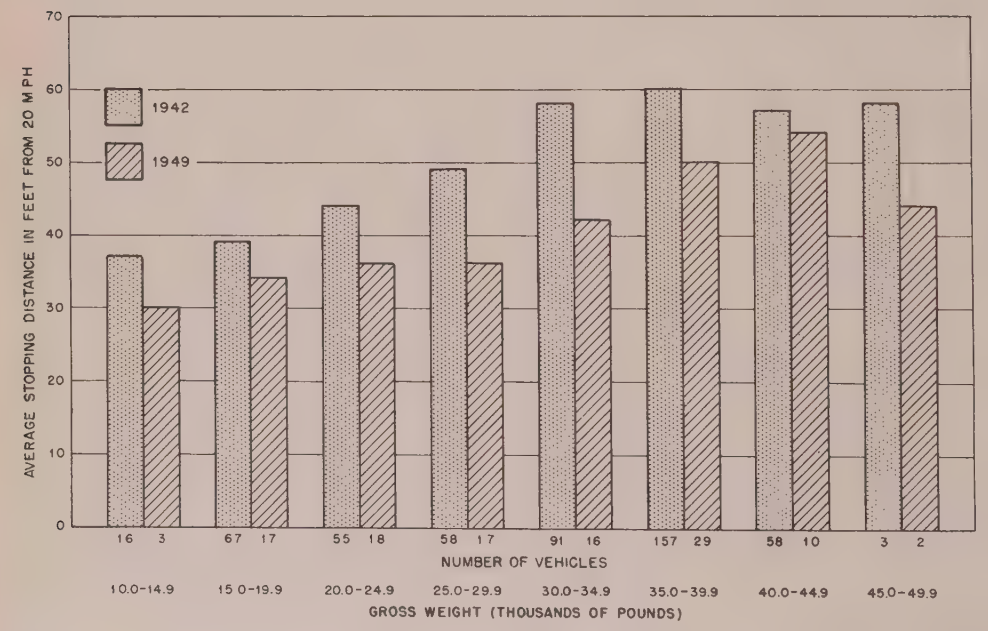

Fig. 6 – Comparison between brake performance observed in 1942 and 1949 for medium 2-axle truck tractors with 1-axle semitrailers selected from everyday traffic

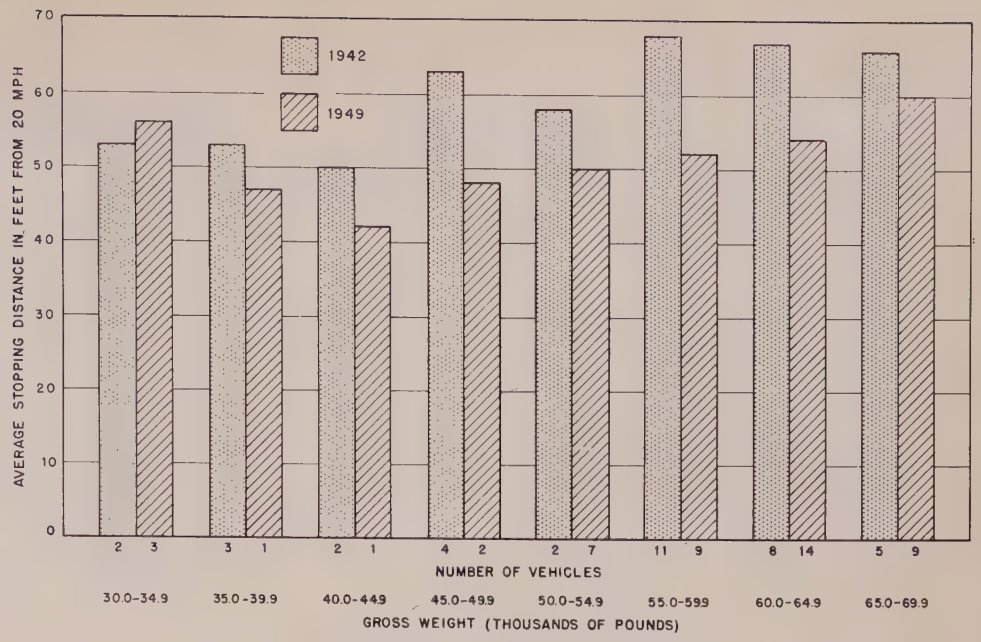

Fig. 7 – Comparison between brake performance observed in 1942 and 1949 for heavy 3-axle truck tractors with 2-axle semitrailers selected from everyday traffic

The amount and manner of improvement was found actually to vary with the magnitude of the stopping distance of the particular vehicle in the condition as first received from service. To illustrate this a simple analysis has been made of the variation of the improvement with the vehicle stopping distance. The results of this analysis are shown in Table 4. First the vehicles were classified according to four groups of vehicle stopping distances. Then the average improvement in per cent was computed for each of these groups. The average stopping distance for each group and the percentage of improvement due both to brake adjustments and to all procedures are indicated together with the number of vehicles in each group.

It is seen in Table 4 that the improvement for the vehicles with stopping distances of 50 ft or more was nearly double that for the 40- to 49-ft group and almost three times that for the other two groups. For the three groups less than 50 ft, the improvement ascribed to brake adjustment is, respectively, 71, 63, and 69% of the total improvement. Since the results of the random tests shown in Fig. 8 show that a large percentage of the commercial vehicles tested on the highway can stop in less than 50 ft, it follows that the rather simple brake adjustment is very important in the improvement of brake performance. However, for the group of vehicles with stopping distances of 50 ft or more, the improvement due to brake adjustment is only about 44% of the total improvement, which definitely means that these vehicles required more than simple brake adjustments to improve materially the brake performance. Based on the average stopping distance as the vehicle was received from service, the improvement attributed to other than brake adjustment averaged less than 2 ft for the vehicles with stopping distances of less than 50 ft, as compared with about 9 ft for those vehicles with original stopping distances of 50 ft or more.

The discussion, so far, has stressed the importance of brake adjustment but not with the idea

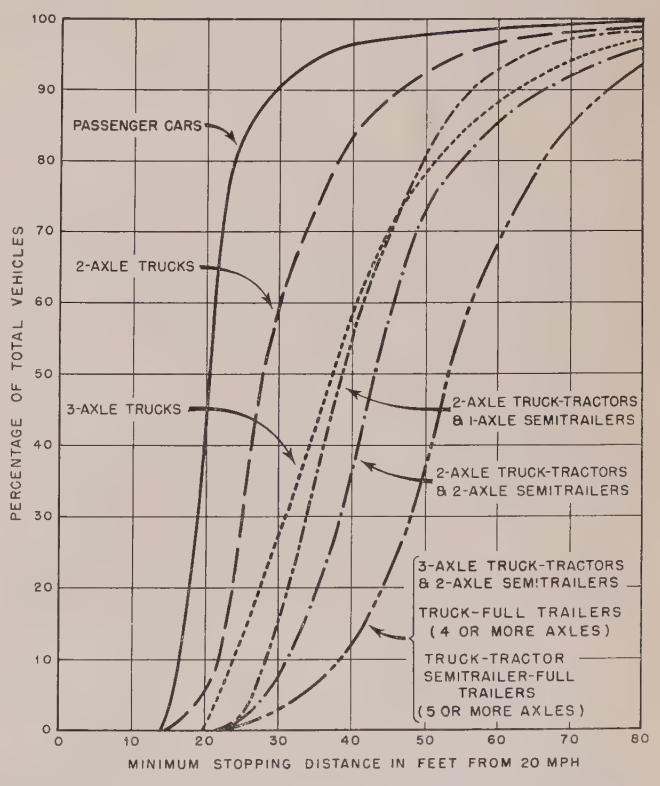

Fig. 8 – Cumulative frequency distribution of vehicle stopping distances of motor vehicles selected from everyday traffic

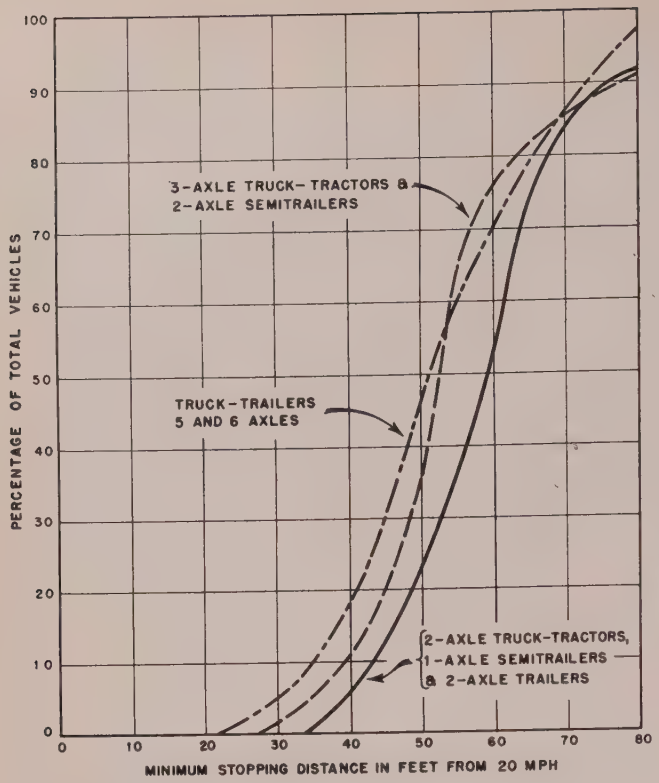

Fig. 9 – Cumulative frequency distribution of vehicle stopping distances of combination vehicles with 5 or more axles selected from everyday traffic

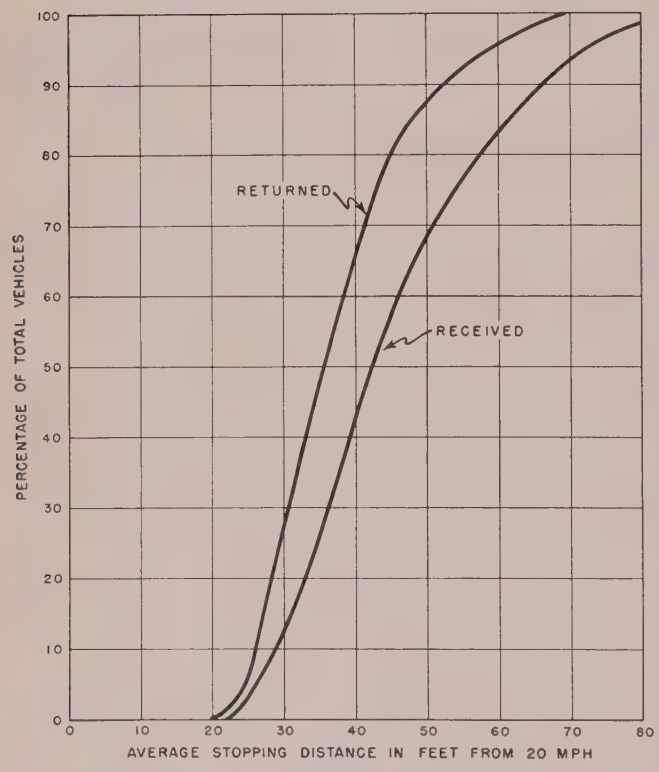

Fig. 10 – Cumulative frequency distribution of vehicle stopping distances measured for all types of trucks and combination units selected from service

Table 5 – Frequency of Maintenance and Repair Work Performed to Improve Vehicle Stopping Ability on 20 Vehicles Requiring 50 Ft or More to Stop from 20 Mph

Description of Work	Number of Vehicles
1. Adjust brakes	19
2. Replace relay valves	9
3. Eliminate elbows, tees, and lengths of line from air or vacuum plumbing system and change sizes of lines	9
4. Increase application pressure through adjustment of pedal stop or control valve linkage	5
5. Increase tank pressure through new governor or adjustment of limits	4
6. Reline brake shoes	4
7. Replace drums	4
8. Remove synchronizing valve	4
9. Replace foot control valve	3
10. Increase brake chamber sizes	2
11. Increase reserve tank capacity	2
12. Replace slack adjustor or slack adjustor arm	2
13. Eliminate leaks	2
14. Increase brake arm lengths	2
15. Connect front wheel brakes	2
16. Lubricate linkage including slack adjustors	1
17. Doctor linings	1
18. Replace brake chambers	1
19. Tighten anchor plates	1
20. Install converter dolly with brakes	1
21. Replace brake camshaft and anchor pins	1

that other procedures should be neglected. For vehicles with stopping distances of less than 50 ft, the study has shown that most major modifications and repairs which are costly in time and money result in only small gains in stopping ability. In many instances additional improvements, although small, could have been made if the equipment could have been held out of service for the required time. On the other hand, for the vehicles with stopping distances greater than 50 ft, it was learned that major repairs were required and necessary. There is no doubt that all of the stopping distances of more than 50 ft from 20 mph could have been reduced to less than 50 ft if the vehicles could have been retained in test status for sufficient time. As it was, 11 of the 20 vehicles requiring more than 50 ft to stop from 20 mph were improved so that the stopping distance was less than 50 ft.

No doubt questions have come to mind concerning the nature and importance of the other maintenance procedures used to improve the performance of the vehicles tested. However, before considering the other maintenance operations, a knowledge of what actually takes place during the stopping of a commercial vehicle with power brakes will be helpful in understanding why certain maintenance operations produced certain results. Fig. 11 is a time-speed record which shows the sequence of events that occur during the stopping of a commercial vehicle with power brakes. There is one period immediately following the instant the braking controls are operated, called "application time," during which the vehicle is not retarded appreciably. This time or distance is required to trans-

Table 6 – Frequency of Maintenance and Repair Work Performed to Improve Vehicle Stopping Ability on 43 Vehicles Requiring Less than 50 Ft to Stop from 20 Mph

Description of Work	Number of Vehicles
1. Adjust brakes	37
2. Eliminate elbows, tees, and lengths of line from air or vacuum plumbing system and change sizes of lines	10
3. Increase tank pressure through new governor or adjustment of limits	7
4. Replace relay valves	5
5. Increase brake arm lengths	5
6. Increase application pressure through adjustment of foot control valve	1
7. Reline brake shoes	1
8. Replace drums	1
9. Replace master cylinder	1
10. Replace foot control valve	1
11. Replace check valve	1
12. Install higher-friction lining	1
13. Remove grease from lining	1
14. Tighten relay mounting	1
15. Remove synchronizing valve	1

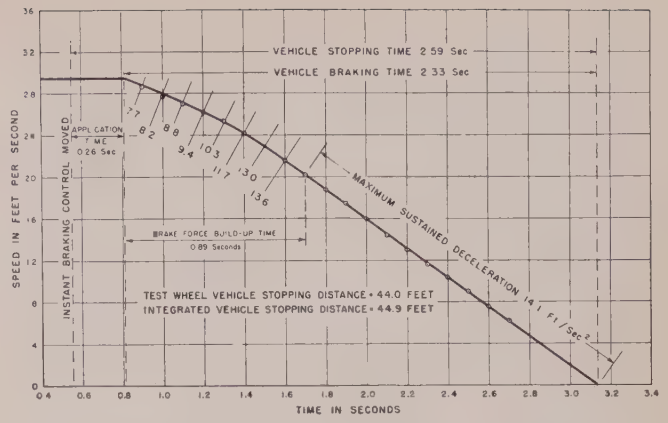

Fig. 11 – Time-speed curve for test vehicle No. 1 stopping from 20 mph showing differentiation for deceleration and illustrating various phases of the stop

mit power to the brake chambers and to overcome frictional resistance in the linkage between brake chambers and shoes and resistance of the brake shoe return springs. The application time is followed by a second period, called the "brake force buildup time," during which the braking force at the wheels is building to a maximum value. The phenomena of application and buildup times are complicated by the fact that they are usually different to some degree on each axle of a vehicle. The time-speed record shows the composite effect of the timing of the forces at the individual axles. The final period of the braking cycle is indicated as "maximum sustained deceleration." It is the period during which the maximum braking force is acting to stop the vehicle.

For the example shown in Fig. 11, the application time is 0.26 sec, the buildup time 0.89 sec, and the period of maximum sustained deceleration 1.44 sec. These times converted to distance traveled are 8 ft, 22 ft, and 14 ft, respectively. It is significant that the combined application and buildup time constitutes only 44.4% of the vehicle stopping time of 2.59 sec but 68.2% of the vehicle stopping distance of 44.0 ft. The importance of reducing application and buildup times to a minimum is readily apparent. If the maximum sustained deceleration of 14.1 ft per sec per sec could have been sustained from the instant the brake control was first moved, the vehicle stopping distance would have been 30.5 ft.

The phenomena shown by Fig. 11 helps to explain why the simple brake adjustment was so effective in reducing vehicle stopping distances. When the clearance between the brake drum and lining is excessive, the mechanism which spreads the brake shoes needs to move a relatively long distance to apply the brakes. Whenever the clearance between the drum and lining is reduced, the distance the operating mechanism moves is shortened, and the time required to apply the brakes is reduced. Since the vehicle is traveling at its greatest speed during the period designated as application time, any reduction in application time will produce a greater reduction in stopping distance than a similar time reduction at any other period during the stop. Also, in the case of air brakes and vacuum brakes, whenever the distance the slack adjuster arm and push-rod must travel is reduced, the amount of air which must pass into or out of the brake chamber is likewise reduced. This, of course, shortens the brake force buildup time, which in turn shortens the vehicle stopping distance.

In order to answer questions concerning the nature and importance of maintenance procedures other than the brake adjustment, the corrective actions taken and the number of vehicles on which each action was performed are summarized in Table 5 for the 20 vehicles which originally required in excess of 50 ft to stop. There is no standard formula for the improvement of brake performance, as each vehicle requires specialized treatment. Usually the improvement effected required a number of actions, and it was often necessary to combine several of the repairs between road tests, making it impossible to define the relative importance of each individual action. For example, the stopping distance of a truck and full trailer was improved 37.5%, 10.9% by brake adjustment and 26.6% by a major repair job wrapped in one package. This major repair job included an entirely new plumbing setup that eliminated unnecessary fittings and tubing, installation of a new-type foot control valve on the truck and two new emergency relay valves on the trailer, relining of the truck front brakes, and connection of the air line to the front brakes. Incidentally, the stop-

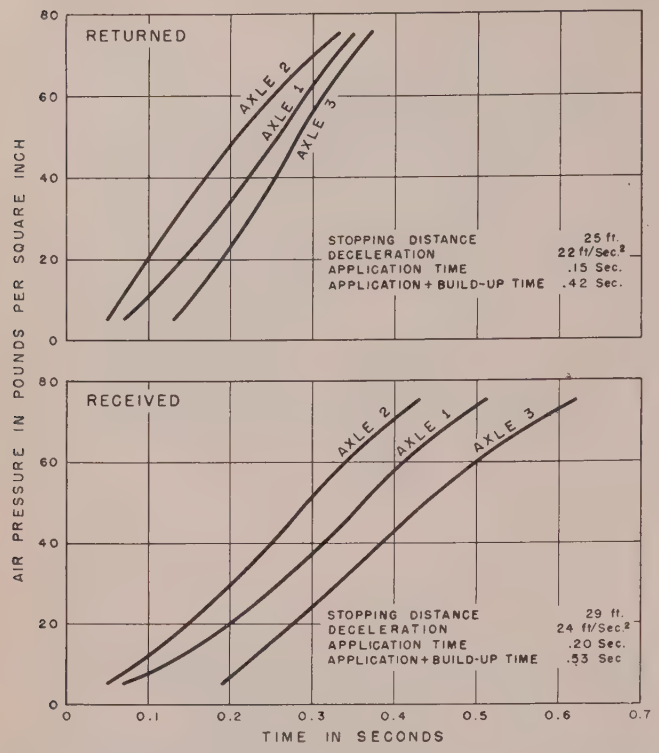

Fig. 12 – Buildup of air pressure at brake chambers of a 2-axle truck tractor and 1-axle semitrailer weighing 40,750 lb obtained from service

ping distance from an initial speed of 20 mph was decreased from 64 to 40 ft.

Although it is not possible to show quantitative results of the improvements effected by individual repair operations, the information in Table 5 indicates that several actions were performed more often than others. Brake adjustments were performed on 19 of the 20 vehicles. The replacement of relay valves and the changes in plumbing setup are next in order and were usually instrumental in reducing application and brake force buildup time.

In replacing relay and control valves and making changes in plumbing on both air-equipped and vacuum-equipped vehicles, an effort was made to eliminate, wherever possible, any condition which would tend to retard the smooth flow of air through the system. This was accomplished (1) by installing properly functioning relay, relay emergency, and brake control valves of adequate capacity; (2) by eliminating all street elbows and by substituting straight fittings for elbows of any type wherever possible; (3) by eliminating unnecessary fittings and lengths of tubing; (4) by replacing any tubing which was pinched or kinked; and (5) by replacing tubing of improper diameter with larger or smaller diameter tubing, as necessary. These actions are not necessarily listed in order of their relative importance as it will vary, depending on the needs of the individual vehicle.

A malfunctioning or sluggish relay, emergency relay, or brake control valve will adversely affect the brake performance of a vehicle making an emergency stop by increasing the application and brake force buildup time and, in some instances, by limiting the maximum braking force. It is imperative that all relay, emergency relay, and control valves function properly and be immediately responsive to any call for action. It is equally important that these valves all have adequate capacity to do the job required of them. A valve of inadequate capacity will stretch out the application and brake force buildup time just as surely as a sluggish valve. There were three instances where the effect of new relay valves on the brake performance could be singled out, the percentage of improvement being 3.3, 5.9, and 19.5%.

When the brakes of an air-brake-equipped vehicle are applied, compressed air flows from a reservoir through a system of tubing, fittings, and valves into the brake chambers where it operates the mechanism which actuates the brake shoes. In a vacuum-brake system air must flow through a series of tubes, fittings, and valves, also; but it flows at less than atmospheric pressure, and, except for vacuum suspended boosters, the direction of flow is reversed. In other words, to actuate the brakes of a vacuum system, air is exhausted from the brake chambers, and it flows *into* a reservoir instead of being forced under pressure from a reservoir into the brake chambers, as in an air-brake system. In either system, the more rapidly the air traverses its course, the shorter the application and buildup time will be.

To hold the application and buildup time to a minimum, the air must travel through the lines at high velocity. Whenever the smooth inner surface of a line is interrupted or its cross-sectional area is abruptly changed, a certain amount of resistance is offered to the rapid flow of air through the line with a resulting increase in application and buildup time. The ordinary pipe street elbow is one of the worst offenders among the fittings which retard the rapid flow of air through a brake system, yet it is very commonly found on vehicles in the everyday traffic. The opening in the small end of a $\frac{3}{8}$-in. ordinary street elbow is no larger than the inside diameter of a piece of $\frac{1}{4}$-in. pipe, and the opening in the small end of a $\frac{1}{4}$-in. street elbow is no larger than the inside diameter of $\frac{1}{8}$-in. pipe. If an elbow must be used, the regular pipe elbow with a close nipple will offer less restriction than the street elbow; but an elbow having a machined inner surface, such as the brass fittings specifically designed for use with copper tubing, is preferable.

Wherever a straight fitting and a fairly long radius bend in the connecting tubing can be used in place of an eblow, there will be some small

increment saved in the application and buildup time. If a fitting can be eliminated completely another small increment of time will be saved. An example of what can happen when elbows are eliminated is illustrated by the work done on a 2-axle truck tractor with single-axle semitrailer and 2-axle full trailer equipped with air brakes. Fifteen elbows of various types were removed from the braking system of this vehicle. Straight fittings were substituted for some, and some were completely eliminated. From 20 mph the stopping distance was reduced by 4 ft, from 30 it was reduced by 9 ft, and from 40 it was reduced by 16 ft. This much improvement is probably not typical of the results which will be obtained by merely removing 15 elbows from a braking system. However, it is a specific example of what has been done. In general the most improvement will be made by removing the restrictions through which the greatest amount of air must pass. In other words, an elbow between a relay valve and a brake chamber would tend to retard brake action considerably more than the same type of elbow in the service line on the top of the relay.

Worth-while savings can sometimes be effected by eliminating unnecessary lengths of tubing. It follows that if the distance the air must travel is shortened, the time will also be shortened. In some instances needless lengths of tubing may be eliminated by making circuitous paths of the lines more direct; and sometimes more strategic placement of various brake components, such as reservoirs and relay valves, is possible. For best brake performance a relay valve should be centrally located among the brake chambers it must serve, and the reservoir should be as near as possible to the relay it serves.

After the discussion of the retarding effect of some fittings, it is hardly necessary to mention the restrictions which can be caused by pinched or kinked tubing. However, such a condition definitely should be corrected whenever discovered.

Another important item to consider in revamping the plumbing system of a vehicle equipped with air or vacuum brakes is the diameter of the tubing used. Different applications require different sizes of lines, but if the correct size line is not used in each location, the best possible results cannot be expected.

Increasing application pressures and tank pressures, relining brakes, replacing drums, removing synchronizing valves, replacing foot control valves, and repairing leaks were also among the more common corrective measures. There were three instances where the improvement made by remodeling the plumbing setup could be definitely assigned as 7.3, 4.4, and 1.6%.

The same type of information shown in Table 5 for those vehicles requiring 50 ft or more to stop from 20 mph is shown in Table 6 for 43 vehicles requiring less than 50 ft to stop. The list of repairs is shorter and the frequency on the basis of percentage is naturally less than for the poorer performers. Although considerable work was performed on the plumbing systems, the results were not startling. The greatest improvement from 20 mph was 3 ft and the average about 1 ft.

It has been stressed that the application time and brake force buildup time were very important segments of the total vehicle stopping distances and were potential areas of improvement. To illustrate that considerable improvement in the application and force buildup times was possible, four examples have been selected and are illustrated in Figs. 12, 13, 14, and 15. In these four figures, time in seconds is plotted as abscissas and air pressure in pounds per square inch or vacuum in inches of mercury as ordinates. A curve for each axle with brakes shows the time required to build up any given pressure from the instant the braking controls are moved. The lower set of curves represents the condition of the vehicle when received from service, and the upper set represents the condition of the vehicle when released from test status. The vehicle stopping distance, deceleration, brake application time, and the combined application and brake force buildup time are shown for each condition of test.

In Fig. 12 the results are for a 2-axle truck trac-

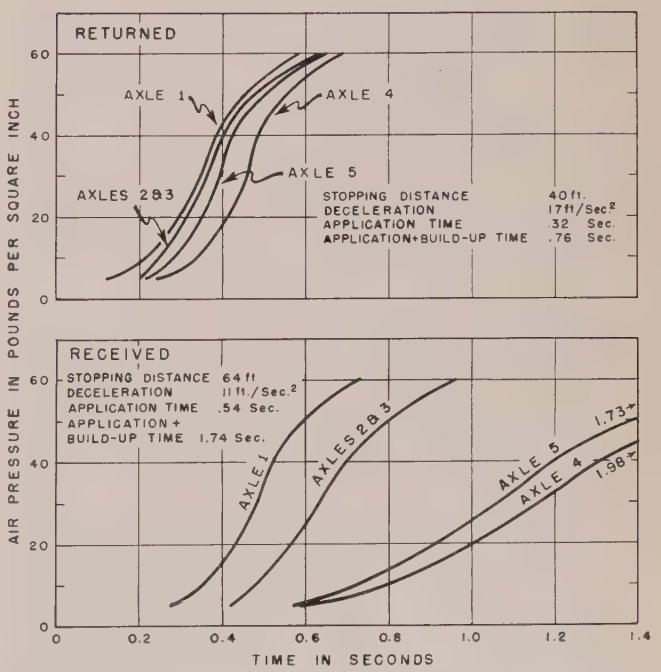

Fig. 13 – Buildup of air pressure at brake chambers of a 3-axle truck and 2-axle trailer weighing 77,740 lb obtained from service

tor with single-axle semitrailer, equipped with air brakes and weighing 40,750 lb. The time required to reach 75 psi air pressure at the brake chambers on axle 3 was originally 0.62 sec and after adjustments and repairs was 0.37 sec. The final stopping distance of 25 ft from 20 mph is exceptionally good. The improvement shown was the combined result of installing a new-type relay emergency valve on the semitrailer, a new relay valve on the truck tractor, changing a ⅜-in. diameter line from the tank to the relay emergency valve on the semitrailer to ½-in. diameter, and taking up the slack between the linings and the drums.

The next example, shown in Fig. 13, is for a 3-axle truck with 2-axle trailer equipped with air brakes and weighing 77,740 lb. There was a considerable variation between the timing of the brakes on the truck and the trailer before taking corrective measures as shown by 0.73 sec being required to obtain a pressure of 60 psi at the brake chambers on axle 1 compared with 1.98 sec at axle 4. When returned to the operator's fleet, the times required to reach 60 psi pressure at axles 1 and 4 were 0.58 and 0.69 sec, respectively. A comparison of the performance data for each condition shows that a sizable improvement was made in the stopping distance, 64 ft reduced to 40 ft. The improvement was effected both by reducing brake application time and force buildup time and by increasing the braking force. In order to make this improvement, brakes were adjusted, all old plumbing on both truck and trailer was replaced by a new setup which eliminated unnecessary fittings and tubing, a new-type foot control valve was installed, two new relay emergency valves were installed on the trailer, and front brakes on the truck were relined and connected. All of this work had to be performed at the same time, so it was not possible to measure the effectiveness of any particular repair operation.

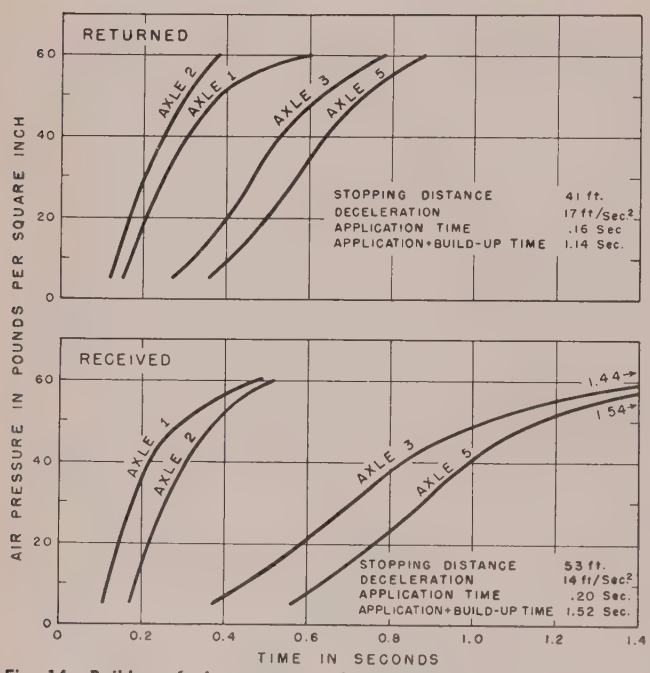

Fig. 14 – Buildup of air pressure at brake chambers of a 2-axle truck tractor, 1-axle semitrailer, and 2-axle trailer weighing 76,150 lb obtained from service

Another interesting example of improvement in air-brake timing is shown in Fig. 14. The vehicle was a 2-axle truck tractor with single-axle semitrailer and 2-axle trailer. The combination weighed 76,150 lb. Very little improvement was made in the application and buildup time of the brakes on the truck tractor, most of the improvement being made in the brakes of the semitrailer and trailer. The stopping distance from 20 mph was reduced from 53 ft to 41 ft. This vehicle did not have brakes on the trailer converter dolly, the first axle of the trailer, when received from service. However, the 41-ft stop was obtained after a converter dolly with brakes had been substituted. Brakes on axle 4 reduced the stopping distance to 41 ft from 43 ft on stops made from 20 mph. The improvement in stopping distance attributed to brakes on axle 4 from 30 and 40 mph was 9 ft and 23 ft, respectively. The application and buildup time of the brakes on this particular dolly was excessive. Had it been more rapid, the improvement in performance, especially from the lower speeds, would have been greater. The total improvement in stopping ability of this vehicle resulted from adjusting brakes, eliminating unnecessary fittings and tubing from the truck tractor and trailers, and using the converter dolly with brakes.

Eight vehicles of the truck tractor-semitrailer-full trailer type averaging 68,400 lb gross weight had an average vehicle stopping distance from 20 mph of 63 ft when received and 48 ft when returned to service. The example just described demonstrates that vehicle stopping distances in the vicinity of 40 ft are not impossible with this type of vehicle.

The fourth example, shown in Fig. 15, considers a 2-axle truck tractor with single-axle semitrailer weighing 40,250 lb. This vehicle had vacuum booster hydraulic brakes on the truck tractor and vacuum mechanical brakes on the semitrailer. Considerable improvement was made in the application and buildup time of the vacuum at the brake chambers on axle 3, but little improvement was possible at the booster unit on the truck tractor. The time required to obtain a vacuum of 12 in. of Hg at axle 3 was decreased from 2.11 to 0.84 sec. The maximum sustained deceleration was increased from 9 to 15 ft per sec per sec indicating that the improvement in stopping distance from 56 to 31 ft

was a result of increasing the braking force as well as reducing the application and buildup time. In order to effect this improvement the following work was performed in the order listed:

1. Adjust brakes.
2. Eliminate leaks in vacuum system on semitrailer.
3. Install new relay valve on semitrailer.
4. Replace brake drums on axle 3.
5. Replace brake cam, shaft, camshaft bearings, and inner wheel bearings on right wheel of axle 3.
6. Replace anchor pins at both wheels of axle 3.
7. Reline brakes on axle 3 with stock lining.
8. Doctor linings on axle 3.
9. Reline brakes on axle 2.
10. Replace ¼-in. rusty pipe control line on semitrailer with ½-in. diameter copper tubing.
11. Reline axles 2 and 3 with high-friction lining.

Considerable emphasis has been placed on the importance of reducing application and brake force buildup time to a minimum. However, it is possible for the brakes of a vehicle to have excellent application and buildup characteristics and still show poor stopping ability when the vehicle is carrying its normal load. Two other very important factors enter into good brake performance. They are braking force and brake capacity. Adequate braking force, in the case of air mechanical and vacuum mechanical systems, is provided by proper selection of brake chamber size and slack adjuster arm length for the axle loads to be carried. Tire size, brake drum diameter, and cam radius must be considered in making this selection. In the case of hydraulic brakes, the correct booster and master cylinder must be selected to provide the necessary braking force.

Brake capacity is a measure of the ability of the basic brake (shoes, lining, and drums) to dissipate the heat generated by braking action. Adequate brake capacity may be obtained by providing the proper drum size and lining size and composition. Insufficient brake capacity is indicated by excessive brake fade, abnormally frequent need for brake adjustment, and poor lining life.

Since the truck operators who provided vehicles for the controlled tests were among the more "brake conscious," there was little need to increase the braking force or brake capacity of the vehicles tested. In a few instances changes were made to provide additional braking force, but other changes were made at the same time, making it impossible to isolate the effect of the added braking force. However, in the tests of vehicles selected at random from the everyday traffic a number of vehicles were observed which obviously had inadequate braking force or capacity or both for the loads carried.

Throughout this paper the selection of proper size or capacity of various brake components has been stressed. The question, "What are the proper sizes and capacities of these components?" has no doubt come to mind. A precise answer will depend upon a number of factors, but the best possible guide to follow is the recommendations of the brake engineers and the practical experience gained by maintenance personnel of fleet operators.

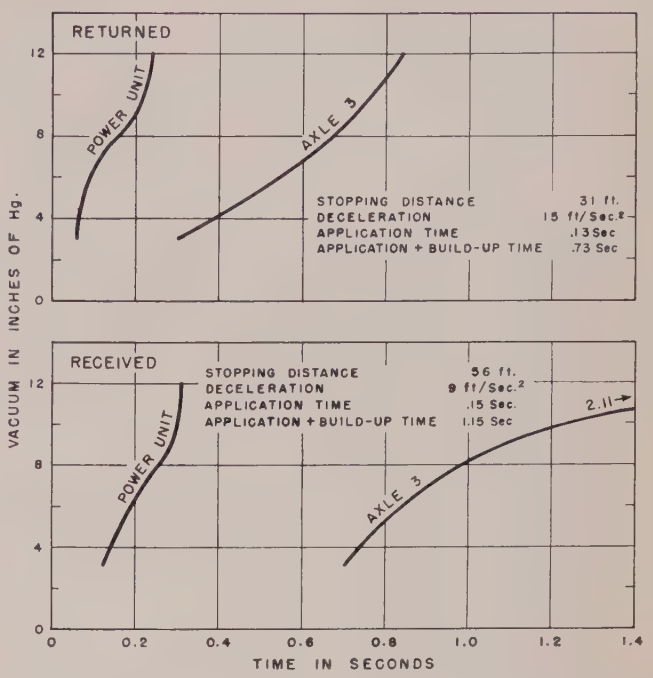

Fig. 15 – Buildup of vacuum at hydraulic power unit of a 2-axle truck tractor and at brake chambers of a 1-axle semitrailer with combined weight of 40,250 lb obtained from service

In summary, the discussion on the improvements made by maintenance procedures in the stopping ability and other integral parts of the stop has indicated that the level of brake performance of the vehicles operating in the everyday traffic, especially those with stopping distances of 50 ft or more from a speed of 20 mph, can be appreciably improved by the adoption of adequate brake maintenance programs. The elimination of slack between linings and drums, the rather simple brake adjustment, is shown to be the most important maintenance operation. However, major repairs are definitely in order for those vehicles which take more than 50 ft to stop. The fact that the controlled tests were conducted on vehicles provided by operators who are "more maintenance minded" than most would lead one to expect that even greater improvement could be effected in many vehicles on the highway.

DISCUSSION ON FOLLOWING PAGES ——→

Suggests Dual Standard For Stopping Requirement

—S. G. Tilden

The Permafuse Corp.

IN setting up standards of brake performance for enforcement by public officials and regulatory bodies, the ability of vehicles now in use to meet or to be made to meet the standards promulgated is of paramount importance. A requirement so stringent that any substantial number of vehicles already in service could not meet or could not be made to meet could obviously never be enforced, for it would mean the scrapping of millions of dollars of equipment and a great financial loss to an important segment of our transportation system.

Building a braking requirement around the "ability to meet" may sound like compromising with safety, but I have seen no reliable statistics which prove that any substantial portion of highway accidents are caused directly by insufficient braking ability.

The ability to stop in a short distance does not make a vehicle safe, per se. Even if all vehicles were made to meet a stringent minimum stopping distance requirement, the wide variation in the reaction time of various drivers would alone cause collisions. This is best illustrated by the chain-reaction rear-end passenger-car collisions becoming somewhat common on our high-speed expressways. Such accidents are seldom due to insufficient braking ability but to inattention and overconfidence of the driver and his plain misjudgment of reaction time.

From Fig. 8 of the author's paper, it is apparent that 90% of passenger cars in the "as found" condition could meet a 30-ft stopping distance requirement from 20 mph, and I think it an accepted fact within the industry that the remaining 10% could be made to meet such a requirement by normal maintenance. In other words, no passenger car as made today would fail to meet a 30-ft minimum stopping distance from 20 mph; and if, say two years from now, the same vehicle could no longer meet the 30-ft requirement, the trouble lies with poor maintenance, not design. If the trouble lies with poor maintenance, it can be cured by good maintenance.

From the author's Fig. 10, it will be noted that only 12% of the trucks and combination units in the "as found" condition could meet a 30-ft-from-20-mph stopping-distance requirement and that after reconditioning the braking system, only 28% could stop in 30 ft. If a 30-ft requirement for all vehicles were to be promulgated, it would immediately rule off the roads the remaining 88% of the trucks and combination trains, only 28% of which could be repaired to meet this requirement.

However, if a 50-ft stopping distance from 20 mph were to be promulgated for the heavier vehicles, some 69% would immediately pass inspection in the "as found" condition and 88% could be repaired and made acceptable. In discussing this point with the author, I was assured that the reason the remaining 12% could not stop in 50 ft is due to the lack of time and parts available in the repair work and that, in the author's opinion, all the vehicles in this class could have been made to stop in 50 ft had the time and parts been available.

The reason why the heavier vehicles cannot stop in 30 ft is apparent from the author's Figs. 12 through 15. Almost all of these vehicles are equipped with power brakes, either air or vacuum. It takes time to transmit power by air or vacuum, and the time taken is consumed while the vehicle is operating at its highest speed, that is, before any retardation has commenced. For this reason, an end deceleration rate considerably in excess of the average is required to meet a certain stopping distance requirement. This is excellently illustrated in the author's Fig. 11 where a maximum sustained deceleration rate of 14.1 ft per sec per sec was achieved which should have resulted in a 30-ft stop. Instead, and due to an application time of 0.26 sec and a brake force buildup time of 0.89 sec, the average deceleration rate achieved resulted in an actual stopping distance of 44 ft. (Note: I do not check with the author's computation of maximum sustained deceleration and vehicle stopping distance for the speed-time given in this example, but the principle illustrates the problem.)

It has been increasingly apparent to those studying this problem, including some members of the SAE Brake Committee, of which I am honored to have been a member for many years, that it might be advisable to set up dual standards of stopping ability: one for passenger cars and light trucks (½ to ¾ ton on a passenger-car chassis) and another for buses and commercial vehicles (including tractor-trailer combinations). At first this may sound discriminatory and capricious and certainly not in accord with a theory that all vehicles on the highway should have the same acceleration and deceleration performance in order to maintain their place in the traffic stream. Such heavy vehicles do not approach passenger cars in their acceleration ability, so why the surprise that they cannot equal passenger-car performance in their deceleration ability? Generally the heavier vehicles are regulated to a maximum speed well below that permitted passenger cars, which somewhat equalizes the actual stopping distances of the two.

Another factor which favors a lower standard of braking requirement for commercial vehicles including buses is the ability of the load carried to accept extremely high deceleration rates without shifting. Such load shifts under fast stops have caused serious and fatal accidents. In the case of buses with standees, high deceleration rates may throw standees violently forward, causing serious and fatal injuries.

Dual standards of braking ability for passenger cars and trucks seem to be a logical answer which is not in conflict with actual highway safety.

Adjust Braking to Impending Skid By Means of Electric Drive System

—A. H. Easton

University of Wisconsin

TO attempt to convince anyone, even though he were familiar with truck operation, that 50% of the trucks could not stop in less than 43 ft would be a difficult task without the supporting data which Mr. Petring has assembled and so clearly presented. Referring to Fig. 13 it is noted that maintenance in this particular case made a vast difference, and yet some vehicles even after maintenance showed very poor characteristics as shown by Fig. 10.

From discussions with those who are concerned with the engineering of brakes, I learned that they are grateful for the help Mr. Petring has given them in emphasizing proper brake maintenance. It is likely that improvements have been made in braking systems since 1949 which should give the later vehicles a considerable advantage. This is borne out by results from our tests on two 1952 units grossing at 56,000 lb which stopped in 34 and 39 ft.

In order to examine the ultimate which we might expect in braking of heavy units, consideration of the three braking distance components may be of value. Everyone is familiar with these components which are perception and reaction distance, brake lag distance, and skid distance.

Inasmuch as perception and reaction times are "built

into" the driver, there is little the engineer can do here to reduce this value except to keep the throttle and brake pedals conveniently near each other and at approximately the same level.

Considering brake lag distance, the distance the vehicle travels between pedal contact and point of maximum braking, the ultimate for a purely mechanical system might be that of a passenger car, which oscillograms show to be in the order of 0.2 sec. In our 1952 vehicles maximum deceleration with a gcw of 56,000 lb was reached in the order of 0.8 sec. Thus at that time there was room for considerable improvement, and I am certain that the challenge has been accepted.

From speeds up to 20 mph with locked-wheel stops, our tests show that the skid distance of a fully loaded straight truck (gvw = 20,000 lb) and a passenger car are very nearly the same. From a speed of 40 mph, however, the skid distance for the truck was 50% greater than that of the passenger car.

The latter hurdle is one which is difficult to cross except by the use of an ideal braking system in which the wheels never slide and yet exert maximum braking torque. A. C. Gunsaulus of Goodyear has already presented an approach to this type of system.[a] A system that could provide ideal braking is the electric drive in which the drive motors are used as generators during braking. This means of braking would automatically adjust to impending skid regardless of the coefficient of friction. I do not propose that it be substituted completely for our present systems but that it might be used in normal braking operations with the present system as a standby. The usual difficulty with an electrical power train is one of weight, but it might be that a reexamination in light of present know-how and materials would reveal that units could be built which would compete with present transmissions through reduction in brake maintenance.

Emphasizes Necessity for Careful Maintenance Procedure

—Ward L. Bennett
Baltimore Transfer Co.

IT is indeed gratifying to learn that there was considerable improvement in the brake performance of motor vehicles between 1942 and 1949. This period, of course, covered three years of World War II, and the balance of it was in the immediate postwar period. Actually, there probably was no great amount of development work being done by the manufacturers during this entire time. It seems quite probable that there has been a much greater improvement made in the years since 1949.

Mr. Petring's field work was most comprehensive. Undoubtedly he has had more opportunities to work with brake problems in various parts of the country than most anybody else in the field of braking work. We, in the Baltimore Transfer Co., had an excellent opportunity to work with Mr. Petring, and the information obtained from these tests has been most helpful in our operations since that time. Our participation in this field testing program clearly demonstrated to us how good maintenance procedures can improve braking performance. Likewise, we also had opportunity to see at first hand how important it is to reduce the application and buildup times.

The question of proper maintenance is one of great importance and it is one that all fleet men are greatly concerned with. The tractors and semitrailers are certainly widely used in all types of truck transportation today. It was this type of equipment that we made available for the test work. The common carrier trucking operators depend almost entirely on this type of equipment for highway use. The majority of such operations call for the ownership of more trailers than tractors. This means that, generally speaking, tractors and trailers are not continuously hooked up together. Because of the frequent switching of vehicles, it is not possible to balance out braking systems between specific tractors and trailers, such as would be possible in many private carrier operations. For this reason, brake maintenance problems with common carriers are considerably complicated.

In such operations where the tractors and trailers are continually being shuttled, it is necessary to follow out a careful maintenance procedure on all tractors and trailers, independently. Even on the tractors, there may many times be a number of drivers on the vehicles in any one 24-hr period, and that again increases the problems.

To meet the problems of the continually changing drivers and trailers, it seems best to set up a regular inspection and adjustment of brakes, rather than to depend on driver's complaints. The air-brake systems are particularly adapted to easy regular adjustment. Unlike the ordinary hydraulic system, the air brakes can be readily adjusted to a standard setting by simple external adjustment. The procedure is as follows: screw the slack adjusters up until the shoes are in full contact with the drum, and then slack them off four notches. This amount of adjustment will generally give sufficient clearance between drums and shoes. Such a program can be recommended to all who operate air-brake vehicles. It will insure the driver that there is a consistent amount of brake available on vehicles at all times. The frequency of adjustment will vary with different operations.

The proper selection of brake linings greatly affects the performance of the braking system. Road testing seems to be the best answer for gaining knowledge as to the best type of brake linings for any particular operation. Linings with a high coefficient of friction may very possibly be no better than those with a low coefficient. High-friction linings may very easily cause the wheels to lock and slide. Once the wheel slides on the pavement, it is not affording the best braking. There is, of course, the continual desire to get a lining which will last the longest time. Many times, however, such linings may be used to the detriment of stopping distance.

Detailed attention should be given to keeping the air lines free of oil and moisture. Automatic moisture ejectors are worthy of consideration and particularly in areas with high humidity. Periodic checking of the trailer emergency relay valves for correct operation is an important item in a good brake maintenance program. Complete servicing and freeing up of all moving parts in the braking system, such as the cams and brake shoe anchor pins, will contribute greatly to the best braking.

The simplification of the piping on the air systems will most certainly improve stopping distance. Many times, comparatively minor improvements could be made on the equipment that is presently in service. Oftentimes, there may be more pipe fittings in a particular line than is necessary, and a few minutes spent in removing several extra fittings will pay dividends in braking performance. In connection with Fig. 12, Mr. Petring mentioned that the increasing of the diameter of the line from the tank to the relay emergency valve on the semitrailer contributed to better stops. This particular modification has been most helpful in improving brakes on equipment in use by the Baltimore Transfer Co.

The majority of the trailer manufacturers set the hose couplings several feet up on the front of their trailers. This means that several 90-deg elbows are used, and these definitely retard the application time. The mounting of the gladhand couplings, with a maximum of one 45-deg fitting just above the fifth-wheel plate, will speed the passage of air to the reservoir tank and thus reduce application time. The tractor manufacturers often use excessive fittings in running the lines from the pedal valves to the trailer brake hoses. Actually, it seems as though they could save money by not using these fittings and, at the same time, give the operator faster brake action. Those in charge of purchasing

[a] See SAE Transactions, Vol. 61, 1953, pp. 189-195: "Rolling Wheels Gather No Skids," by A. C. Gunsaulus.

new equipment can often help to obtain better brakes by specifying such things as simplified piping when buying new vehicles.

The ability to stop a 40,000-lb tractor and trailer within 25 ft at 20 mph is a real testimonial to the effectiveness of the Bureau of Public Roads field testing activities. Quite recently, the Baltimore Transfer Co. has made further tests with a 2-axle tractor and 2-axle trailer. With gross loads of 35,000, 45,000 and then 55,000 lb, stops were within 26½ ft at 20 mph. The measurements were made in a manner similar to those made by Mr. Petring.

These latter tests again bear out the soundness of the points that have been emphasized in the paper. Naturally these tests are made under ideal conditions. However, if the information gained from such tests is utilized in modifying and maintaining the brake systems on all vehicles of a fleet, better brakes are bound to result. Mr. Petring's paper should give fleet operators considerable encouragement in their efforts to gain better braking on their present equipment. Every operator has a great investment in equipment at present, and it is important to know and understand steps that can be taken to improve braking conditions on such equipment. It is well known that the manufacturers are continually striving to improve their new products but it is of utmost importance for all fleet operators to know what they can hope for in the equipment that they now own.

High-Friction Braking Material Reduces Application Buildup Time

– J. V. Bassett
Raybestos-Manhattan, Inc.

OTHER discussers may choose to accent other highlights of this paper, but I want to accentuate the positive as it relates to maintenance. Fig. 10 showed that only 68% of the vehicle sample could stop in 50 ft from 20 mph without some form of maintenance, but after being worked on, 87% of them could stop at 50 ft. This is a tremendous improvement of 59%, figured that of 100 vehicles 68 stopped in 50 ft before correction; 32 did not; but after correction, 19 of these 32 did stop in 50 ft.

Considering, as stated in the text, that three-fifths or 60% of this improvement is due solely to a mere brake adjustment, this surely should spotlight the necessity of a regular, frequent program of brake adjustment. The unit of Fig. 15 surely had little or no regular inspection and maintenance. Regular inspection would have corrected the vacuum leaks as well as the brake adjustment and the necessity for the replacement of items 4, 5, and 6. So far as item 10, replacing the rusty ¼-in. pipe with ½-in. copper tubing, is concerned, the use of iron pipe in my opinion is just plain criminal. It might have been a wartime necessary substitute, but the availability of copper or aluminum tubing has been a fact for many years now, so there is absolutely no excuse for the use of iron pipe for at least the last five years.

Let me establish one basic fact: "A brake is a conversion machine, and a darned efficient machine at that." A brake converts energy units (kinetic energy) into heat units. It is not only impractical to store these heat units in a tremendous mass or weight of brake-drum iron, but it is essential that they be dissipated or radiated into the air stream, otherwise destructive temperatures will be reached in all of the brake components.

Confirmed tests have shown that contrary to mathematical figures, lower drum temperatures and less heat checking is obtained by the use of higher-friction braking materials, giving shorter, safer stops. These high-friction materials by virtue of their higher friction values require less line pressure, either air or hydraulic; therefore, they reduce the application buildup time and give better control and shorter stops with greater highway safety.

In Table 6, Item 13, "Remove grease from lining"—this just can't be done; you remove it from the surface, but the heat of braking draws the absorbed oil or grease to the surface later. If oil- or grease-soaked lining is found, the only thing to be done is to throw it away and reline the unit.

To those of you who have the responsibility of the selection or purchase of vehicles or both, may I offer this advice. Select by the specification book and not by the checkbook, for a vehicle too cheap for the job is definitely the most expensive in the long run.

Must Study the Combination, Not the Separate Vehicles

– Lewis C. Kibbee
American Trucking Associations, Inc.

THIS long-awaited study has pointed out to both the manufacturers and the truck operators some of the shortcomings of our vehicles. It has been a very instructive research in that it has pinpointed some of the things that we need to do to better the stopping ability of our vehicles. This new realization of these joint problems has led to some real action.

Firstly, manufacturers have now realized that we must discuss these vehicles as combinations, as has been pointed out by a previous discusser. This had led to the formation of a joint committee between the Automobile Manufacturers Association and the Truck Trailer Manufacturers Association, whose object is to improve the stopping ability of vehicles in combination.

Secondly, operators have come to realize that the criterion of brake performance for a combination vehicle does not necessarily lie in having the wheels lock up. The time factors in brake lag, which have been so well pointed out in the illustrations presented by Mr. Petring, have indicated that we must now strive to get time lags out of our vehicles. This has also been discussed in some detail by Mr. Bennett in his prepared discussion.

We are still, however, facing some real problems, both as manufacturers and as operators. Braking force in relation to the weight on a given axle of a vehicle still remains a problem. Mr. Petring has indicated that the empty condition of commercial vehicles when making emergency stops really needs some concise study.

As Mr. Tilden has pointed out, there seems to be a desire on the part of enforcement officials and others to adopt a dual standard of brake performance, one for passenger cars and one for commercial vehicles. Such an approach really poses problems to the truck fraternity, and a great deal of discussion is being given to this approach.

Many parties are discussing this approach, among them the D-7 Committee of the American Standards Association, and the Brake Subcommittee of the National Committee on Uniform Traffic Laws and Ordinances. Represented on these two committees are two groups of thinking. One is the truck operators and several of the supplier representatives who feel that a revision of our regulations at this time should look to a realistic standard that can be met by the vast majority of the vehicles on the highways. The other group consists of those who feel that a review of brake performance standards in 1954 should be striving to tighten up brake regulations in view of their not having been reviewed for some 10 years. Somewhere between these two schools of thought there will undoubtedly be some compromising, and this will undoubtedly be the final outcome.

One of our discussers has mentioned the possibility of having the regulations so tightened up that it would restrict a very large proportion of all commercial vehicles from using our highways. This is obviously unrealistic, and any such approach as this does not look at the facts of the situation. We certainly need an open-minded approach from all parties, and I feel that a meeting such as this, where open discussion of these problems can be had, is a great help toward promoting a solution of this very important problem.

The New Look in Lubricating Oils

J. B. Bidwell and R. K. Williams,
Research Laboratories Division, GMC

This paper was presented at the SAE Summer Meeting, Atlantic City, June 9, 1954.

OVER the past 20 years lubricating-oil technologists have maintained as a primary objective the improvement of lubricants both with respect to reduced sludge and varnish formation and to the handling of fuel and lubricant oxidation products which are corrosive to engine components. The development of crankcase oils with the necessary dispersant and corrosion-preventive properties has progressed to the point that most commercial lubricants are now adequate in these important respects.

With the development of engines of higher compression ratio and the increasing cost of higher octane fuels, the petroleum industry has more recently devoted considerable attention to the manner in which selection and compounding of lubricating-oil stocks affect the fuel antiknock requirements of engines. The problem of limiting the increase in antiknock requirements of engines due to combustion-chamber deposits has been studied diligently by many of the marketers of motor oil with the result that a number of improved products promising increased combustion-chamber cleanliness have been introduced during recent months.

For the most part the newer oils differ from conventional lubricants in that they are prepared from distillate oils boiling within relatively narrow ranges. Fractions of low volatility increase combustion-chamber deposit formation, and these, along with the highly volatile components which cause poor oil-consumption characteristics, are generally removed. Since the viscosities of these fractions are considered too low for use in automotive service, viscosity index (V.I.) improvers are usually added to increase the viscosity at engine operating temperatures. The viscosity index of the resulting oils is generally well above 100 and often permits one formulation to meet the viscosity

OCTANE requirement increase and combustion-chamber deposit weights are lower with the new high V.I. oils than with conventional SAE 20-20W oil containing bright stock, according to the authors.

Fuel economy at 30 mph constant speed is slightly better, they found, using the new high V.I. oils than it is when a 100 V.I. lubricant of equivalent Saybolt viscosity at 210 F is used. The high V.I. oils seem to have no advantage in normal suburban highway driving.

Intake-valve deposits are heavier with the new high V.I. oils than with conventional lubricants. Whether these deposits are due to the V.I. improver or to failure of the volatile base stocks to wash the deposits from the valve backs is not known.

The Authors

J. B. BIDWELL (M '54) is assistant head of the Mechanical Development Department of General Motors Research Laboratories. He received his B.S. in Mechanical Engineering in 1942 from Brown University. After graduation he joined the Research Laboratories Division of General Motors and worked on bearings and other engine components. During 1944 and 1945 he worked at the Naval Research Laboratory.

R. K. WILLIAMS (M '52) is assistant head of the Fuels and Lubricants Department of General Motors Research Laboratories. He received his B.S. in Chemical Engineering from Princeton University in 1940. Since that time he has been with the Research Laboratories Division of General Motors Corp.

specifications for several different SAE grades.

Coincident with the development of high V.I. lubricants with reduced combustion-chamber deposit-forming tendencies, the specific power output of automotive engines has increased steadily as have stresses on many of the working parts. This change has placed increased importance upon the ability of the lubricant and sliding metal parts to operate together without metal fatigue or wear. For this reason, engine performance with respect to fatigue and wear when the new high V.I. commercial lubricants are used is of considerable interest both to the petroleum and automotive industries.

As a result of the mounting interest in the new high V.I. lubricants, octane requirement increase, combustion-chamber deposit formation, gasoline economy, and engine wear have been investigated using a number of commercial motor oils of this type.

Effect on Fuel Antiknock Requirement

Until comparatively recently, automotive engineers and petroleum technologists have been unable to agree on the practical importance of lubricant composition relative to knock and surface ignition due to combustion-chamber deposits. Within the last two years, however, a number of investigators[1-4] have shown that important reductions in the harmful effects of combustion-chamber deposits can be made by control of lubricating-oil base stock, volatility, and additive treatment. One of the most important factors in overcoming the reticence of some to recognize the practical importance of these advances in lubricating-oil technology has been proof[5] that proper lubricant choice can cause significant reductions in fuel antiknock requirements of cars in normal customer service.

Because the effects of lubricant composition on knock and surface ignition due to combustion-chamber deposits are now well documented, they will be treated only briefly here to illustrate the benefits of a number of the improved oils now marketed commercially.

The ORI-1 laboratory test, used by the Research Laboratories Division of General Motors Corp. to predict the relative performance of lubricating oils with respect to combustion-chamber deposits and knock, entails the use of 1953 V-8 engine A operated on a light-load dynamometer cycling schedule. The operating conditions for this test are given in Appendix I.

Combustion-chamber deposit weight and octane requirement increase in terms of commercial-type gasolines have been determined for eight commercial lubricants using this test procedure. Oils A, B, and C are graded SAE 10W-30, while oils D, E, and F are graded SAE 5W-20. Oil H is of the improved type meeting the SAE 10W-20 specification.[6] As can be seen from the vacuum distillation data in Appendix II, all of these oils are more volatile than oil G. All contain V.I. improver and, by virtue of their additive treatments, are classified for service MS. SAE 20-20W oil G contains bright stock and was included to illustrate the heavy combustion-chamber deposits and high fuel antiknock requirements caused by some conventional motor oils. Fig. 1 is a plot of octane requirement increase (ORI) in terms of Research octane numbers and combustion-chamber deposit weights averaged for two runs with each oil. ORI with the improved lubricants ranged from 1.5 to 4.2 as compared to 8 for oil G, the conventional oil containing bright stock. It can be seen that among the improved-type lubricants combustion-chamber deposits are generally lowest for oils showing lowest ORI. However, the difference in ORI between oil G and the improved oils is greater than might be expected from the combustion-chamber deposit relationship.

During the ORI-1 tests the observer listens for wild ping, erratic knocking, or other manifestations of uncontrolled combustion each half hour during the full-throttle operating period and records the number of occasions during which these types of surface ignition are observed either prior to or during the measurement of borderline knock spark advance on the 93 Research octane number fuel. While this method of observation leaves something to be desired, it is considered noteworthy that surface ignition was observed on 77 occasions during

---

[1] See SAE Transactions, Vol. 61, 1953, pp. 361-376 + (disc) 376-377: "Combustion-Chamber Deposition and Knock," by H. J. Gibson, C. A. Hall, and D. A. Hirschler.

[2] "Crankcase Oil – An Approach to the Combustion-Chamber Deposit Problem," by R. L. Overcash, W. Hart, and D. J. McClure. Paper presented at SAE Annual Meeting, Detroit, Jan. 14, 1954.

[3] See SAE Transactions, Vol. 62, 1954, pp. 228-242: "Effect of Lubricant Composition on Combustion-Chamber Deposits," by J. G. McNab, L. E. Moody, and N. V. Hakala.

[4] See SAE Transactions, Vol. 62, 1954, pp. 57-65 + (disc) 68-70: "Some Effects of Fuels and Lubricants on Autoignition in Cars on the Road," by R. K. Williams and J. R. Landis.

[5] "Effects of Lubricating Oil on Octane Requirement of Cars in Customer Service," by P. A. Bennett and J. R. Landis. Paper presented at SAE Cleveland Section Meeting, Jan. 18, 1954.

[6] For complete physical properties of all oils discussed in this paper, see Appendix II.

the two runs with oil G and on only three occasions during the entire 14 runs with the improved oils. These observations confirm the results of previous investigations[2, 4] which have shown the marked superiority of distillate oils over those containing bright stock with respect to surface ignition due to combustion-chamber deposits.

Effect on Fuel Economy

Of the advantages claimed for the new-type oils of high viscosity index, one of the most interesting to the automotive engineer is the reduction in gasoline consumption brought about by a reduction in engine friction.

Georgi[7] has shown that fuel economy of fully warmed-up engines operated with oils of comparable Saybolt viscosity is better for oils containing V.I. improver than for straight mineral oils. He has indicated, however, that the average motorist would be unlikely to detect this effect. Galindo and Miller[8] have reported results of road tests showing gains in fuel economy ranging from 5 to 16% for an SAE 10W-30 oil as compared to a conventional SAE 30 oil under low-speed, light-load operating conditions. To provide additional information on the effect of oil V.I. on fuel economy, road tests were conducted at constant speed and under highway conditions.

30-Mph Level-Road Tests – Changes in the effective viscosities of oils in engines should produce greatest effects on gasoline consumption under light-load conditions where friction constitutes a substantial fraction of indicated power. For this reason fuel economy with different lubricants was first investigated in 30-mph level-road tests using two 1953 Hydra-matic-transmission-equipped cars of the same make.

Total fuel to start the engine, accelerate the car to 30 mph, and maintain a constant speed of 30 mph was measured over a distance required to stabilize engine oil and water temperatures at their equilibrium values. Ambient temperature during these tests ranged from 25 to 30 F. The fuel was measured volumetrically at 0.3-mile intervals using a dual system which permitted filling one burette as gasoline was metered through the other.

In each test a commercial oil of the new high V.I. type was compared with a conventional oil without V.I. improver. After conducting observations on a number of days in both cars, the oils were interchanged between cars and an equal number of observations obtained in order to eliminate car differences from the comparisons. Fuel-economy comparisons between pairs of oils run simultaneously were based on the average of the results obtained in both cars. In order to eliminate any effects due to slight variations in the average temperatures under engine starting conditions, comparisons have been made only between oils run on the same days.

Figs. 2 to 4 illustrate the average fuel saving as a function of trip mileage for the higher V.I. oil in three separate 30-mph level-road tests. Oil D used in the comparison of Fig. 2 was a commercial 5W-20 motor oil of 153 V.I. having a viscosity at 210 F of 50.3 SUS. Oil L was a commercial SAE 30 oil of 0 V.I. having a viscosity at 210 F of 62 SUS. The viscosity difference between these oils at 210 F and below was greater than that for any other pair of oils tested, and thus the comparison would be expected to favor the high V.I. oil quite markedly. As shown in Fig. 2 the fuel saving when the high V.I. oil was used decreased sharply from 30%

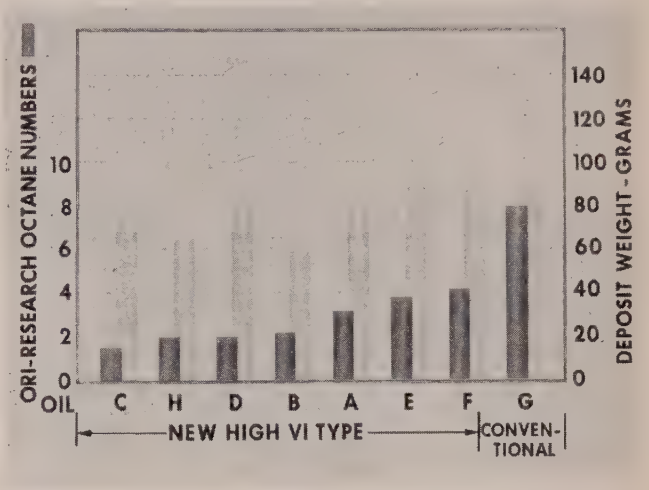

Fig. 1 – Octane requirement increase and deposit weight

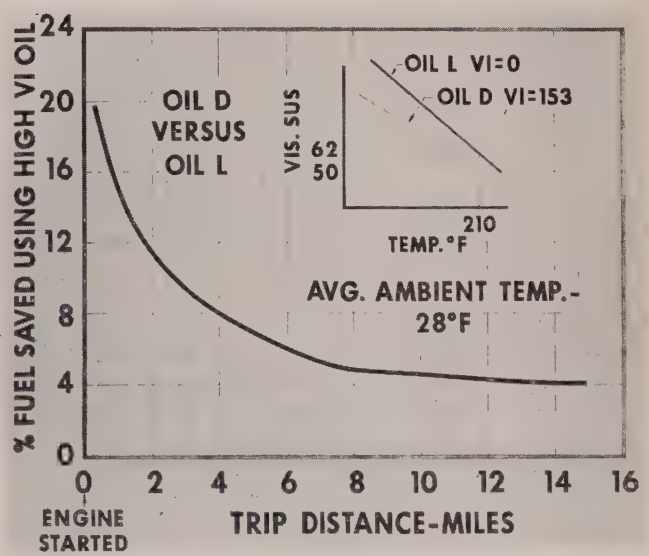

Fig. 2 – Per cent fuel saved, 30-mph level-road test – 153 V.I. SAE 20 oil over 0 V.I. SAE 30 oil

[7] See SAE Transactions, Vol. 62, 1954, pp. 385-389: "Some Effects of Motor Oils and Additives on Engine Fuel Consumption," by C. W. Georgi.

[8] See SAE Transactions, Vol. 62, 1954, pp. 390-391: discussion by H. F. Galindo and J. A. Miller.

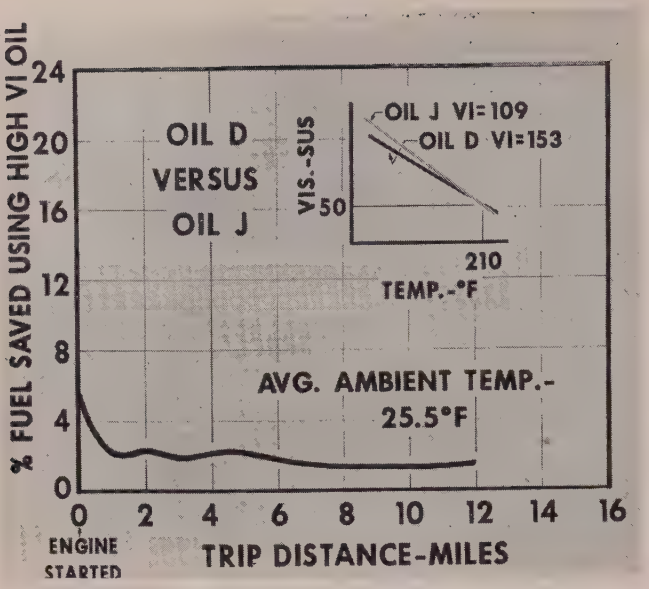

Fig. 3 – Per cent fuel saved, 30-mph level-road test – 153 V.I. SAE 20 oil over 109 V.I. SAE 20 oil

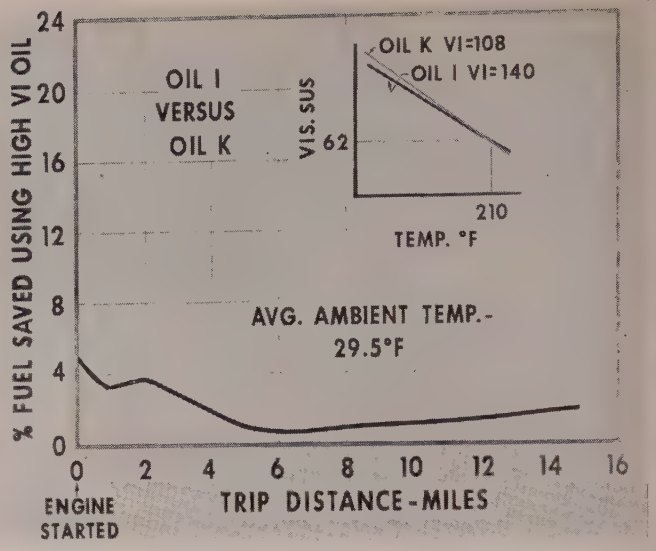

Fig. 4 – Per cent fuel saved, 30-mph level-road test – 140 V.I. SAE 30 oil over 108 V.I. SAE 30 oil

during the starting period to 4% for trip distances greater than 8 miles. The fuel saving shown in the high V.I. oil is in qualitative agreement with the results shown by Galindo and Miller[8] and, for very short distances, with the 15 to 25% advantage claimed for similar oils in some recent advertising.

The results in Figs. 3 and 4 compare oils of the improved types with oils of 100 V.I. containing no V.I. improver and having the same 210 F viscosities as the improved oils. These comparisons are believed to be more nearly representative of motorist experience since the percentage of commercial oils similar to oil L of Fig. 1 is relatively small. In Fig. 3 the fuel saving for oil D as compared to oil J decreases from 6% under starting conditions to 2% or less for trip distances greater than 1 mile. Similar results are shown in Fig. 4 for oil I, a commercial SAE 10W-30 oil of 140 V.I. as compared to oil K, a blend of commercial 100 V.I. oils containing no V.I. improver. The 2 to 6% fuel saving for the oils containing V.I. improver observed under carefully controlled road-test conditions is consistent with the saving indicated by Georgi[7] in dynamometer tests.

Some idea of the fuel saving in miles per gallon for the comparisons in Figs. 2 to 4 may be obtained from Fig. 5. In this figure the average miles-per-gallon saving as a function of trip distance has been determined for the comparisons shown in Figs. 2 to 4. The average economy figures for the two cars operated on all three oils without V.I. improver are used as a basis in computing the savings. These data indicate that the saving to the motorist in the extreme case of oil D versus oil L would be less than 1 mpg and in the more likely cases, as exemplified by the cases of oil D versus oil J and oil I versus oil K, would be less than 0.3 mpg.

Highway Tests – In order to investigate the friction characteristics of oils as reflected by gasoline economy under suburban driving conditions, a second series of tests was run using two 1953 cars incorporating torque-converter transmissions. Since no speed restrictions were placed upon the drivers in these tests, effects due to differences in driving techniques were minimized by alternating drivers between trips which averaged 70 miles. To eliminate effects due to car condition, oils were interchanged between cars at 1200-mile intervals. Since the power absorbed in overcoming engine friction constitutes a smaller percentage of indicated power under these high-speed conditions than in the case of the 30-mph constant-speed tests, it was expected that the fuel-economy differences between oils would be smaller than in the constant-speed tests.

The results obtained with oils D, J, I, and K are shown in Table 1. The average fuel economies indicate no consistent relationship between oil V.I. and fuel economy, and thus it is concluded that there is no advantage in favor of high V.I. oils over conventional oils of comparable 210 F viscosity in this type of service. The 0.3-mpg average advantage in fuel economy for the oils having viscosities of 50 SUS at 210 F as compared to the oils of 62 SUS at 210 F is in good agreement with the effects due to a change of one SAE viscosity grade reported by Georgi.[7]

Dynamometer Tests – In order to shed additional light on the effect of oil viscosity and V.I. on fuel

economy, friction tests were conducted in a single-cylinder engine especially adapted to this work. The principal mechanical elements are identical with those used in a current V-8 passenger-car engine. Motoring friction measurements were made with oils M, N, and O over the speed range from 1000 to 3000 rpm with the water jacket and oil temperatures held constant at 190 F. Oil M was a naphthenic-base oil of low V.I. Oil N consisted of M plus V.I. improver. Oil O was an uncompounded paraffin-base oil which very closely matched the viscosity of oil N over the entire temperature range. The viscosity-temperature relationships for the three oils are shown in Fig. 6.

The absolute viscosities of oils N and O are approximately 50% greater than that of oil M. However, the motoring friction results also shown in Fig. 6 indicate that the complex rubbing surfaces in the engine do not recognize the presence of the V.I. improver, and the motoring frictions for oils N and M, the naphthenic-base oil with and without the V.I. improver, practically coincide over the entire speed range. The motoring friction is approximately 10% less with these oils than with the uncompounded paraffinic oil. This result is not influenced by the engine temperature because the paraffinic oil and the V.I. improved oil have matched viscosities over the whole temperature range.

Measurements of engine friction under conditions when the engine was firing were also made by measuring indicated and brake power. The results are essentially the same as those obtained in the motoring tests. The results are in qualitative agreement with those of Frazier, Klingel, and Tupa[9] who conclude that engine friction is related more closely to viscosity at high shear rate than to viscosity measured at low shear rate. These results raise an important question concerning the minimum base oil viscosity which can be tolerated by engine bearings and other metal parts which subject the engine oil films to high rates of shear and are dependent upon adequate oil film viscosity for satisfactory performance.

Summary of Fuel Economy Tests – Because mechanical friction is related to effective viscosity of the lubricant in the engine, it would be expected that the fuel consumption of engines operated with V.I. improved oils, whose viscosities decrease with rate of shear,[10] would be lower than with oils of comparable viscosity without V.I. improver. The advantage for the oils containing V.I. improver should be dependent on engine operating conditions and should be greatest under light-load conditions where a substantial percentage of indicated power

Table 1 – Fuel Economy of Oils D, J, I, and K

Oil	Viscosity at 210 F, SUS	V. I.	Fuel Economy, mpg		
			Car 466	Car 468	Average
D	50.3	153	14.58	14.85	14.7
J	50	109	14.28	15.29	14.8
Average					14.8
I	62.3	140	14.37	14.35	14.4
K	62.0	108	14.42	14.70	14.6
Average					14.5

[9] See *Industrial and Engineering Chemistry*, Vol. 45, October, 1953, pp. 2336-2342: "Friction and Consumption Characteristics of Motor Oils," by D. Frazier, A. R. Klingel, and R. C. Tupa.

[10] See "Motor Oils and Engine Lubrication," by C. W. Georgi. Published by Reinhold, New York, 1950.

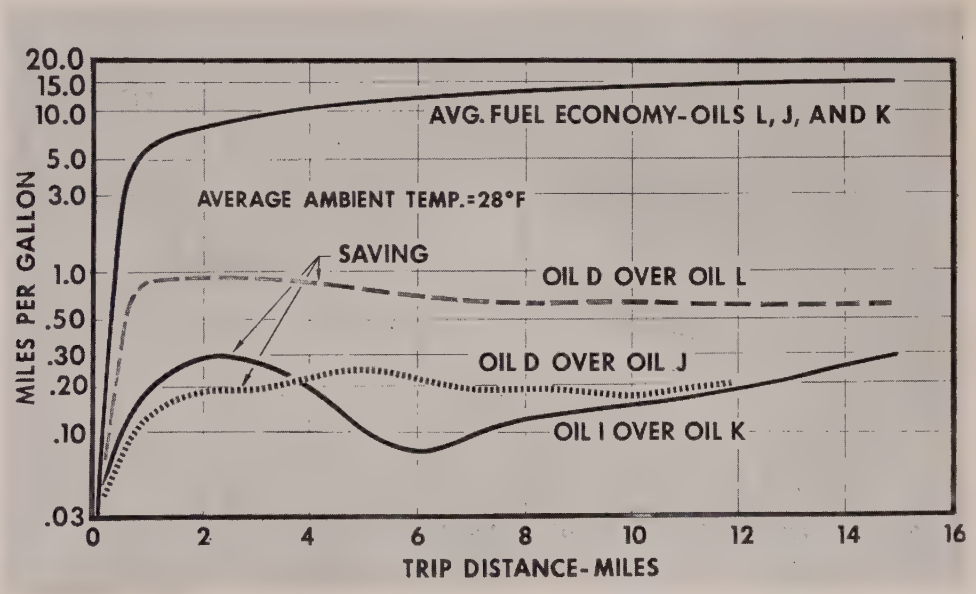

Fig. 5 – Fuel saving in miles per gallon for high V.I. oils, 30-mph level-road test

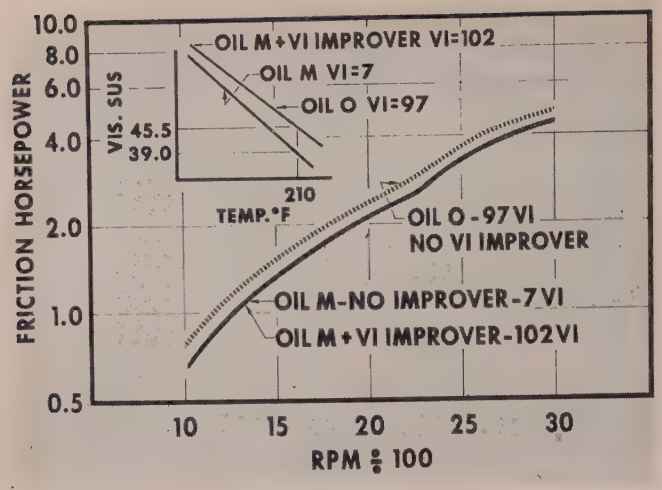

Fig. 6 – Effect of V.I. improver on motoring friction, single-cylinder engine, 6.6 compression ratio, oil and water temperatures 190 F

is required to overcome mechanical friction.

Carefully controlled tests confirm that this is indeed the case but that the advantages for oils containing V.I. improver are of the order of only 2 to 5% under light-load conditions. To detect the still smaller differences that would be expected under city or country driving conditions would require a program of statistical proportions because of the large effects of variations among drivers and traffic conditions. For this reason, it is not surprising that the high V.I. oils did not show any advantage in the highway tests. The results of the constant-speed tests described here and the fact that Frazier et al.[9] have shown "highly significant gasoline mileage differences in favor of oils containing polymers" in statistical field tests indicate that the oil industry's trend to oils containing V.I. improvers should result in a small but definite increase in car miles per gallon of gasoline and a commensurate conservation of our valuable crude-oil reserves.

Effect on Engine Wear

While it is desirable to use a lubricant which will permit fullest utilization of fuel octane numbers and provide the best fuel economy, it is imperative that gains in these qualities be made without sacrifice of the antiwear properties required for long life of the rubbing surfaces in the engine. The extensive efforts by both the oil and automotive industries to improve the wear-reducing properties of lubricating oils are indicative of the importance of the problem.

A number of factors have accentuated the wear problem. Engine designs have made greater demands upon lubricant performance, and the low sound levels in modern automobiles have made the customer more critical of any additional noise resulting from engine wear.

The contact area between the cam and the valve lifter has proven to be one point most sensitive to differences in lubricants, though it is equally dependent upon proper design and metallurgy for satisfactory wear performance. Since the loss of metal from these parts is readily measured and since some correlation with wear of other rubbing surfaces has been demonstrated,[11, 12] the authors have determined the wear-preventive properties of the lubricants discussed in this paper using cam and lifter wear tests.

Test Procedures – Cam and lifter wear tests have been run in two engine designs with three metallurgical combinations. The LS-5 test is run in a 1953 model of engine D, and the LS-6 test uses the 1954 model of the same 6-cyl valve-in-head engine. In the LS-5 test, chilled-iron valve lifters are run with a forged steel camshaft. The LS-6 test is run with six carburized steel lifters and six hardened alloy iron lifters operating on a hardened alloy iron camshaft. Carburized steel lifters and a hardened alloy iron cam are used in the ORI-1 test. The details of all of these test procedures will be found in Appendix III.

Valve Spring Loads – It will be seen from the engine modifications in Appendix III that valve spring load is closely controlled. This load has an important effect upon the type and the degree of failure, and it might appear that the 240-lb static spring loads used in the LS-5 and LS-6 tests are excessive. It must be remembered however that cam and lifter wear problems are most pronounced at low and moderate engine speeds since at higher speeds valve-gear inertia forces tend to reduce the maximum loads at the point of contact. The contact stresses are plotted as a function of the position of the point of contact on the lifter face in Fig. 7 for the standard 160-lb springs used in the 1953 model of engine D both under static conditions and at 3150 rpm where the inertia effects tend to reduce the maximum stress. Also shown are the stresses, including the inertia effects, for the 240-lb springs experienced at 3150 rpm. It is apparent from this comparison that the increased spring load in the laboratory tests does not appreciably increase the maximum stresses over those which would occur with standard springs at low speed where inertia effects are negligible. The increased spring load makes it possible to increase the cycling rate by increasing engine speed while at the same time maintaining a stress magnitude approximating the more severe, low-speed operation conditions. The valve spring load in the LS-6 test is the same as that used in the LS-5 test, but

---

[11] "Engine Wear as Affected by Lubricants," by H. C. Mougey, presented at Symposium on Engine Lubrication, Technical Committee B, ASTM Committee D-2, Atlantic City, July 1, 1953.

[12] See pp. 192-203 of this issue: "Wear, Scuffing, and Spalling in Passenger-Car Engines," by H. A. Ambrose and J. E. Taylor.

it is adjusted to the correct load at 0.060-in. greater deflection. This is necessary to accommodate the greater lift on the 1954 cam. With the modifications given in Appendix III, the contact stresses in the two tests are essentially the same.

In the ORI-1 tests the springs are shimmed to a load of 80 lb at a 0.003- to 0.005-in. valve opening. This is only 19 lb higher than the mean spring load and only slightly greater than the maximum which could result from cumulative tolerances. The maximum spring load is increased by the same increment as the opening load.

Service Correlation – In a previous paper,[13] correlation of LS-5 test results with passenger-car service in car D was established for several lubricants. The LS-6 test, which is performed under essentially the same conditions, indicates wide differences in oil performance, but lack of comparable service tests has precluded correlation with field results. ORI-1 test results indicate excellent duplication of service failures for a limited number of lubricants which have been service tested in car A.

LS-5, LS-6, and ORI-1 Test Results – Tabulated results of cam and lifter wear tests on a number of the new high V.I. crankcase oils are given in Table 2. The properties of these oils are listed in Appendix I. The oils listed in this table are all of the type made from low-viscosity distillate base stocks with large amounts of V.I. improver added to obtain the desired physical properties.

The oils have been listed in order of increasing pitting severity in the LS-5 test. Pitting severity is simply the percentage of rotating lifters which suffer fatigue. Lifter and cam wear are also shown for each of the test procedures. Varying levels and types of additive treatment are represented in this table. Both the type and quantity of additive have a pronounced influence upon the performance of an oil with regard to wear, but with the great variety found in commercial lubricants, it is difficult to separate these materials into a small number of classes. Instead, only two factors have been noted by superscripts after the oil code. The superscript 1 denotes oils which contain some phenol-type material, and 2 appears after lubricants which contain no zinc dithiophosphate. No attempt is made to indicate relative amounts in this rather crude classification.

Examination of the LS-5 results indicates that, in general, both cam wear and lifter length loss increase with pitting severity. The change in length of the chilled-iron lifters has not been called wear since the metal loss in this case is the result of fatigue. Excessive cam wear occurs only after the lifter has become pitted.

The previous reference[13] describes tests in which

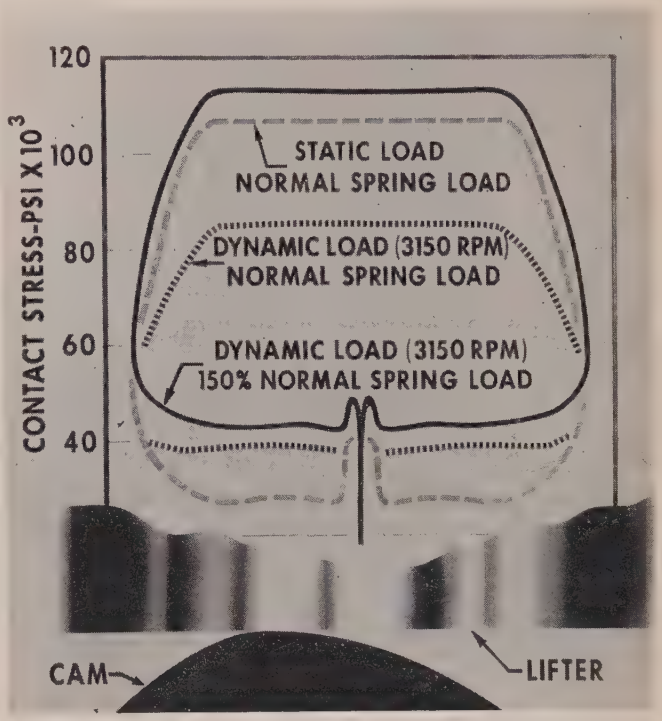

Fig. 7 – Lifter contact stresses

[13] See pp. 211-226 of this issue: "Lifters and Lubricants," by J. B. Bidwell and P. Vermaire.

Table 2 – Cam and Lifter Wear Measurements[a] with New High V.I. Oils

		LS-5 Results			LS-6 Results				ORI-1 Results	
					Steel Lifters		Alloy Iron Lifters			
Oil[b]	SAE Grade	Pitting Severity, %	Lifter Length Loss	Cam Wear	Lifter Wear	Cam Wear	Lifter Wear	Cam Wear	Lifter Wear	Cam Wear
E	5W-20	50	10	13	44	5	7	9	3.6	5.2
A	10W-30	54	17	65	73	11	4	8	4.9	3.8
P	5W	62	26	101	81	498	4	12	—	—
B[1]	10W-30	62	18	94	78	87	8	12	3.7	4.5
C[1]	10W-30	67	28	212	124	18	7	10	21.5	7.5
Q	5W-20	74	22	90	20	6	5	6	—	—
H[2]	10W-20	75	24	96	79	157	8	9	32	56
F[2]	5W-20	92	32	206	157	318	10	10	130	144
I[1]	10W-30	100	31	161	130	22	7	12	—	—
D[1]	5W-20	100	42	340	152	22	8	13	—	—

[a] All wear values are shown in tenths of thousandths of an inch.
[b] Superscript [1] denotes oil that contains some phenol-type additive. Superscript [2] denotes oil that does not contain any zinc dithiophosphate.

selected additive materials were compounded in a single base stock typical of those used for commercial oils. It was shown for the combination of steel cam and chilled-iron lifters that zinc dithiophosphate reduced pitting and wear. Other materials, notably the phenol type, caused severe pitting. Tests were not conducted with mixtures of the two materials, and therefore the performance of these materials in combination is not known. Some of the oils such as B, C, I, and D are of this general type. There is considerable spread in pitting and wear performance which might be explained by the differences in the quantities of the various additives which are involved. The LS-5 test appears to rate materials containing zinc dithiophosphate and some detergent of other than phenol type generally higher than oils of the other types. It should be pointed out that none of the oils in Table 2 gives what is considered a satisfactory LS-5 test and that, with the excessive wear shown, considerable scatter may be expected. The results do, however, check qualitatively those obtained with individual additive components.[13]

The trends indicated in the LS-5 tests are also evident in the LS-6 and ORI-1 results. The high wear experienced with steel lifters and the cams on which they operate when they are run with oils H and F should be noted. These are the only two oils which contained no zinc dithiophosphate. The result applies to the ORI-1 as well as the LS-6 test, though the engine designs and loads are different. Excessive wear also occurs with some of the other oils in the LS-6 tests. Reasonably good correlation is apparent between steel lifter results in the LS-6 and the ORI-1 tests, though the former appears to spread out the results of oils of intermediate quality. As has been previously reported by several investigators, the hardened alloy iron lifters and cams appear to be most tolerant of oil antiwear quality in the LS-6 test. It is felt that greater differences between oils might be obtained after extended running.

While the use of alloy iron lifters and cams appears to solve the valve-gear wear problem, it is believed that the wear shown with other metallurgy combinations in the tests described here is analogous to the wear of other critical engine components. Therefore in order to provide wear protection for these other engine parts, the wear-preventive properties of lubricants should also satisfy the needs of steel and chilled-iron lifters in these tests.

The results tabulated in Table 3 were obtained with conventional oils of higher base oil viscosity and less V.I. improver than the oils in Table 2.

These were selected for comparison of octane requirement and wear with the new high V.I. products. The wear and pitting results indicate that there may be some effect of viscosity upon these failures, though this is somewhat complicated by differences in additive composition and by the inclusion of bright stock in some of these oils. The conclusions to be drawn from these data would be similar to those previously reached. It is apparent that some SAE 10 and 20 oils may be as bad both with chilled-iron and steel lifters as the new high V.I. products. This fact emphasizes the importance of the specific additive composition.

Modified Commercial Oils – None of the commercial oils tested were considered entirely satisfactory from the standpoint of LS-5 and LS-6 wear results. To determine if improvement of some of these commercial oils were possible, three oils were selected and modified. Oils B, P, and F are each compounded with a different type of additive. A sufficient quantity of zinc dithiophosphate was added to each of these finished oils to increase the zinc concentration by about 0.12%. The LS-5 and LS-6 test results are shown in Fig. 8 for the original and the modified oils.

Pitting was completely eliminated from the chilled-iron lifters for all three modified oils. Similar striking reductions were made in lifter length loss and cam wear for the chilled-iron lifter, steel cam combination. In the LS-6 test the tremendous reduction in cam wear is outstanding. Evidently zinc dithiophosphate is a desirable antiwear agent for both the metallurgical combinations used in these tests. Other materials may produce similar beneficial effects. The effect of concentration of zinc dithiophosphate has not been determined, but study of the results obtained with commercial oil

Table 3 – Cam and Lifter Wear Measurements[a] with Conventional Oils

		LS-5 Results			LS-6 Results					
					Steel Lifters		Alloy Iron Lifters		ORI-1 Results	
Oil[b]	SAE Grade	Pitting Severity, %	Lifter Length Loss	Cam Wear	Lifter Wear	Cam Wear	Lifter Wear	Cam Wear	Lifter Wear	Cam Wear
E	20W	42	15	52	—	—	—	—	—	—
S	20W	42	21	64	—	—	—	—	6	3
R[1,2]	20W	50	18	41	52	473	4	10	40	152
X	10W	75	15	89	91	90	8	9	—	—
Z[1]	10W	100	30	100	—	—	—	—	—	—
G[2]	20W	—	—	—	41	10	6	8	5.5	7

[a] All wear values are shown in tenths of thousandths of an inch.
[b] Superscript [1] denotes oil that contains some phenol-type additive. Superscript [2] denotes oil that does not contain any zinc dithiophosphate.

formulations indicates that the quantity required to minimize wear is dependent upon both the type and quantity of the detergent additive used.

Influence of Individual Additive Components – V.I. improver accounts for an appreciable volume of a finished lubricant of 130 to 150 V.I. Accordingly, some tests were conducted to determine the effect of the V.I. improver alone in the base oil. First, the base oil from the commercial lubricant F was run without V.I. improver, oxidation inhibitor, or detergent. The same base stock was then run with the same quantity of V.I. improver as is used in the finished oil but again omitting oxidation inhibitor and detergent. These LS-5 and LS-6 results are shown in Fig. 9 along with the results obtained with the finished oil and also with the finished oil modified with zinc dithiophosphate. LS-5 results were satisfactory with the base oil, but the cam wear running with steel lifters was excessive in the LS-6 test. The addition of the V.I. improver alone caused much poorer LS-5 results, but the steel lifter and alloy iron cam wear in the LS-6 test were greatly reduced.

Further addition of the oxidation inhibitor and detergent to produce the finished commercial oils resulted in very bad performance in both tests. As was shown earlier, addition of zinc dithiophosphate to the finished oil restores antiwear properties to the material. The nature of these results indicates that the particular oxidation inhibitor-detergent combination used in this oil is not desirable from the wear standpoint. The mechanism by which the V.I. improver reduces the wear experienced with the base oil alone in the LS-6 tests is not understood. It would appear to be some type of chemical process, since it has been shown in the section on engine friction that the effective viscosity is about that of the base stock when V.I. improvers are used.

Summary of Wear Tests – Engine tests with three commonly used metallurgical combinations have shown sizable differences in the antiwear performance of several of the new high-V.I. crankcase oils. None of these oils was entirely satisfactory in these tests. This is possibly due to some effect of viscosity but more probably results from particular additive formulations used. The results are in qualitative agreement with previous work using individual additive components. These results have shown the beneficial effects of zinc dithiophosphate additions to commercial oils. Further study of additive combinations including V.I. improver is desirable.

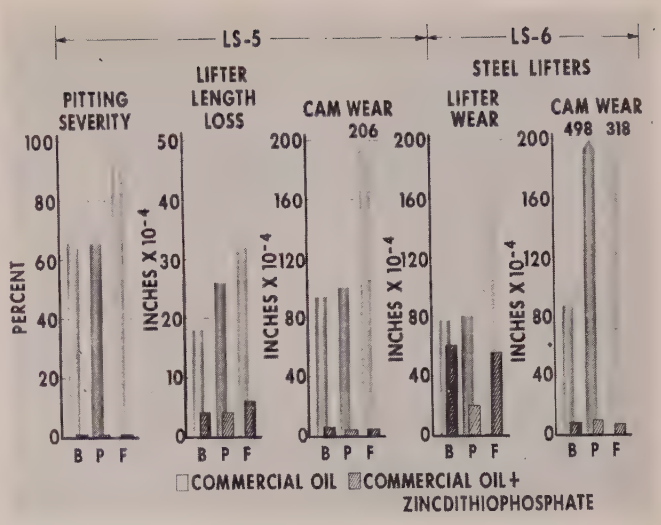

Fig. 8 – Effect of zinc dithiophosphate additions on LS-5 and LS-6 performance of three commercial oils

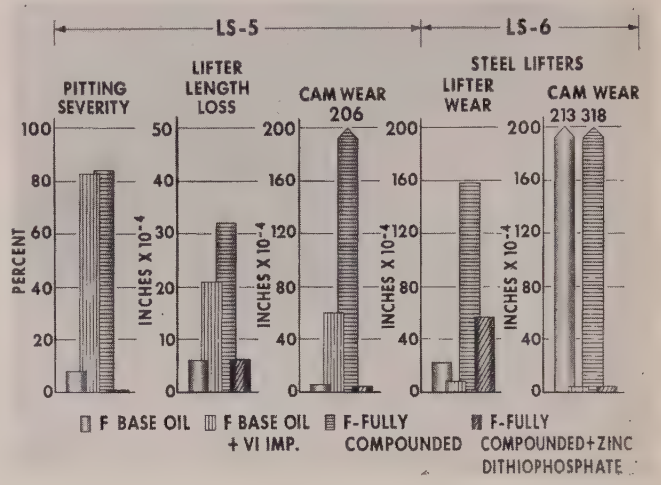

Fig. 9 – Effect of individual additive components on LS-5 and LS-6 performance of commercial oil F

Relation of Pitting to Wear

Havely, Phalen, and Bunnell[14] have reported that with some engine designs and metallurgical combinations, good antiwear materials, such as zinc dithiophosphate, may apparently cause lifter pitting. It is also noted by Ambrose and Taylor[12] that pitting may be encountered when wear is reduced by means of oil additives. Superficially these results appear to be in contradiction to our LS-5 and service test results.

The following discussion is aimed at a better understanding of the relationship between the two common types of lifter failure, pitting and wear. Pitting of the lifter face is the result of fatigue caused by repeated stressing of the material near the lifter surface. Cracks are produced in the metal which propagate approximately parallel to the surface until plates of material are freed. The progress of this type of failure is shown in Fig. 10. The

[14] See pp. 204-210 of this issue: "Influence of Lubricant and Material Variables on Cam and Tappet Surface Distress," by T. W. Havely, C. A. Phalen, and D. G. Bunnell.

wear and surface damage is small until a sufficient number of cycles to cause failure has occurred. Lifter length then changes rapidly, and after the pitting has progressed, the cam wear rate rises.

Loss of metal by wearing is more uniform and continuous. The surface may be relatively smooth even though large amounts of metal have been removed. A badly worn lifter face is shown in Fig. 11.

Metals will fail by fatigue if stressed beyond their endurance limit as measured in the usual fatigue-test apparatus. Further, metals may fail by fatigue even if stressed below their endurance limit as measured in air when the environment promotes corrosion fatigue. A large percentage reduction in endurance limit can result from corrosion fatigue. From LS-5 results, it has been concluded[13] that oils differ in their tendency to promote corrosion fatigue and that zinc dithiophosphate reduces corrosion fatigue. Wear is not a problem in the case of the steel cams and chilled lifters, as evidenced by the low lifter wear obtained with base oils. Since these straight mineral oils will prevent both wear and fatigue under the LS-5 operating conditions, it is also clear that the endurance limit of the material is adequate in the absence of corrosion-fatigue effects.

How may wear influence the occurrence of fatigue? Since fatigue is the result of repeated stressing of material immediately adjacent to the loaded surface, it is clear that, if this surface layer is being worn off at a rate fast enough, no individual particle of the metal will be cyclicly stressed enough times to produce fatigue cracks before it is worn away. New material will always be appearing at the surface and will be removed before fatigue failure occurs. Thus it is possible for an oil which does not prevent wear to prevent fatigue failure. The wear rates necessary to prevent fatigue are dependent upon many factors, but they need not be very high. The stress gradient is so steep that only a thin layer of material is affected. In addition, a large number of stress cycles are required before failure occurs.

It has been pointed out in the case of our LS-5 tests, that zinc dithiophosphate prevents pitting. However, others[12, 14] have reported that pitting tendency may increase when this material is used. This apparent contradiction may be explained if the lifter material were operating beyond its en-

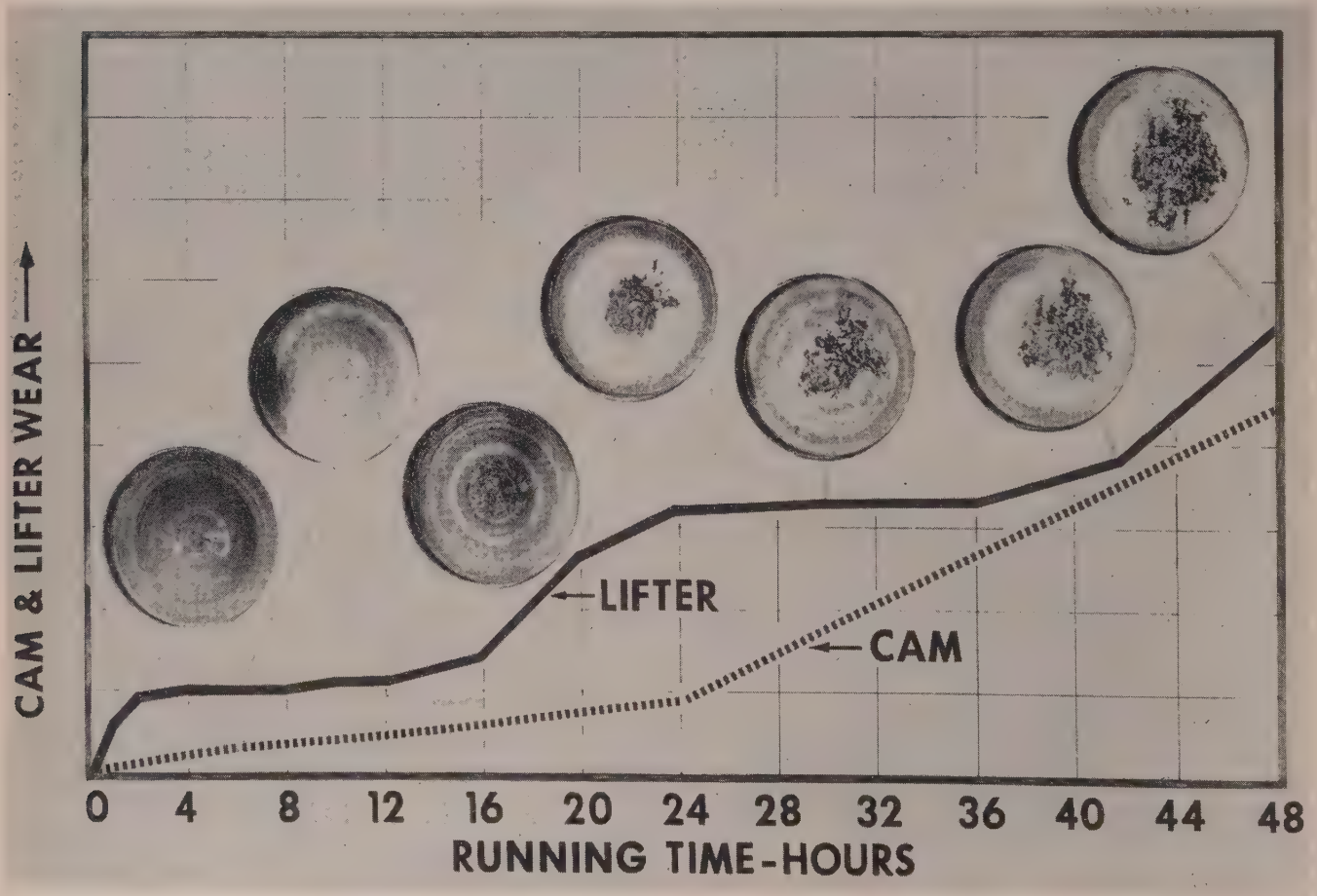

Fig. 10 – Progress of lifter fatigue leading to pitting

durance limit under their test conditions. Under these conditions fatigue would occur in the absence of corrosion fatigue if the wear rate were low. If the wear rate were large and fatigue did not occur, then addition of a wear-reducing agent could cause fatigue. This combination of metallurgy and operating conditions might be expected to be particularly difficult to lubricate since there is a delicate balance between rate of wear and fatigue.

Intake-Valve Deposits

Use of the new high V.I. oils under dynamometer and road-test conditions has usually resulted in exceptional engine cleanliness from the standpoints of varnish and sludge. However, excessive quantities of light, carbonaceous deposits on the backs of intake valves have been observed in road tests. These deposits are considered highly undesirable since they have been known to cause sluggish valve action, power loss, and in serious instances valve burning.

Representative photographs of intake valves from cars operated for 8000 to 10,000 miles under moderate-duty conditions are shown in Fig. 12. Oils B and I are marketed in the SAE 10W-30 grade and are made from volatile base stocks with V.I. improver. Oils G and S are conventional lubricants of lower volatility without V.I. improver. Oils B, I, and S are classified for service MS, while oil G contains a lower level of additive treatment and would fall within the API MM classification. It is quite apparent that the deposits are heaviest with the two new high V.I. oils and are very light with oils G and S.

Table 4 – Total Intake-Valve-Back Deposits

Group I New High V. I. Oils			Group II Conventional Oils		
Oil	SAE Grade	Weight, g	Oil	SAE Grade	Weight, g
A	10W-30	16.8	G	20W	6.9
B	10W-30	15.9	S	20W	5.1
C	10W-30	15.9	R	20W	6.0
D	5W-20	16.6			
E	5W-20	10.0			
F	5W-20	20.2			
H	10W-20	17.0			

Fig. 11 – Badly worn lifter face – steel lifter run on alloy iron cam, LS-6 test

Fig. 12 – Intake-valve deposits

Similar results have been observed in comparing the intake-valve appearance and deposit weights for dynamometer tests using the schedule described in Appendix I. A comparison of the deposit weights from the new-type oils and from conventional oils is given in Table 4.

As indicated by this tabulation the intake-valve deposit weights are, without exception, higher with the new high V.I. oils. While this evidence might suggest that the deposits are associated with the V.I. improver, the base stocks used in the oils in group I are in general more volatile and less viscous than those in group II. Whether the use of V.I. improvers in less volatile base stocks would produce similar effects is not known.

Summary

Performance characteristics in automotive engines have been investigated for several commercial lubricants of the new high V.I. type directing particular attention to octane requirement increase, fuel economy, valve-gear wear, and intake-valve deposits.

Octane requirement increase and combustion-chamber deposit weights were lower with these oils than with a conventional SAE 20-20W oil which contained bright stock.

Fuel economy at 30 mph constant speed was slightly better using the new high V.I. oils than when using a 100 V.I. lubricant of equivalent Saybolt viscosity at 210 F. The advantage in favor of the high V.I. oils decreased from 6% under engine starting conditions to 2% or less for trips greater than 4 miles. No advantage in favor of the high V.I. oils was detected in normal suburban highway driving.

Evidence is presented that the effective viscosities of oils in engines are unaffected by the addition of V.I. improvers. This evidence helps explain the improved fuel economy at light load when oils containing V.I. improver are used. However, it raises a serious question as to the minimum viscosity of the base oil which can be used with V.I. improver if satisfactory engine lubrication is to be maintained.

Cam and valve lifter wear tests indicate large differences in the abilities of these commercial lubricants to prevent wear and metal fatigue. Satisfactory performance with chilled-iron lifters operating on steel cams and carburized steel lifters operating on hardened alloy iron cams is dependent upon oil additive composition. Suitable antiwear agents improve oil performance with both of these metallurgical combinations.

Evidence is presented indicating that intake-valve deposits are heavier with the high V.I. oils than with conventional lubricants. Whether these deposits are due to the V.I. improver or to failure of the volatile base stocks to wash the deposits from the valve backs is not known.

Acknowledgment

The authors wish to express their appreciation to J. R. Altenhoff, J. D. Fleming, W. J. Laita, G. K. Malone, R. E. Osborne, and W. A. Wiese for their help in gathering material for this paper.

APPENDIX I

ORI-1 Test – 1953 Engine A

1. Properties of Fuel Used for Deposit Accumulation:

Research octane number	93
Motor octane number	82
Tel, cc per gal	2.75 ± 0.25
Temperature at 10% evaporated, F	120 ± 15
Temperature at 50% evaporated, F	220 ± 15
Temperature at 90% evaporated, F	335 ± 10

2. Engine Conditions:

Compression ratio	8.25
Engine speed, rpm	2000
Coolant temperature, F	165
Oil temperature, F	180-195
Valve spring loads, lb	80 ± 2 at 0.003- to 0.005-in. opening

3. Cycling Schedule at 2000 Rpm:

(a) Operate 30 min at 12 bhp with spark set at 41 deg btc.

(b) Retard spark 10 deg past previous borderline knock setting.

(c) Open throttle for 5 sec.

(d) Measure borderline knock spark advance.

(e) Retard spark to 5 deg past borderline to complete total of 15 sec at full throttle.

(f) Close throttle to give 12 bhp with spark set at 41 deg btc.

4. Octane Requirement Determination at 2000 Rpm:

At 0 hr and every 10 hr to 100 hr measure borderline knock spark advance with commercial-type reference fuels. Determine engine Research octane number requirement by interpolation between two fuels having borderline knock spark advance bracketing 19 deg btc standard setting.

5. Test Duration:

Continue schedule in step 3 to 110 hr. Inspect, remove, and weigh combustion-chamber deposits.

APPENDIX II

Oil Inspection Data

New oil inspection data are given in Table 5 for oils A-M and in Table 6 for oils N-Z.

APPENDIX III

LS-5 Test Procedure

Engine: 1953 engine D, 6 cylinder, valve in head.

Test Parts: Chilled-iron lifters; forged steel cam; steel rocker shafts; malleable-iron rocker arms.

Operating Conditions:

Speed, rpm	3150
Load, bhp	30
Jacket temperature, F	190-200
Oil sump temperature, F	255

Table 5 – New Oil Inspection Data for Oils A–M

Lub Oil Code	A	B	C	D	E	F	G	H	I	J	K	L	M
SAE Viscosity Grade	10W-30	10W-30	10W-30	5W-20	5W-20	5W-20	20W-20	10W-20	10W-30	20W	20W	30	10W
Viscosity, SUS													
At 100F	333	265	346	176	186	175	347	244	304	242	420	998	122
At 210 F	62.3	58.5	67.6	50.9	50.4	51.3	56.7	55.4	62.3	50.5	62.3	62.3	39
V. I.	138	142	141	153	143	156	108	138	140	112	111	−19	7
Compounding													
Oxidation Inhibitor	Yes	Yes	Yes	Yes	Yes	Yes	Yes	Yes	Yes	Yes	Yes	Yes	No
Detergent	Yes	Yes	Yes	Yes	Yes	Yes	No	Yes	Yes	Yes	Yes	No	No
V. I. Improver	Yes	Yes	Yes	Yes	Yes	Yes	No	Yes	Yes	Yes	Yes	No	No
Sulfated Residue	1.33	2.47	0.88	0.91	1.25	0.58	0.03	1.00	0.70	0.82	0.92	0.06	Nil
Distillation Temperature (10 mm vacuum), F													
Initial	400	347	400	396	414	345	406	352	400	390	390	361	300
50%	463	454	465	457	503	452	550	490	488	510	596	523	419
90%	572	525	521	514	—	522	—	—	495	—	—	593	505
EP	590	530	550	550	605	549	620	555	502	631	653	599	540
% Distilled	93.0	90.5	95.0	91.6	85.0	95.0	66.5	89.5	92.5	80.5	60.5	92.0	97.5
Potentiometric Titration													
Total Acid Number	1.82	1.54	1.59	2.20	1.94	1.60	0.2	1.92	1.66	1.24	1.34	0.24	0.26
Total Base Number	2.94	8.76	0.19	0.49	3.01	0.63	2.40	3.75	2.66	1.89	2.17	0.24	0.04

Fuel — Commercial leaded
Test duration, hr — 24

Modifications: Dual valve springs used. Assembled valve spring load is 240 lb at 0.330-in. valve opening. Rocker shafts inverted.

LS-6 Test Procedure

Engine: 1954 engine D, 6 cylinder, valve in head.

Test Parts: Carburized steel and hardened alloy iron valve lifters; hardened alloy iron cam; steel rocker shafts; malleable-iron rocker arms.

Operating Conditions:

Speed, rpm	3150
Load	None
Jacket temperature, F	190-200
Oil sump temperature, F	255
Fuel	Commercial leaded
Test duration, hr	24

Modifications: Dual valve springs used. Assembled valve spring load is 240 lb at 0.390-in. valve opening. Rocker shafts inverted.

ORI-1 Test Procedure

Engine: 1953 engine A, V-8, valve in head.

Test Parts: Carburized steel lifters; hardened alloy iron cams.

Operating Conditions:

Speed, rpm	2000
Load, bhp	12
Jacket temperature, F	165
Oil sump temperature, F	180-195
Fuel	Commercial leaded
Test duration, hr	110

Modifications: Valve springs shimmed to provide assembled load of 80 lb at 0.003-0.005-in. valve opening.

Table 6 – New Oil Inspection Data for Oils N–Z

Lub Oil Code	N	O	P	Q	R	S	T	U	V	W	X	Y	Z
SAE Viscosity Grade	10W	10W	5W	5W-20	20W	20W	5W-20 base	5W-20	10W-30 base	10W-30	10W	20W	10W
Viscosity, SUS													
At 100 F	185	187	130	200	324	336	109	201	99	243	224	335	192
At 210 F	45.7	45.5	44	55.7	56	55.4	39.7	54.4	39	55.3	48.7	56.6	45.8
V. I.	102	97	142	156	108	104	80	152	84	139	107	110	98
Compounding													
Oxidation Inhibitor	No	No	Yes	Yes	Yes	Yes	No	No	No	No	Yes	Yes	Yes
Detergent	No	No	Yes	Yes	Yes	Yes	No	No	No	No	Yes	Yes	Yes
V. I. Improver	Yes	No	Yes	Yes	No	No	No	Yes	No	Yes	No	No	No
Sulfated Residue	Nil	Nil	1.03	1.32	1.13	1.30	0.01	0.02	0.01	0.01	0.76	0.83	0.79
Distillation Temperature (10 mm vacuum), F													
Initial	309	376	383	373	410	365	136	379	382	373	385	384	414
50%	418	528	471	485	560	571	479	479	466	467	505	538	503
90%	509	592	504	567	650	636	547	547	525	547	698	—	—
EP	511	605	505	587	660	650	590	574	536	566	698	694	570
% Distilled	90.5	90.5	93.0	93.5	92.0	94.0	98.5	98.5	93.0	95.0	90.0	87.0	84.5
Potentiometric Titration													
Total Acid Number	0.28	0.28	1.24	1.06	0.63	1.48	0.25	0.28	0.35	0.45	1.22	1.69	1.12
Total Base Number	0.09	0.09	3.30	2.06	3.99	3.84	0.05	0.07	0.14	0.07	1.74	2.74	3.72

Some Factors Affecting the Fatigue

FOR some time one of the duties of the authors' department in the Research Laboratories has been the appraisal through fatigue-testing procedures of the strength of full-scale steel members. Often a program of this kind has taken the form first of determining the strength of the part as it was initially produced, then following this with an evaluation of gains in strength which might be obtained through the most favorable choice of material, heat-treatment, and processing techniques.

In carrying out programs of this kind, considerable specific information is accumulated. In view of the large number of variables affecting the strength of steel members, the engineer hesitates to take the results of one program and apply them to a different type or scale of structure. On the other hand, this may be unavoidable, at least in the preliminary stages of a design. Over the long term it is hoped that strength data can be better correlated in terms of the influences of certain basic factors, care of course being taken not to generalize over too broad a range of material conditions.

The objectives of this report are first to assemble the results from several test programs for ready reference and secondly to examine them for corroboration of basic factors which have been proposed for predicting strength more accurately.

Only steels through a range from soft to medium hardness are discussed. High hardness, such as used for ball bearings, springs, and most gears, is not considered.

DATA from several fatigue-test programs are examined in this paper for corroboration of basic factors which have been proposed for predicting more accurately the fatigue strength of full-scale steel members. Important among these factors are hardness, service loading, range of stress, and sharpness of the stress gradient at the critical zone.

Although the type of steel is often regarded as a primary factor, its hardness may be more basic, as it correlates better with endurance limit than other physical tests. Test results show that this hardness-strength relationship is useful in evaluating the effect of surface treatments on strength improvement in soft and medium-hardness steels.

Heavy-Duty Crankshaft Studies

While the crankshaft of an automobile is designed primarily for rigidity, that for a truck, bus, or other heavy-duty application must be designed and fabricated for resistance to fatigue failure. Numerous alloys as well as heat and mechanical treatments have been investigated for improving crankshaft strengths and these studies provide the engineer with some of the most extensive data available for determining practical working stresses. The results of fatigue studies of one such shaft, that for a 4¼ x 5 diesel engine, are given in some detail here. This shaft, made of 5046 steel, had 2¾-in. diameter crankpins and fillet radii of 0.145 in. Tests were conducted in both flexure and torsion; the same order of merit for variations in treatment was found in torsion, however, as in

Strength of Steel Members

C. W. Gadd, J. O. Anderson, and David Martin,
Research Laboratories Division, GMC

Paper presented at SAE Golden Anniversary Annual Meeting, Detroit, Jan. 13, 1955.

flexure, and only the latter type loading will be reported.

Flexural studies were first performed by testing single-throw sections in equally reversed bending in a conventional resonant unit operating on the same principle as the "tuning fork" in Fig. 1. Failure occurred along the crankpin fillet, originating at a point in the plane of the throw. Calibration was obtained by 1/16-in. strain-gage measurements at this point. Several measurements may be made here at various angles in order to obtain one as near as possible to the maximum. Once this is done, however, there still remains some doubt when making a calibration of this kind as to whether the gage length employed is sufficiently short to give the true maximum stress in a small fillet.

The question may then be raised as to whether, with a finite gage length of say 1/16 in., the error in elastic stress determination in radii of 3/16 in. or less makes it impractical to even attempt any correlation between theoretical and actual fatigue strength. Results as given in the Appendix of trials of gages in small fillets by the authors have, however, proved quite promising; and such measurements are, therefore, considered in the present study.

Before embarking upon a program of improvement of the crankshaft,[1] it was felt advisable first to take special precautions to establish a valid and repeatable basic *S-N* diagram for the existing production shaft. Straightening was known to be a

The Authors

C. W. GADD is supervisor of vibration and stress analysis in the Special Problems Department of the General Motors Research Laboratories. He received a B.S. degree from M.I.T. in 1937. Since then, he has been with General Motors Corp.

J. O. ANDERSON is a research engineer in the Vibration and Stress Analysis Section of the Research Laboratories Division of General Motors. He received a B.S. in Mechanical Engineering from Michigan College of Mining and Technology in 1951. Immediately afterwards, he became associated with General Motors.

DAVID MARTIN is studying for his M.S. degree at the University of Illinois in the Department of Theoretical and Applied Mechanics. He received a B.S. in Mechanical Engineering from the University of Illinois in June, 1953. He then worked for GM Research Laboratories for several months, before returning to his studies at the University of Illinois.

[1] Carried out in collaboration with J. E. LaBelle of Detroit Diesel-Engine Division, GMC.

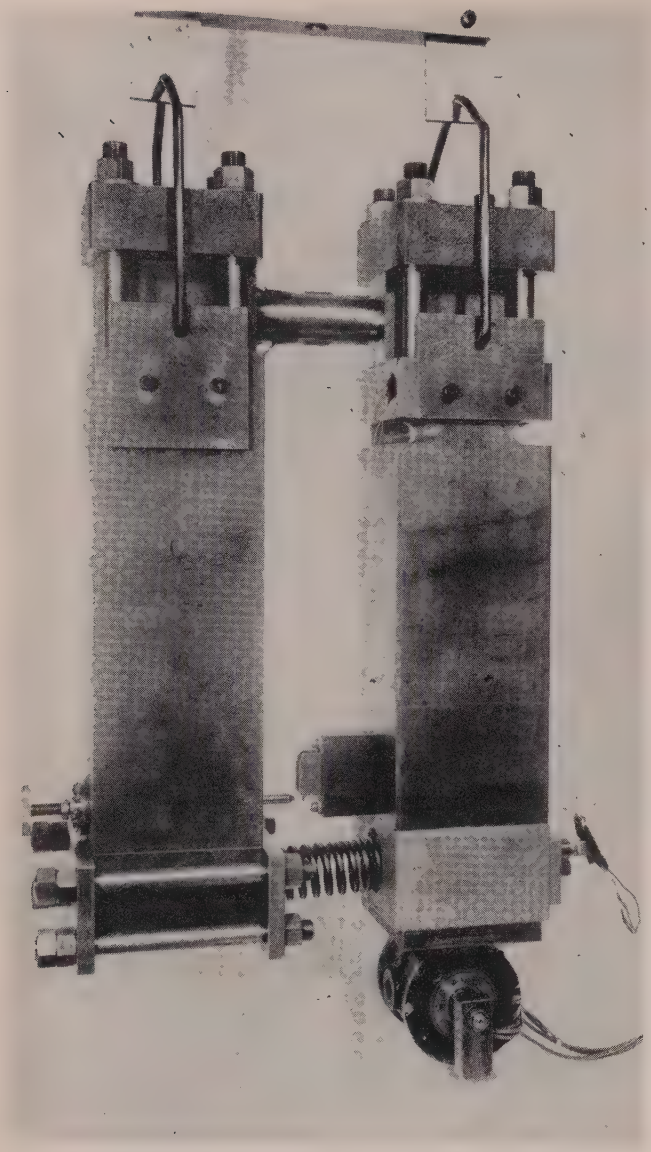

Fig. 1 – Resonant unit for fatigue testing both bar-type and actual crankshaft specimens

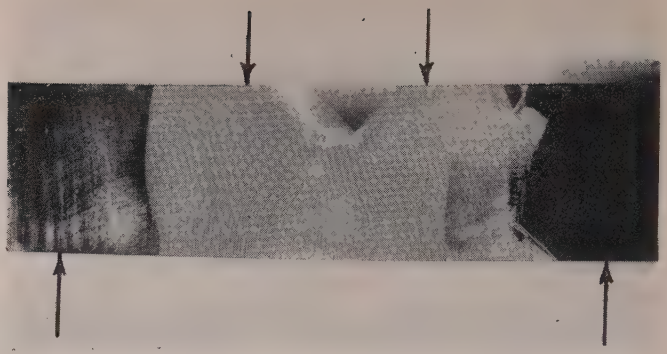

Fig. 2 – Use of brittle coating to show distribution of plastic and elastic strains in a statically loaded notch bar. Plastic flow causes flaking at the root of the notch. Upon removal of the load the root is drawn into tension

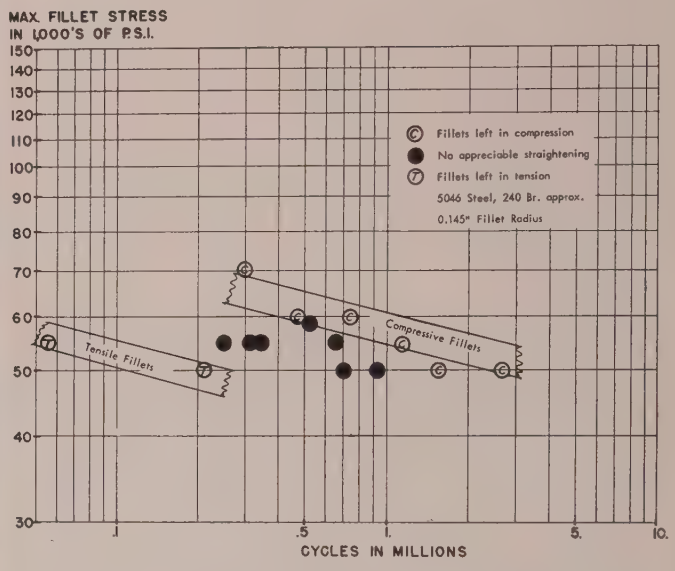

Fig. 3 – Effect of straightening upon flexural fatigue strength of crankshaft of 4¼ x 5 diesel

factor capable of significantly influencing shaft strength[2] and was, therefore, investigated first. This alters the physical properties of the fillets and leaves them in some state of residual stress through plastic flow and subsequent recovery, as illustrated in Fig. 2.

Fillets of the actual shaft varied for better or worse, depending upon their situation relative to the straightening direction, as shown in Fig. 3.

Once this variable could be controlled (finally done in production by taking steps to make it unnecessary even to hot-straighten) it was possible to make comparative studies of alternate materials and treatments as outlined in Fig. 4.

Wide variations in strength were obtained here amounting to as much as 2½/1 in load-carrying capacity. On a life basis even some of the lesser modifications would, for practical purposes, mean an infinite improvement.

The following comments may be made on the diesel crankshaft investigation:

1. Normalized shafts proved almost as strong on the average as the original heat-treatment (not shown) which, over the allowed range of 229 to 269 Brinell, had resulted in considerable scatter.

2. The advantage of the higher-hardness, higher-alloy 4140 steel over the 5046 in the heat-treated, nonrolled condition was not evident.

3. The studies of rolling of this shaft as well as of the 1½-in. bar specimens showed that soft steels respond very well to cold work, provided it is very

[2] See *Luftwissen*, Vol. 9, September, 1942, pp. 263-267: "Bending Fatigue Strength of Machined Crankshafts after Straightening," by R. Schmidt.

intense. Presumably, the greater intensity is required because a relatively greater reliance must be placed upon the work-hardening effect of the treatment than upon the introduction of residual compression. For a given (moderate) degree of rolling, the higher alloys or harder steels responded more favorably than the softer ones.

4. Surface hardening by nitriding produced a relatively large gain as compared with previous tests of specimens having larger fillet radii. The very favorable results obtained from intensive surface treatments here, which offset any greater notch sensitivity effect which might be expected at high hardness, are in conformity with "stress-gradient" theory.

Upon completion of the laboratory flexural and torsional tests, the Detroit Diesel Division rechecked the results by engine test under which loading was exaggerated by opening up one bearing. Since under diesel operation the loading was downward only, this served the very useful purpose as far as basic theory was concerned of providing a comparison of material modifications under reversed as against unidirectional loading. In general, the increases obtained in endurance strength were reasonably consistent, although a quantitative comparison could not be made between the life tests in the engine and the shorter-term laboratory tests run at different amplitudes.

A calibration of the engine test was made by attaching bakelite gages to the crankcheek and statically calibrating them in terms of peak fillet stress. This indicated that the permissible fatigue

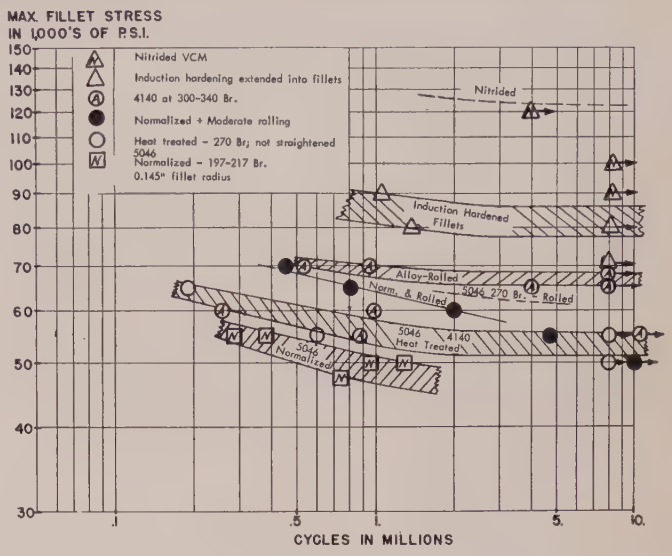

Fig. 4 – Improvements obtained over original strength of the shaft of Fig. 3

range of the shaft was reduced approximately as would be predicted by a Goodman-type diagram.

1½-In. Laboratory Fatigue Testing

Testing with a specimen of about this size has proved advantageous in that the section size as well as range of fillet radii which can be studied bear a close similarity to many actual production parts. If large sections such as those of railroad or marine shafting are of interest, one must still contend with a "size effect," particularly if surface

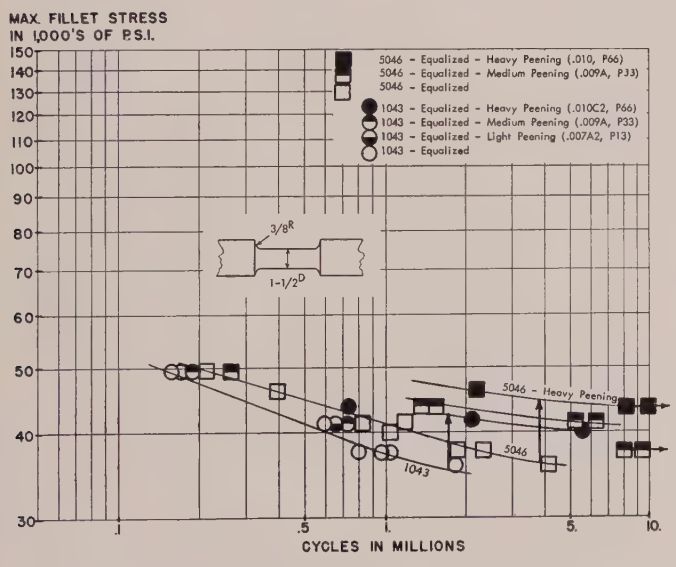

Fig. 5 – *S-N* curves showing the effect of severity of peening upon fatigue strength of 1½-in. bar specimens

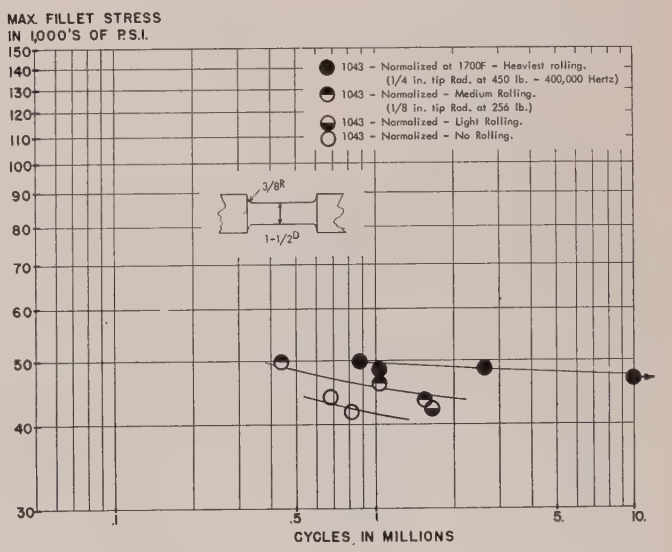

Fig. 6 – *S-N* curves showing the effect of severity of rolling upon fatigue strength of the specimen of Fig. 5

treatments are contemplated. However, the best policy here is felt to be one of conducting at least the earlier tests in the smaller 1½-in. size and applying a scale correction based upon subsurface stress gradient at the critical point.

Typical data obtained from 1½-in.-bar tests are shown in Figs. 5 and 6. Prior to this work a theory of "inherent surface weakness" had been advanced according to which a shallow, relatively light cold-working treatment should be generally superior. This theory has found some support in work with very hard steels. However, one of the results of the tests reported here has been that it does not apply to well-finished steels of low or medium hardness. The 1½-in.-bar tests of Figs. 5 and 6 show a definite upward trend of strength with more severe and deeper treatment.

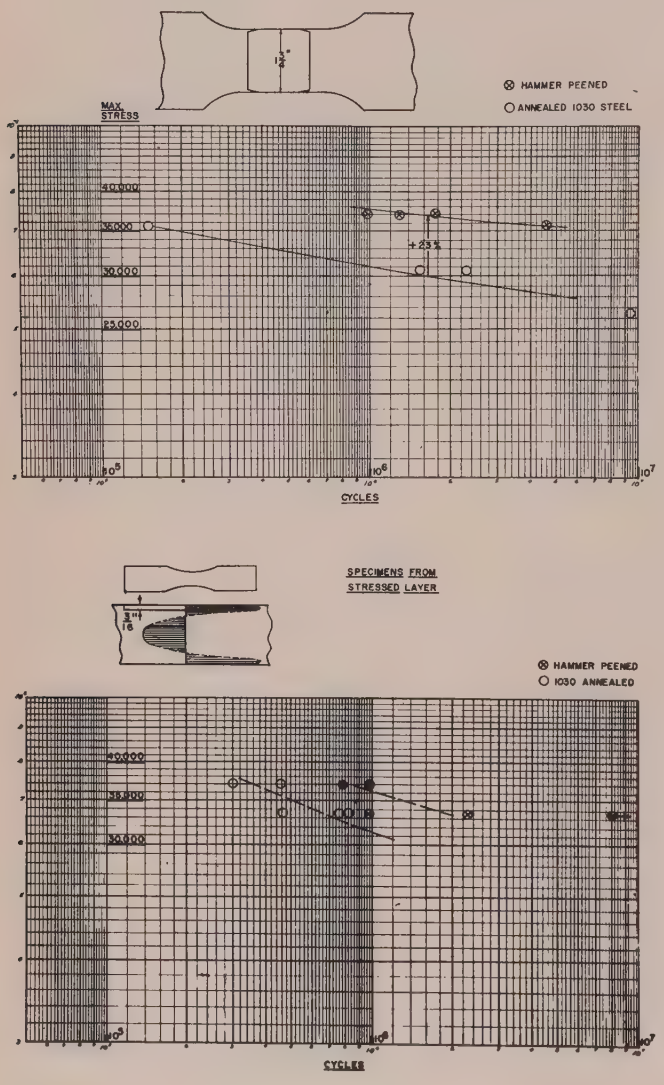

Fig. 7 – Separation of effect of surface cold work from that of residual compression

General Application of Fatigue Data

Once a laboratory fatigue program has been completed, the question arises as to the degree to which the results are applicable to actual field conditions and to what extent they can be extended to other members or structures.

Suppose only steel parts are considered; even with this limitation it has been frequently pointed out that many interrelated factors affect the strength actually obtained. Early in the development of a highly loaded part, however, some kind of estimate of probable strength must be made, and it is axiomatic that this be as sound as possible.

The reasoning upon which the strength estimate is based may be thought of as depending upon a number of basic factors. An important one is the nature of the service loading, particularly as to number of cycles and range of stress involved. These and other phases of working stresses have already been discussed by Schilling.[3]

Another factor which might be regarded as basic is the general type of steel involved. Fortunately, this may not be as basic as its hardness which correlates well with tensile strength[4] as well as to a reasonable degree with fatigue properties. Still other factors which investigators have considered and which appear important are the range of stress and the sharpness of the stress gradient at the critical zone. The extent to which these or other factors are proved to be basic will govern the extent to which it will be possible to select in a given practical case the treatment most likely to succeed.

Range of Stress

There is much evidence that the absolute range of stress as regards percentages of tensile versus compressive stress is a factor. The papers of Almen have considered this extensively. More needs to be done, however. The complexity of the problem is illustrated in a compilation by Smith.[5] Here it is shown that various laboratories had consistently found that a shift of the fatigue range into one predominantly tensile was damaging, but that a shift toward compression was favorable in a rather inconsistent way, depending upon whether or not a notch was present. Improvement was small in unnotched specimens but often large in those having notches. This implies that plastic flow as illustrated in Fig. 2, accompanied by work hardening, contributed to the increase in fatigue strength under superimposed compression.

An unusual opportunity recently presented itself

[3] See SAE *Quarterly* Transactions. Vol. 5, April, 1951, pp. 292-308: "Operational Stresses in Automotive Parts," by R. Schilling.

[4] See p. 116, graph No. 1, 1954 SAE Handbook.

[5] See University of Illinois Bulletin, Vol. XXXIX, No. 26, Feb. 27, 1942, "Effect of Range of Stress on Fatigue Strength of Metals," by J. O. Smith.

to add a little evidence as to the relative importance of elastic compression versus cold work. One and three-quarter in. specimens of annealed 1030 steel had been improved in fatigue strength by hammer peening, as in the first plot of Fig. 7. This treatment was interesting in that it greatly magnified the scale of hardness as well as stress gradients imposed upon the surface, making it possible to study these in considerable detail. It was concluded from the residual stress gradient, which showed large compression to a depth of 3/16 in., that it should be feasible to dissect fatigue coupons of this thickness from the peened surface of the original specimens and thus make possible a separate test of the hardened surface material freed of its residual compression. This was done with the result that in this instance roughly one-half of the response of the steel to peening could be attributed to the work hardening. (The increased slope shown for the *S-N* diagrams for the dissected specimens is in line with the fact that a sharp gradient normally does increase slope.)

In general, range of stress appears to be a factor having its greatest influence when it lies high on the tensile side and when applied to parts of highest hardness. Fortunately, as borne out by the engine tests of the above crankshaft, its influence appears to be relatively consistent through a range of material conditions.

Stress Gradient

This is another factor which, although postulated as having a basic influence upon endurance limit and the effectiveness of surface treatments, has not as yet been thoroughly explored. Since the true stress gradient near the surface cannot often be accurately obtained, it may instead be thought of in an approximate way as being proportional to notch radius in members having high concentration of stress. Looking at it in this way, the response in fatigue to surface treatments has appeared to follow stress-gradient theory but only distinctly in the realm of smallest fillet radii. Here, large gains have been found from strengthening of only the very thin layer actually experiencing high service stress. Tests by the authors on soft and medium-hardness specimens having 1/16- to 3/8-in. radii have shown that a given cold-work treatment produces greater improvement in the smaller radii.

It is so logical to attempt to strengthen a deeper layer when either the fillet radius or net section is large that this is now done immediately, and there is some want of conclusive evidence as to what the actual requirements are. Tests are now under way for determining these in a more systematic way.

Correlation of Fatigue Strength with Hardness

Normal or "par" value of endurance limit for a steel has been found to correlate better with hardness than the other common physical tests. In Fig. 8 (see also Table 1) a number of endurance limit values are given, found from tests by the authors of actual manufactured parts or from tests of full-scale filleted specimens finished, machined, and polished as would be done in production. Endurance limit in each case is based upon measurement of local stress at the nucleus of failure. Results are seen to be relatively consistent even in radii down to 3/32 in. where any failure of a 1/16-in. strain gage to read maximum stress tends to be offset by lower fatigue-notch sensitivity of the steel.

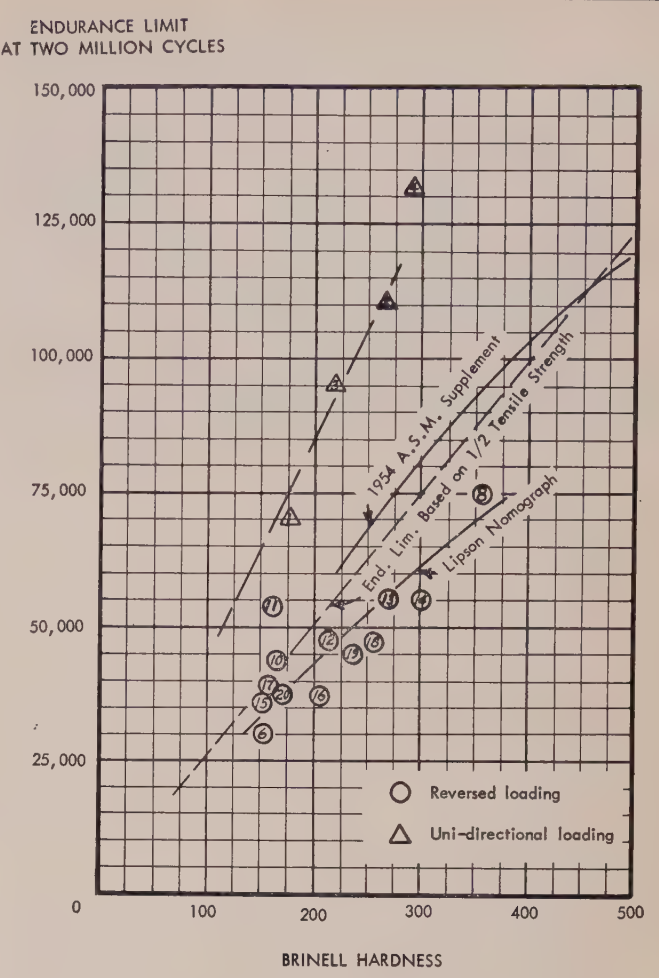

Fig. 8 – Plot of endurance limits versus hardness. Identification of fatigue programs is by number in Table 1

The 1954 ASM Handbook supplement curve (p. 101) predicts values of endurance limit somewhat higher than actually obtained. This is due in some measure to its having been based upon small-specimen tests which do not reflect the "size" effect encountered in medium- or large-scale manufactured parts.

The nomograph[6] was compiled from ground,

[6] See *Product Engineering*, Vol. 20, June, 1949, p. 179: "Surface Finish, Hardness, and Life of Steel Parts," by C. Lipson.

Table 1 – Tabulation of Data Used in Figs. 8 and 9

Test Group No.	Material	Brinell Hardness	Endurance Limit (Fillet Stress)	Net Section, in. dia	Fillet Radius	Loading	Fractional Increase in Hardness[a]	Fractional Increase in Endurance Limit
1	8620	179	70,000	1⅛	⅛	Unidirectional	1.21	1.33
2	8620	269	110,000	1½	⅛	Unidirectional	1.025	1.035
3	86B20	217	95,000	1½	⅛	Unidirectional	1.18	1.16
4	86B20	295	132,000	1½	⅛	Unidirectional	1.0	1.0
5	Cast steel	149	44,000	—	—	Unidirectional	1.31	1.41
6	1030	153	30,000	1¼ sq	⅛	Reversed	1.14	1.23
7	1030	153	31,200	¼	—	Unidirectional	1.14	1.15
8	4140	360	75,000	1½	⅛[b]	Reversed	1.11	1.066
	4140	360	75,000	1½	3/32[b]	Reversed	—	—
9	Spring steel	502	—	3/16	—	Unidirectional	1.04	1.33
10	1045	162	43,500	7/16	2	Reversed	1.17	1.15
11	1045	162	54,000	7/16	1/16-in. notch	Reversed	—	—
12	5046	217	48,000	Crankshaft	0.145	Reversed	—	—
13	5046	270	55,000	Crankshaft	0.145	Reversed	—	—
14	4140	270–340	55,000	Crankshaft	0.145	Reversed	—	—
15	1043	152	35,300	1½	⅛	Reversed	—	—
16	5046	204	37,000	1½	⅛	Reversed	—	—
17	1043	162	39,700	1½	⅛	Reversed	—	—
18	5046	241–277	48,000	6½	⅛	Reversed	—	—
19	1043	234	45,000	6½	⅛	Reversed	—	—
20	1043	168–173	38,000	6½	⅛	Reversed	—	—

[a]—Based on equivalent Brinell.
[b]—Endurance limit same for both radii.

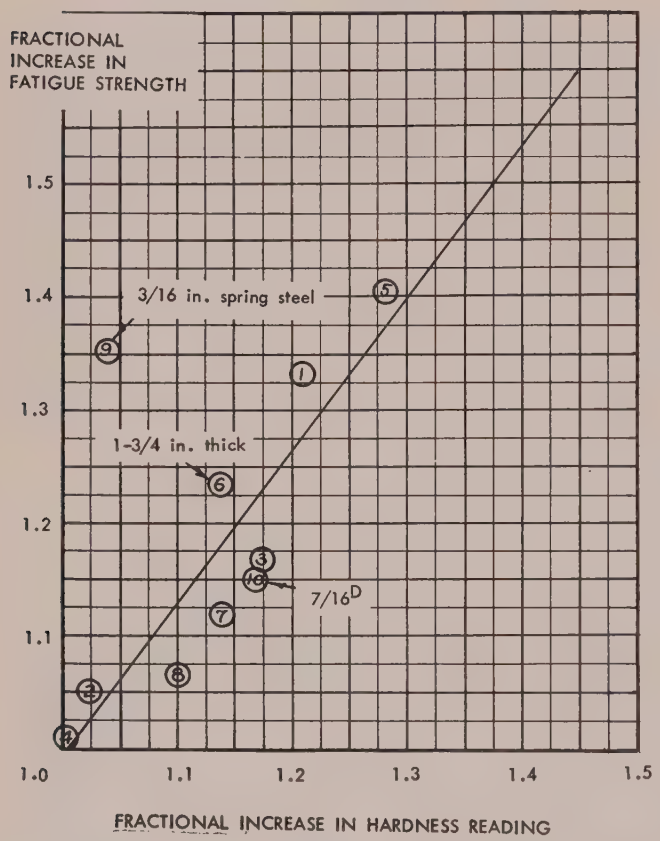

Fig. 9 – Hardness test as a measure of increase in fatigue strength to be expected from surface cold-work treatments. Hardness increases are based on equivalent Brinell. See also Table 1

polished, lapped, and similar surfaces.

Included in Fig. 8 are some limited results for unidirectional loading recently obtained by the use of the preloaded tuning fork. These tests are not extensive enough to justify their use as basic design data, but they are of interest in showing relatively high endurance ranges obtained up to this degree of superimposed tension. They average a permissible stress range equal to that for reversed loading, due in part, at least, to work hardening evidenced by an increase in yield point noted during the progress of the tests.

Appraising Surface Treatments by the Hardness Test

In view of the good correlation of normal endurance limit with hardness, it is logical to try to extend it to the evaluation of improvements to be expected from surface treatments.

A surface hardness reading of a micro type, if necessary, might thus be employed for a quick inspection or appraisal of the improvement to be expected of a given treatment. If, in a particular case, this quick test proved negative, a modification could be made for increasing the probability for success of the treatment before a time-consuming and expensive fatigue program was initiated.

Not only inherent hardness, but to a lesser degree macroresidual stresses contribute to the conventional hardness reading. Therefore, in the case of a part cold worked on its surface, the reading is not strictly a measure of the former but is weighted to some degree by residual stress present.

Since the benefit of peening, rolling, and the like are generally attributed to both cold work and added residual compression, such a reading would appear especially logical for appraisal of the improvement.

In Fig. 9 (see also Table 1) a summary has been compiled showing the degree to which fatigue studies by the authors fall in line with this reasoning. Through a range of soft to medium-hardness steels it is seen that increase in fatigue strength is

roughly proportional to increase in surface hardness reading.

It is believed that this type of analysis provides a better understanding of why in some fatigue studies, indicated by the lowest points on the curve, certain cold-work treatments failed. When they were followed up with heavier treatments, reasonable improvement was often achieved.

The 1¾-in.-thick hammer-peened specimens and the 3/16-in. coupons dissected from their surface, as discussed earlier, are given as points 6 and 7 respectively. In the example for which no increase in strength was obtained, point 4, the lack of response was at first suggested as resulting from the surface already having been in compression from the heat-treatment, prior to the cold working. A residual stress analysis, however, showed that this was not the case.

Standard Rockwell size penetrators have been found satisfactory thus far, although micro indentors are also being tried in the smallest radii. Best results were obtained regardless of type of indentor when readings were taken directly on the surface as opposed to traverse of a cross-section. It is believed that the latter technique, often employed to indicate surface hardening, may fail to give a valid reading sufficiently close to the surface of the specimen.

It should be emphasized that generalizing beyond the realm actually studied is dangerous. The correlation of Fig. 9 extends only from soft through medium hardness, in the neighborhood of 350 Brinell, wherein macrohardness can easily be enhanced by cold work. In parts such as gears, ball bearings, or springs which are left very hard by the heat-treatment, on the other hand, other factors no doubt play a relatively greater role, perhaps on a micro or submicro scale. An instance of an exception to the rule of Fig. 9 is point 9, a leaf-spring section.

Acknowledgment

The tests of cold-worked specimens included herein were done in collaboration with W. S. Coleman, Jr., and other members of the Engineering Mechanics Department of the GM Research Laboratories. Appreciation is also expressed to T. C. Van Degrift, Head, Special Problems Department, under whose supervision this work was done.

APPENDIX

Measurement of Fillet Stresses by Means of Wire Strain Gages

Tests run by the department on the accuracy of strain gages mounted in notches having known concentrations of stress indicate no systematic error for 1/16-in. gages in fillets as small as ⅛ in. in radius, although scatter increases.

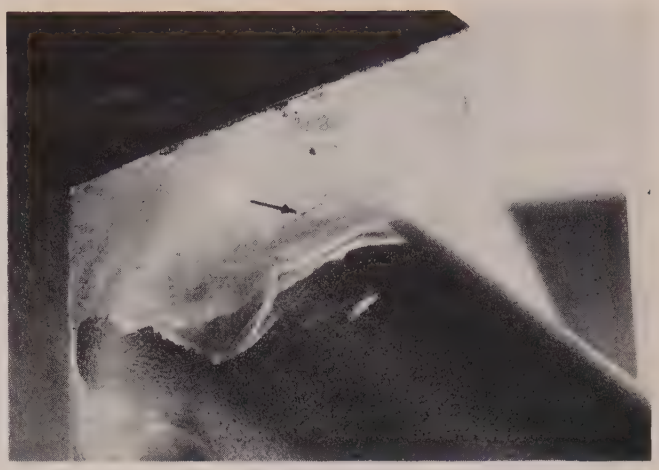

Fig. 10 – Fatigue crack in 1½-in. bar specimens made visible at early stage by Lubriplate

Due to the finite length of the grid, it might be expected that the gage would read a strain value averaged over the gage length rather than maximum strain. It appears, however, that thickness of the paper and cement are such that the grid is raised off the surface of sharp radii in such a way as to increase the reading and thus compensate roughly for the effect of finite gage length.

Method for Detecting Fatigue Cracks

A problem encountered both in laboratory fatigue tests and in service is that of finding a suspected fatigue crack. Commercial inspection methods may be used, although the specimen usually must be removed from the machine to do so. We have, however, for many years used an extremely simple method, more sensitive than most detection systems, consisting of coating the surface of the metal with a thin layer of a white grease such as that known commercially as Lubriplate. If a crack forms, the products of the fretting corrosion at its interface quickly produce a sharp black or dark brown line against the white surface (see Fig. 10) making visible cracks as little as 1/32 in. in length.

After nucleation, the propagation of the crack can also conveniently be followed. An interesting observation was made by this means when studying surface cold work under the magnified scale achieved by hammer peening. In the vicinity of the endurance limit, checks of almost microscopic depth were sometimes observed in the uppermost portion of the cold-worked layer.

In some cases these could be propagated slowly through the subsurface layer of maximum compression if a load, rather than amplitude, control was employed. In other cases no enlargement could be obtained; these would logically be considered as being below the endurance limit.

DISCUSSION ON FOLLOWING PAGES

Present Authors and Previous Investigators in Agreement

— R. J. Miller

Tractor & Implement Division, Ford Motor Co.

THE authors are to be commended in their treatment of a subject that should be of considerable value to design engineers. It is a subject that more engineers should be aware of. The particular value of this paper, of course, is that it treats fatigue in full-scale members. It is regrettable, though understandable, that the information has been condensed to such an extent as to lose some of its effectiveness. The authors have attempted to treat most of the variables that effect fatigue in a relatively short paper, any one of them being worthy of a paper of their own. As the authors have pointed out, there is a complex interplay of factors influencing the fatigue life of structural components, such as:

1. Strength or hardness.
2. Residual stresses.
3. Work hardening.
4. Geometry.
5. Size effect.
6. Notch sensitivity in fatigue.
7. Stress range.

The above variables in themselves are not discrete but may be interrelated, such as work hardening and residual stresses or the residual stresses that are almost always present in steels of high hardness.

As to the authors' comments, they are in agreement in most points with work of a similar nature carried out by ZurBurg and Erickson[a] on fatigue strength of automotive steering knuckles. They were working with material in the same hardness range as the authors, 255-285 Brinell. Their conclusions were:

1. Material composition had no appreciable effect in the hardness range investigated.

2. Fillet radii had a large effect, increasing the fatigue strength 50% when increasing the radius from ⅛ to 0.3 in.

3. Increasing the hardness from 285 to 321 Brinell resulted in a 19% increase in fatigue.

4. Cold rolling the ⅛ fillet (hardness range 255-285 Brinell) increased fatigue strength 48%.

5. Cold rolling the ⅛ fillet (hardness range 285-321 Brinell) increased fatigue strength 67%.

In the same paper is presented data that notch sensitivity of high-strength steels does not increase as the hardness increases but reaches a maximum Q value of 1 at about 30 Rc decreasing to a minimum Q value of approximately 0.56 at a hardness of 55 Rc. These data were determined on notches varying from 0.015 to 0.035 radius.

To sum up, when the existing part fails in fatigue, we are usually restricted to certain factors that cannot be altered such as:

1. Geometry.
2. Stress state.
3. Size effect.

The only direction for improvement is an increase in strength, whether it be by increasing the overall hardness by cold working, such as rolling or shot peening, local heat-treatment by induction or flame hardening, or by conventional heat-treatment to a higher strength level.

Several Comments and Questions for the Authors

— Harry Fall

Caterpillar Tractor Co.

ACQUIRING knowledge of factors affecting the fatigue strength of crankshafts is a very important part of the testing program of the diesel-engine manufacturer. Ideally, the goal of such a program is to acquire sufficient information so that engine operating stresses can be accurately calculated and fatigue strength accurately predicted.

Apparently, the authors have failed to reach such a Utopian state. I must hasten to state, however, that this failure is most certainly not to their discredit. It is somewhat consoling to me to find that they have not as yet been able to make an accurate quantitative correlation between engine tests and specimen tests, for I have been striving to make such a correlation for several years and have similarly failed to do so.

However, even though accurate quantitative solutions cannot be easily obtained, it is helpful to make a qualitative study of those factors affecting the stress level in a crankshaft and those factors affecting the resistance of the crankshaft to these stress levels. The latter problem is the subject under discussion. The authors have studied many factors which influence the fatigue strength of crankshafts, and I would like to comment on a few of these factors.

Hardness and Fatigue Strength

Results of fatigue tests in our laboratory have indicated to us that for hardness levels below Brinell 375 the fatigue strength of notched steel members can definitely be increased by an increase in hardness. It seems to be of little importance whether a given hardness is attained by normalizing or by quenching and tempering. When the authors found little difference in the strength of normalized shafts and shafts of Brinell 229 to 269, I wonder if the hardness ranges were not overlapped? This same comment applies to the comparison of the crankshafts made from 4140 steel (270-340 Brinell) and the 5046 steel (270 Brinell). At any rate, when one considers the statistical nature of fatigue it seems unlikely that the number of points in Fig. 4 for each of these steels is adequate to judge properly the relative strength of the two materials. I am quite surprised that the authors have found a significant difference in the notch sensitivity for these two steels for a fillet radius of 0.145 in. R. E. Peterson's[b] notch sensitivity factor $Q = \dfrac{K_f - 1}{K_t - 1}$ would not change appreciably for a fillet radius of 0.145 and the relatively small hardness difference considered here.

The crankshafts with induction-hardened fillets appear to be very strong even when compared with a rolled fillet.

[a] See "Correlation of Laboratory Tests and Service Performance," by M. F. Garwood, H. H. ZurBurg, and M. A. Erickson. In "Interpretation of Tests and Correlation with Service." ASM, Cleveland, 1951.

[b] See "Stress Concentration Design Factors," by R. E. Peterson. Published by Wiley, New York, 1953.

I am curious about the hardness of these fillets and the state of residual stress.

Shotpeening and Rolling

The beneficial effect on fatigue strength of rolling and peening has been fairly well established. I would like to ask the authors which of these two methods they prefer as a production process and how do they make quality checks on the rolling intensity.

The work aimed at separating the effects on fatigue strength of elastic compression and cold work is very valuable. Much more work is needed on this subject. Because of the scarcity of test points in Fig. 7, I have doubts as to the quantitative effect of these two factors, but there is certainly good evidence that cold work alone is beneficial.

Range of Stress

The data on Fig. 8 show that the safe range of stress for specimens with stress concentration (K_t about 1.4) is very nearly the same for unidirectional loading as it is for reversed loading. For example, at a hardness of 300 Brinell the safe range for unidirectional loading is about 135,000 psi (about 0.9 of ultimate strength) and the safe range for reversed loading is about ±62,000 or a range of 124,000 psi. This apparently is not in agreement with the authors' experience with crankshafts in engine operation. They have stated that the permissible fatigue range of these shafts was reduced approximately as would be predicted by the Goodman-type diagram. I would like to ask the authors what their explanation is for this apparent disagreement.

A unidirectional tensile load of 135,000 psi can be thought of as a cyclic stress of ±67,500 psi superimposed on a tensile mean stress of 67,500 psi. Apparently the mean tensile stress of a significant magnitude had no deleterious effect on the fatigue strength of the specimens.

Hardness and Residual Stress

The work at correlating hardness and residual stress is very interesting. Do the authors feel that the increase of hardness in a compressive stress field is due to a stress state which, with the indentor load, gives a lower shear stress, or is it due to the cold working of the crystals? What is the observed hardness change in a tensile field?

Change Design Rather Than Processing to Improve Strength

– Robert D. Barrett

International Harvester Co.

ANY discussion of fatigue testing sooner or later involves the subject of fatigue life; and predicting fatigue life is just about as controversial a subject as predicting human life. It seems as though the attributes of a clergyman rather than the competence of a scientist would be more applicable to some of the designs I have seen, in that they are released to production with a kiss and a prayer, rather than with sound engineering thinking and intensive test programs. It is with this keynote of sound thinking that we commend the authors on their fine presentation of factors affecting fatigue strength and the facts of life.

At the beginning of the paper, the authors state specifically that they are dealing with full-scale steel members. The theoretical-minded engineer would frown upon the necessity of using full-scale specimens to determine fatigue properties. By merely knowing the metallurgical properties and appraising the geometry, he would predict the $S-N$ curve. Now, by contrast, the practical-minded engineer would realize that there is wide variation in metallurgical properties as well as machining discrepancies, and he would be satisfied with nothing less than a full-scale test. However, I believe our ultimate goal is to attain the theoretical ideal, because the time lapse between the end of design and the start of production is continually being reduced to a point that permits no second guessing.

The authors imply that there is no second guessing in design; and to quote from the paper, "Often a program of this kind has taken the form first of determining the strength of the part as it was initially produced, then following this with an evaluation of gains in strength which might be obtained through the most favorable choice of material, heat-treatment, and processing techniques." They have either consciously or unconsciously omitted the feasibility of a design modification to improve strength and considered only the manufacturing aspects of the problem.

The authors were wise in discussing only soft and medium-hardness steels, primarily because of their response to cold working and improvement by adding desirable residual surface stress, and secondly, because high-hardness steels often have unknown residual stress which confuse the results of fatigue tests.

It is interesting to note the awareness of the authors concerning the effect of residual stress from the straightening operation on a crankshaft. It is even more interesting that they were able to control this variable by eliminating the necessity of straightening in the first place. Therefore, I wish the authors would explain how this feat was accomplished in production.

One of the comments in the paper is that there was no advantage in using a higher hardness obtainable with a higher alloy material. Although there is some reason to be concerned about greater notch sensitivity with higher hardness, we have found from our experience in fatigue testing crankshafts that the endurance limit does increase in proportion to hardness in the region of 200 to 250 Brinell.

Where we are otherwise concerned about notch sensitivity, it is obvious that sensitivity may be alleviated by making a sharp notch less sharp. This principle was applied to crankshafts where a stress-relieving groove was milled perpendicular to the axis of the crankshaft replacing each fillet between the journals and their adjacent cheeks. This design modification resulted in a 30% increase in endurance strength. We rejoiced with this discovery and considered it for patent coverage; however, a search of the literature disclosed that this idea was tried, proved, and published in Germany in 1932.

The year 1958 will be the 100th anniversary of the first publication on the phenomenon of fatigue in metals by A. Wohler in 1858. However, it wasn't until the 1920's that the subject was investigated very extensively when the number of publications on fatigue began to increase at an accelerated pace. Considering what we have learned to date and all that we have yet to discover about fatigue, perhaps, after all, the first 100 years are the hardest.

Discusses Crankshaft Fillet Rolling Operation

– J. E. LaBelle

Detroit Diesel-Engine Division, GMC

A FEW years ago, when our crankshaft fillet rolling program was first started, we were handicapped by two prevailing theories, which the authors have shown to be in error. First, we were of the opinion that the maximum benefit from surface working would be accomplished with a very slight amount of surface deformation. Second, we were also of the opinion that, if cold working was performed in too drastic a fashion, its benefit would be lost, and in some cases the fatigue resistance would actually be lowered as a result of the working. Because of these two theories, our work was conducted on different materials with a fixed fillet rolling procedure, which we felt was correct and not subject to alteration. As a result, the normalized shaft, which the authors referred to as being

slightly inadequate for our operation, was discarded as a production possibility. In its place a hardened and tempered shaft was used. The work of the authors now indicates that the more economical normalized shaft should be reconsidered since, by increasing the amount of cold work, the endurance limit can be raised in proportion.

Another valuable contribution of the authors is the establishment of a work hardening-endurance limit relationship.

Our present method of inspecting crankshafts with rolled fillets in production has been visual. Occasionally, fatigue tests are run, but, since the fatigue tests are time-consuming and costly, such checks are rare. The work of the authors has shown that a more exact evaluation of the fillet rolling process can be made with a hardness test. It is believed that such a test could be devised for use on a production basis. At any rate, spot checks can be occasionally made on scrap crankshafts to make sure that the process is being held at a consistent quality level.

Correlation of Lab and Engine Tests

The tests the authors ran in the laboratory were made on shafts rolled with experimental equipment, while tests run on engines at Detroit Diesel were made on shafts using production rolling equipment. There was a vast difference between the two types of equipment. The experimental equipment utilized an engine lathe with a single rolling tool mounted in the tool holder of the machine. In all, there were 24 fillets on each shaft, and various technical difficulties were encountered, especially in lining up the shaft for rolling the crankpin fillets. The quality of the operation, especially in view of the present work of the authors, is indeed open to question. The production equipment, on the other hand, consists of arms which grip each bearing journal and impresses rollers in each fillet simultaneously under a fixed load. These rollers follow the fillet when the stock is rotated and perform a very uniform operation. It is believed that this difference in procedure also contributed to the better results in engine tests as compared to those of the laboratory tests. In view of this, we feel that the results correlated very well inasmuch as the different types of shafts were rated in the same order of endurance on both tests.

Keeping Shaft Straight

Keeping the shaft straight during processing can be somewhat of a problem. First, the forging is heat-treated and straightened and then stress relieved at a temperature of 1100 F minimum. No straightening is allowed after the stress-relieving treatment at the forge shop. The crankshaft is then centered so that a uniform stock removal will be made during machining. Despite this, some straightening is usually necessary during machining operations. This straightening must be held to very slight amounts to avoid creating high internal stresses. We have found that the straightening causes no reduction in endurance provided it is all done before the fillet rolling operation and none after fillet rolling. If internal stresses are present in the shaft before the fillet rolling operation, run-out will occur during the operation in proportion to the stresses.

It is possible, by processing the forging in the correct manner and restricting straightening in the machine shop, finally to roll the shaft and produce acceptable amounts of run-out after the rolling operation is accomplished. Just how much run-out a particular design can take without causing trouble is something which will have to be determined for each application. There are other problems associated with the process, and even now we do not regard the operation as finalized. The fact remains, however, that the proof of the operation is in the results obtained, and our results have been even better than we originally believed possible.

Authors' Closure To Discussion

IN regard to Mr. Fall's comments, it is agreed that more samples would be needed for evaluating accurately small improvements such as should be expected in going from the normalized condition to the original heat-treatment, or from an average of 217 to an average of 240 Bhn. Comparing trends seen in different laboratories can be valuable in instances of this kind. As for the 4140 alloy, actually, two groups of tests were made; these included the ones plotted that were in the range of 300 to 340 Bhn as well as a second group of five, not plotted, which were close to 270 Bhn and fell consistently along the lower edge of the heat-treated 4140 scatter band. It was felt that sufficient points were obtained here to show an upward trend of strength with hardness, but as for absolute magnitude, a definite lack of advantage from the higher alloy. The 10 samples available showed at least an indication of lower strength at a given hardness than the 5046 steel (as opposed to a definite advantage when rolled). As for the reason, it may be that some other factor entered over and above the admittedly small notch-sensitivity difference that is predicted for this fillet radius.

Extending the induction hardening into the fillets appeared not to be practical at the time of these tests and, unfortunately, little detailed data were obtained. Rolling has been felt most practical for strengthening heavy-duty shafts. As for quality checks on this or other work-hardening treatments, it is hoped that the hardness increase measurement of Fig. 9 will prove useful. Although dissection of a sample is required, the check would only be done at infrequent intervals once the factory technique was finalized.

Considering the complexity of structure and properties of steels, and in view of variations in work-hardening, relaxation, and other effects, it is believed unlikely that the effect of range of stress or residual stress can be closely predicted generally. Work thus far, however, points to a rather small effect in the soft and medium hardness ranges except in the realm of very high superimposed tension. In other words, the Goodman envelope of permissible stress ranges is almost parallel-sided up to the point of pure unidirectional tension. This comment is based on the work of various investigators rather than upon the limited unidirectional data included in the paper. The question raised by Mr. Fall in regard to the high unidirectional ranges shown in Fig. 8 is well taken. Although it was not emphasized in the original paper, they do not necessarily represent the best average for steels in general. The reason for the high value obtained in test No. 4 is not known as yet. The same material has not yet checked under reversed loading.

Sines and Carlson[c] discuss various investigations of the effect of initial stress upon the hardness reading. Experimental results as well as the theoretical combined shear stress indicate a lessening of resistance to the penetrator with superimposed tension as well as an increasing resistance under compression. The effect is greater for tension, which is fortunate in that the greater effect of initial tension than compression upon fatigue strength is thereby more accurately predicted from the hardness reading.

Design modifications were not discussed in the paper, although the authors agree these can be an important factor.

It is gratifying to have the additional hardness correlation experiences of the various discussers included. It is hoped that these data, together with those in the original paper, will provide a better overall picture of strength trends that can be expected.

---

[c] See *ASTM Bulletin*, No. 180, February, 1952, pp. 35-37: "Hardness Measurement for Determination of Residual Stresses," by G. Sines and R. Carlson.

Weighing Vehicles Static and in Motion By Electronic Scales

O. K. Normann,
U. S. Bureau of Public Roads

This paper was presented at the SAE National Transportation Meeting, Boston, Oct. 18, 1954.

VEHICLE weighing is playing an increasingly important part in highway department planning surveys, in addition to its traditional role in helping fleet owners maintain safe loads and in the enforcement of state road load limits.

Described here is a relatively recent electronic method for weighing trucks of all types.

Statically, it can be used for accurate loading of commodities such as cement, at the same time recording empty weight, gross weight, and axle weights. On the road, without the annoyance of weighing stations, it can record truck speed and weight, axle spacing, and individual axle loads.

Constant improvements in equipment, the author reports, eventually will eliminate even the small error now encountered in comparison with static weighing.

THE weighing of commercial vehicles is a much more commonplace operation today than it was a few years ago when about the only vehicles weighed were those hauling coal or other bulk commodities such as grains. Today it is not unusual for the same truck to be weighed several times with the same load on a single day's run.

Many fleet operators have found it profitable to weigh their trucks before leaving the terminals, in order to provide more economical transportation by avoiding breakdowns due to overloaded equipment, as well as to avoid violations of State gross load and axle load regulations. Trucks are also weighed by State agencies in the enforcement of license, tax, and load-limit laws, and for weight classification on toll roads and bridges. Highway departments in their planning surveys weigh vehicles to obtain information on the tonnage of freight carried by the several vehicle types, to determine the magnitude and frequency of axle and vehicle loads for bridge and pavement design purposes, and to obtain other information regarding truck weights, which is prerequisite to a thorough understanding of our national transportation problems. It is in this connection that the Bureau of Public Roads is interested in the development of efficient equipment for the accurate weighing of commercial vehicles.

The use of electronic equipment for weighing vehicles is a comparatively recent development, so

The Author

O. K. NORMANN is chief of the Traffic Operations Section of the Highway Transport Research Branch of the Bureau of Pubic Roads. He is a civil-engineering graduate of the University of Minnesota. He has been with the Bureau of Public Roads since 1928.

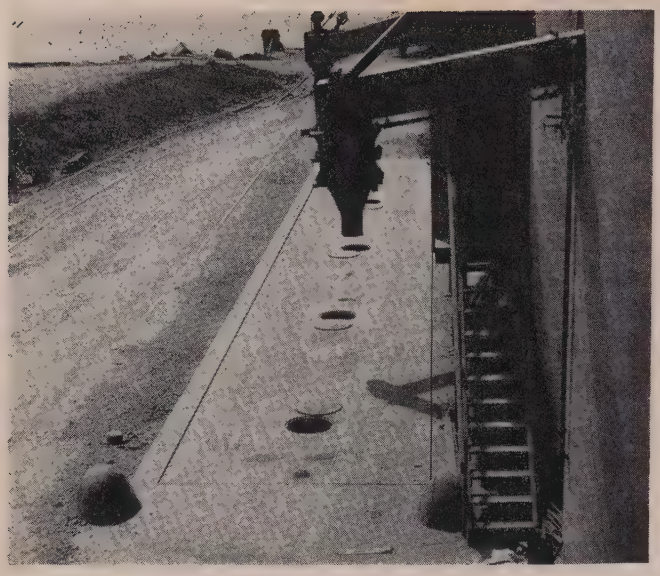

Fig. 1 – Sixty-foot electronic scale used for loading and recording weight of cement trucks

Fig. 2 – Cement truck being loaded at electronic scale

Fig. 3 – Weighing a truck with portable loadometer – one of present sampling techniques, requiring a six-man crew

there are few installations where vehicles are not weighed by the more commonplace mechanical scales with lever arms resting on pivots.

One installation of an electronic scale at Detroit, Mich., is shown in Fig. 1. The scale platform is 60 ft long and 10 ft wide, with a capacity of 150,000 lb. It is used in connection with the loading of cement trucks. A printed and accurate record of the weight of cement loaded on the truck is obtained without the possibility of human error, either intentional or unintentional. As soon as the tractor and semitrailer are positioned on the scale, their empty weight is stamped on a card. This weight is then "zeroed" out, and loading of the cement begins (Fig. 2). When the net weight of cement reaches a preset value, which is usually about 500 lb under the desired load for the semitrailer, the loading mechanism is automatically stopped, and the exact amount of cement is added by jogging the switch to obtain the desired total weight. Pressing a button prints the net weight of the cement on the ticket, after which the gross weight of the tractor and semitrailer is also printed. The combination unit is then pulled ahead and the operation repeated for the full trailer, resulting in additional recordings of the gross semitrailer weight plus the empty weight of the trailer, the net weight of the cement loaded into the trailer, and the gross weight of the combination unit. This is but one example of the many possible applications of electronic weighing in combination with electrical controls for eliminating the possibility of human error in the static weighing of loaded and empty vehicles.

The Bureau of Public Roads has been interested in the development of electronic scales for weighing trucks while in motion, principally for highway planning and design purposes. Present methods generally involve some sampling process. The most common sampling technique employed requires a six-man party equipped with portable loadometers. (See Fig. 3.) Such a party can seldom weigh more than 200 trucks per 8-hr day, at a cost of from $100 to $150. Truck operators object to the delay sometimes encountered at a weighing station, and frequently use circuitous routes to avoid the station, even though the data obtained are used only for highway planning purposes and no law enforcement is connected therewith.

Common practice in enforcement of legal weight limits requires that, at any enforcement station, all trucks be stopped and weighed, excepting perhaps those obviously empty or of very light weight. Inconvenience and sometimes considerable delay to all operators result, even though only a small percentage are overloaded.

An example of the number of trucks that must be stopped and weighed in comparison to the number violating legal weight limits may be obtained from the results at 23 stations in Illinois over a 14-week period. Out of 1,260,871 trucks that were

stopped and weighed, only 2499, or 0.2%, had illegal axle or gross loads.

In realization of the widespread need for a scale which can weigh vehicles at their normal highway speeds, the Bureau of Public Roads during the past several years has investigated the possibility of adapting various types of mechanical and electrical devices to this problem. Of the several devices investigated, the highly perfected resistance-wire strain gage seemed most adaptable to vehicle-weighing requirements.

The first electronic scale for weighing trucks while in motion was constructed in April, 1951, as an experimental project by the Bureau of Public Roads in cooperation with the Virginia Department of Highways and the manufacturer of an aircraft weighing kit. The scale was located on the Shirley Highway about 20 miles south of Washington, D. C.

The basic electrical principle upon which the electronic scale operates is that the resistance of a conductor is proportional to its cross-sectional area. Resistance strain gages are bonded to columns and encased to form a weight-sensitive load cell. Two types of load cell (shown in Fig. 4) were employed in the electronic scale. The two types of cell were used in two separate series of tests in which the accuracy of the scale was determined. The results indicate that the two types are equally satisfactory for in-motion weighing as far as their effect on the accuracy of the scale is concerned.

The electrical circuit of a load cell is a resistance network commonly called a Wheatstone bridge. A load applied to the cell causes the bridge to become unbalanced, resulting in a difference in potential between the output terminals. The value of this potential difference is proportional to the load on the cell.

At the Shirley Highway installation, four of these cells connected in parallel were used to support a 3-ft by 10-ft platform constructed in a traffic lane and even with the road surface. Fig. 5 shows the load cells in place, one on each column in the four corners of the scale pit, and the adjustable

Fig. 4 – Two types of load cell used in electronic scales in tests to determine accuracy of in-motion weighing

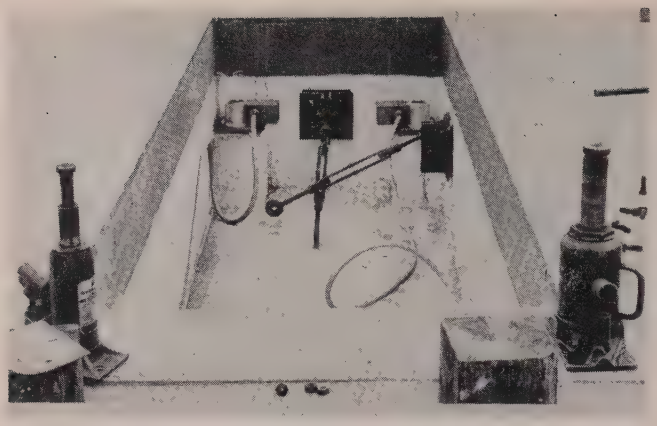

Fig. 5 – Load cells in position at one end of pit

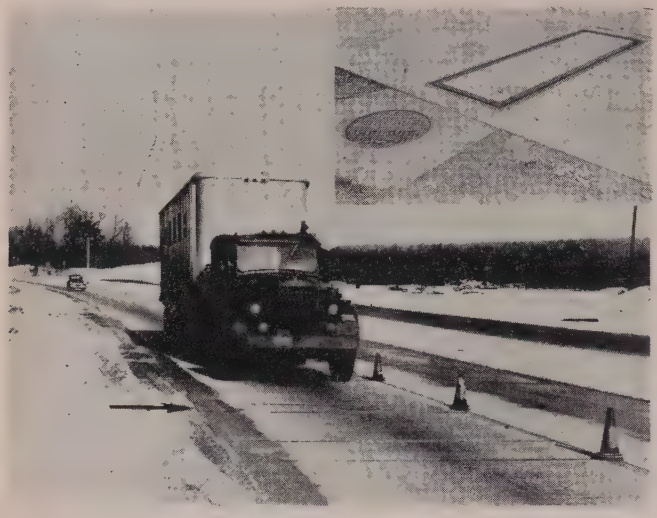

Fig. 6 – Platform in place with truck approaching at normal speed

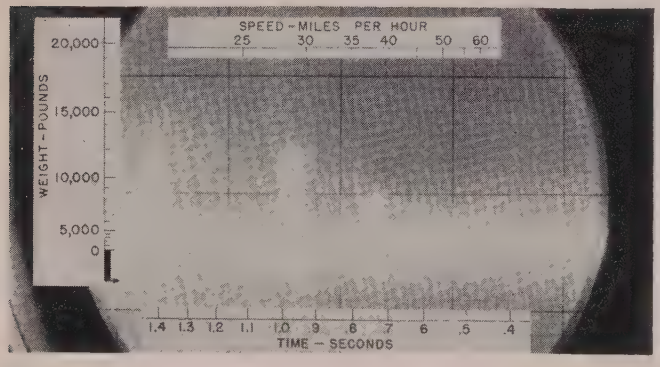

Fig. 7 – Oscilloscope pattern obtained with 3-axle semitrailer. Pattern allows determination of speed, distance between axles, and weight of each axle

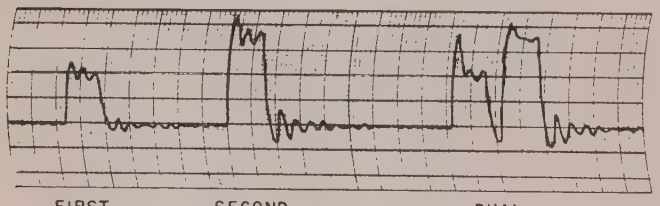

Fig. 8 – Oscillograph chart for 4-axle tractor semitrailer. Peak values represent axle loads

tie-bars used to hold the platform in its proper horizontal position. Fig. 6 shows the platform in place with a truck approaching at its normal speed.

Several types of suspension systems were tried as well as two types of platforms – one made of concrete and steel weighing about 6000 lb and another made of wood weighing about 600 lb. Manufacturers interested in developing a scale have also tried other types of suspension systems, some employing two load cells and in one case only one load cell. The accuracy results presented in this paper are for systems employing the four-cell support. As far as we know, errors with the four-point suspension properly adjusted have so far been no greater than for other suspension systems.

The recording device employed for the major portion of the research in connection with the development of the scale was an oscilloscope. An oscilloscope pattern is shown in Fig. 7.

As a vehicle approaches the scale location traveling at its normal speed, a switch actuated by the impulse received from a rubber tube stretched across the roadway a few feet ahead of the scale starts a point of light moving from right to left across the oscilloscope screen which is similar to a television picture tube. As each axle of the vehicle passes over the scale the point of light is deflected vertically an amount proportional to the weight of the axle. Fig. 7 shows the pattern of a three-axle tractor-semitrailer. From this pattern the speed of the vehicle, the distance spacings between axles, and the weight of each axle may be determined.

While the oscilloscope was probably the best type of recording instrument to use during the development stage, other means of recording the axle weights had to be developed to make the use of the scale more practical. An oscillograph which presents the axle weights on a strip chart was also used to obtain a permanent record. Fig. 8 shows an oscillograph pattern. The equipment is calibrated so that the peak values on the chart represent the axle loads. Equipment manufacturers have recently developed an instrument which records the total truck weight as a certain weight class and automatically records this class in a punch card, together with an indication of any axle weights in excess of a predetermined figure. Equipment shown in Fig. 9 is also available. It sounds a gong or operates other types of electrical apparatus whenever a vehicle with an axle exceeding a predetermined weight crosses the scale. It will probably not be too long before a unit will be available to print the axle weights and total vehicle weights in figures for each truck passing over an electronic scale at its normal highway speed.

Many tests have been conducted to determine the accuracy of the electronic scale located on the Shirley Highway. Weight recordings were made with the trucks traveling at their normal speeds, which averaged 48 mph and varied from 30 to 60 mph. (See Fig. 10.) The weights recorded by the

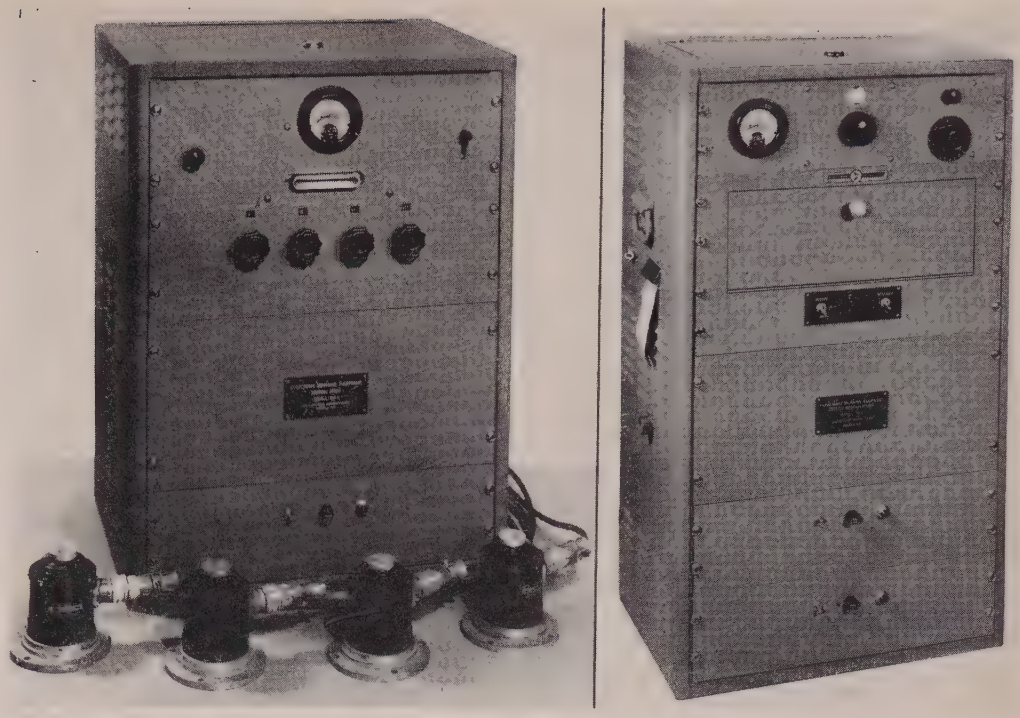

Fig. 9 – Two units for detecting overloaded axles – left: four load cells used for electronic scale with cabinet containing amplifier, detector, and meter indicator; right: axle motion weighing scale. Axle weights, vehicle speeds, and axle spacings are recorded on tape at left

electronic scale were compared with the static weights recorded for the same vehicles at the lever-arm scales operated near Woodbridge, Va., by the Virginia Department of Highways. Fig. 11 shows comparisons for the weights of single axles. The amount that the points are away from the 45-deg line represents the error of the electronic scale, assuming the lever-arm scales to be correct. Most of the points fall on or near the 45-deg line, but in a few cases there is a considerable error.

Fig. 12 shows the results of the accuracy tests for tandem axles. Accurate weights of tandem axles in motion were originally the hardest to obtain by the electronic scale. Apparently, vibrations set up by the first axle of a tandem were still present when the second one crossed the scale. This was soon overcome, however, by proper plates to check the horizontal movement of the platform, so now tandem axles while in motion are weighed with a slightly greater accuracy than single axles.

The accuracy of the total vehicle weights is illustrated by Fig. 13. Sixty per cent of the vehicles are now weighed while traveling at their normal speeds with an error under 5%, and rarely is the error for a vehicle as great as 10%. The total tonnage traveling down a highway can be obtained with an error of only 2%. The electronic scale was, therefore, sufficiently accurate to obtain necessary information for highway planning purposes without inconveniencing the operators by making them stop and wait to be weighed. Any distribution of axle loads or total vehicle weights obtained by using the electronic scale while vehicles are traveling at their normal speeds will be identical with similar weight distributions obtained by stopping

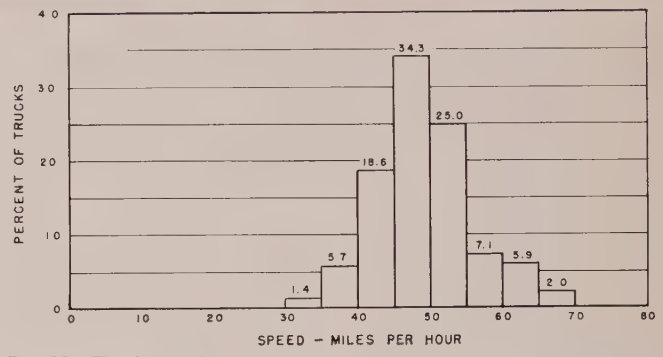

Fig. 10 – Truck speeds recorded at electronic scale on Shirley Highway, south of Washington, D. C.

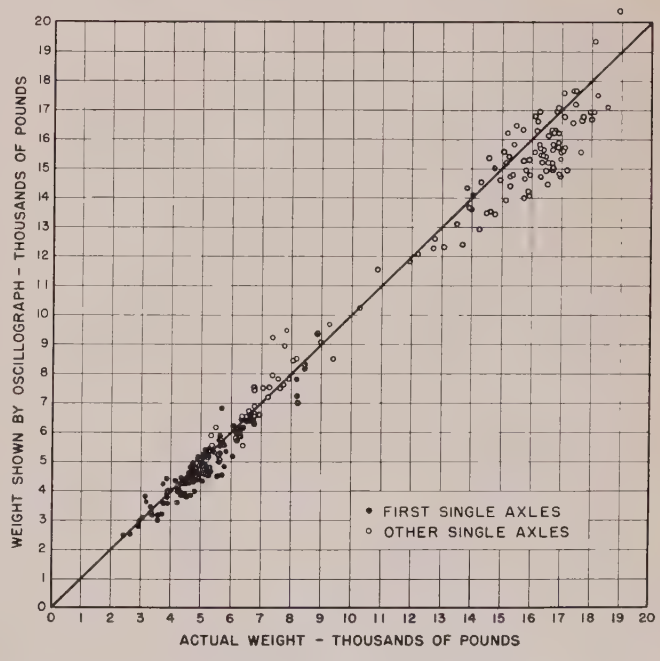

Fig. 11 – Comparison of single-axle weights recorded statically by lever-arm scales, and in motion by electronic scales, near Woodbridge, Va.

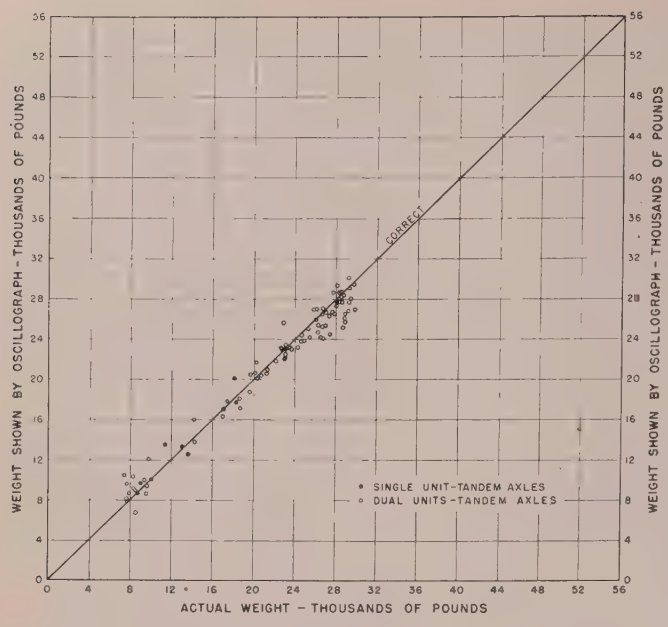

Fig. 12 – Comparison of tandem-axle weights made statically and in motion

the vehicles and weighing them on an accurate static scale.

Since these results were obtained by the use of the first electronic scale constructed for weighing vehicles in motion, more accurate results can be expected by a scale of more recent vintage constructed to embody the changes found to be desirable from both an accuracy and operational viewpoint. The potential uses of such a scale are both varied and extensive, especially since the amplifying and recording apparatus is portable and may be designed so as to be plugged in at a number of different platform locations.

When electronic scales are used in the enforcement of legal weight limits, trucks are weighed while traveling at their normal highway speeds and only the trucks exceeding or near the legal load limits need be stopped. Operators who stay within the legal limits are not penalized by the relatively few violators. It is probably for this reason that such excellent cooperation has been received from the trucking industry during the development of the electronic scale. Trucks with desired loads and axle arrangements that could be operated repeatedly over the scale at different speeds have been supplied by the truck operators without cost.

The results of a study on the Shirley Highway, where a high percentage of the trucks operate at or near the legal limit, show that by employing an electronic scale in connection with the enforcement of weight regulations, over 60% of the vehicles now being stopped to be weighed statically would not need to be stopped. This percentage will, of course, increase as the accuracy of the electronic scale is improved. There is good prospect that the electronic scale will be so improved that its accuracy in weighing vehicles in motion will approach still more closely the accuracy already attained in static weighing.

Many other uses of such a scale will no doubt develop, such as measuring impacts caused by surface roughness or uneven tire wear, and the efficiency of various types of truck suspension systems in reducing impact loads or variations between wheel loads, especially on tandem axles. The electronic scale also has many other potential uses in connection with research projects that could not be undertaken prior to its development.

One interesting application of the electronic scale was conducted during a period when operation of the Virginia scales was suspended for a few days. The Virginia scales are normally operated 24 hr per day, 7 days a week. Unknown to the commercial vehicle operators, the electronic scale was in operation during this period. The results from the electronic scale showed that load-limit violations of the type in excess of the legal limit plus tolerance increased from less than 1% to 5%, about the same percentage as prevailed at the time that the continuous weighing operations were first started several years ago. The magnitude of the violation, however, was not as severe.

The equipment used for electronic weighing also permits the recording of vehicle speeds and axle spacings at the same time. Speeds can be measured to within 1 or 2 mph, and the average error in axle spacing when compared with taped measurements after stopping the vehicles is under 0.5 ft. This is a sufficient accuracy for highway planning purposes and also permits the calculation of legal loads in States where the axle weight limits vary with the spacings between axles.

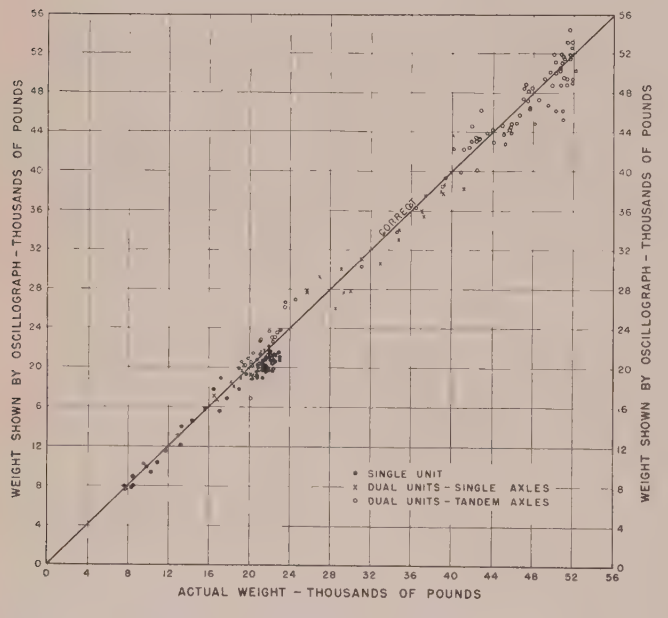

Fig. 13 – Comparison of total vehicle weights. Total tonnage on a highway can be obtained with electronic scale with only 2% error

Reverse Thrust for Jet Transports

Joseph Sutter, Boeing Airplane Co.

This paper was presented at the SAE National Aeronautic Meeting, New York, April 15, 1954.

THE purpose of this paper is to analyze reverse-thrust requirements for jet transports and to discuss the results of some of the design work and testing of jet reversers that have been carried on in this country.

About the time serious design studies of jet transports were started in the United States, a new device for assisting in the landing deceleration of present-day transports was being introduced into everyday airline operation. This was the reversible propeller. At the present time, reverse thrust has been accepted as a well-proven safety feature. The last several hundred transports delivered to the military services and the airlines have reversible propellers as standard equipment.

Why Reverse Thrust Is So Popular

The following figures show why reverse thrust is regarded with such universal enthusiasm. Fig. 1 shows the landing roll for a present-day transport landing on the minimum length runway allowable for the airplane under present airworthiness standards. A dry concrete runway is assumed, and brakes only are used to stop. Under these conditions, an adequate margin in stopping distance exists. Fig. 2 shows a similar condition, except an icy runway is assumed. Here a large part of the margin is used up.

Fig. 3 shows the effect of applying reverse thrust after landing on an icy runway. The margin in stopping distance is more than equal to that achieved on a dry runway using brakes alone.

Requirement for Reverse Thrust for Jet Transports

We now come to the jet transport. Fairly complete design studies have shown that a well-balanced economical jet transport will be able to land and stop in the same distance as contemporary transports on a dry runway. However, any future transport will be required to continue to operate during all types of weather and runway conditions. The incorporation of additional stopping devices in jet transports will be necessary to achieve this "all-weather" capability.

Several methods have been developed to improve stopping capabilities of airplanes without propellers. One of the most noteworthy is the drag chute. Fig. 4 shows a typical chute installation on the B-47 medium bomber. This device has proved to be quite successful in military operations. However, the chute does have limitations which reduce operational flexibility. Not the least of these is that once the chute is deployed, facilities outside the airplane are necessary to handle it. Another disadvantage of the chute is that it has to be de-

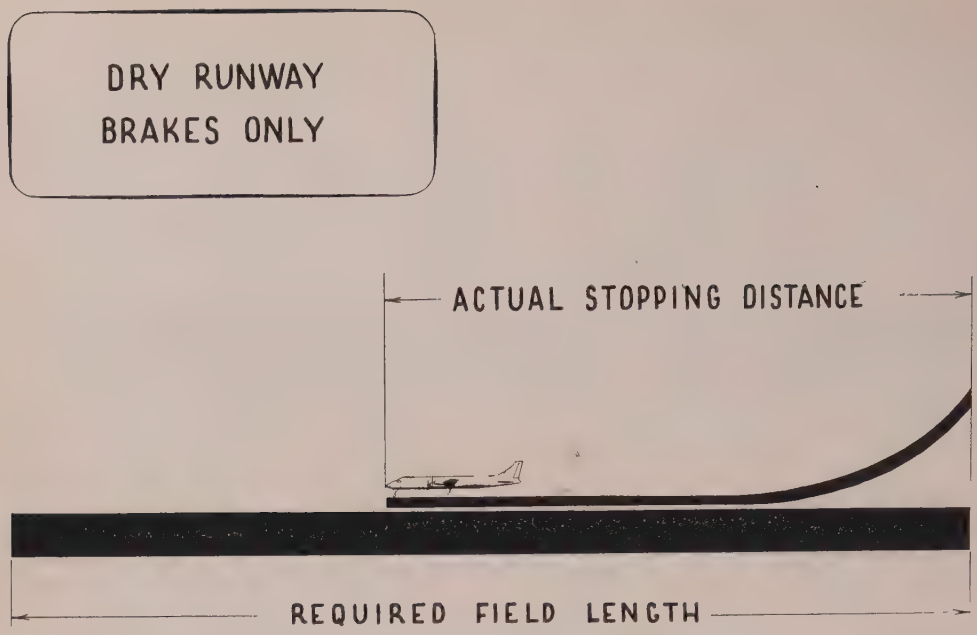

Fig. 1 – Dry runway landing of a reciprocating-engine airplane

ployed quite close to touchdown to be fully effective, since the drag effect is a function of air speed. The chute becomes least effective near the low-speed end of the ground roll, which may be the point at which maximum braking is needed.

After studying various stopping methods, it was concluded that reverse thrust would have to be developed for jet engines if jet transports are to have the operational flexibility of present-day transports.

Design Objectives

At this time a program to develop a jet reverser was instigated with the establishment of a set of design objectives to be followed by the designers. The most important of these are shown in Table 1.

The primary objective was to achieve a device inherently safe and reliable. It was desired that these qualities should be achieved through basic design and simple structural locks. The use of elec-

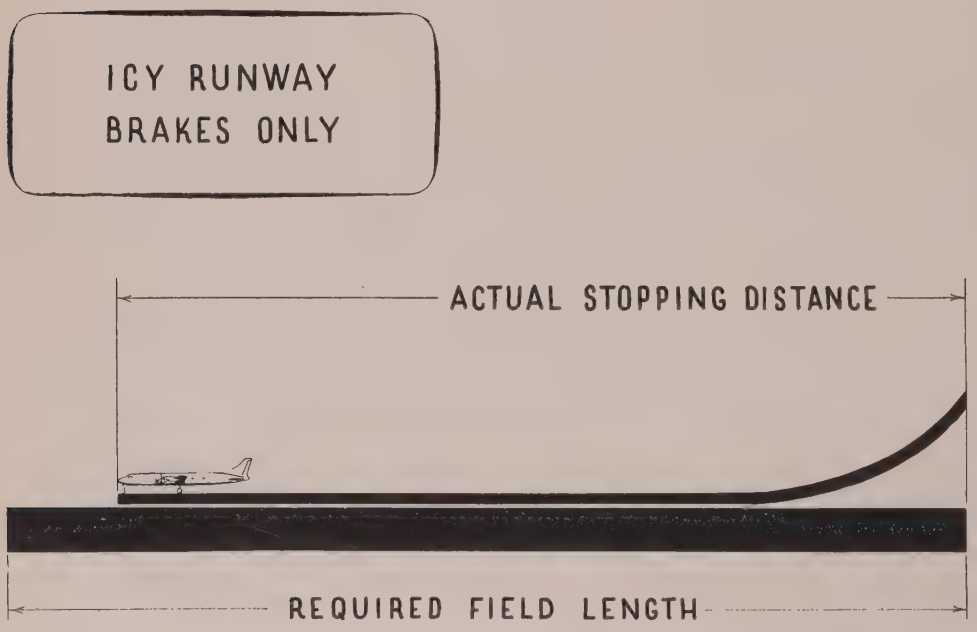

Fig. 2 – Icy runway landing of a reciprocating-engine airplane

A STUDY of various stopping methods indicated, it is explained, that reverse thrust would have to be developed for jet engines if jet transports are to have satisfactory operational flexibility. Requirements for reverse thrust are, therefore, discussed in this paper.

Primary reverser-design objectives are inherent safety and reliability, stopping comparable to present-day equipment, lack of effect on engine operation, and need for ground-run control only. The author shows that a jet transport using reverse thrust has a stopping distance on smooth ice consistent with a dry-runway brakes-alone stop.

The effects of reverser malfunctions on airplane flying characteristics are compared to the effects of reversible-propeller malfunctions.

The Author

JOSEPH SUTTER is with the Seattle Division of the Boeing Airplane Co. He received his B.S. in Aeronautical Engineering from the University of Washington in 1943. For the next three years he worked with the U.S. Navy anti-submarine forces, and later in aviation engineering. Mr. Sutter joined Boeing Airplane Co.'s aerodynamics unit, working on the Stratocruiser certification program. He was assigned aerodynamic group engineer for the Prototype Jet-Tanker Transport project in 1952.

tronic controls and intricate protective devices was to be avoided.

The second objective was that the airplane with jet reversing should have operational flexibility comparable to present transport equipment. It was felt that this would be achieved if, on an icy runway, the airplane could be stopped with brakes and reverse thrust in the same distance it could be stopped with brakes alone on a dry runway. Analysis indicated reverse thrust in the order of 40% of maximum forward thrust would be required to meet this objective. Third, it was specified that reverse thrust should be used for ground-run control only. Using reverse thrust for glide-path control could increase the probability of failure in flight. Since the basic glide-path control of a jet transport can be quite satisfactory, in-flight reverser operation was ruled out to insure the simplest device possible. (Fig. 5 compares the maximum glide paths of a typical jet transport design and a reciprocating-engine transport. Both airplanes are on the landing approach with flaps and gear extended and power off. The jet-transport design shown incorporates aerodynamic drag

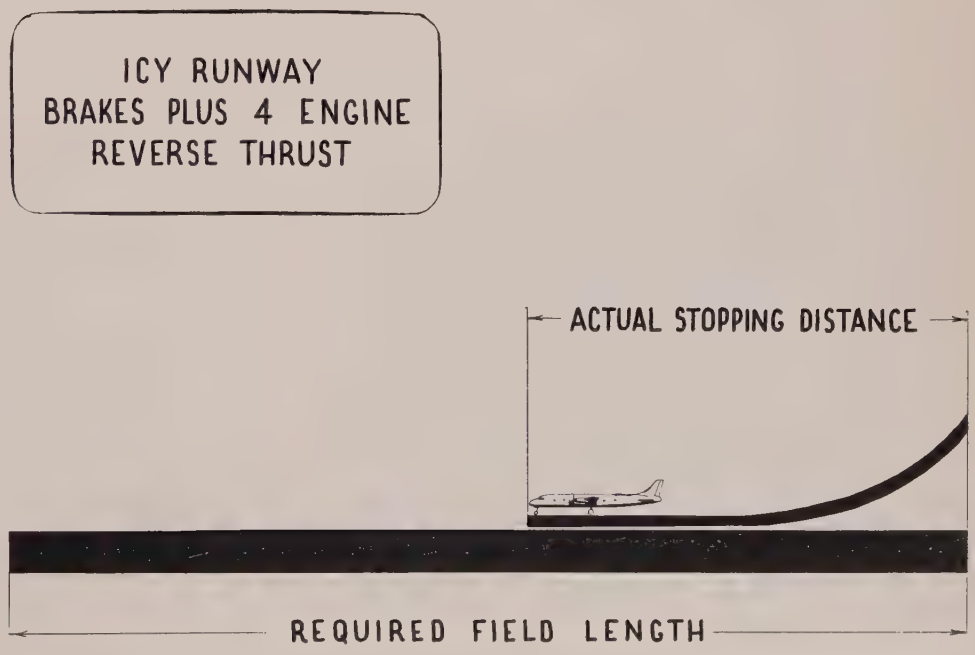

Fig. 3 – Icy runway landing of a reciprocating-engine airplane using reverse thrust

Fig. 4 – B-47 drag-chute installation

brakes which provide increased drag comparable to that available from the windmilling propeller. The glide paths shown are about a slope of 1/5 which is considerably steeper than the normal approach which lies between the ILS approach and a slope of about 1/10.)

The fourth objective requires that the reverser should not affect engine economy when the reverser is not in operation. In addition, the reverser should not adversely affect engine life or engine control characteristics when in operation.

Results of Design and Testing

In proceeding with the design, objectives 1 and 4 immediately indicated a device which, during normal engine operation, would be completely out of the jet blast. Tests of many shapes of likely reversers were conducted using the Boeing nozzle test facility. Some of these are shown on Fig. 6. It might be of interest to note that initial testing was started as early as 1951. A brief summary of test results is shown in Fig. 7. As shown on this plot, about 45 to 50% reversal of the jet blast is possible with reversers that could reasonably fit into the space available near the engine tailpipe. As design and testing progressed, the clam-shell type of reverser showed the greatest promise from the standpoint of meeting the design objectives outlined above and from the standpoints of mechanical simplicity, installed weight, and airplane stowage.

Although the remainder of this paper is primarily concerned with this type of reverser, a great deal of design effort was also expended in developing the V-gutter type of reverser, and the conclusions stated here are applicable to either type of reverser. A typical reverser installation of the clam-shell type is shown in Fig. 8. Details such as linkage arrangement and baffles are shown therein. This type of reverser is shown installed in various airplane-engine combinations in Fig. 9. It is to be noted that this reverser arrangement lends itself to all airplane configurations shown.

During the reverser performance tests, shadowgraphs of the reversed jet blast were made, as shown in Fig. 10. It is seen that reverser effectiveness is proportional to the deflection angle of the blast. It is also apparent that the blast clears the adjacent structure by a considerable margin. Further work is proceeding to determine the effect of the reversed blast on other areas of the airplane and on debris pickup characteristics of the blast. These effects, of course, will be greatly influenced by each particular airplane design.

The clam-shell or V-gutter reverser can have no effect on engine characteristics during normal forward-thrust operation since no part of the device extends into the jet blast. Scale-model tests simulating the reverser also show that engine

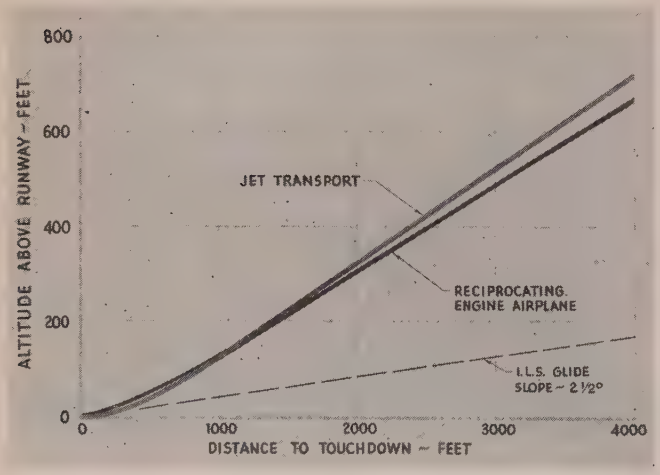

Fig. 5 – Glide-path comparison of jet and reciprocating-engine transports

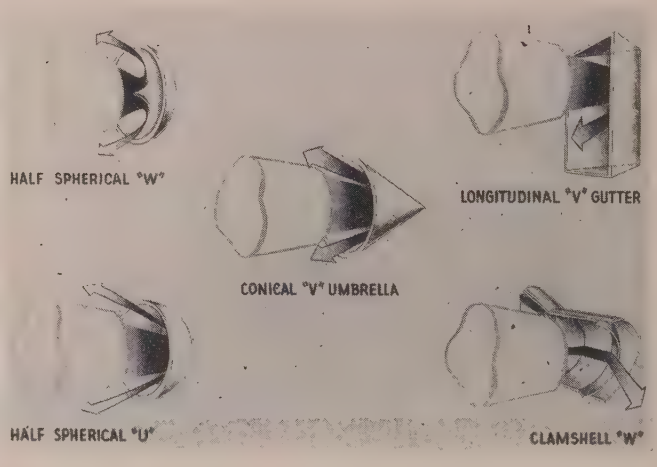

Fig. 6 – Thrust reverser configurations

accelerating characteristics are not affected. Engine operating conditions are not changed in that the effective tailpipe area is unchanged at normal pressure ratios corresponding to full power.

A reverser of the type shown would give a typical jet-transport stopping capability on smooth ice as shown in Fig. 11. It is noted that objective 2 has been achieved – that jet-transport stopping capabilities under all conditions would be consistent with the dry-runway brakes-alone stop.

At this point of testing and design, sufficient progress had been made such that a fairly detailed airplane installation could be developed. Estimates resulting from this work indicate that a four-engine installation would weigh about 800 lb, a two-engine installation about 400 lb. With extensive development and operating experience, this weight could undoubtedly be reduced.

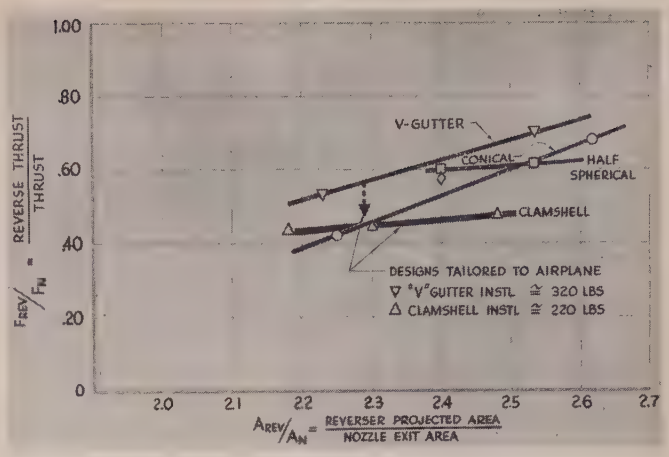

Fig. 7 – Summary of reverser performance

Failure Analysis – Comparison of Jet Reverser and Reversing Propeller

A thorough analysis of the reverser in regard to failures and malfunctions was also made at this time to insure that the reverser would meet the basic objective of safety and reliability.

Those close to the development of the reversible propeller can remember the many difficulties experienced in the early development of this device, which have now been largely overcome. In evaluating the safety and reliability aspects of the jet reverser, it was felt that the jet reverser system should be at least as reliable as the reversible propeller in its present state of development. A failure analysis was therefore made where the two reversing systems are compared. All conceivable types of failure were considered which could be attrib-

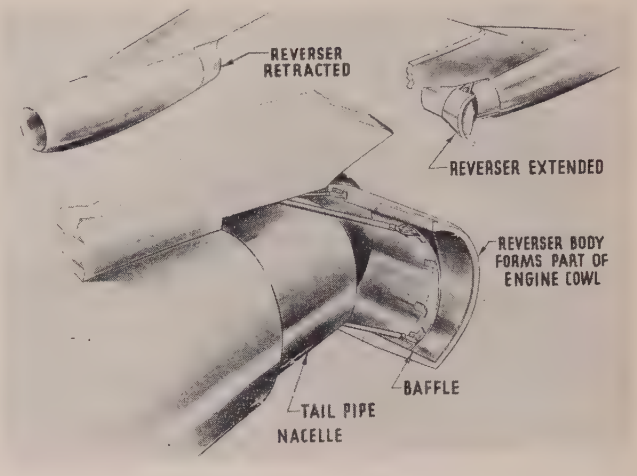

Fig. 8 – Clam-shell type reverser installation

Table 1 – Design Objectives

1. Inherent safety and reliability
2. Stopping comparable to present-day equipment
3. Ground-run control only
4. No effect on engine operation

Table 2 – Failure Analysis – Take-Off

Reversible Propeller		Jet Reverser	
Condition	Severity Factor	Condition	Severity Factor
1. Power fails, prop feathers	1.0	1. Power fails, reverser retracted	1.0
2. Power fails, prop to low-pitch stop	1.2	2. Reverser extended, engine normal	1.55
3. Prop fails, power normal, prop to flat pitch	2.5	3. Power off, reverser extended	1.05
4. Power off, prop to flat pitch	1.9		
5. Prop fails, power normal, prop to reverse pitch	1.4		
6. Power off, prop to reverse pitch	1.3		

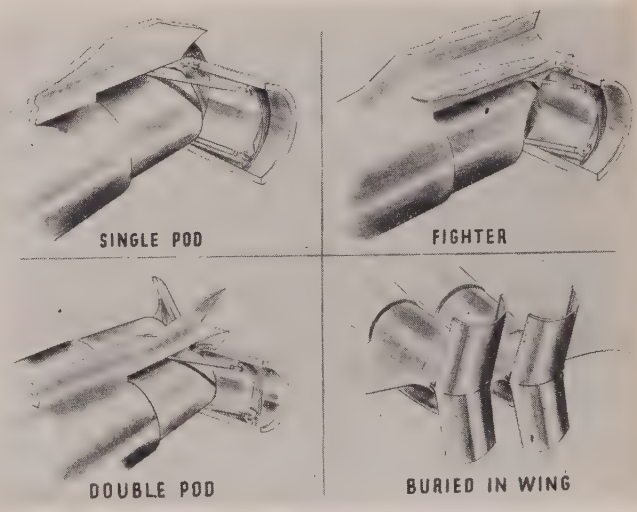

Fig. 9 – Reverser installations in various airplane-engine combinations

Table 3 – Failure Analysis – Cruise

Reversible Propeller		Jet Reverser	
Condition	Severity Factor	Condition	Severity Factor
1. Power fails, prop feathers	1.0	1. Power fails, reverser retracted	1.0
2. Power fails, prop to low-pitch stop	3.2	2. Reverser extended, engine normal	2.1
3. Power fails, prop to flat pitch	15.0	3. Power off, reverser extended	1.3
4. Prop fails, power normal, prop to reverse pitch	5.3		

uted either to the reversible propeller or the jet reverser. It was necessary that a common basis of comparison be available for this analysis. Therefore, the results of the analysis are shown in terms of a "severity factor." A severity factor of unity would mean that for that particular combination of airplane, flight condition, and failure, the effect of the failure would be the same as if a single-engine failure occurred. A severity factor of two would mean that the effect of the failure would be as severe as losing twice the thrust of one engine.

Reversals occurring during take-off and cruise were analyzed. Table 2 covers the take-off situation with the airplane near the "unstick" point. The left-hand column shows the present propeller-driven airplane, the right-hand column the jet airplane. Condition 2 for the propeller case is shown as a reference point since it represents the most severe failure which could occur if reversing were not incorporated in the propeller system. Condition 3 represents the first failure condition involving the reversing feature and is the most critical condition. Not only is the effect on performance and control very severe, being in the order of magnitude comparable to a double-engine failure at take-off, but a very high propeller overspeed would result. Condition 4 shows that cutting power on the engine would alleviate the condition but only slightly, since most of the drag is produced by the high induced lift of the blades in flat pitch rotating at high rpm.

Conditions 5 and 6 show that if the propeller passes through the flat-blade condition, the reversed-propeller condition is somewhat more tolerable. However, the condition is still 30 to 40% more critical than a single-engine failure where the propeller feathers.

Condition 2 for the jet reverser failure represents the most critical failure which can occur with this system. With the engine operating normally, the reverser fully extends into the jet blast. This type of failure is 1½ times as severe as a single-engine failure.

Condition 3 shows the effect of cutting power on the engine with reverser failure. Since the reverse thrust is directly a function of engine power, the consequences of the failure can be readily reduced by this means.

A similar failure analysis is shown for the cruise condition in Table 3. Again, condition 2 in the left-hand column represents the most severe case for a propeller-driven airplane not equipped with reverse thrust. This condition would result in a large reduction in cruising speed to reduce windmilling drag and propeller overspeed. Condition 3 represents the most severe failure with a reversible propeller and would mean a very high overspeed

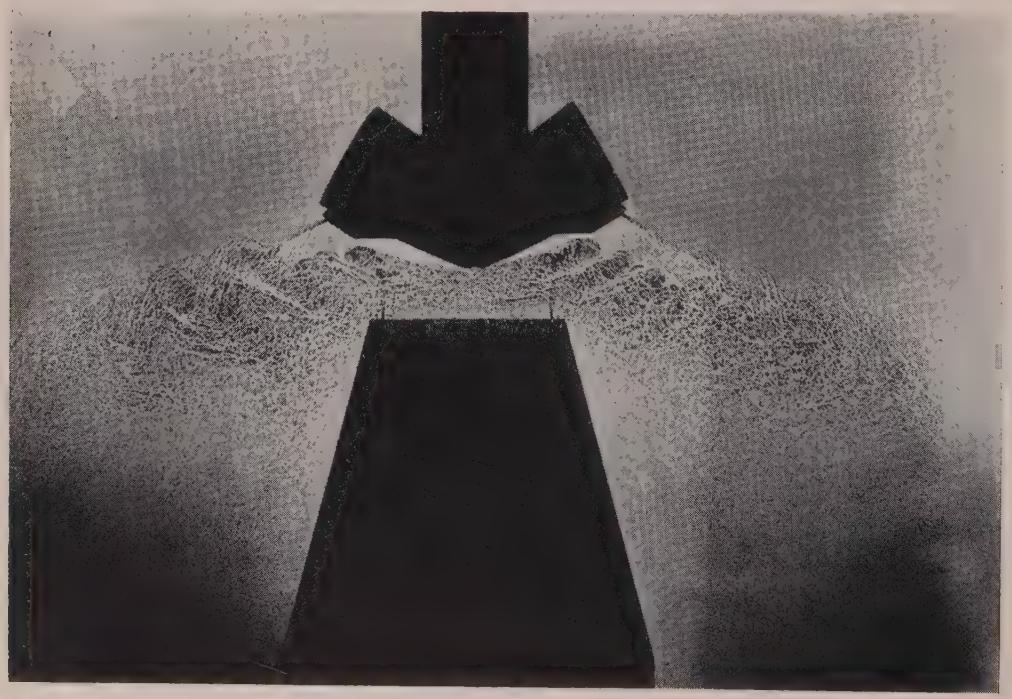

Fig. 10 – Path of reversed jet blast

condition as well as a critical performance and control condition. Condition 4 shows that, after passing through flat pitch, the reversed-propeller condition is still somewhat more critical than the low-pitch stop condition.

The most severe jet reverser failure is that where the reverser fully extends into the jet blast with power on the engine, as shown in condition 2 in the right-hand column. Again, by reducing power on the malfunctioning powerplant, the reverser failure can be reduced in severity to become only 30% more severe than a simple engine failure.

It can be concluded from the foregoing two tables that the jet reverser offers a basically safe method for providing reverser thrust at the proper time. At the same time, the consequences of uncontrolled reversals which might occur due to malfunctions are minimized. The fact that engine throttling is a positive and effective method of further reducing the consequences of failure appears to be one of the attractive features of the jet reverser.

It should be emphasized in studying the above two tables that the failures analyzed have a very low incidence rate, judging by experience gained with reversible propellers during the last few years. However, there are failures which can happen if various serious malfunctions occur. In the case of the reversible propeller, systems which must operate continuously during normal flight are also used to control the reverse-thrust cycle. Therefore, exposure to malfunctions exists during the entire flight. The jet reverser and control are separate from the basic forward-thrust system. Therefore, the system can be effectively disarmed except when reversal is required. Exposure to malfunction can be greatly reduced.

Conclusions

It has been the purpose of this paper to discuss some of the results of the testing and design work leading to the present state of development of jet reversers. It appears that a practical jet reverser installation can be available in the near future which will give jet-type airplanes the operational flexibility enjoyed by present-day reversible-propeller-equipped aircraft.

The type of reverser design discussed herein will not decrease engine fuel economy and can be adapted to a wide variety of engine installations. Because the jet reverser is separate from the basic engine, the consequences of reverser failure are considerably less severe than comparable failures of reversible-type propellers.

Even the most critical type of jet reverser failures will result in conditions which are only slightly more severe than a simple engine failure. Because jet reverse thrust has to be obtained through an additional mechanism rather than through the basic powerplant, a small increase in weight will be necessary to obtain the operational flexibility available through reverse thrust. However, the separation of the forward-thrust system and the reverse-thrust system results in an inherently safe and reliable system. The jet reverser will undoubtedly become the "pilot's friend" in the near future, just as the reversible propeller is today.

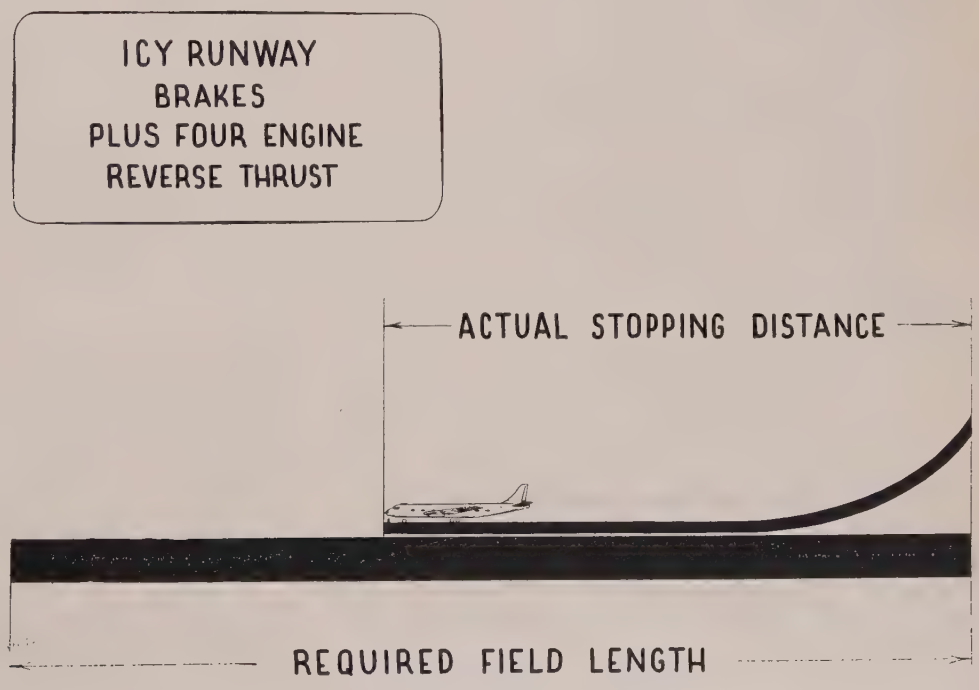

Fig. 11 – Icy runway landing of a jet transport using reverse thrust

RESULTS of tests performed on a modified type F-4 CFR engine show that precombustion reactions in both the fired and motored engine gave the same carbonyl products.

The maximum specific yields of these carbonyls were similar for a given fuel compressed with comparable pressure-time-temperature histories in both motored- and fired-engine tests.

As the motored engine seems to duplicate precombustion reactions occurring in a fired engine under normal operating conditions, the authors of this paper conclude that the motored engine, offering ease of control and sampling, is a convenient and valid tool for combustion research.

Comparison of Formed

NUMEROUS engine-combustion studies in recent years have established that most fuels undergo some chemical reaction during the compression stroke and during the further compression of the unburned end gas prior to the rapid high-temperature oxidation. These initial reactions have been termed variously as early reactions, precombustion reactions, cool-flame reactions, and so forth. It has been shown that a sizable fraction of the heating value of the fuel may be released by the precombustion reaction.[1] These reactions may occur in more than one stage, and under certain conditions they may emit a faint, blue light, or cool flame.[2] Further, there is a definite correlation between the intensity of the precombustion reactions and the tendency for detonation.[3, 4, 5] The hydrocarbons which undergo abundant precombustion reactions are prone to knock, while the engine operating conditions which lead to detonation also are conducive to extensive precombustion reactions.

Attempts have been made to learn more about the phenomenon of detonation by studying precombustion reactions in a motored engine.[6, 7] The motored engine is a convenient research tool because the extent of the precombustion reactions can be controlled by varying the severity of operating conditions. The chemical compounds thus formed are not consumed immediately in a high-temperature flame front since no spark ignition is used and the engine is operated so as to avoid autoignition. Hence, products resulting from the precombustion reactions may be sampled from the exhaust manifold or directly from the cylinder at any desired interval in the cycle.

It was the purpose of this study to determine if the types and concentrations of intermediate-combustion products formed in a motored engine were comparable to those produced by precombustion reactions within the unburned end gas of an engine employing spark ignition and normal combustion.

Test Equipment

The experiments reported herein were performed with a modified Coordinating Fuel Research (CFR) Engine, type F-4. This engine was of the single-cylinder, variable-compression-ratio design and directly coupled to an induction-type dynamometer. The dynamometer was altered to operate at either 900 or 1800 rpm; it also permitted power measurements during the motoring tests and when absorbing power from the engine.

The standard air induction system was used, but a valve was inserted in the induction system for

[1] See SAE *Quarterly* Transactions, Vol. 6, July, 1952, pp. 472-487: "Early Combustion Reactions in Engine Operation," by E. B. Rifkin, C. Walcutt, and G. W. Betker, Jr.

[2] See SAE *Quarterly* Transactions, Vol. 6, July, 1952, pp. 488-508: "Some Effects of Fuel Structure, Tetraethyl Lead, and Engine Deposits on Precombustion Reactions in a Firing Engine," by W. Cornelius and J. D. Caplan.

[3] See SAE *Quarterly* Transactions, Vol. 4, July, 1950, pp. 438-451: "Precombustion Reaction in the Spark-Ignition Engine," by E. R. Retailliau, H. A. Ricards, Jr., and M. C. K. Jones.

[4] See Philosophical Transactions of Royal Society of London, Series A, Vol. 243, July 19, 1951, pp. 463-524: "Study of Reactions that Lead to 'Knock' in Spark-Ignition Engine," by D. Downs, A. D. Walsh, and R. W. Wheeler.

[5] See SAE Transactions, Vol. 61, 1953, pp. 442-450: "Mode of Formation of Lead Deposits in Gasoline Engines," by J. C. Street.

[6] See SAE *Quarterly* Transactions, Vol. 4, October, 1950, pp. 571-587: "Precombustion Reactions in a Motored Engine," by D. L. Pastell.

[7] See SAE Transactions, Vol. 61, 1953, pp. 386-401: "Some Factors Affecting Precombustion Reactions in Engines," by M. W. Corzilius, D. R. Diggs, and D. L. Pastell.

Intermediate-Combustion Products in Engine with and without Ignition

William C. Davis, Marion L. Smith, Earl W. Malmberg, and Jane Ann Bobbitt, Ohio State University.

This paper was presented at the SAE Annual Meeting, Detroit, Jan. 14, 1954.

the purpose of throttling the air to pressures below atmospheric. Air consumption was determined by a sharp-edged orifice and either a U-tube manometer or an inclined-tube draft gage. Manifold air temperature (M.A.T.) was maintained within ± 2 F of a preselected value by the standard thermostatically controlled heaters. A potentiometer and a copper-constantan thermocouple in the air stream before the point of fuel injection provided the means for air-temperature measurement. Two types of fuel injection systems, one for liquid fuels and another for gaseous fuels, were used interchangeably. The liquid injection system included the standard Bosch injection system. Propane and propene were expanded in a pressure-reducing valve and injected into the inlet manifold through a ¼-in. nozzle replacing the Bosch injection nozzle tip. Fuel consumption was measured volumetrically for liquid fuels and gravimetrically for the gaseous fuels. All hydrocarbon fuels used for the experiments reported here were of 99% purity or better.

Methyl alcohol was used as the evaporative coolant for the engine because its low boiling temperature (149 F) could be maintained for both unfired- and fired-engine tests. Ignition was provided by the standard magneto system. Most samples were obtained from a modified CFR type

The Authors

WILLIAM C. DAVIS is research assistant at Ohio State University. He received his bachelor's degree in electrical engineering from Fenn College in 1951, and his master's degree from Ohio State in 1953. Mr. Davis has held his present position since 1952.

MARION L. SMITH (J '48) is assistant professor of mechanical engineering at Ohio State University. He received his B.S. from Louisiana State University, and his M.S. from Ohio State University in 1948. Prof. Smith has been an associate supervisor of a project studying the mechanism of oxidation of hydrocarbons. He joined the staff at Ohio State University in 1947.

EARL W. MALMBERG is assistant professor of chemistry at Ohio State University. He received his B.A. from Gustavus Adolphus College, and his Ph.D from the University of Nebraska in 1947. He was employed as a research chemist with the American Cyanamid Co. from 1947-1948. The following year he was a du Pont postdoctoral fellow at the University of Minnesota.

JANE ANN BOBBITT is a research associate at the Ohio State University Research Foundation. She received her B.S. in chemistry from West Virginia University in 1951. She was employed by the Carbide and Carbon Chemicals Co. in 1951-1952. Miss Bobbitt has held her present position since 1952.

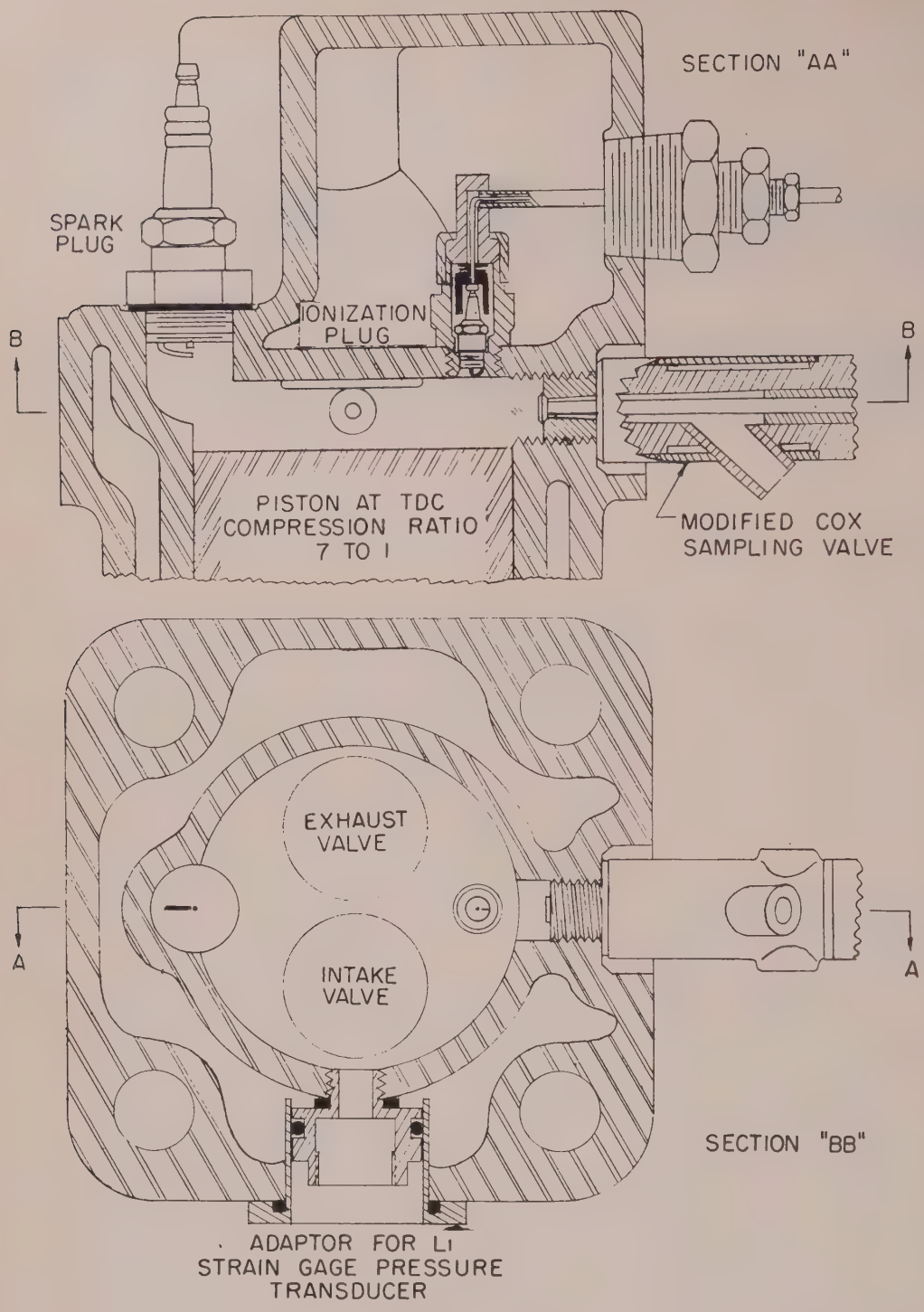

Fig. 1 – Arrangement of instrumentation in cylinder head

F-4 cylinder head with instrumentation located as shown in Fig. 1. Later tests were conducted with a Waukesha model 00109098 cylinder head, which had four openings into the cylinder. Comparable results were obtained with both cylinder heads. The instrumentation used with the standard head included a Cox gas-sampling valve, a pressure transducer, and an ionization plug, which were adapted to the combustion chamber.

The ionization plug, a Champion V-3 spark plug, was mounted on the top of the combustion chamber seven-eighths of the distance across the chamber from the point of spark ignition. Its location was also directly in line with the spark plug and the Cox valve. The purpose of this ionization plug was to detect the presence of the hot-flame front to prevent the sampling of burned gases through the valve during the fired-engine tests. The ionized

gases conducted a small electric current across the plug gap which, when amplified, caused a stroboscopic lamp to flash against a protracted scale marked on the engine flywheel (Fig. 2). This ionization detector was sensitive only to the hot-flame front produced by either normal combustion or autoignition.

Three modifications of the original Cox gas-sampling valve (Fig. 3) were made upon the basis of experience gained at the Ethyl Research Laboratories.

1. A liquid-cooled shank with a short gas-flow passage was designed to replace the standard uncooled shank. Cool tap water was circulated through this jacket in an attempt to retard any reactions that might occur in the gas stream sampled from the combustion chamber.

2. The specified valve displacement of 0.0035 in. was increased to 0.008 in. to permit a larger flow rate of sampled gas. Calibrations indicated that, at a displacement of 0.008 in., the valve remained open about 1.1 milliseconds, or 6 deg of crankshaft rotation at 900 rpm.

3. A debouncing cylinder containing 80 mesh and finer tantalum powder was fastened to the valve stem to permit normal valve operation and eliminate the objectionable bounce of the valve off the valve seat after closing.

The valve was electromagnetically actuated by a timer driven by the engine crankshaft. Thus, a small sample of gas could be withdrawn from the cylinder each cycle during any preselected interval of crank rotation. An electrical impulse from the timer-actuator was used to excite the stroboscopic lamp to flash against the flywheel scale and thereby indicate the valve timing.

The combustion chamber was also provided with an adaptor for a strain-gage-type pressure transducer so that pressure variations within the cylinder could be detected on an oscilloscope.

Experimental Technique

To collect samples for analysis of carbonyl compounds, the gas extracted through the sampling valve was scrubbed in a 2N hydrochloric acid solution of 2,4-dinitrophenylhydrazine. This scrubbing effected a complete removal of the carbonyl content until the reagent solution became saturated with carbonyl product. Detection of saturation in the first scrubber was evidenced by an identical solution in a downstream scrubber which became clouded the moment any carbonyl compounds were carried over from the first scrubber. If saturation occurred in the first scrubber before the end of the test, the carbonyl products carried over to the second were regained by combining the contents of both scrubbers. Thus, the second scrubber, termed an indicator, insured practically 100% collection efficiency.

The gas output from the indicator was measured volumetrically with a wet-test gas meter. Outlet gases from this meter were then expelled to the

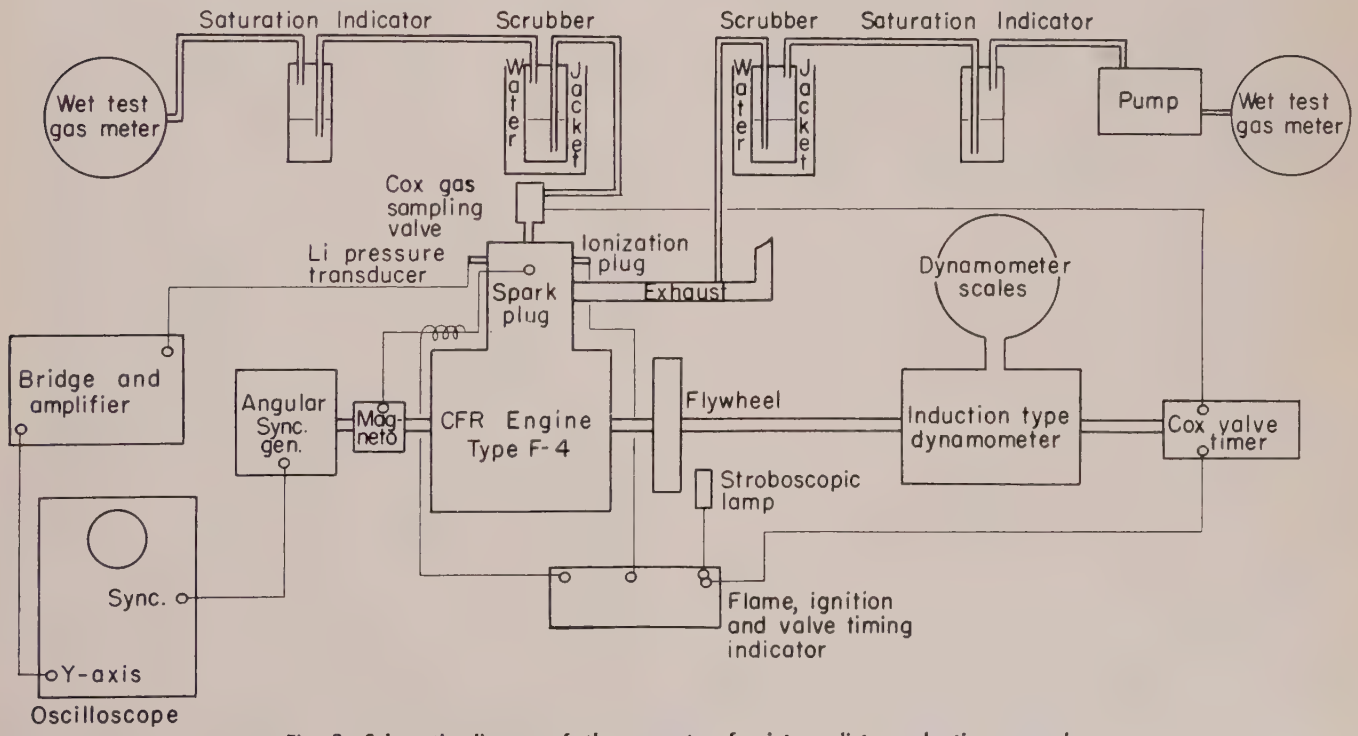

Fig. 2 – Schematic diagram of the apparatus for intermediate-combustion research

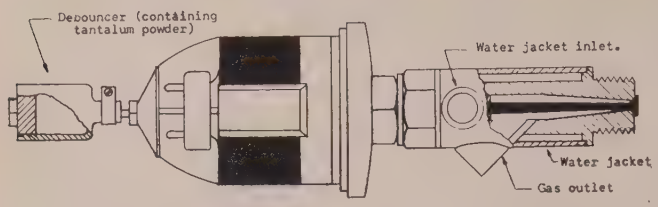

Fig. 3 – Modified Cox gas-sampling valve

atmosphere. To sample the motored-engine exhaust gas, a similar collection system was used except that a pump was added after the two scrubbers to promote the gas flow. The scrubbers were immersed in an ice-water bath during the sampling test and maintained at reduced temperature until chemical analyses were begun. It was thought that, by maintaining the sample at a low temperature, chemical reactions in the scrubber would be minimized. In no case was there a lapse of more than 2 hr between the completion of a test and the initial analysis. Analytical procedures employed for the carbonyl and peroxide compounds are described in the literature.[8, 9]

Analyses were restricted primarily to carbonyl compounds, although a limited study of the hydrogen peroxide and organic peroxides present in the exhaust gas of the motored engine was made. To collect the peroxide products for examination, a portion of the exhaust gas stream was diverted through a condenser maintained at dry-ice temperature. After completion of the test, the condenser was quickly warmed to room temperature, and the reaction products adhering to the condenser surfaces were washed into a collector test tube with benzene. Chemical analysis of this condensate followed immediately to prevent any further decomposition of the unstable compounds.

Prior to every sampling run, the engine was motored without fuel long enough to allow the inlet air temperature and crankcase oil temperature to reach values identical to those maintained during the run. Then test conditions were maintained for a period of 20 to 30 min before sampling was started. The warmup at test conditions had a twofold purpose, to obtain thermal equilibrium and to allow a buildup of a surface coating on the walls of the combustion chamber similar to that which might exist after a longer period of operation.

During tests of a particular hydrocarbon fuel, engine speed, engine jacket coolant temperature, engine oil temperature, manifold air temperature and pressure, exhaust back pressure, spark advance (if fired), and air/fuel ratio were held constant. However, the compression ratio of the motored engine was greater than that of the fired engine. In both cases, the compression ratio was increased as close as possible to the autoignition limit. The purpose of using different compression ratios was to produce an equivalent history of the combined influence of pressure, temperature, time, combustion-chamber-surface effect, and residual-gas effect in both the end gas of the fired engine and the entire charge of the motored engine. Obviously it would be impossible to obtain identical histories in both cases.

The values of the engine parameters held constant for a series of experiments with a particular fuel were selected for various reasons. Engine speed was 900^{+10}_{-5} rpm in every experiment except one, in which the speed was 1800 rpm. The relatively low speed of 900 rpm was chosen primarily because it allowed more time for the production and selective sampling of intermediate-combustion products. Past experience has indicated that the formation of the reaction products is also favored by increasing the temperature of the initial air-fuel charge. Therefore, a relatively high manifold air temperature (280 to 330 F) was maintained during the experiments. Since this work involved a comparison of unfired- and fired-engine samples, an air/fuel ratio in the ignition range of hydrocarbon-air mixtures was dictated. Stoichiometric air/fuel ratio was selected. A 15-deg spark advance was used to permit ample time for the occurrence of preflame reactions before the hot flame consumed the entire charge. The manifold pressure was reduced below atmospheric in the experiments with n-heptane so that extensive precombustion reactions could be produced without autoignition. However, the resistance to autoignition of some other fuels in the motored engine was so great that it was necessary to supercharge the

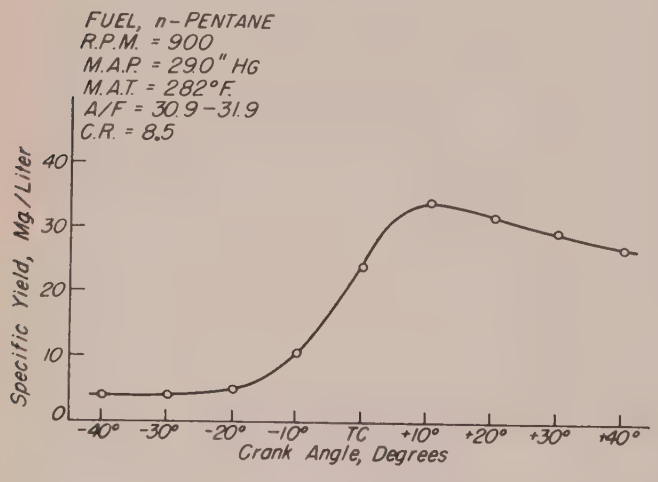

Fig. 4 – Variation of total carbonyl compounds in motored-engine valve samples

[8] "A Chromatographic Study of Carbonyl Compounds Present in a Hydrocarbon-Air Flame," by E. W. Malmberg. Paper presented at American Chemical Society Meeting, Atlantic City, September, 1952.

[9] "Isolation of Alkyl Hydroperoxides from the Combustion Reactions of Hydrocarbons," by E. W. Malmberg, D. L. Fishel, M. L. Smith, and W. C. Davis. Paper presented at American Chemical Society Meeting, Los Angeles, March, 1953.

engine and to use a high compression ratio to approach incipient autoignition.

The presence of chemical reaction in the motored engine could be determined by a reduction in the motoring power requirement, by an increase in the exhaust gas temperature, and by a pressure deviation from the motored-engine pressure-time diagram.

Results

One generally accepted theory concerning the mechanism of hydrocarbon oxidation contends that the first step in the attack of the molecule by oxygen is the formation of an alkyl hydroperoxide. Subsequent reactions may transform the alkyl hydroperoxides to carbonyl compounds and other uninvestigated products. For example, this mechanism may be represented for n-pentane:

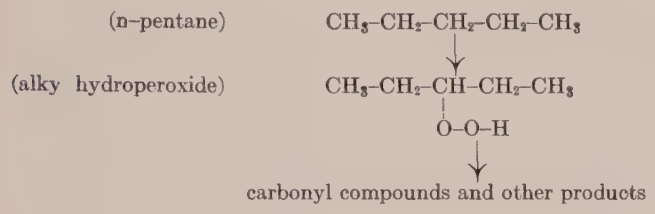

The study of the reaction in this first stage is important because the resistance to knock of a fuel appears to be a function of the formation of peroxides or the conversion of peroxides to other compounds. Although the present oxidation theories involve alkyl hydroperoxides in the reaction mechanism, their presence in oxidation mixtures was never established definitely until the work reported by Malmberg et al.[9] was completed. Pure alkyl hydroperoxides and other organic peroxy compounds were studied to develop chromatographic techniques for identifying such compounds. The chromatographic analyses of samples from the engine indicated many peroxide zones.[10] By polarographic study it was positively established that all of these zones contained alkyl hydroperoxides with the exception of one which, from chromatographic properties, was known to be hydrogen peroxide. Further studies are in progress to determine the chemical structure of these alkyl hydroperoxides isolated from the engine samples.

Inasmuch as the analytical techniques for identifying the alkyl hydroperoxides have been developed only recently and are not yet perfected, the investigation described here has been concerned more specifically with the carbonyl compounds which result after the peroxide formation. Chromatographic analysis of the carbonyl compounds has met with a good degree of success, particularly for studying intermediate-combustion products in the engine samples.

Results with n-Pentane – Data for Figs. 4, 5, and 6 were obtained with lean mixtures of n-pentane. Samples of this series were extracted from the combustion chamber of the motored engine from 40 deg btc to 40 deg atc. During this portion of the cycle the precombustion reactions producing carbonyl products were initiated and then arrested.

Fig. 4 shows the variation with crank angle of the specific yield of total carbonyl hydrazones, in milligrams per liter of gas sampled. Each monocarbonyl (such as formaldehyde, acetaldehyde, and so forth) will have attached to its molecule only one 2,4-dinitrophenylhydrazine residue. Dicarbonyls will have only two, and so forth. The formaldehyde molecule, $H_2C{=}O$, when combined with the 2,4-dinitrophenylhydrazine molecule to form formaldehyde hydrazone is represented by the formula:

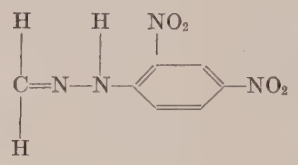

The molecular weight of the hydrazone molecule itself is nearly 200, while the molecular weights of the various pure carbonyl compounds are small in comparison. Therefore the weights of the individual carbonyl hydrazones may be used for a comparison of the relative percentages of the particular carbonyl compounds or class of compounds in the total weight of carbonyl products sampled. Hereafter, for simplicity, reference is made only to the carbonyl product and not to the corresponding carbonyl hydrazone which was the actual substance isolated.

It is evident from Fig. 4 that the carbonyl yield remains relatively constant until 20 deg btc and

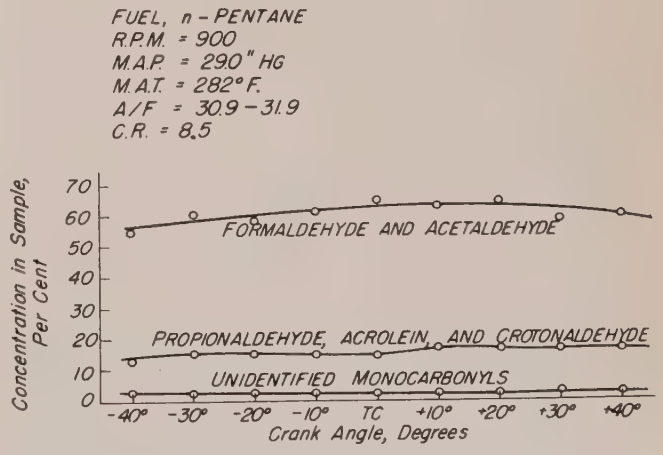

Fig. 5 – Variation of carbonyl compounds in valve samples in the motored engine

[10] A zone in a chromatographic column represents a region locating all molecules having the same tendency to be adsorbed.

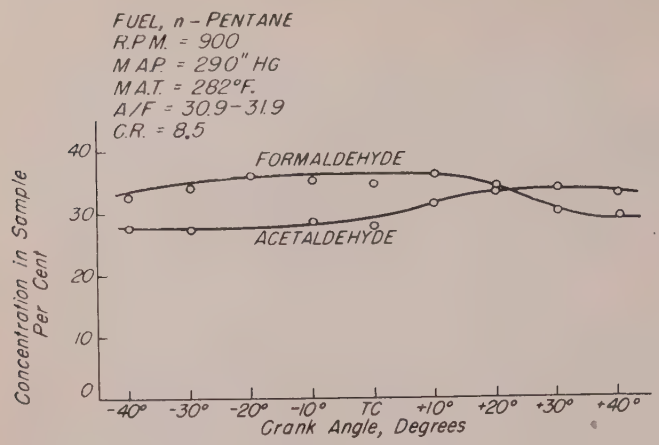

Fig. 6 – Variation in yield of the two principal carbonyl compounds in the motored engine

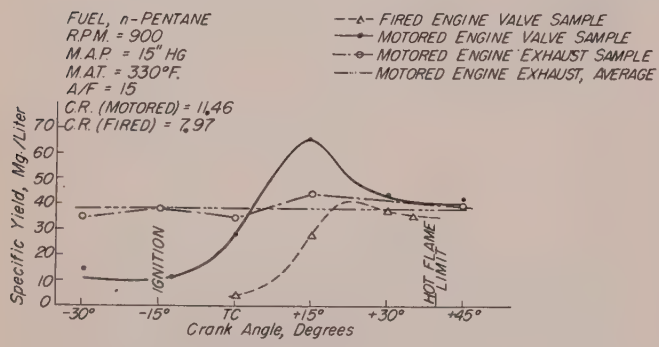

FIG. 7 COMPARISON OF CARBONYL YIELD IN THE FIRED AND UNFIRED ENGINE.

Fig. 7 – Comparison of carbonyl yield in the fired and unfired engine

then rapidly increases to a maximum value at 10 deg atc. Thereafter the yield decreases slightly but levels off later in the cycle. The yields prior to 20 deg btc are believed to represent the carbonyl compounds present in the residual gas which dilutes each new charge. The intermediate-combustion products which survive in the residual gas probably have an important bearing on the initiation of reactions in the fresh fuel-air mixture. One explanation for the slight decrease of carbonyl yield later in the cycle (Fig. 4) is that conversion of carbonyl compounds to other types of reaction product is effected.

Fig. 5 shows the concentration in per cent by weight of the three largest carbonyl groups present in the samples shown in Fig. 4. In this study a carbonyl group represents the compounds which were adsorbed in the same location, or zone, in the chromatographic column.

In all analyses of carbonyl samples, approximately 85% of the carbonyl yield was accounted for in distinct chromatographic zones. About one-third of the remainder was composed of polyfunctional carbonyl compounds which were adsorbed at the top of the chromatographic column; glyoxal and methyl glyoxal, both dicarbonyls, were present in this zone. The rest were minor zones which could not be identified.

Formaldehyde and acetaldehyde constitute the major portion (approximately 60%) of the isolated carbonyl compounds formed from n-pentane in the motored engine. The percentages of each zone remain relatively constant for each crank angle regardless of the rapid formation of carbonyls indicated by Fig. 4. The chromatographic zone containing formaldehyde and acetaldehyde was separated into its components, and the results are indicated in Fig. 6. The percentages of both compounds, referred to the total carbonyl sample, were nearly equal and are relatively constant with the crank angle of sampling. Probably the variations of the curves were caused primarily by experimental error in sampling, combustion control, and analysis.

Additional work (Figs. 7, 8, and 9) with n-pentane at stoichiometric air/fuel ratio and reduced manifold air pressure, correlates closely with the motored-engine series (Figs. 4, 5, and 6), with lean mixtures and manifold pressure of one atmosphere. The curve (Fig. 7) representing the valve samples of the motored engine illustrates the same characteristics as does the similar curve in Fig. 4. The same general comments apply in both cases; however, it is believed that the decreasing yield from 30 deg btc to 15 deg btc indicated by Fig. 7 was the result of experimental variation. In comparing Figs. 4 and 7, it may be noted that the reaction appears to be initiated at approximately the same time in the cycle. However, this was a coincidence because different engine conditions affect the time of initiation of reaction.

The values of yield from the motored-engine exhaust are plotted in Fig. 7 at the crank angles at which valve samples were collected simultaneously. The exhaust samples also served as a check on the constancy of reaction rates during the series of motored-engine experiments. A broken-line curve is drawn through the plotted values because, ideally, the curve should represent a horizontal

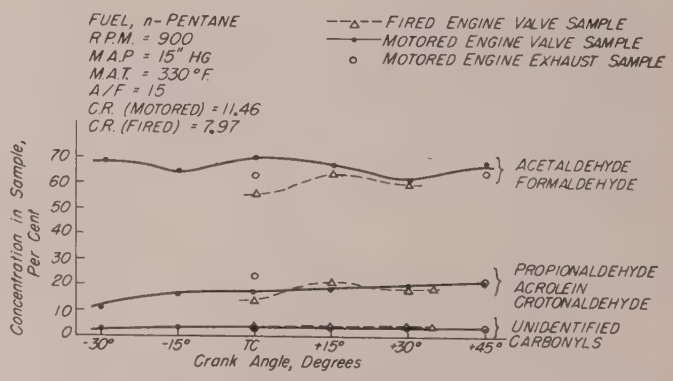

Fig. 8 – Comparison of carbonyl compounds in samples from the fired and unfired engine

line if all reactions and experimental techniques were entirely reproducible. A dotted line at the specific yield which represents the average of the carbonyl yield in the motored-engine exhaust is indicated to illustrate the fact that the yield of compounds in the combustion-chamber gas approached this value late in the cycle.

Results from the fired-engine experiments are also represented in Fig. 7. The shape of this yield curve is very similar to the motored-engine curves of both Figs. 4 and 7, that is, nearly the same rates of formation of carbonyl compounds are indicated. The minimum value of the specific yield in the fired engine is less than in the motored engine, probably because fewer carbonyl compounds survived in the residual gas of the fired engine.

Evidence that equivalent histories of temperature, pressure, and time were produced in both the motored engine and fired engine is indicated by the fact that the specific yield in both cases approached a single value late in the cycle. The maximum yield in the fired engine occurred about 10 deg later in the cycle than in the motored engine. Two logical factors which might explain this phase lag are the lower compression ratio used with the fired engine and the greater concentration of peroxides in the residual gas of the previous cycle in the motored engine. Most of the intermediate compounds in the fired engine are destroyed by the high-temperature combustion. The hot-flame limit indicated in Fig. 7 denotes the crank angle at which the hot flame arrived at the ionization plug in the fired engine. All samples from the fired engine were extracted prior to this point in the cycle to prevent sampling the normal (hot-flame) combustion products.

The results presented in Fig. 8 show the composition by groups of the total carbonyl sample in the motored-engine exhaust, motored-engine valve, and fired-engine valve samples of n-pentane reported in Fig. 7. These results appear similar to

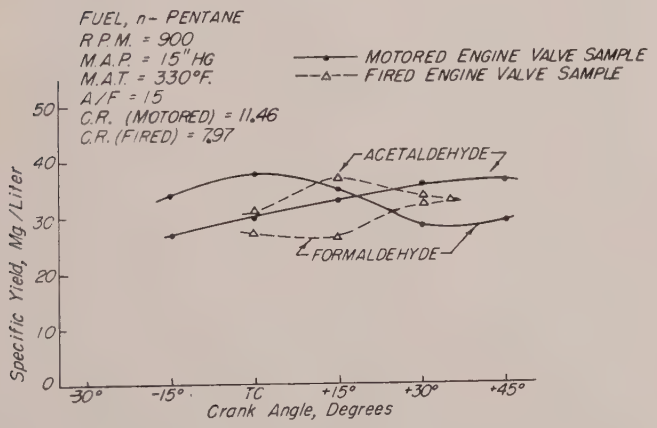

Fig. 9 – Comparison of the two principal carbonyl compounds from the fired and unfired engine

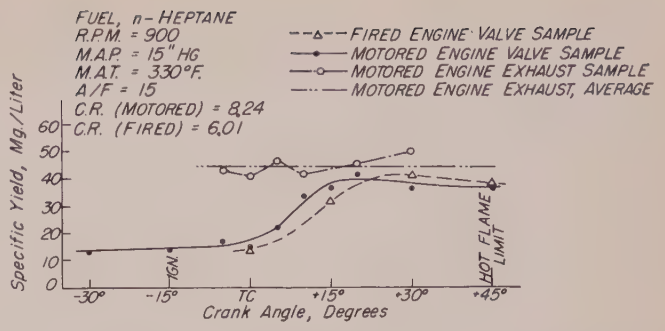

Fig. 10 – Comparison of carbonyl yield in the fired and unfired engine

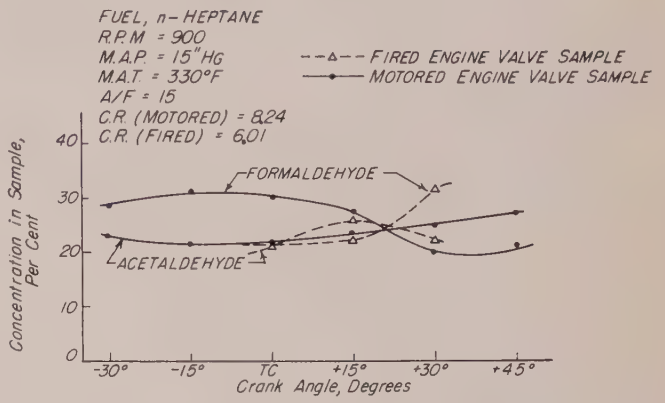

Fig. 11 – Variation in yield of the two principal carbonyl compounds from the fired and unfired engine

those of Fig. 5. No general trend can be ascribed to any of the curves in Fig. 8. However, it seems significant that the respective carbonyl groups from each sample, regardless of the method by which they were obtained, were present in nearly the same percentages. It was also determined that the constituents of each group, irrespective of the method of sampling, were identical and were the same as those described for n-pentane (Figs. 4, 5, and 6). Again, formaldehyde and acetaldehyde comprised about 30 to 40% of the total sample (Fig. 9).

The only deviation from uniformity of results was a discovery of acetone in trace amounts in the fired engine with n-pentane. It is possible that acetone may have been present in the other samples but in such small quantities as to escape detection.

Results with n-Heptane – Results with n-heptane (Figs. 10 and 11), were similar to those obtained with n-pentane. Except for acetaldehyde and formaldehyde, analysis of the carbonyl products in each particular chromatographic zone was not undertaken because of the complexity of the isolated products. However, preliminary infrared analysis of the second and third chromatographic zones gave evidence that they contained the same components identified with n-pentane. Seven chromatographic zones containing monocarbonyl compounds

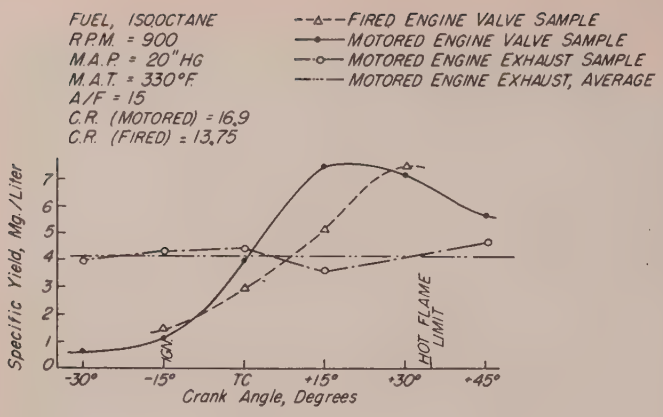

Fig. 12 – Comparison of carbonyl yield in the fired and unfired engine

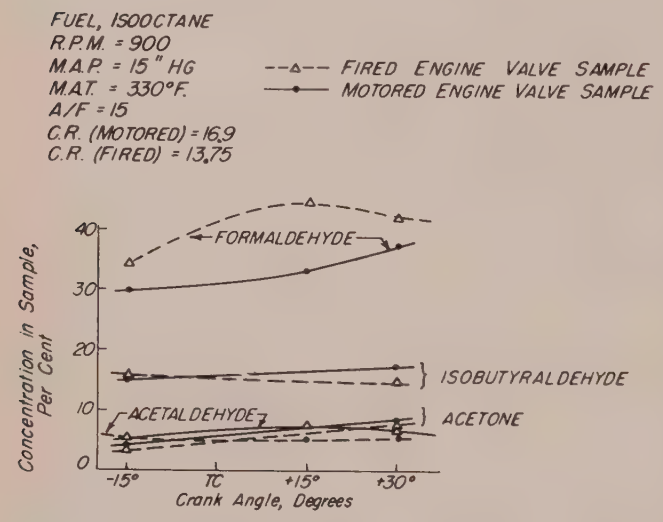

Fig. 13 – Variation of identified carbonyl compounds in the fired and unfired engine

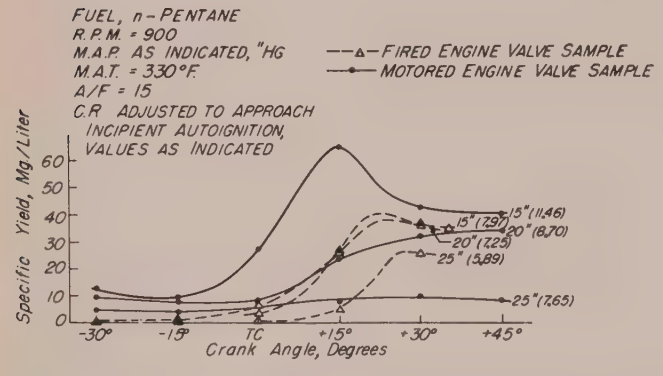

Fig. 14 – Carbonyl yield in the fired and unfired engine as affected by manifold air pressure

were definitely established, whereas only three monocarbonyl zones were present with n-pentane. More numerous carbonyl compounds might be expected from the oxidation of longer molecules. All carbonyl compounds except acetaldehyde and formaldehyde appeared in very small percentages.

Results with Isooctane – In tests with isooctane, the yield curves of carbonyl compounds in samples from the motored engine and fired engine (Fig. 12) are quite similar to those obtained with n-pentane and n-heptane, except for the following differences. Values of specific yield for isooctane were much less, even though more severe engine operating conditions were used in order to approach incipient autoignition. Analyses of both the fired and motored samples indicated that the concentration of acetaldehyde was a small percentage of the total carbonyl compounds (Fig. 13). A small percentage of acetone was present along with isobutyraldehyde and traces of several unidentified monocarbonyl compounds.

The analyses of the motored- and fired-engine samples were nearly identical even though the composition of the isooctane samples differed somewhat from those of n-pentane and n-heptane. As with other fuels, there seemed to be no marked change in composition with crank angle position.

Results with Other Hydrocarbon Fuels – Additional work with propane, propene, and cyclohexane indicated that in the engine, whether fired or unfired, the same general characteristics were exhibited as with the fuels previously discussed. The specific yields with each of these fuels were generally less than the values of specific yield shown for isooctane. As would be expected, the number of monocarbonyl compounds formed with propane and propene was less than with the longer-chain hydrocarbons. With both fuels, formaldehyde, acetaldehyde, propionaldehyde, acrolein, and trace amounts of acetone were present along with a small percentage of polyfunctional carbonyl compounds. No other monocarbonyl compounds appeared.

Again the fired-engine samples were similar to the motored-engine samples in specific yield and composition.

Effect of Engine Operating Conditions – Figs. 14 and 15 show that the same variation in specific yields with crank angle position held for widely different engine operating conditions. In each case the compression ratio was adjusted to approach incipient autoignition for the particular inlet manifold pressure and engine speed. While the values of specific yield of carbonyl compounds changed considerably for the different conditions, the shapes of the yield curves are similar.

Reproducibility – Fig. 16 shows the degree of reproducibility which might be expected in tests of this type. These results from motored-engine valve samples were obtained from two series of test runs, the one made about three months later than the other. As shown on the graph, in one case the compression ratio was limited to 10.99 to eliminate autoignition, whereas in the other test run the compression ratio could be increased to 11.46. The higher compression ratio produced greater specific yields of carbonyl compounds. The fact that engine conditions could not be duplicated exactly may be

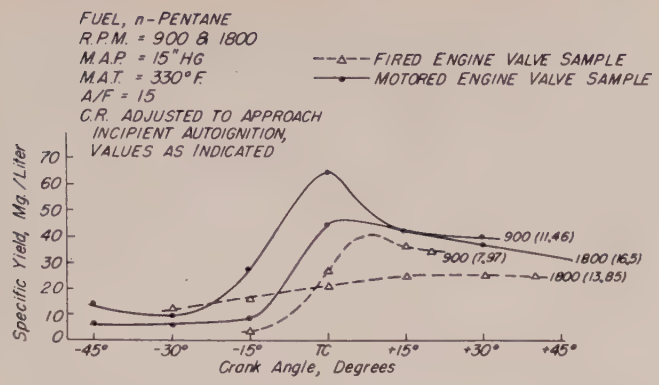

Fig. 15 – Comparison of carbonyl yield with change of engine speed

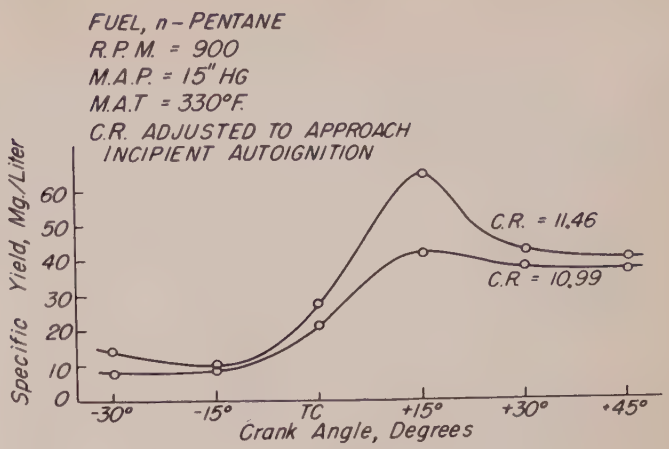

Fig. 16 – Reproducibility of carbonyl yield from the motored engine

an explanation for some of the values of specific yield which appear somewhat erratic. Apparently there is some effect from cylinder deposit, humidity of the intake air, and so forth. In spite of this, many samples with the same fuel were obtained over a period of several months and with two different types of cylinder heads. In most cases the points from later samples fit the trends established by earlier samples. The cylinder head and piston were cleaned periodically, and lead-free fuels were used exclusively.

Conclusions

This work represents progress to date. At the present time, no general theory as to the mechanism of oxidation can be established. However, as a result of this investigation the following conclusions appear evident:

1. The same types of carbonyl products were formed by precombustion reactions in both the motored- and fired-engine tests.

2. The maximum specific yields of these compounds were approximately the same when a given fuel was compressed with comparable pressure-temperature-time histories in both the motored- and the fired-engine tests.

3. The variations of the specific yields of carbonyl intermediates with crank angle position were similar for the motored- and fired-engine tests except for a phase lag of about 10 crank angle degrees.

4. Essentially the same types of intermediate compounds were found with n-pentane, n-heptane, isooctane, propane, propene, and cyclohexane, though the concentrations of the carbonyl compounds formed and the engine operating conditions required to produce vigorous precombustion reactions differed markedly for the several fuels.

5. The motored engine is a convenient and valid tool for combustion research, since apparently it duplicates precombustion reactions which occur in an engine under normal operating conditions. The motored engine offers a much greater degree of control over the reactions and facilitates the sampling technique.

Acknowledgment

This study was conducted in the Departments of Mechanical Engineering and of Chemistry, the Ohio State University, through the Ohio State University Research Foundation, and under the sponsorship of the U. S. Air Research and Development Command, Baltimore, Md. The authors acknowledge with thanks the guidance of Dr. C. E. Boord, project supervisor, and the assistance of Frances Zamnik, spectroscopist.

DISCUSSION

Run Motored Engine at Higher Rpm Than Fired Engine for Comparable Data

– T. J. Schweitzer, O. A. Uyehara, and P. S. Myers
University of Wisconsin

IN their conclusions, the authors state that the yield of carbonyl products was approximately the same in a motored and fired engine when a given fuel was compressed with comparable pressure-temperature-time histories. The discussers would like to point out that it is extremely difficult to obtain comparable pressure-temperature-time histories in fired and motored engines operating at the same rpm.

The difficulties encountered are shown in Fig. A where the compression ratio and temperatures encountered by the unburned gases are shown for a motored engine and for a fired engine. It is seen that the gases in the fired engine are compressed rapidly in the top-center region to a high temperature. In other words, the unburned gases are compressed in the fired engine by two different methods – the piston and the flame front – and it is the combination of the two that determines the pressure-temperature-time history, while the piston alone determines the history of the gases in the motored engine.

This situation is further illustrated in Fig. B where the spark timing was varied while the nominal compression ratio remained fixed. It can be seen here that the compression due to the flame front determines the severity of the

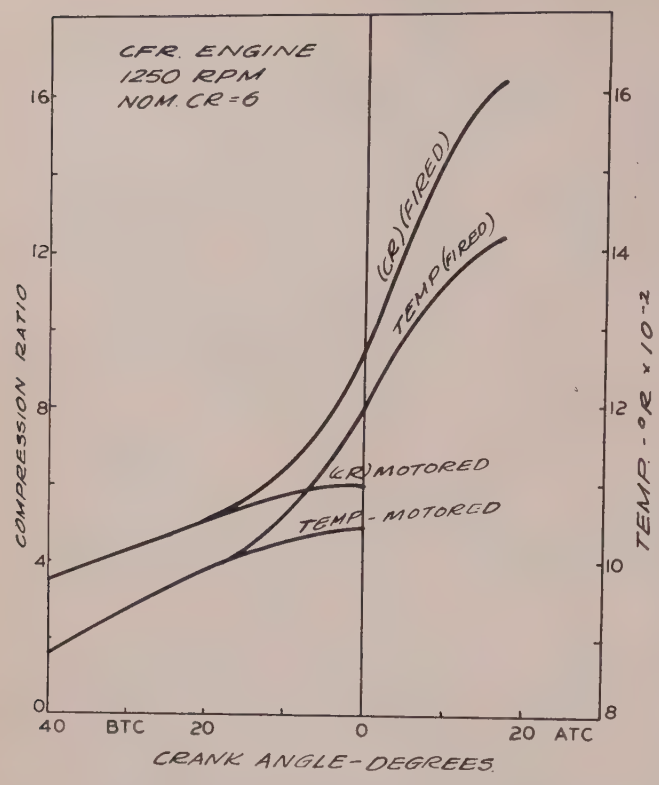

Fig. A – Compression ratio and temperature of unburned gases in a motored and a fired engine

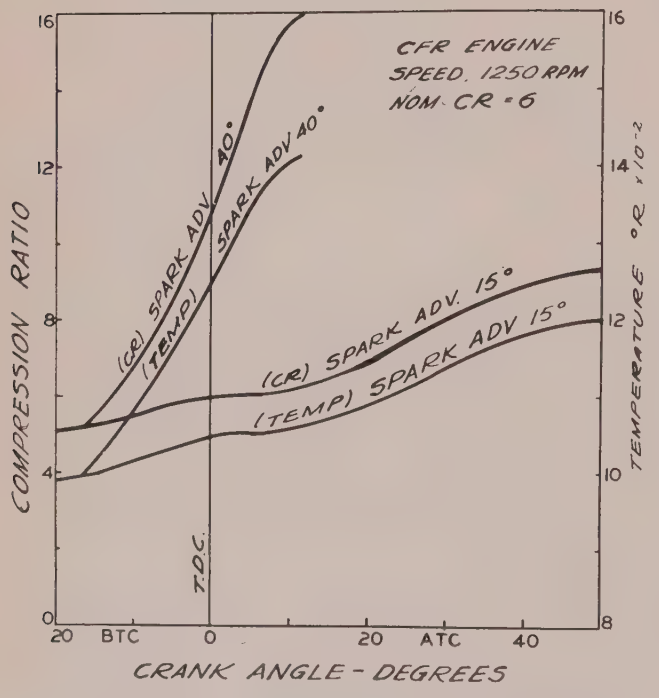

Fig. B – Compression ratio and temperature of unburned gases at varied spark timing

pressure-temperature conditions encountered by the unburned gases.

The temperature conditions encountered by the unburned gases are of interest because they determine the rate of reaction of the fuel and air. Fig. C presents relative rates of reactions of the unburned gases under four different conditions. The first of these is a motored engine having a nominal compression ratio of 6/1. The second is the unburned gases in the same engine when it is fired using 60-octane fuel. The third curve presents calculations for a motored engine with a compression ratio of 10.8/1. These latter data were calculated because Ethyl Corp. found that autoignition occurred at this compression ratio when using 60-octane fuel. It should be noted that a smaller engine and lower rpm were used. The fourth curve is for an engine having a nominal compression of 16.3 and being motored at a speed of 1800 rpm. Similarly these data were used because at this effective compression ratio autoignition occurred in the fired engine (compression ratio = 6).

The item that is probably of interest is not the rate of reaction but the amount of the reaction completed. This quantity is given by the area under the curves of Fig. C and is presented in Fig. D. The relationship between Figs. C and D is comparable to the relationship between velocity and distance.

Fig. D shows very clearly that it is very difficult to achieve the same history for the unburned fuel in a fired and motored engine. It also shows that more nearly similar histories, that is, the same amount of reaction (compare curves 2, 4, and 5), will be obtained when the motored engine is operated at a nominal compression ratio equal to the compression ratio encountered by the end gases in the fired engine and at a higher rpm than the motored engine. It is to be noted that the end points of the curves represent the amount of reaction at the time of autoignition. Confirmation of the foregoing thoughts will be found in the authors' data. They found that the motored engine could be operated at higher nominal compression ratio when higher rpm were used.

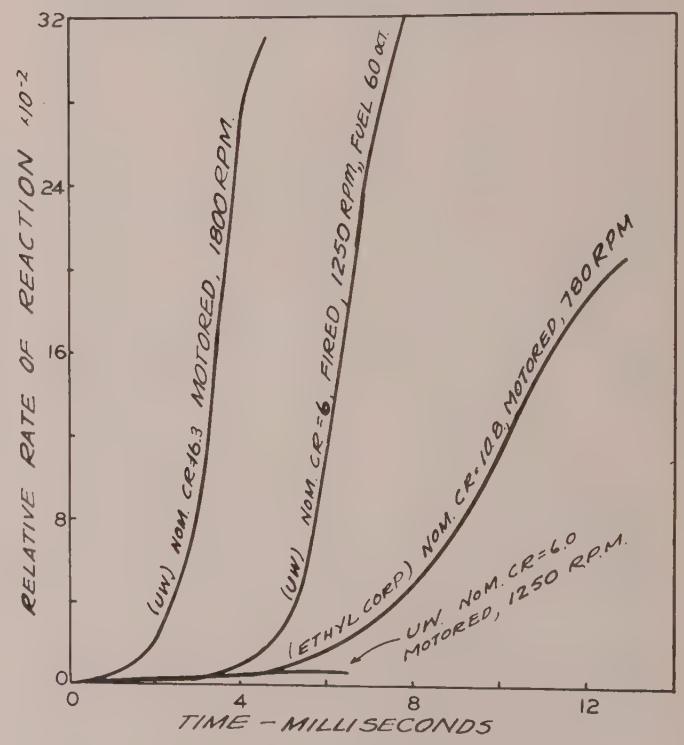

Fig. C - Relative rates of reaction

It may be concluded, therefore, that pressures and temperatures comparable to those achieved in the end gas of the fired engine can be reached in the motored engine only when the time factors are comparable, and the time factors are more nearly comparable when the motored engine is operated at a higher rpm than the fired engine.

Data Show Lack of Correlation Between Carbonyl Yield and Knock

– A. Ross
Ethyl Corp.

IT is generally very difficult to evaluate engine data in terms of the chemical reactions taking place in the combustion chamber because of the very rapid changes in temperature and pressure that occur throughout the cycle. It is for this reason that the authors are to be congratulated on their success in getting into the combustion chamber and obtaining samples which yield consistent and reproducible results. The use of reduced manifold pressures is an especially good technique. It leads to two important consequences. First, it allows the compression ratio to be raised considerably, and thus higher temperatures are reached without leading to knock or autoignition. Secondly, the time interval between ignition and flame arrival at the sampling valve is greatly extended. As a result of both these effects the amounts of the products formed are increased, and thus they are much more easily isolated and identified. A further word of praise is due the authors for the fine work done in working out the analytical methods for the complex mixtures involved here.

There are two comments which should be made concerning the conclusions reached in this work. The first involves the use of the term "equivalent (or comparable) history of pressure, temperature, and time" as applied to the fired and

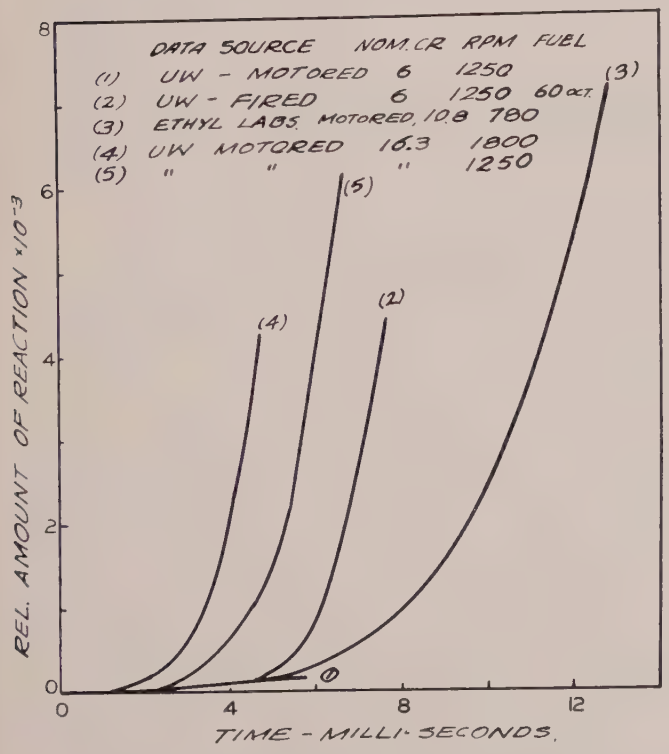

Fig. D – Relative amount of reaction completed

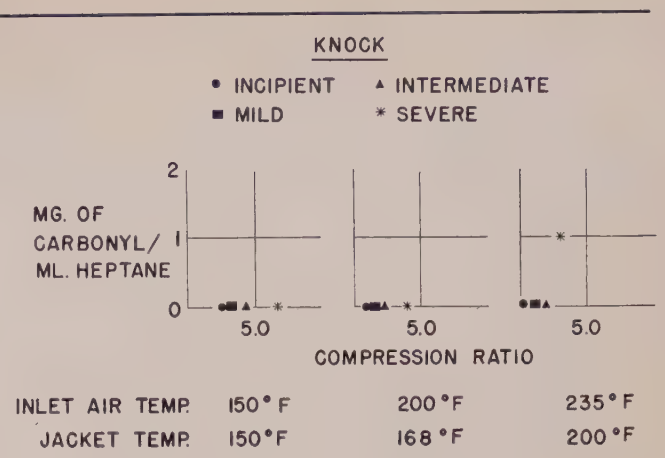

Fig. E – Production of carbonyls in a fired engine; fuel is n-heptane

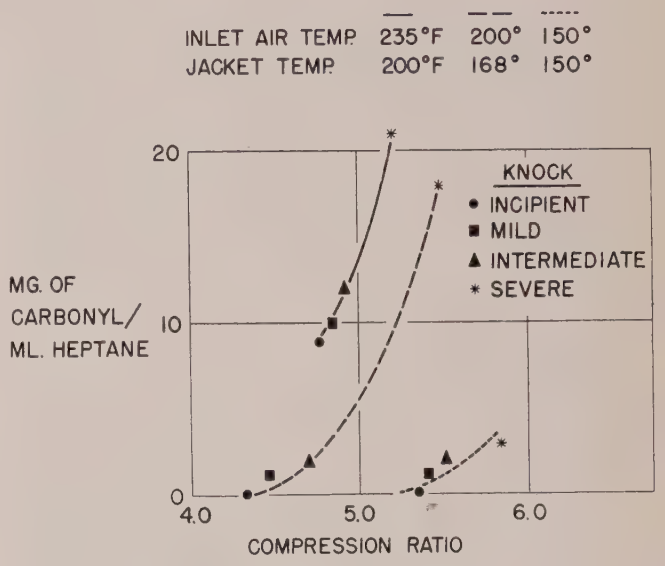

Fig. F – Production of carbonyls in a fired engine; fuel is n-heptane with 3.0 ml tel per gal

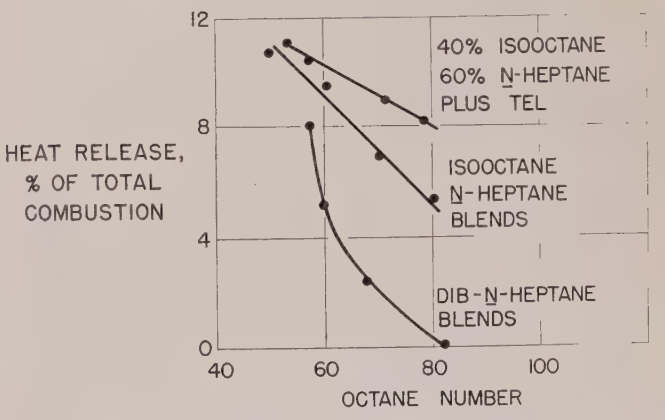

Fig. G – Variation in heat of precombustion

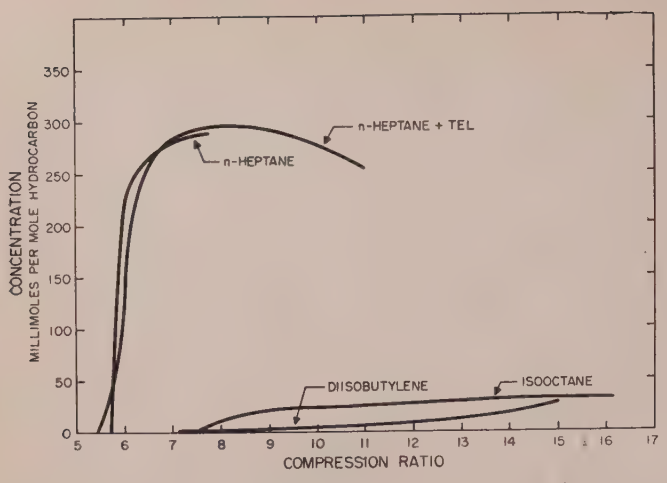

Fig. H – Influence of hydrocarbon structure on higher carbonyl formation

the motored engines. It is important to stress a point that the authors mention, namely, that these are not the **same** histories at all. Even the equivalence of the histories is deduced rather than proved. It can be correctly reasoned that since the products obtained are the same, then, whatever these histories were, they must in some way be equivalent. But the argument cannot then be reversed to say that equivalent histories are shown to produce the same products. In fact, extended studies in the Ethyl Corp. Research Laboratories have not succeeded in giving us accurate time-temperature-pressure histories for fired engines at all, and there is no comprehensive published report of such histories in fired engines for comparison with histories which have been obtained for motored engines.

Secondly, although this work is significant in elucidating the chemistry of fuel combustion, great care should be taken in drawing any correlation between the products found by analysis and the phenomenon called "knock." In our laboratories we have been running experiments similar to those discussed here, using the same techniques of sampling from the end gas. Since we are especially interested in knock, our experiments were run with a normally fired engine, and an attempt was made to associate the formation or presence of the precombustion products with the occurrence of knock. We have analyzed samples obtained from a knocking engine by means of an infrared technique which is very sensitive to carbonyls (Fig. E). The different degrees of knock were set by ear by altering the compression ratio. The samples were taken from the end-gas region as late as possible before flame arrival at the sampling valve. Under normal conditions with n-heptane as the fuel (first graph) there were, at the most, only traces of carbonyls even when the engine was knocking severely. In an attempt to produce more of these intermediates, the engine operating temperatures (inlet air and jacket) were increased stepwise (second and third graphs) but with hardly any evidence of carbonyls being formed except in the one case of heavy knock under the very highest temperature conditions.

We then went to leaded fuels in order to be able to raise the compression ratio and thus further increase the operating temperatures of the engine. In the runs with n-heptane containing 3 ml of tel per gal, we did find carbonyls (Fig. F). It can be seen from these data that with increased engine temperatures the concentration of carbonyls is increased. Also, with any set of operating temperatures, the concentration is increased with compression ratio. It is true that with any one set of engine conditions increased knock gives increased carbonyl, but this is thought to be merely a reflection of the increased compression ratio used to give more severe knocking. With different engine conditions the concentration of carbonyls varies greatly for the same degree of knock. From these experiments it is concluded that temperature and pressure (or compression ratio) are important in carbonyl production, but that the presence of these intermediates does not necessarily result in knock (Fig. F) nor does their absence guarantee the absence of knock (Fig. E). Data on the peroxide concentrations of these samples show the same general variation with engine temperatures and compression ratio and the same lack of correlation with knock. Any apparent discrepancies between the data presented in the paper under discussion and the figures shown here can be attributed to the difference in manifold pressures used. Under reduced-pressure (part-throttle) operation, an abundance of products is observed, but this is not an operating condition where knock is normally observed. In our studies the engines were run at full throttle (atmospheric pressure in the manifold).

These results appear to support earlier work carried out in our laboratories,[a] which has shown that the heat of the precombustion reactions is not related to knock. Fig. G shows that different fuels having the same octane number (and hence the same tendency to knock) vary widely in the amount of heat produced during the precombustion reactions.

A further corroboration of this relationship is to be found in some of the data in the paper under discussion. When isooctane was used as the fuel, the specific yield of carbonyls was found to be greatly reduced even though these runs were made at the same point of incipient knock or autoignition as the other fuels.

In conclusion, it can be said that this paper represents a forward stride in our understanding of the chemistry of fuel combustion, since it successfully shows that the intermediate carbonyl products formed in a motored engine are also produced in a spark-ignited engine. However, great caution is advised in any attempts to relate these products to knock.

Discusses Effect of Hydrocarbon Structure on Carbonyl Formation

– A. J. Pahnke
E. I. du Pont de Nemours & Co., Inc.

THE authors are to be congratulated for their excellent contribution to the understanding of the chemistry of hy-

[a] Same as footnote No. 1 of main paper.

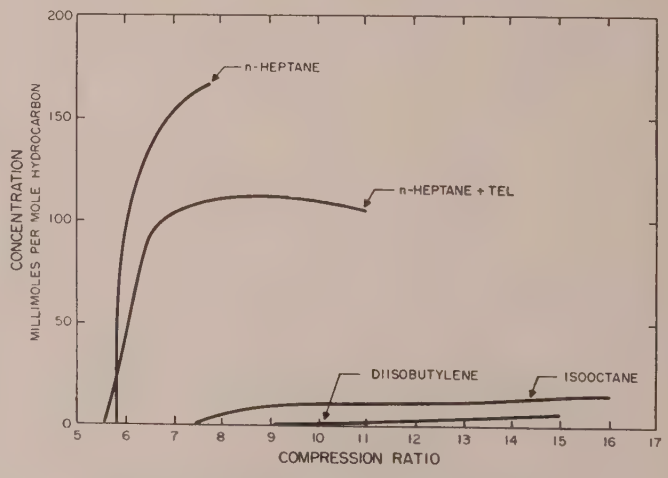

Fig. I – Influence of hydrocarbon structure on formaldehyde formation

drocarbon preflame reactions, particularly for their very detailed study of the carbonyl intermediates formed in these reactions. It is work of this type which may someday lead to an understanding of the knock process. The evidence showing that the chemical reactions taking place in the motored engine are the same as those occurring in the end gas of the fired engine supports the large amount of physical and chemical data validating the use of the motored engine as a research tool.

Hydrocarbon structure has been shown by the authors to have a large effect on the specific yield of carbonyl compounds, n-heptane forming more than ten times the amount produced by isooctane. Studies at the du Pont Petroleum Laboratory also have shown hydrocarbon structure to play an important role in the formation of the carbonyl intermediates. This is illustrated in Fig. H in which the concentration of higher carbonyl compounds found in the exhaust gas of a motored engine is plotted as a function of the compression ratio to which the engine charge was stressed. Experimentally, as the compression ratio is raised the peak cycle temperature is increased and autoignition is approached. The termination of each of the curves corresponds to incipient autoignition conditions.

Considerable differences in both the yield and rate of formation of carbonyl compounds were observed among the three hydrocarbons tested. As found by the Ohio State investigators, n-heptane formed ten times the quantity of carbonyl compounds obtained with isooctane. The magnitude of the preflame process, together with the lower temperature required for initial oxidative attack, explains in part the poor knock resistance of n-heptane.

The concentrations of carbonyl compounds formed from both n-heptane and isooctane rose quite rapidly with increasing compression ratio, then leveled off. Diisobutylene reacted quite differently, since the formation of carbonyl intermediates proceeded very slowly as the compression ratio was increased. This effect indicates an inhibiting action, presumably due to the double bond of the diisobutylene acting as a free radical sink.

Tetraethyl lead has little effect on the reactions of n-heptane leading to the formation of higher carbonyl compounds. It can be seen that the carbonyl concentration curves for leaded and unleaded n-heptane are approximately the same. Other studies have shown tetraethyl lead to function by deactivating simple free radicals formed in part from the decomposition of organic peroxides. Because of the importance of peroxides in the hydrocarbon preflame reactions, the studies in progress at the Ohio State University laboratories on the identification of peroxides are of considerable interest.

The authors have shown that large amounts of formaldehyde are formed in the oxidation of n-heptane and n-pentane. Further evidence of this is shown by the formaldehyde curve for n-heptane in Fig. I. The concentration at incipient autoignition of 165 millimoles of formaldehye per mole of inducted n-heptane was found to represent 35% of the total carbonyl concentration.

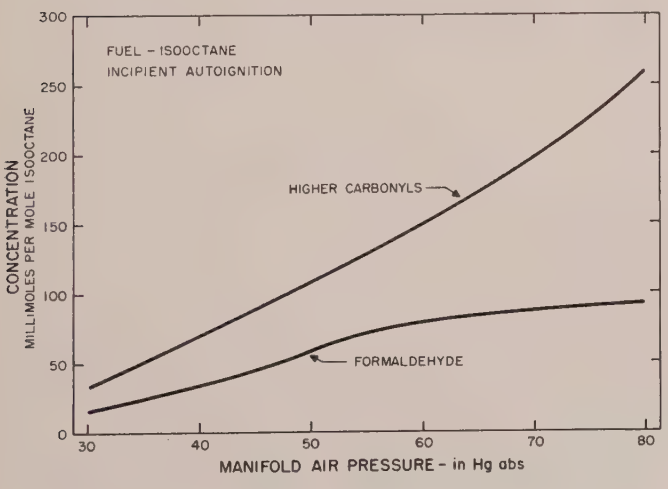

Fig. J – Effect of manifold pressure on carbonyl formation

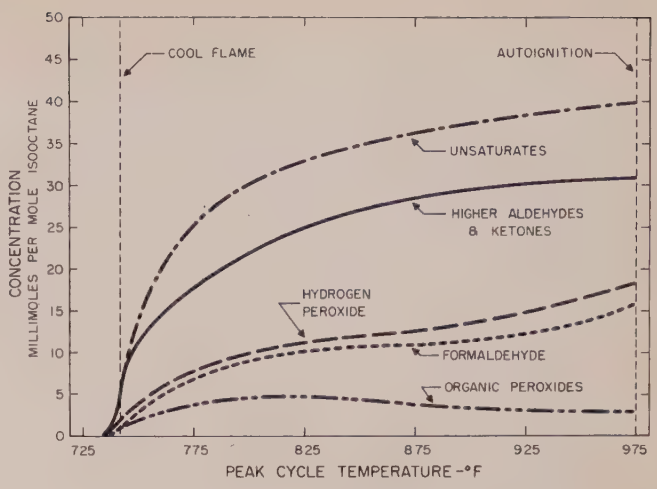

Fig. K – Exhaust gas composition – isooctane

Hydrocarbon structure affects the formation of formaldehyde in a manner similar to that previously discussed for the higher carbonyl compounds. However, the addition of tetraethyl lead produced a marked decrease in the amount of formaldehyde formed in the n-heptane reactions. This indicates that some of the formaldehyde is formed by a reaction mechanism susceptible to interference by the lead antiknock.

The authors have shown that an increase in manifold pressure decreased the specific yield of carbonyl compounds from n-pentane at incipient autoignition. Fig. J shows that isooctane responds differently to changes in manifold pressure. In this figure formaldehyde and higher carbonyl concentrations at incipient autoignition are plotted as a function of the manifold pressure at which the experiments were performed, and it is evident that the carbonyl concentrations increase with the manifold pressure. This increase in the extent of preflame reaction lowers the compression ratio at which autoignition occurs from 16.2 at 30 in. of Hg abs to 7.8 at 80 in. of Hg abs. Since increased pressure conditions exist throughout the entire cycle at the high manifold pressures, these data indicate that the preflame reactions of isooctane are pressure sensitive. A comparison of the curves for the higher carbonyl compounds and for formaldehyde shows that the reactions leading to the formation of higher aldehydes and ketones have greater pressure sensitivity than those leading to the formation of formaldehyde.

As the authors point out, the reactions involving carbonyl intermediates are only part of the overall oxidative mechanism. Other reactions occur simultaneously or consecutively and give rise to the formation of unsaturates, hydrogen peroxide, organic peroxides, and other intermediates. This is shown by concentration curves for isooctane given in Fig. K. The progress of the preflame reactions was followed from initiation to ignition by incrementally raising the peak cycle temperature (by varying the compression ratio). Reactions leading to the formation of unsaturates appear to be extremely important. These may include the decomposition of alkyl peroxy radicals to give unsaturates and an HO_2 radical. Further reactions of the HO_2 radical may account in part for the formation of hydrogen peroxide.

It is hoped that the work of the Ohio State group will be continued along the lines they have indicated for some time to come, since this type of investigation will add materially to the progress of the science of combustion.

The New

THE new Chevrolet engine offers, the authors say, the smallest and lightest commercial V-8 power package for its 265-cu-in. displacement. This has been accomplished by an 0.8/1 stroke/bore ratio, and by weight economies throughout the engine which add up to an assembly lighter by 41 lb than the Chevrolet Six.

New also are its cylinder block casting method, which uses only nine major and three minor cores; its valve-operating mechanism, which features completely independent rocker arms; a lubrication system with short, clean oil passages drilled in the block, none in the cylinder head; and a single intake manifold casting that also forms the top enclosure of the engine and includes provision for hot water heater take-off, cross-over for exhaust heat to the carburetor, distributor mounting, oil filler, thermostat housing, water outlet to the radiator, and water temperature gage hole.

THIS paper describes in detail some of the interesting features of the new Chevrolet V-8 engine (Figs. 1 and 2 and Table 1), and tells the background and development story of some of the designs and components which have attracted considerable attention. For instance, the casting of our cylinder block at the foundry may be of interest because it differs from other methods currently used. This paper also describes the new valve operating mechanism, the lubrication system, and the intake manifold casting, which reduces the number of separate parts generally used.

In our research over a period of years we have investigated many types of V-8 engine. During the early stages, we developed an engine with 231 cu in. of displacement (Fig. 3), but with changing conditions a greater displacement was considered desirable. At one of our group meetings we sketched some basic outlines to indicate just what we wanted in height, displacement, length, and so forth. We began thinking about a 245-cu-in. engine, but when we got further into this study we found we could just as well go to about 260 or 265 with no penalty of extra weight, knowing that ample displacement is fundamentally the most economical way to insure high torque and resultant good performance and economy.

The bore size was discussed at length and 3¾ in. was finally settled upon. The stroke for a 260-cu-in. displacement engine was computed to be 2.93, but to round it off we adopted a 3-in. stroke, which gives us an over-square stroke-to-bore ratio of 0.8/1 and displacement of 265 cu in. (See Fig. 4.)

Now we started to see what could be achieved in the way of compacting the engine. Anything we could slice off the top or bottom of the block, or from the bores, would mean less heavy iron and less water required to cool it. This was one of our prime objectives – to make that basic block just as compact and as light in weight as possible. (See Fig. 5.)

The length of the engine was determined by the length of the crankshaft. After adding the widths of the main bearings, connecting-rod bearings, crank arms, bulkheads, and so on, the length of the crankshaft was computed, and then the length of the block, which is only 21¾ in. long. The distance from the bottom of the block to the head is only 9 in., and the cylinder centers are 4.4 in. apart. (See Fig. 6.)

Cylinder Block

We are well aware of the fact that some of the other manufacturers have their own theories on how the block should be made, but we would like to tell you how we make ours, and why we do it that way.

From a structural point of view, since a V-8 engine is relatively short and inherently stiff, and because of the extremely short couples, a lot of extra ribbing is unnecessary, and we believe it is unnecessary to carry the casting below the centerline of the crankshaft. Fig. 7 shows that we have a drop of only ⅛ in. below the center of the crank-

Chevrolet V-8 Engine

R. F. Sanders, Chevrolet Motor Division, GMC

This paper was presented at SAE Golden Anniversary Annual Meeting, Detroit, Jan. 12, 1955.

shaft. This drop is necessary for locating the main bearing caps in a broached longitudinal slot. By spreading the bolt centers and providing a deep section at the back of the block, we obtain the stiffness necessary to support the transmission and transmission extension, without the penalty of extra weight. (See Fig. 8.)

The cylinder block was designed for high precision in the foundry casting processes and in the machining processes which follow in the manufacturing plant. First, let us take a look at what is done in the foundry. With a lot of cores, there is naturally the problem of variations on every core, and the stackup of those variations during assembly of the cores. Fewer cores mean that our section thicknesses can be controlled much more accurately, and we have less sand to handle. The end result is a precision casting which is lighter, as well as lower in cost.

Our cylinder-barrel cores are formed in pairs. In other words, one left-hand and one right-hand barrel are integral with a crank-chamber core in the form of a Vee (Fig. 9). There are four of these basic cylinder-barrel and crank-chamber cores, which are set on a slab in the drag (Fig. 10). Two one-piece jacket cores are then slipped over the cylinder-barrel Vee cores (Fig. 11). The jacket cores are supported in position and restrained from flotation by the end cores of the block. These end cores, also supported and located on the slab, form the contours of the timing chain case and frontal architecture, and the configurations of the clutch housing attachment. Core prints of generous size project from these end cores to support the jacket

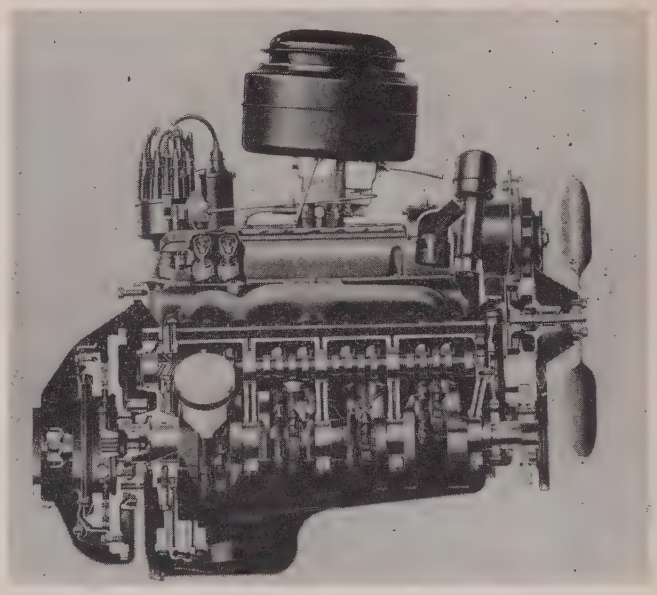

Fig. 1 – Cutaway view of Chevrolet V-8 engine

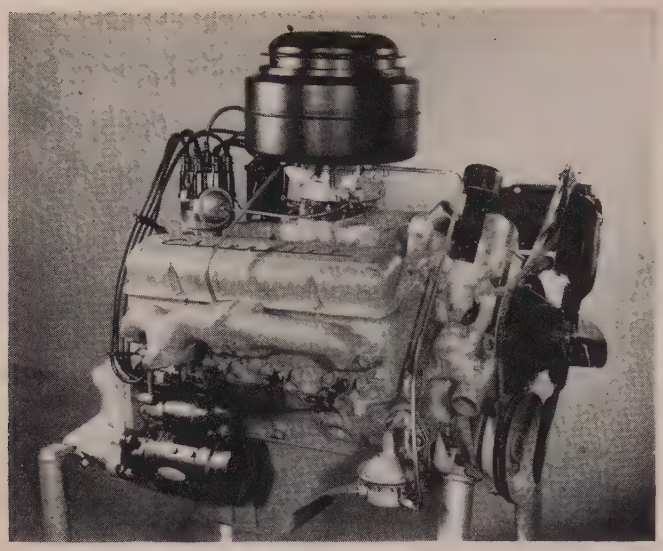

Fig. 2 – Chevrolet V-8 engine

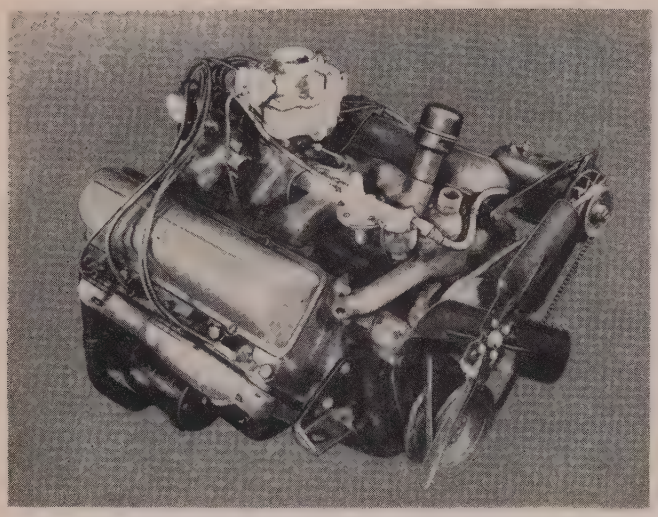

Fig. 3 – Early experimental engine with 231-cu-in. displacement

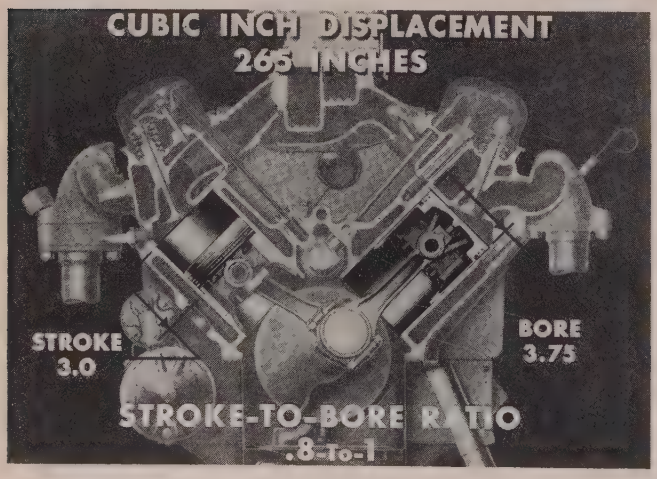

Fig. 4 – Production 265-cu-in. displacement engine with 0.8/1 stroke/bore ratio

Table 1 – General Specifications of Chevrolet Overhead-Valve, 90-deg V-8 Engine

Bore, in.	3.75
Stroke, in.	3.00
Stroke/Bore Ratio	0.8/1
Displacement, cu in.	265
Compression Ratio	8/1
Maximum Gross Horsepower at 4400 Rpm	162
Maximum Gross Torque at 2200 Rpm	257
Maximum Bmep at 2200 Rpm, psi	146
Piston Travel, ft per mile	1339
Engine Weight, lb	531

cores in position, as shown in Fig. 12.

The entire assembly of cores is pasted and gaged on the slab core in a core drying fixture. After drying, it is conveyed to the molding floor, where, after blowing out loose core sand, the entire assembly is lowered into the drag mold in one operation (Fig. 13). Since the simple assembly operation eliminates individual core handling on a moving conveyor and the resultant loose sand in the mold, this process produces a clean, precision casting.

We use only nine major and three minor cores in the casting of our block. By comparison (Fig. 14), another manufacturer uses 22 cores in the casting of a V-8 block. (Four of the cores are not illustrated.) To carry this comparison a little further, Fig. 15 shows the amount of sand required to make our cylinder-block cores, and the amount required to make the cores of another V-8 cylinder block.

Clutch Housing

The clutch housing is bolted directly to the cylinder block, and extends over the flywheel ring gear. The starting motor is located on the clutch housing, and a rigid three-bolt type of mounting has been developed to eliminate all excess weight from mounting surfaces and pads. This housing was designed to be cast entirely in green sand, and weighs 9 lb less than that used on our Six. (See Fig. 16.)

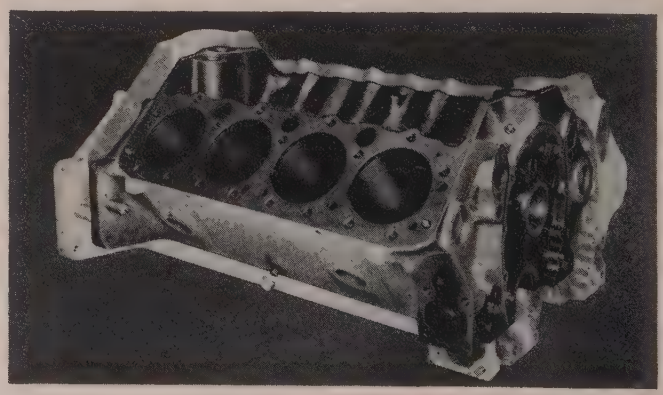

Fig. 5 – Light section shows how block was made compact and weight reduced

The Author

R. F. SANDERS (M '40) is chief passenger-car chassis design engineer for the Chevrolet Motor Division of the General Motors Corp. He received his B.S. in Mechanical Engineering from Michigan State College in 1929. While attending school, he was a part-time apprentice for Federal Drop Forge Co. in 1923, and at Reo Motors from 1923 to 1929. After graduation, he joined the Oldsmobile Division of General Motors, and in 1934 he was assigned to the Chevrolet Division at the General Motors Proving Ground as engineer on special tests.

Each cylinder head is secured to the block with 17 bolts arranged in a pentagon pattern of five bolts around each cylinder. Aside from the advantage of a weight saving through the use of smaller bolts which do not require external ribbing of any consequence, the use of five bolts instead of four around each cylinder bore results in less local distortion. The reason for this is that less torque is required. With four bolts of larger diameter, the higher tension or torque on each bolt would impose local stresses. (See Fig. 17.)

Cylinder Head and Combustion Control

Our main objectives in the casting of cylinder heads were precision, combined with low heat rejection to the coolant, and low weight. The heads are interchangeable, and have the water outlets on the inner face at each end, which eliminates any machine operation or core prints on the front and rear faces of the head. (See Fig. 18.)

The cylinder-head slab core includes the contours of the four combustion chambers (Fig. 19). The lower water jacket core is then set on the slab, as shown in Fig. 20. Next, we add the gas passage cores (Fig. 21), followed by the upper water jacket core (Fig. 22). During assembly, the cores are pasted together at prints and joint surfaces, after

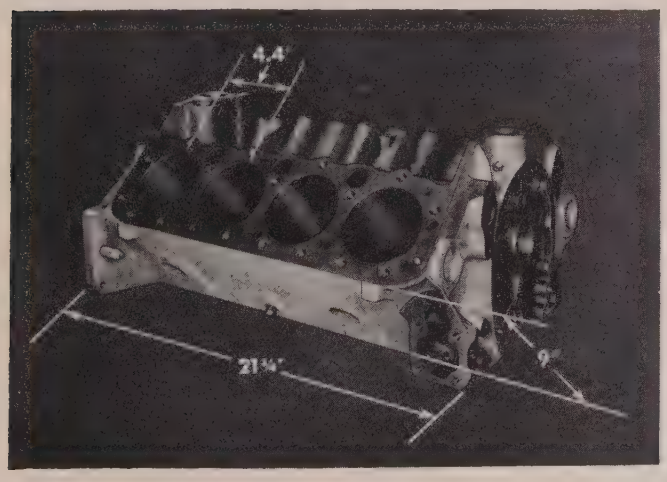

Fig. 6 – Principal dimensions of cylinder block

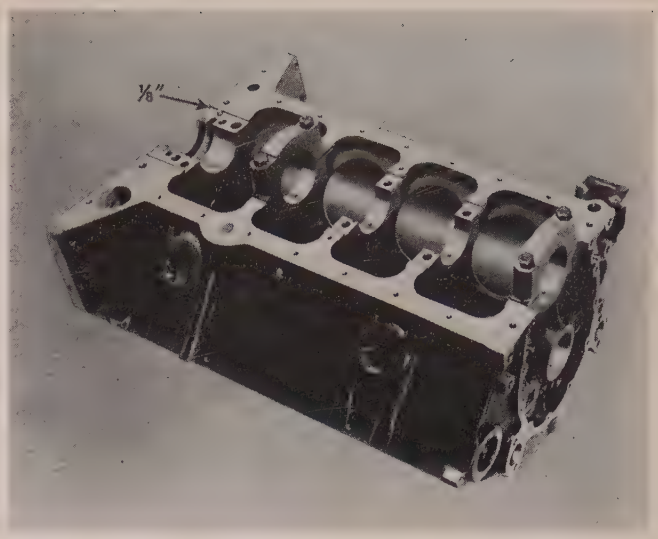

Fig. 7 – Cylinder block structure eliminates necessity for extra ribbing below crankshaft centerline

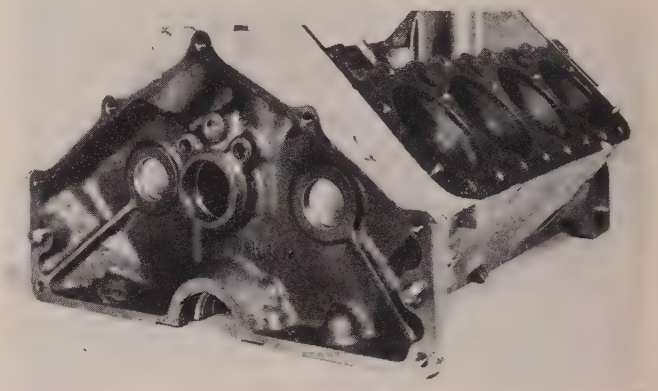

Fig. 8 – Wide bolt centers and deep section at back of block for transmission support

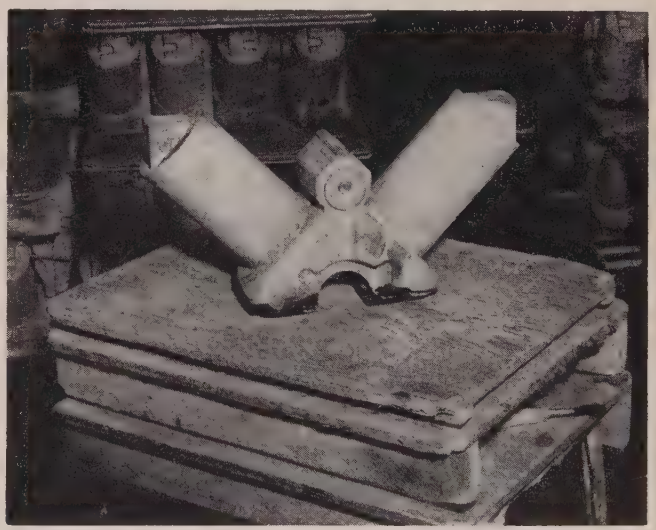

Fig. 9 – Cylinder-barrel cores are formed in pairs integral with crank chamber core

Fig. 10 – Four-cylinder barrel and crank-chamber cores are set on slab

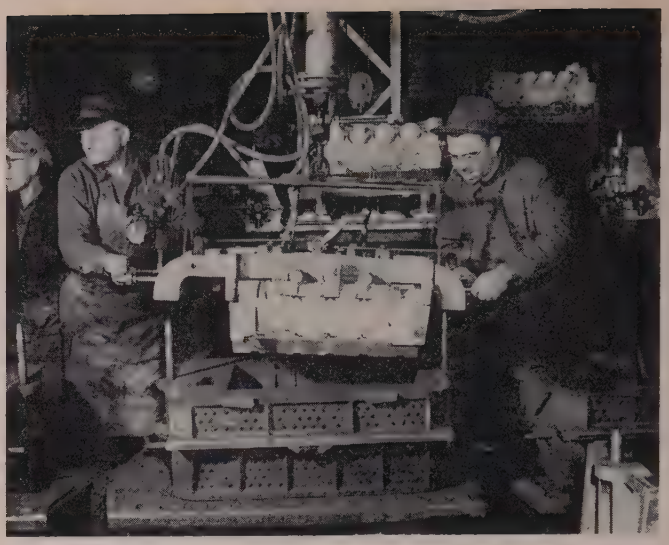

Fig. 13 – Lowering entire core assembly into drag mold

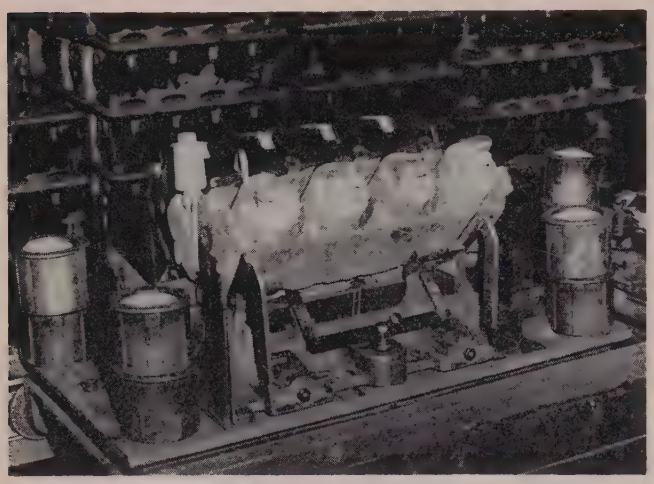

Fig. 11 – One-piece jacket core is slipped over each bank of cylinder-barrel cores

Fig. 14 – Twelve cores are used in casting the Chevrolet block, compared to 22 used by another manufacturer (four not shown)

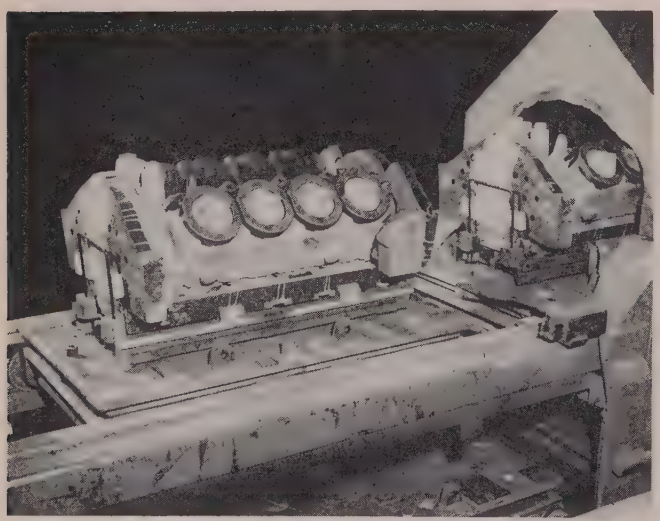

Fig. 12 – End cores, with large projecting core prints, support jacket cores in position

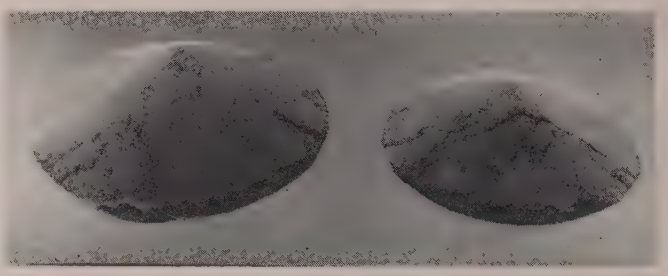

Fig. 15 – Sand required to cast Chevrolet block compared to sand required for another make

which the complete assembly is dried in an oven.

The drag pattern contains the outside contour of the head in the green sand. The dried core assembly is inverted and placed in the drag mold. The slab then acts as a cover core, and is held down by the cope, which contains only the impression for sprue runners and risers. This "upside down"

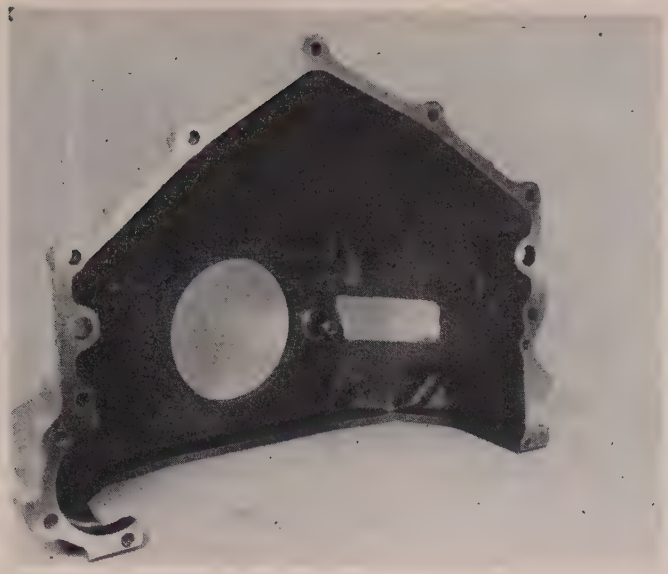

Fig. 16 – Clutch housing

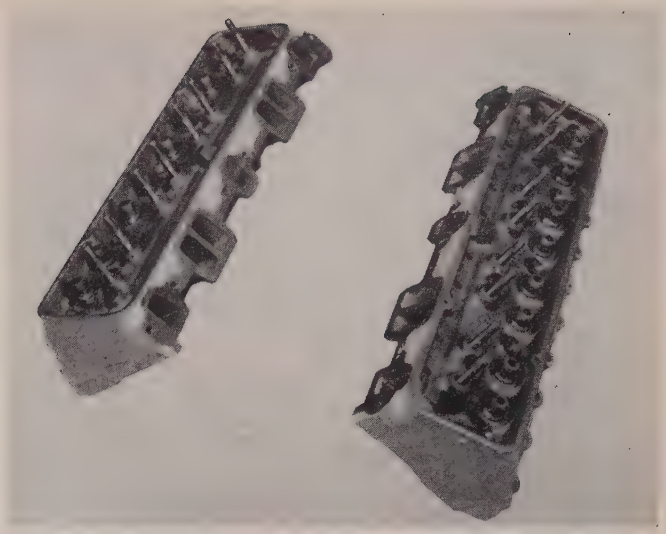

Fig. 18 – Cylinder heads are symmetrical, with water outlets on inner face

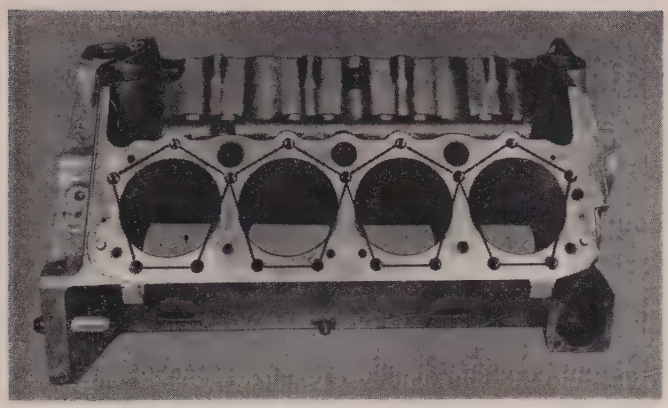

Fig. 17 – Seventeen bolts arranged in pentagon patterns secure cylinder head to block

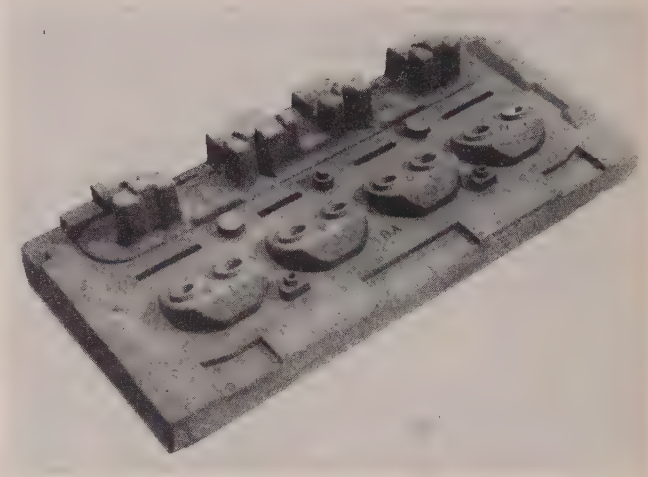

Fig. 19 – Cylinder-head slab core includes contours of the four combustion chambers

method of casting results in harder iron at the bottom of the head and around the valve seats, which is a desirable condition.

Every manufacturer has his own opinion of what makes a good combustion chamber. We settled on the high-turbulence, wedge-type design for combustion control and combustion smoothness, since it controls the rate of pressure rise in the chamber. We feel that the type of chamber which exposes a high volume of the charge early in the burn cycle and then goes out into a quench area gives low octane requirement and smoothness of operation. (See Fig. 23.)

Our combustion chamber is cast to shape, not machined, allowing us to place the volume just where we want it, since we are not limited by a cutter diameter. The only machining necessary in the chamber is for the valves, and even this operation is greatly facilitated because the valves are all in line (Fig. 24).

There are a number of distinct advantages in the

Fig. 20 – Lower water jacket core set on slab

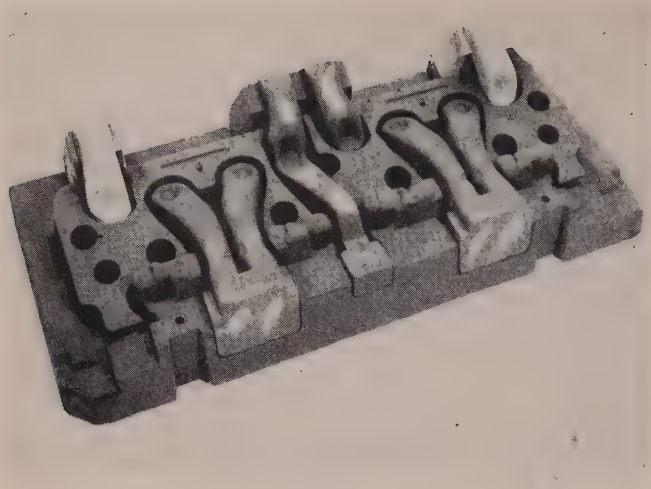

Fig. 21 – Gas passage cores added to assembly

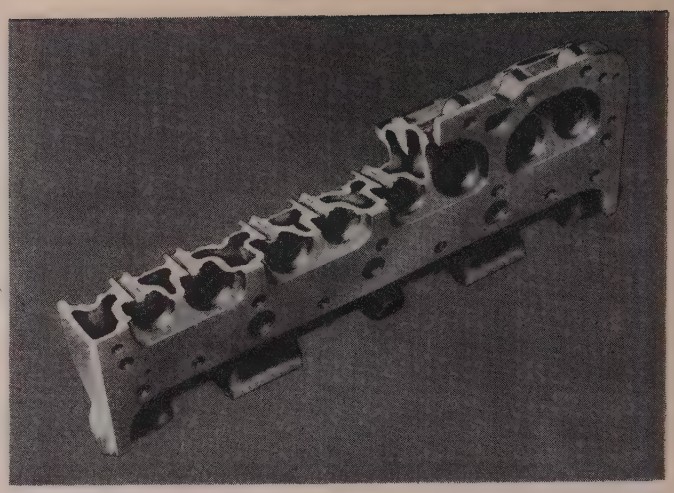

Fig. 24 – Valves are in line

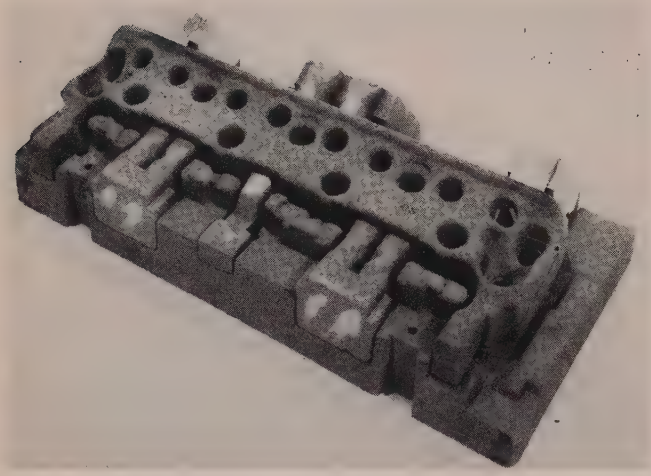

Fig. 22 – Upper water jacket core added to assembly

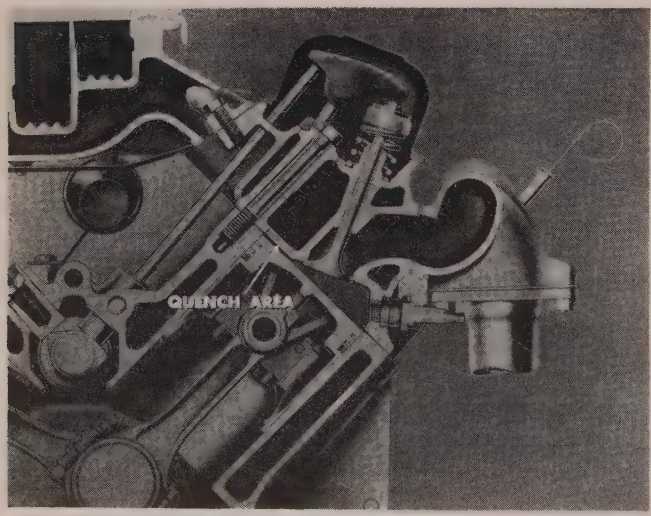

Fig. 23 – High-turbulence, wedge-type combustion-chamber design

compact, wedge-type combustion chamber. For instance, a flat-top piston, which is more economical and prevents excessive head mass, can be used. Our quench area represents 23% piston coverage, and has a nominal thickness of 0.045 in. with the piston at top dead center (Fig. 25).

The compression ratio of 8/1 was selected for acceptable operation in the presence of moderate combustion-chamber deposits on the regular-grade fuels available in most areas. We recognize the fact that in some areas the octane quality of the fuel is below what this engine will require. In those areas, premium-grade fuel can be used, or the spark retarded to permit acceptable operation. We also recognize the fact that, in cases of heavy combustion-chamber deposit accumulations, the octane quality of regular-grade fuel will be below the engine octane requirement. Under these exceptionally severe conditions, premium-grade fuel will be required for acceptable operation.

Most of our octane requirement data have been obtained on cars driven at the GM Proving Ground at Milford on durability schedules. These data show requirements on the Powerglide-equipped cars of 85 to 90 octane number, with 5000 to 25,000 miles of operation, and requirements with the conventional transmission of 88 to 93 octane number (Fig. 26).

Locating the exhaust manifolds near the top of the cylinder heads not only simplified the coring of the job, but it brought the manifolds up out of the way of the steering mechanism. It will be noticed that the short exhaust passages are designed so that they point upward and out, and that the entire length of the ports, both the top side and the under side, are water-jacketed. By completely water-jacketing the exhaust ports, the transfer of distortion loads back to the valve seats is minimized. In all of our testing we have had no valve-burning difficulty, one of the reasons for this being the uniform heat dissipation in this area. Because these exhaust passages are so short, the exhaust-port wall area in

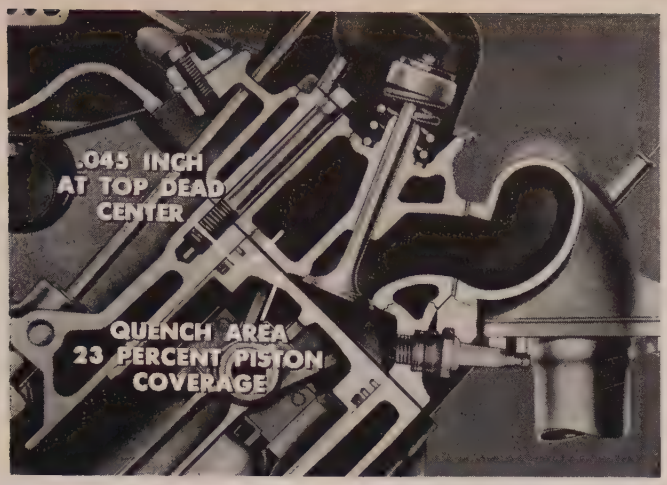

Fig. 25 – Quench area represents 23% piston coverage with a nominal thickness of 0.045 in. with piston at top dead center

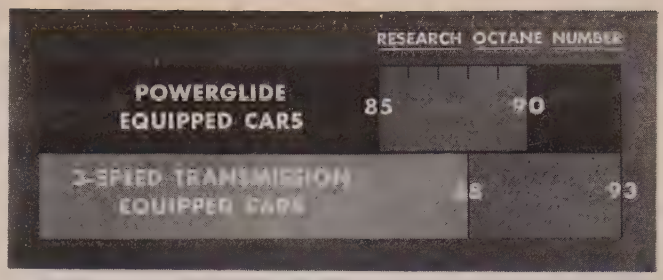

Fig. 26 – Octane requirements

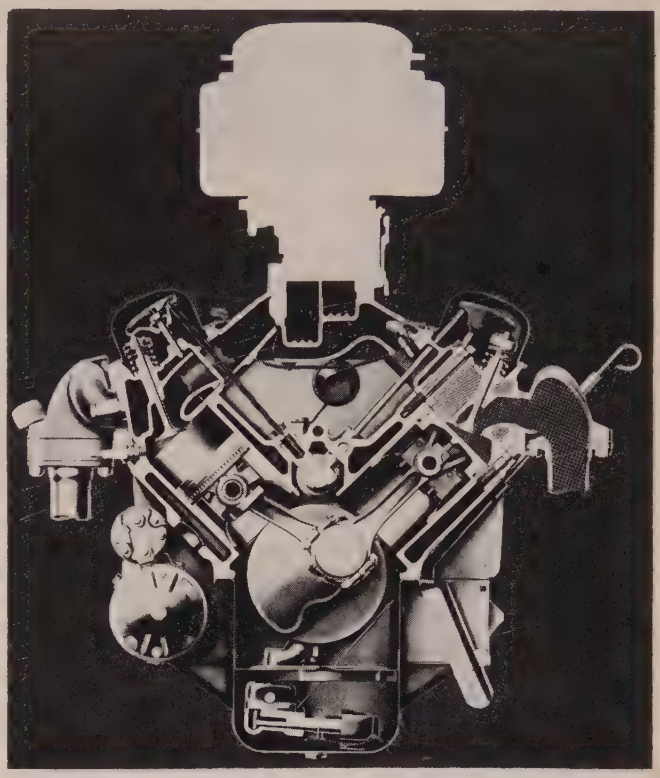

Fig. 27 – Cutaway end view of engine, showing complete water jacketing of cylinders and exhaust ports; and short exhaust passages in head which point upward and out to the exhaust manifolds mounted near top of cylinder head

contact with the water jacket is very small, which accounts for one of the major gains in the feature of low heat rejection to the coolant (Fig. 27).

Even though this engine has a displacement of 30 cu in. more than our 6-cyl engine, and considerably more power output, we are able to use a smaller-size radiator. The radiator core for the V-8 is 21 in. wide, 2 in. less than the radiator for the Six, the frontal area of 357 sq in. is 28 sq in. smaller, and it is 1¼ lb lighter in total weight (Fig. 28). The minimum specific heat rejection is 31 Btu per min per hp at 2800 rpm, and a total rejection to the cooling water of 4800 Btu per min at 4400 rpm.

Complete jacketing provides cooling for the full length and circumference of the short cylinder barrels (Fig. 29). A large drilled-in bypass is provided in the cylinder head, cylinder block, and into the water pump for coolant circulation on cold starts before the thermostat opens. These drilled-in passages eliminate the use of outside piping or hoses (Fig. 30).

A single water pump is used, and the first experimental model had a discharge scroll on the pump to divide the flow of coolant equally to the right and left block. Tests indicated, however, that the contour and position of the water pump inlet had more effect on water distribution to each bank than the discharge scroll. Therefore, the water pump body was simplified by use of a symmetrical plenum chamber design which shaped the inlet of the pump to provide an equal flow of coolant to the right and left bank. The water circulation rate with this pump design in the installed condition, with radiator, is 48 gpm at 4400 engine rpm (Fig. 31).

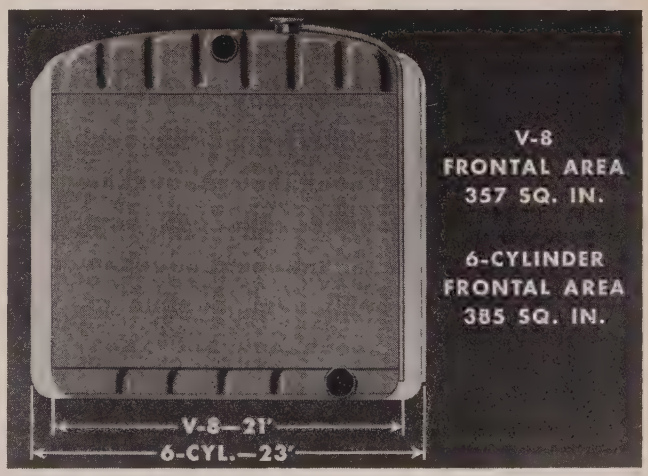

Fig. 28 – V-8 radiator core is lighter and smaller than that of 6-cyl engine

Crankshaft

After a study of both the alloy-iron crankshaft and the pressed-forged-steel crankshaft, pressed forged steel was selected because it has the advantage of a higher modulus of elasticity coupled with

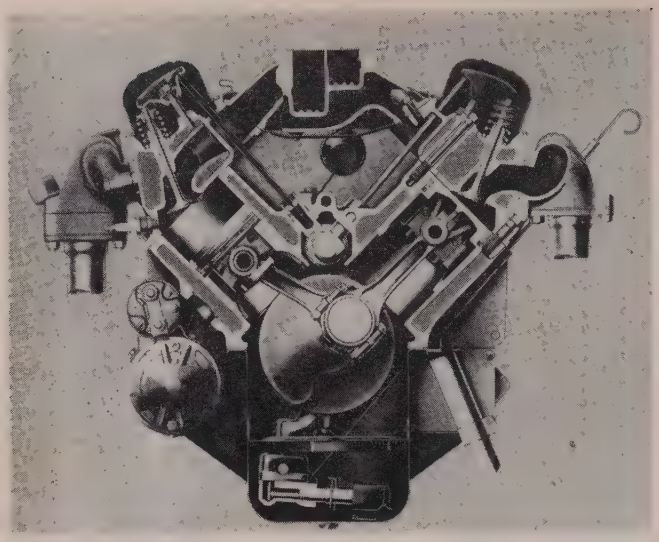

Fig. 29 – Cutaway end view of engine showing complete water jacketing of cylinder barrels

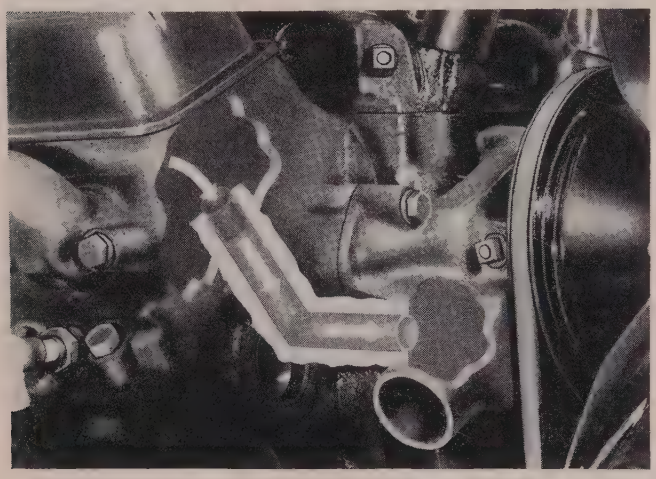

Fig. 30 – Large drilled-in bypass in cylinder head, cylinder block, and into water pump provides coolant circulation on cold starts before thermostat opens

a higher specific gravity, and also because of the vast available forging capacity we have in our manufacturing facilities.

The crankshaft (Fig. 32) was designed with counterweights having the small outside radius of 3.1 in., so disposed that their vectors minimize shaft bending. This is possible because of the short stroke of only 3 in., and the use of the high modulus material and adequate cheek thickness, which gives a stiff shaft.

Full use was made of new forging processes to reduce the draft angles, and therefore the shop problem of cheeking is lessened. Cheeking the sides of the crank arms and counterweights permitted designing for shorter overall length. This cheeking can be held to ± 0.010 in., while cast uncheeked counterweights require a minimum of 0.040 in., which necessitates additional length at each crank arm to allow for grinding-wheel clearance.

Our crankshaft design made it possible to produce what we believe to be the smallest and lightest commercial V-8 power package for its displacement.

Fig. 33 charts crankshaft torsional vibration. With a harmonic balancer we have it below 0.25-deg double amplitude, except at 5200 rpm, where it goes to about 0.3 deg. This is, of course, exceptionally good. The peaks are quite low and not sharp through the general range. From the tests made without a balancer, we concluded it would not be important to crankshaft durability if we did not put a balancer on it, but when the engine was driven in a car we could feel the eighth order at approximately 2700 rpm. With the installation of a harmonic balancer of the rubber and torsional shear type the 0.65-deg double amplitude was dampened to 0.2 deg, and the torsional vibration could no longer be heard or felt in the car.

A new balancing technique is used in our quality control. Not only are all the engine rotating and reciprocating parts precision balanced as individual pieces for use in either production or in service, but when they are brought together as an engine assembly in the plant, we balance the complete assembly. Before the oil pan and heads are installed, the engine is placed on a newly developed machine which motors the engine (Fig. 34), indicates out-of-balance

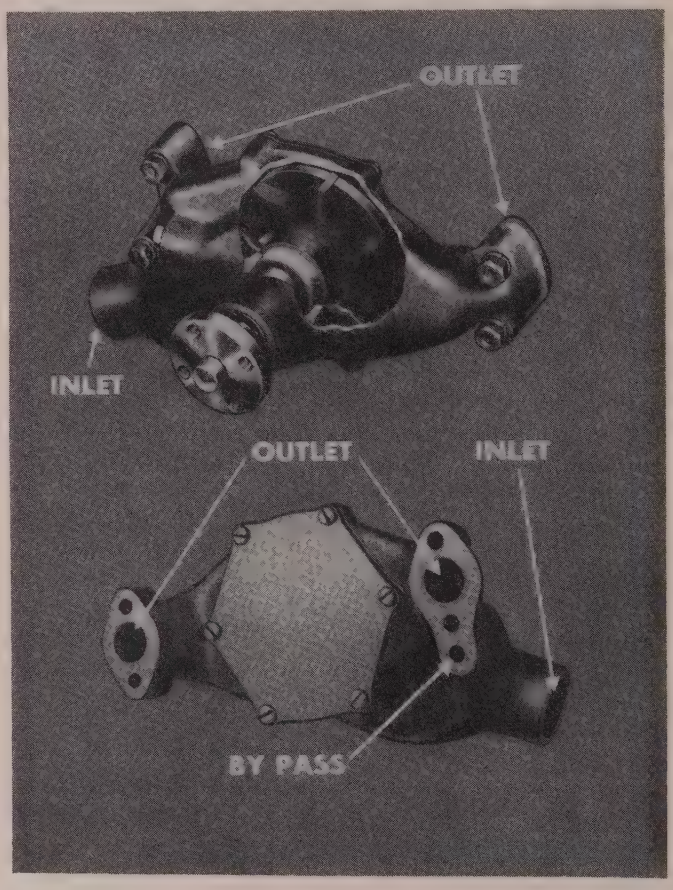

Fig. 31 – Symmetrical plenum chamber design water pump

of the engine assembly (Fig. 35), stops the rotation at the indicated point, and drills the crankshaft front and rear counterweights the required amount (Fig. 36). This reduces any stackup of limits that might normally accumulate in the assembly of an engine, so that our overall result is a completely precision-balanced engine. Through this new equipment every engine is balanced to within ½ in.-oz.

Main Bearings

Our five main bearings are of the same diameter, with the crankshaft thrust taken by the rear bearing. In a short-stroke, high-compression V-8 engine, the maximum main bearing loads are carried in the lower half under most operating conditions. By reducing the maximum oil film loads through the omission of the oil groove in the lower half, the capacity of the main bearings is increased approximately 100%, with the additional benefits of increased durability and greatly reduced wear. Table 2 shows, for instance, that with the grooved bearing, maximum pressure on the front bearing is 2929 psi, and 2414 for the grooveless. On the rear intermediate bearing it is 3820 psi for the grooved bearing, and 3141 for the grooveless.

Fig. 37 shows the oil film distribution for both types of bearings. With the grooveless-type lower bearing, the pounds-per-square-inch pressure goes down compared with the grooved bearing. Since the oil-film thickness is inversely proportional to the load applied, the film of the grooved bearing would be one-half the minimum thickness of the groove-

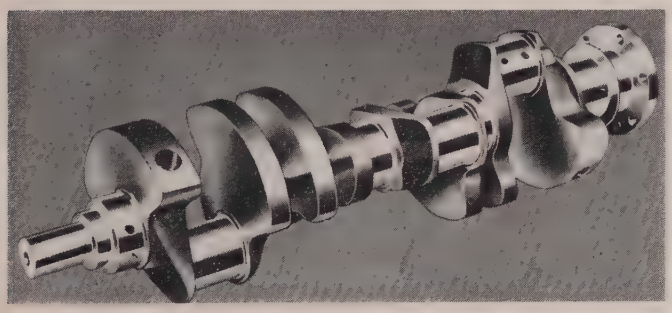

Fig. 32 – Pressed-forged-steel crankshaft

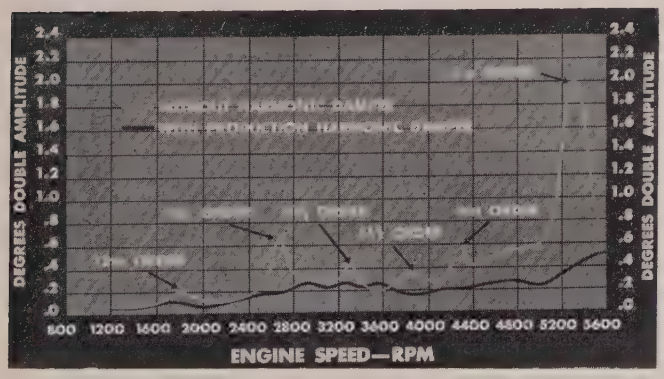

Fig. 33 – Crankshaft torsional vibration characteristics

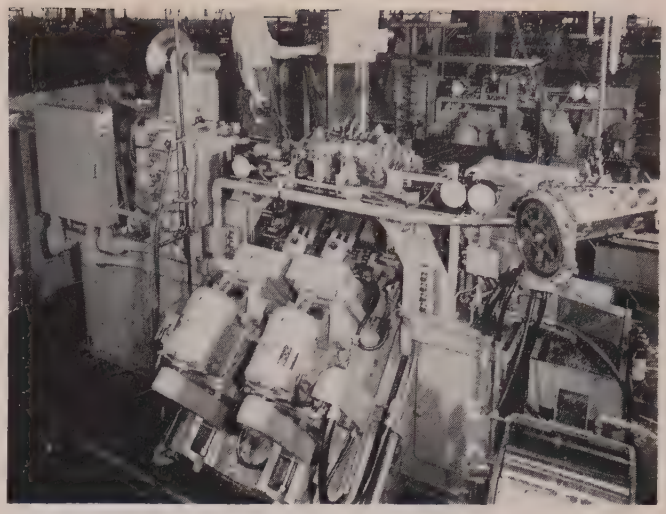

Fig. 34 – All V-8 engines are balanced within ½ in.-oz.

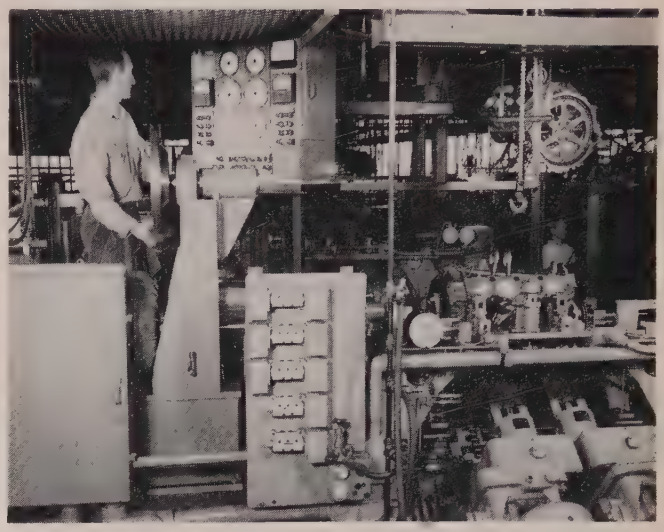

Fig. 35 – Out-of-balance indicator of balancing machine

less bearing. Conversely, with the same minimum film thickness, the bearing without the groove will carry twice the load. The primary reason for this is that the grooved bearing has twice as much side leakage as the bearing without a groove. In tests with experimental engines comparing the grooved lower bearings with the grooveless, it was found that the rate of wear was greatly reduced and the bearing life multiplied with the grooveless bearings. The bearing loads of the engine were not changed, of course. All we did was thicken the oil film.

Connecting Rod

Our standard testing procedure requires a connecting rod to withstand 10,000,000 cycles on a hydraulic fatigue testing machine (Fig. 38). The connecting rods for this new engine were run up to 18,000,000 cycles on the machine. This was under 2400-lb load tension, and 7000-lb compression, which is equivalent to a 10% overload at 4500 rpm

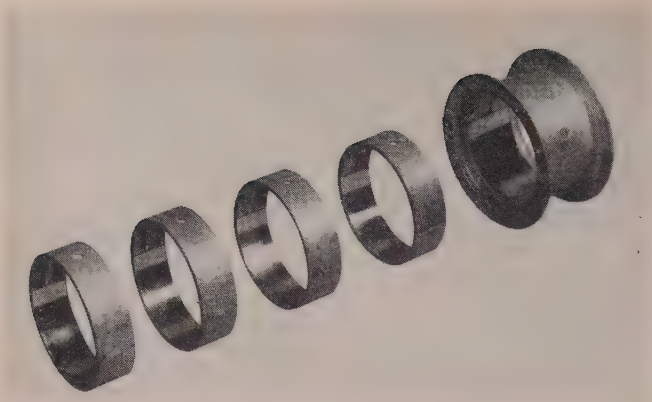

Fig. 36 – Main bearings

Table 2 – Main Bearing Pressures
(Pounds per Square Inch at 4000 Rpm)

	With Groove		Without Groove	
	Max Pressure	Mean Pressure	Max Pressure	Mean Pressure
Front Main Bearing	2929	671	2414	517
Front Intermediate Main Bearing	3402	1022	2792	842
Center Main Bearing	3096	1010	2559	833
Rear Intermediate Main Bearing	3820	1140	3141	939
Rear Main Bearing	1261	275	1125	246

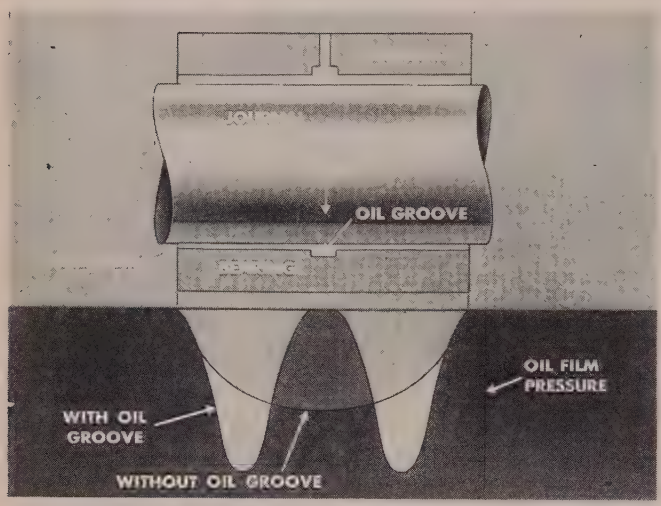

Fig. 37 – Oil film distribution for grooved and grooveless bearings

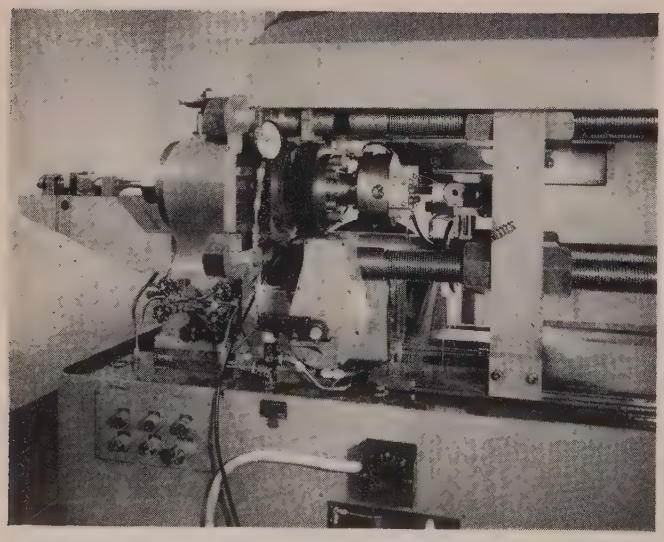

Fig. 38 – Testing connecting rods on hydraulic fatigue testing machine

in tension, and 10% overload at 8/1 compression ratio, at maximum imep. No failures of any type were experienced.

In spite of the large piston, we were able to keep the column section and weight of the rod down, still maintaining high structural rigidity because of the short length. The center distance is only 5.70 in., and length/stroke ratio is 1.9. (See Fig. 39.)

It was decided to use the pressed-in piston pin which is pressed into the rod and proof-tested to withstand a load of 2000-3000 lb. Pressing the pin in not only eliminates the slitting of the rod and the need for a locking bolt, but also relieves the great stress concentration of the clamping method (Fig. 40).

Piston

We use a steel-insert slipper-type aluminum piston of autothermic design (Fig. 41). Through the use of the pressed-pin it was possible to bring the pin bosses close together for efficient use of material. A 5/64-in. offset toward the major thrust face helps to give us freedom from piston slap and allows ample tolerances on piston fits for good manufacturing economy. The skirt is reinforced and the "tails" are made long to reduce deflections and cushion the load transfer during the crossover from minor to major thrust sides (Fig. 42).

Piston Rings

Three piston rings are used. The two compression rings are thick-wall alloy iron, 5/64 in. wide, taper face, and inside bevel. The top ring is flash-chrome-plated and lapped for prevention of scuffing during the break-in and early engine operation (Fig. 43).

One of the problems we encountered was the difficulty common to many of the large-bore, short-stroke V-8 engines of getting good oil control under high-vacuum conditions, such as decelerating down long grades, or in traffic where the engine tends to pull the oil past the oil-control rings. Indications of that are frequently observed in the visible smoking of the exhaust when driving in traffic (Fig. 44).

This smoking seems to be more critical as engines go up in compression ratio and bore size. It

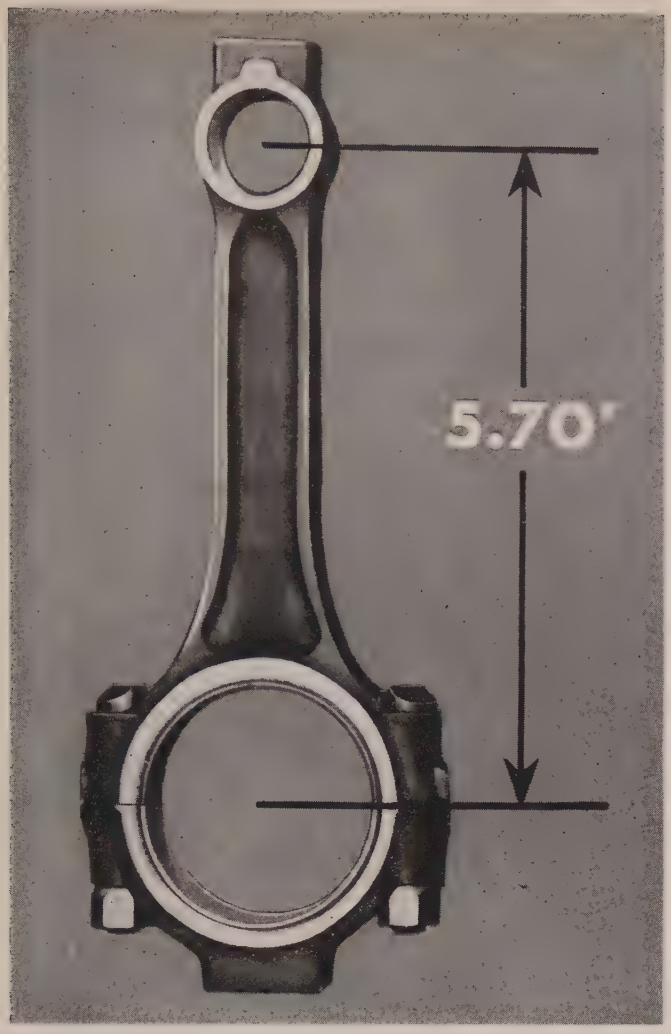

Fig. 39 – Connecting rod. Short length helps keep column section and weight down while maintaining high structural rigidity

Fig. 40 – Pressed in piston pin

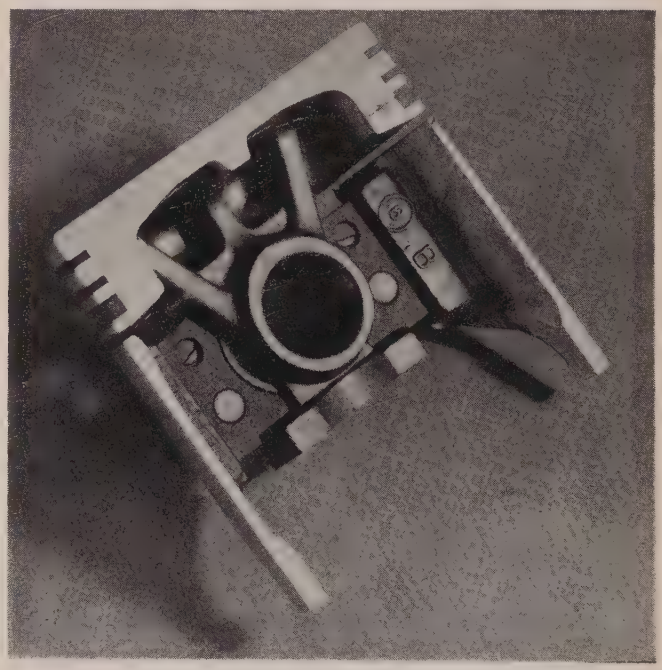

Fig. 41 – Steel-insert, slipper-type aluminum piston

will be noted that at 18 in. of Hg manifold vacuum, oil consumption is 1 qt for 1600 miles, while at 25 in. of vacuum, oil consumption is 1 qt for a little over 200 miles. (See Fig. 45.) These tests were conducted with the vacuum controlled to the values shown.

We believed that the oil loss past the rings was due to their axial displacement from top to bottom in the ring groove through the various phases of the cycle. The solution seemed to be to develop a ring that would give us some side-loading effect, as indicated by the vertical arrows in Fig. 46. This would seal off the passage of oil between the ring and the groove.

Our original premise was that this side-seal principle was good, and we reasoned that the place to use it was in the second compression ring, because the top ring already had enough to do. It had to seal compression as well as to dissipate a lot of heat, and was working as hard as it ought to. The oil ring seemed to be doing all it could, and if there was a ring in the combination that wasn't doing its job it had to be the second one.

We therefore put a spring under the second compression ring to load the ring axially upward against the side of its groove, and found as soon as we started running the first experimental samples that they really did a good job. Spark-plug fouling was down to practically nil on our laboratory high-vacuum cycle and spark-plug fouling schedule, and

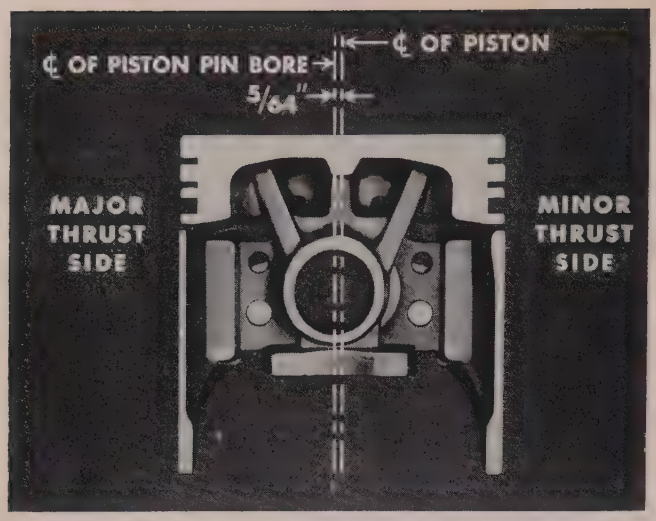

Fig. 42 – Offset of 5/64 in. toward major thrust face of piston helps give freedom from piston slap and allows ample tolerance on piston fits

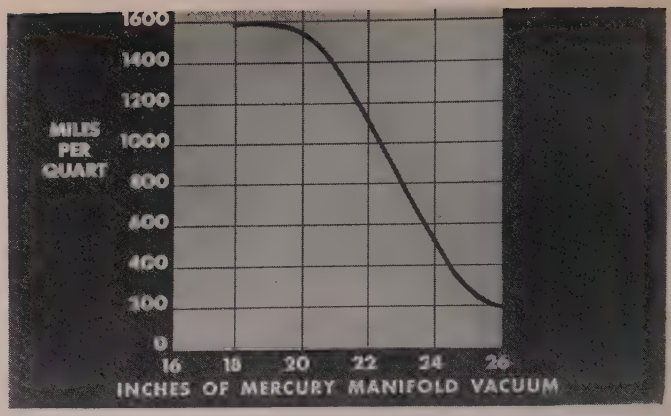

Fig. 45 – High-vacuum oil economy on 7% hill schedule, with vacuum controlled to the values shown

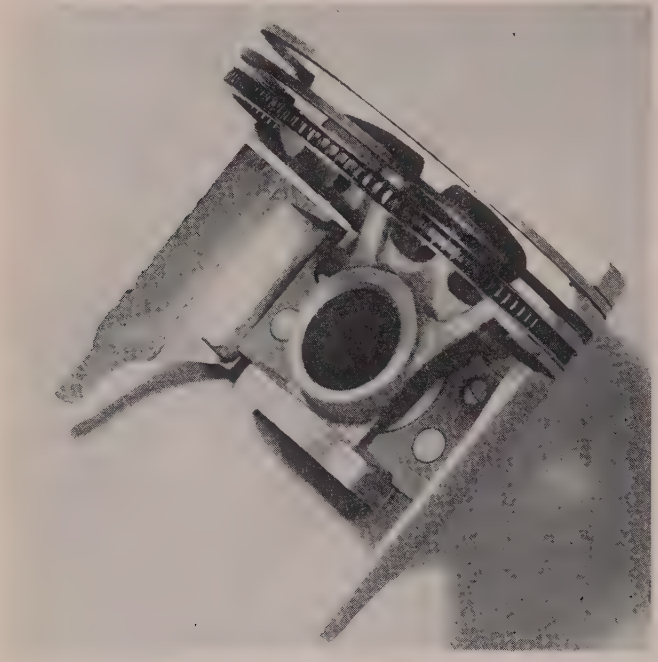

Fig. 43 – Three piston rings are used. Top ring is flash-chrome-plated and lapped; oil control ring is three-piece

Fig. 46 – Side-loading effect (arrows) seals off passage of oil between ring and groove

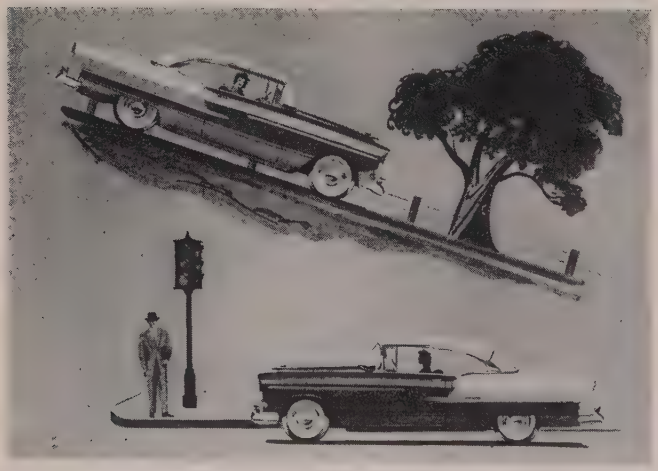

Fig. 44 – Two high-vacuum conditions that make good oil control difficult to attain in many large-bore, short-stroke V-8 engines

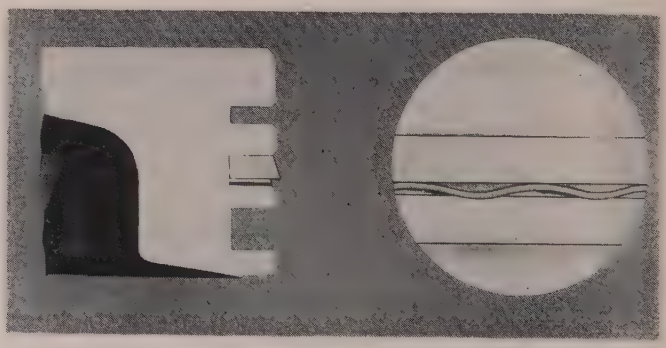

Fig. 47 – Spring placed under second compression ring to load ring axially upward against side of groove presented assembly difficulties and dug into ring groove at each contact point (shown at right)

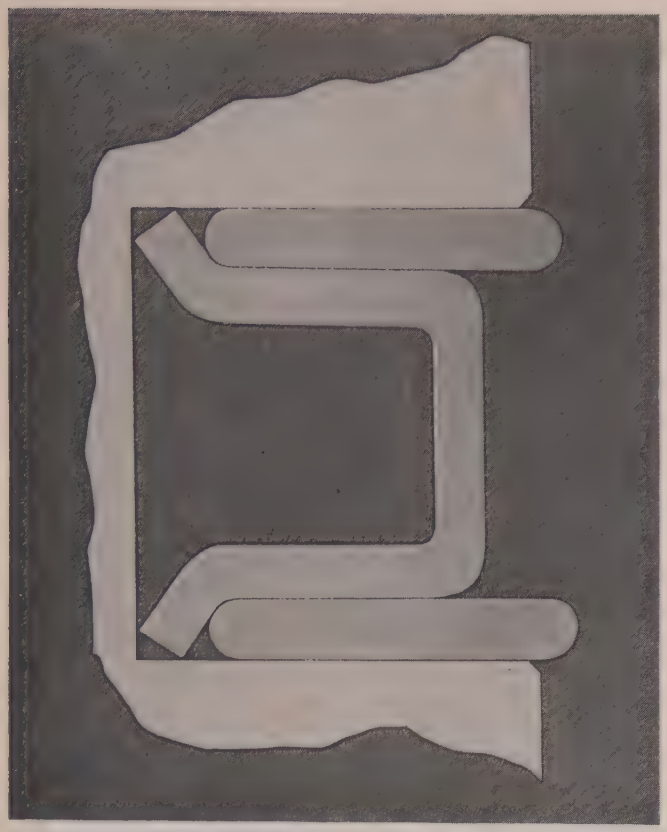

Fig. 48 – Cross-section of new type of expander developed for oil rings

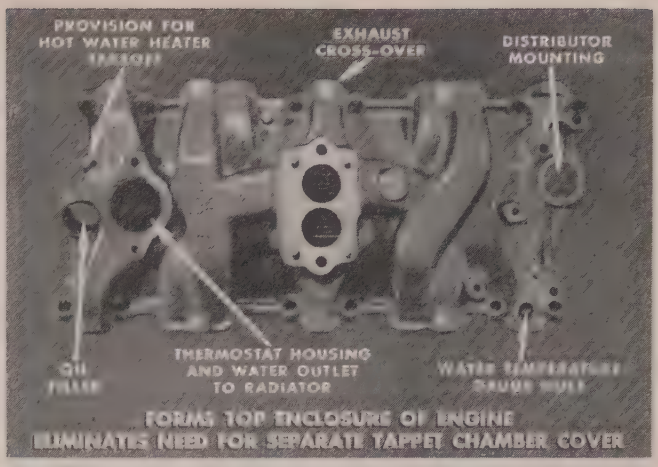

Fig. 49 – Fuel intake manifold

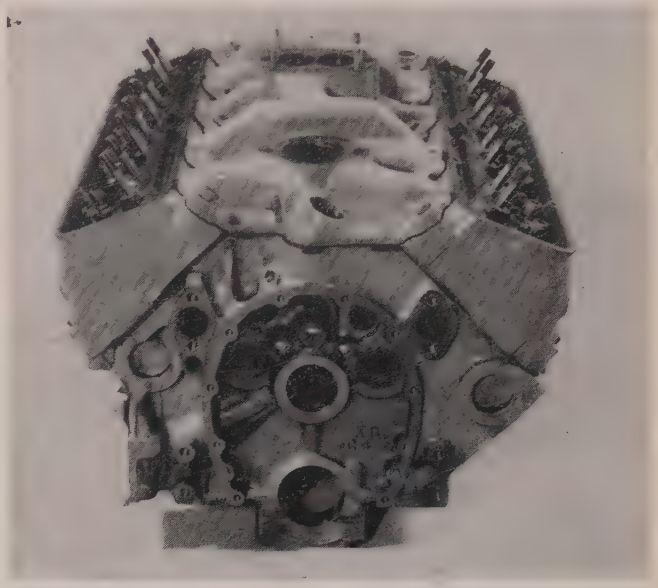

Fig. 50 – Intake manifold installed forms top enclosure of engine

Fig. 51 – Intake manifold raw casting

we obtained some spectacular results on high-vacuum oil economy.

But it also had its failings. For instance, as can be visualized, this spring would be hard to force into the groove. To squeeze this very thin and very stiff spring in the groove alongside the compression ring certainly was an assembly problem. Also, the spring was digging holes for itself in the ring groove of the aluminum pistons at each point of contact (Fig. 47). It looked as though it would take a lot of work and time to make it practical.

We then turned back to the oil ring for control of oil pull-over, and as a result of cooperative test work with several of the ring manufacturers, a new type of expander for the oil rings was developed. The cross-section shown in Fig. 48 illustrates the 12-17-deg angle of the expander which gives an axial force as well as a radial force. It is designed to get the axial support for the rails as far out toward the cylinder-wall end of the ring as possible, and also to provide the side loading for good oil control. The ring design finally adopted incorporates a circumferential expander which not only provides the desired axial load, but provides a uniform radial load of relatively low unit pressure.

Intake Manifold

When it came to the intake manifold, it seemed that this whole area could be greatly simplified, and that some of the separate parts normally used could be combined into one casting or eliminated altogether.

We went into this thoroughly, and the end result (Fig. 49) is that our casting not only acts as the

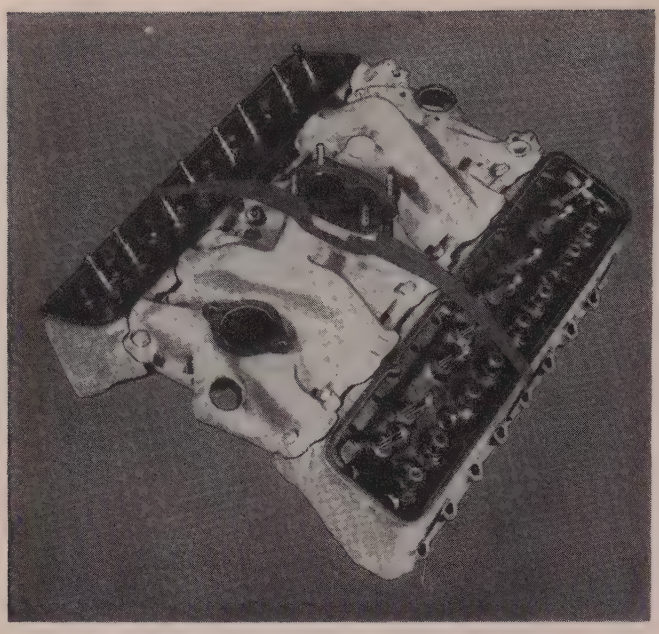

Fig. 52 – Exhaust cross-over for supplying heat to carburetor riser

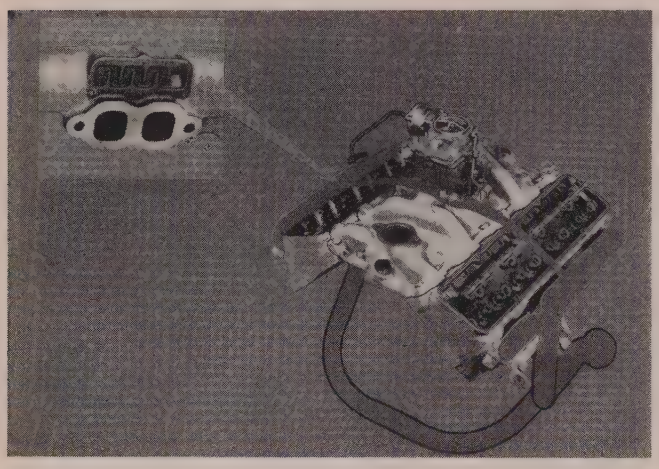

Fig. 53 – Exhaust system consists of left-hand exhaust manifold, cross-under pipe, and right-hand exhaust manifold. Inset: Close-up of automatic-choke heat chamber with cover removed

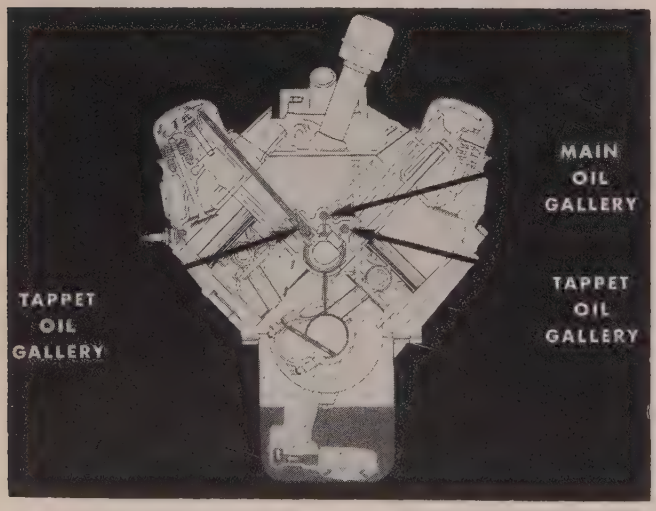

Fig. 54 – Three oil galleries are drill in block

fuel intake manifold, but also includes the following:

1. Provision for hot water heater take-off.
2. Cross-over for exhaust heat to the carburetor.
3. Distributor mounting.
4. Oil filler.
5. Thermostat housing.
6. Water outlet to the radiator.
7. Water temperature gage hole.

In addition, the casting forms the top enclosure of the engine and eliminates the need for a separate tappet-chamber cover. Because of its construction, it is very effective in the suppression of noise; it adds considerable rigidity to the entire engine assembly; and it reduces assembly time. Further, it prevents the passage of cold air under the manifold, which otherwise would reduce mixture temperatures during winter operation, and it gives the engine a clean and finished appearance (Fig. 50). Precision-molded, oil-resistant rubber gaskets are used to seal the ends, and have proved very satisfactory under all limit stack conditions. Molded seals are also used for sealing the oil pan at the front and rear ends.

Touching very briefly on the casting of the intake manifold at the foundry, we find we get a very clean casting because we have webs instead of openings between the branches of the arms. If these webs were not present, the green sand of the cope and drag flasks would have to meet on complicated parting lines which leaves a ragged fin all around, and possibly iron flash over in the open areas. Our manifold is designed so that the flash comes out on the edges of the casting and is removed during machining of the attaching faces (Fig. 51).

Our exhaust cross-over for supplying heat to the carburetor riser is brought from one port only in each cylinder head. Using one port instead of two minimizes valve-seat distortion because of the reduced flame-heated surface in the cylinder head as compared to a siamesed heat take-off. Also, it gives us a more pulsating flow of hot exhaust gas in the cross-over. Two holes in the carburetor flange are drilled down into the exhaust cross-over and index with a cored passage in the carburetor throttle body which passes under the idle jets. The exhaust gases which travel through this circuit prevent carburetor icing during warmup (Fig. 52).

Exhaust System

The exhaust system consists of three basic units, the left-hand exhaust manifold, a cross-under pipe, and the right-hand exhaust manifold. The external exhaust pipe crosses below the front of the engine (Fig. 53). This is very important because in this location it is exposed to the air stream from the fan and the air movement under the vehicle, and this piping reduces the buildup of high temperature under the hood. An automatic choke is standard equipment, its hot-air supply being piped from a cast-in

heat chamber located in the exhaust manifold. The inset shows a close-up of the heat chamber with its cover removed.

Lubrication System

In our lubrication system, all oil passages are drilled in the block (Fig. 54). We have no drilled holes in the cylinder head for high-pressure lubrication. The drilled holes in the block are short, with no sharp angular intersections. This minimizes the chipping of drills and the breaking off of particles of metal at the intersections, which helps to give us a very clean engine internally. Three oil holes are drilled horizontally in the block, one being the main oil gallery and the other two tappet oil galleries.

Except for the rear bulkhead, vertical drilled holes from the main oil gallery pass through the bulkheads, through the centerline of the camshaft opening, and then through the bottom section of the bulkheads to the crankshaft bearings (Fig. 55). Each of the bosses provided in the cylinder block for a camshaft bearing seat has a machined annulus which is covered when the bearing is installed. Oil under pressure in the main gallery moves downward through the drilled hole in the bulkhead and into the annulus under the camshaft bearing shells. Some of the oil is forced from the annulus into the camshaft bearings through a small hole near the bottom of these bearings. The remainder of the oil continues downward through the bottom section of the bulkhead and into a hole in the upper half of each crankshaft main bearing, filling the groove in the upper half of the bearing (Fig. 56).

We developed a way of supplying oil under balanced pressure to the two tappet galleries. A drilled hole from the high-pressure main oil gallery lines up with a small hole in the camshaft rear bearing shell, keeping high-pressure oil on this bearing at all times (Fig. 57). This bearing shell has a similar hole directly to the rear of the first hole and located in line with an annulus machined in the cylinder block. A hole from this annulus is drilled to each of the tappet galleries (Fig. 58).

A metering slot is milled in part of the outside diameter of the camshaft rear journal, just wide enough to cover the distance between the two holes in the bearing shell. Since the front hole is always exposed to high-pressure oil, it keeps the bearing lubricated, and at every revolution of the camshaft, oil from the front hole fills the metering slot with oil under pressure. The oil crosses to the rear hole and down into the annulus, and then, at reduced and equal pressure, through the two drilled holes leading to the tappet galleries. The pressure of the oil in the tappet galleries is controlled through the length of the metering slot milled in the camshaft journal (Fig. 58). Oil flows out the top of the tappets, through the hollow push-rods, and lubricates the rocker arms and the valve stems (Fig. 59).

The crankshaft oil hole to each connecting-rod

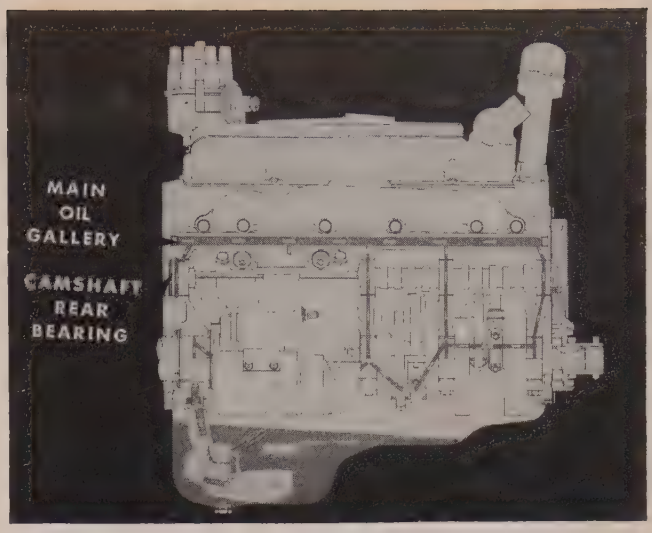

Fig. 55 – Vertical drilled holes from main oil gallery pass through bulkheads, through centerline of camshaft opening, then through bottom section of bulkheads to crankshaft bearings

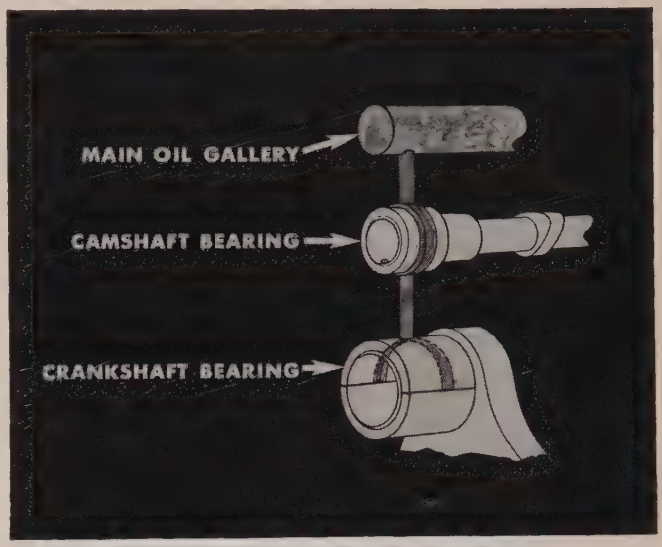

Fig. 56 – Oil (shaded portion) forced from main gallery through bulkhead and into machined annulus under camshaft bearing shells and into camshaft bearings. Remainder of oil goes into a hole in upper half of each crankshaft main bearing, filling groove in upper half of bearing

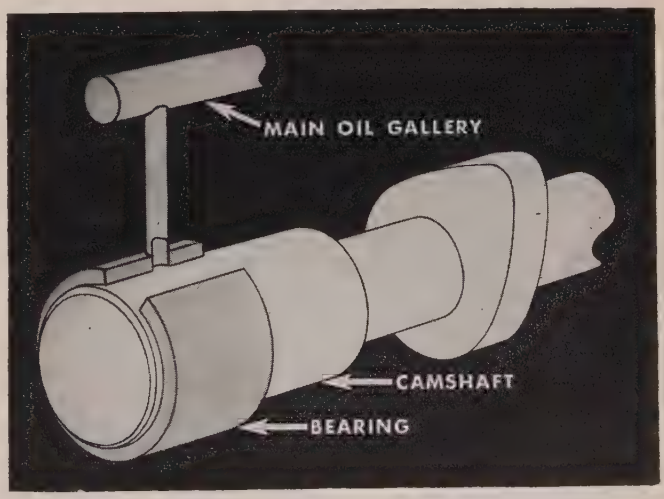

Fig. 57 – High-pressure oil supplied to camshaft rear bearing shell through drilled hole from high-pressure main oil gallery

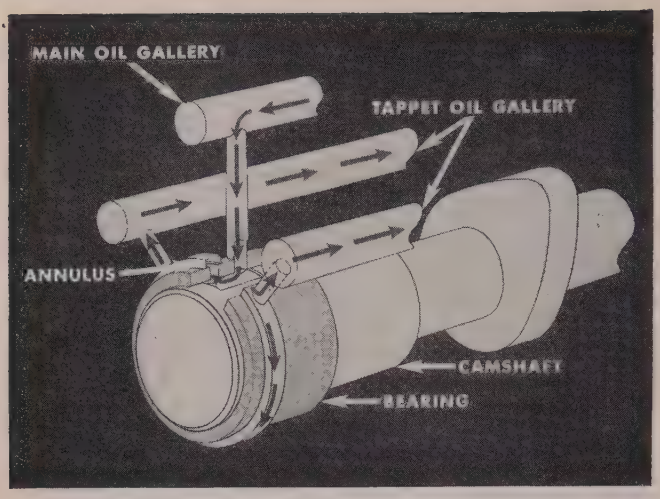

Fig. 58 – Path of oil from main oil gallery through annulus to tappet oil galleries

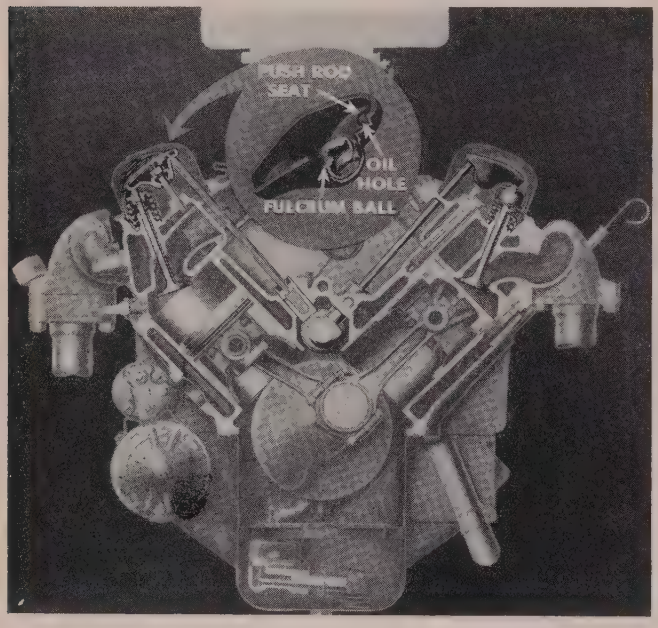

Fig. 59 – Oil flows out top of tappets, through hollow push-rods to lubricate rocker arms and valve stems

bearing leads the top center position of the crankpin by approximately 60 deg, which provides ample lubrication at the right time and position of the stroke, and, furthermore, the oil hole is never in a highly loaded area (Fig. 60). As a matter of fact, considering an engine lugging condition, the load is almost entirely removed at the oil hole position, resulting in a maximum cooling flow of oil from the hole, and providing the bearing with an unbroken surface at the point of load application. This not only increases the relative effective connecting-rod-bearing capacity, but, since the drilling is offset from the main journal, oil pressure required to overcome centrifugal force at the main bearing is reduced approximately 3 lb.

The problem of supplying oil to the pistons under

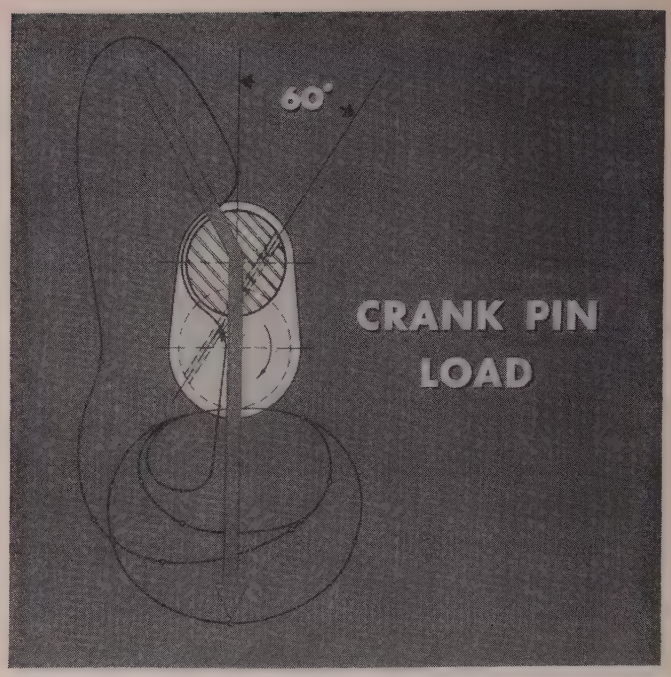

Fig. 60 – Crankshaft oil hole to each connecting-rod bearing leads the top center position of the crankpin by approximately 60-deg

cold operation conditions was thoroughly analyzed. An engine was set up in the laboratory for a stroboscopic analysis of oil flow, and we conducted cold-scuff tests. Oil holes in our connecting-rod-bearing caps at the split line are so oriented that the right-hand bank of rods lubricates the left-bank cylinder walls and the left-hand rods lubricate the right-hand bank of cylinders. (See Fig. 61.)

Valve Train

Turning to the valve operating mechanism, the major development of the system we use was carried out by Pontiac. This system is entirely new. As shown in Fig. 62, the effect one rocker arm may have on another through rocker-shaft deflection is eliminated, since no rocker shaft is used. Each rocker arm is entirely independent of the others.

Our valve rocker arms are stampings of 1010 material, carbonitrided and hardened to a case depth of 0.010-0.020 in., and then surface-treated. This is a precision stamping of high physical characteristics, somewhat resembling an elongated cup with an oval-shaped hole pierced in the bottom. Studs, threaded at the upper end, are pressed into the cylinder heads under a minimum load of 2600 lb. Each rocker arm is assembled over a valve stem and push-rod, and retained by a fulcrum ball and lock nut (Fig. 63). The rocker-arm development included stresscoat analysis which, incidentally, also was used in the development of the crankshaft, connecting rods, crankcase, and other parts.

The push-rods are made from 5/16-in. welded steel tubing, which has been formed and coined on the ends to produce a hemispherical surface. A

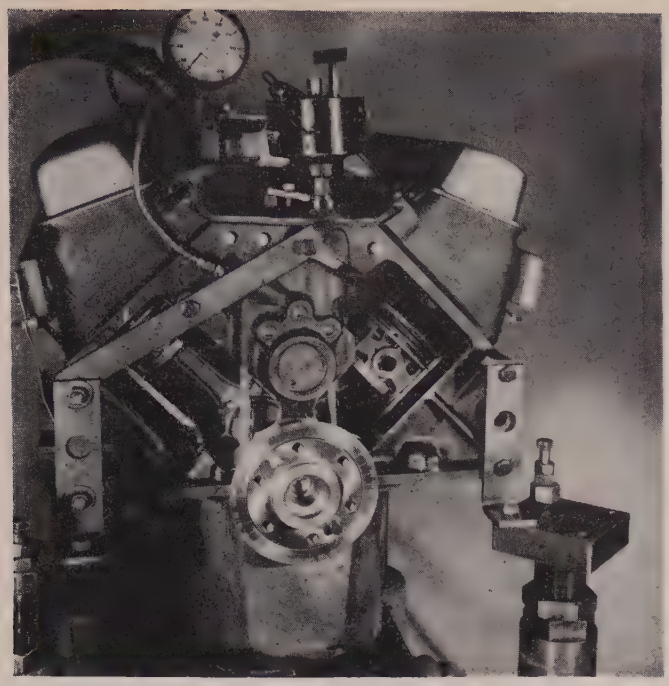

Fig. 61 – Engine setup for stroboscopic analysis of oil flow in cold scuff tests

small opening at each end is provided for the passage of oil from the tappets to the rocker arms.

The valves are lashed by simply turning the nut, whether mechanical or hydraulic lifters are used. (See Fig. 64.) The lash change through the operating range is relatively low for both inlet and exhaust, and we get exceptional uniformity because oil of the same temperature is flowing through all the push-rods.

Electrical System

The relative advantages of the 6-v electrical system and the 12-v system were considered, and when the studies were completed it was found that under the 6-v system there was a deficiency in the voltage required by the spark plugs for good spark-plug life. In our high-compression engine, the secondary voltage available from the 6-v system is barely sufficient to fire new spark plugs with an 0.035-in. gap at speeds of 60 mph and up (Fig. 65). The voltage requirements of used plugs with 0.050-in. gap exceed the voltage available from the 6-v system at around 38 mph and up, resulting in missing. With the 12-v system, the available voltage is sufficient to provide an adequate ignition reserve throughout the entire operating range with either new or used plugs. Tests show that spark-plug gaps may be allowed to grow to 0.055 in. or 0.060 in. before missing is encountered.

There are other definite advantages of the 12-v system over the 6-v, including more efficient generator output, better starting motor operation, and the fact that it permits the use of smaller-gage wires and cables.

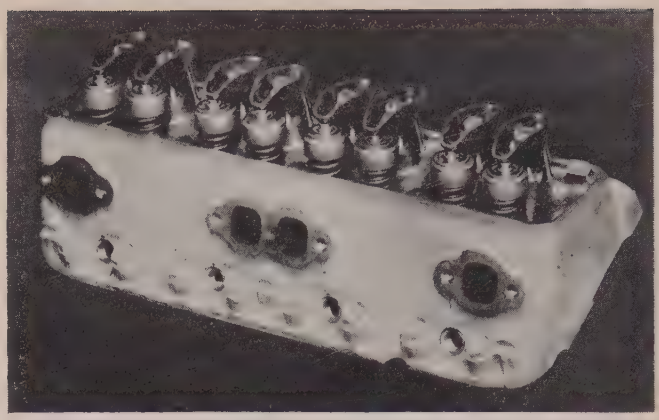

Fig. 62 – Each rocker arm is entirely independent of the others. No rocker-shaft is used

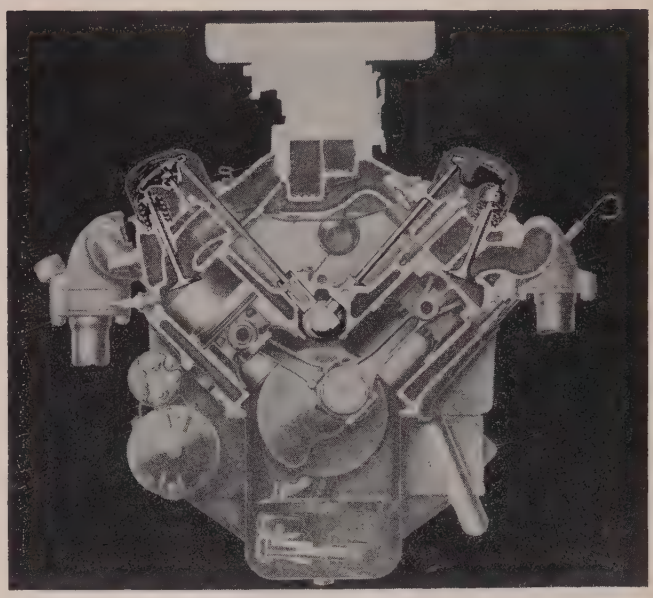

Fig. 63 – Rocker arm is assembled over valve stem and push-rod, and retained on a pressed in stud by a fulcrum ball and lock nut

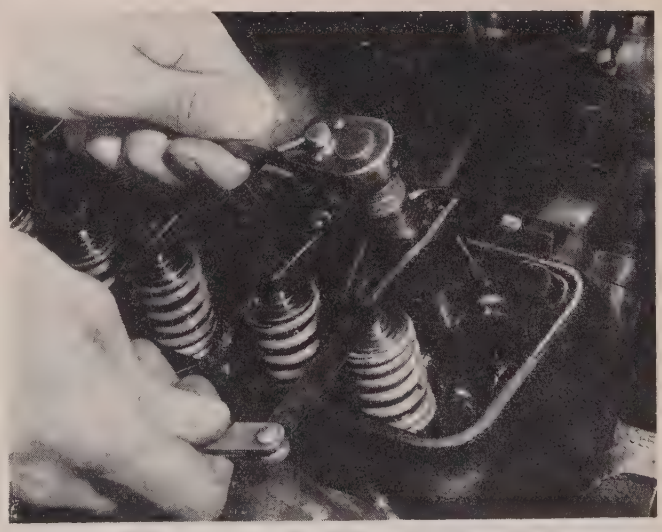

Fig. 64 – Lashing valve by simple turning of nut

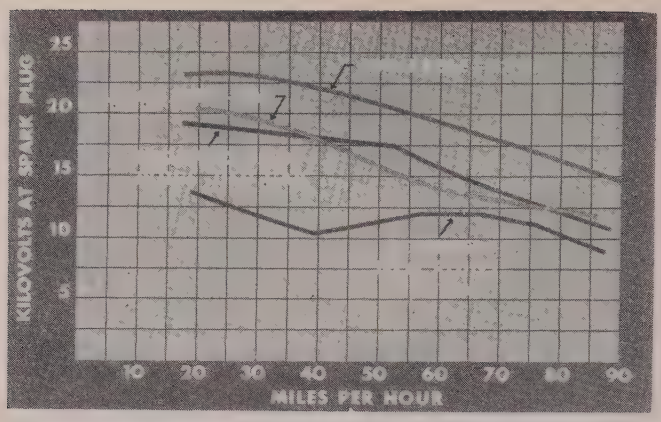

Fig. 65 – Ignition performance of V-8 engine with 12-v and 6-v electrical system

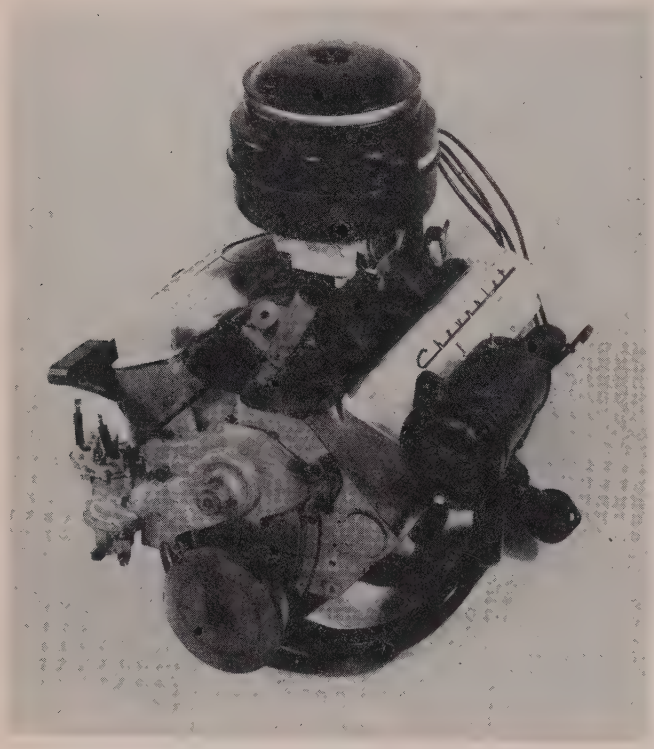

Fig. 66 – Wood mockup of basic engine and accessories

Accessories

The most effective placement of the various accessory parts which are necessarily a part of the engine assembly always presents a problem. This is particularly true in the case of a V-8, since the sides of the engine are so wide apart and also so much shorter than in an in-line engine.

A mockup was made of the basic engine and accessories to determine the best overall relationship of the parts (Fig. 66). For instance, the bracket for mounting the generator is attached to bosses on the front end of the left exhaust manifold. Tests were run which proved the durability of such an arrangement. This location is ideal in that it allows us to mount the power-steering pump on the rear-end frame of the generator (Fig. 67). The offset of the cylinder centers provides enough room to place the fuel-pump push-rod in front of the right cylinder bore, and still have an eccentric to the rear of the camshaft front bearing (Fig. 2).

The advantages of low weight have been stressed throughout this paper. Taking unnecessary weight out of an automobile is the same as putting horsepower in, and results in increased acceleration ability. Tire size and tire life depend, of course, on vehicle weight; and brake size as well as steering effort are closely related to the weight factor.

Our block assembly weighs 147 lb; two cylinder heads, 77 lb; the crankshaft, 47 lb; a set of connecting rods, pistons, and rings, 21 lb; intake manifold, 34 lb; two exhaust manifolds, 17 lb; and the valve actuating mechanism, 18 lb. The total weight of our V-8 engine is 531 lb as compared to 572 lb for our Six. (See Table 3.)

Fig. 68 shows the power curve and the bmep of our engine, which has a two-barrel carburetor. It will be noted that the engine develops 162 gross hp at 4400 rpm, and gross torque of 257 ft-lb at 2200 rpm. Our bmep is 146.0 psi at 2200 rpm.

Fig. 69 shows friction horsepower, friction mean effective pressure, and specific fuel consumption.

Table 3 – Weights of V-8 and In-Line 6 Engines Compared

	V-Eight	Six
Block Assembly	147	163
Cylinder Heads (per Engine)	77	72
Crankshaft	47	79
Connecting Rod, Piston, Rings (per Engine)	21	22
Intake Manifold	34	13
Exhaust Manifolds (per Engine)	17	16
Valve Actuating Mechanism	18	25
Total Engine	531	572

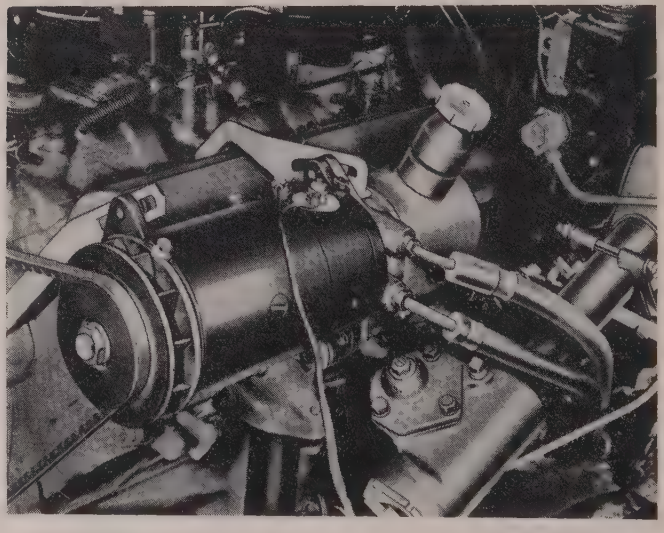

Fig. 67 – Generator mounting bracket is attached to bosses on front end of left exhaust manifold, allowing mounting of power-steering pump on generator rear end frame

Our engine, with its very short stroke, produces the low friction of only 40.6 hp. Note also the low fmep curve. Reducing friction horsepower is another way of adding usable power to an engine. The specific fuel consumption figure of 0.498 lb per hp-hr indicates excellent economy.

Where exceptional acceleration and performance are desired, a four-barrel carburetor and a dual exhaust system are offered as optional equipment (Fig. 70).

Fig. 71 shows that an engine with this equipment turns out 180 hp at 4600 rpm and gross torque of 260 ft-lb at 2800 rpm.

The development of the Chevrolet V-8 engine is the result of the combined effort of all the resources of General Motors, GM Product Study, GM Research, and the Chevrolet Engineering Staff. We recognize that there are many philosophies when it comes to V-8 engine design, and add that the engine we have discussed here represents our best effort. There have been other approaches to this same subject dictated by manufacturing facilities, resources, or other considerations. Our decisions were the outcome of the study of our facilities, our assembly problems, and our merchandising requirements.

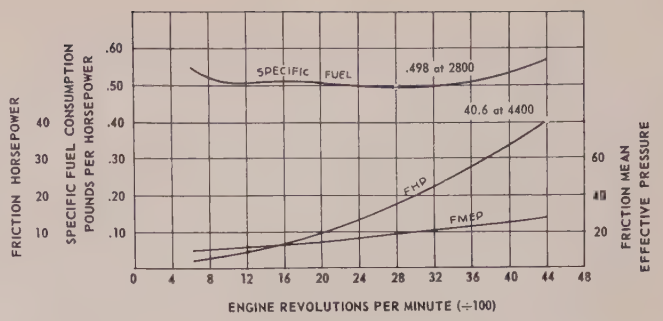

Fig. 69 –Friction horsepower, specific fuel, and friction mean effective pressure

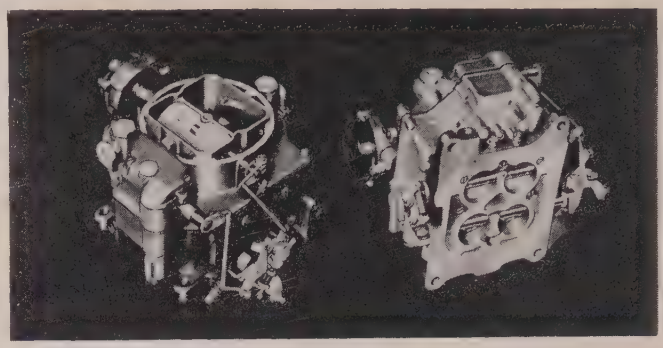

Fig. 70 – Four-barrel carburetor and dual exhaust are offered as optional equipment

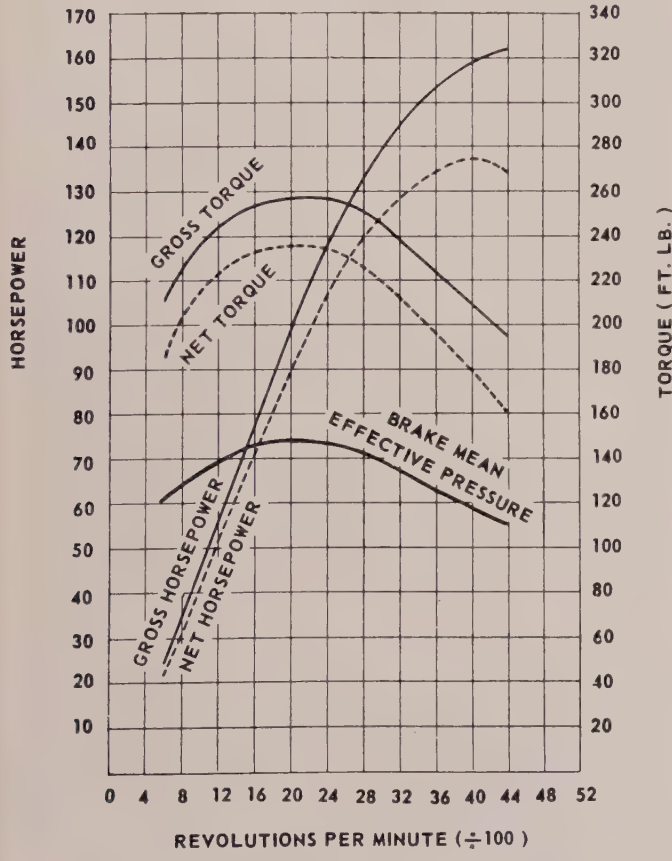

Fig. 68 – Engine performance with 2-barrel carburetor

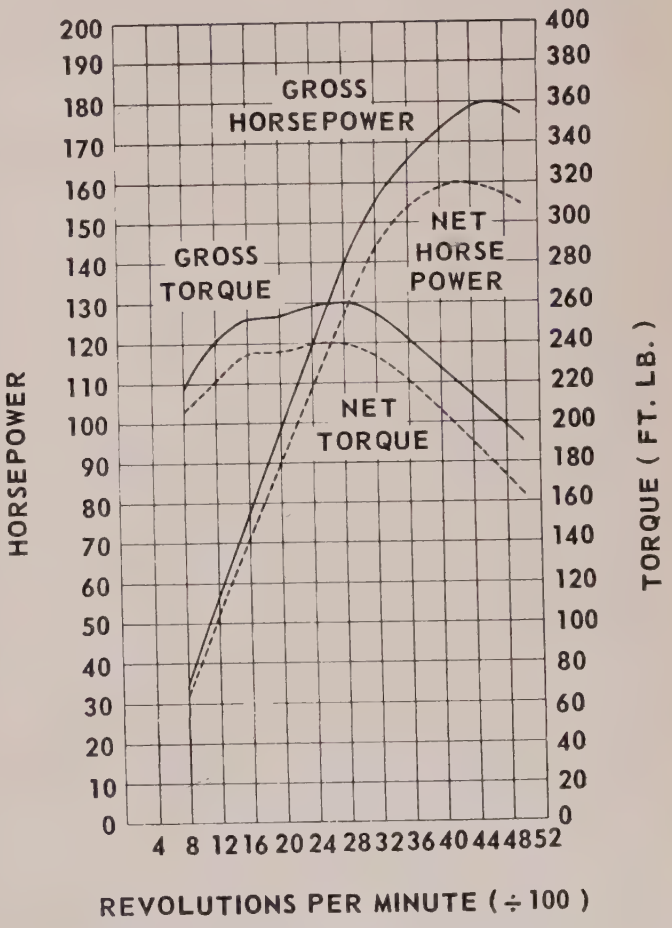

Fig. 71 – Engine performance with 4-barrel carburetor and dual exhaust system

Tractor-Engine

THE subject of best fuel utilization is so broad that it is impossible to treat in a single paper all the aspects of performance and related engine design for the three major types of fuels and their engines used today in our domestic farm tractors.

In the continuous search for improved performance all engine designers have two basic goals in common: greater horsepower per cubic inch of displacement and higher brake thermal efficiency. For the sake of simplifying the approaches to these aims, we can divide our considerations into two broad areas of design application which provide the potential means by which these objectives may be realized. One is basically thermodynamic in character, the other, mechanical. The first deals primarily with those factors providing a greater release of energy in the form of work within the combustion chamber, whereas the latter affects how much of that work is available for use. From a practical point of view, best fuel utilization must necessarily be evaluated by how effectively its potential energy has been transformed into usable work at the flywheel end of the engine's crankshaft. Obviously, any reductions in mechanical losses are direct gains in power and economy. Conversely, the potential gains in power and economy resulting from the application of design elements related to thermodynamic improvement will not be fully attained if abnormal mechanical losses resulting therefrom are not minimized. It is believed, therefore, that continued progress in fuel utilization can only be gained by integrating mechanical improvements along with design factors which take fullest advantage of fuel quality. Unfortunately, in the case of LPG and diesel fuels, the future holds little potential promise of any trend toward improved quality which can be directly translated into progressive increases in power and economy through related engine design.

On the other hand, the past and present gains in power and efficiency of gasoline engines are in large measure the result of progressive engine design being applied to take advantage of the continued upward trend in gasoline antiknock quality. Furthermore, it is generally accepted that this upward trend will continue. This is evidenced by the basic design characteristics found in the new high-performance passenger-car engines developed within the past five years. Such factors as structural rigidity and cylinder proportions have received particular attention to minimize internal friction losses. Also, advances in combustion-chamber design permitting higher compression ratios and designs for increasing volumetric efficiency have been combined to produce power and efficiency gains as fuel antiknock quality has been increased.

The authors recognize that the general effects of these factors on engine performance are well understood by those engaged in tractor engine design. There have been, however, some indications of a feeling that it is not possible to exploit these factors to the same degree in gasoline engines for tractors as has been possible in passenger cars. It has been assumed that much greater compromises must be made in tractor engines because of markedly different operating conditions.

An opportunity to study the performance of a tractor engine incorporating many of these features was recently presented to us by Oliver Corp.'s development of their XO-121 experimental engine. Since we participated in certain phases of their development program, they obligingly loaned us an engine for our studies. Also, our research laboratories have conducted various investigations on the performance gains and fuel requirements related to the increase of compression ratio between 6/1 and 12/1 on several engines. This has made it possible to evaluate certain performance characteristics displayed by the XO-121. Furthermore, through the courtesy of Chrysler Corp. we have been permitted to use published data obtained in their laboratories.

General Description of XO-121

The XO-121 (Table 1) is a 4-cyl, overhead-valve engine having a bore of 3¾ x 4½-in. stroke, which

Table 1 – Major Specifications of XO-121 Engine

No. of Cylinders	4
Cylinder-Head Type	Overhead valve
Bore and Stroke, in.	3.75 x 4.5
Displacement, cu in.	198.8
Governed Speed, rpm	1600 rpm
Compression Ratios	7/1, 9.5/1, 12/1
Voltage of Ignition System	12
Crankshaft	5 main bearings
Main Journal Diameter, in.	3.00
Crankpin Diameter, in.	2.31

Design Requirements

For Best Fuel Utilization

H. T. Mueller and R. E. Gish, Ethyl Corp.

This paper was presented at the SAE National Tractor Meeting, Milwaukee, Sept. 16, 1954.

IMPORTANT gains in passenger-car engine power and efficiency have resulted from design improvements that take advantage of increasing gasoline antiknock quality. Experiments with 7/1, 9.5/1, and 12/1 compression ratio reported in this paper show how similar gains can be achieved in tractor engines by applying the same principles.

Of particular importance to this and future development programs that are to use these principles effectively, the authors say, are:

1. Careful choice of compression ratio for best utilization of antiknock quality of current and possible future fuels.

2. Good combustion-chamber configuration.

3. Good volumetric efficiency.

4. Best possible compromise between friction reduction and reduced thermal efficiency.

5. Control of ignition timing.

6. Control of coolant flow to all parts of jacket.

gives a displacement of 198.8 cu in. The crankshaft is counterbalanced and is carried in five trimetal-on-copper-lead precision-shell-type bearings. Main journals are 3.00 in. in diameter and crankpins 2.312 in. Exhaust valves are 1 11/32 in. and the intake 1½ in. in diameter. Steel-strut solid-skirt pistons of aluminum alloy and tinplated are used, having one 3/16-in. oil and two 5/32-in. compression rings. Both starting and ignition systems are 12-v. The distributor has a single breaker and is controlled only by its centrifugal advance mechanism. Champion C-88-S spark plugs having much wider heat range characteristics than conventional plugs were used at the 12/1 compression ratio. Types EJ-7 and EJ-6 were used for the 9.5 and 7/1 compression ratios, respectively. All three were 14-mm and were shielded.

Engine Performance

Full-Load Power and Fuel Economy – Performance gains in brake horsepower and reduction in brake specific fuel consumption as compression ratio was changed from 7/1 to 12/1 have been determined for two operating speed ranges. These data were obtained with the engine equipped with radiator, fan, generator, and air cleaner to simulate

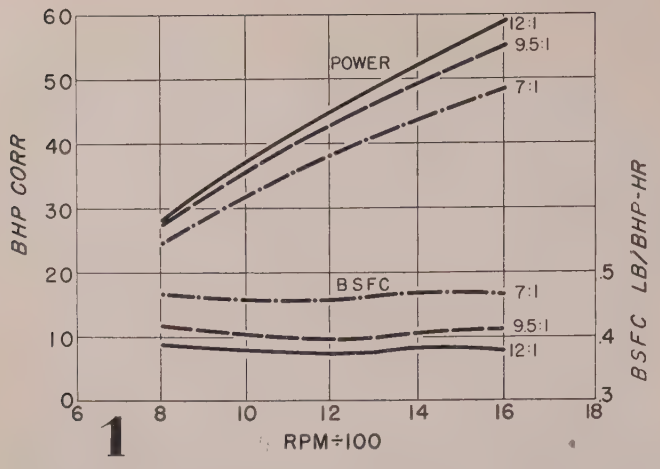

Fig. 1 – Power and fuel economy at three compression ratios as related to engine speed for 800-1600-rpm range. 19-mm carburetor venturi. Engine equipped as installed

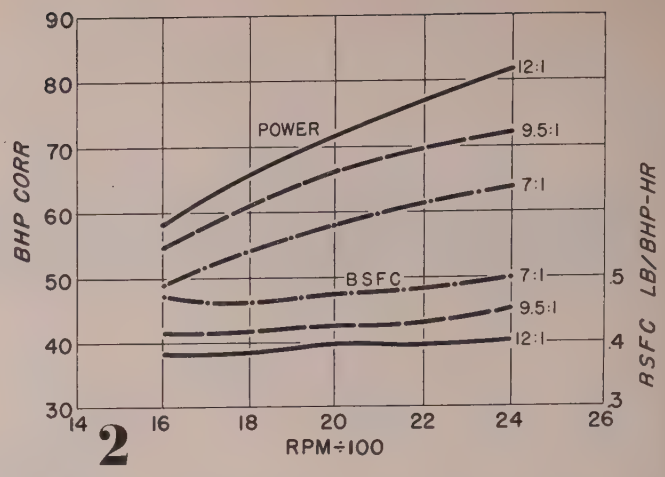

Fig. 2 – Power and fuel economy at three compression ratios as related to engine speed for 1600-2400-rpm range. 21-mm carburetor venturi. Engine equipped as installed

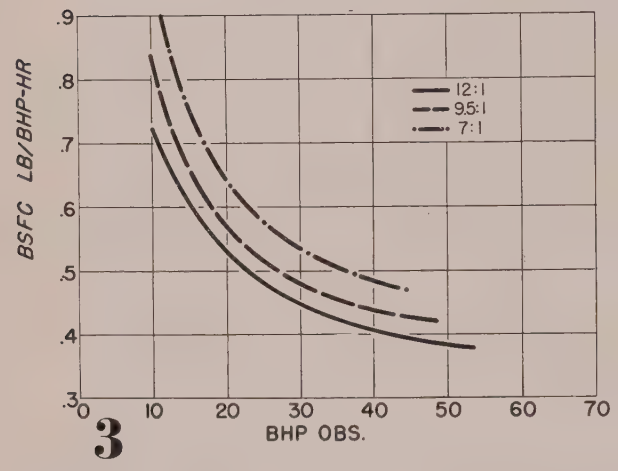

Fig. 3 – Effect of compression ratio on part-load fuel economy. Engine speed 1600 rpm (governed speed). Engine equipped as installed

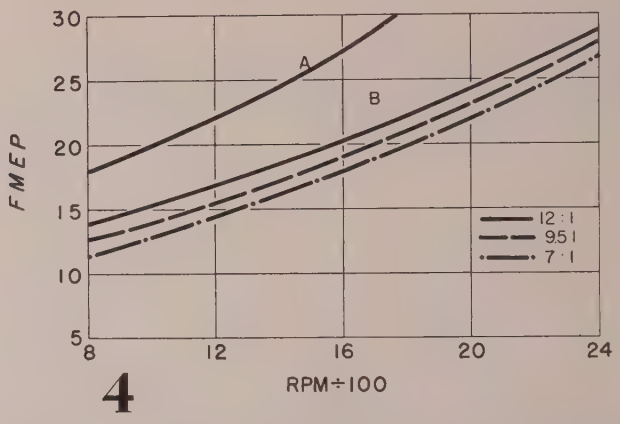

Fig. 4 – Effect on piston and connecting-rod assembly and effect of compression ratio on fmep. Curves A and B show friction obtained with original and final piston and connecting-rod assemblies, respectively, at 12/1 compression ratio. Lower three curves represent friction obtained with final assembly at three compression ratios. Engine equipped as installed

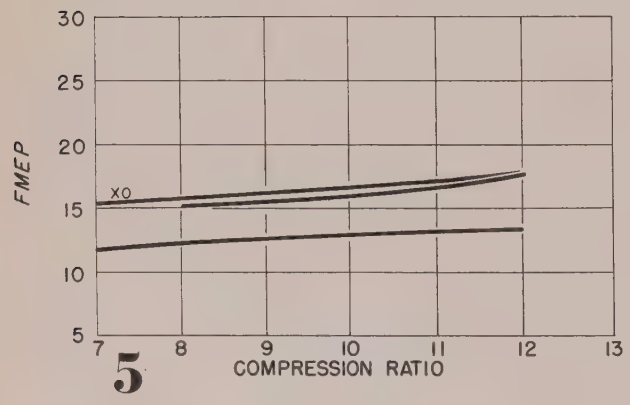

Fig. 5 – Friction related to compression ratio for XO-121 engine and two V-8 passenger-car engines with engine speeds equal. Engine speed 1600 rpm. Engines not equipped with fans

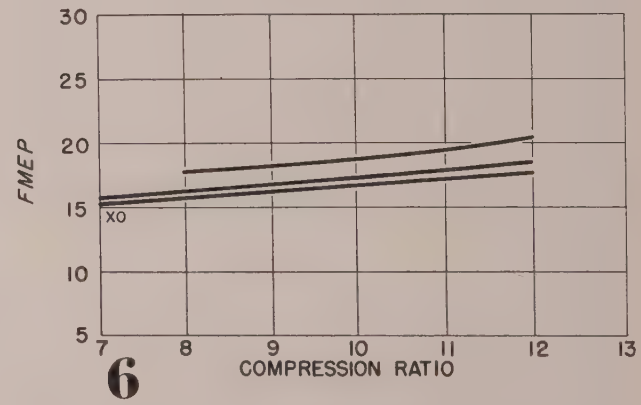

Fig. 6 – Friction related to compression ratio for XO-121 engine and two V-8 passenger-car engines with piston speeds equal. Piston speed 1200 fpm (1600 rpm for XO-121 engine). Engines not equipped with fans

the as-installed condition. Maximum power ignition and maximum economy carburetor settings were used at each condition of speed and compression ratio.

Fig. 1 shows the results at full throttle for speeds of 800 to the present governed point of 1600 rpm. A 19-mm carburetor venturi was used for these runs. It will be noted that a brake specific fuel consumption of 0.378 was obtained on the 12/1 ratio at governed speed. The average improvement in power and fuel economy of the 9.5 and 12/1 ratios over the 7/1 are 12.3% and 17.85%, respectively.

For the purpose of evaluating what gains in power could be realized by shifting the governed speed to a higher level, a second arbitrarily chosen speed range of 1600 to 2400 rpm was investigated. For this work a 21-mm venturi was used. These data are presented in Fig. 2, and, as would be expected, attractive gains in power over that at 1600 rpm were obtained at each of the speeds surveyed up to 2400 rpm. These gains were in the order of approximately 11% at 1800, 20% at 2000, 26% at 2200, and 31% at 2400 rpm. Only relatively minor losses in brake specific fuel consumption accompanied these power gains in this engine. Raising the governed speed in some instances might warrant some consideration when higher power requirements must be met without the immediate possibility of increasing engine displacement. Furthermore, such power gains can usually be obtained at lower fuel octane-number levels than the same gains at lower speeds. These relationships will be shown later.

Part-Load Economy – The part-throttle data obtained at the three compression ratios also display the same trend in improvement as indicated by those at full throttle. They were obtained at maximum economy carburetor setting and with the same spark advance which gave maximum power at full throttle. Fig. 3 shows the variation of brake specific fuel consumption with observed brake horsepower for each compression ratio at the governed speed of 1600 rpm.

The average improvements obtained at constant power levels of 40-30-20-15 for the 12 and 9.5 ratios over the 7/1 was 17.3 and 11.2%, respectively.

Friction – During the initial development stage of the XO-121 engine, it was apparent that higher-than-anticipated friction losses were adversely affecting power and fuel economy levels. To remedy this condition a different combination of connecting-rod and piston assembly was tried. Fig. 4 shows the reduction in fmep resulting from this change (type A to B) at 12/1 compression ratio. It amounts to approximately a straight 23% reduction from 800 to 1600 rpm. The effect of compression ratio on fmep, using combination B, is also shown in Fig. 4. It should be noted that the data shown in this figure were obtained with the engine equipped in the as-installed condition. In spite of the increase in friction as compression ratio was raised, there was actually a slight gain in mechanical efficiency at the higher ratios. At 1600 rpm it varied from 88.3 to 88.8%, and at 2400 rpm from 83.2 to 84.7%. To obtain a realistic appraisal of where the XO-121 actually stands in regard to friction characteristics, comparisons have been made with two high-performance V-8 passenger-car engines. For these comparisons the fan was removed from the XO-121 in order to match the equipment installations of two other engines. Fig. 5 shows the effect of compression ratio on fmep at the same speed of 1600 rpm for all three engines. Since the stroke/bore ratio is considerably larger for the XO-121 than either of the other two units, a comparison on an equivalent mean piston speed basis is shown in Fig. 6. These comparisons would indicate that a lower stroke/bore ratio might improve its present favorable friction level; however, the actual gain could be counteracted by an accompanying decrease in indicated thermal efficiency. One of the important aspects of minimizing friction is its influence on part-throttle economy. Fig. 7 shows the actual effect on brake specific fuel consumption level resulting from the friction reduction made when piston and rod assemblies were changed (refer to Fig. 4). The gain at the 50 hp part-load throttle point at 1600 rpm is about 4%, whereas at 10 hp, or approximately 20% load, it is 11.5%.

Efficiencies – Comparisons of volumetric efficiency and bmep as related to compression ratio have been developed for the XO-121 and one other engine. Both sets of bmep data are corrected to the same conditions of 29.92 in. of Hg and 60 F, and were taken with ignition timing and air-fuel mixtures set for best economy. Fig. 8 shows these comparisons at 1600 rpm, and Fig. 9 at 2400 rpm. It is interesting to note the reversal of position of these two engines with regard to bmep level at these two speeds. The variations in volumetric efficiency of both engines probably account for most of this change.

Brake thermal efficiency and brake specific fuel consumption related to compression ratio are shown in Fig. 10, while indicated thermal efficiency and

The Authors

H. T. MUELLER is manager of the Engineering Service Division, Technical Service Department, Ethyl Corp., where he is engaged in cooperative engine development activities with tractor, commercial vehicle, and accessory manufacturers on problems related to the utilization of fuel. He studied mechanical engineering at the University of Detroit, and joined Ethyl's engineering department in 1929.

R. E. GISH (M '42) is assistant manager in charge of engine development for the Engineering Service Division, Technical Service Department, Ethyl Corp. He received his B.S. in Mechanical Engineering from the University of Southern California in 1935. Mr. Gish joined Ethyl after graduation, and served on the staff of the San Bernardino road test laboratory until 1951.

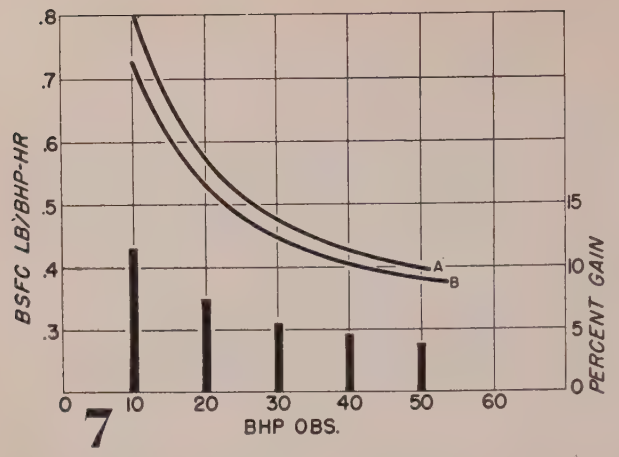

Fig. 7 – Effect of friction reduction on part-load fuel economy. Engine speed 1600 rpm. Curves A and B show bsfc for original and final piston and connecting-rod assemblies, respectively, at 12/1 compression ratio. Bars represent gains due to reduced friction of final assembly at various levels of power. Engine equipped as installed

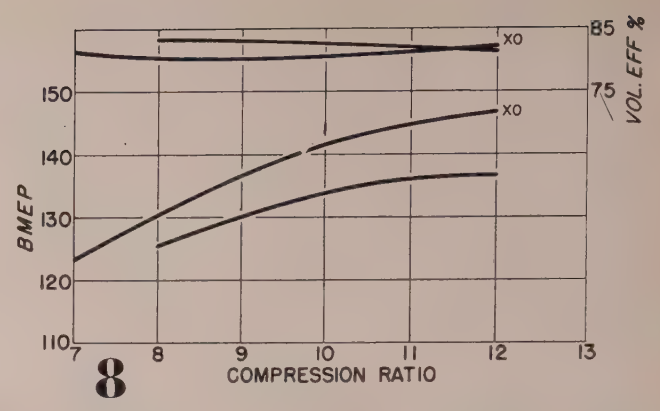

Fig. 8 – Comparison of XO-121 engine and V-8 passenger-car engine with respect to bmep and volumetric efficiency at 1600 rpm. Bmep data are corrected to 29.92 in. of Hg and 60 F and were taken with ignition timing and air-fuel mixture set for best economy. Engine not equipped with fans. V-8 engine equipped with 2-barrel carburetor

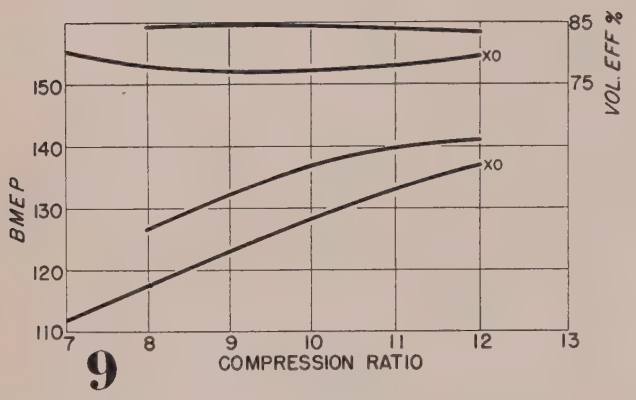

Fig. 9 – Comparison of XO-121 engine and V-8 passenger-car engine with respect to bmep and volumetric efficiency at 2400 rpm. Bmep data are corrected to 29.92 in. of Hg and 60 F, and were taken with ignition timing and air-fuel mixture set for best economy. Engines not equipped with fans. V-8 engine equipped with 2-barrel carburetor

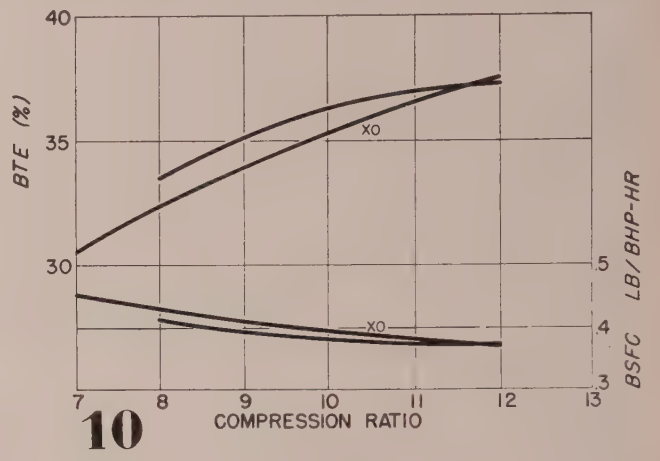

Fig. 10 – Relation of brake thermal efficiency and brake fuel economy to compression ratio for XO-121 engine and V-8 passenger-car engine. Engine speed 1600 rpm. Ignition timing and air-fuel mixture set for best economy. Engines not equipped with fans

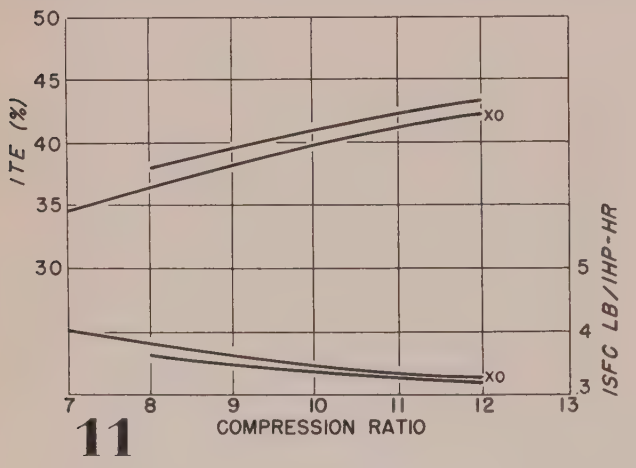

Fig. 11 – Relation of indicated thermal efficiency and indicated fuel economy to compression ratio for XO-121 engine and V-8 passenger-car engine. Engine speed 1600 rpm. Ignition timing and air-fuel mixture set for best economy. Engines not equipped with fans

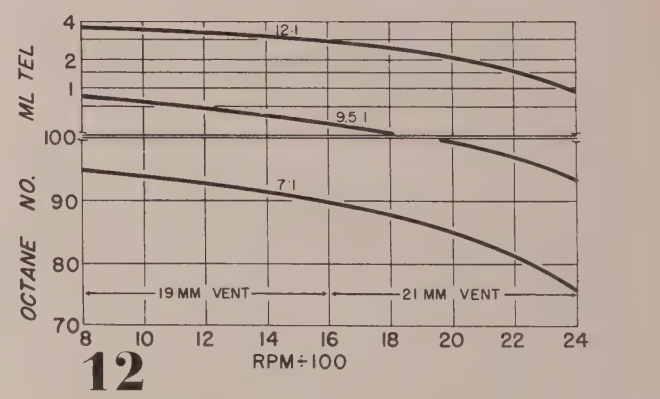

Fig. 12 – Relation of antiknock requirement and engine speed for compression ratios of 7/1, 9.5/1, 12/1, with ignition timing set for maximum power. Data obtained with primary reference fuels. Air/fuel ratio set for maximum economy. Carburetor air temperature 100 F, jacket water 180-185 F. Antiknock values exceeding 100 octane number are expressed as milliliters of tel in isooctane

indicated specific fuel consumption relationships are shown in Fig. 11.

Fuel Antiknock Quality Utilization

Octane-Number Requirement – The fuel antiknock requirements of the engine were evaluated at the three compression ratios with both primary reference fuels and commercial gasolines. In all knock ratings the temperatures of the carburetor air and the jacket water outlet were maintained at 100 F and 180 F, respectively. Air/fuel ratio was held at 15/1 at all speeds in order to evaluate the knocking characteristics at a mixture ratio closely approximating that of maximum economy. Combustion-chamber deposits were accumulated for approximately 100 hr on each compression ratio prior to these tests.

Fig. 12 shows antiknock requirements at maximum power spark timings in the speed range from 800 to 2400 rpm. Values exceeding 100 octane number are expressed in terms of milliliters of tel in isooctane. It will be noted that requirement decreases substantially with speed at all three ratios. This behavior, which is quite typical, should be given consideration in the selection of the speed range for an engine. Since requirements measured at maximum power spark timing are normally high compared to requirements at slightly retarded settings, the power loss and requirement reductions resulting from retarding the spark are shown in Fig. 13 for the 7/1 and 9.5/1 ratios. With spark retarded to give 2% power loss, requirement is reduced about three octane numbers at both ratios. A further retardation to 5% power loss results in a total reduction of about five octane numbers. The same characteristic is displayed by the 12/1 ratio. The requirement reductions, however, cannot be directly related to those of lower compression ratios, as they are based on tel in isooctane instead of octane numbers.

Additional relationships can be obtained from Fig. 13. It can be shown that at the 7/1 compression ratio the power loss on a primary reference fuel of 86 octane number is about 2% at the governed speed of 1600 rpm, and about 6% at the maximum torque speed of 1200 rpm. At 9.5/1 compression ratio the loss on a primary reference fuel of 98 octane number is 2% and 5%, respectively, at 1600 and 1200 rpm. The octane-number requirements at speeds below 1200 rpm are relatively unimportant, since the engine would be operated only intermittently in this range.

Fuel Sensitivity – An important consideration concerning fuel quality utilization deals with the relationship of fuel sensitivity to permissible or knock-limited power output. It may be well at this point to review the meaning and importance of fuel sensitivity. It is defined as the numerical difference between the Motor and Research octane numbers of a fuel as obtained on the standard laboratory

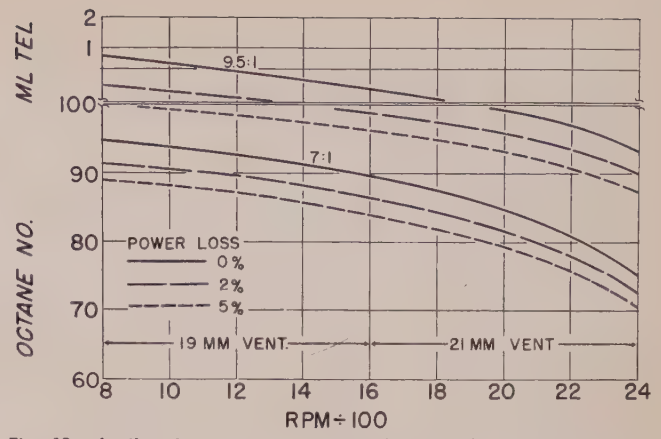

Fig. 13 – Antiknock requirements of 9.5/1 and 7/1 compression ratios with ignition timing set for 0, 2%, and 5% power loss. Data obtained with primary reference fuels. Air-fuel set for maximum economy. Carburetor air temperature 100 F, jacket water 180-185 F. Antiknock values exceeding 100 octane number are expressed as milliliters of tel in isooctane

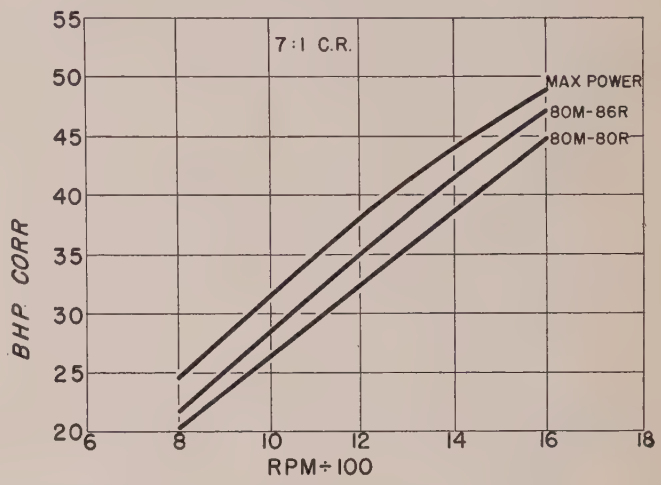

Fig. 14 – Effect of fuel sensitivity on knock-limited power at 7/1 compression ratio. Commercial-type gasolines. Lower curves obtained with ignition timing set for borderline knock on sensitive and insensitive fuels. Upper curve obtained with timing set for maximum power, using nonknocking fuel. Air-fuel mixture set for maximum economy. Carburetor air 100 F, jacket water 180-185 F

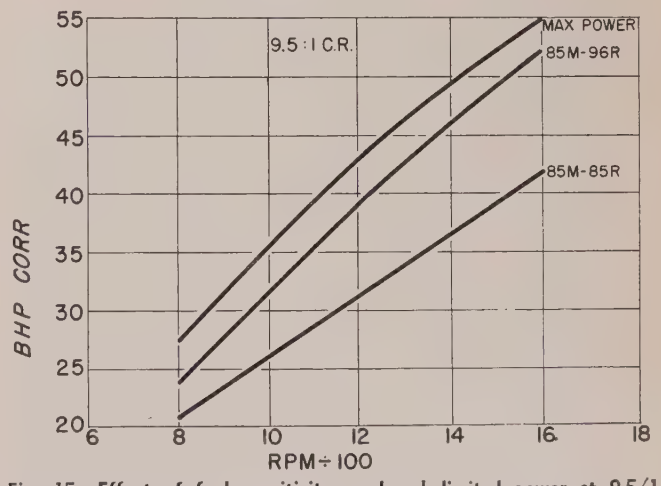

Fig. 15 – Effect of fuel sensitivity on knock-limited power at 9.5/1 compression ratio. Commercial-type gasolines. Lower curves obtained with ignition timing set for borderline knock on sensitive and insensitive fuels. Upper curve obtained with timing set for maximum power, using nonknocking fuel. Air-fuel mixture set for maximum economy. Carburetor air 100 F, jacket water 180-185 F

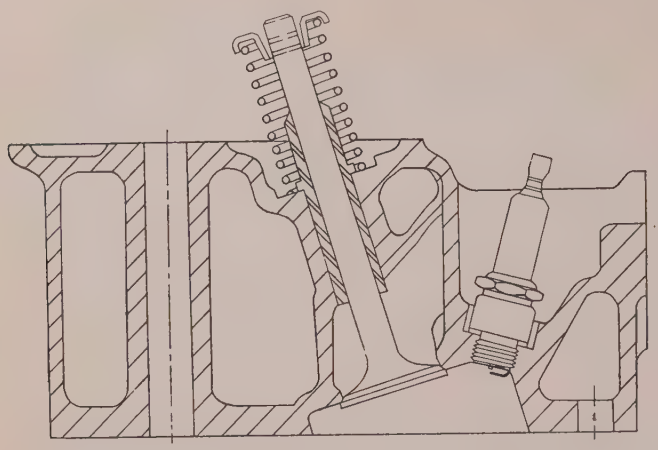

Fig. 16 – Combustion-chamber profile for 12/1 compression ratio

CFR engine. For two fuels having the same Motor Method octane number, the one with the higher Research octane number has greater sensitivity, and generally permits a higher spark timing for borderline knock, thereby producing higher knock-limited power.

Fig. 14 shows the effect of fuel sensitivity on knock-limited power. Data are shown for the 7.0/1 compression ratio across the speed range of 800 to 1600 rpm. The upper curve is at maximum power spark advance and represents the maximum power obtainable with a nonknocking fuel. The lower curve, labelled 80M-80R, is the knock-limited power obtained on an insensitive fuel of 80 octane number Motor and 80 octane number Research. The performance of another fuel with the same Motor octane number but having a six-octane-number sensitivity (the curve labelled 80M-86R) permits substantially higher spark advance, which results in a power gain of 8% at the maximum torque speed of 1200 and 5% at 1600 rpm. This 80-86 fuel is typical of today's commercially available regular-grade gasoline. It will be noted that the 7.0/1 compression ratio on this engine is well suited to the 80-86 fuel, as indicated by the level of power produced in relation to that at maximum power spark advance.

Fig. 15 shows a similar relationship between knock-limited power and fuel sensitivity at 9.5/1 compression ratio. The increase in power between curve 85M-85R and curve 85M-96R is about 23% at speeds of 1200 rpm and above. This increase is due to the high response of the 9.5/1 compression ratio cylinder head to the 11-octane-number sensitivity of fuel 85M-96R. Obviously, the fuel economy gains will be of the same order as the attractive power gains. The sensitive fuel is actually a commercially available premium gasoline. It can be seen that 9.5/1 compression ratio on this engine is reasonably well suited to this particular fuel.

It is evident from the foregoing that maximum fuel quality utilization cannot be attained without the application of designs which fully exploit fuel sensitivity.

Design Considerations

The XO-121 performance data and the various comparisons made with other engines demonstrate that the same thermodynamic and mechanical principles presently exploited in passenger-car engine design can provide equally attractive improvements when applied to a tractor engine. To effectively apply these principles, the following considerations should receive particular attention.

Thermodynamic – (1) Compression ratio should be selected by the proper evaluation of its utilization of the antiknock quality of current fuels with due consideration to the upward trend in this quality.

(2) Combustion-chamber configuration is a highly controversial subject, as evidenced by the wide variety of shapes currently employed. Nevertheless, certain general principles govern good design; namely, compactness; short flame travel; turbulence; high volumetric efficiency (by proper valve size selection and minimum shrouding); uniform cooling; shape that permits full machining of all surfaces so that close control of volume can be maintained at all ratios; and good deposit scavenging.

At this point it might be of some interest to show the configurations for two of the compression ratios used on the XO-121. A profile of the original chamber designed for the 12/1 ratio is shown in Fig. 16. Although it has a simple shape, full consideration was given to the application of the foregoing principles in its design. No profile of the 9.5/1 ratio is shown because of its close similarity to the 12/1. Fig. 17 shows the profile of the 7.0/1 chamber. Because of the relatively large volume required at this ratio, the depth of the cavity had to be greatly increased. As a result, the configuration is markedly different from that of the other two ratios. Although the chamber in its present form is satisfactory from the standpoint of fuel utilization, it is believed that certain modifications in configuration

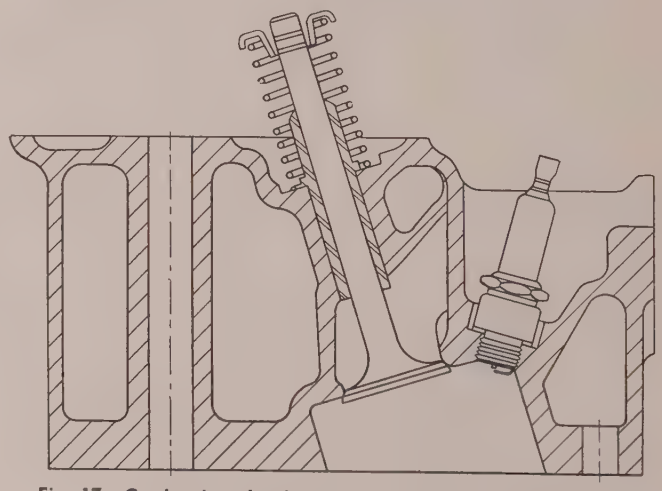

Fig. 17 – Combustion-chamber profile for 7/1 compression ratio

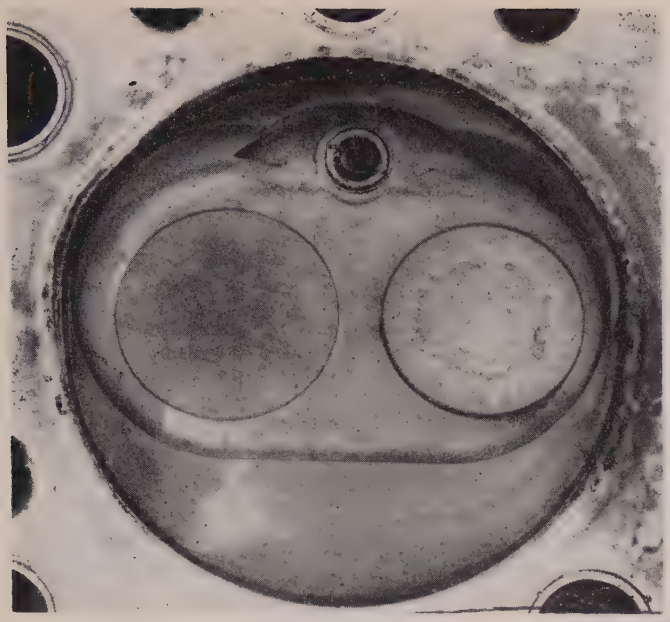

Fig. 18 – Combustion-chamber deposits in cylinder head. Compression ratio 12/1. Condition representative of all cylinders after approximately 600 hr of operation on fuels containing 3-4 ml of tel per gal

might improve it even further. Unfortunately, time did not permit carrying out such an investigation in time for this presentation.

Inasmuch as good deposit scavenging is considered an important characteristic to be sought after in combustion-chamber design, pictures have been taken of the deposits found in the combustion chambers and on the pistons at the conclusion of test work at 12/1 compression ratio. There was no perceptible difference in deposits between any of the cylinders. Figs. 18 and 19 show cylinder head and piston condition of a representative cylinder. The engine had been operated for a total of approximately 600 hr before the cylinder head was removed. Its operation includes belt tests, drawbar tests, field operation by Oliver, and approximately 300 hr of dynamometer testing under a wide range of conditions in our laboratory. Practically all of the operation was on a fuel containing 4.0 ml of tel per gal. We believe this performance is an example of good scavenging resulting from good design application.

(3) Since the full-throttle power output of an engine at any given speed varies substantially in direct relation to the amount of dry air consumed, the improvement of its volumetric efficiency warrants particular consideration. High efficiency can be realized only when the entire induction system and its elements are in proper balance. It is recognized that certain compromises are involved; however, every attempt should be made to widen these by more detailed study and elimination of the barriers involved. Improved valve timing, better manifolding, and cylinder-head porting combined with minimum air-fuel mixture charge heating, are obvious items for investigation.

Mechanical – (1) The importance of structural rigidity for friction reduction or control cannot be overemphasized if the potential benefits of present and future antiknock quality are to be fully realized through the application of higher compression ratios and improved breathing. It has been demonstrated in this program that the predicted gains in power and economy can be obtained by these means when an adequate structure is provided. Furthermore, the substantial adverse effect of unwarranted friction on part-throttle economy has been illustrated.

(2) Cylinder proportions providing lower stroke/bore ratios have received a great deal of attention by the passenger-car engine people as a means for reducing piston friction and providing better breathing at the high-speed ranges in which these engines operate. This factor should not be overlooked regarding its application to tractor engine design. It should be pointed out, however, that the advantages of low stroke/bore ratio may not be as great in a tractor engine because of the lower operating speeds involved. Since combustion chamber surface-to-volume ratio increases as stroke/bore ratio is lowered for a given cylinder displacement, greater heat losses to the combustion-chamber walls are incurred. Therefore a balance must be struck between friction reduction and reduced thermal efficiency to obtain the optimum gains in performance and economy.

(3) One of the most important items required for fullest fuel utilization is control of ignition

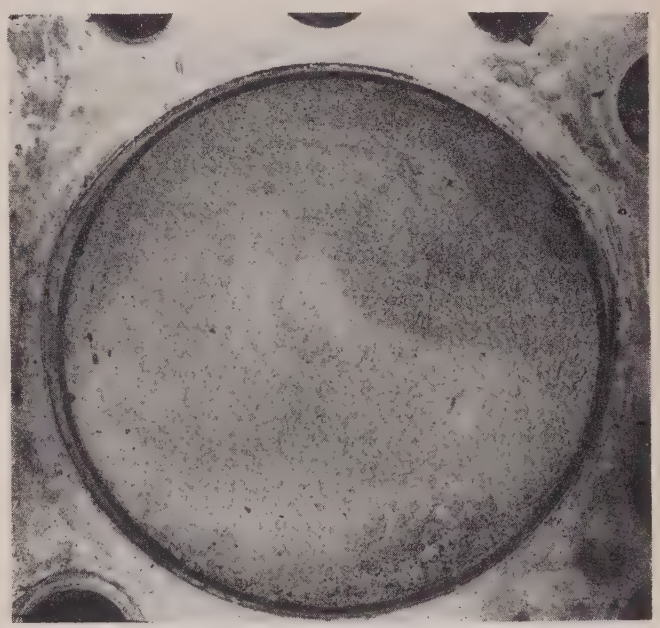

Fig. 19 – Combustion-chamber deposits on piston. Compression ratio 12/1. Condition representative of all cylinders after approximately 600 hr of operation on fuels containing 3-4 ml of tel per gal

timing. When it is realized that in some engines a degree variation in spark advance can raise the fuel requirement by one octane number, it follows that major attention to the distributor advance mechanism is warranted. Of perhaps even greater importance is the matter of drive application to this accessory. Torsional vibrations transmitted to the advance mechanism from the drive can cause serious flutter or fanning of the spark timing. Obviously, such effects must be minimized to control detonation and provide stable operation.

(4) Coolant temperature can have a marked effect on the knocking tendencies of an engine. Usually, local hot-spots cause the trouble rather than high mean temperature of the coolant. Therefore the control of coolant flow to all parts of the jacket is essential if uniform temperatures are to be maintained.

Conclusions

A tractor engine integrating many of the present passenger-car engine design features (high volumetric efficiency, low friction, high compression ratios) is practical and provides similar gains in power and economy, and fuel antiknock quality utilization.

The studies at 7/1, 9.5/1 and 12/1 compression ratios indicate attractive gains in power and economy are possible when advantage is taken of the upward trend in fuel antiknock quality.

As reported by T. H. Morrell, chief engineer of Oliver Corp., "The performance of this engine in a tractor chassis demonstrated that as far as ease of starting, flexibility, and smoothness are concerned, there are no operational problems which limit the use of compression ratios up to 12/1."

DISCUSSION

Emphasizes Importance Of Low Friction Factor

—B. G. Burnside
Ford Motor Co.

THERE are two things on which I wish to comment. The first is fuel economy, and the second is octane requirements.

The realization of better fuel economy based upon lower friction is, to my mind, the most important gain that can be realized by the engine designer today. The present trend in low friction engine design is well illustrated or confirmed by the recent introduction of new engines by automotive engine builders. While it is quite true that the low friction factor is much more important at higher engine speeds, yet we have much to gain at lower engine speeds, and especially so in part-throttle operation. This is clearly shown in Fig. 7 of the authors' paper, for you will note that an appreciable economy gain was realized at the lower or fractional load values. The lower friction values may be realized by several design factors. One is the lower stroke-to-bore ratio, and the others, improved bearing design, low expansion or low friction pistons, and good piston-ring design.

As an example of low stroke-to-bore ratio design, one of our production passenger-car engines having a 0.885 ratio shows 15-psi fmep at 2000 rpm. The reference engine in the authors' paper having a stroke-to-bore ratio of 1.2 shows an fmep of 22 psi at 2000 rpm. Also, a comparison of our present production 4-cyl engine having a stroke-to-bore ratio of 1.025 with our past production engine having a stroke-to-bore ratio of 1.18 shows 17.5-psi fmep at 2000 rpm, which is 12% less than our former engine, and an economy improvement at wide open throttle of 10%.

The second item on which I wish to comment is the octane requirement of the test engine which the authors present in Figs. 12 and 13. In looking at the high requirements for the 7/1 compression ratio, we might well become alarmed. But this characteristic is quite common in dynamometer results obtained on our new engines. However, we believe that we must evaluate the octane requirements on the basis of actual operation, and this suggests that we must develop new techniques for field observations for octane requirements on tractor engines. Our dynamometer method is similar to the method we use for passenger-car engines, and we find a discrepancy of anywhere from five to seven octane numbers between dynamometer and field results. It is my opinion that a similar allowance may be made for octane requirements when tractor engine tests are run on the dynamometer.

Reports Similar Test Program With Compression Ratios to 8/1

—J. H. Eby
International Harvester Co.

IT is assumed that pressure-time data were not obtained with the 9.5/1 and 12/1 ratios, since no mention of them was made in the paper. Comparative peak firing pressures, rates of pressure rise, ignition delay, and preignition tendencies would be of particular interest. Regarding changes made in the connecting-rod and piston assembly, we are wondering what changes could possibly be made to effect a 23% reduction in friction.

We have engaged in a similar development program involving increased compression ratios. However, we limited our investigations to compression ratios expected in the foreseeable future. The basic Super "H" valve-in-head engine was arbitrarily selected as a suitable unit for our program. Since it is generally agreed that basic design characteristics of the engine should be developed prior to starting a program of this kind, certain modifications were made in the cylinder head and induction system which were intended to make the engine fully responsive to increases in compression ratio. To date, information has been obtained with compression ratios of 6.6/1, 7.5/1, and 8/1. The increases in ratio were obtained by using individual cylinder heads all having the same basic shape combustion chamber, but having different volumes as required. A production 6-v battery ignition system and regular spark plugs were used. These tests have shown from 3½% to 5% improvement in economy and horsepower at 7.5/1 ratio, and from 6% to 8½% at 8/1 when compared to the 6.6/1 ratio.

Structural Design of High-Speed Propellers

F. B. Stulen, Propeller Division, Curtiss-Wright Corp.

This paper was presented at SAE National Aeronautic Meeting, Los Angeles, Oct. 9, 1954.

DURING the last few years, high-speed wind-tunnel tests of propellers have shown that, contrary to earlier predictions, good propulsive efficiencies are possible at high subsonic and transonic forward speeds provided the blades are designed with sufficiently low thickness ratios. In addition, detailed aerodynamic analyses of propellers have indicated that satisfactory efficiencies can be expected at supersonic speeds provided very thin profiles are employed along the entire blade

VARIOUS structural problems encountered in the design of high-speed turboprop propellers are discussed in this paper.

Formulas for a number of design factors are also given here. These include:

1. **Blade efficiency.**
2. **Power capacity.**
3. **Advance/diameter ratio.**
4. **Limiting tip speed.**
5. **Periodic lift.**
6. **Propeller normal force and moment.**

The paper also describes two types of vibration occurring with turboprop installations:

1. **First-ordered aerodynamically excited vibration.**
2. **Subsonic stall flutter.**

The author shows how these vibrations may be accurately predicted and controlled by proper design of the propeller blades.

The Author

F. B. STULEN is chief technical engineer with the Propeller Division of the Curtiss-Wright Corp. He received his B.S. in Mechanical Engineering from the Carnegie Insitute of Technology in 1931. The following year he received his M.S. in Aeronautical Engineering from the same school. After being an instructor of mathematics at Westminster College and working for the Gas Industries Co., he joined the Aviation Division of the Pittsburgh Screw & Bolt Corp. In 1939, when this Division was purchased by Curtiss-Wright, Mr. Stulen became its chief blade design engineer.

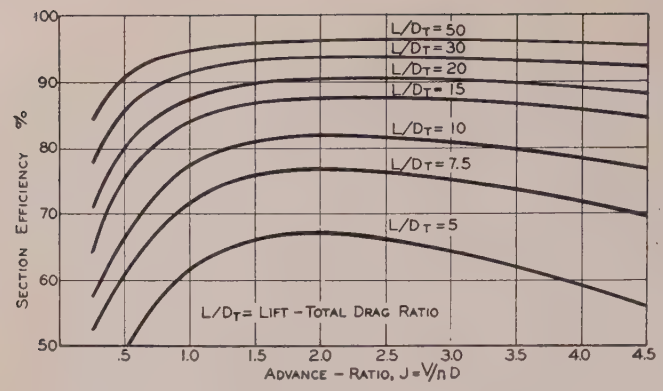

Fig. 1 – Efficiency of the 75% radius section as a function of advance ratio and lift/drag ratio

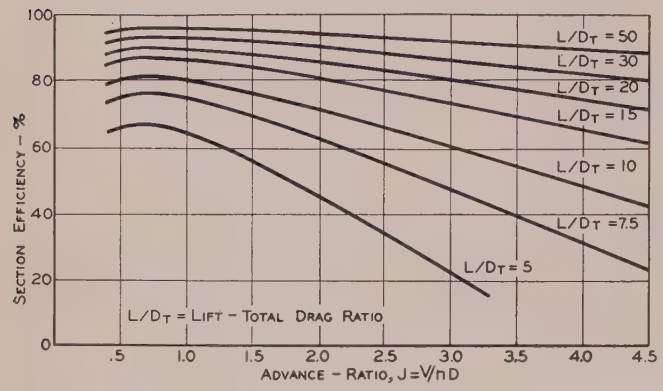

Fig. 2 – Efficiency of the 25% radius section as a function of advance ratio and lift/drag ratio

length. The success of such designs depends, of course, on the stresses which these designs must withstand in service. The structural design of high-speed propellers will be discussed in this paper.

Powered by Turbine Powerplants

High-speed propeller-driven airplanes will be powered by turbine powerplants since these are capable of developing the very large powers required for high-speed flight at low specific weights and at excellent specific fuel consumption. Fortunately, it has been found that there are only a few types of vibrations which may arise in turboprop installations and that these vibrations may be accurately predicted and controlled by proper design. One type is the first-ordered aerodynamically excited vibration, and another which could occur is subsonic stall flutter.

Tests on a number of turbines have shown that there are no major vibratory stresses induced in the blades which are traceable to the turbine itself (although certain high-frequency, low-amplitude vibrations from turbine unbalance and gear tooth passage sometimes cause vibrations of certain components of the pitch-change mechanism). For this reason, the operating stresses of turboprops are readily predictable in contrast to propellers installed on reciprocating engines. Even the most carefully balanced reciprocating engine is capable of generating a large spectrum of vibration frequencies and amplitudes, particularly when malfunctioning operation occurs, and this condition makes it difficult for the propeller designer to foresee all the possible vibratory modes of a new design for installation on a reciprocating engine.

The design of an aircraft propeller involves a compromise between the requirements of good aerodynamic performance and an adequate margin of safety for any operating condition. These structural and aerodynamic requirements are not always compatible; and, for this reason, it is not possible to discuss the structural design of a propeller without first considering its aerodynamic requirements.

Propeller Efficiency

The aerodynamic requirements of a propeller for a specified engine-airplane combination are usually as follows:

1. High propulsive efficiency for the cruise conditions of operation.
2. High take-off and climb thrust.
3. Satisfactory efficiency at the maximum speed condition of the airplane.

The maximum efficiency of a propeller at cruise or maximum speed occurs when the sections of blade in the outer part of the blade are operating at blade angles near 45 deg and are loaded to a point near the maximum lift/drag ratios of these tip sections. However, the blade sections in the inner third of the blade length are oriented at section angles near 90 deg so that the drags of these stations are opposite to the direction of flight and directly decrease the total thrust of the propeller. Furthermore, these inboard drags are roughly independent of the shaft power to the propeller. When a propeller is to operate at its peak efficiency, it is necessary that the power supplied to the propeller be greater than that necessary for the peak efficiency of the outboard sections in order to "mask" the effect of the more-or-less constant drag losses of the inboard sections. That is, the peak efficiency of a propeller corresponds to a load somewhat in excess of that required for the maximum L/D of the outboard sections. This overloading also permits smaller diameter propellers and corresponding weights.

The efficiency of any blade element may be calculated by the formula:

$$\eta = \frac{L/D_T - J/\pi x}{L/D_T + \pi x/J} \qquad (1)$$

where:

η = Section efficiency

L/D_T = Lift to *total* drag of the section

J = Advance ratio of the propeller

x = Proportional blade radius = radius of section divided by the tip radius

The symbol J in the above formula is the well-known advance/diameter ratio, or simply the "advance ratio," and is the major independent parameter commonly used to describe the power and thrust relations of a propeller. This quantity is the distance that the propeller moves forward in one revolution measured in terms of the propeller diameter as a unit of distance. The lift/drag ratio is defined as the ratio of lift to the *total* drag of the blade profile. In subsonic propellers, the total drag is the sum of the section profile drag and the induced drag (similar to the induced drag of wings).

The section efficiency of the 75% radius has been shown as a function of the advance ratio for various lift/drag ratios in Fig. 1. Here it is seen that reasonably good efficiencies are obtained in the outboard or working portion of a blade provided the lift/drag ratio exceeds about 8 to 10 and provided the advance ratio is neither too low nor too high. Although the peak efficiencies of the outboard profiles occur near an advance ratio of about 2.0, a practical high-speed propeller is designed to operate at some higher advance ratio, say from 2.5 to 3.5, as will be discussed later.

The efficiencies of those blade elements located inboard of, say, the 40% radius are generally not high, since these elements must be operated at excessive blade angles. The efficiencies of the 25% radius element are plotted in Fig. 2. The efficiencies are seen to drop rapidly when the lift/drag ratios are less than about 15/1. For this reason, propellers should be designed so that a minimum of power is absorbed in the inner portion of a propeller.

The maximum two-dimensional lift/drag ratios of propeller airfoil profiles have been plotted for various Mach numbers in Fig. 3. Here it is seen that lift/drag ratios in excess of 10 are possible at supersonic speeds provided the thickness ratios of the profiles are not greater than 2 to 3%.

Power Capacity of Propellers

When a propeller is analyzed today for its aerodynamic efficiency, a detailed integration procedure, called "strip analysis," involving the aerodynamic characteristics of the various profiles along the blade length, is undertaken for each important operating condition of the airplane. Although the propeller aerodynamicist can determine the optimum propeller design for any specified operating condition by means of strip analysis, the complexity of this procedure obscures to the airplane designer the fundamental relations involved in propeller selection. To understand the manner in which the basic parameters affect the power capacity of a given propeller, the following formula may be used as a rough guide:

$$HP = K\, q\, D^2\, V_t \left[B \frac{b_{0.7}}{D} \right] C_{L_{0.7}} \frac{1}{\sin \phi_{0.7}} \qquad (2)$$

where:

HP = Shaft horsepower

$q = \frac{1}{2} \rho V^2$, psf

D = Propeller diameter, ft

V = Airplane velocity, fps

V_t = Rotational tip speed, fps

B = Number of blades

$b_{0.7}$ = Chord of the blade at 70% radius

$C_{L_{0.7}}$ = Lift coefficient in the outer part of the blade (70% radius)

$\phi_{0.7}$ = Apparent wind angle at 70% radius

The formula has been found to be reasonably accurate (within about 10% of precise values) and applies only to normal flight conditions (not take-off or early climb). The value of sin $\phi_{0.7}$ is between 0.70 to 0.80 for cruise or high speed. The values of the constants are given in Table 1.

The operating lift coefficient at the 70% radius for maximum efficiency at cruise or high speed is between 0.30 and 0.5 for subsonic propellers and is roughly between 0.15 and 0.25 for propellers designed for supersonic forward speeds.

From an examination of equation (2), it is seen

Table 1 – Values of K

Type of Propeller	Low Blade Angle (25 Deg)	High Blade Angle (50 Deg)
Subsonic	0.00038	0.00035
Supersonic	0.00040	0.00027

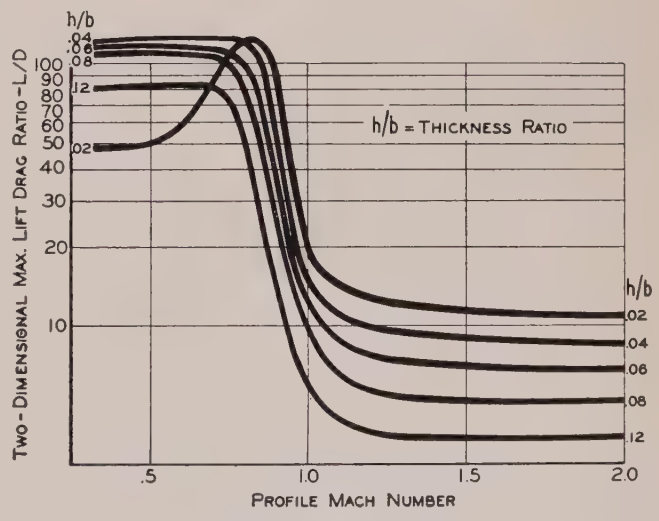

Fig. 3 – Two-dimensional maximum lift/drag ratios for NACA 16 series profiles having optimum design and operating lift coefficients

that the power-absorption capacity of a propeller of a given diameter designed for a given airplane condition is dependent on the *total solidity* $\left(B\frac{b_{0.7}}{D}\right)$ at the 70% radius and not the solidity of one blade. In other words, a propeller of eight blades has roughly the same power capacity as a propeller of four blades having double the chord values. The question, therefore, arises as to the number of blades which a propeller should have for best efficiency. In subsonic propellers, the momentum loss in the slipstream decreases as the number of blades is increased, whereas the total *profile* drag loss remains unchanged if blades having profiles of equal thickness ratios are employed. However, this gain from reduced momentum losses may readily be offset if proper attention is not paid to the design of the inboard sections. If the inboard sections remain the same size and only the outboard profiles are changed in chord, then there is usually a loss in efficiency as the number of blades is increased since the profile drag loss of the inboard sections is increased. There are also a number of other factors to be considered in the choice of the number of blades.

How Prop Diameter Can Be Decreased

Referring again to equation (2), it is seen that the diameter of a propeller can be decreased provided its total solidity is increased. However, the required solidity increases rapidly as the diameter is decreased. Furthermore, the induced or momentum losses increase so that the practical amount of diameter reduction is limited by these two considerations.

Another point of interest to note is that, as the airplane speeds increase, the diameter required to absorb a given power decreases. Since large increases in power are required for transonic and supersonic speeds, the above effect is such that no significant change in the diameters of current propellers is contemplated for transonic and supersonic speeds. In addition, at transonic forward speeds the importance of the value of the diameter on the momentum loss in the slipstream becomes less than that at subsonic speeds. For supersonic and transonic speeds where very large powers are involved, the following methods are contemplated for absorbing these powers using propeller diameters now in current use:

1. Increasing solidity by increased blade chords.
2. Increasing the number of blades by single-rotation tandem units.
3. Increasing the tip speed.
4. Loading the propeller as high as possible without a large sacrifice in efficiency.

One or more of these methods of increasing the power capacity of propellers for high-speed flight is available. Propellers of conventional diameters (13 to 15 ft) having eight or more blades arranged in two rows of four each can efficiently absorb very large powers at high speeds provided the section thickness ratios are maintained at low values along the blade radius. For example, a conventional-size propeller of eight blades of conventional widths will absorb greater than 20,000 hp at forward Mach numbers exceeding 1.5 with reasonably good efficiency at altitude, provided low section thicknesses are used.

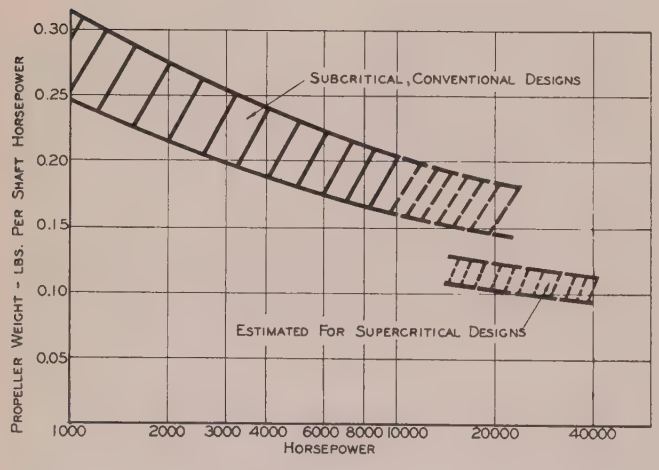

Fig. 4 – Trend in single-rotation propeller weights with shaft powers for conventional shaft mounting

Centrifugal Loads and Weights

As discussed previously, the propeller diameter and solidity for maximum efficiency at cruise or maximum speed, given the power and altitude of operation, are selected so that the operating lift coefficient results in the highest ratio of lift to total drag and so that the advance ratio is in the proper range. In many cases, however, the demand for high static thrust results in a propeller size which is somewhat larger than the optimum for high speed so that the propeller is "underloaded" at high speed. If this compromise is too great in favor of the static thrust, large losses in high-speed efficiency may occur.

Although the advance ratio is one of the major parameters affecting the efficiency of a propeller, as shown in Figs. 1 and 2, it is also a major factor determining the centrifugal stresses and centrifugal loads of the blades. Since the centrifugal stresses and loads vary directly with the square of the rotational speed, it is important to keep the rotational speed as low as possible. This is equivalent to operating the propeller at as high an advance ratio as is practical. For this purpose, the advance ratio may be converted to a more convenient form as follows:

$$J = \frac{V}{nD} = \pi\left(\frac{V}{\pi nD}\right) = \pi\frac{V}{V_t} \qquad (3)$$

where V_t is the rotational speed of the tip of the

propeller in feet per second.

Referring to equation (3), it is seen that increasing the advance ratio for the design condition will greatly reduce the centrifugal loads in the propeller. Referring to Fig. 1, an increase of the advance ratio from 2.0 to 3.0 reduces the efficiency only about 1.2% for an L/D value of 10, whereas the centrifugal stresses and loads are reduced to 44% of their former values. This loss in efficiency can be regained by redesigning the sections to lower thickness ratios as permitted by the lower tip speed. The value of the design advance ratio obviously has a marked influence on not only the design of the blades, hub, and pitch-change mechanism but, as a result, on the propeller weight. Furthermore, the value of the advance ratio has a direct relation to the noise level of the propeller.

As discussed in a previous paragraph, the power capacity of a propeller depends on the *total* solidity and not the number of blades itself. The *total* solidity for the higher powers required for transonic and supersonic speeds may be obtained by a relatively few blades of very high individual solidity or a larger number of blades of lower solidity. In those solid blades contemplated for high transonic and supersonic speeds, the blade weight and centrifugal force are proportional to the square of the blade chords. Also, the centrifugal twisting moment of the blades varies as the fourth power of the chords. For these reasons it is seen that lighter propellers for the very high horsepower class may consist of a relatively large number of blades having relatively narrow chords. These blades may be arranged in tandem fashion.

Since the power capacity of a propeller increases with the forward speed and since there has been a process of continual refinement in design over a period of years, the weights of propellers per horsepower have gradually been decreasing as the powers have increased. This trend of weight is shown in Fig. 4.

Maximum Forward Speed of Propellers

The maximum forward speeds which are possible by propeller-driven airplanes may be estimated from the simple considerations of the maximum practical values of the advance ratio and the centrifugal stress. At high speed, the major steady stress in the blades is the centrifugal stress. This stress depends on the mass distribution along the blade, the density of the blade material, and the square of the tip speed. Although the centrifugal stress depends on the actual design details of the blade, it has been found by experience that the maximum centrifugal stress of practical hollow or solid steel blades is between 25,000 and 35,000 psi when the rotational component of the tip speed is 1000 fps. For other blade materials, the corresponding stress range is found by noting that this stress is proportional to the density of the blade material.

If it is assumed that the maximum centrifugal stress is not to exceed a certain percentage of the ultimate tensile strength of the blade material, the limiting tip speed may be estimated. For this purpose, it will be assumed that the centrifugal stress is not to exceed 60% of the ultimate strength and that the operating stress (for steel) is 25,000 psi for a tip speed of 1000 fps. On this basis, the limiting tip speed, V_t, is as follows:

$$\left(\frac{V_t}{1000}\right)^2 = \frac{0.60\,\sigma_\mu}{25{,}000\,\rho}$$

or

$$V_t = 4.9\sqrt{\frac{\sigma_\mu}{\rho}}$$

where:

V_t = Limiting tip speed

σ_μ = Ultimate tensile strength of the blade material

ρ = Density of the blade material relative to that of steel

This relation is substituted into equation (3) from which the limiting forward speed is found to be as follows:

$$V = 1.56\,J\sqrt{\sigma_\mu/\rho}$$

At supersonic forward speeds, the advance ratio should not exceed 3.5, since higher values cause relatively large losses in the propulsive efficiency.

Table 2 – Maximum Forward Speeds of Propellers

Material	Ultimate Tensile Strength, psi	Relative Density	Maximum Forward Speed, mph	Mach Number at Altitude
Steel, SAE 4340	140,000	1.00	1400	2.1
Steel, SAE 4340	280,000	1.00	2000	3.0
Aluminum Alloy, 76S-T6	75,000	0.36	1700	2.6
Titanium Alloy	180,000	0.58	2100	3.1

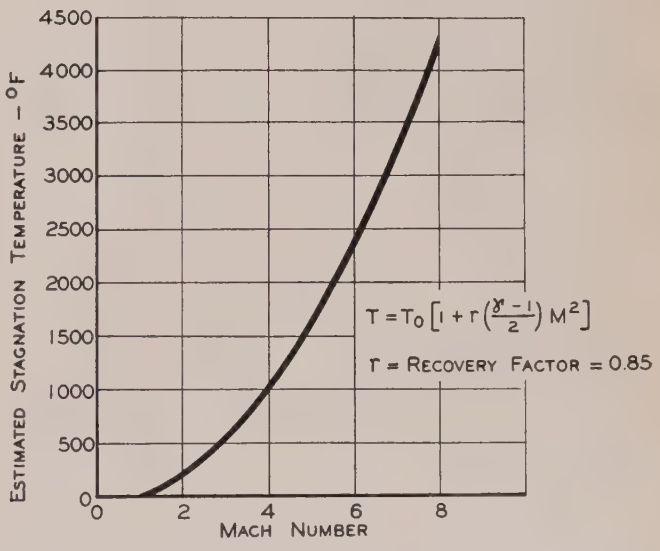

Fig. 5 – Estimated stagnation temperatures for supersonic speeds at altitude

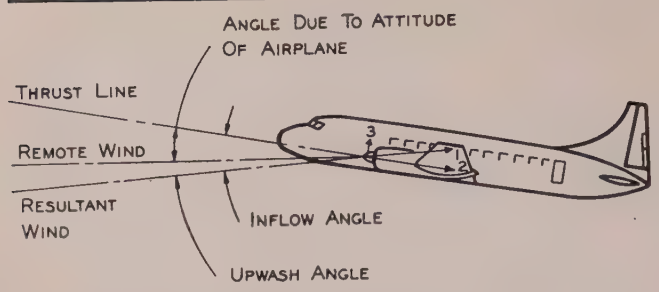

Fig. 6 – The inflow angle and the resolving of the inflow velocity (1) into an axial component (2) and pitch component (3)

Using this limiting value, maximum forward airplane speeds have been estimated and are given in Table 2.

The foregoing simplified analysis demonstrates that the limiting forward speed of a propeller is primarily dependent on the specific strength of the blade materials for the temperatures involved at these high speeds. The stagnation temperature at a forward Mach number of 3.0 is estimated to be 500 F at altitude (see Fig. 5), and this temperature is near the maximum which these materials may withstand at high steady stresses. Above a Mach number of 3.0, the stagnation temperature rapidly increases so that this thermal barrier, in itself, limits the forward speed of propellers using present-day alloys. For these reasons, the maximum forward Mach number of propellers appears to be in the range of 2.5 to 3.5.

The 1x*P* Vibration of Propellers

Prior to about 1946, the major source of vibratory stress in the blades for "clean" tractor airplanes was the reciprocating engine itself. The only major cases where disturbances in the air stream entering the propeller disc were sufficient to excite high vibratory stresses in the blades were pusher installations. When a propeller is mounted behind the wing or the fuselage, the forward disturbance to the airstream may be sufficient to excite undesirable vibratory stresses in certain rpm ranges. After World War II, a type of aerodynamically excited vibratory stress became significant in certain tractor installations. This vibration occurred at a frequency equal to the rotational speed of the propeller and has been designated as the first-ordered, or 1x*P*, vibration (one times the propeller speed). This type of propeller vibration is present when a propeller is operating in a nonuniform airstream, and since this is always true to some degree, 1x*P* blade stresses are always present. This angularity of the airstream into the propeller disc is influenced by the angularity of the thrust line with the direction of flight; by velocity disturbances due to proximity of the fuselage, wing, and nacelle to the propeller; by induced effects of adjacent propellers; and by the actual pitch or yaw attitude of the airplane or both pitch and yaw.

In the past, conventional propellers could satisfactorily handle this vibration in most installations, without particular consideration being given to the airplane configuration. This was due primarily to the fact that former blade designs were of low activity factor and that the thicker inboard blade sections were less sensitive to the lower 1x*P* excitation typical of that time. However, with the increased speed, engine power, and wing loading of present-day aircraft, propeller blades of thinner sections and higher activity factors were required. These factors increase the 1x*P* excitation while the thinner sections and higher activity factor effect an increased sensitivity of the blades to the 1x*P* excitation.

Cause of 1x*P* Vibration

The 1x*P* vibration is caused by the periodic lift forces on the blades induced by the blade sections experiencing an oscillating change in their angles of attack when the propeller shaft is inclined to the direction of flight. In order to obtain a clearer concept of this vibration, the changes in the angle of attack of a blade section will be followed for one complete revolution when the airplane is assumed to be in a climb attitude such that the thrust axis is at a positive angle with the direction of flight.

The local inflow velocity into the propeller disc can be resolved into two components as shown in Fig. 6: one in the plane of rotation and normal to the thrust axis, and the other normal to the propeller disc. The latter vector, being uniform throughout the propeller disc, will not excite vibration; whereas the vertical component will change the relative rotational speed of a given blade section as the blade rotates. It is this upward velocity in the plane of rotation which creates the cyclical lift forces. When the blade is at the horizontal position 1, Fig. 7A, the rotational velocity of the blade is in the same direction as the upward component of velocity; thus the relative tangential velocity of the blade is decreased. It can be seen from Fig. 7A that the effect of a decrease in rotational velocity, shown by the dotted lines, is a decrease in the angle of attack of the blade section. As the blade rotates to the vertical position 2, the blade profile will experience no significant change since the rotational velocity is perpendicular to the upward flow of air. In position 3, when the blade is on its downswing, it opposes the upward current, thus increasing the relative rotational velocity of the blade. A relative increase in rotational velocity, as shown in Fig. 7B, results in an increase in blade angle of attack. Continuing its downswing, the blade arrives at the vertical position 4 and the effect is the same as for position 2 since the two velocities are once again at right angles to one another. Finally, the blade returns to position 1 and the cycle is repeated. Thus, in one

complete revolution of the propeller, each blade section is subjected to an increase and a decrease in lift force, maximum and minimum values occurring at the horizontal blade positions. No significant change in average lift of the blade sections occurs at the vertical positions of the blade. This cyclical change in blade lift induces a bending vibration with a frequency exactly equal to propeller rotational speed.

The equation for the maximum 1xP periodic lift is derived by determining the additional lift due to the maximum change in angle of attack and the change in helical velocity. The oscillating lift caused by the angle-of-attack change may be estimated by means of the steady-state lift formula, substituting for the lift coefficient the maximum change in angle of attack and the slope of the lift curve. The effect of the change in resultant velocity is obtained by taking the derivative of the same lift formula with respect to the resultant velocity. The equation for the maximum periodic lift is then found to be:

$$\Delta L = \frac{A\,q}{57.3}\left[\alpha + 2\,C_L \cot \phi_o\right] b\,\Delta r \qquad (5)$$

where:

ΔL = Alternating lift for blade radius increment, Δr

A = Angularity of airflow into propeller disc, deg

q = Airplane dynamic pressure, psf

α = Slope of lift curve for the blade section including compressibility and inflow effects, radians^{-1}

b = Blade chord, ft

C_L = Average lift coefficient of the blade section

Δr = Incremental blade radius, ft

ϕ_o = Apparent wind angle of the blade section

From this relation for the maximum value of the periodic lift, it is apparent that the resulting 1xP vibratory forces are proportional to:

1. The "Aq" factor where the angle, A, is the air inflow angularity, and the quantity, q, is the dynamic pressure of the airplane, (not the propeller section "q").

2. Blade chord, that is, the wider the blade the greater will be the induced 1xP vibratory forces.

The Aq Factor

The Aq factor in equation (5) is an important parameter to the propeller designer in estimating the magnitude of the 1xP vibration for a given propeller installation. For this reason, it is of primary importance to determine the air inflow angularity into the propeller disc throughout the range of operating conditions for the airplane. Because the vibratory stresses of the blade are proportional to the value of Aq and because this factor is independent of the propeller characteristics, it is called the "excitation factor." The Aq curve for a typical tractor airplane is shown in Fig. 8.

During the initial climb with the use of the full flaps, the Aq values are generally small because the attitude of the airplane is reduced by the flaps. However, for tractor installations with the thrust line below the wing zero lift line, the maximum positive Aq is obtained at the lowest climbing speed without flaps. As the airplane speed is increased, the Aq value decreases steadily until the maximum negative value is reached at the maximum indicated air speed of the airplane.

If the thrust line is oriented at a relatively large angle below the zero lift line, excessive excitation may be incurred when the airplane is flown at maximum indicated air speed and minimum weight. Such a condition would be reached, for example, with a highly loaded bomber on a long-range mission which on returning and descending from high altitude would reach its placard speed at a greatly reduced wing loading. The negative values of Aq resulting from this type of operation can be much larger than those obtained at take-off under maximum loading.

Table 3 – Range of 1xP Excitation Factor

Value of Aq	Relative Magnitude
Less than 1000	Low
1000–1500	Moderate
1500–2000	Moderately high
Above 2000	High

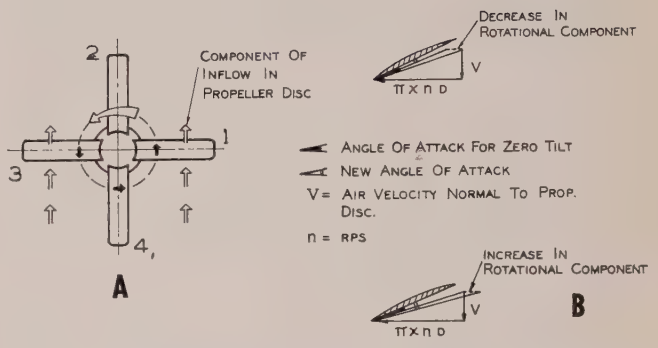

Fig. 7 – (A) Front view of a propeller showing the effect of pitch velocity on the rotational velocity. (B) The effect of change in the rotational velocity on blade angle of attack

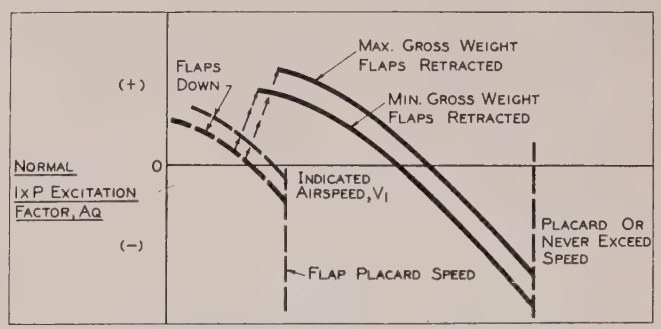

Fig. 8 – The 1xP excitation factor as a function of air speed for a typical airplane

On the other hand, if the thrust line is set near the zero lift line of the wing and the wing loading is large, high 1xP stresses may be expected in the climb condition when the flaps are retracted.

For a well-balanced airplane design, the thrust line should be so chosen that the excitation factor is nearly equal to these two extreme operating conditions. An exception is in the case of military aircraft subjected to high g loads where the Aq at these conditions must be taken into consideration. In Table 3 is shown a range of Aq values and their relative magnitude with respect to one another for evaluating the structural requirements of conventional propeller blades.

In a normal tractor airplane, the excitation factor during climb generally consists of a relatively large inflow angle and a small dynamic pressure. Thus, an error of 1 or 2 deg in the prediction of A causes only relatively small error in the calculated 1xP stresses. However, when the airplane is operating at or near the maximum indicated speed, the 1xP excitation is then the product of a large dynamic pressure and a small inflow angle, ranging from zero to plus or minus a few degrees. For this reason, small errors in the inflow angle will cause large errors in the predicted stresses. For example, suppose that the inflow angle for the placard speed on a certain installation is estimated to be 2 deg, but that the true effective value is 3 deg. This relatively small error of 1 deg would then cause an error of 50% in the predicted 1xP stress values. Therefore, a high degree of precision is necessary for the prediction of the inflow angle and of the corresponding 1xP stresses for high-speed airplanes.

After the excitation factor has been obtained for any given flight condition, the 1xP stresses induced in the propeller blade may be calculated. In order to compute such stresses, the inertia and centrifugal forces in addition to the alternating aerodynamic force must be considered.

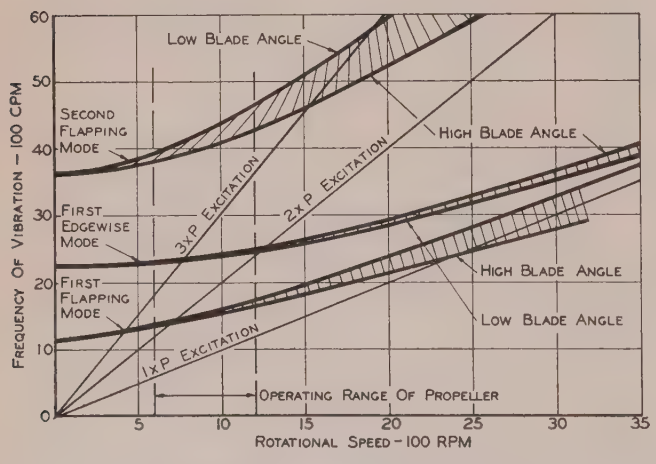

Fig. 9 – Frequency diagram for a conventional subsonic or transonic propeller blade

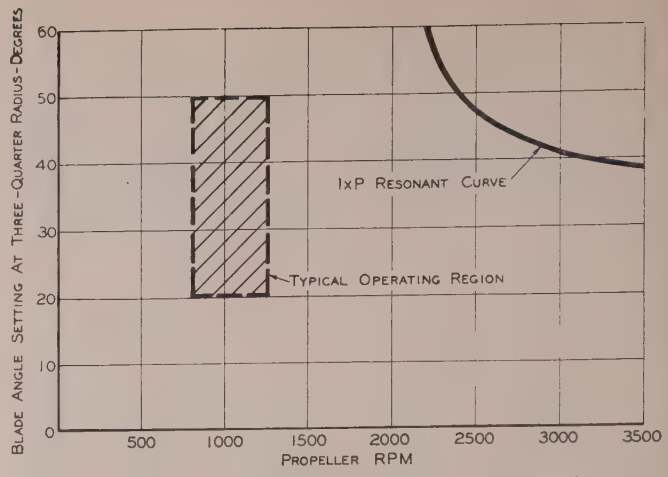

Fig. 10 – Variation in 1xP resonant speed of a conventional subsonic or transonic propeller blade with blade angle setting

A propeller blade is similar to a twisted, tapered cantilever beam subjected to alternating lateral inertia forces as well as centrifugal and aerodynamic forces. The alternating aerodynamic and inertia forces displace the propeller blade sections from the plane of rotation, whereas the centrifugal force and blade stiffness tend to return the blade sections to the plane of rotation. Since the solution for the alternating stresses arising in a vibrating propeller blade is relatively detailed in nature, the method of solution will not be discussed herein.

The magnitude of the vibratory stresses developed in a blade subjected to external alternating forces of a given frequency can be judged by the proximity of the exciting frequency to the frequencies of the natural modes of the blade. As the rotational speed of the propeller is increased, there is additional stiffness of the blades due to the "restoring" action of the centrifugal forces, and hence the natural frequencies continually increase with increasing rotational speeds. A frequency diagram for a conventional propeller design which illustrates the variation of the natural frequencies of the first three modes of vibration with rotational speed and blade angle is given in Fig. 9.

The first-order (1xP) excitation frequency for any given propeller speed is represented by the straight line of unit slope in Fig. 9. In conventional propeller designs, this 1xP excitation line intersects the fundamental natural frequency curve at relatively high rotational speeds and high blade angle settings, and this resonance is usually well removed from the operating speed range of the propeller as indicated in Fig. 10. In conventional propellers the combined dynamic effect is usually small, and the resultant vibratory bending moment acting along the blade is the same order of magnitude as the applied aerodynamic moment. This is illustrated by the curve of Fig. 11, which is a comparison of the

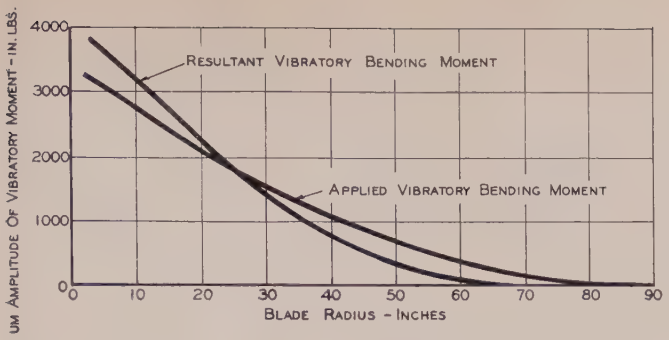

Fig. 11 – Comparison of maximum amplitudes of the applied vibratory bending moment and the resultant vibratory bending moment for a typical subsonic or transonic propeller blade

alternating applied moment along the blade radius to the resultant moment for a conventional propeller operating well below its 1x*P* resonance.

With the trend toward higher-solidity propellers and thinner airfoil profiles required for high-speed flight, the margin between the operating range of the propellers and the location of 1x*P* resonance is gradually reduced. If this margin is reduced significantly the dynamic magnification will become appreciable and excessive vibratory stresses will be encountered. In the design of any propeller blade, it is essential that the 1x*P* resonance of the design be sufficiently removed from the normal operating range of the propeller.

A relatively new type of blade design has been proposed to withstand the high excitation of supersonic propellers. This type of propeller blade, known as a "supercritical" propeller, is designed to operate *above* its 1x*P* resonance throughout its normal range of flight speeds. The basis of this design is that the inertia forces oppose the applied forces (180 deg out of phase) above the resonance, and as a result the "supercritical" design can withstand very high excitation factors and yet be very thin. For this reason, blades of this type are lower in weight relative to an equivalent subcritical design (Fig. 4) and also impose significantly lower centrifugal force and twisting moment loads to the hub and pitch-changing mechanism. A comparison of the applied bending moments to the resultant bending moments for this type of design is shown in Fig. 12.

Propeller "Normal" Force and Moment

The same oscillating 1x*P* aerodynamic lift forces acting on the blade elements which cause the 1x*P* vibration of the blades also create a force perpendicular to the propeller shaft as well as a bending moment on the shaft. This "normal" force and moment are essentially constant with respect to time if there are more than two blades in the propeller. The force has been commonly known as the "side" force, since it is a yawing (or side) force when the airplane is yawed. These quantities are of interest to the airplane designer since they affect the lateral stability of the airplane, particularly at high speed. These quantities are also important in the structural designs of the propeller shaft, the gear reduction housing, the engine mounts, and the nacelle.

The generation of the normal force may be readily visualized by considering the action in a right-hand propeller the axis of which is pitched up in relation to the direction of flight (see Fig. 7). The downswinging blade has a greater-than-average tangential velocity with respect to the air and, therefore, a greater-than-average torque force (which is in the plane of rotation). On the other hand, the upswinging blade has a lower-than-average tangential air speed and, therefore, a lower-than-average torque force. The increment in torque force of one blade and the decrement in torque force of the other are in the same direction and are additive to cause a net lift force on the propeller shaft. These cyclical changes in torque forces are simply components of the corresponding oscillating changes in the lift forces in the blade elements.

There are corresponding oscillating changes in the thrust forces of the individual blades. The downswinging blade generates a correspondingly higher-than-average thrust, while the upswinging blade generates a lower-than-average thrust. This increment in thrust on one blade and the decrement on the opposite horizontal blade create a net bending moment on the propeller shaft. However, there is no significant change in the *total* thrust nor power of the propeller.

Since the blades are vibrating under these conditions, there are alternating inertia forces and resulting inertia moments occurring in the blades. A detailed dynamic study has shown that these inertia forces do not affect the normal force and moment at any operating condition. Another peculiarity of the normal force and moment is that although they are generated by alternating aerodynamic forces they are essentially constant with time (except in two-bladed propellers).

The normal force and moment may be accurately computed by analyzing the aerodynamic forces at each blade element as it rotates through one revolution provided the magnitude and direction of the airflow are known at each point on the propeller disc. Although this integration method is recom-

Table 4 – Values of Constants K_1 and K_2

Planform	K_1	K_2
Round tip	440,000	100,000
Square tip	500,000	125,000

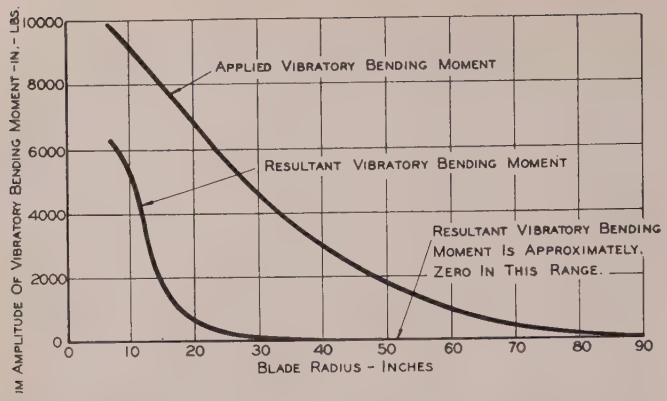

Fig. 12 – Comparison of maximum amplitudes of the applied vibratory bending moment and the resultant vibratory bending moment for a "supercritical" type of supersonic blade design

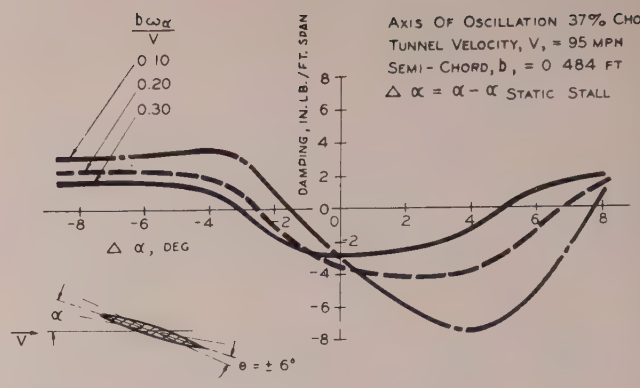

Fig. 13 – Typical variation of work per cycle for pitching oscillation

mended when precise values are required, there are several approximate methods of estimating these quantities for initial studies. One such method has been developed at the NACA and is known as the Ribner method. Another approximate method is given by the following formulas provided the blade planform is essentially rectangular in shape:

$$\left.\begin{aligned} F &= K' \frac{Aq\ B\ AF\ D^2 \sin \beta_{0.7}}{K_1} (\alpha_{0.7} + 2\ C_{L_{0.7}} \cot \beta_{0.7}) \\ M &= K' \frac{Aq\ B\ AF\ D^3 \cos \beta_{0.7}}{K_2} (\alpha_{0.7} + 2\ C_{L_{0.7}} \cot \beta_{0.7}) \end{aligned}\right\} \quad (6)$$

where:

F = Normal force, lb

M = Shaft moment, in.-lb

$\alpha_{0.7}$ = Slope of the lift curve at 70% radius including the compressibility and induced effects

AF = Activity factor of one blade

Aq = 1xP excitation factor, deg-lb per sq ft

B = Number of blades

$C_{L_{0.7}}$ = Operational lift coefficient at 70% radius

D = Propeller diameter, ft

$\beta_{0.7}$ = Blade angle at 70% radius

K' = Constants: 1.10 for moderately stiff blades, 1.20 for blades of normal stiffness, 1.35 for moderately thin blades

The constant, K', represents the contribution from the cyclical torsional deflection of the blade which augments the original cyclical changes in angle of attack. The constants K_1 and K_2 are tabulated in Table 4.

The angle, A, of the inflow is in degrees and is taken at the 70 to 80% radius in computing the shaft moment. For the side force, the inflow angle is chosen at the 50% radius location.

Values as estimated from these formulas for the normal force and moment have been found to agree reasonably well (within ±10%) with available wind-tunnel tests at moderate or high blade angles. The correlation is less accurate at the lower blade angles, that is, angles less than 35 deg at the 75% station.

In dual-rotation propellers, it is generally satisfactory, particularly in preliminary analyses, to assume that the total force is twice that of the front component and that the moments of the two components cancel each other. For more precise values, both components are analyzed, including the mutually induced effects of the components and the time lag in the aerodynamic forces. The inflow angle, A, of the rear component is less than that of the front since the reaction of the front reduces the initial angularity. Tests have shown that the fluctuating forces of the front component are normally somewhat greater, except possibly at low speeds.

Subsonic Stall Flutter

A type of vibration which influences the design of high-speed propellers is subsonic stall flutter. This type of flutter is simply the resonance of the fundamental natural torsional mode of the blades and is not the "classical" flutter encountered in aircraft wings and control surfaces which involves two or more degrees of freedom of the motion. As the name implies, the vibration occurs when the outer blade airfoil sections are operating at angles of attack in the vicinity of their stall angles, and, when it is encountered, it usually occurs at the static take-off and during the early take-off run where the propeller is most heavily loaded. Today, semiempirical methods are available for predicting the regions of occurrence of stall flutter so that the propeller designer can avoid this vibration.

Although the source of the energy which maintains this torsional oscillation of the airfoil is not precisely known, it is believed that this energy is associated with the time lag in the separation of the boundary layer on the airfoil and its reattachment when the angle of attack is lowered sufficiently. Tests conducted on airfoils oscillating torsionally about a spanwise axis in a wind tunnel at low air speeds have shown that energy is required to maintain the torsional oscillation when

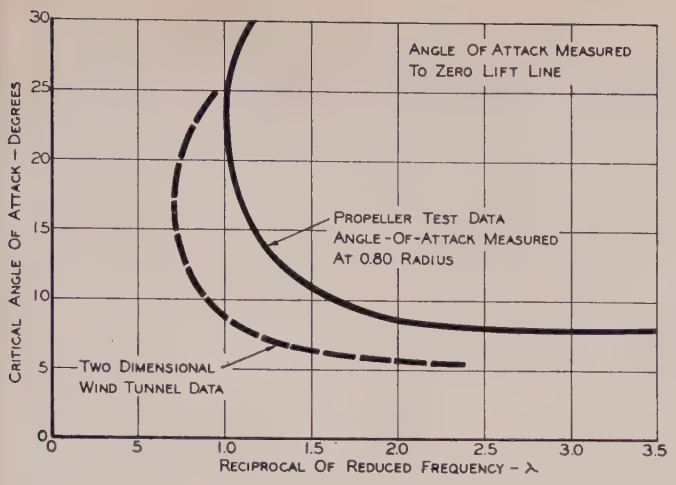

Fig. 14 – Variation of critical angle of attack with modified reduced frequency for stall flutter

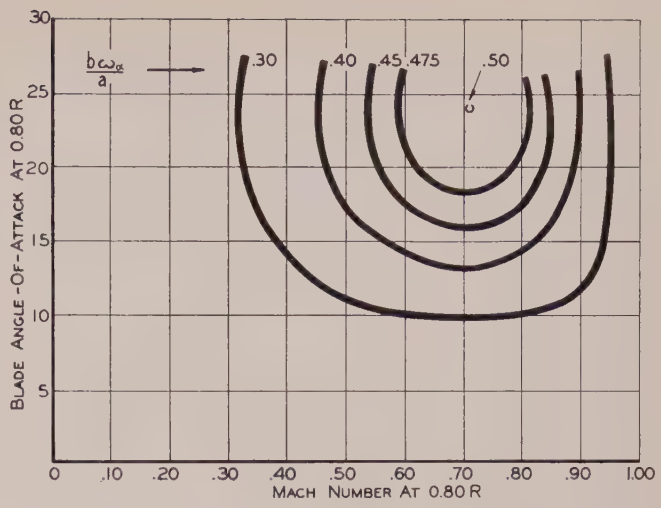

Fig. 15 – Variation of the flutter boundary with the parameter, $b\omega_\alpha/a$

the mean angle of attack is below a certain critical value, whereas energy is absorbed from the airstream when the mean angle of attack is greater than this critical value. Results obtained from one test of this nature are plotted in Fig. 13 where it is seen that the critical angle of attack is also a function of the frequency of vibration.

The cyclical variation of the lift forces on an oscillating airfoil depends on the relative length of the repeating vortex pattern in the wake behind the airfoil as compared to the value of the chord; that is, the number of chords that the vortex pattern moves downstream in one cycle of vibration defines, in part, the forces on the airfoil. This dimensionless parameter describing the geometry of the flow field is called the "reduced frequency" and is defined by:

$$\frac{b\,\omega_\alpha}{V}$$

where:

b = Semichord, ft

ω_α = Frequency of torsional oscillation, radians per sec

V = Air speed, fps

Tests have shown that the critical mean angle of attack at which energy is absorbed from the airstream is a function of this parameter. A plot of the critical angle against the reciprocal of the reduced frequency, λ, is shown in Fig. 14 for a typical airfoil. At high frequency (low λ) the critical angle is substantially greater than the static stall angle, and for a sufficiently high frequency the self-excited vibration will not occur at any angle of attack. The compressible subsonic flow field about an airfoil can be approximated by an incompressible flow field by elongating all distances in the flow direction by the Prandtl-Glauert factor, $1/\sqrt{1-M^2}$, where M is the Mach number of the undisturbed flow. An airfoil in compressible flow,

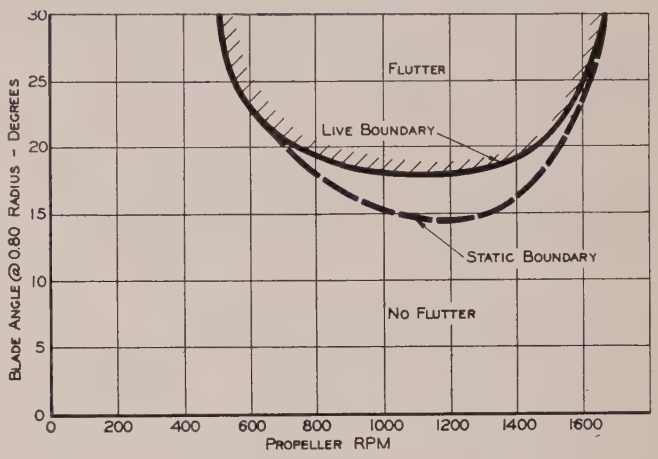

Fig. 16 – Types of flutter boundaries in propeller blades

therefore, behaves as though its semichord were the length, $b/\sqrt{1-M^2}$, and for this reason, the reduced frequency parameter may be replaced by a "modified reduced frequency" equal to:

$$\frac{b\,\omega_\alpha}{V\sqrt{1-(V/a)^2}} \equiv \lambda^{-1}$$

where a is the velocity of sound. This means that Fig. 14 now may be used for subsonic velocities provided the abscissa is replaced by the reciprocal (λ) of the above quantity. The abscissa of Fig. 14 is now no longer a linear function of the airstream velocity. If the chord and frequency of oscillation are given, the curve of Fig. 14 may be transformed into a new curve plotted against the airstream velocity alone. It will be found that each point on the original curve will transform into two points on the new curve. A series of transformed curves are shown in Fig. 15.

Tests have shown that stall flutter of propeller

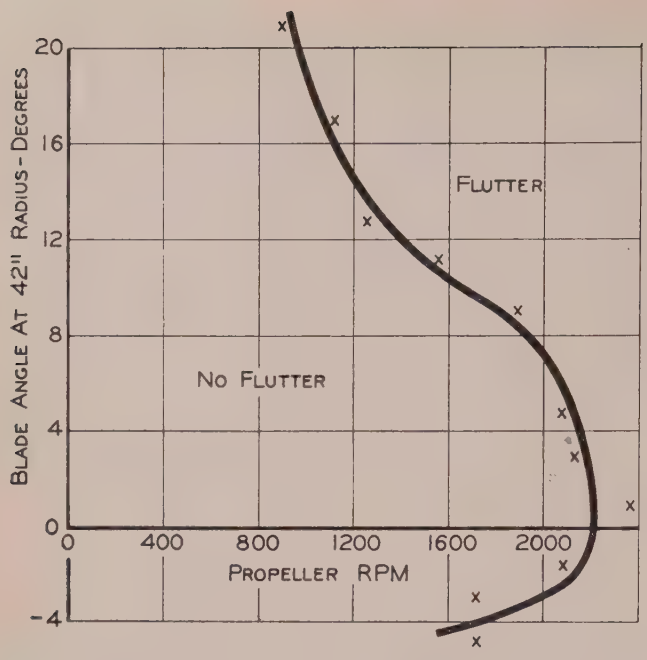

Fig. 17 – Example of closed type of flutter boundary, full-scale propeller test, C644S-B304/109614 supersonic-type propeller

blades usually will not occur if the modified reduced frequency is greater than unity, that is, when:

$$\lambda = \frac{V\sqrt{1-(V/a)^2}}{b\,\omega_\alpha} < 1.0$$

This condition is fulfilled when:

$$b\,\omega_\alpha > a/2 = 560$$

This means that no subsonic stall flutter will be encountered at any angle of attack of the airfoil if the torsional frequency is sufficiently high.

A typical variation of the critical angle-of-attack curve for a two-dimensional airfoil is shown in Fig. 14. The relative position of this curve is influenced by several factors: airfoil characteristics, scale effects, internal damping of the system, and so forth. Correlation with similar curves obtained from propeller tests, also shown in this graph, has shown that such data can be applied to estimate the flutter boundary of a propeller, provided the chord and velocity in the reduced frequency formula are those associated with some representative outboard radius of the propeller. A representative station is that at the 80% radius of the blade. In propeller operation, the blade angle setting with respect to the plane of rotation is a more convenient reference than the angle of attack. This conversion is readily made by correcting for the airflow velocity entering the propeller disc. However, the blade angle corresponding to the angle-of-attack curves of Fig. 14 would represent the live or operating blade angle and is generally further corrected to correspond to the more easily determined static or unloaded blade angle setting by allowing for the torsional twist induced by the thrust and centrifugal forces. Fig. 16 illustrates a normal variation between the live and static flutter boundary. When these corrections are made, a reasonably accurate flutter boundary may be estimated for a given propeller design.

If the blade is exceptionally thin, it will twist up to the stall point under the applied steady aerodynamic and centrifugal loads when a sufficiently high rpm is reached, regardless of the initial blade angle setting. The static boundary at such a condition is called a "closed boundary" and is caused by this torsional divergence. Fig. 17 illustrates the condition of a closed boundary which was discovered several years ago in an experimental supersonic propeller having steel blades with wedge airfoil sections which were only 1½% thick at and near the tip. Such a propeller cannot be operated at the static condition except at very low rpm's.

The foregoing method of computing the flutter boundaries of propellers has been checked for a number of designs. A typical flutter boundary is shown in Fig. 18 where the comparison between the theoretical and experimental values is shown.

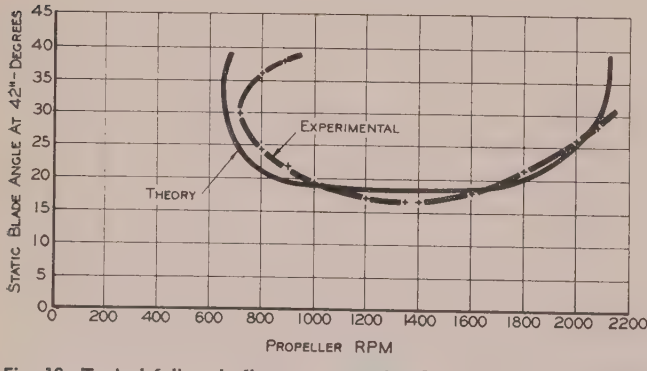

Fig. 18– Typical full-scale flutter test results, Curtiss C544S-A2/109606 propeller, 12 ft 3 in. in diameter (propeller tested as two-way installation)

Other Vibrations

The fundamental and second natural bending modes of propeller blades can be excited by a crosswind when the airplane is operated on the ground with no forward speed. The turbulent condition of the crosswind causes an excitation at a frequency equal to twice the propeller speed, and, hence, these are known as the 2x*P* resonances. The 2x*P* excitation line is shown in Fig. 9 where it is seen to intersect the fundamental curve at a speed near the lower operating speed of a reciprocating engine and of some turbines. This mode can also be excited in flight if there exists sufficient asymmetry of the airstream into the propeller disc.

The location of these undesirable resonances with respect to the operating speed range can be controlled in the initial design of the propeller and are positioned so that they do not occur at the ground idle or take-off rpm's.

Concluding Remarks

This paper has covered the general aspects of the various structural problems encountered in the design of propellers for high-speed installations. As a result of the continued development in the engineering science of propeller design, the propeller designer is now able to predict the structural behavior of designs for installation on modern powerplants with a greater precision than was possible in former years.

Acknowledgment

The author wishes to acknowledge the assistance of his staff at the Propeller Division of the Curtiss-Wright Corp. in the preparation of this paper.

DISCUSSION

Discusses Effects of Engine-Airframe Flexibility

– Robert A. Rogers

Aeroproducts Operations, Allison Division, GMC

MR. STULEN'S very interesting paper covered the parameters that govern the structural design of high-speed propellers. I feel, however, that an additional comment is necessary with regard to the general problem of 1xP propeller vibration and the "normal" forces and moments. This involves the flexibility of the propeller, engine, and airplane combination in both the lateral and vertical directions. This flexibility introduces feedback (the load a function of the deformation) and should be considered in the analyses of propeller blade stresses, "normal" loads and moments, and the effects on aircraft stability.

For illustration purposes, a brief simplified analysis follows in which all induced effects such as wing upwash and fuselage interference are neglected. The airplane is assumed to be in yawed flight.

Symbols used are:

Y_t = Total side load

Y_s = Side load due to spinner

Y_p = Side load due to propeller

θ = Bending angle of propeller hub relative to the undeflected reference line

β = Sideslip angle

β_p = Local propeller side angle of attack

β_s = Local spinner side angle of attack

The total side load is the sum of the propeller and spinner contributions:

$$Y_t = Y_s + Y_p \tag{a}$$

and the local propeller and spinner side angle of attack is given as:

$$\beta_s = \beta_p = \beta + \theta \tag{b}$$

The following relations are assumed to be valid:

$$Y_t/\theta = \partial Y_t/\partial\theta \tag{c}$$
$$Y_s/\beta_s = \partial Y_s/\partial\beta_s$$
$$Y_p/\beta_p = \partial Y_p/\partial\beta_p$$
$$Y_t/\beta = \partial Y_t/\partial\beta$$

Utilizing the previous equation:

$$Y_t = \beta_s \cdot \frac{\partial Y_s}{\partial\beta_s} + \beta_p \cdot \frac{\partial Y_p}{\partial\beta_p}$$

which, by substitution, reduces to:

$$\frac{\partial Y_t}{\partial\beta} = \frac{\partial Y_s/\partial\beta_s + \partial Y_p/\partial\beta_p}{\left[1 - \frac{1}{\partial Y_t/\partial\theta}\left(\partial Y_s/\partial\beta_s + \partial Y_p/\partial\beta_p\right)\right]} \tag{d}$$

This shows that, as the dynamic pressure or indicated air speed increases, the flexibility of the structure plays an increasingly important part in the determination of the side or normal loads as well as the propeller blade stresses. It should also be mentioned that as spinners become larger their contribution in increasing the effective inflow angle at the propeller disc becomes exceedingly important even for an installation with a comparatively high stiffness.

Equation (d) may be used directly to obtain the destabilizing influence of the propeller by means of the propeller stability derivitive, ΔC_{n_β}, thus:

$$\left(\Delta C_{n_\beta}\right)_{\text{prop.}} = \frac{\partial Y_t}{\partial\beta} \cdot \frac{l_p}{S\,q\,b} \tag{e}$$

where:

l_p = Distance from propeller disc to the center of gravity

S = Wing area

q = Dynamic pressure

b = Wing span

In conclusion, this brief analysis may be extended to include the various induced effects in both the pitch and yaw directions. It shows that, not only the flow field at the propeller disc must be known, but that the degree of flexibility as well as the magnitude of the spinner loads must be known and be considered.

ORAL DISCUSSION

Reported by G. H. Arvin

North American Aviation, Inc.

W. Littlewood, American Airlines, Inc.: The charts and equations presented in the paper indicate a calculatable Mach-number limit and a diameter limit for propellers. Is there also a horsepower limit?

Mr. Stulen: Solidity can always be added to the propeller to absorb increased horsepower.

Question: How are take-off conditions at low q taken into account when equation (2) indicates that the horsepower capacity for the propeller is a linear function of q?

Mr. Stulen: The formula I have given is for moderate or high-speed flight only. Different equations are used for take-off or low forward speeds.

M. G. Beard, American Airlines, Inc.: What about the effect on propeller life of nicks and abrasions in regard to supersonic propellers? Airline experience indicates that more material is necessary for adequate life in service operations.

Mr. Stulen: Aerodynamic vibratory stresses of supersonic propellers exist in only about the inboard 10 in. of the propeller blade and are not present in the outboard section of the blade, where nicks and abrasions commonly occur. In turboprop installations, which were the only type discussed in the paper, engine-induced vibrations in the propeller are entirely absent.

Carburetor Icing

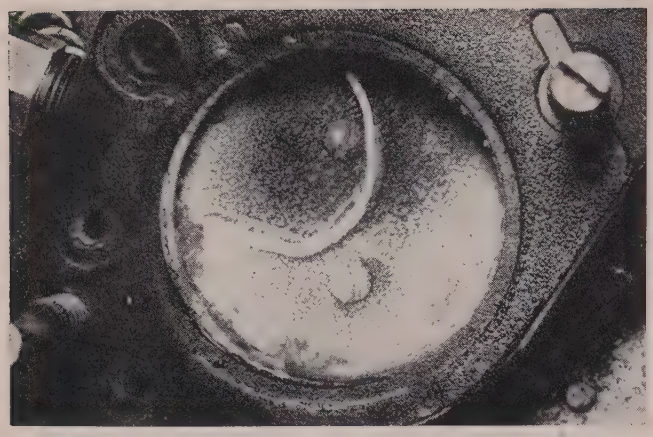

Fig. 1 – Ice formation on throttle blade of engine C

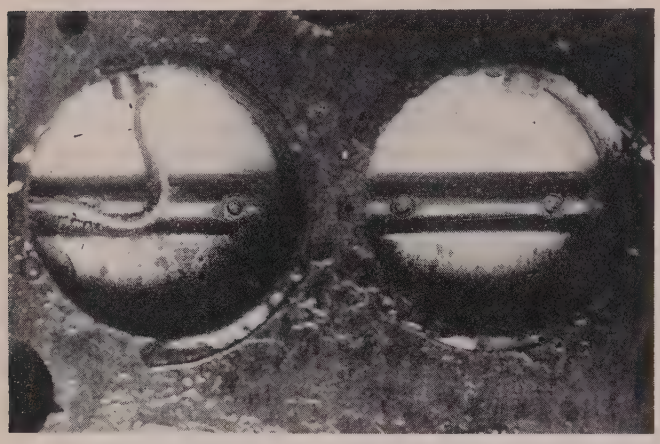

Fig. 2 – Ice formation on throttle blades of engine D

Fig. 3 – Ice formation on throttle blades of engine B

A FACT well known to all those concerned is that the automotive and petroleum industries are constantly striving to improve their products and thus give the motorist more for his money. One item that has received considerable attention over the years is the interrelation of car performance and fuel volatility. For example, the automotive manufacturer has always given careful attention to the starting and warmup performance of his vehicles on commercially available fuels. Conversely, the petroleum refiner has carefully tailored his fuel volatility to suit these vehicles under all climatic conditions.

In recent years, considerable interest has been aroused regarding the interrelation of car performance, fuel volatility, and carburetor icing. Carburetor icing, which, as the name implies, refers to ice formation in the carburetor during warmup, has come into the limelight because its effect – engine stalling – has become more evident in postwar cars. With the advent of automatic transmissions, increased use of automatic chokes, and elimination of the hand throttle, the driver has less control over the engine during the warmup period. Consequently, when ice formation causes the engine to run erratically, there is more opportunity for stalling to occur. Then when the engine does stall, there is the inconvenience of moving the gear selector lever back into neutral and restarting the engine. Under emergency conditions, the time required for this restarting may be partly responsible for an accident.

Conversation with several car and carburetor manufacturers and a study of our own work and that of earlier investigators[1] indicated that when a motorist does encounter stalling due to ice formation during cool, damp weather, it is questionable whether he is aware of the cause. All he knows is

[1] "A New Look at Motor Gasoline Quality—Carburetor Icing Tendency," by J. F. Kunc, Jr., J. P. Haworth, and J. E. Hickok. Paper presented at SAE Annual Meeting, Detroit, Jan. 9, 1951

Tendencies of Some Present-Day Fuels and Engines

W. P. Dugan and H. A. Toulmin
Sun Oil Co. Ethyl Corp.

This paper was presented at the SAE Summer Meeting, Atlantic City, June 11, 1954.

that on certain days and with certain fuels, his car stalls at times during the warmup period. Yet the very next day, on the same fuel, his car operates perfectly. It is quite likely that only when there are a number of days with similar occurrences, will he complain to his car dealer or fuel supplier or both.

As a result of the increased interest in carburetor icing, Ethyl Corp. and Sun Oil Co. decided to conduct a rather extensive investigation of this phenomenon in Ethyl Corp.'s "all-weather" room at their Research Laboratory. The purpose of this paper is to present the results of this work and to try to interpret them in the light of current engine and fuel development.

Stalling Mechanism

The stalling mechanism as described by other investigators[1] was confirmed by this work. This mechanism is as follows. As the fuel evaporates, it removes heat from the surrounding metal parts and considerably lowers their temperature. If the ambient temperature is low enough and if the fuel is sufficiently volatile, their temperature is quickly lowered below 32 F. Any moisture present in the incoming air that comes in contact with these parts immediately begins to form a coating of ice. This ice first appears on the throttle blade and carburetor barrel near the throttle blade. If enough moisture is present in the incoming air, this ice continues to build up until the entire top and edges of the throttle blade are coated. If the throttle is closed, the ice present reduces airflow past the throttle blade until the engine speed is reduced to the stalling point. Although the engine can usually be restarted immediately, the ice formation and the tendency to stall may last as long as 10 to 20 min under the most severe conditions.

Because it is difficult to visualize the appearance and location of carburetor ice, a number of photographs of ice formation were taken. Three of these photographs, showing ice formation in three 1953 passenger-car engines, are included as Figs. 1, 2, and 3. These pictures were taken looking down on the throttle blade. The snake-like object in each picture is a thermocouple wire used in measuring the throttle-blade temperature. In severe cases, this ice formation is great enough that, in order to maintain a given operating speed, it is necessary constantly to increase the throttle opening because

of the buildup around the edges of the throttle blade. In other words, the ice formation is sufficient to restrict airflow even at positions other than closed throttle.

The above discussion has indicated that, for any given engine, a number of things must happen at the same time before stalling due to ice formation can occur. In summary they are: (1) the fuel must be sufficiently volatile, (2) sufficient moisture must be present in the incoming air, (3) the ambient temperature must be low enough so that fuel refrigeration lowers the carburetor metal temperatures below freezing, (4) the engine must be cold, and (5) the engine must be operated in a manner conducive to ice formation and stalling. And, of course, the engine must be one that is subject to stalling in the first place.

When so many things must occur at the same time, it is likely that the carburetor icing problem may not be as extensive as some of the other volatility problems such as starting and warmup, for example. However, since it can and does occur in a good part of the country, any steps taken to eliminate or minimize its effect are worthy of effort.

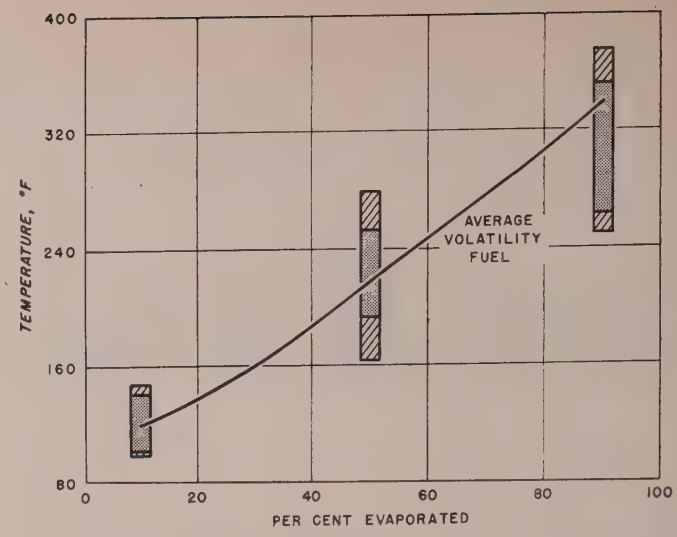

Fig. 5 – ASTM distillation characteristics for volatility reference fuels. The cross-hatched vertical bars represent the range in 10, 50, and 90% points for fuels available in the United States during the winter of 1952-1953. The range in test fuels is shown by the shaded portion of the bars. The fuel distillation curve represents the volatility of the average winter-grade commercial gasoline

Test Procedure and Equipment

After discussing the icing phenomenon with several equipment manufacturers and reviewing our own work and that of earlier investigators,[1] it was decided that a laboratory test program could be laid out that would correlate reasonably well with field results. There was some question as to whether a bare-engine, no-load procedure could be used for this work. To answer this, a brief preliminary program was carried out in which the results obtained on a 1953 passenger car, operated under conditions conducive to ice formation, were compared with those obtained on a bare engine of the same make. This preliminary program indicated good correlation using the following bare-engine, no-load procedure:

1. Start engine.
2. Accelerate to 1500 rpm.
3. Maintain 1500 rpm for 30 sec.
4. Return to idle.
5. Idle for 15 sec.
6. If engine stalls, immediately restart and return to item 2. Otherwise, return to item 2 upon completion of idle period.
7. Continue above cycle until engine performance is satisfactory.

With the procedure difficulties eliminated, the bulk of the program was carried out on six bare engines which were selected either on the basis of sales volume or because of new design features. These engines, which are all 1953 models, are shown in the cold room in Fig. 4, and some idea of the types tested is indicated by Table 1.

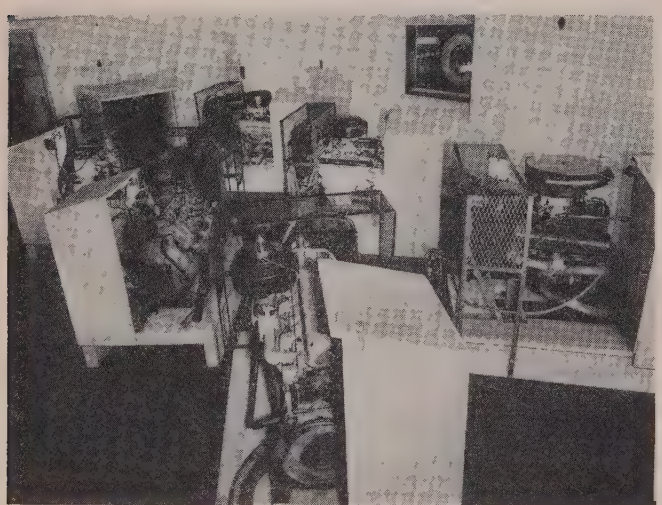

Fig. 4 – Test-engine installations in "all-weather" room. Engines are mounted on portable skids with cooling radiator and fan in place. Air at controlled temperature and humidity is fed into the room through the duct at the rear of the room

Table 1 – 1953 Engine Models Tested

Cylinder Arrangement	Valve Arrangement	Choke Type
6-I	Overhead	Automatic
V-8	L	Manual
6-I	L	Automatic
V-8	Overhead	Automatic
V-8	Overhead	Automatic
V-8	Overhead	Automatic

As will be shown later, the atmospheric conditions most conducive to ice formation were around 40 F ambient with 100% relative humidity, and the bulk of the test work was carried out under these conditions.

Results

General – It has already been stated that carburetor icing does occur in current-model passenger-car engines and that it occurs in amounts sufficient to stall the engine. Its occurrence and effect depend on fuel characteristics, engine design, atmospheric conditions, and operating conditions. The following discussion will treat each of the above items separately and will attempt to point out the most significant relationships in each case.

Fuel Characteristics – In order to define the influence of fuel volatility on carburetor icing, nine test fuels of widely varying volatility were used in this work. One of these fuels was blended to match the volatility of average winter-grade commercial gasoline. Two others were blended to match the extremes in volatility commercially available. The remaining six were designed to determine the effect of 10, 50, and 90% evaporated temperature on icing. Pertinent inspection data on these fuels appear in Tables 2 and 3, while distillation curves are included in Fig. 5.

These tests showed that changes in fuel volatility significantly affect stalling due to icing in some engines. In others, the effect is quite small. The results obtained on all six engines when operating on fuels of high, average, and low volatility are presented in Fig. 6. It is evident from this

A COOPERATIVE study of carburetor icing is described in this paper.

Tests were conducted using 13 fuels of varying volatility in one complete car and six 1953 passenger-car engines. The effects of engine design variables, fuel volatility, alcohol additions to the fuel, and weather conditions were determined.

Ice formation occurred in all engines, but there was a considerable variation in its effect on different engines. As would be expected, fuel volatility significantly influenced carburetor icing, and it is apparent that certain portions of the fuel boiling range exert considerably more influence than other portions. The addition of alcohol to fuels reduced stalling due to carburetor icing. The concentration of alcohol required depended primarily on the volatility of the fuel to which it was added.

The Authors

W. P. DUGAN (J '47) is an automotive research engineer with the Sun Oil Co. He received a B.S. in Mechanical Engineering from the University of Delaware in 1946. That same year he joined the Sun Oil Co.

H. A. TOULMIN (M '44) is supervisor of Vehicle Operations in charge of road testing at the Detroit and San Bernardino Laboratories of the Ethyl Corp. He received his B.S. in Mechanical Engineering in 1942. He worked as a test engineer, and later senior test engineer at Wright Aeronautical Corp. In 1945 he joined Ethyl Corp. as a project engineer.

Table 2 – Fuel Inspection Data

Fuel No.	1	2	3	4	5	6	7	8	9
Inspection Tests									
Initial, F	91	85	92	91	90	88	88	84	96
5 % Evaporated	109	89	111	108	110	100	100	93	101
10%	121	101	141	118	124	117	112	100	150
20%	142	122	183	134	154	145	134	113	202
30%	165	157	208	152	190	179	162	129	227
40%	189	192	218	171	226	201	194	148	239
50%	219	227	226	194	251	213	226	167	250
60%	253	254	233	224	270	222	258	190	261
70%	278	278	245	257	286	230	287	212	280
80%	308	302	272	290	305	239	319	238	313
90%	341	340	342	326	343	262	352	281	364
95%	368	375	398	350	376	287	378	318	391
End Point	441	442	444	384	448	349	430	350	458
Rvp, psi	10.8	13.3	11.2	10.5	9.6	12.5	11.3	14.9	10.3

Table 3 – Variables Investigated – Fuel Distillation Data

Fuels for Studying Varying 10% Evaporated				Fuels for Studying Varying 50% Evaporated				Fuels for Studying Varying 90% Evaporated			
Fuel	10%	50%	90%	Fuel	10%	50%	90%	Fuel	10%	50%	90%
2	101	227	340	4	118	194	326	6	117	213	262
3	141	226	342	5	124	251	343	7	112	228	352

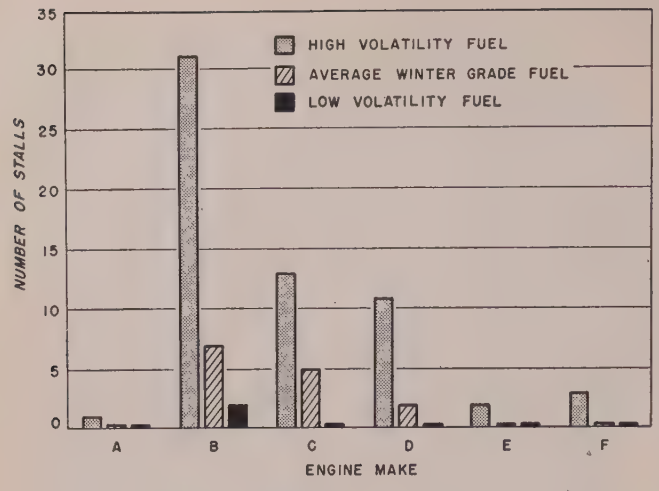

Fig. 6 – Effect of fuel volatility on engine stalling due to carburetor icing in six 1953 passenger-car engines

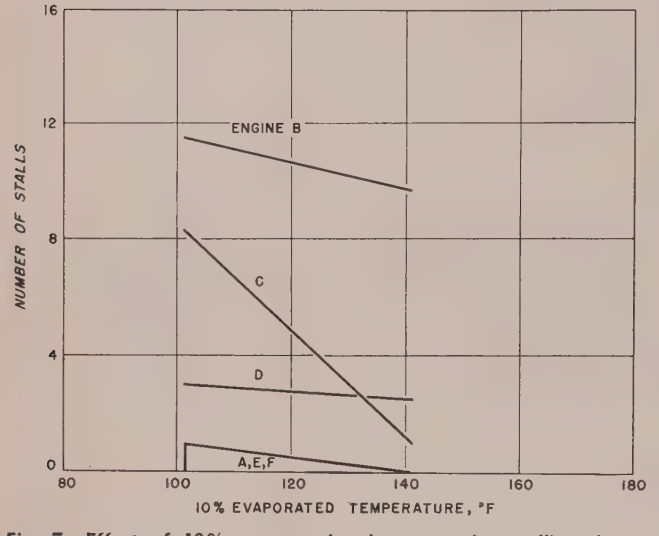

Fig. 7 – Effect of 10% evaporated point on engine stalling due to carburetor icing at 40 F ambient temperature and 100% relative humidity

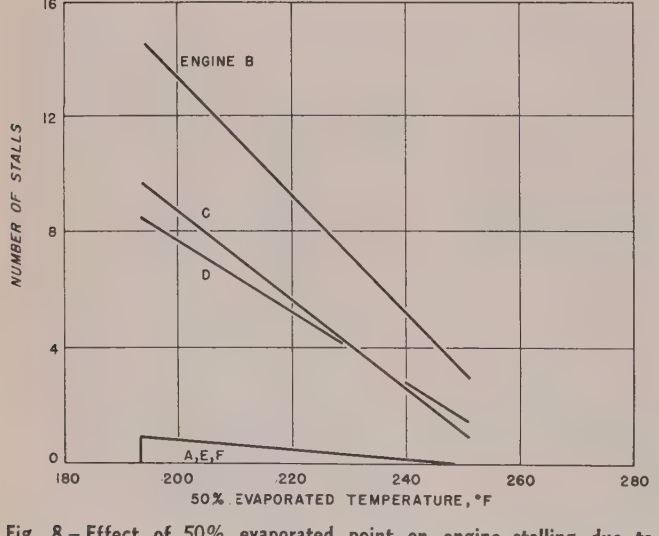

Fig. 8 – Effect of 50% evaporated point on engine stalling due to carburetor icing at 40 F ambient temperature and 100% relative humidity

figure that, not only are there differences between fuels, but there are also differences between the manner in which different engines are affected by fuel volatility. Engine A gives a negligible change in stalling tendency as fuel volatility is decreased. This is because this engine gives so little stalling even on the most volatile fuel that any further reduction in stalling lies within the reproducibility of the test procedure. The stalling tendency of engine B is greatly reduced as fuel volatility is decreased. Engines C and D also show a considerable reduction in stalling as volatility is decreased. Engines E and F give some stalling on the volatile fuel but are stall-free on the average and low volatility fuels. Here again, the stalling tendencies of these latter engines, especially engine E, are so slight that the fuel volatility effects are almost negligible.

The preceding paragraph has clearly indicated that (1) fuel volatility affects stalling due to carburetor icing and (2) the magnitude of this effect varies considerably between engines. Engine stalling can be minimized by fuels of extremely low volatility, but, in making such fuels, the refiner would introduce new performance problems.

Let us now examine the effect of various parts of the fuel boiling range on stalling due to icing. In this work, the effect of 10, 50, and 90% point were independently evaluated in all six engines. The same type of variation occurs here as occurred when changing whole fuel volatility. In other words, some engines give so little stalling that the effect cannot be measured. Others will respond differently to changes in various parts of the boiling range. The effect of 10% point is illustrated in Fig. 7. Engines A, E, and F give negligible stalling and hence a negligible effect. Engines B and D show some decrease in stalling as 10% point is increased, and the stalling tendency of make C is drastically reduced as 10% point is increased. From this, then, it can be said that on engines that are susceptible to stalling, changes in 10% point can influence the number of stalls encountered.

The same reasoning applies to 50% point as is shown by Fig. 8. In this case, however, the influence of 50% is considerably greater as indicated by the fact that all three susceptible engines give a large reduction in stalling with increasing 50% point.

Changes in 90% evaporated temperature also have a slight effect on stalling tendency in the susceptible engines as indicated by Fig. 9, but the magnitude of the effect is considerably less than it was for 50% point and also less than it was for 10% point.

The preceding volatility discussion has shown that some engines are sensitive to fuel volatility and others are not. The sensitive engines show a considerable decrease in stalling tendency as fuel volatility is decreased. These latter engines are also affected by individual changes in 10, 50, and 90%

evaporated temperature; the effect of the 10 and 50% points being greater than that of the 90% point.

One important point to keep in mind is that, although fuel volatility can control stalling due to carburetor icing to some extent, complete control by fuel volatility is not feasible because of other performance considerations.

A second approach available to refiners is the additive route. A detailed investigation of the effect of various additives was not included in this program. However, a limited study in the most critical engines showed that certain additives can help to minimize the problem.

For example, concentrations between 0.5 and 2% of additive A were tried in (1) an average volatility fuel and (2) an extremely volatile fuel. Fig. 10, which presents these data, shows that at the lower concentrations, the additive was most effective in the average volatility fuel. On the other hand, low concentrations had little effect on the high volatility fuel. At the higher concentrations, additive A was equally effective in reducing the number of stalls in both types of fuels.

Engine Design – As pointed out earlier, large differences exist between the stalling tendencies of different engines. Most of these differences were illustrated quite clearly in Fig. 6 in which the number of stalls encountered with each engine on three widely different fuels was compared. It is felt that there are rather clearcut reasons for some of these differences, and the following discussion will point out two of them.

Two items that seem quite significant are fast idle speed and throttle-blade temperature. Fast idle speed is defined as the increased idle speed during the early part of the warmup which is designed to prevent the cold engine from stalling. The fast idle speed is usually maintained by a cam-shaped stop on the throttle linkage controlled by the automatic or manual choke mechanism. A high fast idle speed tends to keep the engine from slowing down enough to stall, and high throttle-blade temperature minimizes the amount of ice formed.

The fast idle speeds of five of the engines are compared in Fig. 11 on a nonstalling fuel. Engine A, which showed excellent antistalling characteristics, has the highest overall fast idle speed. This engine is normally installed with a torque converter, and a high fast idle speed is permissible without undue inconvenience to the driver. It is considered significant that this fast idle speed is maintained over a long period of time because the occurrence of stalling due to icing usually does not occur in the first minute or so of operation. In other words, there is an antistalling advantage to maintaining fast idle for a longer period of time. Engine B was omitted from this comparison, and it will be discussed later.

Engine C, which gave rather poor antistalling

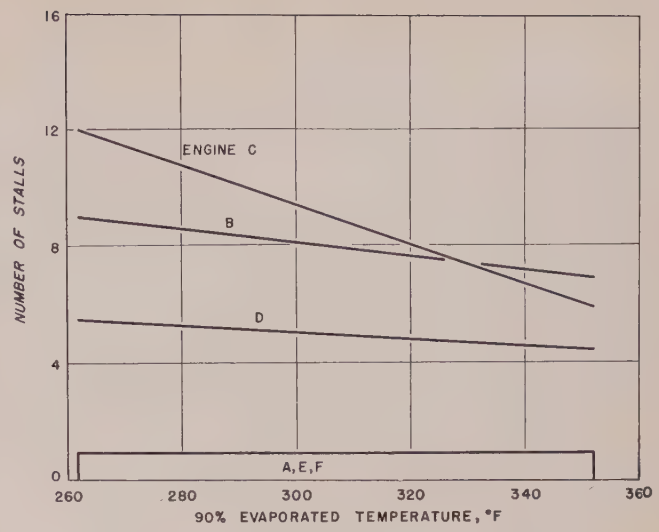

Fig. 9 – Effect of 90% evaporated point on engine stalling due to carburetor icing at 40 F ambient temperature and 100% relative humidity

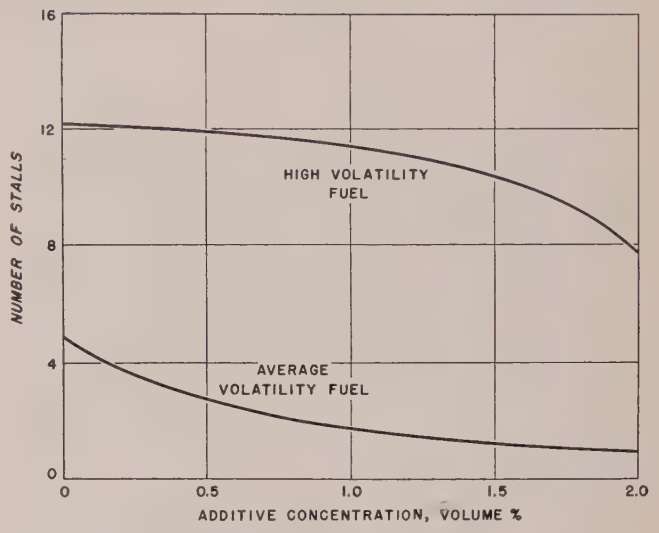

Fig. 10 – Effect of antistalling fuel additive on engine stalling due to carburetor icing. Average data are from two of the most critical engines at 40 F ambient temperature and 100% relative humidity

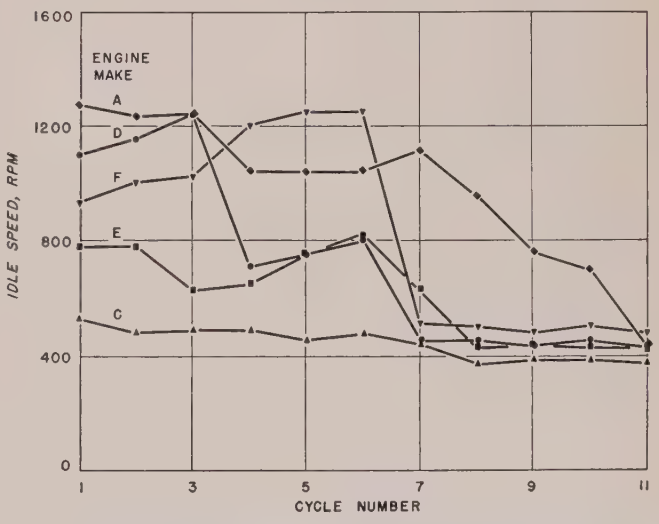

Fig. 11 – Variation in fast idle speed for six 1953 passenger-car engines at 40 F ambient temperature and using nonstalling low volatility fuel

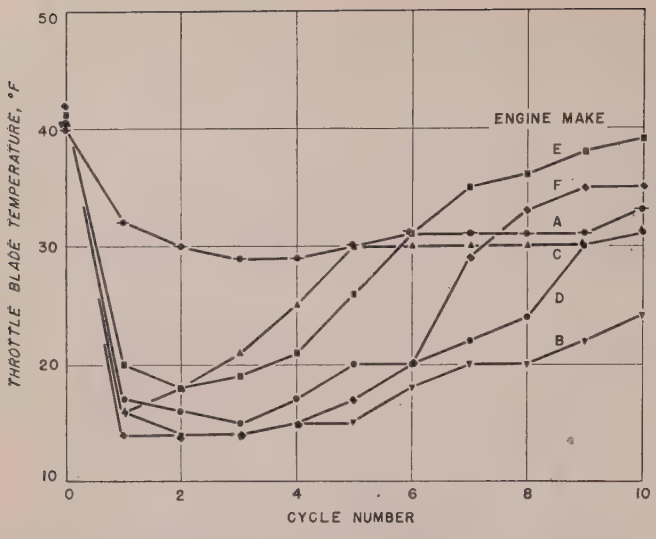

Fig. 12 – Throttle-blade temperatures during carburetor icing test procedure runs for six 1953 passenger-car engines at 40 F ambient temperature and using average winter-grade volatility commercial fuel

performance had a very low fast idle speed. This engine was designed for operation with a standard manual transmission, where it is desirable to maintain fast idle speeds as low as possible. Otherwise, the car speed at closed throttle in third gear would be quite high during warmup. Another engine that gave a fair amount of stalling was engine D. This engine was also designed for operation with a torque converter. The fast idle system of this engine appears to go out of action rather quickly and partially accounts for its poor antistalling characteristics.

Engine E, which had good antistalling characteristics, is normally installed with an automatic transmission, incorporating a fluid coupling and automatic stepwise shifting. Because of this, it is necessary to maintain rather low fast idle speeds. In order to avoid the stalling that usually accompanies such low idle speeds, the carburetor throttle body of this engine is heated during the warmup period. A later discussion will show this mechanism to be quite effective. The last engine, engine F, also showed good antistalling properties. This engine is designed for use primarily with a torque-converter-type transmission. It also has a rather high fast idle speed, although it is brought to normal idle quite soon. Perhaps an explanation of the good performance of this engine can be partially based on the fact that it has an aluminum carburetor throttle body which may have good heat-transfer characteristics. This will be discussed in more detail later.

Engine B was omitted from this comparison because it was equipped with a manual choke. For reasons of reproducibility, the use of the choke was eliminated as quickly as possible. This undoubtedly penalized this engine in one respect, because the choke and fast idle linkage adjustment operate in unison. On the other hand, the elimination of the choke should have decreased the amount of fuel discharging from the main discharge nozzle which should reduce the refrigerating effect of the fuel. To what extent the above two items canceled each other is not known.

Throttle-blade temperature also appears partially to account for differences in antistalling performance between engines. Fig. 12 indicates that the variation in throttle-blade temperature between engines when operating on an average volatility fuel can be quite large. Engine A did not stall on this fuel, and the figure shows that the throttle-blade temperature never dropped below 29 F. The remaining engines gave anywhere from a 20 to almost 30 F maximum drop in blade temperature. Two of the poorer engines, engines B and D, had the lowest overall throttle-blade temperatures. It was indicated earlier that the aluminum carburetor throttle body of engine F might have contributed to its good antistalling performance. Fig. 12 shows that this engine had final throttle-blade temperatures almost as high as those of engine E which was equipped with a carburetor heater.

The effect of fuel volatility on throttle-blade tem-

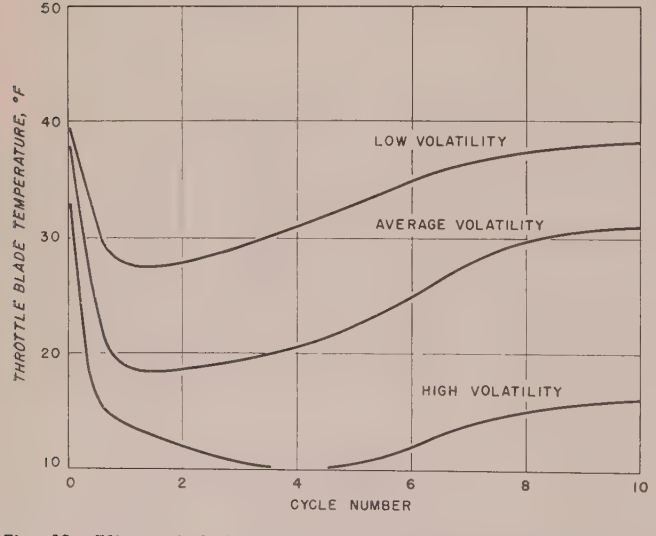

Fig. 13 – Effect of fuel volatility on throttle-blade temperature at 40 F ambient temperature. Data represent six-engine average

Table 4 – Per Cent of Hours in Icing Range, Average 1951 and 1952

	Oct.	Nov.	Dec.	Jan.	Feb.	March	April
Boston	F12	33	29	19	28	39	33
Cincinnati	F19	27	38	33	37	29	29
Detroit	19	26	21	22	11	23	31
Philadelphia	F11	22	31	25	27	28	23
Richmond	F15	31	39	25	31	31	14
Syracuse	22	41	39	32	37	36	40

perature is shown by the six-engine-average data plotted in Fig. 13 for fuels of high, average, and low volatility. Obviously, there is a considerable difference between fuels; and, as would be expected, the least volatile fuels give the smallest temperature drop.

The effectiveness of the carburetor heater in engine E is clearly indicated in Fig. 14. This figure shows a significant difference in throttle-blade temperatures between heat on and off, especially between the sixth and twelfth cycles. The reduction in number of stalls from six to two when heat is added represents a considerable improvement.

The question is sure to arise as to why idle-screw temperatures were omitted from the discussion of carburetor temperatures. They were purposely omitted because in every engine, idle-screw temperatures were well above freezing, yet the engine continued to stall. On account of this, it is most difficult to visualize that ice formation at the idle screw was responsible for stalling during these tests.

The above discussion has indicated some of the reasons for differences between engines and has also indicated why some engines are good and others bad. However, it is not within the scope of this paper to ferret out all the reasons for differences between engines or to explain completely why the so-called "bad" engines cannot be changed into "good" engines.

Weather – The initial stage of this work and work by earlier investigators[1] showed that the atmospheric conditions most conducive to ice formation were between 35 and 40 F ambient temperature at 100% relative humidity. The relation of stalling to ambient temperature on two of the more critical engines is depicted in Fig. 15. Because of equipment limitations, only a limited number of tests were made below 40 F, and therefore the data below that temperature are estimated. However, other data indicate that this estimate should be sound. This plot, then, shows that on a fairly volatile fuel (fuel 4) stalling due to ice formation should cease below about 30 F and above about 50 F. On a fuel of average volatility (fuel 1), the temperature range is slightly narrower.

The manner in which stalling varies with humidity on these same fuels is illustrated in Fig. 16. On the high volatility fuel (fuel 4), stalling ceases below 65% relative humidity; whereas, on an average volatility fuel (fuel 1), it ceases below 75% relative humidity.

Although the above data are limited in that they are based on a two-engine average, the difference between engines was quite small, and therefore the effects are considered significant.

Table 4 is a tabulation of the amount of carburetor icing weather occurring in a number of eastern cities. This table shows that most of the icing weather is encountered during the late fall, winter, and early spring. In interpreting these data, it is

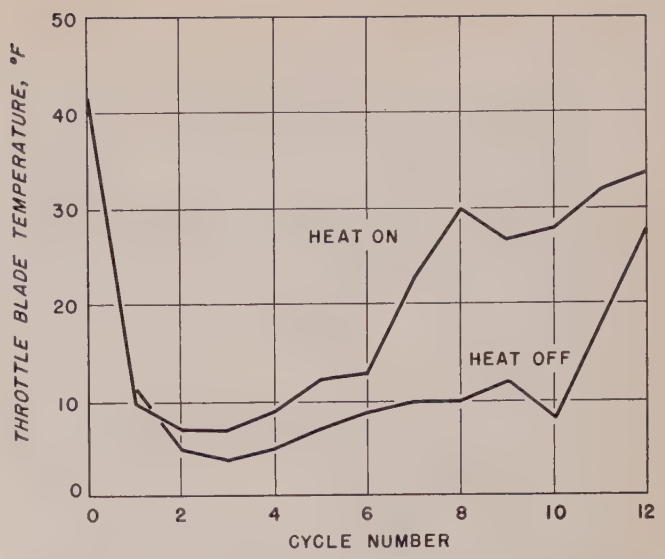

Fig. 14 – Effect of carburetor heater on throttle-blade temperature at 40 F ambient temperature and using high volatility fuel

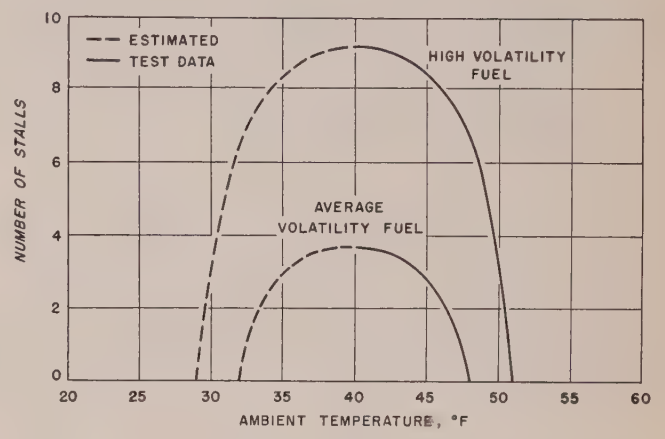

Fig. 15 – Effect of ambient temperature on engine stalling due to carburetor icing at 100% relative humidity. Data are from two of the most critical engines

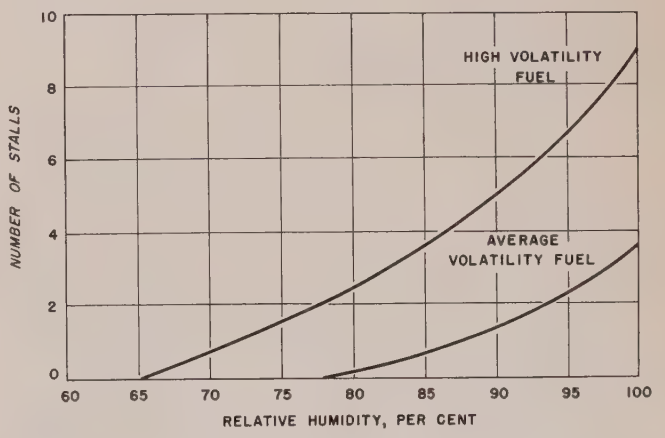

Fig. 16 – Effect of humidity on engine stalling due to carburetor icing at 40 F ambient temperature. Data are from two of the most critical engines

important to remember that (1) these percentage figures include such hours as 2 and 3 a. m. when few cars are in operation and (2) they are based on the weather range of stall-free performance on a volatile fuel. Any tabulation based on (1) a specified time of day, (2) a fuel of average volatility, and (3) a performance level allowing one or two stalls would indicate much smaller percentage figures than those shown here.

Operating Conditions – Obviously, stalling due to ice formation is most likely to occur during idling. If an engine is started and then driven without idling for a 10- to 15-min period, the chance that it will stall due to ice formation is very slim. The type of driving most conducive to ice formation and stalling is about as follows. Assuming that the engine has reached an ambient temperature of about 40 F, let us suppose that the motorist starts his car and drives about 0.2 to 0.3 of a mile at 20 to 30 mph and then stops for a stop sign or traffic light. It is quite possible that his engine will not stall because insufficient refrigeration has occurred. Let us then suppose that he continues on to the next stop light in the same manner. By this time, there is a good chance that a stall will occur, and if it is necessary to continue this type of operation, he may encounter stalls for as much as 2 or 3 miles of operation.

Summary

Engine stalling caused by ice formation in the carburetor does occur. Fortunately, a number of conditions must occur at the same time before an engine will actually stall; and, on that account, the icing problem will not be as evident to the customer as a number of other performance factors that depend on gasoline volatility. However, its limited occurrence can be critical under certain circumstances; and, therefore, any engine or fuel changes aimed at its elimination are worthy of effort.

The amount of stalling varies considerably with fuel volatility and engine design. The fuel supplier has two principal avenues of approach to the solution of the problem. The first is fuel volatility, and the second is the use of additives. The former does not offer a complete solution because the necessary changes are usually accompanied by poor performance in other respects. The use of additives, similarly, may offer a partial solution to the problem. The equipment manufacturer can also help to minimize the problem, as indicated by some of the engines tested in this work. But, here again a compromise must be made between improving antistalling performance and cost and other performance difficulties.

The mechanism of stalling due to ice formation appears to be principally a restriction of the necessary airflow past the throttle blade during the idle period. This restriction is caused by the formation of ice on the blade and the interior of the carburetor barrel during relatively light-load operation.

Acknowledgment

The authors wish to acknowledge the help of their associates, both in Ethyl Corp. and Sun Oil Co., whose complete cooperation made this work possible. They also wish to thank the engine and carburetor manufacturers who were most helpful in supplying test equipment and technical information.

DISCUSSION

Best Solution Is Use of Suitable Anti-Icing Additive

–J. F. Kunc, Jr.
Esso Research & Engineering Co.

IT IS gratifying to note that the results of the work on carburetor icing confirm work done earlier on this problem[a]. The results of both these studies quite clearly demonstrate that engine stalling resulting from carburetor ice formation is influenced by a number of factors. These include the amount of moisture in the air, the temperature of the air, the characteristics of the fuel being used, and the design of the engine involved.

There is not much that can be done about the weather except to talk about it. Some control can be exercised, however, over the characteristics of the fuel used, as well as engine design.

It has been amply demonstrated that increasing fuel volatility, particularly in the mid-boiling range, results in increased engine stalling due to carburetor ice formation. Then why not solve the problem by decreasing the volatility of the fuel? Unfortunately, following this course of action will result in poorer performance in a number of other respects. Decreasing fuel volatility will adversely affect starting ability and rapidity of engine warmup. It will also increase the amount of crankcase-oil dilution which will be obtained. Controlling carburetor ice formation by decreasing fuel volatility, therefore, is a poor solution to the problem. A much sounder approach consists of maintaining the good engine performance which can be realized with high volatility fuels in carbureted engines and using a suitable anti-icing additive to prevent ice from forming on critical parts of the carburetor.

[a] See footnote 1 of main paper.

The work done jointly by Sun and Ethyl as well as the studies conducted by Esso has shown that engines vary widely in their susceptibility to carburetor ice formation. This is good evidence that the engine designer can also contribute to the solution of the icing problem. Most of the mechanical schemes which have been proposed involve bringing additional heat to the carburetor to keep the temperatures above the freezing point of water. This route also leaves something to be desired, since resistance to vapor locking may be sacrificed to some extent when carburetor heating is used to reduce ice formation.

The problem of carburetor ice formation is not restricted to carburetors and engines manufactured in the United States. For example, serious icing difficulties have been reported with several small English cars introduced within the past year or so. In these cars, all of which were equipped with carburetors of new design, ice has been observed to form in the carburetor choke tube in large enough quantities either to completely block or at least restrict severely all flow through the carburetor. In common with the findings for United States cars, ice formation in the English cars in question increases with increasing fuel volatility and can be suppressed by the use of a suitable anti-icing additive.

In contrast to the problem in England, most of the difficulties with carburetor ice formation in the United States involve engine stalling during idling. This is annoying to the driver, but ordinarily it does not pose a serious safety problem. However, cases of carburetor ice formation with considerably more serious aspects have been reported in this country. These involved sticking of the throttle in the open position as the result of ice formation. This is obviously not a comfortable position for the driver of a motor vehicle to be in. It does serve to emphasize, however, that the problem of carburetor ice is serious enough in magnitude to deserve the continued attention of both the automotive and petroleum industries.

Suggests Heating of an Aluminum Carburetor Body During Warmup

—Harry A. Collins
Research Laboratories Division, GMC

A YEAR or so ago, I had the opportunity to see the problem of carburetor icing at first hand in northern Montana, North Dakota, Minnesota, and Alaska. The average owner of an automobile which suffers from this disease does not know what causes stalling of his engine. Owners and operators of filling stations and most service stations do know, though; and the only cure they have to offer is to add alcohol to the gasoline in the car tank. This appears to cut down the number of stalls during warmup, but it also definitely cuts down on vehicle performance after warmup due to a change in fuel volatility by the addition of an overdose of alcohol.

The conditions for carburetor icing vary greatly, and the conditions as are set forth in this report are those which were set up a few years back for laboratory study. The original setup was to operate the engine in an ambient temperature of 40 F and direct all incoming air to the carburetor through a melting ice bath. This assured 100% relative humidity and showed great amounts of ice on the cracked throttle blade without having to search too closely for it.

This test structure allowed for a fixed procedure, and the results of chemical change to fuel or mechanical changes to carburetor and riser were immediately and unmistakably noted.

In actual road use of an automobile, this icing trouble can and does come in an extremely broad range of outer ambient air conditions. This phenomenon has been witnessed during periods of dense fog in a temperature range of —60 F to +50 F. In the Alaskan territory, as far inland as Fairbanks, icing is quite common in an ambient of —60 F during ice fogs or during periods of the "Williwaws." These ice fogs are a phenomena peculiar to Arctic regions because of the warm North Pacific currents impregnating the air with vaporized moisture. It is not uncommon to find a relative humidity of 80-85% at —60 F, the moisture content of the air actually being individual minute grains of ice.

Actually, a vehicle engine in this territory is heated to at least —20 F before it can be started; and, even then, icing-stalling is of greater time duration than anywhere else in the world. A fuel of lessened volatility, in this case, to ward off icing, would really be effective because the engine would never start.

In the lowlands, near bodies of water or marshland anywhere in the United States, this icing phenomenon is witnessed almost regardless of the season or ambient temperature. Naturally, the higher the ambient, the faster the engine warms up and the fewer the stalls due to ice.

This seems to be a problem suffered mostly by city-dwellers. The stop-start driving means more periods of closed throttle and slower engine warmup. The only thing which saves the rural motorist from this same trouble is the fact that as soon as he starts the engine of his vehicle, his running is done in off-idle throttle-blade range, and engine warmup is more rapid.

Contrary to the findings of this report, I have found that engines of the greatest cubic inch displacement suffered most from icing troubles. This is relative, because more moisture laden air is caused to pass over the throttle blade.

Presently, there appear to be two avenues open for continued research and study of this icing problem

1. The use of alcohol additives to the fuel, which would have a tendency to keep the ice formation soft but would also reduce fuel volatility.

2. Use an aluminum lower body on carburetors, and pass a great amount of exhaust heat through the body during warmup only. Heat is to be cut off by thermostatic valving after warmup. Up to this time, the components of the exhaust gases appear to be not too compatible with an aluminum casting.

To gain more complete data, I believe that it would be advisable to run this same study using complete automobiles. The closed hood would tend toward a more rapid engine warmup, thus reducing the number of stalls due to icing.

It is obvious that the engines used for test carried the engine coolant thermostat intended for the use of alcohol, although ethylene glycol was used for coolant. This type thermostat is usually rated at 150 F and would cause the warmup of ethylene glycol to be much slower than if the regular thermostat rated at 175 F were used for ethylene-glycol coolant.

I am glad of having had the opportunity to work with the authors of this important paper and hope that this study may be carried on.

Comments on Effect of Fuel Boiling Range on Icing

—Al Cleveland
Ford Motor Co.

IT is particularly interesting to note the wide variations among engines as to the effect of fuel volatility and stalling. The results, however, appear to be consistent throughout and confirm our previous feeling that this fault is most susceptible to correction with engine design. However, the rapidly decreasing number of stalls of car C with increased temperature of 10% point and the similarly marked effect of 50% point in cars B, D, and C are significant. It is particularly interesting to see that carburetor icing is as much affected by the 50% point. In fact, there even seems to be some effect from the 90% point.

Tractor Seat

THE behavior of a tractor seat suspension as the tractor moves over an irregular surface is a vibration problem. The theoretical investigation and experimental verification of this matter require that the human reaction to vibration be defined in mathematical terms.

Human Reaction versus Mechanical Characteristics

As the result of extensive research conducted during the last three years, sufficient material has been collected and analyzed to permit accurate prognosis. This material will not be discussed here, since it is considered separately elsewhere.[1, 2, 3] It may be stated with reasonable certainty that the criteria of human tolerance of vibration are as follows:

1. Under conditions of severe vibration in the range between 1 and 6 cps, the criterion of human sensitivity or discomfort is "jerk" or the change in rate of acceleration.
2. In the frequency range between 6 to 20 cps this criterion is the value of acceleration itself.
3. In the higher frequency range above 20 cps the velocity of vibration becomes the criterion of discomfort.

As the result of normal spring and tire resonance, the most severe vibrations have been found to occur within the range of 1 to 6 cps. This low-frequency range must, therefore, be given prime consideration in any investigation of vehicle suspensions.

To make possible a theoretical investigation, it is assumed that all vibration patterns are sinusoidal. On this basis, the amplitude of vibration alone determines the values of velocity, acceleration, and "jerk," which limits the calculations to that of establishing the expected amplitude of vibration at the frequency range under consideration.

The same assumption is also used in taking comparative measurements. It will be shown, however, that this may easily result in errors.

Mathematical Study of Vibration

In order properly to analyze the problem under consideration, it is necessary to construct a simplified but equivalent analogy of the complete vibrating system. This is most readily done by considering the human body as an individual vibrating system as shown in Fig. 1.

It is readily apparent that a highly complicated

---

[1] See *Grundlagen der Landtechnik*, Vol. 4, 1933, p. 110: "Über die Beanspruchung des Menschen durch Erschütterungen auf Schleppern und Landmaschinen," by M. Haack.

[2] See *SAE Journal*, Vol. 56, August, 1948, pp. 48-49: "Passenger Vibration Limits," by R. N. Janeway.

[3] See SP-6, "Ride and Vibration Data." Copies available from SAE Special Publications Department. Price: $2 to members, $4 to nonmembers.

THIS paper describes an investigation into the best design of seat suspension for tractors having pneumatic tires with a rigid rear axle.

Test results show that some of the factors entering into a good tractor supension include:

1. A ratio between the natural frequency of the seat and the natural frequency of the tires of about 0.4 to 0.5.

2. A supplementary seat deflection 1½ times the static seat deflection to avoid bottoming.

3. Use of suspensions having nonlinear characteristics in order to hold seat deflection within practical limits.

4. Adjustable seat-spring action to compensate for the varying weights of drivers.

The Author

MAX HAACK is with the Institute for Tractor Research of the Agricultural Research Center Braunschweig-Volkenrode, and is also chief of the motor vehicle department of the German Shell organization. He attended the technical school of the city of Berlin from 1932 to 1934. He served as research engineer at the tractor test station at Bornim, Germany, and the motor vehicle experiment facility of the German Army at Kummersdorf until 1936. In 1939 he obtained the degree Dipl. Ing. from the Technische Hochschule, Berlin – Charlottenburg, and in 1953 he received his doctor's degree in engineering.

Suspensions for Easy Riding

Max Haack, Institute for Tractor Research,
Agricultural Research Center, Braunschweig-Völkenrode

This paper was presented at the SAE National Tractor Meeting, Milwaukee, Sept. 16, 1954.

oscillating system is required if all conditions are to be met to the fullest extent. Considering the limits of human tolerance to vibration in each range, it is possible to simplify this vibrational analogy by considering the driver as a rigid mass. The resulting simplified analogy is shown in Fig. 2 as follows:

1. Consider the body of the tractor driver as a rigid mass connected through the seat spring to the rear axle of the tractor.
2. Damping from the tire is proportional to the velocity, corresponding to viscous damping.
3. The exciting force is truly sinusoidal and the tractor does not "jump," that is, leave the ground.

Thus the equations for the oscillation of both systems are as follows:

$$m_1\ddot{x}_1 + c_1x_1 + c_2\,(x_1-x_2) + k_2\,(\dot{x}_1-\dot{x}_2) + k_1\dot{x}_1 = P_o \sin \omega t$$

and:

$$m_2\ddot{x}_2 + c_2\,(x_2-x_1) + k_2\,(\dot{x}_2-\dot{x}_1) = 0$$

Expressed as complex variables, both equations become:

$$-m_1 \cdot \omega^2 \cdot x_1 + c_1 \cdot x_1 + c_2\,(x_1-x_2) + i\omega k_2\,(x_1-x_2) + i\omega k_1 \cdot x_1 = P_o$$

and:

$$-m_2 \cdot \omega^2 \cdot x_2 + c_2\,(x_2-x_1) + i\omega k_2\,(x_2-x_1) = 0$$

Being interested in the oscillation of the driver (x_2) the two equations above are solved for x_2. After rearrangement and with the application of vector calculus, the solution becomes:

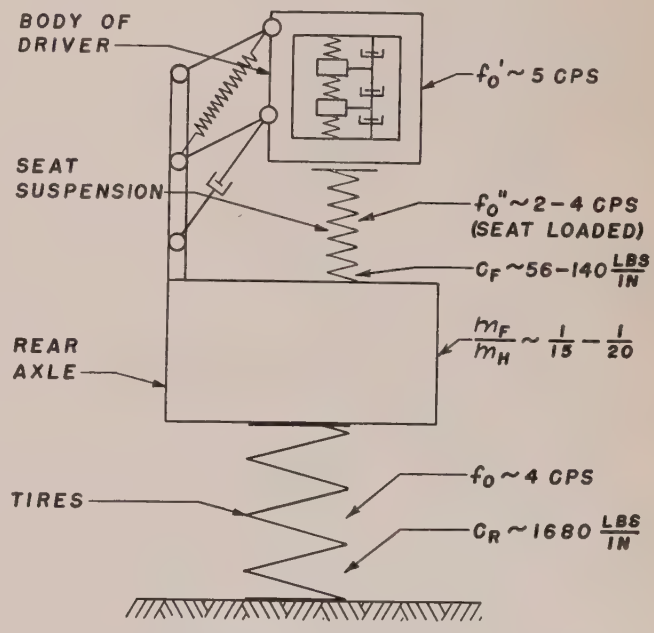

Fig. 1 – Equivalent diagram of human body on tractor seat

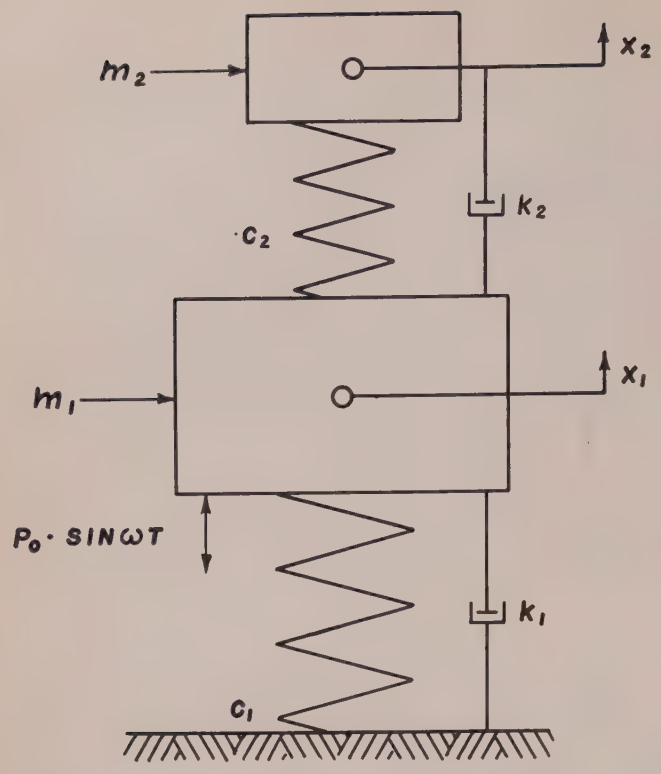

Fig. 2 – Simplified equivalent diagram of rigid man on tractor seat

$$\frac{x_2}{P_o} = \sqrt{\frac{c_2^2 + \omega^2 k_2^2}{[(m_1 \omega^2 - c_1)(m_2 \omega^2 - c_2) - c_2 m_2 \omega^2 - \omega^2 k_1 k_2]^2 + \omega^2 [k_2 (-m_1 \omega^2 - m_2 \omega^2 + c_1) - k_1 (m_2 \omega^2 - c_2)]^2}}$$

To simplify the solution of the equation, the following ratios are substituted:

1. Mass ratio $\mu = \frac{m_2}{m_1}$

2. Ratio of natural frequencies $\nu = \frac{\nu_1}{\nu_2}$

where:

ν_1 = Natural frequency of the tractor with tires

$= \sqrt{\frac{c_1}{m_1}}$

ν_2 = Natural frequency of the driver with seat suspension

$= \sqrt{\frac{c_2}{m_2}}$

3. Frequency ratio for first resonance $w = \frac{\omega}{\nu_1}$

4. Damping ratio $D = \frac{k}{2m\nu}$

5. Vertical displacement of suspension under static load

$x_{1\,st} = \frac{P_o}{c_1}$

6. Static tire loading $P_o = G_1 + G_2$

where:

G_1 = Weight of tractor

G_2 = Weight of operator

Therefore:

$$\frac{x_2}{x_{1\,st}} = \sqrt{\frac{\nu^4 + 4w_2 D_2^2}{[(w^2-1)(w^2-\nu^2) - \mu \nu^2 w^2 - 4w^2 D_1 D_2]^2 + 4w^2 [D_2 (-w^2 - \mu w^2 + 1) + D_1 (-w^2 + \nu^2)]^2}}$$

For a condition of undamped vibration ($D = 0$), the equation is simplified to:

$$\frac{x_2}{x_{1\,st}} = \sqrt{\frac{\nu^4}{[(w^2-1)(w^2-\nu^2) - \mu\nu^2 w^2]^2}}$$

These values approach infinity under the condition where:

$$(w^2-1)(w^2-\nu^2) - \mu\nu^2 w^2 = 0$$

Values of the variables in the above equation fall within the following ranges:

$$\mu = \frac{1}{10} \text{ to } \frac{1}{20}$$

$$\nu = \frac{1.8}{4} \text{ to } \frac{3.5}{4}$$

$$D_1 = D_2 = 0 \text{ to } 0.2$$

$$f_r = 4 \text{ cps (tire frequency)}$$

Substituting the above values in the final equation above, the resulting values are plotted in the curves shown in Fig. 3.

On the assumption that damping is absent, there are two resonance frequencies resulting from the natural frequency of the suspension system. This system is made up of two individual suspension units:

1. The driver and seat.
2. The rear axle and tires.

These curves are of interest only as they define the boundaries of undamped vibration. Actually, considerable damping occurs within the carcass of the tire. (According to E. F. Göbel,[4] calculations may be made on a value of $D_1 \approx 0.2$.) In addition, similar conditions exist in the driver and seat system on account of the damping within the seat suspension material and in the muscular action of the driver. This also may be roughly approximated with a value of $D_2 \approx 0.2$. This justifies assuming the same magnitude of damping for both systems. The resulting curves closely approximate actual conditions and are the basis of further discussion.

Under the assumption that the value of the seat spring rate may be adjusted according to the weight of the driver to retain the same natural frequency (ν = constant), the mass ratio has no significant influence; on the other hand, the frequency ratio has considerable influence. The lowest frequency of the seat (softest spring) which permits satisfactory handling of the operator's controls still gives such a rigid connection between the two vibrating systems that no reduction of displacement appears within the range of frequencies encountered in tractor operation.

The influence of the frequency ratio ν in the equation previously derived is shown in the curves in-

[4] E. F. Göbel, Gummifedern, Bln, 1945.

cluded in Fig. 4. These curves show the effect of progressively increasing the natural frequency of the seat suspension from its lowest practical value of 0.4, that of the tire, to 1.0. The displacement of the seat increases to five times the magnitude of the ground disturbance when the frequency ratio is one and the exciting frequency is equal to the natural frequency of the seat. Increasing the ratio still further results in moving the peaks of resonance to the right and decreasing their magnitude. The limiting case is a rigid connection between the seat and the rear axle of the tractor which results in an increase of the seat displacement of only 2.5 times.

It may, therefore, be stated that a seat suspension with a frequency ratio $\nu > 0.6$ always has a greater maximum displacement than an unsprung (rigid) seat. Reducing the rigidity as previously mentioned is limited by practical requirements to a lower limit value of $\nu = 0.4$. It therefore follows that the best frequency ratio is $\nu \approx 0.5$, that is, the natural frequency of the seat is approximately 2 cps when that of the rear axle is 4 cps.

Furthermore, if the frequency of the rear axle-tire system were decreased with the introduction of softer tires, for example to 3 cps, it becomes necessary to reduce correspondingly the natural frequency of the seat suspension, in accordance with the value of $\nu \approx 0.5$, to 1.5 cps in order to satisfy the optimum condition. For this particular

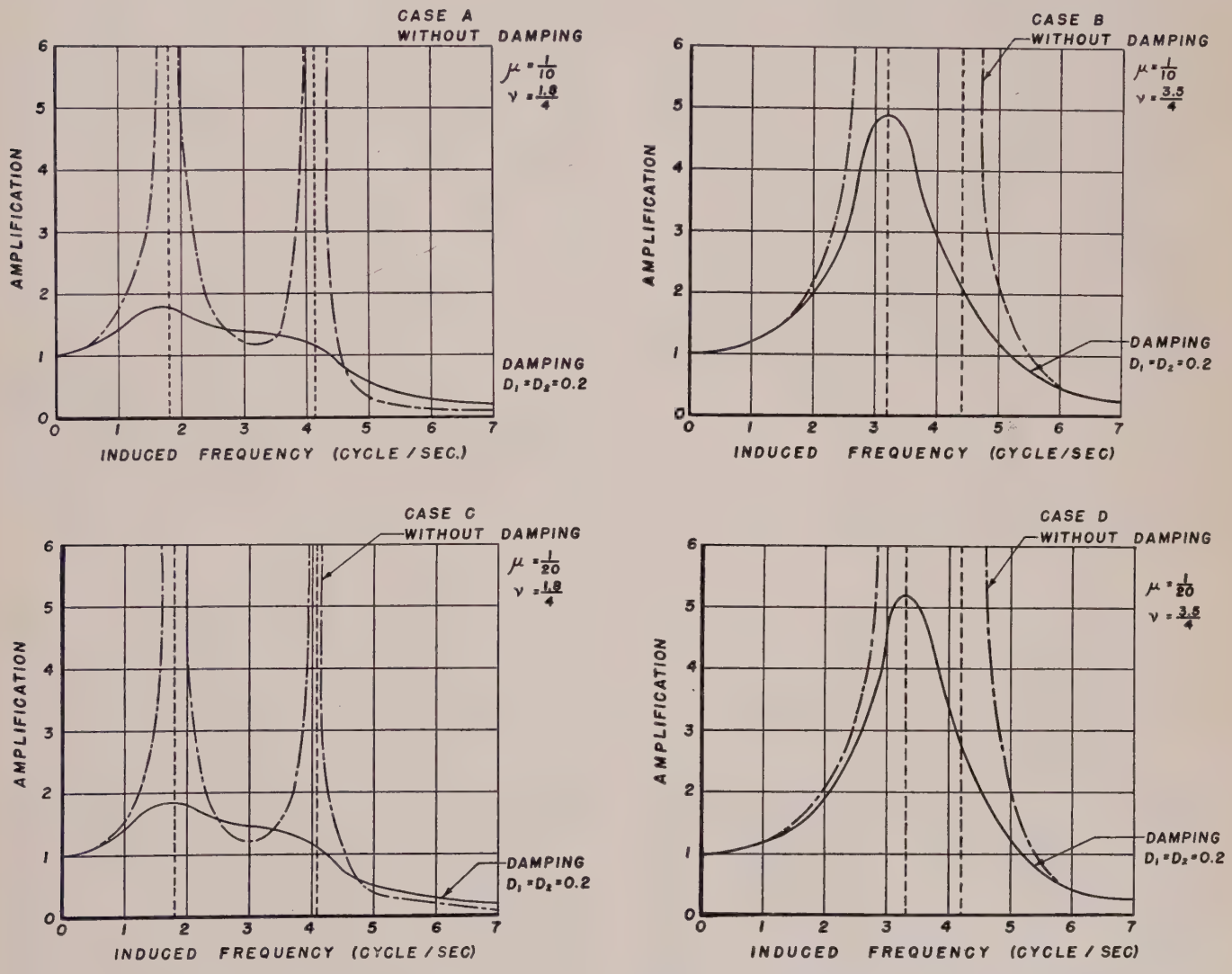

Fig. 3 – Resonance curves of the seat suspension shown at $\mu = \frac{1}{10}$ to $\frac{1}{20}$, $\nu = \frac{1.8}{4}$ to $\frac{3.5}{4}$, and $D = 0$ to 0.2

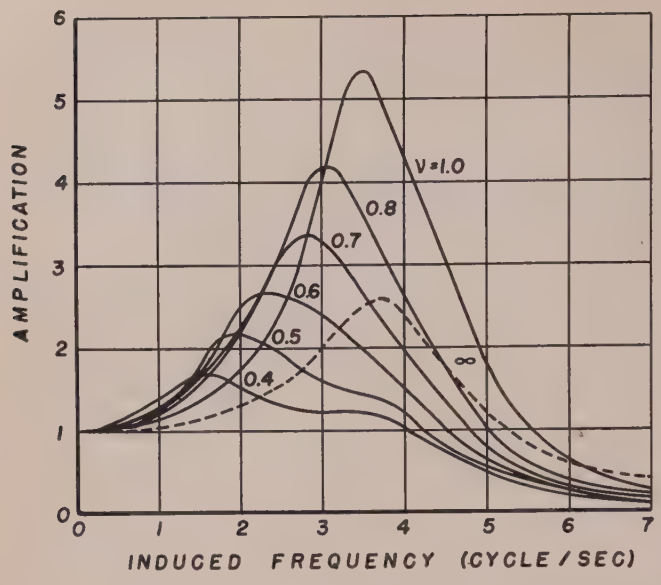

Fig. 4 – Resonance curves of the seat suspension with varying ratios of natural frequencies

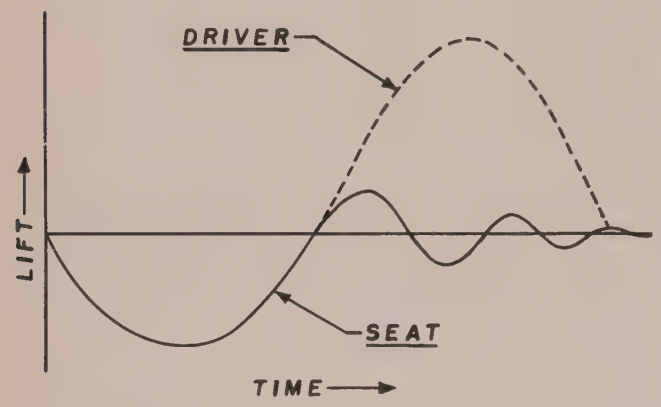

Fig. 5 – Pitching motion of the tractor driver

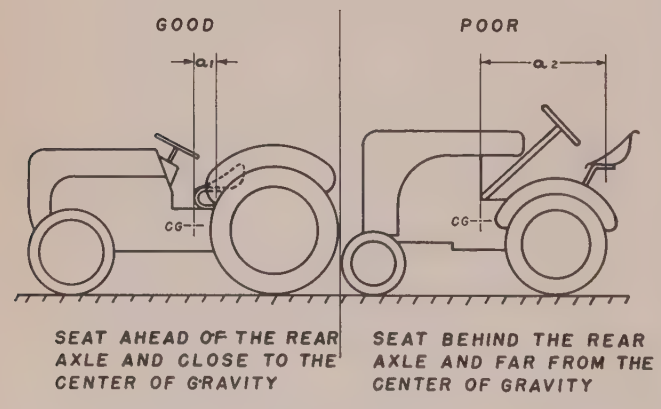

Fig. 6 – Evaluation of seat location with regard to pitching vibration

condition, all seats with a natural frequency exceeding 3 x 0.6 = 1.8 cps are worse than a rigid seat.

To all of this it should be added that the actual vibration is not at all sinusoidal, but it is rather a pitching or jerking oscillation represented by the pseudoharmonic motion shown in Fig. 5.

In this event, the acceleration curve is not similar to the displacement curve due to the strong influence of higher harmonics. It may be added that with the muscles of both his arms and legs, the driver resists any great pitching movement, thus introducing damping of variable intensity. Impacts occur when the driver is pitched from the seat and again when he lands. Such impacts may be significantly amplified by secondary influences such as the natural frequency of the empty seat, which is approximately three times that of the loaded seat. In addition, the pitching of the driver and the movement of the seat may be in opposite directions, resulting in the most unfavorable condition. If seats are not padded, acceleration peaks may be expected which give a greater sensation of vibration than does the amplitude. From these theoretical considerations, two important requirements appear regarding the optimum design of seat suspension:

1. The natural frequency of the seat suspension should be approximately half of the rear axle and tire suspension frequency.

2. The seat should be light and well padded in order to hold to a minimum the impact between the driver and seat as he returns to the seat after being pitched out.

In addition, the free oscillation of the empty seat should be effectively damped (shock absorber, damping effect of spring material, and so forth).

The theoretical requirements listed above were verified experimentally by investigating the riding qualities of 14 different tractor seats.

Suspension Qualities of Tractor Seats

Purpose and Procedure – The purpose of this investigation was to determine quantitatively the nature of the vibrations occurring at the rear axle and driver's seat in tractors with an unsprung rear axle. These experimental data were obtained for the verification of the theoretical analysis.

Use of a vibrating platform supporting the tractor seat was first considered, but the idea was abandoned because it failed to duplicate the actual vibrations (pitching motion) experienced in service. It further failed to include the reflex action of the driver, which significantly influences the nature of the reaction to vibrations.

It was decided that the experiments must be conducted on a moving tractor since it was also necessary to evaluate the influence of the tractor engine vibrations (horizontal, vertical, low- or high-speed engine) together with the location of the seat (in front of or behind the rear axle) on

the total vibrational strain on the driver. It may be stated that engine vibrations can have a noticeable influence only when their exciting frequency is below 1½ times the highest natural frequency occurring in either vibration system (driver-seat and rear axle-tire), that is, 1.5 x 4 = 6 cps. This applies only to engines with a speed below 360 rpm. Engines with so low a speed are no longer built. It was sometimes observed that engines running at a very slow idle speed (250-350 rpm) excited a resonance vibration in the tractor rear axle. This condition is of no significance when driving, because the exciting frequencies at full engine speed are too high to affect vertical vibration of the seat. On the other hand, horizontal vibrations from the engine must be considered since they cannot be effectively isolated from the driver.

In resolving this problem, the difficulties in obtaining satisfactory measurements made it necessary to devise new experimental techniques. The investigation reported below refers only to vibrations originating from the test track.

The ideal fore-and-aft seat location is at the node of the vibration. According to the research of Lehr and Bertschinger,[5] among others, this point is just below the center of gravity. Points located on a vertical line through the center of gravity suffer least from pitching – a factor seriously considered in the design of Ferguson and Ford tractors. (See Fig. 6.) On both tractors it was possible to place the seat close to the center of gravity since only hydraulically controlled integral implements are used and no consideration had to be given to control of trailing implements. In Germany, however, the seat location is determined with respect to the ease of operating trailing implements, in accordance with German Standard DIN 9670. This makes it necessary to locate the seat within a small area above and directly behind the rear axle. It is most unfortunate that a seat location which is so unfavorable from the vibration standpoint must be accepted as standard design for the near future. It may be expected that as hydraulic systems for the control of trailing implements come into more general use, the present limitations on the position of the seat may eventually be revised. The experimental work was conducted without contemplation of such a change.

[5] See *Automobiltechnische Zeitschrift*, Vol. 48, 1946, p. 33: "Über den Zusammenhang zwischen Schwingungseigenschaften and Fahreigenschaften von Kraftfahrzeugen," by E. Lehr and Bertschinger.

Standard Tractor Used in Tests

It was, therefore, decided to use a tractor of standard design throughout the investigation. This tractor was used in investigating 14 different seats, in all cases operating over the same type of surface irregularities.

These included a single obstacle and a periodic set of obstacles (wavy track). Hence, both extremes of suspension behavior were analyzed. Actual driving conditions lie between these extremes, because a road surface consists of an irregular pattern of single bumps as well as those occurring periodically. The particular advantage of this testing procedure is that all tests may be accurately reproduced, which makes it possible categorically to compare test results. A spacing of the periodic obstacles such that the rear-wheel tires are excited into a condition of resonance produces the most severe vibrations to be encountered under normal operating conditions.

At the start of the test, the natural frequency of the rear tires under load was determined approximately from the static deflection of the tire. Considered as a freely oscillating system without damping, the natural frequency was calculated by the following equation:

$$f = \frac{1}{2\pi}\sqrt{\frac{c}{m}}$$

Substituting for $\frac{c}{m}$, the tire deflection under static load, a, (inches)

Table 1 – Average Weights and Tire Deflections for Contemporary Agricultural Tractors

Engine Power	Total Weight, lb	Weight on Rear Axle, lb	Rear Tire Size	Maximum Allowable Capacity at 11.4 Psi, lb	Tire Deflection, in., at Various Inflation Pressures			
					11.4 Psi	14.2 Psi	22.75 Psi	28.4 Psi
15	2420–	1540–	8.00 x 20	880	1.42	1.22	0.99	0.83
	3300	1980	7-30	848	1.22	1.06	0.91	0.75
20	3520–	2200–	9.00 x 24	1430	1.65	1.42	1.06	0.91
	4180	2640	8-36	1100	1.38	1.22	0.91	0.75
25	3960–	2640–	9.00 x 24	1430	1.65	1.42	1.06	0.91
			10-28	1520	1.69	1.46	1.18	1.06
	4400	2860	9.00 x 40	1650	1.77	1.58	1.26	1.06
30	4180–	2640–	11.25 x 24	1760	2.01	1.73	1.34	1.18
			9.00 x 40	1650	1.77	1.58	1.26	1.06
	4840	3080	9.00 x 24	1560	1.61	1.38	1.14	0.95
35	5500–	3300–	12.75 x 28	2420	2.48	2.05	1.58	1.38
	7260	4620	11-28	1815	1.85	1.58	1.38	1.18
40	7040–	4620–	12.75 x 28	2420	2.48	2.05	1.58	1.38
	7700	5060	11-38	2200	2.28	1.97	1.77	1.80
50	7480–	4420–	13-30	2640	2.16	1.93	1.54	1.34
	7920	5060						

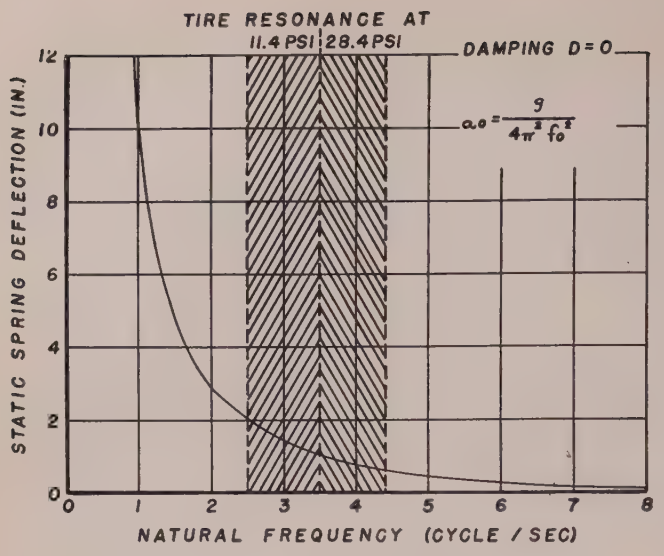

Fig. 7 – Static spring deflection versus natural frequency

$$a_o = \frac{G}{c} = \frac{mg}{c}$$

Whereby:

$$f = \frac{1}{2\pi}\sqrt{\frac{g}{a_o}} = \frac{3.14 \text{ cps}}{\sqrt{a_o}}$$

where:

G = weight of tractor, lb

g = gravity constant, 32.2 ft per sec per sec = 386 in. per sec per sec

It is usual to assume a desired frequency and calculate the desired spring deflection. Further resolution of the above equation gives a result:

$$a_o = \frac{9.86}{f_o^2}$$

This relation of natural frequency to static deflection of the tire is plotted in Fig. 7. Values thus determined are accurate for only very small values of damping. Greater values of damping decrease natural frequency (for example, approximately 4% when $D = 0.2$). This graph shows a rapid increase in spring deflection for frequencies below 2 cps and at the same time indicates the increasingly large resonance amplitudes.

As a tabulation of the relationship between tractor weight and frequency, the average values are shown in Table 1 for contemporary agricultural tractors.

From Table 1, it will be seen that the average "tire constants," that is, pounds loading per inch of deflection (c_m), are as shown in Table 2.

The smaller values of c_m correspond to the smaller tire section, indicating that c_m is more a function of tire width than tire diameter.

These variations of tire deflection result in the shaded ranges of resonance shown in Fig. 7. A decrease in inflation pressure from 28.4 psi to 11.4 psi results in an average frequency change of 1 cps. This difference in tire frequency between the extremes of inflation pressure is not of such a magnitude that two sets of experiments with different air pressures appeared necessary. Therefore, all experiments were conducted with a single air pressure of 22.7 psi, which was chosen as a mean of the pressures used in field and highway work.

Through the use of the deflection-frequency ratios shown in Fig. 7, the expected frequency range of a tire may be estimated. Tire deflection may be determined directly by measuring an available tractor or by interpolation from the load inflation table, assuming that the deflection has a straight-line characteristic.

An important assumption in the calculation is the acceptance of a linear deflection characteristic. For tractors with pneumatic tires, this is only approximate, as in practice the trend is slightly progressive. Actually, the natural frequency will be somewhat higher than that determined by the above approximation. If this error is to be reduced, it should be noted that in the middle range of tire deflection the slope of the load-deflection curve is greater, being approximately 1.2 and 1.4 times the average slope for the entire range at 28.4 psi and 11.4 psi, respectively. Therefore, the tire frequency as determined above must be increased from 10% to 20% over that given by assuming straight-line deflection.

The damping influence of the material in the tire carcass tends to reduce the frequency in the order of 3 to 5%. This small value may be disregarded when other variables change considerably. Due to uncertainties arising in estimating the natural frequency of tractor tires, the calculated values were verified experimentally. For the case investigated, the natural frequency of the tires was found to be approximately 4 cps.

Assuming a natural frequency of 4 cps, the spacing of obstructions along the path of travel necessary to excite resonance can be determined for a speed of 5 to 7.5 mph as follows (Fig. 8):

The period T for one complete cycle of oscillation and the distance between obstructions may be de-

Table 2 – Tire Constants

Inflation Pressure, psi	Lb Loading per In. Deflection, c_m
11.4	615–1120
14.2	730–1370
22.75	895–1680
28.4	1120–2010

termined from a known travel speed as follows:

$$T = \frac{L}{v}$$

$$f = \frac{v}{L}$$

where:

v = Velocity, fps

L = Obstacle spacing, ft

It will be seen that over a speed range of 2 to 14 mph, with obstacles spaced from 8 to 80 in. apart, a condition of resonance can always be induced. The spacing of the obstruction on the test track was such as to develop a vertical vibration without pitching. This condition can be satisfied only when the obstacles are spaced as even fractions of the tractor wheelbase.

This second condition necessitates that spacing of the obstacles be half of the wheelbase. It was expected that tire resonance would occur at a speed of 6¾ to 8 mph. This value was later confirmed experimentally.

The height of the obstacles chosen was 2 in., which corresponds to the depth of holes usually encountered in bad roads.

Test Equipment – (a) Tractor and seats used in test.

A Hanomag 4-cyl Model R 25 diesel tractor, built in 1950, was used as a test vehicle. The front axle was spring mounted, the rear axle unsprung. Its specifications were as follows:

Engine Power, hp	25
Wheel Tread, in.	51.2
Wheelbase, in.	70.9

Tires

Front – Dunlop 6.50 x 20 extra heavy duty, 28.4-psi inflation

Rear – Dunlop 9.00 x 40 Tractor Tires, 22.7-psi inflation

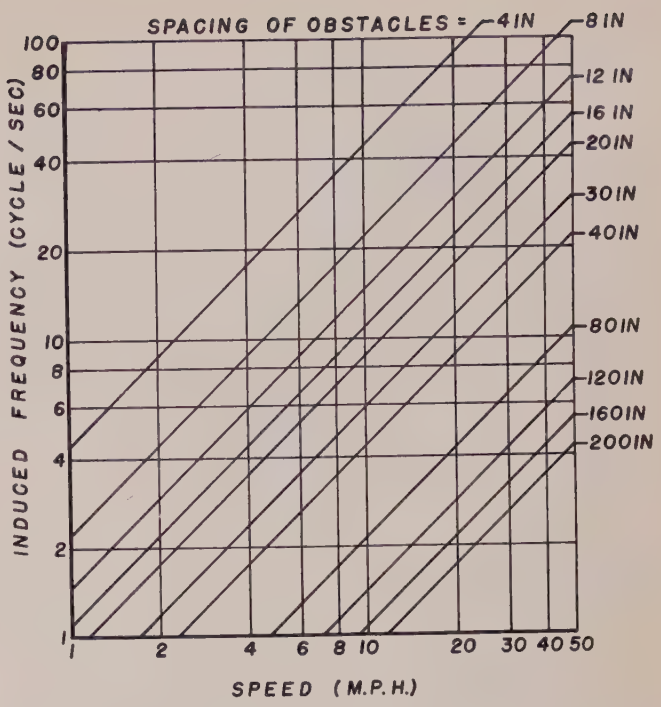

Fig. 8 – Relation of induced frequency to obstacle spacing and speed

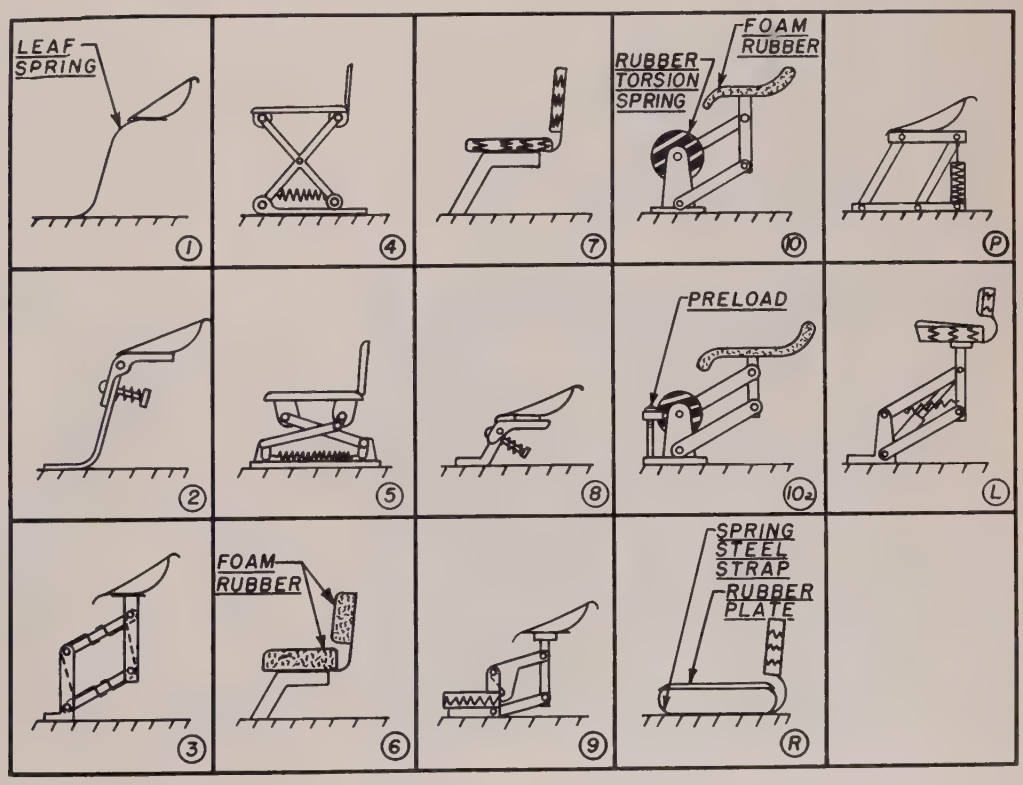

Fig. 9 – Schematic representation of seat designs tested

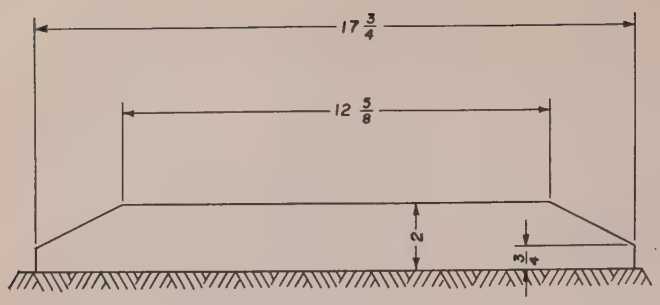

Fig. 10 – Dimensions of obstacle

Weight on Tires, lb.	
Front	
Without Driver	1535
With Driver	1505
Rear	
Without Driver	2675
With Driver	2855
Seat Position, in.	
Behind Rear Axle	13.8
Above Rear Axle	19.7

(b) Seats used in testing.

The 14 different designs of seats used in tests are shown in Fig. 9. From seat 10, an improved version 10a was developed, which included lighter moving parts with a rubber bumper serving as a stop for the supporting arms. Shortly before the end of the tests, a seat supplied by Heinrich Lanz AG, Mannheim, was included in the program. This seat incorporated a damped helical spring and padding.

(c) Test track.

A concrete floor was used as a test track, to which were bolted a single obstacle and a set of regularly spaced obstacles placed in straight rows and having the same shape as the single obstacle. These are shown in Fig. 10. With this fixed arrangement of obstacles, it was possible to reproduce any of the tests and make a reliable comparison of the different seat designs. A track between the rows of obstructions was used as a horizontal reference line for the "feeler" (electrical device for measuring vertical displacements, Fig. 11).

(d) Displacement measurements.

Displacement (oscillation) was measured in two ways. One method employed a photographic camera, with 5 x 7-in. plates, recording simultaneously the displacement curves of the rear axle, seat, and the shoulders of the driver. Electric bulbs (15 w) were mounted at these points to provide the necessary light sources. As the tractor was driven in front of the camera, these bulbs made traces of light on the camera plate and recorded all oscillations.

The vertical scale was obtained by means of a second bulb placed 15.75 in. vertically above the bulb at the end of the rear axle and which had an identical motion. The horizontal distance was established by lights along the ground. Time intervals (0.2 sec) were determined with a slotted disc rotated by a synchronous motor in front of the objective lens of the camera. This made a stroboscopic interruption of the displacement curves (Figs. 12 and 13). In this way, it was possible to record simultaneously and accurately the motions of the principal points essential for investigation of vibrational phenomena. This method has the advantage of employing a comparatively simple procedure and combining in one record all of the oscillations. Its limitations lie in the difficulties of its evaluation, due to unavoidable optical distortion.

Electric displacement measurements were conducted in conjunction with the acceleration measurements described later. Displacements measured as above were verified by means of a three-channel oscillograph together with a "sensing" circuit, so arranged that any change of displacement resulted in a proportional change in electrical current. These varying electrical values were obtained by means of a potentiometer to which a "feeler" was connected to measure any change of height of the rear axle with respect to

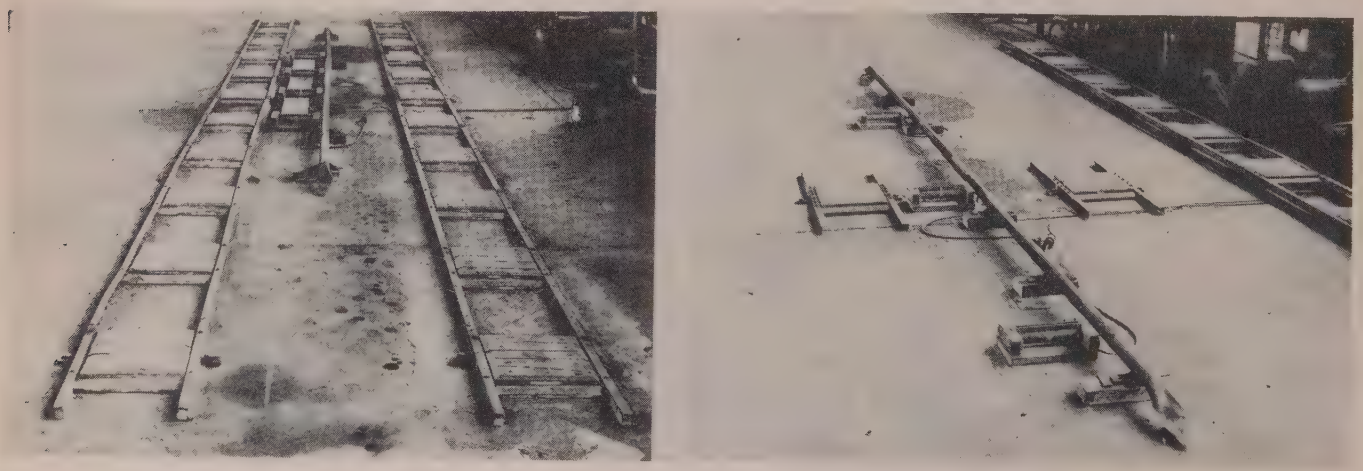

Fig. 11 – Test tracks. Left: single obstacle. Right: periodically spaced obstacles

the ground. A second potentiometer gave an indication of the motion of the driver's shoulders. Both potentiometers were connected to a Wheatstone bridge in such a way that the traces on the oscillograph directly indicated the motion of the driver's shoulders and the tractor rear axle with respect to the ground (Figs. 14 and 15).

(e) Acceleration measurements.

The acceleration of the driver was measured with a carbon-pile accelerometer (Type LFA; total weight, 2.8 lb; oscillating mass, 0.86 lb). The instrument was attached to an aluminum frame mounted on the shoulders of the tractor driver at the height of his shoulder blades (Fig. 14). This location appears to be best, because this portion of the shoulders gave free accessibility, a good mounting area, and a relatively firm support from the bones. Considering the investigations of Békésy,[1] frequencies from 0 to 6 cps are transmitted undiminished to the head, and frequencies as high as 20 cps reached the upper shoulder area. Hereafter, it is assumed that all vibrations are correctly recorded in the frequency range between 0 and 20 cps.

(f) Measurement of distance and time.

Throughout the photographic procedure, travel distance was measured by light markers. In the case of a single obstacle, the center point together with points 86 in. ahead and to the rear were indicated. In the case of the periodically spaced obstructions, light markers were so arranged that from right to left, they showed valley, peak, valley, peak, successively (Fig. 13).

During electrical measurements of displacement, the travel distance was recorded on the oscillogram by means of a photoelectric cell. This photoelectric cell induced electric impulses when the tractor passed lights which were mounted beside the obstruction. In the case of the single obstacle, the center point together with points 70 in. ahead and to the rear were indicated. In the case of the periodically spaced abstructions, the center of the peak was indicated.

In experiments using the photographic procedure, time was measured with power-line frequency using a synchronous motor to drive the slotted disc. In experiments using the oscillograph, a frequency of 50 cps generated electronically by a vibrating tuning fork was superimposed on the 500-cps frequency of the oscillograph circuit.

Experiments Performed – (a) Determination of seat characteristics.

Each of the different seats was investigated to determine the suspension characteristics under static conditions and the natural frequency under load. At first it was thought desirable to determine the natural frequency of the seat from its static characteristics. It was found, however, that due to friction, substantial discrepancies from the calculated values appeared during operation. Thus, it was necessary to determine experimentally the

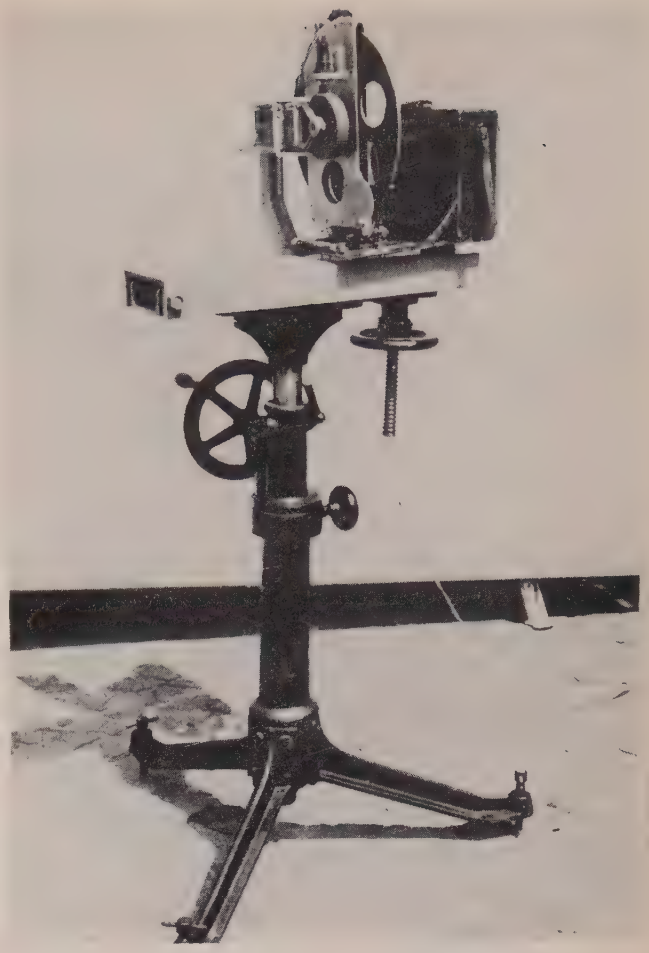

Fig. 12 – Camera with rotating interrupter

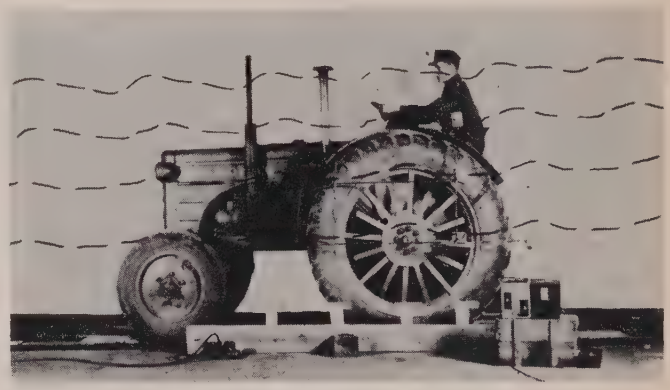

Fig. 13 – Test setup for light tracings

natural frequency under load. Here again difficulties were encountered, since in the case of certain suspensions, a displacing load could not be applied and released by cutting a wire to determine the frequency with a carbon-pile accelerometer. Since seat No. 2 responded readily to this method of test, additional investigations were conducted with it to evaluate the damping influence of the human body (Fig. 16). It was found that the driver's body acted as an effective damper to reduce

Fig. 14 – Measuring vibration at the driver's shoulders

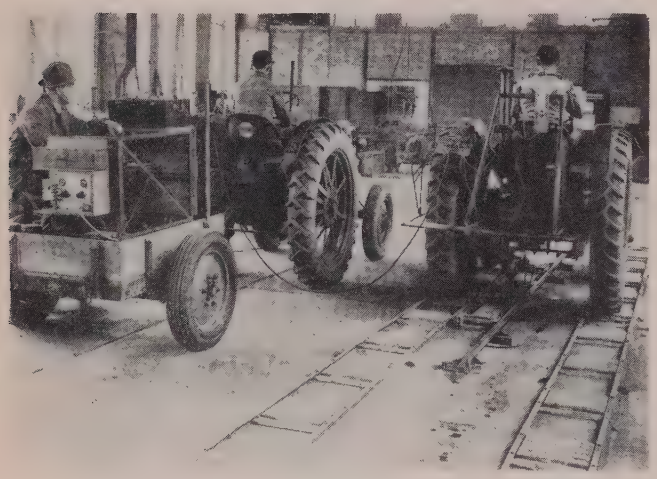

Fig. 15 – Test setup for measuring vibration electrically

seat vibration. In order to determine vibration curves of all seats under the same load, a weight shaped similar to the seat pan, with a magnitude that caused the same seat deflection as the driver does, was dropped from 6 in. onto the seat. The accelerometer was fixed to that weight. The natural frequency of the seat without the damping effect

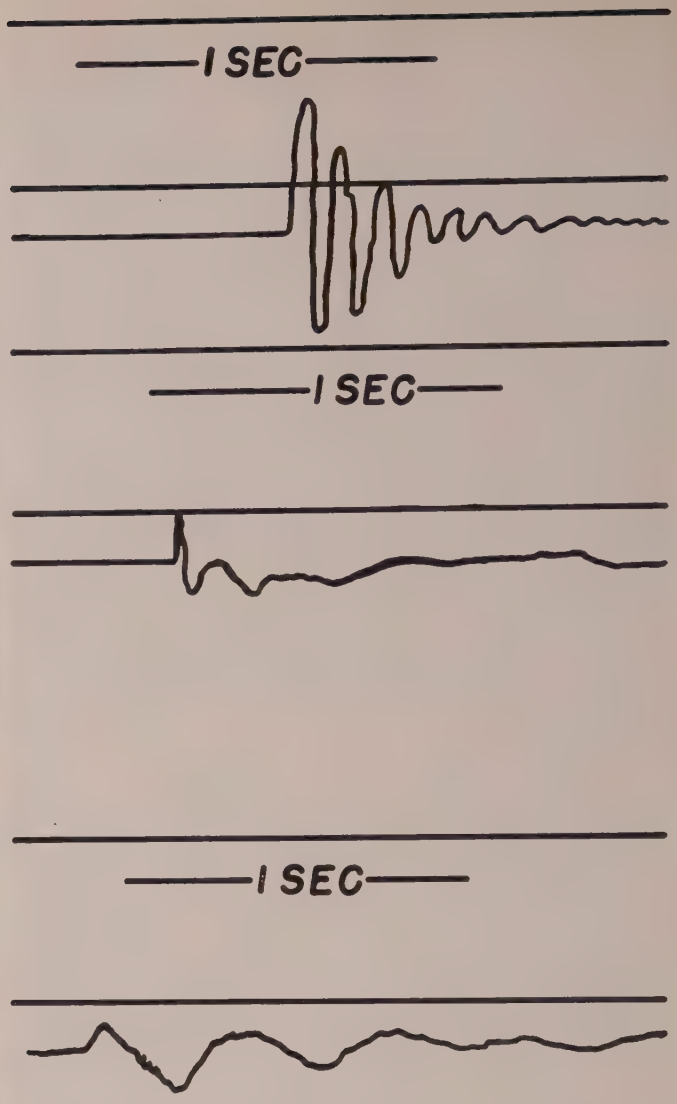

Fig. 16 – Natural frequency of the seat with different loads. Upper trace: empty seat deflected 8 in. Center trace: seat with driver deflected 8 in. Lower trace: seat with rigid mass equivalent to driver's weight deflected 8 in.

of the human body was thus determined.

It should be especially noted that the seat loading does not equal the driver's weight. For a seated person, and especially for a driver whose arms are resting on the steering wheel with his feet on the tractor platform, the weight on the seat is approximately 70% that of the driver's total weight. No change in this ratio with the size of the driver could be established.

It is also important to know what locations to assume for the driver's center of gravity. For a standing human specimen of normal proportions, extensive research data by Braune and Fischer[6] are available. From their carefully determined

[6] See Abhandlungen der mathematisch-physischen classe, der Konigl, sachsischen Gesellschaft der Wissenschaften, Vol. 26, 1889, p. 627: "Über den Schwerpunkt des menschlichen Körpers," by W. Braune and O. Fischer.

values, it is possible to form conclusions regarding a seated person. Fig. 17 presents the weights of the individual body members of a person sitting on a tractor seat. The location of the driver's center of gravity may be assumed to lie in the vicinity of his navel.

A change in position of the seated driver may result in shifting his center of gravity and inertia center as applied to the driver-suspension vibratory system. This means that drivers of equal weight may produce different natural frequencies of the seat, depending upon the position of their bodies. In the same way, the driver may knowingly or unknowingly cause a change in the characteristics of the seat suspension by shifting his body weight. From observation, it has been found that experienced drivers usually sit so that their body is inclined slightly forward, thus placing the center of gravity of the head directly above the resultant center of gravity. This may be considered as an inadvertently correct reaction of the driver, since as a result the head generally oscillates only vertically. It may be mentioned as a comparison that, while walking, the center of gravity of the head is directly above the resultant center of gravity of the human specimen. Considering the strong shock originating with walking, this seems to be a wise adjustment of nature.

(b) Determination of the natural frequencies of the tractor front and rear axles.

As previously mentioned, the natural frequency of the tractor with pneumatic tires was roughly calculated at the beginning of the test program. A more precise evaluation of test results required experimental determination of the natural frequency of the tractor under actual operating conditions. For this purpose, carbon-pile accelerometer pickups were mounted directly on the rear-axle housing and the front frame of the tractor. The tractor was then lifted 4 in. and dropped by severing the lifting wire. The resulting severe impact excited untuned oscillations, with severe higher harmonics appearing during decay, which tended to excite the natural frequency of the accelerometer. This difficulty was largely eliminated by means of a built-in electrical filter, such that the interfering frequencies became negligible as compared to the basic frequencies. The curves thus recorded are shown in Fig. 18.

The measured value of the natural frequency of the rear axle agrees quite well with that calculated. The natural frequency of the front axle is approximately only 10% lower than that of the rear axle, thus creating conditions favorable for the occurrence of pure vertical vibration.

(c) Photographic recording of displacement curve.

The displacement curves of seats 1 to P were recorded as the tractor was driven over both single and periodic obstacles, affording a comprehensive

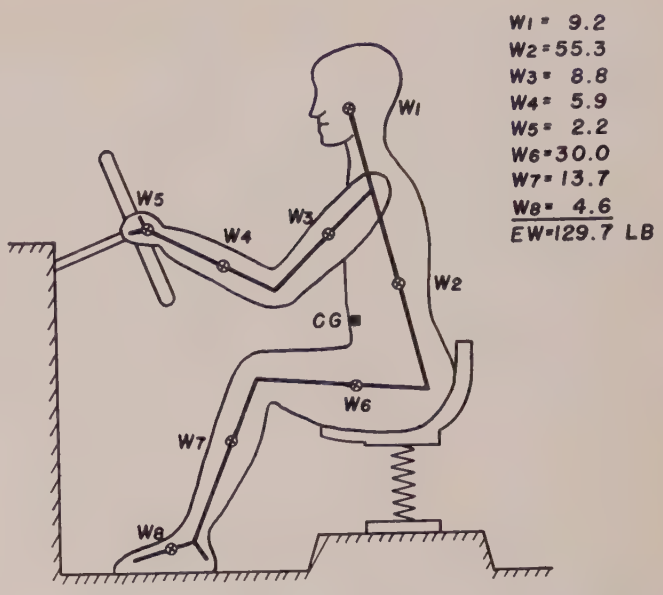

Fig. 17 – Weights of body members according to Braune and Fischer

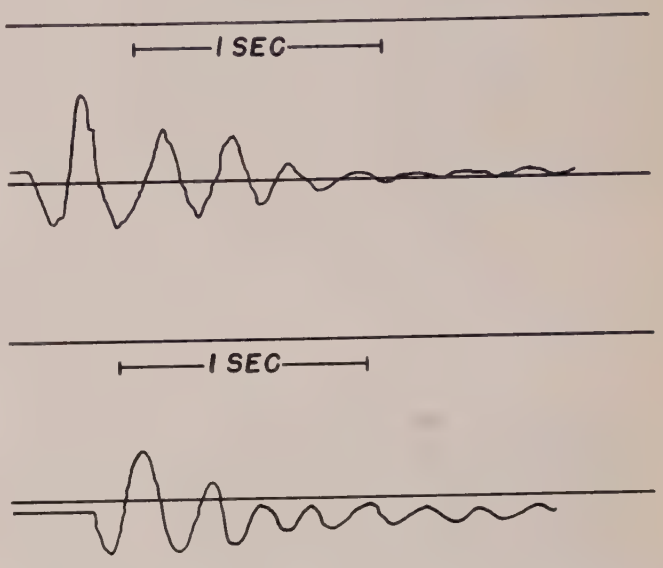

Fig. 18 – Natural frequency of front and rear axles. Upper trace: front axle $f_o = 3.67$ cps. Lower trace: rear axle $f_o = 4.07$ cps

picture of the differing motions of the tractor seat and the driver.

(d) Electrical measurements of displacement and acceleration.

The electrical method was first used to determine the acceleration pattern of the driver. The displacement curve was used only for defining the position of the motion where acceleration peaked. Following this method, all of the seats and seat combinations were investigated by driving over single and periodically spaced obstacles. In addition, accelerations of the rear axle were also determined.

Evaluation – (a) Method.

The displacement curves recorded photo-

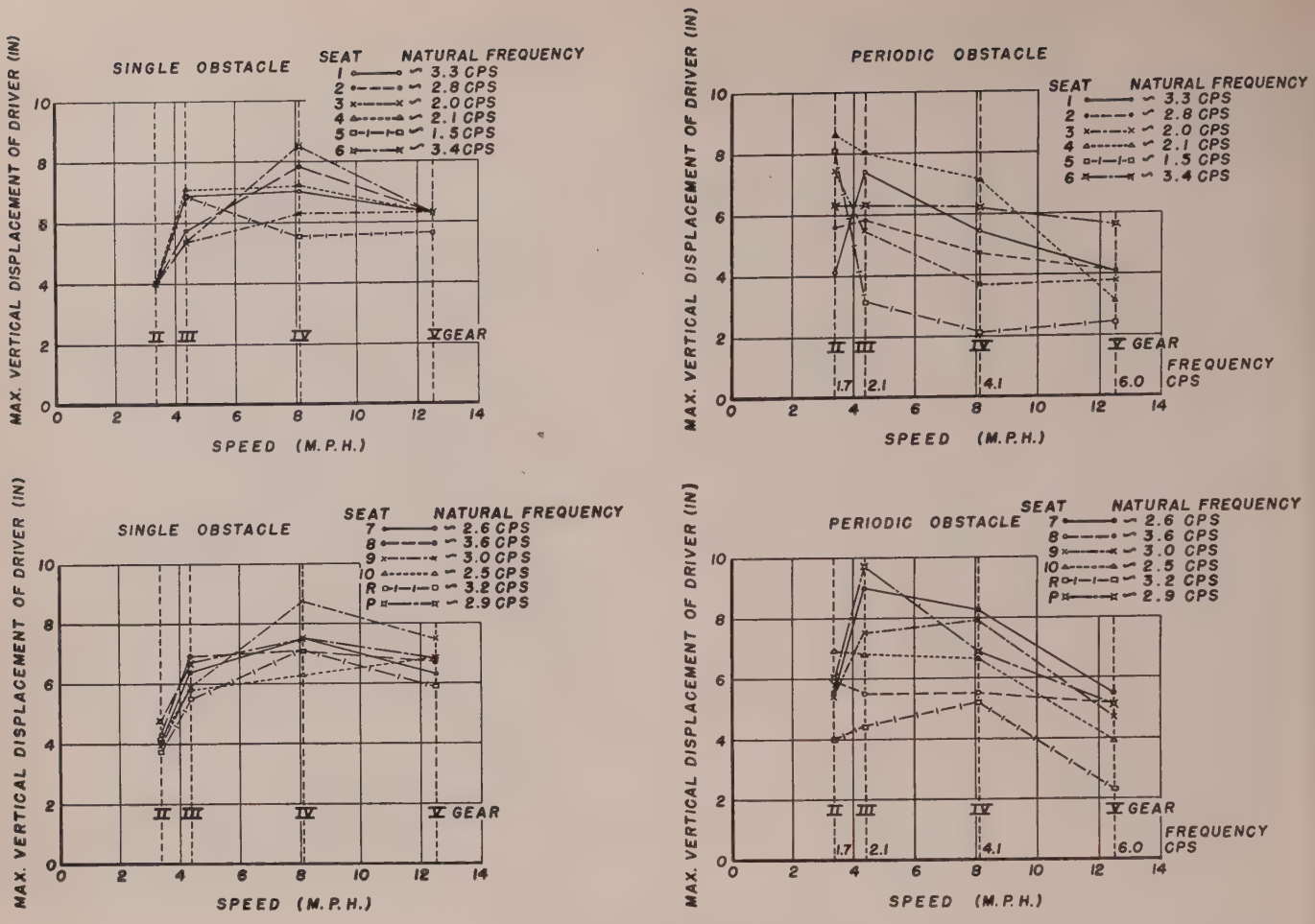

Fig. 19 – Displacement curves

graphically were evaluated on the basis of the greatest displacement between the tractor driver and the horizontal plane of the test track. This was taken as a measure of the stress imposed upon the driver as a result of vibration. These evaluations were compared with the subjective opinion of the driver, which he recorded throughout the tests. In Fig. 19, the measured displacement is shown as a function of tractor speed and frequency of obstacles.

The magnitude of the greatest peaks in acceleration for each gear were evaluated from the displacement and acceleration curves recorded electrically with the oscillograph. Differentiation of the acceleration curves for the purpose of obtaining "jerk" as the actual measure of the sensation of vibration was impractical because of inaccuracies. All curves have the same time and frequency basis (the same tractor speed), thus making it possible to substitute the peak acceleration value for the differentiation of the acceleration curve. The peak acceleration values thus found are presented in Figs. 20, 21, and 22 as functions of tractor speed and frequency of the obstructions.

(b) Results.

A study of the displacement curves recorded photographically (Fig. 19) shows that, in spite of the variations in design of the seat suspensions, displacement of the tractor driver throughout the significant frequency range (between 2 and 6 cps) remains at least equal to the height of the obstacle and is often twice as great. This result confirms predictions based on the earlier study of vibrations recorded in Section B. Any reduction of the amplitude of the movement of the driver as compared with the height of the obstacle is not to be expected for the presently possible seats having a natural frequency in the range of 1.5 to 3 cps, when the frequency of the obstacles ranges from 1 to 6 cps. On the contrary, three- to four-fold amplification may be expected.

These amplifications are actually encountered, but the maximum values of the resonance curves occur, contrary to calculations, more toward the range of the natural frequency of the seat. The difference in the height of the resonance peaks between tight or loose coupling of the system is not evidenced with sufficient clarity. These deviations might be explained as resulting from the rather poor agreement between the simplified anal-

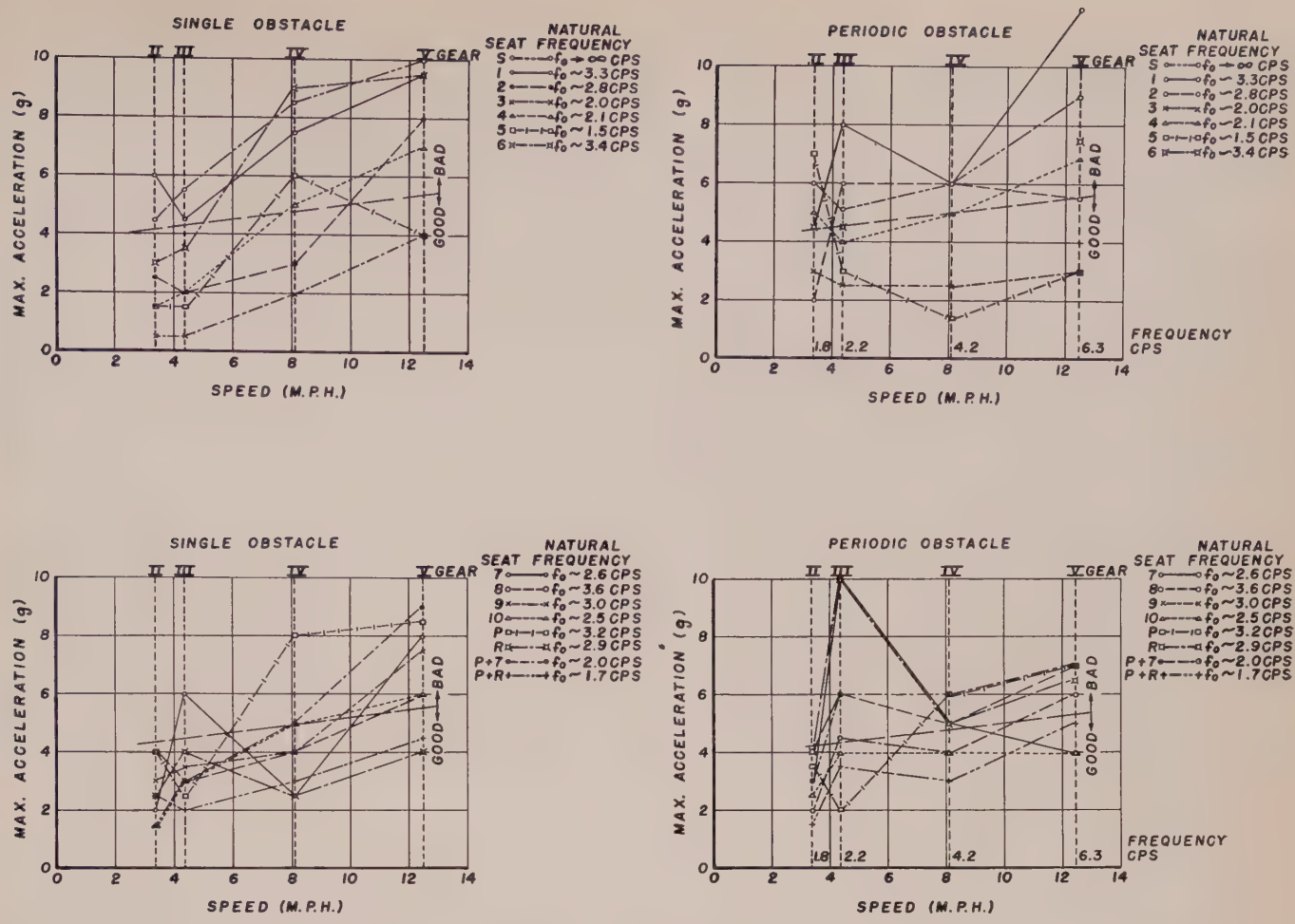

Fig. 20 – Acceleration curves

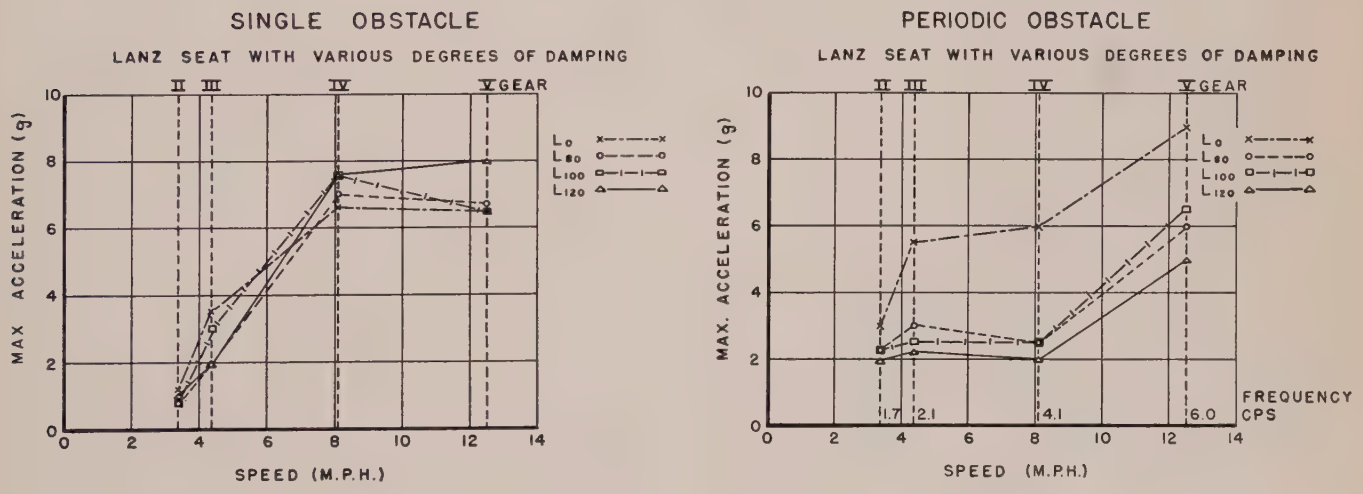

Fig. 21 – Influence of hydraulic damping

ogy system and the actual driver. The tractor driver is definitely not rigidly connected to the seat, which was a basic assumption for the theoretical analysis. Regardless of all this, the trend of the resonance curves obtained when operating on the test track closely agrees with the calculation.

The above statement is particularly true with respect to the extreme case when using the periodically spaced obstacles. The other extreme case, using a single obstacle, shows a deviation of the displacement curve from the theoretical displacement. With periodically spaced obstacles en-

countered at a rate greater than the natural frequency of the seat, the oscillations of the driver are as much as 180 deg out of phase with the rear axle. On the other hand, the single obstacle results in a pronounced cophasal pitching effect, which in turn was actually registered by the tractor driver. It could possibly be explained as follows: for an obstruction height of 2 in., the tire cannot deflect equally, because the static deflection is only about 1.2 in. Furthermore, the deflection characteristic of the tire under dynamic loading does not correspond with that under static loading. Thus the tractor is lifted vertically, and vertical acceleration occurs. This vertical acceleration results in increasing the reaction of the driver's weight and compressing the seat suspension. Energy thus stored is freed as the turning point of the trajectory is reached, tending to pitch the driver upward. With the tractor operating in fourth gear, seats Nos. 4 and 5 gave information regarding the magnitude of the vertical acceleration occurring when the rear axle was lifted and the seats bottomed. Considering the characteristics of seat suspension measured statically, forces of 240 to 285 lb must have been exerted against the seat, corresponding to accelerations ranging from 2.2 to 2.6g. This leads to a design rule that for the ever occurring situation when the tractor tires leave the ground, the seat suspension should provide for an additional deflection of 1½ times the static deflection. Otherwise, it must be expected that the driver will experience the very unpleasant situation of "hitting bottom."

From this, it appears that a progressive seat spring rate may offer a possible advantage. Such a suspension is difficult to calculate and can be made to perform in the desired manner only through lengthy experiments. Therefore, such a seat could not be made in time for these tests.

No difference could be detected between the individual seats as to the height to which the driver was pitched. This may be explained by the fact that the pitching energy is a function of the acceleration of the rear axle and is independent of that resulting from the seat suspension. Any damper built into the seat suspension can be only partially effective in restricting this upward pitching of the driver, since it is effective only on the seat pan and not on the driver.

Regardless of the agreement between the amplitudes measured and calculated for harmonic motions, it is impossible to draw accurate conclusions as to the sensation experienced by the driver

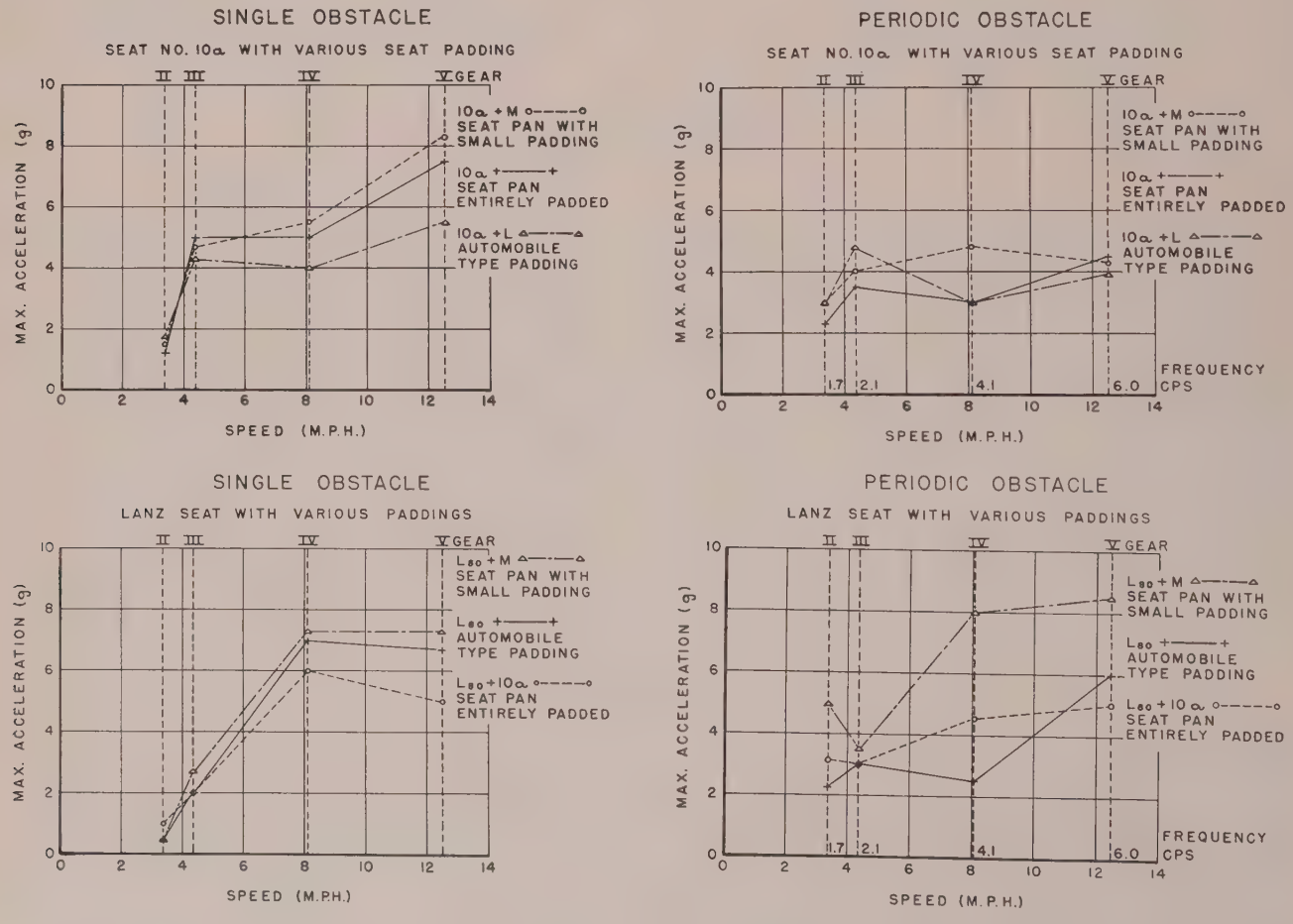

Fig. 22 – Influence of seat padding

as the result of any given amplitude of vibration. It was found that the subjective evaluation of the quality of ride for practically the same amplitudes of vibration ranged from "very poor" to "good." In order to explain this unsatisfactory result, it should be pointed out that the relation of the driver's sensation to vibration resulting from any given amplitude, as stated at the end of Section A, is true only in the case of a pure harmonic motion. Only in so simple a case are the curves of derivatives theoretically equal to the original curve. As a simplified example the influence of the fifth harmonic may be considered theoretically.

The vibrational phenomena may be represented by the following equation for the displacement curve.

$$s = a \sin \phi + b \sin 5\phi$$

where:

$$\phi = \omega t$$

The derivations with respect to time are:

$$\dot{s} = a\omega \cos \phi + 5\, b\omega \cos 5\phi$$

$$\ddot{s} = -a\omega^2 \sin \phi - 25\, b\omega^2 \sin 5\phi$$

$$\dddot{s} = -a\omega^3 \cos \phi - 125\, b\omega^3 \cos 5\phi$$

when:

$$\phi = \frac{\pi}{2}, \text{ that is, } \cos \phi = 1 = \cos 5\phi$$

$$\dddot{s} = -\omega^3 (a + 125b)$$

The result shows that in the presence of a fifth harmonic with an amplitude, for example, of 1/100 of the first harmonic, the effect of the fifth harmonic on vibration sensation is the same as the 100-fold first harmonic.

Any nonharmonic motion, such as that which occurs during pitching, always consists of higher harmonics which cannot be ignored. The displacement curves present only basic information regarding the oscillation and do not permit of any conclusions regarding the riding quality. Thus, for an evaluation of the suspension characteristics (riding qualities) only the acceleration curve need be considered. Recording of the change in rate of acceleration, that is, "jerk," would be better. However, because of the difficulties encountered in measuring, this derivative was disregarded.

Evaluation of the oscillograph records showing displacement and acceleration (Figs. 20, 21, and 22) reveals a close agreement between the factor chosen to represent the ride quality of the suspension, that is, the acceleration peaks, and the subjective driving sensation of the tractor driver.

In Fig. 20, the magnitude of the acceleration peaks are presented graphically as a function of tractor speed. They present an entirely different picture of the individual seat designs as compared to that given by the evaluation of displacement (Fig. 19). The differences in riding qualities (suspension quality) are clearly brought out and are in agreement with those experienced by the driver. By noting the points of the individual designs which were mentioned by the driver as being "poor," it was possible to draw in a line in the diagrams of Fig. 20 which represent the boundary between "good" and "poor." Seat designs having characteristic points which lie above this line must be judged as bad. It is thus possible to prepare an evaluation having three criteria: good (g), still acceptable (a), and poor (p). The middle value, "still acceptable," denotes the ever present borderline cases between "good" and "poor." In Table 3 it will be seen that seats 3, 10, Q, and R have superior ratings. Their natural frequency is approximately 2 cps, whereas seats rated as "poor" have a natural frequency of approximately 3 cps and higher. Natural frequency should not be regarded as the only factor affecting suspension quality (ride characteristics), although the calculations in Section B show it to be an essential fundamental requirement. Seat designs 4 and 5, with natural frequencies of 2.1 cps and 1.5 cps, respectively, had to be regarded as unusable because the useful deflection in the suspension was insufficient to absorb the loads resulting from a single obstacle. Both seats "bottomed" so severely when operating in fourth gear that their otherwise satisfactory performance was overshadowed. Furthermore, the rigid back rests in both seats are regarded unfavorably. The driver's motion is not limited to pure vertical movement, but a horizontal swinging motion due to fluctuations in tractor speed is also present. When this condition prevails, a rigid back rest acts as an unpleasant stop. The acceleration curves confirm the frequently made statement that the most uncomfortable sensation experienced in driving a tractor results primarily from the great increase of acceleration at the time the seat "bottoms." If the acceleration curves are compared with the simultaneously recorded displacement curves of the driver's shoulder with respect to the ground, it is clearly shown that the maximum peaks of acceleration occur when the driver hits the seat at the

Table 3 – Drivers' Subjective Judgment of Seat[a]

Seat Designation	S	1	2	3	4	5	6	7	8	9	10	P	R	P + 7	P + R
Single Obstacle	p	p	a	g	p	p	p	p	g	a	g	p	g	a	g
Periodic Obstacles	p	p	a	g	a	a	p	p	a	a	g	a	p	g	g
Overall Evaluation	p	p	a	g	p	p	p	p	a	a	g	p	p	a	g

[a] Designations used are: g = good, a = still acceptable, p = poor.

lowest point of seat travel, after having been pitched free of it. The impact against the seat which results after the driver is pitched up may be considerably reduced for a given natural seat frequency by padding, by reducing the mass of the oscillating parts, and by damping the natural frequency of the empty seat.

Lanz Seat Tested

A new seat made by Henrich Lanz AG of Mannheim is an example of a design in which all of these points were carefully incorporated. Unfortunately, this seat was not available until the end of the testing period. However, to provide a better understanding of the factors previously discussed, comparative tests were made with this Lanz seat and the No. 10a seat. First, the damping of the Lanz seat was varied, and second, the padding of both the Lanz and the No. 10a seats was varied. The results of these tests are shown in Figs. 21 and 22 and do not reveal any significant influence of the shock absorber when the rear wheels strike a single obstacle. In the case of periodically spaced obstacles, the influence of the shock absorber was quite detectable, as the peak values of acceleration were reduced by over 50%. With regard to padding, the fully padded "pan" seat was practically equivalent to the automobile-type cushion seat. However, the regular pressed steel seat, with a single layer of sponge rubber 13/16 in. thick and used with the Lanz suspension, resulted in considerably higher acceleration peaks than a seat with typical automobile upholstering. With the suspension used with seat 10a, this difference was less pronounced.

To provide an overall view of the accelerations of the rear axle and seat, additional measurements were taken. This confirmed the calculation that the peak acceleration of the seat would be in the range between 2 and 3g when the tractor tires leave the ground. Furthermore, the impact of the driver when landing on the seat produced peaks of seat acceleration higher than that produced on the rear axle as the tires left the ground.

Conclusions

The theoretical investigation and the experimental verification both show that with exciting forces ranging in frequency from 1 to 6 cps vertical displacements of the tractor driver are at least equal to the height of the obstruction, and quite often they are from two to three times larger due to tight coupling between seat and tractor.

Design considerations limit the extent to which the flexibility of the connection between the two oscillating systems, that is, driver-seat suspension and tractor-tire, can be increased. The best conditions prevail when the ratio between the natural frequency of the seat and the natural frequency of the tires amounts to $\nu = 0.4$ to 0.5. Because normally loaded tractor tires have a natural frequency of approximately 4.0 cps, it follows that the natural frequency of the loaded seat should be between 1.6 and 2.0 cps. This conclusion closely agrees with the latest American investigations by Simons.[7] By calculating the extent to which the vibrations of a simple oscillating system may be transmitted, he arrived at the same conclusion. His relatively simple calculations are based on a rough approximation of the resonance behavior of the two existing mass systems. The resonance curves of acceleration actually measured by Simons do not agree entirely with his calculations although they appear comparable with those presented in Fig. 3.

In addition to the static deflection of the seat due solely to the weight of the motionless driver, a supplementary deflection in the order of 1½ times that of the static deflection (assuming linear deflection characteristics) must be available in order to avoid "bottoming."

In order to hold seat deflection within practical limits, it is recommended that suspensions having nonlinear characteristics be used. This will automatically compensate for the differing weights of drivers.

If there is insufficient space to provide for the necessary deflection, then the seat suspension should be discarded and a rigid seat with carefully designed padding used.

As previously mentioned, compensation must be provided for the widely varying weights of the

Fig. 23 – Samples of seat design. Upper: Monroe, FAL. Lower: Ridemaster, Lanz

[7] See *SAE Quarterly Transactions*, Vol. 6, April, 1952, pp. 357-364: "Tractor Ride Research," by A. K. Simons.

drivers. Seat springs should not be preloaded, but their course of action should be varied in such a way that the seat suspension characteristics are changed while the static deflection remains constant. Only in this way can a favorable natural frequency of the seat be maintained.

Due to pitching and as a result of impacts, the oscillations of the tractor and driver are not harmonic. These nonharmonic oscillations have acceleration curves which are not comparable with the displacement curves, and the steep acceleration peaks (change in rate of acceleration) constitute the principal vibration effect on the driver. Consequently, it is of great importance to reduce the impact of the driver as he lands on the seat after being pitched from it. The effective steps to this end include: reduction in the oscillating mass of the seat, padding of the seat, and damping of the seat suspension with a suitable shock absorber or through the use of material having high damping qualities such as rubber (desired damping $D \approx 0.3$ to 0.4).

Seat and suspensions which conform in a large measure with the above listed requirements include those made by Lanz and Monroe, both of which employ the principle of hydraulic damping, and the Ridemaster Seat made by the U. S. Rubber Co., and the experimental design No. 10 made by FAL (Forschungsanstalt fuer Landwirtschaft, Braunschweig-Völkenrode) having torsional rubber springs utilizing the inherent damping of rubber (Fig. 23). An example of a suitable rigid seat is that built by the Dubuque Works of Deere & Co. in the United States (Fig. 24). This padded seat consists of an air cushion which may be inflated in accordance with the weight of the tractor driver, together with a padding approximately 1⅛ in. thick made of animal hair. This hair is dipped in rubber latex, thus binding it elastically together. The air cushion and padding are held together by a thin leather covering. Construction of the air cushion is such that "floating" of the driver does not occur.

Lay-Fischer Results Inapplicable to Tractors

Detailed investigations have been made by W. E. Lay and L. C. Fischer[8] into the design of seats for passenger cars, but they are of only limited value when considering the design of tractor seats. Their report indicates that a back-rest cushion sloping backwards and extended to the height of the operator's shoulders gives the most comfortable sitting position. In the case of the tractor driver, this sloping position is entirely impossible on account of the previously mentioned pitching which occurs when driving over obstructions. The distribution of load acting against the seat of a passenger car does not apply to the seat of a tractor, because in the latter the driver is bending forward. The padding on a tractor seat should not be uniform (of even thickness), but the suspension in the center of the area supporting the driver's weight should be from three to four times stronger than at the sides. The distribution of the pressure on the seat may be assumed to be parabolic.

Furthermore, the position of the seat with respect to the controls and the design of the back rest must be considered in the subjective judgment of a seat. Müller[9] indicates from his investigations of working physiology that the direction of foot pressure should be applied where possible either horizontally or slightly downward. The body must be supported at the pelvis and not at the shoulder blade area because the inherent flexibility of the spine does not afford the necessary rigidity against bending. It will be noted that in our experiments those seats which had a high back rest even with different degrees of resiliency were found by the drivers to be uncomfortable. A low back rest built up to the height of the pelvis seems to be the most favorable design for tractor seats.

Note

The author of this paper has investigated the most favorable design of seat suspension for tractors having pneumatic tires with a rigid rear axle. The findings are presented in his thesis, "Seat Suspension Measurements on Tractors with Pneumatic Tires and Rigid Rear Axles," and are published by permission of the copyright owners, Kuratorium für Technik in der Landwirtschaft, Frankfurt am Main, German Federal Republic. The essential parts of this investigation have been presented herein.

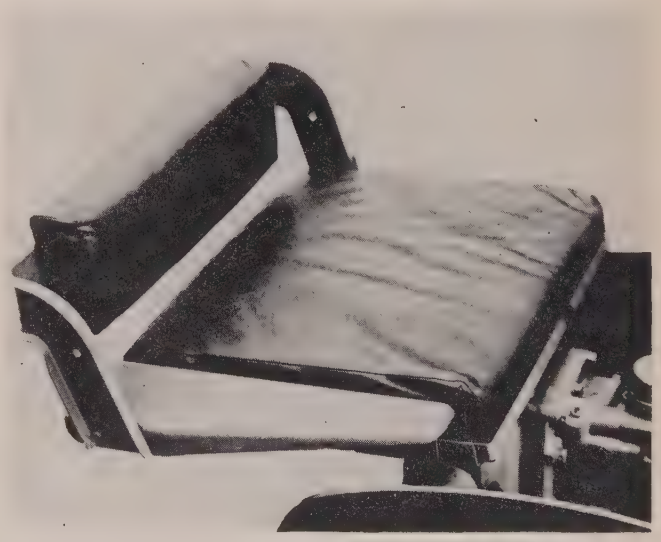

Fig. 24 – John Deere padded seat

[8] See *SAE Transactions*, Vol. 47, pp. 482-496: "Riding Comfort and Cushions," by W. E. Lay and L. C. Fisher.
[9] See *Arbeitsphysiologie*, Vol. 9, 1936, p. 125: "Die günstigste Anordnung im Sitzen betätigter Fusshebel," by E. A. Müller.

DISCUSSION ON FOLLOWING PAGE ⟶

Author's Test Setup Gives Rougher Ride than Real Field Work

– R. N. Janeway
Chrysler Corp.

DR. Haack has done a great deal of painstaking experimental work which strikingly demonstrates the potential brutality of farm tractors as man-carrying vehicles.

Criteria of Human Tolerance for Vibration

At the outset, he subscribes to the precise criteria of human tolerance for vibration, which this writer presented in 1948,[a] based on an analysis of all the available data. It is certainly gratifying to know that these vibration limits have found further verification. However, one would wish that he had included in this paper the approach which led him to accept their validity. Instead, he refers to a discussion of this subject in a previous paper of his own, which is not yet generally available in this country.

The fact is that the intensity of disturbance imposed on the driver in every one of his tests far exceeds the range of the experiments from which these vibration limits were derived. Therefore, such criteria are not applicable to his results except to indicate generally how altogether intolerable such shock levels must be.

This raises a serious question as to whether his results are representative of actual field conditions. Tractor acceleration measurements under actual operation over typical rough farm terrain show a much lower level of primary disturbance on the tractor.[b] Unfortunately, he gives no measurements on the tractor itself but only on the driver. Therefore, his results cannot be directly related to other available measurements. At any rate, it is certain that Dr. Haack's simulated obstacles have exaggerated the tractor disturbance beyond the working range of any of the seat constructions tested. This conclusion is fully borne out by the magnitudes of the test measurements. Consider the maximum displacements of the driver, which vary from 4 to 10 in. These far exceed the possible deflection range of the seats, indicating that the driver is continually being tossed free of the seat. This condition is freely admitted by the author. The natural consequence is that the seat is called upon to function as an impact absorber when the driver falls back upon it. Since the seat suspension does not have sufficient energy-absorbing capacity, the driver ends up by bottoming on the seat. The result is that maximum deceleration measurements up to $10g$ are shown. Under periodic excitation the minimum peak acceleration with the best seat tested was still $2g$.

Threshold of Uncomfortable Disturbance

If we refer to the previously mentioned criteria of human reaction to vibration, we find that the threshold of extremely uncomfortable disturbance at a sinusoidal motion frequency of 3 cps occurs at a displacement amplitude of 0.4 in. This corresponds to a maximum acceleration of 12 ft per sec per sec, or approximately $0.37g$. According to F. J. Meister, on whose work this criterion is based, the human reaction to this level of disturbance is not merely extreme discomfort but "probable injury if sustained." To reach the threshold of discomfort at the same frequency, the peak acceleration must be reduced to one-quarter of this value, or to about $0.1g$. In contrast, even the most conservative measurements of tractor acceleration at 3 cps show accelerations consistently averaging more than $0.6g$, or considerably beyond the very uncomfortable threshold. If the shock level is to be reduced to a safe level by seat design, it is clear that the seat suspension must be capable of attenuating the maximum excitation of the seat support by at least 50% and preferably by 75%. In this connection, emphasis must be placed on the force transmission which directly produces acceleration and jerk. The common tendency to deal analytically only with amplitude ratio can be seriously misleading since it does not bring out the very important component of force transmission introduced by the damping of the system.

It is also evident that the author's mathematical approach to the tractor seat suspension cannot possibly correlate with his experimental results. His derived equations assume a linear vibrating system and an exciting motion of sinusoidal form. To begin with, the tractor wheels readily leave the ground under the conditions of the test, by his own admission. As already pointed out, the driver alternately leaves the seat and bottoms on the suspension. Consequently, there is a wide gap between the characteristics of the real system and the simplified assumptions of his theoretical analysis.

What's Wrong with Present Suspension Systems

If we analyze the suspension system represented by presently accepted farm-tractor construction, we find that it violates a fundamental requirement of any road vehicle intended to be ridden and operated by human beings. In all other vehicles the sprung mass comprises the major portion of the entire vehicle, and the unsprung mass becomes a relatively small fraction of the total. This means that wheel accelerations of $5g$ and higher are commonly required to make the wheel lose contact with the ground. In the tractor used by the author, the condition is both reversed and exaggerated, since the sprung mass represented by the driver amounts to about 1/15 of the unsprung mass on the tires. Obviously, a deceleration rate slightly greater than $1g$ is all that is required to make the wheels hop. When this occurs, the resulting amplitude imposed on the driver's seat is no longer limited by the road irregularity but can and does greatly exceed this primary disturbance.

Until this basic situation is corrected, no seat suspension capable of producing anything approaching "easy riding" is likely to be devised within the practically allowable limits of seat displacement. Instead, all that can be hoped for is to limit the maximum shock on the driver to a point short of potential disablement.

Even if we discount Dr. Haack's results as greatly exaggerated as to the shock intensities normally imposed on tractor drivers, there is ample evidence that the average tractor does subject the driver to a degree of punishment which can lead to permanent disability. A. K. Simons has referred to a number of medical surveys which present startling findings as to the prevalence of certain serious disabilities to tractor drivers in his excellent paper on "Tractor Ride Research."[b] This situation is most certainly serious enough to call for intensive efforts in two directions: first, to alleviate the disturbances by improved design and, second, to establish by scientific investigations the safe limits of shock and vibration with regard to potential injury.

[a] See footnotes 2 and 3 of main paper.
[b] See footnote 7 of main paper.

Flight Load Measurements and Analysis

W. L. Howland and C. J. Buzzetti,
Lockheed Aircraft Corp.

This paper was presented at the SAE National Aeronautic Meeting, Los Angeles, Oct. 7, 1954.

MAN'S progress and ability to fly in heavier-than-air-type vehicles has been closely related to, and to a large extent dependent on, his knowledge of aerodynamic forces and characteristics. It is therefore important to review and describe from time to time the techniques and methods for determining the nature and magnitude of aerodynamic forces. This paper deals with making measurements of loads on actual airplanes in flight and with analyzing the data obtained. This subject has additional interest at the present time due to the present trend in military requirements, which state that load measurements must be made on a prototype airplane before it is accepted for service use. Indications are that CAA may require in-flight load measurements of certain items before certifying high-speed transports.

Theoretical calculations and wind-tunnel measurements have been extremely valuable in contributing to man's knowledge of aerodynamic forces and characteristics; however, both tools have certain fields of application and limitations. For example, the purely theoretical analysis of aerodynamic forces is seriously handicapped when dealing in the transonic speed range; and the wind tunnel has problems with the effect of the wind-tunnel walls on the forces measured, scale effects, and reproducing aeroelastic effects. The theoretical approach and the wind tunnel are both at a serious disadvantage in determining loads during dynamic or nonuniform conditions. Both methods can handle dynamic conditions, but there are serious difficulties and complications. Rapid maneuvers, such as a rolling pullout or a rudder kick, are good examples of where the theoretical approach or wind tunnel have difficulty in predicting loads. Another field in which theory and the wind tunnel are at a serious disadvantage is in such things as buffeting loads, door loads, and landing loads.

Many of the loads imposed on the airplane structure have in the past only been known by their overall effect on the airplane and have seldom been measured directly. A large percentage of all so-called structural measurements performed in the past have been done with accelerometers. Experimental work has been handicapped because of the difficulties of making accurate flight measurements and absence of adequate instruments or methods.

One of the major problems in the structural design of an airplane is the determination of the spanwise wing load distribution. The problem of designing structurally efficient wings has been greatly magnified by the recent trend in high-speed airplane design. Nearly all aerodynamic changes in recent years have been in the direction to make the wing structure more difficult to design and to analyze structurally. The only exception has been the development of laminar flow sections which have a greater thickness over a larger percentage of the chord than the older airfoil sections. Higher and higher speeds have dictated the use of thinner wings and, for the transonic speed range, sweepback. An additional complication to wing design has been the installation of fuel tanks on the wing tips. These trends in design have placed great emphasis on accurately knowing and determining air-load distribution on the wing. In the past, spanwise load distribution has been calculated by several different methods which were based on theoretical calculations and conservative assumptions. More recently, bending-moment distributions have been obtained from wind-tunnel measurements, and the effect of fuselage, nacelles, and external stores on aerodynamic loads on the wings have been determined more accurately.

Several different types of techniques have been

KNOWLEDGE of loads on major structural parts of an airplane while in flight is needed for complete utilization of the airplane's strength and capabilities. Some in-flight measuring techniques and equipment for reducing the data thus obtained are discussed in this paper.

Instrumentation and calibration of strain gages for measuring in-flight air loads are described in detail. Wing bending-moment measurements obtained on a Navy PV-2 airplane are used to illustrate data reduction procedure.

The Authors

W. L. HOWLAND is division engineer in charge of engineering flight testing at Lockheed Aircraft Corp. He received his Ph.D in Aeronautical Engineering from the California Institute of Technology after receiving master degrees in mechanical engineering and aeronautical engineering. Dr. Howland has been with Lockheed since 1939.

C. J. BUZZETTI is a group engineer in charge of the Structural Flight Research Group in the Flight Test Division, Lockheed Aircraft Corp. Following graduation from Curtiss-Wright Technical Institute, in 1939, he joined Lockheed. Mr. Buzzetti has been with the Flight Test Division since 1943.

used in flight test work to determine the loads on various parts of the structure. One of the more common types is that of pressure surveys. On numerous airplanes, multiple-tube manometers have been used to make pressure surveys on such components as a wing, canopy, radome, flaps, and doors. In addition to the manometer, pressure transducers have been used. Many different types and makes of pressure transducers are commercially available. The advantage of a pressure survey is that it gives a direct comparison with wind-tunnel pressure measurements and gives section loading. There are many loads that are best determined by pressure measurements; however, there are numerous disadvantages and limitations to pressure surveys. The pressure measurements can be made with liquid manometers or electrical transducers. Liquid manometers are impractical for anything except level flight conditions. This effectively makes them useless for an air-load survey program that includes maneuvering conditions. The electrical transducer has the disadvantages of requiring calibration, the units are costly, and considerable auxiliary equipment must be used in addition to the transducer. If a large number of pressure measurements are made with transducers, the calibration and data reduction become a major problem. Another basic problem with pressure surveys is the effect of pneumatic lag. At high rates of climb or descent the pneumatic lag, which is a function of the absolute pressure, is a very serious item to evaluate. At low pressure, the pneumatic lag gets so great that it is necessary to install the pressure pickup very close to, if not at, the sensing point. Pressure surveys have been used to determine wing bending-moment distribution in flight, but it has proved to be a colossal job in data reduction work. Numerous integrations were required as well as fairing and cross-fairing of curves. At high speed, pressure measurements have an additional disadvantage because of the sudden change in pressure distribution caused by shock-wave formation and fluctuation. These fluctuations result in a nonstationary pressure field around the wing. This is particularly true in the transonic speed range. The determination of section lift coefficients on a laminar flow airfoil presents difficulties due to the fact that the net airload at a given section is proportional to the difference in area between two faired curves, which corresponds to taking the difference between two large quantities. Thus the resulting accuracy is considerably less than the accuracy of the individual pressure measurements. Near the wing tip, the number of pressure sensing points necessary to determine the net airload precisely is practically prohibitive, and the tip loads have a large effect on the wing bending moment near the root. In addition, trouble is experienced in measuring loads on a tip tank or external stores by means of pressure measurements. Loads on such components as a nacelle behind a rotating propeller, and thus a fluctuating slipstream, come in the same category.

Another technique which has been used a great deal in the determination of flight loads is that of strain-gage measurements. The wire-resistant strain gage is a perfect solution to many of the instrumentation problems connected with load measurements in flight. The advantages of the strain gage are that it is remote reading and its speed of response is excellent. In addition the strain of different members can be accurately integrated electrically, and it gives an indication of load directly. The disadvantages of the strain gage are that it is a very low level output device and requires accurate calibration and a careful check in order to eliminate extraneous effects.

Due to the cost and difficulty of conducting any type of flight test work, it has been the policy at Lockheed to concentrate the in-flight load measurement work on basic quantities instead of to measure such things as detail stress distribution. If the basic external loads on the structure are determined, it is a much easier and simpler job to determine the detail stress distribution on the ground or in the laboratory, rather than in flight. In a few cases, detail stress distributions of various members have been measured; but, in general, basic quantities, such as hinge moment, loads, tip-tank loads, door loads, and spanwise load distribution, have been measured.

Every Lockheed prototype airplane for the past 12 years has had a flight load measurement program conducted on it. These programs have varied greatly in scope depending upon the type and

nature of the airplane. The extent of the program is governed by several factors such as design assumptions used, data available in designing certain items, extent of stress analysis, weight penalties, and safety. On different airplanes, different quantities are measured and to varying degrees. The flight load program is, in general, carried out during the normal flight test program on the airplane; that is, it is sandwiched in with aerodynamic evaluation, engine tests, and stability and control tests. Seldom in the past have flights been made for the specific purpose of measuring air loads. The amount of flight time spent on structural or air-load measurements has actually been a small percentage of the total on any one airplane. This condition is changing. In some instances, airplanes are now assigned exclusively to a structural load measurement program.

The largest costs of conducting flight load measurements are the installation of instrumentation, calibration (which may restrict other work on the airplane), and data reduction. One quantity which has been measured on a large number of airplanes is that of wing bending moment as a function of span. The technique and procedure for instrumenting an airplane for measuring this quantity and the procedure used in analyzing the data will be described in some detail. Before doing this, however, a word will be said about landing load measurements. Landing load measurements have always played an important role at Lockheed; however, in the last few years, these measurements have taken on an even greater importance. This is because the Bureau of Aeronautics now require the first production airplane of a type to go through a series of landings in which the severity is increased until either one landing is made at or above limit conditions or that a certain number of landings are made at a sinking speed above a high percentage of limit. During these tests, it has been of great value to determine the loads on such components as the gear itself, nacelles, external stores, pods, wings, and fuselage. Examples of these types of measurement will not be given in this paper.

Instrumentation and Calibration

The instrumentation for obtaining in-flight load measurements will be described in some detail because of its great importance in obtaining accurate results. The first operation in the installation of load-measuring strain gages in a new wing configuration is to study the wing to determine the desired location to measure the required quantity. This study requires considerable judgment on the part of the engineer in order to determine strain-gage locations in which the output has the desired characteristic.

As a typical example, it will be assumed that shear, torsion, and bending moments are required on a two-spar box-beam structure, as shown in Fig. 1. For the bending-moment measurements, strain gages are located on the front and rear beam caps with two gages on the top cap and two on the bottom cap of each beam. Gages are wired into a bending electrical bridge, as is shown in Fig. 1. (The expression bridge is used because it is an electrical Wheatstone bridge circuit.) For the shear measurement, shear bridges (45-deg V-type installation) are located on the front and rear beam shear webs plus a bending bridge on one beam for canceling bending effects in shear due to taper in depth of the beam. For the torsion measurement, shear bridges and the additional bending bridges are installed identical to those for the shear measurement.

If the beam web where the shear gages are located will buckle at lower than limit load, this buckling has to be eliminated either by reducing the panel size with additional stiffeners or by installing gages on both sides of the web, back to back, in order to cancel out electrically the buckling strains. If the shear bridges are located in a fuel-tank area, the bending load on the panel caused by the fuel has to be eliminated. Generally, it is difficult to install gages inside a fuel tank; so, on occasions, a can has been installed over the beam web in the gage area to keep the fuel pressure off the web at that point.

The bending bridges for making the bending measurements are connected in parallel with the same electrical polarity. The output of the bridge which is most sensitive to torsion effects is reduced so that both bridges have equal but opposite sensitivity to torsion. This output reduction can be accomplished by inserting series resistors of appropriate values in the power input leads to the bridge which is most sensitive to torsion effects.

The front and rear individual shear bridges for making the shear measurement are also connected in parallel with the same polarity; and, like the

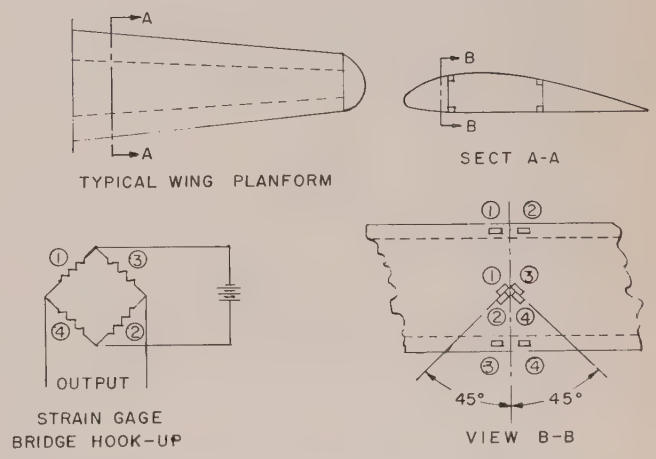

Fig. 1 – Diagram of typical strain-gage installation

bending bridges, the shear bridge most sensitive to torsion load has its output reduced with resistors in the input leads. The bending bridge is also paralleled into the circuit with the polarity arranged to cancel the bending effect on the output of the shear bridges. If the beams have no taper in depth and the bending effect is not present, then a bending cancellation bridge in the shear circuit is not required. In general, the single-beam bending bridge used in the shear circuit will have some torsion sensitivity, so the resistoring of the shear bridge on the bending bridge has to be adjusted so that the net result is cancellation of both bending and torsion effects from the shear measurement. The torsion measurement has the same bridge complement as the shear measurement and is connected in a similar manner, except that the output of the shear bridges are of opposite polarity so as to measure a difference rather than an average. The bridge resistoring is adjusted so that the torsion axis of the gages (that is, the point along the chord of the wing at which an applied shear load produces no output from the paralleled torsion bridges) is located where desired.

The procedure of supplying sufficient individual bridges to make up complete load-measuring bridges as compared with using single bridges at each point and analytically combining their outputs after reading the oscillograph records has the disadvantage of laying and maintaining a large number of strain gages. It also involves a two-part calibration procedure as explained later. But in spite of the disadvantages of complete load-measuring bridges, it is felt that the advantages far outweigh the disadvantages. The advantages are:

1. The recorded traces are a direct measure of the basic load measurement desired, so the action of a given load during a maneuver can be observed directly by looking at the oscillograph record. This is especially true under buffeting conditions where the various natural frequencies of the structure may be excited.

2. The final accuracy is better than that obtained using individual bridges, since the summing of the bridges is done electrically in the paralleling circuits and can be accurately adjusted; thus the inaccuracies involved in the recording, reading, and computing a given load measurement are limited to a single trace rather than including those for two, three, or four traces.

3. Data reduction time is considerably reduced and the number of reading points may be considerably reduced where oscillations are occurring.

All measurements are recorded with a recording oscillograph using no intermediate amplifiers. Sufficient calculations are made using expected strain-gage outputs and known galvanometer sensitivities to insure that the galvanometer trace deflections remain within the linear range. Also, the output unbalance of all bridges for known conditions on the ground are adjusted with fixed high-value shunt resistors so that full use is obtained of the linear portion of the galvanometer trace deflection for the expected loading extremes.

After the strain-gage installation is complete, each strain-gage bridge is statically calibrated by applying known weights or loads on the wing. These loads produce precise shear, torsion, and bending-moment increments at each wing station. During the static calibration process, the strain-gage outputs are read with precision potentiometers. This instrument is 25 to 50 times more sensitive than the oscillograph used in recording the strain-gage output in flight. The calibration of the parallel bridge circuits is divided into two steps: a preliminary and a final calibration. First, all of the individual bridges are calibrated to determine their output for loads applied at various span and chord points; then the resistors required in the battery input leads of the various bridges are computed using this output information. The proper size of the resistors to be used are computed by punching the calibration information obtained from the individual bridge circuits on IBM cards. The cards are then processed, and the linear simultaneous equations are solved using electrical computing equipment. The various circuits are connected in parallel and checked for operation and proper polarity. Final calibration of the parallel circuits is then made using the same loads and load points as used in the preliminary calibration. To calibrate a set of torsion, shear, and bending bridges at a given single-span station involves a minimum of four loading points: two chord points at each of the two span points, as shown in Fig. 2A. If the gage station is near the root of the wing or horizontal tail, carry-over effects from unsymmetrical loads will probably be present and must be evaluated. To gain sufficient information to know how properly to cancel these carry-over effects, the calibration procedure is extended to include loading each side individually and also simultaneously. It should be noted that if cancellation of carry-over effect is required, additional strain-gage bridges are required. Fortunately carry-over effects are generally limited to the local area near the root of a surface.

A diagram of calibration points for a typical

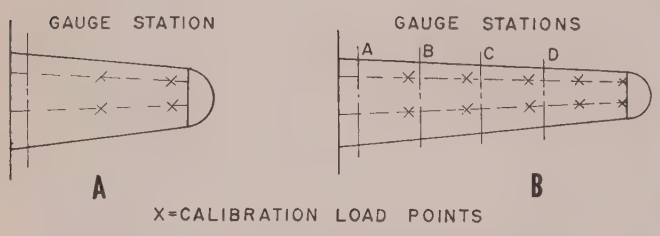

Fig. 2 – Diagram of typical calibration load point locations

wing with four gage stations is shown in Fig. 2B. The load points are arranged so that at least two of the span points are outboard of the most outboard gage location. The remaining span load points are located just inboard of the gage stations in succession but well outboard of the next inboard station. As a general rule, we attempt to keep a load point that will be used to calibrate gages at a given station, a distance outboard of that station which is at least equal to the chord distance between the beams. In the case of a multispar wing, it should be the distance between the front and rear beams. The reason for this general rule is to allow sufficient beam length for the structure to obtain a close-to-normal internal load distribution at the gage station. New wing designs for high-speed airplanes utilizing low aspect ratios will obsolete both the above general rule and also the point loading method. Loads closer than one chord depth will have to be employed, and they will have to be distributed chordwise to simulate approximately chordwise air-load distributions.

For load calibrations where only bending measurements are to be obtained, our experience has shown that accurate calibrations can be obtained using only one span loading point near the tip. Two different chord points are used to determine torsion effects and to arrive at corrections if necessary. An example of calibration results from a typical wing with two different up-load calibrations and one down-load calibration is shown in Fig. 3. Although there is a small offset of the down-load calibration, there is no difference in the sensitivity or slope. At the time of these calibrations, some doubt was expressed as to accuracy of extrapolating calibration data obtained at low loads up to conditions near limit design load. Therefore, a special loading jig was built, and the calibration was carried up to about one-half of limit load. The results agreed with the low-load calibration well within the accuracy of the loads applied during the high-load calibration.

It should be noted in this entire operation that such items as strain-gage sensitivity, modulus of elasticity, or stress analysis are not used. The accuracy of the calibration relies on only fundamental quantities, such as the measurement of input and output voltage, calibrating weights or forces, and their location, which amounts to measuring the distance of the force from some reference point or axis.

After the strain-gage calibrations are obtained, the shunt calibration resistor calibrations are made. These resistors are high-quality precision resistors shunted across one leg of the bridge to produce an output like that of the strain gages under load. From this information, an equivalent load for the calibration resistor can be computed so that, when oscillograph records are obtained switching the shunt resistor across the leg of the bridge, the resulting trace deflection is equal to a known load.

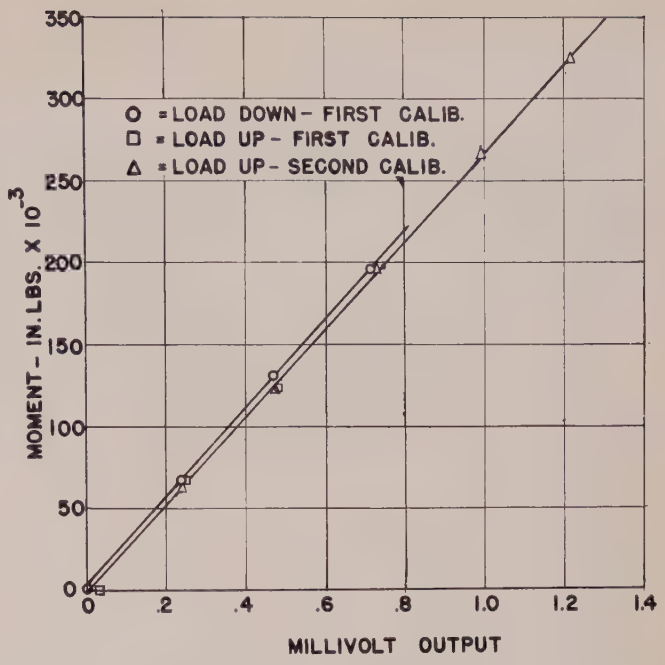

Fig. 3 – Static calibration curves showing bending moment versus millivolt output of strain gages

Thus the trace deflection sensitivity is obtained directly in terms of load.

Wing Load Measurements

The largest share of our flight load measurement work in the past has been concerned with making wing bending-moment measurements. The reason for this is that the wing is the largest single item on the airplane designed mainly by air loads. Therefore, the largest percentage of the structural weight would be affected if the design loads were in error. In addition, if an airplane is to be stretched weight-wise, the wing loads are of primary importance. Measurements being made presently and in the future will include shear and torsion, but we believe that, in general, the quantity of bending measurements will far outnumber shear and torsion measurements. This is because of the greater ease of calibration and the fact that except for the very low aspect ratio wings the largest part of the wing weight is made up of material for resisting bending loads. The procedure used in flight for making wing load measurements consists of a pushover followed smoothly by a pullup and then a let-back to 1g. The maneuver is performed smoothly to minimize maneuvering tail loads yet fairly quickly to keep the change in air speed low. The maneuver is run at various air speeds throughout the desired speed range. An example of the type of oscillograph record obtained during a typical rollercoaster maneuver is shown in Fig. 4.

Reduction of Data

To illustrate the procedure used in data reduction, the wing bending-moment measurements

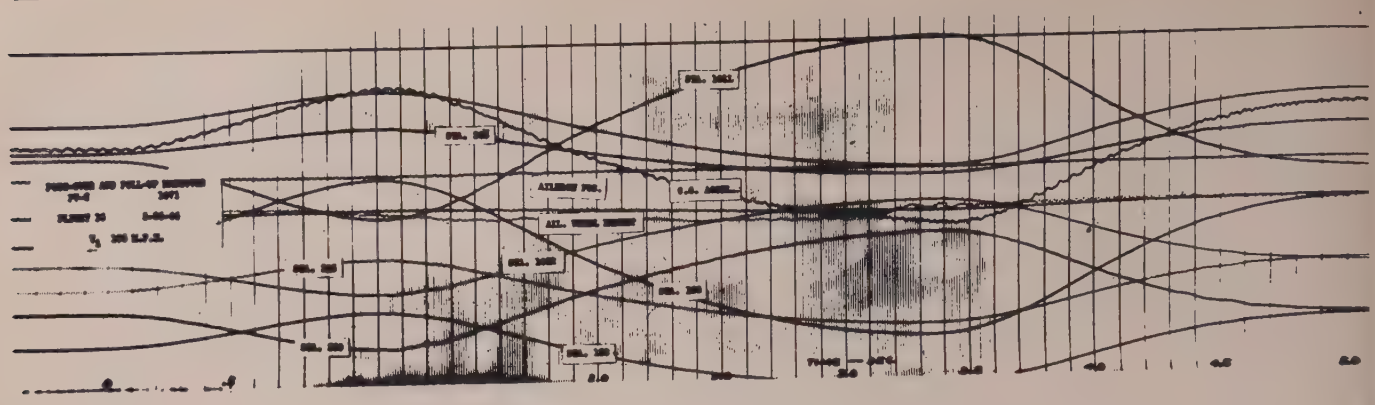

Fig. 4 – Typical oscillograph record of rollercoaster maneuver

obtained on a Navy PV-2 airplane will be used as an example.

The oscillograph records are placed in a Telecomputing Corp. "Telereader" and the "zero" trace positions before and after flight and calibration shunt heights for both zero records and all in-flight records read. The Telereader has associated with it a "Telecorder" and an IBM Summary Punch machine for reading out the cross-hair positions of the Telereader. The data punched in the IBM card is in binary count. The IBM cards are then sent to the Lockheed Engineering Mathematical Analysis Department and processed in an IBM Model 604 computer to convert binary count to inches of trace deflection.

The before- and after-flight zero trace positions are compared and the proper positions determined for use in reducing the records. The zero positions for the wing load measurements are not critical and are used only as an arbitrary starting point; this will be explained later. The zero positions for such items as c.g. acceleration, control forces, positions, and so forth, are critical; and the before- and after-flight zero's give a good indication of the zero stability of each measurement. For average load measurement work, our experience has shown that, if the calibration shunt heights for the before- and after-flight zero records are in close agreement, these values are sufficient for determining the trace sensitivities for the flight records. For wing load measurements where we are looking for better than normal accuracy, calibration shunt heights obtained during the flight records are used to determine the trace sensitivities. Another reason for using the shunt heights obtained on in-flight records for wing load measurements is that the average trace position in flight is different from the on-ground trace position due to the 1g air load in flight. This effect is, of course, most pronounced on transport or patrol airplanes with relatively low design load factors.

While the proper trace zero positions and sensitivities are being determined, the records are being marked for reading. On a rollercoaster type of maneuver we usually read about 40 to 50 points on each maneuver. These points are distributed in approximately even load factor increments throughout the complete maneuver. After marking, the records are placed back in the Telereaders, and all traces desired are read at the points marked. The resulting cards are then sent to the Mathematical Analysis Department for the computing work using an IBM Model 701 high-speed electronic computer. Two types of data are received back. The first type is a straight tabulation of the individual readings showing the trace deflection from the reference line in inches and the load computed from that trace deflection based on the zero position and sensitivity determined previously. This data is useful for later checking of individual points if required. The second type of data is a tabulation of the results of a least-squares analysis to determine the slope in inch-pounds per g and intercept moment at zero g of each wing station bending moment versus c.g. acceleration for

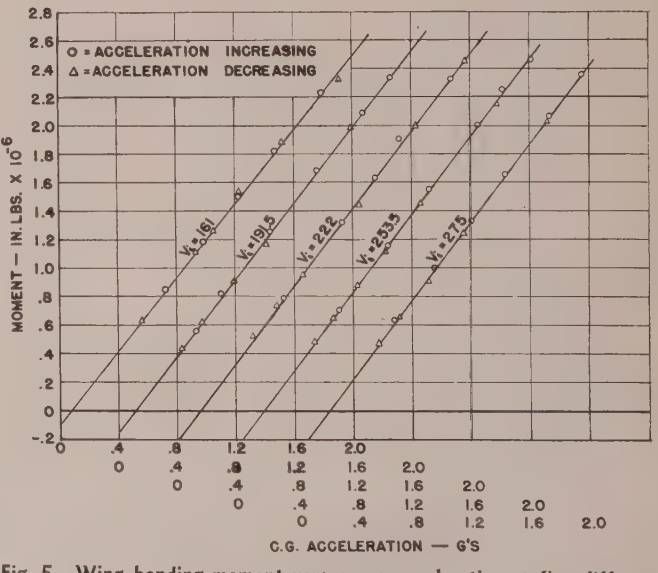

Fig. 5 – Wing bending moment versus c.g. acceleration at five different air speeds

each maneuver. The slope value obtained is independent of the reference point used; thus, temperature effects and zero drift have no effect on the slope value used. An example of some plots of moment versus acceleration are shown in Fig. 5 to illustrate the general scatter of data available for the analysis. The PV-2 data used as an example for the data reduction procedure was done by hand before the reading and computing machines were available, but it is well suited for illustrating the principle involved.

The next step in the data reduction process is to plot the intercept bending moment at zero g for each station against dynamic pressure ($q = \frac{1}{2}\sigma V^2$). These plots show the change in basic moment at each station (that is, moments due to wing lift distribution at zero airplane lift or acceleration) with dynamic pressure. Since the basic C_L lift distribution is assumed a constant in the speed range of the PV-2, the change in basic lift loads and thus the change in basic moments are a linear function of q. Therefore, the basic moment plots are extrapolated linearly to zero q. The moment intercepts obtained at zero q give the correction to the reference values used in obtaining the bending moment versus acceleration curves. This is a very important point, since the entire method is based on the fundamental assumption that at zero dynamic pressure the air loads on the wing must be zero. Fig. 6 shows the measured basic moments and the curve set to zero at zero q. The basic moment measurements obtained on various airplanes have substantiated the assumption of linearity of basic moment with q, but these measurements have been obtained at relatively low Mach numbers. Later tests on higher-speed airplanes have shown that in the high subsonic and transonic speed range the basic moment versus q curves can be nonlinear, but the lower-speed portion of the curve remains linear.

It should be pointed out that basically this method is not dependent on the basic moment being linear with q but rather on being able to make a reasonably accurate extrapolation from the lower q's, at which measurements are made, to zero q. It does not in any way invalidate the general method when the basic moment is nonlinear with q at high speeds.

From the basic moment curves for each station, data is obtained for plotting a spanwise basic moment distribution curve for unit q (that is, M/q). Fig. 7 shows the basic moment curve for a PV-2 with standard configuration and the change that occurred after rigging the ailerons 5 deg up in an attempt to reduce the wing bending moments.

In order to make the data more flexible for calculating the wing moments for various loading conditions, the measured values of inch-pounds per g are converted from net moments to air-load moments by adding in the dead-weight moment values of the wing for the test condition and dividing by the test weight to get air-load moment per g for unit weight (that is, M/GW). These values are plotted against dynamic pressure in Fig. 8.

The wing moment distribution for any design

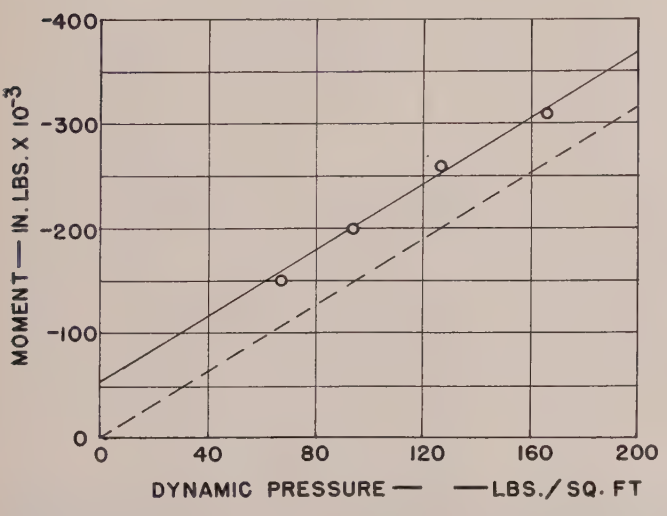

Fig. 6 – Bending moment at zero g versus dynamic pressure (q)

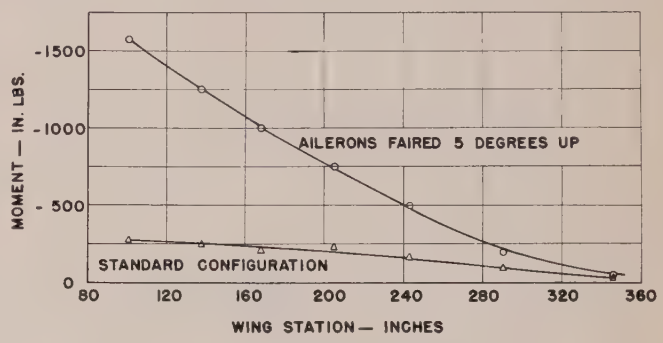

Fig. 7 – Span distribution of basic moment for two different airplane configurations

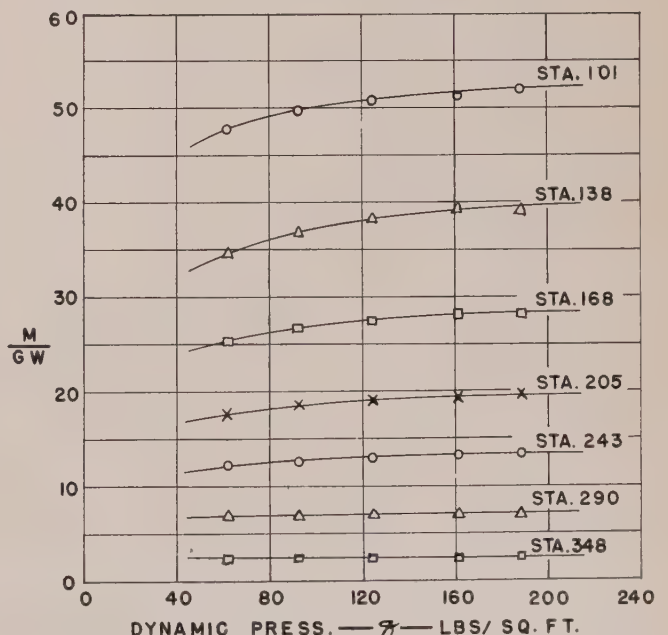

Fig. 8 – Air load M/gW versus dynamic pressure for PV-2 airplane

condition can now be calculated readily using the following procedure:

1. Obtain the basic moment M/q values at the desired stations from the basic M/q distribution plot.
2. Multiply the basic M/q values by the design condition q to obtain the design moments.
3. Obtain the M/GW values at design q for each station from the plots of M/GW versus q.
4. Multiply the M/GW values by the design condition gross weight and center of gravity load factor to obtain air-load moments due to weight and acceleration.
5. Add the design basic moments to the moments calculated by the previous operation to obtain the final design air-load moments.
6. Multiply the dead-weight moment values for the design condition by the design load factor and subtract from the air-load moments to obtain design net moments.

Wing air-load moments computed using the procedure described are compared with design air-load moments in Fig. 9. As a matter of interest, the difference in wing moment due to rigging the ailerons up resulted almost entirely from the change in basic moment. The aileron rigging change had practically no effect on the wing load due to load factor.

An example of the utility of the data reduction procedure outlined and the speed with which it can be applied was obtained recently at Lockheed. During some tests on a particular airplane to develop a tip-tank aerodynamic configuration that would result in a minimum increase in wing loads, a complete analysis of the wing loads at the critical conditions was available within two days after conducting the tests.

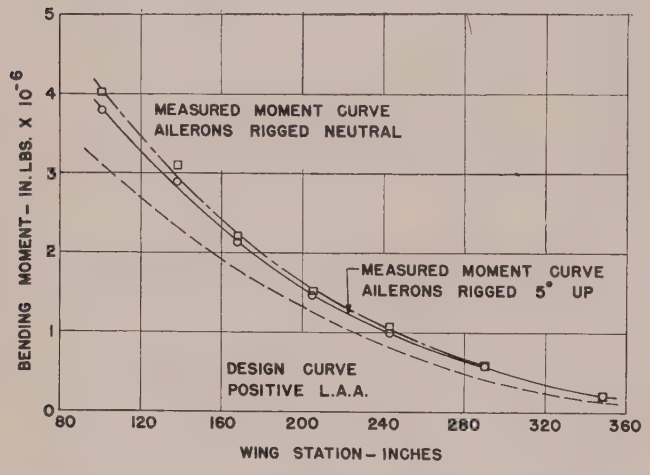

Fig. 9 – Span distribution of air-load bending moment for two different airplane configurations

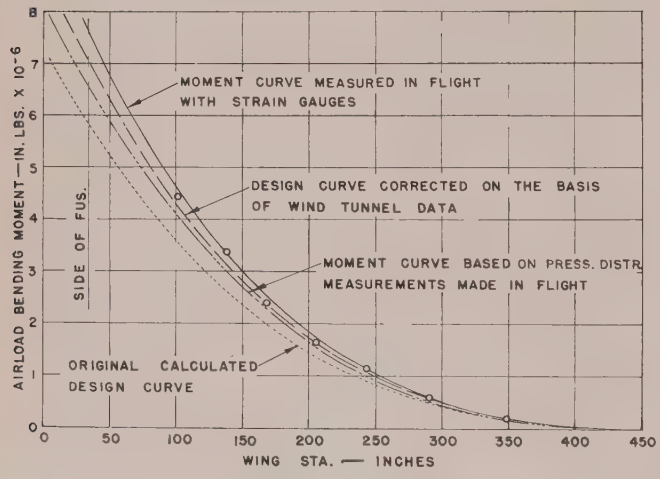

Fig. 10 – Comparison of air-load bending moments for strain-gage measurements, pressure measurements, and design

Strain-Gage Data and Pressure Measurements

In the course of testing the Navy PV-2 airplane mentioned previously, pressure-distribution measurements using a liquid manometer also were obtained. The strain-gage measurements showed the wing loads were considerably greater than design. At that time the use of strain gages for flight load measurements was quite new, and it was decided to make a check independent of the strain gages.

A comparison of span bending-moment distributions obtained by the two measurement methods with the original design curve and the design curve corrected on the basis of more complete wind-tunnel data is shown in Fig. 10. Note that the pressure-distribution measurements are below both the strain-gage data and the corrected design curve. A closer agreement between strain-gage data and pressure-distribution data was obtained when the comparison was based on level flight conditions where the pressure measurements were obtained. These tests showed that pressure dis-

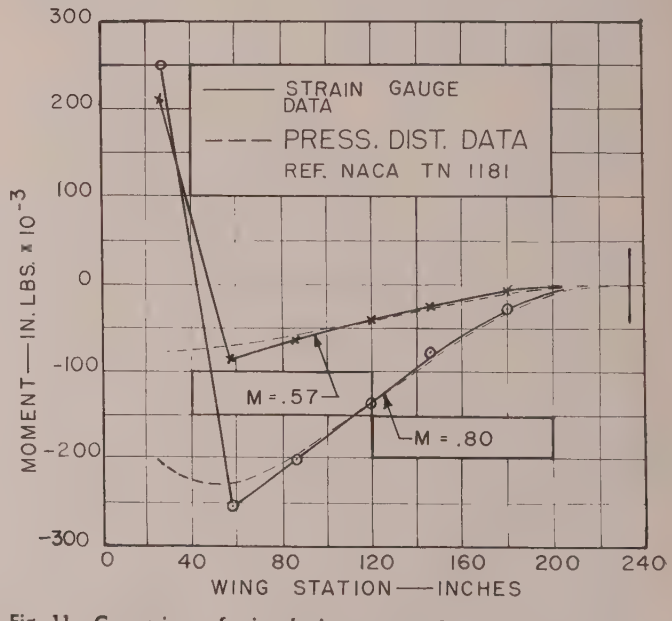

Fig. 11 – Comparison of wing basic moments for strain-gage measurements and pressure-distribution measurements at two different Mach numbers on F-80 airplane

tributions obtained at a given airplane lift coefficient in level flight do not necessarily remain the same for the same lift coefficient in accelerated flight at higher speeds.

Another comparison of strain-gage data with pressure distribution was obtained for the F-80 airplane. The strain-gage measurements were made by Lockheed on one airplane and the pressure-distribution measurements by the NACA on another airplane. The pressure-distribution measurements were obtained during maneuvering conditions using the NACA pressure recording system.

A comparison of wing basic moment at two different Mach numbers for the two methods is shown in Fig. 11. Outboard of station 80 the agreement is very good. The strain gages show a sharp reversal of moment at about station 60. Pressure measurements were not obtained inboard of station 65, thus an accurate comparison near the root cannot be obtained. The pressure data shown near the root is an extrapolation assuming no significant changes in distribution.

A comparison of air-load moments at design load factor for the same two Mach numbers is shown in Fig. 12. At 0.57 Mach number, there is very good agreement between the two methods. At 0.80 Mach number, the strain-gage data is somewhat higher, especially near the root.

Comparison of Measurements for Two Airplanes

Wing moment-distribution measurements obtained on the first Navy Model XP2V patrol bomber showed the measured loads to be lower than design all along the span. It was desired to make use of this information to increase the gross weight of the airplane without accompanying changes in wing strength. Before doing this, it was considered desirable to check the measurements on a different airplane of the same configuration. The reasons for this check were not only to determine the reproducibility of measurements of this type but, in addition, to determine the scatter caused by manufacturing errors in wing contour, such as twist, change in sections, unsymmetry, and the like. The measurements were made almost a year apart with completely different strain-gage installations, calibrations, and equipment.

The comparison of the two airplanes with identical configurations is shown in Fig. 13. Note the excellent agreement all along the span. Over the inner half of the wing the agreement obtained was within 2%. At the outermost station the agreement was within 7%; but in this area of the wing, small differences in aileron float angle could tend to make the agreement not so good.

Tail Load Measurements

Another important field of flight load measurements is that of tail load measurements. In this paper, this will only be covered in a very general way in order to show the nature and type of measurements and the type of information obtained. Actually, a long paper could be written on just this subject of in-flight tail load measurements. The safe conduct of most final demonstration maneuvers requires preliminary tests building up to the final test conditions. A typical example of this is the rudder-kick maneuver. In this maneuver, a specified rudder pedal force or rudder deflection must be applied in a fraction of a second. A maneuver of this type is generally required by both the Navy and the Air Force for structural demonstrations of a new airplane model.

An example of vertical tail load measurements obtained during a demonstration of a Navy P2V airplane is shown in Fig. 14. Note that a peak pedal force of about 470 lb was obtained and that this force occurred before reaching maximum rudder angle. Also note that the torsion load was not affected by the rudder position for a given yaw angle but was a direct function of yaw angle only. In conducting preliminary tests of this type, an adjustable rudder pedal stop device is used which allows the pilot to kick the pedal hard at each test point without danger of overshooting.

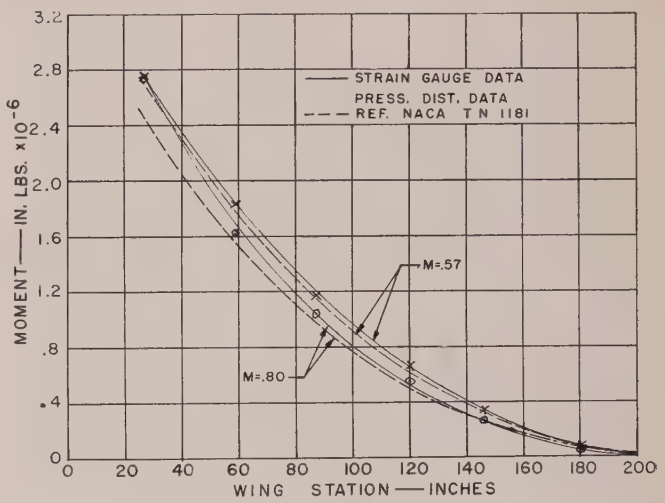

Fig. 12 – Comparison of air-load bending moments for strain-gage measurements and pressure-distribution measurements at two different Mach numbers on F-80 airplane

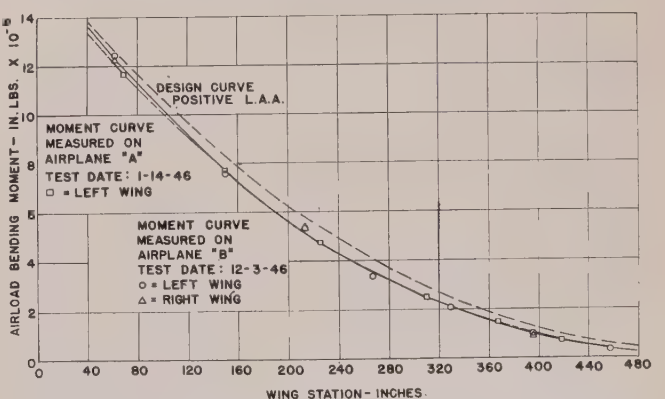

Fig. 13 – Comparison of bending-moment measurements for two different P2V airplanes

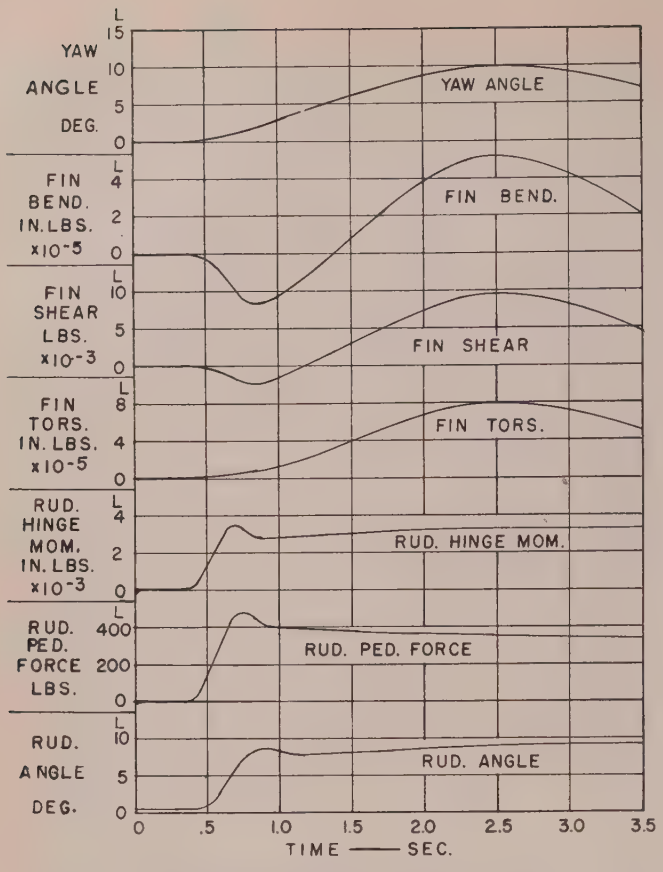

Fig. 14 – Vertical tail load measurements obtained during an abrupt rudder-kick maneuver on a P2V airplane

This stop also allows the pilot to hold the pedal hard up against the stop and maintain a given pedal position during the yaw. The strain gages for measuring rudder pedal force are located beyond the pedal stop in the control system so they measure only that portion of the pilot force that goes into the control system. In the preliminary tests, load measurements are obtained using progressively increasing stop positions up to approximately half the expected deflection. The loads are then plotted against stop position for a given air speed, and an extrapolation is made to show what tail load is expected for a given pedal force or rudder deflection under demonstration conditions.

Discussion and Conclusions

The technique of measuring air loads in flight has definitely developed to the point where accurate reproducible results can be obtained. In this paper, certain aspects of the measuring technique were gone into in considerable detail primarily to illustrate the great importance of various details in obtaining reliable information. Numerous details equally important have not been discussed in this paper. The use of IBM equipment for reducing the data has greatly increased the accuracy and the speed at which final corrected results are available for determining future tests or modifications to be made or both. Another great intangible benefit to be derived from flight load measurements is the confidence and feeling of security which the test pilot or test crew has when running critical or near limit load conditions. This factor can expedite certain programs an immeasurable amount. Valuable design information and high-speed full-scale check on wind-tunnel data, as well as stress-analysis substantiation, can be secured. Flight measurements can definitely tell what loads become critical under maneuvering conditions, as well as the magnitude of the applied loads. Numerous structural failures in flight have been avoided by making measurements during progressive build-up tests. The general conclusion can be drawn that on prototype airplanes, aside from any government or procuring agency requirements, flight load measurements of at least major structural items should be made in order to obtain the full utilization of the airplane's strength and capabilities. On several types of our airplanes, operating capabilities have been extended through flight load measurements.

ORAL DISCUSSION

Reported by G. G. Green
Consolidated Vultee Aircraft Corp.

B. W. Hodges, Boeing Airplane Co.: How high were calibration loads carried, and was it found necessary to recalibrate frequently?

Dr. Howland: The calibration was usually carried to about 20% of limit load depending somewhat on the linearity indicated (and linearity has usually been good). The sensitivity of equipment used in calibration is high compared to that of the flight instrumentation, thus relatively low calibration loads yield acceptable accuracy. Recalibrations are not made as a general rule; however, if the measurements are questioned, a recalibration is made. Also, it depends somewhat on the importance of the test and the time span involved whether a recalibration is made.

L. Hitchcock, Boeing Airplane Co.: How much calendar time was required to calibrate an airplane the size of the Constellation?

Dr. Howland: Actual calibrations of the YC-130 were as fcllows:

Wing – preliminary – 2 days.
Wing – final – 1 day.
Tail and aft fuselage – preliminary – 5½ days (this longer span was due to trouble with the gages in loading rig).
Tail and aft fuselage – final calibration – 2 days.
Forward fuselage – preliminary – 1 day.
Forward fuselage – final – 1 day.
Total actual calibration time – 12½ days.

R. B. Davidson, Northrop Aircraft, Inc.: How were loads measured in unsymmetrical maneuvers such as rolling?

Dr. Howland: The best source of information on such unsymmetrical loads was plotted time histories of the maneuvers.

Jerome Fishler, Douglas Aircraft Co., Inc.: Was the zero *g* bending moment found to change with altitude?

Dr. Howland: Yes, to some degree and apparently in accordance with change of Mach number.

Jerome Fishler, Douglas Aircraft Co., Inc.: Referring to the calibration of the YC-130 being accomplished in one week, how many stations were considered?

Dr. Howland: There were four stations on each side of the fuselage with two chord points per station. The horizontal tail had two stations on each side of the fuselage and two chord points per station. The vertical tail had two stations with two chord points on the upper station and three chord points on the lower.

Correlation of Engine Noises With Combustion Phenomena

Robert Meagher, R. L. Johnson, and K. G. Parthemore, E. I. du Pont de Nemours & Co., Inc

This paper was presented at the SAE Summer Meeting, Atlantic City, June 10, 1954.

THE fact that satisfactory operation of higher-compression-ratio engines is limited in many instances by surface ignition of the air-fuel mixture has caused an intense interest in abnormal combustion phenomena. Although a great deal of work has been done to obtain a better understanding of the surface ignition problem,[1-6] not much effort has been devoted to correlating objectionable engine noises with actual ignition and combustion records. Studies using a highly instrumented single-cylinder engine[6] showed that surface ignition may have several different manifestations. In order to correlate the changes in the combustion process accompanying abnormal ignition with the resulting various engine noises, a modern-type high-compression-ratio passenger-car engine was equipped with rate of change of pressure (dp/dt) pickups in each cylinder.

The type of ignition and the course of combustion were studied by observing the changes in pressure which occurred within the combustion chamber. Using the dp/dt pickups to indicate rates of pressure change, it was possible to detect quite accurately the occurrence of preignition, postignition, knock, or other abnormal combustion phenomena. By photographing simultaneously several oscilloscope screens showing the dp/dt signal from each of the engine cylinders together with a noise signal from a sensitive microphone placed near the engine, the abnormal noises produced by the engine were correlated with the combustion patterns.

This paper presents information which helps to provide a more rational explanation of the noises attendant to abnormal combustion. Several special techniques used in the past to determine the fuel requirements of engines in which surface ignition is occurring also have been examined as a part of this investigation, and an assessment of their merits has been made.

Apparatus and Procedures

A 9/1-compression-ratio overhead-valve V-8 engine on a dynamometer test stand was used to obtain most of the data. The dp/dt pickups were located in the combustion chamber as shown in Fig. 1. The rate of pressure change in all cylinders was indicated on two oscilloscope screens, the images appearing alternately on the screens in the same sequence as the firing order of the engine. These patterns were recorded photographically by means of a medium-speed strip-film camera. Engine noises

[1] See SAE *Quarterly* Transactions, Vol. 6, October, 1952, pp. 724-752: "Flame Photographs of Autoignition Induced by Combustion-Chamber Deposits," by L. L. Withrow and F. W. Bowditch.

[2] See SAE Transactions, Vol. 62, 1954, pp. 40-49: "Deposit-Induced Ignition-Evaluation in Laboratory Engine," by D. A. Hirschler, J. D. McCullough, and C. A. Hall.

[3] See SAE Transactions, Vol. 62, 1954, pp. 50-56: "Occurrence of Preignition in Present-Day Cars in Normal Service," by R. F. Winch.

[4] See Proceedings of API, Vol. 33, No. III, 1953, pp. 137-150: "Preignition in Automotive Engines," by J. R. Sabina, J. J. Mikita, and M. H. Campbell.

[5] See SAE Transactions, Vol. 62, 1954, p. 48: "Some Effects of Fuels and Lubricants on Autoignition in Cars on the Road," by R. K. Williams and J. R. Landis.

[6] See SAE Transactions, Vol. 62, 1954, pp. 32-39: "Investigation of Preignition in Engines," by A. O. Melby, D. R. Diggs, and B. M. Sturgis.

A BETTER knowledge of the nature and causes of preignition and of its frequency during normal engine operation has been obtained by instrumenting a 9/1-compression-ratio engine on a test stand and an engine in an automobile with rate of change of pressure pickups.

Photographic records of the oscilloscope traces produced by this instrumentation have enabled the determination of:

1. The relative tendency for preignition or postignition to occur and the relation of these phenomena to engine or car operating conditions.

2. The physical causes of the noises accompanying the several types of preignition.

3. The effect of retarded spark timing on deposit-induced preignition.

4. The significance of the "key-off" method of fuel rating.

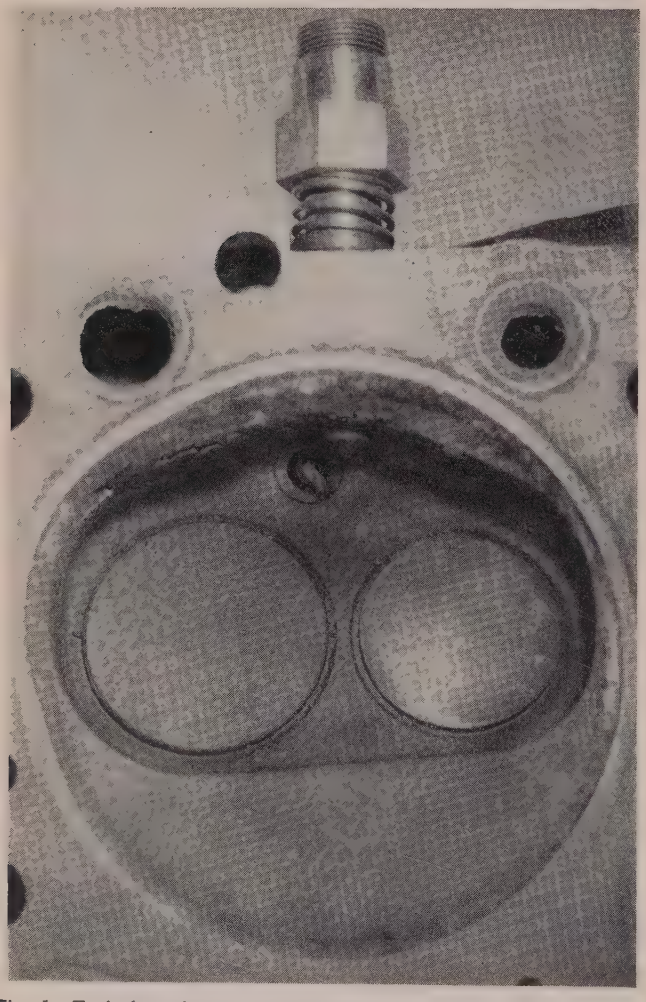

Fig. 1 – Typical combustion chamber of high-compression-ratio engine showing location of *dp/dt* pickup

were observed on another oscilloscope screen which displayed the output from a sensitive microphone placed close to the engine. This latter signal was photographed simultaneously with the rate of pressure change patterns. The arrangement of the test equipment is shown in Fig. 2.

Additional data were obtained employing a similar photographic procedure in a car containing the same type of 8-cyl engine. In the car, however, the *dp/dt* pickups were installed only on the right bank of the engine because the steering column interfered with the installation of the pickups on the left bank. The cylinders containing the *dp/dt* pickups were of 9/1 compression ratio, while the other cylinders had a compression ratio of 7.5/1. With this arrangement the pickups were in the cylinders which were critical from the noise standpoint. A microphone was not included in the car instrumentation. Engine noise was detected aurally and was correlated with the *dp/dt* traces by the observer in the car.

A more complete description of the instrumentation is given in the Appendix.

Records of the combustion patterns and engine noise during knocking and nonknocking combustion in the laboratory engine without deposits were obtained during a series of wide-open-throttle accelerations from approximately 700 to 2000 rpm. During these accelerations the engine was loaded so that the time required to accelerate through this speed range was approximately the same as would be required with the engine installed in the car on the road.

After the clean-engine data were obtained, combustion-chamber deposits were accumulated in the engine by operating on a light-duty cyclic procedure for an extended period. The fuel used for this operation was a blend of 90% catalytically cracked distillate and 10% motor alkylate which contained 3 ml tel as Motor Mix per gallon. The oil was an SAE 20 Mid-Continent distillate and residuum blend containing an antioxidant and a detergent. The engine operating conditions during the cyclic deposit ac-

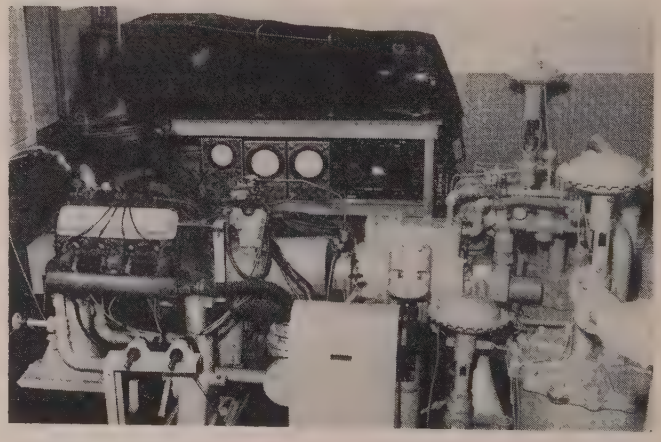

Fig. 2 – Experimental apparatus showing high-compression-ratio overhead-valve engine, microphone location, and recording equipment

cumulation period are shown in Table 1.

Combustion and noise patterns were obtained after 300 hr of deposit accumulation. Some additional data checks were also made after 375 and 400 hr of operation. The reference fuel systems used for rating the engine were of three types: (1) primary reference fuels containing 3 ml tel per gal, (2) CRC severity reference fuels which were unleaded, and (3) blends of full-boiling-range gasolines containing 3 ml tel per gal.

Data were obtained in the road-test car during a series of wide-open-throttle accelerations. The combustion chambers contained deposits which had been accumulated in approximately 3000 miles of low-duty operation with a fuel and lubricant similar to that used in the laboratory tests.

Interpretation of Data Records

Fig. 3 shows typical simultaneous oscilloscope traces of the rate of pressure change and the engine noise as obtained in the clean engine with normal nonknocking combustion at two different engine speeds during an acceleration. The upper trace in both Fig. 3a and Fig. 3b shows the *dp/dt* signals from cylinders 1, 7, 6, and 4, and the lower trace from cylinders 8, 3, 5, and 2. The numbers along the edges of the film record identify the cylinder to which that portion of the *dp/dt* trace applies. The center trace shows the sound pattern recorded by the microphone. The dashed line near the bottom of each figure is a timing mark. The period of successive timing mark pulses is 1/120 sec.

It can be seen by comparing Fig. 3a with Fig. 3b that when engine speed is increased, the spacing between successive combustion patterns on the film record is decreased. At higher engine speeds more engine cycles occur per unit of time, and since the film speed is relatively constant more combustion cycles are recorded per unit length of film. The high-frequency vibration which appears on the *dp/dt* traces of Fig. 3b is the result of the increased vibration accompanying the increased engine speed and is characteristic of all the diagrams obtained at high speeds. Also, the amplitude of the sound trace is greater at the higher engine speed because of the increased engine noise level.

The ignition spark for each cylinder is indicated by the characteristic "blip" identified in Fig. 3. The "blip" appears simultaneously on the upper and lower *dp/dt* traces of both Fig. 3a and Fig 3b. In order to establish a reference point in the firing order, a double "blip" is provided on the upper trace to indicate spark ignition in cylinder 8. This "blip" is also identified in Fig. 3. The *dp/dt* records show that with normal combustion approximately 25 to 40 deg of crankshaft travel are required before maximum rate of pressure rise is obtained.

Abnormal combustion produces characteristic changes in the *dp/dt* patterns as shown in Fig. 4 to 9 inclusive. These figures have been drawn and enlarged to illustrate how the various phenomena ap-

The Authors

ROBERT MEAGHER (A '47) is with the Petroleum Laboratory of E. I. du Pont de Nemours & Co., Inc. He received a Bachelor of Aeronautical Engineering degree from New York University and an M.S. in Mechanical Engineering from the Univerity of Pennsylvania. Mr. Meagher spent nine years as a civilian engineer at the Navy's Aeronautical Engine Laboratory in Philadelphia. He joined du Pont in 1948 as a mechanical engineer.

R L. JOHNSON (M '52) is with the Petroleum Laboratory of E. I. du Pont de Nemours & Co., Inc. He received his B.S in Chemical Engineering, and his M.S. from the University of Texas. Mr. Johnson worked for the Humble Oil & Refining Co. in the Technical Service at the Baytown Refinery in 1944. He joined du Pont in 1947. His work there has included road knock testing of fuels, and study of preignition cars on the road.

K. G. PARTHEMORE is responsible for the design and development of special laboratory instrumentation, and supervision of instrument maintenance at the Petroleum Laboratory of E. I. du Pont de Nemours & Co., Inc. He received his Masters Degree in Electrical Engineering from the University of Delaware in June, 1954. During World War II he was an aviation radio technician with the U. S. Navy. Following his discharge, he worked as a radio and television technician.

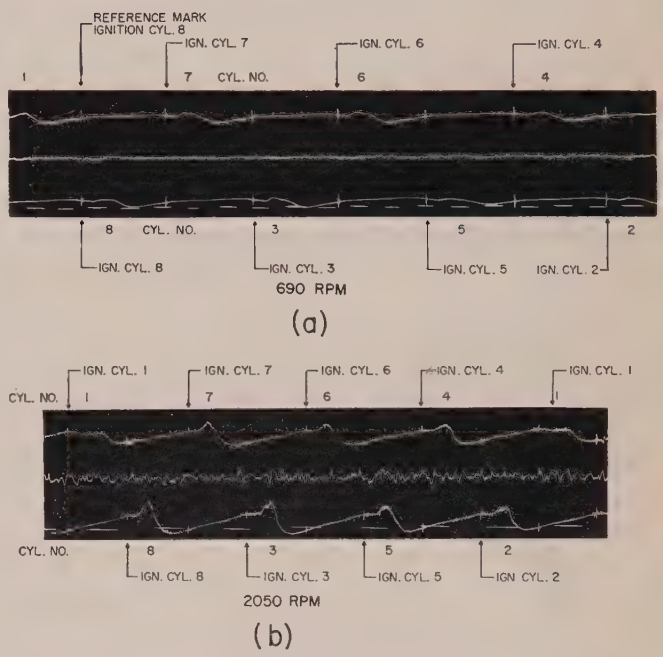

Fig. 3 – Typical *dp/dt* and sound records during normal combustion in a clean engine, with standard spark timing, using 92-octane-number leaded primary reference fuel: (a) low engine speed, (b) high engine speed

Table 1 – Engine Operating Conditions, Light-Duty Cyclic Deposit Accumulation Test

	Idle	Road Load
Cycle Time, sec	30	30
Engine Speed, rpm	500	1500
Bhp	0	15
Manifold Vacuum, in. of Hg	22 (approx)	19½ (approx)
Coolant Temperature, F	160	160
Oil Temperature, F	140	140
Spark Timing, Btdc (Standard), deg	2½	30
Air/Fuel Ratio	Standard	Standard
Carburetor Air Temperature, F	85-95	

pear on the film records. Combustion records from two cylinders are shown in these illustrations.

Fig. 4 shows combustion resulting from normal spark ignition. The upper trace is the *dp/dt* pattern from a given cylinder while the lower trace is the *dp/dt* pattern from the cylinder next in the firing order. The sound trace appears in the middle, while the timing marks are near the bottom of the figure. The time of spark ignition is indicated by the "blips" on the *dp/dt* traces. Also shown in Fig. 4 is the double "blip" indicating the time of spark ignition in cylinder 8 which is used to establish a reference point in the cylinder firing order.

The appearance of the *dp/dt* pattern when autoignition occurs is shown on the upper trace of Fig. 5. Autoignition is indicated by the abrupt change in the *dp/dt* signal vertically upward and also by the high-frequency oscillation shortly after the maximum rate of pressure rise is attained. If autoignition is sufficiently severe, abnormal engine noise, or knock, is produced, and the sound trace is distorted as indicated in Fig. 5. In addition, the accompanying engine vibration is indicated at the same time on the *dp/dt* trace opposite the cylinder in which autoignition occurred. The combustion portion of the *dp/dt* pattern shown on the lower trace of Fig. 5 represents normal combustion.

Fig. 6 shows preignition on the lower *dp/dt* trace and normal combustion on the upper trace. Preignition is indicated by an abnormal rise in the *dp/dt* trace before spark ignition and a somewhat larger than normal maximum rate of pressure rise. The engine noise in the case shown is normal since there is no distortion of the normal sound trace.

Postignition is shown in the lower trace of Fig. 7. The rise in the *dp/dt* trace is similar to that which

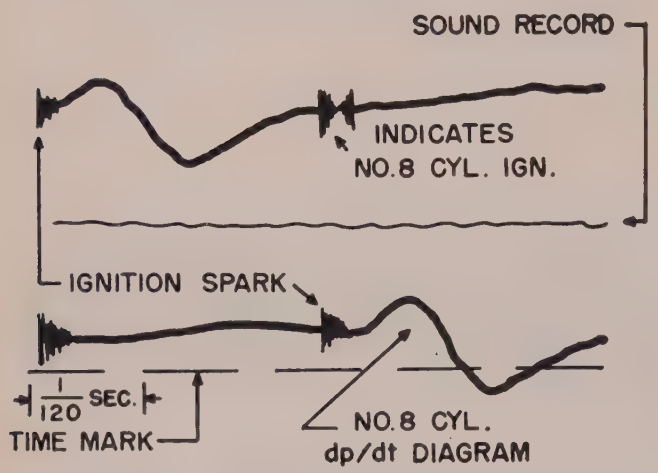

Fig. 4 – Diagram illustrating typical *dp/dt* and sound records with normal spark ignition only in two cylinders. Ignition "blips" for both cylinders, reference mark for cylinder 8, and location and period of time marker are indicated

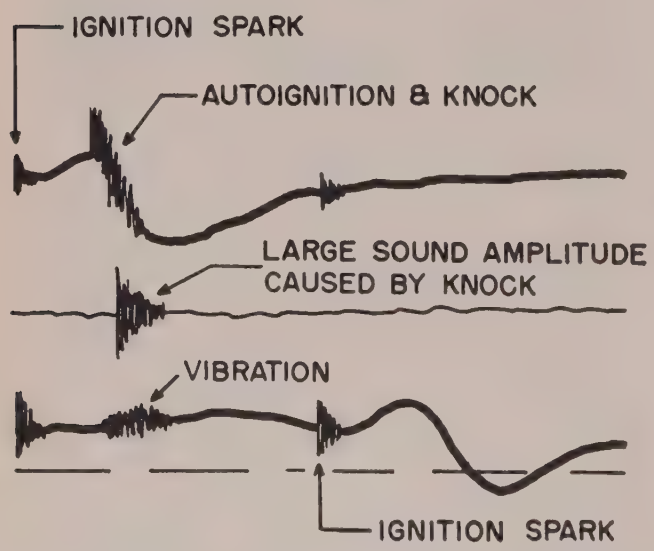

Fig. 5 – Diagram illustrating typical *dp/dt* and sound records for two cylinders, with normal spark ignition in one cylinder and autoignition with knock in the other. Increase in sound amplitude and vibration on accompanying trace are shown

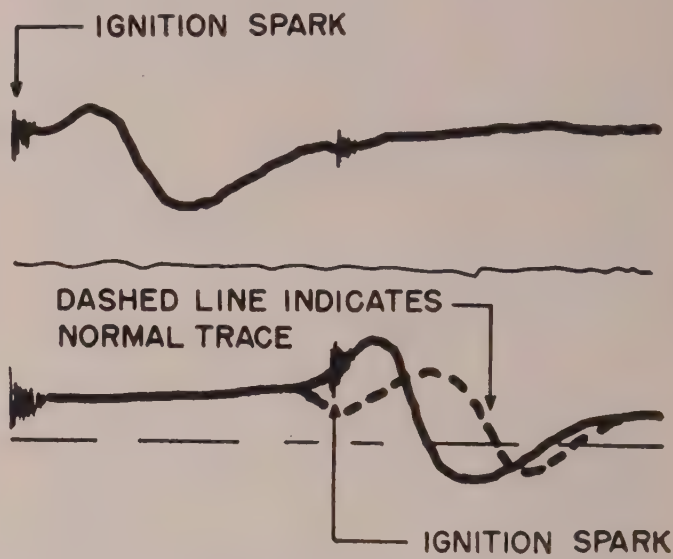

Fig. 6 – Diagram illustrating typical *dp/dt* and sound records for two cylinders, with normal spark ignition in one cylinder and preignition without knock in other. Shift of *dp/dt* diagram due to preignition is indicated

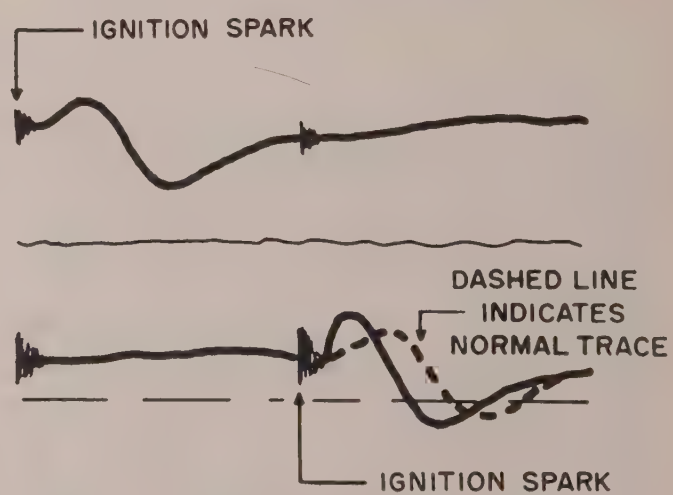

Fig. 7 – Diagram illustrating typical *dp/dt* and sound records for two cylinders, with normal spark ignition in one cylinder and postignition in other. Shift of *dp/dt* diagram due to postignition is indicated

occurs with preignition, but follows immediately after spark ignition rather than before. The maximum rate of pressure rise also tends to be higher than normal when postignition occurs.

A *dp/dt* trace having a large amplitude and one which develops smoothly at a higher than normal rate is identified as multiple ignition. This phenomenon is visualized as ignition of the air-fuel mixture by deposit particles in many locations. This ignition can occur before spark discharge, Fig. 8, or after spark discharge, Fig. 9. Notice that multiple ignition is merely a special case of preignition or postignition depending on the time at which it occurs. The line of demarcation between preignition, postignition, and multiple ignition must, of necessity, be fairly broad since the records indicate only the time of pressure development and not the time of flame initiation.

Combustion in a Clean Engine

No trace of abnormal combustion was observed in the clean laboratory engine using a 92-octane-number leaded primary reference fuel and standard ignition timing. Figs. 3a and 3b, which have been discussed previously, show typical rate of pressure change and sound patterns for normal combustion during an acceleration using this fuel. Variations in the *dp/dt* traces from cylinder to cylinder were slight, and the shape of the *dp/dt* traces was not affected significantly by changes in the engine speed.

Knocking combustion was observed when fuel quality was lowered to 88 octane number. As shown in Fig. 10a, combustion in cylinders 6, 5, and 4 was normal, autoignition was occurring in cylinder 3 without apparent noise as indicated by the normal sound trace, while in cylinders 8 and 7 the autoignition was severe enough to produce a high-frequency noise, or knock, on the sound trace. Severe autoignition may induce sufficient vibration in some part or parts of the engine structure to record on the *dp/dt* pickups in cylinders other than the one in which autoignition occurred. Indications of such vibrations appear on the trace opposite that of the cylinder in which autoignition occurred. Examples of this are shown also in Figs. 10a and 10b.

It is important to note that in the clean engine operated on 88- and 92-octane-number leaded primary reference fuels, there was no indication of surface ignition or any other type of abnormal combustion other than autoignition.

It can be noted in Fig. 10 that a slight upward deflection in the rate of pressure change curve was present in cylinder 8 just after spark ignition in Fig. 10a and just before spark ignition in Fig. 10b. The trace did not continue to rise but paralleled the shape of the normal diagram. Because of the nature and condition of occurrence of this deflection, it is believed that it signals the presence of precombustion reactions. Although this phenomenon was readily observed when using 88-octane-number reference fuel, it was not evident with fuels of higher octane number.

The data discussed in the foregoing paragraphs indicate clearly that in the particular 9/1-compression-ratio engine used in these investigations and in the absence of combustion-chamber deposits, engine noise was the result of knock following normal combustion initiated by the normal spark discharge. There was no evidence of surface ignition.

Surface Ignition in Presence of Deposits

With combustion-chamber deposits present and using a fuel with an antiknock value at or near the octane requirement of the engine, every instance of noise, or knock, was the result of surface ignition. The type of diagram obtained during knocking combustion in the clean engine was never observed in the engine with deposits present.

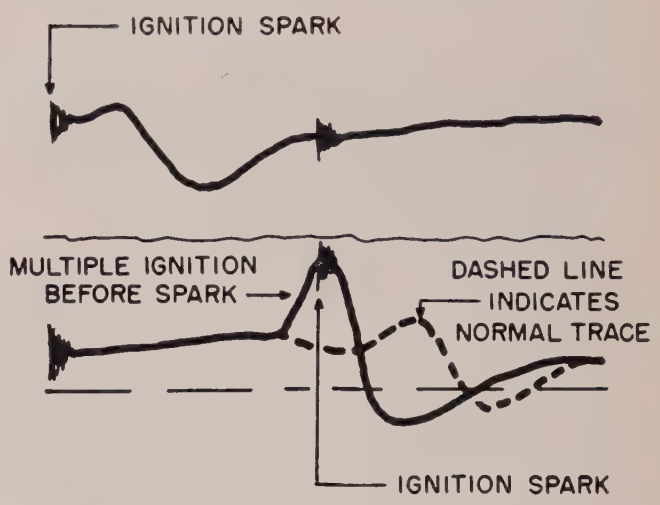

Fig. 8 – Diagram illustrating typical *dp/dt* and sound records for two cylinders, with normal spark ignition in one cylinder and multiple ignition before spark in the other. Increase in amplitude of *dp/dt* pattern is indicated

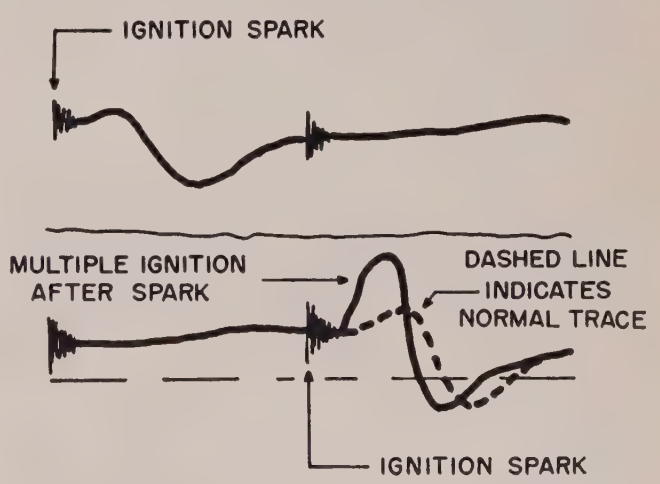

Fig. 9 – Diagram illustrating typical *dp/dt* and sound records for two cylinders, with normal spark ignition in one cylinder and multiple ignition after spark in other. Increase in amplitude of *dp/dt* pattern is indicated

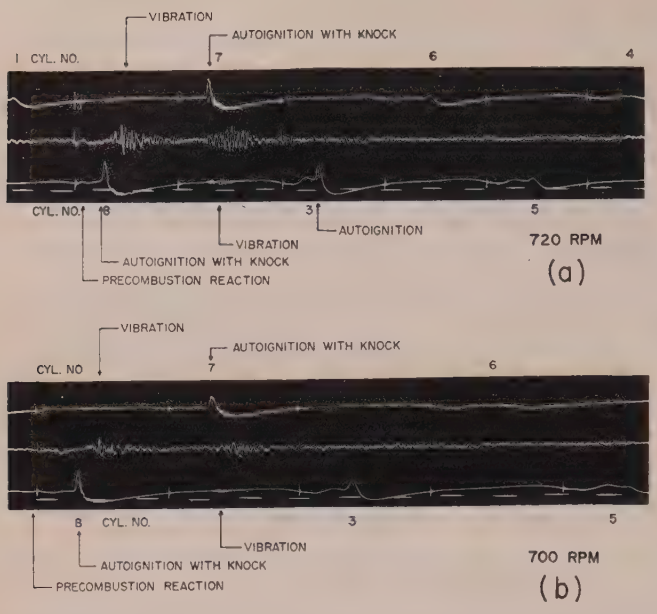

Fig. 10 – Combustion records in a clean engine at low speed, with standard spark timing, using 88-octane-number leaded primary reference fuel: (a) autoignition in cylinder 3, autoignition with knock in cylinders 8 and 7, precombustion reaction after spark in cylinder 8, (b) autoignition with knock in cylinders 8 and 7, precombustion reaction before spark in cylinder 8

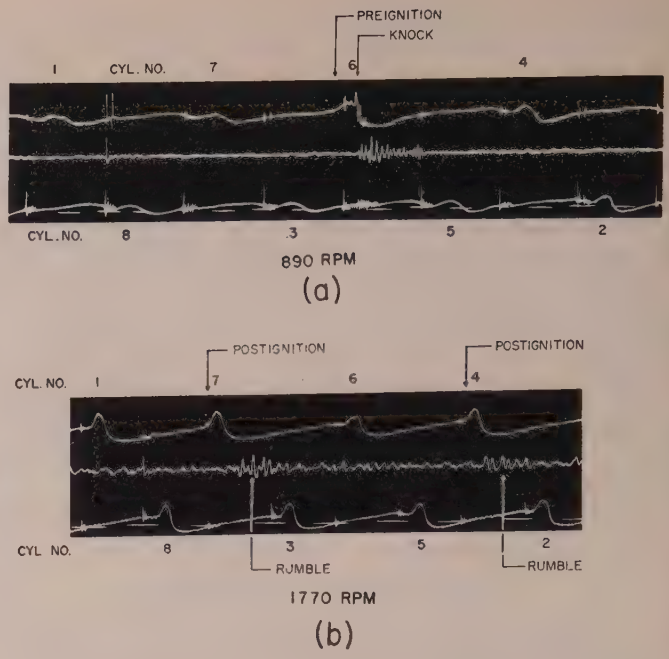

Fig. 11 – Combustion records in the engine with deposits, with standard spark timing, using 108-performance-number leaded primary reference fuel: (a) low engine speed showing knock resulting from preignition in cylinder 6, (b) high engine speed showing postignition in cylinders 7 and 4 producing rumble

Fig. 11 shows the combustion patterns and the noise trace obtained during accelerations using a 108-performance-number leaded primary reference fuel. This fuel was determined so it would just satisfy the requirement of the engine containing deposits accumulated in 300 hr of light-duty cyclic operation. Under these conditions a majority of the cycles exhibited normal combustion patterns; however, in every cycle producing noise there was clearcut evidence of surface ignition. Most of the surface ignition was clearly preignition. As might be expected, this ignition was erratic both in occurrence and in ignition advance. A combustion cycle is shown in which very early surface ignition occurred resulting in a knock noise, and cycles where surface ignition occurred after the spark, termed postignition.

At higher engine speeds there often occurred a low-frequency, continuous noise which has been termed rumble. A combustion diagram for this phenomenon is illustrated in Fig. 11b. This noise is not the result of autoignition and gas vibrations but rather a vibration of some part of the engine structure induced by high rates of pressure rise occurring immediately before or after spark. The cause of the rapid pressure rise appears to be a multiple surface ignition of the charge which occurs at or near the time of normal spark ignition. As shown by the sound trace of Fig. 11b the noise occurs at about 30 deg after spark ignition. Note that there is a complete absence of gas vibrations on the *dp/dt* record. Rumble usually occurs at speeds higher than 1400 rpm. It does not occur in the clean engine. Rumble was disregarded in establishing the fuel requirement of the engine.

Examination of the photographic records taken under the conditions just described showed several instances of isolated, violent knocking brought about by preignition. It is believed that this is the phenomenon which has been termed "wild ping."

Road Tests – Unlike the results obtained in the laboratory engine, knock in the road-test car in the presence of deposits was not positively indicated as resulting from surface ignition. Nevertheless, from careful study of the data, it is believed that surface ignition did occur during the majority of the cycles which gave knock. However, such surface ignition took place after spark ignition, while in the laboratory engine the surface ignition usually occurred before the spark. It is believed that any discrepancy between the laboratory engine and the car on the road was due to the different-type deposits in the combustion chambers. While both the laboratory and car engine deposits were accumulated under mild-duty conditions, with the laboratory engine each small series of accelerations was made with freshly accumulated deposits. On the road the deposit condition deteriorated as a result of the frequency of accelerations.

Fig. 12 shows several *dp/dt* records obtained in the car. The *dp/dt* records for cylinder numbers 4 and 8 are shown in each case on the upper trace – the records for cylinder numbers 6 and 2 are indicated on the lower trace. Spark discharge is indicated by a gap in the *dp/dt* trace. There is no sound trace on this figure, and the dashed line in the

middle is the timing mark trace.

Fig. 12a shows autoignition in all cylinders (numbers 8, 6, 4, and 2) with standard spark advance using 90-octane-number leaded primary reference fuel. That audible knock occurred is indicated by the vibration-type patterns on the trace opposite the knocking cylinders. Fig. 12b shows severe preignition followed by knock in cylinders 6 and 8 with the spark advanced 1½ deg from standard using 96-octane-number leaded primary reference fuel.

It is evident from these data that every instance of noise in the laboratory engine with deposits was the result of surface ignition. The fact that this might not always be so with the car on the road points up the importance of the nature of deposits on the type of fuel failure.

On the basis of the work done to date it is believed that in engines of 9/1 compression ratio operated under average driving conditions, surface-ignition-induced knock may account for a majority of the engine noise.

Routine Techniques for Detecting Surface Ignition

Key-Off Ignition – It is common practice to turn off the ignition key as soon as an engine noise is heard to determine if this noise is the result of surface ignition. If the engine continues to operate or run-on even momentarily, it is usually assumed that the noise was due to surface ignition. In this investigation run-on was obtained even with a clean engine. It will be recalled that in the clean engine during normal combustion with the key on, there was no indication of surface ignition. The *dp/dt* records indicate that opening the ignition switch and interrupting the primary circuit causes a spark discharge of sufficient energy to ignite the charge in many cases. Early spark ignition can occur if the time in the cycle at which the key is turned off is opportune. This difficulty can be eliminated by inserting a switch in parallel with the breaker points so that closing the switch prevents any further spark discharge.

A typical occurrence of "key-off" ignition without the parallel switch is shown in Fig. 13. These data were obtained with a fuel just satisfying the requirement of the engine. Large-amplitude oscillating ignition "blips" on the upper trace indicate positively that the ignition switch has been turned off. The normal ignition "blips" continue to appear, but once the key is turned off these "blips" indicate only the time of breaker point opening. Early ignition by the "key-off"-induced spark occurred in cylinder 3, Fig. 13a, and the resulting violent knocking noise produced a large-amplitude signal on the microphone trace and a vibration signal on the *dp/dt* traces. This early ignition apparently raised the cylinder temperature sufficiently so that on succeeding cycles this same cylinder showed multiple ignition with loud knock. One such cycle is shown in Fig. 13b.

As speed decreased, Fig. 13b, cylinder 8 fired without the spark discharge incident to turning off the key. The ignition in this cylinder, however, occurred after the time at which the normal spark would have passed had the key been turned on. It is likely that such ignition was initiated by a spot in the combustion chamber which, when the

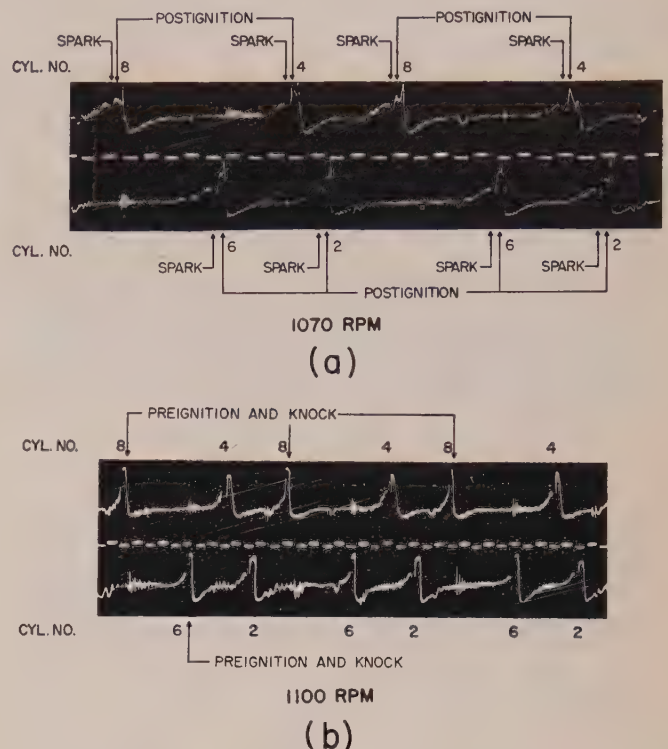

Fig. 12 – Combustion records from road-test car with deposits: (a) knock in cylinders 8, 6, 4, and 2 caused by postignition using 90-octane-number leaded primary reference fuel, with standard spark advance, (b) knock resulting from preignition in cylinders 6 and 8 using 96-octane-number leaded primary reference fuel, with spark advanced 1½ deg from standard

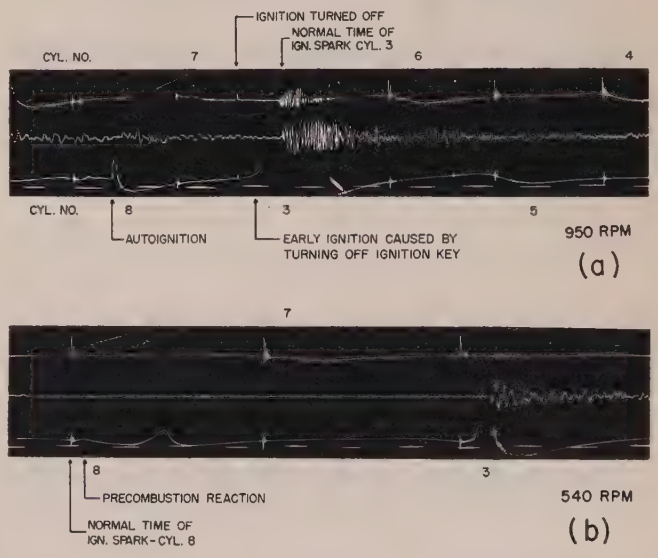

Fig. 13 – Combustion records showing two types of run-on or key-off ignition in a clean engine using 88-octane-number leaded primary reference fuel, with standard spark timing: (a) turning off ignition switch causes spark discharge which initiates early ignition in cylinder 3, (b) engine continues to fire in cylinders 8 and 3 without spark ignition

key was on, was not hot enough to ignite the charge before the mixture in its vicinity was consumed by the primary flame front. However, this spot could cause ignition in the absence of a spark because of the increased time available for ignition reactions to proceed. This is confirmed by the fact that there was no evidence of secondary flame fronts with normal spark ignition. Similar phenomena were observed when combustion-chamber deposits were present.

These data indicate that the "key-off" technique is not always a reliable method for indicating surface ignition in an engine operating with a timed spark. The method may fail for two reasons:

1. Interruption of the primary circuit by turning off the key can cause an electrical discharge at the spark plug and ignition of the charge. If this ignition occurs early in the compression stroke, combustion-chamber temperatures will be raised sufficiently to cause surface ignition in subsequent cycles.

2. Surface temperatures insufficient to cause ignition during the period available with a timed spark can cause ignition during the additional time available in the absence of a spark-initiated flame front.

Table 2 – Effect of Ignition Timing and Reference Fuel Type on Noise Requirement of Engine with Deposits

	Standard Ignition Timing		Ignition Timing Retarded 10 Deg	
Reference Fuel Type	Noise Requirement[a]	Limited by	Noise Requirement[a]	Limited by
Commercial blend + tel	100-104 P.N.	Preignition	98-100 O.N.	Preignition
Primary + tel	108-112 P.N.	Preignition Postignition	93 O.N.	Preignition
Severity	97.5 O.N.	Preignition Postignition	97.5 O.N.	Preignition

[a] P.N. = performance number; O.N. = octane number.

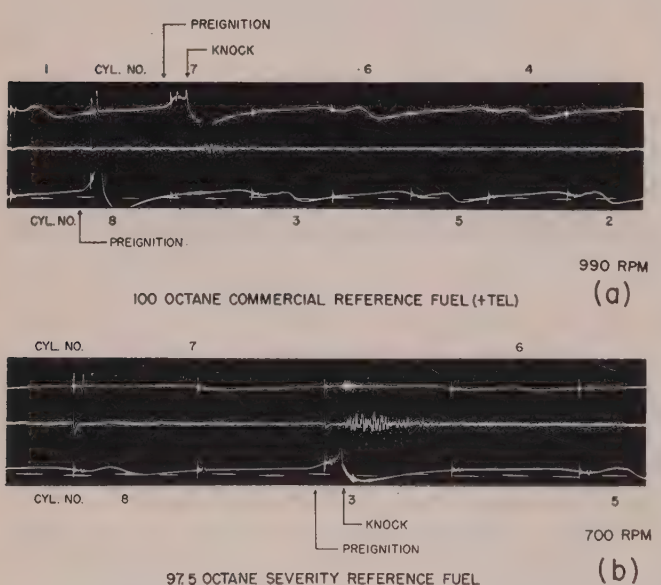

Fig. 14 – Combustion records in the engine with deposits, with standard spark timing: (a) using 100-octane-number leaded commercial blend reference fuel, medium engine speed, showing silent preignition in cylinder 8 and preignition producing knock in cylinder 7, (b) using 97.5-octane-number severity reference fuel, low engine speed, showing preignition resulting in knock in cylinder 3

Effect of Reference Fuel Systems – 1. Ratings at Normal Spark Timing – Data obtained indicate that the types of abnormal combustion which occur in the presence of combustion-chamber deposits, and also the quality level of the fuel required to satisfy the engine, are affected by the choice of the reference fuel system. For example, the engine was satisfied about as well from the standpoint of surface-ignition-induced knock with a 100-performance-number full-boiling-range commercial blend, Fig. 14a, as with a 108-performance-number leaded primary reference fuel, Fig. 11a. Similarly, a 97.5-octane-number CRC severity reference fuel blend, Fig. 14b, also satisfied the engine. Although rumble was not considered when establishing the requirement of the engine, the fuels behaved quite differently in this respect. The commercial blend produced much more rumble than either the leaded primary reference fuel or the CRC severity blend. Furthermore, rumble with the commercial blend started at a lower speed.

2. Ratings at Retarded Spark Timing – It often has been stated that if an engine is surface-ignition-limited, the fuel requirement tends to remain constant when the spark is retarded. To obtain qualitative data relating to this point, photographic records were made during accelerations with the spark timing retarded 10 deg from normal. Fuels from each of the three reference fuel systems were used. This work showed that:

(a) Even though the engine was preignition-limited, the fuel requirement could be decreased substantially by retarding the spark with the engine remaining preignition-limited. The extent of this decrease was dependent on the reference fuel system employed.

(b) In dealing with preignition-limited engines, ratings of engine requirements and fuels per se at retarded spark may lead to results which do not accurately represent the situation existing at normal timing.

Equilibrium noise requirements of the engine using three different reference fuel systems at both standard and retarded spark timing are shown in Table 2.

Retarding the spark reduced the requirement of the engine substantially with leaded primary reference fuels, reduced it slightly with the commercial blends, and did not affect it at all with the CRC severity reference blend. It is important to note that, regardless of the spark timing and the reference fuel system employed, this 9/1-compression-ratio engine was in all cases limited by surface ignition when deposits were present.

In some respects, the data shown in Table 2 are unexpected and contrary to previous experience in lower-compression-ratio knock-limited engines.

For example, it might be expected that the highest fuel requirement would be obtained using either the commercial or severity reference fuel blends. Although this was generally true at retarded timing, it was not true at standard timing. Furthermore, in a preignition-limited engine it might be expected that especially high requirements would be obtained in terms of severity reference fuels because of the presence in these fuels of components usually thought to have low preignition resistance. Because of these discrepancies, the data in Table 2 were carefully checked at a later date by another observer and found to be correct. Analysis of the combustion records did not provide experimental evidence to explain the unexpected behavior of the various type reference fuels. It is reasonable to suppose, however, that this behavior is somehow related to the ignition resistance of the fuels per se and the surface temperature of the deposits. It must be remembered, too, that the deposit temperature is affected by spark timing. It is obvious that previously held concepts on the effect of different reference fuel types on requirements of knock-limited engines can be misleading if applied to preignition-limited engines.

Some of the records taken at retarded spark timing are shown in Figs. 15, 16, and 17. Fig. 15 shows the records for both 94- and 92-octane-number leaded primary reference fuels. Essentially no abnormal noise occurred during the accelerations using the 94-octane-number fuel. However, when the 92-octane-number fuel was used, preignition-induced knock was continuous and the noise was very loud, producing a large-amplitude sound trace and excessive vibration on the *dp/dt* pattern. From these data it was established that the requirement of the engine with the spark retarded 10 deg from normal was 93 octane number in terms of the leaded primary reference fuels. When the leaded primary reference fuels were used, a slight upward deflection was noted in the *dp/dt* traces of several cylinders, either after or before spark. These are indicated in Fig. 15 and have been discussed previously in the section relating to combustion in a clean engine. Once again, it is believed that these deflections are a manifestation of precombustion reactions.

Fig. 16 is the record obtained using the 98-octane-number commercial blend. Fig. 16a shows

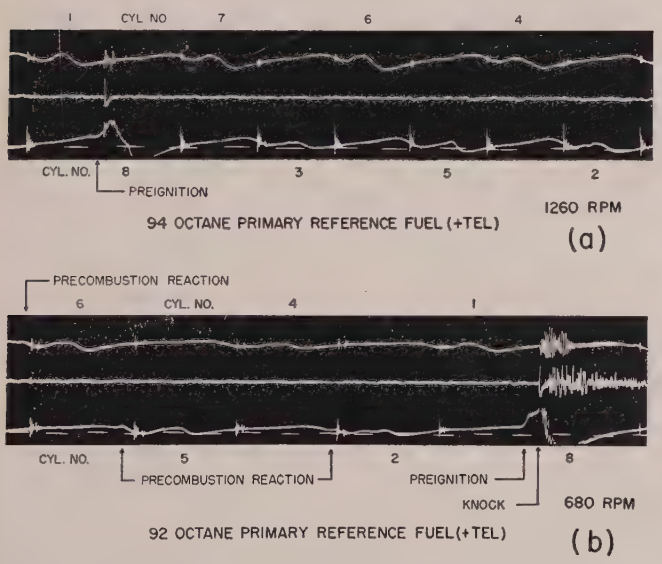

Fig. 15 – Combustion records in engine with deposits, with spark timing retarded 10 deg from standard, using leaded primary reference fuels: (a) 94-octane-number fuel showing preignition in cylinder 8 without knock, (b) 92-octane-number fuel showing preignition with violent knock in cylinder 8, precombustion reactions indicated in cylinders 6, 5, and 2

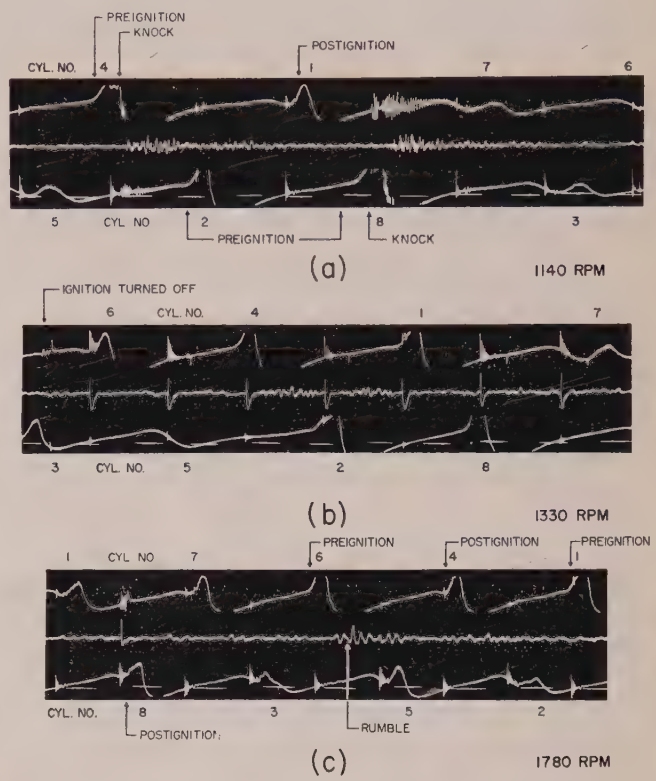

Fig. 16 – Combustion records in engine with deposits, with spark timing retarded 10 deg from standard, using 98-octane-number leaded commercial blend reference fuel: (a) preignition with knock in cylinders 4 and 8, postignition in cylinder 1, preignition without knock in cylinder 2, 1140 rpm, (b) key-off combustion in cylinders 6, 4, 2, 1, 8, and 7, 1330 rpm, (c) preignition without knock in cylinders 6 and 1, postignition in cylinders 8 and 4, rumble after preignition in cylinder 6, 1780 rpm

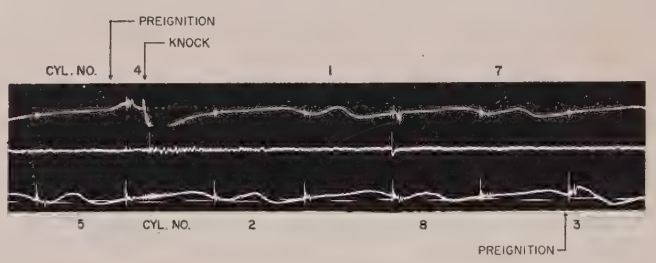

Fig. 17 – Combustion records in engine with deposits, with spark timing retarded 10 deg from standard, using 97.5-octane-number severity reference fuel, at 970 rpm. Preignition with knock in cylinder 4 and preignition without knock in cylinder 3

preignition-induced knock, preignition without noise, and postignition at an engine speed of 1140 rpm. When the speed reached 1330 rpm, Fig. 16b, the ignition was turned off. Run-on was continuous during the interval shown in this record. At a still higher engine speed, with spark ignition on, Fig. 16c, preignition and postignition were observed and rumble also became evident.

Fig. 17 illustrates the data obtained using a 97.5-octane-number severity reference fuel blend. This blend met the requirement of the engine. Surface ignition resulted in trace knock, but there was no run-on and no rumble.

3. Benzene as a Fuel – Benzene is often used in preignition investigations because of its relatively poor resistance to surface ignition and its superior resistance to knock. A series of accelerations was made with combustion-chamber deposits present in the engine using pure benzene as a fuel to determine the types of noise and combustion that would result. A typical record is shown in Fig. 18. Fig. 18a shows preignition without noise, while Fig. 18b shows run-on with the key off accompanied by a harsh rumbling-type noise. Fig. 18c with the ignition on shows preignition with almost continuous rumble.

The data obtained using benzene showed no evidence of ordinary knock. Benzene did, however, cause a very loud, harsh, rumbling-type noise. The *dp/dt* pattern and sound trace showed preignition, postignition, and multiple ignition. The rumble intensity was much greater than that obtained with any other fuel. In addition, it was found that preignition and the resulting loss of power were so severe that the engine would not accelerate beyond 1800 rpm. Subsequent accelerations were made with a reduced dynamometer load. During the accelerations run-on was readily obtained, Fig. 18c, particularly at a high speed. The diagram showing run-on at high speed indicated that combustion continued in a normal manner, as though the spark were still igniting the charge, despite the fact that the ignition system was turned off and no spark was occurring.

Summary

The work reported in this paper relating to combustion in a 9/1-compression-ratio multicylinder engine may be summarized as follows:

1. In the absence of combustion-chamber deposits, engine noise was the result of knock following normal combustion initiated by a normal spark. There was no evidence of any significant preignition, postignition, or other unusual ignition.

2. After deposits had been accumulated in the laboratory engine under light-duty cyclic conditions it was found that, with fuels closely satisfying the requirements of the engine, virtually every instance of fuel failure resulting in engine noise was the result of surface ignition which led to knock. In no case did the *dp/dt* pattern of knock as obtained in the clean engine appear after deposits were accumulated. There were some differences in this respect between the data obtained in the laboratory and the data obtained in the car because of differences in the treatment to which the deposits were subjected while obtaining data.

3. There was no evidence of knock or other gas vibrations on the *dp/dt* records when rumble occurred. The diagrams indicated that rumble was a repetitive pattern of single or multiple surface ignition occurring immediately before or after spark. The noise probably resulted from deflections of some part of the engine structure induced by high rates of pressure rise. Rumble did not occur in the clean engine.

4. The use of the "key-off" technique is not always a reliable method for determining the presence of surface ignition.

5. Information obtained at retarded spark timing in preignition-limited engines may not accurately reflect the operation of the engine at normal timing.

6. The fuel quality level required to satisfy a preignition-limited engine containing deposits varies substantially with the type of reference fuel system employed. In this respect, the response of reference fuels appears to be considerably different from that previously observed in knock-limited engines.

7. The use of pure benzene as a fuel in the presence of combustion-chamber deposits resulted in considerable preignition, postignition, multiple ignition, and a very loud rumble-type noise. Ordinary knock was not observed, and "key-off" ignition was readily obtained.

Acknowledgment

The authors are indebted to D. R. Diggs for his helpful advice in carrying out this work.

Appendix

The display of the outputs of eight *dp/dt* pickups on a single oscilloscope involved a serious overlap of patterns because each pattern covered about 180 deg of crankshaft angle. This problem was overcome by using two oscilloscopes, each unit accommodating four pickups from alternate cylinders in the firing order. In this way 180 deg of crankshaft angle was made available for each pickup pattern on the particular oscilloscope that it was shown.

The use of two oscilloscopes required the use of a two-channel mixer amplifier to convert the outputs of each of the sets of four pickups into suitable composite signals for display on each oscilloscope. A block diagram of the complete instrumentation is shown in Fig. 19. Patterns from cylinders 1, 7, 6, and 4 were shown on "A" oscilloscope, the upper trace, and patterns from cylinders 8, 3, 5, and 2 were shown on "B" oscilloscope, the lower trace.

Each channel of the mixer amplifier had five inputs, four for *dp/dt* pickups and a fifth for an ignition timing signal. The function of the mixer circuit was to provide a single output signal containing all five input signals in proper time sequence. This composite signal was fed into a speed-compensated amplifier which, with the aid of a reference signal from a tachometer generator, prevented the amplitudes of the *dp/dt* signals from changing appreciably with speed. Outputs from the speed-compensated amplifiers were coupled directly into their respective oscilloscopes.

A signal indicating the ignition breaker point opening was connected to the fifth input terminal of mixer amplifier "B," providing an indication of spark ignition on the "B" *dp/dt* trace. For "key-off" studies a switch was provided to disconnect the engine ignition coil and simultaneously connect a dummy coil so that timing indications could be obtained while the engine spark plugs were not firing. These indications were coupled into the fifth input terminal of mixer amplifier "A" causing them to appear on the "A" *dp/dt* traces during "key-off" periods. Normal engine firing was thereby indicated by ignition timing marks on "B" oscilloscope and "key-off" periods by ignition timing marks on "A" oscilloscope. A reference timing signal was also obtained on the "B" trace by capacitively coupling the high-tension lead from No. 8 spark plug into the fifth input terminal of mixer amplifier "B."

Each oscilloscope was connected to a slave tube in a photorecording unit. In this way it was possible to record not only the *dp/dt* signals shown on oscilloscopes "A" and "B" but also the output from oscilloscope "C" which was connected to the microphone suspended over the engine. The microphone was a high-fidelity unit with uniform frequency response from 40 to 15,000 cps. The output was filtered to remove low-frequency noises below 120 cps which tended to obliterate the sound pattern and did not contribute anything to the analysis from the standpoint of combustion phenomena. The microphone was suspended from the ceiling by springs to isolate it from vibration. The camera was a General Radio Co. 35-mm oscilloscope recording camera which recorded streak signals of the three traces from the three slave tubes, and a 60-cps neon timing light which indicated 120 timing marks per second. The speed of the film was approximately 4 fps.

Certain modifications and simplifications were necessary in the car because of space requirements. Spark ignition was indicated by means of a blanking signal obtained by capacitively coupling signals from the spark plug leads into the "Z" input of the oscilloscope. This method was not quite as positive nor as desirable as superimposing a positive ignition trace on the *dp/dt* traces. The film speed in the car was about 2 fps. The rest of the instrumentation was basically similar to that used in the laboratory.

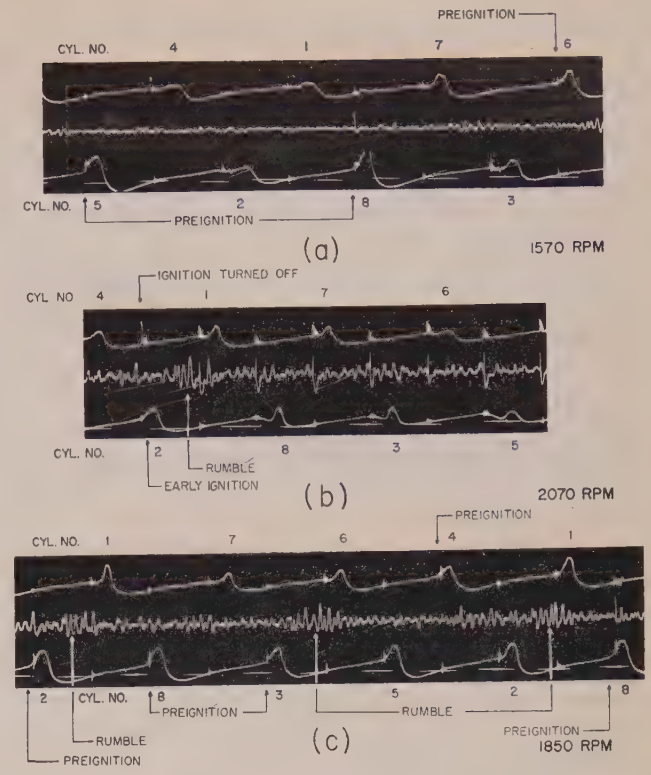

Fig. 18 – Combustion records in engine with deposits, with standard spark timing, using benzene fuel: (a) preignition without knock in cylinders 5, 8, and 6, 1570 rpm, (b) key-off combustion in cylinders 2, 1, 8, 7, 3, 6, and 5, rumble after early ignition in cylinder 2, 2070 rpm, (c) preignition without knock in cylinders 2, 8, 3, and 4. Rumble after preignition in cylinders 2 and 3, 1850 rpm

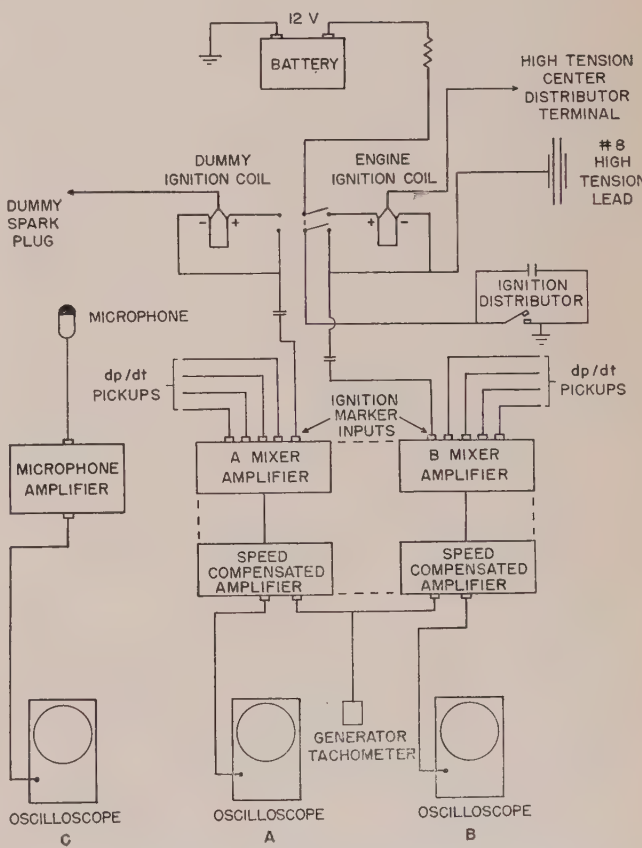

Fig. 19 – Block diagram of instrumentation showing microphone, ignition system components, and *dp/dt* pickup circuits

Manufacture of

THE last few years have added greatly to the knowledge and technique of manufacturing turbine engine parts, and the preferred processing methods have become apparent from present production designs. Many improvements have been made in the original manufacturing methods, and new techniques have been developed, including automation where volume of production has warranted the capital expenditure. We have had sufficient volume to develop many innovations, and in the Korean emergency this pool of know-how was offered to any company chosen by the government to manufacture similar parts.

Print for a part is submitted by the engine manufacturer. The parts specialist studies the print and decides the best method of processing. An engineering service is rendered the engine builder by collaborating on the proposed design, suggesting changes in design for best processing, quality, and lowest cost of the part. Sufficient technical background has now been developed, enabling us to render a valuable engineering consulting service. Data included in this paper represent the knowledge and know-how gained by fabricating approximately 70 million blades and buckets.

This paper covers only the methods of manufacture and the materials used for the following SAE terminology parts:

Blade: A rotating member used to compress gas.

Bucket: A part rotated by hot gas.

Vane: A stationary member used to change gas direction.

We urge the use of this terminology. Considerable confusion results when the term "blade" is used for all these parts, as there is a tremendous variation of physical properties needed in the hot and cold ends of turbine engines.

The manufacturing method used depends upon the material, configuration, component assembly, and specifications for the part. Consideration must be given to tolerances, hardness, grain structure, surface finish, size of the part, operating temperature, and reproducibility, to obtain the required objective, which is dependable aerodynamic performance. (For security reasons, no classified data can be divulged, so only general data are given here.) We used the following methods to make these parts:

Precision forging – airfoil to size.

Rough forging – machine to finish dimensions.

Investment casting (lost-wax) finishing operations only.

Mercast (frozen-mercury) plus finishing operations.

Powder metallurgy – sintered, infiltrated, coined, finished.

Machining from bar stock (prototypes).

Reinforced plastic (development stage).

Compressor Rotor Blades

Materials commonly used for compressor rotor blades are stainless 403, AMS 5616, and aluminum.

Precision Forging of Compressor Rotor Blades and Finishing Operations – Precision forging of blades is one of our developments and our preferred method. By precise control of each detail in forging, the airfoil is forged to finish tolerance, requiring only scale removal and a light polish – the root must be machined. The polishing is done in automatic machines which we developed, 0.0005 to 0.00075 in. being removed from each side of the airfoil, and the polishing done *longitudinally*.

Our technique of precision forging and finishing a typical blade from type 403 stainless steel is as follows:

Slugs are cut from round bar stock, followed by extrusion and blockdown. The slug is approximately 12% heavier than the finished blade. Both the extrusion and blockdown operations are done in the same crank press (see Fig. 1). The slug is heated in an induction furnace and extruded in the first die cavity to a shape resembling an automotive poppet valve – a long smaller diameter stem that becomes the airfoil and a larger diameter knob to be shaped into the root of the blade. Following extrusion, the part is transferred to a second die cavity and blocked down to the general size and shape of the blade.

Several years ago the die life was some 4000 pieces. By detailed attention to lubricants, die surface, die and punch temperatures, and shape of the extrusion, know-how has increased die life to some 20,000 pieces. Improved methods of die making have greatly reduced their cost, and attention to details of forging technique has reduced forging scrap under 3% – which is extremely good for such precision parts. Such improvements have reduced forging costs, although labor rates have risen.

The scale on the blade is removed in a wheelabrator after the hot blockdown operation. The blade is then reheated in an electric furnace and warm

Blades, Buckets, and Vanes For Turbine Engines

A. T. Colwell, Thompson Products, Inc.

This paper was presented at SAE Golden Anniversary Annual Meeting, Detroit, Jan. 12, 1955.

coined in a crank press. While still warm, flash is removed by trimming. The chordal width is now within a tolerance of plus or minus 0.005 in., and other dimensions, such as form and thickness, are now less than plus or minus 0.005 in. See Fig. 2 for the various steps in forging compressor blades: (a) slug of material, (b) extrusion, (c) block-down, (d) coin.

There are two projections on the centerline of gravity of the blade, one at the root and one at the tip of the airfoil. These two projections are locating points for subsequent finishing operations and are of tremendous value. This technique was developed and patented by our chief industrial engineer, Emil Gibian.

After coining, the blade is again blasted to remove scale. The end of the root is then broached, the blade being precisely located by the projections, and subsequent location at the root is made from these broached ends. Broaching the dovetail of the root then follows. These operations could also be done by grinding or milling. However, we favor broaching, and have developed automation in a continuous broaching machine (see Fig. 3), the operator simply feeding the parts into the machine. The angle end of the root is broached in one of these machines – production has been increased some 500% over conventional methods.

After finishing the root, the leading and trailing edges are blended into the airfoil section on a spe-

METHODS of manufacture and materials used for turbine blades, buckets, and vanes are described in this paper.

Precision forging of these turbine parts is the preferred method. Other manufacturing techniques discussed here include the lost-wax, frozen-mercury, and lost-plastic processes and sintered powder metallurgy, casting, and fabrication. Use of specially designed equipment has resulted in vast improvements in some operations.

The paper discusses such new material developments as reinforced plastics, cermets, and titanium in addition to listing the standard alloys used for turbine buckets, blades, and vanes. A description of current British practices is also included.

The Author

A. T. COLWELL (LM '30) is vice-president of Thompson Products, Inc. He is a graduate of the United States Military Academy, and resigned from the Army in 1922 to enter sales work with the Steel Products Co. which later became Thompson Products, Inc. He was appointed chief engineer in 1930 and director of engineering in 1934. Mr. Colwell was appointed vice-president in 1937, and shortly after, became a member of the Board of Directors. Mr. Colwell was president of the SAE in 1941.

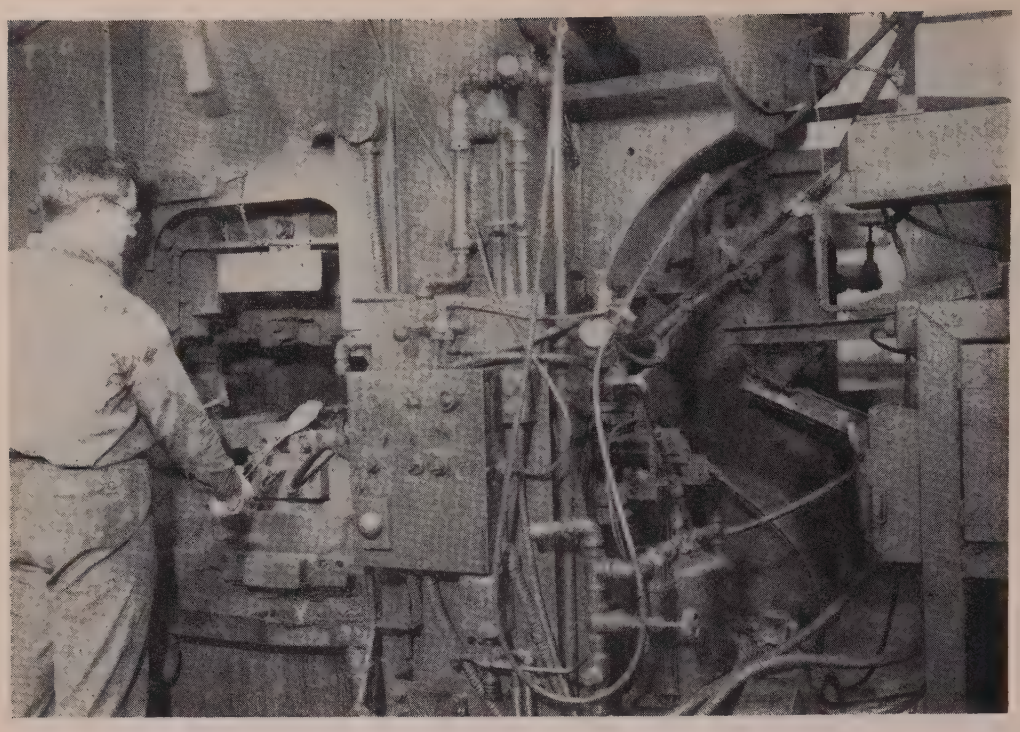

Fig. 1 – Extrusion and block-down forging press

cially developed automatic belt-type grinder (see Fig. 4). This machine evolved from the original method of hand blending through a changing series of special machines, since discarded in favor of the present equipment. The blending of the radii at the intersection of the airfoil and root is done on another machine of our design, which produces a longitudinal polish, thus minimizing stress points.

Next, the only stock removal on the blade airfoil is done on our longitudinal polishing machine. There was no automatic equipment available for this operation, and we therefore invented a machine incorporating five oscillating heads arranged on a rotating turret, Fig. 5.

Fig. 6 shows an operator loading the machine from a central turret; the polished blade is ejected automatically. Three automatic changes of the abrasive polishing cloth are made during the rotation of the turret. The first rough polish removes a maximum of 0.0005 in. per side, followed by a final polish, removing a maximum of 0.00025 in. per side. Final finish is held to 16 microin. or better, and production rate is 900 blades per hour on this equipment.

Inspection of Blades – The guillotine gage (Fig. 7) is at present the most practical method of inspecting blades during the various stages of production. The forging is inspected for airfoil form and twist and visually for surface imperfections. Hardness is checked after forging and heat-treating and before machining. Magnaflux is used to inspect for surface defects, laps, and cracks after rough polish, prior to finish polishing. The machined root is inspected on indicator gages. Locating from the finished root, blade lean and leading edge relationship are checked with indicator gages and in some cases on comparators. The twist is

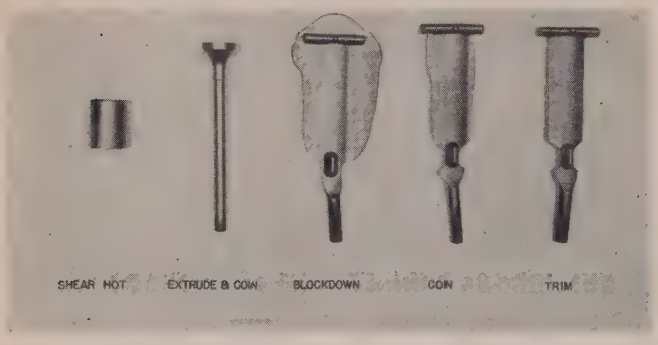

Fig. 2 – Stages in forging compressor blades

Fig. 3 – Continuous broaching machine for compressor blades

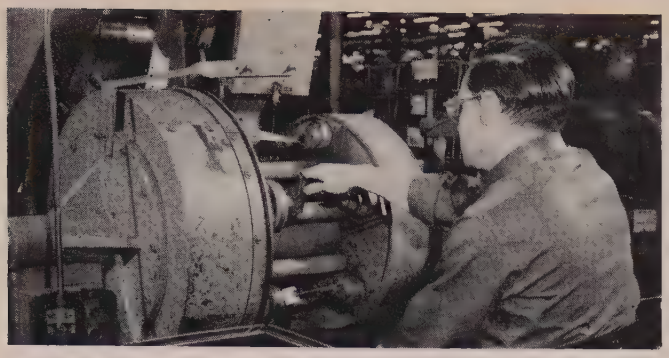

Fig. 4 – Belt-type grinder for finishing leading and trailing edges of blade airfoil

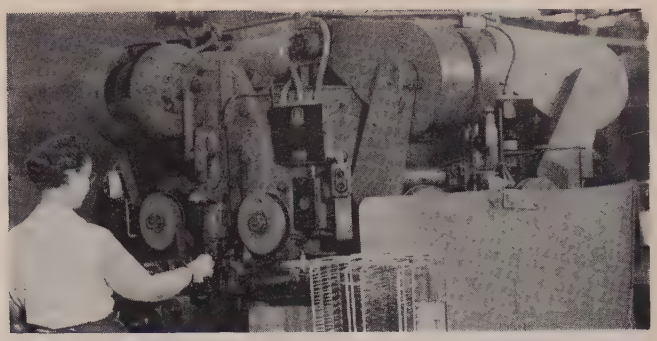

Fig. 5 – Airfoil polishing machine

checked on a specially developed gage (Fig. 8).

Many expensive, slow, and cumbersome attempts have been made for the production checking of these and similar parts. To date the guillotine gage has been the most practical and economical, but some recent developments are being used.

The red-line inspection method (Fig. 9) was developed by General Motors Research at the request of Allison. This is a control check. A finished blade is placed in the machine, and a red line tracing is made of the airfoil contour at definite control points, enlarged five, ten, or twenty times. The master outline on transparent material is then laid over this tracing for any given section. Deviations outside limits can be immediately noted and corrective action taken. Done at frequent intervals, this is a check on production inspection equipment.

A recent development is the Probograph, which can perform inspection at the rate of 6 to 8 pieces per minute and can be used in the production line. This machine has had only limited use, and further experience will be needed for complete evaluation. Electric probes contact the blade contour, at which time a minute electric pulse passes through the probes. The probes are connected through an amplifier to styli which move over a recording paper at a magnified ratio of the probes. A spark passes from the probes to the chart, forming a graph which shows the magnified dimensions of the part.

The well-known Sheffield air gage is also used in production for checking airfoils and roots on buckets.

Listed in Table 1 are typical tolerances which might be specified by the engine designer and must be held by the parts manufacturer.

Other Methods – Blades – also buckets and vanes – can be made by the lost-wax, frozen-mercury, or lost-plastic processes. These processes will be covered in other portions of the paper.

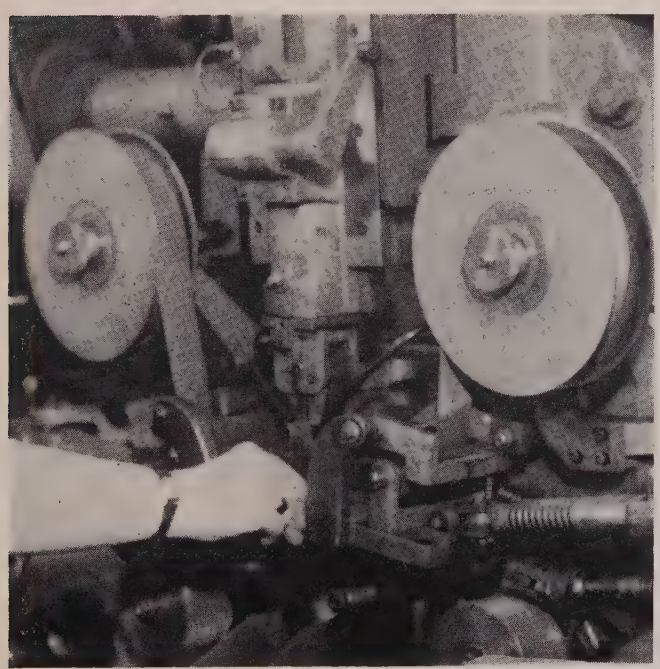

Fig. 6 – Loading the airfoil polishing machine

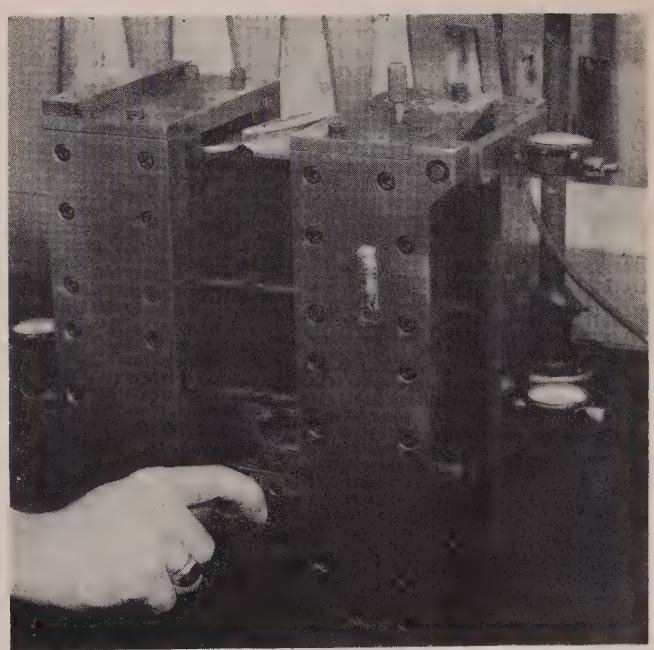

Fig. 7 – Guillotine gage for airfoil checking

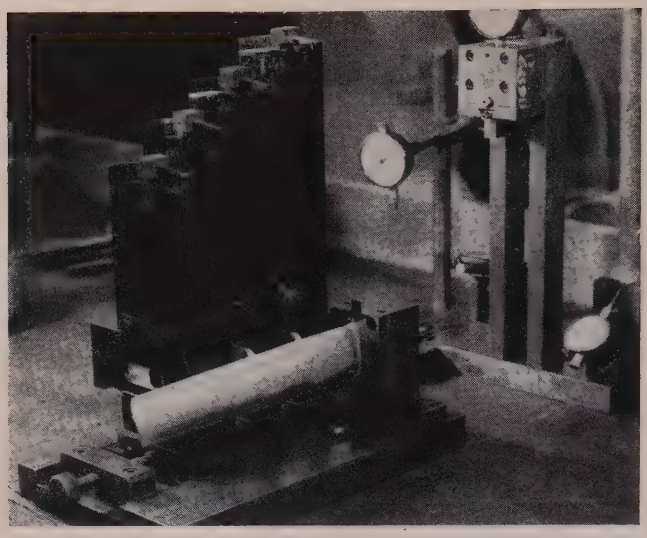

Fig. 8 – Gage for checking airfoil twist

Compressor Stator Vanes

Stator vanes may be made by the precision forging method, described previously, or by sintered powder, casting, or fabrication of rolled strip.

Sintered Powder – We have made over 12,000,000 vanes by this process (known as TP-1), and they have performed exceptionally well. The process was developed when it appeared that the military program would demand 50,000,000 blades per month.

In a serious effort to conserve critical materials, to eliminate the need for heavy forging equipment, and to eliminate mill operations, we developed the powder metallurgy process for the manufacture of vanes. Allison cooperated extensively in this program as a means of eliminating critical materials. TP-1 has been used only for vanes of comparatively small size. The blank can be machined or ground, and the sintered skeleton is made practically 100% dense by infiltration of a copper alloy. After heat-treatment, the blade has good physical properties and exceptional damping qualities, thus reducing stress.

In general the process resembles the making of buttered toast. The powder is compacted (the dough), sintered (baking), and then infiltrated (butter seeping into hot toast).

The various steps are shown in Fig. 10. The powder ingredients are mixed, blended, and sifted for the vanes and also for the pellets and bridges used in infiltration.

The blade is molded in a 250-ton double-acting hydraulic press, the dies forming the blade contour. Experience has developed the correct amount of powder to be used and proper die design to achieve the desired porosity for infiltration. After molding, the vane has cohesive strength, but can be easily broken in one's fingers.

Sintering follows in a controlled-atmosphere furnace (H or dissociated NH_3) at a temperature of 2000 F, well below the melting point of iron. This gives the blade appreciable strength.

Coining is done on a hydraulic press to compress the vane further and to give twist and contour – strength is added, but there is still porosity.

The vane is then infiltrated with a copper alloy in a controlled atmosphere furnace at a temperature above the melting point of copper. The blade is held vertically, sintered iron and copper-alloy pellets are placed on the root, and by capillary

Table 1 – Typical Tolerances of Blades

Lean, in.	± 0.017
Airfoil Thickness, in.	± 0.005
Airfoil Width, in.	± 0.005
Twist, min	±15
Finish, microin.	16 or better
Dimensions on Fastening End Held to, in.	± 0.001

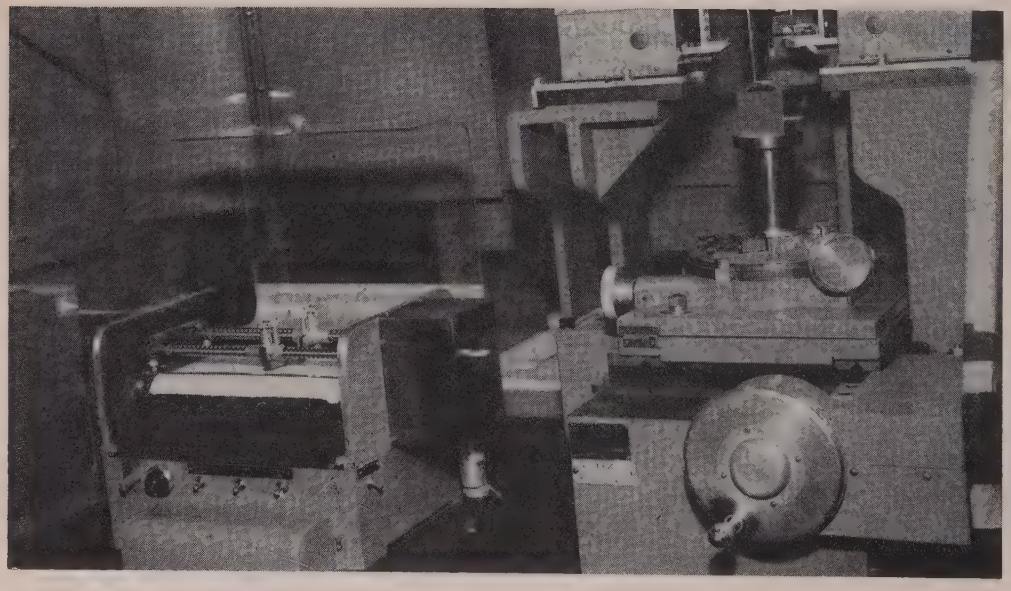

Fig. 9 – Red-line inspection machine

action infiltrated to practically 100% density.

A solution heat-treatment is given, followed by an oil quench. A press straightening operation corrects any warpage that may have occurred. A precipitation hardening treatment provides the final strength properties for the TP-1 vane, with tensile strength over 110,000 psi and ability to take a bend between 40 and 50 deg.

Edge blending, polishing, and broaching are similar to those described for blades. Finally, the vane is electroplated with 0.0005 in. nickel covered by a flash of chromium. This produces a good corrosion-resistant surface, and the blade uses some 12% less chrome than specified for stainless 403.

Fabrication – Hollow inlet guide vanes and stator and diaphragm vanes are also made by fabrication. Sheet metal is formed, and the trailing edges are seam welded, heliarc, or metallic arc welded (see Fig. 11). In some cases a solid trailing edge is welded to the vane and is then machined to finish contour. In some designs strengthening ribs are brazed or spot welded inside the vane. Warm air can be circulated through hollow inlet guide vanes for de-icing.

Vanes of very thin material are best welded by heliarc. Those with greater thickness may be seam welded, while a trailing edge is usually joined by metallic arc. In the case of complicated inlet guide vanes where additions are made to each end, the metallic arc method is favored.

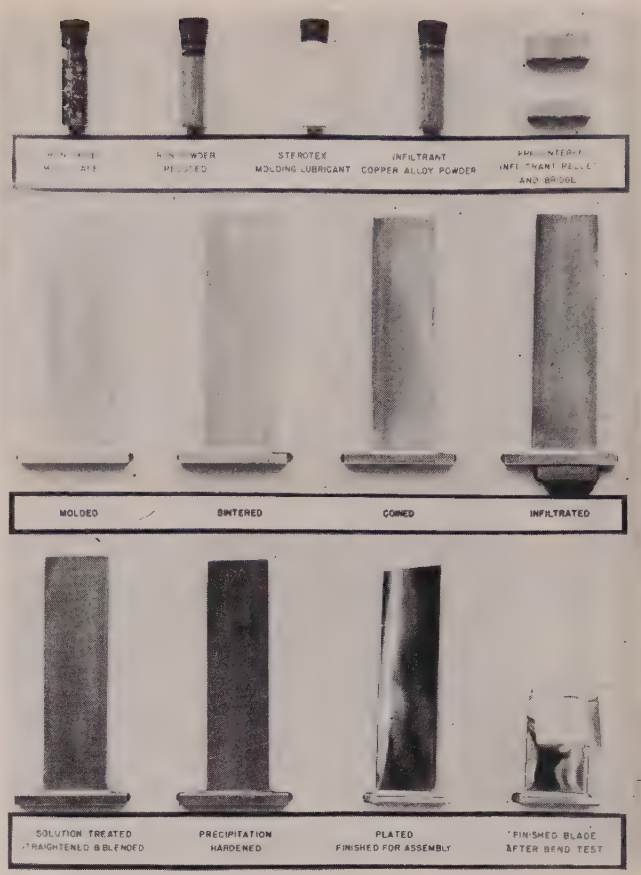

Fig. 10 – Steps in manufacture of TP-1 blade

Turbine Buckets

Precision Forging of Turbine Buckets and Finishing Operations – The precision forging of buckets uses techniques similar to those employed in forging blades. Some modifications are needed because of the higher alloy used and the greater mass of metal to be shaped. Following is a description of the method of fabricating a typical bucket

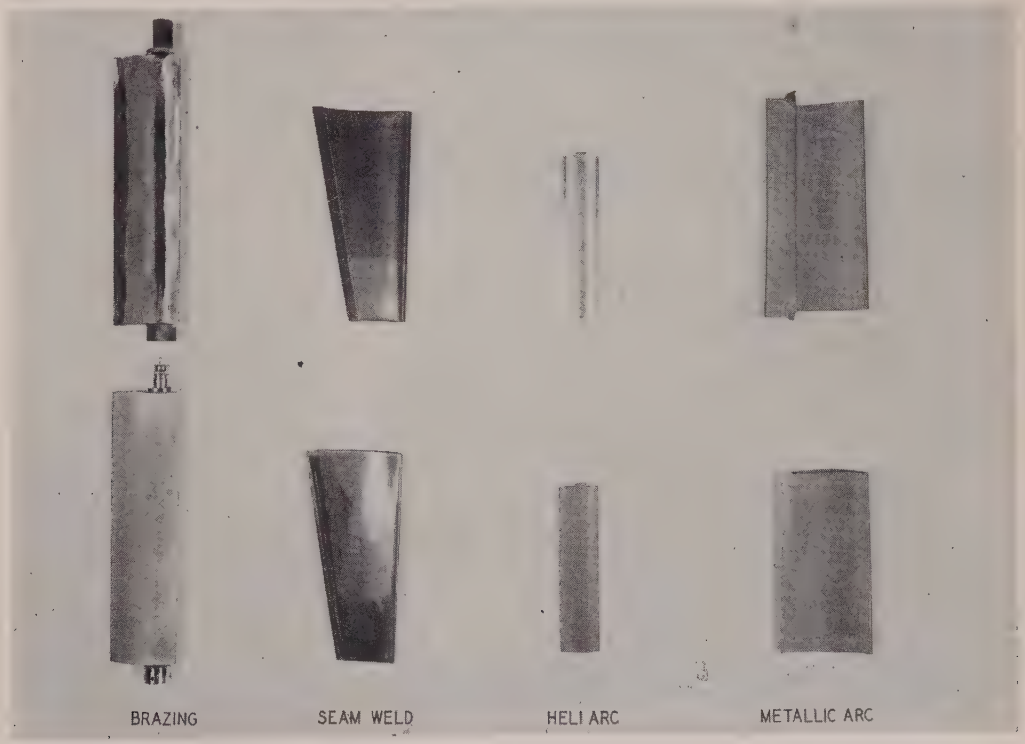

Fig. 11 – Methods of fabricating vanes

from S-816 material:

Ground bar stock is cut into slugs by an abrasive wheel cutoff machine. The slug is then heated in an induction furnace and one end is upset, or "bumped-up," to obtain a gathering of metal. The slugs are then reheated in an electric furnace, atmosphere controlled, and passed through rolls to shape the slug for subsequent forging operations.

Next, the scale is removed from the part by blasting in a wheelabrator, and the bucket is then reheated in a controlled-atmosphere electric furnace for blockdown in a crank press. After the blockdown operation and while the part is still hot, flash is trimmed.

Fig. 12 – Stages of forging turbine buckets

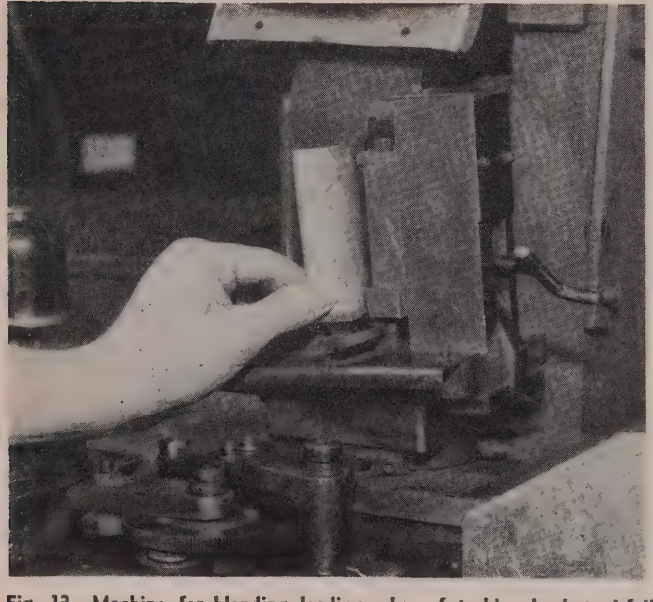

Fig. 13 – Machine for blending leading edge of turbine bucket airfoil

Two more forging operations are then performed on the part, and we call them (1) semi-coin and (2) final coin. Exactly the same equipment and the same procedure (remove scale, heat, forge, and trim) used in the blockdown operation are used in the semi-coin and final-coin operations.

After final coin, the bucket is blasted, reheated in the electric furnace and given one blow on a drop hammer for a final sizing operation. Die design for this operation is critical for the control of grain size. The airfoil of the bucket is now within the limit of the final dimensions required, except the leading and trailing edges which require blending. In shaping the bucket, all forging operations are done in the 2000 F range; and for the hot sizing operation, the bucket is heated in the 1500 F range.

See Fig. 12 for the various steps in forging turbine buckets: (a) slug of material, (b) bumped-up end, (c) rolled slug, (d) blockdown, (e) semi-coin, (f) final coin, (g) hot sizing. Also note the two locating projections used for the same purpose as previously discussed for the blade manufacturing.

After the coining operation and prior to the hot sizing operation, the bucket is solution heat-treated. The aging treatment follows the hot sizing operation and the bucket is again blasted to remove oxidation scale. The first machining operation on the bucket is to finish the fastening end. All finished surfaces on the fastening end of the bucket are broached, including the fir-tree serration. As in the case with blades, we have again exploited the continuous-chain broaching process to machine turbine buckets. The continuous-chain broaching of the fastening end has increased our production approximately 700% over conventional methods of milling, grinding, or vertical broaching.

After the fastening end of the bucket is completely machined, the leading and trailing edges are simultaneously ground between two grinding wheels to establish correct chordal width. The bucket is located from the serrations to locate the airfoil correctly with respect to the root end. To obtain the circular shape on the end of the airfoil, the bucket is held in a rotating fixture, exactly the diameter of the turbine wheel in which the bucket will be used, and ground.

Next, the leading edge is blended on a machine we developed and built ourselves (see Fig. 13). The trailing edge is blended in like manner. This machine utilizes an abrasive belt for stock removal, and the bucket is oscillated about its longitudinal axis to produce the radii. The blending action is in the longitudinal direction to minimize stress lines.

To produce a fine finish on the airfoil, the bucket is next placed in the longitudinal five-headed rotating-turret polishing machine – the same machine that is used to polish the blade airfoil. The surface finish is 16 microin. or better.

Next, the tip squealer is ground by means of

another specially developed machine (see Fig. 14), where the grinding wheel is moved about by cams to follow the airfoil contour. Again, location is done from the finished serrations.

The last operation to complete a turbine bucket is to polish the radii at the intersection of the airfoil and root on the special longitudinal belt grinder previously discussed for blade manufacturing.

Inspection of Buckets – The same inspection techniques are used on the buckets as previously discussed for the blade, with the addition of serration and bucket shelf inspections. The form of the serration is checked on a comparator, and the shelf location is checked by indicator gages. Zyglo is used to inspect for surface cracks, laps, fissures, and other surface imperfections.

Listed in Table 2 are typical tolerances specified for turbine buckets by the engine designer.

Other Methods

Another production method is to forge oversize and then machine the airfoil and root to size. This method was believed necessary for some materials. Such forgings can be produced on presses or hammers, then heat-treated.

One method of machining the airfoil is to use a small milling cutter, machining one side of the airfoil at a time. Ball-nosed milling cutters have been used, as well as the "fast-spiral" method of removing excess material. These operations are tracer controlled from several cams.

Airfoils are ground after machining to get good surface finish. Simple airfoil sections can be controlled with a single cam, but where there is high twist and changing section, four cams may be needed.

Another method is to grind around the entire airfoil with an abrasive belt. This is done from a master, using three to four cams. This machine is a development of the Pratt and Whitney Division of Niles-Bement-Pond Co. (see Fig. 15). After

Table 2 – Typical Tolerances for Buckets

Lean, in. per in. of length (max)	± 0.010
Airfoil Thickness, in.	± 0.005
Airfoil Width, in.	± 0.010
Twist, min	±15
Finish, microin.	20
Dimensions on Fastening End Held to, in.	± 0.001

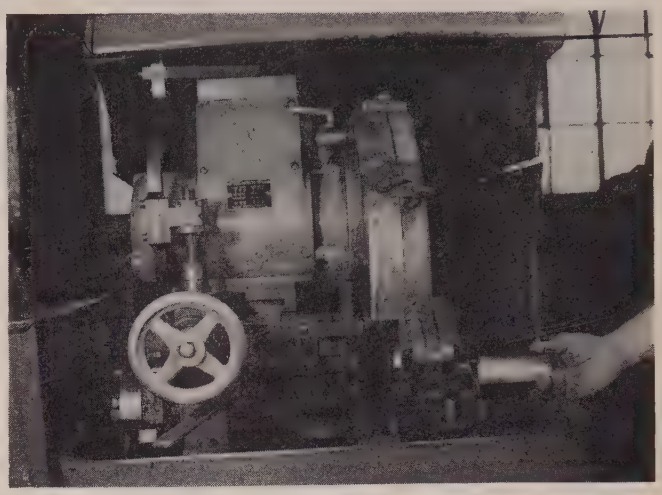

Fig. 14 – Turbine bucket tip squealer grinder

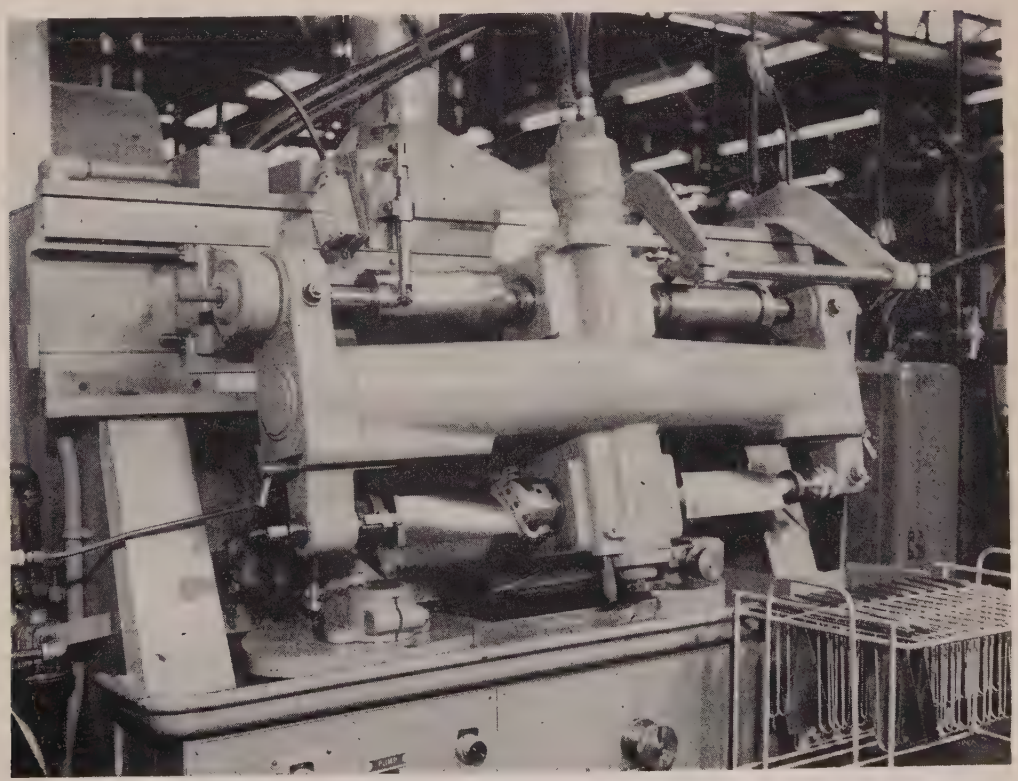

Fig. 15 – Airfoil grinding machine

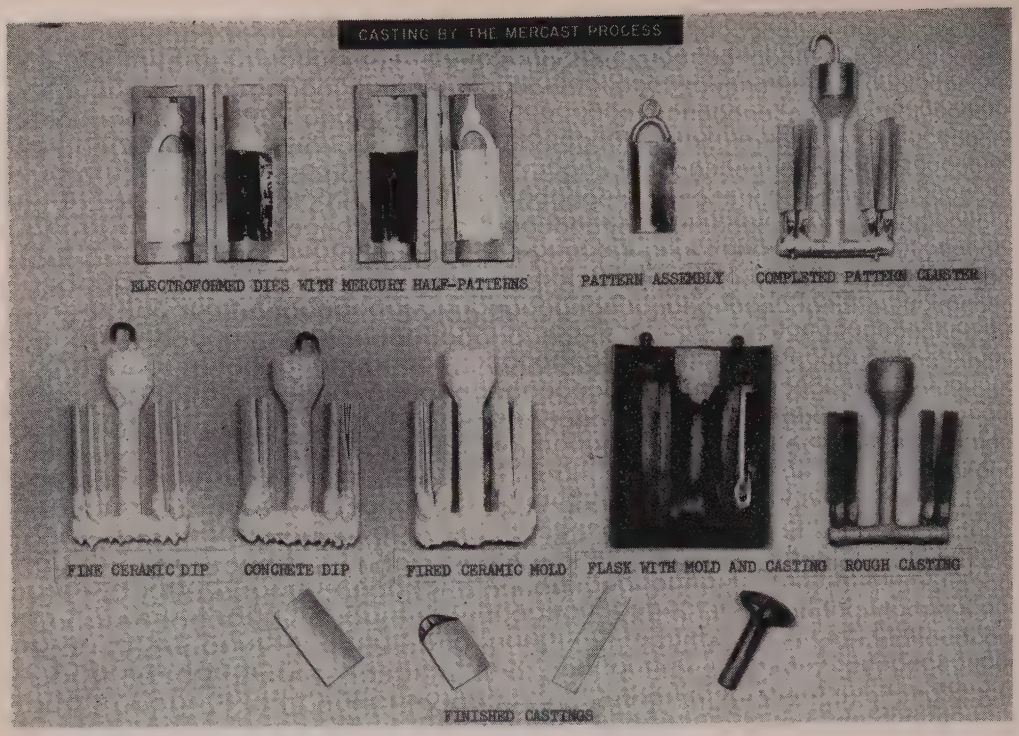

Fig. 16 – Steps in making castings by Mercast process

grinding, final finish is by polishing the airfoil, leading and trailing edges, on abrasive belt grinders duplicating from a master. For blending fillets, a compound motion is used which is actuated by another cam. The root is finished by broaching, milling or grinding. Parts machined all over can be held to close tolerance, but the disadvantages are the time-consuming operations and the tremendous amount of equipment needed for war production.

If the forgings are shrouded, much more machining work is necessary.

Cast Buckets – Parts are made by the lost-wax, lost-plastic, or frozen-mercury process usually when a nonforgeable material is used. Such parts have comparatively large grain size, considered advantageous from the standpoint of high temperature creep but undesirable for high alternating stresses produced by vibration.

Lost-Wax Process – The lost-wax process is adequately covered in the literature. As applied to these turbine engine parts, close tolerances and good surface finish are desirable, but internal soundness is *demanded.* The wax pattern flows slowly at room temperature, and a maximum interval is usually specified between the molding and investing of the pattern. The metal for casting is melted in a small electric indirect arc or electric furnace containing only enough metal to pour one to six pieces, depending upon size. More pieces of very small parts can be made at one pour. Ordinarily, the mold at a temperature of 1200-2000 F is clamped to the furnace and the two quickly inverted to allow the molten metal to run into the mold. In some cases gas pressure is applied to facilitate mold filling. Castings are usually given a stabilizing heat-treatment of about 50 hr. Castings of these turbine engine parts are X-rayed for internal defects, and in general the rejection rate due to surface defects, unsound castings, and distortion is high in this process. Best current practice *can* hold airfoil contour to plus or minus 0.003 in., but average tolerances are greater to reduce rate of rejection. It is not practical to cast trailing edges of 0.015 in. or less, and these edges are cast thicker and reduced to contour by polishing or grinding.

Table 3 – Materials Used for Turbine Rotor Buckets

	AMS-5765 (S-816)	AMS-5382 (Stellite 31)	Nimonic 80A	Nimonic 90	M-252	GMR-235
C	0.37	0.50	0.10	0.10	0.15	0.15
Mn	1.50	1.00	1.00	1.00	1.00	0.25
Si	1.00	1.00	1.00	1.50	0.65	0.60
Cr	20.00	25.50	20.50	19.50	19.00	15.50
Ni	20.00	10.50	Balance	Balance	Balance	Balance
Mo	4.00	....	....	....	10.00	5.25
W	4.00	7.50	....	....	....	....
Co	38.00	Balance	1.00	18.00	10.00	....
Cb	4.00	....	....	....	....	....
Ta	1.00	....	....	....	....	....
Ti	....	....	2.40	2.30	2.50	2.00
Al	....	....	1.20	1.30	0.85	3.00
Other	....	....	Cu-0.50	Cu-0.50	....	B-0.05
Fe	5.00	2.00	2.00	5.00	5.00	10.00
Remarks	Wrought	Cast	Wrought	Wrought	Wrought	Cast

Frozen-Mercury Process – This process uses frozen mercury instead of wax for patterns. Mercury freezes at –40 F, and pattern work is performed at –125 F, either by mechanical refrigeration or by using dry ice. Frozen mercury has the peculiar property of immediately making a strong weld when two pieces are brought in contact. This property makes possible the design and production of complicated assemblies as one piece, as the

Table 4 – Materials Used for Turbine Nozzle Vanes

	AMS-5385 (Stellite 21)	AMS-5532 (N-155)	AMS-5735 (A-286)	AMS-5388 (Hastelloy C)	PWA-651 (Thetalloy)	GMR-235	L-605	Refractalloy 80
C	0.25	0.12	0.08	0.15	0.40	0.15	0.15	0.10
Mn	1.00	1.50	1.50	1.00	2.50	0.25	1.50	0.50
Si	1.00	1.00	0.70	1.00	1.00	0.60	1.00	0.50
Cr	27.00	21.25	14.75	16.50	25.00	15.50	20.00	20.00
Ni	2.75	20.00	25.50	Balance	Balance	Balance	10.00	20.00
Mo	5.50	3.00	1.25	17.00	3.00	5.25	....	10.00
W	....	2.50	....	4.50	7.00	....	15.00	5.00
Va	....	....	0.30	0.40	....	....	....	....
Co	Balance	19.75	....	2.50	12.50	....	Balance	30.00
Cb + Ta	....	1.00	....	....	....	....	....	....
Ti	....	....	2.00	....	....	2.00	....	....
Al	....	....	0.35	....	....	3.00	....	....
N	....	0.15	....	....	....	....	....	....
Other	B-0.007	....	....	....	....	B-0.050	....	....
Fe	3.00	Balance	Balance	5.75	5.00	10.00	3.00	14.00
Remarks	Cast	Wrought and fabricated	Wrought	Cast	Cast	Cast	Wrought and fabricated	Cast

pattern can be built in simple sections and "welded" together. Hollow vanes and buckets with ribbed sections are entirely practical by the frozen-mercury process, as are other parts such as complicated wave guides and nozzle boxes. The process is used for making castings having internal cavities so intricate that withdrawable cores cannot be used. Much larger parts can be made by this process than by lost wax – incidentally, this process is not called "lost mercury" because all the mercury is recovered when it is melted from the pattern. The process gives better surface finish and closer tolerance than other investment processes, but the cost per se is higher – however, the yield is ordinarily much higher than with other processes, rejections being lower, so that on simple pieces it approaches competitive cost. For very intricate pieces it stands alone – hence the name "Intricast." Any castable alloy can be used with this process.

Mercury is poured into steel dies at –125 F to make the pattern. This pattern is then invested with special ceramic slurries at subzero temperature, the initial dip being a very fine-grained ceramic to impart a smooth surface to the casting. The mercury is melted from the mold, which is then fired and set (the molds can be used for centrifugal castings). The molds are then filled with metal from high-frequency induction furnaces, making possible good control of metallurgy and analysis. Molds are then crushed to remove the castings. (See Fig. 16.)

Lost-Plastic Process – Plastics are sometimes used in place of wax as the pattern material. The advantages of polystyrene plastic patterns are: lower cost, good stability, and their handling properties are such that patterns can be inspected before investment.

Costs are reduced (in large-volume production) since plastic patterns can be formed in a multicavity die injection mold. Where volume does not justify the fabrication of a multicavity mold, it is more economical to produce patterns by wax.

The stability of the plastic is good. Also, the plastic patterns can be handled, which permits inspection and gaging before investment.

Because "solid-chills" cannot be used, the shrinkage is greater in heavy sections of plastic patterns than in wax patterns.

Turbine Nozzle Vanes – Nozzle vanes and many turbine buckets are made from nonforgeable materials and are therefore cast by the lost-wax, lost-plastic, or by the Intricast (frozen-mercury) process.

Materials

Tables 3, 4, and 5 are tabulations of materials, not classified by security regulations, used for blades, buckets, and vanes.

New Material Developments

Reinforced Plastic Blades – To keep abreast of new materials and manufacturing techniques, we have been studying plastic blades for the past 18 months. Although the development is still on an experimental basis, the third stage of a compressor rotor was bladed with the fibrous glass-reinforced blades. This development originated with the idea of finding a fast and cheap method of making prototype blades. A 100-hr run at rated engine

Table 5 – Materials Used for Compressor Rotor and Stator Blades

	Type 403	AMS-5628 (Type 431)	AMS-5616 (Greek Ascoloy)	Type 410
C	0.10	0.15	0.15	0.10
Mn	0.55	0.55	0.50	0.45
Si	0.50	0.40	0.50	0.35
Cr	12.25	16.25	13.00	12.50
Ni	0.50	2.00	2.00	0.60
Mo	0.20	....	0.50	0.60
W	....	....	3.00	....
Fe	Balance	Balance	Balance	Balance
Pb	....	....	....	....
Zn	....	....	....	....
Ti	....	....	....	....
Al	0.05	....	0.15	....
Cu	....	....	0.50	....
Sn	0.05	....	0.05	....
Other	....	....	....	....
Remarks	Wrought	Wrought	Wrought	Rolled airfoil section
	Stator and rotor	Stator and rotor	Stator and rotor	Stator

speed was successfully completed on the rotor. Inspection of the blades after disassembly from the rotor showed that they were in excellent condition. There were no signs of erosion or impending failure, and this test indicates continuation of the development (see Fig. 17).

Several properties of the plastic blade make it attractive. One consideration is that the fibrous glass-reinforced plastics are noncritical materials. Also, the plastic blade has a relatively high damping capacity which keeps the stress low and the blade less susceptible to fatigue failure.

Another advantageous characteristic is the lightness. This blade property improves acceleration characteristics of the engine because of the resulting lower moment of inertia, and starting torque also is reduced.

The plastic material exhibits practically no creep, thereby minimizing chances of stress rupture. In spin pit tests at 110% overspeed for 15 min there was no measurable creep on a 30-in. diameter installation (disc plus plastic blade). This compares with steel blades that grew 0.001 to 0.002 in. during the same type of test.

The plastic material's strength/weight ratio is about three times that for a compressor blade steel. Relative to its mass, the plastic's impact strength is equal to that of compressor blade steel.

Disadvantages of the plastic blade are its nonisotropic strength properties. Also, the blade will be difficult to inspect adequately.

It is now possible to produce fibrous glass-reinforced plastic materials with the ability to withstand 500 F. The blades in the 100-hr test ran at about 300 F; however, in the foreseeable future, phenolic-impregnated fibrous glass plastics may be able to withstand approximately 700 F for about 10 hr in a compressor blade application. This would indicate favorable progress in increasing the temperature limitation of the material.

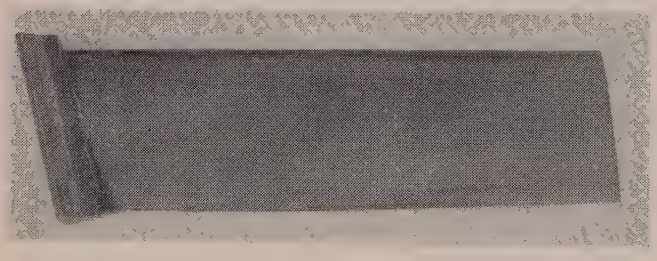

Fig. 17 – Plastic blade

Fig. 18 – Cermet nozzle vane

The molding job for the compressor blade is more difficult than the usual procedure for forming reinforced plastics. Closer control is required in die design of pressures, temperatures, and pre-layup phases. Experimental results to date have been excellent – dimensional uniformity and fine surface finishes are obtained.

The molding process begins with the dry layup, which approximates the shape of the blade. The laminations, cut from phenolic-impregnated fibrous glass cloth, are held together mechanically.

The layup is placed in a male-and-female heated die arrangement in which it is subjected to a pressure forming cycle. When the molded part is removed it is about 90% complete. At this point, the blade is to size and shape. Dimensional control is excellent. A post-curing operation is then required for the resin in the blade to impart the necessary strength properties.

Cermets – Sustained effort is being put into the development of cermets for buckets and nozzle vanes. We have acquired the patent and services of Claus Goetzel for a method somewhat similar to that for making TP-1 blades. At present the product appears to have properties for developing a bucket that will operate in the 2000 F range, and it will be thoroughly evaluated in the jet engine test stand now being built, along with other engine materials. Nozzle guide vanes have completed a 100-hr engine test with encouraging results – vanes are more easily made than buckets. (See Fig. 18.)

Titanium – Titanium metal has not much of a past but a tremendous future, if determination and money are applied. The present cost is prohibitive for anything but military use, and the high cost is occasioned by poor yield at the mill and in the manufacturing of blades and vanes. Also, the titanium scrap cannot be salvaged. The troubles are caused mostly by impurities in the titanium alloy—preponderantly due to hydrogen. Tremendous effort is being expended to improve the material, and progress is being made.

Electrolytic and thermal processes are being tried to replace the Kroll process, which is the only process at present for producing sponge. Titanium must be alloyed for successful use, and some of the alloys have been more troublesome than others.

It has been found that titanium generally requires approximately 30% greater delivered force to effect the same flow pattern as compared with steel. This necessitates careful selection of die block size and hardness. Even so, die life is considerably lower. Die sinking is more critical in that the finish is a controlling factor.

Generally speaking, lower temperatures are employed for forging titanium than are usually employed for the stainless steels. Temperature range is also more closely controlled in order to minimize grain coarsening and the formation of a hard, brittle oxide layer which is known to impart brittleness to titanium. Since no economical atmospheres have been introduced to the industry as yet, we at Thompson employ air atmospheres, using electric-furnace heating exclusively. Because of detrimental effects of surface scale and the possibility of hydrogen pickup, we have realized the necessity of avoiding the use of gas-fired furnaces or industrial atmosphere mixtures.

To date no known commercial-type lubricant has been found satisfactory for the forging of titanium. Thompson employs lubricants which were developed by our research facilities, and we have since made arrangements to secure these mixtures from commercial companies. The best lubes developed to date are still not completely satisfactory, and research is still in progress to secure better lubricants for the various forging operations.

We use centerless ground bar stock to insure satisfactory surface quality. To insure quality further, we employ a stress-relieve operation on slugs to prevent thermal stress cracking at the cut surfaces prior to any forging operations.

The slugs are prepared for the flattening operations by the extrusion process, or gather upset. This extrusion is done in two operations; first, the slug is pointed; and second, the stem is extruded, from which the blade airfoil is formed. Subsequent flat die operations form the airfoil and root end of the blade. A much greater degree of springback is encountered with the titanium alloys, thus increasing the problems of holding bow and twist tolerances. As previously mentioned, a greater force is required on the titanium alloy, and these factors require the use of greater tonnage presses. Experience has shown that a stress-relieving operation after each flattening operation aids somewhat in reducing the bow and twist problems.

A great deal more work is encountered in maintaining good surface conditions when working with the titanium alloys. As an aid in detecting imperfections and to insure the removal of any brittle oxide layers, the parts are pickled after the blockdown and coining operations.

With our present forging techniques, we have found little differences in processing the various grades of titanium alloys. However, with some of the more recent alloys, such as Ti 140A and the MST 5A1 4V, we have discovered that a greater latitude of forging temperatures is permissible without encountering grain coarsening and formations of hard, brittle oxide layers.

Many of the difficulties in the manufacture of titanium parts have been overcome. When good stock is available, satisfactory blades are being made.

Machining Techniques – We have expended the greatest amount of research in the field of broaching. We have found that much greater rigidity in fixturing is required plus the use of slower broaching speeds. The average speed for broaching of titanium is 10-12 fpm, while the speed for broaching the 403 stainless steel is 28-30 fpm. Broach insert materials and coolants are important details in this work.

Final trimming operations on the airfoil edges must be done at comparatively low temperatures to prevent edge cracking. In the belt-type polishing operation, details are again important in order to maintain good surface finishes.

Because of the difference in feeds, speeds, and tool geometry, it will be necessary to maintain a separate machining line to manufacture titanium components.

Fabrication of Large Paddle-Type Blades

Over the past five years, blades have increased three to five times in size. The problems in fabricating these large blades have increased many times.

For example, an older design of blade with a 1-in. chordal width has a specified tolerance of 1 deg or less on the twist. Today, a 3-in. width blade still has a specified tolerance of 1 deg or less on the twist angle. There have been no relaxations in the tolerances as we go to larger blades.

The wide, thin blades also create more problems in machining. Because of their flimsy structure, they are more difficult to fixture for machining.

Also, because of the geometry of the large paddle blades, great care must be exercised in heat-treat to minimize warpage; but definite progress is being made in the manufacture of such parts.

Automation

Certain operations lend themselves to complete or partial automation if there is sufficient volume, and many such installations have been made. One large installation is complete machining of the inside of stator casings. This equipment was designed by Hautau Engineering, and removes 125 lb of metal in 10 min, completing all finishing operations. In case of war, such equipment has tremendous capacity. It was a long, difficult development, but it is now serviceable equipment.

Polishing, broaching, and induction heating have been mentioned in other portions of the paper.

Foreign Practices

Over the past number of years, we have been in close contact with Rolls-Royce on mutual problems of blade and bucket manufacture. Rolls-Royce is now using the precision forging technique of producing blades, and through the courtesy of Lord Hives and A. F. Kelley of Rolls-Royce, the following information on current British practices is available:

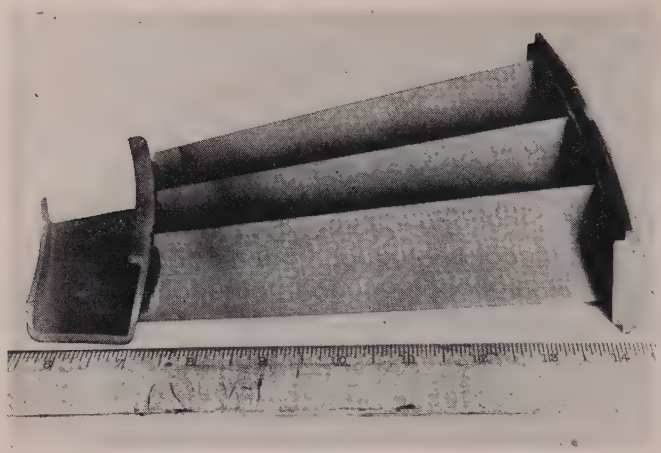

Fig. 19 – Rolls-Royce Avon compressor stator blades

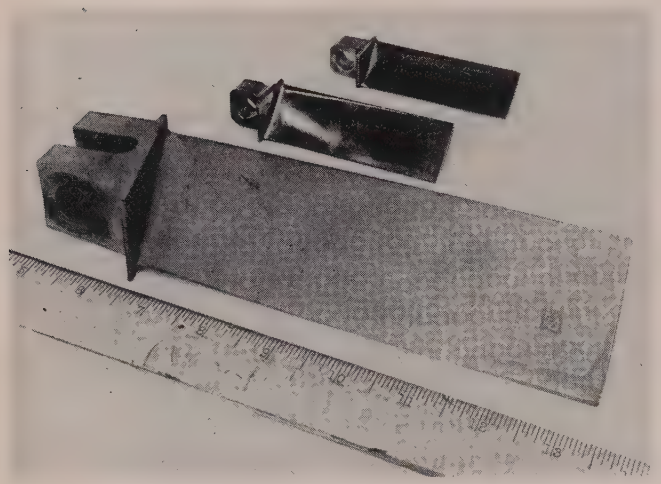

Fig. 20 – Rolls-Royce Avon compressor rotor blades

Rolls-Royce Method of Blade Production

"*Compressor Blades* – Compressor blades are made of three different types of material: (a) aluminum, (b) aluminum bronze, (c) steel.

"Blade Forms – All blade forms are forged to size so that machining is only necessary on the root, tip, and the leading and trailing edge radii.

"Blade Fixing – All stator blades are held by a groove-type fixing, the larger aluminum blades being steadied by shrouds at the inner diameter brazed to the blade tip (see Fig. 19), and for smaller stator blades in aluminum bronze, roots are brazed together to reduce twisting. All rotor blades have a pin-type fixing, the larger aluminum blades having bushed pin holes (see Fig. 20).

"Forging – Precision forging of blades is carried out on crank presses of up to 1200-ton capacity, the uses for these presses being produced by extrusion on machines up to 600-ton capacity. Centerless grinding of the use is carried out to insure uniformity of the surface before forging.

"Machining of Roots – For the aluminum and aluminum bronze blades, the machining of the platform faces is completed on multistation rotary milling machines designed and built by ourselves. Special rotary machines designed by Honsberg of Germany, which reduce the floor-to-floor time from 10 min to 1 min, are used only where production quantities justify the relative inflexibility of such a machine.

"The root of the steel stator blades is finish machined on rotary milling machines, although this will ultimately be broached. The steel rotor blade root is being broached already.

"The leading and trailing edge radius is produced on a special machine which, by a shaving action, blends the two airfoil surfaces by a varying radius.

"Blade Inspection – Nonmagnetic blades are inspected by electrolytic polishing both before and after precision forging. The aluminum blades are anodized before and after machining. Steel blades are magnetically crack tested and are nickel plated to reduce scaling during the forging process.

"After final inspection, rotor blades are graded in relation to their nominal weight to facilitate static balance of each rotor stage; and stator blades are graded according to the circumferential thickness of their roots so that on final assembly in the casing, the joint faces can be made level.

"Strip Blading – This is so far only employed on small engines and only in steel. Stator and rotor blades are cut off from strip rolled to constant airfoil section, the required twist of the blade being produced after cutting to length.

"Stator blades are held in semicircular housings which are punched to receive the blade sections, while the rotor blades are projection welded to the compressor disc which is plunge-milled in the vicinity of the weld to obtain uniform heat dissipation.

"Plastic Blades – Plastic blades are as yet in a fairly early stage of development, the principal difficulty encountered up to now being the establishment of materials with sufficiently high mechanical properties to withstand the aerodynamic loads.

"So far no production application has been found, the work being confined to rig compressor.

"*Turbine Blades* – All engines on production today, with the exception of the Soar and the Nene, have shrouded turbine blades (see Fig. 21). To reduce vibration amplitudes in the Avon, the blades are welded in pairs by Argon-Arc welding.

"Materials – For the Dart turboprop engine, both high-pressure and low-pressure turbine blades are made in Nimonic 80A nickel alloy. All marks of Avon engine have Nimonic 95A high-pressure blades and Nimonic 90 low-pressure blades.

"The composition of Nimonic 90 is:

Carbon: 0.1%
Iron: 5.0%
Manganese: not more than 1.0%
Silicon: not more than 1.5%
Aluminum: not less than 0.8% nor more than 2.0%
Titanium: not less than 1.8% nor more than 3.0%
Cobalt: not less than 15.0% nor more than 21.0%
Chromium: not less than 18.0% nor more than 21.0%
Sulfur content of chromium: not more than 0.5%
Nickel: remainder

"Other properties of Nimonic 90 are detailed in British Specification DTD.747, which is available to the public. Nimonic 95 is still on the secret list.

"General Methods – All Rolls-Royce turbine blades, with the exception of the very small ones used on the Dart turboprop engine (1500 shp), are made from forgings with a small amount of metal to be removed from the blade surface by profile milling. In the case of the Dart, the blades are machined from rectangular pieces of extruded bar, as it is uneconomical to stamp the rough shape.

"The machining of the turbine blade is started by milling location slots and grinding flats on the shroud and platform ends of the blade so that it can be held in broaching machines which finish the fir-tree root and the adjacent neck form. This root is then inspected by 100% shadowgraph check. The inside of the blade form is then rough milled, the finish milling being on an 8-spindled copy miller made by Rigids of Rorschach, Switzerland.

"The outside form is either rough ground or turned on a special lathe of Rolls-Royce design, where two blades are held in pairs and the tool is controlled by a cam to produce the required blade profile, with a face cam to enable the turning to be carried out up to the shroud and platform ends.

"After the machining operations, surplus material is removed by grinding from the shroud end. The final surface finish of the blade is achieved by an abrasive belt which is reciprocated over the surface and held against it by air pressure. The leading and trailing edges are ground on a special machine. The last inspection process is electrolytic polishing.

"Rolls-Royce does not use cast turbine blades on production, although experimental work is proceeding.

"Small blades for the Dart engine will be forged to size so that no more than a polishing operation is necessary on the airfoil section. These forgings are produced on a press up to 2000-ton capacity.

"We are also about to go into production with forged-to-size turbine blades on Avon engines.

"*Nozzle Guide Vanes* – The nozzle guide vanes or stator blades for the turbine are cast by a precision method, either the lost-wax process or, where possible, by shell molding. So far shell molding is only in the early stages of use and has not been used for hollow vanes. The material most commonly used is Crown Max (a high nickel-chrome cast steel), but for more arduous duties C. 130 (a nickel-chrome-molybdenum alloy), is being introduced.

"In all cases the airfoil is cast so that only machining of the platform locations is necessary. Checks of outlet area to the turbine are carried out on final assembly by banana-shaped gages, generally at three points in each blade gap.

"Most new engines use hollow nozzle guide vanes, generally to obviate thermal cracking and in some cases for aircooling. Experiments are also proceeding with fabrication of nozzle guide vanes from sheet metal and solid end pieces."

British Practice Other Than Rolls-Royce

"Other British engine manufacturers, we understand, differ from our practice only in the following main categories:

"(a) Compressor rotor blades are not loosely pin fixed. The rotor blades are either held by a fir-tree root, similar to conventional turbine blade practice, or by a rigid pin fixing.

"(b) Many engines use entirely steel compressor blading, and most of the stages are shrouded at the inner diameters.

"(c) Some steel compressor blades are machined on the airfoil section by the B.R.D. (Blade Research and Development) method. This takes a close forged form, and by application of a moving finishing band over a formed die, it creates the finished airfoil section, apart from the leading and trailing edges. Others are made by the Ex-Cell-O process, with which you are familiar. Otherwise, compressor blades as we understand the situation, are precision forged on the airfoil section in the same way as Rolls-Royce practice.

"(d) Turbine blade construction and manufacture is similar throughout the industry."

Conclusion

The turbine engine has been under wide development in America for only some ten years. We at Thompson Products were of the opinion that this type engine would eventually be widely used, and hence from the start we put concentrated effort on the manufacture of these parts and components. Some of the forging know-how for valves was applied, but much of the other work was entirely new, calling for special machines and processes. Design trend is to larger and more intricate parts as engines increase in thrust, necessitating new and novel approaches to some of the manufacturing problems and materials involved. Quality control is paramount in this work. As of today, we know of no design submitted which cannot be produced.

Acknowledgments

Special acknowledgment is made to Carl Main and Bruce Multhaup for their technical assistance in preparing this paper, and also to Irwin Binder, R. E. Cummings, Robert Paetz, and K. M. Bartlett for their collaboration.

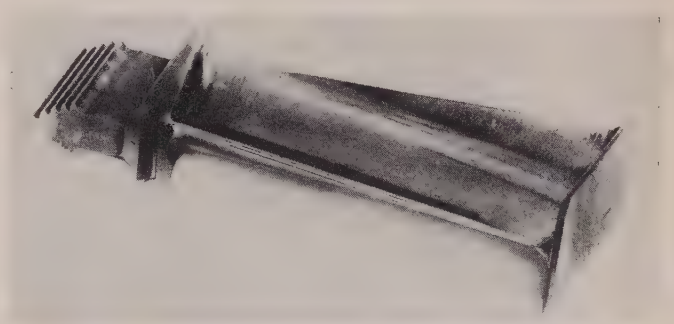

Fig. 21 – Rolls-Royce Avon high-pressure turbine bucket

Wear Rates

THE rate of gear wear varies with speed, load, lubrication, and heat-treatment of the metal used in the gear. Older methods of determining wear consisted of operating a gear under various load and speed conditions and visually observing or measuring the surface of the gear. By this method, little information concerning the rate of wear was obtained. Only those critical loads or speeds where accelerated or destructive wear began were observed.

The radioactive method of measuring gear wear gives a quantitative method of measuring the minutest amount of wear at loads and speeds much below critical destructive conditions. Wear rates as low as 50 micrograms per minute can be detected. Also the amount of metal transferred from a pinion to a mating gear can be detected. Rate of wear can be measured continuously; thus, loads and speeds can be changed frequently and wear rates determined for a large number of operating conditions in a short period of time, many hours being saved in making an extended analysis of gear failure.

Radioactive Method of Measuring Gear Wear

This method for determining gear wear rates consists of activating a sample gear in a nuclear reactor. During the exposure of the gear, some elements in the gear material are changed to other radioactive isotopes, principally FE-59 and FE-55. The half life of FE-59 is 46 days; that of FE-55 is 2.9 years. Iron powder, obtained by grinding the side of the gear, is carefully weighed, wrapped in pure aluminum foil, and inserted in the bore of the gear so that it receives the same exposure in the nuclear reactor as the gear. For purposes of calibration, the activated iron powder is then mixed with a known quantity of oil and circulated in a closed system as shown in Fig. 1. The concentration of radioactive iron is known, and the reading of the detector-ratemeter-recorder unit is a direct measure of the concentration of iron in the oil. By adding successive known amounts of iron to the oil, a calibration curve (Fig. 2), counting rate versus iron concentration, is obtained.

The intensity of radiation from a given weight of iron decreases logarithmically with time. However, by setting aside a small sample of the metal and measuring the activity of this sample periodically, it is possible to correct all the data to zero time. Fig. 3 shows this decay correction curve. There are two sets of data plotted on Fig. 3. The top curve shows the intensity decrease of a sample measured with only air between the detector and specimen. The lower curve shows the intensity decrease with an absorber between the detector and specimen, which is the actual situation when measuring the activity in oil in a closed system with an external detector. Since the slope of the decay correction curve varies according to the material between the radioactive material and the detector, it becomes necessary to measure decay during calibration with the same physical setup as used in the actual tests.

As the radioactive gear is operated under a prescribed load and speed, the particles of iron worn off circulate with the oil. The meter intensity then indicates the concentration of iron in the oil. By plot-

A METHOD is described in this paper by which the rates of gear wear under different conditions can be determined by the use of the radioactive tracer technique. With this method one can measure the minutest amount of wear at loads and speeds much below critical destructive conditions.

This method makes possible the continuous determination of rates of gear wear at all loads and speeds in actual full-scale units. In this investigation, the radioactive tracer technique has been used to determine the rates of gear wear when using a straight mineral oil and when using an extreme-pressure gear lubricant.

The Authors

F. L. SCHWARTZ (M '45) is professor of mechanical engineering at the University of Michigan, and consultant to Continental Motors Corp. He received his B.S. in Mechanical Engineering from Lehigh University in 1928, his M.S. from New York University in 1934, and his Ph.D. from the University of Michigan in 1940. Dr. Schwartz was an engineer with the Aluminum Co. of America from 1928 to 1930. He taught at Pratt Institute and the University of Pittsburgh until 1940, when he came to the University of Michigan.

R. H. EATON (M '51) is a research engineer at the Engineering Research Institute of the University of Michigan. He received his B.S. in Mechanical Engineering from the University of Michigan in 1949, and his M.S. in 1954.

# of Gears

By the Radioactive Method

F. L. Schwartz and R. H. Eaton, University of Michigan

This paper was presented at SAE National Tractor Meeting, Milwaukee, Sept. 15, 1954.

ting a continuous graph of iron concentration versus time, the rate of wear can be measured during any time interval long enough to draw an accurate slope through the plotted data.

A sun gear from a heavy-duty planetary gear set was used in the radioactive-year tests. This sun gear was a standard-width involute gear with a 0.040 modification of the tooth profile. The chemical analysis of this steel is as follows:

C	0.23
Mn	0.85
Si	0.29
Ni	0.48
Cr	0.67
Mo	0.11

After the final manufacturing process, the gear was given a coating of Parker Lubrize 0.001 to 0.003 in. thick.

Another gear from the same steel lot was used to make up the calibration sample. A fine, high-speed grinding wheel was used to grind about 3 g of metal from one end of the gear. This powder was collected by a magnet placed close to the off side of the grinding wheel. Samples of this powder were carefully weighed, wrapped in pure aluminum foil, and placed in the bore of the gear so that the sample and the gear received the same neutron bombardment. A similar sample of the powder ground from the gear was washed with carbon tetrachloride and alcohol to remove all oil film and then photographed under 110 X magnification, Fig. 4. One package contained 113 mg, another contained 311.5 mg, and the third contained 792 mg. The gear and the samples were then sent to Oak Ridge, Tenn., where they were placed in the reactor for 28 days. At the end of this time the gear and samples were returned to the University of Michigan. Daily readings were taken with a Geiger-Müller counting tube and scaler to determine the decay rate. During the first few days the decay rate was high because of the effect of the elements with short half-life periods. After about ten days the activity decreased in a straight-line relationship, and the test was begun.

The calibration oil system, Fig. 1, was calibrated initially with 1 gal of oil in the system, and readings were taken to establish the background level. With the oil still circulating, the smallest package containing 113 mg of the gear-metal powder was added to the system. The calibration system was checked periodically until the activity level became

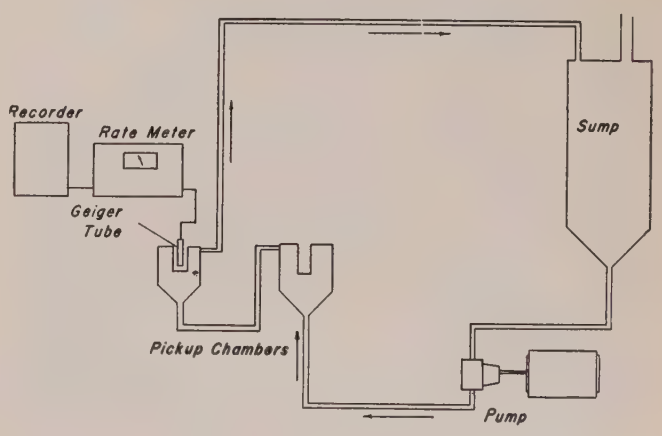

Fig. 1 – Calibration system

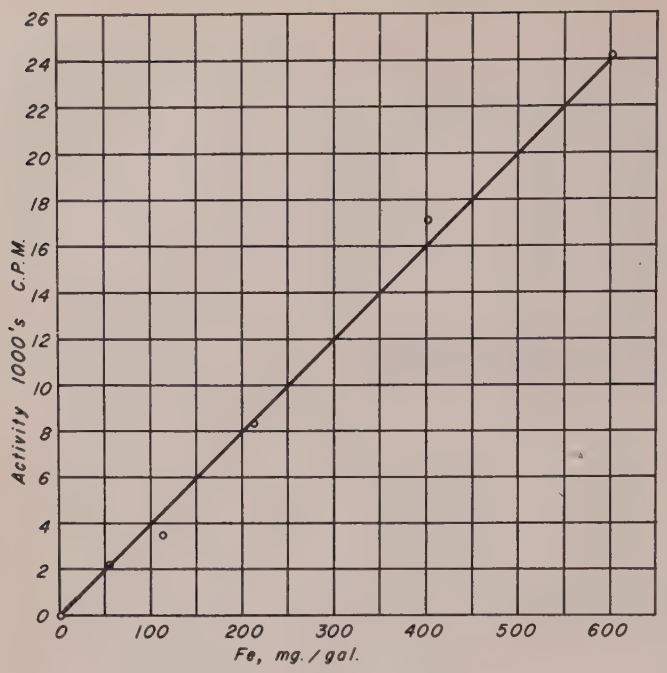

Fig. 2 – Calibration curve

constant, indicating an even distribution of the powder in the oil. This reading was recorded. Next, another gallon of oil was added to the system.

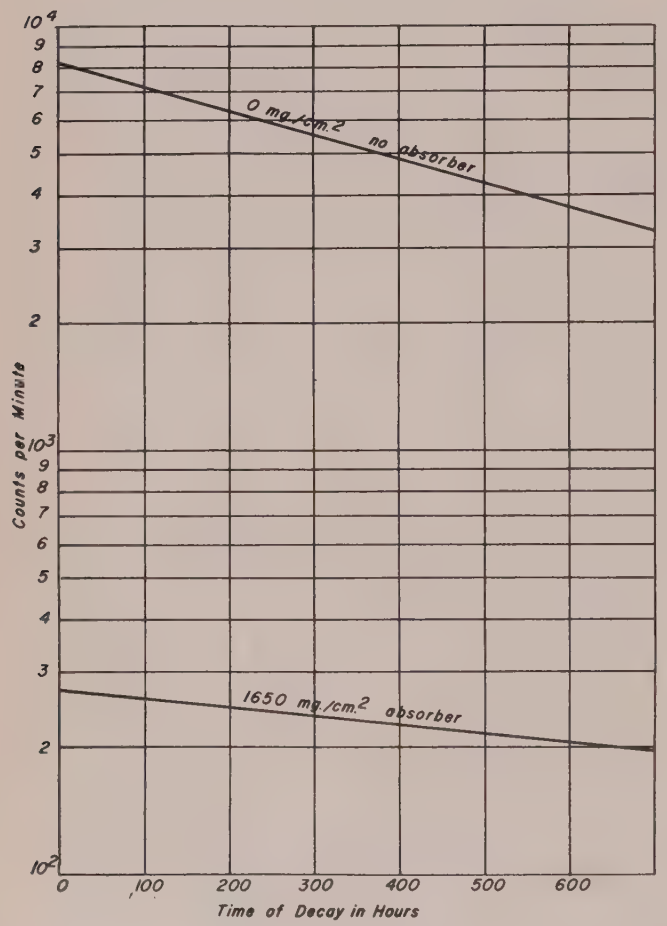

Fig. 3 – Decay chart

After a short time necessary for complete mixing, the system's activity was determined and recorded. Next, the 311.5-mg sample was added to the system making a total of 424.5 mg of metal in 2 gal of oil. This quantity was circulated and a reading taken. Next, the 792-mg sample was added and circulated, and a reading was taken. Another gallon of oil was added and mixed, and a reading was taken. From the above data, the calibration curve of Fig. 2 was made, showing activity versus milligrams of metal per gallon of oil. With this plot, any reading of activity in the identical counting chambers used on the actual oil system (Fig. 5) can be converted to milligrams of metal per gallon of oil. If the tests cover a period of several days, it is necessary to apply corrections for the decay of the radioactivity. This can be done by determining the calibration-system activity and connecting this point with the origin. The resulting curve is the new calibration curve of activity versus weight of metal per gallon of oil. The above calibration procedure was followed for both counting chambers. The larger counting chamber provided an increase in sensitivity by a factor of ten because of the increased amount of radioactive material around the Geiger-Müller tube.

The radioactive sun gear was installed in the gear case by means of special long-handled tongs. The four-square, or locked-torque, testing device was reassembled as shown in Figs. 6 and 7. The oil system was filled with 4 gal of SAE 30 mineral oil. The gears were given a 4-hr break-in run at low speeds and torques. After the break-in run, the gears were run according to the schedule shown in Table 1.

At the end of 10.83 hr run according to the schedule described in Table 1, the sun gear was badly worn. The wear rate had increased until 99 mg of metal were being worn off per minute at a speed of 1200 rpm and a load of 5000 ft-lb. At this point it was decided to see what effect a change to an extreme-pressure type of lubricant would have on this high wear rate of the worn-out gear. The system was flushed thoroughly, checked for residual radioactivity, and refilled with 4 gal of e-p gear lubricant. The worn-out gear was run according to the schedule in Table 1. The wear rate decreased

Table 1 – Gear Test Schedule

Load, ft-lb	Speed, rpm
3000	400
3000	800
3000	1000
3000	1200
4000	400
4000	800
4000	1000
4000	1200
4500	400
4500	800
4500	1000
4500	1200
5000	400
5000	800
5000	1000
5000	1200

considerably due to the use of the e-p gear lubricant. The radioactivity measurements were erratic during the run because of the flaking off of pieces of metal caused by fatigue during the previous run. The average wear rate, however, decreased due to the change to the e-p lubricant.

At this point the entire system was disassembled, cleaned and inspected. New planet gears were installed. The radioactive sun gear was reversed so that the other side of the teeth would now mate with the new set of planet gears. The system was filled with an e-p gear lubricant. The system was reassembled and given a 4-hr break-in run. At the end of the break-in run, the schedule of Table 1 was started. The gears were run over 20 hr at loads up to 5000 ft-lb and speeds up to 1200 rpm.

The wear at this load and speed was so slight, the load was increased to 6000 ft-lb. At this high load the bearing on the planet shaft failed. This failure caused added load on the sun gear, resulting in a fracture through the hub of the gear. The tests were discontinued at this time.

At the conclusion of the wear tests a study was made of the metal transferred to the planet gears which mate with the radioactive sun gear. The planet gears were first cleaned and dried. A strip of Kodak no-screen dental X-ray film was placed in intimate contact with the tooth surface for 24 hr. At the end of this time the film was developed and printed. This procedure was followed on gears from the mineral-oil test and from the e-p lubricant test. The results are shown in Fig. 8. These radiographs indicate a great amount of metal transfer when using a straight mineral oil but comparatively little transfer when using an e-p oil. It should be noted, also, that the gears which had been used with straight mineral oil had only half the running time as the set run with e-p oil but indicated much more transferred metal. In both cases little transfer of metal occurred at the pitch line because of rolling contact.

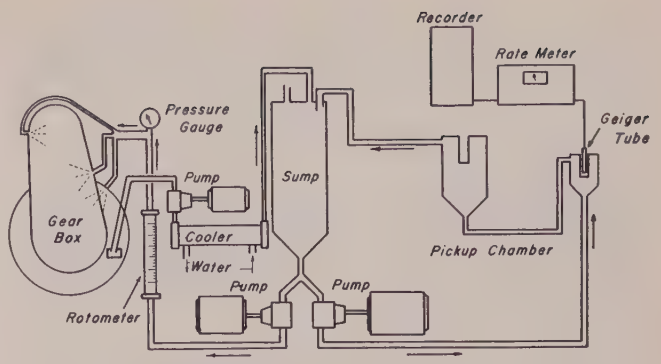

Fig. 5 – Testing system

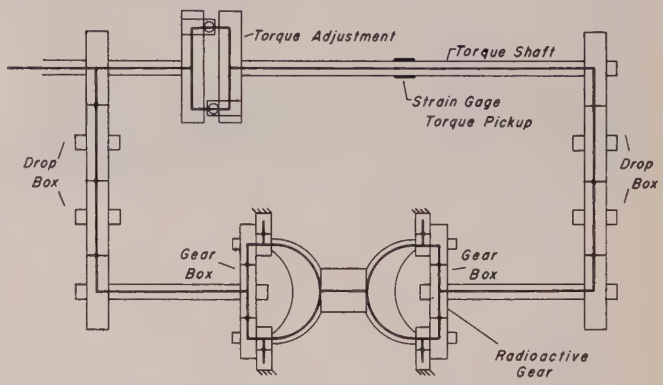

Fig. 6 – Four-square testing arrangement

The particle size of the powder ground from a gear for calibration purposes is of interest. Fig. 4 shows photomicrographs of the particles magnified 110 X. Some of the particles became molten during grinding and congealed into spheres; in others only the ends melted; and others have the form of chips. The largest particles have an average

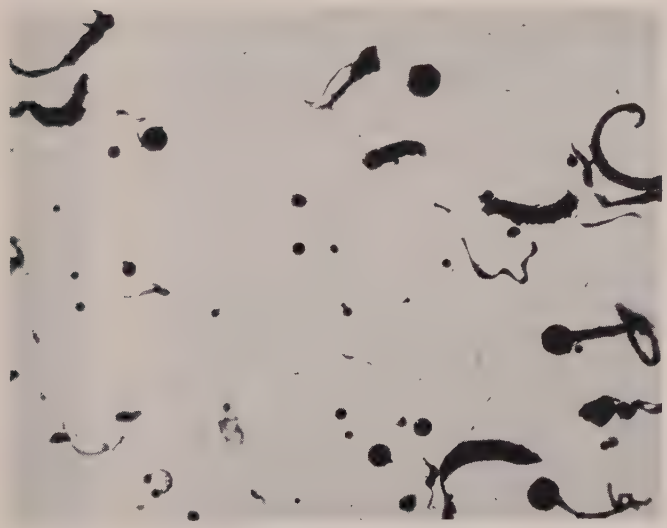

Fig. 4 – Magnified calibration particles

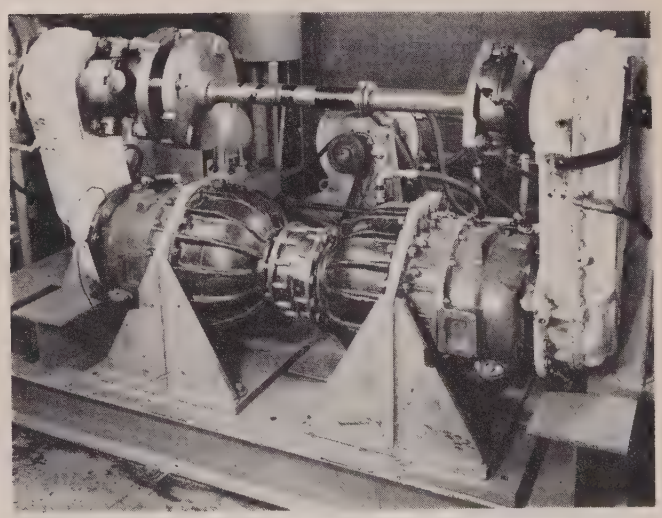

Fig. 7 – Four-square testing arrangement

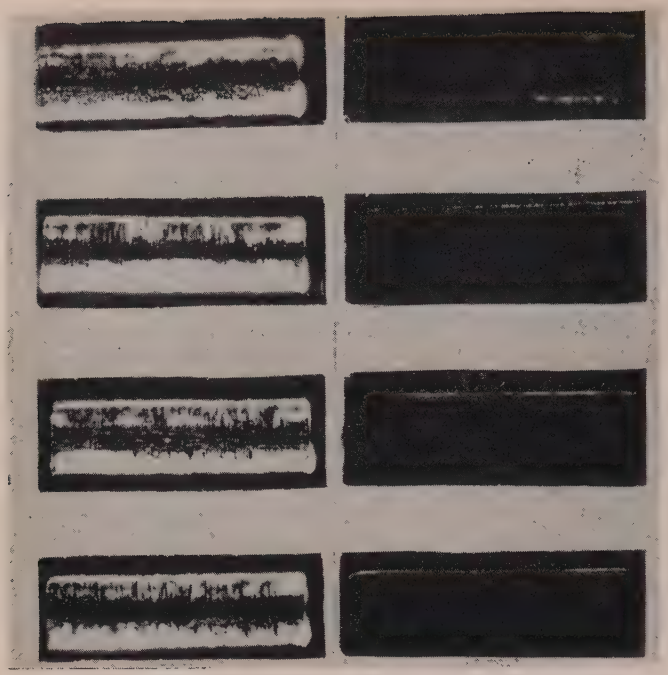

Fig. 8 – Radiographs of transferred metal; left: with SAE 30 oil; right: with e-p oil

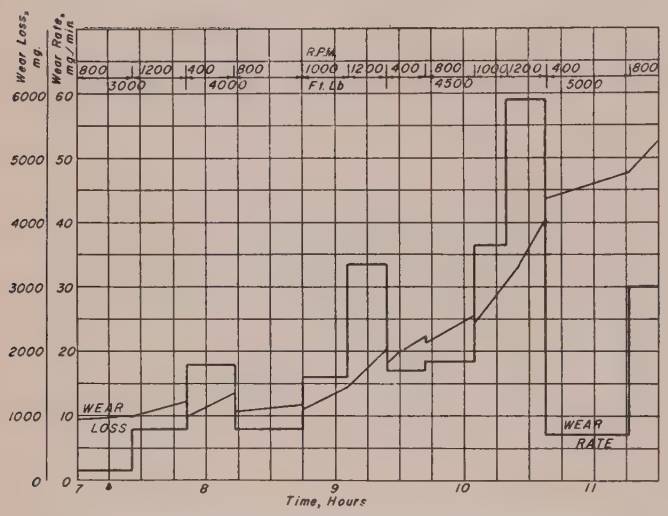

Fig. 9 – Wear data with SAE 30 oil

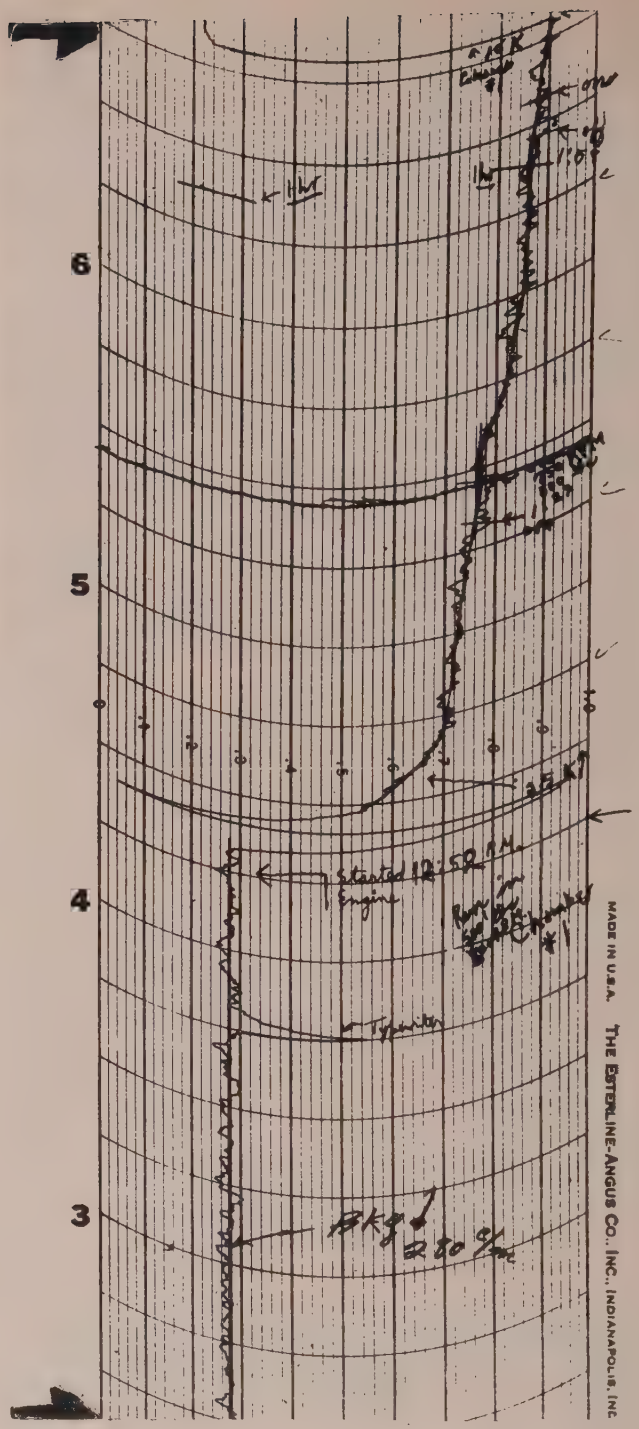

Fig. 10 – Strip chart, break-in period

Table 2 – Wear Rates

Load, ft-lb	Speed, rpm	Mineral Oil, mg per min	E-P Oil, mg per min
6150	400	....	5.7
5000	1200	99.0	4.7
5000	1000	77.7	1.9
5000	800	30.0	1.02
5000	400	14.4	0.21
4500	1200	59.5	
4500	1000	37.0	
4500	800	18.9	
4500	400	18.2	
4000	1200	42.6	
4000	1000	14.8	
4000	800	8.25	
4000	400	27.7	
3000	1200	15.0	....
3000	1000	3.14	....
3000	800	1.67	....
3000	400	1.17	....

dimension of about 0.002 in. It was found necessary to keep a fairly high oil velocity in the calibration system in order to keep the particles in suspension. By placing a Geiger-Müller counter at various points of the calibration system, a check could be made to determine whether there was an accumulation of particles at any point. The tubing, fittings, and counting chambers were designed to prevent the settling of the metal particles. When the oil velocity was maintained above 600 fpm, all

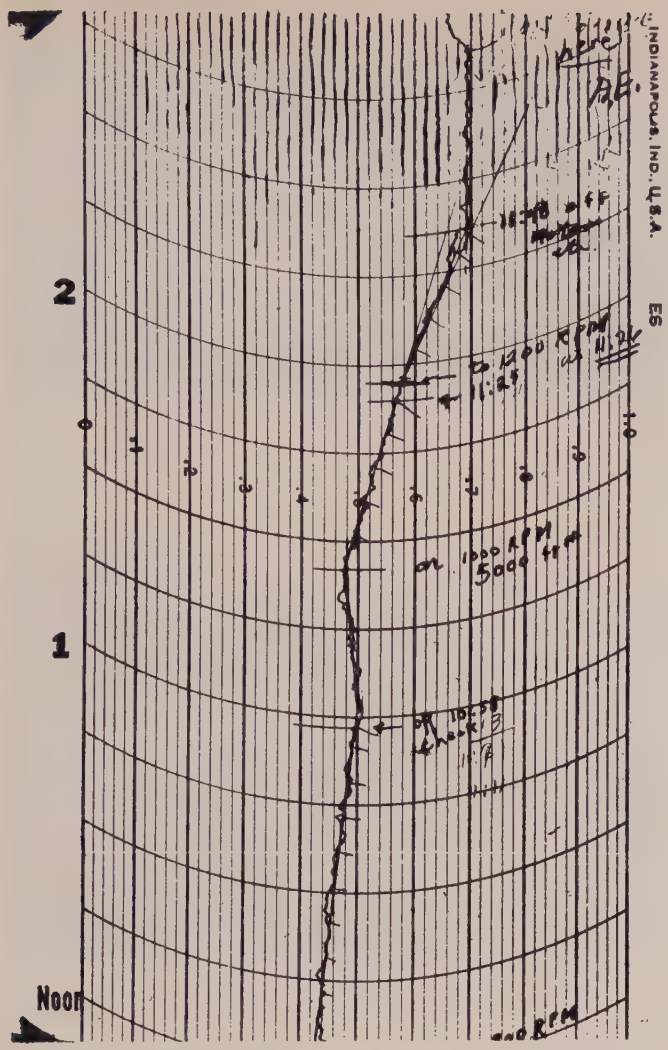

Fig. 11 – Strip chart, typical data

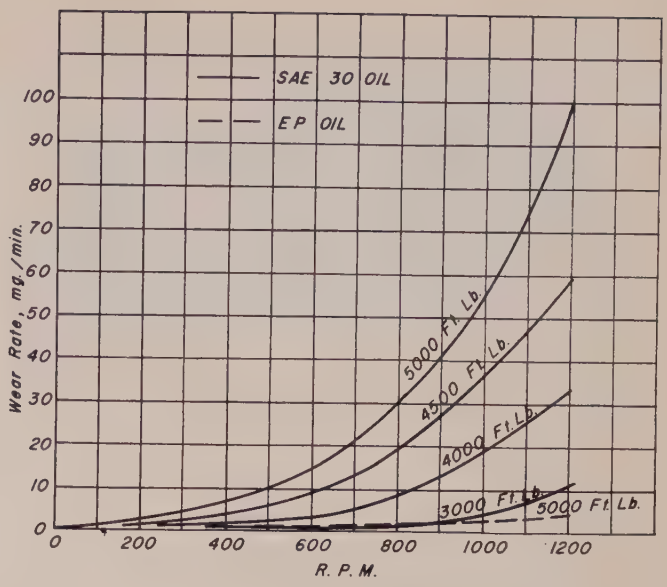

Fig. 12 – Wear rate versus rpm

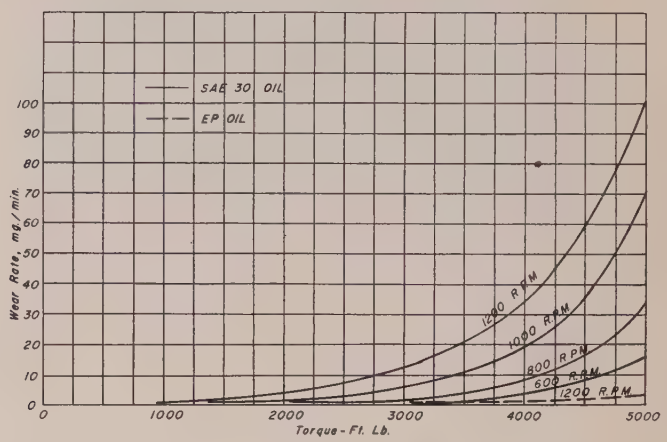

Fig. 13 – Wear rate versus torque

particles remained in suspension. No effort was made to determine the size of wear particles removed from the gear. During normal wear it is reasonable to expect these particles to be very minute, perhaps of molecular size. At very heavy loads with SAE 30 oil, particles of large size, larger than the calibrating particles, broke from the gear face because of surface fatigue. These large particles showed up as erratic readings on the radioactivity chart. When first noticed, these irregular traces on the chart could not be explained satisfactorily. A complete check of all instrumentation proved that all instruments were indicating properly. Further inspection showed that the traces were due to the large particles which spalled off the gear. It should be noted, however, that in spite of the irregularity in the radioactive trace, a definite slope, and therefore wear rate, could be measured. This type of trace was most noticeable after the high loads with SAE 30 mineral oil.

Table 2 gives the wear rates found in the tests. Wear data with SAE 30 oil are plotted in Fig. 9.

The strip chart shown in Fig. 10 shows the background count and the start of the break-in run with straight mineral oil. The rapid initial wear caused the meter to go off scale, requiring a change to a higher scale. The strip chart included as Fig. 11 shows typical data taken during the test. The change in slope under different conditions is easily seen in this photograph.

The wear rates versus load and speed are shown in Figs. 12 and 13. The effect of two kinds of oil on wear rate is clearly demonstrated. Increasing the torque at constant speed or increasing the speed at constant torque increases the wear rate exponentially. With wear rates versus load and speed available, it becomes an easy matter to predict the life of a gear at any load and speed.

The tooth shown in Fig. 14 was broken from the radioactive sun gear. The surface shown in the

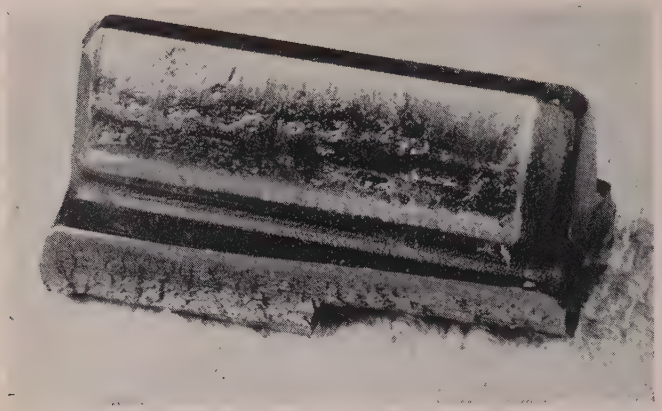

Fig. 14 – Radioactive gear after 10 hr with SAE 30 oil

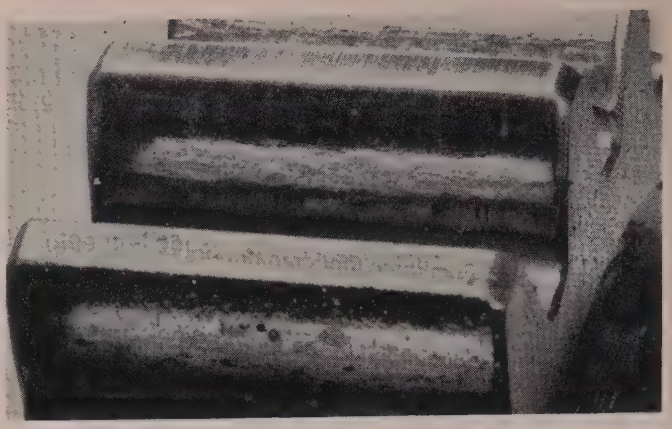

Fig. 16 – Planet gear after 10 hr with SAE 30 oil

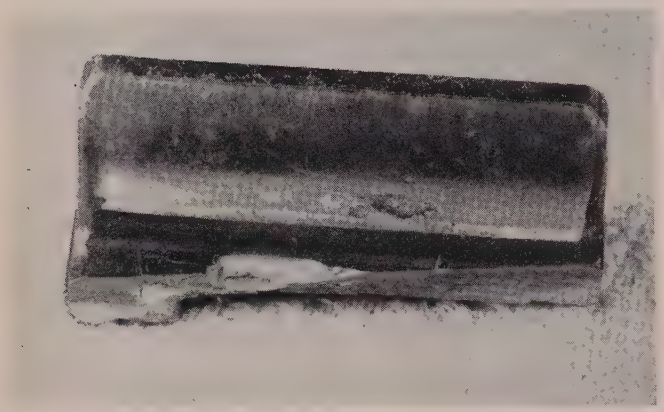

Fig. 15 – Radioactive gear after 20 hr with e-p oil

Fig. 17 – Planet gear after 20 hr with e-p oil

photograph was the result of about 10 hr running with SAE 30 mineral oil. The photograph of Fig. 15 is the opposite side of the same tooth after 20 hr running time using e-p gear lubricant with an even higher maximum load. This surface was not badly worn or pitted. Most of the damage to this surface was caused by the failure of the planet shaft bearing.

The planet gear shown in Fig. 16 ran with the sun gear tooth shown in Fig. 14. The surface was badly worn. The planet gear shown in Fig. 17 ran with the sun gear tooth shown in Fig. 16 using the e-p gear lubricant. This gear still has some of the original tool marks caused by the manufacturing process.

Radiation-Detection Equipment

The special radiation-detection equipment used in these tests can be divided into two categories: (1) required health-protection instrumentation and (2) necessary detection and measurement instrumentation.

The health-protection equipment includes the following:

One model 2611P survey meter from Nuclear-Chicago.

One model SRJ-1 survey meter from Technical Associates.

The first instrument is a low-level detector covering the range of 0 to 20 milliroentgens per hour and is used primarily to check for radioactive contamination. The second is a higher-range instrument covering the range of 0 to 5000 milliroentgens per hour. This instrument is used to evaluate permissible operating times quantitatively in given locations.

Each man in the vicinity of the tests was required to wear a film badge and a quartz-fiber electroscope. The quartz-fiber electroscope gave an immediate check on the exposure to radiation.

The second instrument group includes those required to detect and record quantitatively the activity in the oil system. The instruments used in this work are the following:

Model 6303 detector tubes from Victorsen.

Model SC-34 rate meter from Tracerlab.

Model A. W.-1 MA recorder from Esterline-Angus.

Model L-75 analysis unit from Landsverk.

Acknowledgment

The authors express their appreciation to Ardath H. Emmons, associate radiological safety officer of the University of Michigan, for the assistance and advice he gave in conducting the tests. This work was done as part of a subcontract with Ingersoll Products Division for the Bureau of Ships. Thanks are extended to Code 518, Bureau of Ships, U. S. Navy, and the U. S. Marine Corps for permission to publish the results presented.

DISCUSSION

Complete Data on Gear Wear A Possibility with This Method

— R. Tourret

Admiralty Oil Laboratory, England

I WAS very interested in the authors' experiments on the wear rates of gears using radioactive specimens, especially since so little data has been published so far on this aspect of gear performance.

However, could the authors give more details of the experiments carried out? For instance, what was the time element in the schedule given in Table 1? What heat-treatment was given to the gears? How was the surface of the gears prepared? What was the object of the Parker Lubrize coat?

If the values given in Table 2 are plotted (Fig. A), the curves obtained perhaps do not conform as closely to the ideal as might be thought from consideration of Figs. 12 and 13 of the paper, in which individual test points are suppressed. (And, incidentally, Table 2 refers to results at 400 rpm, whereas Figs. 12 and 13 refer to 600 rpm.) However, the results for 1200, 1000, and 800 rpm appear to lie on straight lines on a logarithmic basis, suggesting that a definite relationship can be established between speed, load, and the wear rate. It is probably safe to assume that the wear-rate results for 4000 and 1500 ft-lb torque at 400 rpm are not representative.

It appears from Figs. 14 and 15 of the paper that the gears operated with the SAE 30 oil (presumably a straight mineral oil?) are "scuffed" (or "scored," I think, in American phraseology). Further, since there are no sudden discontinuities in the wear rates as the torque is increased (Fig. A), the gears must have operated under scuffing conditions throughout the test.

Naturally, when the oil was changed to an e-p type (presumably of the same viscosity?), this afforded protection against scuffing (as indeed an e-p oil is designed to do), and the scuffing and wear rate decreased markedly. The use of an e-p oil, however, can in some circumstances[a] promote pitting, and it is interesting in this connection to observe a large pit in the gear which had been operated with the e-p oil (Fig. 15).

In some ways, it appears that the authors have taken a sledgehammer to crack a walnut, since almost the only result of the use of the highly refined technique of testing radioactive gears appears to be the conclusion that the wear rates were high with an ordinary oil (or that the gears scuff), whereas an e-p oil gives low wear rates (or that the gears did not scuff). It is hardly necessary to use radioactive gears to reach this conclusion — indeed, the IAE Gear Machine and the Ryder Gear Machine have been used for many years on each side of the Atlantic to determine just that.

Our appetite is whetted at the start of the paper by reference to rate of gear wear varying "with speed, load, lubrication, and heat-treatment of the metal used in the gear." In the text, however, it seems that the effects of speed and load are explored over a very small range and then the results idealized and the individual test points suppressed; lubrication is only dealt with by tests on an unspecified SAE 30 oil and an e-p oil of unspecified viscosity, which in any case lead to the obvious conclusion that the e-p oil gives protection against wear when the gears are operated under scuffing conditions; while the heat-treatment of the metal used in the gear is not discussed at all. The authors have a very powerful tool at their disposal — let us hope that sometime in the future they have the opportunity to use it to produce full data on wear rates over a wide range of conditions, using a

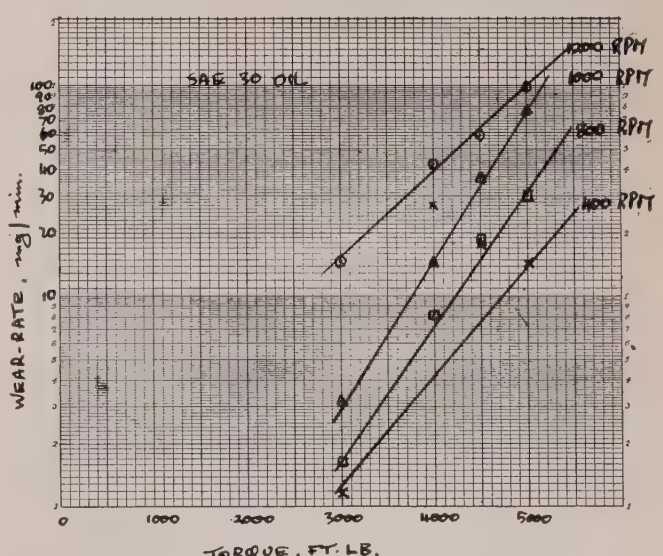

Fig. A — Wear rate versus torque

[a] See *Journal of the Institute of Petroleum*, Vol. 38, No. 344, August, 1952, pp. 652-668: "Wear and Pitting of Bronze Discs Operated under Simulated Worm-Gear Conditions," by L. S. Evans and R. Tourret.

wide range of types of additives used in different proportions in different base oils at different viscosities, and finally used on a range of different gear materials, heat-treatments, and so forth.

Wear Rate per Revolution Increases as Rpm Decreases

– E. E. Shipley
General Electric Co.

THIS paper was of special interest to us, since we have been conducting radioactive gear tests of a similar nature for the past several years. The authors' approach to the problems of setting up the test, running the calibration curves, and then the operation of the test itself was quite thorough and indicates that they have a good working knowledge of the technique of radioactive tracer testing as we know it.

From Table 2 and from the general overall picture, it seems that the gear design was in trouble all the way when using an SAE 30 mineral oil. The minimum wear rate recorded was 1.17 mg per min or 0.002925 mg per revolution, which suggests to me that from the onset the gears were wearing quite heavily, probably scoring. This being the case, then it is not at all surprising that, after 10 hr of operation at various loads, the sun gear was in the condition as shown in Fig. 14. Of course, it is hard to tell from the information given what the face width and pitch of the gears were, thus making it quite difficult to compare test results with what we have on hand.

It is also quite evident that the e-p lubricant helped the situation remarkably. It rescued the gear design from ultimate failure due to inadequate lubrication. Now it seems like the gear design is in danger of failure from being subject to pitting as indicated by Fig. 15. Fig. 8 suggests that even the e-p oil has a slight amount of trouble with the tip and root section. This might not be enough to bother, but perhaps it could be compromised by additional tip modification on both mating elements.

One of the main points that I would like to comment on is the manner in which the data was presented in Figs. 12 and 13. I believe one would get an erroneous opinion of the effects of wear rates. From Fig. 12 it is quite obvious that for a 4500 ft-lb load at 1200 rpm the rate is high or in the order of 58 mg per min; at 800 rpm it is 20 mg per min; and at 400 rpm it is 3.5 mg per min. This progression is logical, as it seems only natural that, if the gears are wearing, the rate of wear will be greater at higher speeds on a time (per minute) basis. However, if one asks the question, "What is the rate of wear per tooth engagement or revolution?" then the above rates become 0.0483 mg per revolution for the 1200-rpm point, 0.025 mg per revolution for the 800-rpm point, and 0.00875 mg per revolution for the 400-rpm point. Again, this progression would tell you that as the rpm was increased from zero the wear rate per revolution or tooth engagement would also be increased.

This is not the case, however, if you take the original data from Table 2 and plot it in a manner as shown in Fig. B. You will notice that for the 4500 ft-lb load the wear rate per revolution for 400 rpm is 0.0455 mg per revolution or almost as high as the wear rate of 0.0495 mg per revolution for 1200 rpm. Again, look at the curve plotted for 4000 ft-lb load. The wear rate for 400 rpm is exceedingly higher than at 1200 rpm. Probably this point should not be quite as high, since in my opinion we are operating in boundary lubrication conditions. At best, things are not too stable, and perhaps the data are a little less reliable. It is not my intention to question the data as such but just the method in which they have been plotted and presented. Fig. B points out that the wear rate on a tooth engagement or a revolution basis increases considerably as the rpm approaches zero, and I believe that if data had been taken at 300, 200, and 100 rpm, these rates would have been increasingly higher than those taken at 400 rpm. One might have the opinion that it is of minor interest that the wear rates do increase at lower values of rpm and that in many applications these higher wear rates would be of little consequence. However, on some equipment, for which the duty cycle includes much starting and stopping, this is a serious problem; for example: gear drives for locomotive and subway application, gas-turbine starters, both industrial and jet engines, and various types of rolling-mill equipment.

As a point of interest to help back up this type of reasoning, some of our own tests show that, when operating the gears below the scoring range, wear rates of any magnitude at all are obtained only at low speeds.

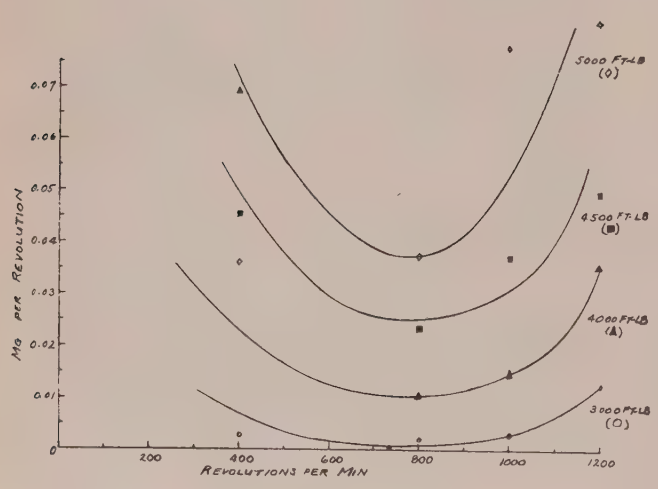

Fig. B – Wear rate per revolution versus rpm, plotted from data of Table 2 of paper

Authors' Closure To Discussion

IN this paper we were trying to emphasize this method of gear wear measurement and to show its great possibilities rather than to explore the whole subject of gear wear. We are planning another research project that will deal with additives in different concentrations and their effect on gear wear.

We agree that the pit seen in Fig. 16 looks like pits found in some gears used with an e-p oil; however, extensive laboratory and field tests have not disclosed any tendency to pit. In this case, the change to an e-p oil was the difference between success and failure for the gear.

The Ryder gear machine is excellent for laboratory use. We would recommend the use of the radioactive gear technique in combination with the Ryder machine in basic studies of gear wear and the variables that affect wear. The radioactive method can measure accurately amounts of gear wear that would be difficult to measure physically. It is difficult, however, always to relate the results obtained from the Ryder gear machine to a specific gear train with different conditions of mounting, cooling, speeds, and lubrication. Wherever possible, we prefer to use the gear train in question for specific studies.

Engine Cranking at Arctic Temperatures

W. E. Meyer and J. J. DeCarolis
Pennsylvania State University

R. L. Stanley
Diesel-Engine Manufacturers Association (formerly, Pennsylvania State University)

This paper was presented at the SAE National Diesel-Engine Meeting, Cleveland, Oct. 26, 1954.

DURING the winter of 1946-1947 the Army decided to investigate the possibility of field operation in the arctic with then current military equipment and materials. That was the first winter in which a fully mechanized Army was to try to live in the field without benefit of normal arctic station accommodations. The temperature for a 14-day period during that winter never rose above –55 F. By the time troops had become established in their field accommodations they found that their mechanized units were practically immobile.

The CRC Group on "Lubricant Requirements under Arctic Temperatures" was requested by the Office of the Chief of Ordnance to assist in determining why the then prescribed cold-weather operational procedures had failed to keep the Army mobile.

Investigation disclosed that one of the reasons that engine lubricants had become solid was that the sudden drop in temperature had prevented the application of the diluting procedures which were prescribed at that time. It simply got too cold too fast to prepare all the equipment properly.

The immobilization of all prime movers in this field exercise emphasized the need for a lubricating oil which did not require field modification. As a result of this and other similar experiences, the Army decided to develop in cooperation with industry a new arctic engine oil for temperatures down to –65 F. The specifications finally agreed on for this oil are stated in Military Specification MIL-O-10295(ORD), which prescribes a pour point of –65 F and kinematic viscosities of not more than 8500 centistokes at –40 F and not less than 5.75 centistokes at 210 F.

For arctic operation a low pour point is required in order that the oil can be easily poured from containers in the field for servicing the engines. The oil must have sufficiently low viscosity to permit satisfactory cranking. During warmup the pumps must be able to deliver a sufficient quantity of oil to the bearings and other points to insure adequate lubrication.

In order to start an engine it must be cranked fast enough to (1) produce combustible mixture

A NEW arctic engine oil, designed to permit cold-weather operation of Army equipment, has been tested to determine required cranking effort. Data obtained are to be used to design new cranking equipment and to estimate the temperature limits of existing cranking equipment.

Tests were conducted on six gasoline engines and five diesel engines using the new oil conforming to MIL-O-10295. Cranking the engines through a torquemeter permitted direct measurement of cranking torque.

The results of the investigation are presented in this paper.

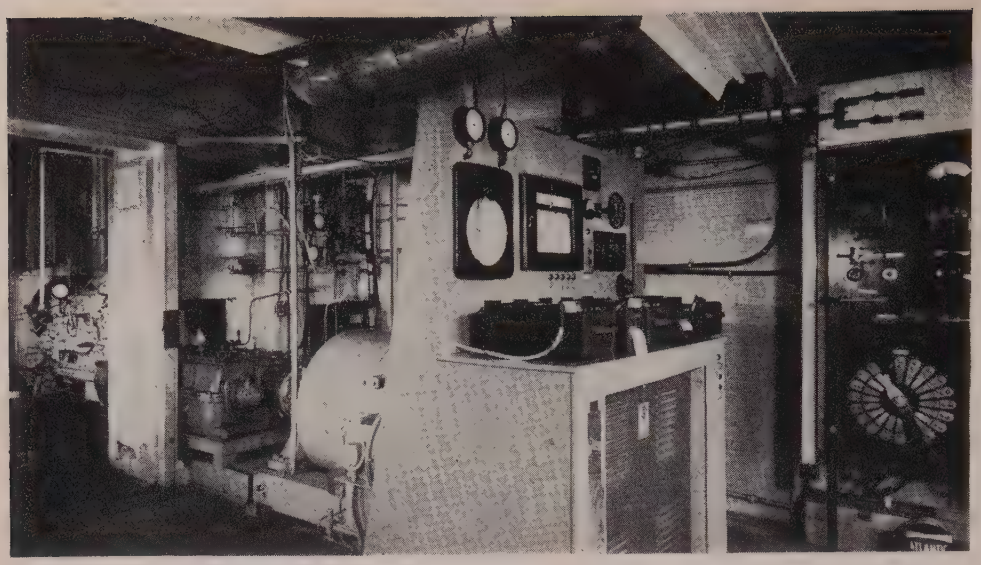

Fig. 1 – Test equipment and instrumentation

in the combustion chambers, (2) develop enough energy to fire the mixture (heat of compression), and (3) enable the engine to develop enough power to continue to fire. Whether or not an engine can be cranked at sufficient speed depends on (1) cranking power available and (2) resistance to cranking offered by the engine. For any given engine the resistance to cranking depends largely upon the viscosity of the oil at the cranking temperature. This in itself would suggest using an extremely low viscosity oil. However, since the same oil must provide adequate lubrication under normal engine operating temperatures, minimum viscosity is dictated by the highest atmospheric temperature that might be encountered during the arctic winter. This viscosity has been established by the military from laboratory tests and field experience as being 5.75 centistokes at 210 F. With this as a fixed point on the viscosity-temperature curve the minimum viscosities at the lower temperature depend on what viscosity index the manufacturers can build into an oil which they can supply economically and in sufficient quantities to meet the needs of the Armed Forces. The maximum viscosity of 8500 centistokes at –40 F specified in MIL-O-10295 has been established with this practical consideration in mind.

Since this arctic oil became available, field and laboratory tests have shown that at elevated temperatures oil consumption remains within acceptable limits and that no excessive engine wear occurs. However, no systematic data on required cranking effort have been available. Therefore, the Engineer Research and Development Laboratories, Ft. Belvoir, Va., sponsored the present investigation in order to obtain data for the design of cranking equipment and for estimating the temperature limits to which presently available cranking equipment would be adequate.

The program which was set up in cooperation with other agencies of the Armed Forces involved the testing of 11 different gasoline and diesel engines. Their major specifications are given in Table 1. The oil used in all tests (with a very few exceptions which are noted in the text) was the same. It conformed to Specification MIL-O-10295 (ORD). The experimentally determined viscosities of this test oil are given in Table 2. The gasoline engines were cranked at 50, 100, and 150 rpm and the diesel engines at 100, 200, and 300 rpm with the ambient and engine temperature stabilized at 0, –25, –40, and –65 F. No fuel was inducted into the engines, but the engines were fully equipped with their standard accessories.

Table 1 – Test Engines

Engine	No. of Cylinders	Displacement, cu in.	Bore x Stroke, in.	Military Rating, hp at rpm
Gasoline				
A	4	134	3 1/8 x 4 3/8	20 at 1800
B	4	134	3 1/8 x 4 3/8	—
C	6	330	4 x 4 3/8	55 at 1800
D	8	540	4 1/2 x 4 1/4	100 at 1800
E[a]	6	895	5 3/4 x 5 3/4	500 at 2800
F	6	1091	5 3/4 x 7	318 at 2200
Diesel				
G	6	230	3 7/16 x 4 1/8	30 at 1800
H[b]	4	284	4 1/4 x 5	100 at 1800
I[c]	4	334	4.4 x 5.5	55 at 1800
J	6	525	4 1/2 x 5 1/2	100 at 1800
K[d]	6	672	4 7/8 x 6	150 at 1800

[a] Aircooled, supercharged.
[b] Two-stroke; with block, cylinder head, and other parts of aluminum.
[c] Designed to be started as a gasoline engine.
[d] Supercharged.

Table 2 – Test Oil, Conforms to Specification MIL-O-10295 (ORD)

Temperature, F	Viscosity,[a] centistokes
210	6.05
100	25.1
0	551
–40	7280[b]
–65	94000[b]

[a] Data obtained with Ostwald viscosimeter.
[b] At these temperatures the oil was cloudy and contained solid particles.

The Authors

W. E. MEYER (M '40) is professor of engineering research and in charge of the Automotive Research Section at Pennsylvania State University. He has been connected with Daimler-Benz A.G. in Germany, the American Bosch Corp., and the Fuel Injection Division of the Bulova Watch Co. Professor Meyer has been on the faculty of Pennsylvania State University since 1947.

J. J. DeCAROLIS is an associate professor at Pennsylvania State University. He received his B.S. and M.S. degrees in mechanical engineering from Pennsylvania State University. Professor DeCarolis joined the University in 1946, following four years in the Air Force.

R. L. STANLEY (M '40) is educational director and Washington representative of the Diesel-Engine Manufacturers Association. He received his B.S. in M.E. in 1936 from Ohio State University, and his M.S. in M.E. in 1939 from Rutgers University. Mr. Stanley has been with the Diesel-Engine Manufacturers Association since 1953.

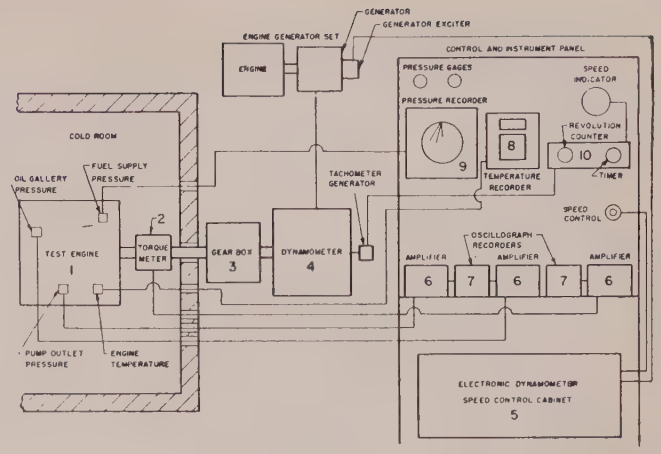

Fig. 2 – Block diagram of low-temperature cranking test equipment

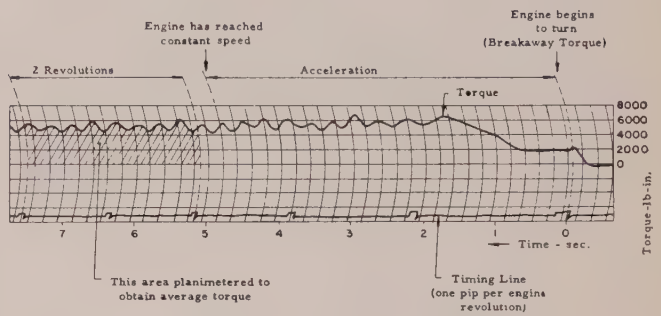

Fig. 3 – Section of a typical torquemeter chart; engine D, 50 rpm, –65 F

Although the necessity for pouring an oil at –65 F will be readily admitted, it may be questioned if it is of practical interest to crank engines with the oil at this temperature. At present, it is necessary to apply heat to the engines long before the ambient temperatures reach –65 F because starts cannot be made reliably without heat with means and methods now available. As long as provision for heating must be made, it is unavoidable as well as logical to apply some of the heat directly or indirectly to the oil, so that in practice cranking never takes place with the oil at –65 F although the air surrounding the engine may be at that temperature. However, progress is being made in lowering the temperatures at which starts can be made without heat application; and, therefore, this investigation was extended down to the limit at which any activities of a field force can be expected to be maintained.

Experimental Apparatus and Procedure

Test Equipment – So as to avoid the inaccuracies and limitations of the method of determining cranking torque by measuring voltage and current to the starting motor, it was decided to crank the engines through a torquemeter in order to obtain a direct measurement of cranking torque. Because the engines had to be power tested prior to the cranking tests, they were set up on an electric dynamometer, and this dynamometer was also used as a cranking motor.

The experimental setup is shown by Figs. 1 and 2. Test engine (1) and the Baldwin SR-4 torquemeter (2) were located inside the cold room. All other equipment was placed outside the cold room. This arrangement was chosen not only for convenience but also in order to reduce the cooling load, since the available refrigeration capacity was just sufficient to reach –65 F without live heat load.

Torquemeter and engine were connected through

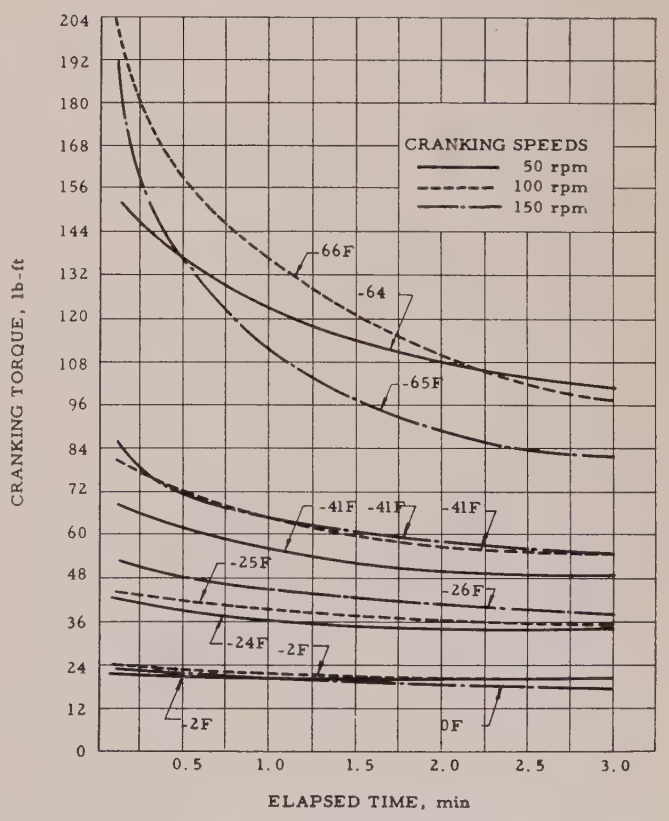

Fig. 4 – Low-temperature cranking torque requirements with MIL-O-10295 lubricating oil – engine A

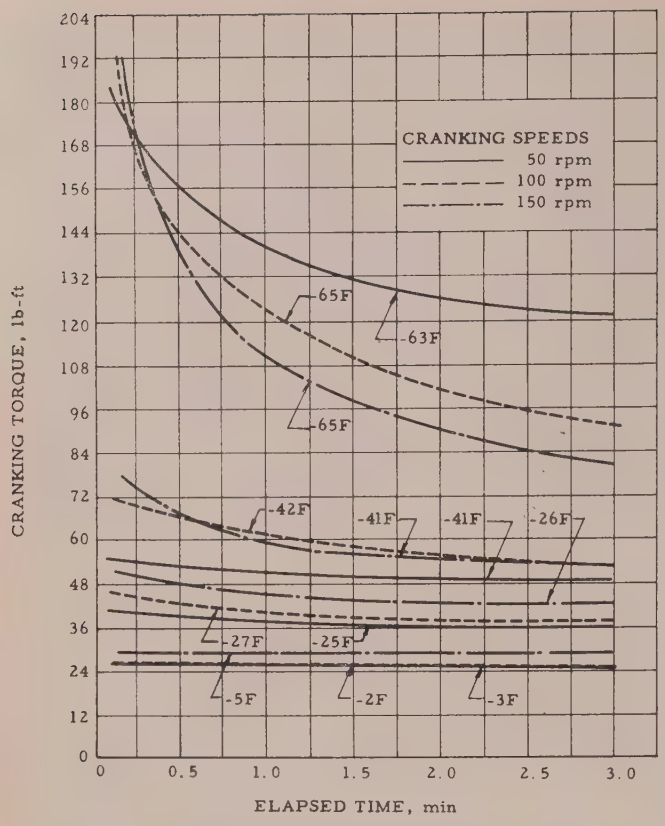

Fig. 5 – Low-temperature cranking torque requirements with MIL-O-10295 lubricating oil – engine B

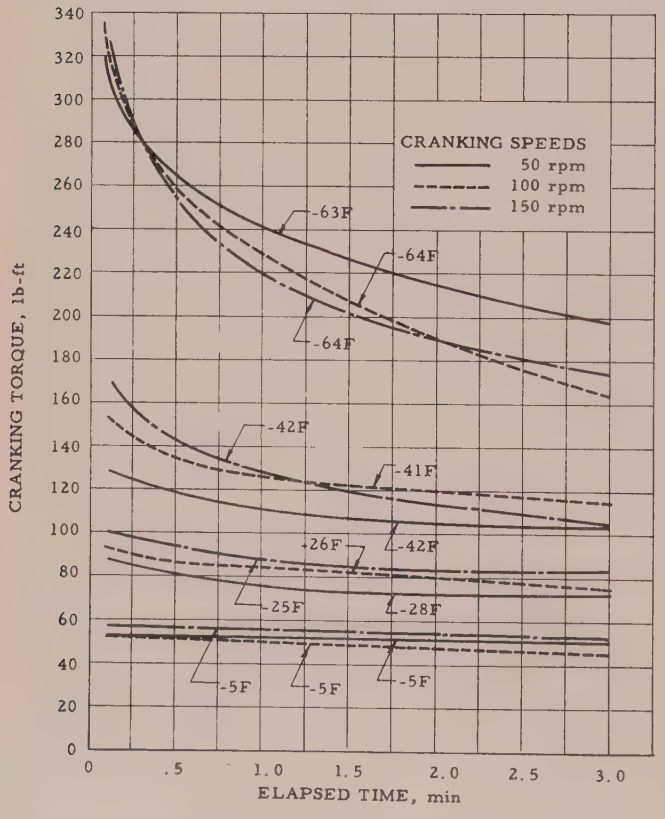

Fig. 6 – Low-temperature cranking torque requirements with MIL-O-10295 lubricating oil – engine C

a Philadelphia Gear Works Type 2S gearbox (3), to a 300-hp d-c dynamometer (4). The gearbox is of the manual shift type and gives either direct drive or 10/1 speed reduction. For power testing and cranking at 300 rpm, direct drive was used; while for the lower cranking speeds the dynamometer was operated at 10 times engine speed in order to get sufficient torque and adequate voltage for control. In cranking tests the dynamometer speed was controlled and maintained at a preset value by a Reliance VSR electronic speed control (5).

Copper coils were installed in the crankcase of every test engine in order to permit heating of the lubricating oil during the reconditioning procedure. A motor-driven pump outside the cold room circulated heated ethylene glycol through the crankcase coils and the engine cooling system.

Instrumentation – Most events and measurements were automatically recorded. Torque was measured by the already mentioned torquemeter (2). Oil pressures were measured near the pump and in the gallery of the engines by strain-gage pressure transducers. The output of these units was fed through amplifiers (6) to direct inking oscillographs (7). A contactor on the engine shaft actuated event markers on the oscillographs which produced a pip per engine revolution on the oscillograph strip charts (Fig. 3). This contactor was so adjusted before each test that it was closed by the slightest motion of the engine shaft, thus indicating on the charts when the engine began to turn.

Copper-constantan thermocouples were installed in several locations on each engine. Generally the following temperature measurements were obtained: coolant in, coolant out, three different levels or locations in the oil sump (crankcase), oil gallery, one of the main bearings, air intake into the manifold, and three locations within the cold room. The main-bearing thermocouple was installed into the lower bearing shell. The wires were introduced through two separate holes drilled into the bearing groove and held by peening. The output of all thermocouples was fed to a 16-point recorder (8) which records one temperature every 2 sec.

Additional pressures were recorded on a Bourdon tube pen recorder (9). A chromotachometer (10) served as speed indicator.

Test Procedure – Prior to the cranking tests, the engines were run in and power tested. After the power tests the oil was drained, the engine flushed, and the crankcase refilled with fresh test oil. This means that all cranking tests were made with oil which had not been subjected to the influences of combustion or to dilution by fuel.

Before every cranking test the engine was cold soaked until the thermocouples in the crankcase oil and bearing had reached the test temperature. The engine was then held at this temperature for

another 4 to 5 hr to insure complete temperature equilibrium.

For a cranking test the engine was accelerated to the desired speed as rapidly as possible (in 5 to 9 sec, depending on the test condition and engine) and cranked at this speed for a total of 3 min. During each test automatic records of torque, pressures, temperatures, and speed were obtained.

After a test the engine was reconditioned by circulating heated ethylene glycol through the coolant jacket and the coils in the crankcase. The engine was then motored for several minutes at about 50% rated speed in order to reestablish oil films as they would exist under field conditions after shutdown. Experience showed that this reconditioning procedure was needed only at the lower temperatures for maintaining reproducibility of the test points. This may be attributed to the fact that no fuel was introduced into the engines during the cranking tests.

Results

The results of the cranking tests are presented in Figs. 4 to 14. These torque-time curves were plotted from the oscillograph strip charts.

A section of a typical strip chart is reproduced in Fig. 3. The upper trace represents the instantaneous cranking torque. The lower trace indicates the number of engine revolutions, one pip per revolution. The first one of these pips identifies the moment at which the engine began to turn and, therefore, serves as the zero point of the time scale. It can be seen that the torque has already reached a finite value at this time. This torque value is referred to in this paper as the "breakaway torque."

During the acceleration period the total torque consists of that required to overcome friction and that needed to accelerate the engine. At constant speed the total torque is equal to the friction torque where this term is to be understood to include the thermodynamic losses during compression and expansion. The chart illustrates that this torque is not constant during any one engine cycle (two revolutions for a 4-stroke engine). The fluctuations represent the cumulative effect of friction, compression and expansion, and inertia of engine and cranking equipment.

The strip charts were analyzed by averaging the torque for two engine revolutions at various points by planimetering the area under the torque curve. From these averages the curves of Figs. 4 to 14 were plotted. The curves begin at the points at which the engines had reached constant speed.

The torque data may be considered reproducible within ± 10%. Numerous reproducibility tests fell within these limits even when such tests were made as the first or last one of a series for a given engine.

It would seem appropriate to say a few more words about "breakaway torque." As used here the term refers to the torque which the dynamom-

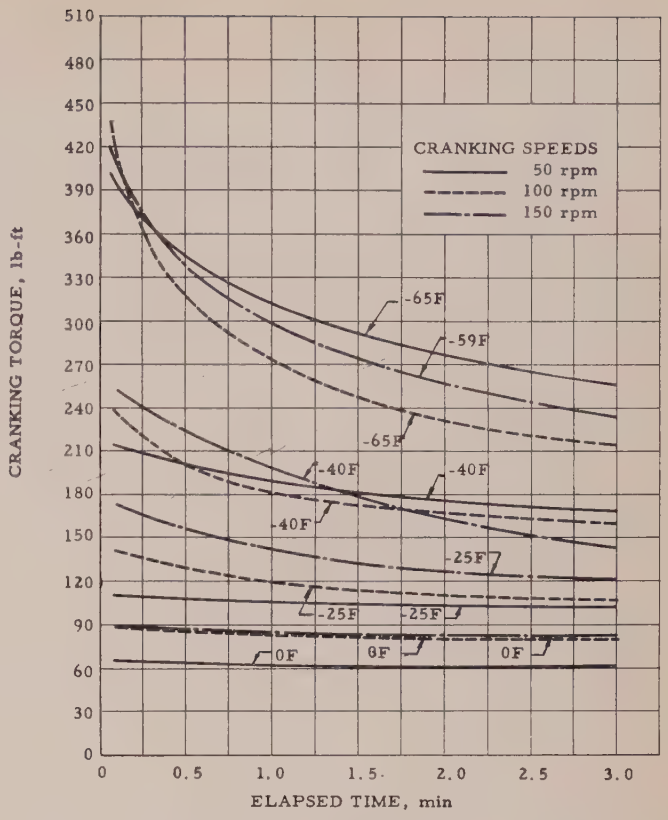

Fig. 7 – Low-temperature cranking torque requirements with MIL-O-10295 lubricating oil – engine D

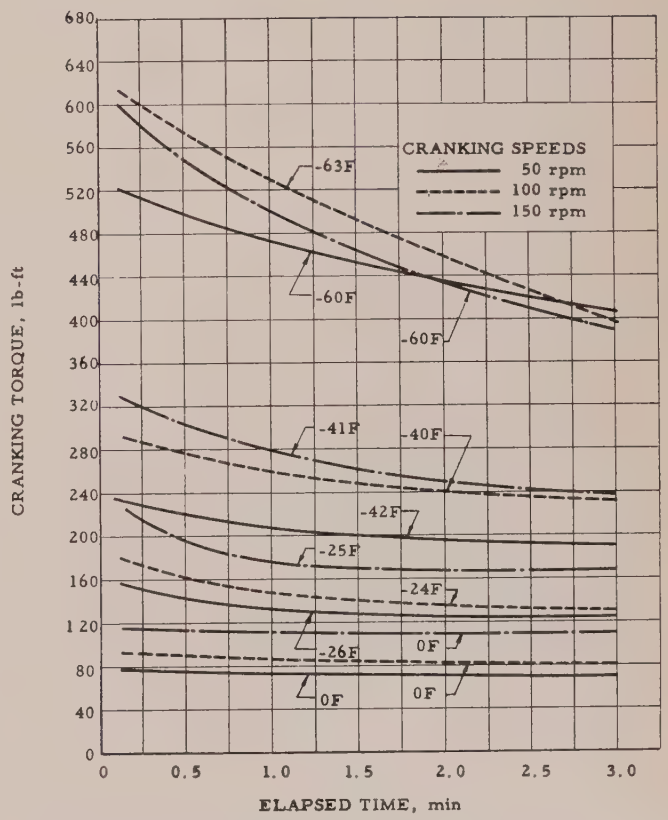

Fig. 8 – Low-temperature cranking torque requirements with MIL-O-10295 lubricating oil – engine E

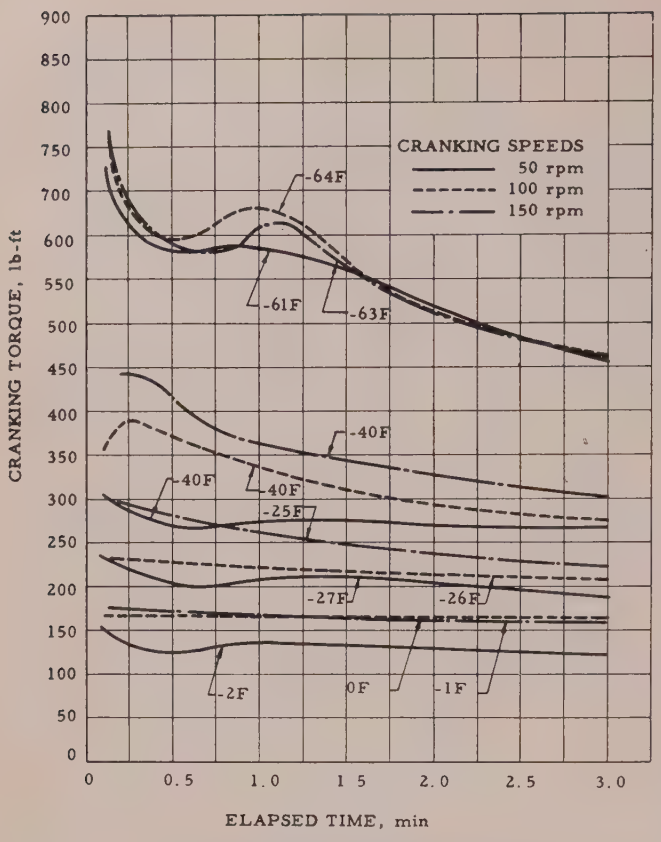

Fig. 9 – Low-temperature cranking torque requirements with MIL-O-10295 lubricating oil – engine F

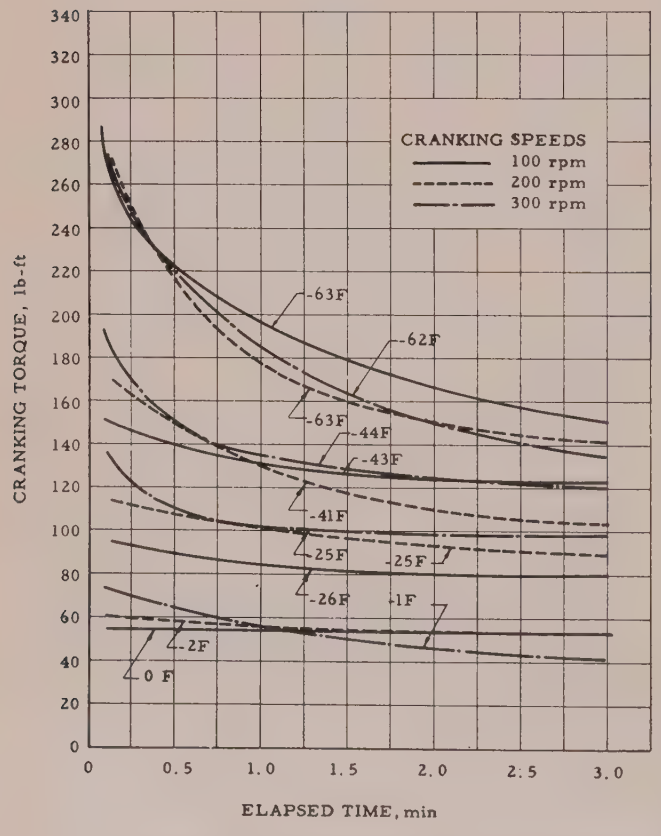

Fig. 10 – Low-temperature cranking torque requirements with MIL-O-10295 lubricating oil – engine G

eter was applying to the engine at the instant at which crankshaft motion could first be observed. The controlled voltage buildup of the dynamometer applied this torque gradually, as the sample chart in Fig. 3 shows. The initial rate of acceleration is also low, so that conditions existed which are quite different from those found when an electric starting motor is used. There a current peak occurs when full voltage is suddenly applied, and the engine is accelerated to full cranking speed in less than one half of a second. This current peak is frequently referred to as "breakaway," although it is not a direct measure of the torque needed to "break the engine loose." It must not be confused with the breakaway torque as defined in this paper.

Discussion

Figs. 4 to 14 show that, in general, the behavior of the eleven test engines was fairly uniform. It can be seen that there is very little change of torque with time at 0 F. As the temperature is decreased the torque increases; but, in addition, there is a progressively greater decrease of torque with cranking time. The initial torque is fairly independent of speed at any one temperature while equilibrium torque generally decreases with increasing cranking speed. The time interval required to reach equilibrium at —65 F seems to vary considerably from engine to engine: in some cases equilibrium was attained within the 3 min of the test, and in others the character of the curves suggests that almost twice that time would have been required. Cranking speed appears to be of relatively minor importance with regard to the time for reaching equilibrium. As the temperature is increased the difference between initial and equilibrium torque becomes progressively less and the time for attainment of equilibrium is reduced.

The decrease of torque with time is due to the increase of the temperature of the lubricant film between the rubbing surfaces. This is illustrated by Fig. 15 which shows the temperature increase at the thermocouple in the bottom of the center main bearing during a series of typical tests.

The oil temperature in the bearings and on the cylinder walls is not only a function of the heat developed and conducted away by the metal but also of the rate at which oil is being replaced. This replacement rate is, in first approximation, a function of the available oil pressure. With the MIL-O-10295 oil which remained fluid down to the lowest test temperature, pressure buildup was very rapid in almost all cases. Fig. 16 shows a set of pressure curves which are fairly typical of those for the majority of test engines. On the other hand, some engines exhibited a quite different behavior with respect to the oil pressure history; see, for instance, Fig. 17.

No attempt will be made here to analyze these curves, but they make one wonder about their influence on the engine cranking friction characteris-

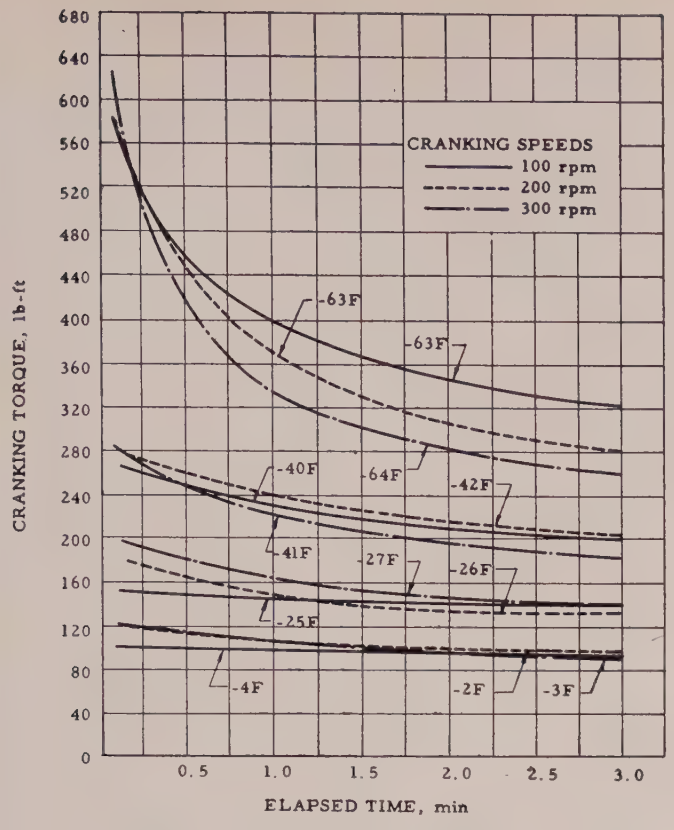

Fig. 11 – Low-temperature cranking torque requirements with MIL-O-10295 lubricating oil – engine H

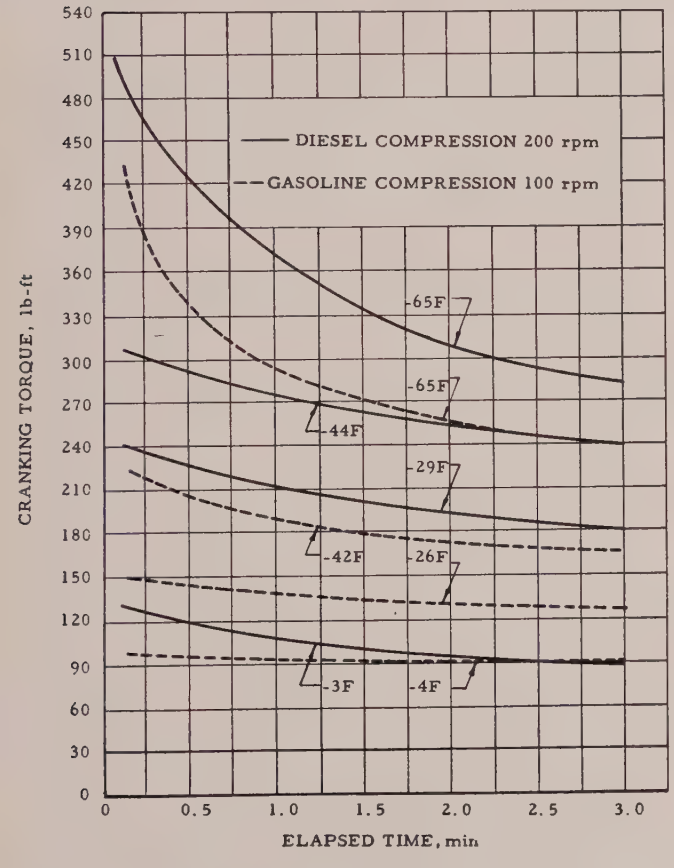

Fig. 12 – Low-temperature cranking torque requirements with MIL-O-10295 lubricating oil – engine I

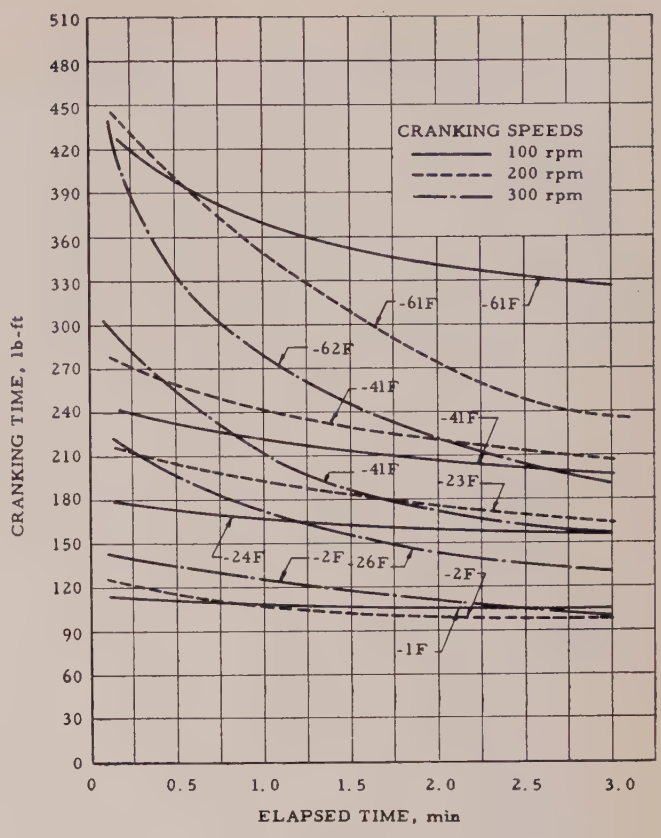

Fig. 13 – Low-temperature cranking torque requirements with MIL-O-10295 lubricating oil – engine J

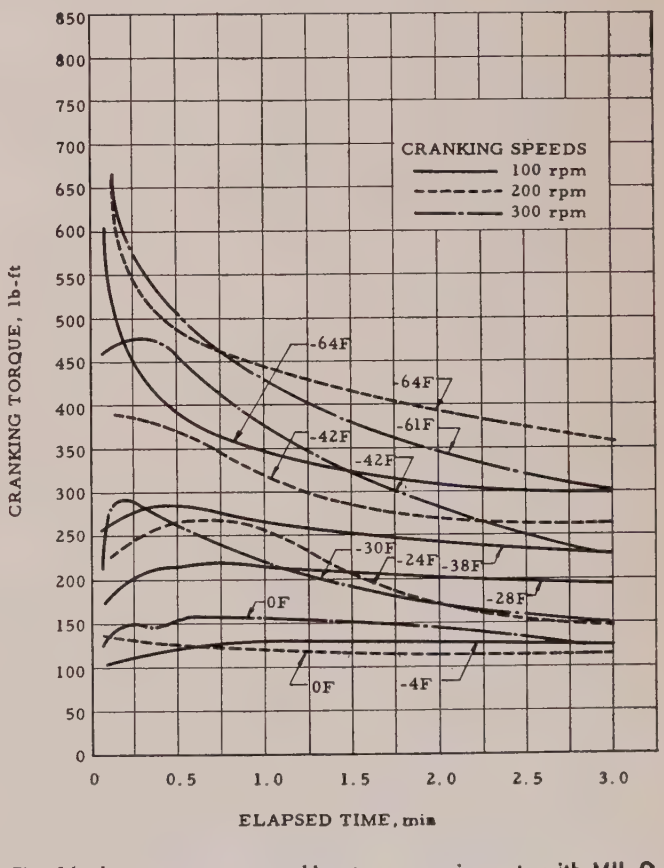

Fig. 14 – Low-temperature cranking torque requirements with MIL-O-10295 lubricating oil – engine K

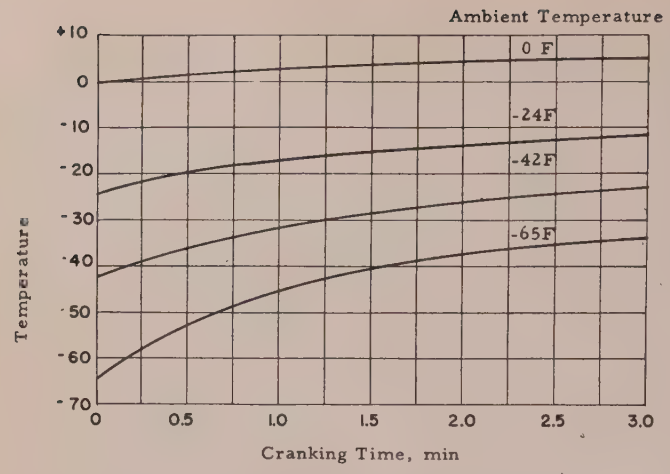

Fig. 15 – Typical bearing temperatures, engine K, 200 rpm. Thermocouple is in the bottom of the center main bearing

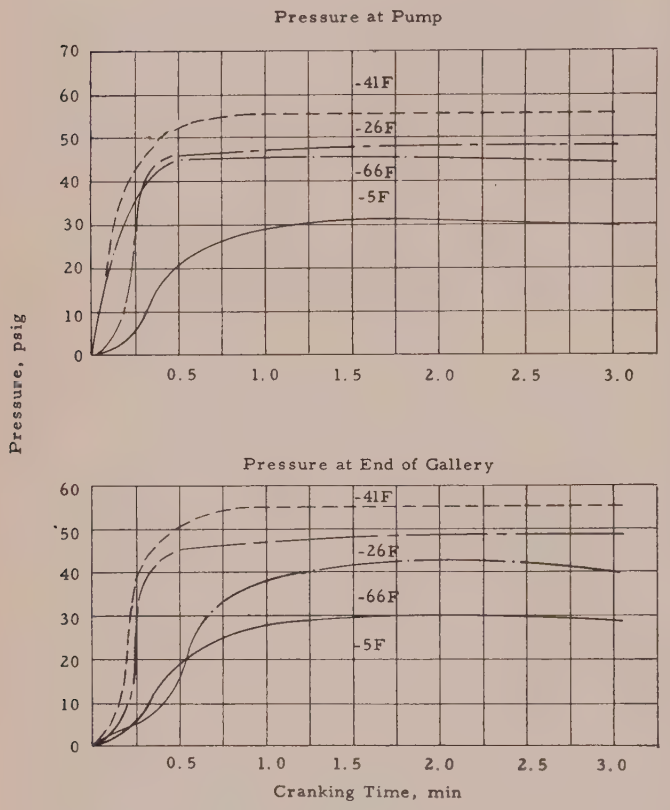

Fig. 16 – Typical lubricating oil pressure curves, engine B, 150 rpm

tics. That there is an interrelation was demonstrated by accident; Curve II in Fig. 18 shows a sudden change in the slope of the torque curve at 1.5 min cranking time. After the test it was found that one of the exterior oil lines to the oil cooler had broken with a consequent loss of pressure. This caused the torque to drop off because the oil in the bearings, and probably also to some extent that on the cylinder walls, was not being replaced by fresh, cold oil. In addition, the torque required by the oil pump was reduced, since considerable energy is required to pump oil of such high viscosities as they occur at these temperatures. This observation lends considerable weight to the possibility that two similar engines may exhibit quite different torque characteristics if the rates of oil flow during the cranking cycle are different.

Attention is also called to the reversals occurring in some of the torque curves of engines F and K shown in Figs. 9 and 14. During the tests no evidence was uncovered which would explain these reversals. The oil-pressure curves provided no clues, nor were the reversals of an accidental nature since they were reproducible.

The breakaway torques are tabulated in Table 3. The values represent averages from the tests at three different speeds, since speed has no influence on breakaway as defined here. In all cases the breakaway torque was substantially lower than the torque at the time at which steady cranking speed was reached.

Some of the data have been replotted in order to show trends and magnitudes. In Figs. 19 and 20 the 100 rpm cranking torque after 8 sec is shown as a function of temperature, and in Figs. 21 and 22 torque at —40 F is plotted against cranking speed. In addition, Table 4 gives the results expressed as frictional mean effective pressure (fmep) for the 8-sec point and for the equilibrium condition. (For the lower temperatures the equilibrium data had to be extrapolated in several cases because equilibrium had not been attained within the 3-min duration of the tests.)

The program did not permit tracking down the sources of certain differences and peculiarities which some of the engines exhibited. However, several remarks and observations can be made on the basis of the available information.

Some investigators who have experimented with engines at low temperatures have expressed the opinion that at extremely low temperatures it may become impossible to crank certain engines because differential expansion may cause misalignment or negative clearances in the bearings. No such observation was made on any of the 11 test engines, despite the fact that engine J had aluminum bearings while engines E and H had crankcases and bearing caps of aluminum.

Others have predicted that cranking at —65 F without preheating would cause serious scuffing of cylinder walls and bearings. When the test engines were returned, the manufacturers were asked to inspect them for any damage which they may have suffered. No damage of any kind was reported, nor was excessive wear reported. It must be remembered, though, that these tests were made without introduction of fuel into the cylinders.

The numerical results of the tests with the MIL-O-10295 oil may be summarized as follows:

1. Breakaway torque is always less than the

initial cranking torque after steady speed has been reached.

2. At O F there is very little change of torque with time, but at —65 F the torque curves show a considerable negative slope during the first few seconds of cranking.

3. General character of torque versus temperature curves is fairly consistent for all engines.

4. Cranking speed has relatively little influence on the 8-sec torque. The general trend is toward an increase with speed.

5. Equilibrium torque at —65 F decreases as the cranking speed is increased. Equilibrium torque exhibits greater variations from engine to engine than does the 8-sec torque.

Unfortunately, only a few experiments with other oils could be fitted into the present program. Figs. 23 and 24 show the results of tests with an SAE 20 W and a very high viscosity oil.

The general character of the curves is similar to those of the same engines when cranked with the MIL-0-10295 oil. The actual torque values do, however, differ somewhat even where the viscosities at the ambient were identical. This disagreement may have a number of causes, one of them being the fact that the ambient temperature defines the temperature of the oil films at zero time only.

Noteworthy is the fact that for the —27 F test of engine A the oil was below the pour point but that this had no noticeable effect on the torque-time relationship. It is, of course, quite possible, in fact likely, that the oil between the rubbing surfaces heated up rapidly enough so that for the recorded portion of the test it was already above the pour point. The breakaway torque was relatively twice that observed with the MIL-0-10295 oil, but it was still below the highest torque value while cranking.

Correlation of Data

Since the accumulation of the presented data required considerable time, effort, and funds, the question arose if they could, in any way, be correlated so as to permit the prediction of the required cranking torque at a given cranking speed

Table 3 – Breakaway Torque at Low Ambient Temperature for Several Gasoline and Diesel Engines When Using MIL-O-10295 Lubricating Oil

Engine	Breakaway Torque, lb-ft			
	Ambient Temperature			
Gasoline	0 F	—25 F	—40 F	—65 F
A	16	33	44	87
B	25	33	43	81
C	23	36	52	154
D	72	73	83	148
E	67	83	83	197
F	80	84	232	400
Diesel				
G	33	36	47	110
H	71	108	181	219
I	73	97	183	240
J	41	58	70	250
K	81	89	158	314

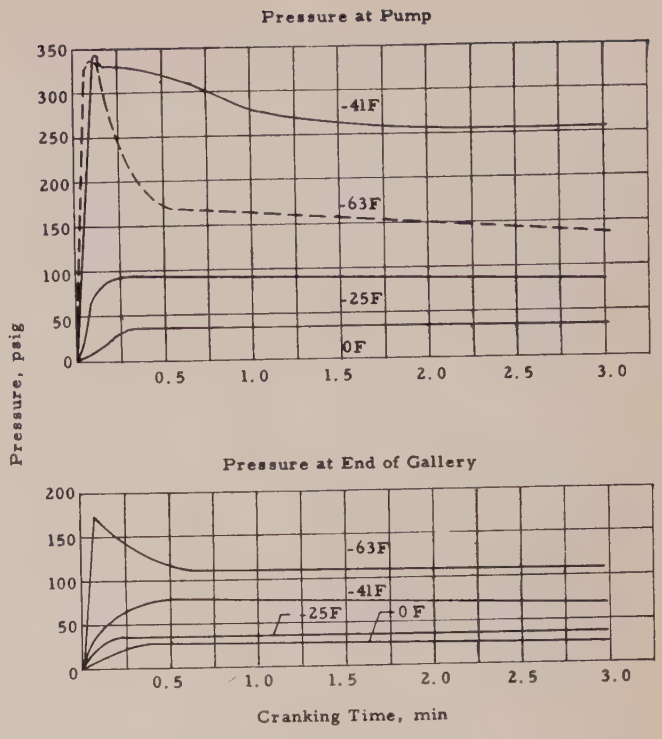

Fig. 17 – Nontypical lubricating oil pressure curves, engine G, 200 rpm

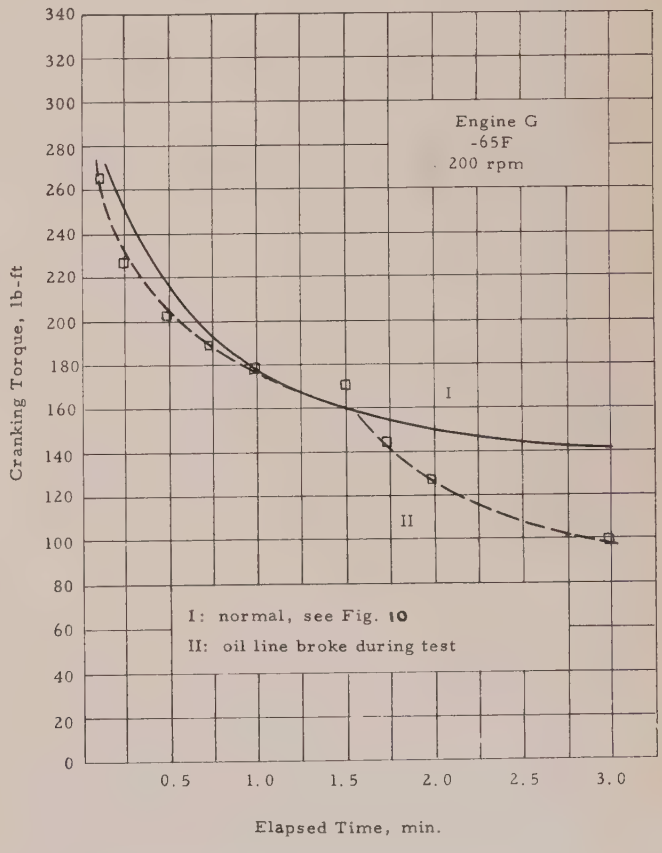

Fig. 18 – Normal and abnormal torque characteristics

Table 4 – Friction Mean Effective Pressures for the Test Engines Using MIL-O-10295 Lubricating Oil

Engine A
Gasoline, 134 cu in., 4 cyl

Fmep, psi	At 0 F	At −25 F	At −40 F	At −65 F
Breakaway	18	37	49	98
8 Sec				
50 Rpm	22	47	75	182
100 Rpm	26	54	88	214
150 Rpm	28	59	94	216
Equilibrium				
50 Rpm	22	36	56	112
100 Rpm	22	39	62	106
150 Rpm	20	45	62	90

Engine B
Gasoline, 134 cu in., 4 cyl

Fmep, psi	At 0 F	At −25 F	At −40 F	At −65 F
Breakaway	28	37	48	91
8 Sec				
50 Rpm	27	43	65	216
100 Rpm	29	50	76	222
150 Rpm	32	59	89	228
Equilibrium				
50 Rpm	28	49	54	135
100 Rpm	28	43	58	101
150 Rpm	20	47	58	84

Engine C
Gasoline, 330 cu in., 6 cyl

Fmep, psi	At 0 F	At −25 F	At −40 F	At −65 F
Breakaway	11	17	24	71
8 Sec				
50 Rpm	21	37	58	146
100 Rpm	22	42	67	151
150 Rpm	24	47	72	155
Equilibrium				
50 Rpm	23	33	48	82
100 Rpm	21	55	50	71
150 Rpm	24	38	48	78

Engine D
Gasoline, 540 cu in., 8 cyl

Fmep, psi	At 0 F	At −25 F	At −40 F	At −65 F
Breakaway	20	20	23	41
8 Sec				
50 Rpm	19	33	56	112
100 Rpm	23	40	64	122
150 Rpm	25	44	70	127
Equilibrium				
50 Rpm	17	29	48	70
100 Rpm	22	30	45	60
150 Rpm	24	33	39	63

Engine E
Gasoline, aircooled, 895 cu in., 6 cyl

Fmep, psi	At 0 F	At −25 F	At −40 F	At −65 F
Breakaway	11	14	14	33
8 Sec				
50 Rpm	12	26	41	102
100 Rpm	16	32	49	108
150 Rpm	19	38	57	112
Equilibrium				
50 Rpm	12	21	32	66
100 Rpm	13	22	39	60
150 Rpm	19	29	40	60

[a] Gasoline compression.

Engine F
Gasoline, 1091 cu in., 6 cyl

Fmep, psi	At 0 F	At −25 F	At −40 F	At −65 F
Breakaway	11	12	32	50
8 Sec				
50 Rpm	19	30	45	98
100 Rpm	22	35	51	100
150 Rpm	24	39	56	104
Equilibrium				
50 Rpm	17	26	37	59
100 Rpm	23	29	37	59
150 Rpm	22	30	41	59

Engine G
Diesel, 230 cu in., 6 cyl

Fmep, psi	At 0 F	At −25 F	At −40 F	At −65 F
Breakaway	22	24	31	72
8 Sec				
100 Rpm	34	62	92	178
200 Rpm	38	75	110	184
300 Rpm	46	87	116	181
Equilibrium				
100 Rpm	36	53	81	94
200 Rpm	36	59	69	92
300 Rpm	28	64	79	85

Engine H
Diesel, 2-stroke, 284 cu in., 4 cyl

Fmep, psi	At 0 F	At −25 F	At −40 F	At −65 F
Breakaway	19	28	42	58
8 Sec				
100 Rpm	26	43	66	155
200 Rpm	29	47	69	157
300 Rpm	31	50	72	161
Equilibrium				
100 Rpm	25	37	53	85
200 Rpm	26	36	53	71
300 Rpm	25	37	48	67

Engine I
Diesel, 334 cu in., 4 cyl

Fmep, psi	At 0 F	At −25 F	At −40 F	At −65 F
Breakaway	33	44	83	108
8 Sec				
100 Rpm	51[a]	77[a]	110[a]	225[a]
200 Rpm	58	91	127	230
Equilibrium				
100 Rpm	39[a]	82[a]	104[a]	127[a]
200 Rpm	41	59	75	104

Engine J
Diesel, 525 cu in., 6 cyl

Fmep, psi	At 0 F	At −25 F	At −40 F	At −65 F
Breakaway	12	17	20	72
8 Sec				
100 Rpm	30	53	71	140
200 Rpm	35	59	78	139
300 Rpm	38	66	84	139
Equilibrium				
100 Rpm	30	46	56	92
200 Rpm	28	49	59	66
300 Rpm	28	39	53	53

Engine K
Diesel, 672 cu in., 6 cyl

Fmep, psi	At 0 F	At −25 F	At −40 F	At −65 F
Breakaway	18	13	36	71
8 Sec				
100 Rpm	23	39	64	121
200 Rpm	29	53	83	149
300 Rpm	33	62	94	162
Equilibrium				
100 Rpm	28	43	51	68
200 Rpm	26	33	61	77
300 Rpm	28	34	50	63

and ambient temperature either from engine parameters, or failing this, from data obtained at other speeds and temperatures or with other oils.

In reviewing cranking data obtained by other laboratories it was first thought that these might be useful in broadening the range of any correlation which the data from the present investigation might yield. However, this was not possible because either not enough was known about test procedures and other pertinent factors or an in-

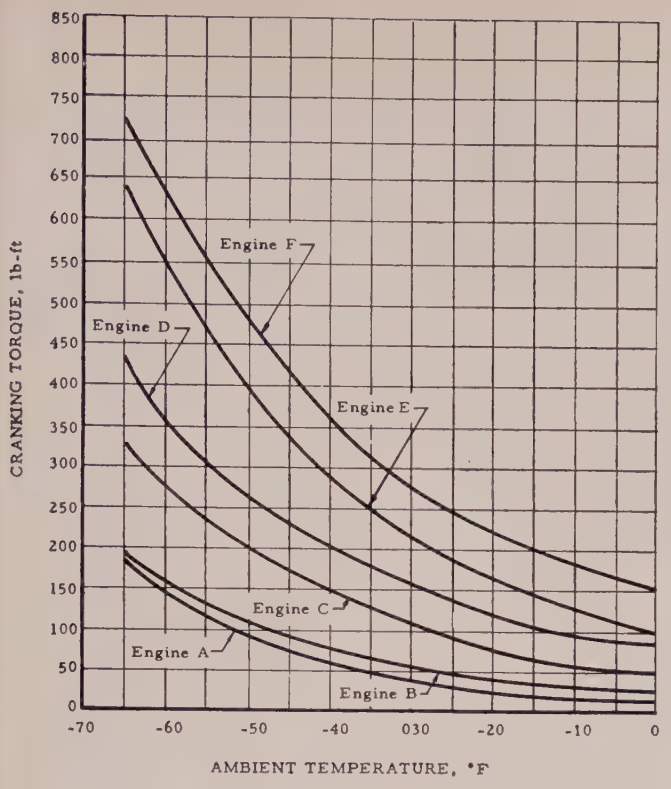

Fig. 19 – Effect of ambient temperature on cranking torque (after 8 sec) for gasoline engines at 100-rpm cranking speed with MIL-O-10295 lubricating oil

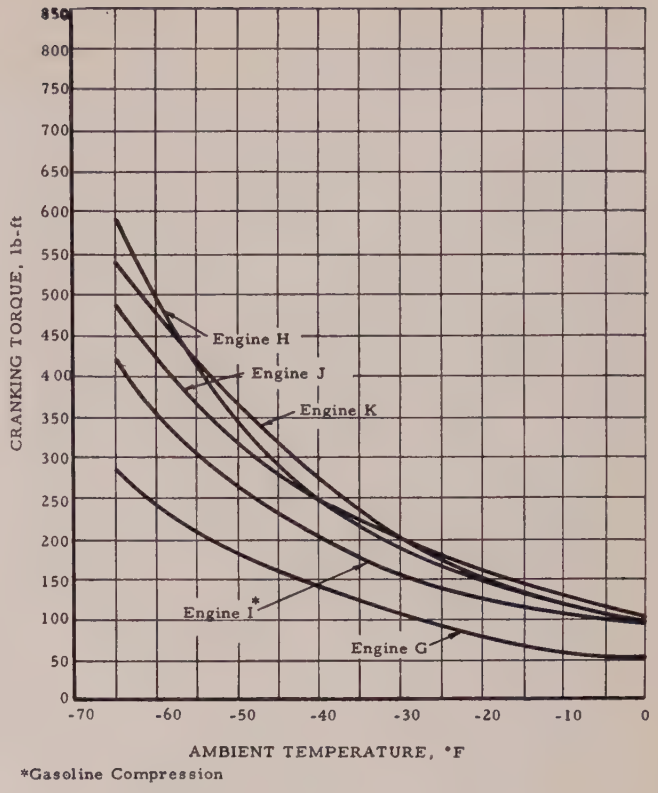

Fig. 20 – Effect of ambient temperature on cranking torque (after 8 sec) for diesel engines at 100-rpm cranking speed with MIL-O-10295 lubricating oil

sufficient number of points was available to make the data significant.

The latter point is an important one, since any correlation to be developed could only be purely empirical because the underlying causes for the character of the cranking torque curves are as yet incompletely understood. On the other hand, if it could be shown that a majority of engines would conform in their cranking behavior to some empirical function, the behavior of the nonconforming engines may shed some light on significant factors.

Various attempts were made to obtain correlations. None of them showed positive correlation for all engines and conditions. Correction factors, taking into account bearing area or other parameters, did nothing to improve the situation. For this reason only two correlations are presented since these two are based on simple relationships and do, within reasonable limits, permit cranking torque predictions and comparisons.

Figs. 25 and 26 show plots of fmep at 100 rpm versus cubic inch displacement per cylinder for all engines tested. The curves were fitted to the points as well as their limited number allowed. In doing so, engine I was not considered because its fmep values are considerably higher than those of all other engines at the same conditions. This leaves 10 points per condition divided into two categories (gasoline and diesel engines) to which to fit one

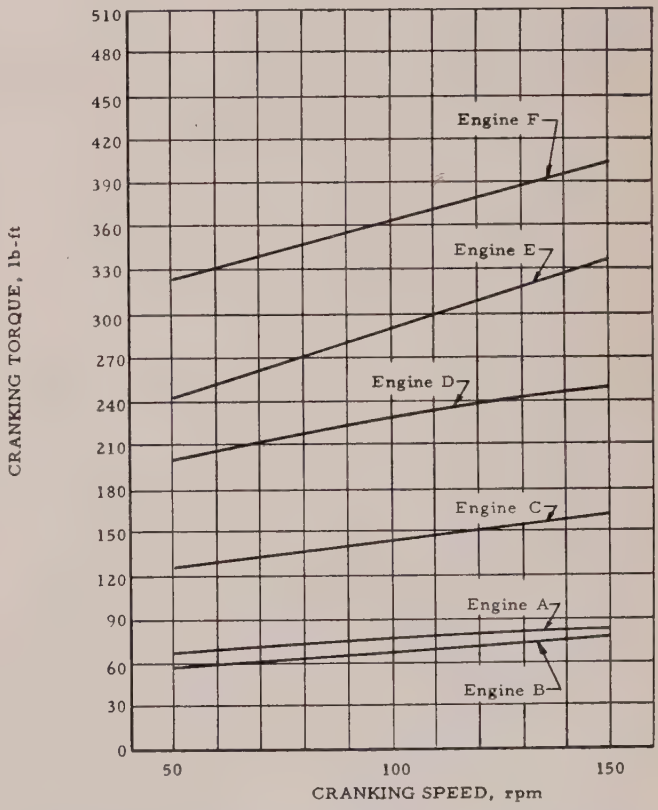

Fig. 21 – Effect of cranking speed on cranking torque (after 8 sec) for gasoline engines at —40 F ambient temperature with MIL-O-10295 lubricating oil

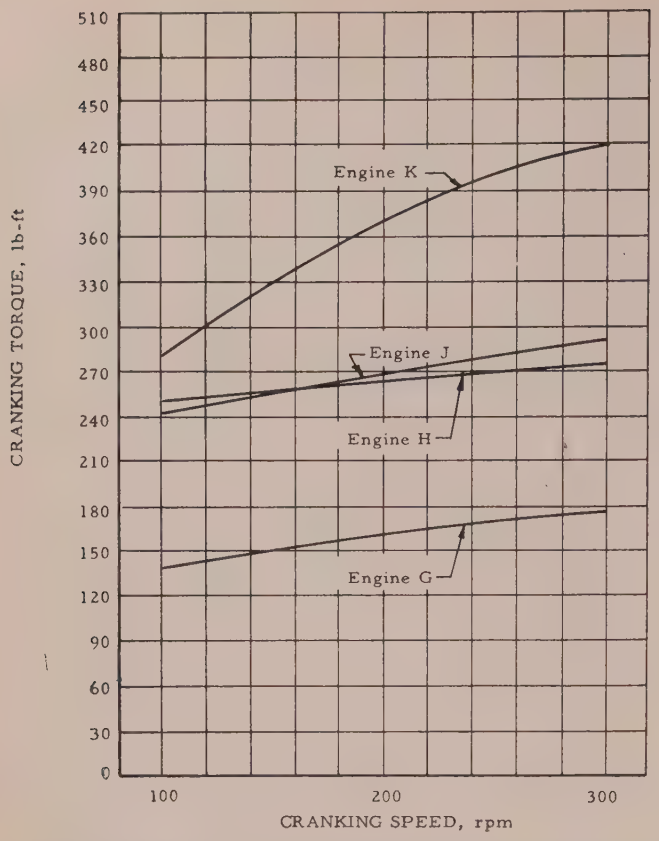

Fig. 22 – Effect of cranking speed on cranking torque (after 8 sec) for diesel engines at —40 F ambient temperature with MIL-O-10295 lubricating oil

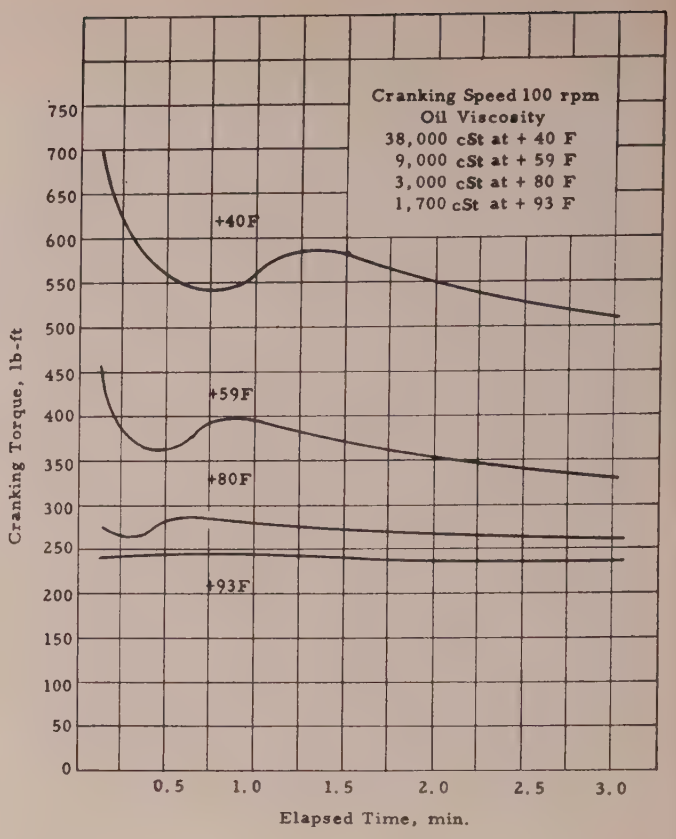

Fig. 24 – Cranking torque requirements with a high-viscosity lubricating oil – engine F

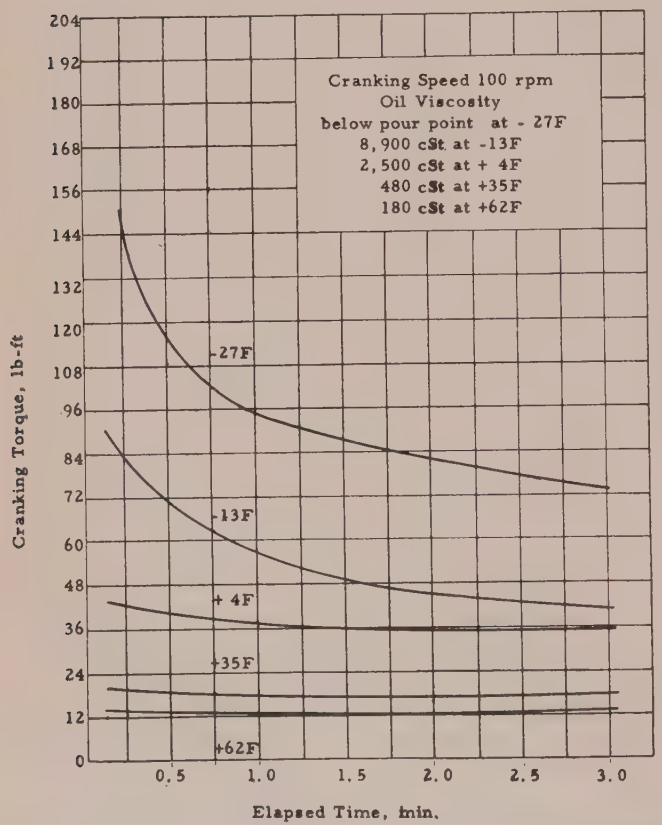

Fig. 23 – Cranking torque requirements with an SAE 20W lubricating oil-engine A

or two curves. Therefore, the curves cannot be considered as more than an attempt to illustrate trends.

The 8-sec curves (Fig. 25) show a fairly consistent trend in that the fmep decreases with displacement up to about 100 cu in. per cylinder and remains fairly constant for larger displacements. Diesel engines have a slightly higher fmep than gasoline engines of the same displacement, as might be expected because of their more liberally proportioned rubbing surfaces on the pistons and in the bearings and their higher compression ratios. Plots for other cranking speeds would give a similar picture because cranking speed in most cases is not an important variable as has been pointed out previously.

The fact that engine I does not conform to the general pattern has already been mentioned. The explanation, no doubt, must be sought in the particularly rugged construction of this engine. It is also noteworthy that the only 2-stroke-cycle engine (engine H) does not exhibit any fundamentally different characteristics than the rest of the engines despite the aluminum construction of this engine. The same applies to the aircooled engine E.

Engines A and B are basically alike in design, although they represent two different models due to differences in valve gear, cylinder head, and so forth. However, their pistons, crankshafts, and

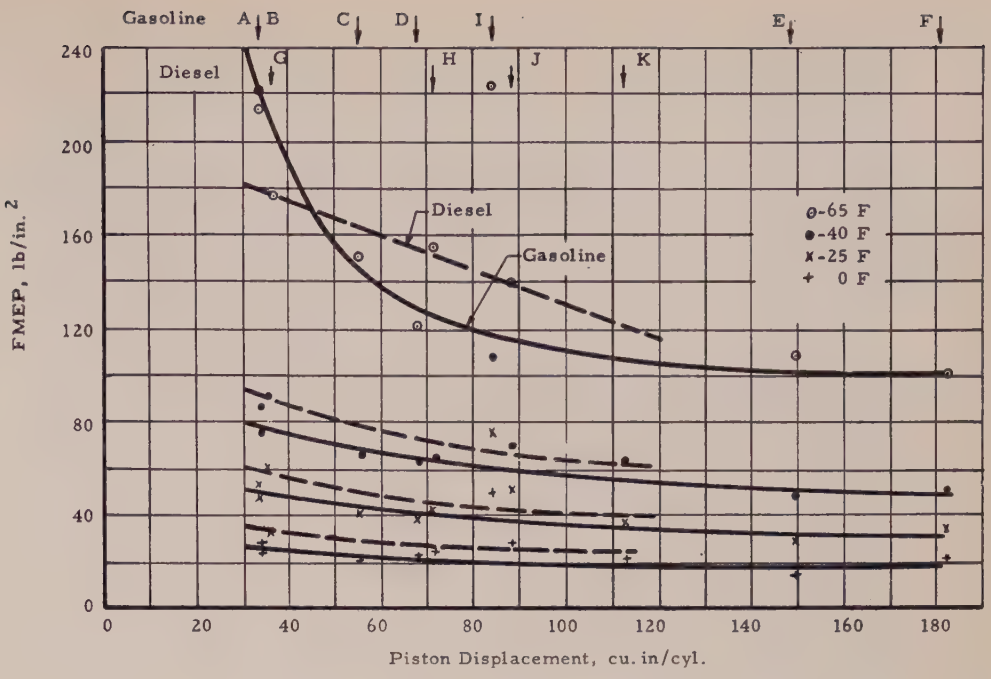

Fig 25 – Frictional mean effective pressure versus piston displacement per cylinder for several engines using MIL-O-10295 lubricating oil; fmep after 8 sec of cranking at 100 rpm

bearings are the same. That engine B shows a somewhat higher fmep than A might be caused by differences in actual clearances between moving parts. Time and circumstances did not permit measurements on any of the engines to ascertain this, but it is evident that, although the design clearances may be the same for two engines, their actual clearances may differ. Other factors could, of course, be contributing. For instance, piston-ring tensions may have differed. There are other possible causes, but not enough is known about them at present to allow an estimate of their probable magnitudes.

The equilibrium fmep plot of Fig. 26 shows more scatter of the test points than the 8-sec graph, and for this reason it was not practical to make a distinction between gasoline and diesel engines in drawing averaging curves. Again engine I is very much out of line. As has been pointed out, the equilibrium torque data are extrapolated and, therefore, not as reliable as the 8-sec data. This may, in part, be responsible for the greater scatter. In addition, one more influence gains prominence at equilibrium: the heat-dissipation characteristics of the engine. They play a major part in determining the temperature level and the time at which equilibrium will be established.

It is unlikely that an engine will be cranked at low temperature until equilibrium is attained. Either the cranking power source will have been exhausted or firing will have taken place. However, an engine which exhibits a more-than-average drop in fmep from the 8-sec point to equilibrium will not only fire earlier than another engine (everything else being equal, of course), but it will also run earlier under its own power. Such an engine very

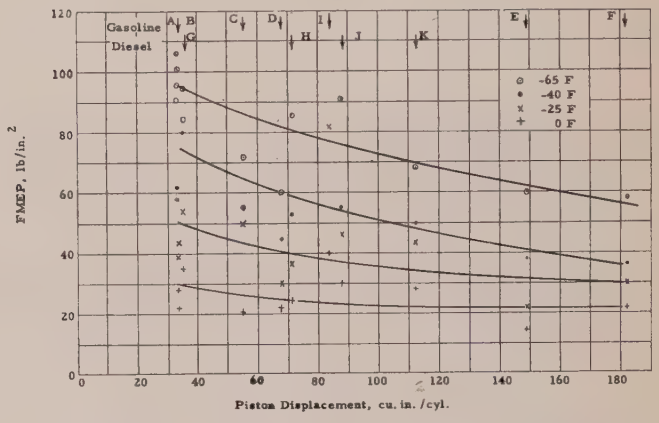

Fig. 26 – Friction mean effective pressure versus piston displacement per cylinder for several engines using MIL-O-10295 lubricating oil; equilibrium fmep at 100-rpm cranking speed

likely rejects less heat from the rubbing surfaces and from the combustion space. This favors ignition. Once heat is being added to the engine not only by friction but also by combustion, the fmep will be reduced more rapidly to the point where the power developed exceeds that consumed by friction. Again the engine with low heat rejection will reach this condition earlier.

Figs. 27 and 28 show log-log plots of the 8-sec cranking torque at 100 rpm against kinematic viscosity of the lubricating oil at the ambient temperatures of the tests. These plots result in very nearly straight lines. Inspection shows the slopes of these lines to be very similar. This suggests that the curves may be represented by an expression of the form $T = AZ^n$, where T is the cranking torque, Z the oil viscosity, n the slope, and A a constant

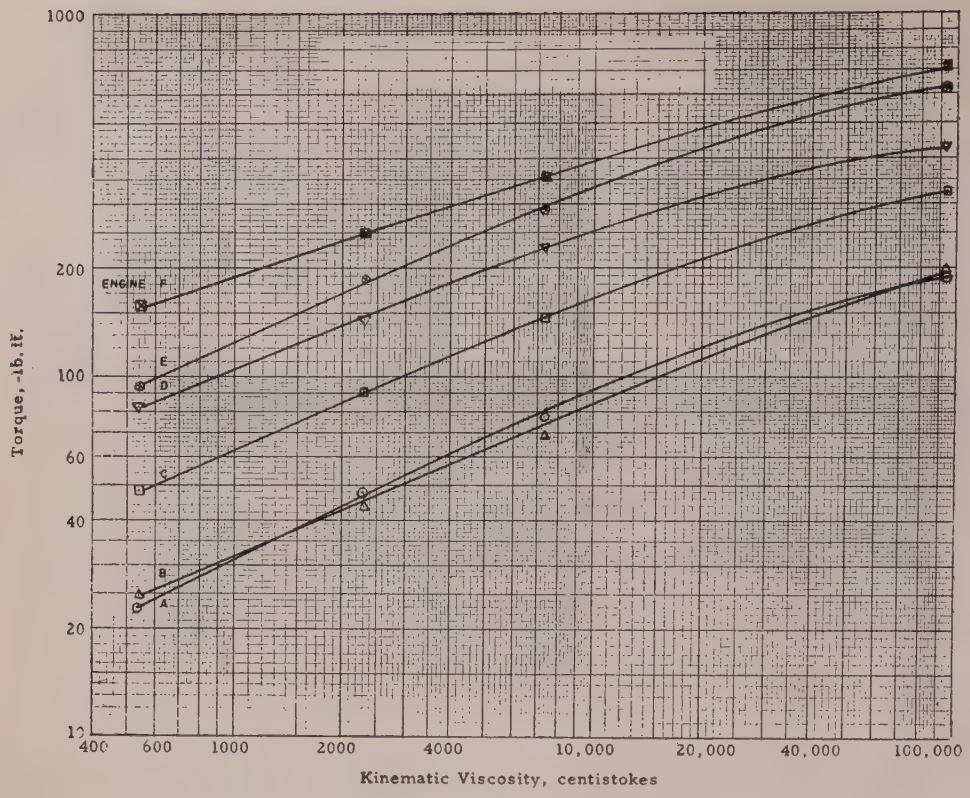

Fig. 27 – Cranking torque versus oil viscosity for gasoline engines at 100-rpm cranking speed using MIL-O-10295 lubricating oil

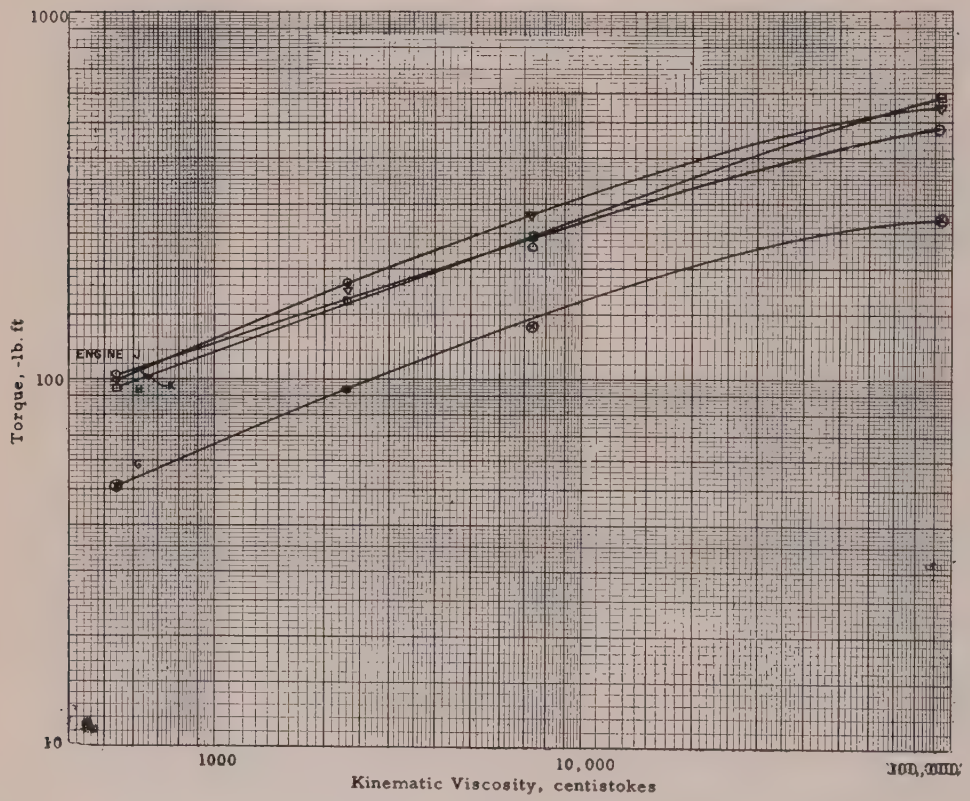

Fig. 28 – Cranking torque versus oil viscosity for diesel engines at 100 - rpm cranking speed using MIL-O-10295 lubricating oil

which denotes the value of T for $Z = 1$ centistoke. By trial and error it was found that $n = 0.365$ for gasoline engines and $n = 0.33$ for diesel engines gave the best compromises. These exponents have been so selected that they equally apply to the other cranking speeds used in this program.

The constant A appears to be a function of engine size, cranking speed, and other factors peculiar

Table 5 – Computed Cranking Torques for Gasoline Engines Using MIL-O-10295 Lubricating Oil

$$T = T_o \left(\frac{1}{Z_o}\right)^{0.365} Z^{0.365}$$

where:

T_o = Experimentally determined cranking torque at 0 F, lb-ft

Z_o = Oil viscosity at 0 F, centistokes

T = Computed cranking torque at desired temperature, lb-ft

Z = Oil viscosity at temperature at which torque is being computed, centistokes

Engine	Cranking Speed, rpm	Actual Torque – O F	−25 F			−40 F			−65 F		
			Computed Torque	Actual Torque	% Error	Computed Torque	Actual Torque	% Error	Computed Torque	Actual Torque	% Error
A	50	20	34	42	−20	51	67	−23	131	162	−19
	100	23	39	48	−19	60	78	−24	150	190	−21
	150	25	42	52	−19	64	84	−23	163	192	−15
B	50	24	40	38	+ 5	62	58	7	157	192	−18
	100	26	44	44	0	67	68	− 1	170	197	−14
	150	28	47	52	−10	72	79	− 9	183	202	− 9
C	50	46	78	81	− 4	118	127	− 7	301	319	− 6
	100	49	83	92	−10	126	146	−14	320	329	− 3
	150	52	88	103	−15	134	158	−15	340	339	0
I[a]	100	96	162	144	+13	247	204	21	638	420	50
D	50	87	113	120	− 6	172	202	−15	438	402	9
	100	88	140	142	− 1	213	250	− 7	543	435	25
	150	88	148	158	− 6	226	252	10	576	456	26
E	50	74	125	154	−19	190	244	−22	484	604	−20
	100	94	159	188	−16	242	290	−17	615	638	− 4
	150	112	189	228	−17	288	340	−16	732	664	10
F	50	140	236	215	+10	360	322	12	918	707	28
	100	160	270	250	+ 8	411	365	13	1046	725	44
	150	178	287	282	+ 2	437	407	7	1111	750	48

[a] Gasoline compression (diesel engine in starting condition).

to any one engine. An attempt was made to obtain an empirical value of A by a correlation between engine parameters and torque at O F. Weighting of the size of the bearings and of piston-ring dimensions and loading gave no overall correlation. The actual clearances for the test engines were not known, and no significant trend could be deduced from the design clearances.

Of all parameters considered, the product of cylinder diameter, stroke, and number of cylinders gave the most positive correlation. Fig. 29 shows that for gasoline engines the use of a thus derived constant would give reasonably accurate results. But for diesel engines such a correlation could hardly be justified unless one would wish to eliminate engines H and I. This may be defensible because engine I fell out of line in the fmep versus displacement plot and engine H is the only 2-stroke among 4-stroke-cycle engines while the other three are engines of similar and conventional 4-stroke design.

Thus, estimation of torque from design data only may be subject to considerable error certainly in the case of diesel engines, since their design has not become as standardized as that of gasoline engines. Therefore, it is a safer approach to make an experimental determination of torque at a high temperature and estimate by means of the mentioned equation the torque at subzero temperatures. For the present data the highest temperature was O F; therefore, estimates for lower temperatures will have to be based on O F. In doing this, constant A becomes $T_o\ (1/Z_o)^n$ where T_o and Z_o are the oil viscosity and the torque at O F, respectively. The

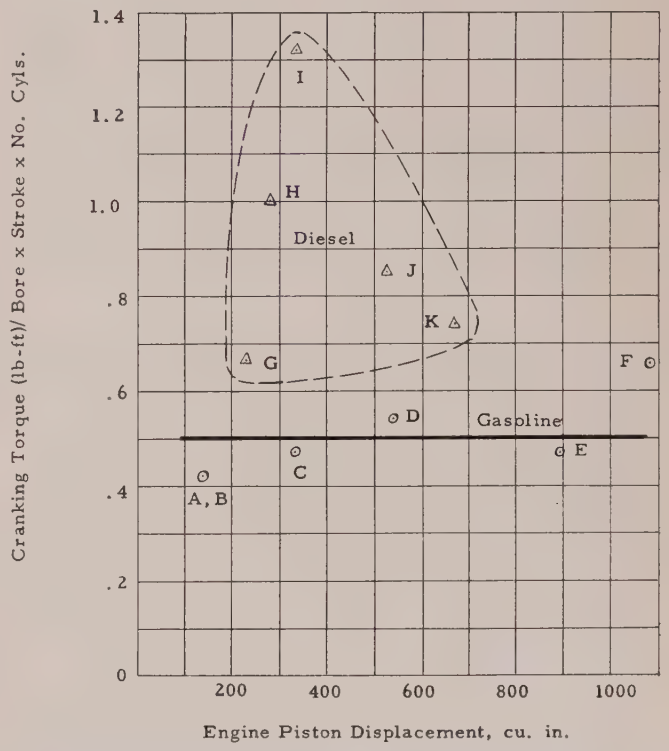

Fig. 29 – Cranking torque divided by product of cylinder bore, stroke, and number of cylinders versus engine piston displacement at O F ambient temperature using MIL-O-10295 lubricating oil. Gasoline engines at 100-rpm cranking speed; diesel engines at 200-rpm cranking speed

Table 6 – Computed Cranking Torques for Diesel Engines Using MIL-O-10295 Lubricating Oil

$$T = T_o \left(\frac{1}{Z_o}\right)^{0.33} Z^{0.33}$$

where:

T_o = Experimentally determined cranking torque at 0 F, lb-ft

Z_o = Oil viscosity at 0 F, centistokes

T = Computed cranking torque at desired temperature, lb-ft

Z = Oil viscosity at temperature at which torque is being computed, centistokes

Engine	Cranking Speed, rpm	Actual Torque – 0 F	–25 F			–40 F			–65 F		
			Computed Torque	Actual Torque	% Error	Computed Torque	Actual Torque	% Error	Computed Torque	Actual Torque	% Error
G	100	51	82	95	–14	120	140	–14	278	272	2
	200	58	93	114	–18	136	167	–18	317	280	13
	300	68	108	132	–17	159	177	–10	368	276	33
H	100	98	157	164	– 4	230	248	– 7	535	588	– 9
	200	108	173	178	– 3	254	262	– 3	590	598	– 1
	300	118	188	192	– 2	277	274	1	644	610	6
I	200	128	205	202	1	301	280	8	699	502	39
J	100	104	167	184	– 9	244	246	– 1	568	488	16
	200	120	192	206	– 7	282	272	4	655	484	35
	300	133	213	228	– 7	313	292	7	728	482	51
K	100	100	160	175	– 9	235	288	–18	548	548	1
	200	130	208	235	–11	306	370	–17	710	660	8
	300	146	233	275	–15	341	420	–19	792	720	10

torque at any lower temperature is then:

$$T = T_o \left(\frac{1}{Z_o}\right)^{0.365} Z^{0.365} \text{ for gasoline engines}$$

$$T = T_o \left(\frac{1}{Z_o}\right)^{0.33} Z^{0.33} \text{ for diesel engines}$$

Tables 5 and 6 compare the thus calculated torque at —25, —40, and —65 F (based on measured torque at O F) with the experimentally obtained values. The agreement is usually much better than 20%. Only at —65 F do some of the engines show greater deviations. This can be considered a good correlation in as much as it applies to 8-sec torque values while the viscosities are those at zero cranking time. The viscosities of the oil films throughout the engine are, of course, lower after 8 sec of cranking, but their magnitudes are unknown.

For estimating the size of cranking motors the above correlations are no doubt adequate since the performance of cranking equipment is subject to many variables so that, in fixing the motor size, a healthy factor of safety must be used in any case. Their chief value will be found to lie in making comparisons and extrapolating available data. However, until further experimental data are available, these correlations cannot be recommended for use with oils which have viscosity characteristics substantially different from the MIL-O-10295 oil.

Acknowledgment

This investigation was carried out in the Department of Engineering Research of the Pennsylvania State University under the sponsorship of the Engineer Research and Development Laboratories, Corps of Engineers, U. S. Army.

Bibliography

1. SAE *Quarterly* Transactions, Vol. 6, October, 1952, pp. 689-709: "Subzero Winterization of Diesel-Engine Power Equipment," by P. W. Espenschade, R. C. Navarin, and W. W. Van Ness.

2. Report of CRC Group on Lubricant Requirements Under Arctic Temperatures. Part I: "Experience with Crankcase Oils in Military Ground Vehicles Under Arctic Temperatures," by Kenneth Boldt. Part II: "Crankcase Oils for Use Under Arctic Temperatures," by H. C. Mougey. Presented at SAE Summer Meeting, Atlantic City, June 12, 1953.

3. SAE Transactions, Vol. 51 (August), 1943, pp. 280-284: "Cranking Power and Torque Requirements at Subzero Temperatures," by H. L. Knudsen.

4. SAE *Quarterly* Transactions, Vol. 4, April, 1950, pp. 161-167: "Light Engine Oils for Improved Subzero Operation," by V. G. Raviolo.

5. *Oil and Gas Journal,* Vol. 48, Nov. 10, 1949, pp. 261, 265-267: "Field Experience with 5W Motor Oils," by A. B. Anglin.

6. *Scientific Lubrication,* Vol. 1, May-June, 1949, pp. 2-4; July-August, p. 11: "Lubricants for Cold Starting," by K. T. Arter.

7. *SAE Journal,* Vol. 57, No. 9, September, 1949, pp. 66-69: "How Oil Viscosity Affects Engine Performance," by J. W. Lane and D. S. Chatfield.

8. *Brennstoff-Chemie,* Vol. 31, April 19, 1950, pp. 111-116: "The Behavior of Automotive Lubricating Oils at Low Temperatures," by R. Holder.

9. Engineer Research and Development Laboratories, Final Report, Part I on Contract No. DA-44-009-eng-765, June 30, 1954, "Low-Temperature Cranking of Gasoline and Diesel Engines," by W. E. Meyer and J. J. De Carolis.

Effects of Operational Factors on Structural Fatigue in Fighter Aircraft

George N. Mangurian and Philip D. Brooks,
Northrop Aircraft, Inc.

This paper was presented at the SAE National Aeronautic Meeting, Los Angeles, Oct. 9, 1954.

OVER a period of years, designers in the air transport field have been able to achieve considerable success in attacking the problem of structural fatigue by establishing good design practices and by defining workable load-life histories for their airplanes. In the fighter aircraft field, fatigue generally has been regarded as a phenomenon of interest but of secondary importance, and until recently, design to static criteria has been an accepted procedure. In the past few years, however, a number of service failures in the primary structure of several fighter and interceptor airplanes have been found to be directly traceable to repeated loads imposed in operational flying. As a result, manufacturers of fighter aircraft are beginning to devote a great deal of attention to environmental conditions affecting life expectancies and to detail analytical, empirical, and design approaches to the fatigue problem.

This paper analyzes the effects of various operational factors on the susceptibility of fighter-type aircraft to fatigue. Its purpose is to enable the designers of these planes to evaluate the significance of such effects in the early design stages. It also should serve as a guide to structural analysts who must set up and carry out a detailed program for defining load-life histories and establishing design criteria.

The operational variables which are significant to structural fatigue are considered herein as divided into two main categories:

1. Those which are a function of airplane or mission characteristics.

2. Those which are a function of the operational environment.

The factors in the first category which are most important include the airplane design limit load factor, the design range, the intended combat and cruising altitude, and the basic type of mission to be flown. Those in the second category include the effects of gust loads, maneuver loads, landing-taxi loads, and the so-called ground-air-ground cycle.

The Authors

GEORGE N. MANGURIAN is chief of structures at Northrop Aircraft, Inc. He received his B.S. and M.S. in Civil Engineering from the Massachusetts Institute of Technology. He was assistant chief structural engineer at the Chance Vought Aircraft Co. from 1935 to 1937. From 1937 to 1950, he worked for the Glenn L. Martin Co. as technical assistant to the chief structural engineer, and supervisor of structures projects.

PHILIP D. BROOKS is supervisor of structures research and stress at Northrop Aircraft, Inc. He received his B.S. in Aeronautical Engineering from the California Institute of Technology in 1941. After graduation he joined Lockheed Aircraft Corp., where he held the positions of stress analyst, stress engineer, and senior stress engineer. He served as an officer in the U. S. Naval Reserve from 1944 to 1946. Mr. Brooks has been with Northrop Aircraft, Inc. since 1946.

FATIGUE life of fighters, as discussed in this paper, is dependent on those variables which are a function of airplane mission characteristics and those which are a function of the operational environment.

The first type of variable includes airplane design limit load factor, design range, combat and cruise altitude, and the basic kind of mission flown. The second class of variable includes gust loads, maneuver loads, landing-taxi loads, and the ground-air-ground cycle.

This paper describes the fatigue damage caused by these factors in the flight histories of two hypothetical fighter aircraft.

These parameters are related to the fatigue damage which they cause in the flight histories of two hypothetical fighter-type aircraft. The design and operating characteristics of these two planes have been arbitrarily chosen as similar to those of aircraft currently being designed in order to provide a means for assessing the effects of such factors on the life expectancies of two representative types having contrasting basic missions.

One example airplane used herein is an all-purpose fighter, designed to a relatively high limit load factor (7.5g), to a probable high-speed Mach number of around 1.6, and assumed to fly the basic short-range mission depicted in Fig. 1. This plane is assumed to spend 50% of its life in the typical high-altitude mission shown and 50% in the low-altitude mission. The two portions are combined in the analysis to give a typical all-altitude, short-range, all-purpose fighter mission. The second example airplane is a long-range interceptor, designed to a lower limit load factor (5.5g), to a probable high-speed Mach number also of around 1.6, and assumed to fly the basic high-altitude long-range mission shown in Fig. 2.

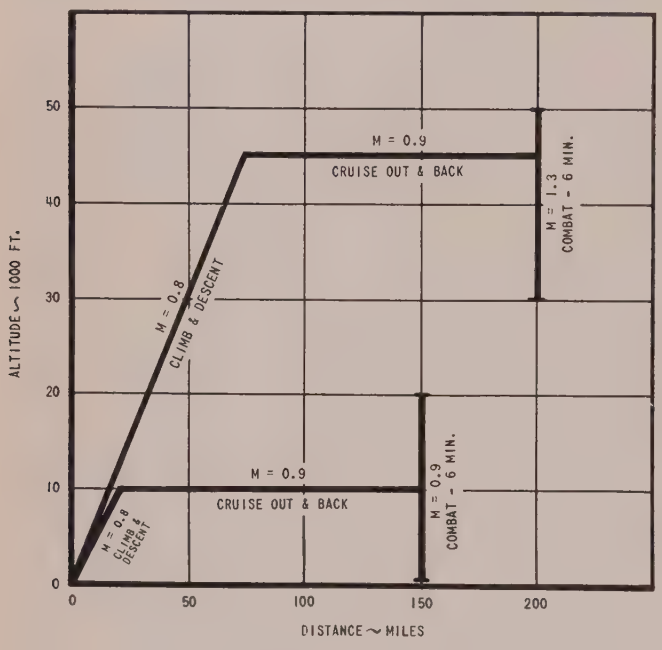

Fig. 1 – Typical missions, all-purpose fighter

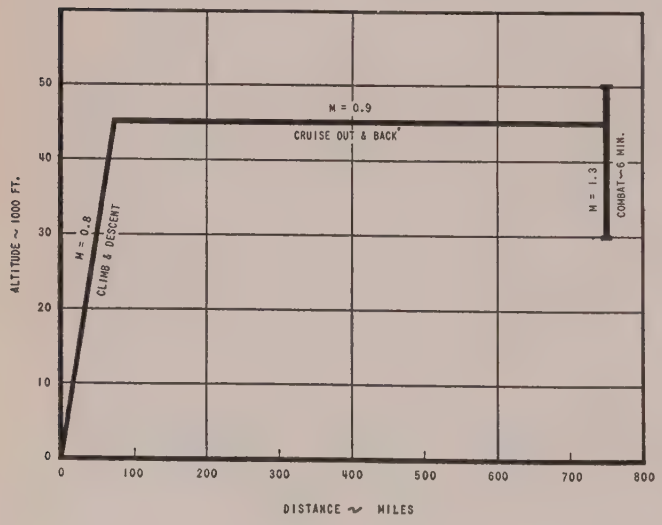

Fig. 2 – Typical mission, long-range interceptor

Assumptions

Several simplifying assumptions have been made in order to allow the reduction of a large amount of data and formulas in a reasonable length of time. The following list contains the most significant of these to serve as a guide for a more rigorous type of analysis which would be necessary in treating an actual case.

1. It has been assumed that stress levels in the portions of the structure which are critical for fatigue damage would be directly proportional to the airplane load factor. This means that the loading in these areas would be zero at zero load factor. Discussion[1] of this effect reveals that it may be an important consideration in the design of an actual airplane. It has further been assumed that the structure is of 75S-T6 aluminum alloy and has been designed to an ultimate net tensile stress of 75,000 psi.

2. In the interests of national security, some mission details and airplane characteristics have been altered so that they do not correspond exactly to current design trends and capabilities. However, the results, which are primarily significant in their comparison of the effects of the various factors studied, are sufficiently typical as to make relative results valid.

3. It has been assumed that gust and maneuver behavior is independent of airplane weight or internal fuel distribution. This would be a significant factor in the case of a plane having wing-tip fuel pods or other form of outboard fuel stowage. In such a case, the fuel loads would subtract from the wing loads, making the structure more susceptible to fatigue damage in the light-weight than in the heavy-weight conditions. The mission would thus have to be divided into portions having significantly different fuel-weight configurations and damage effects assessed independently. This would also be a primary factor in a dynamic response study (see assumption 6 below).

---

[1] "Is the Present Aircraft Structural Factor of Safety Realistic?" by G. N. Mangurian. Presented at IAS Annual Summer Meeting, June 21-24, 1954.

[2] See NACA TN 2663 (1952), "Gust and Gust-Load Experience of a Twin-Engine Low-Altitude Transport Airplane in Operation on a Northern Transcontinental Route," by Harry Press and Robert L. McDougal.

[3] See NACA TN 3041 (1953), "Summary of Revised Gust-Velocity Data Obtained from *V-G* Records Taken on Civil Transport Airplanes from 1933 to 1950," by Walter G. Walker.

[4] See NACA TN 3151 (1953), "Gust Loads and Operating Air Speeds of One Type of Four-Engine Transport Airplane on Three Routes from 1949 to 1953," by Walter G. Walker.

[5] See Boeing Airplane Co. Document No. D-15245 (1954), "Summary of Gust Spectrum Data for ARTC W-76 Fatigue Panel Environmental Conditions Group."

[6] See NACA TN 1684 (1948), "Preliminary Evaluation of Use of Ground Radar for Avoidance of Turbulent Clouds," by Harry Press and E. T. Binckley.

Table 1 – Summary of Speeds, Distances, and Times for Basic Missions

Phase	Altitude Interval, 1000 ft	Mean Alt	All-Purpose Fighter Mission: High-Altitude Portion M	Vt, mph	Ve, knots	Miles per Mission	Hours per Mission	Low-Altitude Portion M	Vt, mph	Ve, knots	Miles per Mission	Hours per Mission	Long-Range Interceptor Mission M	Vt, mph	Ve, knots	Miles per Mission	Hours per Mission
Climb and Descent	0–10	5	0.8	598	482	33.4	0.056	0.8	598	482	40	0.067	0.8	598	482	33.4	0.056
	10–20	15	0.8	576	396	33.3	0.058	...	...	...	...	.....	0.8	576	396	33.3	0.058
	20–30	25	0.8	554	322	33.3	0.060	...	...	...	...	.....	0.8	554	322	33.3	0.060
	30–40	35	0.8	530	256	33.3	0.063	...	...	...	...	.....	0.8	530	256	33.3	0.063
	40–45	42.5	0.8	530	214	16.7	0.032	...	...	...	...	.....	0.8	530	214	16.7	0.032
	Σ					150	0.269				40	0.067				150	0.269
Cruise Out and Back	0–20	10	...	...	...	...	.....	0.9	660	492	260	0.394	...	...	...	...	.....
	40–50	45	0.9	596	227	250	0.420	...	...	...	...	.....	0.9	596	227	1350	2.265
	Σ					250	0.420				260	0.394				1350	2.265
Combat or Intercept	0–10	5	...	...	...	...	.....	0.9	673	542	34	0.050	...	...	...	...	.....
	10–20	15	...	...	...	...	.....	0.9	648	446	32	0.049	...	...	...	...	.....
	30–40	35	1.3	861	416	43	0.050	...	...	...	...	.....	1.3	861	416	43	0.050
	40–50	45	1.3	860	328	43	0.050	...	...	...	...	.....	1.3	860	328	43	0.050
	Σ					86	0.100				66	0.099				86	0.100
					Σ	486	0.789			Σ	386	0.560			Σ	1586	2.634

4. The ratio of wing loading to lift curve slope has been assumed to be a constant, independent of the type of fighter, of altitude, or of Mach number. In actual gust encounters, the effect of the latter parameter, M, would be the most significant. However, the value used in this study has been selected as that corresponding to approximately $0.9M$ because most of the gust damage actually occurs in a Mach range close to this value.

5. The maneuver spectra of the airplanes studied in this paper are based on the assumption that the maneuver histories of any fighter type in terms of per cent of limit load factor would be similar in a given operation regardless of the magnitude of design load factor. In other words, a $5.5g$ limit L.F. (load factor) airplane would pull $5.5g$ the same number of times in a given distance as a $7.5g$ limit L.F. airplane would pull $7.5g$.

6. Neither aeroelastic nor dynamic response effects are taken into account in the numerical calculations. The former would include the shifting of the center of pressure in both chordwise and spanwise directions and the changes in $C_{L\alpha}$ as a function of Mach number and elastic parameters. The latter would involve the consideration of various bending and torsion modes plus load magnification effects resulting from the dynamic characteristics of flexible structure and would become particularly significant where large wing masses are employed. Thus, in an actual case, the stress level at limit load factor in critical fatigue areas would have to be considered a function of Mach number and of the time-magnitude character of the applied loading. For convenience, rigid airplane behavior is assumed herein, and structural stress level is taken as a direct function of airplane load factor.

Basic Mission Study

Table 1 presents a summary of the speeds, distances, and times for the individual segments of each basic mission illustrated in Figs. 1 and 2. This table indicates, for example, that the complete mission for the long-range interceptor lasts 2.634 hr and covers 1586 miles, of which 0.269 hr and 150 miles are spent in climb and descent, 2.265 hr and 1350 miles in the cruise out and return phase, and 0.100 hr and 86 miles in the intercept phase. The high- and low-altitude portions of the all-purpose fighter mission were tabulated in this table as though 100% of the time was spent in each, although the combined fighter mission analyzed assumes 50% of the service life in each portion. The duration of these missions may be seen to be considerably less than for the interceptor (0.789 hr or 486 miles for the high-altitude and 0.560 hr or 366 miles for the low-altitude portion).

Gust Spectrum and Damage

The gust spectrum for each mission was established by applying the gust expectancy curves of Fig. 3 to the actual speeds and distances of each mission segment from Table 1. Fig. 3 was constructed in the following manner:

1. A summary of recorded gust frequency data is presented in Fig. 4 for operation in the 0-10,000-ft altitude interval only, including all types of turbulence history and route or terrain characteristics. On this figure, the average or design gust frequency curve to be used in analysis was selected and drawn in as shown. This curve was then replotted on Fig. 3 as the final curve for 0-10,000-ft altitude.

In Fig. 4:

Curve A presents composite twin-engine transport data at 0-10,000 ft.[2]

Curves B show the envelope of American Transport data.[3, 4]

Curve C presents low-altitude data compiled by Boeing.[5]

Curve D shows thunderstorm precipitation area (radar echo) data[6], and was transformed to total flight miles by the assumption that 5 miles are flown in thunderstorm precipitation every 10,000 total miles.

2. The fraction of time flown in rough air as a function of altitude is shown in Fig. 5. The smooth

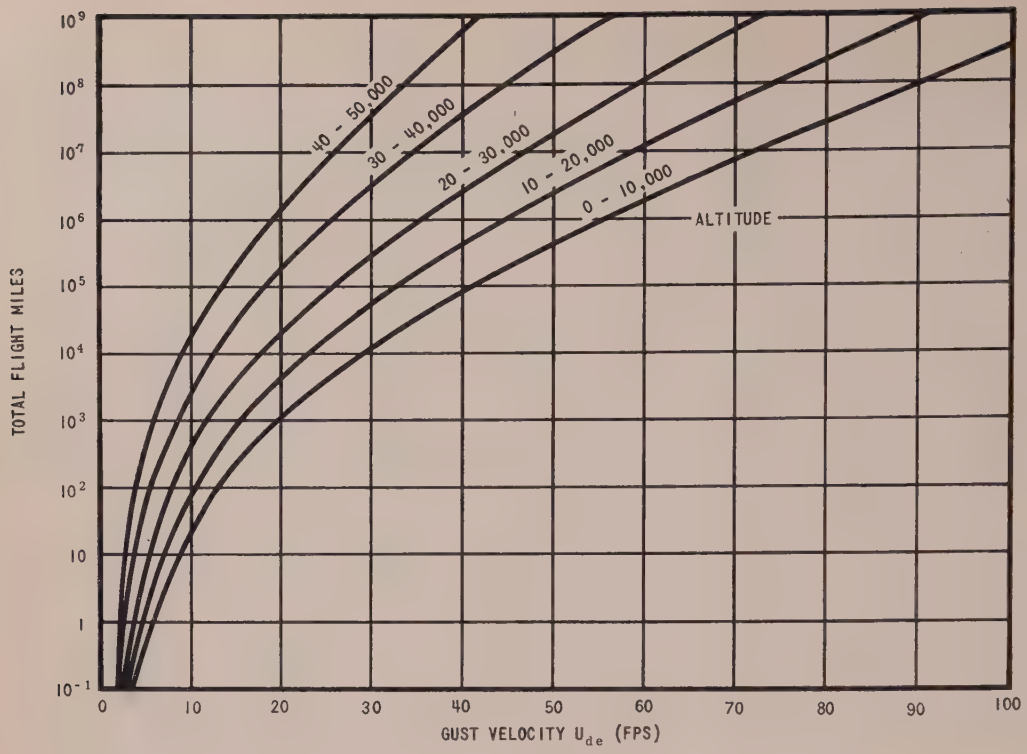

Fig. 3 – Total flight miles to equal or exceed U_{de} twice (one cycle)

curve is a composite plot constructed from data given elsewhere.[7, 8, 9] The superimposed step curve represents the constant values in each altitude interval used in this analysis.

3. Fig. 6 shows gust velocity intensity as a function of altitude. The smooth curve is a plot of the variation of the square root of the air density ratio versus altitude, and the superimposed step curve again represents the constant values in each altitude interval used for analysis. In accordance with recommendations made in several references, it is assumed that $\sigma^{1/2}$ will give a close approximation to the actual ratio of gust velocity at a given altitude to that at sea level. This refers to the equivalent gust velocity used to determine the corresponding incremental acceleration experienced at that altitude, as defined by the rigid airplane formula given herein.

4. Using Figs. 5 and 6, the basic 0-10,000-ft curve selected in Fig. 4 was transformed to give flight mile versus gust velocity values at other altitudes. This enabled plotting of the final curves of gust expectancy for all altitudes presented in Fig. 3.

Using the curves of Fig. 3, together with the values from Table 1, the number of gust cycles which occur in each mission phase and altitude interval were calculated. This analysis and all curves use the gust velocity, U_{de}, defined by Pratt,[10] which is the derived equivalent velocity of an effective gust having a 1-cosine shape. The results of these calcula-

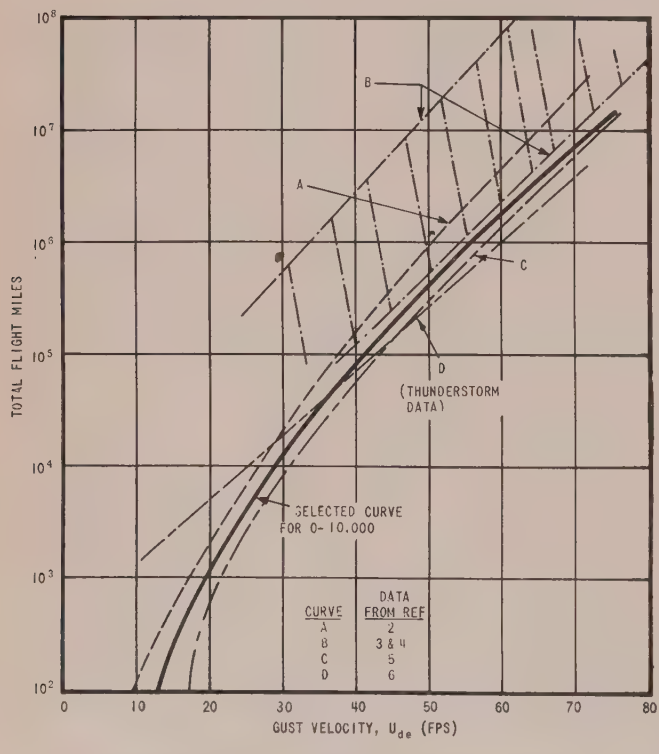

Fig. 4 – Total flight miles at 0-10,000 ft to equal or exceed U_{de} twice (one cycle)

[7] See NACA RM L52L30a (1953), "Summary of Pilots' Reports of Clear Air Turbulence at Altitudes Above 10,000 Ft." by Harry Press, M. H. Schindler, and J. K. Thompson.

[8] See NACA TR 997 (1950), "Summary of Information Relating to Gust Loads on Airplanes," by Philip Donely.

[9] See NACA ARR L4121 (1944), "Frequency of Occurrence of Atmospheric Gusts and of Related Loads on Airplane Structures," by Richard V. Rhode and Philip Donely.

[10] See NACA TN 2964 (1953), "Revised Formula for Calculation of Gust Loads," by Kermit G. Pratt.

tions are shown in Table 2. In this table, values of incremental acceleration (above and below 1.0g) were assumed and the corresponding values of U_{de} calculated from the rigid airplane formula:

$$U_{de} = \left[\frac{2\,(W/S)}{\rho_o\, C_{L\alpha}}\right] \left[\frac{1}{K_g}\right] \left[\frac{1}{V_e}\right] \Delta g$$

where:

U_{de} = Effective gust velocity, fps
W/S = Wing loading, psf
ρ_o = Air density at sea level, slugs per cu ft
$C_{L\alpha}$ = Slope of the lift curve per radian
K_g = Alleviation factor[10]
V_e = Equivalent air speed, fps

In the Pratt paper, K_g is plotted as a function of μ_g, the mass ratio, and in this analysis, μ_g was assumed high enough so that K_g was essentially constant (independent of variation of density with altitude). In this region of the curve the value of K_g is 0.85. In line with assumption 4 previously discussed, the factor $(W/S)/C_{L\alpha}$ was assigned a constant value of 13.0 lb radian per sq ft. This is a reasonable value for the aircraft type considered herein. Substituting $\rho_o = 0.002378$ slugs per cu ft and dividing by 1.689 to enable use of V_e in knots rather than feet per second, the equation becomes:

$$U_{de} = \frac{7600\ \Delta g}{V_e}$$

where:

U_{de} = Effective gust velocity, fps
Δg = Incremental acceleration, g
V_e = Equivalent air-speed, knots

Using these calculated values of U_{de} together with the curves of Fig. 3, the values for flight miles given in Table 2 were obtained. By dividing these values into the number of flight miles per mission for each altitude interval given in Table 1, the number of cycles per mission in that flight segment equaling or exceeding the lower value of $\triangle g$ in the assumed interval were obtained.

By summarizing these cycles for all phases, the total number of cycles occurring per mission which equal or exceed the lower value in each interval was obtained. These are presented in Table 3. Also presented are the net number of gust cycles which occur in each load-factor interval. The latter values actually represent the complete gust loading spectrum for one mission and were obtained by finding the difference between values for total cycles in successive intervals.

These mission spectra were converted in Table 4 to the equivalent spectra for 100 hr of flight, and the resulting fatigue damage was determined using Minor's cumulative damage theory. This table is the first point at which the two portions of the all-purpose fighter mission are combined to give the results for operation based on the assumption of 50% of the life spent in flying the high-altitude portion and 50% in the low-altitude portion.

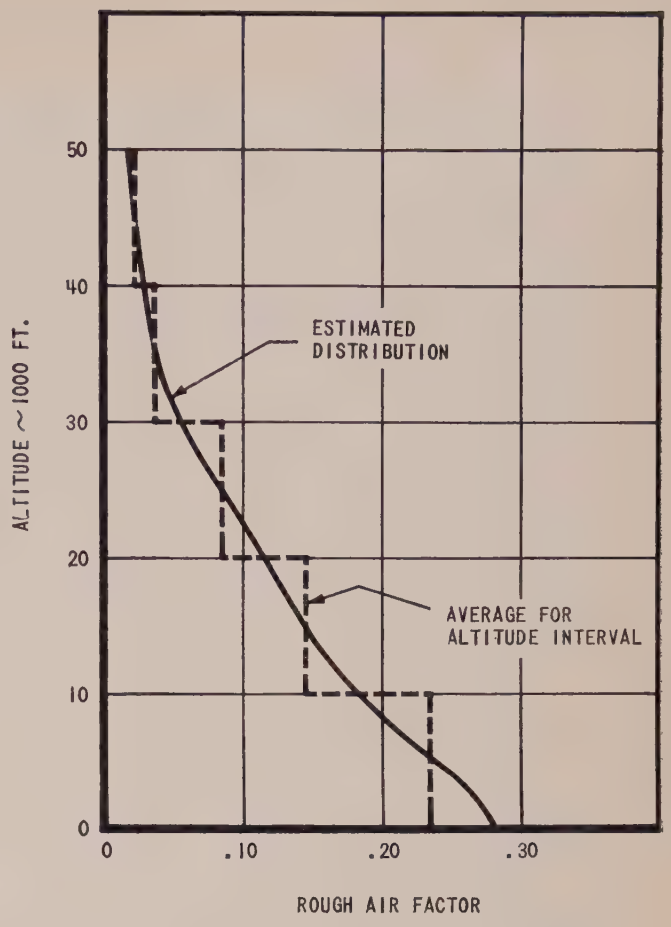

Fig. 5 – Fraction of time in rough air versus altitude

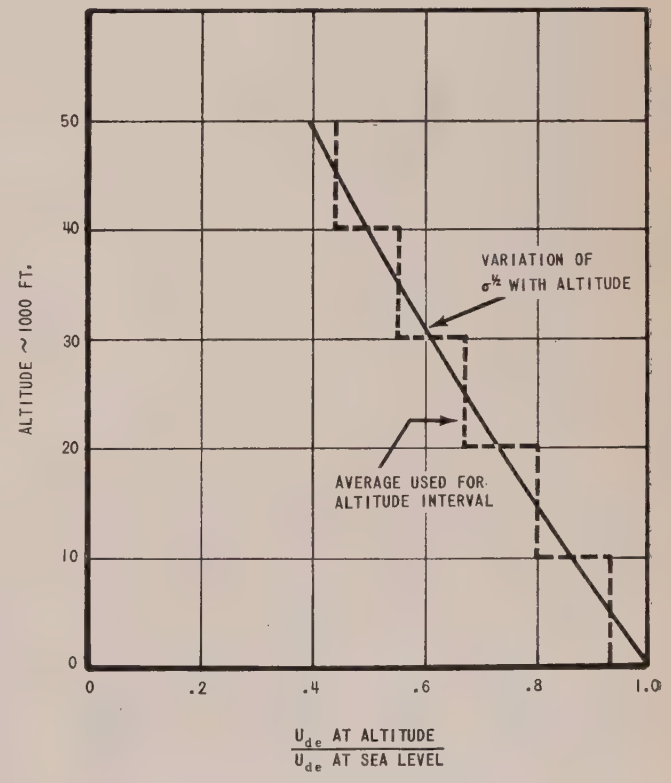

Fig. 6 – Gust intensity variation with altitude

Table 2 – Calculation of Gust Cycle Occurrences per Mission in Each Flight Phase and Altitude Interval

		All-Purpose Fighter Mission								Long-Range Interceptor Mission			
		High-Altitude Portion				Low-Altitude Portion							
Δg Interval	Flight Phase	Altitude Interval, 1000 ft	U_{de} for Lower Δg	Flt Miles to = or Exceed U_{de} Twice	Cycles per Mission Which = or Exceed Lower Δg	Altitude Interval, 1000 ft	U_{de} for Lower Δg	Flt Miles to = or Exceed U_{de} Twice	Cycles per Mission Which = or Exceed Lower Δg	Altitude Interval, 1000 ft	U_{de} for Lower Δg	Flt Miles to = or Exceed U_{de} Twice	Cycles per Mission Which = or Exceed Lower Δg
0.2 to 0.4	Climb and Descent	0–10	3.2	7.0×10^{-2}	4.8×10^{2}	0–10	3.2	7.0×10^{-2}	5.7×10^{2}	0–10	3.2	7.0×10^{-2}	4.8×10^{2}
		10–20	3.8	3.0×10^{-1}	1.1×10^{2}	....	....	.....	.....	10–20	3.8	3.0×10^{-1}	1.1×10^{2}
		20–30	4.7	3.0×10^{0}	1.1×10^{1}	.....	....	.....	.....	20–30	4.7	3.0×10^{0}	1.1×10^{1}
		30–40	5.9	2.1×10^{2}	1.6×10^{-1}	.....	....	.....	.....	30–40	5.9	2.1×10^{2}	1.6×10^{-1}
		40–45	7.1	2.0×10^{3}	8.4×10^{-3}	.....	....	.....	.....	40–45	7.1	2.0×10^{3}	8.4×10^{-3}
	Cruise	40–50	6.7	2.4×10^{3}	1.0×10^{-1}	0–20	3.1	8.0×10^{-2}	3.2×10^{3}	40–50	6.7	2.4×10^{3}	5.6×10^{-1}
	Combat or Intercept	30–40	3.7	1.2×10^{1}	3.6×10^{0}	0–10	2.8	5.0×10^{-2}	6.8×10^{2}	30–40	3.7	1.2×10^{1}	3.6×10^{0}
		40–50	4.6	3.4×10^{2}	1.3×10^{-1}	10–20	3.4	9.0×10^{-2}	3.6×10^{2}	40–50	4.6	3.4×10^{2}	1.3×10^{-1}
0.4 to 0.6	Climb and Descent	0–10	6.3	1.7×10^{0}	2.0×10^{1}	0–10	6.3	1.7×10^{0}	2.4×10^{1}	0–10	6.3	1.7×10^{0}	2.0×10^{1}
		10–20	7.7	1.8×10^{1}	1.8×10^{1}	.....	....	.....	.....	10–20	7.7	1.8×10^{1}	1.8×10^{1}
		20–30	9.4	3.0×10^{2}	1.1×10^{-1}	.....	....	.....	.....	20–30	9.4	3.0×10^{2}	1.1×10^{-1}
		30–40	11.9	7.1×10^{3}	4.7×10^{-3}	.....	....	.....	.....	30–40	11.9	7.1×10^{3}	4.7×10^{-3}
		40–45	14.2	1.5×10^{5}	1.1×10^{-4}	.....	....	.....	.....	40–45	14.2	1.5×10^{5}	1.1×10^{-4}
	Cruise	40–50	13.4	1.2×10^{5}	2.1×10^{-3}	0–20	6.2	3.2×10^{0}	8.1×10^{1}	40–50	13.4	1.2×10^{5}	1.1×10^{-2}
	Combat or Intercept	30–40	7.3	6.0×10^{2}	7.2×10^{-2}	0–10	5.6	8.0×10^{-1}	4.2×10^{1}	30–40	7.3	6.0×10^{4}	7.2×10^{-2}
		40–50	9.3	1.6×10^{4}	2.7×10^{-3}	10–20	6.8	9.0×10^{0}	3.6×10^{0}	40–50	9.3	1.6×10^{4}	2.7×10^{-3}
0.6 to 1.0	Climb and Descent	0–10	9.5	1.8×10^{1}	1.9×10^{0}	0–10	9.5	1.8×10^{1}	2.2×10^{0}	0–10	9.5	1.8×10^{1}	1.9×10^{0}
		10–20	11.5	2.4×10^{2}	1.4×10^{-1}	.....	....	.....	.....	10–20	11.5	2.4×10^{2}	1.4×10^{-1}
		20–30	14.2	3.2×10^{3}	1.0×10^{-2}	.....	....	.....	.....	20–30	14.2	3.2×10^{3}	1.0×10^{-2}
		30–40	17.8	9.0×10^{4}	3.7×10^{-4}	.....	....	.....	.....	30–40	17.8	9.0×10^{4}	3.7×10^{-4}
		40–45	21.3	1.4×10^{6}	1.2×10^{-5}	.....	....	.....	.....	40–45	21.3	1.4×10^{6}	1.2×10^{-5}
	Cruise	40–50	20.1	1.4×10^{6}	1.8×10^{-4}	0–20	9.3	3.3×10^{1}	7.9×10^{0}	40–50	20.1	1.4×10^{6}	9.6×10^{-4}
	Combat or Intercept	30–40	11.0	4.5×10^{3}	9.6×10^{-3}	0–10	8.4	1.0×10^{1}	3.4×10^{0}	30–40	11.0	4.5×10^{3}	9.6×10^{-3}
		40–50	13.9	1.3×10^{5}	3.3×10^{-4}	10–20	10.2	1.3×10^{2}	2.5×10^{-1}	40–50	13.9	1.3×10^{5}	3.3×10^{-4}
1.0 to 1.6	Climb and Descent	0–10	15.8	3.0×10^{2}	1.1×10^{-1}	0–10	15.8	3.0×10^{2}	1.3×10^{-1}	0–10	15.8	3.0×10^{2}	1.1×10^{-1}
		10–20	19.2	3.5×10^{3}	9.5×10^{-3}	.....	....	.....	.....	10–20	19.2	3.5×10^{3}	9.5×10^{-3}
		20–30	23.6	6.1×10^{4}	5.5×10^{-4}	.....	....	.....	.....	20–30	23.6	6.1×10^{4}	5.5×10^{-4}
		30–40	29.7	3.0×10^{6}	1.1×10^{-5}	.....	....	.....	.....	30–40	29.7	3.0×10^{6}	1.1×10^{-5}
		40–45	35.5	8.0×10^{7}	2.1×10^{-7}	.....	....	.....	.....	40–45	35.5	8.0×10^{7}	2.1×10^{-7}
	Cruise	40–50	33.5	1.0×10^{8}	2.5×10^{-6}	0–20	15.4	5.0×10^{2}	5.2×10^{-1}	40–50	33.5	1.0×10^{8}	1.4×10^{-5}
	Combat or Intercept	30–40	18.2	1.0×10^{5}	4.3×10^{-4}	0–10	14.0	1.4×10^{2}	2.4×10^{-1}	30–40	18.2	1.0×10^{5}	4.3×10^{-4}
		40–50	23.2	3.8×10^{6}	1.1×10^{-5}	10–20	17.0	1.6×10^{3}	2.0×10^{-2}	40–50	23.2	3.8×10^{6}	1.1×10^{-5}
1.6 to 2.4	Climb and Descent	0–10	25.2	4.5×10^{3}	7.4×10^{-3}	0–10	25.2	4.5×10^{3}	8.9×10^{-3}	0–10	25.2	4.5×10^{3}	7.4×10^{-3}
		10–20	30.7	7.0×10^{4}	4.8×10^{-4}	.....	....	.....	.....	10–20	30.7	7.0×10^{4}	4.8×10^{-4}
		20–30	37.8	1.5×10^{6}	2.2×10^{-5}	.....	....	.....	.....	20–30	37.8	1.5×10^{6}	2.2×10^{-5}
		30–40	47.5	1.7×10^{8}	2.0×10^{-7}	.....	....	.....	.....	30–40	47.5	1.7×10^{8}	2.0×10^{-7}
		40–45	56.9	$> 10^{9}$	.....	.....	.....	.....	.....	40–45	56.9	$> 10^{9}$	.....
	Cruise	40–50	53.6	$> 10^{9}$	.....	0–20	24.7	8.1×10^{3}	3.2×10^{-2}	40–50	53.6	$> 10^{9}$	10^{-7}
	Combat or Intercept	30–40	29.2	2.6×10^{6}	1.7×10^{-5}	0–10	22.4	2.1×10^{3}	1.6×10^{-2}	30–40	29.2	2.6×10^{6}	1.7×10^{-5}
		40–50	37.1	2.7×10^{8}	1.6×10^{-7}	10–20	27.2	3.1×10^{4}	1.0×10^{-3}	40–50	37.1	2.7×10^{8}	1.6×10^{-7}
2.4 to 3.2	Climb and Descent	0–10	37.8	5.5×10^{4}	6.1×10^{-4}	0–10	37.8	5.5×10^{4}	7.3×10^{-4}	0–10	37.8	5.5×10^{4}	6.1×10^{-4}
		10–20	46.0	1.2×10^{6}	2.8×10^{-5}	.....	....	.....	.....	10–20	46.0	1.2×10^{6}	2.8×10^{-5}
		20–30	56.6	6.4×10^{7}	5.2×10^{-7}	.....	....	.....	.....	20–30	56.6	6.4×10^{7}	5.2×10^{-7}
		30–40	71.3	$> 10^{9}$	.....	.....	.....	.....	.....	30–40	71.3	$> 10^{9}$	.....
		40–45	85.2	$> 10^{9}$	.....	.....	.....	.....	.....	40–45	85.2	$> 10^{9}$	.....
	Cruise	40–50	80.4	$> 10^{9}$	.....	0–20	37.0	1.1×10^{5}	2.4×10^{-3}	40–50	80.4	$> 10^{9}$	.....
	Combat or Intercept	30–40	43.8	8.1×10^{7}	5.3×10^{-7}	0–10	33.6	2.5×10^{4}	1.4×10^{-3}	30–40	43.8	8.1×10^{7}	5.3×10^{-7}
		40–50	55.6	$> 10^{9}$	.....	10–20	40.8	5.0×10^{5}	6.4×10^{-5}	40–50	55.6	$> 10^{9}$	.....
3.2 to 4.0	Climb and Descent	0–10	50.4	4.2×10^{5}	8.0×10^{-5}	0–10	50.4	4.2×10^{5}	9.5×10^{-5}	0–10	50.4	4.2×10^{5}	8.0×10^{-5}
		10–20	61.4	1.5×10^{7}	2.2×10^{-5}	.....	....	.....	.....	10–20	61.4	1.5×10^{7}	2.2×10^{-6}
		20–30	75.5	$> 10^{9}$	.....	.....	.....	.....	.....	20–30	75.5	$> 10^{9}$	.....
		30–40	95.0	$> 10^{9}$	.....	.....	.....	.....	.....	30–40	95.0	$> 10^{9}$	.....
		40–45	113.8	$> 10^{9}$	.....	.....	.....	.....	.....	40–45	113.8	$> 10^{9}$	.....
	Cruise	40–50	107.1	$> 10^{9}$	.....	0–20	49.4	1.0×10^{6}	2.6×10^{-4}	40–50	107.1	$> 10^{9}$	.....
	Combat or Intercept	30–40	58.4	$> 10^{9}$	.....	0–10	44.9	1.8×10^{5}	1.9×10^{-4}	30–40	58.4	$> 10^{9}$	.....
		40–50	74.2	$> 10^{9}$	.....	10–20	54.5	5.1×10^{6}	6.3×10^{-6}	40–50	74.2	$> 10^{9}$	.....
4.0 to 4.8	Climb and Descent	0–10	63.1	2.7×10^{6}	1.2×10^{-5}	0–10	63.1	2.7×10^{6}	1.5×10^{-5}	0–10	63.1	2.7×10^{6}	1.2×10^{-5}
		10–20	76.9	1.4×10^{8}	2.4×10^{-7}	.....	....	.....	.....	10–20	76.9	1.4×10^{8}	2.4×10^{-7}
		20–30	94.5	$> 10^{9}$	.....	.....	.....	.....	.....	20–30	94.5	$> 10^{9}$	.....
		30–40	118.8	$> 10^{9}$	.....	.....	.....	.....	.....	30–40	118.8	$> 10^{9}$	.....
		40–45	142.0	$> 10^{9}$	.....	.....	.....	.....	.....	40–45	142.0	$> 10^{9}$	.....
	Cruise	40–50	134.0	$> 10^{9}$	.....	0–20	61.8	7.0×10^{6}	3.7×10^{-5}	40–50	134.0	$> 10^{9}$	.....
	Combat or Intercept	30–40	73.0	$> 10^{9}$	.....	0–10	56.1	1.0×10^{6}	3.4×10^{-5}	30–40	73.0	$> 10^{9}$	.....
		40–50	92.8	$> 10^{9}$	.....	10–20	68.2	4.0×10^{7}	8.0×10^{-7}	40–50	92.8	$> 10^{9}$	.....

Table 3 – Summary of Cumulative and Net Gust Cycles per Mission in Each Load Factor Interval

		All-Purpose Fighter Mission				Long-Range Interceptor Mission	
		High-Altitude Portion		Low-Altitude Portion			
Δg Interval	Mean Δg	Total Cycles Which = or Exceed Lower Δg	Net Cycles Occurring in Δg Interval	Total Cycles Which = or Exceed Lower Δg	Net Cycles Occurring in Δg Interval	Total Cycles Which = or Exceed Lower Δg	Net Cycles Occurring in Δg Interval
0.2 to 0.4	0.3	605.0	567	4810	4659	606	568
0.4 to 0.6	0.5	38.2	36	151	137	38.2	36
0.6 to 1.0	0.8	2.06	1.9	13.7	12.8	2.06	1.9
1.0 to 1.6	1.3	0.120	0.11	0.91	0.85	0.120	0.11
1.6 to 2.4	2.0	0.00792	0.0073	0.0579	0.053	0.00792	0.0073
2.4 to 3.2	2.8	0.000639	0.00056	0.00459	0.0040	0.000639	0.00056
3.2 to 4.0	3.6	0.0000822	0.000070	0.000551	0.00046	0.0000822	0.000070
4.0 to 4.8	4.4	0.0000122	0.000010	0.0000868	0.000071	0.0000122	0.000010

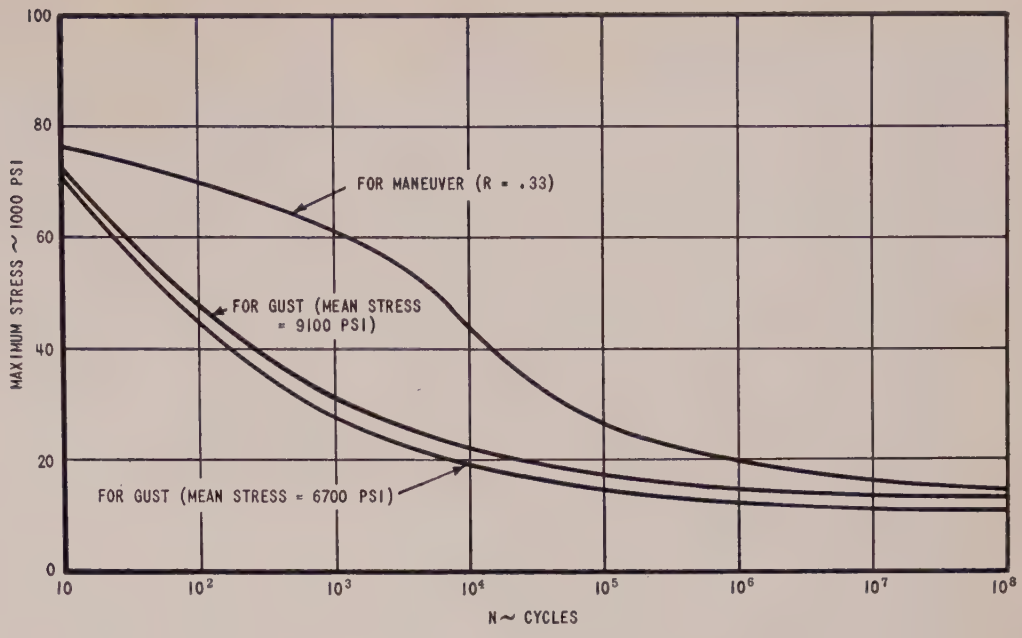

Fig. 7 – Design *S-N* curves for fatigue analysis

The *S-N* curves used for this gust fatigue analysis are shown in Fig. 7 and were constructed from test data of other investigators.[11, 12] The mean stress levels used correspond to 1.0*g* load factor. For the missions based on a design limit load factor of 5.5, the mean stress level is 9100 psi; and for those based on a design load factor of 7.5, the mean stress level is 6700 psi. These curves conform closely to the results of tests of 75S-T6 specimens having a stress concentration factor of 4.0 and employing edge-cut notches.

[11] See NACA TN 2389 (1951), "Fatigue Strengths of Aircraft Materials. Axial Load Fatigue Tests on Notched Sheet Specimens of 24S-T3 and 75S-T6 Aluminum Alloys and of SAE 4130 Steel with Stress Concentration Factors of 2 and 4," by H. J. Grover, S. M. Bishop, and L. R. Jackson.

[12] See NACA TN 3132 (1954), "24S-T3 and 75S-T6 Aluminum Alloy Sheet Specimens with a Theoretical Stress Concentration Factor of 4.0 Subjected to Completely Reversed Axial Load," by Herbert F. Hardrath and Walter Illg.

Table 4 shows that the damage resulting from the gust spectrum in 100 hr of flight for the long-range interceptor (design limit load factor of 5.5), is 0.0014. This means that 0.14% of the total life of this airplane has been used up in 100 hr of flight by the gust spectrum alone. The corresponding damage figure for the all-purpose fighter flying its design mission (limit load factor of 7.5) is 0.0041 or 0.41% of its total life expectancy. The damage values contained in this table are later combined with the damages resulting from the other types of loading spectra to give the total damage incurred in 100 hr of flight and the overall life expectancy values.

Maneuver Spectrum and Damage

The maneuver spectrum for each mission was established by applying the maneuver acceleration

Table 4 – Cumulative Damage Resulting from Gust Spectrum in 100 Hr of Flight
(Stress Level at Limit Load Factor = 50,000 psi)

Mean Δg	Load Factor Range	Max in % Lim L. F.	Stress at Max L. F., 1000 psi	N	All-Purpose Fighter Mission: High-Altitude Portion n	High-Altitude Portion n/N	Low-Altitude Portion n	Low-Altitude Portion n/N	Combined Mission n	Combined Mission n/N	Long-Range Interceptor Mission n	Long-Range Interceptor Mission n/N
For Design Limit Load Factor = 5.5												
0.3	0.7 to 1.3	23.6	11.8	$> 10^8$	7.2×10^4	—	8.3×10^5	—	4.5×10^5	—	2.2×10^4	—
0.5	0.5 to 1.5	27.2	13.6	5×10^6	4.6×10^3	0.00092	2.4×10^4	0.0048	1.4×10^4	0.0028	1.4×10^3	0.00028
0.8	0.2 to 1.8	32.7	16.4	1.1×10^5	2.4×10^2	0.00218	2.3×10^3	0.0209	1.3×10^3	0.0118	7.2×10^1	0.00065
1.3	−0.3 to 2.3	41.8	20.9	1.5×10^4	1.4×10^1	0.00093	1.5×10^2	0.0100	8.2×10^1	0.0055	4.2×10^0	0.00028
2.0	−1.0 to 3.0	54.5	27.3	2.1×10^3	9.3×10^{-1}	0.00044	9.5×10^0	0.0045	5.2×10^0	0.0025	2.8×10^{-1}	0.00013
2.8	−1.8 to 3.8	69.1	34.6	5.2×10^2	7.1×10^{-2}	0.00014	7.1×10^{-1}	0.0014	3.9×10^{-1}	0.0008	2.1×10^{-2}	0.00004
3.6	−2.6 to 4.6	83.7	41.8	1.9×10^2	8.9×10^{-3}	0.00005	8.2×10^{-2}	0.0004	4.5×10^{-2}	0.0002	2.7×10^{-3}	0.00001
4.4	−3.4 to 5.4	98.2	49.1	8.2×10^1	1.3×10^{-3}	0.00002	1.3×10^{-2}	0.0002	7.2×10^{-3}	0.0001	3.8×10^{-4}	—
						Σ 0.00468		Σ 0.0422		Σ 0.0237		Σ 0.00139
For Design Limit Load Factor = 7.5												
0.3	0.7 to 1.3	17.3	8.7	$> 10^9$	7.2×10^4	—	8.3×10^5	—	4.5×10^5	—	2.2×10^4	—
0.5	0.5 to 1.5	20.0	10.0	1×10^9	4.6×10^3	—	2.4×10^4	—	1.4×10^4	—	1.4×10^3	—
0.8	0.2 to 1.8	24.0	12.0	1×10^6	2.4×10^2	0.00024	2.3×10^3	0.0023	1.3×10^3	0.0013	7.2×10^1	0.000072
1.3	−0.3 to 2.3	30.7	15.3	4.6×10^4	1.4×10^1	0.00030	1.5×10^2	0.0033	8.2×10^1	0.0018	4.2×10^0	0.000091
2.0	−1.0 to 3.0	40.0	20.0	7.0×10^3	9.3×10^{-1}	0.00013	9.5×10^0	0.0014	5.2×10^0	0.0007	2.8×10^{-1}	0.000040
2.8	−1.8 to 3.8	50.7	25.3	1.7×10^3	7.1×10^{-2}	0.00004	7.1×10^{-1}	0.0004	3.9×10^{-1}	0.0002	2.1×10^{-2}	0.000012
3.6	−2.6 to 4.6	61.4	30.7	6.2×10^2	8.9×10^{-3}	0.00001	8.2×10^{-2}	0.0001	4.5×10^{-2}	0.0001	2.7×10^{-3}	0.000004
4.4	−3.4 to 5.4	72.0	36.0	2.8×10^2	1.3×10^{-3}	—	1.3×10^{-2}	—	7.2×10^{-3}	—	3.8×10^{-4}	—
						Σ 0.00072		Σ 0.0075		Σ 0.0041		Σ 0.000219

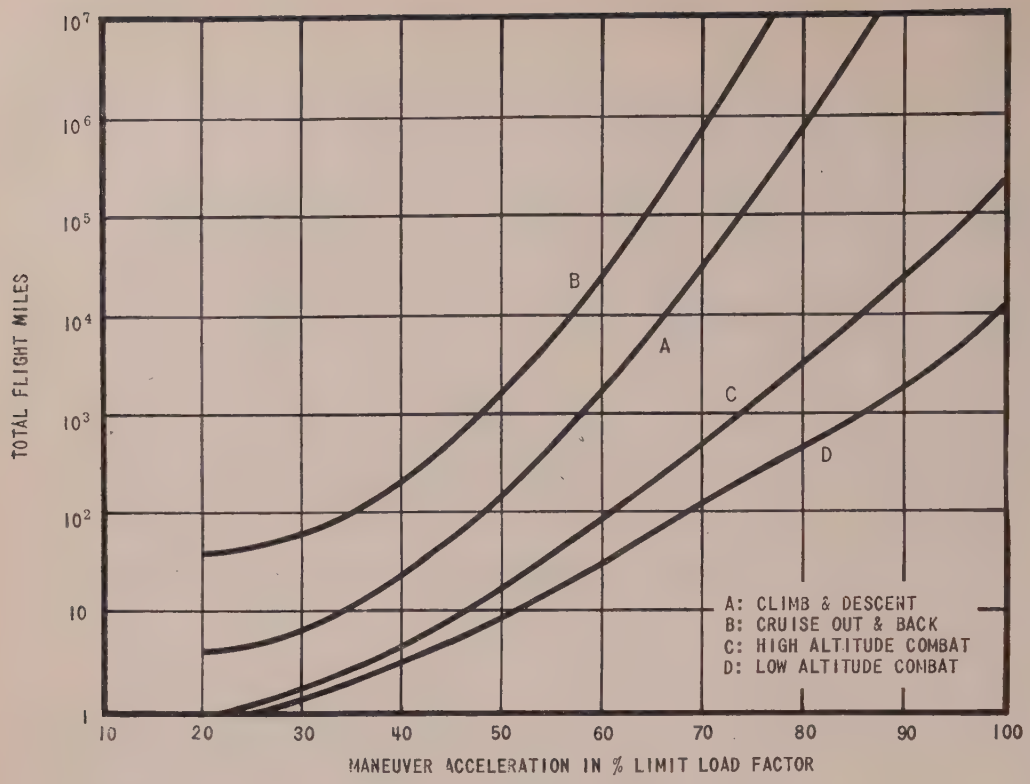

Fig. 8 – Total flight miles to equal or exceed given maneuver acceleration

Table 5 – Summary of Maneuver Acceleration Occurrences per Mission

Max Accel, Interval, % lim L. F.	Mean Value Max Accel, % lim L. F.	Flight Miles to Equal or Exceed Lower Value	Phase	All-Purpose Fighter Mission: High-Altitude Portion: Times in Phase Lower Value Equaled or Exceeded	All-Purpose Fighter Mission: High-Altitude Portion: Times in Mission Lower Value Equaled or Exceeded	All-Purpose Fighter Mission: High-Altitude Portion: Times Accel in Interval Occurred	All-Purpose Fighter Mission: Low-Altitude Portion: Times in Phase Lower Value Equaled or Exceeded	All-Purpose Fighter Mission: Low-Altitude Portion: Times in Mission Lower Value Equaled or Exceeded	All-Purpose Fighter Mission: Low-Altitude Portion: Times Accel in Interval Occurred	Long-Range Interceptor Mission: Times in Phase Lower Value Equaled or Exceeded	Long-Range Interceptor Mission: Times in Mission Lower Value Equaled or Exceeded	Long-Range Interceptor Mission: Times Accel in Interval Occurred
20		2.7	A	5.6×10^{1}			1.5×10^{1}			5.6×10^{1}		
to	25	2.5	B	1.0×10^{1}	166	80	1.0×10^{1}	107	45	5.4×10^{1}	210	104
30		0.80 / 0.80	C/D	1.0×10^{2}			8.2×10^{1}			1.0×10^{2}		
30		6.2	A	2.4×10^{1}			6.4×10^{1}			2.4×10^{1}		
to	35	5.7 x 10	B	4.4×10^{0}	86.4	61	4.6×10^{0}	62	37	2.4×10^{1}	106	75
40		1.5 / 1.3	C/D	5.8×10^{1}			5.1×10^{1}			5.8×10^{1}		
40		2.8 x 10	A	5.4×10^{0}			1.4×10^{0}			5.4×10^{0}		
to	45	2.2×10^{2}	B	1.3×10^{0}	25.6	20	1.2×10^{0}	25.6	17.8	6.1×10^{0}	30.5	24
50		4.5 / 2.9	C/D	1.9×10^{1}			2.3×10^{0}			1.9×10^{0}		
50		1.6×10^{2}	A	9.4×10^{-1}			2.5×10^{-1}			9.4×10^{-1}		
to	55	1.6×10^{3}	B	1.5×10^{-1}	5.89	4.9	1.6×10^{-1}	7.81	5.7	8.4×10^{-1}	6.58	5.5
60		1.8 x 10 / 8.9	C/D	4.8×10^{0}			7.4×10^{0}			4.8×10^{0}		
60		2.0×10^{3}	A	7.5×10^{-2}			2.0×10^{-2}			7.5×10^{-2}		
to	65	3.0×10^{4}	B	8.4×10^{-3}	1.03	0.87	8.7×10^{-4}	2.13	1.62	4.5×10^{-2}	1.06	0.90
70		9.5 x 10 / 3.1 x 10	C/D	9.4×10^{-1}			2.1×10^{0}			9.4×10^{-1}		
70		3.4×10^{4}	A	4.4×10^{-3}			1.2×10^{-3}			4.4×10^{-3}		
to	75	1.0×10^{6}	B	2.5×10^{-4}	0.165	0.140	2.6×10^{-4}	0.511	0.37	1.4×10^{-3}	0.166	0.141
80		5.4×10^{2} / 1.3 x 10^{2}	C/D	1.6×10^{-1}			5.1×10^{-1}			1.6×10^{-1}		
80		8.2×10^{5}	A	1.8×10^{-4}			4.9×10^{-5}			1.8×10^{-4}		
to	85	6.0×10^{7}	B	4.2×10^{-6}	0.0252	0.022	4.3×10^{-6}	0.140	0.101	2.2×10^{-5}	0.0252	0.022
90		3.4×10^{3} / 4.8 x 10^{2}	C/D	2.5×10^{-2}			1.4×10^{-1}			2.5×10^{-2}		
90		4.3×10^{7}	A	3.5×10^{-6}			9.3×10^{-7}			3.5×10^{-6}		
to	95	—	B	—	0.0037	0.0032	—	0.0390	0.028	—	0.0037	0.0031
100		2.3×10^{4} / 1.7 x 10^{3}	C/D	3.7×10^{-3}			3.9×10^{-2}			3.7×10^{-3}		

Table 6 – Cumulative Damage Resulting from Maneuver Spectrum in 100 Hr of Flight (Stress Level at Limit Load Factor = 50,000 psi)

Max Accel, % limit L.F.	Stress Level at Max Accel, psi	Cycles to Failure, N	All-Purpose Fighter Mission: High-Altitude Portion: Load Cycles, n	All-Purpose Fighter Mission: High-Altitude Portion: n/N	All-Purpose Fighter Mission: Low-Altitude Portion: n	All-Purpose Fighter Mission: Low-Altitude Portion: n/N	All-Purpose Fighter Mission: Combined Mission: n	All-Purpose Fighter Mission: Combined Mission: n/N	Long-Range Interceptor Mission: n	Long-Range Interceptor Mission: n/N
25	12,500	$>10^{8}$	1.01×10^{4}	—	8.0×10^{3}	—	9.1×10^{3}	—	3.9×10^{3}	—
35	17,500	3.1×10^{6}	7.7×10^{3}	0.0025	6.6×10^{3}	0.0021	7.1×10^{3}	0.0023	2.8×10^{3}	0.0009
45	22,500	2.7×10^{5}	2.5×10^{3}	0.0093	3.2×10^{3}	0.0118	2.8×10^{3}	0.0104	9.1×10^{2}	0.0034
55	27,500	7.5×10^{4}	6.2×10^{2}	0.0083	1.02×10^{3}	0.0136	8.2×10^{2}	0.0109	2.1×10^{2}	0.0028
65	32,500	3.5×10^{4}	1.1×10^{2}	0.0031	2.9×10^{2}	0.0083	2.0×10^{2}	0.0057	3.4×10^{1}	0.0010
75	37,500	1.8×10^{4}	1.78×10^{1}	0.0010	6.6×10^{1}	0.0037	4.2×10^{1}	0.0023	5.3×10^{0}	0.0003
85	42,500	1.2×10^{4}	2.8×10^{0}	0.0002	1.8×10^{1}	0.0015	1.04×10^{1}	0.0009	8.3×10^{-1}	0.0001
95	47,500	7.4×10^{3}	4.1×10^{-1}	0.0001	5.0×10^{0}	0.0007	2.7×10^{0}	0.0004	1.18×10^{-1}	—
			Σ	0.0245	Σ	0.0417	Σ	0.0329	Σ	0.0085

expectancy curves of Fig. 8 to the speeds and distances of each mission phase as summarized in Table 1. Fig. 8 was constructed using composite data taken from two other reports[13, 14] and shows maneuver accelerations in per cent of limit load factor for each specific phase (cruise, climb and descent, high-altitude combat or intercept, and low-altitude combat). As a result of studies of pilot records and flight time-load histories of several airplanes plus discussions held with several pilots, it was found that maneuver cycles are different from gust cycles in that they do not oscillate about a given constant mean value. A maneuver will usually be started from some initial load factor level which seems to bear a direct relation to the maximum level attained in that particular cycle. It was discovered that the ratio of the initial and maximum levels generally fell close to an average value of one-third. For this reason, the maneuver spectrum used herein was established on the basis of a constant "R" of 0.33 (ratio of minimum to maximum load factor in any one cycle).

Calculations of total maneuver accelerations occurring per mission are presented in Table 5. In this table, the acceleration intervals represent assumed ranges for the maximum load factor levels experienced in maneuvers. For the lower value in each of these intervals, values of flight miles (to equal or exceed that acceleration) were obtained from Fig. 8 for each phase of the flight mission. Using these and the flight distances for each phase from Table 1, the number of times per mission phase that the lower value in the acceleration interval would be equaled or exceeded was obtained. By summarizing for all phases in each interval, the values for total times per mission were obtained, and from these, the net number of occurrences in each interval were found by subtracting successive values of total times in each interval. The net occurrence numbers are actually maneuver loading spectra for one complete mission, with the high and low portions of the fighter mission not yet combined.

These values were converted to 100-hr spectra in Table 6, and the resulting cumulative damage was calculated. For this purpose, the S-N curve in Fig. 7 labeled "For Maneuvers" was used to obtain values of N. This curve was plotted for an R of 0.33 (ratio of minimum to maximum stress in cycle) and was based on test data from other sources.[11, 12, 13]

From this table, the total cumulative damage resulting from the maneuver spectrum for the long-range interceptor is 0.0085 in 100 hr, or a loss of 0.85% of its life expectancy. The total damage for the all-purpose fighter in 100 hr is 0.0329, 3.29% of its life expectancy. It should be noted that these results are independent of the limit load factor to which the airplane is designed, as pointed out previously in assumption 5.

Landing-Taxi Spectrum

An analysis of the expected landing-taxi spectrum was conducted on the basis of data presented in other reports.[15, 16, 17, 18] This study indicated that fatigue damage caused by this loading was negligible in the structural areas critical for gust and maneuver loading. The landing-taxi spectrum would be highly important in a study of landing gear or supporting structure, and could also be significant for wing damage, where large tip masses are employed. For the purpose of this paper, however, fatigue effects resulting from this loading spectrum are not considered further.

Ground-Air-Ground Cycles

The fatigue phenomenon referred to as the ground-air-ground cycle is the one large cycle which occurs each mission as the airplane load level moves from its on-the-ground value to an in-flight value during the mission and back down again. This effect was studied by Boeing and found to contribute a large portion of the total fatigue damage experienced by transport-type airplanes.[19] There has been considerable discussion concerning this cycle, and it is recognized that further study and testing must be done in order to determine correct means for its handling and evaluation. In this paper, the ground-air-ground cycle has been assumed to consist of one oscillation per mission between the dead-weight load level of the aircraft at rest on the ground and the load level corresponding to the mean value of the critical in-flight acceleration cycle which occurs once each mission on a statistical basis.

The calculation of damage resulting from this effect is presented in Table 7 for 100 hr of flight. The critical in-flight loads occurring once each mission are in the maneuver spectrum. Their magnitudes were determined for each mission by plotting accelerations (in per cent of limit load factor) versus the values from Table 5 for the number of times these accelerations were equaled or exceeded per mission and then finding the point where the latter quantity was equal to unity. It was assumed that the minimum stress level in the ground-air-ground cycle was —3500 psi in the area critical for

---

[13] See Northrop Aircraft, Inc. Report No. SRR-33 (1952), "Determination of Expected F-89C Load-Life History and Recommended Spectrum for Repeated Load Tests of F-89C Wing."

[14] "Summary of Flight Load Data Recorded in Tactical and Training Operations During the Period of World War II," by Lawrence B. Reynolds. Presented at IAS Summer Meeting, Los Angeles, July, 1949.

[15] See NACA RM L53E05a (1953), "Some Measurements of Landing Contact Conditions of Transport Airplanes in Routine Operations," by N. S. Silsby and others.

[16] See NACA TN 863 (1942), "Results of Landing Tests of Various Airplanes," by J. A. Hootman and A. R. Jones.

[17] See WADC Project No. 3-S79-E, Midwest Research Institute, "Final Report Prediction of Dynamic Landing Loads," by M. Goland and others.

[18] See Lockheed Aircraft Corp. Report No. 6091 (1947), "Loads and Accelerations Measured During Landing and Taxi Tests," by L. C. Coombs and others.

[19] See Boeing Airplane Co. Document No. D-15305 (1954), "Prediction of the Fatigue Life of Aircraft Structures."

Table 7 – Cumulative Damage Resulting from Ground-Air-Ground Cycle in 100 Hr of Flight

	All-Purpose Fighter Mission			Long-Range Interceptor Mission
	High-Altitude Portion	Low-Altitude Portion	Combined Mission	
Max Maneuver L.F. Occurring Once per Mission, % lim L.F.	60.1	65.4	63.1	60.5
Stress Level at Max Maneuver L.F., psi	30,100	32,700	31,600	30,300
Max Stress Level in Gnd-Air-Gnd Cycle, psi	20,100	21,800	21,100	20,200
Mean Stress Level in Gnd-Air-Gnd Cycle, psi	8,300	9,100	8,800	8,400
N	2.0×10^4	1.1×10^4	1.5×10^4	2.0×10^4
No. of Cycles per 100 Hr = n	127	179	153	38
Damage n/N	0.0063	0.0163	0.0102	0.0019

fatigue. The maximum stress level was taken equal to the mean value of stress occurring in the critical maneuver cycle, or two-thirds of the maximum value of the stress at critical maneuver load (as determined above). In other words, if the critical maneuver cycle occurring once per mission produced oscillation between stresses of 10,000 psi and 30,000 psi ($R = 0.33$), the ground-air-ground cycle maximum value would be the mean of these stresses, or 20,000 psi, which is also two-thirds of the maneuver cycle maximum value.

It will be noted in Table 7 that the mean stress level in the complete cycle is quite close to the value of 9100 psi previously used in checking the 5.5g limit load factor gust spectrum. For this reason the S-N curve in Fig. 7 for a mean stress of 9100 psi was used in calculating cumulative damage for the ground-air-ground cycle.

The damage resulting from this effect in 100 hr of flight for the long-range interceptor is 0.0019, and for the combined all-purpose fighter it is 0.0102. This means that 0.19% and 1.02%, respectively, of the total life expectancies of these airplanes is used up by the ground-air-ground cycle, alone, every 100 flight hr. Since these loads result from maneuvers, the fatigue damage is also independent of the design limit load factor.

Results and Recommendations

A summary of the total damage incurred during 100 flight hr by each hypothetical type of mission and the overall life expectancies are presented in Table 8. The values for the two basic design missions (all-purpose fighter designed to 7.5g and long-range interceptor designed to 5.5g) are shown in this table in italic type.

The results are also depicted graphically in Fig. 9. It may be seen that the life expectancy of the long-range interceptor is roughly four times that of the combined all-purpose fighter when each is flying its design mission. It may also be seen that the largest portion of damage in each case is done by the maneuver loads. If dynamic response effects had been taken into account and if structural flexibility had been assumed, the amount of damage done by gusts would have been larger relative to that done by other loadings.

In Table 9, the individual damages resulting from each phase of the two basic missions are presented in terms of per cent of total damage. This may also be interpreted as representative of the per cent life lost by the two planes in various phases of their overall missions. It may be seen that, because of the predominance of maneuver damage, the largest percentage of life is lost in the combat and intercept phases. The largest relative amount of damage done by gusts occurs in the climb-and-descent phase for the interceptor and in the cruise phase for the all-purpose fighter. The latter circumstance is the result of the large damage done by gusts in the cruise phase of the low-altitude portion of the mission.

The relative damage done by various levels of gust loading is graphically illustrated in Fig. 10 for the combined all-purpose fighter mission. Other missions are not shown; however, they would reflect similar relative damage distributions. It may be seen that the most damage is done by gusts which produce maximum accelerations of between 1.7 and 2.8g, the peak damage occurring at around 2.2g. For a Mach number of 0.9 and an altitude of 10,000 ft (the speed and altitude at which most of the gust damage occurs), this load factor is equivalent to a gust velocity, U_{de}, of 18 fps. There is virtually no damage done by gusts at accelerations above 5.5g (gust velocities of 70 fps).

In Fig. 11, a picture of relative damage similar to that of Fig. 10 is presented for the maneuver spectrum of the combined all-purpose fighter. It may be seen that the largest portion of the damage done by maneuvers occurs in the range of accel-

Table 8 – Summary of Damage Incurred in 100 Hr and Life Expectancies for Each Basic Mission

Design Limit Load Factor	Basic Mission	Gust Damage		Maneuver Damage		Ground-Air-Ground Cycle		Total Damage in 100 Hr	Life Expectancy, hr
		$\Sigma\, n/N$	% Total Damage	$\Sigma\, n/N$	% Total Damage	$\Sigma\, n/N$	% Total Damage		
5.5	Fighter mission, high-altitude portion	0.0047	13.2	0.0245	69.0	0.0063	17.8	0.0355	2820
	Fighter mission, low-altitude portion	0.0422	42.1	0.0417	41.6	0.0163	16.3	0.1002	1000
	Fighter mission, combined	0.0237	35.5	0.0329	49.2	0.0102	15.3	0.0668	1500
	Long-range interceptor mission[a]	*0.0014*	*11.9*	*0.0085*	*72.0*	*0.0019*	*16.1*	*0.0118*	*8470*
7.5	Fighter mission, high-altitude portion	0.0007	2.2	0.0245	77.8	0.0063	20.0	0.0315	3170
	Fighter mission, low-altitude portion	0.0075	11.4	0.0417	63.7	0.0163	24.9	0.0655	1530
	Fighter mission, combined[a]	*0.0041*	*8.7*	*0.0329*	*69.7*	*0.0102*	*21.6*	*0.0472*	*2120*
	Long-range interceptor mission	0.0002	2.0	0.0085	80.1	0.0019	17.9	0.0106	9430

[a] Values for design missions shown in italics.

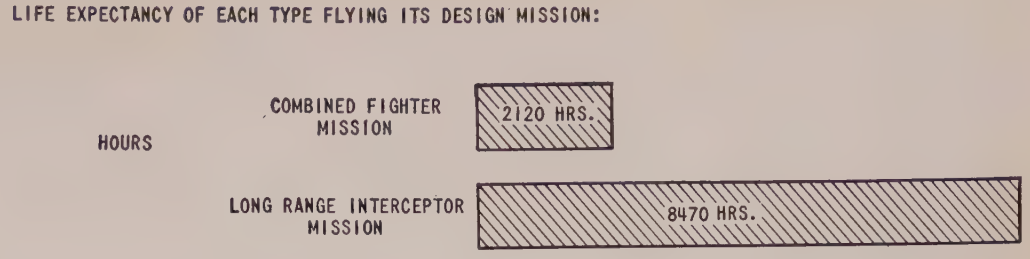

Fig. 9 – Fatigue life and damage comparisons

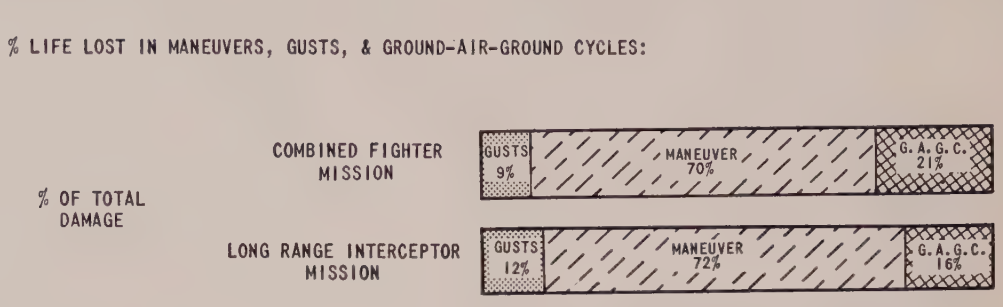

Table 9 – Percentage of Life Lost in Various Flight Phases (Each Fighter Type Flying Its Design Mission)

Flight Phase	All-Purpose Fighter				Long-Range Interceptor			
	Gust	Maneuver	Ground-Air-Ground	Total	Gust	Maneuver	Ground-Air-Ground	Total
Climb and descent	2.0	6.7	4.3	13.0	11.9	11.7	3.2	26.8
Cruise out and back	4.4	2.3	Negl	6.7	Negl	12.0	Negl	12.0
Combat or intercept	2.3	60.7	17.3	80.3	Negl	48.3	12.9	61.2
Total	8.7	69.7	21.6	100	11.9	72.0	16.1	100

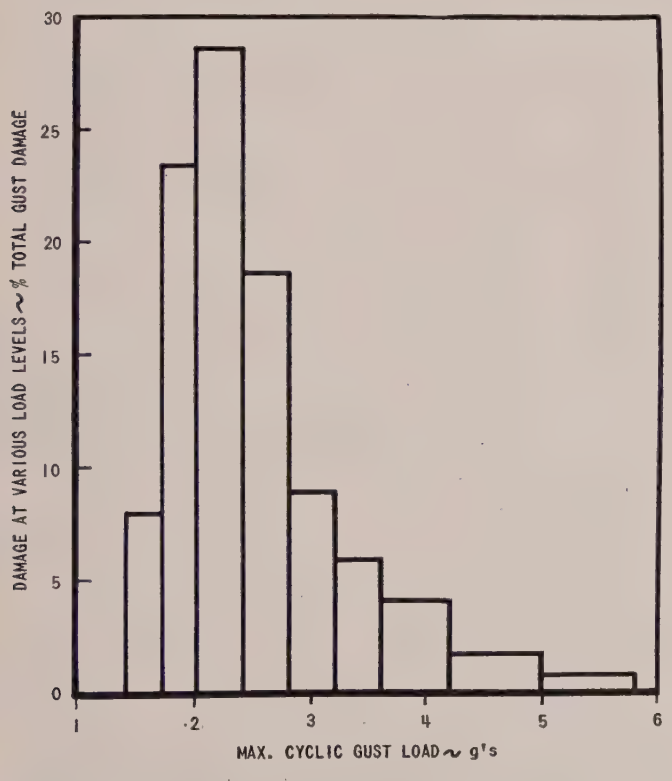

Fig. 10 – Relative damage in gust spectrum (combined fighter mission, design limit load factor – 7.5g)

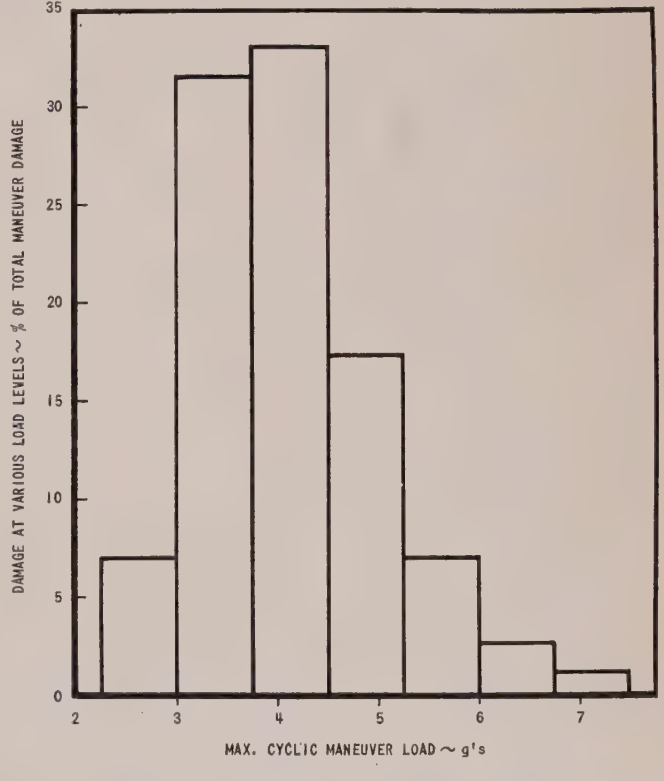

Fig. 11 – Relative damage in maneuver spectrum (combined fighter mission, design limit load factor – 7.5g)

erations between 3.0 and 4.5g (between 40% and 60% of the design limit load factor). The fatigue damage done by higher maneuver accelerations approaching limit load factor is relatively small.

Curves showing the proportion of damage done by gusts as a function of the design limit load factor are presented in Fig. 12. These curves show that the fraction of the total damage inflicted by gusts on planes which are designed for higher load factors (above approximately 7.0g) is quite low. In the lower design load factors, however, gust effects become increasingly significant; and below about 5.5g, gusts may be seen to cause a relatively large amount of the total fatigue damage. At any load factor, the low-altitude and combined-altitude missions show greater relative gust damage than the higher-altitude missions. It may be noted that a plane which is designed to 5.0g, and which flies between 50 and 100% of its lifetime at low altitude, would experience gust damage amounting to around 50 to 55% of the total damage from all causes.

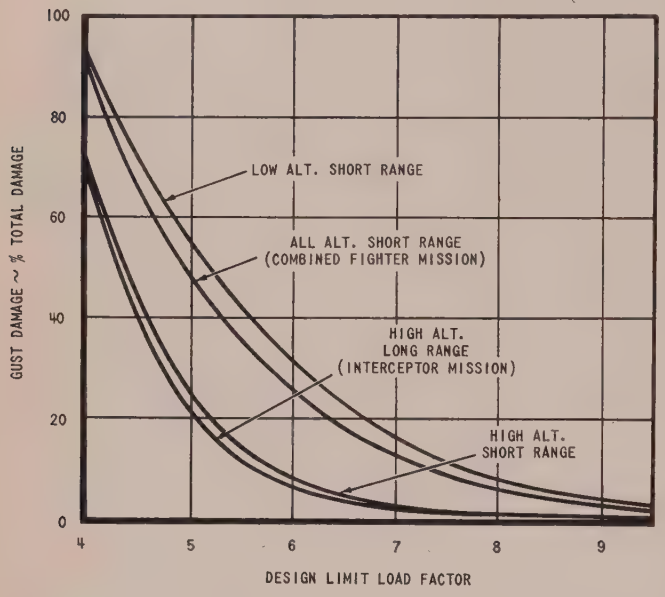

Fig. 12 – Gust damage in per cent total damage versus design limit load factor

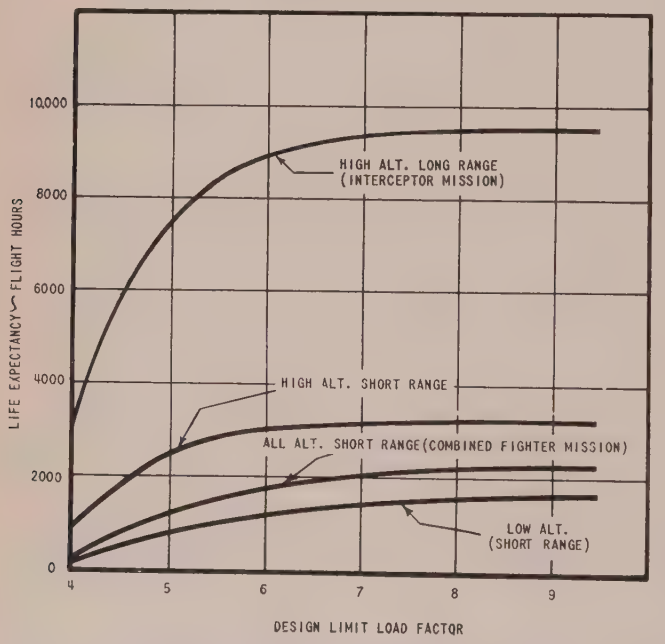

Fig. 13 – Life expectancy in various missions versus design limit load factor

The complete picture of life expectancy for all types of assumed missions as a function of design limit load factor is presented in Fig. 13. As indicated by the leveling off of all curves, the load factor, as a parameter, becomes unimportant above values around 7.5g. On the other hand, it becomes of major importance below about 6.0g. The large difference between the high-altitude long-range curve and the other curves in this figure in the region of high load factors is primarily a result of the difference in range for these missions. This effect is discussed further in connection with Fig. 14.

The curves of Fig. 13 indicate that the example interceptor designed to 5.5g and assumed to fly 100% high-altitude long-range missions at the Mach numbers indicated in Fig. 1 would have a life expectancy of around 8500 hr. If this plane were used entirely in high-altitude but shorter-range missions, its life expectancy would drop to about 2800 hr, a 67% decrease. If it were flown entirely in all-altitude short-range missions, its life expectancy would become approximately 1500 hr, an 82% decrease. This is of major significance in design considerations concerning intended service use of a specific fighter-type aircraft.

The effect of mission range on life expectancy is presented in Fig. 14. These curves were constructed for high-altitude flying only and do not apply to missions involving appreciable flight time at lower altitudes. The effect of range on aircraft life may be seen to be considerable. A plane intended for long-range high-altitude missions but which is used in short-range high-altitude flying may experience a reduction in life expectancy of more than 1000 hr for each 100 miles of decreased range. This is due primarily to the fact that the largest amount of fatigue damage is incurred during combat. A shorter-range airplane encounters combat periods more frequently, resulting in this damage being inflicted more often in a given number of total hours. The life of such a plane would therefore be expended more rapidly in short-range flying than in long-range flying. The effect of design limit load factor on life as a function of range variation may be seen to be relatively unimportant.

The variation of life expectancy with combat altitude is shown in Fig. 15. Although these curves were constructed for short-range missions only, calculations indicate that they are approximately valid for the longer ranges also. The altitude parameter refers specifically to the average combat altitudes at which a given fighter operates. The curves show that a plane which is designed to a limit load factor of 5.5g, and which is intended to fly combat at an average altitude of 40,000 ft (oper-

ating between 30,000 and 50,000 ft), could be expected to have a life expectancy of around 2800 hr. If, however, this plane were actually operated at an average combat altitude of 10,000 ft, its life expectancy would drop to approximately 1000 hr, a decrease of 64%.

The effect of various percentages of increase in applied loading intensity on life expectancy is shown in Fig. 16 for the combined all-purpose fighter. This figure was constructed because of the fact that much of the data used in making the analysis of this paper had a 2/1 or 3/1 spread, even for many miles of accumulated recorded data. It is possible, therefore, that the relative magnitudes used herein for gust or maneuver loads could be considerably exceeded in actual service operation. For example, any type of fighter airplane which is service operated in weather conditions which are 20% more severe than the estimated level used in design may experience a reduction in life expectancy of as much as 50%.

The curves of Fig. 16 specifically reveal that a 10% increase in the gust spectrum alone would result in an 18% reduction in life expectancy, which would amount to 360 hr less life for a 2000-hr airplane. A 10% increase in maneuver loading alone would cause a 38% drop in life expectancy, while a 10% increase in all load levels would decrease the life by about 48%. It should also be noted that the upper curve can be used to find the effect of an increase in the design stress level established for the critical structure. Many companies are finding it desirable to set up a design stress level which may be considerably lower than the actual static allowable of the material or structural configuration.

It is important to note that the results discussed above are based on specific hypothetical cases. It

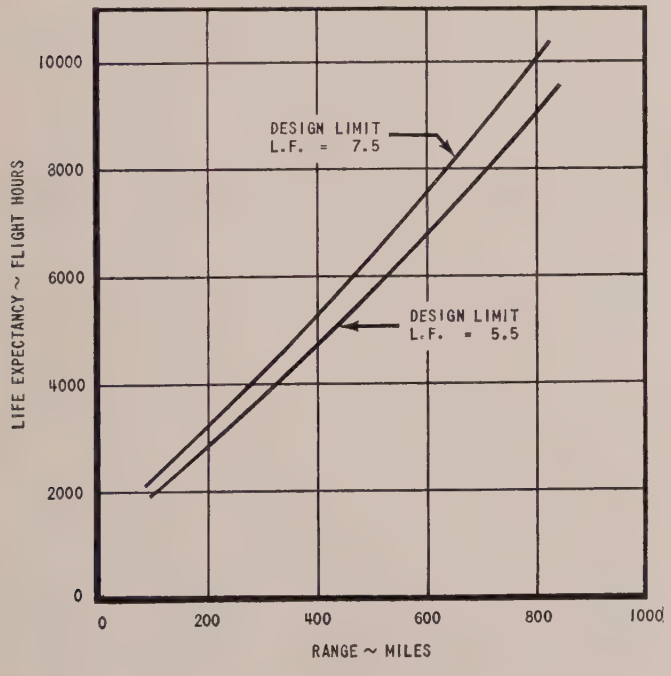

Fig. 14 – Life expectancy range (high-altitude flying only)

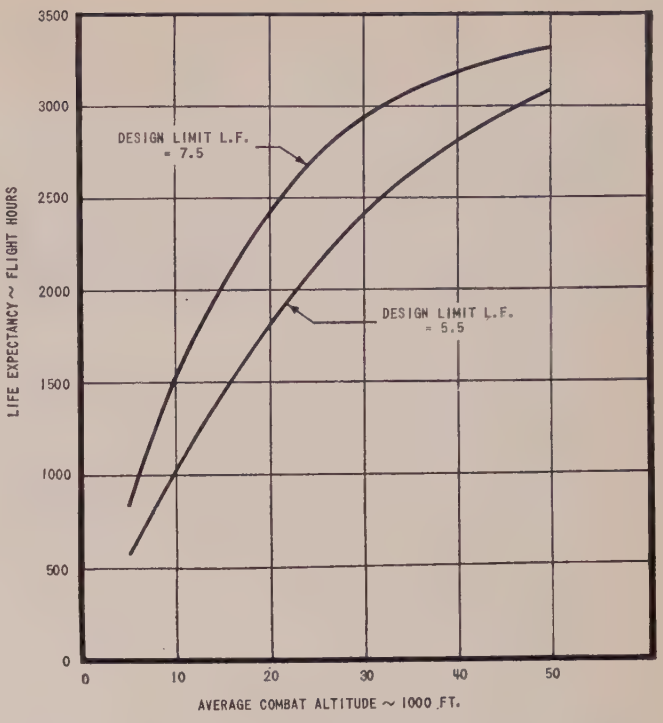

Fig. 15 – Life expectancy versus combat altitude (short-range missions)

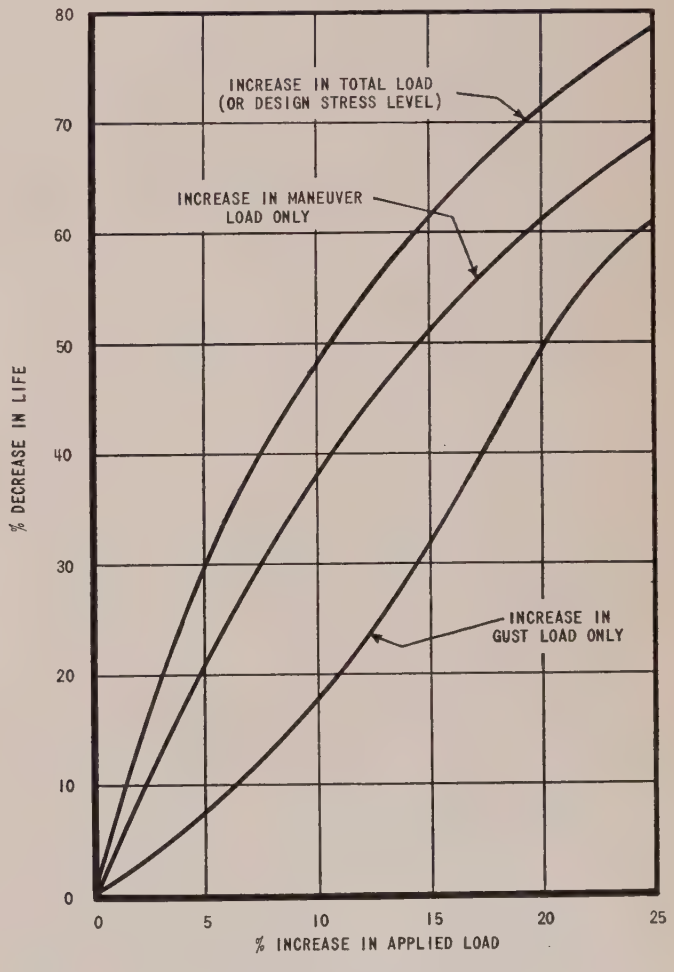

Fig. 16 – Effect of increase in applied load

is felt that the trends they indicate and the relative values used in comparisons are closely representative of typical cases currently being considered in design. However, in establishing loading spectrum, design stress levels, and other specific criteria for new airplanes, careful attention must be given to the actual operational details involved, which collectively could lead to somewhat different numerical results. In such cases, the procedures followed herein should serve as a useful guide in setting up the approach to be used.

Probably the most important single recommendation to be offered as a result of this study is that careful consideration be given in early design stages to the various possible types of operational flying which the airplane may encounter in its service life. As shown by the various curves presented herein, the life can vary considerably, depending on the type of gust or maneuver spectrum encountered and the average range and altitude of the service missions. Since all are directly related to the design limit load factor selected and since adherence to any one specific type of operation cannot be counted on during the entire life of the airplane, the significant effects of these various factors must be carefully evaluated at the earliest possible point in design.

A second recommendation which can be offered is that a detail study be made on the handling of the ground-air-ground cycle. It was found that the theoretical damage caused by this effect was extremely sensitive to the specific assumptions used in setting up the effective levels employed in the cycle. Both analytical and empirical investigations are essential at this point to gain clearer understanding of its action. However, it is clear that the ground-air-ground cycle can contribute a major portion of the fatigue damage encountered in operational flying of many types of aircraft.

In setting up criteria for new design, it will probably become necessary to establish a design stress level in critical areas which is less than the static allowable. If this is done, some feeling for the effect on life expectancy of given percentages of increase or decrease in this level can be gained from the upper curve in Fig. 16. In making a detailed analysis, however, consideration should be given to effects of various factors which were eliminated herein through use of simplifying assumptions. Note especially assumptions 1, 3, and 6.

The results obtained in this study and the methods employed in performing the analysis give a clear indication of the need for increased research and additional data. Several techniques of fatigue analysis other than the cumulative damage method have been proposed recently, and considerable testing and analysis of empirical data must be carried out to evaluate applicability. Also, in connection with all new designs, environmental conditions and potential life-load histories should be studied, and steps should be taken by the individual manufacturer to forestall fatigue trouble by establishing good design practices. The Aircraft Industries Association has set up a fatigue panel (W-76) to investigate these problems and to secure industry cooperation in design and analysis. This panel should serve as a convenient central clearing house for companies needing help on these problems.

Finally, careful handling of structural flexibility effects must be employed in evaluating fatigue characteristics. The dynamic response of wing structures results not only in magnification of specific load levels but also in the superimposing of additional numbers of cycles following each individual load application. This effect can be of major significance in that it will amplify the fatigue damage from both aspects. Specific handling of flexibility effects was not used in the analysis of this paper; however, it is recommended that careful attention be devoted to this factor in the early stages of design and analysis for an actual configuration. It is believed that further development of new techniques, such as the power spectral density method, will contribute in large part to the understanding and control of dynamic effects as related to static and fatigue characteristics.

ORAL DISCUSSION

Reported by G. H. Arvin
North American Aviation, Inc.

L. Hitchcock, Boeing Airplane Co.: Our experience with fatigue analysis has shown that the ground-air-ground cycle accounts for 65 to 70% of the fatigue damage of large airplanes with wing fuel. Because of the high tension stresses from ground loads in such airplanes, the upper surface of the wing has sometimes been known to show a lower life than the lower surface.

Referring to Fig. 13, I would like to know why the fatigue life levelled out between 7.5 and 9g.

Mr. Mangurian: In the case of fighters, which were the subject of this paper, most damage is done by maneuvers. Considering the magnitude of design load factors of fighters, gusts are of relatively little significance.

Mr. Brooks: It was assumed in this study that the maneuver spectrum, expressed in terms of % of limit load, would be the same for any fighter regardless of its design limit load factor. Therefore, up in this higher range (7.5-9.0g), where gust damage is small, the fatigue life curve levels out with increasing design load factor.

Mr. Hitchcock: Why were the two hypothetical airplanes of the paper considered to be subjected to different maximum gust velocities during their lives?

Mr. Mangurian: The difference in gust velocity is due merely to the different design altitudes assumed for the two airplanes.

J. E. Fischler, Douglas Aircraft Co., Inc.: What is the effect on predicted life of the fact that many fighter wings are more critical in the upper surface than the lower?

Mr. Mangurian: In some cases, this consideration could result in an increased life for the airplane, because, although the compression stresses in the upper surface approach the allowable stress for the compression structure, they are low compared to the material allowable stresses. In conjunction with this, the tensile stresses in the lower surface are sometimes inefficiently low since excess material is necessary to provide a sufficient compression strength for inverted flight conditions.

New Pontiac V-8 Engine

C. B. Leach and E. L. Windeler,
Pontiac Motor Division, GMC

This paper was presented at the SAE Golden Anniversary Annual Meeting, Detroit, Jan. 12, 1955.

THE new Pontiac engine is the culmination of nine years of design and development work. In 1946, it became evident that future styling requirements, coupled with the prospects for improved fuels, necessitated the eventual introduction of a more compact, more rigid engine, and an engineering program was initiated with those goals in mind. Other general design objectives established were:

1. Outstanding performance with assured adaptability to future fuels.
2. Proved durability, equaling or excelling its predecessor in all respects.
3. Ready adaptability to displacement increases without major tooling changes and with no compromise to engineering function.
4. Overall simplicity of design for complete ease of manufacturing and convenient servicing.

It is the purpose of this paper to show how these objectives have been realized in the overhead valve V-8 engine introduced in the 1955 Pontiac.

In conformance with the desire for simplicity of design, much attention was given to the effect of fundamental engine arrangement upon the location of all engine components. The general arrangement of the engine as evolved is shown in Fig. 1. The entire exhaust system, including the manifolds and connecting pipe, has been kept low to assure easy access to the spark plugs from the top of the engine, and also to minimize heating of the carburetor air. The generator has been placed on top of the engine, between the cylinder heads, where it is effectively separated from exhaust heat and readily accessible for servicing. This position has been attained with the simplicity of a single belt to drive the generator, water pump, and fan. Also evident in this photograph is the optional full-flow oil filter, which is in a vertical position for ease of servicing without oil spilling.

Fig. 2 illustrates the effect of cylinder bank arrangement upon the fuel pump and distributor drives. The combination fuel and vacuum pump is mounted in the low forward position on the left-hand side, resulting in minimum vapor lock tendency and optimum fuel line connection. The positioning of the right-hand bank of cylinders in the forward position made it possible to place the pump in this corner where it is close to the centerline of the engine, and where it can be driven directly by the eccentric on the camshaft. With the cylinder arrangement chosen, it was also possible to locate the distributor gear on the right-hand side (on the left in the illustration) of the camshaft without cylinder block complication. This location results

PONTIAC'S new V-8 engine, the authors say, fulfills well design objectives of durability, simplicity of manufacture and servicing, and ready adaptability to future fuels and displacement increases.

Important new features include:

1. Simplified casting of cylinder block and cylinder heads.
2. Valve train components designed for long valve gear life, quiet operation, and low cost.
3. A new gusher type of cooling system.
4. An engine ventilation system that scavenges harmful, corrosive diluents from all engine compartments.
5. A more-than-ample 12-v electrical system.
6. A wedge-shaped combustion chamber.

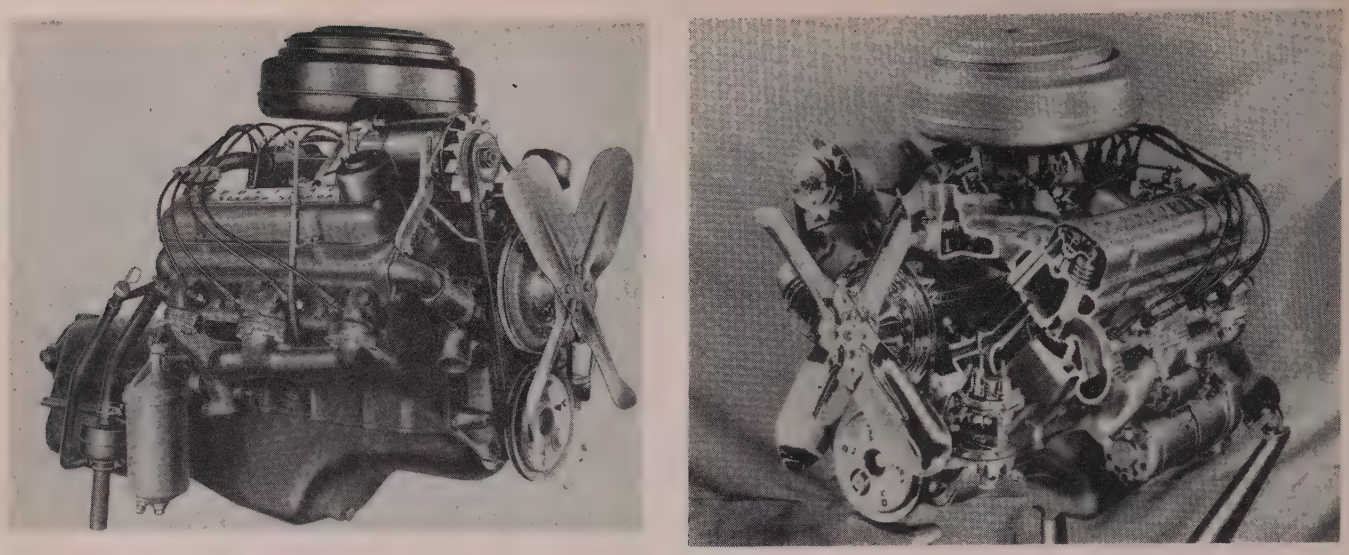

Fig. 1 – General arrangement of new Pontiac V-8 engine

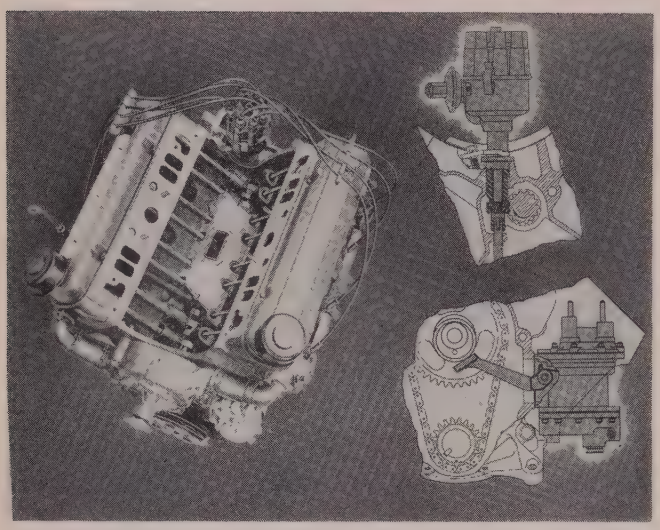

Fig. 2 – Effect of cylinder-bank arrangement on fuel pump and distributor drives

in an upward thrust on the driven gear, and makes a separate thrust surface in the block unnecessary.

Description of Engine

A transverse cross-section of the engine is shown in Fig. 3. The combination of 3.75 in. diameter bore and 3.25 in. stroke was helpful in attaining minimum external dimensions for the 287 cu in. displacement. In addition, the large bore made possible ample valve sizes, and the short stroke resulted in low friction characteristics. The aluminum alloy, steel strut pistons of slipper-type design are tin plated for proper break-in. Three piston rings are employed; the top compression ring is heavily chrome plated (0.004-0.007 in. thick) for durability, the second ring is lubrite coated, while the oil ring is of four-piece, chrome-plated, steel rail design for effective oil control. The four ½-in. bolts per cylinder tie directly into the vertical walls of the block, and are separated from the cylinder walls to assure complete freedom from distortion due to tightening.

The curved sealing surface for the engine top cover made it possible to lower the exhaust heat passage of the intake manifold into this area between the cylinder banks and thereby effect a reduction of engine height. The distance from the centerline of the crankshaft to the top surface of the intake manifold is only 13.9 in. This, combined with a carburetor height of only 5 in., results in a very satisfactory value for the important engine height dimension.

The longitudinal section of the engine (Fig. 4) shows other details of engine construction. The inherent structural rigidity of the cylinder block made possible the placement of the oil pan flange at the centerline of crankshaft. The slanting surface of the cast timing chain cover furnishes a flat sealing contact for the oil pan gasket. This construction also permits the use of a thrust-type seal at the front of the crankshaft. At the rear, a slinger and rope-type seal are employed to prevent oil leakage. The crankshaft has main bearing journal diameters of 2.5 in. and crankpin diameters of 2.25 in., resulting in an overlap of 0.76 in. Its natural frequency of torsional vibration is 350 cps. The five main bearings are supported by rigid bearing caps, doweled in position, and attached to the ribbed bulkheads of the cylinder block.

The mounting surface for the clutch housing is shown in Fig. 5. All of the six attaching screws, including the lower two, enter rigid portions of the cylinder block. The large span between the screws in both the vertical and horizontal directions makes possible a firm support for the clutch housing and transmission. Notice that the two upper screws have been raised approximately 2 in. above the flywheel diameter to increase the important vertical span. This method of attachment provides ample

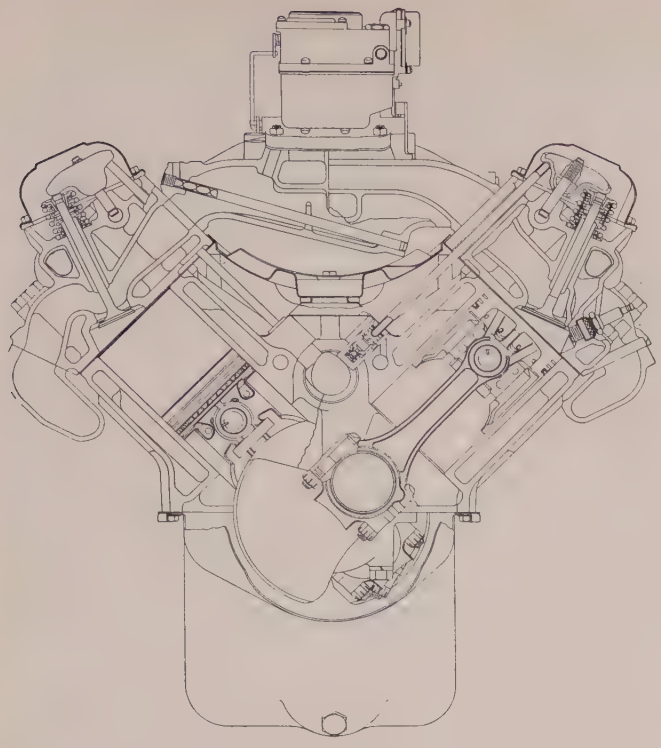

Fig. 3 – Transverse cross-section

rigidity at the transmission, and no resonant vibration is encountered between drive line components throughout the engine operating speed range.

Casting Design

An exceptionally important part of the engineering history of the Pontiac V-8 is the simplification of the casting of the cylinder block and cylinder heads. It is well known that these units are among the most complex items cast by mass production methods. However, because of the many diverse requirements which must be considered during the formative stages of engine design, the tendency is to design for conventional casting procedures.

The 18 cores required to cast an early experimental cylinder block in the conventional manner are shown in Fig. 6. In contrast (Fig. 7), only eight cores are required to cast the block as released for production. This reduction in cores was made possible by careful integration of a new casting concept into the design of the engine.

As shown in the transverse cross-section through the cylinder block mold (Fig. 8), there are no flanges which project into the center area at the top of the cylinder block. This makes it possible to use green sand to form the entire top surface. Also significant is the fact that the barrel cores, which form the cylinders, are an integral part of the crankcase cores.

The longitudinal section through the mold (Fig. 9) shows more details of the casting method. The dry sand core at the rear of the block is the only

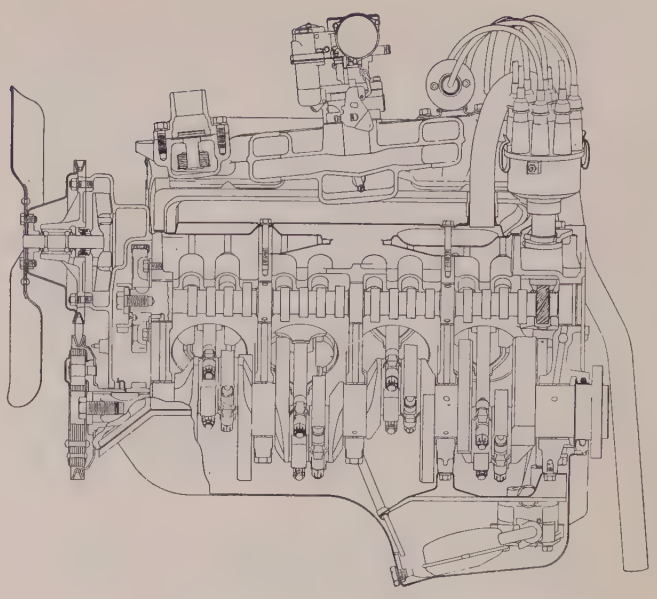

Fig. 4 – Longitudinal cross-section

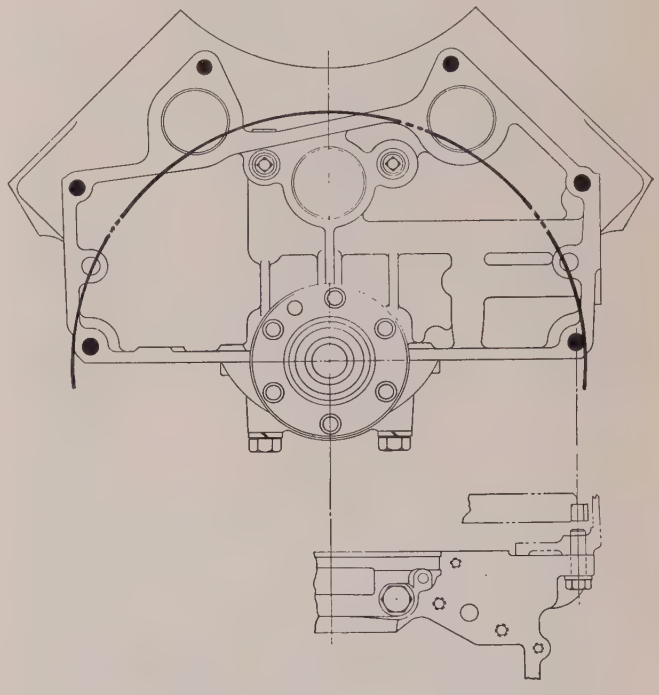

Fig. 5 – Mounting surface for clutch housing

The Authors

C. B. LEACH (M '39) is assistant chassis engineer with the Pontiac Motor Division, General Motors Corp. He received an A.B. degree in mathematics and chemistry from Park College, and attended the GM Institute from 1935 to 1937. Mr. Leach has been with Pontiac since 1937.

E. L. WINDELER (M '41) is supervisor of the Dynamometer Laboratory, Pontiac Motor Division, General Motors Corp. He received a B.S. degree in mechanical engineering from Virginia Polytechnic Institute in 1936. That same year Mr. Windeler joined Pontiac as engineering test driver. Thereafter he occupied various positions with Pontiac until, in 1945, he was appointed supervisor of the Power Development Section.

core required to form an external surface. Separate core assemblies requiring pasting and nailing have been virtually eliminated, and the cores are fixture-set directly into the mold. This casting simplification was found to result in reduced probability of core shift during pouring, and in turn has made possible the lowest weight castings consistent with quantity production.

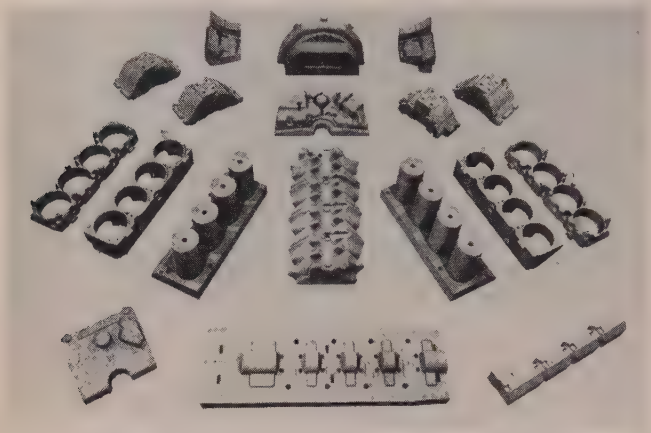

Fig. 6 – Eighteen cores required to cast experimental cylinder block in conventional manner

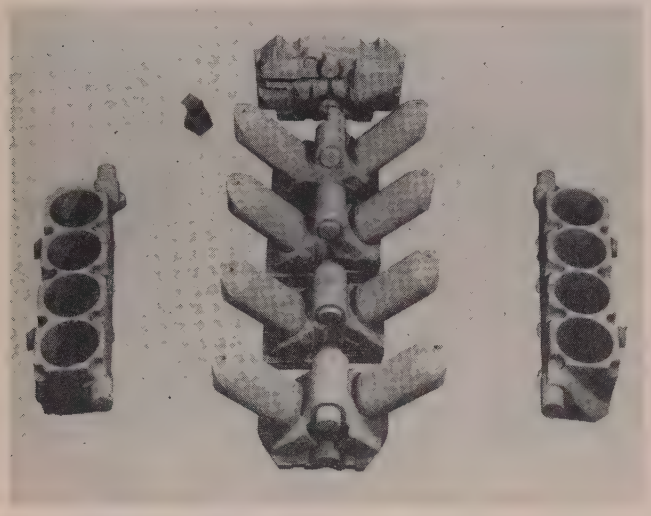

Fig. 7 – Only eight cores required to cast production cylinder block

Another achievement in casting simplification was made on the cylinder heads. Fig. 10 shows the eight cores required to cast an early experimental cylinder head in the conventional manner. Fig. 11 shows the four cores required to cast the production cylinder head. A salient feature is the absence of separate core assemblies requiring the pasting together of water jacket cores. Such pasting may result in the unpredictable occurrence of fins in the water jackets, where they can disturb the flow of coolant and upset temperature balance. In this casting method, all cores are set directly into the mold. Such fins as are necessary are so placed as not to affect the flow of coolant in the critical area between the valves and at the valve guides. Core sections were in all cases kept large enough to assure clean, uniform water jackets free from burned-in iron. Furthermore, the castings tested experimentally have been matched in uniformity by their production counterparts.

The net result of the casting simplification program was to reduce the total number of cores required to cast one cylinder block and two cylinder heads from 34 to 16. The total weight of the dry sand cores was reduced from 320 lb to 158 lb. The ease of casting resulting from this program has resulted not only in manufacturing economies, but also in more uniform castings and a more functional design.

Valve Train

Early in the engine development program it was resolved that every effort would be made to develop valve train components which would result in long valve gear life, quiet operation, and low manufacturing costs. The type of valve train used on the new engine was designed by Pontiac in 1948, and has been successfully proved in the many engines tested since that time.

The ball pivot rocker arm is shown in Fig. 12. The ball is located on a stud which is pressed into the cylinder head. The cyanide-hardened, stamped steel rocker arm pivots on this ball and is able to

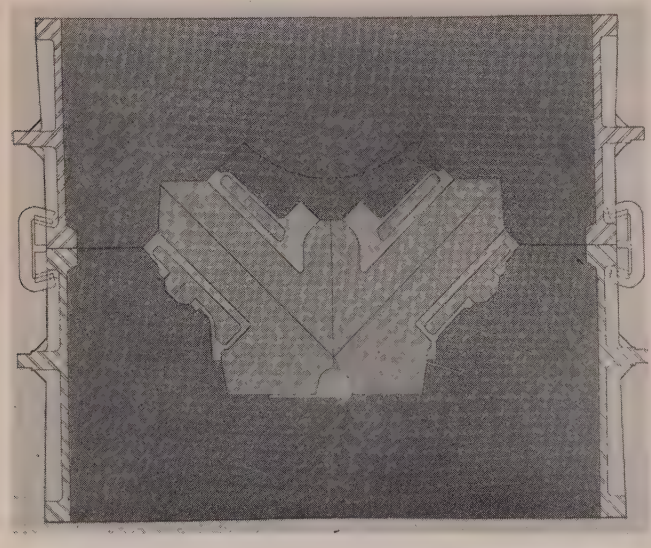

Fig. 8 – Transverse cross-section through cylinder-block mold

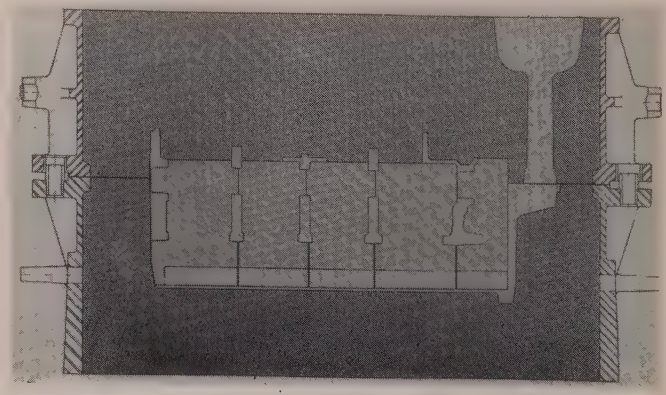

Fig. 9 – Longitudinal cross-section through cylinder-block mold

square itself on the end of the valve stem. This eliminates all misalignment of the rocker arm with the push-rod and valve stem, and minimizes the tendency toward valve cocking. As illustrated, the valve, stud, rocker arm, and push-rod all lie in a single plane for geometrically correct valve gear motion, and sidewise bending moments on the rocker arm are eliminated.

The complete valve train is shown in Fig. 13. The contact of the spherical inner surface of the rocker arm is essentially at the lower surface of the ball, and the entire depth of the rocker arm flanges is available to carry the valve gear load. Positive, pressure lubrication is provided for the ball pivot by oil entering the ball from a drilled hole in the stud which connects with the oil gallery in the head. The hollow, cyanide hardened push-rod is pressure lubricated at each end by oil from the valve lifter.

Hydraulic valve lifters were chosen for the new engine to provide the advantages they afford. It has been possible to use optimum valve timing for high engine output, while maintaining good low-speed idling without engine noise under all operating conditions. The use of dual valve springs and rigid valve gear components has resulted in a valve lifter "pump up" speed of 5000 rpm.

The use of tapered valve guides (Fig. 14) has been continued on the new engine because tests proved their advantages were even more important on the overhead valve engine. The small end of the guide inside diameter is at the top or cool end of the valve. The valves are selectively fitted to the guides to a diametral clearance of 0.0003-0.0006 in. at this point. This close clearance in combination with the shield is helpful in preventing oil flow down the intake valve guide under high vacuum conditions and has contributed to part-throttle-driving oil economy. The larger clearance at the lower end of the valve then allows for expansion of the hot valve stem. In addition, it permits a degree of stem freedom to assure proper valve seating. This self-centering freedom, combined with the reduced cocking tendency of the ball pivot rocker arms, has resulted in reduced valve stem and valve guide wear and has made possible desirable valve seating characteristics.

The intake valve head diameter is 1.781 in. and has a 30-deg seat angle. The exhaust valve diameter is 1.500 in. with a 45-deg seat angle. These valve sizes and the 0.367 in. valve lift have made an important contribution to the engine performance.

Cooling System

The desire for long valve life required low valve seat temperatures, and this consideration had an important bearing on the choice of cooling system for the new engine. Pontiac was the first to introduce the "gusher" type of cooling system to the L-head engine. This system was subsequently adopted by many L-head engine manufacturers.

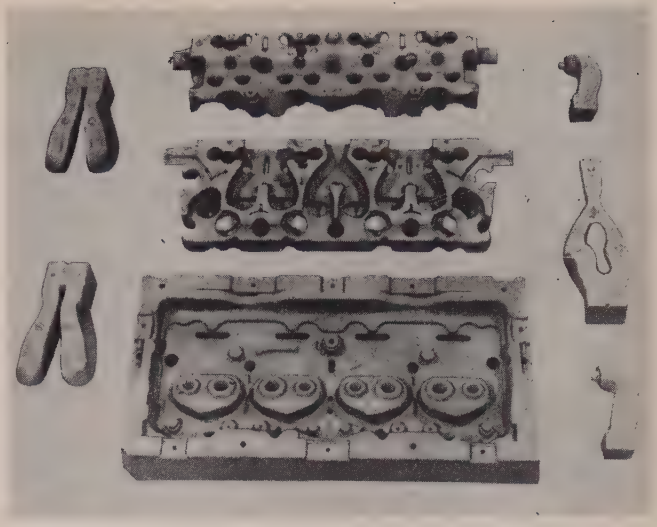

Fig. 10 – Eight cores required to cast experimental cylinder head in conventional manner

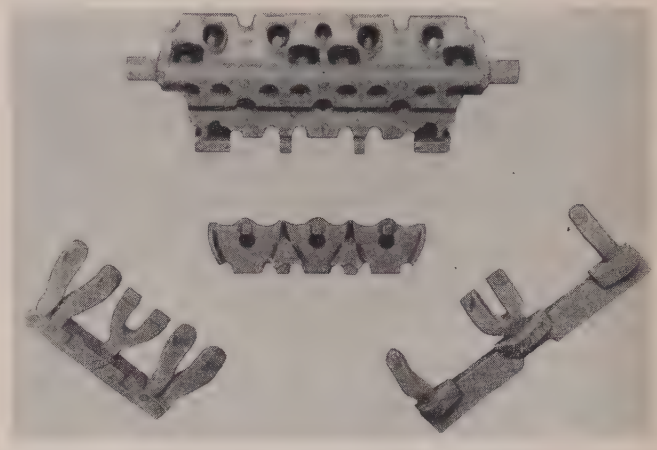

Fig. 11 – Only four cores required to cast production cylinder head

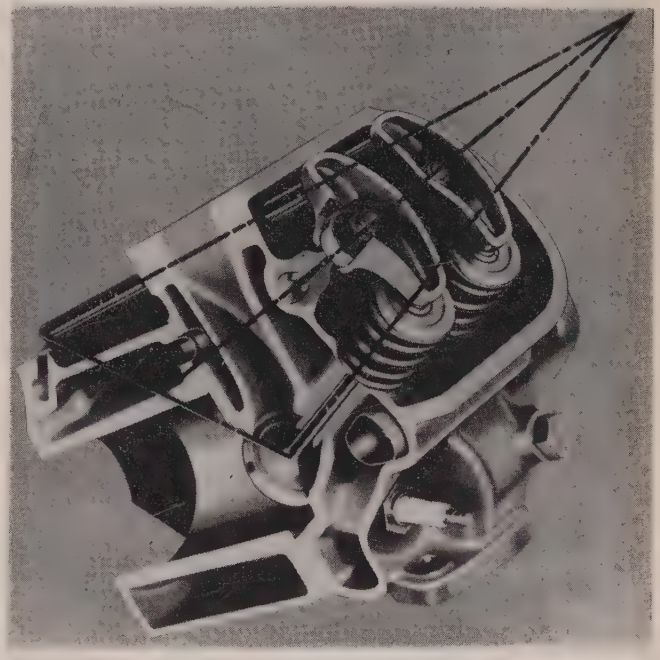

Fig. 12 – Ball pivot rocker arm

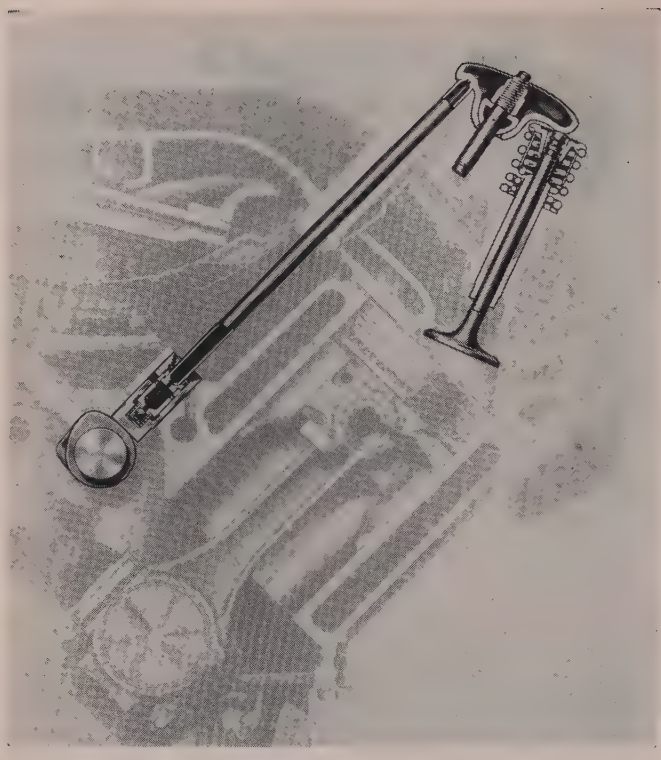

Fig. 13 – Valve train

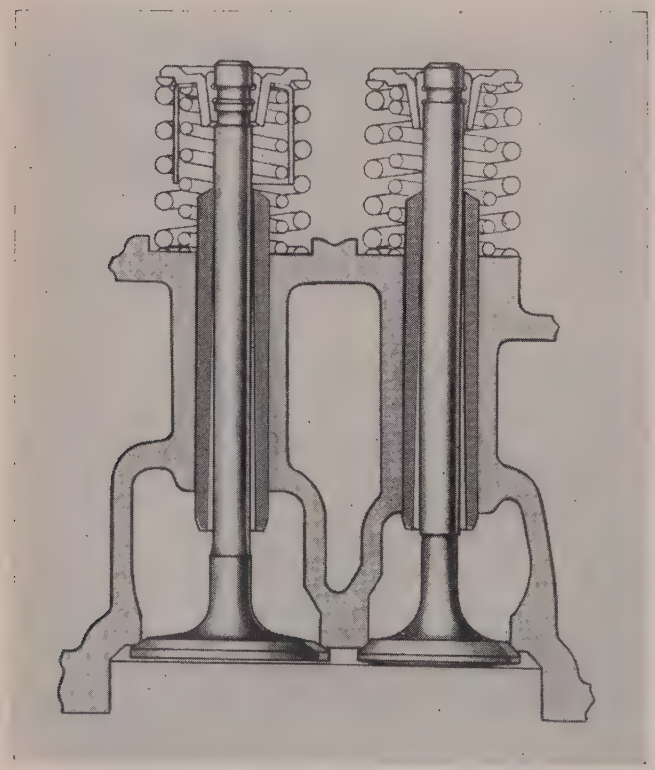

Fig. 14 – Tapered valve guides

The very satisfactory results attained therefrom have prompted the introduction of this feature on the new overhead valve V-8.

The valve cooling is shown in Fig. 15. Cold water is ejected at high velocity from holes in the distributing tube in each cylinder head. This water is directed toward the exhaust valves, where it scours the surface of the valve ports around the seats and absorbs heat therefrom. The possibility of hot, stagnant areas developing around the valve seats is thus completely avoided. In this system, the complete flow from the water pump is used to cool positively the hottest and most critical regions in the engine.

Details of the cooling system are shown in Fig. 16. The single, high-capacity water pump delivers coolant through two outlets which are connected to the front of each cylinder head. From here the water enters the brass distributing tubes which extend the full length of the heads. After the water has been ejected from the holes in the tubes, and has cooled the valve areas, a portion flows downward into the cylinder block through holes surrounding each cylinder. Therefore, no cold water is thrown directly onto any one cylinder at the expense of the others, and virtually complete temperature balance is obtained around the cylinder bores. Through recirculation holes at the front of the block, this water then enters the induction side of the pump. The water which did not enter the block from the heads returns to the radiator by way of a connecting passage at the front of the engine. This passage houses the single thermostat and is cast integral with the intake manifold.

Water flow characteristics are shown graphically in Fig. 17. The flow rate through the radiator core of the 1955 engine has been increased approximately 30% over that of the 1954 in-line engine. The total pump flow, or the amount of water directed toward the valve areas in the cylinder heads, is approximately 90% more than the flow through the radiator core. This difference between the two upper flow curves on the diagram represents the actual amount of recirculation through the cylinder block and induction side of the pump. Cooling of the cylinder block by recirculation of preheated water from the cylinder heads has resulted in water temperatures which are approximately 5 F higher in the block than in the heads. Especially important is the fact that during warmup, when the thermostat is closed, the large amount of recirculation quickly raises the temperature of the cold cylinder walls. Condensation is thus decreased, and lubrication is made more effective during this critical period of operation.

Engine Ventilation

The engine ventilation system (Fig. 18) was not merely designed as a crankcase ventilation system, but has been engineered to scavenge harmful, corrosive diluents from all compartments of the engine. Two air inlet caps, which also serve as oil filler caps, are provided. These caps are located at the front of each rocker arm cover, where they are directly in line with the fan blast. Fresh, filtered air is forced directly into the rocker arm covers,

and its only exit from there is through cast openings connecting to the crankcase at each end of the cylinder heads. Therefore, a portion of the admitted air travels the entire length of the cylinder heads and effectively removes vapors which may have escaped past the valve stems. If positive ventilation is not provided here, the inner surface of the rocker arm covers becomes an ideal place for condensation of such vapors.

After ventilating these compartments, the air passes into the front and rear bulkhead compartments of the crankcase from both cylinder banks. Rotation of the crankshaft assists in thorough ventilation of this area, and also creates a pressure difference at the front which assists in the movement of air through the timing chain cover from a hole at the top of the block.

From the lower part of the crankcase, the air flows upward through the two center compartments, where it exhausts past a cast baffle in the block, into an opening in the center baffle. This opening connects to a large area, low-velocity chamber in the engine top cover. Here, oil is given an opportunity to settle out before the air enters the outlet tube. The high position of the bend in the outlet tube further encourages oil separation, and, in addition, discourages "chimneying" or draw back of dusty air during the cool-down period.

With this system, it has been possible to secure positive, pressurized airflow under all engine operating conditions, with minimum oil loss. Especially important is the fact that the double air inlets permit ample air to enter even during idling and slow-speed operation. These conditions are often encountered during engine warmup, and proper ventilation at this time has been assured.

Lubrication System

The lubrication system of the new engine is shown in Fig. 19. An oil pan baffle completely covers the sump area and minimizes aeration by oil thrown from the crankshaft. Directly under this baffle is the floating oil inlet screen which picks up oil at a controlled distance beneath the top of the oil level. Oil is delivered from the pump to the optional full-flow oil filter, and thence to the left-hand oil gallery. Main crankshaft bearings receive oil through holes drilled into this gallery. Connecting-rod bearings are fed from main bearing journals through drilled holes in the crankshaft. The camshaft journals are lubricated by vertical holes intersecting the main bearing supply holes. The right hand gallery (to the left in the diagram) receives oil from another hole intersecting the two holes at No. 1 main bearing. The two parallel oil galleries supply oil to holes in the lifter bosses, which in turn furnish oil to the valve lifters. Indexed holes in the camshaft journals supply oil at reduced pressure to each cylinder head oil gallery, from which positive lubrication is supplied to the valve train surfaces.

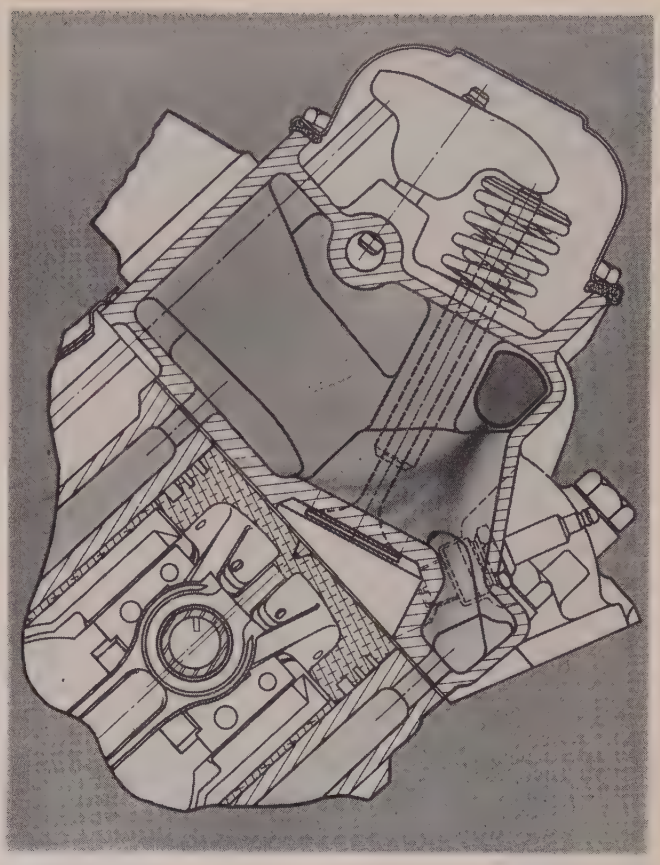

Fig. 15 – Positive valve cooling

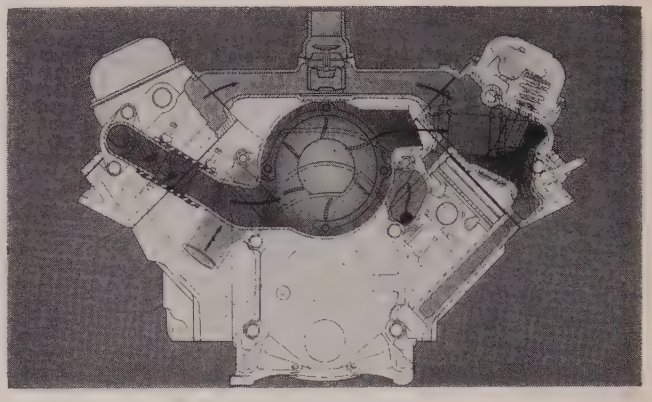

Fig. 16 – Cooling system

The distributor lubrication and oil pump drive are shown in Fig. 20. Lubrication of the distributor lower bushing and drive gear is accomplished by gravity feed. The oil returning from the right-hand cylinder head drains into a hole in the block which aligns with a hole in the distributor pilot. The overflow oil then flows past a flat on this pilot downward to lubricate the distributor drive gear.

The oil pump is driven by an intermediate shaft, which transmits the rotation of the distributor gear through a tongue and groove at each end. Thus, any slight misalignment in the drive line can be tolerated without binding. The swaged projections on the shaft prevent accidental withdrawal through the guide hole when the distributor is removed.

The oil pump utilizes coarse pitch helical gears for high capacity and quiet operation.

Oil pressure regulation (Fig. 21) has been developed to such an extent that very little variation in pressure occurs throughout the speed range. This has been accomplished with the trouble-free operation of a ball relief valve.

Cylinder wall lubrication is accomplished as shown in Fig. 22. A stream of oil is directed onto the upper side of the cylinder wall from the connecting rod of the corresponding cylinder in the opposite bank. This jet of oil is ejected through a groove across the rod at the split line of the connecting rod. This groove indexes with the oil supply hole in the crankpin. Effective lubrication is thereby provided for the cylinder walls immediately after a cold start. The oil also sprays the interior of the piston and lubricates the piston pin.

The lubrication of the timing chain and fuel pump eccentric is shown in Fig. 23. Oil from the camshaft journal is fed intermittently to a groove in the camshaft thrust plate. This groove registers with a groove in the block which directs a stream of oil downward onto the crankshaft sprocket. Positive lubrication of the hardened, stamped-steel fuel pump eccentric is effected by a hole in the camshaft thrust plate, which squirts a stream of oil forward through an indexed hole in the camshaft sprocket.

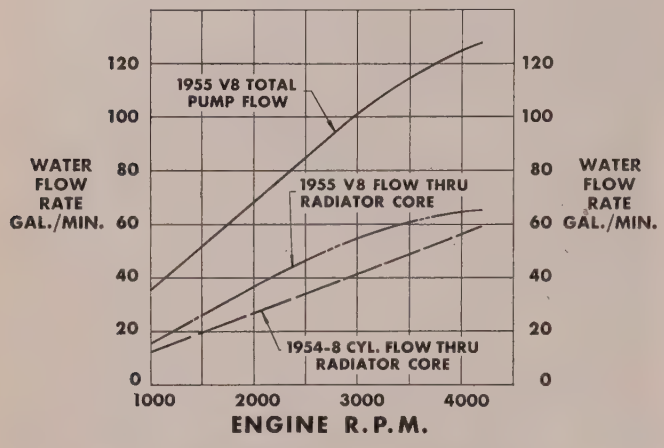

Fig. 17 – Water flow characteristics

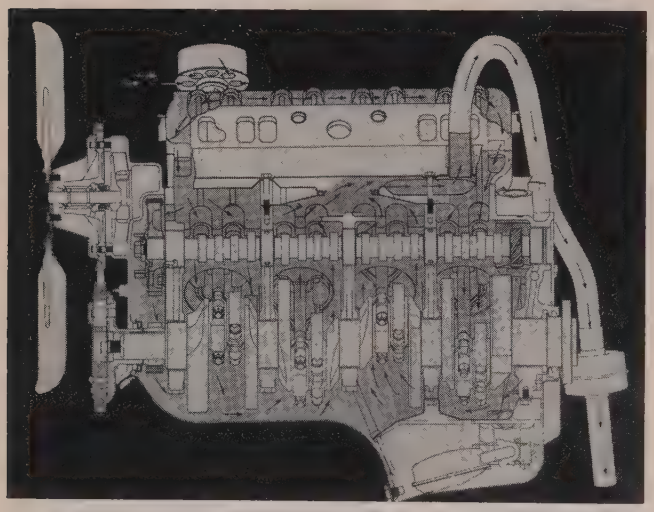

Fig. 18 – Engine ventilation system

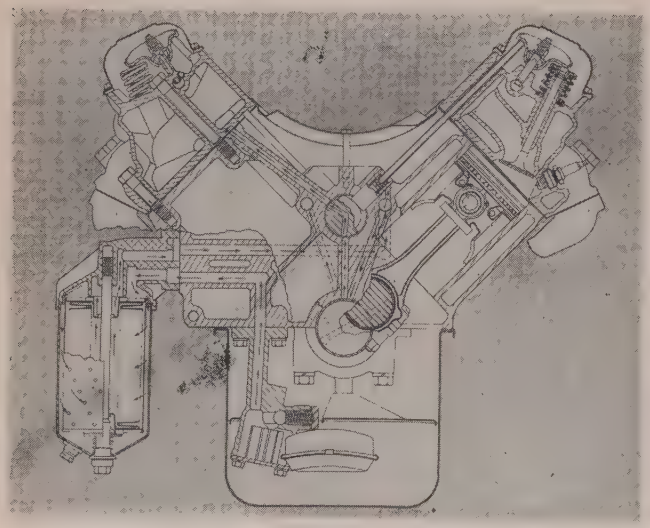

Fig. 19 – Lubrication system

Twelve-Volt Electrical System

The 12-v electrical system has been adopted for the new engine because of its recognized advantages. How well this system has met the demands of the high-output engine is shown in Fig. 24. This illustration compares the secondary voltage required to fire the spark plug with the available voltage, under the conditions shown. Note that the available voltage is always ample to assure proper

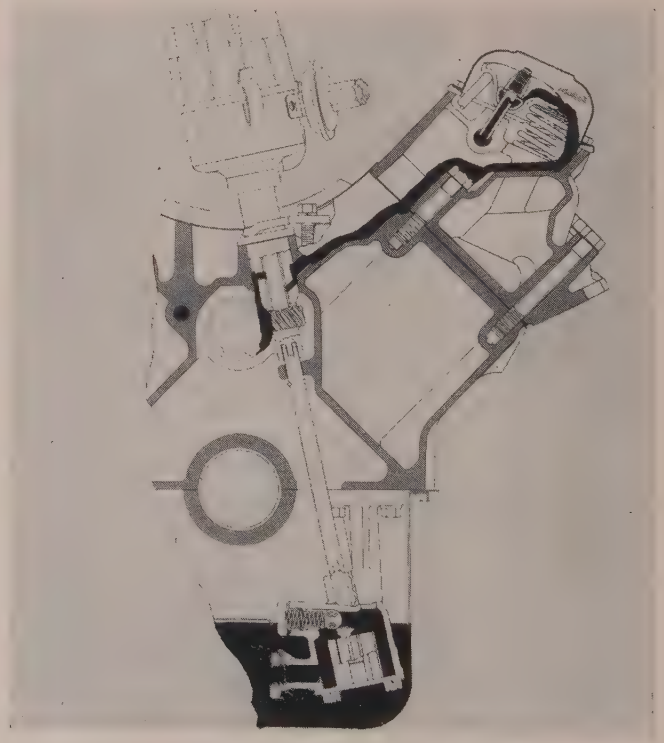

Fig. 20 – Distributor lubrication and oil pump drive

ignition of the charge.

The left-side view of the engine (Fig. 25) shows other details of the electrical system. The coil is mounted on top of the engine in a position close to the distributor. The secondary wires are unshielded, which contributes to the high voltage available at the spark plug, and are well separated to assure immunity from cross-firing. Also evident is the effect of the low position of the exhaust manifold in reducing the proximity of exhaust heat to spark plugs and secondary wiring. The separation of exhaust heat from these parts has negated any possibility of reduced life expectancy from this cause.

The solenoid-actuated starting motor is also visible here. The use of the 12-v system has made possible, at –10 F, a 16% increase in cranking speeds over a 6-v motor of the same size. Statistics concerning the generator further emphasize the advantages of the 12-v system. Power output has been increased from 270 w, developed by the 1954 6-v generator, to 300 w obtained from the new 12-v generator. This 11% increase is accomplished from a generator of the same diameter, but 1 in. shorter than the 1954 6-v model.

Intake Manifold and Carburetor Choke Stove

The intake manifold (Fig. 26) has been designed and developed to obtain optimum distribution of the fuel to all cylinders. Runners are approximately equal in length and are of ample size to match the breathing capacity of the entire induction and exhaust system. During warmup, exhaust gases are forced through the center exhaust passage under the risers to assure vaporization of the fuel. The flow of exhaust gas is regulated by the action of a thermostatically controlled valve located in the right-hand exhaust manifold.

The carburetor choke stove (Fig. 27) is shown in the cross-section through the center exhaust passage of the intake manifold. The tube pressed into this passage transfers heat from the exhaust gas to the air being supplied to the choke by engine vacuum. The use of a helical baffle inside this tube increases the heat transfer to this air, thereby providing sufficient heat to the choke to assure positive operation. In addition, other refinements in the choke itself have increased the precision with which it is made inoperative after warmup. Also evident in this diagram is the compact design of the duplex carburetor. Shown too is the de-icing passage under the idling jets. Exhaust heat is supplied here to prevent ice formation under low temperature, moist air conditions.

Combustion Chamber

The wedge-shaped combustion chamber, Fig. 28, is completely machined for accurate control of compression ratio. The thin-quench area covers 35% of the piston-head area; turbulence is thus promoted, and effective flame travel is shortened. This type of chamber was chosen because it presented the best combination of output and fuel economy of any of the many types of chambers evaluated for this engine. Tests also indicate that this wedge shape offers maximum adaptability to

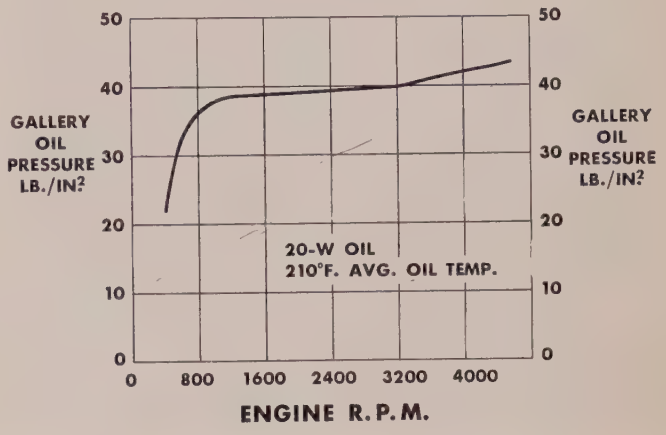

Fig. 21 – Oil pressure regulation

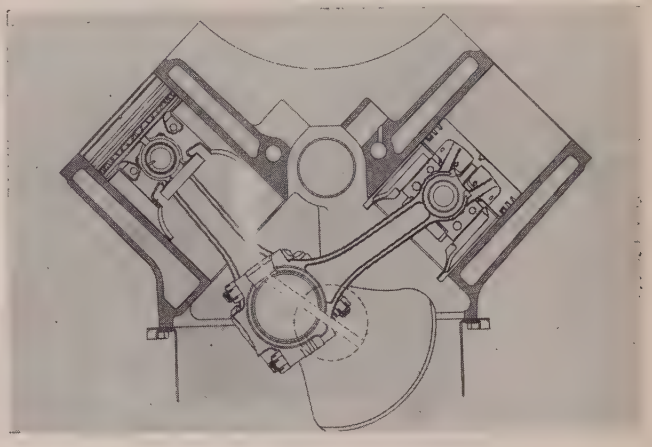

Fig. 22 – Cylinder wall lubrication

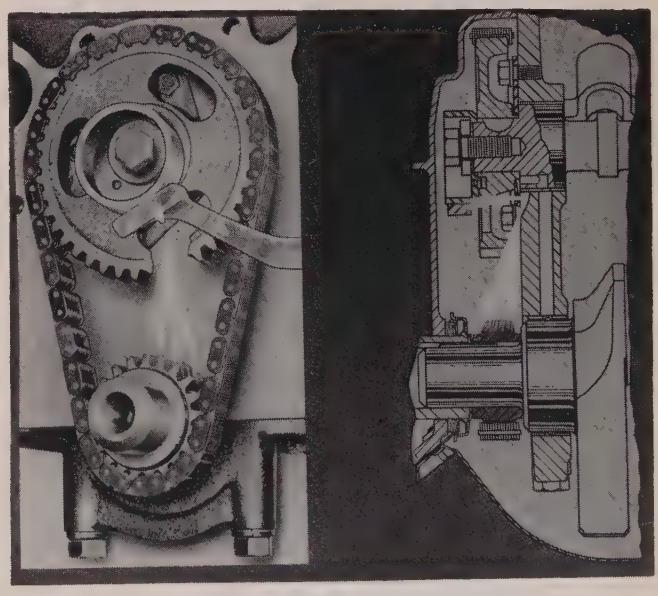

Fig. 23 – Lubrication of timing chain and fuel pump eccentric

future compression ratio increases without combustion harshness. This diagram also shows the large sections of core around the spark plug which assure positive cooling of this unit.

Fig. 29 shows the octane requirements of the 8.0:1 compression ratio engine when used with the Hydra-matic transmission. The operating conditions before evaluation of requirements are such as to encourage deposit buildup. A city-suburban schedule is driven at a speed not exceeding 50 mph at any time. An oil is used which is average in its deposit-forming tendency. The curve shows that in the test range of 3000-7500 miles from clean, 80% of the requirement observations were made without knock when using 93-Research-octane-number fuel. When 96-octane fuel was used, 100% of the requirement observations were made without knock. Since premium fuels in critical areas now have Research octane rating of from 93 to 96, the new engine is well matched to the fuel available. It is felt that a realistic compromise has been reached in the choice of compression ratio which will result in minimum annoyance from abnormal combustion of all types, under varied driving and climatic conditions, while still taking advantage of the potentialities of today's fuels.

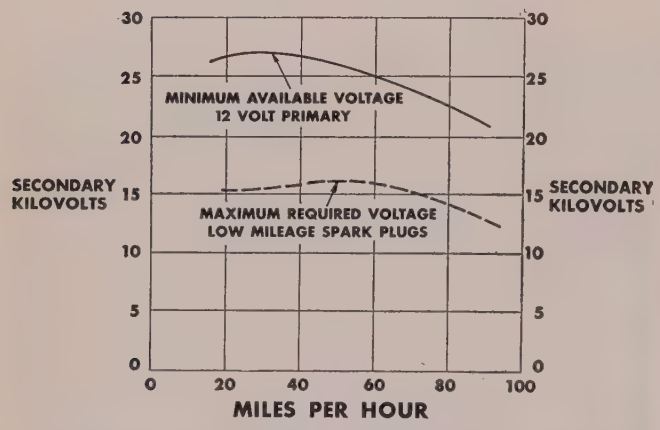

Fig. 24 – Comparison of required and available secondary voltages

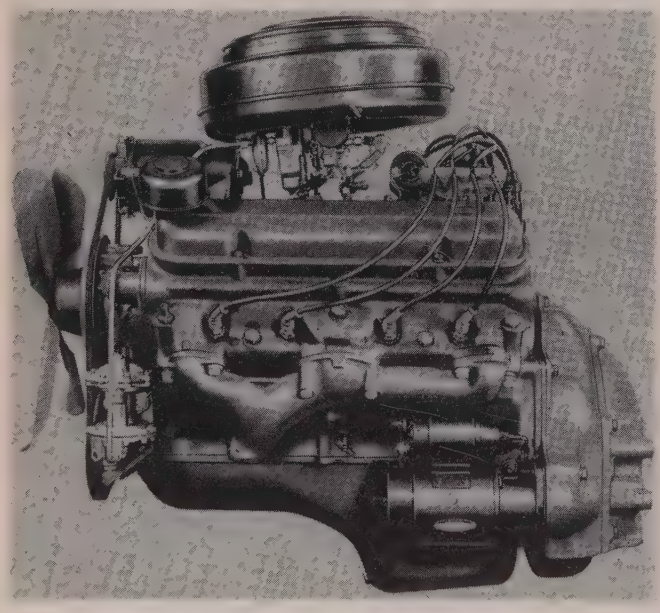

Fig. 25 – Left-side view of engine

Performance

Full-throttle performance of the Pontiac V-8 is shown in Fig. 30. The data presented are from test No. 20 of the General Motors Automotive Engine Test Code. This test is run with spark adjusted for best torque, and the results are corrected to SAE standard conditions of 29.92 in. of Hg atmospheric pressure and 60 F air temperature. As shown, a maximum full-throttle output of 180 bhp is attained at 4600 rpm. The maximum torque of 264 lb-ft at 2400 rpm is developed by a bmep of 139 psi at this speed. The maximum specific output is 0.627 bhp per cu in. of displacement. Minimum brake specific fuel consumption is 0.45 lb per bhp-hr.

Conclusion

The development and testing program made important contributions to the durability characteristics of the new engine. The magnitude of this program is reflected by statistics concerning the number of miles accumulated by experimental engines. Over 3,300,000 miles were run on road test and dynamometer installations prior to the start of production. An additional 300,000 test miles were accumulated on production-built engines be-

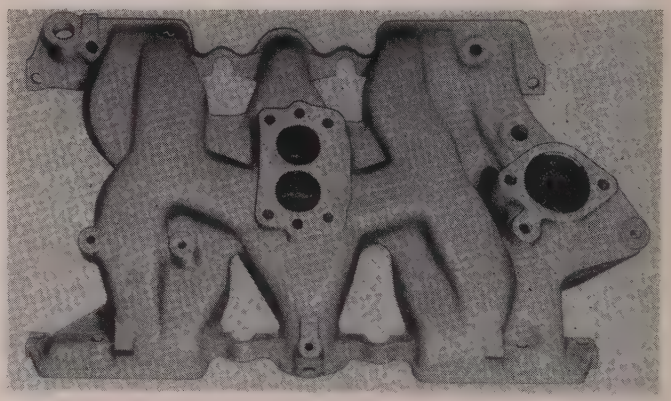

Fig. 26 – Intake manifold

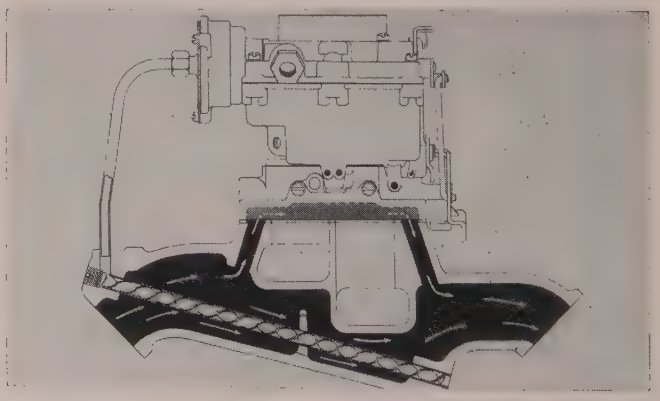

Fig. 27 – Carburetor choke stove

fore new model car assembly was initiated. The final result of this program of design, development and testing is the new Pontiac V-8 engine, which we believe represents, in a large measure, the attainment of our original design objectives.

Appendix

Bore, in.	3.75
Stroke, in.	3.25
Stroke-Bore Ratio	0.866
Displacement, cu in.	287.2
Cylinder Number (Front to Rear):	
Left Bank	1-3-5-7
Right Bank	2-4-6-8
Firing Order	1-8-4-3-6-5-7-2
Compression Ratio	8.0/1
Maximum Bhp Corrected to 60 F (at 4600 Rpm)	180
Maximum Torque, lb-ft (at 2400 Rpm) (Corrected to 60 F), lb-ft	264

Crankshaft:

Weight, lb	5.80
Number of Main Bearings	5
Main Bearing Journal Diameters and Lengths of Bearings	
No. 1, 2, 3 and 4	2.4985 x 0.938
No. 5	2.4985 x 1.560
Bearing Taking Thrust	No. 4
Projected Crankshaft Bearing Area, sq in.	13.22

Connecting Rod:

Length (Center to Center), in.	6.625
Crankpin Bearing Diameter, in.	2.2493
Crankpin Bearing Length, in.	0.881

Pistons, Rings and Pins:

Piston Material	Aluminum alloy (tin plated)
Number of Compression Rings	2
Width of Compression Rings, in.	0.078
Width of Oil Control Ring, in.	0.186
Piston-Pin Diameter and Length, in.	0.980 x 3.02
Type of Piston Pin	Floating
Mean Piston Speed (at 4000 Rpm), fpm	2165

Camshaft:

Material	Alloy iron
Type of Drive	Chain (⅜ in. pitch x 1 in. wide)

Valve Train:

Valve Head Diameters	
Intake, in.	1.781
Exhaust, in.	1.500
Valve Seat Angles, deg.	
Intake	30
Exhaust	45
Valve Stem Diameter, in.	0.341
Rocker Arm Ratio (Mean)	150/1
Valve Lift, in.	0.367
Valve Spring Load, lb.	
Valve Closed—Outer	58
Inner	26
Valve Open—Outer	107
Inner	61
Valve Timing	
Intake Opens, deg btc	22
Intake Closes, deg abc	67
Exhaust opens, deg bbc	63
Exhaust Closes, deg atc	27
Mean Gas Velocity at Intake Valve (at 4000 Rpm), fpm	14,900

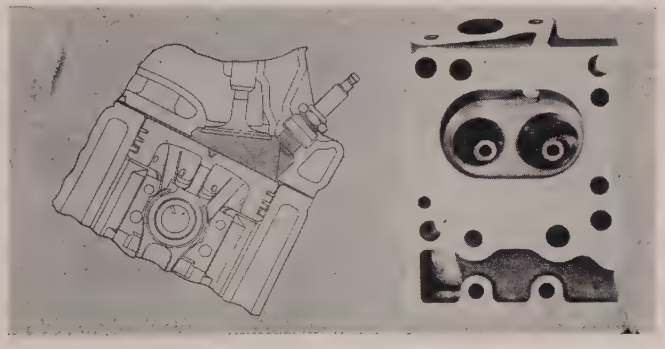

Fig. 28 – Completely machined wedge-shape combustion chamber

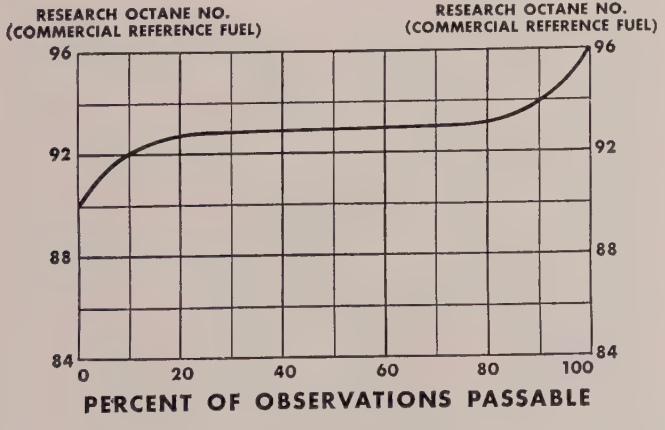

Fig. 29 – Octane requirements

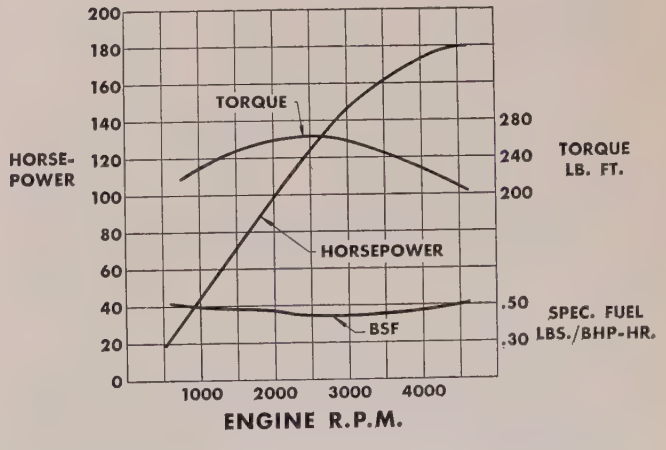

Fig. 30 – Full-throttle engine performance

Temperature

OPERATING temperatures of high-speed rolling-contact bearings are at present limited mainly by lubricants and to a lesser extent by bearing materials.[1, 2] Present-day liquid lubricants are temperature limited by evaporation, thermal decomposition, and oxidation characteristics.[3]

High oil flows to the bearings of a turbojet engine are required to cool the bearings to a temperature level where the oil will not evaporate or break down. Even higher temperature levels are contemplated in future turbojet engines[1] so that attempts to keep bearing temperatures at their present levels would impose a very difficult burden on the available cooling capacity. To reduce the oil-system heat load, bearings must be allowed to operate at higher temperatures. This can be done only if lubricants with better high-temperature stability can be developed. In this regard the possibilities of solid and gaseous, as well as the most promising liquid lubricants, must be thoroughly investigated. In addition, the use of reducing or inert atmospheres might extend the temperature limits of liquid lubricants.

The work reported herein is based on previous investigations[4, 5] and consists of two parts: (a) an investigation of the effectiveness of molybdenum disulfide as a lubricant for 75-mm-bore cylindrical-roller bearings at high speeds and low temperatures, and (b) an investigation of the temperature limitation of various petroleum and synthetic liquids and two solids (graphite and molybdenum disulfide) as lubricants for 20-mm-bore ball bearings at low speeds and high temperatures. The high-speed investigation consisted of a comparison of dry operation, operation with molybdenum disulfide coatings, molybdenum disulfide-air mist, and operation with oil lubrication at *DN* values to 0.975×10^6 under a 368-lb radial load. In the high-temperature investigation, tool-steel ball bearings with either silver-plated beryllium copper or cast Inconel cages were run at increasing temperatures to 1000 F or until failure occurred. Tests were run at 2500 rpm and 110-lb thrust load. Liquid lubricants were introduced in droplet form and solid lubricants in an air stream.

This investigation was conducted at the NACA Lewis Laboratory, Cleveland, Ohio.

Test Equipment

High-Speed Study – The high-speed bearing rig (Fig. 1) is described fully elsewhere.[6] The bearing under investigation was mounted on one end of the test shaft, which was supported in cantilever fashion, for observation of bearing component parts and lubricant flow during operation. The speed range of the test shaft was 800 to 50,000 rpm.

The method of temperature measurement and support-bearing lubrication is described elsewhere.[6] A double felt seal was installed on the shaft between the center support bearing and the test bearing for all dry runs, MoS_2 syrup-bonded film runs and MoS_2-air mist runs. A suction fan was installed between the support bearings to cause a slight flow of air from the test section through the shaft seal. These precautions were taken to prevent oil and oil mist from entering the test-bearing section.

Molybdenum disulfide syrup-bonded coatings[7, 8] were applied to bearings 12, 13, 14, and 15 (Table 1). A new technique was used with bearings 12 and 13. All the surfaces of these two bearings were first liquid honed with number 80 grit before the coating of MoS_2 syrup was applied. This sequence of treatments provided a somewhat more tenacious film of MoS_2 on both the steel and brass surfaces of the test bearings.

Two MoS_2-air mist systems were employed (Fig. 2). The single-opposed-jet system is illustrated in Figs. 2A and 2B, and the modified-single-jet system is shown in Fig. 2C. The operation of bearings 15 (cageless) and 16 (one-piece inner-race-riding cage type) were particularly sensitive to the amount of MoS_2 supplied by the airstream of the

---

[1] See NACA RM 51D20 (1951), "NACA Subcommittee on Lubrication and Wear: Review of Current and Anticipated Lubricant Problems in Turbojet Engines."

[2] See NACA TN 3110 (April, 1954), "SAE Panel on High-Speed Rolling-Contact Bearings: Trends of Rolling-Contact Bearings as Applied to Aircraft Gas Turbine Engines."

[3] See NACA TN 2940 (1953), "Effect of High Bulk Temperatures on Boundary Lubrication of Steel Surfaces by Synthetic Fluids," by S. F. Murray, Robert L. Johnson, and Edmond E. Bisson.

[4] See NACA RM E51G31 (October, 1951), "Preliminary Investigation of Molybdenum Disulfide-Air Mist Lubrication for Roller Bearings Operating to *DN* Values of 1×10^6 and Ball Bearings Operating to Temperatures of 1000F," by E. F. Macks, Z. N. Nemeth, and W. J. Anderson.

[5] See NACA TN 3337 (January, 1955), "Investigation of Temperature Limitation of Various Lubricants for High-Temperature 20-Mm-Bore Ball Bearings," by Z. N. Nemeth and W. J. Anderson.

[6] See NACA TN 2128 (July, 1950), "Investigation of 75-Mm-Bore Cylindrical-Roller Bearings at High Speeds. I – Initial Studies," by E. F. Macks and Z. N. Nemeth.

[7] See NACA TN 1578 (1948), "Friction of Solid Films on Steels at High Sliding Velocities," by Robert L. Johnson, Douglas Godfrey, and Edmond E. Bisson.

[8] See *Metal Progress*, Vol. 50, August, 1946, p. 314: "Molybdenite as Die Lubricant," by T. E. Norman.

Limitations of Petroleum, Synthetic, and Other Lubricants in Rolling-Contact Bearings

Zolton N. Nemeth and William J. Anderson,
NACA Lewis Flight Propulsion Laboratory

This paper was presented at the SAE National Fuels & Lubricants Meeting, Tulsa, Nov. 5, 1954.

single-opposed MoS_2-air mist jet system. This system proved faulty because it did not deliver a constant amount of MoS_2 per unit time when the supply air pressure was maintained constant. The faulty operation was due presumably to the intermittent clogging and breaking away of agglomerations of MoS_2 particles in the feed lines. Accordingly, a modified-single-jet system was designed (Fig. 2C) to disperse the solid MoS_2 particles in such a manner that the larger particles would fall away from the bearing. In order to accomplish this distribution, a second air jet was introduced perpendicular to the MoS_2-air jet. The pressure of this air jet was adjusted so that only the smaller particles were carried to the bearing.

Test Bearings Used for High-Speed Investigation – The physical characteristics of the seven test bearings used in the high-speed rig are given in Table 1. Three types of cylindrical-roller bearings were investigated (Fig. 3). One type was a conventional bearing equipped with 18 rollers, spaced by a one-piece inner-race-riding brass cage. The second type was a conventional bearing equipped with 17 rollers, spaced by a two-piece roller-riding brass cage; and the third type was a cageless bearing equipped with 21 rollers. All three types had the following dimensions: bore, 75 mm; outside diameter, 130 mm; and width, 25 mm. Two each of the first two types of bearing and three of the cageless type were investigated.

High-Temperature Study – The high-temperature bearing rig (Fig. 4) was constructed around a floor-type drill press. The test-bearing housing was supported on an externally pressurized air thrust bearing; the housing was restrained from moving circumferentially by a strain gage which measured friction force. A resistance furnace surrounded the test-bearing housing. Load was applied by means of a lever and dead-weight system which applied load in the axial direction. Temperatures were obtained by thermocouples in the housing and on the shaft. Full details of the rig, furnace, temperature measurement and control, and friction torque measurement are given in another report.[5]

Test bearings were size 204, 18-4-1 tool-steel ball bearings with either two-piece stamped and riveted silver-plated copper beryllium cages or two-piece

STUDIES of 20-mm-bore tool-steel ball bearings operated at 2500 rpm and lubricated with graphite, or molybdenum disulfide-air mist, or one of several liquids (both petroleum and synthetic types) are reported in this paper.

Effective lubrication at 1000 F with graphite, at 850 F with molybdenum disulfide, and at 700 F with a synthetic diester was obtained.

A second investigation of the effectiveness of molybdenum disulfide-air mist as a lubricant for high-speed roller bearings is also reported here. Successful operation of a 75-mm-bore cageless roller bearing at a *DN* of 0.975 x 10^6 (13,000 rpm) with no external heat added was obtained.

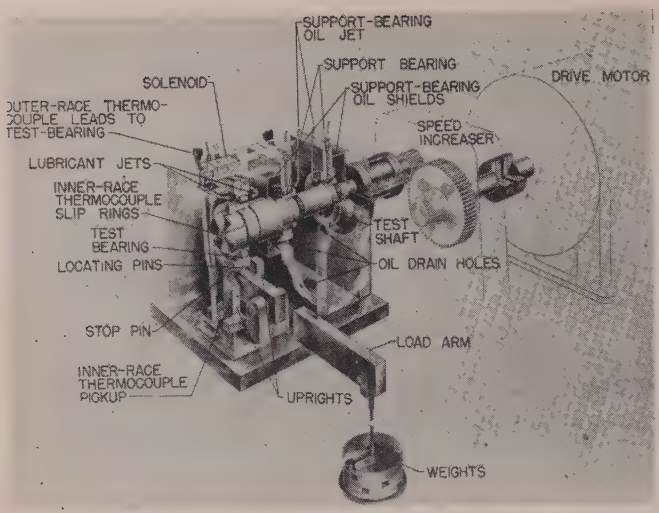

Fig. 1 – Cutaway view of high-speed bearing rig

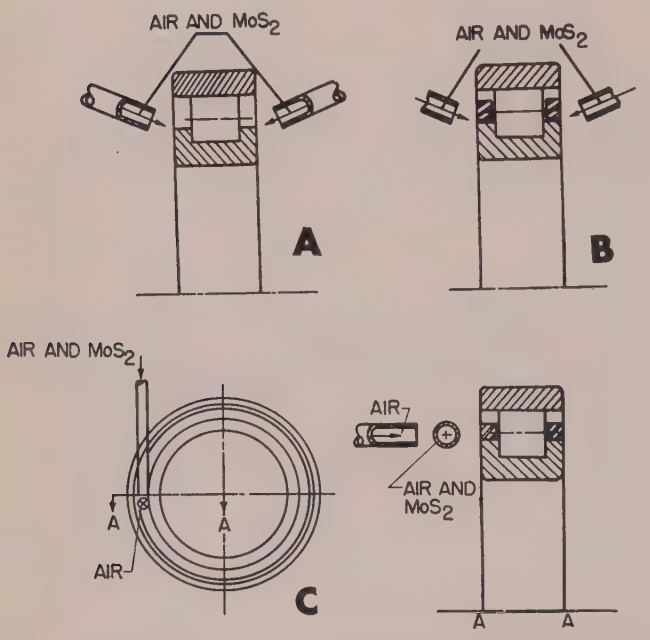

Fig. 2 – Molybdenum disulfide-air mist lubrication techniques for high-speed study. (A) single-opposed-jet lubrication of cageless roller bearing. (B) single-opposed-jet lubrication of inner-race-riding cage-type bearing. (C) modified single-jet lubrication of inner-race-riding cage-type bearing (same technique used for cageless bearing)

machined and riveted cast Inconel cages. All but one of the Inconel cages were immersed in a bath of molten NaOH for 3 hr to produce a nickel oxide coating with good frictional properties.

Petroleum liquids used as lubricants were MIL-O-6081a grade 1010 oil and MIL-F-5624b grade JP-4 fuel. The synthetic oils used were a diester with additives, a phosphonate, and a silicate. Data on liquid lubricants are given in Table 2. Solid lubricants were molybdenum disulfide and graphite, with an average particle size of 25 microns.

Liquid lubricants were introduced in droplet form and solid lubricants in the form of an air mist. The flow rate of liquid lubricants was 0.002 to 0.007 and that of solid lubricants 0.001 to 0.009 lb per hr. Lubricant supply systems are described elsewhere.[5]

Procedure

High-Speed Study – The effect of the various lubricants and lubrication methods on the operating temperatures of three types of roller bearings was determined over a range of *DN* values and at a constant radial load of 368 lb. The one-piece inner-race-riding cage-type bearings were run: (a) lubricated with oil using an 0.089-in.-diameter jet and a lubricant flow of 2.75 lb per min directed perpendicularly to the bearing face and aimed at the cage-locating surface (data from Macks and Nemeth,[6] bearing 6), (b) dry and uncoated, and (c) lubricated with MoS_2-air mist supplied through either single-opposed jets or the modified single jet. The two-piece roller-riding cage-type bearings were run with: (a) MoS_2-syrup coating over conventional bearing surfaces with no other lubrication and (b) MoS_2-syrup coating over liquid-honed bearing surfaces with no other lubrication. The cageless full-complement roller bearings were run: (a) lubricated with oil using an 0.089-in.-diameter jet and a lubricant flow of 2.75 lb per min directed perpendicularly to the bearing face and aimed at the inner-race-flange outside diameter, (b) with MoS_2-syrup coating over liquid-honed bearing surfaces with no other lubrication, (c) with MoS_2-syrup coating over conventional bearing surfaces

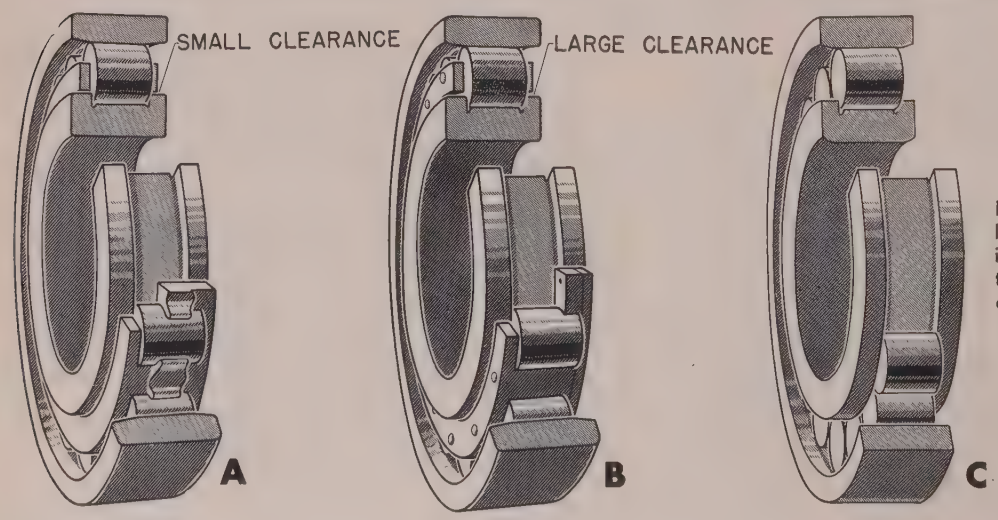

Fig. 3 – High-speed-rig test-bearing types. (A) one-piece inner-race-riding cage. (B) two-piece riveted roller-riding cage. (C) full complement (cageless)

with MoS_2-air mist lubrication, and (d) dry and uncoated.

The lubricating oil used was a commercially prepared blend of a highly refined paraffin base with a small percentage of a polymer added to improve the viscosity index. Its viscosity was 42 centistokes (53×10^{-7} reyns) at 100 F and 8 centistokes (10×10^{-7} reyns) at 210 F.

High-Temperature Study – All runs were conducted at a constant speed of 2500 rpm and 110-lb thrust load over a range of bearing temperatures from 100 F to 1000 F or failure, whichever occurred first. Test-bearing temperatures were raised in increments of 150 F, and test bearings were operated continuously during the time required (about 1 to 1¼ hr) to reach each temperature level and for 2 hr after the designated temperature had been reached. A test was ended when either a lubrication or a bearing failure occurred or when 2-hr successful operation at 1000 F was obtained. Failure was characterized by a combination of high (in excess of 0.5 in.-lb) and unstable bearing friction torque and noisy test-bearing operation. Failure due to cage breakage could be detected by visual inspection during shutdown if other means failed to indicate trouble.

A special run was made using air that had been dried to a maximum dew point of —60 F and graphite that had been baked at 500 F for 2 hr under vacuum to remove moisture to determine the lubricating effectiveness of graphite in the absence of moisture.

Several runs were made using bearings with nickel-oxide coated cast Inconel cages as a pilot evaluation of this material for use in high-speed cages. One run was made with an Inconel cage that had not been treated to form an oxide.

The Authors

ZOLTON N. NEMETH is a research engineer on bearing and lubrication problems for the National Advisory Committee for Aeronautics. In 1944, Mr. Nemeth received a B.S. degree in mechanical engineering from Fenn College in Cleveland, Ohio.

WILLIAM J. ANDERSON is a research engineer on bearing and lubrication problems for the National Advisory Committee for Aeronautics. His work, for the last five years, has been concentrated on high-speed and high-temperature bearing and lubrication problems prevalent in aviation gas turbine powerplants. In 1950, Mr. Anderson received a B.S. degree in mechanical engineering from M.I.T.

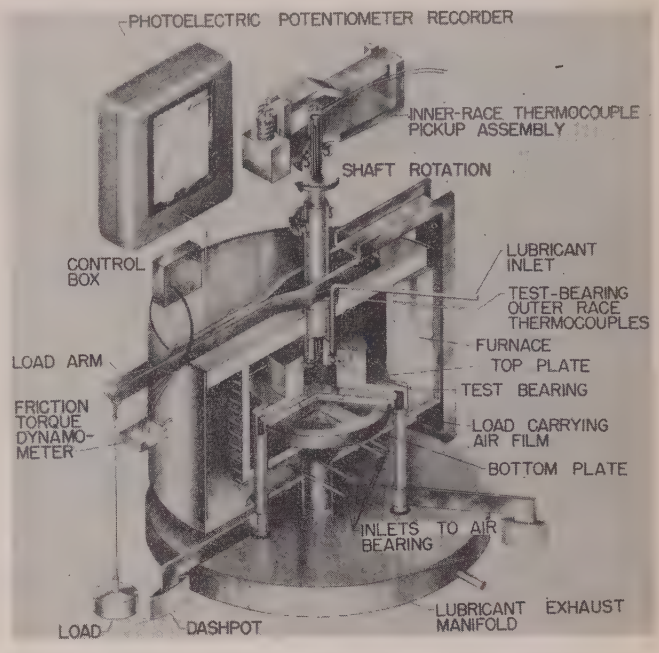

Fig. 4 – Sketch of high-temperature bearing rig showing details

Table 1 – Physical Characteristics of High-Speed Test Bearings and Test Results

Run No.	1[a]	2[b]	3[c]	4[d]	5[e]	6(a)[f]	6(b)[g]	7(a)[h]	7(b)[i]
Bearing No.	10	12	13	14	15	16	16	17	17
Construction	One-piece inner-race-riding brass cage	Two piece roller-riding brass cage	Cageless	Two-piece roller-riding brass cage	Cageless	One-piece inner-race-riding brass cage	One-piece inner-race-riding brass cage	Cageless	Cageless
Pitch Diameter of Bearing, in.	4.036	4.032	4.033	4.032	4.033	4.036	4.036	4.033	4.033
Number of Rollers	18	17	21	17	21	18	18	21	21
Bearing Surface Treatment	None	Liquid honed	Liquid honed	None	None	None	None	None	None
Bearing Coating	None	MoS_2 syrup bonded	MoS_2 syrup bonded	MoS_2 syrup bonded	MoS_2 syrup bonded	None	None	None	None
Type of Lubrication	Dry	Dry	Dry	Dry	MoS_2-air mist	MoS_2-air mist; single-opposed jets	MoS_2-air mist; modified single jet	Oil jet	Dry
Lubricant Flow Rate, Approximate, oz per hr	0	0	0	0	0 to 1.6	0 to 1.6	0 to 1.6	2.75 (lb per min)	0
Lubricant-Air Pressure, in. of Hg	0	0	0	0	0 to 4.0	0 to 4.0	0 to 12.0	0	0
Radial Load, lb	368	368	368	368	368	368	368	0 to 1113	368
Maximum Successful Operating Speed, rpm	5000	....	5000	4000	13,000	9000	12,000	16,000	4000
DNX10^{-6}	0.375	....	0.375	0.30	0.975	0.675	0.90	1.20	0.30
Total Running Time, hr	2.2	0.1	3.2	1.06	11.8	8.4	9.1	9.4	1.1

[a] Failure due to multiple fracture of cage. Excessive brass pickup by rollers.
[b] Bearing ran very hot without showing signs of reaching an equilibrium temperature.
[c] Bearing ran rough and very hot. Wear on roller ends and inner-race lips. No failure.
[d] Failure due to cage wear. Excessive brass pickup by rollers, cage ejected.
[e] Bearing ran rough and hot but no failure; no appreciable wear on any surface.
[f] Bearing ran satisfactorily, but rough and unstable as regards operating temperature.
[g] Run after conclusion of 6 (a). Operation somewhat rough but stable as regards operating temperature. Steel surfaces discolored (dark blue) from heat but no appreciable wear. Wear on cage-locating surfaces but no failure.
[h] Satisfactory operation.
[i] Run after conclusion of 7(a). Bearing failed; damage to roller ends and inner-race guide flanges.

Fig. 5 – Bearing 15 after test

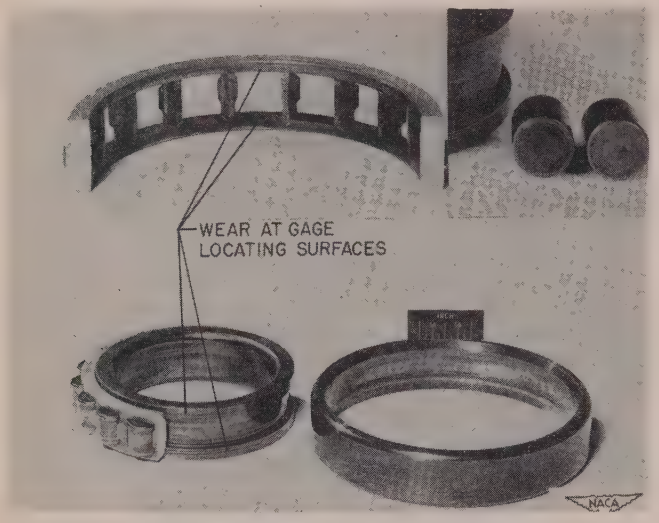

Fig. 6 – Bearing 16 after test

Experimental Results and Analysis

High-Speed Investigation – The high-speed part of the investigation consisted of seven tests. The results of the high-speed investigation are summarized in Table 1 and in Figs. 5-7.

A brief description of each test is given, and the individual high-speed-test results are followed with a general discussion of the relative merits of the various techniques of lubrication.

Test 1 – Bearing 10 (one-piece inner-race-riding brass cage) was run dry and uncoated. The bearing ran successfully at *DN* values of 0.3×10^6 and 0.375×10^6 but failed after having operated for 9 min at a *DN* value of 0.45×10^6. The total running time was 2.15 hr. Failure was due to excessive cage wear in the roller pockets which resulted in a brass buildup on the rollers and in the eventual binding and fracturing of the cage in several places. Bearing running temperatures were not excessive; the maximum temperature read immediately after failure was 201 F.

Test 2 – Bearing 12 (two-piece roller-riding brass cage), which had a syrup-bonded MoS_2 coating after liquid honing, was operated for 6 min at a *DN* value of 0.3×10^6. No indication that the bearing would approach an equilibrium running temperature was apparent. No severe physical damage to the bearing was evident on post-test examination, although some small amount of wear had occurred in the cage-locating pockets causing an increase in the cage diametral clearance.

Test 3 – Bearing 13 (cageless), which had a syrup-bonded MoS_2 coating after liquid honing, was operated without outer-race snap rings and ran rough and very hot at a *DN* value of 0.375×10^6. Although the bearing did not fail, no attempt was made to run at higher *DN* values because of excessively high operating temperatures. The maximum observed bearing temperature was 442 F. Wear was observable on the roller ends and on the flanges of the inner-race track. The total running time was 3.2 hr.

Test 4 – Bearing 14 (two-piece roller-riding brass cage), which had a syrup-bonded MoS_2 coating, ran satisfactorily at a *DN* value of 0.3×10^6 but failed after running for 4 min at a *DN* of 0.375×10^6. Cage wear resulted in the binding of the cage, which, in turn, caused the ejection of the cage cover plate from the bearing. (This bearing had been disassembled for coating.) Total running time was 1.06 hr.

Test 5 – Test 5 was conducted with bearing 15 (cageless) lubricated by the MoS_2-air mist single-opposed-jet system. The bearing was MoS_2 syrup-bonded coated before operation. The bearing was operated without outer-race snap rings. Although operation was somewhat rough and seemingly unstable with respect to operating temperature (Fig. 7), no failure occurred at *DN* values up to and including 0.975×10^6. Total running time was 11.8 hr. Bearing 15 was very sensitive to the amount of solid MoS_2 delivered to it per unit time. Because it was found impossible to keep the flow of

Table 2 – Properties of Liquid Lubricants Used in High-Temperature Investigation

Liquid	Viscosity, centistokes, at −65 F	−40 F	100 F	210 F	ASTM Pour Point, F	COC Flash Point, F	COC Fire Point, F	S.I.T.,[a] F
Petroleum								
MIL-O-6081a (grade 1010)[b]	40,000	....	9.95	2.47	<−70	300	...	500
MIL-F-5624b (grade JP-4 jet-engine fuel)	5	....	0.86	0.51	...	...	...	484
Diester								
Di (2-ethylhexyl) sebacate + additives[c,d,e,f]	16,000	2,700	20.8	5.3	<−75	450	475	...
Phosphonate								
Dioctyl isooctene phosphonate[b]	....	9,003[g]	12.22	2.77	−90	...	...	...
Silicate								
Tetrakis (2-ethylhexyl) silicate + oxidation inhibitor[f,h]	1,400	260	6.8	2.4	<−100	395	450	...

[a] Spontaneous ignition temperature.
[b] Measured values.
[c] 4% methacrylate polymer.
[d] 5% tricresyl phosphate.
[e] 0.5% phenothiazine.
[f] Manufacturer's data.
[g] At −50 F.
[h] Phenyl-α-naphthylamine (1%)

MoS_2 constant at a constant air pressure owing to intermittent clogging in the supply tubes, the operating temperatures varied considerably at a specific *DN* value. A photograph of bearing 15 after test is shown in Fig. 5; no surface damage is evident. In addition, no measurable wear could be detected on any surfaces. Bearing 15 was the only MoS_2-air mist lubricated bearing to operate at very high speeds without showing wear or surface damage.

Test 6(a) – Bearing 16 (one-piece inner-race-riding brass cage) was operated to a *DN* of 0.675×10^6 using the MoS_2-air mist single-opposed-jet lubrication system (Fig. 2B). Again the operation was rough and unstable with regard to operating temperature (Fig. 7), but no failure occurred. Total running time of this test was 8.4 hr.

Test 6(b) – Test 6(b) was conducted with bearing 16, after conclusion of test 6(a), lubricated by the MoS_2-air mist, modified-single-jet system (Fig. 2C). The bearing was operated from a *DN* of 0.675×10^6 to a *DN* of 0.9×10^6. Operation, although somewhat rough, was very stable with respect to operating temperature. As shown in Fig. 7, operating temperatures were considerably lower with the modified-single-jet system than with the single-opposed-jet system. The possibility that the airstream of the modified single jet promoted cooling was eliminated by completely shutting down the airstream for short periods of time. This produced no detectable rises in operating temperature. At the conclusion of the test, the cage diametral clearance had increased from 0.013 to 0.022 in. The bearing was not run to failure, and it is shown in Fig. 6, after test 6(b); there was little evidence of surface damage or wear except at the cage-locating surfaces. The running time of test 6(b) was 9.1 hr. The total running time on bearing 15 was 17.5 hr.

Test 7(a) – Bearing 17 (cageless) was lubricated with oil through a single 0.089-in.-diameter jet aimed perpendicularly to the bearing face and at the inner-race-flange outside diameter. The test bearing operated satisfactorily up to and including a *DN* of 1.2×10^6. Total running time was 9.4 hr.

Test 7(b) – Test 7(b) was conducted without any lubrication on bearing 17 after the conclusion of test 7(a). The bearing operated satisfactorily at a *DN* of 0.3×10^6 for 1 hr and reached a temporary equilibrium temperature of 103 F for both the outer-race maximum and inner-race temperatures. Then, without a change in speed, the bearing temperatures increased slowly until failure occurred 6 min after the temperature had begun to rise. Excessive wear occurred at the roller ends and at the guiding surfaces of the inner-race lips.

Comparison of the High-Speed Lubricating Techniques – Little success was achieved with any of the syrup-bonded MoS_2 coatings. Results were poor in all cases, so that it is evident that a coating alone does not offer promise as a method of lubrication.

The MoS_2-air-mist system does, however, offer promise as a method of lubrication. With this lubrication system a cageless roller bearing was successfully operated at a *DN* of 0.975×10^6.

Parts (a) and (b) of test 6 reveal the superiority of the MoS_2 modified-single-jet lubricating system over the MoS_2 single-opposed-jet system. At a *DN* value of 0.675×10^6, the outer-race maximum temperatures with these two systems were 230 and 355 F, respectively, (Fig. 7); in addition, the operating temperature was very stable with the modified-single-jet system.

Further gains might be effected by refinements in lubricating technique. The results indicate that the MoS_2-air mist was more effective in lubricating

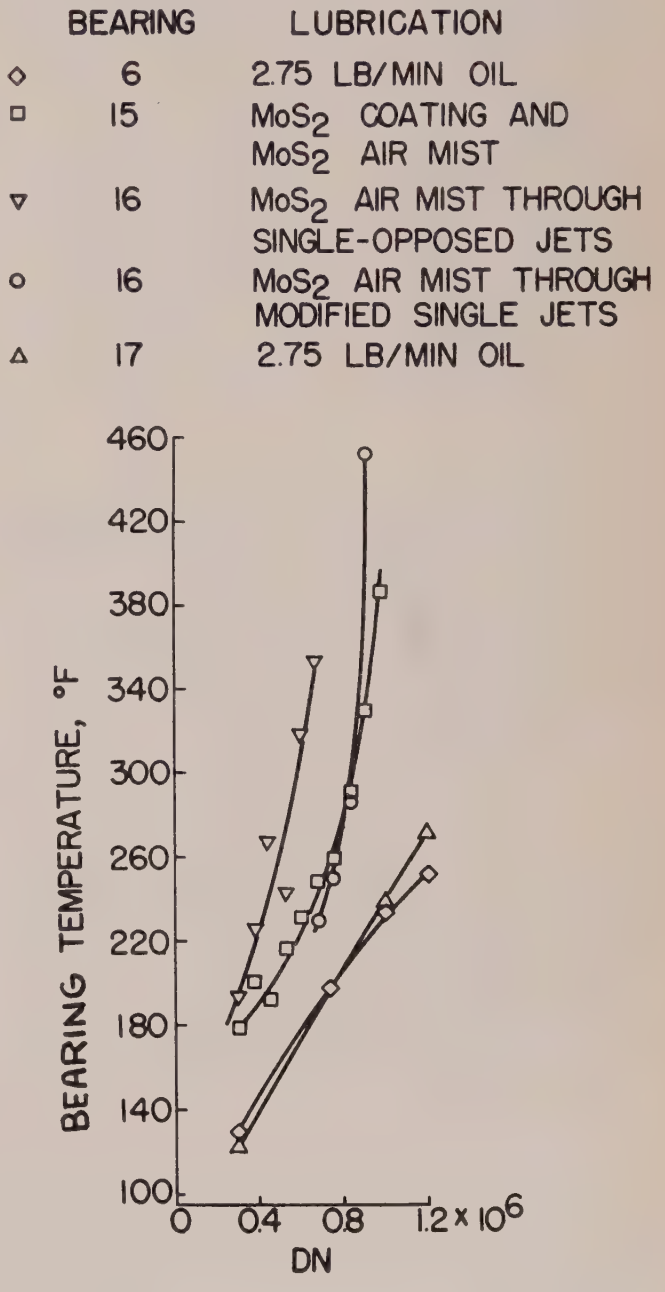

Fig. 7 – Effect of *DN* on outer-race maximum temperature of bearings 6*, 15, 16, and 17. *DN* is 0.3×10^6 to 1.2×10^6; load is 368 lb

Table 3 – Effect of Temperature on Bearing Lubrication

Bearing No.	Bearing Construction	Lubricant Type	Lubricant Flow Rate, lb per hr	Lubrication Method	Airflow Rate, cu ft per hr	Thrust Load, lb	Speed, rpm	Maximum Successful Operating Temperature, F: Ambient	Inner Race	Outer Race	Bearing Torque at Maximum Successful Temperature: Average	Range	Total Running Time, hr	Remarks
101	Stamped and riveted silver-plated beryl copper cage	Dry	.....	.....	.....	110	2500	115	160	130	0.45	0.20–1.30	3.1	Failure; cage broken. Bearing friction torque at failure was just below 5 in.-lb. Inner race, balls, and cage slightly discolored
102	Stamped and riveted silver-plated beryl copper cage	MIL-O-6081a grade 1010 petroleum fluid	55 drops per min to 400 F. 15 drops per min from 550 F and up	Fluid drop	.....	110	2500	656	545	538	0.20	0.11–0.39	14.1	Failure; cage broken in several places. Bearing friction torque at failure was 5 in.-lb. Bearing relatively clean
103	Stamped and riveted silver-plated beryl copper cage	MIL-F-5624b grade JP-4 jet engine fuel	Approximately 0.0014 to 0.002 (20-24 drops per min)	Fluid drop	.....	110	2500	713	664	697	0.20	0.04–0.56	16	Failure; cage broken in several places. Bearing friction torque was low despite failure. Bearing relatively clean but darkened
104	Stamped and riveted silver-plated beryl copper cage	Di (2-ethylhexyl) sebacate + additives a, b, c[a] (PRL-3161)	Approximately 0.007 (55 drops per min)	Fluid drop	.....	110	2500	810	....	710	0.04	0.04–0.19	15.15	Failure; cage broken in several places. Bearing friction torque at failure was 3.44 in.-lb. Bearing clean but darkened
105	Stamped and riveted silver-plated beryl copper cage	Dioctyl isooctene phosphonate	Approximately 0.002 (15 drops per min)	Fluid drop	.....	110	2500	440	402	418	0.11	0.05–0.13	8.5	No failure; cage not broken. Bearing friction torque was 3.5 in.-lb at shutdown. Heavy carbonaceous deposit in bearing
106	Stamped and riveted silver-plated beryl copper cage	Tetrakis (2-ethylhexyl) silicate + oxidation inhibitor d[a]	Approximately 0.002 (15 drops per min)	Fluid drop	.....	110	2500	584	576	548	0.60	0.26 1.04	11.3	No failure; cage not broken, Bearing friction torque was 1.84 in.-lb at shutdown. Slight deposit in bearing
107	Stamped and riveted silver-plated beryl copper cage	MoS_2	Approximately 0.001 to 0.009	Air-mist	Approximately 3.4–14.0	110	2500	1062	938	1001	2.96	1.30–2.96	19.05	Failure; cage corroded and broken on lubricant supply side of bearing. Bearing friction torque very high at last several hours of test. Heavy deposits on bearing
108	Stamped and riveted silver-plated beryl copper cage	Synthetic graphite	Approximately 0.001 to 0.009	Air-mist	Approximately 3.4–14.0	110	2500	1023	882	1000	0.08	0.05–0.10	18.65	No failure; cage not broken. Bearing friction torque only 0.08 in.-lb at 1000 F and was steady. Bearing was clean and free with slight film of graphite on bearing
109	Stamped and riveted silver-plated beryl copper cage	Dried synthetic graphite	Approximately 0.001 to 0.009	Air-mist (dry air)	Approximately 3.4–14.0	110	2500	1037	931	1010	0.09	0.07 0.28	18.5	No failure; cage not broken. Bearing friction torque only 0.09 in.-lb at 1000 F. Bearing was clean and free with slight film of graphite on bearing
110	Two-piece riveted, machined cast Inconel cage, oxide coated	MoS_2	Approximately 0.001 to 0.009	Air-mist	Approximately 3.4–14.0	110	2500	1054	953	1006	1.4	0.64–2.5	20.9	No failure; cage not broken. Bearing friction torque was as high as 2.5 in.-lb at 1000 F. Yellow-white deposit at cage-locating surface
111	Two-piece riveted, machined cast Inconel cage, oxide coated	Synthetic graphite	Approximately 0.001 to 0.009	Air-mist	Approximately 3.4–14.0	110	2500	1018	928	994	0.33	0.20 0.36	19.6	No failure; cage not broken. Bearing friction torque was slightly erratic at all temperature levels. Bearing in good shape and free with slight film of graphite on bearing
112	Two-piece riveted, machined cast Inconel cage, no oxide coating	Synthetic graphite	Approximately 0.001 to 0.009	Air-mist	Approximately 3.4–14.0	110	2500	....	940	1006	0.3	0.06–0.36	18.1	No failure; cage not broken. Bearing friction torque somewhat erratic but low. Bearing in good shape and free and slightly discolored

[a] Additives: (a) approximately 4% methacrylate polymer; (b) 5% tricresyl phosphate; (c) 0.5% phenothiazine; (d) 1% phenyl-α-napthylamine.

bearing 15 (cageless) than in lubricating bearing 16 (one-piece inner-race-riding brass cage). This phenomenon may be due to the fact that (a) the cage acted as a barrier to the MoS_2-air mist and prevented its reaching the cage roller pockets and inner-race roller-guide flange surfaces in sufficient quantity, (b) MoS_2 is more effective in steel-to-steel lubrication than in brass-to-steel lubrication. For example, at a *DN* of 0.6×10^6, the outer-race maximum temperature of bearing 16 was 88 deg higher (Fig. 7) and the inner-race temperature 102 deg higher than were the corresponding temperatures of bearing 15 for similar MoS_2-air mist lubricating techniques; this represents a significant difference in heat generation within the two bearing types.

High-Temperature Investigation – The results of the high-temperature investigation, which consisted of 12 tests, are summarized in Table 3 and in Figs. 8-10. Bearing friction torque was used as the criterion of operation. For comparison purposes bearing number 101 was run dry. Failure occurred after 3 hr and 6 min of operation when the temperature was being raised from 100 to 250 F. During the test, friction torque increased from 0.5 to 5.0 in.-lb (Fig. 9A), and the cage broke. Bearing 101 is shown in Fig. 8C after test.

Petroleum Liquids – The results for 1010 grade turbine oil (bearing 102) and grade JP-4 fuel (bearing 103) are shown in Fig. 9A. For 1010 oil, failure began at 550 F and quickly progressed to a total failure in going from 550 to 700 F. Failure

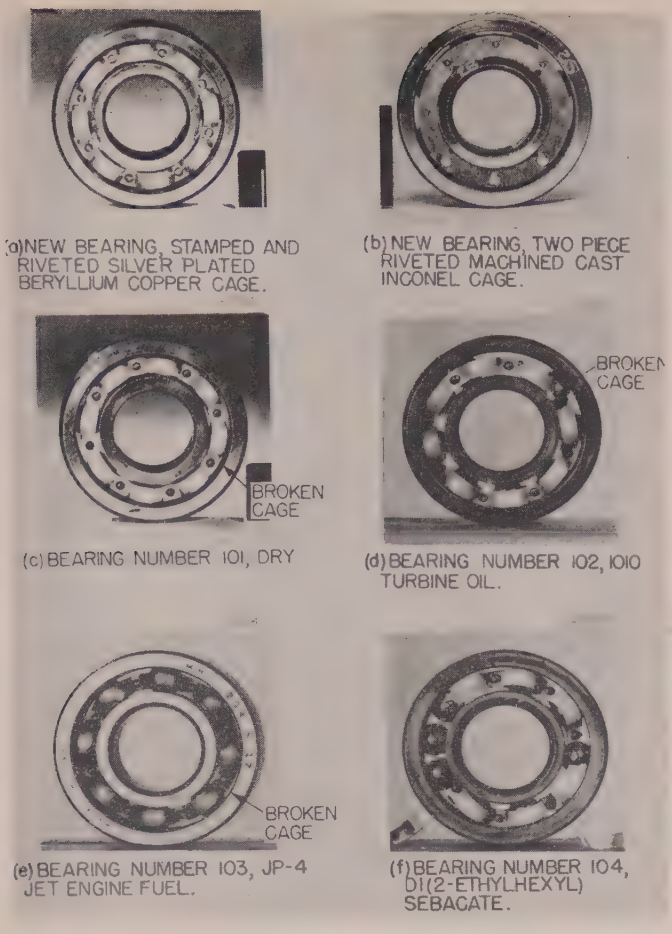

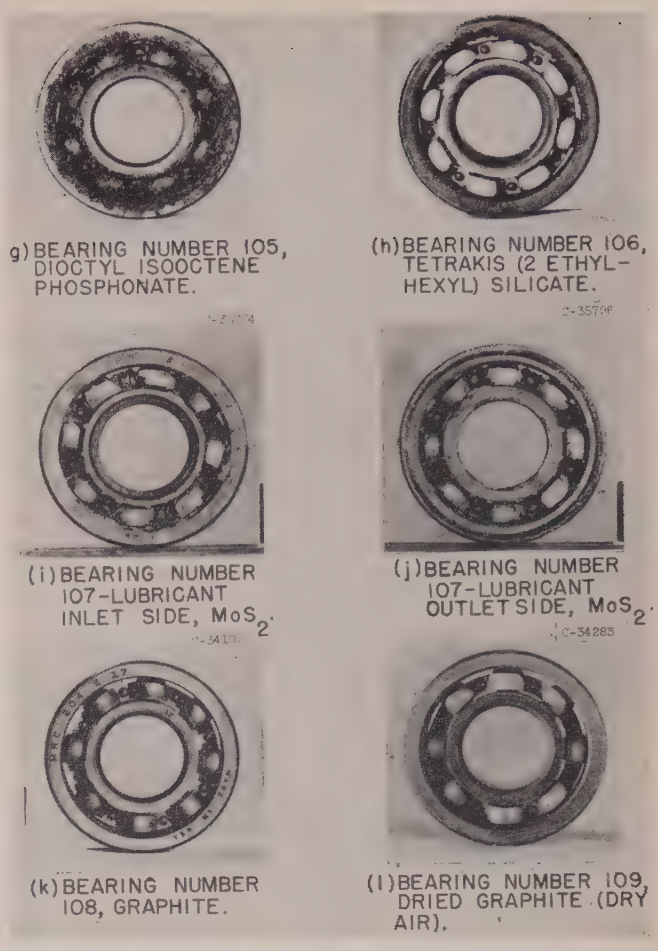

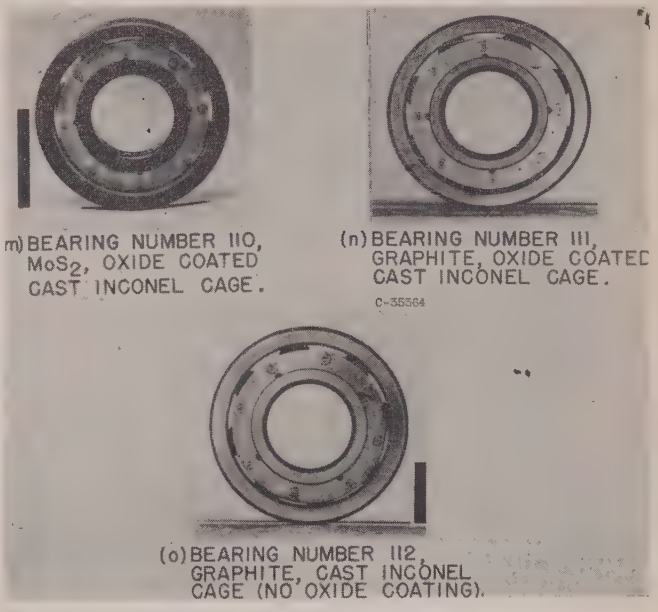

Fig. 8 – High-temperature bearings before and after tests

was evidenced by cage breakage (Fig. 8D). Bearing 102 was fairly clean after the test, with only a slight deposit of varnish. Total running time of bearing 102 was 14.1 hr.

Friction torque values for JP-4 fuel were low at temperatures to and including 700 F (Fig. 9A). Despite the low friction torque, however, fracture of the cage was observed at shutdown (Fig. 8E). It could have occurred during the test, or it is possible that an undetected crack was present in the cage prior to the test. Sulfur present in the fuel may have acted as a solid lubricant at the higher temperatures and may have been responsible for the low friction torque. Total running time with JP-4 fuel was 16 hr. At the conclusion of the test, the bearing was relatively clean but slightly darkened.

Synthetic Oils – The results for the three synthetic oils are shown in Fig. 9B. In this group of lubricants the compounded diester (bearing 104) was best.

The compounded diester, which approaches the requirements of military specification MIL-L-7808, lubricated effectively at temperatures to 700 F, but friction torque rose rapidly when the bearing was being heated from 700 to 850 F (Fig. 9B). The cage was broken, and several sections were missing (Fig. 8F). Bearing 104 was relatively clean. Total running time for bearing 104 was 15.15 hr.

The temperature limits of both the phosphonate (bearing 105) and the silicate (bearing 106) were about 400 F (Fig. 9B), although the silicate did provide somewhat marginal lubrication at 550 F. Neither bearing 105 nor bearing 106 sustained an

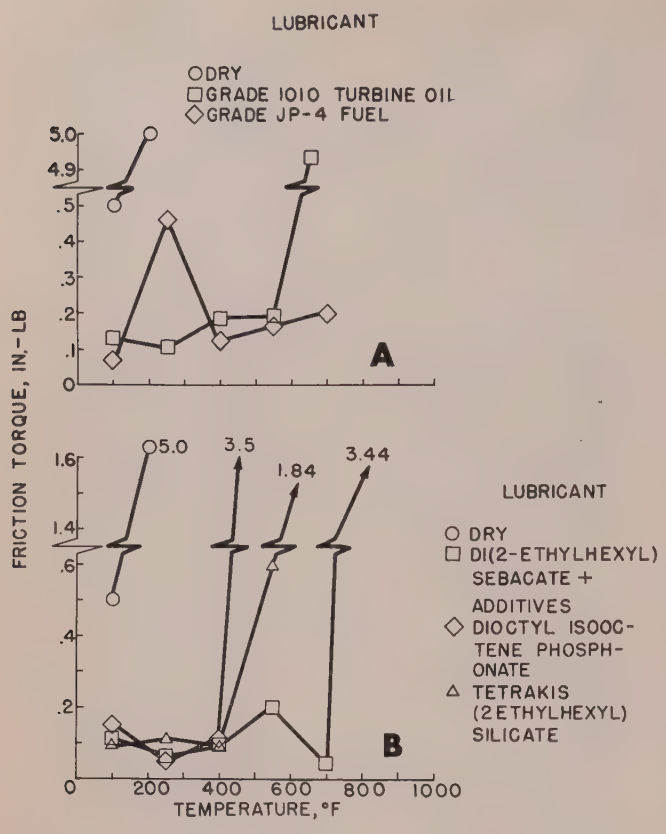

Fig. 9 – Effect of temperature on friction torque of test bearings when lubricated with liquid lubricants. (A) petroleum liquids. (B) synthetics

actual mechanical failure. Bearing 105 was almost completely covered with a heavy carbonaceous deposit (Fig. 8G), while bearing 106 had only a slight brown deposit (Fig. 8H).

Solid Lubricants – The results for the two solid lubricants are shown in Fig. 10A for bearings with silver-plated beryllium copper cages and in Fig. 10B for bearings with cast Inconel cages. Bearing 107 (beryllium copper cage) and bearing 110 (oxide-coated cast Inconel cage) were lubricated with MoS_2. Although both bearings 107 and 110 were operated to 1000 F, friction torque was high and unstable at temperatures above 850 F. The cage of bearing 107 (Figs. 8I and J) showed evidence of damage. At temperatures above 700 F in the presence of oxygen, MoS_2 begins to oxidize and form an abrasive oxide, MoO_3, at a rate which increases with increasing temperature.[9] Bearing 110 showed the same friction torque trend as did bearing 107, but friction torque values at 850 and 1000 F were slightly lower for the bearing with the cast Inconel cage.

Graphite, used with bearings 108, 109, 111, and 112 was the only lubricant that provided effective lubrication at 1000 F (Fig. 10). Bearing 108 (beryllium copper cage) ran smoothly and with low friction torque to 1000 F and showed little evidence of wear at the conclusion of the test (Fig. 8K). A quantity of graphite dried by baking was used to lubricate bearing 109. Specially dried air whose dew point did not exceed —60 F was used. Although the dried graphite was not as effective a lubricant as nondried graphite (Fig. 10A), effective lubrication was provided to 1000 F. It is possible that some moisture seeped into the system despite the extensive precautions taken. Bearing 109 is shown in Fig. 8L after test.

Bearing 111 (oxide-coated cast Inconel cage) showed high friction torque (2.39 in.-lb) at 850 F, while bearing 112 (uncoated cast Inconel cage) operated with low friction torque (less than 0.39 in.-lb) throughout the temperature range (Fig. 10B).

Discussion of Results – For the high-temperature tests of 20-mm-bore ball bearings, the solid-air mist type of lubrication was found to be superior to liquid lubrication at high temperatures and low speeds. Both graphite and molybdenum disulfide gave better results than the best liquid lubricant. Graphite-air mist provided effective lubrication at 1000 F in all four tests in which it was used, while molybdenum disulfide-air mist provided effective lubrication at temperatures to 850 F. The difference in results with graphite and molybdenum disulfide is believed to be due to the properties of the decomposition products of these lubricants. Graphite decomposes to form a gas which could conceivably form a nonoxidizing atmosphere and thus be beneficial to high-temperature bearing performance. Molybdenum disulfide, however, will oxidize in the presence of air at high temperatures, forming an abrasive oxide.[9]

An evaluation of the relative merits of the two cage materials tested is difficult to make because the type of test reported herein may not constitute as severe a test of the cage as would full-scale engine bearing tests at high *DN* values. As a consequence, material weaknesses such as low strength at high temperatures may not be brought to light by tests of this nature. The two cage materials were both tested with graphite and molybdenum disulfide, so they must be compared on the basis of these tests. The Inconel cage showed slightly higher friction torque values at temperatures to 700 F when lubricated with molybdenum disulfide. Above 700 F, however, the copper cage showed higher friction torque values. When lubricated with graphite, both cage types showed comparable values of friction torque at temperatures to 550 F. Friction torque for the oxide coated Inconel cage rose from about 0.2 in.-lb at 550 F to 2.39 in.-lb at 850 F.

The magnitudes of friction torque values in the region of satisfactory lubrication were comparable for both liquid and solid lubricants.

[9] See NACA TN 1882 (1949), "Oxidation Characteristics of Molybdenum Disulfide and Effect of Such Oxidation on Its Role as Solid Film Lubricant," by Douglas Godfrey and Erva C. Nelson.

Summary

Two investigations, one to determine the effectiveness of molybdenum disulfide as a bearing lubricant at high speeds and one to determine the maximum temperatures at which various petroleum and synthetic liquids and molybdenum disulfide and graphite solids would lubricate effectively, are reported herein.

In the high-speed investigation 75-mm-bore cylindrical-roller bearings were run dry and lubricated by: (1) a syrup-bonded coating of molybdenum disulfide applied before running, (2) a molybdenum disulfide-air mist spray during operation, and (3) a combination of (1) and (2). These tests were run at a radial load of 368 lb with no external heat added to the test bearings. A cageless roller bearing provided with a molybdenum disulfide coating before operation and lubricated with molybdenum-disulfide-air mist ran satisfactorily for 11.8 hr at *DN* values from 0.3×10^6 to 0.975×10^6 (13,000 rpm). No signs of wear or damage were present after the test. The maximum bearing temperature was 386 F. Cage-type roller bearings, when lubricated with molybdenum disulfide-air mist, indicated lower limiting *DN* values and showed considerable wear. Syrup-bonded coatings of molybdenum disulfide were not effective in lubricating cylindrical-roller bearings.

In the high-temperature investigation 20-mm-bore tool-steel ball bearings were operated in a test rig at 2500 rpm, 110 lb thrust load, and temperatures of 100 to 1000 F. Friction torque was used as the criterion of operation, and operating temperatures were raised in 150 F increments until failure occurred or until the 1000 F temperature limit was reached. The solid lubricants were found to be better high-temperature lubricants than were the liquids. All tests in which the solid lubricants were used were run to completion at 1000 F without failure, although only graphite provided effective lubrication to 1000 F. Molybdenum disulfide lubricated effectively to 850 F. Of the liquids tested, a compounded diester (di-2-ethylhexyl sebacate) was best. A bearing lubricated with JP-4 fuel operated with low friction torque to 700 F, but the cage was found to be fractured on shutdown. In some test bearings the standard silver-plated beryllium copper cage was replaced by a cast Inconel cage, which has better high-temperature strength. Several bearings with copper cages sustained cage fractures. No Inconel cages sustained fractures.

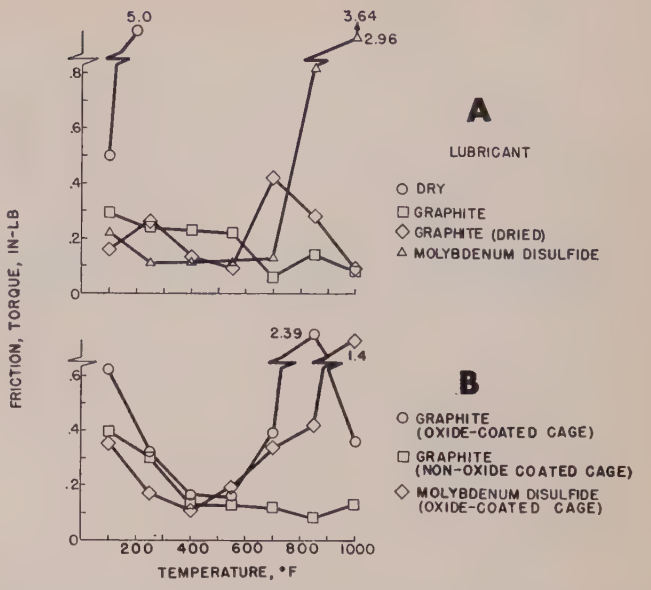

Fig. 10 – Effect of temperature on friction torque of test bearings when lubricated with solid-air mist lubricants. (A) silver-plated beryllium copper cages. (B) cast Inconel cages

DISCUSSION

Number of Cycles Affect Test Results

– D. Roddick
Shell Development Co.

DO the operating techniques involved permit the bearing to be shut down, cooled to ambient temperatures, and then restarted for one or more subsequent cycles of similar operation? Our reason for raising this point is based entirely upon experiences with liquid lubricants wherein we have found that the effective lubrication temperature limit for a given lubricant may be considerably altered if the evaluation is based on a multiple-cycle test instead of a single-cycle test. For example, in tests conducted at 600 F (206 size bearing, 10,000 rpm), two lubricants, a mineral oil and a synthetic, gave almost identical results as judged by bearing condition and a visual rating as to quantity and character of deposits in a single-cycle test. However, in attempting to operate a second cycle after an overnight shutdown, one lubricant gave an early bearing failure while the other permitted satisfactory completion of several subsequent cycles. The explanation in this case appeared to be that the deposit from the successful lubricant was thermoplastic and capable of being plasticized by the parent lubricant, whereas the other deposit remained hard enough to interfere with subsequent bearing operation.

We do not know whether any of the dry lubricants have a tendency to settle in bearing pockets, to agglomerate, or to affect in any other way the bearing in a manner that limits cyclic operation. However, we did wish to point out that an experimental program based on single-cycle tests can sometimes be misleading.

DISCUSSION CONTINUED →

Discusses Turbojet Lubrication Problems

– D. H. McLean
Esso Laboratories

THE work reported in this paper is of great interest and of ever growing importance. The temperatures encountered in the lubrication systems of turbojet aircraft continue to rise as speed of flight and engine power increases.

The ram temperature rise at high speeds also increases the temperature of the engine components including the bearings. As mentioned by the authors, the available cooling capacity is not adequate to reduce the heat load on the oil system. Mechanical refrigeration imposes a weight penalty, and the fuel is efficient as a coolant only under conditions of high fuel flow. Table A illustrates the evolution in lubricant-type which has accompanied the trend in engine design as aircraft have passed the sound barrier. At subsonic speeds, with maximum bearing operating temperatures of about 350 F, a light mineral oil was satisfactory. In the newer designs of engine, however, flying at speeds just below and occasionally above that of sound, bearing temperatures are considerably increased; and it must be remembered also that heat soak-back may raise these temperatures several hundred degrees. Low-temperature performance is also required from the lubricants for these engines. The British requirement is for engine starting at —40 F, and the corresponding United States requirement is —65 F. Ester-type lubricants have been developed for these engines, since no mineral oils possess the required combination of thermal stability and load-carrying ability with low-temperature fluidity.

Supersonic aircraft, however, with bearing operating temperatures up to, say, 750 F and cooled oil-supply temperatures of 300 to 400 F are going to need new developments in lubrication. This work by NACA on alternative mist or solid lubrication is therefore very timely, because we are getting to temperatures where currently known fluids show deterioration.

As shown in Table B, below 350 F thermal stability is very satisfactory. Up to 550 F bearing temperatures, light deposits are found after full-scale engine tests. These deposits do not impair engine operation to any appreciable extent. Above 550 F, however, coke formation limits engine life.

How are we going to resolve these difficulties? Solid lubrication, say in the form of molybdenum disulfide or graphite mists, has the present practical disadvantage that a lot of the other aircraft equipment does not need high-temperature lubrication and has been designed to handle fluid lubricants. If temperatures go up to 800-1000 F in the turbine bearings, however, solid lubricants may be the only solution.

Undoubtedly, more fluid circulation would help to keep bearing temperature down. Keeping the oxygen in the system to a minimum also helps, however. This is illustrated in Table C. A MIL-L-7808 type oil was heated to 400 F bulk oil temperature. When air was excluded, oil degradation was negligible. When air at 600 F was given access to the oil, however, oil deterioration increased with increasing air/oil ratio. Viscosity and acidity increase were particularly marked.

We should like to urge that the type of work reported by the authors be expanded, especially using higher speeds, and that a close tie-in with operating equipment be developed. Even more than is normal in bearing tests, we are getting to conditions where failure of lubricant and failure of bearing due to fatigue may be difficult to distinguish. For that very reason, the NACA work will be invaluable in developing a tool which will help both those who are developing the lubricants and those who are engaged on the metallurgical aspects of the problem.

Table A – Trends in Turbojet-Engine Lubrication System Temperatures

	Engine Designation		
	"Older Design"	"New Design"	"Future Design"
Flight Speed Range	Subsonic	Subsonic and transonic	Supersonic
Maximum Bearing Operating Temperature, F	350	350–550	550–750
Cooled Oil-Supply Temperature, F	200	200–300	300–400
Lubricant Type	Light mineral oil	Ester-type synthetic	Future synthetic

Table B – Full-Scale Performance of MIL-L-7808 Type Synthetic Oil Advanced Design Turbojet Engine

Bearing Temperature, F	Lubricant Performance
<350	Satisfactory
350–550	Light to medium deposits
>550	Heavy deposits, engine life limited by coke formation

Table C – Oxidation of MIL-L-7808 Type Synthetic Oil
(Air Temperature, 600 F; Metal Surface Temperature, 500 F; Bulk Oil Temperature, 400 F; 6-Hr Duration)

		Used Oil Condition	
Air/Oil Ratio	Deposit Weight, g	Viscosity at 210 F, % increase	Neutralization No. Increase
0	0.2	0	0.2
3/100	13.0	10	5.4
12/100	12.0	33	11.8

Authors' Closure To Discussion

MR. RODDICK'S comments on the test method are quite pertinent. A test procedure must always be chosen prior to an experimental investigation, and in this case we chose the one described. The tests, however, were not strictly single-cycle tests, because in all tests where the lubricant was effective at temperatures above 400 F the test was stopped at least once. In no case was a bearing run continuously for more than 8 hr (the length of a work shift). So while the tests are not multiple-cycle tests, neither are they strictly single-cycle tests. It must be emphasized that these tests are merely pilot tests. The most promising of these lubricants are to be evaluated further in tests using full-scale engine bearings run at high speeds, loads, and temperature. Even then, the final answer will come only after actual engine tests.

Mr. McLean's discussion elaborates very nicely on the nature and causes of the high-temperature bearing problem in turbojet engines. Without the use of refrigeration systems, there are available only two fluids (ram air and fuel) to cool the oil. As flight speeds increase, ram-air temperatures increase, and fuel temperatures might increase because of higher skin temperatures. Fuel cooling is limited by the deposition characteristics of the fuel. If heated to too high a temperature, the fuel will deposit and adversely affect nozzle spray patterns. Mr. McLean's data on the effect of oxygen content of the lubricant on neutralization number are extremely interesting. In this regard it might be possible to extend the limiting temperatures of the best liquid lubricants by the use of controlled atmospheres in closed lubrication systems. Partial or total exclusion of oxygen from the lubrication system, since it appreciably lowers the neutralization number, should raise the lubricant limiting temperature.

Distribution and Effects of Automotive Exhaust Gases in Los Angeles

Gordon P. Larson, John C. Chipman, and Erwin K. Kauper,
Air Pollution Control District, County of Los Angeles

This paper was presented at the SAE Golden Anniversary Annual Meeting, Detroit, Jan. 10, 1955.

THE complex mixture of air contaminants that exists in industrial communities may produce a variety of effects. Some of the resultant nuisances are associated with chemical reactions of one or more pollutants in the atmosphere. Under certain atmospheric conditions, the oxidation of sulfur dioxide to sulfur trioxide and the resulting sulfuric acid mist contributes to haze formation.[1] When stable air conditions are such as to provide time for the oxidation of hydrocarbon vapors in the air, aerosols and irritating gases are formed. The particles produced in this photochemical reaction result from the polymerization of the oxidation products of certain unsaturated hydrocarbons.[2] Haze and the consequent reduction in visibility result from these oxidation processes in the air, together with the direct emissions of dust, fumes, and mists from a large variety of sources. On the other hand, the contaminating gases cause damage to vegetation, irritation of the eyes, higher ozone content of the air, and strong odors.[3] Sulfur dioxide, fluorine, hydrocarbons, ammonia, and hydrogen sulfide are prominent among the contaminating gases and vapors found in the atmosphere.

Effects, other than haze formation, have been shown in reactions of hydrocarbons in extreme dilution. Olefinic, branched-chain, and cyclic compounds present in gasoline vapor are readily oxidized in the presence of sunlight and oxides of nitrogen to produce gases which are highly irritating to the eyes and cause damage to vegetation.[4, 5] A byproduct of this chemical reaction is ozone which, in spite of its known activity, leaves residual ozone concentrations sufficiently high to produce rubber cracking during smog attacks.[6] Some of the organic acids, aldehydes, and peroxides resulting from the oxidation of hydrocarbons can be measured in the atmosphere and in test-chamber experiments.

Table 1 presents a classification of important sources and the potential air contaminants from each.[7]

The research studies which developed the role of gasoline vapor as a factor in the Los Angeles smog problem have been extensively reported. Essentially, the work consisted of test-chamber experiments in which the reaction products of oxidized gasoline vapors produced eye irritation and a specific pattern of damage on certain vegetable plants. This type of damage is found extensively in the field on plants after smog attacks. Analyses of the organic aerosol in the atmosphere compared favorably in its chemical and physical properties to the aerosol produced when gasoline vapors are oxidized.

Accompanying these studies was an inventory of the sources of gasoline vapor to estimate the losses of all types of hydrocarbons to the atmosphere. Sampling programs were conducted to determine

---

[1] See Proceedings of Royal Society of Edinburgh, Vol. 32, 1911-1912, pp. 183-215: "Sun as Fog Producer," by J. Aitken.

[2] See *Industrial & Engineering Chemistry*, Vol. 44, June, 1952, pp. 1352-1355: "Composition of Organic Portion of Atmospheric Aerosols in Los Angeles Area," by P. P. Mader, R. D. MacPhee, R. T. Lofberg, and G. P. Larson.

[3] See Proceedings of 44th Annual Convention of Air Pollution and Smoke Prevention Association of America, 1951, pp. 127-137: "Recent Identification of Atmospheric Contaminants in Los Angeles Basin," by G. P. Larson.

[4] See *Industrial & Engineering Chemistry*, Vol. 44, June, 1952, pp. 1342-1346: "Chemistry and Physiology of Los Angeles Smog," by A. J. Haagen-Smit.

[5] See "Second Technical and Administrative Report on Air Pollution Control in Los Angeles County, 1950-1951," Los Angeles County Air Pollution Control District, May, 1952.

[6] See *Air Repair*, Vol. 4, November, 1954, pp. 105-109: "Photochemical Ozone Formation with Hydrocarbons and Automobile Exhaust," by A. J. Haagen-Smit and M. M. Fox.

[7] See Encyclopedia of Chemical Technology, Vol. 12, pp. 558-573: "Smokes and Fumes," by G. P. Larson. Pub. by Interscience Encylopedia, Inc., New York, 1954.

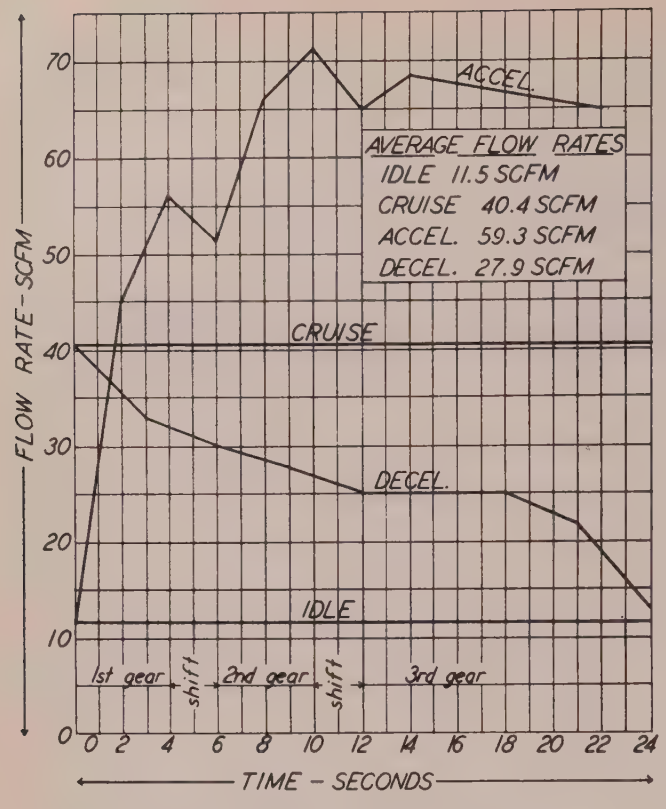

Fig. 1 – Flow rate for 1951 Ford 6

the concentrations of hydrocarbons during smog attacks in close proximity to sources. Samples of air collected in the vicinity of refineries or similar sources of hydrocarbon vapors gave typical smog effects when exposed to sunlight. The extensive work done in connection with hydrocarbons led to studies of the internal-combustion engine. While it could be expected that certain types of hydrocarbons would be found in the exhaust gases, no evidence existed that the mixture of combustion products at the temperatures found in the exhaust would give any of the effects which had been determined in the experiments with pure hydrocarbons or gasoline vapors. As a matter of fact, the exhaust gases do not produce crop damage typical for smog until photochemical reactions take place.

Test Procedure

Since the quantities of contaminants vary for each operating condition, an estimate of total emissions was based on the consumption of gasoline under average driving conditions. Consideration of traffic flow and traffic densities led to the selection of a 39-mile route throughout the community. This route was chosen as representative of average driving conditions in Los Angeles. It includes freeway driving, residential driving, congested city traffic, and industrial areas.

Accumulative stop watches were used to record the time spent in (1) idling, (2) acceleration, (3) cruising, and (4) deceleration, while driving the predetermined route. The cruising cycle recorded was in high gear between 25 and 35 mph at approximately 17 in. of Hg. Deceleration was at closed throttle with a manifold vacuum of between 20 and 24 in. of Hg. Data on acceleration were obtained between approximately 2 and 15 in. of Hg and results from idling were obtained under full stop with a manifold vacuum of about 18 in. of Hg. The average operating time of the test was found to be as follows: idling, 18%; acceleration, 18%; cruising, 46%; and deceleration, 18%.

As an example of the procedure used, a test on a 1951 Ford Six is described. A stainless-steel orifice meter using a 1¼-in. orifice plate was attached to the tail pipe. It was of sufficient size to minimize exhaust back pressure. Orifice pressure differentials were obtained by a standard self-compensating X

Table 1 – Sources and Air Contaminants

Source, Type, or Industry	Aerosol	Specific Gases and Vapors	Vapors
Combustion			
Coal	Dust, fume (smoke, fly ash)	NO_2, SO_2, CO, aldehydes, acids	
Fuel oil and gas	Dust, fume (smoke)	SO_2, NO_2	
Gasoline (motor fuel)	Fume (smoke)	Organic acids, aldehydes, NO_2, CO	Hydrocarbons[a]
Rubbish	Dust, fume (smoke, fly ash)	Organic acids, aldehydes, NO_2, CO	
Petroleum			
Production			Saturated hydrocarbons
Refining	Dust, mist	Mercaptans, SO_2, H_2S, NH_3, CO	Hydrocarbons[a]
Marketing			Hydrocarbons[a]
Chemical and allied products			
Chemicals	Dust, fume, mist	(Process-dependent)	(Process-dependent)
Soap and detergent	Dust	Odor	
Paints and varnish	Mist	Solvent, organic acids	Solvent, organic acids
Fertilizer	Dust	NH_3, odor	
Animal and vegetable oils	Mist	Odor	
Paper and plastics	Dust, mist	Odor, solvent, sulfide (process-dependent)	
Metallurgical and metal fabrication			
Smelters and mills	Dust, fume (smoke)	SO_2, fluorides, CO	
Foundries	Dust, fume (smoke)	Aldehydes	
Fabricators	Dust		
Mineral earth processing			
Ceramic	Dust	Fluorides	
Aggregate and cement	Dust		
Calcining	Dust		
Food products			
Feed and flour	Dust		
Fish and meat	Dust, mist	Odor	
Food processing	Dust, mist	Odor	

[a] Mixtures containing types of hydrocarbons that are readily oxidized in the atmosphere.

The Authors

GORDON P. LARSON is director of the Los Angeles County Air Pollution Control District. A graduate of West Point, he served as a commissioned officer in the army for 12 years, directing and administering major engineering and construction projects. After retiring in 1948 as a lieutenant-colonel, Mr. Larson entered air pollution control work in Los Angeles County as senior inspector. In 1949, he became director of the Air Pollution Control District.

JOHN C. CHIPMAN is head of the source testing section of the Los Angeles County Air Pollution Control District. He received a B.S. in Chemical Engineering from Northeastern University in 1942 and served as an Ordinance Officer for four years in the U. S. Navy. Mr. Chipman joined the Air Pollution Control District seven years ago.

ERWIN K. KAUPER is head meteorologist of the Los Angeles County Air Pollution Control District. He received a degree in physics-meteorology from the University of California in 1944. After serving in the Air Force from 1942-1946, Mr. Kauper was attached to the U. S. Weather Bureau in Los Angeles. He joined the Air Pollution Control District in 1952.

STUDIES of air contamination in the Los Angeles area show that even if all the hydrocarbons coming from sources other than automobile exhausts were removed from the atmosphere, there would still be sufficient concentration of hydrocarbons in certain areas to cause eye irritation and crop damage.

Thus, it is clear that hydrocarbons must be removed from the exhaust gases of automobiles – and with an extremely high efficiency.

The Air Pollution Control District recommends that engineers strive for a 90% removal under conditions of operation experienced in heavy traffic.

This paper is the first in a Symposium on Air Pollution. Discussion of this and the other papers in the Symposium is at the end of the last paper, and starts on p. 618.

gage, which indicated the pressure differentials in inches of water.

Idling exhaust flow was obtained with the engine idling at approximately 450 rpm. (See Fig. 1.) The acceleration cycle consists of accelerating on level terrain in first gear from 0 to 12 mph, then in second gear from 12 to 22 mph, and in high (third) gear from 22 to 35 mph. Orifice differential pressure readings were taken every two seconds through the three forward gears (Fig. 1).

The average exhaust flow rate in first gear was determined by graphically integrating the area under the plotted curve for the first 5-sec increment (to the midpoint of the first shift); the average for second-gear operation was determined from the 5-11-sec increment. The average exhaust flow for the entire acceleration cycle was obtained by graphically integrating the area under the plotted curve for the full 22-sec period (Fig. 1). The average exhaust flow rate for the entire deceleration cycle was obtained by averaging the area under the plotted curve for the entire 0-24-sec interval. The average flow rates are shown in Fig. 1.

Reducing these figures to a ratio of exhaust gas volumes with idling as unity, they become for a 1951 Ford Six:

(1) Idling: 1.00.
(2) Acceleration: 5.15.
(3) Cruising: 3.50.
(4) Deceleration: 2.42.

Collection of Samples

Instantaneous samples for hydrocarbon and Orsat determinations were collected behind the muffler by drawing the exhaust gases into evacuated 300-ml glass mine sampling tubes. Two-liter evacuated flasks were used to collect samples for aldehydes, oxides of nitrogen, and acetylene determinations. The chemical methods that were employed are beyond the scope of this article. The refences are listed separately in Table 2.

During the acceleration cycle, samples were first collected while driving in each of the three forward gears at approximately 6, 17, and 28 mph, respectively. It has been found through experience that the sample taken in second gear at 17 mph represents an average condition of the entire acceleration cycle. For this reason, samples are now taken only in second gear at approximately 17 mph.

During the deceleration cycle, samples were taken originally at 3-sec intervals, corresponding to $0 + 3$, $0 + 6$, $0 + 9$, and so on. The zero time corresponds to the moment that the throttle was closed from a speed of 35 mph. Repeated tests have shown that the sample taken at $0 + 6$ sec represents a suitable average of the entire deceleration cycle. For this reason, only one sample ($0 + 6$ sec) is now taken.

Table 2 – Analytical Methods Used to Evaluate Auto Exhaust Emissions

1. Hydrocarbons – Beckman IR–2 infrared spectrophotometer with a specially constructed 100-cm gas cell. Concentrations are expressed as hexane. (*Analytical Chemistry*, Vol. 24, December, 1952, pp. 1899–1902: "Determination of Small Amounts of Hydrocarbons in Atmosphere," by P. P. Mader, M. W. Heddon, R. T. Lofberg, and R. H. Koehler.)

2. Oxides of Nitrogen – Pheoldisulfonic acid procedure (acid-absorbing solution). (P. 354 of "Analytical Chemistry of Industrial Poisons, Hazards, and Solvents," by M. B. Jacobs. Pub. by Interscience Pub. Co., New York, 1949.)

3. Acetylene and Its Homologs – Copper acetylide method. This method measures acetylene and all mono substituted acetylenes of the type RC≡CH in the form of copper acetylide. (P. 516 of "Analytical Chemistry of Industrial Poisons, Hazards, and Solvents," by M. B. Jacobs. Pub. by Interscience Pub. Co., New York, 1949.)

4. Aldehydes – Sodium bisulfite addition method (Ripper's method). Concentrations are expressed in terms of formaldehyde. (*Industrial & Engineering Chemistry* – Analytical Ed., Vol. 15, 1943, p. 378: "Collection and Estimation of Traces of Formaldehyde in Air," by F. H. Goldman and H. Yagoda.)

5. Carbon Dioxide, Oxygen, and Carbon Monoxide – Orsat method. Results expressed in percentages. For carbon monoxide concentrations less than 0.2%, a Mine Safety Appliance (MSA) sampler is used. (Mine Safety Appliance Co., Pittsburgh, Pa.)

Instantaneous samples are also taken for idling (at approximately 450 rpm) and cruising (level-road load at 35 mph).

For the idling and cruising cycles another sampling technique is frequently substituted for the instantaneous sampling method. When this method is used, samples are drawn through a small orifice restriction into an evacuated 2-l flask. This prolongs the sampling time and tends to give a better average for any fluctuations in the exhaust gas composition due to slight variations in engine operation. Checks made on the two methods, however, have shown no appreciable difference.

Estimated Hydrocarbon Emissions from Auto Exhausts

In 1940, there was a total of 1,160,110 automobiles and trucks in Los Angeles County. By 1954, the total had increased to 2,296,400. Calculations of the total amount of hydrocarbon vapors from automobile exhausts made by the District,[8] and similar calculations by others[9] based on exhaust gas analyses, have shown that about 850 tons[10] of hydrocarbons enter the atmosphere in Los Angeles County each day from automobiles. This calculation is made from the exhaust analyses obtained while driving under moderate traffic conditions.

Table 3 shows the per cent of time the vehicle was operating on the four cycles of the engine, the exhaust gas volumes, and gasoline consumption over a selected driving course through traffic. Using these values with the typical analytical results shown in Table 4, one can estimate the totals for various contaminants and other components on the basis of current gasoline consumption.

Estimated Particulates from Automobile Exhausts

In addition to the analyses for gases and vapors, preliminary data were collected under idling conditions for the solid and liquid aerosols.[11] The weight of particulate matter collected on a filter and electrical precipitator was found to be 3.3 mg per scf. This value may be compared to the hydrocarbon measurements of 1275 ppm or 139 mg per scf, for idling conditions. Theoretical calculations have been made on the quantities of lead and other additives to gasoline which might be emitted. If all of the lead and other compounds added to gasoline were exhausted to the atmosphere, the total for Los Angeles County would be 11 tons per day. The estimated oil consumption is 80 tons per day but only a small fraction of the oil burned would be emitted in particulate form.

The above values for smoke particles, or particulates, emitted in exhaust would lead to estimates ranging from 35 tons per day to 50 tons per day in the Los Angeles Basin. The material collected in tests is known to be extremely small and may be relatively unimportant in reducing the visibility. Air sampling studies are underway to obtain more data on this aspect of exhaust contributions.

Diesels

Only 120,000 gal of diesel fuel are burned per day by buses, trucks, and railroads in Los Angeles County for transportation as compared to 4,500,000 gal of gasoline. From these figures, it is obvious that the quantity of material discharged from diesel exhausts is insignificant from an overall air pollution point of view, as compared to that of gasoline-driven vehicles.

Liquid Petroleum Gas

Preliminary tests on engines using liquefied petroleum products have been made. An insufficient number of tests have been completed to report any valuable data at this time. Analyses appear to show that there is less of the aldehydes when lpg is used than when gasoline is the fuel. This fact may account for the noticeable difference in odor. The analyses for the quantities and types of hydrocarbons must be extended further before conclusions can be reached.

Smog-Producing Hydrocarbons in Exhaust Gases

In order to determine the effect of automobile exhausts, experiments and tests were run exposing leafy vegetables (as indicators) to exhaust gases in fairly low concentration. The hydrocarbons were oxidized with ozone in a test chamber. The results of these tests demonstrated that automobile exhausts could cause typical smog damage to leafy vegetables.

Table 3 – Average Automobile Performance in Los Angeles Traffic

Operating Cycle	% Operation Time – Average Traffic	Exhaust Volume Ratio[a]	Gas Consumption Ratio[b]
Idle	18	1	1
Acceleration	18	4.5	7
Cruising	46	3	4
Deceleration	18	2	2

[a] Values are ratios of exhaust volume to idling exhaust volume of 14 scfm.
[b] Values are ratios of gasoline consumption to idling gasoline consumption of 0.4 gph.

Table 4 – Results of a Typical Analysis of Automobile Exhaust Gases[a]

	Idling	Acceleration	Cruising	Deceleration
Hydrocarbons (C_2-C_9) as Hexane, ppm	1275	410	354	5125
Acetylenic, as Acetylene, ppm	825	18	64	587
Oxides of Nitrogen, as NO_2, ppm	8	4180	1606	18
Lower Aldehydes, as Formaldehyde, ppm	88	1369	264	193
CO_2, %	3.6	0.0	0.4	1.5
CO_2, %	10.0	13.7	12.9	6.1
O_2, %	1.4	1.3	1.1	9.5

[a] "Automotive Exhaust Testing Procedures and Efficiency Studies in the Evaluation of a Catalytic Muffler," Air Pollution Control District, Appendix II, 1954.

[8] See "Atmospheric Pollution from Hydrocarbons in Automobile Exhaust Gases," by F. H. Viets, G. I. Fischer, and A. P. Fudurich. Los Angeles County Air Pollution Control District, 1953.

[9] See Proceedings of Second National Air Pollution Symposium, 1952, pp. 71-74: "Hydrocarbon Constituents of Automobile Exhaust Gases," by P. L. Magill, D. H. Hutchinson, and J. M. Stormes.

[10] Four and one-half million gallons of gasoline, daily consumption in Los Angeles County, used in calculations.

[11] See "Third Technical and Administrative Report on Air Pollution Control in Los Angeles County, 1953-1954," Los Angeles County Air Pollution Control District.

Table 5 – Damage to Vegetation by Automobile Exhaust Gases

Hydrocarbons as Hexane,[a] ppm	Ozone,[b] ppm	Nitrogen Dioxide,[a] ppm	Formic Acid,[a] ppm	Aldehydes,[a] ppm	Exhaust Dilution	Temperature, F	Relative Humidity, %	Damage to Vegetation[a]				
								S	B	O	A	E
5.46	0.19	0.20	0.41	1.67	1:116	83	51	T	T	T	T	T
8.40	0.28	0.17	0.23	1.18	1:116	71	68	T	T	T	T	T
8.60	0.26	0.32	0.23	1.15	1:116	83	53	T	T	T	T	T
35.00	0.33	0.71	ND	1.04	1:29	80	64	T	T	T	T	T
38.50	0.33	1.81	ND	2.69	1:29	82	58	T	T	T	T	T
5.74	0.17	0.23	0.27	1.02	1:116	80	45	T	t	T	t	T
17.40	0.33	0.32	0.33	1.40	1:58	83	58	T	N	t	t	T
16.50	0.33	0.20	0.20	2.15	1:58	87	52	T	t	t	t	N
4.48	0.20	0.25	0.17	0.24	1:232	83	59	N	N	t	N	t
3.01	0.18	0.23	0.07	0.22	1:232	79	60	t	N	N	N	N

[a] As measured in the Plexiglas chamber during the fumigation.
[b] Consumed in the reactions; value obtained equals amounts introduced into the chamber minus amount measured in the chamber after reaction had occurred.
ND: not determined; S: spinach; B: sugar beet; O: oats; A: alfalfa; E: endive; T: typical smog damage; t: typical smog damage in a lesser degree; N: no damage.

Table 6 – Damage to Vegetation by Gasoline

Hydrocarbons as Hexane,[a] ppm	Ozone,[b] ppm	Nitrogen Dioxide,[a] ppm	Formic Acid, ppm	Aldehydes[a]	Temperature, F	Relative Humidity, %	Damage to Vegetation				
							S	B	O	A	E
8.05	0.23	0.86	0.67	1.50	83	54	T	T	T	T	T
10.50	0.19	0.00	ND	1.85	87	53	T	T	t	t	t
12.20	0.21	0.41	0.45	1.64	83	56	T	t	T	T	T
3.08	0.05	0.33	0.25	0.96	92	41	t	t	N	N	N
4.00	0.04	0.36	0.13	0.51	86	45	t	N	t	N	t
15.80	0.25	0.00	ND	1.99	81	54	t	N	N	N	N
2.52	0.11	0.23	0.10	0.35	69	71	t	N	N	N	N
2.87	0.08	0.26	0.15	0.42	88	43	N	t	t	t	t

[a] As measured in the Plexiglas chamber during the fumigation.
[b] Consumed in the reactions: value obtained equals amount introduced into the chamber minus amount measured in the chamber after reactions had occurred.
ND: not determined; S: spinach; B: sugar beet; O: oats; A: alfalfa; E: endive; T: typical smog damage; t: typical smog damage in a lesser degree; N: no damage.

Test-Chamber Experiments

A series of experiments was conducted to learn if constituents found in exhaust gas were capable of producing smog effects. Measured quantities of exhaust gases, mixed with air to dilute the hydrocarbon content, were introduced into the Plexiglas chamber. A controlled amount of ozone was introduced in each fumigation through a separate tube. The outlets of the hydrocarbon and ozone tubes in the chamber were located over a fan to aid the mixing in the atmosphere of the chamber. Earlier experiments in fumigating plants with single hydrocarbons, or gasoline, introduced the ozone directly into the hydrocarbon stream. Air was then introduced to dilute the reaction products for the fumigation experiments.

Damage, typical of that found in the field after smog attacks, was produced on all five indicator plants when the exhaust gases and ozone were introduced into the chamber at separate points. Results are shown in Table 5.[12] A comparison was made of the quantities of equivalent weights of gasoline against hydrocarbons in automobile exhausts to give a minimal damage effect, with the results as shown in Table 6.[12] Borderline damage was obtained with 8.05 parts per million gasoline vapor and with 5.46 parts per million exhaust hydrocarbons. While it is recognized that the concentrations of hydrocarbons used in these experiments are above those found in the atmosphere, the experimental conditions imposed limitations which precluded using concentrations at the dilutions found in the atmosphere. The time for reaction in the chamber, because of its limited size, is only 17 min. The oxidation reaction in the atmosphere is continuous and is difficult to duplicate in an enclosure.

Eye Irritation and Aerosol Formation

During these and other experiments, observations were made for eye irritation and for formation of aerosols from the oxidation of the exhaust gases. Eye irritation was noted in some of the fumigation experiments. The presence of aldehydes in the exhaust gases may account for some of this effect. An experiment, using 4.3 ppm of exhaust hydrocarbons, produced eye irritation when the aldehyde concentration was below the eye-irritating threshold known for formaldehyde. No actual measurements were made of the quantities of aerosols formed from a given amount of hydrocarbons in the exhaust. Observations were made by introducing ozone into the exhaust stream and noting the visual increase of aerosols. Exhaust gases exposed to sunlight in a Plexiglas box showed increases in aerosol formation using a Tyndall beam. From these experiments it was concluded that the exhaust gases from the gasoline internal-combustion engine are as effective in producing

[12] See *Air Repair*, Vol. 4, August, 1954, pp. 31-34: "Detection of Smog-Forming Hydrocarbons in Automobile Exhaust Gases Using Plants as Indicators," by G. R. Cann, W. M. Noble, and G. P. Larson.

Table 7 – Traffic Distribution over 24-Hr Period on Weekdays

Period	% of 24-Hr Traffic
6:00 a.m.–10:00 a.m.	20–25
10:00 a.m.– 4:00 p.m.	30–35
4:00 p.m.– 7:00 p.m.	20–25
7:00 p.m.– 6:00 a.m.	20–25

smog effects as is gasoline vapor when both are oxidized in the presence of NO_2 and ozone.

Automobile Exhaust and Traffic Distribution

Upon completion of the analytical work for the quantities of hydrocarbons, studies were undertaken to determine the hydrocarbon concentrations in the atmosphere which might result from the emissions of automobile exhaust.[11] This project involved a study of the distribution of traffic throughout the basin, measurements in the atmosphere of carbon monoxide, oxides of nitrogen, and hydrocarbons, together with trajectory studies of wind-flow patterns in the area. Since the peak periods of traffic obviously occur during the morning and late afternoon, atmospheric samples were taken prior to and during the period of early morning activity. Studies of air movement had already determined that the pollution would accumulate to the maximum during the early morning hours because of stagnation which occurs at night, followed by a period of low wind velocities.

A study of the traffic flow indicates a distribution over the 24 hr on weekdays as given in Table 7.

Detailed traffic counts show percentages of car miles per day in populated sections of the County.

Fig. 2 shows the traffic distribution in unit areas of approximately 25 square miles each. This distribution indicates approximately 6% of the total traffic miles as being covered in the densely populated downtown Los Angeles section. It can, therefore, be estimated from the analysis of automobile exhausts that 60-75 tons per day of hydrocarbons could reach the air in this area from automobiles.

Atmospheric samples measuring hydrocarbons, carbon monoxide, and nitrogen dioxide taken on several days in the central section of Los Angeles are plotted in Fig. 3 to show the average values obtained. The initial peak for hydrocarbons which occurs between 1:00 and 3:00 a.m. results from the residual pollution in the atmosphere which increases in concentration as the inversion lowers and the air becomes stagnant during the early morning hours. Following sunrise and the increased mixing, the concentration of pollution decreases, to be followed by another peak between 6:00 a.m. and 9:00 a.m. This peak period corresponds well with the influx of traffic to this area. From the studies of the traffic flow in a 24-hr period, it is estimated that 25% of the total emitted in this area for the day would be released during this peak period in the early morning hours. This quantity of hydrocarbons could account for the values measured in the air during the periods that measurements were being taken in this area. The

Fig. 2 – Geographical traffic distribution in Los Angeles County (numbers shown represent percentage of County's daily traffic, car miles, occurring in area)

values for carbon monoxide, and oxides of nitrogen as well, which would be released during a corresponding period, follow a similar pattern and are consistent with the total amount of material released for the period of time involved. A typical example of the traffic flow for a single freeway is shown in Fig. 4.

In order to determine whether or not another source of hydrocarbons could influence the concentrations measured in the downtown area, sampling was carried on in the refinery area, approximately 20 miles south of the Civic Center. At the time these studies were undertaken it was estimated that refinery sources were emitting approximately 300 tons per day of hydrocarbons. Carbon monoxide, and oxides of nitrogen as well, could be expected from sources in the refinery area. It will be observed from the values plotted in Fig. 5 that the carbon monoxide values in the Dominguez area are extremely low as compared to the downtown area. This marked difference in itself indicates a separate source as contributing this material to the Civic Center.

While the peak concentrations for hydrocarbons in the refinery area between 3:00 and 4:00 a.m. might indicate a transfer of this material to influence the later peak in the downtown area between 6:00 and 9:00 a.m., studies of the wind currents on the days when sampling occurs have indicated few occasions when this could occur. A series of studies on days of eye irritation in the Civic Center was made during July, 1952, and January, 1953.[13] For these periods a number of cases of surface wind flow were plotted for each day when eye irritation occurred.

Fig. 6 designates the nighttime stagnation area for the air which was polluted when it reached the Civic Center about 10:00 a.m. The symbols *L, M,* and *H* indicate the degree of eye irritation as light, medium, and heavy, respectively. The square symbols are for those cases where the trajectories passed over the refinery area before the air stagnated. The round symbols show the cases where the air could not have passed over the refinery area.

In the 37 cases of downtown eye irritation studies, there were three instances of air arriving from the west traffic area without stagnating, two cases of air coming from the refinery area without stagnating, and seven indeterminate cases where air passed over both refinery and heavy traffic areas without stagnating. In addition, there were 25 cases where the air stagnated in heavy traffic areas (west 13, southwest 4, south 1, east 2, and northwest 5). Studies of individual cases reveal several where winds both at the surface and aloft could not have brought air from the refinery area to downtown Los Angeles. The intense traffic activity was apparently sufficient in itself to produce the observed moderate to severe eye irritation.

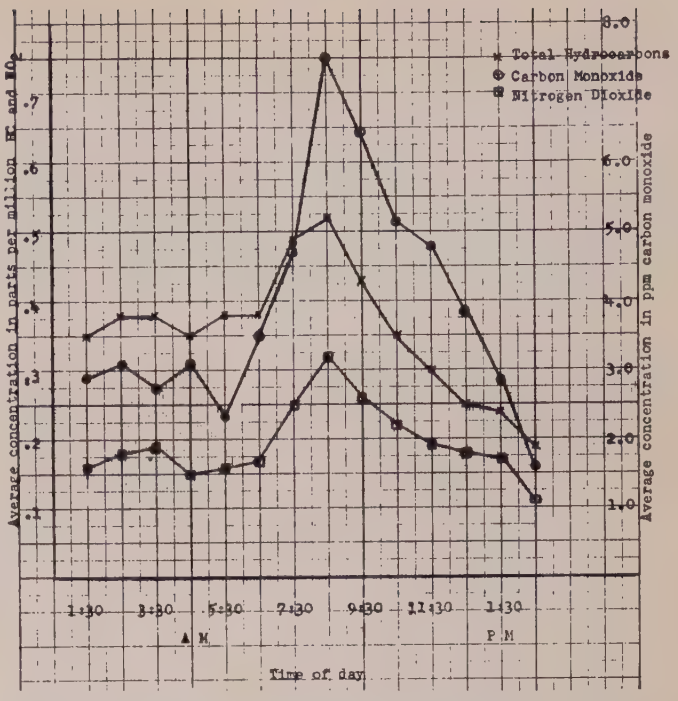

Fig. 3 – Diurnal curves for hydrocarbons, carbon monoxide, and nitrogen dioxide for downtown Los Angeles (days of eye irritation, 1953 and 1954)

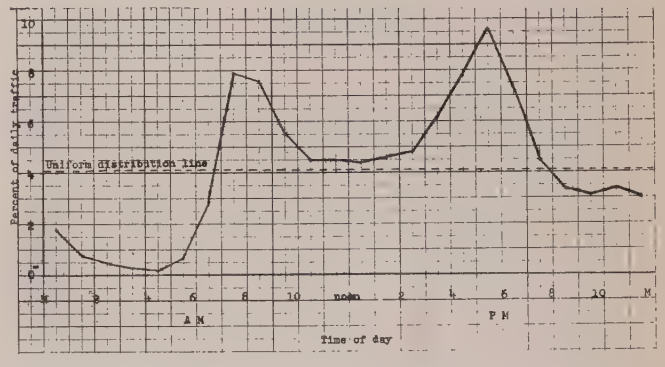

Fig. 4 – Traffic distribution on Hollywood Freeway at Cahuenga Pass (weekday traffic, 1950 and 1951)

Conclusions

The decision to control a source of pollution should be predicated upon studies which show a clear contribution of the source to the detrimental effects caused by polluted air. It could, of course, be conceded without extensive studies that some of the contaminants in auto exhaust contribute to the pollution of the air. Since hydrocarbons or gasoline vapors were known to be an important factor in producing several of the deleterious effects of smog, one question to be answered is whether or not the removal of hydrocarbons from all other sources in the community would relieve the burden on the air sufficiently to avoid any control measures on auto exhaust.

The studies which show that hydrocarbons are present in the exhaust gases and that, under irra-

[13] See Special Report Meteorological Section, Air Pollution Control District of Los Angeles, June 28, 1954.

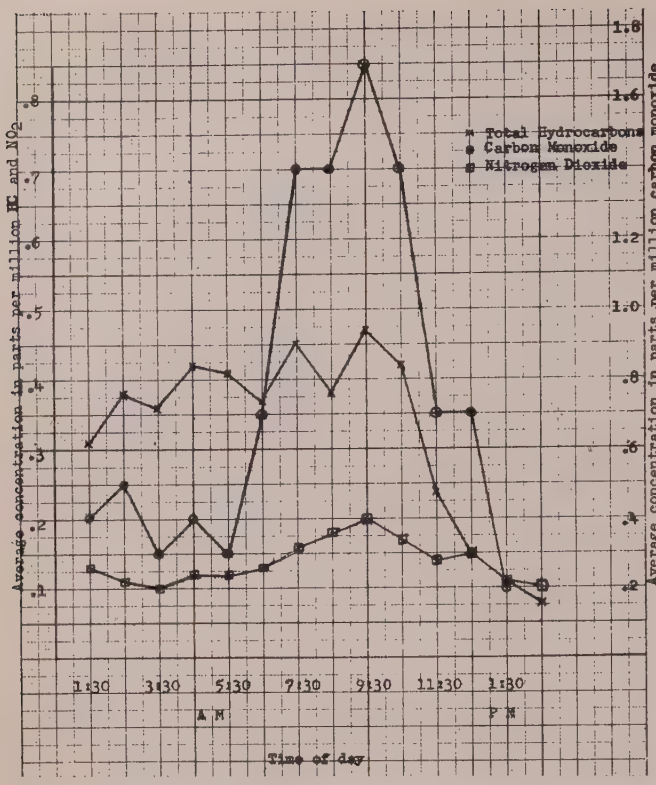

Fig. 5 – Diurnal curves for hydrocarbons, carbon monoxide, and nitrogen dioxide for Dominguez area, Carson Street Station (days of eye irritation, 1953 and 1954)

diation or oxidation with ozone, smog-type damage can be produced on plants, represents only a part of the necessary information to determine whether control measures are necessary. The studies[14] by Dr. A. J. Haagen-Smit at the California Institute of Technology concerning the formation of ozone from hydrocarbons and particularly from auto exhaust is one more step in showing the effects which can be expected under certain conditions. Only when all of these facts are considered along with the measurements of hydrocarbons in the atmosphere and a study of the wind currents, can one conclude that the impact of traffic is significant.

Studies now clearly show that removal of all other sources of hydrocarbons from refineries (Fig. 7) and from the distribution of gasoline will not lower the concentration of hydrocarbons in the downtown area and the north-central section of the County sufficiently to relieve the eye irritation, crop damage effects, and high ozone content of the air in those areas. The marked influence of traffic in the early morning hours increases the concentration of hydrocarbons to levels which cannot be tolerated in the Los Angeles atmosphere. On the basis of the total studies, it has been concluded that the hydrocarbons must be removed from the exhaust gases of the automobile. Furthermore, the efficiency of removal must be extremely high. It is anticipated that the Los Angeles Basin will ultimately serve ten million persons. Because of the topography and the limited atmosphere, it can be anticipated that other areas will be influenced by a dense traffic pattern in the future. Freeway improvement provides easy access to outlying areas and traffic density can be expected to increase. The Air Pollution Control District recommends that engineering studies seeking to remove hydrocarbon vapors from exhaust gases should strive for a 90% overall removal under conditions of operation experienced in heavy traffic.

[14] See *Industrial & Engineering Chemistry*, Vol. 45, September, 1953, pp. 2086-2089: "Ozone Formation in Photochemical Oxidation of Organic Substances," by A. J. Haagen-Smit, C. E. Bradley, and M. M. Fox.

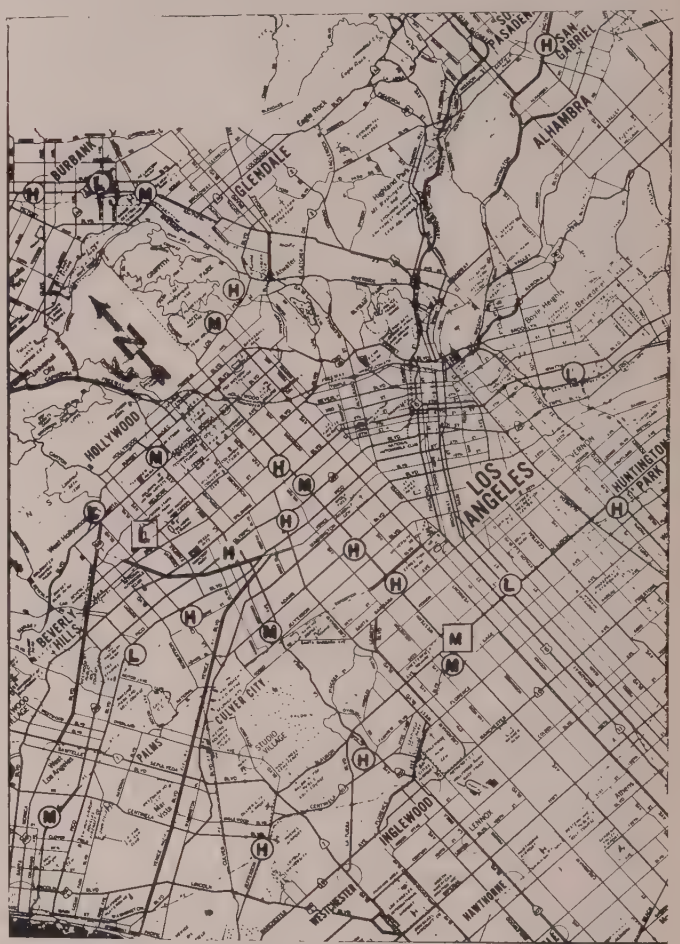

Fig. 6 – Centers of stagnation areas for air arriving at Civic Center at 10 a.m.

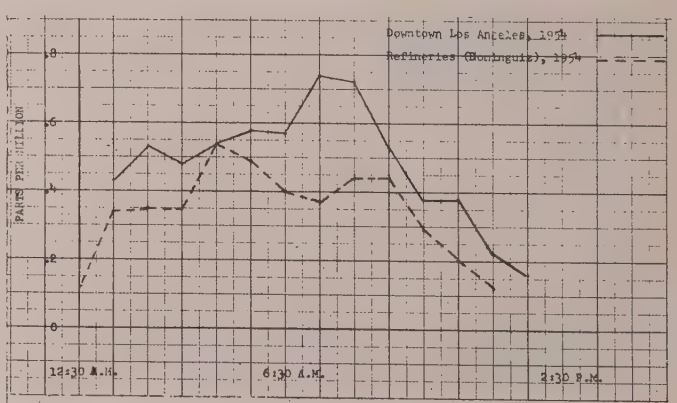

Fig. 7 – Hydrocarbon comparison (average hydrocarbon values for days when inversion base was 1000 ft or lower)

Automobile Exhaust and Ozone Formation

A. J. Haagen-Smit, California Institute of Technology
Margaret M. Fox, Los Angeles County Air Pollution Control District

This paper was presented at the SAE Golden Anniversary Annual Meeting, Detroit, Jan. 10, 1955.

TYNDALL wrote a letter to the Royal Society of London, which reads as follows: "The vapor of nitrite of amyl was permitted to enter an experimental tube while the beam from the electric lamp was passing through it. For a moment the tube was optically empty, nothing whatever being seen within it. But, before a second had elapsed a shower of particles was precipitated on the beam. The cloud, thus generated, became denser as the light continued to act, showing at some phases, iridescence." Tyndall goes on to say: "It is probably the synchronism of the vibration of one portion of the molecule with the incidence waves that enables the amplitude of those vibrations to augment until the chain which binds the parts of the molecule together is snapped asunder."

I think, therefore, that Tyndall was the first man to actually demonstrate the Los Angeles smog, and his explanation of the reaction mechanism still holds, although the modern physical chemist may have more difficult ways of expressing the same thought. Tyndall could have gone further. If he had placed a piece of bent rubber in his experimental tube, he would have seen that after a short while the rubber shows deep cracks resembling those given by ozone.

The most typical characteristic of Los Angeles smog is its strong oxidizing effect. Using the characteristic cracking of rubber as test method, as well as chemical means, it has been established that a substantial part of the oxidant consists of ozone.[1, 2] The ozone concentration rises sharply during smog periods, and values as high as 0.5 ppm (V/V) have been reported, which exceed by a factor of 20 the ozone concentrations found in inhabited areas.

Daily determinations with phenolphthalein reagent have shown that shortly after sunrise the oxidant rises, and reaches a maximum at some time during the day – in Pasadena most often from 1-2 p. m. At about sundown the oxidant decreases considerably, and it is practically absent during the night. We have been measuring these effects for more than a year, and have found that when the oxidant value exceeds a certain level, eye irritation occurs (Fig. 1).

Fig. 2 shows the fluctuation in the daily maximum recorded at the California Institute of Technology in Pasadena. The fluctuations are largely caused by meteorological conditions. However, there is a distinct weekly pattern which shows that Sundays are definitely less smoggy than other days

OZONE has been found to be a substantial part of the oxidant characteristic of Los Angeles' smog. Since automobile exhaust gases are capable of forming ozone in the air, they are considered a definite cause of smog.

In studies reported here, ozone was produced in the laboratory and measured by rubber cracking and chemical tests. Exhaust gases from cruising and accelerating phases of automobile operation were irradiated to form ozone. Exhaust gas from idling and deceleration produced ozone photochemically after addition of NO_2.

Discussion of this paper starts on p. 618.

[1] See *Rubber Chemistry & Technology*, Vol. 24, October-December, 1951, pp. 750-755: "Application of Rubber in Quantitative Determination of Ozone," by C. E. Bradley and A. J. Haagen-Smit.

[2] See *Industrial & Engineering Chemistry*, Vol. 44, June, 1952, pp. 1342-1346: "Chemistry and Physiology of Los Angeles Smog," by A. J. Haagen-Smit.

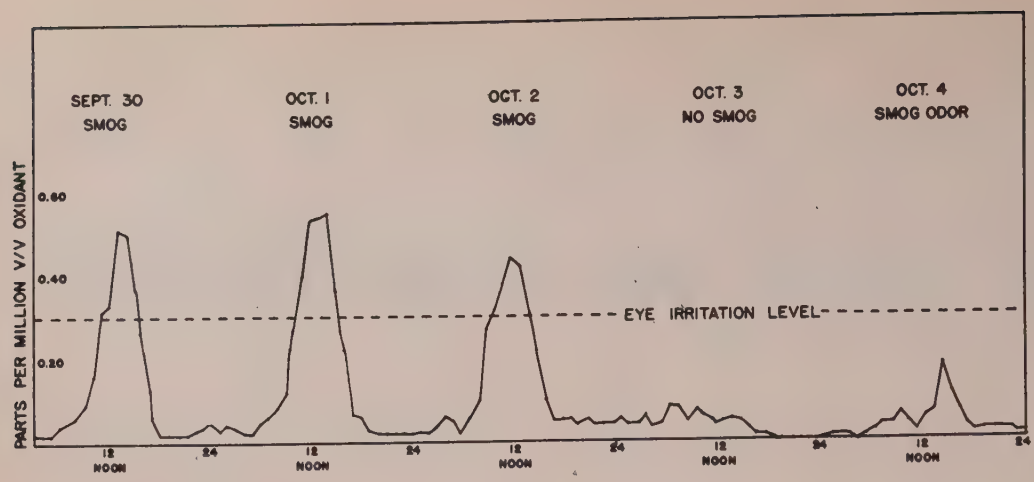

Fig. 1 – Oxidant levels in Pasadena, Calif., over a 5-day period beginning Sept. 30, 1953

of the week, especially Thursdays and Fridays. This phenomenon is not clearly understood. It could be due to reduced activity of industry as well as to a change in the traffic pattern during weekends.

The value of these records lies in the objective estimation of smog intensity, and when continued, the data will aid in judging smog control progress.

From these records we can see that the worst smog period in 1954, from August through October, was not as bad as 1953, either in intensity or in duration (hours per day). Nevertheless, the eye irritation level was exceeded in Pasadena during that time on 65 out of 90 days.

The formation of ozone can be duplicated in the laboratory by exposing hydrocarbon vapors and nitrogen oxides to sunlight at concentrations of reactants which have been found in the Los Angeles air during smog attacks.[3, 4] Ozone formation during photochemical oxidation is not limited to hydrocarbons, but is also shown by their oxidation products – acids, aldehydes, ketones, and alcohols. From a practical point of view, it is important that the irradiation of gasoline vapors in the presence of nitrogen dioxide also leads to the formation of ozone and causes severe rubber cracking, and the Los Angeles County Air Pollution Control District has demonstrated the ozone-forming property of the air near sources of hydrocarbon release.

In duplicating the ozone formation observed in polluted air, it is essential to adhere to a rather narrow concentration range of hydrocarbon and nitrogen dioxide, which was confirmed by a set of experiments in which the hydrocarbons, 3-methylheptane, and the NO_2 concentrations were systematically varied. Artificial light from a bank of Westinghouse 40-w blue fluorescent light tubes was used for the irradiation to eliminate the variable intensity of sunlight. The lamps were arranged in the form of a U, four tubes to a side, and spaced so that when a 5-l flask was placed in the center, the bulbs were approximately ½ in. from the sides and bottom of the flask. An oxygen atmosphere adjusted to 30% humidity and an irradiation time of 10 hr were selected as standards in the experimental procedure. The ozone formed was measured by the cracking observed on bent rubber strips of standard size (8 x 20 x 2 mm) suspended in 5-l flasks during irradiation.

To remove volatile impurities, the rubber strips were exhaustively extracted with carbon tetrachloride at room temperature, and the last traces of solvent were removed in vacuum. It was found advantageous to use as ozone measure the sum of the depth of *all* cracks as measured under the microscope (100 x), using an ocular micrometer. The measurement of crack depth was made on freshly cut surfaces exposed by making longitudinal cuts through test strip 1 mm from the edges.

In the experiments, the rubber was bent and the ends tied together with glass thread used to suspend the test strip in the flask. The calibrations against known ozone concentrations were made in flasks of the same size as those used in the irradiation experiments. In the concentration range used, the total crack depth is proportional to the ozone concentration, 1.0 mm corresponding to 3 ppm of ozone.

When 3-methylheptane in concentrations of 3 ppm and NO_2 concentrations varying from 0-100 ppm are irradiated, it is noticed that cracks begin to appear at a concentration of approximately 0.1 ppm NO_2. The cracking increases with increased NO_2 concentration, until at about 1-3 ppm a maximum is reached. At this maximum, our standard rubber shows 20-30 cracks with a total crack depth of 2.7 ± 0.3 mm. After passing this maximum the rubber cracking diminishes, and at about 5-10 ppm of NO_2, no cracks appear in the 10-hr irradiation. Similar experiments were carried out with concentrations of 0.1, 1.0, 3.0, 10, 20, 40, 150, 400, 2000, and 10,000 ppm of hydrocarbon. The results of

---

[3] See Proceedings of Second National Air Pollution Symposium, September, 1952, pp. 54-56: "Formation of Ozone in Los Angeles Smog," by A. J. Haagen-Smit, C. E. Bradley, and M. M. Fox.

[4] See *Industrial & Engineering Chemistry*, Vol. 45, September, 1953, pp. 2086-2089: "Ozone Formation in Photochemical Oxidation of Organic Substances," by A. J. Haagen-Smit, C. E. Bradley, and M. M. Fox.

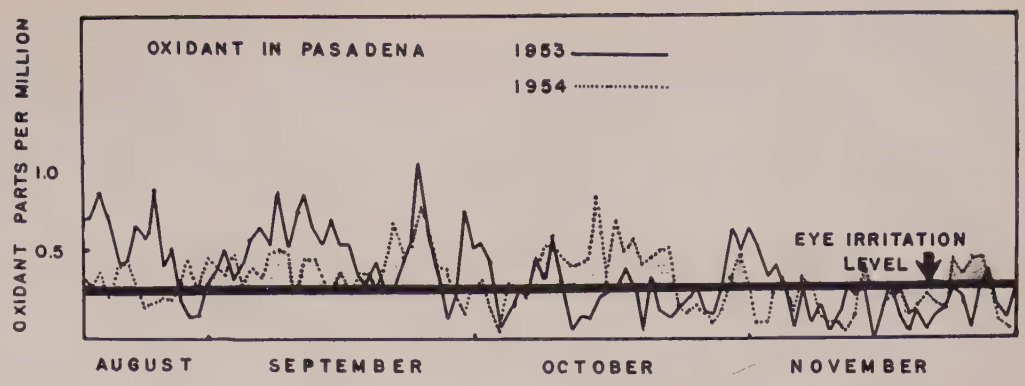

Fig. 2 – Daily oxidant maxima in Pasadena. Fluctuations show the worst smog period in 1954 was not as bad as that in 1953, and reveal a distinct weekly pattern, with Sundays less smoggy than other days of the week

these experiments are compiled in Fig. 3. The approximate area of concentrations of hydrocarbon and NO_2 where rubber cracking takes place in these experiments is indicated by dotted lines. At concentrations higher than 400-1000 ppm of NO_2, the rubber test can no longer be used in irradiation experiments, since NO_2 alone causes rubber cracking in the dark through a direct reaction between the NO_2 and the rubber. This limit is indicated by the dotted line at the right of the ozone-forming area.

The phenomenon that ozone formation is limited to definite relative proportions of hydrocarbon and NO_2, observed with 3-methylheptane, is apparently equally true for other hydrocarbons and their oxidation products. At a concentration of 3 ppm and varying concentrations of NO_2, the hydrocarbons n-butane, n-pentane, n-hexane, n-heptane, n-octane, n-nonane, n-hexene-1 and di-isobutylene gave curves similar to the one obtained with 3-methylheptane, with optimum ozone formation at from 1-3 ppm NO_2. It has been observed that as the length of the carbon chain in the straight chain paraffins increases from C_4 to C_9, the ozone-forming capacity becomes greater. Methane, ethane, and propane were found to be inactive. It is of interest to note that the highly branched hydrocarbon, 2,2,3-trimethylbutane (triptane) does not cause a measurable rubber cracking during the 10-hr irradiation period. This marked effect of branching and also that of the presence and location of double bonds is being further investigated.

While for experimental reasons artificial light and oxygen were used, it was of interest to see if similar results could be obtained with sunlight and air. Fig. 4 shows the similarity of curves obtained by plotting the crack depth obtained from 3 ppm of 3-methylheptane and variable concentrations of NO_2 after 10 hr of irradiation in oxygen in artificial light, and after 3 hr of sunlight irradiation in an atmosphere of synthetic air (80% nitrogen and 20% oxygen of 30% humidity).

The general shape of the curves obtained in these experiments can be attributed to at least two simultaneous reactions: the formation of ozone, and the removal of ozone by NO_2 and the oxidation products of the hydrocarbon. That NO_2

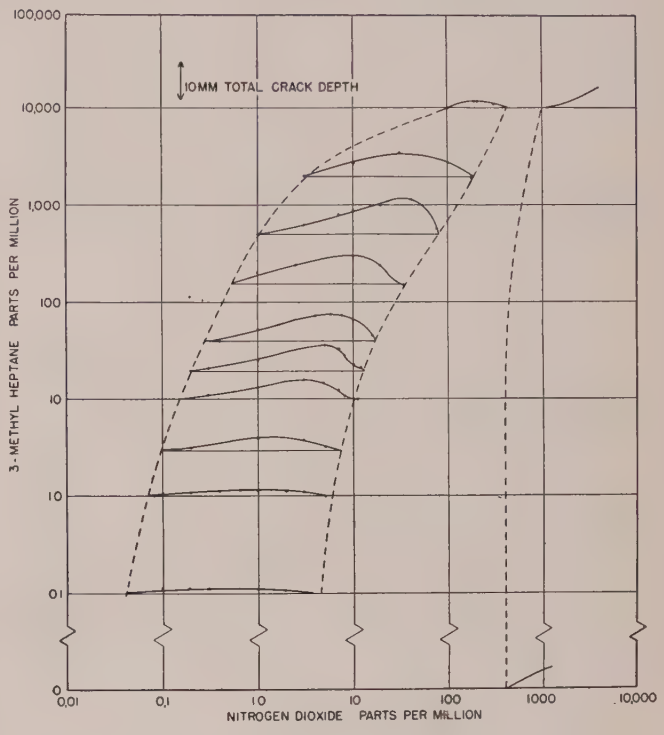

Fig. 3 – Rubber cracking with 3-methylheptane and NO_2

The Authors

A. J. HAAGEN-SMIT is professor of bio-organic chemistry at the California Institute of Technology. He received a Ph.D. in 1929 from the University of Utrecht, the Netherlands. After teaching chemistry at that university, he went to Harvard University for a year as a visiting lecturer. In 1937, Dr. Haagen-Smit became an associate professor at California Institute of Technology and, in 1941, was appointed to a full professorship in bio-organic chemistry. In 1950, he received the American Chemical Society Fritzsche Award. Since 1951, Dr. Haagen-Smit has been a consultant to the Air Pollution Control District.

MARGARET M. FOX is a chemist for the Los Angeles County Air Pollution Control District. In 1940, she received a B.S. in chemistry from Saint Joseph College, West Hartford, Conn. In the following years, her work was concerned with analytical chemistry. Since 1949, Miss Fox has assisted Dr. Haagen-Smit in his research and their work has resulted in the publication of several papers on the formation of ozone through photochemical oxidation of hydrocarbons in the presence of nitrogen oxides.

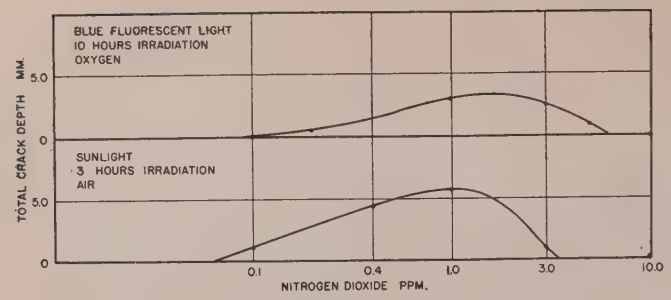

Fig. 4 – Rubber cracking with 3-methylheptane (3 ppm)

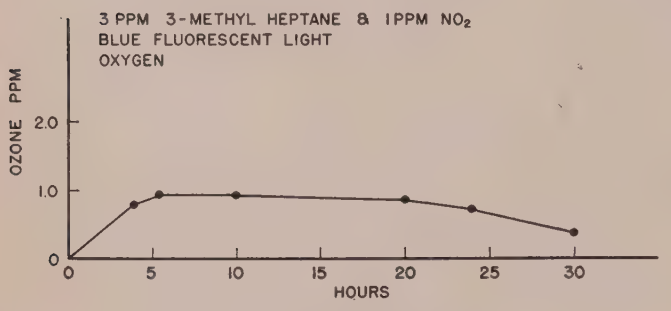

Fig. 5 – Isolation of ozone

does react with ozone is well known, and especially at higher concentration this removal of ozone will play an important role. In our experiments it has been observed that at the upper limits of NO_2 concentrations when no cracking appears after 10 hr, longer irradiation does produce cracking. It is most likely that during this induction period the NO_2 concentration has decreased until it comes within the range of ozone formation. This shift in the composition of the mixture is also brought about by the reaction of NO_2 with the hydrocarbon and its oxidation products. When ozone formation stops, NO_2 is practically absent.

The rubber strip suspended in the flask during the irradiation continually removes the ozone formed, and is in competition with the products that will react with ozone. Although the reaction with the rubber strip takes 20-30 min to remove the ozone nearly quantitatively from a 5-l flask, the rate at which the rubber reacts with the ozone is sufficiently greater than the degradation reaction to be able to show considerable ozone formation. We find that the average rate of ozone formation during the first 10 hr of irradiation of 3-methylheptane (3 ppm) and NO_2 (1 ppm) is about 0.8 ppm per hr. After 100 hr, slight cracking is still observed, and at that time the total crack depth corresponds to 20 ppm of ozone, clearly indicating a chain reaction of considerable extent.

The high values obtained in these experiments are possible only because the rubber strip continuously removes the ozone formed. If, however, the ozone is not removed, it will react with the hydrocarbon and its oxidation products and with the nitrogen oxides. Consequently, the ozone measured, after a certain length of irradiation time in the absence of rubber, will represent the excess of ozone due to the different rates of these reactions. The reaction by which ozone is formed is only slightly faster than those which destroy it. When we attempt to isolate any ozone we isolate only the slight excess resulting from the difference in the rate of these reactions. In the analysis of air samples, it is this excess of ozone which is measured.

In duplicating these phenomena in the laboratory, hydrocarbons and their oxidation products were irradiated in the presence of NO_2, and the ozone determined after exposure for different lengths of time. The ozone concentration was measured in two ways. One was by measurement of the rubber cracking. In these experiments, the rubber was introduced *after* the irradiation, and not during the irradiation as previously described. The second way of determining the ozone was a chemical one, whereby advantage was taken of the difference in vapor pressures of ozone and NO_2. By passing the irradiated mixture through several traps held at —183 C, only ozone passes through, while NO_2, with its higher boiling point (24 C) is trapped. The ozone passing through the traps was determined by both the phenolphthalein and the potassium iodide method. Fig. 3 shows the results of such measurements on irradiated mixtures of 3-methylheptane and NO_2 at concentrations of 3 ppm and 1 ppm, respectively. The experiments were performed with blue fluorescent light in 5-l flasks filled with oxygen at a humidity of 30%.

The ozone present after 4, 5, 10, 20, 24, and 30 hr was determined. Fig. 5 shows that after 5 hr a concentration of 1 ppm of ozone is established, which remains nearly constant for about 20 hr. When duplicate flasks were kept in the dark for 1 hr before measuring the ozone content, the ozone concentration was reduced to one-half the value obtained directly after irradiation. In order to keep the level of ozone concentration at 1 ppm for 20 hr, approximately 14 ppm of ozone must have been formed during that time. The experiments previously described, in which the rubber strips were suspended in the flasks during irradiation, indicated the formation of 12 ppm of ozone during the period between 5 and 25 hr. These experiments, although of a qualitative nature, support the conclusion reached earlier, that a considerably greater amount of ozone is produced than could be expected on the basis of a stoichiometric reaction of 3 ppm of hydrocarbon and 1 ppm of NO_2.

Work is in progress to determine the ozone-forming capacity of mixtures of hydrocarbon and NO_2 in concentrations from 0-3 ppm. It is hoped that from these data it will be possible to determine the reduction in hydrocarbon and NO_2 concentration necessary to bring the oxidant values in the air below threshold concentrations. Because of the practical aspect of this problem, these experiments

are carried out with sunlight and air. Preliminary results have shown that with 3-methylheptane at 2 ppm and NO_2 at 1 ppm, a concentration of 0.6 ppm of ozone is obtained after 4 hr of irradiation. At 1 ppm hydrocarbon and 1 ppm NO_2, 0.3 ppm of ozone is measured after 4 hr of irradiation. These concentrations of hydrocarbon, nitrogen oxides, and ozone formed approximate values actually found in the analysis of Los Angeles smog.

With the knowledge that ozone formation is limited to a definite area of concentration of hydrocarbon and NO_2, problems of a more practical nature, such as the production of ozone from automobile exhaust, could be undertaken.[5] Once the concentration of hydrocarbon and NO_2 in the exhaust is known, the dilution at which ozone formation could be expected to take place can be read from Fig. 6.

The concentrations of hydrocarbon and nitrogen oxides vary with the different phases of automobile operation. Therefore, the exhaust gases from each of these phases – idling, acceleration, deceleration, and cruising – were analyzed for hydrocarbon and nitrogen dioxide, and were diluted to provide concentrations appropriate for ozone formation, using the data collected with pure hydrocarbons as a guide.

In order to obtain a hydrocarbon-NO_2 mixture from cruising and acceleration phases which falls within the area where ozone formation was established with synthetic mixtures, the samples were diluted with air to approximately 1/200 to 1/500 of their original concentration. The gas mixture from deceleration, and especially that from idling, is low in NO_2, and since it was preferred to demonstrate ozone formation at concentrations not exceeding 10 ppm of hydrocarbon, it was necessary to add NO_2 to the reaction mixture. In this manner, concentrations were obtained of 2 ppm hydrocarbon and 1 ppm NO_2 for idling, and 6 ppm hydrocarbon and 1 ppm NO_2 for deceleration. These concentrations are within the range of ozone formation as shown in Fig. 6.

The irradiation was conducted in sunlight, and the ozone concentration was determined after varying periods of time. The atmosphere in the flask was composed of synthetic air (80% nitrogen, and 20% oxygen, of 30% humidity). After irradiation, the contents of the flasks were passed through traps held at —183 C to remove nitrogen oxides, as well as peroxides. The ozone passing through the traps was then determined colorimetrically through its oxidizing effect on reduced phenolphthalein. The results of these experiments are shown in Table 1. In addition, samples of exhaust gas from decelerating and accelerating phases of the cycle were irradiated with artificial light in an oxygen atmosphere under the standard conditions described earlier, using bent rubber strips suspended in 5-l flasks during irradiation. After dilution to 6.6 ppm of hydrocarbon and the addition of 1 ppm NO_2, the exhaust gases from the decelerating phase gave severe cracking of the bent rubber strips, corresponding to an average rate of ozone formation of 1.0 ppm per hr. The exhaust gases of the acceleration phase diluted to 1.1 ppm hydrocarbon and 5.8 ppm NO_2 also gave severe cracking, corresponding to 1.0 ppm of ozone per hr.

It should be noted that during stop-and-go driving, the combination of deceleration, idling, and acceleration furnishes an exhaust mixture which contains hydrocarbons and nitrogen oxides in such proportions that no addition of NO_2 is necessary for ozone formation. This combined mixture has substantially the same composition as that obtained from cruising, and we may therefore expect that, in both driving conditions, ozone formation starts when proper dilution has been reached. This

Table 1 – Ozone Formation with Automobile Exhaust

			Experimental			
Cycle Phase	Original Sample Composition, ppm		Hydrocarbon, ppm	NO_2, ppm	Irradiation Time, hr	Ozone Found after Irradiation, ppm
Cruising	Hydrocarbon	500	0.9	1.1	2.5	0.13
			1.5	2.8[a]	2.75	0.15
	NO_2	611	2.4	3.1	3.1	0.13
			0.9	1.1	5.3	0.15
Decelerating	Hydrocarbon	6,000	6.6	1.1[a]	3.0	1.1
			6.6	1.1[a]	4.1	1.9
	NO_2	75	6.6	1.1[a]	5.0	1.6
Accelerating	Hydrocarbon	600	1.3	6.5	2	0.07
			1.3	6.5	3	0.08
	NO_2	3,090	1.3	6.5	4	0.16
			1.2	6.0	5	0.22
Idling	Hydrocarbon	748	2.4	1.0[a]	2	0.45
			1.9	1.0[a]	3	0.95
	NO_2	0.1	1.9	1.0[a]	4	0.92
			1.5	1.0[a]	5	0.22

[a] 1 ppm NO_2 added.

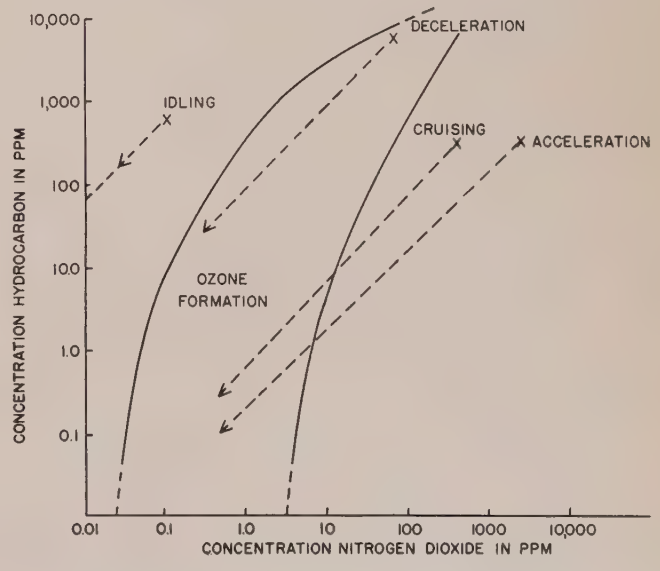

Fig. 6 – Photochemical ozone formation from automobile exhaust

[5] "Formation of Ozone from Automobile Exhaust," by A. J. Haagen-Smit, M. M. Fox, P. Mader, and B. Levy. Unpublished report to Los Angeles County Air Pollution Control District on Project D-34, July, 1954. (Much of its contents appear in *Air Repair*, Vol. 4, November, 1954, pp. 105-109: "Photochemical Ozone Formation with Hydrocarbons and Automobile Exhaust," by A. J. Haagen-Smit and M. M. Fox.

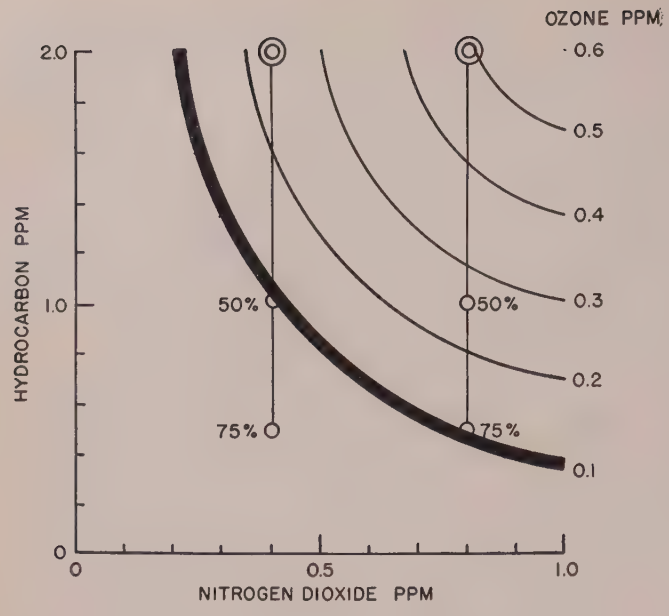

Fig. 7 – Ozone formation with 3-methylheptane and NO_2

condition will prevail at some distance from the emission of the exhaust, and it is estimated that a fifty to one hundred-fold dilution of the exhaust is necessary before ozone can be formed through the action of sunlight.

It is also of interest to note in Fig. 4 that exhaust from idling, either by itself or after dilution, does not lead to the formation of ozone upon irradiation, but that NO_2 addition is necessary from other phases of automobile operation or from extraneous sources. This fact has contributed in the past to many failures in the demonstration of ozone formation from exhaust gas.

The concentration of ozone formed, as well as the concentrations of exhaust gases used, are of the same order as those measured in the Los Angeles atmosphere. These investigations show that automobile exhaust gases are capable of forming ozone in the air, and are therefore to be considered as a definite source of smog.

More recently, we have been studying the effect of oxides of nitrogen on ozone formation in air and sunlight. Fig. 7 illustrates the ozone formation resulting from variable concentrations of hydrocarbon and nitrogen oxides, and represents a closer study of concentrations shown in the lower left-hand corner of Fig. 3, since it is concerned with concentrations of hydrocarbons and nitrogen oxides which have actually been measured during smog periods.

This graph shows the ozone level reached after 4 hr of irradiation with sunlight at varying concentrations of nitrogen dioxide and 3-methylheptane. Notwithstanding the use of a single hydrocarbon in these experiments, the values of ozone found seem to agree well with those found during smog periods, when not only the concentrations of hydrocarbons, but also the concentrations of their oxidation products are used in the computation. This method of computation is necessary because the concentrations of hydrocarbon and NO_2 determined during a smog attack do not represent initial concentrations. Oxidation is continuously going on, reducing the original hydrocarbon and NO_2 concentrations and increasing the concentrations of aldehydes, acids, and other oxidation products.

In the first place, we notice on our graph that the concentration of ozone formed is directly proportional to the product of the hydrocarbon and NO_2 concentrations. An increase of 20% in the hydrocarbon and NO_2 will therefore result in a 44% increase in the ozone formation, and this might well explain some of the increase in ozone levels during the last five years.

The graph also allows us to predict the effect that will be obtained by a reduction in the hydrocarbon. If the initial concentration of hydrocarbon is in the order of 2 ppm, and that of the nitrogen oxides 0.4 ppm, a reduction of 50% in hydrocarbon will enable us to remain just below the threshold of irritation of 0.1 ppm of ozone. However, when the NO_2 concentration is 0.8 ppm, a quantity which has actually been found during severe smog, a 75% reduction in hydrocarbon (from the original concentration of 2 ppm) would be necessary to reach the same threshold. Unfortunately, at present the tendency is toward a steady increase in the NO_2 concentration, which demands greater and greater efficiency in hydrocarbon recovery. The alternative is to reduce the NO_2 concentration as well as that of the hydrocarbons.

Summary

The concentrations of nitrogen dioxide and hydrocarbon at which photochemical ozone formation takes place have been determined, using 3-methylheptane as a standard hydrocarbon. n-butane, n-pentane, n-hexane, n-heptane, n-octane, n-nonane, n-hexene-1, and di-isobutylene showed similar behavior. The ozone formed was determined by rubber cracking and by chemical means. No ozone formation was found with methane, ethane, propane, or 2,2,3-trimethylbutane (triptane).

Experimental proof of the ozone-generating capacity of automobile-exhaust gases was obtained by irradiation of dilute exhaust gases from the cruising and accelerating phases of automobile operation. Exhaust gases from idling and deceleration phases formed ozone photochemically after addition of nitrogen dioxide. The concentrations of ozone formed, as well as the concentrations of exhaust gases used, are of the same order as those measured in the Los Angeles atmosphere. These investigations show that automobile exhaust gases are capable of forming ozone in the air, and are therefore to be considered as a definite smog source.

The control of nitrogen oxide emissions as well as those of hydrocarbons is emphasized.

An Inventory of Automobile Gases

Dale H. Hutchison and Francis R. Holden,
Stanford Research Institute

This paper was presented at the SAE Golden Anniversary Annual Meeting, Detroit, Jan. 10, 1955.

LARGE quantities and many types of impurities are emitted daily into the atmospheres of our cities. The pollutants may be solid, liquid, or gaseous; usually there are combinations of the three types. The magnitude of each pollution problem is a function of many meteorological factors, each contributing to the available capacity of the atmosphere as a dump. Pollution is most troublesome when the air mass becomes stagnant, with great stability for an appreciable period.

Air pollution problems, in the past, have resulted primarily from smoke and fly ash produced by the combustion of fuels used for heating purposes. London, Pittsburgh, Cincinnati, and St. Louis are examples of communities where the major sources of pollution are domestic and industrial heating plants. This type of pollution may be controlled by dust collection, by modification of heating plants, and by restricting the use of high volatility fuel.

Of more recent origin is the type of air pollution represented by Los Angeles smog. In the latter, the smog effects are eye irritation, crop damage, and reduced visibility. These smog manifestations, initiated by sunlight, are caused by the reaction products of combustion effluents, primarily hydrocarbons, and ozone. These gases and vapors are held in place by the topographical and meteorological conditions in the Los Angeles Basin.

The portion of this area generally known as the south coastal basin is bounded by an arc of mountains on three sides, while the ocean with its onshore winds is on the fourth side. During the period from May through November, a mass of air settles over the coast of California from high above the Pacific Ocean. As this mass of air moves downward, it warms to 75 F to 90 F, forming a layer of warm air over the cooler air at ground level. This condition is known as a temperature inversion. The base of the inversion in the Los Angeles area is generally 1000 to 2000 ft above ground level.[1] It rises and lowers depending upon the meteorological conditions. If the inversion is preceded by several days when the daily wind movement is less than the normal 125 miles, the pollutants are held captive. Under these conditions, they accumulate as gases and aerosols, with the latter consisting of a combination of liquid droplets and particles in the submicron range.[2] These materials may react with one another under the influence of sunlight to produce the plant damage and eye irritation so widely associated with smog.[3] In Los Angeles County these conditions exist about 260 days out of the year, and the pollutants may become sufficiently dense to restrict visibility to less than one mile.[4]

Although the entire coastal basin occupies an area of about 1700 square miles, the air pollution is primarily concentrated in an area of 1200 square miles which includes Greater Los Angeles, Pasadena, and Long Beach. The height to which the smog actually rises is unknown, but the upper limit of high concentrations of pollutants is generally considered to be at the base of the inversion, or about 0.2 miles on the average.[1] The volume of smog can be estimated from these figures to be approximately 240 cubic miles.

The major source of air pollution in Los Angeles

TESTS reported here, in which exhaust samples from city-driven test cars were analyzed by mass spectrometer, showed a loss of hydrocarbons out of the exhaust ranging from 5% of the weight of fuel entering the carburetor under steady driving to 19% during deceleration.

It would take about 60% curtailment of exhaust content of hydrocarbons, the authors estimate, to return to the relatively smog-free conditions that existed before 1945.

Discussion of this paper starts on p. 618.

[1] See *American Meteorological Society Bulletin*, Vol. 33, 1952, pp. 247-250: "Some Air Pollution Aspects of Los Angeles Temperature Inversion," by E. Robinson.

[2] See p. 107: "Smog Problem in Los Angeles County," by Stanford Research Institute. Pub. by Western Oil and Gas Association, Los Angeles, 1954.

[3] See Proceedings of Second National Air Pollution Symposium (Stanford Research Institute), September, 1952, pp. 28-34: "Chemical Reactions in Los Angeles Smog," by R. D. Cadle and H. S. Johnston.

[4] See p. 29: "Smog Problem in Los Angeles County," by Stanford Research Institute. Pub. by Western Oil and Gas Association, Los Angeles, 1954.

County is the incomplete combustion of over 50,000 tons of organic materials and fuels each day by the general public and industry. This combustion pours over a million tons of contaminated gas every day into the atmosphere, containing more than 2600 tons of organic materials, aldehydes, ammonia, and oxides of nitrogen and of sulfur.[5] In addition to the organics and other materials put into the air by combustion processes, an amount estimated at 440 tons of hydrocarbons is evaporated into the air each day. Approximately 220 tons of this come from the production, manufacture, and distribution of petroleum products. The other 220 tons come from the evaporation of gasoline from service stations and automobiles.[5]

The Committee on Smoke and Fumes of the Western Oil and Gas Association completed in March, 1954, a survey of losses from petroleum-handling operations and automobiles. (See Table 1.)

Of the more than 3000 tons of organic contaminants emitted to the Los Angeles atmosphere each day by all sources,[5] 1456 tons, or about 50%, are hydrocarbons which arise from the producing, refining, marketing, and automotive usage of petroleum. Of these 1456 tons of hydrocarbons, 1016 tons, or 70%, are the products of automobile exhaust. Automobile exhaust therefore contributes one-third of the total organic contamination of 3000 tons each day, and is the largest single source of pollutants to the Los Angeles atmosphere and also the most effective distribution system.

The importance of hydrocarbons in the atmosphere is related to the strong oxidizing effect of Los Angeles smog. It is reported by Haagen-Smit, Shepherd, and others[6, 7, 8, 9] that unsaturated hydrocarbons (olefins), especially those containing five, six, and seven carbon atoms, can react with nitrogen oxides or ozone in sunlight to produce substances causing the characteristic effects of smog. These products are considered to be ozonized hydrocarbons or peroxides. As is shown in Table 1, automobile exhaust contributes 88% of the olefins found in the Los Angeles atmosphere.

In addition, Haagen-Smit[10] has recently shown that the automobile exhaust gases are capable of forming ozone at concentrations in the same order as those measured in the Los Angeles atmosphere.

Thirty-seven per cent of the nitrogen oxides in the air are emitted to the atmosphere from automobile exhaust,[5] making exhaust one of the major contributors of oxides of nitrogen to the atmosphere.

The amounts of hydrocarbons and nitrogen oxides discharged in automobile exhaust gases daily in Los Angeles County would result in concentrations of 0.25 ppm hydrocarbons and 0.06 ppm nitrogen oxides in the 240 cubic miles of polluted air. These values may be compared with 0-3 ppm hydrocarbons and 0.2-0.4 ppm of nitrogen oxides measured under conditions of intense smog.[5]

The range of measured concentrations of hydrocarbons and nitrogen oxides in the Los Angeles atmosphere demonstrates the variability of smog. It is of interest that the calculated concentrations of the same constituents contributed by automobile exhaust are in reasonable agreement with the measured values. The estimated concentrations assume complete mixing of the exhaust gases in the 240 cubic miles of air. The maximum reported concentration of hydrocarbons is 12 times the calculated average, maximum reported concentration of nitrogen oxides is 6.7 times the calculated average.

It therefore appears that automobile exhaust gases are a substantial source of the hydrocarbons and nitrogen oxides present in the atmosphere during the intense smogs.

As part of the continuing study on the Los Angeles smog problem by Stanford Research Institute, mass spectrometer analyses have been made to estimate the nature and amounts of hydrocarbons exhausted by passenger-car exhausts into the Los Angeles County atmosphere. The ultimate objective of these investigations was to arrive at an estimate of the amount of hydrocarbons released into this atmosphere by gasoline-burning vehicles.

Five prewar and five postwar automobiles were used, chosen at random without regard to the mechanical condition of the motor. The makes of the automobiles and their ages were selected as typical of the automobile population, according to the passenger car count compiled by the Department of Motor Vehicles of the State of California. A rough indication of the mechanical condition of the cars was obtained by measuring the air/fuel ratio, the intake manifold vacuum under idling conditions, and the cylinder pressure. The mechanical condition of the group of cars selected was believed to be roughly representative of the cars on the highway.

Regular-grade, premium-grade, and straight-run

Table 1 – Hydrocarbon Emissions to the Atmosphere from the Producing, Refining, Marketing, and Automotive Usage of Petroleum Products in Los Angeles County

	Total Hydrocarbons		Olefins, Amylenes, and Heavier	
	Tons per Day	Per Cent	Tons per Day	Per Cent
Hydrocarbons from Production, Refining, Marketing	224	15.4	12	3.6
Service Station Operation	52	3.6	6	1.8
Evaporation from Automobile Tanks and Carburetors	164	11.0	20	6.1
Automobile Exhaust	1016	70.0	292	88.5
Total	1456	100.0	330	100.0

[5] See *Industrial & Engineering Chemistry*, Vol. 45, May, 1953, pp. 1070-1074: "Evaluating Sources of Air Pollution," by G. P. Larson, G. I. Fischer, and W. J. Hamming.

[6] See *Analytical Chemistry*, Vol. 23, October, 1951, pp. 1431-1440: "Isolation, Identification, and Estimation of Gaseous Pollutants of Air," by M. Shepherd, S. M. Rock, R. Howard, and J. Stormes.

[7] See *Plant Physiology*, Vol. 27, 1952, pp. 18-34: "Investigation on Injury to Plants from Air Pollution in Los Angeles Area," A. J. Haagen-Smit, E. F. Darley, M. Zaitlin, H. Hull, and W. Noble.

[8] See *Engineering & Science Monthly*, Vol. 14, December, 1950, pp. 7-13: "Air Pollution Problem in Los Angeles," by A. J. Haagen-Smit.

[9] See *Industrial & Engineering Chemistry*, Vol. 44, June 1952, pp. 1342-1346: "Chemistry and Physiology of Los Angeles Smog," by A. J. Haagen-Smit.

[10] See *Air Repair*, Vol. 4, November, 1954, pp. 105-109: "Photochemical Ozone Formation with Hydrocarbons and Automobile Exhaust," by A. J. Haagen-Smit and M. M. Fox.

gasolines were used. The straight-run fuel was especially prepared and contained no unsaturated hydrocarbons. Runs were also made on composite samples prepared from regular- and from premium-grade gasolines produced by six major petroleum companies in the Los Angeles area.

Four driving conditions were considered typical for an automobile operating either in Los Angeles city or suburban traffic:

1. Acceleration (full throttle) – 10 to 30 mph.
2. Steady driving – 30 mph.
3. Deceleration – 30 to 10 mph.
4. Idling – Normal idle.

From inspection of the traffic patterns in the city and in the country, a traffic density of about 30,000 or greater on a 16-hr-per-day basis seemed representative of suburban areas. It was assumed that one-half of the total gasoline was consumed in city driving, and the other half in suburban driving. These densities were arrived at after a study of the traffic counts made annually for Los Angeles County by the Highway Department of the State of California. The division of gasoline consumption was reached by many inspections of traffic density and discussions with informed traffic engineers.

A route was selected in the county as being representative of city and suburban traffic patterns. The amount of gasoline consumed in each of the traffic patterns and under the four driving conditions was determined while the vehicle was in operation in the selected traffic routes. A recording tachometer measured the car speed and the distance travelled.

As the automobiles were operating under the four driving conditions, exhaust samples for analysis by the mass spectrometer were collected by use of an apparatus mounted in a trailer drawn by the test vehicle. (See Fig. 1.)

The automobile exhaust was conducted to the trailer in a double tube to guard against condensation of water. The sample was taken from the inner tube in a 250-ml sample bottle which had previously been evacuated, by raising the pressure in the bottle from 1 to 100 mm mercury with the exhaust gas.

Twenty to 40 samples of exhaust emitted during each driving condition were collected and analyzed to obtain a measure of the variation of results and to permit statistical estimation of the precision.

All samples were analyzed by the Consolidated Engineering Corp., Pasadena, Calif., with a mass spectrometer within 1-3 hr after being collected. A detailed discussion of these analyses is presented in a Stanford Research Institute Report.[11] It has been estimated by the Consolidated Engineering Corp. that the precision of the analyses is ± 0.1 molecular per cent for inorganic gases, and ± 0.01 per cent for volatile hydrocarbons. Statistical analysis of the data confirmed this estimate.

[11] See Proceedings of Second National Air Pollution Symposium (Stanford Research Institute), September, 1952, pp. 71-83: "Hydrocarbon Constituents of Automobile Exhaust Gases," by P. L. Magill, D. H. Hutchison, and J. M. Stormes.

The Authors

DALE H. HUTCHISON is manager, Air Research Section, Stanford Research Institute. After receiving a B.A. in Mathematics and Psychology from Tarkio College in Kansas, he did graduate work in Psychology at Washington University in St. Louis and the University of Kansas. He also studied meteorology at NYU. Before joining SRI in 1951, Mr. Hutchison was with the Landing Aids Express Station, Arcata, Calif. and the Los Angeles Department of Airports.

FRANCIS R. HOLDEN is a senior physical chemist, Stanford Research Institute. In 1930 he received a B.S. in Chemistry cum laude from Hobart College; in 1932, an M.A. in Chemistry from the University of Cincinnati; and in 1934, a Ph.D. in Physical Chemistry. Dr. Holden has been associated with the Industrial Health Conservancy Laboratories and the U. S Naval Radiological Defense Laboratory.

Exhaust sample data for test cars using regular, premium, saturated, and composite gasolines are shown in Fig. 2. It is noteworthy that both saturated and unsaturated gasolines produced almost identical amounts of $C_{5,\ 6,\ 7}$ + olefins in the exhaust gases. In fact, the olefin content was approximately the same for all grades of gasoline used, including

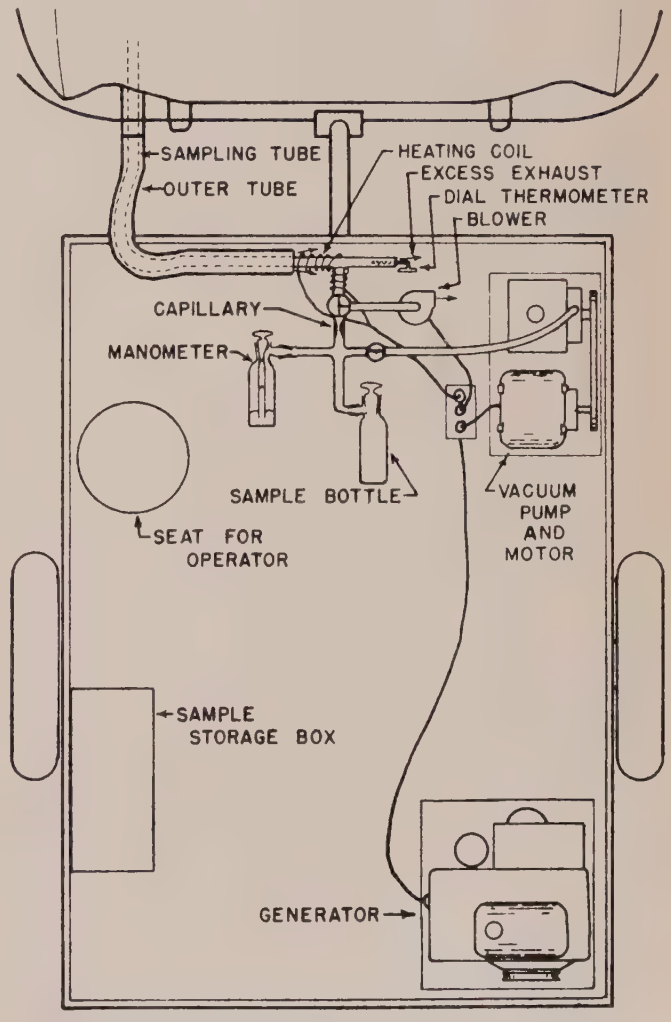

Fig. 1 – Apparatus used for automobile exhaust sampling

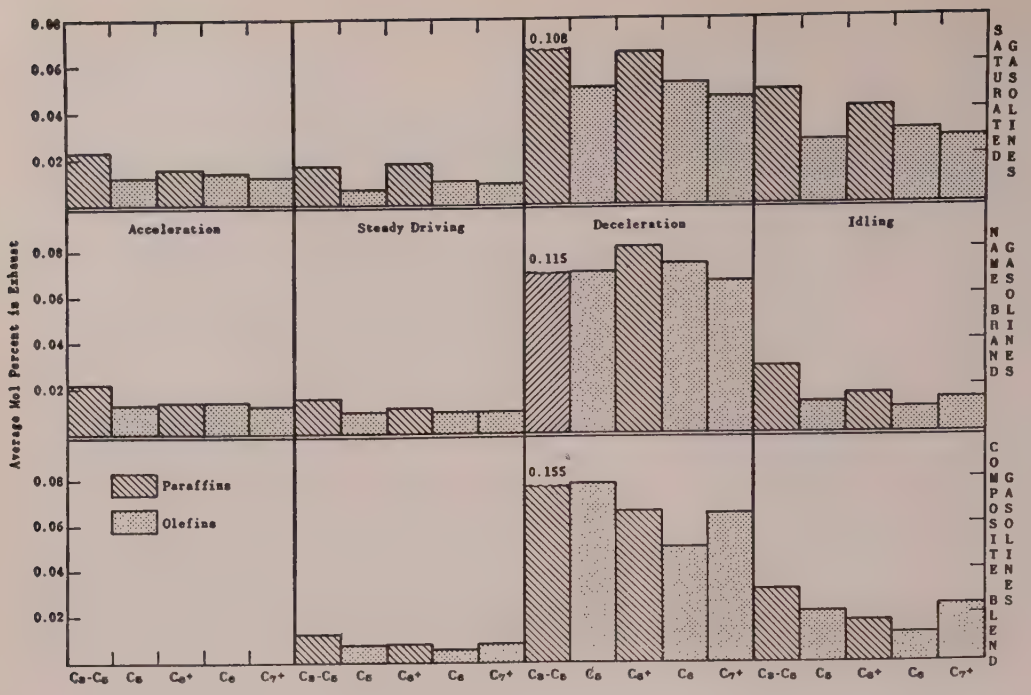

Fig. 2 – Average exhaust analyses for different gasolines

Table 2 – Tons of C_1 to C_7 Hydrocarbons Discharged Daily from Automobile Exhaust

	Molecular Weight	Routes Tested: Figueroa St. Sunset Blvd. to Florence Ave. and Return	Foothill Blvd. from Sunland to U. S. Highway 6	22 Congress St. to Arroyo Seco Pkwy. to Adobe St. and Return
Methane	16	61	54	55
Ethane	30	146	166	165
Acetylene	26	52	36	37
Ethene	28	150	124	127
C_3-C_5 Paraffins	58	116	62	68
C_5 Olefins	70	84	39	43
C_6+ Paraffins	93	128	67	73
C_6 Olefins	84	106	58	64
C_7+ Olefins	100	117	68	73
Benzene	78	17	14	14
Other Aromatics	92	21	16	17
Total		998 (1000)	704 (700)	736 (730)

Table 3 – Gasoline Consumption

Date	State, gal per year	Los Angeles County, %	Los Angeles County, gal per year	Los Angeles County, tons per day
1950	3,391,494,666	40.31	1,365,000,000	11,550[a]
1951	3,694,506,374	40.23	1,485,000,000	12,550
1952	3,965,740,762	40.12	1,590,000,000	13,440
1953	4,172,814,857	40.68	1,700,000,000	14,380

[a] Based on 325.14 gal per 2000 lb, API gravity 60.

blends of six of the leading producers in the area.

The average exhaust composition for all components analyzed by the mass spectrometer for each of the four driving conditions is shown in Fig. 3. Of interest is the result that the concentrations of methane and acetylene produced under idling conditions are greater than those obtained under conditions of acceleration, steady driving, or deceleration. Ethane and ethene do not fall into this pattern.

Using the data that have been obtained, and certain simplifying assumptions, it is possible to obtain an estimate of the amount of hydrocarbon vapors released daily into the Los Angeles atmosphere by approximately 2,000,000 cars[5] burning 12,000 tons (4,000,000 gal) of gasoline. It was assumed that the results were representative of the Los Angeles automobile population during the test period (1951-52), that half of the gasoline was consumed in city driving and half in suburban driving, and that each car produced 1000 cu ft of dry exhaust gas per gallon of fuel burned.

Using these assumptions, the total hydrocarbons emitted to the atmosphere from automobile exhaust were calculated. The tons of exhaust products emitted daily under the four driving conditions are tabulated in a previously published Stanford Research Institute Report.[11] This tabulation shows that over the range of driving conditions encountered in city traffic, there is a loss of hydrocarbons out of the exhaust ranging from 5% of the weight of fuel entering the carburetor under conditions of steady driving, to 19% during deceleration.

Table 2 shows the estimated amount of hydrocarbons discharged daily from automobiles.

If all driving had been done exclusively on one of the three different patterns (Figueroa Street, Arroyo Seco Parkway, and Foothill Boulevard), the emissions would then correspond to 1000 tons, 700 tons, and 730 tons respectively.

It was determined that 700 tons a day represents the minimum daily emission of hydrocarbons into the Los Angeles atmosphere from the automobile exhaust in 1951. The increased gasoline consumption for 1953 indicates that the daily emission would exceed 1000 tons.

The frequency of smog and the severity of its effects have increased markedly during recent years in Los Angeles County, and it is interesting to consider the manner in which this trend follows the increase in gasoline consumption in the county. An effect of smog which has become more exten-

sive and more pronounced each year is injury to vegetable crops and other herbaceous plants. According to Middleton et al.,[12] injury to vegetable leaves was first noted in 1944.

Most of the types of injury observed in the Los Angeles area were duplicated by laboratory fumigations.[13] Typical smog injury was obtained by fumigating plants either with the reaction products of ozone and unsaturated hydrocarbons, or ozone and automobile exhaust, when the reagents were mixed in high concentrations and the products diluted to low concentrations. No other fumigant was found which would produce this type of injury.

In Fig. 4 is shown the number of automobile registrations for the state of California from 1935 to 1953.[14] Thirty-five to 40% of the registrations were in Los Angeles County during this period. Although the County had an increase of 400,000 registrations between 1935 and 1944, there were 1,000,000 more registrations from 1944 to 1953.

The gasoline consumption for California from 1935 through 1953 is shown in Fig. 5. Consumption data for Los Angeles County for the same time period are not available, but Table 3 covers the years of 1950 through 1953.[4]

The tabulated data indicate that the consumption of gasoline in Los Angeles County is approximately 40-41% of the total gasoline consumption for the State of California. It therefore seems reasonable to use the State consumption figures as an index of the consumption of gasoline in Los Angeles County during the period 1935-53.

The data shown in Figs. 4 and 5 may therefore be used for estimating the control of automobile exhaust gases that would be required for return to the relatively smog-free years prior to 1945. Based on the hydrocarbon emission from automobiles shown in this study, it may be estimated that the probable hydrocarbon emission in 1945 was about 600 tons per day. Therefore, automobiles should be equipped with devices which will curtail the exhaust content of hydrocarbons by about 60%. It must be recognized that the addition of more automobiles (the trend is upward) would necessitate curtailment of the hydrocarbon content of automobiles by more than 60%. In no case should the total hydrocarbon emission exceed about 600 tons per day. It is believed that devices can be built that will convert 60% of the unburned or partially burned hydrocarbons to inert gaseous products. Research on devices for the latter purpose seems to be of paramount importance in controlling smog of the Los Angeles type.

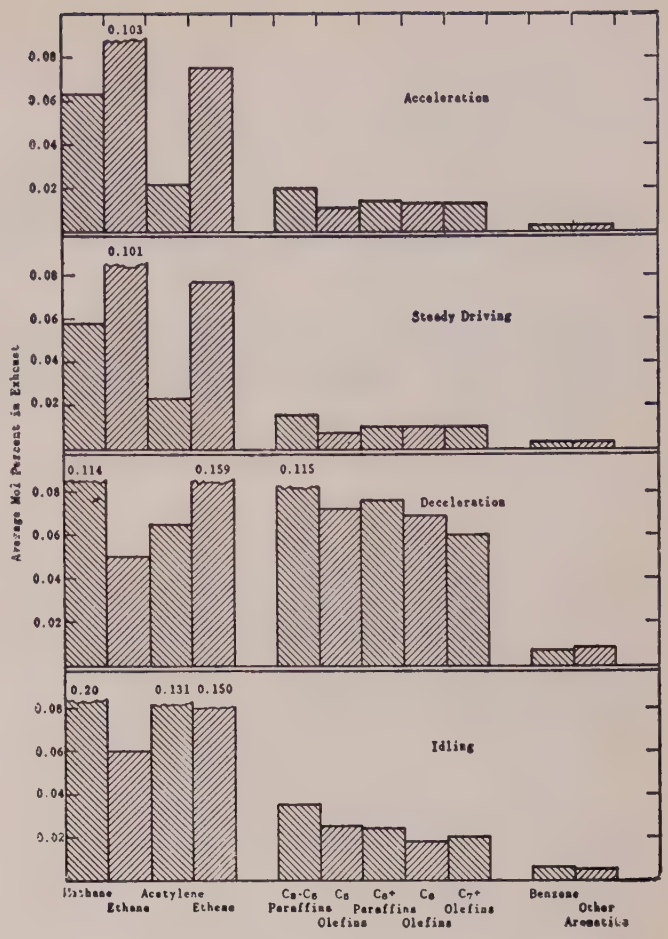

Fig. 3 – Average exhaust analyses under different driving conditions

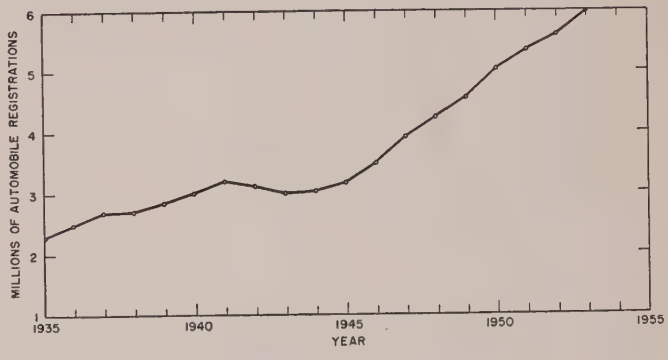

Fig. 4 – California automobile registrations

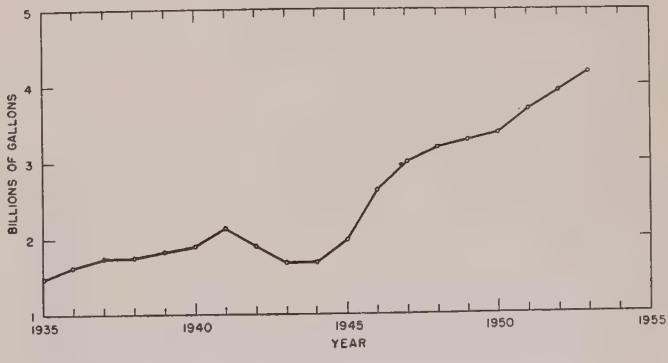

Fig. 5 – Yearly consumption of gasoline in California

[12] See *Plant Disease Reporter*, Vol. 34, 1950, pp. 245-252: "Injury to Herbaceous Plants by Smog or Air Pollution," by J. T. Middleton, J. B. Kendrick, Jr., and H. W. Schwalm.

[13] See p. 64: "Smog Problem in Los Angeles County," by Stanford Research Institute. Pub. by Western Oil and Gas Association, Los Angeles, 1954.

[14] See "Annual Traffic Count," by G. T. McCoy. Pub. by State Printing Office, Sacramento, Calif., 1951.

LIMITED capacity of the atmosphere in the Los Angeles Basin to disperse gaseous wastes accounts for its peculiar susceptibility to smog. While much has been done to determine actual sources of smog, the author contends that nothing has yet been definitely proved. He tells here of the wide variety of investigative programs – covering meteorology, chemistry, combustion products, aerometric surveys, statistics, physical measurements, rubbish disposal, and other vital apects – undertaken by APF, a nonprofit organization sponsored by local industry, business, and civic groups.

Discussion of this paper starts on p. 618.

THE Los Angeles Basin is an industrial community situated in a meteorological environment different from any other large city in the world. Between the strong inversions a great portion of the year and the attendant low wind velocities, the capability of the atmosphere for the dispersion of gaseous wastes is extremely limited.

Shortly after World War II, the smog problem became so great that the community forced State action and formed the first county-wide Air Pollution Control District. This was in 1947. Following the pattern used in other cities, the District first removed a large quantity of particulate matter or smoke from the air and later reduced sulfur dioxide emissions. Reduction of these materials had helped greatly in other cities, but in Los Angeles the smog continued to increase. Research work done at the District indicated that hydrocarbon emissions from the refineries were responsible for eye-stinging smog. Again, control measures were invoked and the emission of hydrocarbons from the refineries was greatly reduced. Even this has not cured the situation. As smog continued, the public demanded direct action by legislation, ignoring the fact that the causes of smog were still unknown. This led to attacks on the Air Pollution Control District, the Board of Supervisors, and participating industries, and finally to dissension between some of these groups. All of this is documented in the press. Air pollution control threatened to become a political football and a campaign weapon. Valid and persistent work by the Air Pollution Control District continued despite the political atmosphere, though impeded by it.

In September, 1953, we had some particularly bad smog days. A group of civic leaders met at the California Club about that time. Remembering how community action had improved the water situation and also the harbor problem, this group of men asked themselves what they, as citizens, could do to aid the Air Pollution Control District in the elimination of smog. It was obvious that more facts concerning the nature and origin of smog were necessary before proper controls could be invoked. These facts, in turn, could only be uncovered through research.

In November of 1953, a group of about 100 civic and business leaders met at the Ambassador Hotel and founded the Southern California Air Pollution Foundation (on Dec. 21, 1955, the Board of Trustees officially changed the name of the Foundation to the Air Pollution Foundation), "an independent scientific organization supported by public-spirited citizens – to help determine the causes of smog and implement its elimination."

The Foundation was incorporated as a nonprofit research organization under the laws of California on Nov. 18, 1953. It is financed by contributions from a cross-section of Southern California industry (ranging from aircraft to zinc), business, and private citizens. The breadth of this civic enterprise may be obtained by examining a list of trustees of the Foundation (Table 1).

The broad base upon which the Foundation was formed may be obtained by looking at the purpose of the Foundation in its "Statement of Policy."

> APF is an independent, nonprofit corporation which has been established for the following purposes:
>
> 1. To cooperate with, and to assist in coordinating the efforts of, governmental agencies, educational institutions, specialized research groups, and medical, legal, and other technologists, so that every phase of air pollution shall be the object of careful study and constructive, remedial action.
>
> 2. To provide for the conduct of research on those phases of the problem not already undertaken or completed by other agencies.
>
> 3. To inform the public periodically concerning the nature and extent of air pollution, progress made in its elimination, and obstacles to such elimination.

The following statements indicate the basic ap-

Table 1 – APF Board of Trustees

Chairman – Fred D. Fagg, Jr., president, University of Southern California
Vice-Chairman – Stephen W. Royce, president and manager, Huntington-Sheraton Hotel, Pasadena
Treasurer – James E. Shelton, president, Security-First National Bank
Raymond B. Allen, chancellor, University of California at Los Angeles
F. M. Banks, president, Southern California Gas Co.
Arnold O. Beckman, president, Beckman Instruments, Inc.
Walter Braunschweiger, executive vice-president, Bank of America
Asa V. Call, president, Pacific Mutual Life Insurance Co.
Edward W. Carter president, Broadway-Hale Stores, Inc.
Lee A. DuBridge, president, California Institute of Technology
Roy M. Hagen, president, California Consumers Corp.
Charles F. Kettering, vice-president and research consultant, General Motors Research Laboratories
John A. McCone, president, Joshua Hendy Corp.
Harvey S. Mudd, president, Cyprus Mines Corp.
William C. Mullendore, chairman of the board, Southern California Edison Co.
Fred B. Ortman, chairman of the board and president, Gladding, McBean & Co.
Alden G. Roach, president, Columbia-Geneva Steel Division and Consolidated Western Steel Division, United States Steel Corp.
Dr. J. Philip Sampson, president, County Medical Association
Reese H. Taylor, president, Union Oil Co. of Calif.
P. G. Winnett, chairman of the board, Bullock's, Inc.

Air Pollution Foundation—

What It Is and What It Does

W. L. Faith, Air Pollution Foundation

This paper was presented at the SAE Golden Anniversary Annual Meeting, Detroit, Jan. 10, 1955.

proach to smog outlined in the Air Pollution Foundation charter:

What the Foundation Proposes to Do

1. To assemble a competent technical staff to organize and direct a broad program of cooperation, research, and public information.
2. To determine, record, and publish what has been accomplished to date by all agencies dealing with the Southern California problem.
3. To determine what remains to be done and to employ experts – through the device of research or service contracts – who will provide information and advice for the shaping of future policies and action.
4. To collect information as to what other municipal areas have done, and are doing, under similar circumstances.
5. To provide and maintain a library of materials pertinent to the subject of air pollution.
6. To consult with, exchange information with, and to suggest to governmental and private agencies those research activities, enforcement methods, or other matters, which have not yet been conducted or tried and which seem to offer promise of air pollution abatement – so that the efforts of all groups and individuals may be coordinated properly.
7. To publish current information – by the most appropriate means – on all phases of air pollution and its abatement.

What the Foundation Does *Not* Propose to Do

1. It will not duplicate services already rendered by governmental or private agencies.
2. It will not conduct research activities directly – unless it appears clear that no existing agency can conduct them as advantageously.
3. It will not expend funds entrusted to it for the constructing or equipping of Foundation laboratories that will duplicate facilities already available.
4. It will not hold public hearings for the purpose of receiving complaints, or in any way substitute for governmental agencies now charged with responsibility for certain phases of the air pollution problem.
5. It will not offer any immediate or ready solution for a very complicated, long-range problem.

The Foundation actually got under way on Feb. 1, 1954, when Dr. Lauren B. Hitchcock was appointed its president and managing director. As the organization chart shown in Fig. 1 indicates, the Foundation is basically a research team of five scientists, supplemented with the necessary related personnel.

The Foundation Program

The first activities of the Foundation were to evaluate the existing situation with respect to air pollution in the Los Angeles Basin. This was done through a series of conferences, among which was a conference on Vehicle Combustion Products and Other Emissions, held in Pasadena on Aug. 19, 20, and 21, 1954. This was a closed session attended by 65 representatives of the automotive and petroleum industries. Other conferences, aimed at evaluating

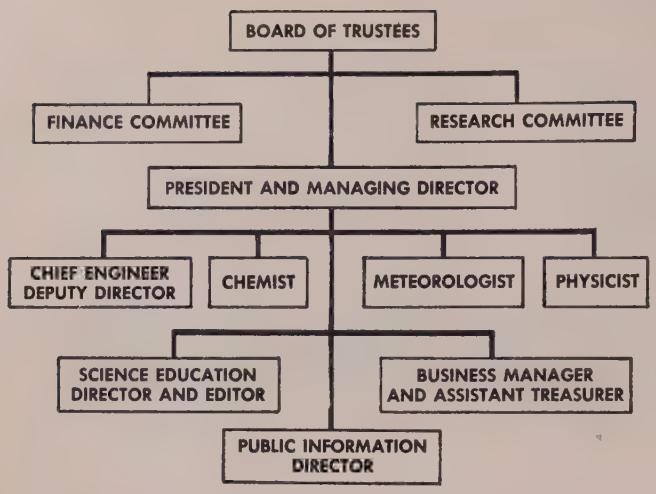

Fig. 1 – APF organization chart

the current situation and determining appropriate courses of action, covered meteorology, atmospheric chemistry, analytical methods, incineration and rubbish disposal, and others.

The evolved research program for 1954 is outlined in Table 2. The highlights of this program are listed below.

Meteorology – "Meteorology of the Los Angeles Basin," by Dr. Morris Neiburger, senior meteorologist of the Foundation, and James G. Edinger, was the first official publication of the Foundation. Based on this review and several meteorological conferences, the current research program was devised. This consists primarily of an air-tracer survey, in which finely divided fluorescent particles are released from various sources and then collected on filters several miles away over a specific period of time. By counting the particles on the various filters, air-particle movements may be traced. A map showing the location of both source and filter for one series of tests is shown in Fig. 2. By means of this technique, it will be possible to determine the reliability of present wind-trajectory techniques of calculating the movement of smog clouds throughout the Basin. Similar studies of the vertical components of air movement are also being made. Historical data of the Weather Bureau are also being studied to learn accurately the amount and characteristics of reduced visibility manifestations in the Basin since 1930.

Chemical Aspects – The chief project in this program is being carried out by Stanford Research Institute at their Air Research Laboratories in Pasadena. Night air in Pasadena usually contains fairly high concentrations of air pollutants, but does not exhibit smog manifestations unless irradiated or treated with small amounts of ozone. Smog-sensitive plants will be subjected to night air, and then irradiated or treated as mentioned to determine the variations of damage that ensue. Air of a similar nature will then be scrubbed with various agents to remove definite classes of air contaminants. The scrubbed air will be mixed with ozone or irradiated and then examined for plant-damaging characteristics. In this way, it is hoped that the precursors of smog will be identified. Other chemical projects include more extended studies on the photochemical reaction between hydrocarbons and NO_2, and further identification of the reaction products.

Combustion Products – A project has been initiated at Midwest Research Institute to explore the smog-forming properties of various components of automobile exhaust, as measured by sensitive plants. Previous data indicate that automobile exhaust damages plants more readily than individual hydrocarbons. It is hoped that, by separating the condensable portion of exhaust into various fractions and testing these fractions for smog manifestations, we may clarify present anomalies. Tests

Table 2 – APF Research Program, 1954

Program	Name
10	Meteorological
20	Chemical Measurements
30	Combustion Products
40	Aerometric Survey
50	Statistics
60	Physical Measurements
70	Disposal of Refuse

Table 3 – Aerometric Survey, 1954 (APF Program 40)

		Stations
1.	Oxidant	12
2.	NO_2	4
3.	Hydrocarbons	2-4
4.	Carbon Monoxide	2-4
5.	Sulfur Dioxide	1-4
6.	Particulate Matter	2
7.	Plant Damage	6
8.	Eye Irritation	10
9.	Upper Air (Oxidant, NO_2)	3
10.	Visibility	4
11.	Temperature & Humidity	4
12.	Meteorological Data	50

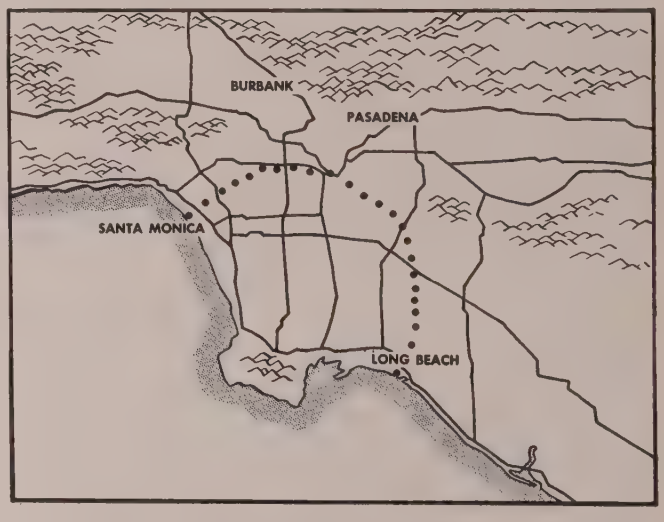

Fig. 2 – Collector stations for air tracer study, with dispersal points (not shown) near center of arc

will be carried out under various motor operating conditions and using several types of fuel. Another combustion project which will be placed shortly will deal with the composition of effluents from backyard incinerators. Current data are both meager and conflicting.

Aerometric Survey – The most extensive project of the Foundation is a 4-month aerometric survey of the Los Angeles Basin. This consists of analyses of the air for contaminants at various locations, and a correlation of air composition with the known manifestations of smog, that is, eye irritation, plant damage, reduced visibility, and high oxidant content. The locations of various sampling stations are shown in Fig. 3. In addition to those shown are one at Santa Barbara, supposedly outside the smog zone, and one at Riverside, about 50 miles inland. The particular measurements being made, and the number of stations involved, are listed in Table 3. Besides the regular measurements at the general stations, we are also sampling the air at various heights above some of the stations. This is being done through the cooperation of the U. S. Navy. A view of a Navy blimp, sampling near the City Hall on a smoggy day, is shown in Fig. 4. Other views taken at various stations are shown in Figs. 5, 6, and 7. The necessary meteorological data are made available by the Los Angeles County Air Pollution Control District, which operates 52 meteorological stations in the Basin. Actually, a large portion of the aerometric survey is financed by the county, and the entire survey is a joint effort with the Control District. The survey is currently yielding about 750 measurements each day. These are recorded on IBM cards and are being correlated on business machines by modern statistical methods.

Statistics – A great many figures have been bandied about concerning the contribution of different sources to air pollution in Los Angeles. These figures are based on someone's estimate of the total amount of fuel used, the number of incinerators in the Basin, and so forth. The Foundation believes that an independent check of reported statistics is necessary, and currently has two projects under way. One of these is an audit by Southwest Research Institute of the petroleum industry's estimate of refinery hydrocarbon emissions. The study has the full backing of the local petroleum industry.

Physical Measurements – Areas of study under consideration in the field of physical measurement include the use of microwave techniques in analyzing the atmosphere for contaminants, the use of carbon isotope techniques to determine the source of certain pollutants, and the measurement of solar radiation at various locations in the Basin. One project under way in cooperation with the U. S. Bureau of Standards is a spectroscopic survey of the Los Angeles atmosphere.

The Author

W. L. FAITH is vice-president and chief engineer of the Air Polluton Foundation. He received a B.S. in 1928 from the University of Maryland, a M.S. from the University of Illinois in 1929, and his Ph.D. in 1932. He has served as special research assistant in chemical engineering at the Engineering Experimental Station, University of Illinois; assistant professor, professor, and later, head of the Chemical Engineering Department at Kansas State College; deputy director in the Office of Production Research and Development, War Production Board, Washington, D. C.; director of development engineering and of the chemical division of the Corn Products Refining Co., Argo, Ill. Dr. Faith joined the Air Pollution Foundation in March, 1954.

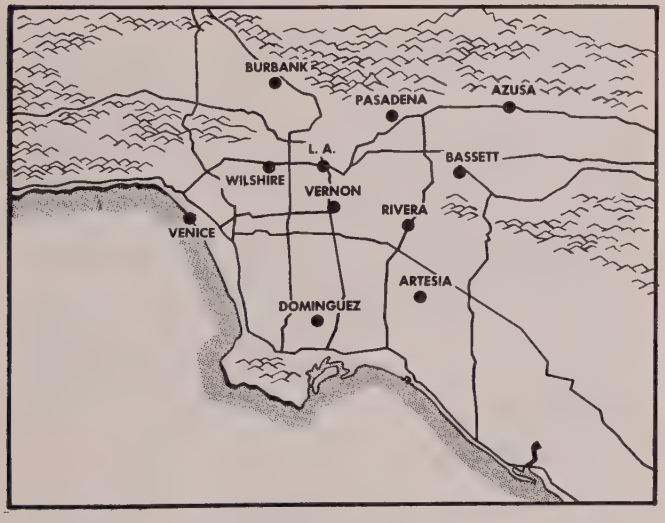

Fig. 3 – Air sampling stations for 1954 aerometric survey

Fig. 4 – Navy blimp sampling near city hall on smoggy day

Rubbish Disposal – A conference on incineration, rubbish disposal, and air pollution has been scheduled for early December, 1954. Participants, many of national prominence, will present available data on incineration, landfill, composting, and other methods of refuse disposal, and point out the areas where further research is necessary.

Where Are We Going?

This program is directed toward only one goal: to get further facts concerning smog. With these facts will come the answers to the important questions in this field. What is smog? Where does it come from? How does it move across the Basin, or does it? Are the same or different phenomena responsible for eye irritation, plant damage, reduced visibility, and high atmospheric ozone concentrations? What is the relative importance of known sources of air pollution?

When we have these answers, we shall not have smog licked. Control devices must still be developed, and we can't wait until the last doubt is erased concerning a specific source before development work begins. There is strong circumstantial evidence that automobile exhaust is a major contributor to Los Angeles smog. Acknowledgment of this situation by the automotive industry has resulted in initiation of actual research work intended to result in reducing the hydrocarbon content of exhaust gases. By this action, the automotive and petroleum industries have given a concrete example of their sense of civic responsibility. The Foundation will do all it can to aid this work and speed it up.

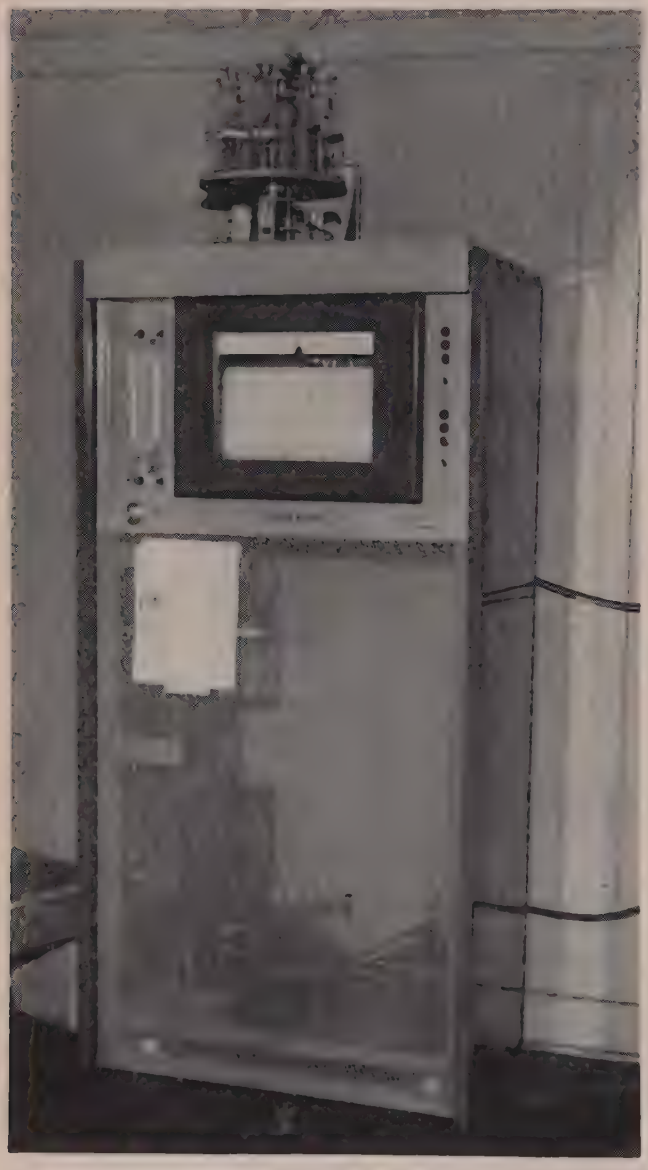

Fig. 5 – NO_2 sample collector (top) and oxidant recorder at Venice aerometric station

Fig. 6 – Closeup of plant box at Pasadena aerometric station

Fig. 7 – Transmissometer sending and receiving equipment at Dominguez aerometric station. Receiver is in lower left-hand corner; light source is bright spot on lower right-hand corner of roof in middle distance

Some Effects of Engine-Fuel Variables On Exhaust-Gas Hydrocarbon Content

F. G. Rounds, P. A. Bennett, and G. J. Nebel,
Research Laboratories Division, GMC

This paper was presented at the SAE Golden Anniversary Annual Meeting, Detroit, Jan. 10, 1955.

SINCE the Twenties it has been known that automotive engine exhaust gases contain hydrocarbons,[1, 2] but the amount has been generally considered too small to be of practical concern. However, recent reports[3, 4, 5] indicate that the amount of hydrocarbons present in exhaust gases under some driving conditions may be significant.

The presence of hydrocarbons in engine exhaust is of interest to the automotive industry for two reasons. The first is air pollution, and particularly the type known as smog encountered in the Los Angeles area. Although no one knows exactly what smog is or how it is formed, some investigators[6, 7, 8] agree that hydrocarbons (particularly olefins), nitrogen oxides, and ozone are important in the mechanism of smog formation.

The second reason for this interest is fuel conservation. The miles per gallon to be gained by utilizing the chemical energy of exhaust-gas hydrocarbons would be small and difficult for the average motorist to detect. However, the nation's gasoline consumption is approaching 3½ million bbl each day, and even a small percentage loss of hydrocarbons in the exhaust gases represents a tremendous waste of fuel.

The present investigation was undertaken to

PROPER maintenance and engine design can do much to reduce exhaust-gas hydrocarbons, the authors say. This conclusion is based on mass spectrometer analyses of engine exhaust from 163 passenger cars, most of them customer-owned, and 8 public-transit coaches, operated at idle, part throttle, and simulated deceleration.

Mixture ratio proved the most important engine-fuel variable affecting hydrocarbon losses at idle; thus the V-8 engine, idling best on a leaner mixture, has lowest hydrocarbon losses.

Manifold vacuum had the most effect during simulated deceleration. Since this depends on engine speed, automatic transmissions and the new lower rear-axle ratios are helpful.

None of the engine-fuel variables tested had any effect at part throttle. Type of fuel and engine type (gasoline, diesel, or LPG) showed no significant influence on hydrocarbon content throughout the tests.

Discussion of this paper begins on p. 618.

[1] See *Franklin Institute Journal*, Vol. 194, November, 1922, pp. 613-644: "Sampling and Analysis of Automobile Exhaust Gas," by A. C. Fieldner and G. W. Jones.

[2] See SAE Transactions, Vol. 38 (March), 1936, pp. 90-98: "Relation of Exhaust Gas Composition to Air-Fuel Ratio," by B. A. D'Alleva and W. G. Lovell.

[3] See Proceedings of Second National Air Pollution Symposium, Stanford Research Institute, 1952, pp. 71-83: "Hydrocarbon Constituents of Automobile Exhaust Gases," by P. L. Magill, D. H. Hutchison, and J. M. Stormes.

[4] See "Hydrocarbon Pollution from Automobile Exhaust Gas, a Report of Test 668 and Associated Work," by F. H. Viets, G. I. Fisher, and A. P. Fudurich. Air Pollution Control District, County of Los Angeles, Sept. 12, 1952.

[5] See Los Angeles County Air Pollution Control District Publication No. 51 (July, 1954): "Automotive Exhaust Testing Procedures and Efficiency Studies in the Evaluation of a Catalytic Muffler."

[6] See *Industrial and Engineering Chemistry*, Vol. 44, June 1952, pp. 1342-1346: "Chemistry and Physiology of Los Angeles Smog," by A. J. Haagen-Smit.

[7] See *Industrial and Engineering Chemistry*, Vol. 44, June, 1952, pp. 1347-1351: "Air Pollution in Los Angeles County – Contribution of Combustion Products," by P. L. Magill and R. W. Benoliel.

[8] See *Industrial and Engineering Chemistry*, Vol. 44, June, 1952, pp. 1352-1355: "Composition of Organic Portion of Atmospheric Aerosols in Los Angeles Area," by P. P. Mader, R. D. McPhee, R. T. Lofberg, and G. P. Larson.

obtain a better understanding of the factors influencing the concentration of hydrocarbons in engine exhaust. Initially, tests were made to determine the fraction of the total fuel supplied to the engine which appeared as hydrocarbons in the exhaust at different driving conditions. Later, more exhaustive tests were made to determine the effect of common engine-fuel variables at each driving condition.

The data presented in this paper are based on mass spectrometer and/or Orsat analyses of exhaust-gas samples obtained from 163 passenger cars and 8 public-transit buses. The test results suggest some practical methods of reducing hydrocarbon losses from motor vehicles.

Test Equipment and Procedure

All five makes of General Motors passenger cars, predominantly 1953 models, were tested. The cars were equipped with V-8, 6-cyl, or line-8 engines, and either standard or automatic transmissions. Of the 163 passenger cars used in this investigation, 11 were test cars and the remainder customer-owned. All the customer-owned cars were tested in the as-received condition. Exhaust-gas samples were also collected from 8 motor coaches used in public-transit service. These commercial vehicles were equipped with either diesel, gasoline, or LPG engines.

Previous investigators have usually divided vehicle operation into four driving conditions: idle, acceleration, cruising, and deceleration. Idle and cruising are essentially steady-state conditions, whereas acceleration and deceleration are not. Since it is very difficult to make quantitative determinations during unsteady-state operation, special test procedures were adopted in the passenger car studies to simulate normal acceleration and deceleration. These operating conditions are:

1. Idle. Idle is operation of the engine at no load with the vehicle stationary. The idle speed of six test cars was arbitrarily held constant at 400 rpm. A total of 152 customer-owned cars was tested.

2. Part Throttle. This condition includes all engine operation at power output equal to or greater than road load. Thus both normal cruising and acceleration are included in this part-throttle condition. To eliminate transient effects, all tests were run at constant engine speeds of 1000 rpm or greater. For this phase of the investigation, seven test cars were used.

3. Simulated Deceleration. Deceleration is characterized by high intake manifold vacuums and decreasing engine speeds. Simulated deceleration data were obtained at constant engine conditions corresponding to those existing momentarily during normal deceleration. These conditions were established by allowing the vehicle to coast downhill at constant speed with closed throttle. It is believed that the data obtained under these simulated conditions are representative of those occurring during normal deceleration, where engine conditions are continually changing. In this work five test cars were operated at constant engine speeds of 1000 and 2000 rpm, whereas 33 customer owned cars were operated in "drive," or highest gear, at a fixed car speed of 30 mph.

The test procedures for the commercial vehicles were somewhat different from those described above. The usual driving conditions of idle, cruising, acceleration, and deceleration were studied. The cruising tests were carried out at 25 mph in high gear, the acceleration tests between 10 and 15 mph in low gear at full throttle, and the deceleration tests beginning at 20 mph.

During this investigation, exhaust-gas samples were collected in evacuated 250- or 500-ml Pyrex bottles from a copper sampling line. In test cars, this sampling line was tapped into the exhaust system just ahead of the muffler. In customer-owned vehicles, the sampling line was pushed up the tailpipe as far as possible. Regardless of the sampling point, the exhaust-gas flow rate was maintained great enough to prevent condensation in the sampling line. The containers were thoroughly cleaned prior to each use to prevent contamination. Stopcocks and rubber tubing were eliminated from the sampling system to prevent possible loss of hydrocarbons by adsorption.

The exhaust-gas samples were analyzed on a Consolidated Engineering Corp. analytical mass spectrometer. The analyses were performed under contract by the Institute of Gas Technology in Chicago, Ill. This method of analysis was selected since the mass spectrometer is capable of measuring the concentration of a large number of individual hydrocarbons. However, the mass spectrometer does have limitations that should

Table 1 – Exhaust-Gas Hydrocarbon Content Ranges

Test Condition	Hydrocarbon Content, weight % of supplied fuel
Idle	1 to 28
Part throttle	1 to 5
Simulated deceleration	1 to 63

Table 2 – Effect of Fuel Type on Exhaust-Gas Hydrocarbon Content at Idle
(Mixture ratio – 80% of theoretical air)

	Fuel Type	Critical Compression Ratio	Hydrocarbon Content, weight % of supplied fuel	
			Total Hydrocarbons	Unreacted Fuel
n-Pentane	Paraffin	4.0	5.4	1.1
Premium Gasoline	Mixed	6.4	5.3	—
Isooctane	Paraffin	7.3	5.1	1.3
100-Octane-Number Gasoline	Mixed	—	5.7	—
Diisobutylene	Olefin	12.0	6.1	0.8
Cyclopentane	Naphthene	12.4	5.9	1.7
Triptane	Paraffin	14.4	5.0	1.3
Benzene	Aromatic	14.0+	2.7	1.2

be recognized. These are discussed in Appendix A. As a result of these limitations, the accuracy of the mass-spectrometer exhaust-gas analyses remains somewhat in doubt. The reported percentages of unburned hydrocarbons are believed to be no more accurate than ±1% by weight of the supplied fuel. In spite of this, the trends shown in this paper are believed to be valid.

Passenger-Car Tests

The ranges of exhaust-gas hydrocarbon contents observed at idle, part throttle, and simulated deceleration for the five makes of passenger cars investigated are shown in Table 1. The hydrocarbon content is expressed as the weight % of the fuel supplied to the engine, a convention that will be used throughout this paper. The detected hydrocarbons included paraffins, olefins, aromatics, and naphthenes ranging from C_1 to C_9. No oxygenated products were reported. The weight % values were calculated from mass spectrometer analyses using a carbon balance. A typical calculation is shown in Appendix B.

There are two features in Table 1 of particular interest to the automotive engineer. First, the hydrocarbon content is markedly affected by driving condition. Secondly, at any one driving condition, the hydrocarbon content may vary considerably. This latter observation points out the need for testing a large number of vehicles if significant averages are to be obtained. It also suggests that a reduction in the hydrocarbon losses may be possible, once the factors responsible for this variation are known.

Idle

Fuel Type – Since the resistance of individual hydrocarbons to oxidation varies with molecular structure, it has been suggested that fuel type might influence the hydrocarbon content of exhaust gas. This is a very important consideration from the petroleum refiners' standpoint, because higher octane fuels are inherently more resistant to oxidation, and thus might be expected to burn less completely. To determine the importance of fuel type, a 1953 model car was operated at idle with several pure hydrocarbons and two gasolines. The results are shown in Table 2, where the fuels are listed in order of increasing critical compression ratio.

For seven of the eight fuels tested, fuel type had little or no effect either on the total hydrocarbon content in the exhaust or on the amount of unreacted fuel. For benzene, however, the total hydrocarbon content was about half that observed with the other fuels, even though the amount of unreacted fuel was about the same. These results suggest that the exhaust gas hydrocarbon content at idle does not correlate with the oxidation resistance of the fuel as measured by the critical compression ratio.

The Authors

F. G. ROUNDS is a senior research engineer in the Fuels and Lubricants Department, Research Laboratories Division, General Motors Corp. After serving two and a half years in the Army during World War II, he received a B.S. in Chemical Engineering from the State College of Washington in 1949. Since that time, he has been engaged in knock, wear, and synthetic lubricant development studies in the GM Research Laboratories.

P. A. BENNETT (J '53) is a research engineer in the Research Laboratories Division of General Motors Corp. After serving three and a half years in the Navy during World War II, he re-entered North Dakota Agricultural College where he received a B.S. in Mechanical Engineering. In 1952, Mr. Bennett obtained his M.S. in Mechanical Engineering from Purdue University. He has recently been engaged in autoignition, vapor lock, and carburetion studies at General Motors.

G. J. NEBEL is also a research engineer in the Fuels and Lubricants Department of the Research Laboratories Division of General Motors Corp. After serving in the U. S. Navy from 1943 to 1946, he re-entered the University of Michigan where he received a B.S. in Chemical Engineering in 1950; and his M.S. in Chemical Engineering in 1951. Mr. Nebel joined General Motors in 1951.

Air/Fuel Ratio – Fig. 1 shows the results of idle tests in which the mixture ratio of test cars was varied over the range for miss-free operation. Additional data from 26 customer-owned cars in the as-received condition are also included. The idle speed of each test car was set at 400 rpm,

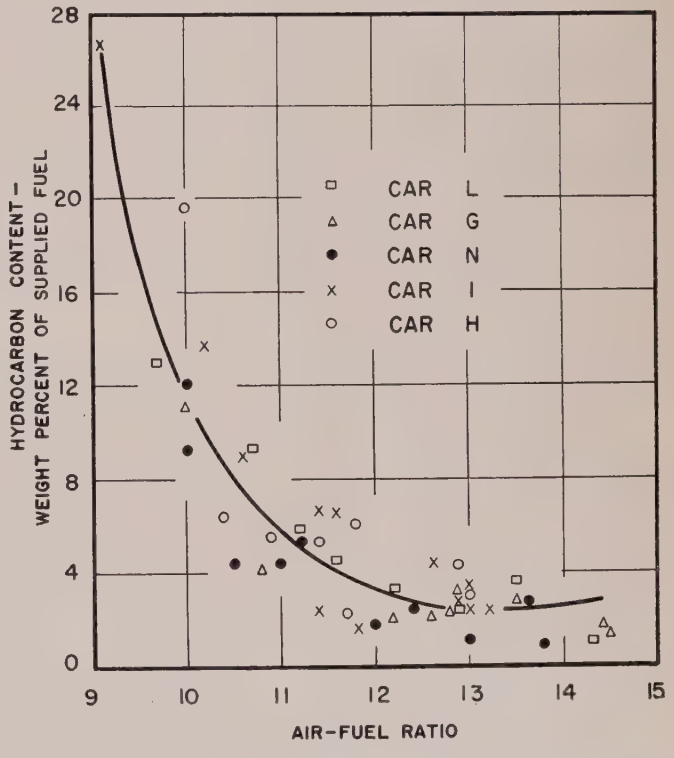

Fig. 1 – Effect of air/fuel ratio on exhaust-gas hydrocarbon content at idle

whereas the idle speeds of the customer-owned cars were found to vary from 280 to 680 rpm. Manifold vacuums varied from 16 to 20 in. of Hg. Although manifold vacuum and engine speed were not comparable in all tests, it appears that the most important variable causing the large effect on exhaust-gas hydrocarbon content at idle was air/fuel ratio.

It has been observed that the mixture ratio range for miss-free idle operation varied with engine design. Since the mixture ratio range for best idle operation generally corresponds to the maximum-power air/fuel ratio, the data illustrated in Fig. 1 indicate that the lowest exhaust-gas hydrocarbon content would also occur at the best idle mixture ratios. To determine how many cars in service are actually operating in the best idle range for the particular engine design, idle air/fuel ratios of 152 customer-owned cars were measured as received. The hydrocarbon content for each customer car was estimated from Fig. 1. Cumulative distribution curves showing these estimates for three basic engine designs are plotted in Fig. 2. These data indicate that the exhaust-gas hydrocarbon content of the compact V-8 engines was less than that for either the line 6's or the line 8's. This results from the fact that the V-8 engines will idle acceptably at leaner air/fuel ratios. In addition, it has been observed that L-head engines require somewhat richer mixtures for satisfactory idle than comparable overhead-valve engines. These observations indicate that the current trend in automotive design towards overhead-valve V-8 engines should result in a reduction in the total hydrocarbon lost during idle operation.

Weighting the data for the 152 customer-owned cars on the basis of 1953 production figures, a single cumulative distribution curve was obtained. The result is shown in Fig. 3 by the solid curve labeled "as received." Assuming equal idle fuel rates for all cars, the average exhaust-gas hydrocarbon content at idle was calculated to be 4% by weight of the fuel supplied to the engine.

The idle mixture ratios of a few of the customer cars were found to be as rich as 10/1, whereas other cars of the same make and model were found to be set as lean as 14/1. Since the exhaust gases from the cars running on the rich mixtures contain appreciably higher hydrocarbon contents than those operating on mixtures in the best-idle range, it would appear that an appreciable reduction in hydrocarbon emission could be achieved by proper maintenance. If the mixture ratio for each car were adjusted to the best idle range, the distribution curve in Fig. 3 would be changed to that shown by the dashed curve. Assuming equal idle fuel consumption rates for all cars, these adjustments would result in a calculated 30% reduction in the total idle hydrocarbon emission. Thus the motorist himself can help to reduce hydrocarbon emission by keeping his motor properly tuned. At the same time he will benefit from improved engine operation.

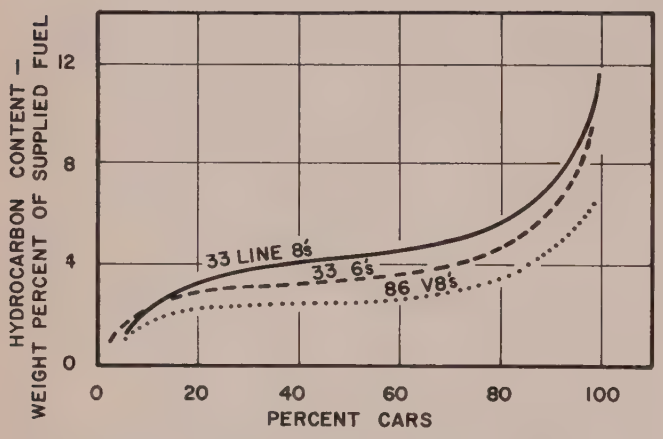

Fig. 2 – Effect of engine type on exhaust-gas hydrocarbon content at idle

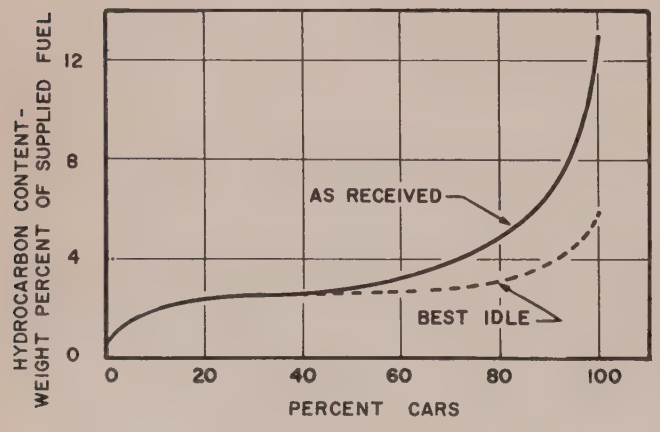

Fig. 3 – Effect of idle mixture adjustment on hydrocarbon content

Part Throttle

Engine Load – The part-throttle operating condition has been defined as all engine operation at power output equal to or greater than road load. Thus, all engine loads from road load to full throttle are included. To determine the effect of engine load, data such as those listed in Table 3 were obtained.

The results of these and other tests indicate little or no effect of engine load on exhaust gas hydrocarbon content.

Fuel Type – To determine the effect of fuel type upon the exhaust-gas hydrocarbon content at part throttle, a 1952 model car and a laboratory single-cylinder engine were operated on several pure hydrocarbons, two leaded isooctane blends, and a commercial gasoline. The results are tabulated in Table 4, where the fuels are arranged in order of increasing critical compression ratio.

The data in Table 4 indicate that neither fuel type nor the presence of tetraethyllead has any

significant effect on the exhaust-gas hydrocarbon content.

Air/Fuel Ratio – Since air/fuel ratio was found to influence the hydrocarbon content at idle, the effect of this variable was investigated at part throttle. The results of 40 tests of five different makes of cars are shown in Fig. 4. The range of air/fuel ratios investigated corresponds roughly to those occurring in normal passenger-car operation. For comparison, the effect of air/fuel ratio at idle previously shown in Fig. 1 has been reproduced in Fig. 4 as the dashed curve. Contrary to the experience at idle, air/fuel ratio has no significant effect on the exhaust-gas hydrocarbon content at part throttle. Included in these tests were cars with engines of all types, which suggests the engine design has little effect on hydrocarbon content under these test conditions.

Engine Speed – To study the effect of engine speed, tests were made employing three different makes of cars as well as a single-cylinder laboratory engine. The results of these tests, covering the speed range from 1000 to 3000 rpm, are shown in Fig. 5. Although there are some minor variations among different engines and duplicate tests on the same engine, it is apparent that a three-fold increase in engine speed has essentially no effect on the exhaust-gas hydrocarbon content at speeds above 1000 rpm.

Compression Ratio – It is well known that the thermal efficiency of an engine increases as the compression ratio is raised. Although this gain is usually explained on the basis of thermodynamic considerations, it was speculated that part of the increased efficiency might result from more complete combustion at higher compression ratios. To check this possibility, tests were conducted on a variable compression ratio single-cylinder engine. The results are given in Table 5.

These data indicate that compression ratio has little or no effect on the exhaust-gas hydrocarbon content. The fuel used in these test, triptane, was selected to permit knock-free operation over the range of compression ratios investigated. Subsequent tests have shown, however, that neither heavy knock nor objectionable preignition influences the hydrocarbon content.

Coolant Temperature – It has been theorized that hydrocarbons are present in exhaust gases either because the fuel/air mixture immediately adjacent to the combustion-chamber walls is too cool to burn, or because the wall destroys certain active radicals necessary for flame propagation. If this were a temperature effect, one would expect the thickness of this layer of unburned gases, and, thus, the hydrocarbon content of the exhaust, to depend upon the wall temperature and indirectly on the coolant temperature. This theory was investigated both in road tests and in single-cylinder laboratory engine tests. In the road tests, exhaust-

Table 3 – Effect of Engine Load on Exhaust-Gas Hydrocarbon Content
(Car I – 1000 rpm)

Manifold Vacuum, in. of Hg	Hydrocarbon Content, weight % of supplied fuel
0.2 (full throttle)	1.4
8.0	1.6
18.0 (road load)	1.5

Table 4 – Effect of Fuel Type on Exhaust-Gas Hydrocarbon Content at Part Throttle
(Maximum-power mixture ratio)

	Fuel Type	Critical Compression Ratio	Hydrocarbon Content, weight % of supplied fuel: Car I – 1000 Rpm, Road Load	Hydrocarbon Content, weight % of supplied fuel: Laboratory Engine – 1000 Rpm, Full Throttle
n-Pentane	Paraffin	4.0	2.4	—
Cyclohexane	Naphthene	4.9	1.9	—
Premium Gasoline	Mixed	6.4	1.8	2.8
Isooctane	Paraffin	7.3	2.8	2.6
Isooctane plus 1 Cc Tel	Paraffin	9.6	—	2.8
Isooctane plus 2.5 Cc Tel	Paraffin	11.0	2.6	—
Diisobutylene	Olefin	12.0	2.3	2.5
Cyclopentane	Naphthene	12.4	2.4	3.0
Triptane	Paraffin	14.4	1.7	2.3
Benzene	Aromatic	14.0+	1.9	2.1

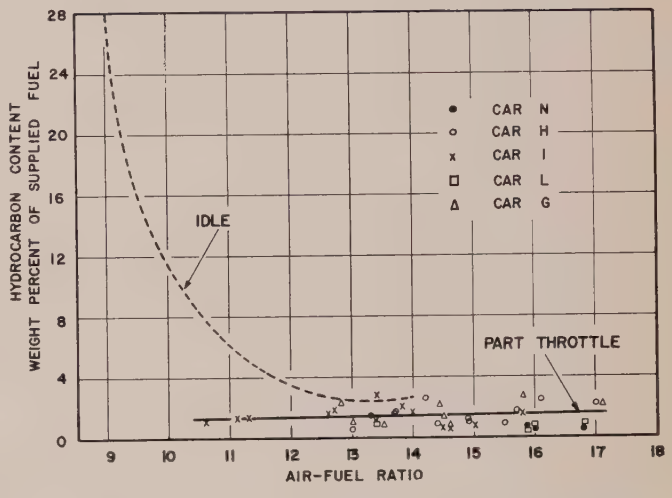

Fig. 4 – Effect of air/fuel ratio on exhaust-gas hydrocarbon content at part throttle

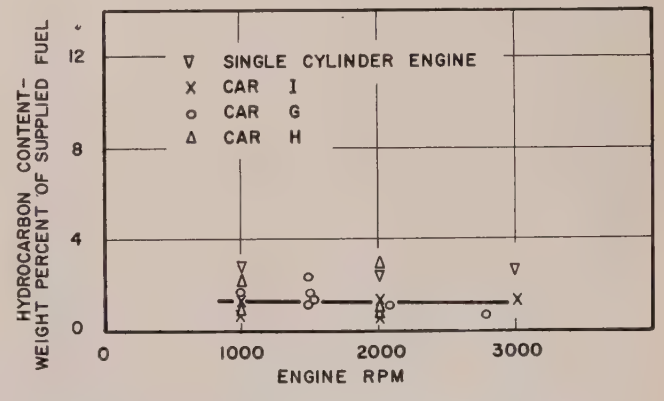

Fig. 5 – Effect of engine speed on exhaust-gas hydrocarbon content at part throttle

Table 5 – Effect of Compression Ratio on Exhaust-Gas Hydrocarbon Content

(1000 rpm – maximum-power mixture ratio)

Compression Ratio	Hydrocarbon Content, weight % of supplied fuel
4.0	2.2
8.0	2.3
12.0	1.9

Table 6 – Effect of Coolant Temperature on Exhaust-Gas Hydrocarbon Content

(Engine speed – 1000 rpm)

	Manifold Vacuum, in. of Hg	Air/Fuel Ratio	Fuel	Temperature, F		Hydrocarbon Content, weight % of supplied fuel
				Coolant	Oil	
Car I	13.0	10.5	Premium gasoline	70	50	5.2
Car I	17.5	13.8	Premium gasoline	215	190	2.1
Car I	0.7	11.0	Premium gasoline	80	112	3.9
Car I	0.2	12.7	Premium gasoline	204	190	1.8
Single-Cylinder Engine	10.1	9.3	Isooctane	9	86	2.3
Single-Cylinder Engine	9.9	10.6	Isooctane	16	93	1.6
Single-Cylinder Engine	9.9	14.2	Isooctane	49	94	1.4
Single-Cylinder Engine	9.6	14.1	Isooctane	103	185	1.2
Single-Cylinder Engine	10.0	16.0	Isooctane	149	182	1.1

Table 7 – Effect of Engine Speed on Manifold Vacuum during Simulated Deceleration at Closed Throttle

Test Car Make	Manifold Vacuum, in. of Hg	
	1000 Rpm	2000 Rpm
L	22.1	24.0
G	22.3	23.8
N	21.8	23.8
I	23.2	24.2
H	24.0	25.0

gas samples were collected from a car soon after starting, and again after thorough warm-up. In the laboratory engine tests, the coolant temperature was regulated by suitable refrigeration. The results of these tests are shown in Table 6.

The car data show somewhat higher hydrocarbon contents immediately after starting than after warm-up. The single-cylinder engine tests, on the other hand, which were conducted under more carefully controlled conditions, indicated little or no effect on the hydrocarbon content as the coolant temperature was reduced. Data shown previously would seem to indicate that the difference between the car and the single-cylinder engine results is not due to a difference in either the fuel or the mixture ratios employed. However, the high values observed in the car tests may have been caused by rich mixtures exceeding the inflammability limit in some cylinders of the multi-cylinder engine.

None of the engine-fuel variables investigated had any significant effect on the exhaust-gas hydrocarbon content at part throttle. Thus, on the basis of present knowledge, there seems very little that the engine designer can do to reduce the hydrocarbon emission at this driving condition. The average hydrocarbon content observed at part throttle was about 1.5% by weight of the fuel supplied to the engine.

Simulated Deceleration

Manifold Vacuum – Simulated deceleration tests were carried out by coasting downhill at various constant engine speeds at closed throttle. The results of these tests, as well as of some part-throttle

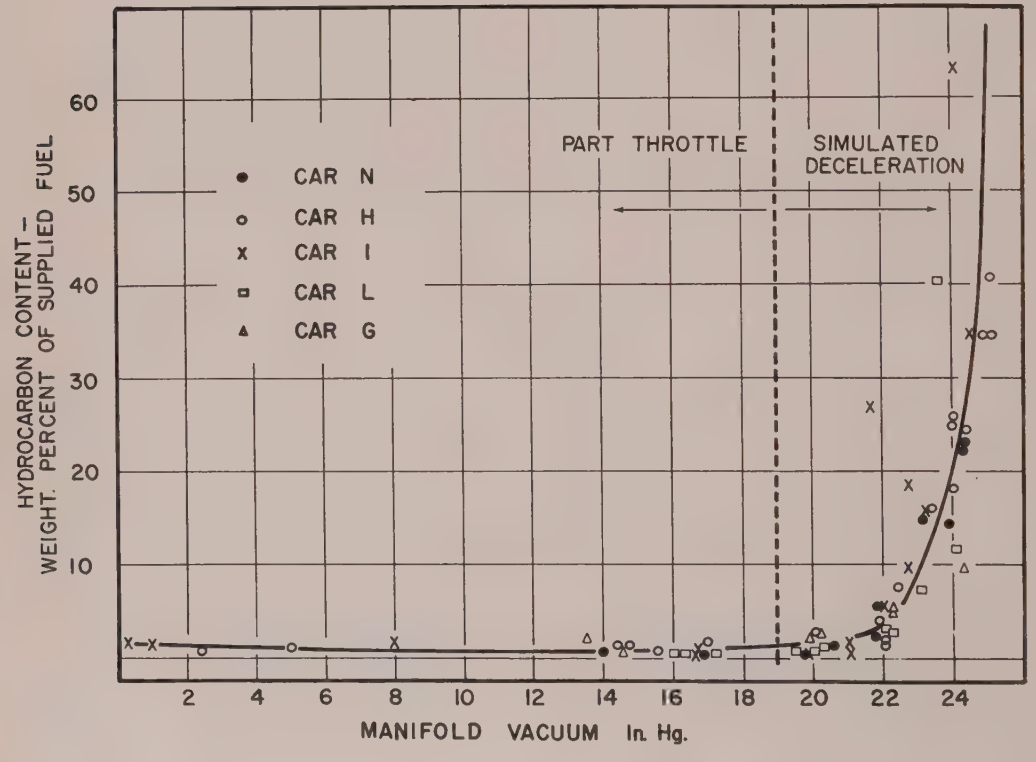

Fig. 6 – Effect of intake manifold vacuum on exhaust-gas hydrocarbon content

tests, are illustrated in Fig. 6 for the five makes of cars investigated. The hydrocarbon content was found to be independent of manifold vacuum below 21 in. of Hg. However, at higher vacuums, the hydrocarbon content increased very rapidly. There was no abrupt change in the observed air/fuel ratios corresponding to this rapid increase in hydrocarbon content. Flame photography studies by Wentworth and Daniel[9] have shown that these high hydrocarbon contents at high manifold vacuums are due to the failure of the flame to propagate throughout the combustion chamber.

The test-car data shown in Fig. 6 were obtained at intake manifold vacuums from 19 to 24 in. of Hg at both 1000 and 2000 rpm. The engine speed and manifold vacuums of the customer-owned cars were those corresponding to 30 mph, closed throttle. The data seem to indicate that neither engine speed nor car make had any effect on hydrocarbon content at any given manifold vacuum. Fig. 6 is very useful, because it permits a reasonable estimation of the exhaust-gas hydrocarbon content to be made for any make or model of car if the manifold vacuum is known.

Engine Speed – The manifold vacuum at closed throttle is dependent upon the engine speed, as shown in Table 7.

Since the manifold vacuum at 2000 rpm was 1-2 in. of Hg greater than at 1000 rpm for all cars, and since all the observed manifold vacuums were greater than 21 in. of Hg, much higher hydro-

[9] See pp. 602-617 of this issue: "Flame Photographs of Light Load Combustion Point the Way to Reduction of Hydrocarbons in Exhaust Gas," by J. T. Wentworth and W. A. Daniel.

Table 8 – Effect of Transmission Type on Estimated Exhaust-Gas Hydrocarbon Content during Simulated Deceleration
(Car speed – 30 mph)

	Number of Cars Tested	Average Engine Speed, rpm	Average Manifold Vacuum, in. of Hg	Estimated Hydrocarbon Content, weight % of supplied fuel
Standard Transmission	10	1405	24.0	22
Automatic Transmission:				
4-Speed Gear Type	15	1130	23.5	17
Torque-Converter Type	8	1075	22.2	7

Table 9 – Effect of Model Change on Hydrocarbon Content during Simulated Deceleration
(Car speed – 30 mph)

	1950-1951 Models	1953-1954 Models
Number of Cars Tested	7	7
Average Axle Ratio	3.82	3.54
Average Engine Speed, rpm	1335	1225
Average Manifold Vacuum, in. of Hg	24	23
Estimated Hydrocarbon Content, weight % of supplied fuel	20.6	13.3

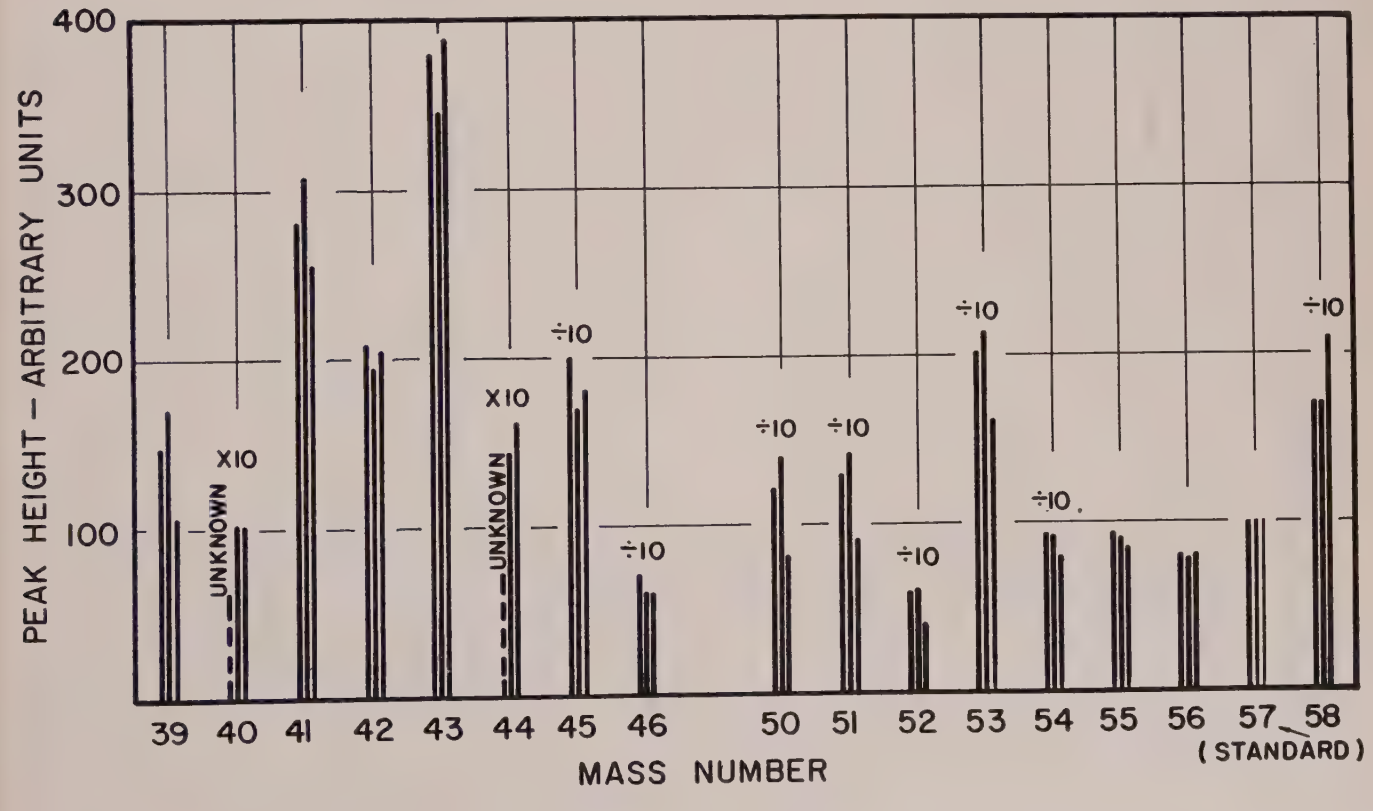

Fig. 7 – Comparison of spectra

carbon contents were observed at the higher engine speed. Thus engine speed affects the exhaust-gas hydrocarbon content as a result of its effect on manifold vacuum.

The manifold vacuum at a fixed engine speed varied from one car to another. Although the cars listed in Table 7 were each of a different make, similar variations have been observed among cars of the same make. These differences are believed to be the result of variations in the idle-speed adjustment and the general mechanical condition of the engine.

Customer Car Survey – The manifold vacuums of a group of 33 customer-owned cars were measured at a constant speed of 30 mph, coasting down hill with closed throttle. With the aid of Fig. 6, the exhaust-gas hydrocarbon content of each vehicle was estimated. Grouping the results on the basis of transmission type or vehicle model year shows some interesting effects of recent automotive design trends.

The effect of the transmission type used in the vehicle on the engine speed and thus the manifold vacuum and exhaust-gas hydrocarbon content during deceleration is shown by the data in Table 8.

The average engine speed, and thus the average manifold vacuum of the cars equipped with standard transmissions, was higher than that of the cars equipped with automatic transmissions. This was due primarily to differences in axle ratios, and to the occurrence of some slip in the automatic transmissions. Thus the use of automatic transmissions, which are becoming increasingly popular with the motorist, should result in lower exhaust-gas hydrocarbon contents during deceleration.

To point out the effect of other recent design changes, a comparison between 1950-51 and 1953-54 cars is shown in Table 9. For each car in the "old" group, which included three makes of cars and three transmission types, there was a corresponding car (same make and transmission type) in the "new" group.

At a constant car speed, lower engine speeds and lower manifold vacuums were generally observed with the newer cars. As a result, the average hydrocarbon content was also lower. Although only a limited number of cars was included in this comparison, the data suggest that the improvement shown was made possible largely because modern high-output engines and improved transmissions permitted the use of lower rear-axle ratios.

Since engine speed and manifold vacuum decrease during normal deceleration, the hydrocarbon content of the exhaust gases changes continuously. Therefore, it is impossible to determine a significant average hydrocarbon content unless all the exhaust products are collected or a continuous sampling procedure is used. The practical application of these methods is very difficult, particularly since many cars should be tested under many different conditions if a truly significant deceleration average is to be obtained. However, an approximate figure is easily obtained from the present simulated deceleration tests, since the tests were carried out under steady-state conditions. The speed, 30 mph, was selected because it is typical of city traffic conditions. The average so obtained, weighted for 1953 car and transmission production figures, was 12.5% by weight of the supplied fuel.

Comparison with Other Work

A comparison of the results of the present work with similar data obtained by other investigators is made in Table 10. All the hydrocarbon contents have been expressed as weight per cent of the supplied fuel, and were calculated from the data of the various investigators.

Each investigator reported the highest hydrocarbon contents at deceleration, the next highest at idle, and the lowest at cruising and acceleration. However, the actual values reported by each differed considerably in some cases. This is not surprising, since different cars, different numbers of cars, different test procedures, and different analytical techniques were employed. The lowest hydrocarbon contents during deceleration and idle were reported in the present work. This may be due in part to the fact that the majority of the cars used in this investigation were 1953 or 1954 models rather than the older models used by the other investigators.

Table 10 – Average Exhaust-Gas Hydrocarbon Content in Weight Per Cent of Supplied Fuel

	McGill, Hutchison, and Stormes[2]	Viets, Fisher, and Fudurich[4]	Los Angeles County Report No. 51[5]	Present Work
Idle	10.7	11.6[a]	5.7[b]	4.0
Acceleration	6.0	1.1[a]	1.8[b]	—
Cruising	5.7	1.1[a]	1.7[b]	1.5[c]
Deceleration	19.2	16.3[a]	29.7[b]	12.5[c]
Cars Tested	10	1	1	7 to 152[d]

[a] Observed values, estimated by Viets, et al., to be 25% low.
[b] All hydrocarbons assumed to be hexane or acetylene.
[c] Simulated deceleration and part-throttle tests.
[d] Based on mass spectrometer and/or Orsat analyses as follows: idle, 152 cars; part throttle, 7 cars; and simulated deceleration, 33 cars.

Commercial Vehicles

Even though gasoline-powered cars, trucks, and buses by far outnumber all other types, the use of diesel- and LPG-powered vehicles in commercial service has grown considerably in recent years. Since there has been considerable discussion of the relative merits of the different engine types in air-pollution-conscious communities, information showing the hydrocarbon content from diesel, LPG, and gasoline engines is of interest to both fleet operators and vehicle manufacturers.

A group of public transit coaches, consisting of two diesel, two gasoline, and four LPG-powered

vehicles, were used for this investigation. However, instead of the steady-state part-throttle and simulated deceleration tests employed in the passenger-car work, unsteady-state acceleration and deceleration as well as cruising conditions typical of bus service were used. The results of the idle, cruising, and acceleration tests are shown in Table 11. It should be pointed out that diesel fuels contain hydrocarbons in the C_{10} to C_{20} range, whereas the mass spectrometer used for the analyses could not detect hydrocarbons heavier than about C_9. For this reason the results for the diesel vehicles may be somewhat low.

The effect of driving condition was similar to that observed in the passenger-car tests. That is, higher hydrocarbon contents were observed during idle than at cruising and acceleration. Also, the similarity of the data for both cruising and acceleration indicates that all engine operation at power output equal to or greater than road load may be combined, as was done with the passenger-car tests. In general, the hydrocarbon contents listed in Table 11 for each driving condition fall within the ranges observed during the passenger-car tests.

The exhaust-gas hydrocarbon content during deceleration for the eight coaches is shown in Table 12. The hydrocarbon content is expressed both as milligrams per standard cubic foot and as the weight % of supplied fuel.

At these particular test conditions, that is, with the deceleration starting at 20 mph, the fuel supply to the diesel engines was not completely shut off. Subsequent tests with Vehicle 1 showed that no fuel was supplied to the engine when the deceleration began at 35 mph. Apparently, the position attained by the injector rack when the foot throttle is closed depends upon the vehicle speed.

On the average, higher hydrocarbon contents were observed during deceleration in the exhaust of LPG vehicles than in that of gasoline vehicles. At first thought, this difference might be attributed to fuel or engine type. However, because the passenger-car tests showed the hydrocarbon content during deceleration to be greatly dependent upon manifold vacuum, it seems likely that this variable was largely responsible for the observed differences. The fact that the highest hydrocarbon contents were observed with vehicles 7 and 8, which were equipped with standard transmissions, lends support to this belief.

Due to the limited number of commercial vehicles tested, definite conclusions concerning the relative merits of the different engine types should be made with caution. Also, it is difficult to compare diesel and carbureted engines with respect to total hydrocarbon emission on the basis of exhaust-gas analyses alone, because the relative air and fuel consumptions vary markedly. However, it is believed that the total amount of hydrocarbon discharged during normal operation would be substantially the same whether the vehicle were equipped with a diesel, gasoline, or LPG engine, provided the overall fuel consumption was comparable.

Summary

These investigations have shown that reductions in exhaust-gas hydrocarbon content can be achieved through proper maintenance and design. Mass spectrometer analyses have indicated that the hydrocarbon content of engine exhaust gas varies appreciably with driving condition, as shown in Table 13.

The most important engine-fuel variable affecting the hydrocarbon content at idle was mixture ratio, with the highest hydrocarbon contents being observed at rich mixtures. A substantial reduction in the average hydrocarbon content could be obtained by adjustment of the idle mixture ratio of all cars to the range resulting in best idle operation. The current trend toward the overhead valve V-8 engine should also help to reduce idle hydrocarbon losses, since these engines will idle acceptably with leaner mixtures than either 6-cyl or

Table 11 – Comparison of Exhaust-Gas Hydrocarbon Content of Diesel, Gasoline, and LPG-Powered Vehicles

	Hydrocarbon Content, weight % of supplied fuel							
	Diesel Coaches		Gasoline Coaches		LPG Coaches			
	No. 1	No. 2	No. 3	No. 4	No. 5	No. 6	No. 7	No. 8
Idle	6.8	15.9	2.0	1.5	1.8	2.9	5.1	3.2
Cruising	1.1	2.6	0.5	0.7	0.9	1.2	0.4	0.6
Acceleration	0.5	1.0	0.4	1.1	0.7	1.3	0.4	0.2

Table 12 – Comparison of Exhaust-Gas Hydrocarbon Content during Deceleration

	Diesel Coaches		Gasoline Coaches		LPG Coaches			
	No. 1	No. 2	No. 3	No. 4	No. 5	No. 6	No. 7	No. 8
Hydrocarbon Content, milligrams per standard cubic foot	21	13	118	130	237	703	839	1515
weight % of supplied fuel	23.9	24.3	8.4	18.7	15.4	31.9	34.1	56.2

Table 13 – Effect of Driving Condition on Exhaust-Gas Hydrocarbon Content

	Hydrocarbon Content, weight % of supplied fuel	
	Observed Range	Average
Idle	1 to 28	4
Part Throttle	1 to 5	1.5
Simulated Deceleration	1 to 63	12.5

line-8 engines. Fuel type was found to have essentially no effect on the exhaust-gas hydrocarbon content.

None of the engine-fuel variables investigated at part throttle was observed to affect significantly the hydrocarbon content. These included mixture ratio, compression ratio, fuel type, coolant temperature, engine type, engine speed, and engine load.

The most important engine-fuel variable affecting the hydrocarbon content during simulated deceleration was manifold vacuum. The hydrocarbon content was found to increase sharply to high values at manifold vacuums above 21 in. of Hg. Since manifold vacuum during a closed-throttle deceleration depends upon engine speed, the trend toward automatic transmissions and lower rear-axle ratios made possible by higher-output engines tends to reduce hydrocarbon losses by reducing engine speed at a given car speed.

Limited studies using gasoline, LPG, and diesel-powered public-transit buses have suggested that there is no significant difference in the total amount of hydrocarbon released to the atmosphere by the three different engines, provided that the overall fuel consumption is comparable.

Acknowledgment

The authors wish to express their appreciation to:

1. The Kansas City Public Service Co., of Kansas City, Mo., and the Leyden Motor Coach Co., of Franklin Park, Ill., for their cooperation in the coach tests.

2. D. V. Kniebes and coworkers of the Institute of Gas Technology for performing the mass spectrometer analyses.

3. The members of the fuels and lubricants department, GM Research Laboratories, for their assistance in running the tests and their criticisms and suggestions during the preparation of the manuscript.

APPENDIX A

In the Twenties and Thirties, several investigators[1, 2] observed small amounts of hydrocarbons in exhaust gases. Since their methods of analysis could not identify individual hydrocarbons, all the hydrocarbon was arbitrarily reported as methane. The development of more suitable analytical instruments, such as infrared and mass spectrometers, made it possible to measure the concentration of individual components of a gas mixture even though present in very small amounts. Both techniques have been successfully applied to the determination of hydrocarbons in exhaust gases.[3, 4]

To decide which of the above two analytical methods would be used in this investigation, several comparable exhaust-gas samples were analyzed by both methods. These tests, and conversations with those familar with the capabilities of each instrument, indicated that the mass-spectrometer method would be the more suitable for this investigation. This decision was reached primarily because the mass spectrometer can quantitatively identify most of the hydrocarbons in exhaust gas. The infrared spectrometer, on the other hand, can identify only those hydrocarbons having characteristic structures, such as methane, ethylene, and acetylene. Other hydrocarbons are grouped together, and one must assume an average molecular weight to make effective use of this information.

The samples were analyzed by the Institute of Gas Technology in Chicago, Ill., and thus several days elapsed between sampling and analysis. It is not known how this delay affected the analyses.

However, the mass spectrometer has limitations that should be recognized. It is difficult to distinguish between carbon monoxide and nitrogen, since both have a parent peak at mass 28, and few characteristic secondary peaks. For this reason, duplicate samples were collected, and the carbon monoxide determined by Orsat analysis. Simple aldehydes have the same molecular weight as the next higher paraffin. Therefore, their parent peaks coincide and, unless both are present in appreciable concentrations, it is difficult to distinguish between the two. Neither aldehydes nor any other oxygenated organic compounds were detected in these analyses. Oxygen, in concentrations greater than 5%, is troublesome because it may attack the tungsten carbide-coated filament in the ionization chamber. In such cases, the mass spectrometer carbon dioxide and carbon monoxide concentrations are questionable, and the Orsat values were assumed to be correct.

Table 14 – Comparison of Mass Spectrometer Exhaust-Gas Analyses Performed by Three Laboratories

(Car H, 1000 rpm downhill, closed-throttle operation)

	Concentration, volume %			
	Laboratory A	Laboratory B	Laboratory C	Orsat
Nitrogen	72.8	75.9	75.6	
Carbon Monoxide	2.6	4.8	5.5	4.5
Oxygen	18.8	13.4	13.3	13.8
Argon	0.90	0.9	0.9	
Hydrogen	0.933	1.5	1.2	
Carbon Dioxide	2.58	2.0	1.6	2.6
Water	—	—	1.0	
Methane	0.173		0.07	
Ethane	0.052		0.06	
Ethylene		0.1		
Acetylene	0.092	0.2	0.1	
Propane		0.01	0.2	
Propylene	0.096	0.1		
Butanes	0.152	0.1		
Butenes		0.05	0.3	
Butadiene	0.490			
Pentanes	0.108	0.1	0.09	
Pentenes	0.055	0.4		
Hexanes	0.044	0.2		
Hexenes	0.022	0.1	0.05	
Benzene		0.005		
Heptanes	0.026	0.1		
Heptenes	0.016	0.005	[a]	
Octanes	0.014			
Octenes		0.005	0.02	
Total Hydrocarbon, volume %	1.34	1.47	0.99[a]	
weight % of supplied fuel	40.7	52.6	31.8	

[a] Probably low because C_7's were present on the spectrum, but not reported in the analysis.

The water vapor in exhaust gas has a strong tendency to condense on or be absorbed by the glass surfaces of the sample containers or of the mass spectrometer inlet system. Most of the analyses were reported on a dry basis because only 5 to 10% of the expected water vapor appeared to reach the ionization chamber and contribute to the spectrum. This was true even though the sample containers were heated to 200 F when transferring the sample to the mass spectrometer. When water condensation occurs, water-soluble oxygenated compounds may be lost, and recent information[10] has shown that hydrocarbons heavier than C_4 may also disappear.

It is difficult to check the accuracy of the mass spectrometer, because no other instrument has the sensitivity required to detect individual hydrocarbons in low concentrations. Although gas mixtures containing various hydrocarbons in low, accurately known concentrations can be prepared, in practice this is very difficult to do. For this reason, it was decided the best approach for this work would be to collect comparable exhaust-gas samples, submit them to several laboratories for analysis, and compare the results.

Exhaust-gas samples were obtained from a 1953 model car coasting downhill at a constant engine speed of 1000 rpm, at the simulated deceleration condition previously described. The samples were not collected simultaneously, but every attempt was made to maintain comparable operating conditions at the times samples were collected. Portions of the mass spectrometer traces of these gas samples as determined by three well-known laboratories are shown in Fig. 7. To make direct comparisons possible, the peak height at mass 57 was arbitrarily assigned a value of 100 in each case, and all other peak heights between 39 to 46 and 50 to 58 scaled accordingly. Considering that each instrument has its own "cracking pattern" for each hydrocarbon, and that one laboratory (C) employed a freeze-out technique, the relative peak heights agree well. This suggests that the true composition of each sample was essentially the same.

The compositions reported by each laboratory differed considerably, however, as may be seen from Table 14. The concentrations of the major constituents agreed fairly well, but there were some large differences in the reported concentrations of individual hydrocarbons. Despite this, the total hydrocarbon content of each sample, expressed as volume per cent or as per cent unburned fuel, were all of the same order of magnitude. Because of the similarity of the spectral patterns, it seems likely that the large variations in the reported concentrations of individual hydrocarbons were due to different interpretations of the spectral patterns.

The conclusion must be reached that the absolute accuracy of mass-spectrometer exhaust-gas analyses remains somewhat in doubt. This is due both to the difficulty of getting a representative sample into the ionization chamber, and the complex problem of deducing the gas composition from the spectral pattern. To help solve these problems the Coordinating Research Council has recently organized a special group to develop improved methods of sampling and analyzing engine-exhaust gas. However, in spite of these difficulties, differences between samples collected in a similar manner and analyzed by one operator on one instrument are significant, and can provide valuable information.

APPENDIX B

The hydrocarbon content of an exhaust-gas sample was calculated from the mass spectrometer analysis of the sample. The weight of supplied fuel was determined from a carbon balance and the carbon/hydrogen ratio of the supplied fuel, assuming that all the carbon in the exhaust-gas sample came from the fuel. A summation of the concentration times the molecular weight for each hydrocarbon gives the weight of unburned hydrocarbons present. The hydrocarbon content in weight % of the supplied fuel is then the ratio of the weight of unburned hydrocarbons present to the weight of supplied fuel. The stepwise procedure is outlined in Table 15.

Table 15 – Calculation of Hydrocarbon Content of Exhaust-Gas Sample from Mass Spectrometer Analysis

(400 rpm idle, 11.7 air/fuel ratio, isooctane)

	Concentration, mole %	× Molecular Weight	= Hydrocarbon, weight per 100 moles of sample	Moles Carbon per 100 Moles of Sample
CO_2	8.63	—	—	8.63
CO	8.5	—	—	8.5
Methane	0.212	16	3.392	0.212
Ethane	0.023	30	0.690	0.046
Ethylene	0.034	28	0.952	0.068
Acetylene	0.096	26	2.496	0.192
Propylene	0.029	42	1.218	0.087
Butanes	0.002	58	0.116	0.008
Butenes	0.013	56	0.728	0.052
Butadiene	0.013	54	0.702	0.052
Pentanes	0.003	72	0.216	0.015
Hexanes	0.002	86	0.172	0.012
Heptenes	0.002	98	0.196	0.014
Octanes	0.041	114	4.674	0.328
Benzene	0.001	72	0.072	0.006
	Total Unburned Hydrocarbon		15.624	
	Total Carbon			18.222

$$\text{Weight of supplied fuel} = \text{Total C} \times 12 + \text{total H} \times 1 = 18.222\,[12 + 2.25\,(1)] = 259.7$$

$$\text{Total hydrocarbon content} = \frac{15.624}{259.7} \times 100 = 6.0\% \text{ by weight of supplied fuel}$$

$$\%\text{ unreacted fuel} = \frac{4.674}{259.7} \times 100 = 1.8\% \text{ by weight of supplied fuel}$$

[10] "Analysis of Automobile Exhaust Gases by Mass Spectrometry," by J. K. Walker and C. L. O'Hara. Presented at Southern California Air Pollution Foundation Meeting, Pasadena, Aug. 18, 1954.

AN investigation to determine why the hydrocarbon content of automobile exhaust gas increases abruptly during deceleration and how this can be prevented is described in this paper.

High-speed motion pictures of the flame, taken through a quartz-window cylinder head, show that residual-gas dilution is the major cause of incomplete combustion under these conditions.

The concentration of hydrocarbons in the exhaust can be reduced either by admitting extra air and fuel to the intake manifold to limit vacuum attained during deceleration or by shutting off the fuel during deceleration.

Flame Photographs To Reduction

THE unburned hydrocarbon content of exhaust gas from engines is of interest for two reasons: (1) the unburned hydrocarbons represent a loss in combustion efficiency, and (2) the unburned hydrocarbons contribute to air pollution. Work published by Viets, Fischer, and Fudurich[1] and also by Magill, Hutchison, and Stormes[2] in 1952 indicated that the largest concentration of unburned hydrocarbons in the exhaust gas of automobiles was found under decelerating conditions. The second largest concentration was found under idling conditions.

In certain important respects engine operation during deceleration and idle differ from engine operation at full throttle. During deceleration and idle operation the intake manifold vacuum is high, the residual-exhaust-gas dilution is high, and the resulting density of reactants in the combustion chamber is lower than during full-throttle operation.

An abrupt increase in the concentration of unburned hydrocarbons in the exhaust gas with an increase in intake manifold vacuum above about 21 in. of Hg has been reported by Rounds, Bennett, and Nebel.[3] The present investigation was undertaken to determine the fundamental reasons for this abrupt increase in hydrocarbon concentration.

Also in the present investigation efforts were made to eliminate the high concentration of hydrocarbons in the exhaust gas of automobiles during deceleration. Two types of carburetor devices designed to reduce the concentration of hydrocarbons in the exhaust gas when an automobile decelerates were tested, and their effectiveness in reducing the concentration of unburned hydrocarbons in the exhaust gas during a closed-throttle deceleration is reported in the present paper.

Combustion Studies Using a Single-Cylinder, Quartz-Window Engine

Equipment – In order to make visual observations and to obtain high-speed motion pictures of the flame, a quartz-window cylinder head was mounted on a CFR crankcase and L-head conversion block assembly as shown in Fig. 1. Also in Fig. 1 can be seen the intake surge tank, carburetor, rotameters, exhaust analysis apparatus, and other equipment grouped around the engine. Fig. 2 is a view through the quartz window showing the location of the piston, valves, and the spark electrodes located directly over the intake valve. The quartz, which forms the top of the combustion chamber, is a 1-in.-thick flat slab and is sloped upwards over the valves. The combustion chamber, therefore, is wedge-shaped.

The engine was coupled to a dynamometer capable of holding the speed within 10 rpm for all conditions used. Engine operating conditions are listed in Table 1.

A speed of 500 rpm was chosen to facilitate the visual observation of the flame. Isooctane was used as the fuel since it was desirable to use an unleaded fuel to keep the window clean. Furthermore, others[2, 3] have shown that there is little or no effect of fuel type on the per cent unburned hydrocarbons in the exhaust gas (weight per cent of input fuel; hereafter referred to as per cent hydrocarbons in exhaust gas). The compression ratio of the engine was 6.7, and a spark timing of tdc was arbitrarily chosen.

The air/fuel ratio was determined from airflow rate and fuel-flow rate measurements. The airflow

[1] See Report of Test 668, Los Angeles County Air Pollution Control District, 1953: "Atmospheric Pollution from Hydrocarbons in Automobile Exhaust Gases," by F. H. Viets, G. I. Fischer, and A. P. Fudurich.

[2] See Proceedings of Second National Air Pollution Symposium, September, 1952, pp. 71-83: "Hydrocarbon Constituents of Automobile Exhaust Gases," by P. L. Magil, D. H. Hutchison, and J. M. Stormes.

[3] See pp. 591-601 of this issue: "Some Effects of Engine-Fuel Variables on Exhaust-Gas Hydrocarbon Content," by F. G. Rounds, P. A. Bennett, and G. J. Nebel.

# of Light-Load Combustion Point the Way of Hydrocarbons in Exhaust Gas

J. T. Wentworth and W. A. Daniel,
Research Laboratories Division, GMC

This paper was presented at the SAE Golden Anniversary Annual Meeting, Detroit, Jan. 10, 1955.

to the engine was controlled and metered by critical-flow nozzles described by Cornelius and Caplan.[4] Fuel-flow rate was measured with a calibrated rotameter.

The intake vacuum was adjusted by regulating the rate at which air was added to the surge tank, and the throttle was always fully open. The large surge tank near the engine served to smooth out pressure fluctuations in the intake system.

Correlation Between Per Cent Hydrocarbon in the Exhaust and Complete Flame Propagation – The procedure used to obtain the data was to wait until the engine had stabilized at a given set of conditions and then to observe whether or not the engine misfired. This was done for many air/fuel ratio and manifold vacuum combinations until a "misfire limit" was determined. By definition a misfire limit condition was taken as approximately one misfire in 50 cycles. The misfire limit thus determined is shown in Fig. 3 as a function of air/fuel ratio and manifold vacuum.

Also shown in Fig. 3 is the range of air/fuel ratios and manifold vacuums within which the flame was observed to burn throughout the combustion chamber. The boundary of the region within which the flame apparently burned throughout the chamber included the range of air/fuel ratios and manifold vacuums within which the flame was observed to burn more than nine-tenths of the mixture.

At the rich boundary of the region within which the flame burned throughout, the flame burned so slowly that it had not completed its travel when the exhaust valve opened at 140 deg atc. With the flame burning out the exhaust port, it could not be determined whether the flame burned throughout the mixture since some burning took place in the exhaust port. The conditions where the flame burned out the exhaust port are indicated in Fig.

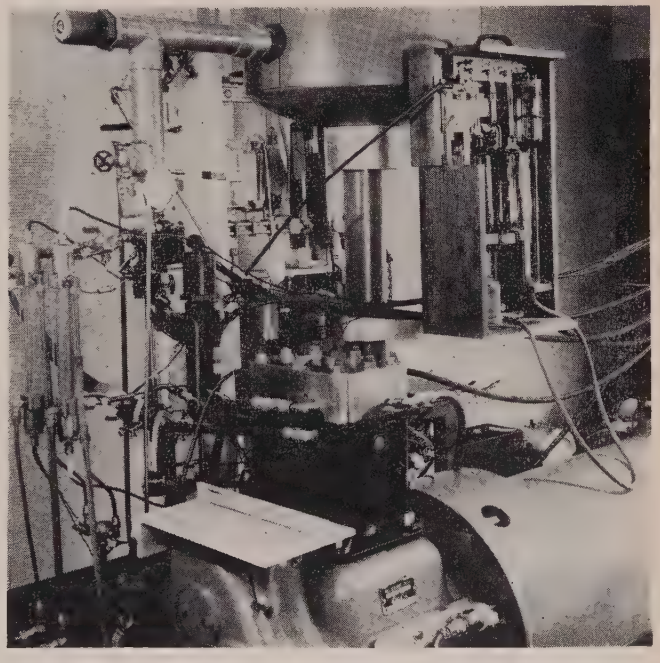

Fig. 1 – Single-cylinder engine and equipment

[4] See SAE *Quarterly* Transactions, Vol. 6, October, 1952, pp. 666-676: "Improved System for Control and Measurement of Air Consumption of Single-Cylinder Engine," by W. Cornelius and J. D. Caplan.

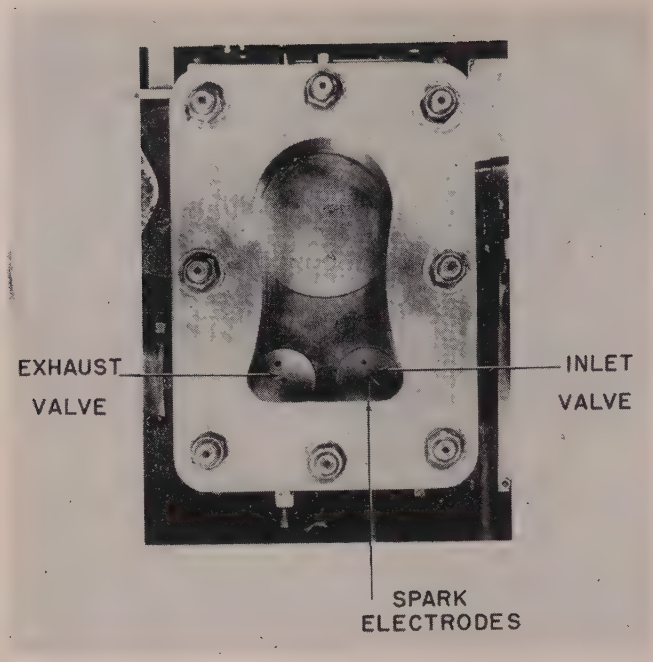

Fig. 2 – Top view of cylinder head

Table 1 – Engine Operating Conditions

Speed, rpm	500 ± 5
Fuel	Isooctane
Compression Ratio	6.7
Spark Timing	Tdc
A/F	Varied from 5 – 17
Intake Manifold Vacuum, in. of Hg	Varied from 16 – 25
Mixture Temperature, [a]F	67 – 130
Oil Sump Temperature, F	102 ± 5
Block Coolant Temperature, F	160 ± 3

[a] No heat was added to the mixture. Temperature varied with air/fuel ratio and manifold vacuum.

3 by a dashed line.

At a constant manifold vacuum the per cent combustion space traversed by flame decreased as the air/fuel ratio decreased from the rich limit of complete inflammation, and at the rich misfire limit less than half of the combustion space was traversed by flame. At lean air/fuel ratios the misfire limit and the boundary of the region within which the flame burned throughout coincided; thus, more than nine-tenths of the combustion space was traversed by flame at the lean misfire limit.

Although most of the observations of the flame were made visually while the tests were being run, a few high-speed motion pictures (400 to 800 frames per sec) were taken at the conditions enumerated in Fig. 4. Flame photographs from the motion-picture sequences are reproduced in Figs. 5 through 8. To obtain these photographs an Eastman high-speed camera was used with Kodak Linagraph Pan film. The film was developed in Kodak SD-19a. In addition it was found necessary to add powdered sodium chloride to the air/fuel mixture to get a good exposure from the flame. The addition of sodium made the flame a bright yellow but did not change the power output of the engine, the exhaust temperature, or the apparent flame speed as determined by observation of the flame through a stroboscopic disc. Thus, it is believed that the flame with sodium added is representative of the flame without sodium.

The Authors

J. T. WENTWORTH (J '54) is a research engineer in the Fuels and Lubricants Department of General Motors. In 1952, he received a B.S. in Mechanical Engineering from the University of Michigan. Mr. Wentworth joined General Motors immediately after graduation.

W. A. DANIEL is a research physicist in the Fuels and Lubricants Department of General Motors. Mr. Daniel received a B.S. in Physics from the University of Texas in 1951 and joined General Motors the following year.

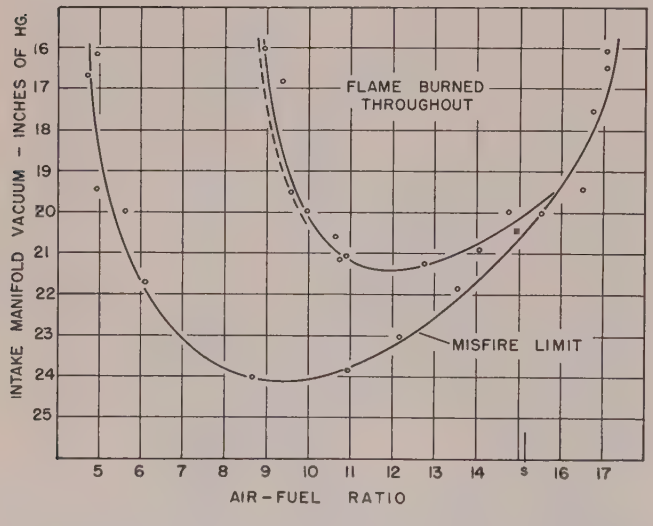

Fig. 3 – Misfire limit and region within which the flame apparently burned throughout the chamber. Engine conditions: speed, 500 rpm; fuel, isooctane; compression ratio, 6.7; spark timing, tdc

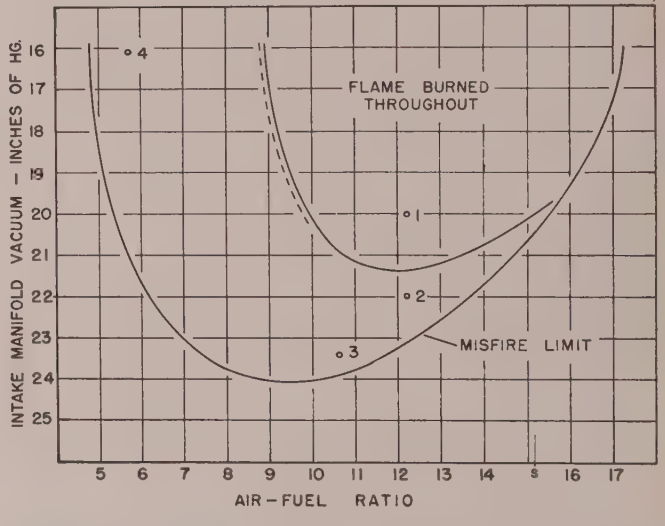

Fig. 4 – Engine conditions at which motion pictures were obtained. Engine conditions: speed, 500 rpm; fuel, isooctane; compression ratio, 6.7; spark timing, tdc

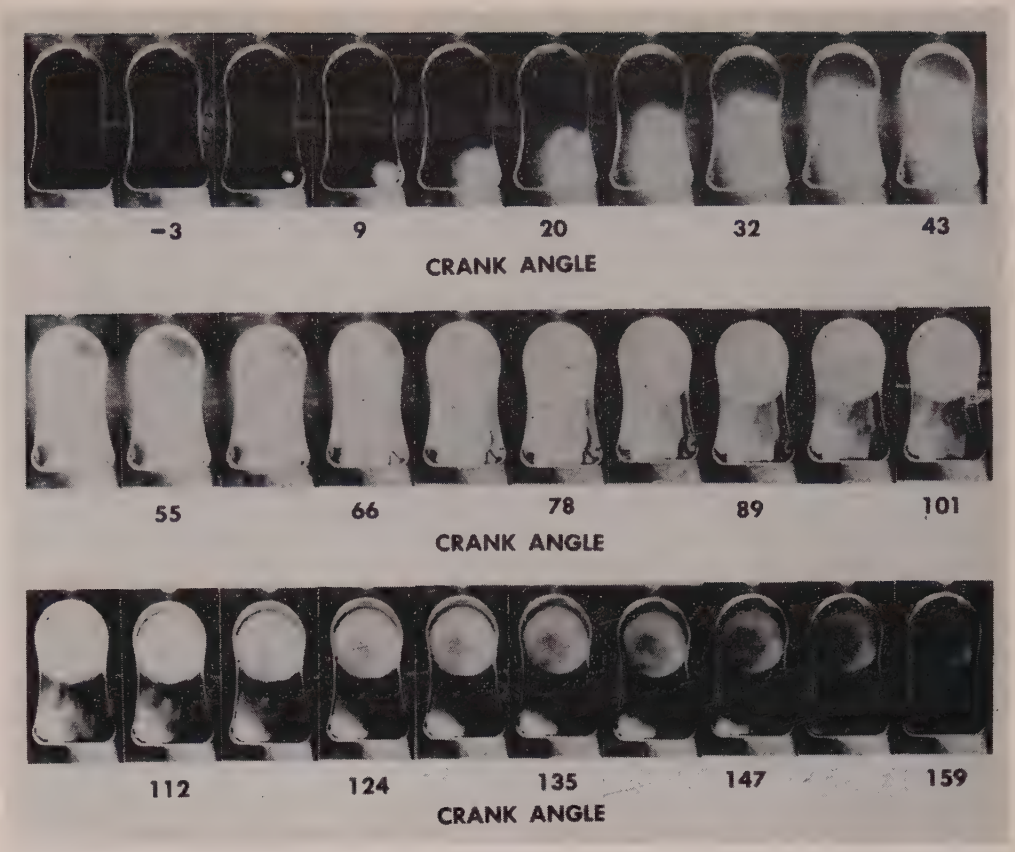

Fig. 5 – Flame photographs for engine conditions of point 1 in Fig. 4. Flame apparently burns throughout. Engine conditions: intake manifold vacuum, 20 in. of Hg; air/fuel ratio, 12.2; spark timing, tdc

In Fig. 5 are shown the flame photographs obtained at engine conditions indicated by point 1 in Fig. 4. Although the accuracy of the crank angles given in the flame photographs was only about ± 2 deg near tdc and about ± 5 deg at 140 deg atc, the lack of accuracy in determining the

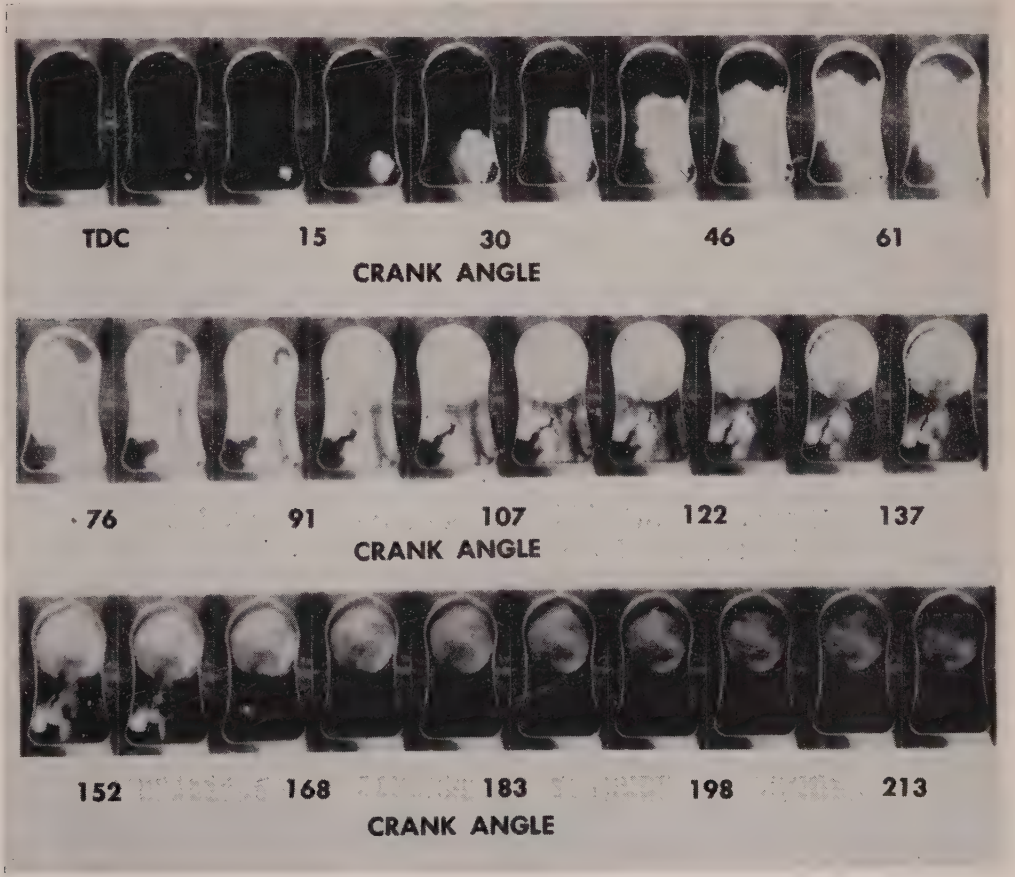

Fig. 6 – Flame photographs for engine conditions of point 2 in Fig. 4. Flame does not burn throughout. Engine conditions: intake manifold vacuum, 21.8 in. of Hg; air/fuel ratio, 12.2; spark timing, tdc

Fig. 7 – Flame photographs for engine conditions of point 3 in Fig. 4. Engine conditions: intake manifold vacuum, 23.4 in. of Hg; air/fuel ratio, 10.6; spark timing, tdc

crank angle for a given frame does not affect the conclusions drawn from the flame photographs. As can be seen from the location of point 1 in Fig. 4, the manifold vacuum and the air/fuel ratio were so adjusted that the flame was expected to burn throughout the combustion chamber. This was verified by the flame photographs shown in Fig. 5.

In Fig. 6 are shown flame photographs which illustrate the effect of increasing the intake vacuum to a point outside the region within which the flame burned throughout. As can be seen in Fig. 6 the flame failed to burn in the exhaust-valve corner. In general, when engine conditions were changed so that the boundary of the region within which the flame burned throughout was crossed, the failure to burn occurred first in the exhaust-valve corner.

The flame photographs shown in Fig. 7 were obtained at the air/fuel ratio and manifold vacuum denoted by point 3 in Fig. 4. These conditions are farther from the boundary of the region within which the flame burned throughout, and the proportion of the combustion space traversed by flame was considerably reduced from that in Fig. 6.

Flame photographs were also taken at the manifold vacuum and air/fuel ratio represented by point 4 of Fig. 4. This sequence is shown in Fig. 8. These engine conditions were near the rich misfire limit, and the flame was green in color. The flame burned in isolated patches, but the patches spread through the chamber in a more or less normal manner. The energy released by the green flame of Fig. 8 was low, as evidenced by the facts that the indicated power was nearly zero and there was approximately 20% oxygen in the exhaust. It is evident that at these conditions the per cent of hydrocarbons in the exhaust would be very high.

The per cent of hydrocarbons in the exhaust gas was determined at a number of different air/fuel ratios and manifold vacuums by means of a combustion Orsat. A description of the method for determining per cent of hydrocarbons in the exhaust gas is given in Appendix I. Briefly, the hydrocarbon was measured by the amount of CO_2 formed when the exhaust gas was passed over a heated catalyst in the presence of excess oxygen. Allowance was made for any CO_2 formed from combustion of CO.

The per cent unburned hydrocarbon values for the points shown in Fig. 9 with air/fuel ratios between 10.4 and 11.0 are plotted in Fig. 10. The curve of Fig. 10 shows the per cent of unburned

Fig. 8 – Flame photographs for engine conditions of point 4 in Fig. 4. Flame at very rich air/fuel ratios. Engine conditions: intake manifold vacuum, 16.1 in. of Hg; air/fuel ratio, 5.7; spark timing, tdc

hydrocarbons as a function of manifold vacuum at an approximately constant air/fuel ratio. The sharp increase in the per cent of unburned hydrocarbons occurring at about 21 in. of Hg vacuum coincides with the failure of the flame to burn throughout the mixture. As the manifold vacuum was increased above 21 in. of Hg, the per cent of combustion space traversed by flame decreased, and the per cent of hydrocarbons in the exhaust increased.

The values of the per cent hydrocarbon in the exhaust gas for the points shown in Fig. 11 for the two manifold vacuum regions of 16.0 to 16.8 in. of Hg and 19.4 to 20.0 in. of Hg are plotted in Fig. 12. The two curves of Fig. 12 show the per cent of unburned hydrocarbons as a function of air/fuel ratio for two approximately constant manifold vacuums. Again the sharp increase in the per cent of hydrocarbons coincides with the failure of the flame to burn throughout the chamber.

From the data of Figs. 10 and 12 it is concluded that when the visual inspection of the flame showed that the flame apparently burned throughout the mixture the per cent of hydrocarbons found in the exhaust was relatively low. When the flame failed to burn throughout the mixture, whether due to the exhaust valve opening before the combustion

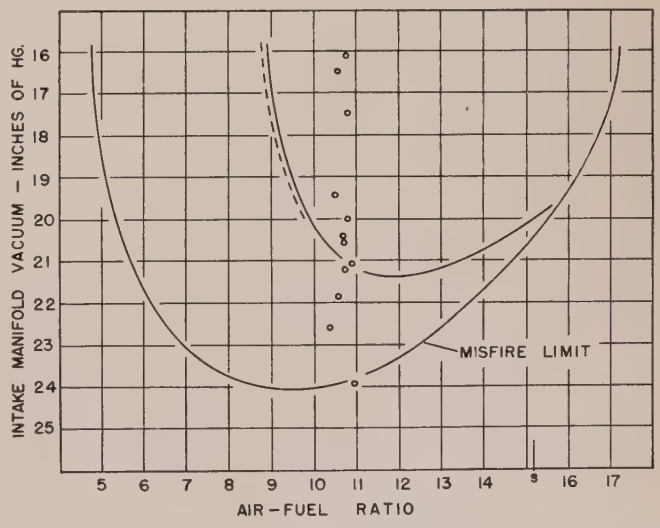

Fig. 9 – Engine conditions used to show effect of intake manifold on per cent hydrocarbons in exhaust. Engine conditions: speed, 500 rpm; fuel, isooctane; compression ratio, 6.7; spark timing, tdc

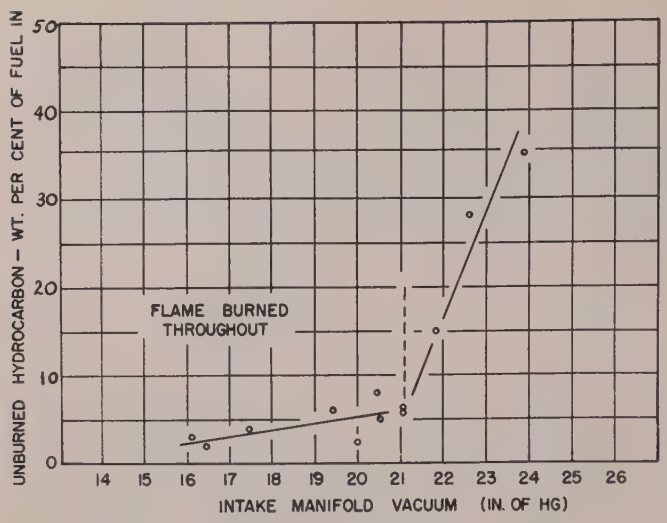

Fig. 10 – Weight per cent hydrocarbons in exhaust gas as a function of manifold vacuum. Engine conditions: speed, 500 rpm; fuel, isooctane; compression ratio, 6.7; spark timing, tdc

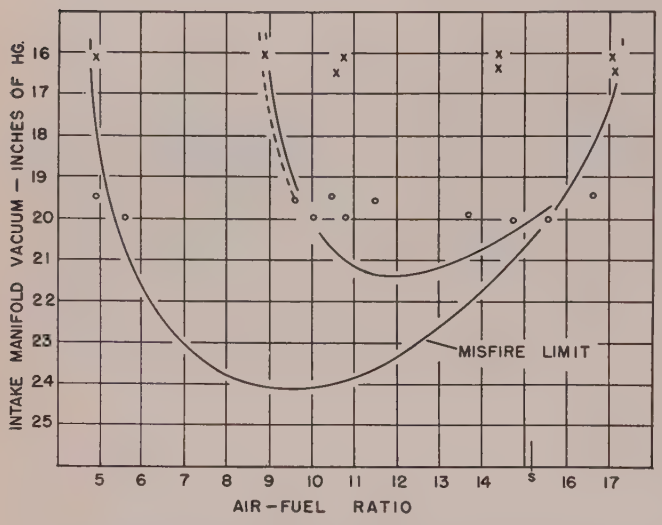

Fig. 11 – Engine conditions used to show effect of air/fuel ratio on per cent hydrocarbons in exhaust. Engine conditions: speed, 500 rpm; fuel, isooctane; compresson ratio, 6.7; spark timing, tdc

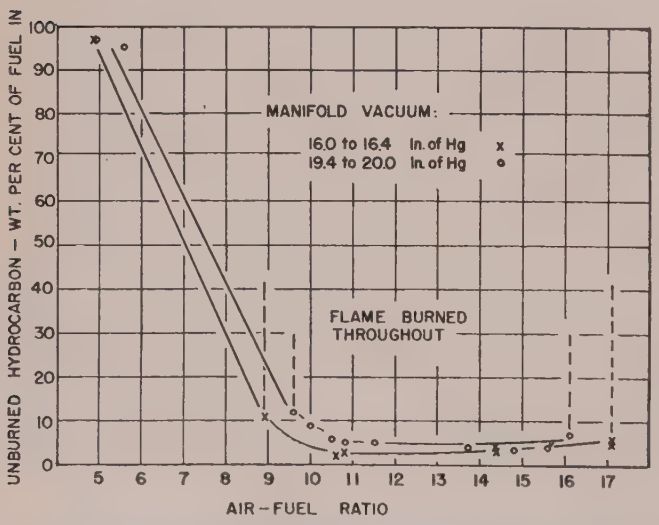

Fig. 12 – Weight per cent hydrocarbons in exhaust gas as a function of air/fuel ratio. Engine conditions: speed, 500 rpm; fuel, isooctane; compression ratio, 6.7; spark timing, tdc

was complete or to too high a manifold vacuum, the per cent of hydrocarbons in the exhaust gas increased.

Effect of Dilution on Flame Propagation and Misfire Limit – At this point an obvious question is: Why does the flame fail to burn throughout the combustion chamber at some engine conditions? It is known[5] that sufficient dilution of a gasoline-air mixture by an inert gas will prevent inflammation of the mixture. It is also known that the residual-gas dilution of the charge in an engine increases with increasing intake manifold vacuum. Accordingly, experiments were conducted to determine whether residual-gas dilution was the cause for the failure of the flame to burn throughout at the higher manifold vacuums.

It has already been noted that when engine conditions were such that a small portion of the mixture was not burned, the unburned portion would be in the exhaust-valve corner. If exhaust-gas dilution were the cause of the failure to burn in this corner, then a determination of the exhaust-gas dilution in the exhaust-valve corner should give the limiting exhaust-gas dilution that would permit combustion.

To determine the residual-gas dilution in the engine, a Cox sampling valve was placed so that the mixture in the exhaust-valve corner could be sampled. The mixture sample was obtained by opening the valve for 130 crank angle deg on the compression-expansion strokes. The valve open time was centered about tdc, and the spark was interrupted on the cycle sampled. Since more than one cycle (3 to 8) had to be sampled to fill a 100-ml burette, a pause was made between the sampled cycles to allow the engine to recover from the effects of the unfired cycle.

The residual-gas weight fraction was determined from the per cent CO_2 in the exhaust and the per cent CO_2 in the mixture sample as outlined in Appendix II.

The particular engine conditions at which the residual fractions were determined are shown in Fig. 13. Each engine condition was chosen to give a small unburned area in the exhaust-valve corner; thus the points would follow the boundary of the region within which the flame burned throughout. At the rich air/fuel ratios and a spark timing of tdc the flame burned so slowly that the exhaust valve opened before the flame passage was complete. At an advanced spark timing, 40 deg btc, the flame no longer burned out the exhaust port, and the engine conditions which gave an unburned area in the exhaust-valve corner are shown by the crosses in Fig. 13. The residual fraction was determined for both spark timings.

In Fig. 14 are shown the residual fractions as

[5] See Bureau of Mines RI, No. 3871 (April, 1946); "Extinction of Gasoline Flames by Inert Gases," by G. W. Jones and W. R. Gilliland.

a function of air/fuel ratio for the points shown in Fig. 13. It can be seen that, for the range of air/fuel ratios commonly used in spark-ignition engines, the richer mixtures tolerated more dilution than the leaner mixtures.

A comparison between the results shown in Fig. 14 and the results of experiments by Jones and Gilliland are shown in Fig. 15. Jones and Gilliland reported the limiting percentages of exhaust gas for inflammability of gasoline-air mixtures of controlled composition in a tube. The data were obtained with the test gases at a reduced pressure and with a spark for ignition. Jones' and Gilliland's data were reported on a volume basis. By assuming an average molecular weight of the gasoline to be 98, their data were changed to a weight basis and plotted in Fig. 15. For air/fuel ratios richer than about 8, the data of Jones and Gilliland show an abrupt boundary between diluted gasoline-air mixtures that will and will not burn; however, at leaner air/fuel ratios the data indicate a spread between the per cent dilution that will burn and the per cent dilution that will not burn. This probably means that within the spread the mixture would burn sometimes and at other times would not.

For air/fuel ratios between 12.5 and 18 and a spark timing of tdc it would appear that the reason the flame does not burn the mixture in the exhaust-valve corner of the engine is because the dilution has reached the upper limit that will permit combustion. Dilution is probably not the cause for the unburned portion of mixture for the air/fuel ratios richer than 12.5 since the measured dilution appears to be well in the range of dilution that should permit combustion. High-speed motion pictures at these conditions have shown that unburned mixture is swept out the exhaust valve when it opens at 140 deg atc. The failure to burn, therefore, has a simple physical explanation – the unburned mixture was swept out the exhaust valve before it had a chance to burn. The advanced spark provides a longer burning time, and a good correlation was obtained between the engine results and Jones' and Gilliland's results for air/fuel ratios as rich as 9.

The fact that the limiting value of the exhaust-gas dilution for a given air/fuel ratio is nearly the same in the tube and in the engine would indicate that residual-gas dilution is a major factor limiting complete inflammation of the mixture in the quartz-window engine operated at high intake vacuums.

Many differences exist between the conditions used in the tube and those present in the engine. One difference is the fuel used. In the engine the fuel was isooctane, and in the tube work the fuel was gasoline. Jones and Gilliland[5] found no effect on the ignition limits when using three different gasolines of widely different octane number and volatility. Pressures also were different in the two cases. The pressures present in the engine ranged

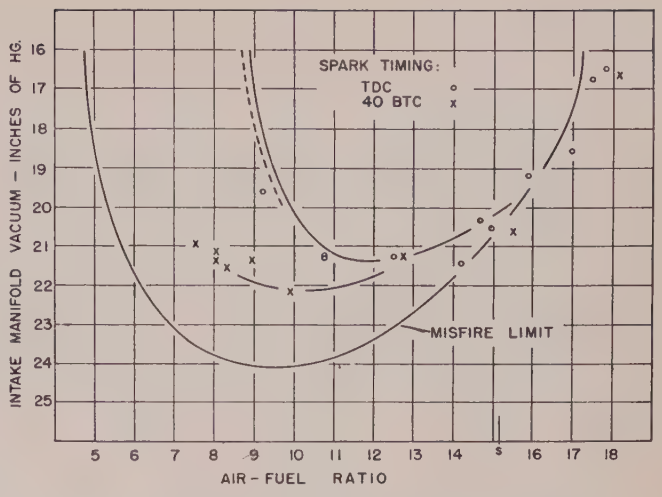

Fig. 13 – Engine conditions at which residual fractions were determined. Engine conditions: speed, 500 rpm; fuel, isooctane; compression ratio, 6.7; spark timing, tdc and 40 btc

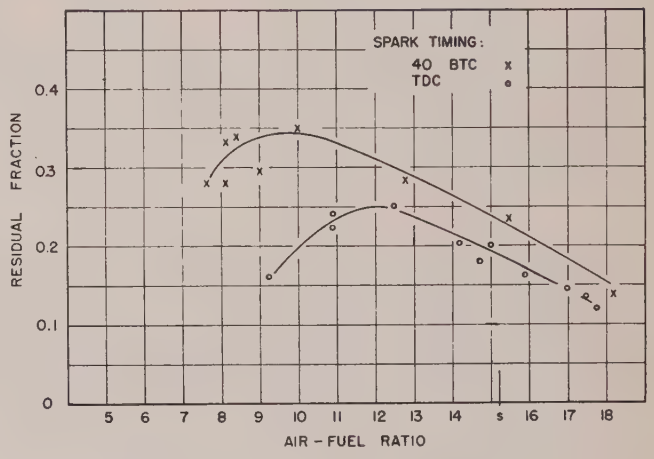

Fig. 14 – Residual-gas weight fraction for points shown in Fig. 13. Engine conditions: speed, 500 rpm; fuel, isooctane; compression ratio, 6.7

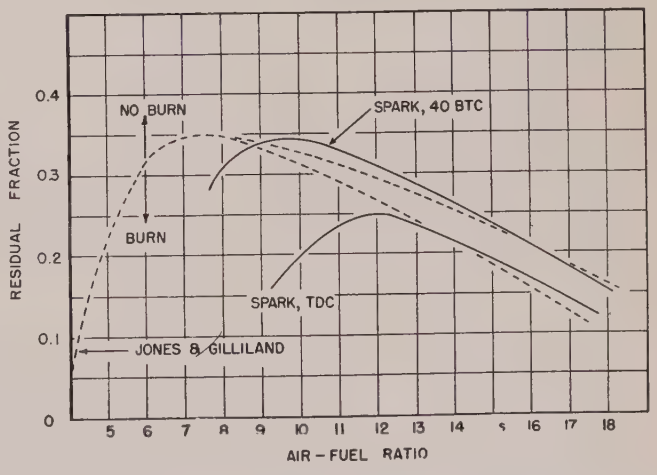

Fig. 15 – Comparison of exhaust-gas dilution in exhaust-valve corner with limiting exhaust-gas dilution in a tube. Engine conditions: speed, 500 rpm; fuel, isooctane; compression ratio, 6.7

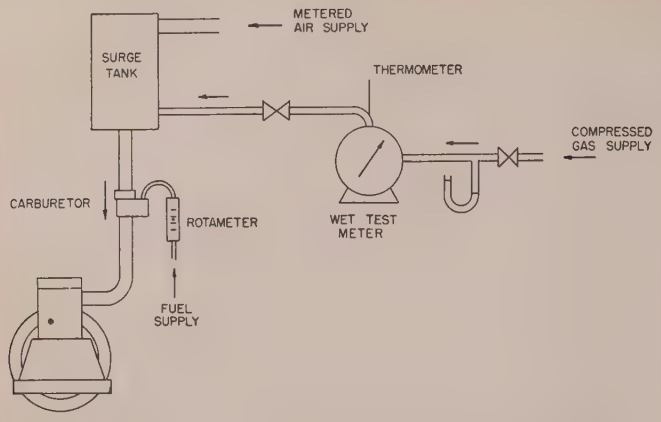

Fig. 16 – Apparatus for adding oxygen or nitrogen to intake air

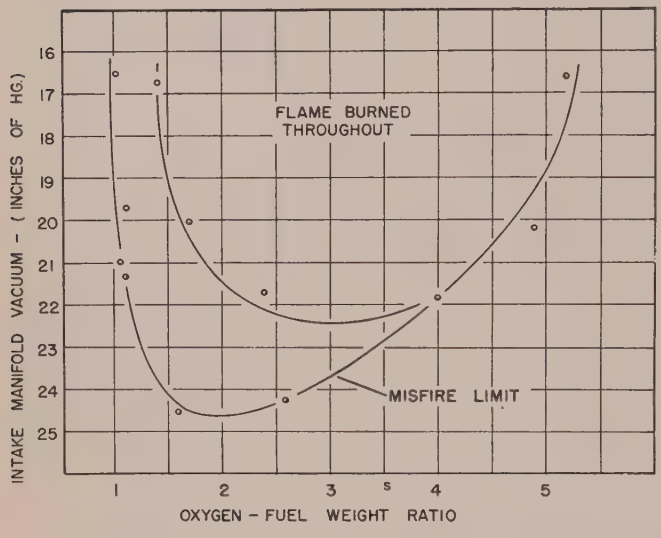

Fig. 17 – Misfire limit and region within which flame burned throughout with extra oxygen added to intake air. Oxygen/nitrogen weight ratio equals 0.44. Engine conditions: speed, 500 rpm; fuel, isooctane; compression ratio, 6.7; spark timing, tdc

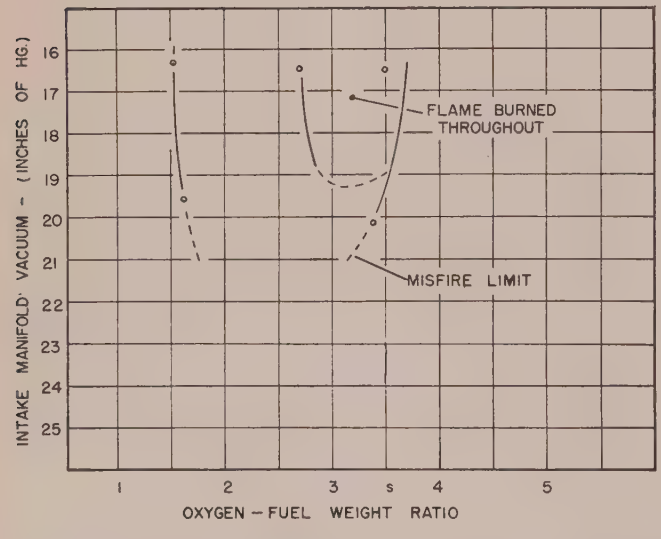

Fig. 18 – Misfire limit and region within which flame burned throughout with extra nitrogen added to intake air. Oxygen/nitrogen weight ratio equals 0.26. Engine conditions: speed, 500 rpm; fuel, isooctane; compression ratio, 6.7; spark timing, tdc

from a maximum of 4.7 atmospheres to a minimum of about 0.25 atmospheres, while the tube experiments were conducted at "reduced pressure." Jones and Kennedy[6] investigated the effect of pressure on the inflammability limits of natural gas-air mixtures with no dilution. The results of this work showed little effect of pressure within the range of pressures used in the engine and in the tube work. Another difference in the two cases is the diluting exhaust gas. In the tube work the exhaust gas was apparently a dry mixture of 85% nitrogen, 15% CO_2 for all air/fuel ratios, while the exhaust-gas diluent in the engine is a mixture containing N_2, H_2O, CO, CO_2, and H_2, depending on the air/fuel ratio. The effect of the differences in exhaust gas in the two cases has not been evaluated, and in particular the effect of the difference in the amount of H_2O present could be significant.

If the boundary of the region within which the flame burned throughout is mainly determined by the limiting dilution that will permit burning, a change in the dilution would cause a corresponding change in the position of the boundary of the region within which the flame burned throughout. The "overall dilution" of the oxygen-fuel mixture in the combustion chamber comes from two sources: (1) the nitrogen which accompanies the oxygen-fuel mixture fed to the engine, and (2) the residual exhaust gas. One way to change the overall dilution of the oxygen-fuel mixture, therefore, would be to change the per cent nitrogen in the intake "air." This was done by adding nitrogen or oxygen to the intake surge tank.

As indicated in Fig. 16 the added gas passed from a gas cylinder through a needle valve to the wet-test meter. From the wet-test meter it passed through a second needle valve into the surge tank of the air system. By adjusting the two needle valves it was possible to obtain the desired rate of flow and to maintain the pressure between the valves at approximately atmospheric.

The procedure followed was to adjust the airflow and added gas flow to obtain a given oxygen/nitrogen ratio in the inlet charge and also to obtain a given manifold vacuum. The fuel flow was then changed to obtain a range of oxygen/fuel ratios to determine the misfire limit and the range of oxygen/fuel ratios within which the flame apparently burned throughout the chamber. By repeating this procedure for several different manifold vacuums a plot of the misfire limit and the region within which the flame burned throughout was obtained. A plot for an oxygen/nitrogen weight ratio of 0.44 (oxygen/nitrogen ratio of air is 0.30) is shown in Fig. 17. A plot for an oxygen/nitrogen ratio of 0.26 is shown in Fig. 18. The plots shown in Figs. 3, 17, and 18 are shown superimposed in

[6] See Bureau of Mines RI, No. 3798 (February, 1945): "Inflammability of Natural Gas; Effect of Pressure upon Limits," by G. W. Jones and R. E. Kennedy.

Fig. 19. It was necessary to change the abscissa of Fig. 3 from air/fuel ratio to oxygen/fuel ratio for Fig. 19.

In Fig. 19 it can be seen that a decrease in the overall dilution of the charge from that given by air, by increasing the oxygen/nitrogen ratio to 0.44, widened and lowered the range of air/fuel ratios and manifold vacuums within which the flame burned throughout. An increase in the overall dilution of the charge by decreasing the oxygen/nitrogen ratio below that of air, narrowed and raised the range of air/fuel ratios and manifold vacuums within which the flame burned throughout. Thus these results appear to confirm qualitatively the hypothesis that the boundary of the region within which the flame burned throughout was primarily determined by the dilution of the mixture.

Reviewing the results of Fig. 19 in more detail, however, yields the following argument: Consider a point on the plot, for example, the bottom point of the boundary for complete burning at an oxygen/nitrogen weight ratio of 0.30 designated by an *X* on the plot. If the oxygen/nitrogen ratio of the charge is changed to 0.26 by replacing some of the oxygen-fuel mixture by nitrogen, it is apparent that at point *X* the nitrogen is now a larger proportion of the charge, but also the concentration of fuel and oxygen (moles/unit volume) has been decreased. Thus, the failure to burn may be due either to the increased dilution or to the lower concentration of reactants. Similarly at point *X*, but with an oxygen/nitrogen ratio of 0.44, the overall dilution is lower and the concentration of reactants is higher. Whether the failure to burn

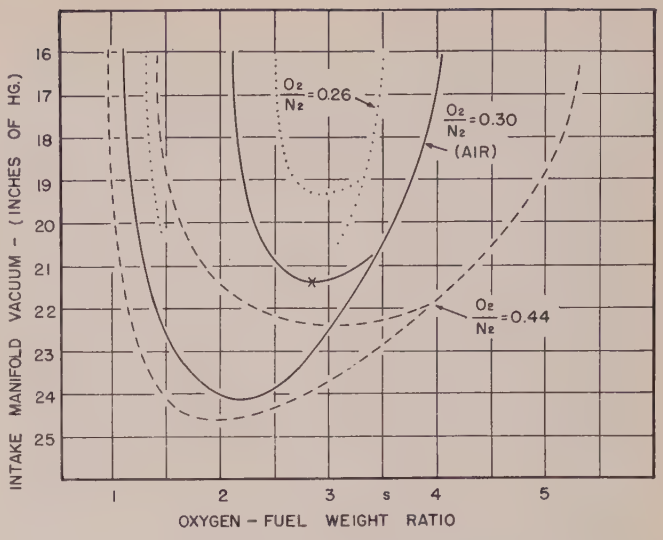

Fig. 19 – The effect of a change in the overall dilution on the misfire limit and on the region within which the flame burned throughout. Engine conditions: speed, 500 rpm; fuel, isooctane; compression ratio, 6.7; spark timing, tdc

Fig. 20 – Sequence showing effect of interrupted ignition on flame propagation. Last cycle before ignition turned off; typical cycle. Engine conditions: intake manifold vacuum, 23.4 in. of Hg; air/fuel ratio, 10.6; spark timing, tdc

then is due to the dilution effect or to the change in the concentration of reactants cannot be determined from the data shown in Fig. 19, although the correspondence between the residual dilution values obtained in the engine and the values of "exhaust-gas" dilution that prevent inflammation in a tube would indicate that the dilution effect is the limiting factor.

In Fig. 19 it may be seen that the misfire limit was affected by a change in the overall dilution in the same manner as the boundary of the region within which the flame apparently burned throughout. Evidently the ignition of the mixture is determined by the same variable or variables that control complete inflammation.

Perhaps the most striking evidence of the role of dilution is given in Figs. 20, 21, and 22. The flame photographs shown in these figures were obtained with a manifold vacuum of 23.4 in. of Hg and an air/fuel ratio of 10.6. These engine conditions, incidentally, are the same as those for point 3 in Fig. 4. At these engine conditions the flame did not normally burn throughout the combustion chamber. Flame photographs of a typical cycle are shown in Fig. 20. The ignition was turned off for four cycles to allow the engine to purge itself of exhaust gas. The ignition was then turned on, and the flame photographs shown in Fig. 21 were obtained from the first cycle after the ignition was turned on. For this cycle the exhaust-gas dilution was low and the flame burned throughout the combustion chamber. It can be noted by comparing Figs. 20 and 21 that the flame was brighter and the apparent flame speed was greater with the low dilution. Flame photographs of the second cycle after the ignition was turned on are shown in Fig. 22. The exhaust-gas dilution in this second cycle is relatively high due to the complete combustion of the preceding cycle. With this high dilution the flame burned only a small portion of the mixture as may be seen in Fig. 22.

Again this experiment did not separate the effects of a change in dilution and a change in concentration of reactants since the manifold pressure was maintained constant while the proportion of reactants and residual in the chamber was varied. Similar to the argument outlined previously, the inflammability of the mixture may have been determined by the concentration of the reactants.

Another experiment was made to determine if a concentration of reactants lower than the concentration of reactants at engine conditions near the bottom of the boundary of the region within which the flame burned throughout could be made to burn. A point at the bottom of the boundary was

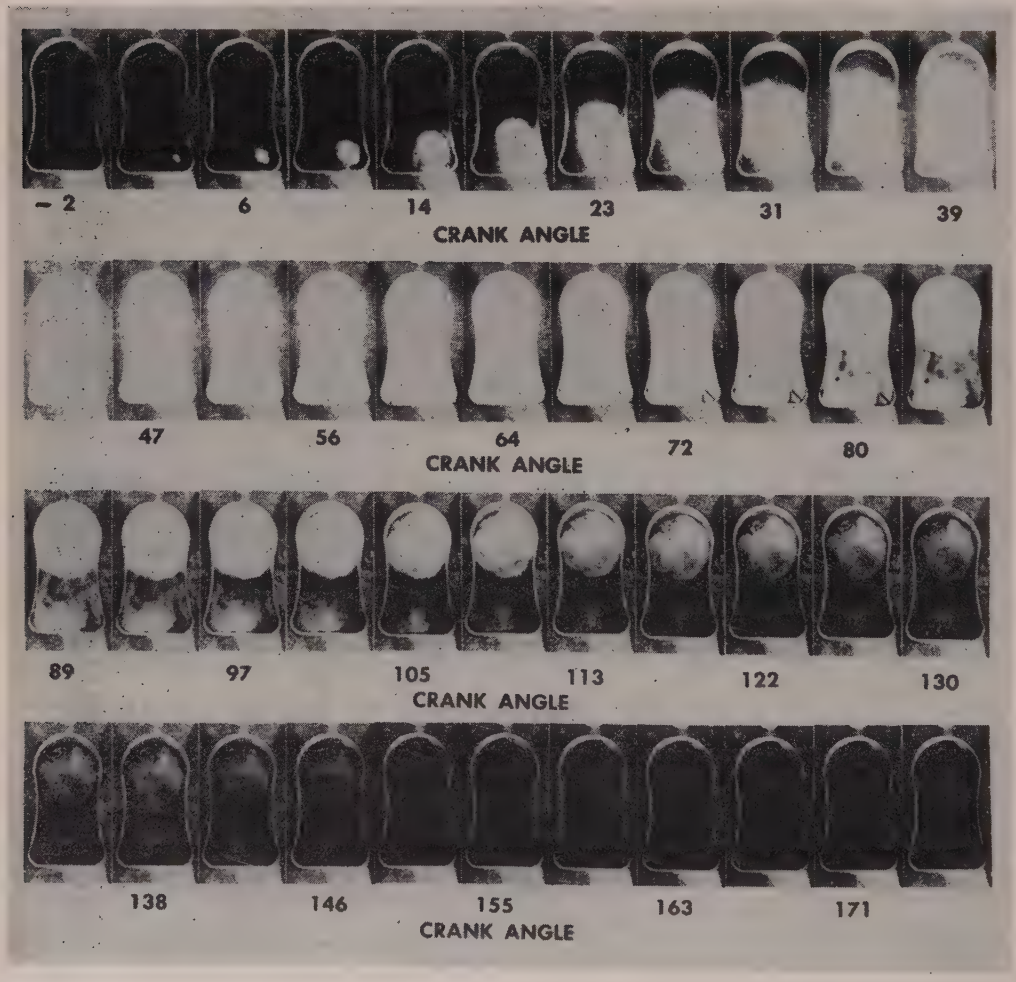

Fig. 21 – Sequence showing effect of interrupted ignition on flame propagation. First cycle after ignition turned on; low dilution. Engine conditions: intake manifold vacuum, 23.4 in. of Hg; air/fuel ratio, 10.6; spark timing, tdc

selected because it would have the lowest concentration of reactants of any point on the boundary and would provide the most critical test. If a mixture with a concentration of reactants lower than the concentration of reactants for the point just mentioned could be made to burn throughout, the possibility that complete inflammation of the mixture in the engine was limited by a critical concentration of reactants could be rejected.

Operating the engine at the highest possible vacuum with no burned-product dilution appeared to afford the best possibility of accomplishing this. Accordingly, the interrupted ignition experiment described above was extended. It was found that when the engine was operated with an intake manifold vacuum of 26.2 in. of Hg (the highest manifold vacuum which the engine could pull) the flame would burn throughout the chamber for one cycle only; thereafter, the engine would not fire for a considerable length of time. The reason for this was that the residual fraction was close to one, and the burned products of the fired cycle oscillated back and forth in the engine and manifolds. If the burned products were cleared from the system, the engine would again fire for one cycle. To aid in clearing the burned products, the exhaust manifold was removed at the block, and the intake manifold was closed about a foot from the block. Fuel was metered through a needle valve into this short section of intake manifold. Upon turning the engine over the intake vacuum rose immediately to 26.2 in. of Hg (1.7 psia). The spark ignition was then turned on, and the fuel flow was adjusted until the engine fired. At an optimum fuel rate the engine would fire every second or third cycle burning the mixture completely. After a cycle in which the flame burned throughout it took about one cycle to replace the residual burned products with sufficient air for combustion since all the air for combustion entered through the exhaust port. Thus it was found that the flame would burn throughout the chamber when the intake manifold pressure and the pressure at the beginning of compression was 1.7 psia.

At an intake vacuum of 21.3 in. of Hg (3.9 psia) and an air/fuel ratio of 12.5 the flame did not burn throughout the chamber when the engine was operated normally as may be seen in Fig. 13. The residual fraction for these engine conditions was 0.24 (from Fig. 14). Therefore, the partial pressure of the reactants at the beginning of compression was about 3 psia.

Making the simplifying assumption that the concentration of the reactants is proportional to the partial pressure of the reactants, it is apparent that the concentration of reactants is less in the

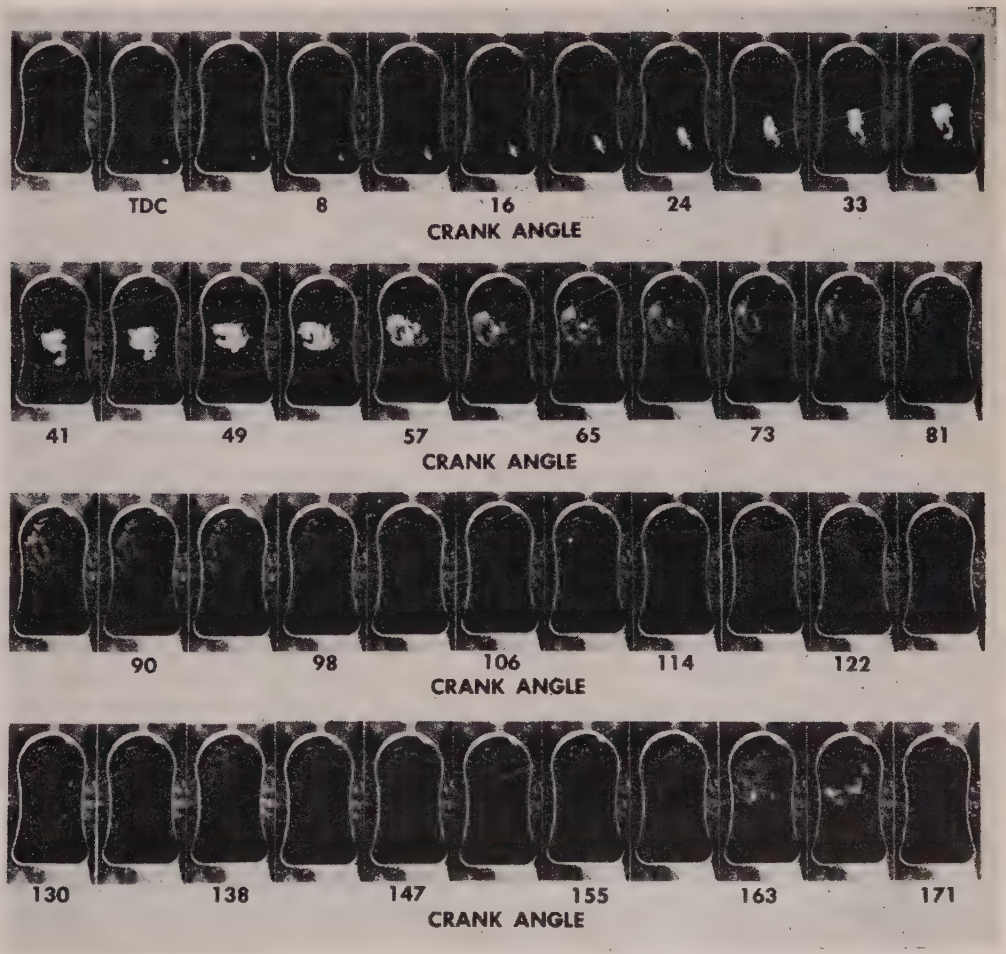

Fig. 22 – Sequence showing effect of interrupted ignition on flame propagation. Second cycle after ignition turned on; high dilution. Engine conditions: intake manifold vacuum, 23.4 in. of Hg; air/fuel ratio, 10.6; spark timing, tdc

case where the partial pressure of reactants was, at most, 1.7 psia than in the case where the partial pressure of the reactants at the beginning of compression was 3.0 psia. Since the flame burned throughout the chamber when the partial pressure of the reactants was 1.7 psia, the failure of the flame to burn throughout when the partial pressure of the reactants was 3.0 cannot be attributed to too low a concentration of reactants.

Similarly, if the partial pressures of the reactants for the conditions considered in Fig. 19 were known, it could be determined whether the effect of the added nitrogen was due to the increased dilution or to the decreased concentration of reactants. Unfortunately, the residual-gas fraction was not determined for these conditions, and therefore the partial pressures of reactants were not known. However, the lowering of the limits when oxygen was added cannot be due to a concentration effect since it has been shown that the concentration of reactants for the "air" curve (oxygen/nitrogen ratio = 0.30) was not a threshold concentration, and with oxygen added (oxygen/nitrogen ratio = 0.44) the concentration of reactants at a given point, X, is greater than that for air.

The experiments described above indicate that dilution is an important factor in preventing the complete inflammation of the mixture; however, the possibility that the incomplete inflammation may be partly due to pressure or other unknown factors or both has not been entirely eliminated.

Two Devices to Reduce Hydrocarbons in Exhaust Gas

Assuming that the plot of the misfire limit and the region within which the flame burned throughout is applicable to present-day automobile engines, the single-cylinder engine investigation indicates that in most cases idle operation is probably within the region in which the flame burns throughout. Idle vacuum is usually between 18 to 20 in. of Hg so it is necessary only to maintain the air/fuel ratio between 10 and 16. In most instances the idle air/fuel ratio is undoubtedly within this range. One would expect, therefore, that the concentration of unburned hydrocarbons in the exhaust at idle would be relatively low.

In addition the single-cylinder investigations confirmed the findings of previous investigators[1, 2, 3] who found that the high concentrations of unburned hydrocarbons in the exhaust gas of engines occur when the engine is operated at high intake vacuums (greater than about 21 in. of Hg vacuum). Usually intake manifold vacuums above 21 in. of Hg can be attained only by deceleration and may be as high as 25 in. of Hg.

Since the highest concentration of hydrocarbons in the exhaust occurs during deceleration, an attempt was made to reduce the concentration during deceleration. There are at least two ways to modify a carburetor in order to reduce the high concentration of unburned hydrocarbons found in the exhaust of an engine during deceleration:

1. The fuel flow may be shut off when the intake manifold vacuum exceeds about 21 in. of Hg.

2. The vacuum may be prevented from reaching the values which give high concentrations of unburned fuel in the exhaust.

Two devices, one operating on each principle, were tested. The device operating on the fuel-flow shutoff principle was installed on the family car of one of the authors. The car was of a 1947 vintage and was equipped with a synchromesh transmission. The mechanical condition of the engine was good, having had an overhaul 10,000 miles or one year before the test. It was found that with the throttle closed (closed to idle position), all of the fuel going into the engine passed through the idle circuit of the carburetor. Therefore to shut off the fuel, it was only necessary to close the idle circuit. It was realized that at higher speeds, deceleration with the throttle held partly open might result in fuel passage through the high-speed circuit, but in view of the facts that the high-speed circuit was more inaccessible and that the contribution to fuel wasted from this source was probably small, it was decided to neglect it.

The second device limited the vacuum attained during deceleration by admitting additional air-fuel mixture to the manifold when the vacuum tended to rise above 21 in. of Hg vacuum. This device was installed on a 1954 model car equipped with a torque-converter type of transmission.

The effectiveness of the two devices was checked by taking exhaust-gas samples in evacuated bottles. A steel line, 3 ft in length, was connected to the exhaust manifold near the exhaust-pipe flange and extended through the fire wall to the sample bottles. For the tests each car was decelerated, with the throttle closed to idle position, from 50 mph, and samples were obtained at 5-sec intervals after the start of the deceleration. Two such runs were made for each car, one with the particular device operative and one with the device inoperative. In every case the samples were analyzed (by the method outlined in Appendix I) on the same day that they were taken.

In Fig. 23 are shown plots of concentration of unburned hydrocarbons in the exhaust gas (lb per cu ft) as functions of elapsed time after the start of deceleration for the two cars with the devices operative and inoperative. Both devices reduced the concentration of hydrocarbons in the exhaust gas to a low value but did not eliminate it. With the devices inoperative the car which was equipped with the synchromesh transmission had the largest concentration of hydrocarbons in the exhaust gas. This car also had a higher intake vacuum at a given car speed than the car with the torque-converter transmission. The difference in the concentration of unburned hydrocarbons in the exhaust of the two cars with the devices inoperative is probably largely due to the difference in intake vacuum. Thus Fig. 23

shows a marked reduction in the concentration of unburned hydrocarbons when either type of device is used and in addition shows an effect of transmission type on the concentration of hydrocarbons in the exhaust of standard cars.

Another consideration that has no bearing on the air pollution problem but would be important to potential owners of automobiles equipped with these devices is the effect of the devices on fuel economy. The device which shuts off the idle circuit during deceleration has been found in preliminary tests to give 2.9% more fuel economy in all-around family driving. The vacuum-limiting device has not been checked for fuel economy, but it is probably lower with the device in operation because more fuel is used during deceleration with the device in use than without it.

The two devices just described were made for experimental purposes in the hope that they would point the way to a practical means of reducing hydrocarbon emission in the exhaust of a decelerating automobile. However, many problems remain to be solved before a device which is effective and economical can appear on automobiles.

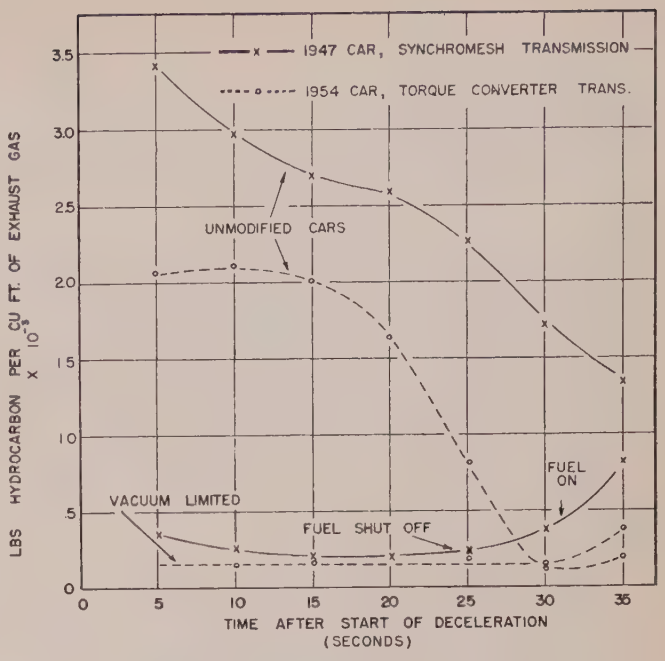

Fig. 23 – Effect of carburetor devices on concentration of hydrocarbon in exhaust during deceleration

Summary

1. It was found that the abrupt increase in the concentration of unburned hydrocarbons in the exhaust gas with an increase in intake manifold vacuum above about 21 in. of Hg corresponded to the initial failure of the flame to propagate throughout the mixture. As the proportion of the combustion space traversed by flame decreased, the per cent of hydrocarbons in the exhaust gas increased.

2. The value of residual-exhaust-gas dilution existing in the engine when the mixture was just failing to burn throughout the chamber was found to correlate well with limiting values of dilution obtained from the literature.

3. Changes in the "overall dilution" of the oxygen-fuel mixture affected the limit of complete inflammation in the same manner that would be predicted if dilution were a factor determining the limit.

4. It was found that the failure of the flame to burn throughout the combustion chamber at the boundary of the region within which the flame burned throughout was not due to too low a concentration of reactants.

5. Therefore, it was concluded that residual-gas dilution was a major factor limiting the complete inflammation of the mixture at engine conditions near the boundary of the region within which the flame burned throughout.

6. The concentration of unburned hydrocarbon emitted in the exhaust gas of automobiles during deceleration was substantially reduced by modifying the carburetor in either of two ways, (a) by admitting additional air and fuel to the intake manifold during deceleration, or (b) by shutting off the fuel during deceleration. The problem of eliminating all the unburned hydrocarbon emission during all driving conditions remains a challenge.

Acknowledgments

The authors wish to thank J. B. Bidwell of Research Laboratories Division, GMC, for making his vacuum-limiting device available for tests. Also, we are indebted to Dr. F. W. Bowditch for his aid in obtaining the flame photographs presented.

APPENDIX I

Method for Determining Per Cent Unburned Hydrocarbons in Exhaust Gas

Conventional Orsat equipment was used to determine the per cent unburned hydrocarbons (weight per cent of input fuel) in the exhaust gas. Exhaust samples were obtained simultaneously in the burettes of two Orsat apparatuses. Sample 1 was analyzed in the usual manner for CO_2, O_2, and CO. Sample 2 was also first analyzed for CO_2. Oxygen was then added to sample 2, and the sample was passed through a catalytic furnace to burn all the combustibles to CO_2 and water. The CO_2 and the remaining O_2 were then absorbed leaving nitrogen. The total amount of CO_2 formed when all of the fuel fed to the engine was completely burned, even though the fuel was burned partly in the engine and partly in the catalytic furnace, was thus determined from the analysis of sample 2. The portion of the fuel burned in the engine was determined from the volume per cent CO and CO_2 from the analysis of sample 1, and the per cent hydrocarbon was determined by means of the following equation:

$$\text{Weight \% unburned hydrocarbon} = \frac{CO_2'' - CO' - CO_2'}{CO_2''} \times 100$$

where:

CO_2'' = Total volume per cent CO_2 obtained from the analysis of sample 2

CO' = Volume per cent CO obtained from the analysis of sample 1

CO_2' = Volume per cent CO_2 obtained from the analysis of sample 1

This method of analysis of the exhaust gas does not differentiate between hydrocarbons and partially oxidized hydrocarbons. The weight per cent of unburned "hydrocarbon" thus obtained includes all carbon-containing compounds, except CO, which burn to form CO_2. The assumptions necessary for this type of analysis are:

1. All of the carbon in the fuel entering the engine leaves the engine in the exhaust gas as some gaseous product.
2. No oil is burned in the engine.
3. The average hydrogen/carbon ratio of the carbon-containing compounds which burned to form CO_2 in the catalytic furnace is equal to the average hydrogen/carbon ratio of the input fuel.

APPENDIX II

Method for Determining Residual-Gas Weight Fraction From Orsat Gas Analyses

The experimental data required to determine the residual-gas weight fraction were the Orsat analysis of the mixture which existed in the combustion chamber after the valves were closed and before ignition and the Orsat analysis of the exhaust gas. In addition air/fuel ratio charts similar to those of D'Alleva and Lovell[7] were used to determine the average molecular weight of the exhaust gas and to determine the volume per cent water in the exhaust gas. The air/fuel ratio of the input charge was determined by measuring the airflow and fuel flow. The sample of the mixture was obtained with a sampling valve on the compression-expansion strokes of a cycle in which the spark was not fired. The mixture sampling was repeated enough times to obtain 100 ml of unburned mixture in an Orsat burette. Next, a sample of exhaust gas was pulled into a second Orsat burette while the engine was firing steadily. Both samples were analyzed for CO_2, O_2, and CO.

The residual-gas fraction, f, is defined as the proportion of residual gas in the mixture of fuel, air and residual exhaust gas:

$$f = \frac{\text{Weight of residual}}{\text{Weight of mixture}} \tag{1}$$

Note that the weight of residual includes water formed due to combustion and will be referred to hereafter as "wet residual." The mixture may be divided into two parts, wet residual and charge, so equation (1) may also be written:

$$= \frac{\text{Weight wet residual}}{\text{Weight wet residual + weight charge}} \tag{2}$$

Air in the charge was assumed to be dry, and the CO_2 in air was considered negligible.

To express f as a function of the CO_2 in the exhaust and the CO_2 in the mixture, assume that the proportion of CO_2 in the residual is the same as the proportion of CO_2 in the exhaust. Thus:

$$\frac{\text{Weight } CO_2 \text{ in residual}}{\text{Weight wet residual}} = \frac{\text{Weight } CO_2 \text{ in exhaust}}{\text{Weight wet exhaust}} \tag{3}$$

or:

$$\frac{\text{Weight } CO_2 \text{ in residual}}{\text{Weight wet residual}} = \text{Weight fraction of } CO_2 \text{ in wet exhaust}$$

Also,

$$\text{Weight fraction } CO_2 \text{ in wet mixture} = \frac{\text{Weight } CO_2 \text{ in wet residual}}{\text{Weight wet mixture}} \tag{4}$$

Divide (4) by (3):

$$\frac{\text{Weight fraction } CO_2 \text{ in wet mixture}}{\text{Weight fraction } CO_2 \text{ in wet exhaust}} = \frac{\dfrac{\text{Weight } CO_2 \text{ in wet residual}}{\text{Weight wet mixture}}}{\dfrac{\text{Weight } CO_2 \text{ in wet residual}}{\text{Weight wet residual}}}$$

or:

$$\frac{\text{Weight fraction } CO_2 \text{ in wet mixture}}{\text{Weight fraction } CO_2 \text{ in wet exhaust}} = \frac{\text{Weight wet residual}}{\text{Weight wet mixture}} \tag{5}$$

therefore, from (5) and (1):

$$f = \frac{\text{Weight fraction } CO_2 \text{ in wet mixture}}{\text{Weight fraction } CO_2 \text{ in wet exhaust}} \tag{6}$$

The numerator of equation (6) may be written:

$$\text{Weight fraction } CO_2 \text{ wet mixture} = \frac{\text{Volume } CO_2 \text{ in mixture} \times 44}{(\text{Volume wet residual})mw_e + (\text{volume charge})mw_c} \tag{7}$$

where

mw_e = Average molecular weight of exhaust

mw_c = Average molecular weight of charge

Similarly the denominator of equation (6) may be written:

$$\text{Weight fraction } CO_2 \text{ wet exhaust} = \frac{\text{Volume } CO_2 \text{ in exhaust} \times 44}{(\text{Volume wet exhaust})mw_e} \tag{8}$$

Substituting (7) and (8) into (6):

$$f = \frac{\dfrac{(\text{Volume } CO_2 \text{ mixture}) \times 44}{(\text{Volume wet residual})mw_e + (\text{volume charge})mw_c}}{\dfrac{(\text{Volume } CO_2 \text{ in exhaust}) \times 44}{(\text{Volume wet exhaust})mw_e}} \tag{9}$$

To express the volume of wet residual and the volume of charge in terms of the volume of wet mixture and to simplify further equation (9), assume that the volume percentage of CO_2 in the residual

[7] See SAE Transactions, Vol. 38 (March), 1936, pp. 90-96: "Relation of Exhaust-Gas Composition to Air/Fuel Ratio," by B. A. D'Alleva and W. G. Lovell.

equals the volume percentage of CO_2 in the exhaust:

$$\frac{\text{Volume } CO_2 \text{ residual}}{\text{Volume wet residual}} = \frac{\text{Volume } CO_2 \text{ exhaust}}{\text{Volume wet exhaust}}$$

or:

$$\frac{\text{Volume } CO_2 \text{ residual}}{\text{Volume wet residual}} = \text{Volume fraction of } CO_2 \text{ in wet exhaust} \quad (10)$$

Also:

$$\text{Volume fraction } CO_2 \text{ in wet mixture} = \frac{\text{Volume } CO_2 \text{ in mixture}}{\text{Volume wet mixture}} \quad (11)$$

Define M as:

$$M = \frac{\text{Volume fraction } CO_2 \text{ in wet mixture}}{\text{Volume fraction } CO_2 \text{ in wet exhaust}} \quad (12)$$

Substituting (10) and (11) into (12),

$$M = \frac{\dfrac{\text{Volume } CO_2 \text{ in mixture}}{\text{Volume wet mixture}}}{\dfrac{\text{Volume } CO_2 \text{ in residual}}{\text{Volume wet residual}}} \quad (13)$$

Since volume CO_2 in mixture equals volume CO_2 in residual, equation (13) may be simplified:

$$M = \frac{\text{Volume wet residual}}{\text{Volume wet mixture}} = \frac{\text{Volume wet residual}}{\text{Volume wet residual} + \text{volume charge}} \quad (14)$$

Therefore,

$$\text{Volume wet residual} = M(\text{volume wet mixture}) \quad (15)$$

and,

$$\text{Volume of charge} = (1 - M)(\text{volume wet mixture}) \quad (16)$$

Substituting (15) and (16) into (9),

$$f = \frac{\dfrac{(\text{Volume } CO_2 \text{ in mixture})44}{M(\text{Volume wet mixture})\text{mw}_e +}}{\dfrac{(1 - M)(\text{volume wet mixture})\text{mw}_c}{\dfrac{(\text{Volume } CO_2 \text{ in exhaust})44}{(\text{Volume wet exhaust})\text{mw}_e}}} \quad (17)$$

or

$$f = \left[\frac{\dfrac{\text{Volume } CO_2 \text{ in mixture}}{\text{Volume wet mixture}}}{\dfrac{\text{Volume } CO_2 \text{ in exhaust}}{\text{Volume wet exhaust}}}\right]\left[\frac{44}{M(\text{mw}_e) + (1 - M)\text{mw}_c}\right] \quad (18)$$

The first term in equation (18) is M, therefore:

$$f = \frac{M(\text{mw}_e)}{M(\text{mw}_e) + (1 - M)\text{mw}_c} \quad (19)$$

M may be expressed in terms of dry volume percentages obtained with the Orsat as follows:

By definition:

$$M = \frac{\dfrac{\text{Volume } CO_2 \text{ in dry mixture sample}}{\text{Volume wet mixture sample}}}{\dfrac{\text{Volume } CO_2 \text{ in dry exhaust sample}}{\text{Volume wet exhaust sample}}} \quad (20)$$

Consider first the denominator of equation (20):

Volume wet exhaust sample = Volume dry exhaust sample + volume of water vapor

Consider first the denominator of equation (20): Volume wet exhaust sample = Volume dry exhaust sample + volume of water vapor

The volume of water may be determined from the volume % of water in burned products, Z:

$$\text{Volume of water} = \frac{100Z}{100 - Z} \quad (21)$$

if a 100-ml dry exhaust sample is assumed. Then the denominator of equation (20) may be written as:

$$\frac{\text{Volume } CO_2 \text{ in dry exhaust sample}}{100 + \dfrac{100Z}{100 - Z}}$$

or:

$$\frac{(100 - Z)(\text{Volume } CO_2 \text{ in dry exhaust sample})}{(100)^2} \quad (22)$$

To simplify the numerator of equation (20) the volume of the wet mixture sample may be expressed in terms of the volume of the dry mixture sample, M and Z.

Volume wet mixture sample = Volume dry charge + volume dry residual + volume water

Assume:

Volume dry charge + volume dry residual = 100

Equation (14) may be written:

$$M = \frac{\text{Volume dry residual} + \text{volume water}}{100 + \text{volume water}} \quad (23)$$

By definition:

$$Z = \frac{\text{Volume water}}{\text{Volume dry residual} + \text{volume water}}(100) \quad (24)$$

Combine equations (23) and (24) to obtain:

$$\text{Volume water} = \frac{100\,MZ}{100 - MZ} \quad (25)$$

and the numerator of equation (20) becomes:

$$\frac{\text{Volume } CO_2 \text{ in dry mixture sample}}{100 + \dfrac{100\,MZ}{100 - MZ}}$$

or:

$$\frac{(100 - MZ)(\text{volume } CO_2 \text{ in dry mixture sample})}{(100)^2} \quad (26)$$

Thus, putting equations (26) and (22) into equation (20):

$$M = \frac{(100 - MZ)(\text{volume } CO_2 \text{ in dry mixture sample})}{(100 - Z)(\text{volume } CO_2 \text{ in dry exhaust sample})} \quad (27)$$

Solving (27) for M:

$$M = \frac{100(\text{volume } CO_2 \text{ in dry mixture sample})}{100(\text{volume } CO_2 \text{ in dry exhaust}) + Z(\text{volume } CO_2 \text{ dry mixture} - \text{volume } CO_2 \text{ dry exhaust})} \quad (28)$$

Substituting equation (28) into (19) and simplifying:

$$f = \frac{[CO_2]_m(\text{mw}_e)}{[CO_2]_m(\text{mw}_e) + ([CO_2]_e - [CO_2]_m)\left(1 - \dfrac{Z}{100}\right)(\text{mw}_c)}$$

where:

$[CO_2]_m$ = Volume CO_2 in mixture sample
$[CO_2]_e$ = Volume CO_2 in exhaust sample
mw_e = Average molecular weight of exhaust
mw_c = Average molecular weight of charge
Z = Volume per cent water vapor in burned products

DISCUSSION STARTS ON NEXT PAGE ⟶

Better Instrumentation Needed to Determine Exhaust Gas Composition

– J. M. Chandler
Ford Motor Co.

IT might be of interest if I were to discuss very briefly some of the activity at Ford Engineering in the field of exhaust gas and air pollution.

Our activities have been centered in two areas: (1) the need for instrumentation for determining the composition of automobile exhaust gas; (2) the effect of engine, fuel, and lubricant variables on exhaust gas composition.

We have long recognized that there are two important objectives in the instrumentation phase of this investigation: one is the need for highly accurate exhaust gas analysis which will identify all of the exhaust gas components; the other is the need for a rugged, easily operated, quick responding instrument which will enable the carburetor or engine engineer to check out changes in engine operation for their effects on exhaust gas composition. To date we don't think either of these needs have been fully met, although instruments like the mass spectrometer are more available for detailed analysis than apparently are the rugged and simpler instruments for more everyday use. We are using both the mass spectrometer and chemical combustion methods for determining exhaust gas composition. Results of this comparative testing program will shortly be presented to a CRC meeting on exhaust gas composition. Those working on altering exhaust gas composition will welcome, however, the early development of a simple, rugged, and preferably continuous analyzer for routine and frequent test work.

The second phase of our overall program, the effect of engine, fuel, and lubricant variables on exhaust gas composition, has also been under careful study. Our work in this area has assumed, for the sake of expediency, that unburned fuel in automobile exhaust may be a contributor to smog formation. We have noted that, according to the published data of the Los Angeles Air Pollution Control District, approximately 60% of the automobiles' contribution of unburned fuel to the atmosphere occurs during the deceleration cycle. There are probably as many methods for reducing unburned fuel during deceleration as there are people working on the problem. We have experimented with several, and have achieved a marked reduction in emission of unburned fuel during deceleration by eliminating fuel flow during most of the deceleration cycle. Unfortunately, however, the engine doesn't always appreciate someone's tinkering with its diet, and as a result several small complications arise when the normal carburetion is disturbed. We feel, however, that as further engineering effort is put into this problem, the emission of unburned fuel during deceleration can be substantially reduced.

Improving combustion efficiency during the other cycles of engine operation is going to be a little more difficult. As has already been pointed out, hydrocarbon emission during idle can easily be improved by tuning the carburetor of every car on the road to the manufacturers' specifications. Acceleration and cruising are already operating near peak combustion efficiency and offer little room for improvement.

We have also experimented with a more volatile commercial fuel blend. An increase in fuel volatility offered no detectable improvement in combustion efficiency as measured by the mass spectrometer.

In conclusion, I would like to emphasize that we, with the rest of the automotive industry, are continually working to improve engine combustion efficiency. With the special effort that the air pollution problem seems to demand, we are confident that required improvements will be engineered into our products as soon as practical.

Reduced Overrichness Claimed with New Gasoline Injection System

– Sidney E. Miller
American Bosch

THE conclusions reached by these authors indicate that the automotive gasoline engine, while idling or decelerating, is the chief offender as a producer of hydrocarbon pollution of the air. Various means of either cutting off fuel flow or limiting manifold vacuum during deceleration are indicated. These are, as mentioned, only laboratory solutions and better and more effective means must be found.

Fortunately, in the last year we have developed a gasoline injection system which has demonstrated on road tests its ability to reduce the idle fuel flow by at least 15%, and the deceleration fuel flow to a value 30% below the idle fuel rate. This system is now being field tested by a leading automobile manufacturer with the plan to offer it in 1956 production. In addition to the obvious performance advantages of gasoline injection engines, this ability to reduce drastically the overrichness of carbureted engines under all conditions of operation can well represent a significant contribution of this new system to the pollution problem.

Often Overlooked Factors Of Idling Cycle Discussed

– F. C. Mock
Bendix Aviation Corp.

IN connection with these very valuable investigations of the incomplete combustion problem, it seems useful to add an explanation of certain often overlooked factors of the idling cycle which cause this to occur.

With our present idle control by having the throttle closed against a fixed stop, the idling airflow through the throttle orifice is usually at a fixed maximum or sonic velocity, and therefore constant per unit of time, at all intake vacuums greater than 15.6 in. of Hg. On present-day carburetors the idling fuel flow follows the airflow and is also constant under these conditions. Therefore, at closed throttle, the intake air and fuel per cylinder charge vary inversely with engine speed.

In contrast, the weight of exhaust residue in the clearance space above the piston (provided there has been previous combustion) tends to be approximately constant. So, during coasting and deceleration, with the throttle closed, the individual air and fuel charges are thinner as the speed is increased, and the per cent of exhaust dilution is greater (see Figs. A, B, and C – from a Stromberg Carburetor booklet of 1916). This is why we have slow and incomplete burning on deceleration with closed throttle.

Note that if combustion in a cylinder does not occur or is incomplete; on the next cycle, the clearance space, instead of having only exhaust gas in it, will contain some air and fuel; as will also the exhaust-valve ports and exhaust manifold. On the next following misfire, this air and fuel content will increase, and again the next time, until finally an ignition can take place in the cylinder (which may be followed by a bang in the exhaust pipe and muffler); after which another miss will result, and the misfiring cycle starts all over again.

As would be expected, this condition is aggravated when exhaust-valve leaks increase the exhaust dilution in certain cylinders; for the additional reason that a rich idling ad-

justment will usually idle such an engine slightly more smoothly than a lean one; which rich setting, of course, increases the hydrocarbon exhaust content on deceleration. Too narrow a gap at the spark-plug terminals also seems to call for a richer idling fuel adjustment, with a similar detrimental result.

A large valve overlap of intake opening before exhaust valve closing, as is common with aircooled aircraft engines, also tends to aggravate this missing, and increase exhaust "torching" on deceleration. In fact, with cylinders cold, this valve overlap is frequently so great that the idling intake vacuum is below sonic flow values, and the idling air intake may increase with engine speed.

Another, and perhaps the major actual, cause of hydrocarbon release in traffic comes from having fuel in the liquid state in the intake manifold at full open throttle. It is fairly well known that below air velocities of about 30 fps, unvaporized fuel is present in considerable quantity on inadequately heated walls of the intake pipe; and that this liquid fuel flashes into fog or vapor when the throttle is closed, giving temporarily a very rich mixture to the cylinders. This difficulty is further augmented with engines having large intake manifolds of low heat supply, whose carburetors require large acceleration pump charges for satisfactory throttle response; so that in the stop-and-go of traffic jams, their hydrocarbon release is high, as we know when we follow heavy vehicles having these characteristics.

The U. S. and foreign patent art on degassers, and the like, is old and extensive, but apparently the public demand, up to now, would not justify their added cost. Perhaps this will soon change in the Southwest, and later in other parts of the country.

For passenger cars, some immediate mitigation would result from educating (and possibly forcibly persuading) the motorist to keep his engine, valves, and ignition in shape to fire steadily without missing, on a carburetor idle adjustment that will give a lean smelling exhaust. Further improvement would result from the application of degassers (which has not been easy or inexpensive with multiple-barrel carburetors). Actually, the degasser feature should not add much to the price of a car, if incorporated in the initial design of the carburetor.

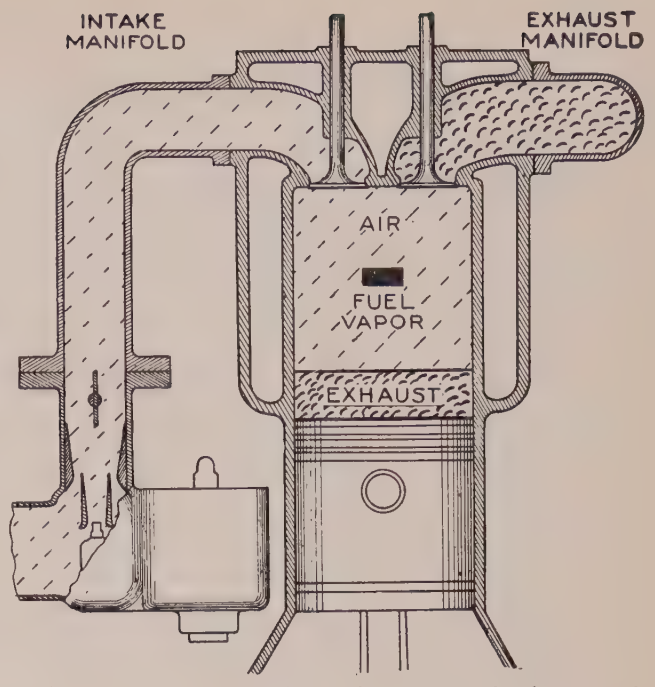

Fig. A – Relative amounts of air, gasoline vapor, and exhaust gas in cylinder at beginning of compression. Full power, full open throttle

For large gasoline truck and bus engines, with cool, low-velocity intake manifolds and big accelerating charges, the alternatives apparently are:

a. Smaller manifolds, more manifold heat, and less acceleration charge, with some resultant loss in maximum power and greater need of high-octane fuel; a degasser, or fuel cut-off on deceleration, would also be necessary.

b. A vacuum-operated auxiliary air port into the intake manifold, which might be difficult to work out satisfactorily.

c. Some form of fuel injection, also with a deceleration fuel cutoff, all of which would probably be quite expensive.

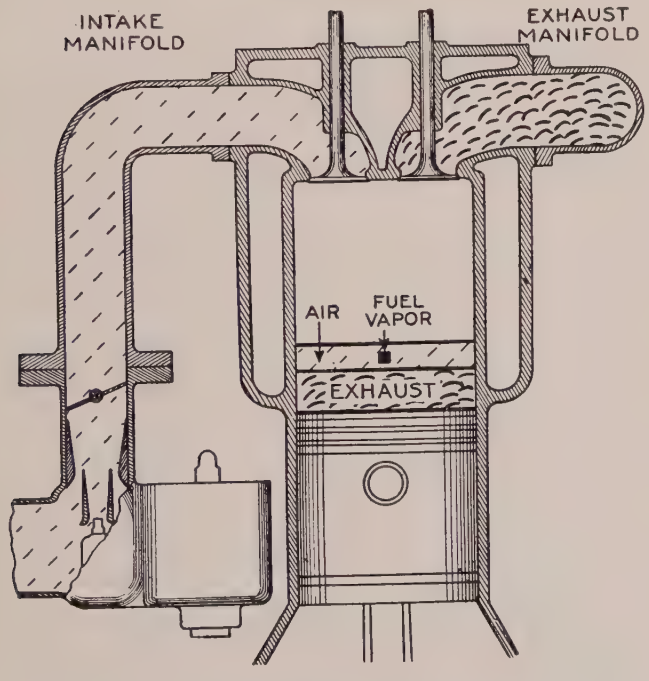

Fig. B – Relative amounts (shown in volumes at atmospheric pressure) of air, gasoline vapor, and exhaust gas in cylinder at beginning of compression. Engine idling, throttle closed (actually, cylinder contents expand to fill whole space at less than half atmospheric pressure)

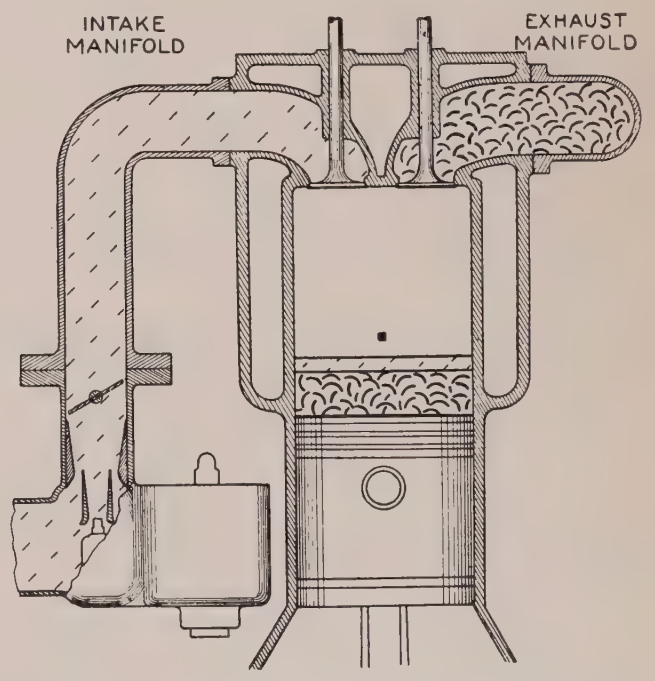

Fig. C – Engine turning over at high speed with throttle closed to low idling position. Note that air and fuel vapor charges are much smaller than with normal idling, as in Fig. B

Some

IN this lecture, which Sir Harry Ricardo gave after receiving the Horning Memorial Award for 1953, he relates some of his early experiences with the internal-combustion engine.

He goes back to the days when, as an undergraduate at Cambridge, he assisted Prof. Bertram Hopkinson in research on rate of flame propagation, preignition, and knock.

He describes his early work with a 2-stroke engine of his own design, which he finally, reluctantly abandoned in favor of the 4-stroke engine. He tells of his investigations of fuels and engines for the British Air Ministry and the Ministry of Munitions during World War I, and how, in 1917, he organized a small private company to carry on his research and development work. The Ricardo variable-compression engine E35, a special fuel for racing cars, and various designs of combustion chamber are only a few of the many accomplishments of this company.

I FIRST met Harry Horning on his visit to England shortly after the end of the First World War, and thereafter we became close friends with identical interests and ambitions. I imagine that it was largely at Horning's instigation that your Society did me the honor of inviting me to New York in January, 1922, to read a paper on the work he had seen being carried out at our then new laboratory at Shoreham. From that date until his sad death in the 1930's we kept in close touch both by correspondence and by the exchange of visits to Waukesha and Shoreham.

Harry Horning was a great enthusiast and a most inspiring man. I always enjoyed greatly and profited by the many long talks we had together on the question of fuels and combustion and their relation to engine design – a subject dear to both our hearts.

Now I am going to claim the privilege of an old man to be reminiscent and to go back to very early days. I am doing this for two reasons. Firstly because I am an old man, and secondly because I am rather out of touch with the latest developments, but old memories can be treacherous guides, for one is apt to recall only the high spots and successes, while a kindly veil of forgetfulness enshrouds the many false trails and failures.

If, in what I am going to say, I give the impression of having leapt from one triumph to another, that would be most misleading, for I missed my foothold and floundered quite as often as anybody else, but all my life I have had rather more than the usual share of good luck and of the generous help of many good friends.

I would like to go right back to the date when your Society was first founded in 1905, for it was my starting point also. At that time I was an undergraduate in my second year at Cambridge, and had just been invited by Prof. Bertram Hopkinson to assist him with research he was then starting on the internal-combustion engine.

Perhaps I might outline briefly the state of the art as I remember it in England in 1905. At that time the gas engine was in the heyday of its triumph; it had ousted the steam engine from all small- and medium-power industrial use and had not yet been ousted in turn by the electric motor. The large and stately diesel engine was also moving from strength to strength, but it was still regarded as rather highbrow.

The automobile had just emerged from a fascinating but wayward mechanical toy to a reliable utility vehicle, and following the lead set by Ford, was being turned out in relatively large-scale production. After 10 years of experimental adventure during which almost every shape and kind of prime-mover had been tried out, its engine was gradually crystallizing into a more or less conventional 4-cyl in-line unit. The surface or wick carburetor had disappeared in favor of the liquid-spray type, but not so its demand upon the fuel, for volatility remained the one and only criterion. The discriminating motorist never bought a drop of gasoline without first dipping his finger in the can and blowing on it to test its volatility.

Two years had passed since the Wright Brothers' first conquest of the air and the development of the aero-engine was perhaps the most fascinating of all for the young engineer of that date.

Hopkinson was, I think, quite the most stimulating research leader I have ever met, with an almost uncanny perception, combined with sound judgment and a thoroughly practical outlook. The pity is that he published so little of his work.

Early Reminiscences

Sir Harry Ricardo, Ricardo & Co., Engineers (1927), Ltd.

This paper was presented at the SAE Golden Anniversary Summer Meeting, Atlantic City, June 13, 1955.

At that time it was the popular belief that the performance of spark-ignition engines was limited as to speed by the slow rate of flame propagation and as to mean pressure by the onset of preignition. Hopkinson was determined first to explore these two factors. As a first step he designed and, in the workshops, we made a most ingenious optical indicator. Within its limitations it proved to be the most accurate and efficient indicator for recording pressure changes, large or small, that I have ever used, once one was practiced in the handling of it, and having made and developed it ourselves we knew its tricks and just how far to trust it.

Our equipment at that time consisted of a large, modern single-cylinder horizontal gas engine with electric ignition and several explosion vessels of various shapes and sizes. For instrumentation, apart from Hopkinson's optical indicator and several pencil indicators, we had only the usual assortment of pressure gages, thermometers, weights, and spring-balances.

As soon as we were satisfied with the behavior of the indicator we started taking diagrams both from the engine and from an explosion vessel, using town gas as fuel for, owing to insurance regulations, gasoline was banned. At the outset Hopkinson pointed out that the rate of pressure rise in the engine cylinder was many times as rapid as in an explosion vessel of about the same capacity. With his usual insight he attributed this to turbulence in the engine cylinder. We therefore fitted up a small electric fan inside the largest of the explosion vessels and found that, with this in operation, we could speed up the combustion to almost any extent; from these simple experiments Hopkinson concluded that, given adequate turbulence, there need be no practical limit, on the score of combustion, to the speed at which an engine could be operated. It so happened that, at about the same time, Sir Dugald Clerk, working quite independently, came to the same conclusions. From these observations, and many others of a similar nature, I became deeply impressed with the importance of turbulence.

Hopkinson always tried to form a mental picture of just what was happening inside the cylinder. To this end we made up an explosion vessel consisting of a strong glass tube about two inches in diameter by about four feet long, with a spark plug at one end. With a strong mixture at atmospheric pressure, the passage of the flame down the tube was too rapid for the eye to follow, but with weak mixtures at reduced pressures it was sometimes possible to slow down the process so as to be able to watch the buildup of a small bubble of flame at the spark-plug points, followed by the passage of a thin filament of flame at a steadily increasing velocity down the length of the tube. This picture has always remained vivid in my memory throughout the last 50 years.

Next, Hopkinson set out to find what really happened when preignition occurred; to this end we projected into the combustion chamber a long steel bolt with a thermocouple buried in its inner end. When the end of the bolt reached a certain temperature autoignition took place. At first there was no perceptible change in the indicator diagram,

but as the temperature rose, ignition crept earlier and earlier till finally the engine came quietly to rest; at no time was there any trace of the high-pitched knock so familiar in the gasoline or kerosene engine and which was popularly attributed to preignition from some hot spot, nor was the rate of pressure rise any different from that when ignition was by timed spark.

In my last term at Cambridge, Hopkinson had borrowed a 4-cyl Daimler car engine of the latest type, and on this we carried out a very complete set of calibration tests on town gas, using the optical indicator with which we were able to get excellent diagrams at speeds up to 1200 rpm – a fairly high speed in those days. Finally, we rigged up a test-bed in a yard outside the laboratory and tested it on gasoline.

With full-power mixture strength and optimum ignition timing it knocked heartily with the familiar high-pitched ringing knock, but ran quite smoothly with a richer mixture or slightly retarded ignition. On attempting to indicate it under knocking conditions, the mirror of the indicator was shattered, a thing that had never occurred before. We made several more attempts but every time, as soon as a knocking condition was reached, the fragile mirror was either shattered or thrown out of its frame. From all these observations Hopkinson concluded that the knocking condition was something quite distinct from preignition and suggested that it might be caused by the setting up of an explosion wave within the combustion chamber; that the tendency to do so was evidently a characteristic of the fuel, and there the matter ended, for the engine had to be returned to its owner, my time at Cambridge was up, and Hopkinson, with a fresh disciple, and at the urgent request of the Admiralty, was turning over to an entirely different line of research, namely, the development of a torsion dynamometer for recording the power of marine steam turbines.

In retrospect, I am amazed at the amount of ground Hopkinson covered in so short a time and at his ingenuity in devising very simple but convincing experiments, involving the absolute minimum of equipment. His lectures and administrative duties left him very little time and there was no grant of money for research. I, too, had to attend lectures and work for my degree, yet we were never in a hurry; we certainly never burned the midnight oil or missed a single meal or entertainment.

The secret, I think, was to be found in two important factors. Firstly, there was no telephone in the laboratory, and secondly, our instrumentation was of the simplest possible kind, which could be checked and calibrated in a few minutes and relied upon with confidence. Today I am appalled by the amount of time spent in setting up, calibrating, and correcting the very elaborate instrumentation upon which we are daily becoming more dependent.

While working with Hopkinson at Cambridge I had designed and built in the workshops a 2-stroke engine in which I had sought to combine a high degree of turbulence with a certain measure of stratification. This engine, upon which I pinned great hopes, was not finished in time to be tested in the laboratory.

On leaving Cambridge I told Hopkinson that I had every intention some day of carrying on with the work he had started and, as a parting present, he gave me his optical indicator, which later proved invaluable.

From Cambridge I joined my grandfather's firm of consulting civil engineers, concerned mostly with the design of bridges, docks, and railways, my job being the mechanical engineering end, the design and development of such specialized equipment as we needed for bridge building, mostly steam, hydraulic, and pneumatic. This I found intensely interesting and instructive, but it was far removed from internal-combustion engines. The production of my cherished 2-stroke engine was taken up by several very small firms and I spent much of my spare time making fresh designs and, where possible, testing such few engines as were produced. But until about 1912, I had nowhere of my own to run an engine, though I had a very small workshop in the basement of our London house where I could make such simple experimental equipment as I needed. During these years I followed closely the progress of the gasoline engine but I had little or no contact with any of the leading designers of such engines, and was much too shy and diffident to approach them or to take part in discussions at meetings.

In particular I was fascinated by the problem of why some engines gave a much better performance than others of generally similar design, and I spent much time searching all the published designs and performance figures I could find in attempts to arrive at the controlling factors. To this end, and greatly helped by H. A. Hetherington, one of my Cambridge friends who had a genius for digging up information, I sought to analyze the performance of contemporary engines under various headings, such as breathing capacity, turbulence, as indicated by spark advance, and mechanical features generally. My main object was to make a commercial success of my 2-stroke engine, which was giving quite a good performance. I had managed to make it very quiet, very flexible, and reasonably economical, but I was dogged all the time by detonation, which I had come to regard as Public Enemy No. 1, for it limited my compression ratio on the gasoline then available to only about 3.5/1.

In 1912 my wife and I moved into a small house in the country about 20 miles from London where, in the garden, I had space to put up a larger workshop and install one of my 2-stroke engines. I had the luck to pick up a second-hand 10-kw dynamo, which I mounted on trunnions to serve as a

swinging-field dynamometer.

From much pondering on the problem of detonation and from my vivid recollections of Hopkinson's teaching and of his experiments in glass tubes, I had come, albeit rather vaguely, to picture the mechanism of detonation as the setting up of an explosion wave by the sudden autoignition or detonation of the last part of the working fluid, due to compression by, and radiation from, the rapidly advancing flame front, but in what manner or to what extent this could be influenced by turbulence seemed to be anybody's guess. On the one hand one could argue that turbulence, by dispersing the end gas, would reduce the tendency to detonate; on the other that by speeding up the advance of the flame front, it would increase the tendency.

Now with an engine of my own on the test-bed and Hopkinson's indicator, I could really get down to studying the problem which had vexed me for so long. Following Hopkinson's technique I first ran the engine on gas and induced preignition by means of a hot wire and found, as in the case of the gas engine at Cambridge, that the engine gradually faded out without any trace of high-pitched knock and that the indicator diagram showed a perfectly normal rate of pressure rise. I had managed in the meantime to strengthen the mirror of the indicator and its attachment so that it could survive at least reasonably severe knocking. I then found that under such conditions the diagram showed a perfectly normal rate of pressure rise until the very last moment, when it shot up abruptly and set the whole thing in vibration as though it had been struck by a light hammer, an observation which seemed to confirm Hopkinson's suggestion of the setting up of a high-velocity explosion wave; also it seemed to fit my picture of the sudden autoignition of the last part and only a very small part of the working fluid near the extreme end of the flame travel.

In my 2-stroke engine I had fitted the indicator on the side of the combustion-chamber opposite to the spark plug. I had noticed that the tendency to knock was much greater when the indicator was in place than when the boss was plugged. The passageway leading to the indicator piston was about 5/16 in. in diameter and about 1½ in. long, and I suspected that the end gas trapped in this passage was the source of trouble.

On the argument that the end gas was unable to get rid of the heat thrust upon it by the advancing flame front, I tried the experiment, first, of water cooling the passage, which gave some improvement; next, I fitted tightly into the passage a twisted copper strip to give additional cooling surface; this proved completely effective, the knocking was now no worse than without the indicator.

This simple experiment brought home to me the importance of giving the end gas every opportunity to get rid of its heat.

By this time I was coming reluctantly to the conclusion that in championing the 2-stroke engine I was fighting a losing battle, so I started out to design and build an experimental 4-stroke engine with a topping-up supercharge through ports in the cylinder wall uncovered by the piston, the air being supplied by using the underside of a crosshead piston to furnish alternately scavenge and supercharge air.

Up to now I had run my engine only on gasoline, which detonated heavily, or on town gas which did not, but I had never tried any other fuels, nor did it occur to me that there was any practical alternative to the gasolines then available which had an octane number ranging from 45 to 50. About this time, however, benzol appeared on the market. On my first run with this fuel I noticed that all trace of detonation disappeared. I could make it preignite readily enough, but I could not make it detonate. I made new pistons for my 2-stroke engine with a compression ratio of over 5/1 and got a greatly improved performance, still without any trace of detonation, but benzol was

The Author

SIR HARRY RICARDO (M '22) is chairman and technical director of Ricardo & Co., Engineers (1927), Ltd., London, England. He is also a consulting engineer to Britain's Air Ministry. His distinguished career as an engineer began at Rugby, where he built a coal-fired steam-powered motorcycle. A few years later at Cambridge, under the inspiration of Prof. Bertram Hopkinson, he built a 4-stroke engine for racing motorcycles, a 2-stroke engine, and began the research in internal-combustion engine development which has lasted for more than a half-century.

In 1907, Sir Harry joined Rendel & Robertson, his grandfather's firm of consulting engineers. As a sideline to designing bridge-building mechanisms, he continued his development of 2-stroke engines, and his studies of detonation. In 1911, he became interested in aviation and built a 4-stroke engine with variable supercharge.

Sir Harry assisted in the secret development of military tanks in 1915. Several of these tank engines incorporated a new form of combustion chamber.

During World War I, Sir Harry continued his studies of the mechanism of combustion. This work eventually led to the development of the famous "Ricardo head."

Sir Harry's improvements on sleeve-valve engines for use as aircraft powerplants resulted in the development of the 9-cyl radial Bristol Perseus and the 14-cyl Hercules. Then, he turned his attention to developing high-speed, high-output diesels both sleeve-valve and poppet-valve types.

In recognition of his many important contributions to engineering, Sir Harry was elected a Fellow of the Royal Society in 1929; in 1944, he received the Rumford Medal; in 1948, he received a Knighthood; in 1953, the Institution of Mechanical Engineers presented him with the James Watt International Medal, and in June, 1955, the Society of Automotive Engineers presented Sir Harry with the Horning Memorial Award.

not everywhere available and my engines in service must run on whatever they could get. From then on I became deeply interested in the behavior of fuels as such.

Early in 1914 I met Hesselmann in Stockholm. Hesselmann at that time was building large diesel engines and was one of the first, if not the first, to make a successful diesel using solid as opposed to air blast injection. In order to bring the air into contact with the fuel sprays he employed an organized air swirl produced by partially masking the inlet valve. We discussed the possibility of small high-speed diesels. He was afraid on mechanical grounds of the very high pressure involved. He favored a relatively low-pressure spark-ignited version, but was deterred by the very low compression ratio to which he was limited with kerosene or gas-oil. I told him of my belief that in such engines detonation was initiated only in the end gas. At once he said, "If that is really the case, then why not use my air swirl to ensure that there is no fuel in the end gas, in other words, inject the fuel a little up-stream of the spark plug." This he did, and that with considerable success, first as a kerosene engine and later using a light diesel fuel. I mention my talks with Hesselmann because I found him so inspiring and learnt so much from him, more especially about the use of an organized air swirl, as distinct from general turbulence in diesel engines, and because, in later years, Horning took up the manufacture of Hesselmann's low-pressure engine, which served as an intermediate stage on the way to the light, high-speed diesel.

War Starts

Within a few days after my return from Sweden, war broke out and I was kept very busy with a lot of fresh mechanical problems. Early in 1915 I received a letter from Hopkinson, with whom I had rather lost touch for some years, saying that he had been appointed a technical director of the newly formed Air Ministry, that since our work together at Cambridge he had grown rather rusty on the subject of internal-combustion engines and asking me to prepare for him a note setting forth my own views on the principal factors governing the design and performance of light, high-speed engines. This was a job after my own heart. Hopkinson was pleased with my effort, but to my horror had it copied and sent not only to some of the Technical Staff of the Ministry but also to the manufacturers of aero-engines, such as Rolls-Royce, Napier, Bristol, and others. On hearing this I shook in my shoes, expecting at any moment to be torn to pieces by outraged designers, but on the contrary I received the most cordial invitations from Royce, from Rowledge of Napier, from Fedden of Bristol, and from the Royal Aircraft Establishment at Farnborough to visit them and discuss their designs. This was almost my first contact with any of the famous designers and was a turning-point in my life. Almost overnight my status had changed from that of an unknown amateur pursuing an innocent hobby, to that of a serious person whose opinion carried weight. One outcome of all this was that for the first time I had some money to spend and could afford the whole-time assistance of a first-rate mechanic, so that I was soon able to complete my new engine as well as various other pieces of simple test equipment. Up to this point I had worked single-handed and had had to make all my own equipment – this was a slow process but a very valuable experience. My new 4-stroke engine turned out to be a very useful instrument for research generally, and particularly so for fuel testing, for by varying the supercharge, I could induce or eliminate knocking over a wide range. Through the help of a friend, an organic chemist, I was now able to procure some reasonably pure samples of benzene, toluene, and xylene, and of some of the paraffin and naphthene series. I soon found that from the point of view of detonation the aromatics were by far the best, with the naphthenes a poor second, and the paraffins in general by far the worst, but my equipment was not precise enough to reveal the more subtle differences.

Early in 1916 I was invited to design, and with the help of my grandfather's firm to organize, the production of engines for tanks, which were then being developed in great secrecy, and for which no suitable engine was available. Except for my single-cylinder experimental engine and my own motorcycle, I had never designed a 4-stroke engine and I felt very diffident, all the more so because the engine was to be built by a group of old established, and very experienced builders of large gas and diesel engines such as Crossley, Gardner, Mirrlees Bickerton & Day, Ruston & Hornsby, and others who might well resent being asked to build to the designs of an inexperienced and virtually unknown young man. They were, however, quite complimentary about my design and contributed from their abundance the experience that I lacked; they did all in their power to bolster up my confidence in what was in many respects a rather unorthodox design. In these engines I employed the same form of combustion chamber as in my experimental engine, for it was the only form with which I had had personal experience and, apart from its proneness to detonate, it gave otherwise a very good performance. Thanks to great goodwill on all sides and to really superb cooperation between the whole group of firms, everything went swimmingly, the engines went straight into large-scale production, and performed quite well.

As a next step I was asked to design a considerably larger engine of 6¾-in. bore for a range of heavier tanks. In this case there was less urgency, and my self-confidence had improved to the extent that I dared put my own pet theories to the test

and ventured on a different design of combustion chamber, which I hoped would be more efficient and less prone to detonate. In this I sought to increase the normal turbulence, to keep the flame travel as short as possible, and to try and ensure that the end gas was so chilled that it could not provoke detonation. To this end I used four horizontally opposed valves opening into a compact rectangular combustion chamber somewhat similar to that of conventional horizontal gas engines, with the spark plugs in the roof close to the exhaust valves. The top of the piston was flat and came into very close contact with the flat overhanging portion of the cylinder head, leaving only a very thin lamina of end gas entrapped between two relatively cold surfaces. I hoped, too, that squish at the end of the compression stroke would set up some additional turbulence.

This form of chamber proved a great success; with a compression ratio of 4.3/1 I got a bmep of 110 psi without the slightest trace of detonation, even when the ignition was advanced well beyond the optimum for maximum torque.

I Appear Before a Government Committee

Early in 1917 I was called upon at short notice to appear before a very high level Government committee dealing with the allocation of fuel to the various services, my function being to plead on behalf of the Tank Corps which had been allocated the lowest grade of gasoline, a ghastly fuel only one step removed from kerosene. In my innocence I asked to be allowed to use benzol of which I understood there were adequate supplies. I was shot down immediately and told that benzol was not a recognized fuel and that I certainly could not have it, that the fuel we were to get was quite good enough for a clumsy contraption that lumbered along at under 4 mph.

The chairman of this committee, a huge and very formidable-looking fellow, turned out to be Sir Robert Waley-Cohen, the head of the Shell organization. He took me aside after the meeting and invited me to dine with him that evening. I told him about my experiments and my beliefs; he was most sympathetic and charming and took me quite seriously. He then asked me to test samples of gasoline from their various oil fields. On testing these in my own engine, one sample stood out far better than all the others – it was a straight-run spirit from an oil field in Borneo. On my reporting this he told me that that particular gasoline was being burnt to waste in the Borneo jungle, because its specific gravity was too high to comply with the existing specification. Sir Robert took action at once and had this fuel shipped to England and used for blending with other light gasolines. Thus began my long and happy association with Shell.

I was still a member of my grandfather's firm but on loan to the Ministry of Munitions and the Air Ministry. My ambition was soaring and I dreamed of forming a small private company with the help of friends and of building up a laboratory and of making a living out of research, royalties, consulting work, designs, and the like. In this project I was much encouraged by the great goodwill of the many firms with whom I had become associated during the war. In 1917 my grandfather died and I was offered a partnership in the firm. At the same time, an old family friend, Campbell Swinton, who had always taken a kindly interest in my career, offered to find the capital necessary to form a small company and to build a small laboratory such as I had often dreamed of. It was a difficult choice to make for one with a wife and family and no private means. The one offered me an assured income but a divorce from the engines I had come to love; the other an occupation after my own heart, but highly speculative.

I consulted Waley-Cohen upon whose wisdom and kindliness I had soon come to rely. He then told me that if I chose the latter course the Shell company would finance a 2-year research program into the problem of matching the fuel to the engine, which would give us at least a good start. His offer clinched matters, but with great generosity, the other partners in my grandfather's firm offered to keep the partnership open for two years in case I should want to return.

A small private company, with Campbell Swinton as chairman, was registered in 1917. We purchased a plot of land at Shoreham and my father – an architect – designed the building of a small test shop, workshop, and drawing office. I had no difficulty, after the war, in collecting together a small staff from among my Cambridge friends and others and we started at Shoreham early in 1919.

Meanwhile, the small workshop in my garden was enlarged and my staff of mechanics increased from one to four, also we rented a small drawing office in London.

For the fuel research I had long wanted to build an engine in which the compression ratio could be varied while running and had schemed out many versions of such. I had discussed this with Waley-Cohen, who fully approved; he also authorized me to design and get built other test equipment including a single-stroke compression machine, which I had also hankered after and which proved very valuable in the earlier stages of our work. He agreed also to our retaining H. T. Tizard and D. R. Pye, two very able physicists who had been members of Hopkinson's staff during the war. Most of the equipment had been made for us by Messrs. Peter Brotherhood, one of the tank-engine group; it was completed early in 1919 and was the first to be installed in our new laboratory at Shoreham. The variable-compression engine type E35 proved to be quite a precision instrument. With it, and after a little practice, we were able with certainty to assess the limiting compression

ratio for any fuel to within 1/20 ratio.

The experiments carried out previously in my own small workshop during the First World War had borne fruit to the extent that Shell was now importing all their Borneo gasoline and using it to blend with the existing aviation fuel, thus raising the octane number of this fuel to about 65, while a narrow cut with an octane number of about 75 was prepared for Alcock and Brown's famous trans-Atlantic flight in 1919 in a Vickers-Vimy biplane with Rolls-Royce "Eagle" engines.

Prior to World War I it had been the practice to extract the aromatics from kerosene in order to avoid burning with a smoky flame, but it was difficult to find a use for these heavy aromatics. As soon as Sir Robert Waley-Cohen realized their value in suppressing detonation, he had arranged for two separate brands of kerosene to be marketed, one aromatic-free for burning in lamps, and one aromatic-enriched for use in vaporizing oil engines, and this practice has continued to the present day.

My previous experience had indicated that of all the fuels I had tried in my own workshop, toluene had proved the best, and some nearly pure samples of heptane the worst. In order, therefore, to provide reference fuels, Shell arranged to set aside a large bulk supply of a light gasoline consisting largely of heptane and from which the aromatics had been removed by sulfonation, also some toluene.

We had decided from the start to express the tendency of a fuel to detonate both in terms of the highest useful compression ratio at which, under certain carefully controlled conditions, it could be used in our variable-compression engine, and also in terms of toluene number, that is, the equivalent proportion of toluene in aromatic-free gasoline. Years later isooctane took the place of toluene and pure heptane that of aromatic-free gasoline.

With the new equipment and very talented assistance we were able to get along very fast, to detect small differences as between the samples from different oil fields, and to do a good deal of fundamental research, which was completed and published in full in 1921.

We continued to carry out routine testing of samples of fuel from every shipment or new source of supply but it was not until some 12 years later and after the chemists had so nobly done their share, that we returned again to fundamental research on volatile liquid fuels.

In the meantime we were invited to carry out a similar research on lubricating oils.

In the course of our research on gasoline fuels we had carried out tests on a number of other fuels, both liquid and gaseous, from which some very interesting side lines emerged.

Our tests on the alcohol group of fuels revealed a very high antiknock value even greater than that of toluene but, in the case of methyl alcohol, a dangerous tendency to preignition. They emphasized also the part played by the high latent heat of evaporation as a means of supercharging by refrigeration.

Special Fuels for Racing Cars

On the strength of these observations we patented in 1920 a special fuel for racing cars and cycles consisting of a mixture of 95% ethyl alcohol, benzol to act as a thermal make-weight, and acetone to give the necessary volatility; we added also 2% of castor oil to provide upper cylinder lubrication and, for fun, we added ½% of bone meal to give a characteristic smell to the exhaust, and also to confuse analysis. This fuel was prepared by the Distillers Co. and marketed jointly by Shell and themselves under the name of "Discol R"; it very soon became the accepted fuel not only for all racing events but also for sports-cars generally, despite its high price. A cheaper version of the same fuel using methyl alcohol instead of acetone and with additional water to check preignition was also supplied.

At the end of World War I there were, in this country, very large stocks of low-grade gasoline with an octane number of about 45; at the same time most of the buses and commercial vehicles were equipped with side-valve engines with conventional flat pancake combustion chambers, the combined effects of which called for compression ratios of under 4/1 and, in consequence, a very heavy fuel consumption. By doping with Power Alcohol as an antiknock and fitting new pistons, we found that we could run safely at a compression ratio of 5/1, but alcohol and gasoline will not mix. In collaboration with H. M. Hobson & Co. we developed a bifuel carburetor in which the alcohol was admitted at or near full torque through a separate jet controlled by the depression in the induction pipe. Two large bus companies, one in the South and one in the Midlands, had their fleets thus equipped and were able to show a net saving of about 10% in fuel cost, but by about 1923 the general, though slight, improvement in the octane number of the fuels, combined with the wide-spread adoption of the turbulent head, allowed compression ratios of 5/1 being used without the addition of alcohol, so the reign of the bifuel carburetor was rather brief, for it required a really large saving in fuel cost to offset the nuisance value of carrying two fuels even in a large and well-organized fleet.

Our tests on ether had shown that this fuel would self-ignite at a very low temperature and that over an extremely wide range of mixture strength; here again this observation proved of value a few years later when, in 1927, we had built for the War Office a large sleeve-valve diesel tank engine but no electric starter at that date would start it from cold. To meet this difficulty we developed an ether carburetor. At starting, the main air supply to the engine was closed off completely, and a very restricted supply drawn through the small ether car-

buretor. This method gave excellent starting even under the coldest conditions; it was forgotten when more powerful starting motors became available, but was reinvented both in England and in the U.S.A. during World War II.

In more recent years advantage has been taken of this peculiar characteristic of ether to make possible the development of very minute so-called diesel engines for model-aircraft.

I had been so pleased with the behavior of the combustion chamber on the larger version of tank engines that I was anxious to see if I could apply the same principles to a small car engine. In those days the side-by-side valve engine was the popular favorite on the grounds of convenience and cost, though it could not compete in performance with the overhead-valve type.

Early in 1918 we bought a small 4-cyl car engine of this type and tested it in my workshop. We found that it was sadly lacking in turbulence and terribly prone to detonate. We therefore made a new cylinder head with the combustion chamber concentrated over the valves but, of course, overlapping the cylinder bore sufficiently to form a slightly restricted port about equal in area to the inlet-valve port, my object being to promote additional turbulence during compression by the passage of the gas through this port.

It was clearly impossible to reduce the total length of flame travel much but, as in the case of the tank engine, I hoped to render the end gas innocuous by reducing it to a very thin lamina between two relatively cool surfaces.

The first results were most encouraging, the bmep was increased by about 10%, the optimum spark advance very much reduced, and there was no trace of detonation with a fuel which had detonated heavily in the original head at the same compression ratio. We had left the deck of the head very thick so that it could be machined down to increase the ratio. This we did progressively and found that we could increase it by nearly one whole ratio. Under these conditions the maximum bmep was increased by nearly 20% at the same gross fuel consumption and the performance generally was about the same as that of a good contemporary overhead-valve engine.

Up to that time, with the exception of Pomeroy of Vauxhall, I had had very little contact with the manufacturers of automobile engines; the war had just ended and most manufacturers were busy with their postwar designs and were somewhat reluctantly planning overhead-valve engines. Pomeroy, however, got very quickly into production with a new side-valve engine with our turbulent or offset head, and made a great success of it. Others quickly followed his example, more especially the makers of commercial vehicles; the side-valve engine came into its own again and held sway for many years after. Not all the designs, however, were so successful; there was a tendency by some makers to overdo the turbulence, causing so rapid a rate of pressure rise as to produce very rough running; others dared not make the clearance between the piston and the flat top of the head close enough to render the end gas innocuous.

Soon after we were established at Shoreham we set up an experimental single-cylinder engine to investigate the effects of varying the turbulence by varying the area of the restricted passage and of varying the clearance between piston and head; we soon arrived at an optimum figure for turbulence giving a rate of pressure rise of 30-35 psi per deg of crank angle. As to the clearance between cylinder head and piston, we found this to be very critical at about $\frac{1}{8}$ in. In one cylinder head we fitted a row of small glass windows extending from near the spark plug to the extreme far side of the cylinder and, overhead, a revolving disc with a narrow slit to act as a stroboscope. With this setup we could watch the spread of flame across the combustion chamber and, by altering the phase of the disc, could time its passage from one window to the next. When detonation occurred a bright yellowish flash could be seen apparently simultaneously in all the windows, but not until the normal flame had traveled almost all the way.

We had patented this form of combustion chamber in 1919 and for many years the royalties so derived from it formed our main source of revenue.

With the advent of much higher octane gasoline in the 1930's and the much higher ratios of compression thus rendered possible, the case for the side-valve engine faded out, for it became impracticable to make a combustion chamber of high ratio without either penalizing the breathing capacity or overdoing the turbulence, or both.

It was during the early days of our work at Shoreham that I first met Harry Horning, who visited us in the Summer of 1920. He was a great crusader, his battle-cry the marriage of the engine and its fuel; over this we soon fell into each other's arms.

We showed him all we were doing and he played lovingly with our variable-compression engine. At that time he was manufacturing at Waukesha a wide range of side-valve gasoline engines. We showed him our turbulent head which had just been adopted by Vauxhall and several other engine-builders. He was very interested and arranged for one of his engines to be sent over for us to test and to fit to it a combustion chamber of our own design. We made and fitted a new head and once again found that with the same fuel we could safely work at a very much higher compression ratio, which, together with more turbulence, gave us a gain of nearly 20% in power and consumption.

Horning's ambition was to create world-wide co-operative research between the oil companies and the engine builders, an ambition which he achieved with triumph, thanks to his energy, his enthusiasm, and the charm of his personality.

Control of

THE residual stresses discussed here are the so-called "macrostresses." They can be determined by mechanical or X-ray diffraction methods as average values within a range of metal thickness of the order of 0.001 to 0.1 in. These stresses are considered a major contributing factor in several types of service failures. In other instances, the introduction of residual stresses may also be an important measure of increasing design strength.

The practical significance of microstresses, which fluctuate over very small distances, has not yet been established. These may be introduced either by coldworking or by differential thermal expansion of the crystal grains.[1]

From the standpoint of the investigator charged with the solution of residual-stress problems these may be subdivided into three classifications, namely: (1) the determination of their magnitude; (2) the recognition and quantitative establishment of their effects on various properties; and (3) their control; in order to arrive at the highest properties.

The greatest portion of research work on residual stresses has been devoted in the past to developing and perfecting methods of measuring residual stresses and to obtaining quantitative and semiquantitative data on the distribution and magnitude of the stresses. The status of knowledge in these respects has been summarized in several books and correlated abstracts on the subject and will not be further evaluated.[2-12]

General Effects of Residual Stresses

The effects of residual stresses depend primarily on their magnitude at exposed surfaces. Therefore, whenever residual stresses are referred to, without further specification, these surface stresses are implied. Generally, residual tensile stresses at the surface are damaging, while residual compressive stresses are beneficial.

Subsurface stresses may also occasionally play an important role. This applies particularly to the fatigue strength of case-hardened parts, which tend to develop cracks underneath the case. It has also been observed that other failure types may be greatly affected by the subsurface condition, such as the season cracking of brass cartridge cases.[13] If the stress gradient near the surface is very high, removal or damage of a thin surface layer may change the surface stresses considerably. Present methods of residual-stress analysis frequently fail to measure high stress gradients.

The effects of residual stresses on various strength properties are not yet fully recognized in spite of the tremendous efforts expended on such problems. This is explained by several basic facts, namely:

1. The effects of residual stresses depend greatly on the particular material and its condition. The susceptibility of different metals to premature failure under service conditions involving residual stresses varies within wide limits.

2. The effects of residual stresses differ widely with the nature of applied loads. They may also be considerably modified by certain chemical environments.

3. Residual-stress patterns are generally very complex and some of their unrecognized or neglected features may be decisive for the occurrence of failures.

4. The magnitude of residual peak stresses is considerably affected by such factors as overstraining, repeated loading, and localized heating of surface layers. Internal changes within the material may also cause a change with time, which may be either a relaxation or an increase of the peak stress.

In general, the effects of residual stresses are fundamentally of the same nature as load stresses. Thus, certain types of failures may be equally

---

[1] See *Nature*, Vol. 153, April 22, 1944, pp. 494-495: "Thermal Fatigue of Metals," by W. Boas and R. W. K. Honeycombe.

[2] See *VDI Zeitschrift*, Vol. 71, Oct. 22, 1927, pp. 1511-1516: "Residual Stresses in Metals," by G. Sachs.

[3] See *Metals & Alloys*, Vol. 5, June, 1934, pp. 131-135; July, pp. 154-158; August, pp. 170-175; September, pp. 196-198; October, pp. 224-226: "Internal Stresses – a Correlated Abstract," by C. S. Barrett.

[4] See pp. 177-228: "Residual Stresses in Metals," by G. Sachs, in Vol. 3, No. 1 of "Handbuch der Metallphysik," edited by G. Masing. Pub. by Akademische Verlagsgesellschaft M.B.H., Leipzig, 1937.

[5] See *Iron Age*, Vol. 148, Sept. 18, 1941, pp. 63-71; Sept. 25, pp. 36-42: "Measurement of Residual Stresses in Metals," by G. Sachs and G. Espey.

[6] See Proceedings of Society for Experimental Stress Analysis, Vol. 2, No. 1, 1944, pp. 147-156: "Critical Review of Various Methods of Residual Stress Measurement," by C. S. Barrett.

[7] See "Symposium on Stress-Corrosion Cracking of Metals." Pub. by ASTM and AIME, Philadelphia and New York, 1945.

[8] See Monographs and Report Series No. 5, "Symposium on Internal Stresses in Metals and Alloys." Pub. by Institute of Metals, London, 1948.

[9] See ASTM Proceedings, Vol. 49, 1949, pp. 539-583: "Residual Stresses in Metals," by W. M. Baldwin, Jr.

[10] See pp. 459-578: "Residual Stresses," by O. J. Horger, in "Handbook of Experimental Stress Analysis," edited by M. Hetenyi. Pub. by Wiley, New York, 1950.

[11] See "Residual Stress Measurements," by R. G. Treuting [and others]. Pub. by ASM,, Cleveland, 1952.

[12] See "Residual Stresses in Metals and Metal Construction," by W. R. Osgood. Pub. by Reinhold, New York, 1954.

[13] See pp. 209-229: "Factors Influencing Stress Cracking of Brass Cartridge Cases," by G. Sachs, G. Espey, and S. M. Clark, in "Symposium on Stress-Corrosion Cracking of Metals." Pub. by ASTM and AIME, Philadelphia and New York, 1945.

Residual Stress in Practice

George Sachs, Syracuse University

This paper was presented at the SAE Golden Anniversary Annual Meeting, Detroit, Jan. 14, 1955.

caused either by load stresses or by residual stresses, or by a combination of both.

Also, there exist border cases which can be classified as either type. The most common of these is a press-fit. Failures resulting from this source (such as that shown in Fig. 1A) are of the same nature as those caused by residual stresses, such as resulting, for example, from grinding (Fig. 1B) or straightening (Fig. 1C).[14]

Classification of Control Measures

The information available to date on the control of residual stresses is rather incomplete. Any specific instance will still frequently require extensive experimentation before residual stresses and their effects can be kept under full control.

The term "controlling" residual stress will be used here in its most general sense. It will relate to any measure that leads to or assists in arriving at highest values of such service properties as are affected by the presence of residual stresses. In general, these measures can be classified from the viewpoint of production as follows:

1. Selection of the most suitable material.
2. Development of processing and heat-treating methods that are conducive to the most favorable residual-stress condition.
3. Close control of finishing operations, such as grinding and straightening.
4. Application of a final mechanical treatment, which favorably affects the residual-stress pattern. These are also called "mechanical-stress relief."
5. Stress-relief annealing.

The most important single factor in regard to intelligent control of residual stresses is that it should, and, in many instances, must, be applied not only to the last stage but also to earlier stages of the production of a part in order to achieve full success. It is a frequent experience that attempts

---

THIS paper discusses the following phases of the residual stress problem, each section containing copious references to work done in the field:

1. General effects of residual stresses.
2. Classification of control measures.
3. Control of residual-stress failures due to mechanical loads plus chemical factors.
4. Control of season cracking and related failures.
5. Control of residual stress to raise fatigue strength.
6. Control in parts loaded statically and in impact.
7. Strengthening of parts by shrinking and overstraining.
8. Dimensional stability and other physical properties.

---

[14] See Wright Air Development Center Report No. 53-254 (1953), "Survey of Low-Alloy Aircraft Steels Heat-Treated to High Strength Levels, Part 3: Failure Cases," by G. Sachs.

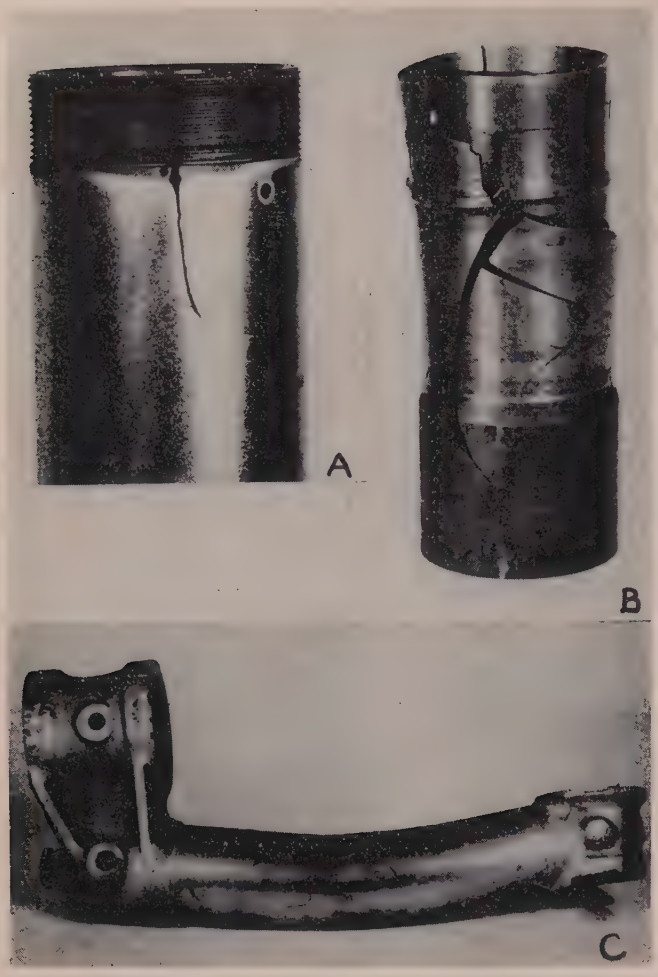

Fig. 1 – Cracking of heat-treated high-strength steel parts on cadmium plating: A. Press-fitted part (cracked after inserting plug). B. Ground part. C. Straightened part

to reduce the magnitude or to change the pattern of residual stresses in the finished part fail to be fully effective. This will be discussed later in detail for several examples.

The extent of using the various control measures greatly depends upon the particular application of the part, that is, the nature of the properties responsible for optimum service performance. These properties are either entirely of a mechanical nature, or they are a combination of mechanical and chemical resistance, or they may be such a physical property as dimensional stability during machining operations.

The control of residual stresses which may cause failures in the presence of additional chemical attack has been studied extensively and, therefore, it will be discussed first, in some detail.

Control of Residual-Stress Failures Due to Mechanical Loads Plus Chemical Factors

It must be emphasized that chemical factors are repeatedly found to be of paramount significance in failure cases where this was not initially suspected.[15] One such example is the longitudinal splitting of aluminum-alloy propellers, which alarmed air transportation about 10 years ago (Fig. 2). While such failures had the appearance of fatigue cracks, load conditions leading to a fatigue failure were absent. The failure was then diagnosed by the author as a slowly progressing fracture resulting from the combination of high residual tensile stresses at the surface of the hub bore resulting from heat-treating and of some unknown, corrosive action of oil. It has been recognized for a long time that the particular type of aluminum alloys used for such propellers is susceptible to stress-corro-

[15] See AIME Transactions (Institute of Metals Division), Vol. 147, 1942, pp. 250-264: "Relief of Residual Stress in Some Aluminum Alloys," by L. W. Kempf and K. R. Van Horn.

Courtesy, Aluminum Co. of America

Fig. 2 – Stress-corrosion failure of aluminum-alloy (76S-T) propeller, which started from surface of bore and slowly developed into longitudinal splitting

The Author

GEORGE SACHS is research professor and director of metallurgical research at Syracuse University. He received his B.S. in C.E. and his doctor's degree in mechanical engineering from a Berlin engineering school. After serving in both teaching and industrial positions in Germany Dr. Sachs, in 1936, came to this country to work for Baker & Co. He later joined the teaching staff of Case Institute of Technology.

sion. The following two measures were suggested for preventing these failures: (1) a slight change in heat-treating resulting in considerably lower stresses and (2) shotpeening of the bore surface, resulting in compressive surface stresses.[16, 17]

Another example of the importance of chemical factors is represented by the repeated failures of landing-gear parts of airplanes, such as that of the large nut illustrated in Fig. 3.[14] Of interest here is the sustained-load failure. It occurs after a considerable time under comparatively low leads, in much the same manner as creep failures at elevated temperatures. However, a sustained-load failure of a heat-treated steel occurs only if it contains hydrogen. This phenomenon is called "hydrogen embrittlement."[18] It may be classified as a particular type of stress-corrosion cracking. Most cases of hydrogen embrittlement, in the past, were caused by applied rather than by residual stresses. This is partly due to the fact that parts loaded with residual stresses crack in the cleaning or plating, when hydrogen is introduced into the steel. However, some observations were made in this laboratory that parts which contained hydrogen and which were subsequently bent, cracked some time thereafter, as shown in Fig. 4.

Cracking due to the combined effect of hydrogen and residual stresses, under conditions where hydrogen is developed rather than retained by the steel, is another type of stress-corrosion cracking. It is illustrated in Fig. 1.

Hydrogen embrittlement and stress-corrosion cracking of aircraft and other steels, heat-treated to high strength levels, is usually controlled by:

1. A stress-relief anneal at a temperature slightly below the tempering temperature.
2. A mechanical surface treatment consisting of shotblasting.

Both measures must be applied prior to the exposure to hydrogen. They eliminate failures associated with the presence of residual stresses.

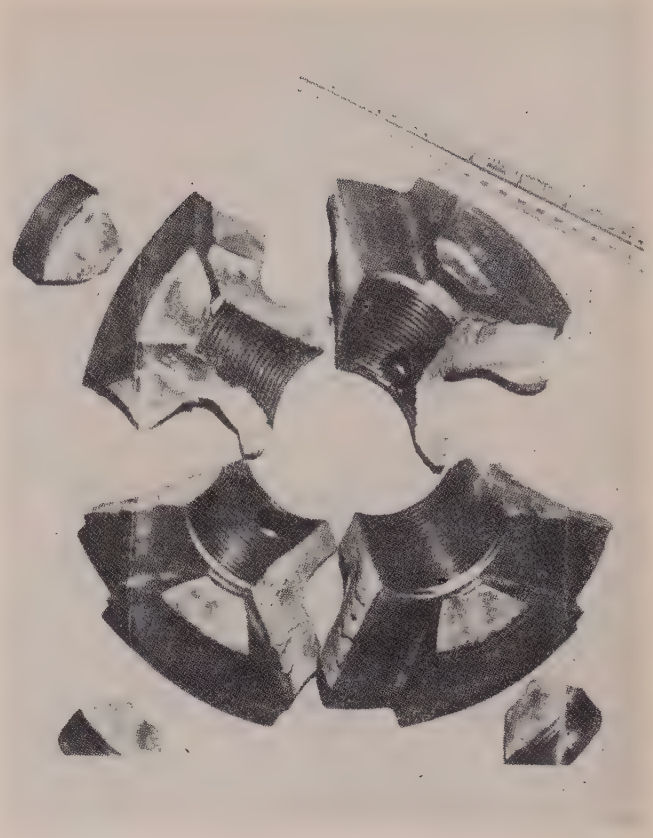

Courtesy, Convair

Fig. 3 – Failure of large nut of landing gear of B-36 bomber

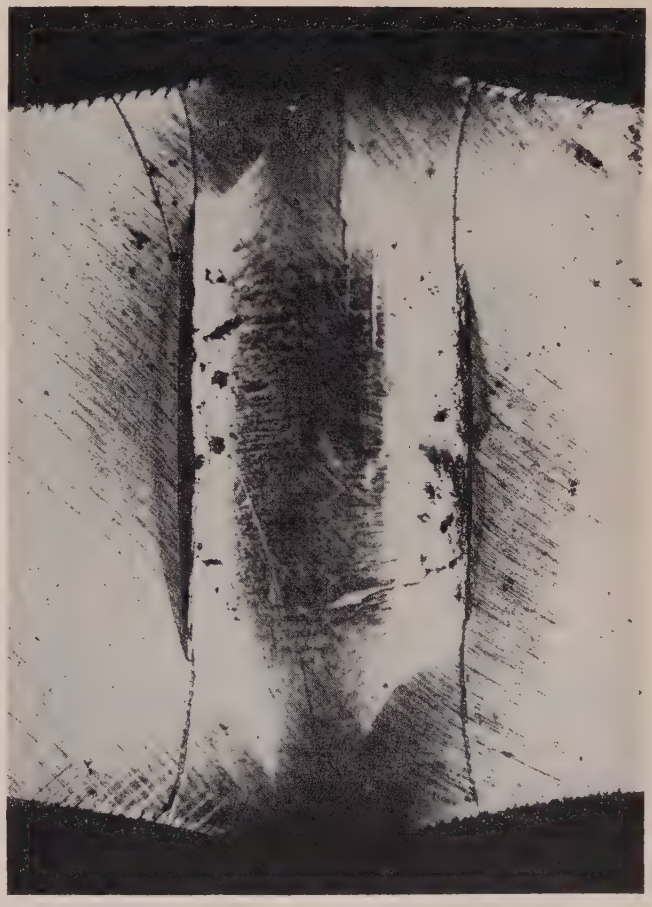

Fig. 4 – Cracks at inside surface, which developed in hydrogen-loaded 4340 steel specimen after plastic bending

[16] See Proceedings of Society for Experimental Stress Analysis, Vol. 3, No. 1, 1945, pp. 40-61: "Study of Certain Mechanically Induced Residual Stresses," by D. G. Richards.

[17] See *Journal of Metals*, Vol. 5, March, 1953, pp. 405-422: "Residual Stresses Introduced during Metal Fabrication," by K. R. Van Horn.

[18] See Wright Air Development Center Report No. 53-254 (1953), "Survey of Low-Alloy Aircraft Steels Heat-Treated to High Strength Levels, Part 1: Hydrogen Embrittlement," by G. Sachs and W. Beck.

However, they do not prevent hydrogen embrittlement due to directly applied loads or to residual stresses developed during assembly. The main control measure, in these respects, is heating to 300-400 F for several hours, or "baking," in order to remove the hydrogen. It appears, however, that full future control of hydrogen embrittlement for aircraft applications must include that of the cleaning and plating procedures. These must either prevent hydrogen embrittlement or result in a permeable coating which renders baking more effective. Furthermore, according to Fig. 5, the danger of hydrogen embrittlement greatly increases with increasing strength of the heat-treated steel. Therefore, selection of a steel possessing lower strength may be the only effective measure of avoiding such failures, in extreme cases.

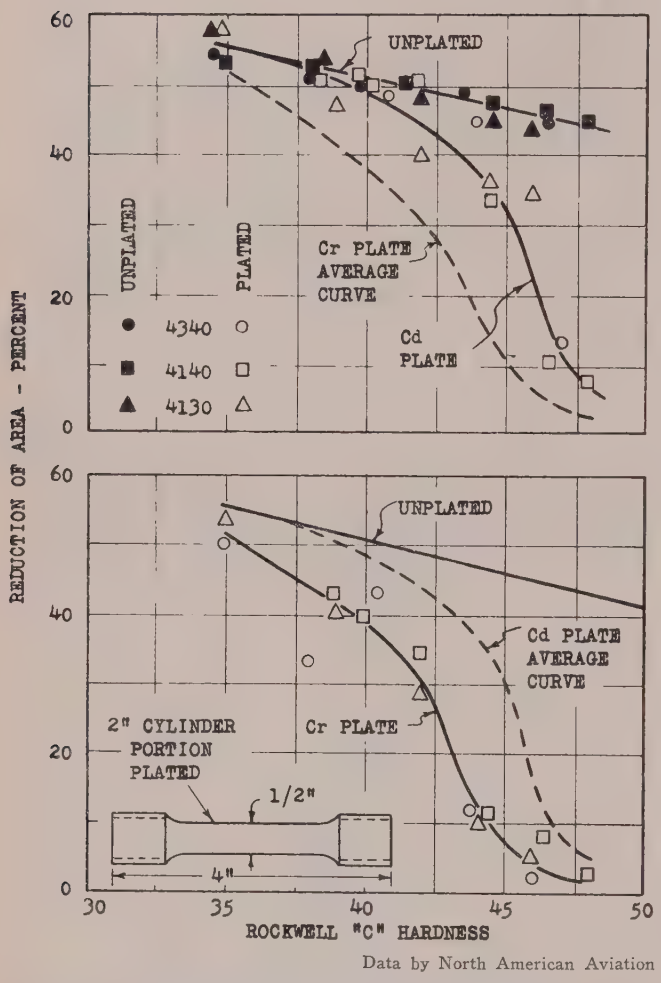

Data by North American Aviation

Fig. 5 – Effects of plating on ductility of various steels heat-treated to hardnesses between 35 and 48 Rockwell[14]

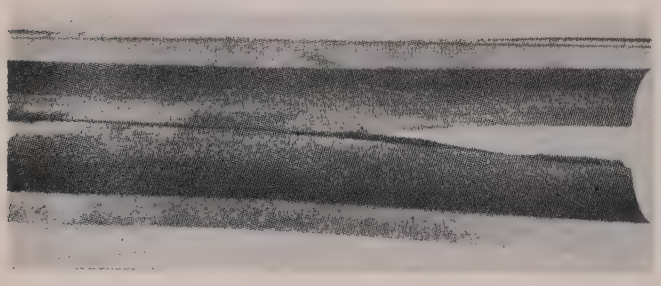

Fig. 6 – Residual stresses causing longitudinal cracks originating from inner tube wall[19]

Control of Season Cracking and Related Failures

The best-known example of stress-corrosion cracking is the "season cracking" of brass and copper-alloy parts which had been subject to drawing or spinning. Very similar stress-cracking phenomena are encountered in many other materials, including carbon and low-alloy steels,[19] stainless steels, and aluminum alloys. Such stress cracking is illustrated for steel tube in Fig. 6.[10] It is explained by the combination of tensile surface stresses and of chemical attack by ammonia in the atmosphere. In order to eliminate season cracking a stress-relief anneal is usually applied, which (according to Figs. 7 and 8) eliminates most of the stresses and the cracking resulting from it, without adversely affecting the hardness.[20-22] However,

[19] See pp. 351-365: "Delayed Cracking in Hardened Alloy Steel Plates," by E. H. Bucknall, W. Nicholls, and L. H. Toft, in "Symposium on Internal Stresses in Metals and Alloys." Pub. by Institute of Metals, London. 1948.

[20] See AIME Transactions (Institute of Metals Division), Vol. 147, 1942, pp. 74-88: "Residual Stress in Sunk Cartridge-Brass Tubing," by G. Sachs and G. Espey.

[21] See *U. S. Bureau of Standards Journal of Research*, Vol. 28, June, 1942 (RP 1477), pp. 755-772: "Relief of Residual Stress in Streamline Tierods," by R. E. Pollard and F. M. Reinhart.

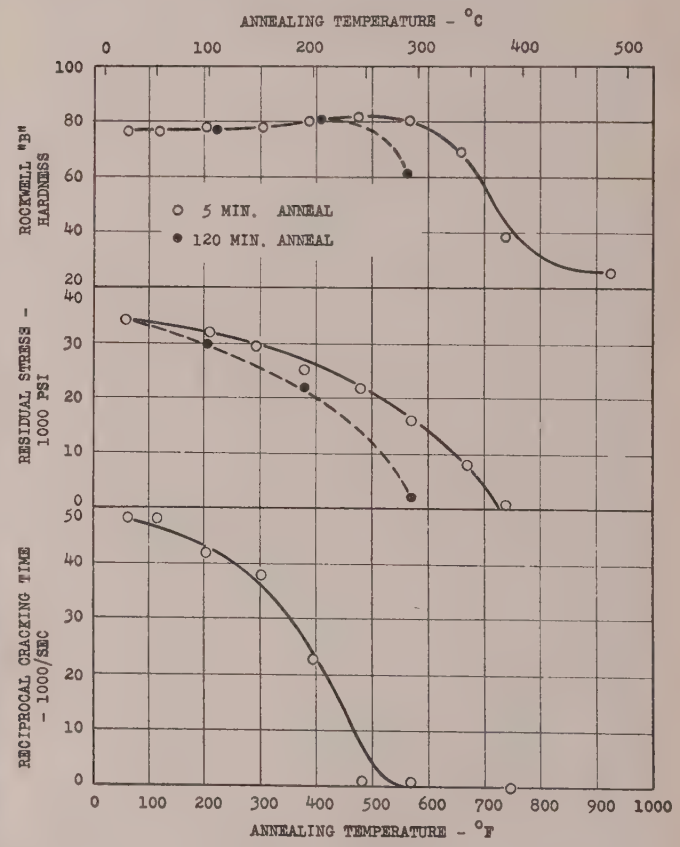

Fig. 7 – Effects of annealing on hardness, residual stress, and cracking tendency of brass tube[20]

there are many instances known where cracking cannot be fully eliminated or prevented by this control measure, such as, for example, the cracking of cartridge cases on firing or in storage.[13]

The cracking of simpler shapes, such as wire, rod, and tube, frequently can be controlled by finishing operations of a mechanical nature. Stretching, or compressing, gradually reduces the residual stresses to very low values, according to Fig. 9.[2, 23-26] Bending and a commercial straightening process, called "reeling" or "polishing," cause a reversal of the surface tensile stresses into compressive stresses, as illustrated in Fig. 10.[2, 27]

However, in the case of tube and wire, the most effective stress-control measures are applied during their production. These are proper selection of tool contour and reductions.[28-31] This is particularly effective for brass tube, where the right combination of wall reduction and diameter reduction produces (according to Fig. 11) very little stress and eliminates the danger of cracking. In the case of stainless-steel boxes, the proper combination of depth and corner radius will prevent such failures, as illustrated in Fig. 12.[32] Occasionally, none of the above-listed control measures will be fully effective. It then may become necessary to change to a material with less tendency to cracking.[28, 32] In the case of austenitic stainless steels, a stabilizing treatment which changes the structure of the alloy is also known to be beneficial in this respect.

Control of Residual Stress to Raise Fatigue Strength

The most publicized measures of controlling residual stresses serve the purpose of increasing the strength of materials subjected to repeated loads. The vast literature on this subject reveals the following important phenomena:

1. Residual stresses are of only slight significance in regard to the fatigue strength and endurance limit at low strength of a particular group of alloys.

2. Residual stresses are also of little significance, in these respects, for polished, smooth, that is, cylindrical and prismatic, sections.

3. The effect of residual stresses, if they exist, becomes more pronounced as the number of cycles to failure increases.

4. The important effects of residual stresses on

---

[22] See *American Foundryman*, Vol. 10, September, 1946, pp. 37-47: "Steel Castings and Weldments, Residual Stress Relief," by C. R. Jelm and S. A. Herres.

[23] See *VDI Zeitschrift*, Vol. 83, Feb. 4, 1939, pp. 129-132: "X-Ray Determination of Stresses in Specimens of Unalloyed Steel in Tensile Tests at above Yield Point," by F. Bollenrath, V. Hauk, and E. Osswald.

[24] See *Journal of Institute of Metals*, Vol. 67, 1941, pp. 87-99: "Quenching Stresses in Aluminum Alloys," by A. von Zeerleder.

[25] See *Zeitschrift für Metallkunde*, Vol. 36, March, 1944, pp. 70-72: "Crystallite Deformation at Surface of Parts Containing Residual Stresses Subjected to Static Tensile and Compressive Loads," by A. Schaal.

[26] See pp. 171-177: "Relief of Internal Stresses in Aluminum Alloys by Cold Working," by W. Betteridge, in "Symposium on Internal Stresses in Metals and Alloys." Pub. by Institute of Metals, London, 1948.

[27] See *Metallwirtschaft*, Vol. 10, Oct. 9, pp. 783-788; Nov. 20, pp. 880-881: "Cracking of Cold-Drawn Steel Bars," by W. Fahrenhorst and G. Sachs.

[28] See A.I.M.E. Transactions (Institute of Metals Division), Vol. 89, 1930, pp. 233-255: "Internal Stress and Season Cracking in Brass Tubes," by D. K. Crampton.

[29] See *Mitteilungen der Deutschen Materialprufungsanstalten*, Vol. 16, 1932, pp. 38-67: "Investigation of Properties of Cold-Drawn Wire and Force Requirements for Wire Drawing," by W. Linicus and G. Sachs.

[30] See *Archiv für das Eisenhüttenwesen*, Vol. 8, May, 1935, pp. 515-516: "Residual Stresses in Burnished Steel Rod," H. Bühler.

[31] See *Archiv für das Eisenhüttenwesen*, Vol. 8, April, 1935, pp. 465-466: "Effect of Die Contour on Residual Stresses and Strength Properties on Cold-Drawn Steel Rod," by H. Bühler.

[32] See "Forming of Austenitic Chromium-Nickel Stainless Steels," by V. N. Krivobok and G. Sachs. Pub. by International Nickel Co., New York, 2nd ed. 1954.

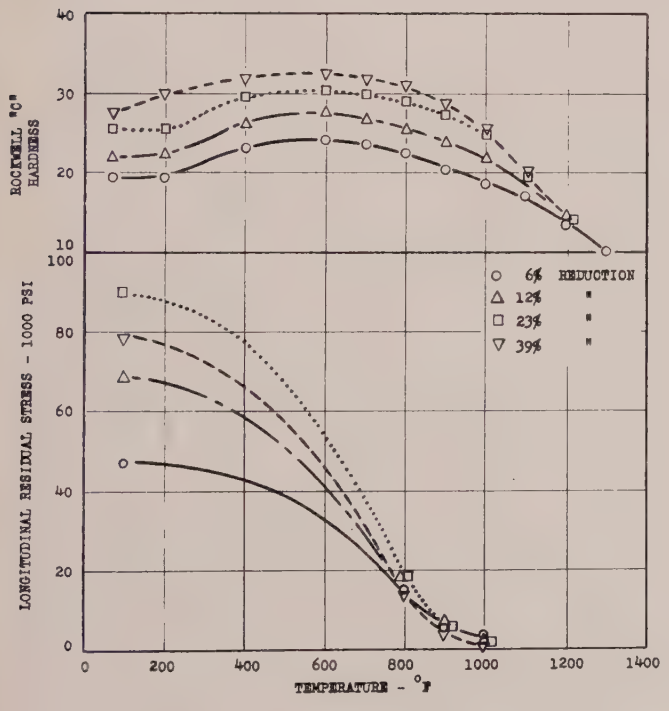

Fig. 8 – Effect of stress relief (2 hr) on hardness and residual stress of cold-drawn 1060 steel bars

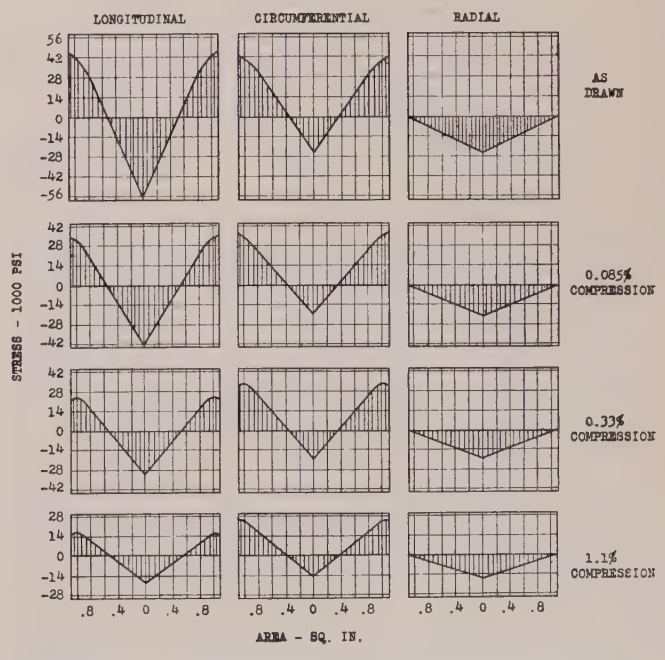

Fig. 9 – Effect of compression on residual stresses in cold-drawn brass rod[2]

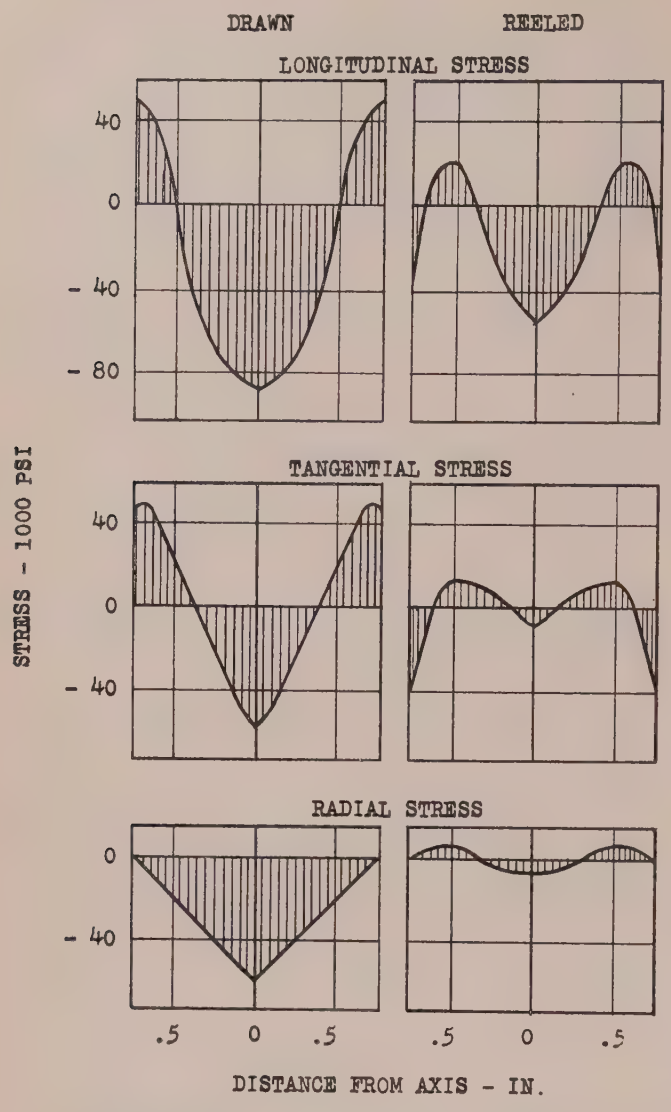

Fig. 10 – Effects of reeling on residual stresses in cold-drawn steel rod[27]

structures which are subjected to repeated loads relate to conditions where the fatigue strength and endurance limit are greatly reduced in comparison to those of polished, smooth sections. This applies (a) to many high-strength materials and particularly to steels, heat-treated to high-strength values and (b) to the fatigue properties in the presence (1) of high stress concentrations, (2) of simultaneous chemical attack, or corrosion fatigue, and (3) of a simultaneous rubbing, fretting, or chafing action.

In general, the question whether residual stresses determine the large variations encountered in regard to fatigue strength is still not completely answered. Undoubtedly, they are of importance, in this respect. However, as already mentioned, the effect is apparently small for uniform, polished sections. In contrast, residual stresses introduced into a reduced section by plastic deformation noticeably affect the fatigue strength, as illustrated in Fig. 13.[33-37] This applies both to direct effects of stretching or compressing and to the indirect effects of localized heating.

The direct damaging effect of tension stresses, however, is rarely observed in practical service. Fatigue failures which are attributable directly or predominantly to residual tensile stresses have only occasionally been reported. One example of this type is the failure of the heat-treated steel piston rods of an ocean liner (Fig. 14[38]). A fatigue failure developed shortly after departure. It started from the surface of a transverse bore where the heat-treating stresses exhibited a maximum value.

Compressive stresses, on the other hand, are associated with the now universally applied mechanical measures which serve to increase the life of high-strength steel parts in reciprocating machinery and vehicles. Such finishing treatments are

[33] See *VDI Zeitschrift*, Vol. 78, Aug. 4, 1934, pp. 921-925: "Increase of Endurance Limit of Notched Structural Parts by Residual Stress," by A. Thum and W. Bautz.

[34] See *VDI Zeitschrift*, Vol. 81, Feb. 27, 1937, pp. 276-278: "Effect of Residual Thermal Stresses on Fatigue Strength," by A. Thum and A. Erker.

[35] See *Welding Journal*, Vol. 22, February, 1943, pp. 63s-78s: "Investigation of Behavior of Residual Stresses under External Load and Their Effect on Safety," by J. T. Norton and D. Rosenthal.

[36] See *Welding Journal*, Vol. 25, May, 1946, pp. 269s-276s: "X-Ray Diffraction Study of Notch-Bend Test," by J. T. Norton, D. Rosenthal, and S. B. Maloof.

[37] See *Welding Journal*, Vol. 25. November, 1946, pp. 729s-735s: "Study of Effect of Residual Compression on Fatigue of Notched Specimens," by J. T. Norton, D. Rosenthal, and S. B. Maloof.

[38] See ASM Transactions, Vol. 27, September, 1939, pp. 821-836: "Internal Stresses in Piston Rods of Large Diesel-Engine Ocean Liner," by G. Sachs.

[39] See *Iron Age*, Vol. 155, March 29, 1945, pp. 40-49, 100: April 5, pp. 66-76, 146, 148-149: "Mechanical and Metallurgical Advantages of Shotpeening," by O. J. Horger.

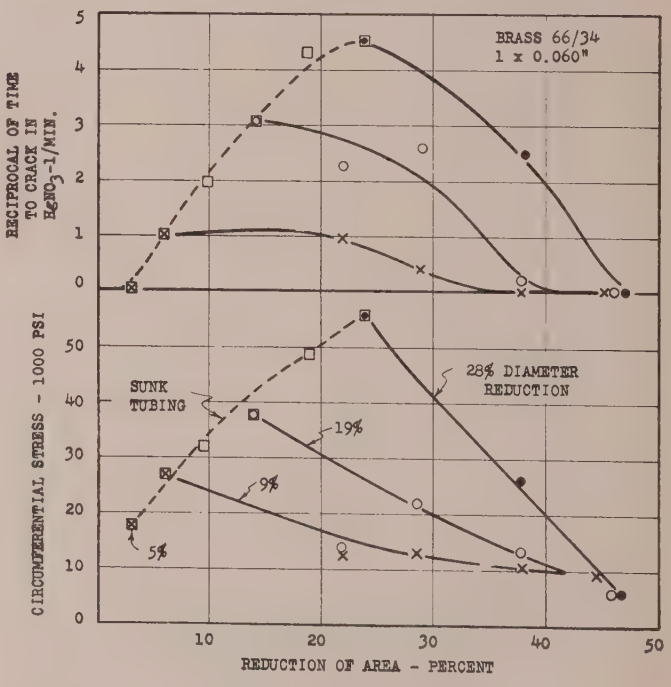

Fig. 11 – Residual stress and corrosion cracking in brass (67% Cu, 33% Zn) tubing drawn different reductions in diameter and wall thickness[28]

shotpeening[39] and surface rolling. The residual-stress pattern introduced by such treatments is illustrated in Fig. 15 for a magnesium propeller.[40] Their effect on the fatigue strength of the hub section which was subjected to fretting is shown in Fig. 16.

Surface Rolling

Surface rolling was already introduced before recognition of the role of residual stresses as "polishing" or "burnishing" to the bearing section of railway axles. Its effect on fatigue strength has been extensively studied.[40-44] The first controlled application of surface rolling was made in Germany to increase the service life of light-alloy propellers, which was determined by the fatigue strength of the hub section. Rolling of threads is another early process which produces the benefits derived from compressive stresses. The rolling of the shoulders of bolts and other parts again is a more recent application of surface rolling.

The control of pressure and coverage are paramount factors in order to achieve success with surface rolling. The control of (fictitious) pressure values derived from Hertz elastic theory has been found useful for surface rolling. These proper values are in the order of 500,000-1,000,000 psi for steels and 250,000-300,000 psi for light alloys.[45] Higher pressures lead to surface damage, lower values lead to a reduced endurance limit. In order to obtain complete coverage, the rolled spirals must overlap. Otherwise, premature failure may occur between the paths covered and protected by the roll indentations.

Control of Shot-Blasting Conditions

The control of shot-blasting conditions is a rather complex matter.[16, 45-50] The spherical shape of the shot must be maintained in order to avoid

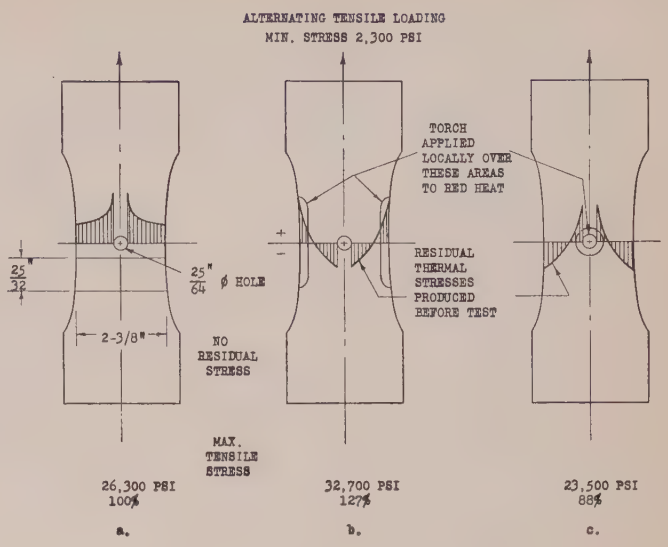

Fig. 13 – Effects of residual stresses induced by local heating on fatigue strength of steel plate with hole[34]

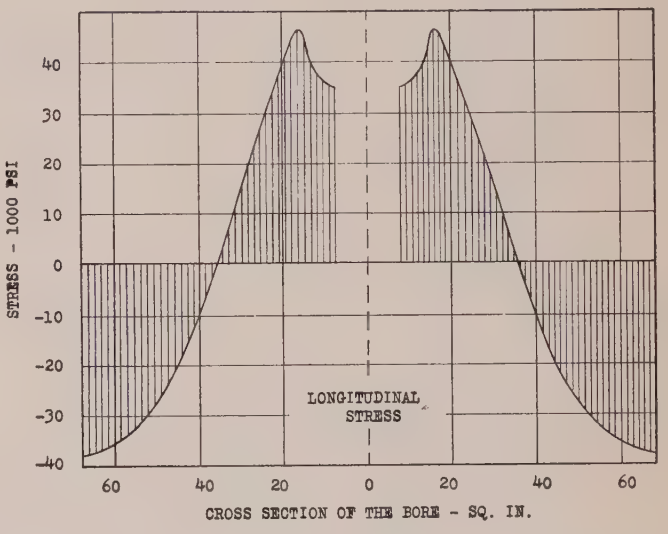

Fig. 14 – Residual-stress pattern in broken piston rod of ocean liner[33]

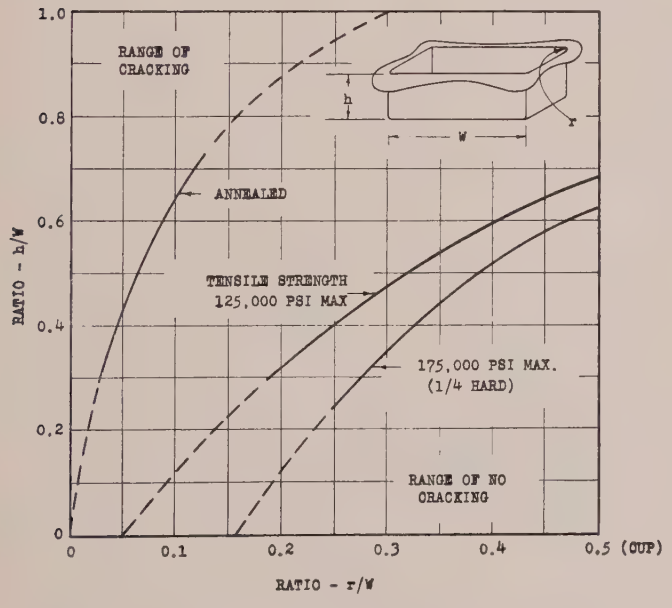

Fig. 12 – Effects of depth, corner radius, and temper on tendency to cracking of austenitic stainless-steel boxes[32]

[40] See *Metals & Alloys*, Vol. 10, January, 1939, pp. 19-23: "Improved Aircraft Propellers by Surface Rolling," by G. Sachs.

[41] See Journal of *Applied Mechanics*, Vol. 2, December, 1935, pp. A128-A136: "Effect of Surface Rolling on Fatigue Strength of Steel," by O. J. Horger.

[42] See pp. 85-142: "Stressing Axles and Other Railroad Equipment by Cold Rolling," by O. J. Horger, in "Surface Stressing of Metals." Pub. by ASM, Cleveland, 1947.

[43] See Mitteilungen des Wöhler-Institute, No. 41 (1948), "Measuring Stresses and Plastic Deformations in Surface-Pressed Test Bars," by H. Föppl.

[44] See *Product Engineering*, Vol. 22, March, 1951, pp. 101-124: "Fatigue Failures Are Tensile Failures," by J. O. Almen.

[45] See pp. 129-204: "Relief and Redistribution of Residual Stresses in Metals," by D. G. Richards, in "Residual Stress Measurements." Pub. by ASM, Cleveland, 1952.

[46] See pp. 261-278: "Shotblasting and Its Effects on Fatigue Life," by F. P. Zimmerli, in "Surface Treatment of Metals." Pub. by ASM, Cleveland, 1941.

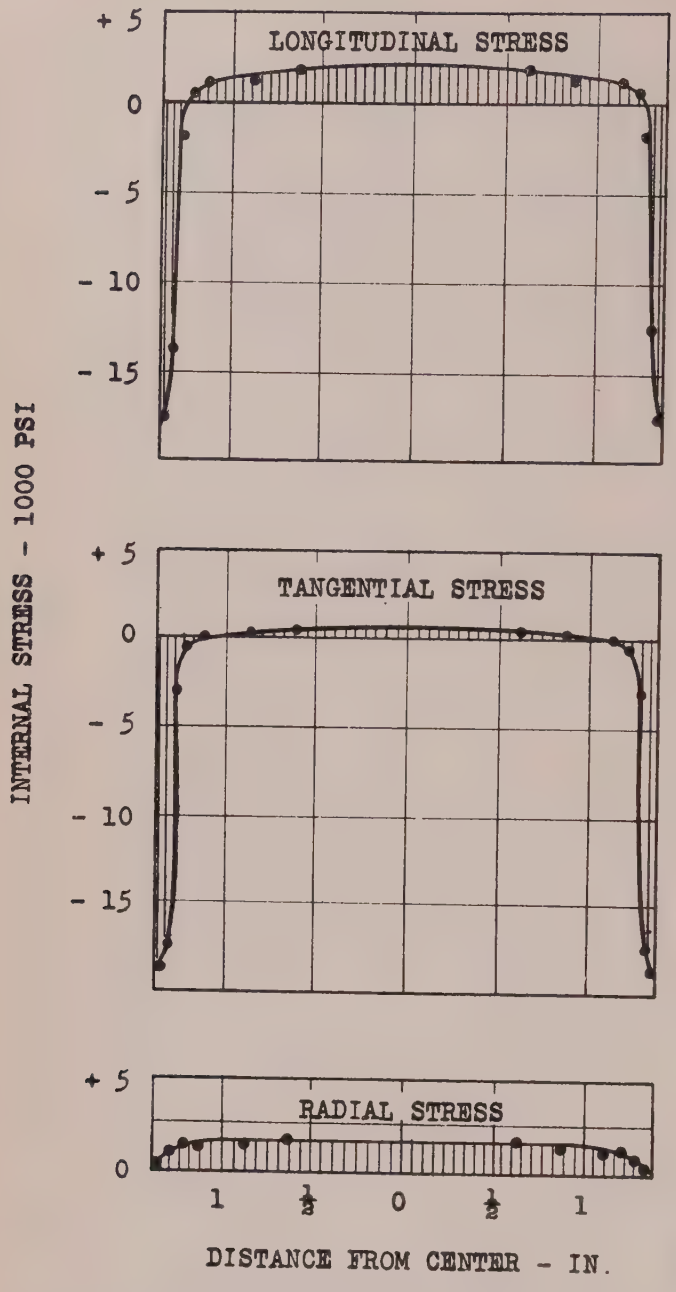

Fig. 15 – Residual-stress pattern in surface-rolled magnesium propeller hub[40]

sharp and deep impressions which may negate the desired effect. Other important items are intensity and coverage. For the control of a desired intensity a thin, flat test specimen has been introduced by Almen, which is widely used. No general control measures for coverage have been proposed to date. If the coverage is incomplete, shotblasting may be ineffective.

If there is a possibility to choose the material the objective of high fatigue properties of a steel part can alternatively be achieved by using case-hardening.[51-53] The high endurance limits of case-hardened steel parts is also attributed to the development of high compressive stresses in the case such as illustrated in Figs. 17 and 18. This applies to flame hardening and induction hardening, as well as to carburizing and nitriding. No definite information appears to be available on the control of case-hardening conditions. Coverage is again an important problem, as, for example, holes cutting through the hardened layer result in a very low endurance limit if their surface is not hardened.[51,54,55]

[47] See Proceedings of Society for Experimental Stress Analysis, Vol. 2, No. 1, 1944, pp. 178-190: "Improving Fatigue Resistance by Shotpeening," by O. J. Horger and H. R. Neifert.

[48] See Proceedings of Society for Experimental Stress Analysis, Vol. 2, No. 2, 1945, pp. 1-10: "Shotpeening to Improve Fatigue Resistance," by O. J. Horger and H. R. Neifert.

[49] See pp. 395-415: "Prevention of Fatigue Failures in Metal Parts by Shotpeening," by J. G. Brookman and L. Kiddle, in "Failure of Metals by Fatigue." Pub. by Melbourne University Press, Melbourne, 1947.

[50] See *SAE Journal*, Vol. 56, November, 1948, pp. 36-39: "Shotpeening," by F. P. Zimmerli and J. Straub.

[51] See *VDI Zeitschrift*, Vol. 82, July 23, 1938, pp. 885-889: "Endurance of Hollow Crankshaft Pins with Internal Reinforcement," by H. Cornelius and F. Bollenrath.

[52] See *Metallurg* (Russian), Vol. 8, 1940, pp. 30-37: "Residual Internal Stresses in Steels Hardened by High-Frequency, Surface-Hardening Process," by I. E. Kontorovich and L. C. Livshits.

[53] See ASTM Technical Publication No. 72 (1947), "Symposium on Testing of Parts and Assemblies," pp. 47-75: "Automotive Rear Axles and Means of Improving Their Fatigue Resistance," by O. J. Horger and C. H. Lipson.

[54] See *Archiv für das Eisenhüttenwesen*, Vol. 12, March, 1939, pp. 445-448: "Influence of Case Hardening on Alternating Bending and Torsion Fatigue Strength of Smooth and Transversely Bored Test Specimens," by H. Wiegand and R. Scheinost.

[55] See *VDI Zeitschrift*, Vol. 84, July 20, 1940, pp. 505-510: "Surface and Fatigue Strength," by H. Wiegand.

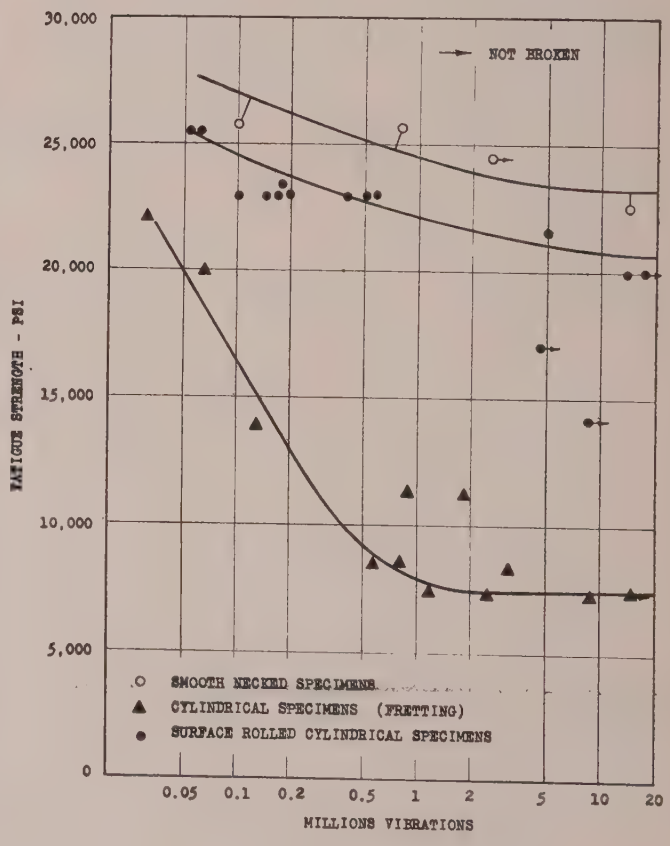

Fig. 16 – Effects of fretting and surface rolling on fatigue strength of magnesium alloy[49]

Failures observed below the case also indicate that extreme changes in residual stress occurring at these locations are harmful, but no definite information is available, in this respect.

Residual stresses developed in conventionally machined and ground parts also affect the fatigue properties.[56-63] As far as machining is concerned, this effect is probably insignificant, in most instances. It even may be beneficial, as dull tools act in much the same way as surface rolling and produce compressive stresses.

Grinding, on the contrary, can be very harmful, as it heats the surface and develops tensile stresses. Careless grinding also results in overheating of the surface layers and frequently in checking and cracking. Control of grinding appears to be one of the most difficult shop problems, in the absence of automatic grinding equipment. With heat-treated, high-strength steels a regular check of surface hardness should be used to prevent grinding damage. Etching has been used to disclose excessive grinding stresses. The influence of grinding on the properties of surface-peened parts is apparently not yet fully clarified.

Adverse effects of electroplating and of subsequent heating on fatigue properties are also ascribed to the development of tensile stresses on

[56] See Transactions of American Society for Steel Treating, Vol. 18, 1930, pp. 423-439: "Stresses and Cracks in Hardened and Ground Steel," by G. R. Brophy.

[57] See Ingeniorvidenskabelige, Skrifter A, No. 43, 1937, "Machining and Residual Stresses," by E. K. Henriksen.

[58] See ASME Transactions, Vol. 73, January, 1951, pp. 69-76: "Residual Stresses in Machined Surfaces," by E. K. Henriksen.

[59] See *VDI Zeitschrift*, Vol. 88, Dec. 23, 1944, pp. 681-686: "Bending Fatigue Strength of Case-Hardened and Nitrided Steels Containing Grinding Cracks," by H. Staudinger.

[60] See *Journal of Technical Physics* (Leningrad), Vol. 16, No. 7, 1946, pp. 791-802: "Residual Stresses Caused by Grinding," by L. A. Glickman and V. A. Stepanov. See also *Engineers' Digest*, Vol. 4, August, 1947, pp. 378-379.)

[61] See ASM Transactions, Vol. 36, 1946, pp. 389-451: "Detection, Causes, and Prevention of Injury in Ground Surfaces," by L. P. Tarasov.

[62] See ASME Transactions, Vol. 73, April, 1951, pp. 337-342: "Residual Grinding Stresses in Mild Steel," by J. Frisch and E. G. Thomsen.

[63] See NACA TN 2324 (1951), "Fatigue Strength of Aircraft Materials; Axial-Load Fatigue Tests on Unnotched Sheet Specimens of 24S-T3 and 75S-T6 Aluminum Alloys and of SAE 4130 Steel," by H. J. Grover, S. M. Bishop, and L. R. Jackson.

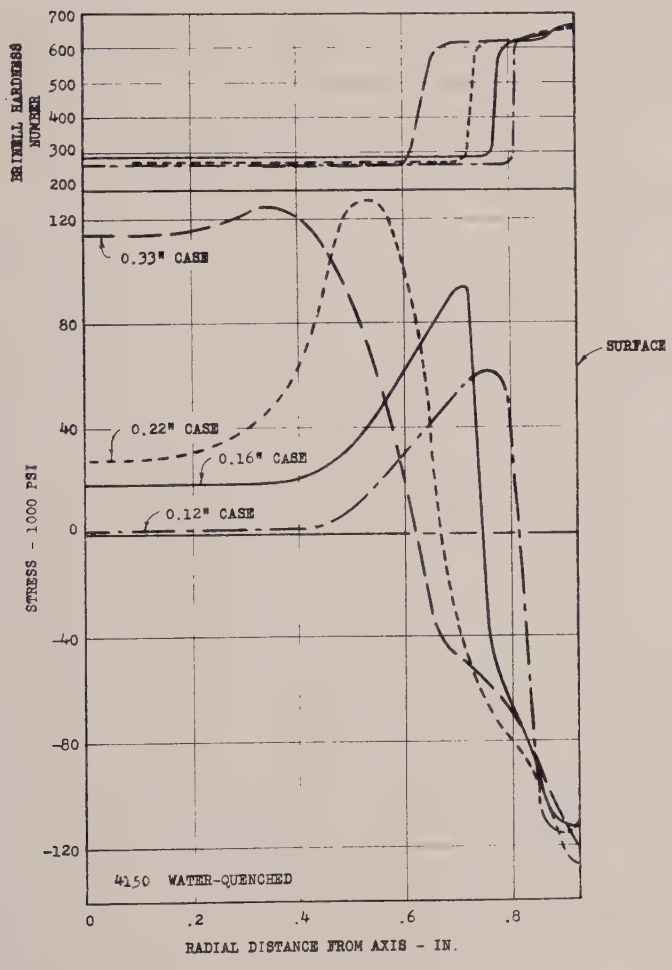

Fig. 17 – Effect of case depth on residual stress of induction-hardened SAE 4150 – normalized and water quenched

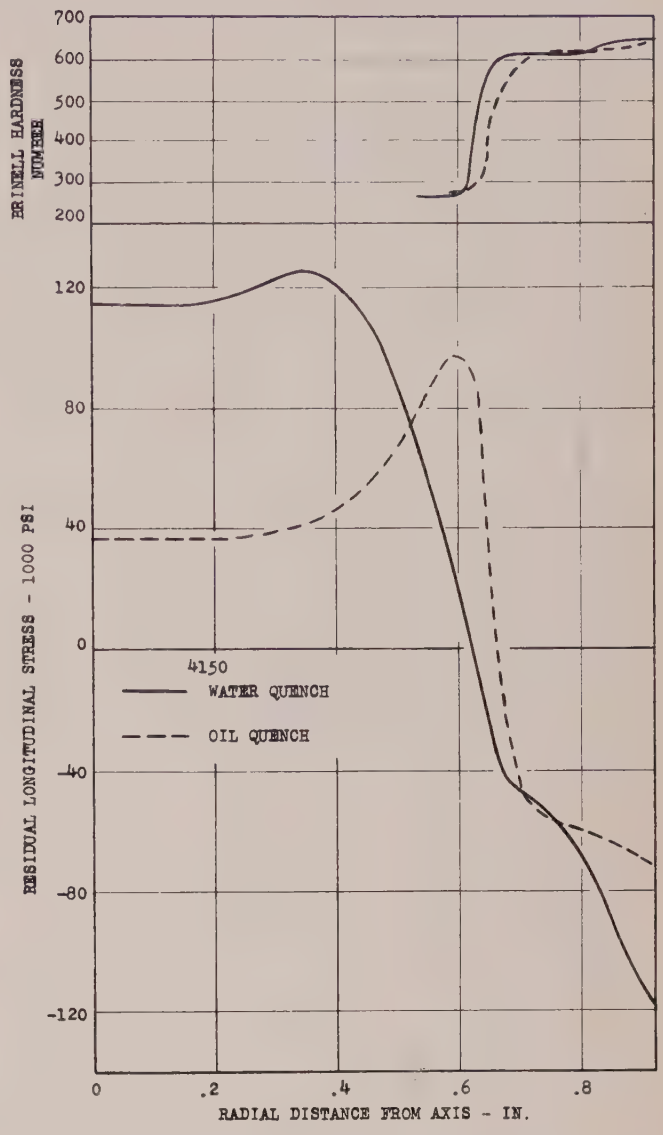

Fig. 18 – Effect of quenching rate on residual stress of induction-hardened SAE 4150 – normalized, case depth 0.33 in.

the electroplate.[64-69] As the plating conditions considerably influence the residual-stress state, efforts are now being made to use plating conditions conducive to low stresses.

Control in Parts Loaded Statically and in Impact

The role of residual stresses in the performance of parts which are loaded statically or a few times only has been little explored. This also applies to static loading followed by holding the load for a long time. Premature static and sustained-load failures with residual stresses being a contributing factor have definitely been observed only under conditions conducive to stress corrosion, as discussed above.

Another effect of residual stresses concerns the stress-strain relations. The presence of such stresses should cause plastic flow to occur earlier. Some tests on welded-steel girders confirmed this theoretically predictable change in the stress-strain characteristics.[70, 71]

The static and impact strength of the normally ductile constructional metals appears not noticeably affected by residual stresses of any type. This is in distinct contrast to the pronounced favorable effect of compressive quenching stresses on the bending strength of a very brittle material, such as glass.[44, 72] The reason for this apparent discrepancy is that metallic materials are usually sufficiently ductile to relieve residual stresses automatically on static and impact straining.

A pronounced influence of weld stresses, however, appears established in static bend tests at temperatures slightly below room temperature on large welded plate provided with saw cuts.[73, 74] Among the measures applied to reduce the magnitude of such weld stresses, a special low-temperature treatment is of particular interest. It consists of heating narrow areas parallel to and about 5 in. apart from the welded bead to 350-400 F, as illustrated in Fig. 19.[75, 76] This, in turn, relieves the stress in the weld and weld-affected zones.[35, 76-78]

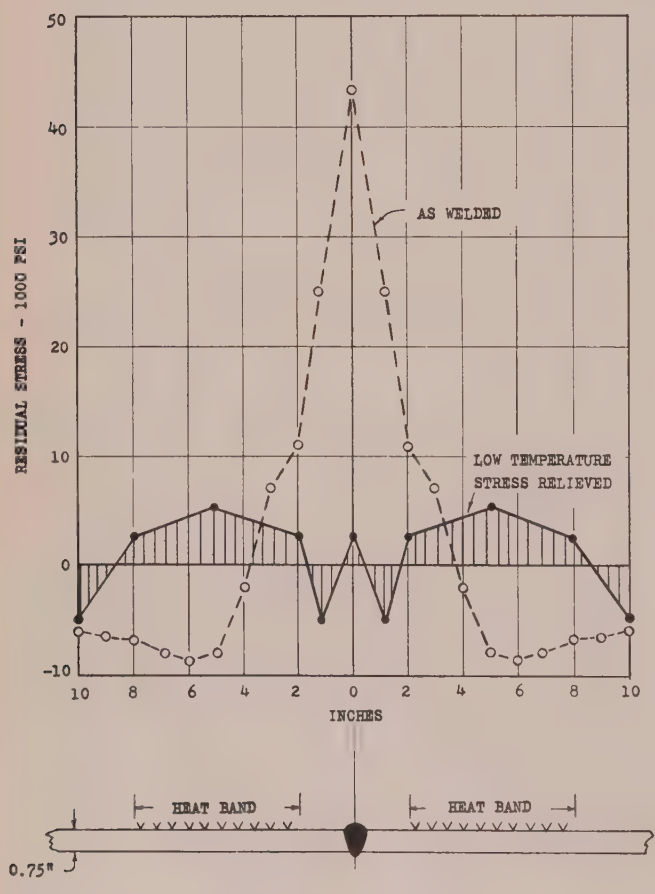

Fig. 19 – Effect of low-temperature stress-relieving on longitudinal residual stresses in surface of 7- by 4-ft weldment[75]

Strengthening of Parts by Shrinking and Overstraining

The stresses introduced by shrinking one part onto another may be classified as residual stresses, considering the two-piece assembly as a unit, as already discussed. These result in a considerable increase in the resistance of the part to plastic deformation and, in the case of a brittle component, to fracture. To obtain maximum strength the geometrical relations between the components of the shrunk part must be closely controlled.[79]

A distribution of residual stress and apparently also strengthening effects similar to those resulting from a shrink fit are also obtained by overloading and expanding a one-piece tube. Such "overstraining" is referred to, in the case of expanded tube, as "autofrettage."[80, 81] The process results in a considerable increase in the yield strength in

---

[64] See *U. S. Bureau of Standards Journal of Research,* Vol. 40, January, 1948 (RP 1854), pp. 31-59: "Physical Properties of Electrodeposited Chromium," by A. Brenner, P. Burkhead, and C. Jennings.

[65] See pp. 107-118: "Stress in Electrodeposited Metals," by A. W. Hothersall, in "Symposium on Internal Stresses in Metals and Alloys." Pub. by Institute of Metals, London, 1948.

[66] See *U. S. Bureau of Standards Journal of Research,* Vol. 42, February, 1949 (RP 1954), pp. 105-123: "Calculation of Stress in Electrodeposits from Curvature of Plated Strip," by A. Brenner and S. Senderoff.

[67] See *U. S. Bureau of Standards Journal of Research,* Vol. 42, February, 1949, (RP 1953), pp. 89-104: "Spiral Contractometer for Measuring Stress in Electrodeposits," by A. Brenner and S. Senderoff.

[68] See *U. S. Bureau of Standards Journal of Research,* Vol. 43 August, 1949 (RP 2011), pp. 101-112: "Effect of Chromium Plating on Endurance Limit of Steels Used in Aircraft," by H. L. Logan.

[69] See *Product Engineering,* Vol. 22, June, 1951, pp. 109-116: "Fatigue Loss and Gain by Electroplating," by J. O. Almen.

[70] See *Welding Journal,* Vol. 28, March, 1949, pp. 89s-97s: "Tests of Large Welded-Steel Box Girders," by A. H. Stang and B. S. Jaffe.

[71] See *Welding Journal,* Vol. 29, September, 1950, pp. 484s-493s: "Distribution of Locked-in Stresses in Large Welded-Steel Box Girder," by J. Vasta.

[72] See pp. 163-168: "Internal Stresses in Glassware," by W. C. Hynd, in "Symposium on Internal Stresses in Metals and Alloys." Pub. by Institute of Metals, London, 1948.

[73] See *Welding Journal,* Vol. 28, May, 1949, pp. 193s-203s: "Evaluation of Effect of Residual Stresses," by T. W. Greene.

[74] See *Welding Journal,* Vol. 30, March, 1951, pp. 135s-145s: "Stress Relieving and Fracture Strength," by D. Swan, A. R. Lytle, and C. R. McKinsey.

[75] See *Welding Journal,* Vol. 25, March, 1946, pp. 171s-185s: "Controlled Low-Temperature Stress Relieving," by T. W. Greene and A. A. Holzbaur.

[76] See *Welding Journal,* Vol. 28, August, 1949, pp. 354s-364s: "Report of Some Recent Research into Measurement and Relaxation of Residual Stresses," by W. Soete.

[77] See University of Illinois Engineering Experiment Station Bulletin, Series 361 (1946), "Residual Stresses in Welded Structures," by W. M. Wilson and C. C Hao.

[78] See *Welding Journal,* Vol. 26, April, 1947, pp. 193s-214s: "Investigation of Influence of Hydrogen on Ductility of Arc Welds in Mild Steel," by A. E. Flanigan.

[79] See Proceedings of Society for Experimental Stress Analysis, Vol. 7, No. 2, 1949, pp. 45-72: "Strength of Inserted Dies," by G. Sachs, J. D. Lubahn, and L. J. Ebert.

respect to further expanding by internal pressure. This is attributed to a redistribution of the induced load stresses, which, in turn, is equivalent to the addition of residual stresses to the load stresses derived from elastic calculations. Other effects of autofrettage, such as in regard to fatigue strength, have not yet been explored.

Another application of overstraining is the presetting, or "scragging," of springs,[80-86] and the expansion of rotating discs at speeds above those present during service.[87-92] The residual stresses induced increase the fatigue strength of the parts. However, these processes apparently have not been sufficiently investigated in order to establish the factors leading to full control of the residual stresses in this respect.

Overstraining is also always associated with microstresses. One of the manifestations of the microstresses is the Bauschingereffect. This term applies to the differences in the yield strength values for tension and compression and for different directions, which result from any plastic deformation.[2, 93] Recent studies indicate that the Bauschingereffect may also be of significance for the distribution of macrostresses and the effects resulting from these.

Dimensional Stability and Other Physical Properties

The presence of residual stresses frequently causes difficulties in production and in service of parts which require high dimensional accuracy and stability.

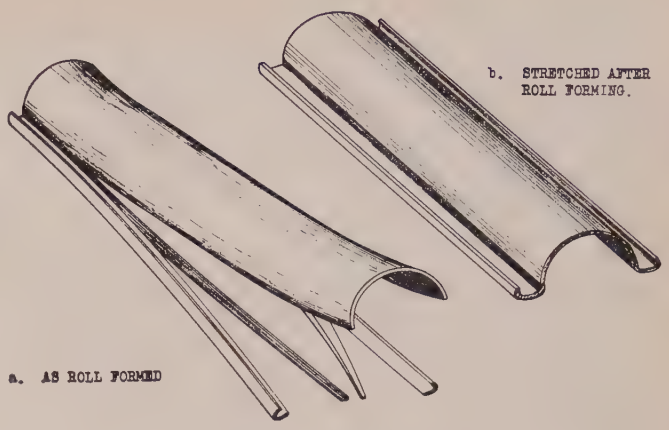

Fig. 20 – Distortion of roll-formed channel on cutting, and its elimination by stretching[94]

Machining and subdivision of metal pieces which contain high residual stresses may result in large distortions, as illustrated in Fig. 20.[94] Small dimensional changes due to changes in the residual-stress pattern have also been observed during storing and heating.[95]

A common measure of minimizing these effects comprises rough machining to almost the final dimensions, allowing the distortions to develop, and then finish-machine the part. However, this will not eliminate any further distortions, which may occur with time, as a consequence of the still retained stresses.

To eliminate such distortions entirely, the residual stresses must be reduced to a minimum. This can be accomplished either by homogeneous stretching (or compressing) or by a stress-relief anneal, as discussed earlier. However, in many instances changes in metal properties result from such control measures, and these cannot always be tolerated.

The effect of stretching which is a common measure of straightening bar, sections, and sheet is illustrated in Fig. 20. However, this causes strain-hardening and thus results in a material with different characteristics. The plastic deformation also introduces microstresses, which may adversely affect the stability of the material in respect to dimensions, elastic properties, electric resistance, and other physical properties.

A stress-relief anneal is the most effective control measure for annealed, normalized, and cold-worked metals. However, it is usually not fully effective for heat-treated alloys without changing their strength characteristics.

Variations in heat-treating practices have been proposed in individual instances, in order to control cracking and distortions on heat-treating and simultaneously to reduce the residual stress.[53, 96]

---

[80] See "Overstrain of Metals and Its Application to Autofrettage Process," by A. E. Macrae. Pub. by H. M. Stationary Office, London, 1930.

[81] See pp. 209-218: "Autofrettage," by A. G. Warren, in "Symposium on Internal Stresses in Metals and Alloys." Pub. by Institute of Metals, London, 1948.

[82] See *Iron & Steel Institute Journal,* Vol. 133, 1936, pp. 427p-442p: "Fatigue Resistance of Spring Steels," by M. L. Becker and C. E. Phillips.

[83] See *Machine Design,* Vol. 17, January, 1945, pp. 107-112: "Utilizing Effects of Cold Setting in Springs," by A. M. Wahl.

[84] See Proceedings of Society for Experimental Stress Analysis, Vol. 4, No. 1, 1946, pp. 64-73: "Measurement of Residual Stresses in Torsion Bar Springs," by H. O. Fuchs and R. L. Mattson.

[85] See *Machinery* (NY), Vol. 52, June, 1946, pp. 152-157: "Utilizing Residual Forming Stresses in Flat Steel Springs," by W. C. Troy.

[86] See pp. 195-207: "Production of Favorable Internal Stresses in Helical Compression Springs by Prestressing," by D. G. Sopwith, in "Symposium on Internal Stresses in Metals and Alloys." Pub. by Institute of Metals, London, 1948.

[87] See *Zeitschrift für Angewandte Mathematik und Mechanik,* Vol. 5, August, 1925, pp. 281-293: "Parts of Rotational Symmetry Rotating in Range of Permanent Deformation," by F. Laszlo.

[88] See *Engineering,* Vol. 168, Oct. 28, 1949, pp. 437-440; Nov. 4, pp. 468-470: "Local Overstraining of Metals," by F. Laszlo.

[89] See *Brown Boveri Review,* Vol. 16, September, 1929, pp. 243-253: "Internal Stresses and Heat Stresses and Their Relation to Steam Turbine Construction," by E. Honnegger.

[90] See SAE Transactions, Vol. 54 (September), 1946, pp. 446-475, 502: "Improving Engine Parts by Direct Measurement of Strain," by R. G. Anderson.

[91] See *Steel,* Vol. 118, June 3, 1946, pp. 104-106, 150: "Prestressing Rotating Discs," by H. Dobkin.

[92] See pp. 139-152: "Some Internal Stresses in Turbine Rotors," by M. C. Caplan, L. B. W. Jolley, and J. Reeman, in "Symposium on Internal Stresses in Metals and Alloys." Pub. by Institute of Metals, London, 1948.

[93] See *Journal of Aeronautical Sciences,* Vol 15, March, 1948, pp. 151-154: "Dependence of Stress-Strain Curves on Cold-Worked Metals upon Testing Direction," by L. J. Klinger and G. Sachs.

[94] See SAE *Quarterly* Transactions, Vol. 3, July, 1949, pp. 480-489: "Design of Aircraft Structures for 'Mass Production,'" by O. A. Wheelon. (Digested in *SAE Journal,* Vol. 57, June, 1949, pp. 62-64.)

[95] See *Zeitschrift für Metallkunde,* Vol. 17, July, 1925, pp. 227-228: "On Removal of Residual Stress by Annealing," by M. Polanyi and G. Sachs.

[96] See pp. 97-128: "Residual Stress States Produced in Metals by Various Processes," by H. B. Wishart, in "Residual Stress Measurements." Pub. by ASM, Cleveland, 1952.

[97] See *Archiv für das Eisenhüttenwesen,* Vol. 8, November, 1934, pp. 219-222: "Superposition of Heat and Transformation Stresses in Quenched Steel Tube," by H. Bühler and E. Scheil.

However, the general picture in this respect is rather obscure.

The residual stresses retained after heat-treating also depend upon the chemical composition. A pronounced effect, in this respect, has been observed in high-nickel steels.[97] It was found that certain combinations of nickel content and section size may result in complete freedom from residual stress.

Acknowledgment

This paper resulted from research work performed under Contract DA-30-115-ORD-376 with Watertown Arsenal. The author is indebted to Watertown Arsenal for granting permission to publish the results of this research and to Dr. R. Beeuwkes, chief scientist, Ordnance Materials Research Office, for many valuable suggestions.

DISCUSSION

Questions on Raising Fatigue Strength

– Ronald F. Brodrick
Lessells & Associates, Inc.

WE should like to see some expansion and clarification of the remarks dealing with the raising of fatigue strength. In particular, this section of the paper posed the following questions:

1. In regard to polished smooth specimens, is it not possible that the apparent small significance of residual stresses is due to their absence, rather than to the lack of roughness or stress concentration? This possibility allows explanation of reduced fatigue properties in cases where the surface is quite smooth, but wherein the polishing procedure has introduced tensile stresses.

2. In regard to the changing effect of residual stress as the number of cycles to failure increases, are we correct in the interpretation that this effect is evidenced as a relocation of the "knee" of the S-N curve? Does the author have an opinion as to the importance of this effect in using the Prot method of accelerated testing?

3. In view of the apparent adverse effects of residual stress in the common practices of grinding and electroplating, as mentioned, is it quite correct to state that the direct damaging effect of tension stresses is rarely observed?

Control of Residual Stress Resulting from Carburizing

– W. S. Coleman, Jr.
GM Research Laboratories Division

I WOULD like to present one or two points of interest involving a project concerned with the investigation and control of the residual stresses resulting from carburizing. The many variables such as material, section size, carburizing temperature, carburizing atmosphere, method of quenching, and tempering – to mention a few – make it a complex picture that we are attempting to draw. The project has two major divisions: (1) carburized gear specimens and (2) carburized laboratory bar specimens. It is hoped that results from the gears will tie in with service and dynamometer data. The bar specimens are also used for investigation because they are cheaper, more easily controlled, and faster to analyze.

Fig. A shows the first phase of the measurement of the residual stresses along the face of a spur-gear tooth. Layout lines are scribed on the tooth surface and the surface curvature in the longitudinal direction is carefully measured. Strain gages are then cemented to the surface within the scribed lines. A rectangular strip is then parted from the tooth, as shown in Fig. B. The sides and back of this strip are carefully surface ground to remove any of the parting wheel stresses that might extend to a significant depth. The strain gages and the surface curvature are then remeasured to obtain parting strains. The combination of these two measurements will give bending and direct stress change data that are used later in constructing the residual stress pattern that existed in the gear tooth before any cutting was done. Fig. C shows how conventional layer removal methods may then be employed to analyze the rectangular strip. The designations primary and secondary cuts are used when layers are removed first from the side opposite to the surface of major interest. This is done to increase sensitivity of the surface measurements.

Fig. D shows the wide range of residual stresses that have been found in carburized gears. Plotted vertically is magnitude of residual stress – tension upwards – compression downwards. Plotted horizontally is depth below the tooth surface. Gear A, it should be pointed out, has a very deep case in comparison to gear B, and the section sizes are considerably different. The investigation of gears of this type is continuing, but the results occasionally are mys-

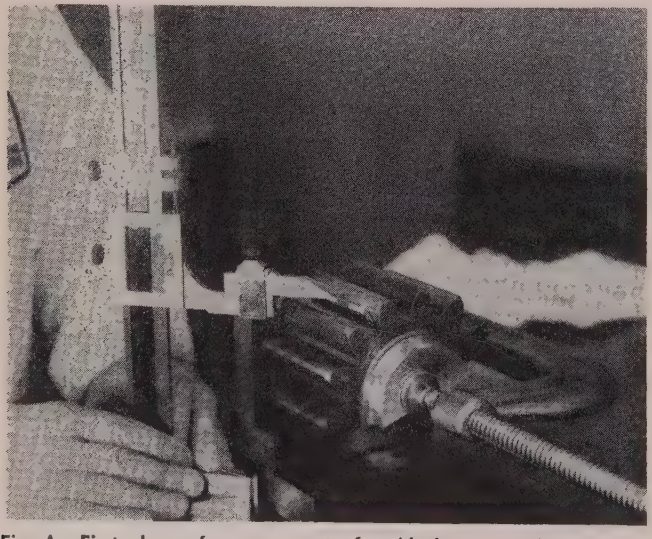

Fig. A – First phase of measurement of residual stresses along face of spur-gear tooth

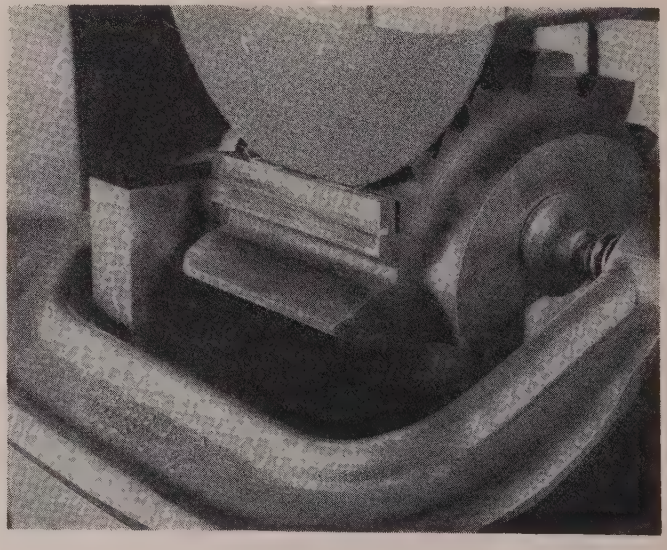

Fig. B – Rectangular strip being parted from tooth

terious, as indicated in Fig. E. Here, two identically processed gears from different heats of steel were analyzed and the results indicated a considerable difference. Fig. F shows a residual stress scatter band for a lot of six laboratory carburized bars which indicates the method of measurement to be reproducible to ±10,000 psi or less.

Residual stresses can be controlled to work for us rather than against us, and if this is done, considerable savings in cost and weight are not far out of reach of the designer.

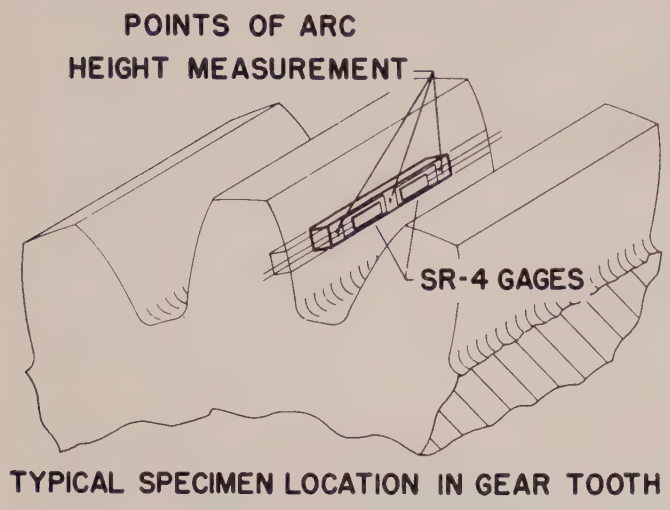

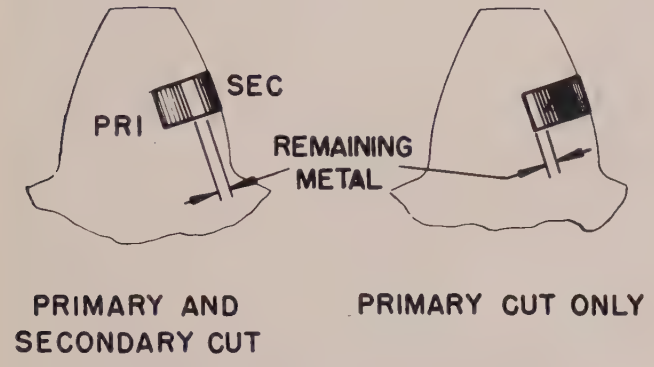

Fig. C – Designation of dissection cuts

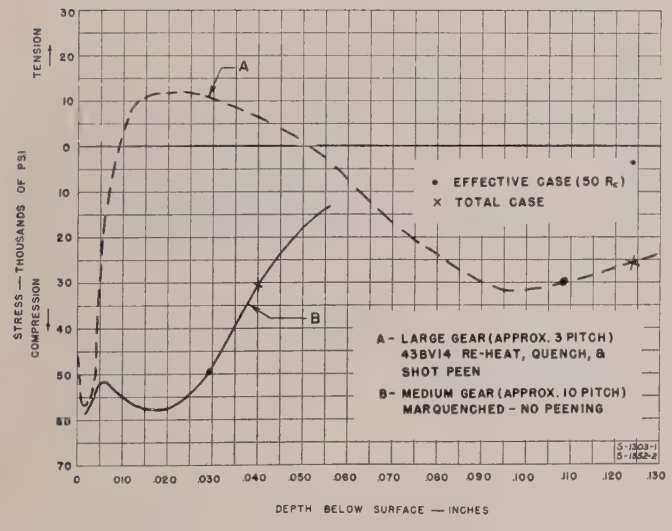

Fig. D – Residual-stress distribution

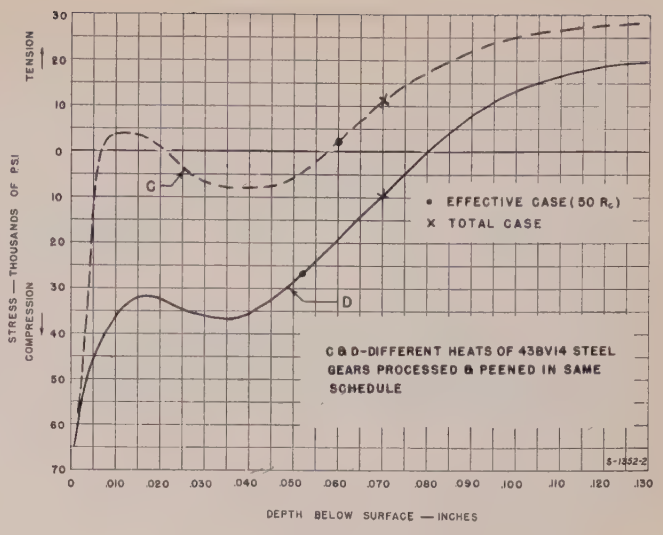

Fig. E – Residual-stress distribution

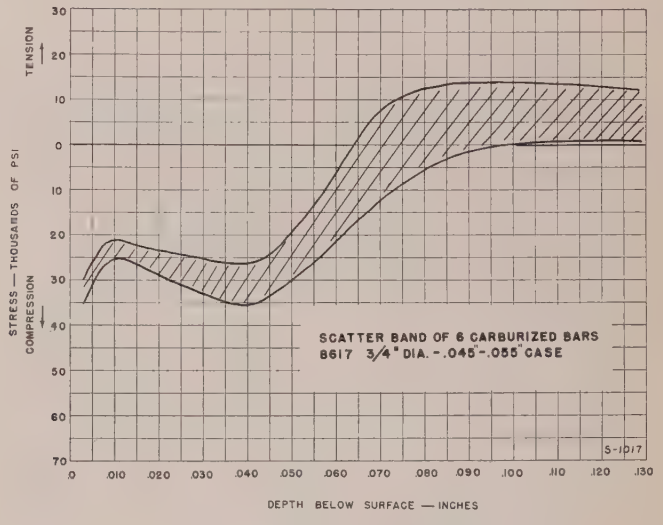

Fig. F – Residual-stress distribution

Author's Closure To Discussion

REGARDING Mr. Brodrick's first question, I would like to clarify my statement that peening or surface rolling of smooth specimens (and presumably also of parts with polished or finely ground surfaces) has been repeatedly found of little effect on the endurance limit in spite of the high compressive stresses developed.

His second question is not quite clear to me. Notching, for example, reduces the fatigue strength to an increasing extent as the number of cycles increases, and this loss may be prevented by peening. I do not know how it would affect the results of the Prot method, but I expect the same effects as on the regular *S-N* curve.

His third question does not appear quite correctly stated, as grinding, in general, has probably little effect on the fatigue strength of smooth specimens. On the other hand, electroplated parts possess a surface that is different from the body, and which may not yield under repeated cycles and thus relieve the stress. Its fatigue strength will then be dependent on the state of residual stress and a crack in the plate will progress into the body.

Mr. Coleman's remarks are very interesting and I hope that the work by GM will be fully successful.

I appreciate the interest in our work expressed by both discussers.

Fuel

HOW commercially available fuels behave in typical aircraft gas turbine combustors was the subject of the investigation discussed in this paper. Data were obtained on full-scale combustion chambers using a wide variety of fuels, with emphasis placed on combustion efficiency and deposit formation.

At low altitudes, combustion efficiencies are high and unaffected by heat output or fuel. An increase in altitude results in an efficiency decrease which is affected by type of fuel under certain conditions.

Combustor design greatly affects location and amount of deposits, but combustor deposits generally increase with decreasing fuel volatility and increasing fuel unsaturation.

IT has been said that the gas turbine engine has an omnivorous appetite for fuel. Although this statement has been repeated enough to have gained some sort of general acceptance, there actually has been little information published to support it. While heat-engine *theory* says that the gas turbine can be run on a wide variety of fuels – say from natural gas to powdered coal – aircraft gas turbines in practice have been operated on only a very limited number of petroleum fuels, with the military services being by far the largest user of these fuels. By way of introduction to the experimental work of this paper, it will be helpful to review briefly the specification turbine fuels which have been used to date.

Early development work was carried out using a kerosene-type fuel (JP-1) which was generally satisfactory from a performance standpoint. It was soon realized, however, that this fuel could not be produced in sufficient quantity to satisfy wartime demand.[1] Accordingly, JP-3 wide-boiling-range-type fuel was developed. Subsequent service experience with JP-3 brought out a serious performance defect – that of high boiling and slugging losses during rapid climb. Another fuel type (JP-4) was, therefore, established. JP-4 maintained most of the wide boiling range of JP-3 except that the percentage of light hydrocarbons was reduced to decrease the fuel vapor pressure. Paralleling this development, the U. S. Navy required that its jet engines run on the standard aircraft carrier fuel, aviation gasoline 115/145. Since this fuel has a vapor pressure comparable to JP-3, a blend stock (JP-5) was created. This stock is used both to reduce the vapor pressure of the gasoline and to conserve gasoline stocks aboard carriers.

It can be seen, therefore, that the primary reasons for the military gas turbine fuels have been logistic ones in which availability is the paramount factor. Now, with increasing application of gas-turbine-powered aircraft to civil aviation, fuel selection gathers new interest, the military basis of selection not being adequate for commercial use.

The Texas Co. has, for several years, been conducting an extensive fuel survey program at its Beacon Research Laboratories. The general objective of this program has been to develop information on the performance of commercially available fuels in typical aircraft gas turbine combustion chambers operating over a wide range of simulated service conditions. It was believed that this work, done independently of any military contracts, might provide information that would normally not be obtained under military development programs.

A complete assessment of the gas turbine fuel picture cannot be covered in one paper of reasonable length. This paper will concentrate on the relative effects of fuels and combustors on combustion efficiency and deposit formation.

Selection of Test Fuels

Eight of the fuels selected for this program were commercially available fuels, covering a range of properties well beyond present turbine fuel limits. These fuels were produced using standard refining techniques and are a good cross-section of a wide variety of existing fuels. The test stocks included:

Aviation gasoline 80
Jet engine fuel MIL-F-5624A (JP-3)
Jet engine fuel MIL-F-5624A (JP-4)
Jet engine fuel MIL-F-5616 (JP-1)
No. 1 fuel oil
Diesel fuel
No. 2 fuel oil
No. 4 fuel oil

[1] Availability of JP-1 fuel is limited primarily by the —76 F freezing-point requirement.

Properties and Jet-Engine Combustor Performance

C. M. Kuhbach, W. F. Ritcheske, and K. H. Strauss, Texas Co.

This paper was presented at the SAE National Aeronautic Meeting, Los Angeles, Oct. 7, 1954.

These fuels were distillate fuels with the exception of No. 4 fuel oil, which is a partly residual material, normally used for industrial heating. Some typical inspection tests are shown in Table 1. ASTM distillation curves are plotted in Fig. 1. These curves indicate the wide volatility range covered in this program. Aviation gasoline (unleaded) is the lightest, most volatile fuel with a distillation end point of slightly over 300F. JP-3 and JP-4 initially boil in the same range as the gasoline but soon pass into the middle distillate range with end points over 500F. One of the major differences between these two turbine fuels is the Reid vapor pressure which was about 5 psi for JP-3 and 2.5 psi for JP-4. JP-1 is a kerosene-type fuel, having a much higher initial boiling point but approximately the same final boiling point as JP-3 and JP-4. No. 1 fuel oil is a somewhat heavier material used in vaporizing home oil burners. The diesel fuel is a type used in railroad and heavy automotive applications. No. 2 fuel oil is a rather heavy distillate material normally burned in atomizing-type residential oil burners. As stated before, No. 4 fuel oil is a cutback residual stock generally used for industrial heating.

In addition to the fuels which have just been described, a series of six special JP-3 and JP-4 turbine fuel blends were evaluated for deposit-forming tendencies. These fuels will be described in a later section of this paper.

Test Equipment and Operating Conditions

Performance data were obtained on full-scale combustion chambers rather than with any small-scale equipment because of the lack of knowledge concerning the effects of various scale factors. Generally speaking, it has been very difficult to translate small-scale burner test data into full-scale results. The test work was carried out in single combustion chambers to keep test-fuel requirements and test equipment to a reasonable size. The "cans" came from a variety of gas turbine engines to check the effects of design differences in the combustion system of these engines. Thus the test program included combustors from axial and centrifugal compressor engines and from turbojet and turboprop engines. Both atomizing

The Authors

C. M. KUHBACH is project leader of Gas Turbine Combustion Studies at the Beacon Laboratories of the Texas Co. He received a B.S. in M.E. from Columbia in 1940 and an M.E. from the same institution in 1941. He has been with the Texas Co. since that time. Mr. Kuhbach is also a member of the CRC Turbine Combustion Group.

W. F. RITCHESKE is assistant supervisor of the Engineering Research Department, Beacon Laboratories of the Texas Co. He graduated from the University of Michigan with a B.S. in M.E. in 1939. He joined the Texas Co. shortly after graduation, and since then has been engaged in a wide variety of fuel and lubricant studies.

K. H. STRAUSS is a mechanical engineer with the Beacon Laboratories of the Texas Co. Since his graduation from the University of Connecticut in 1949 with a B.S. in M.E., he has been doing research on gas turbine fuels and lubricants.

Table 1 – Inspection Tests of Fuels

	Aviation Gas 80	JP-3	JP-4	JP-1	Diesel Fuel	No. 1 Fuel Oil	No. 2 Fuel Oil	No. 4 Fuel Oil	Blend No. 1	Blend No. 2	Blend No. 3	Blend No. 4	Blend No. 5	Blend No. 6
API Gravity, deg	68.0	57.3	54.4	40.7	37.2	41.0	31.6	13.2	56.5	52.7	50.5	47.3	46.9	45.3
ASTM Distillation Temperature, F														
Ibp	113	117	139	316	418	360	392	370	129	139	133	142	125	104
10% evaporated	160	173	190	339	458	408	454	486	216	225	225	229	194	175
20	179	198	212	348	...	...	481	522	265	255	260	263	239	263
50	212	245	293	380	518	459	530	618	393	354	361	382	355	353
90	244	435	421	466	580	538	619	722	483	479	475	467	484	481
Ep	316	480	478	512	617	582	702	...	543	541	539	535	537	525
Rvp, psi	5.3	5.2	2.4	0	0	0	0	0	2.5	2.2	2.1	2.2	5.0	6.2
Aromatics, %	4.5	13.5	10	18	19	10	28.5	80	3	19	27	26	16	22
Olefins, %	0	0	...	1.0	2.5	3.0	6.0	20.2	0.9	1.7	1.7	4.8	2.0	10.1
Sulfur, %	0.019	0.023	0.028	0.053	0.250	0.160	0.240	1.310	0.003	0.021	0.018	0.013	0.070	0.410
Carbon/Hydrogen Ratio	5.56	6.12	5.90	6.35	6.41	6.42	6.62	9.00	5.50	5.92	6.09	6.42	6.39	6.49
Net Heating Value, Btu per lb	18,970	18,650	18,770	18,610	18,420	18,680	18,200	17,270	19,050	18,890	18,770	18,570	18,680	18,540
Smoke Point, mm	45	30	30	19	20	23	12	Unsuitable	42	26	22	18	19	14
Smoke Volatility Index	87	66	66	45	20	26	13	Unsuitable	65	52	51	42	44	41
Freezing Point, F	Below −76	Below −76	Below −76	Below −76	0[a]	−35[a]	+5[a]	−10[a]	Below −76	Below −76	Below −76	Below −76	Below −76	Below −76
Volumetric Average bp, F	208	275	299	391	519	466	533	611	371	353	363	365	347	341
Volumetric % Boiling under 400 F	100	86	86	62	0	7	2	...	54	63	69	57	61	63

[a] Pour point, F.

and vaporizing fuel systems were examined.

To operate a gas turbine combustor independently, air is supplied to the combustor at pressures and temperatures comparable to engine compressor discharge conditions. At the Beacon Laboratories, the test facilities are arranged so that pressure, temperature, and mass flow of the test air can be varied independently. Instrumentation is included for measuring air inlet pressure, mass flow and temperature, fuel flow and temperature, exhaust gas pressure and temperature. Special precautions are taken to obtain accurate measurements of exhaust gas temperature. A minimum of 18 radiation-shielded thermocouples are used for this purpose.

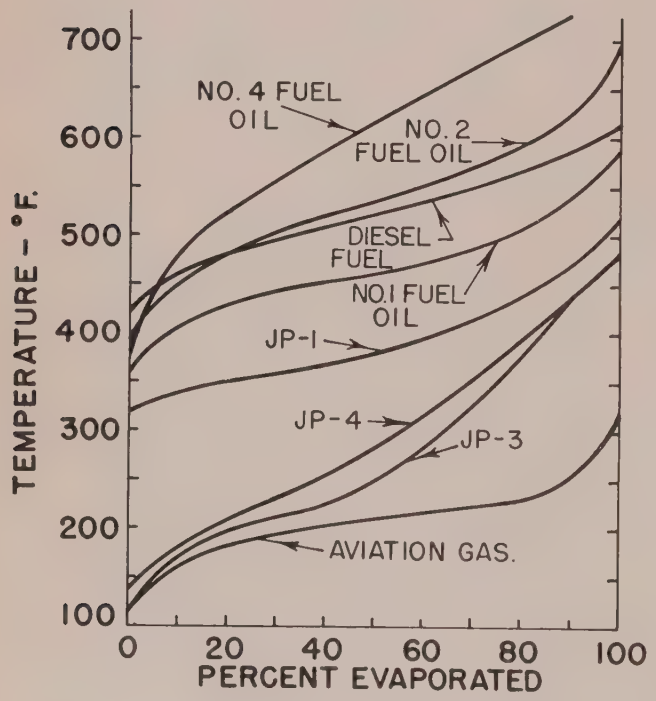

Fig. 1 – ASTM distillation curves of test fuels

In operating an engine over a range of output, speed, and altitude, different equilibrium combinations of compressor discharge pressure, temperature, and mass flow and combustor exhaust temperature exist at each operating point. To simulate operation at constant altitude with varying engine speed or vice versa involves changing all combustor variables for each operating point. To simplify the test control problem, air was supplied to the combustor at constant mass flow, temperature, and pressure while the combustor fuel flow was varied to produce the desired range of exhaust temperatures. Operation along such lines of constant air conditions and decreasing fuel flows simulates engine operation along lines of decreasing altitude and engine speed. A typical set of operating curves for one of the combustors is shown in Fig. 2. It can be seen that fuel evaluations at several fixed combustor inlet pressure conditions cover the spectrum of engine operation reasonably well. The same conditions of air pressure and temperature were used for all the combustors tested. The mass flows were adjusted for each combustor to conform to engine operating characteristics. Limited air capacity prevented operation of combustors at simulated low altitudes and rated engine speeds.

For the deposit runs which are discussed in the last part of this paper, combustor operating conditions were selected to simulate cruise conditions at the lowest altitude (maximum pressure) permitted by the test facilities. Depending on the pressure and mass-flow requirement of the particular combustor under test, the altitude level which was simulated during the deposit test program varied from 20,000 to 30,000 ft. Although there is some evidence to show that deposits increase with combustor operating pressure, these conditions were considered to be more nearly representative of the conditions prevailing during a typical jet flight. The duration of the deposit runs, except as noted otherwise, was 3 hr. This test duration was selected after studies showed that longer running

time, while producing more deposits, resulted in poorer test reproducibility.

Combustor Performance Criteria

In examining the performance of these combustors, the following performance criteria were considered:

1. Combustion efficiency.
2. Combustion deposits.
3. Combustion stability.
4. Ignition characteristics.
5. Pressure drop.
6. Outlet temperature profile.

This paper will be concerned almost entirely with a discussion of the effects of fuels on combustion efficiency and deposits. The test results showed that, except under extreme operating conditions or when operating on a heavy fuel such as No. 4 fuel oil, all of the combustors tested were stable. Pressure drop and outlet temperature profile varied somewhat from one combustor to another but examination of such data did not disclose any consistent fuel effects.

The ignition characteristics were noticeably different from one combustor to another. As might be expected, fuel volatility had an effect on the limiting condition under which a particular combustor could be started. It was found, however, that ignition characteristics could be improved tremendously by resorting to the use of a high-energy system with surface firing plugs. In view of this experience, it is felt that ignition of these combustors is primarily a design problem.

Combustion Efficiency Results

Combustion efficiency is defined as the ratio of the heat rate liberated during combustion to the energy rate supplied in the fuel. Quantitatively this can be expressed as:

$$\eta = \frac{m_{(a+f)}H_e - m_aH_a - m_fH_f}{m_f\,(\mathrm{LHV})}$$

where:

η = Combustion efficiency
m = Mass flow rate, lb per sec
H = Enthalpy, Btu per lb
LHV = Lower heating value of fuel, Btu per lb

Subscripts a, f, and e refer to air, fuel, and exhaust, respectively.

In the above equation, H_e is determined by obtaining an average exhaust temperature and then obtaining an enthalpy as a function of fuel-air ratio from tables.[2] H_a was obtained from the same source.

Since the combustion reaction is not quenched at the combustor exit but is permitted to continue until it reaches the exhaust thermocouples, under certain conditions the exhaust temperatures measured in the experimental setup may be slightly higher than those experienced in an engine. This in turn will cause slightly higher combustion efficiencies for the single combustor results.

A low efficiency indicates that considerably more fuel is being supplied than is being utilized in the engine. Combustion efficiency, therefore, has a very direct bearing on aircraft take-off weight, range, and other important performance factors. Every incentive exists to raise combustion efficiency to maximum values.

The effect of various factors on combustion efficiency at lower altitudes is shown in Fig. 3. In this figure, combustion efficiency is plotted as a function of combustor temperature rise, which is a direct measure of combustor heat output. At this condition a temperature rise of 1300F corresponds to rated engine speed at an altitude of 25,000 ft. Decreasing temperature rise corresponds to simultaneous decreases in engine speed and altitude. The temperature rise region below 600F is well outside of engine operating zones; under such conditions the heat output is insufficient to

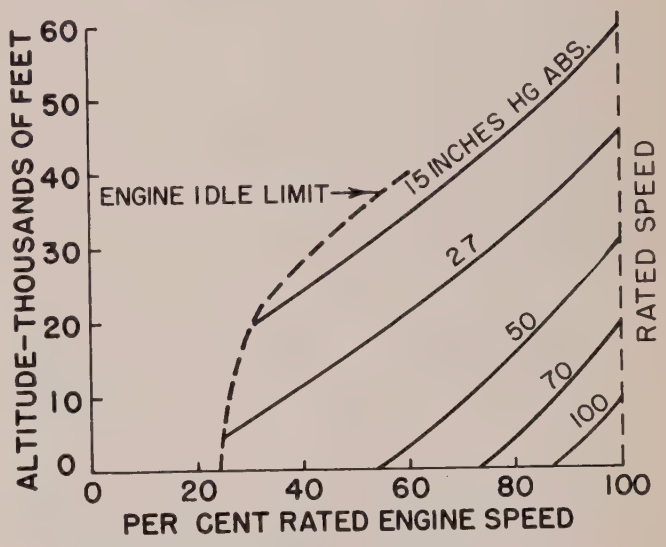

Fig. 2 – Typical combustor operating characteristics

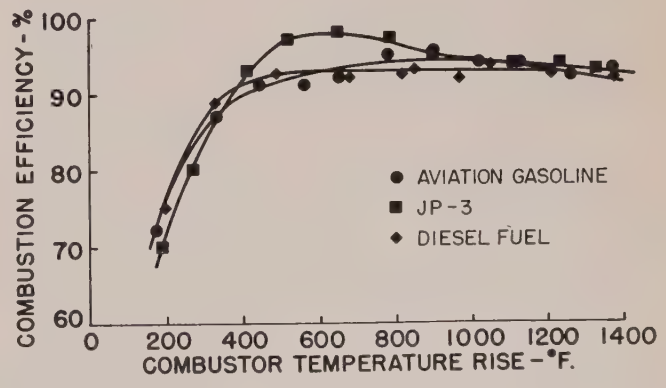

Fig. 3 – Typical low-altitude efficiency for combustor C at inlet pressure of 60 in. of Hg abs

[2] NACA Technical Note 2071.

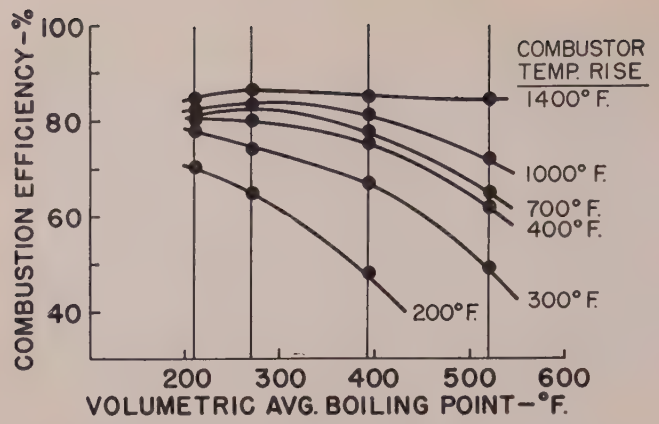

Fig. 4 – Variation of efficiency with volatility for combustor B at inlet pressure of 15 in. of Hg abs

drive the engine compressor. Several facts become clear from this figure. In the normal output range combustor operation is efficient regardless of fuels. Practically no efficiency differences are noticeable between widely different fuels such as aviation gasoline and diesel fuel. The performance in the low-temperature-rise region is of no significance except to indicate the ability of this combustor to operate without blowout at low output levels. With minor variations, these results are typical of those obtained on other combustors under similar conditions.

Considerably different results are encountered after a drastic increase in altitude. Fig. 4 has been arranged to show fuel effects directly. Combustion efficiency is plotted against fuel volumetric average boiling point (volumetric average bp =

$$\frac{10\%\text{ point} + 2\,(50\%\text{ point}) + 90\%\text{ point}}{4}$$

in deg Fahrenheit). Lines of constant temperature rise are indicated. Also shown are the volumetric average boiling points of four fuels, ranging from aviation gasoline to diesel fuel. At this condition the rated temperature rise of 1400F represents an altitude of about 60,000 ft decreasing to an idling limit of about 900F at about 20,000 ft. A general efficiency decrease has taken place compared to lower-altitude performance. Only minor performance differences between fuels exist at rated exhaust temperature. With decreasing temperature rise a slight performance decrease occurs with the lighter fuels. With heavier fuels, however, this decrease is considerably greater, so that the use of heavier fuels significantly penalizes part-throttle operation. In atomizing-type combustors this effect is due largely to lower nozzle pressures which are caused by the reduced fuel requirements of altitude operation, nozzle pressures becoming insufficient to atomize heavy fuels, especially during part-throttle operation.

The full-throttle performance of five fuels in an atomizing combustor over a high-altitude range is summarized in Fig. 5. The general efficiency decrease with altitude is apparent. Fuel effects are

Table 2 – Additional Fuels Used in Deposit Test Program

Fuel Designation	Description
Blend No. 1	A low-deposit JP-4 base fuel prepared from a blend of isoparaffins
Blend No. 2	Fuel blend No. 1 with 15% benzene nucleus aromatics boiling between 230-306 F substituted for isoparaffins of the same boiling range
Blend No. 3	Fuel blend No. 2 with 10% benzene nucleus aromatics substituted for isoparaffins of the same boiling range. The aromatics had an ASTM distillation of 350-570 F with a 50% point of about 370 F
Blend No. 4	Blend No. 2 with 10% naphthalene nucleus aromatics boiling between 465-480 F substituted for isoparaffins of the same boiling range
Blend No. 5	A JP-3 type fuel
Blend No. 6	A referee JP-3 type fuel

not consistent except that JP-3 resulted in generally the best performance over the altitude range while No. 2 fuel oil was poorest. Fuel volatility, however, is not the complete explanation for fuel behavior as is shown by the superior performance of diesel fuel over JP-1. All fuels fall into a relatively narrow performance band.

In Fig. 6 the performance of one fuel, JP-1, in five different combustors has been plotted over the same altitude range. It is obvious that a much greater efficiency spread exists between the five engines on one fuel than in one engine on five widely differing fuels. This clearly illustrates the importance of the mechanical design variable in high-altitude operation.

To determine whether heating the fuel oils would improve their performance by decreasing their viscosity, fuel oil No. 1 and No. 2 were run in one combustor at fuel nozzle inlet temperatures of 70F and 200F. Under these conditions the viscosity of the heated fuel oil No. 2 was lower than that of the unheated fuel oil No. 1. The results are summarized in Fig. 7. Per cent improvement, which is the difference between the heated and unheated fuel efficiencies divided by the unheated efficiency, has been plotted against combustor inlet pressure. In all cases, improvement was greater for the heavier fuel oil No. 2 than for the lighter fuel oil No. 1. At the operating pressures of 50 and 30 in. of Hg these gains brought the heated fuel oil No. 2 to the same performance level as the unheated fuel

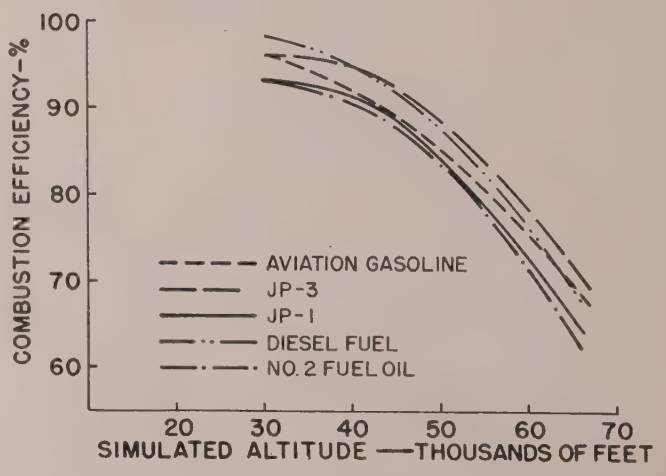

Fig. 5 – Altitude performance of several fuels in combustor D at rated engine speed

Table 3 – Relative Deposit Ratings[a]

Fuel	Combustor D	Combustor E
JP-4	0.2	0.4
JP-1	1.0	1.0
No. 1 fuel oil	2.1	...
Diesel fuel	1.7	4.4
No. 2 fuel oil	2.6	10.2
Blend No. 1	0.5	0.5
Blend No. 2	0.2	1.5
Blend No. 3	0.2	2.3
Blend No. 4	1.7	6.3
Blend No. 5	1.0	3.3
Blend No. 6	...	5.1

[a] JP-1 equals 1.0

oil No. 1. It might be noted that at the lowest pressure the heated fuel oil No. 2 showed higher absolute efficiencies than the unheated fuel oil No. 1.

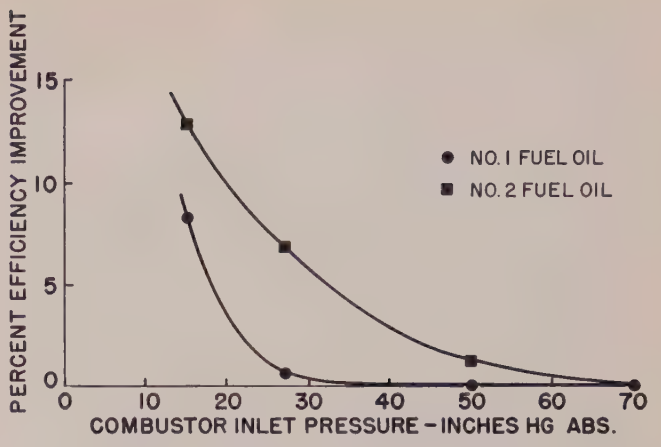

Fig. 7 – Effect of fuel preheating in combustor D at rated engine speed

Results of Deposit Studies

During the early years of aircraft gas turbine development when engines were operated almost exclusively on straight-run fuels, carbon deposition was considered a problem of relatively minor importance. Within recent years, however, this picture has changed considerably. Accompanying the widespread use of JP-3 and JP-4 type fuels and the introduction of many different models of engines into operational service, a number of serious deposit difficulties have been experienced.

The same combustors and many of the same fuels employed in the combustion efficiency tests were used in this portion of the program. In addition to the fuels described previously, the fuels listed in Table 2 were included in the deposit test program.

Some typical inspection tests for these fuels are shown in Table 1. The test apparatus and test conditions were described in an earlier section of this paper.

Before discussing the actual test results, it should be pointed out that there is no single number which can be used to describe completely the severity of deposits. In comparing deposits formed by several fuels in the same engine, deposit weight is probably a fairly good indication of the "dirtiness" of the fuels. However, in comparing the deposits formed in two different engines, the engine having the lighter deposit weight may be in more serious trouble than the one having a much heavier weight of deposit.

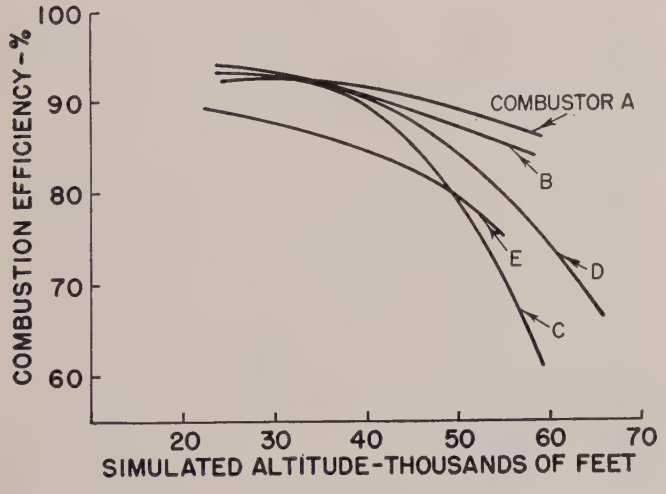

Fig. 6 – Variation of efficiency with altitude with JP-1 fuel at rated engine speed

This point can be illustrated by Figs. 8 and 9, which are photographs of combustor parts from two different engines following a 20-hr run on the same JP-3 fuel. Fig. 8 is a view looking into the liner of combustor A. There is a heavy buildup of deposits in the midsection of the liner. The spark plug, fuel nozzle, and other portions of this combustor were almost free from deposits. The total deposit weight was about 100 g. Checks on performance during the course of the run indicated no loss in combustion efficiency as a result of these large deposit formations. There were indications, however, that the deposits were disturbing the cooling air flow over the liner and that with continued running time the liner would have overheated and failed.

Under similar operating conditions, the liner of combustor B was almost free from deposits, but the fuel nozzle and spark plug had the appearance shown in Fig. 9. Although the deposit weight in combustor A was many times greater than the weight of deposits formed in combustor B, the combustor B deposits had a decidedly detrimental effect on performance. The combustor could not be restarted in the condition shown.

Fig. 10 shows the type of deposit formations observed in a vaporizing combustor. This is a photograph of a vaporizing tube assembly following a 6-hr run on fuel oil No. 2. This quantity of deposit resulted in no loss of performance, nor was there any indication of damage to combustor parts.

From these illustrations, it can be seen that deposits vary considerably in their character and location. Combustor A ran with a relatively clean fuel nozzle and plug but a heavy localized liner de-

Fig. 8 – Combustor A liner deposits with JP-3 fuel after 20-hr cruise operation at 30,000 ft altitude

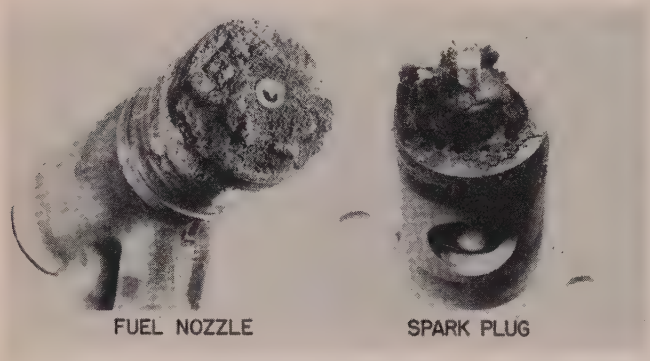

Fig. 9 – Combustor B deposits with JP-3 fuel after 20-hr cruise operation at 30,000 ft altitude

Fig. 10 – Vaporizing-tube deposits with No. 2 fuel oil after 6-hr cruise operation at 20,000 ft altitude

Table 4 – Deposit Weights of Special Blends; Combustor E; Test Duration, 3 Hr

Fuel Blend No.	Aromatics, % Total	Aromatics, % Over 400 F	Deposit Weight, g
1	3	2	0.36
2	19	2	1.11
3	27	4	1.71
4	26	9	4.65
5	16	11	2.40
6	22	19	3.86

posit. Combustor B ran with a relatively clean liner but a fouled plug and dirty fuel nozzle. It is reasonable to assume, therefore, that a combustor can be designed to operate under the same conditions imposed on combustors A and B but without any localized deposit buildup. Considerable progress has been and is being made in this direction by the engine builders.

It has been observed that deposits start to build up in direct proportion to running time. With continued operation of the combustor, the buildup rate begins to fall off, and finally a point is reached where the deposit level remains more or less constant. The relative rate at which deposits are formed at the early stages of a run is considered to be a better indication of fuel cleanliness than is the equilibrium deposit level. After making some preliminary deposit runs for various lengths of time, 3 hr was selected as the duration of a deposit test. This duration was well below the time required for equilibrium deposits, yet it produced a measurable quantity of deposits on the cleanest fuel.

Some typical deposit test results are tabulated in Table 3 for 11 fuels on two combustors, one an atomizing combustor and the other a vaporizing combustor. In order that the results from these combustors can be compared with each other, the data are presented on a relative basis.

Inspection of these deposit test results shows that combustor D is much less sensitive to fuel composition than is combustor E. For example, combustor D rated fuel oil No. 2 only 2.6 times as dirty as JP-1, whereas this factor was 10.2 in combustor E. Neither did these two combustors rate the fuels in the same order. From these results

it can be seen that it will be difficult to develop a single small-scale burning test or rating device suitable for wide ranges of fuels and engines.

Actual deposit weights obtained in combustor E on the six special blend fuels which were described earlier are given in Table 4. This table also contains the experimentally determined total aromatic content of the fuel fraction boiling above 400F. The latter has been suggested as a much better indication of burning quality of a fuel than the total aromatic content. Although there is a rough correlation between the aromatic content of the fuel and deposits, it can be seen that neither the total aromatic content nor the percentage of aromatics boiling above 400F gives an accurate prediction of deposit formation in this combustor.

A review of all the deposit results on combustor E (see Table 3) shows that blend No. 1 was about equal to the commercial JP-4 fuel in deposits. The addition of various aromatics to blend No. 1 kept increasing deposits until blend No. 4 (containing just slightly more aromatics than are permitted by the JP-4 specifications) resulted in more deposits than were obtained in diesel fuel. None of the special blend fuels, however, showed deposits as heavy as fuel oil No. 2.

Within the past few years there has been considerable interest in the development of an inspection test or burning test from which the deposit-forming characteristics of a fuel could be estimated. Within the past year, one such test or factor known as the smoke volatility index (SVI) has been adopted as a requirement of the jet fuel specification MIL-F-5624B. This factor is made up of two terms: (1) the IP smoke point and (2) the volume per cent of the fuel boiling under 400F.[3]

Prior to the adoption of the SVI, the IP smoke point was considered to be a fairly good indication of deposits. Fig. 11 shows a plot of IP smoke point versus combustor E deposit weights. While there is a general correlation, it is apparent that for only a relatively small variation in smoke point in the range from 14 to 24 mm considerable differences in deposit formation occur. Obviously, this smoke point deposit correlation leaves something to be desired.

If the SVI is employed, a picture such as is shown in Fig. 12 is obtained. The commercial fuels line up along one curve, and the special blends arrange themselves on a second curve. Because of the volatility term in the SVI factor, the SVI discriminates heavily between light and heavy fuels which happen to produce the same deposit.

Fig. 13 shows a plot of deposit weight versus SVI for the same fuels run in combustor D. These results differ considerably from those obtained in combustor E. Although the relationship between SVI and deposits is not well defined, there appears to be no differentiation between the two different series of fuels. Discrimination between fuels in the range of chief interest (SVI from 45 to 55) is not entirely satisfactory.

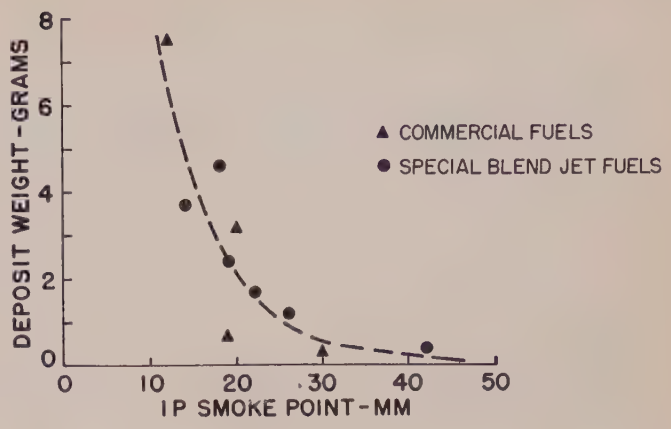

Fig. 11 – Smoke point versus combustor deposits in combustor E with run duration of 3 hr

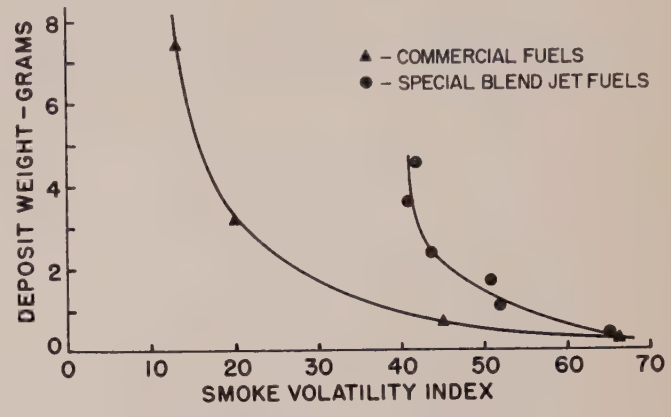

Fig. 12 – Smoke volatility index versus combustor deposits in combustor E with run duration of 3 hr

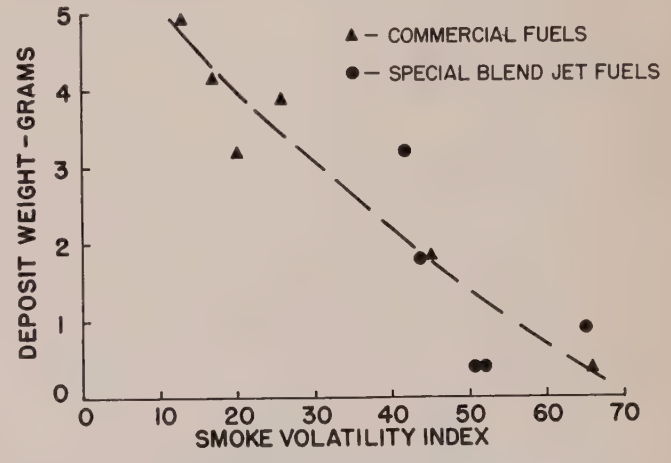

Fig. 13 – Smoke volatility index versus combustor deposits in combustor D with run duration of 3 hr

Summary

The experimental work described herein has shown that at low altitudes (about 25,000 ft and

[3] SVI = IP smoke point + 0.42 volumetric per cent boiling under 400 F.

lower) combustion efficiencies are high and unaffected by output level or fuels; practically no efficiency differences are noted between widely differing fuels such as aviation gasoline and diesel fuel. As altitude is increased a characteristic decrease in combustion efficiency is noted; at rated speed this decrease is only slightly affected by fuel differences, whereas at reduced output, the heavier fuels cause a much greater decrease. There seem to be greater differences among combustors of different designs operating on the same fuel than among different fuels in the same combustor. Combustion performance with heavier fuels can be improved by heating the fuel ahead of the fuel nozzles.

The deposit portion of the program has shown that the location and magnitude of deposits vary considerably from one combustor design to the next. In general, combustor deposits increase with decreasing fuel volatility (heavier fuels) and increasing degrees of fuel unsaturation (more aromatics and olefins). However, combustors have been designed which, under present-day operating conditions, are tolerant of wide ranges of fuel volatility and composition.

It has been shown in this paper that fuels do not behave in the same manner in different combustors. Therefore, methods of deposit predictions based on fuel properties or simple burning tests all have limitations which must be recognized.

As to the future, the prospects are encouraging in that fuel selection need not be limited by combustion requirements. In the final analysis a situation quite parallel to that in the automotive field will prevail. Aircraft turbine fuels can be evolved only through continuous cooperation among the engine builder, the airframe manufacturer, and the fuel supplier.

Acknowledgment

The authors wish to thank all their coworkers who participated in the work described in the paper. They also wish to thank those whose suggestions were helpful in the preparation of this paper.

DISCUSSION

Describes Derivation of Smoke Volatility Index

– D. W. Bedell
Esso Standard Oil Co.

IN 1944 we undertook a similar program to investigate full-scale burner efficiencies and deposit weights as they were affected by design, operating conditions, and fuel characteristics. It is encouraging to note that although burner design has progressed greatly since 1944, the data trends noted in our work are the same as those found by the authors.

The influence of burner design on efficiency under various operating conditions should be emphasized, and the comparatively negligible effect of fuel composition on efficiency noted.

In this paper it is pointed out that such things as aromatic content in the 400F plus fraction, the smoke point of the fuel, and smoke volatility index do something less than a desirable job of correlating with deposit formation in full-scale burners. The derivation of the smoke volatility index should probably be outlined at this point so that its limitations will be more apparent. In our cooperative work with Pratt & Whitney it was learned that per cent aromatics in the 400F plus cut gave a correlation with carbon deposit formation in J-42 burners. An increase from 3 to 22% in this aromatic content brought about an increase from 19 to 84 g of deposit. Since composition specifications are, in general, unpalatable to the refiner and there was a possibility that some high-boiling aromatics might not be contributors to carbon formation, it was decided that a burning test such as the smoke-point test used for burning oils might show the same correlation. Test work was again conducted, and it was learned that the best correlation could be obtained by using the Esso smoke point factor which considers the smoke point of the total fuel, the smoke point of the 400F plus cut, and the per cent of the 400F plus cut. Objections were raised to the necessity of running smoke-point determinations on the 400F plus cut, and on a limited amount of data on JP-3 and JP-4 fuels a mathematical solution for Esso smoke point factor evolved as the smoke volatility index. It is recognized that SVI has limitations and will probably have to be changed as fuel characteristics are changed. No one should attempt to use SVI for rating fuels other than JP-3 or JP-4.

However, the correlation between SVI and service is not as bad as this paper would lead one to believe. Three military surveys – one Air Force and two Navy – and two private surveys conducted by Esso and Pratt & Whitney have shown that an SVI over 54 insures against borderline and unsatisfactory fuels. Four different manufacturers' engines were involved in these surveys as well as about 150 fuel analyses.

Reserve Tractive Ability and Vehicle Drag Test Codes and Comparative Demonstration of Test Equipment

Report of CIMTC Subcommittee XII – Tractor Test Codes

This paper was presented at the SAE Earthmoving Industry Conference, Peoria, Ill., April 13, 1954

The Need for a Test Code and Its Objectives

by

A. J. Rutherford
Engineer Research & Development Laboratories

and

H. L. Rittenhouse
Euclid Division, GMC

IT has been a matter of longstanding recognition that a realistic, comprehensive and unbiased means for judging the true performance capabilities of construction and industrial machinery is needed. The manufacturer is interested in such means because it could provide him with a standard, clearcut basis for competitive claims and the ability to establish and advertise performance values for his product that are valid and mean something to the prospective customer. He also feels the need of something concrete to serve as the ethical guide between manufacturers of similar highly competitive products. The commercial user or contractor is interested because he feels the need for some method of better judging, comparatively, the ability of all the different equipments available for his selection to meet the requirements of his particular operation. He is keenly interested in obtaining the maximum in performance for his monetary investment. The military or government is fundamentally interested in obtaining the highest quality equipment and at the present time has no suitable yardstick for measuring quality. Means for judging the performance capability of equipment will provide the basic engineering information for the government to establish realistic levels of performance. These levels, once established, may be incorporated in procurement specifications, and the means for their establishment then become the standard procedures used by the procurement inspectors to determine compliance of furnished end items with the specification under which they were procured. Recognizing this general area of requirement led the CIMTC of SAE to establish a subcommittee for the purpose of drawing up performance test codes on crawler and wheel-type tractor prime movers.

Subcommittee XII came into being early in 1951.

THIS report of the Tractor Test Codes Subcommittee of the CIMTC consists of separate papers by various members of the subcommittee.

The need for a tractor test code and the objectives of this code are covered in one paper included here. Another paper discussing the instrumentation used in the tests is based on reports about the ERDL dynamometer truck, the Goodyear dynamometer truck, and the Allis-Chalmers dynamometer equipment.

An evaluation of field-test results, discussed in another paper of this report, indicates that there is general accuracy and correlation among the three types of measuring equipment and that the accuracy tolerances given in the code can be met.

The test codes for reserve tractive ability and vehicle drag are also given here.

The original chairman, Arnold Meyer, Heil Co., Milwaukee, Wis., was succeeded by H. L. Rittenhouse, Euclid Road Machinery Co., in 1952.

The primary objective of Subcommittee XII was to establish understandable and uniform testing procedures for evaluating and rating the performance capabilities of the various prime movers used in the earthmoving and construction industry. Since the Corps of Engineers had expressed a vital interest in this field, primary emphasis was given to areas of their greatest needs.

The committee has been an especially ambitious and energetic group with meetings held on the average of once per month since its formation. Loud and long and interesting have been the discussions over the ways and means for solving the many complex problems related to fulfillment of the committee's objective. It was recognized from the start that a step-by-step approach to the development of test codes must be taken. The committee's work was started by first making a survey to ascertain which performance-type tests might be written so as to provide an accurate and understandable method of obtaining useful data on tractor prime movers. Individual requirements for tests were scrutinized to determine if they could be formulated in a way that might broaden out their applicability to other basic types of prime movers. From the committee's standpoint, it was considered that a test code satisfactory for any determination must:

1. Be readily understandable by both the user and manufacturer of the item with which it deals.
2. Be reasonably unrestrictive as to the place and facility required for its application.
3. Be repeatable and controllable within a reasonable tolerance of accuracy.
4. Be a practicable and indicative measure of the test item's true performance capability within its intended field of application.
5. Be impartial in its effect on the judgment of equipment within competitive classes.

Accordingly a format for preparation of test codes was adopted which consisted of parts including:

1. Object.
2. Scope.
3. Facilities, apparatus, and materials.
4. Procedure.
5. Computations and records.

The field of possible tests was narrowed down to those tests which appeared useful and controllable to a degree that made their general application practicable. At the present time test codes are in various stages of completion on tests dealing with:

(a) Reserve tractive ability.
(b) Vehicle drag.
(c) Vehicle fuel consumption.
(d) Speed and acceleration.
(e) Brake ability.
(f) Steering loads and turning.
(g) Gradeability.
(h) Tilt limitations.

In addition, many definitions of the physical characteristics or properties of vehicles such as angle of approach and departure, center of gravity, descriptive dimensions, and descriptive weights have been considered and many agreed upon.

The process of producing a test code which will form an acceptable standard generally requires many hours of painstaking and thoughtful deliberation, plus actual trials, to prove its practicability. Subcommittee XII found it convenient initially to have one or more of the members prepare a draft of a proposed test code in accordance with the outline previously described. Then, with this committee in session, each element of this proposed code is thoroughly discussed and analyzed. After combined thinking has produced what appears to be a theoretically sound and practically workable code, arrangements are made for physically trying out the stipulated procedures and evaluating the results to see what future changes in the original outline are necessary. As you may readily appreciate, the problems of reconciling or eliminating the many variables connected with performance testing is matter for much deliberation and proving. Such factors as the effect of instrument inaccuracies, weather influences, variance in soil conditions, mechanical conditioning of test vehicles, and human behavior factors are only a few salient influences which have to be reckoned with. Subcommittee XII is pleased to be able to submit to you some of the tangible results of its activity to date. It is hoped that we have contributed to better understanding of the problems involved and aided the manufacturer or designer in his aim to represent the performance capabilities of his product in accordance with a fair and just standard; the purchaser or user (military or otherwise) in his aim to judge in a fair and impartial way whether the product he intends to purchase meets the standards of performance he feels are necessary to fulfill the requirements of his job; and the SAE in its aim to disseminate approved standards, sound engineering recommended practices, and general information in a manner helpful to those interested in a particular field of endeavor. It is also hoped that, through this committee report, the engineer who is inexperienced in definitive performance testing (and most of us are) may profit.

Discussion of Instrumentation

by

T. Davidson
Bucyrus-Erie Co.

IN reading the test codes for reserve tractive ability and for vehicle drag (see Appendix) and in

reading the supporting papers, it may surprise you to find such large sections of the codes and so large a part of the discussion dealing with instrumentation. It may look like overemphasis. After all, tractive horsepower is the principal item to be determined, and power requires determination of only tractive force, distance traveled, and elapsed time. Dynamometers to measure pull, tapes to measure distance, and stopwatches to measure time are old and well known and should not require elaborate description.

The reason lies in the conditions under which testing must be done. It is a field job with all the handicaps of weather, wind, and dust. The whole test plant must be mobile with no fixed reference points to tie to, and it must function at speeds up to 10 or 15 mph. Because space is at a premium, the test crew is limited to a driver for the test vehicle and an operator for the towed load, both of whom have their hands full, and at most two observers. These men may be separated by distances of 40 or 50 ft, a cloud of dust, and the noise of a 200-hp open exhaust. Such conditions are far from ideal.

The test must be run on a level, straight roadway which, if dirt, must be scarified, watered, and rolled to as nearly constant surface conditions as possible. It is difficult to get such a road, or a straight and level concrete road, with much over a quarter mile of usable length. Considering that a vehicle at 12 mph will travel a quarter mile in 1¼ min, and considering that the available quarter mile must include acceleration and stabilization of operation, the actual duration of test must be short. The reserve tractive ability code specifies a minimum test distance in feet of 44 times the speed in miles per hour; this means that the instrumentation must be aimed at collecting all necessary data in ½ min.

General

Three sets of test equipment were used in the comparative demonstration at the Engineer Research & Development Laboratories Proving Ground and are described subsequently in this report. It is believed that these equipments incorporate most of the various type components now in use for tractive ability and vehicle drag testing.

The basic principle of all tractive ability testing is to have the test vehicle tow a drag load and measure the towing force, the distance traveled, and the elapsed time. The principle of vehicle drag testing is to tow the test vehicle at suitable speed and measure the towing force.

Two approaches were used in the development of instrumentation at the ERDL demonstration. In one, the equipment was kept as simple as possible and was arranged to be carried in any available pickup truck or station wagon with any available heavy vehicle used for the drag load. In the other, more elaborate instrumentation was adopted to simplify interpretation of data and was permanently mounted in a truck which included a reasonably comfortable cab for observers. This truck carries a large water ballast tank to bring its weight (about 40,000 lb total) to a point where it can supply the total drag load for most tests. The hitch point for the tow cable is arranged to be raised or lowered to match attachment at the test vehicle and so keep the cable horizontal to eliminate any vertical component tending to lift or depress the test vehicle. The truck also is equipped with a cable hitch at the rear so that it can be used to tow the test vehicle for vehicle drag testing.

For occasional tests, the low original cost of the first type is attractive. The greatest convenience and more rapid analysis possible with the second type will justify its greater cost for an extensive program.

Vehicle Weight

The first problem is to weigh the test vehicle. The performance of a purely towing tractor is the result of the weight built into it; there is nothing that can be done about it, and weight is of only academic interest. But if a vehicle carries a payload, the amount of additional weight and its distribution on wheels or tracks can have considerable influence on performance.

The codes specify a "weight measuring device" accurate to ±2½% of the measured load. That may seem like a pretty liberal allowance. But assume that a scale is guaranteed to ±0.1%; that is ±100 lb on a 100,000-lb scale. If you are trying to weigh a 10,000-lb axle load the ±100-lb error becomes ±1%; and when thrust between the axle on the platform and the axle on the ground increases the ±100-lb error, when the scale deteriorates slightly, and when the vehicle is a little out of level, it does not take long to start crowding the ±2.5% tolerance.

If a large enough scale is not available and weighing must be done with jacks or highway scales, this limit may be the best one can hope to meet.

Reserve Tractive Force

The next problem is to impose a load that can be measured "to determine the ability of the vehicle to do useful work beyond that required to move itself on a level test course." Probably everyone uses a tow cable connected through a load-sensing element to a towed load that can be adjusted to resist motion as desired.

The point of attachment of this cable to the test vehicle should duplicate normal operation. If the test is for digging force on a bulldozer or scraper, the cable should be as close to the ground as possible; if a towing tractor is under test, attachment should be at the drawbar. If the data are to be used for gradeability calculations it may be argued that the attachment should be the height of the center

of gravity, but the gain in accuracy probably is not worth this refinement. The need for accuracy in setting this attachment height depends on the vehicle and the test; with a short-wheelbase 4 x 2 tractor operated in first gear a change in attachment height may vary weight on the drive wheels appreciably; but height will be unimportant when a long-wheelbase vehicle is operated in high gear.

The towing load is imposed by a heavy vehicle, on either wheels or tracks, and equipped with engine, transmission, and brakes. The engine, driven as a compressor from the wheels, provides a range of drag loads through the several transmission gears; these loads are supplemented by the brakes for fine adjustment. If one vehicle does not provide enough resistance, more are added.

Three different force-sensing elements were used in the ERDL demonstration.

1. An hydraulic cylinder-piston assembly; this being of known area requires no calibration other than that of the gaging equipment. Piston and rod packing friction tends to make a cylinder read low with increasing loads and high with decreasing loads; but, as the loads are of a more or less vibratory nature, this friction acts as a damper and probably has little effect on the average reading. In order to keep the cylinder to a reasonable diameter, fairly high pressures must be accepted when testing heavy vehicles at a low speed, in this case 1300 psi maximum. The cylinder must be mounted freely, but danger of its hitting the ground with a slack tow cable can be avoided by restraint in the hitch jaws or by a sling cable.

2. An hydraulically loaded diaphragm; this is about frictionless. It is large enough to operate at low pressure, in this case 100 psi maximum. For accuracy, a diaphragm should be calibrated and must be held to a short travel to avoid nonlinearity. A diaphragm may be mounted rigidly, as it is short enough to avoid damage from tow cable off-lead. There is no free mass to whip.

3. Electric strain gages on a calibrated link. This unit is more compact than an hydraulic cylinder. It has the disadvantage of requiring a 110-v a-c power supply and electric amplifiers; but the power supply can be used to advantage in other recording, and it is expected that other advantages, such as direct recording of horsepower, may develop as experience is gained in its use.

When test procedure requires operation at constant tractive force, pressure from the hydraulic sensing element or amplified output from the electric strain gages can be shown by indicating instruments mounted in view of the drag load operator so that he can control the brakes accordingly.

Even on a concrete test course tractive force varies too much to permit visual averaging from an indicating meter, and all units record signals from the force-sensing elements on strip charts which must be integrated to determine the average force imposed during the test. This is a time-consuming process; to avoid it, one of the equipments in the ERDL operation included an automatic integrator so that only one slide rule division is required to determine the actual average tow resistance for the run. Such automatic integration saves analysis time.

The code allows $\pm 2\frac{1}{2}\%$ error in force measurement, which includes errors in the sensing element, recording equipment, and integration. The hydraulic diaphragm unit has a variable-ratio lever system between the tow cable and the diaphragm, which is adjustable to operate the hydraulic system at close to maximum capacity for any force; sizes of hydraulic cylinders and electric strain gage units can be varied to accomplish the same result. This improves accuracy with low forces. The automatic integrator reduces the possibility of an inadvertent error in calculation, but it must be well made since friction and the like may cause unrecognizable random errors.

The tow resistance can be determined by integration and averaging against the time duration of test or against distance traveled. Results will not be the same when wheel slip varies during a test run; but, as only a small variation in slip is permissible for an acceptable run, the difference in results is only a small fraction of a per cent. Integration against time was used on all three units in the ERDL demonstration where recording charts and one element of the automatic integrator were driven at constant speed. In the Nebraska test procedure, on the other hand, the strip chart is driven from the ground and integration is against distance.

Distance and Time

The codes specify the minimum length of test as the feet traveled in $\frac{1}{2}$ min (44 times the speed in miles per hour) but not less than 100 ft. This means 100 ft at $2\frac{1}{4}$ mph, 550 ft at $12\frac{1}{2}$ mph, or more at still higher speeds. The code specifies establishing the test distance to $\pm\frac{1}{2}\%$ and timing accurately to $\pm\frac{1}{2}\%$ in 1 min.

Three approaches to distance and time measurements were available in the ERDL demonstration. In the first the test was run over an established distance; this will be called "fixed distance" for identification later in this discussion. In the second the test was run for a suitable elapsed time; this will be called "fixed time." In the third an extended test was run with the most satisfactory portion of the data selected later; this will be called "variable distance and time."

In the "fixed distance" approach, distance is established by stakes driven in the ground, which can be done to practically absolute accuracy. Time is measured by a stopwatch, interconnected so that all instrumentation is started and stopped simultaneously as the test train passes the stakes. Instrumentation for this approach is the simplest of the three, but the method has two weaknesses.

First, the test run must start and stop at fixed points on the course regardless of how well operation is stabilized. Second, the true distance is not the spacing between stakes, but is the distance covered in the time between starting and stopping instrumentation; additive 6-in. errors at each end of a 200-ft run would make the maximum ½% error permitted by the code; and 6-in. travel, at the 4½ mph required to travel 200 ft in ½ min, takes only 1/13 sec.

Both the "fixed time" and the "variable distance and time" approaches use an odometer wheel for distance measurement. This allows starting the test as soon as operation is stabilized and stopping as soon as requisite time has elapsed. The odometer wheel must be mounted so that it will not jump, it must be accurately calibrated, and counting must register small fractions of a revolution.

The difference between the "fixed time" and the "variable distance and time" approaches is in the method of recording odometer wheel revolutions.

With "fixed time," rotation is registered on an electromechanical counter started and stopped with other recording instruments. In this way test recording can start or be delayed until operation is stabilized and can be stopped as desired.

With "variable distance and time," rotation is registered by marks on the tractive force strip chart. In this way recording can start at any time on an extended length test, and the most satisfactory section of the data can be selected after completion of the run.

The possible recording error of a counter is ±1 count. Therefore, a minimum of 200 counts is required to attain the ±½% accuracy specified in the code, and if any margin is to be left for error in calibration of odometer wheel rotation, this number should be increased to say 400, or 13.3 counts per sec for a ½-min test. (This is approaching the limit for simple a-c counters.) The 400 counts in the minimum 100-ft test run permitted by the code means a count every 3 in. of circumferential travel of the odometer wheel, or 24 counts per revolution of a 2-ft diameter wheel. Even at 12½ mph, 5 counts per revolution are required.

Timing is another matter that should not be considered lightly. Speed regulation of a portable gasoline generation set is not good enough. Stopwatches seem to have a habit of getting out of order. And a governor-controlled d-c motor used in the ERDL demonstration failed because its mounting bolts were too tight. Timers can be compared quite easily with a standard 60-cycle unit, and frequent checking seems necessary for accurate results.

Engine, Output Shaft, and Wheel Speeds

Test procedure may require vehicle operation at a specified engine speed. In this case the code specifies a tachometer with accuracy of ±1%, or a total range of 36 rpm for an 1800-rpm engine, which includes both instrument and reading errors. In addition, recording is used to show the actual number of engine revolutions during the test time either on electromechanical counters for the "fixed distance" and "fixed time" methods, or by marks on the strip chart for the "variable distance and time" method. With ±1 count possible error, a count every four revolutions of an 1800-rpm engine will give slightly less than ±½% accuracy for a 0.5-min test.

When the test vehicle is equipped with a torque converter or electric drive, this instrumentation must be duplicated on the output shaft.

The codes require steering to be held to a minimum during test runs because of its pronounced effect on performance. Excessive steering is indicated by revolutions of the drive wheels or crawler sprockets on the two sides of the machine. The code specifies wheel count accuracy to ±½%, which means about 6-in. circumferential spacing for a minimum 100-ft test or 33-in. spacing for a 550-ft test at 12.5 mph. This amounts to 40 to 8 signals per revolution of a 24.00 x 29 tire. Again these signals are recorded by counters for the "fixed distance" and "fixed time" methods and by marks on the strip chart for the "variable distance and time" method.

Discussion

If there is ±2½% error in the reserve tractive force, ±½% error in the distance traveled, and ±½% error in timing, there can be an error of ±3½% in reserve tractive power, or a variation in reported power from 96.5 to 103.5 hp for a 100-hp vehicle. Coupled with a ±2½% error in weight measurement, this could make a considerable difference in gradeability calculations.

The counters used with the "fixed time" approach have the advantage of direct reading, whereas the strip chart marks used with "variable distance and time" approach must be counted manually, increasing the analysis time and introducing a possibility of error. On the other hand the possible error of ±1 count inherent in any counter system can be reduced 50% or more by interpolation between marks on the strip chart.

Great care must be taken to keep fixed instrument errors to a minimum, and simplicity of calibration should be an important factor in instrument selection. Our hope is that the random errors of observation seldom will be all in the same direction and will diminish with experience.

You will find that the code includes a thermometer and barometer for ambient conditions; readings are to be reported on the summary sheet, but no engine correction is indicated. The data are there if anyone wants to use them, but the actual correction was omitted deliberately because we knew of no reliable formulas to use for engine power and were skeptical of the value of comparative tests run under widely different atmospheric

conditions. In addition so much of the power available at the flywheel may be lost in chassis friction and vehicle drag that a perfect formula for the engine still will be incorrect at the drawbar.

But don't be too discouraged by all this talk about the need for accuracy and the troubles that may be encountered. I believe you will be much more encouraged by a later paper of this report, which shows the degree of consistency obtained in actual comparative tests.

ERDL Dynamometer Truck

by

F. M. Baumgardner
Engineer Research & Development Laboratories

J. H. Meier
Bucyrus-Erie Co.

THE ERDL dynamometer truck (Fig. 1) contains the instruments for a portion of the test code prepared by Subcommittee XII of the SAE Construction and Industrial Machinery Technical Committee. The instrumentation described herein refers to the dynamometer truck as it was applied in the test demonstration of the Society's tentative vehicle tractive ability and vehicle drag procedures at the Engineer Proving Ground, Fort Belvoir, Va., between Oct. 12 and Oct. 15, 1953. Design and fabrication of the instrumentation and test vehicle are the result of the combined efforts of Dr. J. H. Meier, research Engineer, Bucyrus-Erie Co., and technical personnel of the Engineer Research & Development Laboratories.

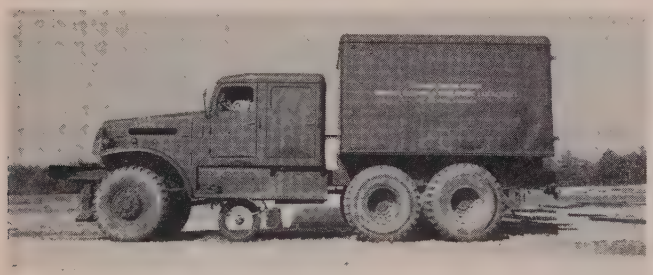

Fig. 1 – View of dynamometer truck with odometer wheel in operating position

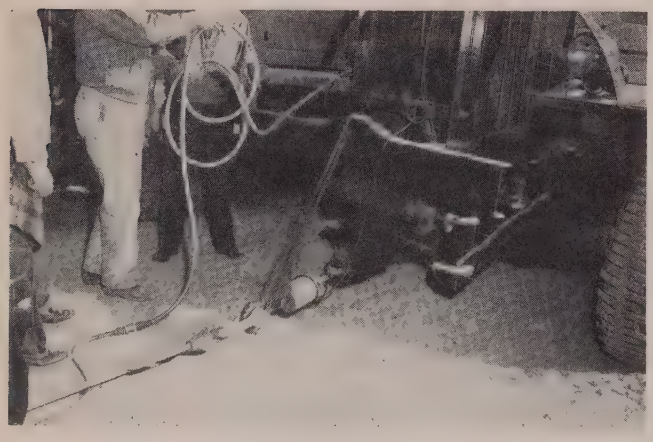

Fig. 2 – SR-4 load cells used in recording force

Objectives

The objectives of the basic instrumentation described herein are to measure vehicle reserve tractive force, reserve tractor power, and vehicle drag. Additional instrumentation was provided for supplementary data, such as engine speed, track or wheel slippage, and torque converter speed. Standard instruments are used for observing temperatures, barometric pressure, and bearing value of the tractive surface conditions.

Dynamometer Truck

Dynamometer Truck Chassis – The dynamometer truck chassis is used for applying a towed load to the test vehicle through the truck brakes, truck engine compression, or both. In addition, the truck is used in measuring vehicle drag by providing the power to tow the test vehicle at selected uniform speeds. It consists of an Army Ordnance 6-ton (6 x 6) White truck chassis equipped with reinforced frame and special front and rear variable-height cable hitches;[1] an oversized cab for the test driver, instruments, instrument operator, and test observer; and a van-type body housing a water ballast tank and a 5-kw, 110-v, gasoline-engine-driven 60-cycle generator. The truck is equipped with Firestone Ground Grip, Type ND, 14.00 x 20 front single and rear tandem dual tires. The 6-wheel service brakes are air actuated, and the parking brake is mechanically applied at the propeller shaft. In addition a 4-forward-speed transmission and transfer case with a high-low range is available for applying a wide range of engine compression loads or for providing a wide range of towing speeds. The truck with full complement of instruments and water ballast has a front axle loading of 9280 lb and a rear tandem axle loading of 31,460 lb. This gives a total gross weight of 40,740 lb. A standard pintle hitch and air outlets for trailer brakes at the rear of the truck permit towing any of a number of loaded machinery trailers to gain additional towing resistance. The angles of approach and departure of the truck are limited by the low ground clearance of the cable hitches; however, this condition is not considered critical for normal highway travel.

Basic Instrumentation – The instrumentation is designed to give a complete and detailed set of data for determining reserve tractive force and reserve tractive power together with considerable additional information such as, for instance, torque converter speed ratio. From the beginning a decision was made in favor of a system that would permit selecting any desired portion of the test run

[1] These hitches are a modified version of those used on the Goodyear Tire and Rubber Co. dynamometer truck.

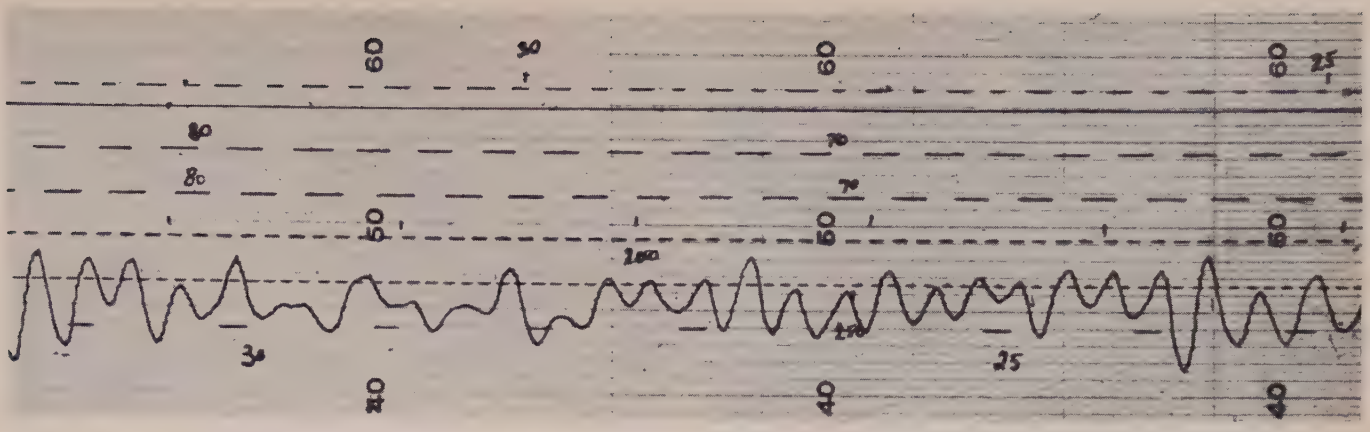

Fig. 3 – Section of strip chart illustrating styli count and pen record of tractive force. Styli from top to bottom are: odometer revolutions, correlation line with Goodyear test record, right driver revolutions, left driver revolutions, torque converter revolutions, engine revolutions, and 1-sec timing marks. Note that four evenly spaced cams are provided on the odometer wheel, giving one mark for each quarter revolution. Similarly, six evenly spaced cams are provided on the left and right drivers, giving one mark for each one-sixth revolution. Suitable reductions are arranged for torque converter and engine output shaft speeds so as to reduce the difficulty of counting. The drawbar pull scale, in this instance, represents a percentage of the nominal SR-4 load cell capacity (20,000 lb)

for final analysis at any time after the record is taken. This requirement results in the choice of a continuous recorder and rules out the possibility of automatic integration and counting devices. Ease and speed of analysis are thus sacrificed in order to obtain completeness of data.

SR-4 load cells[2] (resistance strain-gage type) are used for picking up drawbar pull (Fig. 2); the electrical signal is recorded on a fast self-balancing potentiometer. SR-4 load cells are characterized by very good accuracy and stability and by ease of calibration not only of the cells proper but also of the complete recording mechanism. Event marks, such as revolutions of engine, drive sprocket, and odometer wheel, are recorded by stationary styli, which produce a black mark on the strip chart. It may be seen that the self-balancing potentiometer pen record of tractive force is accurately and conveniently correlated with the event marks on the strip chart (Fig. 3).

Details of Circuitry – Load Cells and Calibration[3] – A complete range of SR-4 cells is available commercially, so that any load up to 100,000 lb can be measured statically to an accuracy of ½% or better. The type used has an output of 2 millivolts per volt input at nominal load. This output voltage can be brought about either by an actual load or by two shunt resistors in opposite arms of the strain-gage bridge. The correct shunt resistors can be determined to good accuracy by means of an SR-4 strain indicator. The tow shunt resistors should always be the same, and for simulating nominal load of the cell, they should be adjusted so that the indicator shows 4000 microin. per in. Similarly, shunt resistances can be determined for any desired fraction of load cell output, so that linearity of the recording setup can be checked at any time.

The shunt resistances required for calibration are nearly the same for all load cells. It is possible, therefore, to prepare one set of shunt resistors for calibration of all load cells and make up a correction table showing the deviations for individual cells. Usually these deviations are within ½%.

For best accuracy, it is necessary to apply the shunt resistances immediately at the load cell and not at the instrument end of the connecting cable (which may be of considerable length). It is convenient, therefore, to make up a small calibration box with the shunt resistors that plugs in near the load cell. By providing an extra plug at the load cell for the calibration box, the necessity of disconnecting the cable can be avoided.

Recording Instrument[4] – Maximum safe input of the load cells is 9 v; the corresponding output is 18 millivolts at nominal load. In order to allow for some range expansion, the instrument sensitivity should be able to produce full-scale deflection at not more than 12 millivolts.

The instrument chosen requires 1.0 sec for the pen to travel across the 11.0-in. chart when a corresponding signal is suddenly applied. Experience indicates that the instrument is sufficiently fast and the chart sufficiently wide. As a matter of fact, under many conditions, tractive force fluctuates considerably, even within such short time intervals as 1 sec. This causes relatively wide excursions of the pen and thus affects unfavorably both the speed and accuracy of analysis. A certain amount of electromechanical damping is thus highly desirable, as this by itself is quite a good means of averaging cyclic load variations. The instrument obtained is a commercially available

---

[2] Baldwin-Lima-Hamilton Co., Philadelphia, Pa.

[3] "Some Phases of the Technique of Recording Performance Data on Large Machines," by J. H. Meier. Presented at the SESA Spring Meeting, Washington, D. C., May, 1951.

[4] Brown Electronik Potentiometer, Strip Chart Recorder, 1 sec, 60 in. per min chart speed, Model 153 x 18, Minneapolis-Honeywell Regulator Co., Industrial Division, Philadelphia, Pa.

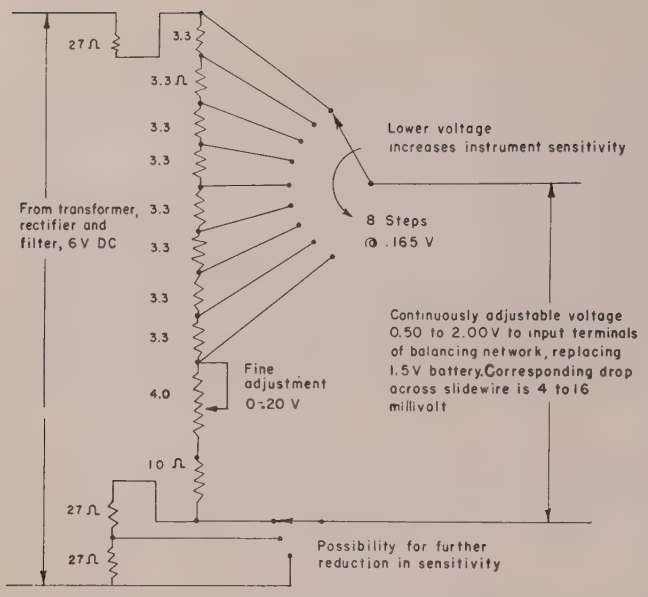

Fig. 4 – Potentiomer for continuously adjustable input to balancing circuit. Output voltages are shown for 6-v input. Supply voltages to load cell and to this potentiometer circuit can be raised without harm to 9 v to obtain better instrument performance

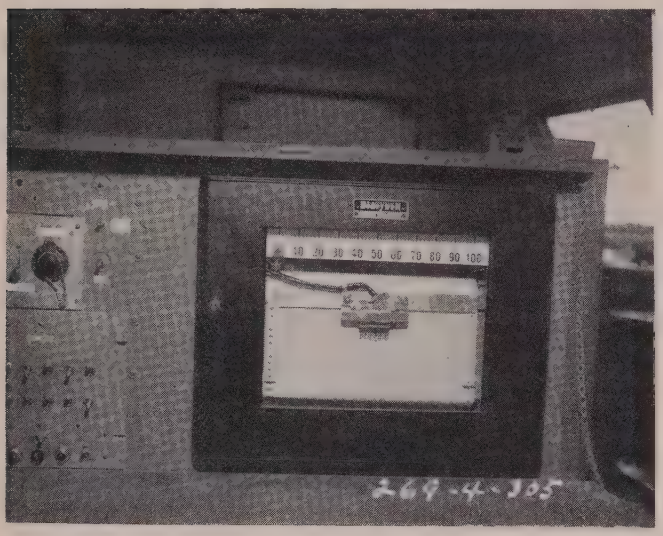

Fig. 5 – Strip chart recorder equipped with Teledeltos paper. Note that styli are placed in the center of the span to avoid an eccentric pull on the chart. The styli are offset to avoid mechanical interference with the pen.

standard millivolt recorder. It is a self-balancing potentiometer and compares the unknown input voltage with an internal balancing voltage derived from a battery and an adjustable slide-wire resistor. The instrument adjusts the position of the slide-wire brush automatically so that the balancing voltage is equal to the input. The position of the brush is then a measure of the input voltage; the recording pen and the visual indicator are mechanically coupled to the slide-wire brush.

Normally, standardization of these instruments is achieved periodically by comparing the voltage of the balancing battery with another internal battery. This second internal battery is of the mercury type and maintains its voltage over long periods of time. For thermocouple pickups, where the output voltage is a function of only one variable (temperature), this arrangement is perfectly satisfactory. However, it becomes cumbersome in the case of load cells, where the output is a function of two variables (input voltage, which cannot be held absolutely constant, and load). In order to avoid the lengthy standardization procedure, it is highly preferable to tie the strain-gage input voltage and the input voltage to the balancing circuit together so that they vary in proportion. In this true null-type circuit, the balancing point is not affected by a change in input voltage, and instrument reading is a function of load only.

The d-c strain-gage input voltage is derived from 115 v alternating current through a stepdown transformer, rectifier, and filter network.[5] An identical voltage source was provided for the input to the balancing circuit. It was loaded exactly the same as the strain-gage supply (120 ohms across the rectifier circuit), and the two units are mounted side by side. They should thus perform exactly in the same fashion, and any possible deviation can be expected to be so slow as not to affect the accuracy of the recorder to a noticeable degree.

The d-c supply is connected to the balancing circuit so that the voltage drop across the slide wire can be adjusted continuously from 4 to 16 millivolts (circuit of Fig. 4). Obviously, the lower the input to the balancing circuit, the further the pen has to travel along the slide wire to match a given signal from the load cell. Adjustment of the input voltage to the balancing circuit thus provides a convenient means of selecting exactly the right overall sensitivity. Calibration resistors are shunted across two opposite bridge arms of the load cell, and the input to the balancing circuit is adjusted so as to bring about the desired response of the recorder.

This circuit has the advantage that the strain-gage circuit is always supplied with the maximum permissible voltage, and the full output signal of this circuit is fed into the recorder. Hence, the signal is at maximum theoretical value for any given load, and best possible accuracy is obtained from the recorder. If the balancing voltage is very low, amplifier performance becomes sluggish; hence, range expansion is limited.

Event Markers – Event markers were to be fast enough to follow microswitches operating at a maximum speed (20 to 25 marks per sec). Mechanical offset-type event markers could thus not be employed, and it was decided to record on Teledeltos[6] paper. This paper is a dry electrolytic, and a black mark is obtained when a current of about 10 ma is passed through a stationary stylus.

[5] D-c power supplies, Ruge-De Forest Inc., consulting engineers, 50 Moulton St., Cambridge 38, Mass.

[6] Western Union Telegraph Co., 60 Hudson St., New York City.

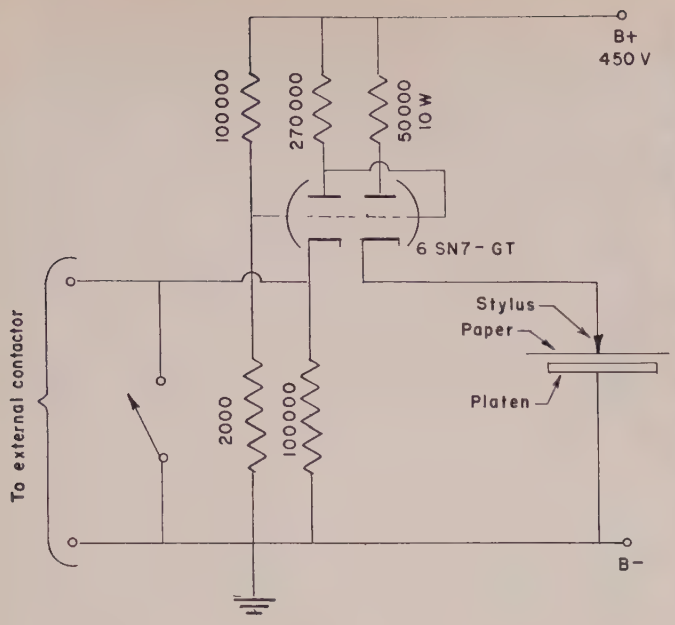

Fig. 6 – Electronic relay for recording on Teledeltos paper. One side of external contactor and paper platen are at ground potential. Open-circuit voltage across external contactors is approximately 30 v, contact current is less than 2 ma.

The styli are placed relatively close together so that a great deal of information is recorded on a small space. Furthermore, if red ink is used for recording the drawbar pull, the event marks are readily distinguished from the load curve, even if they fall on the same spot on the paper. The full chart width is thus available for the load. In order to equalize stylus drag on the paper with respect to the sprockets on the paper drive roll, the styli are placed in the middle of the span (Fig. 5). For dependable operation, about 100 v should be applied to a stylus when it is to produce a mark. The current then is about 10 ma at a paper speed of 1 in. per sec. Open-circuit voltage should be at least twice the writing voltage. It is hazardous to have about 200 v across the switches producing the event marks; therefore, an electronic relay is provided so that there is only about 30 v across the switches. The switches carry less than 2 ma when closed, and the circuit is entirely safe (see Figs. 6 and 7).

Twelve styli are provided, one of which is used to produce a timing mark every second. The remaining eleven are available to record event marks, such as each revolution of an engine camshaft, a torque converter output shaft, the passing of a spoke on a drive wheel, or a cam on the odometer wheel. Figs. 7 and 8 show cam and switch arrangements for recording drive sprocket and drive wheel revolutions.

Timing – A constant-speed d-c timing motor[7] equipped with a cam-operated switch is used in conjunction with the electronic relay and power supply to provide a timing mark on the chart. This instrument is designed for 60 rpm, which provides 1 mark per sec on the chart. It is mounted on the chassis of the electronic relay and power supply

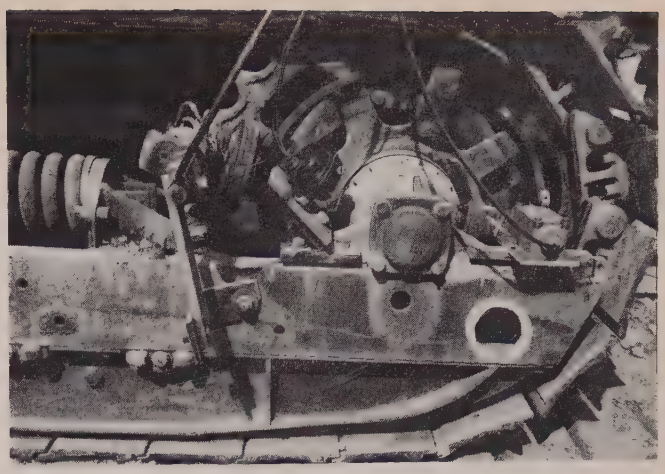

Fig. 7 – Crawler drive sprocket cam and switch for recording drive sprocket revolutions

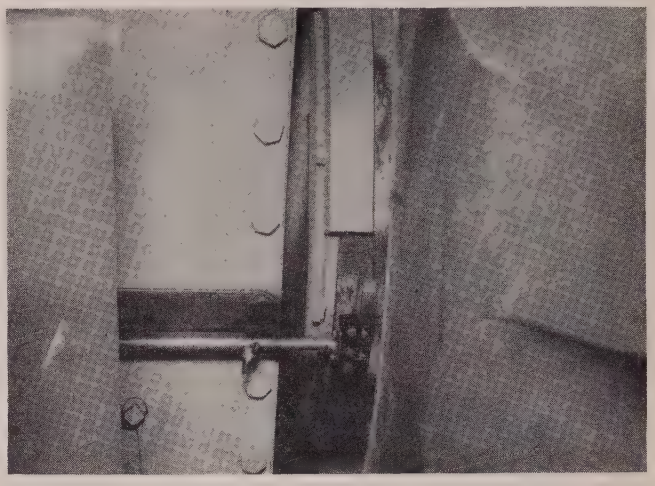

Fig. 8 – Drive wheel cam and switch for recording drive wheel revolutions

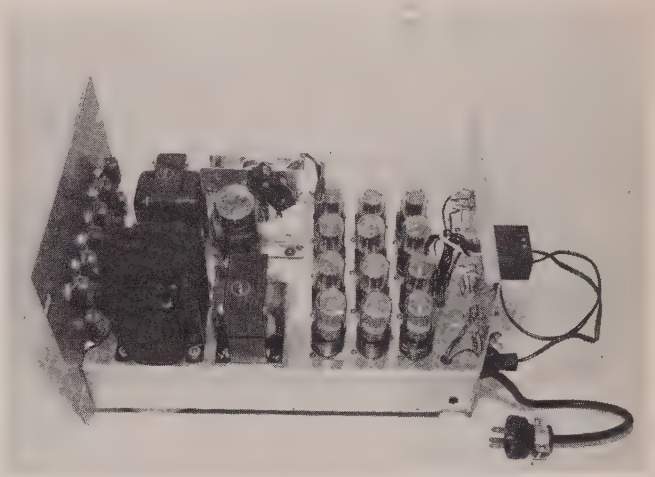

Fig. 9 – Electronic relay and power supply for 12 styli. Note d-c timing motor and cam switch mounted on chassis

[7] Amglo Corp., 4234 N. Lincoln Ave., Chicago, Ill.

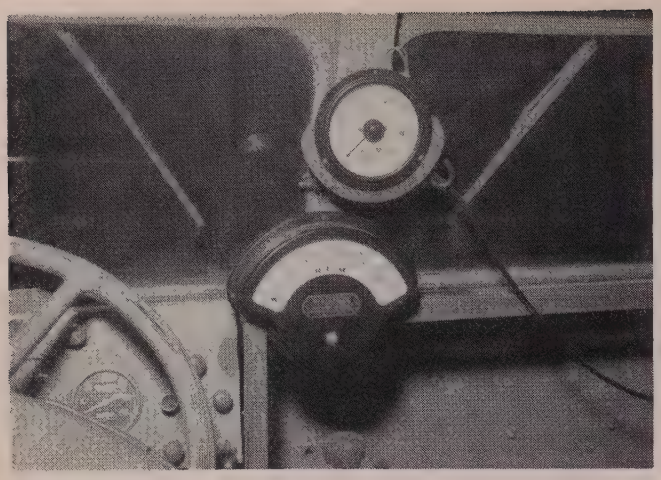

Fig. 10 – Visual indicators of vehicle engine speed (above) and vehicle torque converter output speed (below). The indicators are used by the dynamometer truck driver to control the drawbar load on the test vehicle

with an external 12-v battery power source (see Fig. 9).

Visual Indicators[8] – Two electrical tachometers with remote visual indicators in the truck cab (Fig. 10) are provided for observing test-vehicle engine and torque converter speeds. A positive drive with two flexible couplings is provided for each tachometer generator. Figs. 11 and 12 illustrate installation of these two units.

Supporting Instrumentation

Certain items of instrumentation are made available for recording ambient conditions and tractive conditions incident to testing. A brief description of each of these items is furnished herein. No effort is made to evaluate the data obtained with these instruments, to apply the data to correction formulas, nor to qualify or disqualify tests by the supporting data obtained. It is considered that supporting data might be of possible statistical value at a future time when correction formulas, if any, are made firm.

Thermometers – Two types of thermometers are used. Temperatures of liquid coolant, lubricant, and fuel are obtained with simple laboratory-type mercury thermometers. Ambient temperatures are recorded on a Brown 24-hr circular chart clock-type temperature recorder.[9] The latter thermometer is located in the vicinity of the test course and is considered particularly convenient in that the test recorder needs only to log the time of day and may subsequently refer to this temperature versus time record to obtain the corresponding ambient temperature.

Barometer – Barometric pressures are recorded on a glass-enclosed Taylor barograph.[10] This seven-day clock-type recording instrument offers the same convenience in recording barometric pressure as obtained with the instrument described above.

Anemometer – Wind velocity is recorded with a Taylor Birans-type anemometer[10] equipped with three dials reading to 10,000 ft. This instrument, which records air distance, is used in conjunction with a stop watch for determining average wind velocity.

Hygrometer[11] – Wet and dry bulb temperatures are recorded from an hygrometer consisting of two 120 F thermometers mounted on a metal plate which is free to swing about a wooden handle as an axis.

Hydrometer[11] – An hydrometer with a specific gravity scale from 0.700 to 1.000 is used in testing fuel density. This operation is conducted concurrently with fuel temperature measurement.

---

[8] Weston Electrical Instrument Corp., Newark, N. J.

[9] Brown Instrument Co., Division of Minneapolis-Honeywell Regulator Co., Philadelphia 44, Pa., Model No. 602 x 1E-X-77, O-110 F.

[10] Taylor Instrument Co., Rochester, N. Y.

[11] William Welch Scientific Corp., 1515 Sedgwick St., Chicago, Ill.

Fig. 11 – Installation of generator tachometer and cam switch to hour-meter output shaft for visual engine speed indicator and engine revolutions count, respectively

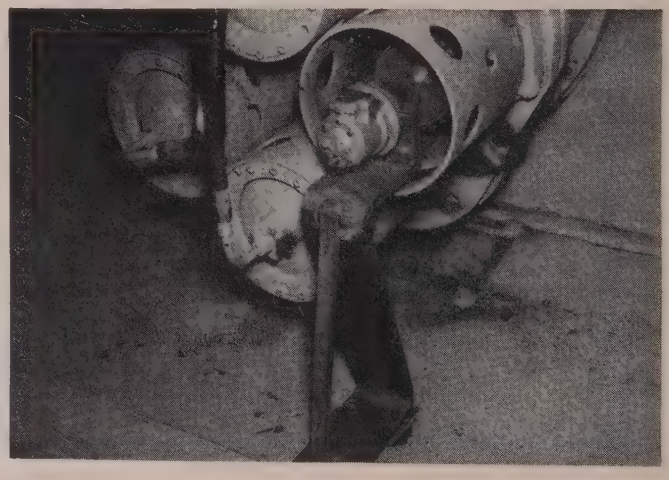

Fig. 12 – Installation of tachometer generator and cam switch to torque converter output shaft for visual torque converter speed indicator and torque converter count, respectively

Platform Scales – Vehicle weights, axle loads, and wheel loads are determined on a commercial 100-ton platform scale. This instrument is graduated in increments of 20 lb. The surface surrounding the platform consists of level concrete.

Tire Pressure Gages – Vehicle tire pressures are measured with a commercial tire valve pressure gage.

Proctor Needle – Earth traction surface bearing values are checked with a Proctor needle.[12] This conveniently portable instrument is capable of rapidly measuring ground bearing values in the range from 10 to 2200 psi (Fig. 13).

Discussion

Tables[13] showing the results of test runs taken simultaneously with the Goodyear, Allis-Chalmers, and ERDL instrumentation reveal remarkably good agreement (Figs. 14 and 15). As a matter of fact, agreement is so good, one is inclined to believe that it is due to coincidence as well as to good accuracy of all three sets of instrumentation. The load cell recording device proved to be remarkably stable, both as to zero position and calibration. A signal corresponding to an accurately known load can be produced and read directly as instrument deflection at any time during the test. Since the self-balancing potentiometer is a true null-type instrument, response does not depend on amplifier sensitivity. Linearity of response depends on the linearity of the slide wire in the balancing circuit. Checks made indicate that the overall accuracy of the recorder is better than $\pm 3/4\%$ of nominal load of the cell.

For best accuracy, cams actuating the event markers' switches should be made so as to produce from 3 to 10 marks per sec. With 10 marks per sec, counting is still relatively easy (paper speed is 1 in. per sec), and the spacing of the marks can readily be interpolated to the nearest 1/5. Hence, over a 30-sec recording period, accuracy of counting is $\pm$ 0.2 marks at each end of 300 marks, that is, the total possible error is $\pm$ 0.13%. (Note that this corresponds to 1500 counts of an automatic counter, which is considerably more than obtained from such counters in 30 sec.) If the marks are too close, counting becomes difficult and interpolation between full marks is no longer feasible, so that accuracy is likely to decrease. Since the instruments are supplied from a nonregulated power source, a special d-c motor with reed-type governor control was used to supply the timing mark. Although this motor was supposed to keep time within a very narrow range, irrespective of some variation in the battery supply voltage, it was realized during the test period that the interval between successive marks gradually decreased. This discrepancy was subsequently attributed to stresses due to improper mounting of the motor. Since there was obviously too much variation, these timing signals were not used for the analysis. Paper speed was established from the correlation mark indicating on the ERDL record the period of integration of Goodyear's recorder. The systems were interconnected through a relay so that a stylus mark was obtained on the ERDL record for the period that the Goodyear recorder was working. A stopwatch was also operated by Goodyear's master switch, and the time indicated by this stopwatch was used as the basis for all analysis. Paper speed was determined individually for each run taken simultaneously by the

[12] Proctor soil plasticity needle, for field and laboratory use, AASHO Method T-99, as described in *Engineering News-Record*, Vol. 111, Sept. 7, 1933, pp. 286-289: "Design and Construction of Rolled-Earth Dams—Description of Field and Laboratory Methods," by R. R. Proctor. See also *Engineering News-Record*, Vol. 111, Aug. 31, 1933, pp. 245-248; Sept. 21, pp.348-351; Sept. 28, pp.372-376: "Design and Construction of Rolled-Earth Dams," by R. R. Proctor.

[13] Tables, Reserve Tractive Ability Tests, Engineer Research & Development Laboratories Dynamometer Truck, Goodyear Dynamometer Truck, and Allis-Chalmers Dynamometer Truck, Oct. 16, 1953.

Fig. 13 – Soil bearing tests with Proctor needle

Fig. 14 – Tractive effort tests conducted in series with Goodyear and Allis-Chalmers dynamometers

Fig. 15 – Vehicle drag test

Goodyear, Allis-Chalmers, and ERDL instruments and also for runs taken simultaneously with the Goodyear and ERDL instruments. The average of these paper speeds was used for analyzing the runs taken simultaneously with the Allis-Chalmers and ERDL instruments.

Analysis of the records is relatively slow and cumbersome, but this is the price one must pay for choice of selecting a portion of the test run for analysis after the records have been taken.

The load curve was averaged by estimating the average load over each inch of paper travel (corresponding to 1 sec) and then averaging the respective numbers over the test period. The 1-sec average was estimated by laying a straight (but not necessarily horizontal) line over the curve and making the areas above and below the curve equal. Intersection of the straight line with the centerline of the interval then gave the estimated average. Somewhat more electromechanical damping of the recorder may be advantageous in that it would produce a smoother curve. The instrument could then be worked in a higher sensitivity range without pen oscillations becoming excessive and rendering analysis difficult. Working with greater (average) pen travel would by itself increase the accuracy of analysis, so that it would become less important to read the curve to very close accuracy.

The tests have indicated that on the more or less uniform tractive pull, there are superimposed oscillations with frequencies of from 1.5 to 4 cps. These oscillations, which may be produced by cyclic irregularities of tires or tracks, or by the elastic system comprising the two vehicles and the rope, appear to be nearly sinusoidal. A somewhat slower instrument would reduce pen excursion for individual cycles without affecting the accuracy of the average to an appreciable degree. Hence, an instrument with 2- or 3-sec full span travel may be preferable to the 1-sec ERDL instrument.

The task of counting closely spaced event marks (such as engine revolutions) can be speeded up, and the chances of errors reduced, by providing two channels of event marks for the same feature and selecting the cam drive so that the second channel records one mark for each 10 or 20 marks of the first channel. Even so, counting up the marks is a tedious task and should be done at least twice to eliminate possible gross errors.

Fig. 16 – Goodyear dynamometer truck

Goodyear Dynamometer Truck

by

R. M. MacFarland

Goodyear Tire & Rubber Co.

FOR a number of years we have operated dynamometer equipment for the purpose of conducting cooperative tests with vehicle manufacturers in order to determine the most suitable type of tire for their equipment and also to use as a tool to aid in the development of tires for specific services.

One of our more recent dynamometer test vehicles and the subject of this discussion is a former U.S. Army truck which we instrumented to test large earth-moving equipment.

A vehicle suitable for this application must inherently have good flotation so that it can operate on relatively soft soils and also have maximum tractive ability of its own. To meet these requirements, an all-wheel drive vehicle was the obvious solution. A 6-ton 6 x 6 vehicle, equipped with a gasoline engine of 202 gross hp, was selected as most nearly meeting our requirements. Fig. 16 shows this vehicle as converted for drawbar pull measurements. The original cab had to be enlarged to provide seating capacity for observers and room for instruments. This required extending the rear of the frame and moving the body back, which allowed the body load to center somewhat behind the bogie, thereby lightening the load on the front axle. This was desirable, as the installation of the front pull-measuring equipment added considerably to the front axle load.

The use of a 6-wheel vehicle provides sufficient brakes so that they may be used as the source of energy absorption during the determination of the drawbar pull of the vehicle being tested. It is, of course, understood that this method of absorbing the energy is limited in that we cannot make long runs at high values of drawbar pull without overheating the brakes. In practice, however, our estimates have proved correct that this type of work does not require absorption of energy by the truck at a rate which is detrimental to the brakes. The original service brake linings are still in use. In addition, the truck has a 4-forward-speed transmission and a high-low transfer case which is available for applying a wide range of engine compression loads or for providing a large range of towing speeds.

A water ballast tank is installed in the center of the body, which enables us to increase the gross weight of the vehicle to a maximum of about 41,000 lb as compared with the unballasted weight of 28,000 lb. On a high friction surface, such as concrete, this will allow the truck unaided to hold back

up to 24,000 lb. Where additional hold-back is required, other vehicles can be attached to a pintle at the rear of the truck.

Basic Instrumentation

The instrumentation is designed to give complete and detailed data for determining reserve tractive force, reserve tractive horsepower, vehicle road speed, engine speed, travel efficiency, vehicle drag, tire rolling radius, and vehicle wheel loads.

For the measurement of force, the hydraulic principle was adopted. Our reasons for this were several. The first was that we had experience with this construction in other dynamometer equipment; and second, we believed this principle of operation to be more suitable for the intermittent and field service in which the vehicle would be required to operate.

A 20,000-lb capacity cell was mounted on the front of the truck to measure the tractive force. This cell was so arranged that it could be shifted beneath a lever to provide three separate ranges, having maximums of 10,000, 20,000, and 40,000 lb. The lever and cell are mounted on a plate which can be raised, or lowered, to adjust the drawbar hitch height from a minimum of 12 in. to a maximum of 27 in. above the ground. This enables us to match more nearly the height of points of attachment on the vehicles we test.

Figs. 17 and 18 show closer views of the front cell and lever mounting. The flexible element of the cell is a rubberized fabric diaphragm spanning an annular gap between the cell base and the load-application foot, and it is limited to a maximum working pressure of 100 psi. The cell is connected to indicating gages, a strip-chart recorder, and an integrator – all mounted in the cab. The volume requirements of these instruments are such that the travel of the load-application foot is quite small. This means that the change in the effective area of the cell with increase in load is negligible, within the limits of accuracy for which we have designed. A similar but smaller cell is mounted under the rear of the truck between the frame members, as can be seen in Fig. 19. This cell is also adjustable with respect to the tee-shaped lever, to provide ranges of 5000, 10,000, and 20,000 lb maximum. Both front and rear cells are connected to the measurement devices through a selector valve, so that either one can be connected to the several indicating and recording instruments.

Fig. 19 also shows the air cylinder which actuates a cam lever, located so as to act upward against the forward end of the tee-shaped lever, thus locking the lever to prevent pressure on the cell when it is not in use. This lock has been found to be very useful in preventing damage to the cell when making vehicle drag tests. It can easily be seen that rapid acceleration or deceleration could produce cell loads in excess of its capacity. When making a vehicle drag run the lock is not released until required vehicle speed is reached; then when sufficient data has been recorded the lever arm is relocked, after which the test train may be brought to a stop or turned around without excessive loading on the cell.

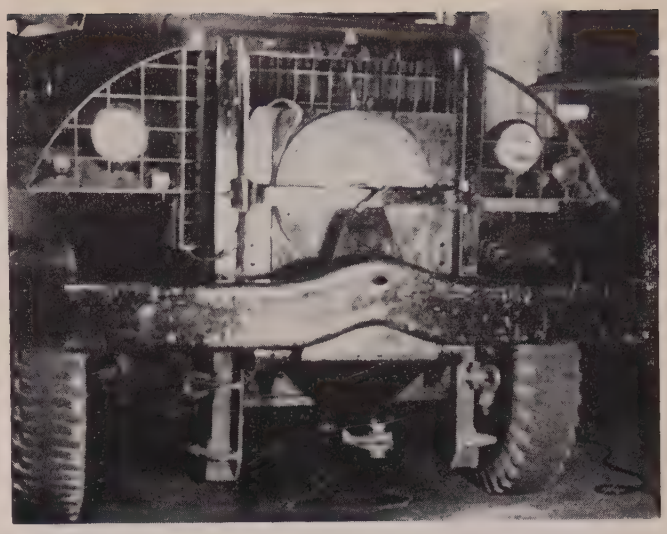

Fig. 17 – Front cell

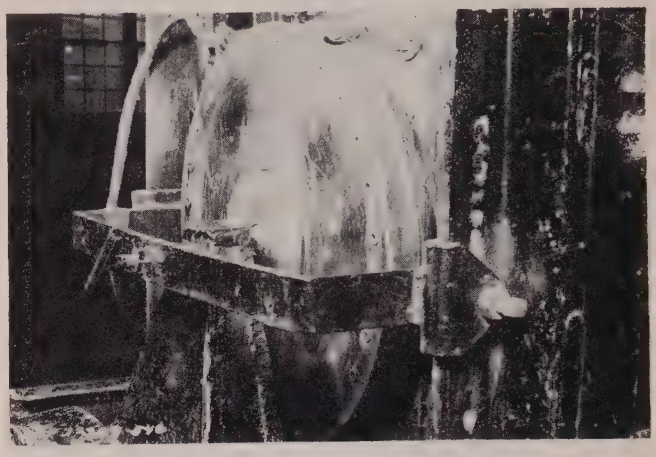

Fig. 18 – Close-up of front cell

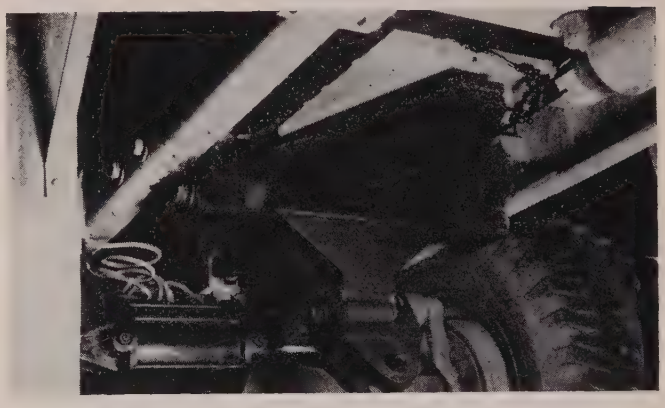

Fig. 19 – Rear cell and locking cylinder

An instrument panel has been built into the cab of the truck on the right side in front of the operator. This is shown in Fig. 20. In the center of the panel is the main indicating gage. This is a 100-psi gage equivalent to maximum pressure allowable in the hydraulic system. It is provided with a set hand adjustable through the glass; this aids the opera-

tor in making a mental integration of the fluctuating drawbar pull. A throttling valve beside the gage allows the operator to damp the gage indication to any desired degree. A similar gage is placed in front of the driver at the left of the cab, as he is the man who, by utilization of the vehicle brakes or engine power, controls the desired drawbar pull.

Also included on the instrument panel is a special low-range speedometer at the lower left and an electrically operated stopwatch at the lower right. Directly above the stopwatch is a mechanical counter driven by a ground wheel to give a measure of distance traveled. Above this is a gage showing the air pressure applied to the vehicle brakes. On the upper left is an indicating tachometer for the engine speed of the vehicle under test, and below this is an electric counter to count engine revolutions.

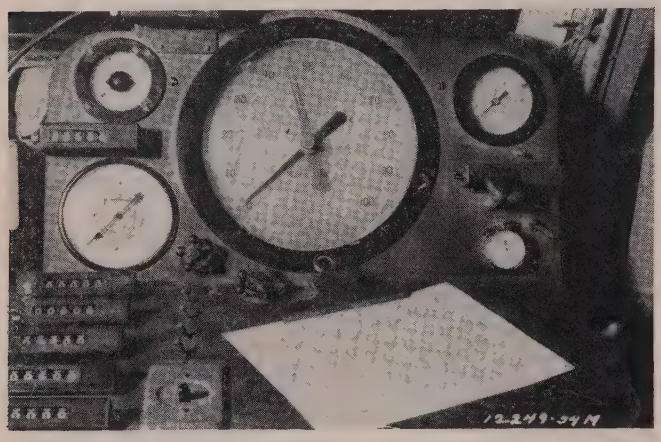

Fig. 20 – Instrument panel

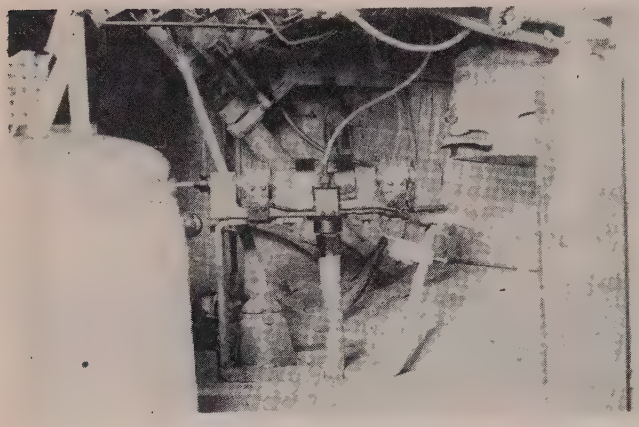

Fig. 21 – Odometer drive divider

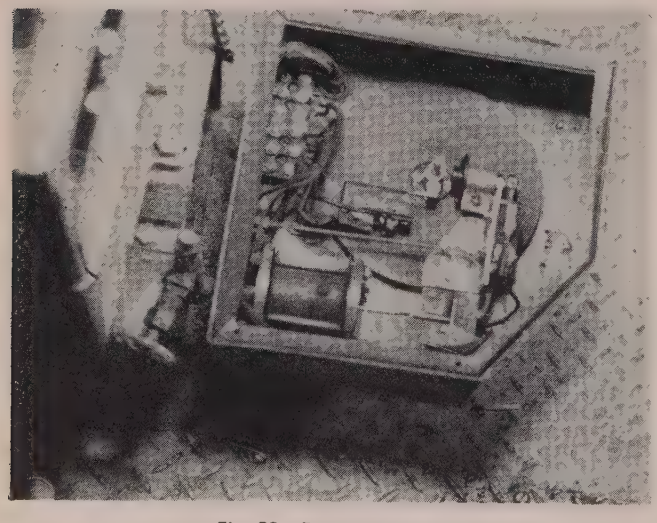

Fig. 22 – Force integrator

On the shelf portion of the instrument panel at the left is a group of five similar electric counters, the first two of which are used in connection with the load integrator; the remaining three and the one at the top left are used to measure slippage of wheels on the test vehicle. The counters, stopwatch, recorder, and integrator can all be started and stopped simultaneously through the use of a master switch which is located at the forward edge of the instrument panel shelf. This enables the operator to start his measurements as conditions become stable and stop them when a sufficient length of run has been made.

Fig. 21 shows a view of the interior of the cab. At the center is shown the drive from the ground wheel coming up through the cab floor and dividing into three separate drives, the one continuing straight up goes to the low-range speedometer, the one to the left to the recorder, and the third one to the ground wheel counter on the instrument panel. The latter two pass through electric clutches, which may be seen on the drive divider. These enable the master switch to control the starting and stopping of the recorder and the ground wheel counter in conjunction with the other phases of measurement.

The integrator has proved to be the most useful instrument of this group, as it allows us to get an average pull reading immediately on completion of a run. This is a difficult thing to accomplish by visual integration of a fluctuating pressure gage, neither can it be quickly gotten from the recorder chart. Fig. 22 shows a close-up view of this integrator, which is essentially a rotating fiber disc, driven at a constant speed, on which rolls a small, hardened-steel knife-edged wheel. This wheel is mounted on the end of a pivoted arm and varies in its radial location on the rotating disc in proportion to pressure input to the pressure element. In this case the pressure element is a sylphon bellows and spring combination, so proportioned that 100 psi hydraulic pressure will distort the bellows to its maximum working value. The motion is then magnified by the lever arm on which the rotating wheel is mounted. The rotation of the disc and wheel opens and closes microswitches which, in turn, actuate a pair of electric counters on the instrument panel.

The integrator is driven by an adjustable-speed d-c motor so that the disc speed may be varied to accomplish the best combination of counter speeds. The counters are limited in their operational speed, so by varying the disc speed to operate faster at low pulls and slower in the higher range, the optimum

combination can be established. This will provide an answer of given accuracy in the shortest interval of time.

Calibration of the integrator may be done by two methods. The first and more cumbersome method is with the use of a spring-type dynamometer whose accuracy has been determined in our Baldwin-Southwark test machine. This spring gage shown in Fig. 23 is placed in an A-frame attached to the front of the truck and linked to the lever arm of the front measuring cell. Then, using additional linkage and an hydraulic jack, a load can be applied to the spring gage which, in turn, applies a load to the hydraulic cell lever arm. This, of course, produces a pressure in the hydraulic system proportional to the load that can be read from the spring dynamometer. The integrator counters are then energized for a short period of time, and the resultant ratio of the integrator wheel counter to the disc counter serves as a basis for the calibration. The load on the spring dynamometer is then varied, and additional ratios are obtained which are essentially a straight-line relationship between the pressure in the system and the load on the cell. After a curve has been established for the load versus the ratio, then any ratio which the integrator may produce during a test may be converted to a load from the established curve.

In the truck body there is mounted a reservoir equipped with an air line which can apply a controlled air head of up to 100 lb pressure to the hydraulic fluid in order to facilitate filling. This air-applied load serves as another method of calibrating the integrator. After the primary Crosby pressure-indicating gage on the instrument panel has been checked with a standard hydraulic gage testing balance, an air load can be placed on the hydraulic system and the value can be read from the primary indicating gage. With this known load the integrator may be operated, and the resultant ratio of the counters can be checked.

Distance is measured by a ground wheel shown in Fig. 24. This is a standard automobile tire-and-wheel assembly mounted on a yoke attached to the running board in such a way that the wheel will track when moving forward. This assembly also has an air cylinder attached so that the truck operator can retract the wheel when backing up. As mentioned earlier the ground wheel is connected by a flexible shaft to the drive divider. The gearing and linkage from the ground wheel to its counter provides a count for about each 4½ in. of forward travel. Vehicle speed may be accurately measured by means of this counter and the electrically controlled stopwatch.

Travel efficiency, or travel reduction, of the driving tires or sprockets of the vehicle under test can be measured by means of slippage measuring wheels shown in Fig. 25. These wheels, which are spring loaded against the sprocket or the sidewall of a tire, serve by their rotation to make and break an electric circuit. This operates one of the electric counters on the test operator's panel. Fig. 26 shows one of these slippage measuring wheels mounted so as to count the revolutions of a crawler sprocket. A range of industrial pneumatic tires of several diam-

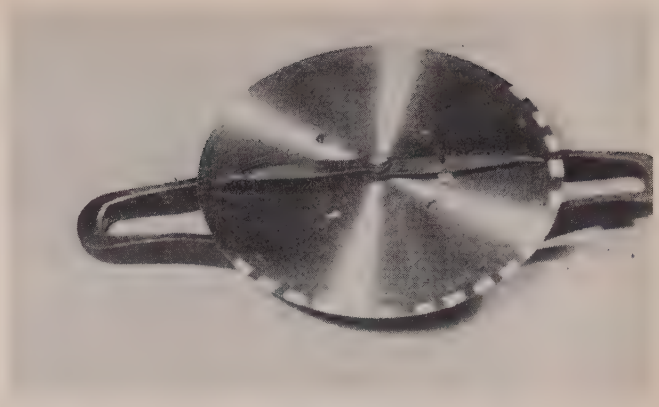

Fig. 23 – Spring dynamometer

Fig. 24 – Odometer or ground wheel

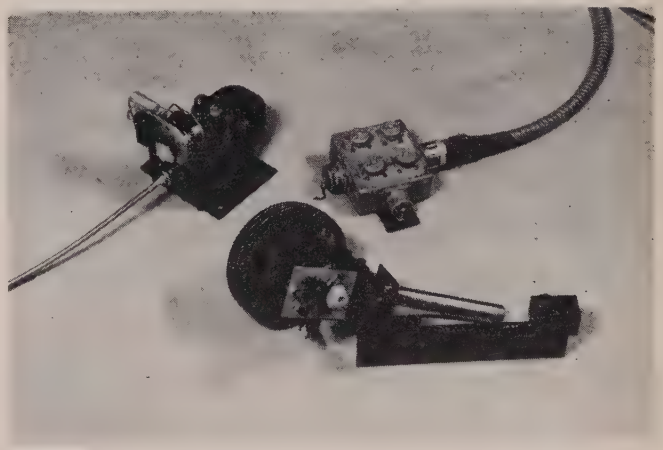

Fig. 25 – Slippage wheel, tachometer generator, and junction box

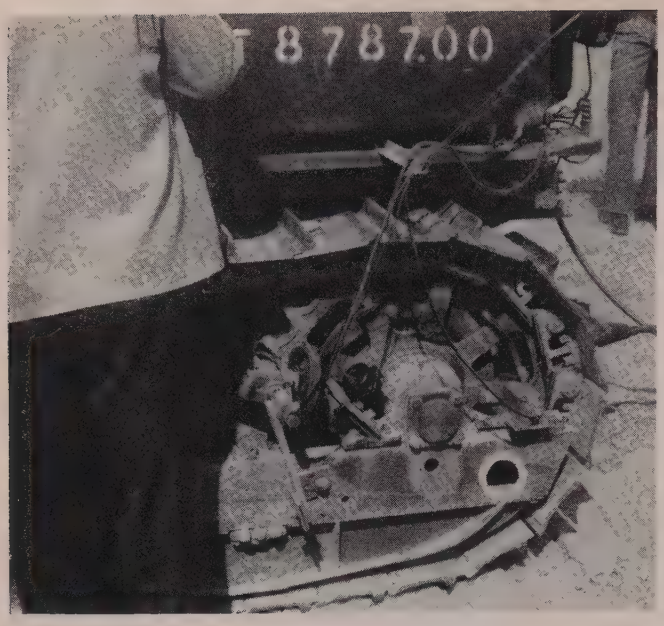

Fig. 26 – Slippage wheel mounted at sprocket

Fig. 27 – Tachometer generator mounted on radiator

Fig. 28 – Vehicle drag test

eters may be used. Also various combinations of contacts per revolution of these tires are available through the use of various cams. Thus, the counters can be operated at approximately their maximum speed for any chosen speed of travel of the test vehicle. This, of course, enables us to get a satisfactory slippage figure in the shortest distance. By comparing these slippage counter readings with the ground-wheel counter reading during the test, and then under conditions where the test vehicle is being towed or driven with no wheel slippage, the vehicle's travel efficiency can be determined. .

We would like to mention at this time that our original slippage wheels energized the counters by means of a commutator and brush arrangement. We have since rebuilt them to use a cam and microswitch circuit breaker. This has proved much more satisfactory and trouble-free.

The rolling radii of tires may also be calculated by the use of these slippage wheels. This may be done by utilizing the counter readings and distance measurements obtained during the vehicle drag tests and, as a constant, the number of counts that are obtained per revolution of the undeflected drive tires. This constant is obtained by jacking up the vehicle wheels and rotating them for a specific number of revolutions while, at the same time, recording the slippage wheel counters.

Mounted on top of the radiator of the crawler in Fig. 27 may be seen the tachometer generator and counter. This can be connected through adaptors to either a tachometer take-off on the engine or to the end of its crankshaft. It will provide both a visual indication of the vehicle engine speed and a total count of the engine revolutions. By the use of suitable couplings it may also be used to determine converter output shaft rpm. The generator has a cam and microswitch circuit breaker similar to those on the slippage wheels. This may be seen in more detail by returning to Fig. 25.

All of the electrical equipment which is attached to the vehicle to be tested is wired to a junction box on the vehicle. From this junction box is attached a Greenfield armored cable which is taped to the drawbar cable and connected to permanent outlet boxes on the truck.

Electric power for the instruments is supplied by the truck's two 6-v storage batteries which, for this purpose, are connected in parallel.

To avoid accidents and damage to the Greenfield cable, it has been found advisable to insure positive draw cable attachment to the vehicle being tested. A welded U or I bolt, drilled hole, or other such closed hitch, coupled to the cable with a screw or pin and cotter key clevis, is desired, rather than chains or cable and clamps.

A standard Bristol roll recording chart is included in the instrumentation. This chart records drawbar force on chart paper driven by the distance-measuring ground wheel.

A stopwatch, graduated in hundredths of a minute, is actuated by a solenoid coil which is energized by the opening of the master switch on the operator's panel.

Fig. 28 shows a typical vehicle drag test run being made, with the draw cable attached to the rear measuring cell.

All recording instruments are wired to the master switch. This simplifies the test to this extent – the test train may be started and brought up to the

required conditions desired for the run; then when the test operator is satisfied with the load or rpm of the vehicle being tested, he can close the master switch. This starts all instruments recording, that is, the integrator, stopwatch, ground wheel counter, engine rpm counter, slippage wheel counters, and Bristol recorder. When sufficient distance has been traveled the switch can be opened and the resultant data recorded. Within a minute or two, slide rule calculations can be made to determine the drawbar force, travel speed, horsepower, average engine rpm, and per cent of travel efficiency. There is a certain value in being able almost instantly to determine these results, because it permits immediate detection of inconsistencies of vehicle performance by comparison with previous runs.

Allis-Chalmers Dynamometer Equipment for Reserve Tractive Ability Tests

by

T. A. Haller
Allis-Chalmers Mfg. Co.

IN supplying equipment for the tests at Fort Belvoir, we proposed to demonstrate how simple the apparatus might be for measuring the reserve tractive ability of a vehicle. It was hoped that this might benefit and encourage those who cannot justify a large expenditure for this work.

List of Apparatus

The principal elements of the apparatus we supplied consisted of the following:

1. Three hydraulic cylinders (see Fig. 29).
2. One recording pressure gage (see Fig. 30).
3. One tachometer (see Fig. 31).
4. Two pair of electrical contactors and counters (see Fig. 32).

Standard instruments available at Fort Belvoir were used for measuring temperatures and atmospheric conditions.

Description and Use of Apparatus

Hydraulic Cylinders – Three sizes of hydraulic cylinder are used, depending on the tractive force to be measured. The 5-sq in. cylinder is used for forces up to about 6000 lb, the 15-sq in. cylinder for forces from about 5000 to 20,000 lb, and the 30-sq in. cylinder for forces from about 15,000 lb to 40,000 lb. In this way, the gage reading is usually in the upper two thirds of the 0 to 1500 psi range of the gage, thus increasing the accuracy of the reading.

An alternate method would be to use one cylinder with a variable leverage arrangement, as used by Goodyear and the University of Nebraska. We believe that the multiple cylinders are preferable, unless the variable leverage is made a permanent part of a dynamometer truck. The multiple cylinders are more direct and eliminate one possible source of error.

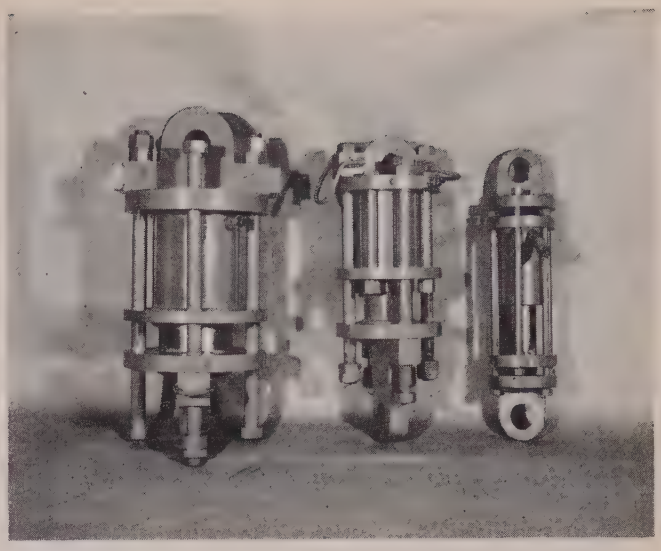

Fig. 29 – Hydraulic cylinders, 30-, 15-, and 5-sq in. piston areas

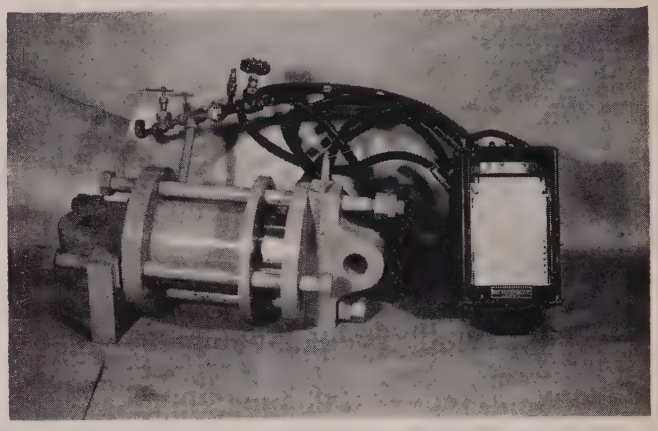

Fig. 30 – Esterline-Angus recording gage connected to 30-sq in. cylinder

Fig. 31 – Tachometer consisting of a Weston generator and voltmeter calibrated to read rpm

The pistons are made to "slip fit" in the cylinders, and no packing is used. The 15-sq in. cylinder has piston rings, but the other two do not. Chrome plating the piston or hardening of the piston and cylinder is desirable for long life but is not necessary. It has been found that, when checked under a static load, these cylinders may show an error of

as much as 4%; but under the varying load encountered in a reserve tractive ability test this error disappears.

The plumbing shown on the cylinder in Fig. 30 is to provide means for bleeding air out of the cylinder and to pump the cylinder full of oil, using a standard grease bucket and a button-head fitting. SAE 90 oil is used in the cylinder.

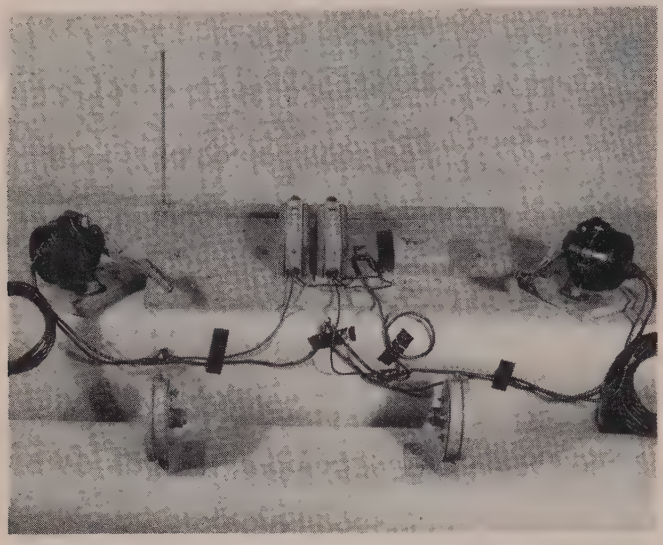

Fig. 32 – Counters and switch (top); lever-type contactors (sides); rotary contactors (bottom)

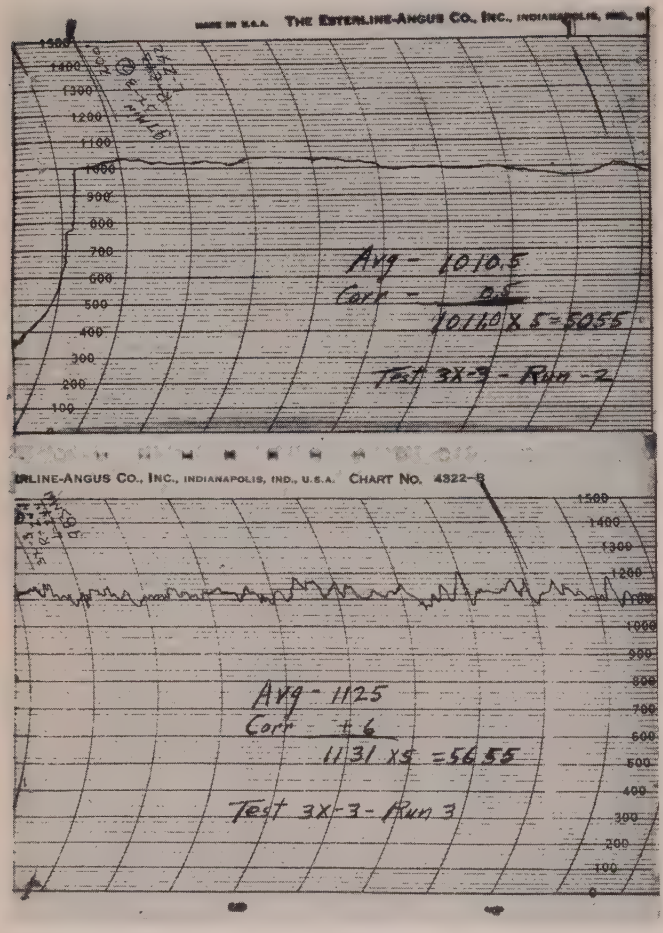

Fig. 33 – Charts showing excessive dampening (upper) and normal dampening (lower)

Recording Pressure Gage – The gage used is an Esterline-Angus Model A.W. having a range of 0 to 1500 psi. Nine chart speeds with a spring-clock drive are provided in this instrument. A chart speed of 6 in. per min is used for runs of 1- to 3-min duration.

A valve is provided at the gage to dampen the recording, to facilitate the determination of the average force, and to shut off the gage when damaging shock loads may be applied during starting or when turning the test train around at the end of the course. However, it has been observed that excessive dampening may cause the gage to read low. During one run at Fort Belvoir the gage was accidentally dampened much more than normal, and we recorded a tractive force 3 to 4% less than Goodyear or ERDL. During the next two runs, under the same conditions but with normal dampening, we checked within 0.3% of the average for the same three dynamometers. The upper chart in Fig. 33 is the one made with excessive dampening, and the lower chart shows the next run with normal dampening.

During the test the chart is marked manually by the observer handling the gage at the start and end of each recorded run. At the end of each run an approximate average gage reading can be obtained by visual inspection of the chart, so approximate results are immediately obtainable. These usually check within ±2% of the final results. A final gage reading is obtained later by estimating the average reading for each ¾ in. of the record and then averaging the numbers so obtained. The gage calibration correction, if any, is then applied and the result multiplied by the cylinder area to obtain the average tractive force.

Tachometer – The tachometer consists of a Weston Model 44 Type C generator and a Model 45 voltmeter with two ranges calibrated for 0 to 1000 rpm and 0 to 2000 rpm.

The generator may be mounted at any convenient location on the test vehicle where it can be either direct coupled or chain driven from the engine crankshaft or a power take-off shaft, having a constant relation to engine speed.

If the test vehicle is equipped with a torque converter, a second tachometer would be required for indicating the converter output shaft speed.

Electrical Contactors and Counters – Two types of electrical contactor are used for operating the wheel or sprocket counters, depending on the type of vehicle being tested. If the vehicle has a live axle, arranged so a connection can be made to the end of it, a direct coupling to a rotary contactor is used as shown at the bottom of Fig. 33. The shaft of this contactor has an easily replaceable cam which operates the standard automotive distributor points which make and break the circuit

(Fig. 34). Cams having four, eight, or sixteen lobes are available as required to obtain at least the minimum of 200 counts required for the ½% accuracy specified in the proposed Test Code A and also to stay within the 600 counts per min speed limitation of the counters.

If the test vehicle does not have a live axle, it is necessary to use a lever-type contactor actuated by obstructions on the wheel or sprocket, or a wheel-type contactor as used by Goodyear. The contactors we used for the test at Fort Belvoir on the Caterpillar D-4 tractor were Veeder-Root, Series No. 1048, as shown at the sides of Fig. 32. These were operated by the sprocket spokes. The rotary contactors were installed on the Tourneau-Dozer, as shown in Fig. 35.

The counters, Veeder-Root, Series No. 1248, are mounted on a board with the switch for operating them at a convenient location for the operator of the test vehicle. The battery of the test vehicle supplies the power to operate the counters, which are arranged for either 6 or 12 v. Also on the board is a vertical rod for sighting on the stakes, indicating the start and end of the measured test course. The counters and a stopwatch are, of course, started and stopped by the operator at these stakes.

When this "measured-course" method is used rather than the odometer wheel, as used by ERDL and Goodyear, two stakes in a line at 90 deg to the course and about 50 ft apart should be placed at each end of the course. If a single stake is used at each end, considerable error may be introduced if the test vehicle is not traveling exactly parallel to the course when the stakes are sighted.

The average wheel or sprocket count, in addition to being used to measure slippage, was used to calculate the engine rpm. While this has proved to be sufficiently accurate under carefully conducted tests, an error may be introduced due to steering when steering clutches are used. The committee, therefore, recently specified in the proposed Test Code A that a separate counter be used for measuring engine rpm. It is agreed that this should give more accurate and reliable results.

Fig. 34 – Internal view of rotary contactor with four-lobe cam. Eight

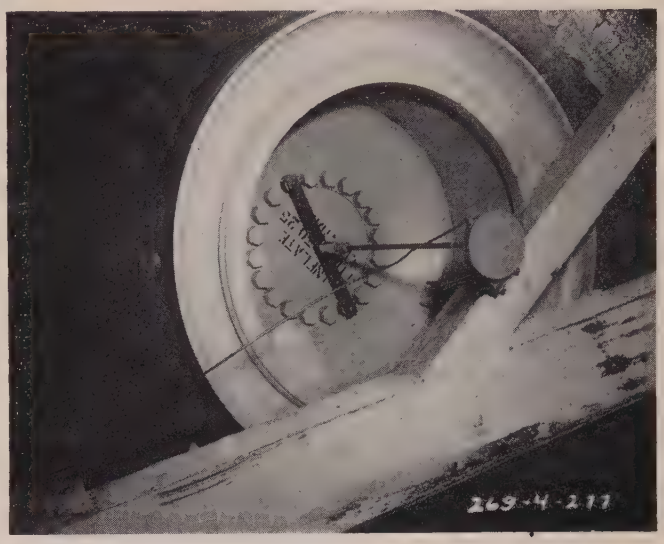

Fig. 35 – Installation of a rotary contactor on a Tourneau-Dozer

Discussion

At Fort Belvoir both the engine speed indicator and recording gage were carried in a light truck which ran beside the test vehicle. Ordinarily, these two instruments would be carried on the vehicle supplying the towed load. The operator of the towed vehicle can then adjust the load to hold either the engine rpm or tractive force as specified.

A vehicle equipped with a 3-stage torque converter has been found nearly ideal for supplying a load. By having the engine running, it is only necessary to set the gearshift lever and adjust the throttle to obtain any desired load within the limitations of the machine. The engine and converter combined act as a stable, infinitely variable absorption dynamometer.

Possible improvements which could be added to this basic equipment for little additional cost would include:

1. A contactor and counter for measuring engine revolutions.
2. An odometer wheel and counter for measuring distance traveled. With the two wheel counters and the engine revolution counter, this would make a total of four counters which should be operated with one switch.
3. The stopwatch could also be operated by the counter switch.

All of this equipment may be easily transported with a light truck or shipped anywhere. It is accurate, rugged, reliable, and easily serviced by field or proving grounds personnel. The total cost should be under $2000. Considering the fact that nearly all of the equipment may be used for other tests, the investment required specifically for reserve tractive ability tests becomes very slight.

REPORT CONTINUED ON NEXT PAGE ——→

Results and Evaluation of Field Tests

by

P. J. Sperry
International Harvester Co.

P. Spennetta
Caterpillar Tractor Co.

D. K. Heiple
LeTourneau-Westinghouse Co.

W. C. Johnson
Goodyear Tire and Rubber Co.

and

B. L. Fisher
International Harvester Co.

OTHER sections of this report have covered what purposes SAE test codes for determining reserve tractive ability and vehicle drag are intended to serve and some of the various types of instrumentation which may be used in determining such values.

Copies of the proposed test codes are given in the Appendix. (It is also included on pp. 1011-1014 of the 1955 SAE Handbook.)

This paper is intended to analyze the results obtained by the use of such equipment in the field to check the codes as written.

Table 1 – Concurrent Measurements

Test	Vehicle and Course	Gear	Measured Function	Measuring Equipment A-C	ERDL	Gdyr	Average	Spread of Values Units	% of Average
3X-2 Runs 1 and 2	Crawler tractor, clay course	5	Reserve tractive force, lb	2000	2010	1945	1985	65	3.3
			Engine speed, rpm	1382	1379	1376	1379	6	0.4
			Ground speed, mph	5.30	5.27	5.27	5.28	0.03	0.6
			Travel efficiency, %	99.2	98.9	99.7	99.3	0.08	0.8
3X-3 Runs 2, 3, and 4	Crawler tractor, clay course	2	Reserve tractive force, lb	5535	5643	5590	5589	108	1.9
			Engine speed, rpm	1356	1355	1355	1355	1	0.1
			Ground speed, mph	2.22	2.21	2.22	2.22	0.01	0.5
			Travel efficiency, %	96.4	96.6	97.1	96.7	0.7	0.7
3X-7 Runs 1 to 5	Pneumatic-tired tractor, portland cement concrete course	3	Reserve tractive force, lb	8889	8867	—	8878	22	0.3
			Converter, rpm	1167	1156	—	1162	11	1.0
			Ground speed, mph	4.42	4.40	—	4.41	0.01	0.2
			Travel efficiency, %	96.9	97.1	—	97.0	0.2	0.2
Runs 8, 10 to 14	Pneumatic-tired tractor, portland cement concrete course	3	Reserve tractive force, lb	—	9185	9145	9165	40	0.4
			Converter, rpm	—	1148	1147	1148	1	0.1
			Ground speed, mph	—	4.35	4.36	4.36	0.01	0.2
			Travel efficiency, %	—	97.1	96.3	96.7	0.8	0.8
3X-9 Runs 1 to 5	Pneumatic-tired tractor, portland cement concrete course	1	Reserve tractive force, lb	14,907	15,221	—	15,064	314	2.1
			Converter, rpm	1961	1926	—	1944	35	1.8
			Ground speed, mph	1.38	1.38	—	1.38	0	0
			Travel efficiency, %	93.8	94.7	—	94.2	0.9	1.0

Table 2 – Summary of Concurrent Measurements

Course	Reserve Force, lb	Spread of Per Cent of Average: Reserve Force	Engine Speed, rpm	Ground Speed	Travel Efficiency
Clay	2000	3.3	0.4	0.6	0.8
Clay	5500	1.9	0.1	0.5	0.7
Portland cement concrete	9000	0.3-0.4	1.0-0.1	0.2-0.2	0.2-0.8
Portland cement concrete	15,000	2.1	1.8	0	1.0
Spread allowed by code	—	5.0	2.0	2.0	Not specified

Specifically, an attempt was made to determine four things:

1. The relative accuracy of the equipment and methods in measuring the quantities demanded in the code.
2. Whether or not the accuracy tolerances specified in the code are within reason.
3. The closeness with which repeat measurements on a clay soil course could be made after the course was reworked.
4. A check on the methods of test procedure written into the code.

Comparison of Measurement Accuracy of the Several Types of Equipment with One Another and with the Code – Three types of measuring equipment were used for these tests. All three were concurrently used for measuring the reserve tractive ability of a crawler tractor (Caterpillar D-4) on a clay course. Tractive ability tests were also run on a pneumatic-tired tractor (LeTourneau-Westinghouse) on a portland-cement concrete course. In this case, however, the tests were made with only two measuring devices operating concurrently.

For the crawler tractor tests, the Goodyear dynamometer truck was used to impose the load, and incorporated in its drawbar were the Allis-Chalmers and Corps of Engineers equipment for measuring reserve tractive effort.

The equipment necessary for measuring the engine speed and travel efficiency[14] by all three methods was attached to the tractor. The results obtained are tabulated in Table 1.

Table 2 is a further summary in which this spread of values expressed as a per cent of the average measurement is shown in comparison with the type of course, the magnitude of the reserve force measurement, and the presently proposed test code tolerance.

Inspection of Table 2 and bar charts in Figs. 36 and 37 show that the measurement methods for reserve tractive force are well within the proposed code limits expressed as $\pm 2\frac{1}{2}\%$ or a spread of 5%. The greatest variation occurred during low pulls on the clay course; however, even under these conditions the spread was considerably under the code limitations. It is quite probable that a systematic error of calibration was present in one or more of these pieces of pull-measuring equipment which would tend to increase the observed spread. Corrections could be made for an error of this nature, and the spreads observed would be even smaller. It is felt, however, that systematic errors are bound to be a part of these measurements and should be included in any expression of expected measurement accuracy.

Engine rpm was measured with accuracy by the

[14] While it has been the custom of industry to use the term "slip" in discussing reduction in vehicle speed resulting from tractive inefficiencies, it is the consensus of the group that travel efficiency is a more pertinent method of reporting and evaluating performance, as travel efficiency is the ratio between observed and theoretical distances of travel.

several types of equipment, and the accuracy of ±1% or 2% spread allowed in the code can evidently be readily met.

Likewise, the 2% spread allowed in the code for the measurement of ground speed was even more easily accomplished.

Travel efficiency, which is the ratio of the distance the vehicle travels while exerting tractive effort under drawbar load to that distance traveled without drawbar load, was determined by the code procedures. Code A in paragraph 4.3 provides that the no-load distance be determined as a general procedure by self-propelling the vehicle, but it also provides an alternate procedure by which the no-load distance can be obtained through pulling or pushing the vehicle. Data reported by Allis-Chalmers and ERDL was obtained by the self-propelling method, while Goodyear results were obtained by towing the test vehicle. Travel efficiencies as determined by the alternate method, that of pulling or pushing the test vehicle, did not show consistent differences when compared with the measurements taken by the self-propelled method. The general accuracy of the results appears to be sufficient for the need of this data, which might be termed supplementary to the main objectives of force, speed, and power.

Repeatability of Tests on Soil Course – During tests, efforts were made to reprocess the soil course to consistent and similar tractive conditions for each successive use. Reworking the course was accomplished by first scarifying the surface with a motorized grader and thoroughly pulverizing it to a depth of 8 in. with a pulvamixer. Moisture was then added, and the course was regraded and compacted with a wobble-wheel roller to uniform surface bearing. Compaction was controlled by taking samples of bearing with a standard Proctor needle. Since the weather was ideal during the period of tests, the effect of extreme changes in temperature, moisture, or other factors which influence the traction strength of the course could not be analyzed. It is understood that this phenomena is a matter of continuing investigation at ERDL.

The results of checks during and subsequent to the test procedure trials show that a maximum spread of 7% occurred in tractive force during any test where the travel efficiency did not vary over 5%. Later studies by ERDL have shown a variation with ±1.5% of average for repeated tests wherein the ultimate strength of the soil was utilized. These results lead us to believe that consistent values may be obtained on fine-grained soil courses which are reprocessed with reasonably close control of bearing strength (as measured by Proctor needle); however, more experience is needed before this can be accepted as an established fact.

Check on Methods and Precautions of Test Procedure as Proposed by Code – It was not intended to ignore well-established practices in conducting the dynamometer work at Fort Belvoir; however,

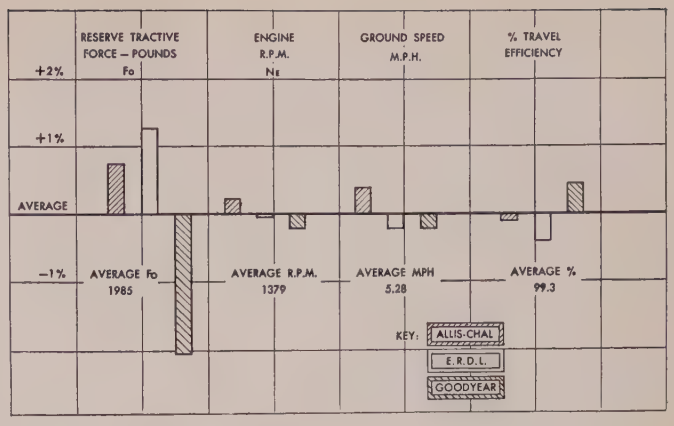

Fig. 36 – Percentage variation in concurrent measurements of crawler tractor in fifth gear

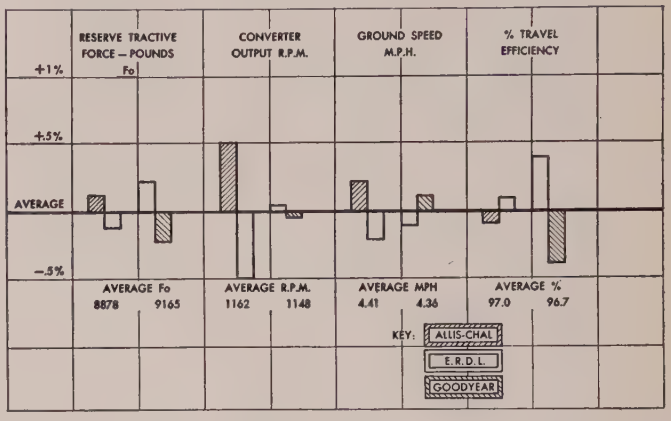

Fig. 37 – Percentage variation in concurrent measurements of wheel tractor in third gear

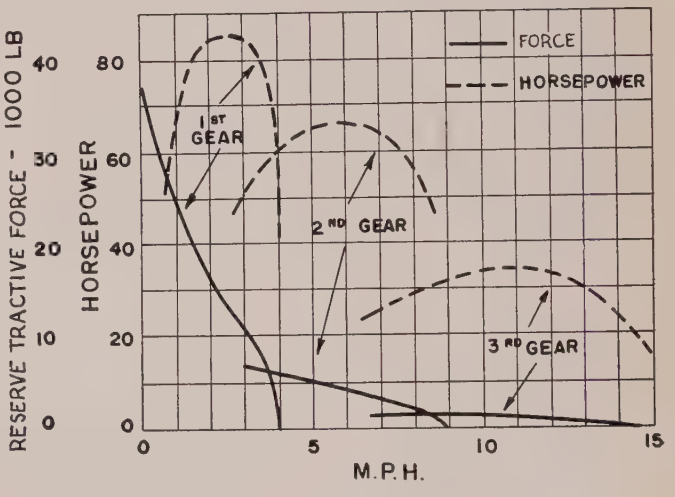

Fig. 38 – Reserve tractive force and horsepower versus speed

the shortage of time did lead into attempting trial runs before the machines were properly conditioned. This gave results which showed the machines were not yet stabilized for test and emphasized the necessity for proper breakin and warmup as set down in the test code.

The results of insufficient conditioning were brought out strikingly in the vehicle drag runs made on the crawler tractor. The tracks, when the

vehicle was first tested, were quite stiff due to storage for a long period of time, and a great deal of power was lost in driving them. Vehicle drag values of over 2000 lb were measured originally. This resistance had been reduced to 1400 to 1500 lb by the time that the official tests were commenced. The vehicle was then blocked up and the tracks run overnight to accomplish further loosening, which reduced resistance to 1100 lb. When measuring the performance of this type of vehicle, it appears that controlling the condition of the tracks may be equally as important as controlling the soil condition in which it is tested.

Under paragraph 4.7 is specified the method of making the test runs. The code states that the value to be controlled during the run should be that of engine speed of the tested vehicle. We quote:

"While traveling over the measured course during any recorded run, the instantaneous engine or drive output shaft rpm should not vary from the specified speed more than ±3%, and the average speed shall not vary from the specified speed more than ±1%, and the average of engine speeds of the four selected runs shall not vary from the specified speed more than ±½%."

This clause is designed to provide a test procedure by which a specified vehicle performance can be checked. For this purpose, engine speed is the best single value to control, and the procedure is designed to give a practical working tolerance for this check test. The field tests indicate that the closeness of speed control specified can be attained with present test equipment.

An alternate procedure has been written into the code for use when available equipment makes controlling the reserve tractive force more desirable. This is carried out by holding the reserve tractive force of the machine steady and keeping the instantaneous speed at the beginning of the recorded run within 3% of that at the end of the run.

Either of these procedures may be used in making a broad study of a machine by obtaining a series of points to form curves such as those shown in Fig. 38. In this case both reserve tractive force and horsepower have been related to vehicle speed.

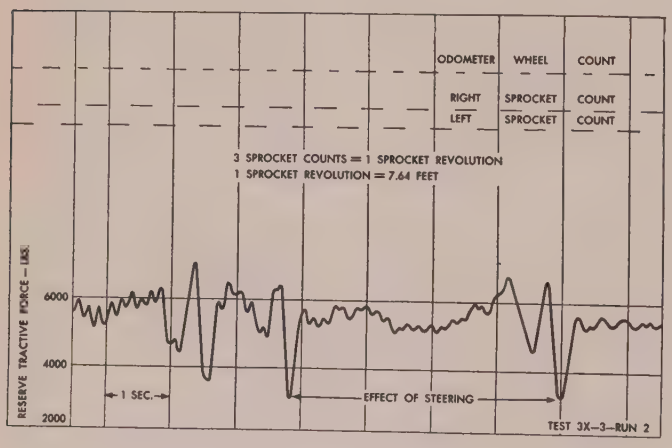

Fig. 39 – Effect of steering on reserve tractive force

Another precautionary note offered in the code is to limit directional changes or steering of the vehicle. The code allows a difference in revolutions of 2% for drive sprockets and 3% for drive wheels. Even though excessive steering corrections to both sides which cancel each other will give results falling within the prescribed limits of the code, the reserve tractive ability of the machine falls off rapidly when steering. For an illustration, look at the large drop in tractive force shown in Fig. 39. This is taken from ERDL record and shows results of one steering correction while running the wheel vehicle.

All results presented have been observed figures with no corrections applied. Since there is reason to doubt the accuracy of current correction factors, as applied to diesel engines, we recommend in the code that any test report state observed reserve tractive effort and observed reserve tractive horsepower. If required, corrected reserve tractive horsepower could be shown as corrected in accordance with the standards set forth in the applicable SAE Engine Test Code.

Appendix

Test Code A – Reserve Tractive Ability

1. *Object* – The object of the reserve tractive ability test is to determine the ability of a self-propelled vehicle to develop tractive force and power, beyond that required to move itself, on a specified course. Reserve tractive ability is reported as "reserve tractive force" in pounds and as "reserve tractive power" in horsepower.

2. *Scope* – This code applies to all types of self-propelled construction and industrial vehicles and their combination with mounted and/or trailed equipment, with or without payload.

3. *Facilities, Apparatus, and Materials* – 3.1 A test course prepared to provide desired conditions of traction and vehicle drag. It may be a loop or a straight course with sufficient room for the test train to turn at the ends. In either case it shall include a straight test zone with a minimum length of 44 times the expected test speed (in mph) or 100 ft, whichever is greater, plus sufficient length to permit stabilization of operation before start of the recorded run. This section of the test course shall be uniform with not over 1% average grade. Its width should be at least twice that of the test vehicle and the crown shall not exceed 1½% slope from the center to the outer edge of the course. The course shall be maintained in a condition consistent with the object of the test.

3.2 One dynamometer for measuring and recording reserve tractive force; overall accuracy

$\pm 2\frac{1}{2}\%$ of the observed force. (To prevent overloading instruments while turning or accelerating, the use of a lockout device is suggested.)

3.3 Suitable towed load controllable to maintain within specified limits either:

(a) Speed of engine or of output shaft of continuously variable drive, if vehicle is so equipped.

(b) Reserve tractive force.

3.4 Means to establish the time duration of test; accuracy $\pm\frac{1}{2}\%$.

3.5 Means to establish the distance transversed during the test; accuracy $\pm\frac{1}{2}\%$.

3.6 Means to establish, during the test, the number of revolutions of the engine and of the output shaft of continuously variable drive if vehicle is so equipped; accuracy $\pm\frac{1}{2}\%$ of total revolutions.

3.7 Tachometer to indicate rpm of the engine or of the output shaft of continuously variable drive, if vehicle is so equipped; accuracy $\pm 1\%$ of reading.

3.8 Means to establish, during the test, the number of revolutions of each drive wheel or sprocket; accuracy $\pm\frac{1}{2}\%$ of total revolutions.

3.9 Means to establish required weights; accuracy $\pm 2\frac{1}{2}\%$ of the weight measured.

3.10 A supply of fuel and lubricants meeting specifications acceptable to the vehicle manufacturer.

3.11 Means to establish specific gravity of fuel; accuracy $\pm\frac{1}{2}\%$.

3.12 Tire pressure gage; accuracy $\pm 3\%$ of reading.

3.13 One steel surveyor's tape, 100 ft.

3.14 One thermometer for ambient temperature; accuracy ± 1 F.

3.15 One barometer; accuracy ± 0.10 in. of mercury.

4. *Procedure* – 4.1 If the vehicle has not recently been used, it should be "limbered up" in a manner recommended by the manufacturer. Any malfunction or maladjustment noted during this "limber up" period should be corrected before proceeding with the test.

4.2 The vehicle shall be given a service check prior to test, to assure that:

(a) All mechanical adjustments (governor, timing, brakes, clutches, and the like) are as recommended by the manufacturer.

(b) Weight and distribution are as specified.

(c) The vehicle is supplied with specified fuel, lubricants, and engine coolant.

4.3 Install the test apparatus and instruments

RESERVE TRACTIVE ABILITY TEST SUMMARY

GENERAL DATA:

Vehicle, Make _____ Model _____ Ser. No. _____

Vehicle Attachment, Type _____

Make _____ Model _____ Ser. No. _____

Engine Make _____ Model _____ Ser. No. _____

Rated rpm _____ Fuel Spec. _____ Gravity ____ at _____°F

Test Track, Location _____

Material _____ Condition _____

Payload or Ballast, Describe _____

Weight _____ Lbs., Location _____

Wheel or Track Location						
Wheel or Track Load						
Tire or Track Size / Type						
Tire Rim Width						
Tire Inflation Pressure						

GROSS VEHICLE WEIGHT _____ Lbs. Hitch Height above Ground _____ in.

AVERAGE DATA ON INDIVIDUAL TESTS:							
Test No.							
Log Sheet Nos.							
Transmission Gear							
Over-all Ratio							
Engine Speed, rpm	n_e						
Output Shaft, rpm	no						
Ground Speed	mph						
Res. Tractive Force	F_o						
Travel Efficiency*	S						
Res. Tractive Power	ThPo						
Ambient Temperature	F						
Barometer	In. Hg.						
Relative Humidity	%						

Signed: _____ Date: _____

*State whether vehicle driven ( ), towed ( ), or pushed ( ) to obtain distance traveled per revolution of drive wheel or sprocket.

VEHICLE DRAG TEST SUMMARY

GENERAL DATA:

Vehicle, Make _____ Model _____ Ser. No. _____

Vehicle Attachment, Type _____

Make _____ Model _____ Ser. No. _____

Test Track, Location _____

Material _____ Condition _____

Payload or Ballast, Describe _____

Weight _____ lbs., Location _____

Wheel or Track Location						
Wheel or Track Load						
Tire or Track Size / Type						
Tire Rim Width						
Tire Inflation Pressure						

GROSS VEHICLE WEIGHT _____ lbs. Hitch Height above Ground _____ in.

AVERAGE DATA ON INDIVIDUAL TESTS:							
Test No.							
Log Sheet Nos.							
Ground Speed	mph						
Vehicle Drag	f_o						
Ambient Temperature	F						
Wind Velocity	mph						

Signed: _____ Date _____

Fig. 40 – Reserve tractive ability test and vehicle drag test summary charts

and operate sufficiently to determine that all function properly.

Note: Attachment of the towed load should duplicate as nearly as possible the normal operation of the test vehicle. If the vehicle normally is used for towing, attachment should be at the towing hitch; otherwise, it should be as close to the ground as practicable. The line of draft should be horizontal unless some particular function of the vehicle dictates otherwise.

4.4 Prior to recording test data, the vehicle shall be operated until functional components and lubricants reach reasonably stable temperatures. Tire inflation on a pneumatic-tired vehicle shall be maintained within limits specified by the vehicle manufacturer.

4.5 Determine the distance the vehicle travels per revolution of the drive wheels or sprockets without tractive load by one of the following methods:

(a) Drive the vehicle in lowest gear with engine throttled to its lowest uniform running speed and without directional correction for a distance not less than 100 ft. Count revolutions of drive wheels or sprockets; divide distance traveled by revolutions to obtain travel per revolution.

(b) If vehicle drag does not exceed 100 lb per ton, the distance traveled per revolution of the drive wheels or sprockets may be determined by towing or pushing the vehicle at the lowest practical uniform speed. Record data and calculate as in method (a).

4.6 Record general data required by test log.

4.7 While traveling test distance with the towed load adjusted to maintain the average speed of drive wheels or sprockets at specified rpm, record:

(a) Reserve tractive force.

(b) Time.

(c) Distance.

(d) Number of revolutions of engine and of output shaft of continuously variable drive, if vehicle is so equipped.

(e) Number of revolutions of each drive wheel or sprocket.

As an alternate procedure, the reserve tractive force may be controlled and held as constant as possible for each run. The same data are recorded. The instantaneous engine and vehicle ground speeds at the end of the test run should be within 3% of the respective values at the start.

Recorded test runs shall cover a minimum time of 0.5 min or a minimum distance of 100 ft, whichever is greater. The average of four runs (two best runs in each direction) shall be used in reporting vehicle performance at each selected speed or load.

There should be a minimum of steering during the recorded runs. Revolutions of the drive wheels on wheeled vehicles shall not vary from each other more than 3%. Revolutions of the drive sprockets on track vehicles shall not vary from each other more than 2%.

During any recorded run the instantaneous speed of engine or of the output shaft of continuously variable drive, if vehicle is so equipped, should not vary more than ±3% from the specified speed. The average speed for any one run shall not vary more than ±1% from the specified speed and the average for the four selected runs shall not vary more than ±½% from the specified speed. To avoid loss of power through engine overspeeding into range of governor regulation, the governor may be set for higher engine speed or the engine may be controlled manually during the recording runs.

Note: The above procedures show vehicle performance under a specified condition. When a broader investigation is desired, a series of recorded runs may be made in any transmission gear under several conditions of speed or reserve tractive force. This data may be plotted to show general performance characteristics on the selected course.

In order to obtain satisfactory readings in low gear on machines having sufficient power to slip their wheels or tracks, it may be necessary to reduce the draft load so that travel efficiency is not less than 85% for wheel vehicles and 93% for track vehicles.

5. *Symbols and Computations* –

F_o = Reserve tractive force, lb (from paragraph 4.7a) averaged for either time or distance

t = Time to travel test distance, min (from paragraph 4.7b)

N_e = Revolutions of engine to travel test distance (from paragraph 4.7d)

N_o = Revolutions of output shaft of continuously variable drive to travel test distance (from paragraph 4.7d)

N_w = Average revolutions of drive wheels or sprockets to travel test distance (from paragraph 4.7e)

s = Test distance traveled, ft (from paragraph 4.7c)

s_s = Average distance vehicle traveled without tractive load per revolution of the drive wheels or sprockets, ft (from paragraph 4.5)

s_o = Average distance vehicle traveled with tractive load per revolution of the drive wheels or sprockets, ft. That is, $s_o = \frac{s}{N_w}$

S = Travel efficiency $= \frac{s_o}{s_s} \times 100\%$

mph = Vehicle speed $= \frac{s}{88t}$ mph

THP_o = Reserve tractive horsepower $= \frac{F_o \times \text{mph}}{375}$

n_e = Average speed of engine, rpm. That is, $n_e = \frac{N_e}{t}$

n_o = Average speed of output shaft of continuously variable drive, rpm. That is, $n_o = \frac{N_o}{}$

Note: Reserve tractive force and reserve tractive power are reported as observed, since the undetermined factors of engine friction, chassis

drive train friction, and vehicle drag make engine correction formulas for atmospheric conditions inapplicable; however, ambient temperature, barometric pressure, and humidity (water vapor pressure) are listed for each test on the summary sheet to show conditions at the time of test as an indication of comparability with data from similar tests.

Test Code B – Vehicle Drag

1. *Object* – The object of the vehicle drag test is to determine the external force required to maintain travel speed on a specified course. Vehicle drag is reported as "vehicle drag force" in pounds.

2. *Scope* – This code applies primarily to towed construction and industrial vehicles, and their combination with mounted equipment and with or without payload. It may be used to determine the resistance to motion of a self-propelled vehicle.

3. *Facilities, Apparatus, and Materials* – 3.1 A test course, prepared to provide desired conditions for vehicle drag and adequate traction for the prime mover. It may be a loop or a straight course with sufficient room for the test train to turn at the ends. In either case it shall include a straight test zone with a minimum length of 44 times the test speed (in mph), or 100 ft, whichever is greater, plus sufficient length to permit stabilization of operation before start of the recorded run. This section of the test course shall be uniform with not over 1% average grade. Its width should be at least twice that of the test vehicle and the crown shall not exceed 1½% slope from the center to the outer edge of the course. The course shall be maintained in a condition consistent with the object of the test.

3.2 One dynamometer for measuring and recording drag force; overall accuracy ±2½% of the observed force. (To prevent overloading instruments while turning or accelerating, use of a lockout device is suggested.)

3.3 Suitable prime mover.

3.4 Means to establish time duration of test; accuracy ±½%.

3.5 Means to establish the distance traversed during the test; accuracy ±½%.

3.6 Means to indicate ground speed.

3.7 Means to establish required weights; accuracy ±2½% of the weight measured.

3.8 A supply of lubricants meeting specifications acceptable to the vehicle manufacturer.

3.9 Tire pressure gage; accuracy ±3% of reading.

3.10 One steel surveyor's tape, 100 ft.

3.11 One thermometer for ambient temperature; accuracy ±1 F.

3.12 Means for measuring wind velocity.

4. *Procedure* – 4.1 If the vehicle has not recently been used, it should be "limbered up" in a manner recommended by the manufacturer. Any malfunction or maladjustment noted during this "limber up" period should be corrected before proceeding with the test.

4.2 The vehicle shall be given a service check prior to test, to assure that:

(a) All mechanical adjustments (brakes, and so forth) are in order.

(b) Weight and weight distribution are as specified.

(c) The vehicle is properly lubricated.

4.3 Install the test apparatus and instruments and operate sufficiently to determine that all function properly.

Note: Attachment of the dynamometer should duplicate as nearly as possible the normal operation of the test vehicle. The line of draft should be horizontal unless some particular function of the vehicle dictates otherwise.

If the test vehicle has a steerable front axle, a bridle hitch or other means will be necessary to maintain directional control.

4.4 Prior to recording test data, the vehicle shall be operated until functional components and lubricants reach reasonably stable temperatures. Tire inflation on a pneumatic-tired vehicle shall be maintained within limits specified by the vehicle manufacturer.

4.5 Record general data required by test log.

4.6 With test vehicle being towed at the selected nominal constant speed over the specified course, record:

(a) Drag force.

(b) Time.

(c) Distance.

Reported test runs shall cover sufficient distance to provide records of at least 0.5-min duration. The average of an equal number of runs in both directions shall be used in reporting vehicle performance.

For any reported test, the ground speeds at start and end of a run shall not differ from each other by more than 2 mph per min of test duration.

Tests shall not be reported for which wind velocity (in any direction) exceeds 15 mph.

5. *Symbols and Computations* –

f_e = Vehicle drag, lb (from paragraph 4.6a), averaged for either time or distance

t = Time to travel test distance, min (from paragraph 4.6b)

s = Test distance traveled, ft (from paragraph 4.6c)

$$\text{mph} = \text{Vehicle speed} = \frac{s}{88t} \text{ mph}$$

Note: Vehicle drag is reported as observed, without correction for atmospheric conditions or wind velocity as available correction formulas are inapplicable to most construction and industrial vehicles; however, ambient temperature and wind velocity are listed for each test on the summary sheet to show conditions at the time of test as an indication of comparability with data from similar tests.

High Supercharging

A THEORETICAL analysis indicated that a charging air system of exhaust-driven turbocharger, engine-driven Roots-type blower, and aftercooler would permit increasing the output of the General Motors Model 16-278A 2-stroke-cycle diesel engine from 1600 to 3000 bhp at 750 rpm. Using a mechanism to control engine compression ratio relative to engine output would further improve thermal efficiency at lower loads.

Tests with a simulated turbocharged installation proved the accuracy of the analysis. Thermal efficiency from 1500 to 3000 bhp was better than that at the original 1600-bhp rating.

Tests are now under way adapting turbochargers to the engine and developing manifolding to duplicate the simulated turbocharged operation.

THERE are diesel engines commercially available in Europe with brake mean effective pressures far exceeding any in this country. Fig. 1 shows the rating of some of those engines in comparison with representative American diesels.

The 2-stroke-cycle section of this figure includes the Gotaverken opposed-piston engine with a continuous rating of 150 psi bmep and a maximum rating of 168 psi bmep. The rating was attained with a supercharging pressure of 20.8 psig, obtained with an exhaust-driven turbocharger. The Napier Nomad, by using its exhaust energy both to drive a turbocharger and to provide added crankshaft power, has an output of 287 psi bmep with a supercharging pressure of 75 psig. In comparison, our most comparable American diesels have outputs not exceeding 90 psi bmep.

The MAN engine shown in the 4-stroke-cycle section has a similar differential over the available American engines in comparable sizes. There, the use of supercharging pressures up to 32 psig, with a 2-stage exhaust-driven turbocharger and an intercooler between stages, permits an output rating of 312 psig bmep with a very high thermal efficiency. Comparatively, American engines are available at a maximum of about 180 psig bmep.

U. S. Navy Interest

The American Navy is the world's largest user of Diesel engines. Despite the improvements in other types of power, such as gas turbines and nuclear powerplants, that condition will undoubtedly exist for many years. Naval service engines desirably should have low specific weight and bulk, but they must maintain outstanding reliability. Not all engines furnished have had sufficient reliability for the severe Naval requirements, and costly improvement is sometimes required.

Since the Naval requirements for low bulk and weight are greater than the normal commercial requirements, it is understandable that the Navy has had to assist in developing suitable engines. This sometimes is done by contracting with a manufacturer to develop an engine to meet specific requirements. More often it is done by buying commercial engines and conducting extensive testing to locate faults and to assist the manufacturer in making the required improvements. A third method is to sponsor or conduct basic investigations. This may be done in an independent laboratory or in government laboratories.

The Navy has been largely interested in 2-stroke-cycle engines because of their lower weight and bulk per horsepower. Their reliability has been generally satisfactory. Recent advances in 4-stroke-cycle engines have again made them competitive in output per size. Inherently, the 2-stroke-cycle engine should maintain its old advantage and will lose it only if its development is neglected. It is advantageous to have the 2-stroke-cycle engine advance equally with the 4-stroke-cycle engine.

Scope of Project

The project described in this paper is one that was conducted in the Navy's own laboratory, the Engineering Experiment Station at Annapolis, Md. It was intended to show the power increase that could be made in a 2-stroke-cycle diesel engine of normal design without any extensive or radical changes in the engine. The information obtained, while serving directly to improve an engine which the Navy owned in very large numbers, would be of greatest value because it would be available to all American manufacturers and should be of assistance to them in increasing the specific output of their engines.

The engine selected for the investigation was the General Motors Model 16-278A. The Navy owns more of that model than of any other large

Development of a GM 16-278A 2-Stroke-Cycle Diesel Engine

Warren G. Payne and Wolfgang S. Lang
U. S. Naval Engineering Experiment Station

This paper was presented at the SAE National Diesel-Engine Meeting, Cleveland, Oct. 27, 1954.

engine. It has been very satisfactory in service and is known to be conservatively designed and rated. It was believed to be amenable to improvement. It has an 8¾-in. bore and a 10½-in. stroke. Operating at 750 rpm, it has been rated at 1600 bhp for submarine and most other types of service, or at 1700 bhp for some types of service. Maximum rating is thus 83.6 to 88.9 psi bmep, about normal for American engines but very conservative compared to the high-output engines mentioned. Specific weight, dry with attached accessories, is 19.4 lb per hp and specific bulk is 0.29 cu ft per hp.

The program included five phases:

1. An analysis of the possible engine air systems, the output that could be obtained with apparent safety, and the engine air requirements under those conditions.

2. Operation with a simulated turbocharger system to determine the actual air requirements of the standard engine at increased outputs without the complications of matching turbocharger and manifolding to the engine.

3. Matching of turbocharger and manifolding to the engine to obtain the airflows previously found necessary.

4. Determination of the improvement in operating conditions that could be obtained if exhaust-valve timing and cylinder charging were varied with engine output.

5. A reliability test of the engine at the new maximum load to locate any unsatisfactory conditions not noted during the development.

Preliminary Analysis

Some limitations were set before the analysis:

1. The engine was to be kept at its present 750 rpm rated speed. Additional power could have been obtained with increased speed, and it was probable the engine would operate satisfactorily. Increased speed might have introduced other complications, and it wasn't necessary. Speed could be increased later after bmep was raised. For purposes of comparision, however, a calculation was also made at 1000 rpm.

2. The existing Roots blower was to be kept on

The Authors

WARREN G. PAYNE (M '40) is a senior mechanical engineer, heading the Experimental Diesel-Engine Branch, Internal-Combustion Engineering Laboratory at the U. S. Naval Engineering Experiment Station in Annapolis, Md. After receiving his M.S. in Mechanical Engineering from the University of Alabama in 1932, Mr. Payne worked for the Electric Boat Co. as a test engineer on diesel engines until 1938, when he joined the Naval Engineering Experiment Station.

WOLFGANG S. LANG is head of the Engines and Combustion Systems Section in the Developments Branch, Internal-Combustion Engines Laboratory, and project engineer in charge of the High Supercharge Development. After obtaining his M.S. in Mechanical Engineering from the Institute of Technology, Munich, Germany, in 1932, Mr. Lang joined the German State Railways. He has also worked for the Junkers Research Institute and Daimler-Benz Co. He has been at the Naval Engineering Experiment Station since 1947.

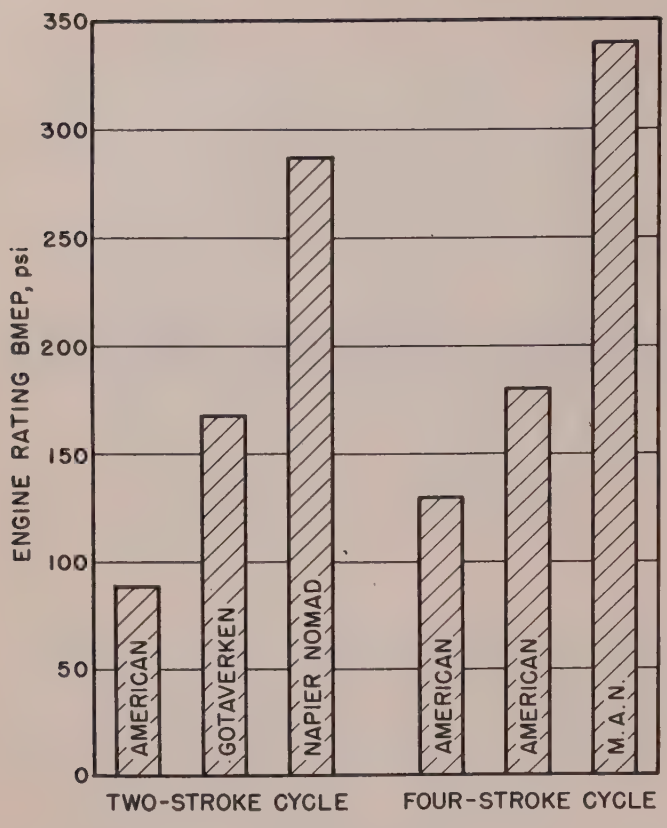

Fig. 1 – Relative rating of representative American diesels and most advanced foreign diesels

the engine and operated at the same speed. Calculations with a larger blower were made for comparison.

3. Intake-port and exhaust-valve areas were to remain unchanged. This was part of the plan to hold to a minimum any engine changes, although it was realized that there would be increasing flow restriction at higher loads.

4. Engine operating conditions had to be kept at safe operating levels. A peak cylinder pressure of 1300 psig and an exhaust temperature of 900 F were selected. Although higher than the normal 1050-1100 psig and 650 F for the engine, they were not considered excessive.

5. The exhaust system must simulate the standard ship's exhaust system with its backpressure of 40 in. of H_2O.

6. The engine must start easily under normal conditions and be capable of being operated under snorkel high backpressure conditions.

7. Airbox temperature must be no lower than could be obtained with sea-water cooling under any sea conditions and a reasonable size of heat exchanger.

The analysis was made both for an engine operating with standard fixed exhaust-valve timing and for an engine with exhaust-valve timing controlled to make the effective piston compression stroke vary with the load carried. Both the rated 750 rpm and an overspeed 1000 rpm were considered. The airflow system included:

1. Conventional engine.

2. Conventional engine with larger mechanical blowers.

3. Lower compression ratios, large mechanical blowers.

4. Lower compression ratios, turbocharger only.

5. Conventional engine with standard blower first stage, turbo second stage.

6. Lower compression ratios, standard blower first stage, turbo second stage.

7. Conventional engine with turbo first stage, standard blower second stage.

8. Lower compression ratio, turbo first stage, standard blower second stage.

9. Snorkel conditions with lower compression ratio, turbo first stage, standard blower second stage.

10. Use of intercoolers, aftercoolers, and various charging conditions to make a total of 37 combinations.

Certain assumptions regarding ambient conditions, airflow restrictions, charging conditions, and heat losses had to be made. Fortunately, the assumptions applied fairly equally to all operating levels considered, and the comparisons remained equitable. The same calculation method was applied to the known standard engine conditions and gave an engine output only 1% from the operating condition.

The calculation method used covered operation with fixed exhaust-valve timing to determine allowable loads and with variable exhaust-valve timing to determine the timing desired and the load which could be carried under the controlled conditions. The main steps in the procedure were:

1. Calculate the effective compression ratio which will give the desired compression pressure with the specified scavenging pressure.

2. (a) Calculate the effective length of stroke (distance back from top center) which represents the calculated effective compression ratio.

(b) Convert length of effective stroke into crank angle to determine exhaust-valve closure timing.

3. Calculate the energy required from the exhaust gas for the turbocharger drive and the energy available in the exhaust gas. (Note: Numerical values cannot yet be obtained, but a relationship can be established based on the pressure differentials at turbine and compressor and the temperature of the gases.)

4. Determine the operating condition (airflow and turbocharger and ducting pressures and temperatures) at which the air delivered by the existing mechanical blower is equal to that required by the engine.

5. Calculate the amount of air retained in the

cylinder charge for the new operating condition as compared to that retained under standard operating conditions.

6. Calculate net brake horsepower available from the new system, based on the amount of air retained in the cylinder, using a constant fuel/air ratio, and the work required to pump that air.

Table 1 summarizes the results of the analysis. Only 18 of the 37 air systems studied are included in the table. The first column is inserted to show the accuracy attained by the method when applied to the standard engine with the known conditions of operation. It indicates that the engine should carry 1584 bhp at 750 rpm with a fuel consumption of 0.405 lb per bhp-hr. In actual operation it developed 1600 bhp with a fuel consumption of 0.408 lb per bhp-hr. The 1% error was less than was expected. The preliminary analysis was intended only to show the way for the experimental development.

The first section of the chart is self-explanatory. Adding an aftercooler, only, to the standard engine gave a denser cylinder charge at very little expense in blower horsepower, and the net output increased 94 bhp, 6%, with as good fuel consumption. Using a larger engine-driven Roots-type blower to increase the supercharging pressure boosted the net output by 60%, but the greatly increased blower horsepower decreased the mechanical efficiency, and specific fuel consumption rose to an amount about 15% more than was desired.

The next two columns include use of an exhaust-driven turbocharger in series with the engine-driven blower. As was anticipated, predicted performance is far superior. Using the engine blower as the first stage, while good, was less desirable than making the turbocharger the first stage. That was because the engine blower, driven at a constant speed, has a definite displacement and, when used as the first stage, provides an increased flow only to the extent of the decreased discharge pressure. The turbocharger as a first stage can supply an increased total airflow and density of charge to the engine blower and use that blower only as a pressure booster. That comparison would not be true if the Roots blower speed could be changed as desired in proportion to the load being carried,

Table 1 – Predicted Performance for Various Supercharging Conditions

	DATA \ ENGINE SYSTEM		STANDARD ENGINE TIMING					CONTROLLED EXHAUST CLOSURE TIMING												
			STANDARD EQUIPMENT	AFTERCOOLER	LARGER MECH. BLOWER – AFTERCOOLER	STD. MECH. BLOWER-TURBOCHARGER-AFTERCOOLER	TURBOCHARGER-STD. MECH. BLOWER-AFTERCOOLER	LARGER MECH. BLOWER – AFTERCOOLER		STD. MECH. BLOWER-TURBOCHARGER-AFTERCOOLER		STD. MECH. BLOWER-INTERCOOLER-TURBOCHARGER-AFTERCOOLER		TURBOCHARGER-STD. MECH. BLOWER-AFTERCOOLER		TURBOCHARGER-INTERCOOLER-STD. MECH. BLOWER-AFTERCOOLER		SNORKEL: TURBOCHARGER-STD. MECH. BLOWER-AFTERCOOLER	TURBOCHARGER AFTERCOOLER	
CONTROLLED CONDITIONS	SCAVENGE AIR	TEMP., °F	140	100	100	100	100	100	100	100	100	100	100	100	100	100	100	100	100	100
		PRESS., psig	3.00	2.90	11.00	11.00	11.00	16.70	16.70	16.70	16.70	16.70	16.70	16.70	16.70	16.70	16.70	14.45	16.70	16.70
	CYLINDER COMPRESSION	TEMP., °F	1145	1038	959	1050	1010	772	885	830	950	830	950	792	909	780	895	972	796	910
		PRESS., psig	594	591	850	850	850	600	850	600	850	600	850	600	850	600	850	850	600	850
	EXHAUST CLOSE °BTC		121.5	121.5	121.5	121.5	121.5	71.3	98	71.3	98	71.3	98	71.3	98	71.3	98	104.7	71.3	98
	EFFECTIVE COMP. RATIO		13.51	13.51	13.51	13.51	13.51	9.06	11.62	9.06	11.62	9.06	11.62	9.06	11.62	9.06	11.62	12.35	9.06	11.62
OPERATING CONDITIONS	INTAKE AIR	TEMP., °F	90	90	90	90	90	90	90	90	90	90	90	90	90	90	90	90	90	90
		PRESS., in. hg.	-1.0	-1.0	-1.0	-1.0	-1.0	-1.0	-1.0	-1.0	-1.0	-1.0	-1.0	-1.0	-1.0	-1.0	-1.0	-3.0	-1.0	-1.0
	CYLINDER CHARGE	TEMP., °F	181	141	110	146	130	110	110	137	137	137	137	120	120	114	114	134	121	121
		PRESS., psig	3.0	2.9	11.0	11.0	11.0	16.7	16.7	16.7	16.7	16.7	16.7	16.7	16.7	16.7	16.7	14.45	16.7	16.7
	INLET PORTS	OPEN, °ATC	129	129	129	129	129	129	129	129	129	129	129	129	129	129	129	129	129	129
		CLOSE °BTC	129	129	129	129	129	129	129	129	129	129	129	129	129	129	129	129	129	129
	EXHAUST OPEN, °ATC		89	89	89	89	89	89	89	89	89	89	89	89	89	89	89	89	89	89
	ENGINE BACK PRESS., psig		1.40	1.50	4.80	9.38	9.10	7.65	7.65	15.08	15.08	15.09	15.09	13.50	13.50	12.50	12.50	12.60	13.90	13.90
CALCULATIONS	VOL. AIR DELIVERED-CFM at STP		5229	5159	10763	5569	6180	13235	13235	5555	5555	5520	5520	7687	7687	8722	8722	5868	7430	7430
	VOL. DELIVERED/VOL. DISPL.		1.191	1.180	2.450	1.270	1.410	3.020	3.020	1.265	1.265	1.260	1.260	1.754	1.754	1.990	1.990	1.340	1.695	1.695
	VOL. RETAINED/VOL DELIVERED		.675	.721	.601	.950	.980	.403	.517	.818	*	.823	*	.646	.828	.587	.754	.993	.661	.852
	RELATIVE CHARGE		0.944	1.000	1.732	1.418	1.620	1.430	1.830	1.219	*	1.219	*	1.330	1.705	1.371	1.760	1.561	1.315	1.695
RESULTS	GROSS OUTPUT, HP		1742	1848	3200	2615	2990	2670	3380	2250	*	2250	*	2455	3145	2535	3250	2880	2425	3130
	BLOWER LOAD, HP		158	170	671	121	125	1132	1133	125	*	135	*	207	207	250	250	328	0	0
	NET OUTPUT, BHP		1584	1678	2529	2494	2865	1538	2247	2125	*	2115	*	2248	2938	2285	3000	2552	2425	3130
	GROSS BMEP, psi		91.2	96.5	167.5	136.8	156.5	138.1	176.9	117.8	*	117.8	*	128.3	164.8	136.7	170.0	150.8	127.0	163.8
	NET BMEP., psi		82.9	87.6	132.3	130.5	150.0	80.4	117.5	111.2	*	110.6	*	117.5	153.3	119.7	157.0	133.5	127.0	163.8
	FUEL CONS., lb/bhp-hr		.405	.403	.466	.386	.383	.640	.553	.390	*	.393	*	.402	.395	.408	.400	.415	.368	.368

* NOT PRACTICAL, INSUFFICIENT AIR DELIVERY FOR COMPRESSION CONDITIONS.

so that its maximum capacity was any amount required but delivery at lower loads would be only the amount needed for that load. The last pressure system had a predicted performance increase of 81% and a reduced specific fuel consumption of over 5%.

This air system of exhaust-driven turbocharger as a first stage, engine-driven blower as second stage, and aftercooler, with an airbox temperature of 100 F, was the one selected for the first test work.

The second section of the chart contains the predicted performance with the effective compression ratio varied to maintain more desirable peak cylinder pressures. The section is labeled "Controlled Exhaust Closure Timing" since it was anticipated that it would be necessary to vary the compression ratio with load in order to obtain the most desirable operation over the wide range of loads. The data are equally true for full-load operation with a constant reduced compression ratio of the amount listed.

Aftercoolers, between the final compressor and the engine airbox, were used in all of the air systems cited. Intercoolers, between first- and second-stage compressors, were included in some cases. The intercooler increased output at a slight cost in fuel economy but not sufficiently to justify use of the added bulk and complexity of equipment.

Increasing the size of the engine-driven blower to obtain a greater charging pressure and to permit use of a lower compression ratio was not successful. The increased power required to drive the blower was greater than the gain in power. Fuel consumption was excessive.

The use of the engine-driven blower as the first-stage compressor and the turbocharger as the second-stage compressor was fairly successful at the lower compression ratios. The limiting capacity of the positive-displacement, fixed-speed first-stage blower prevented full utilization of the engine potential capacity. There was insufficient capacity in the blower to provide the airflow required for the charging pressure desired at the higher compression ratio.

Installation of the exhaust-driven turbocharger as the first-stage compressor and the engine-driven blower as the second stage permitted full utilization of the exhaust energy for pressure boost. Since the engine-driven blower was then supercharged and used only for the pressure boost it would provide, its driving power remained reasonably low. With that arrangement, a predicted output of about 3000 bhp was available with a net thermal efficiency 1 to 2% better than at the original 1600 bhp rating. Also, it could be done with operating conditions which should still provide satisfactory mechanical reliability.

There was another very good reason for this system from the standpoint of Navy requirements. In submarine snorkel service there is a high exhaust backpressure effect on the engine. The exhaust-driven turbocharger alone will not work satisfactorily under those conditions. The arrangement planned will retain the engine-driven blower to take the greatest burden of the air pressure flow. There remains some usable energy for the turbocharger drive, and operation would be improved greatly over present conditions if the variable exhaust-valve timing were used to adjust the compression ratio to meet the requirements.

The snorkel column on the chart contains a predicted net output of 2552 bhp with a specific fuel consumption about 8% better than can now be obtained at 1600 bhp under snorkel conditions. This output is definitely predicated on the use of a variable compression ratio operating system, as it could not be reached with a fixed ratio which was also suitable for normal operation.

The last of the air systems included in the chart has an air arrangement using only an exhaust-driven turbocharger and aftercooler. At the time of the analysis, it was included only for academic interest. First, it did not provide the airflow required during the starting period with a 2-stroke-cycle engine before the exhaust had sufficient energy to make the turbine pick up speed. Second, no turbocharger then available had an efficiency and pressure ratio which would furnish the airflow required with the exhaust energy available.

The data show the desirability of using such a system when it becomes possible. The saving of the engine blower driving horsepower means another 200 hp available for power, and the consequent increase in mechanical efficiency drops the fuel consumption by 7%. This system would be usable only for normal surface operation.

To summarize, predicted performance data show the variable compression ratio system could be used to obtain about 100 bhp greater maximum output with similar limits of operating conditions, it would provide better operating economy over a wider range of loads, and it would make possible increased output under submarine snorkel conditions. It would have the disadvantage of adding a mechanism, probably of moderately complicated design, to the engine. High-pressure supercharging, whether with fixed or variable timing, would permit net brake horsepower to be increased from the present 1600 or 1700 bhp at 750 rpm to about 3000 bhp at the same speed, an increase of about 80%, with a thermal efficiency as good as at the lower rating.

Simulated Turbocharged Tests

Use of an exhaust-driven turbocharger on a diesel engine entails several considerations: most suitable airflow and air pressure to satisfy combustion-chamber requirements for scavenging and charging, engine operating conditions which will provide the exhaust energy for driving the turbocharger, exhaust manifolding to drive the turbo-

charger with the maximum efficiency without causing detrimental backpressure on the engine, air manifolding to transmit the air to the cylinders with the least pressure loss, and a turbocharger with size and characteristics which will match the requirements of the engine under those operating conditions. The problem is especially complex with moderate speed, 2-stroke-cycle engines of high output because of the very limited experience in turbocharging them.

In this project, the application of the turbocharger was divided into two phases to reduce the complicating factors. For the first phase, the turbocharger action was simulated, and tests were made to determine the engine operating characteristics. These requirements were used as specifications for procurement of the turbochargers and as a standard during design of manifolding and matching of turbochargers during a subsequent phase.

The simulated turbocharger installation, shown in Fig. 2, included a valve in the exhaust line to give exhaust backpressures in the ranges that would be caused by current turbochargers. Exhaust line pressure restriction after the valve was the standard 40 in. of H_2O. A motor-driven variable-speed Roots-type blower was installed in the intake air line as a first-stage compressor to take the place of the turbocharger compressor. Valves were installed in the air ducts and after the aftercooler so that the pressure drop would approximate that of the proposed final installation. A salt-water-cooled tubular aftercooler was used. The standard water-cooled engine exhaust manifold was retained in use. The only engine change made for the first tests was installation of fuel injector plungers with 57% additional capacity and a fuel booster pump with 44% larger capacity.

Careful measurement was made of the energy available by adiabatic expansion of the exhaust and of the flow of air to the engine. The relationship of exhaust energy to compressor discharge of airflow for available American turbochargers was determined from manufacturer's data. As long as the exhaust energy actually present was as much or more than the power required to provide the measured airflow, the simulated installation was acting as a turbocharger, and the power used to drive the motor-driven Roots blower could be ignored. The data reported here are for operation with the exhaust energy just sufficient to supply the stated airflow with an overall turbocharger adiabatic efficiency of 62%.

The preliminary analysis had indicated a possible maximum output of 2865 bhp at 750 rpm under standard engine conditions and 2938 bhp at 750 rpm with the later exhaust-valve closure to give a lower effective compression ratio. The controlled exhaust-valve timing mechanism was not installed for the first tests. Instead, a series of tests over a full range of output were made with the standard compression ratio and then a series at the reduced ratio. Comparison of the two curves obtained would show the operation possible at various loads with varied compression ratios. All tests were made with the airbox temperature maintained constant at 100 F.

One mechanical feature which was known in advance to require modification was the fuel injector nozzle tip. The original tip had insufficient orifice area for the higher flow, causing high injection pressure, excessive atomization, and too little penetration. Also, the greater density of oxygen and the necessity for using it more efficiently made it more important for all parts of the combustion chamber to be reached by the atomized fuel. The original single row of orifices was changed to a double row, with total orifice area increased by as much as 70%. Combustion improved, and greater loads could be carried, without exceeding the specified operating limits.

Fig. 3 shows the results obtained from the first tests with the standard engine with change only in the fuel system. The airflow pressure losses through the airbox, intake ports, and exhaust valves were larger than anticipated. It proved necessary to operate at a higher air pressure in order to get the cylinder scavenging and charging desired. The resulting higher pressures caused maximum cylinder pressures to increase rapidly with increase in load.

A net brake output of 2200 bhp at 750 rpm was carried satisfactorily. Fuel consumption at that load was 0.385 lb per bhp-hr as compared to the original 0.408 at 1600 bhp, a reduction of 6% in specific fuel consumption while increasing output 38%. Exhaust temperature was 750 F and maximum cylinder pressure 1300 psig. This was obtained with an airbox pressure of 9.0 psig and an exhaust manifold pressure of 6.9 psig.

Higher pressures, up to 14.5 psig airbox, were tried and caused a decrease to 0.378 lb per bhp-hr fuel consumption and 690 F exhaust temperature,

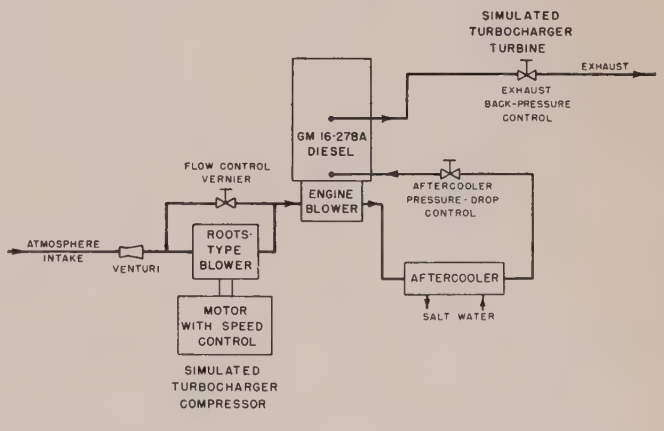

Fig. 2 – System used to simulate turbocharger operation in determining engine air requirements

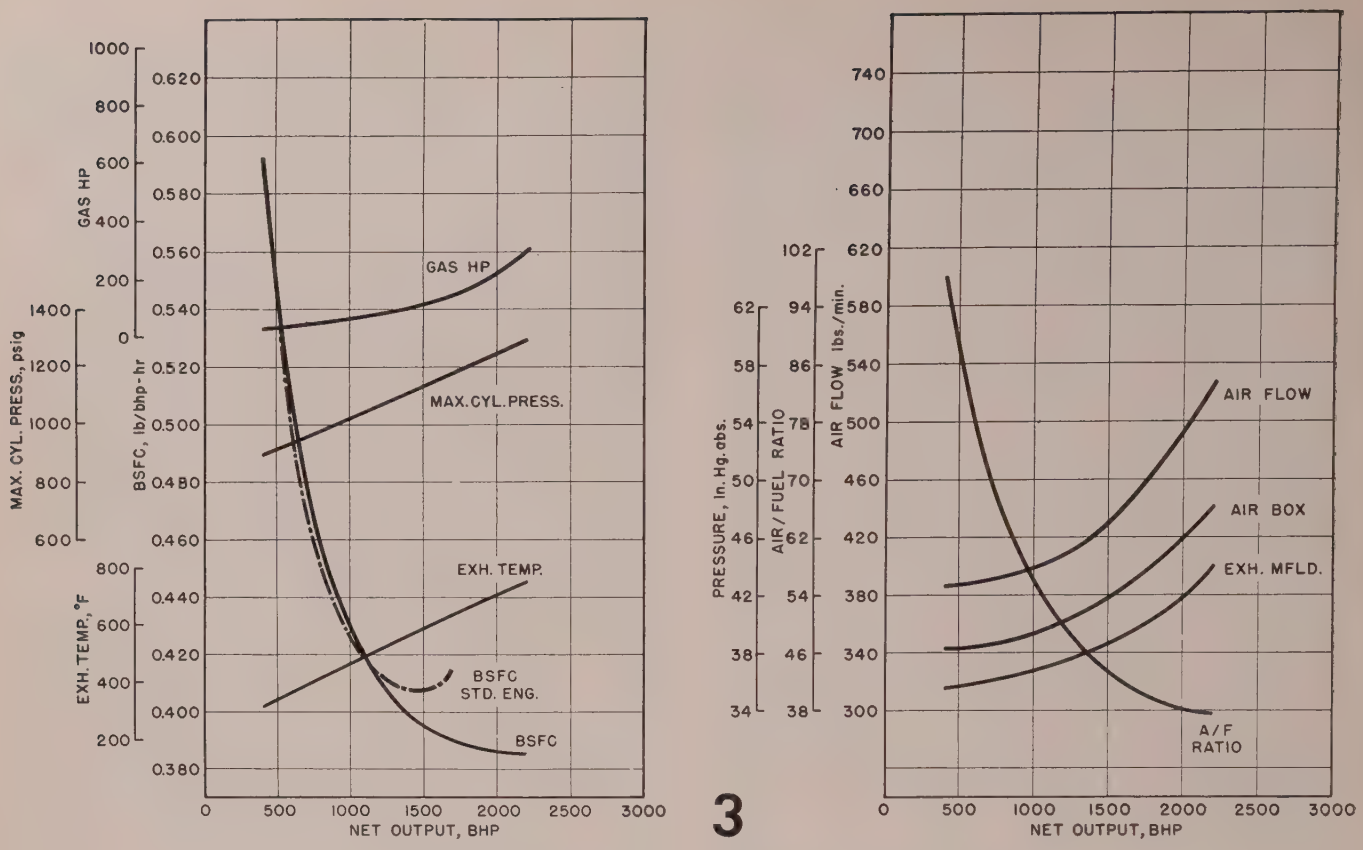

Fig. 3 – Operational data for standard engine with added air supply

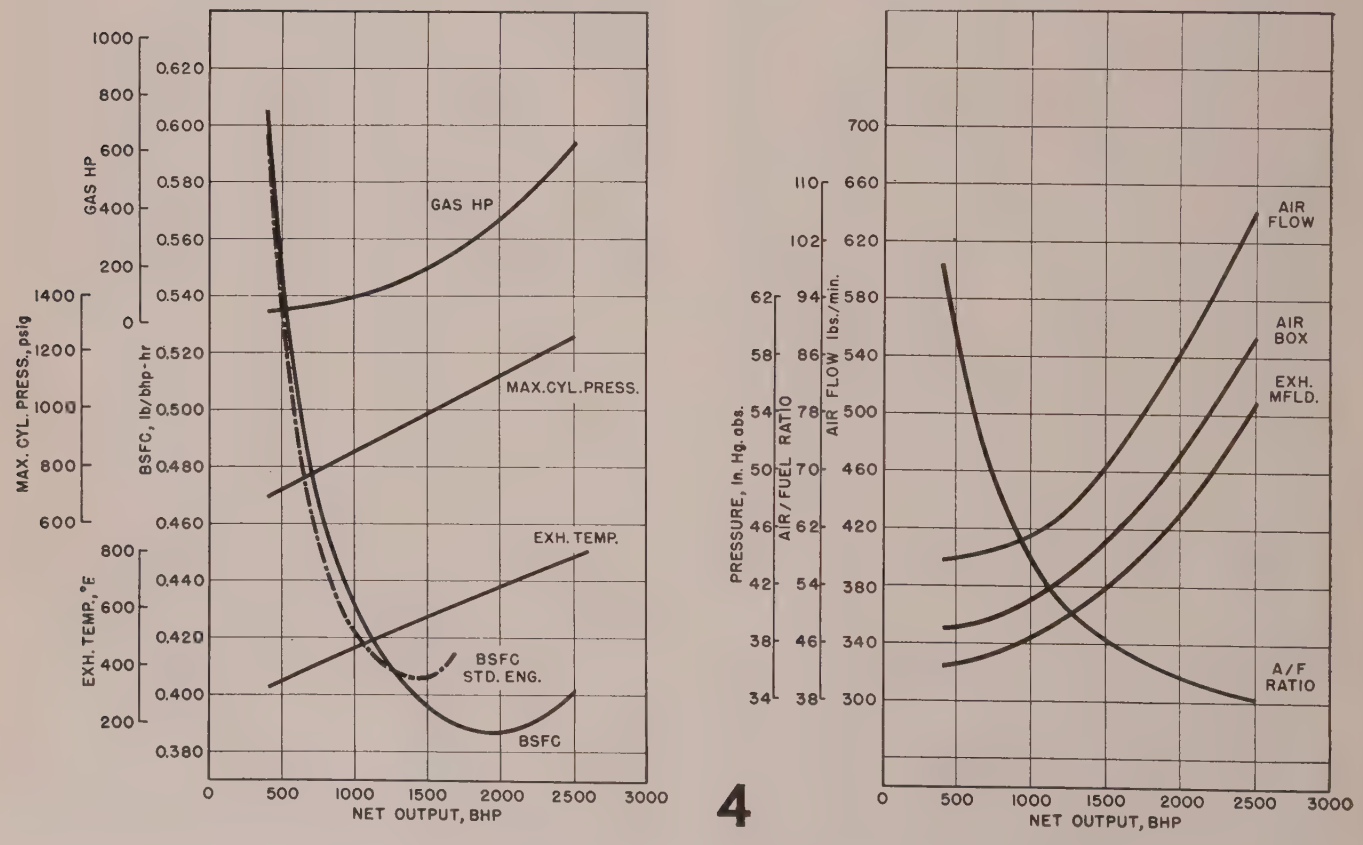

Fig. 4 – Operational data for engine with retarded timing and added air supply

but maximum cylinder pressure rose to 1500 psig. Conversely, lowering the airbox pressure to 5.2 psig reduced maximum cylinder pressure to 1240 psig but at the sacrifice of acceptable thermal efficiency. An output of 2400 bhp was carried at the lower pressure level but with a totally unacceptable specific fuel consumption.

From these tests, data were obtained which would have made possible an immediate conversion of the GM Model 16-278A diesel from a 1600-bhp to a 2200-bhp turbocharged engine.

One change possible to increase output without requiring engine alteration was to change camshaft timing. Moving the driving gear one tooth retarded timing of the exhaust-valve opening from 89 to 94.5 deg atc and the valve closure from 58.5 to 64 deg abc. This gave an extended expansion stroke and a shortened compression stroke. Effective compression ratio was reduced and maximum cylinder pressures lowered. It was anticipated that there would be a slight advantage from the greater expansion ratio. The fuel injection timing should have been retained at the normal timing, but it was impossible to advance it sufficiently to compensate for all of the camshaft retard. The final timing of injection was 3 deg ca later than standard.

Fig. 4 shows the improvement with the retarded timing. Net output increased 300 hp to 2500 bhp at 750 rpm. Fuel consumption, at 0.399 lb per bhp-hr, remained less for 2500 bhp than it was for the original 1600 bhp. Exhaust temperature was 775 F and the maximum cylinder pressure 1270 psig. The top load was obtained with an airbox pressure of 9.5 psig and an exhaust manifold pressure of 7.3 psig. A load of 2600 bhp was carried; but the injectors, because of the depressed plunger position needed to attain the desired timing, would not fill properly at full throttle, and firing was uneven.

These operating conditions, still with no engine design changes, proved that a rating of 2500 bhp at 750 rpm was readily available. They indicated that a change in the fuel injector plunger helix and porting to permit earlier fuel injection would provide satisfactory operation at 2600 bhp, as compared with the predicted output of 2865 bhp. Specific fuel consumption was 4% higher than predicted. Additional minor changes in timing and in fuel spray characteristics would have further improved the output and thermal efficiency. The results obtained, however, were sufficiently satisfactory to show the engine capabilities and permit moving on to the variable compression ratio phase.

As stated earlier, the mechanism for controlling exhaust-valve timing during operation was not installed during the preliminary development. The cylinder head was raised by shimming to increase the combustion-chamber clearance volume while maintaining the chamber shape and the inlet air port timing. This method does not reproduce the controlled valve timing method exactly. The effective compression stroke is longer, so that a lower charging rate is needed to obtain the desired compression pressure. However, the same charging temperature and effective compression ratio used in the preliminary analysis were used in the actual test, and the compression temperature was unchanged. At the 3000-bhp load, under the actual operating conditions, the compression pressure was 910 psig as compared to the predicted 850 psig.

The engine has a normal rated compression ratio of 15.6/1, based on piston displacement. Tests showed that the effective compression ratio is only 13.5/1 because the exhaust valves close later than the intake ports. The increased combustion-chamber clearance volume reduced the rated compression ratio to 13.0/1 and the effective compression ratio to 11.5/1.

Fig. 5 shows the results of operation with the

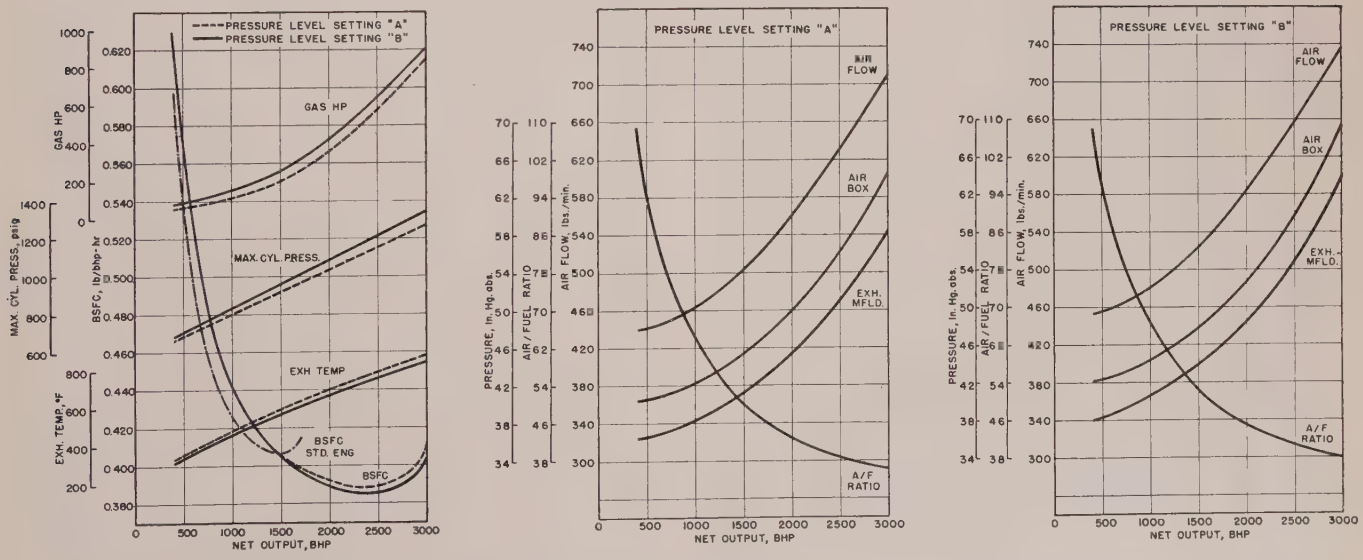

Fig. 5 – Operational data for engine with reduced compression ratio and added air supply (see Appendix)

reduced compression ratio. The original goal of 3000 bhp at 750 rpm, 187% of the present engine rating, was obtained without exceeding the specified operating limits. Thermal efficiency met the predicted performance. The specific fuel consumption from 1450 to 3000 bhp was as much as 5% below the minimum obtained for any load with the standard engine. At lower outputs, below the usual operating range, the specific fuel consumption was slightly higher with the reduced compression ratio. The fuel consumption curve was very flat and was in the 0.385 to 0.400 lb per bhp-hr range from approximately half to full load.

Two sets of data are included. The only change was in the air system pressure level. The higher airbox pressure level setting gave 19.4 psig at 3000 bhp, and the lower setting gave 16.9 psig. A value about half way between the two would provide the desired 1300 psig maximum cylinder pressure. At that condition, fuel consumption would be about 0.405 lb per bhp-hr and exhaust temperature 860 F. The air/fuel ratio varied from 36/1 at 3000 bhp to 51/1 at 1500 bhp and 107/1 at 400 bhp. Maximum airflow would be about 725 lb per min. Energy equivalent to about 875 hp would be taken from the exhaust gas to drive the turbocharger.

These data were highly satisfactory. They closely matched the predicted performance and met the original goals. Again it was realized that further gains could have been made with continued development. For example, the fuel injector plunger helix caused an injection duration of about 23 deg ca at 3000 bhp. Reducing that period would probably have improved combustion without adversely affecting operating conditions.

These tests proved that the engine was capable of developing 3000 bhp with thermal efficiency improved over that at the original 1600 bhp. A net bmep of 157 is possible. Before this output was commercially available, however, it was still necessary to match an exhaust-driven turbocharger to the engine. The exhaust energy present at the engine had to be fed through the turbine without undue energy loss, and the compressed air had to be delivered to the engine equally efficiently. The turbocharger must meet the airflow requirements with the specified 62% efficiency. Commercial sizes of turbochargers were reported by three manufacturers as being suitable to meet the specifications.

The data on Fig. 5 show the operation over a full range from 400 to 3000 bhp at 750 rpm with the constant compression ratio and turbocharger size. The preceding figures have shown similar data for other operating conditions. Fig. 6 shows the performance that could be expected if the compression ratio were changed during operation. Changing the turbocharger characteristics, such as by an adjustable turbine nozzle ring, could cause some further improvement, although these data are all for a constant 62% turbocharger efficiency.

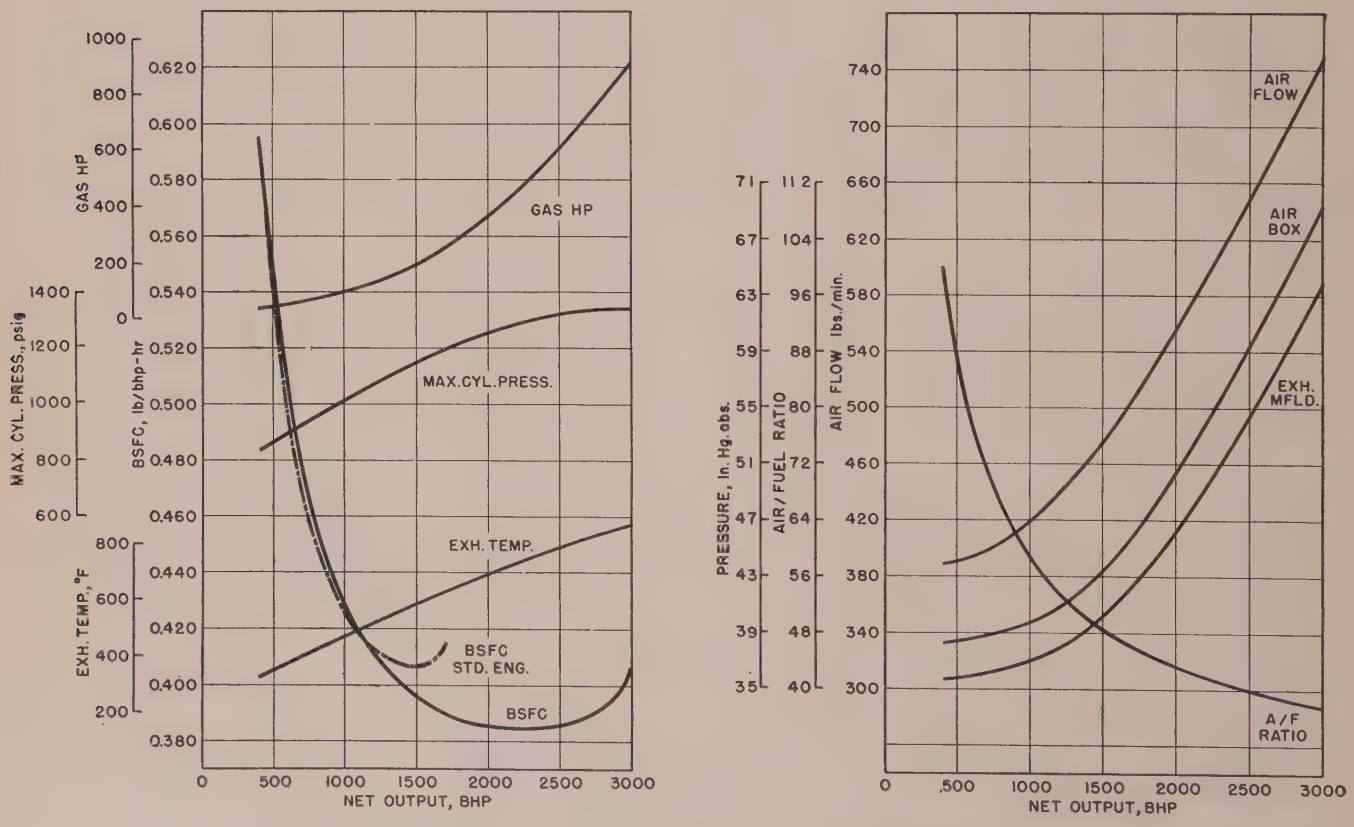

Fig. 6 – Operational data for optimum supercharging conditions with variable valve timing and variable nozzle area

Adjustment of the engine for maximum efficiency at peak load caused some deterioration in performance at lower loads. The compression ratio was too low for best combustion. Variation of the compression ratio in relation to load would permit operation at the lowest of the fuel consumptions shown for each load. Even better combustion than that shown might be obtained at the lowest loads with compression ratios higher than those tested. It is safe to predict that the engine could be operated over the full range of loads up to 3000 bhp at 750 rpm with thermal efficiency at least as good as the best shown.

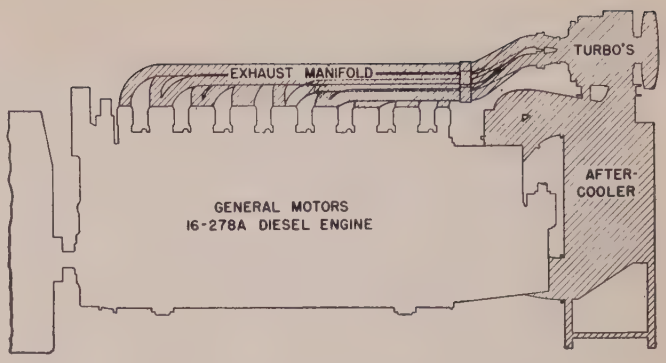

Fig. 7 – Profile of turbocharged engine

Turbocharged Tests

Arrangements were made with three American turbocharger manufacturers to work cooperatively with the Station in adapting turbochargers to the installation. All three had extensive experience with 4-stroke-cycle engines but very limited experience with 2-stroke-cycle diesels. This was realized before the work started, and it was known that a considerable amount of trial-and-error testing would be necessary. There were no illusions about the difficulty in manufacturing manifolding which would provide the needed exhaust and airflows without interfering with the sensitive scavenging process of the 2-stroke-cycle diesel. Also, the need for maintaining the 62% overall efficiency, or higher, with an airflow range from 440 to 725 lb per minute could be met only after some experimentation with turbocharger characteristics.

Two of the manufacturers preferred the use of divided exhaust manifolds with only two cylinders exhausting into each manifold. This system on 4-stroke-cycle engines had shown greatest retention and utilization of exhaust energy. It was therefore desirable that two turbochargers be used for the 16-cyl engine so as to reduce the number of manifolds to each turbocharger. Using two turbochargers also provided a better engine profile because the turbochargers with the aftercooler and ducting could be more easily attached to the existing engine air system. There was a small loss in predicted overall efficiency for two smaller turbochargers as compared to one large one.

The third manufacturer specified a common exhaust manifold but with built-in venturis to permit utilization of much of the exhaust-gas pulse energy. Only one turbocharger was planned for this installation. The turbocharger to be used was a new higher-pressure design which had not been completed at the time the tests were planned.

The installation and tests moved more slowly than planned, in the normal manner for new development work, and the turbocharger adaptation program is not completed at the time of this writing. In fact, the third turbocharger design will not be available before November, 1954. Consequently, the data which can be reported for the actual turbocharger installations is for only the preliminary tests. It does point out the problems and the factors affecting turbosupercharging of 2-stroke-cycle diesel engines.

These preliminary tests were made with the same fixed 13/1 compression ratio, fuel injectors and spray tips, and standard timing of the simulated turbocharger tests. The ducting and intake air aftercoolers were modified to make a more compact installation. Fig. 7 shows the profile of the engine with the turbocharger, aftercooler, and ducting installed. The assembly is less compact than desired because stock coolers were used. It was found that they were larger than necessary. Specially proportioned coolers could have been fitted directly into the ducting. The assembly shown does have the advantage of being available as a self-supported package which could be easily installed on existing engines. The additional weight is 26% and overall bulk 25% for a brake horsepower increase of 87%.

The initial tests showed the value of our simulated turbocharged tests. If it had not been already proved what the engine would do under given air supply and static backpressure conditions, the first data would have been very discouraging.

The first tests were made with eight exhaust manifolds, each taking the exhaust of two cylinders that were timed 180 deg ca apart. The four manifolds from each cylinder bank fed into one turbocharger. The individual manifolds were 3¾ in. ID, a size requested by two turbocharger manufacturers. The manifolds were necessarily rather long, averaging nearly 10 ft. The airbox temperature for all tests was maintained at 100 F.

The dashed lines in Fig. 8 are the results of those tests. Combustion was very poor, being 14% above the predicted fuel consumption at the original rating of 1600 bhp, 750 rpm. It climbed rapidly to 0.484 lb per bhp-hr at 1800 bhp, as compared to the predicted 0.396. Exhaust temperature was correspondingly high and maximum cylinder pressure low. The compression ratio could have been restored safely to its original 15.6/1. Part of the reason for the poor combustion obviously was the deficiency in airflow, which was 5 to 7% less than expected. The turbocharger compressor discharge

pressure was about 1 psi low, but that was partly compensated for by the decreased pressure drop through the new system. Approximate calculations showed that the overall efficiency of this first turbocharger, at these low airflows, was only 56% as compared to the expected 62%.

The deficiency in airflow alone could not account for the entire difference. The airbox pressure was slightly high for the load, and the exhaust backpressure at the cylinders was low. These values are manometer readings of static pressure. The static pressure drop across the cylinders (airbox pressure-exhaust backpressure) was far higher than it should have been for the airflow, and the density of the cylinder charge was much too low.

Oscillograph traces in the airbox and in the exhaust elbows immediately after the exhaust valves were not too definite in indication because of the very low dynamic pressure differential that they showed. In general, they indicated that the exhaust pressure in the manifold was low when the valves opened and that there was a rapid exhaust blowdown, which had reached its peak as the inlet ports opened. For the remainder of the scavenging period the two pressures were practically the same.

The only tenable theory presented was that the ports opened at a time when scavenging flow was too easy and there was a rapid flow through the cylinder. Because of the velocity of the air, there was very incomplete scavenging, and air was wasted in straight-through flow rather than in flushing. After that period, the differential was not sufficiently great. Consequently, airflow was nearly normal, but the cylinder charge was vitiated with exhaust gas. There was no indication of the pressure wave resurging back into the cylinder.

For a quick comparison, the divided manifolds were replaced with the simplest of common manifolds. All 16 cylinders opened into a common header which faired out to a width that permitted attachment to the two turbochargers in parallel. The manifold end was a simple flat plate with no provision for reducing turbulence or assisting airflow.

Fig. 8 shows the results with that manifold, also. Turbine efficiency was reduced appreciably, as much as 21%. Consequently airflow was reduced by 5 to 10%. Despite the reduced airflow, 2000 bhp was carried with a fuel consumption less than that at 1500 bhp with the divided manifolds. Pressure differential across the cylinder was cut in half. Because of the low airflow, combustion was still unsatisfactory and the exhaust temperature remained high, despite the marked improvement.

The next step will be to change to a manifolding which should retain more of the pulse energy of the exhaust to maintain turbocharger efficiency while decreasing or preventing the detrimental backpressure effect on the engine.

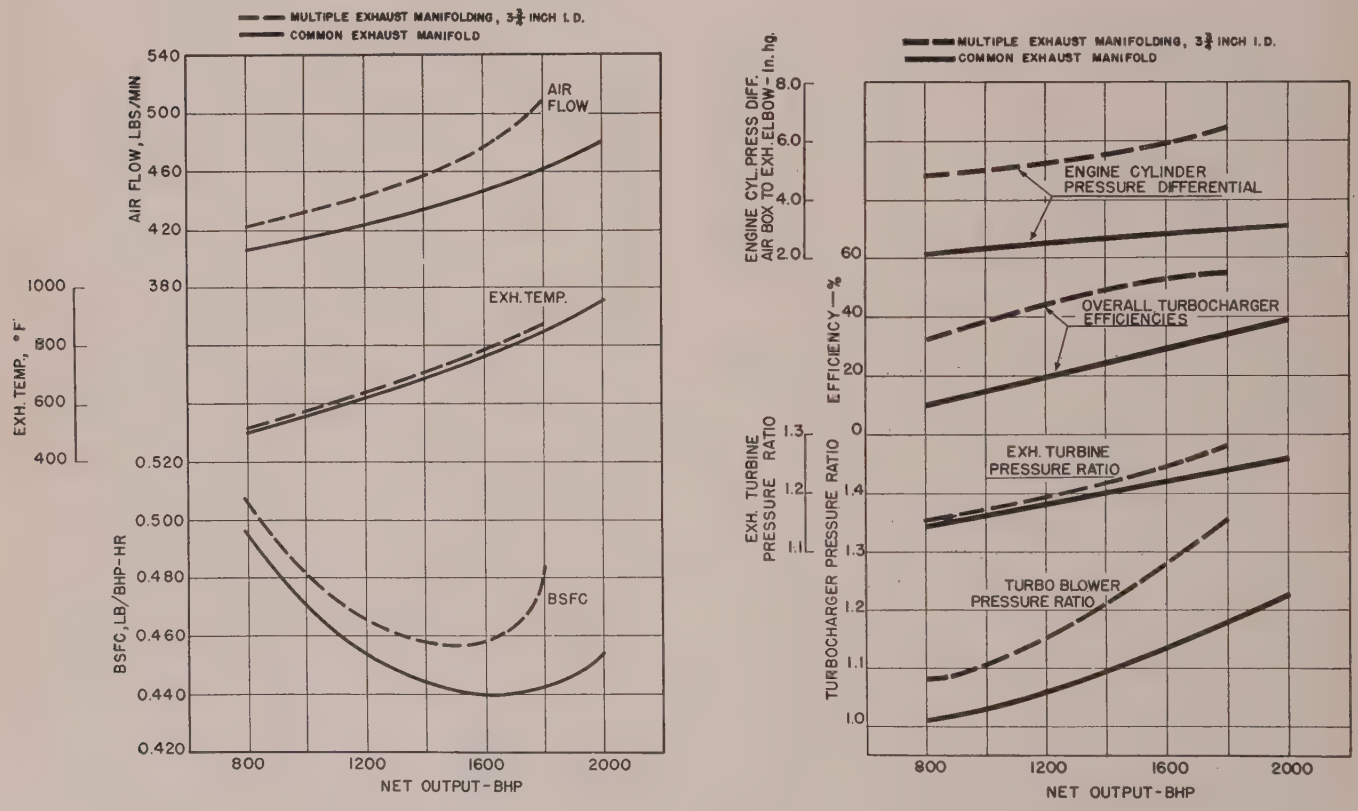

Fig. 8 – Operational data for engine with actual turbocharger operation – standard timing, 13/1 compression ratio

Future Work

Adaptation of the turbosuperchargers to the engine and experimentation with the manifolding will continue until the three turbocharger designs have had an opportunity to show their best efficiency. It is confidently expected that operation will then match the thermal efficiency shown during the simulated turbocharged operation at the peak load of 3000 bhp. Thermal efficiency may be somewhat inferior at the lower loads because the turbocharger efficiency is likely to decrease at lower gas flows. However, the method used for calculating exhaust energy available during the simulated tests, neglecting pulse energy and heat lost in the cooled manifold, will result in somewhat higher exhaust energy being available and may improve over the predicted results.

After the maximum performance has been obtained with the supercharged fixed-compression-ratio engine, the valve timing control will be installed. The improvement should be very little at peak load but should be appreciable at lower loads. The test is intended to show if the improvement is sufficient to justify addition of the timing control mechanism.

It is now intended to complete the project with a run of extended duration to demonstrate that the changes made have not seriously affected the engine's reliability.

Note

The opinions expressed herein are those of the authors and do not necessarily represent the opinions of the Navy Department.

APPENDIX

After the turbochargers were modified to a steady-flow, single-inlet type to suit the common exhaust manifold, and the compressor characteristics were matched to the engine's requirements, the expected 3000 bhp, 157-psi bmep, load was carried again. Brake specific fuel consumption was 2-4% higher than shown in the left-hand graph of Fig. 5. The compression ratio was 13/1 and valve timing was the standard fixed timing. These results were obtained with the standard-size engine-driven Roots blower – necessary for snorkel operation – and back pressure on the exhaust turbine was that required for Navy shipboard installation.

DISCUSSION

Reviews Differences between De Laval Study and This Paper

– Rudolph Birmann
De Laval Steam Turbine Co.

THIS paper brings out clearly the fact that turbocharging of the 2-stroke-cycle engine is a "must" if this type is not to lag behind the 4-stroke-cycle engine in the race for better fuel consumption and more and more output from a smaller and smaller package. Compared with the experimental and experience background of the 4-stroke-cycle engine, turbocharging of the 2-stroke-cycle engine is in its infancy, and furthermore it presents a much more complex problem. For this reason the author's work is of particular value, even though it cannot possibly be expected to cover the subject in such an extensive manner that it leaves no room for a diversity of opinion. Some of the points on which my own opinion does not fully coincide with those expressed by the authors are reviewed herein.

The authors' statement that "it was realized that there would be increasing flow restriction at higher loads" is difficult to understand, because the flow restriction of the engine does not change with load – it is solely a function of the basic engine design. As a matter of fact, a careful analysis of the Engineering Experiment Station's own simulated turbocharged tests of the GM 16-278A engine shows excellent agreement with the theory of flow through a 2-stroke-cycle engine. Theory says that the flow through the engine (Q_E in scfm) is independent of load and depends only on the ambient temperature and pressure (T_0 and P_0), the inlet manifold temperature and pressure (T_1 and P_1), and the exhaust manifold pressure (P_2). All of these variables are related by the expression:

$$Q_E = K \frac{T_0 P_1}{T_1 P_0} \sqrt{T_1} \sqrt{\frac{P_1 - P_2}{P_1}}$$

The simulated turbocharging tests conducted by the Engineering Experiment Station on the GM 16-278A engine showed that K is indeed constant, having the value of 653. This value of K is rather low, which means that the flow restriction of this General Motors engine is high, compared with other 2-stroke-cycle engines. In this connection it might be of interest to point out that there are only two factors to be used in judging the suitability of any 2-stroke-cycle engine for turbocharging – flow resistance and scavenging efficiency. If the flow resistance is low and the scavenging efficiency is high (such as in certain large, very-low-speed European 2-stroke-cycle engines), turbocharging of the 2-stroke-cycle engine is a relatively simple problem, and the turbocharger can become the sole source of air supply to the engine under all conditions of engine load – from idling to full load. On the other hand, if the flow resistance is high and the scavenging efficiency is low, turbocharging becomes a difficult problem, and extremely high turbocharger combined efficiencies are necessary to maintain the turbocharger operative, even in the high-engine-load range. Under these conditions the turbocharger must be given assistance, at least in the light-load range – for example, in the form of a positive-displacement blower operating in series with or in parallel with the exhaust-turbine-driven compressor. As stated before, the flow resistance of the GM 16-278A engine is high; fortunately, however, its scavenging efficiency is known to be good.

The authors specify that high supercharging must be accomplished while adhering to seven sets of engine design and operating limitations. One of these sets of limitations calls for a maximum firing pressure of 1300 psig and a maximum exhaust temperature of 900 F, but the authors place no limitation on the thermal loading. In this connection it should be pointed out that more and more evidence is being collected, almost daily, to prove that high firing pressures are not nearly as detrimental to the reliability and durability of the diesel engine as is high thermal loading. Difficulties with piston rings, liners, valves, cylinder heads, and the like, which at one time were thought to be due to excessive firing pressures, are more often traced to excessive thermal loading. For this reason it is suggested that the authors, in their test and analytical work, should have placed a limit on the thermal loading.

This might have ruled out several of the arrangements investigated, such as the use of low compression ratios in one or two of the systems.

The paper states: "Careful measurement was made of the energy available by adiabatic expansion of the exhaust . . ." In this kind of determination of the energy in the exhaust it is obviously very important to have an exact measurement of the true exhaust temperatures. It is believed that in the tests under discussion these temperatures were measured at the outlet of the standard water-cooled exhaust manifold. In other 2-stroke-cycle engine tests it has been found that the water jackets of the exhaust manifold absorb almost as much heat from the exhaust gases as is rejected to the cylinder jackets. For this reason water-cooling of the exhaust manifold cannot be tolerated in a turbocharged 2-stroke-cycle engine, and it may well be that the exhaust temperatures used by the authors in their analysis are as much as 100 to 150 deg (at full load) lower than they would be in an actual installation, which would completely alter the entire turbocharging picture of the GM 16-278A engine, as presented in the paper.

It is interesting to note that the authors investigated 37 different combinations of engine, mechanical blower, intercooler, and turbocharger, the most promising of which are specifically discussed in the paper. De Laval has made similar investigations, and the conclusions derived therefrom do not entirely check with the findings of the authors. There is no disagreement with regard to the turbocharger-engine-intercooler combination being in many respects the most desirable arrangement, provided the problems of starting, idling, and snorkel operation can be solved. All starting, idling, and high exhaust backpressure problems are eliminated, however, if the positive-displacement blower is retained and the turbocharger arranged to operate in series therewith. With regard to such an in-series arrangement, the authors state that "the engine blower as the first stage, while good, was less desirable than making the turbocharger the first stage." The in-series arrangement of engine blower followed by the turbo was ruled out by the De Laval investigation because of the fact that proper air delivery to the engine can only be accomplished at one engine load point. At a higher load the engine does not get enough air and its fuel consumption becomes very poor; at a light load the engine gets too much air and the positive blower absorbs an excessive amount of power, which again makes the fuel consumption very poor.

There is a similar disagreement between the findings of the authors and those of De Laval with regard to the location of the intercooler in a turbocharger-positive-displacement-blower in-series arrangement. If the intercooler is arranged as recommended by the authors – that is, after the positive-displacement blower, directly ahead of the engine – it can be shown that the engine operating line cannot possibly coincide with the line of turbocharger operation along which best compressor efficiency is obtained over the entire load range. In other words, if the turbocharger, positive-displacement blower, and engine are matched for a certain load, the turbocharger is likely to pulsate at higher engine loads and operate in a bad efficiency region at a lower load. If, on the other hand, the intercooler is placed between the turbocompressor and the positive-displacement blower, the engine operating line falls within the high efficiency region over the entire operating range of the exhaust-turbine-driven compressor. Furthermore, it can be shown that with sufficiently high turbocharger combined efficiency, the positive-displacement blower becomes "unloaded" at a certain engine load; and from there on, as the engine load is increased, it acts as an expander, returning horsepower output to the engine crankshaft. At the same time, if the intercooler is placed ahead of the positive-displacement blower, a refrigerating effect is obtained which lowers the temperature of the air admitted to the cylinders to below the intercooler "out" temperature – a phenomenon which has an extremely desirable effect on the output, the thermal loading, and the fuel consumption of the engine, and one which cannot be obtained if the intercooler is located as preferred by the authors. As a matter of fact, in the latter case, under certain engine operating conditions the intercooler can become a heater.

It is possible that the advantages of the arrangement of turboblower, intercooler, positive-displacement blower, and engine (in that order) were not fully realized by the authors because their investigation was based on retaining the present blower, whereas for proper matching of the aforementioned components a postive-displacement blower having a smaller capacity must be used. Usually approximately 60% of the standard blower capacity can easily be provided by a reduction in the blower speed or by shortening the blower rotor length.

With regard to the actual turbocharger tests, the results of which are presented in Fig. 8, the paper states that the turbocharger overall efficiency was only 56%, as compared with the expected 62%. It is believed that the concept of turbocharger overall or combined efficiency should be clarified. Invariably, efficiency is the ratio of energy output to energy available. It is impossible to determine the amount of energy made available to the turbine merely by measuring mean pressures in the branches of a subdivided exhaust manifold, and therefore it is impossible to base on such mean pressure measurements the determination of the combined efficiency. This is illustrated by the common experience with 4-stroke-cycle engine turbocharger installations where, based on the mean pressure in the exhaust manifolds, the turbocharger combined efficiency is often found to be over 100%, even though the true combined efficiency may only be 50%. Proper determination of the turbocharger combined efficiency must be based on steady flow and pressure, such as measured in the common exhaust manifold, the test results of which are shown by the solid lines of Fig. 8. These tests, under conditions of steady flow and pressure, show that the maximum turbocharger combined efficiency was only 38%. It is realized, of course, that the tests reported in this paper are only preliminary and that better matching of the turbocharger to the engine airflow requirements will result in the attainment of much better turbocharger efficiencies.

The fact that the tests thus far conducted showed much poorer results with the blowdown system (multiple manifold branches) than with the constant-pressure system (single manifold) is not surprising, considering the enormous length of the individual manifold branches (shown by Fig. 7). These great lengths, which mean very large volumes in the individual branches, cause the energy in the exhaust pulsations to be dissipated. If this pulsating energy is to be used effectively, the volume in the individual manifold branches must be reduced to the absolute minimum, since even a very slight increase in the volume causes a great reduction in the amount of pulsating energy made available to the turbine. It is for this reason that the most successful European 2-stroke-cycle engines use one turbocharger for each two or three cylinders, which makes it possible to locate the turbocharger very close to the cylinders and achieve individual exhaust stacks with the smallest possible volumes. Multiple turbocharger installations of this type are, of course, impractical in the case of high-speed engines having a great number of cylinders, such as the GM 16-278A engine. For this reason De Laval has evolved a special pulse-converting type of exhaust manifold for 2-stroke-cycle engines. Tests of this manifold have shown that it combines the advantages of the single manifold (simplicity and steady-flow turbine operation) with those of a good multiple-branched manifold (recovery of the pulsating exhaust energy and elimination of any interference with the scavenging of the various cylinders).

It is hoped that the aforegoing comments will not in any way be construed by the authors as a criticism of their valuable contribution but will be taken as suggestions intended to be of help in their future work.

Suggests Modifications For Turbocharging Setup

– C. A. Chamberlain
Clark Bros. Co.

IT is with much gratification that we note the continually growing interest in the turbocharging of the 2-stroke-cycle engine. The highly developed state of turbocharging in 4-stroke-cycle engines has, indeed, minimized the advantages which the 2-stroke-cycle engines have enjoyed; and, without doubt, it is turbocharging that will restore the 2-stroke-cycle engine to its proper position in the field of internal-combustion engines. Turbocharging is particularly appropriate in the process of increasing the bmep of 2-stroke-cycle engines because the restricting of the engine exhaust provides the only sound means of retaining greater quantities of air in the cylinders which is the prime requisite of increasing bmep. At the same time it removes the parasitic scavenging load (increased in the case of a supercharged engine) which has been inherent in the 2-stroke-cycle engine.

The comparatively large quantities of excess air required to scavenge the 2-stroke-cycle engine have long been considered to make turbocharging impractical. It has only been the increased efficiencies of recent designs of turbocharger equipment that have brought the turbocharging of a 2-stroke-cycle engine into the realm of practicability. Even so, the 2-stroke-cycle engine designer must pay close attention to any possible losses of energy such as occur in pressure drops in the induction system, the exhaust system, or the engine flow passages themselves, or no conceivable turbocharger will perform its functions satisfactorily. The authors have included a mighty hurdle in one of their original design considerations, namely, the 40 in. of water pressure drop which is encountered in the standard ship's exhaust system.

The final column of Table 1 presents the most interesting and promising of the various arrangements studied. There appear, however, to be some inconsistencies among the data of this column. At the risk of having based my conclusions on false assumptions, I should like to discuss these data briefly.

First, the data for compression temperature and pressure indicate an increase in retained air of only 66% over the standard engine data (column 1) rather than the 79% shown. I would expect explosion pressures nearer 1600 psi than the desired 1300 psi if the same fuel injection period is used.

Second, the volume of air delivered, 7430 cfm at 14.7 psia and 492 F, converted to scavenging temperature and pressure is only 3960 cfm compared with 5300 cfm for the standard engine. This raises some doubts as to the potential efficiency of the scavenging process.

Third, the prescribed inlet and discharge pressures for the blower and turbine of the turbocharger and the inlet temperatures would seem to require an overall turbocharger efficiency of nearer 67% rather than 62%.

Respectfully, I would like to submit some modifications to these characteristics which would seem to fit within the framework of the desired operating conditions and still be practicable.

First, I would increase the clearance volume of the cylinders by about 18% and further alter the exhaust-valve closing to retain an effective compression ratio of 11.62/1. I would design for a scavenging pressure of 13.6 psig and 100 F temperature which would result in a compression pressure of 766 psig and temperature of 910 F. This should hold the peak pressure to about 1350 psig at approximately 3130 bhp.

Increasing the clearance volume would, of course, decrease the expansion ratio of the engine. I would estimate the resulting decrease in engine cycle efficiency to be about 3%. This should be more than compensated for by the increase in mechanical efficiency (over and above the increase due to the removal of the scavenging load) in going to the higher horsepower level. At this expansion ratio, the flow of energy to the exhaust at 3130 bhp should be of such a quantity as to raise the temperature of 725 lb per min of air from the 100 F scavenging temperature to the 900 F exhaust temperature. This would mean an airflow of 9000 cfm at stp or 5330 cfm at scavenging conditions. As this is the same flow as the standard engine (measured again at scavenging conditions) it should result in a pressure drop from scavenging to exhaust of no greater magnitude than the standard engine, namely 1.6 psi. This statement is not completely true, as the higher blowdown pressure resulting from the higher peak pressure and lower expansion ratio will somewhat limit the beginning of the scavenging flow, but it is most likely possible that a modification in the porting could overcome this.

With a pressure drop of 1.6 psi, the engine backpressure would be 12.0 psig. These conditions, then, would require an overall turbocharger efficiency of 65.8%. While this is higher than the efficiency figure used in the basic considerations, it is by no means impracticable as it is less than the efficiency of some of the turbochargers we are presently using on Clark Bros. Co. 2-stroke-cycle gas engines. These turbochargers are of the constant-pressure type operating with a simple open-pipe manifold.

Recommends Use of Multiple Manifold

– R. F. Miaskiewicz
Elliott Co.

SIMULATED turbocharger tests, as described in the paper, are certainly a most realistic approach to supercharging this type of engine. Because it is so much more important to match properly turbocharger components for 2-stroke diesel supercharging, the results of such simulated tests make it possible to predict all but manifolding effects for a particular operating condition and consequently to arrive at the proper balance of turbine and compressor components.

From initial engine tests, the authors have conclusively shown an improved engine performance using a common exhaust manifold as compared to a multiple exhaust system. These results were achieved even though turbocharger efficiency suffered appreciably by the transition. Certainly, a turbocharger requires revamping to the new arrangement if optimum turbocharger efficiency is to be expected. I hope that the findings to date are not considered final in regard to multiple versus common manifold. We have had considerable experience to recommend multiple exhaust for many applications. Further, certain modifications from the conventional multiple porting may be achieved to improve engine performance. A common manifold certainly has its advantages. It is desirable from the standpoint of turbine stage efficiency, since it makes possible a full admission wheel. However, in such instance, it should prove advantageous to install individual cylinder diffusers to convert available gas velocity head to pressure before entering the common manifold.

The authors have tabulated various arrangements of controlled exhaust closure timing in Table 1. In each instance, exhaust closure is advanced from the standard timing. With the inlet port arrangement remaining constant, the net effect is to reduce effective compression ratio. This is quite contrary to attempts at retaining maximum cylinder density for self-sustained turbocharger operation and maximum output.

Unless swirl conditions for acceptable combustion requires exhaust closing after inlet closing or exhaust pulse supercharging is desired, it seems reasonable to assume

that exhaust closing could be made to coincide or slightly lead inlet closing to increase engine output at identical maximum cylinder pressure by reducing airbox pressure. This, in effect, would duplicate the existing cylinder charge at the present instant of exhaust closing and achieve a lower engine backpressure. Referring to the standard timing analyses of (1) the standard mechanical blower-turbocharger-aftercooler and (2) turbocharger-standard mechanical blower-aftercooler, a net reduction of 134 gas hp and 149 gas hp respectively would be achieved with a 62% combined efficiency turbocharging system.

Must Consider Effect of Supercharging on Reliability

– C. F. Taylor
Massachusetts Institute of Technology

IT is not surprising that poor results were obtained when the only change was an enlargement of the scavenging blower. Examination of any curve of scavenging efficiency versus scavenging ratio as, for example, Fig. 10 of a paper by Taylor and Rogowski[a] indicates that diminishing returns are certain by this method. It has previously been pointed out that supercharging of 2-stroke engines to any considerable extent is practical only when the **exhaust** pressure, as well as the inlet pressure, is increased. The work of Messrs. Payne and Lang supports this view.

For Table 1 of the paper, I would like to ask how the ratio "Vol Retained/Vol Delivered" was measured and defined? A loss of 2% or less of the scavenging air on a mass basis, as suggested by the ratio 0.98 and 0.993, does not seem possible. In my experience this loss is seldom less than 30%.

The tests reported in the paper are valuable in giving confirmation to results which would be rather easily predictable if two important criteria for scavenging had been known over the operating range of the engine. These criteria are:

1. Mass ratio of air retained to air supplied.
2. Flow coefficient of the engine.

Taylor and Rogowski[a] suggest methods of measuring and predicting these factors.

Of course the big question which remains is the effect of supercharging on reliability and durability of the engine. For example, stresses due to heat flow increase nearly in proportion to the indicated output. If the proposed increase of nearly 100% in power rating can be utilized in service without major structural changes and without sacrifice in reliability, it will be a remarkable tribute both to the ruggedness of the present design and to the conservative nature of the present rating.

Give Data for Other 2-Stroke-Cycle Engines

– A. K. Antonsen and E. L. Dahlund
Fairbanks, Morse & Co.

IT is rather difficult to prepare a discussion on a paper so well founded on theories and experiments as the paper presented by these authors. Our discussion is, therefore, more in the line of offering additional data in support of this very worthy project and less in the way of touching upon controversial data.

One can, however, offer comments to the extent of Fig. 1, which illustrates engine rating of American and foreign diesel engines. We especially refer to the 2-stroke-cycle comparison. Whereas these rating comparisons are valid in the way of accepting published data and perhaps even witnessed data of tests, one can venture to say that the difference will narrow down somewhat in case all these engines were subjected to the same type of service.

One of the engines used in Fig. 1 for comparison of 2-stroke-cycle bmep ratings is an aircraft type of engine which, at a continuous sea-level rating, would have to operate at a greatly reduced brake mean effective pressure.

[a] See SAE Transactions, Vol. 62, 1954, pp. 486-502: "Scavenging the 2-Stroke Engine," by C. F. Taylor and A. R. Rogowski.

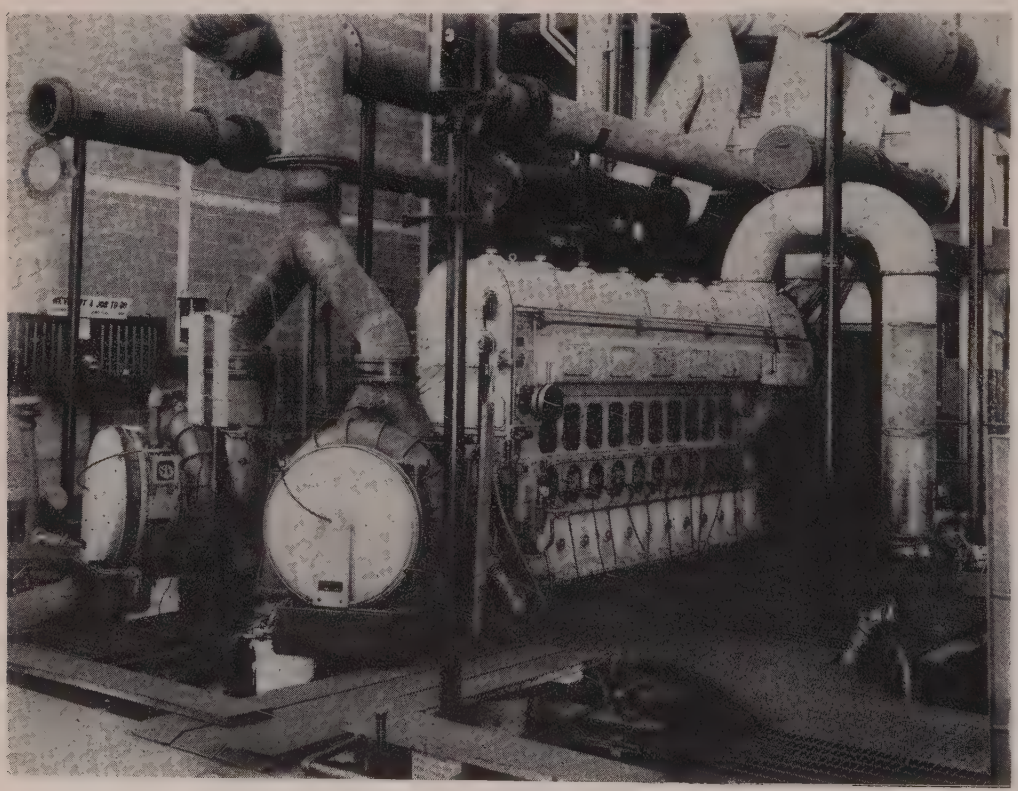

Fig. A – 10-cyl 8⅛ x 10 turbocharged opposed-piston testing arrangement

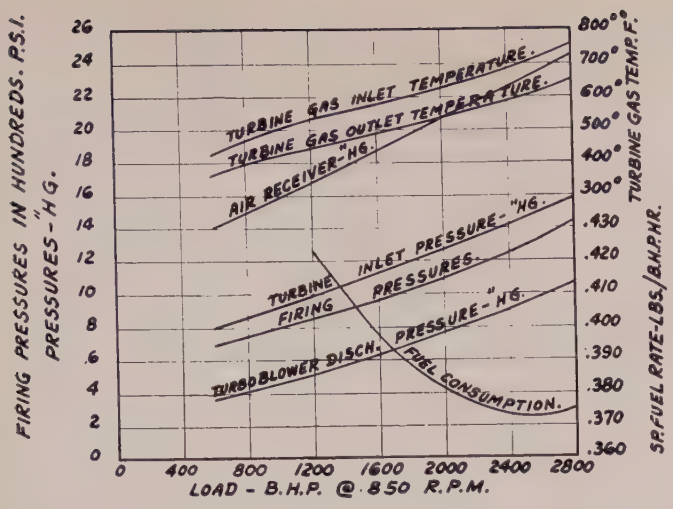

Fig. B – Supercharging of Fairbanks, Morse 10-cyl 8⅛ x 10 opposed-piston engine

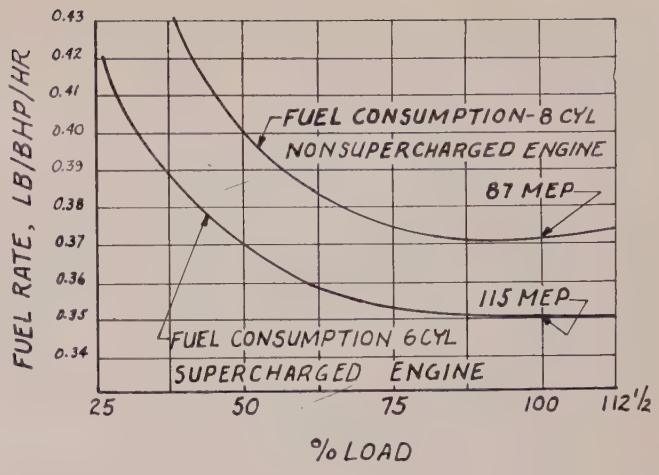

Fig. C – Fuel consumption for 8-cyl nonsupercharged engine and 6-cyl supercharged engine – 100% load, 8-cyl nonsupercharged engine – 100% load, 6-cyl supercharged engine – commercial rating, experimental test data

The other 2-stroke-cycle engine comparison is, to the best of our knowledge, in existence only in the form of a single experimental installation.

Now it would seem to be in order to improve on this comparison by relating heretofore unpublished data of 2-stroke-cycle engines which at the time of obtaining the data were in the same category as the engines being compared.

During the year 1945, there was installed, at the plant of Fairbanks, Morse & Co., a standard 10-cyl 8⅛ x 10 opposed-piston submarine engine for supercharging tests. During these tests, there was no serious attempt made to maintain maximum pressures, but more emphasis was put on maintaining the exhaust-gas temperature. The turbochargers carried out a first stage of compression, and the compressed air was, by way of an intercooler, piped up through the inlet of the normal engine blower. Fig. A illustrates the test arrangement. The intercooler is not visible because it was mounted below the floor level. Fig. B illustrates the general performance characteristic of this experimentally turbocharged engine. Satisfactory operation was maintained up to 2850 hp, which is a 45% increase above even today's nonsupercharged rating or approximately 135 bmep.

At the time of these tests there were available only turbochargers of a low combined efficiency, such as perhaps between 40 and 50%.

Fig. C shows in an indirect manner how turbochargers of higher efficiency at present are partly instrumental in reducing the fuel consumption.

During the year 1945, similar tests were conducted on a 3-cyl 5¼ x 7¼ opposed-piston engine. The test arrange-

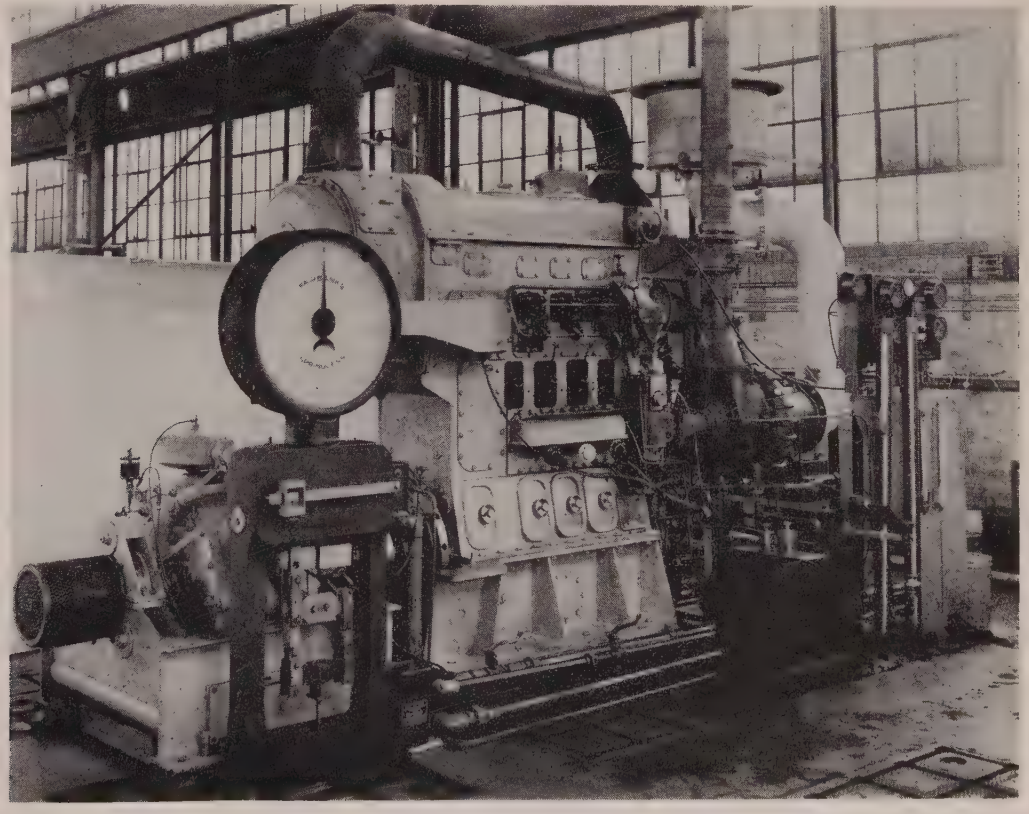

Fig. D – 3-cyl 5¼ x 7¼ turbocharged opposed-piston testing arrangement

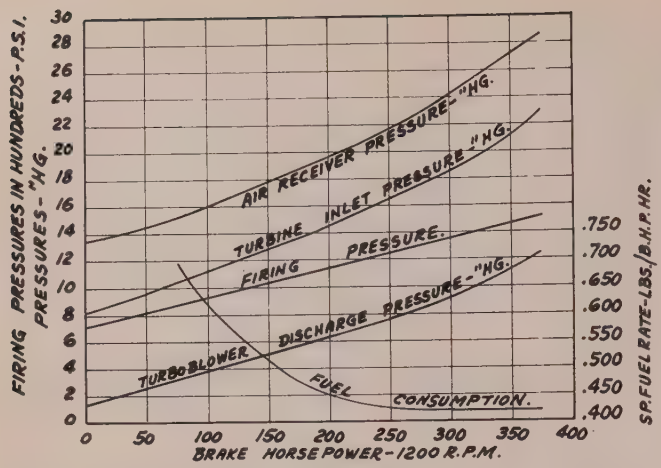

Fig. E – Supercharging of Fairbanks, Morse 3-cyl 5¼ x 7¼ opposed-piston engine

ment of this engine was very similar to the arrangement of the 10-cyl 8⅛ x 10 opposed-piston submarine engine, and the test result was generally comparable with the possibility of a very high power output but at the expense of an excessive cylinder-liner and piston-ring wear. Fig. D illustrates the test arrangement of the small 3-cyl opposed-piston engine, and Fig. E illustrates the general performance at an engine speed of 1200 rpm. The firing pressures in this case went as high as 1500 psi at a brake mean effective pressure of approximately 150 psi.

This 3-cyl experimental test setup also suffered from a low combined efficiency of the turbocharger.

It is felt that the data represented here is not too much out of line with the comparative 2-stroke-cycle engines in Fig. 1. The data presented in this discussion should also add support to the paper presented by Mr. Lang and Mr. Payne to the extent that we feel they will ultimately accomplish what they set out to do.

Authors' Closure To Discussion

MR. BIRMANN'S discussion seems to indicate considerable disagreement with our paper. More careful examination of it, however, shows that there is no basic disagreement, and most of his comments are caused by things we left out or said too briefly in an effort to shorten the paper.

Our statement that there would be increasing airflow restriction at higher loads meant simply that increasing load would give higher turbocharger speed and airflow and that the constant orifice would cause a greater pressure drop. This agrees with Mr. Birmann's formula.

His statement that scavenging efficiency is good is true to a degree, compared with some other types of engine. Any who read Mr. Percival's paper[b] might disagree with its absolute accuracy. That paper showed very bad stratification and actual reverse airflow in similar uniflow cylinders. Our data confirm that. We feel rather that an acceptable combustion has been developed around an existing scavenging condition.

We did not intend that any high-pressure supercharging analysis besides our own would have the same limits we stated. Ours was based on a very specific problem. We wanted to take an existing engine, without any changes in design or attached equipment, and increase its rating while maintaining present reliability and keeping it suitable for snorkel operation. Without those restrictive limits, we might have ended with considerably different results. For example, we know we could have decreased our fuel consumption by at least 30 points by letting maximum cylinder pressure go up to 1800 psi.

We set numerical limits where possible for definitely known restrictive values. We assumed that, to be acceptable, thermal efficiency must be at least as good as for the old maximum rating. Total thermal loading would thus be increased somewhat less than proportional to the load increase. What the limit is, we don't know and feel it can be determined only by operation. That is why we will end up with a reliability test. We do know that maintaining a low charge temperature and thus a low compression temperature, by use of an aftercooler and the variable exhaust-valve timing, will decrease the percentage of heat to cooling and will help us.

Mr. Birmann is correct in stating that we neglected the loss of heat in our water-cooled exhaust manifold and that there would thus be additional exhaust energy available. In fact, that statement is in the paper. That omission was deliberate. Frankly, we don't have too much faith in quoted efficiencies and operating characteristics. We also knew that getting suitable manifolding would be difficult. To keep from getting out on a limb and not be able to live up to our promises, we kept this reserve of energy as far out of our mind as possible.

The 18 air systems mentioned in the paper were not necessarily the best 18. Two are marked impractical because of insufficient airflow, and three others are obviously unsuitable because of excessive fuel consumption. They were representative air systems which could be used as examples to give a connected story in the paper.

We considered the system using the engine-driven blower for the first stage and the turbocharger for the second stage as worthy of consideration. Using our existing engine blower, we could carry one third more load with improved thermal efficiency compared to the standard engine. Combustion at lower loads would be comparable to the standard engine because the turbocharger effect would be very little at the low loads where excess air might be a problem. We also ruled it out, however, because it was so much more suitable to use the turbocharger as the first stage.

In regard to the relative suitability of using an intercooler or an aftercooler, we wouldn't want to make too positive a statement. I can start by conceding that Mr. Birmann knows far more about turbochargers and their characteristics than I do. It is amazingly difficult to get reliable information on turbocharging – that is one reason we are presenting this paper. We would like to know much more about their performance under various pressure and exhaust flow conditions. Our calculations were based on simple operational effects to get the air pressure and temperature best for the engine under controlled conditions. For instance, we plan our combustion on a known air charging temperature. We wouldn't want any uncontrolled refrigeration effect to lower our temperature enough to make ignition difficult. Also, we felt we should maintain the full engine blower capacity because of snorkel requirements, although we would like to have a variable-speed drive on the blower. Under our limitations, it still seems to us that an aftercooler is preferable. I want to assure Mr. Birmann that we will again investigate use of an intercooler and, I hope, make some tests to determine definitely which is best for our requirements.

In regard to turbocharger efficiency, we don't consider the absolute values quoted as too important because we found a difference in calculation methods even among the turbocharger manufacturers. The data prove our point in any case, because we had a higher airflow with the same horsepower and practically the same exhaust temperature when using the divided exhaust manifold. Since then, we have improved the turbocharger efficiency with the same manifolding by changing the turbine nozzle ring area.

b See pp. 737-751 of this issue: "Method of Scavenging Analysis for 2-Stroke-Cycle Diesel Cylinders," by W. H. Percival.

The length of the longest section of manifolding is obviously long, up to 15 ft, but is the same length as the engine. We could reduce it only by relocating the turbochargers and using two or more. That would be awkward because of the difficulty in running the air ducting. A production engine would be more compact than our test installation.

The last point mentioned – loss of pulsating energy – proved to be much different than was expected. Oscillograph records were taken in the exhaust elbows, as close to the cylinder exhaust valves as possible, and in the manifold immediately before the turbocharger exhaust inlet. We would have liked to have used them in the paper because they were very informative, but they were too difficult to reproduce well. The interesting and surprising thing was that there was a pressure peak at the turbocharger which approximately reproduced the pressure peak at each cylinder, with a peak amplitude that was within measuring accuracy of the same value. Rate of pressure change was very close to the same at both locations. The turbocharger peak was 27 deg ca or 0.006 sec later than the peak at the cylinder for a manifold length of about 11 ft.

One thing definitely proved by our tests thus far is that the scavenging and combustion processes in a 2-stroke-cycle diesel are very sensitive and that, in designing manifolding for matching turbocharger to engine, we must think of its suitability for the engine probably even more than its suitability for the turbocharger. The manifolding that gave best turbocharger efficiency and greatest airflow was completely unsuitable for engine combustion. The manifolding design must be a compromise between the two requirements.

We agree with Mr. Chamberlain that straight turbocharging is the ideal arrangement for maximum power and thermal efficiency. As the report stated, its application is limited in Naval usage because of specific ship requirements.

The differences between Mr. Chamberlain's calculations and those from the report are caused by the factors included in the calculation method. We changed the scavenging efficiency factor, based on the pressure level in the air system and the cylinder pressure drop. Our relative charge volume is the relative weight of fresh air, or more specifically oxygen, in the charge and is not the weight of the total gas mixture in the cylinder. Scavenging is not as complete as we desire, and using the full cylinder volume causes some error. Also, our stp comparison is based on 70 F and not 32 F.

The difference in turbocharger efficiency calculations is again a question of calculation method. We use a specific heat of 0.26 for exhaust, based on the analysis, and 0.24 for air. Mr. Chamberlain apparently used 0.24 for both. With those changes, Mr. Chamberlain's calculations agree with ours.

The suggested alternate plan for turbocharging seems very reasonable. The charging conditions are not far different from ours. The total airflow of 725 lb per min, while somewhat higher than our pretest calculations, is the same as we found necessary for the same gross output on our actual tests.

In reply to Mr. Miaskiewicz, we have not reached a conclusion on the relative value of divided and common exhaust manifolds. The common manifold we reported was a simple tube and definitely didn't do justice to the turbochargers. It lost practically all of the pulse energy. The first divided manifolds were very good for the turbochargers, but the engine didn't like them. We are now building another set of divided manifolds which we hope will be a compromise. We would like to save much of the pulse energy without hurting the engine.

The simple common manifold was a temporary expedient. A new design of common manifold now being constructed will have diffusers or pulse converters in the manifold intake.

The variable exhaust valve closure timing does reduce effective compression ratio; and, to get the desired compression pressure and charge density, a higher airbox pressure is required. It has the advantage of reducing compression temperature and, thus, the percentage of heat lost to cooling. In effect, it gives additional air charge cooling but requires a higher-pressure-ratio turbocharger.

We feel that Fairbanks, Morse should be congratulated on the supercharging work for their opposed piston engine reported by Messrs. Antonsen and Dahlund. Other companies are also known to be doing similar good work with their engines and deserve congratulations.

The comparison with foreign engines in our Fig. 1 was selected to show the greatest possible contrast with actual engines. It is true that those engines do not have the reliability and life under sustained operation of the ordinary diesel. They do show standards of efficiency and output which should be our goal but with our present reliability.

Recent improvements in turbocharger design and efficiency have greatly facilitated 2-stroke-cycle engine development.

We are gratified that our work and the Fairbanks, Morse development show such close agreement.

In conclusion, I believe that the paper and discussion have shown very conclusively that high bmep, turbocharged, 2-stroke-cycle diesel engine operation is not only theoretically possible but is rapidly nearing the stage of practical usage. We hope it will not be long before engines are commercially available which will take advantage of these possibilities while maintaining our old diesel reliability. Any part that the Navy has taken in initiating or advancing these developments will be well repaid when the engines become available.

In reply to Professor Taylor, we wish to emphasize the fact that data presented in Table 1 of the paper were obtained from a preliminary theoretical analysis and are not results of actual supercharged operation. Therefore, the values for volume delivered and volume retained (the ratio of the two being the trapping efficiency of the engine) were calculated independently. Unfortunately, at the time of this theoretical analysis several years back, there were neither high scavenge pressure test data nor comprehensive scavenging studies for uniflow-scavenged two-stroke-cycle diesel engines available to us. Whatever information was available had to be extrapolated. As stated in the paper, certain assumptions and limitations were necessary for this preliminary analysis. These assumptions were based on the flow and scavenging characteristics of the engine and its positive displacement blower at low scavenging pressures. In spite of possible deviations, it was felt that these simplifying assumptions were justified since the theoretical analysis served for comparative purposes only. It was found, as expected, from data obtained later from actual engine operation with high-pressure supercharging, that some of the assumptions had to be modified. But the analysis as applied to this particular engine for Navy service gave us the encouragement to enter this new territory.

Professor Taylor's statement in his paper, "Scavenging the Two-Stroke Engine," substantiated our findings that supercharging of two-stroke-cycle engines to any considerable extent is only practical when the pressure level is increased.

As to the question of the effect of supercharging on reliability and durability of the engine, we realize that we do not yet have enough hours of operation to make a final statement. A 1000-hr endurance test is scheduled for the future for that reason. From the hours of operation up to 3000 bhp obtained so far, we found that most parts are in satisfactory condition and wear rates are about normal. No changes were necessary on the engine's cooling and lubrication system including pumps and heat exchangers. How an engine supercharged to develop 80-100% more horsepower will stand up depends on two factors: first, how the turbocharging is applied, and second, how much reliability was originally designed into the engine.

CONTACT wear of diesel-engine cylinder bores and piston rings is the subject of this paper.

The problem of wear is approached through discussion of those conditions most closely associated with wear: the temperature of the moving parts, their materials and design, and the characteristics of the lubricant used on these surfaces.

Effect of

THE purpose of this article is to record some observations of the wear of diesel engines and to discuss this wear with reference to the conditions which seem most intimately related to it: the temperature of the moving parts, their materials and design, and the properties of the lubricant film between the surfaces. Particular attention will be given to the aspect of "contact wear"[1] which can occur only where one metal part touches another. Contact wear, broadly speaking, is most prevalent in engines when loads are high and surfaces are hot, for these are the conditions which minimize the thickness of the liquid film which is intended to separate the moving parts.

To round out the background of the subject, some time will be taken to review the corrosive wear phenomena, which have been shown to appear under cool operating conditions when the liquid film is of ample thickness to prevent contact of metal. As the title of this paper states, discussion will be confined to the wear of cylinder bores and the piston rings which rub against them.

The material presented may be condensed into an outline as follows:

1. Contact wear of cylinders and piston rings in diesel engines occurs when the hydrodynamic cylinder oil film fails to keep the parts separated.

2. The hydrodynamic film will fail when the viscosity of the oil is inadequate or when insufficient oil is retained on the surfaces.

3. Contact wear is not necessarily catastrophic, and it may be produced in varying, stable degrees, related to the quantity and viscosity of oil available to achieve a hydrodynamic separation of the cylinder and rings and the resistance of the metal parts to abrasion after partial hydrodynamic failure.

4. Perfect hydrodynamic conditions never are achieved in an engine cylinder, so that ingenuity of design plays a leading part in ameliorating the inevitable conditions of contact; this involves piston-ring shape and pressure; and it has been shown, also, that compatibility of liner and ring materials are of greatest importance.

5. The nature of lubricating fluids is such that they lose viscosity very rapidly as they are heated; hence, chances of contact wear increase out of proportion to the rise of cylinder-liner temperature.

6. An added invitation to hydrodynamic failure and contact wear when cylinder-liner temperature rises is the loss of fluid from the film by volatilization.

7. The temperature of the cooling water of an engine generally is controlled within a narrow range; *at the same time,* the cylinder-liner temperature can change from safely warm to dangerously hot, depending upon the load, speed, and design of the engine, and the properties of the cooling and lubricating fluids.

8. A detailed method of computing cylinder-liner temperature is given in the text. This brings out clearly the values of all factors which determine cylinder-liner temperature. Comparisons of engine types and operations can be made when these factors are understood.

9. When an engine is forced to operate with lubricating oil which is inadequate, the condition of engine loading at which the hydrodynamic cylinder film begins to fail (and contact wear begins to increase rapidly) can be picked out. Then by experimenting with lubricants which have various viscosities at high temperature and various volatilities, the ruling property can be determined.

10. Viscosity at high temperature was found to be an imperfect indicator of the ability of cylinder lubricants to prevent contact wear.

11. Volatility, if expressed as the amount of oil which will resist vaporization from a hot, thin film, is a reasonably good guide to the quality of an oil to prevent cylinder contact wear.

12. A linear combination of the factors of viscosity at high temperature and film evaporation gave the best agreement with the wear figures provided by the engine.

An ordinary set of pistons and rings is an extraordinary engineering achievement. That it must prevent the leakage of white-hot gas at 1500 psi is taken for granted, but at the same time it must be a liquid metering device of meticulous precision while operating under inertia loads of 200 times the force of gravity. The metering system is required to replace exactly – no more, no less – the

Surface Temperature on Wear Of Diesel-Engine Cylinders and Piston Rings

H. V. Nutt
USN Engineering Experiment Station

E. W. Landen
Caterpillar Tractor Co.

J. A. Edgar
Shell Oil Co.

This paper was presented at the SAE National West Coast Meeting, Los Angeles, Aug. 18, 1954.

amount of oil which is vaporized from the cylinder wall by the hot, turbulent gas on every power stroke. If the film fails, the engine is wrecked; if the rings pass an oversupply of oil, the engine becomes uneconomical. The loss of an occasional particle of metal by corrosion or contact changes the shape of the ring or the bore, so that eventually oil control or sealing effectiveness is lost. The object of design and operation is to reduce the frequency of metal contact, or of corrosive attack, to the point where bores and rings will last as long as any other engine part. Too often this is not accomplished.

While no metal becomes stronger, harder, or more wear resistant when it is heated, most of the blame for contact wear must be placed on the failure of the lubricant. On the other hand, lubricant discoveries have gone a long way toward the elimination of corrosive wear. Therefore, before entering the primary discussion, that of wear at high temperatures, we should remind ourselves of a few of the facts which have been published on the important low-temperature aspects of wear. As early as 1924, Clayden[2] showed that pressure, temperature, and gas composition in a gasoline engine can combine in such a way as to produce dew – liquid water – in the cylinder atmosphere. Since then it has been accepted by many that a sharp increase in wear rate will occur when the dew point has been reached, because then liquid acids will exist, these being the solutions of the inevitable carbon and sulfur oxides of the cylinder gas. Ryan and De Long[3] show an example of this, which is reproduced as Fig. 1. A CFR engine operated on commercial gasoline for 15 hr at each temperature shown in Fig. 1 gave evidence of a critical low-temperature condition at which corrosive wear will begin. This has been attributed to the deposition of liquid water in the cylinder oil film, which combines with carbon, nitrogen, and sulfur oxides to produce corrosive acids.

In Fig. 2, data developed at the U. S. Naval Engineering Experiment Station with a 2-stroke diesel engine operated at a variety of temperatures show rapid wear in the low-temperature range, as with the gasoline engine of Fig. 1; but the transition to low wear at moderate temperature is not abrupt, and the presence of a dew-point effect is not indicated. These observations suggest that there is a regular change with temperature in the amount of water adsorbed as a gas to the iron, there to meet molecules of carbon and sulfur oxides and in combination with them to react with the iron. In passing, it should be noted that the wear shows a tendency to increase at the high-temperature end of the scale, which could be a sign of contact wear. This phenomenon will be a subject of the principal discussion of this paper.

The literature of the last five years is full of descriptions of means which have been applied successfully to reduce corrosive, low-temperature wear. The approach has been to supply, in the lubricating oil, alkaline additives which neutralize the potentially corrosive acids as these attempt to penetrate the cylinder oil film.

Fig. 3 illustrates the power of additives to reduce wear in two types of diesel engines which were op-

---

[1] See ASME Transactions, Vol. 72, July, 1950, pp. 633-645: "Effect of Size on Design and Performance of Internal-Combustion Engines," by C. F. Taylor.

[2] See *SAE Journal*, Vol. 15, July, 1924, pp. 47-50: "Water in Crankcase Oils," by A. L. Clayden.

[3] See API Proceedings, Vol. 33, Sec. 3, 1953, pp. 216-221: "Mechanism of Corrosive Wear in Passenger-Car Service," by J. G. Ryan and B. W. De Long.

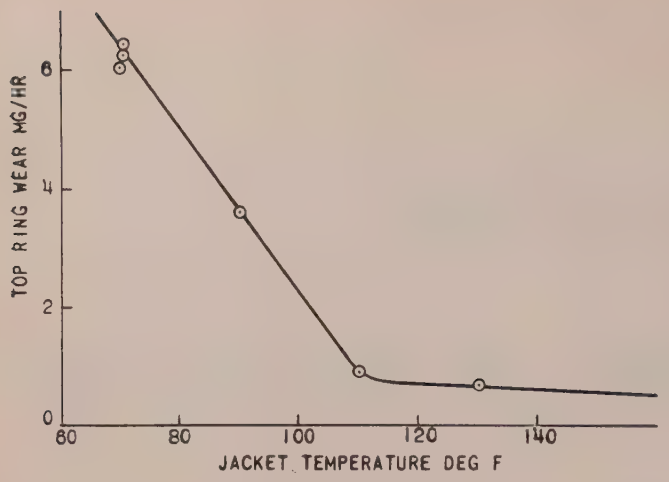

Fig. 1 – Piston-ring wear related to coolant temperature in a gasoline engine

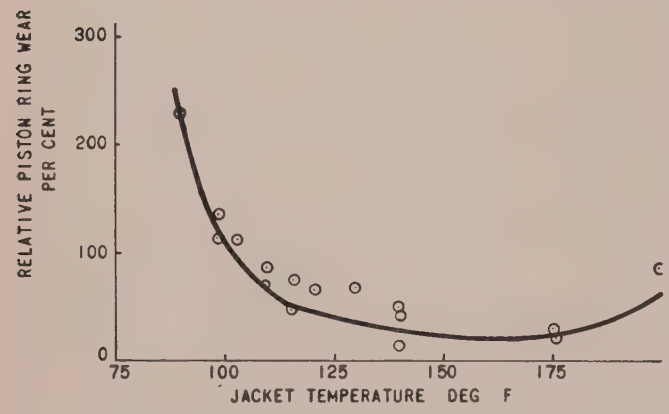

Fig. 2 – Piston-ring wear related to coolant temperature in a 2-stroke diesel engine

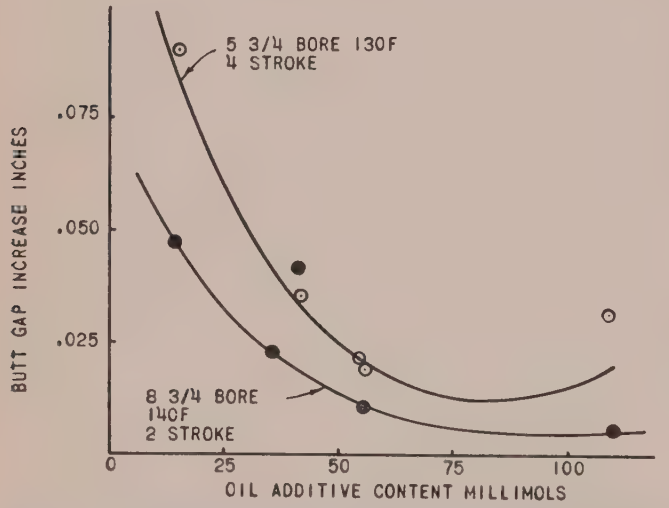

Fig. 3 – Low-temperature corrosive wear is reduced by use of alkaline lubricating oil additives. These tests were of 480-hr duration at water jacket temperatures of 130 and 140 F as noted

erated under low-temperature, corrosive conditions. The general relation of oil alkalinity (total base number, electrometric) to wear rate in another diesel engine is shown in Fig. 4. It is enough to say that corrosive wear in diesels is eliminated for practical purposes by the proper use of modern alkaline compounded oils.[4]

The temperature of the liner depends primarily on the combustion-gas temperature, turbulence, heat conduction of the liner, the type of coolant and its temperature, and the amount and temperature of air used in scavenging the cylinder. The piston rings rubbing on the liner will also contribute somewhat to the temperature, but this is more difficult to evaluate. This friction would undoubtedly influence the ring temperature more than the liner temperature. This part of the paper will indicate how the temperature of the liner is established and also give some values which have been measured.

The hot combustion gases transfer heat to the thin oil film on the liner, which in turn transfers the heat to the liner. The heat flows through the liner and into the coolant where it can be carried away. Fig. 5 shows a simple illustration of a cross-section through the combustion chamber. The barriers to the transfer of heat from the incandescent gases to the water are (1) the boundary layer of stagnant and occluded gas; (2) the oil film; (3) the oil metal liner; if "dry" type there would be an air gap also; (4) the water film boundary. The total temperature gradient may be from 4000 F to 100 F. Temperatures and temperature gradients are illustrated in Fig. 6. This diagram, if to scale, might be several times as high because of the tremendous drop in temperature through the gas boundary and the oil film. It can be seen that the temperature of the hot gases, T_g, of the burning mixture is much higher than that of the oil film and the inner metallic surface of the liner. A mean value of the gas temperature can be evaluated, and it will be designated by $T_{g\,m}$. Another temperature value which we will call the resultant temperature for heat transfer to the cylinder wall will be designated by $T_{g\,res}$. There is a drop in temperature from the hot gases through a gas film close to the oil film, which is on the liner surface. Another drop in temperature through the oil film gives the inner surface a temperature of T_2. It is this region in which we are interested because here the wear occurs on the liner. Conditions in this vicinity should be controlled in such a manner as to reduce the wear. Temperature difference T_2 to T_1 is the gradient through the cylinder liner. There is another film boundary between the outer liner surface and the coolant which drops the temperature from T_1 to T_c. The coolant temperature, T_c, is usually thermostatically controlled and usually is the only temperature which is made known to the operator by means of a thermometer.

We will consider here the variables which affect the value of T_2. The gas temperature T_g is a variable with time of the cycle. During the intake

[4] See SAE Transactions, Vol. 61, 1953, pp. 244-251: "Wear Prevention by Alkaline Lubricating Oils," by J. C. Ellis and J. A. Edgar.

The Authors

H. V. NUTT (M '36) is superintendent of the Fuels and Lubricants Project for the Naval Engineering Experiment Station in Annapolis. A graduate of Iowa State College, Mr. Nutt was affiliated from 1935 to 1938 with the U. S. Diesel Corp., becoming vice-president in 1937. In 1938, Mr. Nutt was employed by the U. S. Naval Engineering Experiment Station. He was commissioned a Lieutenant E-V(S) in the U. S. Naval Reserve in 1943.

E. W. LANDEN (M '53) is staff physicist for the Research Department of the Caterpillar Tractor Co. in Peoria, Ill. In 1938, he received his Ph.D. from the University of Missouri, where he instructed in physics until 1940. After being associated with the Armour Research Foundation, Dr. Landen joined the Caterpillar Tractor Co. in 1943.

J. A. EDGAR (M '37) is chief research engineer of Shell Oil Co.'s Martinez (California) Research Laboratory. After receiving a mechanical engineering degree from the University of California in 1929, Mr. Edgar worked in aerodynamics and structures successively at Wright Field, Dayton, and with the Fokker Aircraft Corp. in West Virginia. Joining the Shell Oil Co. in 1933, he has been with them ever since, except for time out to serve in Naval Aviation from 1940 to 1945.

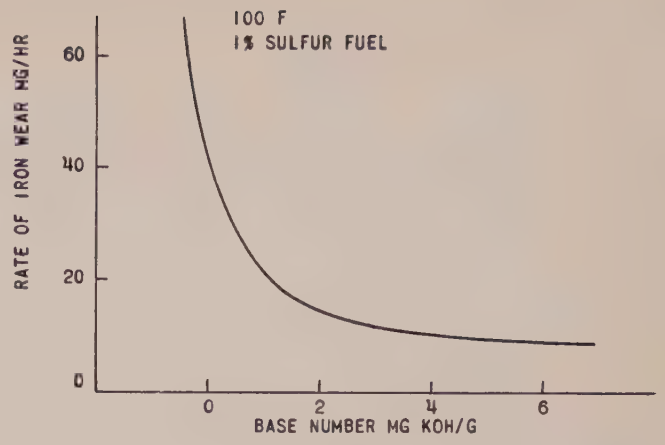

Fig. 4 – Corrosive wear is reduced through use of alkaline oil (indicated by base number) in a 4-stroke diesel engine at full load with a jacket temperature of 100 F

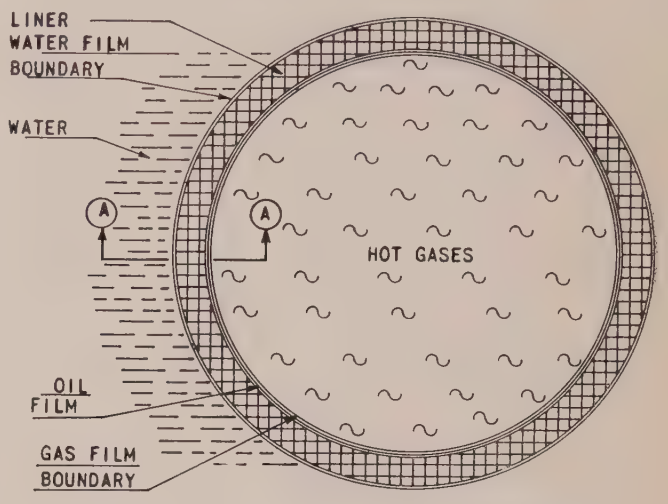

Fig. 5 – Diagrammatical cross-section through an engine cylinder and coolant space

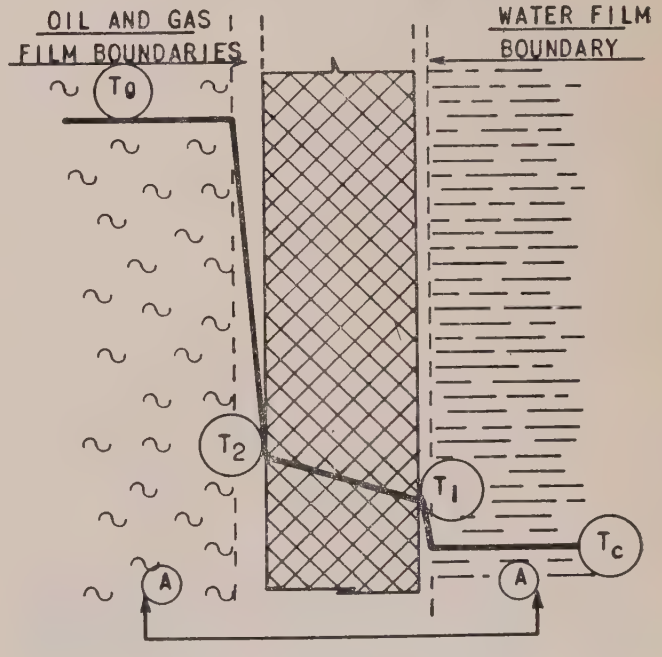

Fig. 6 – Diagram of the temperature drops along the path from the gas to the water

stroke, fresh, cool air is brought in, and T_g is comparatively low. During compression, T_g increases and reaches a maximum during combustion. Then it decreases with expansion until the cycle is ended and the hot gases are exhausted. The conditions of pressure and gas temperature, T_g, during the cycle are shown in Fig. 7 for a 4-stroke engine. The heat transferred to the cylinder wall resulting in T_2 is then known to vary throughout the cycle. G. Eichelberg[5] has made an analytical study of how heat is transferred to the cylinder wall. He has found that the heat-transfer coefficient, A_g, between the hot gases and the cylinder wall is given by the equation

$$A_g = k\sqrt{PT} \qquad (1)$$

where P and T are the instantaneous values of pressure and absolute temperature and k is a turbulence factor which can be expressed by

$$k = c\sqrt[3]{V} \qquad (2)$$

In this equation, c is a constant (and Eichelberg has evaluated it). V is the average piston speed.

We also know that the heat transferred to the cylinder wall is given by equation

$$q = A_{g\,m}\,(T_{g\,res} - T_2) \qquad (3)$$

In this equation $A_{g\,m}$ is the mean value of A_g, $T_{g\,res}$ is the resultant gas temperature for transferring heat to the liner, and T_2 is the temperature of the inner wall of the liner.

The values of A_g and the product $(T_g\,A_g)$ are shown graphically in Fig. 8, and the mean values

[5] See *Engineering*, Vol. 148, Nov. 17, 1939, pp. 547-550: "Some New Investigations on Old Combustion-Engine Problems," by G. Eichelberg.

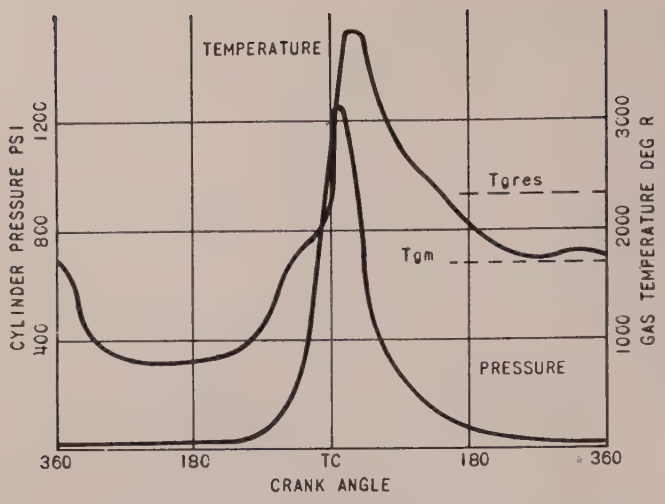

Fig. 7 – Pressure and temperature changes in an operating diesel-engine cylinder during a power stroke

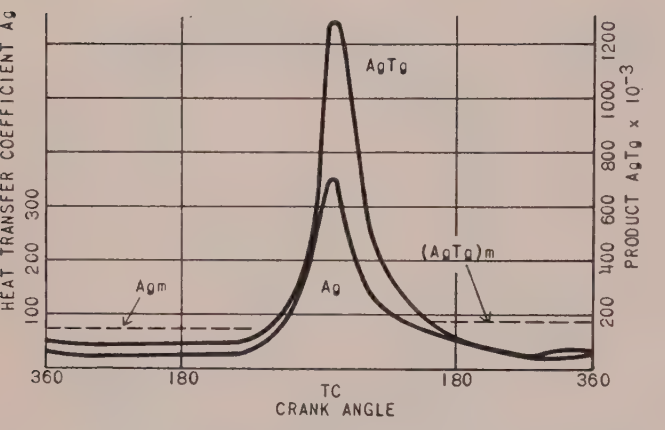

Fig. 8 – Values of heat-transfer coefficient corresponding to the conditions of Fig. 7

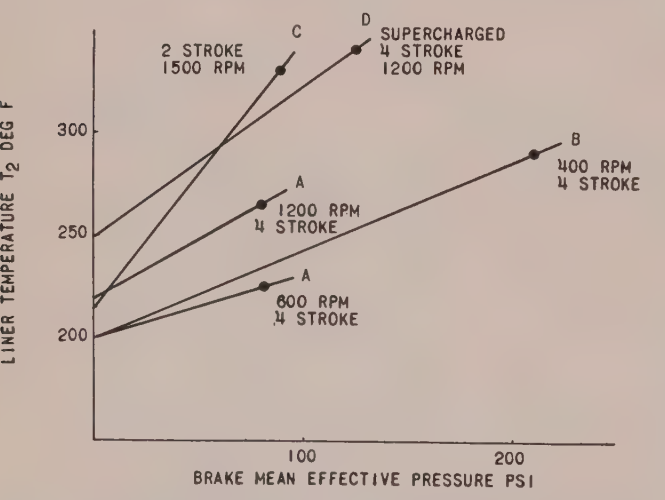

Fig. 9 – Large differences in liner surface temperature result from differences in design and operation. Water jacket temperature was the same in all cases. Rated operating point of each engine is shown by a large dot

$T_{g\,m}$ and $A_{g\,m}$ can be obtained by graphic integration from these curves. The values for this particular engine condition are indicated on the graph. The resultant gas temperature $T_{g\,res}$ is then obtained by the relation

$$T_{g\,res} = \frac{(A_g\,T_g)_m}{A_{g\,m}} \qquad (4)$$

From these equations it can be seen that the factors affecting T_2 from the inside are primarily the gas *temperature, pressure,* and *turbulence* due to piston speed.

The gas temperature and pressure at a given speed depend on the load. The plot of temperature T_2 as a function of bmep for several engines is shown in Fig. 9. It can be seen from this graph that generally as the bmep increases, for a given speed, T_2 increases. Values for engine A are shown for two speeds indicating the effect of speed on the temperature T_2. Engine B is a slow-speed high-output engine which has a rated operating point indicated by the large dot. In each case the large dot indicates the operating point of the engine. Engine D is similar in design to A but is supercharged, and this curve shows the effect of supercharging on the temperature T_2. Engine C which is a 2-stroke-cycle engine shows a steeper curve for T_2 on the bmep scale, as one would expect, since it has one work stroke each revolution.

Excess air scavenged through the engine during valve overlap has an influence on the temperature of the internal surfaces. Heat picked up by the scavenging air can extract heat from the engine parts according to

$$q_1 = C_p M\,(T_o - T_1) \qquad (5)$$

where C_p is the specific heat of air and M is the mass of air, T_1 is the temperature of the air going into the engine and T_o the temperature going out of the engine. The temperature of the air going out would not be the exhaust-gas temperature because as soon as the fresh air reaches a temperature equal to that of the engine parts, it will no longer absorb heat. In fact when the air mixes with the exhaust and becomes hotter than the engine parts, it will again give up heat. The scavenging air would pass through at a time when the exhaust gases are almost all gone. With valve overlap and proper design, it is possible to reject a considerable quantity of the heat normally picked up by the jacket coolant without valve overlap. Engine design would affect the possibility of rejecting heat in this manner. The 2-stroke-cycle engine always requires blow through to obtain a suitable fresh charge. And many 4-stroke-cycle engines have scavenging air blown through, especially with turbocharging.

Large exhaust-valve opening area permits quick expansion and expulsion of the hot gases which would reduce the heat transferred to the liner and, therefore, can have a favorable effect on T_2.

The temperature T_2 can be influenced by the temperature of the coolant T_c, the film coefficient A_c (each coolant has a different value), and the conductivity and thickness of the cylinder wall. As

the coolant temperature is increased, the temperature T_2 is increased. The effect of jacket temperature on T_2 is shown in Fig. 10, an almost linear function of the outlet temperature.

The type of coolant has an effect on the temperature T_2. Fig. 11 shows that with a glycol type of coolant the cylinder temperature is operating at a higher level. This is due to differences in film coefficient, the boiling point of the coolant, and the specific heat of the coolant.

Other engine design features have an effect on the value of temperature T_2. Such factors as combustion-chamber design, compression ratio, pressure charging, intercooling the air, 2-stroke versus 4-stroke cycles, engine speed, liner design, liner scaling, coolant flow all have some influence on T_2.

Thermal stresses and distortions caused by temperature gradients influence the wear, but this is a subject in itself and cannot be considered here.

At this point it is desired to stress that:

1. Water jacket temperature strongly influences cylinder surface temperature, but it alone is not a satisfactory measure of this temperature.

2. A very good comparison of cylinder surface temperatures between various designs of engines can be made by applying the calculations detailed previously.

3. If an engine is inclined toward contact wear of the cylinder and rings, attention to mechanical design features enumerated previously can result in reduced surface temperatures and yield improvement.

4. In view of the efficacy of modern lubricants in reducing corrosive wear, advanced engine design should point toward reduction of cylinder surface temperature; the ideal would be to have cylinder surface temperature as close to coolant jacket temperature as economics would allow, and then adjust jacket temperature just to the desired noncorrosive operating level.

It is easy to visualize a cool cylinder wall, because for a few power strokes after a long shutdown the cylinder wall certainly will be close to the temperature of the rest of the engine and of the cooling water. Soon the wall begins to heat up, and under load it will be much hotter than the jacket water as has been shown. At low load the cylinder-wall temperature will be closer to that of the jacket water, because the flame is cooler, hence the temperature gradient less abrupt. It is very hard experimentally to make a clean separation of corrosive and contact wear in an operating engine cylinder. Conditions can be selected where one type will dominate, but the other process will be present to some extent. A useful approach has been taken by setting up an engine to be motored so that the corrosive influences of fuel gases would be absent. Operating cylinder pressures were made very high by supplying air via inlet ports in the cylinder walls and using no exhaust valves. This mechanism has been operated for many hun-

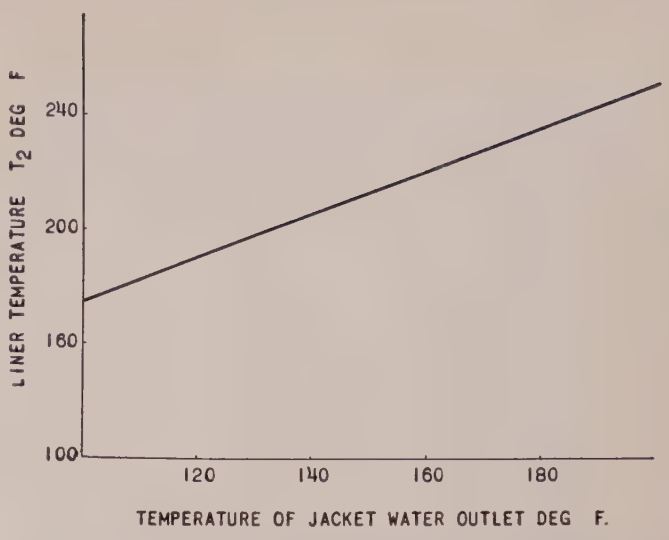

Fig. 10 – In this engine, liner temperature increased between 1½ and 2 times as fast as water jacket temperature, other things being equal. The sense is the same, but the degree may be different in other engine types, as computation would show

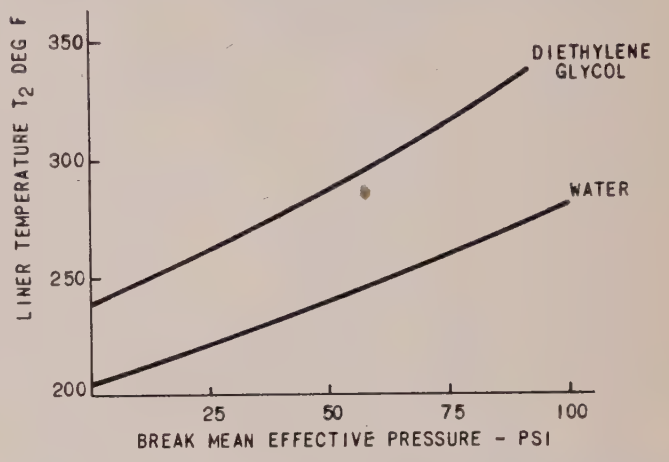

Fig. 11 – Water is a good coolant because of its mobility, favorable film coefficient, and high specific heat. For equal cylinder oil film temperature, permanent antifreeze mixtures must be run at much lower jacket temperature

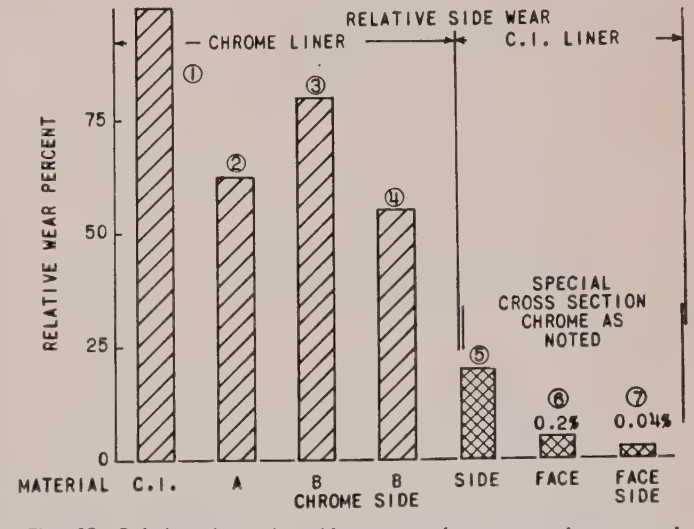

Fig. 12 – Relative piston-ring side wear under noncorrosive, motored operation showing effect of design changes with chrome-plated and cast-iron liners

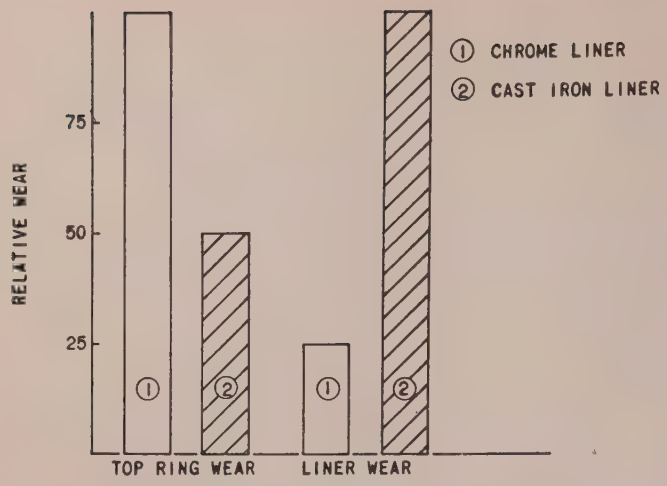

Fig. 13 – Under noncorrosive, motored operation, a cast-iron ring used in a chrome-plated liner resulted in high top ring wear. However, the chrome-plated liner wore only one-fourth as fast as the iron when used with the same rings. Thus, wear can be divided advantageously between rings and liner by choosing suitable combinations of materials

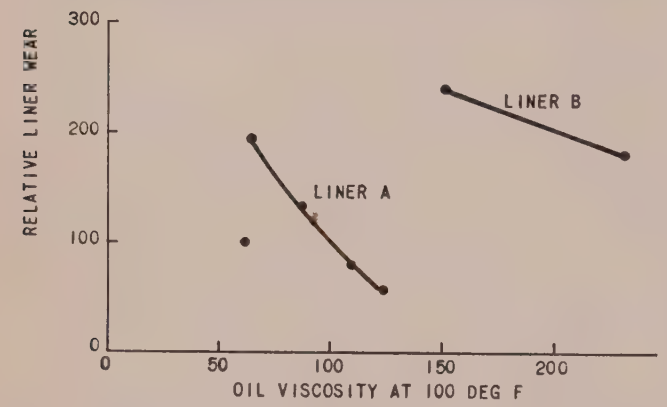

Fig. 14 – Liner wear versus oil viscosity for two different liners used in a 2-stroke engine

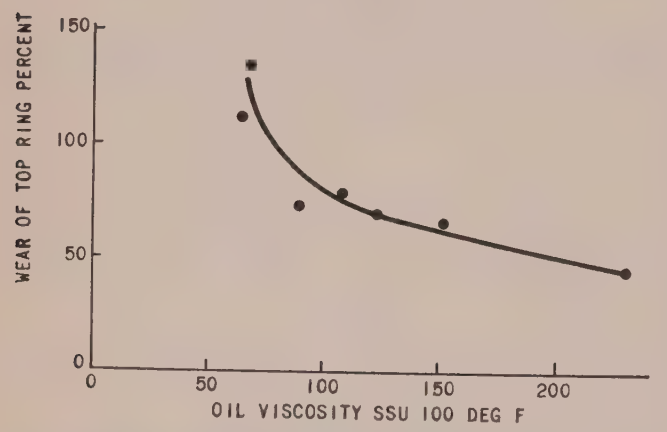

Fig. 15 – Though operated at a low jacket temperature of 117 F, the 2-stroke engine at full load and 1200 rpm showed high ring wear when very light oils were used

dreds of hours at speeds of 2100 rpm and higher and maximum cylinder pressures of about 1500 psi. Excessive contact wear of piston rings and cylinder bores occurred from the very beginning of the operation. This wear was higher than if the engine had been operating normally under its own power. Considerable ring breakage also accompanied the high wear. These effects were attributed to an abnormal shape of the cylinder pressure curve which resulted from compression pressure increases to a value equal to those normally obtained by compression plus combustion.

Considerable effort was spent in reducing the wear rates to normal values by mechanical and metallurgical means. Fig. 12 shows, in the left-hand bar 1, the side wear of the original rectangular cast-iron ring when run in a chrome liner. Ring wear was reduced to the extent shown in the second and third bars by the substitution of other ring materials. The lowest rate of ring side wear in the chrome liner, bar 4, was obtained by chrome plating the sides of a ring made of the material of bar 3. Concurrent changes of ring cross-section and liner surface produced the dramatic reductions of wear shown in bars 5, 6, and 7. The ring base material again was the same as that of bar 3, but the designs as noted were more effective.

Another illustration of how surface combinations can be made to apportion wear between liner and rings was made with the motored engine as shown in Fig. 13. In a chrome-lined engine, the wear of a cast-iron ring was higher than that when iron ran against iron; but the wear of the chrome liner was much less than that of its iron counterpart.

It has been stated earlier that contact wear in the cylinder occurs primarily by lubricant failure. Because known lubricants invariably thin out, volatilize, or decompose as they are heated, the original source of the lubricant failure evidently is the presence of heat beyond the capacity of the oil to withstand. Just as advanced engine design is directed toward the economic elimination of ultrahot surfaces, progress in lubrication is toward improved high-temperature viscosity, decreased volatility, and maximum thermal stability.

Mineral oils are not ideal lubricants (there are no ideal substances as yet), but they are really very good where properly selected to fill the operating requirements. The Engineering Experiment Station shows (Fig. 14) an exploration of wear rate of two different kinds of liners in a 2-stroke diesel engine, where the viscosity of the oil used is the independent variable. An extreme case is shown by the left-hand curve where very light oils were assessed; increased viscosity very rapidly improves the durability of the liner. Surface metallurgy shows its influence in the right-hand curve, but again wear declines as viscosity is increased. A similar systematic improvement of wear property with increased viscosity is shown by the same laboratory in Fig. 15, where piston ring wear was investigated as a function of oil viscosity, other conditions being held constant. A very rapid improvement in oil-film effectiveness is seen as viscosity at 100 F is increased to about 100 SUS, with more gradual benefit wear wise thereafter.

Evidence of this character raises question on how to use mineral oil in arctic operation, where

very light viscosity is required to permit cranking. On demand, full power output of the engines must be produced, and cylinder surface temperature therefore will be as high, or higher, than that prevailing in normal temperature climates, because this temperature is apt to be aggravated by the use of glycol antifreeze, as we have seen (Fig. 11). With these factors in mind, the Bureau of Ships, U. S. Navy, contracted a test program with the Southwest Research Institute, San Antonio, which was designed to reveal the separate contributions of viscosity, initial and average volatility, and residual volatility of the lubricating oil to the prevention of piston-ring wear. Pursuant to the plan, most of the test oils were of Navy 9005 or MIL-O-10295 type, essentially "5W" oils, having viscosities at 210 F of about 45 SUS and viscosity indexes of 140 to 160 in order to be fluid at low temperatures and yet have the viscosity of SAE 20 oils (approximately) at cylinder surface temperature. These were light mineral oils with viscosity-index improvers. In addition an SAE 30 oil, Navy symbol 9030, served as a high-viscosity standard, and a turbine oil based on di-2-ethylhexyl sebacate was included as an example of a more favorable volatility than can be had in a natural oil of like viscosity. In the 9005 oil class, two extremes were represented: first, oils made with well-selected base stock which had the lowest possible volatility commensurate with the desired fluidity; and second, oils made with light naphthenic base stocks which had unfavorable volatility (low boiling points) at the required viscosity. Not to neglect the possible influence of heavy residual components, bright stock was compounded with one of the naphthenic oils.

When used in a 2-stroke diesel engine with all piston compression rings irradiated except the top ring, the oils were found to differ in the power they would permit to be drawn from the engine before ring wear became excessive. Bmep was increased regularly in 14-psi changes at half-hourly intervals with all other factors constant. Wear, indicated by the radioactivity (counts per minute) of the circulating oil, goes on at a fairly low, steady rate until conditions of time and load are reached which tend to produce a considerable increase in wear. If straight lines are drawn representing the average rate of wear before and after this change occurs, characteristic wear patterns such as those shown in Fig. 16 are produced.

In some cases the time and load conditions for rapid wear may approach zero time and load. This is indicated by the curve for oil 624, which is shown to start out in the high-wear stage at a rate of about 1000 counts per min per hr. This rate, if allowed to continue, produced permanent scoring and engine failure. The slopes of the post-knee portions of the curves of the other oils shown are less precipitous, but all rates are intolerably high for good service. Therefore, the knee of the curve is considered the load for failure. Going from left to right, or from bad to good, in Fig. 16, and noting load/time at the knee of each curve, the oils are aligned in order of merit in Table 1. (Because load was not varied in infinitely small steps, it has been necessary in some cases to interpolate, which is to express a greater time at a given load as though it were a greater load only. This is incorrect, but it does not alter the sense of the performance comparison.)

Recalling that these experiments were planned carefully to disclose the independent effects on load-carrying ability of the several prime physical properties of lubricating oils, the materials are listed in Table 1 in their order of performance together with some of their viscosity and volatility characteristics.

Two criteria of volatility are listed in Table 1.

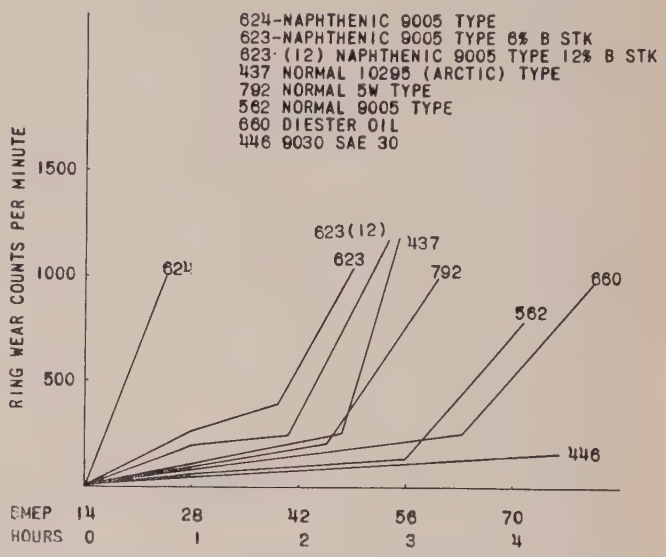

Fig. 16 – Ring wear, as measured by radioactivity of the various oils tested, in a 2-stroke diesel engine. Speed was 1200 rpm, load increased in half-hourly equal steps (hourly values only shown here)

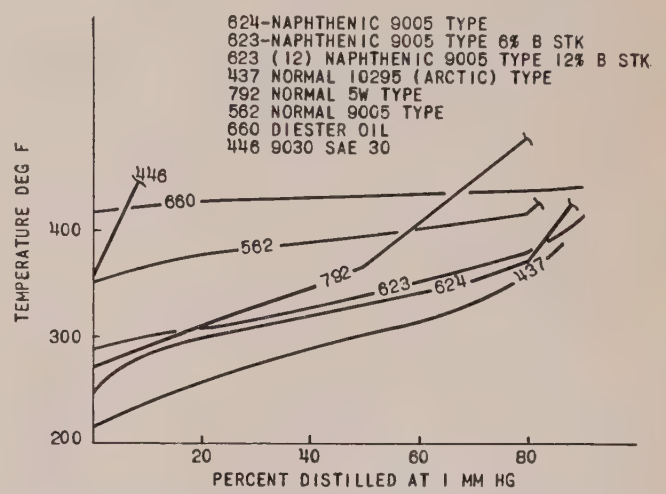

Fig. 17 – Vacuum Engler distillation indicates relative resistance of oils to vaporization, although this test applies only to the more volatile part of the oil and not to the high-boiling residues. Judged by this method alone, the 10295 and naphthenic 9005 oils are the worst and the synthetic oils the best, which is roughly correct

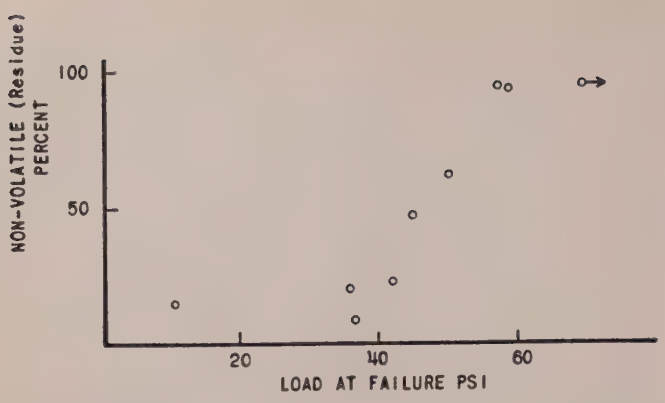

Fig. 18 – Volatility data obtained from thin-film evaporation tests

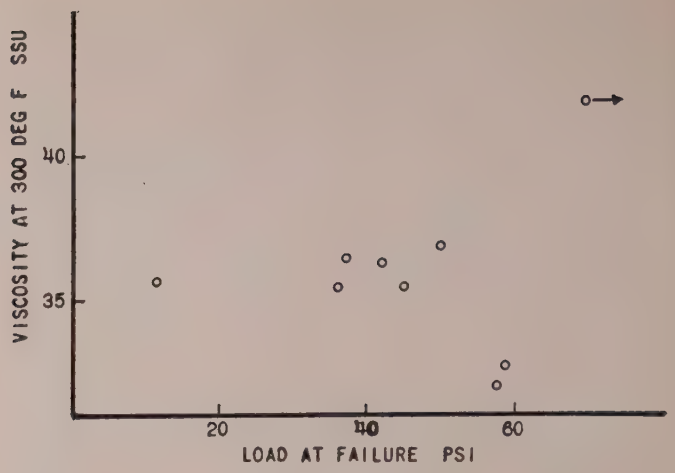

Fig. 19 – These viscosity-versus-load data show that viscosity alone is a poor performance indicator

The first is derived from the property of the oil to vaporize in a "Vacuum Engler" apparatus at a pressure of 1 mm of Hg abs as temperature is increased at a regular rate. In this apparatus it is possible to boil off about 80% of the usual light mineral oil or light synthetic oil before a temperature is reached where the residue begins to decompose and the regularity of the process is disturbed (Fig. 17). The synthetic oils are seen to have high initial boiling points; as much as 50% of the best light mineral oil will have disappeared from the flask before the first drop of the synthetic oil is vaporized. However, this type of assessment evidently emphasizes "initial" volatility, because, as pointed out, it does not tell quantitatively whether a useful residue would remain on the cylinder wall after some or most of the oil had been flashed off. If the 20% evaporated points of the oils are listed, as in Table 1, and compared with engine performance quality, it is seen without plotting that the relation is not regular and that there is at least one important inversion of order. This suggests that an inspection method is needed which will measure the persistence of an oily residue after the oil has been heated in a thin film. "Loss on heating" or its inverse "residue after heating" has been used for this purpose in various lubrication studies, and in this case a large number of combinations of temperature, time, and film thickness conditions were surveyed to develop a reproducible test which would seem to have connection with the engine performance values of the oils. The most suitable conditions found were:

Thickness of oil film, 0.15 mm
Heating condition, (oven, forced draft) 300 F
Time, 2 hr

The last column of Table 1 shows only a roughly systematic performance increase with residue after heating, and minor inversions occur. The degree of correlation is shown better by Fig. 18. The information on oil volatility obtained by vacuum distillation (Fig. 17) can be augmented by a thin-film evaporation test, where the resistance of the oil to loss from a heated dish is measured. In this case the oil film was 0.15 mm thick, the temperature 300 F in air, and the time 2 hr. A good general agreement is seen between the amount of oil remaining after this heat-treatment and the load which the engine would carry before contact wear set in. Load is expressed in bmep at a speed of 1200 rpm.

Whatever the shortcomings of the volatility criterion may be, it is better than a judgment of performance based on viscosity alone. Fig. 19, when compared with Fig. 18, leaves no doubt on this point. If viscosity of oil is considered without reference to its volatility, very poor agreement with the property of cylinder film lubrication results. This observation was made clear in these tests by using oils of greatly differing volatility-viscosity relationships. However, Fig. 18 shows that resistance to evaporation is a better single performance indicator than is viscosity.

As a digression, one asks "Why had viscosity of the oil always been uppermost in mind as the sign of cylinder antiwear property?" The answers:

1. Without viscosity there is no hydrodynamic lubrication; hence, viscosity is emphatically the most important property of the lubricant.

2. In a family of similar mineral oils, volatility becomes better as viscosity increases, so that it is justified to think in terms of the more easily measurable property.

In the results which have been presented in Figs. 14 and 15, viscosity alone was mentioned for the reason just stated.

The wear data under discussion do not decry the importance of viscosity, but they do emphasize:

For cylinder lubrication, low oil volatility is essential; and this property is best recognized by measurement of the quantity which remains after exposure of a film of oil to high temperature.

At the risk of laboring this familiar point, it should be noted that low volatility assures merely that a viscous film will survive the flash evaporation which occurs on the cylinder at each power stroke. Sufficient oil must remain to make a hydrodynamic film, or contact wear will result.

Viscosity and volatility being independent variables, a multiple correlation should be possible. For the tests described, a rather good curve fit is obtained by the simple linear expression:

$$\text{Load Capacity } F = -2 + 0.3R + 0.9V$$

where:

R = Residue after heating, %

V = Extrapolated viscosity, SUS at 300 F

This expression of the wear-test results is plotted in Fig. 20. A linear combination of volatility and viscosity criteria produces a correlation between these properties of oils and their protective value against piston-ring contact wear. "Load at failure" again is expressed in the bmep which could be drawn from the engine at 1200 rpm before evidence of contact wear appeared.

It would not be expected that the terms would apply to all other conditions and engines, but it is confidently proposed that a similar type of correlation will prove to be adequate to compare oils under any situation where the condition of contact cylinder wear may be reached.

Note Concerning H. V. Nutt's Authorship – The opinions given are those of the writer and are not to be construed as official or reflecting the views of the Navy Department or the Engineering Experiment Station.

Additional References

1. "Further Experiments on Cylinder Wear," by C. G. Williams. *Journal of Institution of Automobile Engineers,* Vol. 2, August/September, 1934, pp. 19-34.

2. "Five Ways That Diesels Wear," by J. W. Pennington. *SAE Journal,* Vol. 57, February, 1949, pp. 39-44.

3. "Investigations on Cylinder-Liner Wear," by W. G. Payne and W. E. Joachim. SAE *Quarterly* Transactions, Vol. 3, January, 1949, pp. 51-68.

4. "War on Wear," by H. Blok. *American Society of Naval Engineers Journal,* Vol. 64, November, 1952, pp. 799-806.

5. "Radioactive Tracers Reveal Friction and Wear on Metals," by J. T. Burwell and C. O. Strang. *Metal Progress,* Vol. 60, September, 1951, pp. 69-74.

6. "How Engines Wear," by J. F. Kunc, Jr., D. S. McArthur, and L. E. Moody. SAE Transactions, Vol. 61, 1953, pp. 221-223, 230.

7. "Application of Radioactive Tracers to Improvement of Fuels, Lubricants, and Engines," by P. L. Pinotti, D. E. Hull, and E. J. McLaughlin. SAE *Quarterly* Transactions, Vol. 3, October, 1949, pp. 634-638.

8. "Some Further Work on High-Sulfur Diesel Fuels," by L. A. Blanc. Presented at SAE National West Coast Meeting, San Francisco, Aug. 20, 1948. (Digested in *SAE Journal,* Vol. 56, December, 1948, pp. 53-54.)

9. "Sulfur in Diesel Fuel," by J. J. Broeze and A. Wilson. Institution of Mechanical Engineers Proceedings (Automobile Division), Part 3, 1948-1949, pp. 126-145.

10. "Effect of Lubricating Oil Viscosity on Engine Performance," by J. W. Lane and D. S. Chatfield. Presented at SAE Summer Meeting, French Lick, Ind., June 6, 1949.

11. "Factors Affecting Piston Temperature," by G. B. Fox. Diesel-Engine Users Association Paper S-195, Nov. 27, 1947.

12. "Relation between Dewpoint and Concentration of Sulfuric Acid in Flue Gases," by A. A. Taylor. *Institute of Fuel Journal,* Vol. 16, October, 1942, pp. 25-28.

Table 1 – Viscosity and Volatility Characteristics of Variety of Oils (Arranged in Order from Worst to Best)

Oil No.	Bmep at Failure, psi	Viscosity, SUS at 100 F Measured	Viscosity, SUS at 300 F Extrapolated	V. I.	Volatility: 20% Distilled Temperature, F	Volatility: Residue after Heating, %
624[a]	14 (⅓ rated load)	128	35.7	153	308	15.0
623[b]	35	138	35.6	141	300	20.0
437[c]	37	118	36.4	162	258	8.5
624+12[d]	42	164	36.5	140+	305	23.0
792[e]	45	110	35.4	165	314	47.0
562[f]	50	164	36.8	145	376	61.0
660[g]	56	72	32.0	125	434	93.8
479[h]	59	74	32.7	160	426	92.7
446[i]	Above 70 (full rated load)	582	41.7	100	Decomposed at 430	93.8

[a] Navy 9005 type, naphthenic.
[b] Navy 9005 type, naphthenic, with 6% bright stock.
[c] 10295 type (Army Arctic).
[d] Navy 9005 type, naphthenic like 624 and 623, but with 12% bright stock.
[e] SAE 5W commercial type.
[f] Navy 9005 type.
[g] Diester, di-2-ethylhexyl sebacate.
[h] 7808-type aircraft turbine oil, based on diester.
[i] Navy 9030 type. SAE 30 viscosity, synthetic.

ORAL DISCUSSION

Reported by Paul W. Sheehan
Thompson Products, Inc.

Question: When the rings were plated on the sides and face, which produced the least ring wear, what effect did this have on groove wear?

Answer: The groove wear for all ring combinations was not noticeable when there was only a small amount of ring wear.

Question: Were the pistons in the modified GM model 71 engine in which these tests were run made of aluminum?

Answer: No. Pistons were cast iron.

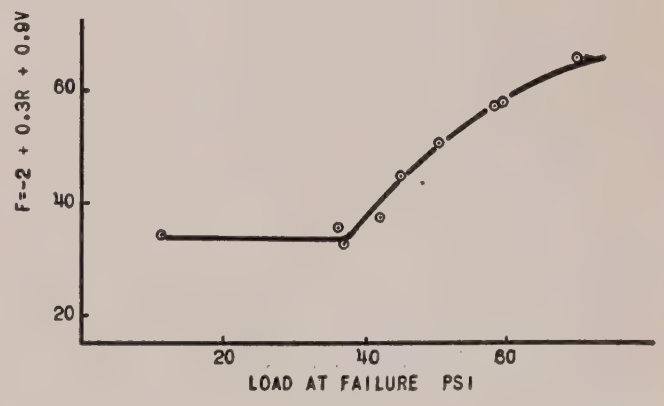

Fig. 20 – Load capacity, a linear combination of volatility and viscosity criteria, versus load at failure

Development

THE highly competitive gas-turbine, jet-engine field has presented metallurgical problems which require new alloys for use as bucket materials at elevated temperatures never before encountered. Development of superior materials for the highly stressed turbine buckets has been the metallurgist's approach in attempts to maintain and improve engine thrust ratings. As the result of a continuing research program, a new nickel-base alloy,[1] designated GMR-235, was developed by the Research Laboratories Division of General Motors for producing cast turbine buckets combining the required high-temperature strength with adequate ductility and low strategic-alloy content. The development has incorporated all metallurgical phases of transfer from laboratory to production operations, including comprehensive manufacturing and quality control procedures governed by realistic engineering specifications.

This paper is intended to describe the salient features of this new super alloy with respect to physical properties, and outline the manufacturing processes required to produce a quality product. Data presented in Table 1 compare GMR-235 with some other commercial alloys in present production and emphasize the combination of high-temperature strength and low strategic-alloy content.

It was this combination which prompted an intense investigation of GMR-235 as a commercial possibility for high-production turbine buckets.

A relatively complete understanding of this cast-nickel-base super alloy must include not only physical characteristics, but the special manufacturing and production controls that are required to produce and maintain the necessary high quality level of gas-turbine parts. Basic data such as chemical composition governed by limits established in correlated laboratory stress-rupture tests constitute effective background information required in maintaining uniformity of product.

Other information which broadens the scope of engineering background includes thermal shock resistance, elevated-temperature fatigue characteristics, and performance of components in actual gas-turbine service.

Chemical Composition

Acceptable composition limits of GMR-235 alloy established as practical production limits controlled within a realistic engineering specification are given in Table 2.

The chemical limitations represent the present preferred compositions which seem to produce the best combination of properties in consideration of strategic-alloy content. Attention is called to the high level of aluminum and titanium contents (6.00% maximum), and the reverse aluminum-to-titanium ratio (1:1 minimum; 2.25:1 maximum), in contrast to the earlier nickel-base alloys. The relatively high percentages of aluminum and titanium as strengtheners in GMR-235, coupled with the major influence of boron on both high-temperature strength and ductility, has resulted in a cast alloy with a desirable combination of properties, even with as high as 12.00% iron.

Physical Properties

Evaluation of high-temperature strength of cast GMR-235 alloy has primarily included stress-rupture and tensile tests at temperatures up to 1700 F. These data have been supplemented by creep-testing shrouded buckets installed on a turbosupercharger wheel used as a B-31 turbobootstrap unit.

The curve data presented in Fig. 1 show the range of ultimate strength, yield strength (0.2% off-set), and per cent total elongation obtained from tensile tests of cast K-2 mold GMR-235 test bars.[2] The K-2 mold is the designation used for a favorable gating arrangement developed at GM Research Laboratories which produces sound test bars. In Fig. 2, typical spread of data obtained in stress-rupture tests is shown in a log-log plot of life and stress at various temperatures, 1300 F through 1700 F. This range of life obtained under all combinations of stress and temperatures results from certain combinations of variables such as chemical composition, control of test conditions, casting soundness, and crystal orientation. For example, creep elongation results covering turbobootstrap operation, shown in Fig. 3, show a measurable spread between buckets of identical materials. In this test, conducted under the direction of W. A. Turunen of our gas turbines department, turbosupercharger buckets measuring 1¼ in. from platform to shroud were tested on a 10-in.-diameter turbine wheel which is run in a B-31 supercharger used as a bootstrap unit with suitable combustion chamber, fuel control, and tailcone accessories.

[1] U. S. Patent No. 2,688,536.

[2] See Transactions of American Foundrymen's Society, Vol. 62, 1954, pp. 293-298: "Technique for Improving Quality of Investment Castings," by D. G. McCullough, F. J. Webbere, and R. F. Thomson.

# of a New Gas Turbine

Super Alloy GMR-235

D. K. Hanink, F. J. Webbere, and A. L. Boegehold,
Research Laboratories Division, GMC

Paper was presented at SAE Golden Anniversary Annual Meeting, Detroit, Jan. 14, 1955.

Normal operation of the bootstrap unit consists of a nozzle-box temperature of 1610 F, resulting in a tailcone temperature of 1425 F at wheel speed of 23,000 rpm.

Generally, a finite life is reached for buckets of other materials tested under these conditions, although no failures have been produced on GMR-235. Information obtained on creep-elongation has indicated a lower spread of results in comparison with other alloys which exhibit lower hot strength.

Effect of Chemical Variations

The influence of boron, the hardeners (aluminum and titanium), and iron on the physical properties of GMR-235 alloy were investigated not only to establish desired chemical limits, but to determine the suitability of cheaper modifications of the GMR-235 alloy base analysis. Accordingly, alloys were produced and tested representing variations in these particular elements to correlate their effect on physical properties either individually or in combinations.

Boron – Relatively minute quantities of boron which are specified in the GMR-235 range of composition can exert a major influence on the ductility of the alloy, and to a lesser extent on the strength.

A series of separate remelt heats were investigated as nickel-boron alloy additions to a base master heat of GMR-235 containing no boron. This series of heats was, therefore, produced with all other elements remaining nominally constant. For example, when the base heat was modified to contain 0.50% boron, it resulted in the chemical changes shown in Table 3.

Fig. 4 illustrates the effect of boron on stress-rupture properties of cast bars tested at 35,000 psi,

Table 1 – GMR-235 Compared with Other Commercial Alloys

Alloy Identification	1953 Materials Strategic Alloy Rating	Stress to Produce Rupture in 100 Hr at 1500 F[a]
S-816	2562	24,000
HS36 (L251)	2527	29,000
HS31 (X40)	2441	28,400
Nimonic 90	896	28,000
Inconel X	849	28,000
Nimonic 80	364	24,000
GMR-235	306	34,000-41,000

[a] From p. 48 of *Metal Progress*, Vol. 66, July 15, 1954.

Table 2 – Composition of GMR-235

Carbon	0.10 – 0.20
Manganese	0.25 max
Silicon	0.60 max
Chromium	14.00 –17.00
Iron	8.00 –12.00
Molybdenum	4.50 – 6.00
Aluminum	2.50 – 3.50
Titanium	1.50 – 2.50
Boron	0.025– 0.100
Nickel	Balance

DESCRIBED here is a new nickel-base alloy offering a combination of high-temperature strength, adequate ductility, and low strategic alloy content.

Used in gas-turbine buckets where extremely high temperatures are encountered, GMR-235 has undergone a program of laboratory testing, development of foundry production and control methods, and extensive field testing with no failures.

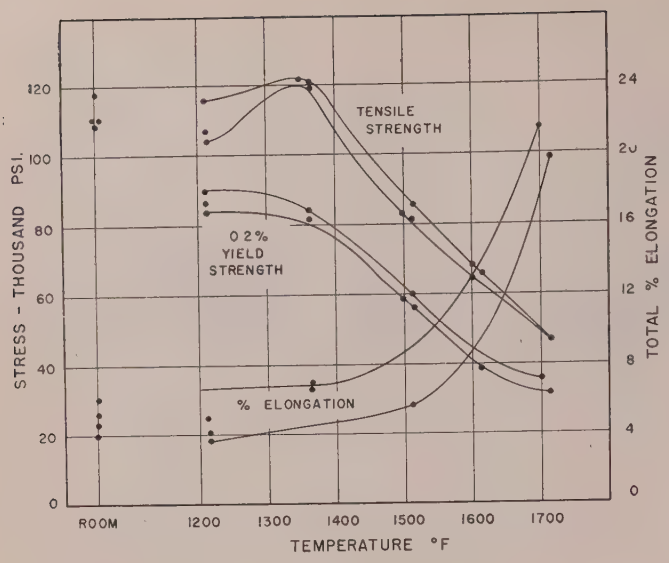

Fig. 1 – Elevated tensile properties of GMR-235 alloy. K-2 investment mold test bars

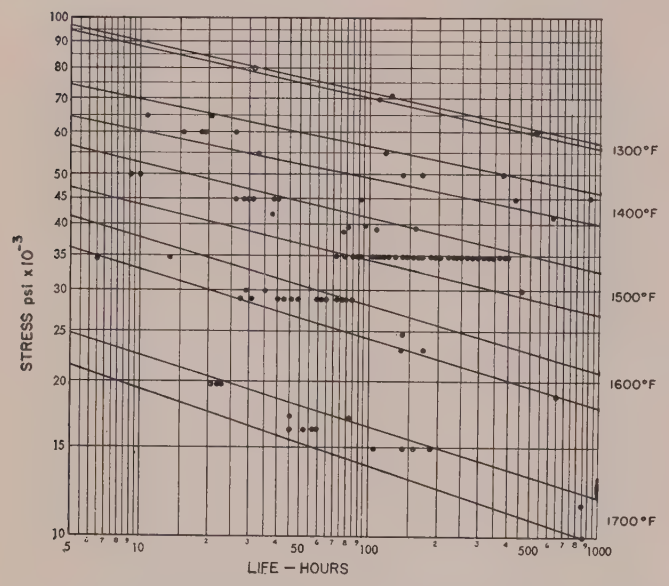

Fig. 2 – Stress-rupture properties of as-cast GMR-235 alloy. K-2 mold test bars

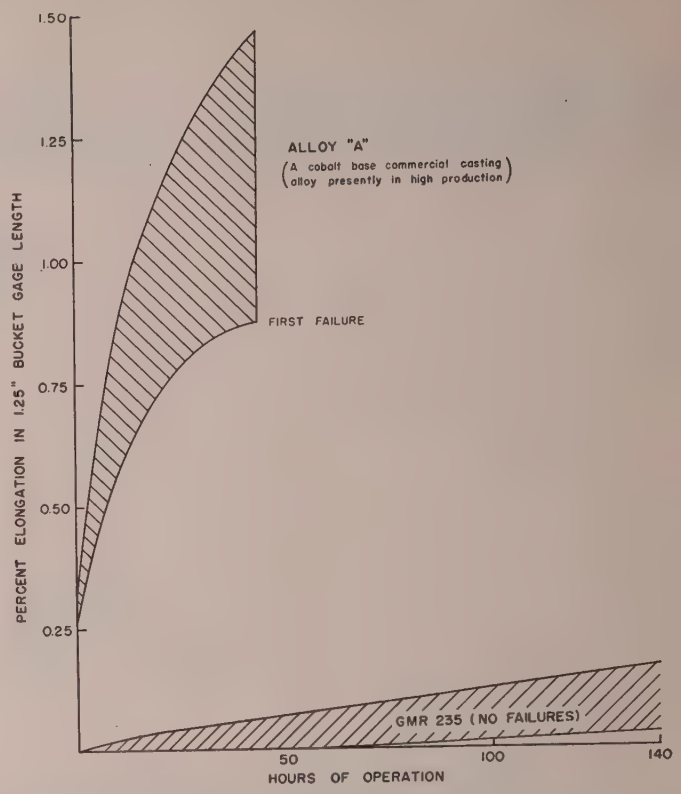

Fig. 3 – Creep spread of turbosupercharger buckets on B-31-type turbobootstrap test – 23,000 rpm, 1425 F tailcone temperature

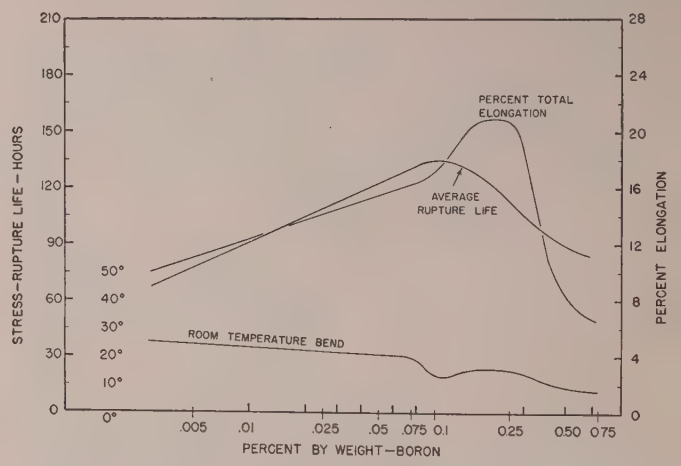

Fig. 4 – Effect of boron content on stress-rupture properties and room-temperature ductility of GMR-235 alloy – 2.5-3.0% aluminum, 1.75-2.00% titanium

Table 3 – Chemical Changes in Base Heat Modified to Contain 0.5% Boron

	MCM-3805 (No Boron Base Master Heat)	MCM-3805 (+0.50% Boron)
Aluminum	2.57	2.57
Titanium	1.92	1.88

1500 F. Rupture elongation in the K-2 mold test bars reaches a maximum at approximately 0.15% boron.

Room-temperature bend tests conducted on $\frac{1}{8}$-in. diameter pins cast in the same molds as the stress-rupture bars have provided information on room-temperature ductility. The angle of bend to first crack formation is shown in the curve so identified in Fig. 4, and indicates a drop-off in ductility when boron exceeds 0.1%. The photographs in Fig. 5 are a further demonstration of the effective embrittling effect at room temperature when boron is increased to as high as 0.15%.

Microstructure changes produced in four different modifications from 0.0% to 0.52% boron are presented in Figs. 6 through 9. The primary change in structure seems to be the amount of grain boundary constituent, resembling Chinese script, and identified as a complex boride phase.

Fig. 5 – Effect of boron on room-temperature ductility of GMR-235 composition – left: standard GMR-235, 0.07% boron; right: modified GMR-235, 0.15% boron

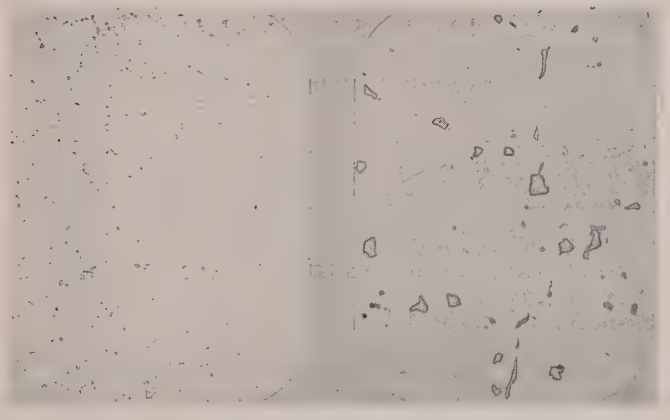

Fig. 6 – Microstructure of cast GMR-235 alloy containing no boron (reduced from photomicrographs taken at: left: 100X; right: 500X)

Titanium and Aluminum – The strengthening effect of titanium and aluminum in combinations up to about 6% is shown in the curve relationship, Fig. 10. The correlated data in these curves were restricted to a minimum of 1% titanium and 2% aluminum contents. Curves which describe the effect of titanium variations with constant aluminum content of 3%, and the effect of aluminum variations with constant titanium content of 2%, are presented in Figs. 11 and 12.

The increased life and elongation of regular

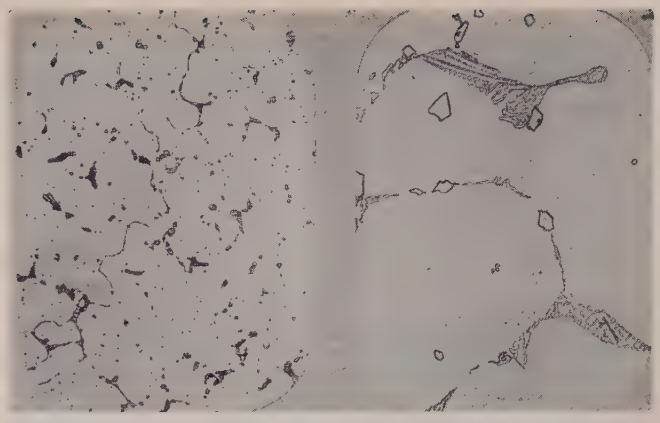

Fig. 7 – Microstructure of cast GMR-235 alloy containing 0.07% boron (reduced from photomicrographs taken at: left: 100X; right: 500X)

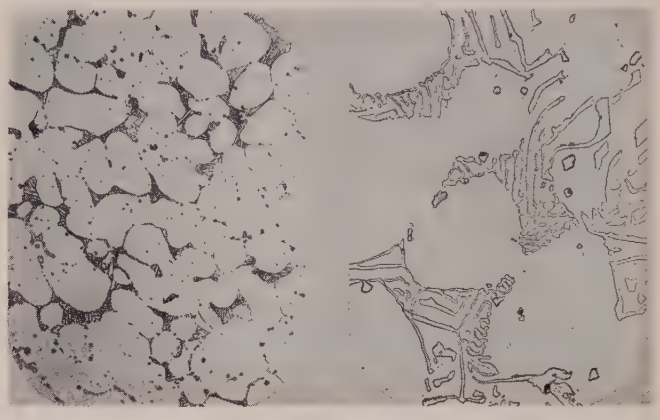

Fig. 8 – Microstructure of cast GMR-235 alloy containing 0.26% boron (reduced from photomicrographs taken at: left: 100X; right: 500X)

The Authors

D. K. HANINK is supervisor of high-temperature alloy research at General Motors Research Laboratories. He received a B.S. degree in Metallurgical Engineering from the University of Michigan in 1942. He received his professional engineer's certificate in Metallurgical Engineering in 1950. Mr. Hanink did laboratory and production control work in the metallurgical department of the Dodge Chicago Plant from 1942 to 1946.

F. J. WEBBERE is supervisor of alloy development and melting at General Motors Research Laboratories. He received a B.S. in Metallurgical Engineering from the University of Wisconsin. He joined the metallurgy department of the GM Research Laboratories Division in 1941. His activities included hardness testing at elevated temperatures and development of high-temperature alloys.

A. L. BOEGEHOLD (M '44) is assistant to the general manager of the General Motors Research Laboratories. He received his B.S. in Mechanical Engineering from Cornell University in 1915. Mr. Boegehold has worked for the Remington Arms & Ammunition Co., the Bridgeport Brass Co., Remington Union Metallic Cartridge Corp., and U. S. Army Ordnance. He was head of the metallurgy department of the Laboratories Division of General Motors Corp. for 27 years.

GMR-235 alloy as a result of increasing aluminum and titanium up to 6.5 combined weight percentage has been related to microstructure changes, examples of which are shown in photomicrographs, Figs. 13 and 14, of standard GMR-235 alloy and modified GMR-235 alloy containing 8.5% total aluminum and titanium content. A new microconstituent identified in the photomicrograph seems to be associated with a decrease in high-temperature properties and accompanying decrease in room-temperature ductility.

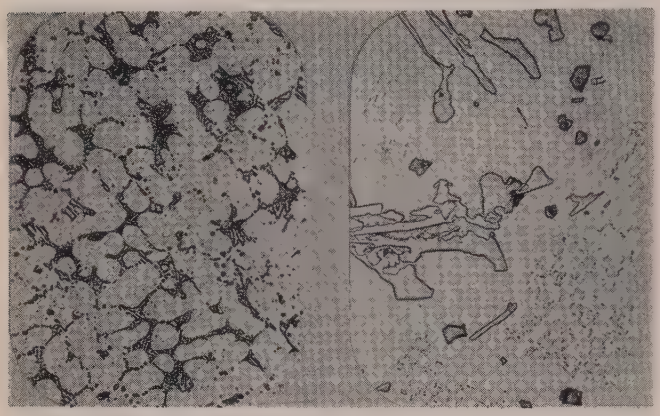

Fig. 9 – Microstructure of cast GMR-235 alloy containing 0.52% boron (reduced from photomicrographs taken at: left: 100X; right: 500X)

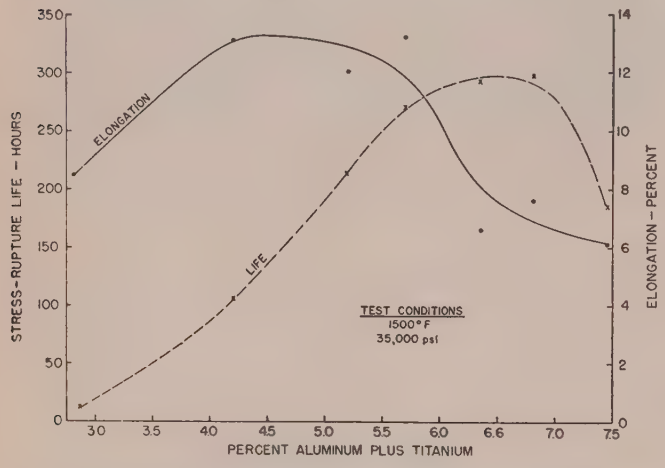

Fig. 10 – Effect of combined aluminum and titanium content on stress-rupture life and elongation of as-cast GMR-235 alloy

Bend tests conducted on cast ⅛-in. diameter cast pins have been used to rate room-temperature ductility. Although results may be influenced by casting soundness, tests show that titanium content up to 2% improves ductility. Larger amounts up to 5.0% have relatively little influence. At the 2% titanium level, however, increasing aluminum contents at levels higher than 4.0% reduce room-temperature ductility below the 15-deg bend to fracture which has been considered an acceptable minimum value in production specifications.

The best combination of properties at both room and elevated temperature seems to be nominal aluminum and titanium contents of 3.5 and 2% respectively.

Heat-Treatment – Preliminary work on heat-treatment of GMR-235 alloy has indicated that a solution treatment of 1 hr at 2100 F followed by air cooling or water quenching can, in some cases, nearly double the stress-rupture life at 1600 F, 28,000-psi stress.

Tests conducted on three typical heats of GMR-235 alloy which were given heat-treatments indicate some advantage in air cooling after solution treatment. Data presented in the bar chart, Fig. 15, indicate that a 16-hr age at 1800 F does not improve properties of solution-treated material.

Some advantages in aging 5 hr at 1800 F from the as-cast condition have been shown in tests covering both cast bars and cast J-33-type turbine buckets. Fig. 16 compares as-cast and as-cast-plus-aging on 0.15-in.-diameter bars cut from buckets as well as cast 1.25-in.-diameter cast bars from K-2 type molds.

The increase in hot strength as a result of this aging heat-treatment coupled with the desirable commercial aspects of eliminating a 2100 F solution treatment make the 1800 F aging treatment a preferred production operation.

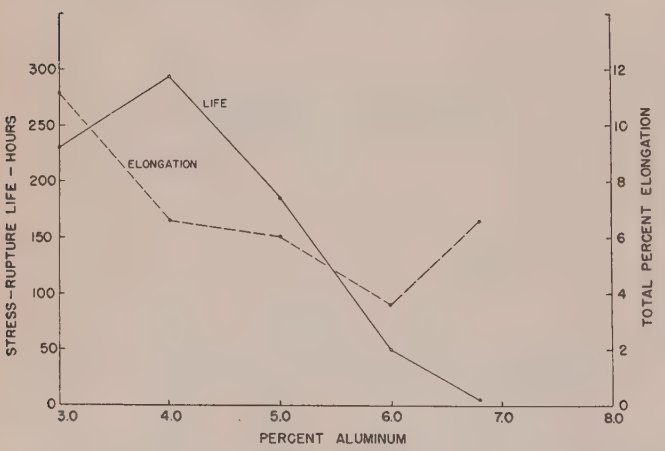

Fig. 11 – Effect of aluminum on the stress-rupture life of cast GMR-235 alloy containing nominal 2.0% titanium

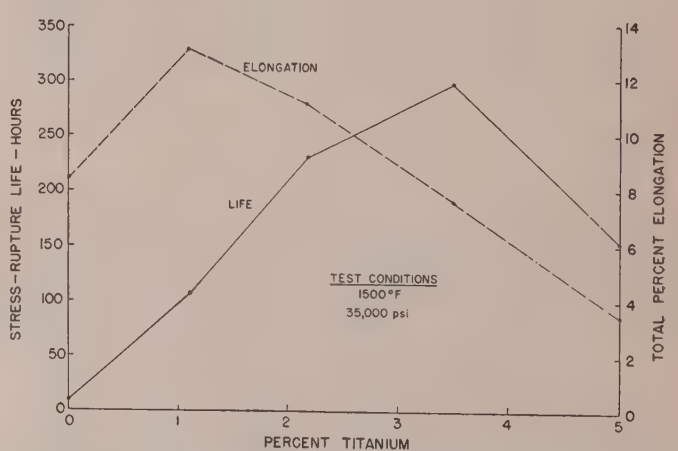

Fig. 12 – Effect of titanium on stress-rupture life of cast GMR-235 alloy containing nominal 3% aluminum

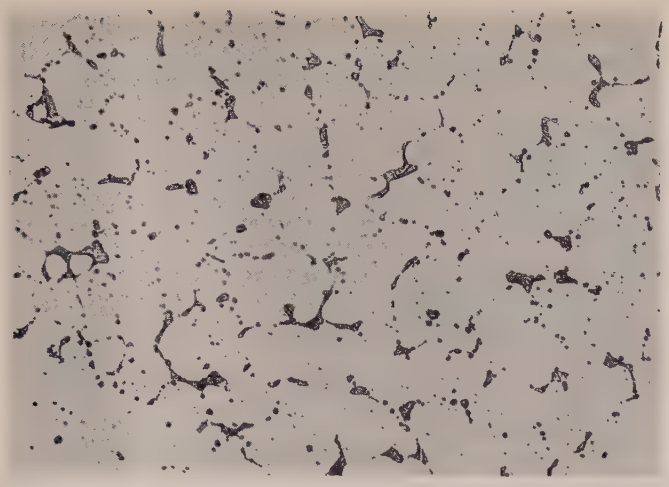

Fig. 13 – Microstructure of standard GMR-235 alloy containing 3.00% aluminum, 2.00% titanium (reduced from photomicrograph taken at 100X)

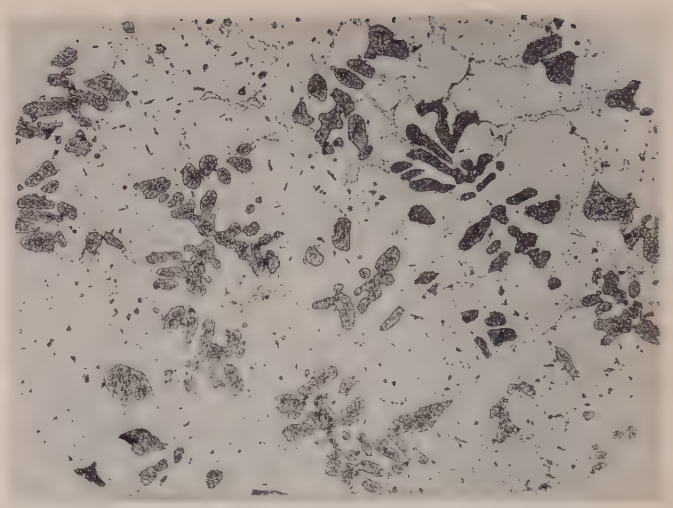

Fig. 14 – Microstructure of modified GMR-235 alloy containing 6.8% aluminum, 2% titanium (reduced from photomicrograph taken at 100X)

Supplementary Physical Tests

Thermal Shock – The effect of sudden temperature changes such as the rapid heating and cooling of turbine-blade edges under cyclic service conditions is considered to be of major importance in determining useful life of promising high-strength super alloys. Cracking at the thin blade edges caused by thermal shock can promote fatigue failure before the potential life based on creep resistance is reached. Thermal shock bench tests, however, were conducted primarily to ascertain any predominant brittle characteristics which might be identified with the material.

The thermal shock test used in this investigation was conducted on NACA-type wedge specimens,[3] a diagram of which is shown in Fig. 17.

These NACA-type wedge specimens are heated by direct flame impingement on the side opposite the wedge tip, and water-quenched selectively at the 1/32-in.-wide tip. Cyclic heating consisted of an 18-min heating period to 1800 F followed by the water quench which cools the tip from 1800 F to room temperature in about 5 sec. Obviously, the high-temperature strength, coefficient of thermal expansion, and thermal conductivity of the alloy determine, to a large extent, the magnitude of forces imposed on the tip during heating and cooling.

[3] See NACA TN 2037 (1950), "Resistance of Six High-Temperature Alloys to Cracking Caused by Thermal Shock," by M. J. Whitman, R. W. Hall, and C. Yaker.

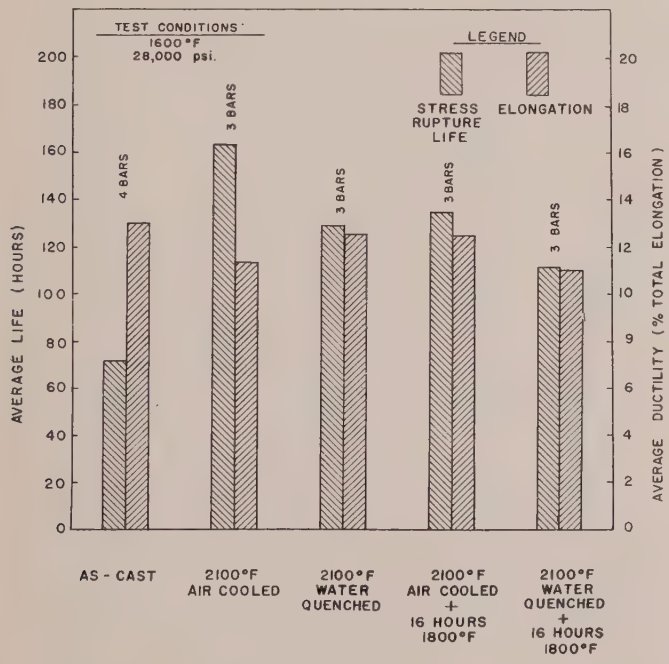

Fig. 15 – Effect of heat-treatment on physical properties of as-cast GMR-235 alloy

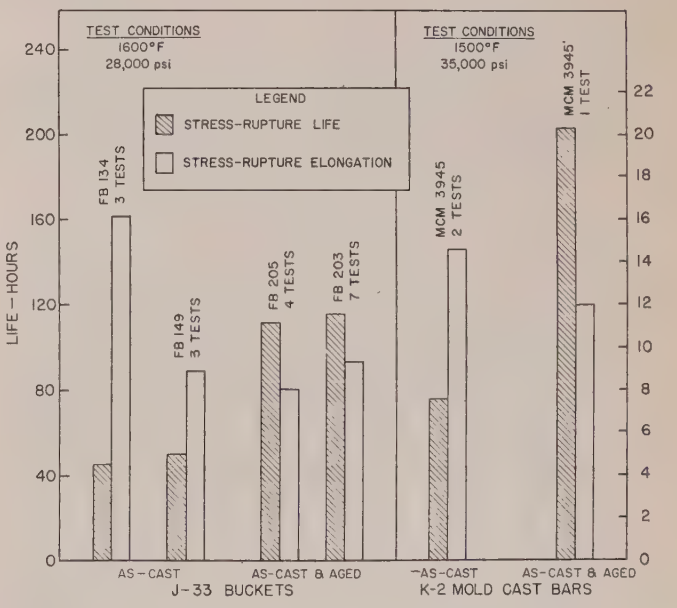

Fig. 16 – Effect of 5-hr, 1800 F age heat-treatment on stress-rupture properties of as-cast GMR-235 alloy

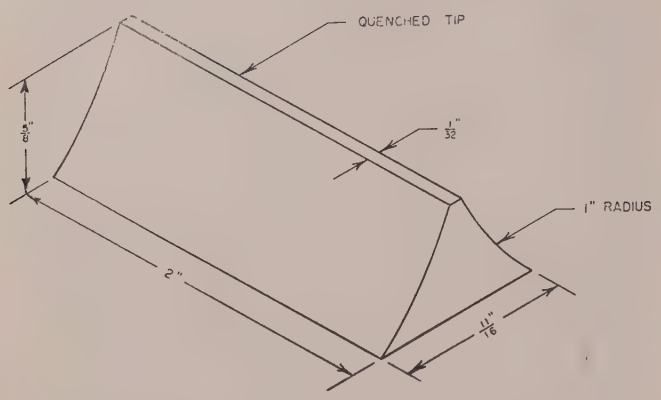

Fig. 17 – Wedge specimen for determination of thermal shock resistance

Wedge specimens which were cycled to produce complete crack propagation across the 1/32-in. edge indicate that GMR-235 alloy will corrugate or warp rather than crack in brittle failure. The distortion is a function of both the hot strength and higher temperature of the thick portion of the wedge during cooling resulting in sudden tensile forces on the restrained edge. As a result, the cooler edge will be shock-loaded beyond the yield point, resulting in permanent deformation. Typical warped specimens after an average of about 80 thermal shock cycles to first complete crack across the 1/32-in. edge are shown in Fig. 18. The degree of distortion does not seem to reflect in the number of cycles run to failure.

Notch Stress-Rupture Tests – Limited tests on notch sensitivity of GMR-235 alloy have established that the material exhibits sufficient plastic flow and is not notch sensitive. Tests were conducted on as-cast bars of the geometry shown in Table 4.

The results given in Table 5 represent test time without failure. The extended test times were specified to determine if long exposure at elevated temperature had a detrimental effect.

Fatigue Tests at Elevated Temperatures

Two types of elevated-temperature fatigue testing have been employed to evaluate qualitatively GMR-235 alloy. The earliest tests were conducted on 11-in.-long, 0.357-in.-diameter, 4-in.-gage-length cast bars under combined static and superimposed dynamic stress at a frequency of 180 cps.[4] More recent tests have employed the vibration of buckets at the first or fundamental mode frequency under controlled amplitudes of vibration at temperatures from 900 F to 1500 F.

Combined Stress Tests – Time elongation curves presented in Fig. 19 compare results of typical static stress-rupture and combined stress-rupture tests conducted on GMR-235 alloy.[4] The dotted curve designated "S-816 alloy," a commercial cobalt-base forged bucket alloy, is shown for comparison purposes to demonstrate that lower-hot-strength materials under approximately the same combined stress test conditions would fail by rapid creep rather than fatigue.

In general, this test has been limited to qualitative correlations directed toward determining the extent, if any, of extreme brittle behavior of materials when subjected to fatigue conditions of static and superimposed dynamic stress.

Bucket Vibration Fatigue Tests – The fatigue characteristics of GMR-235 alloy under resonant vibratory conditions have been investigated on cast buckets at elevated temperatures from 900 F through 1400 F, using a special machine developed by the special problems department for the purpose of vibration-testing full-scale buckets in their fundamental frequency. Vibration is imparted by means of an airstream, directed against the bucket tip, whose amplitude is governed by a servo system controlling air pressure. A second servo system controls the elevated temperature of the test bucket by controlling distance between bucket and flame from a bank of acetylene torches directed against the bucket blade section. Fig. 20 diagrammatically illustrates the bucket vibration at elevated temperature.

This bucket fatigue test, conducted under the supervision of C. W. Gadd of our Special Problems Department, has supplied information on the change in fundamental frequency for a particular bucket design, effect of temperature on internal damping capacity, and the effect of metallurgical changes on endurance limit for a specific bucket geometry.

For example, Fig. 21 compares the effect of temperature on the fundamental frequency and damping capacity of GMR-235 alloy cast and heat-treated buckets with the same bucket forged from S-816. The sudden increase in required air pressure at approximately 1500 F reflects the difficulties connected with obtaining satisfactory vibratory test conditions at this temperature. The curves indicate that increased damping capacity of GMR-235 can be produced by an aging heat-treatment at 1800 F for 5 hr.

The relationship of temperature to energy input required to vibrate buckets of both forged S-816 and cast GMR-235 at their respective endurance stress levels is presented in Fig. 22. The data are correlated in this manner because in gas-turbine operation, effective applied energy of vibration as well as endurance stress level governs durability of buckets in fatigue. The chart also illustrates the type of correlation which can be used to qualitatively evaluate fatigue improvements produced by

[4] See Proceedings of Society for Experimental Stress Analysis, Vol. 9, No. 1 (1951), pp. 211-220: "Combined Stress Test Machine for Evaluating Heat-Resistant Alloys," by W. Foster.

Table 4 – Geometry of As-Cast Bars[a]

Shank Diameter, in.	0.375
Notch Angle, deg	60
Notch Root Radius, in.	0.005
Bar Root Diameter, in.	0.2525

[a] From ASTM Special Technical Publication No. 128 (1953), "Symposium on Strength and Ductility of Metals at Elevated Temperatures," pp. 67-92: "Effect of Notch Geometry on Rupture Strength at Elevated Temperatures," by E. A. Davis and J. J. Manjoine.

Table 5 – Test Results

Test No.	Test Temperature, F	Stress,[a] psi	Notch Test Time, hr	Smooth Bar Rupture Life at Indicated Stress Level, hr
1	1300	70,000	760	125
2	1500	35,000 (stress 45,000 raised)	1,000 510	
			1,510	
3	1500	35,000	1,000	360
4	1600	28,000	743.5	50

[a] Stress calculated from root diameter.

heat-treatment of various GMR-235 alloy cast bucket shapes.

GMR-235 Foundry Technology

The success of a new material is by no means established by favorable performance in laboratory tests, nor by outstanding service in the field. Acceptance of a promising alloy will often depend on the ease with which an end-product can be manufactured by existing processing techniques. It can be fatal to a newly developed material to announce it without having complete mastery of the processing requirements.

GMR-235 has favorably weathered two years of volume production, vindicating the initial enthusiasm with which it was received. The remainder of this paper will consist of a brief description of the techniques which contributed to this success.

Master Heat Melting – This alloy was developed initially as an investment casting alloy and as such it had to be furnished as qualified stock in a form suitable for remelting. Both the high-frequency induction furnace and the direct-arc furnace have proved suitable for master heats. The induction furnace is being used for heats up to 1000 lb, while 6000-lb heats are regularly produced in direct-arc furnaces.

The latter offers the advantage of employing refining techniques. However, up to 90% scrap in the form of gates and risers has been recharged in the induction furnace without detrimental effect on metal quality. No cumulative effect from recharging gates and risers into the induction furnace has been detected in over two years of production without refining. However, low-grade scrap such as ladle skulls and furnace drippings containing a high percentage of non-metallics must be refined in the arc furnace capable of handling a basic slag. The segregation tendency associated with the low density of the aluminum and titanium additions can be controlled within useful limits by careful melting practice.

Shotting – The master heat alloy is produced in shot form for convenience in remelting. Conventional shotting techniques utilizing a drop tower or cross streams of water to break up the molten metal have been used. Suitable melting stock may also be produced as bar or piglet, but the cost is greater, and blending of several heats is ruled out. This is an important consideration, since the con-

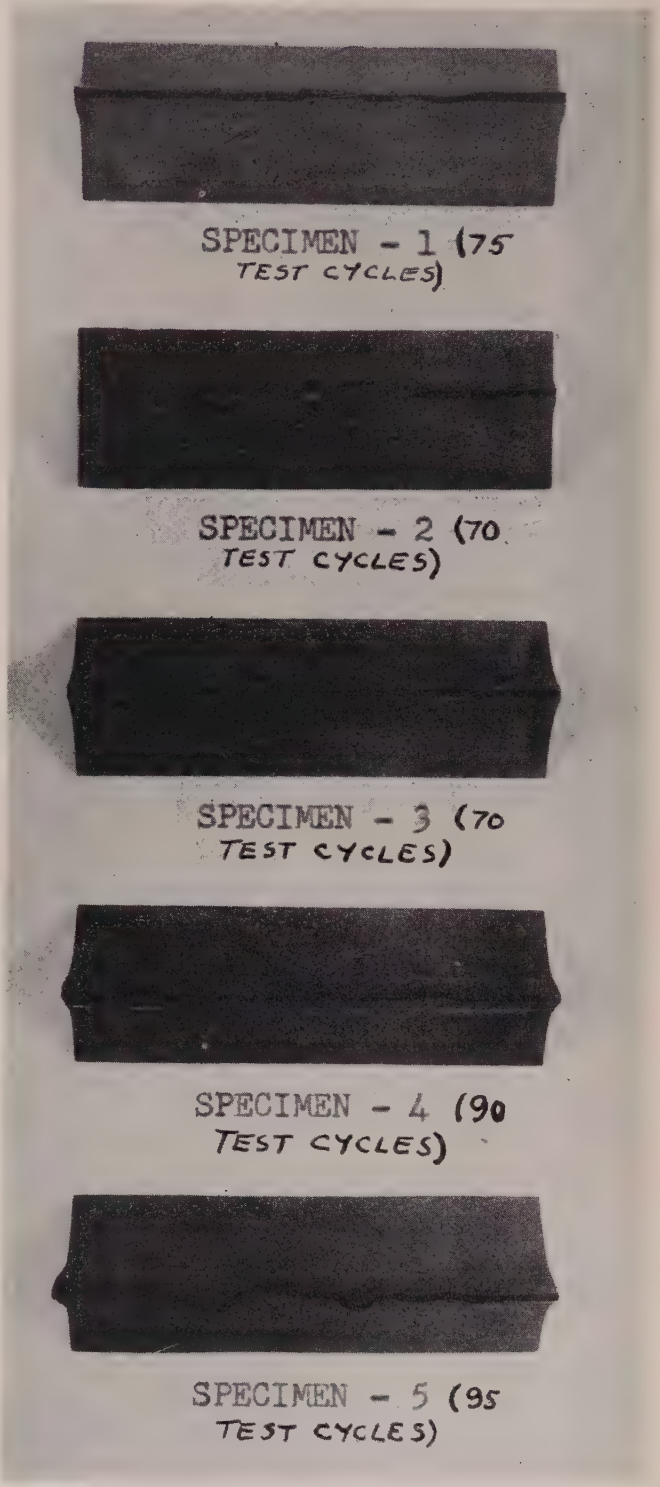

Fig. 18 – Thermal shock test specimens of NACA type (GMR-235 alloy wedge specimens)

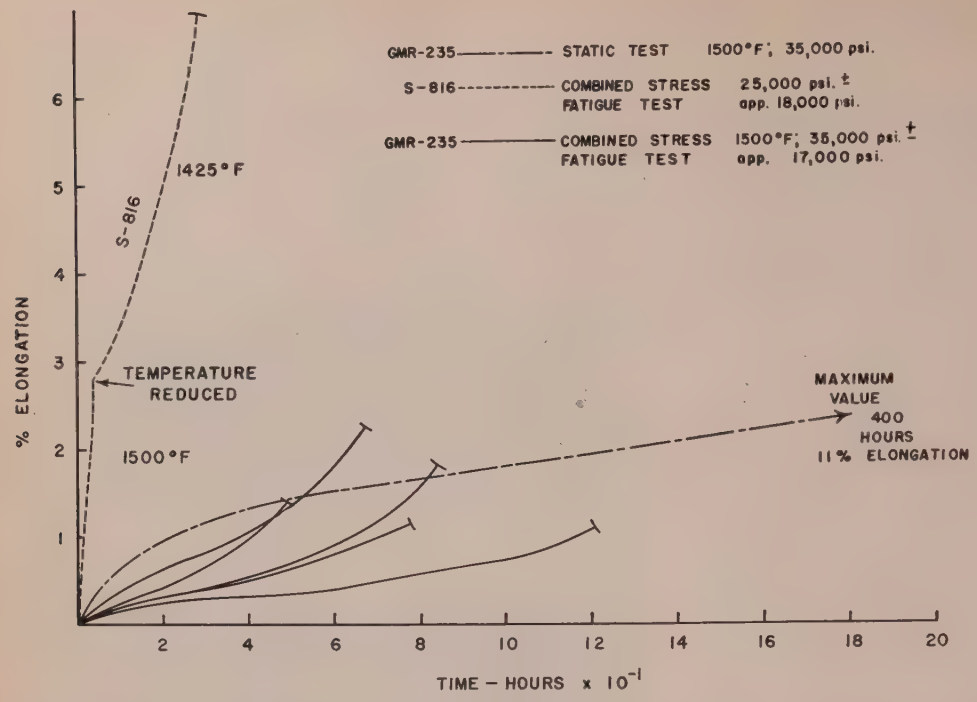

Fig. 19 – Comparison of combined stress-rupture fatigue test with static stress-rupture test

solidation of several heats into one allows significant saving in stress-rupture qualification test time.

Remelting Practice – Although both aluminum and titanium form refractory oxides which may result in surface folds in the casting, this type of defect has been brought under control in the remelting and casting operation. Use of a small furnace for remelting an individual charge just sufficient to fill a single mold allows the inverted mold to be clamped directly to the top of the furnace as shown in Fig. 23. This arrangement, which is common in the investment casting industry, provides for purging of the furnace and mold atmosphere and close control of the pouring operation.

Economical remelting has required the use of the induction furnace. Low thermal conductivity through the shot during initial stages of melting results in unduly long melting time in the indirect arc furnace which has been widely used to produce investment castings. Use of barstock in place of shot and oscillation of the furnace during meltdown allow use of the indirect arc furnace, but the uncertainty of carbon pickup from the electrode and the vigorous stirring achieved in the induction furnace have resulted in exclusive choice of induction melting for the recasting operation. A battery of such furnaces at GMC's Fabricast Division is shown in Fig. 24.

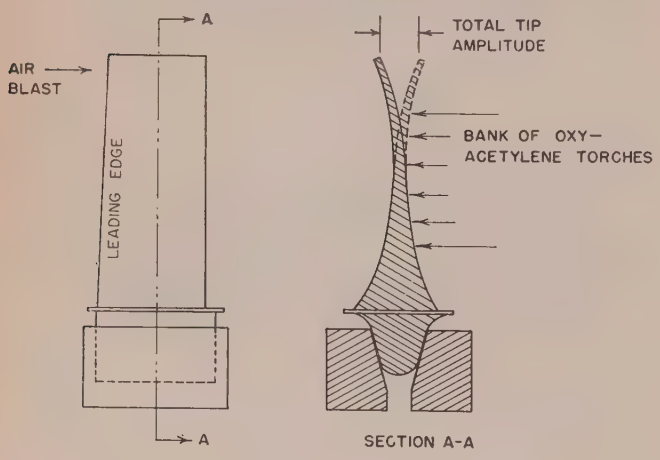

Fig. 20 – Diagrammatic representation of bench vibration test employing controlled torch heating of buckets

It is essential to avoid entrainment of dross as the metal flows into the mold cavity, and to melt clean to assure accurate optical temperature measurements. This is accomplished by melting under a protective blanket of argon, allowing as little back diffusion of air as possible when removing the furnace cover, and placing the mold in position on the casting furnace.

After the inverted mold has been firmly clamped to the top of the furnace, the assembly is rolled over as a unit to transfer the metal from the melting crucible to the mold without exposing the molten metal to air. The speed at which this rollover occurs is important, and should be just fast enough to avoid misruns at the desired casting temperature.

GMR-235 containing both aluminum and titanium has proved to be compatible with silica investment molds when the casting conditions are properly controlled. Excessive metal or mold temperature will promote a reaction between the molten alloy and the silica investment material. Purging of the mold cavity, section size, rate at which the mold is filled, and alloy composition must also be considered. Greater difficulty is experienced

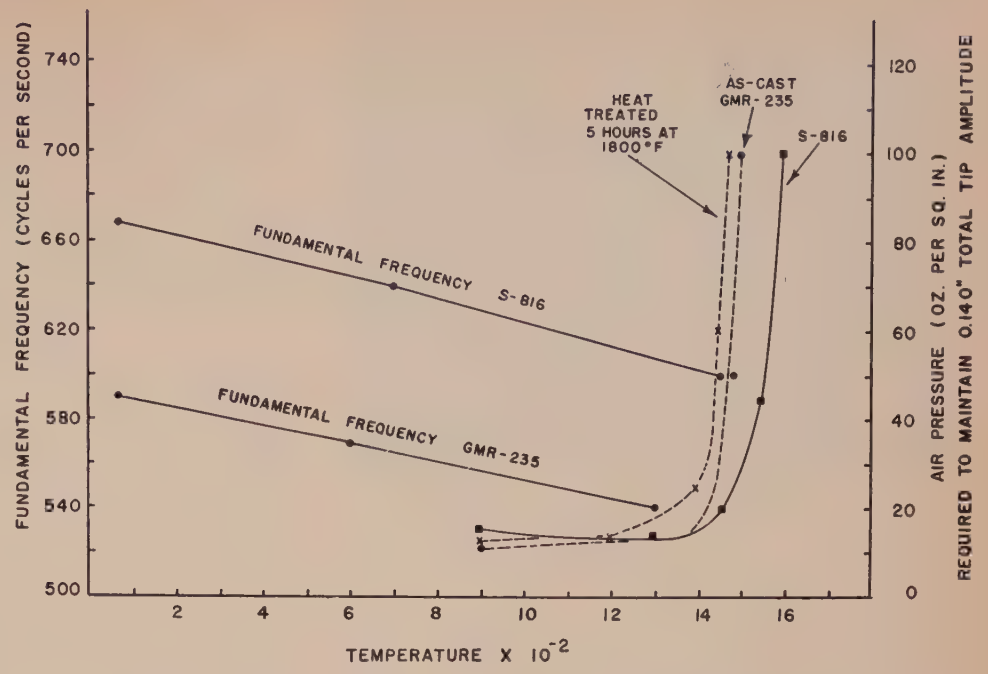

Fig. 21 – Effect of temperature on fundamental frequency and internal damping of GMR-235 and S-816 alloy T40 turbine buckets

with metal-mold reactions when the aluminum content is low (less than 2.5% aluminum).

When the design of the casting requires conditions which may be conducive to metal-mold reaction, alumina precoats may be used. Although there is no reaction tendency with alumina, silica precoats are normally preferred because of decreased cost and improved surface smoothness.

Gating Technique – Inasmuch as GMR-235 is subject to formation of oxide films which show up as surface folds when trapped in the casting, special consideration must be given to gating methods which will eliminate turbulence of the molten metal and entrapment of air. The importance of gating practice was emphasized when redesign of the gating for stress-rupture test bars resulted in an increase in the high-temperature properties comparable to specimens removed from bucket castings.

To arrive at the improved gating system, fluid-flow studies of various gating systems were conducted using water in transparent lucite molds.[2] Application of improved gating techniques to turbine bucket castings have resulted in improved casting recovery. The improved foundry recovery

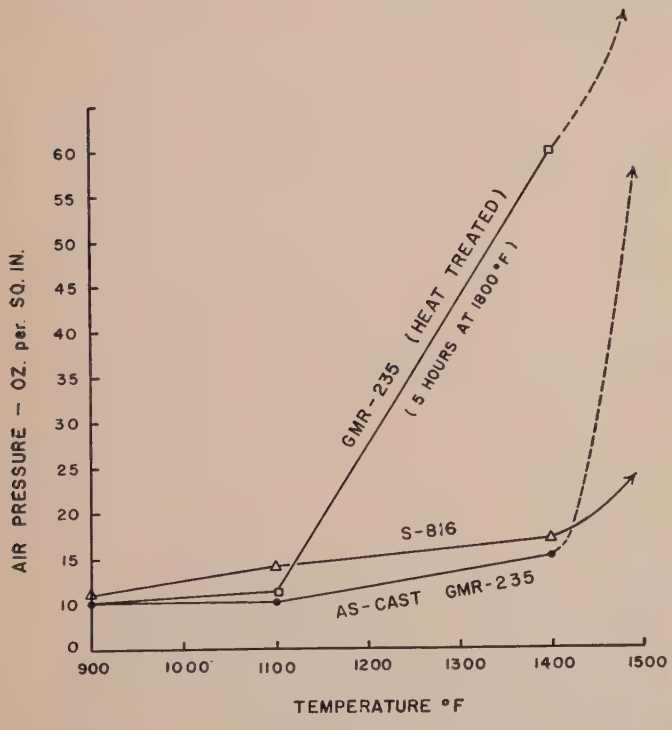

Fig. 22 – Effect of temperature on energy required to vibrate T40 buckets of GMR-235 alloy and S-816 at endurance tip amplitude

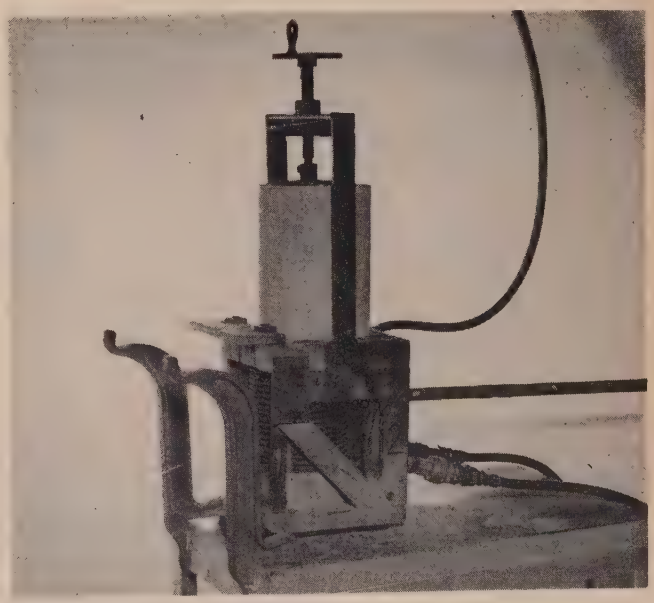

Fig. 23 – Induction furnace and mold assembly used in conjunction with remelt and casting of GMR-235 precision castings

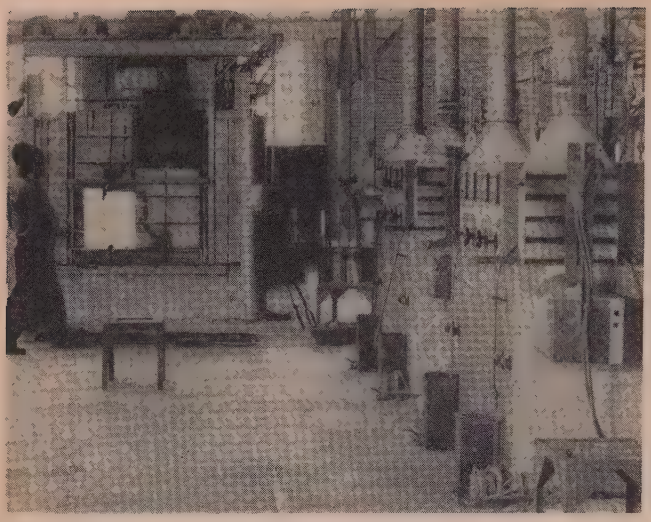

Fig. 24 – Battery of production remelt induction furnaces typical of equipment required in a precision casting foundry for GMR-235 alloy castings

representing adequate inspection controls has resulted in production of turbine bucket castings conforming to aircraft standards.

Conclusion

The complete GMR-235 story has included a coordinated laboratory test and development program coupled with an engineering approach to the production and control methods used in the foundry. A final evaluation of these combined efforts is, of course, reflected in actual field service reports covering engines equipped with GMR-235 alloy.

Over 500 tons of this alloy have been melted and cast into various shapes for gas-turbine service. In flight tests, a control group of 114 engines representing a larger number of production engines equipped with GMR-235 buckets have accumulated an average of 183 hr service time, 56 of which exceed 200 hr of engine service. Twelve sets of buckets have been run more than 500 hr, with maximum time exceeding 800 hr.

This successful field experience without a single bucket failure has resulted in unlimited installation on the engine model covering the above tests, and lends credence to the engineering data constituting the laboratory development work.

Acknowledgments

The success of this research development depended upon the cooperation of all firms engaged in the manufacture of GMR-235. The authors wish to acknowledge the valuable assistance rendered by the many individuals at the GM Allison and Fabricast Divisions and Haynes-Stellite Co., Division of Union Carbide and Carbon Corp.

In particular, the authors wish to thank D. Gerdan, W. S. Broffitt, A. W. F. Green, and C. R. Perry of Allison Division for their cooperation from the standpoint of engine installation. Valuable assistance from D. G. McCullough and R. F. Thomson included the development of improved gating techniques which were successfully applied in production applications. Recognition is also given to S. R. Callaway for his work in establishing the early approximate alloy range.

Important contributions were made by D. G. McLeod in supervising the stress-rupture testing, while significant developments in the field of high-temperature fatigue of buckets were made by C. W. Gadd, J. O. Anderson, and C. E. Sanborn of the special problems department, GM Research Laboratories Division.

DISCUSSION

Asks Further Data From Test Results

– G. D. Dolch
Thompson Products, Inc.

REALIZING that brevity in presentation has undoubtedly prevented the authors from discussing all phases of the program, I feel the following questions are of sufficient industrial worth to warrant their being raised at this time:

1. While this paper reviews the specific application of turbine buckets where mechanical attachment is normally employed, there are undoubtedly other fields of application where welding techniques will be called upon. The writer is under the impression that original investigations in welding GMR-235 alloy to other heat-resistant materials was accomplished with some difficulty. We are interested in knowing

whether the causes for such difficulties have been recognized, and whether developments have been accomplished to cope with this problem.

2. It has been reported that certain of the nickel-base, high-temperature alloys suffer from an intergranular oxidation phenomenon when exposed to high heat-treating temperatures. It would be of interest to know whether the authors have investigated the susceptibility of this material to respond in the same manner during the casting operation or during the heat-treating cycles investigated.

3. The section on heat-treatment indicates that some improvement in the alloy can be accomplished by a solutioning heat-treatment. This improvement presumably is for the chemical composition cited in Table 2 of the paper. Inasmuch as Fig. 4 shows the effect of boron in the as-cast condition on stress-rupture properties, it would be of interest to know whether alloys of high boron content were reinvestigated after heat-treatment to ascertain whether the combination of heat-treatment and high boron could result in a material exhibiting even superior properties to those cited in this paper.

4. The information indicated in the section under heat-treatment would suggest that this alloy is susceptible to an aging phenomenon following solutioning cycles. If the authors have information showing the aging characteristics of this alloy at temperatures below 1800 F, it would be of considerable benefit to have the opportunity to review those properties. I am thinking specifically of applications where this alloy might be subjected to a solutioning-type treatment such as in the heat-affected area of a weldment, when an improper choice of subsequent treatment might result in service behavior less reassuring than information reported in this paper.

5. The section on foundry technology indicates that the production castings used to date have been as the result of remelting master heat alloy shot. If the chemical composition listed in Table 2 represents the chemistry of the master heat, what deviation therefrom have the authors experienced as the result of remelting this material under the practice described later in the paper under the heading "Remelting Practice"? Also, what deviations from the composition cited in the paper would they consider practicable? In the event that the composition cited represents the casting analysis, I believe it would be in order to inquire whether the master heat chemistry must be adjusted to some value other than that listed in order to cope with remelting losses.

6. Are the authors aware of any tendencies toward heat checking during the grinding of this alloy? If such a tendency has been noted, has heat-treatment offered any relief to the condition?

Compares Authors' Work With Other Research Results

– I. S. Servi
Haynes Stellite Co.

IT is felt that the results of previous published work would have greatly improved the significance of this paper, and helped to interpret some of the data reported. For instance, Guy[a] has found that an investment-cast alloy consisting essentially of 10% chromium, 6% aluminum, 5% molybdenum, 2% columbium, 0.5% boron, 0.1% carbon, and the balance nickel, has a 100-hr rupture stress at 1500 F in excess of 45,000 psi. Guy further indicated that a variety of combinations of aluminum, molybdenum, and chromium contents may give origin to alloys having similar strength. Kinsey and Stewart,[b] studying nickel-molybdenum-aluminum cast alloys, suggested compositions for alloys having rupture lives in excess of 150 hr at 1500 F under 35,000 psi, and determined that the intermetallic compound Ni_3Al exists in the structures of such alloys. These results are consistent with those reported in this paper, and with others obtained by the writer on nickel-base cast and wrought alloys.

Regarding the complex boride phase, we have extracted such phases by electrolytic methods and analyzed by chemical methods, finding that they have the compositions of Cr_2MoB_2. However, metallographic observations revealed at least two different constituents in high-boron cast alloys, thus indicating that the complex "Chinese script" may actually consist of a mechanical mixture, such as $Cr_2B + MoB$. As is clearly indicated in Fig. 7, the boride phase does not occur preferentially along the grain boundaries, but along "dendritic boundaries," thus signifying that boron segregates in selected areas, as a consequence of coring. This is further supported by experiments performed at our laboratories showing that the "Chinese script" is completely dissolved after hot-working; no evidence of borides can be found by X-ray methods in wrought alloys containing about 0.05% boron. On prolonged heat-treatment, the "Chinese script" spheroidizes, but does not readily dissolve within reasonable heat-treating times.

The effect of boron reported in Fig. 4, and in general the effect of all elements, should be analyzed in this type of alloy by carefully controlling the amounts of hardening elements, aluminum and titanium. In fact, these elements have very strong effects on strength. Comparing Fig. 4 with Fig. 12, we can see that the titanium range 1.75-2.00% of Fig. 4 corresponds to a life range of 180-210 hr, or 16% of the average life. Although specific data have not been reported, from Fig. 11 it appears that an aluminum range of 2.5-3.00% may correspond to about the same percentage of average life. From Fig. 4, the maximum effect of boron (< 0.005 to about 0.1%) is about 60% of the average life. Although this figure appears significant, its absolute value should be evaluated, as compared with the combined effects of aluminum and titanium, which total about 32% of average life. It should be noted, incidentally, that the values of lives reported in Fig. 12 are not consistent with those of Fig. 4.

During the course of investigations on wrought nickel-base alloys, leading to the development of Hastelloy Alloy R-235,[c] it was found that the combined effects of aluminum and titanium on rupture strength may best be expressed in terms of aluminum + titanium atomic contents. In this case the 100-hr rupture stress at 1500 F as a function of aluminum + titanium contents is nearly linear over a wide span of values, and has a slope of about 4500 psi/atomic content %. We also found that this relationship is valid for several different combinations of titanium and aluminum contents. Deviations occur when the ratio of titanium to aluminum contents (expressed in weight per cents) is larger than about three. This deviation was related to the appearance of the intermetallic compound Ni_3Ti.

In all other alloys, only the Ni_3Al-type compound was found present and positively identified by X-ray methods. This compound, however, is capable of dissolving large amounts of titanium without changing its structure, as indicated by Taylor and Floyd.[d] We found, in general, that titanium-to-aluminum ratios larger than one are beneficial to obtain a good compromise of strength and ductility, and we wonder why the authors specified 3.00% aluminum and

---

[a] See ASM Transactions, Vol. 41, 1949, pp. 125-140: "Nickel-Base Alloys for High-Temperature Applications," by A. G. Guy.

[b] See ASM Transactions, Vol. 43, 1951, pp. 193-225: "Nickel-Aluminum-Molybdenum Alloys for Service at Elevated Temperatures," by H. V. Kinsey and M. T. Stewart.

[c] "Vacuum Melting of High-Alloys Materials," by H. R. Spendelow, Jr., I. S. Servi, and G. A. Fritzlen. American Chemical Society, 1954, in course of publication.

[d] See *Journal of Institute of Metals*, Vol. 81, September, 1952, pp. 25-32: "Constitution of Nickel-Rich Alloys of Nickel-Titanium-Aluminum System," by A. Taylor and R. W. Floyd.

1.75% titanium average contents, whereas Fig. 12 shows that by increasing titanium from 1.75 to 3.5%, the life is almost doubled, and the total elongation at fracture still maintained at a reasonable level.

Authors' Closure To Discussion

The following comments are in reply to Mr. Servi:

The authors fully appreciate the outstanding contributions of Guy, Kinsey, and Stewart in their previous published work covering various alloys developed by them. However, the complex nature of the materials with respect to interaction of the alloying elements, particularly in the cast materials of the same class, may be quite different.

This can be illustrated in a practical way by comparing, for example, the brittle behavior at room temperature of high boron contents such as 0.5% investigated by Guy or the low oxidation resistance of the ternary alloy known as Kinsalloy. This paper emphasizes the importance of other physical properties such as fatigue strength, ductility, and notch sensitivity, in addition to the high-temperature characteristics determined by creep rupture tests.

Of course, many of these properties are largely controlled by castability, which is of prime importance when considering high-volume production. In this respect, the effect of an unsound casting may completely overshadow any influences of the many complex phases formed in the microstructure.

It is further emphasized that the nonequilibrium conditions in the melt during casting many produce different compound phase combinations depending on cooling rate.

The range of stress-rupture life (75 to 500 hr) at 35,000 psi, 1500 F shown in Fig. 2 includes all of the values shown in Fig. 12 within the aluminum and titanium range of the specification. Although the higher titanium content of 3.50% seems to produce a satisfactory strength level with adequate ductility, it was considered advisable to maintain a maximum of 2.50% in view of the greater tendency for reaction with the mold materials currently used in production. Improved melting and casting practice may permit an upward adjustment in titanium and aluminum for higher strength.

As in all other materials, these composition changes require a broad test background incorporating a statistical evaluation on numerous commercial size melts.

In reply to Mr. Dolch, we would like to make the following points:

1. The welding of GMR-235 is currently being investigated to develop a welding rod material which produces a more sound and stress-free weldment. Preliminary results indicate that boron in the material is primarily responsible for the difficulties encountered. A practical approach to counteract the hot shortness caused by this element has been to minimize the amount of melt dilution by the GMR-235 alloy component.

2. When heat-treating GMR-235 at temperatures higher than 1600 F, a protective atmosphere such as argon or helium is recommended. In the casting operation, oxide penetration is normally less than 0.0002 in. and is not considered a problem.

3. Composition modifications and response to heat-treatment is a broad program representing continuing investigation at GM Research. The high boron content modifications representing heats with 0.25% offer some interesting possibilities. Preliminary work has indicated that room-temperature ductility of solution-treated bend test pins will not meet the specification requirements of the engine manufacturer. Ductility at room temperature has been the limiting factor in utilizing as-cast material with boron in excess of 0.10%.

4. The aging characteristics of GMR-235 alloy at temperatures below 1800 F have not been investigated since it was felt that an average condition would be the most beneficial condition in relation to stability of microstructure. Performance of as-cast buckets in the lower temperature range of 1000-1600 F has been satisfactory. Creep rupture strength has been measured on buckets after engine test, and strength appears to be increased as a result of stress aging.

5. Composition limits shown in Table 2 represent the analysis of castings. The remelting practice described in the section, "GMR-235 Foundry Technology," results in the loss of approximately 0.25% aluminum and 0.10% titanium. The master heat should be adjusted accordingly. All other elements appear to be unaffected by remelting.

Allowable deviations will depend upon the end use of the casting. In general, lower carbon is definitely preferred. Minimum values for molybdenum, aluminum, titanium, and boron assure maximum rupture life, and chromium is necessary for oxidation resistance. Iron may be considerably below 8% if desired, but higher values are preferred for economic and strategic reasons. Deviations in manganese and silicon up to 1.0% total have been allowed. Experience has shown that any reasonable deviation can be allowed if the capability tests for each heat or blend of heats meet the engineering requirements.

6. Grinding problems have been brought under relatively good control in the shop using proper feed, speeds, and wheel material. The heat-treatment of GMR-235 has not appreciably altered this picture.

ORAL DISCUSSION

Reported by D. J. Henry
Research Laboratories Division, GMC

HIRAM Brown, Solar Aircraft Co.: (1) Is there danger of oxidation of the alloy above 1850 F? (2) Did you employ a protective atmosphere when heat-treating the alloy above 1800 F, up to 2100 F? (3) Was there a relationship between grain size of GMR-235 and engine failure?

Mr. Hanink: (1) When temperatures exceed 1650 F, stress-rupture failure is usually feared, not oxidation effects. When the stress level permits extended service periods above 1850 F, however, oxidation is severe and protective coatings may be necessary.

(2) Dried and purified argon atmosphere was used for heat-treatment in these temperature ranges of 2100 F.

(3) There has been limited success in controlling grain size; however, to date we have seen no critical requirement for controlling grain size to improve alloy performance.

Paul Eddy, Pratt & Whitney Aircraft: What does the term "bootstrap" mean?

Mr. Hanink: The bootstrap machine is a B-31 turbosupercharger utilized in a configuration comparable to an actual gas turbine engine. Power is derived from combusted gases expanded through the turbine wheel. It is only sufficient to drive the compressor. That is, no external work is delivered. Thus, the greater the fuel burning, the higher the temperature and wheel speed, which further increases power to the compressor, which, in turn, is called upon to supply more air. This operation is termed "bootstrap running."

Mr. Brown: How wide a disparity is encountered in grain size of a GMR-235 bucket casting? How is the pouring temperature of the metal controlled?

Mr. Hanink: We have seen grains ½ in. long at the root of the bucket, and so fine at the tip that they are resolved only at 100X magnification. Temperature measurements are taken on the clear melt surface using an optical pyrometer.

Abrasive Wear of Piston Rings

C. E. Watson, F. J. Hanly, and R. W. Burchell, California Research Corp.

This paper was presented at the SAE Golden Anniversary Annual Meeting, Detroit, Jan. 11, 1955.

THE useful life of an internal-combustion engine is limited by dimensional changes of critical parts, such as piston rings, cylinders, bearings, and cam lobes. When limiting dimensions are reached, the engine must be overhauled or replaced, no matter what the cause of wear of these parts. Major progress has been made during the past 10 years in extending engine life by improved metallurgical techniques, metal alloys, compounded engine lubricating oils, crankcase ventilation, thermostatic temperature control, and, more recently, by fuel additives. Marked reductions have been made in wear from scuffing, rusting, and other corrosion; however, abrasive wear has received only passing attention. Field surveys[1] of engine conditions have indicated the importance of abrasive wear, but relatively little information is available in the literature regarding its mechanism, the influence of particle size on wear, or the effects of concentration and physical properties of abrasives on wear or wear rates. It is the purpose of this paper to present such information, and to describe an experimental method for obtaining data rapidly and reproducibly.

During the development of an improved adhesive for impingement-type air filters in 1951,[2] it became apparent that no quantitative data were available on the relations between properties of airborne abrasives and wear of internal-combustion-engine parts. The information then available could be summarized in the statement "dust causes engine wear." Tests reported as late as 1950[3] and 1951[4] consisted of introducing large quantities of a composite dust with a wide range of particle size into the air induction system of an engine for relatively long periods of time and measuring the resultant dimensional changes of the parts. A more recent (1953) publication[5] showed, for the first time, the effect of size of abrasive particles on piston ring and cylinder wear. The exceedingly high dust concentrations used in this work, however, resulted in ring wear rates in the order of 10 g per hr. Table 1 shows some of the dust concentrations used by various investigators in studying abrasive engine

[1] See SAE Transactions, Vol. 61, 1953, pp. 221-223, 230: "How Engines Wear," by J. F. Kunc, Jr., D. S. McArthur, and L. E. Moody.

[2] See *Diesel Power*, Vol. 32, February, 1954, pp. 37-41: "Increasing Locomotive Air Filter Efficiency," by F. J. Hanly, A. W. Hardy, and B. F. Kline.

[3] See *Petroleum Engineer*, Vol. 22, June, 1950, pp. C7-C12: "Maintenance of Internal-Combustion Engines — Filtration of Air and Oil," by P. H. Moore.

[4] See *Petroleum Engineer*, Vol. 23, July, 1951, pp. C113, C114, C116, C117: "Maintenance of Internal-Combustion Engines — Filtration of Air and Oil," by P. H. Moore.

[5] See *Gas and Oil Power*, Vol. 48, March, 1953, pp. 60-63: "Cleaning of Engine Air," by J. L. Koffman.

MEASURING piston-ring wear by use of irradiated piston rings and modern detection equipment, as was done in tests reported here, is accurate, fast and overcomes any need of disassembling engines.

Tests made with a variety of abrasives showed that size and properties of abrasives influence not only the amount of wear but also its duration.

The same technique would work equally well, the authors say, in studying wear of any irradiated internal engine part in any type of piston engine.

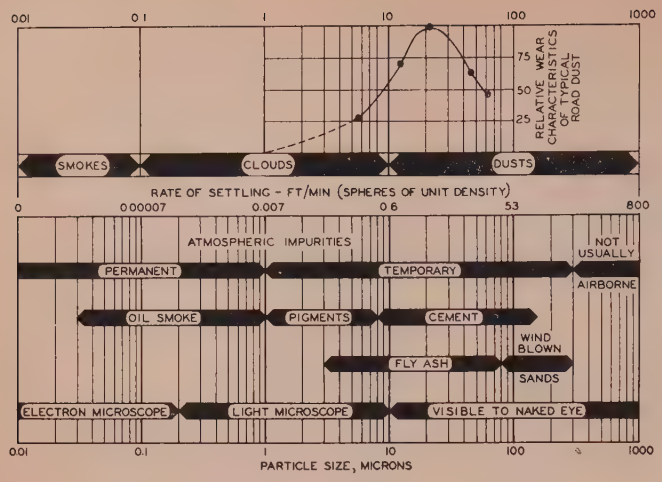

Fig. 1 – Relative size of typical small particles

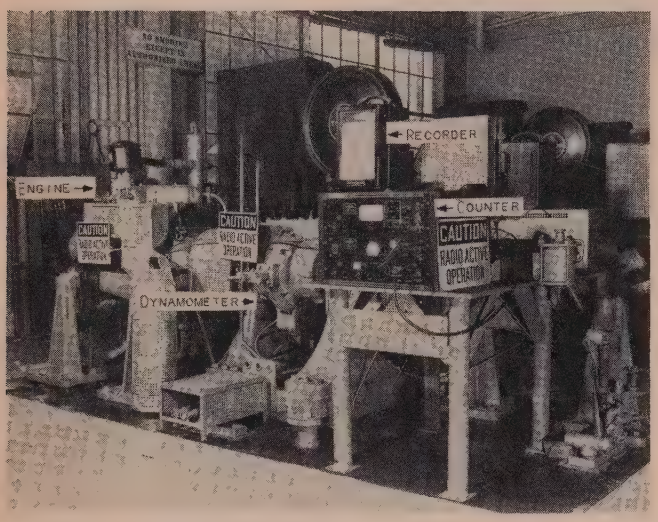

Fig. 2 – Arrangement of equipment for engine abrasive wear studies

Table 1 – Comparison of Airborne Dust Concentrations

Air Dust Condition	Reference	Dust Concentration, mg/1000 cu ft	Weight of Dust Inducted into 6-Cyl Engine, 216 Cu In. Displacement, 2500 Rpm, 45 Bhp, g/hr
"Normal" air	—	5 (est.)	0.04
"Dusty" – maximum likely to be encountered by operating vehicle (nondust storm)	5	10,000	86.7
"Dust storm" – maximum for operating vehicle	5	40,000	347
"Dust storm" – visibility 50 ft	5	35,000-65,000	304-564
"Dust storm" – visibility 20 ft	5	250,000-500,000	2170-4340
Laboratory engine tests	5	1250-5000	10.8-43.4
Farm tractor operation tests	6	930-6070	8.1-52.6
Laboratory engine (gasoline) tests	3	236	2.0
Laboratory engine (diesel) tests	4	33	0.28
California Research Corp. laboratory engine tests, effect of particle size (based on addition over 2-min interval)	Table 2	1088	9.4
Effect of concentration	Fig. 4	4-287	0.03-2.5

Table 2 – Chemical Analysis of Fine Grade Arizona Road Dust Used in Abrasive Wear Tests

	Per Cent by Weight
SiO_2	67-69
Fe_2O_3	3-5
Al_2O_3	15-17
CaO	2-4
MgO	0.5-1.5
Total Alkalis	3-5
Ignition Loss	2-3

Table 3 – Particle Size Distribution of Dust Used in Abrasive Wear Tests

Size, microns[a]	Per Cent of Total Weight
0-5	39 ± 2
5-10	18 ± 3
10-20	16 ± 3
20-40	18 ± 3
40-80	9 ± 3

[a] 1 micron = 0.000039 in.

wear, compared with "normal," "dusty," and "dust storm" concentrations.

Not only must the concentration of the dust in the air be considered, but the particle size distribution within the dust as well. Fig. 1 is presented to clarify the picture of relative particle sizes in terms of familiar materials and their behavior as dusts. This figure was constructed from information published by Koffman.[5] In addition, it shows the specific, relative wear properties of abrasive particles in the critical size range, as determined from the work described below. The largest particle sizes causing wear are well within the range of "temporary" atmospheric impurities, as shown by the relative settling rates. Larson,[6] studying tractor operation, found that at elevations of 3-8 ft above ground level, 90% of the particles were less than 29 microns in diameter, and none was larger than 40 microns.

The purpose of the project reported herein was to investigate the mechanism of abrasive wear caused by dust injected into the induction air and into the crankcase oil. The program was designed to determine the effect on piston-ring wear of abrasive particle size and concentration, abrasive hardness, lubricating-oil viscosity, engine speed, and engine load. Such a program employing previously reported experimental techniques would be prohibitive in time and equipment, because each test point would mean one engine destroyed, and would require approximately three days of operating time. Therefore, the test method adopted was the radioactive piston-ring technique of Pinotti, Hull, and McLaughlin.[7]

Experimental Method

All tests were conducted in a 6-cyl, valve-in-head gasoline engine equipped with a radioactive compression ring installed on No. 1 piston. The crankcase oil was continuously monitored with a Geiger counter. With this system, continuous measure-

[6] "Advantages of a Well-Chosen Air Cleaner Inlet System," by R. E. Larson. Presented at SAE National Tractor Meeting, Milwaukee, Sept. 10, 1952.

[7] See SAE *Quarterly* Transactions, Vol. 3, October, 1949, pp. 634-638: "Application of Radioactive Tracers to Improvement of Fuels, Lubricants and Engines," by P. L. Pinotti, D. E. Hull, and E. J. McLaughlin.

The Authors

C. E. WATSON (M '46) is supervisor, Lubricating Oil Research and Development, California Research Corp. He received a B.S. in Mechanical Engineering in 1933 from the University of California. Mr. Watson has been engaged in petroleum product research and development since 1935, supervising research in lubricating oils from 1947 to 1950 and greases and industrial lubricants since that time.

F. J. HANLY is engaged in the development, field testing, and service performance problems of industrial, marine, and railroad lubricants with the California Research Corp. He received a B.S. in Chemical Engineering in 1937 from the University of California. Mr. Hanly has been with the California Research Corp. since 1937, except for three years with the Navy during the war.

R. W. BURCHELL (M '54) is a research engineer, California Research Corp. He graduated from the University of Idaho in 1942. Mr. Burchell has been engaged in lubricating oil research and development since joining the staff in 1946.

ment and record were made of the radioactive iron suspended in the oil. All tests were conducted without oil filters. Standard engine operating conditions of speed, load, temperatures, and crankcase oil quality were selected to minimize piston-ring wear from causes other than abrasion: speed, 2500 rpm; load, 45 bhp; water jacket temperature, 150 F; crankcase oil temperature, 170 F; crankcase oil quality, MIL-L-2104A compound level, maintained by frequent oil change. Arrangement of the engine test equipment is shown in Fig. 2.

The dust used in these tests is specified in the SAE Air-Cleaner Test Code[8] as the fine grade of Arizona road dust (also termed "standardized fine air cleaner test dust") with the typical chemical analysis shown in Table 2.

The whole dust, fine grade, has the particle size distribution shown in Table 3, as measured with a Roller analyzer.

For the purpose of this test program, the whole dust was separated into the above five nominal size ranges. Spectrographic analysis of the fractions showed the ratios between the major metallic elements to be uniform. It was assumed on this basis that the physical properties of the dust fractions were independent of particle size.

During the initial phases of the program, these road dust fractions were introduced into the air supplied to the engine with equipment supplied by Farr Co., Los Angeles, as shown in Fig. 3. This mechanism was capable of dispensing various size abrasive particles at slow and uniform rates for long periods of time. Fig. 4 shows that the effect of dust concentration upon top compression piston-ring wear rate is linear from 0.0042 to 0.287 g per

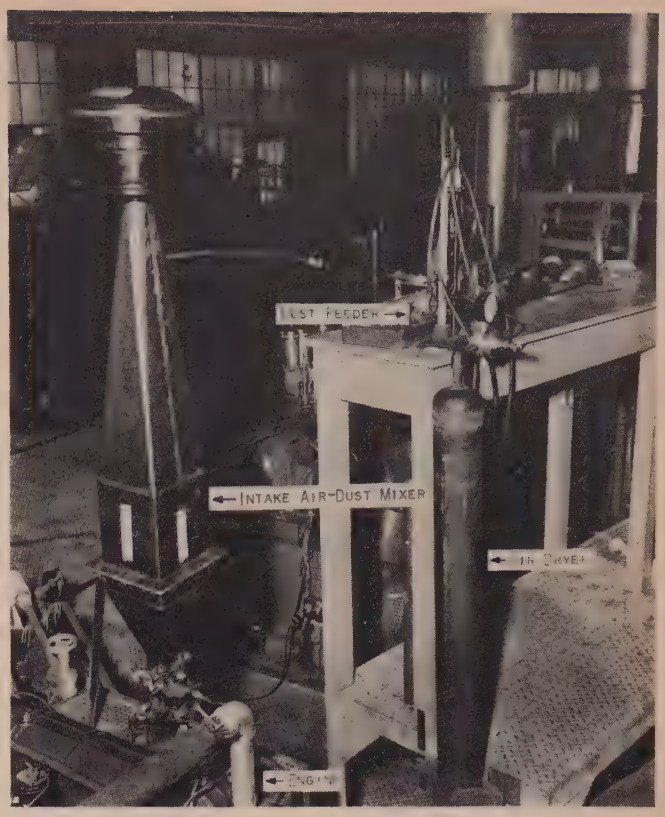

Fig. 3 – Apparatus for introducing dust into engine in controlled concentrations

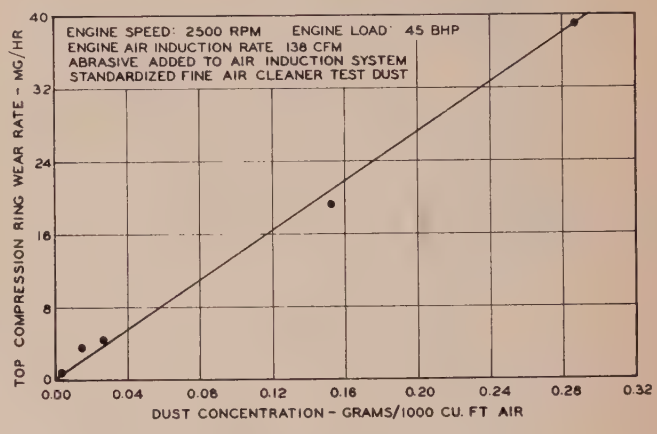

Fig. 4 – Effect of dust concentration on top compression ring wear (0-5-micron dust)

1000 cu ft of induction air. Compared to the dust encountered under normal atmospheric conditions, this wide range of concentration varies from subnormal to more than 50 times normal. Calculations from the relation in Fig. 4 show that piston-ring wear per unit weight of dust injected is a constant. This means that the rate of dust addition is not critical, and selected amounts of abrasive can be injected into the engine over short intervals of time.

Fig. 5 shows the alteration made in the test engine so that the abrasive could be introduced directly into the intake manifold in 2 min rather than the 3 hr used in the concentration tests; the

[8] Classified fractions of standardized fine air-cleaner test dust prepared by AC Spark-Plug Division of GMC from Arizona road dust, as specified by SAE Air-Cleaner Test Code, 1955 SAE Handbook, p. 1030.

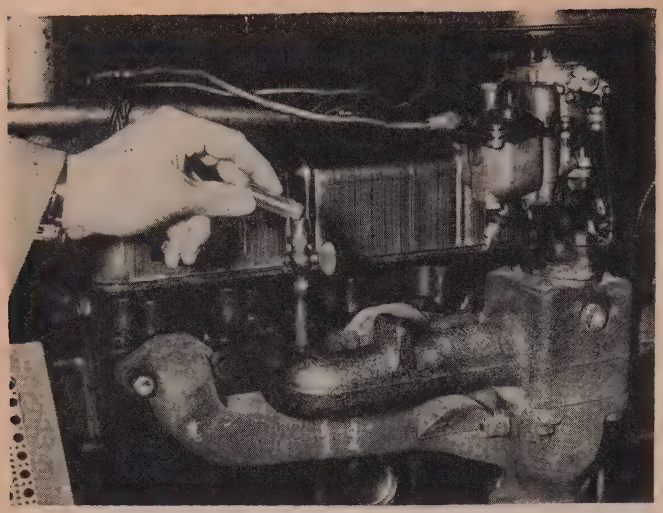

Fig. 5 – Method for rapid addition of abrasive to engine air induction system

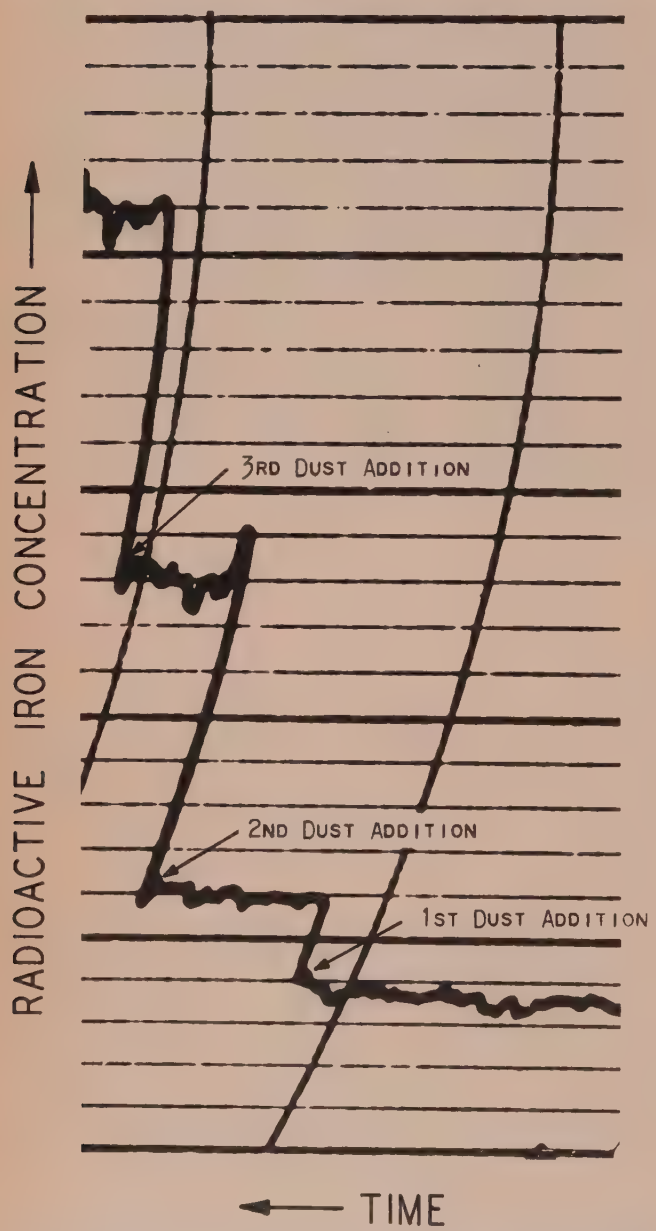

Fig. 6 – Typical recording of change of radioactive iron concentration in crankcase oil when road dusts were added to air induction system

abrasive effects were limited to two cylinders rather than to all six. This modified dust addition procedure was used for the remainder of the work. Repeat tests showed that this method provided data which confirmed values obtained by the slower addition procedure.

Fig. 6 shows a typical recording of radioactive iron concentration in the crankcase oil during three separate additions of road dust of various classifications to the intake air. Wear resulted immediately in each case, but subsequent operation of the engine showed no further abnormal wear. With this method of abrasive dust addition and using the radioactive piston-ring wear technique, it was possible to investigate quickly and reproducibly factors influencing abrasive piston-ring wear.

Consecutive tests in the same engine under the same conditions produced essentially identical results. Tests repeated at different times during the useful life of the engine gave slightly different results; that is, a new engine was more sensitive to abrasive wear and showed higher values of wear per unit weight of abrasive than a worn engine. Thus, wear values obtained on an older engine during the load and speed tests were lower than the values obtained when the effects of particle size and oil viscosity were measured in a relatively new engine.

Considerably more information on the size and distribution of particles was required to interpret the wear data. The particle size distribution for each dust sample was determined by microscope count, which was then converted to weight distribution. The abrasive dusts obtained for this study were found to be mixtures of particles varying over a much wider range of size than was nominally specified. The representative particle size for each dust was selected as the diameter of that particle which represented the midweight per cent of the dust. Fifty per cent of the weight was accounted for by particles of larger size, the remaining 50% weight by those of smaller size. This characteristic dimension for an abrasive sample was termed "diameter of mean weight per cent particle" and was used in tabulating and plotting all data involving abrasive particle size.

Test Results

Effect of Dust Particle Size Upon Top Compression Ring Wear – The five classified fractions of road dust were used in this investigation, with the results shown in Table 4 and plotted in Fig. 7.

The data show that particle size influences wear. The maximum wear effect was obtained with particles of 21.5 microns diameter, decreasing slowly with larger sizes and decreasing rapidly with smaller sizes.

Effect of Engine Speed – Within the range investigated, engine speed was found to have essentially no effect on wear, as shown in Table 5. The speeds selected cover the practical operating limits of the engine for the loading used.

Effect of Engine Load – Abrasive wear results at various loads are tabulated in Table 6 and plotted in Fig. 8. The data show that engine load markedly influences abrasive wear. At low loads, the rate of increase of ring wear is gradual; above 22.5 bhp, the increase is considerably greater.

Effect of Crankcase Oil Viscosity – The possibility that lubricating oil viscosity might influence abrasive piston-ring wear significantly was investigated, but no effect was found in the range of viscosity from SAE 10 grade to SAE 50 grade. This range is not large when considered in absolute viscosity (centipoises), which varied from 2.2 to 5.2, at an estimated cylinder oil film temperature of 300 F. Table 7 and Fig. 9 show the results of these

Table 4 – Effect of Dust Particle Size

Engine speed: 2500 rpm
Engine load: 45 bhp
Abrasive added to air induction system

Nominal Classification Size, microns	Diameter of Mean Weight – % Particle, microns	Diameter of Largest Particle Observed, microns	Top Compression Ring Wear, mg iron per mg dust
0–5	5.7	8	0.09
5–10	12.5	22	0.23
10–20	21.5	51	0.33
20–40	46.0	84	0.21
40–80	62.0	161	0.15

Table 5 – Effect of Engine Speed

Engine load: 45 bhp
Dust classification size: 10–20 microns
Abrasive added to air induction system

Engine Speed, rpm	Top Compression Ring Wear, mg iron per mg dust
1800	0.27
2500	0.27
3200	0.26

Table 6 – Effect of Engine Load

Engine speed: 2500 rpm
Dust classification size: 10–20 microns
Abrasive added to air induction system

Engine Load, bhp	Top Compression Ring Wear, mg iron per mg dust
0	0.02
15	0.04
22.5	0.07
30	0.19
45	0.27

Table 7 – Effect of Crankcase Oil Viscosity

Engine load: 45 bhp
Engine speed: 2500 rpm
Abrasive added to air induction system

Nominal Classification Size, microns	Diameter of Mean Weight – % Particle, microns	Oil Viscosity Grade, SAE No.	Oil Viscosity at 300 F, centipoises	Top Compression Ring Wear, mg iron per mg dust
0–5	5.7	10	2.2	0.07
		30	3.4	0.09
		50	5.2	0.05
5–10	12.5	10	2.2	0.27
		30	3.4	0.23
		50	5.2	0.22
10–20	21.5	10	2.2	0.32
		30	3.4	0.33
		50	5.2	0.32
20–40	46	10	2.2	0.23
		30	3.4	0.21
		50	5.2	0.22
40–80	62	10	2.2	0.14
		30	3.4	0.15
		50	5.2	0.16

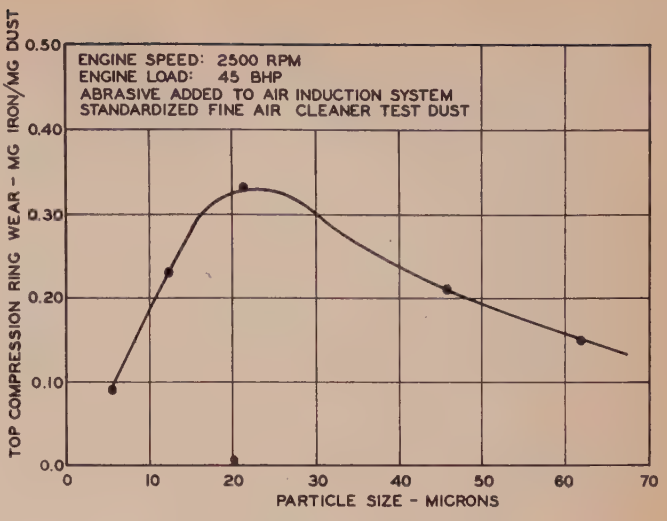

Fig. 7 – Effect of dust particle size on top compression ring wear

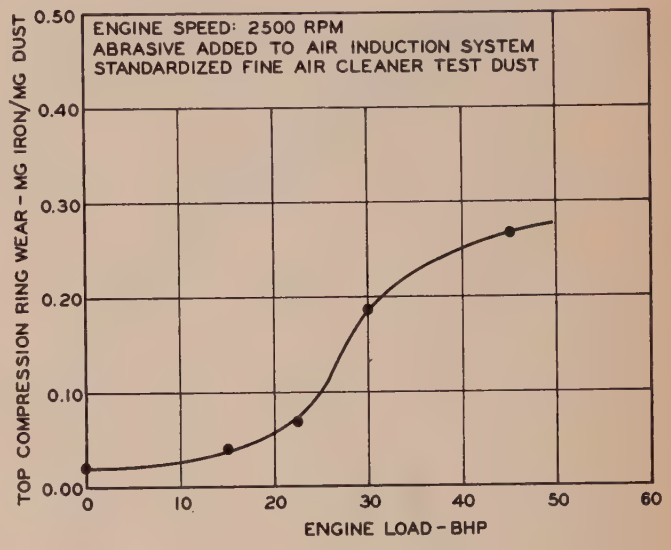

Fig. 8 – Effect of engine load on top compression ring wear – 10-20-micron dust

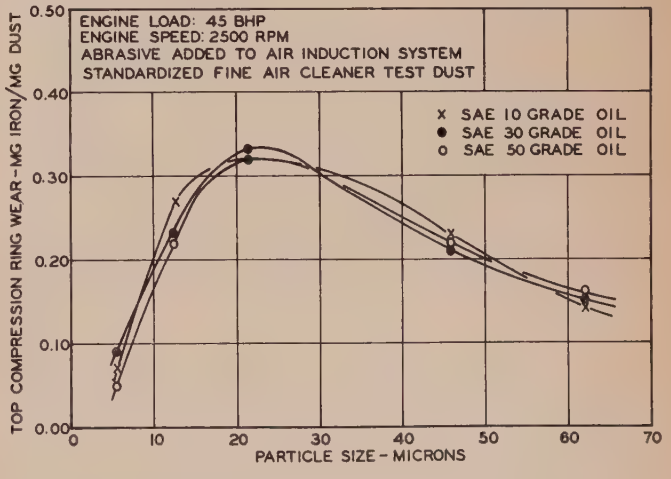

Fig. 9 – Effect of crankcase oil viscosity on top compression ring wear

tests. These results are in agreement with those of previous investigators.[9] Over 70% dilution of an SAE 40 grade motor oil with kerosene (estimated 0.95 centipoise absolute viscosity at 300 F) was required in their work before wear from airborne abrasives increased in rate; without abrasives, the wear rate did not increase until dilution exceeded 90%.

Diamond Dust as the Abrasive – Selected classifications of commercial diamond dusts[10] were introduced into the intake air by the usual procedure, but the amount had to be reduced markedly to maintain the radioactive iron counting system within accurate counting ranges. This series of tests provided two significant facts regarding abrasive wear: the diamond dusts exhibited considerably greater wear per unit weight inducted and, unlike the road dust, continued to cause wear as long as they were in any part of the engine. A typical record of the radioactive iron content of the lubricating oil is shown in Fig. 10, where the fast rise is indicative of the wear

[9] See pp. 30-32 of, "Collected Researches on Cylinder Wear," by C. G. Williams. Pub. by Institution of Automobile Engineers, London, 1940.

[10] "Diamet Hyprez" compounds supplied by Buehler, Ltd., Evanston, Ill. Particle size range and distribution of diamond powders contained in these compounds are governed by Commercial Standard CS 123-49.

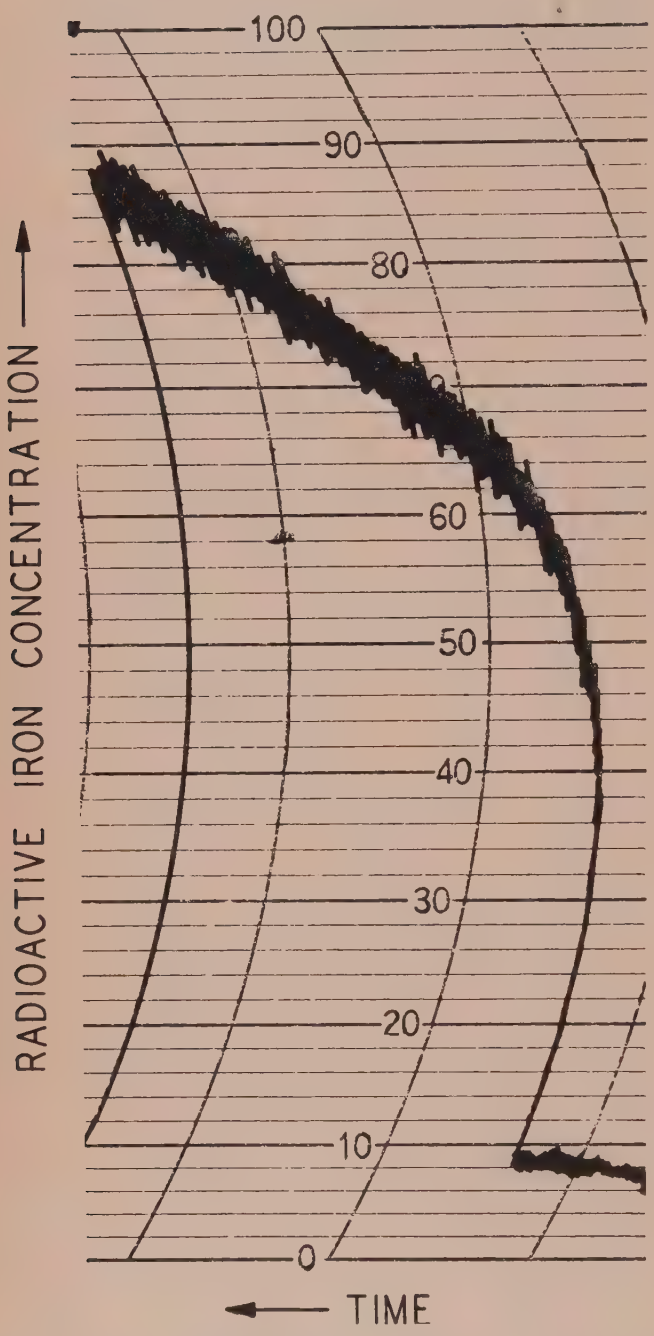

Fig. 10 – Typical recording of change of radioactive iron concentration in crankcase oil when diamond dust was added to air induction system

Table 8 – Effect of Diamond Dust as Abrasive

Engine speed: 2500 rpm
Engine load: 45 bhp Abrasive added to air induction system

Nominal Classification Size, microns	Diameter of Mean Weight – % Particle, microns	Diameter of Largest Particle Observed, microns	Top Compression Ring Wear: Initial Wear, mg iron per mg diamond	Top Compression Ring Wear: Continuing Relative Wear Rate, mg iron per hr
0–0.5	1 (est.)	2.2	0.00	0.084
0–2	1.9	3.7	0.32	0.138
1–5	4 0	8	0.96	0.852
4–8	11 6	17	1.55	1.176
6–10	17	29	2.56	1.656
8–20	31	61	5.92	3.840

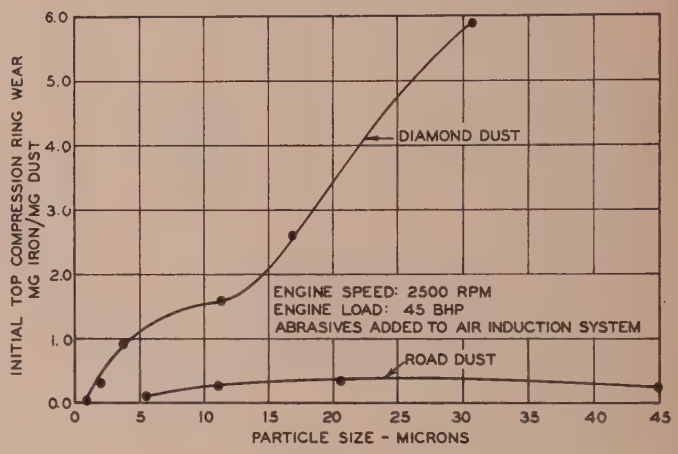

Fig. 11 – Effect of abrasive particle size on top compression ring wear

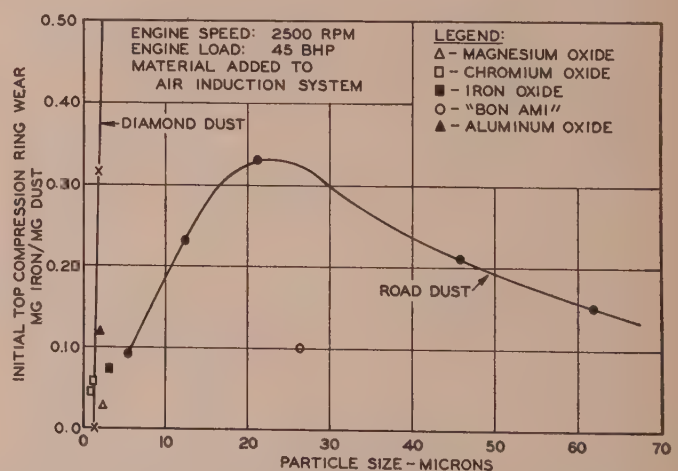

Fig. 12 – Influence of size and physical properties of various materials on top compression ring wear

Table 9 – Influence of Size and Physical Properties of Various Materials on Top Compression Ring Wear

Engine speed: 2500 rpm
Engine load: 45 bhp
Material added to air induction system

	Nominal Classification Size, microns	Estimated Diameter Mean Weight – % Particle, microns	Diameter of Largest Particle Observed, microns	Nominal Hardness – Moh's Scale	Density, gm/cc	Top Compression Ring Wear	
						Initial Wear, mg iron per mg dust	Continuing Relative Wear Rate, mg iron per hr
Magnesium Oxide							
1558 AB Levigated Shamva[a]	1.0	2.5	5.0	4–5	3.7	0.03	Nil
Chromium Oxide							
1564 AB Metpolish No. 3[a]	0.5	1.0	2.0	6	5.2	0.05	0.084
Chromium Oxide							
1563 AB Metpolish No. 1[a]	1.0	1.2	2.4	6	5.2	0.06	0.096
Iron Oxide							
1559 AB Jewelers Rouge[a]	3.0	2.8	5.7	6	5.2	0.07	0.042
Bon Ami Scouring Powder	—	27	55	5	—	0.10	Nil
Aluminum Oxide							
1552 AB Gamma Polishing Alumina No. 3[a]	0.1	2.1	4.3	9	3.7	0.12	0.11
Diamond							
1546 R AB Diamet Hyprez Compound[a]	0–2	1.9	3.7	10	3.5	0.32	0.14

[a] Numbered abrasives supplied by Buehler, Ltd. (see footnote 10) and described in the company's catalog, "Polishing Cloth and Abrasives," January, 1962.

caused by the initial passing of the diamond dust past the piston rings into the crankcase oil, and the subsequent constant wear rate by the small amount of abrasive circulating in the oil system. Two flushings of the oil system reduced the wear rate to normal, showing that the diamond dust was not embedded in the piston rings or cylinder walls of the engine. Table 8 summarizes test data obtained with diamond dust as the abrasive material.

Fig. 11 is a plot of the wear data obtained with the diamond dusts in comparison to the road dusts. The wear with diamond dust is considerably greater than that for equivalent size road dust and, unlike that with road dust, continues to increase with particle size throughout the range investigated.

Other Materials as Abrasive Dusts – To obtain a broad experience with abrasives and determine the physical properties which influence abrasive wear, the variety of materials shown in Table 9 was evaluated for wear characteristics, both for initial wear and for continuing wear rates.

The data show a large variation in the wear-inducing characteristics of different materials. Also, a few generalizations can be made regarding physical properties which influence wear. Particles which are very hard cause high initial wear and a continuing higher-than-normal wear rate, indicating that they remain intact as long as they are in the engine. Particles of softer materials appear to be disintegrated during the initial wear process, and become incapable of causing further wear. Fig. 12 shows the wear characteristics of the several abrasive dusts.

Addition of Abrasives to the Crankcase Oil – Fig. 7, as discussed above, shows the influence of abrasive particle size on top compression ring wear when road dust was added to the airstream. Under this condition, it could be reasoned that only a portion of the particles impinged on the cylinder walls to cause wear, while most of the abrasive remained airborne and passed out the exhaust. To examine this effect, the radioactive top piston ring was exchanged with the second compression ring, and the oil control ring was removed from the piston. The abrasive material was mixed thoroughly with a quart of fresh crankcase oil and added to the operating engine. Under this condition, the radioactive ring encountered an abrasive-laden oil film on the cylinder wall on each downstroke of the piston. Introducing abrasive to the crankcase oil assured that all particles remained in the engine. However, all engine parts lubricated by the crankcase oil were then exposed to the abrasive particles, and only a small amount of the total wear could be identified with the radioactive piston ring. Each test involved the addition of 2 g of abrasive to the crankcase oil, which at the start of the tests averaged 7 qt in volume. Fig. 13 shows a typical recording of the wear-time relation for road dust. Total wear was not immediate, as in the case of airborne dust, nor was the wear rate uniform; but piston-ring wear followed a curve of constantly decreasing wear rate. Data obtained in a series of tests with road dusts are shown in Table 10.

Fig. 14 shows a plot of total wear with various fractions of road dust after 30 min of operation. This curve shows a maximum wear characteristic for road dust particles of 21.5 microns diameter, and is quite similar to Fig. 7, where the abrasive was airborne. For smaller sizes, the wear decreased rapidly with decreasing particle size; but for larger particles, the decrease was very gradual as the diameter was increased. Examination of the used crankcase oils showed the ratio of radioactive iron to inert iron averaged 1 to 120. Calculations showed that given weights of abrasives added to the crankcase oil caused about 10 times as much wear as equivalent weights of airborne abrasive, confirming the opinion that the major amount of airborne abrasive blows out the exhaust without impinging on the cylinder walls.

Discussion

From the foregoing data and from experience gained in operating engines with radioactive piston rings under abrasive wear conditions, the following history is given of an abrasive particle which enters an engine with the induction air or which

Table 10 – Effect of Adding Road Dust to Crankcase Oil

Engine speed: 2500 rpm
Engine load: 45 bhp
Two grams road dust added to crankcase oil

Nominal Classification Size, microns	Diameter of Mean Weight - % Particle, microns	Second Compression Ring Wear, mg iron			
		0 Min	15 Min	30 Min	60 Min
0-5	5.7	0	4.5	9.0	15.3
5-10	12.5	0	17.2	32.7	—
10-20	21.5	0	26.2	45.6	65.6
20-40	46.0	0	26.8	43.0	62.8
40-80	62.0	0	27.2	41.0	58.4

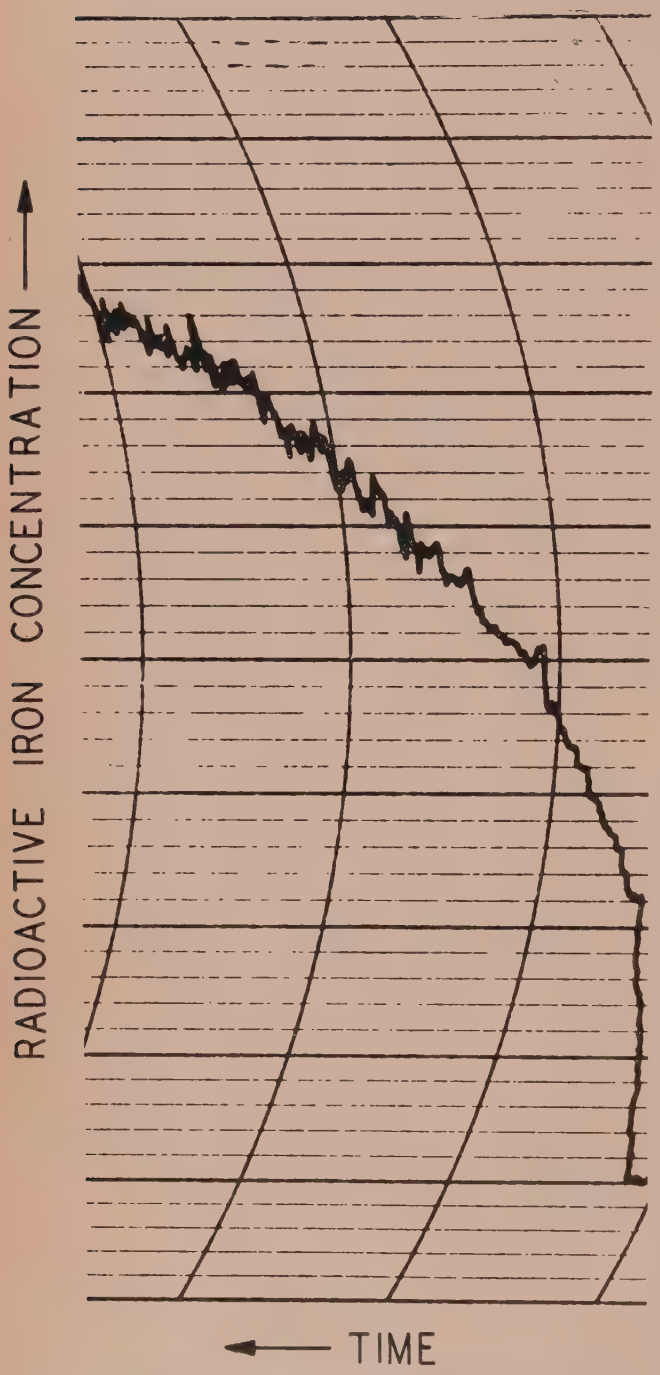

Fig. 13 – Typical recording of change of radioactive iron concentration in crankcase oil when road dust was added to crankcase oil

is introduced into the crankcase oil.

Airborne Abrasive Particle Entering Air Induction System – When an abrasive particle enters an engine cylinder during the intake stroke, there is a high probability that it will remain airborne because of the extreme turbulence, and that it will leave the combustion chamber during the next exhaust stroke. If the particle impinges on the cylinder wall oil film during the intake or power stroke, there is a high probability that it will cause wear of the piston ring and cylinder wall during the next upstroke of the piston. The amount of piston-ring wear occurring depends upon the size of the particle and its physical properties.

If the abrasive is reduced in size as it causes wear, the amount of wear is relatively low for a given particle size. The wear occurs immediately, and there is no tendency to cause continuing wear. Road dust, Bon Ami scouring powder, and magnesium oxide (1558 AB Levigated Shamva) fall in this classification. With these materials, wear is limited almost exclusively to the top compression ring. The abrasive wear debris is washed into the crankcase oil; but microscopic examination of used crankcase oils from tests with road dust in the intake air failed to show any particles larger than five microns diameter, regardless of the size of abrasive used in the tests.

If the abrasive has sufficient strength to resist the high compression loads imposed during wear, its size does not change while it is in the engine. Diamond, aluminum oxide (1552 AB Gamma Polishing Alumina No. 3), chromium oxide (1563 AB Metpolish No. 1 and 1564 AB Metpolish No. 3), and iron oxide (1559 AB Jewelers Rouge) fall into this classification. These abrasive materials cause high wear of all piston rings, and after entering the crankcase oil continue to cause high wear rates. The only way to stop this type of wear is to remove the abrasive from the crankcase oil by filtration, oil change, or loss through leaks or oil consumption. It is indeed fortunate that very few natural, airborne dusts fall in this classification.

Airborne Abrasive Particle Entering Engine Crankcase Oil System – If an abrasive particle contaminates the crankcase oil, there is a very high probability that it will cause wear unless it is removed. Unlike an abrasive entering a cylinder with the intake air, wear is not immediate but depends upon the probability that the particle enters a zone where it can cause wear. This probability increases with the number of particles, engine speed, and the ratio of the volume of oil in the critical wear zones to the crankcase oil volume.

With abrasive particles of sufficient size and high internal strength, the probability of wear remains constant because the number of particles does not change. Therefore, wear of all internal parts subject to abrasive wear is continuous.

When a low-internal-strength abrasive is in the crankcase oil, wear also depends upon the prob-

ability of the abrasive entering a critical wear zone. In this case, however, each time a particle causes wear it is reduced in size until it is no longer capable of causing further wear. For this reason, wear rate decreases constantly as the number of potential wear-causing particles decreases, and the total wear is related to the number of original abrasive particles in the oil and to their original size and strength. Small amounts of abrasives of this type cause initially high wear of the oil-control ring, with essentially no wear of the compression rings. Continued introduction of abrasive to the oil progressively causes excessive wear of the lowest compression ring, and then proceeds upward on the piston to the remaining compression rings as the lower rings lose tension and are less subject to wear. Typical road dust has the wear characteristics described above and illustrated in Fig. 13.

Hydrodynamic Lubrication of Engine Piston Rings – While results of extensive work have been published regarding the hydrodynamic lubrication of journal bearings, and more recently on tilting pad bearings, there is little information available in the literature devoted to studies of the lubrication of piston rings or related machine parts where corollaries could be drawn. It has not been established in the literature whether piston rings in an engine operate under conditions of boundary or of fluid-film lubrication. It is believed that the data obtained during this study of abrasive wear lend support to the concept that piston rings operate under hydrodynamic conditions, the fluid film being very thin as compared with values reported for operating journal bearings or tilting pad bearings.

Fig. 7 shows the relation between wear characteristics and particle size of road dust. If this curve is continued to the abscissa, it is found that no abrasive wear occurs at a particle size of 1 micron (0.000039 in.). This extrapolation indicates that road dust particles below 1 micron in diameter do not cause wear of the piston ring in the test engine. A plausible explanation of this critical dimension is that the lubricant film separating the piston ring from the cylinder wall is 1 micron thick, and particles too small to bridge the film cannot cause wear. Arguments could be presented that the critical dust dimension exists because airborne particles of a smaller size cannot impinge on the cylinder wall under the turbulent condition existing in the cylinder. This argument can be refuted, however, by reference to Fig. 14, where the abrasive is known to be present in the crankcase oil. Extrapolation of this curve also gives a critical size of approximately 1 micron.

A piston ring subjected to abrasive wear was examined under high magnification. Fig. 15 shows a typical cross-section of the outer ring surface in which the wear track cross-sections are nearly hemispherical. Measurement of the width and depth of many of the tracks showed that the depth was consistently less than the width, indicating that the center of the abrasive particle causing the wear track was above the surface of the ring. This effect requires that the ring and cylinder be separated except in a case where the cylinder material was somewhat softer than the ring material, which is not the condition in the test engine.

The data thus indicate that engine piston rings operate under hydrodynamic conditions, and in the absence of abrasives are separated from the cylinder wall by a finite clearance determined by the factors influencing film formation and dimensions.

Conclusions

1. Abrasive materials cause wear of piston rings, the amount of wear depending upon the size and properties of the abrasive and the method by which the abrasive enters the engine.
2. Some abrasives cause only limited wear, while others continue to wear as long as they are in the engine. This characteristic is related to the physical properties of the abrasive.
3. There is evidence that piston rings are separated from the cylinder walls by finite distances, this separation apparently being caused by formation of a hydrodynamic oil film.
4. The method described for measuring piston-ring wear by use of irradiated piston rings and

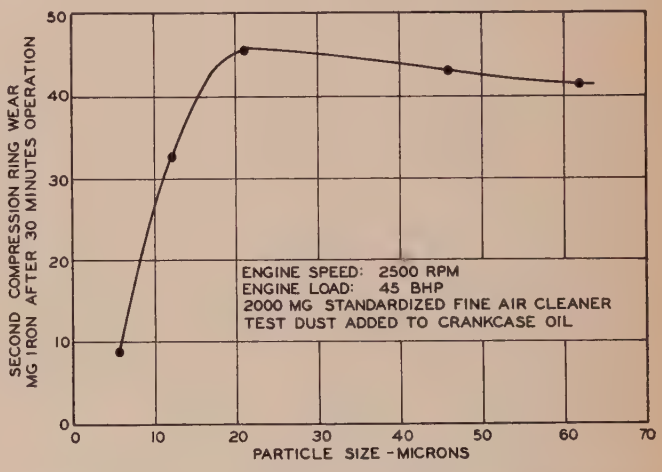

Fig. 14 – Effect of dust particle size on second compression ring wear

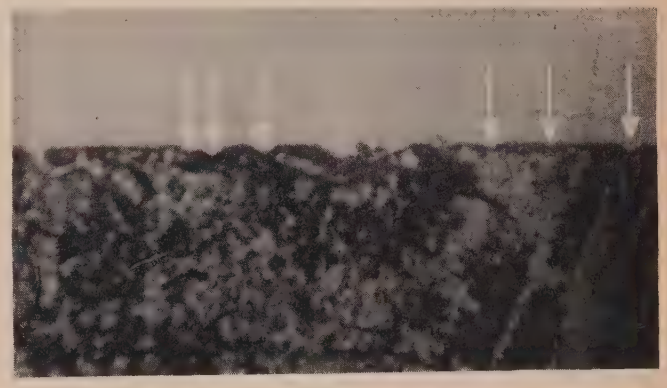

Fig. 15 – Typical cross-sections of wear tracks on face of piston ring after abrasive wear (reduced from photomicrograph taken at 1200X)

modern detection equipment is both accurate and fast. It also overcomes objections to previous methods involving disassembly of the engine after each test or the use of separate engines to obtain each test value.

5. While these studies involved abrasive wear of piston rings, the method could be used readily to study normal or abnormal wear of any internal engine part if irradiated. The effectiveness of air or oil filters could be determined by the same method.

6. The above conclusions can be expected to apply not only to gasoline engines but to diesel engines, air compressors, or any mechanism involving pistons, piston rings, and cylinder combinations.

7. Maximum piston ring life is obtained when abrasive wear is reduced to a minimum and corrosive wear is controlled by adequate compounding of the crankcase oil.

Acknowledgment

The authors are indebted to S. F. Duncan and A. W. Hardy of the Farr Co. for providing equipment, materials, technical advice, and help in carrying out parts of this investigation.

DISCUSSION

Feels Oil Viscosity Might Be Factor in Abrasion

– C. M. Heinen
Chrysler Corp.

IN spite of the increase in surfaced roads, major abrasive wear is encountered often enough to be more than a nuisance, and minor abrasive wear is always with us.

The test methods used by the authors, while not completely unique, showed considerable ingenuity, and certainly yielded excellent data. The methods selected allowed the authors to use realistic dust concentrations and yet achieve results within a reasonable time. I venture to say that the task of obtaining data such as those showing the effect of various abrasives in an engine would have awed the average investigator who had to rely on engine teardowns and measurements in order to establish trends.

I concur wholeheartedly with the main conclusions of the paper, but would like to discuss three items.

1. The conclusion that crankcase oil viscosity is not a factor in engine wear appears premature when it is considered that the temperature at the top ring is certainly not representative of that obtained elsewhere in the engine or even the rest of the ring line-up.

The evidence which the authors presented to show that rings operate under hydrodynamic conditions would argue that viscosity should have an effect on abrasive wear at some temperatures. Before reaching a general conclusion, other rings and parts of the engine should be checked. In short, I believe a more accurate conclusion would be that "viscosity of crankcase oil does not affect the abrasive wear of the top ring." This would be coupled with a recommendation for further work on other areas.

2. My second comment is more in the nature of a plea. Table A shows some results obtained in our 10,000-mile dust tests in the Southwest. A quick calculation will show that the dust conditions were somewhere between those defined by the authors as "dusty" and "dust storm." It is apparent that properly operating air cleaners and oil filters are very effective in reducing the abrasive dust to the engine. Based on the results obtained by the authors, it is evident that a ten-fold reduction in top-ring abrasive wear can be expected from these devices.

My plea is directed at those who can effect the proper servicing of these units. They can do the motorist a real favor by pushing these items at service centers.

3. Finally, I should like to second the authors' suggestion that further work on abrasive wear be done using the techniques which they have developed. I look forward, as I am sure everyone does, to further excellent papers on this important subject from them and from others who follow their lead.

Tests Show Air Filters Must Handle Quantity of Dust

– M. J. Caserio
AC Spark Plug Division, GMC

THE authors have developed a technique which gives reproducible results on the measurement of the effect of particle size on the wear of engine parts.

Previous testing on this subject had given conflicting results, and there has been up to this time a distant difference of opinion regarding the size of particles which an engine may "digest" without harmful results.

The results reported by the authors show that dust in the 20-micron range is the most destructive to piston rings; however, it is shown that dust particles both above and below this size are definitely harmful.

Although it is obvious that without the protection provided by adequate air cleaners, by far the greatest quantity of dust entering an engine would come in with intake air, the authors have made it clear that a large portion of this dust would not be harmful since it would be carried away with the exhaust; and therefore that dust entering the crankcase of the engine by other paths may also be a great cause of engine wear. This indicates that careful consideration must be given to the prevention of dust entering the crankcase directly, such as through the crankcase ventilation inlet.

It is, therefore, also necessary to have adequate oil

Table A – Dust Tests in the Southwest
(All values expressed in grams)

	Car No. 550		Car No. 512		Car No. 568		Car No. 569	
	First Test	Second Test	First Test	Second Test	First Test	Second Test	First Test	Second Test
Oil Filter	35.1	35.6	—	30.0	63.5	38.3	65.5	34.0
Oil Gallery	0.065	0.11	—	0.23	0.26	0.13	0.28	0.12
Oil Drain	1.17	1.27	—	2.18	4.43	0.74	4.26	0.74
Air Cleaner	167.6	144.9	—	208.6	143.0	137.3	187.8	214.6
Crankcase Vent Air Cleaner	—	—	—	—	4.22	4.04	6.44	3.51
Crankcase Vent Outlet Pipe Air Cleaner	—	—	—	—	—	1.92	—	2.34

Table B – Dust Concentrations at 49 Cfm Airflow (30–50 Mph)

	Lead Car Distance	Road Surface	Location	Maximu mor Minimum Encountered	G per Cu Ft of Air	Miles per 100 G	
1	None	Various	Michigan	Minimum	None	Never	
2	None	Various	Michigan	Maximum	0.000035	47,000	
3	None	Various	Arizona	Minimum	0.0000015	1,000,000	
4	None	Various	Arizona	Maximum	0.000025	55,000	
5	75 ft	Pavement	Michigan	Minimum	0.0000015	1,000,000	
6	75 ft	Pavement	Michigan	Maximum	0.000009	166,000	
7	75 ft	Pavement	Arizona	Minimum	0.000008	200,000	
8	75 ft	Pavement	Arizona	Maximum	0.0003	5,000	
9	75 ft	Dry gravel	Michigan	Minimum	0.0033	400	Occasional zero visibility
10	75 ft	Dry gravel	Michigan	Maximum	0.0036	370	
11	75 ft	Dry gravel	Arizona	Minimum	0.0117	131	Driving considered hazardous
12	75 ft	Dry gravel	Arizona	Maximum	0.0124	112	
13	Up to 1 mile	Dry gravel	Arizona	—	0.0032	548	Safe driving in fringe of dust cloud

filtration if minimum practical wear is to be obtained. This is borne out by the authors' calculation that abrasives in the crankcase oil caused 10 times as much wear as carburetor airborne abrasives, and also by their Fig. 13 showing that wear caused by road dust in the crankcase oil continues with the passage of time. Their Fig. 6, on the other hand, shows that road dust introduced into the intake manifold caused no subsequent wear after its initial effect.

In testing oil filters, we use a standardized oil filter test contaminant concentrated from used oil having particle size distribution as follows: 0-2 microns, 60%; 2-5 microns, 37%; over 5 microns, 3%.

Tests using this contaminant show that 96 to 98% of the contaminant is removed. This is particularly interesting in view of the fact that 97% of the particles in this contaminant are 5 microns or less. The reason behind this is the filtering assistance provided by the deposition on the filter of the initial layers of contaminant.

The rather surprising results which indicate that the "Standardized Air Cleaner Test Dust," when introduced through the intake system, loses its abrasive properties once it has been subjected to the action of the piston rings, indicates that interesting information could be gained by further experimenting with the abrasive qualities of various types of materials. We recall that the test by Schudt and O'Hara of Allis-Chalmers in 1943 indicated considerable variation in the rate of wear caused by dust from various parts of this country. Perhaps one of the reasons why some materials seem to lose their abrasive qualities after contact with the piston rings is indicated by the fact that the two materials in Table 9 which did lose this property – magnesium oxide and Bon Ami – have good cleavage planes, which may be responsible for their relatively easier destruction. The major constituent of the Standardized Test Dust used by the authors is quartz, which has a hardness of 7, compared to iron oxide's hardness of 6. According to Table 9, the iron oxide did not lose all of its abrasive properties, whereas the Test Dust did. Therefore, it is not necessarily the hardness of the particle which controls its resistance to destruction by the piston rings. The Standardized Test Dust is prepared from natural dust collected in the vicinity of Phoenix, Ariz., and is intended to be typical of dust encountered in field operations. There is some reason to believe that natural dusts of this nature have some properties different from pure abrasive crystals due to large amounts of colloidal materials mixed with them in their natural state, each dust particle being coated with a film of the colloidal materials. The colloidal materials apparently aid in keeping the dust particles relatively uniformly dispersed throughout their carrying medium, while the pure abrasive particles have a greater tendency to adhere one to another. Perhaps this is another reason why the Bon Ami powder seemed to operate in similar fashion to the Test Dust, since Bon Ami also contains a colloidal soap coating each of its individual particles. In order to understand more clearly the phenomenon of the breaking up of the Test Dust particles, it might be desirable to run comparative tests using similar-size particles of pure quartz, which is the major constituent of the dust.

We have collected some figures on the dust concentrations which a passenger car might encounter. Although these figures in no way dispute the results of the authors' wear test, they do seem to differ to some extent from those quoted by the authors in Table 1. Our data were obtained by driving a passenger car 100 miles under each condition, and passing the carburetor air through an absolute filter which was weighed to determine the amount of dust collected. Tests were conducted both in Michigan and in Arizona in order to obtain a range of climate. Several tests were run under each condition, and Table B reports the minimum and the maximum amounts of dust collected under each condition. In this chart we show both the grams of dust per cubic foot of air and also the miles which would have been traveled under each condition in order to collect 100 g. The 100-g figure was used since it is a commonly used quantity of dust for determining the plugging or restriction build-up of a passenger car air cleaner. It will be noticed that with no lead car preceding the test vehicle, only very minor dust concentrations were encountered under any conditions of road surface. It will be noticed, however, that when a lead car was used on gravel roads very high concentrations were encountered, and particularly in Arizona we approached the condition of collecting 1 g of dust per mile. Under these conditions, however, driving was extremely hazardous and it was found that dropping back of the lead car a sufficient distance to obtain safe driving conditions, but still remaining in the dust cloud, it was necessary to remain as far back as one mile. The dust

concentration was still appreciable, however, and we were approaching the condition of collecting 1 g of dust each five miles. It is therefore evident that air cleaners must not only prevent dust from entering the engine, but that they also must be able to handle large quantities of dust.

Questions Authors' Extrapolation of Curves

– Robert E. Kennemer
Caterpillar Tractor Co.

IT might be well to comment on the chemical analysis of the dust which was shown. The analysis indicated that the material was made up largely of oxides of silicon, iron, and aluminum. However, it should be noted that the exact materials shown in the analysis were not necessarily present in the dust (various combinations of these materials were present). This analysis was reported in the manner which is familiar to most chemists, but not well understood by many engineers. The pure forms of the three oxides mentioned above are all quite hard and should have caused continuing wear, as noted in the latter part of the paper. However, in the mineral forms actually present in the dust, the materials were much softer, and apparently deteriorated during operation of the engine until the rate of wear was greatly reduced.

Table C – Oil Ring Wear Rates

Ring Face Material	Dust Feed, AC Fine, g/1000 cu ft air	Relative Wear Rate, Gap Increase
Iron	None	1
Iron	0.1	50
Chrome	0.1	4

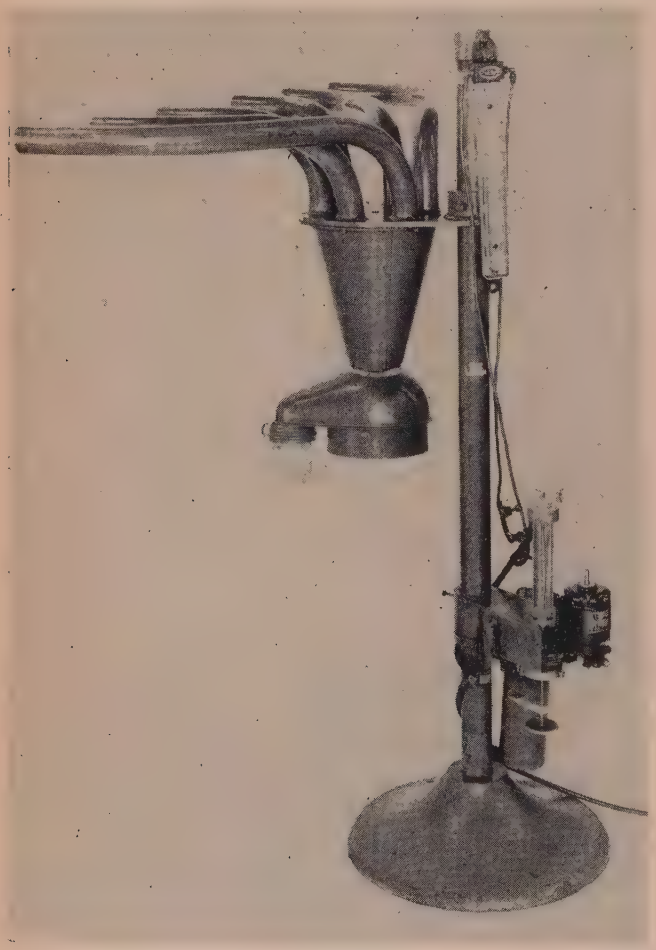

Fig. A – Motor-driven dust feeder used in abrasive wear tests

In our laboratory, abrasive wear tests have been conducted over a period of more than six years, using a motor-driven dust feeder of the type shown in Fig. A. In the past few years, the precleaner and conical mixing chamber, which operate above the dust feeder with separate air-transfer pipes to each intake port, have been used. AC fine dust has been used in most of our tests, although in some cases, we have used 0-5 micron dust separated from the AC fine dust. In all cases, wear figures have been determined by dimensional changes. In most tests, we have investigated the effects of various materials and design factors on the rates of wear of the pistons, rings, and cylinder liners.

We were interested to note the linearity of rate of wear with rate of dust feed which was shown. We had suspected that rate of wear increased with rate of dust feed, at least above some critical rate of dust feed. The possibility of inducing scuffing with high rates of dust feed was the factor which we had suspected might cause exceptionally high rates of wear with high rates of feed.

We can verify the effect of load on the rate of abrasive wear, and we have also noted that dust in the 0-5 micron range causes less top ring wear than the same weight of AC fine dust.

At one point, the authors commented that with road dust or other relatively soft abrasives, the wear was limited almost exclusively to the top compression ring. Table C shows the oil ring wear rates which we have determined with and without dust feed, and also compares iron and chrome plated rings. It can be noted that the iron oil rings, when subjected to abrasives in the intake air, wore at a rate 50 times as high as when operated with clean air. However, when chrome-plated oil rings were used, a great improvement in oil-ring wear rate was obtained. This demonstrates that with soft abrasives wear is not limited to the top compression rings in a diesel engine.

The authors have concluded that piston rings are separated from the cylinder walls by finite distances, based on extrapolations of the curves relating wear to dust particle size and on the cross-sections of wear tracks on the face of a piston ring after abrasive wear. Extrapolation of wear curves of the type shown cannot be expected to provide accurate information, since each plotted point for particle size is only an arbitrary point selected to represent the many particle sizes contained in each sample. The form of the wear tracks shown might be explained in other ways:

1. The abrasive particles are not necessarily spherical in form, but may have one axis longer than others.

2. Abrasive particles may temporarily embed in a soft constituent of **either** wearing surface, even though the measured hardness values might not indicate this possibility.

Other investigators have found by direct measurements of piston-ring friction, and by electrical resistance measurements between a ring and cylinder, that the lubrication between a piston ring and cylinder is partially hydrodynamic and partially boundary. The greatest likelihood is that there is hydrodynamic lubrication of a ring during the time when the relative velocity between the ring and cylinder is high, and boundary lubrication at the ends of each stroke. In view of the extremely low rates of wear of rings and cylinders which may occur under clean conditions with low sulfur fuel, it seems apparent that the rings must be well lubricated most of the time, but it also seems unlikely that rings are hydrodynamically lubricated at all times.

References

1. "Analysis of Lubrication between Piston Rings and Cylinder Wall of Running Engine," by J. S. Courtney-Pratt and G. K. Tudor. Proceedings of Institution of Mechanical Engineers, Vol. 155, 1946, pp. 293-322.

2. "Direct Measurement of Piston-Ring Friction in an Internal-Combustion Engine," by J. C. Livengood. American Society of Lubrication Engineers, 1949.

Antiknock Requirements of Passenger Cars—1953 CRC Survey

H. W. Best Yale University
H. A. Bigley Gulf Research and Development Co.
R. K. Williams Research Laboratories Division, GMC

This paper was presented at the SAE National Fuels and Lubricants Meeting, Tulsa, Nov. 5, 1954.

SINCE 1948 the Coordinating Research Council, Inc. (CRC) has conducted annual surveys of the octane-number requirement of postwar vehicles in order to assist the petroleum and automotive industries in the evaluation of their products.

Survey Technique Revised

Prior to the accelerated trend to fuels of higher octane quality and the introduction of engines and transmissions of new design, these surveys consisted of measurements of requirements of a sample of the total car population chosen as to make and model according to national registration figures. While these surveys have provided a sound basis for measuring trends in octane-number requirement, they do not lend themselves to the study of individual car makes. Rapid developments in the fields of fuels, engines, and transmissions have created a need for surveys of individual models. Such surveys can be used to evaluate the effects of engine and transmission design changes and to establish trends which may be helpful in predicting future fuel requirements.

Consequently, in 1951 a few new-design models were tested in sufficient number to obtain a relatively accurate estimate of their octane-number requirement level. In 1952 and 1953 the CRC surveys were devoted exclusively to new-design models. Twenty-four laboratories participated in the 1953 survey, results of which are discussed in this paper.[1]

Test Vehicles

A total of 235 cars representing nine 1953 models was tested. All of the cars tested were in the condition as received from the owner. The minimum number of each model was 22 and the maximum was 30. The makes and models investigated are given in Table 1.

Test Fuels

Requirements were measured in terms of three series of fuels: primary reference fuels, severity reference fuels, and a series of full-boiling-range gasolines.

RESULTS of the 1953 CRC survey of octane-number requirements are presented in this paper. This 1953 survey initiated the use of a new technique, which included both full- and part-throttle procedures.

Nine new-design models, represented by 235 cars, were tested using primary reference fuels, severity reference fuels, and a series of full-boiling-range gasolines.

It differed from the previously used technique in that accelerations were made at a series of constant intake manifold vacuums from 10 in. of Hg to wide-open throttle.

[1] Complete results on the 1953 survey are contained in the CRC report entitled "Octane-Number Requirement Survey, 1953."

Table 1 – Makes and Models of Cars Investigated

Car Make	Transmission
Buick Model 50	Dynaflow
Buick Model 70	Dynaflow
Cadillac	Hydra-matic
Chevrolet	Powerglide
Chevrolet	Synchromesh
Dodge V-8	Gyrotorque and Gyromatic
Ford 6	Synchromesh
Lincoln	Hydra-matic
Oldsmobile	Hydra-matic

Table 2 – Composition of Severity Reference Fuels

	Composition, %			Average Rating	
Blend No.	SR-10	n-Heptane	Isooctane	Motor O. N.	Research O. N.
1-S-51	15.3	35.0	49.7	72.9	75.0
2-S-51	22.9	36.4	40.7	74.4	77.5
3-S-51	32.2	38.0	29.8	75.7	80.0
4-S-51	36.2	36.7	27.1	77.2	82.5
5-S-51	38.9	34.5	26.6	78.7	85.0
6-S-51	41.8	32.2	26.0	80.1	87.5
7-S-51	44.9	29.7	25.4	81.4	90.0
8-S-51	46.1	26.5	27.4	82.9	92.5
9-S-51	43.6	21.9	34.5	84.7	95.0
10-S-51	40.8	16.9	42.3	86.6	97.5
11-S-51	37.9	11.6	50.5	88.3	100.0

Table 3 – Composition of Full-Boiling-Range Gasolines

		Average Rating	
Blend No.	Composition	Motor O. N.	Research O. N.
1-C-53	RMFD 54-53	73.4	75.2
2-C-53	50/50 RMFD 54-53 and 55-53	74.7	77.6
3-C-53	RMFD 55-53	76.0	79.6
4-C-53	50/50 RMFD 55-53 and 56-53	77.6	82.3
5-C-53	RMFD 56-53	79.5	85.1
6-C-53	50/50 RMFD 56-53 and 57-53	80.7	87.5
7-C-53	RMFD 57-53	81.5	89.8
8-C-53	50/50 RMFD 57-53 and 58-53	83.1	92.5
9-C-53	RMFD 58-53	84.5	94.9
10-C-53	50/50 RMFD 58-53 and 59-53	85.7	97.6
11-C-53	RMFD 59-53	86.8	99.7

The primary reference fuels were ASTM isooctane and n-heptane blended in 2.5-octane-number increments to cover the range of 75 to 100 octane numbers.

The severity reference fuels were prepared by blending diisobutylene (SR-10) and ASTM isooctane and n-heptane in 2.5-octane-number increments to cover the range of Research-method octane numbers from 75 to 100. The composition of these reference fuels is identical to the severity reference fuels of previous surveys and is given in Table 2.

Six full-boiling-range gasolines covering the range of Research-method octane numbers from 75 to 100 in 5-octane-number increments were cross-blended to provide increments of approximately 2.5 octane numbers. The identification and average octane-number ratings of the resulting blends are given in Table 3.

Inspection data for the six full-boiling range gasolines used for these blends are given in Table 4.

In addition to the reference fuels, the fuel in

The Authors

H. W. BEST (M '24) is associate professor of mechanical engineering at Yale University's School of Engineering, where he has been teaching since 1927. He was associated with the experimental engineering department of Mack from 1923 to 1927, and holds degrees both from M.I.T. and Yale.

H. A. BIGLEY, JR. (M '38) is section head in the Automotive Engineering Division of the Gulf Research and Development Co. After graduating in 1935 from the University of Pittsburgh with a B.S. in Aeronautical Engineering, he taught for a brief period. Mr. Bigley joined Gulf as a test engineer in 1936. Except for a five-year tour of duty with the U. S. Army from 1941 to 1945, he has been with Gulf since that time, assuming his present position in 1953.

R. K. WILLIAMS (M '52) is assistant head, Fuels and Lubricants Department, Research Laboratories Division, General Motors Corp. He received a B.S. in Chemical Engineering from Princeton University in 1940. Mr. Williams has been with General Motors since 1940, where he was engaged first in rubber and plastics research and later in research in the fields of fuels and lubricants.

Table 4 – Properties of Full-Boiling-Range Fuels

Fuel, RMFD	Octane Number		API Gravity, deg	Rvp, psi	Tel, ml per gal	Induction Period, min	ASTM Gum, mg per 100 ml	ASTM Distillation Temp, F at % evap					Composition
	Research	Motor						Ibp	10	50	90	Ep	
54-53	75.9	72.2	61.5	5.8	0.82	836	3.1	114	156	226	338	412	40% 250 ep st run 50% th reformate 10% heavy st run
55-53	79.9	75.2	60.8	5.8	1.23	681	3.1	112	150	224	338	428	30% 250 ep st run 70% th reformate
56-53	85.7	80.0	61.4	8.5	2.22	780	1.4	102	131	222	318	388	16% cat. cracked 18% th cracked 52% st run 14% light ends
57-53	90.0	80.9	60.1	7.6	2.49	600+	3.0	110	141	219	353	428	52.6% cat. cracked 41.5% st run 4.2% th cracked 1.7% n-butane
58-53	95.0	84.5	61.5	6.9	2.75	969	2.0	100	142	214	362	416	26% aviat st run 10% dib (SR-10) 64% fluid cat. cracked
59-53	100.0	86.8	60.9	6.1	2.44	871	1.5	105	152	225	354	420	20% H. F. alkylate 20% dib (SR-10) 60% fluid cat. cracked

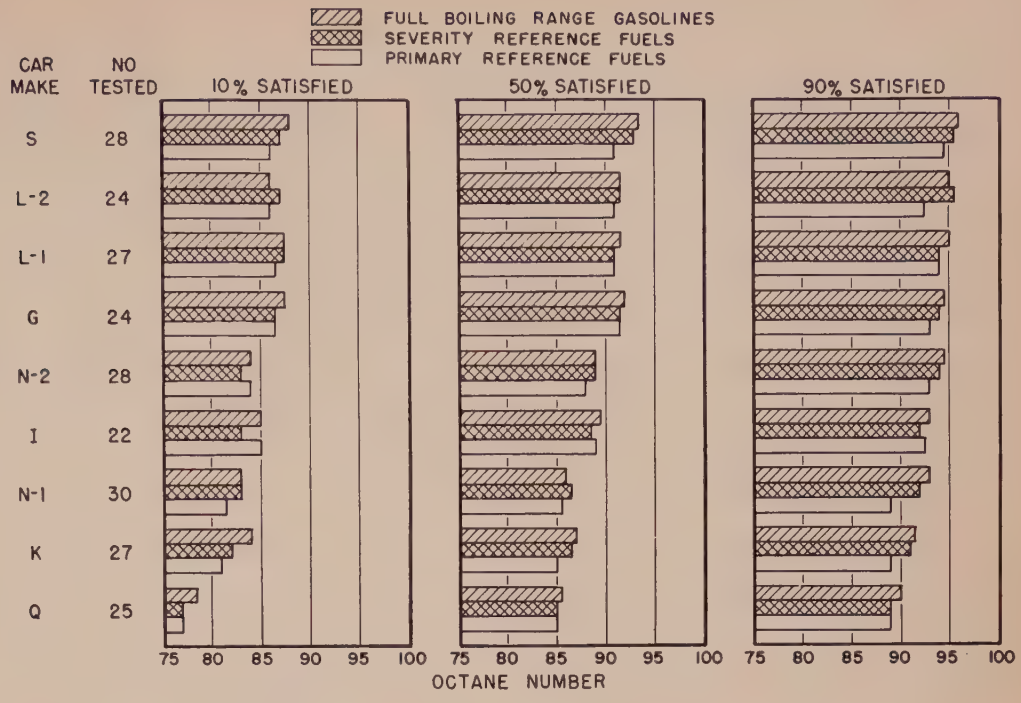

Fig. 1 – Octane-number requirement at 10, 50, and 90% satisfied points

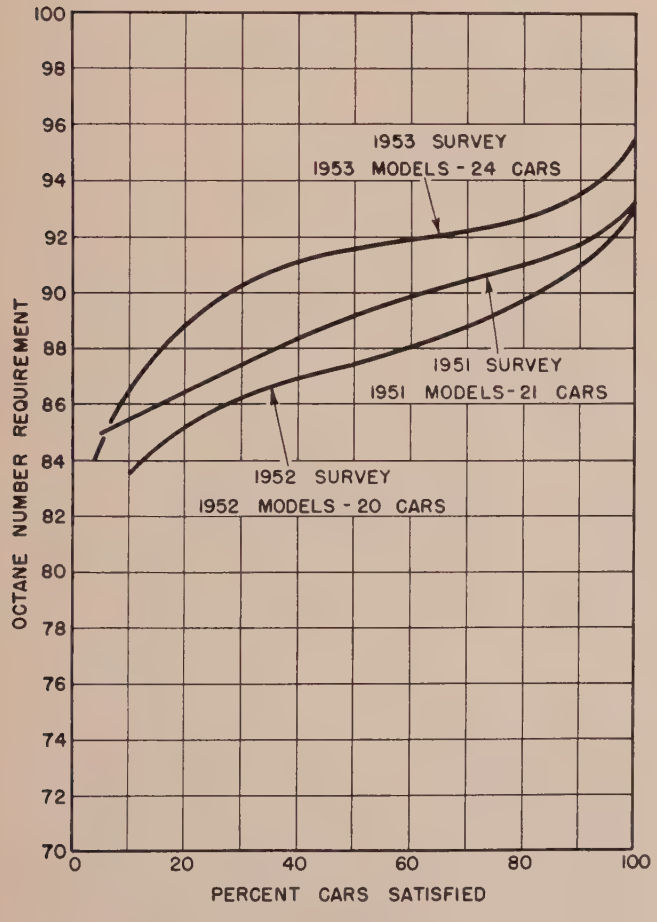

Fig. 2 – Comparison of maximum requirements of 1953 with earlier models of car G – primary reference fuels

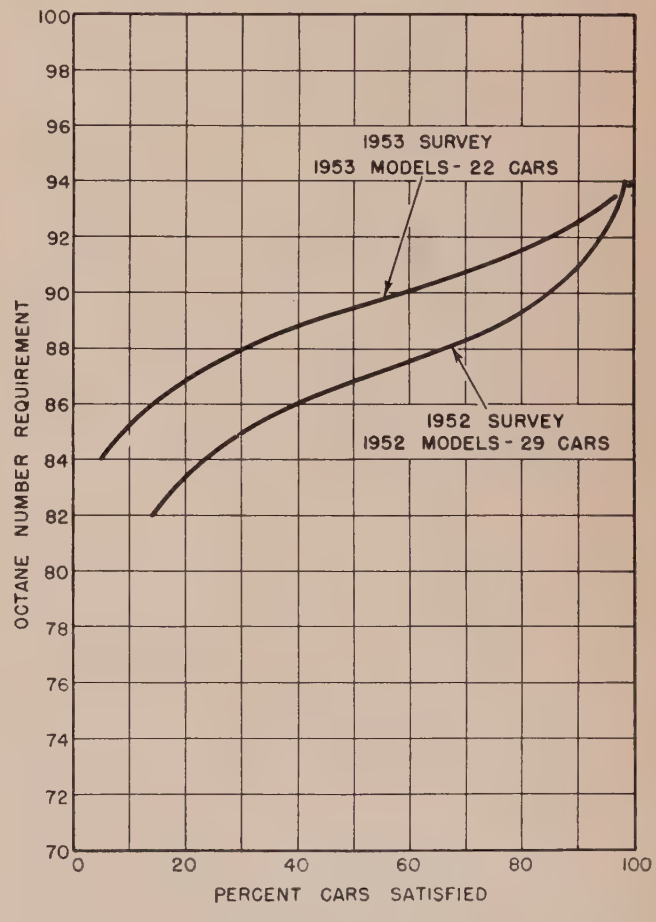

Fig. 3 – Comparison of maximum requirements of 1953 with earlier models of car I – primary reference fuels

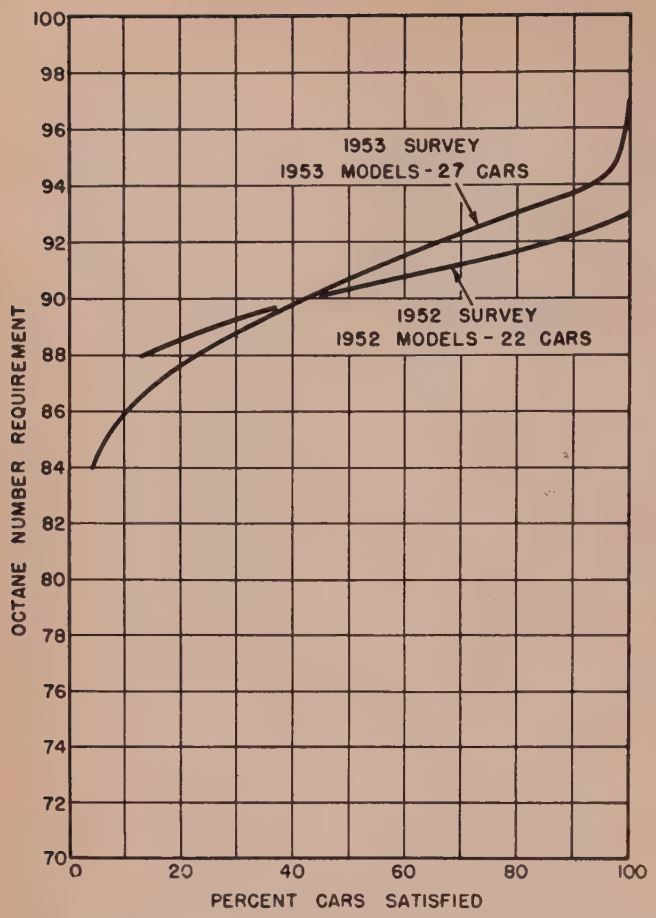

Fig. 4 – Comparison of maximum requirements of 1953 with earlier models of car L-1 – primary reference fuels

Table 5 – Research-Method Octane Number for Indicated Per Cent of Models Satisfied

Car Make	No. Tested	10% Satisfied			50% Satisfied			90% Satisfied		
		PR[a]	CR[a]	SR[a]	PR	CR	SR	PR	CR	SR
S	28	86	88	87	91	94	93	94	96	95
L-2	24	86	86	87	91	92	92	92	95	96
L-1	27	88	88	88	91	92	91	94	95	94
G	24	87	88	87	91	92	91	93	94	94
N-2	28	84	84	83	88	89	89	93	94	94
I	22	85	85	83	89	89	88	92	93	92
N-1	30	82	83	83	85	86	87	89	93	92
K	27	81	84	82	85	87	86	89	92	91
Q	25	77	79	77	85	86	85	89	90	89

[a] PR = primary reference fuels; CR = full-boiling-range reference fuels; SR = severity reference fuels.

Table 6 – Part-Throttle Knock – Primary Reference Fuels

Car Make	No. Tested	Per Cent Having Maximum Requirements at Part Throttle	Part-Throttle Requirement Minus Full-Throttle Requirement	
			Maximum	Average[a]
G	24	50	2	1
I	22	95	10	4
K	27	7	2	2
L-1	27	37	5	2
L-2	24	17	2.5	0.5
N-1	30	3	2	2
N-2	28	0	—	—
Q	25	64	Greater than 8	5
S	28	47	5.5	3

[a] Based only on those cars having maximum requirement at part throttle.

the vehicle tank was also tested.

Test Techniques

Octane-number requirement investigations were conducted under level-road conditions at engine speeds ranging from 750 rpm (or the lowest practical engine speed if 750 rpm could not be attained) through 2500 rpm.

For this survey a new technique which included both full- and part-throttle procedures was used. It differed from the previously used technique in that accelerations were made at a series of constant intake manifold vacuums from 10 in. of Hg to wide-open throttle. Thus, for the first time a uniform part-throttle as well as full-throttle technique was used. The detailed technique can be found in the 1953 CRC survey report.[1]

Discussion of Results

Octane-Number Requirements – The Research-method octane numbers of the 1953 reference fuels which satisfy 10, 50, and 90% of each of the nine models are given in Table 5 and Fig. 1. The models are listed in order of decreasing requirements at the 90% satisfied points, using full-boiling-range gasolines.

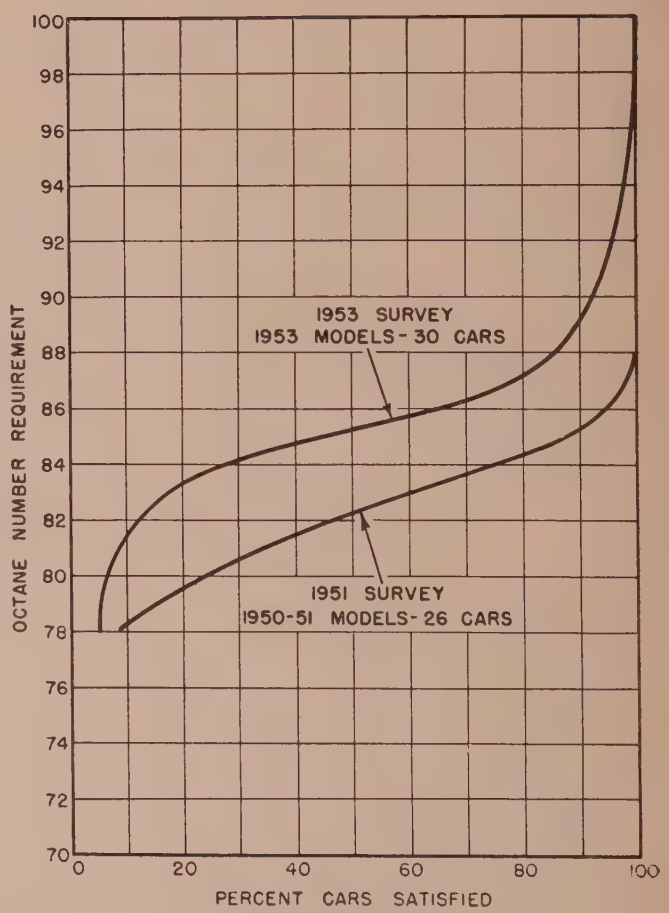

Fig. 5 – Comparison of maximum requirements of 1953 with earlier models of car N-1 – primary reference fuels

The relative Research-method octane-number requirements with the three sets of reference fuels varied among different models. Fig. 1 indicates that Research-method requirements with full-boiling-range gasolines were from 0 to 3 octane numbers higher than the primary-reference-fuel requirements at 10 and 50% satisfied and 1 to 4 octane numbers higher at 90% satisfied. In general the severity-reference-fuel requirements were within the range covered by the primary and full-boiling-range fuels.

The spread between the primary-reference-fuel requirements at the 10 and 90% satisfied points for the different car makes varied from a minimum of 6 octane numbers for makes G and L-2 to a maximum of 12 octane numbers for make Q. Thus, a given change in octane number would effect a greater change in per cent cars satisfied for makes G and L-2 than for make Q.

Comparison of 1953 with Earlier Models – Six of the 1953 model cars tested in the 1953 survey were of the same make as those tested in either the 1951 or 1952 surveys. Figs. 2 through 7 compare the maximum primary-reference-fuel requirements of 1953 and earlier models. The five 1953 models in which design changes had been made showed higher requirements above the 50% satisfied point than the earlier models. The greatest change was found in the 1953 model of make S (Fig. 7) which showed an increase in requirement from 88.5 to 94.5 octane number at the 90% satisfied point and from 83 to 91 octane number at the 50% satisfied point. Make Q (Fig. 6), having no significant design changes between 1952 and 1953 models, showed substantially the same requirements from the 50% satisfied point upward.

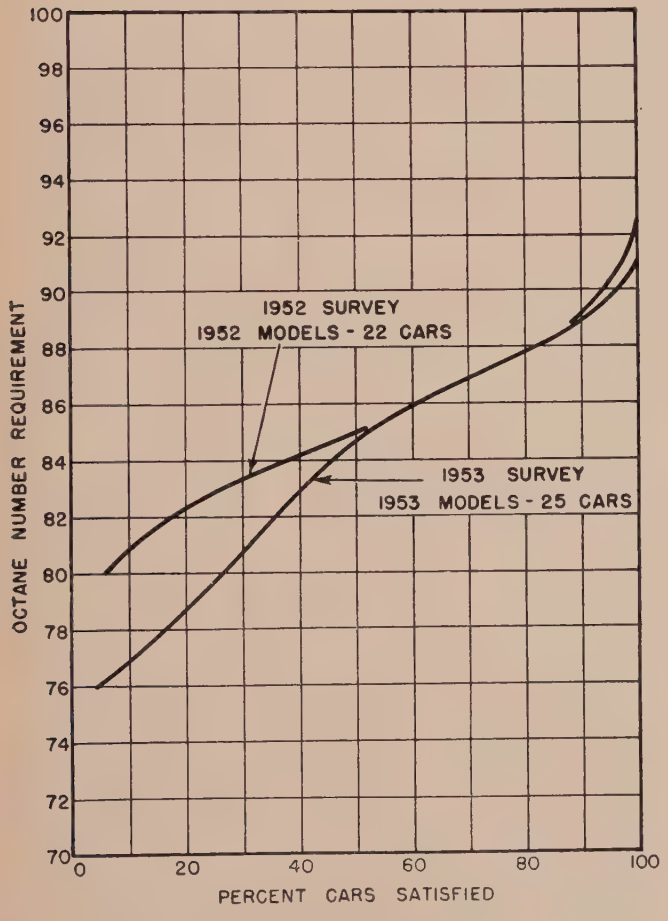

Fig. 6 – Comparison of maximum requirements of 1953 with earlier models of car Q – primary reference fuels

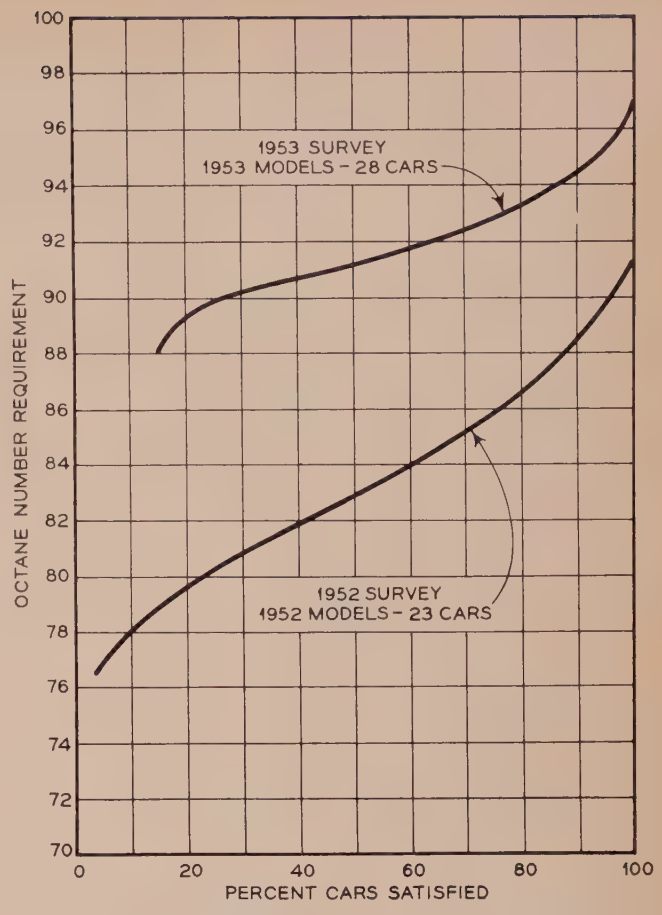

Fig. 7 – Comparison of maximum requirements of 1953 with earlier models of car S – primary reference fuels

Part-Throttle Knock – In the 1953 survey, for the first time, a uniform part-throttle test technique was used. When the maximum requirement was at part throttle, both full- and part-throttle requirements were reported in the present tests.

Table 6 summarizes the effect of part-throttle knock when primary reference fuels were used in nine different makes of cars—235 cars in all being used in the tests.

The percentages of cars having maximum requirements at part throttle show considerable variation, ranging from 95% for make I to 0% for make N-2. For the cars having maximum requirements at part throttle the average dif-

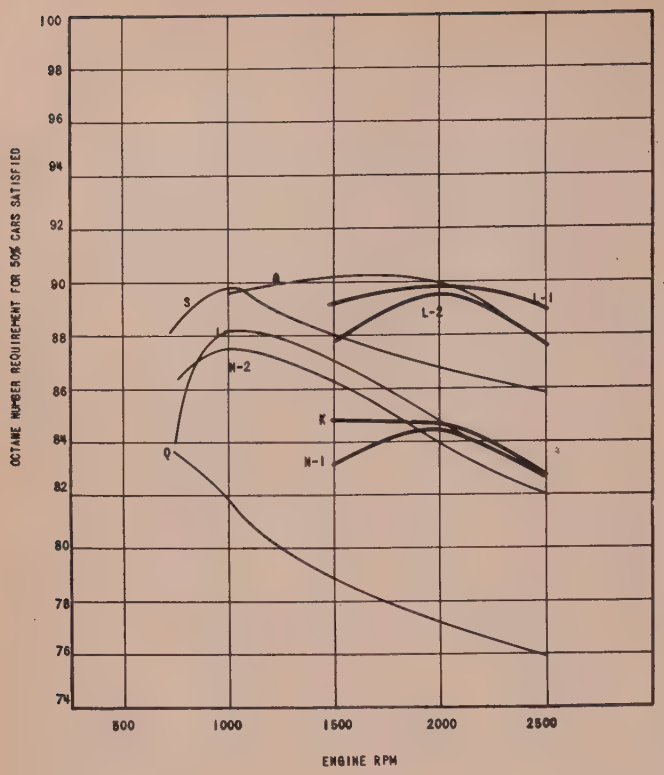

Fig. 8 – Effect of engine speed on requirement for individual car makes – primary reference fuels

ference between part- and full-throttle requirements varied from 0.5 octane numbers for make L-2 to 5 octane numbers for make Q. In individual cars this difference was as great as 10 octane numbers.

Effect of Engine Speed on Octane-Number Requirement – Characteristic curves of octane-number requirement versus engine speed for the individual car makes are shown in terms of primary reference fuels in Fig. 8 and in terms of full-boiling-range fuels in Fig. 9. These curves show the octane number at each speed required to satisfy 50% of the cars at that speed.

The per cent of cars of each make which developed maximum requirement at the various speeds is given in Table 7.

Surface Ignition – This survey was not designed specifically to investigate surface ignition; however, the test operators were requested to report any manifestations of uncontrolled combustion, such as wild ping or erratic knocking with the ignition off. The number of cars showing surface ignition on reference fuels at or above the maximum requirement level and on the tank fuel is given in Table 8.

The tank fuel and reference fuel data are not directly comparable since in some cases tank fuels were considerably above and in other cases were considerably below the octane-number requirement of the car. Of the 16 cars having surface ignition on the tank fuel, 14 were high-requirement cars using premium-grade gasoline.

Tank Fuel – For each car the observer first tested the fuel found in the tank to determine whether or not knock occurred and obtained a sample of the tank fuel for Motor- and Research-method ratings. In addition each car owner was questioned as to the grade of gasoline in the vehicle fuel tank and whether or not he had encountered knock with this fuel.

The percentages of the cars that operated without knock on the tank fuel and the corresponding percentages reported knock-free by the owners are shown in Table 9 for this and previous surveys.

In the 1951 and 1952 surveys the percentages of observers and owners reporting knock were nearly equal. In 1949 and 1953, however, the percentage of cars found knock-free by the observers was appreciably less than reported to be knock-free by the owners.

Table 7 – Per Cent of Cars Having Maximum Requirement at Engine Speed Indicated

Car Make	750 to 999 Rpm	1000 to 1399 Rpm	1400 to 1799 Rpm	1800 to 2199 Rpm	2200 and Over Rpm
Primary Reference Fuels					
G	0	20	51	29	0
I	23	72	5	0	0
K	0	11	47	34	8
L-1	0	0	30	50	20
L-2	0	0	23	67	10
N-1	0	3	56	38	3
N-2	46	51	3	0	0
Q	70	20	5	5	0
S	47	39	6	5	3
Full-Boiling-Range Gasolines					
G	0	5	40	51	5
I	13	68	14	0	5
K	0	12	38	30	20
L-1	0	0	39	52	9
L-2	0	9	13	55	23
N-1	0	0	50	47	3
N-2	41	48	7	4	0
Q	78	17	5	0	0
S	45	45	7	3	0
Severity Reference Fuels					
G	0	5	43	52	0
I	19	57	19	0	5
K	0	12	37	35	16
L-1	0	0	38	50	12
L-2	0	9	18	64	9
N-1	0	0	43	36	21
N-2	29	52	19	0	0
Q	72	28	0	0	0
S	40	44	8	4	4

Table 8 – Cars Having Surface Ignition At or Above Maximum Requirement Level

Car Make	No. of Cars Tested	Number of Cars with Surface Ignition: On Tank Fuels	Number of Cars with Surface Ignition: On Ref Fuels At or Above Max Octane Req Level
G	24	2	3
I	22	3	6
K	27	1	0
L-1	27	2	1
L-2	24	4	5
N-1	30	0	0
N-2	28	4	5
Q	25	0	0
S	28	0	0
Total	235	16	20
% of total cars		7	9

Comparison of Hill-Climbing and Level-Road Requirements – Four laboratories obtained maximum primary-reference-fuel requirements of 32 cars under hill-climbing as well as level-road conditions. The technique used consisted of operating the vehicle at constant speed under maximum knock conditions. The procedure is described in detail in the CRC report,"Octane-Number Requirement Survey, 1953." With the exception of one car, which showed no increase in requirement, the maximum requirements under hill-climbing conditions were higher than those obtained on the level road. The average increase in maximum requirement was 2.4 octane numbers.

One laboratory tested 14 of the above cars using all three types of reference fuels. The results with the severity and full-boiling-range reference fuels were similar to those with the primary reference fuels and did not differ from the results obtained in the 32-car sample.

Confidence Limits – The question frequently arises regarding the significance of distribution curves based on a 20- or 25-car sample. To help clarify this question the standard deviation and the confidence limits for 95% certainty in terms of octane numbers for the nine models tested in the 1953 survey have been calculated from the primary reference fuel test data and are shown in Table 10. The method of calculation is given later, in the appendix.

The confidence limits depend not only on the sample size but also on the spread in requirement, that is, the slope of the distribution curve. For example, for make Q, where the spread between the 10 and 90% points was 12 octane numbers (Fig. 1) the 95% confidence limits were ± 2.4 at the 50% satisfied point. For make G where the spread was only 6 octane numbers the confidence limits were ± 1.4.

In a previous paper by Best, Raymond, and Williams,[2] it was reported that "the confidence limits for 95% certainty based on a 20-car sample are approximately ± 3 to 4 octane numbers between the 10% and 90% satisfied points." In that paper, the confidence limits were based on a spread of 14 octane numbers between the 10 and 90% points of the curve for all cars given in Fig. 1 of the CRC report "Octane-Number Requirement Survey, 1951."

The confidence limits in Table 10 are less than those reported by Best et al. This is to be expected, since the spread in requirement among cars of a single model will in general be less than the spread for several models. Therefore, for results of equal significance, a survey involving cars of only one make will usually require a much smaller sample than one including all makes.

Table 9 – Per Cent of Cars Knock-Free on Tank Fuel

Year	Observers	Owners
1949	52	62
1951	63	64
1952	65	69
1953	46	60

Table 10 – Standard Deviation and 95% Confidence Limits, Primary Reference Fuels

Car Make	Number Tested	t Factor	Standard Deviation, Octane Numbers	95% Confidence Limits at 50% Satisfied, Octane Numbers ±
S	28	2.052	2.68	1.3
L-2	24	2.069	2.74	1.4
L-1	27	2.056	2.77	1.4
G	24	2.069	2.64	1.4
N-2	28	2.052	3.18	1.5
I	22	2.080	2.60	1.5
N-1	30	2.045	3.92	1.8
K	27	2.056	3.12	1.5
Q	25	2.064	4.63	2.4

Summary

During the 1953 CRC Octane-Number Requirement Survey, 24 laboratories obtained data on a total of 235 cars, representing nine 1953 models having new-design engines or transmissions. Octane-number requirements were obtained in the cars as received from the owners, using primary and severity reference fuels and a series of full-boiling-range gasolines. The sensitivity (Research-

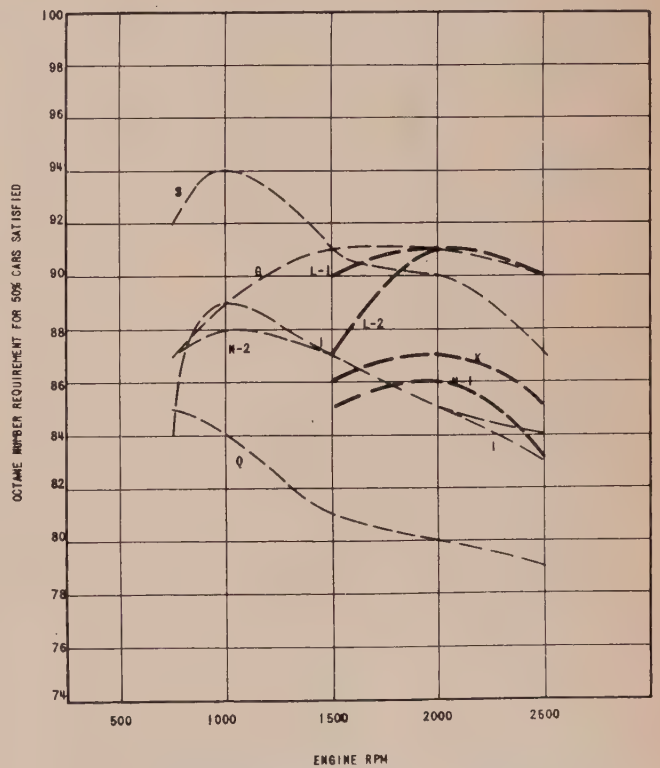

Fig. 9 – Effect of engine speed on requirement for individual car makes – full-boiling-range reference fuels

[2] See SAE Transactions, Vol. 62, 1954, pp. 288-297: "Anti-knock Requirements of Passenger Cars – 1951-1952," by H. W. Best, L. Raymond, and R. K. Williams.

method minus Motor-method rating) of the severity and full-boiling-range fuels varied with octane level in a manner similar to commercial gasolines.

The following results were obtained:

1. The Research-method ratings of full-boiling-range gasolines required to satisfy 50% of the cars varied from 86 to 94 octane number for the nine models tested. The Research-method rating required to satisfy 90% of the cars of a given model ranged from 90 to 96 octane number.

2. The requirements of the nine individual models with full-boiling-range gasolines were from 0 to 3 octane numbers higher than the primary-reference-fuel requirements at 10 and 50% cars satisfied and 1 to 4 octane numbers higher at 90% cars satisfied.

3. In general, the severity-reference-fuel requirements were within the range covered by the primary and full-boiling-range fuels.

4. Six of the 1953 models tested were of the same make as those tested in previous surveys. One model, with no significant design changes between 1952 and 1953, showed substantially no change in requirement in the 50 to 90% satisfied range. The other five models which did have significant design changes showed increases from 2 to 6 octane numbers over previous models.

5. The 95% confidence limits of the distribution curves for the nine models ranged from ± 1.3 to ± 2.4 octane numbers at the midpoint of the curve (50% satisfied). Only two of the nine models tested had confidence limits greater than ± 1.5 octane numbers.

6. The maximum requirement occurred at part throttle in 95% of the cars of one model, the other models ranging from 0 to 64%. For cars having maximum requirements at part throttle, the average difference between part- and full-throttle requirement varied from 0.5 to 5 octane numbers for the different models. The maximum increase observed in any one car was 10 octane numbers.

7. The speed at which the majority of the cars of an individual make showed maximum requirement varied from 750 to 2000 rpm.

8. Test observers reported 46% of the cars to be knock-free on the tank fuel while the owners reported 60% of the cars to be knock-free.

9. Thirty-two of the cars were tested under hill-climbing conditions. The average requirement of these cars under hill-climbing conditions was 2.4 octane numbers higher than the level-road requirement.

10. Surface ignition was observed in 9% of the cars when operating on reference fuels at or above the maximum requirement level and in 7% of the cars operating on the tank fuel.

Acknowledgment

The authors acknowledge the work done by the representatives of the cooperating organizations who obtained the data as well as those who analyzed the results.

The organizations which contributed data were: Atlantic Refining Co.; California Research Corp.; Chrysler Corp.; Continental Oil Co.; E. I. du Pont de Nemours & Co., Inc.; Ethyl Corp.; Ford Motor Co.; General Motors Corp., Research Laboratories Division; General Petroleum Co.; Gulf Research and Development Co.; Pan American Refining Corp.; Phillips Petroleum Co.; Pure Oil Co.; Richfield Oil Corp.; Shell Oil Co.; Sinclair Research Laboratories, Inc.; Standard Oil Development Co., N. J.; Standard Oil Co. (Ind.); Standard Oil Co. (Ohio); Sun Oil Co., Pa.; Texas Co., and Universal Oil Products Co.

APPENDIX

Determination of Standard Deviation and Confidence Limits

The standard deviation for each make was calculated from the primary-reference-fuel maximum requirement test data using the formula:

$$s = \sqrt{\frac{\Sigma(x - \bar{x})^2}{N - 1}} \qquad (1)$$

where:

s = Standard deviation
x = Individual car octane-number requirement
$\bar{x}$ = Average octane-number requirement
N = Number of cars tested

In order to obtain some estimate of the standard deviation at the 50% decile, the following formula, taken from Kendall's "Advance Theory of Statistics," Vol. 1, p. 225, was used:

For 50% satisfied:

$$S_{50} = \frac{1.2533s}{\sqrt{N}} \qquad (2)$$

It should be pointed out that equation (2) was derived from data having a normal distribution. Since the octane-number-requirement data obtained during the 1953 CRC survey did not have a normal distribution, there is some doubt as to the validity of using an empirical formula such as Kendall has derived to compute the confidence limits of a segment of the distribution curve. However, the authors have taken the calculated risk that this formula which is based on normal distribution gives a reasonably accurate picture for the survey data.

The 95% confidence limits were computed using the following formula:

For 50% satisfied:

$$U_{50} = t(S_{50}) \qquad (3)$$

where:

U_{50} = Confidence limit

t = A factor taken from standard statistical tables for the 95% certainty level. The values of t vary slightly with sample size, as shown in Table 10.

Method of Scavenging Analysis for 2-Stroke-Cycle Diesel Cylinders

W. H. Percival, Research Laboratories Division, GMC

This paper was presented at the SAE National Diesel-Engine Meeting, Cleveland, Oct. 26, 1954.

EVERY builder of 2-stroke-cycle diesel engines is faced with the problem of how to improve the scavenging of his cylinder, especially as the customer keeps demanding more power but no more smoke. He may try increasing engine speed or he may try pumping more air through the cylinder, but in either case, the power, fuel economy, and smoke conditions could be further improved by purging more of the residual gas and trapping more fresh air.

The builder has a choice of two general methods to improve scavenging:

1. He can study the design factors of his engine; that is, port shape and angle, valve and port timing, scavenging ratio, airbox size, exhaust system. After comparing these factors with similar engines and studying the recommendations of authorities on 2-stroke scavenging, he can make changes in his engine and run tests to see if improvements have been made.

2. He can investigate the flow conditions inside the cylinder. This second method can be further divided into dynamic and static investigations.

The dynamic investigation involves instrumentation, such as sampling valves and gas analysis apparatus, and requires considerable experience to operate successfully.[1, 2] It does give an answer as to how well the cylinder is scavenged, but it does not tell how the air is going through the cylinder nor how the scavenging can be improved. Another dynamic method employs high-speed motion-picture photography to study the path of the inlet air and exhaust gas within the cylinder. This method may give a qualitative answer as to how well the cylinder is scavenged and also may point to how the scavenging can be improved. However, it requires elaborate equipment and requires considerable modification of the cylinder, which might be impossible in some cases. In addition, there is the problem of presenting the results. Unless one is able to study the motion pictures thoroughly, he may find it difficult to understand the flow process. Where three-dimensional flow is present, the method is not well suited.

The static analysis involves studying the flow in a cylinder under steady-flow conditions. The cylinder is usually mounted on a flow bench with the piston fixed in one position uncovering the ports.

HOW to go about improving scavenging efficiency in 2-stroke-cycle diesel engines through use of a static method of analysis is discussed here. Briefly, the steps are:

1. Determine airflow pattern in the existing cylinder design by means of instrumentation, and find the synthetic scavenging efficiency by plotting axial and tangential velocity components.

2. Decide what should be improved and the method of accomplishing this improvement, such as using a different port shape and angle.

3. Test the new design on the flow bench and compare with the original design for scavenging efficiency, tangential velocity distribution, and pressure drop.

4. Test the improved design in the engine.

[1] See SAE Transactions, Vol. 62, 1954, pp. 486-502: "Scavenging the 2-Stroke Engine," by C. F. Taylor and A. R. Rogowski.

[2] See "Scavenging of 2-Stroke-Cycle Diesel Engines," by P. H. Schweitzer. Pub. by Macmillan, New York, 1949.

More quantitative information can be gained about the flow path through the cylinder by this method, and it usually requires less elaborate equipment. However, the question arises as to whether the flow picture is the same as in a running engine.

At General Motors Research Division, all the methods described have been used over the past 20 years in studying the 2-stroke engine.

The design factors such as port shape, angle, and timing were evolved by extensive testing of single and multicylinder engines. The thoroughness of scavenging was determined by electrically operated sampling valves. In spite of the sampling difficulties due to high pressures and lack of an homogeneous mixture, sufficient information was gained to show us that an improvement could be made in scavenging the 2-stroke cylinder.

In addition, high-speed motion pictures have been made of flow through a glass cylinder in a motoring engine. However, the interpretation of these films left much to be desired. Only a rough estimate could be made of the velocities, while the "plane" of the picture was practically unknown.

Static Method

We are now pursuing the static method for studying scavenging. We feel that this method gives a reasonably accurate picture of airflow through a cylinder, especially when the effect of piston position is not significant, as in uniflow scavenging. It is believed that the scavenging flow profile, after the exhaust blowdown period, is determined only by the geometry of the cylinder, while the scavenging pressure differences determine the magnitude of the profile—the fact that the process takes place in a very short interval of time and at higher temperatures in a running engine does not, in our opinion, change the flow picture appreciably.

The method has not been applied to cross- or loop-scavenge designs because there is some indication that the flow path is dependent on the piston position relative to the inlet ports.

What we were striving for as the "ideal" scavenging process was a 2-stroke cycle which functioned like a 4-stroke cycle; in other words, a moving piston of fresh air driving out before it a column of exhaust gas. We were certain this was not the case, but other than that we did not know what was going on inside the cylinder.

The first attempt consisted of a water analogy. Under conditions where gravity does not influence the flow and the density changes are relatively small, water can be used in a model to simulate air in the prototype. A transparent plastic cylinder was made geometrically similar to the prototype cylinder and the Reynolds number maintained in the same order of magnitude as in air. This enabled us to decrease the water velocity until it was possible to observe the flow by eye instead of resorting to photography.

The setup is shown in Fig. 1. The water-pump inlet was placed downstream of the cylinder head with straightening vanes between. Fig. 2 is a view inside the tank showing the adjustable ports made from ball bearings.

From this installation we gained some useful information about helical flow through a cylinder. We learned that, for a particular port configuration, reverse flow existed along the wall as well as at the core of the cylinder, but that the quantity flowing in the core was negligible in comparison to that along the wall. By changing the port angles we were able to study the effect on the reversed-flow regions qualitatively. Also noted were radial-flow components as well as axial and tangential. It was apparent that to measure these three velocity components would require a rather special instrument. The water-flow method had served its purpose, but it was believed that the use of air would be more suitable for studying flow in greater detail.

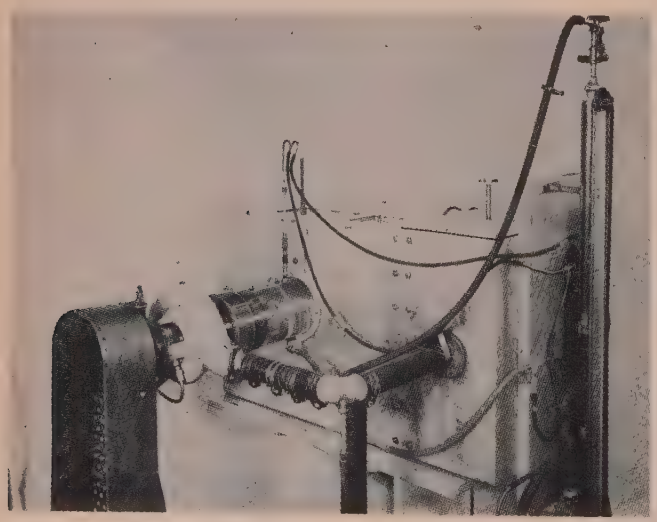

Fig. 1 – Water analogy

Fig. 2 – Ball ports

The Author

W. H. PERCIVAL (M '48) is senior research engineer in the Research Laboratories of General Motors Corp. in Birmingham, Mich. He received a B.S. in Mechanical Engineering from Iowa State College in 1942. After serving in the A.A.F. in the Pacific area during the Second World War, Mr. Percival received his M.S. in Mechanical Engineering from M.I.T. in 1947. Since then, he has been connected with the General Motors Research Laboratories.

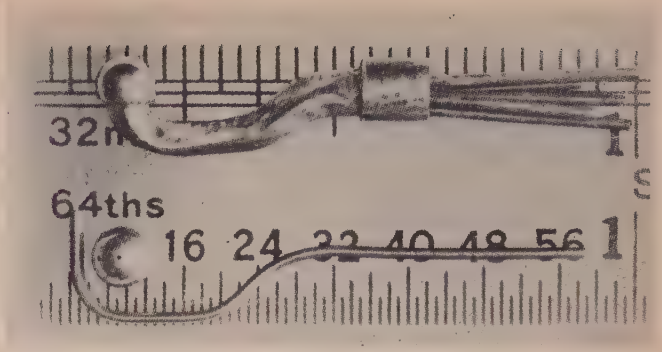

Fig. 3 – Pitot sphere head

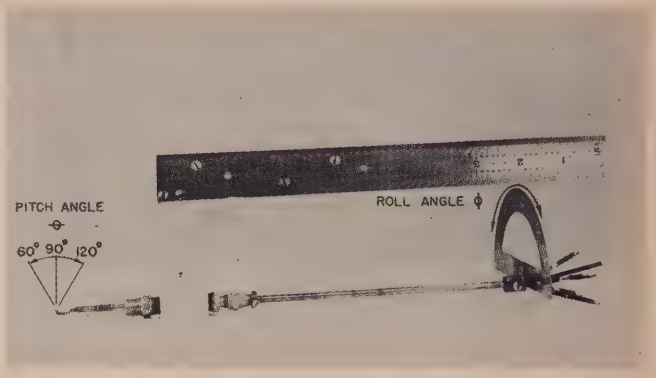

Fig. 4 – Pitot sphere instrument

Instrumentation

A survey was made of "point" pressure recording instruments including the pitot static tube, pitot claw, pitot cylinder, Cole pitometer, and others.[3, 4] None seemed to be suited for measuring three-dimensional flow, where the stream lines are helical, without a complicated traversing and rotating mechanism. In addition, some were too bulky and others subject to errors due to change in turbulence intensity and transverse flow along the supporting shaft.

The instrument which most nearly satisfied the requirements appeared to be the pitot sphere.[5, 6] It was developed by the Dutch in 1928 and was commercially available in Germany before the war in sizes as small as 8 mm. A model developed at the Research Laboratories is shown in Figs. 3 and 4. The instrument head is a brass hemisphere 0.1-in. in diameter supported at the rear by a gooseneck arrangement which permits it to be inserted through a 0.20-in. opening. One 0.008-in. hole is drilled in the center, while four holes are each drilled approximately 42 deg from the center hole, two in the plane of the support shaft and two at 90 deg to this plane. These five holes lead to five 0.020-in. OD by 0.014-in. ID brass tubes which transmit the pressure and serve as the support for the hemisphere. These five tubes are soldered into five 0.032-in. brass tubes which lead up the 0.156-in. steel support shaft. At the top are five radial tubes to which are attached the manometer connections using 1/16-in. surgical tubing. Fig. 5 shows the necessary plumbing and manometers.

This instrument has the following advantages over other point flow measuring devices:

1. It can be calibrated in a low-turbulence wind tunnel and then used inside a cylinder where the turbulence intensity is high without appreciable error.

2. The error due to transverse flow along the support shaft is negligible.

3. The error when traversing through a steep velocity gradient is not serious because of the small diameter. However, this is the major error and results in an apparent increase in flow through the cylinder. Integration of the velocity profile gives a 2 to 4% increase over the actual flow measured by an orifice meter. In a typical cylinder the difference in velocity across the 0.1-in. diameter sphere can amount to 8 fps, with the flow angle changing as much as 10 deg.

How the Pitot Sphere Is Used

How is the Pitot sphere used? From Fig. 4 can be seen the two angles which must be determined in order to locate the velocity vector. The roll angle ϕ is found by merely rotating the instrument shaft until the pressures measured at holes 4 and 5 (see Fig. 5) are equal. Either a U-tube manometer or sensitive diaphragm-type gage can be used for this purpose. Finding angle ϕ locates the velocity vector in a plane passing through the instrument axis. In order to find angle θ, the pitch angle, the instrument must be calibrated beforehand. This was done by holding the instrument in a compound rest with the instrument head in an open airstream. The calibrating setup is seen in Fig. 6. The instrument shaft was set at various pitch

[3] See NACA TM 969 (1941), "Experiences with Flow Direction Instruments," by B. Eckert.
[4] See SAE Quarterly Transactions, Vol. 2, January, 1948, pp. 104-116: "Instrumentation for Development of Aircraft Powerplant Components Involving Fluid Flow," by S. J. Markowski and E. M. Moffatt.
[5] See *VDI Zeitschrift*, Vol. 82, Jan. 8, 1938, pp. 52-53: "Spherical Probe of Small Diameter for Pressure and Velocity Measurements," by K. Strauss.
[6] See NACA TM 688 (1932), "Speed and Pressure Recording in Three-Dimensional Flow," by F. Krisam.

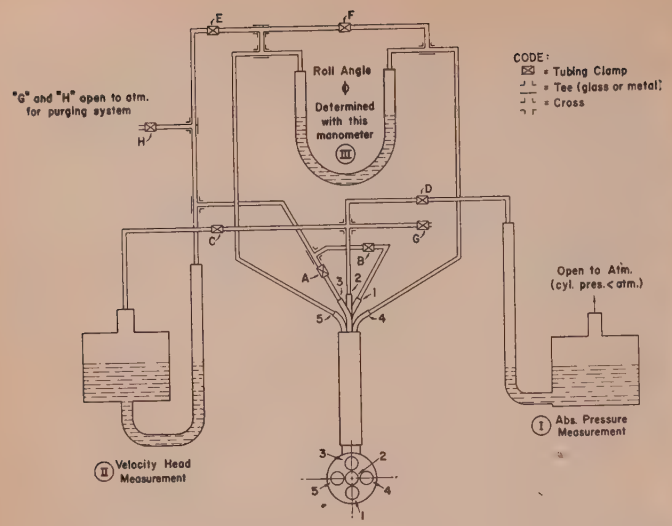

Fig. 5 – Manometer layout for pitot sphere

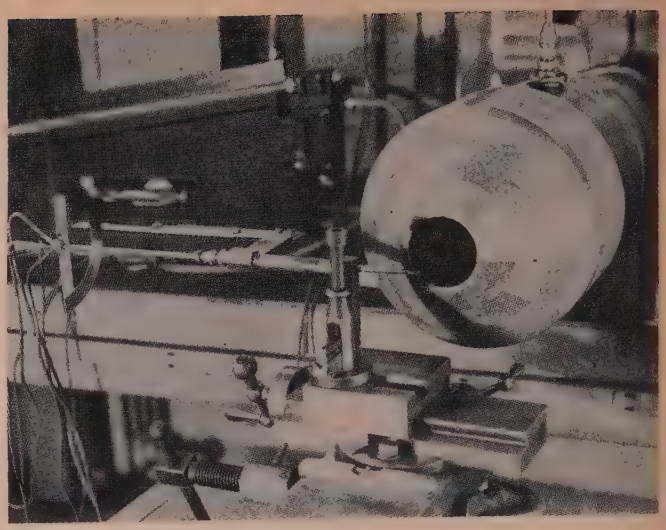

Fig. 6 – Calibration setup

angles from 45 to 135 deg, while the instrument head was kept at the same point in the airstream. At 5-deg intervals the following dimensionless ratios were determined:

$$P_{tr} = \frac{P_{\text{total}} - P_2}{P_2 - P_{4,5}}$$

$$P_{sr} = \frac{P_2 - P_{\text{static}}}{P_2 - P_{4,5}}$$

$$\theta_r = \frac{P_2 - P_3 \text{ (or } P_1)}{P_2 - P_{4,5}}$$

These values were then plotted, and the resultant curves can be seen in Fig. 7. Note that in finding θ_r, the pressure P_1 is used where the angle θ is less than 90 deg, and P_3 when greater than 90 deg. This was done in order to maintain the small holes 1 and 3, on the surface of the hemisphere, always within about 45 deg of the airstream. Beyond an angle of 45 deg the error in measuring θ increases rapidly due to the influence of turbulence and Reynolds number.

With the instrument calibrated, it can then be used to explore an unknown three-dimensional flow within a cylinder, providing the pitch angle is within the calibration range. The instrument is inserted through a hole tapped in the cylinder wall perpendicular to the cylinder axis. Any plane can be chosen, provided it is not too close to the ports or the cylinder head where extreme radial flow may exist. It has been found satisfactory to traverse a plane located about midway between the ports and the valves in order to obtain a representative scavenging picture. Here the radial-flow component is small, the pitch angle usually ranging from about 75 to 105 deg.

Fig. 8 is a view of the airflow bench being used at present. The components are as follows:

1. Test cylinder (inverted).
2. Pitot sphere instrument.
3. Plenum chamber.
4. Segmental orifice meter.
5. Flow control valve.
6. Housing enclosing centrifugal blower (7½ hp).

The cylinder is connected to the inlet side of the blower instead of the outlet as in an engine installation. This was done in order to insure quiescent air surrounding the cylinder ports and to facilitate installing the instrument.

The cylinder was usually placed on a dummy head with open valves to simulate the actual cylinder geometry, although the effect of a downstream disturbance on the velocity profiles is very slight.

Cylinder sizes traversed have been from 4¼ to 8½ in. in diameter, but 16-in. cylinders could be studied by traversing from both sides. Near the cylinder wall, readings are taken at about ⅛-in. intervals, increasing to about ⅜ in. near the center. It requires from 5 to 10 min to get the data for one point in the cylinder because of the restricted airflow through the small holes and tubes.

When coefficient θ_r is computed for each point across the cylinder, the pitch angle θ follows from Fig. 7. Then the corresponding values of P_{tr} and P_{sr} can be found for that angle, and the value $P_{\text{total}} - P_{\text{static}}$, the velocity head, can be computed. The velocity follows from the relation $V = 18.3\sqrt{P_t - P_s/\rho}$ where V is in fps, $P_t - P_s$ in in. of H_2O, and ρ in lb per cu ft. For the velocity profiles presented here an average density was used, but for more precise work the decrease in density toward the center of the cylinder should be taken into account in computing velocity at each point as well as volume flow.

As was mentioned, the velocity vector usually has components in the axial, tangential, and radial

directions, although the radial are small. Those in the axial and tangential directions only are of interest, the axial as a measure of how well the cylinder is being scavenged and the tangential as a measure of the residual swirl which is necessary for proper mixing of the air and fuel spray. The question of swirl is discussed later.

Scavenging Profiles

Fig. 9 shows a typical axial velocity profile across a 6½-in. cylinder diameter with ports inclined 10 deg to the radial, all in a plane perpendicular to the cylinder axis. The pitot sphere was traversed twice across the midplane of the cylinder with the inlet ports and exhaust valves full open. Note that the two profiles taken at 90 deg to one another are very nearly matched. Because of this, one traverse is usually sufficient unless it is noted that there is considerable difference in the profiles between one half of the cylinder and the other. Fig. 10, giving the tangential velocity distribution, shows the center of rotation to be slightly off the cylinder axis. Note in the tangential velocity profile the abrupt change from a form of "wheel" rotation near the wall to a free vortex at a radius of about 2½ in.

Figs. 11 and 12 present the axial and tangential velocity distributions for three planes, near the ports, the midplane, and near the cylinder head for a 6½-in. cylinder. The cylinder port geometry was slightly different from that of Figs. 9 and 10, and the port angle was 11 deg. The axial plot, Fig. 11, shows similarity between the three positions except for the valve end of the cylinder where less reverse flow occurs. The tangential velocity distribution indicates an energy loss as the air moves down the cylinder from the ports to the valves. This is apparently due to internal shear between the adjacent layers of gas rotating at different speeds and at different angles. The effect of wall

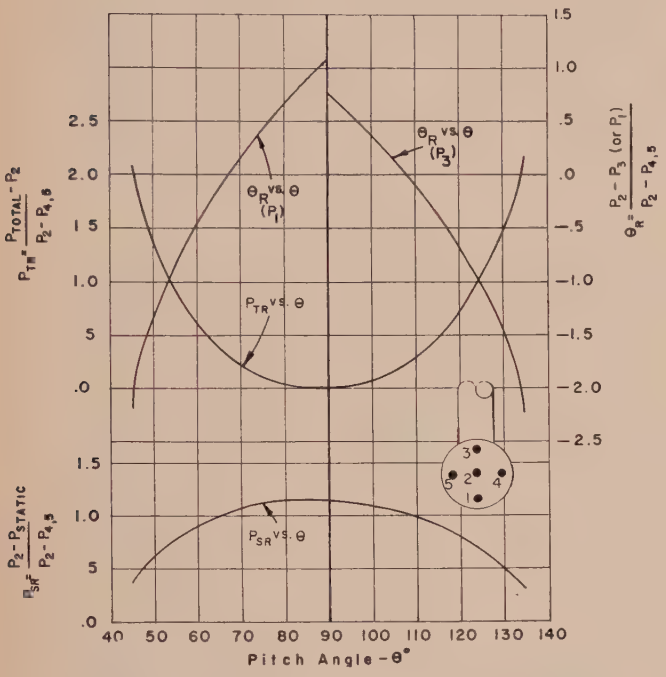

Fig. 7 – Calibration of pitot sphere No. 2 for pitch angle, static pressure, and total pressure

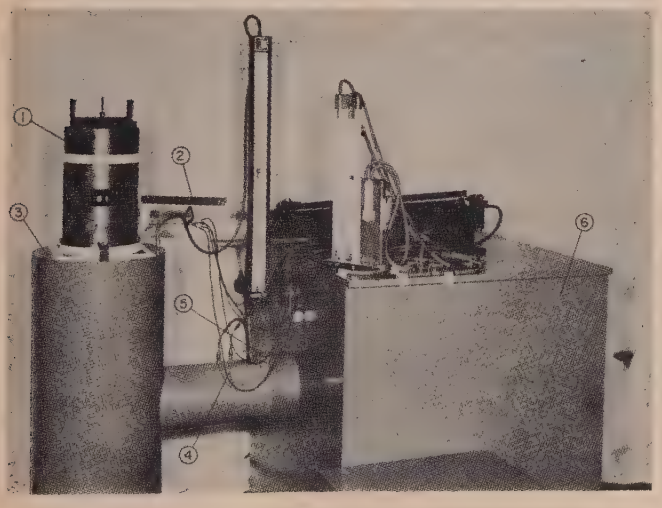

Fig. 8 – Airflow bench

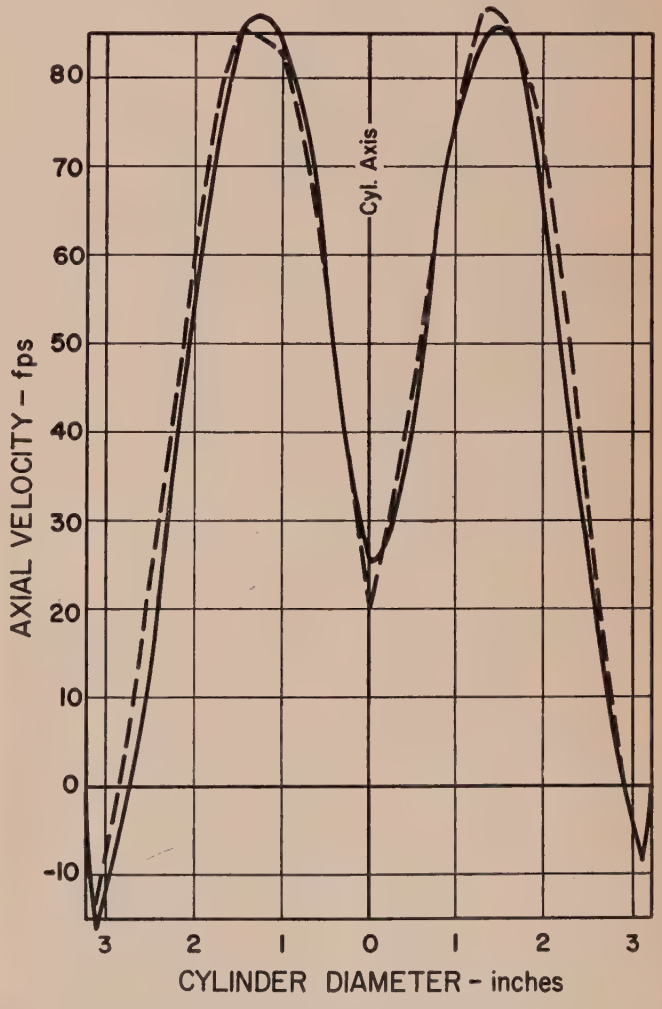

Fig. 9 – Axial velocity distribution across cylinder

friction does not appear to be so significant as internal friction.

Figs. 13 through 17 present the effect of port entry angle on the axial velocity distribution. These tests were run on a series of six identical liners, each having two rows of holes drilled at angles from 4 to 40 deg (measured from the radius). These holes had a length/diameter ratio of approximately 1 and an area ratio (cylinder/ports) of 6. The point of maximum velocity appears to move radially outward as the angle increases until it reaches the cylinder wall at about 30 deg. The tangential velocity distributions, which are not shown, are similar to those of Figs. 10 and 12, beginning as a free vortex, evolving into a combination of a free vortex and a forced vortex, until finally at about 30 deg the forced vortex or "wheel" rotation predominates. The axial and tangential distributions for 40-deg ports appear to be very similar to those found in "cyclone" dust collectors.[7]

How the pressure drop varies for equal mass flow through the cylinders is shown in Fig. 18. The pressure drop was measured between atmosphere and a point downstream of the cylinder where no rotating flow was occurring. It can be seen that for angles beyond 16 deg the pressure drop increases rapidly. This is apparently the result of an increase in internal shear as the tan-

[7] "Cyclone Dust Collector Design," by Melvin W. First. Paper No. 49-A-127 for meeting Nov. 27-Dec. 2, 1949.

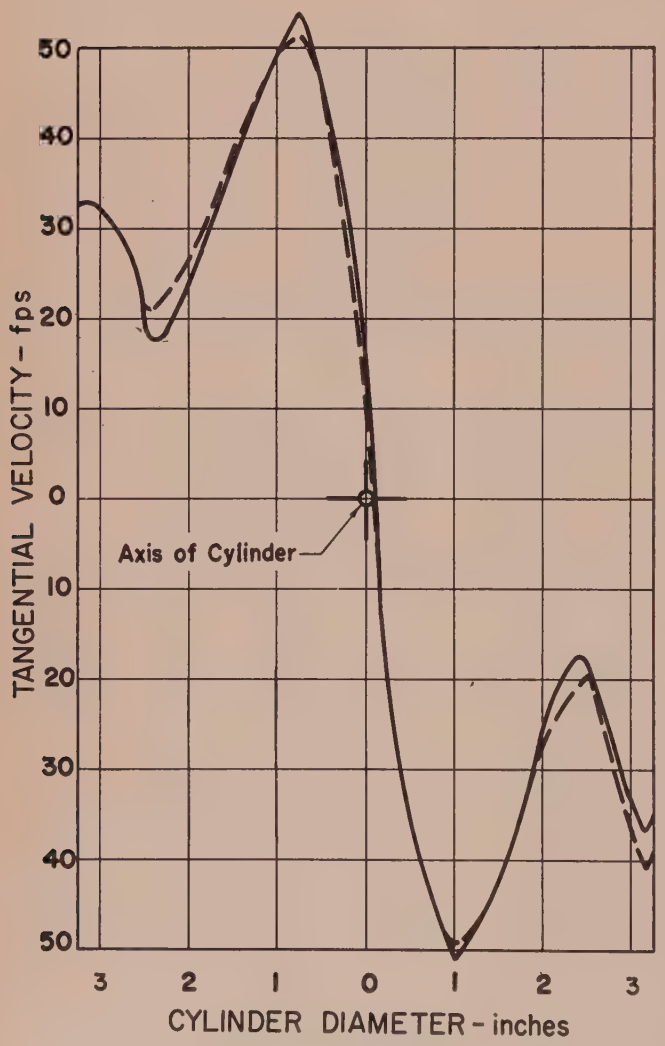

Fig. 10 – Tangential velocity distribution across cylinder

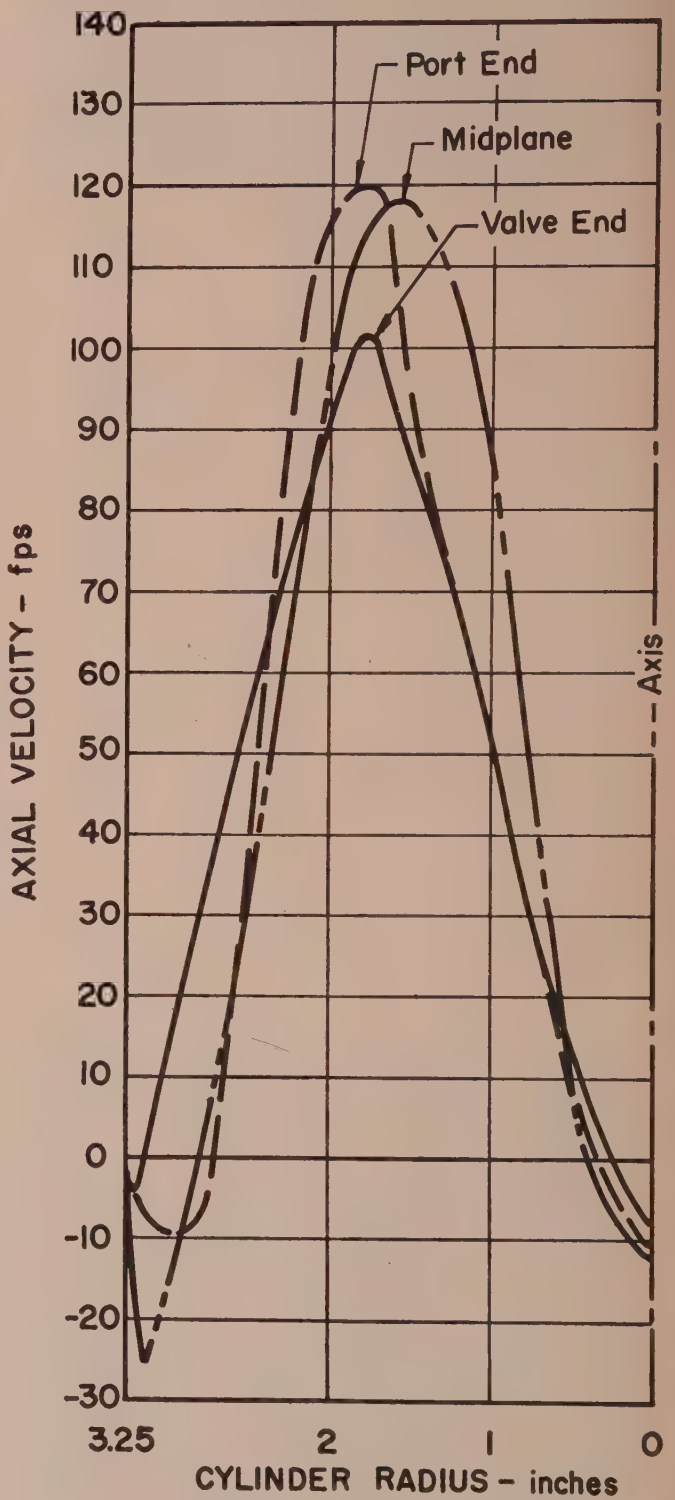

Fig. 11 – Axial velocity distribution across cylinder at three planes

gential distribution gradually changes from a free vortex to a forced vortex.

Synthetic Scavenging Efficiency

After the data for axial and tangential velocity have been plotted for a number of cylinders, it becomes necessary to establish some rational basis for comparison. A method has been developed, based on integrating the axial velocity profiles, which might be termed a synthetic scavenging analysis. It is as follows:

From the axial velocity profile, the net volume of revolution is found by the use of an Amsler integrating machine. This represents the flow through the cylinder at the particular plane traversed. Then the mean axial velocity line is drawn on the profile. This distance from the "zero" velocity line to the mean velocity line may be thought of as the length of a fictitious cylinder. For a scavenging efficiency of 100% the axial velocity profile would be represented by the mean velocity line. In order to judge how well the cylinder is scavenged, the volume of revolution of the positive area under the mean velocity line and enclosed by the "envelope" of the axial velocity profile is derived by integration as before. This volume of "flow" is expressed as a percentage of the mean flow and is termed the synthetic scavenging efficiency, η_s.

The area enclosed by the curve above the mean axial velocity line is considered to be "lost" air. The value of scavenging efficiency obtained in this manner is, therefore, based on a scavenging ratio (or delivery ratio) of unity.

Fig. 19 presents the synthetic scavenging efficiency for three simple velocity profiles having triangular "envelopes." These profiles approximate some of the actual profiles noted in Figs. 13-17, except that no reverse flow is present.

How reverse flow is treated is shown in Fig. 20. On the left of the cylinder axis is a velocity profile with no reverse flow, while on the right is another arbitrary velocity profile with reverse flow but having the same net flow volume. The reversed flow represented by area D is found by integration, and the ratio of it to the net flow might be used as a second criterion of scavenging.

This synthetic scavenging method appears to be independent of the flow rate and cylinder size but is somewhat dependent on the particular plane traversed, so that the same plane should be chosen when comparing geometrically similar cylinders

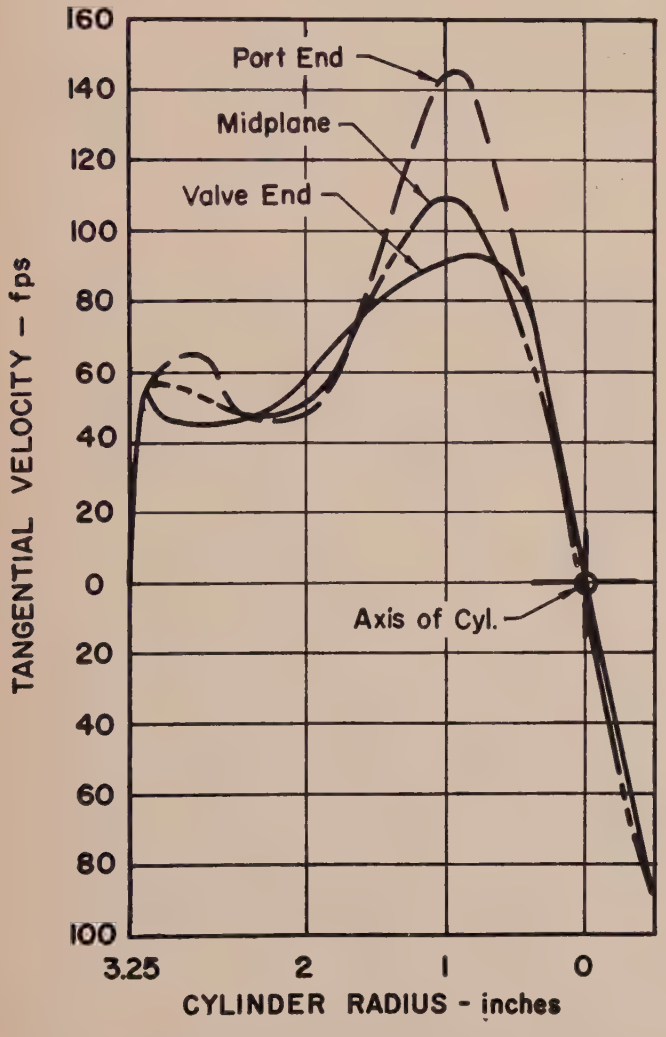

Fig. 12 – Tangential velocity distribution across cylinder at three planes

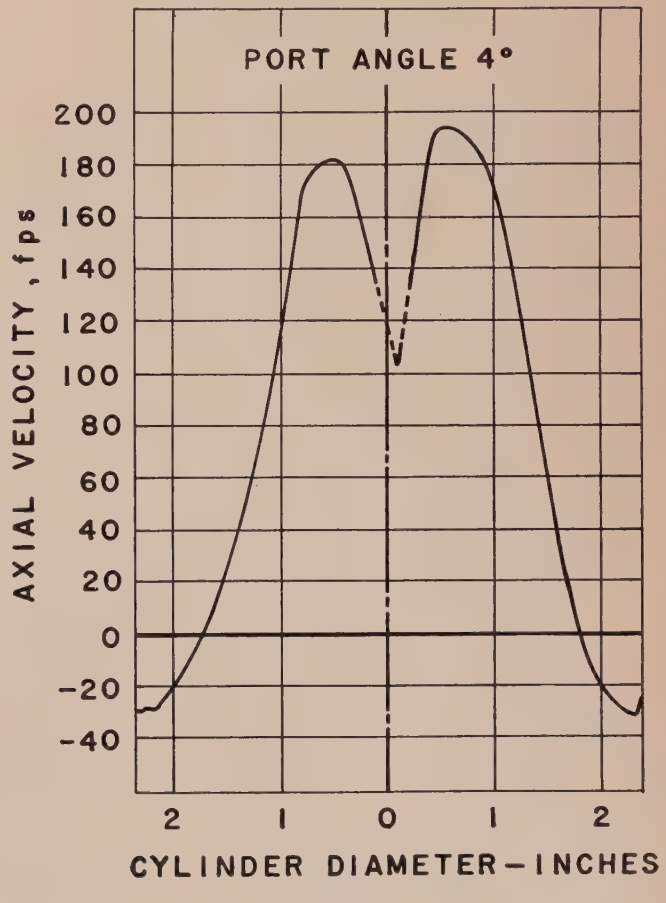

Fig. 13 – Axial velocity distribution for port angle of 4 deg

with different port configurations.

The synthetic scavenging efficiency for port angles from 4 to 40 deg is shown in Fig. 21. These are the values obtained by integrating the profiles seen in Figs. 13 through 17, in addition to several not shown. The efficiency rises to a maximum at around 30 deg after which it decreases slightly. This is seen to be the same trend as indicated by the geometrical profiles in Fig. 19, except that the reverse flow has reduced the efficiency values.

The curves in Figs. 18 and 21 should not be considered conclusive since they represent only one series of tests, although considerable care was taken to insure accuracy in machining the ports and in running the pitot sphere traverses. Our future program calls for repeating this series of tests with different cylinders. These will be traversed in at least three planes for comparison with the method now being used. Maier and Lutz in Germany have run similar tests on opposed-piston-type cylinders in which as many as ten planes were traversed, but the labor must have been prodigious.[8]

Correlation with Engine Performance

One might ask if there is any correlation between the synthetic scavenging efficiency and actual engine scavenging efficiency as measured by sampling valves? From a limited amount of engine data based on gas analysis of an expansion sample, the scavenging efficiency for valve-in-head uniflow-scavenged engines ranges from 65 to 70% for a scavenge ratio of one.[1] These values are somewhat dependent on engine speed and load, but the exact relationship is not known.

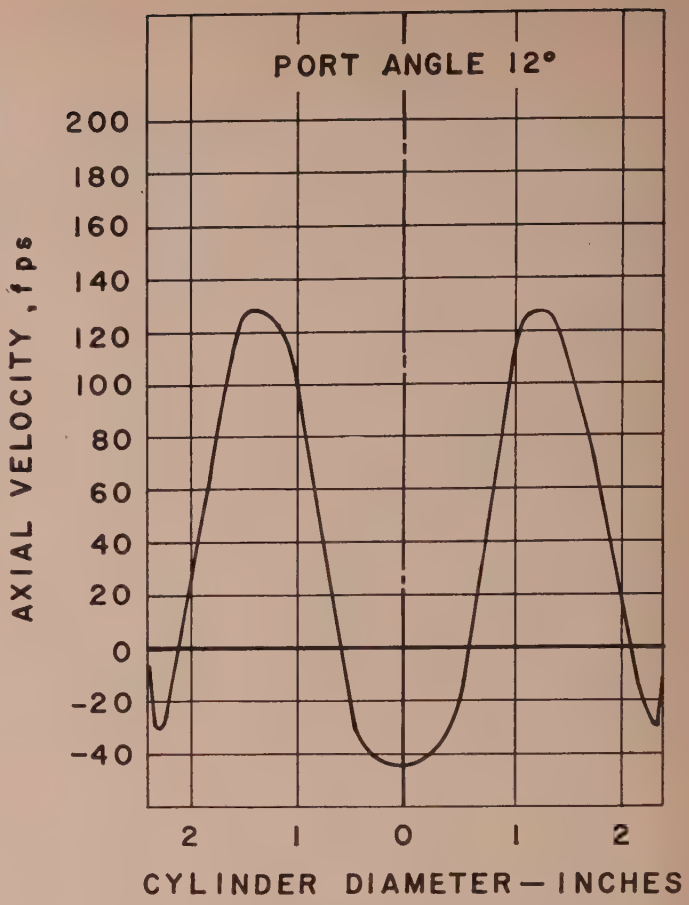

Fig. 15 – Axial velocity distribution for port angle of 12 deg

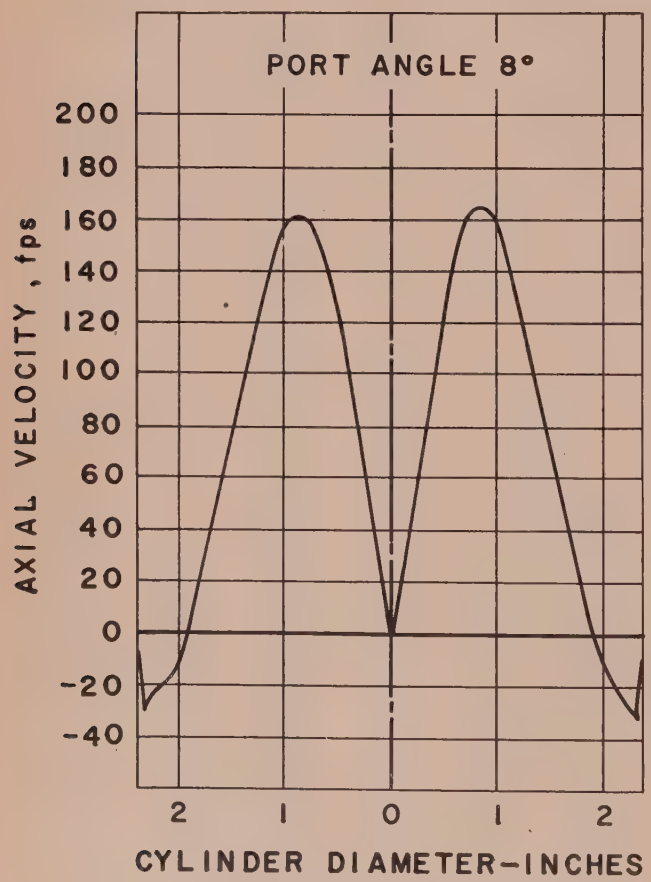

Fig. 14 – Axial velocity distribution for port angle of 8 deg

Scavenging efficiency and ratio are defined as follows:

$$\text{Scavenging efficiency} = \frac{\text{Weight of air trapped per cycle}}{\text{(Total cyl volume) (density)}}$$

$$\text{Scavenging ratio} = \frac{\text{Weight of air pumped per cycle}}{\text{(Total cyl volume) (density)}}$$

Density is based on airbox temperature and exhaust pressure.

As a comparison, Fig. 21 indicates that for port angles from 12 to 20 deg, which is the range covered by most uniflow-scavenged engines, the synthetic scavenge efficiency lies between 60 and 70%. It should be pointed out that some engines may have a greater port angle, but the *effective* angle

[8] See "Investigations Concerning Scavenging of 2-Stroke-Cycle Engines," by Otto Lutz. Pub. by K. Wittwer, Stuttgart, Germany, 1931.

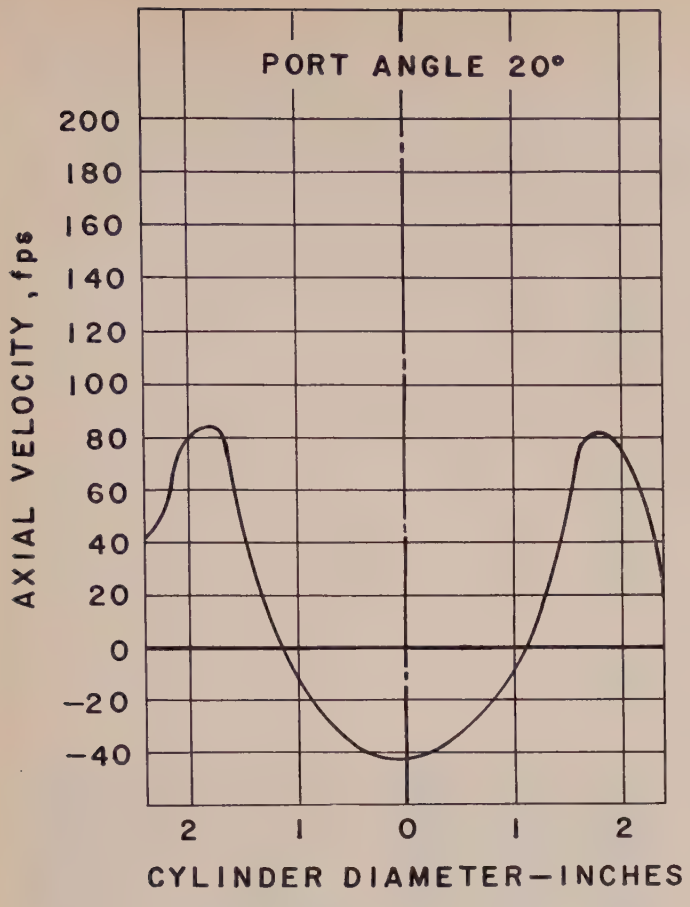

Fig. 16 – Axial velocity distribution for port angle of 20 deg

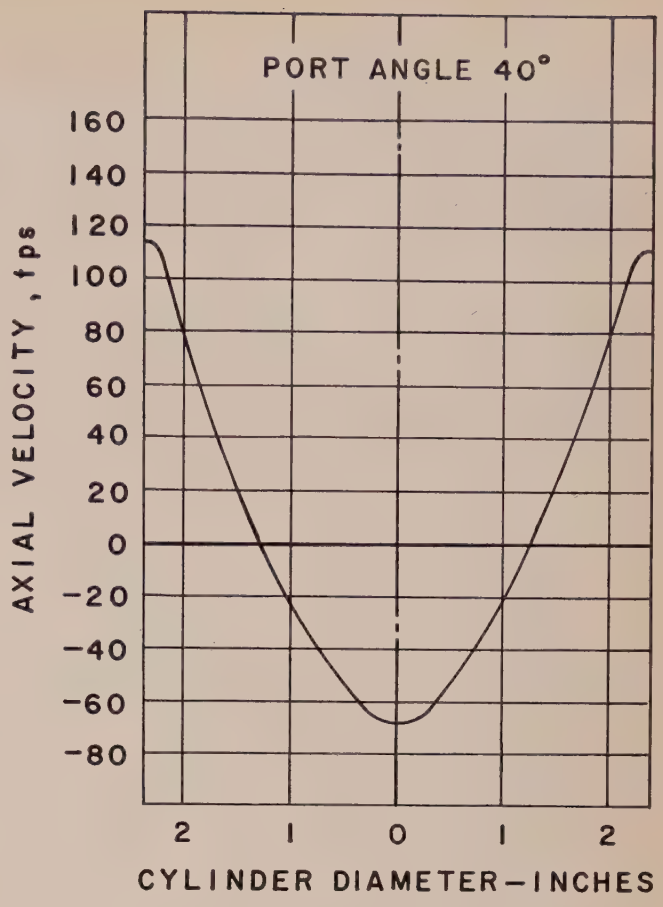

Fig. 17 – Axial velocity distribution for port angle of 40 deg

may be much less due to a small depth/width ratio of the port.

Some attempt has been made to correlate the synthetic scavenge efficiency with the performance of a running engine. A single-cylinder test engine having a separately driven blower was made available. It had a rather unique port ring which could be readily removed from around the cylinder liner and another substituted. Six different port configurations were constructed on the basis of our own studies and of several foreign designs. These were tested on the steady-flow bench for synthetic scavenging efficiency and in the engine to see if any change in power and fuel consumption could be detected. The air consumption was maintained constant for each port ring.

Four of these experimental port rings turned out very similar results, both on the flow bench and in the engine, the best on the flow bench being slightly superior in engine performance. Among the other two, one consisted of 0-deg (radial) ports and this was decidedly the worst of the six in both tests. The other, however, was satisfactory on the bench test but inferior in the engine. This may have been the result of an unfavorable tangential velocity distribution which gave the wrong swirl and adversely affected combustion. By swirl is meant the residual rotation of the air remaining after the ports close, which persists throughout the remainder of the cycle. How the tangential

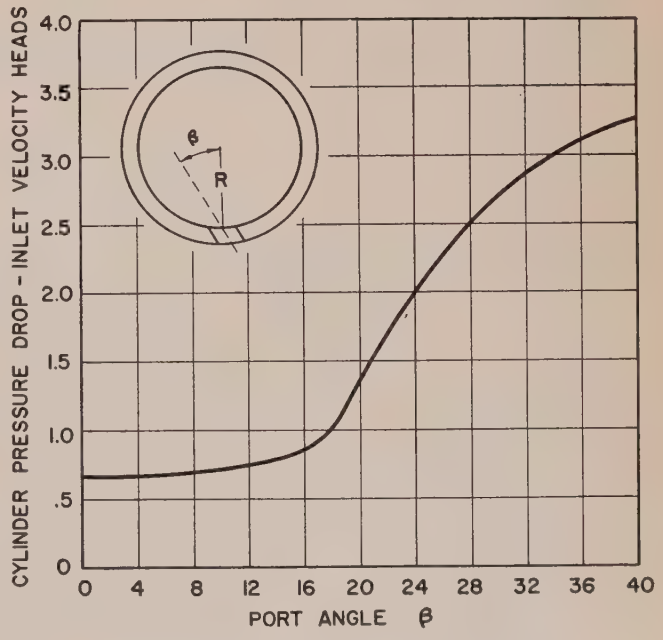

Fig. 18 – Pressure drop versus port angle

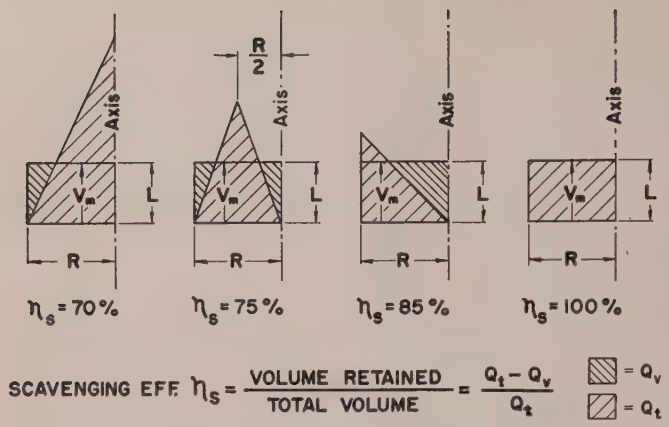

Fig. 19 – Synthetic scavenging efficiency

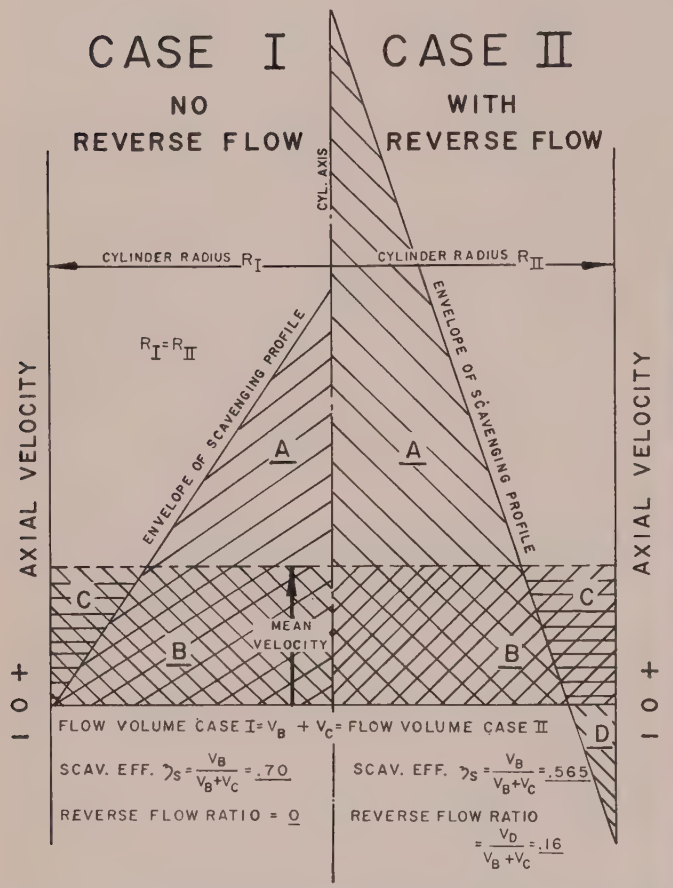

Fig. 20 – Comparison of synthetic scavenging efficiencies based on two scavenging profiles

velocity distribution changes as the piston moves up is not known.

With open combustion-chamber engines as well as so-called "swirl"-chamber engines there appears to be an optimum swirl rate which depends on such factors as engine speed, number of injector orifices, spray pattern, and rate of injection. In some engines a change in the effective port angle of only 2 deg from the optimum results in a noticeable increase in fuel consumption.

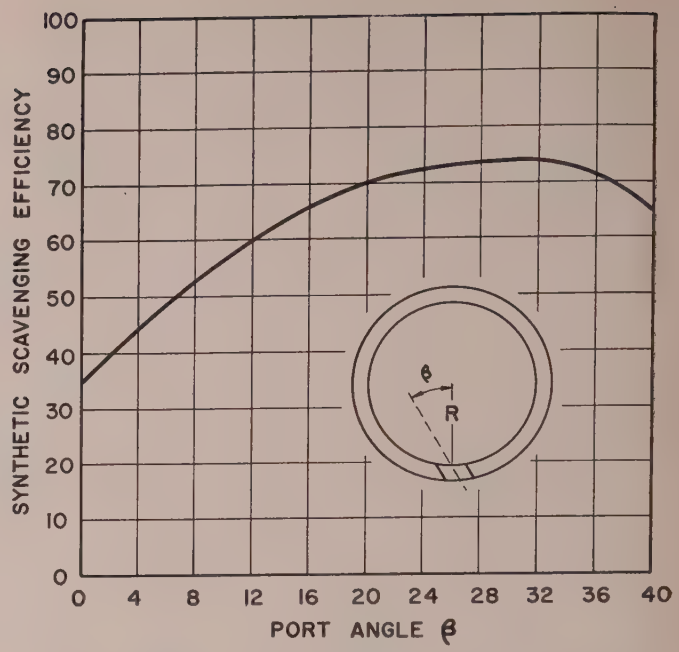

Fig. 21 – Synthetic scavenging efficiency versus port angle

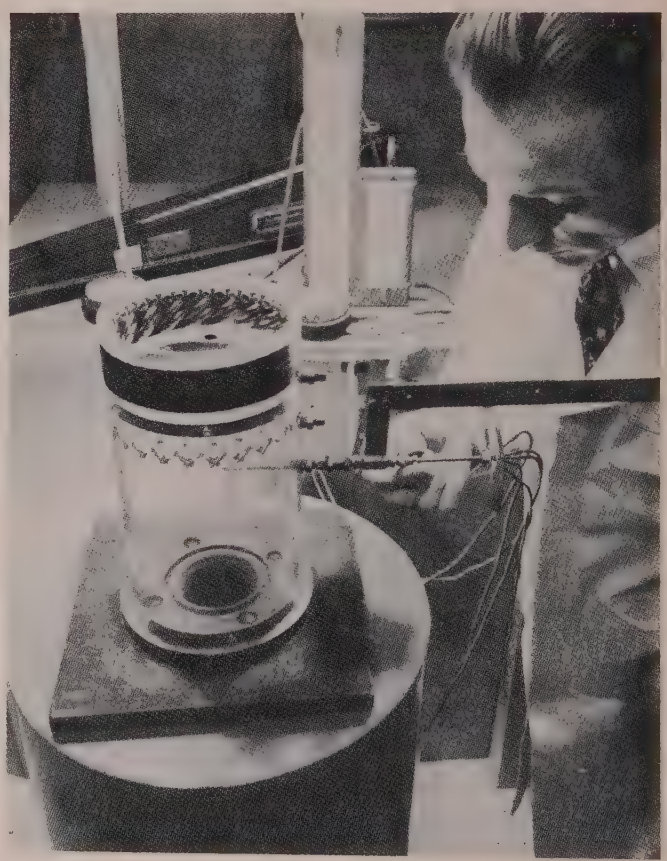

Fig. 22 – Traversing experimental cylinder

Conclusions

In attempting to improve an engine design, if one were to select a new port angle which gave a

maximum synthetic scavenging efficiency according to Fig. 21, without changing any other variable, the result might be (1) a higher pressure drop and therefore a lower scavenging ratio, (2) more heat loss during compression due to the effect of swirl on heat transfer, (3) poor fuel and air mixing resulting in increased smoke and fuel consumption. This emphasizes the need of the engine builder to keep in view the entire engine design when he attempts to improve scavenging efficiency, whether by means of increasing the scavenging ratio or by changing port configuration.

Changing the port angle uniformly and in one plane, as was done for Figs. 13-17, is not the only solution by any means. For example, several commercial uniflow engine designs show unsymmetrical port configurations. Compound angles, multiple rows of holes, and special deflectors are some of the other possibilities now under study. What we are looking for is a design which will show an improved axial velocity profile without increasing the pressure drop nor radically changing the tangential velocity distribution (having higher or lower angular momentum than the prototype).

In addition to scavenging the cylinder efficiently, it is obviously desirable to strive for as much port area and exhaust-valve area as possible and for a maximum flow coefficient.

In conclusion, our approach to the problem of improving the 2-stroke-cycle uniflow-scavenged engine can be summarized as follows:

1. Determine the airflow pattern in the present cylinder design by means of instrumentation. Plot the axial and tangential velocity components at the midplane diameter and find the synthetic scavenging efficiency.

2. After determining what should be improved, ideas are brought forth as to how it can be accomplished – as for example, a different port shape and angle.

3. The new idea is tested on the flow bench and compared with the original design for scavenging efficiency, tangential velocity distribution, and pressure drop. Fig. 22 shows a rather unorthodox design being tested – one which did *not* offer any improvement!

4. Test the improved design in the engine.

The technique described has certain limitations, especially as to methods of correlating results. However, we feel that it is the best approach so far to *understanding* the scavenging process. Eventually it may help solve this problem which has confronted engine builders ever since 1878 when Dugald Clerk first conceived the 2-stroke-cycle engine.

DISCUSSION

Steady-Flow Data Can't Predict Actual Operation

– C. F. Taylor
Massachusetts Institute of Technology

THERE are still many unknown factors concerning the scavenging of 2-stroke engines, and it is always gratifying to know that good work is being done in this field. The "pitot sphere" appears to be a useful instrument in studying nonuniform flow, and the data obtained in this way by Mr. Percival are most interesting.

The basic objective of scavenging a 2-stroke engine is to supply as much retained air as possible for a given expenditure of pumping power. While a high ratio of retained air to scavenge air is desirable, it must not be obtained at the price of ports which require too much pumping power. Thus, a port arrangement giving large flow areas is often more effective than an arrangement with smaller ports which gives a more attractive pattern in a steady-flow apparatus.

The power required to scavenge may be computed from a flow coefficient based on piston area, as suggested by Taylor and Rogowski.[a] If model tests could be developed which would predict values of both scavenging efficiency and flow coefficient under engine operating conditions, such tests would be of great practical value in the design and development of 2-stroke engines. However, experience at M.I.T. indicates that it is very difficult to translate the results of steady-flow measurements into predictions of performance in operating engines.

Mr. Percival explains the rise in pressure drop versus crank angle shown in Fig. 18 by the increase in an internal shear. Is not this increase in pressure drop more likely to

[a] See footnote 1 of main paper.

be due to the decrease in effective flow area accompanying an increase in port angle? Or was the effective flow area kept constant as the port angle was increased?

Discusses Theory Of Reversed Flow

– P. H. Schweitzer
Pennsylvania State University

I AM very happy that someone had the courage to come forward with a paper on scavenging tests. I know that a lot of work has been done lately on scavenging studies, and I suspect it was less secrecy which prevented the investigators from publishing their results but lack of confidence in their results and their interpretation. Credit is due to Mr. Percival and General Motors Corp. for presenting this analysis.

The instrumentation employed – the five-orifice pitot tube – is rather delicate and the evaluation of the readings admittedly laborious. In order to decide whether the method is justified, we compared the results with those obtained at Penn State with much simpler means.[b] In studying stationary flow the total nondirectional air velocity was measured by a hot-wire anemometer, its direction by a probe with a small flag and a protractor, the angular velocity by rotating vanes in various distances from the cylinder axis. Neglecting the radial velocity of the air particles, which is negligible, this method should give identical results with the Percival method.

Well, our results agree fairly well with those of the paper.

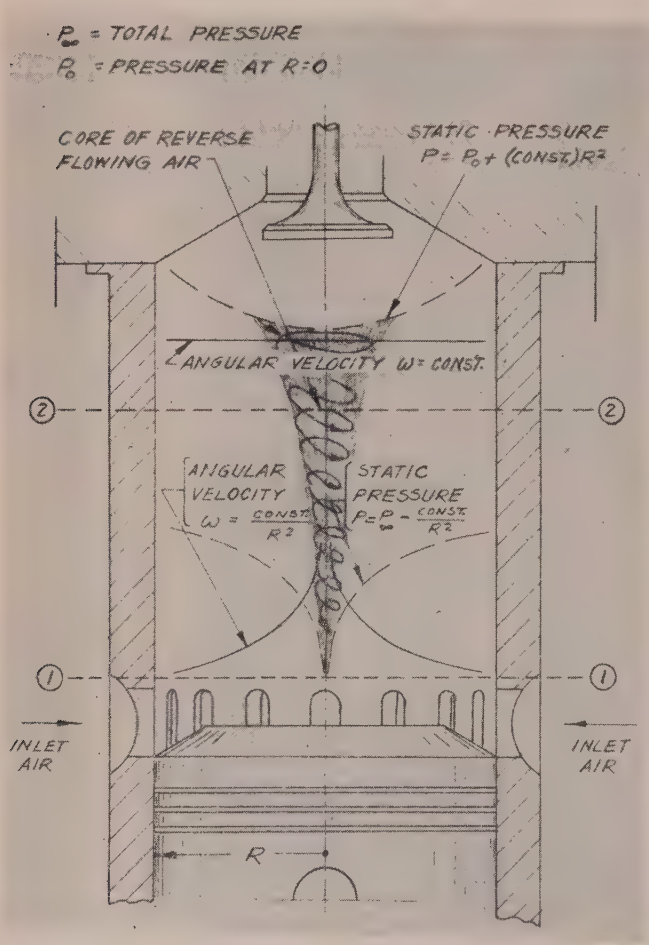

Fig. A – Schematic diagram of reverse-flow theory

A significant result is that even a very small angle of the inlet ports produces a relatively stagnant core near the center of the cylinder and even reversed flow. The popular notion that uniflow scavenging can be visualized as an air piston driving out the burnt gases is false.

You may be interested in Philip Barkan's theory of the reversed flow illustrated in Fig. A.

When the air enters the cylinder through angular ports the swirl velocity distribution will approach that of a free vortex, complying with the law of constant angular momentum, $\omega R = \text{Constant}$. With this velocity distribution and assuming potential flow, the pressure distribution will be as shown. However, the free vortex type of flow is not stable because a shearing force proportional to $(\partial\omega/\partial R)$ develops between circular layers which slows the fast-rotating inner layers and accelerates the slow-rotating outer layers. If this trend is carried to its limit, the rotational velocity becomes constant across the cylinder. As the air rises from the ports to the cylinder head the irrotational flow changes and begins to approach the rotational flow with a static pressure distribution as shown.

The absolute pressure in the center of the cylinder is therefore higher near the head than near the ports. The result is a reverse flow in the center which is unkind to good scavenging.

Our answer has been: radial ports on the bottom and angular ports higher up, or twisted ports. Swirl is needed for good combustion. You may think by using radial-flow ports at the bottom you sacrifice some swirl in favor of better axial velocity distribution. We have found that no such sacrifice is involved. The swirl is just as good with radial ports at the bottom and angular ports on top as with ports of a single angle. We have come to the conclusion that single-angle ports are unsuitable for diesel engines.

I should mention the few instances where our results

[b] "Scavenging Study for Uniflow Engines," by John A. Sobel III. Pennsylvania State University thesis for master's degree, August, 1953.

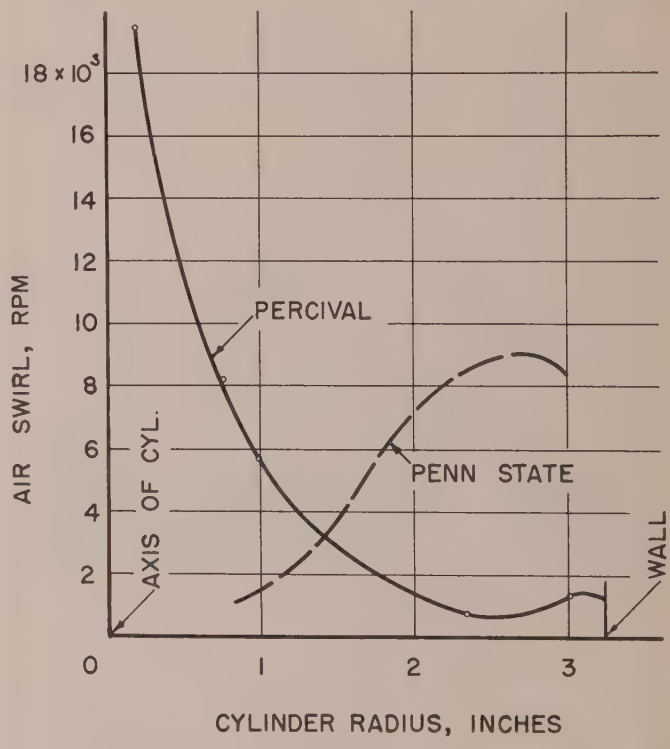

Fig. B – Replot of author's Fig. 10 to swirl rpm's, compared with Penn State results

show discrepancies from those of Mr. Percival. If you replot his Fig. 10 to angular velocities or swirl rpm's, as shown in Fig. B, you find very high swirl, 18,000 rpm, near the center and low swirl, 1000 rpm, near the wall. Our readings in a similar case look like the dashed line. We know our measurements are falsified by the friction of the vane bearings and make no claim for their accuracy.

In axial velocity distribution our results are much closer, as shown in Fig. C. For these the concept of "synthetic scavenging efficiency" might become quite useful. Only I would call it "synthetic trapping efficiency." If Percival's Fig. 16 is replotted using radial area for abscissa, instead of radius, Percival's synthetic efficiency is

$$\frac{\text{area } D}{\text{area } D + \text{area } C}.$$

He compared the figures with experimentally determined scavenging efficiencies (I call it charging efficiency) on engines and found satisfactory agreement. I believe that to be an accident. If the cylinder length is doubled and the air delivery cfm remains the same, the synthetic efficiency will remain substantially the same while the engine scavenging (charging) efficiency, as defined in the paper, will be much less. This can be avoided by defining engine trapping efficiency as

$$\eta_{tr} = \frac{\text{air retained}}{\text{air delivered}}$$

and steady flow trapping efficiency

$$\eta_{st} = \frac{\text{area } D}{\text{area } D + \text{area } C}.$$

A puzzling discrepancy pertains to Fig. 18, showing that the pressure drop across the cylinder increases 400% when the port angle is increased from 0 to 40 deg. Replotting that to volume flow basis, the flow coefficient would drop to less than half because of the port angle. Our measurements did not show such drastic change in flow coefficient.

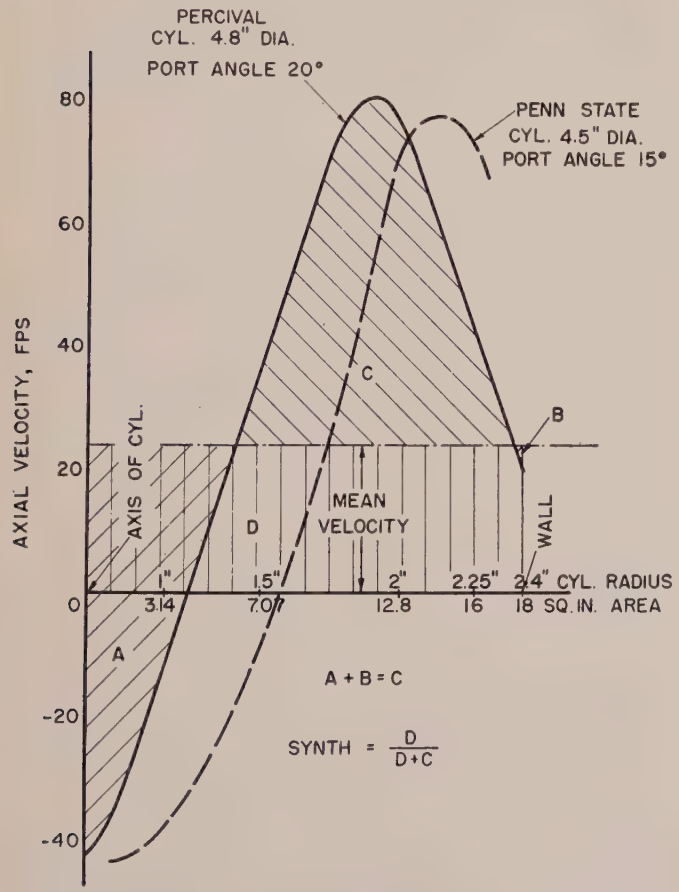

Fig. C – Author's axial velocity distribution results compared with Penn State results

Author's Analysis Explains Some Actual Engine Results

– Warren G. Payne
U. S. Naval Engineering Experiment Station

MY comments on the paper will be primarily observations on scavenging peculiarities we have observed in similar engines which tend to confirm the accuracy of Mr. Percival's methods.

The methods used appear logical and could be expected to give a close approximation of the actual airflow. Of course, as the author has stated, there is always the question of reproducibility of static observations in a working engine. As he indicates, the only certain way of doing that is to run an engine and measure the effect. I would feel that the methods would be an aid in preliminary design, but that they would have maximum value in helping to explain what is actually happening to the engine, so that corrections could be made in the final design. They certainly help in explaining peculiarities we have already noted.

We have done combustion development work on an engine of similar design in a somewhat larger cylinder size. The combustion did not respond in the way we thought it should to certain manifolding designs. Based on the indications, we evolved a theory as to why that action was occurring. The axial velocity diagrams in Mr. Percival's paper confirm that theory.

We were using a divided manifold with each section taking the exhaust from two cylinders which were timed 180 deg ca apart. Oscillograph records showed very desirable conditions. There was a very low pressure in the manifold at the time of exhaust-valve opening. The pressure wave traveled nearly intact to the turbocharger and provided good turbocharger efficiency and airflow. There was no resurgence of exhaust into the cylinder. Despite these apparently ideal conditions, there was very inferior combustion. Static pressure drop from the airbox to the exhaust manifold was out of proportion to the airflow.

A very simple common manifold, with a nearly constant, higher pressure level for the exhaust to discharge into, and no pulsating energy to the turbocharger, gave much poorer turbocharger efficiency and a lower airflow. Despite these apparently inferior conditions, the engine carried an increased 400 hp with the same thermal efficiency.

At a previous period, we had sampled, with a timed sampling valve, and analyzed the gas from the cylinder and manifolds. The exhaust manifold showed the proper low oxygen content during the beginning of the scavenging period and a higher oxygen content toward the end. The oxygen never did get up to atmospheric. That feature did not worry us too greatly, however, as it was probable that there was dilution in the volume of gas in the manifold elbow. Trying to obtain a gas sample in the cylinder proved very frustrating. The only opening we had was in the cylinder head surface about 1 in. from the cylinder wall. During the compression stroke, oxygen never rose above 20% by volume and during the combustion stroke didn't go below 16%. We knew that must be wrong, because we measured down to 4% in the exhaust manifold and the average oxygen in the exhaust stack was as low as 8%.

Examining all of the evidence, we decided that there must be a positive flow of air through the cylinder from the intake ports to the exhaust valves in the form of a hollow truncated cone. The gas near the cylinder edge was not being purged by the airflow and, furthermore, was not entering properly into the combustion process. This action was true with all airflows. When airflow was increased and,

simultaneously, the manifolding design provided very low back pressure for the exhaust to discharge against, the air velocity increased, the thickness of the wall of the conical path was decreased, and the fresh air sluiced through the cylinder with a minimum of purging of the exhaust gas. Thus, according to our theory, too high a cylinder pressure differential and airflow velocity decreased scavenging efficiency and hindered combustion.

The axial velocity plots in Mr. Percival's paper show positive pressure paths along the lines we had theorized. Negative flow paths are shown along the cylinder wall. It seems that the volumes of gas where the negative pressures are shown are only diluted and not cleaned out during the scavenging period. His static analysis confirms our interpretation of actual engine results.

Another point in the paper helping to explain our results is the explanation of the increase in cylinder airflow pressure drop. The author states that the greater angularity of ports increased internal shear and caused a rapid increase in pressure drop. We increased our tangential velocity by increasing airflow rate and apparently got the same effect. Our scavenging efficiency was affected by a combination of airflow rate and exhaust-valve backpressure level.

I would like to learn from Mr. Percival if he has confirmation of this lack of scavenging of the cylinder volumes where negative axial flow is present.

There is another factor which should enter into the scavenging efficiency problem. Too free an airflow, as by increased exhaust-valve area, may adversely affect the cylinder charging density. We have found the charge density a very critical factor in high bmep work. I would caution restraint in increasing the valve area for the sake of scavenging efficiency alone, unless a turbocharger or restricted exhaust pipe will be used to provide the necessary backpressure. It would be desirable for the scavenging investigation to be done under the desired conditions of charging density.

I realize that Mr. Percival's paper is on a method of scavenging analysis rather than on actual scavenging performance. It is too great a temptation to resist to try to obtain some additional information on actual application of scavenging to an engine. I have two questions:

1. In 4-stroke-cycle diesels we find that, fairly early in the scavenging period, the exhaust is cleared away and fresh air is blowing through. Except for the cooling effect, the valve overlap period on many 4-stroke-cycle engines need be no longer than 60 deg, instead of the 130 deg or more often used. In uniflow 2-stroke-cycle diesels, we haven't found that complete flushing of the exhaust. Has GM Research found that they are getting complete scavenging on any 2-stroke-cycle engine?

2. Have they followed their scavenging swirl as the piston compresses the cylinder charge? Does our difficulty in using the air near the cylinder wall for combustion agree with their experience?

Suggests Approach to Similar Study of Loop Scavenging

– R. J. McCrory
Battelle Memorial Institute

THE research described is of the type that is essential if the 2-stroke-cycle engine is to realize its potential; for, although the scavenging system is the heart of a 2-stroke-cycle engine, very little is known about the mechanics of the scavenging process.

It was noted with interest that the author considers the static analysis techniques which were effectively applied to uniflow scavenging not too well suited to research on loop-scavenged engines. Unfortunately, the steady flow of air through a static model does not indicate the effects on loop scavenging of exhaust blowdown, piston motion across the ports, or in most cases airflow velocity through the ports, three important factors in the mechanics of loop scavenging.

It is suggested that a research technique might be applied to loop-scavenging development that utilized a dynamic model which would permit a qualitative observation of scavenging flow and a quantitative determination of the effectiveness of the scavenging process. This dynamic model could be designed to accomplish this during a single scavenging cycle. The cycle would be traversed in such a way that blowdown, piston velocities, and flow velocities closely simulated those of a running engine.

Previous investigators have attempted to realize some of these objectives by the rapid start-and-stop mechanical actuation of the piston. A more applicable method of actuating the pistons through a single scavenging cycle would be by pneumatic means. For example, with the piston held at a predetermined position above the port belt, heated carbon dioxide could be introduced into the cylinder at a pressure and initial volume that, upon release of the piston, would result in a piston velocity and blowdown pressure, at exhaust port opening, similar to that of the running engine. A properly designed piston-rebound mechanism could cause the piston to have the proper velocity schedule across the ports, while air at a simulated manifold pressure scavenged the carbon dioxide from the cylinder. Upon rebound of the piston onto its compression stroke, it could be retained at its uppermost position while the charge of the cylinder was sampled and analyzed. During the scavenging process, simultaneous high-speed photographs from two directions matched frame to frame could indicate clearly the characteristics of the scavenging flow through the cylinder, even to the extent of tracing the flow through a single port.

Although the final development of any scavenging system must be on a running engine, the use of the dynamic-model technique provides a means of screening the many possible scavenging system designs without resorting to costly engine tests. Furthermore, it indicates paths of improvement in scavenging design which are not readily apparent in engine tests.

Presents Some Improvements for This Method of Scavenging Analysis

– D. S. Sanborn
Consulting Engineer

THE author clearly brings out the bitter truth: that there is no such thing as uniflow scavenging in engines of current production proportions. A similar investigation to determine if the very-long-stroke carefully-ported Junkers aircraft engine cylinders exhibit corresponding reverse flow patterns would be of considerable interest. It would appear that the so-called uniflow cylinder will be fraught with counterflow problems as long as the cylinder cross-sectional flow area exceeds the inlet-port area. Inlet ports simply do not make a good diffuser against a positive pressure gradient. In this respect it seems dangerous to draw conclusions from tests with wide-open ports—especially for uniflow scavenging. The inlet velocity and accompanying tendency either to form a jet or follow a potential flow pattern depend upon the relative inlet-port, cylinder, and exhaust-port flow areas.

The difficulties in making a cylinder "uniflow" lend encouragement to those of us who champion the mechanically simpler loop-scavenged cylinder. If the inlet stream traverses the cylinder twice rather than only once, the theoretical diffusion of the stream required to fill the flow cross-section is cut in half and the scavenging efficiency should be improved. This highly idealized picture assumes that the flow can be directed by the inlet ports, guided by the cylinder wall, and has sufficient kinetic energy to make the

circuit without being shortcircuited by the pressure gradient urging it toward the exhaust ports. It is probable that the velocities required to move the required air through the inlet ports in the time available in a modern high-speed engine will satisfy the kinetic energy requirement if favorable proportioning of inlet and exhaust areas is incorporated.

1. Static investigation with wide-open ports leaves doubts about the flow configuration changing with inlet- and exhaust-port openings.

2. A static study with the piston systematically moved to correspond to various crank angles would satisfy the objection in (1) but leave in doubt the carryover effect of vortex systems built up during the scavenging process.

3. Tests with a motored engine would eliminate the objections of (2) but still leave residual effects from the exhaust blowdown.

4. If compressed air is admitted by a timed valve near the top center piston position, the blowdown process can be simulated, and the actual scavenging process will be represented except for minor effects of differences in temeprature.

5. A special motoring test engine could be arranged to duplicate the actual piston motion during the scavenging process but limit its travel to a height only slightly above the ports.

6. The NACA has developed small multielement hot-wire anemometer probes with lag compensating networks for determining direction and velocity of fluctuating airflows.

7. With such equipment Mr. Percival's survey method could be applied to either uniflow- or loop-scavenged cylinders under conditions representative of actual operation, and a time history for each velocity vector could be obtained as well.

8. A test engine several times actual size, or substitution of water as the scavenging medium (with an auxiliary accumulator to take the compression), or both would permit maintaining the Reynolds number at lower cyclic speed and simplify instrumentation and observation.

9. It would seem that a computer circuit could be devised that would take the necessary information from the "pitot sphere" (or hot-wire anemometer), automatically solve for axial, tangential, and radial components of velocity, and plot them as a function of cylinder diameter as the bore is traversed by the probe. A considerable portion of the "coolie labor" must be eliminated before the author's method of scavenging analysis can appeal to engineers who are too lazy to take two extra strokes per cycle.

Author's Closure To Discussion

AS Prof. Schweitzer believes, the radial flow components can be neglected for symmetrical port angles from about 2 to 8 deg and also from about 20 to 60 deg. This means that the pitch angle is between 80 and 100 deg for these particular port angles. However, for radial ports and for port angles from about 10 to 18 deg, the pitch angle can range from about 60 to 120 deg or more for certain portions of the cylinder.

It is true that the synthetic scavenging efficiency will remain the same while the engine scavenging efficiency will be less if the cylinder length were doubled and the air delivery remained the same. But once we have defined the synthetic scavenging efficiency on a basis of a scavenging ratio of one, then for the actual engine cylinder we must also maintain a scavenging ratio of one. Therefore, if we double the cylinder length, we must also double the air delivery, which would result in an engine scavenging efficiency of the same magnitude as with the shorter cylinder.

The 400% increase in pressure drop is calculated from the actual measured values for a port/cylinder area ratio of one sixth. For a ratio of one third, which is nearer the actual condition for a uniflow engine, the pressure drop increases by about 235% from 0 to 40 deg, but the shape of the curve remains the same as noted in the paper.

In reply to Mr. Payne's question on lack of scavenging with negative axial flow, the negative flow at the wall, for example, implies a circulation of residual exhaust gas which becomes entrained by the air coming through the ports. These gases tend to become mixed at their interface. As scavenging continues the residual gases become more diluted by fresh air, and a portion of the residual is carried into the main stream of fresh air and may pass out of the cylinder. One might expect the wall portion of the cylinder to have a higher proportion of residual gas at the instant of port closing than the region where the airflow is positive.

In answer to Mr. Payne's other questions, we are not getting complete scavenging on any 2-stroke-cycle engine. Also, we follow only the swirl near top dead center during combustion by means of high-speed photography.

Prof. Taylor has asked about the effective flow area accompanying an increase in port angle. The flow area was kept constant and, so far as could be determined, the individual port flow coefficient was not altered as the angle increased, except for the slight effect of increased port length.

Mr. Sanborn asked about opposed-piston uniflow-scavenged cylinders. We have traversed types similar to the Junkers aircraft cylinder and found the axial velocity profiles to be very similar to those for valve-in-head uniflow cylinders. So far as the "coolie labor" involved, we have recently eliminated much of it by using the IBM 701 computer for reducing the data. Formerly, the calculations for one traverse of a cylinder required about 4 hr, while the total time for the IBM is about 10 min.

Mr. McCrory's suggestion of a dynamic model for loop-scavenging development would seem to be in the right direction and I would be very interested in learning if such a device is contemplated by Mr. McCrory and his associates in the near future. I assume by high-speed photographs that he refers to the schlieren method.

ORAL DISCUSSION

Reported by C. G. Goohs

Cleveland Diesel-Engine Division, GMC

Gordon Millar, Ford Motor Co.: Has any work been done on intermixing of radial and tangential ports in one plane?

Mr. Percival: Yes. It has been found that according to the steady-flow tests the effect of such ports is very similar to symmetrical ports having some intermediate angle. For example, if half the ports are radial with the remainder located between the radial ports at a 20-deg angle, the axial and tangential profiles are very similar to a uniform 12-deg port angle.

E. W. Spannhake, Le Tourneau-Westinghouse Co.: What is the effect of the very small holes on instrument accuracy under conditions of extreme turbulence?

Mr. Percival: The principal error is not the result of turbulence so much as traversing a steep velocity gradient. The manometers record the root mean square of the velocity gradient and not the mean velocity across the face of the instrument.

Simon K. Chen, International Harvester Co.: What is the effect of tipping the ports toward the piston or toward the cylinder head?

Mr. Percival: The effect of tipping the ports up or down 10 deg is very slight, so far as synthetic scavenging efficiency goes. In an actual engine, the ports tipped toward the piston seem to be better, performance wise, than those tipped toward the head.

Symposium—

EXPERIENCE with new plastics for truck bodies reported by these five authors yields a complexity of pros and cons.

Among advantages claimed are:

1. High strength-weight ratio.
2. High impact strength and ability to absorb punishment and return to original condition without permanent damage.
3. Ease of maintenance, repair, and cleaning.
4. Good thermal insulation.
5. Resistance to chemical or electrolytic attack or deterioration.
6. Ease of bonding.
7. Adaptability to mass production techniques.

Disappointments reported by various users include:

1. High cost of raw materials.
2. Low modulus of elasticity.
3. Low endurance limit.
4. Fractures from internal abrading of reinforcement.
5. Weakening and failure of structures because of poor adhesion between plastic and its reinforcement.
6. Inadequate and faulty engineering knowledge of the subject.

Agreement is general, however, that plastics for trucks have a bright future, once the many problems have been ironed out.

Across-the-Board Look at Plastics for Truck Bodies

– Hiram McCann

MY purpose is to introduce a new material for automotive construction and to describe its properties in order to paint a background for the more specialized papers that follow.

A candle and a hard-boiled egg are two items representing the two main types of plastics. The thermoplastics, like the candle, melt in conditions of heat and harden when the heat is withdrawn, and may be melted and molded over and over again. The hard-boiled egg represents the thermoset materials, which fuse or cure under conditions of heat and may not be melted again.

Naturally, the thermoset materials in the main have greater heat resistance than the thermoplastics.

We need not discuss the thermoplastics at any great length here because, with few exceptions, they would not be used as structural materials. The thermoplastics include styrene, which is found in toys and housewares; the acrylics, used in escutcheons and tail lights; the vinyls, found in truck and other automotive upholstery and also in safety glass; the cellulosics, which include cellulose acetate butyrate in the form of steering wheels; polyethylene, used for squeeze bottles, film, and coaxial cable coating, nylon, found in bearings, gears, and grommets, and the fluorocarbons which are high-heat-resistant thermoplastics used for industrial applications.

In many cases the industry has found that the basic thermoplastic polymer or resin may be improved by fusing it chemically or alloying it mechanically with another resin. So we have the copolymers and the alloys, mainly of styrene, wherein acrylonitrile (this resin is known as orlon in textiles) and butadiene (a synthetic rubber) are combined with styrene to form a new resin, which is then extruded into sheets. These may be vacuum-formed into door liners, kick plates, cab ceilings, body-floor surfacing, instrument panels, and many other automotive parts.

The styrene copolymer or alloy plastics have tremendous scuff resistance, good tensile properties, high impact strength, and adequate chemical resistance, and have the further advantage that they may be vacuum-formed from sheet on relatively simple tools at much lower tool cost than would be required for molding.

In the thermoset field are urea, which is used chiefly in buttons and cosmetic closures; the phenolics, used in distributor caps and electrical components; the melamines, which turn up in high-pressure laminates as well as in ignition harness; the epoxies, found in adhesives, coatings, and pottings; and the polyesters, which are the resins we want chiefly to discuss here.

Of these thermoset materials, all of which in simple resin form are rather brittle, the polyesters and the epoxies have got the imagination of truck and transportation designers and engineers because of three things:

1. They are very compatible with fibrous glass reinforcement, which is the strongest reinforcement one could use.
2. These resins may be catalyzed to produce a cure, thereby obviating the use of outside heat in the making of a molding.
3. Since they may be thus cured, they can be

Plastics for Truck Bodies

Hiram McCann
Modern Plastics

David S. Brown
Brodix Corp.

Stanley S. Wulc
Strick Co.

Walter R. Herfurth
United Parcel Service

Henry Jennings
Fleet Owner

This symposium was presented at the SAE Golden Anniversary Annual Meeting, Detroit, Jan. 14, 1955.

molded with reinforcement at very low pressures and, in many cases, on low-cost tubes.

These three factors, peculiar to the polyesters and the epoxies, make it possible to mold out of these resins, reinforced with glass and filled with some inorganic matter, huge sizes and complicated shapes.

There are other advantages:

1. They have high inherent corrosion resistance.
2. They are basic thermally and electrically insulated.
3. They have a relatively high strength-weight ratio.
4. They are colorable in both opaque and translucent form, permitting them to be used for both bodies, where capacity is needed, and roofs, where translucency is required.
5. They are bondable with proper adhesives.
6. They may be given good finish in the mold or may be painted after molding.

The polyesters are, of course, considerably lower in cost than the epoxies, and the technology of the polyesters reinforced with fibrous glass is better known.

With all these economic and functional advantages, it is little wonder that the excitement and enthusiasm accruing to the reinforced plastics is so intense and widespread. You can hardly think of a product that would not appear to gain from being made out of reinforced plastics. Boats, buildings, pipes, housings, furniture, tanks, sports cars, and trucks are obvious markets for these materials.

Then why haven't reinforced plastics, particularly polyesters, zoomed to colossal market size? To

The Authors

HIRAM McCANN is editor of *Modern Plastics Magazine* and "Modern Plastics Encyclopedia." In 1929, he received a degree in political economics from MacMaster University. During World War II, he was chief of the Industrial Magazines Division of Consolidated Press, Ltd., in Toronto. Mr. McCann also served as executive secretary to the Food Conservation Board of the Dominion of Canada.

DAVID S. BROWN is president and chief engineer of the Brodix Corp. He was assistant traffic manager and fleet manager for the Dairymen's League Cooperative Association. Mr. Brown has also been assistant staff engineer in the Transportation Department of Johns Manville Corp.

STANLEY S. WULC is general manager of the Plastics Division of the Strick Co. He received a B.S. in Mechanical Engineering and an M.S. in Applied Mechanics from Virginia Polytechnic Institute. Mr. Wulc has taught engineering mechanics at NYU.

WALTER R. HERFURTH (M '29) is assistant to the vice-president in charge of equipment for the United Parcel Service of America, Inc. He has been actively engaged in various phases of the automotive industry since completing his mechanical engineering training at M.I.T.

HENRY JENNINGS (M '37) is technical editor of *Fleet Owner*. For eight years he was associated with the Society of Automotive Engineers where he handled the activities of the Transportation and Maintenance Technical Committee and the Truck and Bus Technical Committee.

answer that we must look at the negative factors involved:

1. These are composite materials made of glass or from other reinforcing material in fiber form, plus a liquid resin, plus inert filler, plus catalyst, plus reaction inhibitors, plus colorant in many cases. And being composite materials, literally created on the job, one is faced with human, mechanical, and chemical uncertainty at every stage of that creation.

2. Our chemistry is probably 10 years ahead of our mechanical engineering in this field, and we lack both definitions and standards relating to the composite materials and to the methods of molding and fabricating.

3. We need greater flame resistance than has so far been provided by chemical additives.

4. We need a better understanding on the part of automotive engineers and designers of the simple fact that each change in design creates a new engineering problem of both a chemical and mechanical nature.

5. We have an industry geared to too little capital, too inept management, and possibly too much misplaced enthusiasm at processor or molder level.

The overcoming of the problems occasioned by these negative factors is not, I submit, a job for the plastics industry alone – at either resin- or reinforcement-maker level or at processor level. And I further submit that the job of overcoming these problems will be sooner accomplished by statesmanship than by salesmanship coupled with spot service to individual plants.

There are, to my knowledge, 43 manufacturers of polyester resins, and at least five manufacturers of epoxy resins. There are five or six producers of fibrous glass, about 20 weavers of glass, and at least six companies engaged in coating or impregnating glass, cloth, or mat with resin on either a custom or a proprietary basis. On molder level we have about 130 companies ranging from two-man shops in empty garages to fair-sized companies employing 300 or more people.

Now, if each of the engineers in the truck industry and their purchasing agents were to be bombarded by any major portion of these people who constitute the reinforced plastics industry, they would spend their time doing nothing but listening and getting more and more confused.

Fortunately, the Reinforced Plastics Division of the Society of the Plastics Industry has already established a modus operandi for intra-industry cooperation designed to produce usable engineering data and standards. And I submit that the statesmanlike approach to the situation would be to have a subcommittee of the SAE Truck & Bus Technical Committee sit down with a committee selected from interested engineers in the Reinforced Plastics Division of SPI and set up a program for the evaluation of composites made in various ways and in various component balances.

An example of what such a program might prevent is found in the sports car body, first bag-molded and now press-molded in metal tools. Originally, nearly everyone in both the automotive and the reinforced-plastics industries had an idea that a rigid polyester resin would be most suitable for this application. The few technologists who disagreed were ignored and months were wasted – until the automobile manufacturer set up his own program for the competitive evaluation of resins and composite structures, whereby it was proved conclusively that a semiflexible resin was the proper thing to use.

The automotive engineer has long been accustomed to working with metals about which engineering data has been long established and readily available. And while the properties of the reinforced plastics and even the economics of reinforced plastics over the life of a vehicle are intriguing; while the present rather weird molding and fabrication methods for reinforced plastics constitute a challenge to any engineer, I think we can prevent headaches, waste of money and time, and heartbreak by taking the statesmanlike approach to the problem and setting up intra-industry engineering committees.

Anyone can dream. Anyone can visualize not only big reinforced plastics standard truck-building establishments, geared to quantity production, but also possibly hundreds of small custom truck-body-building plants across the country, capable of quickly providing specialized truck bodies for standard chassis. The markets will be worth the effort.

And as the revolution proceeds in methods and means of freight distribution in this country, as the pick-a-back becomes effective on more and more railroads, as our highway system is expanded to provide faster truck routes, as decentralization of industry and suburbanization of population proceed, these presently obvious opportunities for the use of reinforced plastics in trucks will again be greatly expanded.

On the part of the reinforced plastics industry I believe I can say this: expansion of present processor or molder facilities, amalgamation of others, and the entry of bigger capital into the industry at that level is going to give the automotive engineer a stronger technical and business body with which to work. And I can also say that the resin makers themselves are trying their level best to simplify and standardize the fantastic range of specialized materials now available, with a view to obtaining engineering efficiency in application as well as more economic materials.

Use of Reinforced Plastics for the Construction of Transport Tanks

– David S. Brown

OF all the uses of fibrous-glass reinforced plastic in the transportation industry, the adaptation

of this material to the construction of liquid transportation tanks will undoubtedly prove to be of major importance. The movement of commodities in bulk has grown tremendously in the past few years, and as we continue to develop and synthesize new materials, the necessity for a light-weight, corrosion-resistant, durable liquid-transport unit is of ever-increasing importance.

Of the many characteristics which make fibrous-glass reinforced plastic an admirable material for liquid transportation units, the following are of prime importance:

1. Its high impact strength and its ability to absorb tremendous blows and return to its original condition without permanent damage.
2. Its high strength-to-weight ratio.
3. Its resistance to chemical or electrolytic attack or deterioration.
4. By recently developed processes, the ability to mold at low pressures to sizes and strengths limited merely by the physical capacity of the plant.
5. The ease of maintenance and the quickness with which repairs may be effected without any attendant fire hazard.
6. Its adaptability to mass production methods.

While the use of reinforced plastics for the construction of tanks for transporting liquids by rail and highway has long been considered feasible, their use has not progressed as one might imagine, considering all of the previously listed advantages. A large part of this delay has been due to misused glamor phrases such as "miracle," "indestructible," and "corrosion-proof" by overambitious manufacturers who did not have a clear understanding of the requirements of liquid-transportation equipment. An example of the confusion brought about by such glamor phrases is the term "corrosion-proof." While in itself this statement is approximately correct, it is meaningless, since the term corrosion should never be applied to plastics or nonmetallic products. Such confusion discourages many competent transportation engineers from considering these materials for handling corrosive liquid, or any other liquid for that matter. Since companies successful in the production of liquid-transportation equipment are characteristically conservative, as their success is based on long-term performance, they have been hesitant to utilize these reinforced plastics.

The progress of tank construction of fiber-reinforced plastics has been beset by numerous failures which have been due largely to the fact that manufacturers attempted to adhere to the designs originated for steel – merely substituting laminated plastics in their stead. The use of any new material brings about the necessity of re-evaluating all present designs, properly delineating the exact problems to be solved, and approaching them on the basis of these new materials. The dilemmas resulting from frequent product misapplication have practically destroyed some technically weak firms, and have in the past jeopardized the future of the entire industry. Among the many problems encountered in the construction of liquid-holding tanks have been:

1. Weeping or permeability of the finished tank.
2. Fractures of the material due to internal abrading of the fibrous-glass reinforcement.
3. Weakening and failure of the structure due to the poor adhesion between the fibrous-glass reinforcements and the plastic itself.
4. Inadequate and faulty engineering.

Various methods used in the construction of transport tanks to date may be divided into three main classes: hand lay-up with mat or glass cloth; matched die formation of sections later assembled; and the dry lay-up method of forming entire tank units. While the hand lay-up method has produced the largest number of transport tanks in use, they have done little or nothing to advance the position of plastic tanks in the liquid transportation picture, because of:

1. The impracticability of incorporating new designs.
2. Non-attainment of full utilization of the strength of the materials and resultant lower weights.
3. High cost of this type of construction.
4. The inability to have complete quality control over a situation which relies entirely upon the craftsmanship of the individual concern.

In the second method, that of matched-die preformed section assembly, the tanks have more commercial appearance, have better chemical and moisture resistance, higher strength, and lower weights; the costs have been higher than one would normally expect to pay in the market place, since a great deal of hand labor is needed to assemble the sections into a finished product. This method can best be utilized for small-size tanks where assembly can be kept to a minimum. The dry lay-up method at the present time seems to lend itself to this better than either of the preceding two. In this method, the entire tank assembly, including valve fittings, manhole fittings, fittings for attachment to running gear, brakes, and lights, is laid up into the mold and the resins introduced and the pressure applied. After a short cure period, the entire unit is ready for removal from the mold, and is ready for service upon the attachment of its running gear, valves, and lights. This method, more than either of the other two, lends itself to better quality control and more uniform structure.

While we have discussed fibrous-glass reinforced plastics in general up to this point, I believe it would be wise to point out that as of the present time the polyester resins are most widely used. However, there is every indication that they may have to share this field with some of the silicones and some of the epoxies, and perhaps an alloy of either one of the foregoing with some of the more recently developed rubber compounds. By this method, resistance to almost any known chemical

should be obtainable while retaining the high strength and low weight of the plastic tank. By this same method, we may expect to see the flame resistance of these materials greatly improved.

One of the more important of the many problems besetting the user of a plastic tank when various commodities are to be carried is the possible absorption of the liquid by the plastic and its subsequent contamination of other products. To overcome this, one manufacturer has been utilizing a light-gage, stainless-steel liner which furnishes the necessary liquid opacity, corrosion resistance, and sanitary surface, allowing the tank to be used interchangeably for any chemicals or commodities, but relying on the high-strength, low-weight fibrous glass reinforced plastic for its strength. This same design has utilized a sandwich wall to provide excellent insulating characteristics as well as the lowest possible strength-to-weight ratio. Sandwich wall, as defined by the American Society for Testing Materials, is: "A laminated construction comprising a combination of alternating dissimilar or composite materials assembled and intimately fixed in relation to each other so as to use the properties of each to attain specific structural advantages to the whole assembly." In simpler terms, a sandwich wall may be described as a composite structure consisting of thin skins which are separated and stabilized by a relatively thick low-density material. This sandwich construction, when made of fibrous-glass reinforced outer surfaces with a low-density expanded plastic cellular core will, I believe, be the best practicable answer to a low-weight, high-strength, high-capacity general purpose transportation tank.

Plastics for Trailer Bodies

– Stanley S. Wulc

TEN years ago we undertook an extensive research and development program in glass-reinforced plastic as applied to trailer structure. The new "wonder" material so widely publicized by the raw materials manufacturers also stirred our interest. It took us many years and a lot of money to separate the wild claims from the actual truth. And the truth is that reinforced plastic has advantages, but also has disadvantages; it should not be used indiscriminately just because it is fashionable; and it must be carefully evaluated and intelligently applied. I do not wish to create the impression that I want to discredit the cause of reinforced plastic. On the contrary, I am interested in its promotion, but the only way to achieve it is by a realistic approach.

For us, the desirable qualities of glass polyester laminates are: low weight, lack of corrosion, good thermal insulation, and light transmission. On the other hand, however, there are the low modulus of elasticity, relatively low endurance limit, high cost of raw materials, and expenses involved in the tedious process of producing uniform and strong laminates. Strength is a very important factor in our application.

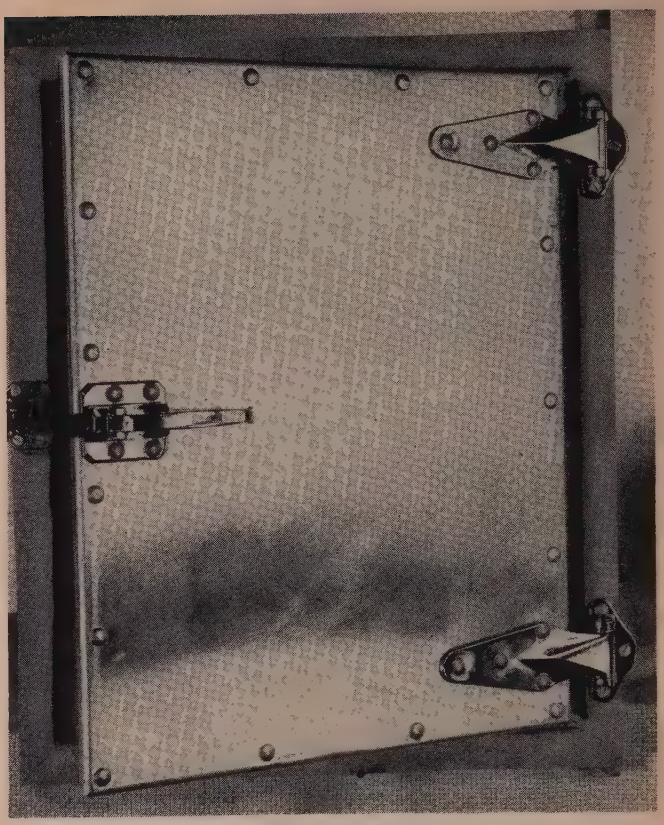

Fig. 1 – Small plastic refrigerator door

The engineer in the trailer industry must work within a very narrow frame of specifications imposed upon him by state regulations and customer requirements. While states are limiting the maximum permissible overall weight of the vehicle, axle location, and physical dimensions, customers are demanding a vehicle of maximum carrying space and minimum weight. Thus, three basic conditions in the design of a trailer must be taken into account:

1. Low weight and high strength.
2. Maximum volume within permissible dimensions.
3. Axle and kingpin location.

It is obvious, therefore, that a superior trailer can be designed only when all the critical forces in static as well as dynamic conditions are known, and the corresponding stresses are computed. Since we specialize in frameless trailers, in which side panels are load-carrying elements, our engineer has to deal with instability problems as well as the frequent fatigue failures.

In order to improve our product and create a still finer vehicle, we have searched continuously for new and better materials. We were the first to pioneer an all-aluminum trailer. We were again the first to pioneer reinforced plastics for trailers. We realized the potentialities offered to industry by

Fig. 2 – Plastic parts of refrigerator door: frame, pan, and insulating material

Fig. 3 – Plastic refrigerator pan door

this material, in spite of its drawbacks previously mentioned. We were attracted by its low weight, high strength, resistance to corrosion, and excellent insulating properties.

This material was tried out in building doors and linings for our refrigerated trailers.

Wooden insulated doors had many disadvantages. Quite frequently they could not provide an effective air seal, as they would warp and swell under the action of moisture, making closure difficult or downright impossible. Moreover, they retained odors, were difficult to clean, and required a great deal of maintenance. They were also heavy.

Metal doors, too, had many drawbacks. They were good thermal conductors, and they corroded easily. It was difficult to construct a metal door which, while light in weight, would simultaneously have good impact characteristics and resistance to local deformation under a concentrated load.

The use of polyester-glass-reinforced laminates has solved these problems. Plastic doors were designed and produced (Figs. 1-4). They have better insulating properties, present no problem with deformation by moisture, and are light in weight (240 lb as compared with 420 lb for wooden doors). Pigments are incorporated into the laminates, and maintenance, cleaning, and repairing are very easy.

Before we introduced plastic linings for trailers, the industry was using either plywood or metallic ones. The former were unsatisfactory for the same reasons mentioned above in connection with the wooden doors. The latter were inferior in absorbing impacts of the shifting cargo, and of loading and unloading, since they were made out of thin sheets to save weight; they were good heat conductors; when made of stainless steel they were too heavy; when of aluminum, they turned the meat black.

Reinforced-plastic laminate has solved all these problems at once. Designed with corrugation to provide space between the cargo and the inner

Fig. 4 – Interconstruction of refrigerator door

surface, plastic linings (Fig. 5) allow better air circulation necessary to maintain uniform low temperatures in every part of the interior. They are stronger and lighter than the metallic or wooden liners, having at the same time excellent insulating properties. They are sanitary, as they have no open joints and no plywood interlining to rot, to absorb odors, or to harbor maggots or bacteria. Plastic linings can be steamed out without deteriorating effects, and repaired in case of damage.

Our next step in the development was the introduction of skylight roof trailers (Fig. 6). One or two reinforced-plastic panels, 8 x 4 ft, unpigmented, were built into the roof. The plastic panels let enough light into the trailer to make reading of the shipping labels possible, and thus considerably speed up the loading and unloading processes.

The skylight roof trailers became very popular with the customers. At present, three out of every four trailers produced by Strick, which turns out a completed unit every 20 min, have skylight roofs.

Encouraged by our customers' reception of the first uses of plastics in trailers, and backed up by favorable reports from the field, we began to nurse the idea of designing a complete plastic-refrigerated trailer.

If such a trailer could be built, we thought, it would save weight, cut maintenance, and provide effective insulation. To achieve this plan it was necessary to establish exact material specifications, since a trailer is a highly stressed structure. Material specifications, however, depended not only upon the basic quality and type of raw materials used, but also upon the hundreds of variables involved in manufacturing laminates. It was necessary to develop standards and establish rigid quality control.

Besides establishing material specifications, we had to solve another tough problem – that of joining. Extensive studies were made on an effective joint design.

For some time we had several requests from customers for trailers with plastic side panels. Though we wanted to make them completely out of plastic, we soon found out that this was not possible without reducing the available cubic capacity. Aluminum posts could not be economically replaced by plastic ones of the same depth because of the small modulus of elasticity of the laminates. We decided, therefore, to build trailers with plastic panels and aluminum posts.

The trailer of this type (Fig. 7) has plastic side panels 3/32 in. thick, except for a 3-ft area at

Fig. 5 – Plastic-lined refrigerated trailer

Fig. 6 – Skylight roof of trailer

Fig. 7 – Plastic trailer

Fig. 8 – Plastic side panel with aluminum posts

the bottom which is built up to ⅛ in. for added strength. Posts are made out of aluminum (Fig. 8). "Plastic" vehicles, because of their resistance to acids and alkalis, are used for hauling corrosive materials. Some customers use them for transportation of perishable foods for relatively short-distance hauling, as they provide the insulation and the sanitary conditions required for this type of cargo.

Our next goal and logical step forward was a completely plastic refrigerated trailer. The need for such a vehicle was very urgent. The conventional refrigerated trailer was heavy, its cargo space not fully utilized. It was actually a modified van-type trailer. The modification consisted, among other details, of installation of wooden stringers acting as spacers between the inner skin and the customary outer structural panel. In the space thus provided, insulation was laid.

Its floor area was one of the greatest sources of heat transfer. The exposed floor cross members were acting as huge fins, and their action was especially detrimental in motion. This inefficient structure was necessitated by a lack of materials which could be used for structural members having good heat insulating properties and simultaneously low weight.

The new refrigerated trailer we produced (Figs. 9 and 10) has structural members made out of reinforced plastic. Each member serves also as a spacer between the inner corrugated plastic and the outer smooth skins. The space between them is filled with insulation. The subframe, composed of plastic cross members and insulation, is sandwiched between aluminum extruded floors and plastic sheets.

Creation of this vehicle was possible by "Lamicor," very special glass-reinforced laminates developed by Strick. (The average physical properties of Lamicor are listed in Table 1.)

Summarizing, the chief outstanding advantages

Table 1 – Physical Properties of Lamicor Polyester Mat Laminates

1. Flexural Strength

Five test specimens were prepared from each sample and tested in accordance with Federal Specification L-P-406b, Method No. 1031.1.

Flexural Strength, psi

	Sample No. 1	Sample No. 2	Sample No. 3	Sample No. 4	Sample No. 5	Average
3/16 In	38,500	42,100	31,900	36,100	31,300	36,000
¼ In.	38,000	35,500	40,000	38,100	36,900	37,700
⅜ In.	28,400	31,900	31,400	34,800	29,500	31,200

2. Compressive Strength, Edgewise

Five test specimens were prepared from each sample and tested in accordance with Federal Specification L-P-406b, Method No. 1021.1.

Compressive Strength (Edgewise), psi

	Sample No. 1	Sample No. 2	Sample No. 3	Sample No. 4	Sample No. 5	Average
3/16 In.	31,900	33,600	34,800	34,000	30,800	33,000
¼ In.	35,100	37,300	33,900	33,500	36,100	35,200
⅜ In.	37,100	33,500	32,700	32,100	35,100	34,100

3. Shear Strength (Double Shear)

Five test specimens were prepared from the ¼-in.-thick material and tested in accordance with Federal Specification L-P-406b, Method No. 1041.

Shear Strength (Double Shear), psi[c]

	Sample No. 1	Sample No. 2	Sample No. 3	Sample No. 4	Sample No. 5	Average
¼ In.	7800	8000	8300	8300	8500	8200

4. Tensile Strength and Modulus of Elasticity

Five test specimens were prepared from the ¼-in.-thick material and tested in accordance with Federal Specification L-P-406b, Method No. 1011.

Tensile Strength, psi

	Sample No. 1	Sample No. 2	Sample No. 3	Sample No. 4	Sample No. 5	Average
¼ In.	30,100	25,200	30,900	27,100	25,100	27,700

Modulus of Elasticity in Tension, psi × 10^6 (Young's Modulus)

	Sample No. 1	Sample No. 2	Sample No. 3	Sample No. 4	Sample No. 5	Average
¼ In.	1.98	1.78	1.98	1.81	1.80	1.87

5. Impact Strength

Five test specimens were prepared from the ¼-in.-thick material and tested in accordance with Federal Specification L-P-406b, Method No. 1071.

Impact Strength (Notched Izod), ft-lb per in. of notch

	Sample No. 1	Sample No. 2	Sample No. 3	Sample No. 4	Sample No. 5	Average
¼ In.	17.86	15.98	16.14	18.42	16.76	16.99

Fig. 9 – Plastic refrigerated trailer

Fig. 10 – Rear view of plastic refrigerated trailer

of the plastic refrigerated trailer are as follows:

1. Weight saving factor of about 20%.
2. Gain in cubic capacity.
3. Durable, maintenance-free construction.
4. Completely effective insulation.

The future of glass-reinforced plastics seems to be bright. But it will be so only if its properties are honestly and impartially appraised, and its characteristics intelligently evaluated and competently applied in design.

Fibrous-Glass Reinforced-Plastic "Door-to-Door" Delivery Truck Bodies

– Walter R. Herfurth

THERE appears to be an ever-increasing interest by delivery truck operators and manufacturers in the use of fibrous-glass reinforced plastic for the construction, either partially or wholly, of delivery-truck bodies. This composite material is comparatively new, as were steel, aluminum, and magnesium at one time. Each of the latter has had its period of trial and error, as will fibrous-glass reinforced plastic. As we have heard from Mr. McCann, the physical, mechanical, and production characteristics of this modern miracle material differ in many respects from the other metal or composite materials.

As with other materials and methods based on the sciences of chemistry and electronics, there is considerable glamor and fascination associated with reinforced plastic. There is no limit to the potential applications of the material in the minds of the enthusiasts. This is not all illusion, however, and there is no doubt that each of the hardheaded, dollar-conscious truck operators who has been venturesome enough to subsidize or completely finance the construction of delivery truck bodies anticipates with good reason some economic advantage from the utilization of one or more of the characteristics of the material.

We believe we will realize a number of short-range and long-range economies, and some intangible value, by the use of this material in our parcel delivery body. They are as follows:

1. No greater and possibly less initial investment, eventually.
2. Less weight.
3. Reduced fender and body damage.
4. Longevity.
5. Less repair and rebuilding expense.
6. Reduced appearance-rehabilitation expense.
7. Heat insulation.
8. Translucency.
9. Shape design freedom.

The assumption on which we base our hope for less initial cost is that the total labor cost of fabrication, assembly, and mounting about 20 moldings per body, plus amortization of design and tooling cost over a limited production, as compared to the same items of expense involved in the several hundred individual parts required for a metal body, will be less – and therefore offset the difference in cost of the raw materials. If this end is not achieved immediately, the outlook is that it may be eventually. The slope of the fibrous-glass and resin price curve is downward. Improved materials and manufacturing methods have been developed in the short period since our pilot model was produced and will no doubt continue to be developed. The cost outlook with this material is down rather than up.

Fig. 11 – Interior of body showing diffused illumination provided through translucent roof section

The strength-weight ratio of properly made fibrous-glass laminates results in less total weight, notwithstanding the requirement for thicker sections. Although we are not in the type of business which would involve gvw limitations, there is at least the prospect of reduced fuel consumption and tire wear. It is conceivable that for a given size body and payload a lighter weight chassis could be used. Anything that reduces the ratio of tare weight to payload should favorably influence the ratio of income to outgo. Another condition developed in our pilot model which we had not anticipated was that the center of gravity of the vehicle was lowered, which our drivers said improved the riding quality and roadability. The advantage of this quality may be questioned because, although the chance of upset is reduced, it may tend to make our drivers take corners faster than they do now.

Reduced fender and body damage should be experienced as a result of the flexibility and energy-absorbing ability of fibrous-glass laminates. That which does not dent or take a permanent set does not have to be straightened, therefore, good appearance is maintained at no cost.

As far as we now know, the life of the body is

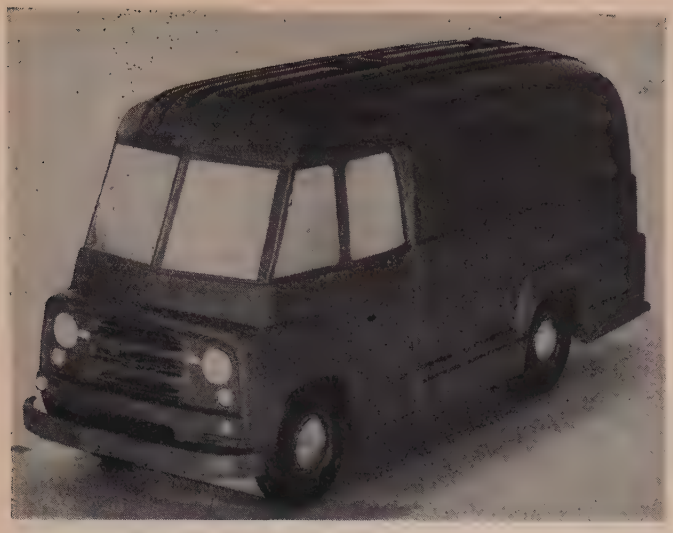

Fig. 12 – One-tenth-scale clay model of plastic truck

Fig. 13 – Completed prototype of plastic-bodied United Parcel vehicle

limitless. We will not have to be concerned with corrosion, electrolysis, dryrot, or decay, as we have with aluminum, steel, or composite bodies. The body will not require undercoating.

If sections of the fenders or body are broken out or cracks develop due to forcible contact with another object, we are assured that repairs will be easy and inexpensive.

In order to maintain our appearance standards, it has been necessary to adopt a policy of sanding down and applying a coat of color about once a year. This is principally because of tree branch scratches. Our plastic bodies will have a highly scuff-resistant pigmented outer coating over the fibrous glass. It is hoped that this will obviate the necessity for refinishing for several years. Cleaner vehicles and less washing expense may result, since it will be feasible to use washing solutions with greater detergency without fear of damage to the surfaces.

Of intangible value to us is the low heat conductivity. Our drivers say the plastic body is cooler to work in on hot summer days than others, even with insulated roofs, that we operate. Less fatigue and exhaustion should result and therefore, we hope, more production.

The translucency of the unpigmented laminate permits us to incorporate a skylight in the entire area of the load-compartment roof merely by blocking off the pigment from that area (Fig. 11). There are no joints to leak or glass to break. For loading and reading of addresses we have thoroughly diffused shadowless lighting even on cloudy days. Less drain on the battery will also result, since body lights will not be used as much.

Liberties in design to obtain a modern, pleasing, and attractive appearance can be taken when designing for molded fibrous glass that are not permitted when designing moderate-production bodies in any other material. There appears to be quite general agreement that we succeeded in producing

Fig. 14 – Plastic truck, showing plastic sliding doors and low entrance steps. Grill is hinged at bottom and is removable for access to radiator

Fig. 15 – Rear door of truck, a thin panel of fibrous-glass reinforced plastic that slides on tracks into roof

a modern attractive body (Figs. 12, 13, and 14). What this is worth in hard cash is difficult of determination. In our case, however, we were able to design into our body, in addition to appearance, certain dimensional features which we could not

obtain in vehicles purchased off the shelf, without considerable additional modification expense.

It may be pertinent to acquaint you with some of the features we have for years designed into our bodies, including the plastic body, which we have learned reduce our delivery expense. The load space in our body is 137 in. long, and averages about 72 in. wide and 74 in. in height, which results in a capacity of about 375 cu ft. We find the ample head room permits our loaders and delivery men to work in an upright position, resulting in less fatigue and greater efficiency. The vehicle is 76 in. in overall width. This is dictated by the size and spacing of the package bins in our delivery stations. The rear portion of the floor is depressed about 10 in. to the level of the rear step and bumper. This is at the same height as the delivery station platforms. In combination with a 70-in.-high rear body door (Fig. 15), this permits our loaders to walk into the body with an armful of packages without stooping.

Lunn Laminates, Inc., Huntington, L. I., N. Y., constructed the pilot model and are at present in the process of building 19 more to our order. Possibly by this time next year we will be in a position to tell whether any of our fond hopes have been realized. The industrial designing firm of Walter Dorwin Teague Associates was engaged to aid us in the design of the body.

Plastic Bodies Can Be Repaired

– Henry Jennings

A FEW months ago we started out to get an article on the repair of fibrous-glass reinforced plastic bodies. The purpose of the article was to tell the shop superintendent who was totally unversed in fibrous-glass reinforced-plastic lore what he would be up against when one of these bodies arrived at his shop for repairs as a result of accidental damage.

For once our position for this investigation was correct. We did not have to make any preliminary investigation because our knowledge of the subject was casual – well, meager, perhaps, or, if you want it straight, almost nonexistent. This put us just about where we wanted to be – that is, on a par with the shop superintendent whom we were trying to serve. We felt that if we could understand the process of repair, we could transmit the information to him in a manner so that he could understand it.

The Strick Trailer Co. very kindly agreed to demonstrate a method of repair. They guaranteed to make us understand what we saw and what we were trying to record. I believe they did.

Our conclusion after preparing the article is that fibrous-glass reinforced plastic is an easy, if not the easiest, body material to repair. Very little training and experience is indicated for the mechanical crew before they become very proficient.

As usual, some difficulty arose. First we were unable to locate a damaged panel. This meant that we would have to deliberately punch a hole in a good panel. This we did, although they were somewhat scarce at the time and I understand they had to tie up the production man while we damaged a piece of his handiwork.

To create our own accident, we gave the largest mechanic in the shop a 3-lb hammer and let him whale away at a new panel intended for use in a truck body. Repeated blows netted us only a few superficial scratches. So, impatient to be on with the job, we gave the man a large nail which he

Fig. 16 – Cleaning area around break in fibrous-glass reinforced plastic panel in preparation for repair

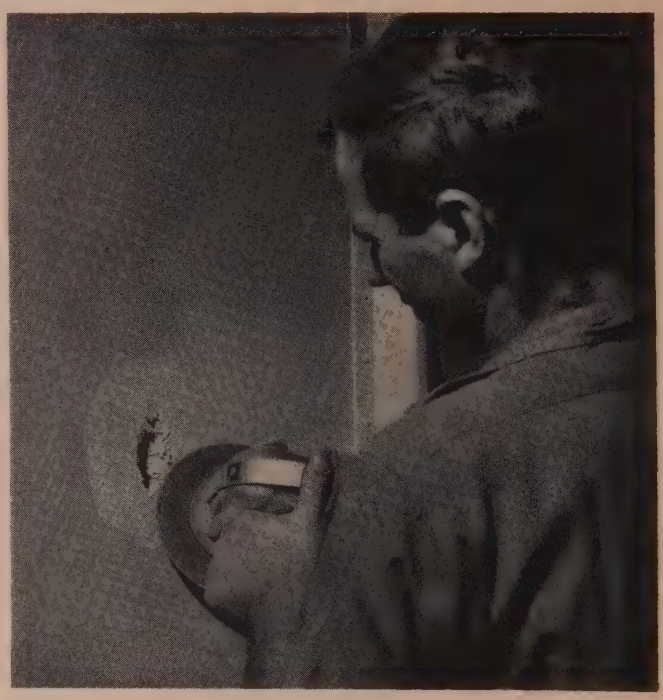

Fig. 17 – Sanding area of break

succeeded in driving into the panel. With this as a starter, we enlarged the hole to about 4½ x 1½ in. This damage was repaired in the following steps.

First, an area extending 12 in. from the break in all directions was thoroughly cleaned with a standard shop solvent (Fig. 16). There is no reason to believe that any of the cleaning fluids found around an automotive shop will not be satisfactory.

Next step was to sand an area extending about 6 in. from the hole on all sides (Fig. 17). The size of this tapered area may vary, with 6 in. from the fracture being about the maximum distance. The sanding should be deeper at the hole to give a Vee or scarving effect.

At this point the fibrous-glass cloth patches are cut with ordinary shears or a shop knife (Fig. 18). The first patch should be cut to overlap the break about 2 in. in all directions. Other patches should be cut in graduated sizes to fill out the sanded area. The number of patches depends upon the thickness of the panel – one patch for each 0.025 in. of thickness of the panel.

Before mixing the resin the patches should be weighed (Fig. 19). This will determine the amount of the batch. About ⅔ as much resin as cloth by weight will be required. Since the resin mixture is temperature-sensitive, it is practice to mix a small

Fig. 18 – Cutting fibrous-glass cloth patches in graduated sizes to cover sanded area

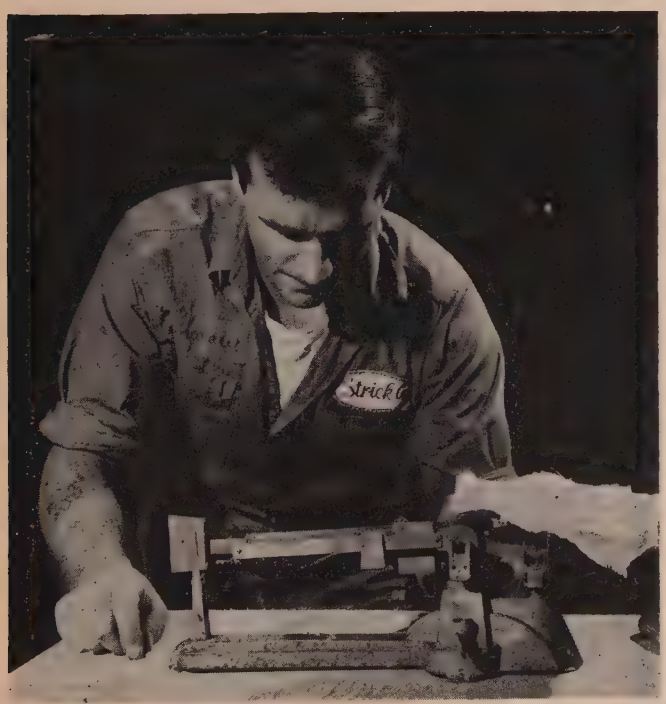

Fig. 19 – Weighing patches to determine amount of resin needed

Fig. 20 – Painting area of first patch with resin

Fig. 21 – Repeating painting process for subsequent patches

quantity in a waxed-paper cup and time the setting period. The target is 20 min at 70 F. If the temperature is higher, slightly less of an ingredient known as promoter is used. Roughly, the mixture is 100 parts of resin to 50 parts of pigment to 3 parts of catalyst to 3 parts of promoter.

When the batch is mixed in correct quantity, the procedure is to paint a coat on the area roughly covered by the first patch (Fig. 20). Then when the first patch is laid in, the painting process is repeated (Fig. 21), and so on until all the patches have been applied.

When all the patches have been applied, a sheet of cellophane is laid over the injured area and, with an ordinary squeegee or scraper, the area is smoothed out with all strokes starting at the center and working towards the outer edges (Fig. 22).

When the smoothing-out process is completed, any smooth pressure plate which more than slightly covers the injured area is applied with a very gentle pressure (Fig. 23). This pressure is kept applied for about one hour.

At the end of this time, the fixture and the cellophane are removed from the panel (Fig. 24). When this is done, the operator can tell how good a job of smoothing out he did.

Sanding the area will compensate for the shortcomings of the smoothing out process (Fig. 25). If the panel has a sheen, it is recommended that another coat of resin be applied and then buffed

Fig. 22 – Cellophane laid over injured area, and squeegee used for smoothing

Fig. 23 – Smooth pressure plate applied gently for about 1 hr

Fig. 24 – Plate and cellophane removed

Fig. 25 – Sanding of finished repair

with a power tool.

When the work is done well and carefully you wind up with a panel looking like that in Fig. 26. Frankly, we took before and after pictures, and we could not tell them apart after they got mixed up except by number.

It is recommended that when a fracture is accessible on both sides the same treatment be given both sides. I do not wish to fly in the face of these recommendations made by men who know a lot more about plastic bodies than I do, but I am willing to hazard a guess that there are going to be a lot of repairs made on one side only. It is further recommended that repairs to holes without extended cracks, up to the size of a dime, be made without applying the fibrous-glass patches. This

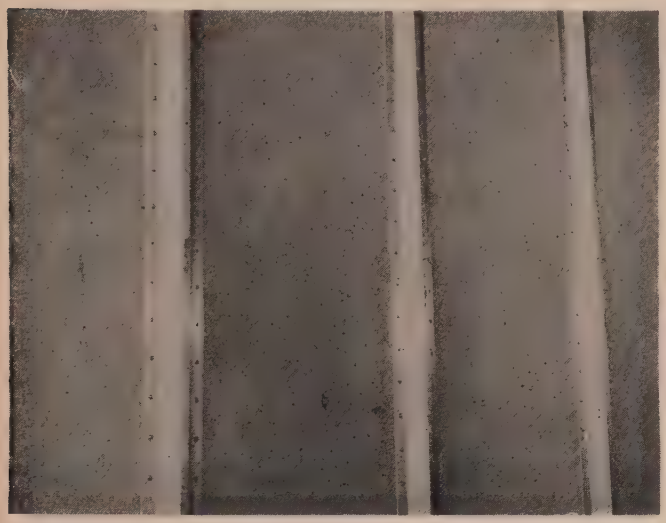

Fig. 26 – Panel with repair work completed

Fig. 27 – Damaged fibrous-glass fender

Fig. 28 – Broken area cleaned with sander and cracks Veed out

Fig. 29 – Four separate cracks revealed after cleanup, each to be repaired individually

Fig. 30 – Fibrous-glass cloth patches applied

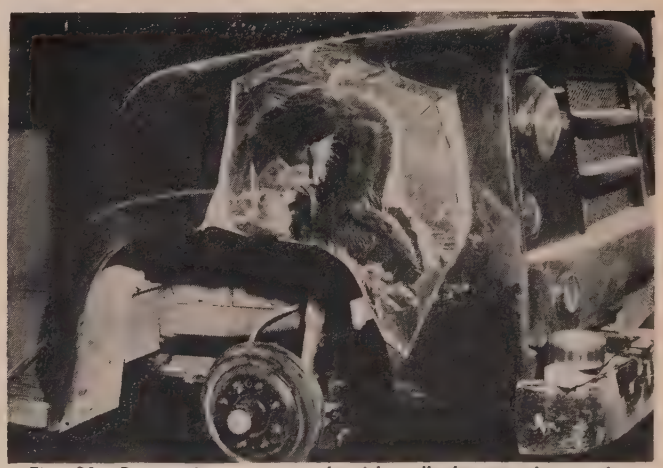

Fig. 31 – Damaged area covered with cellophane and smoothed

Fig. 32 – Cellophane removed and area sanded

Fig. 33 – Surface prepared or painting

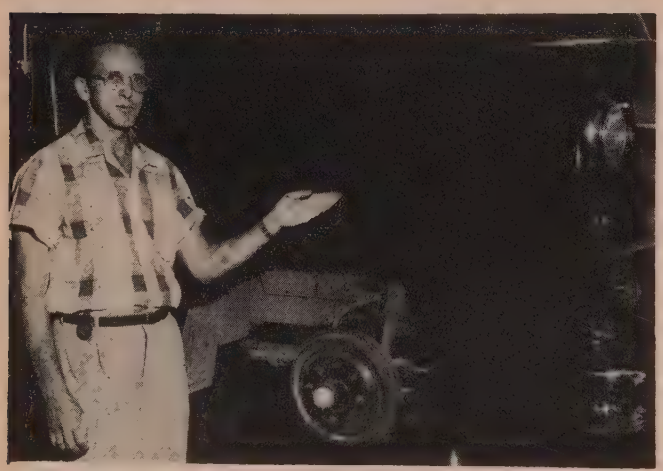

Fig. 34 – Finished repair job

recommendation need scarcely be made, as plenty of shop superintendents will find out about this by themselves.

About the time we finished our investigation, United Parcel Service banged a fender against a support column in one of their garages. This particular surface was painted, and that accounts for the large scarred area (Fig. 27). This body and fenders were fabricated by Lunn Laminates, and this repair was made by that company.

Figs. 28-34 illustrate the similarity in the methods of repair.

First the area is cleaned up with a sander and the cracks are Veed out (Fig. 28). You will note that the vehicle is jacked up and the wheel removed. The other side of the fender is accessible, and the repair is to be made on both sides.

The clean-up and inspection discloses that there are four separate cracks which must be repaired (Fig. 29). Each one of these receives individual but identical treatment.

Next the fibrous-glass cloth patches are applied. In Fig. 30 they are held in place by strips of adhesive tape mostly for photographic purposes.

When the application of the patches has been completed, the damaged area is covered with cellophane. Fig. 31 shows the damaged area ready for the smoothing process with the scraper.

After the curing time has elapsed and the cellophane cover has been removed, the sanding operation smooths out the hills and valleys (Fig. 32). I have the impression that this material responds to sanding more readily than some other materials.

Now the surface is prepared for paint (Fig. 33). Remember that this particular fender was painted. That accounts for the patches of discoloration.

After painting, the restored fender is ready to go (Fig. 34). This job was the United Parcel Service original. Subsequent trucks have the pigment mixed into the resin and are not painted, which eliminates one step in repair as well as in original construction.

DISCUSSION

Emphasizes Need for Much More Knowledge

– Woldemar Schultz
Ford Motor Co.

MR. McCann's classic comment in the introduction of the very useful compendium entitled "Fiberglas Reinforced Plastics," by Ralph H. Sonneborn of the Owens-Corning Fiberglas Corp., I, for one, cannot forget: "In the course of their development, reinforced plastics have suffered somewhat from misunderstanding on the part of designers and users, caused by too-glib definition and oversimplification of techniques. At one time they were called 'low-pressure plastics' simply because the resins may be catalyzed to cure at low pressures with the application of little or no heat. Today, however, it is known that both heat and pressures are required to produce good parts with satisfactory densities and finishes. It is known, also, that these new structural materials are not cheap nor are the methods of their processing. They are economical in competition with other materials only when properly designed and engineered, and properly produced."

Since Henry Ford engineered a plastic car development almost 20 years ago, a great many valiant efforts have been made to utilize late discoveries to facilitate use of plastics as against conventional materials, and progress is being made.

This business is full of surprises. Small wonder, then, to observe several hundred plastic materials being sold under more than a thousand trade names.

We would like to use more plastics, but they must give us better performance, better economy, better appearance.

Mr. Brown's paper on transport tanks presents a matter-of-fact story that separates the sales picture from the engineering aspect. It also emphasizes, in general, inadequate and faulty engineering which has been a serious threat to progress of fibrous-glass reinforced plastics.

Its high strength-to-weight ratio is to an extent problematical, that is, it is obtained at a price.

The four problems encountered in constructing liquid holding tanks are, of course, common shortcomings, but they are under constant improvement and some corrections have already been accomplished.

Not being familiar with the requirements of tanks, my comments are limited to generalities of fibrous-glass reinforced plastics.

For the other disadvantages Mr. Brown listed, such as result from engineering problems, high costs, or manufacturing troubles, one must agree that pioneering has its handicaps.

A most promising note appears at the end of this paper in the last paragraph. It points to the future: "... construction when made of fibrous-glass reinforced outer surfaces with a low-density expanded plastic cellular core will, I believe, be the best practicable answer to a low-weight, high-strength, high-capacity, general-purpose transportation tank."

Mr. Wulc's paper is a rather interesting presentation of fibrous-glass reinforced plastics used in conjunction with other materials, like aluminum. This makes for greater weight saving.

However, if it were possible to separate more strictly the sales viewpoint from engineering, pure and simple, we would get to the heart of the matter.

Since fibrous-glass reinforced plastics cannot actually be considered a substitute for steel or aluminum, especially on large-volume production, they might, in this case, fit the requirements of special-purpose vehicle bodies of relatively low-volume manufacture, mostly because of the initially lower cost of tooling.

The large-volume automotive competitive system must operate from a sound economic base, particularly in a competitive economy, and that, of course, calls for quality at lowest possible costs, and, for one thing, for progressive automation.

It is therefore an accomplishment for a new material like fibrous-glass reinforced plastic – still in its infancy – to compete with the long-established materials.

This paper gives a good picture of the known advantages versus the known disadvantages, and later we might learn about the unknown parts. The complexity of factors controlling strength, for instance, is vexing. Neither the economic aspects (man-hours, for instance), nor engineering design have as yet been completely resolved.

It is to Mr. Wulc's credit that he calls attention to the "hundreds of variables involved in manufacturing laminates," and it is good news that the physical properties of fibrous-glass reinforced plastics, like creep and flow under stress; moisture absorption as it affects modulus of rupture; tension and compression, shear, fatigue, extremes of cold and heat distortion, not to mention quality control, are still in a state of flux, with so many factors governing the strength of laminates.

In the final analysis, a comparison could be made of expensively built vehicles, or else with a standard product of the automotive industry. It depends on the yardsticks, like performance, costs, and appearance.

Mr. Herfurth reports that venturesome truck operators appreciate light-weight parcel-delivery vehicles for special-purpose trucking as against standard vehicles. But let it suffice to say that in the present state of the plastic art, the average plastic body does not represent competition for a well-engineered and economically produced body of steel or aluminum.

This body is being advertised as heavy duty and light in weight, and it features widely dissimilar materials, like fibrous-glass reinforced plastics, aluminum and wood. This means that a composite construction appeared desirable for the sake of lessening tool costs and perhaps weight. This may or may not outweigh the greater cost of materials. Longevity, climatologically considered, cannot yet be guaranteed except on expensive materials. We share Mr. Herfurth's hopes, but we remember that the average automotive body can be assembled by spot welds in fewer minutes than the number of fingers on your hands; however, this is an unfair comparison.

Actually, fibrous-glass reinforced-plastic parts could gain enormously by the saving grace of integration – combining many pieces into one molding, similar to die casting zinc alloys, and supplemented by plastic foam stabilizers of the cellular type, as mentioned by Mr. Brown; or by other types of structures designed for plastics, as aircraft is developing new designs by utilizing expanded foamed or molded-in stiffeners of light weight.

Translucency is desirable, particularly when daylight comes in, but the elimination of inert fillers and pigmentation does not help costs or resin shrinkage, because it exposes the fibers. If we knew how many bodies of this type passed the test of time and various types of climate, it would greatly enhance the state of the art and further promote the use of fibrous-glass reinforced plastics.

We agree with Mr. Jennings' title: "Plastic Bodies Can Be Repaired." However, it is one operation that relies entirely upon the craftsmanship of the individual, and, incidentally, the same applies to repair of more conventional materials.

Sheet-steel metal finishers have been trained for some time; but, unfortunately, we have not yet started the training of fibrous-glass reinforced-plastic "patchers and finishers."

And we don't mind the length of time required for curing, or the fact that pressures might have to be applied for one hour, because the finishing of a metal body might take longer. At any rate, further development of the processes of patching reinforced-plastic bodies could boost the do-it-yourself business and possibly bring down the high cost of glass-cloth patches.

My question is – should we apply this method of repair to dented or torn steel fenders as well, and use epoxy resins rather than lead? But I don't want to be facetious; I rather hope for fewer repairs. I'd rather promote **Frp dent- and rustproof fenders** and Frp all over, for my crystal ball calls for better things to come. A few examples follow:

1. Atomic energy has been put to use converting thermoplastic into thermosetting materials, and it is possible that radiation from an atomic pile might be destined to become a major new tool. Radiation actually changes the molecules of a substance, and can be compared to catalysts now widely used in improving the output of chemical and oil refining plants. One trouble is that the price and sources of radioactivity are still costly. Radioactive cobalt-60 is priced at $5.00 per curie.[a]

2. Fibrous-glass reinforced plastic goes into submarine superstructures, radomes, flying missiles, turbines, and rockets, and does right by their requirements, at a price, of course. Fibrous-glass reinforced plastics are almost ideal for marine applications, like boats.

3. The U. S. Department of Agriculture survey of fabrics and fibers used in passenger cars is making promising headway.

4. Strong plastic laminates from furane resins produce low pressure panels with flexural strength of 65,000 psi,

[a] 1920 price, according to Dr. V. L. Parsegian, director of research, AEC.

and edgewise compressive strength up to 40,000 psi.[b] This resin can be made from such noncritical materials as corncobs and other vegetable byproducts (PB-111418).

5. A glass-filled silicone (#301) developed for molding high-temperature plastics, pulled hot, without cooling, will take high-bake enamels up to 450 F and approach a new class of engineering materials with a most unusual combination of properties. A chemical hybrid, it comes close to a cross between the organic and the inorganic. Silicones are organo-silicon-oxide polymers, and, as such, chemical cousins of glass.

6. Integration of many parts into one, die-casting-wise; premix compounds with fiber orientation to simulate direction of structural grain, unidirectionally; postforming; special means of reinforcing secondary bonds; and so forth, are in the background of many new developments; this cannot be overemphasized.

Commends Current Progress in Plastics

– A. J. Carter
Chrysler Corp.

ALL automotive engineering divisions are ever on the alert to find better and cheaper materials for their products. Keen competition makes this a necessity. We are very familiar with polyester-reinforced plastics, and do understand the simple fact that each part must be designed for the material to be used. It is true that to get a quick indication of how a part might function, we will use an existing mold or form to make a part from a new material, but in our final evaluation we certainly keep in mind the fact that the part would be improved by design changes.

To give you some idea of our work with this material, let me point out that in 1944 we started an intensive program to evaluate the physical and chemical properties of reinforced-polyester plastics and to fabricate some automotive parts in order to determine where this new material might be utilized in our industry. The following parts were made: Chrysler rear deck lid, Chrysler station-wagon door, Plymouth right rear fender, Plymouth turret top, DeSoto rear deck lid, DeSoto hood, DeSoto rear fenders, and DeSoto instrument panel.

The average weight saving in these parts was 48%. They were all painted, and considering the methods used in their fabrication, their appearance was acceptable. All parts performed successfully on road-test cars. The DeSoto left rear fender and deck lid were damaged in service, but the damage was considered less serious than it would have been had the corresponding metal parts been involved.

Since this initial program, we have worked closely with the resin and fiber manufacturers and fabricators, and have considered many applications for this material. Chrysler's release of an all-plastic heater-housing assembly for their 1955 models represents the results of such a joint effort. Cooperation of this nature goes a long way toward insuring satisfactory performance. This is the largest volume usage of polyester resins in the automotive field today.

The SPI has done an outstanding job in promoting and standardizing reinforced plastics, and ASTM is now becoming active in this field. Committee D-20 on plastics has created Section 18 to prepare specifications on glass-reinforced rods and tubes, sheets, corrugated sheets, resins, and fibers. This effort will further promote use of these materials.

The use of reinforced plastics for transport tanks appears to be a natural application for this material. We do agree with Mr. Brown that the major problem will be contamination due to absorption of liquids by the plastic. There is every reason to believe that this problem will be overcome by the use of specially formulated interliners. These interliners may be either organic coatings or metals.

The development work of the plastics division of Strick Co. is very interesting, and they are to be congratulated for the progress made. Certainly their efforts have contributed and will contribute much to hastening the time when reinforced plastics will be used for truck cabs and bodies. The experiences of United Parcel Service with reinforced-plastic delivery bodies will also be carefully watched and evaluated.

Such pioneering programs will go a long way in establishing the quality and cost of reinforced plastic bodies and will give some insight into the type and amount of equipment necessary to meet production line requirements of the automotive industry. It will show what fabricating and assembling techniques are most practical for a satisfactory body, and will establish the type of cemented and mechanical joints necessary to adequately hold the various parts together. Another important question answered will be the amount of sanding and reworking of the exterior surface necessary to get the quality paint job now considered essential in the automotive field.

Before closing, a few words should be said on the subject of reinforced-plastic tooling for sheet-metal parts versus reinforced-plastic parts. Much has been written and said concerning the utilization of reinforced plastics for low-volume parts because of the low tooling costs. Today, however, because of the rapid strides being made in the plastic-tooling field, it appears to be advisable to carefully investigate and compare the economics and practicability of these two production methods. Plastic tooling has one decided advantage, in that it enables the manufacturer to utilize his own existing equipment in fabricating the parts. Considerable time can also be saved, since plastic tools can be made in only a fraction of the time required for steel tools.

Describes Details of Corvette Body Construction

– E. J. Premo
Chevrolet Motor Division, GMC

MR. McCann's introduction of the two main types of plastics, comparing the thermoplastic type to a candle which can be softened by the application of heat and remolded; and comparing the thermosetting type, which is used for body panels, to a hard-boiled egg which cannot be returned to the previous condition, is an excellent explanation of the basic difference between the two types of plastic. I wish that I had thought of that explanation during the question period of an SAE meeting last spring, when asked if the Corvette body could be melted and put back in the bottle.

His suggestion that an SAE committee meet with an SPI committee to set up a program of evaluating reinforced plastic as an automotive material, is very timely and merits consideration.

Mr. Brown's report on the use of a reinforced plastic for liquid-transportation tanks and Mr. Wulc's and Mr. Herfurth's applications to the construction of trailers and delivery bodies very ably pointed out many advantages and disadvantages of this material, which we also have experienced.

Their recommendation that potential users recognize the pitfalls as well as the favorable aspects to gain the maximum benefits of its use is good advice.

We are interested in the development of reinforced plastics as we are in any other automotive material that will result in improved passenger cars and trucks. Our responsibility to the motoring public demands this interest.

An opportunity to explore the potential of reinforced plastic as a body material occurred when GM management decided to produce an American sports car (Fig. A). Our assignment was to complete a design and tool it for production in five months. The only practical means of accomplishing this objective was by use of reinforced plastic.

The hand-lay process of manufacture was used (Fig. B) to obtain limited production quickly, regardless of the high

[b] Wright Air Development Center.

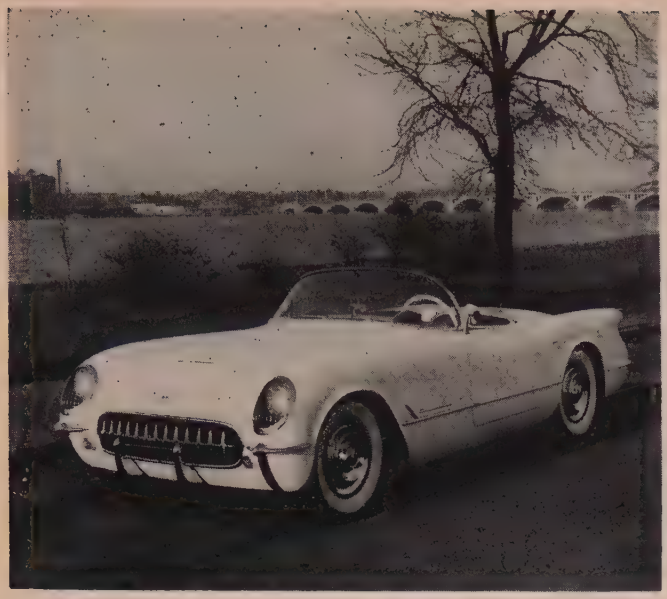

Fig. A – Chevrolet Corvette

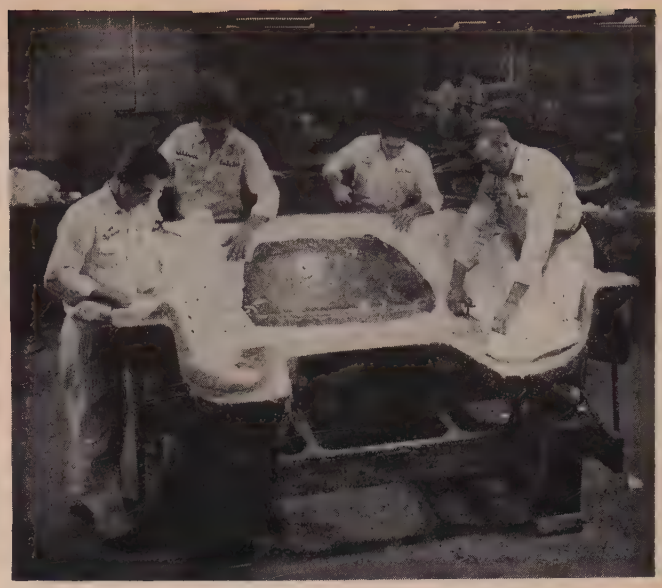

Fig. B – Hand-lay process – fitting fibrous glass cloth and mat to mold

piece-cost involved. The reinforcement utilized consisted of a sandwich of woven fibrous-glass cloth filled with mat.

The vacuum bag process (Fig. C), which used fibrous-glass mat only, followed; this increased production and reduced piece cost in the interim until the matched metal dies, which resulted in the highest production and lowest piece cost, could be completed.

The matched metal die process used for Corvette parts utilized preforms made of fibrous-glass roving which is machine cut in short lengths and deposited on a screen shaped to the inside contour of the finished part. The fibers are retained on the rotated screen by suction, and a small amount of resin is sprayed on to hold the resulting preform together (Fig. D).

The preform and screen are then passed through an oven to cure the resin binder (Fig. E).

To obtain a smooth surface suitable for exterior panels, very fine filaments of fibrous glass are deposited on the outer surface of the preform when it is made, or a fine-textured-surface mat is laid in the metal die (Fig. F).

The preform is then added and a measurable amount of resin poured on it (Fig. G).

The die is closed for a curing cycle of 2-3 min, after which it automatically opens for removal of the completed part (Fig. H). This process yields 15-25 parts per hr per mold, the quantity being governed by the size and shape of the part.

We have followed the rapid development of reinforced-plastic production processes with keen interest. A method of making preforms for use with matched metal dies observed recently is known as the "Slurry" preform process.

Reinforcing materials used include cellulose and fibrous glass. These fibers are mixed and treated, in the tank shown in the background of Fig. I, to assure a uniform blend and to prevent balling. The resin necessary to hold the preform together is applied in this operation.

After the prepared fiber is separated from the liquid treating agents, it is added to a continuously agitated mixture of water and fiber in the lower main tank, as necessary to maintain a consistent fiber content.

The preform screen is mounted on a platform (Fig. J), which can be raised and lowered hydraulically, and an air hose is connected below the screen.

As the platform is lowered into the tank, air under pressure is forced through the screen to clean it, and then vacuum is applied, resulting in a filtering process which deposits a uniform layer of fiber on the screen (Fig. K).

The amount deposited depends on the density of the mix-

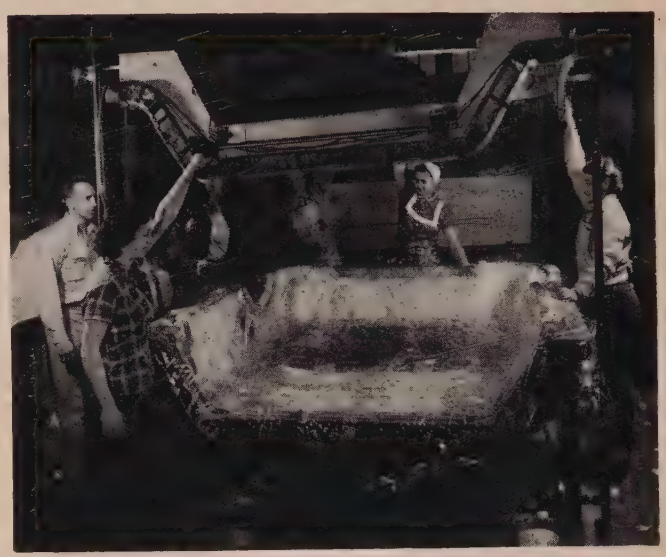

Fig. C – Vacuum bag process – closing mold for curing cycle

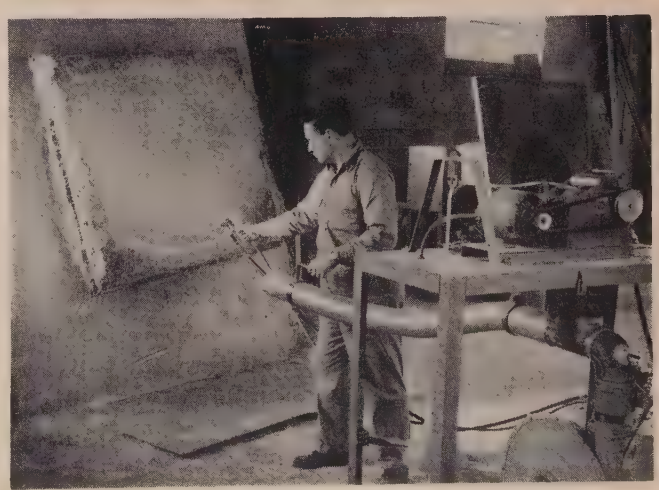

Fig. D – Making preform for use with matched metal mold process

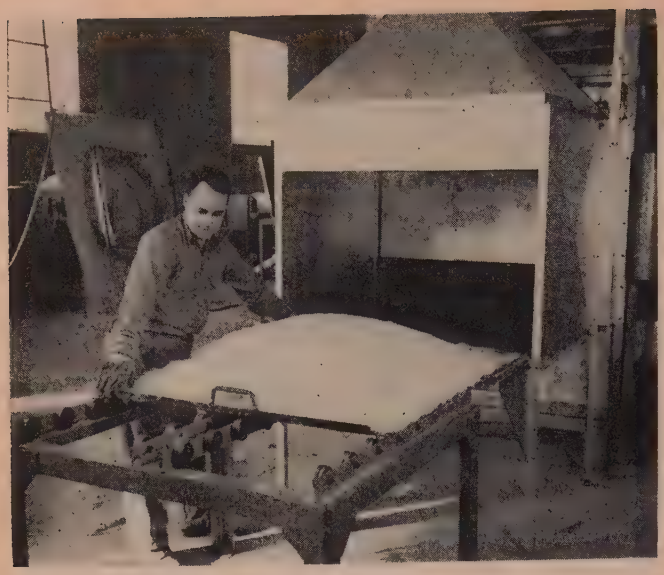

Fig. E – Preform is passed through oven to cure binder

Fig. H – Completed part is removed after 2-3-min curing cycle

Fig. F – Fine textured fibrous-glass surface mat is laid in matched metal die

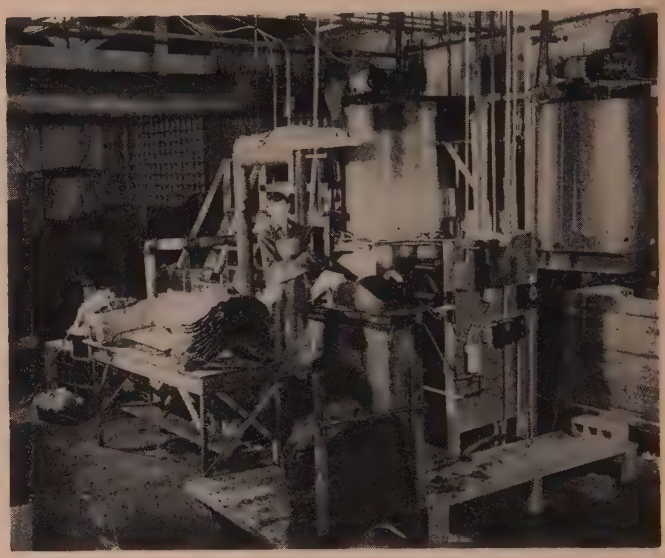

Fig. I – Equipment used to make preforms by Slurry method

Fig. G – Preform is added to surface mat and resin poured on

Fig. J – Preform screen for chair seat mounted on platform with air hose connected below screen

Fig. K – Preform screen lowered in tank containing mixture of liquid and fiber reinforcement

Fig. M – Rubber sheet spread over preform to remove excess liquid

Fig. L – Uniform layer of fiber is deposited on screen by filtering process – vacuum applied below screen

Fig. N – Preform placed on heated drying die to remove remaining moisture and cure resin binder

ture and the duration of the filtering action, which is controlled by an automatic cycling mechanism (Fig. L).

The vacuum remains on as the platform is raised and a sheet of rubber is spread over the preform, applying atmospheric pressure to remove excess water and compact the fibers (Fig. M).

The preform is then placed in a drying die (Fig. N), where the remaining moisture is removed and the resin binder cured.

The matched metal die molding process employed (Fig. O) is identical with that previously described, and the rate of production is the same. By using a percentage of cellulose in combination with fibrous glass, the part cost is reduced. This combination is suitable when the higher strength and lower water absorption of all-glass reinforcement is not required.

The mixture of reinforcing materials results in rather unique patterns when the fibers are dyed different colors and clear resin is used. For example, the distinctive appearance of the darker part in the foreground of Fig. P is obtained by using brown cellulose fiber, white glass fiber, and clear resin.

The idea of utilizing semicured formable sheets of reinforced thermosetting plastic (Fig. Q) in a process similar to that employed for forming sheet steel was suggested some years ago as a way of obtaining higher production of reinforced-plastic parts. It was thought that physical properties could be better controlled and hand work greatly reduced by this means.

Such a material is now being manufactured.

The desired thickness of this material is produced by laminating basic layers which are approximately 0.008 in. thick (Fig. R). Manufacture of the basic layer is a continuous process. Filaments of glass are impregnated with a prepared resin mixture, and rolled on a mandrel (Fig. S), together with a layer of paper to separate the plies. Epoxy is being used as the resin for this material at the present time because it is best adapted to current uses and sheets up to 48 in. wide are available with thicknesses ranging from 0.075 in. to ½ in. Storage times of 30 days at 75 F and 150 days at 40 F are practical.

Sheets may be used with either the vacuum bag, pressure bag, or matched metal die processes.

When used with matched metal dies (Fig. T), the material is handled very much like sheet steel. Parts up to 8 in. in depth can be formed.

Although the resulting part strengths are very high – over 40,000 psi tensile strength, and 64,000 psi flexural strength – a substantial reduction of mold time and cost will be necessary to increase use of this material (Fig. U).

Fig. O – Adding polyester resin to preform in matched metal mold

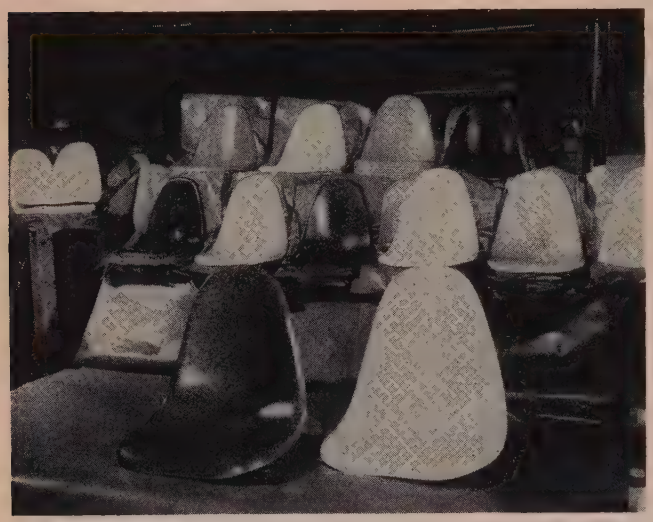

Fig. P – Completed parts. Variety of colors and patterns achieved by dyeing fibers

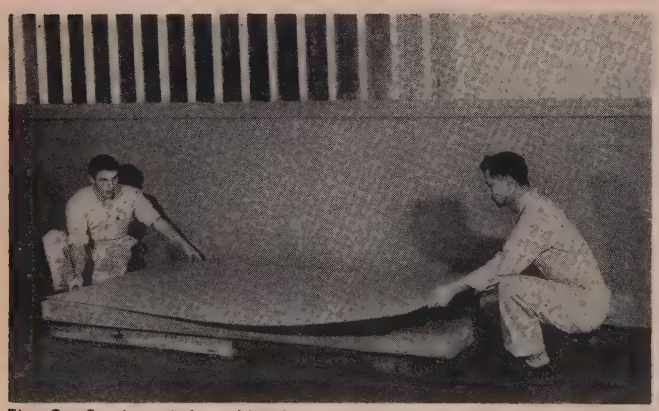

Fig. Q – Semicured formable sheets of reinforced thermosetting plastic for use in matched metal molds

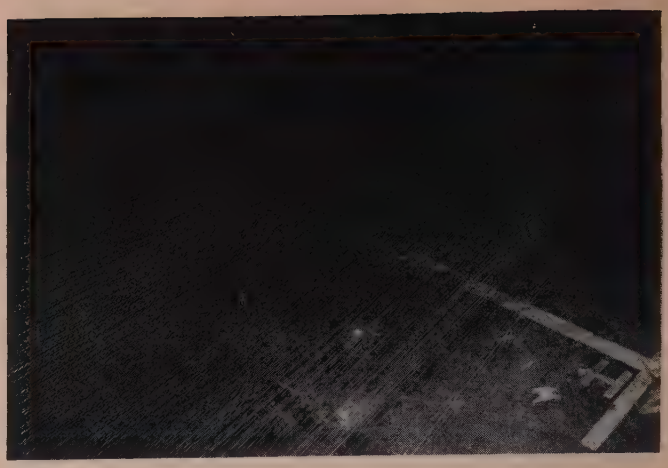

Fig. R – Filaments of glass to be impregnated with prepared resin mixture

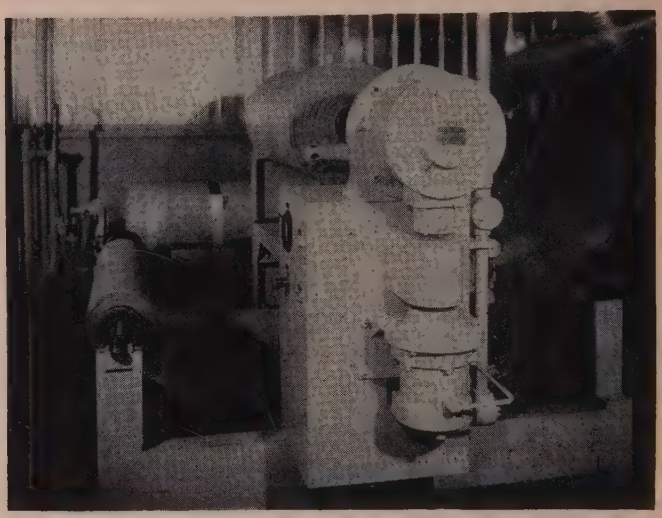

Fig. S – Single layer of material rolled on mandrel with paper separator. Sheets are made up of several layers of this material

Fig. T – Formable sheet inserted in matched metal mold

Another method, which has been employed extensively, is known as the Premix molding or Gunk process.

Over 1,000,000 lb per month of reinforced-plastic automotive parts are being produced by one manufacturer alone. Fig. V shows some examples.

The intricate shapes that can be molded by this process make it particularly adaptable to interior trim panels, arm rest foundations, and heater ducts (Fig. W). High structural strengths are not usually required for these parts, and sisal or other low-cost reinforcement may be used along with

Fig. U – Finished parts made of formable sheet

Fig. V – Variety of shapes produced from premixed resin and reinforcement

Fig. W – Intricate shapes molded by Premix process

Fig. X – Mixer for preparing reinforcement and resin Premix

fibrous glass to reduce cost.

The reinforcement and premixed resin, which includes colored pigment as desired, is thoroughly mixed and then transferred to an extruder where billets, of the size necessary to make the part, are formed (Fig. X). The bulk material or billets may be stored up to 3 months at room temperature and up to 6 months at 50 F.

A billet, and metal clips or local fibrous glass reinforcement, if necessary, are placed in a heated matched metal die (Fig. Y), which is then closed for a curing period varying from 30 sec to 1 min, depending on the thickness of the part.

Pressure of 400-600 psi is used to produce a smooth finish and reduce porosity. A temperature of 290 F assures completion of the cure by the time the part has cooled (Fig. Z).

When sidewalls are undercut or recesses required, slides or retractable cores are used, and residual flash is trimmed in much the same manner as is used in the zinc die-casting industry.

This process yields up to 40 parts per hr or 140,000 parts per year on a two-shift basis, per mold (Fig. A_1).

Equal in importance to every automobile manufacturer, to producing a desirable new product, is the essential requirement that the product reach the used-car market in good condition.

All too often, however, in spite of the precautionary measures taken by the manufacturer, a car reaches this stage with rusted-out body areas (Fig. B_1) which are difficult to repair by conventional metal patch and solder finishing methods.

To overcome this difficulty, a process of repair using reinforced plastic has been developed, which is related to that just described. The first step in this process is to remove loose material and sand the surrounding area (Fig. C_1) to assure a good bond.

Edges of the metal are then depressed to permit a buildup of the repair material and to allow smooth feathering out of

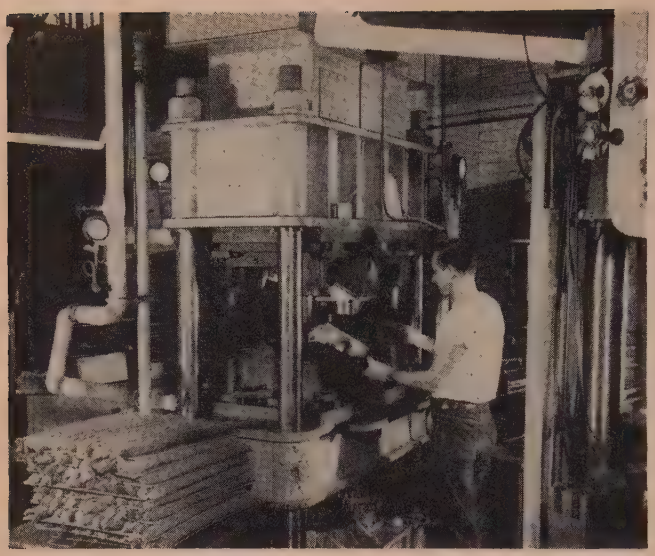

Fig. Y – Billet of premix being placed in matched metal mold

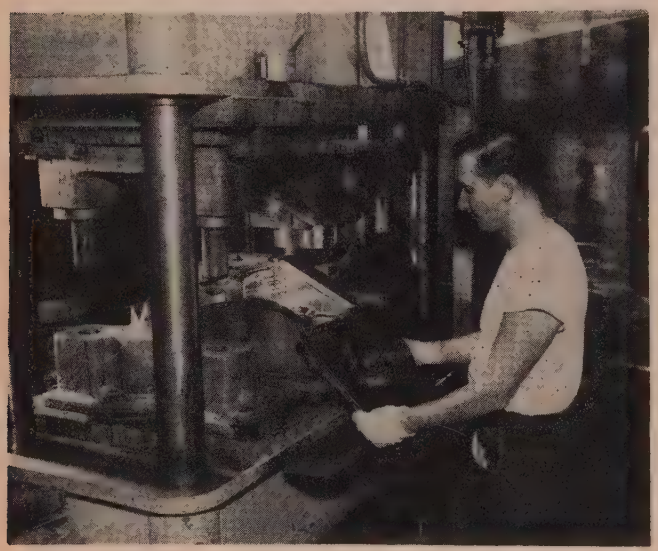

Fig. Z – Part molded in less than one minute

Fig. A_1 – Premix process produces high-volume parts production

Fig. B_1 – Rusted-out body area to be repaired with reinforced fibrous glass

Fig. C_1 – Loose material is removed and area sanded

the patch (Fig. D_1).

Heat lamps are applied to dry out the area thoroughly while the epoxy resin used is being mixed with hardener, and patches of fibrous-glass cloth are cut (Fig. E_1).

The metal is then coated with mixed resin and successive layers of cloth and resin are applied until the surface is built up enough to allow finishing to the required contour (Fig. F_1).

Air bubbles and excess resin are removed with a squeegee rubber during this process, in the interest of maximum strength.

Fig. D_1 – Depressing edges of metal to permit buildup of repair material

Fig. E_1 – Area being dried out with heat lamps while resin is mixed with hardener and patches of fibrous glass cloth are cut

A film of transparent material is then spread over the repaired area to assist final smoothing out of the surface and heat lamps are applied to promote the cure (Fig. G_1).

After the patch has hardened, it is sanded to contour and edges are feathered to the metal surface (Fig. H_1). Imperfections are filled with a paste mixture of fibrous glass and resin, allowed to harden, and sanded smooth.

Conventional painting operations then follow; priming, putty-glazing, finish painting, and rubbing to obtain a high luster.

The repair cannot be detected (Fig. I_1) and usually possesses greater strength and durability than surrounding areas.

Our experience with reinforced plastic as a body material has justified our confidence in using it for the Corvette body (Fig. A).

Fig. F_1 – Successive layers of resin and fibrous glass reinforcement are applied to build up area to required thickness

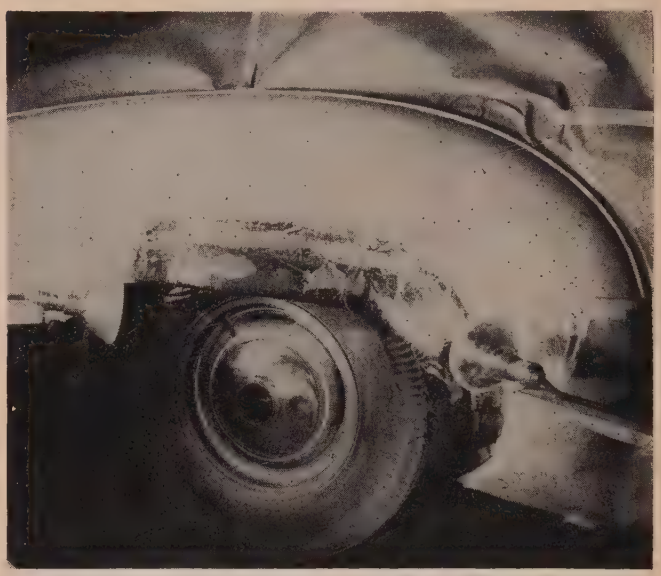

Fig. G_1 – Transparent film is used to assist in removing air bubbles and smoothing out surface. Heat lamps are used to accelerate cure of resin

We continue to consider reinforced plastic for use wherever the physical characteristics are suitable and the volume requirements result in favorable economics.

Improved technical knowledge and manufacturing methods have increased the use of reinforced plastic in the automotive industry during the past year.

Continued progress in these fields resulting in stronger laminates at lower costs, together with availability to the automotive engineer of the technical data enabling him to use the material intelligently, should result in a promising future for the reinforced-plastic industry.

Calls Integration Important To Plastics' Break-Even Point

– Robert S. Ames
Goodyear Aircraft Corp.

THE phrase coined by Mr. Schultz, ". . . the saving grace of integration . . ." deserves considerable attention. Every-

Fig. H_1 – Sanding to desired shape

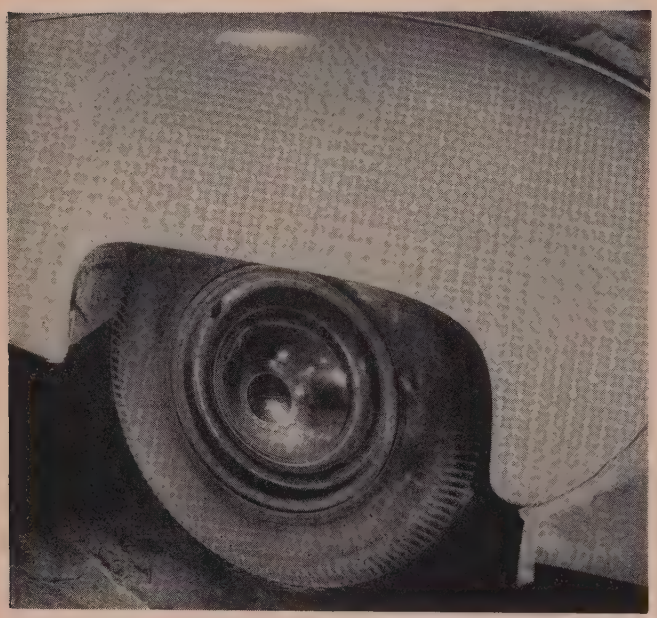

Fig. I_1 – Repaired area cannot be detected after finish painting

one is familiar with the fact that plastics parts must be engineered, and that the simple substitution of plastic for metal is neither feasible nor economical, but not everyone appreciates fully how far integration of parts should be carried. We feel that this can have an enormous influence on what is commonly described as the break-even point.

It is generally understood that reinforced plastics are more expensive materials, and that parts cost will be higher than is the case with metal stampings. However, tooling costs are thought of as being lower and, therefore, there is a break-even point. This is widely understood, but from our experience we have reached the conclusion that there can be an enormous difference in the break-even point between what might be called a moderately well-designed plastic part, and an assembly that really integrates a large number of parts. The difference between these figures may well be 2 to 1. That is, an assembly that really does a good job of integration makes possible a very dramatic reduction in the number of parts and the number of tools, and the result is to increase the quantity at which plastics are the equivalent in cost to a metal assembly.

The question was put to Mr. Premo as to what he considered the economic point, and he answered that he believed that it was in the neighborhood of 15,000 parts. Another commentator indicated that it was perhaps somewhat higher. Naturally, every part will have its own break-even point in this type of analysis, but the point to be emphasized is that when assemblies are considered, and integration is optimized, the break-even point may be raised substantially.

ORAL DISCUSSION

Reported by

Murray Simkins

Commercial Car Journal

Walter Neumann, Willett Co.: What about fade with plastic panels impregnated with color?

Mr. Premo: There is difficulty with fading when repairs are made on panels into which color has been fused. The difficulty of matching up panels, strips, and moldings has precluded the use of color-fused plastic panels in the Corvette. It is difficult to conceal joints, especially where bodies are fabricated with materials from multiple sources. It is not practical to use color in the panels.

H. A. Schwartz, Montpelier Mfg. Co.: How about the abrasive resistance of the plastic when applied to flooring?

Mr. Wulc: Stripping used in conjunction with the plastic has eliminated problems of abrasion in the Strick construction methods.

Mr. McCann: Spraying of the flooring with a vinyl would improve the abrasive resistance of the plastic floor.

Mr. Ames, Goodyear Aircraft Co.: The "saving grace of integration" is important in the design of plastic bodies. Plastic is not a substitution, but should be considered a new type construction, while engineering methods should enable the designer and user to get the ultimate from its inherent advantages over other materials. How do the economics of plastic-body fabrication apply to the Corvette?

Mr. Premo: While the plastic material itself is more costly than comparable materials, plastic dies can help to reduce costs. Tooling costs in making dies are lower. As many as 15,000 units can be obtained from a single tooling.

Question: "What will the operator or user pay for weight-saving?"

Frank DeFrance, Balsam & DeFrance Petroleum Trans: The economics would be determined by comparing the available extra payload with the fleet revenue. In our own operation we can haul 500 gal of gasoline with a new design tank that has reduced dead weight. At 2½¢ per gal freight, this has resulted in an additional revenue of $12 to $15 per day.

Emil Gohn, Atlantic Refining Co.: Study of our own fleet experience places the weight saving figure at approximately 80¢. Thus we could pay as much as 80¢ for every pound of weight saved in payload. Other figures have been set at $1.00 per pound.

Robert Morris, Molded Products Co.: With matched metal dies of simple design, and with improvements in fabricating technique, the cross-over point in the type of construction used in the Corvette could be placed 5000 units higher. Thus one might conceivably be able to produce up to 20,000 units with matched dies more economically than with stamping. After this point is reached, however, it becomes more economical to use standard fabricating methods. I estimate that molding costs of plastic material could be placed between 65¢ and 70¢ per lb.

E. N. Hatch, Nassau County: How critical is the proportion of fibrous glass to resin in repair?

Mr. Wulc: The material should be mixed in the same proportion as that of the original panel. The strength is a factor of the glass, while the resin acts only as a bond. Thus, the higher the percentage of glass used, the better the strength of the repaired area.

Control of Low-Temperature Sludge In Passenger-Car Engines

R. L. Willis and E. C. Ballard,

E. I. du Pont de Nemours & Co., Inc.

This paper was presented at the SAE Golden Anniversary Annual Meeting, Detroit, Jan. 11, 1955.

EARLY in 1954, Biswell, Catlin, Froning, and Robbins[1] reported the discovery of a new class of detergents for hydrocarbon systems. These new detergents, which are nitrogen-containing polymers, appeared to be particularly effective in controlling sludge formation in engines operated at low or moderate temperatures. These are the operating conditions encountered by most passenger cars.

In order to discover the reason for this unusual detergent activity, a study was made of several factors affecting the dispersancy and solubilization of solid particles in hydrocarbons. This study showed differences in behavior between the new and older types of detergents which provided important leads to a better appreciation of the way in which detergents function. It is the purpose of this paper to describe the results of this investigation and to relate them to engine performance.

Action of Detergents

Over the past several years, considerable attention has been given to determining the mechanism by which detergents function in lubricating oils. While this mechanism is not yet completely understood, sufficient information has now been developed to permit a rational explanation of most of the phenomena observed.

Materials which function as detergents in lubricating oil must possess at least one polar and one nonpolar group. The nonpolar group provides oil solubility for the molecule, while the polar group is of such a nature that it is attracted to the particles of sludge. These detergent molecules tend to cluster together to form micelles containing many molecules. Fig. 1 shows electron photomicrographs of two samples of new oil. One sample is a carefully filtered neutral, and the other sample is the same filtered base oil to which a barium petroleum sulfonate has been added. The micelles of the detergent are clearly visible in the additive-containing sample. They are 2 to 4 millimicrons in diameter and 5 to 20 millimicrons in length.

One way in which a detergent functions is by keeping sludge particles in suspension. The available evidence indicates that the detergent molecules or micelles orient themselves around the sludge particles which develop in the oil, and that this coating of detergent prevents the particles from agglomerating. During the service life of the oil, the number of sludge particles gradually increases, while the number of unattached detergent molecules or free-floating micelles decreases.[2] The sludge particles may or may not possess an electrical charge attributable to the detergent. There

THIS paper evaluates a new class of detergents, specially effective in controlling sludge formation at the low or moderate temperatures most often encountered in passenger-car operation.

This new Detergent C (a copolymer of lauryl methacrylate plus diethylaminoethyl methacrylate) has undergone extensive bench and laboratory tests in comparison with three other major classes of detergent. It exhibits, among other attributes:

1. Complete solubilization of sludge.
2. Complete carbon suspension under both wet and dry conditions.
3. Residual detergency, as indicated by dispersancy in blotter tests under wet and dry conditions.
4. Ability to prevent agglomeration and precipitation of sludge formed during oxidation of lubricating oils, with and without presence of water.
5. Effective sludge suspension after 40-hr laboratory tests, and after several months of storage.

[1] "New Class of Polymeric Dispersants for Hydrocarbon Systems," by C. B. Biswell, W. E. Catlin, J. F. Froning, and G. B. Robbins. Presented at National ACS Meeting, Kansas City, Mo., 1954.

[2] "An Electron Microscope Study of Performance of Detergent Oil," by J. B. Peri. Presented at SAE National Fuels & Lubricants Meeting, Chicago, November 5, 1953.

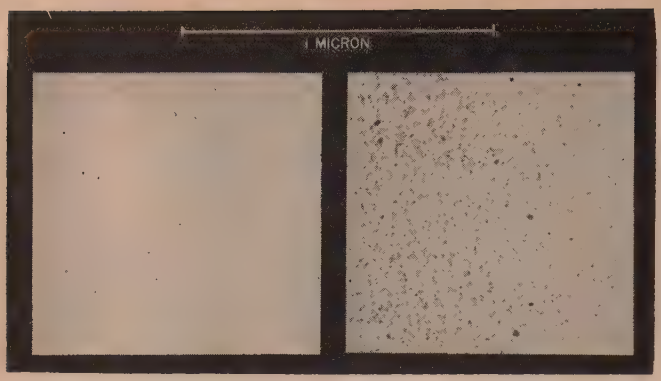

Fig. 1 – Electron photomicrographs of oils without additive (left) and with barium sulfonate (right). Micelle formation is visible in oil containing detergent. Pictures were taken at 17,000x and enlarged to 90,000x (shown here somewhat reduced in size)

is some disagreement in the literature as to whether these charges are responsible for the stability, or lack of stability, exhibited by the sludge dispersions.[3, 4, 5]

Fig. 2 shows photomicrographs of oil samples withdrawn from a passenger-car engine operated in the laboratory on an oil containing 0.5% active ingredient of a barium petroleum sulfonate. The first picture shows the oil before it was placed in the engine, while the others show samples of the oil after 5, 15, and 40 hr of operation. It can be seen that as small particles of sludge are formed, the micelles of detergent cluster around each particle and tend to keep them dispersed. As the oil continues in use, the micelles are gradually depleted, and agglomeration of particles proceeds.

Some detergents are capable of keeping the size of sludge particles so small that, for all practical purposes, it can be said that the particles are in solution. This solubilization of sludge is the most effective way in which a detergent can function. As shown by Spindt and Wolfe,[6] engine sludge in suspension in the lubricating oil does not tend to deposit on engine parts until the concentration becomes excessive. The deposition tendency of this sludge is reduced if the sludge is solubilized by the detergent.

Many laboratory engine tests and also road tests have indicated that not all detergents perform adequately under low or moderate temperature operating conditions. The foregoing concepts of detergency are inadequate to explain these differences in performance. For this reason, bench and engine tests were conducted with representative examples from four different classes of detergents having known differences in low-temperature performance. The detergents studied were a basic barium phenate, a basic barium petroleum sulfonate, a metal-containing experimental detergent, and a nitrogen-containing polymeric detergent. This last detergent, an example of the new class of materials,[1] is a copolymer of lauryl methacrylate and diethylaminoethyl methacrylate having the structure shown in Fig. 3. It will be referred to as Detergent C. The sulfonate and phenate selected for this work had the best low-temperature laboratory engine performance of the five or six of each class investigated.

---

[3] See *Journal of Institute of Petroleum*, Vol. 39, 1953, pp. 677-687: "Detergency of Carbon Black, VI," by F. H. Garner, C. W. Nutt, and M. F. Mohtadi.

[4] See *Journal of Physical Chemistry*, Vol. 48, 1944, p. 125: "Study of Colloidal System Carbon Dispersed in Xylene," by V. R. Damarell and A. Urbanic.

[5] See *Journal of Physical and Colloid Chemistry*, Vol. 55, 1951, p. 1527: "Electrophoresis in Non-Aqueous Media," by M. Hayek.

[6] "Why and Wherefore of Engine Deposits," by R. S. Spindt and C. L. Wolfe. Presented at SAE National West Coast Meeting, Seattle, Aug. 15, 1951.

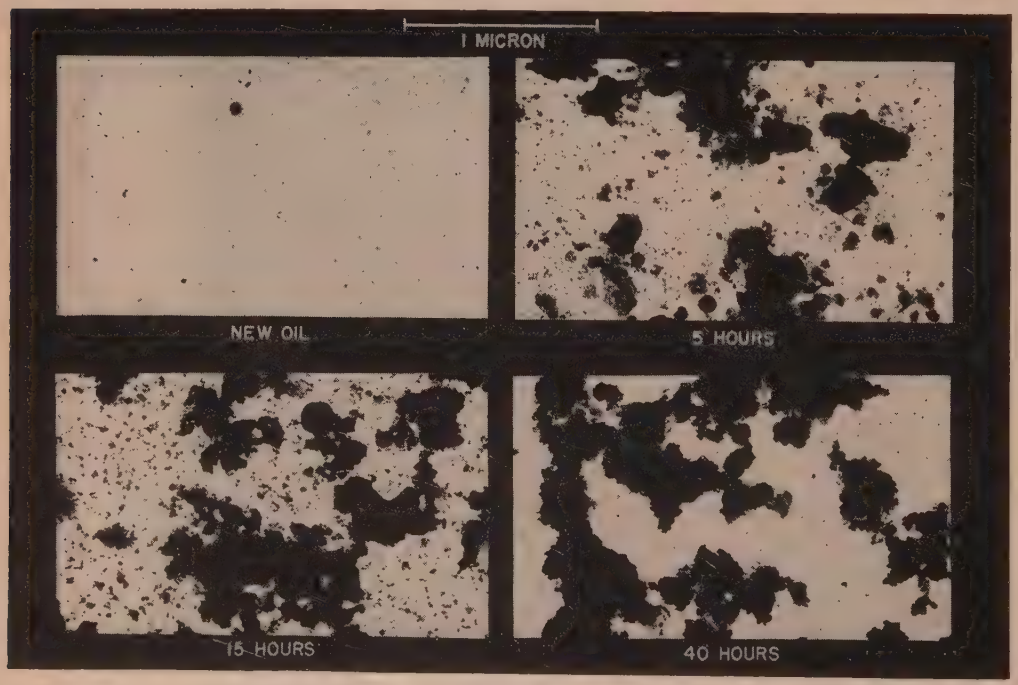

Fig. 2 – Electron photomicrographs at 38,000x showing barium petroleum sulfonate micelle depletion in oil samples taken from multicylinder engine test (shown here somewhat reduced in size)

Bench Test Performance of Detergents

Sludge Suspension – The ability of the four detergents to suspend sludge was examined using a test described by Biswell et al.[1] This interesting technique measures the ability of detergents to suspend oil-insoluble sludge when the sludge is precipitated in the presence of the detergent. It is carried out by adding a benzene solution of the oil-insoluble resins from oxidized oil to a kerosene solution of the detergent. The benzene is then evaporated under controlled conditions, leaving behind the original kerosene. The physical state in which the sludge appears in the benzene-free kerosene is determined by the effectiveness of the detergent present in the system. Fig. 4 illustrates the differences in performance of the four detergents when evaluated at a concentration of 0.5 weight-percent active ingredients in this test. The photographs show the sample vials as they appeared 5 hr after the evaporation of the benzene. When no detergent was present, all the sludge settled to the bottom of the vial. Detergent A showed some suspending ability, while Detergents B and D failed to keep the sludge in suspension. Detergent C gave complete solubilization of the sludge. Discrete sludge particles could be detected in all vials except that containing Detergent C, which remained bright and clear for several months. Even at electron microscope magnifications of 10,000x, no sludge could be seen in the Detergent C system.

Carbon Suspension – In addition to the organic sludge which must be kept dissolved or in suspension, carbon from partially burned fuel must be prevented from depositing in the lubrication system. For this reason, a test was carried out to determine the ability of the four detergents, at a concentration of 0.5 weight per cent active ingredient, to suspend a finely divided carbon in kerosene under both wet and dry conditions. The performance of detergents in the presence of water is considered to be important, because water is present in crankcase oils during low-temperature engine operation. This water enters the crankcase either as condensate from blowby gas during engine operation,[7] or as condensate which forms as a result of engine breathing during periods in which the engine is not in operation.

For these experiments, a fine carbon black was milled into a heavy white oil on an ink mill. A sufficient amount of the carbon-oil paste was dispersed in each kerosene-detergent solution with a Waring Blendor to form a suspension containing 0.5 weight per cent of carbon. As shown in Fig. 5, Detergents B and C maintain complete suspension of the carbon for more than six days, whereas Detergents A and D lose their suspending power in less than one day. The suspending ability of Detergent B is lost when one volume per cent water is present in the kerosene. Under these conditions, Detergent C retains its effectiveness. These results are shown in Fig. 6. Photographs of these mixtures, taken after settling for one day, are shown in Fig. 7. The effect of water on the performance of the detergents is evident.

Several samples of detergents of the types represented by Detergents A and B were found to exhibit suspending ability for carbon in both wet and dry kerosene. However, detergents of these types

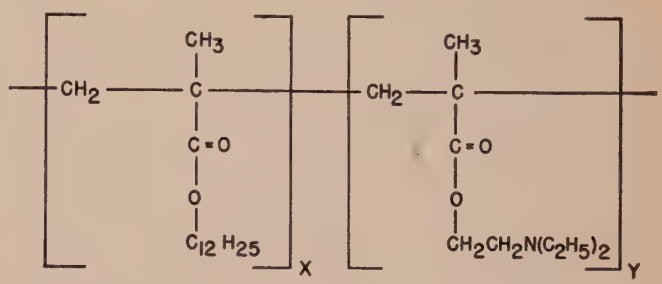

Fig. 3 – Chemical structure of Detergent C (lauryl methacrylate diethylaminoethyl methacrylate)

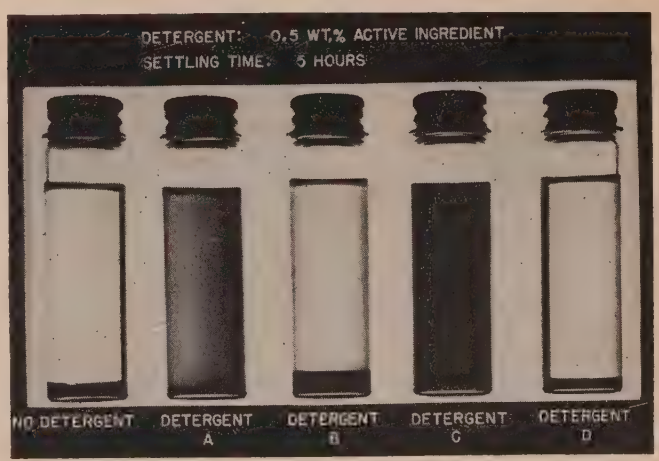

Fig. 4 – Sample vials containing kerosene-sludge systems, showing wide range in sludge-suspending ability of detergents

[7] "Oil Filtration Problems with High Detergency Lubricants," by H. M. Gadebusch, R. T. Karr, and W. B. Bassett. Presented at SAE National Fuels & Lubricants Meeting, Chicago, Oct. 31, 1951.

The Authors

R. L. WILLIS (M '52) is a research chemist in the Petroleum Laboratory of E. I. du Pont de Nemours Co., Inc. He received a B.S in Chemical Engineering from the University of Pennsylvania in 1941 and a chemical engineering degree from Princeton University in 1942. Mr. Willis joined du Pont in 1942 as a production supervisor on the Manhattan Project, assuming his present position in 1946. His work is primarily concerned with lubricating oils and additives.

E. C. BALLARD (M '55) is a supervisor of research on lubricating oils and lubricating oil additives in the Petroleum Laboratory of E. I. du Pont de Nemours Co., Inc. He received a Ph.D. in Organic Chemistry from the University of Minnesota in 1940. Prior to becoming associated with the Petroleum Laboratory in 1950, Dr. Ballard did research and development work on pigments, synthetic rubber, petrochemicals and tetraethyl lead in other laboratories of du Pont.

were generally not very effective in the presence of water.

Because crankcase oils eventually become acid during the normal use period, the carbon-suspending ability of several detergents of various types was determined in the presence of two volume per cent of a 10 weight per cent hydrochloric acid solution. The quantity of acid was sufficient to more than neutralize the basicity of the kerosene-detergent system. Under these conditions, Detergent C was the only effective dispersant.

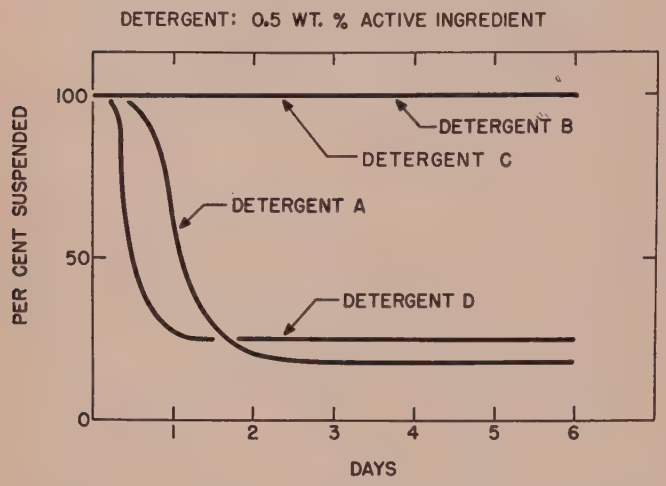

Fig. 5 – Effect of detergent on suspension of carbon in dry kerosene

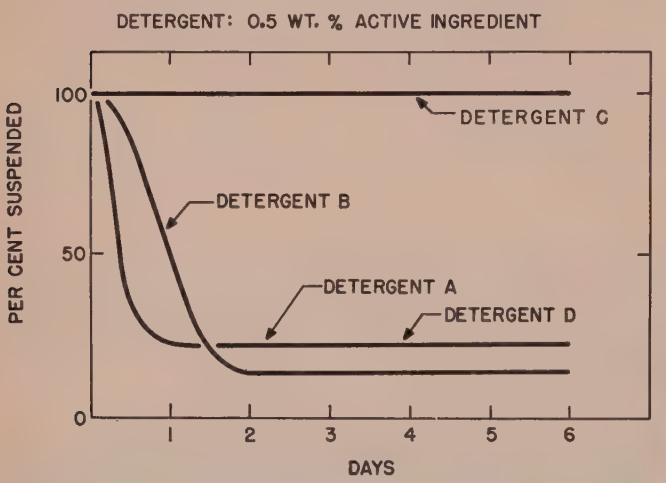

Fig. 6 – Effect of detergent on suspension of carbon in wet kerosene

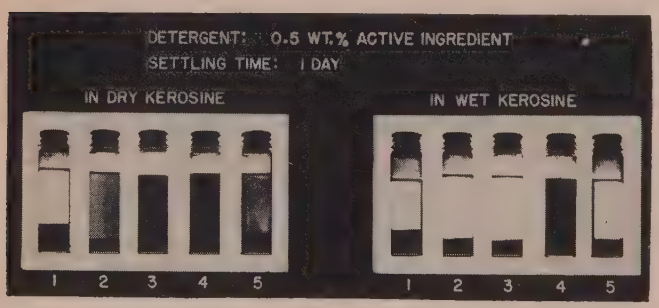

Fig. 7 – Sample vials containing kerosene suspensions of carbon, showing dispersant performance of representative detergents in presence and in absence of water. 1: no detergent, 2: Detergent A; 3: Detergent B; 4: Detergent C; 5: Detergent D

"Blotter" Tests – Gates and co-workers[8] have recognized the importance of water, and have reported that the effectiveness of a detergent oil can be neutralized by engine-coolant leakage into the crankcase, and also by the presence of aqueous blowby condensate in the oil. Gates and also Edgar[9] have used "blotter" or filter-paper spot tests to evaluate the residual detergency of used engine oils. In such tests, when a drop of the oil containing an effective detergent is placed on a piece of filter paper, the dispersed sludge flows out with the oil into the paper, giving a large, dark oil spot. If the detergent properties of the oil have been exhausted, the sludge remains in its original position on the paper, and only clear oil spreads out into the paper. The blotter test performance of used oils formulated with the four different detergents has been determined. The essentially water-free used oils for this experiment were taken from Buda diesel engines operated for 50 hr at 175 F oil temperature and 195 F coolant temperature. The oil spots illustrated in Fig. 8 show the residual detergency of the used oils as well as the effect of the addition of 0.5% water. In the dry systems, Detergents A, B, and C all show good detergency as indicated by the large black spots, while Detergent D is marginal in performance. One-half per cent water neutralizes the Detergents A and D and decreases the efficiency of Detergent B. Water has no effect on the dispersancy of Detergent C.

Oxidation Tests – The ability of the detergents to prevent the agglomeration and precipitation of sludge formed during the oxidation of lubricating oils was determined using the MacCoull test equip-

[8] "On-the-Spot Testing of Used Lubricating Oils," by V. A. Gates, R. F. Bergstrom, T. S. Hodgson, and L. A. Wendt. Presented at SAE National West Coast Meeting, Los Angeles, Aug. 17, 1954.

[9] "High Additive Oils in the City, on the Long Lines, and Off the Road," by J. A. Edgar. Presented at SAE National West Coast Meeting, Seattle, Aug. 14, 1951.

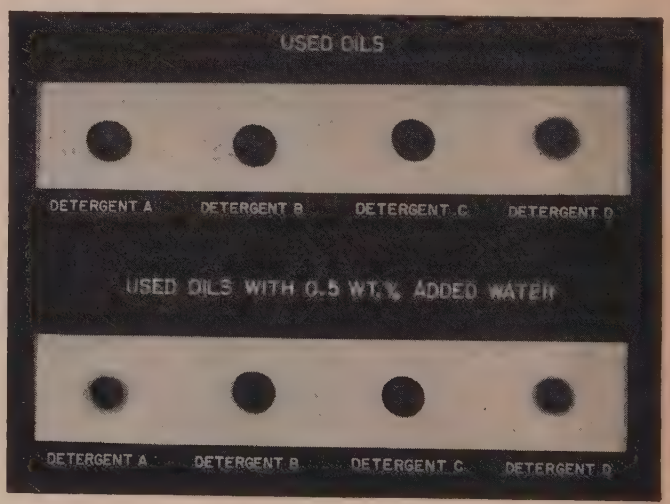

Fig. 8 – Used-oil spot tests, indicating that water neutralizes effectiveness of Detergent A, harms that of Detergent B, and has no effect on that of Detergent C. Detergent D exhibits little, if any, residual detergency even in dry oil

ment.[10] The base oil used was an SAE 10W Midcontinent solvent-refined neutral, carefully filtered to remove tramp solids. The detergents were added at a concentration of 0.5 weight per cent active ingredient. Duplicate samples of these treated oils were oxidized at 200 F, and 2 ml of water was added every 30 min to one set of samples. Oxidation was not extensive even after 60 hr in the test equipment. However, examination of the oxidized oils under the electron microscope did show that the type of detergent present exerts considerable influence on the nature and the extent of sludge formation. This study also demonstrated that water increases the rate at which sludge develops. These results are illustrated in Fig. 9. The electron photomicrographs show plainly the effect of water on the quantity and particle size of the sludge. The peculiar feathery sludge particles formed in the presence of Detergent B were obtained repeatedly; they were not present in the unoxidized oil. The ability of Detergent C to minimize sludge formation, and the insensitivity of the polymer system to water, are illustrated quite clearly by these photomicrographs, which were selected to represent the typical, or average, of approximately 10 pictures taken on each oil. In turn, the 10 pictures were typical of some 25 to 40 visual observations made on each oil.

Effect of Detergents on Sludge Development in Lab Engines

Certain of the techniques used in the bench test work have been applied to an engine study of these detergents. The gradual loss of oil detergency during a series of FL-2[11] engine tests was followed by observing the sludge settling rates of small oil samples removed periodically from the engine. In addition, the gradual development and growth of the sludge particles was followed by an examination of these used-oil samples with an electron microscope. The base oil used in these tests was a solvent-refined Midcontinent neutral of 140 SUS at 100 F. It was carefully filtered to remove tramp particles which might otherwise have been mistaken for sludge. One weight per cent of a zinc dialkyldithiophosphate antioxidant and 0.5 weight per cent, on an active ingredient basis, of the required detergent were added to this filtered oil. The concentration of the detergent was set at a value lower than used in service, in order that depletion of the detergent would be appreciable during the course of the 40-hr engine test. The tests were all started without the separate break-in, using 6 qt of oil rather than the customary 4 qt. This procedure prevented contamination of the test oil with sludge from the break-in period, and also provided sufficient oil for completion of all the tests without further oil additions. The engine was operated on a non-leaded fuel. A representative 15 ml sample of oil was withdrawn from the crankcase each hour. These small samples were used in sludge settling tests and electron microscope studies, after gradual detergent depletion.

The engine scores obtained from these tests are summarized in Table 1. It is evident that at equal concentrations the different types of detergents vary widely in their effect on piston varnish and overall engine score. Detergent C, as might be predicted from the previously discussed bench test results, was very effective in minimizing sludge and varnish formation. Although the oil containing Detergent A actually gave a lower piston score than the base oil, it did show some improvement in overall engine cleanliness. Detergents B and D had little effect on the oil performance under these conditions.

The tendency of the sludge to settle out of the used oils was studied visually following vigorous shaking of the samples. These settling tests were repeated several months later on the same samples with the same results, indicating that once the oils were removed from the engine their detergent qualities were quite stable. The settling rates obtained indicate that Detergent A loses its effectiveness after 6-8 hr of engine operation, Detergent B at approximately 15 hr, and Detergent D at 4 hr. Detergent C effectively suspends sludge for the complete 40-hr test. The results obtained are illustrated in Fig. 10, which shows photographs taken after four days of settling of the oil samples taken after 0, 3, 6, 10, 15, and 40 hr of engine operation. The base oil showed no tendency to suspend sludge, and, therefore, samples of it were not photographed. The physical appearance of the sludge at the 10- and 40-hr points of the tests is illustrated by the electron photomicrographs in Fig. 11. Small sludge particles can be observed in the 10-hr samples of all four detergent oils. The 40-hr photographs indi-

[10] See SAE Transactions, Vol. 50 (August), 1942, pp. 338-345: "An Oil Corrosion Tester," by N. MacCoull, E. A. Ryder, and A. C. Scholp.
[11] "Laboratory Engine Tests of Sulfur in Motor Gasoline Field Test Fuels." Report of Coordinating Research Council, Inc., January, 1950.

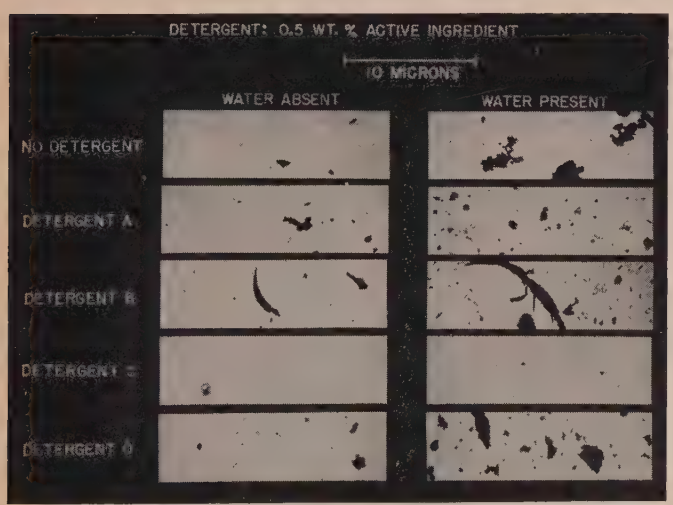

Fig. 9 – Electron photomicrographs at 3800x of sludge from oils oxidized at 200 F in MacCoull apparatus. Water accelerates oxidation and formation of sludge particles

Table 1 – FL-2 Engine Test Scores Obtained in the Sludge Development Study

Oil: Solvent-refined SAE 10W + antioxidant
Fuel: 10% alkylate. 90% catalytic cracked, unleaded

Detergent	Active Ingredient, weight %	Piston Score (10 = Clean) No. 1 Piston	Piston Score (10 = Clean) Average Piston	Engine Score (50 = Clean) Varnish	Engine Score (50 = Clean) Sludge
None	—	3.5	5.0	30	38
A	0.5	1.0	3.7	33	44
B	0.5	4.5	6.0	32	37
C	0.5	7.0	8.3	39	47
D	0.5	4.5	5.8	35	35

Table 2 – FL-2 Engine Performance of the Four Different Detergents

Oil: Solvent-refined SAE 30 + antioxidant
Fuel: 100% thermal reformate + 3 ml tel/gal

Detergent	Active Ingredient, weight %	Piston Score (10 = Clean) No. 1 Piston	Piston Score (10 = Clean) Average Piston	Engine Score (50 = Clean) Varnish	Engine Score (50 = Clean) Sludge
None	—	4.5	5.9	29	39
A	1.2	2.5	4.1	30	40
B	1.0	5.5	7.5	38	41
C	1.0	8.0	9.3	42	43
D	1.0	7.0	8.3	41	43

cate that in the case of Detergents A, B, and D the small particles have agglomerated very extensively, whereas in the oil containing Detergent C there has been little change in particle size, although the number of particles has increased somewhat. Much of the sludge from the 10-hr samples of the detergent oils is small enough to pass through efficient lubricating oil filters. At 40 hr, however, such filters would trap most of the sludge in all of the oils except that containing Detergent C. In this oil, only a few of the particles are of filterable size – that is, larger than 1 to 2 microns in diameter.[7]

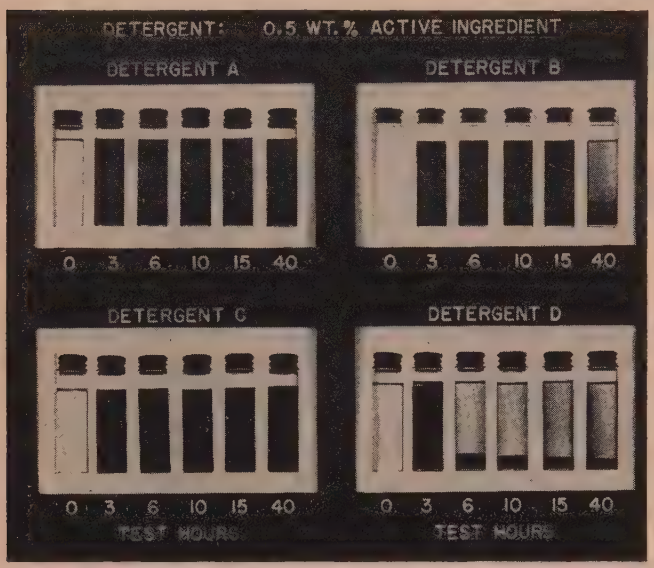

Fig. 10 – Used-oil samples, showing detergent depletion and gradual failure of the oils to suspend sludge

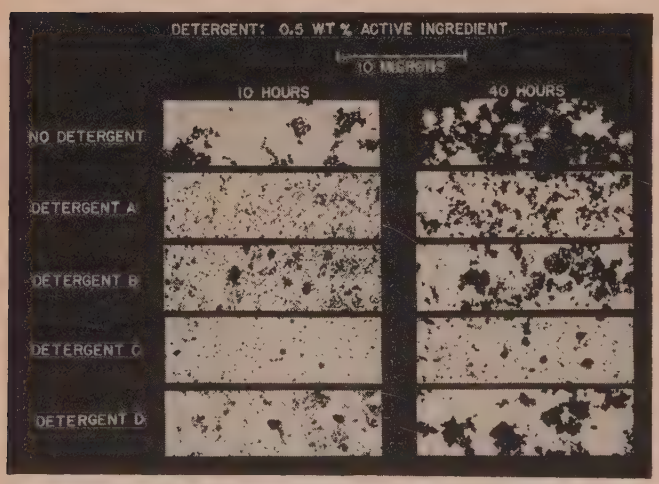

Fig. 11 – Electron photomicrographs at 3800x of sludge from used oils, showing that all four detergents have some ability to minimize particle size during first 10 hr of engine operation. Differences in performance become apparent after 40 hr (shown here somewhat reduced in size)

Representative samples of sludge were photographed again through the electron microscope after the samples had been stored for several months. No observable change in particle-size distribution or particle shape occurred during this storage period. This result suggests that growth or agglomeration of sludge particles normally occurs only during periods of engine operation as the detergent is gradually depleted. Agglomeration can also occur in the presence of some detergents during periods of nonoperation, if the water content of the oil is increased by condensation or coolant leakage into the crankcase.

Performance of Detergents in Lab Engine Tests

The four detergents were evaluated in a Mid-continent solvent-refined SAE 30 base oil at a concentration of approximately 1% active ingredient, using both the FL-2 and EX-3 procedures. The first of these is a steady-duty 40-hr test with low coolant temperature, which offers an accelerated means for evaluating fuel or lubricant performance at low engine temperatures. The second is a cyclic 96-hr procedure, currently under development by the Coordinating Research Council, which has incorporated into it periods of operation under both high- and low-temperature conditions. The results of these engine tests, summarized in Tables 2 and 3, indicate that engine cleanliness is a function of the type of detergent used. Detergent A has little effect on overall engine cleanliness in either test, but increases varnish formation on the pistons. Detergents B and D decrease piston and engine varnish in the FL-2 test, but allow somewhat more varnish to form than with the base oil in the EX-3 procedure. In both procedures, engine cleanliness is improved by Detergent C. In addition to the variation that these detergents exhibit in their ability to control varnish and sludge formation, they also show differences in their ability to control the plugging of the narrow slotted oil rings used in the EX-3 procedure. Detergent C, and to a lesser extent Detergents B and D, reduced oil-ring plugging in this procedure.

Table 3 – EX-3 Engine Performance of the Four Different Detergents

Oil: Solvent-refined SAE 30 + antioxidant
Fuel: 100% thermal reformate + 3 ml tel/gal

Detergent	Active Ingredient, weight %	Average Piston Score (10 = Clean)	Engine Score (50 = Clean)		Narrow Slot Oil Ring, % plugging
			Varnish	Sludge	
None	—	5.2	30	35	38
A	1.0	3.5	26	40	29
B	1.0	4.2	24	38	14
C	1.0	8.6	40	43	7
D	1.0	4.5	23	36	12

Table 4 – Effect of Type of Detergent on the Sludge Content of Used Oils

Test: FL-2
Oil: Solvent-refined SAE 30 + antioxidant
Fuel: 100% thermal reformate + 3 ml tel/gal

Detergent	Active Ingredient, weight %	Number of Tests	Average Sludge Content of Oils[a]		
			n-Pentane Insolubles, weight %	Benzene Insolubles, weight %	Insoluble Resins, weight %
None[b]	—	27	1.94	1.16	0.78
None	—	5	1.87	1.22	0.65
A Type	1.2	4	1.91	1.23	0.68
B Type	1.5	5	2.43	1.63	0.80
C	0.5	56	1.17	0.83	0.34
C	1.0	11	0.86	0.67	0.19
C	1.5	3	0.61	0.55	0.06
D Type	1.0	4	2.33	1.02	1.31

[a] ASTM Method - D893-52T.
[b] No antioxidant.

Sludge analyses on the used oils from the above engine tests show that oils containing Detergent C contain less oil-insoluble material than any of the other oils. This information is substantiated by the analytical results from a large number of FL-2 tests which are presented in Table 4. These data strongly suggest that the type of detergent influences the benzene insolubles and the insoluble resin content of the oil. Detergents of Type D structure appear to increase the insoluble resins in the used oil to a level higher than that found in the base oils, whereas detergents similar to A and B have but little effect on these resins. Detergent C markedly decreases the insoluble resin content of the used oil. In the case of this last detergent, sufficient data are available to illustrate the effect of detergent concentration on the sludge content of the oil; as the detergent dosage increases, the sludge content decreases. The low sludge content of used oils containing Detergent C may be related to the ability of this detergent to solubilize sludge, as was demonstrated in the sludge suspension tests already described. It is possible that Detergent C also decreases the rate of the condensation and polymerization reactions which transform low molecular weight fuel and oil oxidation products into varnish and sludge. The low level of benzene-insoluble material encountered in the engine oils with low insoluble resins suggests a relationship between the two materials. Indeed, it seems quite likely that the same reactions that lead to insoluble resins can continue and convert these resins into higher-molecular-weight, benzene-insoluble materials. Confirmation of the data shown in Table 4 has been obtained from analysis of used oils from EX-3 tests and L-4[11] high-temperature engine tests.

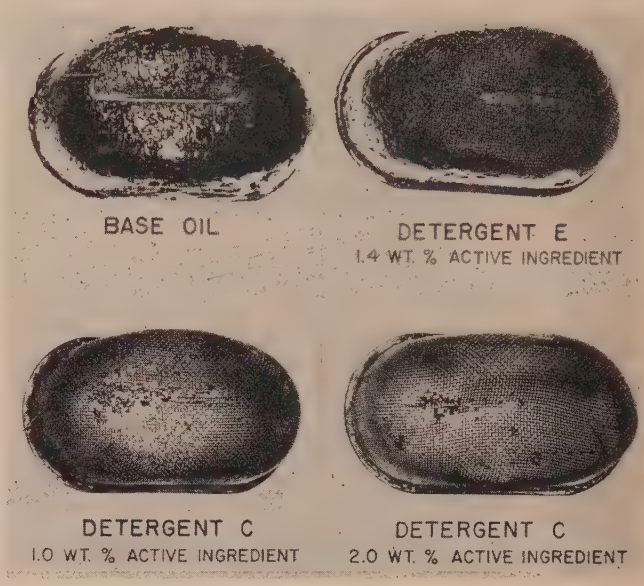

Fig. 12 – Oil screens from extended service test

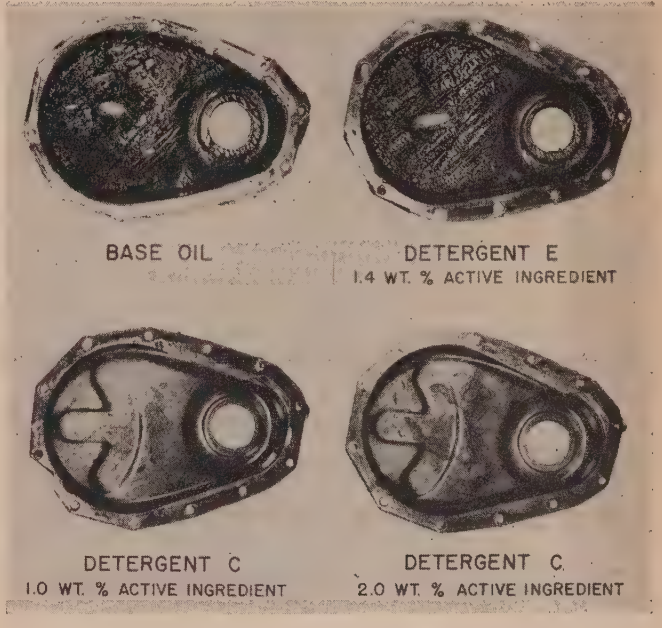

Fig. 13 – Timing gear covers from extended service test

Field Performance of Detergents

The data from bench tests and laboratory engine tests indicate that considerable differences in low-temperature performance exist among different types of detergents. These results have been substantiated by several road tests. One of these road tests involved both city and country driving in convoy for 40,000 miles, and was run using Mid-continent solvent-refined SAE 30 oils containing Detergent C in two cars and Detergent F (a deter-

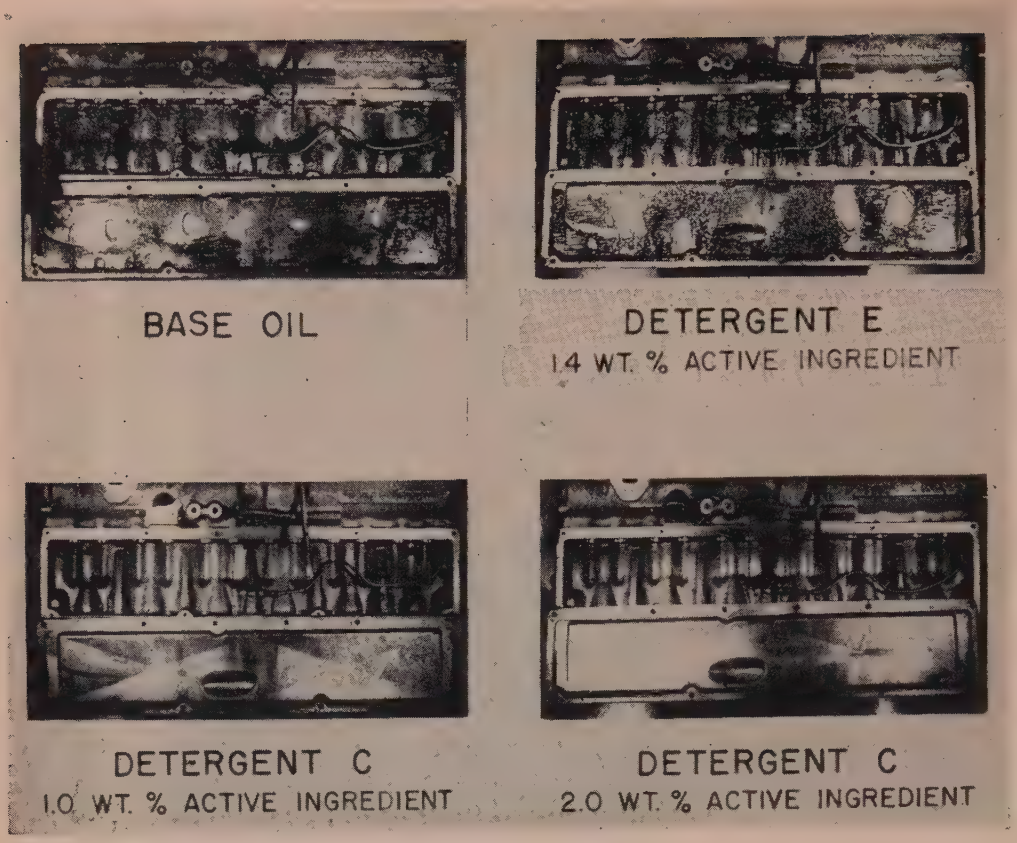

Fig. 14 – Blocks and side plates of engines from extended service test

gent similar to Detergent A) in two others. Average analyses of used oils taken from this test are given in Table 5. The oil drain period was 2500 miles, and the results presented in the table are the averages obtained after analyzing the individual used-oil samples from every drain period of each car. The performances of the two cars on each oil were in good agreement, and the differences between the two oils were clearcut; Detergent C minimized insoluble-resin formation to a much greater extent than did Detergent F. The reduction of the benzene-insoluble contents from 0.97 and 1.16 weight per cent with the oil containing Detergent F to 0.45 and 0.42 weight per cent with Detergent C also was significant.

Another field test involved extended urban and suburban operation. The results of this test agree with the laboratory engine tests and show that Detergent E (a detergent similar to Detergent A), at an active ingredient level of 1.4 weight per cent, did not markedly improve engine cleanliness during low and moderate temperature operation over that obtained with the base oil. In contrast to the appearance of the engines lubricated with the base oil or oil containing the Detergent E, all of the engines lubricated with oils containing Detergent C were clean. Photographs of parts from representative engines at the end of the test on the base oil, an oil containing Detergent E, and two oils containing Detergent C are shown in Figs. 12, 13, and 14.

Table 5 – Effect of Detergents on the Sludge Content of Road Test Oils

Oil: Solvent-refined SAE 30 + antioxidant
Test: 40,000 miles per vehicle
2,500-mile drain periods

	Vehicle			
	1	2	3	4
Detergent C, weight % Active Ingredient	—	—	1.5	1.5
Detergent F, weight % Active Ingredient	1.3	1.3	—	—
New Oil Ash, weight %	0.28	0.28	0.09	0.09
Used Oil Analysis[a]				
n-Pentane Insolubles, weight %	1.73	2.05	0.59	0.57
Benzene Insolubles, weight %	0.97	1.16	0.45	0.42
Insoluble Resins, weight %	0.76	0.89	0.14	0.15

[a] ASTM Method D893-52T. Each value is the average of the analyses of the 16 oil drain samples obtained during the 40,000 miles of operation.

Summary and Conclusions

1. Various types of detergents, including a new ashless, polymeric type, have been evaluated for their performance at low engine temperatures.

2. Detergent types vary widely in their ability to maintain engine cleanliness under low-temperature conditions.

3. Detergents which are effective at high engine temperatures are not necessarily effective at low engine temperatures.

4. Bench tests show that many detergents lose their effectiveness when evaluated in systems containing small amounts of water. The performance of detergents in low-temperature engine service is believed to be related to their sensitivity to water.

5. Bench tests and analytical data from used en-

gine oils indicate that the benzene insolubles and the insoluble resin content of used oils is influenced by the type and the amount of detergent in the oil.

6. Extensive low-temperature service tests have confirmed the conclusions reached in the laboratory.

DISCUSSION

Commends Attention to Stop-and-Go Driving Needs

– J. G. Moxey
Sun Oil Co.

THE new additive described by these authors has been aimed specifically at the low and intermediate temperature ranges that are so typical of passenger-car service, and I think it has been almost inevitable that eventually the path of motor-oil additive development would turn in this direction.

Most of the oils we now have were developed primarily to provide protection at the high-temperature, severe-duty end of the scale. We've been very fortunate, however, in that these same oils have done a pretty good job of protection at the low-temperature end. Such features as low-temperature corrosion and wear resistance are a very important part of our current oils. Whether it was planned that way or not, I don't think any of us need to be too apologetic about the performance of the oils that are now being used commercially in passenger-car service.

But that doesn't mean that we shouldn't continue to make progress. And it makes sense to me that we should include in our additive development programs the search for materials aimed specifically at typical stop-and-go passenger-car operation.

I don't believe the du Pont people intend that their new additive should be a replacement for all of the materials that are now used. There are many performance features that these polymers make no attempt to provide. But they apparently have made a real advance in providing engine cleanliness under the temperature conditions that we have to contend with in passenger-car operation.

My other thought is in connection with the performance of the additive. We've been doing work with it, as I imagine most oil companies have. Our results have been pretty much the same as those of the authors.

Table A shows results from a modification of the EX-3 procedure that we've been using in our laboratory. The three oils all used the same type of base stock. The first column is for a nondetergent oil containing only an antioxidant. The second is a typical Series I product. And the last column is an oil incorporating the du Pont additive, Detergent C. The differences are of the same order of magnitude as those described in the paper.

Fig. A illustrates the solubilizing properties of the additive. These are drain samples from duplicate FL-2 tests on three different oils as indicated. They've been allowed to settle for 24 hr, and the ability of the polymer to maintain the contaminants in suspension is quite apparent.

Corroborates Findings With Ashless Detergent C

– R. I. Potter
Standard Oil Co. (Ohio)

THE authors have presented a most important and timely paper, first, because it has developed a new approach in studying and defining sludge particle size growth by means of the electron microscope, and second, because their research has revealed another of nature's secrets in the creation of an ashless detergent dispersant, seemingly unaffected by moisture under low-duty engine operating conditions. This ashless detergent appears to have a long period of effectiveness even under most adverse conditions of laboratory, bench, and field test operation. If what they have discovered can be substantiated by further field testing with resultant clean engines, then this discovery portends to be one of the most important in the field of automotive motor oils since oxidation inhibitors were used to produce clean and corrosion free L-4 tests.

Table A – 72-Hr Modified EX-3 Engine Test

	Nondetergent	Series I Detergency	Detergent C
Piston Rating	2.3	3.5	7.0
Total Varnish	24.3	27.5	40.5
Oil Screen	2.0	3.0	9.0
Total Sludge[a]	15.8	20.6	27.5
Total Engine	40.1	48.1	68.0

[a] Corrected to $\frac{5}{9}$ of total numerical sludge rating.

The paper is timely because the problem of low-temperature sludge formation in V-8 engines is becoming more acute as engine horsepowers go up and the distance between stoplights becomes less.

In the winter of 1953, we did some work which confirms the authors' contention that wide differences exist in the ability of various detergent additives to minimize sludge formation in engines. Our objectives were:

1. To determine the effect of oil drain periods on varnish

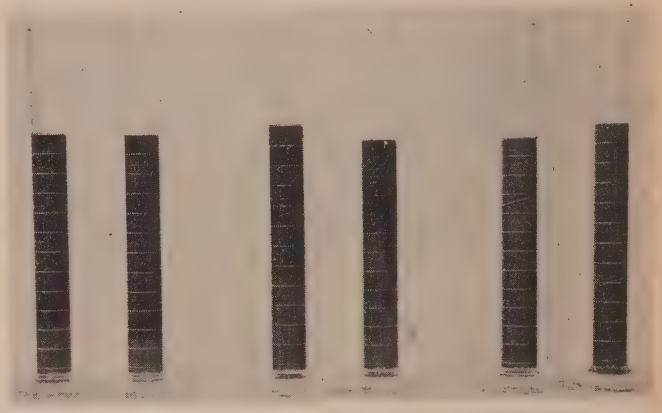

Fig. A – Dispersion of drain samples after 24-hr settling—left pair: MIL detergency, middle pair: Series 1 detergency, right pair: Detergent C

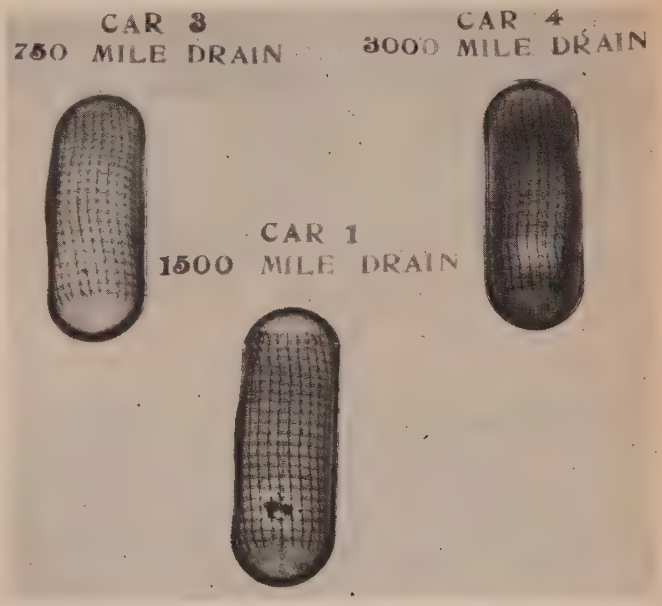

Fig. B – Oil screens from test cars after 750-, 1500-, and 3000-mile drain periods

Table B – Used Oil Analyses

Car No.	Drain Interval, Miles	Detergent	Rating
1	750	Metallic	82.6
3	1500	Metallic	80.3
4	3000	Metallic	72.0
2	3000	Ashless	77.0

Note: All of these engines were in reasonably clean condition because of the low mileage operated – 3000.

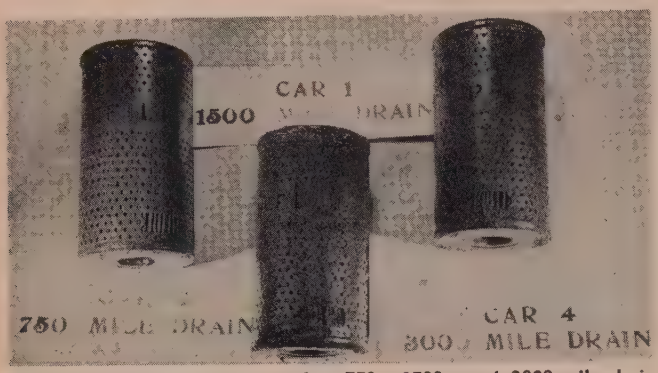

Fig. C – Filters from test cars after 750-, 1500-, and 3000-mile drain periods

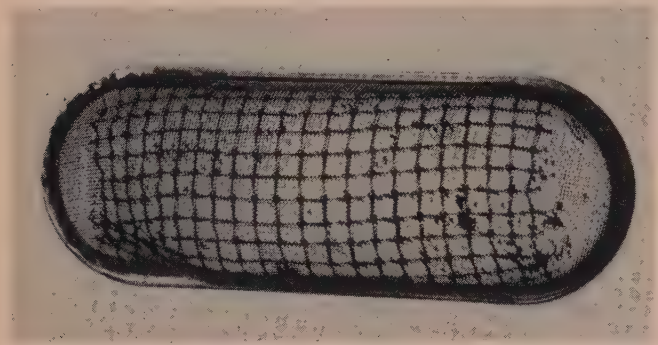

Fig. D – Oil screen from test car operated on oil treated with experimental additive C after 3000 miles

Fig. E – Oil filter from test car operated on oil treated with additive C after 3000 miles

Fig. F – Sludge-settling behavior of used motor oils in 15-month test. Left to right: premium, MIL-L-2104A, S-2, and Ashless Detergent C

and sludge formations under stop-and-go driving conditions, using a common test fuel and an oil containing a sizable amount of metallic detergent.

2. To compare the effectiveness of a metallic detergent with an experimental ashless detergent of the same type as Detergent C referred to by the authors.

Engine Buildup

Four 1952 overhead-valve V-8 engines of a well known make were carefully rebuilt after about 25,000 miles of operation. New hydraulic valve lifters, new oil filters, and clean filter cases went into each test engine. Then the engines were reassembled in a completely clean condition. Ethylene glycol-type permanent antifreeze was used as coolant in conjunction with 156 F thermostats.

Operations

Cars were parked outside at all times. Long trips were avoided. Driver assignments were changed each week. Car travel averaged about 25 miles per day, and oil was drained while hot. Total mileage was 3000 miles.

Three oil drain periods for respective cars were used: 750-, 1500-, and 3000-mile intervals.

Test Results

Figs. B and C show how the drain periods affected the oil screens and filters from cars 1, 3, and 4. They offer visible proof that the filter elements from the 1500- and 3000-mile drain period cars weighed almost ½ lb more than did the filter from the 750-mile drain period car.

It can be seen from this test that a vehicle operated under these severe home-to-work conditions, using a common winter grade fuel and oil containing a sizable amount of metallic detergent, should be drained either once a month or after 1000 miles of operation. This conclusion relates favorably with the API Committee recommendation that "crankcases should be drained after not over 60 days, or 500 miles of travel in this type of service."

Ashless Detergent Results

Concurrently with the three cars already described, a fourth car, No. 2, was operated on an oil treated with an experimental ashless type Additive C without drain for a 3000-mile period. Figs. D and E show the oil screen and filter from this engine, which compare favorably in condition with the screen and filter of the 750-mile drain operation using the metallic detergent (Car 1).

Combined Sludge and Varnish Ratings

The used oil analyses (Table B) indicated that the ashless detergent oil was capable of suspending some three to seven times as many oil contaminants as the metallic detergent – probably due to the fine dispersion of these solids, as pointed out by the authors.

This property of sludge and insoluble contaminant suspension is further observed in another of our tests, as shown in Fig. F, where four used oil samples of the qualities premium, MIL-L-2104A, S-2, and Ashless Detergent C were settled for a 15-month period. Each of these oils was operated under stop-and-go city driving conditions for over 4000 miles without draining. The amount of settling appears to vary proportionately with the detergent dispersant quality of the oil – the premium oil on the left containing the least detergent shows the most settling, and the ashless type, Detergent C treated oil on the right, shows very little separation.

We can conclude then with the authors that the use of an electron microscope to determine the effectiveness of detergents to prevent sludge particle size growth in oil is a much more effective and novel method than waiting for used oil samples to settle. Although the work described here is limited and a great deal more road testing is necessary, the results substantiate that large differences exist between the metallic and ashless type C detergents in their ability to keep filters, oil screens, and engine parts free from sludge under low-temperature operating conditions.

Tire Thump: Its Mechanism and Measurement

David C. Apps and George M. Vanator,
General Motors Proving Ground

This paper was presented at the SAE Golden Anniversary Passenger-Car Meeting, Detroit, March 1, 1955.

TIRE thump has gained prominence as passenger cars have become quieter and roads smoother. Studies at the GM Proving Ground dating back to 1940 have shown thump to be a very complex example of the simple phenomenon that combining two closely spaced frequency components will produce a certain beat.

Here the authors detail what has been learned about the physical characteristics of car and tire which go into producing thump of various frequencies and loudnesses. They also describe a newly developed portable instrument which measures the depth of modulation of the beat between two frequencies, thus serving as a uniform standard of tire thump severity.

AS modern motor cars become quieter and roads become smoother, it frequently happens that noises and disturbances previously of no great concern are gradually forced into prominence. Tire thump and tire roughness are examples of such disturbances. Although the phenomena of tire thump and tire roughness are closely related, each is a subject within itself. We shall, therefore, confine our attention to the tire thump problem.

The term "tire thump" refers to that tire disturbance which occurs at wheel rotational speed, and sounds like a boot in the tire. It is heard most strongly in the speed range of 20-50 mph, and is most pronounced on smooth sheet tarvia roads. The audible effect is usually, but not always, more apparent than the corresponding feel or vibration.

Although the disturbance originates from the tires, it is known that various makes and types of cars exhibit varying degrees of sensitivity to a given tire or set of tires; therefore, both tire and car manufacturers are giving attention to the problem.

Tire thump first came to our attention in 1940. Since that time, it has been recognized throughout the automotive industry and, in some model years, has been a major problem.

In order either to measure tire thump or make an intelligent approach toward the solution to the tire thump problem, it is essential that we understand the nature of the phenomenon – that is, the mechanism of tire thump. Let us list, therefore, some of the things we need to know to understand the mechanism:

1. What is the nature of the acoustic disturbance we hear?
2. Why is thump louder at some speeds than others?
3. Why, at a given speed, does thump periodically increase and decrease in intensity; that is, what causes phasing?
4. Why do we hear only one thump per wheel revolution, when it is known that the car has more than one thumping tire?

A clue to the nature of the acoustical disturbance we hear was obtained from our tests in 1940. Fig. 1 is a reproduction of an oscillogram taken during these tests. It is an oscillogram of sound picked up by a microphone inside a car operating at 37.5 mph with a thumping tire. The lower trace is a 60-cps timing wave. This oscillogram shows the presence of beats, and led directly to a hypothesis

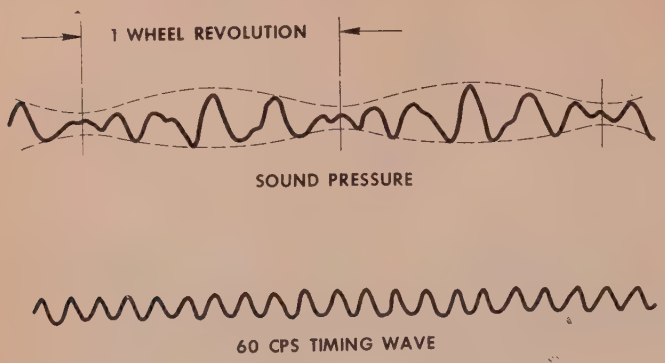

Fig. 1 – Oscillogram of noise inside a car, showing presence of beats that result from thumping tire. Car speed: 37.5 mph

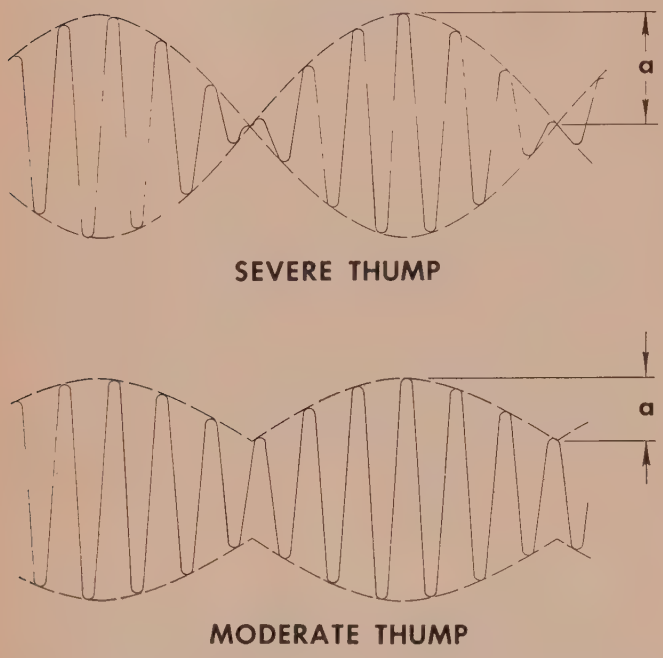

Fig. 2 – Beat or modulation resulting from combining two closely spaced frequency components. Upper trace: both components have equal amplitudes; lower trace: both components have unequal amplitudes

concerning the nature of tire thump which has since been confirmed. The oscillogram also shows that the component frequencies involved in this example of tire thump lie in the 30-40 cps range, and that the beat frequency, that is, the rate of occurrence of the bulges in the envelope, is 7.5 cps, identically equal to wheel rotational rate.

As a result of this and subsequent studies at the Proving Ground, it has been determined that tire thump is due to the simultaneous excitation of at least two audio frequency sound components which are adjacent harmonics of wheel rps, and which have approximately equal sound-pressure amplitudes. These components interfere with each other and produce a beat frequency equal to wheel rps, which is heard as tire thump. The production of beats by the combining of two closely-spaced frequency components, as exemplified by tire thump, is a practical example of a simple phenomenon discussed in texts on elementary physics.

It is interesting to note that the mechanism described is a means by which a sub-audible frequency is made audible; that is, the ear cannot detect a tone of frequency 7.5 cps, but it can hear a variation at the rate of 7.5 cps of tones of several times that frequency. The component terms serve as true carrier frequencies in a literal sense.

Having identified the phenomenon of beats taking place in the structure of the car and in the air inside the body, interest naturally turns to the characteristics of the tire which produce this disturbance.

As the tire rolls, variations of such parameters as tire stiffness, crown thickness, radial runout, lateral runout, and so forth, cause force variations to be fed into the wheel spindle. These force variations are a complex function of time, but regardless of their complexity the fundamental period is equal to the tire rotational period, and the function may be expressed as a Fourier series of harmonically related components. The coefficients of these harmonic terms, however, do not in general maintain their relative values as the speed changes.

As an example of the manner in which these harmonic tire forces combine to produce thump in the car, let us assume a car speed of 35 mph, which, for an average tire size, means a wheel rotational speed of 7 rps. The frequencies of the various Fourier terms are then 7, 14, 21, 28, 35, 42, 49, . . . cps. Unless a study is made of a specific tire, the coefficients of these Fourier terms are not known. Let us assume, however, that due to some peculiar frequency-response characteristic of the car in question the 6th and 7th harmonics, 42 and 49 cps, are the predominant noise components excited in the air cavity of the body. The 42 and 49 cps components beat together, producing a beat repetition rate equal to their difference, 7 cps. This is, of course, the assumed wheel rotational speed. The result is audible tire thump.

When the amplitudes of the individual sound pressure components are equal, the envelope of the interference pattern goes to zero (see Fig. 2). The modulation, or beat envelope, then has a large amplitude, and we say that thump is "severe." On the other hand, if only one component has a large amplitude, and either of its neighbors has a small amplitude, the modulation envelope is small and the thump is "light."

Let us next look at the peculiar frequency-response characteristics of a car that causes certain of the harmonics of tire excitation to predominate over others. This brings us to our second question: Why is thump louder at some speeds than others; that is, why do we experience a number of

thump periods as car speed is changed?

An answer to this question was obtained from studies conducted on a chassis dynamometer. For this study, a thumping tire was placed on one of the front wheels, and only that wheel rotated. Then at discrete wheel speeds, taken in ¼-rps steps, a complete analysis was made of the amplitude and frequency of each of the harmonic components of noise in the car that were excited by the complex force function of the tire. That is to say, we make a Fourier analysis of the noise at each speed. When these data are plotted, they appear as shown in Fig. 3. The coordinate system of this chart is frequency in cps along the abscissa, sound pressure expressed in arbitrary linear units along the left-hand ordinate, and wheel speed in rps with corresponding mph along the right-hand ordinate. The plotted curves represent noise level with order of wheel speed as a parameter. The diagonal lines labeled "Order 3," "Order 4," and so forth, were added to simplify interpretation of the data.

For example, the horizontal dotted line at 8.45 rps of the wheel intersects these order lines at points which represent the frequency of that order at this wheel speed. These frequencies are 25.35, 33.8, 42.25, 50.7, and 59.15, for Orders 3, 4, 5, 6, and 7, respectively. Vertical lines drawn from these points of intersection to the corresponding noise curve for that order gives the amplitude of each of these noise frequency components. In this case, it is 340, 380, 330, 120, and 16 units of sound pressure for Orders 3, 4, 5, 6, and 7, respectively.

It is interesting to note in this particular example that we have three adjacent harmonics of the wheel rotational rate (8.45 rps) that give approximately equal noise response in the car and which predominate over the other harmonics. These three harmonics will combine to produce a beat, the rate of which is equal to their common difference, 8.45 cps, and produce thump in the car.

Obviously, then, from this set of curves we can choose any wheel speed and determine what the relative amplitude of noise is for each of the harmonics of wheel speed, and how severe we might expect thump to be at this speed with respect to any other wheel speed.

More important, however, are two other bits of information that these curves reveal:

1. That the coefficients of the Fourier terms of the complex tire excitation force do not maintain their relative values as the speed changes; otherwise, the curves in this family would quite probably have been uniformly spaced and not cross each other, as they frequently do in this plot.

2. That there are numerous resonances, or modes, of vibration in the car structure that serve to amplify certain frequencies more than others.

While individual resonances are not too clearly defined by these curves, it is obvious that there is at least one major resonance in the frequency range of 38 to 48 cps, and another in the range of 50 to 56 cps. It is, however, these many resonances that cause the thump severity to change as car speed is varied. It is clear, then, that thump severity is the combined effect of tire excitation and response characteristics of the car in question. Also of interest is the fact that only those frequencies in the band 20-70 cps need be considered to obtain a quantitative measure that will correlate with a personal reaction to tire thump.

Thus far we have considered what happens when only a single thumping tire is on the car. Let us again put our car on the dynamometer, but this time place a thumping tire on each front wheel and rotate both front wheels. While it has not as yet been spelled out, it is a fact that with only one thumping tire and speed adjusted to a thump period, the thump severity will not change with time. However, with two thumping tires, operating at the same road speed, the thump severity will be observed to increase and decrease periodically; that is, phasing occurs. This brings us to the third question: What causes phasing?

To study this question, we will attach a two-

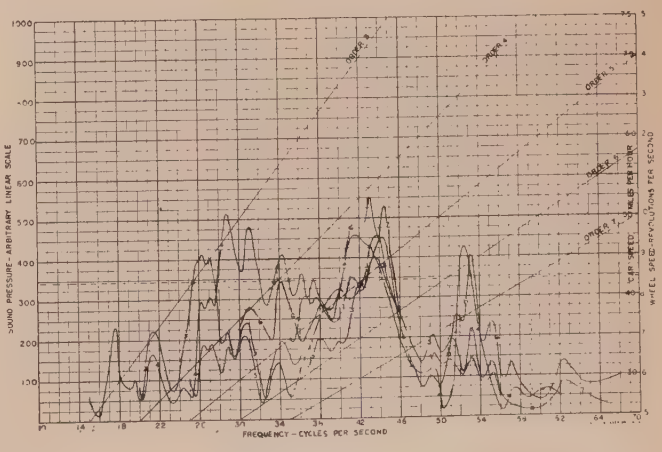

Fig. 3 – Harmonic analyses of noise frequency components for various orders of wheel speed

The Authors

DAVID C. APPS (M '52) is department head of the Noise and Vibration Laboratory of General Motors at their Proving Ground in Milford, Mich. He graduated from the University of Michigan in 1934 with a B.S. in Electrical Engineering. At present, Mr. Apps is chairman of the Truck Noise Subcommittee of the Motor Truck Technical Subcommittee of the Automobile Manufacturers Association, and also an editorial advisor of the new publication, "Noise Control."

GEORGE M. VANATOR is assistant department head of the Noise and Vibration Laboratory at General Motors Proving Ground in Milford. Mr. Vanator received a B.S. degree in 1939 and in 1941, a M.S. from Ohio State University. Since that time he has been connected with General Motors first as a technician and later as a project engineer.

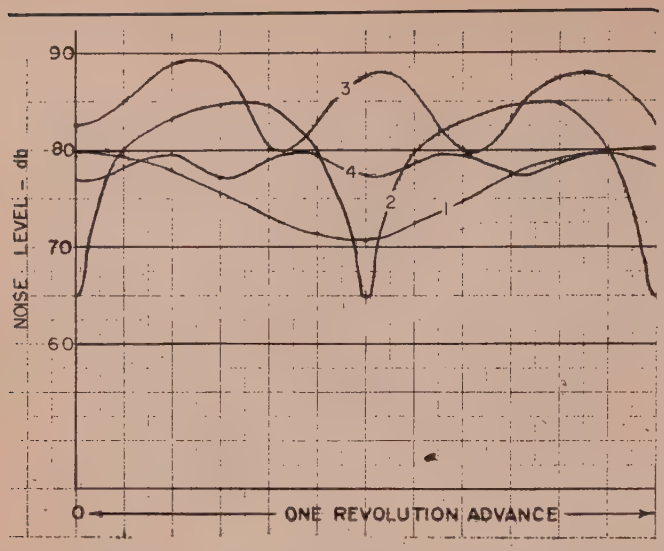

Fig. 4 – Graphic level recording of amplitude variation of the first, second, third, and fourth harmonics of wheel speed (2-wheel excitation) during one complete revolution advance of one wheel over the other

phase generator to one of the front wheels and use its output to drive the circular sweep of a polar oscilloscope. The rate of this circular sweep will then be synchronized with that wheel. To the other front wheel we will attach a contact that will cause a sharp pip to occur on the radial deflection of the polar oscilloscope each time that wheel makes a complete revolution. As long as the pip maintains a fixed angular position, the two wheels are exactly synchronized in speed. Any difference in wheel speed will cause the pip gradually to move around the circular trace on the oscilloscope. With this device, it is easy to demonstrate that phasing occurs only when there is a difference in speed between the two wheels and that the rate, or how rapidly this phasing occurs, is directly proportional to their speed difference.

Assume next that we have adjusted the dynamometer speed to a thump period, and adjusted tire pressure so that one wheel rotates slightly faster than the other by perhaps 1 rpm, as indicated by the polarscope. We will again analyze the noise in the car. This time, we will turn the analyzer to a particular harmonic of wheel speed, say Order 3, and record on a graphic level recorder the rms amplitude of this component. We will start the recorder at a predetermined relative position of the two wheels, and continue it until one wheel has advanced one complete revolution over the other. We then rewind the chart and in the same manner start a second recording of a different order. By repeating this process until all the important harmonics have been recorded, we obtain the graph shown in Fig. 4. The coordinates of this chart are time along the abscissa, and sound pressure level in db along the ordinate. The parameter of course is order, or harmonic, of wheel speed.

Note that in these curves Order 1 periodically increases and decreases in intensity once per wheel advance, Order 2 two times per wheel advance, and so forth. We can generalize this statement and say that any harmonic order (N) of wheel speed will periodically increase and decrease in intensity (N) times per wheel advance; and, indeed, this is true.

From this it is clear that with two thumping tires on the car we have, in effect, two complex excitation sources, each producing integral harmonics of their rotational rate. The difference in rotational rates, however, is very small, so that the frequencies of corresponding harmonics are very nearly the same. For example, let us assume that the rotational rate of one of the wheels is 7 rps and that the time required for the other wheel to advance one complete revolution is 1 min. The rotational rate of the other wheel is then 7.0166 rps. If we now consider some harmonic of these wheel speeds, say Order 6, the corresponding frequencies would be 42 and 42.1 cps. Their difference frequency is 6 cpm. From the preceding discussion of beat phenomena, it is then obvious that these two Order 6 components will combine in the car to produce a resultant Order 6 component of noise that will "beat," or periodically increase and decrease in intensity, 6 times per minute or, more specifically, 6 times for each complete revolution advance of one wheel over the other.

This same line of reasoning applied to any other harmonic will readily confirm our previous statement that any harmonic order (N) of wheel speed will periodically increase and decrease in intensity (N) times per wheel advance.

It is also generally true that the coefficients of corresponding Fourier terms for the complex force functions of two individual tires will not be the same. For example, the Order 4 curve in Fig. 4 shows only a 3 db variation in amplitude. This means that the 4th harmonic generated by one tire is much stronger than the 4th harmonic generated by the other tire. The two second harmonics, on the other hand, are more nearly equal, for their phasing amplitude is nearly 20 db.

How Thump Phasing Is Produced

Let us next examine how this phasing of the individual harmonics operates in the car to produce thump phasing. Fig. 5 is a noise recording of the phasing cycles of the 5th, 6th, and 7th harmonics of wheel speed. It had previously been determined that these were the principal harmonics involved in the thump period at the speed in question. The lower recording is of our thump meter output and shows how thump severity changes during a complete advance of one wheel over the other. Note that in this case the thump intensity has phased in and out seven times during the one complete revolution advance, but that only once during this period does a thump phasing cycle reach maximum intensity. Note also that at the time when maximum thump occurs, all three harmonics are also at approximately maximum amplitude.

If you examine these curves closely, you will find that at some times during a phasing period, that is, one complete wheel advance, the thump you hear will be composed primarily of a beat between Orders 6 and 7, at other times between Orders 5 and 6, and again, at other times, of a beat between all three orders.

It is obvious, therefore, that one might expect to observe any number of phasing cycles during one complete wheel advance, depending upon which harmonics are involved in the thump period in question. Also, we find that in general the character, or quality, of the thump heard continually changes as we progress through each cycle of a phasing period. In any event, however, the cycle of events will exactly repeat itself each time one wheel advances a complete revolution over the other.

From the preceding discussion, it should now be clear that when there is more than one thumping tire on a car, the resultant effect on the car, except for phasing, is no different than with a single thumping tire and we should, therefore, hear no more than one thump per wheel revolution.

Many will probably wonder at this point what happens in the example of Fig. 5 at the times when Orders 5 and 7 are approximately equal in amplitude and Order 6 is relatively low. When this occurs, these two orders will combine in the car to produce a beat, the rate of which is twice the rotational rate of the wheels. This beat occurs too rapidly to associate it with wheel speed, and is called "tire roughness." This is but one of many observable types of tire roughness. While we normally associate tire roughness with speeds above 50 mph, it can, and frequently does, occur at speeds below 50 mph.

With this understanding of the mechanism of tire thump, we are ready to design an instrument with which it can be measured. The principle of the tire thump meter is based on measuring the amplitude, or "depth of modulation," of the beat between two frequencies. It was reasoned that this depth of modulation, represented by distance "a" in Fig. 2, might be directly related to one's personal rating of thump. Fortunately, this is in general true, and a thump meter was designed and built that measures this modulation depth on an arbitrary scale of 1 to 10.

The principal components of the meter are shown in block diagram in Fig. 6. The microphone placed at a passenger's ear position inside the car senses the total incident sound, and produces a voltage which is a facsimile of the sound. In general, there will be many other sounds totally unrelated to thump, such as engine noise, transmission noise, and so forth, which must be rejected by the instrument. These extraneous sounds are filtered out by the 20-70 cps bandpass filter so that, after filtering, the familiar beat pattern is apparent. Next, this signal is demodulated and passed through a 10-cps lowpass filter. This removes the "carrier," so to speak, leaving the desired modulation envelope, which is measured by a voltmeter circuit with a long time-constant.

It should be noted that the meter rejects all pure tones regardless of frequency, as it should, because they do not constitute tire thump.

At first glance, this appears to be a rather simple

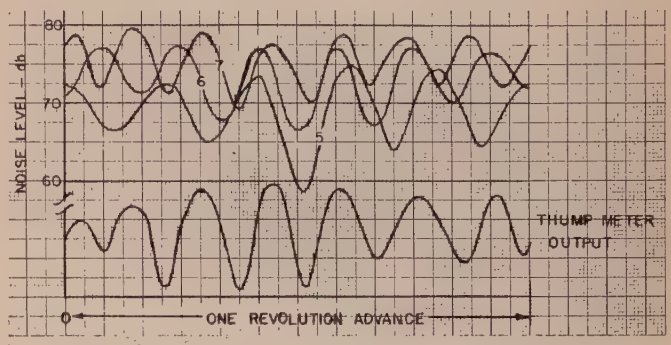

Fig. 5 – Graphic level recording of amplitude variation of the fifth, sixth, and seventh harmonics of wheel speed and of thump severity (2-wheel excitation) during one complete revolution advance of one wheel over the other

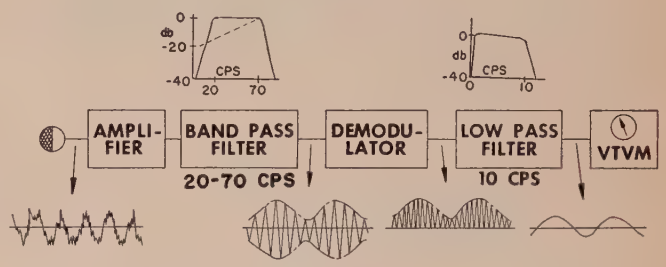

Fig. 6 – Block diagram of principal elements of tire thump meter

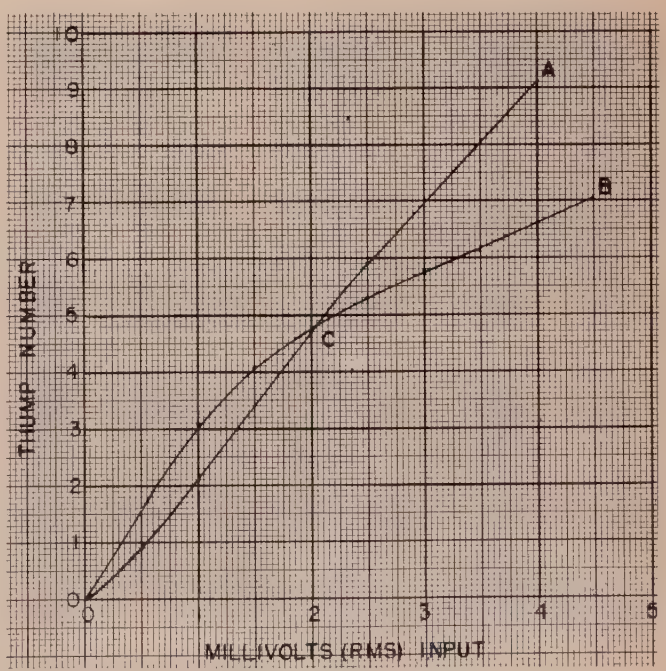

Fig. 7 – Response characteristics of thump meter ratio network. A: response required for equal amplitude signals; B: response required for unequal amplitude signals

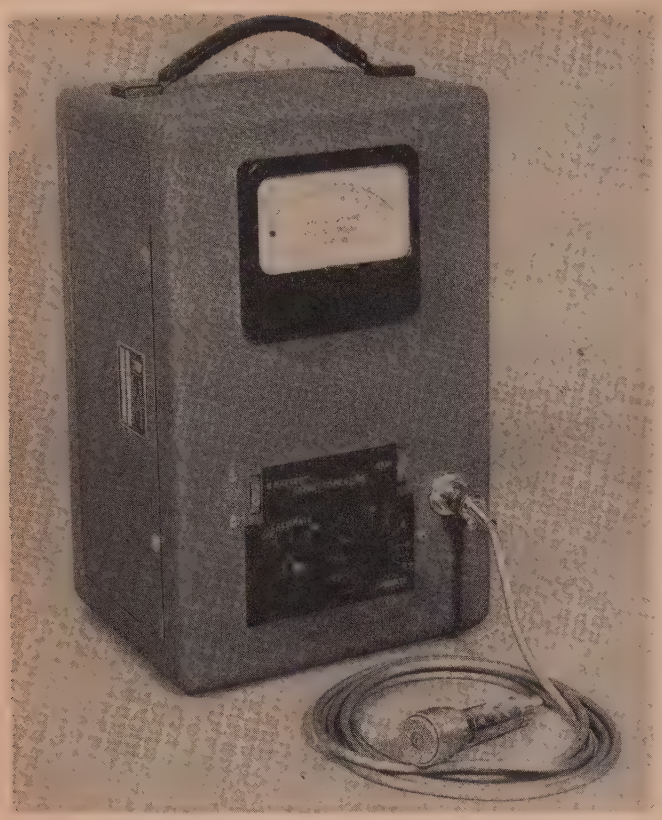

Fig. 8 – Tire thump meter

instrument, and basically it is. However, on the basis of a number of psychoacoustic tests, it was found necessary to incorporate several rather unusual response characteristics in the various circuit components. This again is a subject within itself, so we will discuss only the two most important considerations.

The first of these is the shape of the frequency response curve of the 20-70 cps bandpass filter. Rather than a flat-topped response curve shown by the heavy line in Fig. 6, it was necessary to have a response curve represented by the dotted line. This curve rises at the rate of 9 db per octave between the frequency limits of 20-70 cps.

The second consideration is in the demodulator circuit. Fig. 7 is a response curve of this circuit. Earlier it was stated that one's personal rating of tire thump was directly related to the depth of modulation of the beat envelope. Unfortunately, this is strictly true only when two frequency components producing a beat are equal in amplitude and the beat pattern, or modulation envelope, goes to zero. In this case, when the depth of modulation is doubled by doubling the amplitude of both components, the impression of thump severity is doubled, and the demodulation response should follow the straight line "A" of Fig. 7.

On the other hand, when the two frequency components producing a beat are not equal in amplitude, the impression of thump severity is not directly proportional to the depth of modulation, but is a function of both the ratio of the two signal amplitudes and the depth of modulation. It is easy to show mathematically that with two signals of unequal amplitude the depth of modulation is always equal to the amplitude of the smaller signal. If then, with a linear demodulator, we start at point "C" in Fig. 7 and hold one component fixed and increase the other, the output should not increase; but again, starting at point "C," if we hold one component constant and decrease the other, the output should decrease approximately along Curve A. Typical ear response measurements for unequal components, however, dictate that the demodulator response should follow along Curve C for unequal components. It was necessary, therefore, to add a ratio network to the circuit to produce a dual-response characteristic – one that follows the straight-line response of Curve A for components of equal amplitude, and one that follows Curve B for components of unequal amplitude. Although these requirements for bandpass filter and demodulator response characteristics seem severe, they are necessary to obtain good instantaneous correlation between personal impression of thump in the car and meter reading.

The final thump meter which incorporates these features is shown in Fig. 8. This instrument has been successfully used to rate tire thump on a good many cars, and to evaluate year-to-year progress in controlling tire thump.

A calibration level has been set such that components of 45 and 50 cps, each having sound pressure levels of 95 db, result in a reading of 10 on the thump meter. Equal components of one-half that pressure, or 89 db, then give a reading of 5, and so forth.

In making this meter commercially available, the thought in mind was to provide a single uniform standard of tire thump severity for the automotive and tire industries, with the obvious advantages that a common yardstick affords.

DISCUSSION

Calls 35-55 Cps Most Important Range

– C. D. Miller
Battelle Memorial Institute

GOODYEAR is sponsoring a rather intensive study of tire thump and tire roughness at Battelle, which began just one year ago. Our primary purpose is to find out as much as we can about how the tire manufacturer can reduce or eliminate thump produced by his tires. Our effort has supplemented studies that have been going on over a period of years in the Goodyear laboratories. The purpose of our participation has been to bring a fresh viewpoint to the problem.

Although our primary objective has been means of com-

bating thump in the tire-producing plant, a necessary preliminary part of our work has been a study of what thump is, how it is produced, and how it can be measured. We are now in an intermediate stage of our work, in which we believe we have a clear idea as to what thump is and how it is produced, and we have several promising lines of attack which we are investigating by which a tire manufacturer may be able to reduce or to eliminate the thumping characteristics of his tires.

Much of what we have learned about the mechanism by which thump and roughness are produced, and means of measuring the magnitude of thump and roughness, is identical with the material presented in this excellent paper. Realizing that our differences will be of more importance to this meeting than our coincidences of findings, I shall not dwell on the points of agreement, but shall simply take the basic mechanism and method of measurement as outlined by the authors for granted and shall proceed directly to a discussion of our differences and a discussion of facets of the thump mechanism that have been of particular interest to us.

We have found modulated carrier waves of frequencies extending throughout the entire range shown in Fig. 3. However, in our tests, the carrier frequencies in the range 35-55 cps have been incomparably more important than carrier waves of frequency below 35 cps or those of frequency above 55 cps. I would emphasize this statement to such an extent as to say that, so far as our tests indicate, elimination of all the carrier frequencies in the range from 35 to 55 cps would place any tire we have examined within the no-thump classification.

Our indication of the predominant importance of the carrier-frequency range from 35 to 55 cps is based not upon a measurement of sound pressures for each frequency component, nor upon the response of the human ear to one frequency as compared with another. Instead, we have listened to rendition by a speaker of the transmission through a narrow bandpass filter, of just sufficient width to show the modulation produced by two adjacent harmonics, and have found the audible thumping effect tremendously more pronounced throughout the 35-to-55-cps range than above or below this range.

We have particular interest in the carrier range from 35 to 55 cps because we have considerable indication that a multi-degree-of-freedom vibratory system exists within the tire-wheel assembly that would produce strongly modulated signals within this range.

At present, our theory of the multi-degree-of-freedom system is only partly proved, and I shall present it here on a tentative basis, for consideration.

Mass elements involved in our tentative multi-degree-of-freedom system are:

1. The moment of inertia of the wheel upon which the tire is mounted (not including the tire itself);

2. The mass of the wheel in its vertical motion (not including the mass of the tire); and

3. The mass of the tire in vertical motion.

These three mass elements are interlinked by spring forces existing solely within the tire itself. These mass elements are also linked with two solid foundations through the spring force of the tire: 1. the road surface, and 2. the wheel suspension in its rigid resistance to fore-and-aft movement.

As the multi-degree-of-freedom system postulated contains no spring forces except those of the tire, the system is nonlinear. That is, restoring forces are not proportional to displacement, and resonant frequencies increase with increasing amplitude. With a considerable degree of nonlinearity, wide differences can exist in the magnitudes of exciting forces with only slight changes in the amplitudes of the resulting vibrations. In this regard, it is interesting to note, in Fig. 3, that sound pressures for all harmonics within the range from 38 to 48 cps are much more nearly uniform than on any other part of the chart.

Fig. A illustrates a simple two-degree-of-freedom system. The two masses, M_1 and M_2, are interconnected with a comparatively weak spring, and each of the masses is linked with a rigid foundation through a comparatively strong spring. The system is shown in Fig. A(a) in an assumed condition of equilibrium, without vibration. If the mass M_1 is held in the equilibrium position while the mass M_2 is displaced, as illustrated in Fig. A(b), and if both masses are then released, the two masses will undergo a series of modulated vibrations as shown in Fig. A(c). First, at position A in Fig. A(c), the mass M_2 will oscillate with maximum amplitude while the mass M_1 remains stationary. The energy of the oscillation will then gradually be fed to mass M_1 until, at position B, the mass M_1 is undergoing an oscillation at maximum amplitude and mass M_2 is stationary. With damping neglected, the process will then continue indefinitely, with a continual feeding of energy of vibration back and forth from one mass to the other.

The essential requirement for a multi-degree-of-freedom

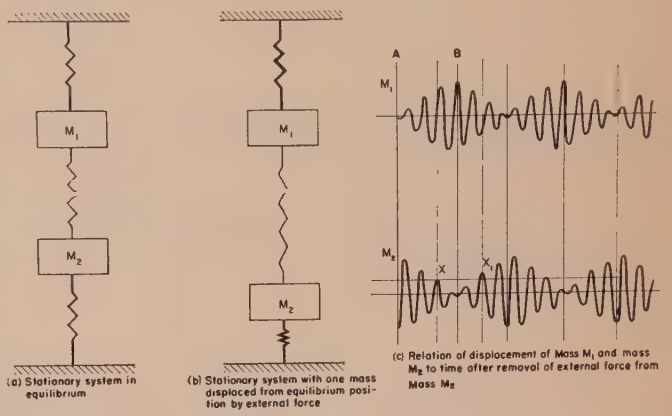

Fig. A – Simple mechanical system capable of vibration with two degrees of freedom, and type of motion of each mass that can result from a single impulse

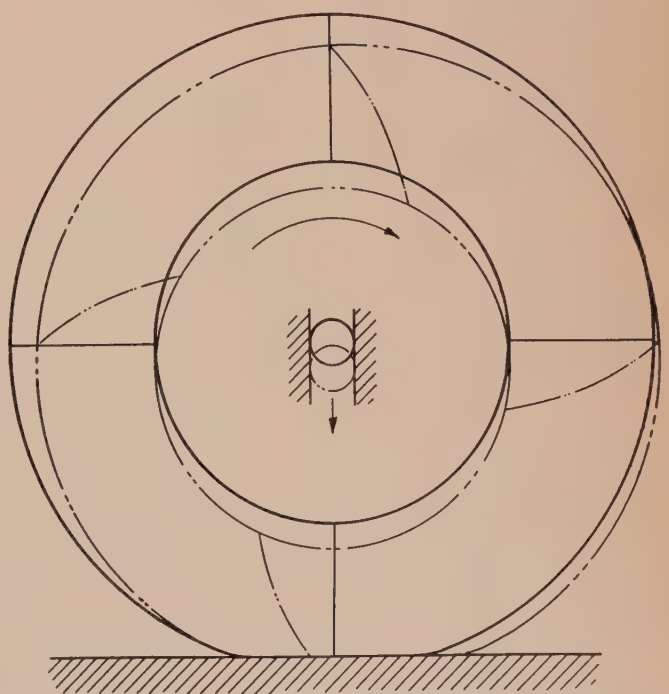

Fig. B – Linkage between rotational oscillation of wheel upon which thumping tire is mounted, and linear oscillation of same wheel in vertical direction

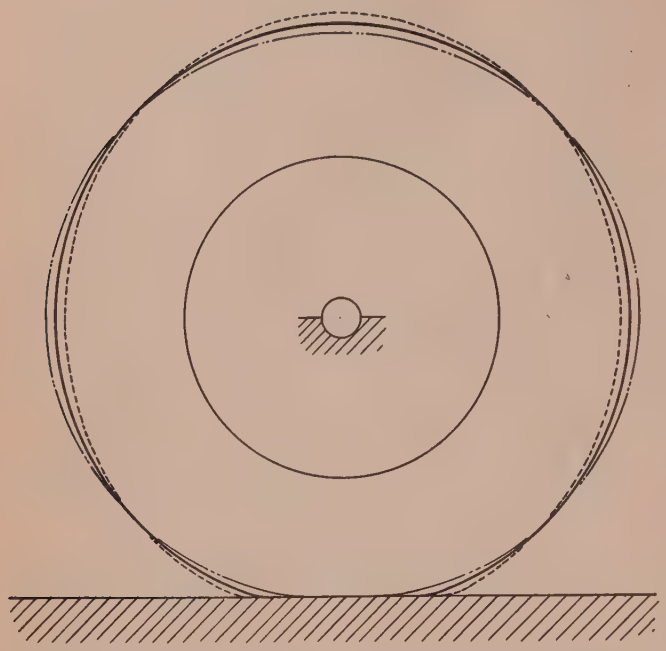

Fig. C – Mode of oscillation of tire on nonoscillating wheel, associated with postulated multi-degree-of-freedom oscillating system

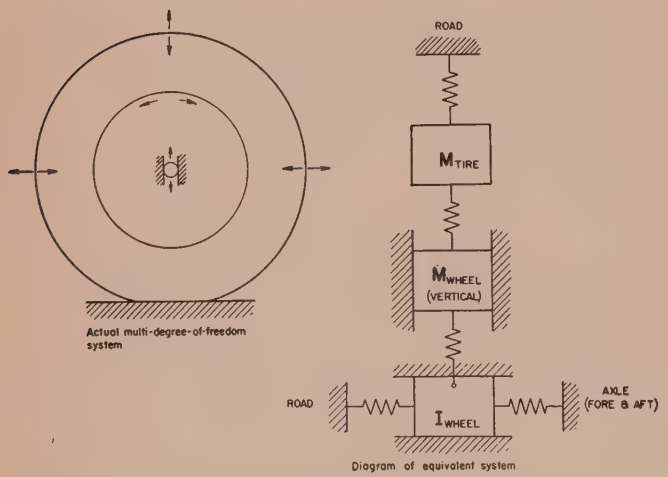

Fig. D – Actual multi-degree-of-freedom system and equivalent diagrammatic system

system is the existence of two or more mass elements interlinked with springs of such comparative strengths that two or more modes of vibration exist with nearly equal frequencies.

Fig. B illustrates the type of linkage that exists between rotational oscillation of the wheel on which a thumping tire is mounted and the associated up-and-down oscillation of the same wheel. The solid lines indicate the positions of tire and wheel with the wheel undeflected rotationally. Now let us assume, as the tire rolls along the road toward the right, that the wheel forges ahead somewhat, rotationally, producing a clockwise displacement relative to the tread of the tire. The four lines indicated radially along the sidewall of the tire, with the wheel undeflected rotationally, are now distorted as indicated by the dash-dot curves. As these lines will retain approximately their original length, their radial components are diminished. Consequently, the wheel and axle descend to the level indicated by the dash-dot outlines. Now, as the rotational oscillation of the wheel relative to the tread of the tire goes into the counterclockwise direction and returns the wheel to the undeflected position, the wheel will rise again to its original level. Then, as the counterclockwise part of the rotational oscillation continues to its extreme limit, the radial lines are distorted in the opposite direction, but with the same effect as before, that the wheel and axle drop to a lower position relative to the surface of the road. Hence, it is apparent that the wheel will oscillate up and down through two complete cycles for every one cycle of the rotational oscillation.

With accelerometers mounted on the wheel to indicate rotational acceleration, and with accelerometers mounted on the axle to indicate vertical accelerations, the filtered output with thumping tires has shown both the rotational oscillation of the wheel, with 100% modulation, at a carrier frequency between 40 and 50 cps, and the vertical oscillation of the axle at twice that frequency. With a stationary wheel, mounted on a flat surface with normal loading, we have determined a resonant frequency for the rotational oscillation of the wheel in the range of 40 to 50 cps. Of course, this resonant frequency varies with the amplitude.

The rigidity of the wheel suspension relative to fore-and-aft movement of the axle does not allow such movements to occur with large amplitude. However, the rotational oscillation of the wheel relative to the tread of the tire necessarily involves accelerating torques. These torques must be countered by reactions consisting of fore-and-aft forces exerted between the tread and the road, coupled with fore-and-aft forces exerted by the axle against the wheel suspension. These fore-and-aft forces against the wheel suspension are transmitted to the chassis and in turn to the body parts, where corresponding vibrations may be set up.

Fig. C illustrates another important mode of vibration in our postulated multi-degree-of-freedom system. In this case, let us assume that the wheel axle is held rigid relative to the road. Let us further assume that the mass of the tire vibrates up and down in the manner illustrated, involving spring force of the tire, both between the mass of the tire and the road, and between the mass of the tire and the rigidly held wheel axle. In a test machine, we have found resonant frequency for this type of vibration of a 7.10 tire to lie within the range from 90 to 100 cps. Note that this range lies very near the frequency of the vertical oscillation of the wheel associated with its rotational oscillation at 40 to 50 cps.

Fig. D illustrates our postulated multi-degree-of-freedom system diagrammatically, alongside the actual system. The crosshead-restrained mass element in the diagrammatic system, representing the moment of inertia of the wheel, vibrates from side to side against powerful spring forces linking it with the rigid foundations, the road surface and the fore-and-aft rigidity of the wheel suspension. This mass element is linked through another powerful spring with the mass of the wheel, in its vertical motion, in a toggle arrangement providing double the frequency for the vertical movement. And then we have the vertical mass of the wheel interconnected with a strong spring to the mass of the tire, which in turn is connected through a strong spring with the road surface.

In view of the fact that a frequency of 90 cps in all of the vertical oscillations of the system is equivalent to a frequency of 45 cps in the vibration of the horizontal element, our determinations of resonant frequencies for vibration of the mass of the tire and for the rotational oscillation of the wheel satisfy the condition of near equivalence necessary for a beating two-degree-of-freedom system. To what extent the vertical movement of the mass of the wheel affects this system, we do not yet know. This motion of the wheel

represents a necessary medium for transmission of energy from the rotational oscillation of the wheel to the vertical bouncing of the tire.

All of the springs in this system are composed of the tire as a whole or particular parts of the tire. These springs are all more or less nonlinear. Irregularities of the tire can impart impulses to any one of the three mass elements of the system. It might be expected that some types of irregularity would impart greater impulses to one of the mass elements, and other types greater impulses to another of the mass elements.

Now let us return to Fig. A and consider some of the peculiar characteristics of a two-degree-of-freedom system. If we construct a vertical line at a position such as X, crossing over the curves of Fig. A(c) representing the oscillation of the two masses, we can construct a corresponding vertical line X_1, at which the energy distribution between the two masses will be the same. The only difference existing between the conditions at X and X_1 is in the phasing of the oscillation of the two masses. For the total energy of oscillation involved, and the distribution of this energy between the two masses that exist, only two phasings are possible, the one existing at X and the one existing at X_1.

As we go on beyond the point in question, either X or X_1, whether energy will feed from the oscillation of mass M_2 to the oscillation of mass M_1, or the reverse, will depend on which of the two possible phasings exists. If, at the point X, we were to strike the mass M_2 a blow of exactly the right momentum and at exactly the right phase of the oscillation of this mass, we might avoid making any change in the amplitude of the oscillation of mass M_2, but might shift the phase of that oscillation, relative to the oscillation of mass M_1, to the condition existing at X_1. If we were to do so we would eliminate the portions of both curves between the vertical lines X and X_1.

In Fig. E, in the upper curve, we see six cycles of the oscillation of the mass M_2 as those oscillations would exist if they persisted after an initial impulse, by inertia, without the imparting of any further impulses to either mass. Now let us assume at point A an impulse is imparted to mass M_2 that changes the amplitude of its oscillation, and the phasing of its oscillation relative to mass M_1, to that which would normally exist at point X. The result would be that the portion of the curve between the lines A and X would be omitted. By another impulse at point B we might strike out the portion of the curve between lines B and Y, and so on. The resulting curve, the lower curve of the figure, would represent a quite haphazard modulation of the carrier wave. This type of modulated curve has been recorded many times in our tests with nonthumping tires. A typical example of such a recording appears in Fig. F.

We believe with an absolute regularity of impulses at each wheel rotation, with an absolutely constant rotational speed, this pattern eventually irons out into a regular pattern that repeats itself at each wheel rotation. However, with nonthumping tires, we have found that the wheel rotation rate must be kept constant over a considerable length of time, sometimes as long as 1 or 2 min, for the pattern to become regular.

Modulation of a strong carrier wave of this irregular nature might doubtless be interpreted as a type of roughness. However, in our opinion, for any given average amplitude of modulation, the effect produced by a carrier modulated in this manner will be much less objectionable than if the same degree of modulation existed with a pattern repeated regularly at wheel-rotation rate.

We have designed and built an experimental thumpmeter whose reading is a function of both average amplitude of modulation and regularity of modulation. We are investigating the correlation of results with this meter with the audible effect upon occupants of an automobile with thumping and nonthumping tires. As this thumpmeter has just been completed, we cannot yet report any results as to the degree of correlation.

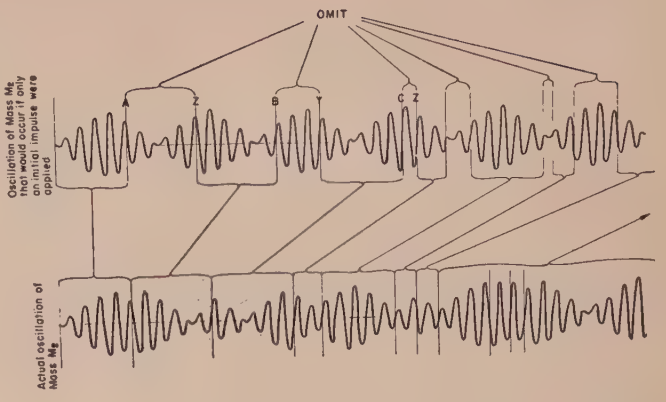

Fig. E – Effect of a postulated series of impulses applied to mass M_2 of Fig. A. A,B,C: points of application of impulses. X,Y,Z: amplitudes and phasings of oscillation of mass M_2, relative to mass M_1, created by impulses

Fig. F – Irregularly modulated carrier frequency recorded by filtering total noise signal received by microphone within automobile, with nonthumping tire turning on test drum

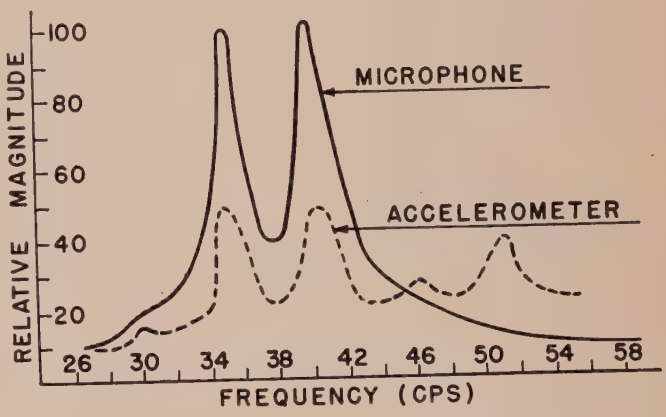

Fig. G – Sound intensities (rear seat) versus spindle vibrations as a function of frequency

Both Sound and Feel Contribute to Thump

– John W. Liska
Firestone Tire and Rubber Co.

IT is interesting to note that our approach to the problem of thump, which was based largely on vibration studies, has led us to many of the same conclusions which were reached by the authors on the basis of sound analyses. In some of our early experiments, which were designed to evaluate the relative importance of sound and mechanical vibrations in the evaluation of thump, we observed that the driver of the car was, in general, much more critical in evaluating severity of thump than any of the other observers. This was attributed to the vibrations he received through the steering wheel. We later verified this point by designing and building

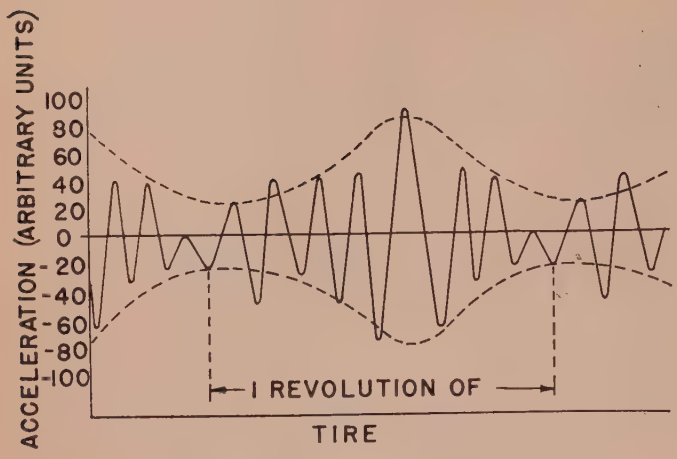

Fig. H – Spindle acceleration pattern during severe thump

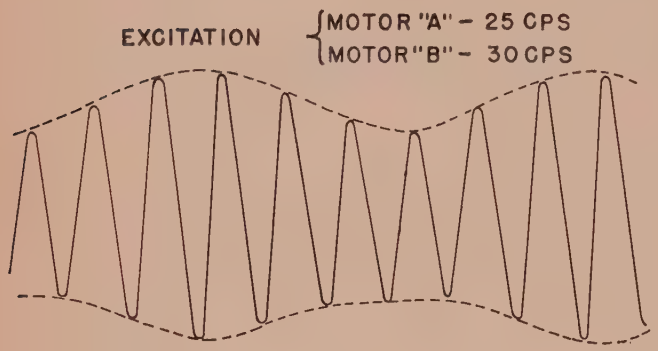

Fig. I – Door panel accelerations excited by two motors with off-center weights

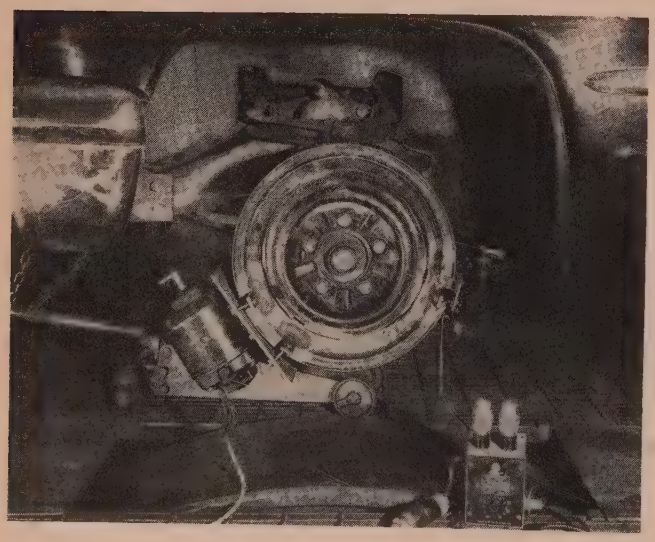

Fig. J – Two variable-speed motors mounted on car wheel

a resilient mounting for a steering wheel. With such a device, it was found that the driver was no longer the most sensitive observer. Also, in our early tests, we enlisted the services of a deaf mute as a thump observer. We found that his evaluations were usually in agreement with those of an observer with good hearing. In another series of tests, we fastened a contact microphone to various parts of the inside of a car, amplified the output, and fed this signal to a loudspeaker situated in a room outside the dynamometer location. The mechanical vibrations picked up were thus transformed into sound waves of the same characteristics. Observers were able to rate the thump characteristics of the system without hearing the sounds actually present in the car. On the other hand, we found it possible to observe thump by having the observer place his head through one of the open side windows of the car while one wheel was rotating on a dynamometer, thus demonstrating that sound is also a factor, in agreement with the authors. In this event, it was not possible for the observer to "feel" any of the vibrations produced. The dual nature of thump was also demonstrated by making complete vibration and sound analyses on the same car. The results obtained are shown in Fig. G. Here it can be seen that, in many cases, the same frequencies are present in both mechanical vibrations of the car and in sound waves in the car. It should also be noted, however, that the relative intensities, at the various frequencies studied, are not the same in the sound and vibration patterns. Thus it is seen that the contributions to thump arising from sound and vibration may be the result of different sets of frequencies.

Despite the basic difference in our approach to this problem, we arrived independently at very similar conclusions regarding the nature of the problem, particularly with respect to the explanation of thump in terms of beat phenomena, in the case of a single tire, and phasing, in the case of more than one tire. Fig. H shows the variation in vibration accelerations of a car spindle as a function of wheel rotation. This illustrates the beat phenomenon which gives rise to thump in exactly the same way as does Fig. 1.

Fig. I also shows the development of beats from vibrations giving rise to thump. In this case, however, the pattern shown was obtained by removing three of the four wheels, supporting the car on two stands, and recording the vibrations of the left front door panel. The tire was removed from the fourth wheel, and in its place two small electric motors were mounted. On each of the motor shafts a small eccentric weight was attached, as shown in Fig. J, so that vibrations of frequencies corresponding to the rotational speeds of the motors could be transmitted to the car door panel. When both motors were operated simultaneously at slightly different speeds, the vibration pattern which was obtained varied as is shown in Fig. I, and a blind-folded observer was able to sense or evaluate thump. All this took place with the car stationary and with no tires on the wheels. This illustrates the fact that the car itself contributes to the overall thump problem, as is mentioned briefly by the authors. It is believed that some additional observations along this line would be of some interest. We found, for instance, that the same set of four tires mounted on several makes of cars received variable ratings covering almost the entire range of thump – from very good to very poor. In fact, the same set of tires mounted on several individual cars of the same make, year, and model were often rated quite differently – from good to poor. All of the above "car" tests were conducted with the position of each tire the same on each of the test cars. Further variations in the thump ratings of a given set of four tires could also be introduced by switching the positions of the four tires on the same car.

The above comments confirm and amplify the remarks and explanations given by the authors, illustrating the complexity of the problem both from the standpoint of the tire, which initiates the vibrations and/or sounds which give rise to thump, and from the standpoint of the car, which amplifies the sounds and vibrations produced.

Various methods of isolating the vibrations induced in the unsprung mass system of a car and preventing their transmission to the car body and frame were attempted. Such a vibration isolator was designed, built, and tested in the lower control arm of the steering mechanism of a test car. It accomplished its design purpose, in reducing the degree of thump with any given set of tires, but unfortunately it also introduced some steering instability, and hence was not pursued further as a practicable solution to the thump problem. Various other methods of modifying the car body and/or frame to reduce the degree of thump were also tested, with varying degrees of success. The steering wheel vibration isolator has already been mentioned. Another fairly effective method is the use of additional resilient padding under the floor mats and on the seats, back, and sides of the interior, any of which reduces the amount of vibration transmitted to the observer or passenger. Another method is to stiffen frame members by additional braces (to increase the natural frequency of vibration of the given member) or to damp out panel vibrations by adding mastic (which would lower the natural frequency of the panel). As in the earlier instance mentioned, some degree of success can be achieved, but usually the net gain (considering extraneous effects which are introduced, such as cost and weight) is small.

The tire vibrations which produce observable thump in a car, incidentally, are of an extremely small magnitude. This was demonstrated by running a tire which was essentially thump-free on a car at a speed of 30 mph on a single-wheel dynamometer drum (the other three wheels remaining stationary). One of the nonrotating tires was then tapped moderately lightly with the handle of a screw driver at a frequency corresponding to once-per-revolution of the rotating wheel. An impression indistinguishable from thump was received by an observer seated in the car.

When the beat frequency theory of thump was first developed in our laboratories, several possible solutions to the problem became immediately apparent. One of the more obvious solutions was to introduce slight disturbances which would break up the rhythmic pattern of vibration or possibly even "cancel" the tire vibrations giving rise to thump. It was soon learned that cancellation of vibration by the creation of an additional vibration of exactly equal amplitude and frequency, but exactly 180 deg out of phase, was not very practicable. However, the introduction of additional vibrations to break up the original pattern is somewhat more successful, though as the authors point out, this solution is at best only partially successful, since roughness of ride is usually introduced at the same time.

A number of attempts were made to correlate thump with conventional tire quality measurements. Positive correlations were found between thump and center gage variation (Fig. K) and also between thump and difference in shoulder gage (side to side) in a tire (Fig. L). No direct correlation was found between thump and either balance (Fig. M) or loaded rolling radius variations (Fig. N). As a result of a great many such observations, it was concluded that thump is produced in a car by a number of tire factors, no single factor being outstandingly responsible. In all cases, even where positive correlations were obtained, there were enough extreme exceptions to rule out the possibility of using any one particular quality measure as a means of rating individual tires for thump severity. Some combinations of such measures were found to be effective for this purpose. For example, tires which have unbalance, radial runout, and center-gage variations each below certain maximum limits could be quite reliably selected as being relatively free from severe thump. Other combinations of quality ratings could probably also be devised. It appears that only an overall improvement in all the conventional quality measures of tires can be expected to reduce thump incidence or severity significantly. This means precision and uniformity in tire constructoin are essential. Recently, reports have been circulated throughout the automotive industry, and have even been included in advertisements, to the effect that

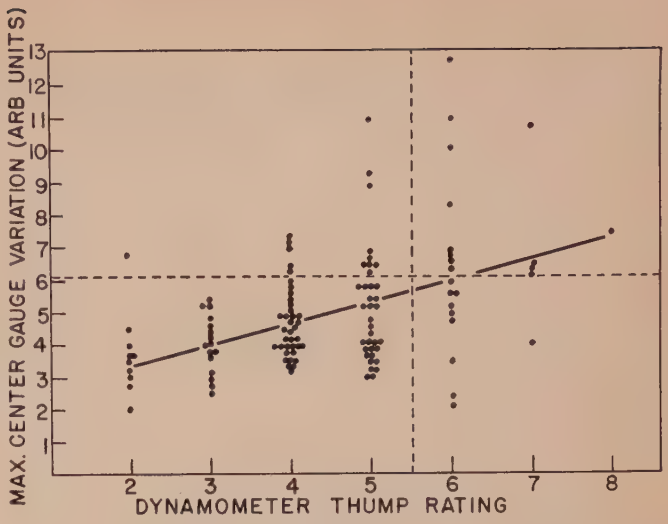

Fig. K – Relation between thump rating and maximum center gage variation

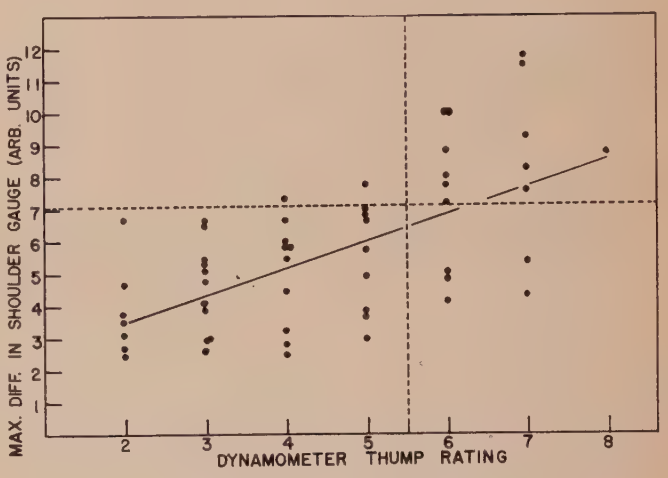

Fig. L – Relation between thump rating and maximum difference in shoulder gage

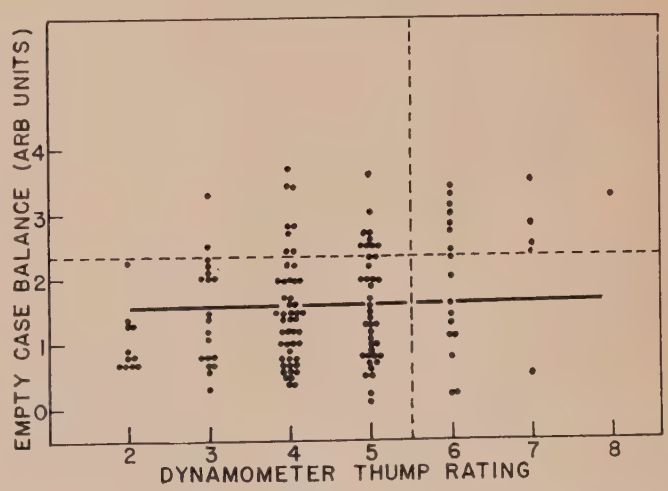

Fig. M – Relation between thump rating and empty case balance

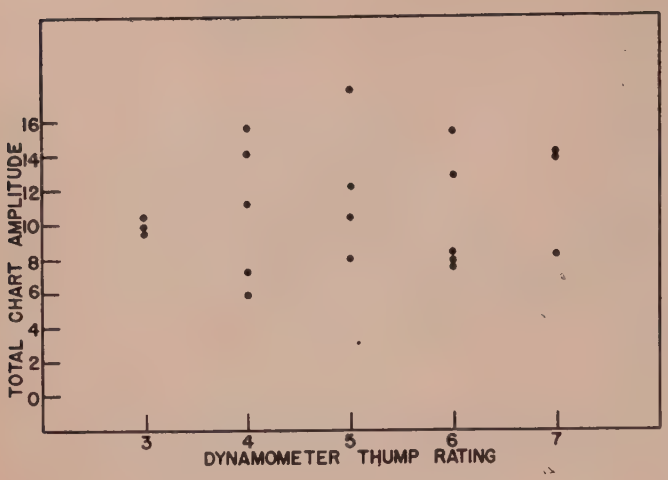

Fig. N – Relation between thump rating and maximum variation in loaded rolling radius

thump-free tires can be produced on a quantity production basis simply by making the tread splice in a very special manner. Our experience does not support this claim at all. A high degree of precision in the tire bodies is also required.

What Do Precision and Uniformity Mean?

Just what do we mean by precision and uniformity? Specifically, in the case of the tire tread, one of the steps which is necessary is to produce a tread which is uniform in width and gage, not only along its length but also from side to side. The two shoulder regions must match each other as perfectly as possible. The uniformity of tread length at the time of application must be increased, and precise methods of applying the tread to the unvulcanized tire body must be used. One of the commonly suspected causes of thump is the nonuniform tread splice. Though, as we have said before, our studies do not indicate that this is the dominant cause of thump, we believe it is one of a number of causes, and hence a uniform tread splice is essential.

So far we've talked only about the treads, and we have already said that tread and tread splice uniformities are not enough, that the tire bodies also contribute to the generation of tire vibrations which, in turn, cause thump. How must the tire body be handled? We find that both the number and the bulk of the ply splices must be reduced to a minimum. Furthermore, constant attention must be paid to the matter of splice spacing, to avoid the difficulties mentioned earlier in the discussion. Increased ply-gage uniformity is required despite the fact that, because of the economics involved, this is already a very closely controlled tire component. Cord angle and cord density (or the number of cords per inch of fabric) must also be controlled to a high degree of uniformity throughout the tire, as still another contribution to the achievement of a substantial reduction in both thump incidence and degree.

It must be realized that all of the foregoing items, calling for increased precision and uniformity, require additional care and time in manual operations in the factory, and therefore represent a significant increase in cost which will have to be borne by the consumer who is sufficiently disturbed by thump to be willing to pay the necessary premium.

Wheel specifications, too, will have to be tightened, since even the most precisely built tire will register undesirable radial runout if it is mounted on an eccentric wheel or one whose bead seats vary with respect to each other.

The authors describe the periodic increase and diminution of sound or phasing as the result of having two or more tires on a car, each of which is capable of producing thump by itself. We have also observed this phenomenon, but in addition have found that when tires are tested in pairs they may produce a more severe thump than when tested singly. It is thus seen that it is possible for two or more very slight sets of impulses to add up to a degree of thump which could be termed severe. On this account, thump ratings of tires obtained on single-wheel dynamemeter tests must be interpreted with caution.

Our Experience with Thump Meter

Our experience with the GM thump meter has been favorable to a degree. However, there apparently are a few refinements which need to be worked out. We find a rather good, general correlation between the thump meter readings and the ratings of a trained group of three or more observers, who incidentally do not always agree among themselves. Specifically, we found a correlation coefficient of + 0.76 on an indoor, single-wheel dynamometer test between the two, which is certainly very good as a general index. However, as a positive method of rating single tires this degree of correlation is not adequate, since there are sometimes rather wide differences in individual tire ratings between the observer rating and the thump meter reading. It is suggested that, at least in some cases, this difference is a result of the fact that the thump vibrations are affecting the observers' reactions, while having no effect on the microphone or sound pickup of the thump meter. In tests on highways, even on relatively smooth pavement, the galvanometer needle varied considerably (despite its damped design) so that, as a result of car motion, precise readings were difficult to obtain. Passing or intercepting vehicle noise was also observed to have a disturbing effect on the apparent stability of the thump meter system. It is possible, in this case, that the sounds of the two vehicles involved combine to produce a wave form to which the thump meter is responsive even though the electronic circuits described should and do filter out the high frequency sounds produced by the individual cars. The desirability and need for a single, uniform standard of thump severity is, of course, obvious.

Tire Thump Isn't Always the Trouble

There is still considerable uncertainty in the field detection or interpretation of thump, particularly among individual car owners and service station attendants. A number of customer complaints about tire thump, for example, were ultimately traced to mechanical vibrations in the car. Other cases were found to be due to faulty mounting of the tires, such as improperly seated beads or safety diaphragms. A number of cases of reported severe thump were corrected simply by inflating the tires to 40 or 50 psi, running the car for a few blocks, then reducing the pressure to normal. On the other hand, it has been reported that some sets of tires developed thump after 1000 miles of operation. Some such cases were attributed to uneven wear due to wheel misalignment or other severe conditions. These examples serve to illustrate the extremely small magnitude of the disturbances which originate in the tire and then are transmitted to and amplified by the car to produce thump.

What we have tried to do in this discussion of the authors' excellent paper is to amplify some of the points to which they referred briefly, to point out the dual nature (sound and feel) of thump, to describe in more detail the effects on thump of both cars and tires, and to illustrate the extreme complexity of the problem in both car and tire. Just as no single, simple change can be made in a car to reduce its sensitivity to thump or its tendency to amplify the offending vibrations, no single, simple change in tire construction, composition, design, or cure has been found which will eliminate or even significantly reduce thump incidence or severity.

The experimental data and conclusions given in this dis-

cussion were summarized from the results of extensive tests conducted by a group of investigators including F. S. Conant and G. L. Hall of our research laboratory, and W. D. Sollinger of our development department staffs.

Question for Authors

We have talked about the necessity of improving the precision and uniformity of tires all the way along the line. We have also talked about conducting a few tests on the car itself. Admittedly, we have performed only a limited number of tests compared with what the car manufacturers have done.

Have you noticed whether it has been possible to add up some of these improvements we have talked about? We did notice a reduction in thump by several of the expedients we tried, but we did not try to add them all up to see if they will combine into a substantial reduction. It is true enough that no one thing we did was a howling success.

Compares Meter Readings With Human Observations

– Gerald Klaasen
Chrysler Corp.

I WOULD like first to make a few comments on the mechanism of thump. We feel that the authors have done an excellent job in delineating what is happening during thump. We have done a lot of work in our own laboratory, and have found nothing to refute their ideas, and have substantiated many of their points by means of our tests.

The authors allude to the frequency response characteristics of a car, but choose not to expand their views on what components of the car might be responsible for the significant part of this response with regard to tire thump. At this point it might be instructive to mention some of the schools of thought on this matter of resonance. There are those who hold the view that the principal resonance involved is a torsional one, that in which the rotational inertia of the wheel assembly acts against the tangential flexibility of the tire, and against fore-and-aft flexibility in the suspension. Thump probably occurs, they say, when this single resonant system so amplifies a harmonic of the exciting force as to bring it approximately equal in intensity to an adjacent harmonic. There are others who hold that there are two main resonances involved – one similar to that just described, and the other a resonance involving the inertia of the wheel assembly acting against lateral flexibility in the tire and suspension. These two resonances, they say, are in the neighborhood of 40 cps, but are spaced just far enough apart so that they amplify adjacent harmonics of the exciting force above all other harmonics. There are others who have suggested body cavity resonance as a possible offender, and others who have suggested major body panels. The fact that open convertibles often have bad thump would seem to discredit the first notion. Those who have studied the forced vibrations of body panels will, I think, agree that there are so many sizes and shapes of panels in the body which can adjust their mode of vibration so readily to accommodate whatever the impressed frequency may be, especially in the frequency range between 20 and 100 cps, that the overall response is not likely to exhibit any outstanding peaks.

It is difficult to isolate the responsible resonances by means of vibration pick-ups, because the vibrations associated with thump are transmitted generally throughout the car. For example, the beat vibration characteristic of thump has been picked up in the roof panel, instrument panel, hood panel, steering column, rear seat pan, and rear spring, as well as in other suspension parts. It appears, therefore, that if the resonance is to be identified, it must be done by changing the damping or tuning of suspected components, and showing that such an alteration also changes the thump characteristics of the car.

Table A – Comparison of Thump Rating by Jury and Thump Meter

Turns of Screw	Jury Average	GM Thump Meter
0	5	2.8
4	5⅔	3.0
7	7⅔	3.2
4	5½	3.4

Measurement of Thump

Turning now to the measurement of thump, the authors have undertaken a very formidable job. Measuring noise in its subjective aspects is almost always a difficult job. When you add to this the fact that this particular noise called tire thump is unusually complex, it is appreciated that the problem is a very difficult one. The authors have attacked the problem in a thorough and systematic manner, and have produced an instrument which is small and conveniently portable, and which is also easily read. After using the instrument for some time on tire thump work, however, we are forced to conclude that our results with the meter were not completely successful.

It has been our practice to use juries in evaluating thump. This is usually done with two cars, one being used as a control car. In these tests a rating scale of 1-10 is used, 10 being extremely bad thump and 1 being undetectable thump. By depending upon quick comparisons, we find it possible to get quite precise evaluations. This method has its disadvantages, of course, the most serious of which is the comparatively high cost in man-hours. A comparison of the results obtained by jury evaluations and by thump meter was disappointing.

A typical test is one in which a car was equipped with three nonthumping tires and one tire in which the thump was adjustable. This was accomplished by threading a screw through the bead flange of the wheel. By turning this screw in and out, it could be made to produce various amounts of distortion in the bead, and hence various amounts of thump. A jury of old hands at tire thump was asked to rate this car by means of a secret ballot during four runs in which the thump was adjusted to various amounts unknown to them. During the same runs readings were taken on a thump meter. The results are shown in Table A.

Immediately after this test, the meter and microphone were completely checked in the laboratory to make sure that they were functioning as intended, and were found to be in good order.

We are unable to say exactly why the correlation was not better, but we can think of a couple of possibilities. The first of these is that the meter, in spite of its two filters, still does not appear to be selective enough in what it indicates. There probably are noises other than those associated with a thumping tire which are in the 20-70 cps frequency range and which undergo considerable modulation, however, in a random pattern rather than in a pattern associated with wheel turns. These extraneous noises would also be indicated by the meter, and may be covering up the noise we are trying to measure. Then too, the impression we receive of thump is not all received by means of our ears. In some instances a considerable portion of the impression is received through the hands, feet, and seat. The proportion varies from car to car, and varies with position in a given car. Our experience is that, generally, thump is heard to a greater extent in the rear seat than in the front seat, and felt to a greater extent in the front seat than in the rear seat. It seems to us that the meter must take these

factors into account before it can do the job expected of it.

Perhaps my remarks on the tire thump problem up to this point have not been very constructive. Maybe a few remarks along the lines of what can be done about tire thump would be a little more in the direction of something helpful.

In the light of our present knowledge of tire thump, there are at least three angles of attack which might be used to reduce it. The first thing to consider is the reduction of the excitation of the tire. This is the source of our problem and is, of course, the province of the tire manufacturers who have been working very intensively to reduce irregularities in their tires. There seems to be no doubt that standards of precision in tire manufacturing higher than those now in use will be a prerequisite of any substantial improvement in thump. Statistical analysis of the thump characteristics of batches of tires from different manufacturers, from different plants of the same manufacturers, of different tire sizes, and so forth, has shown that improvement is possible. As an interesting sideline to the matter of improving the tire, I would like to mention that some have suggested that the solution from the tire maker's standpoint may be in putting more irregularities in the tire rather than reducing the irregularities which now exist, but at the same time controlling the location of the irregularities to produce specific, calculated, favorable results. The danger in this approach lies in the possibility of introducing in place of thump another problem which is at least as serious, namely, tire roughness.

As automobile manufacturers we may have to make use of two other lines of attack, namely, alter or destroy the resonant system or systems involved, or isolate the disturbance from the passenger compartment. Before the resonant system or systems involved can be altered or destroyed they must first be identified and, as pointed out earlier, this is not easy. Isolation is also difficult because the frequencies are low, and high deflections are necessary to attenuate low frequencies.

We are able to report that our work has indicated that more fore-and-aft flexibility in the front suspension is beneficial to thump. We are not prepared to say at this time whether the reduction in thump was due to detuned resonant systems or to better isolation of the thump vibrations. The trick in introducing fore-and-aft flexibility, of course, is to do it without sacrificing directional stability or other important suspension requirements.

We can also report that reductions in thump have been achieved by the use of softer mountings between the body and frame. In this area, too, a compromise is involved. The body and frame depend upon each other for support, and if the tie is weakened, either considerably more metal will have to be used, or excessive shake will result. The solution may lie along the lines of more carefully controlling the direction of body mounting and suspension stiffnesses.

Suspension Insulation Effective Against Thump

– P. H. Kuhn
Ford Motor Co.

WHEN I received the invitation to participate in this discussion on the premise of basic car design contribution to the problem of tire thump, I was first confronted with several negative complications. First of all, the average car in recent years has, by quieter, smoother performance, complicated the problem rather than assisted it. Secondly, to the best of my knowledge, the basic car design is not established and developed around a thumping tire. While this last statement sounds harsh, it is honest. Third, I do not have any positive answers. The overall noise level of our automobiles, however, has received considerable attention, and increasing activity is evident in this direction. Considerable success in reducing the noise level and the extended usage of smoother roads have aggravated the problem of tire thump.

The reduction of car sensitivity and awareness of tire thump to the passengers of the automobile is as illusive and difficult to establish as the answer to the problems of tire thump itself. That the tire industry is aware of the complexities of the problem is attested to by the tremendous amount of research and development activity currently engaged in and programmed for the future. The automobile industry is very cognizant of the problem and, from the standpoint of car design, is very interested in any development which contributes to the reduction of car sensitivity and awareness to tire thump. As the complaint increased, expanded car activity was engaged in to provide such assistance as was thought possible by the car manufacturer.

The nature of thump has been adequately described and defined by the authors and other discussers. Since the vibrations are apparently carried and amplified to the interior of the vehicle by the various car components, it first seemed reasonable to merely insulate or tune the offending area. With the multiplicities of insulators, deadeners, and dampening devices that has been experimentally applied to entire chassis and body panels, tire thump has continued on without much response to this kind of treatment.

Individual components of the car were segregated and investigated in every conceivable manner as to any possible dampening or isolation effect that they might contribute to the reduction of the problem. None of these areas has satisfactorily responded to the desired degree.

One Area of Possible Relief

At this point I am forced to acknowledge that I have very little to offer as positive information; however, in reviewing investigations to date, I feel that one immediate area in the car offers some promise of slight relief. This area is the body insulation from the chassis through the body mounts themselves. The use of large, soft, low-rate body mounts has, by seat-of-pants feel and car detection, effected a noticeable improvement in some test activity to date. The difficulty encountered in this direction has been excessive shake on rough roads; however, by providing lateral control capacity to the body mount insulator, a satisfactory shake compromise has been established. I do not imply that this modification has resulted in a correction of the problem – it merely reduces the degree of thump awareness within an acceptable range of shake performance as tailored to the vehicle.

In reviewing past car performance with regard to thump for any clue to reduce road noise, tire thump, and overall noise, I would like to point out that suspension design, or rather the ability to insulate the front and rear suspensions from the chassis, can be very influential and beneficial in reducing tire thump and road noise. An example of this type of suspension insulation was the 1948 Lincoln. The transverse front and rear spring arrangement on this car lent itself quite readily to low-stress rubber isolation of the suspensions from the frame. It is generally conceded by tire engineers that this car was outstanding for its quietness of tire operation and thump-free characteristics.

When using some of these vehicles as mechanical suspension prototypes and eliminating the large, widely spaced insulators, a very considerable increase in general road harshness and thump was apparent. Low stress insulation of present suspensions to the same degree as employed on this vehicle is not readily accomplished; however, it does indicate that the possibility exists for improvement in this direction if such design considerations could be applied to present-day suspensions.

In final summary, it appears, at least for the time being, that there is very little to offer to the solution of tire thump problems from the standpoint of car design, except continued effort.

Use of Single Meter Can Give Confusing Results

– Paul Wang
Houdaille-Hershey Corp.

THE authors have very admirably presented a case explaining the mechanics of tire thump in a manner commendable for the endorsement of all who may be engaged in this subtle science of applied acoustics in one way or another. The focal point involved in this given problem is the use of a single meter to rate the audible stimulus received and heard in a car body. That the same stimulus is also detectable by means other than sound transmission simply means that it has the same origin as some vibration phenomenon which a deaf person can feel rather than hear. Tire thump is an audible noise of low frequency components whose thumping severity depends on the frequency rotation of one thumping wheel, and also on the beating amplitudes of two components at the same frequency apart; that is, the beating frequency. These components were given for one illustration as 42 and 49 cps, which were not in the subaudible range. It is the writer's opinion that when audibility of a noise is rated from the indication of one single meter, very confusing results are often obtained.

When an audible noise is measured or analyzed, the spectrum pressure level is generally the basic reference, and is expressed in decibels referring to 0.0002 dyne/cm^2. The loudness level is not the same physical unit, but represents, instead, a subjectively determined level, using for comparison a reference tone of 1000 cps whose loudness level is arbitrarily designated as n phons at a pressure level of n db. Tones at other frequencies which may sound to us with the same loudness as the reference tone at n phons are also designated as n phons loud, whatever the pressure levels may be. Perhaps some confusion could be avoided at this very point, if we would always specify sound pressure levels in decibels and loudness levels in phons. A pure tone of 40 cps at 60-db pressure level is only 4 phons in loudness level when a 1000-cps tone is 60-phons loud at the same pressure level, if both are heard in the same very quiet room.

Rating Loudness of Complex Noise

In rating the loudness of a complex noise, such as tire thump, complications are immediately introduced, because it contains more than one pure tone and because it is also heard in the presence of a noisy background whose influence on the audibility and severity of the signal noise (tire thump, in this case) is exceedingly large.

It seems reasonable to expect, therefore, that a simple meter basically indicating spectrum pressure levels or modifications thereof would not be sufficiently indicative over a wide range of loudness level, which is really how a noise signal is rated. It also seems proper to consider the following questions before proceeding further with our problem:

1. Is the noise heard in the presence of another noise?
2. Does the presence of the background noise decrease the loudness stimulus of the signal noise whose loudness rating is being sought?
3. What do the spectrum analyses of both signal and background noise show?

If it is assumed that the background noise does not decrease the loudness of the signal, it is possible to calculate the latter from a knowledge of the analysis of the signal. Many published articles on this subject have appeared in the **Journal of the Acoustical Society of America** over the past years.

If it is considered that the background noise does decrease the loudness of the signal noise, as it usually does, the relationship of the loudness of the signal to the sound pressure level and analysis of the background noise must then be studied at great length. The result for one kind of signal noise in a particular background can take the form shown in Fig. O. It is observed that for a signal at 60-db pressure level in a background noise of 60 db, its loudness is equivalent to that of the same signal, but only at 50 db, in a quiet field, whereby its loudness can then be calculated. If the background noise is raised to 80 db, the 60-db signal would then be equivalent in loudness to that of 7 db in quiet field. If the pressure level of the signal drops down to 59 db in a noise field of 80 db, it would most likely be inaudible. This, of course, applies only to the particular noises used, and must not be considered as general data for qualitative comparison in other cases.

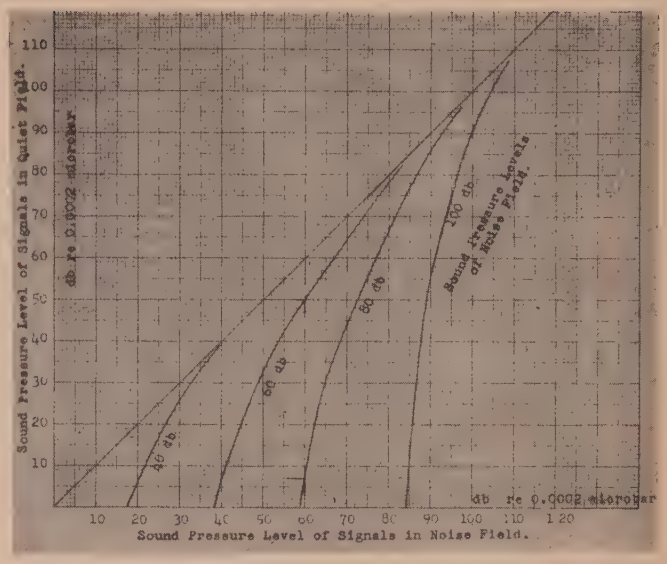

Fig. O – Equivalent loudness of signals

In the case of tire thumps, the background noise involved is probably the low band (20-75 cps) component, which is generally about 80-90 db, a latitude that is of sufficient magnitude to make the thump audible in one case and inaudible in another, as well as to affect its degree of audibility or severity. The solution of rating tire thumps does not, therefore, lie in the device or calibration of a single meter whose indication is neither the pressure level nor the loudness rating.

Authors' Closure To Discussion

MR. MILLER states that they find tire thump carrier frequencies in the 35-55-cps range to be the most important. This may indeed be so, especially if one concerns himself with a limited number of observations on a limited number of cars. We have had the opportunity to analyze a good many cars. As a result, we feel that even the 20-70-cps band limitation is a compromise. For example, we found one car with a carrier frequency component as low as 15 cps. We feel, therefore, that to extend the upper cutoff to 35 cps would indeed impose a serious limitation on the correlation that we could expect from the meter. We can only say that there is an honest difference of opinion as to the required band of component frequencies that are important.

Dr. Liska suggests that we are concerned with vibrations rather than sound. We have no major disagreement with this concept. We choose to work with sound, however, because it is quite easy to determine where to place the microphone, and that is by the observer's ear. If we choose to use vibration pickups, we would have to decide, first, from a

great many possible locations, just where the pickup should be placed and, second, how the pickup should be oriented, since it is sensitive along one axis only. That is not to say, however, that a suitable location and orientation for a vibration pickup cannot be found that will give correlation and satisfactory answers.

In so far as using the meter to classify tires is concerned, we say "No," particularly if it is desired to classify tires on one car and use them on other cars. This is because of the particular response characteristics of a given car such as the one represented in Fig. 3. A given set of tires may excite the 38-45-cps resonances in this car, yet the same tires which have been selected with great confidence on that car could very well excite another series of frequencies in a different car. We do not recommend, and have never proposed, using the meter to select tires. The meter reads the combined effect of the tires and the car, and will do nothing else.

Mr. Klaasen's remarks regarding the possible resonances involved in tire thump are extremely interesting, particularly the one involving the amount of inertia of the wheel on the fore-and-aft elasticity of the tire. The possibility of this resonance had not occurred to us. Regarding the lack of correlation with our tire thump meter, we think we know why. Our filter cuts off at 20 cps, and you can remember the qualms we experienced when we cut it off that high. Now we believe it makes sense, analytically at least, that to put a single bump on a tire, as represented by this rather abnormal condition, will excite the Order 1 component more strongly than the others. If Order 1 is to pass through the filter, then the lower cutoff limit of the filter will have to be way below 20 cps. As it is, Order 1 will only pass through the filter at 100 mph. If we wanted to read down to 25 mph and include Order 1, such as put in by this tire by this rather abnormal condition, the lower cutoff limit would have to be 5 cps. This would introduce another problem which cannot be easily solved: A 5-cps carrier component upon demodulation has a strong second order which is 10 cps, and this will pass through the second filter and read thump represented by a pure tone of 5 cps. We do not believe this is desirable. We believe this is the explanation, in theory at least, why you did not get correlation. Our viewpoint is that this is a rather artificial and nontypical cause of thump. Back in 1940, everyone might agree that it might have been a rather typical case where thump happened mostly because of a bad tread splice. Then you got the strong Order 1 component. Today, the tire people do not build tires that bad.

We have no comments regarding Mr. Kuhn's remarks. He has been rather modest, as we are afraid we have to be. We do not know what the answer is or what we can do to a car to improve the situation, so we look to the tire people at this stage of the game.

We agree with Mr. Wang that in the usual run of noise measurements one cannot place too much confidence in a single meter reading, whether that reading be sound pressure level, sound level, loudness level, or anything else. Indeed, it is for this reason that at our proving ground we conduct all noise comparison tests using a binaural record-playback procedure in conjunction with a sound jury.

Measuring Audible Tire Thump

The problem of the measurement of audible tire thump, however, is distinctly different from that of measuring other automotive noise disturbances (and those from other fields of endeavor) in at least two important ways: (1) Tire thump is confined to an extremely limited frequency band, 20 to 70 cps, and (2) tire thump is characterized by a beating or interfering phenomenon which is not the distinguishing characteristic of other types of noises usually measured.

At the outset, it was clear to us that the successful measurement of this disturbance could never be done according to the concepts or instrumentation adequate for these commoner types of noise. At first, we devised a measuring system which evaluated a single and simple physical quantity: the amplitude of the modulation envelope. At that point in the development, it is clear that we had the equivalent of the sound level meter, which also measures only physical quantities. (The various weighting networks available on ASA sound level meters demand a slight qualification of the foregoing remark.)

However, we were not entirely satisfied with an objective type of meter and, accordingly, we proceeded to run a series of psycho-acoustic tests, limited though they were, in order to design a meter which would give a reading in terms of subjective response, that is, one which would read closely to a rating given by a sound jury. Needless to say, a considerable portion of the total time was spent in making these psycho-acoustic tests and subsequently making correlation tests between the readings obtained on the improved thump meter and personal evaluations. The present thump meter devised for the measurement of the relatively simple disturbance called thump really has, at present, no counterpart or equivalent for obtaining the loudness, by a direct meter reading, of a complex noise of any of a variety of spectra.

Regarding Mr. Wang's comments about the loudness of thump in the presence of background noise, no attempt whatsoever was made to rate tire thump in terms of the way it will be heard in the presence of one of a myriad of possible background masking noises. This would, indeed, be a herculean task, the time and cost for which would be out of proportion to its inherent value. We have taken a much simpler approach: We rate our tire thump on a smooth sheet asphalt road (which removes road rumble), at times when the ambient wind velocity is low (which eliminates wind noise), and under coasting conditions if necessary (to remove engine and drive line noise).

Additional Comments By Vanator

DR. LISKA'S question is a pertinent one, but we have not had occasion to determine whether the various improvements are cumulative or not.

Although the subject of tire thump has been pretty well covered, I can relate some of our experiences in running tire thump measurements and correlation work.

It was suggested during the discussion that to make the tires more nonuniform might be an answer to the tire thump problem. We had an example similar to this with one car in which we were trying to measure tire thump. We actually obtained a thump measurement, but were unable to recognize, either physically or aurally, the presence of tire thump. The answer in this case was the phasing characteristics of the tires. Actually, we had four tires that were producing thump, but phasing very rapidly, and not until we had adjusted tire pressures to slow down the phasing rate were we able to correlate the meter reading with our physiological impression of tire thump. It is possible, therefore, to arrive at conditions where the phasing will occur so rapidly as to obscure the impression of tire thump, both physically and aurally.

Our attempts to reduce tire thump by introducing rubber isolation in front suspensions have not been successful. In general, such isolation has increased, rather than decreased, tire thump. In other words, softening the suspension, particularly by isolation at the frame, increases the response of the car to low frequencies, thereby increasing its sensitivity to tire thump.

In another experiment we attempted to increase drastically the amount of damping and stiffening in the floor areas, but by so doing changed the car from one with roughness at 60 mph to one with thump at 30-40 mph. The reason for the change from roughness to thump was not investigated.

Developments in Explosion- and Fire-Suppression Techniques

George Grabowski, Simmonds Aerocessories, Inc.

This paper was presented at a meeting of the SAE Metropolitan Section, New York, Dec. 14, 1954.

ANY review of the field of explosion- and fire-suppression techniques should certainly begin by acknowledging the original work done by the English, specifically by Glendinning and MacLennan at Farnborough prior to 1951. It is appropriate, also, to note here that these gentlemen are not only responsible for the original work in this field, but that they devoted considerable time and effort to making their invention known to the American aircraft industry. In 1951 they visited the United States under the sponsorship of their government and described their work in detail to our own Air Force authorities, to CAA officials, and to the principal United States aircraft manufacturers. In that year they presented a very complete paper on the subject at the annual meeting of the National Fire Protection Association. In view of their efforts in making their invention available to the United States aircraft industry, it is gratifying to note that official recognition of their pioneer work has been accorded in the form of basic patents covering explosion- and fire-suppression systems, which have been issued both in the United States and in England.

In accordance with its well-established custom, the British Government has granted to the inventors the rights to the development of this device in the aircraft and industrial fields. The inventors, in turn, have assigned these rights to the Graviner Mfg. Co., Ltd. of England, of which our company is the sole United States licensee.

DEVELOPMENT of an explosion- and fire-suppression system is described here.

The system consists of two components, a detector and a capsule, which are placed in the volume to be protected. The explosions encountered in aircraft fuel tanks can be started by either high- or low-energy ignition sources, necessitating a wide range of detection times. Therefore, three types of explosion detectors have been designed, two visual, and one pressure rate of rise. Each of these detectors has a particular advantage, making it possible to meet any requirement for a particular installation.

When ignition occurs, the detector senses the explosion, causing an electric current to flow to the capsule. This sets off an explosive charge, which supplies the force to burst the capsule and disperse the suppressing agent.

Of the many fire-extinguishing agents that have been studied, the new halogenated compounds have been found to present the most desirable characteristics. These compounds such as dibromodifluoromethane, monobromotrifluoromethane, and monobromomonochlorodifluoromethane, are outstanding for their low toxicity and corrosiveness.

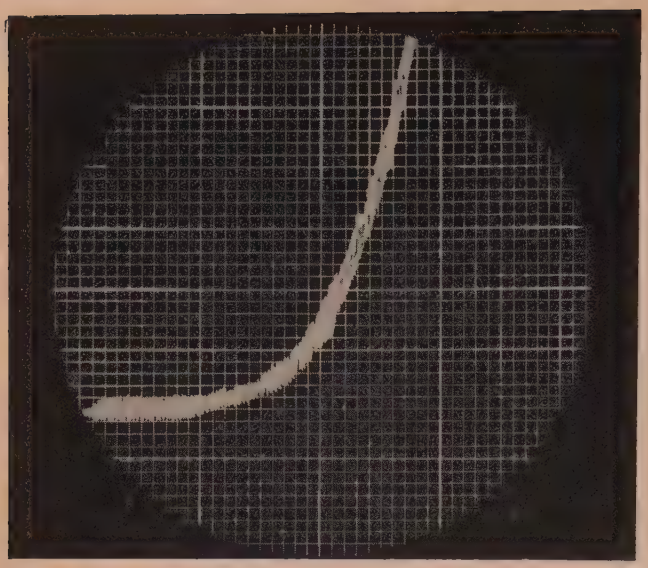

Fig. 1 – Oscillograph record – typical unprotected explosion

Systems Developed by American Companies

In the evaluation of design criteria for explosion- and fire-suppression systems, Chance Vought, Republic Aviation, Northrop, and Lockheed have all played a leading part. Working with these manufacturers, we have concentrated on an extensive study of the nature of explosions, on the characteristics of suppressant fluids, as well as on the design of system components for production purposes. Certain phases of this work have been aided by a development contract from the USAF. Our company has also completed the installation of explosion- and fire-suppression systems on three advanced types of combat aircraft. Recently, I had an opportunity to study an installation by Graviner now being completed on one of the newer British combat planes. The data which are being obtained from the flight service of these installations are adding immeasurably to our knowledge of the problems ahead. Unfortunately, however, these projects are classified and therefore cannot be discussed in this paper.

Combustion Data Not Applicable

At the start of our program an intensive survey of published data revealed that, although considerable research had been done on studying the characteristics of combustion, these data were not applicable to explosion- and fire-suppression techniques, since, prior to the work of Glendinning and MacLennan, the dimension of time was not adequately considered. As a consequence, test work was then started to study explosions of aircraft fuel mixtures by measuring the pressure-time curve in various tanks and under a number of environmental conditions.

Study of Aircraft Fuel Mixture Explosions

Each explosion was studied by recording the pressure increase with transducers and a recording oscilloscope. A typical record of an explosion is shown in Fig. 1. With these data it was possible to obtain the effect of the various factors on the characteristics of the explosion. The two main characteristics to be considered are the maximum explosive pressure and the rate of pressure rise. The maximum explosion pressure in a closed vessel depends on the composition of the mixture and the pressure and temperature in the system prior to ignition. It is not appreciably dependent on the size of the vessel or the nature or intensity of the igniting source, except in a vessel where the energy release is comparable with that of an explosion. This last statement is very important, as will be shown later.

Effect of Mixture Composition and Initial Pressure

The effect of the mixture composition and initial pressure may be seen in Fig. 2. Starting with the lean limit of flammability, the peak explosive pressure will increase to a maximum which occurs at the stoichiometric mixture and then decrease as the mixture increases into the rich range. From these curves, it can be seen that the ratio of maximum explosive pressure to initial pressure changes very slightly, being approximately 8.5 for the sea-level condition and 8.0 for the 30,000-ft condition. This ratio can be assumed constant throughout the normal altitude range for present-day aircraft. The reduction in the rich limit for the 30,000-ft range does not necessarily reflect the reduction in the limits of flammability, but does reflect the change

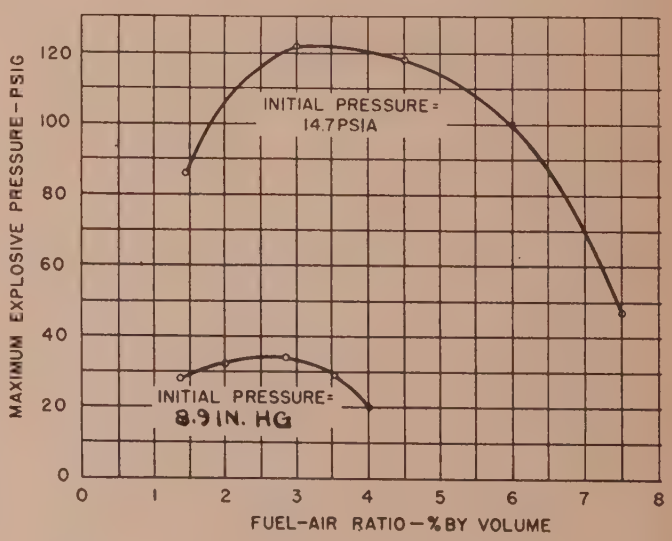

Fig. 2 – Effect of fuel-air ratio on maximum explosive pressure

in the limits of ignitability for this particular test condition.

The rate of pressure rise in a closed vessel such as an aircraft fuel cell is a function of the flame speed, vessel size, and nature of ignition source. In turn, the flame speed is dependent on the mixture strength and the temperature and pressure before ignition. The effect of the mixture strength on the flame speed is reflected in the curves shown in Fig. 3 for sea level. The maximum flame speed occurs at the stoichiometric mixture represented by 2.70% in this chart. The effect of the initial pressure can be seen in Fig. 4 which shows pressure-time curves at the 30,000-ft altitude condition. The effect is identical to that of the sea-level condition, but the curve for the stoichiometric mixture is considerably slower. Since the flame speed of a fuel-air mixture is generally considered constant for these pressures, the change in the time is directly a function of the mass of the air.

Pressure-Time Relationship Determined

Using these curves and assuming that the flame speed remains constant during the early stages of the explosion, we determined that a definite relationship exists between the pressure and the time. With this relationship, the variation of pressure rate of rise can be developed for various volumes. Fig. 5 shows the effect of the volume on the pressure-time curve of an explosion. This shows that the larger the volume, the greater the time becomes for actuation of an explosion-suppression system.

The effect of the ignition source can be shown by an example of the change in time when a number of point sources replaces a single point source. Each source will have a sphere of burnt gases and while the individual spheres do not encroach on each other, it is possible to determine the time difference to reach a given pressure. For example, if a single low-energy ignition source is used and 28 millisec is necessary to reach 1-psi increase, with 10 low-energy ignition sources, only 13 millisec would be necessary to reach a pressure of about 1 psi.

Two Classes of Explosions Found

These data on ignition effect, along with those obtained during tests performed at Republic, confirmed our belief that the problem of suppression of explosions in aircraft must be divided into two classes. One class deals with explosions ignited by low-energy sources such as electrical sparks or heated particles, and the other with those ignited by high-energy sources such as incendiary projec-

The Author

GEORGE GRABOWSKI is a safety device design engineer at Simmonds Aerocessories, Inc. Prior to his association with Republic Aviation as a research engineer and Glenn L. Martin as a stress analyst, Mr. Grabowski was graduated from Brooklyn Polytechnic Institute and the Academy of Aeronautics.

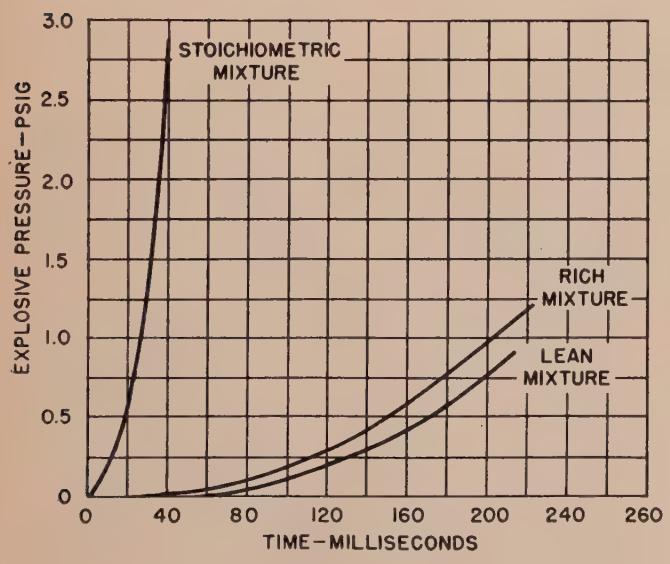

Fig. 3 – Explosion curves for jet fuel. Initial pressure = 14.7 psia

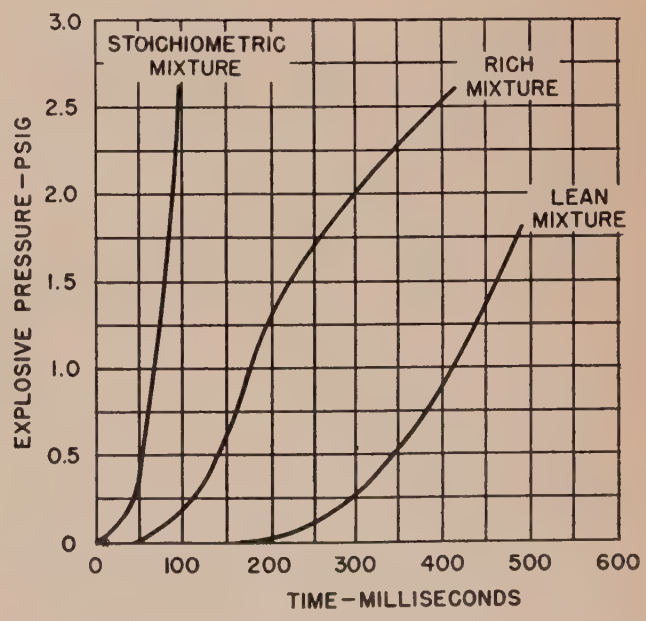

Fig. 4 – Explosion curves for jet fuel. Initial pressure = 8.9 in. of Hg

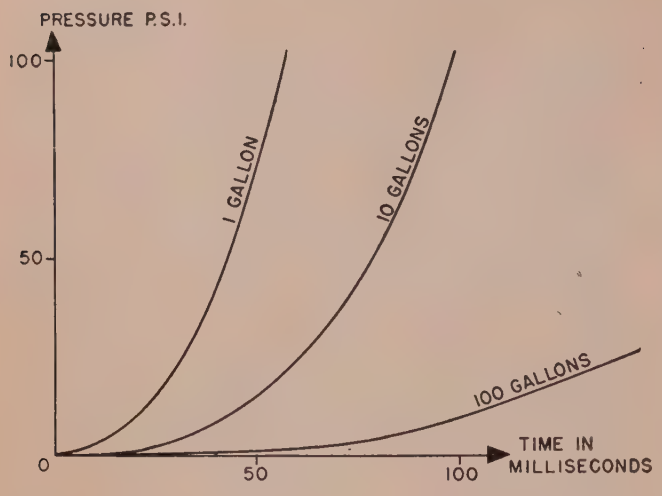

Fig. 5 – Typical pressure – time curves for vessels of various volumes

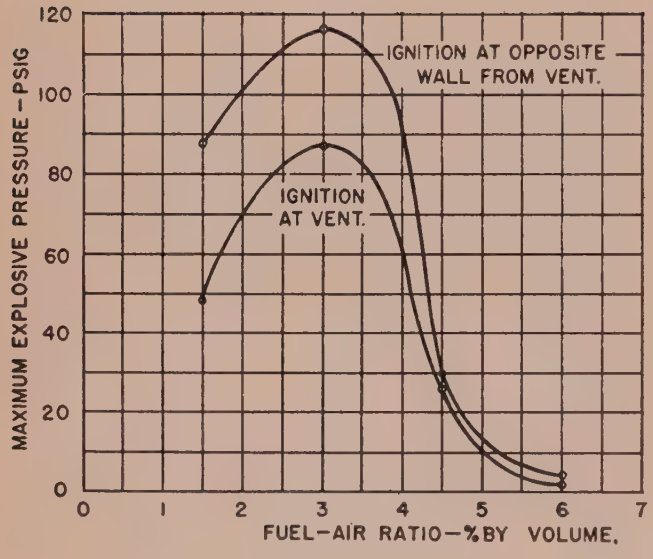

Fig. 6 – Effect of ignition location

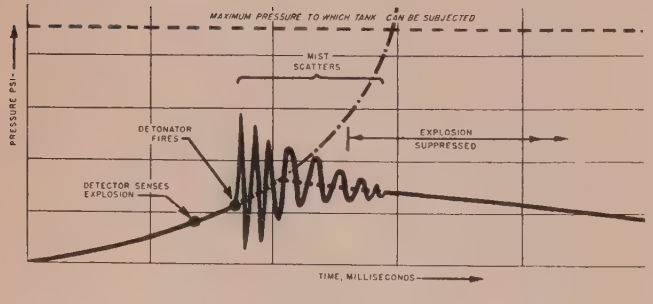

Fig. 7 – System operation

tiles. The terms high- and low-energy ignition sources are, however, relative in that the volume of the tank to be protected must be taken into consideration. An ignition source would be considered as having high energy if the energy released by the explosion is comparable to that of the ignition source. A 1000-joule ignition source, though being high compared with normal ignition sources, would still be considered a low-energy source when the explosion itself releases 100,000 joules. Thus, the classification of the energy source is a relative comparison between the ignition and explosion energy.

Effect of Vent Size

Another factor which was considered by us was the effect of the vent size on the explosion characteristics. The majority of aircraft tanks have vent systems which vary in size and length. These vents will change the characteristics of explosions, as can be seen in Fig. 6. This shows the effect of the ignition position on the peak pressure for a particular vent area. In general, vents will tend to narrow the fuel-air ratio range over which the explosion is destructive.

With all of this information available on explosions, it was then possible to consider the design aspects of the system. First let us consider the operation of the system, as shown in Fig. 7. The two components, detector and capsule, are placed in the volume to be protected, and when ignition occurs the detector senses the explosion and allows current to flow to the capsule. Further illustration of this operation is shown in Fig. 8, where the operation points of the components are marked. The time and pressure scales have been left off this graph since they will change according to all the

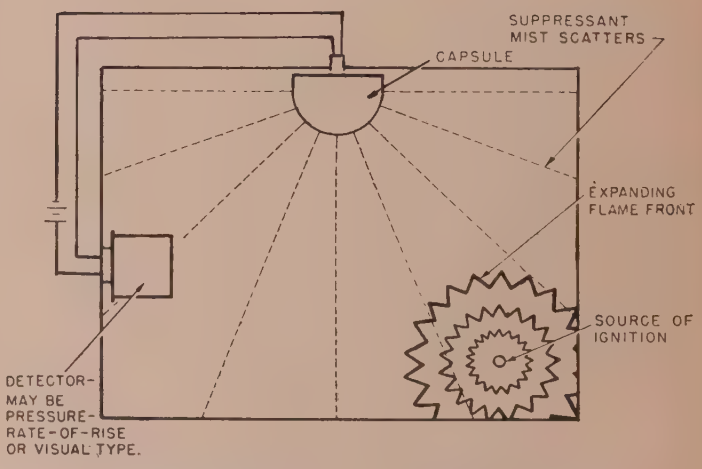

Fig. 8 – Basic elements of explosion suppression system

variables that have been mentioned previously. However, for explosions starting with high-energy ignition, the detection time necessary could be as low as 200 microsec. For explosions started by low-energy ignition, the minimum detection time would be 10-15 millisec.

These values show that the term "comparatively slow rate of pressure rise" can be a misleading phrase, since the entire system operation must take place in fractions of a second. Particular emphasis has been placed on the detector since its operation must occur at a sufficiently low pressure to allow suppression.

Wide Range of Detection Times Needed

The explosions that are encountered in aircraft fuel tanks can be started by either high- or low-energy ignition sources, necessitating a wide range of detection times, as mentioned previously. Therefore, we have felt it necessary to design three types of explosion detectors, two visual, and one pressure rate of rise. Each of these detectors has a particular advantage making it possible to meet any requirement for a particular installation.

Visual Detectors

The design of the visual detectors, one type of which is shown in Fig. 9, required considerable research to determine the optimum means of detection, for the specifications set by us for these detectors required that they be more than the usual light-sensitive device. Our specifications required that these detectors also be capable of seeing any explosion throughout the entire flammability range. We required also that the detectors not be designed to see only the ignition source, since it is possible that the source could be hidden from the view of the detector, or could be of sufficiently low energy to escape detection. This made the problem more difficult, for only 10% of the energy of an explosion is emitted, this being extended over a wide range of the spectrum. Spectral studies had to be made taking into consideration the fuel-filtering effect, in order that these detectors be capable of detection when submerged. High temperature also required considerable study, since the majority of the light-sensing devices are affected

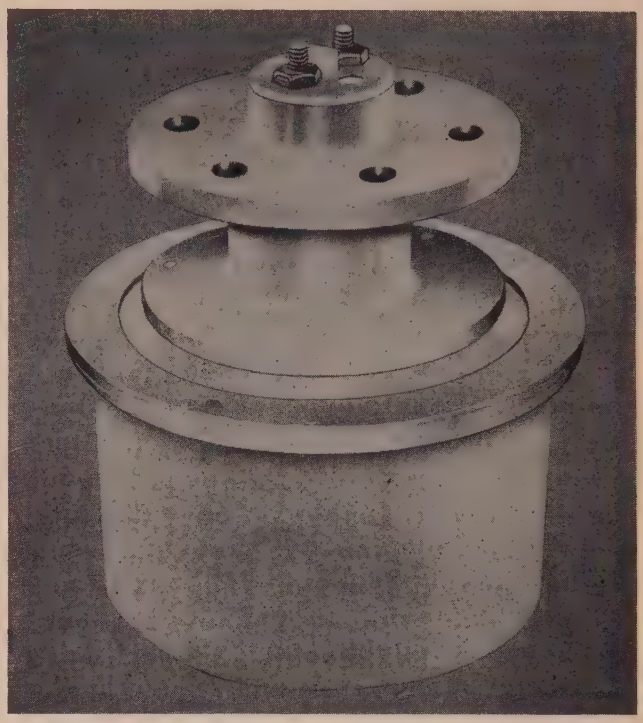

Fig. 10 – Rate of pressure rise detector

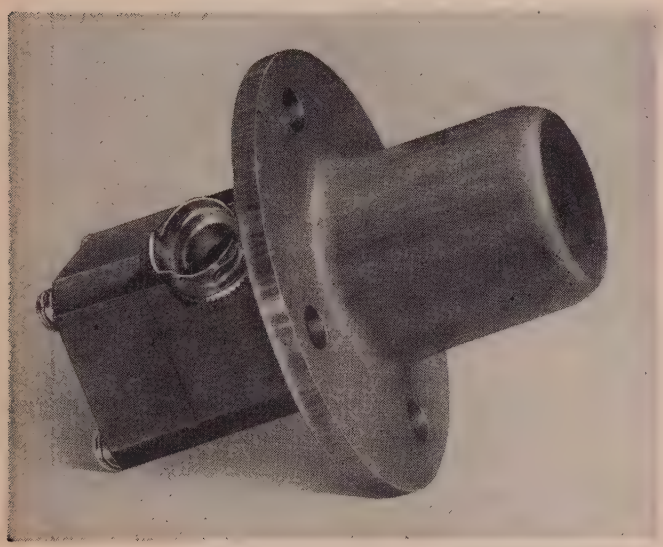

Fig. 9 – One type of visual detector

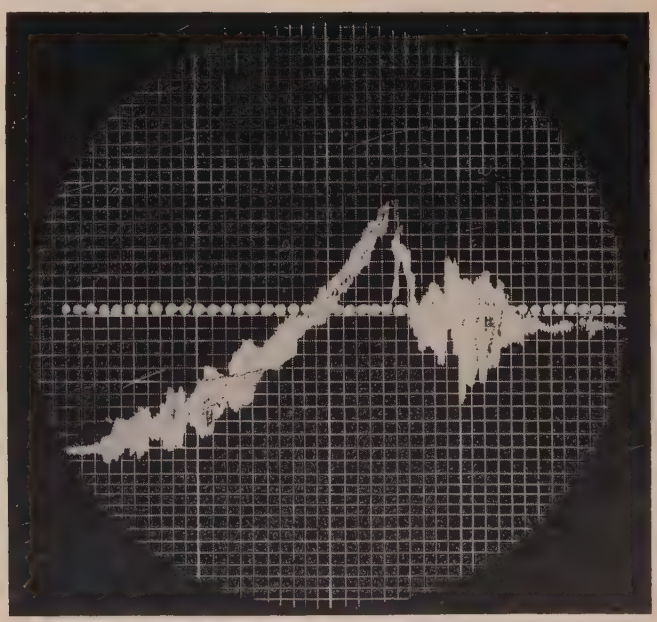

Fig. 11 – Oscillograph record – typical protected explosion

Table 1 – Characteristics of Fire-Extinguishing Agents

	Methyl Bromide	Carbon Tetra-chloride	Bromo-chloro-methane	Dibromo-difluoro-methane	Mono-bromo-trifluoro-methane
Chemical Formula	CH_3Br	CCl_4	CH_2BrCl	CBr_2F_2	$CBrF_3$
Halon No.	1001	104	1011	1202	1301
Molecular Weight	94.94	153.83	129.40	209.8	148.9
Liquid Density at 70 F, g/cc	1.73	1.595	1.93	2.28	1.567
Boiling Point at Sea Level, F	40	170	152	76.1	−76
Vapor Pressure at Room Temperature, psig	12	0	0	0	235
Vapor Pressure at 160 F, psig	110	0	3	45	550
% by Volume to Render Hexane Nonexplosive	7.05	9.7	6.35	3.55	4.9
Toxicity	Class 2	Class 3	Class 3	Class 4	Class 6
Corrosiveness (Most Inactive = 1)	4	3	5	2	1

by heat. The necessary data were obtained and furnished sufficient information for the design of these visual detectors.

Pressure Rate of Rise Detector

The pressure rate of rise detector, as shown in Fig. 10, is primarily used for low-energy explosions. This detector has been used to suppress explosions in various sizes and shapes of tanks, with results similar to the oscilloscope record shown in Fig. 11. The peak pressure in this test was approximately 2.5 psi. The oscillations after the bursting of the capsule are typical of all suppressions and are probably due either to an excitation lag in the molecules of the gas or to pressure waves set up by rapid contraction.

After the detector senses the explosion, the capsule disperses the agent. Each capsule consists of an explosive charge for supplying the bursting force and a frangible reservoir for containing the agent. These capsules must be capable of withstanding the vapor pressure of the suppressing agent and still be capable of rapid bursting action. These and all the other requirements made it necessary to conduct an extensive program for investigating all the variables that exist in the capsule design. During this program, the spray pattern of a large number of capsules was studied by means of high-speed photography. Such shapes as hemispherical, spherical, cylindrical and many others were tested. Materials such as nylon, Kel-F, phenolic, phenolic laminate, and metals were used for manufacture. A typical capsule is shown in Fig. 12. Each shape and material has a particular advantage, and for any specific installation all of these must be considered to determine the optimum type. When capsules of faster action are required, several types have been developed where the initial rate of travel of the agent is several times faster than the 300 fps characteristic of the earliest capsule designs. Where fragments are undesirable, capsules which burst but have no fragments have been developed. It is possible from all these types to select a capsule capable of meeting all of the requirements of any type of installation.

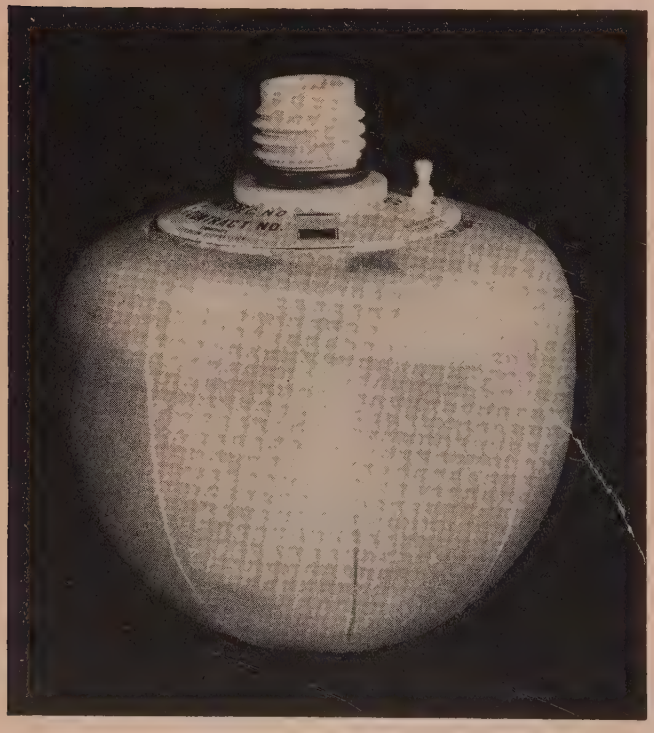

Fig. 12 – Typical capsule

Characteristics of Extinguishing Agents

As is true in all aircraft installations, weight is a primary problem. Since in an explosion or fire-suppression system 50-80% of the weight of the entire system is the liquid agent, investigations have been carried on to determine the most weight-efficient type. This has included carbon tetrachloride, methyl bromide, bromochloromethane, and the new halogenated compounds such as dibromodifluoromethane, monobromotrifluoromethane, and monobromomonochlorodifluoromethane. Of these, the latter agents present the most desirable characteristics due to their lower toxicity and corrosiveness, as shown in Table 1. All of these characteristics have been considered during this evaluation.

Using these newer agents, tests have shown that the initial criterion of 8 cc per gal of vapor space necessary for suppressing explosions has been greatly reduced. Present installations are being made using concentrations close to the theoretical value of 2 cc. It was during these tests that carbon tetrachloride was found to be ineffective at concentrations of less than 4 cc per gal and is generally no longer considered for explosion- and fire-suppression systems. Newer agent theories are being investigated which will possibly reduce further the system weight.

Index to SAE Transactions

Volume 63—1955

Page

ACCIDENTS AND ACCIDENT PREVENTION (AIRCRAFT)
Developments in Explosion- and Fire-Suppression Techniques, George Grabowski ... 803
ADDITIVES, FUEL
Practical Yardsticks for Deposit Effects, C. A. Hall, J. A. Warren, and J. D. McCullough ... 53
Some Concepts of Knock and Antiknock Action, B. M. Sturgis ... 253
ADDITIVES, OIL
Control of Low-Temperature Sludge in Passenger-Car Engines, R. L. Willis and E. C. Ballard ... 777
Designing New Performance into a Special Motor Oil, L. Raymond and J. F. Socolofsky ... 132
Influence of Lubricant and Material Variables on Cam and Tappet Surface Distress, T. W. Havely, C. A. Phalen, and D. G. Bunnell ... 204
Lifters and Lubricants, Joseph B. Bidwell and Paul Vermaire ... 211
The New Look in Lubricating Oils, J. B. Bidwell and R. K. Williams ... 349
Wear, Scuffing, and Spalling in Passenger-Car Engines, H. A. Ambrose and J. E. Taylor ... 192
AERODYNAMICS
Flight Load Measurements and Analysis, W. L. Howland and C. J. Buzzetti ... 471
Structural Design of High-Speed Propellers, F. B. Stulen ... 429
Why Do Airplanes Make Noise? Arthur A. Regier ... 275
AIRCRAFT ACCESSORIES AND EQUIPMENT
Developments in Explosion- and Fire-Suppression Techniques, George Grabowski ... 803
Reverse Thrust for Jet Transports, Joseph Sutter ... 379
AIRCRAFT DESIGN AND PERFORMANCE
Control of Propeller Noise in Turboprop Installations, Joern Schmey and Ralph M. Guerke ... 295
Effects of Operational Factors on Structural Fatigue in Fighter Aircraft, George N. Mangurian and Philip D. Brooks ... 531
Flight Load Measurements and Analysis, W. L. Howland and C. J. Buzzetti ... 471
Simulated Jet Transport Operation, R. D. Kelly and H. B. Kaster ... 36
AIRCRAFT PROPELLERS
Control of Propeller Noise in Turboprop Installations, Joern Schmey and Ralph M. Guerke ... 295
Structural Design of High-Speed Propellers, F. B. Stulen ... 429
Why Do Airplanes Make Noise? Arthur A. Regier ... 275
AIR POLLUTION
Air Pollution Foundation—What It Is and What It Does, W. L. Faith ... 586
An Inventory of Automobile Gases, Dale H. Hutchison and Francis R. Holden ... 581
Automobile Exhaust and Ozone Formation, A. J. Haagen-Smit and Margaret M. Fox ... 575
Distribution and Effects of Automotive Exhaust Gases in Los Angeles, Gordon P. Larson, John C. Chipman, and Erwin K. Kauper ... 567
Flame Photographs of Light-Load Combustion Point the Way to Reduction of Hydrocarbon in Exhaust Gas, J. T. Wentworth and W. A. Daniel ... 602
Some Effects of Engine-Fuel Variables on Exhaust-Gas Hydrocarbon Content, F. G. Rounds, P. A. Bennett, and G. J. Nebel ... 591
AIRPORTS AND AIRWAYS
Aircraft Noise Problem in Airport Vicinities, C. E. Rosendahl ... 289
AIR TRANSPORT
Aircraft Noise Problem in Airport Vicinities, C. E. Rosendahl ... 289
Application of Airborne Radar to Airline Operations, Edgar A. Post ... 227

Page

Simulated Jet Transport Operation, R. D. Kelly and H. B. Kaster ... 36
AMBROSE, H. A.
Wear, Scuffing, and Spalling in Passenger-Car Engines (Co-author J. E. Taylor) ... 192
AMES, ROBERT S.
Discussion of "Symposium—Plastics for Truck Bodies" by Hiram McCann, David S. Brown, Henry Jennings, Walter R. Herfurth, and Stanley S. Wulc 775
ANDERSON, J. O.
Some Factors Affecting the Fatigue Strength of Steel Members (Co-authors C. W. Gadd and David Martin) ... 362
ANDERSON, WILLIAM J.
Temperature Limitations of Petroleum, Synthetic, and Other Lubricants in Rolling-Contact Bearings (Co-author Zolton N. Nemeth) ... 556
ANTONSEN, A. K.
Discussion of "High Supercharging Development of a GM 16-278A 2-Stroke-Cycle Diesel Engine" by Warren G. Payne and Wolfgang S. Lang ... 690
APPS, DAVID C.
Tire Thump: Its Mechanism and Measurement (Co-author George M. Vanator) ... 787
AVIATION, MILITARY
Effects of Operational Factors on Structural Fatigue in Fighter Aircraft, George N. Mangurian and Philip D. Brooks ... 531
Flight Load Measurements and Analysis, W. L. Howland and C. J. Buzzetti ... 471
AXLES
Design, Evaluation, and Selection of Heavy-Duty Rear Axles, K. W. Gordon ... 5

BALLARD, E. C.
Control of Low-Temperature Sludge in Passenger-Car Engines (Co-author R. L. Willis) ... 777
BARRETT, ROBERT D.
Discussion of "Some Factors Affecting the Fatigue Strength of Steel Members" by C. W. Gadd, J. O. Anderson, and David Martin ... 371
BASSETT, J. V.
Discussion of "Improvement in Stopping Ability of Trucks in Use on the Highway" by F. William Petring ... 348
BATCHELOR, CLYDE S.
Discussion of "When Are Brakes 'Adequate'?" by J. G. Oetzel ... 252
BAUMGARDNER, F. M.
Tractor Test Codes—ERDL Dynamometer Truck (Co-author J. H. Meier) ... 656
BEARINGS AND BEARING MATERIALS
Temperature Limitations of Petroleum, Synthetic, and Other Lubricants in Rolling-Contact Bearings, Zolton N. Nemeth and William J. Anderson ... 556
BEDELL, D. W.
Discussion of "Fuel Properties and Jet-Engine Combustor Performance" by C. M. Kuhbach, W. F. Ritcheske, and K. H. Strauss ... 650
BENDZ, W. I.
Discussion of "ABC's of Ultrasonic Inspection" by Edward F. Weller, Jr. ... 188
BENNETT, P. A.
Some Effects of Engine-Fuel Variables on Exhaust-Gas Hydrocarbon Content (Co-authors F. G. Rounds and G. J. Nebel) ... 591
BENNETT, WARD L.
Discussion of "Improvement in Stopping Ability of Trucks in Use on the Highway" by F. William Petring ... 347
BEST, H. W.
Antiknock Requirements of Passenger Cars—1953 CRC Survey (Co-authors H. A. Bigley and R. K. Williams) ... 729

Page

BIDWELL, JOSEPH B.
Lifters and Lubricants (Co-author Paul Vermaire).. 211
The New Look in Lubricating Oils (Co-author R. K. Williams) 349
BIGLEY, H. A.
Antiknock Requirements of Passenger Cars – 1953 CRC Survey (Co-authors H. W. Best and R. K. Williams) 729
BIRMANN, RUDOLPH
Discussion of "High Supercharging Development of a GM 16-278A 2-Stroke-Cycle Diesel Engine" by Warren G. Payne and Wolfgang S. Lang..... 687
Discussion of "Napier Nomad Aircraft Diesel Engine" by Herbert Sammons and Ernest Chatterton..... 125
BOBBITT, JANE ANN
Comparison of Intermediate-Combustion Products Formed in Engine with and without Ignition (Co-authors William C. Davis, Marion L. Smith, and Earl W. Malmberg)..... 386
BODIES
A Cradle for New Power – Chassis Features of the Firebird, Robert Schilling..... 63
Across-the-Board Look at Plastics for Truck Bodies, Hiram McCann 752
Fibrous-Glass Reinforced-Plastic "Door-to-Door" Delivery Truck Bodies, Walter R. Herfurth..... 760
Plastic Bodies Can Be Repaired, Henry Jennings... 762
Plastics for Trailer Bodies, Stanley S. Wulc..... 756
Size, Structure, and Shape of European Automobiles, Laurence Pomeroy..... 159
Use of Reinforced Plastics for the Construction of Transport Tanks, David S. Brown.....
Who is the Designer – the Stylist or the Engineer? Duncan McRae and Kenneth E. Coppock..... 145
BOEGEHOLD, A. L.
Development of a New Gas Turbine Super Alloy GMR-235 (Co-authors D. K. Hanink and F. J. Webbere).. 705
BOLT, RICHARD H.
Basic Facts about Noise as Related to Aviation (Co-author Adone C. Pietrasanta)..... 265
BRAKES
A Cradle for New Power – Chassis Features of the Firebird, Robert Schilling..... 63
Coordination of Electric With Other Braking Systems, F. C. Hile..... 98
Improvement in Stopping Ability of Trucks in Use on the Highway, F. William Petring..... 334
When Are Brakes "Adequate"? J. G. Oetzel..... 242
BRODRICK, RONALD F.
Discussion of "Control of Residual Stress in Practice" by George Sachs..... 640
BROOKS, PHILIP D.
Effects of Operational Factors on Structural Fatigue in Fighter Aircraft (Co-author George N. Mangurian) 531
BROWN, DAVID S.
Use of Reinforced Plastics for Construction of Transport Tanks 754
BRYAN, H. F.
Discussion of "Lifters and Lubricants" by Joseph B. Bidwell and Paul Vermaire..... 223
BUNNELL, D. G.
Influence of Lubricant and Material Variables on Cam and Tappet Surface Distress (Co-authors T. W. Havely and C. A. Phalen)..... 204
BURCHELL, R. W.
Abrasive Wear of Piston Rings (Co-authors C. E. Watson and F. J. Hanly)..... 676
BURNSIDE, B. G.
Discussion of "Tractor-Engine Design Requirements for Best Fuel Utilization" by H. T. Mueller and R. E. Gish..... 428
BUZZETTI, C. J.
Flight Load Measurements and Analysis (Co-author W. L. Howland)..... 471

CAMS AND CAMSHAFTS
Influence of Lubricant and Material Variables on Cam and Tappet Surface Distress, T. W. Havely, C. A. Phalen, and D. G. Bunnell..... 204

Page

Lifters and Lubricants, Joseph B. Bidwell and Paul Vermaire 211
CARBURETORS AND CARBURETION
Carburetor Icing Tendencies of Some Present-Day Fuels and Engines, W. P. Dugan and H. A. Toulmin 442
CARTER, A. J.
Discussion of "Symposium – Plastics for Truck Bodies" by Hiram McCann, David S. Brown, Henry Jennings, Walter R. Herfurth, and Stanley S. Wulc 768
CASERIO, M. J.
Discussion of "Abrasive Wear of Piston Rings" by C. E. Watson, F. J. Hanly, and R. W. Burchell.... 726
CASTING
Manufacture of Blades, Buckets, and Vanes For Turbine Engines, A. T. Colwell..... 492
New Pontiac V-8 Engine, C. B. Leach and E. L. Windeler 545
CHAMBERLAIN, C. A.
Discussion of "High Supercharging Development of a GM 16-278A 2-Stroke-Cycle Diesel Engine" by Warren G. Payne and Wolfgang S. Lang..... 689
CHANDLER, J. M.
Discussion of "Distribution and Effects of Automotive Exhaust Gases in Los Angeles" by Gordon P. Larson, John C. Chipman, and Erwin K. Kauper... 618
CHATTERTON, ERNEST
Napier Nomad Aircraft Diesel Engine (Co-author Herbert Sammons) 107
CHIPMAN, JOHN C.
Distribution and Effects of Automotive Exhaust Gases in Los Angeles (Co-authors Gordon P. Larson and Erwin K. Kauper)..... 567
CLEVELAND, AL
Discussion of "Carburetor Icing Tendencies of Some Present-Day Fuels and Engines" by W. P. Dugan and H. A. Toulmin..... 451
COLD WEATHER OPERATION
Engine Cranking at Arctic Temperatures, W. E. Meyer, J. J. DeCarolis, and R. L. Stanley..... 515
COLEMAN, W. S., JR.
Discussion of "Control of Residual Stress in Practice" by George Sachs..... 640
COLLINS, HARRY A.
Discussion of "Carburetor Icing Tendencies of Some Present-Day Fuels and Engines" by W. P. Dugan and H. A. Toulmin..... 451
COLWELL, A. T.
Manufacture of Blades, Buckets, and Vanes For Turbine Engines 492
COMBUSTION
Comparison of Intermediate-Combustion Products Formed in Engine with and without Ignition, William C. Davis, Marion L. Smith, Earl W. Malmberg, and Jane Ann Bobbitt..... 386
Correlation of Engine Noises With Combustion Phenomena, Robert Meagher, R. L. Johnson, and K. G. Parthemore 481
Flame Photographs of Light-Load Combustion Point the Way to Reduction of Hydrocarbon in Exhaust Gas, J. T. Wentworth and W. A. Daniel..... 602
Fuel Properties and Jet-Engine Combustor Performance, C. M. Kuhbach, W. F. Ritcheske, and K. H. Strauss 642
COMBUSTION CHAMBERS
Fuel Properties and Jet-Engine Combustor Performance, C. M. Kuhbach, W. F. Ritcheske, and K. H. Strauss 642
COMPRESSORS, TURBINE ENGINE
Manufacture of Blades, Buckets, and Vanes For Turbine Engines, A. T. Colwell..... 492
CONSTRUCTION AND INDUSTRIAL MACHINERY
Allis-Chalmers Dynamometer Equipment for Reserve Tractive Ability Tests, T. A. Haller..... 667
ERDL Dynamometer Truck, F. M. Baumgardner and J. H. Meier..... 656
Goodyear Dynamometer Truck, R. M. MacFarland... 662
Reserve Tractive Ability and Vehicle Drag Test Codes and Comparative Demonstration of Test Equipment – Report of CIMTC Subcommittee XII – Tractor Test Codes 651

Page

The Need for a Test Code and Its Objectives, A. J. Rutherford and H. L. Rittenhouse 651
Tractor Test Codes – Discussion of Instrumentation, T. Davidson 652
COOLING, ENGINE
Effect of Surface Temperature on Wear of Diesel Engine Cylinders and Piston Rings, H. V. Nutt, E. W. Landen, and J. A. Edgar 694
New Pontiac V-8 Engine, C. B. Leach and E. L. Windeler 545
COPPOCK, KENNETH E.
Who is the Designer – the Stylist or the Engineer? (Co-author Duncan McRae) 145
CORROSION
Control of Residual Stress in Practice, George Sachs 628
CRANKSHAFTS
Some Factors Affecting the Fatigue Strength of Steel Members, C. W. Gadd, J. O. Anderson, and David Martin 362
CROCKER, B. E.
Acoustic Design and Performance of Turbojet Test Facilities (Co-author R. O. Fehr) 284
CROSTHWAIT, R. E.
Discussion of "Lifters and Lubricants" by Joseph B. Bidwell and Paul Vermaire 220
CYLINDERS
Effect of Surface Temperature on Wear of Diesel-Engine Cylinders and Piston Rings, H. V. Nutt, E. W. Landen, and J. A. Edgar 694
Method of Scavenging Analysis for 2-Stroke-Cycle Diesel Cylinders, W. H. Percival 737

DAHLUND, E. L.
Discussion of "High Supercharging Development of a GM 16-278A 2-Stroke-Cycle Diesel Engine" by Warren G. Payne and Wolfgang S. Lang 690
DANIEL, W. A.
Flame Photographs of Light-Load Combustion Point the Way to Reduction of Hydrocarbons in Exhaust Gas (Co-author J. T. Wentworth) 602
DAVIDSON, T.
Tractor Test Codes—Discussion of Instrumentation.. 652
DAVIS, WILLIAM C.
Comparison of Intermediate-Combustion Products Formed in Engine with and without Ignition (Co-authors Marion L. Smith, Earl W. Malmberg, and Jane Ann Bobbitt 386
DeCAROLIS, J. J.
Engine Cranking at Arctic Temperatures (Co-authors W. E. Meyer and R. L. Stanley) 515
DEPOSITS, ENGINE
Comparison of Intermediate-Combustion Products Formed in Engine with and without Ignition, William C. Davis, Marion L. Smith, Earl W. Malmberg, and Jane Ann Bobbitt 386
Control of Low-Temperature Sludge in Passenger-Car Engines, R. L. Willis and E. C. Ballard 777
Designing New Performance into a Special Motor Oil, L. Raymond and J. F. Socolofsky 132
Fuel Properties and Jet-Engine Combustor Performance, C. M. Kuhbach, W. F. Ritcheske, and K. H. Strauss 642
Practical Yardsticks for Deposit Effects, C. A. Hall, J. A. Warren, and J. D. McCullough 53
The New Look in Lubricating Oils, J. B. Bidwell and R. K. Williams 349
DETONATION
Comparison of Intermediate-Combustion Products Formed in Engine with and without Ignition, William C. Davis, Marion L. Smith, Earl W. Malmberg, and Jane Ann Bobbitt 386
Correlation of Engine Noises With Combustion Phenomena, Robert Meagher, R. L. Johnson, and K. G. Parthemore 481
Some Concepts of Knock and Antiknock Action, B. M. Sturgis 253
Some Early Reminiscences, Sir Harry Ricardo 620
DOLCH, G. D.
Discussion of "Development of a New Gas Turbine Super Alloy GMR-235" by D. K. Hanink, F. J. Webbere, and A. L. Boegehold 714

Page

DUGAN, W. P.
Carburetor Icing Tendencies of Some Present-Day Fuels and Engines (Co-author H. A. Toulmin) 442
du PONT, STEPHEN
Discussion of "Jet Noise" by John M. Tyler and Edward C. Perry 320
DYNAMOMETERS
Allis-Chalmers Dynamometer Equipment for Reserve Tractive Ability Tests, T. A. Haller 667
ERDL Dynamometer Truck, F. M. Baumgardner and J. H. Meier 656
Goodyear Dynamometer Truck, R. M. MacFarland... 662
Tractor Test Codes – Discussion of Instrumentation, T. Davidson 652
Tractor Test Codes – Results and Evaluation of Field Tests, P. J. Sperry, P. Spennetta, D. K. Heiple, W. C. Johnson, and B. L. Fisher 670

EASTON, A. H.
Discussion of "Improvement in Stopping Ability of Trucks in Use on the Highway" by F. William Petring 346
Discussion of "When Are Brakes 'Adequate'?" by J. G. Oetzel 252
EATON, R. H.
Wear Rates of Gears By the Radioactive Method (Co-author F. L. Schwartz) 506
EBY, J. H.
Discussion of "Tractor-Engine Design Requirements for Best Fuel Utilization" by H. T. Mueller and R. E. Gish 428
EDGAR, J. A.
Effect of Surface Temperature on Wear of Diesel-Engine Cylinders and Piston Rings (Co-authors H. V. Nutt and E. W. Landen) 694
ELECTRICAL EQUIPMENT
Coordination of Electric With Other Braking Systems, F. C. Hile 98
ELECTRONICS
Weighing Vehicles Static and in Motion By Electronic Scales, O. K. Normann 373
ENGINES, AIRCRAFT (JET AND TURBINE)
Acoustic Design and Performance of Turobjet Test Facilities, R. O. Fehr and B. E. Crocker 284
An Airplane Manufacturer's Progress With Noise Suppression Devices, Robert E. L. Fogle and Holden W. Withington 303
Basic Facts about Noise as Related to Aviation, Adone C. Pietrasanta and Richard H. Bolt 265
Development of a New Gas Turbine Super Alloy GMR-235, D. K. Hanink, F. J. Webbere, and A. L. Boegehold 705
Fuel Properties and Jet-Engine Combustor Performance, C. M. Kuhbach, W. F. Ritcheske, and K. H. Strauss 642
Jet Noise, John M. Tyler and Edward C. Perry 308
Napier Nomad Aircraft Diesel Engine, Herbert Sammons and Ernest Chatterton 107
Reverse Thrust for Jet Transports, Joseph Sutter... 379
Why Do Airplanes Make Noise? Arthur A. Regier... 275
ENGINES, AIRCRAFT (RECIPROCATING)
Napier Nomad Aircraft Diesel Engine, Herbert Sammons and Ernest Chatterton 107
ENGINES, COMPOUND
Napier Nomad Aircraft Diesel Engine, Herbert Sammons and Ernest Chatterton 107
ENGINES, DIESEL
Effect of Surface Temperature on Wear of Diesel Engine Cylinders and Piston Rings, H. V. Nutt, E. W. Landen, and J. A. Edgar 694
Engine Cranking at Arctic Temperatures, W. E. Meyer, J. J. DeCarolis, and R. L. Stanley 515
High Supercharging Development of a GM 16-278A 2-Stroke-Cycle Diesel Engine, Warren G. Payne and Wolfgang S. Lang 676
Method of Scavenging Analysis for 2-Stroke-Cycle Diesel Cylinders, W. H. Percival 737
Napier Nomad Aircraft Diesel Engine, Herbert Sammons and Ernest Chatterton 107

Page

ENGINES, GASOLINE
Engine Cranking at Arctic Temperatures, W. E. Meyer, J. J. DeCarolis, and R. L. Stanley..... 515
Some Early Reminiscences, Sir Harry Ricardo..... 620

ENGINES, GENERAL
Some Early Reminiscences, Sir Harry Ricardo..... 620

ENGINES, JET AND TURBINE (NONAIRCRAFT)
Pinwheels or Pistons? – A Progress Report on Automotive Gas Turbines, W. A. Turunen..... 72

ENGINES, PASSENGER CAR
Antiknock Requirements of Passenger Cars – 1953 CRC Survey, H. W. Best, H. A. Bigley, and R. K. Williams 729
Carburetor Icing Tendencies of Some Present-Day Fuels and Engines, W. P. Dugan and H. A. Toulmin 442
Control of Low-Temperature Sludge in Passenger-Car Engines, R. L. Willis and E. C. Ballard..... 777
Correlation of Engine Noises With Combustion Phenomena, Robert Meagher, R. L. Johnson, and K. G. Parthemore 481
Influence of Lubricant and Material Variables on Cam and Tappet Surface Distress, T. W. Havely, C. A. Phalen, and D. G. Bunnell..... 204
Lifters and Lubricants, Joseph B. Bidwell and Paul Vermaire 211
New Pontiac V-8 Engine, C. B. Leach and E. L. Windeler 545
Pinwheels or Pistons? – A Progress Report on Automotive Gas Turbines, W. A. Turunen..... 72
Some Concepts of Knock and Antiknock Action, B. M. Sturgis 253
Some Effects of Engine-Fuel Variables on Exhaust-Gas Hydrocarbon Content, F. G. Rounds, P. A. Bennett, and G. J. Nebel..... 591
The New Chevrolet V-8 Engine, R. F. Sanders..... 400
Wear, Scuffing, and Spalling in Passenger-Car Engines, H. A. Ambrose and J. E. Taylor..... 192

ENGINES, TRACTOR
Tractor-Engine Design Requirements For Best Fuel Utilization, H. T. Mueller and R. E. Gish..... 420

ENGINES, TRUCK AND BUS
Pinwheels or Pistons? – A Progress Report on Automotive Gas Turbines, W. A. Turunen..... 72

EXHAUST SYSTEMS AND EXHAUST GASES
Air Pollution Foundation – What It Is and What It Does, W. L. Faith..... 586
An Inventory of Automobile Gases, Dale H. Hutchison and Francis R. Holden..... 581
Automobile Exhaust and Ozone Formation, A. J. Haagen-Smit and Margaret M. Fox..... 575
Distribution and Effects of Automotive Exhaust Gases in Los Angeles, Gordon P. Larson, John C. Chipman, and Erwin K. Kauper..... 567
Flame Photographs of Light-Load Combustion Point the Way to Reduction of Hydrocarbon in Exhaust Gas, J. T. Wentworth and W. A. Daniel..... 602
Some Effects of Engine-Fuel Variables on Exhaust-Gas Hydrocarbon Content, F. G. Rounds, P. A. Bennett, and G. J. Nebel..... 591

FAITH, W. L.
Air Pollution Foundation – What It Is and What It Does 586

FALL, HARRY
Discussion of "Some Factors Affecting the Fatigue Strength of Steel Members" by C. W. Gadd, J. O. Anderson, and David Martin..... 370

FARM MACHINERY
Designing Adjustable-Speed V-Belt Drives for Farm Implements, William Spencer Worley..... 321
Tractor Seat Suspensions for Easy Riding, Max Haack 452

FEHR, R. O.
Acoustic Design and Performance of Turbojet Test Facilities (Co-author B. E. Crocker)..... 284

FISHER, B. L.
Tractor Test Codes – Results and Evaluation of Field Tests (Co-authors P. J. Sperry, P. Spennetta, D. K. Heiple, and W. C. Johnson)..... 670

Page

FLEET OPERATION
Weighing Vehicles Static and in Motion by Electronic Scales, O. K. Normann..... 373

FLYNN, GREGORY, JR.
Discussion of "Napier Nomad Aircraft Diesel Engine" by Herbert Sammons and Ernest Chatterton..... 127

FOGLE, ROBERT E. L.
An Airplane Manufacturer's Progress With Noise Suppression Devices (Co-author Holden W. Withington) 303

FOREIGN DESIGN AND OPERATION (AIRCRAFT)
Manufacture of Blades, Buckets, and Vanes For Turbine Engines, A. T. Colwell..... 492
Napier Nomad Aircraft Diesel Engine, Herbert Sammons and Ernest Chatterton..... 107

FOREIGN DESIGN AND OPERATION (NONAIRCRAFT)
Size, Structure, and Shape of European Automobiles, Laurence Pomeroy 159

FORGING
Manufacture of Blades, Buckets, and Vanes For Turbine Engines, A. T. Colwell..... 492

FOX, MARGARET M.
Automobile Exhaust and Ozone Formation (Co-author A. J. Haagen-Smit)..... 575

FUELS, AVIATION
Fuel Properties and Jet-Engine Combustor Performance, C. M. Kuhbach, W. F. Ritcheske, and K. H. Strauss 642

FUELS, MOTOR
Antiknock Requirements of Passenger Cars – 1953 CRC Survey, H. W. Best, H. A. Bigley, R. K. Williams 729
Carburetor Icing Tendencies of Some Present-Day Fuels and Engines, W. P. Dugan and H. A. Toulmin 442
Comparison of Intermediate-Combustion Products Formed in Engine with and without Ignition, William C. Davis, Marion L. Smith, Earl W. Malmberg, and Jane Ann Bobbitt..... 386
Practical Yardsticks for Deposit Effects, C. A. Hall, J. A. Warren, and J. D. McCullough..... 53
Some Concepts of Knock and Antiknock Action, B. M. Sturgis 253
Some Effects of Engine-Fuel Variables on Exhaust-Gas Hydrocarbon Content, F. G. Rounds, P. A. Bennett, and G. J. Nebel..... 591
Tractor-Engine Design Requirements For Best Fuel Utilization, H. T. Mueller and R. E. Gish..... 420

GADD, C. W.
Some Factors Affecting the Fatigue Strength of Steel Members (Co-authors J. O. Anderson and David Martin) 362

GEARS
Design, Evaluation, and Selection of Heavy-Duty Rear Axles, K. W. Gordon..... 5
Wear Rates of Gears By the Radioactive Method, F. L. Schwartz and R. H. Eaton..... 506

GISH, R. E.
Tractor-Engine Design Requirements for Best Fuel Utilization (Co-author H. T. Mueller)..... 420

GORDON, K. W.
Design, Evaluation, and Selection of Heavy-Duty Rear Axles 5

GORSKY, R. J.
Buick's Twin Turbine Dynaflow Transmission..... 42

GRABOWSKI, GEORGE
Developments in Explosion- and Fire-Suppression Techniques 803

GUERKE, RALPH M.
Control of Propeller Noise in Turboprop Installations (Co-author Joern Schmey)..... 295

HAACK, MAX
Tractor Seat Suspensions for Easy Riding..... 452

HAAGEN-SMIT, A. J.
Automobile Exhaust and Ozone Formation (Co-author Margaret M. Fox)..... 575

HALL, C. A.
Practical Yardsticks for Deposit Effects (Co-authors J. A. Warren and J. D. McCullough)..... 53

Page

HALLER, T. A.
Tractor Test Codes – Allis-Chalmers Dynamometer Equipment for Reserve Tractive Ability Tests.... 667
HANINK, D. K.
Development of a New Gas Turbine Super Alloy GMR-235 (Co-authors F. J. Webbere and A. L. Boegehold) 705
HANLY, F. J.
Abrasive Wear of Piston Rings (Co-authors C. E. Watson and R. W. Burchell)..... 676
HAVELY, T. W.
Influence of Lubricant and Material Variables on Cam and Tappet Surface Distress (Co-authors C. A. Phalen and D. G. Bunnell)..... 204
HEAT TREATMENT
Control of Residual Stress in Practice, George Sachs. 628
HEINEN, C. M.
Discussion of "Abrasive Wear of Piston Rings" by C. E. Watson, F. J. Hanly, and R. W. Burchell.... 726
HEIPLE, D. K.
Tractor Test Codes – Results and Evaluation of Field Tests (Co-authors P. J. Sperry, P. Spennetta, W. C. Johnson, and B. L. Fisher)..... 670
HERFURTH, WALTER R.
Fibrous-Glass Reinforced-Plastic "Door-to-Door" Delivery Truck Bodies..... 760
HILE, F. C.
Coordination of Electric With Other Braking Systems 98
HOLDEN, FRANCIS R.
An Inventory of Automobile Gases (Co-author Dale H. Hutchison) 581
HOWLAND, W. L.
Flight Load Measurements and Analysis (Co-author C. J. Buzzetti)..... 471
HUTCHISON, DALE H.
An Inventory of Automobile Gases (Co-author Francis R. Holden)..... 581

INSTRUMENTS
ABC's of Ultrasonic Inspection, Edward F. Weller, Jr. 176
Flight Load Measurements and Analysis, W. L. Howland and C. J. Buzzetti..... 471
Practical Yardsticks for Deposit Effects, C. A. Hall, J. A. Warren, and J. D. McCullough..... 53
Weighing Vehicles Static and in Motion by Electronic Scales, O. K. Normann..... 373
IRON AND STEEL
Control of Residual Stress in Practice, George Sachs 628
Manufacture of Blades, Buckets, and Vanes for Turbine Engines, A. T. Colwell..... 492
Some Factors Affecting the Fatigue Strength of Steel Members, C. W. Gadd, J. O. Anderson, and David Martin 362

JACKMAN, C. W.
Discussion of "When Are Brakes 'Adequate'?" by J. G. Oetzel..... 251
JAMES, W. S.
Discussion of "Lifters and Lubricants" by Joseph B. Bidwell and Paul Vermaire..... 222
JANEWAY, R. N.
Discussion of "Tractor Seat Suspensions for Easy Riding" by Max Haack..... 470
JENNINGS, HENRY
Plastic Bodies Can Be Repaired..... 762
JOHNSON, R. L.
Correlation of Engine Noises with Combustion Phenomena (Co-authors Robert Meagher and K. G. Parthemore) 481
JOHNSON, W. C.
Tractor Test Codes – Results and Evaluation of Field Tests (Co-authors P. J. Sperry, P. Spennetta, D. K. Heiple, and B. L. Fisher)..... 670

KASTER, H. B.
Simulated Jet Transport Operation (Co-author R. D. Kelly) 36
KAUPER, ERWIN K.
Distribution and Effects of Automotive Exhaust Gases in Los Angeles (Co-authors Gordon P. Larson and John C. Chipman)..... 567

Page

KELLY, R. D.
Simulated Jet Transport Operation (Co-author H. B. Kaster) 36
KENNEMER, ROBERT E.
Discussion of "Abrasive Wear of Piston Rings" by C. E. Watson, F. J. Hanly, and R. W. Burchell..... 728
KIBBEE, LEWIS C.
Discussion of "Improvement in Stopping Ability of Trucks in Use on the Highway" by F. William Petring 348
KLAASEN, GERALD
Discussion of "Tire Thump: Its Mechanism and Measurement" by David C. Apps and George M. Vanator 799
KOLK, F. W.
Discussion of "Napier Nomad Aircraft Diesel Engine" by Herbert Sammons and Ernest Chatterton..... 130
KUHBACH, C. M.
Fuel Properties and Jet-Engine Combustor Performance (Co-authors W. F. Ritcheske and K. H. Strauss) 642
KUHN, P. H.
Discussion of "Tire Thump: Its Mechanism and Measurement" by David C. Apps and George M. Vanator 800
KUNC, J. F., JR.
Discussion of "Carburetor Icing Tendencies of Some Present-Day Fuels and Engines" by W. P. Dugan and H. A. Toulmin..... 450

LaBELLE, J. E.
Discussion of "Some Factors Affecting the Fatigue Strength of Steel Members" by C. W. Gadd, J. O. Anderson, and David Martin..... 371
LANDEN, E. W.
Effect of Surface Temperature on Wear of Diesel-Engine Cylinders and Piston Rings (Co-authors H. V. Nutt and J. A. Edgar)..... 694
LANG, WOLFGANG S.
High Supercharging Development of a GM 16-278A 2-Stroke-Cycle Diesel Engine (Co-author Warren G. Payne) 676
LARSON, GORDON P.
Distribution and Effects of Automotive Exhaust Gases in Los Angeles (Co-authors John C. Chipman and Erwin K. Kauper)..... 567
LEACH, C. B.
New Pontiac V-8 Engine (Co-author E. L. Windeler) 545
LICHTY, L. C.
Discussion of "Napier Nomad Aircraft Diesel Engine" by Herbert Sammons and Ernest Chatterton 130
LISKA, JOHN W.
Discussion of "Tire Thump: Its Mechanism and Measurement" by David C. Apps and George M. Vanator 795
LUBRICANTS AND LUBRICATION (AIRCRAFT)
Temperature Limitations of Petroleum, Synthetic, and Other Lubricants in Rolling-Contact Bearings, Zolton N. Nemeth and William J. Anderson..... 556
LUBRICANTS AND LUBRICATION (NONAIRCRAFT)
Abrasive Wear of Piston Rings, C. E. Watson, F. J. Hanly, and R. W. Burchell..... 676
Control of Low-Temperature Sludge in Passenger-Car Engines, R. L. Willis and E. C. Ballard..... 777
Designing New Performance into a Special Motor Oil, L. Raymond and J. F. Socolofsky..... 132
Effect of Surface Temperature on Wear of Diesel-Engine Cylinders and Piston Rings, H. V. Nutt, E. W. Landen, and J. A. Edgar..... 694
Engine Cranking at Arctic Temperatures, W. E. Meyer, J. J. DeCarolis, and R. L. Stanley..... 515
Influence of Lubricant and Material Variables on Cam and Tappet Surface Distress, T. W. Havely, C. A. Phalen, and D. G. Bunnell..... 204
Lifters and Lubricants, Joseph B. Bidwell and Paul Vermaire 211
Practical Yardsticks for Deposit Effects, C. A. Hall, J. A. Warren, and J. D. McCullough..... 53
The New Look in Lubricating Oils, J. B. Bidwell and R. K. Williams..... 349

Page

Wear Rates of Gears by the Radioactive Method, F. L. Schwartz and R. H. Eaton 506
Wear, Scuffing, and Spalling in Passenger-Car Engines, H. A. Ambrose and J. E. Taylor 192
LUNDQUIST, W. G.
Discussion of "Napier Nomad Aircraft Diesel Engine" by Herbert Sammons and Ernest Chatterton 129

MacFARLAND, R. M.
Tractor Test Codes – Goodyear Dynamometer Truck 662
MACHINING
Control of Residual Stress in Practice, George Sachs 628
Manufacture of Blades, Buckets, and Vanes for Turbine Engines, A. T. Colwell 492
MALMBERG, EARL W.
Comparison of Intermediate-Combustion Products Formed in Engine with and without Ignition (Co-authors William C. Davis, Marion L. Smith, and Jane Ann Bobbitt) 386
MANGURIAN, GEORGE N.
Effects of Operational Factors on Structural Fatigue in Fighter Aircraft (Co-author Philip D. Brooks) .. 531
MARTIN, DAVID
Some Factors Affecting the Fatigue Strength of Steel Members (Co-authors C. W. Gadd and J. O. Anderson) 362
MARTIN, E. A.
Discussion of "Lifters and Lubricants" by Joseph B. Bidwell and Paul Vermaire 220
McCANN, HIRAM
Across-the-Board Look at Plastics for Truck Bodies 752
McCRORY, R. J.
Discussion of "Method of Scavenging Analysis for 2-Stroke-Cycle Diesel Cylinders" by W. H. Percival 750
McCULLOUGH, J. D.
Practical Yardsticks for Deposit Effects (Co-authors C. A. Hall and J. A. Warren) 53
McLEAN, D. H.
Discussion of "Temperature Limitations of Petroleum, Synthetic, and Other Lubricants in Rolling-Contact Bearings" by Zolton N. Nemeth and William J. Anderson 566
McRAE, DUNCAN
Who Is the Designer – the Stylist or the Engineer? (Co-author Kenneth E. Coppock) 145
MEAGHER, ROBERT
Correlation of Engine Noises with Combustion Phenomena (Co-authors R. L. Johnson and K. G. Parthemore) 481
MEIER, J. H.
Tractor Test Codes – ERDL Dynamometer Truck (Co-author F. M. Baumgardner) 656
METALS
Development of a New Gas Turbine Super Alloy GMR-235, D. K. Hanink, F. J. Webbere, and A. L. Boegehold 705
MEYER, W. E.
Engine Cranking at Arctic Temperatures (Co-authors J. J. DeCarolis and R. L. Stanley) 515
MIASKIEWICZ, R. F.
Discussion of "High Supercharging Development of a GM 16-278A 2-Stroke-Cycle Diesel Engine" by Warren G. Payne and Wolfgang S. Lang 689
MILLER, C. D.
Discussion of "Tire Thump: Its Mechanism and Measurement" by David C. Apps and George M. Vanator 792
MILLER, M. M.
Discussion of "Jet Noise" by John M. Tyler and Edward C. Perry 319
MILLER, R. J.
Discussion of "Some Factors Affecting the Fatigue Strength of Steel Members" by C. W. Gadd, J. O. Anderson, and David Martin 370
MILLER, SIDNEY E.
Discussion of "Distribution and Effects of Automotive Exhaust Gases in Los Angeles" by Gordon P. Larson, John C. Chipman, and Erwin K. Kauper ... 618
MOCK, F. C.
Discussion of "Distribution and Effects of Automotive Exhaust Gases in Los Angeles" by Gordon P. Larson, John C. Chipman, and Erwin K. Kauper ... 618

Page

MORGAN, NORMAND E.
Discussion of "Designing Adjustable-Speed V-Belt Drives for Farm Implements" by William Spencer Worley 330
MOXEY, J. G.
Discussion of "Control of Low-Temperature Sludge in Passenger-Car Engines" by R. L. Willis and E. C. Ballard 785
MUELLER, H. T.
Tractor-Engine Design Requirements for Best Fuel Utilization (Co-author R. E. Gish) 420
MYERS, P. S.
Discussion of "Comparison of Intermediate-Combustion Products Formed in Engine with and without Ignition" by William C. Davis, Marion L. Smith, Earl W. Malmberg, and Jane Ann Bobbitt 395

NEBEL, G. J.
Some Effects of Engine-Fuel Variables on Exhaust-Gas Hydrocarbon Content (Co-authors F. G. Rounds and P. A. Bennett) 591
NEMETH, ZOLTON N.
Temperature Limitations of Petroleum, Synthetic, and Other Lubricants in Rolling-Contact Bearings (Co-author William J. Anderson) 556
NICKEL AND ALLOYS
Development of a New Gas Turbine Super Alloy GMR-235, D. K. Hanink, F. J. Webbere, and A. L. Boegehold 705
NOISE
Acoustic Design and Performance of Turbojet Test Facilities, R. O. Fehr and B. E. Crocker 284
Aircraft Noise Problem in Airport Vicinities, C. E. Rosendahl 289
An Airplane Manufacturer's Progress with Noise Suppression Devices, Robert E. L. Fogle and Holden W. Withington 303
Basic Facts About Noise as Related to Aviation, Adone C. Pietrasanta and Richard H. Bolt 265
Control of Propeller Noise in Turboprop Installations, Joern Schmey and Ralph M. Guerke 295
Jet Noise, John M. Tyler and Edward C. Perry 308
Why Do Airplanes Make Noise? Arthur A. Regier ... 275
NORMANN, O. K.
Weighing Vehicles Static and in Motion by Electronic Scales 373
NUTT, H. V.
Effect of Surface Temperature on Wear of Diesel-Engine Cylinders and Piston Rings (Co-authors E. W. Landen and J. A. Edgar) 694

OETZEL, J. G.
When Are Brakes "Adequate"? 242
OLLEY, MAURICE
Discussion of "Size, Structure, and Shape of European Automobiles" by Laurence Pomeroy 174

PAHNKE, A. J.
Discussion of "Comparison of Intermediate-Combustion Products Formed in Engine with and without Ignition" by William C. Davis, Marion L. Smith, Earl W. Malmberg, and Jane Ann Bobbitt 398
PARTHEMORE, K. G.
Correlation of Engine Noises with Combustion Phenomena (Co-authors Robert Meagher and R. L. Johnson) 481
PASSENGER CAR DESIGN AND PERFORMANCE
A Cradle for New Power – Chassis Features of the Firebird, Robert Schilling 63
Size, Structure, and Shape of European Automobiles, Laurence Pomeroy 159
Who Is the Designer – the Stylist or the Engineer? Duncan McRae and Kenneth E. Coppock 145
PAYNE, WARREN G.
Discussion of "Method of Scavenging Analysis for 2-Stroke-Cycle Diesel Cylinders" by W. H. Percival 749
High Supercharging Development of a GM 16-278A 2-Stroke-Cycle Diesel Engine (Co-author Wolfgang S. Lang) 676
PERCIVAL, W. H.
Method of Scavenging Analysis for 2-Stroke-Cycle Diesel Cylinders 737

Page

PERRY, EDWARD C.
Jet Noise (Co-author John M. Tyler) 308
PETRING, F. WILLIAM
Improvement in Stopping Ability of Trucks in Use on the Highway 334
PHALEN, C. A.
Influence of Lubricant and Material Variables on Cam and Tappet Surface Distress (Co-authors T. W. Havely and D. G. Bunnell) 204
PIETRASANTA, ADONE C.
Basic Facts About Noise as Related to Aviation (Co-author Richard H. Bolt) 265
PISTONS AND RINGS
Abrasive Wear of Piston Rings, C. E. Watson, F. J. Hanly, and R. W. Burchell 676
Effect of Surface Temperature on Wear of Diesel-Engine Cylinders and Piston Rings, H. V. Nutt, E. W. Landen, and J. A. Edgar 694
Lifters and Lubricants, Joseph B. Bidwell and Paul Vermaire 211
Wear, Scuffing, and Spalling in Passenger-Car Engines, H. A. Ambrose and J. E. Taylor 192
PLASTICS
Across-the-Board Look at Plastics for Truck Bodies, Hiram McCann 752
Fibrous-Glass Reinforced-Plastic "Door-to-Door" Delivery Truck Bodies, Walter R. Herfurth 760
Manufacture of Blades, Buckets, and Vanes for Turbine Engines, A. T. Colwell 492
Plastic Bodies Can Be Repaired, Henry Jennings ... 762
Plastics for Trailer Bodies, Stanley S. Wulc 756
Use of Reinforced Plastics for the Construction of Transport Tanks, David S. Brown 754
POMEROY, LAURENCE
Size, Structure, and Shape of European Automobiles 159
POST, EDGAR A.
Application of Airborne Radar to Airline Operations 227
POTTER, R. I.
Discussion of "Control of Low-Temperature Sludge in Passenger-Car Engines" by R. L. Willis and E. C. Ballard 785
PREIGNITION
Correlation of Engine Noises with Combustion Phenomena, Robert Meagher, R. L. Johnson, and K. G. Parthemore 481
Some Early Reminiscences, Sir Harry Ricardo 620
PREMO, E. J.
Discussion of "Symposium – Plastics for Truck Bodies" by Hiram McCann, David S. Brown, Henry Jennings, Walter R. Herfurth, and Stanley S. Wulc 768
PRODUCTION (AIRCRAFT)
ABC's of Ultrasonic Inspection, Edward F. Weller, Jr. 176
Control of Residual Stress in Practice, George Sachs 628
Development of a New Gas Turbine Super Alloy GMR-235, D. K. Hanink, F. J. Webbere, and A. L. Boegehold 705
Manufacture of Blades, Buckets, and Vanes for Turbine Engines, A. T. Colwell 492
PRODUCTION (NONAIRCRAFT)
Control of Residual Stress in Practice, George Sachs 628
New Pontiac V-8 Engine, C. B. Leach and E. L. Windeler 545
The New Chevrolet V-8 Engine, R. F. Sanders 400

RADAR
Application of Airborne Radar to Airline Operations, Edgar A Post 227
RADIOACTIVITY
Abrasive Wear of Piston Rings, C. E. Watson, F. J. Hanly, and R. W. Burchell 676
Wear Rates of Gears by the Radioactive Method, F. L. Schwartz and R. H. Eaton 506
RAVIOLO, V. G.
Discussion of "Lifters and Lubricants" by Joseph B. Bidwell and Paul Vermaire 223
RAYMOND, L.
Designing New Performance into a Special Motor Oil (Co-author J. F. Socolofsky) 132
REGIER, ARTHUR A.
Why Do Airplanes Make Noise? 275

Page

RICARDO, SIR HARRY
Some Early Reminiscences 620
RICHARDSON, E. A.
Discussion of "Some Concepts of Knock and Anti-knock Action" by B. M. Sturgis 264
RICHARDSON, G. A.
Discussion of "Some Concepts of Knock and Anti-knock Action" by B. M. Sturgis 264
RITCHESKE, W. F.
Fuel Properties and Jet-Engine Combustor Performance (Co-authors C. M. Kuhbach and K. H. Strauss) 642
RITTENHOUSE, H. L.
Tractor Test Codes – The Need for a Test Code and Its Objectives (Co-author A. J. Rutherford) 651
ROGERS, ROBERT A.
Discussion of "Structural Design of High-Speed Propellers" by F. B. Stulen 441
ROSENDAHL, C. E.
Aircraft Noise Problem in Airport Vicinities 289
ROSS, A.
Discussion of "Comparison of Intermediate-Combustion Products Formed in Engine with and without Ignition" by William C. Davis, Marion L. Smith, Earl W. Malmberg, and Jane Ann Bobbitt 397
ROUNDS, F. G.
Some Effects of Engine-Fuel Variables on Exhaust-Gas Hydrocarbon Content (Co-authors P. A. Bennett and G. J. Nebel) 591
RUTHERFORD, A. J.
Tractor Test Codes – The Need for a Test Code and Its Objectives (Co-author H. L. Rittenhouse) 651

SACHS, GEORGE
Control of Residual Stress in Practice 628
SAMMONS, HERBERT
Napier Nomad Aircraft Diesel Engine (Co-author Ernest Chatterton) 107
SANBORN, D. S.
Discussion of "Method of Scavenging Analysis for 2-Stroke-Cycle Diesel Cylinders" by W. H. Percival 750
SANDERS, R. F.
The New Chevrolet V-8 Engine 400
SCHALL, M. M.
Progress of Torque Converters (Co-author E. W. Zingsheim) 84
SCHERGER, T. A.
Discussion of "Lifters and Lubricants" by Joseph B. Bidwell and Paul Vermaire 223
SCHILLING, ROBERT
A Cradle for New Power – Chassis Features of the Firebird 63
SCHMEY, JOERN
Control of Propeller Noise in Turboprop Installations (Co-author Ralph M. Guerke) 295
SCHULTZ, WOLDEMAR
Discussion of "Symposium – Plastic for Truck Bodies" by Hiram McCann, David S. Brown, Henry Jennings, Walter R. Herfurth, and Stanley S. Wulc ... 766
SCHWARTZ, F. L.
Wear Rates of Gears by the Radioactive Method (Co-author R. H. Eaton) 506
SCHWEITZER, P. H.
Discussion of "Method of Scavenging Analysis for 2-Stroke-Cycle Diesel Cylinders" by W. H. Percival 748
SCHWEITZER, T. J.
Discussion of "Comparison of Intermediate-Combustion Products Formed in Engine with and without Ignition" by William C. Davis, Marion L. Smith, Earl W. Malmberg, and Jane Ann Bobbitt 395
SERVI, I. S.
Discussion of "Development of a New Gas Turbine Super Alloy GMR-235" by D. K. Hanink, F. J. Webbere, and A. L. Boegehold 715
SHIPLEY, E. E.
Discussion of "Wear Rates of Gears by the Radioactive Method" by F. L. Schwartz and R. H. Eaton 514
SMITH, MARION L.
Comparison of Intermediate-Combustion Products Formed in Engine with and without Ignition (Co-authors William C. Davis, Earl W. Malmberg, and Jane Ann Bobbitt) 386

Page

SOCOLOFSKY, J. F.
Designing New Performance into a Special Motor Oil (Co-author L. Raymond) 132
Discussion of "Lifters and Lubricants" by Joseph B. Bidwell and Paul Vermaire 220
SPENNETTA, P.
Tractor Test Codes – Results and Evaluation of Field Tests (Co-authors P. J. Sperry, D. K. Heiple, W. C. Johnson, and B. L. Fisher) 670
SPERRY, P. J.
Tractor Test Codes – Results and Evaluation of Field Tests (Co-authors P. Spennetta, D. K. Heiple, W. C. Johnson, and B. L. Fisher) 670
SPRINGS AND SUSPENSIONS
A Cradle for New Power – Chassis Features of the Firebird, Robert Schilling 63
Tractor Seat Suspensions for Easy Riding, Max Haack 452
STANLEY, R. L.
Engine Cranking at Arctic Temperatures (Co-authors W. E. Meyer and J. J. DeCarolis) 515
STRAUSS, K. H.
Fuel Properties and Jet-Engine Combustor Performance (Co-authors C. M. Kuhbach and W. F. Ritcheske) 642
STRESSES
Control of Residual Stress in Practice, George Sachs 628
Flight Load Measurements and Analysis, W. L. Howland and C. J. Buzzetti 471
Some Factors Affecting the Fatigue Strength of Steel Members, C. W. Gadd, J. O. Anderson, and David Martin 362
STULEN, F. B.
Structural Design of High-Speed Propellers 429
STURGIS, B. M.
Some Concepts of Knock and Antiknock Action 253
SUPERCHARGING
High Supercharging Development of a GM 16-278A 2-Stroke-Cycle Diesel Engine, Warren G. Payne and Wolfgang S. Lang 676
SUTTER, JOSEPH
Reverse Thrust for Jet Transports 379

TAYLOR, C. F.
Discussion of "High Supercharging Development of a GM 16-278A 2-Stroke-Cycle Diesel Engine" by Warren G. Payne and Wolfgang S. Lang 690
Discussion of "Method of Scavenging Analysis for 2-Stroke-Cycle Diesel Cylinders" by W. H. Percival 747
TAYLOR, J. E.
Wear, Scuffing, and Spalling in Passenger-Car Engines (Co-author H. A. Ambrose) 192
TILDEN, S. G.
Discussion of "Improvement in Stopping Ability of Trucks in Use on the Highway" by F. William Petring 346
TIRES AND RIMS
Tire Thump: Its Mechanism and Measurement, David C. Apps and George M. Vanator 787
Tractor Seat Suspensions for Easy Riding, Max Haack 452
TOULMIN, H. A.
Carburetor Icing Tendencies of Some Present-Day Fuels and Engines (Co-author W. P. Dugan) 442
TOURRET, R.
Discussion of "Wear Rates of Gears by the Radioactive Method" by F. L. Schwartz and R. H. Eaton 513
TRANSMISSIONS, AUTOMATIC
Buick's Twin Turbine Dynaflow Transmission, R. J. Gorsky 42
Progress of Torque Converters, E. W. Zingsheim and M. M. Schall 84
TRUCK DESIGN AND PERFORMANCE
Improvement in Stopping Ability of Trucks in Use on the Highway, F. William Petring 334
TRUCK TRACTORS AND TRAILERS
Coordination of Electric with Other Braking Systems, F. C. Hile 98
Improvement in Stopping Ability of Trucks in Use on the Highway, F. William Petring 334

Page

TURUNEN, W. A.
Pinwheels or Pistons? – A Progress Report on Automotive Gas Turbines 72
TYLER, JOHN M.
Jet Noise (Co-author Edward C. Perry) 308

UYEHARA, O. A.
Discussion of "Comparison of Intermediate-Combustion Products Formed in Engine with and without Ignition" by William C. Davis, Marion L. Smith, Earl W. Malmberg, and Jane Ann Bobbitt 395

VALVES AND GEAR
Influence of Lubricant and Material Variables on Cam and Tappet Surface Distress, T. W. Havely, C. A. Phalen, and D. G. Bunnell 204
Lifters and Lubricants, Joseph B. Bidwell and Paul Vermaire 211
Wear, Scuffing, and Spalling in Passenger-Car Engines, H. A. Ambrose and J. E. Taylor 192
VANATOR, GEORGE M.
Tire Thump: Its Mechanism and Measurement (Co-author David C. Apps) 787
VERMAIRE, PAUL
Lifters and Lubricants (Co-author Joseph B. Bidwell) 211
VIBRATIONS
Structural Design of High-Speed Propellers, F. B. Stulen 429
Tractor Seat Suspensions for Easy Riding, Max Haack 452

WANG, PAUL
Discussion of "Tire Thump: Its Mechanism and Measurement" by David C. Apps and George M. Vanator 801
WARE, MARSDEN
Discussion of "Napier Nomad Aircraft Diesel Engine" by Herbert Sammons and Ernest Chatterton 129
WARREN, J. A.
Practical Yardsticks for Deposit Effects (Co-authors C. A. Hall and J. D. McCullough) 53
WATSON, C. E.
Abrasive Wear of Piston Rings (Co-authors F. J. Hanly and R. W. Burchell) 676
WEBBERE, F. J.
Development of a New Gas Turbine Super Alloy GMR-235 (Co-authors D. K. Hanink and A. L. Boegehold) 705
WELLER, EDWARD F., JR.
ABC's of Ultrasonic Inspection 176
WENTWORTH, J. T.
Flame Photographs of Light-Load Combustion Point the Way to Reduction of Hydrocarbons in Exhaust Gas (Co-author W. A. Daniel) 602
WILLIAMS, R. K.
Antiknock Requirements of Passenger Cars – 1953 CRC Survey (Co-authors H. W. Best and H. A. Bigley) 729
The New Look in Lubricating Oils (Co-author J. B. Bidwell) 349
WILLIS, R. L.
Control of Low-Temperature Sludge in Passenger-Car Engines (Co-author E. C. Ballard) 777
WINDELER, E. L.
New Pontiac V-8 Engine (Co-author C. B. Leach) 545
WITHINGTON, HOLDEN W.
An Airplane Manufacturer's Progress with Noise Suppression Devices (Co-author Robert E. L. Fogle) 303
WORLEY, WILLIAM SPENCER
Designing Adjustable-Speed V-Belt Drives for Farm Implements 321
WULC, STANLEY S.
Plastics for Trailer Bodies 756

YOWELL, H. L.
Discussion of "Lifters and Lubricants" by Joseph B. Bidwell and Paul Vermaire 221

ZINGSHEIM, E. W.
Progress of Torque Converters (Co-author M. M. Schall) 84

DATE DUE

GAYLORD			PRINTED IN U.S.A.